Cule - H62925-11-P 0244438

AJR

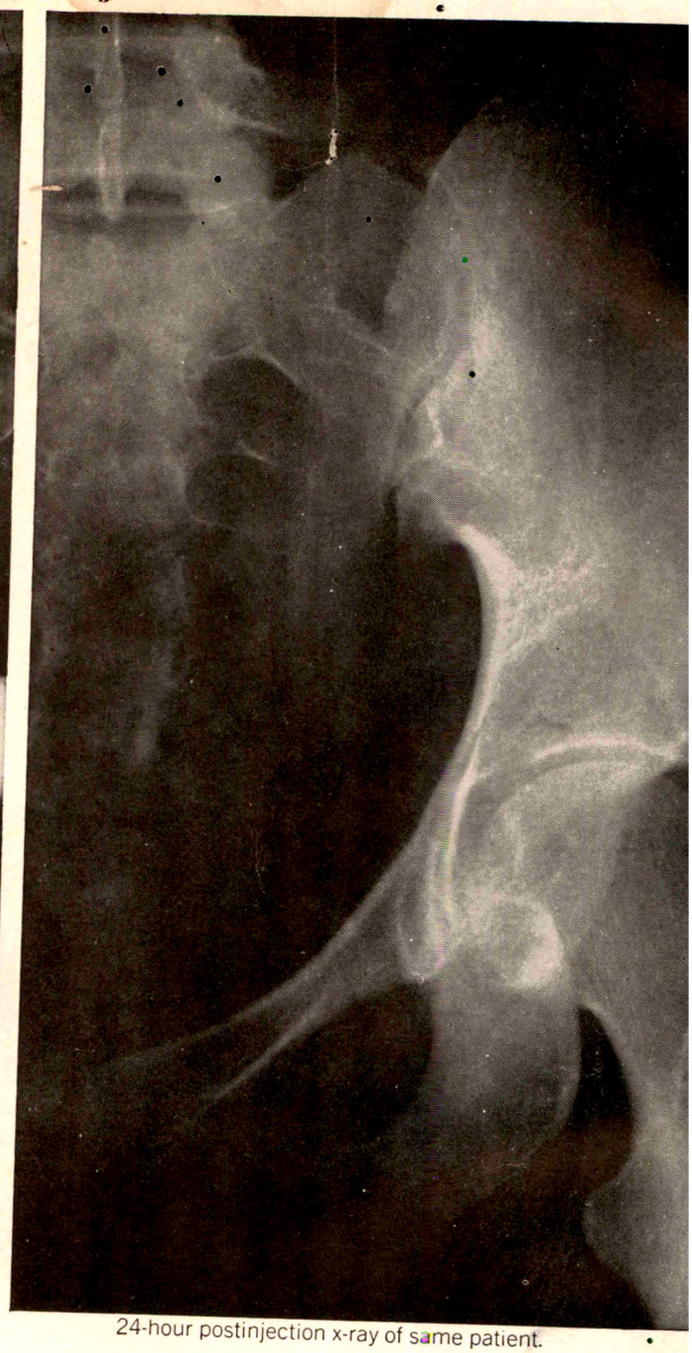
(11)

American
Journal of
Roentgenology

January 1979



Hysterosalpingogram with Salpix Contrast Medium.



24-hour postinjection x-ray of same patient.

now you see it

now you don't

With Salpix as your contrast medium, your gynecologic patient needn't undergo the 24-hour postinjection x-ray usually required with iodized oils. Water-soluble Salpix leaves virtually no irritating radiopaque residue to produce foreign-body reactions, yet it provides the viscosity needed for adequate visualization.

Contraindications: Contraindications to hysterosalpingography include the presence of severe vaginal or cervical infections, existing or recent pelvic infection, marked cervical erosion or endocervicitis, and pregnancy. The procedure is contraindicated during the immediate pre- or post-menstrual phase.

Sensitivity Test: If indicated in the patient's history, an intracutaneous skin test or sublingual absorption observation may be done with 0.1 cc Salpix.

Warning: Not for intravenous use.

CONTRAST MEDIUM

Salpix

TRADEMARK

EACH CC CONTAINS:
sodium acetrizoate 0.53 g and
polyvinylpyrrolidone 0.23 g.

Ortho

© ORTHO PHARMACEUTICAL CORPORATION 1970

ORTHO PHARMACEUTICAL CORPORATION • RARITAN, NEW JERSEY 08869

Official Journal
American Roentgen Ray Society
American Radium Society

P24.438

AJR

American Journal of Roentgenology

Diagnostic Imaging • Radiation Oncology
Related Sciences

Editor Melvin M. Figley

Associate Editor Rosalind H. Troupin

Assistant Editor John D. Harley

Contributing Editor E. Frederick Lang

Consulting Editorial Board Luther W. Brady • Kent Ellis
E. Robert Heitzman • Donald L. King • N. Thorne Griscom
Eugene C. Klatte • Kenneth Krabbenhoft • John G. McAfee
Russell H. Morgan • Thomas H. Newton • Robert G. Parker
Stewart R. Reuter • William B. Seaman • Robert J. Shalek
John Storer • Michel M. Ter-Pogossian • Joseph P. Whalen,
David M. Witten

Editorial Staff K. A. Murray, manager • M. J. Leonard,
manuscript editor • J. Anderson, assistant manuscript
editor • C. P. Kaiser, secretary

Published monthly by The Williams & Wilkins Co., 428 East Preston St., Baltimore, Maryland 21202. All correspondence, except editorial office business, should be addressed to the publisher. Annual subscription rates: $40 ($20 for residents with letter of verification) plus appropriate mailing surcharge (see note next page). Single copies, $5. Undelivered or damaged copies replaced within 60 days of publication; 90 days for foreign subscribers. Allow 90 days for address changes. © 1979 by American Roentgen Ray Society. Second-class postage paid at Baltimore, Maryland, and at additional mailing offices. Printed in U.S.A. ISSN 0361-803X

American Roentgen Ray Society

President: Harry Z. Mellins
President Elect: Paul A. Riemenschneider
1st Vice-president: Joseph D. Calhoun
2nd Vice-president: Charles E. Bickham, Jr.
Secretary: James F. Martin
Treasurer: Harley C. Carlson

COMMITTEES 1977–1978

Executive Council: H. Z. Mellins, P. A. Riemenschneider, J. D. Calhoun, C. E. Bickham, Jr., J. F. Martin, H. C. Carlson, M. M. Figley, R. G. Evens, B. G. Brogdon, R. A. Gagliardi, E. Gedgaudas, G. A. Kling, T. F. Leigh, S. F. Ochsner, J. F. Wiot, R. E. Buenger, E. C. Klatte, J. P. Tampas, J. L. Gwinn, chairman

Finance and Budget: A. E. James, E. C. Klatte, R. McLeeland, J. P. Tampas, R. G. Evens, chairman

Publications: M. P. Capp, K. Ellis, F. F. Ruzicka, Jr., E. R. Heitzman, R. A. Gagliardi, chairman

Editorial Policy: M. M. Figley, E. F. Lang, R. H. Troupin, E. R. Heitzman, K. Ellis, F. F. Ruzicka, Jr., M. P. Capp, R. A. Gagliardi, chairman

Advisory Committee on Education and Research: J. E. Youker, G. Wilson, G. W. Hartman, L. F. Rogers, E. Gedgaudas, chairman

Scientific Exhibits: T. C. Beneventano, G. Dodd, B. G. Brogdon, chairman

Constitution and Bylaws: J. H. Walker, W. M. Whitehouse, J. P. Tampas, chairman

American Board of Radiology Representatives: J. F. Roach, R. W. McConnell, S. W. Nelson

Program Committee: H. Z. Mellins, J. F. Martin, J. L. Gwinn, M. M. Figley, R. A. Gagliardi, B. G. Brogdon, E. Gedgaudas, G. A. Kling, P. Riemenschneider, chairman

Instruction Courses: E. Gedgaudas, director; G. W. Hartman, associate director

American College of Radiology Board of Chancellors Representative: W. B. Seaman

Annual Meeting: March 25–30, 1979, Sheraton Centre, Toronto, Canada

Scientific Program: P. A. Riemenschneider, president elect, Cottage Hospital, Santa Barbara, California 93105

Manager Annual Meeting: George A. Kling, Harper Hospital, Detroit, Michigan 48201

Membership: John L. Gwinn, 4650 Sunset Blvd., Los Angeles, California 90027

Business Office: Keith W. Gundlach, comptroller, American College of Radiology, 20 North Wacker Drive, Chicago, Illinois 60606

American Radium Society

President: Frederick W. George, III
President Elect: Alfred S. Ketcham
1st Vice-president: Julian P. Smith
2d Vice-president: Edwin M. Jacobs
Secretary: Norah duV. Tapley
Treasurer: Simon Kramer

COMMITTEES 1978–1979

Executive: A. S. Ketcham, J. P. Smith, E. M. Jacobs, N. duV. Tapley, S. Kramer, L. W. Brady, R. H. Jesse, F. W. George, F. Rutledge, chairman

Public Relations: V. Marcial, J. Vaeth, C. Honaker, ex-officio, and F. George, chairman

Publication: K. L. Krabbenhoft, D. Hussey, A. Raventos, I. Fix, L. W. Brady, chairman

Scientific Program: R. Parker, J. Durant, A. S. Ketcham, M. S. Mitchell, G. Murphy, F. Rutledge, M. Griem, W. E. Powers, M. Apuzzo, F. George, chairman

Local Arrangements: L. Davis, J. Vaeth, J. Nolan, R. McKenna, J. Slater, J. Stein, J. Scallon, S. Kramer, J. Helsper, chairman

Constitution and Bylaws: A. S. Glicksman, P. J. DiSaia, K. L. Krabbenhoft, chairman

Audiovisual: C. R. Bogardus, J. Helsper, R. Schweitzer, R. H. Jesse, C. Perez, J. Glassburn, A. M. Nisar Syed, R. Young, B. Herrington, F. George, chairman

American Board of Radiology Representatives: J. J. Stein, R. E. King, N. duV. Tapley

American College of Radiology Board of Chancellors Representative: L. W. Brady

American College of Radiology Council Representative: J. del Regato

Editorial Board of AFCOS Newsletter Representative: J. Vaeth

National Council on Radiation Protection and Measurements Liaison Representative: L. W. Davis

Annual Meeting: March 4–8, Los Angeles, California

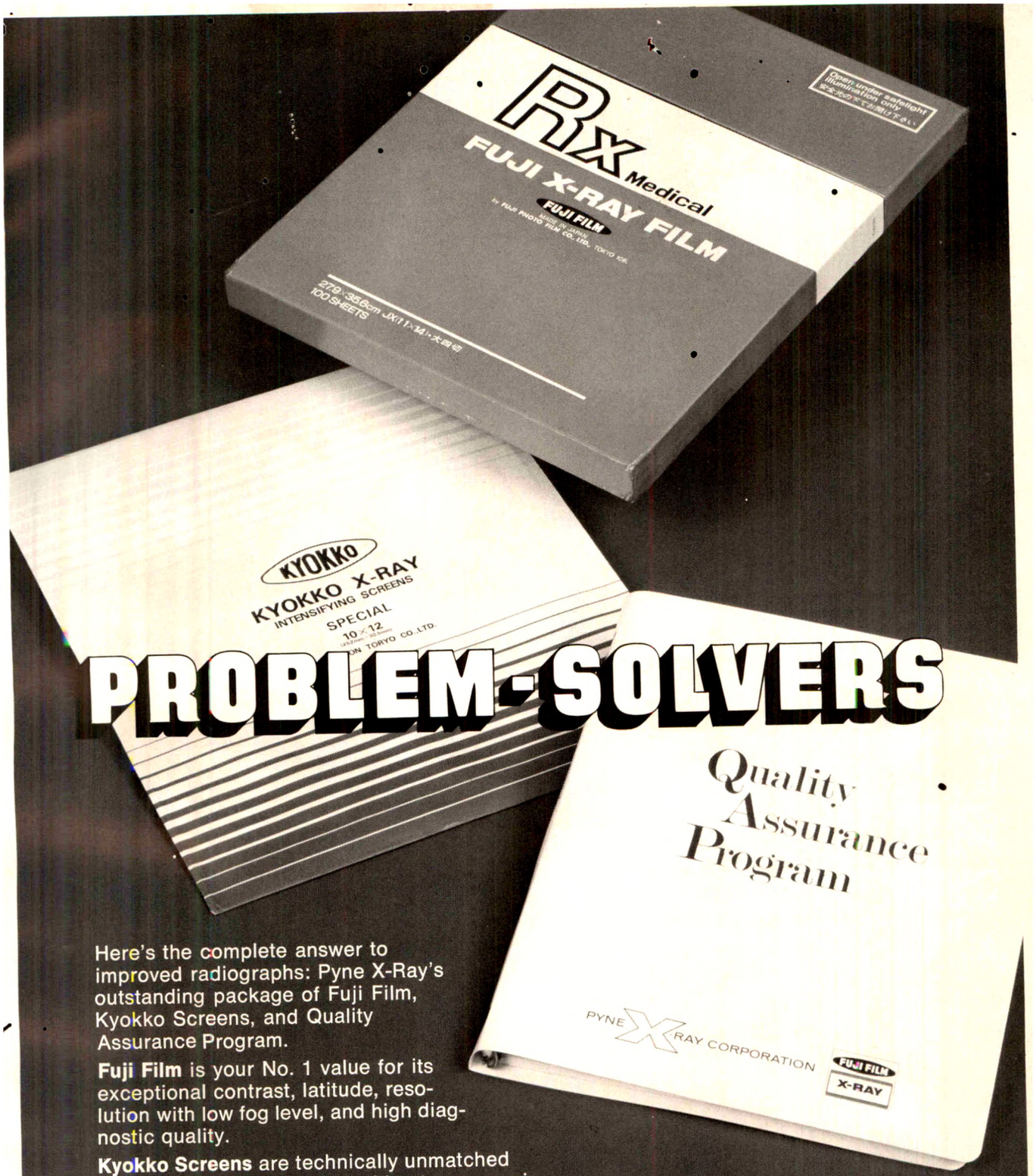
Scientific Program: F. W. George, III, University of Southern California School of Medicine, Los Angeles, California 90033

Local Arrangements: James Helsper, Pasadena, California

Membership: Norah duV. Tapley, secretary, M. D. Anderson Hospital, 6723 Bertner Avenue, Houston, Texas 77030

Business Office: N. V. Jordan, c/o R. H. Jesse, M. D. Anderson Hospital and Tumor Institute, 6723 Bertner Avenue, Houston, Texas 77030

Mailing note.—Mailing surcharges: U.S. and possessions, none; European countries, $25; Japan, $45; other, $10. European rates apply to Algeria, Austria, Belgium, Czechoslovakia, Denmark, Finland, France, Germany, Great Britain, Greece, Hungary, India, Iran, Ireland, Israel, Italy, Kenya, Luxembourg, Netherlands, Nigeria, Norway, Portugal, Romania, South Africa, Spain, Sweden, Switzerland, Turkey, Uganda, Yugoslavia. All subscriptions to Japan and European countries are delivered by air freight; there is no option for surface mail.



PROBLEM-SOLVERS

Here's the complete answer to improved radiographs: Pyne X-Ray's outstanding package of Fuji Film, Kyokko Screens, and Quality Assurance Program.

Fuji Film is your No. 1 value for its exceptional contrast, latitude, resolution with low fog level, and high diagnostic quality.

Kyokko Screens are technically unmatched for providing higher speed without compromise to superior resolution.

Quality Assurance Program developed by Pyne X-Ray has set a new standard in providing technical assistance to insure consistent radiographic quality.

For details, call your nearest Pyne X-Ray representative.

QUALITY PRODUCTS PLUS PERSONAL SERVICE

KYOKKO

FUJI FILM X-RAY

Distributed throughout the U.S.

PYNE X-RAY CORPORATION

NEW YORK
20 North Avenue
Larchmont, New York 10538
(914) 834-4567

CHICAGO
1211 West Norwood Avenue
Itasca, Illinois 60143
(312) 773-3360

LOS ANGELES
1639 Gardena Avenue
Glendale, California 91204
(213) 240-0280

Liquid Polibar with Super XL

A Total System

For double-contrast examination of the colon.

Satisfactory results in the double-contrast examination of the colon require special attention to two aspects of the procedure.

First, the barium sulfate formulation. Our Liquid Polibar (56% w/w) is a bubble-free, non-precipitating uniform suspension formulation ... with proper flow and coating characteristics. No blending required and once routines are established, you can rely on its consistency.

The second concern is with the proper apparatus. The E-Z-EM system is unique in that 1/2" lumen tubing attached to the enema bag is utilized — for freer, more uniform flow. Miller Air Retention Tip, with or without optional cuff completes the system.

A total system for ease of administration and consistently reliable radiological results. For additional literature, write:



Multiple pseudo polyps in the splenic flexure in longstanding ulcerative colitis.
Film courtesy of Richard Palmer Gold M.D. Columbia Presb. Medical Center N.Y.

E-Z-EM

7 Portland Ave.
Westbury, New York 11590
(516) 333-8230

International Affiliates: E-Z-EM Rooster B. V., Infirmeriestraat 6-8, Rotterdam 16, Netherlands
E-Z-EM De Mexico, S. A. de C. V., Calz. Azcapotzalco La Villa No 882, Zona Industrial Vallejo, Mexico 16 D. F.

7/78

clear, clean colon

X-Prep® Liquid

(standardized extract of senna fruit)

versatile bowel evacuant for diagnostic procedures



Versatile in indications

May be used prior to:

G.I. radiography
Urologic radiography
Colonoscopy
Sigmoidoscopy
Other diagnostic bowel procedures

Versatile in administration

May be used:

Alone, in a single dose
Alone, in divided doses, particularly in elderly or debilitated patients
With adjunctive use of citrate of magnesia, laxative suppositories and enemas, as required
As part of other regimens, such as hydration

X-PREP Liquid is formulated specifically for effective bowel evacuation prior to diagnostic procedures. It induces peristalsis through virtually colon-specific action. X-PREP Liquid has been found effective in cleansing the colon for diagnostic evaluation in 95% of 749 patients prepared for barium enemas, intravenous pyelography, or colonoscopy.* Its pleasant taste meets with high patient acceptance, and its ease of administration is appreciated by the patient and nursing staff.

Supplied: X-PREP Liquid (standardized extract of senna fruit) in 2½ fl. oz. bottles (alcohol 7% by volume). X-PREP Powder (standardized senna concentrate) in ¾ oz. containers. **Now Available:** X-PREP™ Bowel Evacuant Kit. Each kit contains: two SENOKOT® S Tablets (standardized senna concentrate and dioctyl sodium sulfosuccinate), one bottle of X-PREP® Liquid 2½ fl. oz., and one RECTOLAX™ Suppository (bisacodyl 10 mg), plus easy-to-follow patient instructions for hydration, clear liquid diet, and the correct time sequence of administering the above laxatives.

* Bibliography available upon request

Colonoscope, courtesy of Olympus

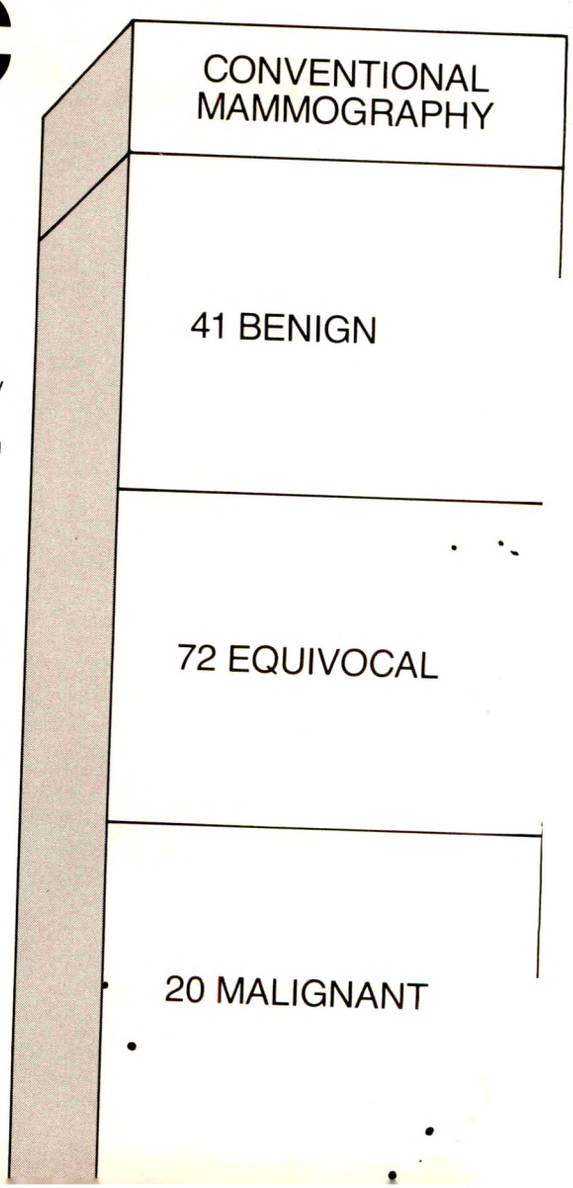
Gray Pharmaceutical Co., Affiliate
The Purdue Frederick Company

© Copyright 1978, Gray Pharmaceutical Co. Norwalk, CT 06856

A9047 194578

A New Study Confirms...

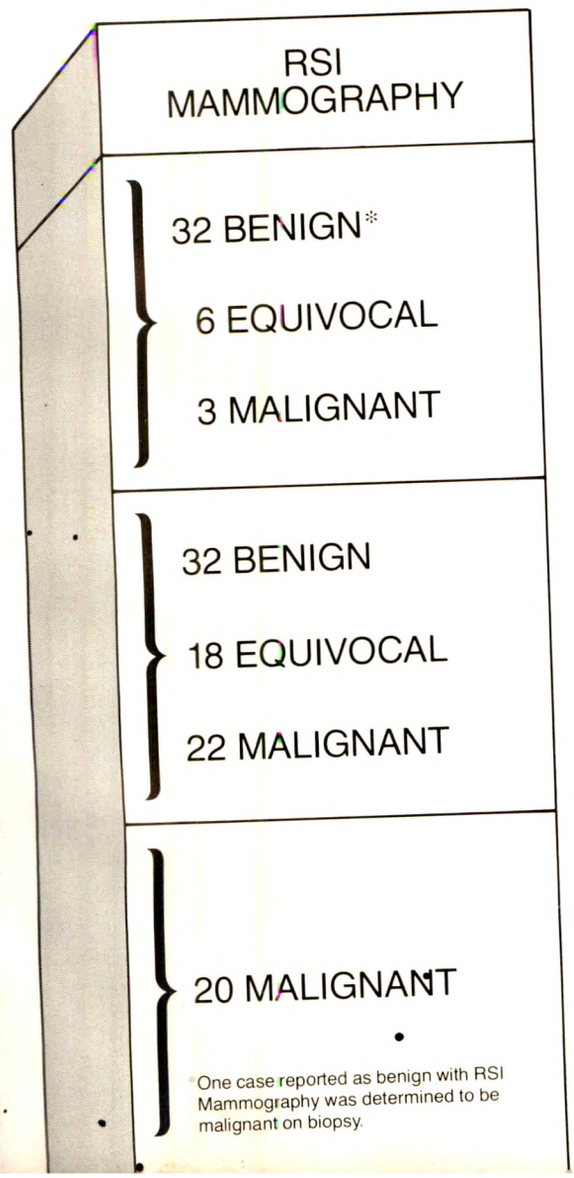
THE RSI MAMMOGRAPHIC SYSTEM **INCREASES DIAGNOSTIC ACCURACY**



Take a good look at the chart. You'll see the remarkable results of a study published by Dr. Edward A. Sickles, making a clinical comparison of 133 patients who received both conventional mammography and RSI Magnification Mammography. The results were confirmed with pathological diagnosis.*

This new study confirms just how accurate RSI Mammography really is. In fact, Dr. Sickles wrote in 1977, that magnification mammograms are "...clearly superior both quantitatively and qualitatively to conventional contact mammograms."[1]

Diagnostic Accuracy in Mammographic Examinations[2]
Clinical Data of Edward A. Sickles, M.D.
Assistant Professor of Radiology, University of California, San Francisco
Clinical Comparison of 133 Cases



Out of 41 cases diagnosed as benign with conventional mammography, RSI Mammography determined that 3 of these cases were, in fact, malignant. In addition, with conventional mammography alone, 72 cases were diagnosed as equivocal and direct magnification mammography (RSI System) was able to differentiate these as: 22 malignant, 32 benign, and only 18 remained equivocal. This revealing clinical comparison clearly shows that RSI Magnification Mammography increases the certainty in diagnosis, decreases the time between examination and confirmation, and may even reduce the need for biopsy.

In a radiologic symposium presented in New York City, Dr. Sickles remarked, "...in dealing with difficult cases, we considerably improved our diagnostic accuracy [with RSI Magnification Mammography]."[2]

These more accurate diagnoses are the direct result of the capability of the RSI Mammography's System to give you—

- Clearer definition of mass borders
- Improved image sharpness and resolution
- Resolution of malignant microcalcifications often not discernible by conventional mammography
- Delineation of trabecular patterns

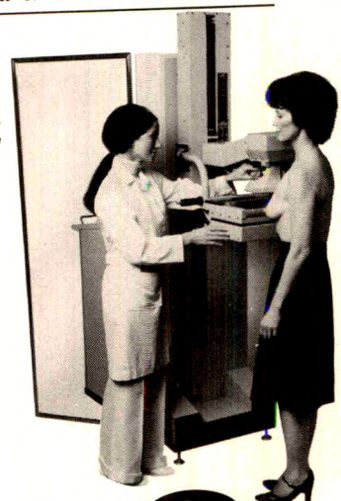
The RSI Mammography System offers high-detail resolution in the magnification mode as well as the conventional contact mode. The superior image which results from the exceptionally uniform focal spot provides a new level of confidence in the detection of breast cancer.

For more detailed information on the RSI Mammographic System and a reprint of the study published by Sickles *et al* in 1977, please write or call, Radiologic Sciences Inc., a subsidiary of Pfizer Inc., 235 East 42nd St., New York, N.Y. 10017 (212) 573-7941.

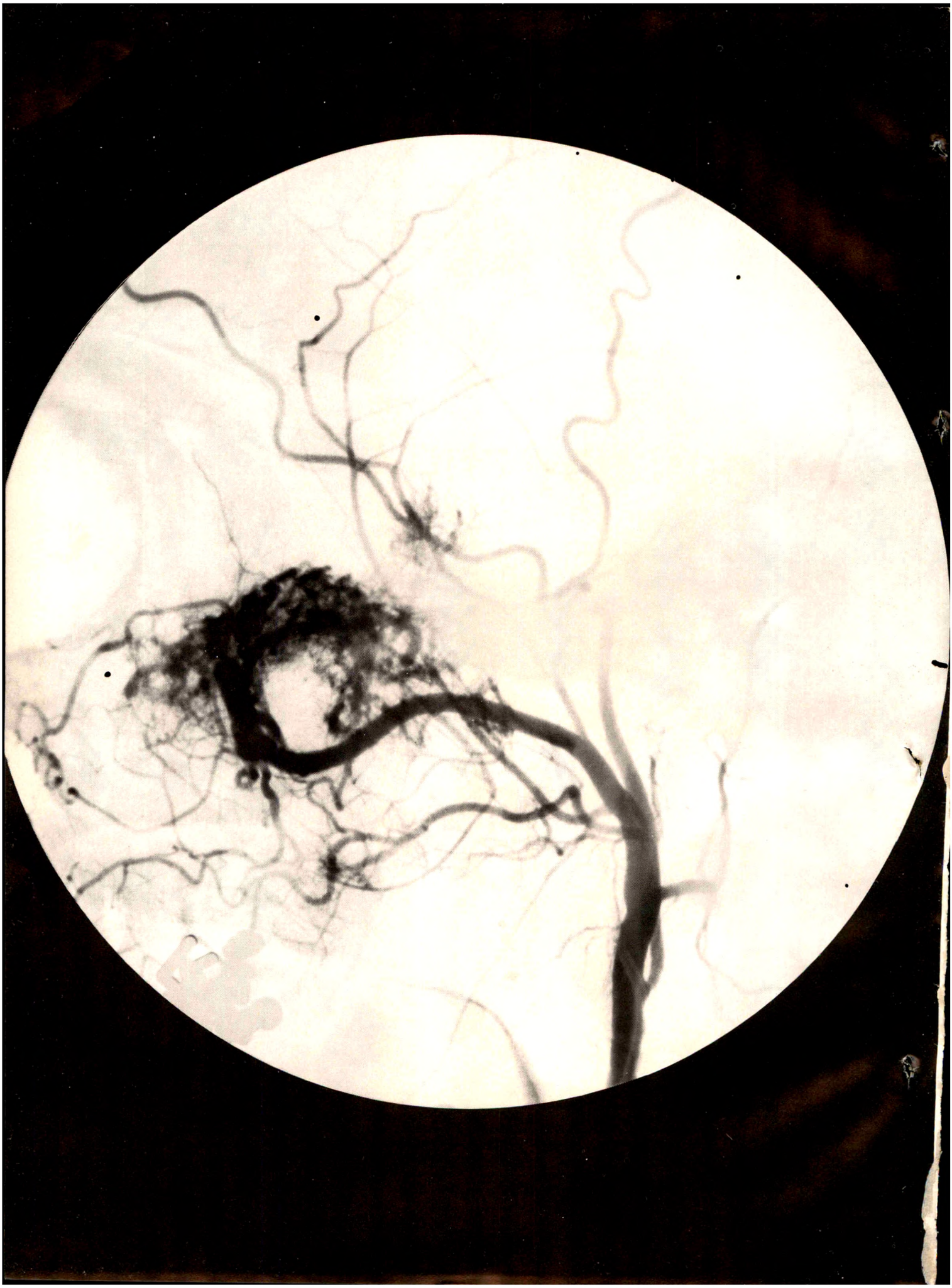
References: 1. Sickles, E.A.; Doi, K.; Genant, H.K.: *Radiology* 125:69-76, October 1977. **2.** Sickles, E.A.: *Microfocal Spot Magnification Mammography.* Presented at a Symposium, New York City, June 1, 1978.

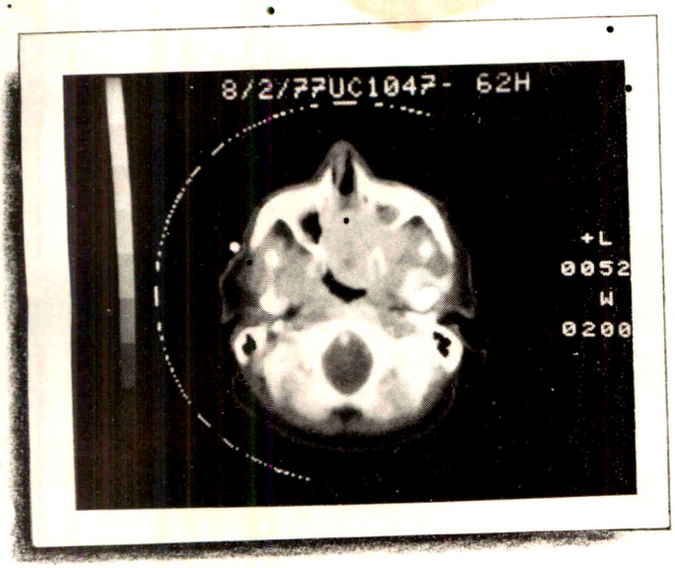
THE RSI MAMMOGRAPHIC SYSTEM

INCREASES DIAGNOSTIC ACCURACY



RADIOLOGIC SCIENCES INC. Pfizer
A subsidiary of Pfizer Inc., New York, N.Y. 10017





Diagnosis:
Angiofibroma involving Ethmoid and Sphenoid Sinuses.

Clinical Data:
32 year old man with an eight month history of nasal congestion.

CT Scan:
A large soft tissue mass is noted in the nasopharynx extending upward into the sphenoid sinus and distorting the normal airway. Destruction of the medial and posterior walls of the left maxillary sinus is noted. Following intravenous contrast infusion, slight contrast enhancement is noted.

Selective Right External Carotid Arteriogram:
Study shows a highly vascular neoplasm in the nasopharynx extending upward into the sphenoid sinus. The angiographic appearance is typical for an angiofibroma.

The external carotid artery was embolized following which the angiofibroma was surgically excised.

The arteriogram and the CT scan reproductions are both reduced to 79% of their original size.

Angiography and CT scanning.

Each has its own special diagnostic advantages in this era of expanding imaging technology.

Angiography and Elema-Schonander.

For diagnostic specificity.

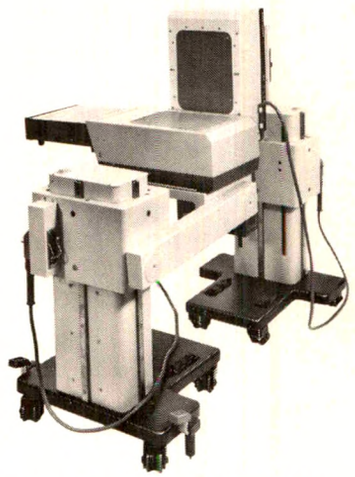
While CT has proved to be a highly sensitive diagnostic technique, angiography, in many cases, is necessary to make a specific diagnosis. And, no matter what your angiographic applications are, Elema-Schonander has a sheet-film changer to meet your requirements.

PUCK Models: Where increased magnification, mobility, and compactness are important considerations, 20-film capacity PUCK Model film changers are available to accommodate either 35cm x 35cm (14″ x 14″) or 24cm x 30cm sheet-film sizes. They operate at film exposure rates of up to 3 exp/sec in single plane or simultaneous biplane mode. When biplane alternating mode is chosen to eliminate cross-fogging, PUCK Models change film at 1.5 exp/sec. per plane.

AOT-S Models: Six exp/sec, 30-film capacity Model AOT-S film changers are available for the same sheet-film sizes. They also can be used for single plane, or biplane simultaneous or alternating sequences.

All Elema-Schonander sheet-film changers feature convenient, accurate punch card control (PDA), and are equipped with a newly developed carbon-fiber reinforced plastic (CFRP) compression plate that minimizes x-ray attenuation, while maintaining intimate film contact, year after year.

Call or write for brochures describing the PUCK and AOT-S sheet-film changers. Elema-Schonander, Inc., 699 Lively Blvd., Elk Grove Village, IL 60007. (312) 593-6770.

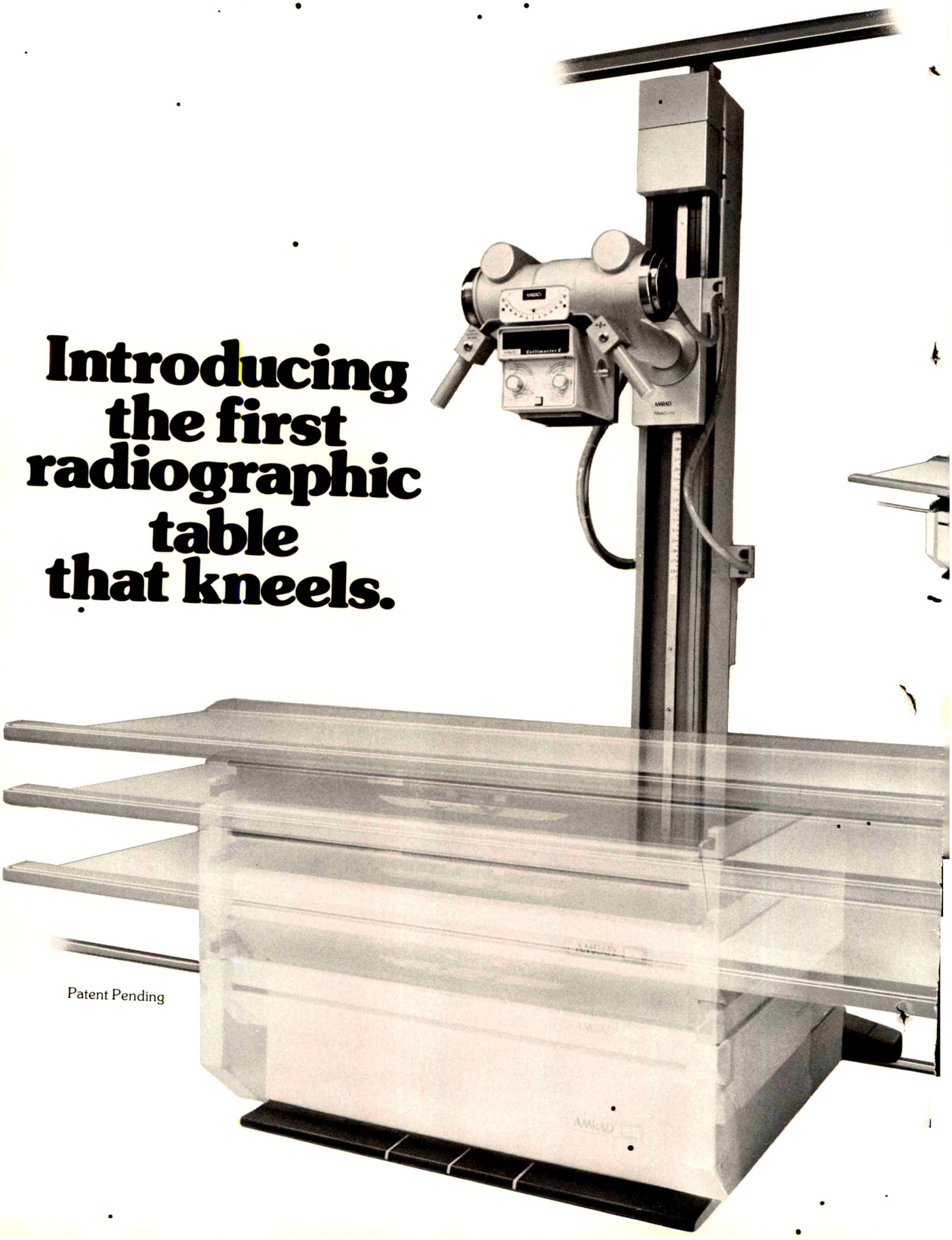


Biplane PUCK U24/30 installation
on PUCKWOP 24/35 Universal Stands

elema·schonander

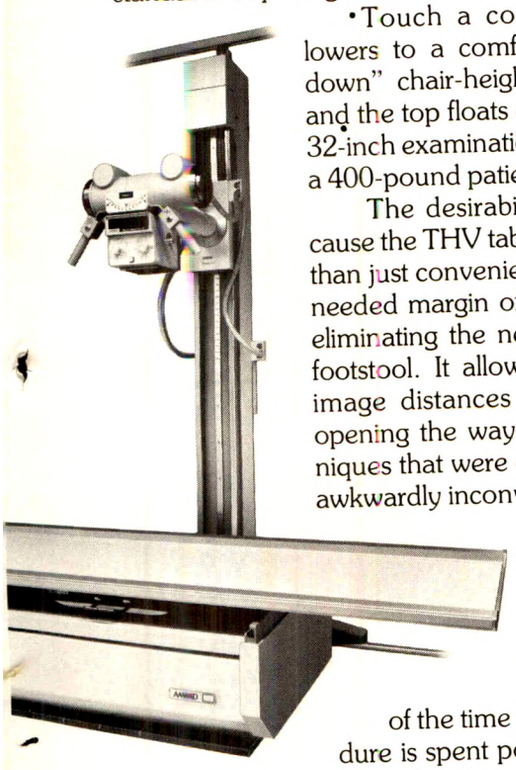
78212

Introducing the first radiographic table that kneels.



Patent Pending

Amrad's new THV table literally obsoletes every horizontal radiographic table on the market—including, unfortunately, some of our own. "THV," you see, stands for *Top Height Variable*.

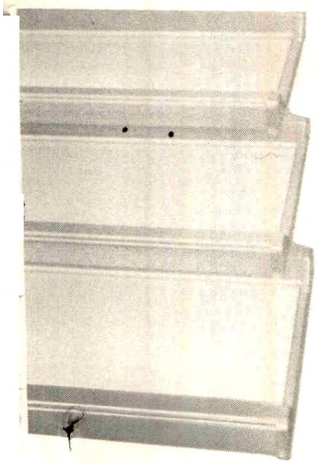


•Touch a control and the top lowers to a comfortable, "please-sit-down" chair-height. Touch it again, and the top floats effortlessly back to a 32-inch examination height, even with a 400-pound patient aboard.

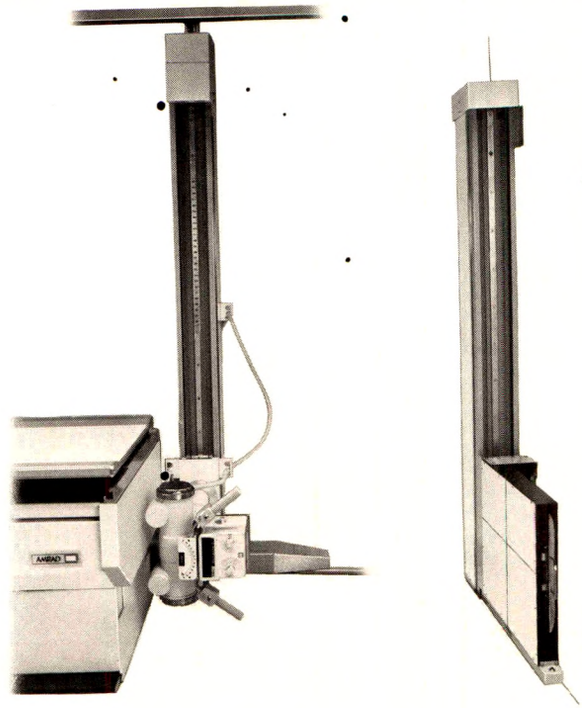
The desirability is obvious. Because the THV table offers much more than just convenience. It adds a much needed margin of safety—completely eliminating the need for a hazardous footstool. It allows extended source-image distances of 55″ or more—opening the way to many new techniques that were either not possible or awkwardly inconvenient before.

And with today's spiraling costs, the Amrad THV table offers an important *savings of time*. After all, most of the time for an average procedure is spent positioning the patient. Procedures are often complicated by patient feebleness or incapacity—certainly a common problem in every radiographic facility. Throughout the day, extra people must be available to help the technologist with those instances.

But not with the Amrad THV table. An Amrad THV room allows fewer people to perform more examinations in less time.



That high-volume capacity is augmented by the now-famous Amrad four-way floating top—the one that travels as far or farther in every dimension than that of any other radiographic table—no matter what the price. After initial positioning, there is no possible coverage, head to toe, side to side, that could require scooting or sliding the patient.



The table is augmented by the Amrad tubestands—the ones where the tube and vertical bucky combination *goes all the way to the floor*—allowing weight-bearing procedures to be handled with a minimum of dangerous and bulky platform accessories. And by the superb Craig-series of 600 MA generators—the ones with the small, remote-control console connected with low-voltage telephone cable. The ones that have earned a near-perfect record of reliability.

And so Amrad's new THV table makes possible the first radiographic room that is designed around people, instead of machines. Surprisingly, it's not expensive—costing little or no more than obsolete tables. Phone collect for the name of your local Amrad dealer.

And go sit down on the first radiographic table that kneels.



AMRAD®

A Raytheon Company

The common-sense people in x-ray

2020 North Janice Avenue
Melrose Park, Illinois 60160
(312) 865-2600

What's new in contrast media for excretion urography?

Renovue®
Iodamide Meglumine
is new!



Fast opacification

Maximal opacification of renal passages may begin as early as one minute following injection of Renovue-65 (Iodamide Meglumine Injection) and within five minutes after start of infusion of Renovue-DIP (Iodamide Meglumine Injection 24%).

High contrast density

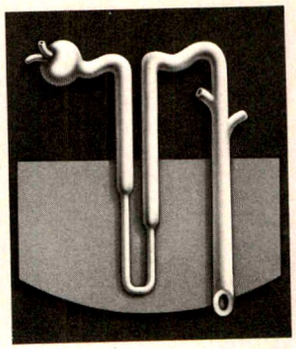
Iodamide meglumine produces dense opacification of calyces, renal pelves and ureters.

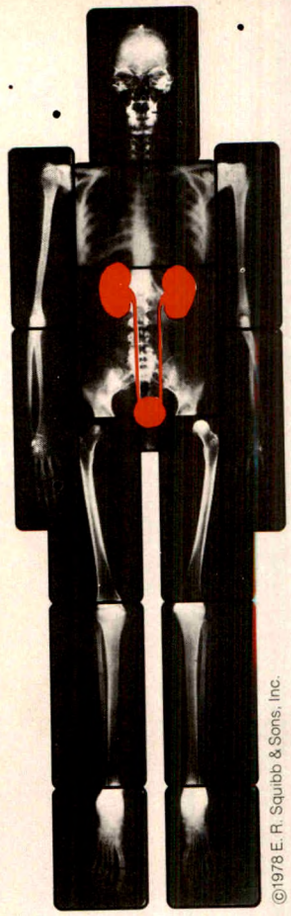
Rapid urinary excretion

Contrast medium is excreted essentially unchanged in the urine, principally by glomerular filtration, but *at least one-third is secreted by renal tubules.*









©1978 E. R. Squibb & Sons, Inc.

Renovue®-65
Iodamide Meglumine Injection

65% iodamide meglumine with approximately 30% (300 mg/ml) organically bound iodine.
Available in 50 ml single-dose vials.

Renovue®-DIP
Iodamide Meglumine Injection 24%

Useful when routine pyelography would not be expected to be, or has not been, satisfactory for diagnosis.
24% iodamide meglumine with approximately 11% (111 mg/ml) organically bound iodine.
Available in 300 ml single-dose bottles.

See next page for brief summary.

SQUIBB®



RENOVUE®-65
odamide Meglumine Injection
Renovue®-DIP
odamide Meglumine Injection 24%

ESCRIPTION: Renovue-65 (Iodamide Meglumine Injection) and Renovue-DIP (Iodamide Meglumine Injection 24%) are radiopaque rographic contrast agents supplied as sterile, nonpyrogenic, queous intravenous solutions. Renovue-65 provides 65% odamide meglumine with approximately 30% (300 mg/ml) organically bound iodine with 0.01% edetate disodium as a sequestering abilizing agent. *Renovue-65 contains approximately 0.0124 mg 0.0005 mEq) sodium per ml.* Renovue-DIP provides 24% iodamide eglumine with approximately 11.1% (111 mg/ml) organically ound iodine with 0.00368% edetate disodium as a sequestering abilizing agent. *Renovue-DIP contains approximately 0.0046 mg .0002 mEq) sodium per ml.*

ONTRAINDICATIONS: No absolute contraindications; however, e WARNINGS.

ARNINGS: Because of the great possibility of producing transient fatal renal failure, a definite risk exists with excretion urography in tients with multiple myeloma. The risk in these patients is not a ntraindication to the procedure; however, avoid dehydration in eparing these patients since this may predispose to precipitation protein in the renal tubules.

Administer radiopaque materials to patients known or suspected have pheochromocytoma only if the physician deems that the ssible benefits outweigh the considered risks and then only with reme caution while keeping the volume of drug at an absolute nimum. Assess blood pressure throughout the procedure and ve measures for treatment of a hypertensive crisis available.

ntravenous contrast media have been shown to promote sickling persons homozygous for sickle cell disease. Perform urography extreme caution in presence of anuria or severe concomitant patic and renal disease. Although not an absolute contraindication to use of iodamide meglumine, a history of sensitivity to iodine *se* or to any contrast agent calls for extreme caution in administion.

ECAUTIONS: *General*—Since all procedures utilizing contrast dia carry a definite risk of producing side effects, carefully evalte the risk-benefit factor before undertaking a procedure bese life-threatening and fatal reactions may occur without warnConstantly have available a fully equipped emergency cart (or ivalent supplies and equipment) and personnel competent in gnizing and treating all degrees of adverse reactions to the or to the procedure. Immediately discontinue administration of contrast agent if a serious reaction occurs. Keep competent sonnel and emergency facilities available for at least 30 to 60 utes after administration to cope with severe delayed reactions. nal toxicity has been reported in a few patients with liver unction who were given oral cholecystographic agents fold by urographic agents; therefore, if known or suspected he or biliary disorder exists, administration of iodamide meglne preparations should be postponed following the recent inon of cholecystographic agents. Exercise caution with use of ast media in severely debilitated patients and in those with ed hypertension. Consider the functional ability of the kidneys e injecting iodamide meglumine preparations. Bear in mind ossibility of thrombosis or other complications due to mechanauma of the intravenous procedure. Collect urine before or two re days after administration of the drug since contrast agents ere with some chemical determinations made on urine speci. Perform PBI and radioactive iodine uptake studies, if such ndicated, prior to administration of the drug since iodinening contrast agents may alter thyroid function test results. If an antihistamine for premedication or treatment of an adverse on is considered, recognize that admixture of an antihistamine contrast agent may result in a precipitate; because of this, nt sites should be used to administer the antihistamine and ntrast agent. Use of a diuretic prior to the examination in order rease the urinary concentration of the contrast agent is not ble; dehydration may predispose to a greater incidence of, or severe, reactions. Consider the increased osmotic load asso with *drip infusion* pyelography in patients with congestive failure; the diuretic effect of drip infusion pyelography may hinder assessment of residual urine in the bladder. Do not exceed recommended rate of infusion (appropriate volume infused in approximately 10 minutes) of Renovue-DIP (Iodamide Meglumine Injection 24%).

Sensitivity Testing—Severe, life-threatening reactions often resemble hypersensitivity phenomena. A personal or family history of asthma or allergy or a history of a previous reaction to a contrast agent warrants special attention and may predict more accurately than pretesting the likelihood of a reaction although not the type nor severity of the reaction in the individual. The value of any pretest is questionable. The pretest most performed is the slow I.V. injection of 0.5 to 1.0 ml of the preparation prior to injection of the full dose; however, the absence of a reaction to the test dose does not preclude the possibility of a reaction to the full diagnostic dose. Should the test dose produce an untoward response, the necessity for continuing the examination should be carefully re-evaluated; if deemed essential, the examination should proceed with all possible caution. In rare instances, reaction to the test dose may be extremely severe; therefore, close observation and facilities for emergency treatment are essential.

Usage in Pregnancy—No teratogenic effects attributable to iodamide meglumine preparations have been observed in mouse, rat, and rabbit reproduction studies. Safety for use during pregnancy in humans has not been established. Although there is no clearly defined risk, the possibility of infrequent or subtle fetal damage cannot be excluded. Iodamide meglumine should be used in pregnant women only when clearly needed.

Pediatric Use—Safety and effectiveness for pediatric use have not been established.

ADVERSE REACTIONS: In clinical studies, adverse reactions occurred in approximately 9.5 to 13% of patients. Nausea and/or vomiting, urticaria, pruritus, a rise or fall in blood pressure, sneezing, and sensation of warmth occur most frequently (individually occurring at a frequency of approximately 1 to 5% and usually mild). The following occur less frequently: generalized flushing, lacrimation, headache, edema of the eyelids, coughing, retching, bitter or metallic taste, pharyngeal burning sensation, nasal congestion, hoarseness, sweating and weakness, malaise, perianal burning sensation, pain and erythema at injection site due to faulty technique, bradycardia, hyperpnea, flank tenderness, chills, syncope, pulse rate increase, shortness of breath, chest pain, tachycardia, hemiparesis, and shock. Other reactions to iodinated contrast media include fever, dizziness, restlessness, lightheadedness, pallor, choking, laryngeal or pulmonary edema, dysphagia, facial or conjunctival petechiae, rash and other eruptions, wheezing, asthmatic reaction, cramps, tremors, anxiety, hematomas and ecchymoses around injection site due to faulty technique, vein cramp, partial collapse of injected vein, thrombophlebitis and cellulitis following injection, neutropenia, transient proteinuria, hysterical reaction and numbness of head and neck, and convulsions. "Iodism" (salivary gland swelling) has been reported infrequently; immediate or delayed rigors sometimes with hyperpyrexia has occurred rarely. Antihistaminic agents may be of benefit in event of adverse reactions. Adverse reactions may be severe enough to require discontinuation of injection of Renovue-65 (Iodamide Meglumine Injection) or infusion of Renovue-DIP (Iodamide Meglumine Injection 24%).

Severe reactions, which may require emergency measures, may take the form of a cardiovascular reaction characterized by peripheral vasodilatation with resultant hypotension and reflex tachycardia, dyspnea, agitation, confusion, and cyanosis progressing to unconsciousness. Cardiac arrest, ventricular fibrillation, cardiac arrhythmias, hypertension, temporary renal shutdown or other nephropathy may occur rarely. The histamine-liberating effect of an iodinated contrast agent may induce a reaction ranging in severity from rhinitis or angioneurotic edema to laryngeal or bronchial spasm and, rarely, anaphylactoid shock.

For full prescribing information, consult package inserts.

HOW SUPPLIED: Renovue-65 (Iodamide Meglumine Injection) is available in 50 ml single-dose vials. Renovue-DIP (Iodamide Meglumine Injection 24%) is available in 300 ml single-dose infusion bottles (designed to be suspended from an I.V. stand).

SQUIBB® "The Priceless Ingredient of every product is the honor and integrity of its maker."™

©1978 E. R. Squibb & Sons, Inc. 658-501

new Section 4: Golden's Diagnostic Radiology Series RADIOLOGY OF THE HEART AND GREAT VESSELS, 3rd edition

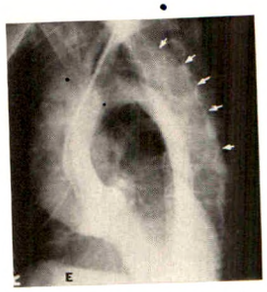


Fig. 517. Type I dissecting aneurysm (hematoma) with origin in the ascending aorta. (E) Injection into lumen. A large hematoma is seen in aortic wall (arrowhead) and the lumen of the aorta is narrowed.

By **Robert N. Cooley, MD,** Professor of Radiology; and **Melvyn H. Schreiber, MD,** Professor and Chairman, Department of Radiology; both of University of Texas Medical Branch, Galveston.

Completely rewritten and updated, RADIOLOGY OF THE HEART AND GREAT VESSELS will soon be the cornerstone of the radiologist's working library as well as the one book heart and chest specialists will turn to for method, technique, and interpretation in the roentgenologic study of the heart and great vessels.

- the authors cover every facet of both acquired and congenital heart disease from clinical, anatomical, and radiologic points of view.
- the style is succinct and to the point.
- the 734 illustrations, nearly all radiographs, have been chosen as much for their interpretive value as for their outstanding precision and clarity.
- the illustrations are carefully labeled with clear, helpful legends.
- the excellent bibliography allows quick and easy reference and has been updated to include the latest work in the specialty.
- the rigid standards of the world-renowned reputation of the Golden's Diagnostic Radiology Series have been met with both radiologic expertise and excellence.

This new third edition, with its complete revision reflects the very latest developments in cardiac radiology, including the newest techniques of cardiography and nuclear imaging. RADIOLOGY OF THE HEART AND GREAT VESSELS is virtually the definition of the field.

CONTENTS

PROCEDURES: Fluoroscopy. Chest Films. Body Section Radiography. Cardiac Catheterization. ANGIOCARDIOGRAPHY: History. Patient Preparation. Venous Angiocardiography. Selective Angiocardiography. Thoracic Aortography. CONTRAST SUBSTANCES: Toxicity. Factors Governing Injection. Injectors. Dosage. Reactions. EQUIPMENT: Cinefluorographic. Film Changers. EMBRYOLOGY OF HEART AND GREAT VESSELS: Interior of Heart. Blood Vessels. ROENTGENOLOGIC APPEARANCE: Contours and Topography of Normal Heart. Pulsations of Normal Heart & Great Vessels. Relation of Esophagus to Cardiovascular Contours. Normal Angiocardiogram. Cardiac Catheterization. Normal Ventriculogram. MEASUREMENT OF HEART AND GREAT VESSELS. GENERAL SYMMETRICAL AND ASYMMETRICAL CARDIAC ENLARGEMENT—CHANGE IN SIZE OF SPECIFIC CHAMBERS—ABNORMAL PULSATIONS. DISEASES OF PULMONARY VASCULAR SYSTEM: Anatomy & Physiology. Obstructions. Dilatation. Alterations in Vascular Permeability. Intralobar Sequestration. RHEUMATIC HEART DISEASE: Acute Rheumatic Carditis and Valvulitis. Chronic Rheumatic Heart Disease. Mitral Valvular Disease. Aortic Stenosis and Calcific Aortic Stenosis. Combined or Multiple Valvular Disease. Radiologic Changes after Surgery. CONGENITAL ANOMALIES: Classification. Obstructions. Abnormal or Persistent Openings Between Right & Left Sides of Circulation. Congenital Malpositions of Heart or Cardiac Chambers. Anomalies of Great Vessels without Significant Circulation Changes. HYPERTENSIVE HEART DISEASE: Cardiac Compensation. Isolated Left Ventricular Failure, Combined Left and Right Heart Failure. Drug Effects. Hypertension with Nephritis. Bernheim's Syndrome. ATHEROSCLEROTIC CHANGES: CORONARY ARTERIOSCLEROSIS: MYOCARDIAL INFARCTION: Valves. Cardiac Aneurysm. Heart Rupture. CORONARY ARTERIOGRAPHY. CARDIOMYOPATHIES. SYPHILITIC HEART DISEASE. MUCOID OR MYXOMATOUS CHANGES IN CARDIAC VALVES. TUMORS OF THE HEART. THE HEART IN SYSTEMIC DISEASE: Endocrine Disorders. Anemia. Nutritional Deficiency States. Rhythm Abnormalities. IMPLANTABLE CARDIAC PACEMAKERS. CALCIFICATION WITHIN HEART AND PERICARDIUM. TRAUMA TO HEART AND GREAT VESSELS. HEART DISPLACEMENT. DISEASES OF THE PERICARDIUM. DISEASES OF THORACIC AORTA AND ITS BRANCHES. VALVE REPLACEMENTS. Index.

December, 1978/676 pages/734 illustrations/$65.00

Yes, please send me _____ copy(ies) of RADIOLOGY OF THE HEART AND GREAT VESSELS, 3rd edition, (#2103-6) at $65.00 each, on 20-day approval.

name

address

city state zip code

All orders sent on 20-day approval. Maryland residents please add 5% sales tax. Prices subject to change without notice.
TOLL-FREE TELEPHONE ORDERING
(9am to 4pm), call: 1-800-638-0672; Maryland residents call collect: 528-4221.

☐ Check enclosed ☐ VISA ☐ MasterCharge ☐ Bill me

card# expiration date

Williams & Wilkins P.O. Box 1496 Baltimore, Md. 21203

Leadership in Micro-Focus Technology

Magnification techniques for all radiography . . . routine studies as well as special procedures

☐ **Power** for stopping motion
for penetrating thick body sections

☐ **Resolution** for finest detail
for several times magnification

Available in these micro-focus x-ray tubes:

	Focal Spot	Power
Dynamax 78	.13/.6	10/57 KW
Dynamax 78	.23/1.3	15/100 KW
Dynamax 69	.3/1.2	10/100 KW
Dynamax 68	.3/.6	13/35 KW
Dynamax 68	.3/1.0	13/87 KW
Dynamax 65	.3/.6	18/60 KW

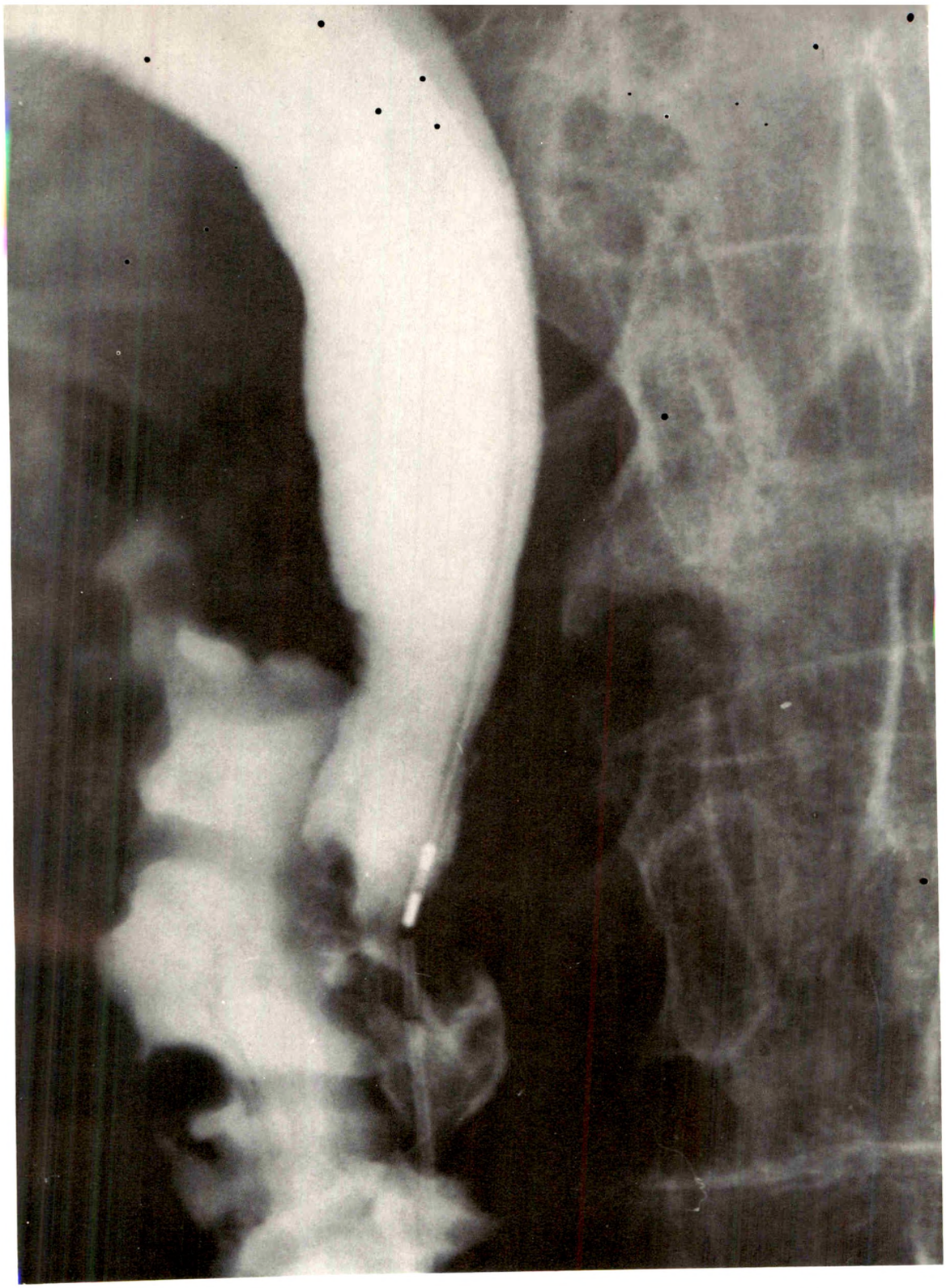
Biasing can be used to further improve resolution.

MACHLETT

The Machlett Laboratories, Incorporated
1063 Hope Street
Stamford, Connecticut 06907
Telephone: (203) 348-7511

A Raytheon Company

Machlett has the power . . .



54-year-old male, referred for removal of retained common duct stones, missed at prior surgery which included exploration of the common bile duct. Four post-operative T-tube cholangiograms and two pre-operative Upper G.I. series failed to show any of the pathological features that were subsequently revealed on the 4.5X magnification catheter cholangiogram (above).

These findings include (a) irregular shelf-like wall defect, irregular intraluminal mass and mucosal destruction typical of malignancy; (b) soft tissue mass extending beyond the duct to compress adjacent duodenal wall; (c) compression and effacement of duodenal mucosa from tumor extension; (d) microcalcifications from chronic pancreatitis.

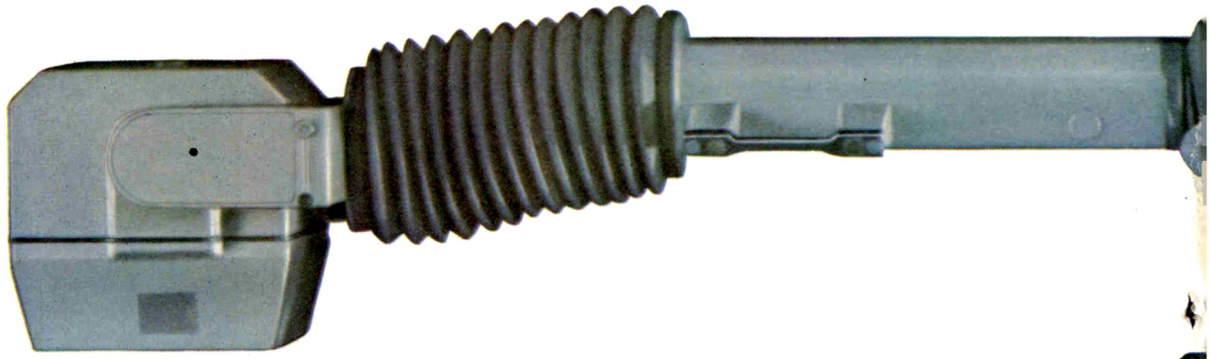
These radiographic features suggested the correct diagnosis of primary bile duct carcinoma with extension to the duodenal wall and associated pancreatitis, all documented at subsequent surgical resection.

These films were obtained with a Dynamax 78E x-ray tube with a double-biased micro-focal spot of 120 by 160 microns (FWHM measurement with a 10-micron pinhole camera) at 7.5 kW. FFD: 46". Instantaneous output of 100 mA at 75 kVp was used, with 83 msec exposure in an angiographic type run to follow the dynamic flow of contrast medium through the ductal system. This power capability allowed easy penetration of the abdomen of this 180 pound man, when used in conjunction with several different rare-earth screen-film combinations.

M cilett i stie r esolutic n

SIEMENS





Introducing the MOBIL XR: A revolutionary concept in X-ray systems

Siemens has taken the concept of mobile X-ray systems and redesigned it from top to bottom. The result is total freedom of positioning, exceptional maneuverability, and ease of operation seen only in the MOBIL XR.

Only the MOBIL XR simplifies positioning.
Its innovative flexible extender arm provides a height and distance capability over and above any other mobile X-ray system. Without moving the unit from the foot of the patient's bed, the operator can easily maneuver the X-ray tube housing into any position, including lateral. Typically, at a bed height of 32 inches, the MOBIL XR will allow a 60-inch source-image distance. No other mobile unit can offer this capability.

Only the MOBIL XR has complete computerized organ programming.
By simply activating the push-button controls, the operator can select specific organ programs, reprogram the unit for specialized application techniques, or switch to manual settings. And for functional security, a digital readout displays the Kv, mAs, and battery condition of the unit.



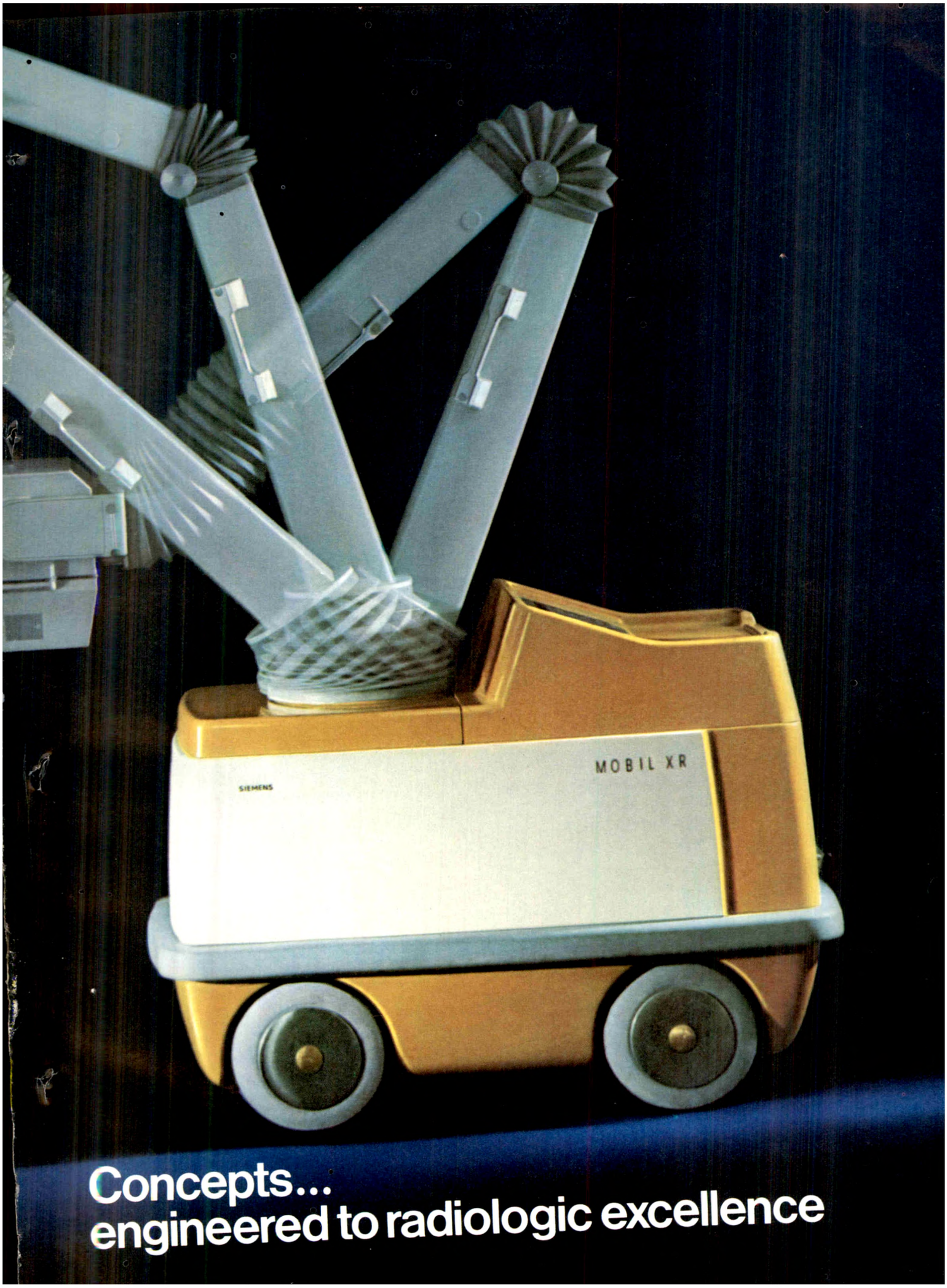


Only the MOBIL XR has a custom-designed cassette tunnel.
It establishes and maintains the proper perpendicular relationship between X-ray tube and film cassette to provide optimum geometric positioning accuracy.

Only the MOBIL XR is easy to clean and keep aseptic.
That's because its design is free of corners, ridges, and hidden surfaces. Bacteria has no place to hide on the smooth fiberglass body of the MOBIL XR.

The Siemens family of mobile X-ray units extends beyond the MOBIL XR to include the KONDIAMOBIL 125 and the SIREMOBIL 2U. All are products of the quality engineering that reflect Siemens' standard of excellence in the field of radiological equipment.

For further information, please contact your local Siemens Representative or Siemens Corporation, Medical Systems Division, 186 Wood Avenue South, Iselin, New Jersey (201) 494-1000. In Canada: Siemens Canada Limited, P.O. Box 7300, Pointe Claire 730 P.Q.

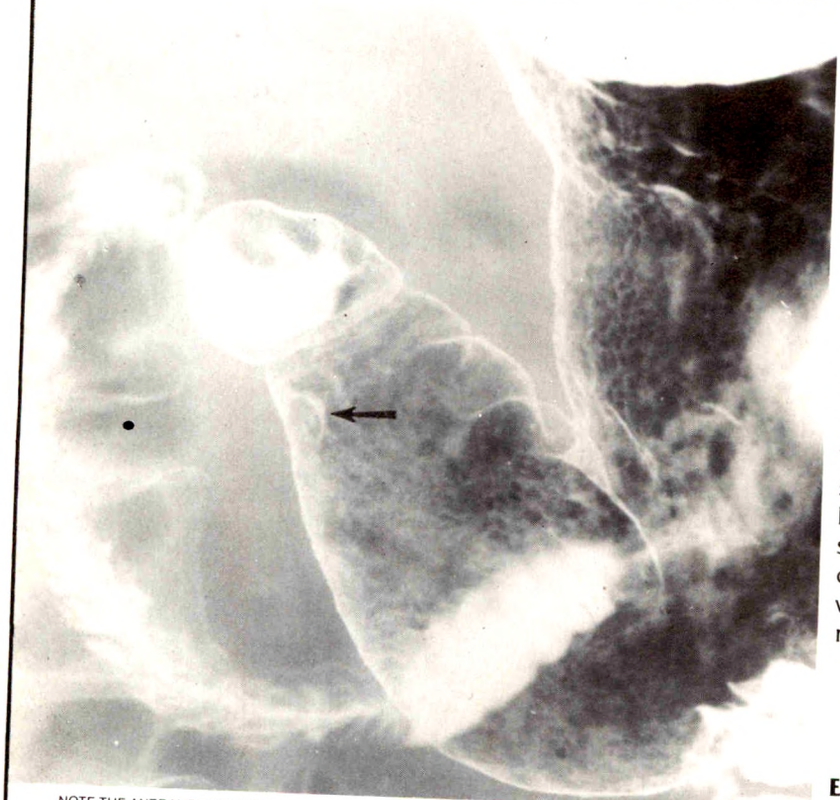


Concepts...
engineered to radiologic excellence

For Double Contrast Stomachs, Use

E-Z-HD™

High Density with High Fluidity Barium Sulfate for Suspension



NOTE THE ANTRAL POLYP (ARROW) AND THE LACELIKE AREAE GASTRICAE IN THE BODY OF THE STOMACH. Film, courtesy of Robert E. Koehler, M.D. Washington University, Dept. of Radiology, St. Louis, Missouri.

Double contrast radiography appears to offer the potential for significant improvements in diagnostic accuracy.

Double contrast studies of the stomach best demonstrate the surface pattern of the stomach (areae gastricae). This leads to improved detection of superfical erosions and ulcers, malignancies, polyps and other benign tumors, and ulcer scars.

E-Z-HD barium sulfate provides the basic ingredient necessary for good double contrast of the stomach.

The higher the density of the barium suspension, the better the coating. E-Z-HD allows for the highest density suspension of any commercial product on the market today: 85% w/w, 250% w/v. E-Z-HD achieves this density while remaining fluid for ease of administration.

- High density
- High fluidity
- Palatable
- Unit dose convenience.

E-Z-HD — The barium for the double contrast examination of the stomach and duodenum.

Optimal Density & Fluidity for the Modern Double Contrast Examination of the Stomach and Duodenum

Refrences:

David W. Gelfand: The Japanese-Style Double Contrast, Examination of the Stomach, Gastrointest Radiol. 1, 7-17 (1976)

Igor Laufer: The Diagnostic Accuracy of Barium Studies of the Stomach and Duodenum — Correlation with Endoscopy, Radiology 115: 569-573, June 1975

Roscoe E. Miller: The Air Contrast Stomach Examination: an overview. Radiology 117: 743-744 Dec. 1975

E-Z-EM

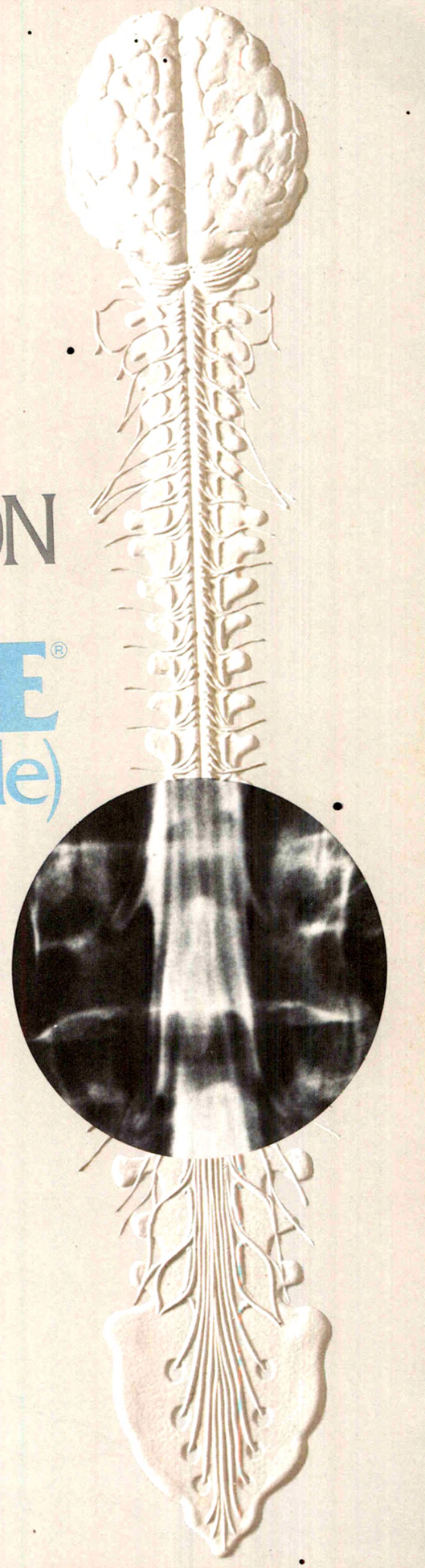
For Further Information Write:

7 Portland Ave.
Westbury, New York 11590
(516) 333-8230

9/77

DISCOVER MORE WITH CLEAR DEFINITION

new AMIPAQUE® (metrizamide)

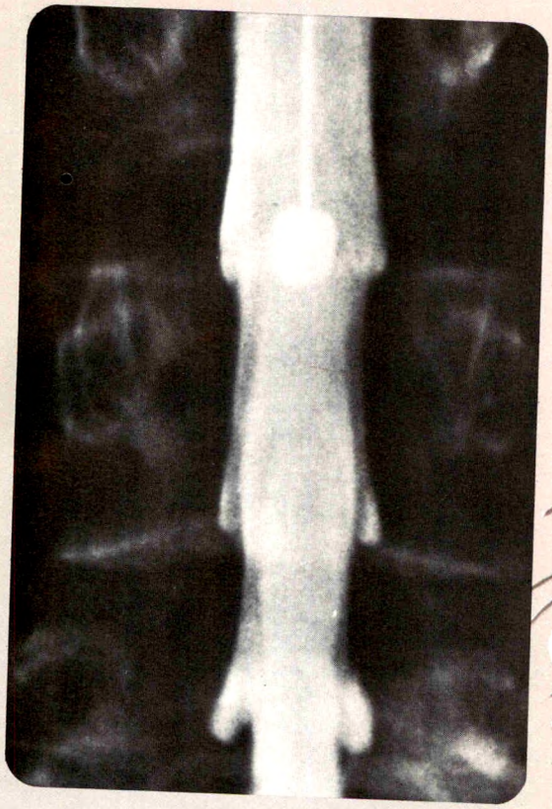


See last page for important product information including warnings, adverse reactions, and prescribing and precautionary recommendations.

COMPARE RADIOGRAPHS

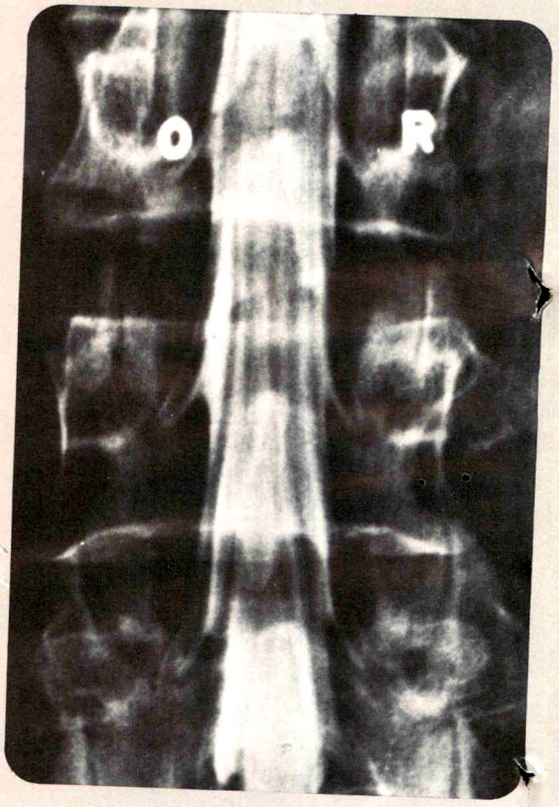
iophendylate

Lumbar myelogram of 27-year-old female (anteroposterior view): Note high-density shadows and failure of contrast medium to adequately fill nerve-root sheaths.



AMIPAQUE (metrizamide)

Lumbar myelogram of 20-year-old male (anteroposterior view): Note graded density of shadows and filling of nerve-root sheaths by the low-viscosity, water-soluble contrast medium.



See last page for important product information including warnings, adverse reactions, and prescribing and precautionary recommendations.

CLEARER VISUALIZATION

Water-soluble, low viscosity

- ☐ Miscible with CSF for more uniform distribution around structures in subarachnoid space.[1,2]
- ☐ Flows into and through narrow subarachnoid spaces, fills slender cavities of nerve-root sheaths.[1,3]
- ☐ Usually diffuses around all except total obstructions with a single injection.
- ☐ Radiographic contrast provides nonobscured view of fine details.

Slightly hyperbaric

- ☐ Allows control of contrast distribution during initial phase of radiologic study, if desired.[1,3]

SIMPLIFIED MYELOGRAPHY

Nonionic... does not dissociate in solution

Isotonic with CSF at concentrations most frequently used (170 mgI/ml).

Low viscosity

- ☐ Allows use of narrow-bore needle (22-gauge).
- ☐ Less chance of CSF leakage... less chance of trauma to dura.

Resorbed and excreted mainly via kidneys in 48 hours

- ☐ No need for aspiration or second puncture... lessens potential for neurologic damage.
- ☐ No needle left in place during procedure... facilitates patient manipulation.

PATIENT TOLERANCE

- ☐ In general, the types of adverse reactions following subarachnoid injection of AMIPAQUE are not substantially different from those seen after lumbar puncture alone.
- ☐ The most frequently occurring reactions are headache, nausea, and vomiting.
- ☐ Rarely have reactions been severe or persistent beyond 24 hours.
- ☐ Although metrizamide is relatively safe and, in comparative studies, less toxic than other compounds for these indications, side effects ranging from headache and nausea to epileptic fits, convulsions, slow wave patterns on EEGs, petit mal states, paralysis, and arachnoiditis have occurred with the use of such compounds. Neurologic examinations were performed before and at intervals after the procedures in 1,495 of 1,850 cases. No clinically significant changes were found.

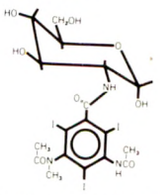
INDICATIONS: lumbar, thoracic, cervical, and total columnar myelography; and for use in computerized tomography of the intracranial subarachnoid spaces following spinal subarachnoid injection.

new **AMIPAQUE**® (metrizamide)

More fully investigated before introduction than any other subarachnoid contrast agent

☐ 158 published reports ☐ 5 years in clinical research ☐ 2 years in U.S. medical centers

Description: Metrizamide, 2-[3-Acetamido-2,4,6-triiodo-5-(N-methylacetamido) benzamido]-2-deoxy-D-glucopyranose, is a compound derived from metrizoic acid and glucosamine. It is a nonionic water-soluble contrast medium with a molecular weight of 789 (iodine content: 48.25%). The chemical structure is as follows:



AMIPAQUE (metrizamide) is provided as a sterile, white lyophilized powder. Each 3.75 g/20 ml vial contains 3.75 g metrizamide (1.81 g organically-bound iodine) and 1.2 mg edetate calcium disodium. Each 6.75 g/50 ml vial contains 6.75 g metrizamide (3.26 g organically-bound iodine) and 2.16 mg edetate calcium disodium.

Each 20 ml vial of sterile aqueous diluent contains 0.05 mg/ml sodium bicarbonate in water for injection, pH is adjusted with carbon dioxide, USP, if necessary.

When AMIPAQUE is reconstituted to the lowest recommended concentration (170 mgI/ml) it has a specific gravity of 1.184 at 37°C, is hyperbaric to cerebrospinal fluid, is isotonic with CSF, and has a pH of approximately 7.4.

Clinical Pharmacology: AMIPAQUE is absorbed from cerebrospinal fluid into the bloodstream. Approximately 60 percent of the administered dose is excreted unchanged through the kidneys within 48 hours.

The initial concentration and volume of the medium, in conjunction with appropriate patient manipulation, will determine the extent of the diagnostic contrast that can be achieved. This can be monitored by fluoroscopy.

Following spinal subarachnoid injection, conventional radiography will continue to provide diagnostic contrast for approximately an hour. At 4 to 5 hours contrast is hazy and none is detectable at 24 hours.

Following subarachnoid placement, irrespective of the position the patient has maintained, upward diffusion of AMIPAQUE takes place through the CSF.

After introduction into the lumbar subarachnoid space, computerized tomography (CT) shows CSF contrast enhancement in the thoracic region in about one hour, in the cervical region in about 2 hours, and in the basal cisterns in 3 to 4 hours.

When low doses of AMIPAQUE (see DOSAGE AND ADMINISTRATION) are introduced into the lumbar CSF and moved cephalad under gravity control and examined by CT scanning, they will provide immediate CSF contrast in the basal cisterns. Depending on the specific technique used, the lateral, third, and fourth ventricles may also be visualized. The contrast in this area will markedly diminish at 6 hours and disappear by 24 hours. CSF enhancement will be evident at the cortical sulci and interhemispheric fissures at 6 hours. Between 12 and 24 hours the surfaces of the cerebrum and cerebellum, in contact with the subarachnoid spaces, will develop a "blush" effect on the scan which will normally disappear in 36 to 48 hours. The rate, time, extent of diffusion, and the disappearance or stasis of AMIPAQUE as demonstrated with CT scanning, can be used to detect or infer the presence of CNS abnormalities.

Indications and Usage: AMIPAQUE is indicated for lumbar, thoracic, cervical, and total columnar myelography and for use in computerized tomography of the intracranial subarachnoid spaces following spinal subarachnoid injection.

Contraindications: AMIPAQUE should not be administered to patients with a known hypersensitivity to metrizamide.

Warnings: If grossly bloody CSF is encountered, the possible benefits of a myelographic procedure should be considered in terms of the risk to the patient.

Usage in pregnancy. No teratogenic effects attributable to AMIPAQUE have been observed in reproduction studies in animals. However, before administration of AMIPAQUE to women during pregnancy, the benefit to the patient should be carefully weighed against the possible risk to the fetus.

Until further experience is gained in children younger than 12 years, administration of AMIPAQUE in this age group is not recommended.

Fatal reactions have been associated with the administration of water-soluble contrast media. Although no fatal reactions have been associated with AMIPAQUE, it is of utmost importance that a course of action be carefully planned in advance for the immediate treatment of serious reactions, and that adequate and appropriate facilities and personnel be readily available in case of a severe reaction.

Precautions: Caution is advised in patients with a history of epilepsy, severe cardiovascular disease, chronic alcoholism, multiple sclerosis, or with a history of bronchial asthma or other allergic manifestations.

Before a contrast medium is injected, the patient should be questioned for a history of allergy. Although a history of allergy, including asthma, may imply a greater than usual risk, it does not arbitrarily contraindicate the use of the medium. Premedication with antihistamines to avoid or minimize possible allergic reactions may be considered. No conclusive relationship between severe reactions and antigen-antibody reactions or other manifestations of allergy has been established.

Patients who are receiving anticonvulsants should be maintained on this therapy. Should a seizure occur, intravenous diazepam or sodium phenobarbital is recommended.

Prophylactic anticonvulsant treatment with barbiturates or diazepam orally for 24 to 48 hours should be considered in patients with evidence of inadvertent intracranial entry of a large or concentrated bolus of the contrast medium since there is an increased risk of seizures in such cases.

Any drugs, such as neuroleptics, including phenothiazine derivatives, which lower the seizure threshold should be avoided. These drugs should not be used as premedications. If possible, they should be withdrawn at least 48 hours before the examination and not used for at least 12 hours postprocedure.

In patients with severe renal insufficiency or failure, the drug is excreted by the liver into the bile at a much slower rate. Patients with hepatorenal insufficiency should not be examined unless the possibility of benefit clearly outweighs the additional risk. Reexamination should be delayed for five to seven days.

Adverse Reactions: In general, the adverse reactions following subarachnoid injection of AMIPAQUE are not substantially different from those seen after lumbar puncture alone. The most frequently occurring adverse reactions are headache, nausea, and vomiting. These reactions occur 3 to 8 hours postinjection, almost all occurring within 24 hours. They are usually mild to moderate in degree lasting for a few hours and disappearing within 24 hours. Rarely have the headaches been severe or persisted beyond 24 hours.

Backache, neck stiffness, numbness and paresthesias, leg or sciatic-type pain occurred less frequently, often in the form of a transient exacerbation of preexisting symptomatology. Temperature elevations and dizziness have also been reported.

Rarely, muscle spasm or generalized convulsions have occurred 4 to 8 hours following injection and in some cases were attributed to a history of epilepsy, medication with neuroleptic drugs, or inadvertent overdose. In all cases, treatment with intravenous diazepam or sodium phenobarbital has provided rapid control.

Transient alterations in vital signs may occur, the significance of which is difficult to assess since these parameters may be affected by the procedure or the patient's physical or emotional state.

Other rarely occurring adverse reactions include the following:

Allergy or Idiosyncrasy: chills, pruritus, urticaria, nasal congestion, and dyspnea.

CNS: mild and transitory perceptual aberrations such as hallucinations, depersonalization, anxiety, depression, hyperesthesia, visual and speech disturbances, confusion and disorientation. In addition, malaise, weakness, EEG changes, and meningismus have occurred.

Cardiovascular: chest pain, tachycardia, bradycardia, and arrhythmia.

Other: diarrhea.

Dosage and Administration: The dosage and concentration of AMIPAQUE will depend on the degree and extent of contrast required in the area(s) under examination and on the equipment and technique employed. Concentrations which are approximately isotonic (170 to 190 mgI/ml) are recommended for examination in the lumbar region. For movement of the medium to distant target areas, higher concentrations are recommended to compensate for dilution of AMIPAQUE with CSF.

A total dose of 3000 mg of iodine should not be exceeded.

The recommended usual and maximum doses of AMIPAQUE are summarized in the following table:

DOSAGE TABLE

Procedure	Conc. of Solution (mgI/ml)	Usual Recommended Dose* (ml)	Max. Dose Total (mgI)
Lumbar myelogram	170-190	10-15	2850
Thoracic myelogram	220	12	2640
Cervical myelogram (via lumbar injection)	250-300	10	3000
Cervical myelogram (via lat. cervical inj.)	220	10	2200
Total columnar myelography	250-280	10	2800
CT cisternography (via lumbar inj.)	170-190	4-6	1140

*Refer to RECONSTITUTION TABLE for preparation of Solution.

PATIENT MANAGEMENT

PREPROCEDURE: Anesthesia is not necessary. Premedication sedatives or tranquilizers are usually not needed. The use of neuroleptic drugs, including phenothiazine derivatives, should be avoided and such medication should be discontinued, when possible, 48 hours before the procedure (see PRECAUTIONS). Epileptic patients should be maintained on their anticonvulsant medication.

INSTRUCTIONS FOR PREPARATION OF THE SOLUTION: Contents under vacuum. Use only if vacuum is present as evidenced by diluent being drawn into vial when stopper is punctured.

1. Fill a sterile syringe with the exact volume of diluent as indicated in the following RECONSTITUTION TABLE to obtain the desired iodine concentration. *Examples: a.* For vials containing 3.75 g AMIPAQUE: To obtain 170 mgI/ml, use 8.9 ml of diluent; to obtain 190 mgI/ml, use 7.8 ml of diluent. *b.* For vials containing 6.75 g AMIPAQUE: To obtain 170 mgI/ml, use 16.1 ml of diluent; to obtain 190 mgI/ml, use 14.0 ml of diluent.

RECONSTITUTION TABLE

Conc. of Solution (mgI/ml)	Volume of Diluent to be Added 3.75 g Vial (ml)	6.75 g Vial (ml)
170	8.9	16.1
180	8.3	15.0
190	7.8	14.0
220	6.5	11.7
250	5.5	10.0
260	5.2	9.4
270	5.0	9.0
280	4.7	8.5
290	4.5	8.1
300	4.3	7.8
	The volume of the final solution will equal the volume of the diluent + 1.7 ml	The volume of the final solution will equal the volume of the diluent + 3.1 ml

The volume of the final solution will exceed the amount required to achieve the recommended dosage. For precise volume for injection refer to DOSAGE TABLE.

2. Inject the diluent into the vial, and leave the syringe and needle in place.
3. Gently swirl the vial (without shaking) until its contents are dissolved (approximately 3 to 10 minutes). The solution should be clear and colorless to slightly yellow.

Use immediately after reconstitution (see DOSAGE AND ADMINISTRATION). Discard any unused portion.

As with any lumbar puncture, sterile technique must be employed. The lumbar puncture is usually made between L3 and L4, but if pathology is suspected at this level the interspace immediately above or below may be selected. A lateral cervical puncture may also be used.

POSTPROCEDURE: The lumbar puncture needle may be removed immediately following injection since it is not necessary to remove AMIPAQUE after injection into subarachnoid spaces.

Management of the patient is similar to that used following simple lumbar puncture. Maintaining the patient recumbent in bed with the head raised 15° to 30° for 8 hours may reduce the rate of upward dispersion of the medium. The patient may then remain horizontal for a further 16 hours at the discretion of the physician.

How Supplied: *Kits, each containing:* one-3.75 g/20 ml single-dose vial of AMIPAQUE with 1 vial of diluent (NDC 0024-0044-01); or one-6.75 g/50 ml single-dose vial of AMIPAQUE with 1 vial of diluent (NDC 0024-0046-01).

Combination packs, each containing: five-3.75 g/20 ml single-dose vials of AMIPAQUE with 5 vials of diluent (NDC 0024-0044-12); or five-6.75 g/50 ml single-dose vials of AMIPAQUE with 5 vials of diluent (NDC 0024-0046-12).

Protect vials of AMIPAQUE from light.

References: 1. Grainger RG, Kendall BE, Wylie IG: Lumbar myelography with metrizamide—a new non-ionic contrast medium. *Br J Radiol* 49:996-1003, 1976. **2.** Peeters FLM: Myelography with metrizamide. *Radiol Clin* 46:203-213, 1977. **3.** Hindmarsh T: Myelography with the non-ionic water-soluble contrast medium metrizamide. *Acta Radiol [Diagn] (Stockh)* 16:417-435, 1975.

new **AMIPAQUE®** (metrizamide)

from the originators of the broad line of contrast media

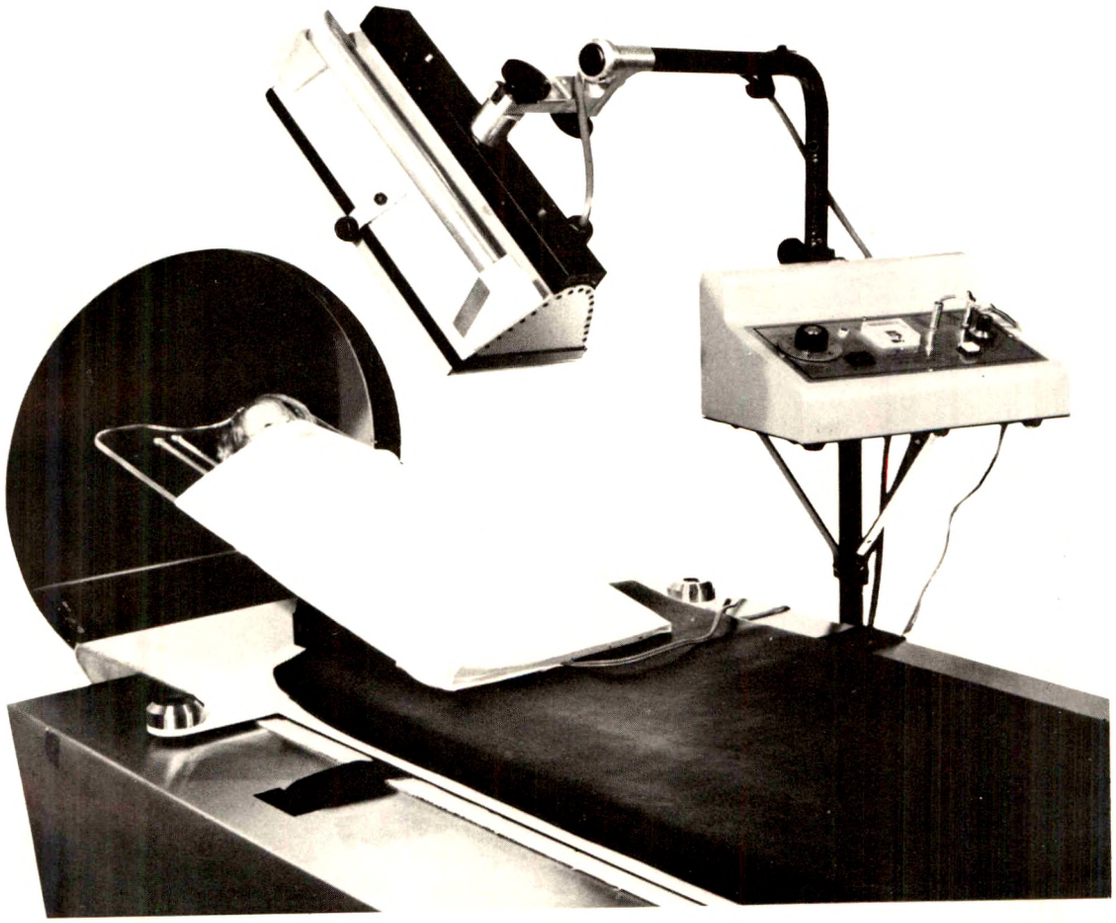
Winthrop

Winthrop Laboratories
New York, N.Y. 10016

4023

temp • guard™

temperature stabilizer



- coverless temperature support system for complete accessibility
- mobile and versatile
- for use in fluroscopy, special procedures, c.t. and ultrasound
- feed back probe which provides accurate temperature control and readout display
- fail safe instrumentation

call direct 716 882-0862

or write

gordon consultants, inc. 361 dewitt st. • buffalo, new york 14213



NEW *KODAK* AUTOMIXER PUTS *KODAK* CHEMICALS TO WORK FOR YOU.

FAST. EASY. EFFICIENTLY.

There are at least seven important reasons to use this new mixer with your automatic processors. You may discover others.

To be sure of consistent processing results, your chemicals should be fresh and accurately mixed. The new KODAK Automixer handles this chore for you with astonishing ease. One automixer will feed two processors.

1. Easy to load. The convenient batch size (5 gallons each for developer and fixer replenishers) makes it easy for the operator—no heavy chemical containers to lift. Dispenser automatically breaks seals, meters in the correct amount of water, while uniformly mixing the fresh replenisher.

2. Safe. The plastic openers are permanently mounted. They do not move. Dispenser shapes are such that they will accept only the correct chemical containers.

3. Fast. Mix takes from 2 to 3½ minutes, depending on local water pressure. Far faster than manual operation.

4. Fresher chemicals. With a total 10-gallon capacity, chemical oxidation is reduced, keeping chemicals at full potency.

5. Easy to teach. Because operation is so simple, personnel training time is minimal. And because handling is neat, simple, and quick, department personnel can easily attend to it.

6. Automatic. The automixer protects against accidental refills with water alone. An automatic signal tells you when levels are low.

7. Accessible. Outlets on the tanks will accept standard replenisher hoses from any processors.

Ask your Kodak Technical Sales Representative to tell you more about the new KODAK Automixer. It's the fast, easy, efficient way to put KODAK Chemicals to work. Or write: Eastman Kodak Company, Dept. 740-B, Rochester, New York 14650.

TURNING ENERGY INTO IMAGES

Kodak

COMPUTED TOMOGRAPHY • NUCLEAR MEDICINE
ULTRASOUND • RADIOGRAPHY • THERMOGRAPHY

AJR Guidelines for Authors

Address manuscripts and correspondence to the Editorial Office, American Journal of Roentgenology, 403 Pacific National Bank Building, 4545 15th Avenue N.E., Seattle, Washington 98105; telephone (206)633-2754.

Publication Policy

The Journal publishes original and timely contributions to the advancement of radiologic diagnosis and treatment. Although the content is predominantly clinical, laboratory investigations are accepted when their relevance to clinical practice is demonstrable. In prospective clinical investigations, authors should indicate if informed consent from patients was obtained. Decisions on manuscripts are based on the opinions of at least two outside reviewers. Reviewers receive manuscripts without title pages to protect the identity of authors and to ensure an unbiased review; names of reviewers, in turn, are not revealed to authors. Statements within an article are the responsibility of the authors and not the Journal or its publisher.

It is understood that material submitted has not been published and is not currently submitted elsewhere. Portions of the data or illustrations from previously published works may be included if permission release forms accompany the manuscript and such material is clearly credited in the text. Prior publication of abstracts will not prejudice publication of the complete study.

Copyright Information

In accordance with Journal implementation of the 1976 U.S. Copyright Law, authors must release first and subsidiary rights to their manuscript at submission. A dated cover letter, containing signatures of all authors, should state: "We, the authors, assign first and subsidiary rights to the American Roentgen Ray Society in the event that our manuscript (title) is published by AJR." The Journal, in turn, grants authors the right to use portions of their manuscript, without charge, in books or articles of which they are authors or editors.

Manuscript Form

Manuscripts should be typed double-spaced throughout, including references, tables, and figure legends. Tables, footnotes, and figure legends should be on separate sheets, and a separate title page should be provided. In addition to the original typewritten copy, a duplicate copy complete with figures, tables, and references is required. Authors' names should be on title page only and should not be on figures so that author anonymity can be maintained during the review process.

Figures should be submitted as 13 × 18 cm glossy prints, untrimmed and unmounted. Labels and arrows must be of professional quality and should be removable from the prints. Each figure should be numbered to correspond with figure legends, and the top should be indicated. Specific permission for publication of facial photographs of patients is required. Line illustrations and graphs should be drawn in black ink on white background.

References should be cited in the text by number (e.g., [3, 4]). The bibliography should be arranged in the numerical order that references are cited in the text and typed double-spaced throughout. Data for each reference should be arranged according to the uniform style on bibliographic citations adopted by many biomedical journals. Provide all authors' names and inclusive pages. Abbreviations for titles of medical periodicals should conform to those published in *Index Medicus*. Examples:

1. Miller RE, Chernish SM, Skucas J, Rosenak BD, Rodda BE: Hypotonic roentgenography with glucagon. *AJR* 121:264–274, 1974
2. Boijsen E: Superior mesenteric angiography, in *Angiography*, edited by Abrams H, Boston, Little, Brown, 1971, pp 1091–1119

Organization

Title page. Titles should be brief and specific. Include addresses for each author and acknowledgment of grant support when appropriate.

Abstract. A description of the purpose, methods, results and conclusions of the study is required.

Introduction. Clearly state the purpose of the investigation including necessary background facts.

Materials and methods. Decribe the protocol clearly. Use standard abbreviations as presented in the *Council of Biology Editors Style Manual*, 3d ed. Metric measurements should be used throughout.

Results. Present results in logical sequence.

Discussion. Interpret the results to lend meaning and importance to the observations. Hypotheses and speculation based on the results are encouraged. When results differ from those of previous investigators, an attempt should be made to explain the discrepancy.

References. Only include references which provide adequate background and present fairly any opposing evidence and concepts. Accuracy of reference data is the responsibility of the author.

Legends. Legends should be brief but should provide sufficient description to interpret the figure.

Special Communications

Case Reports. Concise case reports are accepted if they present unusual experiences that are medically important and educational. Clarity and brevity are essential. After preliminary screening by an editor to determine whether the requirement of medical significance has been met, qualifying papers will undergo the same peer review as major papers.

Technical notes. Brief descriptions of new techniques or significant modifications of older ones which are directly applicable to clinical practice will be accepted.

Letters to the Editor. Letters are subject to editing and condensation. Criticism of published articles should be objective and constructive. Letters may also discuss matters of general interest to radiologists.

Radiographic Manifestations of Burkitt's Lymphoma in American Patients

N. REED DUNNICK,[1] GREGORY H. REAMAN,[2] GORDON L. HEAD,[1] THOMAS H. SHAWKER,[1] AND JOHN L. ZIEGLER[2]

Radiographic manifestations of Burkitt's lymphoma in 40 American patients are presented. Pleural effusions were the most common intrathoracic abnormality and were correlated with abdominal ascites more often than with intrathoracic tumor. Tumor involved bone in four patients, and in two instances included the mandible. Twelve patients had intrinsic bowel involvement; nine instances were in the ileum. Intrinsic renal tumor was seen in only two patients. Both ultrasound and computed tomography were useful.

Undifferentiated Burkitt's type malignant lymphoma is a distinct entity with well defined clinical, immunologic, histologic, and cytochemical features [1]. Patients from endemic areas in Africa differ clinically from patients from nonendemic areas [2]. Americans with Burkitt's lymphoma have a lower incidence of jaw tumors, but a higher incidence of abdominal tumors, pleural effusions, and peripheral lymph node involvement [3, 4]. While radiographic manifestations of Burkitt's lymphoma from endemic areas in Africa have been presented [5–8], only a few Americans with Burkitt's lymphoma have been reported [9–12]. We studied 40 previously untreated patients admitted to the Pediatric Oncology Branch of the National Cancer Institute since March 1974. Radiographic findings at admission are described.

Subjects and Methods

Forty consecutive patients referred to the National Institutes of Health Clinical Center for evaluation and treatment of Burkitt's lymphoma since March 1974 underwent pretreatment evaluations to determine the extent of disease. Age range was 2–38 years (median, 12) (fig. 1); 30 were male and ten were female. All were American; 39 were Caucasian and one was of Oriental descent.

Clinical and histological material for all patients was reviewed to confirm the diagnosis. All radiographs performed here were reviewed by two of us (N. R. D. and G. H.). In many cases outside studies were also available for review. In three cases, outside radiographs could not be retrieved, so the reports were used for this study. Ultrasound examinations were performed on a Picker Gray Scale Echoview [6] System. Computed tomography was performed on an EMI CT 5000 body scanner.

Findings

Abdominal pain or palpable abdominal mass was the initial complaint of 28 of the 40 patients; six of these were localized to the pelvis. Adenopathy in the neck (six patients) or nasopharynx (four) were the other major complaints. One of these patients was found to have Burkitt's lymphoma localized to the tonsil after tonsilectomy. Bone pain was the initial complaint of only two patients, one shoulder and the other mandibular.

Chest

All 40 patients had chest radiographs, and abnormalities related to Burkitt's lymphoma were present in 12 (table 1). Pleural effusion, the most common abnormality, was present in nine patients and associated with ascites in seven patients.

Pleural effusions were bilateral in five patients (fig. 2), while in four patients the effusion was limited to the right side. Two patients had mediastinal adenopathy and one patient had both mediastinal and bilateral hilar adenopathy; however, none of these three had pleural effusions. In addition, soft-tissue neck masses were visible on chest radiographs in two patients and axillary masses were identified in two others. No full lung tomograms were performed.

Abdomen

Plain films of the abdomen demonstrated ascites in nine patients, and in one it was seen on abdominal ultrasound. Seven of these ten patients had associated pleural effusions. Abdominal plain films were also useful in detecting abdominal masses (four cases), pelvic masses (six), small bowel obstruction (four), splenomegaly (three), and hepatosplenomegaly (one).

Gastrointestinal Tract

Nine patients had radiographic evidence of intrinsic involvement of the gastrointestinal tract: one in the stomach, seven in the small bowel, and one in the colon. No cases involved the esophagus. In addition, 11 patients had evidence of tumor masses appearing as extrinsic compression on the small bowel or colon.

Tumor involvement of the bowel was most common in the terminal ileum (six cases) (fig. 3). In four cases this was seen on the small bowel films where the tumor mass and an irregular mucosa indicating tumor invasion were identified. In two patients the tumor involved the terminal ileum and was seen only on the barium enema, since a small bowel series was not performed.

In addition, three patients had evidence of small bowel obstruction on plain abdominal films. At surgery two of

Received September 27, 1977; accepted after revision September 26, 1978.

[1] Department of Diagnostic Radiology, Building 10, Room 6S211, Clinical Center, National Institutes of Health, Bethesda, Maryland 20014. Address reprint requests to N. R. Dunnick.

[2] Division of Cancer Treatment, Pediatric Oncology Branch, National Cancer Institute, National Institutes of Health, Bethesda, Maryland 20014.

0361–803X/79/1321–0001 $0.00

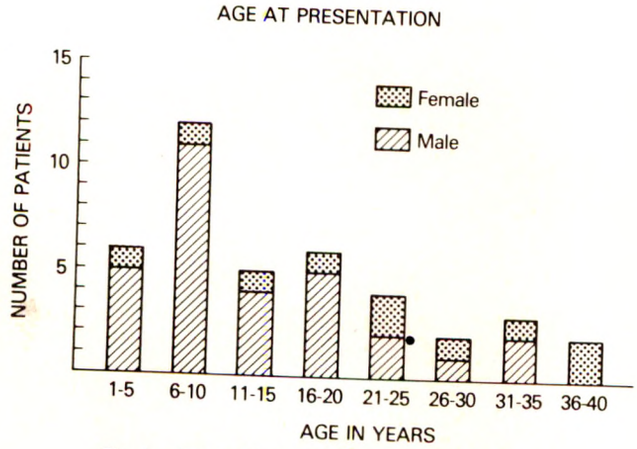


Fig. 1.—Age and sex distribution of the 40 patients.

TABLE 1
Tumor Distribution

Location	No. Patients
Chest:	
Pleural effusion	9
Adenopathy	3
Parenchymal	0
Abdomen:	
Hepatomegaly	1
Splenomegaly	4
Ascites	10
Gastrointestinal tract:	
Stomach	1
Small bowel	10
Appendix	1
Colon	1
Genitourinary tract:	
Renal tumor	2
Ureteral obstruction	6
Ovarian mass	3
Bone:	
Mandible	2
Other bones	4
Adenopathy:	
Cervical	6
Nasopharyngeal	4
Retroperitoneal	0

these patients had intussusceptions and one had a mass in the terminal ileum causing distal small bowel obstruction.

In one patient an intragastric mass believed to be lymphomatous involvement was seen on an upper gastrointestinal series (this was not surgically confirmed). Tumor in the colon, separate from the terminal ileum, was seen only once. This appeared as a retroperitoneal tumor invading the transverse colon, and was also shown on arteriography.

Genitourinary Tract

Two patients had evidence of intrinsic renal involvement. In one an intrarenal mass confirmed on ultrasound regressed after chemotherapy (fig. 4). The second case was confirmed on selective renal arteriography and subsequent nephrectomy (fig. 5).

Excretory urography was abnormal in 14 of 34 cases. In addition to the two cases of intrinsic renal involvement, six patients had ureteral obstruction. In seven

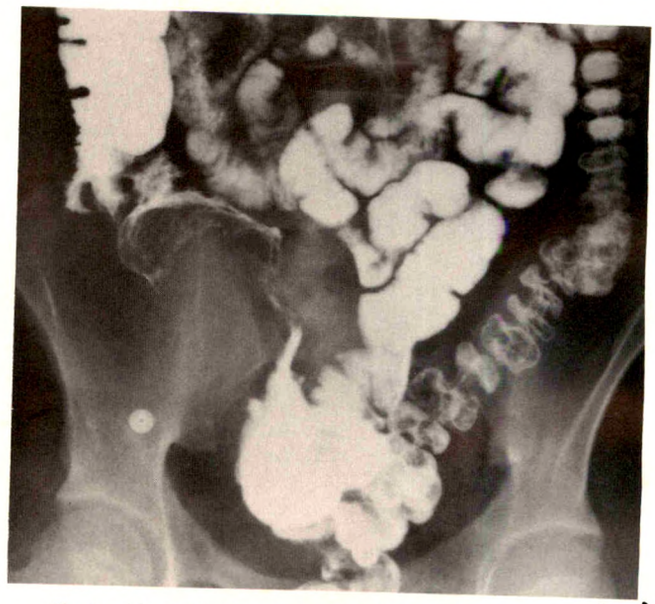


Fig. 3.—17-year-old boy. Large intrinsic mass in terminal ileum.

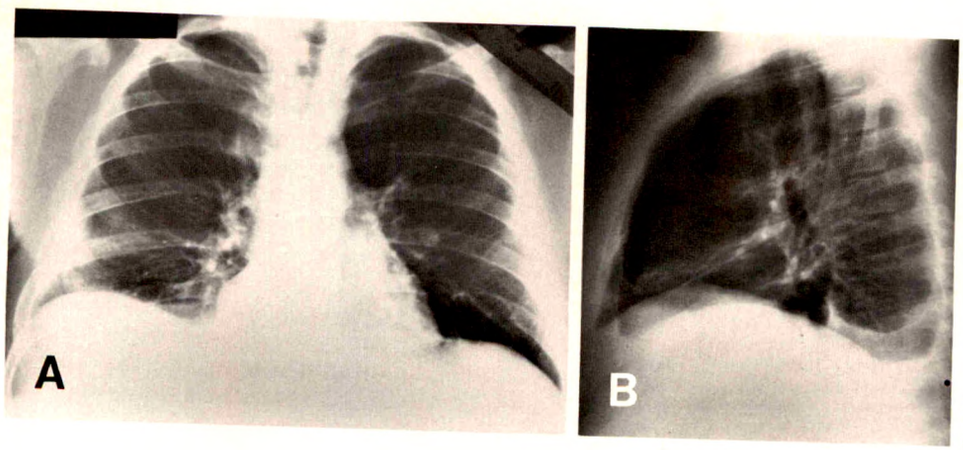


Fig. 2.—16-year-old boy. Bilateral pleural effusions. Bilateral subpulmonary effusions suggested in **A** are easily recognized in **B**.

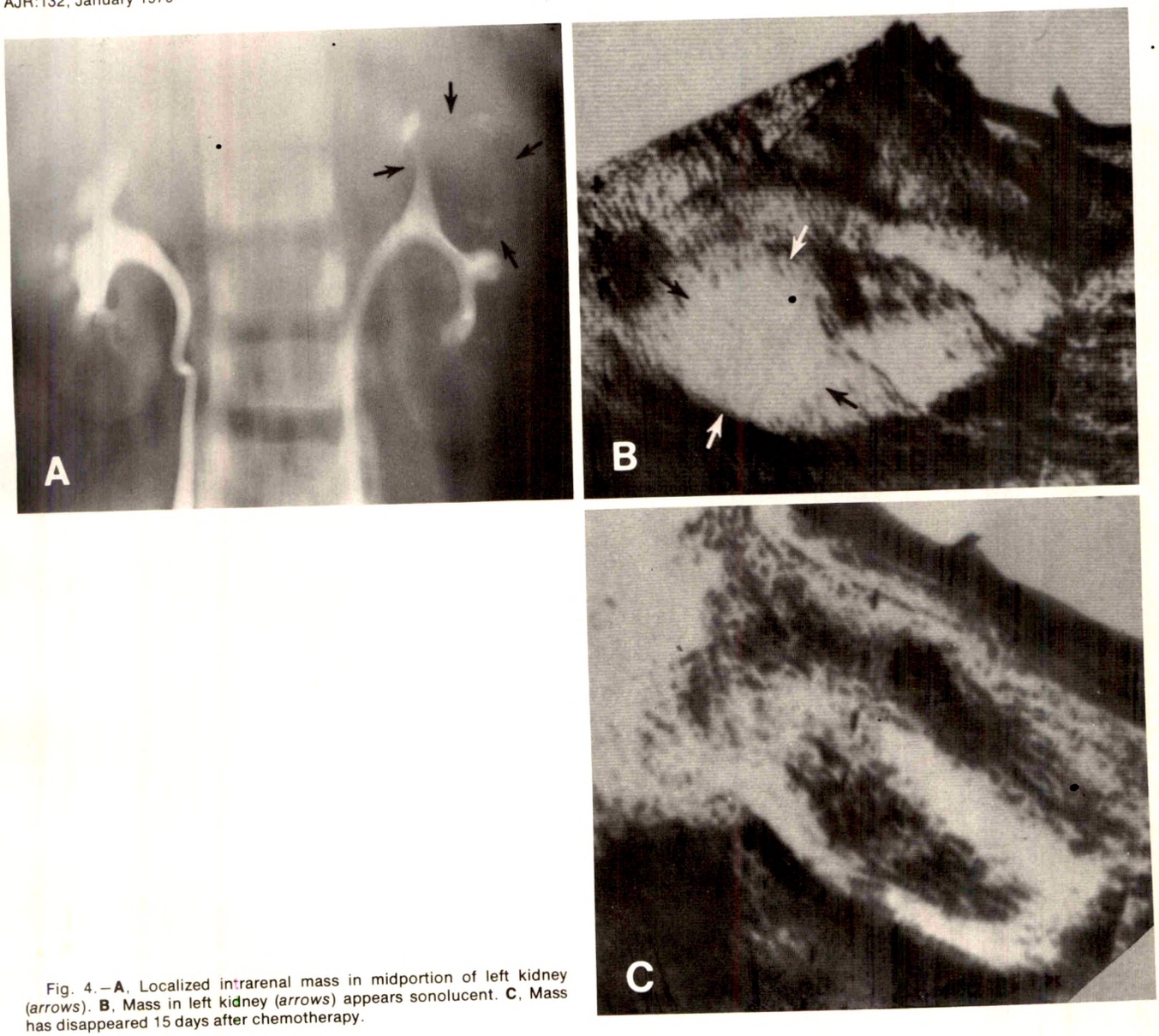


Fig. 4.—**A**, Localized intrarenal mass in midportion of left kidney (*arrows*). **B**, Mass in left kidney (*arrows*) appears sonolucent. **C**, Mass has disappeared 15 days after chemotherapy.

patients (including one who also had ureteral obstruction), a pelvic mass caused extrinsic compression upon the bladder. Three of these had Burkitt's lymphoma involving the ovaries.

Bone

Four of the 40 patients had radiographic evidence of bone involvement. Bone lesions were permeative without local expansion or soft-tissue masses. The two patients with mandibular involvement also had evidence of other bone disease. The humerus was the most commonly involved bone (three of four cases) (fig. 6). The cranial vault, tibia, and ribs were also sites of tumor infiltration.

Additional Studies

Arteriography was performed on two patients. In one patient (fig. 4B) arteriography demonstrated a large hypervascular intrarenal mass in which the vessels were stretched and splayed, but no encasement, venous laking, or arteriovenous shunting was seen. In a second patient arteriography demonstrated a relatively avascular retroperitoneal mass invading the transverse colon that was also confirmed at laparatomy. Bipedal lymphography performed on three patients was normal.

Abdominal sonography was performed in nine patients prior to therapy, and six showed abnormalities consistent with Burkitt's lymphoma. Two had pelvic masses,

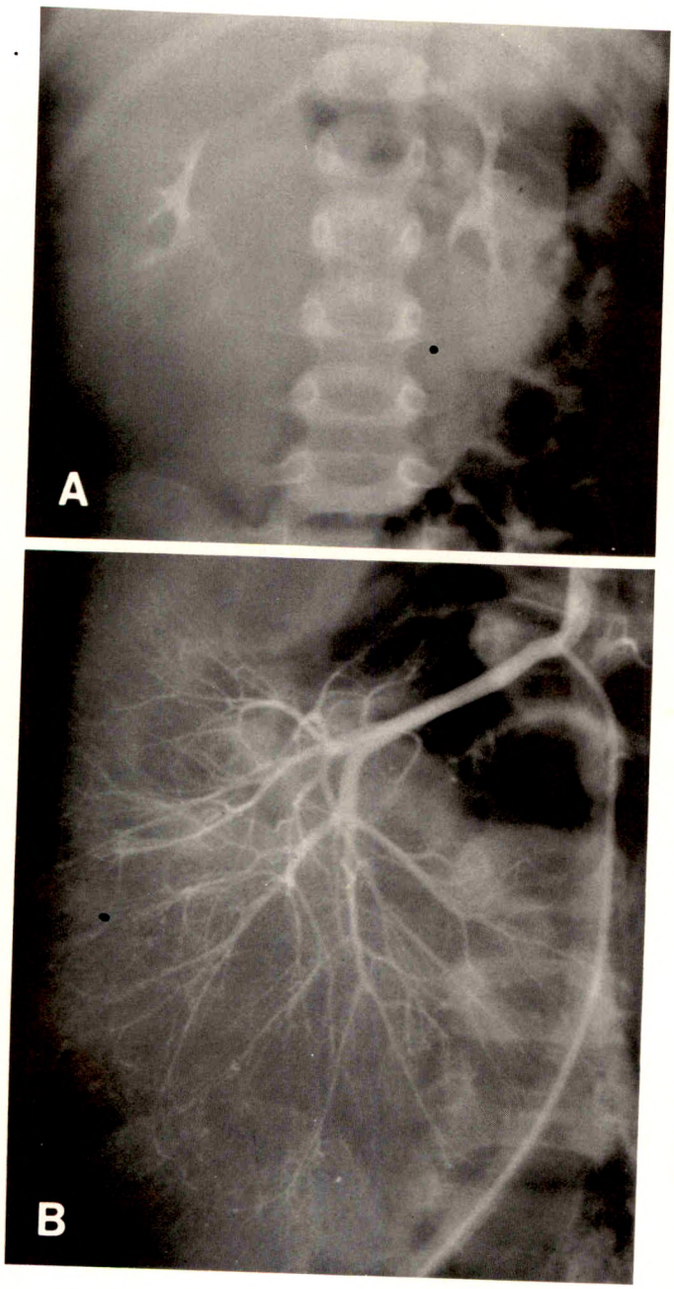


Fig. 5.—2-year-old boy. **A**, Large mass in right kidney. **B**, Kidney diffusely infiltrated with tumor (later confirmed surgically).



Fig. 6.—30-year-old woman. Burkitt's lymphoma involving humerus. Bony lesions have permeative lytic appearance; mandibular involvement also present.

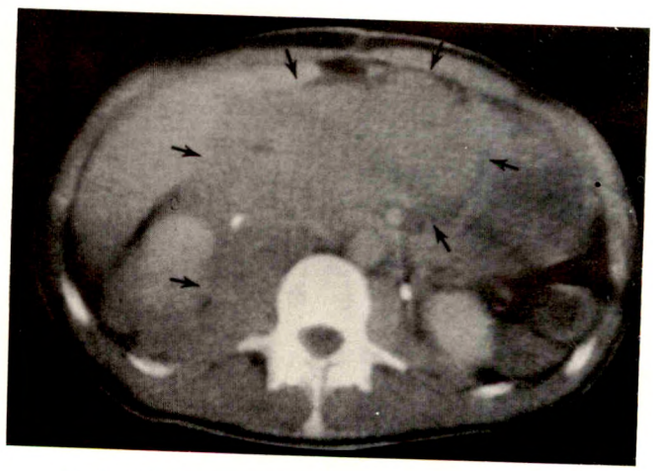


Fig. 7.—33-year-old man. Diffuse abdominal tumor (*arrows*).

one had an abdominal mass, and one had several intrarenal masses. In each instance the mass was relatively sonolucent, almost "cystic." However, in most cases a poorly delineated posterior wall demonstrated its solidity. Ascites was demonstrated in two patients, one of whom also had splenomegaly.

Computed tomography was used to evaluate the presence and extent of tumor in six patients. Large retroperitoneal masses were seen in two patients, one of whom also had splenomegaly (fig. 7). A pelvic mass was seen in one patient and a mediastinal mass previously seen on chest radiography was confirmed in another patient. No evidence of tumor was found in the other two patients.

Discussion

Burkitt's lymphoma is a clinically and histologically distinct tumor first described in African children. It arises from B-lymphocytes, has a rapid doubling time, but responds dramatically to combination chemotherapy [13]. Although endemic in tropical Africa, it is now recognized worldwide. Occurrence of Burkitt's lymphoma in endemic locations and its association with Ebstein-Barr virus has evoked much interest in a possible viral etiology. Clinical findings in patients from nonendemic areas of Africa and other parts of the world differ from those in endemic areas. Predilection for tumors of the jaw in patients from endemic areas is not seen in patients from nonendemic areas where there is a higher incidence of abdominal disease and peripheral nodal involvement. An earlier report from this institution described clinical and pathologic findings in 30 American patients with Burkitt's lymphoma [14, 15].

Pleural effusion is an uncommon initial manifestation of non-Hodgkin's lymphoma with an incidence of less than 10% [16]. When pleural effusion does occur, it is usually a manifestation of intrathoracic lymphoma, either mediastinal or hilar adenopathy, a pleural-based mass, or parenchymal involvement. With Burkitt's lymphoma [17], pleural effusion was present in 23% of the patients, but was associated with abdominal ascites and probably represents passage of ascitic fluid through diaphragmatic communications.

The reverse is true of mediastinal and hilar adenopathy. While it is a common initial finding for patients with non-Hodgkin's lymphoma [18], it appeared in only 7.5% of our patients with Burkitt's lymphoma.

Abdominal and pelvic masses were the most common initial findings in our patients. Many were visible on plain abdominal films, and intrinsic or extrinsic involvement of the genitourinary or gastrointestinal systems was demonstrated on specific studies. As with other non-Hodgkin's lymphomas, the terminal ileum was the most common site of gastrointestinal involvement; but it occurred with much higher frequency in patients with Burkitt's lymphoma.

While renal involvement is commonly found at necropsy in patients with Burkitt's lymphoma or other non-Hodgkin's lymphomas, it is unusual at presentation. Goffinet et al. [16] found only two cases of initial intrinsic renal involvement in a series of 423 consecutive patients with non-Hodgkin's lymphoma. We demonstrated tumor in two of 40 patients (5%), suggesting a higher incidence of renal involvement.

Radiographic evidence of bone involvement was more common in Burkitt's lymphoma than in other non-Hodgkin's lymphomas. We found bone involvement in 10% of our cases at presentation, while it is present in less than 4% of non-Hodgkin's lymphomas. Furthermore, each of our four cases consisted of poorly defined permeative lesions. The sclerotic lesions occasionally seen in other types of malignant lymphomas were not present.

Most radiographic reports of Burkitt's lymphoma describe patients from endemic areas [5–8]; only scattered reports have described North American patients. A patient with both mediastinal and abdominal masses was described in Canada [9]. An intrarenal mass that resolved on therapy was reported in an American patient [10]. The radiographic findings in three American patients with Burkitt's lymphoma were reported, and lesions involving the gastrointestinal tract and mandible, as well as mediastinal adenopathy and pleural effusion, were presented [11]. These findings concur with our series.

More recently reported was a series of 12 American patients with Burkitt's lymphoma [12]. The study described the course of the illness showing the disease process altered by combination chemotherapy. However, as in our series of previously untreated patients, the predilection of intraabdominal tumor sites in American patients with Burkitt's lymphoma was demonstrated.

REFERENCES

1. Berard C, O'Connor GT, Thomas LB, Torloni H: Histopathological definition of Burkitt's tumor. *Bull WHO* 40:601–607, 1969
2. Mann RB, Jaffe ES, Braylan RC, Nanba K, Frank MM, Zeigler JL, Berard CW: Non-endemic Burkitt's lymphoma, a B-cell tumor related to germinal centers. *N Engl J Med* 295:685–691, 1976
3. Cohen MH, Bennett JM, Berard CW, Ziegler JL, Vogel CL, Sheagren JN, Carbone PP: Burkitt's tumor in the United States. *Cancer* 23:1259–1272, 1969
4. Ziegler JL, De Vita VT, Graw RG Jr, Herzig G, Leventhal BG, Levine AS, Pomeroy TC: Combined modality treatment of American Burkitt's lymphoma. *Cancer* 38:2225–2231, 1976
5. Cockshott WP: Radiologic aspects of Burkitt's tumor. *Br J Radiol* 38:172–180, 1965
6. Whittaker LR: Burkitt's lymphoma. *Clin Radiol* 24:339–346, 1973
7. Whittaker LR: Intravenous pyelography in Burkitt's tumor. *Australas Radiol* 14:197–199, 1970
8. Whittaker LR: The radiologic appearance of Burkitt's tumor involving bone. *Australas Radiol* 13:307–310, 1969
9. Davidson JW: Radiographic findings in "Burkitt type" lymphoma. *J Can Assoc Radiol* 19:121–125, 1968
10. Dunnick NR, Cunningham JJ: Burkitt's lymphoma involving the kidney: urographic findings before and after therapy in an American child. *J Urol* 112:394–395, 1974
11. Ferris RA, Hakkal HG, Cigtay OS: Radiologic manifestations of North American Burkitt's lymphoma. *AJR* 123:614–620, 1975
12. Alford BA, Coccta PF, L'Heureux PR: Roentgenographic features of American Burkitt's lymphoma. *Radiology* 124:763–770, 1977
13. Ziegler JL: Treatment results of 54 American patients with Burkitt's lymphoma are similar to the African experience. *N Engl J Med* 297:75–80, 1977
14. Arseneau JC, Carellos GP, Banks PM, Berard CW, Gralnick HR, De Vita VT: American Burkitt's lymphoma: a clinicopathologic study of 30 cases. I. Clinical factors relating to prolonged survival. *Am J Med* 58:314–321, 1975
15. Banks PM, Arseneau JC, Gralnick HR, Canellos GP, De Vita

VT, Berard CW: American Burkitt's lymphoma: a clinicopathologic study of 30 cases. II. Pathologic correlations. *Am J Med* 58:322–329, 1975

16. Goffinet DR, Warnke R, Dunnick NR, Castellino RA, Glatstein E, Nelsen TS, Dorfman RF, Rosenberg SA, Kaplan HS: Clinical and surgical (laparotomy) evaluation of patients with non-Hodgkin's lymphomas. *Cancer Treat Rep* 61:981–992, 1977
17. Aderele WI, Seriki O, Osunkoya BO: Pleural effusion in Burkitt's lymphoma. *Br J Cancer* 32:745–746, 1975
18. Filly R, Blank N, Castellino RA: Radiographic distribution of intrathoracic disease in previously untreated patients with Hodgkin's disease and non-Hodgkin's lymphoma. *Radiology* 120:277–281, 1976

Hepatocellular Carcinoma: Clinical and Angiographic Findings and Predictability for Surgical Resection

WILLIAM M. MARKS,[1] RICHARD P. JACOBS,[1, 2] PHILIP C. GOODMAN,[1] AND ROBERT C. LIM, JR.[3]

Demographic, clinical, and angiographic data were reviewed for 63 consecutive patients with hepatocellular carcinoma. Angiography remains the critical examination in determining extent of disease and potential surgical cure. Angiographic findings were correlated with surgical or autopsy findings for 26 of the patients. The absence of venous invasion and lack of involvement of at least one hepatic segment favor resectability. Selective hepatic injections and oblique views accurately answered these questions in more than 80% of our patients. Pitfalls to angiographic accuracy include vascular invasion by very small tumor masses, hypovascular or diffuse hepatocellular carcinomas, metastatic disease, and involvement of the left lobe.

The prognosis of hepatocellular carcinoma is dismal, with 5-year survival rates reported at only 4%–8% [1]. Surgical resection of this tumor is the only treatment known to effect a cure; however, the surgery is intricate and requires as precise an estimate of tumor site and extent as possible. Such diagnostic methods as radionuclide scanning, CT scanning, and ultrasonography can locate liver tumors and demonstrate whether they are solitary or multicentric. Needle biopsy can allow for histologic definition. However, only angiography can distinguish the lobes and segments of the liver and thus provide the information needed by the surgeon to perform hepatic resection.

We retrospectively studied 63 patients with proved hepatocellular carcinoma to obtain general information on the incidence, survival rate, predisposing factors, extent, and resectability of the disease; to ascertain the frequency of the angiographic findings in hepatocellular carcinoma; and to establish angiographic findings that would help predict the resectability of the tumor.

Materials and Methods

The medical records of all 63 patients with proved hepatocellular carcinoma seen at our institution from January 1965 through January 1977 were reviewed and analyzed regarding age, sex, race, clinical background, and course and outcome of treatment. In 13 patients, diagnosis was made by histologic examination of a liver specimen obtained by percutaneous needle biopsy. In the remaining 50 patients, diagnosis was made by histologic examination of a surgical or autopsy specimen of the liver; this latter group consisted of the patients analyzed for extent and resectability of disease.

Of the original 63 patients, 26 had preoperative angiograms which we reviewed to determine the frequency of radiographic findings. Of these 26 patients, 23 had findings available from surgery or autopsy which we used to attempt to establish angiographic findings that would predict the resectability of hepatocellular carcinoma. Finally, comparison was made between the survival rates of patients who underwent attempted curative surgery and those who did not.

Results

Clinical Findings

Of the 63 patients, 57 were men and six women. The largest racial subgroup was Chinese (43% of patients). Patients' ages ranged from 24 to 93 years. Average age at diagnosis was 58 years: 54.1 years for Chinese, 60.9 years for non-Chinese.

Cirrhosis, the most frequent disease associated with hepatocellular carcinoma, was present in 57% (36 of 63) of all patients, 72% (26 of 36) of non-Chinese, and 37% (10 of 27) of Chinese patients. In most of the non-Chinese group (21 of 26) the cirrhosis was nutritional, whereas in most of the Chinese group (8 of 10) it was macronodular. Other primary malignancies were found in six patients; three patients had *Clonorchis sinensis (Opisthorchis sinensis)*; and one patient had two brothers who died from hepatocellular carcinoma.

Of the 50 patients assessed for extent and resectability of the disease, 37 had evidence of either vascular invasion or distant metastases and thus the tumor was considered not resectable. Of those 39, 30 exhibited vascular invasion (23 by gross examination and seven microscopically). The other nine patients (22%) had distant metastases (e.g., to regional and hilar nodes, lung, peritoneum, or chest wall) without demonstrable vascular invasion.

Follow-up information was available for 60 of the original 63 patients. The 1-year survival rate for the entire group was 12% (7 of 60); the 5-year survival rate was 5% (3 of 60).

Of the 60 patients for whom there were follow-up data, 14 underwent attempted curative surgery. The 1-year survival rate in this group was 43% (6 of 14); the 5-year survival rate was 21% (3 of 14). Five of the 14 patients were found to have tumor involvement of both lobes of the liver. Two of these five had three of the four segments involved; they underwent extended hepatic resection and were able to survive longer than 1 year. One of the 14 patients had vascular invasion by tumor which was demonstrated both angiographically and surgically; he

Received June 8, 1978; accepted after revision September 28 1978.
[1] Department of Radiology, University of California School of Medicine and San Francisco General Hospital, San Francisco, California. Address reprint requests to P. C. Goodman, Department of Radiology, Room 1X55, San Francisco General Hospital, San Francisco, California 94110.
[2] Present address: Department of Radiology, Children's Hospital, 3700 California Street, San Francisco, California 94118.
[3] Department of Surgery, University of California School of Medicine and San Francisco General Hospital, San Francisco, California 94110.

AJR 132:7–11, January 1979
0361–803X/79/1321–0007 $0.0
© 1979 American Roentgen Ray Society

nevertheless underwent attempted curative resection and died within 9 months.

Angiographic Findings

In the 26 patients who underwent visceral angiography, the most common angiographic findings were mass effect, hypervascularity, and neovascularity (table 1). The two patients without angiographic evidence of mass effect were found at necropsy to have diffuse hepatic neoplasia. Tumors in five patients showed no greater vascularity than that of surrounding hepatic parenchyma. All five patients had severe macronodular cirrhosis, distorted vascular architecture, and regenerating nodules. No neovascularity was seen angiographically in the tumors of three patients; two of the tumors were found to have diffuse neoplasia and the other was relatively hypovascular.

Comparison of angiographic with surgical or autopsy findings in 23 patients provided two items of information. First, angiographic and histologic findings were in agreement with respect to distribution (extent) of malignancy in 19 patients (83%); the four errors were in interpretation of the left lobe of the liver. Second, angiographic and histologic findings were in agreement with respect to the presence or absence of vascular invasion by tumor also in 19 patients (83%); eight of these angiographic interpretations were true positives. The four misinterpretations were false negatives (i.e., no angiographic demonstration of the vascular invasion subsequently shown at necropsy).

Of the four patients misdiagnosed regarding extent of the tumor, two were thought to have tumor in the medial segment of the left hepatic lobe where it abuts the right lobe; at surgery, tumor was disclosed to be confined to the right lobe. Another patient had angiographic findings of a hypervascular nodule in the lateral segment of the left lobe, which at autopsy was found to be granulation tissue probably related to a prior splenectomy. The fourth patient demonstrated tumor limited to the right lobe angiographically; at laparotomy the left lobe was disclosed also to be involved. This was our only false negative interpretation regarding extent of the tumor. Thus we agreed with others regarding the difficulty of angiographic examination of the left lobe[2].

TABLE 1

Angiographic Findings in 26 Patients with Hepatocellular Carcinoma

Finding	No. Patients
Mass effect	24
Hypervascularity*	21
Neovascularity	23
Encasement of large arterial vessels	7
Portal hypertension	5
Threads and streaks sign	7
Arteriovenous shunting	5
Evidence of intravascular tumor without streaks	1
Extent of disease:	
Both lobes	17
Right only	6
Left only	1
Indeterminate	2

* Three patients had areas of necrosis.

Discussion

Except for a more pronounced male-to-female predominance (9:1), our results agree with those from other studies of hepatocellular carcinoma [3, 4] as to race, age, and sex distribution. The large percentage (43%) of our patients who were Chinese probably reflects the population base (San Francisco Bay Area) and the underlying predilection of this group for hepatocellular carcinoma. We do not know what percentage of these patients were first-generation Chinese. It is known that Orientals acquire the tumor at a younger age [4].

In 57% (36 of 63) of the patients, cirrhosis was present when hepatocellular carcinoma was diagnosed—somewhat less than the 64%–85% reported by others [5]. Although patients with this carcinoma often have a history of alcoholism [3], our findings of a large number of patients with actual nutritional cirrhosis contradict the usual predominance of macronodular cirrhosis, or cirrhosis that occurs after hepatitis [3, 5, 6]. We do not know whether this represents an actual change in associated conditions, a combination of different types of cirrhosis that was not previously appreciated, or is due to the patient population of our institution. The association of hepatocellular carcinoma with *Clonorchis sinensis* is well known.

Because surgical resection of the liver is today the only curative form of treatment for patients with hepatoma, precise information regarding tumor extent and basic liver anatomy must be available to the surgeon. The liver is divided into lobes, segments, and divisions by ramifications of the hepatic arteries, portal veins, and biliary tracts [7]. This anatomic organization permits removal of individual hepatic lobes, segments, or divisions. Survival is possible even after three of the four hepatic segments have been removed, provided the remaining segment(s) is normal. For technical as well as anatomic reasons, this surgery is usually an extended right hepatectomy (or trisegmentectomy), leaving only the lateral segment of the left lobe (fig. 1) [8].

CT scanning, radionuclide scanning, and ultrasonography cannot demonstrate intrahepatic anatomy precisely enough to preoperatively determine the extent of tumor in relation to the total hepatic mass. Hepatic angiography is the critical diagnostic procedure in patients with hepatocellular carcinoma to determine whether the tumor is resectable (potentially curable) or nonresectable. In defining extent of tumor involvement, the limitations of the procedure must be known. Vascular invasion by a small tumor mass, involvement of the left lobe, and hypovascular hepatocellular carcinoma were the most troublesome areas. Metastatic disease might also escape detection. However, in the 22% of our clinical series with distant disease, the lesions were found before angiography (e.g., malignant ascites, positive chest radiographs).

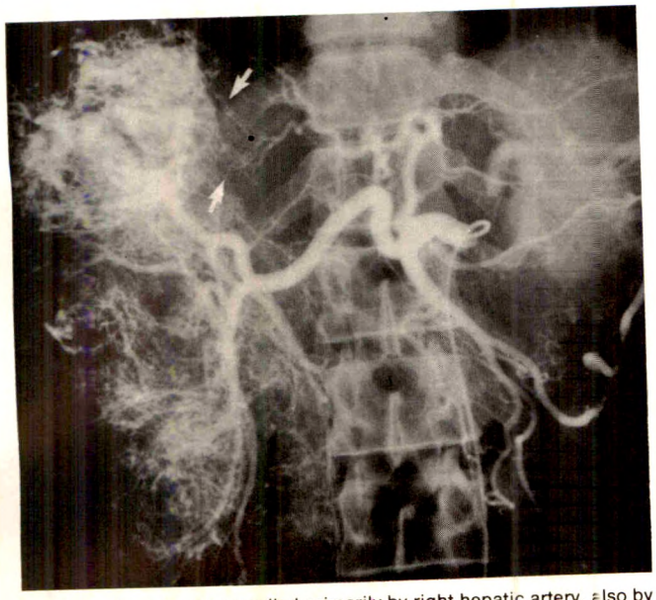


Fig. 1.—Large mass supplied primarily by right hepatic artery, also by branches of left hepatic artery (*arrows*) to medial segment of left lobe. Patient is free of disease 2 years after extended right hepatic resection.

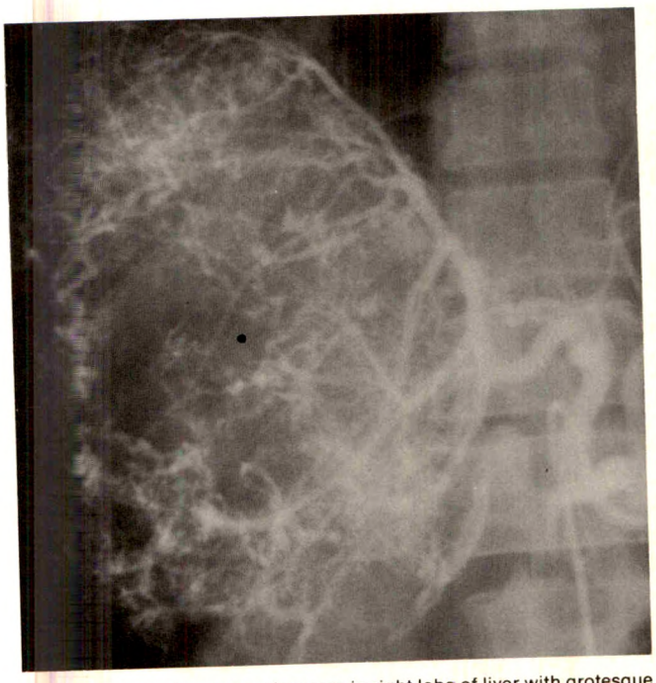


Fig. 2.—Large hypervascular mass in right lobe of liver with grotesque neovascularity and arteriovenous shunting. Patient underwent right hepatectomy and has survived more than 6 years.

Celiac or selective hepatic injections, or both, must be performed in both anteroposterior and right posterior oblique views. If all segments of the liver are obviously involved, no additional views are needed. When doubt arises, more selective injections may be necessary. In particular, superselective catheterization of the left and right hepatic arteries may be required to ascertain whether the vascular supply of the tumor crosses intralobar segments. We find oblique views mandatory to decide which right hepatic branch supplies the anterior segment and which the posterior segment of the right lobe. In a few cases, the anatomy was so distorted that this determination could not be made.

The angiographic appearance of typical hepatocellular carcinoma has been described [3, 9, 10]. Hepatoma can present as a focal bulky type or as a diffuse infiltrative type. The single, massive, tumefactive type was by far the more common in our series (fig. 2). Although this type of hepatocellular carcinoma is characteristically hypervascular, it can be mimicked by hypervascular metastases (renal cell carcinoma, choriocarcinoma). The differential diagnosis can be confidently made if the clinical setting is appropriate (Oriental patient, cirrhotic liver, no other known primary tumor). If any therapy is planned, histologic diagnosis is of course mandatory. Hypovascular hepatocellular carcinoma is rare, and very difficult to diagnose and assess (fig. 3). In such cases, biopsy becomes more critical and operative evaluation may be necessary because of the less reliable angiographic findings.

Okuda et al. [11] recently described "threads and streaks" seen in hepatocellular carcinoma thrombus growing within veins of nine of 112 (8%) patients with hepatocellular carcinoma. We observed this sign in 27% of our cases. Whenever it was seen, histologic follow-up study confirmed vascular invasion by tumor; there were no false positive interpretations. In our series the portal veins were the most common sites of these threads and streaks (fig. 4), although less commonly hepatic venous invasion showed the same sign. This angiographic sign, therefore, has great value in determining which patient should, or should not, undergo hepatic surgery for tumor resection. Review of the literature and of cases seen at our institution of cholangiocarcinoma and hepatic metastases from extrahepatic sources failed to disclose a single case in which this sign was exhibited. When confined to the portal or hepatic veins, and associated with other positive angiographic findings in the liver, the threads and streaks sign is highly specific for hepatocellular carcinoma.

It has been widely held that the diameters of lobar and segmental arteries supplying this type of carcinoma increase with increased blood flow to the tumor [12]. We tried to determine if these arteries enlarged consistently enough to be useful in determining tumor extension. By comparing the size of affected hepatic branches to normal hepatic branches as well as to the aorta and renal arteries we hoped to detect selectively increased caliber. However, only three of our 26 patients who underwent angiography demonstrated significant enlargement of the arteries supplying the tumor mass. Therefore, we found increased caliber to be of little diagnostic benefit.

Large and medium sized tumor nodules often show avascular areas (fig. 5), which we and others [13] have interpreted as areas of tumor necrosis. Investigation of the surgical specimens and review of the clinical histories, however, disclose that such eccentric, avascular zones are actually areas of spontaneous hemorrhage from or within the tumor mass. Since exsanguination is

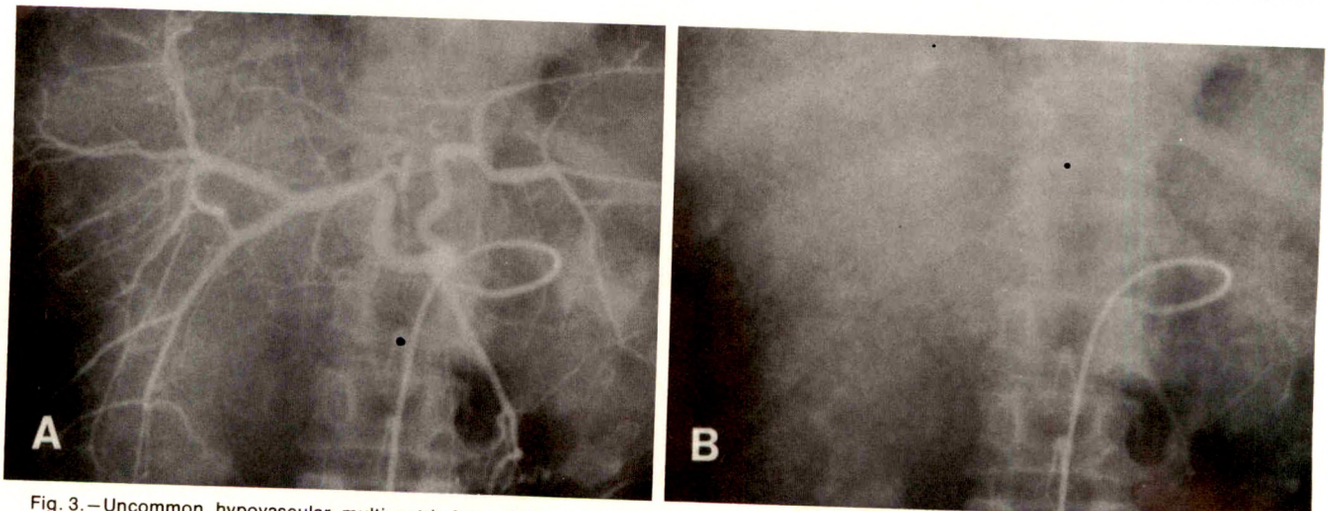


Fig. 3.—Uncommon, hypovascular, multicentric form of hepatocellular carcinoma. Angiographically this cannot be distinguished from cirrhosis.

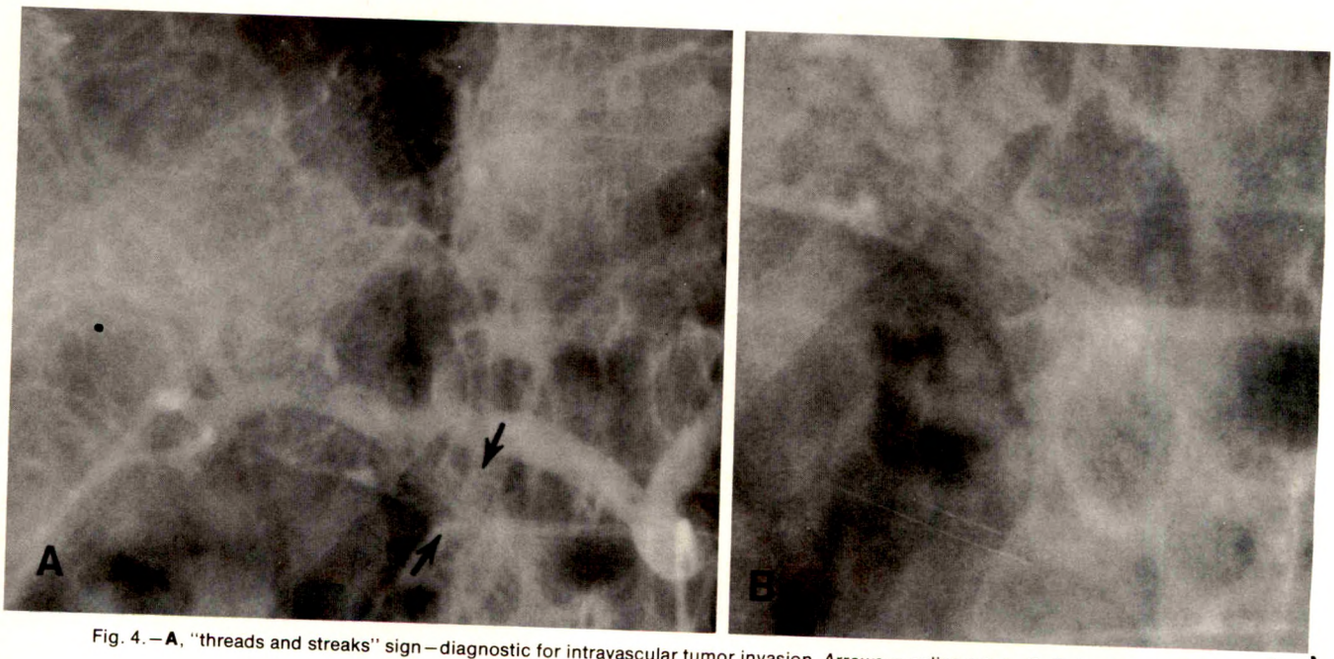


Fig. 4.—**A**, "threads and streaks" sign—diagnostic for intravascular tumor invasion. *Arrows* = celiac artery. **B**, Enlargement of **A**.

a common cause of death in patients demonstrating these nodules, and since surgeons must approach these delicately tamponaded hematomas with great caution, knowledge of their presence and site is therapeutically valuable.

By present standards, angiography is the pivotal examination for the evaluation of hepatocellular carcinoma. Gammill and associates [14, 15] emphasized the necessity of angiography when considering a patient for hepatic resection. The threads and streaks effect is a common and reliable angiographic sign. Hemorrhage, rather than simple necrosis, accounts for the eccentric avascular zones seen within tumor masses. Our study affirms the angiographic accuracy in assessing the extent and, thus, the resectability of hepatocellular carcinoma. Superselective studies may further improve the accuracy rate of angiography. Although ultrasonography, radionuclide scanning, and computed tomography are valuable for the detection and gross assessment of hepatocellular carcinoma, currently angiography remains the only modality that can demonstrate the surgical anatomy of the liver.

ACKNOWLEDGMENT

We thank Shirley Soucie for assistance in manuscript preparation and Drs. Morton M. Glickman and Sidney Wallace for thoughtful review and criticisms.

REFERENCES

1. Seidheim H, Silverberg E, Holleb AI: Cancer statistics 1976. *CA* 26:22–28, 1976

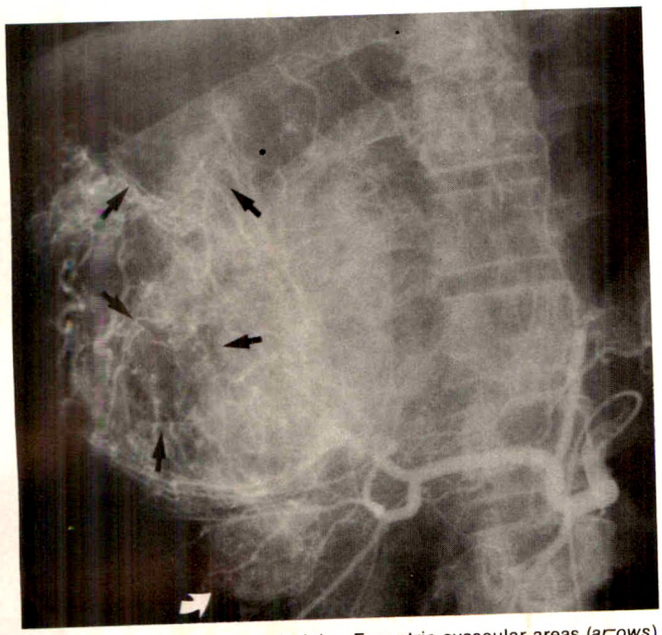


Fig. 5.—Large mass in right lobe. Eccentric avascular areas (*arrows*) represent regions of hemorrhage. Intrahepatic metastasis or second primary tumor (*white arrow*) also visible.

2. Bartley O, Edlund Y, Helander CG: Angiography in primary hepatic carcinoma. *Acta Radiol* [*Diagn*] (Stockh) 6:81–90, 1967
3. Sherlock S: *Diseases of the Liver and Biliary System*, 5th ed. Oxford, Blackwell Scientific Publications, 1975, pp. 665–698
4. Edmondson HA, Steiner PE: Primary carcinoma of the liver: a study of 100 cases among 48,900 necropsies. *Cancer* 7:462–503, 1954
5. Gall EA: Primary and metastatic carcinoma of the liver. *Arch Pathol* 70:226–232, 1960
6. Boijsen E, Abrams HL: Roentgenologic diagnosis of primary carcinoma of the liver. *Acta Radiol* [*Diagn*] (Stockh) 3:257–277, 1965
7. Michels NA: Newer anatomy of the liver and its variant blood supply and collateral circulation. *Am J Surg* 112:337–347, 1966
8. Starzl TE, Bell RH, Beart RW, Putnam CW: Hepatic trisegmentectomy and other liver resections. *Surg Gynecol Obstet* 141:429–437, 1975
9. Fredens M, Egeblad M, Holst-Neilsen F: The value of selective angiography in the diagnosis of tumors in pancreas and liver. *Radiology* 93:765–769, 1969
10. Kido C, Sasaki T, Kaneko M: Angiography of primary liver cancer. *AJR* 113:70–82, 1971
11. Okuda K, Musha H, Yoshida T, Kanda Y, Yamakazi T, Jinnouchi S, Moriyami M, Kawaguchi S, Kubo Y, Shimokawa Y, Kojiro M, Kuratomi S, Sakamoto K, Nakashima T: Demonstration of growing casts of hepatocellular carcinoma in the portal vein by celiac angiography: the thread and streaks sign. *Radiology* 117:303–309, 1975
12. Reuter SR, Redman HC: *Gastrointestinal Angiography*, 2d ed. Philadelphia, Saunders, 1977, p. 145
13. Okuda K, Obata H, Jinnouchi S, Kubo Y, Nagasaki Y, Shimokawa Y, Motoiki Y, Muto H, Nakajima Y, Musha H, Yamazaki T, Sakamoto K, Kojiro M, Nakashima T: Angiographic assessment of gross anatomy of hepatocellular carcinoma: comparison of celiac angiograms and liver pathology in 100 cases. *Radiology* 123:21–29, 1977
14. Gammill SL, Takahashi M, Kawanami M, Font R, Sparks R: Hepatic angiography in the selection of patients with hepatomas for hepatic lobectomy. *Radiology* 101:549–554, 1971
15. Gammill SL, Takahashi M, Jingu K, Stumpe W, Font R: A comparison of scans and angiograms in selecting patients with hepatomas for hepatic lobectomy. *AJR* 123:522–530, 1975

ARS Presidential Address:

The Surgeon Looks at Recurrences After Unsuccessful Radiation Therapy

RICHARD H. JESSE[1]

Head and neck cancer surgeons operating on patients with recurrent cancer after supposedly curative radiation therapy are often asked the following:

1. Do you really believe you will cure this patient's cancer and, if you do, what quality of life will the patient have?
2. How are length of surgery and hospitalization related to outcome?
3. Can you identify patients with recurrent cancer at certain sites and staging for whom you can achieve a reasonable degree of success?
4. Can a group of patients be defined by site and stage of cancer for whom no effort should be expended?

This presentation attempts to determine answers to these questions from data acquired by the Head and Neck Surgical Service of the University of Texas System Cancer Center.

Subjects and Methods

From 1971 through 1975, surgery was performed on 126 patients who had received unsuccessful "curative" radiation therapy for primary cancer at M. D. Anderson Hospital. Also seen, but excluded from analysis were irradiated patients whose cancer was thought to be inoperable, those whose surgical procedures were part of a sequential treatment plan, those who developed second primary cancers, and those whose recurrences were in the neck only but not at the primary site.

Five primary sites, vocal cord, oropharynx, oral cavity, supraglottic larynx, and hypopharynx, were selected. Recurrent primary cancer was staged according to its extent at surgery. Also evaluated were: (1) the length of time from completion of radiation therapy to recurrence, (2) the hours of operating time, (3) the duration of hospital stay, and (4) the patient's quality of life. M. D. Anderson Hospital is an acute care hospital and patients are not hospitalized beyond the time required to move them home or to a secondary care area. In an analysis to determine the causes for radiation failure, the cases were divided between those who received radiation therapy at M. D. Anderson Hospital and those treated elsewhere to see if there was a difference in survival. Patients were followed 2–7 years.

Results

Of the 126 patients, 69 (55%) had successful surgical treatment for cancer, although 12 died of other causes during the follow-up period. Surgery was successful for 44 of 62 patients staged T1 and T2 and for 25 of 64 patients staged T3 and T4 (fig. 1). Three of the latter 25 successfully treated patients were staged T4.

The 33 patients with recurrent vocal cord cancer had the greatest longevity, and only three died after surgery (fig. 2). Operable, advanced stage recurrent vocal cord cancers can usually be surgically treated with results equal to those for early stage disease.

Of 27 (44%) patients with recurrent oropharynx cancer, 12 survived (fig. 3). Of the T1 and T2 patients, 67% survived, in contrast to only 27% of the T3 and T4 groups. The survival rate for patients with recurrent oral cavity cancer was 16 of 46 (35)% (fig. 4); 58% of the T1 and T2 patients survived in contrast to 19% of the T3 and T4 groups.

Seven of 12 (58%) patients with recurrent supraglottic larynx cancer survived (fig. 5) and four of eight (50%) patients with recurrent hypopharynx cancer survived (fig. 6). The numbers in these samples are too small to determine the effect of advanced staging on longevity.

The time from completion of radiation therapy to recurrence has a definite correlation to patient survival. Of the patients who died, 84% developed recurrences within 12 months after radiation therapy, whereas only 50% of the successfully treated patients had recurrence within 12 months (table 1). This finding was unrelated to the original size of the primary cancer.

The mean duration of surgery was 4.5 hr for surviving patients and 7.5 hr for patients who later died; mean numbers of procedures were 1.5 and 2.4, respectively. From an economic standpoint, almost twice the number of acute care hospital days were required for those patients who had unsuccessful treatment (mean length of stay: 17 versus 32 days). Only six of the successfully treated patients were hospitalized longer than 40 days, in contrast to 11 of the patients who later died.

An evaluation of the initial radiation therapy showed an error either in dose or field size for 37 of the 126 patients. The lesion was considered too large for single-method treatment for 22 patients. Of the 67 remaining patients, no reason was found for radiation therapy failure in 48 of them, and in 19 the failure could not be determined. When plotted against mortality, the only factor that made a difference was if the cancer was too big for single-method treatment. The incidence of this

Received June 23, 1978; accepted after revision October 9, 1978.
Presented at the annual meeting of the American Radium Society, New Orleans, 1978.
[1] Section of Head and Neck Surgery, University of Texas System Cancer Center, M. D. Anderson Hospital and Tumor Institute, 6723 Bertner Drive, Houston, Texas 77030.

0361-803X/79/1321-0013 $0.0

AJR 132:13–15, January 1979
© 1979 American Roentgen Ray Society

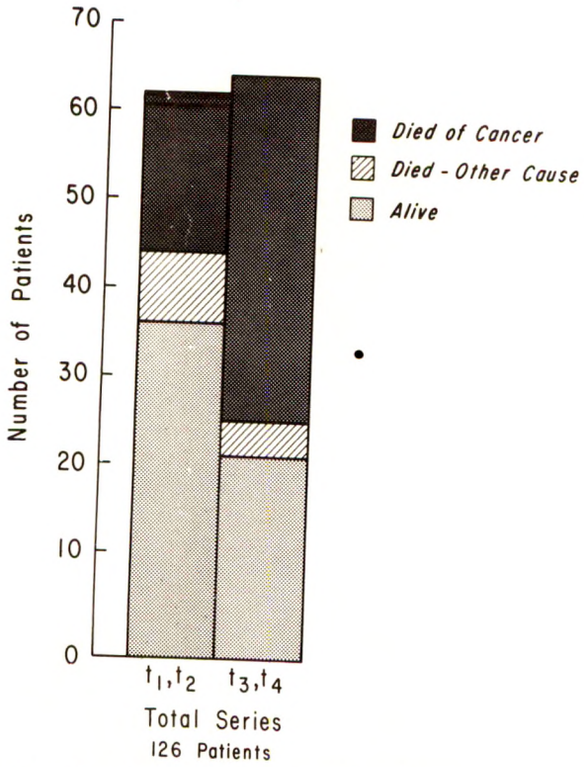


Fig. 1.—Postsurgical survival in 126 patients relative to stage of primary recurrence.

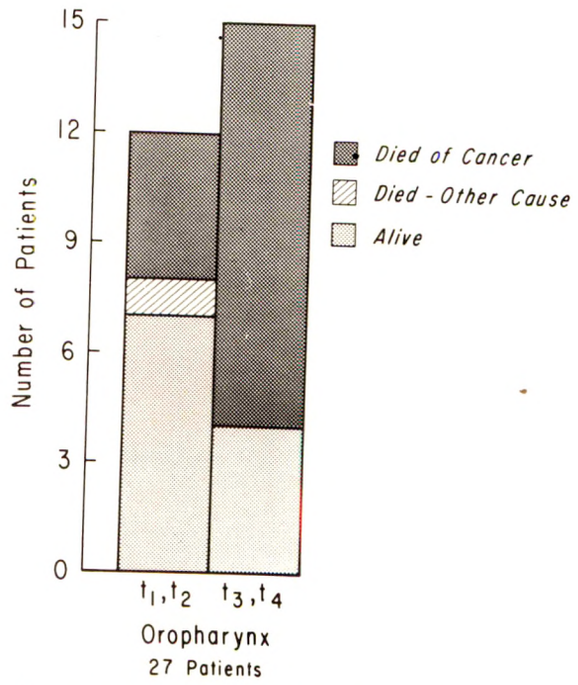


Fig. 3.—Postsurgical survival in 27 patients with oropharynx cancer relative to stage of primary recurrence.

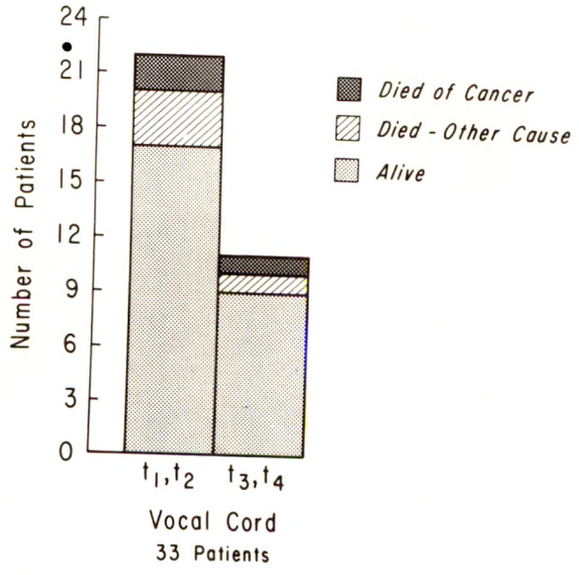


Fig. 2.—Postsurgical survival in 33 patients with vocal cord cancer relative to stage of primary recurrence.

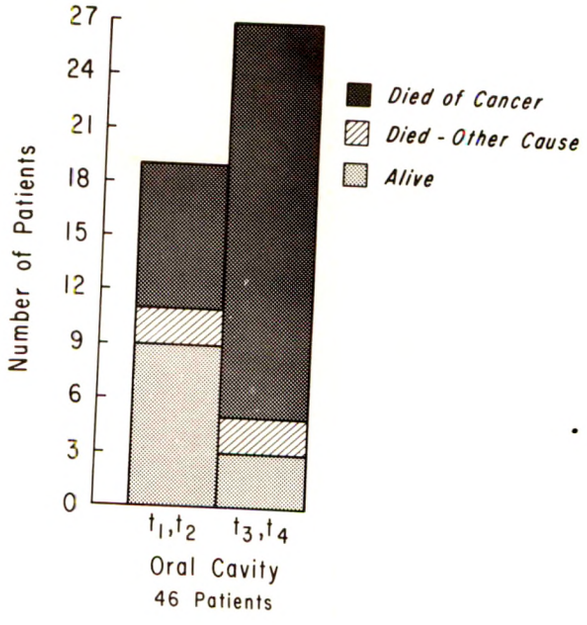


Fig. 4.—Postsurgical survival in 46 patients with oral cavity cancer relative to stage of primary recurrence.

factor was 2 times greater among patients who died of cancer.

Quality of life was evaluated on a scale of 1 to 5: 1 = a patient who performed in a near normal manner; 2 = mild to moderate cosmetic deformity or a slight to moderate functional deficit; 3 = a lack of adequate verbal communication, moderate to severe functional deficit, or cosmetic defect, but still able to function within his community; 4 = pain, nonhealing fistula, or a severe cosmetic or functional defect forcing him to stay at home most of the time; 5 = severe pain or treatment-related hemiplegia, and mostly bedridden.

The distribution of the quality of life ratings is shown in table 2. Most of the patients having successful treatment had a reasonable quality of life rating, but 10 of the 69 patients had severe handicaps. Most of the patients

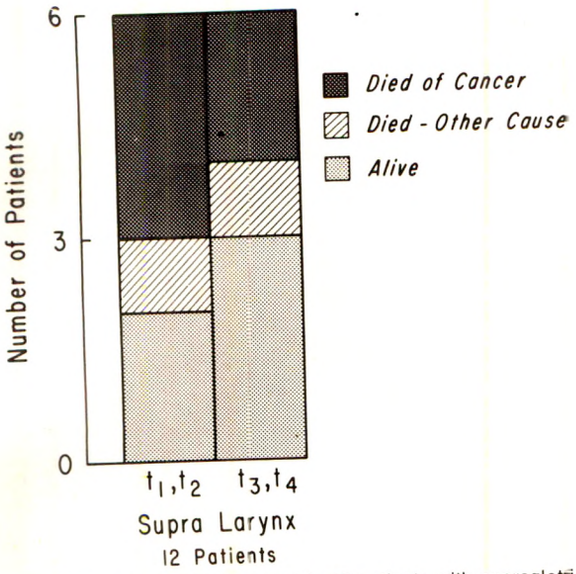


Fig. 5.—Postsurgical survival in 12 patients with supraglottic larynx cancer relative to stage of primary recurrence.

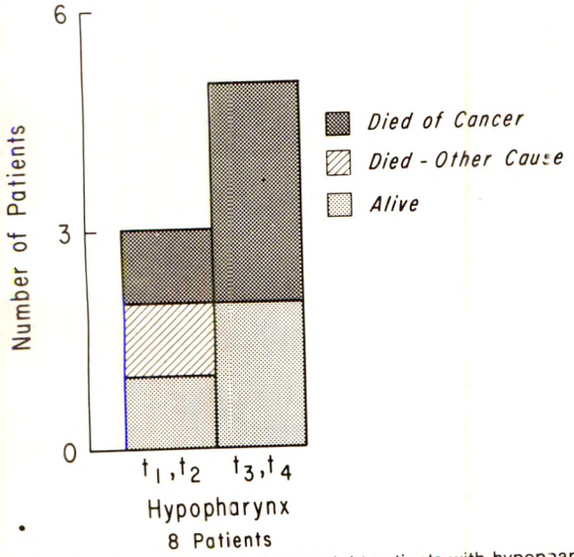


Fig. 6.—Postsurgical survival in eight patients with hypopharynx cancer relative to stage of primary recurrence.

who had unsuccessful surgical treatment had severe handicaps for most of their remaining life much of this related to their cancers.

Discussion

Surgical success was the same for patients irradiated at M. D. Anderson Hospital as it was for those irradiated elsewhere. We suspect our surgeons were more likely to operate on our failures than on those from elsewhere; thus, the actual effectiveness of surgery for patients after unsuccessful radiation therapy elsewhere may be lower than the statistics indicate. The population base of patients with cancer recurring after radiation therapy is not determinable when patients treated elsewhere are included. The patients whose radiation therapy elsewhere failed were already subjected to a selection process by the family physician, radiotherapist, the patient, and the patient's family, and only a portion of them were referred to us for treatment. The surgeon further refines the population by including only those patients whose primary cancers and neck metastases are resectable, those who have reasonably good general health, and those who do not have metastases below the clavicle. Although the survival figures are low for a total population, they reflect what can be accomplished in a selected group of patients by highly skilled head and neck cancer surgeons.

From these data we conclude that patients with recurrent laryngeal cancer and those with T1 and T2 lesions of the oropharynx, oral cavity, and hypopharynx are definitely candidates for surgical treatment. On the other hand, surgery for T3 and T4 cancers offers only moderate hope of success. Patients who do least well are those with T4 staged cancer of the oropharynx, oral cavity, or hypopharynx. However, since the survival rates for patients with cancer at these three sites are 18% for T4 and 25% for T3, obviously one should not deny patients who are operable their right to live.

TABLE 1

Time from Irradiation Until Primary Recurrence Related to Postsurgical Survival

	More than 12 mo. (%)	Less than 12 mo. (%)
Living patients (N = 69)	50	50
Dead patients (N = 57)	16	84

TABLE 2

Quality of Life After Surgery

Quality Scale	Living Patients (N = 69)	Dead Patients (N = 57)
1	20	0
2	39	4
3	7	15
4	1	20
5	2	18

Primary Mediastinal Seminoma

STANLEY M. POLANSKY,[1] KENNETH W. BARWICK,[2] AND CARL E. RAVIN[3]

Four new cases of primary mediastinal seminoma are presented, and the 103 previously reported cases reviewed. All of the tumors occurred in the anterior mediastinum, and generally appeared as lobulated noncalcified masses on chest radiography. Most patients were in the third and fourth decades, and about 30% were asymptomatic at the time of initial diagnosis. Although mediastinal seminoma is not commonly considered a cause of superior vena caval obstruction, about 10% of patients experience it. The tumors are radiosensitive and potentially radiocurable. A striking reduction in size of the tumor may be noted after radiation therapy. Prognosis is generally good, with a 5-year survival rate of 75%. The controversy surrounding histogenesis of this tumor is reviewed, and the pathologic criteria for making the diagnosis presented.

Primary mediastinal seminoma is an uncommon lesion, with only 103 cases previously reported in the English literature [1–31]. All of these tumors have occurred in the anterior mediastinum, and the vast majority have occurred in males. As a result, there has been some controversy as to whether these tumors arise primarily in the mediastinum or represent metastases from gonadal primaries [11, 23, 26, 29, 32]. This issue has been addressed by serial sectioning of the gonads at autopsy [7, 9, 11, 16, 23, 29] and by prolonged follow-up during which gonadal primaries have not become evident [4, 9, 13, 16, 19–21, 27, 29, 30]. It is now widely accepted that germinal cell tumors can arise primarily in the mediastinum.

We recently studied four such tumors; one of these was particularly unusual as it occurred in a woman who had signs and symptoms of superior vena caval obstruction. Although this association has not been stressed previously, review of the literature shows that mediastinal seminoma causes superior vena caval obstruction in about 10% of cases [4, 12, 16, 17, 21, 25, 27, 28].

Case Reports

Case 1

A 49-year-old woman was studied because of signs and symptoms of superior vena caval syndrome. Chest radiography demonstrated a large noncalcified mass involving the anterior and superior portions of the mediastinum (fig. 1). There was no associated hilar adenopathy. Laboratory tests were normal except for an elevated sedimentation rate. Bilateral arm venography confirmed superior vena caval obstruction. Gallium scanning demonstrated intense uptake in the mediastinal mass. Thoracotomy with biopsy demonstrated seminoma.

A split course of 4400 rad to the mediastinum was delivered over a 40-day period. The superior vena caval obstruction abated clinically. Chest radiography revealed a slight decrease in the size of the mediastinal mass. The patient is doing well at 6-month follow-up.

Case 2

An 11-year-old boy was evaluated for complaints of chest pain. Physical examination, including careful examination of the testes, was entirely normal. Chest radiography demonstrated a large mass in the anterior mediastinum (fig. 2). Metastatic survey, bone scan, liver/spleen scan, and lymphangiography were negative. Mediastinal exploration showed that the mass adhered to the tracheobronchial tree and great vessels. The lymph nodes were invaded, although a segment of the thymus was histologically uninvolved. Biopsy specimens demonstrated seminoma.

A split course, totalling 3700 rad, was delivered to the mediastinum over 30 days. Chest radiography demonstrated marked decrease in the size of the mass. Prophylactic radiation of the periaortic nodes was also given. The patient has been asymptomatic without evidence of residual tumor for a follow-up period of 18 months.

Case 3

A 22-year-old man was evaluated for complaints of severe back pain associated with progressive leg weakness and a 4.5 kg weight loss. Physical examination was unremarkable except for lower extremity hyperreflexia and ankle clonus. The testes were normal. Chest radiography revealed a large noncalcified anterior mediastinal mass with lobulated margins (fig. 3A). Subsequent mediastinoscopy revealed a histologically typical seminoma. The leg weakness proved secondary to a metastases to the D11 vertebra. Radiation therapy of 3900 rad delivered to the chest over 40 days resulted in marked shrinkage of the mass 5 days after the start of therapy (fig. 3B). However, the patient followed a progressive downhill course with development of pulmonary metastases. Despite chemotherapy, he expired 8 months after the initial diagnosis.

Case 4

A 24-year-old man was evaluated because of 2 months of laryngitis and hoarseness. Left vocal cord paralysis was noted on laryngoscopy. Physical examination, including examination of the testes, was normal except for left anterior cervical lymphadenopathy. Chest radiography revealed a large anterior mediastinal mass predominantly to the left of midline with associated elevation of the left hemidiaphragm thought to be

Received June 23, 1978; accepted after revision September 28, 1978.

[1] Department of Diagnostic Radiology, Yale University School of Medicine, New Haven, Connecticut 06510. Present address: Department of Diagnostic Radiology, Hospital for Sick Children, Toronto, Ontario M5G 1X8, Canada.

[2] Department of Pathology, Yale University School of Medicine, New Haven, Connecticut 06510. Present address: Department of Pathology, Memorial Sloan Kettering Cancer Center, New York, New York 10021.

[3] Department of Diagnostic Radiology, Yale University School of Medicine, New Haven, Connecticut 06510. Present address: Department of Radiology, Box 3808, Duke University Medical Center, Durham, North Carolina 27710. Address reprint requests to C. E. Ravin.

0361–803X/79/1321–0017 $0.0

AJR 132:17–21, January 1979

© 1979 American Roentgen Ray Society

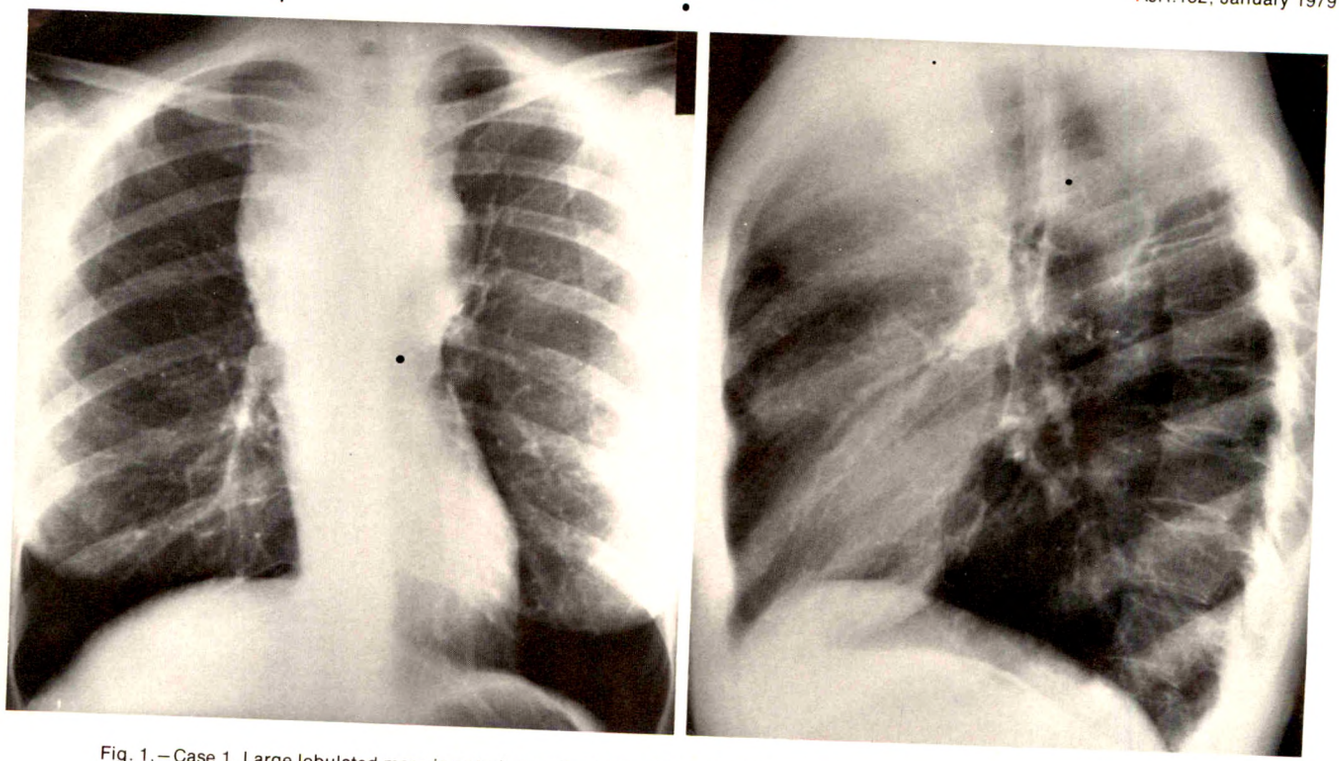


Fig. 1.—Case 1. Large lobulated mass in anterior mediastinum. Patient had signs and symptoms of superior vena cava syndrome.

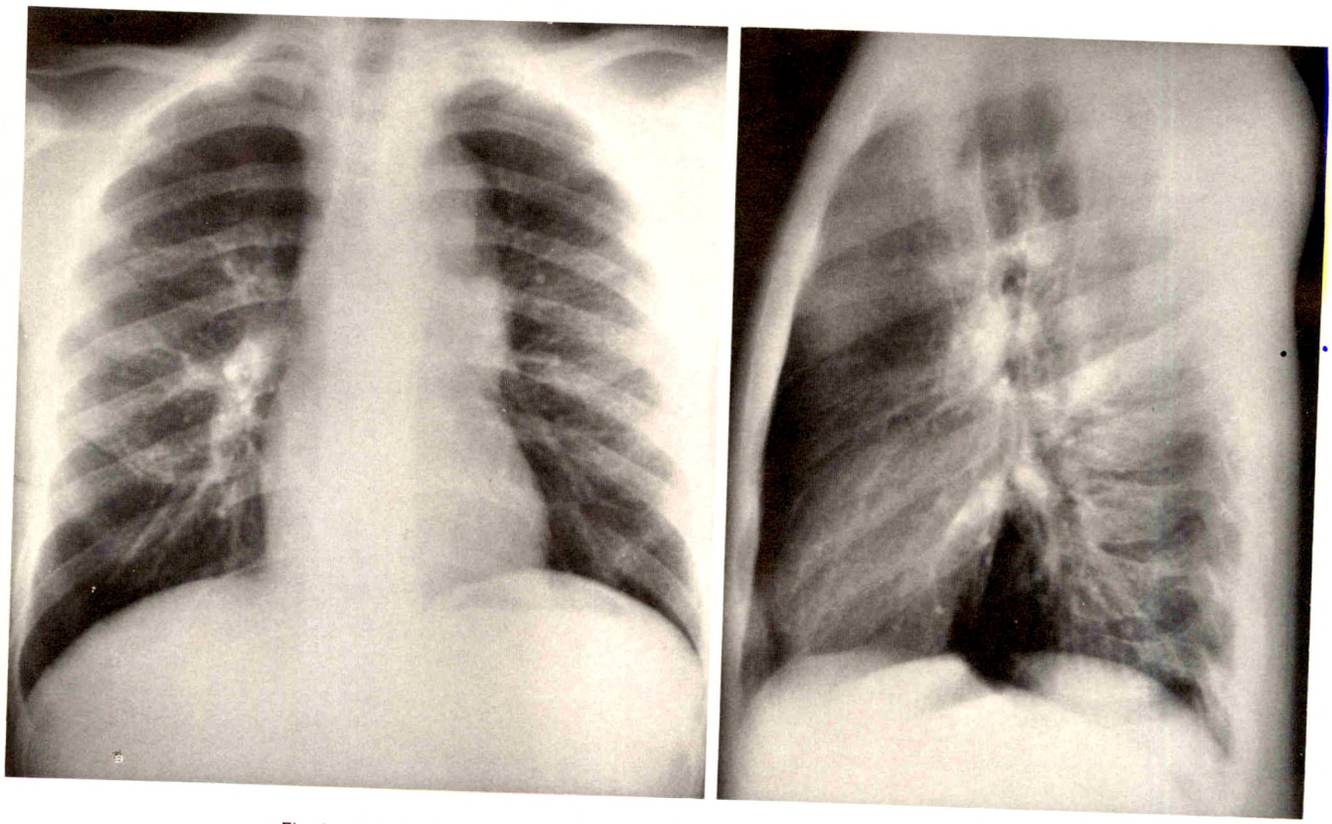


Fig. 2.—Case 2. Moderately large lobulated mass occupying anterior mediastinum.

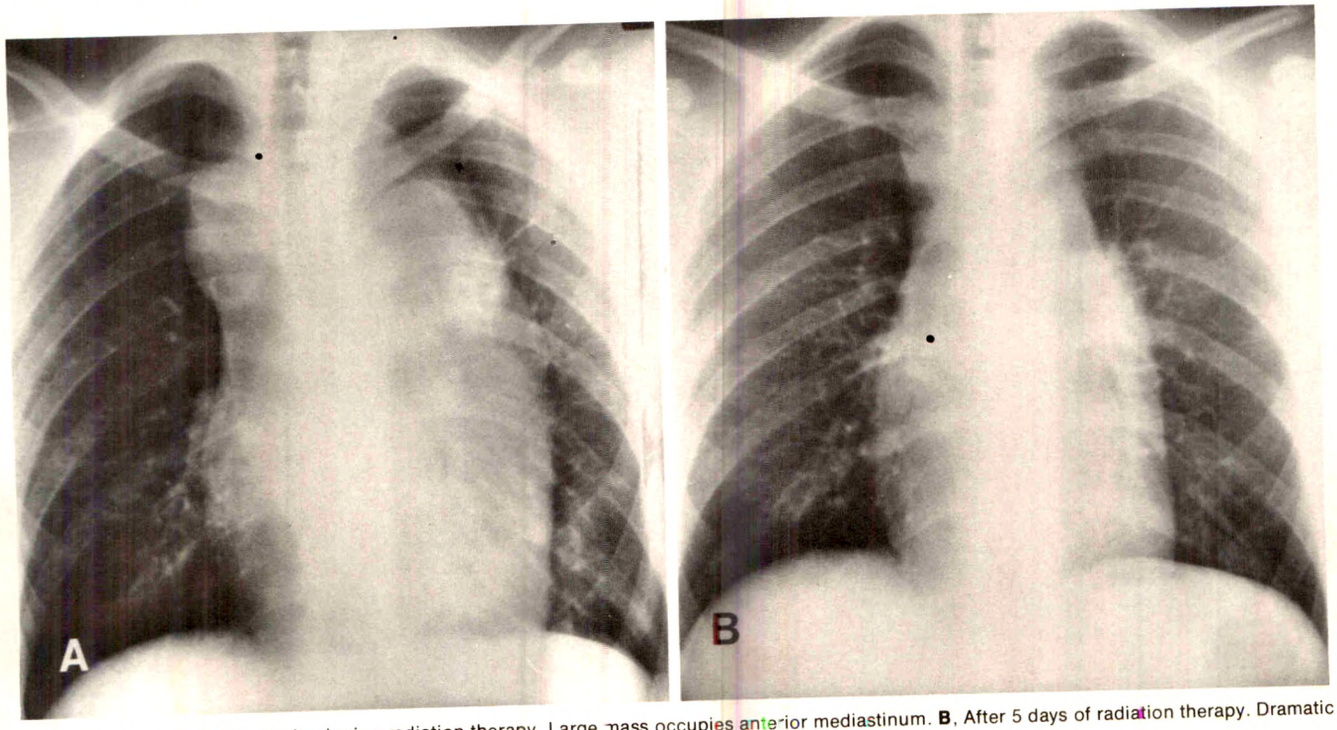


Fig. 3.—Case 3. **A**, Prior to beginning radiation therapy. Large mass occupies anterior mediastinum. **B**, After 5 days of radiation therapy. Dramatic shrinkage of mass.

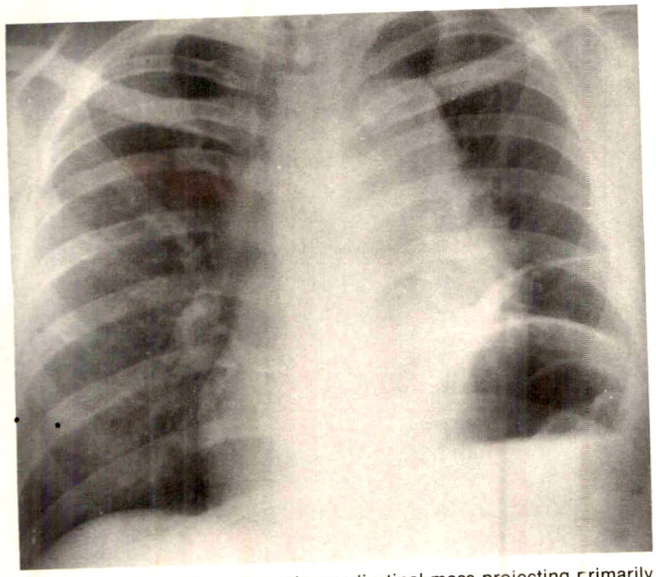


Fig. 4.—Case 4. Large anterior mediastinal mass projecting primarily into left hemithorax. Associated elevation of the left hemidiaphragm and discoid atelectasis at left lung base. (Case courtesy of Dr. Raymond M. Abrams, St. Mary's Hospital, Waterbury, Conn.)

secondary to phrenic nerve paralysis (fig. 4). Lymphar giography demonstrated equivocal involvement of several paraaortic nodes. Liver/spleen scan showed hepatosplenomegaly without specific filling defects. Left scalene node biopsy revealed seminoma.

A split course of 5000 rad to the mediastinum was delivered over a 50-day period and 3500 rad to the paraaortic region over a 30-day period. There was prompt shrinkage of the mediastinal mass, although the paralysis of the left vocal cord and left hemidiaphragm did not improve. One year after the initial diagnosis, the patient developed metastases to the left femur and skull. These were treated with local irradiation and systemic chemotherapy. The patient has been asymptomatic without evidence of further recurrence for a follow-up period of 18 months.

Pathology

Each of the four cases had a similar histologic pattern of nests of large atypical cells with abundant clear cytoplasm divided by fibrous bands (fig. 5). The tumor cells contained large nuclei with thick nuclear membranes, coarse chromatin stippling, and irregularly shaped nucleoli. Mitoses were not frequent in three tumors, but were moderate in number (7 per 10 high power fields) in case 4. Mature lymphocytes were numerous in three cases, predominantly along the fibrous bands, but were scant in case 1. This case also differed in that the large tumor cells occasionally overran the fibrous trabeculae, creating a diffuse pattern, and in that localized areas of necrosis were present. Glycogen was demonstrated in the cytoplasm of all four lesions but was scanty in case 1. A well formed granulomatous background with giant cells was present in cases 2–4; in case 1, giant cells were absent, but aggregates of epitheloid histiocytes were present.

Electron microscopy was performed in case 1 to clarify the findings at light microscopy. The individual tumor cells contained round to oval nuclei with evenly dispersed chromatic clumps. The cytoplasm was relatively simple without abundant organelles and contained moderate amounts of glycogen. Blunted cytoplasmic extensions were manifested by some cells. Rare desmosomes were encountered, but tonofilaments were absent. Nucleoli were prominent, manifesting a meshwork pattern at times, but a complex filamentous arrangement was not demonstrated. These findings confirmed the diagnosis of seminoma.

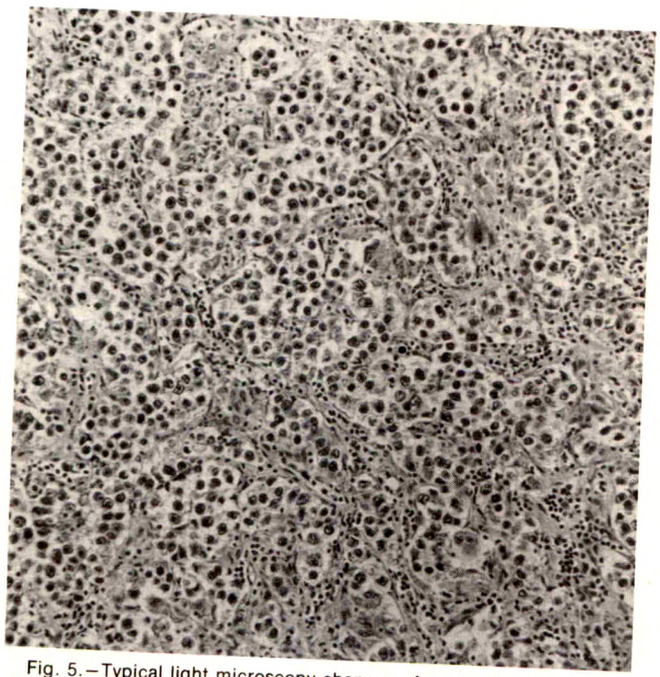


Fig. 5.—Typical light microscopy changes of mediastinal seminoma. Uniform tumor cells with abundant clear cytoplasm and large nuclei having prominent nucleoli and nuclear membranes. Tumor cells are divided into lobules by delicate fiber strands containing numerous lymphocytes (H and E × 100).

Discussion

Primary extragential seminoma has been documented arising in the mediastinum [1–31], retroperitoneum [18, 23], and pineal body [18, 23, 33]. Of these extragonadal locations, the mediastinum has been by far the most common [18, 23]. The histogenesis of these extragenital germ cell tumors remains controversial. Of the several theories which have been advanced, two have gained widest acceptance: (1) origin through faulty thymic embryogenesis (somatic aberration) [34] and (2) origin from germ cells [33]. Somatic aberration, originally proposed by Schlumberger [34], suggests that extragonadal germ cell tumors develop as a result of dislocation of germ cell layers during embryogenesis and that the mediastinal tumors derive from the thymic anlage, thus constituting an abnormality in thymic development. The common occurrence of most germ cell tumors and thymomas in the anterior portion of the mediastinum has been offered in support of this concept [19]. However, primary mediastinal seminoma is not associated with diseases normal incidence of thymic tumors (i.e., myasthenia gravis, erythrocyte agenesis, acquired agammaglobulinemia, and Cushing's syndrome) [12]. The germ cell theory proposed by Friedman [33] hypothesizes that the tumors originate from the primordial germ cells which migrate to midline structures, including the mediastinum, during embryogenesis. The pathway of these cells is from their origin in the yolk sac to the gonadal folds [24], but they have been shown to locate at extragonadal sites. This hypothesis may explain intracranial germ cell tumors, in that these wandering germ cells have been demonstrated to locate in the head of the embryo. The ultrastructural similarity of seminoma cells to primordial germ cells, gonocytes, and normal human spermatogonia [24] further supports the germ cell theory.

Pathologic distinction of seminoma from other mediastinal tumors, particularly thymoma [8, 24] and lymphoma [27], may be exceedingly difficult [17, 24] and on a small biopsy may be impossible. Helpful histologic features of seminoma are subdivision of the tumor into numerous islands by fine reticulum fibers, frequent presence of granulomatous inflammation, cytoplasmic glycogen, and nuclei with coarse chromatin stippling. In cases where pathologic distinction by light microscopy is not possible, electron microscopy will often resolve the problem [24]. The most useful ultrastructural features of seminoma are a paucity of desmosomes and absent tonofilaments, complex bizarre nucleoli, and short cytoplasmic processes [24].

A total of 103 cases of primary mediastinal seminoma has been reported in the English literature. (A review of the literature in tabular form has been deposited with a documentation service.*) Only five of these 103 patients were female [3, 16, 27, 29]. Our case 1 is the sixth female reported. Patients tend to present in the third and fourth decades, averaging 29 years of age (range, 11 years (case 2) to 63 years)[21]. About 30% of the patients are asymptomatic and have a mediastinal mass noted on routine chest radiography. When present, signs and symptoms are nonspecific and are identical to those seen with any slowly invasive or expanding mediastinal tumor [3, 9, 12, 22, 30]. The initial symptom may be a sensation of pressure in the chest or pain [4, 6, 9, 13, 16, 17]; the pain may be localized to the retrosternal area or radiate to the neck and arms. Other complaints include exertional dyspnea [9, 13], cough [1, 4, 9, 15], hoarseness [11], and dysphagia [6]. Systemic symptoms [1, 22] of weight loss and easy fatigability may be noted but endocrinopathies have not been associated with this tumor. In 10 of the 80 patients for whom complete clinical records were available, the first symptoms were those of superior vena caval syndrome [4, 12, 16, 17, 21, 25, 27, 28]. Although not commonly considered a cause for superior vena caval obstruction, primary mediastinal seminoma should be included in the differential diagnosis.

The radiographic findings of primary mediastinal seminoma unfortunately do not allow it to be reliably distinguished from other tumors occurring in a similar location. It is invariably found in the anterior mediastinum and is usually large with lobulated borders when initially noted. If of sufficient size, the mass can cause posterior angulation of the trachea [4, 10, 14] and deviation or compression of bronchi [14, 20, 26]. Calcification within mediastinal seminoma has not been demonstrated on either plain films or tomograms, nor has it yet been reported on pathologic examination. Rapid shrinkage of this lesion during radiation therapy [6, 16, 20] may be

* See National Auxiliary Publications Service document no. 03360 for one table of supplementary material. Order from ASIS/NAPS, c/o Microfiche Publications, P.O. Box 3513, Grand Central Station, New York, New York 10017.

seen as in case 2. Other mediastinal neoplasms which may show marked regression in response to radiation therapy are lymphomas and small cell undifferentiated carcinomas of the lung. However, the natural history of these entities serves to distinguish them from seminoma.

All pure seminomas, regardless of their site of origin, are radiosensitive and, if localized, potentially radiocurable [3, 6, 15, 19, 26, 29]. The therapeutic recommendations of El-Domeiri et al. [16] are total surgical excision if possible, followed by irradiation at a suitable dosage to the mediastinum. Schantz et al. [21] also advise adding the supraclavicular, intraclavicular, and low cervical lymph nodes to the radiation portals. Metastatic spread does not preclude the possibility of cure [9, 17, 21, 26]. In advanced cases, radiotherapy plus chemotherapy gives good palliation [27, 30, 31].

Metastases have been reported in 16 [1, 4, 7, 9, 12, 16, 17, 25, 27–29] of the 80 patients with complete clinical records. Spread of tumor is most common within the thorax [7, 12, 16, 17, 25, 27, 29] both to the lungs and regional lymph nodes. Occasionally the hilar nodes are involved at initial study [20, 26]. The skeletal system is the next most frequent site of metastases [1, 4, 9, 16, 27, 29] and metastases to liver [27], spleen [7], tonsils [7], thyroid gland [9], adrenal glands [7], skin [1], spinal cord [16], and brain [27] have also been reported. The average follow-up time in the literature is 6.3 years and the longest survival time has been 24 years [27]. There have been 23 deaths in the group of 80 well documented cases: three deaths related to surgical complications [21, 28, 31], 18 attributable to the neoplasm [11, 12, 16, 17, 23, 27, 29], and two unrelated to the neoplasm [14, 16]. Prognosis is generally good [3, 15, 21], with a 5-year survival rate of 75%, for patients with primary mediastinal seminoma.

REFERENCES

1. Woolner LB, Jamplis RW, Kirklin JW: Seminoma (germinoma) apparently primary in the anterior mediastinum. *N Engl J Med* 252:653–657, 1955
2. Effler DB, McCormack LJ: Thymic neoplasms. *J. Thorac Surg* 31:60–82, 1956
3. Iverson L: Thymoma. A review and reclassification *Am J Pathol* 32:695–719, 1956
4. O'Gara RW, Horn RC Jr, Enterline HT: Tumors of the anterior mediastinum. *Cancer* 11:562–590, 1958
5. Inada K, Nakano A: Germinoma of the mediastinum: a case report with special reference to the histogenesis of mediastinal teratoma. *Dis Chest* 36:438–441, 1959
6. Rovinson BW: Germinal neoplasia of extragenital origin. *J Natl Med Assoc* 52:162–165, 1960
7. Steinmetz WH, Hays RA: Primary seminoma of the mediastinum: report of a case with an unusual site of metastasis and review of the literature. *AJR* 86:669–672, 1961
8. Lattes R: Thymoma and other tumors of the thymus. An analysis of 107 cases. *Cancer* 15:1224–1260, 1962
9. Kountz SL, Connolly JE, Cohn R: Seminoma-like (or seminomatous) tumors of the anterior mediastinum. Report of four cases and a review of the literature. *J Thorac Cardiovasc Surg* 45:289–301, 1963
10. Oberman HA, Libcke JH: Malignant germinal neoplasms of the mediastinum. *Cancer* 17:498–507, 1964
11. Pachter MR, Lattes R: "Germinal" tumors of the mediastinum: a clinico-pathologic study of adult teratomas, teratocarcinomas, choriocarcinomas and seminomas. *Dis Chest* 45:301–310, 1964
12. Shields TW, Fox RT, Lees WM: Thymic tumors. Classification and treatment. *Arch Surg* 92:617–622, 1966
13. Nazari A, Gagnon ED: Seminoma-like tumor of the mediastinum. A case report with 7 year follow-up. *J Thorac Cardiovasc Surg* 51:751–754, 1966
14. Kleitsch WP, Taricco A, Halsam GJ: Primary seminoma (germinoma) of the mediastinum. *Ann Thorac Surg* 4:249–255, 1967
15. Edland RW, Levine S, Serfas LS, Flair RC: Seminoma-like tumor in the hyperplastic thymus gland. A case report and literature review. *AJR* 103:25–31, 1968
16. El-Domeiri AA, Hutter RVP, Pool JL, Foote FW Jr: Primary seminoma of the anterior mediastinum. *Ann Thorac Surg* 6:513–521, 1968
17. Bagshaw MA, McLaughlin WT, Earle JD: Definitive radiotherapy of primary mediastinal seminoma. *AJR* 105:86–94, 1969
18. Utz DC, Buscemi MF: Extragonadal testicular tumors. *J Urol* 105:271–274, 1971
19. Benjamin SP, McCormack LJ, Effler DB, Groves LK: Primary tumors of the mediastinum. *Chest* 62:297–303, 1972
20. Nickels J, Franssila K: Primary seminoma of the anterior mediastinum. *Acta Pathol Microbiol Scand [A]* 80:260–262, 1972
21. Schantz A, Sewall W, Castleman B: Mediastinal germinoma. A study of 21 cases with an excellent prognosis. *Cancer* 30:1189–1194, 1972
22. Besznyak I, Sebesteny M, Kuchar F: Primary mediastinal seminoma. A case report and review of the literature. *J Thorac Cardiovasc Surg* 65:930–934, 1973
23. Johnson DE, Laneri JP, Mountain CF, Luna M: Extragonadal germ cell tumors. *Surgery* 73:85–90, 1973
24. Levine GD: Primary thymic seminoma—a neoplasm ultrastructurally similar to testicular seminoma and distinct from epithelial thymoma. *Cancer* 31:729–741, 1973
25. Cha EM: Ectopic seminoma (germinoma) in the retroperitoneum and mediastinum: with emphasis on the lymphangiogram. *J Urol* 110:47–49, 1973
26. Larmi RJI, Karkola P: Mediastinal seminoma. *Ann Chir Gynaecol* 63:351–357, 1974
27. Martini N, Golbey RB, Hajdu SI, Whitmore WF, Beattie EJ Jr: Primary mediastinal germ cell tumors. *Cancer* 33:763–769, 1974
28. Ximenes-Neto M, Agostini AA: Primary seminoma of the mediastinum. *Int Surg* 59:425–427, 1974
29. Cox JD: Primary malignant germinal tumors of the mediastinum. A study of 24 cases. *Cancer* 36:1162–1168, 1975
30. Sterchi M, Cordell AR: Seminoma of the anterior mediastinum. *Ann Thorac Surg* 19:371–377, 1975
31. Das PB, Deodhare SG: Giant mediastinal seminoma (germinoma). *Int Surg* 61:563–565, 1976
32. Meares EM Jr, Briggs EM: Occult seminoma of the testis masquerading as primary extrogonadal germinal neoplasms. *Cancer* 30:300–306, 1972
33. Friedman NB: The comparative morphogenesis of extragenital and gonadal teratoid tumors. *Cancer* 4:265–276, 1951
34. Schlumberger HG: Teratoma of the anterior mediastinum in the group of military age. A study of sixteen cases, and a review of theories of genesis. *Arch Pathol* 41:398–444, 1946

D24,438

Oat Cell Carcinoma Manifesting as a Bronchocele

DIXIE J. ARONBERG,[1] STUART S. SAGEL, R. GILBERT JOST, AND ROBERT G. LEVITT

Three cases of oat cell carcinoma appearing as a bronchocele on the chest radiograph are described. A bronchocele as the major radiologic manifestation of oat cell carcinoma has not been emphasized previously. Such a bronchocele may be filled with neoplastic cells rather than only inspissated mucus. Needle aspiration biopsy was definitive in two of the cases when conventional diagnostic methods failed.

A bronchocele or bronchial mucocele is a dilated mucus-filled bronchus which has a characteristic radiographic appearance [1–3]. Bronchoceles may be caused by abnormal or excessive mucus production, such as cystic fibrosis or bronchial asthma. In the latter condition, an allergic reaction to aspergillosis may be responsible for the excess mucus formation. Mucoid impaction is a term often used for bronchocele formation in which no anatomic obstruction is present.

A bronchocele may also result from segmental or subsegmental bronchial occlusion caused by congenital atresia or inflammatory stricture. Although rare, bronchial neoplasm may be the underlying etiology of a bronchocele [2, 4]. In association with malignancy, a mucocele has been understood as a dilated mucus-filled bronchus distal to an obstructing mass. On the basis of the following cases, this concept should be enlarged to include tumor impaction within a bronchus. Recent reviews of oat cell carcinoma [5, 6] have not described a bronchocele as an initial radiographic feature.

This report demonstrates that a bronchocele may be the sole finding or part of the tumor complex seen on radiographs in oat cell carcinoma. During the past 3 years, we have studied three such cases. During this same time period, two cases of bronchoceles associated with bronchogenic carcinoma of the squamous cell type were seen. In addition, we point out that such a bronchocele may be filled with neoplastic cells rather than only inspissated mucus, and that needle aspiration biopsy [7] can achieve a diagnosis when standard techniques (sputum analysis, fiberoptic bronchoscopy) fail.

Case Reports

Case 1

A 54-year-old man had a 4-week history of a productive cough and night sweats. Chest radiography (fig. 1A) revealed oval densities in the left mid-lung field, suggestive of bronchocele formation, and an enlarged ductus lymph node. Sputum cytologies were negative. Fiberoptic bronchoscopy showed patent major airways, and washings were negative. Bronchography (fig. 1B) demonstrated nonfilling of the superior segmental bronchus of the lingula, corresponding to the region of bronchocele formation. Cytologic specimens from concomitant brushing of this area under fluoroscopic control disclosed malignant cells (specific cell type could not be characterized). After a negative mediastinoscopy, thoracotomy with a left pneumonectomy was performed. The pathologic specimen showed a dilated superior segmental bronchus filled with both oat cell carcinoma and mucus. Metastatic neoplasm in an enlarged ductus lymph node and in several smaller hilar lymph nodes was also found.

Case 2

A 66-year-old man with a 100 pack per year smoking history experienced marked weakness. Chest radiography (figs 2A and 2B) revealed a mass density near the left hilum. Tomography (fig. 2C) defined a well circumscribed elliptical left perihilar mass, consistent with a bronchocele, and left hilar lymph node enlargement. The major bronchi were patent. Sputum analysis and fiberoptic bronchoscopy and washings were negative. Bronchography demonstrated narrowing of the superior segment of the lingular bronchus, but brushings from the area were negative. Cytologic specimens from an aspiration needle biopsy of the bronchocele were positive for oat cell carcinoma. The patient was referred for radiation therapy.

Case 3

A 71-year-old man with a heavy smoking history had a productive cough and weight loss. Chest radiography (figs. 3A and 3B) demonstrated ovoid shadows adjacent to the left hilum. Tomography in the left posterior oblique projection (fig. 3C) defined a bilobulated density radiating into the left upper lobe, consistent with a bronchocele. Sputum analysis and fiberoptic bronchoscopy and washings were negative. Cytologic specimens from a needle aspiration biopsy of the lobulated left upper lobe mass showed oat cell carcinoma. The patient was treated with combined chemotherapy and radiation therapy.

Discussion

The three cases described have in common the appearance on chest radiographs of lesions consistent with bronchocele formation. Theoretically, bronchoceles might be expected to occur in association with oat cell carcinoma since this type of bronchogenic carcinoma frequently involves the proximal bronchi. Yet this manifestation has not been demonstrated in recent comprehensive articles [5, 6].

These cases emphasize that bronchoceles caused by bronchial neoplasm may not have a proximal obstructing mass within the reach of a fiberoptic bronchoscope. Histologic examination of the bronchocele in the first case revealed the unexpected finding of oat cell carcinoma mixed with mucus. Prior to this case, we had not used needle aspiration in the evaluation of a bronchocele, assuming that any etiologic obstructing neoplasm

Received July 19, 1978; accepted after revision October 9, 1978.

[1] All authors: Mallinckrodt Institute of Radiology, Washington University School of Medicine, 510 South Kingshighway Boulevard, St. Louis, Missouri 63110. Address reprint requests to D. J. Aronberg.

© 1979 American Roentgen Ray Society

0361-803X/79/1321-0023 $0.00

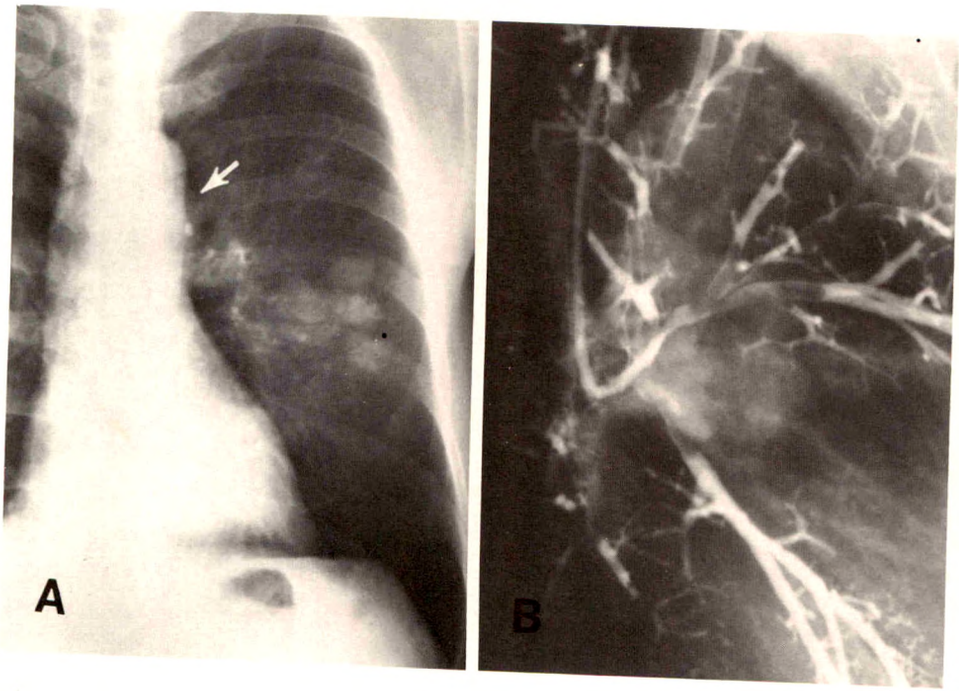


Fig. 1.—**A**, Oval densities in left mid lung field and enlarged ductus lymph node (*arrow*). **B**, Nonfilling of superior segment of lingular bronchus.

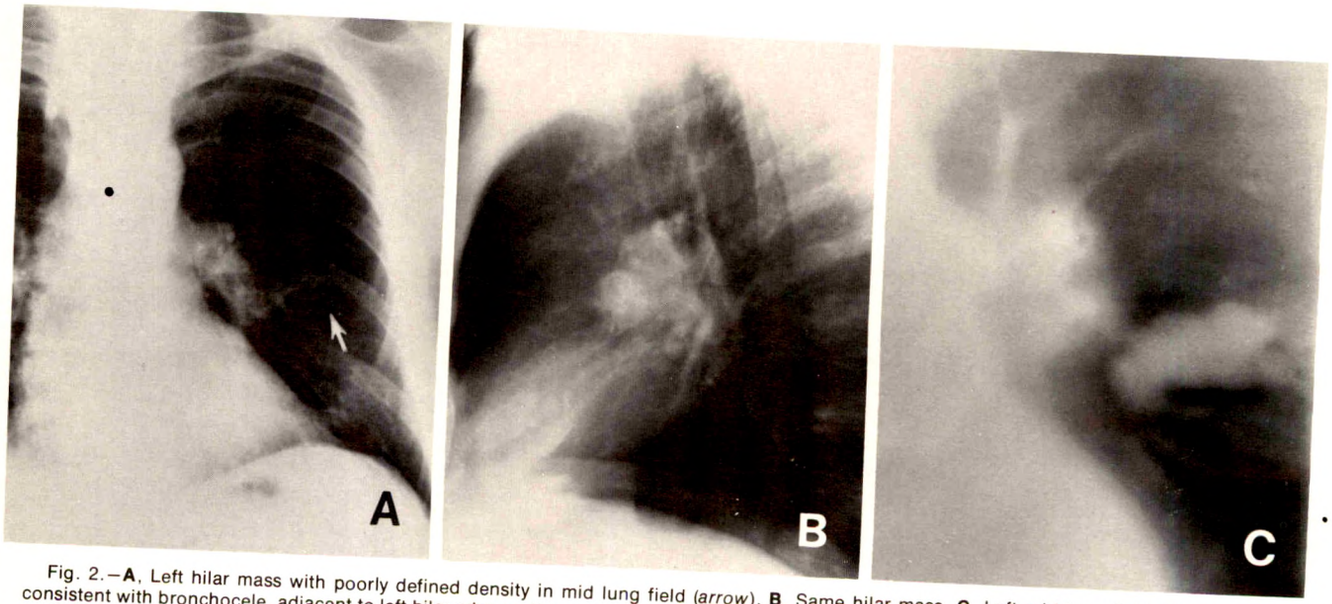


Fig. 2.—**A**, Left hilar mass with poorly defined density in mid lung field (*arrow*). **B**, Same hilar mass. **C**, Left mid lung field. Fingerlike density, consistent with bronchocele, adjacent to left hilar adenopathy.

would be too small to successfully biopsy. As cases 2 and 3 illustrate, needle aspiration biopsy may confirm neoplasm to be the cause of an observed bronchocele when standard diagnostic methods fail. We have used needle aspiration biopsy to establish a diagnosis in another instance of bronchocele due to malignancy (other than oat cell) when other methods were not revealing.

A specific diagnosis of oat cell carcinoma usually can be determined by needle aspiration biopsy, even though other cell types frequently cannot be distinguished by this method [6, 7]. Ascertaining the cell type of a suspected malignant pulmonary lesion prior to a contemplated thoracotomy may be extremely important, as resection of an oat cell carcinoma will almost always prove futile [8].

REFERENCES

1. Lemire P, Trepanier A, Hebert G: Bronchocele and blocked bronchiectasis. *AJR* 110:687–693, 1970
2. Levitt RG, Forrest JV, Sagel SS: Roentgenographic recognition of bronchoceles. *South Med J* 69:1556–1558, 1976
3. Talner LB, Gmelich JT, Liebow AA, Greenspan RH: The

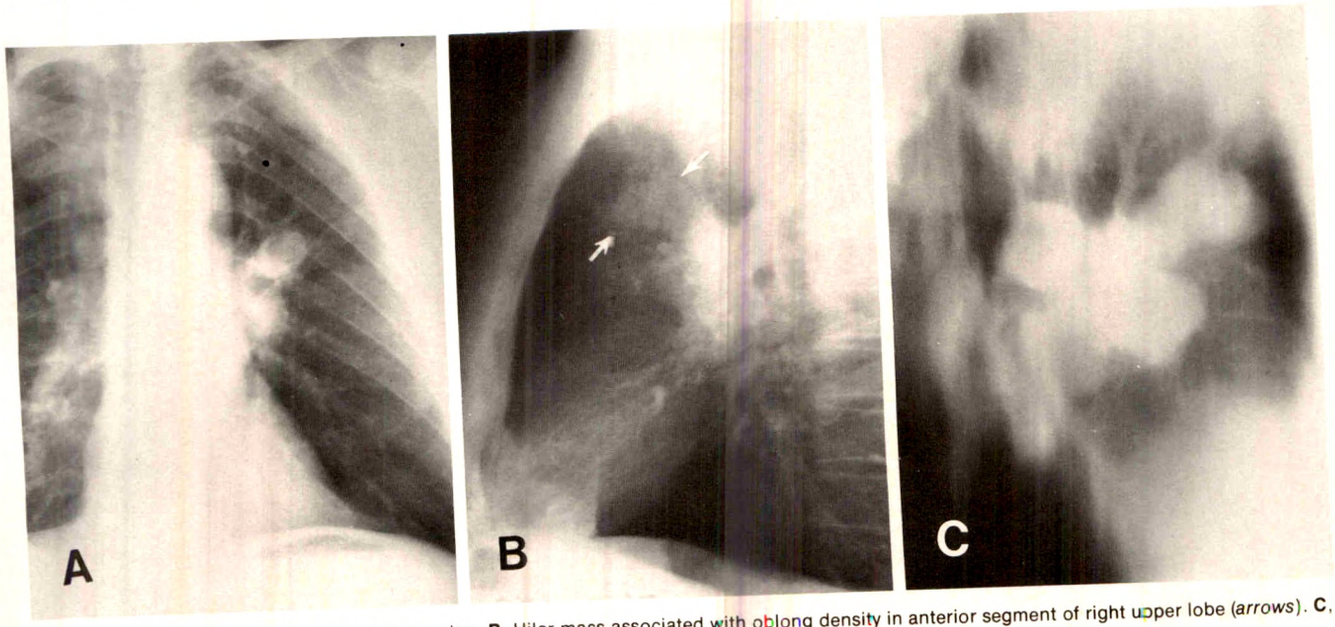


Fig. 3.—**A**, Ovoid densities in left perihilar region. **B**, Hilar mass associated with oblong density in anterior segment of right upper lobe (*arrows*). **C**, Hilar adenopathy with anterior lobulated density extending to lung periphery, suggesting bronchocele.

syndrome of bronchial mucocele and regional hyperinflation of the lung. *AJR* 110:675–686, 1970
4. Rees DO, Ruttley MST: The bronchocele in bronchial neoplasm. *Clin Radiol* 21:62–67, 1970
5. Byrd RB, Miller WE, Carr DT, Payne WS, Woolner LB: The roentgenographic appearance of small cell carcinoma of the bronchus. *Mayo Clin Proc* 43:337–341, 1968
6. Sinner WN, Sandstedt B: Small-cell carcinoma of the lung. Cytological, roentgenologic, and clinical findings in a consecutive series diagnosed by fine needle aspiration biopsy. *Radiology* 121:269–274, 1976
7. Sagel SS, Forrest JV: Fluoroscopically assisted lung biopsy techniques, in *Special Procedures in Chest Radiology*, edited by Potchen EJ, Philadelphia, Saunders, 1976, p 22–69
8. Scannell JG: The problem of oat cell carcinoma. *N Engl J Med* 282:98–99, 1970

Antrochoanal Polyps

RICHARD TOWBIN,[1] J. S. DUNBAR,[2] AND KEVIN BOVE[3]

The antrochoanal polyp, a benign solitary polypoid lesion, usually arises in a maxillary sinus, opacifying and enlarging the sinus cavity without bone destruction. It passes through the ostium of the sinus into the choana, and from there into the posterior nasopharynx. The soft tissue mass does not erode or destroy contiguous soft tissue or bony structures. In this sequence of events, its radiologic findings are characteristic. Five case reports are presented, and the differential diagnosis is discussed.

The antrochoanal polyp, usually a solitary benign growth, arises from the maxillary antrum of a nonatopic patient. It grows by extension from the antrum through its ostium into the middle meatus, then into the posterior choana and may extend into the nasopharynx.

Antrochoanal polyps are known to otolaryngologists and have been frequently reported in the otolaryngologic literature after Killian's excellent description in 1906 [1]. In the radiologic literature, the antrochoanal polyp has been largely ignored. Since it has distinctive features which allow radiologic diagnosis, we present five cases and discuss the diagnosis and differential diagnosis.

Case Reports

Case 1

H. B. (female) was followed by an otolaryngologist since 19 months of age because of recurrent otitis media and its complications. During this interval physical examinations revealed no nasal polyp. No history of allergy was elicited. At 6 years of age, she was admitted to Children's Hospital Medical Center for observation after incurring a linear skull fracture. Radiography showed a linear frontal fracture and opacification of the left maxillary antrum. The antrum was slightly expanded without bone destruction. A water-density mass extended from the posterior choana into the nasopharynx, but was not appreciated at that time. At age 7 a large polyp filled the left naris and extended into the nasopharynx. An antrochoanal polyp (8.0 × 1.5 × 1.2 cm) was removed by snare avulsion.The antrochoanal polyp recurred 11 months after removal. The polyp was then removed at its base in the antrum by a Caldwell-Luc procedure.

Case 2

P. S., a 12-year-old white boy, was admitted for evaluation of left nasal obstruction which had gradually progressed over the previous year. There was no history of allergic disease. Because of changes in his voice and a feeling of something in the back of his throat, otolaryngologic consultation was requested. Examination of the pharynx revealed a nasopharyngeal mass at the level of the velum. On radiologic examination, the left maxillary antrum was shown to be slightly enlarged and completely opacified (figs. 1A–1C). A water-density mass in the posterior choana protruded into the nasopharynx. There was no bone destruction. A Caldwell-Luc procedure was performed and a 5 × 2.2 × 1.4 cm granular gray mass, arising from the maxillary antrum and extending into the nasopharynx, was removed (fig. 1D).

Case 3

S. W., a 12-year-old white girl, was admitted with a 5 week history of increasing left nasal obstruction. No pain or discharge was present. There were no known allergies. Physical examination was unremarkable except for a large, glistening, soft and fleshy, nonpulsatile mass in the left nostril. It was not seen in the nasopharynx. Sinus radiography showed opacification of the left maxillary antrum with minimal expansion but no bone destruction. The lateral view demonstrated a water-density mass in the posterior choana (fig. 2). A left Caldwell-Luc procedure with partial ethmoidectomy was performed. The mass arose in the left maxillary sinus and extended into the nasopharynx. The pathologic findings were consistent with an antrochoanal polyp.

Case 4

J. M., an 11-year-old white boy, developed an upper respiratory infection associated with right epistaxis 2 weeks before admission. One day before admission, his mother noted tissue protruding from the right naris with swallowing. On physical examination there was complete obstruction of the right naris by a fleshy mass. The mass extended into the oropharynx, appeared multilobular, and was cystic to palpation. No adenopathy was present. Radiography showed complete opacification of the right maxillary antrum, with enlargement but no bony destruction. A water-density mass in the right naris extended into the nasopharynx (fig 3). A mucus retention cyst was incidentally noted on the floor of the left maxillary antrum. At surgery, a biopsy was followed by a right Caldwell-Luc procedure. An antrochoanal polyp which originated in the right maxillary antrum and extended into the posterior choana was removed. The left maxillary antrum was not investigated.

Case 5

J. B., a $10^{5}/_{12}$-year-old white boy, was seen in the emergency room with epistaxis and an autoamputated polypoid mass from his left naris. For the previous 2 months he had had recurrent epistaxis and a sensation of a left nasal blockage. He had no allergic history. Examination of the nasopharynx revealed mucopurulent discharge and a polypoid mass exiting from the middle meatus and extending into the nasopharynx. Radiography of the sinuses demonstrated mucoperiosteal thickening of the right maxillary antrum, and opacification and slight expansion of the left antrum. A soft-tissue mass extended into the nasopharynx. Pathologic examination of the autoamputated 3.0 × 0.9 × 0.3 cm polyp was consistent with the diagnosis of antrochoanal polyp.

Received June 22, 1978; accepted after revision October 2, 1978.
[1] Division of Roentgenology, Pediatrics, Children's Hospital Medical Center, Cincinnati, Ohio 45229.
[2] Division of Roentgenology, Pediatrics, University of Cincinnati College of Medicine, Children's Hospital Medical Center, Cincinnati, Ohio 45229.
Address reprint requests to J. S. Dunbar at Children's Hospital.
[3] Departments of Pediatrics and Pathology, Children's Hospital Medical Center Cincinnati, Ohio 45229.

0361–803X/79/1321–0027 $0.00

AJR 132:27–31, January 1979
© 1979 American Roentgen Ray Society

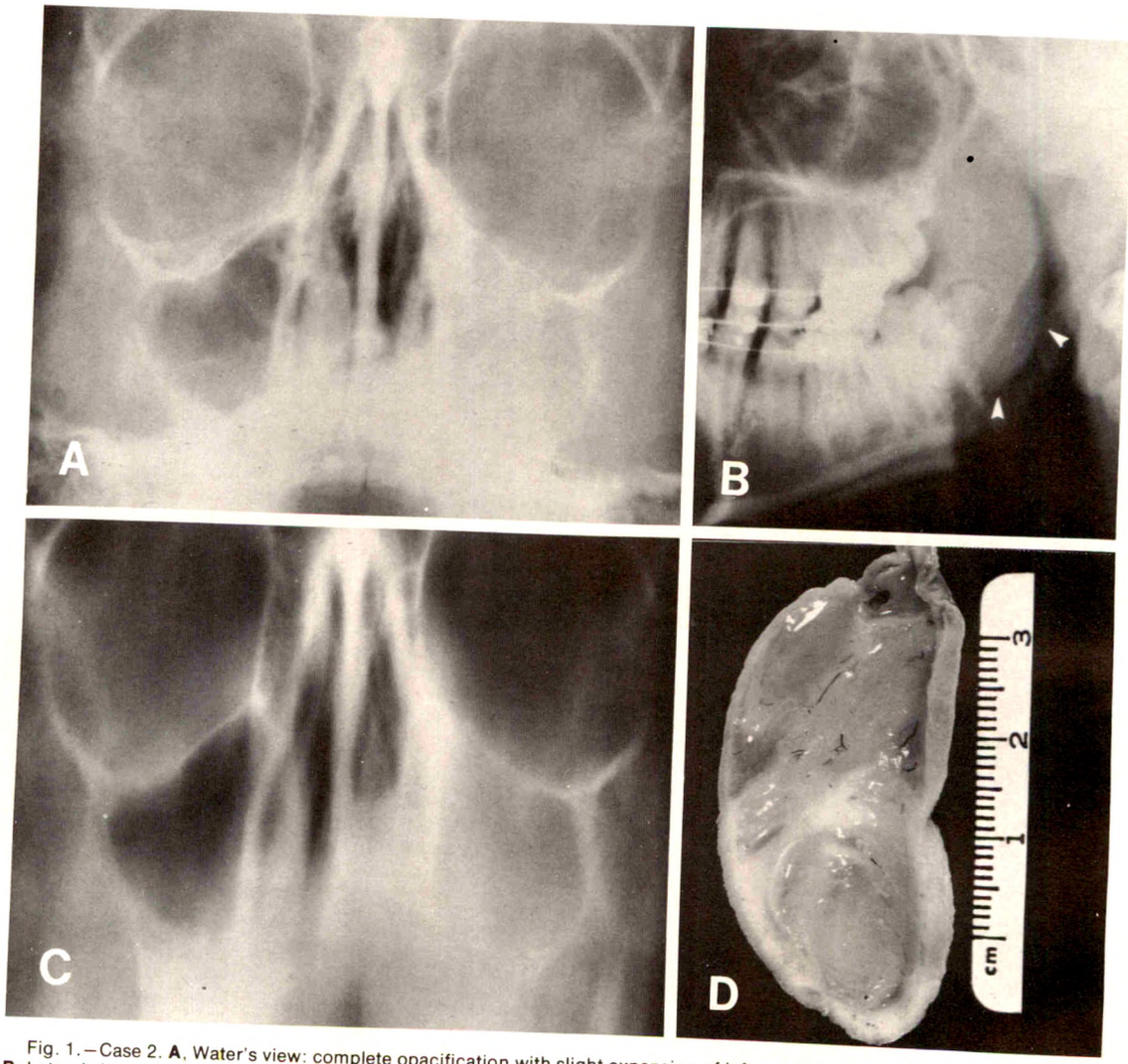


Fig. 1.—Case 2. **A**, Water's view: complete opacification with slight expansion of left maxillary antrum. No bony destruction. **B**, Lateral view: a large, rounded water-density mass extends into nasopharynx (*arrows*). **C**, Tomogram: left maxillary antrum is opacified and enlarged, without bony destruction. **D**, 5.0 × 2.2 × 1.4 cm polyp on stalk. Typical appearance of choanal polyp.

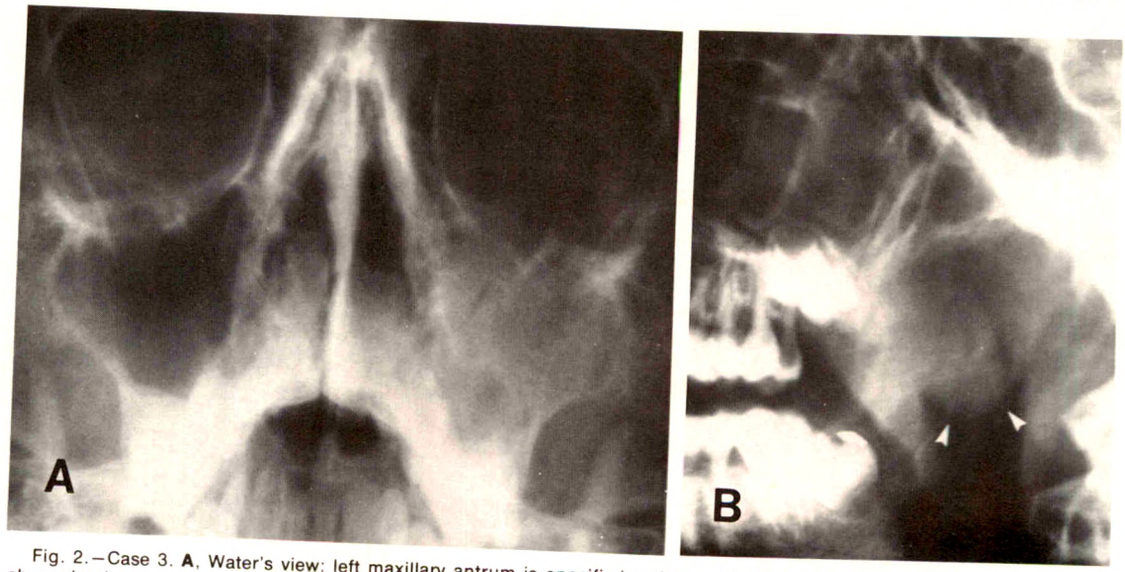


Fig. 2.—Case 3. **A**, Water's view: left maxillary antrum is opacified and expanded. No bony destruction. **B**, Lateral view: choanal polyp (*arrows*) extends into upper nasopharynx. Pterygoid plates and posterior wall of maxillary sinus are unaffected.

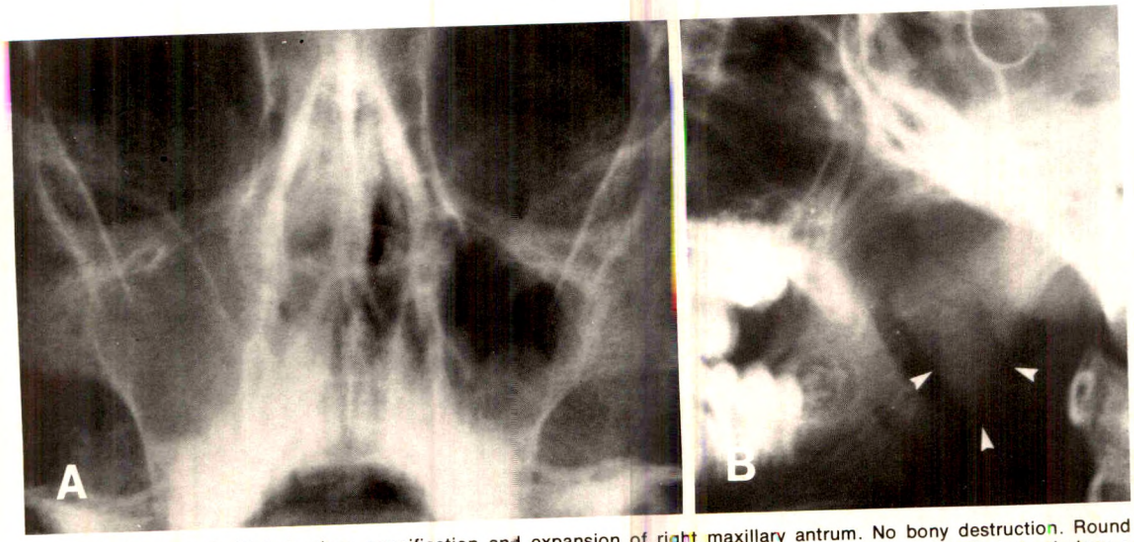


Fig. 3.—Case 4. **A**, Water's view: opacification and expansion of right maxillary antrum. No bony destruction. Round water density mass in inferomedial aspect of left maxillary antrum, representing mucus retention cyst. **B**, Lateral view: a polypoid mass extends into nasopharynx (*arrows*).

Discussion

The first description of antrochoanal polyps was by Palfyn in 1753 [2]. He reported a female in whom a nasopharyngeal polyp extended to the level of the uvula. The tumor was round, smooth, whitish, insensitive, and soft. She had difficulty speaking and could only breath through her mouth. Throughout the nineteenth century there were scattered reports of removal of antrochoanal polyps. However, in 1906 Killian [1] first accurately described the natural history of the antrochoanal polyp, including its true site of origin in the maxillary sinus. Prior to this time, it had been thought that the antrochoanal polyp arose in a posterior choana. However, Killian did not confirm the maxillary antrum origin of the lesion by opening or dissecting the antrum. This documentation is credited to Ino Kubo in 1909. Since then, there have been many reported cases, most arising from a maxillary antrum, but occasionally from the ethmoid or sphenoid sinuses.

The benign inflammatory or allergic polyp is the most frequent new growth in the nasal fossa and the paranasal sinuses. The antrochoanal polyp is infrequent. Syme [3] found 26 (3%) of 878 patients with antral disease to have antrochoanal polyp. Myers [4], in over 25,000 ear-nose-throat examinations during 3 years in the military, found only three cases of antrochoanal polyp. In the series of Heck et al. [5], 56 of 1720 patients (3.7%) with nasal polyps had antrochoanal polyp. In the large experience of 118,374 patients examined over 13 years at Helsinki University Central Hospital, 1,295 cases of nasal polyps were discovered [6]. Of the latter there were 80 cases of antrochoanal polyp. Thus, the incidence of antrochoanal polyp was 0.07% of otolaryngologic cases and 6.2% of nasal polyps in the Helsinki series. Data from three well documented series [5–7] indicate that about 71% of patients with antrochoanal polyps are 10–39 years of age. Also noted was a 1.3 to 1 male-to-female ratio.

Radiographic Features

In the series of Heck et al. [5], radiography of the sinuses was performed in 61 of 64 patients with antrochoanal polyp. In only one instance was the examination negative. In 57.4% there was evidence of a unilateral lesion on the involved side, and 42% showed bilateral involvement of the maxillary or other sinuses. A nasopharyngeal soft tissue mass was demonstrated in 7 (11.4%) of the 61 patients.

In Hardy's series [7], interpretation of radiographs was made in only 13 of 31 cases. In comparison with Heck et al. [5], a large number (69.2%) showed involvement of one or more sinuses on the side of the polyp, and a smaller number (23%) showed bilateral involvement. In only one instance was a choanal mass demonstrated. No examination failed to indicate an abnormality.

In all of our patients there was evidence of slight but definite expansion of the involved maxillary antrum. Hiranandani and Melgiri [8] and Chhangani [9] described this phenomenon; the latter also documented erosion of the lateral nasal wall in one of his patients. This complication was believed to result from failure of the polyp to pass posteriorly after it had traversed the maxillary ostium into the choana; it had therefore expanded and eroded contiguous structures.

Differential Diagnosis

The diagnosis of antrochoanal polyp is strongly suggested when an opacified maxillary antrum is expanded and there is a nasopharyngeal mass. Other possible diagnoses include the following.

Normal or hypertrophied inferior turbinates. The inferior turbinate projects into the nasopharyngeal fossa. This normal finding is sometimes misinterpreted as a nasopharyngeal mass, but should easily be recognized for what it is [10, 11].

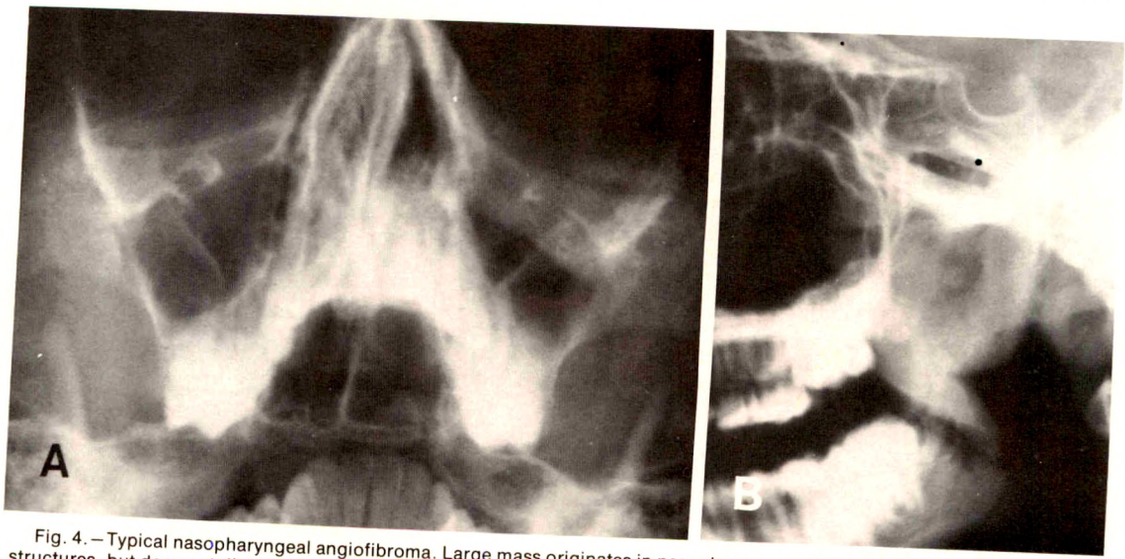


Fig. 4.—Typical nasopharyngeal angiofibroma. Large mass originates in nasopharynx, and invades and displaces contiguous structures, but does not distend antra.

Chronic hypertrophic polypoid rhinosinusitis. This condition affects the upper respiratory epithelium. It is characterized by vasomotor instability, polypoid mucosal hypertrophy, and superimposed infection. Numerous etiologies are associated with vasomotor instability of the upper respiratory tract and include drugs, infection, endocrine imbalance, and psychogenic factors. Allergy is often a factor, especially when the changes are bilateral [12].

The hypertrophic polyps may be unilateral or bilateral, most frequently occurring in the nose and ethmoid sinuses, although no sinus is spared. Expansion of the sinus lumen or nasal cavity may occur and occasionally is so marked as to produce hypertelorism and widening of the nasal bridge [13]. When nasal polyps are seen in children, cystic fibrosis of the pancreas should be considered. However, in our experience, no nasopharyngeal component occurs.

Juvenile nasopharyngeal angiofibroma. This is a highly vascular, benign neoplasm with potential for local destruction; most occur in the nasopharynx or posterior nasal cavity of pubescent males. The symptoms can be epistaxis, nasal obstruction, or a mass in the nasopharynx.

The radiologic features (fig. 4) of this tumor are (1) a large soft-tissue mass in the nasopharynx extending into the areas of the parapharyngeal structures; (2) anterior bowing of the posterior wall of the maxillary antrum of the involved side, best seen on lateral projection; (3) bony erosion of contiguous structures—erosion of the sphenoid bone above the sphenooccipital synchrondrosis, the hard palate, one or both pterygoid processes, and the medial wall of the maxillary sinus may occur; and (4) displacement of the nasal septum. When necessary, carotid angiography and computed tomography can be performed to demonstrate the tumor.

Mucus retention cyst. This lesion is common within sinus cavities, particularly in the antra. It is a well defined, smooth, mucus-filled epithelial cyst arising from the floor or one of the walls of the cavity. It does not extend into the choana, nor enlarge the sinus cavity.

Mucocele. This represents an interstitial mucin pool resulting from rupture of glands or ducts [15, 16]. The mucocele usually occurs in the frontoethmoid region, and only rarely in the maxillary sinuses. It causes enlargement (sometimes severe) of the cavity in which it occurs, erosion or sclerosis of the walls of the cavity, and sometimes sclerosis of the surrounding bone. However, it does not extend into or through the choana when the maxillary sinus is involved.

Malignant tumors of the nasopharynx. These tumors account for about 1% of all malignancies [17–20]. These neoplasms may cause difficulty in differential diagnosis. However, they tend to cause destruction of contiguous bony structures, airway obstruction, enlargement of the adenoidal tissue outside of its normal confines, or invasion into the paranasal sinuses. Tomography may be necessary to evaluate the extent of the neoplastic involvement. The most common malignant tumors of the nasopharynx in childhood are lymphoma, rhabdomyosarcoma, lymphoepithelioma, olfactory neuroblastoma, and chordoma. These usually cannot be differentiated by radiographic means.

Pathology and Treatment

Grossly the antrochoanal polyp is a large, solitary, gray-white, smooth polyp with a stalk of variable length. Both the antrochoanal polyp and nasal polyps are myxoid and both are lined by ciliated pseudostratified columnar epithelium, the characteristic mucosa of nasal passages and paranasal chambers.

Reports indicate that the histology of antrochoanal polyp does not differ substantially from that of the nasal polyp. Heck et al. [5] stated that antrochoanal polyp was less likely to contain eosinophils and mucus glands. The latter may be a function of local differences in density of

mucus glands, but the disparity in content of eosinophils suggests differing pathogenesis. Hyperplasia of surface epithelium is, in our series, more prominent in antrochoanal polyp. We concur that nasal polyps exhibit greater density of submucosal glands, more mucus retention, and more eosinophils. However, the validity of such distinction has not been established.

It would seem that the best results occur when the Caldwell-Luc operation is used. If simple polypectomy by snare and avulsion is performed, there is a recurrence rate of about 20% [5, 7].

ACKNOWLEDGMENTS

We thank Dr. Corning Benton for his thoughtful suggestions and N. Woolum for her fine secretarial work.

REFERENCES

1. Killian G: The origin of choanal polyps. *Lancet* 2:81–82, 1906
2. Palfyn J: *Anatomie Chirurgicale*. Paris, 1753
3. Syme WS: Choanal polyps. *J Laryngol Otol* 31:515–518, 1916
4. Myers D: Obstruction of the nasopharynx secondary to choanal polyp of antral origin. *Arch Otolaryngol* 44:328–333, 1946
5. Heck WE, Hallberg OE, Williams HL: Antrochoanal polyps. *Arch Otolaryngol* 52:538–548, 1950
6. Sirola R: Choanal polyps. *Acta Otolaryngol* (Stockh) 61 42–48, 1965
7. Hardy G: Choanal polyps. *Annals Otol* 66:306–326, 1957
8. Hiranandani LH, Melgiri RD: Expansion of antrum by antrochoanal polypus. *J Laryngol Otol* 80:175–177, 1966
9. Chhangani DL, Agarwal KK, Popli SP: Expansion of antrum and erosion of lateral nasal wall: antrochoanal polypus. *J Laryngol Otol* 81:1049–1051, 1967
10. Capitano MA, Kirkpatrick JA: Upper respiratory tract obstruction in infants and children. *Radiol Clin North Am* 6:265–277, 1968
11. Dunbar JS: Upper respiratory tract obstruction in infants and children. *AJR* 109:227–245, 1970
12. Wilson M: Chronic hypertrophic polypoid rhinosinusitis. *Radiology* 120:609–613, 1976
13. Rulon JT, Brown HA, Logan CB: Nasal polyps and cystic fibrosis of the pancreas. *Arch Otolaryngol* 78:94–101, 1963
14. Holman CB, Miller WE: Juvenile nasopharyngeal fibroma. *AJR* 94:292–298, 1965
15. Samuel E: The radiology of the paranasal sinuses, in *Textbook of X-Ray Diagnosis, Head and Neck* (vol 1), 4th ed., edited Shanks SC, Kerley P, Philadelphia, Saunders, 1969, pp 613–614
16. Dubois PJ, Schultz JC, Perrin RL, Dastur KJ: Tomography in expansile lesions of the nasal and paranasal sinuses. *Radiology* 125:149–158, 1977
17. Dehner LP: Tumors of the mandible and maxilla in children. I. Clinicopathologic study of the 46 histologically benign lesions. *Cancer* 31:364–383, 1973
18. Floyd JH: Tumours of the head and neck, in *Tumours of Infancy and Childhood*, edited by Jones PG, Campbell PE, Philadelphia, Lippincott, 1976, pp 343–364
19. Jaffe BF, Jaffe N: Head and neck tumors in children. *Pediatrics* 51:731–740, 1973
20. Donaldson SS, Castro JR, Wilbur JR, Jesse RH: Rhabdomyosarcoma of the head and neck in children. *Cancer* 31:26–35, 1973

Computed Tomography Diagnosis of Mesenteric Masses

MICHAEL E. BERNARDINO,[1] BAO S. JING, AND SIDNEY WALLACE

The computed tomographic findings of 30 mesenteric masses are presented. To delineate the mesentery accurately, oral contrast material must fill the entire small bowel. Of the masses, 23 were secondary to non-Hodgkin's lymphoma. These masses were irregular in shape and homogeneous in their tissue attenuation. Two of the 23 had a normal lymphangiogram in the upper paraaortic area. Both lymphangiography and CT were necessary to define the extent of disease in such patients. The six mesenteric metastases were irregular in shape. Four of these had areas of decreased attenuation eccentrically located within the mass which may be secondary to necrosis. One mesenteric cyst had a circular shape with smooth, sharp borders, and a centrally located area of decreased attenuation.

Cross sectional imaging using computed tomography (CT) has greatly facilitated the diagnosis of abdominal masses involving the kidneys, liver, and retroperitoneum [1–5]. However, only a few reports have mentioned CT with mesenteric masses [6, 7]. We reviewed our experience with CT in diagnosing and characterizing mesenteric masses.

Subjects and Methods

The CT scans of 30 patients with mesenteric masses were reviewed. Patients rangec in age from 36 to 68 years. Seventeen patients were male; 13 were female. Table 1 shows the types of mesenteric masses reviewed. The masses were confirmed by surgery in eight patients, ultrasound in 15, and barium studies or angiography in three.

All patients were examined on an EMI 5005 scanner, utilizing an 18 sec scan time, 320 × 320 matrix, and 13 mm collimator. Scans were obtained at 2 cm intervals or less through the abdomen after the intravenous infusion of 300 ml of 30% meglumine diatrozoate. A 300 ml mixture consisting of 15 parts water to one part Gastrografin was given orally 20–30 min prior to scanning. Antoher 200 ml of this mixture was administered just prior to the procedure in order to delineate the small intestine. Glucagon (1 mg) or Pro-banthine (15 mg) was administered intravenously to reduce intestinal motility. This was repeated if more than 8–10 slices were necessary. Images were recorded by matrix camera at various window widths and levels.

CT Features

The mesenteric masses delineated ranged in size from 1 cm to greater than 20 cm. Smaller rounded masses were difficult to distinguish from unopacified bowel. However, these were usually in a cluster pattern and/or adjacent to a larger mesenteric or retroperitoneal mass (fig. 1). Larger masses were difficult to distinguish from retroperitoneal disease when contrast-filled bowel did not separate the two areas (fig. 2). Also, when masses occupied a large portion of the mesentery, the bowel loops appeared splayed and compressed (fig. 3).

Non-Hodgkin's Lymphoma

The 23 non-Hodgkin's lymphoma mesenteric masses had shapes ranging from tiny round densities to irregular, bulky masses. However, all demonstrated a homogeneous tissue attenuation throughout. Of the 23 non-Hodgkin's lymphoma patients with mesenteric masses, 21 demonstrated retroperitoneal and mesenteric disease. Of these 21, 11 had contiguous spread of the lymphomatous mass from the retroperitoneum along the root of the mesentery into the abdomen. This was sometimes best observed on sequential scans. In the remaining two non-Hodgkin's lymphomas (both nodular undifferentiated lymphocytic variety), the only sign of abdominal disease was the mesenteric mass alone, since both CT and lymphangiography showed no evidence of retroperitoneal disease (fig. 4).

Metastatic Masses

The six patients with metastatic carcinoma demonstrated retroperitoneal and mesenteric disease in two cases and mesenteric disease alone in four. The latter were totally or almost totally surrounded by contrast-filled bowel. In the patient with a carcinoid of the small bowel, CT also demonstrated additional tiny nodules with kinking and angulation of the bowel loops (fig. 5). Four of the six patients with metastases had areas of decreased tissue attenuation within the mesenteric masses. All of these relatively lucent areas were eccentrically located (fig. 6). At surgery, in one of the four patients, a recurrent renal cell carcinoma, the area of decreased attenuation corresponded to an area of necrosis.

Mesenteric Cyst

The only benign lesion was a mesenteric cyst within a well circumscribed fibroconnective tissue capsule and an area of centrally located decreased attenuation within it (fig. 7). At surgery, this area of decreased attenuation was filled with a yellow, thick creamy material.

Discussion

The most common neoplasms to involve the mesentery are metastases and lymphoma, usually seen in disseminated disease. Primary mesenteric neoplasms are rare but commonly benign and of fibrous origin [8–10]. Our series supports this data since metastatic cancer and

Received July 6, 1978; accepted after revision October 5, 1978.

[1] All authors: Department of Diagnostic Radiology, M. D. Anderson Hospital and Tumor Institute, University of Texas System Cancer Center, Houston, Texas 77030. Address reprint requests to M. E. Bernardino.

0361-803X/79/1321-0033 $0.00

AJR 132:33–36, January 1979

© 1979 American Roentgen Ray Society

TABLE 1

Etiology of Mesenteric Masses

Types of Masses	No. Patients
Non-Hodgkin's Lymphoma:	
Diffuse histiocytic	16
Nodular undifferentiated lymphocytic	6
Burkitt's	1
Metastatic masses:	
Metastatic colon carcinoma	2
Recurrent renal cell carcinoma	1
Metastatic testicular carcinoma	1
Metastatic leiomyosarcoma	1
Metastatic carcinoid	1
Benign:	
Mesenteric cyst	1
Total	30

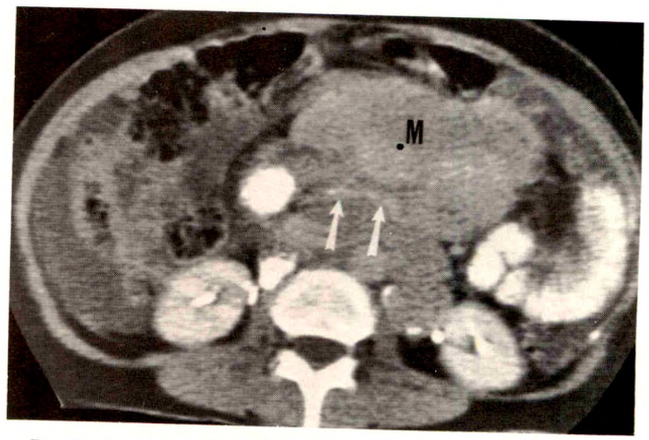


Fig. 2.—Large mesenteric lymphoma mass (M), difficult to separate from retroperitoneal disease except for faint visualization of oral contrast within compressed small bowel (*arrows*).

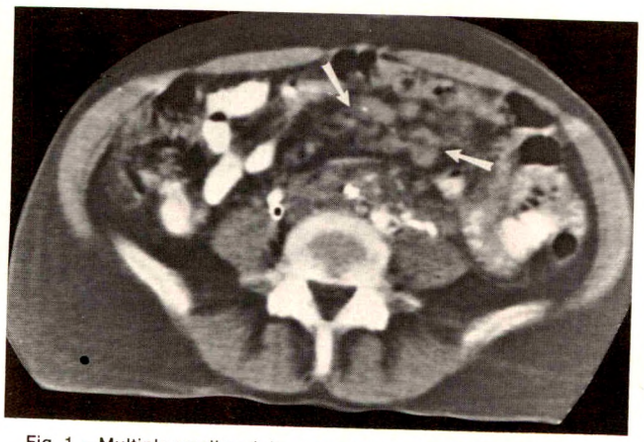


Fig. 1.—Multiple small nodular masses (*arrows*) are in cluster pattern. These were confirmed by ultrasound and would be difficult to distinguish from unopacified small bowel. Note associated retroperitoneal disease.

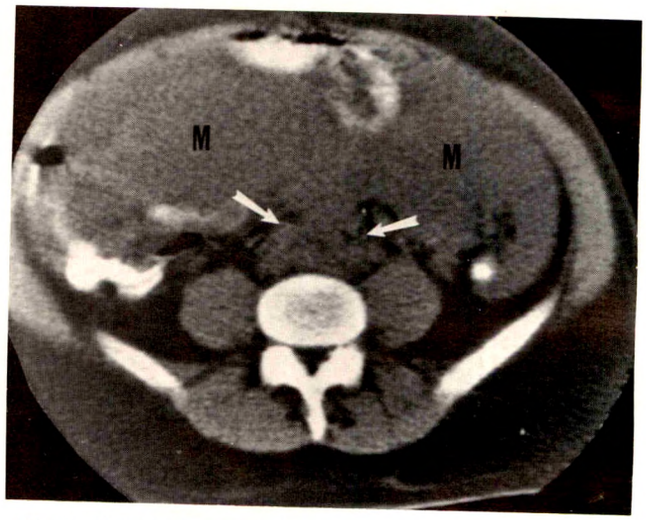


Fig. 3.—Massive mesenteric lymphoma mass (M) grossly displaces contrast-filled small bowel loops. Mass is contiguous with root of mesentery (*arrows*).

lymphoma accounted for all but one of our mesenteric masses.

The root of the mesentery extends from left of the upper lumbar spine, a distance of 15 cm, across the great retroperitoneal vessels inferiorly to the right sacroiliac joint [11]. This area along with the lymph nodes above cisterna chyli and at the hepatic or splenic hila are not opacified by pedal lymphangiography. Lymphangiography is best suited to diagnose architecturally abnormal nodes in the region of the iliac and retroperitoneal great vessels [6]. However, the areas not seen by lymphangiography are easily visualized by CT. Since 61% of all non-Hodgkin's lymphomas will have positive mesenteric nodes at presentation, the true extent of disease will be missed if lymphangiogram alone is used for diagnosis and staging [12]. This contrasts with Hodgkin's disease, in which only 5% of the patients will have mesenteric involvement. Also, two patients with nodular undifferentiated lymphocytic lymphoma had mesenteric masses while the paraaortic lymph nodes were normal by lymphangiography. Although lymphangiography is limited in its area of evaluation, it is generally more sensitive and more specific than CT. Subtle changes in the status of the opacified nodes are more readily appreciated on follow-up lymphangiography. These examinations can be performed readily by conventional radiography of the abdomen every few months as long as contrast remains in the lymph nodes. This type of reevaluation is significantly less expensive than repeated CT examinations. Thus, initially, we feel both CT and lymphangiography should be performed on all non-Hodgkin's lymphoma patients since these methods are complementary.

The only benign lesion, a mesenteric cyst, was a mass with a central area of decreased attenuation. It had a sharply defined margin which distinguished it from the metastatic or lymphoma masses. The metastatic lesions were irregular in shape and four had eccentrically located areas of decreased attenuation. None of the non-Hodgkin's masses had areas of decreased attenuation, but all were irregular in shape. The shape of a mesenteric mass or location of an area of decreased attenuation

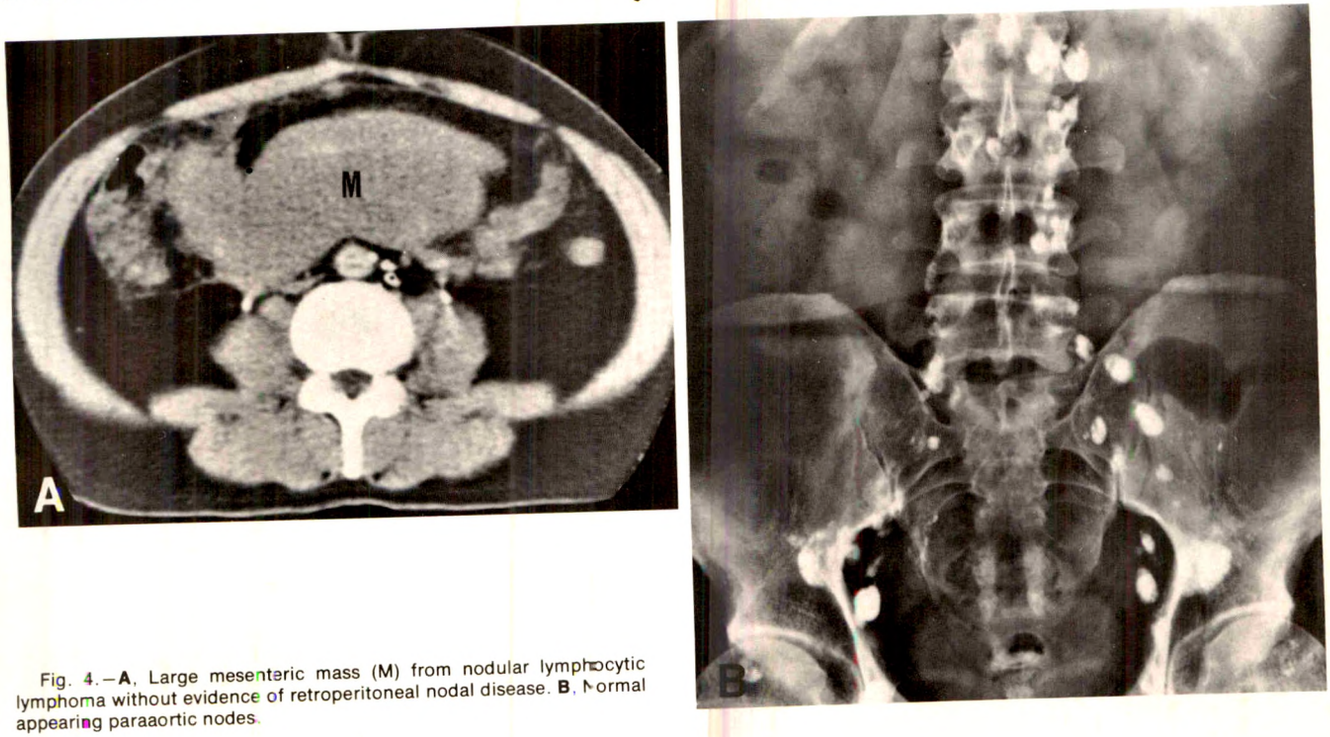


Fig. 4.—**A**, Large mesenteric mass (M) from nodular lymphocytic lymphoma without evidence of retroperitoneal nodal disease. **B**, Normal appearing paraaortic nodes.



Fig. 5.—Large irregular mesenteric mass (*arrows*) secondary to carcinoid is almost totally surrounded by small bowel. Area of decreased tissue attenuation, eccentrically within mass, felt to be due to necrosis.

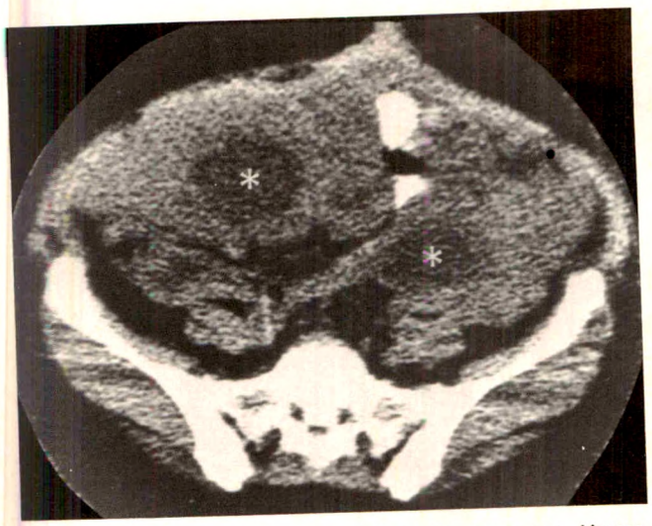


Fig. 6.—Large mesenteric masses due to leiomyosarcoma. Masses have areas of decreased attenuation (*) located eccentrically within them.

within a mass may be criteria for distinguishing benign from malignant disease by CT. However, a larger CT experience with both benign and malignant masses is needed before such a statement can be made with certainty.

The use of oral contrast material is extremely important in the CT diagnosis of a mesenteric mass, since unopacified bowel loops may be mistaken for a mesenteric lesion [6]. The oral contrast agent should be given 20–30 min before the first scan in order for it to reach the terminal ileum. Thus, when a mass is totally or almost totally surrounded by contrast-filled bowel and separate from the retroperitoneum, it must lie within the mesentery. This was noted in the majority of metastatic masses and roughly half the lymphomatous masses (fig. 8). The other lymphomatous mesenteric masses could be traced on serial scans to the retroperitoneum.

REFERENCES

1. Levitt RG, Sagel SS, Stanley RJ, Jost RG: Accuracy of computed tomography of the liver and biliary tract. *Radiology* 124:123–128, 1977
2. Stephens DH, Sheedy PF II, Hattery RR, MacCarty RL: Computed tomography of the liver. *AJR* 128:579–590, 1977

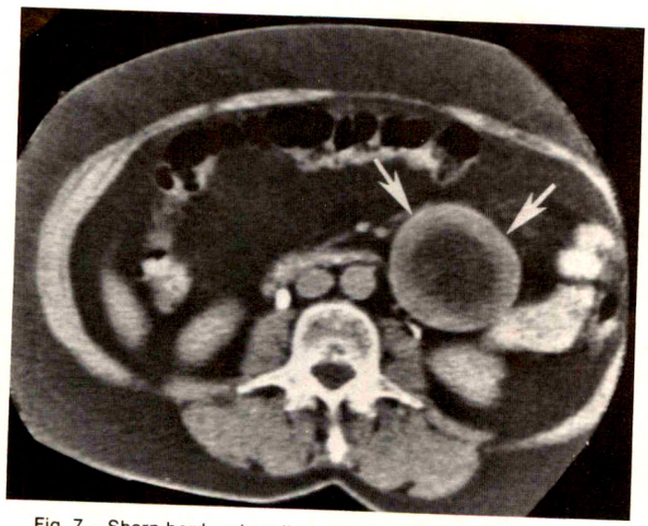


Fig. 7.—Sharp bordered, well circumscribed mass (*arrows*) with centrally located area of decreased attenuation. Surgery showed mass was mesenteric cyst.

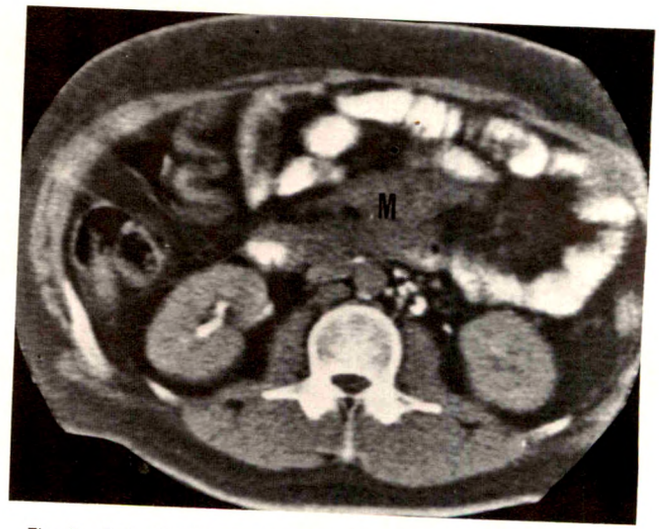


Fig. 8.—Patient with non-Hodgkin's lymphoma. Irregular mesenteric mass (M) is surrounded by contrast-filled bowel.

3. Sagel SS, Stanley RJ, Levitt RG, Geisse G: Computed tomography of the kidney. *Radiology* 124:359–370, 1977
4. Alcorn FS, Mategrano VC, Petasnick JP, Clark JW: Contributions of computed tomography in the staging and management of malignant lymphoma. *Radiology* 125:717–723, 1977
5. Stanley RJ, Sagel SS, Levitt RG: Computed tomographic evaluation of the pancreas. *Radiology* 124:715–722, 1977
6. Breiman RS, Castellino RA, Harell GS, Marshall WH, Glatstein E, Kaplan HS: CT-Pathologic correlations in Hodgkin's disease and non-Hodgkin's lymphoma. *Radiology* 126:159–166, 1978
7. Redman HC, Glatstein E, Castellino RA, Federal WA: Computed tomography as an adjunct in the staging of Hodgkin's disease and non-Hodgkin's lymphomas. *Radiology* 124:381–385, 1977
8. Hashmonai M, Hampel N, Auslaender L, Schramek A: Acute abdomen due to torsion of a pedunculated mesenteric fibroma. *Surgery* 78:665–667, 1975
9. Malt RA, Vickery AJ: Abdominal mass in a 62-year-old man. Report of a case, Massachusetts General Hospital. *N Engl J Med* 295:214–218, 1976
10. Yannopoulos K, Stout AP: Primary solid tumors of the mesentery. *Cancer* 16:914–927, 1963
11. Meyers MA: Metastatic seeding along the small bowel mesentery. *AJR* 123:67–73, 1975
12. Goffinet DR, Castellino RA, Kim H, Dorfman RF, Fuks Z, Rosenberg SA, Nelsen T, Kaplan HS: Staging laparotomies in unselected previously untreated patients with non-Hodgkin's lymphomas. *Cancer* 32:672–681, 1973

Bilateral Concurrent Renal Neoplasms: Report of Eleven Cases

L. STIGSSON,[1] L. EKELUND, AND W. KARP

Eleven patients with concurrent bilateral renal neoplasms are presented, including one case with dissimilar tumor histogenesis. In four cases urography showed only unilateral expansive lesions. The importance of high-dose nephrotomography and bilateral selective renal angiography is stressed. Literature review revealed 57 patients with concurrent bilateral renal cell carcinoma, indicating that this entity may be more frequent than previously believed.

Bilateral renal malignant tumors are being reported with increasing frequency, though they are still considered to be rare. Wilms' tumor, with a reported incidence of 3.6%–18.3% [1] is the most common primary renal neoplasm with synchronous bilateral appearance. In a recent review of 1,746 cases, 4.4% were bilateral [2]. Bilateral renal adenocarcinomas have a reported occurrence of 1.8% [3]. However, most of these tumors were not concurrent. Viets et al. [4] recently reported nine cases of bilateral renal cell carcinoma, five of which had bilateral synchronous disease, accounting for an incidence of 3.8%. In another recent report [5], incidence was estimated at 1.4%. While bilateral primary malignant renal tumors of similar histogenesis are relatively uncommon, those with dissimilar histogenesis are extremely rare. In a 1967 literature review, Villegas [6] found only two cases and added two more. Jozsi et al. [7] reported another case in 1976. Secondary renal tumors are more than twice as common as primary ones, but they are rarely diagnosed in vivo because of lack of symptoms [8, 9]. At autopsy bilateral renal metastases are more frequent than unilateral disease [10–12].

Viets et al. [4] recently suggested that the incidence of bilateral renal cell carcinoma seems to be increasing. During 1969–1977 some 220 cases of renal carcinoma were diagnosed by angiography in our department; among them were 11 cases of concurrent bilateral renal neoplasms. Ten of these patients had bilateral concurrent renal adenocarcinoma; in the remaining case a renal adenocarcinoma was found in the right kidney and a transitional cell carcinoma of the pelvis in the contralateral kidney. Since only 27 cases of angiographically demonstrated bilateral renal tumors have been reported, it is worthwhile to present our experience with these 11 patients.

Subjects and Methods

The eleven patients (four female and seven male) were 40–82 years old (mean, 57). Of the seven patients with macroscopic hematuria, two also had flank pain. Two had only flank pain, one had polycythemia, and another one had skeletal metastasis with histology suggesting primary renal carcinoma. Urography, performed in all patients, was followed by transfemoral abdominal aortography and bilateral selective angiography of the kidneys. Histologic diagnosis was obtained from five patients who underwent bilateral nephrectomy or heminephrectomy. Bilateral fine needle biopsy was performed in one case and unilateral fine needle biopsy guided by ultrasonography in two cases. In three cases, no histologic diagnosis was obtained.

Results

There was no evidence of bilateral renal tumor in any patient at physical examination. As shown in table 1, two patients had unilateral palpable mass at the site of the kidney, and further investigations in both cases showed large tumors. At urography four patients had only unilateral expansive lesions, while bilateral masses were diagnosed in the remainder.

Angiography showed bilateral tumors in all 11 patients, although a few small tumors were not found until autopsy or surgery. Six patients (cases 3, 5–8, and 11) showed one tumor in each kidney, and most of the tumors were larger than 5 cm (fig. 1). In case 7 the right-side tumor also infiltrated the liver. Cases 1, 4, and 9 showed one large tumor in one kidney and multiple small tumors in the contralateral one (fig. 2). Bilateral multiple small tumors were found in cases 2 and 10 (fig. 3). In case 2 the primary urographic finding was a 10 cm large cyst in the upper pole of the left kidney. All expansive lesions except the left renal pelvic tumor (case 11) were hypervascularized and had angiographic features of renal carcinoma.

Seven of the patients died 6–36 months after diagnosis. Two of these had had bilateral nephrectomy; one, right nephrectomy and left heminephrectomy; one patient, only fine needle biopsy of the right kidney. In three of the patients no biopsy, surgery, or autopsy had been performed, and thus no histologic diagnosis received. Four of the patients had lung or other metastases at diagnosis; the other three developed pulmonary metastases later.

Four of the patients were still alive 8–36 months after diagnosis. One of these had a right heminephrectomy and left nephrectomy; one had bilateral nephrectomy; one had bilateral fine needle biopsy; and another had only left-side fine needle biopsy. Three of these patients had no metastases at diagnosis; the other had multiple pulmonary metastases.

Bilateral histological diagnosis was obtained in six cases. In three cases no histologic diagnosis was obtained because neither surgery nor autopsy was performed. Only ultrasonographic unilateral fine needle

Received April 28, 1978; accepted after revision September 11, 1978.
[1] All authors: Department of Diagnostic Radiology, University Hospital, S-221 85, Lund, Sweden. Address reprint requests to L. Stigsson.

0361–803X/79/1321–0037 $0.00

AJR 132:37–42, January 1979
© 1979 American Roentgen Ray Society

TABLE 1
Summary of Findings

Case No.	Age and Sex	Signs and Symptoms	Urography	Angiography	Histology	Follow-up
1	....45, M	Hematuria; no palpable mass	Bilateral expansive lesions: left, 7 cm; right, 2 cm	Another 2 cm tumor, right; 5 cm adrenal metastasis	Bilateral nephrectomy: renal carcinoma, same histology	No initial lung metastases; died 12 months after diagnosis
2	....70, F	Flank pain, left; no palpable mass	Expansive lesion, left	10 cm cyst, three small tumors left; two small tumors, right	Bilateral fine needle biopsy: renal carcinoma, same histology	No metastases; Still alive 36 months after diagnosis
3	....61, F	Polycytemia; no palpable mass	Expansive lesion, left	Tumors: left, 11 cm; right, 3 cm	Left heminephrectomy, right nephrectomy: renal carcinoma, same histology	No lung metastases; thoracic spine metastasis; died 24 months after diagnosis
4	....46, M	Hematuria; no palpable mass	Expansive lesions: right, 3 cm; left, 10 cm	2.2 and 3 cm tumors, right; large tumor, left	Bilateral nephrectomy: renal carcinoma, same histology	No initial metastases; later liver and lung metastases; died 36 months after diagnosis
5	....82, M	Fracture through renal cell carcinoma metastasis; no palpable mass	5 cm expansive lesion, left; possible expansive lesion, right	Tumors: left, 6 × 9 cm; right, 8 × 9 cm	Right ultrasound-guided fine needle biopsy: renal carcinoma (no autopsy)	No initial metastasis; died 22 months after diagnosis
6	....54, M	Hematuria; no palpable mass	Large expansive lesions bilaterally	Tumors: left, 17 cm; right, 7 × 10 cm	No histology (no autopsy)	Single lung metastasis initially; died 8 months after diagnosis
7	....44, F	Flank pain, right; no palpable mass	Large expansive lesions bilaterally	10 cm tumor infiltrating liver, right; 7 × 10 cm tumor, left	No histology (no autopsy)	Lung metastases; died 6 months after diagnosis
8	... 51, M	Hematuria; palpable mass, left	Large expansive lesions bilaterally	Large tumors bilaterally	Two urine specimens suggesting carcinoma; no other histology (no autopsy)	No initial metastases; died 36 months after diagnosis
9	....64, M	Hematuria and flank pain; palpable mass, left	10 cm expansive lesion, left; normal finding, right	Large tumor, left; three small tumors, right	Left ultrasound-guided fine needle biopsy suggesting angiomyolipoma	Newly developed pulmonary metastases; still alive 8 months after diagnosis
10	...40, M	Hematuria and flank pain, right no palpable mass	Multiple bilateral expansive lesions; cysts (?)	Multiple 5 × 5 to 7 × 8 cm tumors bilaterally	Bilateral nephrectomy: renal carcinoma, same histology	No metastases; still alive 9 months after diagnosis
11	...70, F	Hematuria; no palpable mass	4 × 3 cm pelvic defect, left; normal finding, right	3 × 4 cm pelvic tumor, left; 3 × 5 cm tumor, right	Left nephrectomy: transitional cell carcinoma; right heminephrectomy: renal carcinoma	No initial metastases; still alive 35 months after diagnosis.

biopsy was performed in two cases. In one of these cases, although cytologic diagnosis was angiomyolipoma, the patient's recently developed pulmonary nodules made this diagnosis suspect. In all the other histologically verified cases, diagnosis was renal cell carcinoma, excluding case 11 in which the lesion in the left renal pelvis showed a papillary transitional cell carcinoma.

Discussion

In a 1968 literature survey, Small et al. [13] found 11 proven cases of concurrent renal adenocarcinoma and added one case which was only the second reported case preoperatively diagnosed. In a recent literature review, we found an additional 45 cases (4, 5, 14–31) excluding three cases from the present series that were also reported earlier [32, 33]. Of the 57 cases of synchronous bilateral renal carcinomas previously described, 27 underwent angiography. Our 11 patients have all had transfemoral aortography and selective bilateral renal angiography. Case 11 is the sixth reported case with bilateral renal tumors of dissimilar histogenesis [6, 7].

When renal adenocarcinomas are bilateral, von Hippel-Lindau disease must be considered, since this disease usually involves both kidneys [30]. In cases of angiomyolipoma, it is generally impossible to angiographically exclude malignancy [34, 35]. In tuberous sclerosis bilateral renal angiomyolipoma is reported as high as 50%–89% [36, 37]. None of our patients had von Hippel–Lindau disease or tuberous sclerosis.

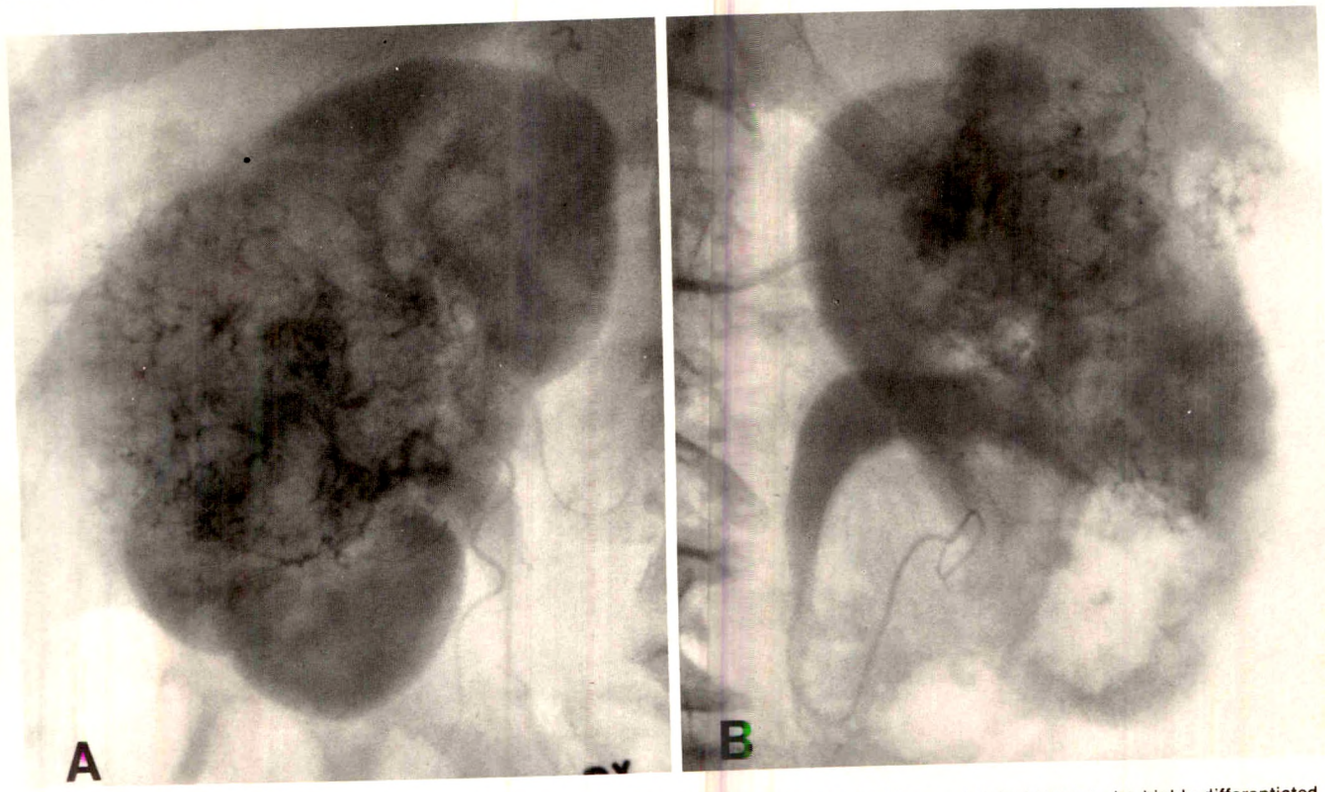


Fig. 1.—Case 5, 82-year-old male with bilateral solitary renal carcinoma proved by fine needle biopsy of right kidney to be highly differentiated carcinoma.

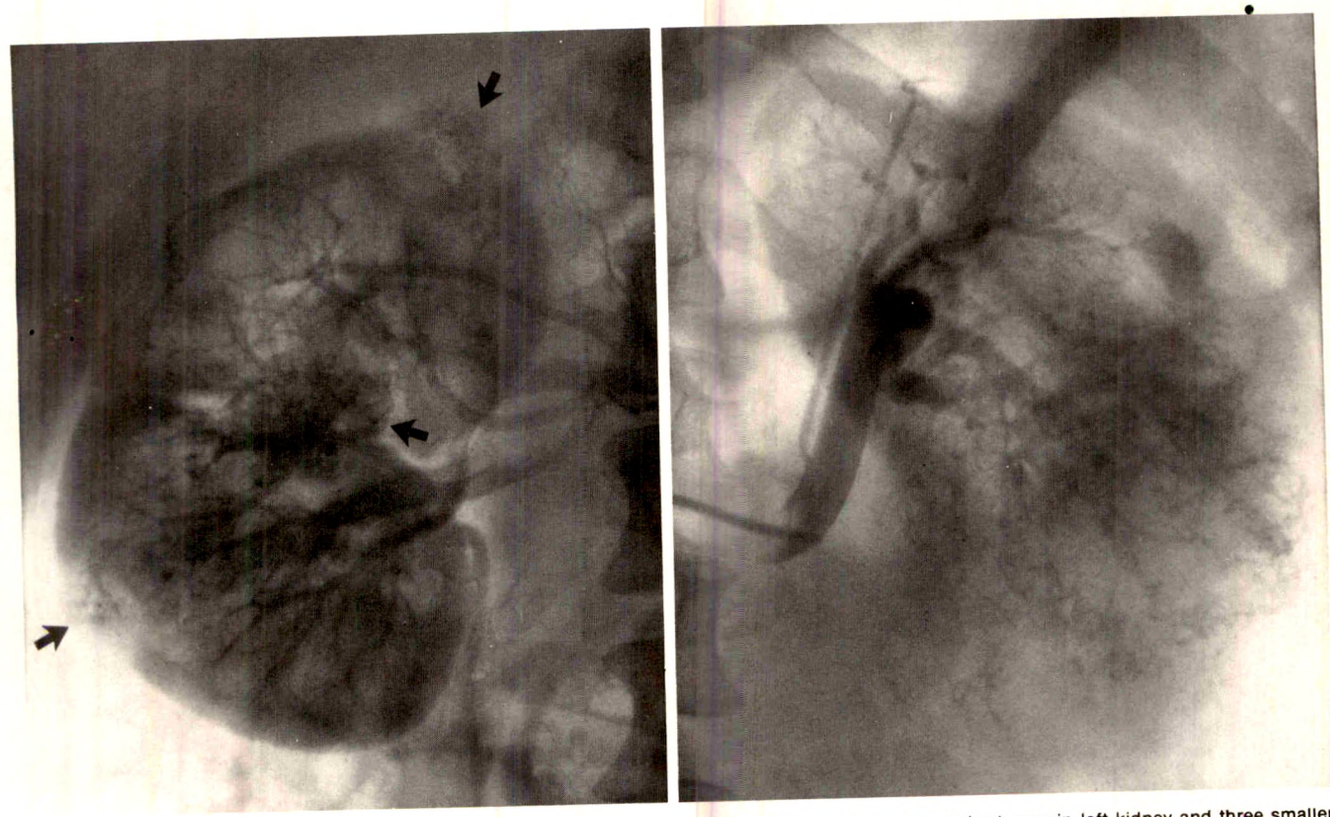


Fig. 2.—Case 4, 46-year-old male. Bilateral selective renal angiograms demonstrating large hypervascular tumor in left kidney and three smaller hypervascular tumors in right kidney (*arrows*). Bilateral nephrectomy showed renal carcinomas; on sectioning two more small tumors were found in right kidney.

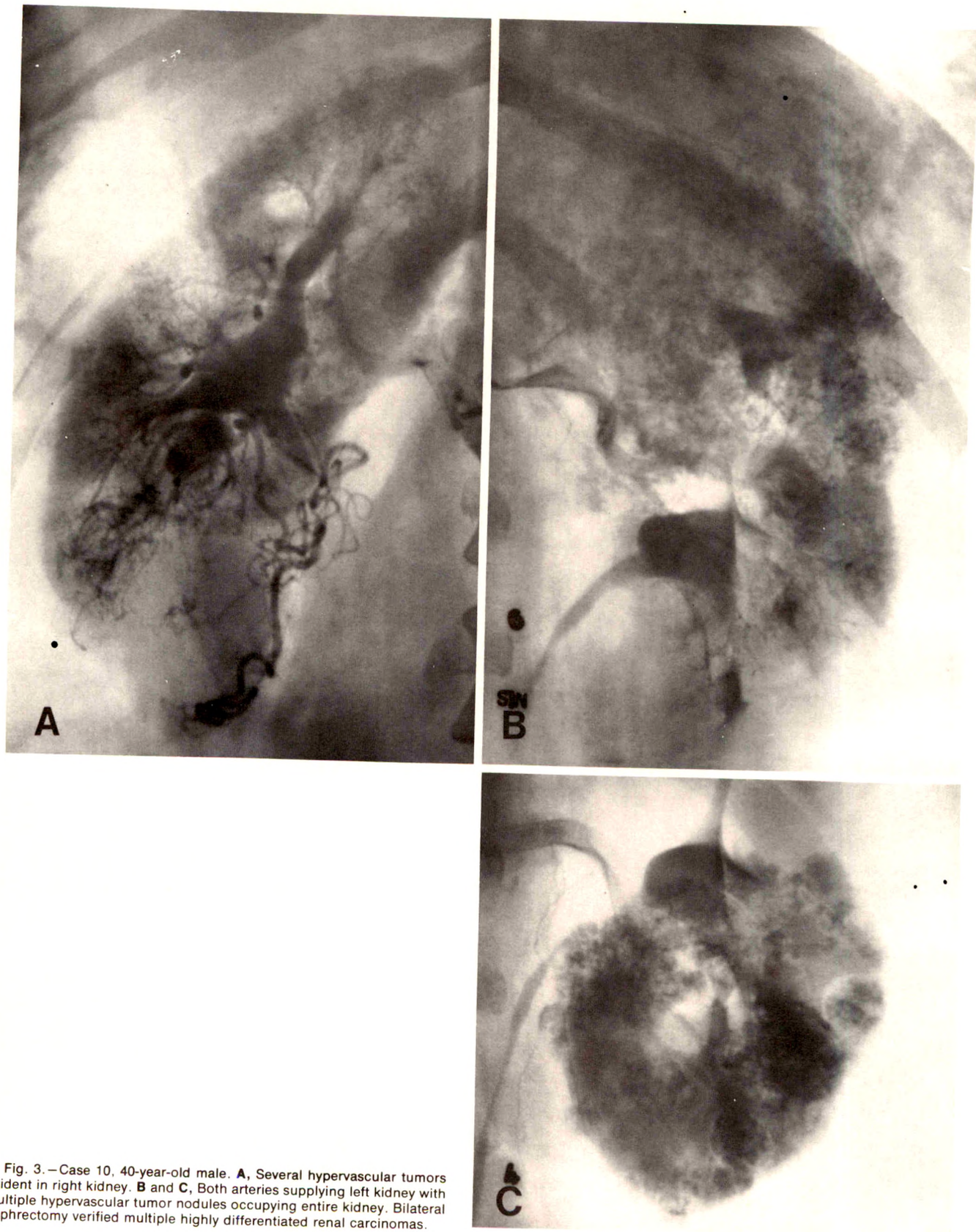


Fig. 3.—Case 10, 40-year-old male. **A**, Several hypervascular tumors evident in right kidney. **B** and **C**, Both arteries supplying left kidney with multiple hypervascular tumor nodules occupying entire kidney. Bilateral nephrectomy verified multiple highly differentiated renal carcinomas.

Clinical suspicion of bilateral renal cell carcinoma seems very rare. Diagnosis, therefore, is radiographic, and the first step is to show an expansive lesion at urography. In 11 of 26 cases of unilateral renal neoplasms verified by autopsy, Berge et al. [38] found that even 5–10 cm tumors were not recognized urographically. Since two-thirds of their cases had purely cortical tumors, it is clear that optimal urographic technique is very important in identifying the kidney margins. High dose nephrotomography has greatly increased the ability to demonstrate renal lesions [39]. In our cases (2, 3, 9, and 11) where urography showed only unilateral expansive lesions, angiography revealed small tumors (up to 3 × 4 cm) in the contralateral kidney. In case 2 the single expansive lesion found at urography was demonstrated to be a cyst at angiography, while the small tumors were not even suspected at urography. In another patient (case 4) angiography revealed two additional small (2 cm) tumors. In one patient with multiple bilateral tumors, diagnosis at initial urography was supposed to be polycystic disease of the kidneys.

The importance of angiography in detecting small renal tumors is emphasized by Viets et al. [4] who had two of nine cases in which tumors were inapparant before angiography. They recommend that bilateral selective renal arteriography be performed in all patients with a renal mass lesion, since abdominal aortography may not show small lesions that could be demonstrated by selective angiography, and we agree.

The complication rate for selective catheterization of renal arteries was studied by Jonsson et al. [40] who found a 0.9% incidence (five of 583 patients) of subintimal deposits of contrast medium. We believe this is an acceptable risk. The extra volume (8 ml) of contrast medium selectively injected results in no significant additional risk to the kidney.

An important question concerning patients with bilateral renal carcinomas is whether the contralateral tumor is metastatic or primary. Clinical studies have shown metastatic growth of 1.24% in the opposite kidney, while autopsy studies have shown contralateral metastases in 4%–29.5% [41–44]. Various criteria have been suggested to diagnose bilateral primary tumors [13, 45]. Hyman et al. [20] offer the following to help identify primary bilateral kidney tumors: (1) the tumors should preferably appear simultaneously; (2) there should be only one tumor in each kidney (multiple lesions suggest metastases); (3) each tumor should show at least partial encapsulation; and (4) the basic histology should be different in each lesion.

However, it has also been suggested that the presence of multiple bilateral renal lesions of the same histologic appearance and the absence of any other evidence of metastatic growth would favor bilateral origin of the lesions [25]. Obviously, no characteristics exclusively distinguish bilateral primary renal cell carcinoma from unilateral tumor metastasizing to the opposite side. The question of multicentric primary tumors versus primary neoplasms with metastatic deposits is speculative and cannot be proved in the single case.

The 11 cases here exhibit the whole range of combinations from one large tumor in each kidney to one large tumor in one kidney with multiple small tumors in the contralateral to multiple small tumors in both kidneys (figs. 1–3). In five cases there were initially no known metastases outside the kidneys, while in the other cases metastases were found in the lungs or elsewhere.

REFERENCES

1. Pay R, Brosman S, Williams DI: Bilateral nephroblastoma. *J Urol* 110:119–124, 1973
2. Ragab AH, Vietti TJ, Perez C, McAllister W: Bilateral Wilms' tumor. *Cancer* 30:983–988, 1972
3. Skinner DG, Vermillion CD, Colvin RB: The surgical management of renal cell carcinoma. *J Urol* 107:705–710, 1972
4. Viets DH, Vaughan ED Jr, Howards SS: Experience gained from the management of 9 cases of bilateral renal cell carcinoma. *J Urol* 118:937–940, 1977
5. Johnson DE, Von Eschenbach A, Sternberg J: Bilateral renal cell carcinoma. *J Urol* 119:23–24, 1978
6. Villegas AC: Bilateral primary malignant renal tumors of dissimilar histogenesis: report of 2 cases and review of the literature. *J Urol* 98:450–455, 1967
7. Jozsi BP, Wise HA II, Quilter TN, Evans WE: Bilateral simultaneous kidney tumors of dissimilar cell type: a case report with emphasis on operative approach. *J Urol* 116:655–657, 1976
8. Zinke H, Furlow WL: Metastatic squamous cell epithelioma of the kidney: report of a case of bilateral involvement and review of the literature. *J Urol* 109:971–973, 1973
9. Ben-Menachem Y, Marcos J, Wallace S, Medellin H: Angiography of renal metastases. *Br J Radiol* 47:869–874, 1974
10. Willis RA: *The Spread of Tumor in the Human Body*, 2d ed. London, Butterworth, 1952
11. Olsson CA, Moyer JD, Laferte RO: Pulmonary cancer metastatic to the kidney—a common renal neoplasm. *J Urol* 105:492–496, 1971
12. Klinger ME: Secondary tumors of the genito-urinary tract. *J Urol* 65:144–153, 1951
13. Small MP, Anderson EE, Atwill WH: Simultaneous bilateral renal cell carcinoma: case report and review of the literature. *J Urol* 100:8–14, 1968
14. Kobayashi A, Hoshino H, Ohbe Y, Sawaguchi S, Shimizu K: Bilateral renal cell carcinoma. *Arch Dis Child* 45:141–143, 1970
15. Kölln CP, Boldus RA, Brandon DNK, Flocks RH: Bilateral partial nephrectomy for bilateral renal cell carcinoma: a case report. *J Urol* 105:45–48, 1971
16. Marchetti LJ, Gonick P, Ciavarra V: Partial nephrectomy in bilateral renal carcinoma: discussion and case report. *J Urol* 106:818–819, 1971
17. Franksson C, Bergstrand A, Ljungdahl I, Magnusson G, Nordenstam H: Renal carcinoma (hypernephroma) occurring in 5 siblings. *J Urol* 108:58–61, 1972
18. Vermillion CD, Skinner DG, Pfister RC: Bilateral renal cell carcinoma. *J Urol* 108:219–222, 1972
19. Calne RY: Treatment of bilateral hypernephromas by nephrectomy, excision of tumour, and autotransplantation.

Report of three cases. *Lancet* 2:1164–1167, 1973
20. Hyman RA, Voges V, Finby N: Bilateral hypernephroma. *AJR* 117:104–107, 1973
21. Ochsner MG, Brannan W, Pond HS III, Goodier EH: Renal cell carcinoma: review of 26 years of experience at the Ochsner clinic. *J Urol* 110:643–646, 1973
22. Roberts PF: Bilateral renal carcinoma associated with polycystic kidneys. *Br Med J* 3:273–274, 1973
23. York WN, Mawn TJ: Aggressive surgical management of bilateral adenocarcinoma of the kidney. *Cancer* 31:1160–1163, 1973
24. Phelippot JL, Lange D, Valentin F, Lange J: Cancer bilatéral du rein chez l'adulte. *J Urol Nephrol* (Paris) 80:742–745, 1974
25. Stroup RF, Shearer JK, Traurig AR, Lytton B: Bilateral adenocarcinoma of the kidney treated by nephrectomy: a case report and review of the literature. *J Urol* 111:272–276, 1974
26. Wright FW: Bilateral renal cell carcinoma. *Radiology* 115:543–550, 1975
27. Behara D, Block NL, Politano VA: Simultaneous surgical management of bilateral hypernephroma: an alternative therapy. *J Urol* 115:648–650, 1976
28. Finkbeiner A, Moyad R, Herwig K: Bilateral simultaneously-occurring adenocarcinoma of the kidney. *J Urol* 116:26–28, 1976
29. Amarjit S, Singh A, Sehgal RK, Kaur B: Bilateral hypernephroma in a child. *J Urol* 118:323–324, 1977
30. Fetner CD, Barilla DE, Scott T, Ballard J, Peters P: Bilateral renal cell carcinoma in von Hippel–Lindau syndrome: treatment with staged bilateral nephrectomy and hemodialysis. *J Urol* 117:534–536, 1977
31. Tegtmeyer CJ, Cail W, Wyker AW Jr, Gillenwater JY: Angiographic diagnosis of renal tumors associated with polycystic disease. *Radiology* 126:105–109, 1978
32. Olsson O: Multiple expanding renal lesions. *Acta Radiol [Diagn]* (Stockh) 17:481–492, 1976
33. Ekelund L, Jonsson K: How is renal carcinoma detected? *Int Urol Nephrol* 9:3–10, 1977
34. Becker JA, Kinkhabwala M, Pollack H, Bosniak M: Angiomyolipoma (hamartoma) of the kidney: an angiographic review. *Acta Radiol [Diagn]* (Stockh) 14:561–568, 1973
35. Owman T: Renal angiomyolipoma versus renal carcinoma. Is an angiographic differential diagnosis possible? *Fortschr Geb Roentgenstr Nuklearmed* 121:315–320, 1974
36. Golji H: Tuberous sclerosis and renal neoplasms. *J Urol* 85:919–923, 1961
37. Crosett AD Jr: Roentgenographic findings in the renal lesion of tuberous sclerosis. *AJR* 98:739–743, 1966
38. Berge T, Hellsten S, Wehlin L: Njurcancerdiagnostik—erfarenheter från ett obduktionsmaterial. *Lakartidningen* 71:260–262, 1974
39. Bosniak MA: Nephrotomography: a relatively unappreciated but extremely valuable diagnostic tool. *Radiology* 113:313–321, 1974
40. Jonsson K, Lunderquist A, Pettersson H, Sigstedt B: Subintimal injection of contrast medium as a complication of selective abdominal angiography. *Acta Radiol [Diagn]* (Stockh) 18:55–64, 1977
41. Bastable JRG: Bilateral carcinoma of the kidneys. *Br J Urol* 32:60–68, 1960
42. Riches E: Tumors of the kidney and ureter, in *Monographs on Neoplastic Diseases,* edited by Smothers DW, Baltimore, Williams & Wilkins, 1964, p 283
43. Lucké B, Schlumberger HG: Tumors of the kidney, renal pelvis and ureter, in *Atlas of Tumor Pathology,* Section VIII, fascicle 30, Washington, D.C., Armed Forces Institute of Pathology, 1957, p 43
44. Hajdu SI, Thomas AG: Renal cell carcinoma at autopsy. *J Urol* 97:978–982, 1967
45. Billroth T, von Winiwarter A: Die allgemeine chirurgische Pathologie und Therapie in einundfünfzig Vorlesungen, in *Ein Handbuch für Studierende und Aerzte,* vol 14. Berlin, Reimer, 1889, p 908

Computed Tomography in Adrenal Tumors

N. REED DUNNICK,[1] EVERETT G. SCHANER,[1] JOHN L. DOPPMAN,[1] CHARLES A. STROTT,[2] JOHN R. GILL,[3] AND NASSAR JAVADPOUR[4]

Computed tomography (CT) was used to evaluate 26 patients with a variety of adrenal lesions. Surgical proof was available in 22 patients and clinical confirmation with a variety of other studies in the other four patients. Nine patients had aldosterone-producing adrenal adenomas and CT correctly identified seven. Four patients had cortisol-producing adenomas and five patients had cortisol-producing carcinomas. CT identified each of these tumors. Prominent but normal shaped glands were seen in each of the four patients with adrenal hyperplasia. Adrenal metastases from malignant melanoma in two patients were identified. Only one of two pheochromocytomas in two patients could be seen on CT. CT is a noninvasive method of localizing adrenal tumors and may be helpful in distinguishing adenomas from adrenal hyperplasia.

Adrenal venography with samples for laboratory analysis is a valuable technique for functioning adrenal cortical lesions [1–3]. However, in addition to being an invasive procedure with the risk of adrenal infarction, the right adrenal vein may be difficult to catheterize selectively and sample. Whole body computed tomography (CT) has proved most valuable in the evaluation of retroperitoneal structures difficult to image by conventional means. Several reports describe the CT manifestations of normal adrenal glands and adrenal tumors [4–6]. Thus, there is much interest in the use of CT as a means of detecting and lateralizing adrenal tumors. We performed CT scans on 22 patients with a variety of adrenal tumors, and four patients with bilateral adrenal hyperplasia who were initially seen for Cushing's syndrome. The spectrum of CT findings in these adrenal lesions is presented and correlation is made with both catheterization data and surgical results.

Subjects and Methods

A total of 26 patients (14 male, 12 female) ranging in age from 17 to 67 years was examined. Nine patients were studied for primary aldosteronism, 13 for Cushing's syndrome, two for adrenal metastases, and two for biochemical evidence of a pheochromocytoma (table 1).

Bilateral adrenal venography with sampling was performed in 12 patients. Arteriography was performed in the two patients with pheochromocytomas and in six patients who had either adrenal carcinomas or metastases to the adrenal gland. Surgical confirmation was obtained in 22 of the 26 patients.

The CT scans were performed on an EMI 5000 whole body scanner with an 18 sec scan time and a 320 × 320 matrix display. Adjacent but not overlapping 13 mm cuts were routinely obtained after injection of intravenous contrast material. More recently we have taken additional overlapping cuts at 7 mm intervals after initially localizing the adrenal glands on routine scans.

Results

Aldosteronoma

Nine patients had CT scans as part of their evaluation of primary aldosteronism; CT identified the adrenal adenoma in seven (figs. 1–3). Five had confirmation of the suspected adrenal adenoma by adrenal vein catheterization and all seven had subsequent surgical proof. At surgery, these adrenal adenomas ranged from 1 to 6 cm in diameter. Of the two CT failures, one patient had an adrenal adenoma only 0.5 cm in diameter which was diagnosed by venous sampling and surgically confirmed. The other patient had an adrenal adenoma localized by venous sampling, but has refused surgery.

Cushing's Syndrome

Of 13 patients studied for Cushing's syndrome, five had adrenal carcinomas, four had adrenal adenomas, and four had bilateral adrenal cortical hyperplasia. Of the four patients with adrenal adenomas, CT correctly identified all four and each was surgically confirmed. The smallest of these adenomas was 2 cm. The CT examination correctly identified the tumor masses in all five cases of adrenal carcinoma and each of these cases was surgically confirmed. Adrenal masses were not seen in any of the four cases of adrenal hyperplasia. Instead the adrenal glands were prominent but maintained a normal configuration (fig. 4).

Metastatic Tumor

Two patients with malignant melanoma were studied for adrenal metastases. CT correctly identified both of these tumors, and both were surgically confirmed (fig. 5).

Pheochromocytoma

Two patients were studied for suspected pheochromocytoma. CT identified an adrenal mass in one of these cases and surgical proof was obtained. The other patient had a 3 cm right adrenal pheochromocytoma not identified on CT. The paucity of retroperitoneal fat in this patient made delineation of retroperitoneal structures impossible on CT.

Received April 13, 1978; accepted after revision October 5, 1978.

[1] Diagnostic Radiology Department, Clinical Center, National Institutes of Health, Building 10, Room 6S211, Bethesda, Maryland 20014. Address reprint requests to N. R. Dunnick.

[2] Reproductive Research Branch, National Institute of Child Health and Human Development, National Institutes of Health, Bethesda, Maryland 20014.

[3] Hypertension Endocrine Branch, National Heart, Lung and Blood Institute, National Institutes of Health, Bethesda, Maryland 20014.

[4] Surgery Branch, National Cancer Institute, National Institutes of Health, Bethesda, Maryland 20014.

0361–803X/79/1321–0043 $0.00

TABLE 1

Diagnostic Methods in Patients with Adrenal Tumors

Reason Seen and Case No.	Venous Sampling	Angiography		Radionuclide Scan	CT	Surgery	Pathology and Final Diagnosis
		Venogram	Arteriogram				
Aldosteronism:							
1.	+	+	NP	NP	+	+	Adenoma, Aldosteronoma
2.	+	+	NP	NP	+	+	Adenoma, Aldosteronoma
3.	+	+	NP	NP	+	+	Adenoma, Aldosteronoma
4.	+	–	–	NP	+	+	Adenoma, Aldosteronoma
5.	NP	NP	NP	+	+	+	Adenoma, Aldosteronoma
6.	+	+	NP	NP	+	+	Adenoma, Aldosteronoma
7.	NP	NP	NP	+	+	+	Adenoma, Aldosteronoma
8.	+	–	NP	NP	–	+	Adenoma, Aldosteronoma
9.	+	–	NP	NP	–	NP	NP, Aldosteronoma
Cushing's syndrome:							
10.	+	+	+	+	+	+	Adenoma
11.	NP	NP	NP	+	+	+	Adenoma
12.	+	+	+	NP	+	+	Adenoma
13.	NP	NP	NP	+	+	+	Adenoma
14.	–	–	–	NP	–*	–	Hyperplasia
15.	–	–	–	NP	–*	NP	NP, Hyperplasia
16.	–	–	NP	NP	–*	NP	NP, Hyperplasia
17.	NP	NP	NP	–	–*	NP	NP, Hyperplasia
18.	NP	+	+	NP	+	+	Carcinoma
19.	NP	NP	+	NP	+	+	Carcinoma
20.	NP	NP	+	NP	+	+	Carcinoma
21.	NP	+	+	NP	+	+	Carcinoma
22.	NP	+	+	NP	+	+	Carcinoma
Melanoma:							
23.	NP	NP	+	NP	+	+	Metastasis
24.	NP	NP	NP	NP	+	+	Metastasis
Hypertension:							
25.	NP	NP	+	NP	–	+	Pheochromocytoma
26.	NP	NP	+	NP	+	+	Pheochromocytoma

Note. – + = positive for adrenal tumor; – = negative for adrenal tumor; NP = not performed.
* Hyperplasia rather than tumor.

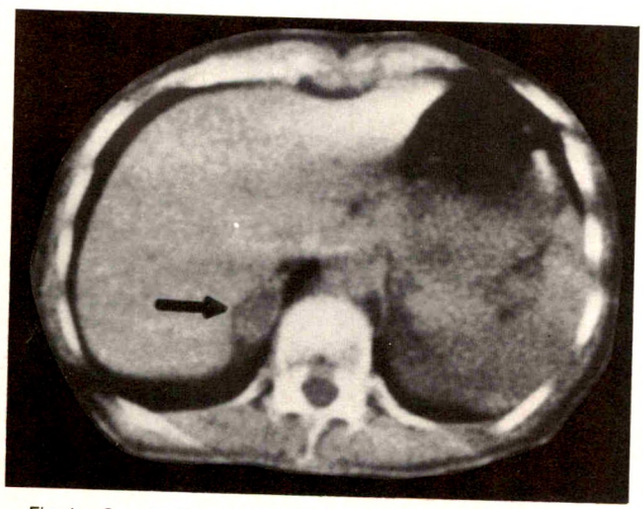


Fig. 1.—Case 5, 47-year-old woman with primary aldosteronism. Right adrenal mass. Subsequent surgery demonstrated 1.3 × 1.0 × 0.5 cm right adrenal adenoma.

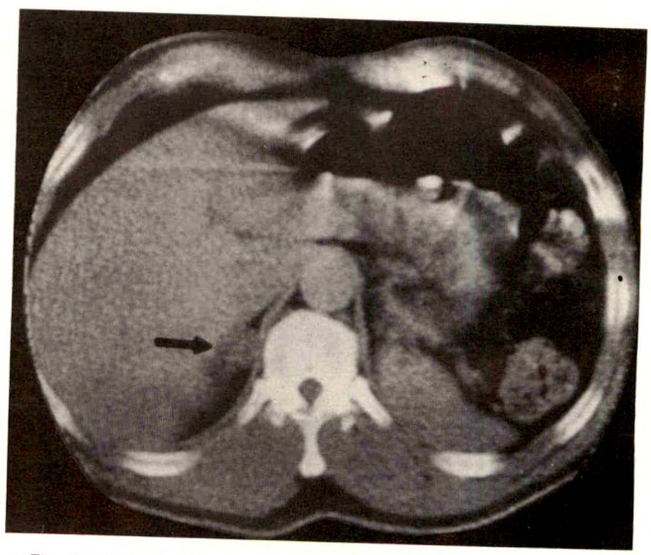
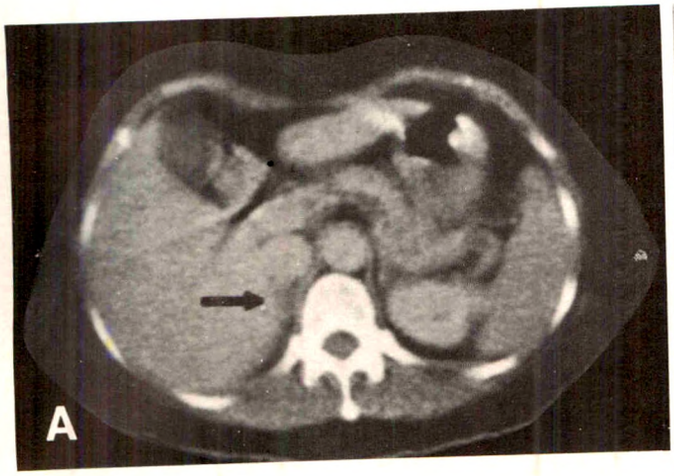


Fig. 2.—Case 7, 49-year-old man with primary aldosteronism. Right adrenal mass. Confirmed by iodocholesterol scan and subsequent surgery.

Discussion

This series of patients demonstrates the value of adrenal venography with venous samplings for the evaluation of hormone-producing adrenal lesions. However, adrenal venography is an invasive procedure which requires skilled angiography. Even an experienced angiographer may not be able to sample successfully both adrenal glands in all patients.

The normal adrenal glands are commonly identified on CT scans of the upper abdomen by their characteristic shape and location. The left adrenal gland is routinely



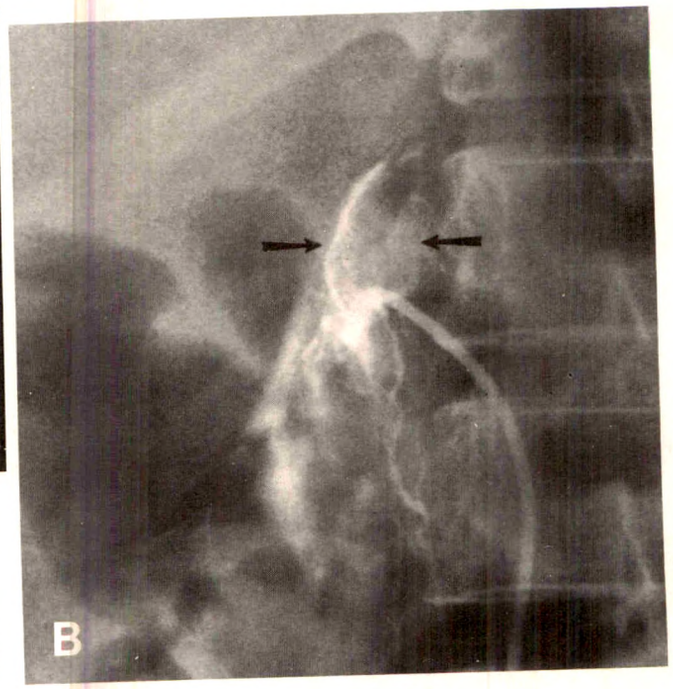


Fig. 3.—Case 3, 55-year-old woman with primary aldosteronism. **A**, Right adrenal mass (*arrow*). **B**, Mass (*arrow*) confirmed by adrenal venogram and venous sampling. Subsequent surgery removed 1.6 × 1.5 × 1.2 cm right adrenal adenoma.

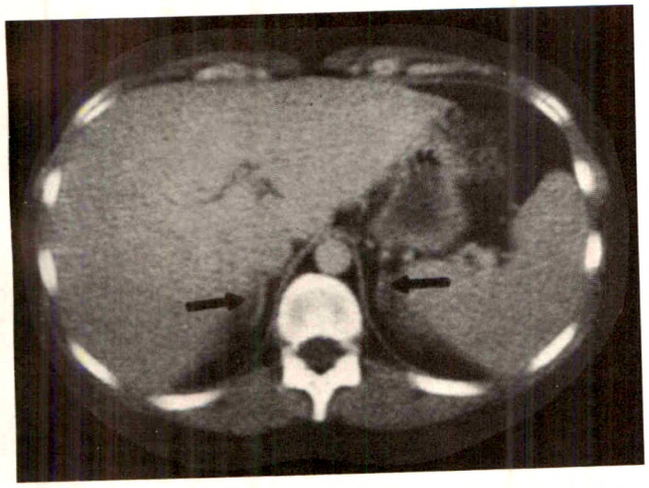


Fig. 4.—Case 16, 26-year-old woman with Cushing's syndrome. Prominent but normally shaped adrenal glands bilaterally (*arrows*). Adrenal vein samples confirmed impression of bilateral adrenal hyperplasia.

visualized at the same level, or one cut above the top of the left kidney. It is shaped like an inverted V, one arm of which may be slightly longer than the other. The right adrenal gland is seen medial to the liver and also has an inverted V shape. The posterior arm is much longer than the lateral arm, and we frequently visualize only the longer posterior arm. It is located immediately behind the inferior vena cava, slightly above the top of the right kidney, and parallels the right diaphragmatic crus.

Adrenal tumors appear as discrete masses in the adrenal gland. If the tumor is small, a portion of normal gland may also be identified. When the tumor is large, the adrenal etiology may be suspected by the clinical presentation, anatomic location, and absence of a normal adrenal gland. As we have stressed in an earlier report [6], many adrenal tumors have a low absorption coefficient even after intravenous contrast material.

CT correctly identified 11 of the 13 steroid-producing adrenal adenomas, and there were no false positives. The smallest tumor identified was 1 cm in diameter. Two adenomas were missed, one was surgically confirmed (0.5 cm) while the other was diagnosed by venous sampling (of unknown size). CT identified the absence of tumors in the four patients with bilateral adrenal hyperplasia. Although both adrenal glands are slightly enlarged in bilateral adrenal hyperplasia, we have not been able to distinguish these glands from normal glands on CT. However, a normal adrenal scan in Cushing's syndrome provides reliable, though indirect, evidence of adrenal hyperplasia. CT correctly identified all seven of the malignant tumors involving the adrenal glands, and demonstrated one of the two adrenal pheochromocytomas.

Thus, there was an overall accuracy of 89% (23 of 26). However, both of the errors were false negatives. In every case in which CT identified an adrenal lesion, the diagnosis was confirmed by other studies, usually angiography and surgery. The false negative rate of 11% (3 of 26) is a result of a small lesion (0.5 cm) or lack of retroperitoneal fat.

In patients with biochemical findings of either Cushing's syndrome or primary aldosteronism, CT may localize the functioning tumor and thus provide lateralization for the surgeon. Two other noninvasive methods currently provide similar information: isotopic adrenal scanning with an iodinated cholesterol compound [7–9] and diagnostic ultrasound [10–11]. Isotopic scanning is a prolonged procedure with a rather high radiation dose. The resolution of gray scale ultrasound is continuing to improve; however, the adrenal glands are difficult to image, especially in large patients where a lower fre-

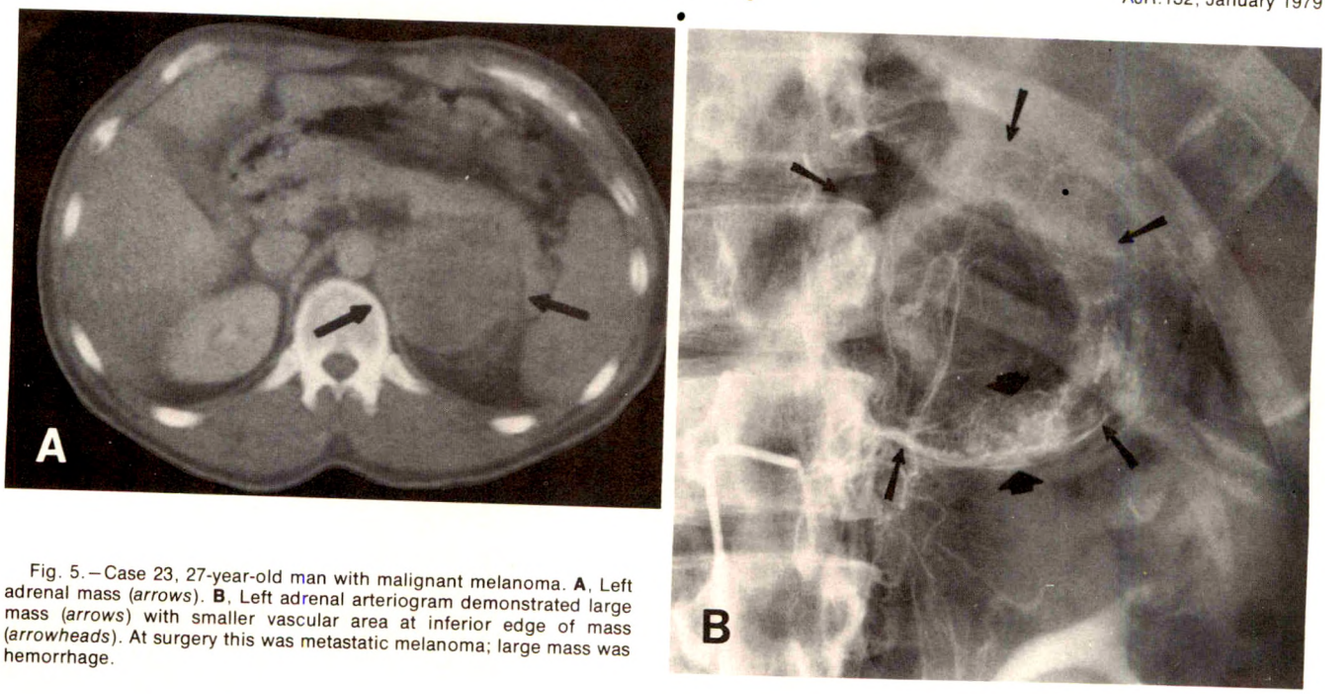


Fig. 5.—Case 23, 27-year-old man with malignant melanoma. **A**, Left adrenal mass (*arrows*). **B**, Left adrenal arteriogram demonstrated large mass (*arrows*) with smaller vascular area at inferior edge of mass (*arrowheads*). At surgery this was metastatic melanoma; large mass was hemorrhage.

quency transducer is required. At present, we feel CT provides the best anatomic information in the presurgical evaluation of adrenal lesions.

REFERENCES

1. Scoggins BA, Oddie CJ, Hare WSC, Coghlan JP: Preoperative lateralization of aldosterone-producing tumours in primary aldosteronism. *Ann Intern Med* 76:891–897, 1972
2. Mitty HA, Nicolis GL, Gabrilovh JL: Adrenal venography: clinical-roentgenographic correlation in 80 patients. *AJR* 119:564–575, 1973
3. Lecky JW, Wolfman NT, Modic CW: Current concepts of adrenal angiography. *Radiol Clin North Am* 14:309–352, 1976
4. Schaner EG, Head GL, Kalman MA, Dunnick NR, Doppman JL: Whole-body computed tomography in the diagnosis of abdominal and thoracic malignancy: review of 600 cases. *Cancer Treat Rep* 61:1537–1560, 1977
5. Brownlie K, Kreel L: Computer assisted tomography of normal suprarenal glands. *J Comput Assist Tomogr* 2:1–10, 1978
6. Schaner EG, Dunnick NR, Doppman JL, Strott DA, Gill JR Jr, Javadpour N: Adrenal cortical tumors with low attenuation coefficients: a pitfall in computed tomography diagnosis. *J Comput Assist Tomogr* 2:11–15, 1978
7. Moses DC, Schteingart DH, Sturman MF, Beirwaltes WH, Ice RD: Efficacy of radiocholesterol imaging of the adrenal glands in Cushing's syndrome. *Surg Gynecol Obstet* 139:201–204, 1974
8. Hogan MJ, McRae J, Schambelan M, Biglieri EG: Localization of aldosterone-producing adenomas with I-131-19-iodocholesterol. *N Engl J Med* 294:410–414, 1976
9. Parthasarathy KL, Bakshi S, Ackerhalt RE, Villa M, Diae R: Adrenal scintigraphy utilizing I-131-19-iodocholesterol. *Clin Nucl Med* 1:150–155, 1976
10. Kehlet H, Blichert-Toft M, Hancke S, Pedersen JF, Kristensen JK, Efsen F, Dige-Petersen H, Fogh J, Lockwood K, Hasner E: Comparative study of ultrasound, I-131-19-iodocholesterol scintigraphy, and aortography in localizing adrenal lesions. *Br Med J* 2:665–667, 1976
11. Sample WF: A new technique for the evaluation of the adrenal gland with gray-scale ultrasonography. *Radiology* 124:463–470, 1977

Ultrasonic Characteristics of Chronic Atrophic Pyelonephritis

CHESTER J. KAY,[1,2] ARTHUR T. ROSENFIELD,[2] KENNETH J. W. TAYLOR,[2] AND MURRAY A. ROSENBERG[1]

Six cases of chronic atrophic pyelonephritis were studied with gray scale ultrasound. The findings are analogous to those seen pathologically, namely a focal or multifocal process with loss of renal parenchyma, retraction of one or more calyces, decrease in renal size, and increased echoes from fibrosis. In the proper clinical setting, the diagnosis of chronic atrophic pyelonephritis can be made using ultrasound technique.

Ultrasound is capable of demonstrating fine anatomic detail in the kidney. The renal parenchyma consists of the cortex, which produces low-level echoes; the pyramids, which are sonolucent; and the arcuate vessels, which are seen in cross-section as punctate zones of intense echoes at the corticomedullary junction [1, 2]. The calyces and infundibula, when seen, are best defined as sonolucent structures within the renal sinus surrounded by echogenic urothelium. The remainder of the renal sinus contains dense echoes [3].

Most of the literature concerning renal inflammatory disease has dealt with cases studied using bistable display [4]. This paper demonstrates the ultrasound findings of chronic atrophic pyelonephritis. These are analogous to the urographic signs and permit the diagnosis to be made in the proper clinical setting.

Case Material and Findings

Six cases of chronic atrophic pyelonephritis were studied whose diagnoses have been established by clinical history and radiographic criteria. Case material was collected over a 3 month period and included patients 7–59 years old. Scans were performed in the prone and supine positions on a Picker Echoview VI unit using a 2.25 mHz transducer.

All six patients had focal loss of parenchyma and small kidneys. All but one patient had a local area of increased echogenicity, and four of six patients showed retraction of calyces from the renal sinus.

Representative Case Reports

Case 1

E. B., a 59-year-old woman, had a 3 week history of fatigue, chills, and sweating. She suffered "damage" to the right kidney 36 years earlier during pregnancy. She was treated intermittently with sulfisoxazole. White blood cell count was 13,600 on admission. Urine had 4–6 white cells per high power field. Blood urea nitrogen and serum creatinine were normal. Intravenous urography (fig. 1A) showed focal areas of clubbing and loss of renal parenchyma. Sonography (fig. 1B) showed focal loss of renal parenchyma, extension of the calyces peripherally from the renal sinus, a slight increase in parenchymal echoes in the upper pole, and a decrease in renal size. The perinephric space was maintained.

Case 2

C. T., a 59-year-old woman, had chest and shoulder pain. She had a long history of urinary tract infections treated with periodic urethral dilatations. Blood urea nitrogen and serum creatinine were within normal limits. Urography showed chronic pyelonephritis predominating in the upper pole, consistent with reflux nephropathy (fig. 2A). The ultrasound study (fig. 2B) showed increased echoes in the involved areas of the upper and lower poles, and associated loss of renal parenchyma. The perinephric space is intact.

Case 3

S. T., an 18-year-old woman, had abdominal pain for 1 week. Excretory urography (fig. 3A) showed scarring of the lower pole of the right kidney with a duplicated right collecting system. The ureters inserted separately into the bladder. There was clubbing of the middle and lower pole calyces. White blood cell count was 14,600 with a shift to the left. Urine had 15–20 white cells per high power field. Bacterinuria was present. Ultrasound study (fig. 3B) demonstrated loss of renal parenchyma in the lower pole, increased echogenicity, and a normal upper pole.

Discussion

Chronic atrophic pyelonephritis has several etiologies. Hodson [5] described it as a focal or multifocal process with normal intervening areas of kidney. The process may involve the full thickness of the kidney with retraction of the papilla, dilatation of the surrounding calyx, depression of the surface, and loss of the renal parenchyma. The involved kidney is often small and the adjacent tissue is normal. This constellation of findings can be induced by several processes, most commonly vesicoureteral reflux. Clinical correlation is essential.

The ultrasound findings of chronic atrophic pyelonephritis reflect the pathologic alterations. Focal loss of parenchyma can be appreciated. Collagen is considered to be a major source of echoes [6]. Focal fibrosis manifested by increased echoes can be demonstrated in the involved area of the cortex and medulla (fig. 4). The retracted calyx, if not distended with fluid, appears as an echogenic zone extending beyond the normal area of the renal sinus. When distended with urine, sonolucent fluid within the calyx or infundibulum may be appreciated. One of our patients had a dense fibrous band in the parenchyma (fig. 1). The entire scarring process, if advanced, may be global rather than focal.

The focal abnormalities are in contrast to a group of

Received June 29, 1978; accepted after revision September 29, 1978.
[1] Department of Radiology, Park City Hospital, Bridgeport, Connecticut 06602. Address reprint requests to C. J. Kay.
[2] Department of Radiology, Yale University School of Medicine, New Haven, Connecticut 06510.

© 1979 American Roentgen Ray Society

0361–803X/79/1321–0047 $0.00

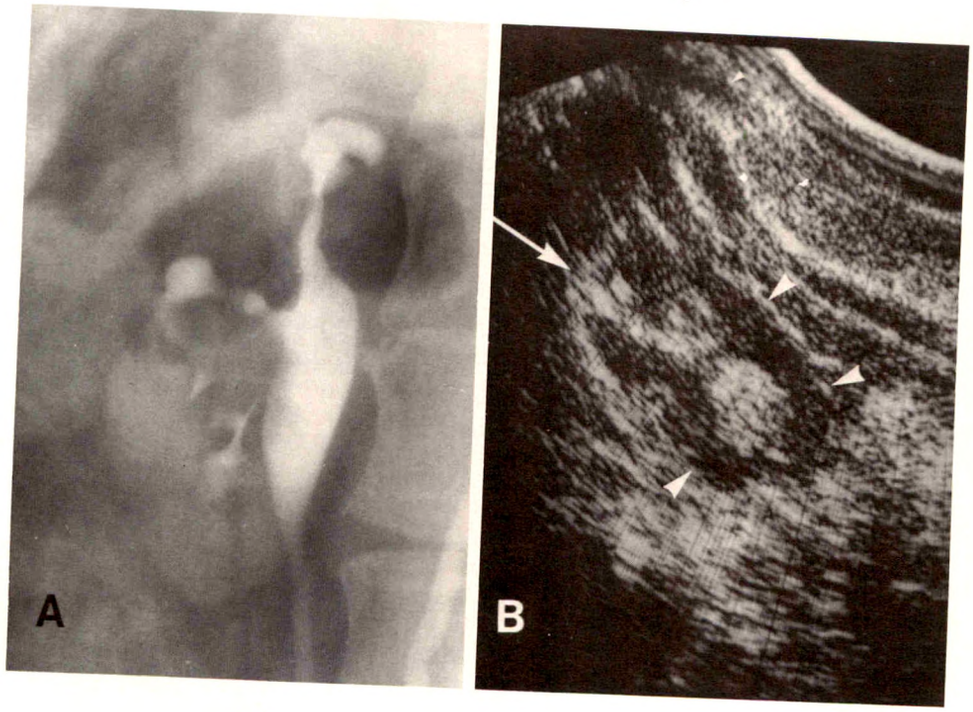


Fig. 1.—Case 1. **A**, Focal scarring and calyceal retraction in upper pole of right kidney, typical of chronic atrophic pyelonephritis. **B**, Right kidney (*arrowheads*) with patient prone. Focal loss of parenchyma, extension of calyx from renal sinus to renal margin, and associated focal increased echogenicity due to fibrosis (*arrow*) in upper pole.

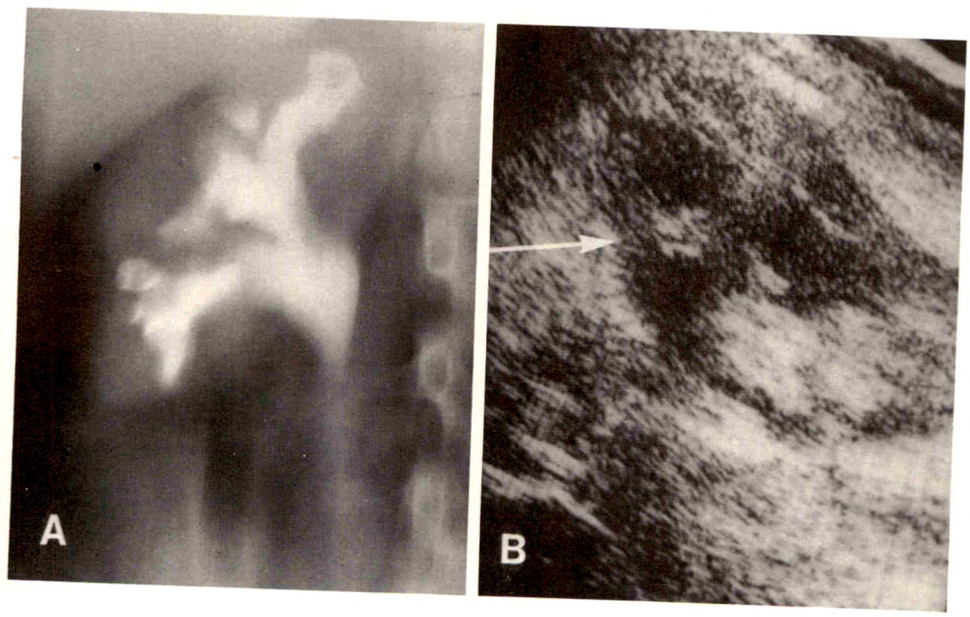


Fig. 2.—Case 2. **A**, Focal scarring in both upper and lower poles of right kidney with associated calyceal blunting. **B**, Right kidney with patient prone. Focal scarring and extension of renal sinus to renal margin in upper pole of right kidney (*arrow*) and increased echogenicity and loss of parenchyma in lower pole.

diseases which produce a generalized increase in cortical echoes and preserve the sonolucent medulla leading to an accentuation of normal renal anatomy. These entities include acute or chronic glomerulonephritis, diabetic glomerulosclerosis, acute tubular necrosis, and Alports Disease [1, 2, 7]. In one case of renal infarction studied with ultrasound [8] there was a focal zone of intense echoes in the involved renal parenchyma, but no abnormality in the renal sinus. Renal tuberculosis, papillary necrosis, and possibly focal postobstructive atrophy would be expected to produce a sonographic appearance similar to chronic atrophic pyelonephritis.

Technical artifacts from an overlying rib may appear to produce loss of parenchyma. The ultrasound findings should be technically reproducible, since the transducer, not being perpendicular to the kidney, can produce some of the above described findings.

Intravenous urography usually precedes ultrasonic evaluation in cases of suspected urinary tract infection. It adequately displays morphologic abnormalities and is preferable to ultrasound in most cases as the primary method of evaluation. However, the ultrasonic patterns should be familiar, since it may be used initially to evaluate the abdomen or may be the procedure of choice

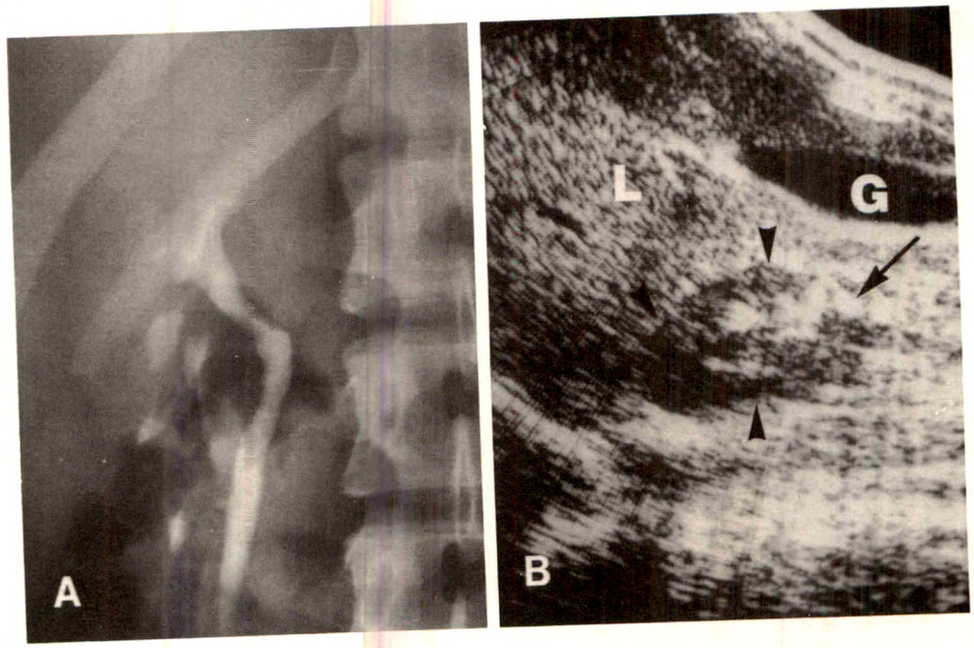


Fig. 3.—Case 3. **A**, Duplicated collecting system on right with scarring and calyceal blunting involving lower moiety of duplex system. **B**, Parasaggital section through liver (L), gallbladder (G), and right kidney (*arrowheads*) with patient supine. Focal loss of renal parenchyma in lower pole with zone of increased echoes (*arrow*) in adjacent region from both fibrosis and calyceal retraction.

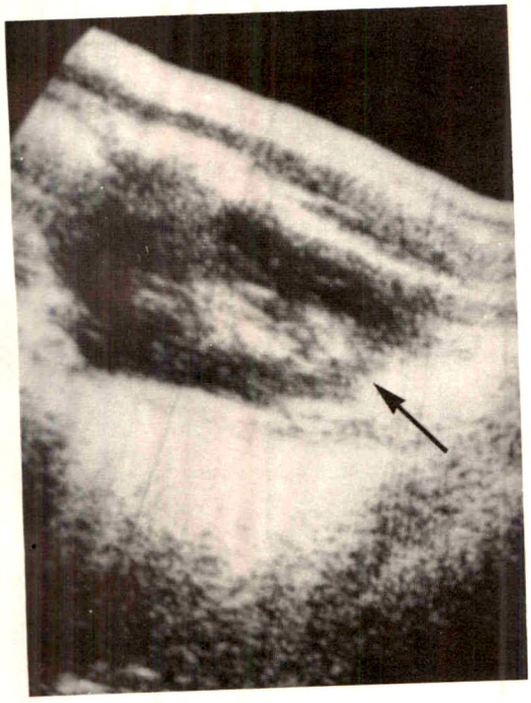


Fig. 4.—Prone section through left kidney of 7-year-old girl with chronic atrophic pyelonephritis. Focal scar in lower pole (*arrow*) with associated increased echogenicity at this site and in upper pole.

in certain clinical situations, such as pregnancy or in patients with a history of allergy.

ACKNOWLEDGMENTS

We thank Dr. C. J. Hodson for comments on the manuscript and Patricia Donnelly for technical assistance.

REFERENCES

1. Cook JH III, Rosenfield AT, Taylor KJW: Ultrasonic demonstration of intrarenal anatomy. *AJR* 129:831–835, 1977
2. Rosenfield AT, Taylor KJW, Crade M, DeGraff C: Anatomy and pathology of the kidney by gray-scale ultrasound. *Radiology* 128:737–744, 1978
3. Sanders RC, Conrad MR: The ultrasonic characteristics of the renal pelvicalyceal echo complex. *JCU* 5:372–377, 1977
4. Schneider M, Becker JA, Staiano S, Campos E: Sonographic-radiographic correlation of renal and perirenal infections. *AJR* 127:1007–1014, 1976
5. Hodson CJ: The radiological contribution toward the diagnosis of chronic pyelonephritis. *Radiology* 88:857–871, 1967
6. Taylor KJW, Carpenter DA, Hill CR, McCready VR: Gray scale ultrasound imaging: the anatomy and pathology of the liver. *Radiology* 119:415–423, 1976
7. Le Quesne GW: Ultrasonic demonstration of glomerular disease. Presented at the annual meeting of the Society for Pediatric Radiology, Boston, Mass., September 1977
8. Rosenfield AT, Taylor KJW: Gray scale nephrosonography: current status. *J Urol* 117:2–6, 1977

Persistent Gallbladder Opacification after Iopanoic Acid Cholecystography: Diagnostic Implications for Acalculous Cholecystitis

MARC P. BANNER,[1,2] MICHAEL H. BLESHMAN,[1,3] AND JERRY M. SPECKMAN[1]

Recent reports in the surgical literature state that persistent dense visualization of an otherwise normal-appearing gallbladder 36 hr after the administration of iopanoic acid is highly suggestive of acalculous cholecystitis. To determine the incidence and significance of persistent gallbladder visualization, 324 patients and 66 asymptomatic controls were evaluated. An equal percentage (about 10%) of both groups showed persistent dense gallbladder opacification 36 hr after iopanoic acid ingestion. The results do not support the contention that patients with acalculous cholecystitis can be identified by simply obtaining an additional abdominal radiograph the day after oral cholecystography.

Introduction

The radiographic diagnosis of acalculous cholecystitis has been, and remains, elusive. All radiologists have examined patients with convincing and often persistent symptoms of gallbladder disease whose oral cholecystograms appear normal, often on repeated occasions. Barium gastrointestinal examinations are also usually normal or do not account for the patient's symptoms. The development of a reliable method of separating patients with acalculous cholecystitis from those with other abdominal disease would be an important adjunct to clinical diagnosis.

Adams and Foxley [1] recently reported 26 patients with persistent symptoms compatible with biliary tract disease and normal oral cholecystograms who had dense visualization of their gallbladders 36 hr after ingestion of 3 g iopanoic acid (Telepaque, Winthrop Labs., New York, NY). A control population of 22 patients with symptoms related to gynecologic or gastrointestinal organs other than the gallbladder was studied preoperatively and had normal cholecystograms at 12 hr with no gallbladder opacification at 36 hr. The 26 patients showed histologic evidence of cholecystitis while the 22 control patients had normal gallbladders by inspection and palpation at laparotomy.

Nora et al. [2] studied 14 patients with chronic gallbladder symptomatology by oral cholecystography and fatty meal. Their cholecystograms were reportedly normal except for prolonged gallbladder visualization at 24 hr to 7 days. All of these patients had cholecystectomy and histologic evidence of acalculous cholecystitis and/or hyperplastic cholecystosis.

We undertook a prospective study to determine the incidence of persistent gallbladder opacification after oral cholecystography and its relation to symptomatology in patients and presumed normal subjects.

Subjects and Methods

All patients with visible gallbladders by oral cholecystography during a 6 month period in 1976 were asked to return 24 hr after their initial examination for one additional radiograph of the gallbladder. A total of 324 patients with diagnostic gallbladder visualization returned. A minority of both in- and outpatients was unable to return for a variety of reasons; these patients were questioned about abdominal symptoms associated with gallbladder disease. There were 185 patients (57%) evaluated with 3 g iopanoic acid ingested 12–14 hr prior to filming, and 139 patients (43%) with 6 g ingested during the 36 hr prior to initial filming [3].

Initial prone and prone oblique radiography of the right upper quadrant was followed by erect and supine fluoroscopic compression spot films of the gallbladder at 70–75 kVp. Follow-up filming at 24 hr (36 hr after ingestion of iopanoic acid) consisted of a single upright fluoroscopic spot film of the gallbladder duplicating the previous day's technique.

A commercial fatty meal (Lipomul Oral, Upjohn, Kalamazoo, MI) was given to 152 patients (47%) with further filming 30–45 min after ingestion, a much higher percentage of fatty meals than we normally administer in regular clinical practice. Whenever feasible, all patients studied during an even-numbered month received a fatty meal while those examined during odd-numbered months did not. This randomization was adhered to as closely as possible, regardless of findings on initial cholecystogram films. Irrespective of month, however, all patients whom we believed needed a fatty meal to establish a radiographic diagnosis received one.

Upon completion of initial cholecystography all patients were instructed to resume their normal diet and to have breakfast before returning for the follow-up film. Ingestion of some fatty food was encouraged, though specific diets were not prescribed and dietary information was not obtained at the time of follow-up filming.

Gallbladder visualization at 24 hr was compared to the initial cholecystogram. Visualization was noted as good, faint, or absent. Unchanged gallbladder density was designated persistent good visualization; a change from initial good to subsequent faint opacification was designated prolonged visualization of the gallbladder. Defined this way, persistent good visualization was apparently the criterion used by Adams and Foxley [1] to establish a diagnosis of acalculous cholecystitis.

In addition to 324 patients, 66 healthy and asymptomatic control subjects (all members of our department) were examined 14 hr after ingestion of 3 g iopanoic acid. A single prone oblique radiograph of the right upper quadrant was obtained after which a fatty food was given to each subject. Normal dietary patterns were resumed. Filming was repeated at 24 hr intervals, with identical radiographic technique, until the gallbladder shadow was no longer seen. To our knowledge, no patient with a normal-appearing gallbladder underwent cholecystectomy.

Received April 13, 1978; accepted after revision September 26, 1978.

[1] Department of Radiology, Wilford Hall USAF Medical Center, Lackland Air Force Base, Texas 78236.
[2] Present address: Department of Radiology, Hospital of the University of Pennsylvania, 3400 Spruce Street, Philadelphia, Pennsylvania 19104. Address reprint requests to M. P. Banner.
[3] Present address: Department of Radiology, Phoenixville Hospital, Phoenixville, Pennsylvania 19460.

0361–803X/79/1321–0051 $0.00

TABLE 1
Comparison of Gallbladder Opacification with Cholecystographic Findings

Gallbladder Visualization (36 hr after Ingestion of Iopanoic Acid)	Patient Population*				Control Population
	Normal Oral Cholecystogram	Gallstones	Hyperplastic Cholecystosis	Total	
Persistent good visualization	26 (9.4)	5 (13.9)	1 (8.3)	32 (9.9)	7 (10.6)
Prolonged visualization	134 (48.6)	17 (47.2)	7 (58.4)	158 (48.8)	24 (36.4)
No visualization	116 (42.0)	14 (38.9)	4 (33.3)	134 (41.3)	35 (53.0)
Total	276	36	12	324	66

Note.—Numbers in parentheses are percentages.
* Patients with and without fatty meal considered together in each diagnostic category. Patients receiving 3 and 6 g iopanoic acid also considered together in each diagnostic category.

Results

Gallbladder Appearance

Of the 324 patients with diagnostic gallbladder visualization, 276 (85.2%) had cholecystograms which appeared normal, 36 (11.1%) had gallstones, and 12 (3.7%) showed changes of hyperplastic cholecystosis. At 24 hr, persistent good visualization was noted in 32 patients (9.9%) and prolonged visualization in 158 (48.8%) (table 1).

Persistent good visualization was seen in 26 patients (9.4%) with normal cholecystograms, in five (13.9%) of those with gallstones, and in one patient (8.3%) with hyperplastic cholecystosis. Prolonged visualization was present in 134 (48.6%), 17 (47.2%), and seven (58.4%) patients with normal cholecystograms, gallstones, and cholecystosis, respectively. Of the 150 patients who received 3 g iopanoic acid, 15 (10.0%) had persistent good visualization and 65 (43.3%) prolonged visualization; of the 126 patients who ingested 6 g, 11 (8.7%) had persistent good visualization and 60 (54.8%) prolonged visualization. The relatively small numbers of patients with gallstones and cholecystosis precluded statistical comparison between 3 and 6 g dose cholecystography.

Of the 66 control subjects, seven (10.6%) showed persistent good visualization and 24 (36.4%) prolonged visualization 36 hr after ingestion of 3 g iopanoic acid. The seven control subjects with persistent good visualization were restudied in identical fashion 1–3 weeks after their initial participation. Three of the seven controls again showed persistent good visualization, three had prolonged visualization, and one showed absence of visualization 36 hr after iopanoic acid ingestion. Two of the seven had discernible gallbladder opacification for 4 days. All controls showed diagnostic gallbladder visualization after 3 g iopanoic acid and no gallbladder abnormalities were demonstrated. At reexamination, the control subjects with persistent good visualization also had upright fluoroscopic compression spot films of the gallbladder to exclude small gallstones which might have been overlooked on the overhead radiographs. No stones or other abnormalities were found.

Response to Fatty Meal

Films after a fatty meal in the patient population usually demonstrated gallbladder contraction of varying degrees, though an occasional unchanged gallbladder was noted. Of 131 patients who received a commercial fatty meal 12 (9.2%) had persistent good visualization and 58 (44.3%) prolonged visualization. Of 145 patients who were not given a fatty meal, 14 (9.7%) showed persistent good visualization and 76 (52.4%) prolonged visualization.

All control volunteers had a fatty breakfast after the first day's filming and, like the patient population, resumed their normal diet. Persistent good visualization was noted as frequently in the controls (10.6%) as it was in the patient groups who did or did not receive a commercial fatty meal. However, fewer controls (36.4%) showed prolonged visualization than did patients (48.8%) who did or did not receive a fatty meal. Again, too few patients with gallstones and hyperplastic cholecystosis were studied with and without fatty meals to allow valid comparison with "normal" patients and controls.

Symptomatology

Table 2 compares patient symptomatology with gallbladder appearance. With normal cholecystograms no statistical difference among the three appearance groups (persistent good visualization, prolonged visualization, no visualization at 36 hr) was noted with regard to abdominal pain located in the epigastrium or right upper quadrant, radiation of pain to the right scapula, nausea and/or vomiting associated with pain, or intolerance to fatty or spicy food. Abdominal pain and associated nausea and/or vomiting was reported as frequently by the normal cholecystogram group as it was by those with gallstones. However, the latter indicated specific pain radiation to the right scapula more frequently than the former. Those with hyperplastic cholecystosis tended to have symptoms more often than either of the other two groups. Too few patients gave a history of prior jaundice to allow statistically significant comparison of the various groups. The control population, as noted above, was asymptomatic.

TABLE 2

Comparison of Patient Symptomatology with Cholecystographic Findings and Gallbladder Visualization after Iopanoic Acid Ingestion

Symptom	Normal Oral Cholecystogram				Gallstones	Hyperplastic Cholecystosis
	Regardless of Visualization at 36 hr	Persistent Good Visualization at 36 hr	Prolonged Visualization at 36 hr	No Visualization at 36 hr		
Epigastric or right upper quadrant abdominal pain	197 (71.4)	17 (65.4)	100 (74.6)	80 (69.0)	25 (69.4)	10 (83.3)
Radiation of pain to right scapula	63 (22.8)	6 (23.1)	34 (25.4)	23 (19.8)	11 (30.6)	4 (33.3)
Nausea or vomiting associated with pain	121 (43.8)	12 (46.2)	64 (47.8)	45 (38.8)	16 (44.4)	8 (66.7)
Fatty or spicy food intolerance	159 (57.6)	18 (69.2)	77 (57.5)	64 (55.2)	21 (58.3)	9 (75.0)
Jaundice	12 (4.3)	2 (7.7)	5 (3.7)	5 (4.3)	3 (8.3)	0
Total	276	26	134	116	36	12

Note.—Numbers in parentheses are percentages.

Discussion

Mechanisms postulated for prolonged gallbladder visualization include (1) failure of the gallbladder to empty after cholecystography and (2) enterohepatic recirculation of conjugated iopanoic acid with refilling of the gallbladder. Goldberg et al. [4] demonstrated that conjugated iopanoic acid is absorbed by the bowel and that 19%–53% of the drug undergoes enterohepatic recirculation. Though it was not possible for us to study recirculation in our patients, one observation seems worthy of speculative comment. Patients with normal cholecystograms who ingested 6 g iopanoic acid had a greater incidence of prolonged gallbladder visualization (54.8%) than did those who ingested 3 g (43.3%). Though it has not been determined, to our knowledge, that the amount of enterohepatic recirculation of iopanoic acid is dose related, it is not unreasonable to assume that, for a given percentage of recirculation, the higher the ingested dose, the more prolonged gallbladder visualization would be.

The alternate postulate for prolonged gallbladder visualization, that is, failure of gallbladder emptying after cholecystography, was examined using the fatty meal. Administering a fatty meal, as well as having patients and controls resume a normal diet after the initial day's filming, provided the needed stimulus for gallbladder emptying. A virtually identical incidence of persistent good visualization (about 10%) in patients who received a fatty meal, those who did not, and control subjects as well as a lack of correlation of fatty meal administration with degree of subsequent gallbladder opacification imply that failure of gallbladder emptying is not the sole cause of persistent good or prolonged visualization.

It became obvious during our 6 month study that identification of patients with normal cholecystograms and persistent good visualization was not sufficient to recommend surgery for these patients, as many were subsequently shown to have upper gastrointestinal pathology which could account for their symptomatology. Even cholecystectomy with pathologic confirmation of acalculous cholecystitis in the 9.4% of patients with persistent good visualization of a normal-appearing gallbladder would not support the reports in the surgical literature that acalculous cholecystitis can be accurately identified by oral cholecystography. Validation would require cholecystectomy in all 276 patients with normal cholecystograms, histologic confirmation of cholecystitis in the above-mentioned 9.4%, and absence of inflammatory changes in the 42% of patients whose gallbladders were no longer seen at 36 hr (table 1). Such a procedure would obviously be impossible.

For these reasons a control population was studied. The results obtained from our patient population were reproduced in our control population. The latter, aside from being asymptomatic and healthy, was younger on the average than the patient population and, therefore, less likely to harbor gallbladder disease. The equal percentage of controls and patients with persistent good visualization 36 hr after iopanoic acid ingestion and the inconstancy of persistent visualization in controls tend to invalidate, at least by inference, the published reliability of persistent good visualization in identifying patients with acalculous cholecystitis. We realize that our patients with normal cholecystograms and persistent good visualization did not have surgery and could have had acalculous cholecystitis. Nonetheless, we conclude that neither persistent good visualization nor prolonged visualization would distinguish them from those with otherwise normal oral cholecystograms. Prolonged gallbladder opacification after ingestion of another contrast agent, iocetamic acid (Cholebrine, Mallinckrodt, St. Louis, MO), also seems to be common and is undependable as a criterion for the diagnosis of cholecystitis [5].

Prolonged or persistent good gallbladder visualization is, at present, an incompletely understood observation. In the presence of a normal diet, sluggish gallbladder emptying does not seem to be a major factor. Enterohe-

patic recirculation is the most likely basis for this radiographic finding, possibly related in some degree to dose of ingested contrast material. This latter possibility merits further investigation.

REFERENCES

1. Adams TW, Foxley EG Jr: A diagnostic technique for acalculous cholecystitis. *Surg Gynecol Obstet* 142:168–170, 1976
2. Nora PF, McCarthy W, Sanez N: Cholecystokinin cholecystography in acalculous gallbladder disease. *Arch Surg* 108:507–511, 1974
3. Burhenne HJ, Obata WG: Single-visit oral cholecystography. *N Engl J Med* 292:627–628, 1975
4. Goldberg HI, Lin SK, Thoeni R, Moss AA, Brito A: Recirculation of iopanoic acid after conjugation in the liver. *Invest Radiol* 12:537–541, 1977
5. Koehler RE, Stanley RJ, DiCroce J: Proionged gallbladder opacification after oral cholecystography. *Radiology* 128:601–604, 1978

Double Blind Comparison of Meglumine Iotroxate (Biliscopin), Meglumine Iodoxamate (Endobil), and Meglumine Ioglycamate (Biligram)

V. TAENZER[1] AND V. VOLKHARDT[2]

Two new intravenous cholegraphic agents, iotroxate and iodoxamate, hold a lower general toxicity, lower protein binding, and claim a higher rate of biliary excretion. Both compounds proved to be equally effective in opacifying the gallbladder and the bile ducts in a double-blind clinical study comprising 400 cases. Iotroxate gave significantly earlier good or adequate visualization as a result of its higher excretion rate by the liver ($P < 0.05$). Side effects were observed in fewer patients in the iotroxate group (11.6%) compared with the iodoxamate group (16.4%, $P > 0.05$). In a second double-blind study, an iotroxate group of 97 patients who received two thirds of the overall content of iodine (3.6 g) was compared with a group of 98 patients, who received ioglycamate (5.3 g). Visualization was equal in the two groups, while side effects were significantly reduced to 10.3% in the iotroxate group against 20.4% ($P < 0.05$). The higher biliary clearance of iotroxate permits a reduction of the amount of iodine.

Meglumine iotroxate (Biliscopin, Schering AG, Berlin/Bergkamen) and iodoxamate (Endobil, Bracco SpA, Milan) are new contrast media for intravenous cholangiography. Like iodipamide and ioglycamate, iotroxate and iodoxamate are dimeric molecules. The link between the two iodine-bearing aromatic nuclei has been lengthened in both substances in comparison to iodipamide (fig. 1). In addition, oxygen has been incorporated in the link. In both the enlarged molecules this resulted in a reduction of protein binding [1], a reduction of the general toxicity in animal experiments [2, 3] and a higher rate of excretion into bile by the liver of dogs compared with iodipamide at equimolar infusion rates [4]. With iotroxate, a remarkable reduction of the neural toxicity was also observed in animal experiments [5].

Reports on clinical experience with iotroxate and comparative pharmacokinetic data have been published [1, 6], as have reports on the biotransformation of the two cholegraphic agents under discussion [7]. These studies demonstrated a statistically significant improvement both in tolerance and in contrast quality on visualization of the gallbladder and, in particular, the bile ducts for iotroxate in comparison with ioglycamate.

This report presents the results of two double-blind comparisons of the two agents with respect to radiographic quality and clinical tolerance. In the first study, these parameters were investigated in a comparative double-blind trial using the same amount of iodine in each preparation. A second double-blind study, also in a group of unselected patients, was conducted to decide whether the higher excretion rate of iotroxate would permit a reduction of the total amount of iodine and thus a further decrease of the rate of side effects in comparison to ioglycamate.

Subjects and Methods

The two double-blind studies were conducted as controlled clinical trials, each with two independent treatment groups. Unselected patients with indications for intravenous cholangiography were allocated to the individual groups with the aid of a random number generator.

As in previous studies [6, 8], the radiologic contrast density was assessed by classification into four groups by one of us, having knowledge of neither the contrast agent used nor the patient's history: (1) good contrast; (2) adequate contrast; (3) poor contrast (inadequate for definite diagnosis); and (4) no contrast. The gallbladder and bile ducts were assessed separately.

A radiologist assessed the quality of the demonstration independent of another, who performed the examination. Patients under 18 years of age, pregnant women, and patients with IgM gammopathy were excluded from the study. All patients were asked specifically about allergic reactions in their history, such as hay fever, asthma, and hypersensitivity to drugs, but were not excluded from the study if the answers were positive. No studies of the serum enzymes, bilirubin, alkaline phosphatase, and creatinine before and after injection or progress controls to assess the liver toxicity of the substances were performed, since results in this respect have been published [1, 9].

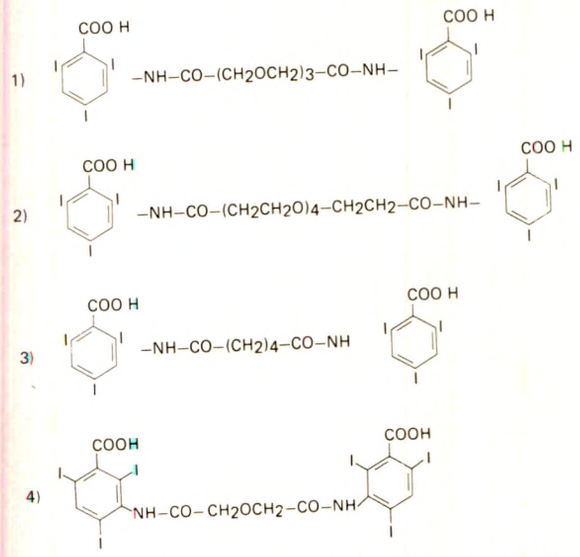


Fig. 1.—Molecular structure of iotroxate (1), iodoxamate (2), iodipamide (3), and ioglycamate (4).

Received March 22, 1978; accepted after revision August 16, 1978.
[1]Department of Roentgendiagnosis, Krankenanstalten Moabit, Turmstrasse 21, D-1000 Berlin 21. Address reprint requests to V. Taenzer.
[2]Department of Clinical Research, Schering AG, Müllerstrasse 170–178, D-1000 Berlin 65.

0361–803X/79/1321–0055 $0.00

AJR 132:55–58, January 1979
© 1979 American Roentgen Ray Society

TABLE 1
Quality of Radiologic Visualization in Patients with Gallbladder

	Gallbladder		Bile Ducts	
	Biliscopin	Endobil	Biliscopin	Endobil
Good	85 (47.7)	86 (47.3)*	77 (43.3)	73 (40.1)*
Adequate	29 (16.3)	36 (19.8)*	60 (33.7)	60 (33.0)*
Poor	16 (9.0)	16 (8.8)*	30 (16.8)	38 (20.9)*
None	48 (27.0)	44 (24.2)*	11 (6.2)	11 (6.0)*
Total	178 (100)	182 (100)	178 (100)	182 (100)

Note.—Numbers in parentheses are percentages. Significance was determined using the Chi square test ($\chi^2 = 0.889$ for the gallbladder; $\chi^2 = 1.004$ for the bile ducts). In one patient with gallbladder, radiographs were not technically satisfactory.
* $P > 0.05$.

All side effects, whether trivial or serious, were recorded according to the nature, time of occurrence, and duration, and were classified as mild or severe. Trivial reactions which did not require any treatment were classified as mild. These were mainly sensations of heat and taste, and nausea. Reactions which required further intensive supervision or even therapeutic measures were regarded as severe.

Administration of Contrast Material

In the first study, 400 patients referred for intravenous cholangiography received an intravenous injection of 30 ml meglumine iotroxate (iodine content, 180 g/l; total iodine, 5.4 g) or of 30 ml meglumine iodoxamate (iodine content, 183 g/1; total iodine, 5.5 g). In accordance with the randomization scheme, each substance was administered to 200 patients. The injection was given over 5 min.

In the second study, 195 patients received an injection of 30 ml meglumine iotroxate at low concentration (iodine content, 120 g/l; total iodine, 3.6 g) or 30 ml meglumine ioglycamate (iodine content, 176 g/l; total iodine, 5.3 g). In accordance with a randomization scheme, 97 patients received iotroxate and 98 ioglycamate. To avoid falsification of the side effects rate due to uneven or too rapid an injection, the contrast media were administered with an Injectomat at a constant rate within 6 min [10–12].

Radiographic Technique

Serial films of the right upper abdomen were made at 30, 60, 90, and 120 min after administration, and also after 3, 6, and in some cases 24 hr if no demonstration had been achieved by 120 min. In addition tomographic films were made if the opacification of the biliary tract was unsatisfactory or in the event of overshadowing by intestinal gas.

Results

Iotroxate versus Iodoxamate

The degree of randomization achieved in the two groups can be seen in the distribution of the sexes: 113 women and 87 men were examined with Biliscopin, and 116 women and 84 men with Endobil. There were 21 patients in the Biliscopin group and 18 in the Endobil group who had undergone cholecystectomy.

Contrast quality. The quality of the visualization for the contrast media iotroxate (Biliscopin) and iodoxamate (Endobil) is shown in table 1. Visualization in patients without gallbladders is assessed in table 2. No statistically significant difference was established. Good and

TABLE 2
Quality of Radiologic Visualization in Patients without Gallbladder

	Biliscopin	Endobil
Good	9 (42.9)	6 (33.3)
Adequate	8 (38.1)	5 (27.8)
Poor	3 (14.3)	6 (33.3)
None	1 (4.8)	1 (5.6)
Total	21 (100)	18 (100)

Note.—Numbers in parentheses are percentages.

adequate visualization of the gallbladder was achieved in 64% of cases after Biliscopin injection and in 67.1% after Endobil injection. The figures for the bile ducts are 77% and 73.1%, respectively. No visualization of the gallbladder was achieved in 27% of cases after Biliscopin injection and in 24.2% after Endobil injection; nonvisualization of the bile ducts was 6.2% and 6.0%, respectively. The findings tended to be different only in the groups of cholecystectomized patients, but this could not be confirmed statistically: good and adequate visualization was observed in 81% of cases after Biliscopin injection and in only 67% of cases after Endobil injection. Good or adequate visualization of the gallbladder was frequently observed earlier ($P < 0.05$) after Biliscopin injection than after Endobil injection (table 3).

Side effects. Side effects were observed in 16% of patients after Endobil injection and in 11.6% after Biliscopin injection ($P > 0.05$) (table 4). Severe side effects occurred in only three patients: respiratory complaints (wheezing) and collapse after Endobil injection (in one case each) and allergic skin reactions after Biliscopin injection (one case).

Iotroxate versus Ioglycamate

This study comprised 112 women and 83 men. There were 11 patients without gallbladder in the iotroxate (Biliscopin) group and 15 in the ioglycamate (Biligram) group.

Contrast quality. Despite the reduced amount of iodine in the Biliscopin group, assessment of contrast quality was the same for the gallbladder and better for the bile ducts after Biliscopin injection (table 5). The result was

TABLE 3

Earliest Film with Good or Adequate Visualization in Patients with Gallbladder

Time of film (min after injection)	Gallbladder		Bile Ducts	
	Biliscopin	Endobil	Biliscopin	Endobil
30	53 (46.5)	7 (14.2)*	123 (86.6)	116 (82.9)**
60	47 (41.2)	66 (55.0)	14 (9.9)	17 (12.1)
90	14 (12.3)	37 (30.8)	5 (3.5)	7 (5.0)
Total	114 (100)	120 (100)	142 (100)	140 (100)

Note.—Numbers in parentheses are percentages. Significance was determined using the Chi square test ($\chi^2 = 31.948$ for the gallbladder; $\chi^2 = 0.815$ for the bile ducts).
*$P < 0.05$.
**$P > 0.05$.

TABLE 4

Distribution of Side Effects Rate

	Biliscopin	Endobil	Biliscopin (3.6 g)	Biligram
Number of patients	200 (100.0)	200 (100.0)	97 (100.0)	98 (100.0)
Patients with side effects	23 (11.6)	32 (16.0)*	10 (10.3)	20 (20.4)**
Nausea	4 (7.4)	10 (5.0)	2 (2.1)	7 (7.1)*
Vomiting	6 (3.2)	7 (3.5)	2 (2.1)	3 (3.1)
Sensation of heat	5 (2.5)	18 (9.0)	3 (3.1)	4 (4.1)
Circulatory reaction	3 (1.5)	4 (2.0)	1 (1.0)	1 (1.0)
Skin reactions	6 (3.0)	6 (3.0)	1 (1.0)	4 (4.1)
Respiratory complaints	1 (0.5)	4 (2.0)	1 (1.0)	1 (1.0)

Note.—Numbers in parentheses are percentages. Significance was determined using Fisher's test.
*$P > 0.05$.
**$P < 0.05$.

TABLE 5

Quality of Radiologic Visualization in Patients with Gallbladder

	Gallbladder		Bile Ducts	
	Biliscopin 3.6 g	Biligram	Biliscopin 3.6 g	Biligram
Good	40 (46.5)	40 (48.2)*	50 (58.1)	37 (44.6)*
Adequate	17 (19.8)	14 (16.9)*	25 (29.1)	26 (31.3)*
Poor	10 (11.6)	12 (14.4)	9 (10.5)	17 (20.5)
None	19 (22.1)	17 (20.5)	2 (2.3)	3 (3.6)
Total	86 (100)	83 (100)	86 (100)	83 (100)

Note.—Numbers in parentheses are percentages. Significance was determined using the Chi square test ($\chi^2 = 0.530$ for the gallbladder; $\chi^2 = 4.572$ for the bile ducts).
*$P > 0.05$.

similar in the comparison of cholecystectomized patients (table 6, $P > 0.05$).

Side effects. Side effects were observed in 20.4% of patients after ioglycamate injection, and in 10.3% of patients after iotroxate injection ($P < 0.05$). All side effects were mild.

Discussion

As a radiologic method, intravenous cholangiography has been accompanied by a high rate of abortive examinations and undesired side effects. Researchers have tried to optimize the most important parameters of quality in cholangiography (opacification and the rate of side effects) by modifying the examination technique. An attempt was made with the infusion technique to adapt the dose of contrast medium administered per unit of time to the capacity of the vehicle substances in plasma and the functional excretory capacity of the liver. Although the high rate of side effects in cholangiography was reduced by this protracted application of contrast

TABLE 6

Quality of Radiologic Visualization of the Biliary Tract in Patients without Gallbladder

	Biliscopin 3.6 g	Biligram
Good	7 (63.6)	5 (33.3)
Adequate	4 (36.4)	5 (33.3)
Poor	0	3 (20.1)
None	0	2 (13.3)
Total	11 (100)	15 (100)

Note.—Numbers in parentheses are percentages.

medium, no convincing improvement in the quality of the films has been achieved even by increasing the dose of contrast medium [9, 13, 14].

Two new substances, iodoxamate [11, 15–19] and iotroxate [1, 4–7, 9], are now available for cholangiography. In comparison with the older agents (iodipamide, ioglycamate) they are superior with regard to the hepatobiliary excretion rate (and thus opacification on the film) and also with regard to tolerance. The present double-blind comparative study of these new cholegraphic agents, which was conducted in a large study population of 400 patients, showed that the diagnostic effectiveness of both substances is very good.

No differences could be demonstrated with regard to the quality of the opacification in the gallbladder, but a higher percentage of good and satisfactory visualizations was achieved by iotroxate in opacification of the bile ducts of cholecystectomized patients ($P > 0.05$). We are currently checking this result in a double-blind study in a larger population of cholecystectomized patients. Our results suggest that smaller differences are detectable in the cholecystectomized patients.

Distinct differences between the two agents can also be observed by comparing the earliest time points at which good and satisfactory demonstrations are achieved. Optimal visualization of the bile ducts and particularly of the gallbladder is achieved earlier after injection of iotroxate. Contrast quality in the gallbladder was good or adequate only 30 min after injection of iotroxate in 46.5% of cases, while the same quality was achieved at the same time in only 14.2% after injection of iodoxamate ($P < 0.05$). This improved speed of excretion by the liver could result in a shorter, less expensive examination.

The frequency of side effects for the two new preparations is distinctly reduced in comparison with previously reported results [6, 9, 11, 15–19]. The nature and type of the side effects are basically the same after injection of both agents. However, side effects were recorded in only 11.6% of cases after injection of iotroxate and in 16% after injection of iodoxamate ($P < 0.05$). When comparing these figures with those of other workers, it must be remembered that trivial side effects were included in both studies. We have already demonstrated the clear superiority of iotroxate over the older substance ioglycamate in an earlier series of studies [6].

Although decreasing the standard dose of 5 g iodine for ioglycamate would lead to a loss of contrast quality [14], the higher excretory rate of iotroxate compensates and yields superior results even when the dose of iodine is reduced by a third. The quality of the image of the gallbladder remains equivalent, while that achievable in the bile ducts is improved. The degree of opacification achieved in noncholecystectomized patients is described as good in 58.1% using the smaller iotroxate dose, and only 44.6% after ioglycamate injection ($P > 0.05$). The corresponding figures in cholecystectomized patients are 63.6% and 33.3%, respectively ($P > 0.05$).

A very low overall rate of side effects was achieved by using the even, protracted contrast medium administration of an Injectomat [10, 12]. However, it should be noted that side effects were twice as frequent with ioglycamate as with iotroxate. While providing the same or, for the bile ducts, even better opacification, the advantages of iotroxate permit a reduction of the overall dose of iodine and thus a decrease in the dose-dependent side effects in comparison to ioglycamate.

REFERENCES

1. Taenzer V, Speck U, Wolf R: Pharmakokinetik und Plasmaeiweißbindung von Iotroxinsäure. *Fortschr Geb Roentgenstr Nuklearmed* 126:262–267, 1977
2. Lasser EC: Metabolic basis of contrast material: toxicity—status 1971. *AJR* 113:415–422, 1971
3. Lasser EC, Lang JH: Contrast-protein interactions. *Invest Radiol* 5:446–451, 1970
4. Loeb PM, Barnhart JL, Berk RN: Iotroxamide: a new intravenous cholangiographic agent. *Radiology* 125:323–329, 1977
5. Speck U, Düsterberg B, Mannesmann G, Siefert HM: Pharmakologie der Iotroxinsäure, eines neuen intravenösen Cholegraphicums. II. Tierexperimentelle Untersuchungen zur Verträglichkeit. *Drug Res.* In press, 1978
6. Taenzer V, Blumenbach L, Heitzeberg H, Kolb KH, Speck U, Wolf R: Intravenöse Cholegraphie mit Chologram. *Fortschr Geb Roentgenstr Nuklearmed* 123:414–418, 1975
7. Mützel W, Taenzer V, Wolf R: Biotransformation of ioglycamic acid, iodoxamic acid and iotroxic acid in man. *Invest Radiol* 11:598–601, 1976
8. Taenzer V, Herms HJ: Intravenöse Cholegraphie mit Biligram: klinische Pharmakologie. *Fortschr Geb Roentgenstr Nuklearmed* 114:102–107, 1971
9. Stillger E, Persigehl M, Frik W: Klinische Erfahrungen bei der Infusionscholegraphie mit Iotroxamid (Biliscopin ®). *Roentgenblaetter* 30:414–420, 1977
10. Hoenle R, Kölling K: Maschinell optimierte Injektionstechnik bei der Cholegraphie. *Röntgenpraxis* 29:87–90, 1976
11. Kölling K, Hoenle R, Korsten FW: Beitrag zur Nebenwirkungsrate hepatotroper Kontrastmittel. Klinische Vergleichsuntersuchung von Iodoxamat (Endomirabil) und Ioglycamid (Bilivistan). *Radiologe* 17:70–73, 1977
12. Schlesinger L, Liberty MN: Single-dose intravenous cholangiography with minimal visceral reaction. *Radiology* 119:478, 1976
13. Scholz FJ, Johnston DO, Wise RE: Intravenous cholangiography. *Radiology* 114:513–518, 1975
14. Taenzer V, Rühl U: Intravenöse Cholegraphie—Einfluß der Kontrastmittelmenge auf Bildgüte und Nebenwirkungen. *Fortschr Geb Roentgenstr Nuklearmed* 115:808–813, 1971
15. Moss AA: Double-blind comparison of iodipamide and iodoxamate using direct and drip infusion intravenous cholangiography. *AJR* 128:931–933, 1977
16. Robbins AH, Sargent EN, Vincent ME, Boswell W, Meyers HI: Double-blind comparison of meglumine iodoxamate (Cholovue) and meglumine iodipamide (Cholografin). *AJR* 127:257–260, 1976
17. Sargent EN, Schulman A, Meyers HI, Gütler RB, Nicoloff JT, Difazio LT: A new contrast medium for cholangio-cholecystography: meglumine iodoxamate. *AJR* 125:251–258, 1975
18. Schmerwitz W, Rösch E: Infusions-Cholegraphie—Der Einfluß von Kontrastsubstanz und Kontrastmittelkonzentration sowie Infusionszeit auf Kontrastmittelausscheidung und Nebenwirkungen. *Roentgenblaetter* 30:71–78, 1977
19. Schmerwitz W: Injektions-Cholegraphie—Der Einfluß von Kontrastsubstanz und Injektionszeit auf Kontrastmittelausscheidung und Nebenwirkungen. *Roentgenblaetter* 30:64–70, 1977

Significance of Intrapancreatic Gas Demonstrated by CT: A Review of Nine Cases

GASTON MENDEZ, JR.[1] AND MICHAEL B. ISIKOFF[1]

Nine patients with intrapancreatic air were encountered among 450 patients evaluated for pancreatic pathology. Eight of these patients had surgically proven pancreatic abscesses. The ninth had spontaneous perforation of a pancreatic pseudocyst into the gastrointestinal tract as an explanation of the intrapancreatic air. Computed tomography has been found to be very helpful, not only in the initial diagnosis of pancreatic abscesses, but also in the evaluation of distant spread of the infection. The presence of intrapancreatic air in our experience is the most reliable sign of a pancreatic abscess.

Pancreatic abscesses are collections of pus and necrotic debris within the pancreas. They are due to secondary infection of a devitalized pancreas produced as a general rule by necrotizing pancreatitis. Occasionally, a preexisting pseudocyst will become secondarily infected. About 4% of patients with pancreatitis will form abscesses [1, 2].

Due to the extremely high mortality associated with pancreatic abscesses (50%–70%), it is essential the diagnosis be made as rapidly as possible and appropriate surgical drainage performed. We recently studied six cases of surgically proven pancreatic abscesses which were diagnosed initially by computed tomography (CT). The outstanding feature in each case was the presence of intrapancreatic gas. Although this finding has been discussed with conventional radiography, its recognition by CT should be emphasized as well. We also identified the significance of gas in the postoperative pancreas and at least one noninfectious cause of intrapancreatic air.

Materials and Methods

In the last year 450 patients with suspected pancreatic pathology were evaluated in our institution. Six patients with pancreatic abscesses were correctly diagnosed preoperatively by CT. All scans were performed on a General Electric CT/T total body scanner with a scanning time of 4.8 sec and a slice thickness of 1 cm. Multiple scans were performed at 1.5 cm intervals in the area of the liver and pancreas. In most patients 10–12 slices were sufficient to cover the area of interest. A dilute mixture of Gastrografin and water was administered to all patients before the examination. Intravenous contrast material, although not used routinely, was used in many patients when it was felt to be of value.

Results

In nine patients air was demonstrated within the pancreas. In six of these cases, subsequent surgery revealed the presence of a pancreatic abscess. Two patients were evaluated in the postoperative period after surgical drainage of a pancreatic abscess. Their postoperative scans continued to reveal intrapancreatic air. The ninth patient also had gas within the pancreas but since he was not clinically ill a presumptive diagnosis of spontaneous perforation of a pancreatic pseudocyst into the duodenum was based on the clinical course and CT study.

CT was found to be very helpful, not only in the diagnosis of pancreatic abscesses but also in preoperative planning of the surgical treatment. CT was able to demonstrate spread of the abscess into the groin, subphrenic space, and retroperitoneal region. The presence of air within the pancreas in a patient who has had previous drainage of a pancreatic abscess does not necessarily indicate a recurrent process. Two of the patients in our series did quite well with conservative management, even though pancreatic gas was identified on follow-up CT scans done over several weeks. The following cases demonstrate the significance of intrapancreatic gas.

Illustrative Case Reports

Case 1

H. W., a 48-year-old man with history of alcohol abuse, had distention and acute abdominal pain. The admission abdominal film was interpreted as normal. In retrospect, there was obliteration of the right psoas profile, which at initial reading was thought to be due to slight rotation of the patient. An ultrasound examination of the pancreas was nondiagnostic due to overlying bowel gas. After 4 days, the patient became septic and a right groin swelling was noted on physical examination. A CT scan performed on hospital day 5 demonstrated gas in the pancreas consistent with a pancreatic abscess (fig. 1). The patient subsequently underwent an emergency laparotomy with draining of a pancreatic abscess.

Case 2

I. C., a 67-year-old West Indian man, was transferred from Aruba where he had been in good health until he was admitted for acute pancreatitis. Five days later he underwent exploratory laparotomy and was found to have hemorrhagic pancreatitis. The patient continued to have fever spikes to 39.4°C, at which point he was transferred to our institution. Abdominal films revealed dilatation of the large and small bowel compatible with adynamic ileus. An abdominal CT scan was interpreted as consistent with a pancreatic abscess (fig. 2). Since the patient had become afebrile on antibiotics, his physician elected to treat him medically. Nine days later, his temperature spiked to 40°C and he was taken immediately to surgery. An exploratory

Received August 8, 1978; accepted after revision October 12, 1978.
To be presented at the annual meeting of the American Roentgen Ray Society, Toronto, March 1979.
[1] Department of Radiology, University of Miami School of Medicine, Department of Radiology (R130), P. O. Box 016960, Miami, Florida 33101. Address reprint requests to G. Mendez, Jr.

0361-803X/79/1321-0059 $0.00

AJR 132:59–62, January 1979
© 1979 American Roentgen Ray Society

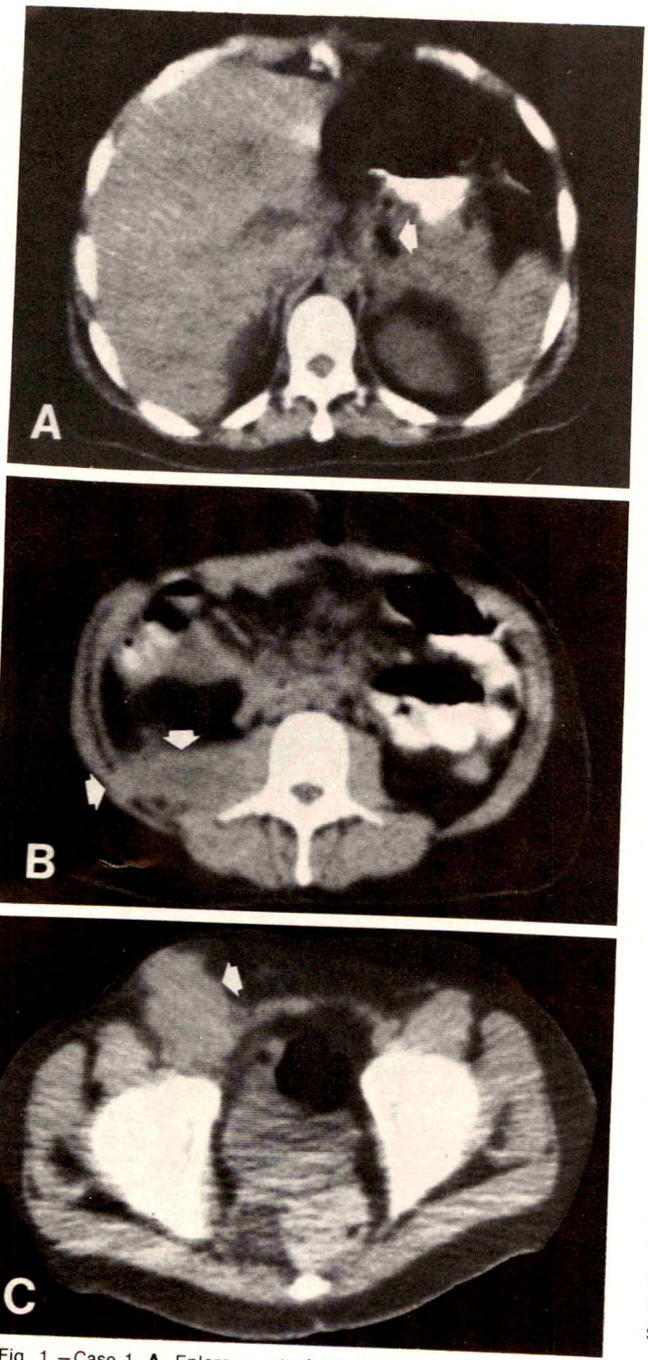


Fig. 1.—Case 1. **A**, Enlargement of tail of pancreas associated with intrapancreatic air (*arrow*). **B**, Just below level of kidneys. Spread of infection into posterior pararenal space with involvement of psoas and lateral extension into abdominal wall (*arrows*). **C**, Low in pelvis. Spread of infection into right groin (*arrow*).

laparotomy revealed a diffusely necrotic pancreas containing multiple bubbles of gas. *E. coli* was isolated from the cultures.

Case 3

S. A., a 67-year-old white woman, was transferred to Jackson Memorial Hospital in acute distress with a presumptive diagnosis of pancreatitis. About 2½ weeks after admission, she began complaining of nausea and vomiting. At that time her temperature was 40.6°C. An abdominal film was normal. Chest radiography revealed a left pleural effusion. A CT scan on hospital day 8 was felt to be consistent with a pancreatic abscess (fig. 3). Laparotomy revealed diffuse necrosis of the pancreas with intrapancreatic gas.

Case 4

T. C., a 55-year-old white male alcoholic, had a diagnosis of pancreatic abscess. Exploratory laparotomy with drainage of an abscess in the head of the pancreas was performed on day 2. One week after surgery, the patient's temperature rose to 39.4°C. An upper gastrointestinal examination demonstrated a narrowed second portion of the duodenum and retrogastric air bubbles, which were thought to be in the area of the pancreas. A CT scan confirmed a large collection of air in the head and body of the pancreas. Because of his reasonably stable clinical status, the patient was continued on antibiotic treatment and showed slow but steady improvement over the next several weeks. The patient was discharged in good condition, even though subsequent CT scans continued to demonstrate intrapancreatic air.

Case 5

L. J., a 60-year-old black woman, had abdominal pain and a history of pancreatitis. On admission she had a markedly elevated urinary amylase. An abdominal film at admission was normal. A CT scan on hospital day 5 was interpreted as consistent with either a pancreatic pseudocyst or abscess which had perforated into the second portion of the duodenum (fig. 4). A repeat abdominal film after the CT examination showed an abnormal collection of air in the upper abdomen, outside the bowel loops. The patient remained afebrile throughout her hospital stay making the diagnosis of a pancreatic abscess extremely unlikely. Unfortunately, before an upper gastrointestinal series could be performed to confirm the CT findings, the patient was discharged.

Discussion

The origin of bacterial contamination in the pancreas has not been definitely established. Current theories include invasion from infected bile, hematogenous seeding, spread along lymphatics from the gallbladder or colon, and right transmural passage of organisms from the transverse colon [3]. The most commonly cultured organisms are coliforms, *E. coli, Klebsiella,* and other enteric species. While gram-positive organisms may occasionally be seen, this is somewhat unusual. Frequently multiple organisms are recovered from pancreatic abscesses [4].

The abscess may remain confined to the pancreas or it may spread to adjacent organs within the anterior pararenal space. This may include either the ascending or descending colon depending on the site of infection. Infections arising in the head of the pancreas may also involve the duodenum or biliary tree [5]. Dissection along the ascending colon into the pelvis and eventually into the groin may occur (case 1). Although the infection may spread from the anterior to the posterior pararenal space, it generally does not involve the perirenal space, indicating that the intact perirenal fascia is a barrier against the spread of infection [6]. The process may also dissect anteriorly into the lesser sac from which it can spread to the subphrenic space, stomach, or intraperi-

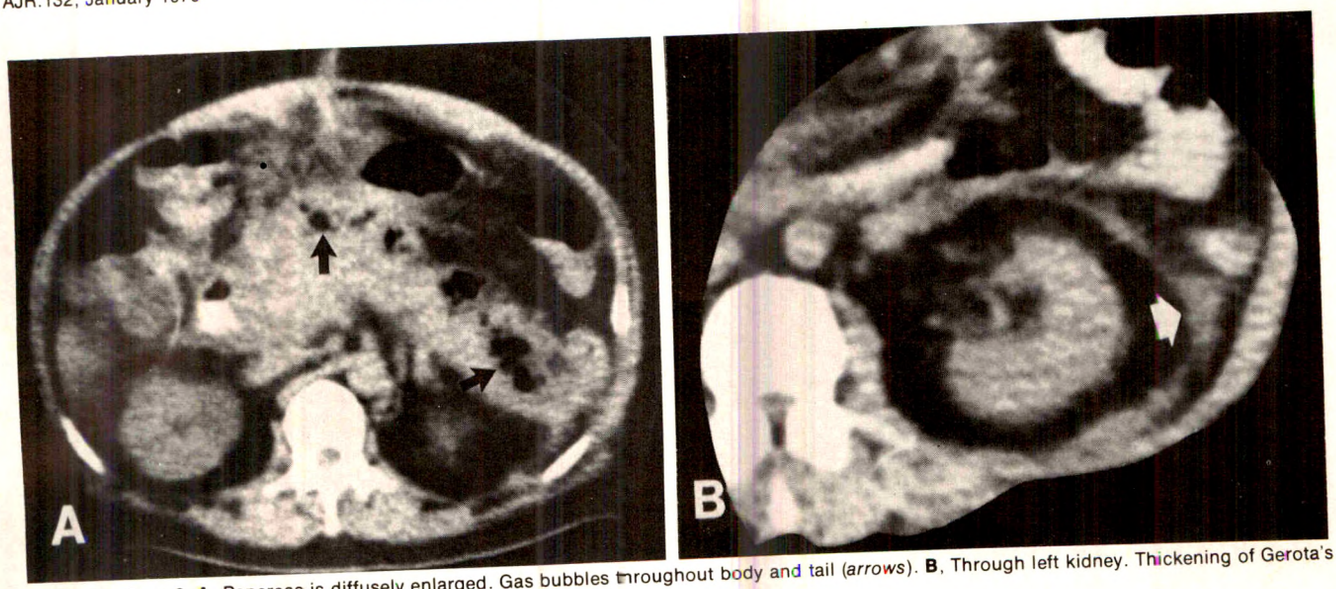


Fig. 2.—Case 2. **A**, Pancreas is diffusely enlarged. Gas bubbles throughout body and tail (*arrows*). **B**, Through left kidney. Thickening of Gerota's fascia and small amount of fluid in anterior pararenal space (*arrow*).

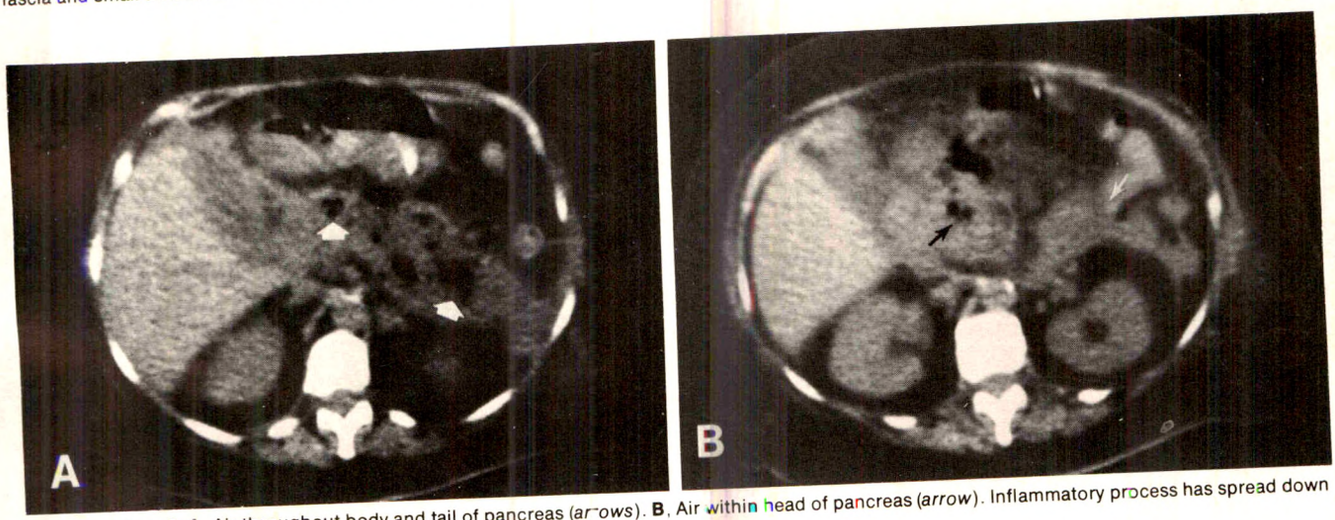


Fig. 3.—Case 3. **A**, Air throughout body and tail of pancreas (*arrows*). **B**, Air within head of pancreas (*arrow*). Inflammatory process has spread down anterior pararenal space in front of left kidney (*white arrow*).

toneally. Most perforations, rather than serving as useful drainage tracts, are generally associated with massive hemorrhage due to erosion into a major artery [7]. Perforations into the mediastinum, bronchi, and pleura have also been reported [2].

The CT findings of a pancreatic abscess have been described by Moss and Kressel [8]. They stated that pancreatic abscesses not containing gas usually have higher attenuation numbers and more variability in the attenuation coefficient than a pseudocyst. After intravenous contrast administration the walls of an abscess tend to increase significantly in density. In their experience, pancreatic abscesses tend to be somewhat more irregular in shape and have a thicker rim than a true pancreatic pseudocyst. However, since pancreatic abscesses frequently arise in preexisting pseudocysts, we have not found these signs to be completely reliable. When the process is localized to the pancreas and only a mass is seen on CT, the diagnosis can only be inferred from the clinical situation. In doubtful cases an aspiration under ultrasound or CT guidance may be diagnostic. The differentiation of a sterile phlegmonous pancreatitis from an early pancreatic abscess can at times be difficult.

In our series the most reliable sign of a pancreatic abscess was the presence of gas within the pancreatic parenchyma. In only one case could a true fluid collection be demonstrated. The seven remaining cases demonstrated only intrapancreatic gas and at surgery the pancreas was necrotic, but no well formed cavity was identified. CT is important not only in establishing the diagnosis but also in planning the surgical approach. It is helpful to be aware of the routes of spread of the pancreatic abscess prior to undertaking surgical intervention. After surgery, CT may be helpful in following the patient, although the presence of intrapancreatic air

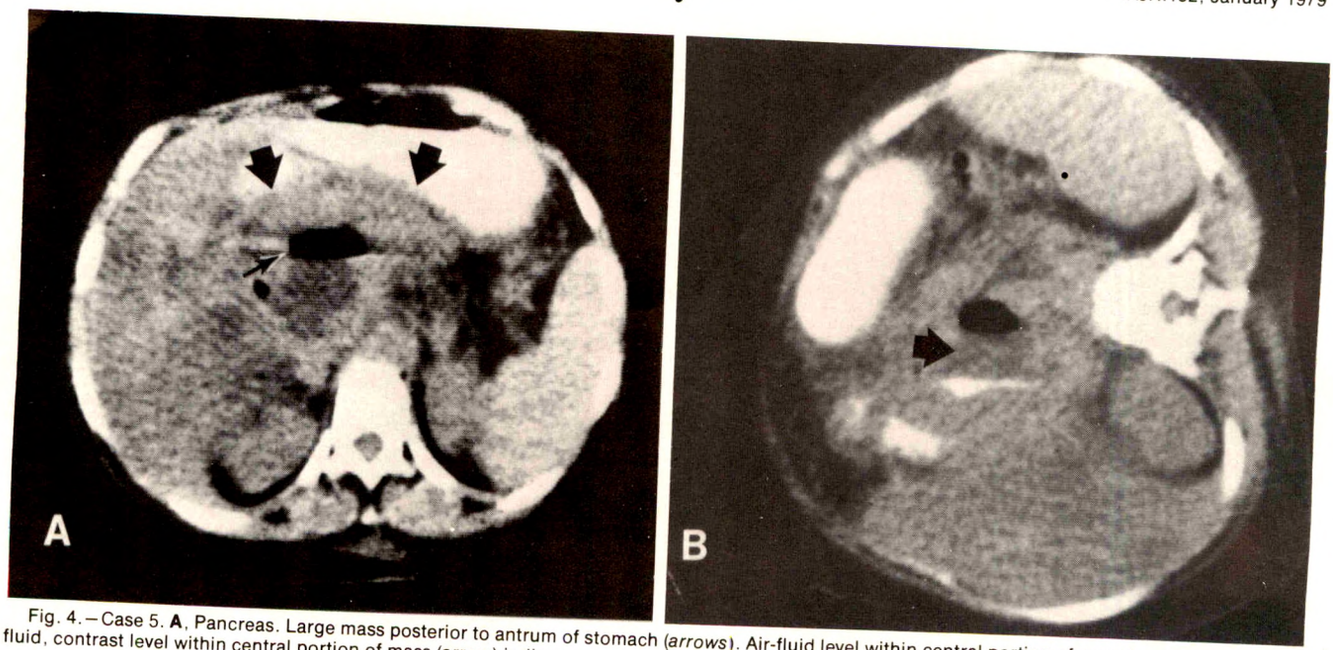


Fig. 4.—Case 5. **A**, Pancreas. Large mass posterior to antrum of stomach (*arrows*). Air-fluid level within central portion of mass (*small arrow*). **B**, Air, fluid, contrast level within central portion of mass (*arrow*) indicates communication with gastrointestinal tract.

postoperatively does not necessarily indicate a recurrent abscess.

ACKNOWLEDGMENT

We thank Cynthia Bellinger for secretarial assistance.

REFERENCES

1. Warshaw AL: Pancreatic abscesses. *N Engl J Med* 287:1234–1236, 1972
2. Altemier WA, Alexander JW: Pancreatic abscess, a study of 32 cases. *Arch Surg* 87:80–89, 1963
3. Warshaw AL: Inflammatory masses following acute pancreatitis. *Surg Clin North Am* 54:621–630, 1974
4. Carey LC: Acute and chronic pancreatitis. *Surg Clin North Am* 55:325–338, 1975
5. Farringer JL Jr, Robbins LB II, Pickens DR Jr: Abscesses of the pancreas. *Surgery* 60:964–970, 1966
6. Meyers MA: *Dynamic Radiology of the Abdomen.* New York, Springer, 1976
7. Berne TV, Edmonson HA: Colonic fistulization due to pancreatitis. *Am J Surg* 3:359–363, 1966
8. Moss AA, Kressel HY: Computed tomography of the pancreas. *Am J Dig Dis* 22:1018–1027, 1977

Neonatal Intestinal Opacification Secondary to Transplacental Passage of Urographic Contrast Medium

JEREMIAH KELLEHER,[1] PETER J. FECZKO,[1] MARY ANN RADKOWSKI,[1] AND N. THORNE GRISCOM[2]

Neonatal intestinal opacification in five infants (one set each of triplets and twins) after maternal excretory urography is described, and mechanisms leading to this phenomenon are discussed. Transplacental passage of urographic contrast medium with subsequent excretion by the fetal kidneys and possibly liver and small bowel seems to explain the radiographic appearance. Although the contrast medium probably does not harm the fetus, it should be distinguished from other more sinister causes of colonic opacification in the neonate.

Extrarenal excretion of urographic contrast medium is well recognized, and excretion by the liver [1], small bowel mucosa [2], and salivary glands [3] has been described. Such vicarious excretion can occur with either normal or impaired renal function [4]; it is probably related to blood levels and thus to the contrast medium dose administered. Transplacental passage of contrast medium producing a fetal pyelogram [5] and intrauterine opacification of the fetal small and large bowels after two maternal urograms on successive days [6] have been reported.

We report five infants, a set each of triplets and twins, whose mothers received intravenous contrast medium a few days before delivery. Abdominal radiography of these infants after delivery showed intestinal opacification due to the presence of contrast medium in the bowel. We believe this is the first documentation of this phenomenon in the literature.

Case Reports

Case 1

A white woman, 31 weeks pregnant with triplets, was admitted to Boston Hospital for Women in June 1975 complaining of left costovertebral angle pain and gross hematuria. Physical examination revealed pedal edema. There was no proteinuria; blood pressure was 130/90 mm Hg; blood urea nitrogen was 37 mg/dl, but rose to 53 mg/dl after 2 days; serum creatinine was 2.0 mg/dl. A single film 30 min after injecting 120 ml of Renografin-60 on the second day showed faint opacification of the maternal pelvicaliceal systems and bladder, but no evidence of stones or urinary obstruction. A clinical diagnosis of hemolytic-uremic syndrome was made.

Four days after excretory urography, triamniotic, trichorionic triplets were delivered by cesarean section. All three infants developed respiratory distress; chest and abdominal radiography revealed abnormal opacification of the small intestine and colon (fig. 1). The three infants had severe hyaline membrane disease, but two survived. Those two had normal bowel movements and easily cleared the abnormal opacities from their bowels.

Case 2

A 27-year-old white woman, 30 weeks pregnant with twins, was admitted to the University of Chicago Hospitals and Clinics in January 1978 with abdominal pain. During modified excretory urography 2 days later, 120 ml of Renografin-60 (34.5 g iodine) was injected intravenously. Blood urea nitrogen was normal at 12 mg/dl, and serum creatinine was slightly elevated at 1.5 mg/dl (normal, 0.5–1.4). Abdominal radiography 15 min after injection showed poor opacification of the maternal pelvicaliceal systems and, though both sides were slightly dilated, it was considered compatible with pregnancy; calculous obstruction was excluded.

Attempts to delay labor by intravenous isoxsuprene (Vasodilan, Mead Johnson Labs.) were abandoned, and twins (a male weighing 1,650 g and a female weighing 1,755 g) were delivered after 27 hr. Both developed respiratory distress and radiography within a few hours after birth confirmed the clinical impression of hyaline membrane disease. However, abnormal opacification of the small and large bowels (figs. 2 and 3A) was noted in both twins.

Both infants had normal bowel movements. Although abdominal radiography of the female infant 3 days after delivery showed almost total clearing of the abnormal colonic opacification, she died of severe hyaline membrane disease 1 day later. The male infant survived and serial radiography for 6 days after delivery showed persistent opacification of the colon, initially of the cecum and ascending colon and then progressing to the descending colon. The opacification seemed more dense with time, presumably because of further reabsorption of water (fig. 3B).

Discussion

Abnormal opacification of the neonatal bowel in the absence of orally or rectally administered contrast medium is unusual. Although routinely seen after amniography if the fetus is healthy [6], it is otherwise most often due to inspissated meconium secondary to bowel obstruction or atresia [7], or imperforate anus with rectourinary fistula [8]. Our cases showed a homogenous faint opacification of the colon unlike either the typical "bubbly" appearance of meconium or punctate calcification described with bowel atresia [8]. Though faint, the radiographic appearance resembled that of a water-soluble contrast enema.

There are several ways for maternal intravenous contrast medium to reach the fetus. It could pass across the placenta into the fetal circulation [9], be excreted by the fetal kidneys into the amniotic fluid [5], and then be swallowed by the fetus. Once in the fetal intestinal tract, it would be concentrated by resorption of water [10].

Received June 30, 1978; accepted after revision October 5, 1978.
[1]Department of Radiology (Box 429), University of Chicago, 950 East 59th Street, Chicago, Illinois 60637. Address reprint requests to J. Kelleher.
[2]Department of Radiology, Children's Hospital Medical Center, 300 Longwood Avenue, Boston, Massachusetts 02115.

0361-803X/79/1321-0063 $0.00

AJR 132:63–65, January 1979
© 1979 American Roentgen Ray Society

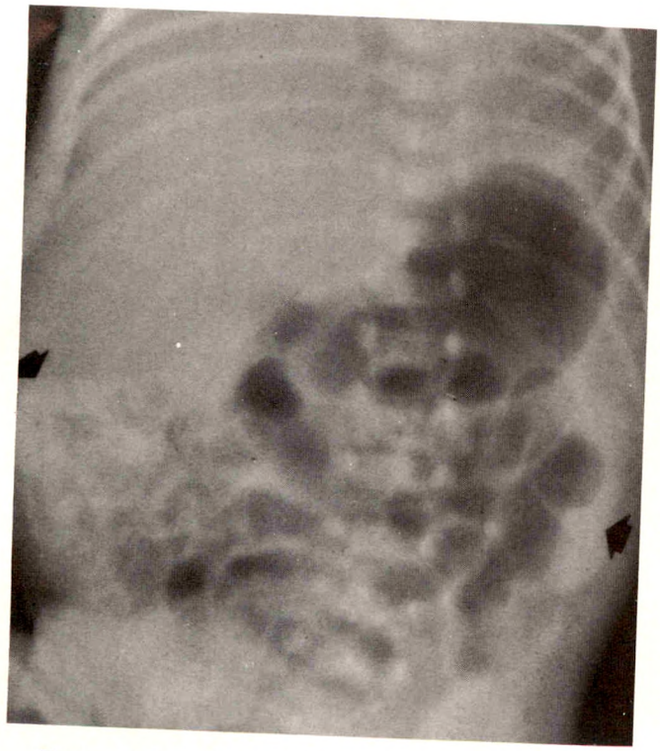


Fig. 1.—Triplet no. 2. Contrast medium within ileum and ascending and descending colon (*arrows*). Lungs show extensive changes of hyaline membrane disease. Similar radiographic findings were seen in other triplets.

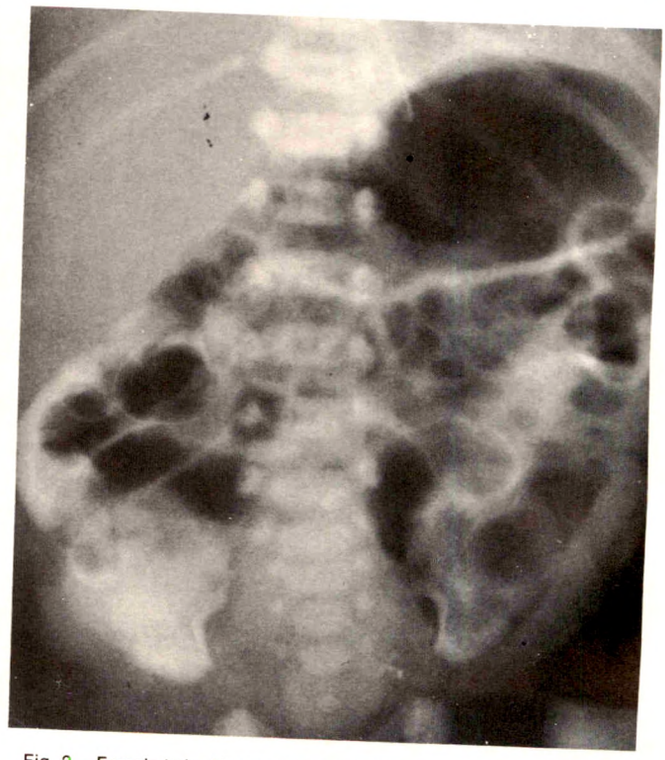


Fig. 2.—Female twin. Homogenous opacification of ascending colon.

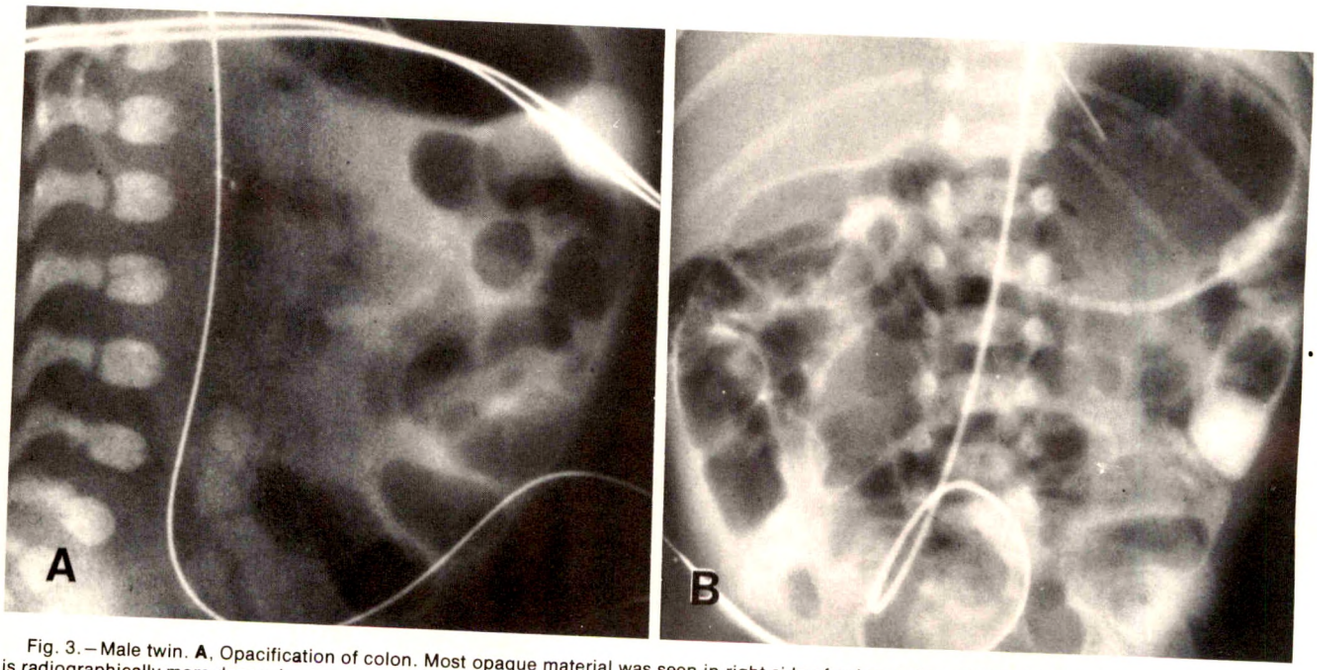


Fig. 3.—Male twin. **A**, Opacification of colon. Most opaque material was seen in right side of colon on frontal film. **B**, After 3 days contrast medium is radiographically more dense due to water resorption.

Less likely is that vicarious excretion by the fetal liver or gut occurs once the contrast is in the fetal blood stream. Alternatively, contrast medium from the maternal circulation may equilibrate directly into the amniotic fluid by transudation, and this fluid is then swallowed by the fetus.

It is not surprising that urographic contrast agents administered to the pregnant female pass to the fetal

circulation in view of the relatively low molecular weight of most urographic contrast media (molecular weight 614–809, Squibb, personal communication) and the known permeability of the placental barrier to molecules of this size [11]. Contrast medium in blood, though ionized, shows little protein binding, a factor which favors transplacental passage [11, 12].

These observations suggest that intravenous urographic contrast agents probably enter the fetal circulation whenever they are administered to the mother during pregnancy. The amount is probably related to the maternal blood level achieved and the duration of that level. No harmful effects of urographic contrast medium in utero have been reported, and it is unlikely that there was any damage in our cases. Two of the infants died from prematurity complications.

Diatrizoate compounds have been used for many years in amniography without reported complications. One study has shown that the lecithin-sphingomyelin ratio actually increases after administration of diatrizoate during amniography [13], but this is almost certainly an artifact due to interference by the agents in the estimation of the various amniotic fluid constituents. Even though our two cases occurred in multiple pregnancies, we believe multiple pregnancy does not cause this phenomenon; the effect has also been described in a single pregnancy complicated by ureteral obstruction [6].

With changes in pharmacology, intrauterine contrast examinations of the fetus might be possible after maternal injection, a subject that has been reviewed by one of us [6]. Furthermore, these cases are an added reminder that many drugs absorbed or injected into the maternal blood stream also reach the fetus, with largely unknown effects.

REFERENCES

1. Chamberlain MJ, Sherwood T: The extrarenal excretion of diatrizoate in renal failure. *Br J Radiol* 39:765–770, 1966
2. Salzman E, McClintock JT: Opacification of the small bowel with intravenously administered contrast medium. *Radiology* 80:748–751, 1963
3. Talner LB: Urographic contrast media in uremia. *Radiol Clin North Am* 10:421–432, 1972
4. Becker JA, Gregoire A, Berdon W, Schwartz D: Vicarious excretion of urographic media. *Radiology* 90:243–248, 1968
5. Thomas CR, Lang EK, Lloyd FP: Fetal pyelography—a method for detecting fetal life. *Obstet Gynecol* 22:335–340, 1963
6. Griscom NT: Possible radiological approaches to fetal diagnosis and therapy. *Clin Perinatol* 1:435–464, 1974
7. Martin CE, Leonidas JC, Amoury RA: Multiple gastrointestinal atresias, with intraluminal calcifications and cystic dilatations of bile ducts: a newly recognized entity resembling "a string of pearls." *Pediatrics* 57:268–271, 1976
8. Selke AC, Cowley CE: Calcified intraluminal meconium in a female infant with imperforate anus. *AJR* 130:786–788, 1978
9. Longo LD: Disorders of placental transfer, in *Pathophysiology of Gestation*, vol 2, edited by Assali NS, Brinkman CR III, New York, Academic Press, 1972
10. Berdon WE: Gastrointestinal activity and water absorptive capacity in the fetus, in *Diagnosis and Treatment of Fetal Disorders*, edited by Adamsons K, New York, Springer, 1969
11. Mirkin BL: Drug distribution in pregnancy, in *Fetal Pharmacology*, edited by Broeus LO, New York, Raven, 1973, pp 2–5
12. Cattell WR: Excretory pathways for contrast media. *Invest Radiol* 5:473–486, 1970
13. Knox E, Todd K, Cassady G: The effect of amniography on amniotic fluid L/S ratio. *Obstet Gynecol* 49:154–155, 1977

Scintiangiographic Diagnosis of Acute Mesenteric Venous Thrombosis

R. WESLEY SMITH[1] AND JOHN B. SELBY[2]

Scintiangiographic findings of prolonged mesenteric activity in a case of acute mesenteric thrombosis is described and 105 cases with abdominal scintiangiography are reviewed. Usual peak mesenteric blush occurred 5–15 sec after initial visualization of the aorta. Normal clearance of this activity was 15–30 sec. Future cases should confirm the importance of this observation in early diagnosis of mesenteric venous thrombosis.

Some lesions are often evaluated with ^{99m}Tc sulfur colloid liver-spleen imaging. Dynamic scintigraphy has primarily been used for differentiating vascular and avascular lesions involving the liver [1–4]. A case of portal, splenic, and superior mesenteric venous thrombosis is reported in which abdominal scintiangiography with a large field of view camera was useful in demonstrating the abnormality. To our knowledge, this has not been described before.

Case Material and Findings

Of 105 patients who had liver-spleen scans with flow studies at the Charleston Veterans Administration Hospital, visualization of a characteristic mesenteric "blush" was seen in 75. This appeared as a localized area of increased activity that was more than the expected renal "show-through." This blush was usually localized to the left mid and lower quadrants of the abdomen. Occasionally, right lower abdominal patterns were seen. The usual peak mesenteric blush determined from initial visualization of the abdominal aorta varied from 5 to 15 sec. Maximal clearance of activity from this region was 15–30 sec. Residual body background from recirculation contributed to a persistent low level of activity that did not interfere with interpretation. Visualization of the portal vein to the porta hepatis could sometimes be demonstrated, as well as an occasional splenic artery or vein and mesenteric veins. Less often, the inferior vena cava could be demonstrated, usually if the aorta was tortuous and deviated to the left (fig. 1A). Problems with visualization of mesenteric flow arose mainly from poor bolus injection, poor positioning, thin patients with marked renal "show-through," marked cirrhosis with ascites, and poor arterial filling of unknown cause. In patients with findings suggesting portal hypertension, such as hepatomegaly with patchy uptake, and splenomegaly with increased nuclide trapping, the scintiangiographic findings showed no clear pattern. The presence of ascites in these patients tended to diminish scintiangiographic quality, and normal patterns of mesenteric flow were frequently encountered. However, no patterns of persistent increased mesenteric activity were seen in this group.

Representative Case Report

A 49-year-old formerly alcoholic man was admitted with muscle weakness, dyspnea, increasing abdominal girth, weight loss, and a change in bowel habits over the previous month. Physical findings included a distended abdomen, hepatomegaly, and 4+ pedal edema. Laboratory tests revealed elevated alkaline phosphatase and decreased serum potassium and albumin. Total bilirubin was 1.1 mg/100 ml. Abdominal paracentesis revealed ascitic fluid with a markedly elevated amylase. Initial oliguria was subsequently controlled, and believed caused by hypovolemia from diarrhea and dehydration. Abdominal radiography demonstrated only ascites. Carcinoma of the pancreas was suspected, and a liver-spleen scan with scintiangiography was performed to exclude hepatic metastases.

The dynamic phase of the study consisted of 5 sec sequential scintiscans obtained after rapid intravenous injection of 4.5 mCi of ^{99m}Tc sulfur colloid with the patient supine and the camera positioned over the abdomen. With the large field of view camera, a low energy, all-purpose parallel hole collimator gives adequate area coverage with good quality and resolution. (A diverging collimator can be used with standard cameras, but will exhibit poorer resolution.)

An unexpected area of increased activity, or "blush," was revealed in the midabdominal area that lasted more than 50 sec after initial visualization of the aorta (fig. 1B). Subsequent static images demonstrated mild hepatomegaly and ascites without splenomegaly. The patient died of cardiorespiratory failure 5 days after admission. Autopsy revealed thrombosis of the superior mesenteric, portal, and splenic veins, chronic pancreatitis with pseudocyst formation, chemical peritonitis, and massive ascites (14) without gangrenous changes of the bowel.

Discussion

Mesenteric venous thrombosis is not rare and accounts for about 10% of bowel ischemia cases [5]. Portal vein thrombosis is often the origin of the more diffuse type of mesenteric venous thrombosis [6]. This type can lead to bowel infarction, although collateral development may preserve flow [5]. Splenoportography is required to exclude obstruction in preoperative evaluation of optimal shunt procedures [7, 8]. However, good success has been reported with superior mesenteric artery injection augmented with tolazoline [7].

Severe forms of mesenteric venous occlusion can occur with polycythemia and hypercoaguable states, carcinoma, portal hypertension, sepsis, tumor compression, direct injury, and contraceptive pills [9]. An agnogenic or spontaneous form, which is usually segmental,

Received June 6, 1978; accepted after revision October 5, 1978.

[1] Department of Radiology, Medical University of South Carolina, Charleston, South Carolina 29401. Present address: Department of Radiology, St. Francis Xavier Hospital, 135 Rutledge Avenue, Charleston, South Carolina 29403. Address reprint requests to R. W. Smith.

[2] Nuclear Medicine Service, Veterans Administration Hospital, Charleston, South Carolina 29403.

0361-803X/79/1321-0067 $0.00

AJR 132:67–69, January 1979

© 1979 American Roentgen Ray Society

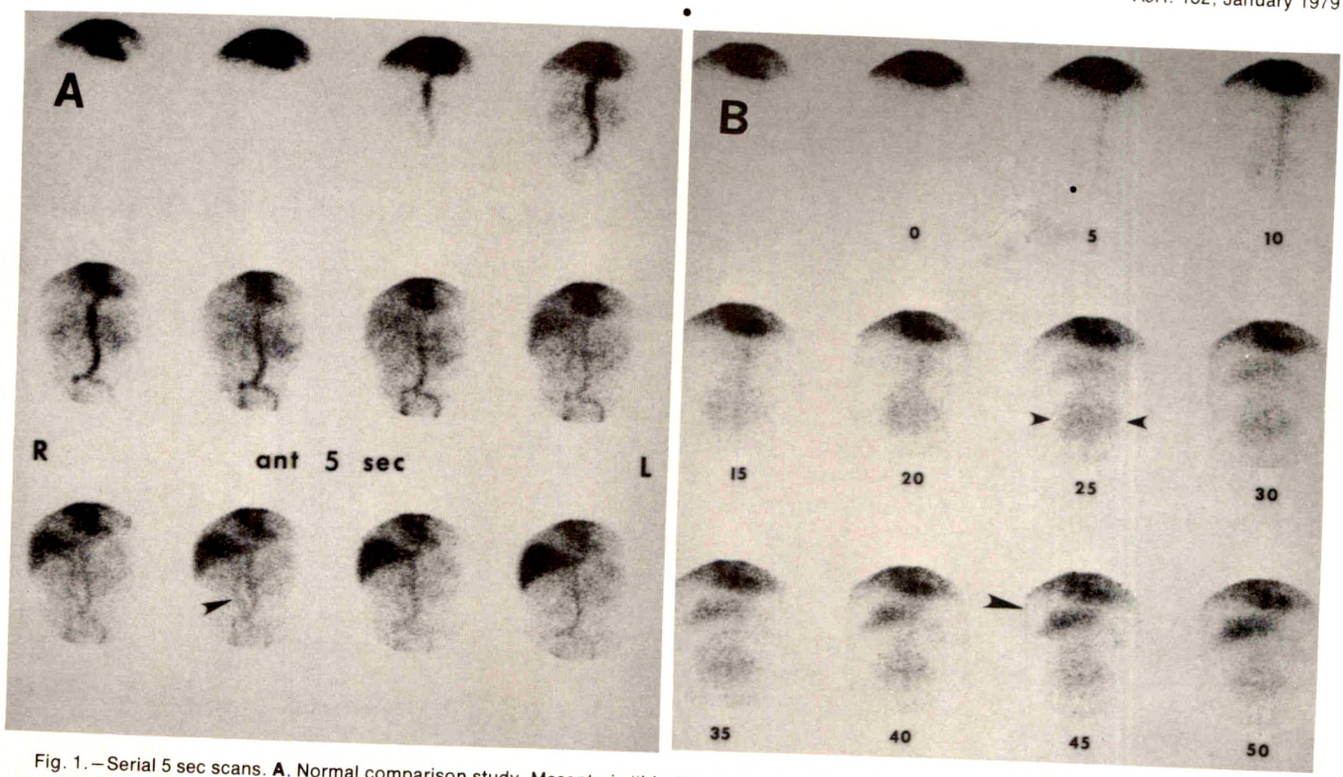


Fig. 1.—Serial 5 sec scans. **A**, Normal comparison study. Mesenteric "blush" with rapid disappearance by 30 sec after visualization of aorta; inferior vena cava is adjacent to tortuous aorta (*arrowhead*). **B**, Patient with mesenteric thrombosis. Persistent midabdominal "blush" (*small arrowheads*) up to 50 sec and evidence of ascites (*large arrowhead*).

has a gradual onset of poorly defined abdominal discomfort, anorexia, and changes in bowel habits over 7–10 days. In these instances, early diagnosis and appropriate intervention is essential if the high mortality rate of this disease is to be reversed [10, 11].

Radiographic plain film diagnosis of mesenteric venous occlusion has been well described [12–16]. A simple, quick, noninvasive procedure (e.g., mesenteric scintiangiography) may be useful, especially in critically ill patients, before subjecting them to more invasive procedures. To our knowledge, scintiangiographic findings in mesenteric venous occlusion have not previously been reported.

This case illustrates thrombotic occlusion of the superior mesenteric, portal, and splenic veins secondary to chronic pancreatitis, which in itself is a rare phenomenon [17]. The poorly defined symptomatology may have hindered diagnosis and appropriate treatment. The massive ascites was believed to be caused by chronic pancreatitis and chemical peritonitis [18], since portal hypertension alone is rarely a cause [19]. Despite the massive ascites, visualization of the mesenteric blush was not hindered, and was seen to occur within 20–25 sec in this patient, with little clearance throughout the duration of the flow study. This prolonged and increased radiocolloid activity correlates well with angiographic findings in mesenteric venous thrombosis with slow or absent flow on selective superior mesenteric arterial injection [12]. The etiology of the intense radiocolloid accumulation in this region is probably related to slow washout in acute stages prior to collateral development. The validity of this preliminary observation should be tested by future experience with similar cases. In patients with chronic occlusion of the mesenteric vein, collateral development would probably allow rapid clearance of the radiocolloid and a positive study would not be obtained.

With a dose of 4–5 mCi of ^{99m}Tc sulfur colloid useful information on the mesenteric venous drainage as well as the vascularity of liver-spleen lesions could be obtained. Therefore, we believe this should be routine protocol for liver-spleen imaging, especially if mesenteric venous thrombotic disease is suspected.

REFERENCES

1. Freeman LM, Mandell CH: Dynamic vascular scintiphotograph of the liver. *Semin Nucl Med* 2:133–138, 1972
2. Waxman AD, Apau R, Siemsen JK: Rapid sequential liver imaging. *J Nucl Med* 13:522–524, 1972
3. DeNardo GL, Stadalnik RC, DeNardo SJ Raventos A: Hepatic scintiangiographic patterns. *Radiology* 121:135–141, 1974
4. Stadalnik RC, DeNardo SJ, DeNardo GL, Raventos A: Critical evaluation of hepatic scintiangiography for neoplastic tumors of the liver. *J Nucl Med* 16:595–601, 1975
5. McDonald WC, Taylor HE, Johnstone FRC, Walsh GC, Bogoch A: Diseases of the liver, in *Gastroenterology*, edited by Bogoch A, New York, McGraw-Hill, 1973, pp 833
6. Spiro HM: Small intestinal disorders, in *Clinical Gastroenterology*, edited by Spiro HM, New York, McMillan, 1977, pp 449
7. Turcotte TG, Child CG: Ideopathic extrahepatic portal hypertension in adults. *Am J Surg* 123:35–42, 1972
8. Aldrete JS, Slaughter RL, Han SY: Portal vein thrombosis

resulting in portal hypertension in adults: *Am J Gastroenterol* 65:236–243, 1976
9. Williams LF: Vascular insufficiency of the intestines. *Gastroenterology* 61:757–777, 1971
10. Roberson G: Mesenteric venous occlusion. *J Arkansas Med Soc* 64:143–148, 1967
11. Naitove A, Weismann RE: Primary mesenteric venous thrombosis. *Ann Surg* 161:516–523, 1965
12. Clemett AR, Chang J: The radiologic diagnosis of spontaneous mesenteric venous thrombosis. *Am J Gastroenterol* 63:209–215, 1975
13. Hessen I: Roentgen examination in cases of occlusion of the mesenteric vessels. *Acta Radiol* (Stockh) 44:293–305, 1955
14. Nelson SW, Eggleston W: Findings on plain roentgenograms of the abdomen associated with mesenteric vascular occlusion with a possible new sign of mesenteric venous thrombosis. *AJR* 83:886–894, 1960
15. Wang CC, Reeves JD: Mesenteric vascular disease. *AJR* 83:895–908, 1960
16. Dunbar JD, Nelson SW: Nonangiographic manifestations of intestinal vascular disease. *AJR* 11:127–135, 1967
17. Longstreth GF, NewComer AD, Green PA: Extrahepatic portal hypertension caused by chronic pancreatitis. *Ann Intern Med* 75:903–908, 1971
18. Donowitz M, Kerstein MD, Spiro HM: Pancreatic ascites. *Medicine* (Baltimore) 53:183–195, 1974
19. Sherlock S: The portal venous system and portal hypertension, in *Diseases of the Liver and Biliary System*, edited by Sherlock S, London, Blackwell Scientific, 1975, pp 161

Chronic Impairment of Leg Muscle Blood Flow Following Cardiac Catheterization in Childhood

JAN ŠKOVRÁNEK[1] AND MILAN SAMÁNEK[1]

In 99 patients with congenital heart defects or chronic respiratory disease without clinical symptoms of disturbances in peripheral circulation, resting and maximal blood flow in the anterior tibial muscle of both extremities were investigated 2.7 years (average) after cardiac catheterization. The method used involved ^{133}Xe clearance. Resting blood flow was normal and no difference could be demonstrated between the extremity originally used for catheterization and the contralateral control extremity. No disturbance in maximal blood flow could be proved in the extremity used for catheterization by the venous route only. Maximal blood flow was significantly lower in that extremity where the femoral artery had been catheterized or cannulated for pressure measurement and blood sampling. The disturbance in maximal flow was shown regardless of whether the arterial catheterization involved the Seldinger percutaneous technique, arteriotomy, or mere cannulation of the femoral artery. The values in the involved extremity did not differ significantly from the values in a healthy population.

The reported incidence of disturbances in blood flow in the peripheral arterial bed after catheterization and angiography of the arterial system range from 0% to 100% [1–9]. The principal cause of this scatter is differences in the manner of determining such complications and their evaluation. Clinical investigation reveals only very crude disturbances of arterial patency. More sensitive methods include oscillometry [1, 5, 9–12] or the Doppler technique [12]. A more objective evaluation of disturbances in function which result from puncture catheterization or angiography is measurement of blood flow in the involved extremity [10–12]. Plethysmographic methods after catheterization have shown a significant decrease in blood flow to the calf, increased resistance, and decreased venous blood volume. Repair to these changes took about 1 week [10]. Unfortunately, measurement limited to resting blood flow does not reveal slight disturbances in blood supply [13–15] or inadequate blood supply during periods other than resting conditions.

We studied late disturbances in peripheral blood flow resulting from catheterization. The method allowed us to measure this parameter in any selected muscle, not only at rest but also with increased muscle demands on the blood supply. The investigated group included only those patients with congenital heart defects or with severe respiratory disease, in whom catheterization and angiocardiography had been carried out in childhood and in whom clinical investigation and, in suspect cases, oscillometry had not revealed any disturbance of blood flow to the lower extremity following the investigation. Because of discordant views on the incidence of complications related to arterial catheterization technique, we attempted to evaluate differences between the two basic technical approaches—percutaneous Seldinger technique and surgical insertion of the catheter. Two further subgroups were formed by patients in whom left heart catheterization was carried out transseptally and the femoral artery was not involved or only cannulated to measure pressure and sample blood.

Subjects and Methods

Muscle blood flow in the lower extremities was measured in 99 patients (52 male and 47 female) in whom cardiac catheterization had been performed between 2 months and 16 years of age (mean, 8.1 years). The mean age at the time of investigation of muscle blood flow was 10.8 years (range, 3–21 years). The shortest time interval from cardiac catheterization was 5 months; the longest, 11 years. The mean time interval between cardiac catheterization and investigation of muscle blood flow was 2.7 years.

In all cases cardiac catheterization had been indicated for diagnostic purposes, in 80 children for clinical suspicion of a congenital cardiac defect and in 19 for severe pulmonary disease. In 57 of these children we had demonstrated a congenital cardiac defect with a left-to-right shunt; in seven children, a right-to-left shunt. In the remaining 16 patients with congenital cardiac disease without a shunt, pulmonary artery stenosis and congenital mitral insufficiency predominated. The most frequent lung disease which served as an indication for cardiac catheterization and angiography was idiopathic interstitial pulmonary fibrosis and lung hypoplasia, followed in incidence by situations in which pulmonary resection had been done for bronchiectasis.

The investigated group included those patients in whom only vessels of one lower extremity were used for catheterization. In all patients we carried out complete catheterization of the right heart after introduction of the catheter percutaneously through the femoral vein by the Seldinger technique, and in children up to age 2 years, after surgical preparation of the saphenous vein. In 15 children only the venous route was used for cardiac catheterization without touching the femoral artery. However, in the majority of cases the femoral artery was involved. In 31 children, the femoral artery was only cannulated for the purpose of sampling arterial blood and measuring pressure. Puncture of the femoral artery in children younger than 1 year was carried out after previous surgical dissection of the superficial femoral artery, but percutaneously in the older children. In 36 patients the catheter was introduced in the femoral artery percutaneously using the Seldinger technique. Red and gray Kifa catheters (AB Kifa, Solna, Sweden) were used. If angiography using a closed-tip catheter was indicated, we began with arteri-

Received May 2, 1977; accepted after revision September 13, 1978.

[1] Cardiopulmonary Laboratory, Center of Pediatric Cardiology and Cardiac Surgery, University Hospital Motol, 150 06 Prague, Czechoslovakia. Address reprint requests to M. Samánek.

AJR 132:71–75, January 1979

© 1979 American Roentgen Ray Society

0361–803X/79/1321–0071 $0.00

TABLE 1
Catheterization by the Venous Route

Blood Flow	Reference Values (n = 60)		Lower Limb						
			Affected		Intact		Difference Affected to Intact		
	Mean	SD	Mean	SD	Mean	SD	%	t	P
Resting	3.2	1.7	3.3	1.6	4.0	2.4	−17.5	1.7630	NS
Maximal	78.6	27.0	92.3	33.9	88.0	25.0	+4.9	0.5491	NS

Note.—Data on 15 patients reported in milliliters per 100 g per minute. NS = not significant.

otomy. Later on, such a procedure was reserved for children only in the first year of life. This group included 17 patients after femoral arteriotomy.

Angiography formed a part of the investigation in all cases. The contrast material used was salts of substituted tri-iodinated benzoic acids (Conray 60%, Bracco/Industria Chimica S.p.A., Milan, Italy; Verografin 76%, Spofa/United Pharmaceutical Works, Prague, Czechoslovakia) in total dose of 1–4 mg/kg body weight.

All patients received 5–20 mg of Heparin (Spofa/United Pharmaceutical Works, Prague, Czechoslovakia). After removal of the cannula from the femoral artery, bleeding was prevented by several minutes of manual compression. After the Seldinger percutaneous puncture, this manual compression lasted longer than with needle puncture alone. After arteriotomy, manual compression was not carried out. In all cases the patients were returned to the ward after cessation of bleeding and we never applied a compressive bandage or sandbags as weight at the site of puncture.

Muscle blood flow was measured simultaneously in both lower extremities in reclining patients by means of ^{133}Xe muscle clearance. The solution of ^{133}Xe was injected into the anterior tibial muscle in a dose of 50–100 μCi in a volume of 0.1 ml. The clearance of the radionuclide was measured by two scintillation detectors containing 5 cm sodium-iodide thalium-activated crystals with cylindrical collimators 7 cm long (Duovigraph, Ateliers de constructions életriques de Charleroi, Charleroi, Belgium). The head of the collimator was located 10 cm over the region to be measured. By means of an analyzer-amplifier (ISN 10A, Ateliers de constructions életriques de Charleroi, Charleroi, Belgium) only the 81 keV emission was selected and recorded on a stripchart two-channel pen recorder (Recti/riter, Texas Instruments) at a paper speed of 3.75 cm/min. The time constant was 1 sec.

The wash-out curve of ^{133}Xe from the muscle during resting conditions was recorded for 15 min. Then cuffs placed around both thighs were inflated to pressure values of 200 torr, and the patients lifted a 1 kg weight attached to an ergometer. The rate of exercise was maintained at 60 strokes/min. After the occurrence of intensive ischemic pain in both lower extremities, usually after 3 min, the cuffs were rapidly deflated and the curves of decline of radioactivity in the phase of postischemic hyperemia were recorded. By using this method, maximal muscle blood flow is reached in all cases [16, 17].

Muscle blood flow is calculated [16]:

$$\dot{Q}_M = 100 \cdot \lambda \cdot \frac{1n\ 2}{T^{1}/_{2}} / \text{ml/100 g/min/},$$

where $\dot{Q}_M$ is muscle blood flow, λ is muscle-to-blood partition coefficient corrected for hematocrit [18], and $T^{1}/_{2}$ is the time interval during which the clearance curve in a semilog plot decreased to one half of the initial value. For calculation of resting flow, values of $T^{1}/_{2}$ were put into the equation as read off from the clearance curves recorded at rest. For calculation of maximal muscle blood flow we used values of $T^{1}/_{2}$ from curves obtained during postischemic hyperemia. The details of this measurement are presented elsewhere [13, 14, 17]. Differences measured between the catheterized and the intact extremity were evaluated for each patient separately by a paired t test. As reference values we used the values of 60 measurements in 54 young patients (30 male and 24 female), obtained by the same technique [14]. The mean age of this control group was 11 years (range, 5–17 years). The significance of differences of mean values in the separate groups from reference values was evaluated by Student's t test.

Results

Catheterization, Venous Route, Without Touching Femoral Artery

The venous route of inserting a catheter was used in 15 children (nine boys and six girls) without cannulation or puncture of the femoral artery. The mean age at time of the investigation was 5.3 years (range, 4 months to 14 years). The mean age at investigation of muscle blood flow was 8.3 years (range, 4.5–17 years). The mean time interval from catheterization was 3.0 years (range, 8 months to 11 years).

Resting muscle blood flow was normal in both extremities (table 1). Maximal muscle blood flow in the catheterized extremity did not differ from that in the control contralateral extremity. Both values were within the limits of the normal range.

Catheterization or Cannulation of Femoral Artery

Blood flow to the anterior tibial muscle was evaluated first in the entire group of 84 patients without regard to the methods of catheterization (table 2).

Resting muscle blood flow in the catheterized extremity did not differ from that in the control extremity. Values measured in both lower extremities in these patients also did not differ from the normal control group. Maximal muscle blood flow in the catheterized extremity was significantly lower than in the control extremity ($P < 0.001$), whereas values of maximal muscle blood flow on the catheterized side did not differ significantly from the norm. Values measured in the control extremity were raised over the norm ($P < 0.02$).

Femoral arteriotomy (table 3). From a group of 84 patients, 17 (eight boys and nine girls) had retrograde

TABLE 2

Catheterization or Cannulation of the Femoral Artery

Blood Flow	Reference Values (n = 60)		Lower Limb				Difference Affected to Intact		
			Affected		Intact				
	Mean	SD	Mean	SD	Mean	SD	%	t	P
Resting	3.2	1.7	3.2	1.9	3.4	2.2	−5.9	0.9122	NS
Maximal	78.6	27.0	75.1	25.7	90.1*	29.1	−16.7	6.0286	<0.001

Note.—Data on 84 patients reported in milliliters per 100 g per minute. NS = not significant.
* Difference from reference values $P < 0.02$.

TABLE 3

Femoral Arteriotomy

Blood Flow	Reference Values (n = 60)		Lower Limb				Difference Affected to Intact		
			Affected		Intact				
	Mean	SD	Mean	SD	Mean	SD	%	t	P
Resting	3.2	1.7	3.4	2.6	4.1	3.6	−17.1	1.2736	NS
Maximal	78.6	27.0	64.4	29.8	94.9	39.6	−32.2	4.3944	<0.001

Note.—Data on 17 patients reported in milliliters per 100 g per minute. NS = not significant.

TABLE 4

Percutaneous Seldinger Technique

Blood Flow	Reference Values (n = 60)		Lower Limb				Difference Affected to Intact		
			Affected		Intact				
	Mean	SD	Mean	SD	Mean	SD	%	t	P
Resting	3.2	1.7	3.6	1.9	3.4	1.5	+5.9	0.4799	NS
Maximal	78.6	27.0	73.4	21.7	79.2	20.9	−7.4	2.0670	<0.05

Note.—Data on 36 patients reported in milliliters per 100 g per minute. NS = not significant.

catheterization through the femoral artery after surgical preparation and arteriotomy. After the investigation, the artery was sewn with atraumatic sutures and subsequently both proximal and distal segments of the artery were observed to determine if they were normally patent. The mean age of the patients at time of the catheterization was 4.5 years (range, 2 months to 16 years). The mean time interval from catheterization to investigation was 4.2 years (range, 2–7 years). The mean age at muscle blood flow investigation was 8.7 years (range, 3–21 years). In 16 cases the arteriotomy was on the right side, and in one case, on the left.

Resting muscle blood flow in both lower extremities did not differ from one another. There were also no differences from the healthy normal control group. Maximal muscle blood flow in the catheterized extremity was significantly decreased when compared with the control extremity in the same patient ($P < 0.001$). However, the lower values on the catheterized side and the higher values on the control side did not differ from the normal control group.

Percutaneous Seldinger catheterization of the femoral artery (table 4). The Seldinger technique of introducing a catheter into the femoral artery was used in 36 patients (18 boys and 18 girls). The mean age at catheterization was 10.5 years. The youngest patient was 3 and the oldest 15 years of age. The mean time interval from catheterization was 2.8 years (range, 8 months to 7 years). The mean age of this group at investigation of muscle blood flow was 13.4 years (range, 5–19 years). In 31 cases, catheterization involved the right femoral artery, in 5 cases, the left.

Resting muscle blood flow on the catheterized side did not differ from values on the other or from healthy controls. Maximal muscle blood flow in the muscles on the catheterized side in comparison with the contralateral side was significantly decreased ($P < 0.005$). The values from either side did not differ from the healthy normal controls.

Cannulation of the femoral artery (table 5). Venous catheterization with needle or cannula puncture of the femoral artery for blood sampling and pressure measurements was carried out in 31 patients (17 boys and 14 girls) of mean age 8.7 years (range, 4–15 years). The time

TABLE 5
Cannulation of Femoral Artery

Blood Flow	Reference Values (n = 60)		Lower Limb				Difference Affected to Intact		
			Affected		Intact				
	Mean	SD	Mean	SD	Mean	SD	%	t	P
Resting	3.2	1.7	2.7	1.4	3.0	1.7	−10.0	1.3489	NS
Maximal	78.6	27.0	82.9	26.0	100.1*	27.0	−17.2	4.6257	<0.001

Note.—Data on 31 patients reported in milliliters per 100 g per minute. NS = not significant.
* Difference from reference values $P < 0.001$.

interval from catheterization was 1.5 years on the average. The shortest interval was 5 months, the longest, 4 years. The mean age at investigation of muscle blood flow was 10.2 years (range 5–17 years). In 29 cases the right femoral artery was punctured, in the remainder, the left.

Resting muscle blood flow in both anterior tibial muscles did not differ from another or from the normal control group. Maximal muscle blood flow on the catheterized side was significantly lower than on the control side ($P < 0.001$).

Maximal muscle blood flow in the individual patients. Decrease in the maximal muscle blood flow in the catheterized limb higher than 25% of the control value was found in 33% of the 84 patients studied after catheterization or cannulation of the femoral artery (table 6). The highest incidence was found after femoral arteriotomy, the lowest after percutaneous Seldinger catheterization of the femoral artery. Reduced maximal blood flow was also shown in a high percentage of patients after cannulation of the femoral artery. There was no significant difference in the participation of main types of congenital heart diseases or respiratory diseases between patients with a significant reduction in maximal muscle blood flow and the others.

Correlation of the measured-deviation of maximal muscle blood flow from the control value with the age of the patient at the time of catheterization or with the time interval from catheterization to the investigation was statistically insignificant. We also did not prove any relation between the size and type of catheter used and the relative decrease in maximal muscle blood flow.

TABLE 6
Significant Decrease in Maximal Muscle Blood Flow

Catheterization Technique	No. Patients	Decrease in Maximal Blood Flow*	
		No.	%
Arteriotomy	17	11	65
Seldinger	36	6	17
Cannulation	31	11	35
Total	84	28	33

* More than 25% from the control value.

Discussion

These results show that resting muscle blood flow is not affected by interference with the femoral vein and artery during cardiac catheterization and angiocardiography. This finding is in agreement with the report of Vyden et al. [10] who used a different measuring technique. The measurement of resting blood flow alone is not suitable for revealing disturbances of blood supply to the muscles of the extremity. This is shown by the fact that normal values of resting blood flow can be measured even with complete tying-off of an artery supply an extremity, such as in the Blalock-Taussig operation [13] or in patients with obliteration of arteries of the lower extremity of various etiology [15]. A very different situation occurs when the tissue demands in the lower extremity for blood supply are increased. Measurement of maximal blood flow produced by muscle exercise under ischemic conditions has shown significant differences between mean values in the extremity on which there was interference with a femoral artery in comparison with extremities with an intact arterial system.

The analysis of the individual data has confirmed the tendency which was revealed by testing the average values among three groups, differing in terms of the methods used during catheterization. Since the oldest patient was 21 years at the time of investigation, there is a strong probability that atherosclerosis did not play a role in these changes of blood flow, and the latter are related to the manipulation with the artery.

There is still lack of agreement on the problem of the relation between complications following catheterization and the catheterization technique used. Mortensen [6] stressed the advantages of arteriotomy over the Seldinger technique; Hohn and Crenen [5] maintained the opposite view. The present results of a significantly decreased maximal flow in ischemic exercise-induced hyperemia show that this change occurs both after the percutaneous Seldinger technique and after arteriotomy. The decrease of blood flow, expressed in the percentage of a control value, was more pronounced after arteriotomy than after the Seldinger technique.

It was most surprising that a disturbance in maximal blood flow could be shown even in those cases in which the femoral artery was only cannulated without a catheter having been introduced. These findings indicate that even the simple procedure of cannulation can have the same negative long-term sequelae. It can be argued that puncture, in addition to damage to vessel wall, can also

alter arterial blood flow by changes in the area of the puncture associated with hematoma, which more or less always accompanies any arterial puncture. These changes around the site of a puncture can be manifest in particular when the artery is punctured after surgical preparation.

Since in all cases included in the present series the great saphenous vein was dissected or the femoral vein entered percutaneously, we can assume that such procedures in the immediate area of the femoral artery could also play a role in the development of blood flow disturbance. The role of venous catheterization itself without interference with the femoral artery in disturbances of blood supply to tissues of the lower extremity was shown to be negligible. In patients in whom only catheterization through the saphenous or femoral vein had been carried out, disturbances of blood supply to the muscles of the affected extremity were not revealed at rest or after ischemic exercise. The present results convincingly show the worsened condition in blood flow to the extremities on the side where the femoral artery was catheterized or punctured, as compared with the contralateral extremity with intact vessels.

The increased mean value of maximal blood flow in the intact extremity (89.77 ± 28.38 ml/100 min, $P < 0.02$) in the present series (99 patients) in comparison with reference values can be explained by the high proportion of congenital heart disease with a left-to-right shunt in the total patient group. Previous work has shown that in such cases maximal muscle blood flow is highly significantly increased [20]. Also differences in mean values of maximal blood flow in the intact extremity among the groups, differing in terms of the method used during catheterization, can be explained by uneven representation of respiratory disease and hemodynamically different types of congenital heart defects in the various groups.

From the view of potential functional disturbances, it is fortunate that the blood flow in the involved extremity did not differ significantly from normal values. From this point of view, we did not show any difference among the groups following arteriotomy, percutaneous catheterization, or puncture of the femoral artery. It can therefore be argued that disturbances in blood flow, seen after a mean time interval of 2.7 years after catheterization, should not produce any defect of function of the involved extremity in patients with respiratory diseases or congenital heart diseases without a left-to-right shunt. After repair of the malformation in the latter patients, disturbances in the muscle blood supply may appear in response to increased tissue demands. Our findings should stimulate the search for a method which would minimize these problems and their potential clinical sequelae.

REFERENCES

1. Berman MA, Fishbone G: Femoral arteriography after percutaneous left heart catheterization in infants and children. *Circulation* 45, 46 (suppl 2):II-131, 1972
2. Beckmann CH, Dooley B: Complications of left heart angiography. A study of 1,000 consecutive cases. *Circulation* 41:825–832, 1970
3. Hauf G, Amplatz K: Complication rates of transfemoral and transaortic catheterization. *Surgery* 63:594–596, 1968
4. Kirkpatrick SE, Takahashi M, Petry EL, Stanton RE, Laurie PR: Percutaneous heart catheterization in infants and children. II. Prospective study of results and complications in 127 consecutive cases. *Circulation* 42:1049–1056, 1970
5. Hohn AR, Craenen J: Arterial pulses following percutaneous catheterization in children. *Pediatrics* 43:617–620, 1969
6. Mortensen JD: Clinical sequelae from arterial needle puncture, cannulation, and incision. *Circulation* 35:1118–1123, 1967
7. Izukawa T, Varghese PJ, Rowe RD: Topical papaverine in arteriotomies in infants and children: effect on incidence of thrombosis. *J Pediatr* 72:853–854, 1968
8. White JJ, Talbert JL, Haller JA Jr: Peripheral arterial injuries in infants and children. *Ann Surg* 167:757–766, 1968
9. Real FJP, Scarpelli EM, Ruttner N, Rudolph AM: Arteriotomy and local circulation in children: the value of oscillometry. *J Pediatr* 69:372–377, 1966
10. Vyden JK, Nagasawa K, Graettinger W, Spencer HS, King B: The effect of transfemoral catheterization on blood flow in the extremities. *Circulation* 50:741–746, 1974
11. Jacobson B, Paulin S, Schlossman D: Thromboembolism of leg following percutaneous catheterization of femoral artery for angiography. Symptoms and signs. *Acta Radiol [Diagn]* (Stockh) 8:97–108, 1969
12. Barnes RW, Hafermann MD, Peterson J, Krugmire RB Jr, Strandness DE Jr: Noninvasive assessment of altered limb hemodynamics and complications of arterial catheterization. *Radiology* 107:505–511, 1973
13. Škovránek J, Goetzová J, Šamánek M: Changes in muscle blood flow and development of the arm following the Blalock-Taussig anastomosis. *Cardiology* 61:131–137, 1976
14. Goetzová J, Škovránek J, Šamánek M: Muscle blood flow in children measured by ^{133}XE-clearance method. *Cor Vasa* 19:161–164, 1977
15. Lindbjerg I, Munck O, Lassen NA: Skeletal muscle blood flow determined by intramuscular injection of xenon-133 in *Radioaktive Isotope in Klinik und Forschung*, vol 6, edited by Fellinger K, Höfer R, Munich, Urban & Schwarzenberg, 1965, pp 222–231
16. Lassen NA, Lindbjerg J, Munck O: Measurement of bloodflow through skeletal muscle by intramuscular injection of xenon-133. *Lancet* 1:686–689, 1964
17. Šamánek M, Goetzová J, Fišerová J, Škovránek J: Differences in muscle blood flow in upper and lower extremities of patients after correction of coarctation of the aorta. *Circulation* 54:377–381, 1976
18. Corman LA, Flickinger FW, Sokoloff J, Nodine JH: Radioactive xenon tissue clearance: standardization for measurement of peripheral blood flow. *J Nucl Med* 11:233–238, 1970
19. Jacobson B, Schlossman D: Thrombolism of leg following percutaneous catheterization of femoral artery for angiography. Predisposing factors. *Acta Radiol [Diagn]* (Stockh) 8:109–118, 1969
20. Škovránek J, Šamánek M, Goetzová J: Blood flow through muscles of the extremities in congenital heart defects (in Czech), *Cas Lek Cesk* 116:1080–1084, 1977

Role of Radionuclide Imaging in Osteoid Osteoma

ROBERT LISBONA[1, 2] AND LEONARD ROSENTHALL[1]

Radiophosphate bone scans readily disclosed osteoid osteomas in 20 symptomatic patients, including nine patients whose radiographic findings had been negative. In five of the nine patients adjuvant radiogallium imaging was performed, and four showed a disproportionately low uptake relative to radiophosphate. When this occurs, osteoid osteoma can be distinguished from subacute osteomyelitis, which is particularly helpful if the radiograph is equivocal. Radiophosphate bone imaging's generally accepted excellent sensitivity in disclosing obscure symptom-producing focal bone disorders makes it the screening procedure of choice, especially if osteoid osteoma is considered in the differential diagnosis. Only abnormal areas need to be radiographed to add specificity and more precise delineation.

Osteoid osteomas have certain well recognized radiographic features. The characteristic appearance is a small central nidus that is usually radiolucent, although occasionally it is calcified. It generally exhibits a sclerotic reaction and cortical thickening in the surrounding bone, reflecting the histology of an osteoid nidus with immature, irregularly mineralized trabeculae of nascent bone forming in a substrate of highly vascularized osteogenic connective tissue. The adjacent host bone microscopically exhibits slightly thickened to densely sclerotic bone.

However, the interval between onset of symptoms and radiographic diagnosis may last up to 2 years or more. During this time radiographs may be normal, or the changes are too subtle and escape detection even with tomography [1, 2]. There have been scattered case reports on the excellent sensitivity of radiophosphate imaging in disclosing and localizing osteoid osteomas [3–6].

We studied 20 patients with histologically proved osteoid osteomas who had both radionuclide and radiographic studies prior to surgery. This rather large radionuclide experience with osteoid osteoma stemmed from the difficulty encountered in radiographically determining a lesion's existence, particularly in areas like the axial skeleton, wrist, femoral neck, and tarsus. Also, nondescript radiographic lucencies were frequently of questionable significance relative to the patient's symptomatology. Because radionuclide bone imaging discloses the bony metabolic reaction to an active disorder, sound theoretical reasoning predicts it would be sensitive to the presence of a symptom-producing osteoid osteoma, regardless of its radiographic features. This proved to be true in this series.

Materials and Methods

Seven osteoid osteomas were found in the axial skeleton, four in the femur, five in the tibia, and one each in the tarsal navicular, cuboid, trapezium, and ulna (table 1). Block resection of the lesion and histology substantiated osteoid osteoma in all patients.

The 20 patients, 7–28 years old, were imaged with ^{99m}Tc methylene diphosphonate (^{99m}Tc-MDP). The dose was scaled down in the pediatric group according to the relationship $A(X + 1)/(X + 7)$, where A denotes the adult dose (20 mCi) and X the child's age. Scanning was started 2 hr or more after intravenous delivery of ^{99m}Tc-MDP.

Five of the 20 patients were also imaged with ^{67}Ga-citrate after the ^{99m}Tc-MDP study. A 5 mCi ^{67}Ga-citrate adult dose (again reduced depending on age) was intravenously administered and the area of interest scanned 24 or 48 hr after injection.

In order to present the results in the context of the patient's clinical investigation, only the nucleographic and radiographic diagnoses in the patient's hospital records are detailed in table 1.

Results

Positive ^{99m}Tc-MDP nucleograph was obtained in each of the 20 patients (table 1). By contrast, plain films of the area of interest identified a lesion in only 11 of the 20 patients on original interpretation. Failures occurred in the axial skeleton, wrist, tarsus, and femoral neck. Tomography disclosed most of the missed lesions, except for two patients, one with osteoid osteoma in the articular facet of L3 and one, the tarsal navicular. These patients underwent surgery based on a strongly positive bone scan and characteristic symptomatology. Excluding the subcapsular femoral neck (case 8), routine radiography readily identified osteoid osteomas in the long bones, and since all bone scans were strongly positive, tomography was usually not performed.

Of the five patients studied with ^{67}Ga-citrate, four had minimal concentration within the confines of the lesion. The fifth patient demonstrated a significant accumulation of ^{67}Ga-citrate that in some respects resembled osteal infection [8].

Representative Case Reports

Case 2: Osteoid Osteoma of T5 Pedicle

A 10-year-old boy complained of having pain in the left scapula for 4 months. Initial radiography only demonstrated a scoliosis. The patient was reexamined after 7 months for persistent scapular pain, which then intensified at night and was relieved

Received March 14, 1978; accepted after revision August 28, 1978.

[1] Division of Nuclear Medicine, Montreal General Hospital, 1650 Cedar Avenue, Montreal, Canada H3G 1A4. Address reprint requests to L. Rosenthall.

[2] Present address: Royal Victoria Hospital and Jewish General Hospital, Montreal, Canada.

AJR 132:77–80, January 1979

© 1979 American Roentgen Ray Society

0361–803X/79/1321–0077 $0.00

TABLE 1
Summary of Cases

Case No.	Site	Age and Sex	Duration of Symptoms	Bone Scan	Plain Films	Tomography
1	C3 pedicle	18, M	1 yr	+	–	+
2	T5 pedicle	10, M	4 mo	+	–	+
3	T10 pedicle	19, M	6 mo	+	–	+
4	L3 facet	28, F	2 yr	+	–	–
5	L4 transverse process	18, F	4 mo	+	+	+
6	L4 pedicle	7, M	2 mo	+	+	+
7	L4 pars interarticularis	17, M	8 mo	+	–	+
8	Femoral neck	7, M	1 yr	+	–	+
9	Femur, distal	21, M	3 mo	+	+	ND
10	Femur, distal	19, M	8 mo	+	+	ND
11	Femur, distal	11, M	1 yr	+	+	ND
12	Tibia, proximal	17, F	1 yr	+	+	ND
13	Tibia, proximal	21, M	8 mo	+	+	ND
14	Tibia, distal	8, M	3 mo	+	+	+
15	Tibia, distal	21, M	1 yr	+	+	ND
16	Tibia, distal	12, F	4 mo	+	+	ND
17	Tarsal navicular	11, M	3 mo	+	–	–
18	Cuboid	20, F	6 mo	+	–	+
19	Trapezium	19, F	6 mo	+	–	+
20	Ulna	25, M	3 mo	+	+	+

Note.—+ = positive study; – = no abnormalities; ND = not done.

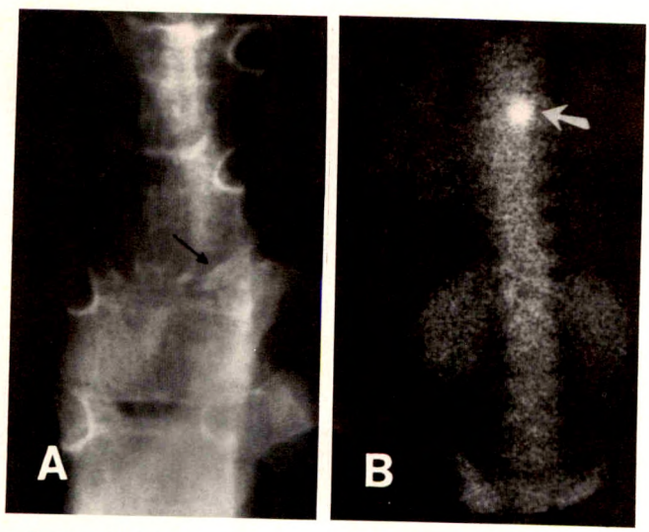


Fig. 1.—Case 2, osteoid osteoma of T5 pedicle. **A**, Lesion (*arrow*). **B**, ^{99m}Tc-MDP scan demonstrating scoliosis and intense concentration in osteoid osteoma (*arrow*).

by aspirin. Radiography (fig. 1A) showed further scoliosis and also suggested an abnormal T5 pedicle. The ^{99m}Tc-MDP scan (fig. 1B) was strongly positive, as were ensuing tomograms.

Case 8: Subcapsular Femoral Neck Osteoid Osteoma

A 7-year-old boy complained of left hip pain atypical of osteoid osteoma for over a year. Radiography (fig. 2A) showed some osteopenia of the left hip region. Radiophosphate images (fig. 2C) depicted an intense abnormal concentration in the left femoral capital epiphysis, neck, and intertrochanteric region, while radiogallium scan showed only a slightly higher uptake than normal. This combination mitigates against an infectious process. Tomography (fig. 2B) of the left hip after the radionuclide study disclosed a nidus partially encompassed by a rim of bony sclerosis.

Case 11: Osteoid Osteoma of Distal Right Femur

An 11-year-old boy complained of pain in the area of the distal right femur for about 1 year. Lateral and anterior radiography (fig. 3A) of the right limb showed bony sclerosis and cortical thickening in the distal diaphysis. There was a possible small radiolucent nidus, but tomography was not performed for elucidation. Abnormal concentrations were found with ^{99m}Tc-MDP and ^{67}Ga images (fig. 3B), similar to subacute osteomyelitis (fig. 4).

Comparison Case: Subacute Osteomyelitis of Proximal Tibia

A 13-year-old boy complained of local pain, not entirely unlike that encountered in osteoid osteoma. Radiography (figs. 4A and 4B) depicted sclerosis and thickened cortex in the proximal diaphysis. No definite nidus could be identified, although a nondescript radiolucent seam was seen in lateral projection. The ^{99m}Tc-MDP scan (fig. 4C) demonstrated abnormal concentration in the corresponding area that indicated an active process, and the degree of enhanced ^{67}Ga uptake was interpreted as compatible with an osteomyelitis (cf. fig. 3). The patient underwent surgery on the presumed diagnosis of osteoid osteoma, but a nidus was not found. Gross and histologic features suggested subacute osteomyelitis. Treatment was by curettage; since causative organism was not found, no antibiotics were postoperatively administered.

Discussion

Our experience with radiophosphate imaging in osteoid osteomas clearly attests to its exquisite sensitivity in disclosing the presence of an active bone process, regardless of radiographic appearance. All 20 patients depicted a patently abnormal concentration at the site of

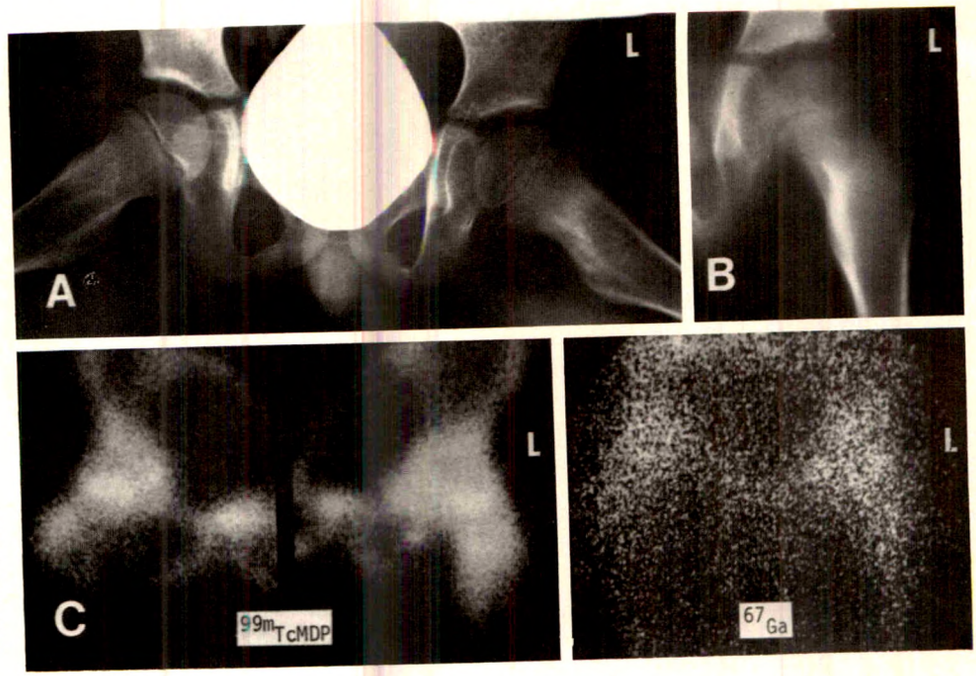


Fig. 2.—Case 8, osteoid osteoma in left femoral neck. **A**, Osteopenia of left hip region. **B**, Nidus and some reactive sclerosis. **C**, Markedly enhanced uptake in left femoral capital epiphysis, neck, and intertrochanteric zone with ^{99m}Tc-MDP, while ^{67}Ga scan exhibits only slightly higher uptake.

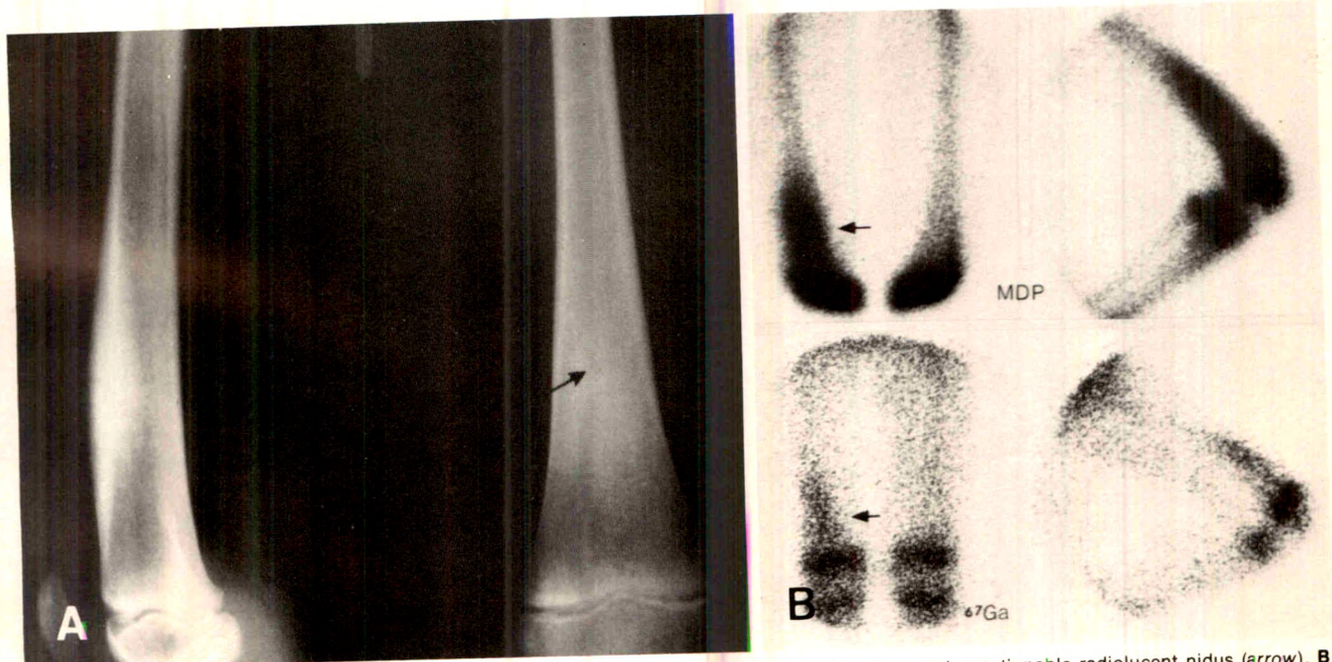


Fig. 3.—Case 11, osteoid osteoma of distal femoral diaphysis. **A**, Sclerosis, cortical thickening, and questionable radiolucent nidus (*arrow*). **B**, Abnormal concentration similar to subacute osteomyelitis in figure 4.

the osteoid osteoma, whereas corresponding radiographic appearances varied from normal to characteristic features. A report [7] of a densely sclerotic lesion, allegedly an osteoid osteoma, was negative by bone scan, but no mention was made whether the lesion was symptomatic.

Subacute osteomyelitis (fig. 4) can be difficult to radiographically distinguish from osteoid osteoma, and supplemental ^{67}Ga imaging may be helpful. Radiogallium is known to concentrate in inflamed bone [8], and we found that osteoid osteomas are associated with a little or low-grade uptake, despite an intense radiophosphate deposition in four of five cases; thus, the two entities can be distinguished provided the radiogallium concentration is minimal. The studies must be clinically interpreted since very low gallium uptakes are also registered in fractures, infarctions, chronic osteomyelitis, and acute osteomyelitis under treatment with antibiotics [8, 9].

Although not reviewed specifically here, radiophosphate bone scanning has proven useful in ruling out an

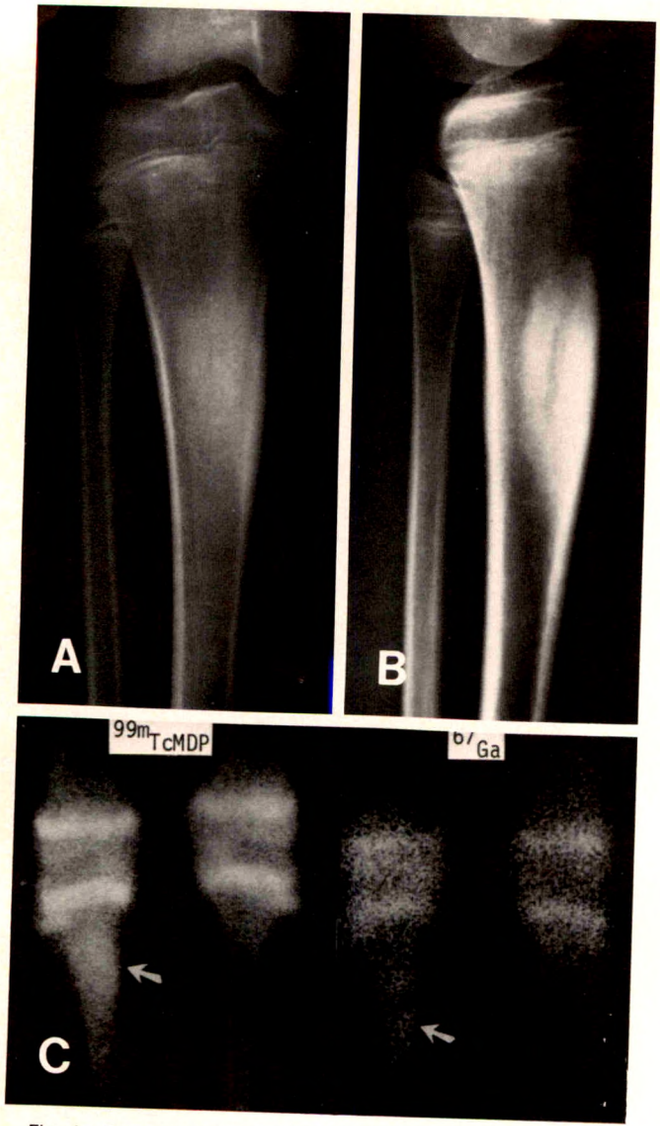


Fig. 4.—Comparison case, subacute osteomyelitis of right proximal tibia. Frontal (**A**) and lateral (**B**) radiographs showing sclerosis and cortical thickening apparently containing radiolucent seam. **C**, Enhanced uptake in corresponding area.

active process when there is a coincidental occurrence of pain and a featureless lucency or sclerosis at radiography.

Experience with radiophosphate bone imaging in general (in malignant disease, infection, infarction, trauma, etc.), in addition to osteoid osteoma, has proved it to be very sensitive, but equally nonspecific, in detecting lesions. The primary noninvasive screening procedure for skeletal pathology is understandably radiophosphate scanning, whether for osteoid osteoma or any other focal disorder. A normal study virtually excludes the presence of an active symptom-producing process, particularly osteoid osteoma. Statistics support the use of radiography adjuvant to nucleography, and not the reverse, and if a single screening procedure for an obscure symptom-producing bone lesion is preferred, it is nucleography. Fewer negative and superfluous radiographic examinations will result. An area abnormal by scan should be radiographed, including tomography if necessary, to characterize the lesion and add specificity.

An alternate scheme, of radiographing the patient initially, often results in unnecessary duplication and marginal benefit. If a characteristic lesion is found, radiophosphate bone scanning is unnecessary. If a nondescript bone change is present, a bone scan is needed to establish whether it is active and, if so, whether it is unifocal or multifocal. In addition, negative radiography requires radionuclide bone imaging to disclose an occult lesion, particularly in regions such as the axial skeleton, wrists, feet, and subcapular portions of the femurs. Failing tomographic detection of the active process, the scan can still aid in directing surgical intervention, as occurred in two of our patients (cases 4 and 17).

REFERENCES

1. Orlowski JP, Mercer RD: Osteoid osteoma in children and young adults. *Pediatrics* 59:526–532, 1977
2. Editorial: Osteoid osteoma. *Br Med J* 3:395–396, 1975
3. Gilday DL: Diagnosis of obscure childhood osteoid osteomas with bone scan (abstr). *J Nucl Med* 15:494, 1974
4. Winter PF, Johnson PM, Hilal SK, Feldman F: Scintigraphic detection of osteoid osteoma. *Radiology* 122:177–178, 1978
5. McCombs RK, Olson WH: Positive ^{18}F bone scan in a case of osteoid osteoma. *J Nucl Med* 16:465–466, 1975
6. Gore DR, Mueller HA: Osteoid osteoma of the spine with localization aided by ^{99m}Tc-polyphosphate bone scan. *Clin Orthop* 113:132–134, 1975
7. Telfer N: Nuclear medicine in the management of musculo skeletal tumors. *Orthop Clin North America* 9:1011–1021, 1977
8. Lisbona R, Rosenthall L: Radionuclide imaging in septic joints and their differentiation from periarticular osteomyelitis and cellulitis in pediatrics. *Clin Nucl Med* 2:337–343, 1977
9. Majd M: Radionuclide imaging in early detection of childhood osteomyelitis and its differentiation from cellulitis and bone infarction. *Ann Radiol* (Paris) 20:9–18, 1977

"Step-off" Vertebral Body: Gaucher's Disease Versus Sickle Cell Hemoglobinopathy

ALAN M. SCHWARTZ,[1] MARC J. HOMER,[2] AND ROY G. K. McCAULEY[1]

Two patients with Gaucher's disease and radiographic findings in the spine similar to sickle cell hemoglobinopathy are reported, making a total of four known patients with Gaucher's disease who have these steplike vertebral endplate deformities. Serial films of a patient having Gaucher's disease compared with patients having sickle cell hemoglobinopathy suggest that different events lead to formation of the vertebral deformities. In Gaucher's disease, there is an initial collapse of the entire vertebral body with subsequent growth recovery peripherally. In sickle cell hemoglobinopathy, the endplate deformity is nontraumatic and is caused by an underlying growth arrest.

Introduction

The "H" or "step-off" vertebra is considered characteristic of sickle cell hemoglobinopathy [1–4]. The vertebral configuration is a central depression with an abrupt transition to the more normal periphery. It is different from the "cod-fish" or "fish-mouth" vertebra, in which a smooth, concave depression of the endplate extends from corner to corner, secondary to collapse of usually osteopenic bone (e.g., senile osteoporosis).

Occasional reports indicate the "step-off" deformity is not limited to sickle cell disease. Hansen and Gold [5] recently reported that a patient with Gaucher's disease had central depression of the vertebral endplates similar to sickle cell hemoglobinopathy. We found one other documented case [6] and Moseley [2] anecdotally referred to a third case. In one report [7] the "step-off" vertebra was seen in a patient with thalassemia major and in another it was seen in two patients without hemoglobinopathy [8]. In the latter report, one patient had hereditary spherocytosis; the other, osteopenia. Both had very minimal radiographic changes.

In 1966 Reynolds [3] hypothesized that circulatory stasis and ischemia retard growth in the central portion of the vertebral cartilaginous growth plate in sickle cell anemia. The periphery of the growth plate, with a different blood supply [13], continues to grow at a more normal rate, resulting in the characteristic "step-off" de-

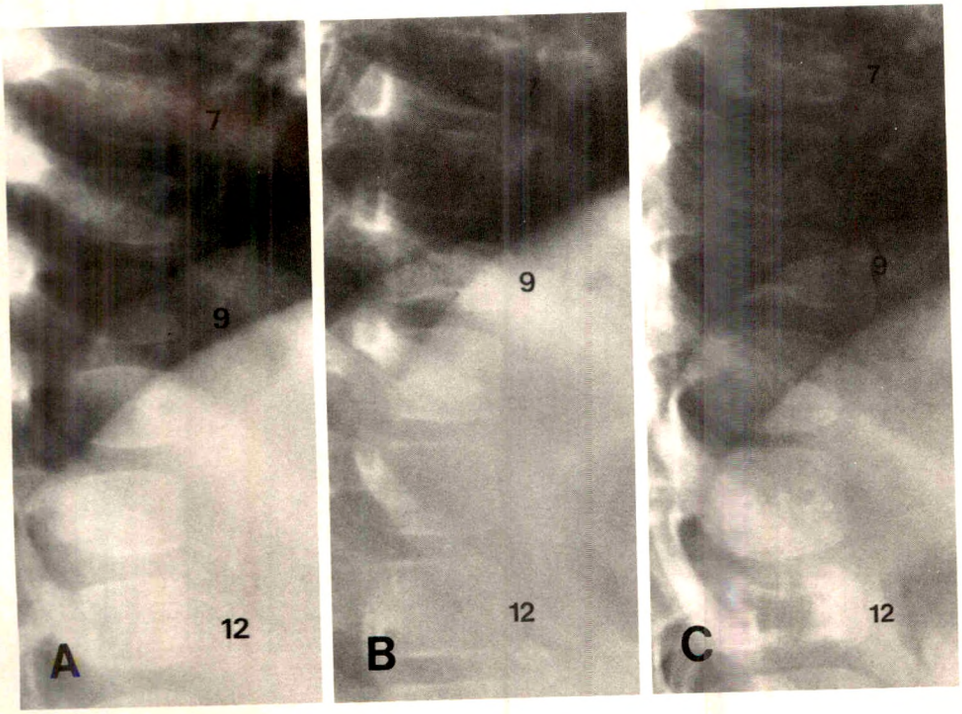


Fig. 1.—Patient with Gaucher's disease showing dorsal spine T7–T12. **A,** At age 2½. **B,** At 8½, there is rectangular collapse of T9 with beginning "step-off" formation. **C,** At 11, T7 and T9 show collapse with "step-off" vertebral formation; T12 shows collapse with reactive sclerosis parallel to endplates.

Received April 28, 1978; accepted after revision October 9, 1978.
[1]Department of Radiology, Boston Floating Hospital, Tufts New England Medical Center Hospital, 171 Harrison Avenue, Boston, Massachusetts 02111. Address reprint requests to A. M. Schwartz.
[2]Department of Radiology, Pratt Diagnostic Clinic, Tufts New England Medical Center Hospital, Boston, Massachusetts 02111.

0361-803X/79/1321-0081 $0.00

AJR 132:81–85, January 1979
© 1979 American Roentgen Ray Society



Fig. 2.—T12 in same patient as fig. 1, age 14½, showing "bone within a bone" appearance caused by sclerotic densities parallel to vertebral contours.

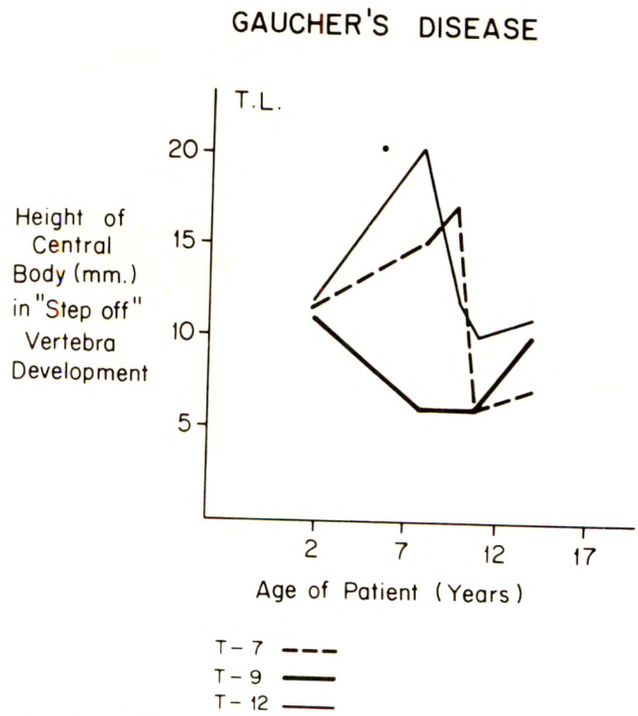


Fig. 3.—Collapse of central bodies in Gaucher's disease with slight growth recovery; collapse not limited to central portions, but more growth recovery occurred peripherally with radiographic appearance of "step-off" vertebrae.

formity. However, there were no sequential films with direct measurement to support this theory.

This paper tests Reynold's theory that central endplate depressions are due to growth arrest by studying the sequence of events in two patients with Gaucher's disease and two patients with sickle cell hemoglobinopathy who have "step-off" vertebral deformities.

Subjects and Methods

We reviewed the records of the two patients with Gaucher's disease. In one, serial films showed progressive disease over 10 years. We also reviewed the records of seven other patients with Gaucher's disease (five adults and two children), but none showed similar changes in the spine. For comparison, we reviewed the records of 16 patients with either homozygous sickle cell disease, sickle cell beta-thalassemia, or sickle-C disease. In two of the seven with radiographic spinal changes of sickle cell hemoglobinopathy, serial films showed definite progressive changes. In one of these initial films were normal.

Fine pointed calipers were used to measure changes in height over time of the central vertebral bodies in the three patients with serial changes. Although it is possible that slightly different points were measured on successive examinations in the same patient, the central vertebral endplate depressions were flat enough so that this was not a significant problem.

Results

The patient with Gaucher's disease had been filmed over a 12-year period (figs. 1–3). Three vertebral bodies were easily measurable and comparable. Initial films from 1965 were normal (fig. 1A). Each of the vertebral bodies involved showed an initial collapse with some central growth recovery (figs. 1B and 1C). However, initial collapse was not limited to the central endplates; the entire vertebral body was involved. As the "step-off" vertebral bodies were formed, there was simply less growth centrally than peripherally. In all three instances, the initial visible event was of collapse or fracture (fig. 3).

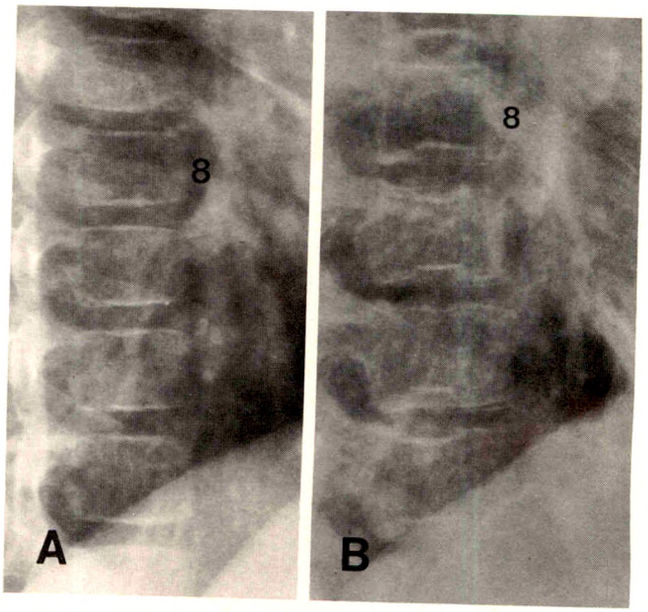


Fig. 4.—Sickle cell beta-thalassemia. **A**, Age 7, normal spine. **B**, Age 14, multiple areas of typical central depression.

One patient with sickle cell beta-thalassemia had early normal films of the spine. In films spanning 6 years (fig. 4), there was at most, 1 mm of diminished height (fig. 5) versus 6–10 mm difference in the patient with Gaucher's disease. The 1 mm difference could be related to differences in projection or error in measurement. The abnor-

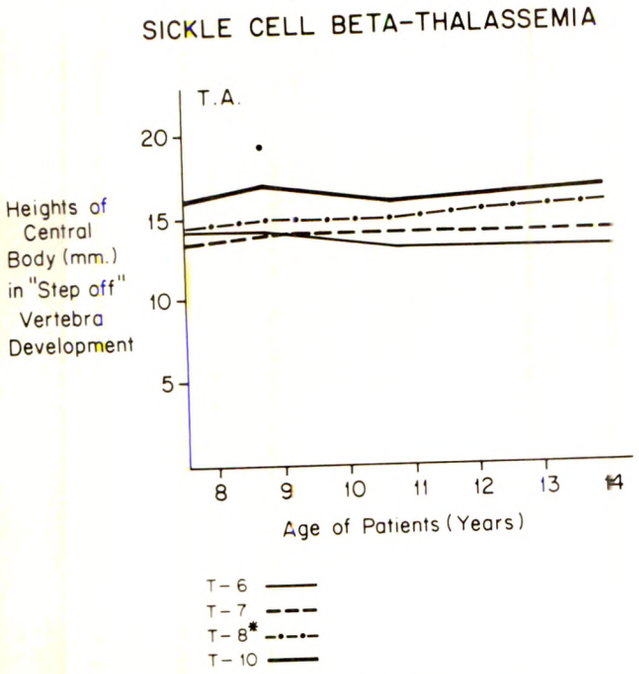


Fig. 5.—Same patient as fig. 4 showing flat curves compared to Gaucher's disease. Height loss of 1 mm possibly secondary to differences in projection and errors in measurement, rather than collapse. One normal endplate and 2 mm growth in T8.

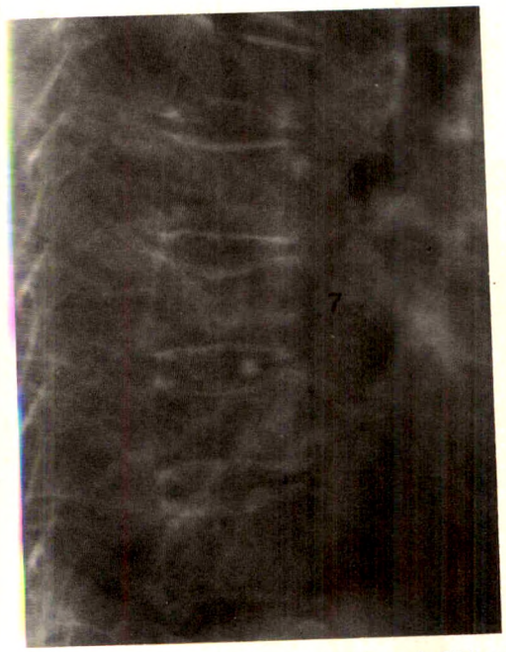


Fig. 6.—Sickle cell beta-thalassemia; only T5 has definite "step-off" vertebral appearance on one endplate and shows steady growth. T7 and T9 have more concave appearance of compression fractures and show height loss. T8 not measured but also shows biconcave compression.

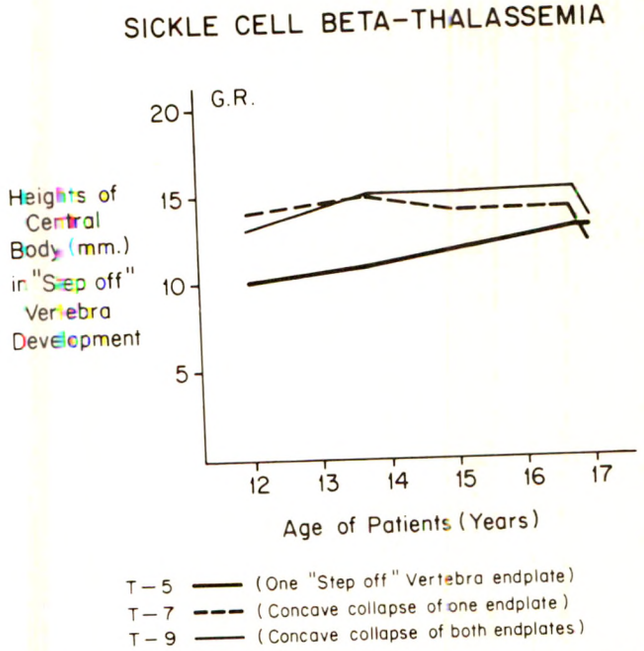


Fig. 7.—Same patient as fig. 6; variable curves reflect variable radiographic appearances.

mal vertebral body that showed some continued growth (T8) had only one vertebral endplate with a "step-off" deformity; the other appeared normal and could have had normal growth. Rather than the dramatic collapse or fracture of Gaucher's disease, there was simply a growth arrest of the central endplate with continued peripheral growth resulting in the central depression. The other patient with sickle cell beta-thalassemia had more variable radiographic appearances and measurements (figs. 6 and 7).

Discussion

Though the "step-off" vertebra in Gaucher's disease is similar to the vertebral deformities of sickle cell hemoglobinopathies, the pathogenesis seems different. nitial collapse of the entire vertebral body is followed by differential growth recovery. In addition, though the "step-off" vertebral body is radiographically similar, other radiographic qualities are sometimes different. In our two patients with Gaucher's disease and in the patient reported by Hansen and Gold [5], there was reactive sclerosis parallel to the endplates in some of the vertebral bodies.

In one vertebral body in each of our patients with Gaucher's disease, there was both horizontal and vertical sclerosis giving a "bone within a bone" appearance (figs. 2 and 8). Modeling defects sometimes present in adjacent vertebral endplates were probably due to alteration of forces on adjacent vertebral discs and cartilaginous growth plates and resulted in growth disturbances.

The reactive sclerosis somewhat resembles a healing infarct, supported by the fact that all four of the reported patients with "step-off" vertebral bodies had other areas of aseptic necrosis. Perhaps infarction of the entire vertebral body weakens the bone, which then collapses under normal weight-bearing forces. As a result of differences in blood supply to the central portions of the body and the periphery, more growth recovery occurs in the periphery.

Reynolds [3] hypothesized that circulatory stasis and

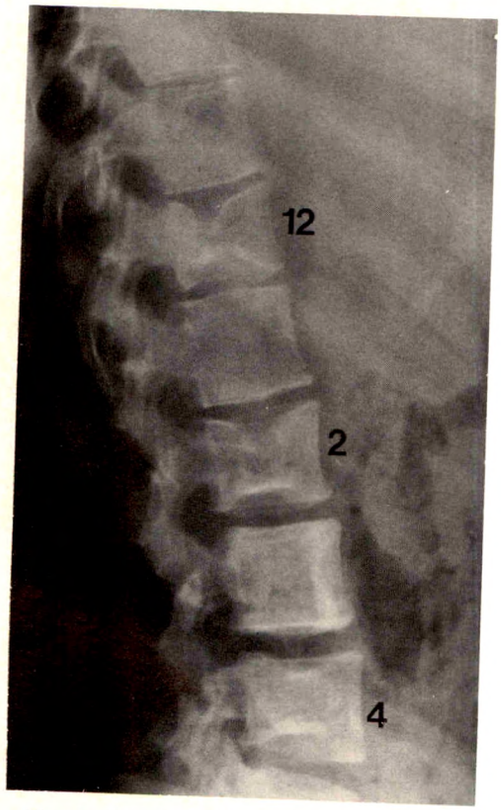


Fig. 8.—Gaucher's disease in 37-year-old male showing deep depression and sclerosis of T12. L2 has "bone within a bone" appearance and L3, which has recovered enough to have normal shape, exhibits linear sclerosis. L4 has "step-off" vertebral appearance. Even at birth, central vertebral body is larger than deepest depression in T12. Some collapse must have occurred, since Gaucher's disease victims have normal spines at birth.

ischemia cause growth retardation in the central portion of a cartilaginous vertebral endplate in sickle cell anemia. He compared the cartilaginous growth plate of a vertebral body to the epiphyseal plate of a long bone, which when injured in toto (e.g., by radiation) resulted in oddly shaped epiphyses and cupped metaphyses with greater growth peripherally. Similar to a long bone metaphysis, the central portion of the vertebral body and adjacent cartilaginous growth plate receives its blood supply from nutrient arteries, which are radially distributed and have a long course through the marrow (fig. 9) [13]. The periphery of the growth plates are supplied by short perforating periosteal arteries, so that sickling and its effects might be more pronounced in the central portions.

Reynolds et al. [4] found a gross correlation between the level of hemoglobin S in erythrocytes and skeletal changes. All five of their patients with hemoglobin S levels greater than 77% had characteristic bone changes, while those with less than 67% had no bone changes. Patients with levels between 67% and 77% formed a mixed group. Since bone changes of homozygous sickle cell disease and sickle cell beta-thalassemia are identical, it is tenable to apply the findings in our sickle cell

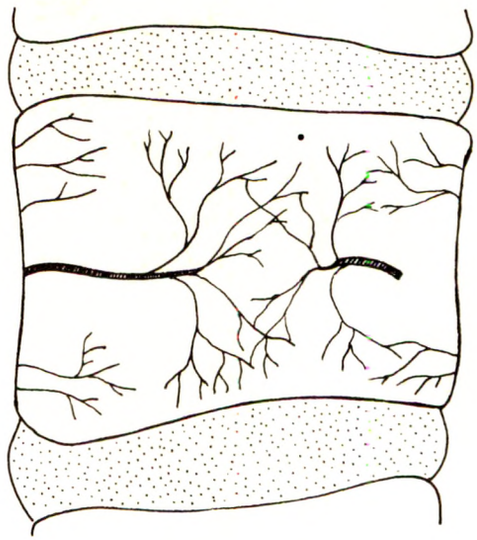


Fig. 9.—Single vertebral body with adjacent discs; central body and growth plates supplied by radially distributed vessels, while periphery supplied by short periosteal branches.

beta-thalassemia patients to those with homozygous sickle cell disease. This is further supported by the hemoglobin S levels in sickle cell beta-thalassemia. The thalassemia gene suppresses the synthesis of normal beta chains required for hemoglobin A. As a result, the percentage of hemoglobin S in the sickle cell beta-thalassemia red blood cells increases.

In the production of the "step-off" deformity in our patients with sickle cell hemoglobinopathy, there was no initial collapse, but simply a failure of growth centrally that confirmed Reynold's theory. There was no evidence of the infarction, sclerosis, or collapse of Gaucher's disease.

While the exact incidence of the "step-off" vertebra in Gaucher's disease is unknown [2, 5, 9–12], we suspect that it may be more common than anticipated if a large series of patients were examined specifically for this radiographic finding. Our two patients make a total of four cases documented in the literature.

ACKNOWLEDGMENT

We thank Nancy Martin for help in typing the manuscript and preparing the graphs.

REFERENCES

1. Carroll DS: Roentgen manifestations of sickle cell disease. *South Med J* 50:1486–1490, 1957
2. Moseley JE: Skeletal changes in the anemias. *Semin Roentgenol* 9:169–184, 1974
3. Reynolds J: A re-evaluation of the "fish vertebra" sign in sickle cell hemoglobinopathy. *AJR* 97:693–707, 1966
4. Reynolds J, Pritchard JA, Ludders D, Mason RA: Roentgenographic and clinical appraisal of sickle cell beta-thalassemia disease. *AJR* 118:378–400, 1973
5. Hansen GC, Gold RH: Central depression of multiple verte-

bral endplates: a "pathognomonic" sign of sickle hemoglobinopathy in Gaucher's disease. *AJR* 129:343–344, 1977
6. Junghagen S: Rontgenologische Skelettveranderungen bei morbus Gaucher. *Acta Radiol* 5:506–516, 1926
7. Cassady JR, Berdon WE, Baker DH: The "typical" spine changes of sickle cell anemia in a patient with thalassemia-major. *Radiology* 89:1065–1068, 1967
8. Rohlfing BM: Vertebral endplate depression: report of two patients without hemoglobinopathy. *AJR* 128:599–600, 1977
9. Greenfield GB: Bone changes in chronic adult Gaucher's disease. *AJR* 110:800–807, 1970
10. Rourke JA, Hesler DJ: Gaucher's disease: roentgenologic changes over twenty year interval. *AJR* 94:621–630, 1965
11. Amstutz HC, Carey EJ: Skeletal manifestations and treatment of Gaucher's disease. *J Bone Joint Surg [Am]* 48:670–700, 1960
12. Strickland B: Skeletal manifestations of Gaucher's disease with some unusual findings. *Br J Radiol* 31:246–253, 1958
13. Ehrenhaft JL: Development of vertebral column as related to certain congenital and pathological changes. *Surg Gynecol Obstet* 76:282–292, 1943

Gray Scale Ultrasonography in the Diagnosis of Endometriosis and Adenomyosis

JAMES W. WALSH,[1,2] KENNETH J. W. TAYLOR,[1] AND ARTHUR T. ROSENFIELD[1]

Ultrasound findings in 25 patients with surgically proven endometriosis are presented. Of the 31 lesions characterized at ultrasound examination, 17 were described as cystic, four as polycystic, five as mixed, and four as solid. Nine patients had a diagnostic pattern of sonolucent zones within the uterus representing blood lakes (adenomyosis) associated with extrauterine masses. In the remaining 16 patients, ultrasound alone could not differentiate endometriosis from diseases such as tubovarian abscess, ruptured ectopic pregnancy, ovarian cyst(s), or tumor. Clinical history contributed to proper diagnosis in these patients.

About 15% of all women develop endometriosis during their active menstrual life [1], and it is discovered in about 20% of gynecologic laparotomies [2]. Gray scale ultrasound findings in 25 surgically proven cases of endometriosis are reported, and one ultrasound pattern specific for diagnosing endometriosis is described.

Subjects and Methods

Over a 2 year period, 325 consecutive female patients with suspected pelvic masses were referred for ultrasound study. Surgery confirmed endometriosis in 25 patients. Conservative surgery consisting of resection of the endometrioma was performed in 21 patients and hysterectomy in four. One patient was 60 years old and the others ranged from 22 to 46.

Ultrasound examinations were performed with commercially available gray scale equipment at a transducer frequency of 2.25 or 3.5 MHz, depending upon the patient's size. The pelvis was routinely scanned using the full bladder technique with multiple transverse and sagittal sections. Ultrasonograms were correlated with pathologic morphology and organ site of disease.

Results

The masses were characterized by four different ultrasound patterns: cystic, polycystic, mixed, and solid. In the 25 patients, 31 lesions were classified.

In 13 patients, 17 cystic lesions with an average size of 4–8 cm were noted. In 10 of these lesions, the inner wall of the cyst was irregular and shaggy. In seven cysts, the mass had a smooth, well defined inner wall. Fifteen cysts were acoustically sonolucent and two had internal septation. In 13 cases the masses were located in the adnexae and in four cases, the cul-de-sac (fig. 1). In one patient, a cystic endometrioma was present in an enlarged left ovary and a right ovarian endometrioma was located in the cul-de-sac (fig. 2). The uterus closely adhered to the cystic mass and formed part of the outer cyst wall in eight patients.

Four patients were classified as having a polycystic pattern. All had an enlarged ovary with three to five small cystic cavities separated by septations (fig. 3). In each patient, the excised ovary had multiple small chocolate cysts lined by endometrial cells. In two cases the uterus adhered to the adnexal mass.

Three patients had a mixed pattern. In one patient the mass was predominantly cystic with focal clusters of irregular echogenic tissue lining the cyst wall and projecting centrally (fig. 4). In two patients with bilateral ovarian endometriosis at surgery, the ovaries could not be distinguished when reviewing the ultrasonograms. In both patients the cul-de-sac was filled with confluent cystic masses with focal clusters of echogenic debris (fig. 5). The uterus was incorporated into the mass in all three patients.

Classic ultrasound criteria suggested solid lesions in five patients. In four of these patients the 4–7 cm adnexal mass was round with fine, homogeneous, light to medium gray-toned echoes uniformly filling the lesion. In one patient a 9 × 12 cm endometrioma extended from the left true pelvis to the umbilicus (fig. 6). The pathologic specimen in each patient was an endometrioma of the ovary filled with characteristic, brown altered blood.

Nine patients were noted to have uterine changes including those in a subserosal location. It was most commonly associated with cystic adnexal or cul-de-sac masses. On ultrasonogram, this abnormality was characterized by 5–7 mm irregular cystic spaces disrupting the normal fine, speckled echo pattern of the uterus (figs. 1, 2, and 5). The focal honeycomb appearance of the myometrium was due to these blood-containing cavities (adenomyosis). This was only confirmed by pathologic examination in four of nine patients; in the others the uterus remained in situ.

Discussion

When external endometriosis involves the ovary, fallopian tubes, and the pelvic peritoneum, gray scale ultrasound may promote the correct diagnosis when combined with a characteristic clinical history or physical examination. When ultrasonography shows uterine adenomyosis (internal endometriosis) combined with any of the four described endometriosis patterns, endometriosis can be diagnosed.

Received June 2, 1978; accepted after revision September 29, 1978.

[1] Department of Diagnostic Radiology, Yale University School of Medicine, 333 Cedar Street, New Haven, Connecticut 06510. Address reprint requests to K. J. W. Taylor.

[2] Present address: Department of Diagnostic Radiology, Medical College of Virginia, Richmond, Virginia 23298.

0361-803X/79/1321-0087 $0.00

AJR 132:87–90, January 1979

© 1979 American Roentgen Ray Society

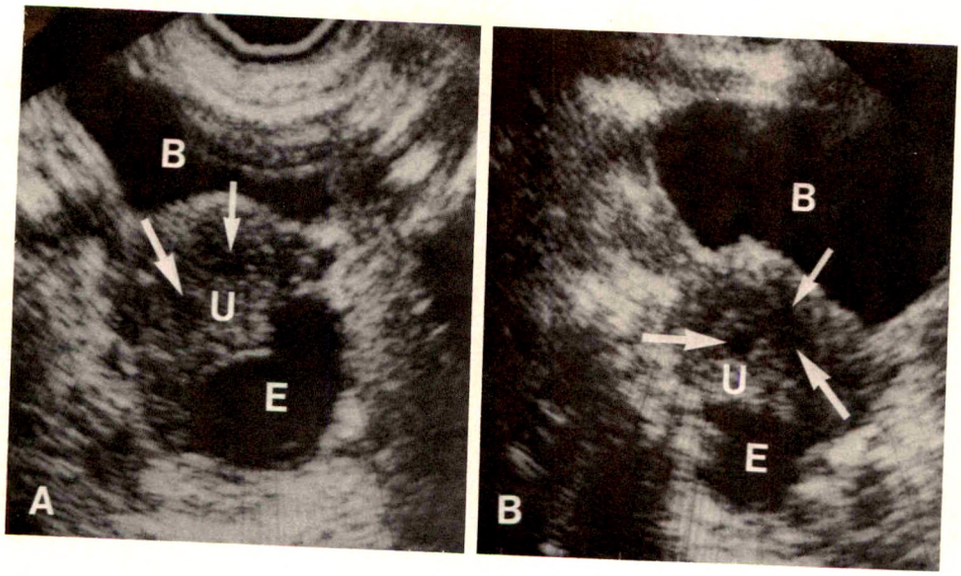


Fig. 1.—**A**, Transverse section through true pelvis revealing 3 cm bilobed cystic mass (E) behind uterus (U) in pouch of Douglas. Sonolucent areas (*arrows*) in uterus represent adenomyosis. B = bladder. **B**, Midline sagittal section through bladder (B) demonstrating adenomyosis (*arrows*) in uterus (U); endometrioma (E) located in cul-de-sac.

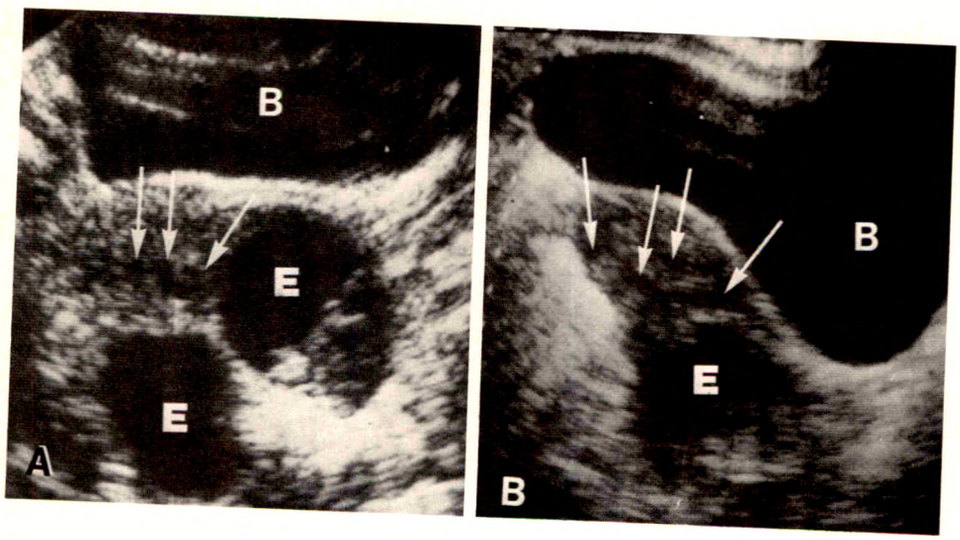


Fig. 2.—Bilateral endometriomas. **A**, Transverse section through bladder (B) 6 cm above symphysis pubis showing cystic masses (E) in left adnexa and cul-de-sac. Irregular cystic spaces in uterus (*arrows*) represent adenomyosis. **B**, Sagittal section through bladder (B) 1 cm left of midline demonstrating cystic spaces from adenomyosis throughout uterus (*arrows*). Right ovarian chocolate cyst (E) located in pouch of Douglas.

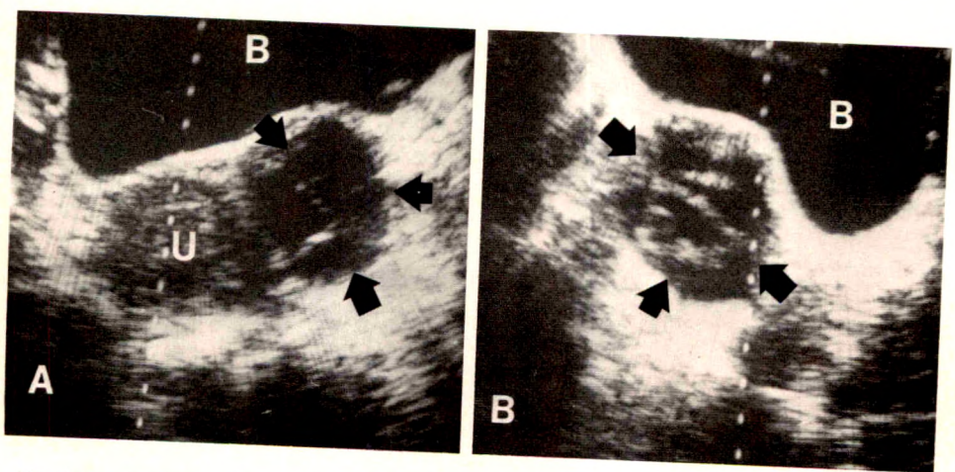


Fig. 3.—Multiple endometrial cysts. **A**, Transverse section through bladder (B) 2 cm above symphysis pubis revealing 5 cm mass (*arrows*) left of uterus (U). Multiple chocolate cysts found in left ovary at surgery. **B**, Longitudinal section through bladder (B) 3 cm left of midline showing multiple oblong cysts in left ovary (*arrows*) separated by septations.

Uterine adenomyosis is characterized by ingrowths of endometrium into the myometrium, and the presence of glandular and stromal tissue among the uterine muscle fibers [3]. Cystic blood-containing spaces in the uterus are caused by dilated glands filled with menstrual products [2]. Pathologically, adenomyosis may be localized or diffuse, and usually involves the posterior uterine wall. On ultrasonography, these dilated glands appear

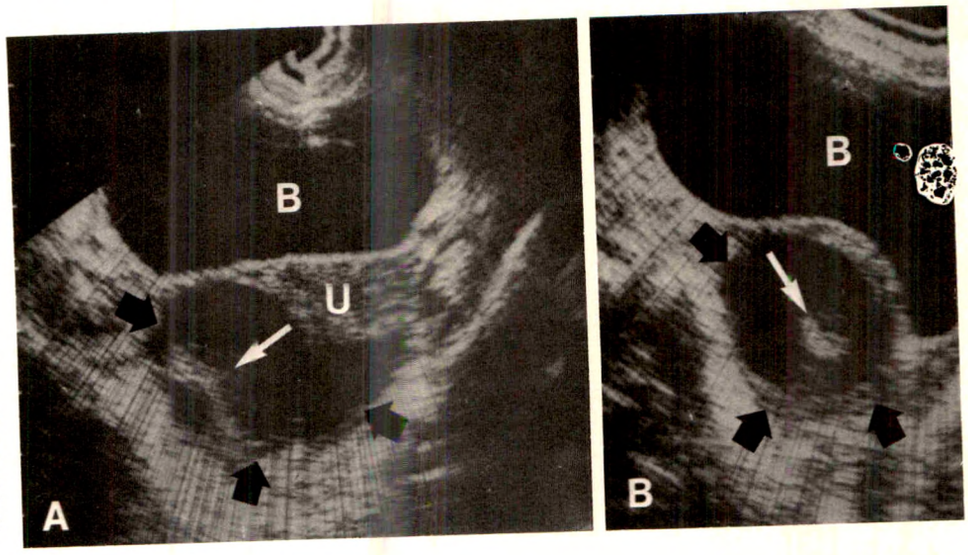


Fig. 4.—**A**, Transverse section through bladder (B) revealing complex cystic mass (*black arrows*) filling right adnexa and cul-de-sac behind uterus (U). Solid tissue (*white arrow*) lines posterior wall. **B**, Sagittal section through true pelvis revealing cystic mass (*black arrows*) behind bladder (B) with central solid component (*white arrow*).

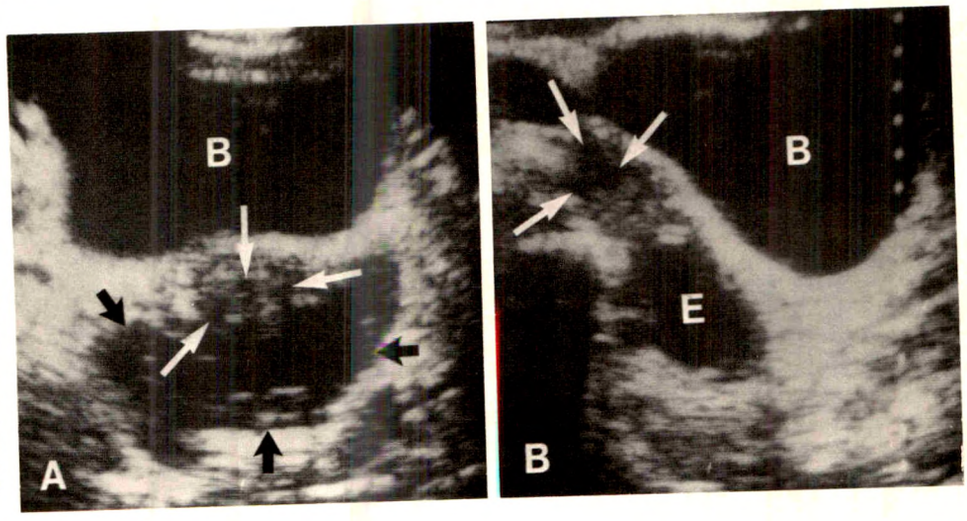


Fig. 5.—Frozen pelvis. **A**, Transverse section through bladder (B) 4 cm above symphysis pubis revealing confluent cystic mass (*black arrows*) filling pelvic floor and pouch of Douglas. Multiple sonolucent spaces in uterus (*white arrows*) represent adenomyosis. **B**, Longitudinal section through bladder (B) 1 cm left of midline revealing irregular cystic mass (E) in pouch of Douglas. Confluent cystic spaces (*arrows*) due to adenomyosis in uterine fundus.

as irregular cystic spaces through the myometrium [4]. The incidence of this ultrasound pattern was 36% in these patients. This coincidence of adenomyosis with endometriosis is higher than is reported in pathologic literature. Typically, adenomyosis is described as distinct from endometriosis, although associated with it in 13% [5]. It is said to occur in older women who have had more children. However, it is also described as the "hidden" disease and, as in this series, the uterus is not always removed to allow pathologic examination. The higher incidence found in this series may be real, although because of the small subject population further study is needed.

We observed endometrial lesions with a cystic, mixed, or solid pattern similar to those previously reported [6]. In addition, four patients had a unilateral enlarged polycystic ovary. An ovary with multiple benign follicular or inclusion cysts may mimic this pattern of endometriosis. This ultrasonic appearance was similar to bilateral polycystic ovaries we observed in the Stein-Leventhal syndrome.

The solid echo pattern noted in five chocolate cysts was presumably due to organized blood and fibrin deposition. Although difficult to distinguish from solid ovarian tumors, these endometriomas had a uniform, homogeneous, low-level echo pattern with good through transmission. In our experience, ovarian neoplasms have been inhomogeneous, mixed with cystic elements, highly echogenic, and sound attenuating.

The uterus was adherent, border forming, or incorporated into the adnexal or cul-de-sac endometriosis deposits in 13 of 25 patients. Cyclic hemorrhage into the lesions probably resulted in a fibrotic reaction and cicatrization between pelvic organs.

Primary differential diagnoses are tuboovarian abscess and ruptured ectopic pregnancy. Cystic collections of purulent material or blood (endometriosis or ruptured ectopic pregnancy) may have identical ultrasonic appearances. Evaluation of the uterine echo pattern can be the key to correct diagnosis. In patients with tuboovarian abscess, the uterus should have a normal echo pattern; fever and an exquisitely tender pelvic examination are adjunct clinical data. In patients with ectopic pregnancy, the uterus may contain clusters of high amplitude echoes

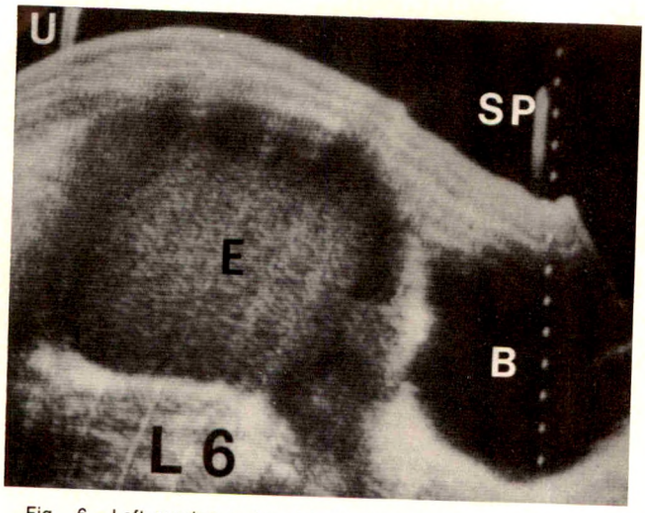


Fig. 6.—Left ovarian endometrioma. Longitudinal section through bladder (B) 6 cm left of midline revealing 9 × 12 cm mass (E) extending from 4 cm above symphysis pubis (SP) to umbilicus (U). Mass filled with homogeneous echoes.

due to increased vascularity of the myometrium or to a decidual reaction [7]. A positive urine chorionic gonadotropin or beta subunit blood result is important clinical information. In patients with endometriosis, the uterus may contain small cystic lakes of blood due to adenomyosis. A history of dysmenorrhea, menorrhagia, chronic pelvic or sacral pain, or dyspareunia also contributes to proper diagnosis.

Gray scale ultrasound is a valuable tool in the evaluation of patients with endometriosis. Specific diagnosis is possible when adenomyosis is present or a typical clinical history is obtained.

REFERENCES

1. Jenkinson EL, Brown WH: Endometriosis. *JAMA* 122:349–354, 1943
2. Browne JCM: *Postgraduate Obstetrics and Gynecology*. London, Butterworths, 1973
3. Dewhurst CJ: *Integrated Obstetrics and Gynaecology for Postgraduates*. Oxford, Blackwell Scientific Publications, 1976
4. Taylor KJW: *Atlas of Grey Scale Ultrasonography*. Edinburgh, Churchill Livingstone, 1978
5. Benson RC, Sneeden VD: Adenomyosis: a reappraisal of symptomatology. *Am J Obstet Gynecol* 76:1044–1061, 1958
6. Sandler MA, Karo JJ: The spectrum of ultrasonic findings in endometriosis. *Radiology* 127:229–231, 1978
7. Maklad NF, Wright CH: Grey scale ultrasonography in the diagnosis of ectopic pregnancy. *Radiology* 126:221–225, 1978

Doppler Evaluation of Extracranial Cerebrovascular Disease

ANDREW B. CRUMMY,[1] WILLIAM J. ZWIEBEL,[1] PATRICIO BARRIGA,[1] CHARLES M. STROTHER,[1] JOSEPH F. SACKETT,[1] WILLIAM D. TURNIPSEED,[2] FREDERICK JARRETT,[2] AND HERBERT BERKOFF[2]

The carotid Doppler examination is an accurate means of screening the extracranial carotid system for stenotic lesions. Comparison of 100 patients (200 vessels) examined by the Doppler method and arteriography showed agreement in 90% of the vessels and a significant error rate in only 3.5%.

Extracranial occlusive cerebrovascular disease is the major cause of stroke and a leading cause of death and disability in the United States. Of the patients with an ischemic stroke, 40% have segmental occlusions of the extracranial carotid system. Of these individuals, 75% have one or more surgically accessible obstructive lesions in the carotid system [1]. Spencer and associates [2, 3] described a noninvasive Doppler ultrasound technique for the evaluation of cervical cerebrovascular system. In an effort to assess the accuracy of their method for the evaluation of the cervical carotid system, we compared our results using this technique with the arteriographic findings in 100 patients who have undergone both examinations.

Technique

The subject lies supine on a firm table, with his head immobilized by sandbags. A sharply focused, continuous wave Doppler ultrasound transducer connected to a mechanical scanning arm is used for mapping the carotid artery in the neck. The probe's location is sensed by circuitry that positions multiple spots on a storage oscilloscope in a position corresponding to the arterial flow in the patient's neck. The scanning pattern is determined by the operator; after repeated passes over the vessel of interest, a two-dimensional image is developed (fig. 1). The image may then be photographed for use as a permanent record. Simultaneous with the mapping of the vessel the Doppler audiofrequency signals are recorded on magnetic tape. A strip chart tracing of the pulse contour may be made.

Changes in audiofrequency indicate variations in the velocity of blood flow and thus indirectly reflect alterations of the arterial lumen. The anatomic site from which the audiosignal is recorded is determined by referring to the oscilloscopic image of the artery being evaluated.

After evaluation of the carotid bifurcation, the probe is removed from the scanning arm and placed over the eye to determine the direction of blood flow within the ophthalmic artery. The eye is closed in order to eliminate artifacts of muscular activity. An experienced technologist can perform the entire examination in 20–30 min.

Results

Examination of 100 patients included both selective common carotid angiography and the Doppler ultrasound examination as described. Of these, 50 had signs or symptoms of cerebral ischemia, but no carotid bruits; 23 had a bruit over one or both carotid arteries as well as signs or symptoms of cerebral ischemia; while 27 had asymptomatic bruits.

Both the Doppler study and the arteriogram were evaluated by an experienced radiologist who was unaware of the findings provided by the other study. A decision was made as to whether the carotid bifurcation: (1) was normal; (2) had evidence of nonobstructive wall disease; (3) showed evidence of a nonhemodynamically significant stenosis (less than 90%); (4) had a hemodynamically significant stenosis (greater than 90%); or (5) was occluded. The findings of the two examinations were then compared to assess the accuracy of the Doppler technique for detecting arteriographically demonstrable disease. The findings obtained by the two methods were in agreement in 180 (90%) of the carotid arteries. In 13 arteries, the degree of stenosis was overestimated by the Doppler technique, and in seven it was underestimated. However, in only five patients was the magnitude of the false positive and in two the magnitude of the false negative finding such that inappropriate therapy would have been undertaken had the Doppler examination been considered definitive. In most instances of error, the degree of stenosis was slightly overestimated by the Doppler; for example, minimal stenosis was interpreted on the Doppler study while only nonobstructive wall disease was demonstrated by arteriography. Thus, the Doppler study had a significant error rate of 3.5% and an overall error rate of 10%.

Discussion

We believe these data confirm the findings of Barnes and associates [4, 5] and indicate that the Doppler examination provides an accurate and practical means of screening the extracranial carotid system for occlusive disease. The detection of nonobstructive plaques is not as certain as is the determination of stenosis. Thus, the method as currently performed is of limited utility in the evaluation of patients with transient ischemic attacks. In our opinion, this does not represent a significant limitation as we feel that all such patients, if candidates for corrective surgery, should be evaluated with arteriography.

The arterial images obtained are relatively crude and two dimensional; however, resolution is sufficient to reflect the presence of a gross stenosis which compromises the lumen from either side (figs. 2A and 2B). Plaques on the portion of the arterial wall not perpendic-

Received March 17, 1978; accepted after revision September 29, 1978.

[1] Department of Radiology, University of Wisconsin Center for Health Sciences, 1300 University Avenue, Madison, Wisconsin 53706. Address reprint requests to A. B. Crummy.

[2] Department of Surgery, University of Wisconsin Center for Health Sciences, Madison, Wisconsin 53706.

0361-803X/79/1321-0091 $0.00

AJR 132:91–93, January 1979

© 1979 American Roentgen Ray Society

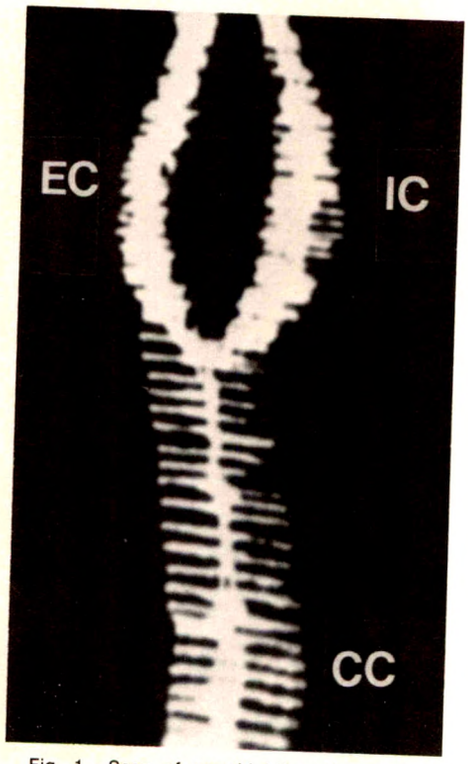


Fig. 1.—Scan of carotid bifurcation. Internal carotid artery is, by convention, positioned to right of scan. EC = external carotid; IC = internal carotid; CC = common carotid.

ular to sound beam may not be well shown. In addition, the presence of calcium within atherosclerotic plaques interferes with sound transmission, and may produce "nonsounding" areas. This artifact results in voids in the image which may be erroneously interpreted as areas of stenosis. We believe that this pitfall may be minimized by obtaining xeroradiographs of the neck to detect the presence of vascular calcification. The most important use of a visual image is to determine the site or origin of an abnormal audiosignal and thus allow anatomic localization of the segment of the vessel involved by disease. This localization is essential for accurate assessment of the significance of a demonstrated stenosis. For example, the importance of an isolated high-grade stenosis in the external carotid artery is very different from that of a similar lesion located in the common or internal carotid artery.

Changes in the character of the audiosignal are the most important aspect of the examination. The velocity of blood flow increases at an area of narrowing. The Doppler signals from blood cells with a greater velocity have a higher frequency. Therefore, a high-frequency signal indicates an area of stenosis. In general, the change in the signal is rather abrupt and quite characteristic. Turbulence and coarse tones indicate the wall irregularity associated with nonobstructive plaquing. A shortcoming of the examination is that ulceration of the plaques cannot be determined.

Calcified plaques may also complicate the evaluation of the audiofrequency signal. As previously stated, calcification may result in "nonsounding" areas because of interference with the transmission of sound waves. In the area of a void in the image, there will be a similar void in the audiosignal. Generally if the stenosis is significant, the velocity of the cells is increased distal to the area of calcification and the high-frequency Doppler signal can be detected downstream allowing the diagnosis of a stenosis.

The direction of flow in the ophthalmic artery can be determined from the pulse tracing obtained as previously described. Reversed or biphasic ophthalmic artery flow is indicative of decreased pressure in the carotid siphon. Of our 100 patients, 17 had reversed ophthalmic artery flow. Of these, 12 had occlusion of the internal or common carotid artery; four had hemodynamically significant stenoses in these vessels; and one was normal. Thus, in our experience, reversal of flow in the ophthalmic artery is very significant and substantiates the findings of obstruction to flow in the extracranial carotid artery.

The Doppler examination is useful in detecting occult, high-grade carotid artery stenoses. The detection of these lesions may be important in identifying individuals who are at increased risk in undergoing major surgical procedures such as coronary artery bypass or resection of an abdominal aortic aneurysm. In addition, the Doppler ultrasound technique should prove useful in clarifying the problem of the significance of an asymptomatic bruit. With the use of this method, the hemodynamic significance of the stenosis causing the bruit can be determined. Because of its noninvasive nature and accuracy, the Doppler test is the ideal way of following patients with bruits and should afford us an opportunity to determine the natural history of these lesions.

The Doppler technique has utility in the evaluation of patients after carotid endarterectomy. After surgery, the absence of a bruit can indicate either a successful surgical result or total occlusion of the vessel. Heretofore, this distinction could only be made definitively with arteriography. The Doppler examination provides a noninvasive approach to this problem (fig. 2C). In addition, postoperative patients may be followed at appropriate intervals to assess the possibility of recurrence of stenosis.

A potential source of significant error with the Doppler examination is the totally occluded internal carotid artery. When the internal carotid occlusions are located 1 cm or more from the carotid bifurcation, interruption of the visual image and alteration in the audio signal may be erroneously attributed to the change in position of the artery which normally occurs near the angle of the mandible. If the obstruction is at the take-off of the internal carotid artery and no stump remains, the proximal portion of the external carotid artery may be misinterpreted as a portion of the common carotid artery and hypertrophy of one of the external branches may simulate the bifurcation of the common carotid artery. Reversal of the flow in the ophthalmic artery should alert the examiner. Unfortunately, reversal of flow in the presence of a severe stenosis or occlusion does not always occur.

Spectral analysis of the audiofrequency signals in a few of our patients showed that the changes in the visual

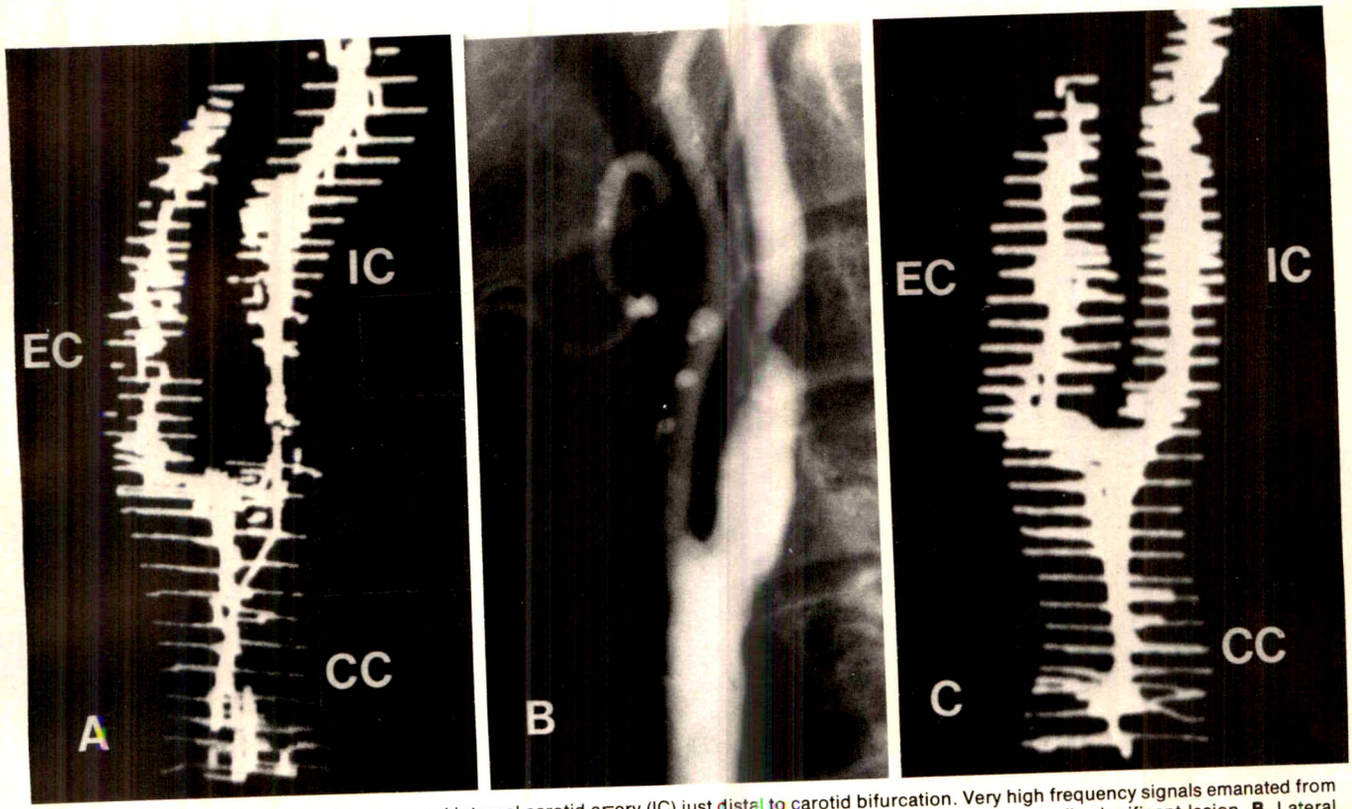


Fig. 2.—**A**, Abnormal scan showing narrowed internal carotid artery (IC) just distal to carotid bifurcation. Very high frequency signals emanated from area of stenosis. Flow in left ophthalmic artery was reversed, thereby confirming audio impression of hemodynamically significant lesion. **B**, Lateral selective common carotid arteriogram confirming interpretation of Doppler examination. **C**, Scan after endarterectomy showing that area of narrowing is no longer present. EC = external carotid; CC = common carotic.

audiospectrum parallel those heard with the audio format. We are currently investigating the possibility that a visual display might allow establishment of objective criteria for the presence of a significant stenosis and thereby reduce the subjectivity associated with interpretation of the sound signal. The use of the visual display might also result in a reduction of the amount of physician and technician time required for the examination. This would greatly enhance the value of this technique for mass screening.

REFERENCES

1. Fields WS, North RR, Hass WK, Galbraith JG, Wylie EJ, Ratinou G, Burns MH, McDonald MC, Meyer JS: Joint study of extracranial arterial occlusions as a cause of stroke. *JAMA* 203:153–158, 1968
2. Reid JM, Spencer MP: Ultrasonic Doppler technique for imaging blood vessels. *Science* 176:1235–1236, 1972
3. Thomas GI, Spencer MP, Jones TW, Endmark KW, Stauney LS: Noninvasive carotid bifurcation mapping. Its relation to carotid surgery. *Am J Surg* 128:168–174, 1974
4. Barnes RW, Bone GE, Reinertson J, Slaymaker EE, Hokanson DE, Strandness DE: Noninvasive ultrasonic carotid angiography: prospective validation by contrast arteriography. *Surgery* 80:328–335, 1976
5. Baker WH, Barnes RW: The cerebrovascular Doppler examination in patients with non-hemispheric symptoms. *Ann Surg* 186:190–192, 1977

A Second Look at the Utility of Radiographic Skull Examination for Trauma

ARTHUR A. DeSMET,[1] DENNIS G. FRYBACK,[2] AND JOHN R. THORNBURY[3]

A prospective study tested the hypothesis of Bell and Loop (1971) that 21 high yield findings are significantly associated with the presence of a skull fracture and can be used to decide which patients need skull radiography. In our study, 17 fractures were detected in 594 patients who had skull radiography because of trauma to the head. Six of these fractures occurred in children who had none of the 21 Bell and Loop high yield findings. These six patients were asymptomatic except for superficial injury at the site of trauma. Had the Bell and Loop criteria been used to decide which patients had skull radiography, 35% (all in children) of the fractures would have gone undetected. Thus, in our study population, the Bell and Loop high yield findings were not satisfactory criteria for the decision about obtaining skull films in children.

In 1971 Bell and Loop [1] reported a large series, 93 fractures in 1,500 patients (6.2%), in which 21 "high yield findings" were significantly associated with the presence of a skull fracture. If these findings had been used as criteria to define the need for skull radiography, 29% of the films would not have been obtained. Only one clinically insignificant skull fracture out of 93 would have been overlooked. With increasing concern over rising medical costs and overutilization of radiography [2], it is surprising that no clinical use of these criteria has been reported. In fact, the frequency of detected skull fractures in reported series continues to decrease; 14.3% in 1956 [3], 8.6% in 1969 [4], 6.2% in 1971 [1], and 4.0% in 1975 [5].

The large patient volume seen in a military branch dispensary was felt to be an ideal population to evaluate for potentially unnecessary radiographs. A prospective study was therefore initiated to determine if Bell and Loop's high yield findings would be useful in screening the population to be filmed for skull fracture in this clinical setting. The question we wished to answer was: "In a patient population different from Bell and Loop's, what proportion of skull fractures would be missed if patients having head trauma were evaluated using the Bell and Loop criteria for the decision to order skull radiography?"

Subjects and Methods

The Admiral Joel T. Boone Clinic, a branch dispensary of the Portsmouth Naval Regional Medical Center, is a full service outpatient medical facility with emergency room coverage 24 hr/day. Over 66,000 patients are seen yearly in the emergency room and about 55,000 radiologic examinations are performed yearly in the radiology department. The emergency room is staffed by general medical officers and board-certified or board-eligible internists or surgeons.

In this clinical setting, prior to ordering skull films on head trauma patients, the physicians filled out a form using the 21 high yield findings of Bell and Loop [1] (fig. 1). The physicians then used their customary indications for deciding which patients should have skull radiography. Study data was collected from November 1976 to October 1977.

The first 112 cases were collected using what proved to be an ambiguous question for the last item, the physician's probability estimate of fracture. For this reason, the answers to this item were discarded in the analysis of these 112 cases. For the subsequent 482 cases, the ambiguous original question was replaced by the form indicated in figure 1 for the probability estimate. All equivocal findings were considered negative (as in the original Bell and Loop study).

Skull films were obtained in the posteroanterior, Chamberlain-Towne, and both lateral projections. For each case, the films were evaluated by the radiologist for skull fracture and shift of the pineal from the midline. Interpretation was done at the time films were obtained and with knowledge of the clinical history and the data on the study form.

At the conclusion of the 11 month study, the medical records of all patients with fractures were reviewed to determine the accuracy of the data on the study forms, the accuracy of radiographic diagnosis, and the outcome of subsequent diagnosis and treatment. In addition, the participating physicians individually estimated the total number of fractures they would expect to occur in such a population as had been seen during the study. All information was keypunched on data cards and correlations between the Bell and Loop high yield findings and skull fractures were determined. For comparison of our data with that from the Bell and Loop study, Drs. Bell and Loop kindly sent us a copy of their data in the form of IBM keypunched data cards.

Results

During the 11 month study, 17 skull fractures were detected out of 594 cases (2.9%) radiographed because of trauma to the head. Of the fractures, 15 were linear and two were depressed. Pineal shift was not present. Retrospective review of the medical records indicated that none of the original radiographic diagnoses of skull fracture were incorrect.

An additional 68 patients had skull films for head trauma during the study period, but no study forms were filled out by physicians on these patients. Subsequent

Received August 8, 1978; accepted October 12, 1978.
This work was supported by U.S. Navy CIP grant 7-08-1108PS. The views expressed herein are those of the authors and not necessarily those of the United States Navy or the Department of Defense.

[1] Radiology Service, Naval Regional Medical Center, Portsmouth, Virginia 23708. Present address: Department of Diagnostic Radiology, University of Kansas Medical Center, Kansas City, Kansas 66103. Address reprint requests to A. A. DeSmet.
[2] Department of Preventive Medicine, University of Wisconsin, Madison, Wisconsin 53706.
[3] Department of Radiology, University of Michigan Medical Center, Ann Arbor, Michigan 48109.

AJR 132:95-97, January 1979
© 1979 American Roentgen Ray Society
0361-803X/79/1321-0095 $0.00

SKULL EXAMINATION FOR TRAUMA

NAME: _____ AGE: _____

SSN: _____ SEX: _____

DATE: _____

	YES	NO
A. HISTORY:		
>5-minutes of unconsciousness		
>5-minutes of retrograde amnesia		
Vomiting		
Focal weakness or sensory defect by history		
Accident at work or gunshot wound		
B. PHYSICAL EXAMINATION:		
Palpable bony malalignment		
Discharge from ear		
Discharge from nose		
Ear-drum discoloration		
Bilateral black eyes		
C. NEUROLOGIC EXAMINATION:		
Stupor, semiconsciousness or coma		
Breathing irregular or apneic		
Babinski reflex present		
Other reflex abnormality		
Focal weakness		
Sensory abnormality		
Anisocoria		
Other cranial-nerve abnormality		
D. ESTIMATION OF SEVERITY OF HEAD INJURY:		
Head injury considered "severe"		
Examination because "fracture seriously suspected"		

What is the chance of a fracture being present?

<1% 1% 5% 10% 25% 50% 75% 90% 95% 99% >99%

Requesting Physician _____

Fig. 1.—Data collection form.

retrospective review of these patients' skull films showed that none had skull fractures.

Among the 17 detected skull fractures were seven cases in which the study forms were negative for all the Bell and Loop high yield findings. These patients were age 2 months, 7 months, 10 months, 1 year, 8 years, 10 years, and 16 years. The 16-year-old boy, besides having a negative data form, presented at the emergency room with the unique finding of expressive dysphasia. This specific finding was not included in Bell and Loop's original list of 21 high yield findings. He had been struck on the head with a claw-hammer and had a depressed skull fracture on skull films. After surgery his dysphasia improved.

All of the 17 patients with fractures were examined by a staff neurosurgeon upon transfer for hospitalization to the Portsmouth Naval Regional Medical Center. These neurosurgical evaluations confirmed that none of the Bell and Loop high yield findings were present in the seven cases with negative study forms. In addition, no clinical clues of any kind (with the exception of the dysphasic 16 year old) were present that would have raised the suspicion of skull fracture.

Thus, the entirely asymptomatic six children were

admitted to the hospital for observation solely because of radiographic evidence of a skull fracture. One patient was treated with antibiotics because the fracture line extended into the frontal sinus. Another patient had a 3 mm depressed fracture which did not require surgery. Subsequent outpatient follow-up revealed no head trauma sequelae in these six children.

The association of the Bell and Loop high yield findings with detected skull fractures was determined for the entire population and for various population subgroups. This correlation data from our study was also compared with Bell and Loop's original data (table 1). A significant P value of 0.1 or less for the overall data (All Ages, table 1) was achieved in our study for only one of the high yield findings (no. 20): serious suspicion of fracture. When subdivided by age, no significant P values were found for children, and only one (no. 20) was significant for patients over 12 years of age.

The present results deviate substantially from the Bell and Loop data in the over 12 age group. However, our sample of fractures in this group is small. The present data agree with Bell and Loop's in the younger age group, but our data show a significantly lower proportion of fractures ($P < 0.01$) in this group than do the corresponding Bell and Loop data.

It should be noted that the copy of the data sent to us by Drs. Bell and Loop from their original study was the total data from their collection. They reported the first 1,500 cases (93 fractures), whereas their entire data totaled 1,564 cases (98 fractures).

There was considerable overestimation by the physicians of the probability of a fracture (table 2). Table 3 shows the increasing relationship between physicians' estimated probability of fracture and the number of positive findings. The poststudy physicians' subjective estimates of the number of fractures actually found in the study population showed a mean estimate of 13.1 (range, 0–60; SD 11.8). Seventeen fractures actually occurred.

Discussion

The intent of Bell and Loop's original study was to find a method for decreasing the number of skull films and still maintain a minimum of undetected fractures. Using their high yield findings as criteria for the decision to order skull radiography, 92 of 93 fractures would have been detected in their study population of 1,500 head trauma patients having skull films.

The results from our study reveal three differences from those of Bell and Loop: (1) a lower incidence of fracture (2.9%); (2) a larger proportion of fractures would have gone undetected (7 of 17); and (3) general lack of significant association of the high yield findings with the presence of fracture.

The lower incidence of fracture in our study could be due to several reasons. First, and foremost, the type of facility where our study was done could well be expected to deal with a patient population having a greater overall proportion of less severe head injuries than the facilities in which Bell and Loop collected their data. In addition, the "free medical care" environment of the military facility where our study was done may have resulted in more clinic visits and more skull films for less significant head injuries.

Regarding fracture nondetection, seven of 17 fractures in our study would not have been detected if skull films had been obtained only when one or more of Bell and Loop's high yield findings had been positive on the data form. Assuming that the 16-year-old dysphasic boy would have had radiography anyway, six of the 17 fractures (over one-third) still would have gone undetected. In contrast, in Bell and Loop's study, only one of 93 fractures would have gone undetected.

This discrepancy can be explained by the significant difference in the proportion of children and adults with fractures in our study population from that of Bell and Loop (table 1). Our fracture population was 55% preadolescent compared to Bell and Loop's 9.7%. Our reanalysis of Bell and Loop's original data (table 1), dividing their study population into two age groups, 12 years or less and over 12 years, revealed that their results actually do agree with ours in the 12 years or less age group. Only one of the high yield findings, serious suspicion of fracture (no. 20), achieved a significant P value of 0.1 or less. This small noncorrelating children's group was not discovered in the original Bell and Loop study, since their original results were calculated for all of their patients as a group, children and adults.

Nevertheless, Bell and Loop sensed the possibility that their high yield findings might be invalid in children. They stated that the threshold for ordering skull radiography may have to be lowered in children [1]. The observed lack of correlation between high yield findings and presence of fracture in children 12 years of age or less in our study and theirs may simply be a reflection of the difficulty in obtaining history from and evaluating children [6].

In our study, the correlation of high yield findings with presence of skull fracture is poor as well for patients over 12 years of age. Only one P value of 0.10 or less was achieved. This was a subjective judgmental finding, serious suspicion of fracture (no. 20). However, in view of the small number of fractures, five in this age group in our study, we are reluctant to generalize this statement.

The analysis of the physicians' intuitive judgments, under the category of Estimation of Severity of Head Injury (fig. 1), provided paradoxical results. These three items were: (1) classification of head injury as severe or not severe; (2) presence or absence of "fracture seriously suspected"; and (3) subjective probability estimate of the presence of fracture.

Of these three judgmental items, only "serious suspicion of fracture" correlated significantly with the presence of fracture (table 1). The noncorrelation of "severity of injury" (no. 19) is not surprising in view of the observed noncorrelation of items 1 through 18, findings resulting from history and physical examination. Again, it just seems very difficult to evaluate children for skull fracture.

The lack of correlation between the physicians' probability estimates of fracture and presence of fracture

TABLE 1
Significance (*P*) for High Yield Findings for Selected Subpopulations of Present Data Set and Bell & Loop's Data

Finding	All Ages		12 yrs or less		Over 12 yrs	
	Present Study*	Bell & Loop	Present Study*	Bell & Loop*	Present Study*	Bell & Loop
1 .....> 5 min unconscious	0.70	<0.001	1.0	0.61	0.38	<0.001
2 .....> 5 min retro amnesia	.34	<.001	.48	.42	.39	<.001
3 .....Vomiting	.39	<.001	.29	.31	1.0	<.005
4 .....Focal weakness by history	.46	<.02	.17	.46	1.0	<.025
5 .....Accident/gunshot	1.0	<.001	1.0	1.0	1.0	<.001
6 .....Bony malalignment	.32	<.001	1.0	.37	.13	<.001
7 .....Discharge from ear	1.0	<.001	.31	.37	1.0	<.001
8 .....Discharge from nose	.41	<.05	1.0	1.0	1.0	<.025
9 .....Eardrum discolored	1.0	<.001	1.0	.58	1.0	<.001
10 .....Bilateral black eyes	1.0	<.001	.34	1.0	1.0	<.005
11 .....Stupor, coma, semiconscious	.52	<.001	1.0	.42	1.0	<.001
12 .....Breathing irregular or apneic	1.0	<.001	.11	1.0	1.0	<.001
13 .....Babinski reflex present	.21	<.001	1.0	.82	1.0	<.001
14 .....Other reflex abnormal	1.0	<.001	1.0	.46	1.0	<.001
15 .....Focal weakness	1.0	<.01	1.0	1.0	1.0	<.005
16 .....Sensory abnormality	1.0	<.08	1.0	1.0	1.0	<.05
17 .....Anisocoria	1.0	<.001	1.0	.26	1.0	<.001
18 .....Other cranial nerve abnormality	1.0	<.001	1.0	.01	1.0	<.001
19 .....Injury "severe"	.64	<.001	.43	.20	1.0	<.001
20 .....'Fracture seriously suspected"	.03	<.001	.28	.02	.02	<.001
No. fractures in group	17	98	12	11	5	87
Total cases in group	594	1564	330	151	264	1413
Proportion of fractures	0.029	.063	.036	.073	.019	.062

* Probabilities computed using Fisher's exact probability test, and are the probability of the observed data, or a distribution more extreme, favoring a *positive* association between the indicator and skull fracture. Fisher's test was used because low expected cell frequencies made the chi-squared test unreliable. Chi-squared was used in the other columns.

TABLE 2
Clinician-estimated Probability of Fracture: Correspondence to Radiographic Results

Physicians' Probability of Fracture (%)	No. Fractures	Total Cases	Fractures (%)
<1	1	119	0.8
1	5	178	2.8
5	3	100	3.0
10	1	37	2.7
25	1	25	4.0
50	1	19	5.3
75	0	1	0
90	0	1	0
95	0	0	–
99	1	2	50
Ambiguous item 21 cases	4	112	3.6

TABLE 3
Relation Between Physicians' Probability Estimates and Number of Clinical Criteria Checked Positive

Physician's Probability Estimate (%)	No. Cases	Forms Entirely Negative (%)	Forms With More Than One Positive Criterion (%)
<1	119	70.6	6.7
1	178	66.3	7.3
5	100	52.0	17.0
10	37	35.1	40.5
25	25	16.0	52.0
≥50	23	17.4	60.9

(table 2) is somewhat surprising at first glance. Preliminary data from the American College of Radiology Efficacy Study [7] suggests that our physicians' probability estimates of skull fracture in individual cases should have been more accurate than we observed.

To some extent, this noncorrelation reflects the rather vague sense the physicians had of the actual incidence of skull fractures in the 594 head trauma patients seen by them in the course of our study. The physicians' poststudy subjective estimates of the total number of fractures that occurred in the study population ranged from 0 to 60. The mean estimate was 13.1 (SD 11.8). In actuality, 17 fractures occurred.

Furthermore, reasonably accurate diagnostic predictions of uncommon events (in this instance, 17 skull fractures in 594 head trauma patients) requires prior knowledge by the diagnostician of proven case outcomes from his or her own experience. It is quite doubtful that our physicians individually had a large enough *proven case* experience with this specific clinical problem to permit them to make valid probability estimates. Of course, at the heart of the probability estimate noncorrelation is the basic result of our study: there were no correlatable "high yield findings" for the diagnosis of skull fracture in our population, particularly in children.

One of the most important implications of our study results is the demonstration of the inherent danger in casually transferring the decision strategy based on valid findings in an original study population to a new and potentially *different* population. Variations between populations must be known (or tested) and taken into ac-

count before this transfer can be made in valid fashion.

There may well be a subgroup of patients (not fitting the overall group's valid decision criteria) which was submerged in the original study's data analysis. This was the case in our investigation. Furthermore, the development of an impressively valid check list of "high yield findings" for one patient population may well give the physicians using it in their own patient populations a false sense of security. That is, until the diagnostic errors indicating a mismatch come back to surprise the unwary physician!

In view of our results, it seems that future research on how to optimize the decision about ordering skull radiography may be centered more profitably on the treatment consequences of demonstrating skull fractures. Indeed, previous studies have shown that the presence of a skull fracture rarely affects the management of a patient [4,8]. In concentrating on diagnosis instead of treatment, investigators may well have been "barking up the wrong tree" when it comes to containing costs of unnecessary skull films.

REFERENCES

1. Bell RS, Loop JW: The utility and futility of radiographic skull examination for trauma. *N Engl J Med* 284:236–239, 1971
2. Hall FM: Overutilization of radiological examinations. *Radiology* 120:443–448, 1976
3. St. John E: Role of emergency skull roentgenogram in head trauma. *AJR* 76:315–319, 1956
4. Roberts F, Shopfner CE: Plain skull roentgenograms in children with head trauma. *AJR* 114:230–240, 1972
5. American College of Radiology Bulletin 31:11, 1975
6. Dowman CE: Early management of head injuries in children. *South Med J* 63:992–997, 1970
7. Lusted LB: Relationship between initial probabilities and subsequent fraction of positive diagnoses, section 4.10, in *A Study of the Efficacy of Diagnostic Radiologic Procedures: Final Report on Diagnostic Efficacy*, Efficacy Study Committee of the American College of Radiology, May 1977, pp 78–92
8. Harwood-Nash DC, Hendrick EB, Hudson AR: The significance of skull fractures in children. *Radiology* 101:151–155, 1971

Progress in Radiology:

Preoperative Localization of Nonpalpable Breast Lesions

FERRIS M. HALL[1] AND HOWARD A. FRANK[2]

Surgeons are increasingly required to resect nonpalpable breast lesions only detected by mammography. Methods for preoperative localization of such lesions were reviewed with emphasis on invasive radiologic techniques using injection, needle, and wire markers. Invasive localization of nonpalpable breast lesions is a relatively simple procedure that should be available wherever breast biopsies and mammography are performed. Its precision and success relate to the radiologist's experience in marker placement and to close cooperation between the radiologist and surgeon.

Widespread use of mammography has resulted in the detection of increasing numbers of suspicious, but nonpalpable, breast lesions. Such lesions represented over one-half of the detected cancers in a recent breast screening project report [1]. Excisional biopsy of lesions identified only by mammography may be unsuccessful because the shape and position of the breast during compression mammography are very different from that seen during surgery. This is especially a problem in large or pendulous breasts, but even in small breasts imprecise surgical localization may result in an unnecessarily large biopsy or in failure to find the lesion. Radiographically guided invasive preoperative localization of nonpalpable breast lesions is a simple procedure that permits expeditious and accurate surgery, often under local anesthesia; it should be available wherever mammography and breast biopsies are performed.

Nonpalpable breast lesions consist of focal microcalcifications and/or relatively small masses. The latter may remain nonpalpable during surgery and even on examination of the specimen. Specimen mammography is mandatory to document removal of the suspicious area and to direct histologic examination.

Noninvasive Localization Techniques

Noninvasive techniques for localization of mammographically suspect breast areas include simple visual estimates, coordinates plotted on a diagram of the breast [2–4], radiopaque markers taped to the skin during mammography [5–7], stereomammograms [8], perforated grid compression devices [9], and use of a stereotaxic instrument [10]. Many nonpalpable breast lesions, particularly those located superficially and/or adjacent to the nipple, can be adequately localized preoperatively by visual estimates. However, all noninvasive geometric techniques lack precision, and surface or depth distances can be markedly distorted when the appearances on compression radiographs are extrapolated to the breast in the surgical recumbent position. The surgeon's experience and confidence will, in the final analysis, determine how often invasive localizing procedures are employed.

Invasive Localization Procedures

Occult breast lesion localization is improved by invasive techniques that involve inserting one or more radiopaque markers (usually small gauge needles) into the breast. Subsequent mammography determines the proximity and relation of the marker to the lesion. These procedures are usually performed by the radiologist in the radiology department. Preoperative medication is generally not recommended because an alert and cooperative patient is desired during postinsertion mammography, usually performed in the sitting position. Local anesthesia is used in the skin and subcutaneous tissue, but is unnecessary in the breast parenchyma.

The needle is usually inserted with the patient recumbent, although we have found that more precise needle placement can sometimes be achieved with the patient semierect and the breast lifted to simulate the craniocaudad mammography position. In theory, localization should be more accurate when the patient is in the sitting mammographic position, or perhaps even during actual breast compression, because the needle adjustment would be predominantly in a single plane. However, this is awkward for the operator and might be uncomfortable and stressful for the patient. In the recumbent method, the needle is introduced perpendicular to the skin at the site estimated to directly overlie the lesion. Traction of the breast away from the chest wall facilitates mammographic depth measurements, but may preclude accurate localization in other dimensions. This is particularly true for a deeply situated lesion where even slight misangulation at skin entry directs the needle tip progressively away from the target.

Successful application of breast localization procedures requires cooperation between the surgeon and radiologist and, when specimen mammography is needed, with the pathologist. We agree with Bigongiari et al. [11] that lack of communication and mutual understanding among these parties is the greatest potential cause of failure to remove a nonpalpable lesion after

Received July 18, 1978; accepted after revision October 10, 1978.

[1]Department of Radiology, Harvard Medical School, Beth Israel Hospital, 330 Brookline Avenue, Boston, Massachusetts 02215. Address reprint requests to F. M. Hall.

[2]Department of Surgery, Harvard Medical School, Beth Israel Hospital, Boston, Massachusetts 02215.

0361-803X/79/1321-0101 $0.00

AJR 132:101–105, January 1979

© 1979 American Roentgen Ray Society

apparently adequate invasive localization. In our department, breast localization procedures are not scheduled by the radiologist until the mammograms have been reviewed, preferably with the surgeon. This review may show the area of suspicion to be of doubtful clinical significance, or to be definitely seen in only one projection and therefore possibly artifactual. When indicated, mammography is repeated before scheduling localization and subsequent surgery. We often obtain a single projection mammogram immediately before needle localization to confirm the presence of the suspicious area and/or to check exposure factors.

Radiologic-surgical consultation continues after the breast localization. Postlocalization mammograms are not sent to the operating room until the radiologist knows the surgeon understands the film orientation and the relation of the suspicious area to the localization marker. If that marker is relatively distant from the lesion, a joint decision must be made whether to introduce an additional marker with repeat mammograms.

Injection (Spot) Localization

Injection (spot) localization was first described by Simon et al. [12] and has been subsequently modified and successfully used by others [13–16]. On the basis of initial mammography, a needle is inserted into the breast in the estimated area of the lesion. The position of the needle tip relative to the lesion is ascertained by standard craniocaudad and lateral mammograms, and the needle position may then be readjusted or occasionally a second needle is placed and a second set of mammograms is obtained. When more than one needle is used, they must be both visually and radiologically distinguishable. After final adjustment of the needle position, 0.05 ml [13, 15] or 0.1 ml [12, 14, 16] of methylene blue [14] or Evans blue [12, 13, 15] dye and an approximately equal amount of radiopaque water-soluble contrast medium [13, 16] are injected together by tuberculin syringe. Oily contrast medium, originally recommended by Simon et al. [12], may interfere with the visualization of microcalcifications on specimen mammograms and if not removed could result in formation of foreign body granulomas within the breast. The solutions are fully expelled from the needle by injecting a small amount of gas. After needle withdrawal postinjection mammograms are obtained. Egan et al. [14] do not inject contrast medium and omit postinjection mammograms because they believe the needle position does not change after placement. Using a microinjector they also inject an additional 0.015–0.03 ml of dye along the tract as the needle is removed to further guide the surgeon.

The contrast medium seen on mammography and the dye seen surgically are landmarks that help localize the breast lesion. As in all invasive localizing procedures, it is ideal, but not essential, for the marker to be immediately adjacent to the suspicious area. Once the dye is intraoperatively identified the relative position of the lesion to the dye should be evident from examining the postlocalization mammograms. The injection method of breast localization has been uniformly successful, and without described complications, in 12 cases [13], 160 cases [14], and 70 cases [15].

Although we have not used this technique, we are aware of potential pitfalls, some of which are inherent in all invasive breast localization procedures. Unless the needle has been placed perpendicular to the coronal plane of the breast (which is often not the shortest distance from the skin surface to the lesion), subsequent compression in one or both projections may cause the needle to withdraw or bend, or conceivably to advance or break. Even with the needle hub taped to the skin, some peripheral needle displacement frequently occurs both during mammographic compression and in patient movement to and from the supine and sitting positions. In the injection technique, the needle itself is not the surgical marker, and therefore postmammographic needle displacement can be eliminated by injection of the dye and contrast medium immediately after radiography. However, a second "spot" marker cannot be applied without potential confusion both on the mammograms and at surgery. Furthermore, the dye gradually diffuses circumferentially within the breast parenchyma after spot localization, and it has been recommended that biopsy be carried out within 4 hr [15] or 30 min [16] after injection. The latter recommendation presumes immediate availability of an operating room and expeditious handling of the patient. A more serious pitfall, over which there is little control, is the possibility of dye entering ducts within the breast parenchyma, which results in rapid and widespread dispersion of the dye with the original spot not clearly defined at surgery.

Needle Localization

Needle localization of nonpalpable breast lesions was first described by Dodd et al. [17] but was only employed extensively with widespread use of screening mammography [11, 16, 18–22]. Like other invasive techniques, this procedure introduces one or more needles into the breast in the estimated area of the lesion. The needle tip rarely transfixes the lesion, but rather its position and distance relative to the suspicious area serve as a guide during biopsy. As the needle tip and the lesion become farther apart in a mammographic projection, the perpendicular projection reflects an increasing parallax and distortion of their relative positions. When the needle tip and lesion are greater than 2–3 cm from one another, a second needle placement and repeat mammography, using the first needle as a guide, may be desirable. If more than one needle is introduced before mammography, they must be visually and radiologically distinct from one another. Usually only the needle closest to the lesion on postlocalization mammograms is left in place to guide the surgeon.

Using preoperative needle localization for nonpalpable breast lesions, Lipshitz et al. [21] reported 100% successful surgical removal of 83 lesions, and Bigongiari et al. [11] reported a 90% success rate in 90 similar patients. Neither report, nor those using the injection technique for localization, contained a control group of patients undergoing breast biopsy for nonpalpable lesions with-

out preoperative invasive localization. In addition, none states how often more than one biopsy was necessary before removing the suspicious area or how often the lesion was readily palpable during surgery. In the former instance, preoperative localization should probably be considered unsuccessful, and in the latter instance localization was possibly noncontributory. The presumed diminution of the biopsy specimen needed to remove the suspicious area is a major rationale for using breast localization procedures, but it is difficult to objectively assess.

The need for compression mammography in two perpendicular projections after introducing one or more needles places restraints both on the planes of needle introduction and the positioning of the breast for mammography. Because of the often subtle mammographic appearance of nonpalpable breast lesions, the technique must not be compromised by the localization method. Furthermore, unless the needle axis is perpendicular to the coronal plane of the breast, compression in one or both projections may impose stresses likely to move the needle. We have observed needles extruded from the breast both during mammographic compression and when the patient lies down. To minimize needle motion, previous authors [11, 19, 21] have advocated inserting the needle to its hub (presumably using needles of varying lengths) and taping it to the skin after insertion. However, this does not prevent changes in the relation of the needle tip to the lesion during changes in breast shape and position. Because a nonmalleable needle could endanger the patient, assisting personnel must be alerted, particularly if the patient is confused or drowsy from medication. Breakage or conceivably even advancement of the needle into the thorax could result from turning such a patient.

Self-retaining Wire Localization

Two major problems of needle localization, the nonmalleability of the guide and its potentially variable relation to the lesion with breast compression and patient movement, are obviated by using a wire guide with self-retaining tip developed by us [23]. This flexible guide is inserted into the breast inside a needle with internal caliber usually equal to the wire. If desired, a larger caliber, less flexible needle can introduce the marker wire. The needle is immediately withdrawn leaving the guide in place with its tip fixed in proximity to the lesion. A self-retaining wire can be fashioned by removing the hub of the stylet of a 25 gauge spinal needle and bending its tip back upon itself. A sterile prepackaged guide wire and needle designed for this purpose, with a depth marker and insulation against contact with an electrosurgical instrument, is commercially available (Randal Faichney Corp., Avon, Mass.) (figs. 1 and 2). This technique is occasionally useful in nonmammographic radiologic localization, such as for removing foreign bodies.

Local anesthesia is used and a tiny stab incision helps introduce the needle and protruding wire tip. If more than one guide is required, the wires can be visually and radiologically distinguished by acutely bending one of them near the skin surface. Introducing the second guide through a separate skin incision precludes the rare occurrence of radiologic overlapping at the site of skin entry. Because of its self-retaining feature, the guide wire is not readily withdrawn or redirected once it enters the breast parenchyma and, presuming it is in close proximity to the lesion, its tip is excised with the specimen. A poorly placed guide can be extracted during localization or surgery by steady traction on its protruding end. Some minor tissue damage probably occurs along the wire tract as the hooked distal portion of the marker partly straightens. It returns to its original molded configuration after removal. Because the guide is introduced into the breast at a point estimated to be closest to the lesion, surgical approach is usually along the axis of the wire.

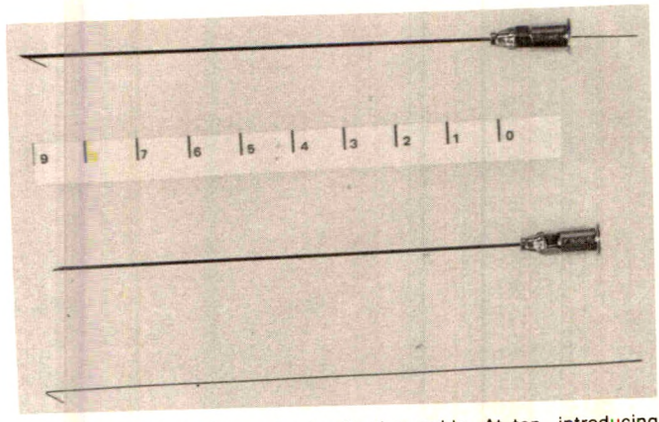


Fig. 1.—Self-retaining wire localization guide. At top, introducing needle and marker wire assembled together; below, separated. Acutely bent wire tip is self-retaining within tissue. Centimeter ruler with "9" against skin helps assess marker depth.

The effectiveness of the self-retaining feature in maintaining the proximity of the guide tip to the lesion is demonstrated by the frequent retraction of a deeply placed wire during mammographic compression or change in body position. It is therefore important to use a long guide and not to cut off excess wire outside the breast before mammography or biopsy. If the guide is inadvertently introduced into the underlying pectoralis musculature, its self-retaining feature may make it retract completely into the breast from arm motion or change in body position, occasionally receding out of the mammographic field. Therefore, if a lesion adjacent to the chest wall is being localized, we momentarily place a hemostat on the outer tip of the wire until it is certain there is no undue retraction. Taping the wire to the skin is unnecessary and will even prevent the normal motion of the wire during changes in position or compression. No dressings are used during mammography; the skin area and exposed guide are covered with a sterile drape before transfer to surgery.

We performed breast wire localization in 40 patients during a 3-year period. In 28 cases the lesion remained nonpalpable during surgery and subsequent specimen mammography definitively documented its removal or nonremoval. One of us (F. M. H.) performed or was present at all localization procedures, but the biopsies were

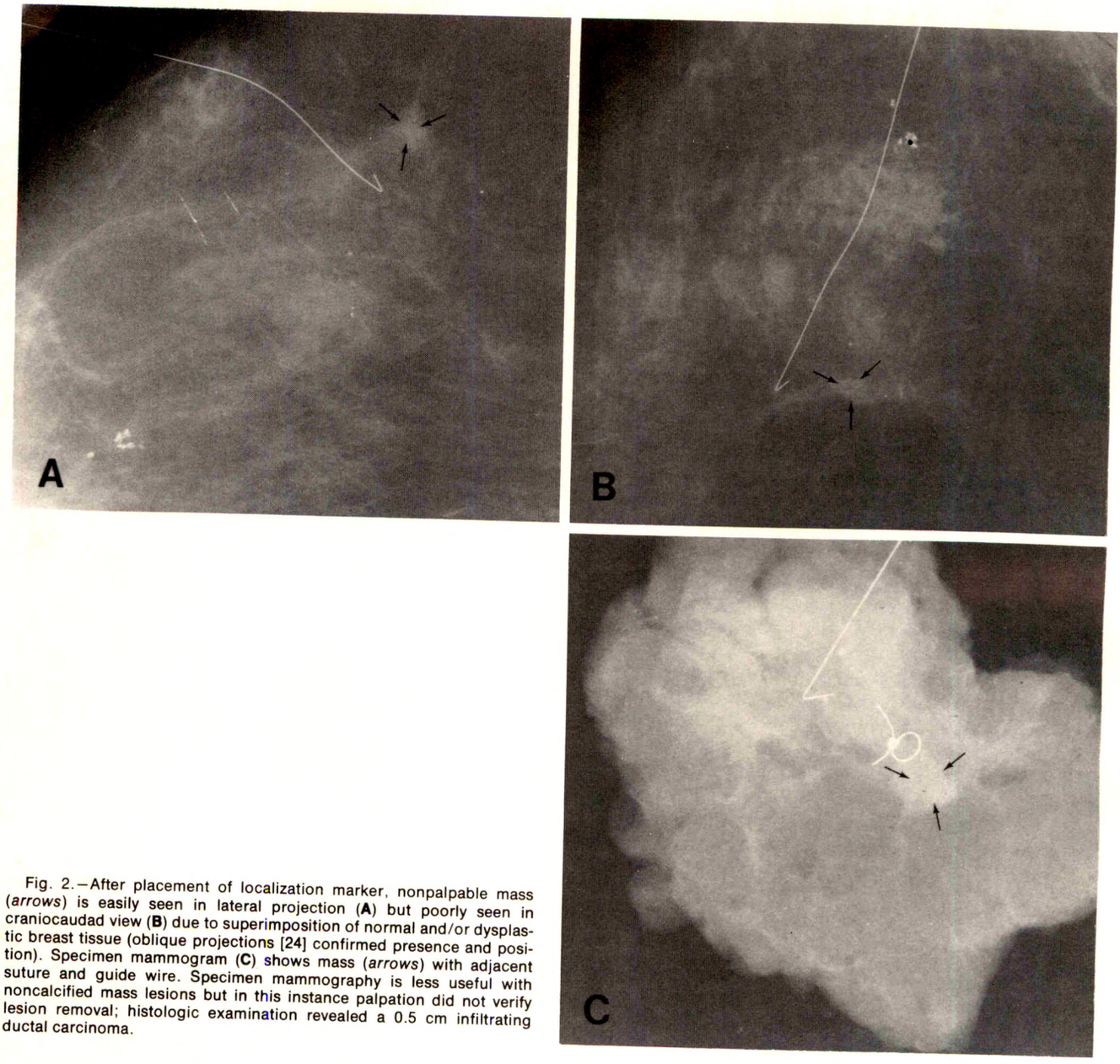


Fig. 2.—After placement of localization marker, nonpalpable mass (*arrows*) is easily seen in lateral projection (**A**) but poorly seen in craniocaudad view (**B**) due to superimposition of normal and/or dysplastic breast tissue (oblique projections [24] confirmed presence and position). Specimen mammogram (**C**) shows mass (*arrows*) with adjacent suture and guide wire. Specimen mammography is less useful with noncalcified mass lesions but in this instance palpation did not verify lesion removal; histologic examination revealed a 0.5 cm infiltrating ductal carcinoma.

performed by various members of the surgical staff, in many instances their first experience with the localizing method. In 24 of 28 procedures the suspicious area was completely or almost completely removed with the first biopsy; in two of 28 the suspicious lesion was excised on a second or third biopsy; and in two of 28 it was not removed during the initial operation. Carcinoma was diagnosed in nine of these 28 specimens, three of which showed no histologic invasion. During this same 3-year period, six patients underwent biopsy and diagnostic specimen mammography at our hospital for similar nonpalpable lesions without preoperative wire localization. Despite multiple biopsies, the suspicious area was not removed in two of six patients and only partially removed in a third. In one of these three cases, the radiologist considered preoperative localization unnecessary because the suspicious area was superficial and paraareolar.

The success of any invasive breast localization procedure in facilitating removal of a suspicious area, decreasing the operating time, or diminishing the size of the biopsy specimen obviously increases with the experience of the radiologist and the surgeon and how close to the lesion they insist on having the localizing marker. One-third of our cases have had a second wire marker placed with a second postlocalization mammographic examination. The relative ease and rapidity of this procedure with increasing experience has encouraged the authors to more frequently place a second marker, and in some instances a third marker. Radiologists can comfort themselves when more than one wire is required for localization by presuming that without a preoperative

marker similar difficulties would likely occur under more adverse operating conditions.

ACKNOWLEDGMENTS

We thank Betty Ann Tangney for help in preparing this manuscript and Dr. Clinton Koufman for surgical correlation.

REFERENCES

1. Sayler C, Egan JF, Raines JR, Goodman MJ: Mammographic screening. *JAMA* 238:872–873, 1977
2. Berger SM, Curcio BM, Gershoncohen J, Isard HJ: Mammographic localization of unsuspected breast cancer. *AJR* 96:1046–1052, 1966
3. Curcio BM: Technique for radiographic localization of nonpalpable breast tumors. *Radiol Technol* 42:155–160, 1970
4. Stevens GM, Jamplis RW: Mammographically directed biopsy of nonpalpable breast lesions. *Arch Surg* 102:292–295, 1971
5. Frankl G, Rosenfeld DD: Breast xeroradiography: an analysis of our first 17 months. *Ann Surg* 178:676–679, 1973
6. Frankl G, Rosenfeld DD: Xeroradiographic detection of occult breast cancer. *Cancer* 35:542–548, 1975
7. Malone LJ, Frankl G, Dorazio RA, Winkley JH: Occult breast carcinomas detected by xeroradiography: clinical considerations. *Ann Surg* 181:133–136, 1975
8. Price JL, Butler PD: Stereoscopic measurement in mammography. *Br J Radiol* 44:901, 1971
9. Mühlow A: A device for precision needle biopsy of the breast at mammography. *AJR* 121:843–845, 1974
10. Bolmgren J, Jacobson B, Nordenström B: Stereotaxic instrument for needle biopsy of the mamma. *AJR* 129:121–125, 1977
11. Bigongiari LR, Fidler W, Skerker LB, Comstock C, Threatt B: Percutaneous needle localization of breast lesions prior to biopsy: analysis of failures. *Clin Radiol* 28:419–425, 1977
12. Simon N, Lesnick GJ, Lerer WN, Bachman AL: Roentgenographic localization of small lesions of the breast by the spot method. *Surg Gynecol Obstet* 134:572–574, 1972
13. Shepard D, Soder P, Cooper D, Eaton B, Godwin JT: Mammography: an aid in the treatment of carcinoma of the breast. *Ann Surg* 179:749–755, 1974
14. Egan JF, Sayler CB, Goodman MJ: A technique for localizing occult breast lesions. *CA* 26:32–37, 1976
15. Horns JW, Arndt RD: Percutaneous spot localization of nonpalpable breast lesions. *AJR* 127:253–256, 1976
16. Hoeffken W, Lanyi M: *Mammography*. Philadelphia, Saunders, 1977, pp 309–312
17. Dodd GD, Fry K, Delany W: Pre-operative localization of occult carcinoma of the breast, in *Management of the Patient with Cancer*, edited by Nealon TF, Philadelphia, Saunders, 1965, pp 88–113
18. Rosato FE, Thomas J, Rosato EF: Operative management of nonpalpable lesions detected by mammography. *Surg Gynecol Obstet* 137:491–493, 1973
19. Threatt B, Appelman H, Dow R, O'Rourke T: Percutaneous needle localization of clustered mammary microcalcifications prior to biopsy. *AJR* 121:839–842, 1974
20. Dodd GD: Pre-operative radiographic localization of nonpalpable lesions, in *Early Breast Cancer—Detection and Treatment*, edited by Gallager HS, New York, Wiley, 1975, pp 151–152
21. Libshitz HI, Feig SA, Fetouh S: Needle localization of nonpalpable breast lesions. *Radiology* 121:557–560, 1976
22. Kalisher L: An improved needle for localization of nonpalpable lesions. *Radiology* 128:815–817, 1978
23. Frank HA, Hall FM, Steer ML: Preoperative localization of nonpalpable breast lesions demonstrated by mammography. *N Engl J Med* 295:259–260, 1976
24. Hall FM, Berenberg AL: Selective use of the oblique projection in mammography. *AJR* 131:465–468, 1978

Case Reports

Radiographic Findings in the Mucocutaneous Lymph Node Syndrome

ANTHONY COOK[1] AND PHILIPPE L'HEUREUX[1]

The mucocutaneous lymph node syndrome was first described in English in 1974 by Kawasaki et al. [1]; before that time more than 6,000 cases had been reported in Japan. The syndrome has been clinically confused with the Dubin-Johnson syndrome and scarlet fever. Most patients are younger than 5 years and about half are younger than 2. The main features of mucocutaneous lymph node syndrome are fever lasting about 1–2 weeks that does not subside with antibiotics, congestion of the ocular conjunctivae, reddening of the lips and oral cavity, and swelling of cervical lymph nodes. After 3–5 days a macular, erythematous skin eruption with pronounced reddening begins on the palms and soles and rapidly spreads over the trunk. During the second week an unusual desquamation begins at the junction of the nails and skin, followed by recovery in most patients. In some individuals, however, the heart and systemic arteries are significantly involved, as in the patient described here.

Case Report

J. H., an 8-month-old white boy, was admitted to the University of Minnesota Hospitals in October 1977. The patient had fever 4 weeks before admission followed by a macular, erythematous rash on his face after 24 hr that progressed to his trunk and extremities. The conjunctivae were congested, and eventually the erythema also involved the conjunctivae, tongue, lips, palms, and soles. It progressed to desquamation of the palms and soles and was gone within 96 hr. However, the fever did not abate despite treatment with intramuscular penicillin. White blood cell count was 23,500 with a polymorphonuclear cell predominance. The patient did not respond to treatment with ampicillin or cephalosporin. At hospitalization his hemoglobin was 9.4 and white blood cell count 25,200 with 54% polymorphonuclear cells and 19% band forms. Sedimentation rates were 125 and 96 on two separate determinations. Lumbar puncture was unremarkable; cultures of nose, throat, blood, and cerebrospinal fluid showed no growth of normal flora. Negative laboratory tests included direct and indirect Coombs, rheumatoid factor, mononucleosis spot test, and fluorescent test for toxoplasmosis. Antibiotic therapy was stopped and the fever continued. Admission chest radiography was normal, although later films showed progressive cardiomegaly. Electrocardiography showed depressed S-T segments and variability of the voltage of the R waves across the midprecordial leads, consistent with ischemia but without evidence of infarction.

After transfer to the University of Minnesota Hospitals the patient was febrile, tachypneic, and tachycardic. A 1 × 1.5 cm anterior cervical node was palpated on the left side of the neck. Relevant laboratory findings were hemoglobin, 7; white blood cell count, 19,600; and erythrocyte sedimentation rate, 91. Urinalysis was unremarkable; lymph node culture was negative; and chest radiography (fig. 1A) showed marked enlargement of the cardiac silhouette.

A pericardotomy was performed because of the persistent tachycardia and tachypnea. At surgery the pericardium was tensely distended and about 100 ml of straw-colored fluid was aspirated. A pericardial segment was removed to create a window. Pathologic examination (including electron microscopy) of the pericardium revealed changes compatible with mild chronic inflammation. There was no evidence for an immune complex disease. Protein in the pericardial fluid was 4–8 g/100 ml; it was sterile for viral and bacterial cultures. The patient's temperature decreased after surgery but rose again after 10 days. White blood cell count and erythrocyte sedimentation rate increased again. Repeat blood and urine cultures showed no growth.

The patient was given prednisone and promptly became afebrile. Expansile masses thought to be bilateral arterial aneurysms were felt in the patient's axillae 2 days after steroids were started. Peripheral pulses were not affected, nor was there any evidence of hypertension. Angiographic findings prompted antiplatelet therapy, in addition to continuing steroid therapy. All convalescent antibody titers of viruses were negative. The patient was discharged 1 month after admission with the diagnosis of mucocutaneous lymph node syndrome. He was maintained on aspirin, dipyridamole, and prednisone therapy; his blood pressure was normal at discharge.

The patient has shown good progress at follow-up. He remains afebrile and has a normal electrocardiogram. There is no evidence of residual cardiac damage. Blood pressure is normal. Prednisone dosage is being tapered, and he is being maintained on dipyridamole and aspirin.

Findings

Admission chest film (fig. 1A) showed marked enlargement of the cardiac silhouette consistent with a pericardial effusion. The cardiac silhouette decreased in size after pericardotomy (fig. 1B). A peculiar "lump" just inferior to the pulmonary artery segment was evident.

Received February 14, 1978; accepted August 21, 1978.
[1] Department of Radiology, University of Minnesota Medical School, Box 292 Mayo Memorial Building, 420 Delaware Street Southeast, Minneapolis, Minnesota 55455. Address reprint requests to P. L'Heureux.

AJR 132:107–109, January 1979
© 1979 American Roentgen Ray Society

0361–803X/79/1321–0107 $0.00

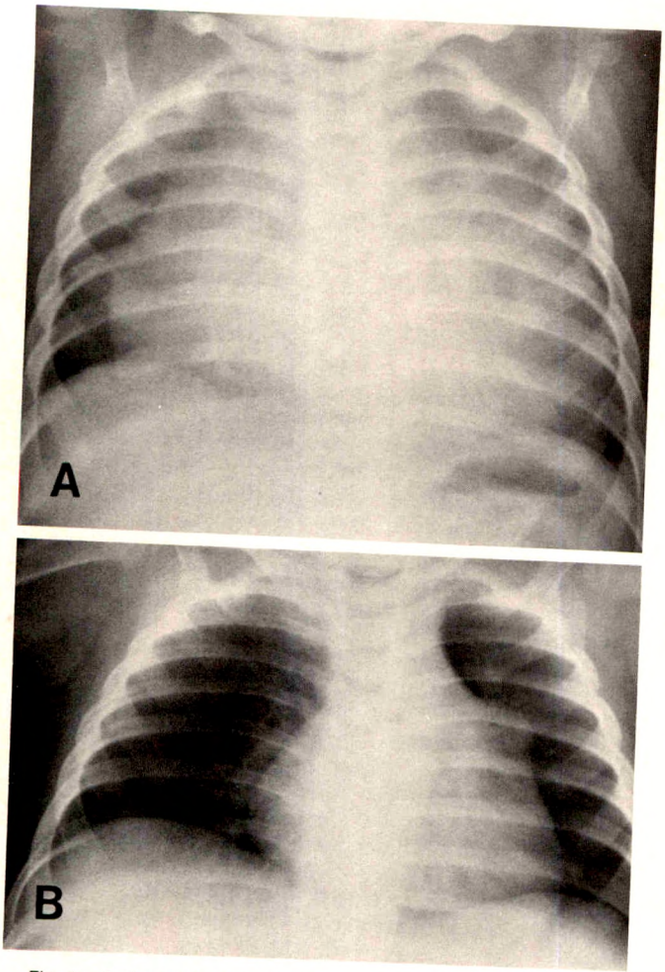


Fig. 1.—**A**, On admission. Marked enlargement of cardiac silhouette; fluoroscopy showed markedly reduced cardiac pulsation. **B**, After pericardotomy. Reduction in size of cardiac silhouette with abnormal contour of left heart border.

Thoracic angiography (fig. 2A) showed complete occlusion of the right coronary artery. There was a fusiform, partly clotted aneurysm of the left coronary artery, particularly in the circumflex branch. This dilated artery accounts for the abnormal contours on the left heart border on the chest film. There were long fusiform aneurysms of both subclavian and axillary arteries.

Abdominal aortography (fig. 2B) showed aneurysms involving a right intercostal artery, both iliac arteries, and the left renal artery. The aneurysms were both sacular and fusiform and some intraluminal clotting could be seen, particularly in the iliac arteries. Serial films showed these were not completely occluded, however, and renal perfusion was normal.

Discussion

Many questions about this unusual disease are unanswered. Epidemiology and geographic distribution are puzzling. Although many cases have now been reported in Europe and North America, the majority have been diagnosed in Japan. This is perhaps because the disease was recognized earlier in Japan, and physicians there

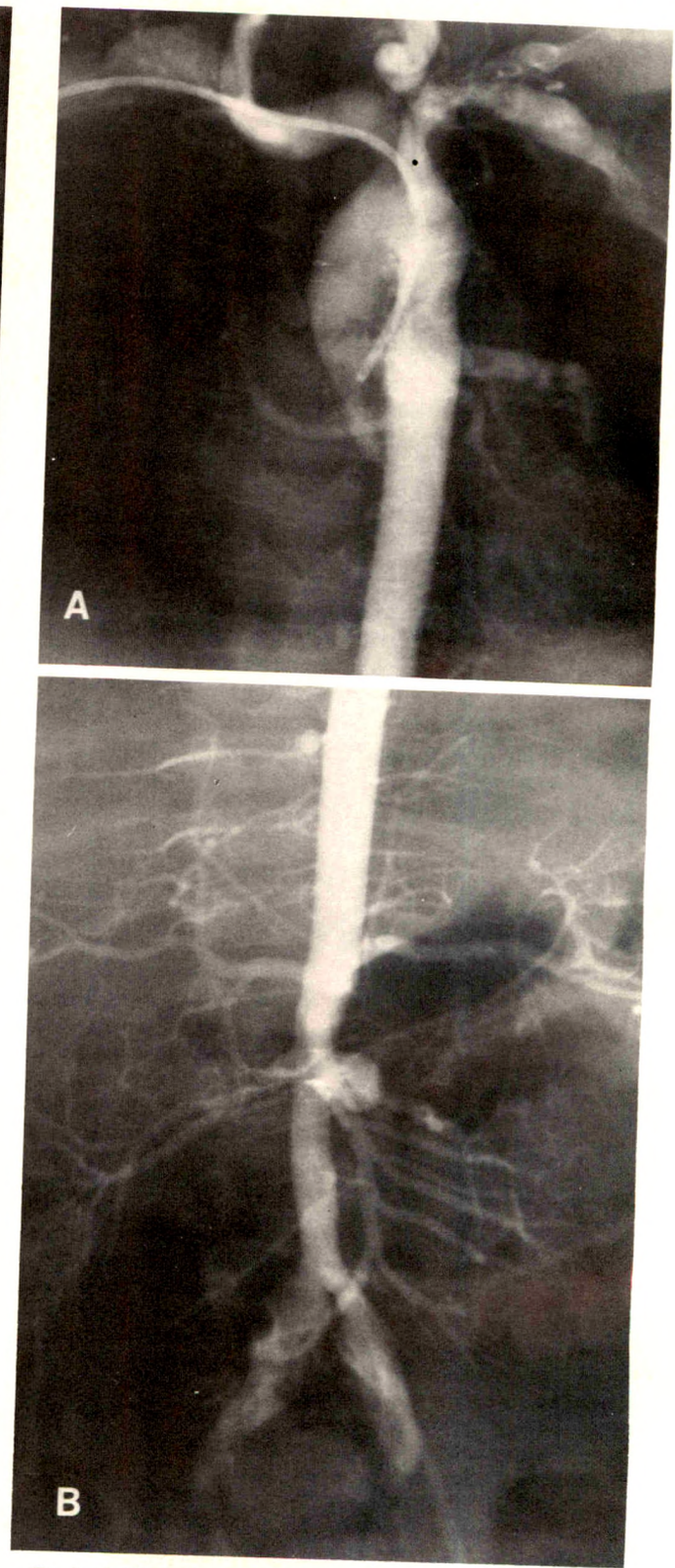


Fig. 2.—**A**, Thoracic aortogram. Completely obstructed right coronary artery and aneurysmal dilatation of circumflex branch of left coronary artery with partial thrombosis. Aneurysms also involve both subclavian and axillary arteries. Large bronchial artery anastomosing with upper intercostal arteries evident on right side. **B**, Abdominal aortogram. Sacular aneurysm in lower right intercostal artery and large aneurysm at origin of left renal artery. Aneurysmal dilatation of both common iliac arteries with thrombus formation evident.

are more aware of this entity, but it could reflect a geographic predeliction.

The etiology of this disease remains unclear; like other "new" diseases such as Lassa fever and kuru, it may be infective with a viral etiology. Rickettsial bodies have been found in the lymph nodes of several patients and elevated levels of IgE immunoglobin have been reported [3, 4]. Kegel et al. [5] believe mucocutaneous lymph node syndrome is probably the disease previously diagnosed as infantile periarteritis nodosa.

Although mucocutaneous lymph node syndrome tends to be a benign, self-limiting disease, its mortality rate is reported to be 1%–2%. Deaths are usually related to the cardiovascular system (myocardial infarction or fatal arrhythmia). Kato et al. [6] recently reported the results of coronary arteriography in 20 patients who survived the illness. Coronary angiograms were abnormal in 12 of the 20, including seven with coronary artery aneurysms. Two patients showed complete regression of these aneurysms [6–8].

Although diagnosis of mucocutaneous lymph node syndrome is often discovered clinically by process of elimination, radiologists are sometimes involved in the workup of these patients at different points in their clinical course. This disease should be considered whenever pericardial effusions or cardiomyopathies are detected in young children, especially under age 2. Diagnosis may be suggested after the vasculitis associated with this disease leads to hypertension and multiple, primarily fusiform aneurysms are detected at abdominal arteriography. Radiologists should be aware of the marked predilection of this disease for involving coronary arteries, and of the potential hazards of such involvement.

Vasculitis is rare in children of this age. Differential diagnosis includes the juvenile form of periarteritis nodosa (usually in older children), which typically involves the medium and small arteries of the kidneys, liver, spleen, and viscera. These aneurysms may vary in size, but are rather uniformly distributed [9]. Another diagnosis to be considered is Takaysu's arteritis in children [10], where the disease affects the aorta and its major branches, and may produce stenosis of these vessels, as well as aneurysms. These angiographic features, as well as the differing clinical pattern, should readily distinguish Takayasu's arteritis from mucocutaneous lymph node syndrome.

ACKNOWLEDGMENT

We thank Susan Marthaler for help in preparing the manuscript.

REFERENCES

1. Kawasaki T, Kosaki F, Okawa S, Shigematsu I, Yanagawa H: A new infantile acute febrile mucocutaneous lymph node syndrome (MLNS) prevailing in Japan. *Pediatrics* 54:271–276, 1974
2. Editorial: Mucocutaneous lymph node syndrome: a new disease. *Br Med J* 1:511, 1977
3. Hamashima Y, Kishi K, Tasak K: Rickettsia-like bodies in infantile acute febrile mucocutaneous lymph node syndrome. *Lancet* 819:42, 1973
4. Kusakawa S, Heiner D: Elevated levels of immunoglobin E in acute mucocutaneous lymph node syndrome. *Pediatr Res* 10:108–111, 1976
5. Kegel S, Dorsey T, Rosen M, Taylor W: Cardiac death in mucocutaneous lymph node syndrome. *Am J Cardiol* 40:282–286, 1977
6. Kato H, Koike S, Yamamoto M, Ito Y, Yano E: Coronary aneurysms in infants and young children with acute febrile mucocutaneous lymph node syndrome. *J Pediatr* 86:892–898, 1975
7. Darby C, Kyong C: Mucocutaneous lymph node syndrome. *JAMA* 236:2295–2299, 1976
8. Yanagisawa M, Kobayashi N, Matsuya S: Myocardial infarction due to coronary thrombo-arteritis following acute febrile mucocutaneous lymph node syndrome (MLNS) in an infant. *Pediatrics* 54:277–280, 1974
9. Abrams H: Renal angiography in hypertension, in *Angiography*, edited by Abrams H, Boston, Little, Brown, 1971, pp E78–879
10. Golding R, Perri G, Cremin B: The arteriographic manifestations of Takayasu's arteritis in children. *Pediatr Radiol* 5:224–230, 1977

Bone Imaging of the Heel in Reiter's Syndrome

IRAJ KHALKHALI,[1] ROBERT C. STADALNIK,[1] KENNETH B. WIESNER,[2] AND ROBERT F. SHAPIRO[2]

Classic Reiter's syndrome, which affects young adult males, is characterized by arthritis, conjunctivitis, and nongonococcal urethritis. Since Hans Reiter's description of the syndrome in 1916, other features of probably equal significance, added to the original triad, include circinate balanitis, shallow ulcerations of the buccal mucosa, and a dermatitis (keratodermia blennorrhagicum). Reiter's arthritis is usually asymmetrical and tends to involve lower extremity joints. Talalgia, or heel pain, is an often underrated characteristic feature of the arthritis [1, 2].

With an incidence of 50% [3], talalgia can be localized to either the posterior aspect of the heel (along the achilles tendon, its insertion, or in the area of the subachilles bursa) or to the plantar surface of the heel (at the insertion of the plantar aponeuroses on the calcaneus). Radiographic alterations in these regions are common in patients with recurrent or chronic disease, but are infrequent or minimal in patients with acute Reiter's syndrome [3]. Recent observation of a young male with Reiter's syndrome suggests that bone imaging may help substantiate this clinical feature before radiography reveals calcaneal spurs.

Case Report

R. N., a 20-year-old white man referred to the Rheumatology Clinic at Sacramento Medical Center of the University of California at Davis in May 1975, had a 6 week history of back pain and polyarticular arthralgias involving the ankles, knees, hips, shoulders, and wrists. About 4 weeks before admission he developed "red eyes" associated with photophobia. He also had a painful erythematous area in the roof of his mouth and dysuria associated with a urethral discharge. Additional systemic symptoms included low-grade fever, anorexia, and weight loss. There was no history of anterior uveitis, inflammatory bowel disease, or psoriasis. Family history did not include arthritis, inflammatory bowel disease, psoriasis, peripheral arthritis, or axial joint disease.

Physical examination revealed an ill-appearing male with bilateral conjunctival hyperemia. Hard palate mucosa demonstrated painless yellow-white ulcerations with red borders. Heart examination revealed a grade 2 out of 6 systolic ejection murmur. Musculoskeletal examination showed evidence of synovitis involving the right shoulder, wrist, knee, and ankle, with sausage toe deformities of the right toes. There was marked tenderness of the left heel at the attachment of the plantar aponeurosis to the calcaneus.

Objective laboratory data included a markedly elevated Westergren sedimentation rate, and negative rheumatoid factor and antinuclear antibody studies. Histocompatibility antigen HLA-B27 was present. Joint fluid analysis revealed an inflammatory fluid characterized by increased levels of complement and the presence of characteristic cells [4]. Radiography of the sacroiliac joints and of the feet was normal (fig. 1).

During the next 1.5 years the patient had recurrent episodes of large, lower extremity asymmetric joint disease. In October 1976 he developed acute anterior uveitis of the right eye requiring local, as well as systemic, steroids for eventual control. In December 1976 he was seen for complaints of bilateral talalgias at both the Achilles tendon insertion and the plantar aponeurosis attachment, as well as increasing arthralgias and swelling in some of the interphalangeal joints of his toes and ankles.

On heel examination, the plantar aponeurosis insertions were slightly bulging, faintly erythematous, and markedly tender on direct pressure. The posterior aspects of the heels were also very tender and erythematous. Soft tissue swelling at the margins of the Achilles tendons was thought to represent sub-Achilles bursitis. There was swelling and tenderness of both ankles and the first and second interphalangeal and metatarsal phalangeal joints of the right foot.

Follow-up radiography of the heels again failed to demonstrate any erosive or proliferative changes of the calcaneus on lateral views of either heel. Radionuclide bone scan was performed. After intravenous injection of 15 mCi ^{99m}Tc pyrophosphate, total body bone images were obtained with additional static anterior and lateral views of both feet using a low energy, high resolution collimator. Images showed increased activity bilaterally around the sub-Achilles bursa and in the right first and second tarsophalangeal and proximal interphalangeal joints. In addition, diffuse increased activity was noted in the right tarsal, left tarsal, and left proximal metatarsal bones (fig. 2). No other joint or bony abnormalities were noted on bone imaging.

Discussion

It is not unexpected to find enhanced ^{99m}Tc pyrophosphate radionucleotide uptake in the region of the sub-Achilles bursa in a patient with Reiter's syndrome. In chronic recurring Reiter's syndrome accompanied by objective physical evidence of plantar fasciitis, sub-Achilles bursitis, and Achilles tendonitis, the radiographic and xeroradiographic features are characteristic [2, 3]. They include small erosions and bony proliferation at the posterosuperior surface of the calcaneus, tendon thickening, erosions on the plantar aspect of the calcaneus, and fluffy, irregular plantar-calcaneal spurs that become more sharply defined on subsequent radiographs.

Anatomically, the synovial lining of the sub-Achilles bursa (also called the retrocalcaneal bursa) extends over both the Achilles tendon and the inferior limit, and is the pre-Achilles fat pad [2]. Cadaver studies in both rheumatoid arthritis and ankylosing spondylitis have demon-

Received May 11, 1978; accepted after revision September 7, 1978.
R. C. Stadalnik is a Picker Scholar of the James Picker Foundation.
[1] Department of Nuclear Medicine, Sacramento Medical Center, University of California, 4301 X Street, FOLB I, Sacramento, California 95817. Address reprint requests to R. C. Stadalnik.
[2] 2222 Sierra Boulevard, Suite E26, Sacramento, California 95825.

© 1979 American Roentgen Ray Society

0361-803X/79/1321-0110 $0.00

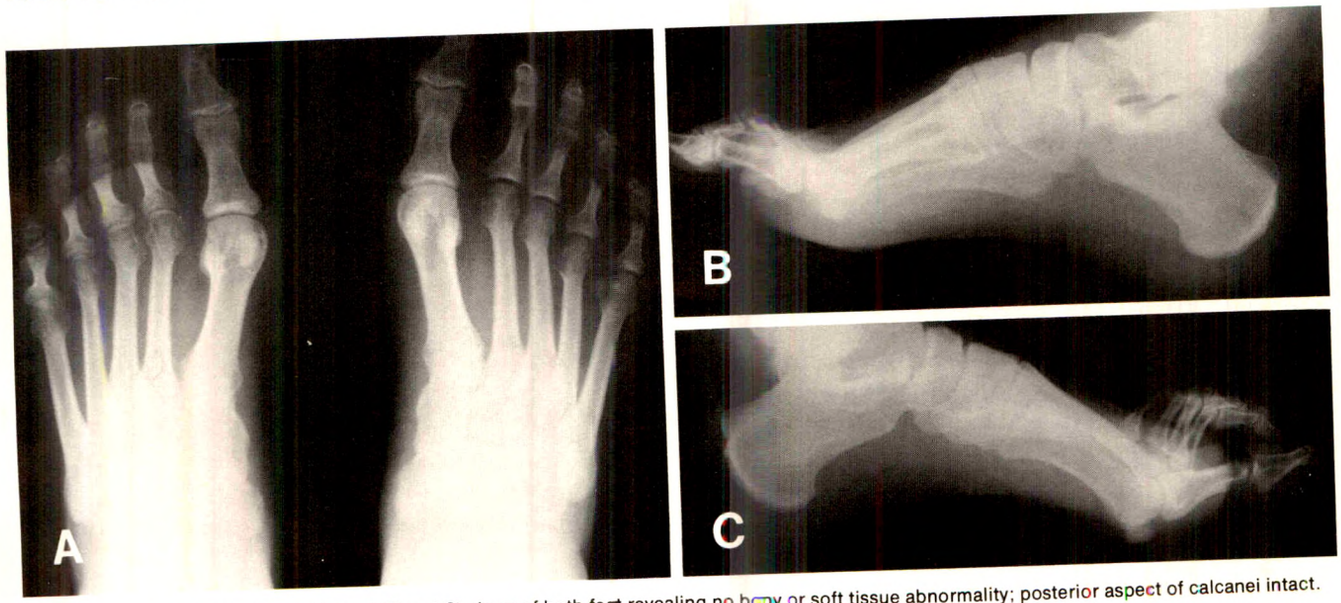


Fig. 1.—Anteroposterior (**A**) and lateral (**B** and **C**) views of both feet revealing no bony or soft tissue abnormality; posterior aspect of calcanei intact.

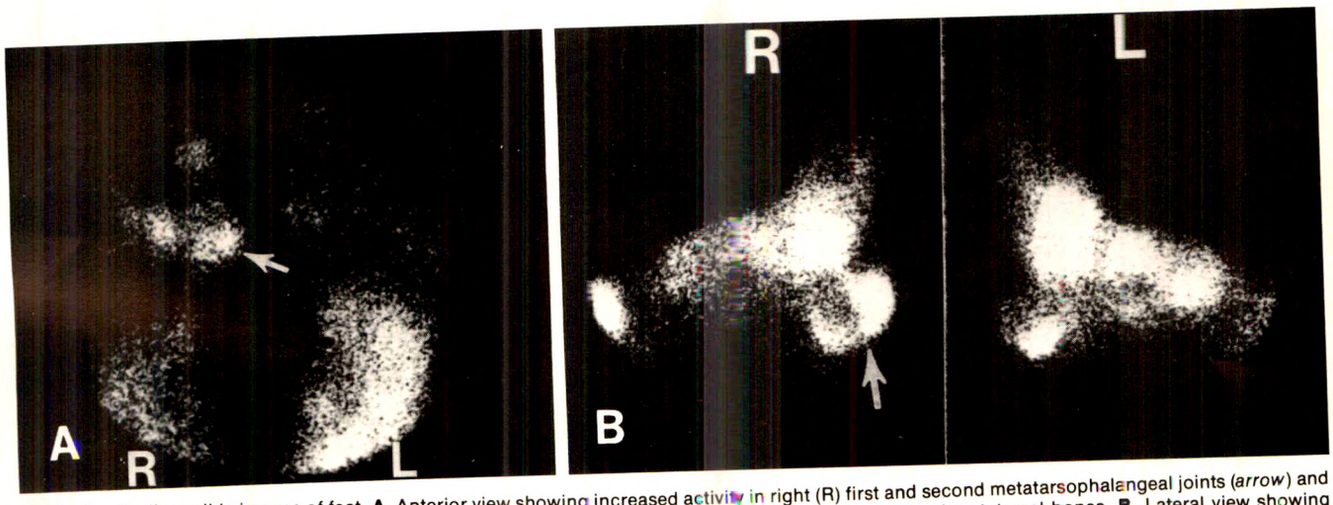


Fig. 2.—Radionuclide images of feet. **A**, Anterior view showing increased activity in right (R) first and second metatarsophalangeal joints (*arrow*) and proximal interphalangeal joints; diffuse increased activity in right tarsal bones, left tarsus, and proximal metatarsal bones. **B**, Lateral view showing previously described abnormal areas and increased activity in area of subachilles bursa bilaterally (greater on the right side, *arrow*).

strated inflammation of the bursa synovial lining fluid production within the bursa, and cartilage and osseous destruction on the posterior surface of the calcaneus. On the plantar surface, fibrinoid-containing tissue with cellular proliferation was found in the plantar aponeurosis. Similar pathologic changes within these anatomic structures would be expected in Reiter's syndrome, which is characterized by a type of arthropathy radiographically similar to ankylosing spondylitis [5].

Since observing that primarily bone-seeking ^{99m}Tc-labeled phosphate compounds localize in or near articular structures in patients with joint disease, they have been effectively used in disclosing synovitis before radiographic and in some cases objective physical findings [6]. The mechanism of increased concentration of ^{99m}Tc pyrophosphate around inflamed joints is considered secondary to the increased bone blood flow contributed by branches of synovial vessels; there is also evidence that ^{99m}Tc pyrophosphate binds to immature collagen of inflamed synovium and articular cartilage [6].

Therefore finding enhanced ^{99m}Tc pyrophosphate near an inflamed sub-Achilles bursa in a patient with Reiter's syndrome is to be expected on the basis of previous observations. Since other "rheumatoid variant" disorders (the arthropathies associated with ankylosing spondylitis, psoriasis, and inflammatory bowel disease) are clinically and radiographically similar to Reiter's syndrome, they might exhibit similar bone imaging findings at the heel.

REFERENCES

1. Ford DK: Reiter's syndrome. *Bull Rheum Dis* 20:588–591, 1970
2. Resnick D, Feingold ML, Curd J, Miwayama G, Goergen

TG: Calcaneal abnormalities in articular disorders: rheumatoid arthritis, ankylosing spondylitis, psoriatic arthritis, and Reiter's syndrome. *Radiology* 125:355–366, 1977

3. Gerster JC, Vischer TL, Bennani A, Fallet GH: The painful heel: comparative study in rheumatoid arthritis, ankylosing spondylitis, Reiter's syndrome and generalized osteoarthrosis. *Ann Rheum Dis* 36:343–348, 1977
4. Pekin TJ, Malinin TI, Zvaifler NJ: Unusual synovial fluid findings in Reiter's syndrome. *Ann Intern Med* 66:677–684, 1967
5. Resnick D, Niwayama G: On the nature and significance of bony proliferation in "rheumatoid variant" disorders. *AJR* 129:275–278, 1977
6. Rosenthall L, Hawkins D: Radionuclide joint imaging in the diagnosis of synovial disease. *Semin Arthritis Rheum* 7:49–61, 1977

"Sinking Pellet" Sign of Bladder Perforation

M. R. CONRAD,[1] C. BAZAN,[1] T. ALLEN,[2] AND R. SCHOENVOGEL[2]

Preoperative diagnosis of urinary bladder perforation due to penetrating missile injury may be difficult to establish. Although retrograde cystography usually demonstrates extravasation, it may be normal on occasion [1]. In shotgun blast wounds, metallic pellets are usually distributed randomly throughout the abdominal cavity, but clumping of pellets in the pelvis on the plain film of the abdomen suggests that they may be lying in a hollow viscus such as the bladder. We present two cases with this finding.

Case Reports

Case 1

A 23-year-old white man received a shotgun wound to the right upper quadrant of the abdomen, left buttock, and left hemiscrotum. The patient was hypotensive and had gross hematuria. Excretory urography showed normal upper tracts with poor opacification of the bladder. Numerous metallic pellets were present in the pelvis and left side of the abdomen, and there was a large clump of pellets in the lower pelvis (fig. 1A). Retrograde cystography was normal (fig. 1B). At exploratory laparotomy a large hole in the posterior wall was repaired along with multiple perforations of the sigmoid colon. Numerous pellets were removed from the bladder. A diverting colostomy was performed and a suprapubic tube was placed in the dome of the bladder.

Case 2

A 39-year-old white man suffered a shotgun wound to the lower abdomen. Physical examination revealed multiple abdominal pellet wounds, decreased pulses in the left leg, and an 8 cm hematoma in the left inguinal area. Urinalysis showed gross hematuria. The plain film of the abdomen revealed scattered metallic pellets in the right side of the abdomen with a clump of pellets in the lower pelvis. Excretory urography showed extravasation from the bladder (fig. 2). At surgery multiple bowel perforations were oversewn, and a partial colectomy was done because of nonviable bowel. Several pellets were removed from the bladder, but no evidence of perforation was found on examination of the exterior or interior of the bladder.

Discussion

In order to minimize the mortality and morbidity of traumatic bladder perforation, early diagnosis and surgical repair is required [2]. In cases of penetrating missile injury, retrograde cystography may be falsely negative [1, 2] as illustrated in case 1. The inherent elasticity and contraction of the highly muscular bladder wall can effectively seal off puncture wounds of 0.5 cm or less [3]. Urine and/or contrast medium extravasation may also be prevented by the heat-searing effect of the blast injury, bladder spasm, and perivesicle tamponade due to urine leakage and/or hematoma formation.

Although numerous metallic pellets may be present in the pelvis following a shotgun wound, clumping of pellets can only occur when they are within the lumen of a hollow viscus such as the bladder. Under the influence of gravity, the pellets sink and clump in the dependent portion of the bladder. The presence of this "sinking

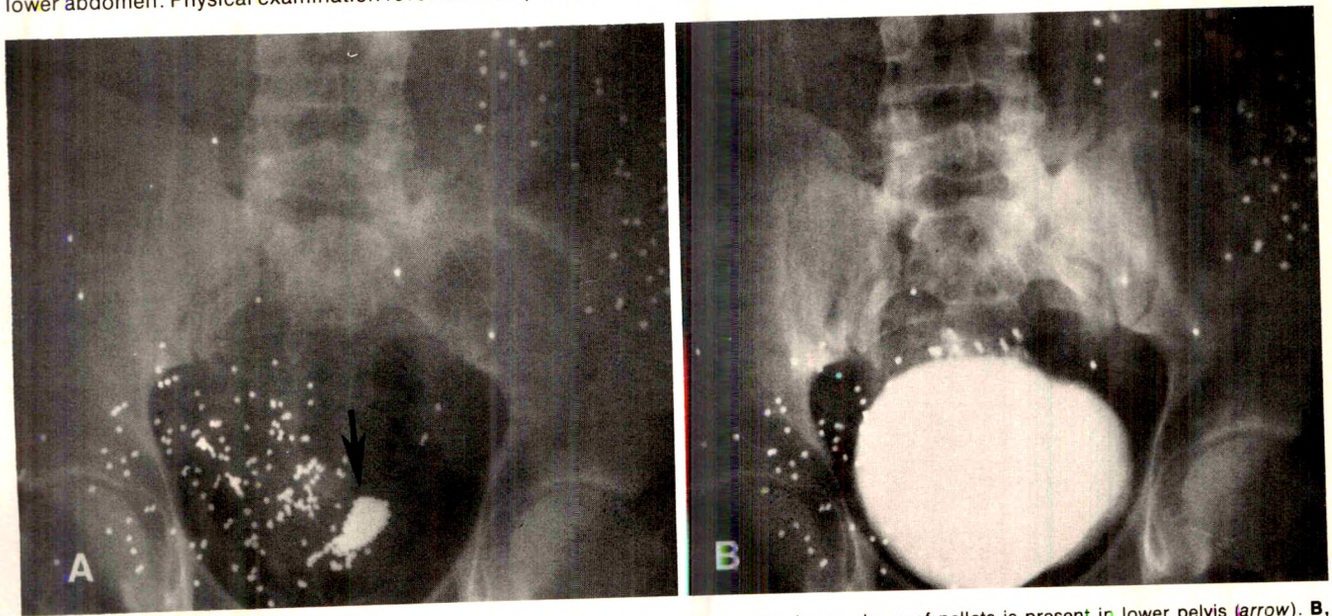


Fig. 1.—Case 1. **A,** Excretory urogram showing scattered metallic pellets in pelvis. Large clump of pellets is present in lower pelvis (*arrow*). **B,** Retrograde cystogram showing normal bladder without evidence of extravasation.

Received July 14, 1978; accepted August 28, 1978.
[1] Department of Radiology, Parkland Memorial Hospital, 5201 Harry Hines Boulevard, Dallas Texas 75235. Address reprint requests to M. R. Conrad.
[2] Department of Urology, Parkland Memorial Hospital, Dallas, Texas 75235.

AJR 132:113–114, January 1979
0361–803X/79/1321–0113 $0.00
© 1979 American Roentgen Ray Society

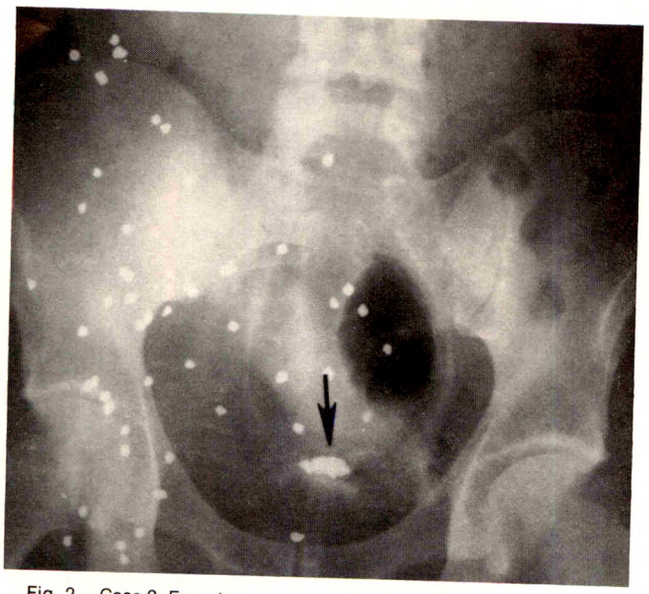


Fig. 2.—Case 2. Excretory urogram showing extravasation of contrast material in pelvis. Note clump of pellets (*arrow*) in region of bladder.

pellet" sign in the region of the bladder indicates that the bladder has been penetrated even if retrograde cystography fails to show extravasation.

ACKNOWLEDGMENTS

We thank Mary Nell Ryals, Mary Starling, and Nancy Schreiber for assistance in the preparation of this manuscript.

REFERENCES

1. Rieser C, Nicholas E: Rupture of the bladder: unusual features. *J Urol* 90:53–57, 1963
2. Lichtenheld FR, Lancaster JM: Intraperitoneal bladder rupture. *J Trauma* 2:457–464, 1962
3. Weyrauch HM, Peterfy RA: Tests for leakage in the early diagnosis of the ruptured bladder. *J Urol* 44:264–273, 1940

Real Time Ultrasound in the Diagnosis of Acute Dissecting Aneurysm of the Abdominal Aorta

M. R. CONRAD,[1] G. M. DAVIS, C. E. GREEN, AND T. S. CURRY, III

The value of ultrasound in evaluation and diagnosis of an abdominal aortic aneurysm has been well established [1]. Diagnosis of dissecting abdominal aortic aneurysm using sonography is less well established. The importance of using real-time ultrasound in diagnosis of an acute dissection of the abdominal aorta is illustrated by the following case. Correct diagnosis would not have been made using static B-scan ultrasound.

Case Report

A 51-year-old black woman with a history of malignant hypertension developed acute chest pain radiating from the midscapular region to the retrosternum, back, and legs. Physical examination revealed a pulse rate of 120, blood pressure 320/150–160, and a grade II/IV systolic ejection murmur at the left sternal border. The abdomen was normal to palpation. Electrocardiography demonstrated left axis deviation and left atrial overload. Chest radiography showed a tortuous aorta and a normal mediastinum.

Despite antihypertensive medication and decrease in blood pressure to 150/75, the back pain and abdominal discomfort increased and the urine output decreased. Real-time sonography, using a linear transducer array (Advanced Diagnostic Research), showed a fine longitudinal "flaplike" structure within the abdominal aorta which appeared to have a normal diameter (2.0 cm) and contour. The "flap" extended inferiorly from the level of the superior mesenteric artery throughout the lower abdominal aorta and vividly undulated in unison with systolic pulsation (fig. 1). On the initial static B-scan the aorta appeared normal (fig. 2A), but careful scanning along the left lateral margin of the aorta revealed the "flap" which appeared to be within the aortic lumen (fig. 2B). Arteriography confirmed a type III dissecting aneurysm of the entire thoracoabdominal aorta (fig. 3) which began immediately distal to the left subclavian artery.

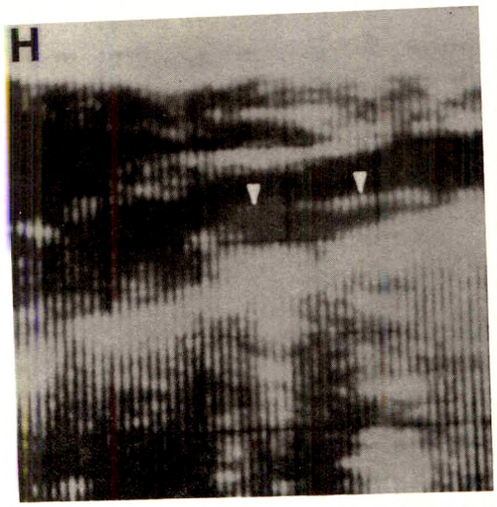


Fig. 1.—Longitudinal real-time scan of abdominal aorta showing normal contour and apparent intraluminal linear echo (*arrowheads*) which undulated in unison with systolic pulsation. H = head end.

Discussion

The estimated incidence of dissecting abdominal aortic aneurysm is 0.28%–1.1% based on autopsy series [2]. Cystic medial necrosis is the most common etiology [3]. Although the symptom of severe, radiating thoracoabdominal pain is characteristic of dissecting aneurysm, confusion with other abdominal conditions, such as cholecystitis, pancreatitis, or renal colic, is possible [2].

Winsberg et al. [4] reported the diagnosis of eight cases of dissecting aneurysm of the abdominal aorta using real-time ultrasound. A "second sonolucent channel" anterior or posterior to the aneurysmal abdominal aorta represented the false channel. In our case of an acute dissection, frank aortic aneurysm formation evidenced by deformity of the contour of the abdominal aorta was not present. Although the intimal flap due to the dissection was imaged, it was not immediately obvious that an extraluminal false channel was present. The true lumen of the abdominal aorta was markedly compressed by the intimal flap which had a "pseudointraluminal" appearance on the sonogram due to preservation of the contour of the abdominal aorta. Had only static B-scanning been done, it is doubtful that the undulating intimal flap would have been diagnosed because of its rapid pulsatile motion and lateral location. Curati et al. [5] described characteristic undulating movement of the intimal flap in a dissecting aneurysm of the ascending aorta using echocardiography. To our knowledge this has not been described in the abdominal aorta.

When sonography is performed in the presence of suspected dissecting abdominal aortic aneurysm, real-time ultrasound should be done. If static B-scanning is to be done, then it should be done very carefully in order to image the delicate intimal flap.

ACKNOWLEDGMENTS

We thank Mary Nell Ryals, Mary L. Starling, and Nancy Schreiber for assistance in the preparation of this manuscript.

Received June 1, 1978; accepted after revision September 8, 1978.

[1] All authors: Department of Radiology, University of Texas Health Science Center, Parkland Memorial Hospital, 5201 Harry Hines Boulevard, Dallas, Texas 75235. Address reprint requests to M. R. Conrad.

AJR 132:115–116, January 1979
© 1979 American Roentgen Ray Society

0361-803X/79/1321-0115 $0.00

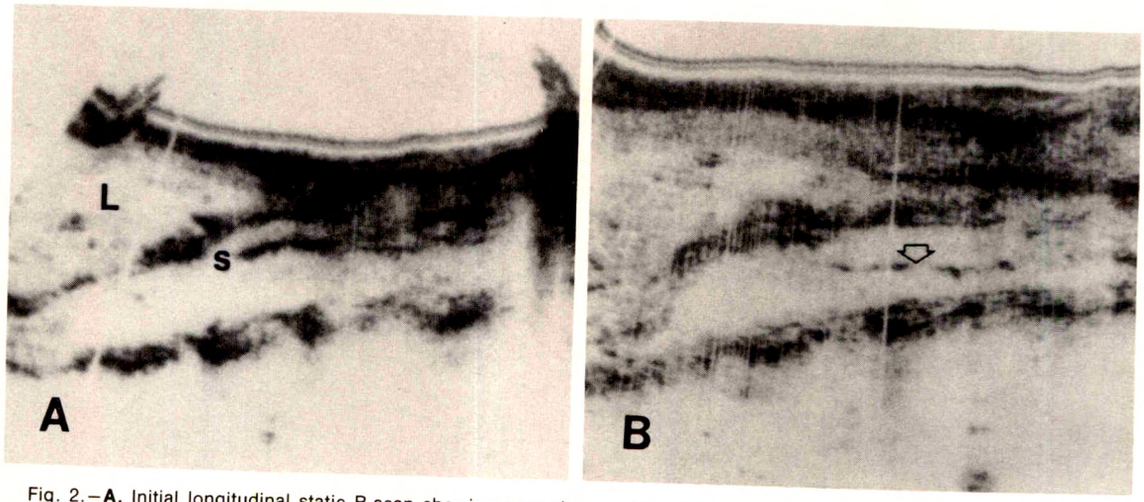


Fig. 2.—**A,** Initial longitudinal static B-scan showing normal-appearing abdominal aorta. S = origin of superior mesenteric artery; L = left lobe of liver. **B,** Repeat static B-scan through left lateral portion of aorta showing delicate intraluminal-appearing "flaplike" structure (*arrow*).

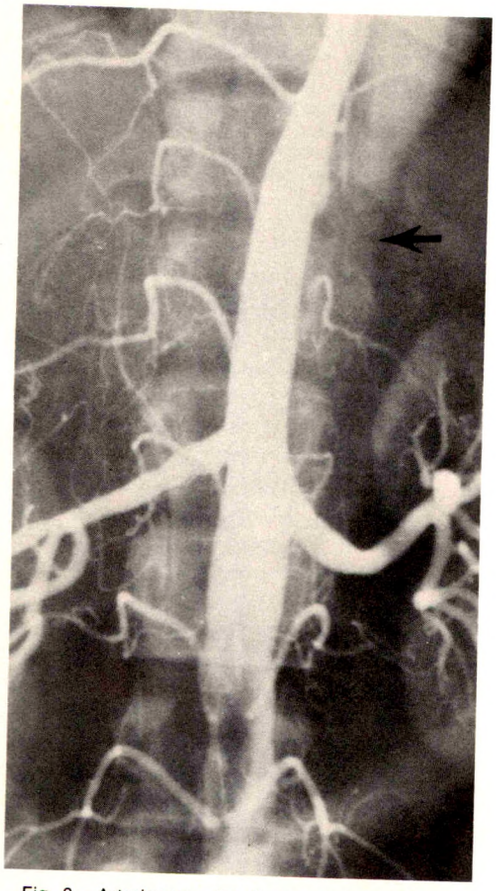


Fig. 3.—Arteriogram showing compressed true lumen of abdominal aorta and faint opacification of false lumen (*arrow*).

REFERENCES

1. Kristensen JK, Holm HH, Rasmussen SN: Ultrasonic diagnosis of aortic aneurysm. *J Cardiovasc Surg* 13:168, 1972
2. Hume DM, Porter RR: Acute dissecting aortic aneurysm. *Surgery* 53:122–153, 1963
3. Burchell HB: Aortic dissection (dissecting hematoma; dissecting aneurysm of the aorta). *Circulation* 12:1068–1079, 1955
4. Winsberg A, Cole-Beuglet C, Mulder DS: Continuous ultrasound "B" scanning of abdominal aortic aneurysms. *AJR* 121:626–633, 1974
5. Curati WL, Peticlerc R, Dyrda I, Winsberg F: Echographic demonstration of mobility of the dissecting flap of an aortic aneurysm. *Radiology* 123:173–174, 1977

Radioisotopic Diagnosis of False Left Ventricular Aneurysm

PATRICK J. PERKINS[1]

Noninvasive diagnostic techniques in cardiovascular nuclear medicine are reliable [1, 2] and are becoming more widely available. Wall motion studies to evaluate regional and global left ventricular function and determine ejection fraction provide information formerly available only from cardiac angiography. This report confirms the utility of this technique in diagnosing false aneurysm of the left ventricle and illustrates its diagnostic features at radioisotope cardiovascular imaging.

Case Report

A 71-year-old woman with a long history of hypertension and adult-onset diabetes was first seen 3 days after onset of chest pain. On admission she was conscious, with systolic blood pressure of 70 mm Hg; electrocardiography indicated acute anterolateral myocardial infarction. She rapidly became obtunded and responded only to painful stimuli. Initial laboratory data revealed serum creatinine greater than 10 mg/dl; blood urea nitrogen, 91 mg/dl; and hematocrit 35%. Cardiac enzymes were markedly elevated. Renal function was normal prior to the present illness.

With support, her consciousness level improved remarkably and blood pressure returned to normal. Peritoneal dialysis was instituted; cardioversion was required four times during the next 17 days to eliminate episodes of rapid artrial fibrillation.

Electrocardiogram-gated cardiac blood pool imaging was then accomplished by in vivo labeled red blood cells according to the method of Pavel et al. [3]. A high resolution gamma camera interfaced to a microcomputer and electrocardiogram gate (Ohio Nuclear Series 100 gamma Camera, Solon, Ohio; ADAC Clinical Data System, ADAC Laboratories, Sunnyvale, Calif.; Brattle Physiological Synchronizer, Brattle Instrument Corporation, Cambridge, Mass.) was used for imaging and data collection and processing. A 45° left anterior oblique radioangiocardiogram displayed retarded progression of activity in the central circulation; initial appearance of activity in the left ventricle revealed only a dilated chamber. Activity persisted in the left ventricle and thoracic aorta over several cardiac cycles. The left ventricle was visualized 14 sec after activity appeared in the main pulmonary artery; 8 sec later focal activity became evident and persisted at the inferoapical border of the left ventricle (fig. 1). Subsequent end-systolic and end-diastolic electrocardiogram-gated blood pool images likewise demonstrated abnormal focus of activity at cardiac apex; a "bottleneck" configuration at the junction with the cardiac chamber extended farther inferiorly and posteriorly. Left ventricle wall motion was poor with little contractility other than high at the posterior and lateral wall (fig. 2). Ejection fraction from equilibrium data was 13%. Diagnosis was false ventricular aneurysm.

While still in congestive heart failure, the patient was transferred to the University of Oregon Health Sciences Center. The next day an intraaortic balloon was inserted to aid circulation. Cardiac catheterization showed occlusion of the midleft anterior descending artery and no visualization of its distal extent. A large false aneurysm filled from near the cardiac apex on ventricular injection (fig. 3).

The false aneurysm was then surgically resected. Recovery was rapid; serum creatinine was normal by postoperative day 5. After discharge and 50 days after surgery the patient died from extension of the anterior infarction.

Discussion

Aneurysm of the left ventricle is not uncommon after myocardial infarction. Mourdjinis et al. [4] recorded a 16% incidence in 112 consecutive coronary care admissions. Incidence reports range from 5% [5] to 38% [6]. The overwhelming majority of postinfarction aneurysms are of the "true" type, which was defined by Schlichter et al. [7] as "a localized outpouching of the cavity of a cardiac chamber, with or without outward bulging of the external surface." "True" ventricular aneurysm has a wide mouth opening to the ventricular cavity and a wall principally composed of fibrous connective tissue, interspersed with myocardial elements, that has replaced infarcted myocardium [7]. Because of its noncontractility, the aneurysm compromises ventricular function [8, 9]; aneurysm is also associated with angina, tachyarrythmias, and systemic embolism [7, 10, 11].

"False" aneurysm results from rupture of the ventricular wall; the junction of the aneurysm and ventricular wall shows a sharp loss of continuity of myocardium. The aneurysm orifice is small relative to its diameter [12], which causes the delay in filling the aneurysm after delineation of the left ventricle. A similar phenomenon is observed at angiography with true aneurysms, such as those occurring intracranially [13]. Pericardium helps contain the false aneurysm; pericardial adhesions may prevent death from hemopericardium with attendant cardiac tamponade [8, 14]. Already mentioned complications associated with "true" aneurysm occur also with "false" aneurysm [11, 12]. False aneurysm, however, contrasted with true aneurysm [4, 7], has an increased tendency for delayed rupture [8, 14, 15]. The larger the diameter of the aneurysm, the greater the force on its wall [16], and thus the greater the likelihood to rupture. Therefore, it is important to diagnose the aneurysm when it is still small, although even small false aneurysms can rupture [15].

Diagnosis of false aneurysm has been rare preoperatively or before postmortem examination [8]. With current radioisotopic techniques, however, this diagnosis can be made noninvasively. Focal and diffuse ventricular

Received March 10, 1978; accepted after revision August 21, 1978.

[1]Departments of Radiology and Nuclear Medicine, University of Oregon, Health Sciences Center, Portland, and Department of Nuclear Medicine, Salem Hospital, 665 Winter Street Southeast, Salem, Oregon 97301. Present address: Department of Diagnostic Radiology, Samuel Merritt Hospital, 350 Hawthorne Avenue, Oakland, California 94609.

AJR 132:117–119, January 1979
0361–803X/79/1321–0117 $0.00

© 1979 American Roentgen Ray Society

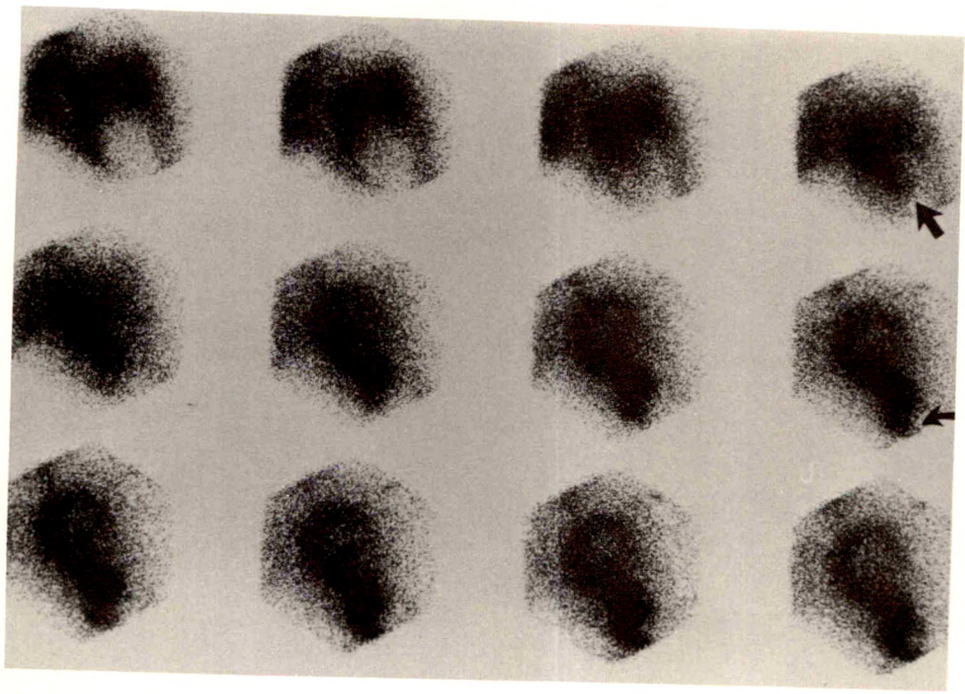


Fig. 1.—45° left anterior oblique radioangiocardiogram showing sequential 2 sec images. Top left: activity in lungs 8 sec after pulmonary artery fills. Top right (*arrow*): left ventricle appearing 6 sec later. Middle right (*curved arrow*): 8 sec later false aneurysm fills. Bottom: aneurysm showing persistently.

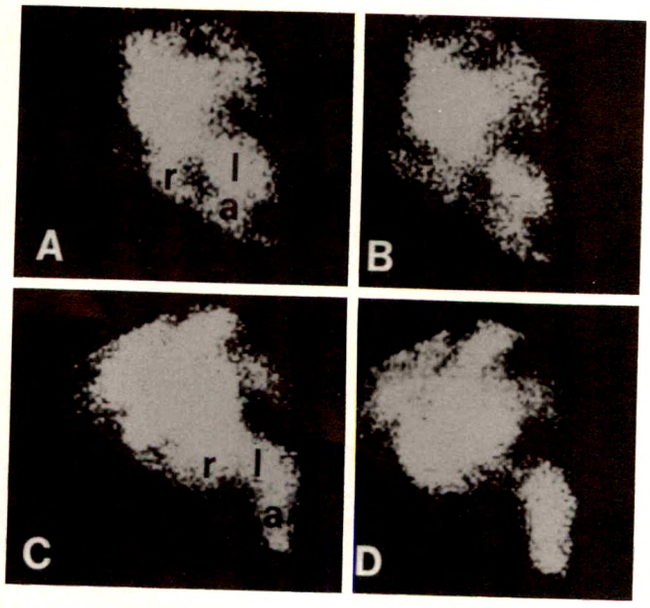


Fig. 2.—Cardiac blood pool images of 45° left anterior oblique views in end-diastole (**A**) and end-systole (**B**), and 5° right anterior oblique views in diastole (**C**) and systole (**D**) shown after background subtraction and contrast enhancement (r = right ventricle; l = left ventricle; a = false aneurysm.) False aneurysm extends from inferior apical aspect of left ventricle (**C** and **D**). **A** and **B** show "bottleneck" connection between false aneurysm and left ventricle. Little wall motion occurs except high laterally and posteriorly.

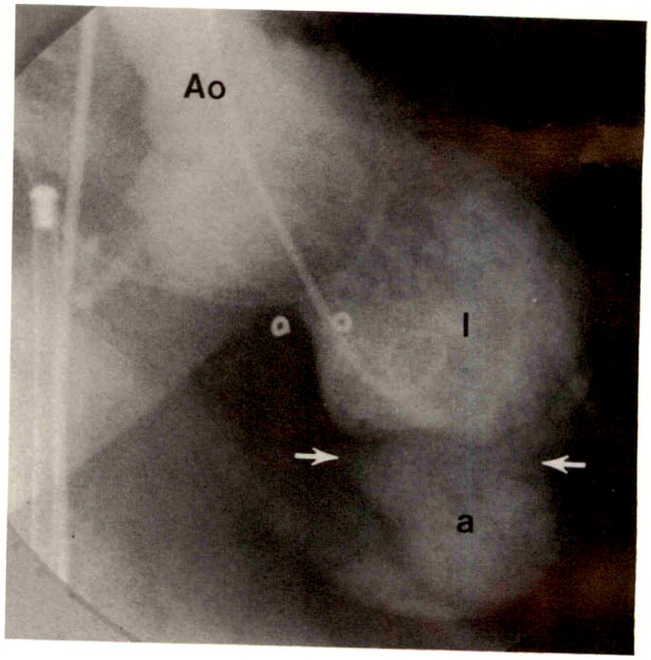


Fig. 3.—Left ventriculogram showing opacified left ventricle in right anterior oblique projection (Ao = aorta root; l = left ventricle cavity; a = false aneurysm). Note "bottleneck" connection between aneurysm and left ventricle (*arrows*).

dysfunction are reliably differentiated with electrocardiogram-gated cardiac blood pool imaging, and the results of this imaging method favorably compare with standard invasive contrast ventriculography [2, 17, 18]. Recognition of false ventricular aneurysm is important both as a cause of left ventricular dysfunction and also because of the increased tendency to delayed rupture. As in true aneurysm, false aneurysm is amenable to surgical therapy [8, 19, 20].

Differential diagnosis should include a large true aneurysm with mural thrombus; this could produce a negative defect in the blood pool activity of the ventricle. How-

ever, the progression of activity from the left ventricle proper through the "bottleneck" of the false aneurysm and subsequent filling of the aneurysmal cavity, as well as the presence of the "bottleneck" on multiple views at blood pool imaging should exclude this possibility. A case reported by Botvinik et al. [21] had characteristics at radioisotopic imaging similar to this case.

ACKNOWLEDGMENTS

We thank Drs. Bradley Harlan, Division of Cardiopulmonary Surgery, and Josef Rösch, Department of Diagnostic Radiology, University of Oregon Health Sciences Center, Portland, Oregon for providing details of the surgical record and the cineventriculogram, respectively, and Drs. C. Patrick Moore and James Devorss, Salem Hospital, for permission to study this patient.

REFERENCES

1. Zaret BL, Strauss HW, Martin ND, Wells HP Jr, Flamm MD Jr: Noninvasive evaluation of myocardial perfusion with potassium 43: study of patients at rest, exercise and during angina pectoris. *N Engl J Med* 288:809–812, 1973
2. Rigo P, Murray M, Strauss HW, Pitt B: Scintiphotographic evaluation of patients with suspected left ventricular aneurysm. *Circulation* 50:985–991, 1974
3. Pavel DG, Zimmer AM, Patterson UN: In vivo labelling of red blood cells with 99m Tc: a new approach to blood pool visualization. *J Nucl Med* 18:305–308, 1977
4. Mourdjinis A, Olsen E, Raphael MJ, Mounsey JPD: Clinical diagnosis and prognosis of ventricular aneurysm. *Br Heart J* 30:497–513, 1968
5. Lisa JR, Ring A: Myocardial infarction or gross fibrosis: analysis of 100 necropsies. *Arch Intern Med* 50:131–141, 1932
6. Applebaum E, Nicholson GHB: Occlusive disease of the coronary arteries; analysis of pathological anatomy in 168 cases with electrocardiographic correlation of 36 of these. *Am Heart J* 10:662–680, 1935
7. Schlichter J, Hellerstein HK, Katz LN: Aneurysm of the heart: a correlative study of one hundred and two proved cases. *Medicine* (Baltimore) 33:43–86, 1954
8. Gueron M, Wanderman KL, Hirsch M, Borman J: Pseudoaneurysm of the left ventricle after myocardial infarction. *J Thorac Cardiovasc Surg* 69:736–742, 1975
9. Greenwood WF, Aldridge HE, Wigle ED: The nature of the disorder of function in chronic post infarction aneurysm of the left ventricle. *Can Med Assoc J* 92:611–614, 1965
10. Graber JD, Oakley CM, Pickering BN, Goodwin JF, Raphael MJ, Steiner RE: Ventricular aneurysm—an appraisal of diagnosis and surgical treatment. *Br Heart J* 34:830–838, 1972
11. Dubnow MH, Burchell HB, Titus JL: Post infarction ventricular aneurysm. *Am Heart J* 70:753–760, 1965
12. Van Tassell RA, Edwards JE: Rupture of heart complicating myocardial infarction. *Chest* 61:104–116, 1972
13. Allcock JM: Aneurysms, in *Radiology of the Skull and Brain* vol II, book 4, edited by Newton TH, Potts DG, St. Louis, Mosby, 1974, p 2437
14. Ersek RA, Chesler E, Korns ME, Edwards JE: Spontaneous rupture of a false left ventricular aneurysm following myocardial infarction. *Am Heart J* 77:677–680, 1969
15. Vlodaver Z, Coe JI, Edwards JE: True and false left ventricular aneurysms. *Circulation* 51:567–572, 1975
16. Compton RA: Bursting forces within the human body. *Radiology* 107:77–80, 1973
17. Zaret BL, Strauss HW, Hurley PJ, Natarajan TK, Pitt B: A noninvasive scintiphotographic method of detecting regional ventricular dysfunction in man. *N Engl J Med* 284:1165–1170, 1971
18. Strauss HW, Pitt B: Common procedures for noninvasive determination of regional myocardial perfusion, evaluation of regional wall motion and detection of acute infarction. *Am J Cardiol* 38:731–738, 1976
19. Effler DB, Groves LK, Favaloro R: Surgical repair of ventricular aneurysm. *Chest* 48:37–43, 1965
20. Basta LL, Takeshita A, Theilen EO, Ehrenhaft JL: Aneurysmectomy in treatment of ventricular and supraventricular tachyarrhythmias in patients with post-infarction and traumatic ventricular aneurysms. *Am J Cardiol* 32:693–699, 1973
21. Botvinik EH, Shames D, Hutchinson JC, Roe RB, Fitzpatrick M: Noninvasive diagnosis of a false left ventricular aneurysm with radioisotope gated cardiac blood pool imaging. *Am J Cardiol* 37:1089–1093, 1976

Nuclear Scan of Pulmonary Hemorrhage in Idiopathic Pulmonary Hemosiderosis

THEODORE MILLER[1] AND TOSHIYUKI TANAKA[2]

Idiopathic pulmonary hemosiderosis, a disease of unknown etiology most often occuring in children, is characterized by recurring episodes of alveolar consolidation. Exacerbations of pulmonary hemorrhage coincide with episodes of alveolar filling; repeated episodes lead to progressive interstitial fibrosis and eventually to cor-pulmonale [1].

Serial nuclear scans of the lungs after injection of radiolabeled red blood cells should parallel the pathologic and radiographic findings. We observed the accumulation of radiolabeled red blood cells in the lungs on scan images, a finding not previously reported.

Case Report

A 2-year-old Mexican girl was admitted because of recurrent episodes of dyspnea with hemoptysis. Chest films on admission revealed diffuse alveolar consolidation without cardiomegaly or pleural fluid. Initial hospitalization was 2 months earlier for bilateral "pneumonitis," thought secondary to mycoplasma pneumonia. At that time she had severe iron deficiency anemia, jaundice, and hemoptysis. Transfusion, iron supplement, and a course of erythromycin was effective. Current admission studies revealed iron deficiency anemia due to both chronic and acute blood loss. Urinalysis and blood chemistry levels were normal. Direct Coombs was negative. Admission hematocrit was 11.6%; hemoglobin, 4.6 gm; reticulocyte count, 6%. Bilirubin levels were 1.2 mg/100 ml total and 0.3 mg/100 ml direct. Sputum for hemosiderin-laden macrophages was negative. She was transfused with 400 ml of packed cells, which raised the hematocrit to 30.2%. Iron supplement (6 mg/kg/day) and erythromycin (20 mg/kg/day) were given with good clinical results. By hospital day 3, the chest film showed progression of the alveolar consolidation; subsequent films showed marked resolution of the infiltrates. Hematocrit dropped to 17.7 with concurrent dyspnea and hemoptysis 1 week later. Chest radiography showed recurrent alveolar consolidation, followed by clearing over the next 6 days (fig. 1A). After administration of ^{99m}Tc-labeled red blood cells (fig. 1B) scans showed activity largely centered in the heart, liver, and spleen. Symptoms of dyspnea and hemoptysis recurred the next morning with radiographic alveolar consolidation (fig. 1C). A scan at this time without additional radionuclide (fig. 1D) showed markedly increased activity in both lungs. The patient was placed on steroids with symptomatic improvement. Follow-up films for more than 1 year after cessation of steroid therapy revealed bilateral lung volume loss with diffuse interstitial pattern consistent with hemosiderosis.

Discussion

Idiopathic pulmonary hemosiderosis, first recognized by Virchow in 1864, was described in children by Ceelen in 1940 (cited in [2]). The disease is characterized by recurrent intrapulmonary hemorrhage manifested by hemoptysis, iron deficiency anemia, and pulmonary insufficiency [3]. Diagnosis is confirmed primarily by demonstrating hemosiderin-laden macrophages in lung biopsy, sputum samples, or gastric washings. Clinical manifestations, laboratory indices, and radiographic changes can support this diagnosis. Confirming hemorrhage as the cause of lung infiltrates can be done by injecting ^{51}Cr-labeled red blood cells and demonstrating high activity in the lung fields by profile counting with an external detector [1, 4]; ^{59}Fe produces similar results [5, 6]. Another means of confirming alveolar hemorrhage is based on retention of inhaled carbon monoxide by blood cells deposited in the alveoli. Carbon-15–labeled carbon monoxide clearance test has shown delayed clearance from the lungs in cases of pulmonary hemorrhage; however, the test requires a nearby cyclotron for ^{15}C production [11]. The profile counting is a numerical representative. An image of the intrapulmonary hemorrhage should be readily demonstrated by abnormal accumulation of ^{99m}Tc-labeled red cells in the lungs.

Blood pool scanning had been chiefly limited to ^{99m}Tc-labeled human serum albumin, but this agent is a marker for albumin space and not vascular space. In vivo labeling of red blood cells by sequential intravenous injection of stannous tin compound and ^{99m}Tc pertechnetate is simple and effective with a 78% average of injected dose in red blood cells [7, 8]. Scanning is limited to about 24 hr after injecting ^{99m}Tc pertechnetate because of its short 6 hr half-life. Our patient received 2.6 mg reconstituted stannous pyrophosphate followed by 2 mCi ^{99m}Tc pertechnetate.

Blood pool imaging using in vivo labeling of red blood cells with ^{99m}Tc pertechnetate and "cold" pyrophosphate was also performed on two adult patients with suspected myocardial infarction studied for evaluation of cardiac wall motion. A blood pool image obtained 24 hr after injection of ^{99m}Tc pertechnetate showed normal cardiac chambers and minimal pulmonary activity. Examination of red blood cells in adult patients revealed labeling of 99% during the first 1/2 hr after injection and 95% at 24 hr, and correspond well with previously reported results [9].

Nuclear scan image of the blood pool revealed increased accumulation of radiolabeled red blood cells correlating directly with the radiographic and clinical changes. This method offers a direct image of the pathophysiology; however, the short half-life necessitates opportunistic timing of this diagnostic procedure for demonstrating acute hemorrhage. The reliability of labeled red blood cells as a blood pool imaging agent has been proven [10]. The lack of pulmonary uptake in delayed images of patients without pulmonary hemorrhage is documented. The study can be performed in any

Received February 10, 1978; accepted after revision August 16, 1978.

[1] Division of Pediatric Radiology, Charles R. Drew Postgraduate Medical School and Martin Luther King, Jr. General Hospital, 12021 South Wilmington Avenue, Los Angeles, California 90059. Address reprint requests to T. Miller.

[2] Division of Nuclear Medicine, Charles R. Drew Postgraduate Medical School and Martin Luther King, Jr. General Hospital, Los Angeles, California 90059.

© 1979 American Roentgen Ray Society

0361–803X/79/1321–0120 $0.00

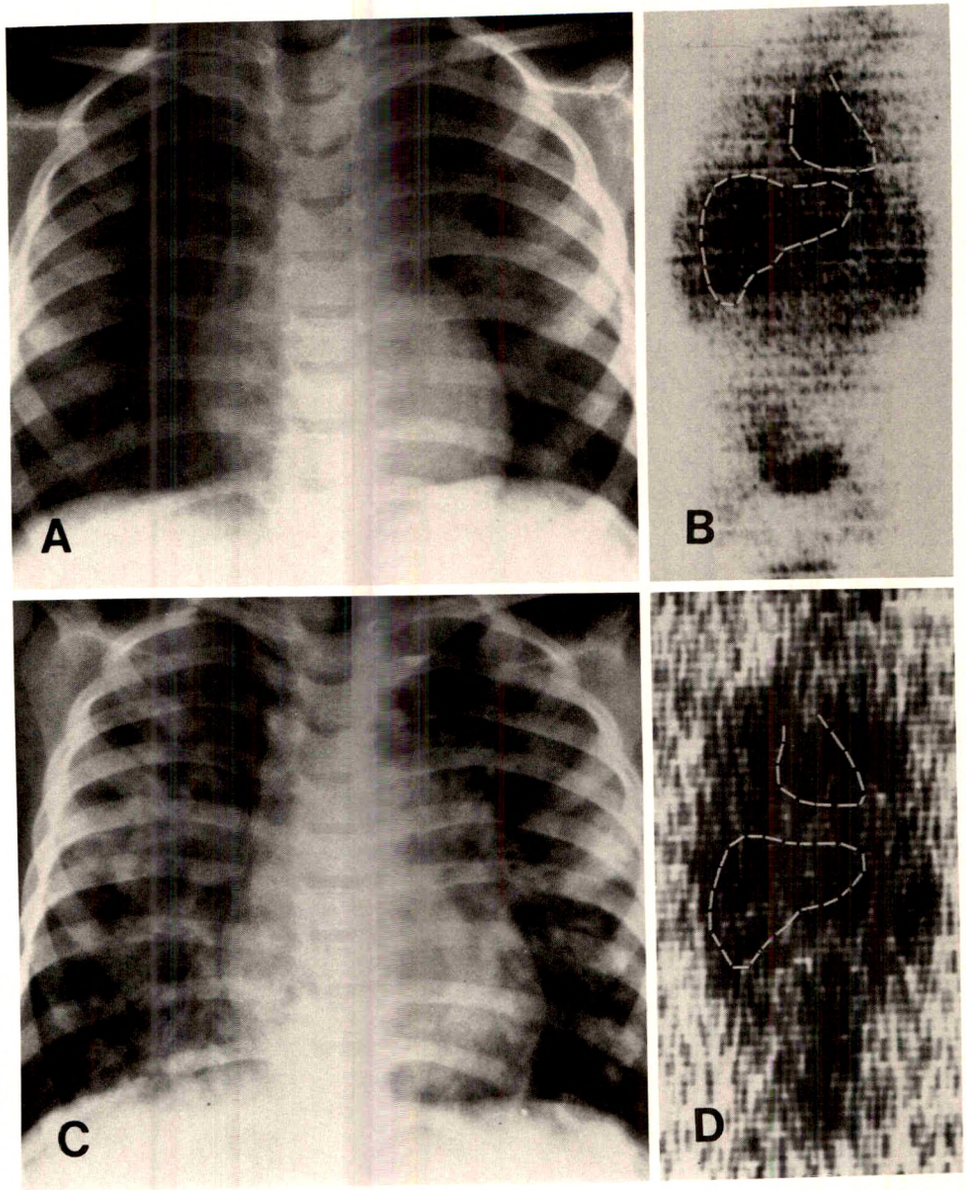


Fig. 1.—**A,** Relatively normal lungs after episode of alveolar consolidation. **B,** 3 hr after administration of ^{99m}Tc, ^{64}Tc; patient in remission. Activity centered in heart, liver, and spleen. **C,** Exacerbation of disease; alveolar consolidation. **D,** Same time as **C**; activity shifted to lungs. Boundary of lungs with heart and liver obscured by intrapulmonary hemorrhage.

nuclear medicine laboratory with an imaging device, bone kit, and ^{99m}Tc pertechnetate, all readily available.

ACKNOWLEDGMENTS

We thank Dr. Fred Mishkin and Candace Chandler for assisting in manuscript preparation.

REFERENCES

1. Fraser RG, Pare JA: *Diagnosis of Diseases of the Chest*. Philadelphia, Saunders, 1970
2. Jiji V, Hofkin CA: Case report: idiopathic pulmonary hemosiderosis. *South Med J* 67:488–491, 1974
3. Soergel KH, Sommers SC: Idiopathic pulmonary hemosiderosis and related syndromes. *Am J Med* 32:499–511, 1962
4. Samuels LD, Bass JC: ^{51}Cr lung scan in idiopathic pulmonary hemosiderosis. *J Nucl Med* 16:106–107, 1969
5. Azen EA, Clatanoff DV: Prolonged survival in Goodpasture's syndrome. *Arch Intern Med* 114:453–460, 1964
6. De Gowin RL, Sorenson LB, Charleston DB, Gottschalk A, Greenwald J: Retention of radio iron in the lungs of a woman with IPH. *Ann Intern Med* 69:1213–1220, 1968
7. Jones AG, Davis MA, Uren RF, Shulkin P: In vivo red cell labeling with Tc-99m (abstr). *J Nucl Med* 18:637, 1977
8. Parker JA, Uren RF, Jones AG, Maddox DE, Zimmerman RE, McNeil JM, Homan BL: Radionuclide left ventriculography with the slit hole collimator. *J Nucl Med* 18:848–851, 1977
9. Pavel DG, Zimmer AM, Patterson VN: In vivo labeling of red blood cells with 99m-Tc: a new approach to blood pool visualization. *J Nucl Med* 18:305–308, 1977
10. Theros EG, Reeder MM, Eckert JF: Case of the month from the AFIP. *Radiology* 90:784–791, 1968
11. Ewan PW, Jones HA, Rhodes CG, Hughes JMB: Detection of intrapulmonary hemorrhage with carbon monoxide uptake. *N Engl J Med* 295:1391–1396, 1976

Myoblastoma of the Breast

LAWRENCE W. BASSETT[1] AND HARVEY C. COVE[2]

Among conditions clinically, mammographically, and pathologically confused with breast carcinoma are fat necrosis [1], plasma cell mastitis, and sclerosing adenosis [2]. Myoblastoma (granular cell tumor) of the breast may also suggest a carcinomatous lesion. To our knowledge, this is the first report of myoblastoma of the breast in the radiology literature.

Case Report

R. D., a 53-year-old woman, had noted a mass in her left breast for 3 weeks. Medical history was noncontributory. Physical examination revealed 1 cm hard mass in the upper outer quadrant of the left breast. There was no skin retraction. Attempted needle aspiration produced no fluid.

Mammography showed a 1 cm nodular density in the upper outer quadrant of the left breast (fig. 1A). It had sharp margins except for tendrillike extensions into adjacent breast tissue. There was no evidence of calcifications or skin retraction. The mammographic impression was "nodular density in the left breast suspicious for malignancy."

The biopsy specimen was a 4.5 × 4.5 × 1.3 cm portion of breast tissue. Centrally it contained a 1.0 × 1.0 × 1.3 cm firm, gritty nodule. Histologic sections demonstrated a tumor of cordlike plump cells with round central nuclei and an eosinophilic granular cytoplasm (fig. 1C). No mitoses were noted. The tumor appeared to expand by replacing adjacent fat which marginated the nodule (fig. 1B).

Discussion

Myoblastoma, or granular cell tumor, was first described by Abrikossoff in 1926 [3]. Mulcare [4] published a comprehensive review of these tumors in 1926. These lesions most commonly occur in the tongue or subcutaneous tissue. Only about 6% of myoblastomas occur in the breast [5]. About thirty cases have been reported in the surgical literature. Haagensen [6] stressed the importance of distinguishing myoblastoma from carcinoma to avoid unnecessary mastectomy. These tumors can produce all the signs and gross characteristics of mammary cancer including hardness, fixation, poorly defined outlines, and inflammation and ulceration of the skin. However, there are no proven cases of malignancy in myoblastoma of the breast, and local resection is adequate treatment. As demonstrated by this case, myoblastoma can also appear mammographically as a lesion suspicious for carcinoma. The apparent invasion of surrounding breast tissue on mammography is explained by inspecting the biopsy specimen.

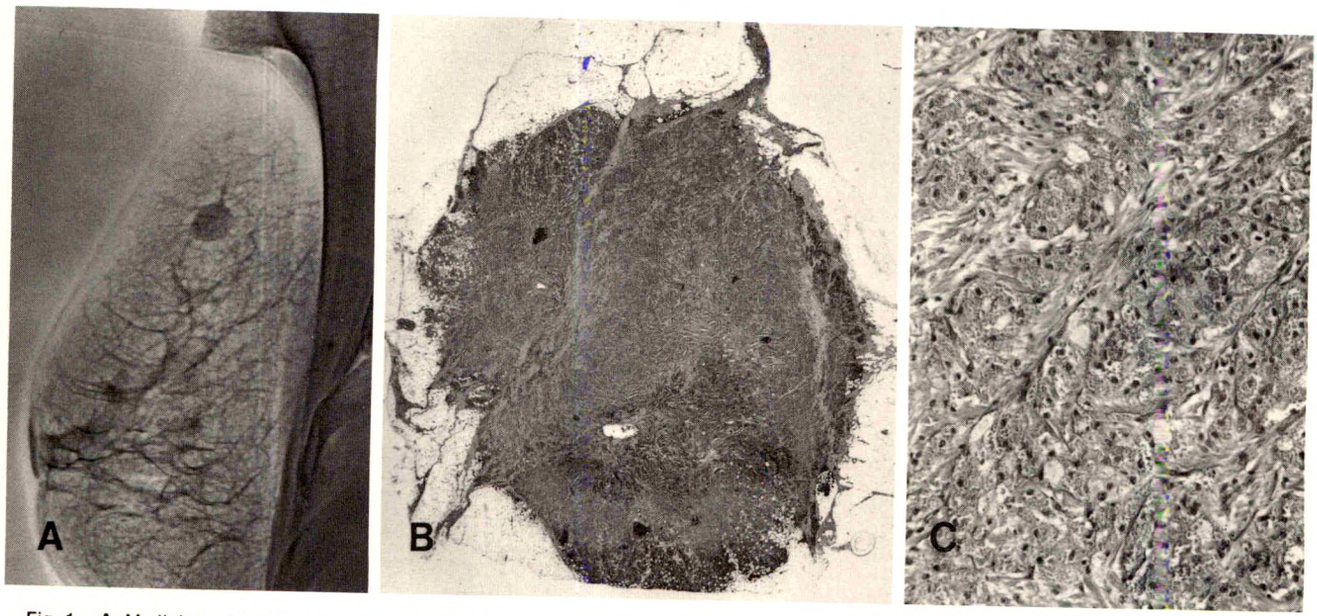


Fig. 1.—**A,** Mediolateral xeromammogram demonstrating 1 cm nodular density in upper portion of left breast. Margins sharp except for extensions into surrounding breast tissue. **B,** Low power section demonstrating whole nodule and surrounding adipose tissue. Note marginal extensions of tumor into surrounding fat. **C,** Histologic section. Cordlike arrangement of plump cells showing granular cytoplasm.

Received June 13, 1978; accepted after revision September 7, 1978.

[1] Department of Radiological Sciences, University of California School of Medicine, Los Angeles, California 90024. Address reprint requests to L. W. Bassett.

[2] Department of Pathology, University of California School of Medicine, Los Angeles, California 90024.

© 1979 American Roentgen Ray Society

0361–803X/79/1321–0122 $0.00

REFERENCES

1. Bassett LW, Gold RH, Cove HC: Mammographic spectrum of traumatic fat necrosis: the fallibility of "pathognomonic" signs of carcinoma. *AJR* 130:119–122, 1978
2. Gold RH, Montgomery CK, Rambo ON: Significance of margination of benign and malignant infiltrative mammary lesions: roentgenographic-pathological correlation. *AJR* 118:881–894, 1973
3. Abrikossoff AI: Über Myome, Ausgehend von der quergestreiften willkurlichen Müskulatur. *Arch Pathol Anat* 260:215, 1926
4. Mulcare R: Granular cell myoblastoma of the breast. *Ann Surg* 168:262–268, 1968
5. Colberg JE, Hubay CA: Granular cell myoblastoma, a problem in diagnosis. *Surgery* 53:226–237, 1963
6. Haagensen CD: *Diseases of the Breast*. Philadelphia, Saunders, 1956

Isolated Dextrogastria: Report of Two Cases

J. GEORGE TEPLICK,[1] ROBERT J. WALLNER,[2] ARNOLD H. LEVINE,[1] MARVIN E. HASKIN,[1] AND STEVEN K. TEPLICK[1]

Isolated situs inversus of the stomach with otherwise normal position of the thoracic and abdominal viscera is an extremely rare anomaly occurring in two distinct forms [1, 2]. Because of its close relationship to the liver, the right-sided stomach may produce interesting and confusing changes in the liver scan. Two cases illustrate the radiologic features of the two principal types of isolated congenital dextrogastria and the effect of one type on the liver scan.

Case Reports

Case 1

E. M., a 50-year-old woman, was hospitalized for cardiac catheterization. She had been increasingly dyspneic for several years, and 1 week before admission had an acute attack of substernal pain lasting several hours. A total thyroidectomy for thyroid carcinoma had been performed 15 years earlier, and she had been on a maintenance dosage of thyroid extract. Family history was noncontributory.

A systolic murmur extending into the neck and a 2 cm node on the right side of the neck were the only significant physical findings. Blood pressure was normal. All biochemical and blood studies were within normal range. Chest radiography was negative with no apparent cardiac abnormality. Cardiac catheterization disclosed evidence of obstructive cardiomyopathy with an 80 mm gradient and evidence of mild aortic and mitral insufficiency. Coronary arteries were normal.

Because of the neck node, radionuclide scans were made of the thyroid gland and liver to rule out local recurrence of thyroid carcinoma or liver metastasis. No functioning thyroid tissue could be demonstrated with radioiodine. The ^{99m}Tc sulfur-colloid liver scan revealed an atypical filling defect in the inferolateral right lobe (fig. 1A). A band of decreased activity extended along the superior liver margin to merge with the inferolateral defect in the posterior view (fig. 1B). A broad band of decreased activity appeared to separate the posterior liver from splenic activity in the lateral view (fig. 1C).

Because these scan abnormalities suggested possible metastatic disease, the gastrointestinal tract was radiographically investigated. Barium enema study revealed a normal colon with a low-lying transverse colon. A gas shadow high in the right upper quadrant resembled the gastric fundus. Barium meal study (figs. 1D and 1E) disclosed a completely right-sided mirror-image stomach that was entirely retrohepatic. The duodenal bulb, duodenal loop, ligament of Treitz, and small intestine were in normal anatomic position.

The liver scan was reevaluated during and after ingestion of ^{99m}Tc pertechnetate in water. Serial studies performed during deglutition demonstrated progressive radionuclide filling of the inferolateral hepatic defect (fig. 1F). Postingestion static scans clearly demonstrated the retrohepatic stomach.

Case 2

J. L., a 65-year-old woman, was an outpatient seen because of pain in the left shoulder and anterior chest that was relieved by vomiting. Occasional dysphagia has been noted for many years. Medical history included rheumatic fever at age 3, hysterectomy at age 41, and occasional attacks of angioneurotic edema.

Electrocardiography showed left ventricular hypertrophy and myocardial damage. Chest and upper gastrointestinal tract radiography (fig. 2) showed an enlarged heart shadow and a density in the right lower chest with an air-fluid level. Barium studies disclosed a completely right-sided stomach lying posteriorly under an eventrated portion of the right diaphragm above the liver. The lower esophagus was somewhat tortuous as it entered the elevated right-sided stomach. The duodenal bulb, ligament of Treitz, small bowel, and liver were normally located. Studies of the colon and gallbladder revealed no abnormalities of position. The hepatic flexure of the colon was slightly low, apparently due to a low-lying liver. On a liver scan, the liver appeared normal in contour except for a slight decrease in activity at the posterosuperior margin caused by extrinsic pressure from the adjacent stomach.

Discussion

The incidence of complete transposition of all the viscera (situs inversus totalis) is about 1:6000–1:8000 [2]. Partial or isolated visceral transposition, also rare, most often involves the heart (congenital dextrocardia). Isolated dextrogastria is the rarest of all visceral transpositions and can occur in two distinct forms. The stomach may lie completely behind the liver (here called type I) or may lie above the liver in association with eventration of the right diaphragm (type II). In both forms, the ligament of Treitz and all other viscera are in their usual position. Embryologically, failure of the foregut to normally rotate results in type I dextrogastria; if there is associated failure to complete descent of the foregut from the chest, dextrogastria with eventration (type II) will occur [3–5].

Only isolated cases of either type have been reported. Type I [2, 5–9] is apparently even rarer than type II (3, 10–13) having an incidence less than 1:100,000 [3]. Generally, both types of dextrogastria produce no symptoms and are accidentally discovered. Eventration of type II causes abnormalities on routine chest radiography (fig. 2A) and may simulate abscess, right-sided hiatal hernia, or other pathology at the right base [3, 14]. The normal left-sided gastric gas shadow is absent.

In type I, the chest film is normal but the gastric gas shadow is absent on the left side and may be identified

Received April 10, 1978; accepted after revision September 7, 1978.

[1]Department of Diagnostic Radiology, Hahnemann Medical College and Hospital, 230 North Broad Street, Philadelphia, Pennsylvania 19102. Address reprint requests to J. G. Teplick.

[2]Department of Nuclear Medicine, Hahnemann Medical College and Hospital, Philadelphia, Pennsylvania 19102.

© 1979 American Roentgen Ray Society

0361–803X/79/1321–0124 $0.00

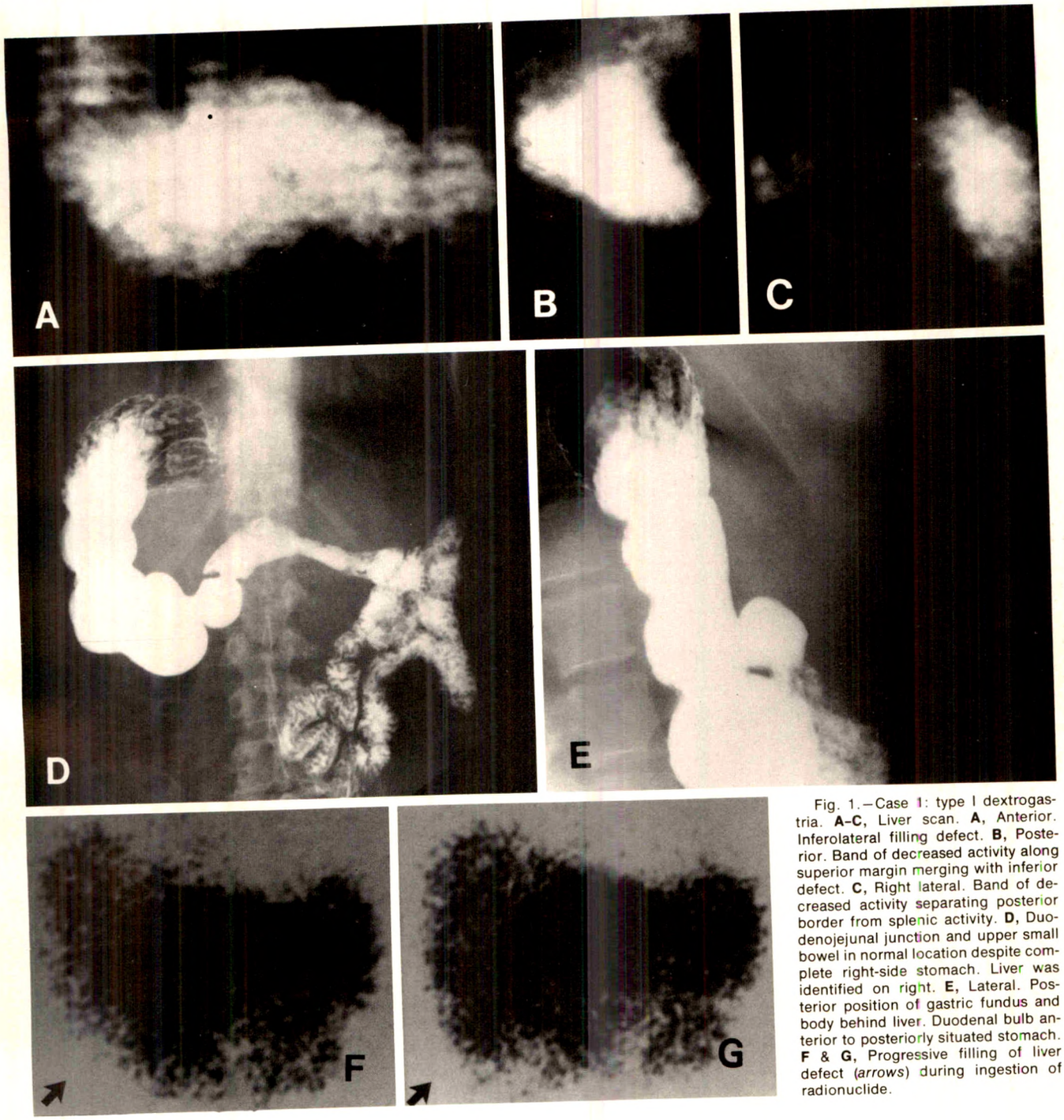


Fig. 1.—Case 1: type I dextrogastria. **A–C,** Liver scan. **A,** Anterior. Inferolateral filling defect. **B,** Posterior. Band of decreased activity along superior margin merging with inferior defect. **C,** Right lateral. Band of decreased activity separating posterior border from splenic activity. **D,** Duodenojejunal junction and upper small bowel in normal location despite complete right-side stomach. Liver was identified on right. **E,** Lateral. Posterior position of gastric fundus and body behind liver. Duodenal bulb anterior to posteriorly situated stomach. **F & G,** Progressive filling of liver defect (*arrows*) during ingestion of radionuclide.

on the right side below the diaphragm. Contrast studies may show redundancy of the lower esophagus in type II with the high position of the stomach (fig. 2). In both types, the gastric fundus and body are posteriorly located and appear as mirror-image reversal on frontal projection. The duodenal bulb loop, duodenojejunal junction, and small and large bowels are all in their usual locations.

Changes in the liver scan from a type I dextrogastria (fig. 1) were also presented in a case report by Chadhuri

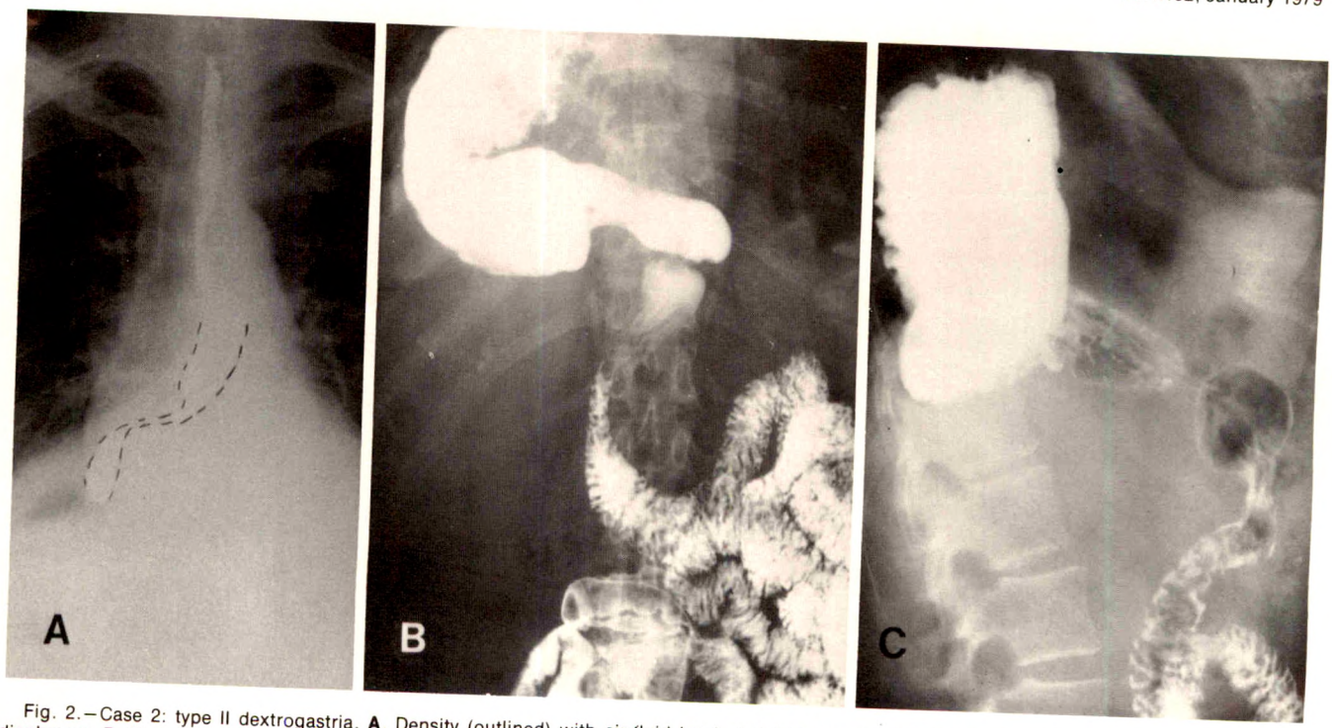


Fig. 2.—Case 2: type II dextrogastria. **A**, Density (outlined) with air-fluid level at right base; normal gastric air bubble not seen under the left diaphragm. **B**, Stomach, on right with mirror-image configuration, lies above liver; posterior right diaphragm markedly elevated. Note normal location of entire duodenum and small bowel. **C**, Lateral view showing posterior location of elevated stomach beneath elevated posterior right diaphragm. Bulb is located anteriorly.

[9], but no posterior scan was shown. In this view, the major component of the defect will be posterior and such findings might suggest dextrogastria.

REFERENCES

1. Lassrich MA, Bruns HA: Anomalies of stomach, duodenum, and small and large bowel in children (in German). *Radiologe* 7:12–26, 1967
2. Almy MA, Volk FH, Graney CM: Situs inversus of stomach. *Radiology* 61:376–378, 1953
3. Nayer HR: Right-sided stomach associated with eventration of diaphragm simulating hydropneumothorax. *AJR* 64:50–52, 1950
4. Dott NM: Anomalies of intestinal rotation. *Br J Surg* 11:251–286, 1923
5. Anton JI, Panoff CE, Spiegel MB: Segmental abdominal heterotaxy. *Am J Surg* 54:446–456, 1941
6. Risel W: Literature of partial situs inversus of stomach (in German). *Zentralbe Allq Pathol* 20:673–734, 1909
7. Buis J: Transposition of the stomach. *Nebr Med J* 10:20–27, 1925
8. Rosselet A, Mengis O: A congential anomaly of the stomach. *Acta Radiol* (Stockh) 15:438–442, 1934
9. Chandhuri TK: False-positive liver scan caused by dextrogastria. *J Nucl Med* 17:1109–1110, 1976
10. Kinney LC: Congenital non-rotation of the stomach. *AJR* 8:383–385, 1921
11. Harris LI, Stivelman BP: Non-rotation of the stomach simulating spontaneous hydropneumothorax. *JAMA* 89:1836–1837, 1927
12. Greenwald HM, Kaufman J: Congenital non-rotation of stomach with eventration. *Am J Dis Child* 35:641–652, 1928
13. Kinzer RE, Cook JC: Lesions of the diaphragm with special reference to eventration. *AJR* 52:611–614, 1944
14. Teplick JG, Macht SH: Right-sided thoracic stomach. *AJR* 58:196–202, 1947

"Circumscribed" Glioblastoma Multiforme: the Role of Computed Tomography in Two Cases

ROBERT B. GEEHR,[1] GEORGE J. DOHRMANN,[2] AND STEPHEN L. G. ROTHMAN[1]

Radiographic, pathologic, and clinical characteristics of intracranial glioblastoma multiforme are well known. However, a few of these tumors, termed "circumscribed" glioblastoma by Davidoff and Feiring [1], may even be misdiagnosed intraoperatively because of their superficial, well circumscribed nature and dural attachment [2]. Since invasion of the dura by gliomas stimulates desmoplastic response, vascular proliferation, and subsequent meningeal blood supply to the lesion [3–5], it is not surprising that these tumors are often misdiagnosed by angiography as meningiomas, particularly if they lack an identifiable pial blood supply. We discuss "circumscribed" glioblastoma, emphasizing the role of computed tomography (CT) over more conventional radiographic techniques in arriving at correct preoperative diagnosis.

Case Reports

Case 1

A 32-year-old right-handed male had a 6 month history of seizures, during which his head turned to the left. A CT scan 2 months before admission appeared normal. Shortly before admission he began to develop weakness of his left arm and leg and an increasing headache.

Physical examination revealed left hemiparesis. Skull films were normal. Repeat CT scan demonstrated a low density area in the right frontal lobe near the midline on the noncontrast study. Contrast material enhanced the major portion of this lesion (fig. 1A), but multiple low density areas were present throughout the mass. Right internal carotid angiography (fig. 1B) demonstrated an avascular mass in the right posterior frontal, parasagittal region. However, examination of the external carotid artery on the right (fig. 1C) showed vascular supply to this tumor by hypertrophied branches of the middle meningeal artery. A later film demonstrated tumor stain (fig. 1D), believed to be a right parasagittal meningioma.

Right frontoparietal craniotomy was performed. In the region of the motor strip (figs. 1E and 1F), a reddish, well circumscribed tumor was seen; it was firm except for a quite friable central area. The neoplasm adhered to the dura near the superior sagittal sinus, but the sinus was not invaded by tumor. Though there was an apparent capsule along much of the tumor margin, a small portion of the surgical plane disappeared laterally into abnormal brain.

Pathologic examination of the resected specimen revealed a densely cellular malignant glial tumor composed of markedly pleomorphic cells with hyperchromatic nuclei and numerous mitotic figures. Areas of necrosis as well as endothelial proliferation were noted. Focal areas of early sarcomatous change were also present. Pathologic diagnosis was glioblastoma multiforme with early sarcomatous change.

Case 2

A 58-year-old right-handed female had a 1 year history of recurrent left focal motor seizures, involving her arm and leg, and progressive left side weakness. She was oriented, though drowsy, on examination and had a marked left hemiparesis.

Skull films were interpreted as normal. CT scan (fig. 2A) demonstrated a poorly defined mass in the right frontal region close to the midline that enhanced only slightly with contrast material. Right carotid angiography (figs. 2B and 2C) showed a mass in the right parasagittal, prerolandic region lacking demonstrable tumor stain. However, a hypertrophied middle meningeal branch led to the region of the tumor, and branches of the right anterior cerebral artery demonstrated an ipsilateral shift. Preoperative diagnosis was right parasagittal meningioma.

Right frontoparietal craniotomy revealed a raised, reddish gray area in the posterior frontal region that was gelatinous and grossly well circumscribed (figs. 2D and 2E). The tumor partially adhered to the dura.

Pathologic examination revealed a densely cellular malignant glial tumor with pleomorphic cells, bizarre nuclei, and many mitotic figures. Endothelial proliferation was also noted. Pathologic diagnosis was glioblastoma multiforme.

Discussion

In 1940 Scherer [6] reported that certain glioblastomas seem to maintain a fairly narrow zone of infiltration, even at detailed postmortem examination. Davidoff and Feiring [1] categorized similar tumors appearing as superficial, grossly circumscribed lesions often attached to the dura as "circumscribed" glioblastomas. Scherer hoped such lesions would yield better surgical results than more infiltrative glioblastomas; Davidoff and Feiring found no such difference in mortality between the two groups.

In 1969 Jelsma and Bucy [2] showed improved surgical results in patients with this type of tumor compared with those of a more macroscopically invasive nature. They concluded that prognosis in glioblastoma multiforme is favorably affected, in part, by the gross appearance of circumscription. However, they were less optimistic about the ability to preoperatively diagnose "circumscribed" glioblastomas.

The two cases in this report illustrate the difficulties of correct preoperative diagnosis. The cases demonstrate the angiographic findings typical of parasagittal meningioma. At angiography both cases had hypertrophied middle meningeal branches supplying the tumors secondary to dural invasion. In addition, case 1 had a dense

Received April 25, 1978; accepted after revision September 7, 1978.
[1]Department of Diagnostic Radiology, Yale University School of Medicine, 333 Cedar Street, New Haven, Connecticut 06510. Address reprint requests to R. B. Geehr.
[2] Division of Neurosurgery, University of Chicago Medical Center, Chicago, Illinois 60637.

AJR 132:127–129, January 1979
0361–803X/79/1321–0127 $0.00
© 1979 American Roentgen Ray Society

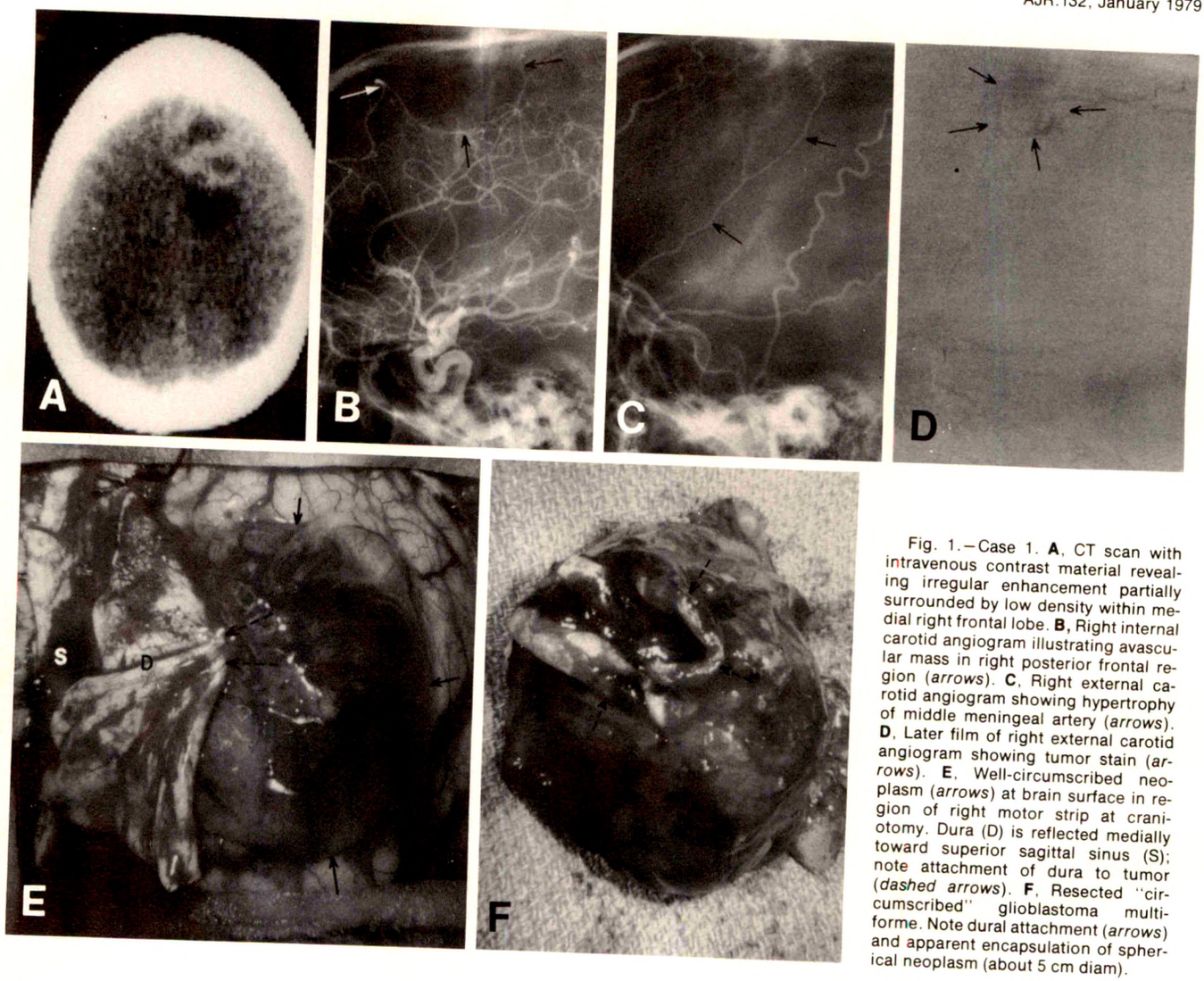


Fig. 1.—Case 1. **A**, CT scan with intravenous contrast material revealing irregular enhancement partially surrounded by low density within medial right frontal lobe. **B**, Right internal carotid angiogram illustrating avascular mass in right posterior frontal region (*arrows*). **C**, Right external carotid angiogram showing hypertrophy of middle meningeal artery (*arrows*). **D**, Later film of right external carotid angiogram showing tumor stain (*arrows*). **E**, Well-circumscribed neoplasm (*arrows*) at brain surface in region of right motor strip at craniotomy. Dura (D) is reflected medially toward superior sagittal sinus (S); note attachment of dura to tumor (*dashed arrows*). **F**, Resected "circumscribed" glioblastoma multiforme. Note dural attachment (*arrows*) and apparent encapsulation of spherical neoplasm (about 5 cm diam).

tumor stain. Case 2 also showed an ipsilateral shift of anterior cerebral branches, probably resulting from the superficial position of the tumor. It seems that in cases of superficial "circumscribed" glioblastoma with dural invasion, angiography is often nondiagnostic or even misleading.

In case 2 CT demonstrated a slightly enhanced poorly defined lesion near the midline. Though this type of enhancement is often seen with low grade gliomas [7, 8], it is not characteristic of meningiomas, which usually display striking homogeneous enhancement and sharp definition [7, 9].

Case 1 illustrates a different CT pattern, with initial low density followed by marked contrast enhancement with low density areas within the tumor. Although most characteristic of malignant lesions [7, 8, 10], cystic meningiomas may mimic this appearance [9, 10].

In each case, meningioma was entertained as the primary preoperative diagnosis because of the misleading angiographic findings. In retrospect the CT appearance makes the diagnosis of meningioma unlikely; however, the possibility of a low grade glioma in case 2 or of a rapidly growing malignant neoplasm other than glioblastoma in case 1 cannot be eliminated. Therefore, CT, though not absolutely diagnostic, with divert attention from a meningioma and may suggest a more aggressive lesion.

REFERENCES

1. Davidoff LM, Feiring EH: "Circumscribed" gliobastoma multiforme. *J Neuropathol Clin Neurol* 1:161–167, 1951
2. Jelsma R, Bucy PC: Glioblastoma multiforme: its treatment and some factors effecting survival. *Arch Neurol* 20:161–171, 1969
3. Cairns H, Russell DS: Intracranial and spinal metastases in gliomas of the brain. *Brain* 54:377–420, 1931
4. Silverberg GD, Hanbery JW: Meningeal invasion by gliomas. *J Neurosurg* 34:549–554, 1971
5. Enestrom S: Meningeal relations of primary brain tumors. A

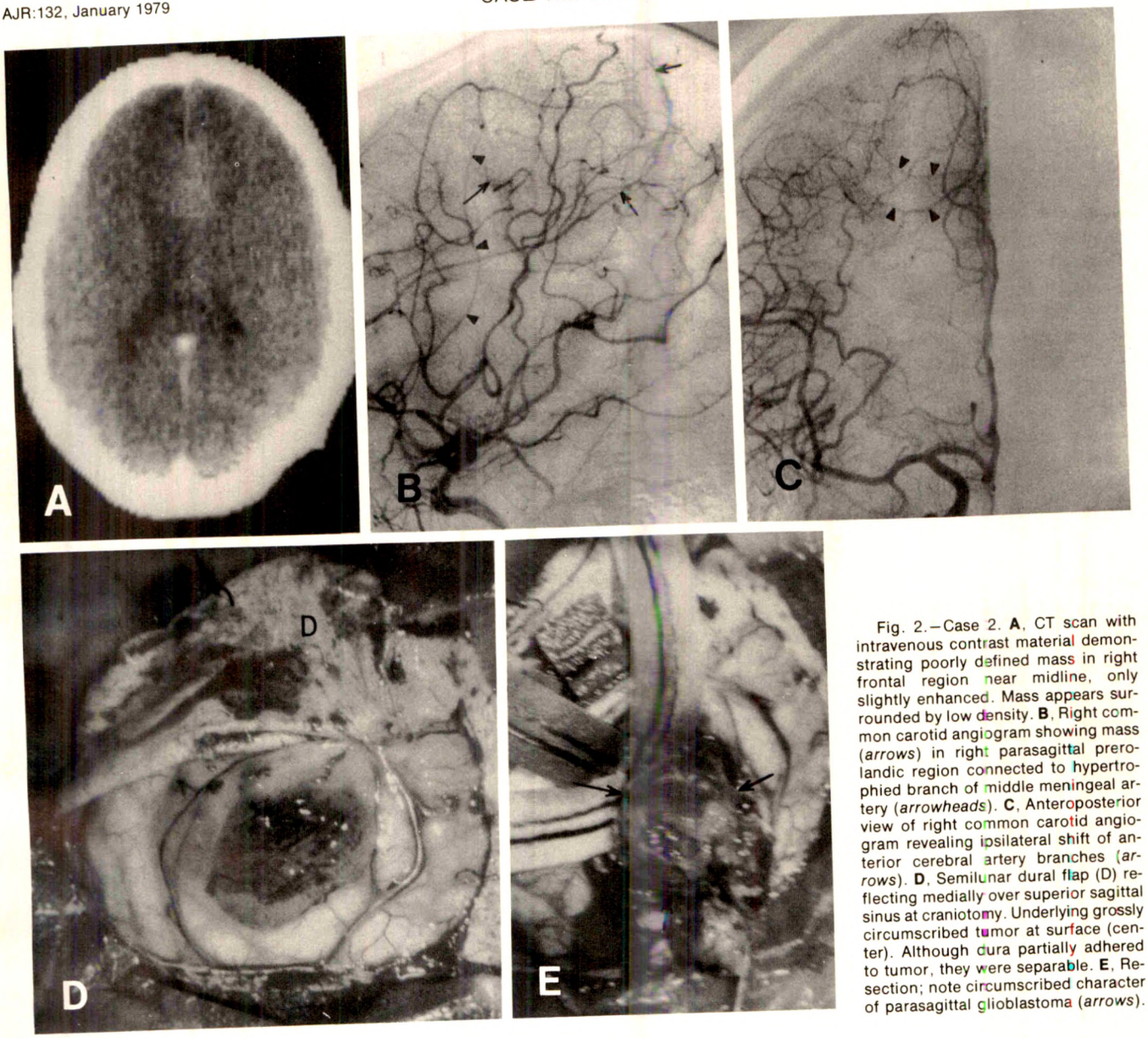


Fig. 2.—Case 2. **A**, CT scan with intravenous contrast material demonstrating poorly defined mass in right frontal region near midline, only slightly enhanced. Mass appears surrounded by low density. **B**, Right common carotid angiogram showing mass (*arrows*) in right parasagittal prerolandic region connected to hypertrophied branch of middle meningeal artery (*arrowheads*). **C**, Anteroposterior view of right common carotid angiogram revealing ipsilateral shift of anterior cerebral artery branches (*arrows*). **D**, Semilunar dural flap (D) reflecting medially over superior sagittal sinus at craniotomy. Underlying grossly circumscribed tumor at surface (center). Although dura partially adhered to tumor, they were separable. **E**, Resection; note circumscribed character of parasagittal glioblastoma (*arrows*).

histological study. *Cancer* 19:1117–1123, 1966
6. Scherer HJ: The forms of growth in gliomas and their practical significance. *Brain* 63:1–35, 1940.
7. Davis DO: CT in the diagnosis of supratentorial tumors. *Semin Roentgenol* 12:97–103, 1977
8. Thomson JLG: Computerised axial tomography and the diagnosis of glioma: a study of 100 consecutive histologically proven cases. *Clin Radiol* 27:431–441, 1976
9. Claveria LE, Stutton D, Tress BM: The radiological diagnosis of meningiomas, the impact of EMI scanning. *Br J Radiol* 50:15–22, 1977
10. Steinhoff H, Lanksch W, Kazner E, Grumme T, Meese W, Lange S, Aulich A, Schindler E, Wende S: Computed tomography in the diagnosis and differential diagnosis of glioblastomas. A qualitative study of 295 cases. *Neuroradiology* 14:193–200, 1977

Agenesis of the Internal Carotid Artery with a Primitive Transsellar Communicating Artery

PAUL C. JANICKI,[1, 2] JOHN P. LIMBACHER,[1, 3] AND FAUSTINO C. GUINTO, JR.[4]

Agenesis of the internal carotid artery is an unusual developmental anomaly which occurs before the 24 mm stage of embryologic growth. In the majority of reported cases, collateral circulation to the intracranial arteries is from the contralateral internal carotid artery and the vertebrobasilar system via the circle of Willis. We present a case of an unusual collateral pathway in the presence of agenesis of the left internal carotid artery. Three instances of a similar anomalous pathway in the presence of agenesis of the right internal carotid artery have been reported, although none had tomographic studies that demonstrated absence of the ipsilateral bony carotid canal [1–3]. We believe this to be the first instance of this anomaly reported in the radiologic literature.

Case Report

A 47-year-old white man was seen in the emergency room after the sudden onset of numbness and weakness in his right arm. Earlier he had experienced a severe headache in the left parietal area, unlike any other he had previously experienced. This was followed by lightheadedness, blurred vision, and right arm heaviness. The headache had resolved when the patient was first examined. He was alert, oriented, and appeared in good health. Neurologic examination revealed a mild weakness of dorsiflexion at the right wrist, and mild hyperesthesia to pin prick over the right arm and shoulder. The remainder of the neurologic evaluation was unremarkable. The left carotid pulse was significantly less than the right, and no bruits were noted. A lumbar puncture produced normal manometric measurements. Cerebrospinal fluid cell count and chemistry were also normal. The patient was scheduled for arch and carotid angiography for evaluation of transient cerebral ischemia.

Findings

Arch aortography revealed normal origins and courses of the right carotid and both vertebral arteries. A 3 cm atheromatous narrowing of the right internal carotid artery near its origin was demonstrated. Another remarkable finding was an absent left internal carotid artery (fig. 1).

A large intersellar communicating artery connecting the intracavernous portion of the right and left internal carotid arteries was demonstrated on selective injection of the right internal carotid artery (fig. 2). This served as the main collateral to the left middle cerebral artery circulation; a selective injection of the right vertebral artery filled only the posterior fossa. Selective injection of the left "common carotid" artery revealed only external carotid artery branches with no transdural collateral circulation.

Tomography of the sella showed a prominent carotid sulcus on the right. A vascular impression on the sellar floor was also well visualized (fig. 3). Tomography of the petrous bones showed an absent carotid canal on the left side (fig. 4).

Anteroposterior and lateral views of the right internal carotid plaque revealed an almost 90% stenosis not evident on the arch study. In view of the absence of collateral supply from the vertebrobasilar system, this was thought to be the cause of the patient's symptoms and an endarterectomy was performed.

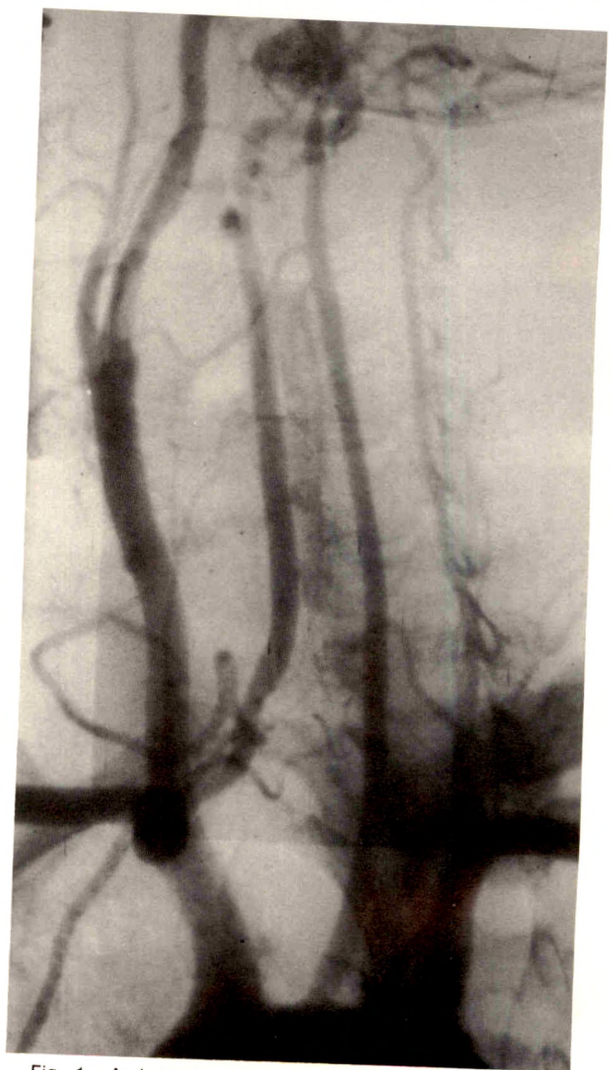


Fig. 1.—Arch aortogram. Right carotid and both vertebral arteries have normal origins and courses. Left external carotid artery originates directly from aorta. Left internal carotid artery is absent.

Received April 18, 1978; accepted after revision August 21, 1978.

The opinions or assertions contained herein are the private views of the authors and are not to be construed as reflecting the views of the Department of the Army or the Department of Defense.

[1] Department of Radiology, Brooke Army Medical Center, Fort Sam Houston, Texas 78234. Address reprint requests to Chief, Department of Radiology, Brooke Army Medical Center, Fort Sam Houston, Texas 78234.

[2] Present address: Department of Radiology, Cleveland Clinic, Cleveland, Ohio 44106.

[3] Present address: Department of Radiology, Tripler Army Medical Center, Honolulu, Hawaii 96823.

[4] Department of Radiology, University of Texas Health Science Center, San Antonio, Texas 78284.

0361-803X/79/1321-0130 $0.00

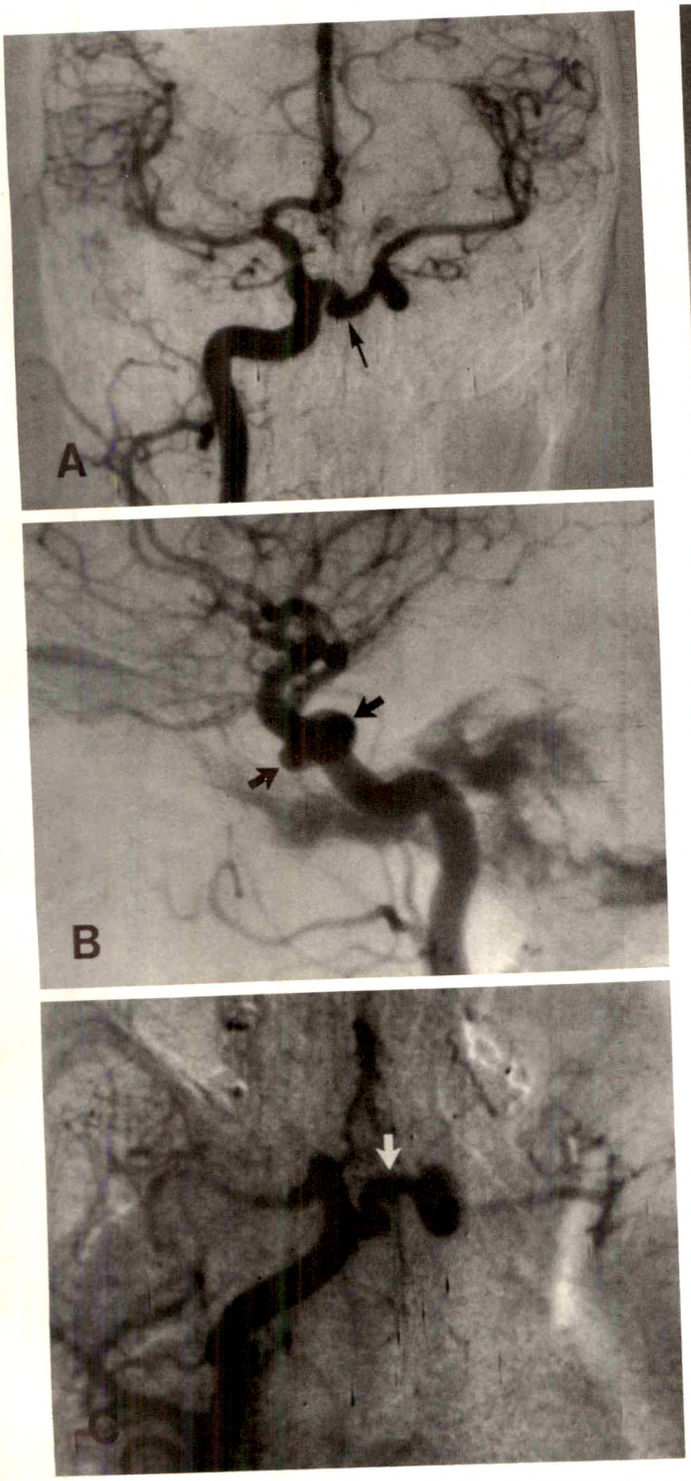


Fig. 2.—Right carotid arteriogram. **A**, Anteroposterior projection showing normal right carotid arterial pattern. Large persistent primitive maxillary artery (*arrow*) bridges right and left carotid siphons. **B**, Lateral projection showing primitive maxillary artery (*arrows*). **C**, Base view of primitive maxillary artery (*arrows*).

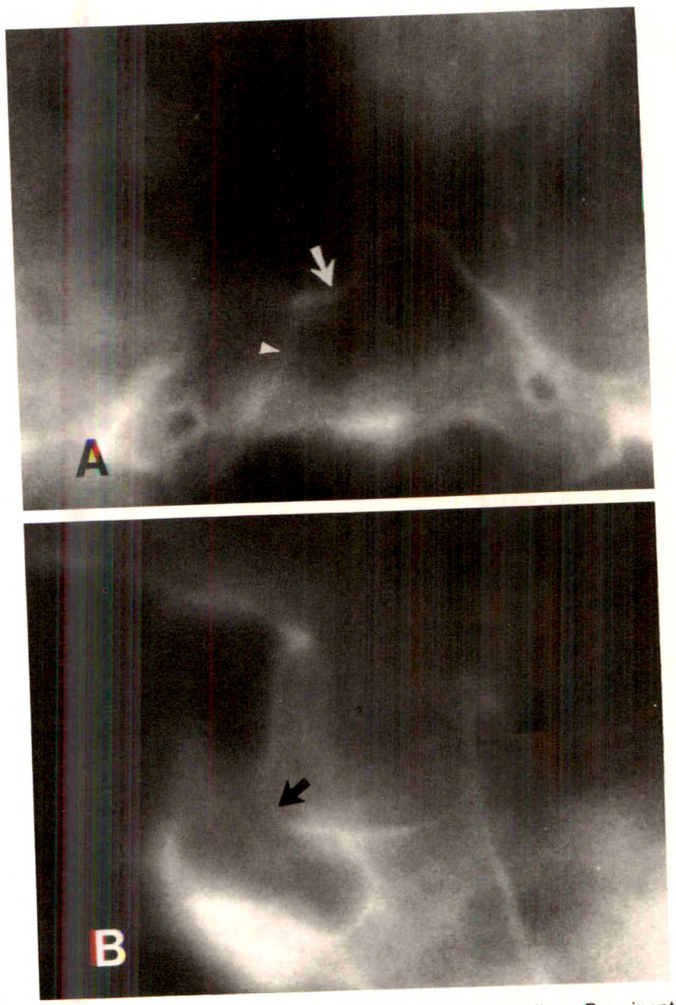


Fig. 3.—**A**, Coronal tomogram through anterior sellar floor. Prominent carotid sulcus along right lateral wall of sphenoid sinus (*arrowhead*). Depression along right aspect of sellar floor (*arrow*) due to impression of primitive maxillary artery. **B**, Lateral tomogram through right lateral aspect of sellar floor. Localized depression along sellar floor (*arrow*) corresponds to impression of primitive maxillary artery.

Discussion

This case demonstrates absence of the left internal carotid artery with collateral circulation via an anomalous communicating transsellar artery between the intracavernous portions of the internal carotid arteries. It is similar to three previously reported cases [1–3], yet differs in several ways. The other cases all involved the opposite internal carotid artery; the anastomotic arteries were described as crossing either behind the clivus or at the level of the dorsum sella. Tomography of our patient showed that the communicating artery ran along the anterior floor of the sella. Moreover, tomography of the petrous pyramids demonstrated absence of the carotid canal on the left. The absence of a bony canal is more indicative of agenesis than aplasia.

Lie [2], in reporting the first case of this anomaly, defined agenesis of the internal carotid artery as total absence of the entire length of the artery. He used the term "aplasia" when a remnant or a portion of the internal carotid artery remained, such as the carotid siphon. Lack of angiographic demonstration does not by itself either establish agenesis or exclude a fibrous remnant or aplasia. Since in our patient the left carotid siphon was intact, using Lie's criteria, the term "aplasia" might be used in describing this anomaly. However, we feel that the absence of the left carotid canal demon-

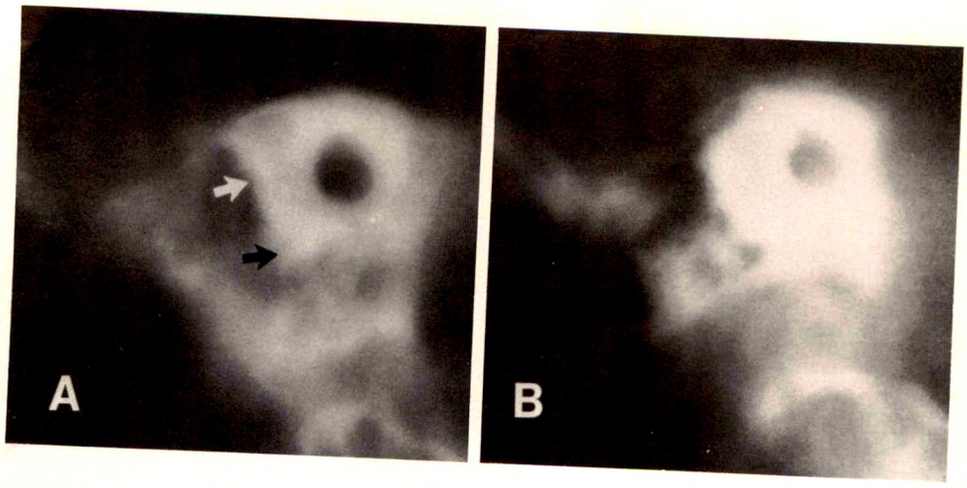


Fig. 4.—**A**, Normal lateral tomogram of right temporal bone through plane of carotid ridge. Carotid canal is sharply defined (*arrows*). **B**, Lateral tomogram of left temporal bone in same plane and orientation as **A**. Carotid canal is absent.

strated by polytomography favors the true absence of at least the cervical and petrous portions of the internal carotid artery, and thus have used the term "agenesis" in describing it.

The embryogenesis of this anomaly is open to interpretation. This anomaly has never been observed in the fetus or developing embryo, but Padget [4] described a plexiform network of vessels in the 4–5 mm embryo which originates from the internal carotid arteries, and which communicates with one another around Rathke's pouch. Unfortunately, no other observation of this plexus in the fetus has been made. It would seem reasonable, however, that this anomaly represents either the persistence of one of these primitive channels or hypertrophy of a normally developing blood supply to the floor of the sella.

One possibility is that the artery represents hypertrophy of a capsular artery. The capsular artery, as described by Parkinson [5], originates from the intracavernous carotid artery 2–3 mm anterior to the origin of the meningohypophyseal trunk, and anastomoses with the artery from the opposite carotid extradurally within the sella turcica. McConnell [6] described the inferior capsular artery as originating from the inferomedial aspect of the internal carotid artery, halfway along the course of the cavernous carotid artery, and coursing medially in the dura covering the inferior surface of the anterior lobe of the hypophysis. It anastomoses with branches of the inferior hypophyseal artery, giving branches to the floor of the sella.

Another possibility is that the artery represents a persistent primitive maxillary artery. Padget [4] noted the primitive maxillary artery originates from the cavernous internal carotid artery lateral to the base of Rathke's pouch in the 3–4 mm embryo. Its primary role at this stage of development is to supply the prosencephalon and the optic vesicle, but the artery normally involutes by the 12 mm stage; by the 24 mm stage, only the stem remains. This is apparently incorporated into the formation of the inferior hypoglossal artery, a branch of the meningohypophyseal trunk which supplies the posterior lobe of the pituitary gland and the dura of the floor of the sella. The communicating artery in our patient did not, however, originate from the meningohypophyseal trunk. Although conjectural, it is most likely that the primitive maxillary artery or one of its branches persists, resulting in this unusual anomaly.

ACKNOWLEDGMENT

We thank Yvonne Arispe and Dorothy Budd for secretarial assistance.

REFERENCES

1. Harispe L, Creissard P, Martinez G, Metzger J: An abnormal communicating artery between the two intracranial internal carotid arteries. *J Radiol Electrol Med Nucl* 51:759–762, 1970
2. Lie TA: *Congenital Anomalies of the Carotid Arteries*. Amsterdam, Excerpta Medica, 1968
3. Smith RR, Kees CJ, Hogg ID: Agenesis of the internal carotid artery with an unusual primitive collateral. *J Neurosurg* 37:460–462, 1972
4. Padget DH: The development of the cranial arteries in the human embryo. *Contrib Embryol* 32:205–261, 1948
5. Parkinson D: Collateral circulation of cavernous carotid artery: anatomy. *Can J Surg* 7:251–268, 1964
6. McConnell EM: Arterial blood supply of human hypophysis cerebri. *Anat Rec* 115:175–203, 1953

Occult Bronchogenic Carcinoma Masquerading as Recurrent Pulmonary Embolism

ROBERT J. ROSEN[1] AND LAWRENCE R. GOODMAN[1]

The antemortem diagnosis of pulmonary embolism can be elusive. Autopsy series reveal that up to 60% of pulmonary emboli are unsuspected during life [1]. Conversely, many patients believed to have pulmonary embolism on clinical grounds do not when studied by perfusion scans and pulmonary angiography. We report a patient with an occult bronchogenic carcinoma who was mistakenly diagnosed over an 8 month period as having recurrent pulmonary emboli.

Case Report

A 66-year-old man was admitted with complaints of dizziness and palpitations. He had been admitted 8 months earlier with identical symptoms. On the previous admission chest radiography revealed changes consistent with chronic obstructive pulmonary disease, but no other significant abnormalities. A perfusion scan at that time revealed defects in the left lower lung field. Blood gas studies at that time revealed a pO_2 of 77 and a pCO_2 of 34. A diagnosis of pulmonary embolism was made and the patient placed on heparin therapy. Paroxysmal atrial fibrillation noted on electrocardiography was felt to be the result of the pulmonary embolism and the cause of the symptoms. This arrhythmia subsided spontaneously. Serial perfusion lung scans revealed marked improvement in the perfusion defects and the pO_2 rose to 82. No source for pulmonary emboli could be found despite an extensive investigation.

On the present admission, a perfusion scan revealed complete absence of flow to the left lung (fig. 1A). Radiography of the chest again demonstrated bilateral changes of obstructive lung disease and a new small left pleural effusion. A tentative diagnosis of recurrent pulmonary embolism was made and the patient again was placed on heparin therapy. The mild symptoms, a pO_2 of 83, and the unusual lung scan were felt to be inconsistent with a pulmonary embolism, although similar cases have been reported [2]. A weight loss of 4.5 kg was also noted over the previous year. No cardiac arrhythmia was present at this time.

Pulmonary arteriography was performed. The overpenetrated scout film suggested fullness in the left infrahilar region which was confirmed on a well penetrated posteroanterior radiograph (fig. 1B). The arteriogram revealed a normal right pulmonary circulation but stasis of contrast in the left pulmonary arterial tree (fig. 1C). Repeat selective injections into the left pulmonary artery revealed no intrinsic filling defects, compression, or evidence of vascular invasion. However, delayed filming to about 20 sec failed to demonstrate a pulmonary capillary phase or visualization of any pulmonary veins on the left (fig. 1D). Subsequent hilar tomography and bronchoscopy revealed the presence of a squamous cell carcinoma partially obstructing the left lower lobe bronchus, but no evidence of obstruction in the remainder of the bronchial tree. The heparin was discontinued and a course of radiation therapy and chemotherapy was begun. The patient developed widespread metastatic disease and expired 4 months later.

Discussion

Unilateral absence of perfusion is a relatively infrequent pattern in lung scanning, occurring in 13 of 607 abnormal scans in one series. Pulmonary embolism is an unusual cause of this scan abnormality [3]. Other causes include lung carcinoma, parenchymal lung disease, and congenital heart and lung anomalies.

It is well known that bronchogenic carcinoma, and hilar lesions in particular, may markedly alter pulmonary blood flow, thus causing abnormalities in perfusion scans of the involved lung [4–9]. Rarely, cases of hilar tumors have been reported in which marked perfusion defects were noted in the absence of any radiographic evidence of tumor [7]. These cases have led some authors to recommend routine lung scanning in patients suspected of having bronchogenic carcinoma with negative chest films [7, 8].

It is generally believed that there are three mechanisms which may be responsible for the disproportionate scan defects associated with bronchogenic carcinoma. The most direct cause is invasion or compression of the pulmonary artery by tumor; this finding has been well demonstrated by pulmonary arteriography in many of these cases [4, 7, 9, 11, 12]. Another direct mechanism, also well documented, is replacement of the normal pulmonary arterial flow by bronchial arterial circulation through tumor masses [5, 13]. The arteriographic findings in this case excluded either of these two mechanisms.

There are many cases in which no direct vascular involvement can be demonstrated at pulmonary arteriography or at autopsy, despite markedly abnormal perfusion scans [3–5]. In these cases it has been postulated that reflex redistribution of pulmonary vascular flow due to obstructed ventilation of the involved area by tumor is responsible for the scan defects [13]. Unexplained slow flow in the regional pulmonary arterial circulation has previously been reported to occur in the presence of bronchogenic carcinoma [15]. Wagenvoort and Wagenvoort [13] noted medial hypertrophy and intimal fibrosis of the pulmonary arteries in the presence of bronchogenic carcinoma, particularly in the involved lobe; a response to the high pressures of shunting from bronchial circulation was postulated as the causative factor in these cases.

In the present case, pulmonary arteriography showed no pulmonary artery compression or invasion, but did reveal almost complete cessation of forward flow on the left. Since tomography and bronchoscopy revealed tumor partially obstructing only the left lower lobe bron-

Received March 2, 1978; accepted after revision August 29, 1978.
[1] Department of Diagnostic Radiology, Hahnemann Medical College and Hospital, 230 North Broad Street, Philadelphia, Pennsylvania 19102. Address reprint requests to L. R. Goodman.

AJR 132:133–135, January 1979
© 1979 American Roentgen Ray Society
0361–803X/79/1321–0133 $0.00

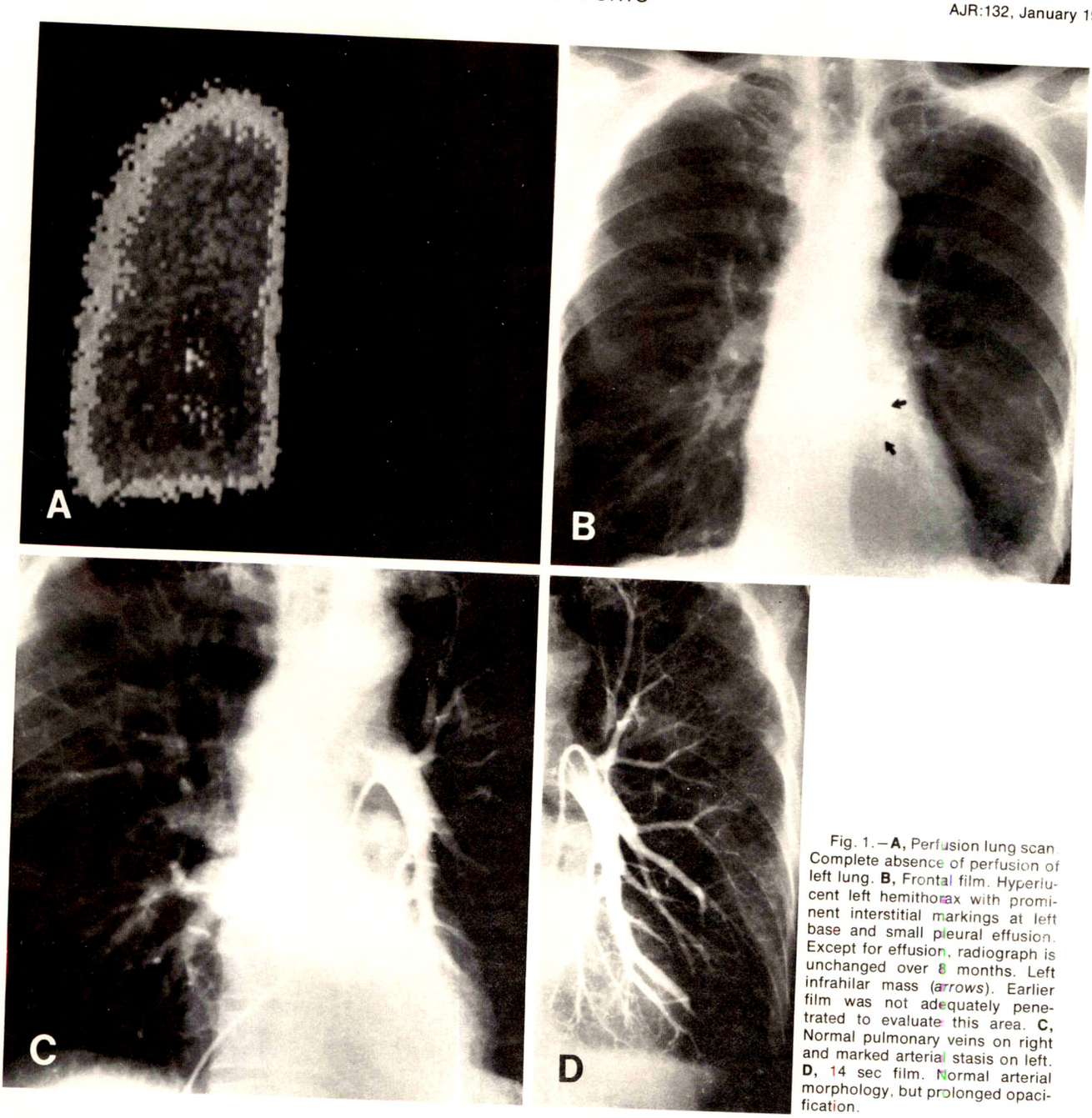


Fig. 1.—**A,** Perfusion lung scan. Complete absence of perfusion of left lung. **B,** Frontal film. Hyperlucent left hemithorax with prominent interstitial markings at left base and small pleural effusion. Except for effusion, radiograph is unchanged over 8 months. Left infrahilar mass (*arrows*). Earlier film was not adequately penetrated to evaluate this area. **C,** Normal pulmonary veins on right and marked arterial stasis on left. **D,** 14 sec film. Normal arterial morphology, but prolonged opacification.

chus, the cause of a complete lack of flow angiographically and by perfusion scanning was not clear. One explanation for these findings could be invasion or compression of the left pulmonary veins, preventing emptying of the pulmonary circulation on this side and thus resulting in cessation of forward flow. The infrahilar location of the mass at tomography would be appropriate to obstruct pulmonary venous inflow into the left atrium. In reported cases of pulmonary venous obstruction (due to primary venoocclusive disease), the angiographic picture has been one of pulmonary vascular dilatation [16], not found in this case.

Another intriguing aspect is the changeable nature of the scan defects over the preceding year. With a steadily expanding mass, a correspondingly steady decrease in perfusion would be expected. In this case, however, follow-up scans on the first admission showed improved perfusion. Three possible mechanisms could account for this finding. First, the original episode may have represented a straightforward case of pulmonary embolism, unrelated to the present problem, which responded to heparin therapy (this seems unlikely). Second, recurrent thrombotic episodes related to the presence of tumor occurred over this period of time. Wagenvoort and Wagenvoort [13] reported an increased incidence of in situ thrombus formation in the pulmonary arteries of lungs with bronchogenic carcinoma which may be related to the intimal fibrosis previously mentioned. The absence of filling defects in the pulmonary arteries in this case casts doubt on this mechanism, although

recanalization remains a possibility. Third, intermittent mucous plugging of the partially obstructed bronchus, with consequent reflex changes in perfusion, is a possible mechanism.

Two important points are raised by this case. First bronchogenic carcinomas (especially hilar) inapparent on routine chest films may be associated with marked defects on perfusion scans. Thus, routine scanning probably is indicated where bronchogenic carcinoma is a diagnostic possibility in the absence of radiographic evidence of tumor. Second, dramatic perfusion defects on lung scans may be present without direct involvement of the pulmonary artery by tumor and in patients who are only mildly symptomatic. Reflex redistribution of flow due to obstructed ventilation may be an alternative mechanism; however, this redistribution need not correspond closely to the specific area of compromised ventilation.

ACKNOWLEDGMENTS

We thank Drs. A. Wilson and J. Conroy for their assistance.

REFERENCES

1. Freiman DG, Suyemoto J, Wessler S: Frequency of pulmonary thromboembolism in man. *N Engl J Med* 272:1278–1280, 1965
2. Parmley LF, Senior RM, McKenna DH, Johnston GS: Clinically deceptive massive pulmonary embolism. *Chest* 58:15–23, 1970
3. White RI, James AE, Wagner HN: The significance of unilateral absence of pulmonary artery perfusion by lung scanning. *AJR* 111:501–509, 1971
4. Hatch HB, Maxfield WS, Ochsner JL: Radioisotope lung scanning in bronchogenic carcinoma. *J Thorac Cardiovasc Surg* 50:634–639, 1965
5. Johnson PM, Sagerman RH, Jacox HW: Changes in pulmonary arterial perfusion due to intrathoracic neoplasia and irradiation of the lung. *AJR* 102:637–644, 1968
6. Macumber HH, Calvin JW: Perfusion lung scan patterns in 100 patients with bronchogenic carcinoma. *J Thorac Cardiovasc Surg* 72:299–302, 1976
7. Maxfield WS, Hatch HB, Ochsner JL: Perfusion lung scanning in evaluation of patients with bronchogenic carcinoma. *Surg Clin North Am* 46:1389–1398, 1966
8. Maynard DC, Cowan RJ: Role of the scan in bronchogenic carcinoma. *Semin Nucl Med* 1:195–205, 1971
9. Walker RHS, Provan JL: Scintillation scanning of lungs in preoperative assessment of carcinoma of the bronchus. *Br Med J* 3:327–330, 1969
10. Ito H, Ishii Y, Sakamoto T, Suzuki T, Fujita T, Hamamoto K, Torizuka K: Radionuclide studies in bronchogenic carcinoma of the hilum. *AJR* 125:640–650, 1975
11. Nabatoff RA: Contrast visualization of the pulmonary vessels as an aid in the early diagnosis of pulmonary neoplasms. *Ann Surg* 133:270–271, 1951
12. Neuhof J, Sussman ML, Nabatoff RA: Angiocardiography in the differential diagnosis of pulmonary neoplasms. *Surgery* 25:178–183, 1949
13. Wagenvoort CA, Wagenvoort N: Pulmonary arteries in bronchogenic carcinoma. *Arch Pathol* 79:529–533, 1965
14. Wagner HN, Lopez-Majano VL, Tow DE, Langan JK: Radioisotope scanning of the lungs in early diagnosis of bronchogenic carcinoma. *Lancet* 1:344, 1965
15. Bookstein JJ, Silver TM: The angiographic differential diagnosis of acute pulmonary embolism. *Radiology* 11:25–33, 1974
16. Scheibel RL, Dedeker KL, Gleason DF, Pliego M, Kieffer SA: Radiographic and angiographic characteristics of pulmonary veno-occlusive disease. *Radiology* 103:47–51, 1972

Ultrasound Demonstration of a Thyroid Carcinoma Within a Benign Cyst

FRANK H. ALLEN,[1] PETER M. KROOK,[1] AND WALTER P. H. DE GROOT[2]

Cystic lesions of the thyroid, generally considered benign, are managed differently from solid lesions. To our knowledge, this is the first reported case in which gray scale ultrasound identified a pedunculated carcinoma within the lumen of an otherwise benign cyst.

Case Report

A healthy 49-year-old woman with no history of thyroid abnormality or radiation exposure had a painless, nontender mass in the left lobe of the thyroid. At physical examination, the mass felt smooth and cystic with slight firmness at its lower edge. Routine laboratory studies were normal. The mass was nonfunctional on ^{131}I scanning. Gray scale ultrasonography revealed a 5–6 cm oval cystic structure with a 1.5–2 cm pedunculated mass projecting into the lumen (figs. 1B and 1C). Subsequent surgery and subtotal thyroidectomy revealed a left lobe mass resembling a benign cyst containing clear fluid. However, a fingerlike projection extended into the lumen of the cyst and the adjacent thyroid was firm and yellowish. Figure 1A was rendered from the surgeon's description of the mass (no photographs were taken before biopsy and sectioning).

Frozen and permanent sections of the mass demonstrated a partially collapsed benign cystic lesion and fibrous capsule with inflammatory infiltrate. An accompanying papillary carcinoma was growing in a "small portion" of the cyst wall, extending up to 2 cm into the surrounding thyroid with a partly necrotic, pedunculated extension into the cyst's center. There was no evidence of local recurrence of metastasis at follow-up 9 months after surgery.

Discussion

Cystic thyroid nodules are managed differently from solid nodules. About 20% of solitary thyroid lesions are simple cysts rarely associated with an occult malignancy within or adjacent to them and most clinicians confidently treat these nodules with repeated aspirations, as necessary [1–3]. However, since 10%–20% of all solitary thyroid nodules subjected to surgery [4] are found to be carcinomatous, exploration of solid or partly solid lesions in the uninodular gland is warranted. About 2% of primary thyroid carcinomas contain fluid. The possibility of misdiagnosis and the fear of seeding a needle tract are responsible for use of additional diagnostic maneuvers, especially ultrasound, in evaluating solitary nodules.

Several thyroid ultrasound imaging techniques have been described. This study used a 5 MHz, 6 mm diameter, near-zone focused transducer, mineral oil coupling, and multiple images in transverse, longitudinal, and longitudinal oblique planes. The time gain control curve was nearly flat to optimize near field imaging. An alternate and recently advocated technique [5] is to use a water bath against the skin. This procedure permits use of the best focused zone of the ultrasound beam. In our lab, water bath scanning has not been found necessary since high quality images are routinely obtained with the 5 MHz transducer, and contact scanning permits finer control of the position of the ultrasound beam within the lesions. This assures closely spaced serial sectioning and permits better normalization of the ultrasound beam to reflecting surfaces.

Despite careful techniques, solid nodules may appear as sonolucent masses (23% in Blum's series [2]). Differentiation of a cyst from a solid lesion is aided by the presence or absence of fine internal echoes on A-mode, as well as B-mode, gray scale images. Particular attention to beam attenuation and far-wall enhancement may help distinguish a simple cyst from a masquerading homogenous sonolucent solid mass [6–8].

Because of occasional inability in differentiating cystic and solid lesions, we feel that diagnosis of thyroid cyst should be confirmed. This is easily accomplished by aspiration, which should result in the disappearance of the mass. The combination of physical examination, ultrasound imaging, and aspiration provides excellent assurance of benignity and avoids unnecessary surgical exploration.

ACKNOWLEDGMENTS

We thank the Virginia Mason Medical Art Section for artwork and Cindy Denney for secretarial help.

REFERENCES

1. Crile G Jr: Treatment of thyroid cysts by aspiration. *Surgery* 59:210–212, 1966
2. Blum A, Golman AD, Herskovic A, Hernberg J: Clinical applications of thyroid echography. *N Engl J Med* 287:1164–1169, 1972
3. Miller J, Zafar S, Karo J: The cystic thyroid nodule. *Radiology* 110:257–261, 1974
4. DeGroot L: Diseases of the thyroid gland, in *Textbook of Medicine*, edited by Beeson P, McDermott W, Philadelphia, Saunders, 1971
5. Sackler J, Passalaqua A, Blum M, Amorocho L: A spectrum of diseases of the thyroid gland as imaged by gray scale water bath sonography. *Radiology* 125:467–472, 1977
6. Chilcote WS: Gray scale ultrasound of the thyroid. *Radiology* 120:381–383, 1976
7. Taylor K, Carpenter B, Barrett J: Gray scale ultrasonography in the diagnosis of thyroid swellings. *JCU* 2:327–330, 1974
8. Crocker E, McLaughlin A, Kosoff G, Jellins J: The gray scale echographic appearance of thyroid malignancy. *JCU* 2:305–306, 1974

Received September 6, 1977; accepted after revision September 5, 1978.
[1] Department of Radiology, Mason Clinic, 1100 Ninth Avenue, Seattle, Washington 98111. Address reprint requests to F. H. Allen.
[2] 1019 Madison Street, Suite 240, Seattle, Washington 98104.

© 1979 American Roentgen Ray Society

0361-803X/79/1321-0136 $0.00

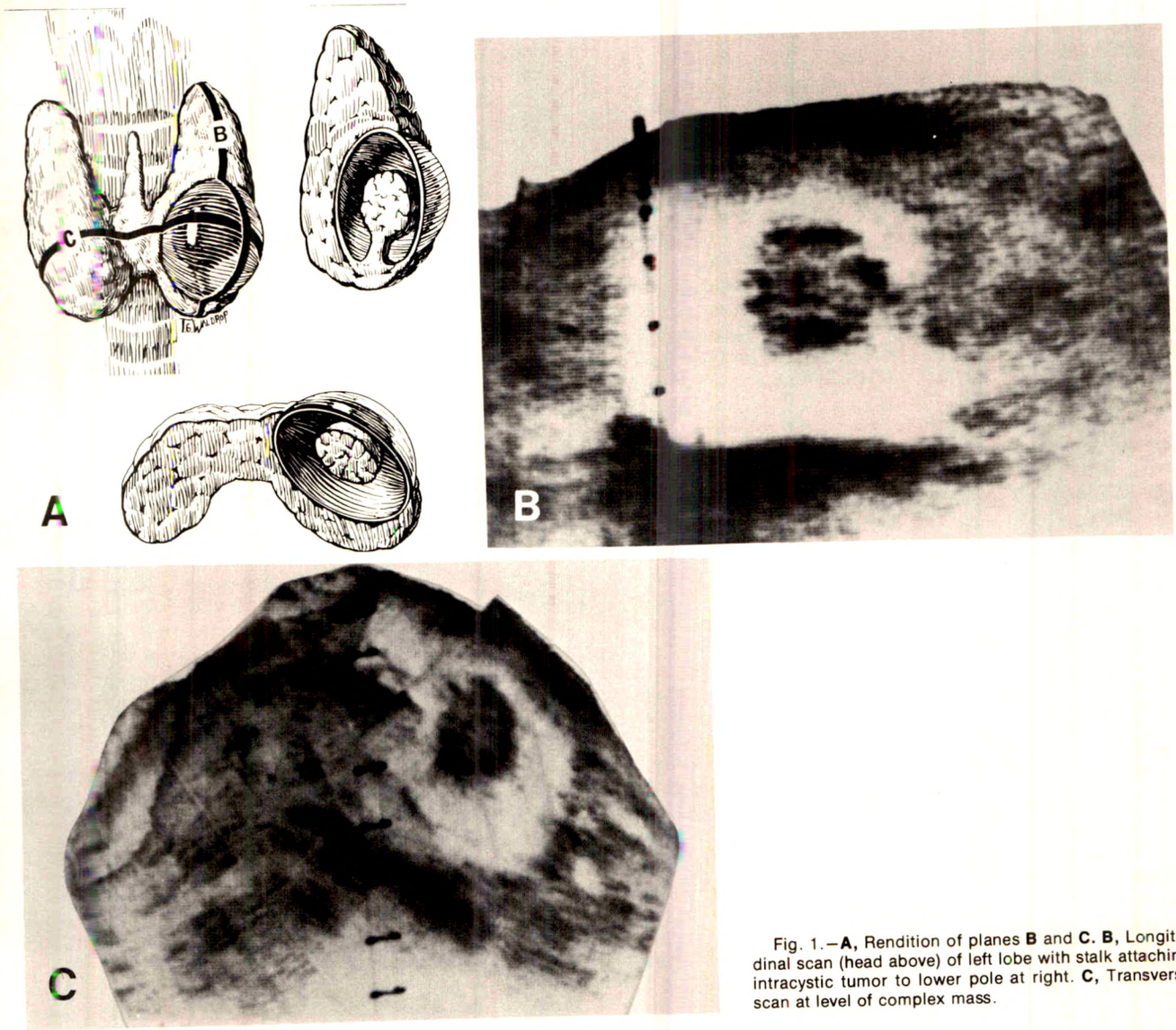


Fig. 1.—**A,** Rendition of planes **B** and **C. B,** Longitudinal scan (head above) of left lobe with stalk attaching intracystic tumor to lower pole at right. **C,** Transverse scan at level of complex mass.

Radiographic Presentation of Spinal Abscess in the Subdural Space

NICHOLAS J. PATRONAS,[1] WILLIAM J. MARX,[1,2] AND EUGENE E. DUDA[1]

Purulent infections of the spinal canal can be devastating, whether involving the epidural or the subdural spaces. Since first described by Bennett and Keegan [1], only 11 cases of spinal subdural abscess have appeared in the literature, and only one of these contained a detailed myelographic description. The additional case reported here stresses the important radiographic features of spinal subdural abscess. Once diagnosis is confirmed, treatment consists of prompt surgical drainage and appropriate antibiotic therapy.

Case Report

A 39-year-old black man had back pain for 1 month, and then developed episodic chills and fever that lasted 1 week.

On admission to University of Chicago Hospitals and Clinics, symptoms included spinal ache, radicular pain, persistent chills and fever, paraparesis, and incontinence. Physical examination demonstrated a right gluteal abscess, sensory loss, and weakness in the buttocks and legs; there was no percussion tenderness over the spine.

Attempted lumbar puncture at L4–L5 drained thick pus; stains showed gram-positive cocci. No cerebrospinal fluid was obtained, suggesting that the needle had entered an epidural or subdural abscess. Myelography performed through a C1–C2 puncture showed a complete block at the T8 level. The interface of the block showed a gradual transitional zone with nodular irregularities projecting into the pantopaque column. A dorsal defect of the subarachnoid space was seen at the level of the block (fig. 1), but there was neither displacement nor compression of the cord. Diagnosis of spinal abscess was made.

A 12-level laminectomy (D6–L5) was performed. The dura, opened the full length of the laminectomy, revealed grossly purulent material. The arachnoid was not breached; however, venous thrombosis was seen on the surface of the spinal cord in the low dorsal area. The pus was aspirated and the subdural space thoroughly irrigated. The right gluteal abscess was also drained. *Staphylococcus aureus* was cultured from the surgical sites, and the patient was intravenously treated with 2 g methicillin every 4 hr and 100 mg gentamycin every 8 hr. The patient showed steady improvement 3 wk after surgery, regaining sensation and strength in the legs.

Typical initial symptoms of spinal subdural abscess are spinal ache, radicular pain, and fever. Concurrent or prior remote infection is also common, as are Kernig's and Lasègue's signs (lower motor neuron signs) and paraparesis, which may progress to paraplegia [2, 3]. Localized spinal percussion tenderness is conspicuously absent [4]. Mild pleocytosis and elevated protein levels in the cerebrospinal fluid suggest meningeal irritation rather than intraarachnoidal infection. Diagnosis of spinal subdural abscess is confirmed by myelography.

A distant source of infection predated the onset of spinal disease in ten of the 12 spinal subdural abscess cases in the literature [1, 2, 4–8]. Three mechanisms are implicated in the pathogenesis of the disease: (1) hematogenous spread from a distant infectious source; (2) contamination following spinal puncture [5]; and (3) direct extension from contiguous infection [6]. In most cases hematogenous spread seems to explain the disease. *Staphylococcus aureus* was isolated from the spinal subdural abscess in seven cases, hemolytic streptococcus in two cases, and pneumococcus in one case; there were no bacteriologic reports for the two other cases.

In contrast to epidural abscess, osteomyelitis of the vertebrae is not associated with spinal subdural abscess, and therefore no plain film abnormalities have been shown [4].

Myelography was performed in seven of the reported cases. In six of these a complete block was shown. In the other case the abscess was located in the lowest part of the dural sac. However, detailed myelographic description was recorded in only one case other than ours. In both cases there was a gradual transitional zone between the normal subarachnoid space and the block. In the transitional zone there were irregular defects at the interface of the block reminiscent of the pattern seen in arachnoiditis. This pattern, caused by thick pus projecting into the oil column, is the most specific myelographic finding in spinal subdural abscess and helps to distinguish subdural from epidural abscesses. In our case there was also a dorsal defect of the subarachnoid space placing the lesion in an extraarachnoid location. Finally the spinal cord was neither expanded nor displaced.

Because of possible transmission of the infection to the subarachnoid space, a cisternal puncture is performed in patients with suspected lumbar or dorsal involvement. A lumbar puncture is permissible if cervical disease is suspected [9]. If pus is obtained during the puncture, this material is collected for bacteriology, but no contrast medium is injected. A remote site is punctured and a few milliliters of spinal fluid is obtained for analysis prior to instilling a small volume of contrast for the block study.

If a spinal tap reveals pus, the major differential consideration is spinal epidural abscess. Spinal epidural abscess is far more common than spinal subdural abscess. Although spinal epidural abscess causes signs and symptoms nearly identical to subdural abscess [10], its distinguishing features are the presence of local spinal tenderness, vertebral osteomyelitis, and cord compression. In contrast to spinal epidural abscess, the most specific myelographic finding for spinal subdural abscess is the gradual transitional zone of nodular irregularities leading to a complete block. Another consideration might be acute transverse myelitis, which is more typically characterized by sudden onset and paralysis [11]. The myelogram is usually normal, although cord swelling and partial block may be seen.

Although arachnoiditis is generally diffuse, it may appear myelographically as a complete block indistinguishable from spinal subdural abscess. Displacement of the arachnoid membrane similar to that in extradural masses is not seen. The clinical setting and the cerebrospinal fluid findings may help to separate these diseases.

Received May 30, 1978; accepted after revision September 21, 1978.

[1]Department of Radiology (Box 429), University of Chicago, 950 East 59th Street, Chicago, Illinois 60637. Address reprint requests to N. J. Patronas.

[2]Present address: Department of Radiology, Swedish American Hospital, Rockford School of Medicine, University of Illinois, 1316 East Charles Street, Rockford, Illinois 61108.

© 1979 American Roentgen Ray Society

0361–803X/79/1321–0138 $0.00

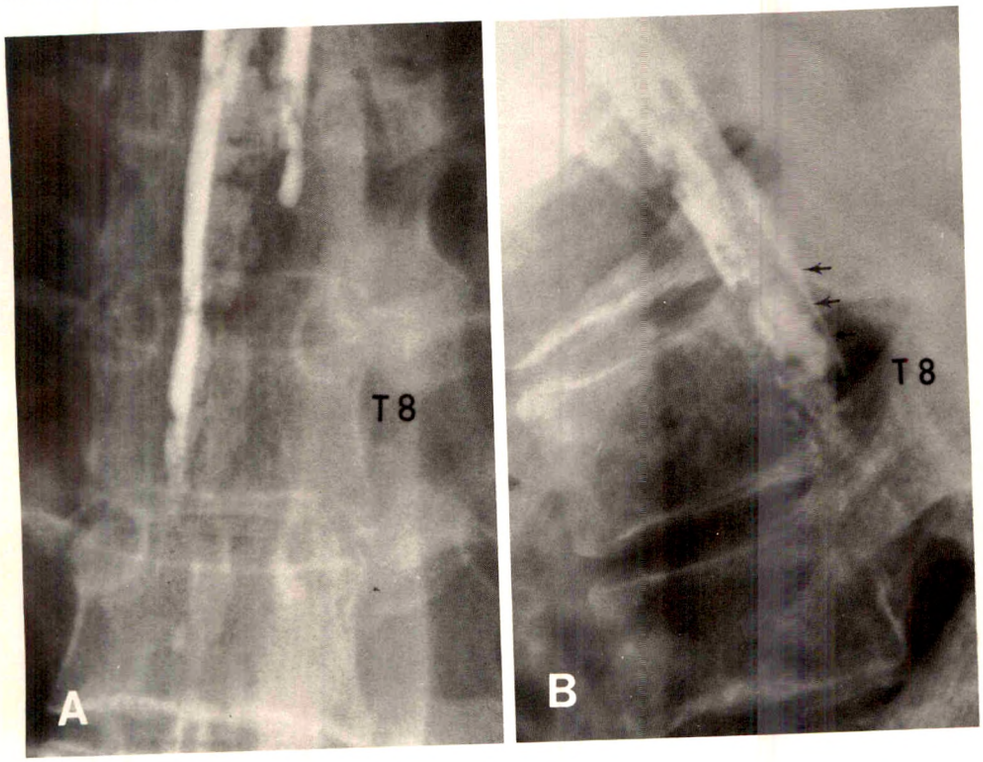


Fig. 1.—Midthoracic region. **A**, Gradual transitional zone (T7–T8) to complete block. Irregular filling defects in oil column reminiscent of arachnoiditis. **B**, Dorsal defect in subarachnoid space (*arrows*), placing lesion in extraarachnoid location. Irregularities appear in transitional zone.

Herniated nucleus pulposus and spinal stenosis may cause neurologic findings similar to spinal subdural abscess, but the infectious manifestations are absent. The cerebrospinal fluid is usually normal, and the myelogram shows typical extradural defects.

REFERENCES

1. Bennett AE, Keegan JJ: Circumscribed suppurations of the spinal cord and meninges: report of a case of subdural abscess with functional recovery following operation. *AMA Neurol Psychiatr* 19:329–333, 1928
2. Schiller F, Shadle OW: Extrathecal and intrathecal suppuration: report of two cases and discussion of the spinal subdural space. *Arch Neurol* 7:33–36, 1962
3. Abbott KH: Acute subdural spinal abscess. *Bull Los Angeles Neurol Soc* 5:227–231, 1940
4. Fraser RF, Ratzan K, Wolpert SM, Weinstein L: Spinal subdural empyema. *Arch Neurol* 28:235–238, 1973
5. Negrin J, Clark RA: Pyogenic subdural abscess of the spinal meninges. *J Neurosurg* 9:95–100, 1952
6. Chi CY: Intraspian subdural abscess. *Chin Med J (Engl)* 50:921–926, 1936
7. Freedman H, Alpers BJ: Spinal subdural abscess. *AMA Neurol Psychiatr* 60:49–60, 1948
8. Reddy DR: Pneumococcal subdural spinal abscess. *J Postgrad Med* 19:190–192, 1973
9. Dus V: Spinal peripachymeningitis (epidural abscess): report of eight cases. *J Neurosurg* 17:972–983, 1960
10. Baker AS, Ojemann RG, Swartz MN, Richardson EP Jr: Spinal epidural abscess. *New Engl J Med* 10:463–468, 1975
11. Altrocchi PH: Acute spinal epidural abscess vs. acute transverse myelopathy: a plea for neurosurgical caution. *Arch Neurol* 9:17–25, 1963

Technical Notes

Percutaneous Replacement of Biliary T Tubes

VICTOR G. MILLAN,[1] DEEPAK M. BRAMHAVAR, OUN J. KWON, AND ROBERT E. PAUL, JR.

A method for reinsertion of a new T tube was described by Crummy and Turnipseed in 1977 [1]. In our laboratory we devised a modification of their technique, which has been successfully used 18 times since March 1977. The method requires some expertise with angiographic techniques.

The indications for insertion of a new biliary T tube are (1) for cholangiography after stone extraction [2]; (2) for subsequent remanipulation when an unsuccessful stone extraction must be terminated prematurely [3]; (3) to replace a deteriorating T tube in patients with bile duct carcinoma, sclerosing cholangitis, or benign strictures requiring chronic drainage; (4) after percutaneous dilatation of biliary strictures [4]; and (5) when a T tube has been inadvertently removed.

Technique

A Teflon-coated J guide wire (0.089 cm) is passed through the stem and into the limb (preferably the upper limb) of the T tube in situ. With gentle traction, the tube is then removed, leaving the guide wire in place. The new no. 14 French T tube is prepared by shortening the T limbs (fig. 1A). The lower limb length will vary (1–3.5 cm) depending on the *diameter* of the common bile duct. The upper limb length is determined by the *length* of the common hepatic duct. The new T tube is snugly mounted on a firm catheter (RPX054 Formocath, outside diameter 2.38 mm) and introduced over the guide wire. The assembly is passed along the fistulous tract (fig. 1B), facilitated by the presence of bile. After both limbs of the T have entered the common hepatic duct (fig. 1C), the assembly is pulled back and, if necessary, rotated to enable the lower limb to drop into the common bile duct. The inner catheter and guide wire are then slowly removed in short increments, leaving the new T tube in place (fig. 1D).

If a no. 12 French T tube is to be used, it should be mounted on a smaller, firm catheter (BDRPX047 Formo-

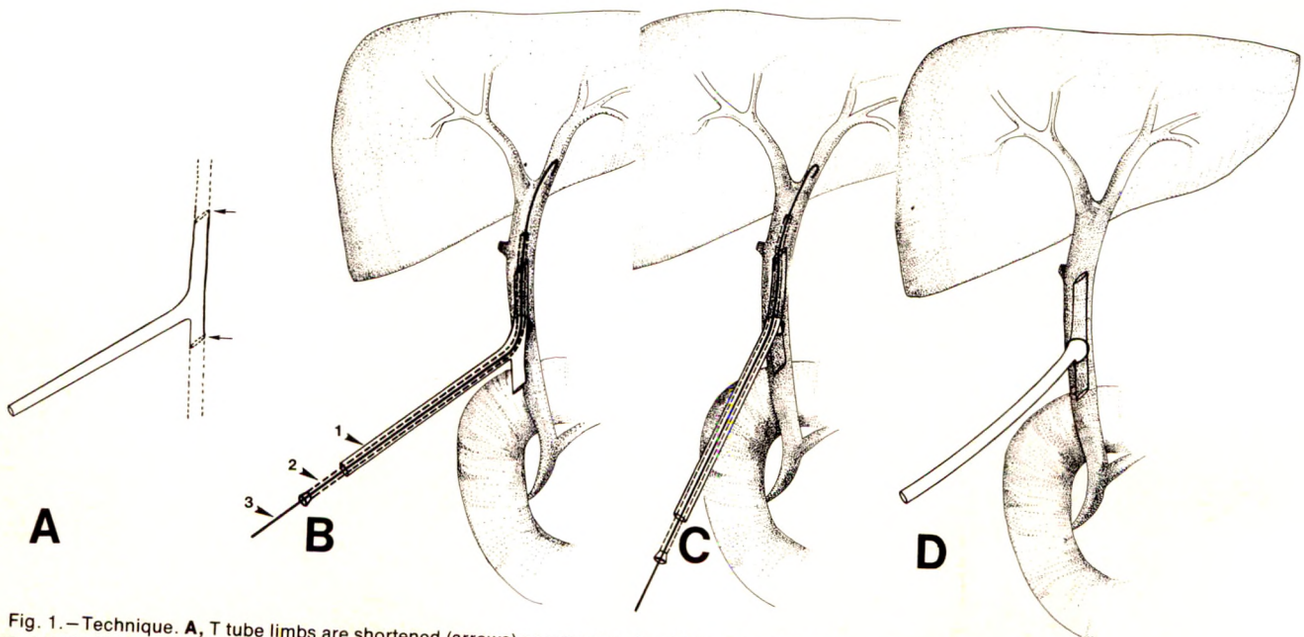


Fig. 1.—Technique. **A,** T tube limbs are shortened (*arrows*) commensurate with lengths of common hepatic and common bile ducts. **B,** Mounted on firm, snugly fitting catheter (2), T tube (1) is passed over guide wire (3) through fistula and into common hepatic duct. **C**, T tube assembly further advanced until lower limb is within duct. Gentle pullback causes lower limb to drop down into common bile duct. **D**, New T tube in place after removal of catheter and guidewire.

Received July 25, 1978; accepted September 29, 1978.

[1] All authors: Department of Radiology, Tufts University School of Medicine, New England Medical Center Hospital, 171 Harrison Avenue, Boston, Massachusetts 02111. Address reprint requests to V. G. Millan.

© 1979 American Roentgen Ray Society

0361-803X/79/1321-0140 $0.00

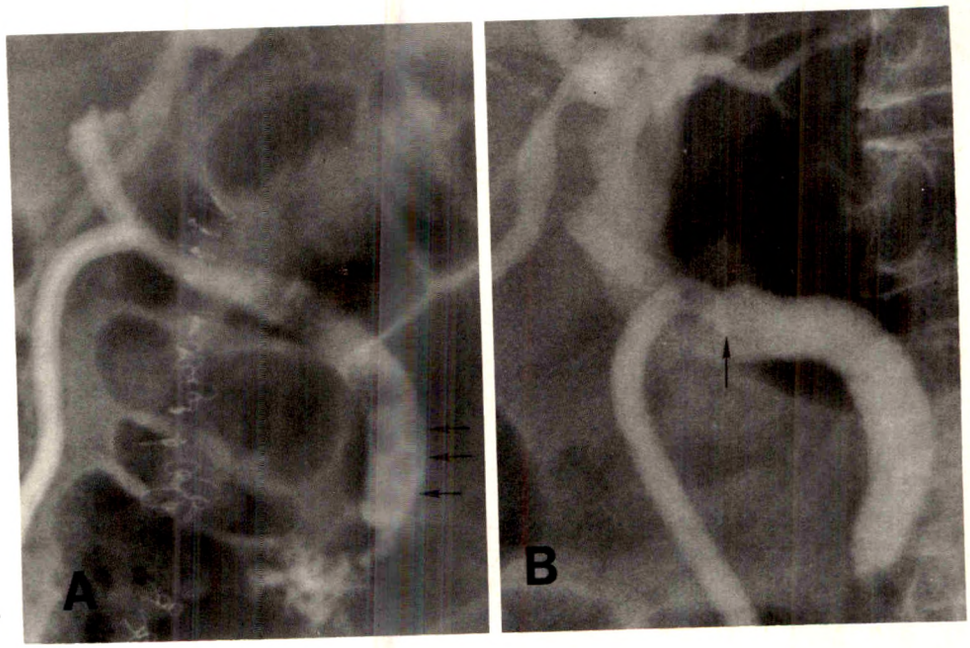


Fig. 2.—T tube replacement after stone retrieval. **A**, Original T tube in situ and four stones (*arrows*) in common bile duct; all were removed. **B**, New no. 14 French T tube in place. Length of T limbs and ends are trimmed obliquely to facilitate insertion and secure retention. Distal limb (*arrow*), less than 1 cm, was too short, later fell out, and was replaced.

cath, outside diameter 2.18 mm). T tubes smaller than no. 12 French are not recommended, as their use will result in narrowing of the fistulous tract, subsequently preventing passage of a retrieval catheter if retained stones are found. T tubes over no. 14 French are unnecessarily large.

When the fistulous tract is too small to accept the T tube or if manipulation has caused perforation or disruption of the tract, it may be impossible to advance a new T tube. Nevertheless, a straight rubber catheter can always be introduced [5, 6]. The largest possible size must be used, and if necessary, the catheter can be changed using increasing sizes on successive days until a size 16 French is obtained. A T tube can then be inserted.

Results

Since March 1977, this method has been successfully used 18 times in 12 patients. A typical example of before and after T tube replacement after removal of a retained common bile duct calculus is shown in fig. 2. Another patient with lithogenic bile required five T tube reinsertions over a 10 month period because of recurrent stone formation. The technique was also used in a patient with cholangiocarcinoma, who required percutaneous dilatation of a bile duct stricture and replacement of a disintegrating T tube. One patient seen at the departmental office had the T tube in his pocket; it had fallen out during the night because the distal limb was of insufficient length and had therefore not been well anchored in a rather capacious common bile duct. A new T tube was inserted through the fistulous tract.

In summary, this method for the percutaneous replacement of T tubes is routinely used in all of our patients undergoing bile duct manipulation. This technique has represented an important factor in the successful management of our patients on biliary drainage.

REFERENCES

1. Crummy AB, Turnipseed WD: Percutaneous replacement of a biliary T-tube. *AJR* 128:869–870, 1977
2. Carter BL, Millan VG, Sarno RC: Percutaneous common duct stone removal. *J Abdominal Surg* 20:60–65, 1978
3. Burhenne HJ, Richards V, Mathewson JC, Westdahl PR: Nonoperative extraction of retained biliary tract stones requiring multiple sessions. *Am J Surg* 128:288–292, 1974
4. Burhenne HJ: Nonoperative roentgenologic instrumentation technics of the postoperative biliary tract: treatment of biliary stricture and retained stones. *Am J Surg* 128:111–117, 1974
5. Bolich PR, Crummy AB: Extravascular use of angiographic technique to establish drainage. *JAMA* 227:655–656, 1974
6. Razzaque MA, Malhotra C, Wise RE, Whitcomb FF Jr: Treatment of T-tube obstruction by catheterization. *Radiology* 110:739, 1974

Audiovisual Problems at Scientific Meetings: An Appeal from the Conference Floor

JAMES B. MASTERSON[1]

Poor audiovisual quality and mechanical problems often mar the presentation of scientific papers at conferences. This paper outlines some commonly recurring problems and suggests simple remedies.

Room

The floor area required to seat various sized audiences can be computed from tables published by Eastman Kodak Company, Rochester, N.Y. 14650 [1, 2]. Room shape is important in determining how many people can be seated in a given area within satisfactory distance and viewing angle of the screen [3]. A room with a length-width ratio of 2:1 can seat more people with a comfortable viewing angle to the screen than a room with a 4:3 length-width ratio for the same floor area. For example, a room 14.6 m long and 11 m wide has a floor area of 160.6 m^2 and seats 129 persons within a 50° viewing angle of the screen, whereas a room 17.1 m long and 8.5 m wide has an area of 146 m^2, but seats 132 persons within a 50° viewing angle [1].

Aisles in the center of the audience waste optimum viewing space. If ordinances limit the length of seat rows, aisles should be located at the sides.

Screen

Screen size

Desirable screen size is closely related to room dimensions:

1. No one should be at a greater distance from the screen than 8 times the height of the screen image.
2. The person nearest the screen should be at a distance away from it at least twice the height of the projected image.
3. The lower edge of the screen should be at least 1.2 m above floor level so that the heads of the seated audience do not obstruct the image; however, it should not be so high that the viewing angle to screen center is more than 15° for people in the front row [4].
4. The screen should preferably be square, and its size should be 1½ times the image height of a horizontal slide to accommodate either vertical or horizontal projection.

Screen type

The standard for determining ideal screen type is "gain." "Gain" is the ratio of observed luminance (ft-lamberts) to incident illumination (ft-candles). An ideal white matte surface would have a luminance of 1 ft-lambert/1 ft-candle, or a gain of 1.

Screen design also affects gain. When viewed from near the center of the projection axis, a screen surface that can focus light reflected from it can have a gain of up to 200; however, the viewing angle at which the brighter image can be seen always decreases (fig. 1) [5].

Commonly available screen types are:

Matte white. This category includes painted matte or plastered wall and has a uniform gain of 0.85–0.9. Its wide angle (up to 45°) of acceptable image brightness is somewhat offset by its image contrast, which is badly degraded by ambient light.

Aluminized. Aluminized screens can be either smooth or textured. Gain from 1–12 is possible for a smooth screen depending on the design. The viewing angle is relatively narrow at 25°–28°; however, stray light incident at steep angles does not degrade the image contrast significantly. Textured screens have a relatively high gain (1–8) and the textured surface increases the satisfactory viewing angle to about 30°.

Lenticular. This screen has a vertical ribbed pattern like corduroy, a 1–2 gain, and fairly wide viewing angles (up to about 45°).

Beaded. Although peak gains of 1.5–3 may be obtained, the viewing angle falls to about 25°.

A matte white or lenticular surface is usually desirable since the rapid fall-off of image brightness outside the "satisfactory" viewing angle of aluminized and beaded screens may create seating problems. However, in certain circumstances (e.g., where a high ambient light level cannot be avoided), these more directional screens may be more appropriate.

Projection Equipment

The projector should be aligned to the screen so that the center of the projected image strikes the center of the screen at a right angle. Tilting the projector up or down relative to the screen produces a "keystone" distortion of the image, where one end of the image is longer than the other and vertical lines diverge. The projector should have an appropriate focal length lens to produce the desired image size, and it should produce adequate image brightness.

The absolute brightness of a projected image is measured by U.S. standard PH 22.124–1961. For indoor theater screens, the standard luminance is 16^{+4}_{-6} ft-lamberts in a darkened room with the projector turned on and no slide in the gate. Compliance with this recommendation depends on the absence of ambient light. Specification sheets for projectors outline the luminance of the screen for different image sizes; however, additional factors should be considered:

Maximum aperature of projection lens. This is analagous to the "f" stop on a camera. A f 2.8 projector lens allows 1.27 as much light through as an f 3.5 lens.

Slide frame or mask. A 135 slide, with a larger picture area, allows more light through than a 126 slide.

Glass surfaces. Each clean glass surface reflects 4% of the light striking it. Thus, if glass mounted transparencies are used and the projection booth has a glass

Received November 29, 1977; accepted after revision September 29, 1978.

[1]Department of Radiology, University of Chicago, 950 East 59th Street, Chicago, Illinois 60637. Present address: Department of Radiology, St. Laurence's Hospital, North Brunswick Street, Dublin 7, Ireland.

© 1979 American Roentgen Ray Society

0361-803X/79/1321-0142 $0.00

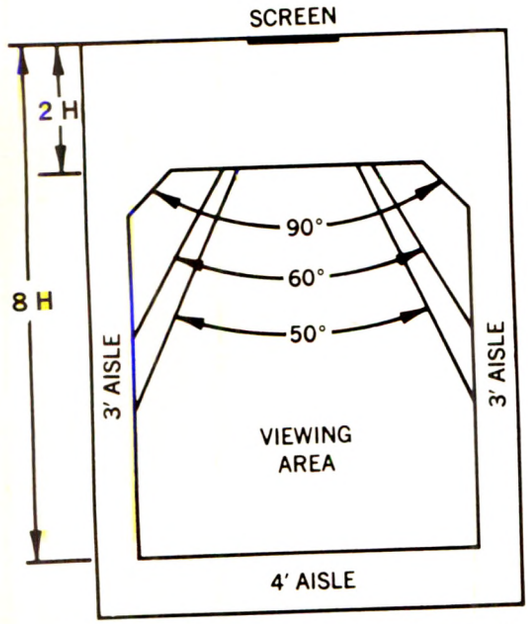


Fig. 1.—Conference room floor plan showing audience distribution relative to screen height (H) and screen material. Beaded screens provide good viewing up to a 50° angle, aluminized to 60°, and matte white surface and some lenticular screens up to 90°. (Reproduced with permission from Eastman Kodak Company.)

window, only 78% of the light will be transmitted to the screen.

Line voltage. Manufacturers specifications assume a line voltage of 120 V. The actual line voltage may be lower than this and result in decreased lamp brightness.

Stray Light

Stray light, caused by inadequately blacked out windows, note-taking lights, open doors, and light reflected from the screen back onto the screen by white walls, degrades the projected image.

Stray light reflected from the screen can seriously reduce image contrast. The ratio of image light to stray light reflected from the screen is the "brightness ratio." The degree of contrast required depends on the subject matter. Pictorial subjects (such as slides of radiographs) require a brightness ratio of 100:1; printed matter requires a brightness ratio of 25:1. Doubling the stray light striking the screen requires a doubling of image brightness to maintain the brightness ratio. If an arc lamp projector is required to correct the problem, projector cost could multiply 6 times.

If possible, handouts of important information should be distributed to eliminate the need for note-taking lights. If essential, the lights should be designed to light the audience area only and be extinguishable when slides requiring a high brightness ratio are shown.

Controls

The projectionist should be able to control the room lights from his station and should be able to hear the speaker's request for diminished room lighting, slide advances, etc. Ideally the speaker should be able to control the advance and focus of the slides. If more than one projector is used at a time, blank slides or duplicate slides should be used and both projectors advanced simultaneously, rather than risk confusing the order of advancing the projectors relative to each other.

A pointing device, either simple rod or light pointer, should be supplied. If a light pointer is used, one that operates from house current rather than batteries is suggested for adequate brightness.

Sound

To assess the need for a loudspeaker system, the obvious acoustical problems, such as noisy ventilation, a nearby kitchen, or construction work, should be predetermined.

Microphones often cause problems at scientific meetings. If the microphone is attached to the rostrum, the lecturer's voice becomes inaudible when he turns toward the screen. A halter-type microphone worn around the neck is awkward and dangerous because of the trailing cord. An attractive alternative is the radiomicrophone, which is worn as a halter, but contains a small radio transmitter and does not need a cable.

High-pitched feedback whines frequently accompanying lectures are caused by the spatial relation between the microphones and the loudspeakers, or to too high a gain setting on the amplifier. This can be prevented by placing the loudspeakers in front of the lecturer, directed away from him, and close to his level. Ideally, the loudspeakers are near the front of the hall directed toward the back, at a height of about 1.5–18 m above ground. Feedback whine is also much less likely if a directional microphone is used, coupled with an amplifier not set at too high a gain. If possible, microphones should be distributed in the aisles so that people asking questions from the floor can be heard by the audience. The spatial relation of the locutor to the loudspeakers makes feedback whine more likely in this situation, and the use of a directional microphone will minimize this danger.

Timing

The chairman should help lecturers complete their presentation in the allotted time. Simple timing devices issue an alarm only audible to the lecturer, or a warning light on the lectern can be turned on at a specified interval before the paper is scheduled to end. A speaker exceeding his allowed time reduces discussion time, which to many people is the most important part of a scientific meeting.

Slides

Slides are a very important component of radiology presentations. Experimental evidence [6] suggests that pictorial memory is almost unlimited and that pictures are remembered by a quite different mechanism than linguistic material. It seems that pictures are directly committed to long-term memory, while verbal or numeric

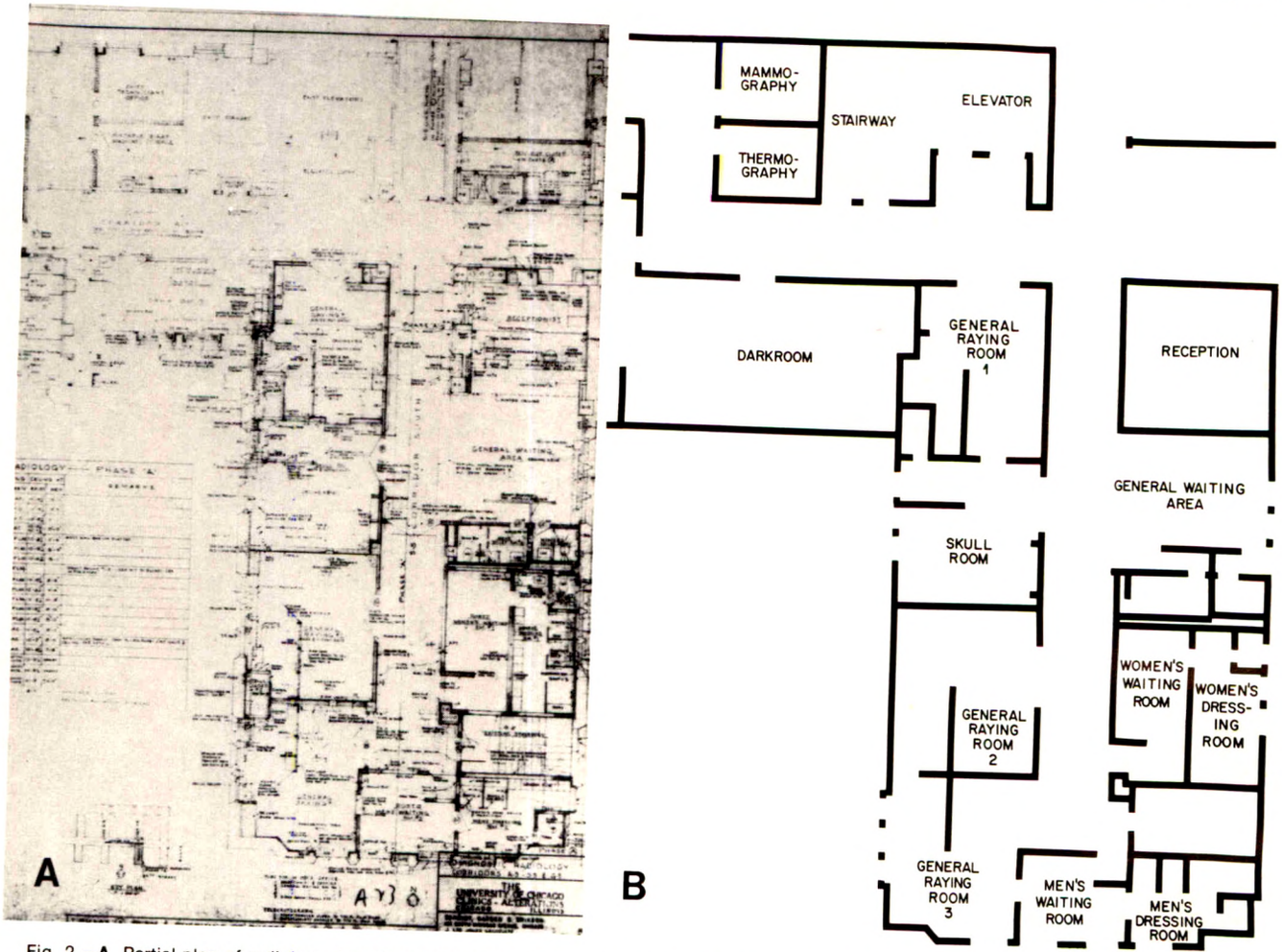


Fig. 2.—**A,** Partial plan of radiology department. Excessive detail, narrow lines, and small print make this almost useless as a slide. **B,** Simplified drawing with clearly visible print and lines that retain all details necessary for discussion.

data are remembered by a much more complicated mechanism, in which short-term memory is followed by conceptualizing the data and than transferring it to long-term memory. Several factors concern slide preparation for scientific presentations:

Materials. I believe that black and white reversal film is best for making slides of radiographs. Adequate slides can be made with color reversal film, but often the overall hue is aesthetically displeasing. Reversal films, (such as Kodak S0185) can be processed in automatic processors in radiology departments, other films are professionally processed.

Reversal film used for tables and graphs leaves large areas of white and emphasizes any small pieces of dust on the slide. On high contrast negative film, such as Kodalith, the scripts of drawings appear as white on a black background, which gives a pleasing effect and diminishes any dust marks. In addition, Kodalith is processible in a standard 90 sec radiograph film processor.

Lettering on diagrams and tables should be drafted, although quite acceptable results are achieved with press-on lettering such as Letraset Instant Lettering (Arthur Brown & Brothers, Inc., New York, N.Y. 10036) or Geotype (Geographics, Inc. Salt Lake City, Utah 84119), or an electric typewriter with a carbon ribbon. Table and data presentation can be enhanced by color slides. Eastman Kodak [7–9] booklets outline various means of producing titles or presenting material in graph or prose form. When color material is reproduced from books or other sources, the type of color slide film should be matched to the light source (either tungsten light or daylight).

Mounting. Glass-mounted slides are simple to clean and store, but can develop Newton rings, colored rings rather similar to those in oil spills. They are not caused by moisture between the slide and the glass cover, but are related to the actual distance between slide and cover. The rings produce a distracting and unsightly screen image. Special anti-Newton glass slide mounts can be used or anti-Newton powder can be lightly dusted between the slide and the glass mount.

Another problem with glass-mounted slides is that they do not fit into the Kodak Carousel trays designed to take 140 slides. Slides mounted in cardboard are more easily damaged by finger marks, but a special film cleaning fluid is available in most photography stores.

Content. Two common problems encountered in the presentation of slides of radiographs are (1) the abnormality is not convincingly demonstrated because it occupies too small a part of the image or because it is poorly photographed and (2) people interested in a particular abnormality often show too many examples of that abnormality even though each succeeding slide adds no further information. Although it may be necessary to show a slide of a large part of a radiograph for orientation purposes, it should be followed by a close-up view of the area of interest.

Unique cases are sometimes encountered in studies using inferior radiographic technique. LogEtronics system (LogEtronics, Inc., Springfield, Va. 22150) can enhance the radiograph for photographic purposes. It is not widely available at present, but is worth researching. A less sophisticated method called "blurred-under subtraction" gives excellent results and is described by Kattan et al. [10].

The often transgressed rule concerning layout of written material on a slide is worth repeating: "Not more than five words per line and not more than five lines per slide." Another simple rule is that if the graphs or tables can be read or the lesion can be clearly seen without magnification when the slide is held up to the light, then the information can also be seen by audience members (fig. 2). If possible, only a single idea should be conveyed on each slide. Above all, long tables of differentials or graphs showing numerous different parameters should not be used. If it is necessary to compare five or six different parameters, they should be introduced singly with the composite slide at the end.

Care. Slides should be stored away from direct light and extremes of temperature and humidity. Conditions comfortable for people are comfortable for slides. Inspect and clean slides prior to presentation.

Since Kodak Carousel trays are used so often at conferences, they are convenient for transporting slides, despite their bulk. If a Carousel tray is used, it is even more necessary to preview the slides before the conference to ensure correct orientation and sequence. A preview room at conferences reassures the lecturer and projectionist, and allows the lecturer to explain any special requirements for projecting his slides.

Conclusion

Attention to detail by conference planners and participating lecturers will minimize the artifacts, distractions, and frustrations which interfere with communication and will enable speakers and audience to concentrate on the scientific content of the message.

REFERENCES

1. *Projection Calculator and Seating Guide*. Kodak Publication No. S16
2. *Audiovisual Projection*. Kodak Publication No. S-3
3. Weiss H: Optics, in *Display Systems Engineering*, New York, McGraw-Hill, 1968, pp 165–209
4. *Designing for Projection*. Eastman Kodak Co., 1970
5. Vlahos P: Film-based projection systems, in *Display Systems Engineering*, New York, McGraw-Hill, 1968, pp 277–318
6. Haber RN: How we remember what we see. *Sci Am* 222: 104–113, 1970
7. *Planning and Producing Slide Programs*. Kodak Publications No. S-30
8. *Effective Lecture Slides*. Kodak Publication No. S22
9. *Legibility—Artwork to Screen*. Kodak Publication No. S24
10. Kattan KR, Caplan MC, Felson B: A method for improving roentgenographic illustrations for publication—blurred under subtraction (BUS). *Med Radiogr Photogr* 49:21–22, 1973

Editorial

The Old Order Changeth

Beginning with this issue, the Journal will be published by the Williams & Wilkins Company of Baltimore, Maryland.

Introducing the January 1930 issue of the Journal, Dr. Lawrence Reynolds used similar words to announce the transfer of publishing responsibilities from the Paul B. Hoeber Company of New York to the Charles C Thomas Company of Springfield, Illinois. After 49 years of friendly and fruitful association, the American Roentgen Ray Society has chosen to ask new publishers to assume the challenges of the years ahead.

The role of the publisher in the production of any journal is too often dimly understood. It is usually the editor and the editorial staff who receive either the credit or the blame for the product the reader receives each month. From its beginning in 1906 as the *American Quarterly of Roentgenology* to the *American Journal of Roentgenology* of 1979, the list of editors has included the leaders in our specialty. Drs. Preston Hickey, James Case, H. M. Imboden, Arthur Christie, Lawrence Reynolds, Merrill Sosman, Traian Leucutia, Frederick Lang, and Melvin Figley have all been exceptional individuals. They have been radiologic scholars with the additional skill of communication of their own scholarship and that of others to the radiological community. Each has left his own mark on the contents and appearance of the Journal.

Our publishers have been fewer but have had equally impressive credentials in their area. When the Journal was first formed as the *American Quarterly of Roentgenology*, it was published by the American Roentgen Ray Society, and then became the property of Paul B. Hoeber Company of New York until 1929. Since 1930, when the Society reacquired ownership of the Journal, it has been published by the Charles C Thomas Company. The publisher, as well as the editor, leaves a mark on the Journal, although it may be less apparent to the reader.

The publisher of the Journal does more than collect subscription payments. It is his responsibility not only to obtain suitable printing and distribution services, but also to solicit advertising that has an educational as well as commercial content. The publisher provides for subscription fulfillment, deals with postal and foreign distribution services and offers appropriate advice regarding technical problems and editorial content. Since it is the continuing goal of the Editorial Office to provide the most prompt transmission of radiologic communications to its readers, the liaison between Editor and Publisher is an intimate and demanding one. When the Journal subscription was $10 per year and was half the size of our present volume, the Paul B. Hoeber Company listed the following information in each issue:

> Subscribers are invited to make the office of the publishers their headquarters. Mail, packages, or bundles may be addressed in our care. Hotel reservations will gladly be made for those advising us in advance; kindly notify us in detail as to requirements and prices. A list of operations in New York hospitals on file in our office daily.

Unfortunately, these services of a simpler time are no longer available to the subscriber, and the complexities of contemporary publication have placed an even greater strain on the production of a quality product. As a result of production problems in mid-1977 quite beyond the control of the Thomas Company, the Journal was forced on short notice to seek a new printer. Waverly Press responded admirably to this urgency and has since continued to satisfy the Editorial Office and Publications Committee. To enhance this association and to seek more aggressive distribution the Society has chosen the publisher associated with Waverly Press.

The new publisher, Williams & Wilkins, is one of the oldest and most respected publishers of medical books and journals in the world. The *American Journal of Roentgenology* is one of the oldest and most respected radiologic publications in the world. It is to be expected that this union will fulfill the expectations of a critical and demanding readership, adding more bright chapters to an already bright history.

In his editorial of 1930, Dr. Reynolds went on to say: "As may be seen, these changes represent no great departure from the well established policy of the Journal but such changes as have been made we hope will improve the Journal in certain minor details. The business arrangement which the Publication Committee has made with the Publisher enables the Society to have a more direct concern in the earnings of the Journal." These words are also appropriate for the new agreement that has been consumated. The old order changeth but our immediate and long-term aspirations for excellence remain in the great tradition of those who have gone before.

R. A. Gagliardi
Chairman, Publications Committee
880 Woodward Avenue
Pontiac, Michigan 48053

Editor's Note

With becoming modesty Dr. Gagliardi has not described his crucial role in directing the search for a publisher and effecting a smooth transition of responsibilities from old to new. The Journal is the largest financial enterprise of the American Roentgen Ray Society, accounting for the majority of the income that assures continuity of services to the radiologic

public. Sound financial management of the Journal is essential for the Society's continuing educational role in our specialty.

In choosing Dr. Gagliardi as Chairman of the Publications Committee, the Executive Council was quite aware that renewal of the publishing contract would come during his term. Its trust in his commitment to the task and his skill in handling such matters was rewarded by an excellent contract providing for both the requirements of the Society and the expectations of the new publisher. With ultimate fairness to all aspirants and special consideration for both the Thomas Company and Williams & Wilkins, Dr. Gagliardi has placed the Society in a very favorable position as it looks ahead to improving its educational efforts at a time of rising costs. The Society and all the Journal readers are indebted to Dr. Gagliardi for his successful fulfillment of a very important task.

MMF

ARRS Meeting, Toronto, Canada, March 25–30

The annual meeting of the American Roentgen Ray Society will be March 25–30 in Toronto, Canada. Nonmembers as well as society members are very welcome. The headquarters hotel and meeting site will be the **Sheraton Centre.** In some previous AJR issues, the hotel was incorrectly identified as the Four Seasons Sheraton.

The October 1978 issue of AJR carried a meeting section which included colored forms for registration for the meeting, hotels, instruction courses, and social events. In addition, the special categorical course on neuroradiology was described. The series of registration forms was repeated in the November 1978 issue.

AJR plans to carry additional meeting information in the February and March 1979 issues.

In February, a list of titles of papers selected for the scientific program will appear; the refresher course schedule will be repeated. AJR will also carry a synopsis of the U.S. Internal Revenue Service rules regarding allowable deductions of expenses for attending conventions in foreign countries. The program for the Society of Photo-Optical Instrumentation Engineers will be listed. SPIE meets in conjunction with ARRS. The program for spouses will again be briefly described.

The March issue of AJR will list papers selected for presentation at the Society for Pediatric Radiology meeting. This society also meets in conjunction with ARRS.

President's Invitation

American Radium Society Meeting, March 4–8

Dear Colleague:

It is with great pleasure that I invite you to attend the sixty-first annual meeting of the American Radium Society, March 4–8, in Los Angeles. As you know, the American Radium Society in 1916 first unified the various medical disciplines into one oncologic society, and since that time has provided a unique opportunity for senior oncologists to interact and exchange information valuable to their participation in national cancer programs. This year the theme, "Interdisciplinary Cancer Patient Management Emphasizing New Approaches", will provide a forum for the most important recent advances in every major area of oncology.

The scientific program will again emphasize papers submitted by society members. Discussants will be identified for each paper, primarily from disciplines other than that of the essayist. The morning scientific sessions will be far ranging in scope, covering new approaches in urologic, gynecologic, immunologic medical, surgical, and radiation oncology. Optional minisymposia on genitourinary cancer, colorectal cancer, malignant melanoma, central nervous system tumors, and pediatric oncology are also planned to ensure good multidisciplinary representation. Workshops in scientific writing, the impact of federal regulatory and funding agencies, and other topics are planned.

At this writing, final paper selection has not occurred, however, titles submitted include: renal artery occlusion; breast cancer and the dysplastic breast; Scribner-Broviac shunts; long-term adjuvant chemotherapy; integrated therapy for bladder cancer; aspiration cytology; malignant melanoma; cloagenic carcinomas; gestational choriocarcinoma; pyriform sinus cancer; iridium-192 brain implants; and hyperthermia.

The presentation of new programs of cancer management to an interdisciplinary forum where they are critically reviewed and evaluated from both the antagonistic and protagonistic points of view is an important process in optimizing new approaches to cancer treatment. The accelerated development of multidisciplinary treatment and evaluation, and the increasing intervention of governmental agencies into their use has underscored the need for close collaboration between professional, commercial, and governmental organizations for the most efficacious delivery of cancer patient care. In this connection, the American Radium Society has long recognized commercial and governmental organizations as a major resource to the professional community responsible for the management of the cancer patient, and extends a special invitation to encourage their participation in an expanded role in this and future meetings.

The meeting will take place at the Los Angeles Bonaventure Hotel which provides easy access via pedestrian bridges to the Los Angeles Tennis and Racquet Club, the Music Center, and other major attractions. Dr. James Helsper assures me that the social and recreational program is innovative, varying, and exciting, ranging from the elegance of the old masters at the Huntington Museum and Library to the diverse attractions of Disneyland and Marineland.

We expect the diversity and high quality of presentations at the meeting to be outstanding. Your participation is all that is needed to guarantee a truly memorable meeting of our nation's senior oncologic society. We will make you most welcome; please plan to attend.

Inquiries regarding meeting registration and program should be directed to me at the University of Southern California School of Medicine, 2025 Zonal Avenue, Los Angeles, California 90033; telephone (213) 226-5017.

Sincerely,

Frederick W. George, III
American Radium Society
Office of the President

John Caffey, 1895–1978



John Caffey

Dr. John Caffey died the morning of September 2, 1978, at Presbyterian-University Hospital in Pittsburgh, Pennsylvania after a brief illness. He was 83 years old and had worked until the morning of his admission to the hospital.

Dr. Caffey was regarded throughout the world as the father of pediatric radiology. His classic textbook, *Pediatric X-Ray Diagnosis*, which was first published in 1945, has become the recognized bible and authority in its field. The seventh edition of this book was completed several months before Dr. Caffey's death, and will have been published before this memorial appears. It has been among the most successful books of its kind in the medical field.

Dr. Caffey was born in Castle Gate, Utah on March 30, 1895, the same year that Roentgen discovered the x-ray. Dr. Caffey was graduated from the University of Michigan Medical School in 1919, following which he served an internship in internal medicine at Barnes Hospital in St. Louis. He spent 3 years in Eastern Europe with the American Red Cross and the American Relief Administration, and returned to the United States for additional training in medicine and in pediatrics at the Universities of Michigan and Columbia, respectively.

While in the private practice of pediatrics in New York City at the old Babies Hospital of Columbia University College of Physicians and Surgeons, he became interested in radiology and was charged with developing a department of pediatric radiology in 1929. He frequently expressed appreciation and admiration for the late Ross Golden, Chairman of Radiology at Columbia Presbyterian Hospital, who allowed him to develop a separate department of diagnostic radiology without undue interference, and who was always available to help and advise him.

Dr. Caffey's keen intelligence and inquiring mind quickly established him as the leader in the field of pediatric x-ray diagnosis; recognition became worldwide almost instantaneously with the publication of his book in 1945.

Dr. Caffey received numerous awards in recognition of his achievements. Outstanding among these were the Mackenzie Davidson Medal of the British Institute of Radiology in 1956, the Distinguished Service Award of the Columbia Presbyterian Medical Center in 1962, the Outstanding Achievement Award of the University of Michigan in 1965, the Howland Award of the American Pediatric Society in 1967, the Jacobi Award of the American Medical Association in 1972, and the Gold Medal Award of the American College of Radiology in 1975. He had been a member of the editorial board of *Pediatrics* and of the consulting editorial board of the *American Journal of Roentgenology*. He was a counselor of the Society for Pediatric Radiology and was an honorary member of the European Society for Pediatric Radiology.

Dr. Caffey's contributions to the pediatric radiologic literature were many. He was instrumental in directing attention to the fact that a prominent thymic shadow was a sign of good health and not of disease, an observation that literally spelled the end to the practice of thymic irradiation in infancy. Infantile cortical hyperostosis was described by him and is called "Caffey's Disease." Dr. Caffey in 1946 first recognized the telltale radiographic changes that characterize the battered child, and his students helped disseminate his teachings about these findings. It was Dr. Caffey who first recognized and

described the characteristic bony changes in vitamin A poisoning. He recognized and described the findings associated with prenatal bowing of the skeleton.

In 1963, 3 years after his retirement from Babies Hospital, he joined the staff of the Children's Hospital of Pittsburgh as associate radiologist and as Visiting Professor of Radiology and Pediatrics at the University of Pittsburgh School of Medicine. Although Dr. Caffey came to Children's Hospital and the University of Pittsburgh in an emeritus position, he worked daily and on weekends throughout the years he was there. In Pittsburgh, he made four major new contributions to the medical literature. He described the entity, "idiopathic familial hyperphosphastasemia." He recognized and described the earliest radiologic changes in Perthes's Disease. He called attention to the potentially serious effects of shaking children, and used this as the subject of his Jacobi award lecture. He described, with the late Dr. Kenny, a hitherto unrecognized form of dwarfism which is now known as the Caffey-Kenny dwarf.

The John Caffey Society, which includes as its members pediatric radiologists who have been intimately associated with Dr. Caffey, or who have been trained by his students, was established in 1961. This society is now among the most prestigious in the field of radiology. His book and the society named in his honor will live on as important memorials to this great man.

His greatness was obvious to all who worked with him. He was warm, kind, stimulating, argumentative, and above all, honest in his approach to medicine and to x-ray diagnosis. His dedication to the truth was expressed in his abiding interest in the limitations of radiologic signs in pediatric diagnosis and in his interest in normal variations in the growing skeleton. He was concerned with the written and spoken word, and was a skilled semanticist. His book and his articles are masterpieces of language and construction. He stimulated and was stimulated and loved by all who had the privilege of working with him. Radiology and Pediatrics have lost a great man, but they shall ever have been enriched by his presence.

Dr. Caffey is survived by a sister, Mary E. of Salt Lake City, a brother, Paul, of Philadelphia, and by a legion of close friends, colleagues, students, and associates.

Bertram R. Girdany
Pittsburgh, Pennsylvania

Abstracts of Current Literature

Chest

The chest radiograph in Legionnaires' disease. Dietrich PA, Johnson RD, Fairbank JT, Walke JS (University of Vermont College of Medicine, Burlington, Vermont 05401). *Radiology* 127:577–582, June 1978

The chest radiographs of 24 patients with documented Legionnaires' disease were evaluated. Twenty-two of the 24 patients had positive findings for the disease initially. There was unilateral involvement in 68% and the most common lung shadows were poorly marginated round opacities (46%), diffuse patchy (25%), and peripheral opacities (21%). At peak, 70% of patients had a lobar shadow. Pleural effusions were present in 39% of cases but could be explained by underlying congestive heart failure or renal failure in seven of the nine. Although the findings are not specific, the radiologist should consider this diagnosis in a patient with compatible clinical history, a pneumonia of obscure etiology and these radiographic manifestations.

Author Abstract

Visualization of the pulmonary arteries in pseudotruncus by pulmonary vein wedge angiography. Nihill MR, Mullins CE, McNamara DG (Pediatric Cardiology, Texas Children's Hospital, Houston, Texas 77030). *Circulation* 58:140–147, July 1978 (by permission of the American Heart Association)

Pulmonary venous wedge angiography revealed the anatomy of the mediastinal and parenchymal pulmonary arteries in 22 patients with obstruction of the right ventricular outflow tract, proximal pulmonary arteries or branch pulmonary arteries, when conventional angiographic methods had failed. Nine of these patients had pseudotruncus-type anatomy and had no previous surgery. One pulmonary artery was not visualized in 13 of the 22 patients because of post-operative occlusion in 10, congenital "absence" of the left pulmonary artery in two, and suspected sequestration of the left lower lobe in one.

Retrograde pulmonary wedge angiograms were obtained by wedging an end-hole catheter in a pulmonary vein and slowly injecting, by hand, 0.2 to 0.45 ml/kg of contrast material followed by a flush of dextrose solution (1-2 ml/kg). In seven of the nine patients without previous surgery, the confluence of the pulmonary arteries in the mediastinum could be seen clearly by this method. Nine patients had a previous systemic-to-pulmonary anastomosis, and only the ipsilateral pulmonary arteries were visualized by aortography. Venous wedge angiography filled the pulmonary arteries of the nonopacified lung up to the point of obstruction in the mediastinum in each patient. Eight patients were able to have a systemic-to-pulmonary shunt because of the visualization of the previously unseen pulmonary arteries.

We conclude that pulmonary venous wedge angiography is a valuable adjunct to the current angiographic methods of investigating patients with pulmonary atresia and related conditions. In some cases, it may be the only way to determine the presence of surgically accessible pulmonary arteries.

Author Abstract

Radiographic manifestations of broncholithiasis. Vix VA (Indiana University School of Medicine, Indianapolis, Indiana. *Radiology* 128:295–299, August 1978

Calcifications within the lung may produce symptoms when they erode surrounding tissue and move. Lithoptysis, hemoptysis, or symptoms related to bronchial obstructions may occur. Under these circumstances, careful attention should be paid to evidence of movement of a calcific focus and its relationship to the bronchi. Six examples are described. Tomography and bronchography are useful. Histoplasma organisms can be demonstrated in most broncholiths in an endemic area. In other areas this entity is becoming unusual, probably because of the declining incidence of tuberculosis. Not all hilar or parenchymal calcifications are innocuous.

Author Abstract

Cardiovascular

Venous-phase angiography in subclavian-steal syndrome. Nalbantgil I, Yigitbaşi Ö, Çağatay G, Kiliççioğlu B, Atabay G (Aegean University, Izmir, Turkey). *Radiology* 128:411–413 August 1978

The value of demonstrating the venous phase of angiography in patients with subclavian-steal syndrome was evaluated in 17 patients. In patients with mild symptoms, there was no difference between the left and right jugular-vein opacification, but minimal or no opacification was observed in patients with severe symptoms. The authors believe evaluating venous phases in angiography in patients with subclavian-steal syndrome is useful because the findings correlate well with the severity of the symptoms.

Author Abstract

Nitroglycerin and nitrate esters. Warren SE, Francis GS (Department of Internal Medicine and Clinical Investigation Center, Naval Regional Medical Center, San Diego, California). *Am J Med* 65:53–62, July 1978

This review updates the physiologic basis and clinical indications for use of nitroglycerin and other nitrate esters in the treatment of angina pectoris and other conditions related to myocardial ischemia. Nitroglycerin remains the drug of choice for the management of anginal pain. It relieves most patients within 3 min with the exception of those having a myocardial infarction. Nitroglycerin may aggravate symptoms due to idiopathic hypertrophic subaortic stenosis and may also be deleterious to patients with ischemic chest pain due to severe anemia, aortic stenosis, hypotension, and tachyarrhythmias. It is contraindicated in glaucoma.

Recently, nitroglycerin has been tried as a therapy to reduce the size of myocardial infarctions. It has also been tried for the treatment of acute congestive failure. In both of these situations, it shows some promise although nitroprusside appears to be the more promising agent in acute congestive failure. Nitroglycerin has also been tried even in patients with myocardial infarction because of experimental observations that it may reduce arrhythmias and also because it may reduce spasm within the coronary vessels in certain patients. Long-acting nitrates have been used for many years but are now increasingly popular. This is particularly true for patients with frequent anginal attacks and angina occurring at night. Isosorbide dinitrate and nitroglycerin paste are especially popular. Many other important points about the use of these common drugs are made in this excellent review.

David C. Dale
Department of Medicine
University of Washington

AJR 132:151–161, January 1979
© 1979 American Roentgen Ray Society

0361-803X/79/1321-0151 $0.00

Doppler ankle systolic blood pressure. Prognostic value in vein bypass grafts of the lower extremity. Corson JD, Johnson WC, LoGerfo FW, Bush HL, Menzoian JO, Kumaki DJ, Nasbeth DC (Boston University and Tufts University Schools of Medicine, Boston, Massachusetts 02118). *Arch Surg* 113:932–935, Aug 1978

The application of the transcutaneous Doppler technique to indirectly measure arterial pressure in an extremity has proved to be an extremely useful, easy, reliable, inexpensive, and accurate means of measurement of ankle blood pressure in the lower limb. The ankle systolic pressure index, calculated by dividing the highest ankle pressure of the involved limb by the highest brachial artery pressure, has been shown to correlate significantly both with severity of symptoms and with extent of disease in patients with atherosclerotic vascular occlusive disease of the lower extremity.

In this study, the prognostic value of Doppler derived ankle systolic pressure indices for predicting the patency of vein bypass grafts in the lower extremity was analyzed in 126 vein bypass grafts performed for limb salvage. Although a vein bypass in a limb with a preoperative ankle systolic pressure index less than 0.5 had a higher chance of early failure than a vein bypass in a limb with a preoperative pressure index greater than 0.5 (25% versus 3.0%), there was no statistical linear relationship between early or late vein graft failure and the preoperative pressure index. The authors state that a low preoperative index should not be used as a contraindication to an attempt at limb salvage by vein bypass grafting.

A postoperative ankle systolic pressure index less than 0.7 at 24–48 hr, or an increase in the index of less than 0.4 were prognostic signs of early vein graft failure, and are considered indications for angiography and/or reexploration of the graft. Periodic follow-up Doppler evaluation of patients with vein bypass graft is recommended, since stenotic lesions may develop at the proximal or distal anastomoses of the graft. A deterioration in the last postoperative Doppler pressure index is a strong indication for arteriography.

Reiley Kidd

Physician and patient exposure during cardiac catheterization. Rueter FG (Analysis and Evaluation Branch, Division of Training and Medical Applications, Bureau of Radiological Health, Food and Drug Administration, HFX-70, Rockville, Maryland 20857). *Circulation* 58:134–139, July 1978 (by permission American Heart Association)

Physician eye exposures of approximately 20 mR/cardiac catheterization procedure were measured, which suggested a limit of five procedures/week for physicians. Although the average patient skin entrance exposure of 28 R is high, as is the 12 mR gonadal exposure; they are accepted because of the possible benefits of the procedure.

Robert Frech

Histopathological study of arterial encasement in pancreatic carcinoma (in Japanese). Sumida M, Takagi T, Fukuda Y, Ariyama J, Ikenobe H, Kurosawa A, Ohashi K, Kawai S, Shirata I, Shimagushi H, Shirakabe H, Hashimoto K (Juntendo University, Tokyo, Japan). *Jpn J Clin Radiol* 23:445–461, April 1978

Arterial encasement has been reported as a specific finding of pancreatic carcinoma, but histopathologic background of this finding has not been evaluated yet. Authors performed angiography of specimens in three cases and histopathologic study was carried out thereafter. Angiograms of specimens and in vivo were compared to histologic study. Results indicated that infiltration of the arterial wall by carcinoma cells was limited to the elastica externa and was accompanied by marked perivascular fibrosis. These findings are specific for arterial encasement. It is concluded that the pathogenesis of arterial encasement is incomplete dilatation and constriction of the artery due to the evoked perivascular fibrosis.

Hozumi Arii

Echocardiographic features of the interventricular septum in chronic constrictive pericarditis. Candell-Riera J, Garcia del Castillo H, Permanyer-Miralda G, Soler-Soler J (Servicio de Cardiologia, Departamento de Medicina, Ciudad Sanitaria de la Seguridad Social, Paseo del Valle Hebron s/n, Barcelona, Spain). *Circulation* 57:1154–1158, June 1978 (By permission American Heart Association)

Echocardiographic characteristics of the interventricular septum have been studied in eight patients with chronic constrictive pericarditis. Values of septal thickening were clearly below normal in all cases. Interventricular septal systolic motion was normal in four cases, hypokinetic in three, and paradoxical in one. In seven of eight patients, an early interventricular septal diastolic motion (IVSDM) consisting of a sudden anterior displacement followed by a brisk posterior rebound was recorded. The beginning of this anomalous movement was coincident with the pericardial knock in the phonocardiogram and its peak was coincident with the simultaneously recorded deep "y" trough in the jugular pulse tracing. The tendency toward normality of IVSDM observed after pericardiectomy in six of seven patients suggests that this peculiar interventricular septal systolic motion may be a frequent and probably specific echocardiographic finding in constrictive pericarditis.

Author Abstract

Hemodynamically significant primary anomalies of the coronary arteries: angiographic aspects. Levin DC, Fellows KE, Abrams HL (Harvard Medical School, 25 Shattuck Street, Boston, Massachusetts 02115). *Circulation* 58:25–32, July 1978 (by permission American Heart Association)

Hemodynamically significant primary anomalies of the coronary arteries are those which alter myocardial perfusion. There are four major types: coronary artery fistulae, origin of the left coronary artery from the pulmonary artery, congenital coronary stenosis or atresia, and origin of the left coronary artery from the right sinus of Valsalva, with subsequent passage of the vessel between the aorta and right ventricular infundibulum. The angiographic features of these lesions are discussed.

Author Abstract

The posterior left atrial echocardiogram of mitral regurgitation. Patton R, Dragatakis L, Marpole D, Sniderman A (Division of Cardiology, Royal Victoria Hospital, 687 Pine Avenue West, Montreal, Quebec H3A 1A1, Canada). *Circulation* 57:1134–1139, June 1978 (By permission American Heart Association)

The motion of the posterior wall of the normal left atrium has not been studied systematically. The superoposterior portion of the left atrium is adynamic throughout the cardiac cycle, whereas the inferoposterior portion is displaced posteriorly with left atrial filling during ventricular systole. In the present study, the left atrial diameter (LAD), the left atrial systolic motion (LASM), and the left atrial systolic velocity (LASV), were determined in the following groups of patients: 34 normals; eight patients with either coronary artery disease or aortic stenosis; six patients with aortic insufficiency; and three patients with ventricular septal defect. The results obtained were compared to 15 patients with angiographically documented mitral regurgitation. In the last group, the LAD (4.2 ± .19 cm) and LASV (12.3 ± 1.23 cm) and LASM (1.2 ± .04 cm) were significantly greater reflecting the early accentuated filling of the left atrium induced by mitral regurgitation. As well, the product of these three parameters was greater in the mitral regurgitation group (63.2 ± 7.34 cm^3/sec) than in the other groups and patients with mild to moderate regurgitation had a significantly lower value

than those with moderate to severe regurgitation (45.7 ± 4.1 vs 78.5 ± 10.9, $P < 0.102$). The left atrial echocardiogram, therefore, is an aid in the diagnosis of mitral regurgitation and provides a rough index of the severity of the lesion.

Author Abstract

Gastrointestinal

Retained intrahepatic stones. Use of the U-tube during repeated non-operative stone extractions. Burhenne HJ, Peters HE (University of British Columbia, Vancouver, Canada). *Arch Surg* 113:837–841, July 1978

The U-tube is an alternative biliary drainage system in which a single polyvinyl or latex tube enters the abdominal wall, lies in the intrahepatic biliary tree and common bile duct, and exits the latter to the abdominal wall as does the more usual T-tube; thus a U is formed, following which the two external ends of the U-tube are connected, preventing its inadvertent extraction and permitting normal activities, such as showering. The operative placement of U-tubes has been used with success in (1) the palliation of bile duct carcinoma and (2) the longterm treatment of strictures; side-holes above and below the point of potential obstruction decompress the biliary system internally, and the U configuration allows nonoperative replacement of a bile plugged U-tube in a "pull through" fashion or over a guide wire.

This article discusses the operative or postoperative percutaneous placement of a U-tube in a third setting: in patients with retained intrahepatic stones in whom multiple nonoperative extraction procedures under fluoroscopic control may be required, especially when stricture dilatation must precede stone extraction. Three illustrative cases are presented.

Reiley Kidd

The transjugular technique of hepatic venography and biopsy, cholangiography, and obliteration of esophageal varices. Goldman ML, Gonzalez AC, Galambos JT, Gordon IJ, Oen K-T (Grady Memorial Hospital, Emory University Affiliated Hospitals, Atlanta, Georgia). *Radiology*, 128:325–331, Aug 1978

Transjugular examinations were performed in 105 patients. Biopsy was obtained in 63 patients, cholangiography performed in 16, portal venous study with obliteration of coronary vein in four patients, hepatic venous studies in nine, with failure of the procedure in 13. In 33 patients prothrombin time was 4 sec over the control. Thirty patients had bilirubin levels greater than 5 mg/cc. The authors utilized this modality in patients with severe ascites, marked obesity, or defective hemostasis.

When cholangiography was to be performed, antibiotics were given prophylactically. The authors used oral ampicillin at a dose of 500 mg every 6 hr for 24 hr prior to the study and 48 hr following.

Sedation was achieved by use of oral Serax 15 mg and oral Phenergan 12.5–25 mg. These were given 2–4 hr prior to the study. Atropine was used when thought necessary. If additional sedation was necessary it was achieved by intravenous injection of 2–3 mg of morphine sulfate which could be repeated at 10 min intervals. During the study there was a continuous EKG monitoring.

Needle puncture is performed 1–2 cm below the angle of the mandible and approximately 1 cm lateral to the carotid pulse. Skin and subcutaneous tissues are separated with a hemostat. Generally puncture of the right internal jugular vein was preferred. An 18 gauge open end needle is used with continuous aspiration through a partially saline-filled syringe and extension tubing. Once free flow is achieved, a 0.89 mm (0.035 inch) J-shaped guide wire is advanced through the right atrium and inferior to the hemidiaphragm. During this time there is continuous EKG and fluoroscopic monitoring. A No. 9 French dilator is used following which a 9 French Teflon catheter is advanced over the guide wire. Following removal of the guide wire and flushing, the catheter is positioned just at the orifice of the hepatic vein. The guide wire is reintroduced and the catheter is advanced over it following into the hepatic vein. At this stage venography can be performed. For biopsy, cholangiography, or portal venography a modified Ross needle is advanced through the catheter tip.

Complications of hepatic biopsy which require transfusion occurred in two patients; transient bacteremia in one, and aneurysm of the intrahepatic branch of the hepatic artery occurred in one patient. Cholangiography performed in 16 patients resulted in sepsis in three. Portal venography performed in four patients resulted in perforated liver capsule requiring transfusion in two patients. Venography performed in 94 patients had no complications. Among the limitations of this modality are patients with a small cirrhotic liver and sharp angle between the vena cava and hepatic vein which did enable the passage of the stiff Ross needle. The cirrhotic liver may be fibrotic and thus samples are inadequate. The authors feel that there is a great need for a more flexible biopsy instrument in order to further increase the versatility of this technique.

Asher Nov

Transverse folds in the human esophagus. Gohel VK, Edell SL, Laufer I, Rhodes WH (Hospital of the University of Pennsylvania, Philadelphia, Pennsylvania). *Radiology* 128:303–308, Aug 1978

Fine transverse folds can be seen by double contrast technique in the human esophagus which are similar to those seen regularly in the feline esophagus. These folds are transient in nature and possibly represent contraction of the muscularis mucosae. This fold pattern can be seen in patients with gastroesophageal reflux and in those with no symptoms of esophageal disease. The marginal serration should not be mistaken for diffuse ulceration on barium filled views of the esophagus. Distortion of interruption of the normal fold pattern can be seen in patients with superficial ulceration due to reflux esophagitis or other invasive mucosal lesions. Although the pathophysiologic significance of this phenomenon is uncertain, the demonstration and recognition of these folds allows for better definition of mucosal surface abnormalities.

Author Abstract

Therapeutic applications of catheter cholangiography. Ring EJ, Oteaga JA, Freiman DB, Husted JW, Lunderquist A (Hospital of the University of Pennsylvania, Philadelphia, Pennsylvania). *Radiology*, 128:333–338, Aug 1978

Thirty-five patients underwent percutaneous transhepatic cholangiography; in 31 patients obstruction was noted. In 24 of the patients, catheter introduction was attempted. Cause of obstruction was pancreatic carcinoma in 10 patients, benign stricture in seven patients, obstructing stones in two, metastatic carcinoma encasing the porta hepatis in four and carcinoma of the gallbladder in one.

Technique consisted of percutaneous introduction of a Chiba needle in the supine position with cholangiography which confirmed the presence of obstruction. If drainage was decided upon, an 18 gauge needle with a thin polyethylene sheath was introduced. A single pass was performed with manipulation and gentle aspiration to confirm intraluminal position. Once this was established the needle was withdrawn and a special guide wire with a curved tip (enabling engaging of the obstructed tract) was introduced (Kifa, Sweden). If the guide wire could not be advanced the catheter was left in place at that point allowing for external drainage. A second attempt was performed 48 hr following the drainage. When the guide wire could be advanced beyond the obstructed lesion, a 7.1 French pigtail catheter was advanced over it with the pigtail formation allowing for anchorage against the papilla in order to prevent accidental withdrawal of the catheter. Sideholes are formed prior to introduction of

the catheter with attention to their presence only in the intraductal region.

Surgical decompression of malignant obstruction carries a mortality rate of 13%–21%. Patients with malignant biliary obstruction who are candidates for transcatheter therapy include those with: (1) surgically proved unresectable tumors which proceed to obstruct the common bile duct; (2) metastatic tumors encasing the porta hepatis; (3) primary bile duct tumors in the intrahepatic biliary radicals; (4) obstructing tumors shown to be unresectable; (5) resectable tumors with severe jaundice (bilirubin levels greater than 20 mg/100 ml). If long term palliative drainage is considered, the authors recommend a No 12 French catheter with large side holes which can be made using a scalpel.

Asher Nov

Rapid diagnosis of pancreatic carcinoma: an algorithmic approach. Freeny PC, Ball TJ (Mason Clinic, Seattle, Washington). *Radiology* 127:627–633, June 1978

An algorithmic approach for radiological evaluation of suspected pancreatic carcinoma was applied in more than 200 patients. Outpatient ultrasonography and barium studies of the upper gastrointestinal tract were followed by inpatient endoscopic retrograde cholangiopancreatography, angiography, and percutaneous biopsy. Evaluation took no more than 2 hospital days and exploratory laparotomy was not needed. Twenty-five patients had carcinoma. The diagnostic accuracy of the algorithm was 96%. Although this method did not increase the diagnosis of resectable tumors, it did result in rapid, accurate diagnosis of pancreatic carcinoma at relatively low cost and with minimum patient discomfort. Hopefully, these results will eventually lead to earlier diagnosis and improved survival.

Author Abstract

Radiological features of vascular compression of the duodenum occurring as a complication of the treatment of scoliosis (the cast syndrome). Griffiths GJ, Whitehouse GH (University of Rochester Medical Center, Rochester, New York 14642). *Clin Radiol* 29:77–83, Jan 1978

The application of a body cast or the surgical correction of scoliosis may be complicated by acute obstructive vascular compression of the duodenum. If untreated, death may eventually ensue. This report describes the clinical and radiological features in a group of 10 patients, mean age 17 years and with a female preponderance, who all manifested abdominal distension and vomiting, while epigastric pain was present in 50%. In three cases plain films of the abdomen demonstrated duodenal distension, with little gas in the remainder of the bowel. In the absence of pathognomonic signs or as a confirmatory study, an upper gastrointestinal series following aspiration of the stomach, was performed. The findings in eight patients were dilatation and retention of barium in the duodenal loop, extrinsic linear compression of the third portion of the duodenum with an intact mucosa, and regurgitation of barium into a slightly hypotonic stomach with moderate gastric retention and delay in emptying. Mild ileus is a complication in most patients following spinal instrumentation and this is thought to be an important predisposing factor to the development of the "cast syndrome." Other factors recently stressed include an acute origin of the superior mesenteric artery from the aorta with an unusually short supraduodenal course and exaggeration of the lumbar lordosis by hyperextension with displacement of the intestine into the pelvis causing traction on the mesentery and vessels.

These patients all recovered with nonoperative treatment, which included nasogastric suction, intravenous fluids, and nursing in the prone position. Adoption of this position, also, usually relieved duodenal obstruction during a barium study. These authors emphasize the inappropriateness of the term "cast syndrome." Vascular compression of the duodenum may be seen in the absence of a cast following spinal surgery, in acute pancreatitis, in burns, and in severe trauma.

T. Noel K. Allan

Combined radiation therapy and surgery in the treatment of carcinoma of the esophagus. Gary-Bobo J, Pujol H, Solassol C, N'Guyen M, Gary-Bobo A (Centre Paul-Lamarque, Clinique Saint-Eloi, Avenue Professor-Grasset, F 34000 Montpellier, France). *J Radiol Electrol Med Nucl* 59:343–345, 1978

Cancer of the esophagus remains the most deadly of cancers. Early diagnosis is often difficult. By the time the diagnosis is made, treatment is relatively ineffective. In a series of 755 cases of cancer of the thoracic esophagus treated at the Centre de Montpellier, 530 received radiation therapy alone, 131 surgery, 32 combined radiation therapy and surgery, 17 chemotherapy, and 45 patients received no treatment.

Surgical treatment consisted of complete resection of the tumor and reconstruction of the esophagus. In carcinoma of the upper third of the esophagus the 6 months to 5 years survival was zero. In carcinoma of the middle third of the esophagus, survival leveled off from 56% at 1 year to 29% at 2 years to 16% at 5 years, and in carcinoma of the lower third the survival rate was 43%, 31%, and 15%, respectively. Thus the survival rate for both groups was about the same. Those receiving radiation therapy for the most part had been rejected from surgery as inoperable. In this group the 5 year survival after cobalt^{60} for carcinoma of the upper third was 5.7%; for carcinoma of the middle third 1.4%; and for the lower third, 2.7%. The lower survival rate in this series is attributed to the advanced stage of disease.

In an attempt to improve the overall results, a program of combined radiation therapy followed by surgery was tried in a series of 143 patients. A tumor dose of 4,000 rads was administered in 8 days followed within 4–6 days by surgical resection of the tumor. In 53 patients the extent of the tumor and regional metastasis was such that only a simple exploratory operation was performed. This was followed by 2,000 rads delivered postoperatively. In this group the survival rate was 24% at 1 year and 4% at 2 years. However, in the 90 patients who received intensive preoperative radiation followed by successful surgery there was a 3 year survival of 29% and 28% for cancer of the middle and lower thirds respectively, and a 5-year survival of 18% and 25% respectively.

In those patients with considerable metastatic disease, both local and distant—pulmonary and hepatic, the prognosis remains very poor and the results so far obtained are most discouraging.

Would the addition of chemotherapy improve the results? This is the question raised by the authors.

William H. Shehadi

Evaluation and follow-up of pancreatic arteriograms. A new role for angiography in the diagnosis of carcinoma of the pancreas. Herlinger H, Finlay DL (Department of Radiology, St. James's University Hospital, Leeds, England). *Clin Radiol* 29:277–284, May 1978

Of over 300 pancreatic arteriograms done in this hospital group adequate follow-up was possible in only 103 patients, with carcinoma in 35 of them. Based on the prospective report there were three false negatives and seven false positive carcinoma diagnoses, an overall accuracy rate of 90.3%. A retrospective review could eliminate all but one false negative and one false positive diagnosis. Angiographic findings are reviewed separately for periampullary and true pancreatic carcinoma. Subselective catheterization and adequate opacification of the arterial network of the pancreas allows the reliable demonstration or exclusion of even 1–2 cm carcinomas, provided the clinical presentation of the patient has not been that of jaundice or pancreatitis. Taking into account the availability of newer noninvasive imaging techniques, clinical situations are

listed in which the angiographic diagnosis of carcinoma is no longer required. The new purpose of angiography in pancreas carcinoma diagnosis is the demonstration of small and still curable lesions, the prerequisite for this being a much earlier clinical suspicion of the disease and an earlier referral for angiography.

Author Abstract

Genitourinary

Urinary diagnostic indices in acute renal failure: a prospective study. Miller TR, Anderson RJ, Linas SL, Henrich WL, Berns AS, Gabow PA, Schrier RW (Department of Medicine, University of Colorado Medical Center, Denver, Colorado). *Ann Intern Med* 89:47–50, July 1978

It is often difficult, if not impossible, to recognize the cause of acute renal failure. This interesting prospective study was conducted to determine which indices of renal function most accurately predict the basic etiology of an acute deterioration in renal function. The study included all adult patients with acute renal failure evaluated during a 1-year period at the University of Colorado hospitals. Patients with chronic renal failure and those with an obvious cause for abnormal renal function tests, such as diuretic therapy, glycosuria, adrenal insufficiency or cirrhosis, were excluded. The tests determined the urine osmolality, urine sodium concentration, urine to plasma urea nitrogen ratio, urine to plasma creatinine ratio, and a renal failure index determined by dividing the urinary sodium by the urine to plasma creatinine ratio.

These investigators found that acute renal failure is probably due to a prerenal cause when the urine osmolality is greater than 500, the urine sodium less than 20 meq/liter, the urine to plasma urea nitrogen ratio is greater than 8, and the renal failure index is less than 1. Oliguric acute renal failure is suggested by a urine osmolality of less than 350, a urine sodium of greater than 40 meq/liter, a urine to plasma urea nitrogen ratio of less than 3, and a renal failure index of greater than 1. Although there are some patients, particularly those with acute nonoliguric renal failure, in whom these indices of renal function do not accurately predict the cause of the renal failure, in general these tests are highly reliable. This article provides valuable clinical data which can be extremely helpful in managing patients in whom the urine output has suddenly fallen.

David C. Dale
Department of Medicine
University of Washington

Urinary tract after abdomino-perineal resection. Barbaric ZL, Wolfe DE, Segal AJ (University of Rochester Medical Center, Rochester, New York). *Radiology* 128:345–348, Aug 1978

Uroradiological examinations on 33 patients subjected to abdominoperineal resection were analyzed. The most common finding was medial displacement of both ureters, with the right one frequently crossing the midline. Bladder deformity, sometimes severe, was present in all patients. Localized ureteral narrowing due to stricture or recurring neoplasm was found in 30% of the patients examined. Other common complications included retrovesical abscesses, periurethral abscesses, urethral fistulas and strictures, and bladder retention. All these findings were more prominent in men.

Author Abstract

The angiography of intrarenal leiomyoma. Costello P, Zinman L, Michaud J (New England Deaconess Hospital, Boston, Massachusetts 02215). *J Can Assoc Radiol* 29:134–135, June 1978

Renal leiomyomas constitute 5.2% of asymptomatic renal nodules. The authors state that a search of the literature reveals that only three renal leiomyomas have been studied angiographically. Two cases were predominately avascular, and one vascular. The authors add one more case to the literature, that of a 26-year-old female who presented with complaint of a dull epigastric ache. Initial investigation revealed a solid right upper lobe renal mass. Selective renal arteriography demonstrated a very vascular mass with numerous irregular and dilated vessels and a dense inhomogeneous tumor stain.

Jack M.A. Tishler

Renal medullary necrosis in infants and children. Kozlowski K, Brown RW (Royal Alexandra Hospital for Children, Camperdown 2050, New South Wales, Australia). *Pediatr Radiol* 7:85–89, 1978

Decreased renal perfusion or exposure to nephrotoxic substances may result in tubular, medullary, or cortical necrosis. In infancy, anoxia is the most common precipitating cause. The authors present two infants with renal medullary necrosis, and a review of 24 autopsy cases. The radiologic appearance varies with the stage and severity of involvement. Early, the excretory urogram may be normal, or there may be enlargement of the kidneys with dense opacification of the medullary zones of the whole kidney. Late changes are divided into the medullary or papillary types. In the medullary variety, sinus formation and central intrapapillary cavitation occur. In the papillary type, contrast is seen between the viable and necrotic portions of the papilla with a ring formation. With sloughing of the papilla, filling defects may be seen.

B. J. Wood

Musculoskeletal

Calcific tendinitis of the neck. Newmark H III, Forrester DM, Brown JC, Robinson A, Olken SM, Bledsoe R (Century City Hospital, 2070 Century Park East, Los Angeles, California 90067). *Radiology* 128:355–358, Aug 1978

Rupture of a calcific deposit in the longus colli muscle causes acute tendinitis with pain and spasm. These may mimic infectious spondylitis or meningitis. The longus colli originates from the anterior surface of T1, 2, 3 and C7, 6, 5. It inserts on the anterior tubercle of the atlas C2, 3, and 4. The longus colli muscle along with the longitudinal ligament form a 3–4 mm soft tissue density anterior to the cervical vertebral body as seen on the lateral view. Symptomatic patients typically will show soft tissue swelling anterior to the vertebral bodies with amorphous calcification just inferior to the anterior arch of C1. Differential diagnosis would include avulsion fracture due to hyperextension injury and extraossicle as a developmental anomaly.

Asher Nov

Morphology of the acetabulum in congenital dislocation of the hip. Ponseti IV *J Bone Joint Surg* [Am] 60:586–599, July 1978

The author discusses the autopsy findings of the hips of six infants who had unilateral congenital hip dysplasia. He stresses that many of the newborn infants previously examined may have slight "clicks" of the hip but the diagnosis of a dislocation should only be made when there is a "jolt" over the acetabular ridge causing a true positive Ortolani sign.

Well described cases and excellent pictures along with histology highlight the anatomic findings.

The article is well written and presents an interesting approach to understanding the basic cases of congenitally dislocated hips and is of value to orthopedic and radiology specialists who have occasion to evaluate this difficult problem. An excellent list of references is offered for those who wish to pursue this problem.

Gerald R. Smith

Proximal focal femoral deficiency. Goldman AB, Schneider R,

Wilson PD Jr (Hospital for Special Surgery, New York, New York). *J Can Assoc Radiol* 29:101–107, June 1978

The authors discuss the wide spectrum of conditions characterized by a partial absence and shortening of the proximal femora, thought to be a disturbance in mesenchymal growth, and referred to as proximal focal femoral deficiency (PFFD). This group of congenital limb deficiencies are generally recognized at birth and are characterized by shortening of the femur and partial absence of the proximal diaphysis. More severe cases may also involve the trochanters, femoral neck and head, and the acetabulum.

PFFD is a congenital but not hereditary disorder, occurring in both males and females and is not associated with any specific prenatal complication. The lesion is bilateral in 9%–16% of cases, the degree of severity in bilateral cases usually being unequal. The differential diagnosis for these groups of diseases includes septic hip, congenital hip dislocation, Morquio's disease, cleidocranial dysostosis, developmental coxa vara, and multiple epiphyseal dysplasia.

Jack M.A. Tishler

Skeletal manifestations of hyperthyroidism. Chevrot A, Pallardy G, Ledoux-Labard G (G. Pallardy, Service de Radiologie B, Hopital Cochin, 27 Rue du Faubourg-Saint Jacques, 75674 Paris, France.) *J Radiol Electro Med Nucl* 59:29–32, 1978

Skeletal changes in hyperthyroidism receive little attention by the radiologist. However, an awareness of the clinical history and symptoms should enable early recognition of the skeletal changes, when present.

Hyperthyroidism affects the metabolism of bone with an increase in the excretion of calcium and phosphorus resulting in osteoporosis. There is increased reticulation of the spongiosa and thinning of the cortex involving mostly the hands, feet, long bones and vertebrae. Spontaneous fractures, or fractures following minor trauma may occur in 5%–10% of cases. In the adult, hyperthyroidism with osteoporosis is most likely to occur in females past age 50, especially with a prolonged history of hyperthyroidism. Clinical manifestations which may be present are exophthalmus, pretibial edema, and swelling of the extremities. Additionally scapulo-humeral periarthritis, hypercementosis, oncholysis, and less frequently, thyroid acropathy may occur. In children hyperthyroidism is usually recognized early and treatment is instituted without delay. Thus skeletal manifestations are rare. Linear bone growth may be accelerated, with early fusion of the epiphysis. The authors' report is based on a study of 1,200 adults and 35 children at the hopital Cochin. Excellent radiographs illustrate the described changes.

William H. Shehadi

Computed tomography scanning for the measurement of bone mineral in the human spine. Weissberger M, Zamenhaf R, Aronow S, Neer R (Physics Research Laboratory, Massachusetts General Hospital, Fruit Street, Boston, Massachusetts 02114). *J Computer Assisted Tomography* 2:253–262, July 1978

This study considers the sensitivity and reproducibility of CT scanning examination of the vertebral column in order to determine whether or not accurate and reproducible measurement of small (1%–2%) changes in mineral content of the vertebral column is possible. Theoretical calculations using a glucose solution phantom in a water bag CT unit shows that (as a model of osteomalacia) the particular scanning unit in use would be marginally able to measure 1% changes in the mineral content of a vertebra. It was also determined that bone mineral measurement is both density and composition dependent in the vertebral body. This complicates interpretation as other pathologic processes (fracture, neoplasia, etc.) could produce an apparent change in bone mineral by this technique. Despite these problems, this technique appears to offer a unique method of measuring in vivo bone mineralization.

Michael J. Meagher

The double-contrast shoulder arthrogram. Goldman AB, Ghelman B (Hospital for Special Surgery, New York, New York). *Radiology* 127:655–663, June 1978

Experience with double contrast arthrography indicates it is superior to the single contrast technique. First, the double contrast study provides additional information on the width of rotator cuff tears and on degeneration in the tendons. This information is valuable in choosing surgical candidates and electing the best surgical incision. Second, the air-distended capsule permits visualization of the entire intraarticular portion of the biceps tendon. Third, improved visualization of the articular cartilage is important in evaluating patients with previous anterior shoulder dislocations or inflammatory arthritis.

Author Abstract

Nervous System

Risk factors in complications of aqueous myelography. Eldevik OP, Haughton VM (Milwaukee County General Hospital, Medical College of Wisconsin, Milwaukee, Wisconsin). *Radiology* 128:415–416, Aug 1978

The adverse reactions from aqueous myelography in 88 primates were reviewed to determine what factors increase the risk of complications. Seventy-four iocarmate (Dimeray) myelograms were obtained on 41 animals, and 90 metrizamide (Amipaque) myelograms were obtained on 47 animals. The risk of seizures and death from iocarmate myelography was higher than from metrizamide myelography. In animals that had previous myelograms or showed evidence of arachnoiditis, the risk of complications from aqueous myelography was higher. Additional precautions may be indicated if aqueous myelography is performed in patients with arachnoiditis.

Author Abstract

Rational management of the asymptomatic carotid bruit. Brewster DC, Schlaen HH, Raines JK, Abbott WM, Darling RC (Harvard Medical School, Boston, Massachusetts 02114). *Arch Surg* 113:927–930, Aug 1978

The benefits of carotid angiography and carotid endarterectomy in the symptomatic patient have been well established. More controversial, however, is the role of angiography and surgery in the asymptomatic patient whose only abnormality is a carotid bruit.

It is now clear that a carotid bruit may be the only manifestation of a significant carotid bifurcation occlusive lesion. Documentation of its severity and importance, however, requires the use of cerebral angiography, which, despite increasing safety, is not without occasional morbidity and mortality, and is also relatively expensive and time consuming. Modern rational management of an asymptomatic carotid bruit therefore demands noninvasive screening techniques that will allow identification for angiography and surgery. In recent years, a wide variety of noninvasive methods for evaluation of the cerebrovascular system have been developed. Each method, however, has limitations; most provide different information; and no single technique has emerged as totally reliable.

For these reasons, a noninvasive cerebrovascular evaluation has been devised that combines three separate but complimentary procedures: ocular pneumoplethysmography (OPPG), carotid audiofrequency analysis (CAA), and cerebral Doppler analysis. This evaluation has proven particularly useful in examination of the asymptomatic carotid bruit, and the management of such patients is aided by noninvasive testing. Patients with a poorly compensated stenosis (reduced OPPG) are all considered candidates for angiography and surgery. For patients with a well-compensated (normal OPPG) but surgically important stenosis (abnormal CAA or Doppler), angiography and surgery are recommended in selected patients. Angiography and/or surgery are believed safely withheld in all remaining patients as long as they remain asymptomatic. The reliability and effectiveness of this approach is evaluated in a series of 100 consecutive

patients with an asymptomatic carotid bruit. There were no false-positive results and only one known false negative interpretation.

Reiley K dd

The apical artifact: elevated attenuation values toward the apex of the skull. DiChiro G, Brooks RA, Dubal L, Chew E (Clinical Center, Building 10, National Institutes of Health, Bethesda, Maryland 20014). *J Computer Assisted Tomography* 2:65–70, Jan 1978

An artifact that can cause an elevation in CT numbers of as much as 20 Hounsfield units toward the apex of the head is described. This artifact was first noted on the EMI CT 1010 scanner but has been observed in other scanners as well. Phantom studies of this artifact have revealed that its primary origin is the beam hardening distortion due to the large amount of bone present in apical cuts. This has been verified by computer simulations. An intuitive explanation of the origin of the artifact is also presented.

Author Abstract

Comparative efficacy of contrast agents in computed tomography scanning of the brain. Norman D, Enzmann DR, Newton TH (University of California, San Francisco, California 94143). *J Computer Assisted Tomography* 2:319–321, July 1978

A number of intravenous contrast agents utilizing both sodium and meglumine cations as well as iothalamate and diatrizoate anions are compared in a small group of patients with documented gliomas. Measurement of the changes in attenuation coefficient of the brain after contrast infusion showed no clinically observable differences between the meglumine and sodium salts or between iothalamate and diatrizoate anion. Comparisons of so-called "dilute" agents and "concentrated" agents showed no significant differences in the degree of tumor enhancement when an equal total iodine dose is given.

Michael J. Meagher

Giant intracranial aneurysms simulating brain neoplasms on computed tomography. Baird S, Bentson J, Winter J, Wilson G, Joyce P, O'Connor L (UCLA, Center for Health Sciences Los Angeles, California 90024). *J Computer Assisted Tomography* 2:303–307, July 1978

Three patients are discussed in whom intracranial aneurysms of greater than 2.5 cm in size were misdiagnosed as neoplasms. In each case, the lesion presented on the precontrast scan as an area of increased density without surrounding edema. After contrast enhancement, the lesion markedly increases in density. Two types of aneurysms are demonstrated. The globoid aneurysm contains little clot within the ectatic vessel and the entire area of increased density on the precontrast scan increases further in density after contrast infusion. In the case of a serpentine aneurysm, large amounts of thrombus and a relatively small vascular channel are present. On precontrast scan, the margins of the ectatic vessel usually are of higher density than adjacent brain tissue with the central area within the ectatic vessel often being of similar density to surrounding brain tissue. Following contrast enhancement, both the wall and the lumen of the vessel increase in density. This corresponds to the histologic finding of small vessels within the adventitial wall of giant serpentine aneurysms.

The authors emphasize that giant aneurysms must be considered in the differential diagnosis when CT scanning shows a well circumscribed area of increased density without surrounding edema. Further differentiation requires angiography.

Michael J. Meagher

Radiation necrosis of the brain: correlation between computed tomography, pathology, and dose distribution. Mikhael MA (Washington University School of Medicine, 510 South Kingshighway Boulevard, St. Louis, Missouri 63110). *J Computer Assisted Tomography* 2:71–80, Jan 1978

The authors describe four histologically confirmed cases of delayed radiation necrosis. Three of the patients had primary brain tumors which were treated by surgery and radiation, the fourth patient had received radiation followed by surgery for maxillary sinus carcinoma. All patients received 6,000–6,750 rads and presented 9 to 19 months later with severe neurological symptoms which included confusion, lethargy, aphasia, hemiparesis, and seizures. The patients were scanned on an EMI scanner with a 160 × 160 matrix with and without contrast enhancement. CT findings were similar in all cases. A low density lesion with mass effect was seen before contrast enhancement. The mass enhanced in an irregular fashion either in the center or at the periphery. In one of the cases, the original tumor did not show enhancement. CT findings alone could not discriminate between recurrent tumor which is the usual cause of recurrent symptoms and delayed radiation necrosis. Angiography showing an avascular mass and radionuclide studies showing areas of increased uptake are also nonspecific. The authors stress that one must correlate the findings on CT scanning and the zones of high radiation dose on dose reconstruction plans to differentiate between delayed radiation necrosis and recurrent tumor. They found in all cases that the areas of the brain which received 6,000 or more rads during therapy were the areas in which radiation necrosis occurred. Three of the patients underwent surgery with subsequent clinical improvement.

Paul M. Chikos

Relative detectability of intracranial calcifications of computed tomography and skull radiography. Norman D, Diamond C, Boyd D (University of California School of Medicine, San Francisco, California 94143). *J Computer Assisted Tomography* 2:61–64, Jan 1978

Phantom studies comparing "plain film" skull radiography and CT scanning using an EMI water bag unit show that the relative sensitivity of CT scanning versus skull x-rays for intracranial calcifications is dependent on the size of the calcium deposits. In general, the CT scan appeared to be five to 15 times more sensitive than skull radiographs in detection of intracranial calcifications. However, under certain circumstances, the plain skull radiograph could be more sensitive than the CT scan in demonstrating intracranial calcification.

Michael J. Meagher

Computed tomography of the orbit with special emphasis on coronal sections: Part I. Normal Anatomy. Tadmor R, New PFJ (Massachusetts General Hospital, Boston, Massachusetts 02114). *J Computer Assisted Tomography* 2:22–34, Jan 1978

The authors describe their experience with an EMI CT 5000 prototype scanner modified with a 6 mm collimator and scanned in the axial plane at zero degrees to Reid's base line and in the direct coronal plane at 70 to 80 degrees to the same line. Scans were viewed as a 160 × 160 matrix display having matrix elements of 1.5 × 1.5 mm and also as a direct enlargement of the 320 × 320 matrix display having elements of .8 × .8 mm. The normal anatomy of the orbit is illustrated both with CT scans and drawings and described in detail. The authors comment that on coronal sections each ocular muscle was individually discernible except for the inferior oblique which was not visualized. The CT illustrations included the elongated appearance of the optic nerve on slightly rotated coronal sections, tortuosity of the optic nerve, partial visualization of opthalmic vein in a noncontrast enhanced study and a partial visualization of the opthalmic artery following contrast enhancement.

Paul M. Chikos

Computed tomography of the orbit with special emphasis on coronal sections: Part II. Pathological Anatomy. Tadmor R,

New PFJ (Massachusetts General Hospital, Boston, Massachusetts 02114). *J Computer Assisted Tomography* 2:35–44, Jan 1978

Using the techniques described in the preceding article, the authors illustrate the pathologic changes seen with a mucocele, mucopyocele, dermoid cyst, blowout fracture, undifferentiated carcinoma, lymphoma, metastasis, meningioma, and optic glioma. The authors feel that direct coronal scans significantly improve the appreciation of orbital pathology. Contrast enhancement was found helpful in evaluating intracranial tumor extension but generally did not contribute to the establishment of a specific histologic diagnosis. All tumors were well visualized without administration of contrast. The authors feel that CT evaluation of the orbit in cases of blowout fracture has merit and it is possible to define entrapment of the inferior rectus muscle. They also comment that further improvement in spatial resolution is limited by the radiation dose and that the lens dose is undesirably high when x-ray tube rotation is such that the orbits receive the entry dose rather than the exit dose.

Paul M. Chikos

Steroids and apparent cerebral atrophy on computed tomography scans. Bentson J, Reza M, Winter J, Wilson G (UCLA Center for the Health Sciences, Los Angeles, California 90024). *J Computer Assisted Tomography* 2:16–23, Jan 1978

In a retrospective analysis of 7,000 CT scans performed on an EMI 160 × 160 matrix head unit, 15 relatively young patients (8–40 yrs old) were found to have varying degrees of apparent cerebral atrophy not expected for their age. The common factors in these 15 patients were autoimmune diseases and long term corticosteroid treatment. There seemed to be a relationship between the degree of apparent cerebral atrophy and the current corticosteroid dosage. In two of the cases the CT appearance improved after the steroid dosage was lowered. This group of patient was also unusual because they suffered far less neurologic impairment than would be predicted on the basis of the CT scan. The pharmacologic action of corticosteroids on the brain includes steroid-induced protein catabolism and loss of brain volume secondary to a loss of water. The authors advised caution in attributing apparent cerebral atrophy to the underlying disease in patients who have been on long term corticosteroids.

Paul M. Chikos

Computed tomography in the evaluation of encephaloceles in infants and children. Byrd SE, Harwood-Nash DC, Fitz CR, Rogovitz DM (D.C. Harwood-Nash, Hospital for Sick Children, 555 University Avenue, Toronto, Ontario, Canada M5G 1X8). *J Computer Assisted Tomography* 2:81–87, Jan 1978

The authors report their findings in 20 infants and children with encephaloceles who were scanned on an Ohio Nuclear Delta scanner. A standard axial projection was obtained with and without contrast and supplemented by contrast enhanced coronal projection. The cursor was routinely used to measure the attenuation values of the brain and encephalocele contents. The authors caution that the attenuation values are only accurate in the axial projection. They also found that viewing the image in the reverse mode with bone being black was helpful in defining the precise bony abnormalities. Determination of the attenuation value of the substance of the encephocele fully delineated the cerebral spinal fluid cavity from one which contained cerebellar or cerebral tissue as well. In their experience the only disadvantage with CT was that cerebral angiography was still required in those patients who were selected for surgery to better define the major arteries and draining dural venous sinuses.

Paul M. Chikos

Pediatric Radiology

Bowel stenosis as a late complication of acute necrotizing enterocolitis. Costin BS, Singleton EB (Texas Children's Hospital, Houston, Texas). *Radiology* 128:435–438, Aug 1978

The present survival rate in necrotizing enterocolitis is 75%–80%. The late complication of bowel stenosis has been previously described and is caused by cicatricial changes that coexist with healing. The authors describe a series of 10 infants. Average age at diagnosis was 38 days; ages ranged from 13 to 93 days. The period between diagnosis of necrotizing enterocolitis to development of stricture was a mean of 33 days; range of 11–72.

Patients receiving medical management tended to show a single stricture whereas those surgically treated showed a higher number of cases of two or more strictures. Distribution of the acute disease process was predominantly in terminal ilium whereas distribution of stricture is mainly in the left colon. There was a predominance of necrotizing enterocolitis as well as stricture formation in males.

The authors stress that their series is small and their findings may not be statistically significant. Differences between the medically and surgically managed patients may be a manifestation of severity rather than management. Difference in distribution of acute disease process as compared with late sequela may again be a manifestation of severity of the disease process with the more malignant form not achieving healing and sequela.

Asher Nov

Gastroesophageal reflux in infants and children: correlation of radiological severity and pulmonary pathology. Darling DB, McCauley RGK, Leonidas JC, Schwartz AM (New England Medical Center Hospital, 171 Harrison Avenue, Boston, Massachusetts 02111). *Radiology* 127:735–740, June 1978

Symptoms of gastroesophageal reflux (GER) in the infant and child consist of esophageal stricture, esophagitis, vomiting, dysphagia, failure to thrive, and pulmonary complications. A total of 507 barium studies were analyzed in 77 cases. Radiographic pulmonary abnormalities were noted within a period of 1 month prior to or following the barium study.

Gastroesophageal reflux with hiatus hernia, as well as pulmonary abnormalities were noted in 54 patients (68.4%). Gastroesophageal reflux with hiatus hernia were present in 154 patients showing no pulmonary symptoms or 36.4%. Twenty-five patients had no evidence of gastroesophageal reflux with hiatus hernia (31.6%), while gastroesophageal reflux and hiatus hernia were negative with negative chest radiographs in 269 or 63.6%, a total of 79 patients with pulmonary radiographic abnormalities as opposed to 423 patients without pulmonary abnormalities.

Reflux was divided into "minor reflux," which defined reflux as limited to the thoracic esophagus in hiatal hernia. "Major reflux" was defined as retrograde flow of barium to the level of the clavicles with or without aspiration of the contrast material. Pulmonary disease was defined as protracted or transitory. Among the groups showing major reflux a total of 33 patients with 11 showing transitory pulmonary findings and 22 showing protracted pulmonary findings. In the minor reflux group, 14 patients had transitory pulmonary findings and six had protracted findings. In the group showing no reflux there were 17 cases of transitory pulmonary findings and seven cases of protracted findings for a total of 24. Their findings suggest that major reflux and pulmonary findings are related until proven otherwise.

Asher Nov

Spondylometaphyseal dysplasia in two sibs of normal parents. Gustavson KH, Holmgren G, Probst F (Department of

Pediatrics, University Hospital, S-90187 Umea, Sweden). *Pediatr Radiol* 7:90–96, 1978

Two siblings with short-limbed dwarfism of the spondylometaphyseal dysplasia variety are described. Both parents were normal, and the mode of inheritance in these cases best fits autosomal recessive, in contrast to previously described familial cases which appeared to be autosomal dominant. Included in the article is a table differentiating features between achondroplasia, metatropic dwarfism, spondylometaphyseal dysplasia, and pseudoachondroplastic dysplasia.

B. J. Wood

Segmental colonic gangrene: a surgical emergency in the hemolytic-uremic syndrome. Schwartz DL, Becker JM, So HB, Schneider KM (1300 Union Turnpike, New Hyde Park, New York 11040). *Pediatrics* 62:54–56, 1978

The number of patients with hemolytic-uremic syndrome developing acute surgical abdomen is small. The authors present a 2½-year-old female admitted with a 4-day history of fever, diarrhea, and abdominal pain. On physical examination, she had an abdominal mass in the epigastrium and signs of peritonitis. No petechiae were seen initially. The stool was 3+ guaiac-positive. At operation, a segment of gangrenous colon in the transverse and proximal descending portion was encountered. Massive petechial hemorrhages were seen in the mesenteries, peritoneum, and serosal surfaces. Histologically, the resected bowel showed gangrene and extensive vascular occlusions. Following surgery, the BUN rose and the platelet count fell. The child developed oliguria. The intestinal manifestations of the hemolytic-uremic syndrome are discussed.

B. J. Wood

Nonsurgical management of renovascular hypertension in the neonate. Adelman RD, Merten D, Vogel J, Goetzman BW, Wennberg RP (School of Medicine, Department of Pediatrics, 4301 X Street, Sacramento, California 95817). *Pediatrics* 62:71–76, 1978

Over an 18-month period, nine infants in a neonatal intensive care unit developed hypertension (blood pressure, 115/88 to 280/140 mm/Hg) at 2–45 days of age. Eight of the nine infants had indwelling umbilical artery catheters prior to onset of hypertension; six of the nine infants had evidence of a patent ductus arteriosus. Peripheral plasma renin activity was 300 ng/ml/3 hr in six of eight infants. Angiograms were abnormal in six of seven infants and computerized renal scans were abnormal in all nine infants. One infant had congenital renal artery stenosis. Eight of nine infants had evidence of unilateral or bilateral renal artery thrombi which were felt to have emanated from an umbilical artery catheter or a ductus arteriosus. Hypertension in all infants was successfully controlled medically (follow-up of 3 to 27 months; mean 14.4 months). Blood pressures remained normal when medication was discontinued. In our experience, neonatal renovascular hypertension is no longer uncommon, responds to aggressive medical management, and rarely requires early nephrectomy. Neonatal renovascular hypertension was usually associated with umbilical artery catheters positioned above the level of the renal arteries.

Author Abstract

Necrotising entero-colitis following umbilical vein catherisation. Shah KJ, Corkery JJ (Children's Hospital, Birmingham, England). *Clin Radiol* 29:295–301, May 1978

Fifteen cases of neonatal necrotising enterocolitis (NEC) following umbilical vein catherization are reported. Their clinical and radiological features are briefly described and the proper course of a catheter through the umbilical vein-ductus venosus-inferior vena cava segment is demonstrated. The significance of malposition of the catheter and its association with NEC is discussed. It is suggested that the abdominal radiographs be taken in the anteroposterior and lateral projections with a portable x-ray machine to check the position of the radiopaque catheter prior to the commencement of transfusion or infusion.

Author Abstract

Cerebral echinococcosis, a pediatric disease: report of two cases with one successful five-year follow-up. Pearl M, Kotsilimbos DG, Lehrer HZ, Ao AH, Fink H, Zaiman H (Metropolitan Hospital Center, 1901 First Avenue, New York, New York 10029). *Pediatrics* 61:915–920, 1978

Cerebral involvement with echinococcosis is uncommon, occurring in only 1%–2% of cases of *E. granulosa*. One-half to 75% of these cases, however, occur in children. The authors present two patients, one of whom died before treatment could be instituted, and the other who is alive and well 5 years after surgical resection of both cerebral and liver cysts. A new nontoxic antihelmintic, Mebendazole, promises help in medical therapy. It has been highly effective in animals and in a few human patients who have been treated.

B. J. Wood

Pulmonary lesions in atypical measles. Laptook A, Wind E, Nussbaum M, Shenker IR (Division of Adolescent Medicine, Long Island Jewish-Hillside Medical Center, New Hyde Park, New York 11040). *Pediatrics* 62:42–46, 1978

Three children are reported who developed atypical measles 9–13 years following immunization with killed measles vaccine. All three had pulmonary involvement which consisted of pneumonic consolidation followed by shrinking and resolution of the pneumonia but with residual pulmonary nodules. The nodules have persisted on follow-up films 3.5 to 5 months later. Diagnosis was confirmed by elevated antibody titers to rubeola. The occurrence of pulmonary nodules is characteristic of atypical measles pneumonia and it is important to recognize that the nodules may persist for prolonged intervals.

B. J. Wood

Miscellaneous

The detection of inferior vena caval thrombosis with computed tomography. Steele JR, Sones PJ, Heffner LT Jr (Emory University School of Medicine, Atlanta, Georgia). *Radiology* 128:385–386, Aug 1978

The authors present two cases; the first, a 34-year-old with recurrent pulmonary emboli in whom a CT scan done for unrelated purposes demonstrated thrombosis in the inferior vena cava. The second case was a 35-year-old man in whom a CT scan was performed for tumor staging and demonstrated thrombosis within the inferior vena cava and left renal vein. Thrombi were detected following intravenous contrast injection. They appear as low density filling defects within the caval lumen and surrounded by higher density blood following the contrast enhancement. The authors propose that detecting such a finding may have application in the staging of abdominal neoplasms, in particular adrenal cell carcinoma.

Asher Nov

Narcotics smuggling: the double condom sign. Merrille PF, Ducas J, Ruggere MD (Queen Mary Veteran's Hospital, Montreal, Quebec, Canada). *J Can Assoc Radiol* 29:79–81, June 1978

The authors describe a new sign on the plain film of the abdomen which may aid in the identification of narcotics smug-

glers who have ingested their precious cargo to avoid detection. Hashish is radioopaque and may be identified on the plain film of the abdomen, but cocaine, morphine, and heroin are radiolucent. In order to prevent intoxication and to present their valuable cargo, the smuggler may wrap each narcotic ball in two condoms, folding each on itself. This may trap air between the condom layers and this gas may present as a ring-like density on abdominal film. No hidden narcotics were found in seven suspected smugglers with normal abdomen films, but narcotic laden condoms were eventually passed per rectum in five patients in whom a positive ring sign was demonstrated on the abdominal plain film.

Jack M.A. Tishler

Skeletal diseases associated with angiomatosis. Macpherson RI, Letts RM (Children's Rehabilitation Centre, University of Manitoba, Winnipeg, Manitoba, Canada). *J Can Assoc Radiol* 29:90–100, June 1978

The authors discuss the clinical and radiologic features of skeletal diseases associated with angiomatosis. These represent basically two groups of diseases, Maffucci's syndrome, where angiomatosis is associated with enchondromatosis and congenital angiectatic hypertrophy, where angiomatosis is usually associated with hypertrophy of underlying bones, soft tissues, and occasionally viscera.

Jack M.A. Tishler

Ultrasonics

Ultrasonography of necrotic hepatic metastases. Wooten WB, Green B, Goldstein HM (M. D. Anderson Hospital and Tumor Institute, Houston, Texas 70030). *Radiology* 128:447–450, Aug 1978

Twelve patients with sonolucent hepatic metastases studied with gray scale ultrasonography are presented. Extensive necrosis presumably accounts for the sonolucent appearance of the hepatic lesions. The spectrum of ultrasonographic features and correlations, particularly with computed tomography, are presented. The similarity between anechoic hepatic metastases and benign conditions of the liver is emphasized.

Author Abstract

Computed tomography and gray scale ultrasonography of the adrenal gland: a comparative study. Sample WF, Sarti DA (University of California School of Medicine, Los Angeles, California 90024). *Radiology* 128:377–383, Aug 1978

The anatomy of the normal and pathologic adrenal gland is demonstrated using computed tomography and gray scale ultrasonography. A number of potential anatomic pitfalls specific to one or both modalities are noted. These include the posteromedial aspect of the fundus of the stomach which is very close to the left adrenal gland and can be mistaken for a mass. This can usually be delineated with dilute iodinated oral contrast using CT. Oral contrast can also be used to identify the second and fourth portions of the duodenal sweep which reside slightly caudad to the adrenal glands. Another potential pitfall seen with ultrasound is the esophagogastric junction which lies anteriorly and to the left of the aorta. Vascular structures can be confused with the left adrenal. These include the left renal artery and vein and a tortuous splenic artery.

Stephen J. Carter

Ultrasonographic identification of dilated intrahepatic bile ducts and their differentiation from portal venous structures. Laing FC, London LA, Filly RA (University of California, San Francisco, California 94143). *J Clin Ultrasound* 6:90–94, April 1978

The appearance of dilated intrahepatic bile ducts was evaluated on ultrasonograms of 50 patients with proven extrahepatic biliary obstruction. Five characteristic changes allowed differentiation between biliary and portal venous systems. These changes included: (1) alteration in the anatomic pattern adjacent to the main right portal venous segment and the main portal vein bifurcation; (2) irregular walls of dilated bile ducts; (3) stellate confluence of dilated bile ducts; (4) acoustic enhancement by dilated bile ducts; (5) peripheral location of dilated bile ducts. Many patients exhibited more than one of these findings. Parasagittal scans of the main right portal vein were the most sensitive for detection of intrahepatic ductal dilatation. Recognition of the characteristic changes and knowledge of the portal venous anatomy makes it possible to diagnose extrahepatic biliary obstruction with a high degree of confidence.

Author Abstract

Echography in the examination of abdominal lymphadenopathies. Vadrot D, Laval-Jeantet M, Vadrot M, Delmas PF, Bouzac H (M. Laval-Jeantet, Service de Radiologie, Hopital Saint-Louis, 2 Place du Docteur Alfred Fournier 75010, Paris, France). *J Radiol Electrol Med Nucl* 59:399–406, 1978

In a study of abdominal lymph nodes, lymphography is limited because only the retroperitoneal lymph nodes are opacified. Furthermore, both normal and abnormal lymph nodes may not be opacified at all or may be only partially opacified. Thus their true size and structure cannot be determined. Also, in some cases lymphography may be contraindicated or technically impossible to perform.

In 20% of cases, echography will give additional information that could not be obtained from lymphography and will identify retroperitoneal lymph nodes not opacified by lymphography. Additionally, lymph nodes not accessible to lymphography—mesenteric, celiac, and other abdominal nodes, can be readily identified. Echography provides an excellent method for evaluation of the extent of regression of lymph nodes involved in primary (Hodgkin's lymphoma) or metastatic disease following radiation therapy or chemotherapy. While echography will demonstrate the changes in the size of the nodes, lymphography will give more information about the structure and architecture of the lymph nodes when they are opacified.

This report is based on a study of 100 patients on whom both lymphography and echography were performed. The simultaneous application of both procedures gives a greater yield of positive results and diagnostic accuracy than either procedure performed alone.

William H. Shehadi

B-mode ultrasonography of prosthetic vascular grafts. Gooding GA, Herzog KA, Hedgcock MW, Eisenberg RL (University of California School of Medicine, San Francisco, California 94143). *Radiology* 127:763–766, June 1978

The role of contact B-mode ultrasonography in demonstrating prosthetic vascular grafts was assessed in 24 patients (27 grafts). All grafts were well delineated. End-to side bypass grafts could be separated from end-to-end replacement grafts by their characteristic appearance. Patent and occluded grafts could not be distinguished either in vivo or in vitro. However, B-mode ultrasonography was ideally suited to the detection of other complications of vascular prosthetic grafts: hematoma, infection, and false aneurysm formation.

Author Abstract

Radiation Oncology

The effectiveness of prophylactic brain irradiation in small cell carcinoma of the lung. Moore TN, Livingston R, Heilbrun L, Eltringham J, Skinner O, White J, Tesh D (Southwest Oncology Group, Operations Office, 3500 Rainbow Boulevard, Suite 100, Kansas City, Kansas 66103). *Cancer* 41:2149–2153, June 1978

The results of a prospective SWOG study involving the use of prophylactic whole brain irradiation in patients with oat cell

bronchogenic carcinoma extending from December 1974 through November 1976 are presented. Three hundred fifty-eight patients were fully or partially evaluable. Most patients received the protocol prescribed: central whole brain tumor dose of 3,000 rads in 10 increments over 2 weeks. Of the 152 patients with extensive disease who received prophylactic brain irradiation, only six have suffered a clinical central nervous system relapse. Of the 88 fully or partially evaluable patients with limited disease who were given prophylactic brain irradiation, six subsequently developed clinical brain symptoms. The respective percentages of failure were 3.9% (6/152 patients) and 6.8% (6/88). The morbidity of whole brain irradiation was minimal. There was no statistically significant difference in survival demonstrated in this report although there appeared to be a trend toward improved median survival in protocol treated patients. The authors feel that prophylactic brain irradiation is of benefit.

Herbert C. Berry

Frozen autologous platelet transfusion for patients with leukemia. Schiffer CA, Aisner J, Wiernik PH, *N Engl J Med* 299:7–12, July 6, 1978

For this study, 25 patients with acute nonlymphocytic leukemia, many of whom had become alloimmunized from previous platelet transfusions, had their platelets removed and frozen in dimethylsulfoxide anticipatory to an episode of thrombocytopenia from therapy for their leukemia. Using very specialized techniques, the investigators were able to show that the platelets could be stored for several months, could be freeze-thawed with only a 13% loss, and gave good increments of increase in the platelet count after their transfusion. In many of the patients, the transfusion requirement could be met by the use of the frozen platelets. This technical advance may be the forerunner for the development of improved methods for blood cell transfusions for many other conditions.

David C. Dale
Department of Medicine
University of Washington

Carcinoma of the prostate. Harisiadis L, Vennema RJ, Senyszyn JJ, Puchner PJ, Tretter P, Romas NA, Chang CH, Lattimer JK, Tannenbaum M (Division of Radiotherapy, Columbia-Presbyterian Medical Center, 622 West 168th Street, New York, New York 10032). *Cancer* 41:2131–2142, June 1978

The authors retrospectively review the results of external radiotherapy in the treatment of 146 patients with prostate cancer treated between 1964–1976. There were 13 stage A patients, 21 stage B patients, 112 stage C patients with respective 5 year survival rates of 88.2%, 86.8%, and 58%. Patients with undifferentiated tumor had significantly lower survival rates in the stage C group ($p = 0.008$). Patients with obstructive changes on excretory urography had a 5-year survival of 24.1% versus 71.3% ($p = 0.001$) for those with a normal excretory urogram. Patients receiving adjuvant hormonal treatment did not do statistically significantly better than those who did not. A delay of more than 6 months in starting radiation therapy from the time of diagnosis correlated with a decrease in 5-year survival rate from 70.3% to 31.9% ($p = 0.003$). Patients receiving tumor doses greater than 6,500 rads had a 5-year survival rate of 86.7% versus 57.1% for those receiving tumor doses less than 6,500 rads ($p = 0.009$). Of the patients, 8.2% developed complications attributed to radiation therapy, six of these growing in the intestinal tract. The authors feel that external radiotherapy rather than brachytherapy appears to be the treatment of choice for cancer of the prostate with indications for radiotherapy.

Herbert C. Berry

Pericarditis following wide field irradiation of the mediastinum for Hodgkin's Disease. Dana M, Colombel P, Bayle-Weissberger C, Teillet F, Desprez-Curely JP, Bernard J, Chotin G (Service de Radiotherapie, Hopital Saint-Louis, 75010 Paris, France). *J Radiol Electrol Med Nucl* 59:335–341, 1978

The authors report on the incidence of postradiation pericarditis in a series of 579 patients with Hodgkin's disease treated with $Cobalt^{60}$, using a mantle field. The pericardium is a critical organ being more sensitive to radiation than the other mediastinal structures. The development of pericarditis as a complication of radiation therapy depends on the total dose delivered to the mediastinum and the relative distribution through the anterior and posterior fields. The size of the field and the thickness of the patient are relatively unimportant factors compared with the total dose delivered. The incidence of pericarditis is zero when the dose to the mediastinum is less than 4,000 rads, 3% when the dose is 4,000 rads, 9.2% when the dose is 4,500 rads and 20% when the dose is 5,000 rads. The incidence is double in children under 15 years of age, otherwise age plays no significant role. The incidence is essentially the same in both sexes. A dose distribution of 60% to the anterior field and 40% to the posterior field is optimal.

In a series of 579 patients treated by the authors, there were 35 cases of pericarditis. In five patients pericarditis was due to Hodgkin's disease which preceded radiation therapy. In six patients there was probable involvement of the pericardium by Hodgkin's disease during the period of observation. Twenty-four patients developed pericarditis as a result of radiation therapy, an over all incidence of 4.4%. None of the patients who received a dose under 4,000 rads developed pericarditis.

The authors believe that successful administration of a course of chemotherapy prior to radiation therapy will obviate the necessity of administering doses above 4,000 rads. In a little over half the cases the clinical manifestations of pericarditis were retrosternal pain, dyspnea, muffling of the cardiac sounds, at times a friction rub, and enlargement of the cardiac silhouette. These cases responded favorably to corticosteroid therapy. In the remaining patients, the symptoms were less pronounced and consisted of vague pains and slight dyspnea. Serial chest films showed progressive increase in the size of the heart shadow. Three patients developed constrictive pericarditis which required pericardectomy. The other patients responded well to corticosteroid therapy as did the first group.

William H. Shehadi

Extrapelvic metastases in carcinoma of the cervix. Berkmen YM (New York Medical College-Metropolitan Hospital Center, New York, New York 10029). *Revista Interamer Radiol* 3:155–160, July 1978

Cervical carcinoma spreads beyond the pelvis through the lymphatics and blood with an instance varying from 15% to 58% in different series. Direct extension involves the parametrium, rectum, and urinary bladder. Invasion of the pelvic bones by contiguity is similarly common. Nodal implants in the external iliac and hypogastric lymph chain can extend to the lymphatics of the utero-sacral ligament, sacral and lumbar nodes of the promontory, the aortic lymph nodes, and cisterna chyli. Thus, the tumor can propagate through these lymphatics to the retroperitoneal space, mediastinum, and to the left supraclavicular nodes. The tumor can extend from lymph nodes and invade the adjacent organ. Thus outward growth from paraaortic lymph nodes can destroy lumbar vertebrae, obstruct the ureters, or invade other retroperitoneal organs. Destruction of the vertebrae is usually unilateral and occasionally may involve the intervertebral disc. The duodenum and pancreas can be invaded by extension from retroperitoneal nodes.

Blood-born metastases are second in frequency of occurrence. Malignant cells easily reach the venous circulation via abundant pelvic and vertebral venous plexuses which freely communicate with the inferior vena cava or via the thoracic duct. Thus the lungs become the most common site of hematogenous metastases. Retrograde propagation of the tumor cells from the mediastinal lymph nodes may be a major mechanism for lymphangitic dissemination to the lungs. Bony metastases via hematogenous route is less common than involvement by direct invasion or extension from the lymph nodes.

Charles M. Nice, Jr

Book Reviews

Bone Tumors: General Aspects and Data on 6,021 Cases, 3d ed. By David C. Dahlin. Springfield, Ill. Thomas, 445 pp., 1978. $32.75

This new edition of a popular work on bone tumors reflects the author's experience over the past decade of collating an additional 2,234 cases of bone tumors referred to the Mayo Clinic. This edition follows the same format as the previous one with an introductory chapter on general aspects of bone tumors followed by separate chapters on specific lesions. The classification follows that of Lichtenstein.

Significant changes in the new edition are reflected in the addition of four chapters and about 160 additional pages. Several entities taken from previous classifications are treated separately. These include benign and malignant histiocytomas, telangiectatic osteosarcoma, hemangioendothelioma, hemangiopericytoma, ossifying fibroma, giant cell reactive lesions, and mesenchymoma of the chest wall.

Once again each entity is outlined by its incidence, sex distribution, age distribution, localization, symptoms, physical findings, radiologic findings, gross and histologic pathology, treatment, and prognosis. Particularly helpful is the continuation of this format in the chapter on conditions that simulate primary neoplasms of bone. This establishes continuity throughout the book.

The most welcome change is the use of a larger type face in both the text and the legends for illustrations. This makes the reading considerably easier. Other improvements include a better distribution of illustrations to follow the text more closely and the addition of a considerable amount of pathologic material. As expected, the bibliography has been updated to 1976.

One of the more popular features of previous editions, the illustrations depicting the skeletal, age, and sex distribution of individual lesions, has been changed slightly to reflect half-decade intervals in the age graph. This reviewer, who was familiar with the old illustrations, initially found the new graphs slightly confusing. However, after study, it became apparent that the new format represented a further breakdown of the age distribution.

The text itself is basically unchanged from the previous edition. It does, however, reflect the differences which the addition of new case material has provided and the conclusions the author has reached based on his exhaustive analysis of these cases.

I have two criticisms, however, one minor and one major. The minor criticism is in the placing of tables II and III. Each of these requires two pages. In the previous edition, the tables were placed so that the reader could see the entire table with the book open. It is now necessary to turn the page to see the second part of the table. For table II it is necessary to keep turning the page back to know exactly which tumor one is dealing with.

The major criticism of the book and perhaps its greatest shortcoming is in the quality of the illustrations. The majority of the radiographs and indeed much of the pathologic material are either too contrasty, or too "muddy" resulting in a loss of detail which is disappointing in a work of this scope. Those illustrations which have been carried over from the previous edition have suffered the most in clarity of reproduction. However, even the new illustrations are not entirely adequate. (I showed the book to several colleagues who agreed on the quality of illustrations.) Judging from the quality in the previous edition, I would surmise that the fault is the printer's rather than the author's.

If one can overlook the deficiencies in the illustrations, this book represents an excellent compendium regarding every aspect of bone tumors. The reader will find it well organized and easily comprehensible. Anyone with an interest in bone tumors will certainly want to add this book to his library.

Richard H. Daffner
Veterans Administration Hospital
Durham, North Carolina 27705

Cardiac Catheterization and Angiography, 3d ed. By David Verel and Ronald G. Grainger. New York: Churchill Livingstone, 239 pp., 1978. $29.50

The third edition of this text provides a basic introductory book outlining the place of cardiac catheterization and angiographic methods in the study of cardiac disease. Initial chapters outline methods of recording, measuring pressure, shunt detection, and calculation of data. A chapter on echocardiography has been added. Radiologic equipment, contrast media, and general principles of angiography are discussed. The body of the text is largely devoted to principles of right and left heart catheterization and coronary angiography. Concluding chapters include anesthesia and complications of cardiac catheterization.

This text reads easily and largely fulfills its intended purpose. Certain sections of the book are especially well written, particularly those discussing methods of left and right heart catheterization, catheter courses, and problems in the use of guide wires. The thoughtful and critical discussion of the assessment of catheterization results and pitfalls in interpreting pressure and oximetry data is excellent.

While this introductory text could not be expected to cover everything in detail, certain deficiencies are evident. There is little emphasis on techniques of pediatric cardiac catheterization especially through the umbilical artery, although there is a brief discussion of umbilical vein catheterization. There is no discussion of the techniques of percutaneous catheterization in the neonate utilizing the newer types of balloon angiography catheters, and septostomy catheters, pulmonary artery catheterization in patients with transposition, and bronchial artery catheterization in patients with pulmonary atresia. The angiographic approach to the diagnosis of complex cyanotic congenital heart disease especially complex transposition and angiographic methods of volume determination are not discussed. Similarly there is no mention of methods of His bundle recordings.

The added chapter on echocardiography is the weakest section, and is probably inappropriate in a book discussing the principles of cardiac catheterization and angiography. A large number of echocardiograms are of poor technical quality and do not demonstrate the described abnormalities well. A serious

limitation is the lack of discussion of echocardiographic systolic time intervals in the evaluation of pulmonary arterial hypertension.

The recently recognized value of axial angiography is briefly discussed in the evaluation of coronary artery disease, but is not illustrated. Similarly, the technique of axial cineangiography in the evaluation of complex congenital heart disease is not discussed or illustrated. Systemic heparinization of adults and children, prevalent in the United States, is not mentioned.

The text concludes with an atlas of 161 illustrations of congenital and acquired heart disease. Although the printed radiographs are high in contrast, most adequately demonstrate the described lesions with a few exceptions. The figures illustrating coronary artery disease are poor, do not illustrate the abnormalities well, and should be replaced by more adequate radiographs representing newer angiographic techniques. The small section on normal and abnormal catheter positions is good. Unfortunately, common aortic arch anomalies including those causing vascular rings are not illustrated. The illustrations of hypertrophic obstructive cardiomyopathy do not correctly discuss or illustrate the cause of left ventricular outflow tract obstruction.

Despite these limitations, the text is useful as an introduction for residents and fellows in the place of cardiac catheterization and angiographic methods in the modern study of cardiac disease.

Richard B. Jaffe
Garth S. Orsmond
University of Utah
Salt Lake City, Utah 84132

Echocardiography: Interpretation and Diagnosis. By Jack J. Kleid with Stephen B. Arvan. New York: Appleton-Century-Crofts, 460 pp., 1978. $36.50

This monograph briefly summarizes the current status of ultrasound as a diagnostic tool in cardiology. It is clinically oriented, with chapters devoted to specific disease entities such as endocarditis and aortic dissection as well as chapters discussing the evaluation of particular anatomic structures. Its strongest features are the clinical correlations, discussions of differential diagnosis of echocardiographic findings, and explanation of some of the potential pitfalls and sources of confusion.

Although the book is generally quite readable, up-to-date, and well referenced, there are a number of significant lapses. The "obligatory" chapter on ultrasound physics is confusing and misleading, and the chapter on equipment is abstracted entirely from the operator's manual of one commercial unit.

In several instances, the author makes unsupported statements and it is unclear whether he is merely expressing an opinion. For example, the statement that premature mitral valve closure is common in acute aortic insufficiency but never occurs in chronic aortic insufficiency would have had greater weight if backed by a reference to the literature.

The illustrations are copious and pertinent. For the most part, they are good demonstrations of the described pathology. A few of the echograms, however, do not seem to agree with the text, and at least one illustration seems to refute the author's statement in the text.

This is a reasonably good survey of the present status of cardiac ultrasound, but would have benefited greatly from more careful editing.

Michael Grossman
University of California, Irvine
Orange, California 92668

Diagnostic Ultrasound in Clinical Obstetrics and Gynecology. Edited by Horace E. Thompson and Richard L. Bernstine. New York: John Wiley & Sons, 192 pp., 1978. $25

This book is a concise compilation of the current utilization of ultrasonography in clinical obstetrics. Despite its title, the text gives only cursory coverage to gynecologic ultrasonography.

The authors make a chapter by chapter presentation of ultrasonographic methods of examination, normal and gravid pelvic anatomy, principles of fetal mensuration, placental localization, and the complications of pregnancy, including diagnosis of fetal death. Two chapters, one at the beginning and one at the end, are dedicated to physics and instrumentation. An additional chapter is dedicated to the radiation hazards of ultrasonography (or the absence thereof).

The greatest value of this monograph is the chapter on fetal mensuration by Dr. Thompson. Its contents and presentation reflect the well assimilated and extensive experience of the author in this particular field. Dr. Thompson emphasizes the technique, clinical use, value, and limitations of fetal mensuration. This discussion includes not just the often-used biparietal diameter determination, but also the systematic use of crown-rump, trunk, and maternal uterine volumes. A great deal of perspective and sound clinical guidance can be obtained from this chapter. I believe it is one of the best references on the subject.

Rather little of new significance has been added to the literature in obstetrical ultrasonography since it became widely used in the first half of this decade. This is reflected in the chronology of the authors' references at the end of each chapter. Accordingly, one may question the justification for another textbook on the subject. However, this text emphasizes the clinical impact of ultrasonography in obstetrical practice. This correlation can be of particular value to the ultrasonographer.

Ironically, the more challenging gynecologic ultrasonography is less extensively discussed. Though the authors state that diagnostic ultrasound is of utmost assistance to the gynecologist, they fail to demonstrate why or how it is such a valuable procedure. The few chapters alloted to the subject are short. The discussion of many problems of gynecologic differential diagnosis, such differentiation among various types of ovarian tumors, is incomplete and presented in a fragmented manner.

Likewise the chapters on physics and radiation biology add little new to previous textbook presentations. The authors fail to point out the comparative resolution value of some of the instruments they discuss, and thus give a rather deceptively favorable impression of "real time" or rapid imaging systems. Of interest is the detailed index for the physics subtitles. The index for the book contains 117 major headings, 37 of these are in reference to physics and instrumentation (including "X-axis and Y-axis," and excluding clinical listings such as "ovarian malignancy," "teratoma," or "fetal weight").

In general, this book will be a welcome addition to any already extensive library on the subject. However, it is recommended only for a few specific aspects of obstetric ultrasonography not as a comprehensive, or working-desk, reference text.

Antonio C. Gonzalez
Grady Memorial Hospital
Atlanta, Georgia 30303

Ultrasound: Its Application in Medicine and Biology, parts I and II. Edited by F. J. Frey. (Series: Methods and Phenomena 3.) Amsterdam and New York: Elsevier Scientific Publishing, 745 pp., 1978. $72.75

The interaction of man-made ultrasound with biologic systems is discussed by 15 authors and coauthors in this two-part volume. This topic is quite complex and touches on many fields, ranging from basic physics of acoustics to the therapeutic and diagnostic applications of ultrasound in clinical medicine. It is presented in 14 chapters, with each standing on its own and contributing to a particular aspect of the material. The majority of chapters present their subjects in great depth, addressing the reader with considerable background in mathematics and physics, but other articles are understandable without such an extensive scientific background.

This volume can be used and recommended as a textbook and reference source for bioscience and bioengineering students and professionals as well as for the interested radiologist and ultrasonographer. For the clinically oriented physician, however, the subject presentation may well be too theoretical to be of real interest.

Peter F. Winter
Allgemeines Krankenhaus St. Georg
2 Hamburg 1
Lohmuehlenstrasse 5
West Germany

An Atlas of the Human Brain for Computerized Tomography. By Takayoshi Matsui and Asao Hirano. Tokyo and New York: Igaku-Shoin, 570 pp., 1978. $54.50

This book consists of black and white photographs of brains cut at 0°, 10°, 15°, 20°, 25°, 30°, 40°, 50°, 60°, 80°, 110°, and 140° from the canthomeatal line. There are accompanying line drawings for all pictures and computed tomographic correlations for the 15° and 20° sections only. Other than to explain the method of sectioning and the organization of each picture on each page, there is no text. The bibliography is a good overview of the major CT articles to 1977. The index is detailed and helpful.

The pathologic specimens in this atlas were prepared with meticulous care. All brain photographs are crisp and fill each page. The line drawings for each picture are labeled in detail. However, the CT sections, when present, are of poor technical quality.

As an atlas of pathologic brain sections, this book appears complete. However, its application for computed tomography is limited by the absence of bony landmarks in the cut brain specimens. Bony reference points would be especially helpful at the foramen magnum, temporal bone, and sella turcica. In addition, larger, technically better, and more plentiful correlative CT sections are needed to make each pathologic brain specimen more meaningful. Certainly, CT sections at 0° and in the coronal plane would be appropriate.

This atlas would seem to have greatest appeal as a reference source for those doing research projects in computed tomography of the brain.

Edward Grayson
Memorial Hospital
Hollywood, Florida 33021

Secondary Spread in Breast Cancer, vol. 3 in the series, New Aspects of Breast Cancer. Edited by Basil A. Stoll. Chicago: Year Book Medical Publishers (distributor), 245 pp., 1977. $12.95

The third volume in this series provides the specialist physician with an authoritative and balanced interpretation of new scientific findings and thinking specifically oriented toward the possible application to a clinical problem. As expected from a multiauthor volume, some contributions are outstanding, while others are less impressive. Likewise, in a field where theory and practice move rapidly, as in the adjuvant chemotherapy of breast cancer, the time required for publication makes it impossible to be entirely timely. Therefore, the latest report of Bonnadonna's work dates back to February 1976, and the criticism of Dr. Stjernsward's "Examination of Adjuvant Radiation Therapy" could not be included.

While the majority of the contributions contain a review of the knowledge in the field of factors influencing the spread of breast cancer and the appearance of metastasis in relation to treatment, some original data are presented. Of special value are the sections dealing with conclusions and possible future applications of basic science research to the treatment of human breast cancer which follow each of the 13 chapters. This volume will give the specialist physician an understanding of the status of basic research in the spread of breast cancer as of 1977, and it will give the scientists working in a specific area an understanding of other work that is taking place. The cost of the book seems reasonable, and the production is beyond reproach.

H. Gunter Seydel
Thomas Jefferson University Hospital
Philadelphia, Pennsylvania 19107

Breast Cancer Management: Early and Late. Edited by Basil A. Stoll. Chicago: Year Book Medical Publishers (distributor), 237 pp., 1977. $17.95

This book was published in 1977 by William Heinemann Medical Books, and is distributed in this country by Yearbook Medical Publishers. The editor is Dr. Basil A. Stoll, honorary consultant physician to Radiotherapy and Oncology Departments, St. Thomas' Hospital and Royal Free Hospital, London. The contributors are principally American and British, with one each from Wales, Australia, and Canada. Dr. Michael Baum of Cardiff, Wales, introduces the book with a discussion of prognosis related to the biology of breast cancer, and argues that breast cancer should be considered a systemic disease until proven otherwise. The case for radical surgery is presented by Dr. Guy Robbins, Chief of the Breast Service at Memorial Hospital of New York City, with a good summary of the results from Memorial Hospital. Dr. George Crile of Cleveland continues his campaign for doing less surgery, and, as usual in his papers, he describes performing partial mastectomy for selected cases, but then uses his follow-up statistics as if the results were derived from unselected cases. It would have been helpful to include a chapter by Dr. Crile's principal critics, Drs. Thomas Anglem and Robert Leber of Boston, since Dr. Crile presents his data like an attorney arguing a case before a jury, rather than as a clinical scientist objectively analyzing data.

Dr. Paul Strickland has written a good chapter on radical radiation therapy for locally advanced disease, discussing overall results with primary radiation therapy. Included is a section on the morbidity of high dose radiation to the breast, for

example, the rare instances of brachial neuritis, radiation damage to the myocardium, and secondary carcinomas resulting from high dose radiation therapy. It is unfortunate that there is little discussion of the ongoing trials of radiation therapy for early operable breast cancer. Although these trials (e.g., the Harvard study) are not yet extensive enough to draw final conclusions, they do show promise in early cases of breast cancer in which the patient refuses surgery.

There is a good summary of the clinical trials conducted by the National Surgical Adjuvant Breast Project under the direction of Dr. Bernard Fisher. He summarizes the project's protocols no. 5 through no. 10, which are presently ongoing in that group, as well as similar trials conducted by other cooperative groups in the United States and Europe. His emphasis is on the results with combined modality therapy, especially adjunctive chemotherapy.

One chapter discusses sequential systemic therapy, including hormones and ablation, as well as radiation therapy for metastatic disease. There are several good chapters on specific problems with breast cancer, including management of pleural metastases, hypercalcemia, management in pregnancy, treatment of arm edema, and cancer of the male breast. Another difficult problem, the management of the contralateral breast, is discussed by Dr. John McCredie.

There is no mention of breast reconstruction after radical surgery, especially useful when modified radical mastectomy can be done and the pectoralis major muscle preserved.

The book offers much worthwhile information; it is clearly written, fairly concise, and has a bibliography following each chapter. It should be useful to any surgeon, radiation therapist, or chemotherapist who participates in the care of breast cancer patients at any stage of their disease.

Robert F. Jones
Department of Surgery
University of Washington
Seattle, Washington 98195

Psychosocial Care of the Dying Patient. Edited by Charles A. Garfield. New York: McGraw-Hill, 430 pp., 1978

The author has put together an anthology that includes eight parts, one preface, an introduction, and epilogue. He was assisted by 39 contributors and he borrowed heavily from published materials in journals in order to construct an impressive textbook on the psychosocial care of the dying patient. The eight parts include: Guidelines for Terminal Patient Care; Patients and Families Facing Life-threatening Illness; Doctor-Patient Relationships: Emotional Impact; Psychological Needs: Recognition and Action; Counseling the Patient's Family; Specific Issues; and Care of the Dying Patient: Recent Developments.

Dr. Garfield's personal input and a good number of contributions are of excellent taste, well written, and stimulating. The style and message of a few contributions are poor and uninformative.

Some 39 topics or chapters are discussed. For example in part seven, Specific Issues, these topics are included: Reflections on Life and Death, Human Sexuality and Serious Illness, Adaptation to Open Heart Surgery: A Psychiatric Study of Response to the Threat of Death, and Survival by Machine: The Psychological Stress of Chronic Hemodialysis. A few illustrations of good taste are used to separate one part of the book from the next, and a number of tables and linear drawings help to present the subject.

Dr. Garfield is the Director of the Shanti Project and uses this book to inform the reader of this humane alternative or complement to the concept of a hospice.

All professional oncologists and medical professionals, including people in allied health services that come in contact with cancer patients, could benefit from reading this book

Ruheri Perez-Tamayo
Department of Radiation Therapy
Loyola University Hospital
Maywood, Illinois 60153

Cancer Therapy by Hyperthermia and Radiation. Edited by C. Streffer, D. van Beuningen, F. Dietzel, E. Rottinger, J. E. Robinson, E. Scherer, S. Seeber, and K.-R. Trott. Baltimore: Urban & Schwarzenberg, 344 pp., 1978. $39.50

This book reports the Proceedings of the Second International Symposium on Cancer Therapy by Hyperthermia and Radiation held in Essen, Germany in June 1977. The editor, Prof. Christian Streffer, is associated with the University of Essen Institute for Medical Radiation Physics and Radiation Biology.

Included are the complete texts of the 11 main lectures presented by invited speakers. All are excellent, comprehensive reviews. The remainder of the book includes 82 short proffered papers in nine subsection topics. As is frequently the case with books reporting the proceedings of a conference, there are numerous rather unsophisticated, perhaps even inaccurate or misleading, papers. The publication has had no real scientific editorial review.

Although hyperthermia research is in its infancy, a number of important physiologic principles and biologic concepts are already known; most are reviewed in this monograph. Nevertheless, many of the reported studies apparently have not taken sufficient cognizance of the importance of significant physiologic changes which occur with heating in vivo, but are unlikely to be seen in in vitro experiments. This is not to say that complicated in vitro studies may not help in explaining mechanisms of actions, but findings in vitro may not have the applicability of in vivo situations. This is particularly important when considering important matters such as sequencing of the heating with other therapeutic measures (like irradiation), alteration of responses during a fractionated treatment regimen, and, of course, the crucial concept of therapeutic gain in vivo.

Cancer therapy by combined hyperthermia and radiation as implied in the title, is not actually dealt with except from a theoretical standpoint. There are 15 papers on clinical studies; all but four of these relate to whole body heating rather than localized or regional heating which is considered most appropriate in conjunction with irradiation.

Despite these shortcomings, this monograph is still essential for anyone interested in the current state of the art of hyperthermia in cancer therapy. So much is currently being done investigationally in the area that it is virtually impossible to remain abreast in the field; this book summarizes the essential findings and state of the art as of mid-1977.

William L. Caldwell
Division of Radiation Oncology
University of Wisconsin
Center for Health Sciences
Madison, Wisconsin 53706

Noncoherent Optical Processing. By Gordon Leonard Rogers. New York: John Wiley & Sons, 176 pp., 1977

With the recurrence of interest in use of noncoherent or incoherent optical techniques in optical data processing, and the general interest in data processing systems that can handle high data rates, this book is of particular interest. The work of Professor Rogers in the optics literature is well known. Therefore, one would be interested in any compendium by this author for a good overview of the field and possible base for an appropriate tutorial entrée into this field.

This book, however, appears not to meet these expectations. In general, the work has not been brought above the level of professional journal papers. The reader is assumed to understand a great deal about the field, the terms used, and the specialized phraseology. The presentation is terse and nonpedagogical. Specifically, the historic perspective is rarely presented, terms are introduced without definition, and fundamental contributions of other works are excluded, such as the Kovaznay Correlator, the Hanbury-Brown Twiss experiment, the excellent work of Bromley et al., and others.

Although it may be appropriate in professional journals, the use of specialized terms without definition or reference is undesirable. Examples are terms like the following: spectral luminosity, correlation, convolution, polar diagram, lenticular, coherence, etc. It would seem that in a textbook, the pedagogical style would predominate.

In the description of techniques, terminology like "negative intensity" detracts from the technical credibility of the material. In addition, the reference to COS ( ) being a period is inappropriate descriptive material. A more direct statement of the definition of period is desirable.

Although the first four chapters are brief and lacking in style and completeness, the latter chapters are much better. The author persists, however, in writing for a selected audience and leaves definitions and terms to guesswork. This creates problems for some readers, such as radiologists, who would be frustrated in understanding material which will some day be of importance to them.

The book is timely and interesting, and I enjoyed reading about the clever techniques that enable simple data processing tasks (chapters 9 and 10). It is lamentable that the author did not expand the material to appeal to a broader and less specialized audience. This is particularly important today, since noncoherent optics is emerging as an exciting area for study and research.

F. Paul Carlson
Vice President
Oregon Graduate Center for Study and Research
Beaverton, Oregon 97005

News

National Breast Cancer Conference

The eighteenth National Conference on the Detection and Treatment of Breast Cancer will be held in Atlanta, March 5–8. The conference, devoted to progress in the detection and treatment of breast cancer, will feature internationally recognized authorities in the fields of radiology, surgery, pathology, obstetrics and gynecology, epidemiology, and other medical and nonmedical specialties.

Emphasis will be on the team approach to cancer management and the involvement of the various specialities in major problem areas including: high-risk benign disease, minimal breast cancer, radiation risks, detection programs, invasive cancers, the relationship of gynecological disease and breast disease, and rehabilitation.

The conference will be sponsored by the American College of Radiology. AMA Category I continuing medical education credit is available.

For further information contact: American College of Radiology, 6900 Wisconsin Ave., Chevy Chase, MD 20015; telephone, (301) 654-6900.

Radiation Therapy Seminar

The University of Florida Division of Radiation Therapy will hold its Ninth Annual Clinical Research Seminar April 26–28, in Gainesville. This is a clinical oncology conference emphasizing multidisciplinary decision making and radiation therapy techniques with one day devoted to case presentations and two days to clinical research papers. Guest professor will be Samuel Hellman. Direct inquiries to: Dr. Rodney R. Million, Radiation Therapy Division, Box J-385, J. Hillis Miller Health Center, Gainesville, FL 32610.

Conference on CT, Ultrasound, Nuclear Medicine

A conference, CT, Ultrasound, and Nuclear Medicine: A Correlation, will be February 23–25 in Albuquerque, New Mexico. Fee is $125; 16 hr continuing education credit wil be available. For information contact: Dr. F. A. Mettler, Jr., Cancer Research and Treatment Center, University of New Mexico, Albuquerque, NM 87131.

Symposium: Computerized Tomography of the Brain

A symposium on computed tomography of the brain has been scheduled for September 20–22 in Bordeaux, France. Organizers are Professors J. M. Caille and G. Salamon under the guidance of the University of Bordeaux II and INSERM (the French National Institute of Health and Medical Research). Primary topics will be the physical data of computed tomography; CT normal images and correlations; the neutron scanner-emission scanner. Registration fee is 500 francs. For additional information, write: Secretariat du Professor J. M. Caille, Service de Neuroradiologie, Hôpital Pellegrin Tripode, 33076 Bordeaux, France.

Gastrointestinal Radiology

A postgraduate course, Gastrointestinal Radiology, will be April 5–7 in New York City. Sponsor is the William Black Post-Graduate School of the Mount Sinai School of Medicine. Course directors are R. H. Marshak and J. G. Rabinowitz. Guest faculty will include: S. Baum, T. C. Beneventano, G. W. Friedland, H. G. Jacobson, E. Kazam, W. B. Seaman, S. C. Sommers, and J. P. Whalen. Other faculty will be: A. H. Aufses, C. Bloch, H. D. Jancwitz, M. T. Khilnani, D. Maklansky, J. D. Waye, and H-C Yeh.

This course will meet the criteria for 16¼ hr AMA Category I credit. Applications and inquiries should be directed to: Director, Page and William Black Post-Graduate School of Medicine, Mount Sinai School of Medicine, 1 Gustave L. Levy Place, New York, NY 10029; phone, (212) 650-6737.

Bone Radiology Course

The Medical College of Virginia, Virginia Commonwealth University, will host its fifteenth annual radiology postgraduate course, Bone Radiology, March 4–8 in Williamsburg, Virginia. Tuition is $250; $125 for those in training. Continuing education credit is available.

Guest faculty will include: J. W. Bowerman, Johns Hopkins; H. K. Genant, University of California, San Francisco; J. J. Kaye, Vanderbilt; T. E. Keats, University of Virginia, Charlottesville; J. E. Madewell, Armed Forces Institute of Pathology, Washington, D.C.; R. O. Murray, Royal National Orthopaedic Hospital, London, England; J. F. O'Connor, Boston City Hospital; D. L. Resnick, University of California, San Diego; and C. D. Teates, University of Virginia, Charlottesville.

Participating from the Medical College of Virginia will be: M. C. Beachley, program director; A. C. Brower and I. Yaghmai, chairpersons; J. A. Cardea, T. A. Hazra, M. B. Kodroff, M. P. Neal, Jr., G. U. Rao, J. L. Steinfeld, and F. S. Vines.

For additional information and complete program information, contact: Department of Continuing Medical Education, Medical College of Virginia, Box 91, Richmond, VA 23298; phone (804) 786-0496.

Aspen Radiology Conference

The Ninth Annual Aspen Radiology Conference, designed as a postgraduate course for practicing radiologists and other physicians interested in diagnostic radiology, CT scanning, nuclear medicine, and diagnostic ultrasound, will be February 25–March 3 in Aspen, Colorado. Sponsor is the Beth Israel Hospital, Denver.

Independent refresher courses will be offered in diagnostic radiology on bone, gastrointestinal tract, interventional angiography, and myelography; in nuclear radiology on bone, gastrointestinal tract, brain, and cardiac; in diagnostic ultrasound on abdomen, retroperitoneal structures, obstetrics and gynecology, and new technology. Two days will be devoted to CT scanning of abdomen and brain, comparing this modality with diagnostic ultrasound and nuclear radiology.

A total of 20 hr continuing education credit will be available.

For information contact: Dr. E. Salzman, Beth Israel Hospital, West 17th Avenue and Lowell Boulevard, Denver, CO 80204; phone (303) 825-2190, extension 350.

Diagnostic Imaging Seminar

A 2-day seminar, Diagnostic Imaging, Correlation of Ultrasound, Computed Body Tomography, and Nuclear Medicine, will be presented in Philadelphia by the Department of Radiology, Hospital of the University of Pennsylvania, March 6 and 7. Course directors are P. Arger and C. Mulhern. The faculty will include: A. Alavi, P. Alderson, P. Arger, S. Baum, B. G. Coleman, M. J. Eymontt, B. Green, J. Haaga, E. R. Heitzman, E. Kazam, H. Y. Kressel, and C. Mulhern. The seminar will consist of lectures that will correlate and integrate the use of ultrasound, computed body tomography, and nuclear medicine in the chest and abdomen. A total of 14 hr AMA Category I credit is available. Registration fee is $150; $75 for residents.

Additional information may be obtained from Mrs. C. Reynolds, Department of Radiology, Hospital of the University of Pennsylvania, 3400 Spruce Street, Philadelphia, PA 19104; (215) 662-3049.

Abdominal Ultrasound and CT of the Trunk

An Integrated Approach to Abdominal Ultrasound and Computerized Tomography of the Trunk is a seminar slated for May 24–26 in Dallas. Sponsor is the Department of Radiology, Southwestern Medical School. A total of 18 hr AMA Category I credit is available. For additional information, contact L. W. Kiker, Department of Radiology, Southwestern Medical School, 5323 Harry Hines Boulevard, Dallas, TX 75235.

Boston University Reunion

The Department of Radiology, Boston University Medical Center, is planning a reunion during the spring of 1980. Because of the difficulty in locating past residents and staff of the department, those who have been affiliated with teaching programs at Boston City and Massachusetts Memorial hospital are asked to send their names and current addresses to: Dr. J. H. Shapiro, Department of Radiology, University Hospital, 75 East Newton St., Boston, MA 02118.

Nuclear Medicine: Spring Meeting

The Central Chapter of the Society of Nuclear Medicine will host its annual spring meeting February 22–24 in Chicago. Topics will include: Pediatric Nuclear Medicine, Practical Computer Applications, Unusual Clinical Procedures, and Radioreceptor Assays. This meeting will be a conjoint meeting of physicians, physicists, and technologists. There will also be a commercial exhibit.

For complete information, write: D. A. Churan, Executive Director. Central Chapter of the Society of Nuclear Medicine, P. O. Box 160, Cyrstal Lake, IL 60014.

Aspen Seminar: Chest and Abdominal Radiology

The Second Annual Aspen Seminar on Chest and Abdominal Radiology—Imaging and Current Topics will be March 5–9 in Aspen, Colorado. Sponsor is the Department of Radiology, Loyola University of Chicago. Emphasis will be on a comparison of CT, computer assisted radionuclide studies, and gray scale ultrasound, with conventional and invasive radiographic examinations. The course will carry 24 hr AMA Category I credit. Attendance is limited to 300. Fee is $250; $200 for residents. Information is available from Mrs. L. Gunzburger, Division of Continuing Medical Education, Loyola University of Chicago Medical Center, 2160 South First Ave., Maywood, IL 60153.

Diagnostic Ultrasound Workshop

A postgraduate workshop in diagnostic ultrasound will be presented weekly by the Department of Radiology, Baylor College of Medicine through December 14, 1979. The course will be at Ben Taub General Hospital in Houston. For information contact: Office of Continuing Education, Baylor College of Medicine, Texas Medical Center, Houston, TX 77030; telephone (713) 790-4941.

Cardiac Imaging Refresher Course

The Sixth Annual Refresher Course in Cardiac Imaging will be April 23–26 at Hilton Head Island, South Carolina. Sponsor is the North American Cardiac Radiology Society. For details contact Dr. L. P. Elliott, University of Alabama Hospitals, 619 South 19th St., Birmingham, AL 35233.

Diagnostic Ultrasound Training Programs

A series of training programs are being offered by the Downstate Medical Center, State University of New York, for physicians interested in learning the basic techniques of ultrasound scanning and interpretation, and for those who wish to upgrade their skills. A comprehensive, highly structured 1 week session in obstetrics/gynecology and abdominal ultrasound is the main offering. One day programs will also be available. In addition to faculty from the Downstate Medical Center, outstanding guest lecturers will be scheduled weekly. Cost is $350 for a 1-week session; $100 for 1 day sessions. Category I credit is available.

For information contact: Department of Radiology, Box 1192, State University of New York, Downstate Medical Center, 450 Clarkson Avenue, Brooklyn, NY 11203; telephone (212) 270-1602.

National Conference on Urologic Cancer

The American Cancer Society's National Conference—Urologic Cancer—1979 will be April 4–6 in Los Angeles. Purpose is to improve the care of the urologic cancer patient by bringing the best available information to the attention of the general medical community. Emphasis will be on specific areas where advances in understanding and management are occurring. Presentations will be multidisciplinary and objective in orientation. Attendance is open to physicians and medical students; 15 1/2 hr AMA Category I credit is available. There is no fee. For information, write: Urologic Cancer Conference, American Cancer Society, 777 Third Ave., New York, NY 10017.

Eighth Congress, European Society of Neuroradiology

The Eighth Congress of the European Society of Neuroradiology will take place September 7 and 8 in Strasbourg, France. The program will consist of invited and proffered papers. For information, write: Society President, Professeur A. Wackenheim, Service de Neuroradiologie, C.H.U. de Strasbourg, B.P. 426, 67091 Strasbourg Cedex, France.

Tahiti Diagnostic Radiology Seminar

The seventh annual International Diagnostic Radiology Seminar will be in Tahiti, March 16–24. This program, sponsored by Extended Programs in Medical Education, University of California, School of Medicine, San Francisco, is approved for 32 hr

Category I credit. The conference will provide an opportunity for radiologists from Australia, New Zealand, and North America to meet and discuss recent advances in diagnostic radiology. The course utilizes lecture and seminar format with limited group sizes. Early registration is advised.

Guest speakers from the faculty of the University of California, San Francisco, will be: R. Filly, ultrasound; C. A. Goodin g, pediatric; G. W. Gooding, ultrasound; H. Minagi, emergency room radiology; A. Moss, gastrointestinal; T. H. Newton, neuroradiology; and D. Norman, computed tomography. Others will include W. Hare, University of Melbourne, genitourinary, and E. Milne, University of California, Irvine, chest.

For information, contact: Diagnostic Radiology Seminars, 200 South Ridgewood Road, Kentfield, California 94904; phone (415) 461-9746.

Meeting and Course Review

For reader convenience, a summary of upcoming meetings and courses is provided. Detailed listings of these events appeared in journal issues indicated in parentheses.

CT in Radiotherapy, workshop, March 28–30, Geneva, Switzerland (June).

Courses in Ultrasound, 8-week postgraduate course, beginning April 2, Winston-Salem, N. C. (July).

General Diagnostic Radiology, course, February 5–9, Puerto Rico (July).

Adjuvant Therapy of Cancer, conference, March 28–31, Tucson (July).

Body CT Course, February 26–March 1, San Diego (September).

Current Concepts in Diagnostic Radiology, course, February 12–16, Acapulco, Mexico (September).

Computed Tomography, Ultrasound, and X-ray, course, January 29–February 2, San Francisco (September).

Two Courses: Snowbird and Park City, January 28–February 3, Snowbird, Utah, and February 24–March 3, Park City Ski Resort, Utah (September).

XII Interamerican Congress of Radiology, July–August 1979, Quito, Ecuador (October).

Sixth Congress of Radiation Research, May 13–19, Tokyo (October).

Noninvasive Imaging in Medicine, symposium, June 6–9, Lund, Sweden (October).

Conferences on Medical and Biological Engineering and Medical Physics, August 19–24, Jerusalem (October).

L. H. Gray Conference, September 10–14, Cambridge, England (October).

Asian Oceanian Congress of Radiology, October 28–November 3, Singapore (October).

Diagnostic and Therapeutic Angiography, course, March 21–25, Puerto Rico (October).

Research Training Fellowships, deadline January 31, International Agency for Research on Cancer (October).

Diagnostic Ultrasound Preceptor Training Programs, San Diego, one month programs (October).

Double Contrast Techniques in GI Radiology, seminar, March 8–10, Philadelphia (November).

Diagnostic Ultrasound Courses, series, Philadelphia (November).

Abdominal Real Time Sonography Courses, March 12–16, June 11–15, July 16–20, August 6–10, December 9–13, 1979, Winston-Salem, North Carolina (November).

LSU Diagnostic Radiology Seminar, March 15–17, New Orleans (November).

Aspen Uroradiology Seminar, February 18–23, Aspen, Colorado (November).

Fleischner Society Ninth Symposium (and course), June 11–13, Stockholm, (November).

Musculoskeletal Course and Cruise, April 28–May 5, Carribean (November).

CT, Ultrasound, and X-ray, course, January 29–February 2, San Francisco (November).

Diagnostic Radiology Course, March 12–16, San Francisco (November).

International Symposium and Course on CT, April 16–20, Las Vegas (November).

Gastrointestinal Radiology, Update '79, seminar, March 9–11, San Diego (November).

Selected Topics in Neuroradiology, seminar, February 7–9, San Diego (November).

European Cardiovascular Radiology Congress, May 3–5, Nuremberg, West Germany (November).

LA Bone and Joint Conference, continuing once monthly course, Los Angeles, (November).

Diagnostic Ultrasound Seminar, April 21 and 22, New York City (November).

San Diego Postgraduate Courses, 1 and 2-week programs (November).

San Francisco Cancer Symposium, March 23 and 24 (November).

American Board of Radiology, oral and written examination dates for and locations 1979 and 1980 (December).

1979 Midwinter Radiological Conference, January 26–28, Los Angeles (December).

AFIP Diagnostic Radiology Seminars, series, May 7–11, August 27–31, November 12–16, Washington, D.C. (December).

Course Slated for Mexico City, February 5–8 (December).

Radiation Biology in Cancer Research, symposium, February 27–March 2, Houston (December).

Nuclear Medicine Computer Council Symposium, January 21 and 22, Phoenix (December).

AFIP Alumni Course, March 1–4, Deerfield Beach, Florida (December).

Clinical Advances in CT, seminar, March 10 and 11, Washington, D.C. (December).

Big Sky (Montana) Radiology Conference, February 6–9 (December).

Canadian Radiologists Annual Meeting, June 24–28, Vancouver (December).

Multidisciplinary Aspects of Brain Tumor Therapy, June 8–10, Lake Garda, Italy (December).

Radiology of Bone and Chest Diseases, course, April 23–27, San Diego (December).

Radiology of the Chest, course, April 2–6, Durham, North Carolina (December).

Skeletal Radiology Course, May 14–18, New York City (December).

Controversies in Radiology and Medicine, course, March 4–9, Vermont (December).

General Diagnostic Radiology, February 15–17, Dallas (December).

Spring Physics Seminar, April 23–25, Las Vegas (December).

Nuclear Radiology Workshop, May 4 and 5, Ann Arbor, Michigan (December).

A Public Service of this magazine & The Advertising Council Ad Council



Your Business can be one, too.

Red Cross needs individual volunteers, and donors of blood and money, by the millions.

But we need even more help. We need the solid support of American Business. And we never needed it more.

If your business is already helping, by organizing blood drives, and by supporting payroll deductions—either directly for the Red Cross, or through the local combined fund drive—the whole community owes you thanks. And we thank you, too.

Last year, with help from our friends, we offered major aid at over 30,000 disasters—from typhoons, to local (but just as devastating) house fires.

We were able to help the elderly with practical programs, we helped veterans by the hundreds of thousands, we taught people by the millions to swim or swim better. And that's just the tip of the iceberg.

Think of America without The American Red Cross.

And you'll know why we need your business as a Red Cross Volunteer. In your community. And all across America. Contact your local Red Cross Chapter to see how your company can become a volunteer.

Red Cross. The Good Neighbor.

"How many people do you know who have been cured of cancer?"

Almost everybody knows someone who has died of cancer. But the fact is about two million living Americans have been cured. Not only cured but leading active, normal lives. Another fact is millions more could be.

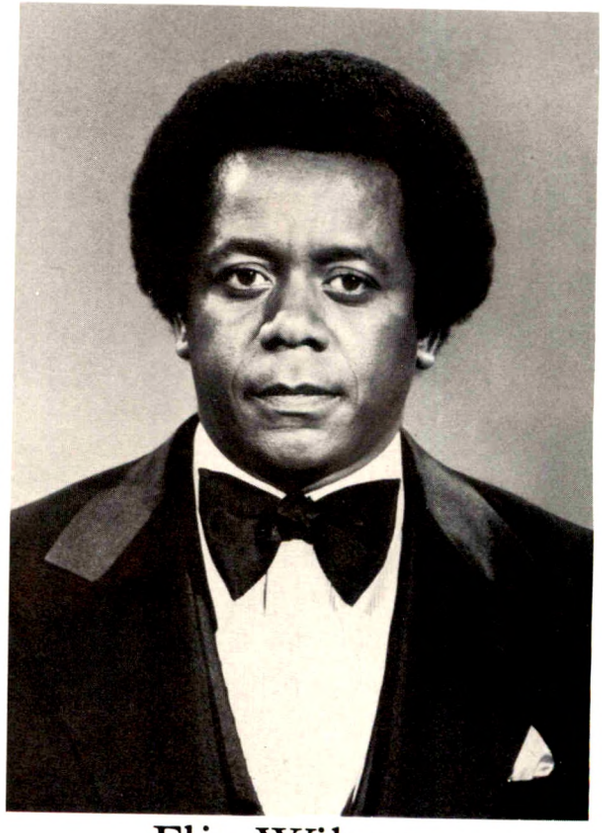
By getting to the doctor in time.

By availing themselves of the most effective methods of treatment today.

By advances made through cancer research. Research made possible with the help of the American Cancer Society.

However, there's much more to be done. To help save more people, the American Cancer Society needs more money. So, please, give. We want to wipe out cancer in your lifetime.

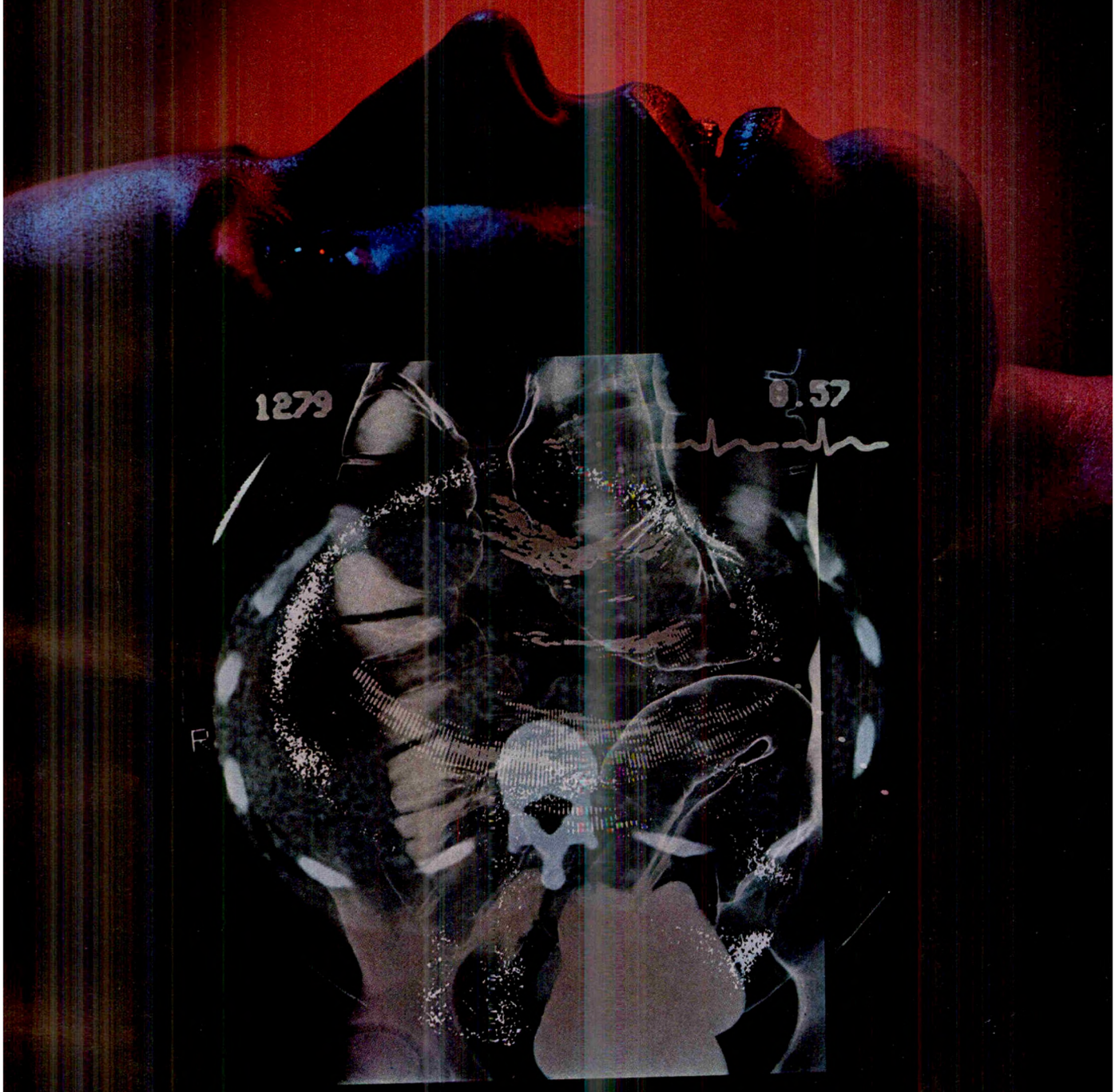
American Cancer Society



Flip Wilson,
National Crusade Chairman

This space contributed by the publisher as a public service.

For Total Imaging



TOSHIBA
MEDICAL SYSTEMS

At Toshiba, the concept has always been total imaging. It is the reason the world looks to us for all four types of imaging systems in use today.

From modular radiology and fluoroscopy systems, to the world's first super high resolution large field gamma camera, six decades as medicine's international imaging leader goes into every system we make.

Two things make Toshiba Medical Systems the image to look for, resolution and human engineering.

As an example, both have contributed equally to making Toshiba's Ultrasound Sonolayergraph series the finest available to modern clinical medicine.

Backing Toshiba Medical System's 60 years of medical imaging experience, is Toshiba Corporation's position as a leader in electronic and computer integrated systems of all types.

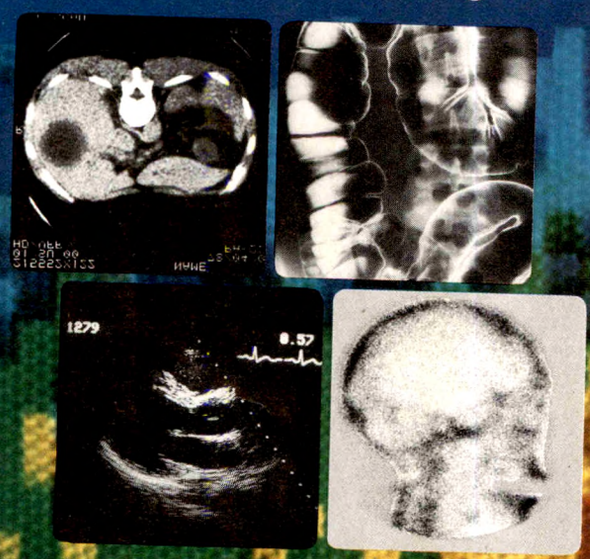
This kind of technical capability enabled Toshiba to incorporate the latest advances from a wide range of fields, to produce a new level of computer tomography with Toshiba's whole body CT scanner.

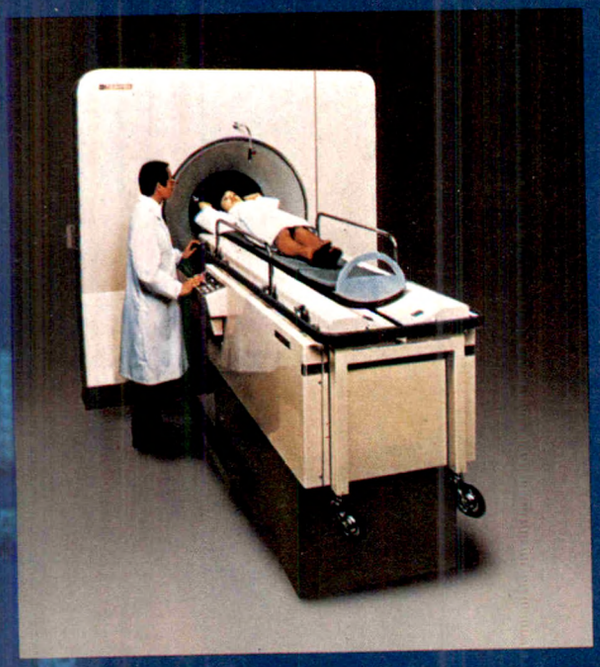
As medicine goes forward, you can be assured Toshiba Medical Systems will be there to give you the most useful diagnostic image you can get. That's because our commitment to giving you the finest imaging is as deep as your commitment to the good health of your patients.

Look to us, we are your total imaging company.

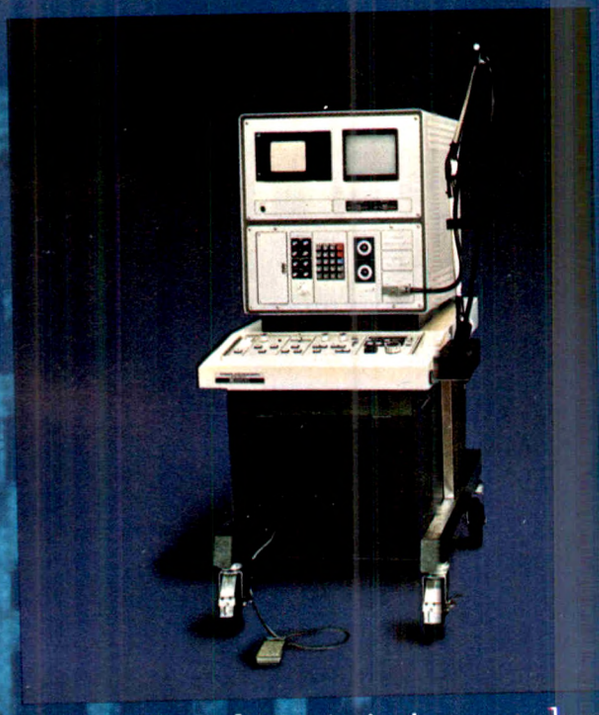
Toshiba is Your Total Image,

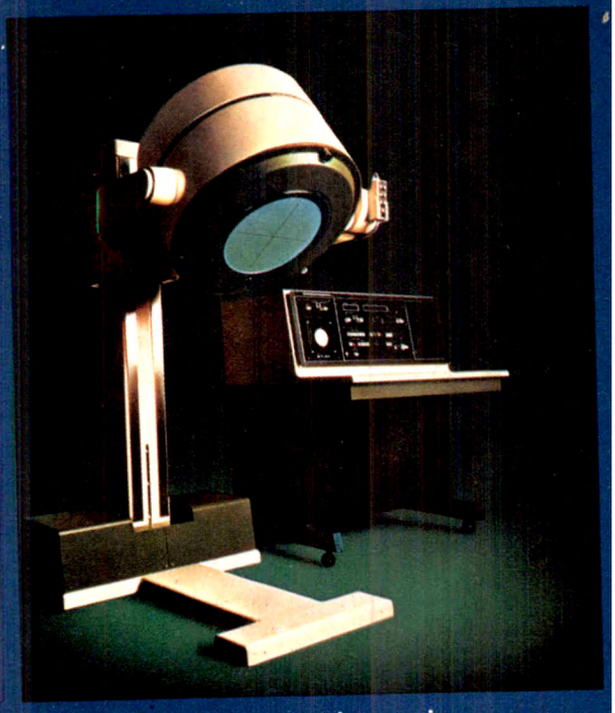
manufacturing the total gamut of imaging systems.











The ultimate in image clarity and human engineering for Radiology and Fluoroscopy, Ultrasound, Computer Tomography and Nuclear Medicine.

EXTENDED SERVICE PLANNING

Toshiba Medical Systems is also your total service company. With engineering personnel and logistics support that span the globe, Toshiba is committed to provide around the clock service and support anywhere in the world.

Toshiba Medical Systems sales and service headquarters around the world:

Argentina, Buenos Aires
Australia, Sydney
England, London
Hong Kong, Hong Kong
Iran, Teheran
Mexico, Mexico City
The Netherlands, Amsterdam
New Zealand, Wellington
Philippines, Manila
Republic of South Africa, Johannesburg
Taiwan, Taipei
Thailand, Bangkok
Venezuela, Caracas

Toshiba Medical Systems

Division of Toshiba International, Corporation, U.S.A. — Los Angeles, California

Atlanta, Georgia
Boston, Massachusetts
Chicago, Illinois
Cincinnati, Ohio
Cleveland, Ohio
Dallas, Texas
Detroit, Michigan
Houston, Texas
Kansas City, Missouri
Los Angeles, California
Memphis, Tennessee
Miami, Florida
New Orleans, Louisiana
New York, New York
Philadelphia, Pennsylvania
Phoenix, Arizona
San Francisco, California
Seattle, Washington
Tampa, Florida
Washington, D.C.
Ontario, Canada

Toshiba Medical do Brasil, Ltda. — Sao Paulo, Brazil









Toshiba

TOSHIBA

Toshiba Corporation, Tokyo, Japan

When it comes to keeping up-to-date with advances in diverse areas of your specialty —

THE MEDIASTINUM: Radiologic Correlations with Anatomy and Pathology. By E. Robert Heitzman, M.D. This book provides the foundation for a more analytic and deductive approach to radiological evaluation of the mediastinum. It emphasizes that such an evaluation depends on a thorough understanding of basic principles of anatomy and pathology and their correlations. The author offers a new anatomical classification of the mediastinum; provides a new radiological classification of the lymph nodes of the mediastinum; and stresses the value of computed tomography in the study of this area. 1977, 356 pp., 595 illus. **Price, $39.50.**

New Volume IV! **RADIOLOGY OF THE SKULL AND BRAIN: Ventricles and Cisterns.** Edited by Thomas H. Newton, M.D. and D. Gordon Potts, M.D.; with 15 contributors. The once-in-a-lifetime series — **RADIOLOGY OF THE SKULL AND BRAIN** — nears completion with this final volume. In it, the ventricles and cisterns are displayed by anatomical techniques, ventriculography, and pneumoencephalography. As in previous volumes, distinguised contributors offer valuable insights into their specific area of expertise. You'll read individual chapters on the third ventricle, the aqueduct, the fourth ventricle, the lateral ventricles, and subarachnoid cisterns. Order your copy today! October, 1978. Approx. 704 pp., 1,369 illus.. **About $59.50.**

A New Book! **RADIOGRAPHIC FUNDAMENTALS AND TECHNIQUE GUIDE.** By Terry R. Eastman. Concise, convenient, and completely up-to-date, this guide details the essentials of quality x-ray production. Chapters cover minimal exposure technique, radiographic quality, grids, intensity screens, darkroom, calibration, automated exposure and clinical quality control. You'll particularly appreciate a valuable pediatric technique chart. Order your copy today! May, 1979. Approx. 200 pp. **About $12.00.**

New 3rd Edition! **TEXTBOOK OF NUCLEAR MEDICINE TECHNOLOGY.** By Paul J. Early, B.S.; Muhammed A. Razzak, M.D.(Cairo), M.B.Ch., D.M., F.A.C.P.(U.S.A.); and D. Bruce Sodee, M.D., F.A.C.P. Help your staff review basic fundamentals with this comprehensive new 3rd edition. The first of two parts provides pertinent new information on nuclear science including the tri-linear chart of the nuclides plus phosphors, films, photographic devices, and film characteristics. The MIRD concept of dosimetry has been expanded to include "S" factors. Part II then deals with clinical nuclear medicine including tests, interpretations, and main sources of errors. Updated information on current radiopharmacuticals is also featured. May, 1979. Approx. 550 pp., 275 illus. **About $21.95.**

5th Edition! **Ackerman and del Regato's CANCER: Diagnosis, Treatment, and Prognosis.** By Juan A. del Regato, M.D. and Harlan J. Spjut, M.D. The classic in its field, this thoroughly revised and updated 5th edition continues to provide you with an integrated view of all aspects of cancer diagnosis and treatment. Beginning chapters offer current information on such general topics as cancer reseach, pathology, and radiotherapy. Subsequent chapters examine specific disorders, classified according to body systems or organs. You'll particularly value two new chapters on chemotherapy and tumors of the central nervous system. 1977, 1,028 pp., 805 illus. **Price, $57.50.**

rely on Mosby.

For faster service, or if coupon has been removed, CALL US! Dial toll-free (800) 325-4177 and ask for extension 10; in Missouri, call collect (314) 872-8370 during our regular business hours. A90035 26 05

Mail this coupon today and you'll have 30 days to evaluate your selections.

YES! I want to inspect an on-approval copy of the book(s) I've checked below.

_____ THE MEDIASTINUM, (3646-9) $39.50.
_____ RADIOLOGY OF THE SKULL AND BRAIN: Ventricles and Cisterns (3661-2) $59.50*.
_____ RADIOGRAPHIC FUNDAMENTALS AND TECHNIQUE GUIDE, (1493-7) $12.00*.
_____ TEXTBOOK OF NUCLEAR MEDICINE TECHNOLOGY, (1488-0) $21.95*.
_____ CANCER, (1250-0) $57.50.

*Estimated price, subject to revision prior to publication.

☐ Bill me ☐ Payment enclosed
☐ mastercharge # _____
☐ VISA # _____
Name _____
Address _____
City _____
State _____ Zip code _____

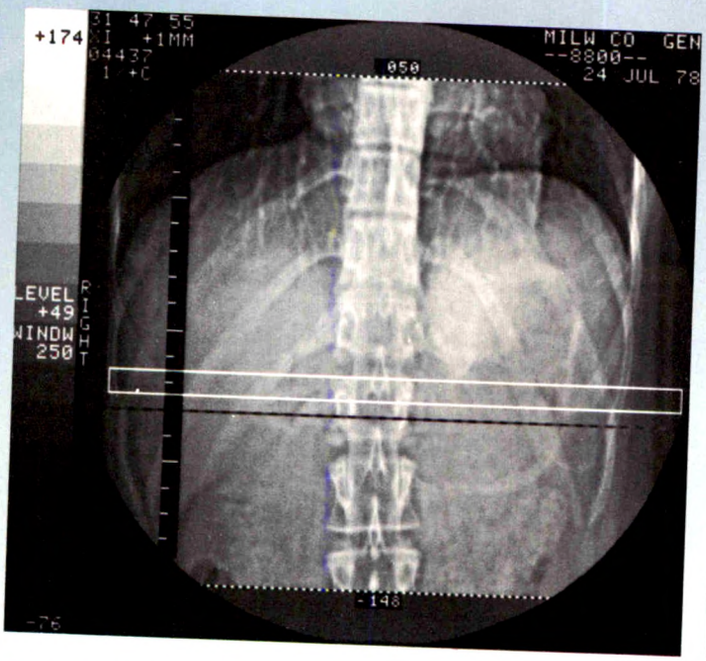
30-day approval offer good in U.S. and Canada.
Prices effective in U.S. only. A90035 26 05

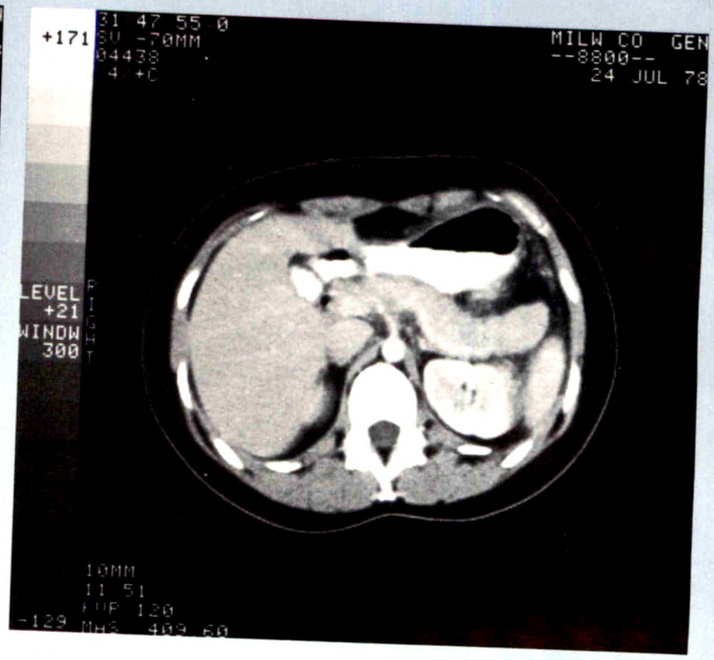
Complete and mail to: The C. V. Mosby Company, 11830 Westline Industrial Drive, St. Louis, Mo. 63141.

MOSBY
TIMES MIRROR

THE C. V. MOSBY COMPANY
11830 WESTLINE INDUSTRIAL DRIVE
ST. LOUIS, MISSOURI 63141

New imaging versatility.





These images demonstrate how ScoutView imaging simplifies pancreatic localization. An axial slice taken at the mid to lower L-1 vertebral level is almost invariably at the takeoff of the superior mesenteric artery from the abdominal aorta, and the body of the pancreas will be included in the same slice. The scan sequence can then be monitored both above and below this level to ensure that the complete pancreas has been studied. Unnecessary slices resulting from attempts to define the level of the pancreas from external landmarks are thus avoided.

The image at the right was taken at the level indicated by the box on the ScoutView image. In this case, the patient has a horizontally oriented pancreas, and the slice taken at this level, following an intravenous bolus injection of 25 cc of Renographin 60, clearly demonstrates the splenic vein and superior mesenteric vein, in addition to the superior mesenteric artery on the posterior surface of the pancreas. Note the obliteration of the spleno-renal angle due to pancreatitis. Gas is present within the distal common bile duct secondary to a previous sphincteroplasty on the ampulla of Vater.

Clinical documentation of ScoutView's usefulness in diagnostic procedures is provided in a new 4-page Medical Systems Report. It's yours for the asking from your GE Medical Systems representative, or write ScoutView, P.O. Box 414 (W-512), Milwaukee, WI 53201.

New operator's console, one part of the ODC package, lets you initiate ScoutView imaging, then position a cursor on the image to select scan locations and plan gantry angulation. The new console also allows set up and control of axial scans, plus viewing of the last slice. When the physician's console is not in use, image analysis can be controlled at the operator's console.



SDC physician's console (far right), standard with CT/T systems, provides complete axial, sagittal and coronal scan image manipulation and analysis capability. With the optional ODC package, this console also displays ScoutView images, which can be analyzed with magnification, angle measure and grid/annotate.

You'd expect it from GE.

GE's new Optional Diagnostic Capability package (ODC) offers these key features:

- **New operator's console with image viewing, manipulation and recording capability**
- **Improved, coordinated anatomical reference system utilizing new table electronics**
- **1.5 mm contiguous axial slice capability**
- **ScoutView™ localization imaging—AP/PA, lateral and oblique**
- **Easily installed on existing CT/T 7800 and 8800 systems**

ScoutView localization provides important new benefits for the CT/T operator. The scanner actually generates a radiograph-like image that is used to accurately plan first and last slice locations, plus the exact gantry angulation needed. Each axial scanning procedure is thus tailored precisely to the anatomy of the individual patient, since the ScoutView image and the axial scans share a coordinated anatomical reference system.

A ScoutView procedure is performed in just 5 to 10 seconds, and the image is reconstructed in less than 40 seconds. Dosage is low, varying from 6 mR to 600 mR depending on technic and patient size.

At the operator's console, ScoutView images and the last slice may be viewed without interrupting diagnostic activity at the physician's console. And when the physician's console is not in use, the operator can perform virtually all image manipulation and recording functions at the operator's console.

ScoutView images can also be displayed, manipulated and analyzed at the physician's console. Because of the coordinated reference system, axial scans can be selected for viewing according to their locations on the ScoutView image.

This new package is further evidence of GE's Continuum concept: to provide important options without major systems changes. This cost-saving concept has brought you GE's fast-reconstruct option, X-2 ultra-high resolution detector, and the Independent Diagnostic Console. And now the ODC with ScoutView imaging.

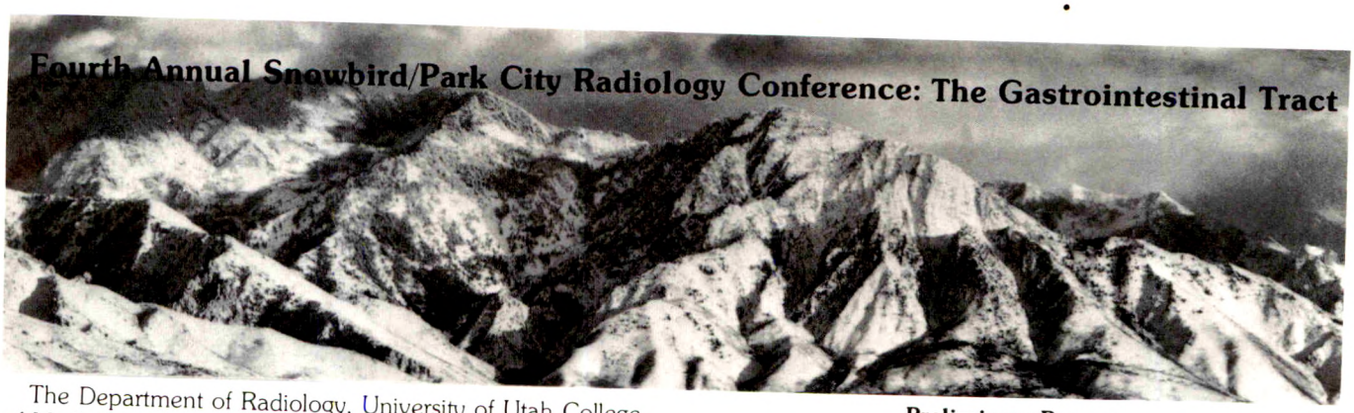
That's just what you'd expect from GE. The best images and best value...now and in the future.

General Electric Medical Systems,
Milwaukee, Toronto, Madrid.



GENERAL ELECTRIC

Fourth Annual Snowbird/Park City Radiology Conference: The Gastrointestinal Tract



The Department of Radiology, University of Utah College of Medicine, is sponsoring a postgraduate course in Gastrointestinal Radiology, January 27 - February 3, 1979 at the Snowbird Ski Resort, Snowbird, Utah and a second similar meeting at the Park City Ski Resort from February 24 - March 3, 1979.

Registration fee is $230.00 for each meeting and includes breakfasts and coffee breaks. A limited number of residents will be accepted at a registration fee of $150.00 if accompanied by a letter of endorsement from their departmental chairman. Cancellations will be accepted up to January 4, 1979 for the Snowbird course and up to February 4 for the Park City course, subject to a $30.00 handling fee. Rooms have been secured at Snowbird and Park City and will be held until November 28 and December 24, 1978, respectively. After that time, reservations will be accepted on the basis of availability.

The course has been accredited for 20 hours AMA - CME Category I credit.

FACULTY:

David G. Bragg, M.D.
Professor and Chairman, Radiology

R. Edward Coleman, M.D.
Associate Professor, Radiology

Virgil R. Condon, M.D.
Associate Professor, Radiology

William B. Cutcliff, M.D.
Assistant Professor, Radiology

James W. Freston, M.D., Ph.D.
Professor, Medicine and Pharmacology

John R. Haaga, M.D.
Staff Radiologist, Cleveland Clinic

Richard B. Jaffe, M.D.
Associate Professor, Radiology

P. Ruben Koehler, M.D.
Professor, Radiology

Timothy G. Lee, M.D.
Associate Professor, Radiology

Patrick D. Lester, M.D.
Associate Professor, Radiology

William J. McSweeney, M.D.
Professor and Chairman, Radiology
Children's Hospital National Medical Center

Franklin J. Miller, Jr., M.D.
Associate Professor, Radiology

D. Edward Mineau, M.D.
Instructor, Radiology

Frank G. Moody, M.D.
Professor and Chairman, Surgery

James A. Nelson, M.D.
Associate Professor, Radiology

G. William Nixon, M.D.
Associate Professor, Radiology

Patrick F. Sheedy, M.D.
Associate Professor, Radiology
Mayo Clinic

Edward B. Singleton, M.D.
Professor, Radiology
Texas Children's Hospital

Karl T. Wickstrom, M.D.
Assistant Professor, Radiology

Preliminary Program

Sunday Evening

7:00 - 9:00 — Film Reading Session

Monday

7:30 - 9:30 a.m. — Contrast Examination of the Biliary Tract
Drs. Mineau, Moody, Nelson, Wickstrom

4:30 - 6:30 p.m. — CT and Ultrasound of the Biliary Tract
Drs. Haaga*, Lee, Sheedy*

Tuesday

7:30 - 9:30 a.m. — Ultrasound and CT of Abscess; Contrast Studies in Oncologic Entities
Drs. Koehler and Bragg

4:30 - 6:30 p.m. — Plain Film and Barium Studies Technique
Drs. Freston, Mineau, Nelson, Wickstrom

Wednesday

7:30 - 9:30 a.m. — Liver Imaging and Interventional Techniques
Drs. Coleman, Haaga*, Miller, Sheedy*

4:30 - 6:30 p.m. — Pediatric Lower GI Tract: Part I
Drs. Cutcliff and Jaffe

Thursday

7:30 - 9:30 a.m. — Pediatric Upper GI Tract: Part I
Drs. Condon, Lester, McSweeney*, Singleton*

4:30 - 6:30 a.m. — Pediatric Upper GI Tract: Part II
Drs. Condon, Nixon, McSweeney*, Singleton*

Friday

7:30 - 9:30 a.m. — Pediatric Lower GI Tract: Part II
Drs. Condon, Lester, McSweeney*, Singleton*

afternoon — Free Time

* Drs. Haaga and McSweeney at Park City Conference, Drs. Sheedy and Singleton at Snowbird Conference.

REGISTRATION FORM

FOURTH ANNUAL SNOWBIRD/PARK CITY RADIOLOGY CONFERENCE
GASTROINTESTINAL RADIOLOGY

Check course(s) desired:

☐ Snowbird Ski Resort January 27 - February 3, 1979
☐ Park City Ski Resort February 24 - March 3, 1979

NAME: _____

ADDRESS: _____

_____

CITY, STATE: _____ ZIP: _____

TELEPHONE: _____

Fee: $230.00

Checks payable to:
Department of Radiology
University of Utah

Return with registration fee to:
Franklin J. Miller, Jr., M.D.
Department of Radiology
University of Utah Medical Center
50 North Medical Drive
Salt Lake City, Utah 84132

(801) 581-8188

Upon receipt of registration, hotel and ski information will be forwarded. Lodging guaranteed until November 28, 1979 for Snowbird course and December 24, 1979 for Park City course. After these dates, lodging on availability basis only.

In just one second we'll show you something in CT imaging no one else can.



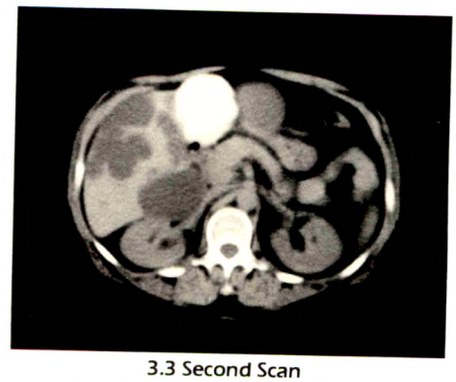
PICKER®
ONE OF THE CIT COMPANIES

For high-quality CT body scans,



1 Second Scan

The advantages of speed in body scanning are evident in the absence of artifacts due to physiological motion. Note the well-defined loops of bowel in the above scan. Other structures seen are the kidneys and the renal arteries.



3.3 Second Scan

The above image demonstrates polycystic disease of the liver. Note the clear delineation of the pancreas, superior mesenteric artery and renal arteries. In addition, the left colic or splenic flexure can be seen.



Faster is better.

To achieve high-quality body scans, faster is better. Synerview is the fastest scanning CT system presently available. It can routinely perform high-quality scans, as fast as 1 second.

Because of the natural involuntary motions that occur within the human body, fast-scanning capabilities are necessary for clear images in body scans. The faster your CT scanning capabilities, the more you can minimize motion artifacts caused by peristaltic, muscular, respiratory, and cardiovascular actions.

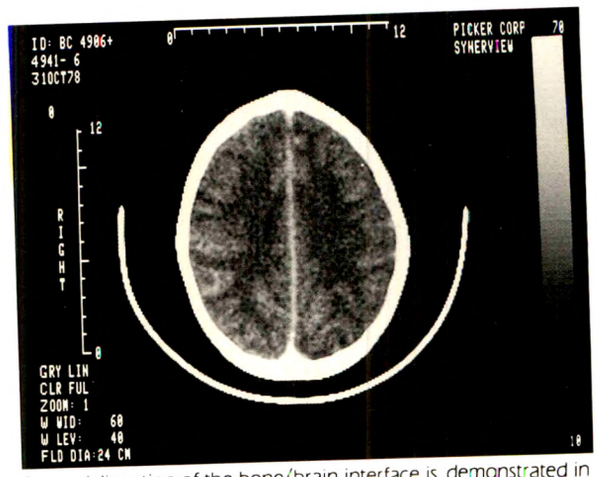
And for CT diagnosis to be effective for uncooperative, unconscious, pediatric or geriatric patients, you need 1-second scanning.

Ready to advance the state-of-the-art for CT. An investment in Synerview is the best way to obtain a high-quality CT scanner and minimize the obsolescence factor. Other manufacturers have reached the limit of their CT capabilities with the technology employed in their present systems. But Synerview, based on the proven Stationary Detector principle, has the potential to advance state-of-the-art for CT. Synerview is ready to expand its capabilities when new technology becomes available.

Synerview performance features. Synerview has features that help make CT operation fast and convenient. Our unique patient transport is one example. It lets you prepare a patient for scanning almost anywhere in the hospital. And to maximize your patient throughput, Synerview combines fast patient-data entry and scanning selection protocol with processing as fast as 25 seconds.

Superb software capabilities bring added dimensions to your CT operations. Synerview can display sagittal and coronal reconstructions in less than 5 seconds. Our bone correction software provides better visualization of the bone/brain interface. In addition, Synerview's optional therapy treatment planning feature can be supplied either for economical shared use, or for more versatile independent use.

And a field size of 48 cm means Synerview can perform body scans with even your larger patients.



Sharp delineation of the bone/brain interface is demonstrated in the above image. Note the white and gray matter separation.



In this contrast-enhanced image taken through the body of the lateral ventricles we see enhanced choroid plexus, torcula, and vein of galen. Note the white and gray matter differentiation as well as cortical sulci.

Head to head, there's no one better. We have the latest technology and the images to prove it.

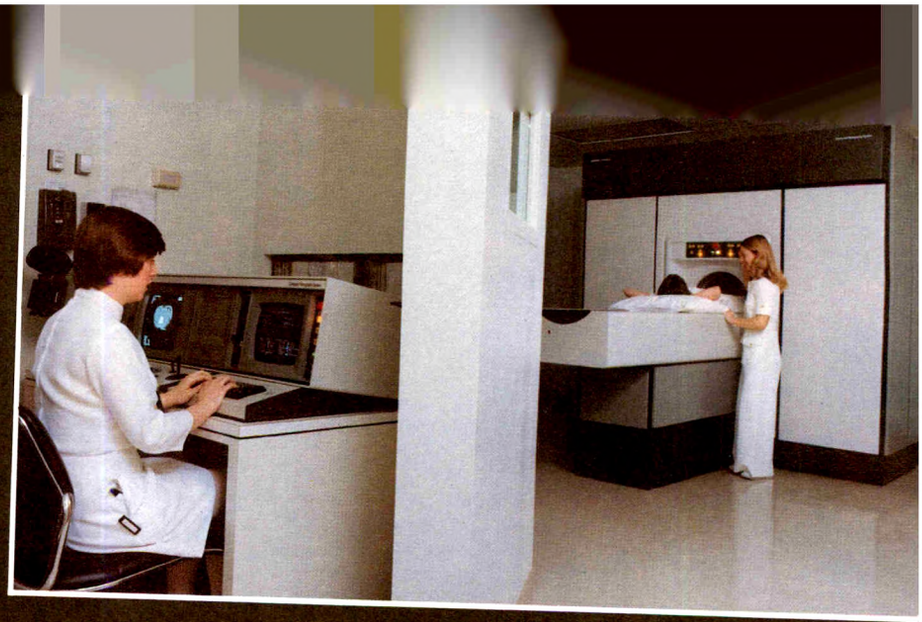
A large portion of any CT caseload involves head scans. It's of particular significance to know that Synerview brings you high-quality head scans in addition to high-quality body scans. It's also important that you can position your patient's head easily with Synerview. You can get the right scan — the first time. And, for accurate Towne's projections, Synerview's ultra-stable gantry can tilt ± 20 degrees.

There's only one 1-second CT system. Synerview.

PICKER
ONE OF THE CIT COMPANIES

Synerview. Developing a fine image.

The Synerview installations pictured are currently in operation and producing optimum diagnostic results. Our various CT systems include the Synerview 120, which utilizes Translate/Rotate geometry, and the Synerview 300 and 600, both of which employ the Stationary Detector method.



Carlisle Hospital, Carlisle, PA

We have the experience and the resources to help you acquire the right CT system for your needs.

Certificate of Need Assistance. Picker CT representatives work with you to help you acquire your Synerview. From acquisition to installation, we can help. And that includes Certificate of Need counseling and room-layout planning.

Financial Assistance. Through our parent CIT Financial Corporation, we can arrange your financing. Our financial arrangements can be as flexible as your financial needs. If and when they change, our arrangements can too.

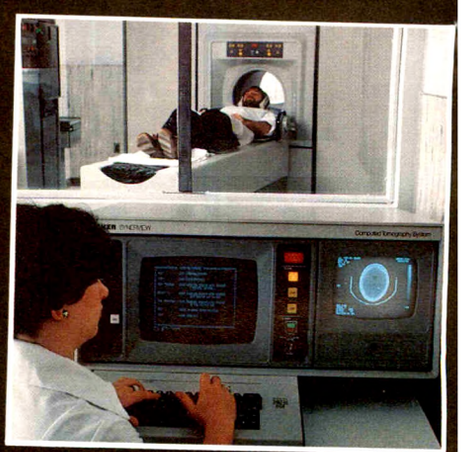
Training and Installation. We train you on the same Synerview you purchase. So, before operation begins, you are familiar with all the features of the CT system you'll use every day. And installation is usually accomplished in seven to ten days in a prepared room. When you're ready to start full CT operations, so is Synerview.

Service. Your local Picker representative's service engineers undergo rigorous training. Upon completion of this training, each Synerview service engineer is assigned to a system and follows it through the final tests at the factory. The Synerview is then escorted to its installation site, where the installation checkout and performance certification are performed before turnover to you. The service engineer is then assigned to the area to provide swift, professional service. In addition, there is always a team of specialists, based at Picker, to further support your Synerview.

Over 62 years of diagnostic imaging. When you think about computed tomography, it makes sense to think about Picker. Picker's dedication to the total field of diagnostic imaging emerged from a strong X-ray background. That experience and knowledge helped us develop the world's first 1-second CT scanner. Synerview.



Princess Margaret Hospital, Toronto, Canada



Akron City Hospital, Akron, OH

For a free portfolio of Synerview head and body scans, contact your local Picker representative, or call collect 216/461-9100, CT Marketing, extension 332. Picker Corporation, 595 Miner Road, Cleveland, OH 44143.

PICKER®

ONE OF THE CIT COMPANIES

Caffey's PEDIATRIC X-RAY DIAGNOSIS, 7th Ed.

The appearance of the 7th edition of this classic represents a major event in medical literature. The long awaited revision of this work will more than satisfy those familiar with the book and readily fulfill the expectations of those who come upon it for the first time. Indeed, few medical books in any field command the respect and approval of this volume.

By **John Caffey, A.B., M.D., M.D.(Hon.)**, University of Torino, Italy; Visiting Professor of Radiology at Children's Hospital of Pittsburgh; Professor Emeritus of Radiology, College of Physicians and Surgeons, Columbia University; Consulting Radiologist, Columbia Presbyterian Medical Center in New York City.

- ★ In Two Volumes
- ★ About 2,000 Pages
- ★ Approx. 6,000 Illustrations
- ★ $115.00*

*See coupon for money saving offer!!

- ☐ **Each section rewritten, expanded and up-dated by leading authorities in the field.**
- ☐ **Over 300 additional pages, covering all the new developments in the last five years.**
- ☐ **More than 900 new illustrations—a reference and atlas combined.**
- ☐ **Revised to include new clinical trends such as computed tomography, ultra-sound imaging, radionuclide scintigraphy, standard angiography.**

It's been nearly 5 years since publication of the last edition, and those 5 years have been marked by numerous advances. To keep up with these developments, every section has been completely rewritten and expanded. Along with the book's excellent coverage of x-ray technics, you will find thorough discussions of newer modalities such as computed tomography, ultra-sound imaging, radionuclide scintigraphy, and standard angiography, to name a few. The authors add this material while maintaining the features that established the book's reputation. Anatomical variants which may simulate disease continue to be explored through detailed discussion. The authors never hesitate to take sides on controversial issues and apply their personal expertise. And, of course, the book is still written in such a way that both the beginner and the expert practitioner will find it readily applicable to clinical situations.

Pediatric Radiology

By **Jack G. Rabinowitz, M.D., F.A.C.R.**, Professor and Chairman, Department of Diagnostic Radiology, College of Medicine, University of Tennessee Center for the Health Sciences; and Chief of Radiology, City of Memphis Hospitals, Memphis.

516 Pages. 885 Illustrations.
Published July 1978. $50.00*
***See coupon for money saving offer!!**

PEDIATRIC RADIOLOGY helps the clinician and radiologist to grasp the fundamentals while developing a productive overall approach to film reading. Deviating from the classical presentation centered around disease descriptions, the format of this radiology text is more closely aligned with the actual thought processes and discussion which accompany the interpretation of radiographs.

Ten chapters organize the fact-filled material by area of interest (abdomen, heart, skull, etc.) and age of presentation (newborn, infant, and child). Within each chapter, an outline of the possible diseases underlying each radiographic finding is followed by a discussion of their distinguishing features, associated signs and symptoms, and incidence among young patients-all supplemented by clear, well-annotated radiographs of the normal conditions and disease entities.

Modern Radiation Oncology

Classic Literature & Current Management

Edited by **Harvey Alan Gilbert, M.D.**, Staff Radiotherapist, and **A. Robert Kagan, M.D.**, Chief Radiotherapist, Southern California Permanente Medical Group.

712 Pages. 49 Illustrations.
Published September 1978. $42.00*
***See coupon for money saving offer!!**

The purpose of this book is to bring together 29 American experts in radiation oncology to lay a foundation for the use of curative radiation therapy in modern clinical practice. For each tumor site the contributing author begins with an exact reproduction of the modern classic article from the radiation literature. This article states the fundamental rationale for the dose field size and treatment principles that govern the use of magavoltage radiation therapy. An annotated bibliography abstracts the critical findings of other key literature. This review is followed by a personal overview prepared by the contributing author in his field of expertise. This overview links the classic radiation literature and modern multidisciplinary therapy.

Radiobiology for the Radiologist, 2nd Ed.

By **Eric J. Hall, Ph.D.**, Professor of radiology, College of Physicians and Surgeons, Columbia University.

300 Pages. 195 Illustrations.
Published August 1978. $25.00*
***See coupon for money saving offer!!**

This book is intended primarily for Radiology residents preparing for their board certification. It covers the subject matter needed by residents in diagnosis, therapy and nuclear medicine. The effects of radiation on living things are described simply, but in detail. With the radiotherapist in mind, dose fractionation, model tumor systems, tumor kinetics, radiation sensitizers and new radiation modalities such as neutrons, pions and heavy ions, are some of the topics covered. For the residents in diagnostic radiology and nuclear medicine, the area of radiobiology which is most pertinent is the study of late effects. Radiation induced non-specific life shortening carcinogenesis and genetic mutations are discussed, as well as radiation effects on the developing embryo.

ORDER FORM

When you enclose payment with your order we ship your books at LOW SALE PRICES.
Act Now! This offer expires February 28, 1979.

☐ Please ship at the Sale Prices shown. Payment is enclosed.*
☐ I prefer to be billed. Please ship at regular prices plus postage & handling.

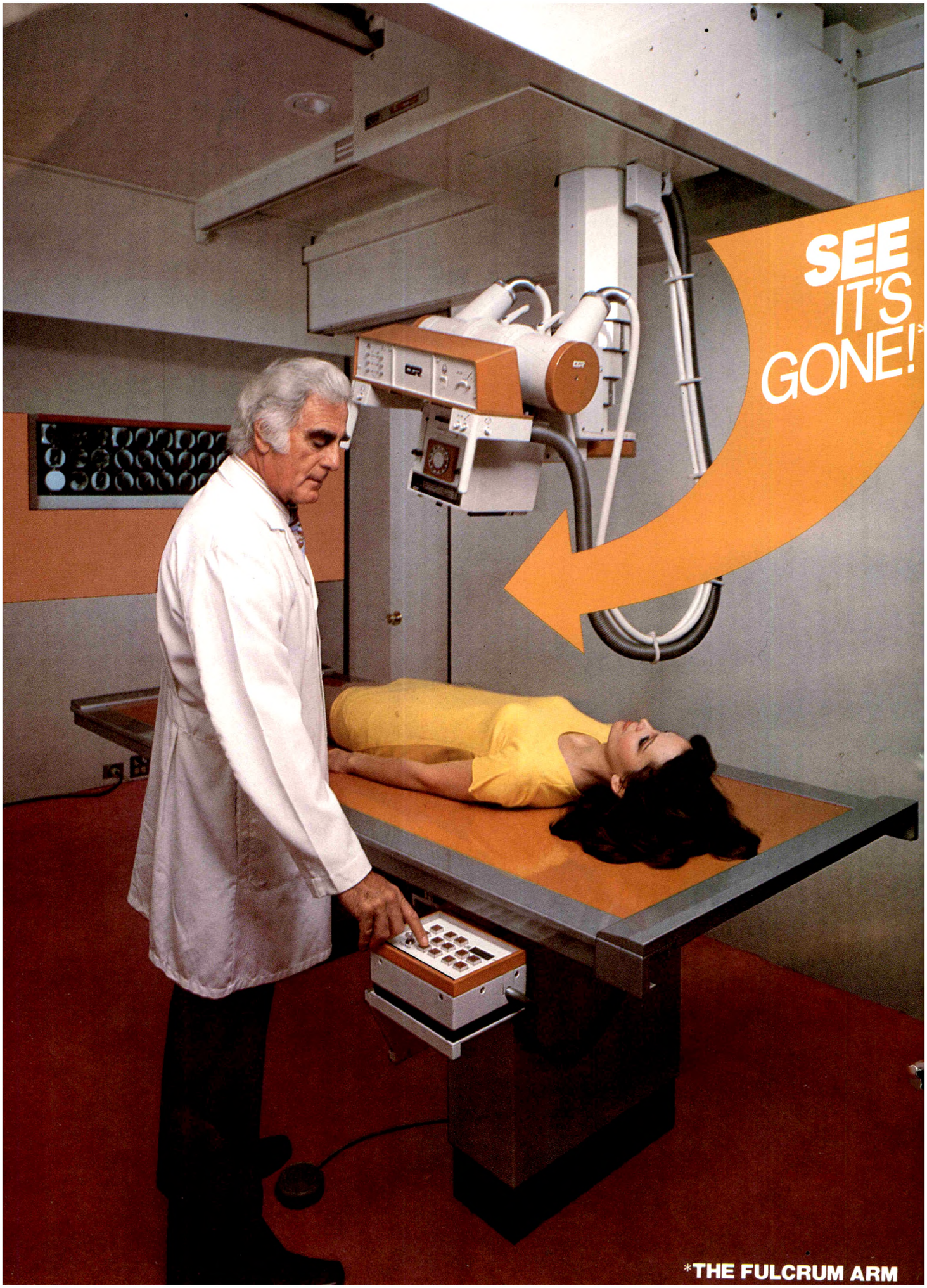
	Sale Price	Reg. Price
____ Caffey's Pediatric X-Ray Diagnosis.	105.00	115.00
____ Pediatric Radiology	45.00	50.00
____ Modern Radiation Oncology.....	37.50	42.00
____ Radiobiology for the Radiologist ...	22.50	25.00

*New York State Residents Please Add Appropriate Sales Tax.

Name _____
Address _____
City _____ State _____ Zip _____
Phone No. _____
Signature _____

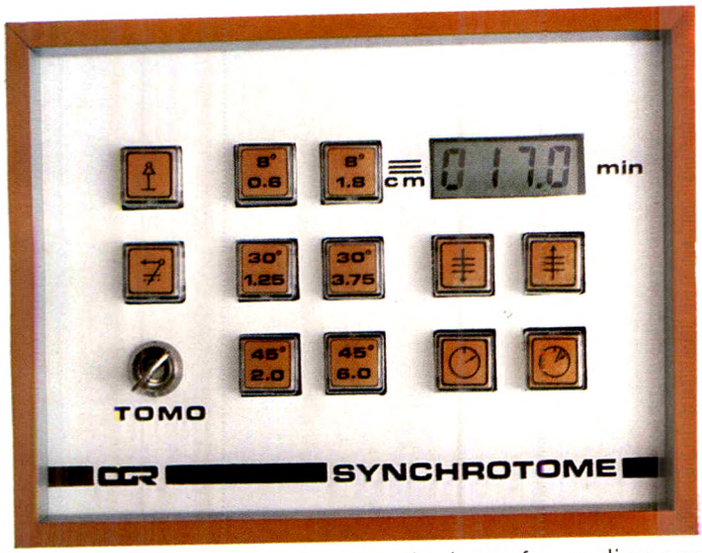
Professional Book Service
496 Clarkson Avenue
Brooklyn, New York 11203

IN A HURRY? CALL!
(212) 467-1292
Sorry - No Collect Calls.


SEE
IT'S
GONE!*
*THE FULCRUM ARM

COMPACT/ SYNCHROTOME.™

CGR'S NEW RADIOGRAPHIC/ TOMOGRAPHIC SYSTEM THAT'S TOTALLY "FULCRUM ARM FREE."



It's a totally new approach to radiography and linear tomography. Starting right out with a superior table: The Compact.

The Compact table gives you an island approach to examination. Complete, obstruction-free access to every side. The large, four-way, floating table top accommodates patients of any size and has extended longitudinal and transverse movement. Table-to-film distance is only 1.6". And the table has an ultra-fast Bucky and your choice of a radiographic grid. Phototiming is optional.

Synchrotome completes the system. The first "fulcrum arm free" linear tomography in the industry. A revolutionary approach using microcomputer electronics. No mechanical linkage whatsoever. Combined with its suspension system it offers complete examination versatility.

Compact/Synchrotome. CGR's cost effective breakthrough in economical radiography/linear tomography.

Your CGR representative has all the details.



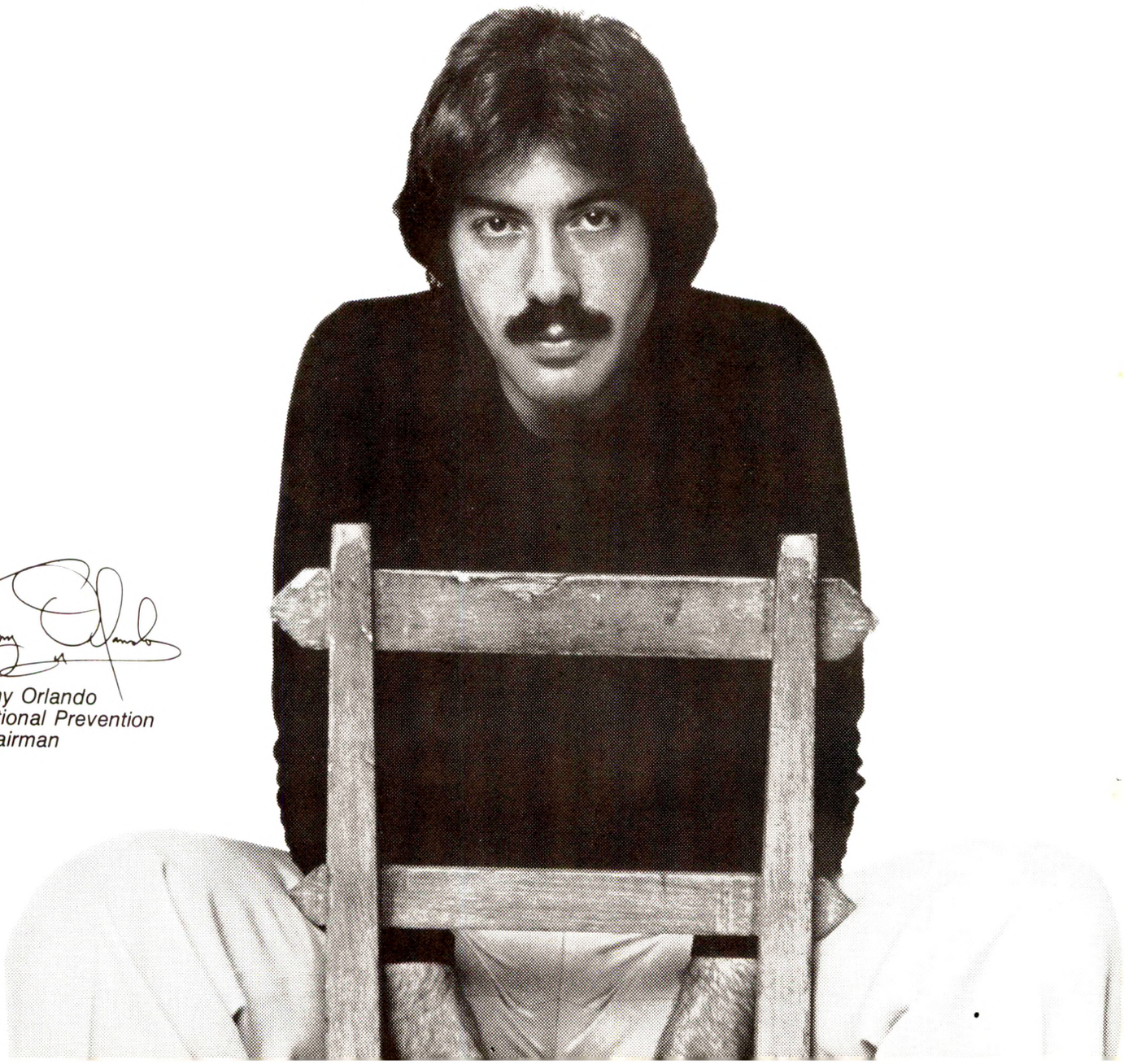
CGR MEDICAL CORPORATION 2519 Wilkens Ave
Baltimore, Maryland 21223 (301) 233-2300
CGR CANADA LTÉE-LTD. 500 Boulevard de l'Aéroparc,
Lachute, Québec, Canada, (514) 562-8806
CGR 13 Square Max Hymans,
75741 Paris, France 273-8200

Mental retardation is not a household word.

And we don't want it to become one.

Only you can prevent mental retardation in your family. We'll give you the facts.

Write me . . . at the National Association for Retarded Citizens, P.O. Box 6109, Arlington, Texas 76011



Tony Orlando
National Prevention
Chairman

The Second Announces A First

Advanced regional learning seminars on radiographic imaging. From the second largest producer of photographic products in the world, the Agfa-Gevaert Group.



Introducing

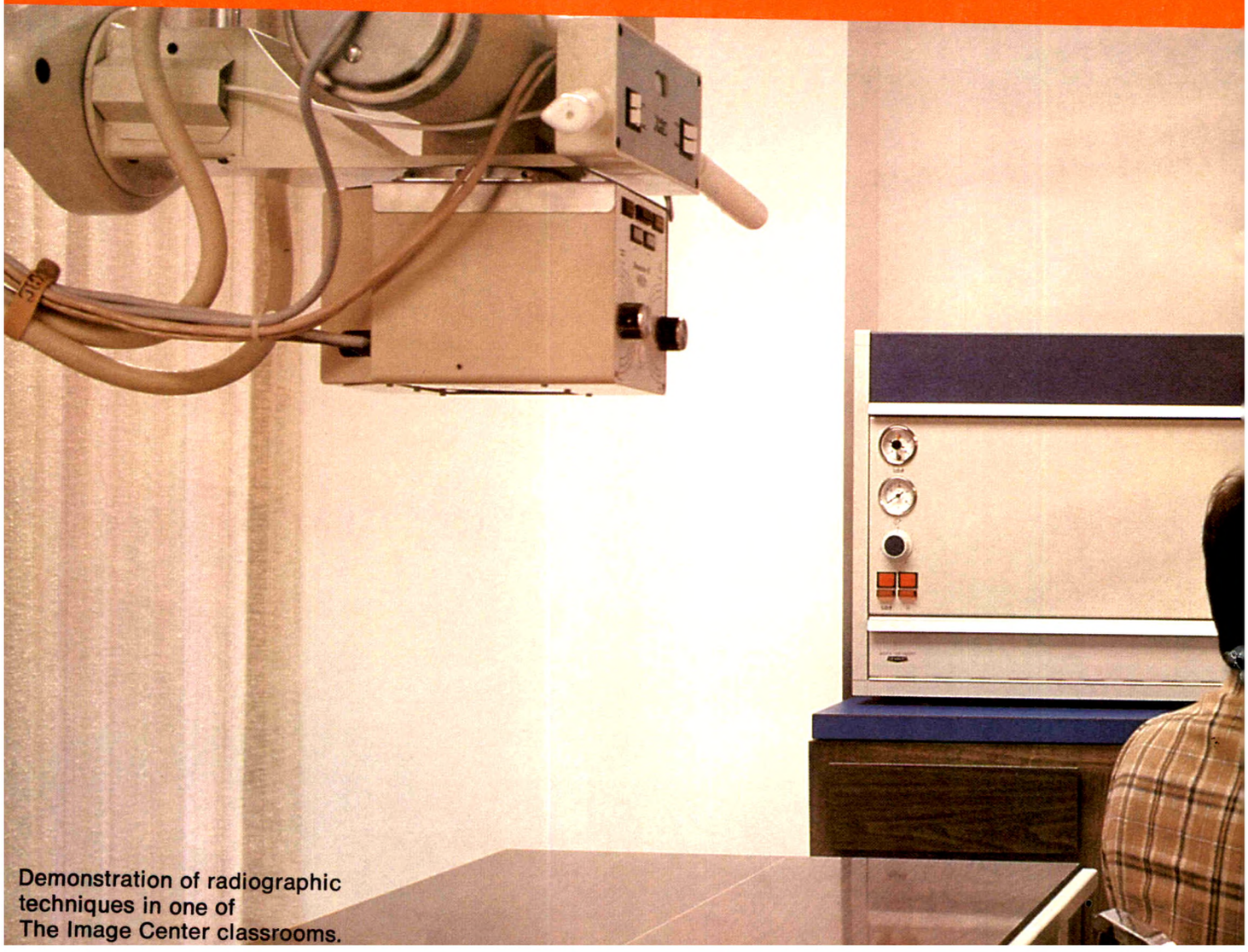
The Image Center

Advanced learning seminars on radiographic imaging.

A unique Resource Center.
Now, Radiology Departments throughout the country will have regional facilities to provide the most up-to-date information available on radiographic imaging: The Image Center. An educational resource where ideas can be exchanged. A resource that offers the opportunity to discuss new systems and techniques with recognized experts. A resource that provides continuing education credits in selected subject areas.

Located throughout the country.
These state-of-the-art centers, located in major cities in the U.S. including Los Angeles, Atlanta, San Francisco, Chicago, Dallas and metropolitan New York, contain classrooms, conference rooms and fully equipped radiographic rooms. Designed specifically for study and practice of new radiographic techniques, The Image Center provides hands-on experience with the latest equipment and imaging technology.

For the Radiologist.
The Image Center is a forum for bringing physicians together to exchange the latest ideas, procedures and information. Speakers who are experts in their field will conduct seminars on relevant topics in medical imaging. Business, government and legal aspects of radiology will be discussed . . . topics not readily available from other sources.



Demonstration of radiographic techniques in one of The Image Center classrooms.

AGFA-GEVAERT REX INC.

A subsidiary of Agfa-Gevaert Group, the second largest film maker in the world. White Plains, N.Y. Tel. 914 682-5650

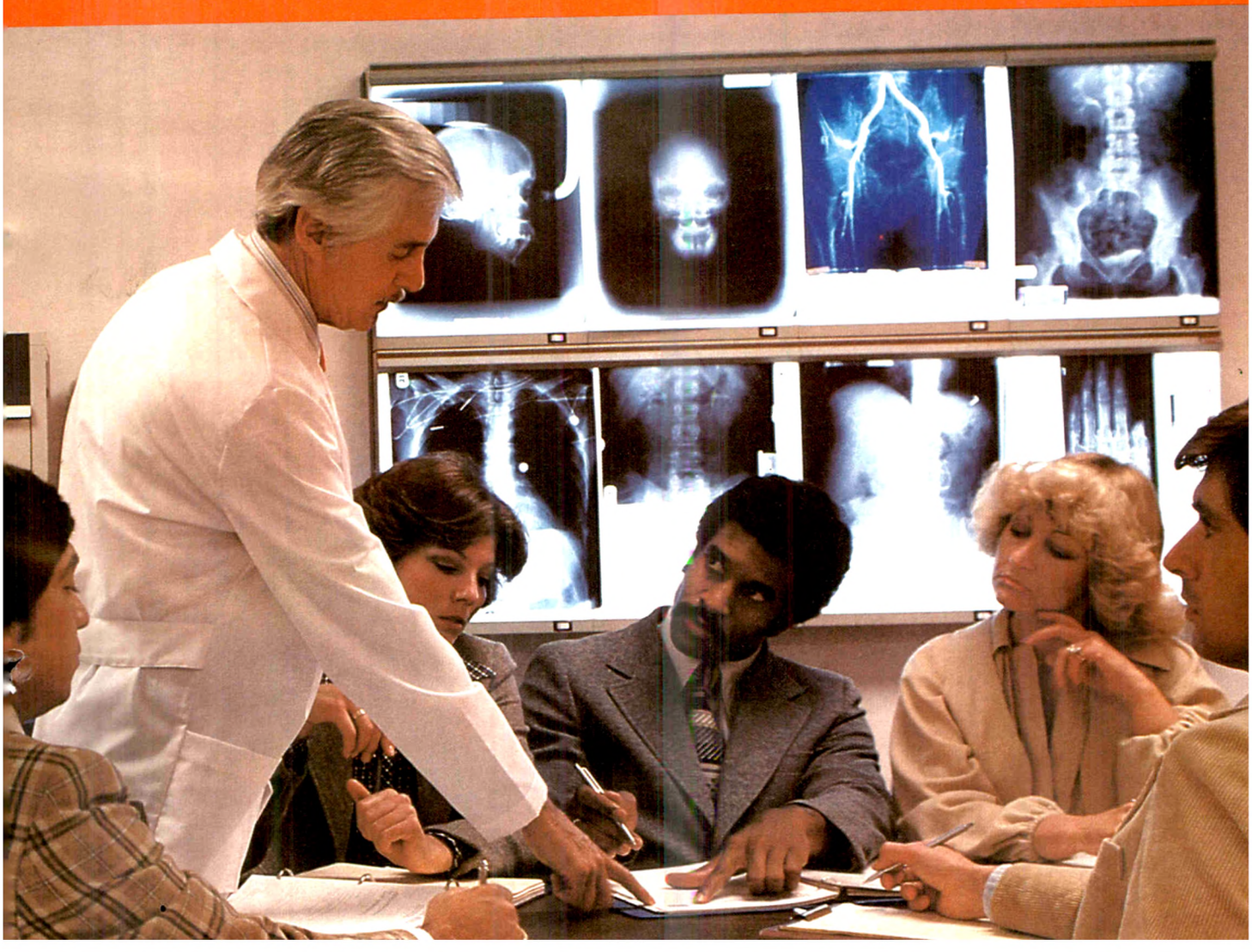
For the Radiologic Technologist.
The Image Center is an educational resource for teaching and keeping technologists up-to-date on current techniques and trends in medical radiography. It is a technical, in-service, educational program with emphasis on key factors affecting diagnostic quality of the finished radiographs. Laboratory sessions will provide the opportunity to use a variety of imaging and processing systems and to discuss related technical problems.

For the Resident.
Whether it's sensitometry, conventional radiography, CRT imaging or ultra-sound, The Image Center offers a broad range of educational seminars. Latest advances in radiographic imaging will be covered and many seminars qualify for Continuing Education credits.

For the Department Administrator.
Special seminars on cost effectiveness, business and financial management workshops are all available at The Image Center.

For the Physicist.
Physicists will receive information directly related to basic aspects of X-ray film and chemistry. Technical seminars will cover relevant R & D subjects and new products under development.

Contact your Agfa-Gevaert Rex representative for more information about scheduled seminars and programs being offered at The Image Center servicing your area.



X-RAY IMAGE INTENSIFYING SYSTEMS

precise optics

IT MAY SURPRISE YOU.....

. . . to know that the people at Precise Optics have been supplying X-Ray Image Intensifying Systems since 1954. Precise specializes in Imaging, and offers a complete line of systems to meet requirements ranging from the private office to the special procedures room, at a cost savings over comparable units, without sacrificing quality.

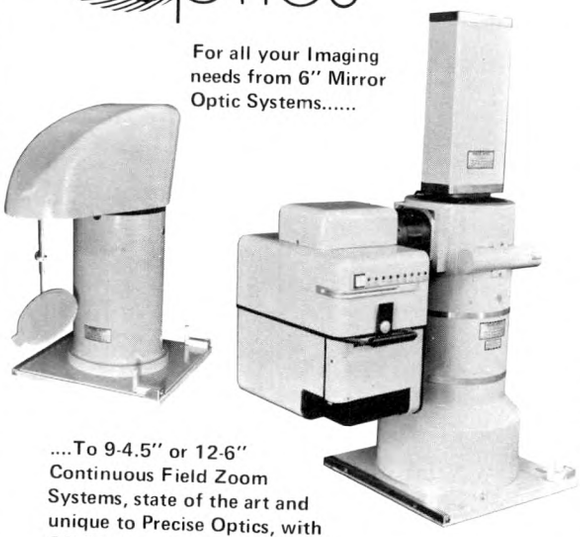
EVERY SYSTEM CONTAINS a guaranteed optimal performance cesium iodide image tube and field-proven solid-state power supply, covered by a two-year warranty.

THE PRECISE CCTV SYSTEM uses x-ray rated separate mesh vidicons, selected for high resolution and low-lag characteristics. Brightness compensation is an excellent 10,000:1, assuring the correct light level despite large variations in body densities.

THE NEW 105mm SPOT/RAPID SEQUENCE CAMERA (roll film, 6 frames per second maximum) utilizes the same digital electronics package and many of the mechanical sections of our other reliable 105mm cameras, while incorporating a rapid-load film transport and daylight receiving cassettes.

ACCESSORIES AVAILABLE INCLUDE: TWO-AND THREE-PORT LIGHT DISTRIBUTORS for spot and cine filming capabilities, ABS SYSTEM with automatically variable kV and selectable mA, SPOT FILM ADAPTERS compatible with any spot film device, CEILING SUSPENSION UNITS with smooth vertical and horizontal movements, CCTV MONITOR CARTS that are lightweight and easily mobile.

For all your Imaging needs from 6" Mirror Optic Systems.....



....To 9-4.5" or 12-6" Continuous Field Zoom Systems, state of the art and unique to Precise Optics, with CCTV and 105mm Spot/Rapid Sequence Cameras.

PRECISE OPTICS/PHOTO MEDIC EQUIPMENT, INC.
239 SO. FEHR WAY
BAYSHORE, N.Y. 11706
TEL. (516) 242-6600
TWX 510-227-9837

JOIN THE AIR FORCE, PRACTICE AT HOME.

The Air Force has a new Hometown Assignment Program for physicians. If you have the right specialty and if you live in or near a city where an Air Force hospital is located, you could qualify.

You would receive a direct commission, possibly as high as Lt. Colonel, and all the benefits of an Air Force Officer. At the same time you could maintain your present home. Your children could stay in the same schools. You could even take a paid vacation—4 weeks a year!

Here's what you would *lose*.

You wouldn't have to pay malpractice insurance. "Boss" an office staff. Or worry about the thousands of details a small businessman has to deal with.

You could concentrate on practicing medicine.

Get all the details. Talk to your Air Force Recruiter. Or mail in this coupon.

It's a great way of life!

AIR FORCE

Medical Professional Opportunities CJR019
Box 1776, Valley Forge, PA 19481

I would like more information about training and career opportunities in the Air Force Medical Service. I understand there is no obligation.

Name_____ Sex ☐ M ☐ F

Address_____ Apt. #_____

City_____

State_____ Zip_____

Phone_____ Birth Date_____

School_____

Yr. of Degree_____ Specialty_____

PHILIPS TOMOSCAN 300

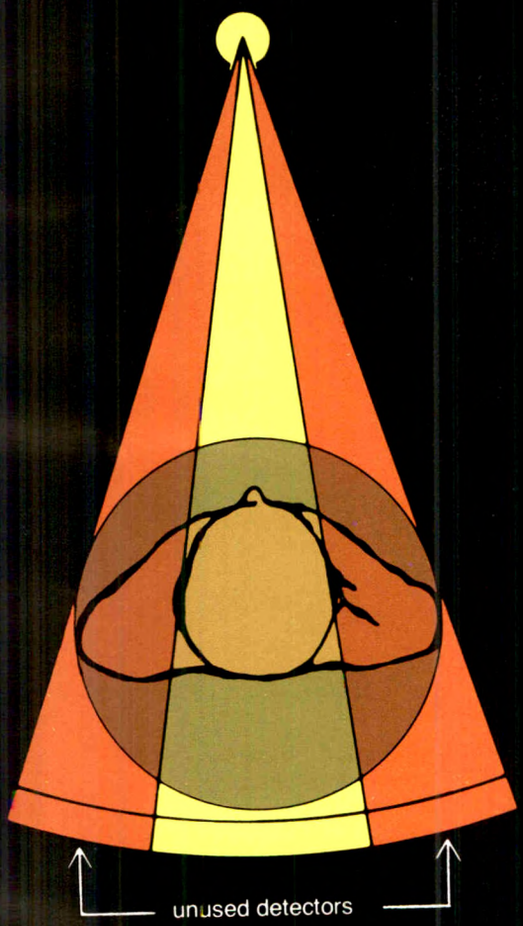
Philips Tomoscan 500

the only fast
scanner with variable
geometrical enlargement
–and full use of every
Xenon detector.

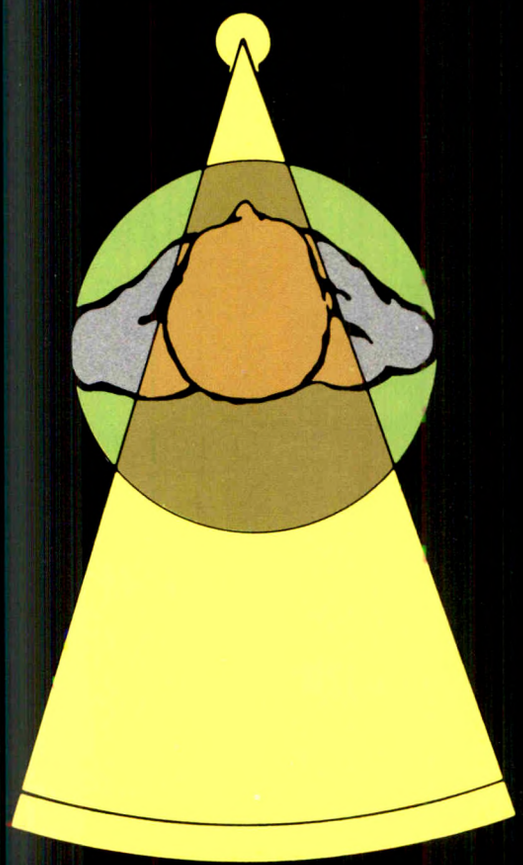
You're entitled to your points of view... all 172,800 of them.

Today's scanners are missing the points, especially for cerebral and pediatric studies. Philips isn't. Judge for yourself.

The problem: unused detectors



Philips' solution: geometrical enlargement



Only Philips makes full use of all detectors all the time. Why? Because the number of detector channels used and the number of pulses per scan create a data profile of image points which the computer reconstructs into an image. The more detectors used, the more image points. And the more "points of view," the closer the image comes to maximum spatial resolution and a better diagnostic result.

Philips Tomoscan 300 produces a superb image every time.

Actually, it's good old fashioned logic: waste not, want not.

While everyone else built scanners frantically, Philips built the best—on medical basics, not medical gimmickry.

Turn the page. We've got more of the best to offer.

PHILIPS®

TOMOSCAN 300

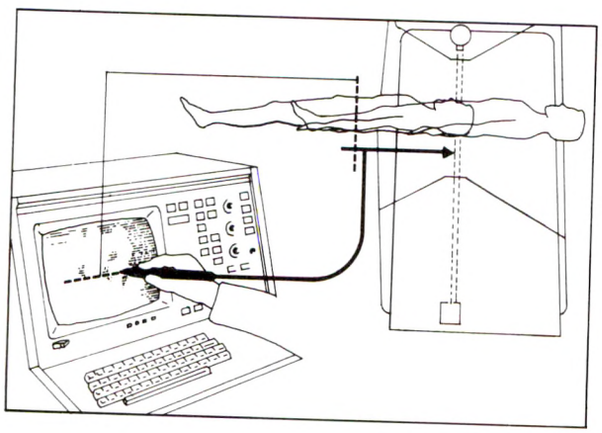
A 4.2 second whole body CT scanner

The concept was developed slowly and methodically—right in the middle of an industry-wide frenzy to sell systems that, in many cases, were outdated before installation was complete.

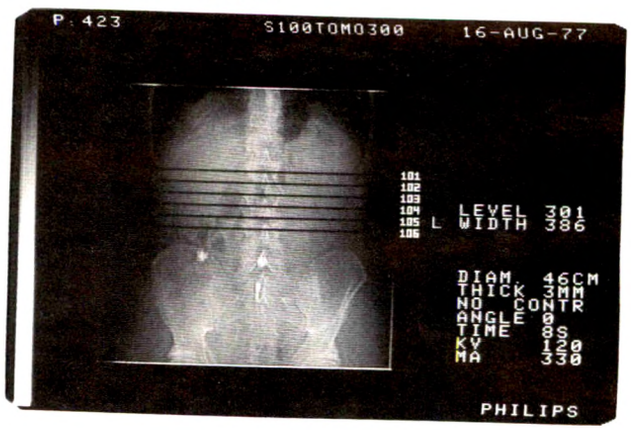
Philips did it differently. In close consultation with medical professionals worldwide, we evaluated *real* clinical needs. We said "No" to the unnecessary gadgetry that gives scanners a futuristic look. Instead, we returned to basics and developed a scanner with a future.

The result is our TOMOSCAN 300, a truly universal fast-scanner designed first and foremost as a medical instrument. Its features, like its specifications, stem from an appraisal of the system's medical application. Consider just some of the key reasons why you'll want to select TOMOSCAN 300.

THE SCANOGRAM



AN ACTUAL SCANOGRAM



- Computerized patient positioning for survey studies at very low dose exposures. The Scanogram provides lines that identify each slice by number and location of the body for lightpen selection of the exact scan location. The touch of a button brings the area of interest into the scan plane. The Scanogram eliminates trial scans and unnecessary radiation. Automatic patient positioning can also be done with a lightbeam.
- Rapid image reconstruction time (15 seconds)
- Wide choice of scanning parameters for precise adaptation to applicational requirements. For example:

——variable scanning speed—from 2.6s to 4.2s
——variable slice diameters—from 25cm (10″) to 48cm (19″)
——variable slice thickness—3, 6, 9 or 12mm

- Outstanding image quality
- Extraordinary range of viewing facilities, including:

——slow and fast window level control
——11-step window width control
——calculation capability for average attentuation, standard deviation and number of pixels for three regions of interest of both irregular and circular regions
——enlargement, image reversal and distance measurement between any two pixels
——Stand-alone physician's viewing console with lightpen

There's more, much more . . . because Philips considers *your* point of view.

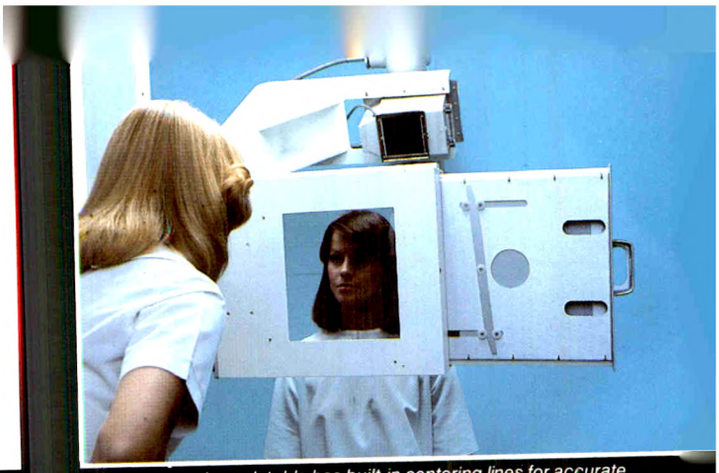
PHILIPS MEDICAL SYSTEMS, INC.
710 Bridgeport Avenue, Shelton, Conn. 06484

® TM N.V. Philips of Holland

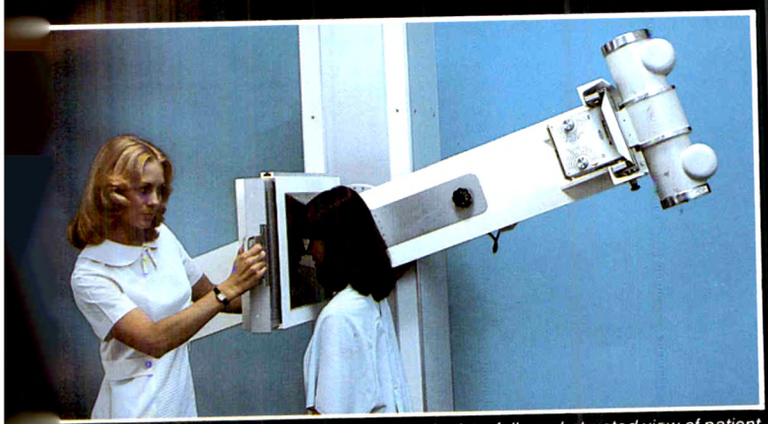
KATUM Rx 40

Radiographic Head Stand

Contemporary design... efficient operation



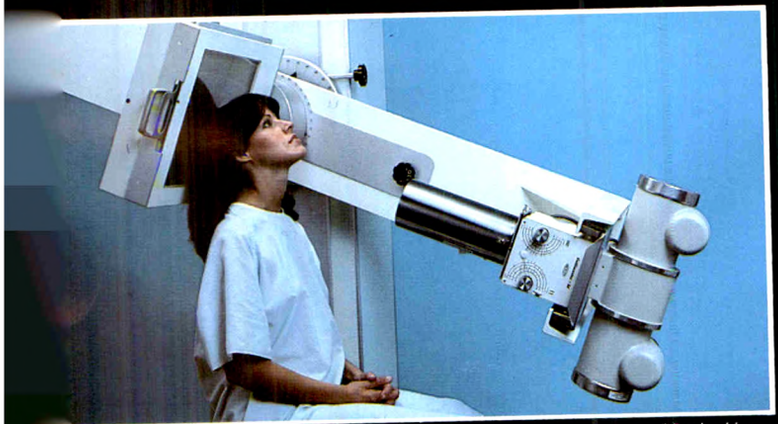
Full-view, see-through table has built-in centering lines for accurate patient positioning. Optional phototimer slides out of field when not in use.



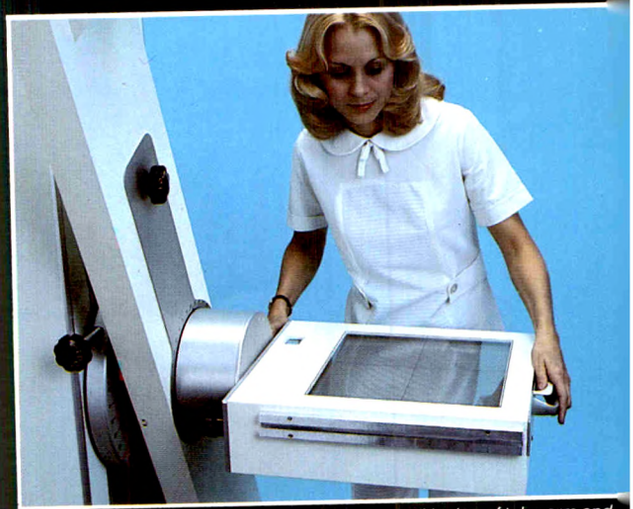
lide-away grid and cassette tray allow technologist a full, unobstructed view of patient.



Unobstructed work area and simple, conveniently-located controls provide fast, precise setup.



able and tube arm can be rotated independently or together; feature positive locking. ntricate setups are easy to handle and replicate.

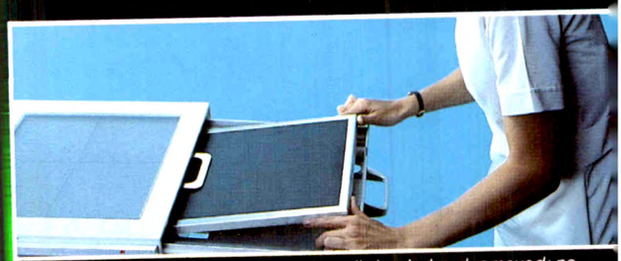


Large, easy-to-read scales and fast, fingertip positioning of tube arm and table make setups easy and precise.

Precise, reproducible radiography
Fast setup . . . easy operation
Versatile—fits large or small departments

he Katum Rx 40 is the contemporary response to the needs of very busy Radiology Department. Its versatility, efficiency and simplicity mean faster setups—reduced technologist t me. Its advanced design and easy, precise positioning mean high quality, replicable radiographs—fewer retakes. Its clean styling means less patient anxiety. It incorporates a fast (1/60 sec) bucky, 40-inch SID and removable grid and/or cassette tray. The Rx 40 is a system technologists love to use . . . produces quality that radiologists appreciate.

Call your X-ray supplier or write for details.



Unique, self-centering cassette tray is easily loaded and removed; no pinched fingers.

KATUM Longmont, Colorado 80501 • 303/772-2283
DIVISION OF
H.G. FISCHER, INC. 3816 N. Carnation Street, Franklin Park, Illinois 60131 • 312/671-5275

"Productivity is up 10% to 20%"

"Lower absenteeism"

"You can tell by their attitude—the workers who participate are happier, more cooperative, much sharper"

"We can identify direct savings of $2,000,000 per year"

"The program has had a distinct bearing on staff performance. Our engineering people now have a camaraderie with their counterparts in other departments"

"It started in headquarters. By next year we hope to have it in all our factories and research facilities"

These are actual quotes from executives of large and small companies and organizations in Denver, Omaha, Birmingham, and Greenwich. They're talking about company fitness programs. That's right, many employers now provide facilities or opportunities for exercise for their employees. They are glad they did.

Most began with a concern for employee health and well being. What they have found is a variety of additional benefits. These benefits add up to *increased productivity*—so much so that several companies can demonstrate that the fitness program pays for itself. Add to this improved morale, better internal communications, and employee health. How can you lose? Write us now for more information:

The President's Council on Physical Fitness and Sports
Department B
Washington, D.C. 20201

Employee Fitness: In the long run you will be the winner.

dedicated to progress . . .

The National Conference on Breast Cancer
18th Annual Conference on
Detection and Treatment

Atlanta, Georgia
March 5-8, 1979

The American College of Radiology
6900 Wisconsin Avenue, Chevy Chase, Maryland 20015
(301) 654-6900



Protect your patient's eyes from over-exposure and potential cataractogenic doses during special x-ray procedures

RADILENS® Eye Lens Shield

• *Lead-glass shield reduces eye lens dose approximately 90%**

Inadequate protection of a patient's eye lens during diagnostic x-ray exams in the cranial region can lead to cataracts or other eye damage. Therefore, the eyes should be covered with a Radilens Shield. Its cup-shaped, lead-glass lenses have x-ray absorption characteristics equivalent to 1 mm lead. Each lens is contoured to fit the outer eye orbits snugly and protect the eyes, even in the lateral projection. The lenses are held by a cord which stretches to fit any patient. Since the shields are transparent, the subject's pupils can be observed when necessary.

When the Radilens is used in carotid angiography in projections that do not obscure the vascular regions to be evaluated, such as in lateral and A-P. I projections, the dose rate to the eye lens is reduced to about 10%. The Radilens is also used widely to reduce radiation exposure during tomographic exams of the temporal bone.*

56-500CR Radilens Eye Lens Shield **$125.00**

VICTOREEN

NUCLEAR ASSOCIATES
Division of VICTOREEN, INC.
100 Voice Road • Carle Place, N.Y. 11514 • (516) 741-6360

**Copies of references and dosimetry data are available on request. Ask for Bulletin 144-C.*


MPX
120
500
400
125
90
00
GENERAL ELECTRIC
RPX Navigator



A classic breakthrough.

GE's new R&F system saves you time, space, money and dose. And gives you excellent images.

Here's a totally new R&F system that offers you many advantages over existing units—it's a major breakthrough in classical R&F. Let's take a closer look at each component.

Fluoricon® L300 suspensionless intensifier gives you 9" triple field performance, high frame rate photospot capability and improved imaging in a new lightweight package.

Diagnostic detail is exceptional—with advanced video camera technology and high resolution, high contrast ratio image tubes.

User-selectable dose rate and video gain let you add video gain for imaging obese patients, and provide the lowest dosage for young or thin patients.

When you choose the computerized technic management option at the spotfilmer, unique values of kVp, mA and focus are stored for each spotfilm and photospot procedure. Patient size selection includes pediatrics down to the neonate range.

And the new suspensionless design allows ample clearance for an overhead tube, facilitating radiography and attachment of an optional tomograph. The compact design fits into smaller, problem-sized rooms, giving you large room R&F capability.

RFX™ table and spotfilmer, with user-selectable grids, combines lower dose fluoro and high kVp spotfilms in one easy-to-use system.

The spotfilmer's unique, effort-sensing power assist simulates the feel of an unpowered fluoroscopic screen.

Two-per-second spotfilming with sequence anticipation allows two to four manually sequenced spotfilms without cassette return. Load from the front or rear, with pushbutton changeover.

Diagnostic advantages include automatic masking to format with full field, 2-on-1 vertical or transverse, or 4-on-1 formats. Masking is internal, allowing full field fluoro with the cone in place.

Additional RFX features include: (1) cone lockout for myelography; (2) automatic cassette return; (3) rapid access spotfilming (.75 sec.); (4) arthrographic collimation and ion chamber compensation for 9-on-1 or 6-on-1 formats; and (5) improved radiation protection at all routine angulations.

MPX computerized generator, with Quantamatic™ tx technic management, stores all of your department's standard radiographic settings.

The operator simply presses the appropriate anatomical selection buttons. The microprocessor instantly displays all technic parameters, including kVp, mA, mAs, time, focal spot size and AEC status. And the operator may raise or lower factors to suit special patient situations.

With over 200 programmed AEC and fixed-time technics (on or off the table) available, you can handle virtually every patient size. From infant to obese adult. And any body part, including extremities.

Quantamatic tx technic management gives you consistent, high-quality films. Throughput increases. Costly retakes due to technic error are virtually eliminated. And programmed constant load design extends tube life by optimizing tube loading.

You'd expect it from GE.

Contact your GE representative to get all the facts on this important R&F breakthrough. Fluoricon L300/RFX/MPX....it's a classic.

General Electric Medical System
Milwaukee, Toronto, Madrid

GENERAL ELECTRIC

HARVARD MEDICAL SCHOOL,
DEPARTMENT OF CONTINUING EDUCATION
AND DEPARTMENT OF RADIOLOGY,
MASSACHUSETTS GENERAL HOSPITAL

ANNOUNCE

ANGIOGRAPHY:

CURRENT METHODS AND BASIC PROBLEMS

A practical course on therapeutic applications of Angiography, including "hands on" workshops on transluminal angioplasty and transcatheter embolizations.

APRIL 19–21, 1979

AT THE PARKER HOUSE, BOSTON

Under the direction of

C.A. Athanasoulis, M.D. and
A.C. Waltman, M.D.

For information contact: Department of Continuing Education, Harvard Medical School, 25 Shattuck St., Boston, MA 02115

A Public Service of This Magazine
& The Advertising Council

Ad Council

Some-
body
needs
you.

Red Cross.
The Good
Neighbor.

Index to Advertisers

In Alphabetical Order

Agfa-Gevaert Rex, Inc.
American College of Radiology
AMRAD, a Raytheon Company
CGR Medical Corporation
Dunn Instruments, Inc.
Eastman Kodak Company
Elema-Schonander, Inc.
E-Z-EM Company
H. G. Fischer, Inc.
General Electric Company
Gordon Projectors
Harvard Medical School
Machlett Laboratories
C. V. Mosby Company
Nuclear Associates
Ortho Pharmaceuticals
Philips Medical Systems, Inc.
Picker Corporation
Precise Optics
Professional Book Service
Purdue Frederick Company
Pyne X-Ray Corporation
Radiologic Sciences, Inc.
Raven Press Publishers
Siemens Corporation
E. R. Squibb & Sons, Inc.
Toshiba Medical Systems
United States Air Force
University of Utah
Williams and Wilkins Company
Winthrop Laboratories

Journal of Computer Assisted Tomography

A RADIOLOGICAL JOURNAL DEDICATED TO THE BASIC AND CLINICAL ASPECTS OF TRANSMISSION AND EMISSION RECONSTRUCTIVE TOMOGRAPHY

Editor: Giovanni Di Chiro, M.D.
National Institutes of Health

CONTENTS

Volume 3 Number 1 February 1979

Functional Anatomy by Cranial Computed Tomography
Mokhtar Gado, Joseph Hanaway, and Robert Frank

The Use of Iodolipids in Hepatosplenic Computed Tomography
J. L. Lamarque, J. M. Bruel, R. Dondelinger, B. Vendrell, O. Pelissier, J. P. Rouanet, J. L. Michel, and P. Boulet

Development and Experimental Evaluation of a Contrast Medium for Computed Tomographic Examination of the Liver and Spleen
Michael Vermess, Dulal C. Chatterji, John L. Dopoman, George Grimes, and Richard H. Adamson

Computed Tomography of Calcified Liver Metastases
Michael E. Bernardino

An Analysis of the Spatial Distribution of Attenuation Values in Computed Tomographic Liver and Spleen Scans
R. T. Ritchings, B. R. Pullan, S. B. Lucas, R. A. Fawcitt, I. Isherwood, and A. I. Morris

Computed Tomography in the Evaluation of Abdominal Trauma
Edward M. Druy and Bruce E. Rubin

Computed Tomography of the Prostate
J. M. A. Van Engelshoven and Louis Kreel

Computed Tomography Reconstruction from Hollow Projections: An Application to *In Vivo* Evaluation of Artificial Hip Joints
Th. Hinderling, P. Rüegsegger, M. Anliker, and C. Dietschi

Computed Tomography in Bone and Soft Tissue Pathology of the Extremities
George Hermann and Judith S. Rose

Computed Tomography in Unilateral Extremity Swelling of Unusual Cause
E. Mark Levinsohn and Patrick J. Bryan

Two Methods for Calculating Regional Cerebral Blood Flow from Emission Computed Tomography of Inert Gas Concentrations
I. Kanno and N. A. Lassen

Optimal Processing of Computed Tomography Images Using Experimentally Measured Noise Properties
Robert E. Alvarez and J. Peter Stonestrom

Theoretical Resolution of Computed Tomography Systems
Gary H. Glover and Robert L. Eisner

Lissencephaly (Agyria) on Computed Tomography
Kousaku Ohno, Takao Enomoto, Jun Imamoto, Kenzo Takeshita, and Masataka Arima

Multiple Cystic Encephalomalacia of Infancy: Computed Tomographic Findings in Two Cases with Associated Intracerebral Calcification
Philip J. Dubois, E. Ralph Heinz, Henry B. Wessel, and Barbara W. Zaias

Posttraumatic Intracranial Meningiomas: Recognition by Computed Tomography in Three Cases
Denis Gardeur, Rachid Allal, Jean-Pierre Sichez, and Jean Metzger

Computed Tomography in a Primate Stroke Model Using Selective Balloon Catheter Arterial Occlusion
Paul H. Pevsner

CASE REPORTS

The Iron Rim Sign
Peter M. Som, Sureshchandra Patel, Hiroshi Nakagawa, and Paul J. Anderson

Diagnosis of Pick's Disease by Computed Tomography
Robert E. McGeachie, John O. Fleming, Leroy R. Sharer, and Roger A. Hyman

Preoperative Localization of a Parathyroid Adenoma Using Computed Tomography and Thyroid Scanning
Robert R. Shimshak, Gary J. Shoenrock, Howard P. Taekman, Paul Cianci, and Richard F. Chambers

Computer Assisted Tomographic Evaluation of a Ganglioneuroblastoma in an Adult
Eric J. Mannes, James W. Walsh, Joseph F. Simeone, and Susan L. Putnam

Renal Oncocytoma
J. Wejtowicz, A. Karwowski, J. Knokiewicz, and B. Lukaszewski

Extreme Hydronephrosis Versus Echinococcal Cyst of the Liver: Computed Tomography Evaluation
Pierre A. Schnyder and Georges Candardjis

TECHNICAL NOTES

Recognition of Head Motion During Cranial Computed Tomography
Isamu Mano and Masao Kaneko

Water Cylinder for Cerebral Computed Tomography of Premature Neonates
M. Banna, C. Porteous, and M. Molot

Optimal Computed Tomography Technique for Bone Evaluation
Ali Shirkhoda, R. Eugene Johnston, Edward V. Staab, and William H. McCartney

ABSTRACTS OF ARTICLES ON COMPUTED TOMOGRAPHY FROM NON-RADIOLOGICAL JOURNALS

SUBSCRIPTION ORDER FORM

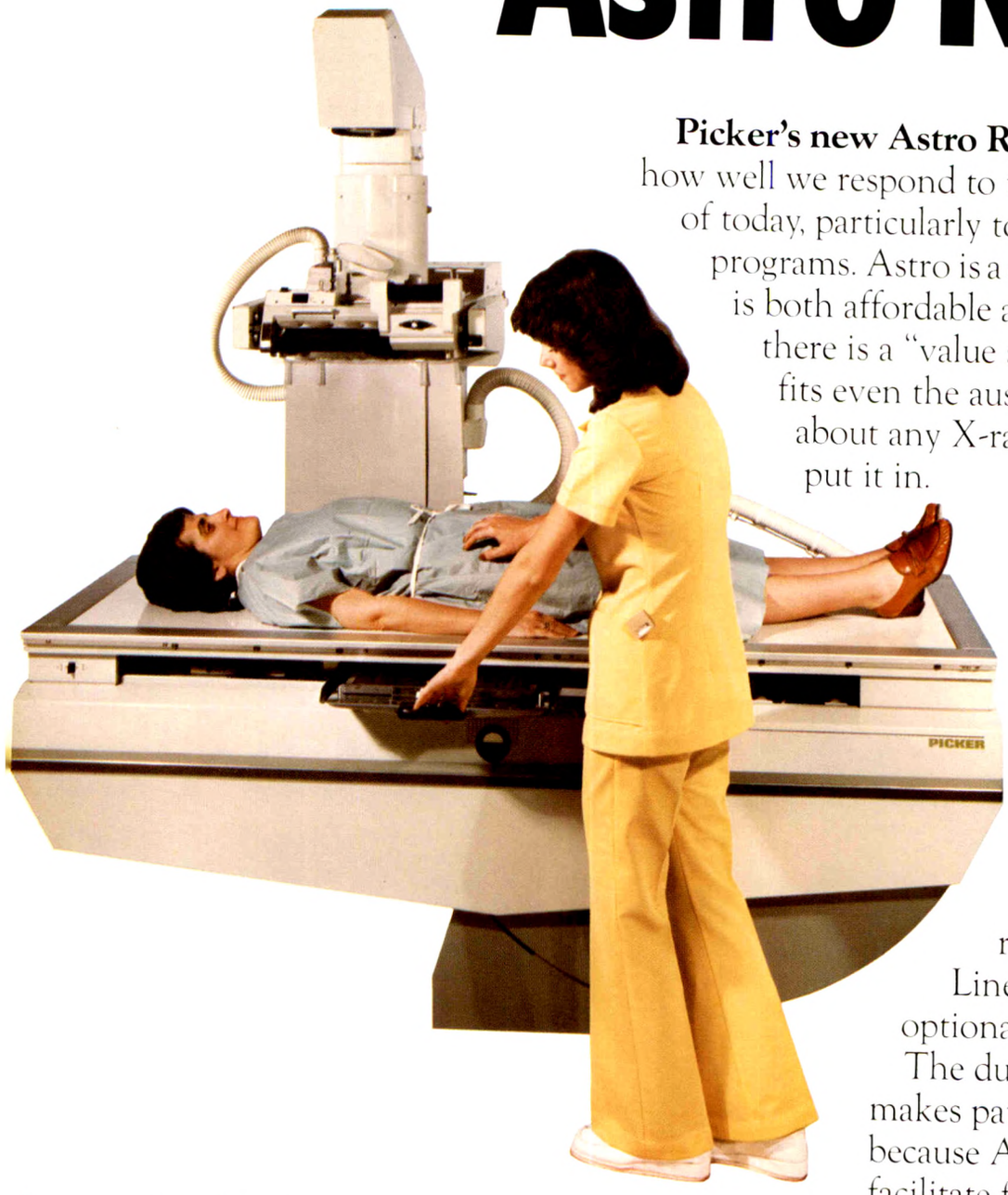
Please enter my subscription for Volume 3 (1979).
Published bimonthly.
Personal subscription rates: U.S. $68; Elsewhere $78.
Library and institutional rates: U.S. $78; Elsewhere $88.

I enclose payment by check □.
Name _____
Address _____
_____
_____

Make checks payable to Raven Press. JR

RAVEN PRESS /1140 AVENUE OF THE AMERICAS/NEW YORK CITY 10036

Astro R&F is



Picker's new Astro R&F system demonstrates how well we respond to the health-care needs of today, particularly to cost-containment programs. Astro is a quality R&F system that is both affordable and compact. So now there is a "value system" for R&F that fits even the austere budget—and just about any X-ray room you choose to put it in.

We built Astro to do the job in small hospitals and clinics without cutting corners on quality. This top-notch system has the necessary features to deliver quality R&F results including mammography and arthrography. Linear tomography is optional.

The durable Astro 102 table makes patient handling a snap because Astro is designed to facilitate fast operation. With a low-profile table for rapid throughput of both ambulatory and stretcher patients, Astro also features a two-way power top for positioning ease.

With Astro you can choose either a front or back-loading spotfilmer. Convenience features include: spotfilm automatic exposure control...longitudinal power assist of spotfilmer...and selections of up to nine exposure patterns on a 9½ x 9½" cassette. Human engineered operator controls are conveniently located for fast spotfilming.

We offer a choice of either Astrocon TV or Astroview mirror viewing. Both viewing systems are readily interchangeable. Either imaging system is integrally mounted for quick installation, and centers at 67 in. (1700 mm) above the floor for complete upper GI coverage of your taller patients.

just plain value.

Our 600 mA single-phase generator assures ample power for all your examinations. Also, you have the option of designating conventional or simple mAs technique selection.

A rigid counterpoised telescoping tubemount supports the radiographic tube, minimizing sag and vibration. For precise X-ray field centering and reduction of penumbra, Astro is equipped with Picker's automatic collimator.

Another feature is the "mini-centroid" concept—computer-prewired interconnecting cables to ensure a speedy, accurate installation.





An Astro system can normally be installed in a week's time. Because Astro uses 100% Picker made components, spare parts backup through our worldwide service organization assures you of continued operation.

The affordable Astro R&F—the value system. When you measure what you really need for R&F, it fits. Contact your local Picker representative or write Picker Corporation or Picker Internationa 595 Miner Road, Cleveland, OH 44143.

PICKER

ONE OF THE CIT COMPANIES

better

The 600 Beta Series Camera



Nice looking. The camera, we mean.

No need to pout. This camera won't let you make any careless mistakes, like forgetting to pull the dark slide.

Easy access. Takes the pain out of installation and service.

How do you name the heir to a classic?

We needed a way to tell the world that our new generation of 600 Series cameras was part of the original family of multi-format, video display cameras. But different. Totally redesigned for improved performance. But recognizably the same. So we picked the second letter of a classic alphabet – the Greek – and called it the Beta camera. It's second, but not second best. In fact, it's better.

Better than the camera that established the concept of multiple image hard copy on 8"×10" x-ray film? (And has the patent to prove it.) That has sold more units in this country and abroad than any of its numerous imitators? Hard to believe . . . hard to achieve. But true.

Better operating, for one thing. Single-handed front loading. Film cassette and dark slide interlocks that keep you from taking a picture when you shouldn't. Automatic Reset when a new film is loaded so you operate the camera almost without thinking.

We still offer the proven formats. And all the proven features, like flash card data entry, spot meter exposure system and footswitch remote operation. Our components will always be the finest available, including a new, high performance video monitor, Schneider lens and CMOS electronics.

This all pays off where it counts – in image quality. And when you see our images, you'll know for sure that Beta's not only better. It's best.

For more information, call collect or write: Dunn Instruments, Inc., 544 Second Street, San Francisco, CA 94107, (415) 957-1600

Dunn Instruments

The 600 Beta Series Camera



Single-handed front loading. Lets you install the Beta anywhere you like and load it on the run.

Ho hum. Simplified front panel controls make picture-taking a breeze

Where Beta's best – superb clinical images in any format, positive or negative.

American Journal of Roentgenology

Vol. 132 January 1979 No. 1

DIAGNOSTIC IMAGING

1 **Radiographic Manifestations of Burkitt's Lymphoma in American Patients.** *Dunnick NR, Reaman GH, Head GL, Shawker TH, Ziegler JL*

7 **Hepatocellular Carcinoma: Clinical and Angiographic Findings and Predictability for Surgical Resection.** *Marks WM, Jacobs RP, Goodman PC, Lim RC Jr*

13 **The Surgeon Looks at Recurrences After Unsuccessful Radiation Therapy.** *Jesse RH*

17 **Primary Mediastinal Seminoma.** *Polansky SM, Barwick KW, Ravin CE*

23 **Oat Cell Carcinoma Manifesting as a Bronchocele.** *Aronberg DJ, Sagel SS, Jost RG, Levitt RG*

27 **Antrochoanal Polyps.** *Towbin R, Dunbar JS, Bove K*

33 **Computed Tomography Diagnosis of Mesenteric Masses.** *Bernardino ME, Jing BS, Wallace S*

37 **Bilateral Concurrent Renal Neoplasms: Report of Eleven Cases.** *Stigsson L, Ekelund L, Karp W*

43 **Computed Tomography in Adrenal Tumors.** *Dunnick NR, Schaner EG, Doppman JL, Strott CA, Gill JR, Javadpour N*

47 **Ultrasonic Characteristics of Chronic Atrophic Pyelonephritis.** *Kay CJ, Rosenfield AT, Taylor KJW, Rosenberg MA*

51 **Persistent Gallbladder Opacification after Iopanoic Acid Cholecystography: Diagnostic Implications for Acalculous Cholecystitis.** *Banner MP, Bleshman MH, Speckman JM*

55 **Double Blind Comparison of Meglumine Iotroxate (Biliscopin), Meglumine Iodoxamate (Endobil), and Meglumine Ioglycamate (Biligram).** *Taenzer V, Volkhardt V*

59 **Significance of Intrapancreatic Gas Demonstrated by CT: A Review of Nine Cases.** *Mendez G Jr, Isikoff MB*

63 **Neonatal Intestinal Opacification Secondary to Transplacental Passage of Urographic Contrast Medium.** *Kelleher J, Feczko PJ, Radkowski MA, Griscom NT*

67 **Scintiangiographic Diagnosis of Acute Mesenteric Venous Thrombosis.** *Smith RW, Selby JB*

71 **Chronic Impairment of Leg Muscle Blood Flow Following Cardiac Catheterization in Childhood.** *Škovránek J, Šamánek M*

77 **Role of Radionuclide Imaging in Osteoid Osteoma.** *Lisbona R, Rosenthall L*

81 **"Step-off" Vertebral Body: Gaucher's Disease Versus Sickle Cell Hemoglobinopathy.** *Schwartz AM, Homer MJ, McCauley RGK*

87 **Gray Scale Ultrasonography in the Diagnosis of Endometriosis and Adenomyosis.** *Walsh JW, Taylor KJW, Rosenfield AT*

91 **Doppler Evaluation of Extracranial Cerebrovascular Disease.** *Crummy AB, Zwiebel WJ, Barriga P, Strother CM, Sackett JF, Turnipseed WD, Jarrett F, Berkoff H*

95 **A Second Look at the Utility of Radiographic Skull Examination for Trauma.** *DeSmet AA, Fryback DG, Thornbury JR*

101 **Preoperative Localization of Nonpalpable Breast Lesions.** *Hall FM, Frank HA*

CASE REPORTS

107 **Radiographic Findings in the Mucocutaneous Lymph Node Syndrome.** *Cook A, L'Heureux P*

110 **Bone Imaging of the Heel in Reiter's Syndrome.** *Khalkhali I, Stadalnik RC, Wiesner KB, Shapiro RF*

113 **"Sinking Pellet" Sign of Bladder Perforation.** *Conrad MR, Bazan C, Allen T, Schoenvogel R*

115 **Real Time Ultrasound in the Diagnosis of Acute Dissecting Aneurysm of the Abdominal Aorta.** *Conrad MR, Davis GM, Green CE, Curry TS III*

117 **Radioisotopic Diagnosis of False Left Ventricular Aneurysm.** *Perkins PJ*

120 **Nuclear Scan of Pulmonary Hemorrhage in Idiopathic Pulmonary Hemosiderosis.** *Miller T, Tanaka T*

122 **Myoblastoma of the Breast.** *Bassett LW, Cove HC*

124 **Isolated Dextrogastria: Report of Two Cases.** *Teplick JG, Wallner RJ, Levine AH, Haskin ME, Teplick SK*

127 **"Circumscribed" Glioblastoma Multiforme: the Role of Computed Tomography in Two Cases.** *Geehr RB, Dohrmann GJ, Rothman SLG*

130 **Agenesis of the Internal Carotid Artery with a Primitive Transsellar Communicating Artery.** *Janicki PC, Limbacher JP, Guinto FC Jr*

133 **Occult Bronchogenic Carcinoma Masquerading as Recurrent Pulmonary Embolism.** *Rosen RJ, Goodman LR*

136 **Ultrasound Demonstration of a Thyroid Carcinoma Within a Benign Cyst.** *Allen FH, Krook PM, deGroot WPH*

138 **Radiographic Presentation of Spinal Abscess in the Subdural Space.** *Patronas NJ, Marx WJ, Duda EE*

TECHNICAL NOTES

140 **Percutaneous Replacement of Biliary T Tubes.** *Millan VG, Bramhavar DM, Kwon OJ, Paul RE Jr*

142 **Audiovisual Problems at Scientific Meetings: An Appeal from the Conference Floor.** *Masterson JB*

146 **Editorial: The Old Order Changeth.** *Gagliardi RA*

149 **Memorial**

151 **Abstracts of Current Literature**

162 **Book Reviews**

167 **News**

Acc.
30.8.79

AJR

American
Journal of
Roentgenology

UNIVERSITY OF MEDICINE & DENTISTRY OF N.J.
LIBRARY

February 1979



Hysterosalpingogram with Salpix Contrast Medium.



24-hour postinjection x-ray of same patient.

now you see it

now you don't

With Salpix as your contrast medium, your gynecologic patient needn't undergo the 24-hour postinjection x-ray usually required with iodized oils. Water-soluble Salpix leaves virtually no irritating radiopaque residue to produce foreign-body reactions, yet it provides the viscosity needed for adequate visualization.

Contraindications: Contraindications to hysterosalpingography include the presence of severe vaginal or cervical infections, existing or recent pelvic infection, marked cervical erosion or endocervicitis, and pregnancy. The procedure is contraindicated during the immediate pre- or post-menstrual phase.

Sensitivity Test: If indicated in the patient's history, an intracutaneous skin test or sublingual absorption observation may be done with 0.1 cc Salpix.

Warning: Not for intravenous use.

© ORTHO PHARMACEUTICAL CORPORATION 1970

CONTRAST MEDIUM

Salpix

TRADEMARK

EACH CC CONTAINS:
sodium acetrizoate 0.53 g and
polyvinylpyrrolidone 0.23 g

Ortho

ORTHO PHARMACEUTICAL CORPORATION • RARITAN, NEW JERSEY 08869

Official Journal
American Roentgen Ray Society
American Radium Society

AJR

American Journal of Roentgenology

Diagnostic Imaging • Radiation Oncology
Related Sciences

Editor Melvin M. Figley

Associate Editor Rosalind H. Troupin

Assistant Editor John D. Harley

Contributing Editor E. Frederick Lang

Consulting Editorial Board Luther W. Brady • Kent Ellis
E. Robert Heitzman • Donald L. King • N. Thorne Griscom
Eugene C. Klatte • Kenneth Krabbenhoft • John G. McAfee
Russell H. Morgan • Thomas H. Newton • Robert G. Parker
Stewart R. Reuter • William B. Seaman • Robert J. Shalek
John Storer • Michel M. Ter-Pogossian • Joseph P. Whalen
David M. Witten

Editorial Staff K. A. Murray, manager • M. J. Leonard, manuscript editor • J. Anderson, assistant manuscript editor • A. C. Van Dyck, secretary

Published monthly by The Williams & Wilkins Co., 428 East Preston St., Baltimore, Maryland 21202. All correspondence, except editorial office business, should be addressed to the publisher. Annual subscription rates: $40 ($20 for residents with letter of verification) plus appropriate mailing surcharge (see note next page). Single copies, $5. Undelivered or damaged copies replaced within 60 days of publication; 90 days for foreign subscribers. Allow 90 days for address changes. © 1979 by American Roentgen Ray Society. Second-class postage paid at Baltimore, Maryland, and at additional mailing offices. Printed in U.S.A. ISSN 0361-803X



American Roentgen Ray Society

President: Harry Z. Mellins
President Elect: Paul A. Riemenschneider
1st Vice-president: Joseph D. Calhoun
2nd Vice-president: Charles E. Bickham, Jr.
Secretary: James F. Martin
Treasurer: Harley C. Carlson

COMMITTEES 1977–1978

Executive Council: H. Z. Mellins, P. A. Riemenschneider, J. D. Calhoun, C. E. Bickham, Jr., J. F. Martin, H. C. Carlson, M. M. Figley, R. G. Evens, B. G. Brogdon, R. A. Gagliardi, E. Gedgaudas, G. A. Kling, T. F. Leigh, S. F. Ochsner, J. F. Wiot, R. E. Buenger, E. C. Klatte, J. P. Tampas, J. L. Gwinn, chairman

Finance and Budget: A. E. James, E. C. Klatte, R. McLeeland, J. P. Tampas, R. G. Evens, chairman

Publications: M. P. Capp, K. Ellis, F. F. Ruzicka, Jr., E. R. Heitzman, R. A. Gagliardi, chairman

Editorial Policy: M. M. Figley, E. F. Lang, R. H. Troupin, E. R. Heitzman, K. Ellis, F. F. Ruzicka, Jr., M. P. Capp, R. A. Gagliardi, chairman

Advisory Committee on Education and Research: J. E. Youker, G. Wilson, G. W. Hartman, L. F. Rogers, E. Gedgaudas, chairman

Scientific Exhibits: T. C. Beneventano, G. Dodd, B. G. Brogdon, chairman

Constitution and Bylaws: J. H. Walker, W. M. Whitehouse, J. P. Tampas, chairman

American Board of Radiology Representatives: J. F. Roach, R. W. McConnell, S. W. Nelson

Program Committee: H. Z. Mellins, J. F. Martin, J. L. Gwinn, M. M. Figley, R. A. Gagliardi, B. G. Brogdon, E. Gedgaudas, G. A. Kling, P. Riemenschneider, chairman

Instruction Courses: E. Gedgaudas, director; G. W. Hartman, associate director

American College of Radiology Board of Chancellors Representative: W. B. Seaman

Annual Meeting: March 25–30, 1979, Sheraton Centre, Toronto, Canada

Scientific Program: P. A. Riemenschneider, president elect, Cottage Hospital, Santa Barbara, California 93105

Manager Annual Meeting: George A. Kling, Harper Hospital, Detroit, Michigan 48201

Membership: John L. Gwinn, 4650 Sunset Blvd., Los Angeles, California 90027

Business Office: Keith W. Gundlach, comptroller, American College of Radiology, 20 North Wacker Drive, Chicago, Illinois 60606

American Radium Society

President: Frederick W. George, III
President Elect: Alfred S. Ketcham
1st Vice-president: Julian P. Smith
2d Vice-president: Edwin M. Jacobs
Secretary: Norah duV. Tapley
Treasurer: Simon Kramer

COMMITTEES 1978–1979

Executive: A. S. Ketcham, J. P. Smith, E. M. Jacobs, N. duV. Tapley, S. Kramer, L. W. Brady, R. H. Jesse, F. W. George, F. Rutledge, chairman

Public Relations: V. Marcial, J. Vaeth, C. Honaker, ex-officio, and F. George, chairman

Publication: K. L. Krabbenhoft, D. Hussey, A. Raventos, I. Fix, L. W. Brady, chairman

Scientific Program: R. Parker, J. Durant, A. S. Ketcham, M. S. Mitchell, G. Murphy, F. Rutledge, M. Griem, W. E. Powers, M. Apuzzo, F. George, chairman

Local Arrangements: L. Davis, J. Vaeth, J. Nolan, R. McKenna, J. Slater, J. Stein, J. Scallon, S. Kramer, J. Helsper, chairman

Constitution and Bylaws: A. S. Glicksman, P. J. DiSaia, K. L. Krabbenhoft, chairman

Audiovisual: C. R. Bogardus, J. Helsper, R. Schweitzer, R. H. Jesse, C. Perez, J. Glassburn, A. M. Nisar Syed, R. Young, B. Herrington, F. George, chairman

American Board of Radiology Representatives: J. J. Stein, R. E. King, N. duV. Tapley

American College of Radiology Board of Chancellors Representative: L. W. Brady

American College of Radiology Council Representative: J. del Regato

Editorial Board of AFCOS Newsletter Representative: J. Vaeth

National Council on Radiation Protection and Measurements Liaison Representative: L. W. Davis

Annual Meeting: March 4–8, Los Angeles, California

Scientific Program: F. W. George, III, University of Southern California School of Medicine, Los Angeles, California 90033

Local Arrangements: James Helsper, Pasadena, California

Membership: Norah duV. Tapley, secretary, M. D. Anderson Hospital, 6723 Bertner Avenue, Houston, Texas 77030

Business Office: N. V. Jordan, c/o R. H. Jesse, M. D. Anderson Hospital and Tumor Institute, 6723 Bertner Avenue, Houston, Texas 77030

Mailing note.—Mailing surcharges: U.S. and possessions, none; European countries, $25; Japan, $45; other, $10. European rates apply to Algeria, Austria, Belgium, Czechoslovakia, Denmark, Finland, France, Germany, Great Britain, Greece, Hungary, India, Iran, Ireland, Israel, Italy, Kenya, Luxembourg, Netherlands, Nigeria, Norway, Portugal, Romania, South Africa, Spain, Sweden, Switzerland, Turkey, Uganda, Yugoslavia. All subscriptions to Japan and European countries are delivered by air freight; there is no option for surface mail.



Revitalize Your Tired R-F Equipment.

Add a Machlett Cesium Iodide Image Intensifying System

- **IRIS 100** TV Viewing & 100mm Spotfilming
- **DYNAVISION** TV Viewing
- **DYNAVIEW** Optical Viewing

Superior performance at the right price. Ask your x-ray dealer for complete information or contact:

MACHLETT

Machlett Laboratories, Incorporated
1063 Hope Street
Stamford, Connecticut 06907
(203) 348-7511

A Raytheon Company



KODAK FILM: CONSISTENCY MAKES IT A LOGICAL CHOICE.

TURNING ENERGY INTO IMAGES

COMPUTED TOMOGRAPHY • NUCLEAR MEDICINE
ULTRASOUND • RADIOGRAPHY • THERMOGRAPHY

clear, clean colon

X-Prep® Liquid

(standardized extract of senna fruit)

versatile bowel evacuant for diagnostic procedures



Versatile in indications

May be used prior to:

G.I. radiography
Urologic radiography
Colonoscopy
Sigmoidoscopy
Other diagnostic bowel procedures

Versatile in administration

May be used:

Alone, in a single dose
Alone, in divided doses, particularly in elderly or debilitated patients
With adjunctive use of citrate of magnesia, laxative suppositories and enemas, as required
As part of other regimens, such as hydration

X-PREP Liquid is formulated specifically for effective bowel evacuation prior to diagnostic procedures. It induces peristalsis through virtually colon-specific action. X-PREP Liquid has been found effective in cleansing the colon for diagnostic evaluation in 95% of 749 patients prepared for barium enemas, intravenous pyelography, or colonoscopy.* Its pleasant taste meets with high patient acceptance, and its ease of administration is appreciated by the patient and nursing staff.

Supplied: X-PREP Liquid (standardized extract of senna fruit) in 2½ fl. oz. bottles (alcohol 7% by volume). X-PREP Powder (standardized senna concentrate) in ¾ oz. containers. **Now Available:** X-PREP™ Bowel Evacuant Kit. Each kit contains: two SENOKOT® S Tablets (standardize senna concentrate and dioctyl sodium sulfosuccinate), one bottle of X-PREP® Liquid 2½ fl. oz., and one RECTOLAX™ Suppository (bisacodyl 10 mg), plus easy-to-follow patient instructions for hydration, clear liquid diet, and the correct time sequence of administering the above laxatives.

* Bibliography available upon reques

Colonoscope, courtesy of Olympus

Gray Pharmaceutical Co., Affiliate
The Purdue Frederick Company

© Copyright 1978, Gray Pharmaceutical Co. Norwalk, CT 06856

A9047 194578

better

The 600 Beta Series Camera



Nice looking. The camera, we mean.

No need to pout. This camera won't let you make any careless mistakes, like forgetting to pull the dark slide.

Easy access. Takes the pain out of installation and service.

How do you name the heir to a classic?

We needed a way to tell the world that our new generation of 600 Series cameras was part of the original family of multi-format, video display cameras. But different. Totally redesigned for improved performance. But recognizably the same. So we picked the second letter of a classic alphabet – the Greek – and called it the Beta camera. It's second, but not second best. In fact, it's better.

Better than the camera that established the concept of multiple image hard copy on 8"×10" x-ray film? (And has the patent to prove it.) That has sold more units in this country and abroad than any of its numerous imitators? Hard to believe . . . hard to achieve. But true.

Better operating, for one thing. Single-handed front loading. Film cassette and dark slide interlocks that keep you from taking a picture when you shouldn't. Automatic Reset when a new film is loaded so you operate the camera almost without thinking.

We still offer the proven formats. And all the proven features, like flash card data entry, spot meter exposure system and footswitch remote operation. Our components will always be the finest available, including a new, high performance video monitor, Schneider lens and CMOS electronics.

This all pays off where it counts – in image quality. And when you see our images, you'll know for sure that Beta's not only better. It's best.

For more information, call collect or write: Dunn Instruments, Inc., 544 Second Street, San Francisco, CA 94107, (415) 957-1600

Dunn Instruments

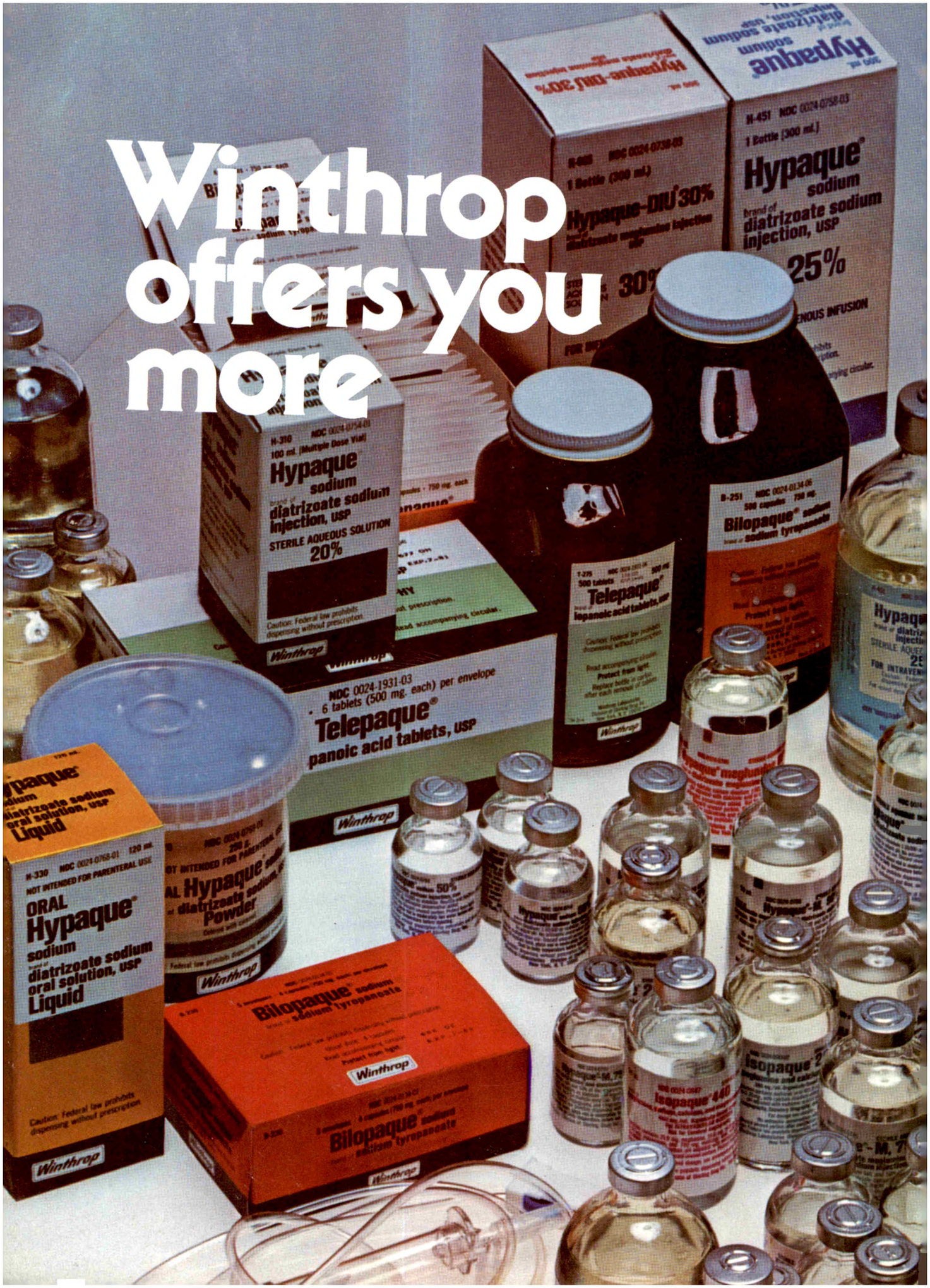
The 600 Beta Series Camera



Single-handed front loading. Lets you install the Beta anywhere you like and load it on the run.

Ho hum. Simplified front panel controls make picture-taking a breeze.

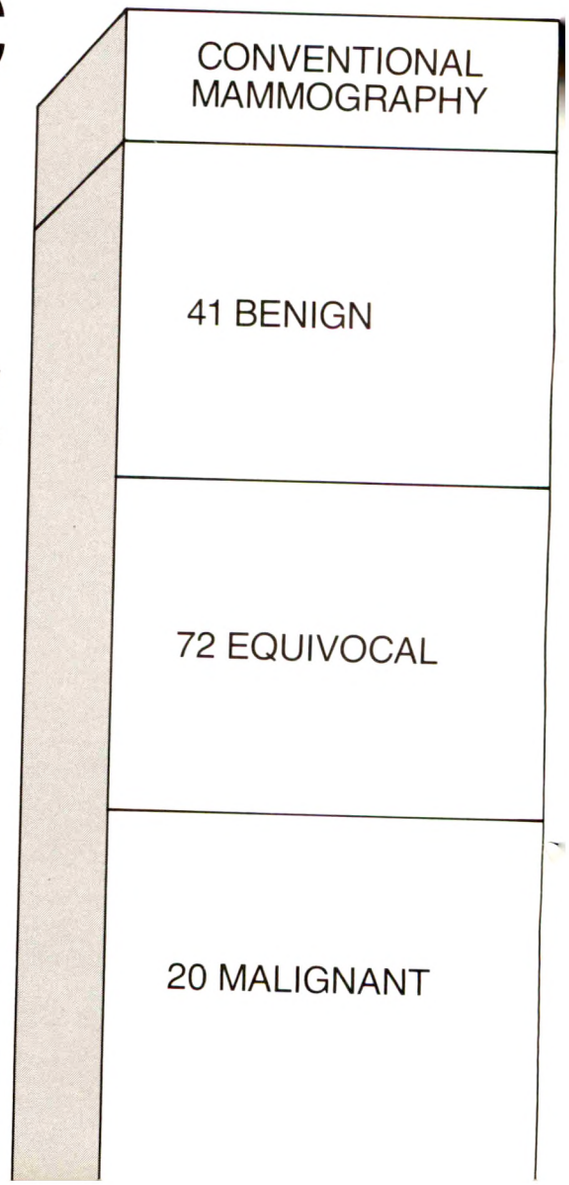
Where Beta's best – superb clinical images in any format, positive or negative.


Winthrop offers you more
Hypaque sodium
diatrizoate sodium injection, USP
25%
Hypaque-DIU 30%
Hypaque sodium
diatrizoate sodium injection, USP
STERILE AQUEOUS SOLUTION
20%
Telepaque
panoic acid tablets, USP
Bilopaque sodium
sodium tyropanoate
ORAL Hypaque sodium
diatrizoate sodium oral solution, USP
Liquid
Caution: Federal law prohibits dispensing without prescription.
Winthrop


Winthrop
Hypaque-Cyste
30%
Hypaque-DIU 30%
Hypaque-M 75%
H-341
10 vials
NDC 0024-0786-02
50 ml.
Hypaque® meglumine 60%
H-581
10 vials
NDC 0024-0746-02
50 ml.
Hypaque® sodium 50%
H-361
10 vials
NDC 0024-0766-02
50 ml.
STERILE AQUEOUS INJECTION
...the originators
Winthrop Laboratories, New York, NY 10016
4040

A New Study Confirms...

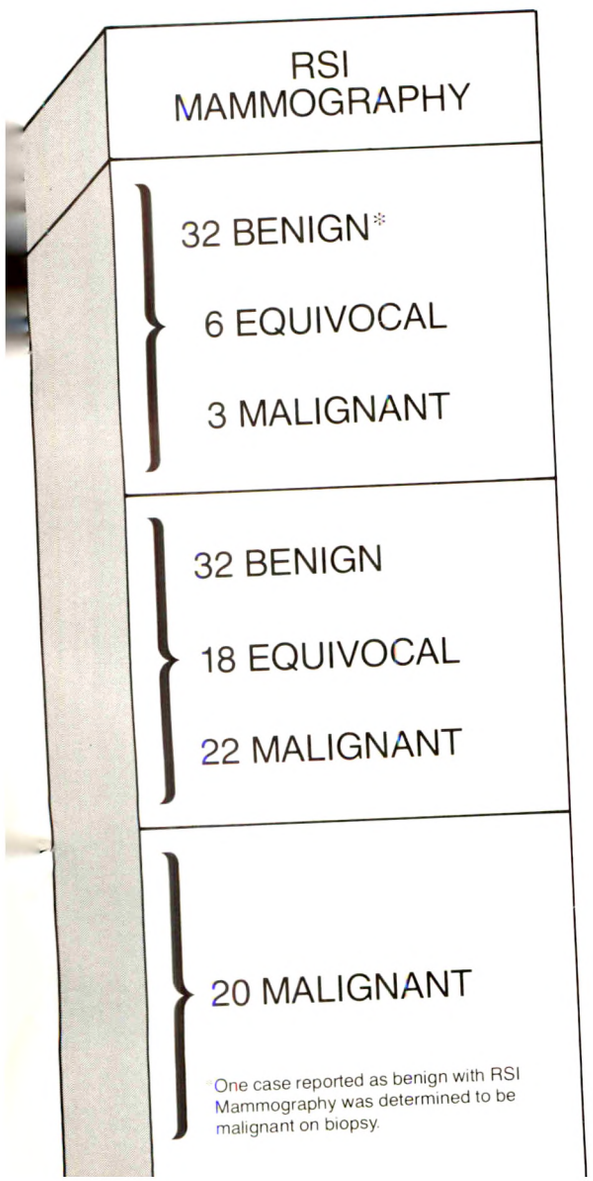
THE RSI MAMMOGRAPHIC SYSTEM **INCREASES DIAGNOSTIC ACCURACY**



Take a good look at the chart. You'll see the remarkable results of a study published by Dr. Edward A. Sickles, making a clinical comparison of 133 patients who received both conventional mammography and RSI Magnification Mammography. The results were confirmed with pathological diagnosis.*

This new study confirms just how accurate RSI Mammography really is. In fact, Dr. Sickles wrote in 1977, that magnification mammograms are "...clearly superior both quantitatively and qualitatively to conventional contact mammograms."[1]

Diagnostic Accuracy in Mammographic Examinations[2]
Clinical Data of Edward A. Sickles, M.D.
Assistant Professor of Radiology, University of California, San Francisco
Clinical Comparison of 133 Cases



Out of 41 cases diagnosed as benign with conventional mammography, RSI Mammography determined that 3 of these cases were, in fact, malignant. In addition, with conventional mammography alone, 72 cases were diagnosed as equivocal and direct magnification mammography (RSI System) was able to differentiate these as: 22 malignant, 32 benign, and only 18 remained equivocal. This revealing clinical comparison clearly shows that RSI Magnification Mammography increases the certainty in diagnosis, decreases the time between examination and confirmation, and may even reduce the need for biopsy.

In a radiologic symposium presented in New York City, Dr. Sickles remarked, "...in dealing with difficult cases, we considerably improved our diagnostic accuracy [with RSI Magnification Mammography]."[2]

These more accurate diagnoses are the direct result of the capability of the RSI Mammography's System to give you—

- Clearer definition of mass borders
- Improved image sharpness and resolution
- Resolution of malignant microcalcifications often not discernible by conventional mammography
- Delineation of trabecular patterns

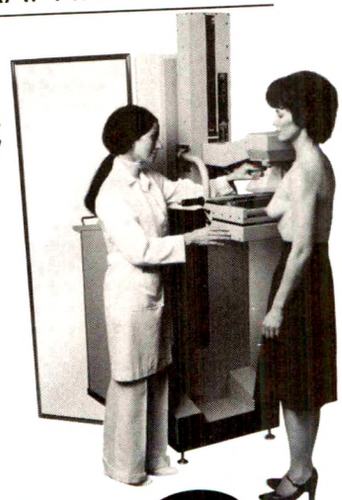
The RSI Mammography System offers high-detail resolution in the magnification mode as well as the conventional contact mode. The superior image which results from the exceptionally uniform focal spot provides a new level of confidence in the detection of breast cancer.

For more detailed information on the RSI Mammographic System and a reprint of the study published by Sickles *et al* in 1977, please write or call, Radiologic Sciences Inc., a subsidiary of Pfizer Inc., 235 East 42nd St., New York, N.Y. 10017 (212) 573-7941.

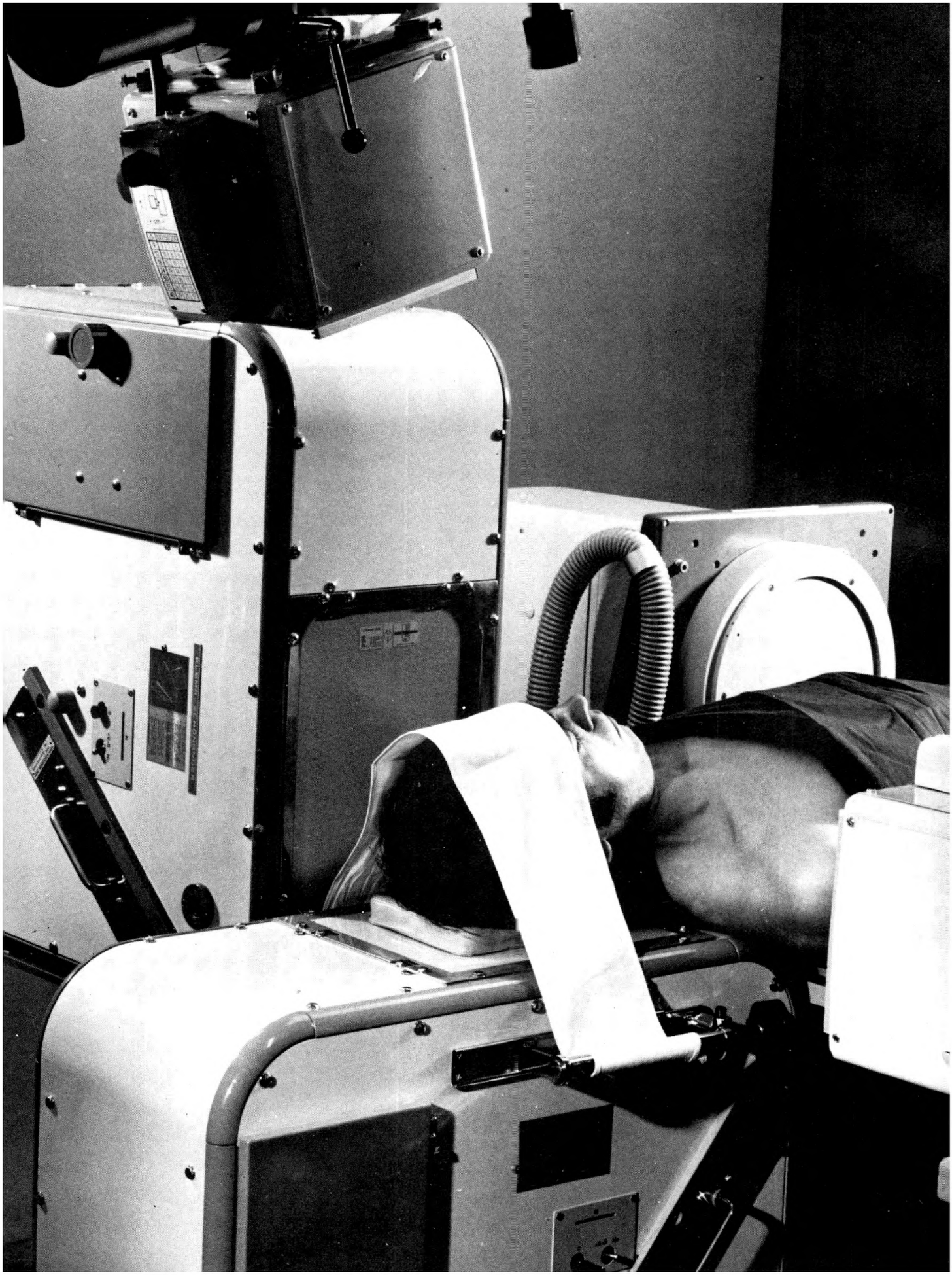
References: 1. Sickles, E.A.; Doi, K.; Genant, H.K.: *Radiology* 125:69-76, October 1977. **2.** Sickles, E.A.: *Microfocal Spot Magnification Mammography.* Presented at a Symposium, New York City, June 1, 1978.

THE RSI MAMMOGRAPHIC SYSTEM

INCREASES DIAGNOSTIC ACCURACY



RADIOLOGIC SCIENCES INC. Pfizer
A subsidiary of Pfizer Inc., New York, N.Y. 10017

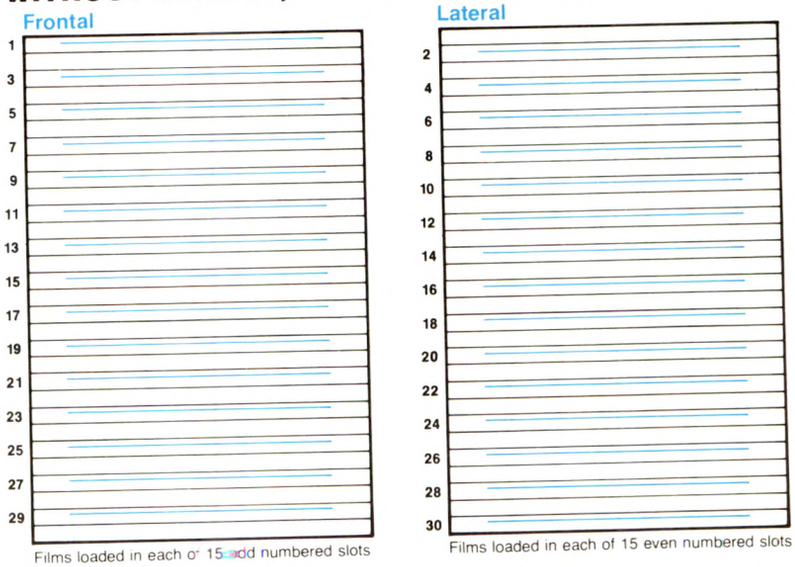


Eliminate cross-fogging*, simplify Alternate Biplane Angiography with the new LOAD-30

LOW FOG ALTERNATING DEVICE for AOT® CHANGERS.

- No cross-fogging of film (as with simultaneous biplane angiography).
- No film waste (as with roll-film changers).
- No skip-loading.
- Operates automatically when alternating mode is selected.
- 30 exposures at 3 exp/sec in each plane with ample exposure time for each exposure.
- Available for new and most existing AOT Film Changers.
- Eliminates loading errors and saves darkroom time.

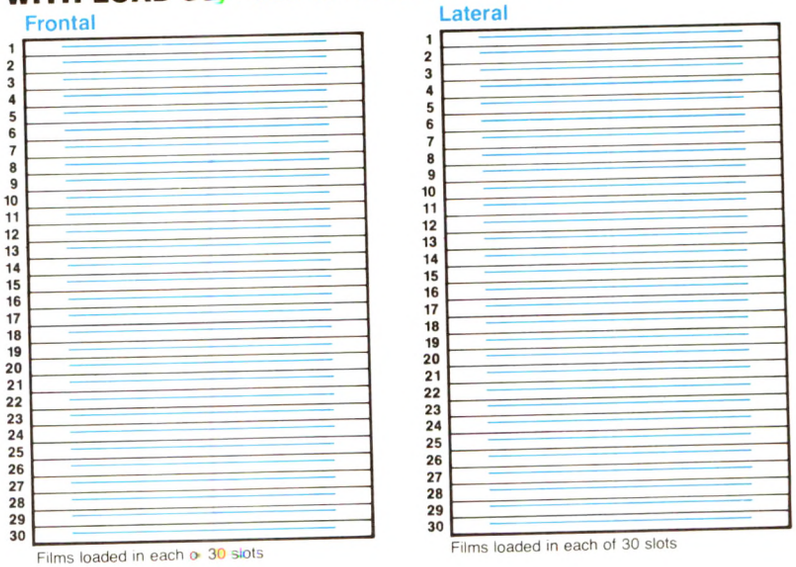
WITHOUT LOAD-30, SKIP-LOADING REQUIRED



Films loaded in each of 15 odd numbered slots

Films loaded in each of 15 even numbered slots

WITH LOAD-30, FULL CAPACITY LOADING



Films loaded in each of 30 slots

Films loaded in each of 30 slots

The above diagrams are schematic representations of the AOT magazines for illustrative purposes only.

For more information on the LOAD-30 Low Fog Alternating Device for AOT Film Changers, call or write:
Elema-Schonander, Inc., 699 Lively Blvd.
Elk Grove Village, Illinois 60007
(312) 593-6770

*"Cross-fogging" is a term commonly used to describe the increased film fogging which occurs in simultaneous biplane angiography due to the fact that the film in each plane is hit by scattered radiation from two exposures.

elema·schönander

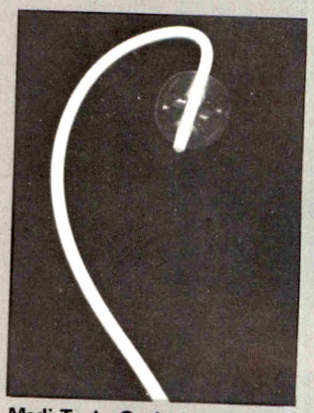
PROBLEM: Reflux and Migration of Embolic Agents

SOLUTION: MEDI-TECH Occlusion Balloon Catheters

REF: Greenfield, A.J.; Transcatheter Embolization: Complications and Prevention With Balloon Catheters. PROGRAM OF THE AMERICAN ROENTGEN RAY SOCIETY: Seventy-eighth Annual Meeting, September 26-30, 1977, Boston, Mass.



Arteriogram performed with balloon inflated prior to embolization



Medi-Tech Occlusion Balloon Catheter OB/7/2/65 (also used in X-Ray at left)

When carrying out therapeutic embolization, the risk that embolic agents will be carried to non-intended locations should be considered.

REF: Woodside, J.; Schwarz, H.; Bergreen, P.: Peripheral Embolization Complicating Bilateral Renal Infarction With Gelfoam. American Journal of Roentgenology: Vol. 126: 1033-1034, 1976.

Gang, D.L.; Dole, K.R.; Adelman, L.S.: Spinal Cord Infarction Following Therapeutic Renal Artery Embolization. JAMA: VOL. 237, No. 26, June, 1977.

Bradley, E.L.; Goldman, M.L.: Gastric Infarction After Therapeutic Embolization. SURGERY: Vol. 79, No. 4, April, 1976.

With the development of the MEDI-TECH Occlusion Balloon Catheters this risk has been significantly reduced.

MEDI-TECH offers the only balloon catheter available today with a polyethylene catheter body. Unlike polyvinyl chloride (PVC) which softens at body temperature, polyethylene retains its torque and holds pre-set curves. This enables selective placement of the balloon either with or against the blood flow.

The smooth tip profile and large I.D. (.038" in the 7F) allow percutaneous introduction by Seldinger Technique over a .035" guide wire.

(For more information fill out the coupon below and mail, or call Toll Free 800-225-3238).
In Massachusetts 617-923-1720.

CATHETERS AVAILABLE

Catalog Number	French	Lumens	Balloon Dia. (mm)	Tip I.D. (.000")	Usable Length (cm)
OB/7/2/65	7	2	12	38	65
OB/7/2/100	7	2	12	38	100
OB/5/2/65	5	2	8.5	27	65
OB/5/2/100	5	2	8.5	27	100

MEDI-TECH
Div. of Cooper Scientific Corporation
372 Main Street • Watertown, Massachusetts 02172

☐ I'd like more information sent
☐ I'd like a representative to call

Name _____ Dept. _____
Hosp. _____
Address _____
City _____ State _____ Zip _____
Phone _____ ( ) Area Code

THIS BOOK TELLS A LOT ABOUT US ...WITHOUT ONCE MENTIONING OUR NAME

OR OUR PRODUCTS

The name of this volume is *Certificate of Need: An Expanding Regulatory Concept.* Not once in its 944 pages does the name Pfizer appear.

Yet, despite this, we are proud to offer this book to several hundred people in the health care field, with our compliments, as part of an important, new Pfizer program called the Certificate of Need Assistance Program.

A Total C.O.N. Assistance Program

Pfizer's C.O.N. Assistance Program is designed to aid you in the increasingly regulated climate in which medicine now operates. As one of the health care industry's leaders for 129 years, Pfizer feels a responsibility not only to provide quality products but also to join the medical community in its current search for effective ways to comply with these regulations. Typical of these requirements is the Certificate of Need, or C.O.N., which is required in most cases where federal funding is involved in paying for major equipment or plant expansion.

Toll-free C.O.N. Assistance Service

Applying for the C.O.N. can be a complicated process—sometimes confusing, always time-consuming. The Pfizer C.O.N. Assistance Program can help. The two main components of this program are the book, *Certificate of Need: An Expanding Regulatory Concept,* and the toll-free C.O.N. Telephone Service to answer questions about the cost effectiveness of diagnostic equipment, as well as how this information relates to C.O.N. requirements.

To use our C.O.N. Telephone Service just phone 800-221-4688, from 9 a.m.-5 p.m. Monday through Friday. (In New York State, please call 212-573-2030, collect.)

Complimentary Books to Administrators and Radiologists

Many hospital administrators have already received copies of the book. We have also offered it to chief radiologists throughout the country and to certain other medical and administrative personnel who are involved in the purchase of diagnostic equipment.

(Incidentally, if you have not personally received *Certificate of Need: An Expanding Regulatory Concept,* and you take part in major purchasing as a hospital executive or radiologist, you are welcome to a complimentary copy. To receive it, just send us your request on your official letterhead.)

The book, as its title suggests, is a comprehensive, state-by-state compilation of current C.O.N. requirements. We feel that it makes a substantial contribution to understanding this very complex subject. And it is a subject in which we feel a special responsibility, since CT Scanners usually require this document.

Full Range of Pfizer Radiological Services

Now that we have told you how we're making it easier for you to meet the regulatory requirements for buying diagnostic equipment, we'd like to tell you why you should want to.

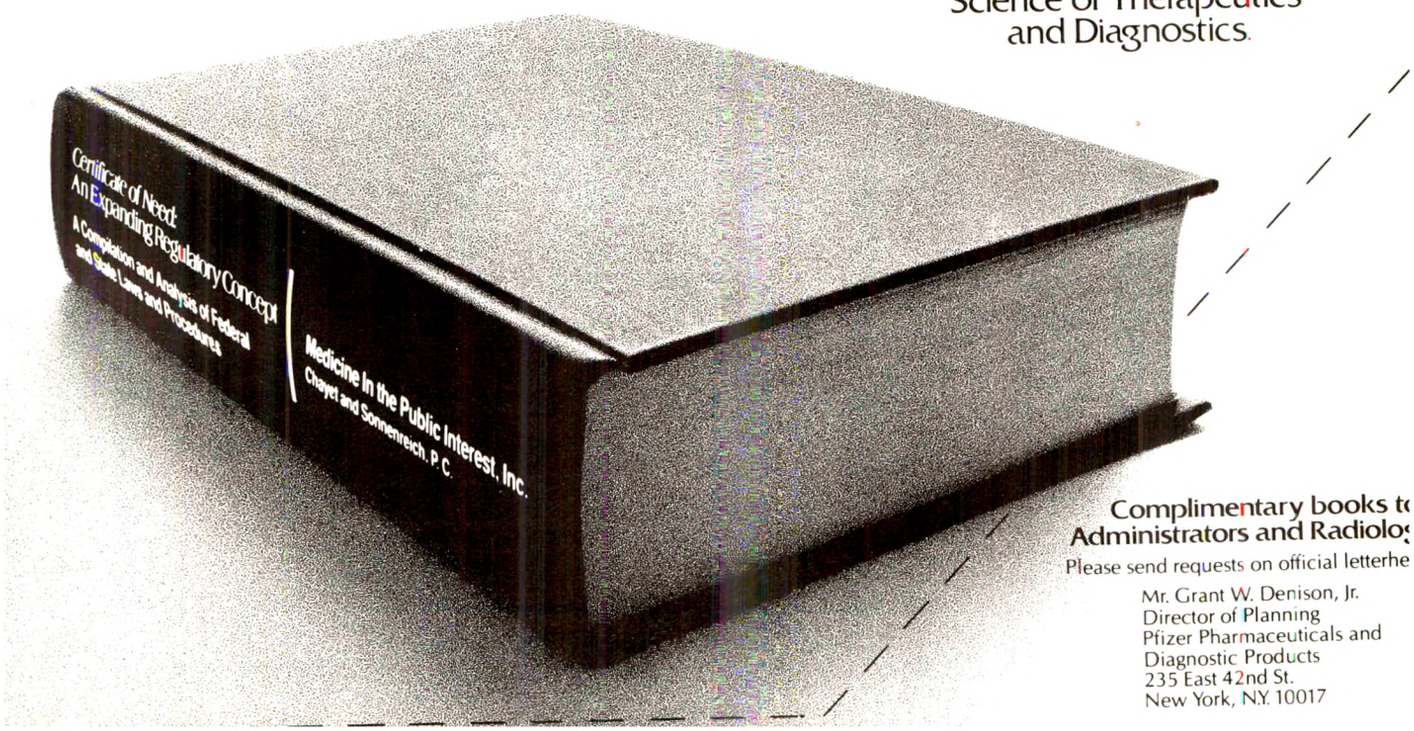
There's an expert specially qualified to do just that: the Pfizer Medical Systems or Radiologic Sciences Technical Representative.

He'll give you useful, specific information on the one subject that isn't included in the C.O.N. Assistance Program.

Our Products.

Pfizer Inc.
235 East 42nd St.
New York, N.Y. 10017

Advancing the Science of Therapeutics and Diagnostics.



Complimentary books to Administrators and Radiolog

Please send requests on official letterhe

Mr. Grant W. Denison, Jr.
Director of Planning
Pfizer Pharmaceuticals and Diagnostic Products
235 East 42nd St.
New York, N.Y. 10017



PYNE X-RAY CORPORATION

Proudly Announces

FUJI FILM

RX-M

Developed for use with multi-format imaging systems designed for CT Scanners, Nuclear Diagnostic Equipment, or Ultrasonic Diagnostic Equipment.

An orthochromatic, single-emulsion film, Fuji RX-M is also excellent for mammography, as it offers high speed plus superior contrast and resolution.

RX-M is available for immediate delivery. Please contact your nearest Pyne X-Ray office or your local authorized Fuji Film dealer.

PYNE X-RAY CORPORATION

Distributed throughout the U.S. by:

NEW YORK
20 North Avenue
Larchmont, New York 10538
(914) 834-4567

CHICAGO
1211 West Norwood Avenue
Itasca, Illinois 60143
(312) 773-3360

LOS ANGELES
1639 Gardena Avenue
Glendale, California 91204
(213) 240-0280

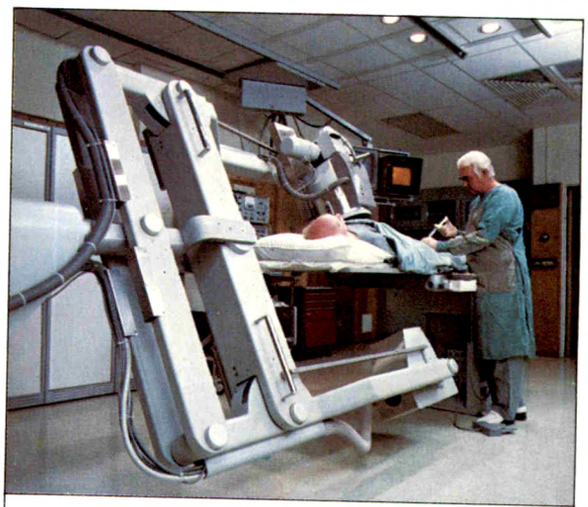
Philips Angiography Systems.

TOTAL BODY COVERAGE WITH THE BROADEST RANGE OF EQUIPMENT

. . . from the only company offering all the choices you need!



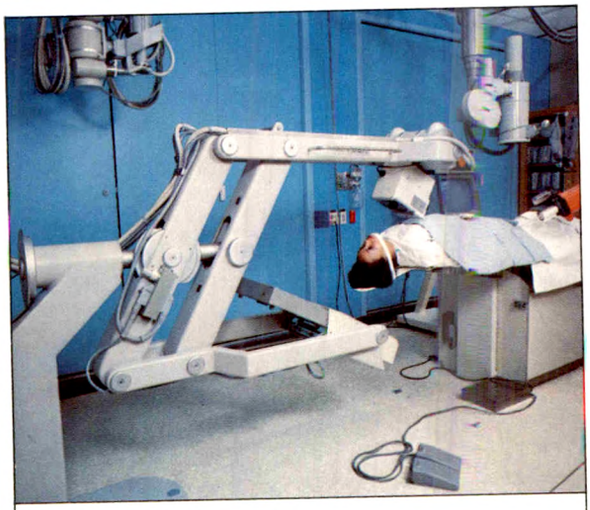
Poly Diagnost C



The parallelogram construction of the Poly Diagnost C permits the patient to remain stationary, leaving the physician more relaxed and able to concentrate fully on the procedure. Insuring maximum safety for both patient and operator, the Poly C provides both routine and cranio-caudal views that insure clear, unobstructed views of overlapping vessels. Stenoses which might have been obscured can be detected with a high degree of efficiency and operational ease.

Designed for both the brachial and femoral techniques of cardiac angiography, the Poly C is also successfully used in abdominal and thoracic studies.

Poly Diagnost N

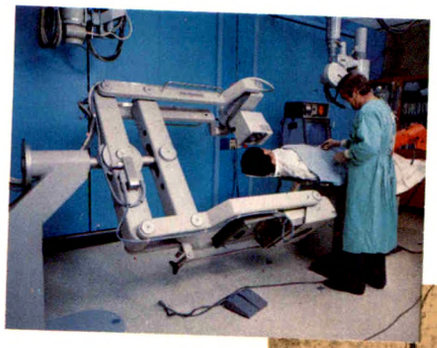


Designed specifically for cerebral angiography at 2:1 magnification, the Poly Diagnost N easily provides views of the patient previously difficult (or impossible) to achieve. The parallelogram construction allows full rotation around the long axis of the body *and* the maximum desirable head-to-foot angulation. The unique construction insures all motions are isocentric and all results are distortion free.

Designed for use in single or bi-plane operation with a Puck rapid film changer, the Poly N lends itself to extensions for more dedicated requirements, such as the latest configuration with a quickly interchangeable image intensifier and a rapid film changer.

PHILIPS MEDICAL SYSTEMS, INC.
710 Bridgeport Avenue, Shelton, Conn. 06484

Philips Angiography Systems.



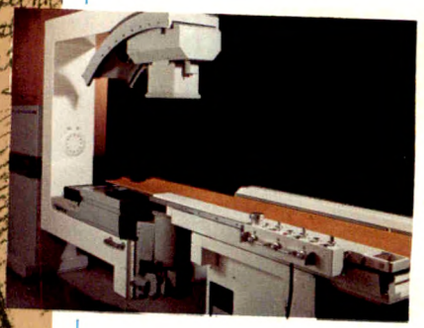
Poly Diagnost N

The first in Philips' family of dedicated cerebral angiography systems with parallelogram construction. For optimum results with isocentric patient positioning for all projections.



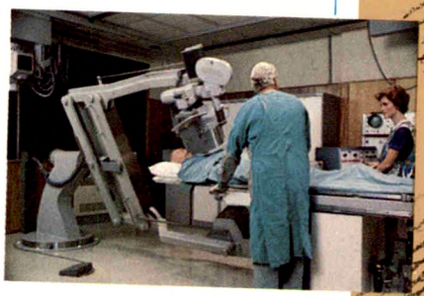
Poly Diagnost UPI

Philips' new universal angiography system for the most flexible filming of cerebral, thoracic, abdominal and peripheral angiography, with full provision for occasional cardiovascular examinations.

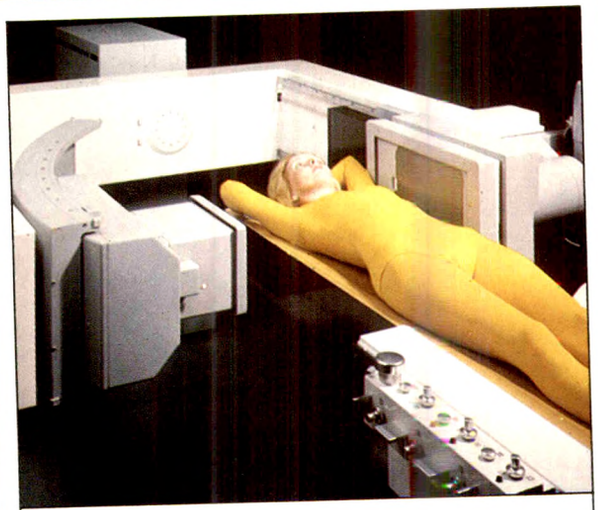


Poly Diagnost C

An extension of the U-arm principle first developed by Philips in the Cardio Diagnost, the Poly C is a dedicated cardiovascular system. Parallelogram construction provides routine and cranio-caudal views without moving the patient, making the Poly C widely used for imaging the thoracic and abdominal areas.



Poly Diagnost UPI



A universal system with revolutionary design, the Poly Diagnost UPI features a rotating U-arm that carries the X-ray tube and an image intensifier and rapid film changer which are quickly interchangeable.

A new experience in examination convenience, the Poly UPI is a masterful combination of system features: free choice of oblique, cranio-caudal and caudo-cranio projections; rapid changeover from fluoroscopy to film changer work; automatic control of object-film distance; motorized height adjustment of both table and U-arm, which provides contact and up to 2:1 geometric enlargement; and a unique boating movement that keeps the object centered in the beam while the object-film distance is automatically controlled in every projection. It's the ideal universal system for angiography!

PHILIPS®

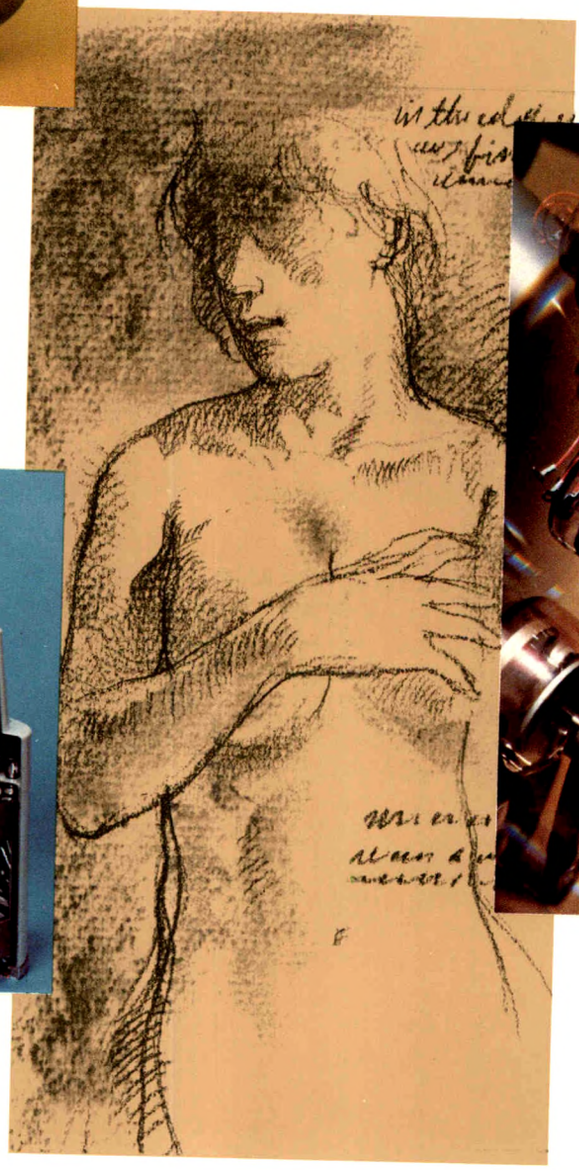
® TM N.V. Philips of Holland

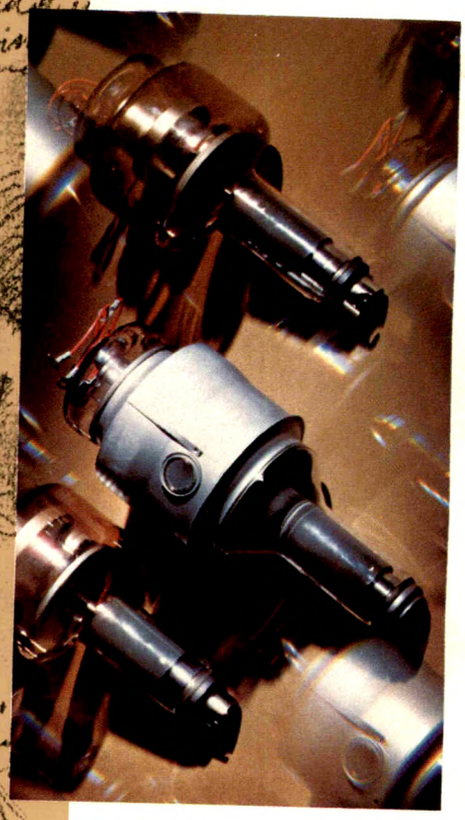
A COMPLETE FAMILY OF IMAGE INTENSIFICATION SYSTEMS, X-RAY TUBES AND GENERATORS FOR PHILIPS ANGIOGRAPHIC EQUIPMENT.

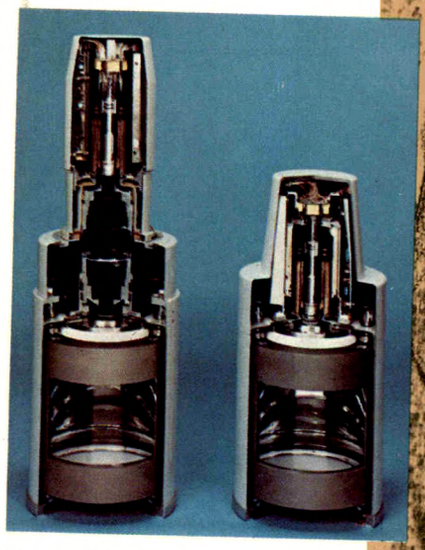


The 14″ Triple-Mode Image Intensifier
Another first from Philips! An amazingly lightweight 14″ image intensifier for highly detailed surveys with outstanding results.

Super Rotalix and Trinodex X-ray Tubes
Preferred for exceptional image quality and reliable performance in sustained operation, Philips' tubes are designed for high loadability and superbly efficient heat dissipation.



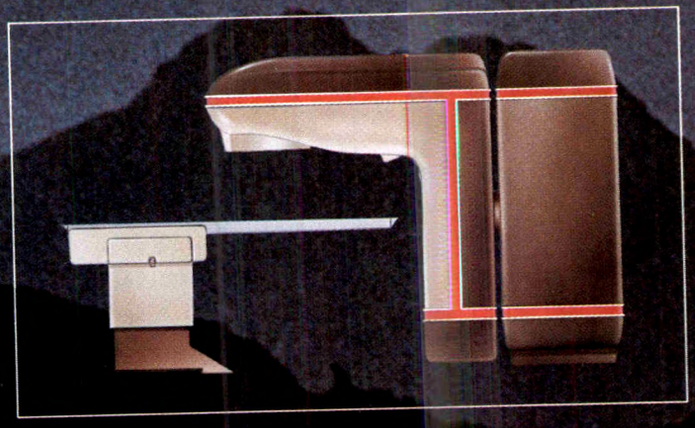




Conventional or Fiber Optic Image Intensifiers
Select from a full range of fields in conventional image intensifiers . . . or Philips' Exclusive Fiber Optic Image Intensification System. Fiber optics provides 30:1 contrast ratio for greater detail, uniform image quality over the entire screen, optimum image transfer and compactness for easy maneuverability.

PHILIPS®
the most reliable family of systems and people in the industry.

A Full Range of Generators
From the very affordable three-phase, high output Classic line, to a full range of Modular Generators, to the computerized Optimus M200, Philips' family of generators combines quality, performance and price for your every examination need.



Therac 6
Linear Accelerator. Teletherapy beyond Cobalt 60.

With an energy output of 6 MeV photons, the AECL Therac 6 Linear Accelerator offers the full advantages of mega-voltage therapy while demonstrating significant improvements over Cobalt 60. Possessing superior dose uniformity and depth dose characteristics, Therac 6 provides the maximum of control. And, for added safety, record and verify feature is standard. Compact, self-contained, Therac 6 is easily installed with limited modification to existing cobalt facilities required. Without doubt, Therac 6 is the cost effective way of acquiring the advanced technology of linear acceleration. For full details, contact AECL.

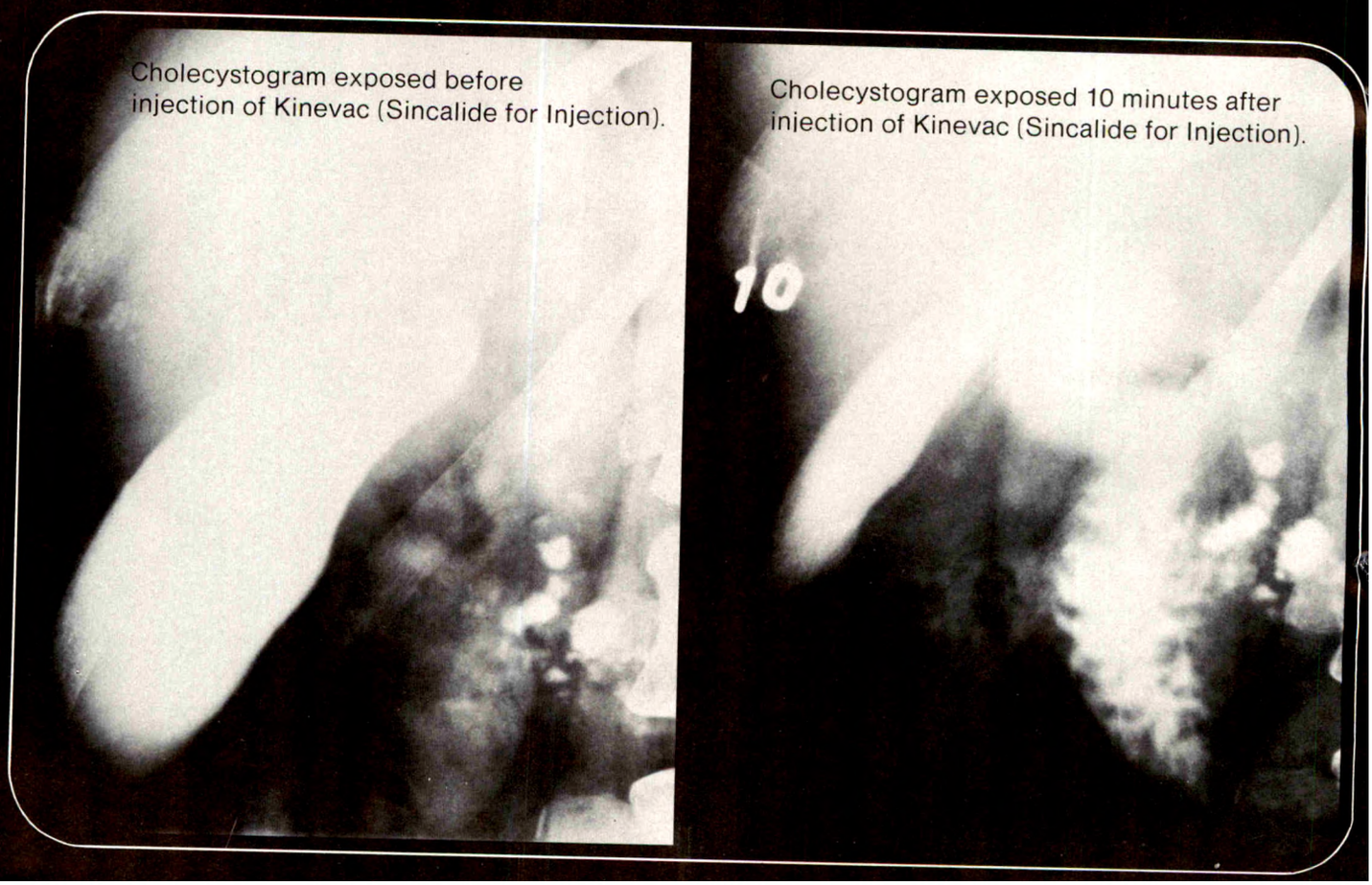
Atomic Energy of Canada Limited
Commercial Products

P.O. Box 6300, Ottawa, Canada K2A 3W3. Tel.: (613) 592-2790. Cable Nemota. Telex: 053-4162.
In the United States: Chicago: (312) 593-2242. Philadelphia: (215) 441-5952. Atlanta: (404) 987-9280. Dallas: (214) 233-0920. Los Angeles: (714) 989-20

a significant advance in postevacuation cholecystography

Kinevac®
Sincalide for Injection

- a convenient alternative to the fatty meal
- optimal gallbladder contraction in 5 to 15 minutes
- complete physician control



Cholecystogram exposed before injection of Kinevac (Sincalide for Injection).

Cholecystogram exposed 10 minutes after injection of Kinevac (Sincalide for Injection).

Rapid, predictable gallbladder contraction

In cholecystography, Kinevac produces diagnostically satisfactory gallbladder contraction in 5 to 15 minutes.

A convenience to physician and patient

Provides the physician with an alternative to the fatty meal or fatty meal substitute when such a choice is desirable, gives greater control, permits a barium meal examination immediately following cholecystography, and results in an economy of time and personnel.

Valuable adjunct in diagnosis of diseases

Kinevac provides a sample of gallbladder bile that may be aspirated from the duodenum for analysis. In conjunction with secretin, it stimulates pancreatic secretion for analysis of its composition and examination of its cytology.

A significant scientific achievement

Sincalide, the C-terminal octapeptide of cholecystokinin synthesized in The Squibb Institute for Medical Research, reproduces all the known biological activity of the intact cholecystokinin molecule.

Kinevac®

Sincalide for Injection



KINEVAC (Sincalide for Injection)

DESCRIPTION: Kinevac (Sincalide for Injection) is a sterile, lyophilized, white powder of the synthetic C-terminal octapeptide of cholecystokinin. Each vial provides 5 mcg. sincalide with 45 mg. sodium chloride as a carrier; sodium hydroxide or hydrochloric acid may be added during manufacture to adjust the pH to 5.5 to 6.5. When reconstituted with 5 ml. of Sterile Water for Injection U.S.P., each ml. contains 1 mcg. sincalide and 9 mg. sodium chloride.

CONTRAINDICATIONS: Contraindicated in patients sensitive to sincalide.

WARNINGS: Usage in Pregnancy—Although no teratogenic or antifertility effects were seen in animal studies, data are inadequate to determine the safety of sincalide in human pregnancy. Accordingly, sincalide should be used in pregnant women only when, in the judgment of the physician, the benefits outweigh the possible risk to the fetus.

Usage in Children—The safety of sincalide for use in children has not been established.

PRECAUTIONS: The possibility exists that stimulation of gallbladder contraction in patients with small gallbladder stones could lead to the evacuation of the stones from the gallbladder, resulting in their lodging in the cystic duct or in the common bile duct. The risk of such an event is considered to be minimal because sincalide, when given as directed, does not ordinarily cause complete contraction of the gallbladder.

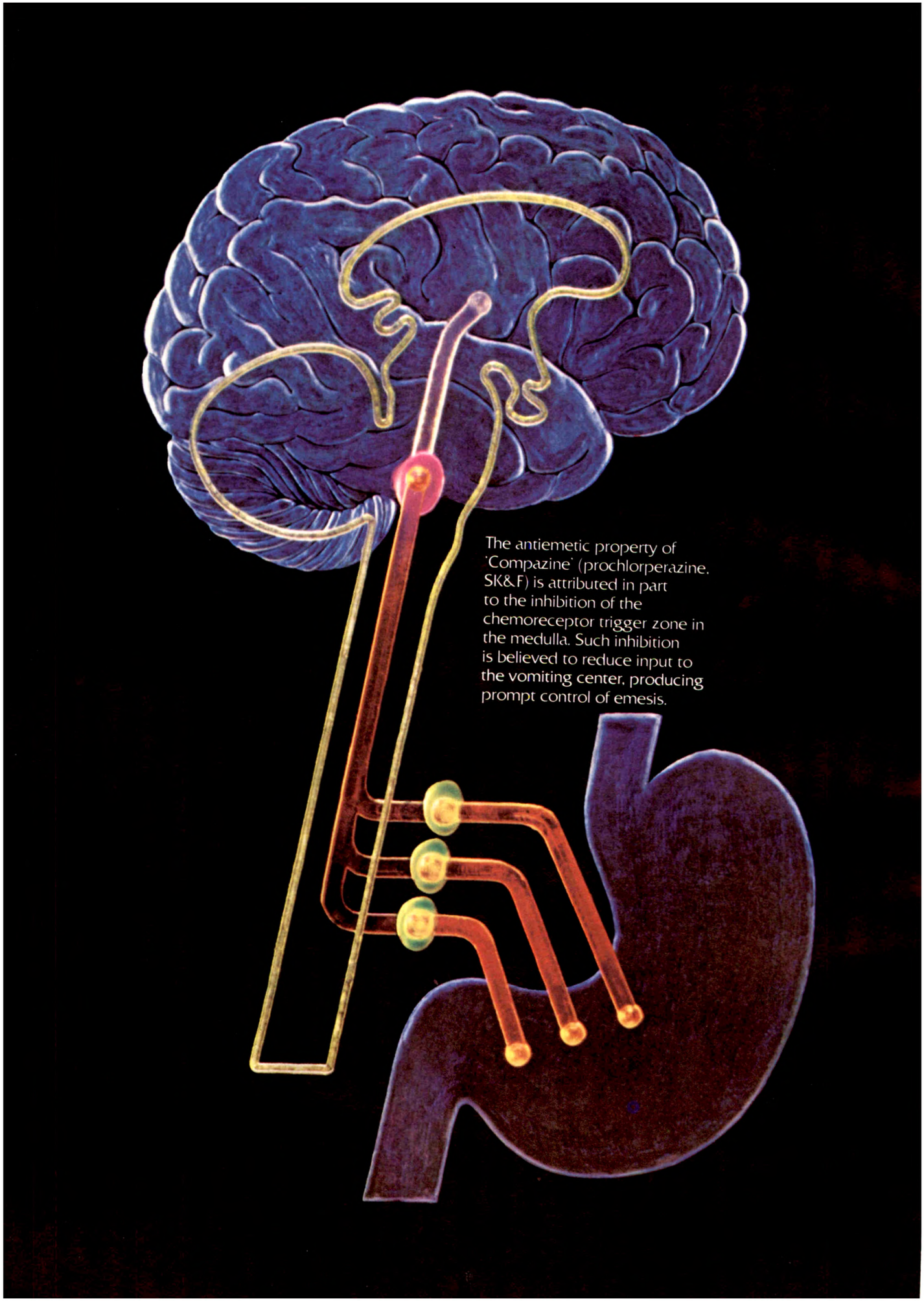
ADVERSE REACTIONS: G.I. symptoms such as abdominal discomfort or pain, and an urge to defecate, frequently accompany the injection of sincalide. These phenomena are usually manifestations of the physiologic action of the drug, which include delayed gastric emptying and increased intestinal motility, and are not to be construed as necessarily indicating an abnormality of the biliary tract unless there is other clinical or radiologic evidence of disease. Nausea, dizziness, and flushing occur occasionally.

For full prescribing information, consult package insert.

HOW SUPPLIED: Kinevac (Sincalide for Injection) is supplied in cartons of 10 vials, each vial containing 5 mcg. of sincalide.

SQUIBB® contrast media™ The leader in radiologic diagnostics

©1977 E. R. Squibb & Sons, Inc. H637-501


The antiemetic property of
'Compazine' (prochlorperazine,
SK&F) is attributed in part
to the inhibition of the
chemoreceptor trigger zone in
the medulla. Such inhibition
is believed to reduce input to
the vomiting center, producing
prompt control of emesis.

Compazine®

Injection 5 mg./ml.
disposable syringe

brand of
prochlorperazine

Shouldn't it be your first choice for severe nausea and vomiting that often accompany cancer therapy?

- **Unsurpassed antiemetic action**
- **12 dosage forms and strengths**

Before prescribing, see complete prescribing information in SK&F literature or PDR. The following is a brief summary.

Indications: Management of the manifestations of psychotic disorders; management of psychoneurotic patients displaying primarily symptoms of moderate to severe anxiety and tension; and for control of severe nausea and vomiting.

'Compazine' has not been shown effective in the management of behavioral complications in patients with mental retardation.

Contraindications: Comatose or greatly depressed states due to C.N.S. depressants; bone marrow depression; pediatric surgery.

Warnings: The extrapyramidal symptoms which can occur secondary to 'Compazine' may be confused with the central nervous system signs of an undiagnosed primary disease responsible for the vomiting, e.g., Reye's syndrome or other encephalopathy. The use of 'Compazine' and other potential hepatotoxins should be avoided in children and adolescents whose signs and symptoms suggest Reye's syndrome.

Avoid using in patients hypersensitive (e.g., blood dyscrasias or jaundice) to any phenothiazine. Caution patients about activities requiring alertness (e.g., operating vehicles or machinery) especially during the first few days' therapy. Prochlorperazine may intensify or prolong the action of other C.N.S. depressants. Not recommended for children under 20 pounds or 2 years of age.

Use in pregnancy only when potential benefits outweigh hazards.

Precautions: The antiemetic action of 'Compazine' may mask the signs and symptoms of overdosage of other drugs and may obscure the diagnosis and treatment of other conditions such as intestinal obstruction, brain tumor and Reye's syndrome (See WARNINGS). Postoperative aspiration of vomitus has occurred in a few surgical patients who received prochlorperazine as an antiemetic. Deep sleep and coma have been reported, usually with overdosage. Patients on long-term therapy, especially high doses, should be evaluated periodically for possible adjustment or discontinuance of drug therapy. **In children with acute illnesses or dehydration, use only under close supervision.**

Adverse Reactions: Drowsiness, dizziness, amenorrhea, blurred vision, skin reactions. Hypotension. Cholestatic jaundice, leukopenia, agranulocytosis. Fatty changes in the liver have been observed in a few patients who died while receiving the drug (no causal relationship has been established). Neuromuscular (extrapyramidal) reactions: motor restlessness, dystonias, pseudo-parkinsonism, persistent tardive dyskinesia. Contact dermatitis is a possibility with concentrate and injectable forms.

Other adverse reactions reported with Compazine (prochlorperazine, SK&F) or other phenothiazines: Some adverse effects are more frequent or intense in specific disorders (e.g., severe hypotension in mitral insufficiency or pheochromocytoma).

Grand mal convulsions; altered cerebrospinal fluid proteins; cerebral edema; prolongation and intensification of the action of C.N.S. depressants, atropine, heat and organophosphorus insecticides; dryness of mouth, nasal congestion, headache, nausea, constipation, obstipation, adynamic ileus, inhibition of ejaculation; reactivation of psychotic processes, catatonic-like states; hypotension (sometimes fatal); cardiac arrest; pancytopenia, thrombocytopenic purpura, eosinophilia; biliary stasis; lactation, galactorrhea, gynecomastia, menstrual irregularities, false-positive pregnancy tests; photosensitivity, itching, erythema, urticaria, eczema up to exfoliative dermatitis; asthma, laryngeal edema; angioneurotic edema, anaphylactoid reactions; peripheral edema; reversed epinephrine effect; hyperpyrexia; a systemic lupus erythematosus-like syndrome; pigmentary retinopathy; with prolonged administration of substantial doses, skin pigmentation, epithelial keratopathy, and lenticular and corneal deposits.

EKG changes have been reported, but relationship to myocardial damage is not confirmed. Discontinue long-term, high-dose therapy gradually.

NOTE: Sudden death in patients taking phenothiazines (apparently due to cardiac arrest or asphyxia due to failure of cough reflex) has been reported, but no causal relationship has been established.

Supplied: Tablets – 5, 10 and 25 mg., in bottles of 100; Spansule® capsules – 10, 15, 30 and 75 mg., in bottles of 50; Injection – 5 mg./ml. in 2 ml. ampuls, 10 ml. vials, and 2 ml. disposable syringes; Suppositories – 2-1/2, 5 and 25 mg.; Syrup – 5 mg./5 ml.; Concentrate (intended for institutional use only) – 10 mg./ml.; Single Unit Packages of 100 (intended for institutional use only) – 5 and 10 mg. tablets; 10, 15 and 30 mg. 'Spansule' capsules.

SK&F
a SmithKline company

Smith Kline &French Laboratories
Philadelphia, PA

AJR Guidelines for Authors

Address manuscripts and correspondence to the Editorial Office, American Journal of Roentgenology, 403 Pacific National Bank Building, 4545 15th Avenue N.E., Seattle, Washington 98105; telephone (206)633-2754.

Publication Policy

The Journal publishes original and timely contributions to the advancement of radiologic diagnosis and treatment. Although the content is predominantly clinical, laboratory investigations are accepted when their relevance to clinical practice is demonstrable. In prospective clinical investigations, authors should indicate if informed consent from patients was obtained. Decisions on manuscripts are based on the opinions of at least two outside reviewers. Reviewers receive manuscripts without title pages to protect the identity of authors and to ensure an unbiased review; names of reviewers, in turn, are not revealed to authors. Statements within an article are the responsibility of the authors and not the Journal or its publisher.

It is understood that material submitted has not been published and is not currently submitted elsewhere. Portions of the data or illustrations from previously published works may be included if permission release forms accompany the manuscript and such material is clearly credited in the text. Prior publication of abstracts will not prejudice publication of the complete study.

Copyright Information

In accordance with Journal implementation of the 1976 U.S. Copyright Law, authors must release first and subsidiary rights to their manuscript at submission. A dated cover letter, containing signatures of all authors, should state: "We, the authors, assign first and subsidiary rights to the American Roentgen Ray Society in the event that our manuscript (title) is published by AJR." The Journal, in turn, grants authors the right to use portions of their manuscript, without charge, in books or articles of which they are authors or editors.

Manuscript Form

Manuscripts should be typed double-spaced throughout, including references, tables, and figure legends. Tables, footnotes, and figure legends should be on separate sheets, and a separate title page should be provided. In addition to the original typewritten copy, a duplicate copy complete with figures, tables, and references is required. Authors' names should be on title page only and should not be on figures so that author anonymity can be maintained during the review process.

Figures should be submitted as 13 × 18 cm glossy prints, untrimmed and unmounted. Labels and arrows must be of professional quality and should be removable from the prints. Each figure should be numbered to correspond with figure legends, and the top should be indicated. Specific permission for publication of facial photographs of patients is required. Line illustrations and graphs should be drawn in black ink on white background.

References should be cited in the text by number (e.g., [3, 4]). The bibliography should be arranged in the numerical order that references are cited in the text and typed double-spaced throughout. Data for each reference should be arranged according to the uniform style on bibliographic citations adopted by many biomedical journals. Provide all authors' names and inclusive pages. Abbreviations for titles of medical periodicals should conform to those published in *Index Medicus*. Examples:

1. Miller RE, Chernish SM, Skucas J, Rosenak BD, Rodda BE: Hypotonic roentgenography with glucagon. *AJR* 121:264–274, 1974
2. Boijsen E: Superior mesenteric angiography, in *Angiography*, edited by Abrams H, Boston, Little, Brown, 1971, pp 1091–1119

Organization

Title page. Titles should be brief and specific. Include addresses for each author and acknowledgment of grant support when appropriate.

Abstract. A description of the purpose, methods, results and conclusions of the study is required.

Introduction. Clearly state the purpose of the investigation including necessary background facts.

Materials and methods. Decribe the protocol clearly. Use standard abbreviations as presented in the *Council of Biology Editors Style Manual*, 3d ed. Metric measurements should be used throughout.

Results. Present results in logical sequence.

Discussion. Interpret the results to lend meaning and importance to the observations. Hypotheses and speculation based on the results are encouraged. When results differ from those of previous investigators, an attempt should be made to explain the discrepancy.

References. Only include references which provide adequate background and present fairly any opposing evidence and concepts. Accuracy of reference data is the responsibility of the author.

Legends. Legends should be brief but should provide sufficient description to interpret the figure.

Special Communications

Case Reports. Concise case reports are accepted if they present unusual experiences that are medically important and educational. Clarity and brevity are essential. After preliminary screening by an editor to determine whether the requirement of medical significance has been met, qualifying papers will undergo the same peer review as major papers.

Technical notes. Brief descriptions of new techniques or significant modifications of older ones which are directly applicable to clinical practice will be accepted.

Letters to the Editor. Letters are subject to editing and condensation. Criticism of published articles should be objective and constructive. Letters may also discuss matters of general interest to radiologists.

Complement and Coagulation: Causative Considerations in Contrast Catastrophies

E. C. LASSER,[1] J. SLIVKA,[1] J. H. LANG,[1] W. P. KOLB,[1,2] S. G. LYON,[1] A. E. HAMBLIN,[1] AND G. NAZARENO[1]

Earlier studies suggest that adverse reactions to injected radiographic contrast media are idiosyncratic. In an attempt to gain a better understanding of pathophysiologic events underlying these reactions, rabbit models injected with lethal dose ranges of a cholangiographic contrast material were studied. These animals showed activation of both the complement and coagulation systems. Externally applied heat potentiated complement consumption and increased mortality. Depleting complement components C3–C9 by cobra venom factor did not prevent activation of coagulation or diminish mortality. However, depleting fibrinogen diminished complement activation and markedly diminished mortality. Heparin, administered at several hourly intervals after contrast challenge, also diminished mortality. These studies suggest that the adverse effects of contrast media in this model system are mediated chiefly by the coagulation system, and that complement, if it participates deleteriously, must involve components up to, but not including, C3. A logical role for the inhibitor of C1 esterase in adverse contrast reactions is considered.

Introduction

The pathogenesis of contrast media reactions has not yet been clearly defined. Potential factors considered to date include the development of a true allergy or hypersensitivity [1–4], contrast-induced histamine release [5, 6], anxiety [7], chemotoxicity [8], and activation of the complement and coagulation sequences [9–15].

While the nature of the anaphylactoid responses occurring in systemic reactions to injected contrast media make it naturally attractive to consider that these occur on the basis of a true allergy or hypersensitivity, there are several factors that mitigate against this. In the first place, attempts to induce circulating antibodies against contrast media injected alone or conjugated to serum proteins have been unsuccessful. On the other hand, Brasch and colleagues [1, 2], working with analogues of contrast media and binding these haptens to keyhole-limpet hemocyanin, were successful in producing antibodies of both the IgG and IgE classifications in immunized rabbits. These same workers, using radioimmunoassay, demonstrated significant elevation of antibodies directed against contrast media in a number of patients suffering severe reactions in comparison with controls. However, the significance of these findings is uncertain. Many of the patients demonstrating reactions did not show elevated binding levels, and a number of patients in the control series with binding levels equivalent to those noted in the reactor group did not show evidences of reaction. Furthermore, the occurrence of previous exposure to contrast media was as common among the controls as among the reacting patients. In addition, there has not yet been any clear evidence for the development of an anti-contrast material IgE-class antibody in humans receiving contrast media of the urographic type. It is this particular class of immunoglobulins that has been most commonly associated with anaphylactoid-type reactions.

Wakkers-Garritsen et al. [4], using passive transfer skin test techniques, demonstrated the presence of an IgE-antibody directed against a cholangiographic material. By virtue of their chemical structure, the cholangiographic media could function as divalent haptens and would be more likely to effectively bind to IgE antibodies than would the univalent haptens that characterize the structure of the urographic media. Nevertheless, at this time a true hypersensitivity in some reactions occurring after injections of urographic media cannot be excluded.

Our own attention was drawn to the possible role that activation of the complement and coagulation sequences might play in acute contrast reactions for several reasons. Activation of the complement system has been noted in association with shock and systemic anaphylaxis in numerous circumstances in man and in animal experiments [16–18]. Laboratory and clinical evidence of intravascular coagulation was observed in a number of cases, both in our own institution and in cases sent to us for consultation, in patients sustaining acute systemic reactions to contrast media. Furthermore, some case reports [19–21] have correspondingly indicated that anaphylactoid reactions to contrast media were accompanied by thrombocytopenia, fibrinogenopenia, and other findings suggesting that the coagulation system had been activated in the course of the reaction.

In the past few years we have documented that contrast media can activate both the complement and coagulation systems. (Activation of the complement system has been shown both in vitro and in vivo, and activation of the coagulation system in vivo only.) Our in vivo studies concentrated on two animal models. In one of these, dogs injected daily with urographic contrast me-

Received April 25, 1978; accepted after revision November 6, 1978.
This work was supported by U.S. Public Health Service grant GM-22794 from the National Institute of General Medical Sciences, Bethesda, Maryland 20014.
[1]Department of Radiology, University of California School of Medicine, San Diego, California 92093. Address reprint requests to E. C. Lasser.
[2]Present address: Department of Biochemistry, University of Texas Health Science Center, San Antonio, Texas 78284.

0361-803X/79/1322-0171 $0.00

AJR 132:171–176, February 1979
© 1979 American Roentgen Ray Society

dia at dosages equivalent to those used in clinical practice developed idiosyncratic reactions characterized clinically by an anaphylactoid response and in the laboratory by a fall in total complement levels and by evidence of intravascular coagulation [10]. In the second model, rabbits injected with lethal-range doses of iodipamide, a cholangiographic contrast material, showed corresponding changes [11, 12]. While the canine model is perhaps somewhat more satisfactory from the standpoint of comparison with adverse reactions demonstrable in humans, the logistics and economics of extensive testing in these models have led us to more intensive use of the rabbit model. Use of the rabbit model entails the presumption that some contrast media reactions are idiosyncratic in nature, and that information gleaned from these very high dosage challenges might be applicable to that small segment of the animal or human population programmed for idiosyncratic responses. These studies, then, must be viewed in the perspective of two assumptions, either of which could be challenged by future data: (1) that some contrast media reactions at least are idiosyncratic and, hence, data elicited as a consequence of massive dosages might be applicable to those few individuals who respond to customary clinical dosages in the same fashion that other individuals respond to massive dosages; and (2) that information concerning the effects on the complement and coagulation systems in rabbits can be carried over to humans. Mindful of these assumptions, we undertook the following studies.

Materials and Methods

White New Zealand male rabbits, weighing 1.5–3 kg, obtained from one supplier, were used in all studies. Most rabbits weighed 2–3 kg, and test and control rabbits in each series were matched for size and development. Test and control rabbits in each study were similarly caged and fed.

The challenging contrast material in each instance was meglumine iodipamide in the form of 52% Cholografin (provided by Squibb). The rabbits were injected intravenously in the marginal ear vein. All blood samples were obtained from the central artery of the ear, and were immediately placed in plastic tubes containing sodium citrate. Samples were centrifuged at 3,000 rpm for 15 min and were assayed within 2 hr. A Harvard infusion pump was used to regulate the rate of administration. No sedation was administered. Dosages varied from 7.5 ml/kg to 7.8 ml/kg. Infusion rates were established to allow for either infusion of the total dose over 5 min, or for an injection rate of 2.0 ml/min. Dosages were selected to provide an estimated LD_{30} to LD_{100}. Earlier studies in this laboratory indicated that there was a sharp rise in the lethality curve between dosages of 7.0 ml/kg to 8.0 ml/kg, and that lethality in this dose range was to some extent dependent on a factor, or factors, in the external environment during the period in which the study was undertaken. Since earlier studies showed a protective effect of adrenocorticosteroids in these test animals [11] and since the activity of the rabbit adrenal cortex is known to be dependent, in part, on environmental temperature and humidity [22], it is conceivable that these laboratory factors which varied throughout the year were responsible.

Significant differences between test and control parameters for all studies were determined at the 95% confidence level by two-sided *t*-test analysis and mortality differences by chi-square analysis.

Study 1: Effect on Coagulation and Complement Systems

Six rabbits were infused with 7.5 ml/kg of iodipamide over a total of 5 min. Plasma samples were obtained before injection and at 1, 2, and 3 hr after injection, and were assayed for factor XII of the intrinsic coagulation system, activated partial thromboplastin time, prothrombin time, total hemolytic complement (CH50), and iodipamide concentrations.

Factor XII assay was carried out using factor XII–deficient human plasma (George King Biomedical, Salem, N. H.). Kaolin was used as the activating agent in these assays. All studies were done using two dilutions and duplicates were run at each dilution. Test runs were compared to a standard pooled rabbit citrated plasma. Control factor XII determinations done in 20 rabbits produced a mean factor XII of 92.9% ± 6.9% (all cited figures in this report are ± SE). Prothrombin time was measured using the one-stage technique and thromboplastin supplied by Ortho Diagnostics, Raritan, New Jersey. For partial thromboplastin time assays, a test kit supplied by Hyland Division, Travenol Labs., Costa Mesa, California, was used. Total complement (CH50) and iodipamide concentrations were assayed by methods previously reported [15].

Study 2: Effect of Externally Applied Heat

Rabbits were placed in a restraining cage and were enveloped in a small commercial heating pad (General Electric). The heating pad was switched to a medium range "on" position for 30–35 min, and rectal temperatures were continuously monitored until an approximate elevation of 2°C was noted. Next each animal was infused with 7.8 ml/kg of iodipamide at a rate of 2.0 ml/min. After completion of the infusion, the rabbits were maintained in the cage, enveloped in the heating pad, for an additional 15 min. These animals showed a mean peak rectal temperature elevation of 1.92 ± 0.08°C above the baseline temperatures obtained prior to application of the heating pad. Nineteen rabbits were used in the study and a control group of 14 rabbits was similarly examined. However, the control rabbits did not have the heating pad switched to the "on" position. Both groups were observed for mortality in 24 hr; for changes in total complement (CH50) in plasma samples obtained at death or 2 hr after challenge, whichever came first; and for plasma concentrations of circulating iodipamide at the same postchallenge times.

Study 3: Effect of Complement Depletion

Nine rabbits were pretreated by intraperitoneal injections of cobra venom factor (prepared by W. P. K.). Five grams of dried cobra venom (Biological Unlimited, Baltimore, Md.), obtained from the cobra *Naja naja kaouthia*, was diluted into 50 ml of 50 mM sodium acetate buffer at pH 5.5 and dialyzed against the same buffer. This was then loaded onto a 5 × 100 cm CM-32 column and equilibrated with the same buffer. The column was washed with 4 liters of the same buffer and the cobra venom factor activity eluted with a linear sodium chloride gradient. Venom factor–containing fractions were pooled and concentrated by Amicon ultrafiltration to a volume of 5.0 ml. This pool was applied to a 2.5 × 100 cm Biogel A-05 M column, which was equilibrated with phosphate-buffered saline at pH 7.4. The flow rate was 2.5 ml/hr. Fractions of 1.5 ml were collected.

The venom factor–containing fractions were pooled and this pool contained about 1.5 mg/ml in a volume of 25–30 ml. This

TABLE 1

Changes in Coagulation Parameters and Total Hemolytic Complement After Meglumine Iodipamide Injection

	Factor XII (preinjection %)	Partial Thromboplastin Time (sec)	Prothrombin Time (sec)	Total Complement, CH50 (preinjection %)	Iodipamide (mM)
Preinjection (6)	100 (6)	32.8 ± 8.4 (6)	7.1 ± 0.4 (6)	100 (6)	0 (6)
1 hr (6)	68 ± 8 (6)*	152 ± 18 (6)*	8.0 ± 0.5 (6)	79 ± 4 (5)*	6.2 ± 0.5 (5)
2 hr (6)	75 ± 9 (6)	130 ± 40 (6)*	8.6 ± 0.6 (6)*	77 ± 4 (5)*	4.9 ± 0.6 (5)
3 hr (5)	81 ± 10 (5)	156 ± 51 (5)*	9.2 ± 1.5 (5)	80 ± 5 (4)*	3.1 ± 0.4 (4)

Note.—(N) = number of rabbits. Each rabbit was injected with 7.5 ml/kg of meglumine iodipamide over 5 min.
* Significant difference from preinjection level ($P < 0.05$).

process results in a 200–250-fold purification. Activity was assayed as reported by Cochrane et al. [23]. One unit of activity corresponded to 3–5 μg of cobra venom factor. The venom factor was given at a dose of 160 U/kg over 24 hr. This resulted in complete depletion of total hemolytic complement in all but one animal. In that animal, complement was reduced to 5.8 CH50 units before challenge. (Control rabbits had a mean CH50 level of 25.6 ± 1.7.)

After depletion of complement, the rabbits were injected with iodipamide at a dose of 7.8 ml/kg at a rate of 2.0 ml/min. The rabbits were observed for mortality over a 72 hr period for changes in partial thromboplastin time, fibrinogen, and platelet levels, and for circulating iodipamide concentrations at 2 hr after iodipamide challenge. A control group of 10 rabbits was pretreated by injections of normal saline in equivalent quantities to those used for the cobra venom factor injections, and then was similarly challenged with iodipamide and assayed for the same pre- and postchallenge parameters.

Study 4: Effect of Fibrinogen Depletion

Ten rabbits were pretreated with 1.2 U/kg of Ancrod given as a 30 min infusion on two occasions, 17 hr apart. Ancrod is crude venom of the Malayan pit viper *Aghristrodon rhodostoma*, prepared in solution of 114 U/ml (supplied by A. O. Geiszler of Abbott Labs., Chicago, Ill.). Two hours after the second infusion the rabbit was challenged with 7.8 ml/kg of iodipamide injected at 2.0 ml/min. Ten control rabbits were similarly injected with a volume of 5% dextrose in water equivalent to the infused Ancrod. Animals were observed for mortality over 72 hr. Total complement (CH50) was determined in blood drawn immediately before iodipamide challenge and at about 2 hr after completion of the challenge. Prechallenge fibrinogen levels (total clottable protein) and the concentration of circulating iodipamide at 2 hr after challenge were also determined.

Study 5: Effect of Heparin Anticoagulation

Eleven rabbits were challenged with 7.5 ml/kg of iodipamide given at 2.0 ml/min. At 1, 3, and 5 hr after challenge, rabbits were given 100 U of heparin (aqueous sodium heparin, Riker Labs.) intravenously. Ten control rabbits were similarly challenged, but received normal saline instead of heparin. Animals were observed for mortality at 72 hr. No other parameters were evaluated in this group.

Results

Study 1: Effect on Coagulation and Complement Systems

The intravenous injection of rabbits with meglumine iodipamide at 7.5 ml/kg over 5 min produced the results shown in table 1. It may be noted that significant differences from preinjection parameters occurred in one or more of the three hourly sampling periods for each of the factors assayed. For factor XII, a significant difference from preinjection levels was noted at the 1 hr sampling interval. Partial thromboplastin time showed significant increments at each of the three hourly sampling periods in comparison with preinjection values. Prothrombin time showed a significant increment over preinjection values at the 2 hr sampling interval. Since the reduction in factor XII is modest in this experiment, one might consider that the prolonged partial thromboplastin and prothrombin times could have occurred on the basis of a circulating inhibitor or inactivator, rather than on the basis of consumed coagulation factors. However, appropriate control studies carried out in six additional rabbits challenged with iodipamide at 7.6 ml/kg suggested that a circulating inhibitor, if present, played only a minor role. (Prechallenge partial thromboplastin times averaged 52.3 sec. They were greater than 600 sec in all six rabbits at 1 hr after challenge; whereas a 1:1 mixture of prechallenge plasma and the 1 hr sample prolonged the prechallenge times by an average of only 136 sec. Incubation of these samples for 1 hr at 37°C did not produce any appreciable change.)

Significant depressions in total hemolytic complement were noted at each of the sampling intervals in comparison with preinjection values. Earlier studies indicated that the change in total complement could not be ascribed solely to the presence of circulating iodipamide at the concentrations noted at each interval [15]. Hence, complement activation in vivo is presumed to occur by a somewhat different mechanism than in vitro activation.

Study 2: Effect of Externally Applied Heat

The results of this study are summarized in table 2. In two of the animals in the control series, blood samples could not be obtained from the central artery of the ear and cardiac punctures were used. Both of these animals died immediately after the cardiac puncture and were eliminated from mortality considerations. It is clear that heating the animals before injection of contrast material resulted in a marked increase in mortality, accompanied by significantly increased complement depletion and significantly increased iodipamide residual concentrations. However, these must be regarded in perspective. Since the average death in the heated rabbit series occurred at 42 min, it is expected that the higher residual

TABLE 2

Effects of Temperature Elevation on Complement and Mortality After Meglumine Iodipamide Injection

	Mean Temperature Before Contrast (C°)	Mean Drop of Total Complement, CH50* (%)	Mean Iodipamide Concentration* (mM)	Mortality 24 hr (%)
Heated rabbits (19)	40.6 ± 0.1 (19)†	72.2 ± 4.1 (19)†	11.2 ± 0.7 (18)	100 (19)‡
Control (sham-heated) (14)	38.6 ± 0.1 (14)	19.4 ± 2.6 (14)	5.5 ± 0.5 (14)	25 (12)

Note.—(N) = number of rabbits in assay.
* CH50 determinations and iodipamide concentrations were done at death or 2 hr after injection, whichever came first.
† Significant difference from control ($P < 0.05$).
‡ Significant difference from control ($P < 0.01$).

TABLE 3

Effects of Pretreating Rabbits with Cobra Venom Factor to Deplete Complement Factors C3–C9 Before Iodipamide Challenge

	Mean Total Complement, CH50, Before Iodipamide	2 hr Mean Increase, Partial Thromboplastin Time† (sec)	2 hr Mean Fall Platelets (%)	2 hr Mean Fall Fibrinogen (%)	Mortality, 72 hr (%)
Cobra venom factor rabbits (9)	* (8)	480 ± 80 (8)	71 ± 6 (8)	48 ± 9 (6)	78 (9)
Controls (10)	25.6 ± 1.7 (10)	392 ± 59 (10)	75 ± 5 (10)	61 ± 6 (8)	80 (10)

Note.—(N) = number of rabbits in assay. No significant differences ($P > 0.05$) between cobra venom factor rabbits and control for any parameter other than CH50. Prechallenge partial thromboplastin time, fibrinogen, and platelets were not statistically different ($P > 0.05$) in cobra venom factor rabbits and controls.
* All CH50 levels immeasurably low except for 5.8 value in one animal.
† Times of less than 10 min were treated as 10 min for these compilations.

TABLE 4

Effects of Pretreating Rabbits with Ancrod to Diminish Fibrinogen Concentrations Before Iodipamide Challenge

	Fibrinogen Concentration Before Iodipamide* (mg/100 ml)	2 hr Mean Fall, CH50, After Iodipamide (%)	2 hr Increase O.D. 541	Mortality, 72 hr (%)
Ancrod rabbits (10)	43 ± 6 (10)†	33 ± 4 (10)†	0.52 ± 0.1 (10)†	10 (10)‡
Control rabbits (10)	280 ± 31 (10)	47 ± 3 (10)	1.18 ± 0.3 (10)	100 (10)

Note.—(N) = number of rabbits in assay.
* Values of less than 30 mg/100 ml were treated as 30 mg/100 ml for this compilation.
† Significant difference from control ($P < 0.05$).
‡ Significant difference from control ($P < 0.01$).

iodipamide concentrations and complement activations are due, at least in part, to the earlier sampling periods. The rabbits in the control group had residual iodipamide concentration sampled at 2 hr.

Study 3: Effect of Complement Depletion

Depleting the rabbits of complement (C3–C9) had no significant effect on mortality, fall in platelets or fibrinogen, or prolongation of partial thromboplastin time in comparison with controls. Specific values for each of these parameters are given in table 3. In addition, the 2 hr iodipamide plasma concentrations do not differ between the treated animals and the control group (5.03 ± 0.7 mM for cobra venom factor rabbits; 5.39 ± 0.3 mM for controls). The earliest deaths in both the treated and control groups in this study occurred at 1¾ hr.

Study 4: Effect of Fibrinogen Depletion

Table 4 indicates that there was a marked diminution in mortality in the rabbits pretreated with Ancrod. The majority of control rabbits died within 2–3 hr after challenge. The single mortality in the fibrinogen-depleted group also occurred in the same period. In addition, the mean fall in total complement in the pretreated rabbits was about 30% less than in the control rabbits, and the increase in O.D. 541 (a measure of induced hemolysis) was more than 50% less in the pretreated animals. There were significant differences in the 2 hr iodipamide concentrations in the rabbits pretreated with Ancrod in contrast to controls. Mean values for the 2 hr iodipamide concentrations were as follows: Ancrod-treated rabbits, 3.84 ± 0.4 mM; controls, 5.64 ± 0.3 mM.

Study 5: Effects of Heparin Anticoagulation

Animals treated with heparin at 1, 3, and 5 hr after iodipamide challenge had a 9% mortality. Control rabbits treated with normal saline rather than heparin had a 50% mortality. The majority of deaths occurred within 12 hr, but one rabbit survived more than 48 hr. These mortality values for the two groups were significantly different ($P < 0.01$).

Discussion

From these studies it is evident that rabbits injected at lethal dose range levels of one contrast material—iodipamide, a cholangiographic substance—activated both the complement and coagulation systems. The procoagulative effect seems to involve both the intrinsic coagulation pathway and the extrinsic pathway. The precise mechanism of death in these animals is uncertain. Some exhibited convulsive activity, some had profuse diarrhea, some showed marked lateral nystagmus, and all showed hind limb weakness and marked lethargy immediately preceding death. They were not specifically examined for bronchospasm or hypotension, but cardiovascular collapse might be inferred from the frequent difficulty in obtaining blood samples from the central ear artery in the challenged animals as they grew weaker.

The fall in total hemolytic complement paralleled results noted in earlier rabbit studies [11, 12], and substantiated the idea that in vivo activation by contrast media considerably exceeded in vitro activation at similar contrast concentrations. Earlier we noted that preinjecting rabbits with very small doses of endotoxin prior to iodipamide challenge considerably diminished renal excretion of iodipamide, and increased total hemolytic complement activation and mortality [12]. At that time we did not know to what extent these augmented effects were assignable to simple temperature elevation, and to what extent such effects might be assigned to endotoxin-induced blockade of the reticuloendothelial system, depressing clearance of activated coagulation factors. The present study, using external heat to increase internal body temperature, also resulted in a marked increase in mortality, circulating iodipamide levels, and total complement consumption, suggesting that temperature elevation alone could account for the augmented effects. Furthermore, preliminary observations in this laboratory indicate that endotoxin in the dosages used in the previous study produced no significant blockade of the reticuloendothelial system as measured by half-time clearances of ^{99m}Tc-labeled sulphurcolloid (E. C. Lasser and N. Alazraki, unpublished data).

From what has been mentioned thus far, it would be difficult to determine whether the mortality noted in any of the rabbit groups challenged with the high iodipamide dose was related principally to activation of the complement system, activation of the coagulation system, or both. The augmented activation of the complement system noted in both the endotoxin-treated and the externally heated rabbits does not help in this regard. In some of these rabbits succumbing to the iodipamide challenge, there was microscopic evidence of partial or complete plugging of the renal glomeruli and other capillary systems by fibrin deposits [12]. While we did not undertake a systematic histologic examination of the renal areas in all of the rabbits that succumbed after iodipamide challenge, the increased iodipamide retention noted in these animals, and in similar studies reported earlier, suggested either mechanical plugging or circulatory failure as a basis for the diminished glomerular excretion of iodipamide. On this basis, it might be expected that an increased retention of circulating iodipamide would result in an augmentation of its complement-activating effects.

In recent years, increasing evidence of multiple interrelationships between the complement and coagulation systems has appeared [24–29]. Among these, a particularly strong case has emerged for the significance of a modulator exerting its influence at a point earlier than C3 of the complement sequence, and factor X of the intrinsic coagulation sequence. Particular attention has been paid to the role of the $C\bar{1}$ esterase inhibitor, a protein that exerts important regulatory activities on the complement, coagulation, and kinin systems [30, 31]. This particular protein is considerably diminished or absent in the congenitally determined abnormality termed hereditary angioedema, and it is believed that the absence of this inhibitor provides the basis for the production of a C2 derivative under conditions of stress, that accounts for the symptoms exhibited by these patients [31]. Since angioedema is a frequent occurrence in patients exhibiting systemic reactions to contrast media, and since there are also later components in the complement sequence (especially C3 and C5) that have the potential to produce edema-producing products on activation, it was thought worthwhile to attempt to sort out the relative roles that might be assigned to these various factors in contrast material toxicity. Toward this end, the cobra venom factor studies and the Ancrod studies were undertaken.

The cobra venom factor study suggested that complement activation, at least from C3 to C9, was not necessary to produce the mortality or procoagulant effects noted. On the other hand, the rabbits with depleted fibrinogen levels induced by Ancrod gained marked protection and showed diminution of complement activation and hemolysis. Diminished 2 hr iodipamide plasma levels in these animals may reflect diminished fibrin deposition in renal glomeruli.* The protective effects produced by heparin therapy further strengthened the notion that coagulant effects played a greater role than did complement activation in the rabbit lethality of iodipamide at these high concentrations. However, one could not eliminate in these studies a role for complement components preceding C3, particularly for the $C\bar{1}$ esterase inhibitor, since any circumstance that might diminish the level of the inhibitor would not only provide the potential for the production of permeability producing C2 products, but would also potentiate the effects of any induced activation of the coagulation, fibrinolysin, and kinin systems, as well as the complement system itself. [30].

These studies and accumulated clinical data thus suggest the possible importance in contrast reactions of this

* All these studies showed a close correlation between induced hemolysis and 2 hr iodipamide retention levels (presumably reflecting fibrin glomerular plugging). Control studies showed considerable induction of hemolysis in rabbits depleted of C3–C9 prior to combined heat and iodipamide challenge. Therefore, we assume that a major part of the induced hemolysis is microangiopathic, since the terminal components of the complement sequence are those concerned with the production of hemolysis.

critical inhibitor. For this reason we are currently examining early complement components (with particular emphasis on the $C\bar{1}$ esterase inhibitor) in patients manifesting reactions to injected media. Preliminary data suggest that, prior to injection, reactors as a group have lower mean concentrations of the inhibitor than do nonreactors, and that severe reactions may be characterized by partial consumption of the inhibitor and activation of the remainder of the complement sequence.

REFERENCES

1. Brasch RC, Caldwell JL: The allergic theory of radiocontrast agent toxicity: demonstration of antibody activity in sera of patients suffering major radiocontrast agent reactions. *Invest Radio* 11:347–356, 1976
2. Brasch RC, Caldwell JL, Fudenberg HH: Antibodies to radiographic contrast agents: induction and characterization of rabbit antibody. *Invest Radiol* 11:1–9, 1976
3. Kleinknecht D, Deloux J, Homberg JC: Acute renal failure after intravenous urography: detection of antibodies against contrast media. *Clin Nephrol* 2:116–119, 1974
4. Wakkers-Garritsen BJ, Houwerziji J, Nater JP, Wakkers PJM: IgE-mediated adverse reactivity to a radiographic contrast medium. *Ann Allergy* 36:122–126, 1976
5. Rockoff SD, Kuhn C, Creplyvy M: Contrast media as histamine liberators. V. Comparison of in vitro mast cell histamine release by sodium and methylglucamine salts. *Invest Radiol* 7:177–181, 1972
6. Lasser EC, Walters AJ, Reuter SR, Lang JH: Histamine release by contrast media. *Radiology* 100:683–686, 1971
7. Lalli AF: Urography, shock reaction, and repeated urography. *AJR* 125:264–268, 1975
8. Lang JH, Lasser EC: Nonspecific inhibition of enzymes by organic contrast media. *J Med Chem* 14:233–236, 1971
9. Lasser EC: Contrast media activation of serum complement system (letter). *Invest Radiol* 9:6A, 1974.
10. Lasser EC, Sovak M, Lang JH: Development of contrast media idiosyncrasy in the dog. *Radiology* 119:91–95, 1976
11. Lasser EC, Lang JH, Sovak M, Kolb WP, Lyon SG, Hamblin AE: Steroids: theoretical and experimental basis for utilization in prevention of contrast media reactions. *Radiology* 125:1–9, 1977
12. Slivka J, Lasser EC, Lang JH, Lyon SG, Hamblin AE: Effect of endotoxemia on contrast media reactions. *Invest Radiol* 13:21–25, 1978
13. Arroyave CM, Bhat KN, Crown R: Activation of the alternative pathway of the complement system by radiographic contrast media. *J Immunol* 117:1866–1869, 1976
14. Heideman N, Jacobsson B, Lindholm N: Activation of the complement system by water-soluble contrast media. *Acta Radiol [Diagn]* (Stockh) 17:733–736, 1976
15. Lang JH, Lasser EC, Kolb WP: Activation of the complement system by x-ray contrast media. *Invest Radiol* 11:303–308, 1976
16. Schur PH: Complement activation in septic shock. *N Engl J Med* 293:1261–1262, 1975
17. Tannenbaum H, Ruddy S, Schur PH: Acute anaphylaxis associated with serum complement depletion. *J Allergy Clin Immunol* 56:226–234, 1975
18. Ruddy S, Gigli I, Austen FK: The complement system of man (first of four parts). *N Engl J Med* 287:489–495, 1972
19. Trinkner RL, Perkins HA: Severe acute fibrinogenopenia apparently caused by reaction to drugs. *JAMA* 189:158–160, 1964
20. Bishopric GA: Athrombocytosis following oral cholecystography. *JAMA* 189:771–772, 1964
21. Zeman RK: Disseminated intravascular coagulation following intravenous pyelography (letter). *Invest Radiol* 12:203–204, 1977
22. Chowers I, Conforti N, Superstine E: Effects of changing levels of glucocorticosteroids on heat exposure in rabbits. *Jpn J Physiol* 25:655–676. 1975
23. Cochrane CG, Müller-Eberhard HJ, Aikin BS: Depletion of plasma complement *in vivo* by a protein of cobra venom: its effect on various immunologic reactions. *J Immunol* 105: 55–69, 1970
24. Brown DL: Complement and coagulation, in *Progress in Immunology II*, vol 1, edited by Brent L, Horborow J, Amsterdam, North Holland Publishing, 1974, pp 191–200
25. Zimmerman TS, Müller-Eberhard HJ: Blood coagulation initiation via complement-mediated pathway. *J Exp Med* 134:1601–1607, 1971
26. Dodds WJ, Pickering RJ: The effect of cobra venom factor on hemostasis in guinea pigs. *Blood* 40:400–411, 1972
27. Zucker NB, Grant RA, Alper CA, Goodfokofsky I, Lepow IH: Requirement for complement components and fibrinogen in the zymosan-induced release reaction of human blood platelets. *J Immunol* 113:1744–1751, 1974
28. Kalowski S, Howes EL Jr, Margaretten W, McKay DG: Effects of intravascular clotting on the activation of the complement system. The role of the platelet. *Am J Pathol* 78:525–536, 1975
29. Tomar RH, Kolchins D: Complement and coagulation. *Thromb Diath Haemorrhag* 27:388–395, 1972
30. Schreiber AD, Kaplan AP, Austen FK: Inhibition by $C\bar{1}$ INH of Hageman factor fragment activation of coagulation, fibrinolysis, and kinin generation. *J Clin Invest* 52:1402–1409, 1973
31. Hadjiyannaki K, Lachmann PJ: Hereditary anglo-edema: a review with particular reference to pathogenesis and treatment. *Clin Allergy* 1:221–233, 1971

Percutaneous Transhepatic Portography. I. Technique and Application

FLEMMING BURCHARTH[1]

Percutaneous transhepatic portography with selective catheterization of the portal vein and its tributaries was performed on 120 patients, of whom 71% had cirrhosis of the liver. The technique was improved by ultrasonically guided puncture, and the procedure was successful in 96% of the examinations. Collateral veins were visualized in 81% and esophageal or gastric varices in 69% of the patients with portal hypertension. The procedure was performed with little risk and discomfort, and portograms of high quality were obtained. Other applications of percutaneous transhepatic catheterization of the portal vein system are discussed.

Radiologic visualization of the portal venous system through injection of contrast medium has been performed by direct puncture during celiotomy [1], splenoportography [2, 3], exposures of the venous phase of celiac and mesenteric arteriography [4], percutaneous transhepatic puncture of the portal system [5, 6], injection via the reopened umbilical vein [7], and by transjugular transhepatic puncture of the portal vein [3]. Percutaneous transhepatic portography has attracted increasing attention during recent years [9–15].

In cirrhosis of the liver, percutaneous transhepatic portography evaluates hemodynamic changes, visualizes varices and other collateral systems, demonstrates the patency of the portal and splenic vein, and checks the patency of surgically established portocaval shunts [9, 13–15]. The examination is also indicated in hepatomegaly, splenomegaly, and suspected tumors along the splenoportal pathway [16].

Catheterization of the portal venous system may also be used for nonoperative obliteration of esophageal varices [17, 18]. Recently the procedure has been used to diagnose and localize endocrine pancreatic tumors [19–21]. We have used the percutaneous transhepatic portography since 1972.

Subjects and Methods

Percutaneous transhepatic portography was performed with a 27-cm-long, smooth polyethylene catheter fitted with a metal mandrin (Wiechel-Stille, Sweden), 1.00 mm ID/1.45 mm OD. It was introduced under local anesthesia in the right midaxillary line under fluoroscopic control with the patient supine. To improve the success rate of portal vein puncture, the porta hepatis was localized by ultrasonic scanning prior to portography [12]. From the ultrasonic scan, surface coordinates were marked on the patient (fig. 1). The aim was to puncture a hilar portal vein, usually the right branch. If unsuccessful, the procedure was repeated by slightly altering the direction of the catheter without completely withdrawing it from the liver. Using a flexible guide wire (PE 160) with slightly curved tip, the catheter was conducted from the intrahepatic portal vein into the branches of the portal system.

The first exposures were ordinarily made with the tip of the catheter in the splenic hilum. Sodium methylglucamine diatrizoate 76% was injected at a rate of 6 ml/sec (30 ml total). Films were exposed at one per second for 10 sec and then one every other second for 10 sec.

Portal pressure was recorded on a water manometer with the catheter tip in the main portal vein. The reference level was the midaxillary line; the recorded pressure was the mean of three readings.

Selected patients had sclerotherapy with injection of hydroxypolyaethoxy-dodecane (Aethoxysklerol, Kreussler, West Germany) in selectively catheterized varices (fig. 2). During injection, blood flow in the varices was stopped by inflation of a Sengstaken-Blakemore tube.

In patients with endocrine pancreatic tumors, the pancreatic veins were catheterized selectively and blood sampled for hormone assay. Blood samples for reference values were obtained from a percutaneous transhepatic catheterized hepatic vein.

At the end of examination, the catheter was clamped and retracted until the tip of the catheter was left in the liver parenchyma. It was withdrawn gradually during the next 6–12 hr.

From 1972 through 1978, 120 patients, 36 female and 84 male (median age, 52 years; range, 1 month to 87 years) were studied with percutaneous transhepatic portography. Eight patients were studied twice (128 total investigations). Diagnoses are shown in table 1. Two cases of portal vein thrombosis were secondary to cirrhosis.

In the evaluation of results the following definitions were used:

Successful transhepatic portography was defined as catheterization and visualization of the portal veins.

Direction of the flow in the portal vein was defined as *hepatopetal* if all contrast medium flowed through the liver, *complete hepatofugal* if contrast medium flowed to collateral veins with no flow through the liver, and *partial hepatofugal* if a great part of contrast medium flowed through collateral veins.

Liver size was defined as *normal* if the hepatogram reached the costal margin, the L1 vertebra, and the cardia; as *less than normal* if the liver was clearly within these limits; and as *enlarged* if the liver exceeded one or more of these boundaries. *Left lobe hypertrophy* denoted a liver extending far into the left hypochondrium.

Portal hypertension was defined as portal venous pressure above 20 cm of water.

Results

Percutaneous transhepatic portography was successful in 123 of the 128 investigations (96%). The main portal vein was catheterized in 106 (83%), and the splenic

Received May 30, 1978; accepted after revision October 30, 1978.
This work was supported by grant no. 512-10468 from the Danish Medical Research Council.
[1] Departments of Surgical Gastroenterology and Radiology, Gentofte Hospital and Herlev Hospital, University of Copenhagen, 2730 Herlev, Copenhagen, Denmark. Address reprint requests to author at Herlev Hospital.

© 1979 American Roentgen Ray Society

0361-803X/79/1322-0177 $0.00

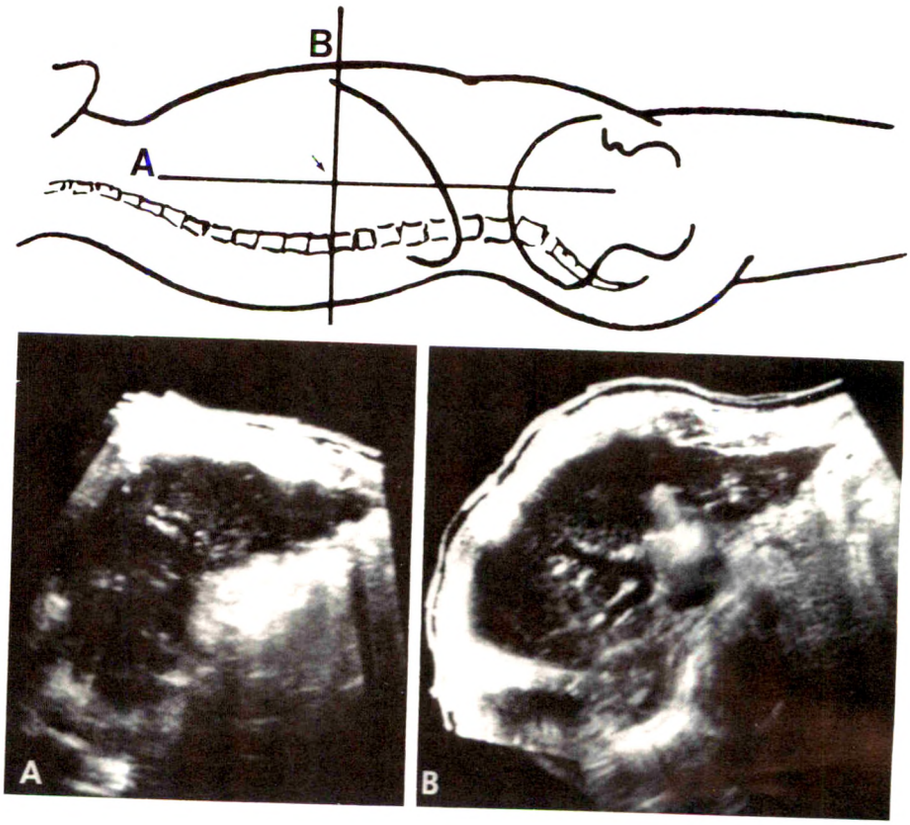


Fig. 1.—Puncture site (*arrow*) determined by scans used for localization of porta hepatis. Branching of right portal vein is shown.



Fig. 2.—Selective catheterization of coronary vein shows esophageal and fundic varices.

vein in 98 (77%). Portal vein catheterization was unsuccessful in six cases due to portal vein thrombosis. In an additional 11 cases the guide wire could not be passed from tortuous intrahepatic portal veins into the main portal vein.

TABLE 1
Diagnosis

Diagnosis	No. Patients
Intrahepatic obstruction (cirrhosis):	
Alcoholic	61
Cryptogenic	11
Chronic hepatitis	9
Primary biliary	2
Secondary biliary	2
Extrahepatic obstruction (thrombosis):	
Portal vein	6
Hepatic veins	1
Inferior vena cava	1
Biliary obstruction:	
Chronic pancreatitis	4
Pancreatic carcinoma	3
Common duct stenosis	2
Common duct stone	1
Lymphoma in porta hepatis	1
Toxic hepatitis (intrahepatic bile duct obstruction)	1
Biliary atresia	1
Other:	
Gastrinoma	12
Suspected gastrinoma	1
Insulinoma	1
Total	120

The direction of blood flow could be estimated in 106 patients; it was hepatopetal in 35, partial hepatofugal in 59 (fig. 3), and complete hepatofugal in 12 (fig. 4). All patients with hepatofugal flow had intra- or extrahepatic obstruction.



Fig. 3.—Widespread collateral veins from coronary vein, splenic hilum veins, and inferior mesenteric vein. Catheter lies in main portal stem. Flow in portal vein system is partial hepatofugal. Only sparse filling of intrahepatic portal veins. (Same patient as in fig. 2).

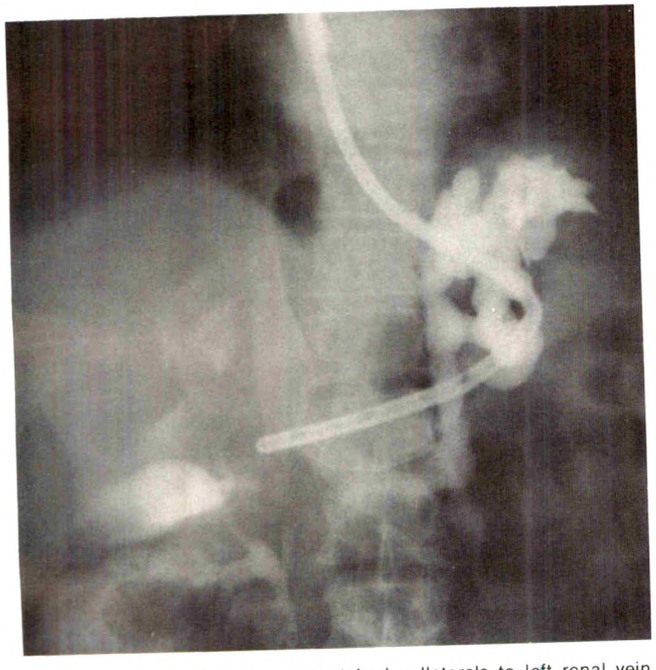


Fig. 4.—Retroperitoneal, paravertebral collaterals to left renal vein and inferior vena cava. Flow is complete hepatofugal.

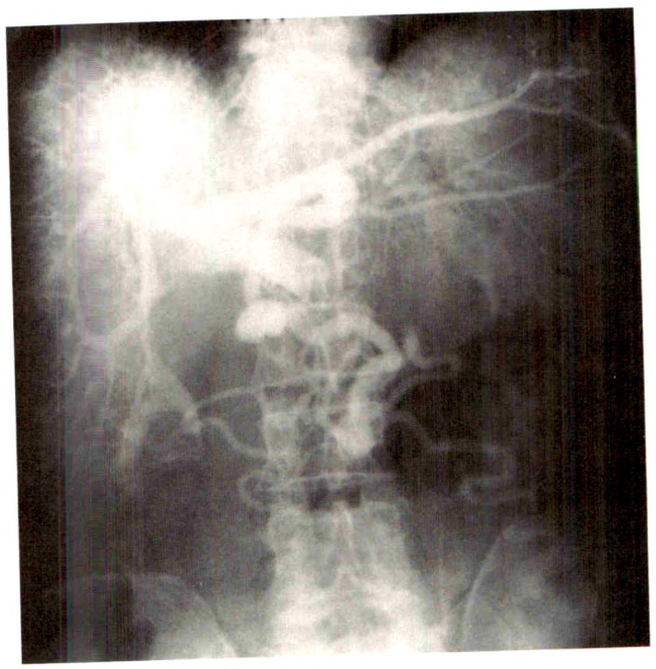


Fig. 5.—Recanalized umbilical vein connecting left portal branch and veins in abdominal wall (Caput Medusae). Left hepatic lobe is hypertrophied. Irregular and deviating intrahepatic portal vessels.

TABLE 2

Visualization of Collateral Vein System in Patients with Portal Hypertension

Type of Collateral Vein System	No. Patients (N = 94)
Coronary	60
From inferior mesenteric vein	38
Short gastric	22
Retroperitoneal-paravertebral	22
Recanalized umbilical	19
From superior mesenteric vein	13
From splenic hilum	12
From liver hilum	11
To abdominal wall	7
To left renal vein	4
Other	19

The type and number of collateral veins are shown in table 2. In 18 of the patients with cirrhosis or extrahepatic obstruction no collaterals were visualized. The most commonly observed collateral pathways to the superior vena cava were the coronary veins, short gastric veins, and esophageal venous plexus (figs. 2 and 3). Next most frequently observed were collaterals to the inferior vena cava via the inferior mesenteric vein (fig. 3), followed by retroperitoneal veins (fig. 4), and recanalized umbilical veins (fig. 5). Less frequently collaterals via the superior mesenteric vein (fig. 6) and other types of collaterals were seen. Most patients with collateral veins had two or more collateral systems visualized. In nine patients the vena cava could be seen (fig. 4).

Of the patients with intra- or extrahepatic obstruction, 63 (69%) had visible varices. Esophageal varices alone were seen in 16 patients, and gastric varices alone in nine patients. Both esophageal and gastric varices were seen in 38 patients.

All the patients with extrahepatic portal obstruction had them demonstrated by the transhepatic portography. Stenosis of the main portal vein was demonstrated in six patients (fig. 7). The diagnoses are shown in table

3. Four of these patients had minor collateral veins, but pressures below 20 cm.

In 79 of the patients with intra- or extrahepatic obstruction, the portal venous pressure was measured. The mean portal pressure was 34.5 cm water (SD 9.6). The highest pressures were found in patients with marked collaterals to the superior vena cava. In 16 of the patients with biliary obstruction or endocrine pancreatic tumors, the mean portal pressure was 15.9 cm water (SD 5.1).

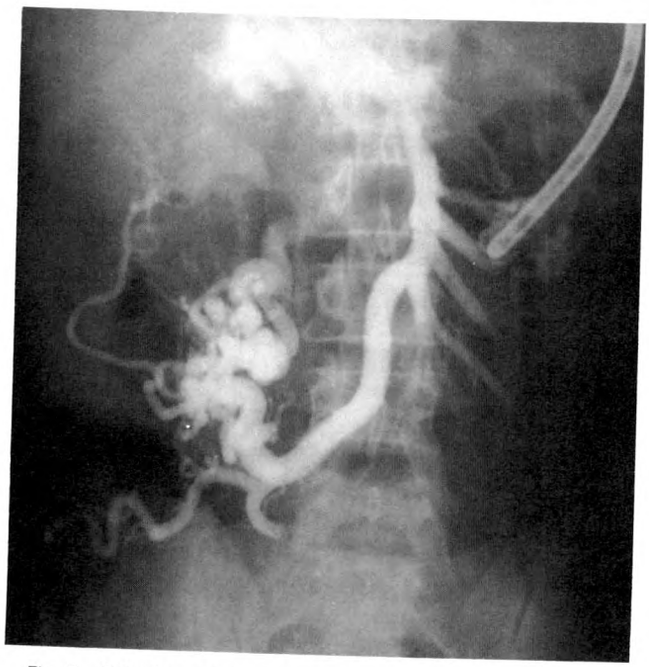


Fig. 6.—Selective catheterization of superior mesenteric vein. Collaterals around cecum and ascending colon.

The liver size could be estimated in 108 patients (90%). In 75 of the patients with cirrhosis the liver size could be estimated. The liver was normal in 40 (53%), smaller than normal in 24 (32%), and enlarged in 11 (15%); 22 (29%) had left lobe hypertrophy (fig. 5). In 33 patients without cirrhosis the liver size was normal.

In four patients 4–10 ml of 3% Aethoxysklerol was injected selectively into esophageal varices. A few minutes after injection, contrast medium flow stopped in the varices. Two of the patients had the catheter left in the coronary vein for repeated injection of Aethoxysklerol for 2 days. All patients suffered rebleeding from esophageal varices 2–4 weeks later, and portography showed recanalization of varices and formation of new collaterals to the varices.

The results of localization of the endocrine pancreatic tumors will be published elsewhere [21].

One patient had inadvertent puncture of the right flexure of colon causing no symptoms. Otherwise no complications were recorded.

Discussion

Percutaneous transhepatic puncture is the most direct route to catheterization of the portal venous system. Portography by this approach is probably the superior method for radiologic delineation of the portal venous system [22].

In normal subjects the porta hepatis is placed about 3 cm right of the vertebral spine and about the width of a vertebral body anterior to the T12 vertebra. Our portograms showed that this prediction may be as much as 7 cm off in cirrhosis. By the ultrasonic scanning method for localization of the porta hepatis, the number of puncture attempts can be reduced significantly [12].

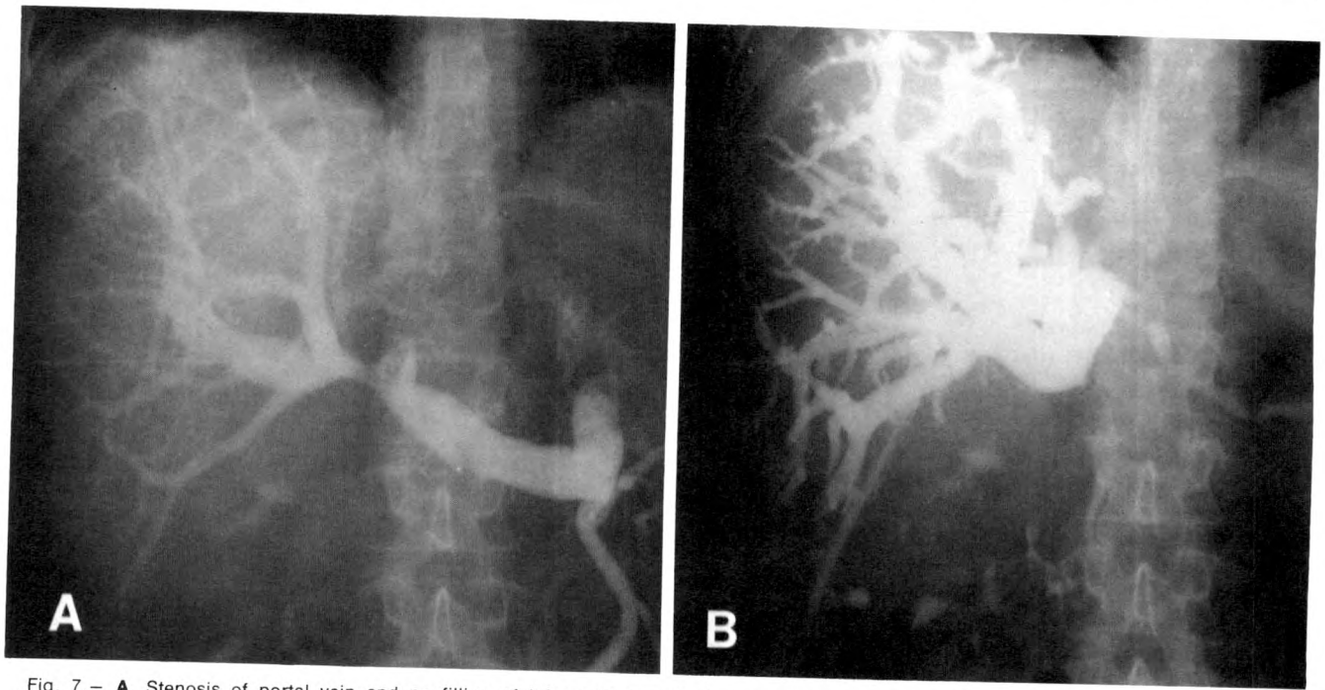


Fig. 7.— **A**, Stenosis of portal vein and no filling of left portal branch due to lymphoma in porta hepatis. **B**, Percutaneous transhepatic cholangiography. Total obstruction in porta hepatis.

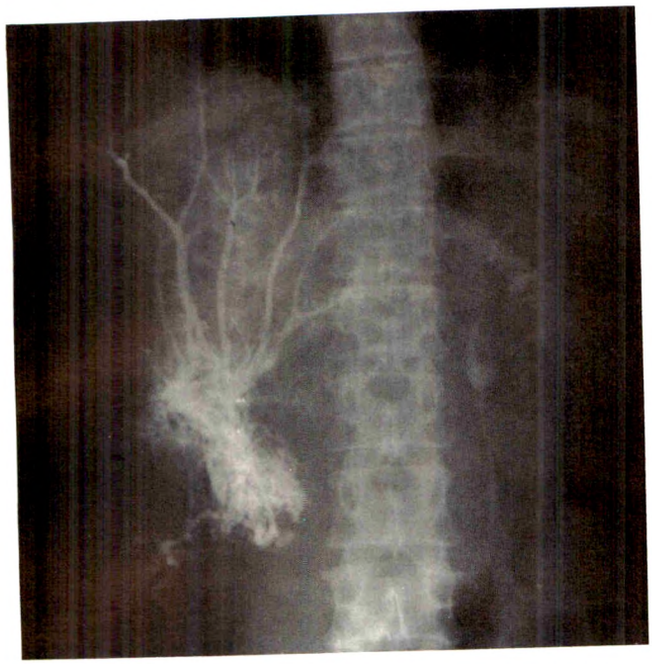


Fig. 8.—Occlusion of extrahepatic portal vein. Paraportal tortuous collaterals and some normal intrahepatic portal veins.

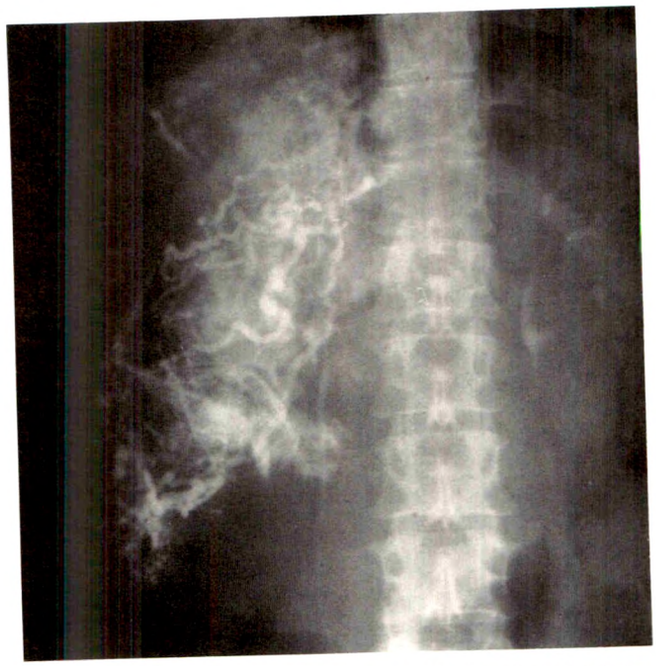


Fig. 9.—Occlusion of hepatic veins (Budd-Chiari syndrome). Intrahepatic tortuous collaterals.

TABLE 3

Diagnoses in Patients with Visualization of Stenosis of Main Portal Vein

Diagnosis	No. Patients
Carcinoma in head of pancreas	1
Gastrinoma in head of pancreas	1
Lymphoma in porta hepatis	1
Chronic pancreatitis	1
Postoperative iatrogenic stenosis	2
Total	6

Other investigators have used cholecystography or the venous phase of celiac and mesenteric arteriography to establish the anatomic position of the right portal vein [14, 15], but these methods are more cumbersome or invasive.

Puncture in the right midaxillary line secures a convenient angle of entry into the right portal branch, provides more parenchymal thickness for protection from bleeding, prevents injury of other intraabdominal organs, and eases manipulation of the catheter and guide wire.

In cirrhosis the intrahepatic portal veins are often irregular with a course markedly deviating from the normal (fig. 5) making catheterization of the extrahepatic portal system impossible in some cases. The left portal branch is often dilated, because of collateral circulation via the umbilical vein [23] or hypertrophy of the left lobe (fig. 5).

Location, number, size, and flow pattern of the collateral veins in relation to the portal venous pressure may have therapeutic implications [24]. Communications to the superior vena cava through gastroesophageal varices and a high portal pressure seem to be correlated with severe bleeding from the varices. Large communications to the inferior vena cava through retroperitoneal collaterals with opacification of the inferior vena cava and a less elevated portal pressure are correlated with minor or no gastroesophageal varices. These communications represent the most desirable route of natural decompression. Unfortunately they are a less frequent collateral system.

Extrahepatic obstruction of the portal vein is usually caused by thrombosis. With complete obstruction, the radiologic diagnosis is made by demonstration of paraportal tortuous collaterals (fig. 8). Obstruction may also be caused by tumors along the vein; it is usually incomplete and its exact site and extent can be demonstrated (fig. 7). Obstruction of the hepatic veins should be suspected when tortuous intrahepatic collaterals (fig. 9) accompany decreased or hepatofugal flow in the portal veins.

The preliminary results of obliteration of esophageal varices [17, 18] were promising, but recanalization occurred after a few weeks in about 80% of the patients [25]. The method can be used to stop actual bleeding and has been successful in about half of the cases [17, 18, 25].

The preliminary results of selective catheterization of pancreatic veins with blood sampling and hormone assay for localization of endocrine pancreatic tumors have been encouraging. The number of patients examined is still small. The largest group consists of patients with gastrinomas, in whom the localization was successful in about 80% [21].

Catheterization of the portal venous system may also be valuable in pharmacologic, metabolic, and hemodynamic studies. It is possible to leave the catheter in the portal venous system for several days for such studies.

The most often reported complications with transhe-

patic catheterizations are intraperitoneal bleeding and bile leakage from the puncture site. To avoid these, the puncture canal can be sealed with an acrylate compound [26], or by injection of autologous clots, thromboplastin, or gelatin foam [14, 15]. We have used gradual withdrawal of the clamped catheter over 6–12 hr, which allows the puncture canal time to seal. We use the same procedure in percutaneous transhepatic cholangiography. In 200 investigations, we have had two cases with bleeding episodes and two with bile leakage. However, in all four patients the catheter retracted completely in immediate connection with the procedure.

REFERENCES

1. Blakemore AH, Lord JW Jr: The technic of using vitallium tubes in establishing porta-caval shunts for portal hypertension. *Ann Surg* 122:476–489, 1945.
2. Boulvin R, Chevalier M, Gallus P, Nagel M: La portographie par voie splénique transperiétale. *Acta Chir Belg* 50:534–544, 1951
3. Leger L, Albot G, Arvay N: La phlébographie portale dans l'exploration des affections hépato-spléniques. *Presse Med* 59:1230–1232, 1951
4. Ödman P: Percutaneous selective angiography of the coeliac artery. *Acta Radiol [Suppl]* (Stockh) 159:1–168, 1958
5. Bierman HR, Steinbach HL, White LP, Kelly KH: Portal veinpuncture. A percutaneous, trans-hepatic approach. *Proc Soc Exp Biol Med* 79:550–552, 1952
6. Bierman HR, Kelly KH, White LP, Coblentz A, Fisher A: Transhepatic venous catheterization and venography. *JAMA* 158:1331–1334, 1955
7. Carbalhaes OG: Portography: a preliminary report of a new technique via the umbilical vein. *Clin Proc Child Hosp* 15: 120–122, 1959
8. Rösch J, Hanafee WN, Snow H: Transjugular portal venography and radiologic portacaval shunt: an experimental study. *Radiology* 92:1112–1114, 1969
9. Silva L, Thiago JBS, Ferrarini E, Goffi FS: The percutaneous transhepatic approach of the portal vein in man in the determination of patency of splenorenal shunts. *Surgery* 50:473–477, 1961
10. Wiechel KL, Kulling KG, Marions O, Erwald R, Lindberg K: Direkt portografi. *Nord Med* 86:1255–1256, 1971
11. Von Deimer E: Die perkutane hepatographie. *ROEFO* 114: 84–102, 1971
12. Burcharth F, Nørby Rasmussen S: Localization of the porta hepatis by ultrasonic scanning prior to percutaneous transhepatic portography. *Br J Radiol* 47:598–602, 1974
13. Nabseth DC, Widrich WC, O'Hara ET, Johnson WC: Flow and pressure characteristics of the portal system before and after splenorenal shunts. *Surgery* 78:739–748, 1975
14. Viamonte M Jr, LePage J, Lunderquist A, Pereiras R, Russell E, Viamonte M, Camacho M: Selective catheterization of the portal vein and its tributaries. Preliminary report. *Radiology* 114:457–460, 1975
15. Okuda K, Suzuki K, Musha H, Arimizu N: Percutaneous transhepatic catheterization of the portal vein for the study of portal hemodynamics and shunts. *Gastroenterology* 73: 279–284, 1977
16. Russell E, LePage JR, Viamonte M, Levi JU, Meier WL: An angiographic approach to hepatobiliary diseases. *Surg Gynecol Obstet* 143:414–424, 1976
17. Scott J, Dick R, Long RG, Sherlock S: Percutaneous transhepatic obliteration of gastro-oesophageal varices. *Lancet* 2:52–55, 1976
18. Pereiras R, Viamonte M Jr, Russell E, LePage J, White P, Hutson D: New technique for interruption of gastroesophageal venous blood flow. *Radiology* 124:313–323, 1977
19. Ingemansson SG: Pancreatic and intestinal vein catheterization with hormone assay. *Bull Dept Surg Univ Lund* (Sweden) 13:1–31, 1977
20. Turner RC, Morris PJ, Lee ECG, Harris EA: Localization of insulinomas. *Lancet* 1:515–518, 1978
21. Burcharth F, Stage JG, Stadil F, Fischermann K, Jensen LI: Localization of gastrinomas by transhepatic portal catheterization and gastrin assay. *Gastroenterology*. In press, 1979
22. Burcharth F, Nielbo N: Percutaneous transhepatic portography. Comparison with splenoportography in 67 patients with portal hypertension. *AJR* 132:183–185, 1979
23. Kam-Hansen L, Burcharth F: Omphalocaval shunt: A procedure for portal decompression in Cruvielhier-Baumgartens syndrome. *Acta Chir Scand* 143:493–494, 1977
24. Nunez D Jr, Russell E, Yrizarry J, Pereiras R, Viamonte M Jr: Portosystemic communications studied by transhepatic portography. *Radiology* 127:75–79, 1978
25. Lunderquist A, Simert G, Tylén U, Vang J: Follow-up of patients with portal hypertension and esophageal varices treated with percutaneous obliteration of gastric coronary vein. *Radiology* 122:59–63, 1977
26. Georgakakis A: Experimental investigation of the use of cyano-acrylate adhesive to prevent biliary leakage in percutaneous transhepatic cholangiography. *Br J Surg* 60: 115–116, 1973

Percutaneous Transhepatic Portography. II. Comparison with Splenoportography in Portal Hypertension

FLEMMING BURCHARTH,[1] NIELS NIELBO,[2] AND BJØRN ANDERSEN[1]

Percutaneous transhepatic portography and splenoportography were compared in 67 patients with portal hypertension. Portograms were evaluated without knowledge of the identity of patients. Factors evaluated included technical success of the examination; visualization of the portal vein, splenic vein, and other tributaries; contrast medium density, portal blood flow direction; presence and type of collaterals and varices; and liver size and configuration. Percutaneous transhepatic portography proved superior with regard to delineation of the portal venous system and esophageal varices. A definite diagnosis of portal vein thrombosis was possible only with the transhepatic approach.

The standard methods for radiologic visualization of the portal venous system are venous phase arteriography and splenoportography, whereas percutaneous transhepatic portography is used infrequently. Since 1972 we have performed both splenoportography and transhepatic portography in 67 consecutive patients with portal hypertension in order to compare the methods.

Subjects and Methods

From 1972 through 1976, 20 female patients (median age, 59 years; range, 9–75) and 47 male patients (median age, 53 years; range, 26–74) with portal hypertension were investigated with both transhepatic portography and splenoportography. The study was approved by the local committee of ethics. Informed consent was obtained. The diagnoses are shown in table 1.

Percutaneous transhepatic portography was performed with the technique described previously [1]. Splenoportography was performed under local anesthesia with a 15 cm catheter similar to that used for transhepatic portography. The contrast medium was 30 ml of 76% sodium methylglucamine diatrizoate, as in transhepatic portography. Otherwise the procedure was as described by others [2–4]. All procedures were performed by us, transhepatic portography by F. B. and splenoportography by N. N.

Patient identification was (temporarily) removed from the films of the two types of portography. Each series was separately evaluated in random order by an independent colleague. His evaluations subsequently formed the basis for paired, within-patient comparison of the two methods. In the evaluation the following definitions were used:

Successful transhepatic portography was defined as catheterization and visualization of the portal veins, and a successful splenoportography as puncture of the splenic pulp with passage of contrast medium to the splenic vein or collateral veins from the spleen.

Density of the contrast medium was ranked as *high* when the veins were completely filled and produced a homogeneous white shadow on the films, as *medium* when the shadow was less intensive (gray), and as *low* when contrast filling was incomplete.

Direction of the flow in the portal vein was defined as *hepatopetal* if all contrast medium flowed through the liver, *complete hepatofugal* if contrast medium flowed to collateral veins with no flow through the liver, and *partial hepatofugal* if a great part of contrast medium flowed through collateral veins.

Grading of esophageal or gastric varices was *0* if no varices were visible, *1* when small varices were just visible, *2* when varices were distinct, and *3* when large varices were seen.

The *liver size* was defined as *normal* if the hepatogram reached the costal margin, the L1 vertebra, and the cardia; as *less than normal* if the liver was clearly within these limits; and as *enlarged* if the liver exceeded these boundaries. *Left lobe hypertrophy* denoted a liver extending far into the left hypochondrium.

The sign test, Pratt's test, and Spearman's rank correlation coefficient were used for the statistical analyses.

Results

All splenoportographies were successful; transhepatic portography was unsuccessful in five cases (7%). The following results are based on the 62 patients in whom both methods succeeded. The splenoportography procedure lasted 0.5–1 hr (mean 0.5 hr), and the transhepatic portography 0.5–2 hr (mean, 1 hr).

Visualization of the portal vein was superior in transhepatic portography (table 2) ($P < 0.05$, sign test), while the visualization of the splenic vein was best in splenoportography (table 2) ($P < 0.01$, sign test). In 13 investigations splenoportography indicated portal vein thrombosis, but transhepatic portography proved that the

TABLE 1

Diagnoses

Diagnosis	No. Patients
Intrahepatic obstruction (cirrhosis):	
Alcoholic	46
Cryptogenic	9
Chronic hepatitis	6
Primary biliary	1
Secondary biliary	2
Extrahepatic obstruction:	
Thrombosis of portal vein	1
Thrombosis of hepatic vein	1
Lymphoma in porta hepatis	1
Total	67

Received May 30, 1978; accepted after revision October 30, 1978.
This work was supported by grant no. 512-10468 from the Danish Medical Research Council.
[1]Department of Surgical Gastroenterology, Gentofte Hospital and Herlev Hospital, University of Copenhagen, 2730 Herlev, Copenhagen, Denmark. Address reprint requests to F. Burcharth at Herlev Hospital.
[2]Department of Radiology, Gentofte Hospital, University of Copenhagen, Copenhagen, Denmark.

© 1979 American Roentgen Ray Society

0361-803X/79/1322-0183 $0.00

portal vein was patent in 11 of these patients (table 2) (fig. 1).

The intravascular contrast density was vastly superior in transhepatic portography ($P << 0.01$, sign test), as was the density of the hepatogram phase.

The direction of the portosystemic blood flow is shown in table 3. In eight cases the flow was deemed partial hepatofugal by transhepatic portography, but hepatopetal by splenoportography ($P < 0.01$, sign test). The estimation of flow direction by the two methods agreed in 69% of the 62 patients with successful studies.

Transhepatic portography offered a better and more detailed picture of collateral veins than splenoportography. Collateral pathways involving the superior and inferior mesenteric veins and collaterals from the liver hilum, especially, were more often seen by transhepatic portography ($P < 0.05$, sign test). Only collaterals from the splenic hilum were better demonstrated by splenoportography ($P << 0.01$, sign test). However, in four patients transhepatic portography demonstrated splenic hilum collateral veins not apparent on splenoportography. The vena cava was visualized by transhepatic portography in three patients and by splenoportography in one.

Visualization of gastric and esophageal varices by the two methods correlated well (table 4) ($P < 0.001$, Spearman's analysis). However, the diagnosis of esophageal varices was much better by transhepatic portography than by splenoportography (table 4) ($P < 0.01$, Pratt's test). In 16 investigations esophageal varices were seen on transhepatic portography, but not on splenoportography, and the varices seen by both methods were better presented with transhepatic portography. In the four patients in whom splenoportography showed varices not found by transhepatic portography, the catheter could not be advanced beyond the porta hepatis, but according

TABLE 2

Degree of Visualization of Portal and Splenic Veins

Transhepatic Portography	Splenoportography			Total
	Complete	Partial	None	
Portal vein:				
Complete	**43**	2	11	56
Partial	1	**0**	1	2
None	2	1	**1**	4
Total	46	3	13	62
Splenic vein:				
Complete	**29**	4	1	34
Partial	15	**2**	0	17
None	7	3	**1**	11
Total	51	9	2	62

TABLE 3

Flow Direction

Transhepatic Portography	Splenoportography				Total
	Hepatopetal	Partial Hepatofugal	Complete Hepatofugal	Unclarified	
Hepatopetal	**2**	0	0	1	3
Partial hepatofugal	8	**31**	7	0	46
Complete hepatofugal	0	3	**7**	0	10
Unclarified	1	2	0	**0**	3
Total	11	36	14	1	62

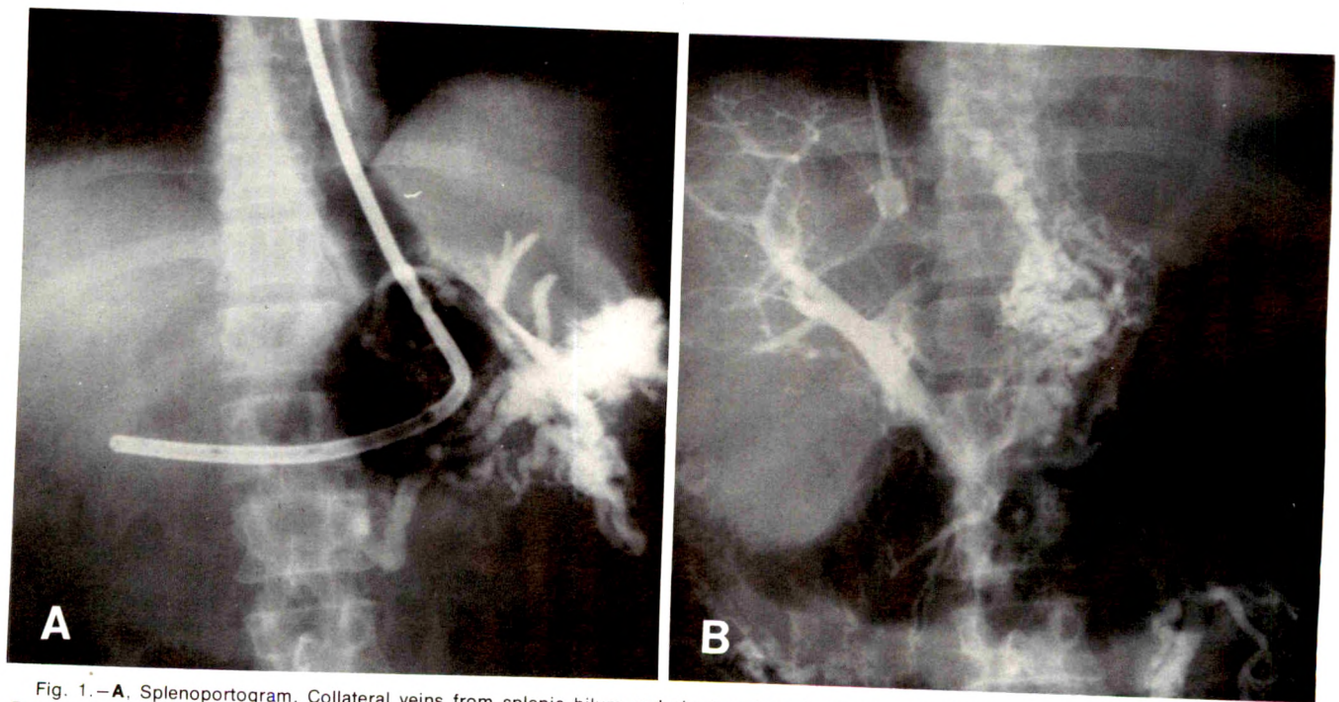


Fig. 1.—**A**, Splenoportogram. Collateral veins from splenic hilum and short and small splenic vein. Suggestive of portal vein thrombosis. **B**, Percutaneous transhepatic portogram. Open portal vein, huge collateral vein system, and esophageal varices.

TABLE 4

Visualization of Esophageal and Gastric Varices

Transhepatic Portography (grade)	Splenoportography				Total
	0	1	2	3	
Esophageal varices:					
0	**15**	1	2	1	19
1	9	**3**	2	0	14
2	4	9	**3**	0	16
3	3	2	4	**4**	13
Total	31	15	11	5	62
Gastric varices:					
0	**13**	6	1	2	22
1	6	**4**	1	1	12
2	2	9	**6**	2	19
3	1	1	3	**4**	9
Total	22	20	11	9	62

to our definitions the investigations were considered successful. The frequency with which a diagnosis of gastric varices was made did not differ significantly between the two methods (table 4) ($P > 0.10$, Pratt's test).

The registered liver size was the same in the two types of investigations, but left lobe hypertrophy was more readily seen in transhepatic portography ($P < 0.01$, sign test).

All transhepatic portographies were performed without complications. Two patients had clinical signs of intraabdominal bleeding after splenoportography; both patients recovered without surgery after blood transfusion.

Discussion

Splenoportography is the quickest and simplest method of delineating the portal vein anatomy. Transhepatic portography presents more technical problems and is more time consuming. Our study indicates that transhepatic portography provides more detailed anatomic information. This is especially important in the planning of portacaval shunt surgery.

The value of splenoportography has been studied retrospectively [2–4], but the two methods have not previously been compared. As soon as we mastered the technic of transhepatic portography [1] we started the present trial.

The high success rate and the low frequency of complications were probably due to the fact that the same persons performed all the investigations, and that ultrasonic localization of the porta hepatic was used in the transhepatic approach [5].

Transhepatic portography visualized the main portal vein better than splenoportography, and revised in 11 investigations the splenoportographic diagnosis of portal vein thrombosis by demonstrating a patent portal vein. In these cases the hepatofugal flow in huge collateral veins from the splenic hilum drained the contrast medium away from the main portal vein. Since surgical portacaval anastomoses may be incorrectly considered impossible because of apparent portal vein thrombosis on splenoportography, this procedure should be replaced by transhepatic portography in the workup of these patients.

The intravascular contrast medium density was highest in transhepatic portography, because of the more direct application of contrast medium. This also accounts for a denser hepatogram phase in transhepatic portography.

Reversed circulation in collateral veins was demonstrated in 95% of patients by transhepatic portography and in 78% by splenoportography. The difference was due to the more detailed visualization of the collateral vein system by transhepatic portography. Apart from diagnosis of varices, demonstration of collaterals and flow direction is of value in estimation of the degree of spontaneous portosystemic shunt.

Esophageal varices were more frequently and better demonstrated by transhepatic portography. Gastric varices were visualized equally well with both methods. Gastric varices without concomitant esophageal varices were seen only in five patients.

In four patients the transhepatic catheter could not be advanced into the portal vein and visualization of the extrahepatic portal system was impossible (tables 2 and 4). In 10 patients the splenic vein was not catheterized and consequently not visualized (table 2). Splenic vein thrombosis cannot be ruled out by transhepatic portography if the splenic vein is not catheterized.

In conclusion, percutaneous transhepatic portography was found superior to splenoportography in delineation of the portal vein system, and in the diagnosis of esophageal varices. A reliable diagnosis of portal vein thrombosis can only be made by transhepatic portography. Transhepatic portography with selective catheterization technique makes visualization of the entire portal system possible, and is recommended as the method of choice in radiologic investigation of portal hypertension.

REFERENCES

1. Burcharth F: Percutaneous transhepatic portography. Technique and application. *AJR* 132:177–182, 1979
2. Bergstrand I: Splenoportography, in *Angiography*, 2d ed, vol 2, edited by Abrams HL, Boston, Little, Brown, 1971, pp 1029–1072
3. Foster JH, Conkle DM, Crane JM, Burko H: Splenoportography. An assessment of its value and risk. *Ann Surg* 5:773–781, 1974
4. Panke WF, Bradley EG, Moreno AH, Ruzika FF Jr, Rousselot LM: Technique, hazards, and usefulness of percutaneous splenic portography. *JAMA* 169:1032–1037, 1959
5. Burcharth F, Rasmussen SN: Localization of the porta hepatis by ultrasonic scanning prior to percutaneous transhepatic portography. *Br J Radiol* 47:598–602, 1974

AJR Guidelines for Authors

Address manuscripts and correspondence to the Editorial Office, American Journal of Roentgenology, 403 Pacific National Bank Building, 4545 15th Avenue N.E., Seattle, Washington 98105; telephone (206)633-2754.

Publication Policy

The Journal publishes original and timely contributions to the advancement of radiologic diagnosis and treatment. Although the content is predominantly clinical, laboratory investigations are accepted when their relevance to clinical practice is demonstrable. In prospective clinical investigations, authors should indicate if informed consent from patients was obtained. Decisions on manuscripts are based on the opinions of at least two outside reviewers. Reviewers receive manuscripts without title pages to protect the identity of authors and to ensure an unbiased review; names of reviewers, in turn, are not revealed to authors. Statements within an article are the responsibility of the authors and not the Journal or its publisher.

It is understood that material submitted has not been published and is not currently submitted elsewhere. Portions of the data or illustrations from previously published works may be included if permission release forms accompany the manuscript and such material is clearly credited in the text. Prior publication of abstracts will not prejudice publication of the complete study.

Copyright Information

In accordance with Journal implementation of the 1976 U.S. Copyright Law, authors must release first and subsidiary rights to their manuscript at submission. A dated cover letter, containing signatures of all authors, should state: "We, the authors, assign first and subsidiary rights to the American Roentgen Ray Society in the event that our manuscript (title) is published by AJR." The Journal, in turn, grants authors the right to use portions of their manuscript, without charge, in books or articles of which they are authors or editors.

Manuscript Form

Manuscripts should be typed double-spaced throughout, including references, tables, and figure legends. Tables, footnotes, and figure legends should be on separate sheets, and a separate title page should be provided. In addition to the original typewritten copy, a duplicate copy complete with figures, tables, and references is required. Authors' names should be on title page only and should not be on figures so that author anonymity can be maintained during the review process.

Figures should be submitted as 13 × 18 cm glossy prints, untrimmed and unmounted. Labels and arrows must be of professional quality and should be removable from the prints. Each figure should be numbered to correspond with figure legends, and the top should be indicated. Specific permission for publication of facial photographs of patients is required. Line illustrations and graphs should be drawn in black ink on white background.

References should be cited in the text by number (e.g., [3, 4]). The bibliography should be arranged in the numerical order that references are cited in the text and typed double-spaced throughout. Data for each reference should be arranged according to the uniform style on bibliographic citations adopted by many biomedical journals. Provide all authors' names and inclusive pages. Abbreviations for titles of medical periodicals should conform to those published in *Index Medicus*. Examples:

1. Miller RE, Chernish SM, Skucas J, Rosenak BD, Rodda BE: Hypotonic roentgenography with glucagon. *AJR* 121:264–274, 1974
2. Boijsen E: Superior mesenteric angiography, in *Angiography*, edited by Abrams H, Boston, Little, Brown, 1971, pp 1091–1119

Organization

Title page. Titles should be brief and specific. Include addresses for each author and acknowledgment of grant support when appropriate.

Abstract. A description of the purpose, methods, results and conclusions of the study is required.

Introduction. Clearly state the purpose of the investigation including necessary background facts.

Materials and methods. Decribe the protocol clearly. Use standard abbreviations as presented in the *Council of Biology Editors Style Manual*, 3d ed. Metric measurements should be used throughout.

Results. Present results in logical sequence.

Discussion. Interpret the results to lend meaning and importance to the observations. Hypotheses and speculation based on the results are encouraged. When results differ from those of previous investigators, an attempt should be made to explain the discrepancy.

References. Only include references which provide adequate background and present fairly any opposing evidence and concepts. Accuracy of reference data is the responsibility of the author.

Legends. Legends should be brief but should provide sufficient description to interpret the figure.

Special Communications

Case Reports. Concise case reports are accepted if they present unusual experiences that are medically important and educational. Clarity and brevity are essential. After preliminary screening by an editor to determine whether the requirement of medical significance has been met, qualifying papers will undergo the same peer review as major papers.

Technical notes. Brief descriptions of new techniques or significant modifications of older ones which are directly applicable to clinical practice will be accepted.

Letters to the Editor. Letters are subject to editing and condensation. Criticism of published articles should be objective and constructive. Letters may also discuss matters of general interest to radiologists.

Infusion Hepatotomography for Evaluation of Obstructive Jaundice

WON S. CYNN,[1] BARRY L. LEVIN, PATRICIA A. GUREGHIAN, AND ARNOLD CHAIT

Total body opacification with high doses of a urographic contrast agent demonstrated dilated intrahepatic biliary ducts as branching or rounded lucencies in all of 18 patients with obstructive jaundice. Dilated extrahepatic ducts were seen as tubular lucencies in 11 of 16 patients with distal common bile duct obstruction. In seven patients with nonobstructive jaundice and in a control group of 25, the biliary ducts were either normal or not seen. Gallbladder size was also evaluated. The site of obstruction could be predicted by the size of the gallbladder and visualization of the biliary ducts.

Since O'Connor and Newhauser's description [1], total body opacification during urography with high doses of contrast material has been used for the differentiation of solid from cystic abdominal and pelvic masses [2]. Infusion tomography has also been used to determine gallbladder size and wall thickness [3, 4]. Infusion nephrotomography for evaluation of renal mass lesions has been widely used [5]. Infusion tomography for evaluation of intrahepatic masses and liver disease has also been reported [6]. We used a similar technique to determine whether the intra- and extrahepatic biliary ducts could be visualized in a control group and in patients with obstructive and nonobstructive jaundice.

Subjects and Methods

Two groups, 25 jaundiced patients (serum bilirubin levels of 5–17 mg/100 ml) and 25 control patients, were studied with infusion hepatotomography. The control patients, requiring infusion nephrotomography for renal problems, had no hepatobiliary symptoms. All the patients had survey radiography including tomography of the right upper quadrant of the abdomen in the right posterior oblique projection. Linear tomograms with an arc of 45° were obtained at the midplane; 1, 2, and 3 cm above; and 1 cm below the midplane.

Diatrizoate meglumine (Renografin) was used as the contrast agent. Three different combinations of iodine concentration and total contrast dosage were tried. One jaundiced and five control patients received 300 ml of Reno-M-Dip (141 mg I/ml; total, 42.3 g I). One jaundiced and five control patients received 190 ml of Renografin 76 (370 mg I/ml; total, 70.3 g I). The rest of the patients received a mixture of 300 ml of Reno-M-Dip and 40 ml of Renografin 76 (168 mg I/ml; total, 57.1 g I). Through a 19-gauge butterfly needle, the contrast was infused in an anticubital vein as fast as hydrostatic pressure allowed.

When about two-thirds of the contrast material had been infused, linear tomography and routine radiography were performed to include the area of the gallbladder and liver. The films were immediately checked and additional tomograms were obtained if necessary. To evaluate the density and duration of the hepatogram, in five patients, additional radiographs were obtained when about one-half of the contrast material had been infused, at the completion of the infusion, and then at 10, 20, and 30 min after infusion.

Results

Among the 25 jaundiced patients, 18 had obstructive jaundice proven by either subsequent percutaneous transhepatic cholangiography, surgery, or autopsy. Of these 18, 15 patients had distal common bile duct obstruction from carcinoma of the pancreas, one had cholangiocarcinoma at the porta hepatis, and two (with previous cholecystectomy) had chronic pancreatitis. In all 18, dilated intrahepatic ducts were visualized as branching or rounded lucencies on the tomograms (fig. 1) and, in many of these patients, even on the plain radiographs. Of the 15 patients with carcinoma of the pancreas, 11 also showed dilated extrahepatic biliary duct and a distended gallbladder (figs. 2–4). Tubular lucencies identified the dilated extrahepatic ducts, two of which were bordered by parallel, thick opaque lines. A twelfth patient with distal common bile duct obstruction from carcinoma of the pancreas showed a normal-sized gallbladder and dilated intrahepatic ducts. The other three patients with carcinoma of the pancreas causing common bile duct obstruction showed dilated intrahepatic ducts only. The patient with cholangiocarcinoma showed only dilated intrahepatic ducts; the extrahepatic ducts and the gallbladder were not visualized on several tomograms (fig. 5).

Of the seven patients with nonobstructive jaundice, five did not show any biliary ducts with infusion tomography, while a sixth had a dilated gallbladder and a seventh showed normal-sized intrahepatic ducts. Five of the seven proved to have hepatocellular jaundice at biopsy or autopsy. In the other two patients, the bilirubin became normal without any specific treatment.

In the 25 control patients, the extrahepatic ducts were not seen. The intrahepatic ducts were either not seen or appeared as thin, linear, branching lucencies in the area of the porta hepatis.

We found that the infusion of 300 ml of Reno-M-Dip alone did not produce a sufficiently dense hepatogram, even though the gallbladder and dilated intrahepatic ducts could usually be recognized in the obstructed patients. Renografin 76 (190 ml) yielded a good hepatogram; however, one of our control patients receiving this dose developed violent nausea, vomiting, and shaking chills. The mixture of 300 ml of Reno-M-Dip and 40 ml of Renografin 76 produced a hepatogram clearly seen for

Received March 18, 1977; accepted after revision November 9, 1978.
[1]All authors: Department of Radiology, Graduate Hospital, Philadelphia, Pennsylvania 19146. Address reprint requests to B. L. Levin.

0361-803X/79/1322-0187 $0.00

AJR 132:187–190, February 1979
© 1979 American Roentgen Ray Society

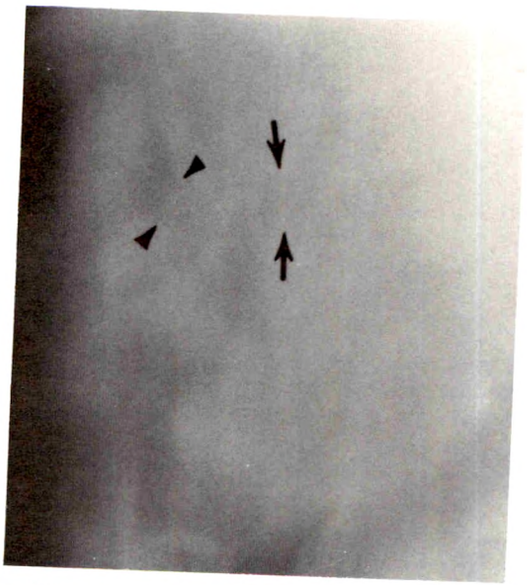


Fig. 1.—Tubular (*arrowheads*) and oval (*arrows*) lucencies representing dilated intrahepatic biliary ducts.

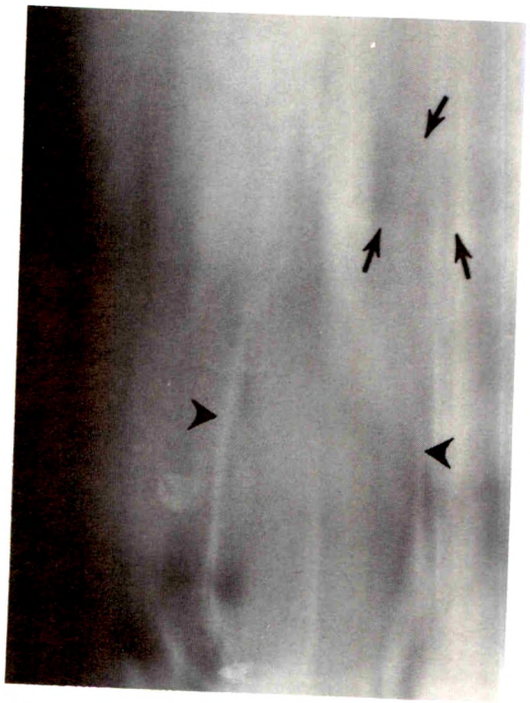


Fig. 2.—Tubular 2.3 cm lucency (*arrows*) represents dilated extrahepatic duct from carcinoma of pancreas. Also note distended gallbladder with thick wall (*arrowheads*).

about 15 min after completion of the contrast infusion and was tolerated well by all patients who received it.

Discussion

There are many radiologic techniques to differentiate obstructive from nonobstructive jaundice. Angiography



Fig. 3.—Dilated extra- (*arrows*) and intrahepatic 1.0 cm biliary ducts. Note thickened wall of duct (*arrowhead*). Patient had carcinoma of pancreas.

[7], endoscopic retrograde cholangiopancreatography, ultrasound [8, 9], computed tomography [10], and skinny needle percutaneous transhepatic cholangiography have succeeded in demonstrating dilated biliary ducts. Visualization of dilated biliary ducts by total body opacification has been reported [6, 11], but the extrahepatic duct and gallbladder were not mentioned. We found that infusion hepatotomography also can demonstrate dilated intra- and extrahepatic ducts and can simultaneously provide information about gallbladder size. During total body opacification, only the vascular compartments are opacified. The biliary ducts, which are nonvascular, will be lucent as seen against the vascular hepatogram; the gallbladder, too, is lucent as its wall becomes opacified. Dilated extrahepatic ducts are seen as tubular lucencies in contrast to the opacified wall and surrounding tissue, while intrahepatic biliary ducts are branching lucencies, or rounded lucencies if seen on end. Occasionally, the walls of the extrahepatic duct are seen as thick, parallel, opacified lines presumably representing a thickened wall secondary to inflammatory changes. Biliary ducts may be seen in plain films as parallel lucent lines if there is prominent peribiliary fat [12–14].

In the majority of our patients, we found that the distended gallbladder is visualized when the common bile duct is obstructed. However, it is interesting to note that one patient with distal common bile duct obstruction from carcinoma of the pancreas had a normal-sized gallbladder, but dilated intrahepatic ducts. In one nonobstructed jaundiced patient, the gallbladder was markedly dilated but the biliary duct was not seen.

Thus, in our experience, dilated extra- and intrahepatic ducts are seen on infusion tomography only in

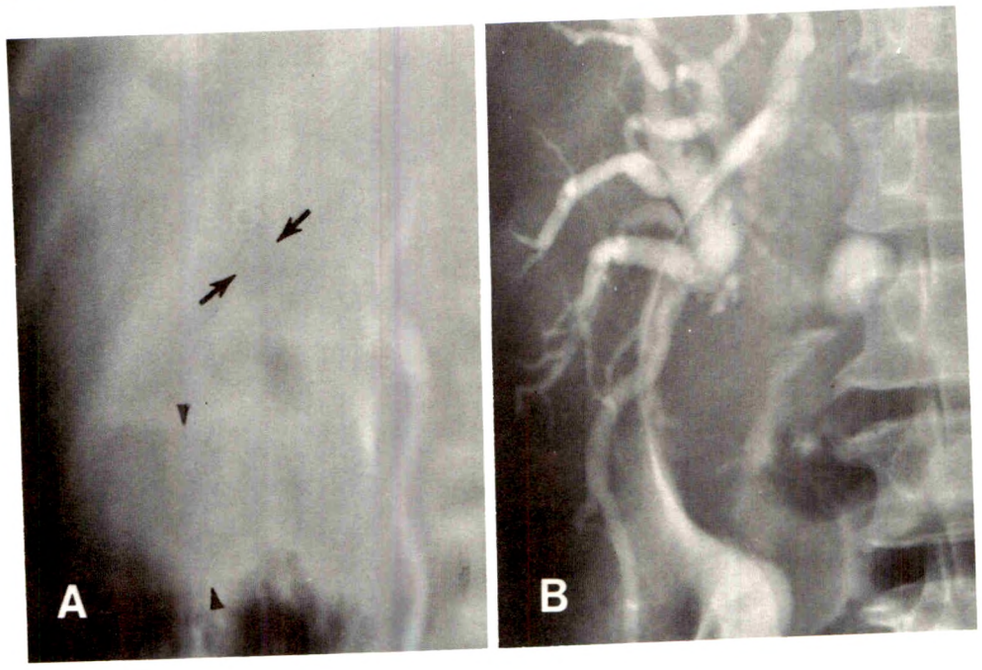


Fig. 4.—**A**, Dilatation of intrahepatic ducts (*arrows*). Enlarged gallbladder with thickened walls (*arrowheads*). (Ring above arrows is photographic artifact.) **B**, Confirmed obstruction of common hepatic duct and dilatation of intrahepatic radicles. Carcinoma of pancreas was found at operation.



Fig. 5.—Dilated intrahepatic duct (1.2 cm) (*arrows*) with thick wall. Gallbladder and extrahepatic duct were not seen with several tomograms. Cholangiocarcinoma at porta hepatis found at operation.

the presence of extrahepatic duct obstruction. When a distended gallbladder is also seen, the obstruction is distal to the cystic duct insertion. However, gallbladder distention in the absence of dilated ducts is not diagnostic of obstructive jaundice. When dilated intrahepatic ducts and a normal-sized gallbladder are seen, we find that the site of obstruction cannot be identified. But in our patients, finding dilated intraphepatic ducts without visualization of the gallbladder localized the obstruction to the porta hepatis.

Our technique for infusion hepatotomography used low kilovoltage to obtain maximum contrast. The mixture of 300 ml of Reno-M-Dip plus 40 ml of Renografin 76 gives a satisfactory hepatogram and enough time to repeat tomography if the initial films are not satisfactory.

Infusion hepatotomography can help to differentiate between obstructive and nonobstructive jaundice and to determine the site of biliary tract obstruction. Simple and noninvasive, this technique can be done in any radiology department equipped with linear tomography.

REFERENCES

1. O'Connor JF, Newhauser EBD: Total body opacification in conventional and high dose intravenous urography in infancy. *AJR* 90:63–71, 1963
2. Peck AG, Yoder OC, Pfister RC: Tomography of pelvic abdominal masses during intravenous urography. *AJR* 125: 322–330, 1975
3. Moncada R, Cardoso M, Danley R, Rodriquez J, Kimura K, Pickleman J, Brandly J: Acute cholecystitis: 137 patients studied by infusion tomography of the gallbladder. *AJR* 129:583–585, 1977
4. Rabushka SE, Love L, Moncada R: Infusion tomography of the gallbladder. *Radiology* 109:549–552, 1973
5. Bosniak MA: Nephrotomography: a relatively unappreciated but extremely valuable diagnostic tool. *Radiology* 113:313–321, 1974
6. Dalla Palma L, Bacarini L, Bazzocchi M: The use of abdominal contrast tomography in liver disease. *Br J Radiol* 50: 483–488, 1977
7. Sprayregen S, Messinger NH: Angiography of the jaundiced patient, with emphasis upon the angiographic appearance

of biliary duct dilatation. *AJR* 122:335–355, 1974
8. Goldberg BB: Ultrasonic cholangiography: gray-scale B-scan evaluation of the common bile duct. *Radiology* 118: 401–404, 1976
9. Malini S, Sabel J: Ultrasonography in obstructive jaundice. *Radiology* 123:429–433, 1977
10. Harvilla TR, Haaga JR, Alfidi RJ, Reich NE: Computed tomography and obstructive biliary disease. *AJR* 128:765–768, 1977
11. Morin ME, Baker DA, Marson RZ: Demonstration of dilated biliary duct by total body opacification. *Radiology* 121:307–309, 1976
12. Giovoni AF, Meyers MA: Pseudopneumobilia. *Radiology* 118:526, 1976
13. Shaub MS, Birnbaum WW, Meyers HI: Peribiliary fat: a new roentgenographic finding. *AJR* 123:330–337, 1975
14. Smith TR: Tomographic visualization of the common bile duct without contrast media. *Invest Radiol* 9:412–414, 1974

Significance of the Nonopacified Gallbladder in Endoscopic Retrograde Cholangiography

CHARLES A. ROHRMANN, JR.,[1] HOWARD J. ANSEL,[2] ROBERT L. PROTELL,[3] FRED E. SILVERSTEIN,[3] STEPHEN E. SILVIS,[3] AND JACK A. VENNES[4]

Failure to visualize the cystic duct and gallbladder during endoscopic retrograde cholangiography, while obtaining satisfactory opacification of the rest of the biliary system, is a radiographic sign of undetermined meaning. The diagnostic implication of this finding was analyzed in 63 patients with pathologically proven diagnoses. One patient was normal at surgery. Three groups of abnormal patients had: (1) obstructing lesions of the distal common bile duct (35 patients); (2) primary lesions of the cystic duct or gallbladder (19 patients); or (3) obstructing lesions about the common hepatic/cystic duct junction (8 patients). The results indicate that obstructing lesions of the distal common bile duct may cause stasis of bile within the biliary system, increased biliary pressure, and sludge formation that prevent the flow of contrast material through the cystic duct and into the gallbladder, which can cause nonopacification. If the extrahepatic biliary system is of normal caliber without evidence of an obstructing process, nonfilling of the cystic duct and gallbladder is highly predictive of pathology.

TABLE 1

Diagnoses

Diagnosis	No. Patients
Carcinoma of pancreas or periampullary region	19
Cystic duct or gallbladder stones	14
Common bile duct stones only	5
Carcinoma of proximal common hepatic duct	5
Metastases to or lymphoma of common bile duct	4
Chronic pancreatitis with common bile duct stenosis	3
Gallbladder empyema or chronic obliterative cholecystitis	3
Gallbladder carcinoma	2
Carcinoma of distal common bile duct	2
Papillary fibrosis or stenosis	2
Metastases to common hepatic duct or cystic duct	1
Posttraumatic common hepatic duct stenosis	1
Polycystic liver disease	1
Normal	1
Total	63

Endoscopic retrograde cholangiography is well established as a primary method for evaluating both the extra- and intrahepatic biliary systems in jaundiced patients [1–5]. When outlined by contrast material, calculi within the gallbladder and cystic duct may be confidently diagnosed. Failure to opacify the gallbladder or cystic duct during retrograde injection may imply an abnormality, but current information does not permit assessment of

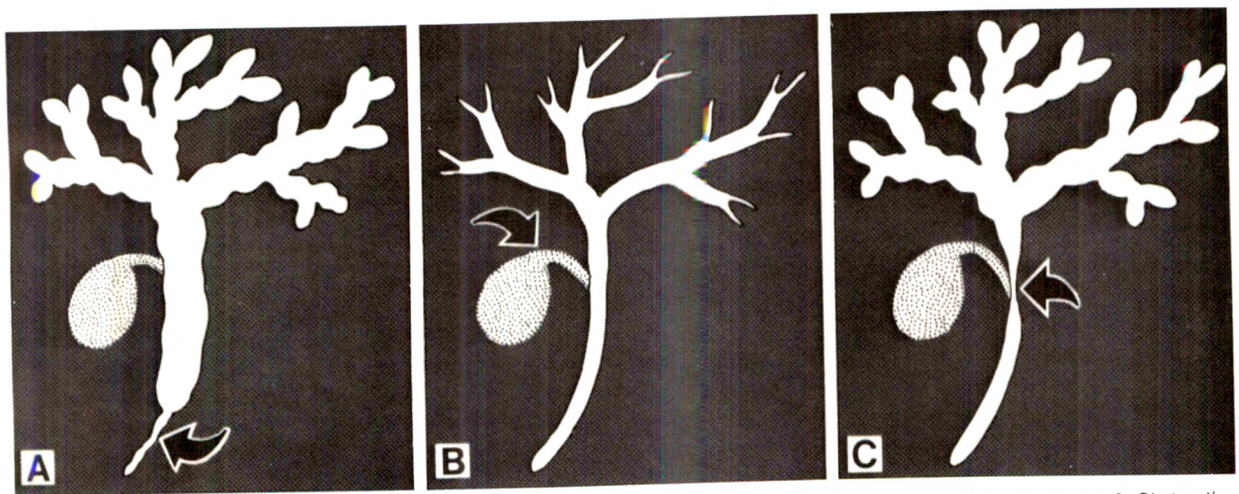


Fig. 1.—Groups of lesions that produce nonfilling of gallbladder and cystic duct at endoscopic retrograde cholangiography. **A,** Obstruction of distal common bile duct (*arrow*) with dilatation of intra- and extrahepatic systems. **B,** Primary cystic duct or gallbladder lesions (*arrow*) have normal intra- and extrahepatic biliary systems. **C,** Obstruction about cystic duct/common hepatic duct junction occludes cystic duct (*arrow*).

Received August 28, 1978; accepted November 3, 1978

[1]Department of Radiology, SB-05, University of Washington, School of Medicine, Seattle, Washington 98195. Address reprint requests to C. A. Rohrmann, Jr.

[2]Department of Radiology, Veterans Administration Hospital and University of Minnesota, Minneapolis, Minnesota 55455.

[3]Division of Gastroenterology, Department of Medicine, University of Washington, School of Medicine, Seattle, Washington 98195.

[4]Special Diagnostic and Treatment Unit, Veterans Administration Hospital and Department of Medicine, University of Minnesota, Minneapolis, Minnesota 55455.

© 1979 American Roentgen Ray Society

0361-803X/79/1322-0191 $0.00

TABLE 2

Classifications of Diagnoses

Lesions	No.
Distal Biliary Lesions:	
Carcinoma of pancreas or ampulla	19
Common bile duct calculi	5
Metastases to common bile duct	4
Chronic pancreatitis	3
Periampullary fibrosis or stenosis	2
Carcinoma of common bile duct	2
Subtotal	35
Primary Cystic Duct or Gallbladder Lesions:	
Cystic duct or gallbladder calculi	14
Gallbladder empyema or chronic obliterative cholecystitis	3
Gallbladder carcinoma	2
Subtotal	19
Proximal Biliary Lesions:	
Carcinoma of common hepatic duct	5
Metastases to common hepatic duct	1
Inflammatory stenosis of the common hepatic duct	1
Polycystic liver disease	1
Subtotal	8
Normal	1
Total	63

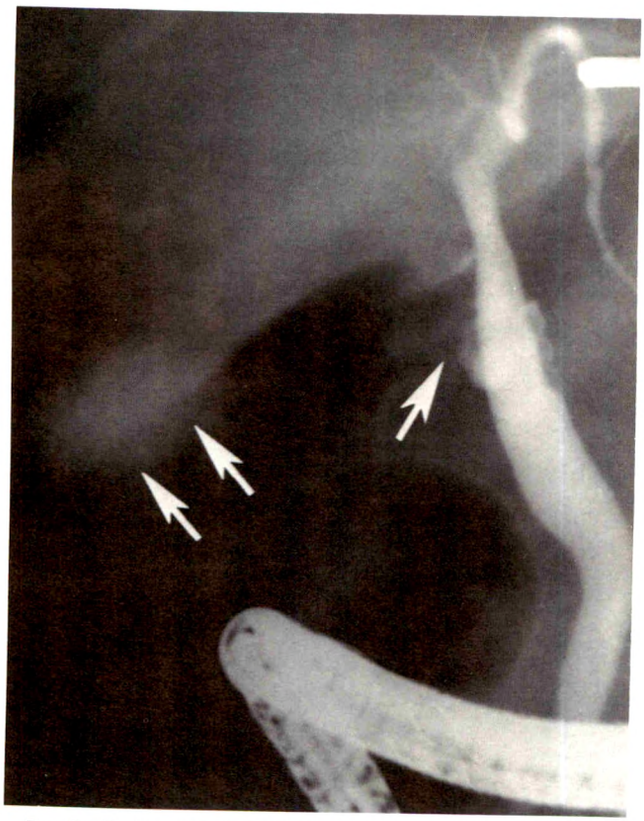


Fig. 2.—During retrograde injection, contrast fills cystic duct and gallbladder (*arrows*), accompanied by synchronous filling of intrahepatic system.

the diagnostic significance of this finding. This investigation was designed to establish the diagnostic implications of failure of the cystic duct and gallbladder to opacify at endoscopic retrograde cholangiography.

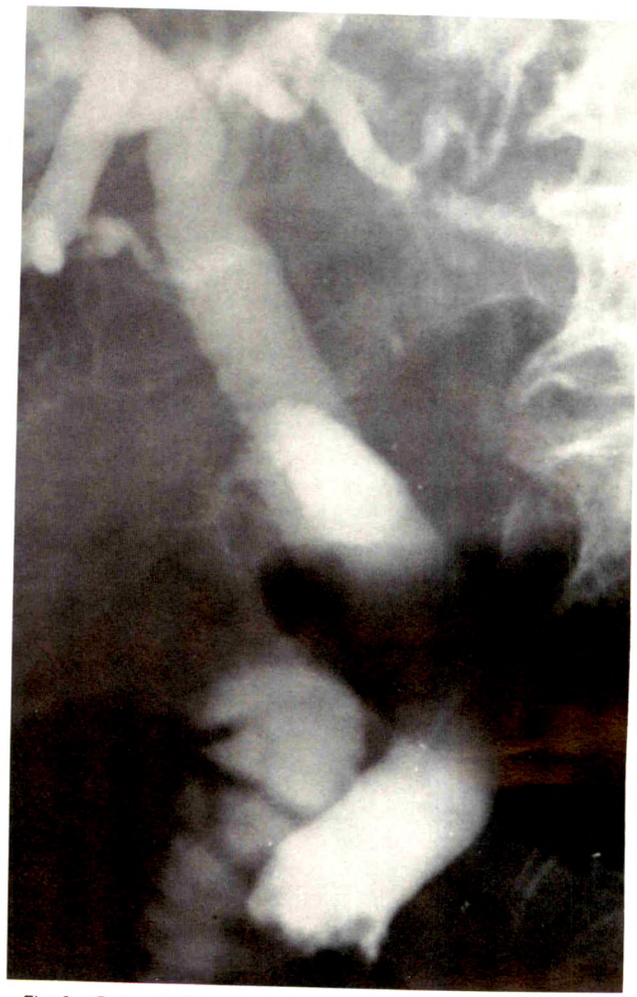


Fig. 3.—Periampullary carcinoma produces nearly total obstruction of distal common bile duct. Intra- and extrahepatic systems are dilated; cystic duct only partially filled.

Materials and Methods

Using the combined endoscopic retrograde cholangiography experience of 1,400 cases at Minneapolis Veterans Administration Hospital and University of Washington Hospital, 63 patients were defined who had not undergone cholecystectomy and in whom a technically adequate endoscopic retrograde cholangiogram failed to demonstrate opacification of the gallbladder or cystic duct. The final surgical or autopsy diagnosis was compared with the radiographic findings of endoscopic retrograde cholangiography. Cholangiograms were retrospectively evaluated for adequacy of filling the intra- and extrahepatic systems, location of obstructing lesions of the extrahepatic system, ductal dilatation, and associated pancreatic or duodenal abnormalities.

Results

Final diagnoses of the 63 patients are summarized in table 1. At surgery, one patient was found to be normal. The other 62 patients were divided into three groups depending on site of abnormality (fig. 1). At surgery or autopsy 35 patients had no obstructive or primary abnormalities of the cystic ducts or gallbladder, but 19 of these

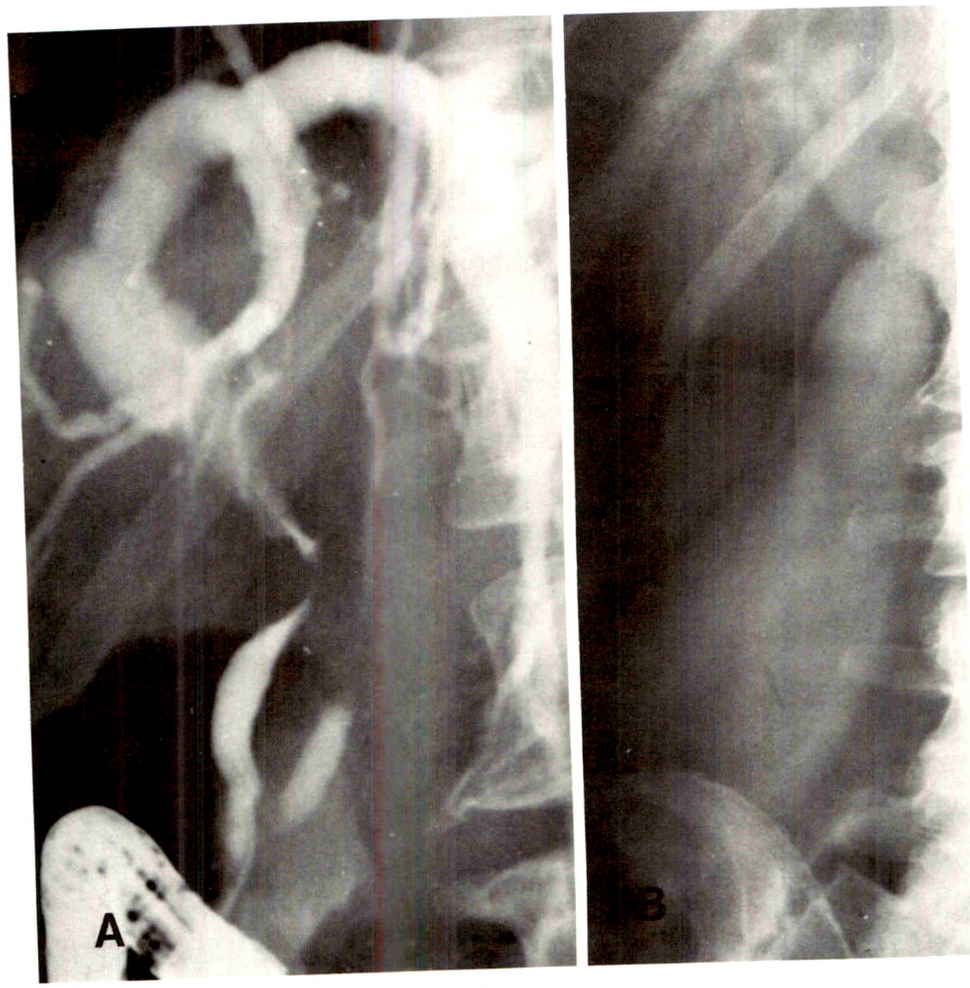


Fig. 4.—Carcinoma of pancreas with common bile duct obstruction and delayed opacification of distended gallbladder. **A,** Obstruction of the pancreatic duct and high-grade stenosis of common bile duct as it traverses pancreatic head. Prestenotic dilatation and dense filling of intrahepatic biliary system. No gallbladder or cystic duct opacification. **B,** 5 hr after endoscopic retrograde cholangiography, contrast retained in dilated biliary system and distended gallbladder, resulting from gradual diffusion of contrast into distended gallbladder.

had distal common bile duct obstruction from pancreatic or periampullary carcinoma, five had common bile duct stones, and four had metastases partially obstructing the common bile duct. Chronic pancreatitis, periampullary stenosis and common bile duct carcinoma accounted for the remaining seven patients with these findings (fig. 1A). In the second group, 19 patients had actual obstructing lesions of the cystic duct or gallbladder, such as calculi (in 14), inflammatory disease (in three), and carcinoma (in two). Common bile ducts and common hepatic ducts were normal (fig. 1B). The third group (eight patients) had proximal obstructing lesions of the biliary tree at the confluence of the cystic duct and common hepatic duct; five patients had cholangiocarcinoma, and three had metastases, inflammatory stenosis, and polycystic liver disease, respectively (fig. 1C). The three groups of abnormalities and the specific lesions in each group are presented in table 2.

Discussion

Failure of the gallbladder to opacify during intravenous cholangiography is highly indicative of cystic duct obstruction [6–10], although distal biliary obstructive lesions may also be responsible [8]. The implication of this sign is disputed, whether in endoscopic retrograde cholangiography (1, 11, 12) or percutaneous transhepatic cholangiography [13].

In the nonpathologic state, endoscopic retrograde injection of the biliary system usually results in synchronous opacification of the cystic duct and main intrahepatic ducts (fig. 2). As the injection is continued, there is progressive opacification of the gallbladder and intrahepatic ducts. This normal sequence is aided by appropriate patient positioning, which includes the right decubitus or Trendelenberg positions. Prolonged injection time or repeat injection may be necessary to obtain a cholangiogram of high technical quality, which is determined by dense opacification of the extrahepatic ducts with filling of the third-order intrahepatic branches. If these conditions do not result in filling of the gallbladder, a pathologic process should be suspected.

Table 2 demonstrates the variety of diagnoses associated with nonopacification of the gallbladder at endoscopic retrograde cholangiography, which can be categorized into three groups of lesions (fig. 1). The first group is characterized by a distal common bile duct abnormality, either stenosis or intraluminal filling defect, that causes subtotal obstruction with dilatation of the biliary system and stasis of bile within the ductal system (fig. 3). As noted in this series, a variety of processes can



Fig. 5.—Obstructing cystic duct stone; normal, well opacified intra- and extrahepatic duct systems. Adequate filling pressure documented by filling of third- and fourth-order intrahepatic branches. Only small portion of cystic duct visualized.

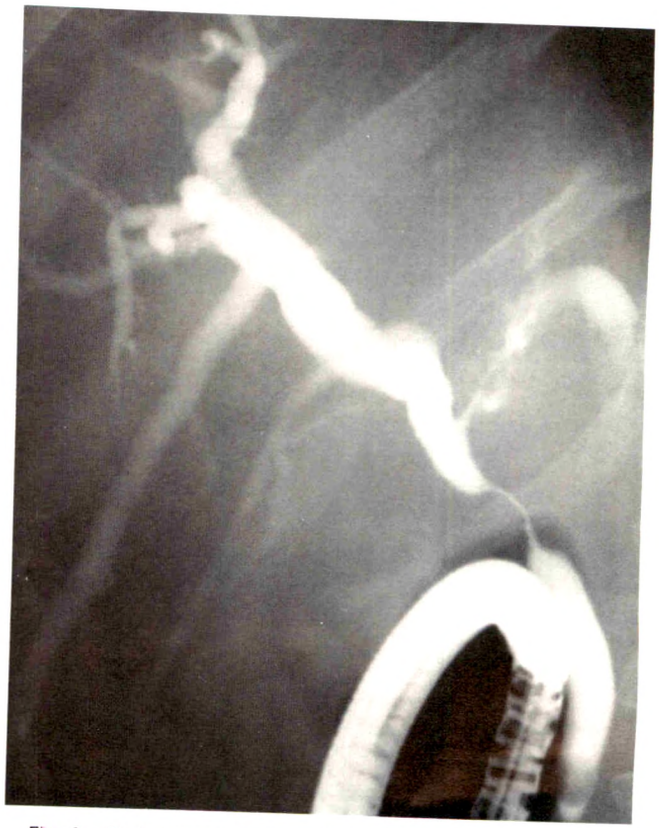


Fig. 6.—Cholangiocarcinoma obstructs cystic duct at junction with common hepatic duct; no gallbladder opacification and narrowing of the left hepatic duct. Air bubble is in normal distal common bile duct.

produce these findings. All cases in this group had evidence of obstruction with biliary ductal dilatation. Operative manometry has shown that obstructing lesions of the distal common bile duct elevate biliary pressure and increase ductal diameter [14, 15], which implies that gallbladder distension, stasis, and sludging of bile occur and inhibit retrograde flow of contrast. During injection at endoscopic retrograde cholangiography, gallbladder opacification is not obtained; if injection is continued or if delayed films are obtained, the contrast may gradually diffuse into the distended system and faint delayed opacification of the gallbladder may occur (fig. 4). The large number of patients in this study with extrahepatic obstructive lesions is due to the large number of jaundiced patients studied by endoscopic retrograde cholangiography. Jaundiced patients studied by percutaneous transhepatic cholangiography with distal obstructing lesions may show a similar incidence of nonopacification of the gallbladder for similar reasons [13].

The second most numerous group contains lesions that actually obstruct or obliterate the gallbladder and cystic duct (fig. 5), such as calculi, inflammation (chronic cholecystitis, empyema), and gallbladder carcinoma. The least numerous group of lesions includes those that affect the common hepatic duct where it joins the cystic duct. Both malignant and benign processes may occlude or stenose both ducts at this junction (fig. 6).

Analysis of the radiographic features accompanying these lesions suggests that:

1. Only if technical adequacy of the cholangiogram has been documented by dense opacification of the extrahepatic system, third-order intrahepatic visualization, change in patient position to enhance gallbladder filling, or prolonged injection time can radiographic appearances be confidently interpreted.

2. Obstructing lesions of the distal common bile duct may cause stasis of bile within the biliary system, increased pressure within the gallbladder, and biliary sludge formation. These factors, alone or in combination, prevent the flow of contrast through the cystic duct and into the gallbladder. Therefore, since nonopacification can result from lesions that do not primarily affect

the cystic duct or gallbladder, nonopacification of the gallbladder in the presence of distal biliary obstructing lesions does not necessarily imply gallbladder or cystic duct disease.

3. Stenosing or obstructing lesions at the cystic duct/common hepatic duct junction can occlude the cystic duct, prevent reflux of contrast, and therefore prevent gallbladder visualization.

4. If the the extrahepatic biliary system is of normal caliber without evidence of an obstructing process at the distal common bile duct or at the cystic duct/common hepatic duct junction, nonfilling of the cystic duct and gallbladder is highly predictive of pathology within the cystic duct or gallbladder.

REFERENCES

1. Cotton PB: Progress report: ERCP 1977. *Gut* 18:316–341, 1977
2. Vennes JA, Jacobson JR, Silvis SE: Endoscopic cholangiography for biliary system diagnosis. *Ann Intern Med* 80: 61–64, 1974
3. Falkenstein DB, Ruiobond C, Sidhu G, Abrams RM, Seliger G, Zimmon DS: The endoscopic intrahepatic cholangiogram—clinico-pathologic correlation with postmortem cholangiograms. *Invest Radiol* 10:358–365, 1975
4. Ayoola EA, Vennes JA, Silvis SE, Rohrmann CA, Ansel HJ: Endoscopic retrograde intrahepatic cholangiography and liver diseases. *Gastrointest Endosc* 22:156–159, 1976
5. Rohrmann CA, Ansel HJ, Ayoola EA, Silvis SE, Vennes JA: Endoscopic retrograde intrahepatic cholangiogram: radiographic findings and intrahepatic disease. *AJR* 128:45–52, 1977
6. Wise RE, O'Brien RG: Interpretation of the intravenous cholangiogram. *JAMA* 160:819–827, 1956
7. Wise RE, Johnston DJ, Salzman FA: The intravenous cholangiographic diagnosis of partial obstruction of the common bile duct. *Radiology* 68:507–525, 1957
8. Wise RE: Current concepts of intravenous cholangiography. *Radiol Clin North Am* 4:521–523, 1966
9. Johnson HC Jr, McLaren JR, Weens HS: Intravenous cholangiography in the differential diagnosis of acute cholecystitis. *Radiology* 74:790–796, 1960
10. Weens SH, Clements JL Jr: The radiologic diagnosis of acute cholecystitis. *Semin Roentgenol* 11:245–247, 1976
11. Oi I: Retrograde cholangiography in biliary and hepatic diseases, discussion in *Endoscopy of the Small Intestine with Retrograde Pancreato-Cholangiography*, international workshop at Erlangen 1972, edited by Demling L, Classen M, Stuttgart, Thieme, 1973, p 89
12. Block MA, Schuman BM, Weckstein ML: Interpretative problems in endoscopic retrograde cholangiopancreatography. *Am J Surg* 129:29–33, 1975
13. Johnson GH, Halls J, Douglas AP: The significance of the non-visualized gallbladder at transhepatic cholangiography (abstr). *Clin Res* 25:110A, 1977
14. Hopton D, White TT: An evaluation of manometric operative cholangiography in 100 patients with biliary disease. *Surg Gynecol Obstet* 133:949–954, 1971
15. White TT, Waisman H, Hopton D, Kavlie H: Radiomanometry, flow rates and cholangiography in the evaluation of common bile duct disease. *Am J Surg* 23:73–79, 1972

Predictability of Rectal Incontinence on Barium Enema Examination

EDWARD T. STEWART[1] AND WYLIE J. DODDS[1]

The aim of this study was to determine if digital assessment of anal sphincter tone predicts whether a rectal balloon is needed to prevent incontinence during a barium enema examination. During an 8 month period, 306 patients scheduled for barium enema examination were evaluated. Immediately before each examination rectal sphincter tone was scored on digital examination as good, fair, or poor. The barium enema was then performed in a conventional manner. Leakage of even small amounts of barium was scored as rectal incontinence. Ability to retain the barium enema correlated closely with the strength of rectal bone, regardless of patient sex or age. For different sphincter tones the incidence of rectal incontinence was: good, 2%; fair, 30%; and poor, 90%. From these findings it is recommended that, irrespective of patient age and sex, the use of rectal balloon catheters be limited to patients with poor or fair rectal tone.

On barium enema examination, inflated rectal balloon catheters are commonly used to prevent rectal leakage of barium in patients with suspected rectal incontinence. However, no data exist that enable the examiner to accurately predict which patients are likely to have rectal incontinence during a barium enema. We evaluated patient variables which might have value in predicting the likelihood of rectal incontinence during a barium enema examination. We anticipated such information might provide a rationale for appropriate use of inflatable rectal balloons for barium enema examinations in patients with a high probability of having rectal incontinence of barium.

Subjects and Methods

All patients undergoing a single-contrast barium enema examination by either of two staff radiologists at the Milwaukee County General Hospital formed the study. A total of 306 patients was studied during an 8 month period. Observer A examined 204 patients and observer B examined 102 patients. Of the 306 patients studied, 142 were male and 164 were female. No significant age difference existed between the two sexes; the men were 55.8 ± 17 SD years and the women 56.0 ± 17 SD years (fig. 1).

Immediately before each barium enema, the quality of rectal tone in each patient was subjectively scored by digital examination as good, fair, or poor by one of the two radiologists participating in the study. The following scoring system was used:

1. *Good*—The anal sphincter offered substantial resistance during digital insertion and maintained a hard, steady-state squeeze on the inserted finger. A substantial increase in anal tone occurred during a voluntary rectal squeeze.

2. *Fair*—The anal sphincter offered only moderate resistance to digital insertion, but maintained a moderately firm squeeze on the inserted finger. A voluntary rectal squeeze produced a modest increase in anal tone.

3. *Poor*—The anal sphincter offered negligible resistance to digital insertion, and felt flaccid on palpation. Resting sphincter tone was negligible and showed little if any increase during a voluntary squeeze.

Despite the subjectivity of the scoring system, interobserver scoring error was minimal. For 10 patients examined independently by the two observers, only one scoring difference occurred between the two examiners, a good vs. a fair.

To further validate the digital scoring method, rectal tone was scored digitally in 25 patients, and then quantitated manometrically using an infused-catheter recording system. The 6-mm-diameter manometric assembly had four side-hole recording sites at the same axial level. Each recording lumen was perfused with water at the rate of 0.5 ml/min using a minimally compliant hydraulic-capillary infusion system [1]. This system provides high-fidelity recording from gastrointestinal tract sphincters [2, 3]. We measured resting rectal tone by inserting the recording assembly into the rectum and withdrawing the perfused recording sites across the anorectal sphincter in 0.5 cm intervals, pausing 30 sec or longer at each station. This procedure was repeated and at the station giving the highest basal pressure, active change in sphincter tone was recorded during voluntary anal squeeze. Subsequently, the tracings were evaluated without knowledge of the digital score of rectal tone. Basal rectal sphincter tone was taken as the average of the maximal pressure recorded by the four radial catheters during an anal pull-through, using atmospheric pressure as zero reference. Voluntary anorectal squeeze was scored as the change in sphincter pressure above its basal value.

After data on rectal tone, age, and sex were recorded, conventional barium enema examinations were performed with liquid barium (15% wt/vol) using 91 cm of hydrostatic pressure. A plastic enema tip was used for 250 studies and a noninflated balloon catheter (Bardex) in 56 studies. Any leakage of barium during the study, even small amounts, was scored as rectal incontinence. In those patients with a balloon catheter, the rectal balloon was inflated only after demonstration of rectal incontinence. Data from the study was subsequently analyzed for statistical significance by the students *t* test or chi square analysis.

Results

Analysis of the manometric data demonstrated a direct correlation between basal rectal sphincter pressure and digital scores of sphincter tone (table 1). Patients with good rectal tone had significantly higher basal rectal sphincter pressure than subjects with fair rectal tone. Similarly basal sphincter pressure was significantly

Received July 25, 1978; accepted after revision November 9, 1978
Presented in part at the annual meeting of the Society of Gastrointestinal Radiologists, Hamilton, Bermuda, September 1976.
This work was supported in part by U.S. Public Health Service grant AM 15540.
[1]Department of Radiology, Medical College of Wisconsin, Milwaukee County Medical Complex, 8700 West Wisconsin Avenue, Milwaukee, Wisconsin 53226. Address reprint requests to E. T. Stewart.

0361-803X/79/1322-0197 $0.00

AJR 132:197-200, February 1979
© 1979 American Roentgen Ray Society

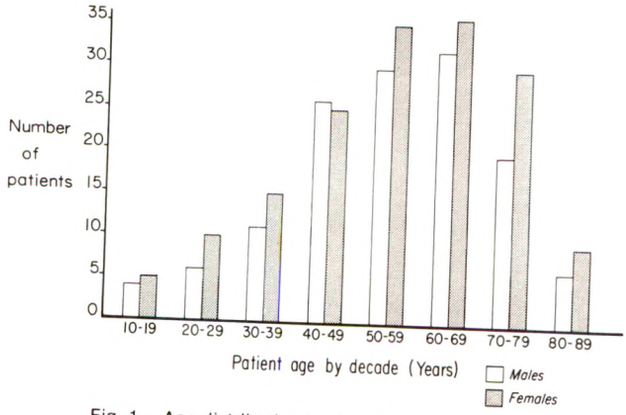


Fig. 1.—Age distribution by decade of 306 patients.

TABLE 1

Rectal Sphincter Pressure Compared with Subjective Rectal Sphincter Tone

Rectal Sphincter Tone	Rectal Sphincter Pressure			
	Basal (mm Hg)	Comparison	Squeeze (Δ mm Hg)*	Comparison
Good	94 ± 31		93 ± 66	
		$P < 0.01$		$P < 0.2$
Fair	59 ± 11		63 ± 55	
		$P < 0.05$		$P < 0.2$
Poor	44 ± 6		28 ± 18	

Note. — Values given as x ± 1 SD. Difference in basal and squeeze pressures between good and poor tone were significant at $P < 0.001$ and $P < 0.05$, respectively.
* Increase in pressure above basal sphincter pressure.

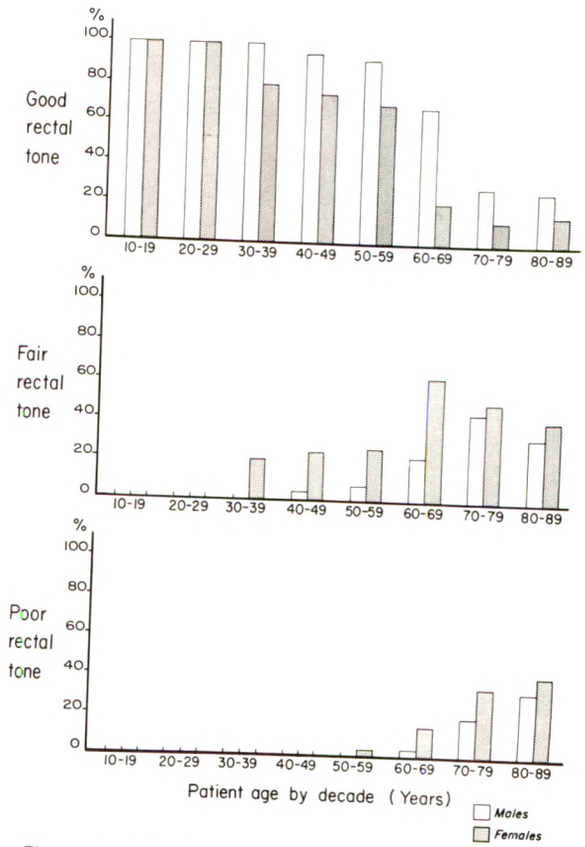


Fig. 2.—Relation between digital scores of rectal tone and patient age.

higher in subjects with fair rectal sphincter tone than in subjects with poor sphincter tone. Increases in rectal sphincter pressure elicited by voluntary rectal squeeze were less discriminating. The difference in squeeze pressure was significantly different between patient groups with digital scores of good or poor; but the differences between good and fair, and fair and good were not significant.

For the patients in this study, rectal sphincter tone was good in 63%, fair in 27%, and poor in 10%. The quality of rectal tone was inversely related to patient age ($P < 0.01$). Patients with good tone averaged 48.0 ± 16 SE years; patients with fair tone averaged 64.9 ± 12 years; patients with poor tone averaged 74.9 ± 9 years of age.

The relation of gender to rectal tone is shown in fig. 2. Until age 30, rectal sphincter tone was invariably good in both sexes. Beginning in the fourth decade, however, female patients demonstrated a greater incidence of decreased rectal tone (either fair or poor) than did male patients. The pattern of poorer rectal tone for the women held into the ninth decade.

The incidence of rectal incontinence was about 10% or less until age 60, after which it increased progressively for each additional decade of age (fig. 3). Women showed a significantly ($P < 0.05$) higher incidence of incontinence than men until after age 80, at which time the incidence of incontinence climbed to about 50% for

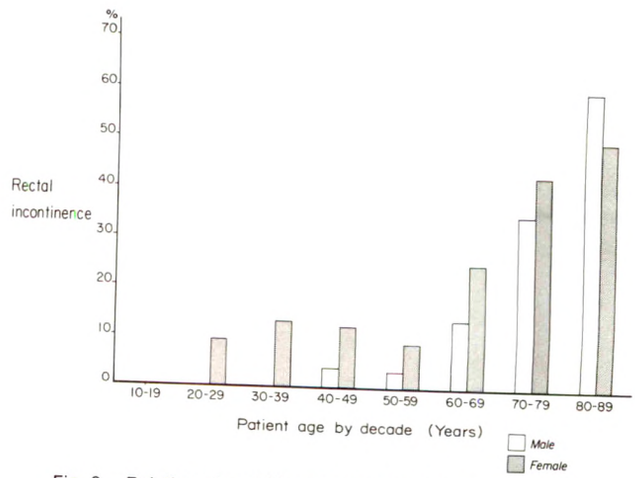


Fig. 3.—Relation of rectal incontinence to patient age and sex.

both sexes. Considering age and sex together, the following facts were determined about the probablility of rectal incontinence during barium enema examination: (1) in men under 60, incontinence occurs in less than 5%; (2) in women under 60, incontinence occurs in 10%–12%; (3) after age 60, the incidence of incontinence increases progressively by decade for both sexes; and (4) for patients in the ninth decade, the incidence of rectal incontinence is about 50% for both sexes.

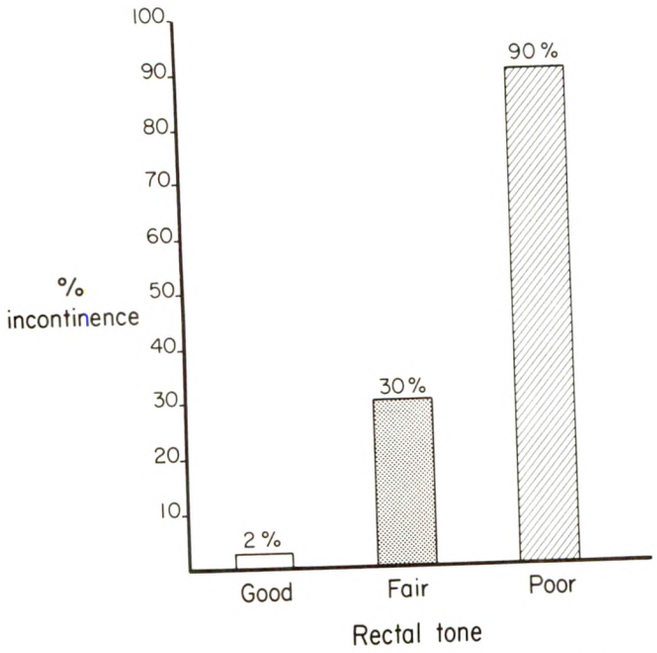


Fig. 4.—Relation between rectal incontinence and digital scores of rectal tone.

The study findings demonstrated a strong inverse relation between the strength of rectal sphincter tone and rectal incontinence (fig. 4). Incontinence occurred in only 2% of patients with good rectal tone, but in 90% of patients with poor tone. Because 73% of the patients had either good or poor rectal tone, rectal continence, or incontinence, respectively, could be predicted with at least 90% confidence in three of every four patients. In patients whose rectal tone was fair, incontinence occurred in about 30%. Consequently, predictions concerning rectal continence in this group of patients could be made only with a 70% accuracy.

Discussion

Currently more than three million barium enema examinations of the colon are performed each year in the United States [4]. For these examinations inflated rectal balloons are used, commonly, in some practices even routinely, to prevent rectal leakage of barium. However, over-use of the rectal balloon should be avoided. Inflation of a rectal balloon should be used only in those patients with demonstrable rectal incontinence or a high probability of rectal incontinence. Minimal use of balloon catheters is desirable because inflated rectal balloons may obscure low-lying rectal lesions which are potentially detectable on radiography [5, 6] and rectal balloon inflation is associated with a small, but definite risk of rectal perforation [7, 8].

In our study, manometric measurement of anal sphincter pressure demonstrated that subjective digital assessment of anal sphincter tone correlated closely with quantitative values of resting sphincter pressure. We interpret this finding as validation of the digital scoring method which is readily applied clinically. The discrepancy between the adequacy of rectal sphincter pressure measured under resting condition and during voluntary anal squeeze is not really surprising. Involuntary resting pressure is governed primarily by the smooth muscle of the internal anal sphincter [9–11], whereas voluntary anal squeeze is generated by the external anal sphincter composed of striated muscle [9]. The latter measurement depends on patient cooperation and effort as well as the status of the striated muscle sphincter. Assessment of resting basal tone of the internal sphincter seems to be adequate for predicting the probability of rectal incontinence.

We studied the value of patient sex, age, and rectal tone in predicting rectal incontinence during barium enema examination. From the third to eighth decades of life, women demonstrated a higher incidence of rectal incontinence and poorer rectal sphincter tone than men. The precise reason for this finding is not known, but pregnancy and vaginal delivery likely contribute to rectal incompetency in women. However, our data collection was not designed to permit an analysis of these factors.

Our results establish the anticipated finding that rectal incontinence increases with age. Rectal incontinence occurred in 5% or less of young to middle-aged males and about 10% of young to middle-aged females, but increased sharply after age 60. By the ninth decade, the incidence of incontinence rose to about 50% for both sexes. Although these results provide some information about the likelihood of rectal incontinence, patient age and sex serve as relatively poor indicators for accurately predicting rectal incontinence in an individual patient, especially for patients beyond middle age. A more useful indicator is digital assessment of rectal sphincter tone. Regardless of age or sex, patients with good sphincter tone almost invariably held the barium enema (98%), whereas patients with poor rectal sphincter tone were almost always incontinent (90%). Fair intermediate sphincter tone was associated with a 30% incidence of incontinence. These results should not be surprising. Previous studies using quantitative manometric methods demonstrate an inverse relation between the strength of rectal sphincter tone and rectal incontinence [12, 13].

Although our patients were not routinely questioned for previous history of rectal incontinence, we did form certain impressions from talking with many of the patients after completion of their barium enema. In our opinion, information about continence during previous barium enemas or their recent cleansing enema had minimal value in predicting incontinence for the current barium enema examination.

On the basis of our findings, we suggest the following rationale for using rectal balloon catheters in patients undergoing radiographic examination of the colon. Rectal sphincter tone should be assessed on digital rectal examination by the radiologist immediately prior to a barium enema. A conventional plastic enema tip is used for all patients with good rectal tone. For patients with poor or fair rectal tone, we insert a balloon catheter into

the rectum. Under fluoroscopic control the rectal balloon is inflated at the onset of the examination in patients with poor rectal tone; in patients with fair rectal tone, the balloon remains uninflated so long as the patient remains continent (about 70% of such patients). With this method, an inflated rectal balloon was needed for barium enema examination in only about 15% of all our patients. Of course, this percentage will vary depending on the age profile of the patient population being examined, and would probably be much lower in office practice.

The approach described here, now routine in our department, has markedly reduced the need for inflated rectal balloons to prevent rectal incontinence. This concept is readily taught to residents who quickly become expert in assessing rectal tone and predicting the probability of rectal incontinence. We believe that it is the radiologist's responsibility to evaluate the requirement for a rectal balloon catheter, because the technologist and the patient often cannot satisfactorily predict continence. By using the very simple approach suggested here, the use of balloon catheters can be reduced to a minimum. Selection of the appropriate enema tip and inflation of a rectal balloon, when indicated, should be the responsibility of the examiner and not the technician. The unsupervised insertion and inflation of balloon catheters by persons other than the radiologist is to be discouraged.

The digital rectal examination is useful not only for quantitating rectal tone, but also for excluding significant rectal disease, such as a stricture or tumor, which would increase the hazard of rectal balloon inflation. In addition each year we discover several rectal lesions on digital rectal examination which were not detected on rectal examination by the referring clinician and occasionally even missed by proctoscopy.

REFERENCES

1. Arndorfer RC, Stef JJ, Dodds WJ, Linehan JH, Hogan WJ: Improved infusion system for intraluminal esophageal manometry. *Gastroenterology* 73:23–27, 1977
2. Dodds WJ, Stef JJ, Hogan WJ: Factors determining pressure measurement accuracy by intraluminal esophageal manometry. *Gastroenterology* 70:117–123, 1976
3. Dodds WJ: Instrumentation and methodology for intraluminal esophageal manometry. *Arch Intern Med* 136:515–523, 1976
4. Dodds WJ: Roentgenographic examination of the colon: relevant questions (letter). *Invest Radiol* 7:63, 1972
5. Miller RE: Barium-enema examination with large-bore tubing and drainage. *Radiology* 82:905–911, 1964
6. Laufer I, Smith NCW, Mullens JE: The radiological demonstration of colorectal polyps undetected by endoscopy. *Gastroenterology* 70:167–170, 1976
7. Nathan MH, Kohen R: The bardex tube in performing barium enemas: evaluation of its use and safety. *AJR* 84: 1121–1124, 1960
8. Noveroske RJ: Perforation of the rectosigmoid by a bardex balloon catheter: report of 3 cases. *AJR* 96:326–331, 1966
9. Bennett RC, Duthie HL: The functional importance of the internal anal sphincter. *Br J Surg* 51:355–357, 1964
10. Duthie HL: Progress report. Anal continence. *Gut* 12:844–852, 1971
11. Schuster MM: The riddle of the sphincters. *Gastroenterology* 69:249–262, 1975
12. Harris LD, Winans CS, Pope II CE: Determination of yield pressures: a method for measuring anal sphincter competence. *Gastroenterology* 50:754–760, 1966
13. Wheatley IC, Hardy KJ, Dent J: Anal pressure studies in spinal patients. *Gut* 18:488–490, 1977

Ultrasonographic Evaluation of Pericholecystic Abscesses

ALAN B. BERGMAN,[1] HARVEY L. NEIMAN, AND BESSIE KRAUT

Pericholecystic abscess formation is a serious complication of cholecystitis that develops after gallbladder perforation and is usually associated with acute inflammatory signs and symptoms. Ultrasonographic findings in three surgically proven cases of pericholecystic abscess are reported. The findings ranged from a well defined band of low-level echoes around the gallbladder to multiple, poorly defined hypoechoic masses surrounding an irregular, indistinct gallbladder outline. The former situation correlated with a well encapsulated pericholecystic inflammatory process, while the latter was associated with extensive abscess formation resulting from gallbladder rupture. Cholelithiasis was identified in two of the three cases. Ultrasound for preoperative detection of pericholecystic abscess is discussed.

The use of gray scale ultrasound in evaluating gallbladder disease is well established. Several investigators have discussed the diagnostic criteria and accuracy of sonographic findings in cholelithiasis and cholecystitis [1–4]. This report describes the findings associated with one of the potentially serious complications of acute cholecystitis, pericholecystic abscess formation. Sonographic and surgical findings were correlated in three patients.

Materials and Methods

Ultrasound studies were done with commercially available gray scale equipment. Depending on patient size, either a 2.25 or 3.5 MHz long-focus transducer was used. The images were recorded on a multiimage camera. Scans were performed over the right upper quadrant and epigastric regions in transverse, longitudinal, and oblique planes. Both the supine and left lateral decubitus views were used to assess changes resulting from positional maneuvers.

Case Reports

Case 1

A 77-year-old white man with polycythemia vera had chills, fever, and intermittent right upper quadrant pain for 10 days. Physical examination on admission disclosed minimal right upper quadrant tenderness and fever of 39.8°C. White blood cell count was 16,400 with left shift. Bilirubin and liver enzymes were within normal limits.

Shaking chills and fevers continued despite intravenous antibiotics. Abdominal ultrasonography of the right upper quadrant region demonstrated a discrete halo of low-level echoes surrounding the gallbladder. High-level echoes associated with prominent acoustic shadowing were also noted in the gallbladder neck, consistent with cholelithiasis (fig. 1). No evidence of biliary ductal dilatation was identified.

On day 10 exploratory laparotomy revealed cholelithiasis, thickened gallbladder wall, a small mural perforation, and a walled-off pericholecystic abscess. Cholecystectomy and drainage of the abscess were performed, and the patient recovered uneventfully.

Case 2

A 30-year-old white woman with a long history of systemic lupus erythematosus and chronic renal failure had chills, fever, and right upper quadrant pain for 1 month. She had had similar symptoms 1 year earlier, along with a nonvisualizing gallbladder on oral cholecystography. At that time, cholecystitis was diagnosed, but surgery was not performed due to the patient's compromised immune status.

Physical examination at admission disclosed right upper quacrart rebound tenderness, a palpable mass in the same area, and fever of 40°C. Bilirubin and liver enzymes were within normal limits.

The major sonographic finding was a thick hypoechoic band surrounding the gallbladder wall (fig. 2A). A small area of high-level echoes also noted within the dependent portion of the gallbladder lumen was believed to represent a calculus (fig. 2B). A trial of parenteral antibiotic therapy failed to alter the septic course, and exploratory laparotomy was performed on day 14. Surgical findings included a moderately thickened gallbladder wall and a small perforation. A well defined abscess was found in the region of the gallbladder bed, along with a calculus in the gallbladder lumen. Cholecystectomy was performed, and the patient's postoperative course was satisfactory.

Case 3

A 46-year-old black woman was admitted after having upper abdominal fullness, vomiting, right upper quadrant pain, and jaundice for 1 week. At admission, physical examination dis-

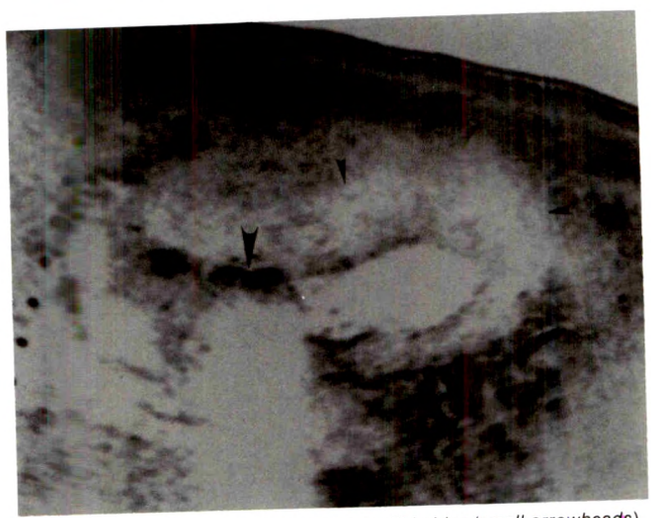


Fig. 1.—Hypoechoic band surrounds gallbladder (*small arrowheads*). Prominent acoustic shadowing is from gallstone (*large arrowhead*).

Received July 9, 1978; accepted after revision October 30, 1978.

[1] All authors: Department of Radiology, Northwestern Memorial Hospital, Northwestern University Medical School, 250 East Superior Street, Chicago, Illinois 60611. Address reprint requests to H. L. Neiman.

0361-803X/79/1322-0201 $0.00

AJR 132:201–203, February 1979

© 1979 American Roentgen Ray Society

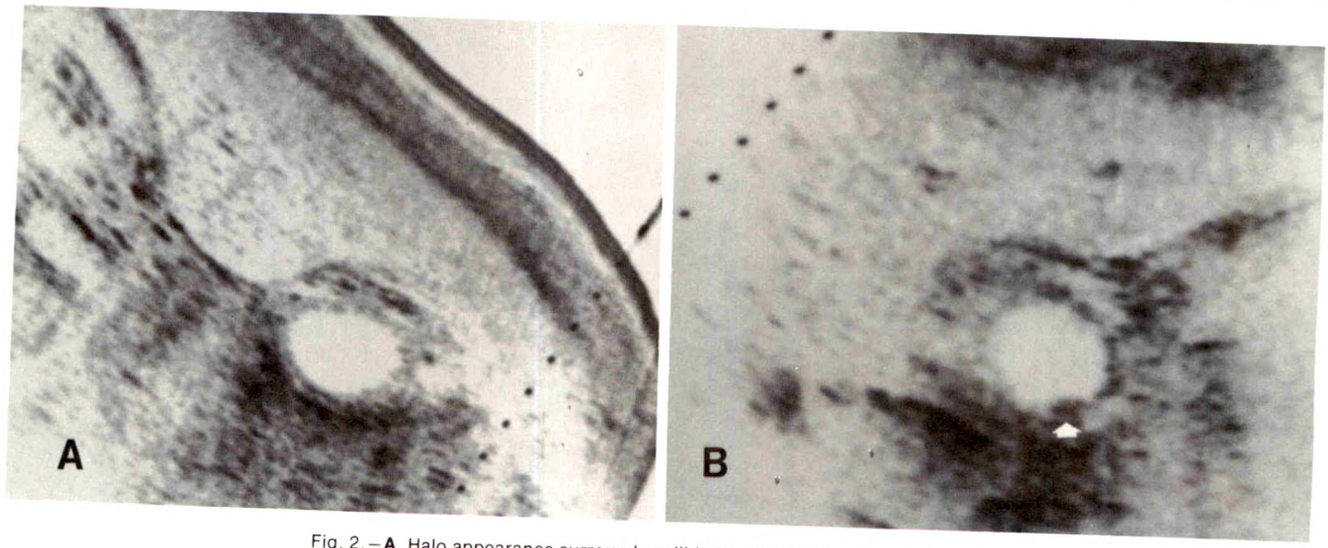


Fig. 2.—**A**, Halo appearance surrounds gallbladder. **B**, Single gallstone (*arrow*).

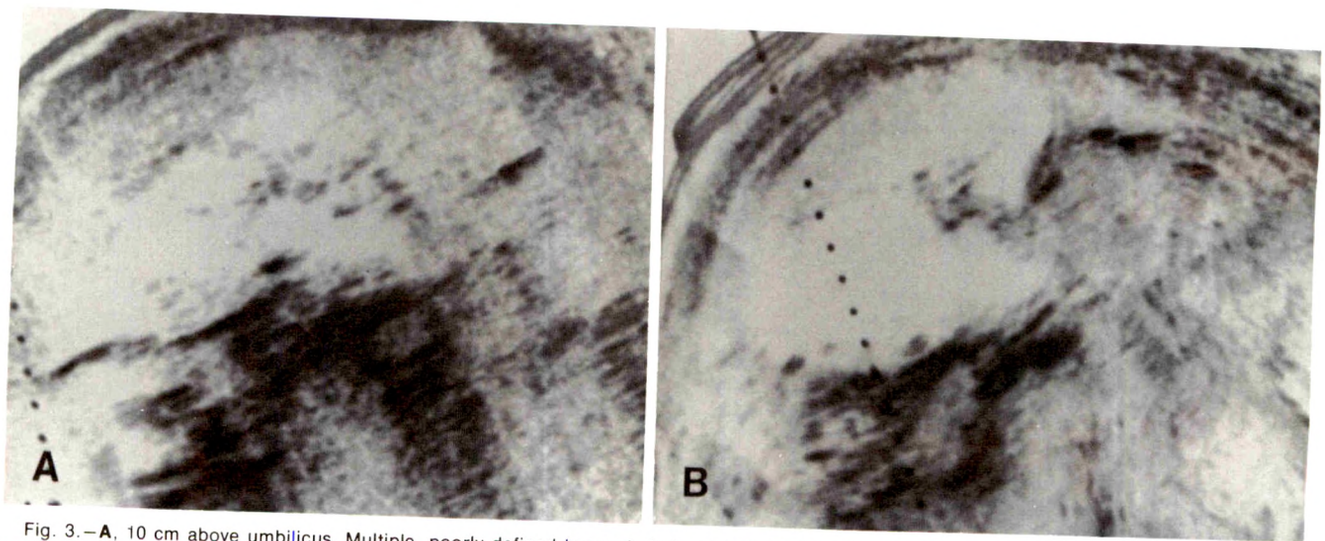


Fig. 3.—**A**, 10 cm above umbilicus. Multiple, poorly defined hypoechoic loculation. Gallbladder cannot be separately identified. **B**, 4 cm above umbilicus. Multiple hypoechoic masses comprise pericholecystic inflammatory reaction.

closed a fever of 40°C, tenderness in the right upper quadrant, and a questionably palpable mass in the same region. White blood cell count was 12,500 with left shift; bilirubin, 12.4 mg/100 ml; alkaline phosphatase, 450 units; lactic dehydrogenase, 378 units; and SGOT, 78 units. Chest radiography and plain films of the abdomen were unremarkable.

Blood cultures grew alpha hemolytic streptococcus. The fever did not subside despite parenteral antibiotics. Sonographic examination of the abdomen on day 4 revealed multiple, irregular, somewhat poorly defined hypoechoic masses in the right upper quadrant. Although difficult to identify, the gallbladder appeared to have a slightly thickened wall. Linear low-level echoes within several of the hypoechoic areas were believed to represent areas of septation and loculation (fig. 3). A distinct calculus was not identified. Exploratory laparotomy revealed evidence of acute cholecystitis with an edematous gallbladder wall. A calculus had perforated through the gallbladder and the common bile duct. Bile was found in the peritoneal cavity along with multiple abscess pockets in the gallbladder bed. Cholecystectomy, common bile duct exploration, and repair were performed. The patient did well postoperatively and was discharged 10 days later.

Discussion

Perforation of the gallbladder after an episode of acute cholecystitis usually occurs at an area of gangrene or infarction in the wall. There are three basic types of perforation: (1) acute free perforation causing bile peritonitis; (2) subacute walled-off perforation causing pericholecystic abscess; and (3) chronic perforation resulting in the formation of an internal biliary fistula [5]. The risk of perforation increases with each day of an attack of cholecystitis and is, therefore, unusual before 48 hr after onset of symptoms. With localized perforation, the formation of a pericholecystic abscess may be a gradual process and not suspected until a tender right upper quadrant mass and high fever signal its presence. According to Dowdy [6], 5%–10% of patients with acute

cholecystitis develop this complication. Unfortunately, preoperative clinical diagnosis of this lesion is not frequently made and, as a result, the associated morbidity of the subsequent surgical procedure is increased. Therefore, pericholecystic abscess is an uncommon, but serious, complication of cholecystitis.

The sonographic findings in this series of patients represent a spectrum of severity. In the first two cases, where scans demonstrated a halo effect around the gallbladder wall, surgery disclosed a well contained walled-off abscess associated with mild pericholecystic edema. The perforation in each case was also noted to be small when the gallbladder was examined directly. The findings in case 3, on the other hand, consisted of multiple hypoechoic masses surrounding a markedly irregular gallbladder. In this situation, a far more extensive pericholecystic inflammatory reaction was found. Therefore it seems that the halo appearance is indicative of a relatively well confined, more mature postperforation lesion. Since this ultrasonographic appearance has also been described in association with chronic cholecystitis and a thickened gallbladder wall without abscess formation, it does not necessarily signify a perforation has occurred [7]. However, when clinical symptoms are relatively acute, this sign should suggest gallbladder perforation with abscess formation.

Case 3 lies at the other end of the continuum of subacute gallbladder perforations. The absence of the halo appearance in this particular situation is not surprising, since the perforation was much more extensive than in the first two cases. The irregularity and indistinctness of the gallbladder outline in this case was due to adhesions and severe inflammatory edema involving the gallbladder bed. In such cases, the abscess may also involve adjacent structures such as the duodenum and colon, which become bound by the inflammatory process.

Detection of a pericholecystic abscess may be difficult. Since the abscess is usually not well delineated by routine radiography, in the past diagnosis has been largely clinical. From the cases described in this report, we feel that ultrasonographic examination may provide important information to the clinician suspecting the presence of this lesion.

Perforation and abscess formation should be suspected in those patients with acute cholecystitis who deteriorate rapidly or who become increasingly toxic for unexplained reasons. Such patients should undergo ultrasonographic examination to detect possible pericholecystic abscess. Hopefully, early diagnosis will reduce the surgical morbidity and mortality of this serious complication.

REFERENCES

1. Doust BD, Maklad NF: Ultrasonic B-mode examination of the gallbladder. *Radiology* 110:643–647, 1974
2. Lawson TL: Gray scale cholecystosonography: diagnostic criteria and accuracy. *Radiology* 122:247–251, 1977
3. Berk RN, Clemett AR: *Radiology of the Gallbladder and Bile Ducts*. Philadelphia, Saunders, 1977
4. Arnon S, Rosenquist CJ: Gray scale cholecystosonography: an evaluation of accuracy. *AJR* 127:817–818, 1976
5. Niemeier OW: Acute free perforation of the gallbladder. *Ann Surg* 99:922–924, 1934
6. Dowdy GS: *The Biliary Tract*. Philadelphia, Lea & Febiger, 1969
7. Marchal G, Crolla D, Baert AL, Fevery J, Kerremans R: Gallbladder wall thickening: a new sign of gallbladder disease visualized by gray scale cholecystosonography. *JCU* 6:177–179, 1978

Ultrasonic Appearance of the Falciform Ligament

BRUCE J. HILLMAN,[1] CARL J. D'ORSI,[1] EDWARD H. SMITH,[1] AND ROYAL J. BARTRUM[2]

In transverse liver scans an echogenic focus was commonly encountered at the junction of the right and left hepatic lobes. This finding was variable in prominence, but could be identified in 22 of 25 patients with otherwise normal livers in whom it was specifically sought. Correlation of ultrasound and CT examinations indicate that these echoes represent the falciform ligament. This normal anatomic structure can be differentiated from an intrahepatic mass by attention to its consistent location and alteration of its configuration by experimenting with the transducer axis during the examination.

The falciform ligament is a normal anatomic structure that extends from the umbilicus to the diaphragm in a parasagittal plane, containing between its layers the ligamentum teres and the umbilical vein remnant. In the anteroposterior axis, the ligament extends from the right rectus muscle anteriorly to the bare area of the liver, where its reflections separate to contribute to the hepatic coronary ligament and attach to the undersurface of the diaphragm [1].

Transverse ultrasound scans through the normal liver frequently show an echodense focus in the expected area of the falciform ligament. Occasionally this structure may be unexpectedly prominent, raising the suspicion of a solid hepatic mass [2]. This study correlates the echographic appearance of the falciform ligament with its appearance on computed tomography (CT). Recognition of the ultrasonic appearance of the ligament should aid in avoiding misinterpretation of this normal structure.

Materials and Methods

Hepatic ultrasonography was performed on 25 patients with no clinical evidence of liver disease, using a commercially available phased-array scanner. Conventional gray scale scans were also performed for illustrative purposes on selected patients, in the area identified as containing the falciform ligament. All studies were done with the patient supine.

All scans were recorded on Polaroid film and evaluated for the presence of an echogenic focus in the expected region of the falciform ligament. Each patient's body habitus was subjectively evaluated as thin, normal, or obese.

Two patients undergoing abdominal examination by CT had the location of the falciform ligament, as identified by CT, marked on their skin. Ultrasound examination of this region was then performed as previously described.

Results

The falciform ligament was identified as a distinct entity in 22 of the 25 patients. Its degree of prominence was highly variable and was unrelated to body habitus. Figure 1A shows a particularly large, echogenic ligament, and demonstrates how this normal structure might be confused with an intrahepatic mass.

In both patients in whom CT localization of the falciform ligament was performed before ultrasound examination, the ligament's typical, echodense configuration could be found at the expected site.

Discussion

The frequent finding of a round, echogenic focus in transverse liver scans of otherwise normal patients has been described by Bartrum and Crow [2]. Noting its consistent position at the junction of right and left hepatic lobes, they suggested that it must represent a normal structure and warned of misinterpreting particularly prominent examples as intrahepatic masses (fig. 1A). Indeed, recent reports have indicated that both primary and metastatic hepatic malignancies may commonly present just such an ultrasonic appearance [3; B. Hillman, E. H. Smith, J. Gammelgard, H. H. Holm, unpublished data]. We have demonstrated that this focus may represent the falciform ligament.

Experimenting with the orientation of the transducer frequently converted the ligament's typically round appearance in transverse scans to a more linear structure (fig. 1B). This served to differentiate it from either a mass or the tubular-appearing portal vein branches which may simulate the ligament when seen on end (fig. 1C). A scan of a patient with ascites (fig. 1D) demonstrates the anatomic relations of the falciform ligament to the right and left hepatic lobes and helps explain how this change in appearance with alteration of the transducer axis might occur. Localization by CT similarly confirms that the echoes represent the position of the falciform ligament (fig. 1E). It is interesting that the hepatic round ligament—which forms the falciform ligament's free edge—may also be a source of confusion on conventional abdominal radiographs when, surrounded by a large amount of fat, it is subject to misinterpretation as a biliary duct or portal vein gas [4].

On ultrasound examination, consideration of the falciform ligament's typical location and attempts to view a suspicious focus of echoes in multiple scan planes seem the best means of differentiating the falciform ligament from an intrahepatic mass or a vascular structure.

ACKNOWLEDGMENTS

We thank Drs. Douglass Adams and Samuel Hessel for use of figure 5, and Deborah Sawyer for preparation of the manuscript.

Received August 1, 1978; accepted after revision October 20, 1978.
This work was supported in part by Fogarty grant no. FO6-TW0014601.
[1] Department of Radiology, Harvard Medical School; Sidney Farber Cancer Institute; Peter Bent Brigham Hospital, 721 Huntington Avenue, Boston, Massachusetts 02115. Address reprint requests to C. J. D'Orsi.
[2] Department of Radiology, Dartmouth Medical School; Hitchcock Clinic, Hanover, New Hampshire 03755.

0361-803X/79/1322-0205 $0.00

AJR 132:205-206, February 1979
© 1979 American Roentgen Ray Society

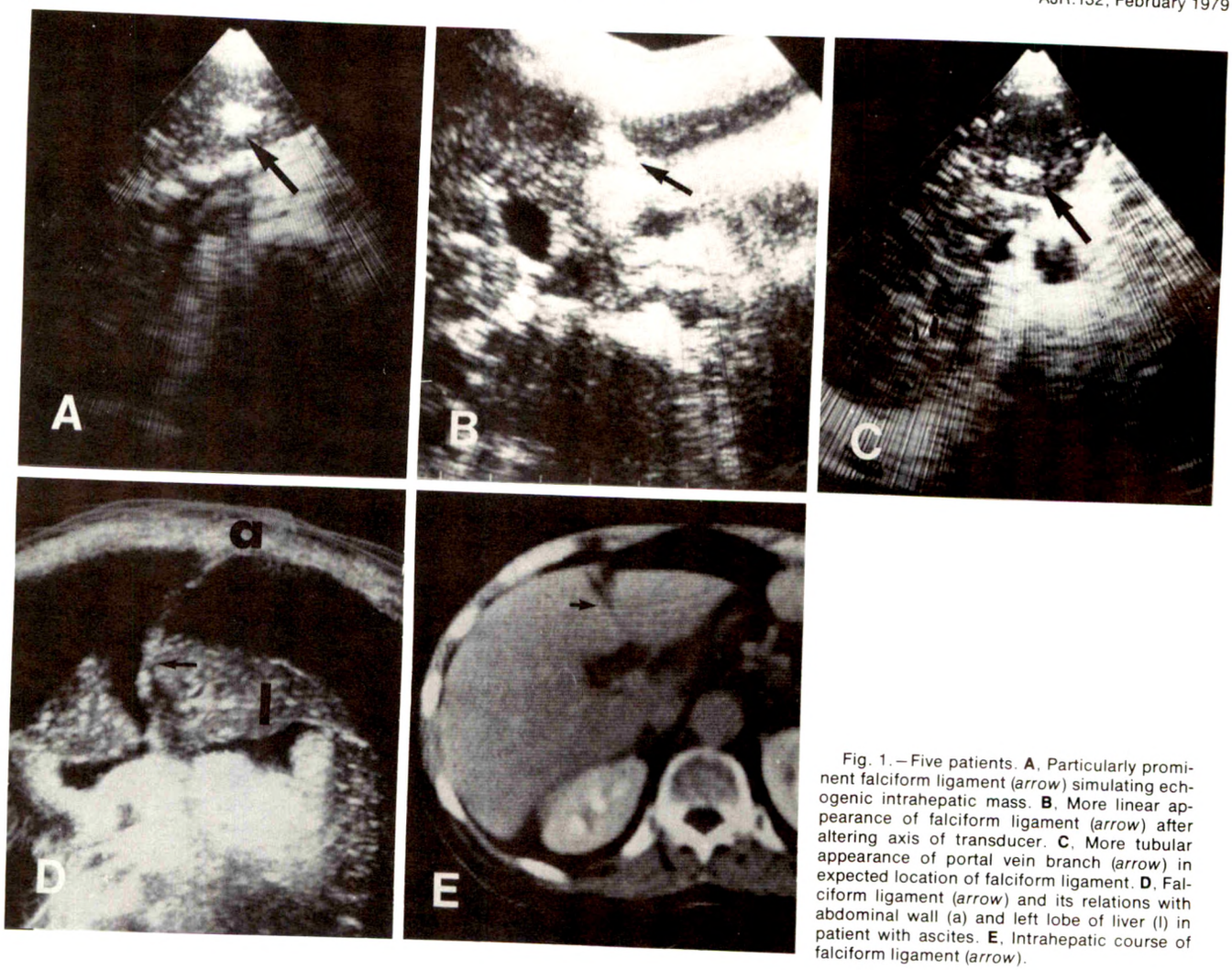


Fig. 1.—Five patients. **A**, Particularly prominent falciform ligament (*arrow*) simulating echogenic intrahepatic mass. **B**, More linear appearance of falciform ligament (*arrow*) after altering axis of transducer. **C**, More tubular appearance of portal vein branch (*arrow*) in expected location of falciform ligament. **D**, Falciform ligament (*arrow*) and its relations with abdominal wall (a) and left lobe of liver (l) in patient with ascites. **E**, Intrahepatic course of falciform ligament (*arrow*).

REFERENCES

1. Gray H: *Anatomy of the Human Body*, 29th American ed., edited by Goss CM, Philadelphia, Lea & Febiger, 1973
2. Bartrum RJ, Crow HC: *Gray Scale Ultrasound: A Manual for Physicians and Technical Personnel*. Philadelphia, Saunders, 1977
3. Scheible W, Gosink BB, Leopold GR: Gray scale echographic patterns of hepatic metastatic disease. *AJR* 129:983–987, 1977
4. Haswell DM, Berne AS, Schneider B: Plain film recognition of the ligamentum teres hepatis. *Radiology* 114:263–267, 1975

Calibrated Leak Balloon Microcatheter: A Device for Arterial Exploration and Occlusive Therapy

CHARLES W. KERBER,[1] WILLIAM O. BANK,[2] AND LAURENCE D. CROMWELL[3]

In quest of an endarterial treatment for intracranial arteriovenous malformations and fistulas, a microcatheter which can be flow-guided into third- and fourth-order branches of the intracranial arteries was developed. This permits controlled deposition of a vascular occlusive polymer (isobutyl-2 cyanoacrylate). Goals and experimental techniques are reviewed and clinical experience on the first 25 patients is presented. Complications included one stroke and three catheters glued in place, but refinements in technique have permitted avoidance of complications over the 14 months before this report.

Arteriovenous malformations of the central nervous system are difficult lesions to treat. Located within vital structures, even the surgical approach to them can be dangerous. Recently nonsurgical methods of therapy such as radiographically controlled endarterial deposition of balloons [1, 2] and flow directed particulate emboli [3–11] have developed. We conceived a third method based on the fluoroscopically controlled percutaneous delivery of a tissue adhesive polymer into the malformation.

Arteriovenous malformations are usually high-flow abnormalities, and thus the arteries feeding them become large and tortuous. Unless occluding material passes deep into the substance of the malformation, treatment is only palliative since other feeding vessels subsequently enlarge. Doppman et al. [12] emphasized the need to fill the substance of the lesion—its smallest vessels—in order to effect a cure.

We felt that there were three problems to solve:

1. Identify a suitable plastic to form an intravascular cast. The plastic should polymerize on contact with the abnormality, and then cause a mild inflammatory reaction to ensure fibroblastic response. It should be permanent and radiopaque, neither causing continuing tissue damage, nor possessing carcinogenic properties. Viscosity should be low so it can pass through microcatheters.

2. Develop experimental models. These models should duplicate conditions found in human malformations and fistulas. They should have pulsatile high-flow and large-calibre tortuous vessels. The models should be inexpensive and easy to make.

3. Develop a method to deliver the plastic to the abnormality. The delivery system should be extremely soft and flexible to negotiate tortuous vessels and to avoid injury to thin intracranial arteries. The catheter should be small enough to allow penetration to third- and fourth-order intracranial branches. A balloon tip on the catheter would not only add guidance to high flow abnormalities, but inflation of the balloon could slow or stop the blood flow during deposition of the polymer. The lumen of the catheter should be large enough to permit adequate control of the balloon while giving the operator easy control for the delivery of large or small volumes of occluding material or contrast agent.

Materials and Methods

Polymer

Isobutyl-2 cyanoacrylate (IBCA) was chosen because of Zanetti and Sherman's work [13]. They injected IBCA both directly through needles and indirectly through polyethylene catheters to occlude canine renal arteries, vein pouch aneurysms, and artificial arteriovenous shunts. IBCA can be made opaque by the addition of tantalum dust and Pantopaque. It polymerizes on contact with ionic materials (blood, blood vessel wall) in a few seconds. It excites a modest inflammatory response (fig. 1), has low viscosity, and passes readily through microcatheters.

Models

A plastic and glass device (fig. 2) was designed with a rubber-capped blind loop to allow the catheter to be placed within the system using the Seldinger technique. The study segment was usually made of cadaver vessel. A heart pump provided pulsatile flow, and a downstream reservoir allowed determination of the amount of IBCA lost through the shunt. With this model we assembled the appropriate adapters and tubings which would keep the system perfused with heparinized saline, yet still allow manipulation of the balloon microcatheter and coaxial catheter.

After encouraging preliminary experience with this model, a malformation in animal subjects was created with the most difficult therapeutic characteristics. A short-segment high-flow arteriovenous fistula was made from a canine carotid artery to the adjacent external jugular vein (fig. 3). The 19 shunts created remained patent in all but two animals. Blood flow through these varied from 450 to 1,350 ml/min, and all dogs developed cardiac enlargment. We hoped that successful occlusion of these high flow fistulae would facilitate treatment of the slower flow abnormalities in man.

Delivery system

For flexibility, inertness, and elasticity silicone catheters and balloons were used. Fabrication was relatively easy; the only

Received August 8, 1978; accepted after revision October 20, 1978.
Presented in part at the annual meeting of the American Society of Neuroradiology, Bermuda, March 1977, as the outstanding paper of the year. Also presented at the annual meeting of the American Roentgen Ray Society, Boston, September 1977.

[1] Department of Radiology, Section of Neuroradiology, University of Pittsburgh School of Medicine, Presbyterian-University Hospital, DeSoto at O'Hara Street, Pittsburgh, Pennsylvania 15261. Address reprint requests to C. W. Kerber.
[2] Department of Radiology, University of California School of Medicine, San Francisco, California 94143.
[3] Department of Radiology, University of Washington School of Medicine, Seattle, Washington 98195.

0361-803X/79/1322-0207 $0.00

AJR 132:207–212, February 1979
© 1979 American Roentgen Ray Society



Fig. 1.—Artery occluded with tantalum-impregnated cyanoacrylate. Cyanoacrylate appears on H and E stains as refractile material. Irregular black clumps within are agglutinations of tantalum dust. Arterial wall surrounding plug shows little inflammatory change.

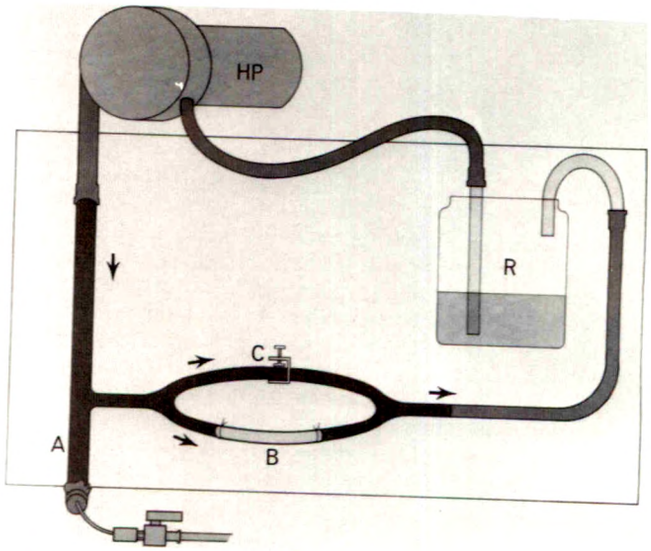


Fig. 2.—Plastic model. Blind loop (A) ending in rubber dam allows introduction of catheter by Seldinger technique. Heart pump (HP) supplies pulsatile fluid flow. Study segment (B), generally cadaver vessel, is placed in system. Catheter may be directed to this point and blood flow stopped with balloon or polymer may be introduced without any modification of blood flow. Screw clamp (C) allows variation in flow and pressure through study segment. Downstream reservoir is used to determine how much polymer embolizes distally. (Reprinted with permission from [14].)

difficulty was the avoidance of a double lumen system. Until our development, flow-guided balloon-tipped catheters needed two lumens: one lumen inflated the balloon; the other delivered material distal to the balloon. But decreasing catheter lumen size by one-half increases the resistance to flow through the catheter 16 times, and when microcatheters are used, a double lumen system carries a high penalty in terms of slow fluid delivery and balloon response. We solved that problem by developing a balloon with a calibrated leak at its tip [15]. A single lumen could thus carry a fluid which first caused the balloon to inflate. Additional pressure by the operator then delivered contrast agent, adhesive, or drugs distal to the balloon tip (fig. 4).

With this background and these tools, we began a cautious exploration of intracranial vessels. A no. 6 French Cordis sheath (501-606, Cordis Co., Miami, Fla. 33137) was placed into the left femoral artery. (The axillary or carotid artery may be used but are less preferred.) Through the sheath a no. 5.8 French thin-wall catheter (P5.8-NT-100-P-NS-0, Cook, Inc., Bloomington, Ind. 47401) was directed with fluoroscopic control into the appropriate cranial artery. A second no. 5 French catheter was placed into the opposite groin and directed into the same cranial artery to allow localizing injections of contrast agent.

Through the first catheter, the balloon microcatheter was squirted into the intracranial circulation, the balloon inflated, and the final position determined fluoroscopically and with cut films.

Results

With our model of plastic tubes we worked out and assembled all of the necessary tubings, adapters, wires, and connectors used to make the system operational. Manipulating various catheters in such a model developed proficiency, and allowed the team to learn under low stress conditions.

In 17 dogs, 17 shunts were occluded simply by placing a straight catheter into the proximal shunt and injecting about 0.3-0.4 ml IBCA. Two dogs died within 2 days of treatment from embolization of polymer to the lungs with resultant acute cor pulmonale. Even though the other animals remained asymptomatic, IBCA was found in their pulmonary arteries at postmortem examination. The cyanoacrylate introduced slowly into rapidly flowing blood expanded, captured blood elements, and produced particulate emboli far in excess of the expected quantity. It was obvious that a balloon was needed to stop flow during cyanoacrylate deposition.

In humans, we found that the balloon microcatheter passed through the carotid siphon and into third- and fourth-order intracranial branches and allowed sufficient flow rates for satisfactory superselective angiography. Passage into the posterior cerebral arteries by a femoral-vertebral artery approach was accomplished as well. We have not found these angiograms to be of clinical diagnostic utility yet, except for the precise localization of the balloon prior to adhesive deposition (fig. 5).

As expected, we found that neurologic deficits could be readily produced in patients. These have been transient except for one permanent stroke (described later). These temporary ischemic strokes appear gradually, generally after about 20-30 sec of occlusion by the balloon. They clear after balloon deflation or removal in another 20-30 sec.

Surprisingly, some deficits were produced within seconds of injection of the microcatheter or balloon inflation. These also cleared rapidly. Inadvertent entry into the posterior inferior cerebellar artery of one patient produced an immediate tonic movement of the head to that side, with striking left lateral nystagnus and a feeling of panic (in both patient and angiographer). Injection of contrast agent in another patient's posterior inferior cerebellar artery, also inadvertent, caused the patient to

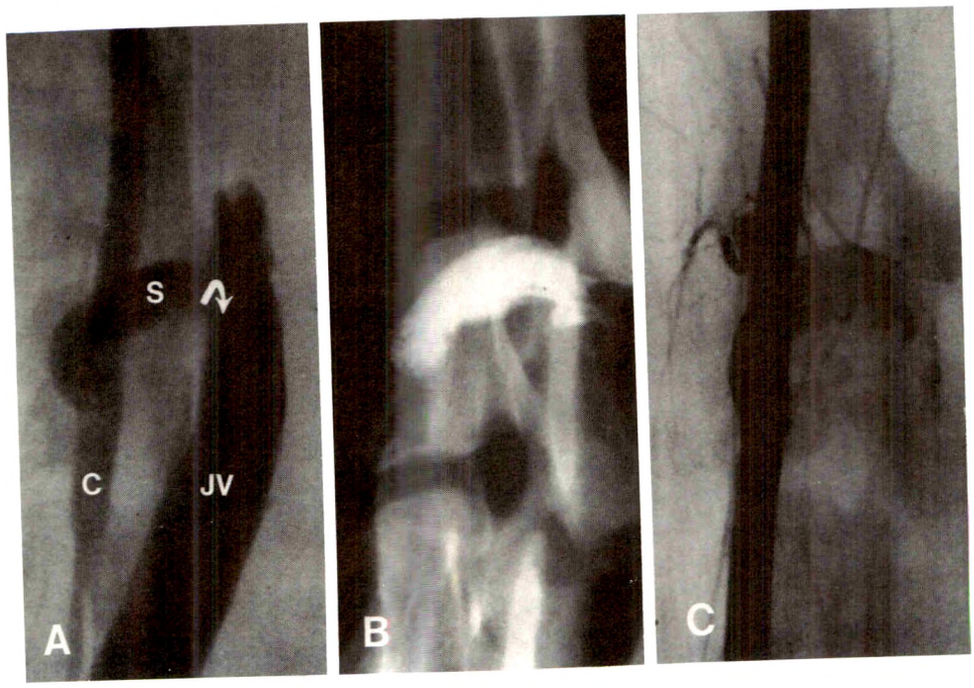


Fig. 3.—Dog 21-331. **A**, Short segment shunt(s) created between carotid artery (C) and external jugular vein (JV). Contrast agent is dilute, and does not fill small branches of external carotid artery. **B**, Small catheter was placed coaxially at orifice of fistula and tantalum-impregnated isobutyl-2 cyanoacrylate was deposited completely occluding flow. **C**, Closure of shunt and good filling of carotid artery radicals.

feel impending death but was without focal neurologic deficit and cleared quickly.

We have not found it possible to predict functional loss from the occlusion of a specific artery except in a general way. The branches of the middle cerebral artery seem to vary considerably in their functional distribution. We were not able to detect spasm caused by the microcatheter, nor were any of these thin-walled feeding vessels ruptured.

The balloon was placed in arteries supplying spinal cord arteriovenous malformations in three patients (fig. 6). Perfusing the feeder for 10 min with contrast agent gave some idea of the likelihood of causing permanent neurologic deficit and was performed as a provocative test in both the spinal and intracranial patients.

Treatment of intracranial arteriovenous malformations has been successful in part, but no complete cure has resulted. However, palliation of signs and symptoms has been encouraging. Our longest follow-up is $3\frac{1}{2}$ years: that patient had two subarachnoid hemorrhages and complained of roaring in her ears. Occlusion of the left posterior cerebral artery feeders stopped the painful noise. (She died from a pelvic malignancy and no autopsy was performed.) To date we have injected more than 85 balloons into the central nervous system of 25 patients. Cyanoacrylate has been deposited 28 times either as presurgical or primary treatment of arteriovenous malformations and fistulae. These include two iatrogenic and one traumatic carotid cavernous fistulae with preservation of flow through the internal carotid artery. Those patients remain asymptomatic. A detailed report of these patients is the subject of a paper in preparation.

Even with large fistulae and shunts only 0.2–0.4 ml of cyanoacrylate is needed for one treatment.

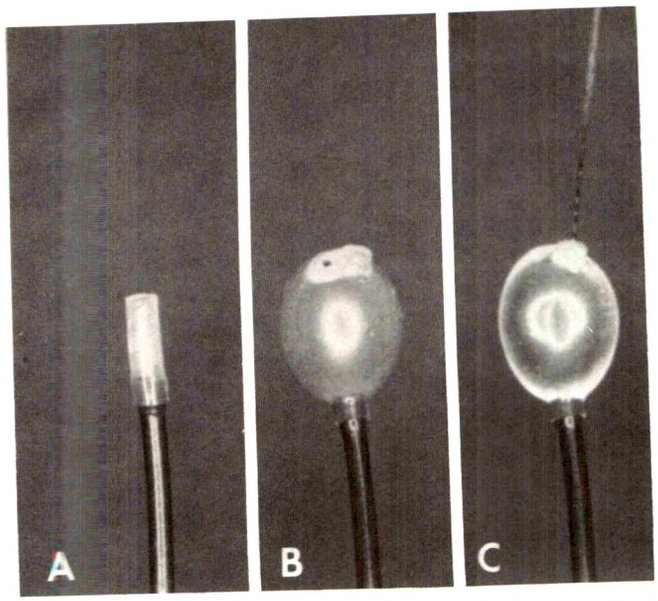


Fig. 4.—Calibrated-leak balloon microcatheter. **A**, Uninflated, widest diameter of balloon is 1 mm. **B**, Balloon may be inflated to allow it to be flow directed. **C**, With greater pressure, liquid squirts through calibrated leak placed at reinforced tip. (Reprinted with permission from [15].)

Complications

One profound parietal stroke occurred during the provocative test perfusion of a temporal arteriovenous malformation with contrast agent. Recovery of this patient was not complete, as he had persisting parietal signs and slight weakness. The cause of his stroke is unclear but will be commented upon in the discussion.

Three catheters were glued in place. None of these have caused further symptoms. One was removed 2 days

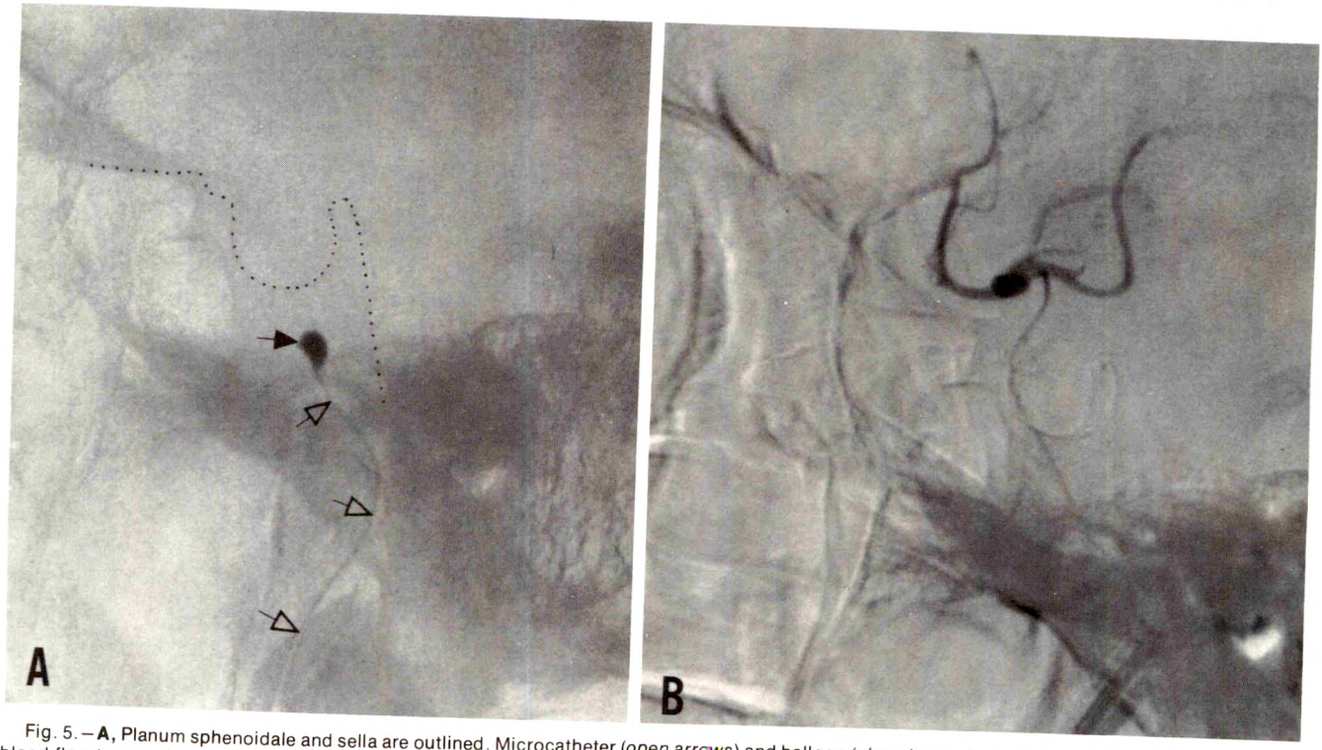


Fig. 5.—**A**, Planum sphenoidale and sella are outlined. Microcatheter (*open arrows*) and balloon (*closed arrow*) are visible. Inflation of balloon causes blood flow to carry it through carotid siphon. **B**, Balloon carried into branches of middle cerebral artery.

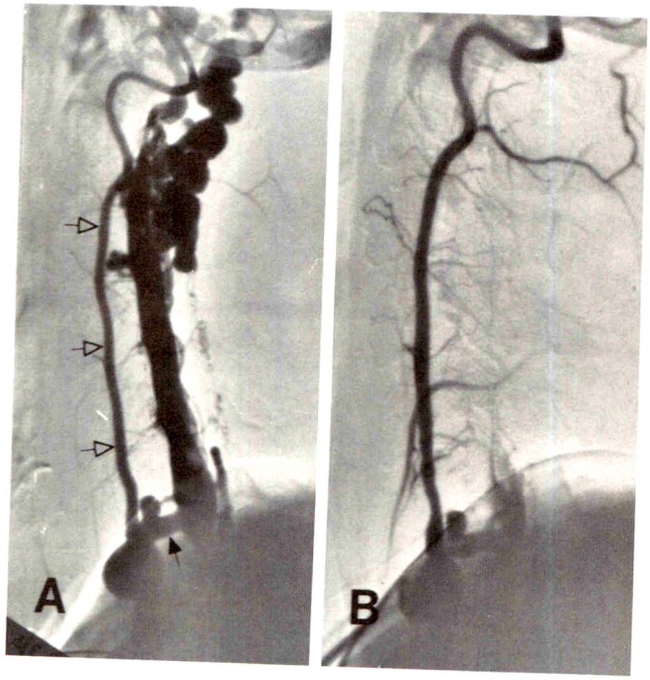


Fig. 6.—**A**, Short segment arteriovenous malformation between vertebral artery and vessels about cord. Vertebral artery (*open arrows*); fistula (*closed arrow*). Treatment was carried out in three stages. After first two, there was little apparent change in flow through fistula, and procedure was considered a failure. Futher deterioration of neurologic status prompted third attempt. **B**, After last treatment, flow through malformation has slowed considerably. Patient subsequently had lesion removed surgically.

later by percutaneous techniques; another was partially removed percutaneously and still remains within that patient's patent internal carotid and middle cerebral arteries. The patient continues to do well and returns periodically for follow-up angiography. A third catheter was removed from a middle cerebral artery branch during subsequent surgical excision of his arteriovenous malformation.

There has been neither infection nor other discernible problem associated with this treatment. We have found no evidence of embolization to the lungs on postprocedural follow-up chest films or lung scans done on the last six patients.

One of the patients treated for carotid cavernous fistula had a seizure 2 weeks after polymer deposition. Films showed cyanoacrylate in at least three branches of her middle cerebral artery. She has been asymptomatic since.

Discussion

Isobutyl-2 cyanoacrylate is a reasonable but not an ideal polymer. It is a powerful adhesive and sets quickly. Special care must be taken not to glue the catheter in place. Experience has shown that the catheter must be lubricated with an inert silicone grease (Dow-Corning stopcock grease, Fisher Scientific, Pittsburgh, Penn.) before its introduction and removed quickly after injection. IBCA is not an approved drug and one must have federal permission before using it in humans.

Models

Although the models are tedious to construct, they provide the only way to develop the necessary teamwork and proficiency to use this adhesive. The deposition of adhesive intracranially is a formidable undertaking and

is truly a team effort. We found the animal practice invaluable.

Delivery System

The balloon catheter made of silicone is inert, flexible, and has allowed exploration of arteries throughout the body that previously have been difficult to catheterize. Even the intracranial arteries seem to tolerate this system well, and no spasm has been noted about the catheter tip. No vessel has been inadvertently ruptured by its use, even though arteries supplying intracranial arteriovenous malformations are thin walled. The delivery system introduces the microcatheter in only a few seconds. It is so rapid that if the microcatheter does not enter the desired vessel immediately, rather than expending time and effort to advance it, we remove it and replace it with another. Complete details concerning its introduction and use have been reported [16].

The system may be used to correlate blood flow and anatomic function, to perform superselective pharmacoangiography and to study regional blood flow. Our studies in these areas are primitive, as we have been concerned primarily with avoiding injury to the patient. The production of acute neurologic deficits was stressful to the team. That these deficits appeared after about 30 sec of occlusion was disturbing but expected; their resolution in another 30 sec was a relief. We were surprised by ischemic deficits which developed in some patients almost instantly after occlusion of a particular vessel. Apparently there are portions of the brain which have no reserve before decreased function appears, or, less likely, there is a rapidly reversible toxic affect of the contrast agent.

We do not suggest that this system of catheter therapy is ideal. The polymer hardens so rapidly that it is sometimes not possible to get the desired penetration of cyanoacrylate into the arteriovenous malformation, and the intravascular cast is not always complete. Fortunately it is possible to delay polymerization; a modification to do this is the subject of a subsequent report [17]. However, rapid polymerization of IBCA is valuable in treating short segment shunts and carotid cavernous fistulae. The polymer has also been useful for the palliation of patients with inoperable arteriovenous malformations. These patients have had no progression of their symptoms and have actually improved.

One specific indication for polymer embolization may be emphasized: surgical candidates with angiomas supplied by both the posterior cerebral and middle cerebral arteries may benefit from preoperative cyanoacrylate occlusion of the deep posterior cerebral feeders, a procedure which is not difficult. Subsequently, the surgeon may control the middle cerebral opercular branches with direct vision with no concern about the deep supply.

We do suggest one caution: our experience has shown that rapid total occlusion of blood supply to a large arteriovenous malformation may lead to cerebral edema. Presumably the normal intracranial vessels have lost, at least temporarily, their normal homeostatic responses. Sudden correction of the intracranial shunt presents these vessels with a large pressure load and cerebral edema results. We routinely prepare all patients with dexamethasone (24 mg orally in divided doses the day before the treatment, 12 mg orally the morning of the treatment, and 24 mg/day for the next 3–4 days) and do the occlusions in a minimum of two stages.

Complications

That there were few complications reflects not basic simplicity and safety of the procedure, but that we selected our patients with great care and attempted cyanoacrylate occlusion on only a few of them.

Our major complication was a profound parietal lobe stroke during manipulation of the microcatheter in the middle temporal lobe branches. On reconsideration, we believe we either damaged the internal carotid artery with the outer coaxial catheter or perfused the coaxial catheter poorly during the procedure. We now take great care not to introduce the polyethylene catheter much higher than C2 and use constant infusion of heparinized saline to keep the coaxial catheter free of clot.

Since cyanoacrylate is a powerful adhesive, it is no surprise that three catheters were glued in place. This likelihood is lessened by placing an inert silicone grease on the catheter tip before its introduction and watching carefully with fluoroscopy for the placement of the cyanoacrylate. When there is no more forward progression of the tantalum-impregnated cyanoacrylate, the balloon is quickly deflated and removed.

Finally, we suggest that the visceral angiographer may have more use for this system than the neuroangiographer. We have done only a few abdominal cases, but have found this system of occlusive therapy much easier to use in the abdominal vessels than in the brain. We have used it to occlude renal arteries supplying hypernephromas and have treated successfully one renal arteriovenous fistula [18].

Exploration of the intracranial vessels is a formidable undertaking. The brain is an unforgiving organ and the production of stroke is not only disabling to the patient but traumatic to the radiologist unaccustomed to doing high risk procedures. The introduction of a catheter for therapeutic rather than diagnostic purposes is a departure from his usual mental set. Whether that departure turns out to be good for patients will depend on how well the radiologist is prepared with the skills required and for the risks involved.

REFERENCES

1. Serbinenko AF: Balloon catheterization and occlusion of major cerebral vessels. *J Neurosurg* 41:125–145, 1974
2. Debrun G, Lacour P, Caron JP, Hurth M, Comoy J, Keravel Y, Loisance D: Traitment de fistules artérioveineuses et d'anevrysmes par balloon gonfable et largable. *Nouv Presses Med* 4:2315–2318, 1975
3. Newton TH, Adams JE: Angiographic demonstration and non-surgical embolization of spinal cord angioma. *Radiology* 91:873–876, 1968
4. Boulous R, Kricheff II, Chase NE: Value of cerebral angiography in the embolization treatment of cerebral arteriove-

nous malformation. *Radiology* 97:65–70, 1970
5. Djindjian R, Cophignon J, Rey A, Theron J, Merland JJ, Houdart R: Superselective arteriographic embolization by the femoral route in neuroradiology. Study of 50 cases. III. Embolization in craniocerebral pathology. *Neuroradiology* 6:143–152, 1973
6. Djindjian R, Cophignon J, Rey A, Theron J, Merland JJ, Houdart R: Superselective arteriographic embolization by the femoral route in neuroradiology. Study of 50 cases. II. Embolization in vertebromedullary pathology. *Neuroradiology* 6:132–142, 1973
7. Djindjian R: Superselective internal carotid arteriography and embolization. *Neuroradiology* 9:145–156, 1975
8. Luessenhop AJ, Gibbs M, Velasquez AC: Cerebrovascular response to emboli. *Arch Neurol* 7:264–274, 1962
9. Luessenhop AJ, Kachmann R, Shevlin W, Ferrero AA: Clinical evaluation of artificial embolization in the management of large cerebral arteriovenous malformations. *J Neurosurg* 23:400–417, 1965
10. Luessenhop AJ, Presper JH: Surgical embolization of cerebral arteriovenous malformations through internal carotid and vertebral arteries. *J Neurosurg* 42:443–451, 1975
11. Wolpert SM, Stein BM: Catheter embolization of intracranial arteriovenous malformations as an aid to surgical excision. *Neuroradiology* 10:73–85, 1975
12. Doppman JL, Zapol W, Pierce J: Transcatheter embolization with a silicone rubber preparation. Experimental observations. *Invest Radiol* 6:304–309, 1971
13. Zanetti PH, Sherman FE: Experimental evaluation of tissue adhesive as an agent for the treatment of aneurysms and arteriovenous anomalies. *J Neurosurg* 36:72–79, 1972
14. Kerber CW: Experimental arteriovenous fistula. Creation and percutaneous catheter obstruction with cyanoacrylate. *Invest Radiol* 10:10–17, 1975
15. Kerber CW: Balloon catheter with a calibrated leak. *Radiology* 120:547–550, 1976
16. Kerber CW: A system of catheter occlusive therapy. *Invest Radiol* 11:370, 1976
17. Cromwell LD, Kerber CW: Cyanoacrylate properties for therapeutic embolization. *AJR*. In press, 1979
18. Kerber CW, Freeny PC, Cromwell LD, Margolis MT, Correa RJ: Cyanoacrylate occlusion of a renal arteriovenous fistula. *AJR* 128:663–665, 1977

CT Detection of Demyelinated Plaques in Multiple Sclerosis

VICTOR M. HAUGHTON,[1] KHANG-CHENG HO,[2] ALAN L. WILLIAMS,[1] AND O. PETTER ELDEVIK[1]

CT images and anatomic slices of two brains containing numerous demyelinated plaques were correlated. Demyelinated plaques smaller than 0.7 cm were not detected by CT. Some larger plaques were misinterpreted as normal structures. These and other considerations suggest that chronic cerebral demyelination cannot be excluded by negative nonenhanced CT scan.

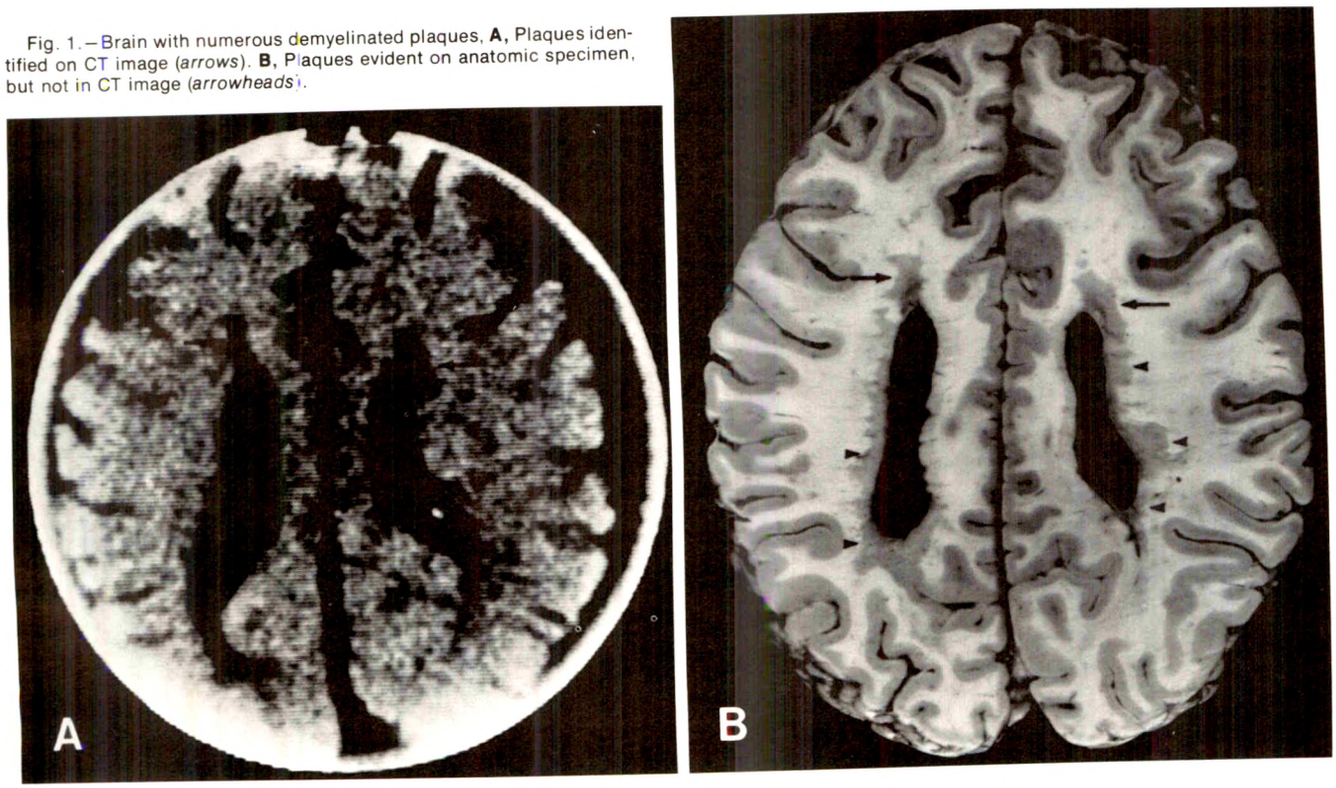
Computed tomography (CT) demonstrates focal abnormalities in one-third of patients with clinically diagnosed multiple sclerosis [1–11]. In two-thirds of these patients, cerebral demyelinated plaques are either not present, isodense, too small for resolution, or not recognized by the radiologist reviewing the images. To determine what factors affect CT detection of demyelinated plaques, we correlated CT and anatomic findings in brains from two cadavers with multiple sclerosis.

Materials and Methods

The brains of two cadavers with a clinical diagnosis of multiple sclerosis were removed and immediately placed in a polyethylene container filled with physiologic saline. Air within the brain or container was extracted [12] and the container was placed in the head holder of a General Electric CT/T 8800 scanner. Consecutive CT sections were made at 5 mm intervals parallel to the base of the brain. Technical factors included a 5 mm cut thickness, 9.6 sec scan time, 600 mA, and 120 Kv. Three radiologists studied the display console and hard copy images, and tried to identify the location and size of any low attenuation abnormality.

The brains were subsequently fixed and sectioned with an electric slicer into 5 mm thick axial sections parallel to the base of the brain. The pathologist then identified the location and size of each demyelinated plaque visible on the surface of the sections and the pathologically identified lesions were correlated with those identified radiographically. To compare these

Fig. 1.—Brain with numerous demyelinated plaques, **A,** Plaques identified on CT image (*arrows*). **B,** Plaques evident on anatomic specimen, but not in CT image (*arrowheads*).



Received July 25, 1978; accepted after revision November 6, 1978.

[1]Department of Radiology, Medical College of Wisconsin and Milwaukee County Medical Complex, 8700 West Wisconsin Avenue, Milwaukee, Wisconsin 53226. Address reprint requests to V. M. Haughton.

[2]Department of Pathology, Medical College of Wisconsin and Milwaukee County Medical Complex, Milwaukee, Wisconsin 53226.

© 1979 American Roentgen Ray Society

0361-803X/79/1322-0213 $0.00

TABLE 1

CT-Detected Demyelinated Plaques

Lesion Size (cm)	Location	Detection*
Brain 1 (of 31 lesions):		
2.8 x 0.6	Paraventricular	3
2.1 x 0.7	"	3
1.5 x 0.9	"	3
3.0 x 0.8	"	2
1.2 x 0.6	"	2
3.2 x 1.6	"	R
2.1 x 0.5	"	R
1.7 x 0.6	"	R
1.6 x 1.1	"	R
1.2 x 0.4	"	R
1.2 x 0.2	"	R
Brain 2 (of 39 lesions):		
0.6 x 0.7	Epiventricular	3
0.7 x 0.3	Paraventricular	2
1.4 x 0.6	Subcortical	1

* Number of radiologists (of three) who detected demyelinated plaques or to plaques detected retrospectively (R).

observations with in vivo imaging, attenuation numbers of the demyelinated plaques in the cadaver brain images and in patients with presumed multiple sclerosis were measured with a region-of-interest cursor.

Results

In the first brain, 31 demyelinated plaques were found (table 1). Five of these plaques, all larger than 1.0 cm, were initially detected by one or more of the radiologists. Six additional lesions 1.6–3.2 cm in greatest diameter and located immediately adjacent to the ventricle, were detected only after the anatomic specimens and the CT images were compared (fig. 1). The remaining 20 lesions, 0.2–1.6 cm in greatest diameter, were not detected prospectively or retrospectively. All lesions in this brain were paraventricular (near the ventricle) or epiventricular (over the ventricle).

In the second brain, 39 demyelinated plaques were found on pathologic examination. Only three of these plaques, 0.6–1.4 cm in greatest diameter, were detected in the CT images (table 1). The other 36 lesions, all less than 1 cm in diameter, were missed by CT scanning both prospectively and retrospectively. Of the 39 plaques in brain 2, 36 were paraventricular.

Pathologic examination showed the plaques in both brains to be old, except for two plaques that were undergoing organization. The two largest demyelinated plaques in the first brain had average attenuation numbers of 27.2 and 23.6 units (table 2, fig. 2). A living patient with multiple sclerosis (fig. 3) had plaques measuring 16–25 units. Attenuation of white matter in cadaver brains averaged 35.3 units compared to 32.6 units in the living patient with multiple sclerosis.

Discussion

CT-detected abnormalities in multiple sclerosis patients include: (1) nonspecific findings such as atrophy [1, 3, 9]; (2) transient focal contrast-enhancing or low-density lesions [2, 5, 6, 8–10]; and (3) chronic low attenuation lesions without contrast enhancement [3, 5, 11]. The third abnormality, presumably an organized demyelinated plaque, is the subject of this study.

The Resolving capacity of the scanner affects detection of small low-contrast lesions, such as demyelinated

TABLE 2

Attenuation in Brain No. 1

	Attenuation No.	SD	Area (cm^2)
Lesion:			
Area 1	27.2	2.4	0.30
Area 2	23.6	2.8	0.44
Gray matter:			
Area 1	43.8	3.8	0.43
Area 2	45.0	2.6	0.39
White matter:			
Area 1	34.8	2.4	1.68
Area 2	35.8	2.4	1.47

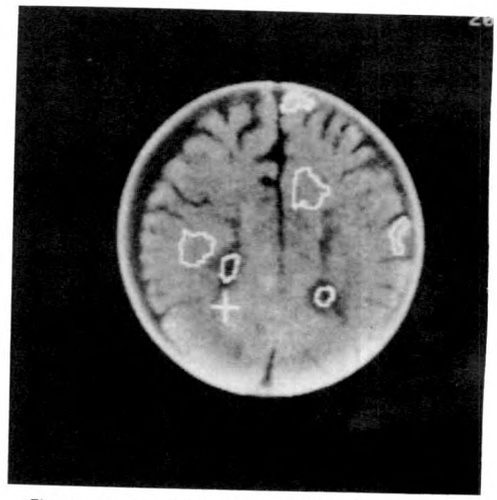


Fig. 2.—Two regions of gray matter, two regions of white matter, and two regions of demyelinated plaque in which average attenuation coefficients were measured.

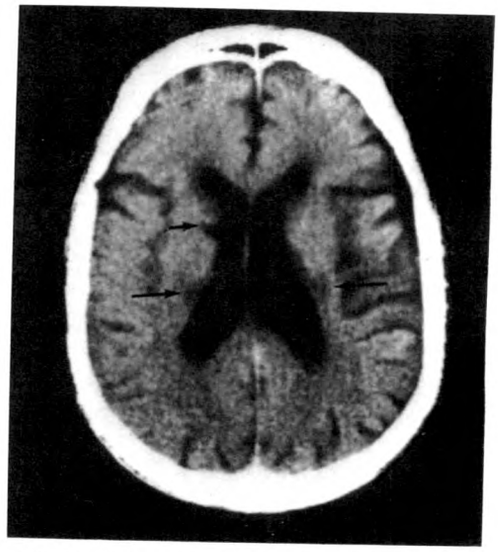


Fig. 3.—Attenuation in periventricular low density lesions (*arrows*) measured 16–23 units in patient with presumed disseminated sclerosis.

plaques. A 3 mm diameter cylindrical phantom differing by 5 units from the surrcunding substance may be detected in a CT/T 8800 tomographic slice obtained perpendicular to the cylinder [13]. However, a 3 mm chronic demyelinated plaque differing from cerebral white matter by 5 units is not distinguished in the same scanner. In fact, plaques smaller than 7 mm were not detected in vitro. These undetected demyelinated plaques are probably hypodense (since their pathologic and histologic appearance is identical to the larger hypodense plaques), yet presumably they are not detected by CT because of irregular, rounded margins that result in partial volume averaging. Whether xenon contrast enhancement of cerebral white matter permits more accurate detection of these plaques is under investigation [14, 15]).

Plaques larger than 7 mm are sometimes disregarded on a CT scan if they simulate normal structures. Paraventricular plaques in the occipital lobe may simulate occipital horn, and plaques in the corpus callosum may simulate lateral ventricle; confluent paraventricular lesions may appear as enlargement of the ventricle; subcortical lesions may simulate sulci or fissures, or when detected as an abnormality on CT may suggest infarct rather than a demyelinating process.

The study would have been more valuable if the brains had also been scanned when living. However, differences in CT appearance between cadaver and living brains are mainly related to the cortex. The attenuation numbers of cadaver white matter and demyelinated plaques agree well with in vivo measurements by the same scanner and with published data [16]. We conclude that the minimum size of chronic cerebral demyelinated plaques detectable with the CT techniques we used is 7 mm, and that plaques larger than 7 mm may be missed when they simulate a normal structure. Therefore, cerebral involvement cannot be ruled out in a patient with presumed demyelination, even though the CT scan is negative.

REFERENCES

1. Cala IA, Mastaglia FL: Computerized axial tomography in multiple sclerosis. *Lancet* 1:689, 1976
2. Cole M, Ross RH: Plaques of multiple sclerosis seen on computerized transaxial tomograms. *Neurology* (Minneap) 27:890–891, 1977
3. Gyldensted C: Computer tomography of the brain in multiple sclerosis. A radiologic study of 110 patients with special reference to demonstration of cerebral plaques. *Acta Neurol Scand* 53:386–389, 1976
4. Jacobs L, Kinkel WR: Computerized axial tomography in multiple sclerosis (abstr). *Neurology* (Minneap) 26:390–391, 1976
5. Weinstein MN, Lederman RJ, Rothner DA, Duchesneau PM, Norman D: Cranial computed tomography in multiple sclerosis. Paper presented at the annual meeting of the Radiological Society of North America, Chicago, November, 1977
6. Aita JF, Bennett DR, Anderson RE, Ziter F: Cranial appearance of acute multiple sclerosis. *Neurology* (Minneap) 28: 251–255, 1978
7. Robertson WC, Gomez MR, Reese EF, Okazaki H: Computerized tomography in demyelinating disease of the young. *Neurology* (Minneap), 27:837–842, 1977
8. Aita JF, Bennett D, Anderson R, Ziter F: Cranial CT appearance of multiple sclerosis. *Neurology* (Minneap) 28:251–255, 1978
9. Campbell BA, Pedley TA: Computerized tomography in cerebral diseases of white matter. *Neurology* (Minneap) 28: 534–544, 1978
10. Aita JF: Cranial CT and multiple sclerosis: contrast enhancing lesions (letter). *Arch Neurol* 35:183, 1978
11. Eyerman DL, Archer CR, Mayer B Jr: Multiple sclerosis in brain and optic nerves seen by standard and high resolution CT (abstr). *Neuroradiology* 12:52, 1976
12. Binder GA, Haughton VM, Ho DC: Computed tomography of anatomic specimens. *J Comput Assist Tomogr* 2:506–508, 1978
13. Di Bianca FA, Edelheit LS, Eisner RL, Glover GH, Keyes GS: The contrast-detail-dose diagram as a measure of CT image quality. Paper presented at the International Symposium and Course on Computed Tomography, Miami Beach, Florida, March 1978
14. Haughton V, Harrington G, Schmidt J, Scanlon G: Xenon contrast enhancement for computed tomography scanning in multiple sclerosis (abstr). *J Comput Assist Tomogr* 1:271, 1977
15. Arimitsu T, DiChiro G, Brooks RA, Smith PB: White-gray matter differentiation in computed tomography. *J Comput Assist Tomogr* 1:437–442, 1977
16. Radue EW, Kendall BE: Iodine and xenon enhancement of computed tomography (CT) in multiple sclerosis (MS). *Neuroradiology* 15:153–158, 1978

Computed Tomography of Intracerebral Leukemic Masses

LYLE R. WENDLING,[1] LAURENCE D. CROMWELL,[2] AND RICHARD E. LATCHAW[3]

Five patients with differing types of leukemia had clinical symptoms of a localized intracerebral leukemic mass. Computed tomography (CT) demonstrated a mass of equal or increased density relative to normal brain; a zone of surrounding edema was variable. In each case, the mass showed evidence of relatively uniform contrast enhancement. CT appearance of leukemic masses is consistent and quite different from the findings in other central nervous system complications of leukemia and its aggressive treatment.

Until recently, the central nervous system was the site of frequent relapse in leukemic patients in hematologic remission. This was especially true for childhood acute lymphocytic leukemia, in which 50% of initial relapses occurred in the central nervous system [1, 2]. Introduction of chemotherapy protocols, which included prophylactic central nervous system irradiation and intrathecal methotrexate, has reduced the incidence of central nervous system relapse to 5%–10% for acute lymphocytic leukemia [3, 4]. In this type of recurrence, usually manifested as infiltration of the leptomeninges with sheets of leukemic cells, frank intracerebral mass resulted only infrequently [5]. This report deals with five patients with intracerebral leukemic masses examined by computed tomography (CT).

Case Reports

Case 1

R. R., a 74-year-old white man, had watery diarrhea, anorexia, weakness, and diaphoresis for 2 weeks. White blood cell count was 15,000/mm³ and blood smear demonstrated polychromatophilia, nucleated red blood cells and highly atypical lymphocytes. Hemoglobin was 11.7 g/100 ml and hematocrit 36%. Diagnosis of acute lymphoblastic leukemia was made on a bone marrow biopsy. Treatment with cytoxin and prednisone produced prompt remission. After induction, he was placed on maintenance chemotherapy and was seen as an outpatient. A year later, he was readmitted in apparent hematologic remission because of a change in mental status. Neurologic consultation revealed weakness, lethargy, and confusion, but there were no lateralizing signs. White blood cell count this time was 3,800/mm³; hemoglobin was 9.6 g/100 ml and hematocrit was 28.1%. Over the next several days he had several fever spikes and became more confused and disoriented. CT scan (fig. 1) demonstrated an irregular area of slightly increased density in the left basal ganglia region adjacent to the anterior horn of the left lateral ventricle. Enhancement was uniform after administration of contrast material. The patient was subsequently comatose and died 14 days after admission. Lymphoblastic leukemia infiltrating multiple organ systems was revealed at autopsy. Neuropathologic examination demonstrated solid sheets of leukemic cells infiltrating the region of the left putamen and globus pallidus.

Case 2

J. B., a 29-year-old woman, had a sore throat that did not respond to antibiotics. White blood cell count was 250,000/mm³. Bone marrow examination showed cell forms typical of acute myelogenous leukemia. After treatment with a modification of the chemotherapy protocol developed by Glucksberg et al. [6], she had a prompt remission and was maintained with multiple courses of "consolidation" chemotherapy.

The patient was still considered in remission 2 years later when she complained of increasingly severe headaches, vomiting, dizziness, and staggering gait. Physical examination demonstrated numerous focal neurologic signs that pointed to a mass in the left cerebellar hemisphere. Lumbar puncture was unremarkable, and routine analysis of the spinal fluid showed no abnormal cells. CT scan (fig. 2) demonstrated a large left cerebello pontine mass which enhanced uniformly with contrast material. Angiography revealed an avascular mass lesion. At posterior fossa craniotomy an intrinsic left cerebellar hemispheric mass lesion was removed. Pathologic examination confirmed the presence of the leukemic mass. After postoperative treatment of 2,400 rad in combination with intrathecal methotrexate, the patient has improved clinically.

Case 3

T. B., a 3-year-old girl, was diagnosed as having acute lymphoblastic leukemia. Chemotherapy treatment showed good results, but over the next 6 years she was hospitalized on several occasions for recurrent episodes of central nervous system leukemia. Four years after diagnosis, she was treated with radiation calculated at 2,300 rad in a midplane dose, and was given multiple doses of intrathecal methotrexate.

Almost 3 years later, she developed severe headaches, lethargy, a right hemiparesis, and decreasing vision in the right eye. With steroid treatment, she gradually improved over the next 2 weeks, and neurologic examination at hospitalization was normal. Analysis of cerebrospinal fluid obtained from a spinal puncture revealed 200 abnormal lymphocytes per high power field. CT scan (fig. 3) demonstrated a mass of increased density in the right cerebellar hemisphere that displaced the fourth ventricle to the left and resulted in an obstructive hydrocephalus. There was uniform enhancement of the mass. Angiography confirmed the presence of an avascular rightside cerebellar lesion. Craniotomy and neurohistopathologic examination confirmed the presence of a leukemic mass.

Case 4

C. J., a 21-year-old man, was diagnosed with acute lymphocytic leukemia. Analysis of cerebrospinal fluid 2 years later

Received July 18, 1978; accepted after revision October 19, 1978.
Presented at the annual meeting of the American Society of Neuroradiology, New Orleans, Louisiana, February, 1978.
[1] Department of Radiology, Sacred Heart Medical Center, West 101 Eighth Avenue, Spokane, Washington 99203. Address reprint requests to L. R. Wendling.
[2] Department of Radiology, University of Washington Hospitals, Seattle, Washington 98195.
[3] Department of Radiology, University of Minnesota Hospitals, Minneapolis, Minnesota 55455.

0361-803X/79/1322-0217 $0.00

AJR 132:217–220, February 1979
© 1979 American Roentgen Ray Society

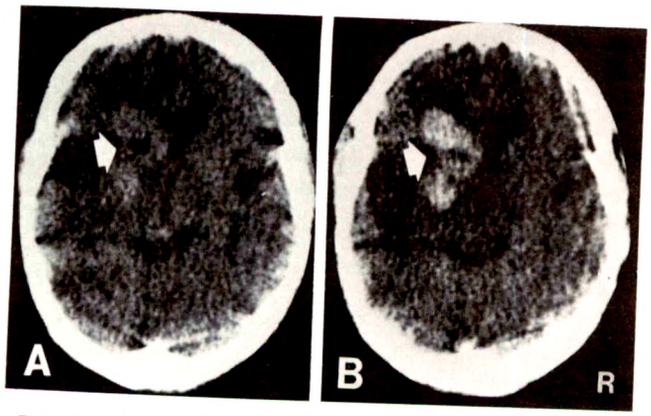


Fig. 1.—**A**, Unenhanced scan. Irregular area of increased density in left basal ganglia region (*arrow*). **B**, Uniform enhancement of leukemic mass after administration of contrast material (*arrow*).

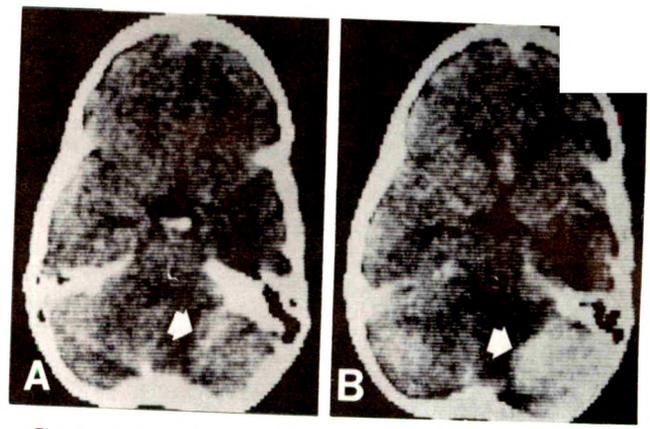


Fig. 3.—**A**, Area of increased density in right cerebellar hemisphere (*arrow*) with displacement of fourth ventricle from right to left. **B**, Mass enhances uniformly (*arrow*).

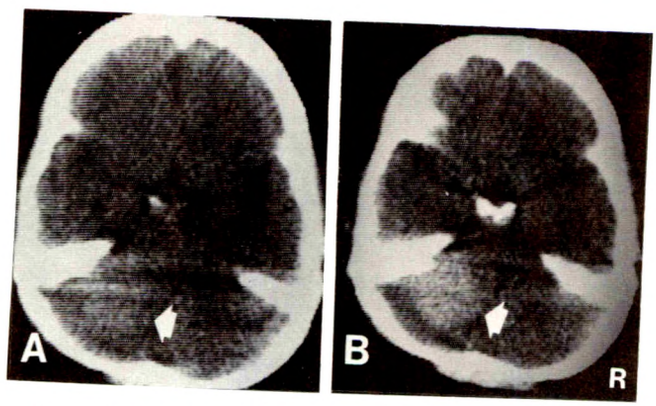


Fig. 2.—**A**, Unenhanced scan. Mass lesion in left cerebellar hemisphere (*arrow*). **B**, Cerebellar hemispheric mass enhances after administration of contrast material (*arrow*).

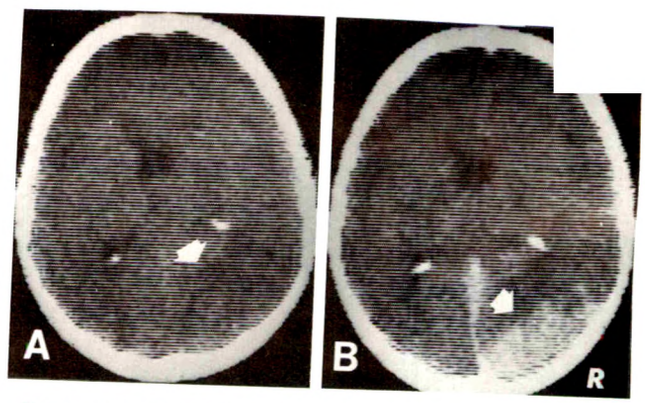


Fig. 4.—**A**, Isodense right parietooccipital mass lesion with surrounding zone of edema (*arrow*). **B**, Isodense mass enhances uniformly (*arrow*). (Reprinted with permission from [7].)

demonstrated abnormal cells. He was treated with radiation therapy combined with intrathecal methotrexate. After 15 months, he complained of bitemporal headaches and visual blurring, and a left homonymous hemianopsia was found. No abnormal cells were found on cytocentrifuge examination of the cerebrospinal fluid. Radionuclide brain scan was positive in the right parietooccipital area, but CT scan at the same time was normal. Angiography demonstrated irregular vessels with early draining veins in the right parietooccipital area. The patient seemed to improve with repeated intrathecal methotrexate therapy. Three lumbar punctures were performed 1 month later and, although suspicious, cytocentrifuge examination of the cerebrospinal fluid was not definitely positive for leukemic cells.

The next month, the patient again complained of blurred vision and was admitted for placement of an Ommaya reservoir. CT scan (fig. 4) demonstrated an isodense right parietooccipital mass lesion with a surrounding zone of edema and there was uniform contrast enhancement. At craniotomy, a greenish mass extending 5–10 mm deep to the cortex was removed and histopathologic examination demonstrated extension of leukemic tissue into the brain parenchyma. The Ommaya reservoir was tapped several times after surgery, and in each case cerebrospinal fluid was positive for leukemic cells. The patient was treated with further radiation therapy and intraventricular methotrexate, but he died 2 months after surgery.

Case 5

D. P., a 4-year-old boy, was diagnosed with acute lymphocytic leukemia. Remission was induced by a combination of vincristine, prednisone, and asparaginase. Maintenance chemotherapy consisted of 6-mercaptopurine and methotrexate. Neither prophylactic intrathecal methotrexate nor craniospinal radiation were given.

His first episode of central nervous system leukemia occurred 1 year later and was treated with cranial irradiation (total dose 3,000 rad) and 4 doses of intrathecal methotrexate. During a second episode of central nervous system leukemia 9 months after the first, he was referred to Children's Orthopedic Hospital in Seattle, Washington for placement of an Ommaya reservoir. He received intraventricular methotrexate every 4 weeks for 2 years.

Four months after end of treatment, he suffered his first bone marrow relapse and five-drug therapy was reinduced; maintenance chemotherapy consisted of methotrexate, vincristine and asparaginase. A third central nervous system relapse 4 months later was treated with intraventricular doses of methotrexate. After another 4 months, he developed truncal ataxia, bifrontal headaches, intermittent obtundation, nystagmus, and a seizure-like episode. CT scan (figs. 5A and 5B) demonstrated a posterior fossa mass with uniform enhancement. Cranial irradiation to 1,200 rad, in addition to dexamethasone and multiple taps of his Ommaya reservoir to reduce cerebrospinal fluid pressure,

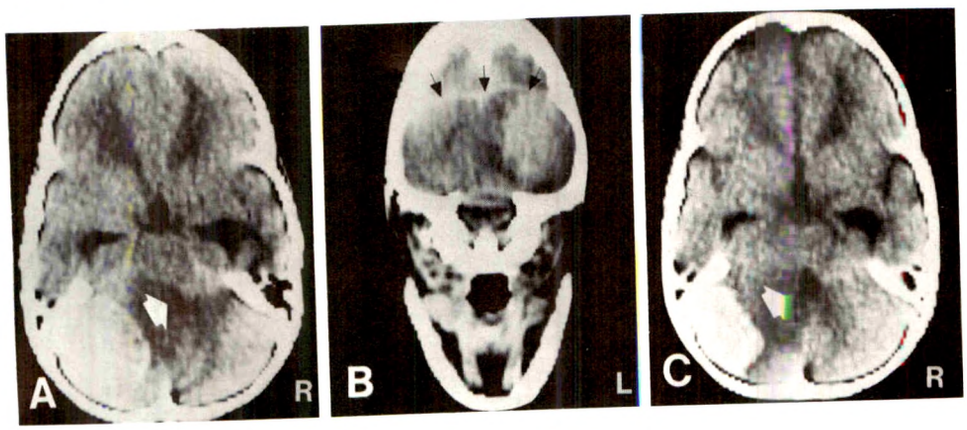


Fig. 5.—**A**, Area of increased density in left cerebellar hemisphere displaces fourth ventricle (*arrow*) from left to right. **B**, Coronal scan after intravenous injection of contrast material. Leukemic mass lesion inferior to tentorium (*arrows*). **C**, Follow-up scan after 1-week of radiation therapy. Fourth ventricle (*arrow*) returned to more normal location. Diminution in size of cerebellar mass lesion.

was given. Cytocentrifuge examination of the cerebrospinal fluid was positive, even though the unspun specimen contained only five white cells per high power field. The patient improved quite promptly with his radiation therapy and was clinically well within a week (fig. 5C). Shortly before bone marrow transplantation 2 months after CT, the patient received an additional 1,000 rad of total body irradiation. Currently, the boy is doing well and there is no evidence of recurrent disease.

Discussion

Before effective chemotherapy protocols, leukemic involvement of the central nervous system was common, and fatal intracerebral hemorrhage frequently occurred in association with the blastic crisis. In 117 consecutive autopsy cases, Moore et al. [8] found leukemic infiltration of the dura in 70% of patients with acute lymphocytic leukemia and in 50% of patients with acute myelongenous leukemia. Death resulted from fatal intracerebral hemorrhage in 20% of these patients, and from leukemic infiltrates in the arachnoid in 30%.

Another autopsy series by Price and Johnson [5], after development of effective combined chemotherapy, showed 56% of patients with acute lymphocytic leukemia had leukemic infiltration of the arachnoid at autopsy. At that time, 50% of initial leukemic relapses occurred in the central nervous system. In response to this and other types of "sanctuary disease", more aggressive therapy protocols for all types of leukemia have evolved. In the case of acute lymphocytic leukemia, this now includes routine central nervous system prophylaxis with low dose cranial or craniospinal radiation therapy in combination with intrathecal methotrexate.

Price and Johnson [5] detailed the pathophysiology of central nervous system leukemia. Infiltration of leukemic cells first appears in the walls of superficial arachnoidal veins. As the disease progresses, more extensive infiltration of the arachnoid occurs until the cerebrospinal fluid channels are contaminated with leukemic cells. After the normal pia-glial membrane is destroyed, invasion of neural tissue eventually occurs.

Leukemic infiltration of the arachnoid is manifested in the central nervous system in a number of ways. Leukemic cells may fill the arachnoid space and cause hydrocephalus. More extensive arachnoid infiltration may result in venous compression and obstruction with secondarily increased intracranial pressure and occasionally venous infarction. Intracerebral hemorrhage may occur immediately adjacent to an area of extensive leukemic infiltrate or in a region of gram-negative bacterial arachnoid vasculopathy. Dural infiltration may result in either local mass effect or increased intracranial pressure. Invasion of neural tissue through a disrupted pia-glial membrane leads to the development of the intracerebral leukemic mass.

Intracerebral leukemic masses seem to have a relatively consistent CT appearance. All of our patients demonstrated uniform enhancement of a mass equal or slightly greater in density than normal brain on precontrast study. A zone of adjacent edema was a variable finding independent of the leukemic cell type. However, Danzinger et al. [9] recently reported two cases of intracerebral leukemia with conflicting CT findings. In a patient with acute lymphocytic leukemia, a low attenuation mass enhanced with contrast material. Another patient with acute mylogenous leukemia had a mass of high attenuation that did not enhance. Gold and Latchaw (personal communication) also report a case of diffuse cortical and leptomeningeal leukemic infiltration in which the CT scan mimicked the CT appearance of "methotrexate leukoencephalopathy."

In the appropriate clinical setting, we believe the CT appearance described here strongly suggests intracerebral leukemia. Leukemic masses should be readily differentiable from the large areas of decreased attentuation and infrequent areas of enhancement seen with methotrexate leukoencephalopathy [9–11]. Similarly, the large scalloped zones of decreased attenuation seen in the centrum semiovale in patients with progressive multifocal leukoencephalopathy [9, 12–14] should be readily distinguishable from a leukemic mass. CT examination of the leukemic patient with catastrophic hemorrhage would show a typical high attenuation coefficient lesion characteristic of an intracerebral hematoma.

The CT appearance of leukemic mass of the posterior fossa seen in our patients could be confused with other lesions, notably acoustic neuroma [15, 16] and medulloblastoma [17]; confusion with other posterior fossa masses seems unlikely. Similarily, a small percentage of basal ganglia or hemispheric primary neoplasms, as well

as meningioma and certain metastases, could appear similar to the leukemic masses in our patients. The CT findings described by Danziger et al. [9] for central nervous system leukemia could be easily confused with intracerebral hematoma, or any one of a variety of lesions resulting in areas of decreased attenuation that subsequently enhance after administration of contrast material. Further experience is needed to determine the frequency of this appearance versus the "typical" CT appearance in our patients.

The work of Price and Johnson [5] provides little doubt that intracerebral leukemic masses are the secondary result of arachnoid leukemia. It has been well demonstrated that in most circumstances the combination of intrathecal methotrexate and whole brain irradiation effectively eradicates leukemic cells in the central nervous system sanctuary [3, 4]. However, in certain instances local obliteration of portions of the arachnoid space may effectively isolate foci of leukemia from the therapeutic agent. Blasberg et al. [18] demonstrated that, at a distance of 3.2 mm from the brain surface, the concentration of methotrexate is only 1% that of the cerebrospinal fluid. This may partially explain why three of our patients developed progressive enlargement of an intracerebral mass in the face of ongoing intrathecal or intraventricular methotrexate therapy. Indeed, in case 5, intraventricular methotrexate may not have even reached the subarachnoid space in the posterior fossa because of aqueductal obstruction produced by the mass.

Cytocentrifuge examination of the cerebrospinal fluid has been the standard method of diagnosing central nervous system leukemia. In this series only two of the four patients studied in this manner (case 1 did not undergo lumbar puncture) had positive cerebrospinal fluid examinations for leukemic cells. Case 2 had no abnormal cells in the cerebrospinal fluid, while case 4 had multiple suspicious but not diagnostic centrifuge examinations. Case 5 had only a few cells on routine examination; however, cytocentrifuge study was positive for leukemic cells. This implies that if lumbar puncture is done when CT suggests obstructive hydrocephalus and an intracranial mass, one should be wary of the occurrence of "false negative" cerebrospinal fluid for leukemic cells.

While only limited conclusions can be drawn from our small series of patients, it seems that the five patients discussed here demonstrate a fairly consistent CT appearance of intracerebral leukemic mass. This appearance in association with confirmatory cytocentrifuge examination of the cerebrospinal fluid specimen resulted in a presumptive diagnosis of leukemic mass in our case 5. The remarkable response to radiation therapy made surgical intervention unnecessary. The neuroradiologist and attending physician should be aware of the atypical cases discussed, as well as the possibility of a false negative cerebrospinal fluid analysis for leukemic cells.

ACKNOWLEDGMENT

We thank Dr. Mack Jones, Good Samaritan Hospital, Portland, Oregon for supplying the scans in case 3 and Dr. John Isom for permission to report clinical details of case 3.

REFERENCES

1. Evans AE, Gilbert ES, Zandstra R: The increasing incidence of central nervous system leukemia in children. *Cancer* 26:404–409, 1970
2. Melhorn DF, Gross S, Fisher BJ, Newman AJ: Studies on the use of "prophylactic" intrathecal amphopterin in childhood leukemia. *Blood* 36:55–61, 1970
3. Aur RJA, Simone JV, Hustu HO, Verzosa MS: A comparative study of central nervous system irradiation and intensive chemotherapy early in remission of childhood acute lymphocytic leukemia. *Cancer* 29:381–391, 1972
4. Hustu HO, Aur RJA, Verzosa MS, Simone JV, Pinkel D: Prevension of central nervous system leukemia by irradiation. *Cancer* 32:585–597, 1973
5. Price RA, Johnson WW: The central nervous system in childhood leukemia. I. The arachnoid. *Cancer* 31:520–533, 1973
6. Glucksberg H, Buckner C, Fefer A, DeMarsh Q, Coleman D, Dobrow R, Huff J, Kjobech C, Hill A, Dittman W, Neiman P, Cheever M, Einstein A, Thomas E: Combination chemotherapy for acute non-lymphoblastic leukemia in adults. *Cancer Chemother Rep* 59:1131–1137, 1975
7. Latchaw R, Gold L: Computerized tomography of intracranial tumors. *Minn Med* 60:554–559, 1977
8. Moore EW, Thomas LB, Shaw RK, Freireich EJ: The central nervous system in acute leukemia. A postmortem study of 117 consecutive cases with particular reference to hemorrhages, leukemic infiltrations and the syndrome of meningeal leukemia. *Arch Intern Med* 105:451–468, 1960
9. Danziger J, Wallace S, Handel SF, Leavens ME: The radiographic appearance of intracranial leukemia and lymphoma. Abstract presented at the annual meeting of the American Society of Neuroradiology, New Orleans, February 1978
10. Lane B: Computed tomography of cerebral white matter disease. Abstract presented at the international symposium on computer assisted tomography in non-terminal diseases of the brain, spinal cord and eye, National Institutes of Health, Bethesda, October 1976
11. Peylan-Ramu N, Poploch DG, Blei CL, Herdt JR, Vermess M, DiChiro G: Computer assisted tomography in methotrexate encephalopathy. *Comput Tomog* 1:216–221, 1977
12. Bjorgen JE, Gold LHA: Computed tomographic appearance of methotrexate induced necrotizing leukoencephalopathy, *Radiology* 122:377–378, 1977
13. Carroll BA, Lane B, Norman D, Enzmann D: Diagnosis of progressive multifocal leukoencephalopathy by computed tomography. *Radiology* 122:137–141, 1977
14. Conomy JP, Weinstein MA, Agamanolis D, Holt WS: Computed tomography in progressive multifocal leukoencephalopathy. *AJR* 127:663–665, 1976
15. Paxton R, Ambrose J: The EMI scanner. A brief review of the first 650 patients. *Br J Radiol* 47:530–565, 1974
16. Glydensted C, Lester J, Thomsen J: Computed tomography in the diagnosis of cerebellopontine angle tumors. *Neuroradiology* 11:191–197, 1976
17. Zimmerman RA, Bilaniuk LT, Pahlajani H: Spectrum of medulloblastomas demonstrated by computed tomography. *Radiology* 126:137–141, 1978
18. Blasberg RG, Patlak C, Feustermacher JD: Intrathecal chemotherapy: brain tissue profiles after ventriculo-cisternal perfusion. *J Pharmacol Exp Ther* 195:78–83, 1975

Unsuspected Aortic Dissection: The Chronic "Healed" Dissection

MARJORIE A. AMBOS,[1] MURRAY ROTHBERG, RICHARD S. LEFLEUR, SYDNE WEINER, AND DOROTHY I. McCAULEY

Of all aortic dissections, 10% are chronic. Typically they arise distal to the left subclavian artery and have reentry points into the true lumen. Pain may be minimal or absent and patients often present with cardiac failure. Chronic dissections are more likely to appear radiographically as atherosclerotic aneurysms on a chest film than are acute dissections. Four cases of chronic dissections found incidentally during angiography are presented.

Aortic dissections typically present as acute catastrophic events. Patients may have sudden tearing chest pain and loss of pulses, and may rapidly go into shock. Angiography is performed in order to confirm the clinical impression, and to show the location and extent of the dissection. However what is well known in the medical literature, but has not been adequately stressed in the radiologic literature is that approximately 10% of aortic dissections are chronic (i.e., the patient has survived more than 6 weeks). Chronic dissections often have findings different from acute ones. Congestive heart failure and minimal or atypical pain are the commonest presentations [1, 2]. Chronic dissections may even be discovered incidentally during angiography, surgery, or autopsy. Of the last 15 aortic dissections studied by angiography at our institution, four (27%) were found during arteriography done for other medical reasons. This paper presents these four cases and discusses the clinical and radiographic findings in chronic aortic dissections.

Case Reports

Case 1

A 62-year-old man was admitted with a 2 year history of microscopic hematuria. Eight months earlier he had a suprapubic prostatectomy for benign prostatic hypertrophy. He denied any thoracic or abdominal pain, dyspnea, or orthopnea. For several years before admission, he had mild hypertension which was controlled with diuretics. Physical examination revealed a blood pressure of 140/70 and equal pulses in all extremities. No cardiac murmurs were heard. Pertinent laboratory findings included blood urea nitrogen, 22 mg/100 ml; creatinine, 0.9; and +1 proteinuria. Admission chest radiography showed left ventricular enlargement and a tortuous descending aorta (fig. 1A).

Intravenous urography was normal, as was ultrasound of the kidneys. Angiography was then done to rule out a small renal tumor or an arteriovenous malformation as the cause of the persistent microscopic hematuria. A DeBakey type III aortic dissection was found with a reentry point in the abdominal aorta (fig. 1B). Subsequent work-up led to the diagnosis of focal glomerulonephritis as the cause of the hematuria.

Case 2

A 54-year-old man was admitted for angiography to rule out a renal artery lesion as the cause of hypertension. The hypertension, which he had had for 10 years, had recently become increasingly difficult to control with medication. Angiography done elsewhere 4 months before this admission was reported as showing renovascular disease (films not available for review). The patient denied having any chest or abdominal pain or dyspnea at present; however, 8 months before this admission, he had a documented myocardial infarction. His blood pressure on admission was 190/110; all pulses were present and equal. Blood urea nitrogen was 26 mg/100 ml and creatinine, 2.4. Chest radiography showed an 8 cm aneurysm of the descending thoracic aorta and left ventricular prominence. A DeBakey type III aortic dissection extending distally to the iliac arteries was discovered during angiography (fig. 2). It was felt that surgery was not indicated and the patient was discharged on antihypertensive medication. Renin studies were not performed.

Comment. Primary systemic hypertension is found in 70%–85% of patients with aortic dissections and is the most common predisposing factor for this condition [2–4]. Sudden worsening of chronic hypertension has been reported in some patients when they develop aortic dissections [5].

Case 3

A 63-year-old man was followed for 5 years for a slowly enlarging, asymptomatic aneurysm of the thoracic aorta. It had originally been discovered on a routine chest radiography. No history of chest or abdominal pain was elicited; however, the patient was moderately hypertensive and had a history of mild congestive heart failure, treated with digoxin for the past 7 years. The admission blood pressure was 150/100 and pulses were equal bilaterally. A systolic ejection murmur was present, but no diastolic murmur was heard. Admission chest radiography showed an 8 cm aneurysm of the descending thoracic aorta. There was a faint linear calcification in the wall of the aneurysm (fig. 3A). Overall cardiac size was normal.

Angiography showed a diffuse aneurysm of the thoracic aorta with a DeBakey type III dissection extending into the abdominal aorta. The dissection involved the brachiocephalic vessels. Since the ascending aorta was not dissected, and since a dissection beginning within the arch itself was unlikely, the dissection presumably began distal to the left subclavian artery and extended proximally (figs. 3B and 3C). A definite reentry point could not be seen (fig. 3D). It was felt that surgery was not indicated and the patient was discharged.

Comment. Congestive heart failure may be the only symptom in patients with chronic aortic dissections, and rapidly worsening failure may be the reason for angiography [6, 7]. In patients

Received August 14, 1978; accepted after revision November 9, 1978.

[1]All authors: Department of Radiology, New York University Medical Center, 560 First Avenue, New York, New York 10016. Address reprint requests to M. A. Ambos.

0361-803X/79/1322-0221 $0.00

AJR 132:221–225, February 1979

© 1979 American Roentgen Ray Society

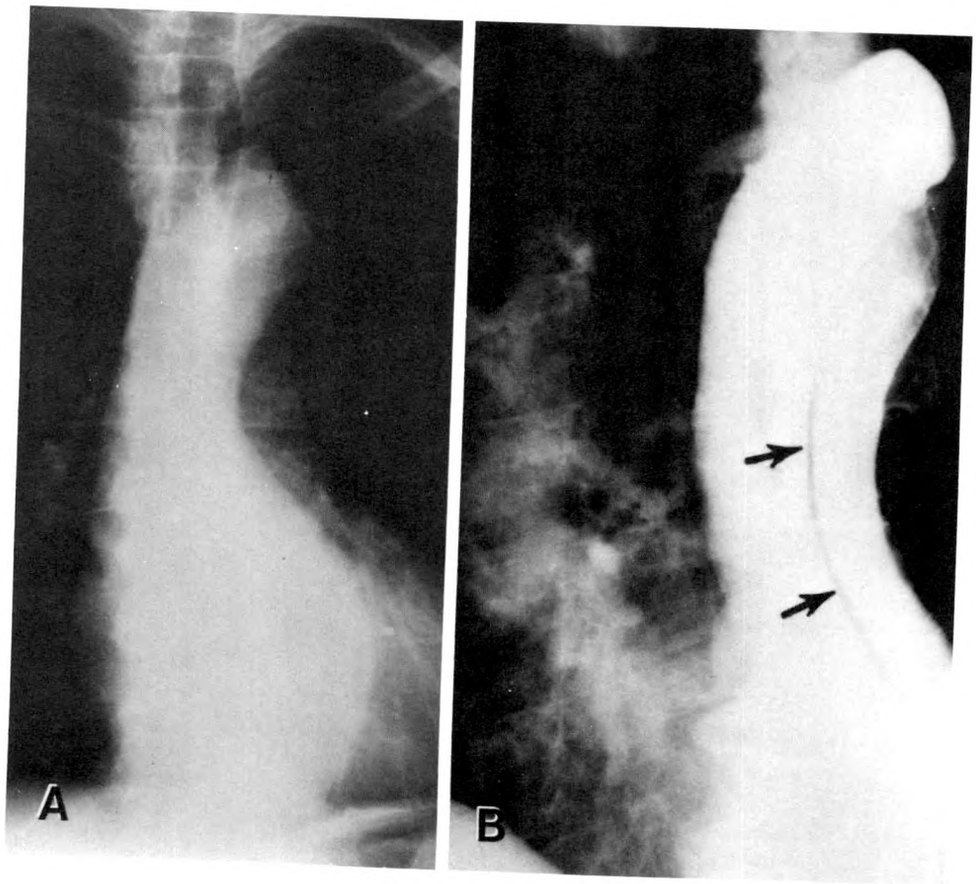


Fig. 1.—Case 1. **A,** Left ventricular prominence and tortuosity of descending thoracic aorta. **B,** Type III dissection with filling of both true and false lumen, and prominent intimal stripe between them (*arrows*).

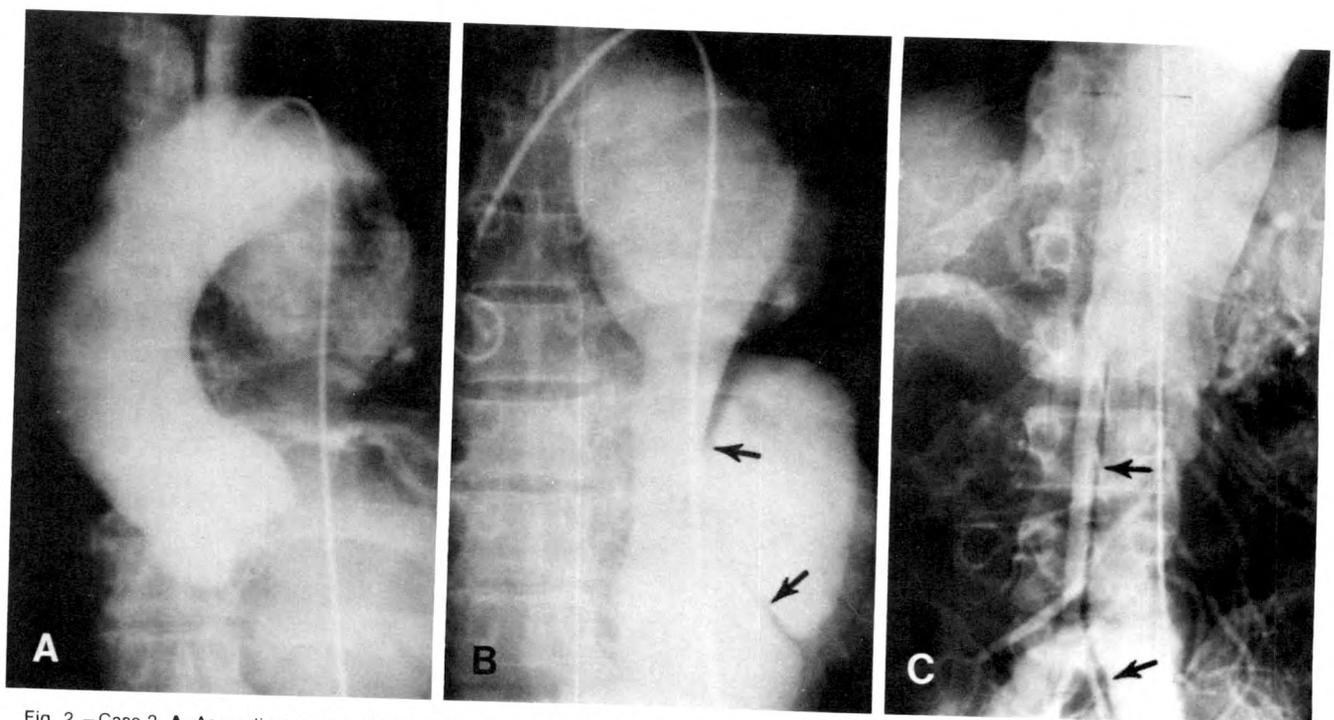


Fig. 2.—Case 2. **A,** Ascending aorta well visualized down to level of aortic valve. No dissection. **B,** Dissection begins past origin of left subclavian artery. Prominent intimal flap (*arrows*). **C,** Good filling of both channels and visceral branches. Dissection extends into both iliac arteries. Intimal flap (*arrows*). Poor visualization of renal arteries; flow through them appears diminished.

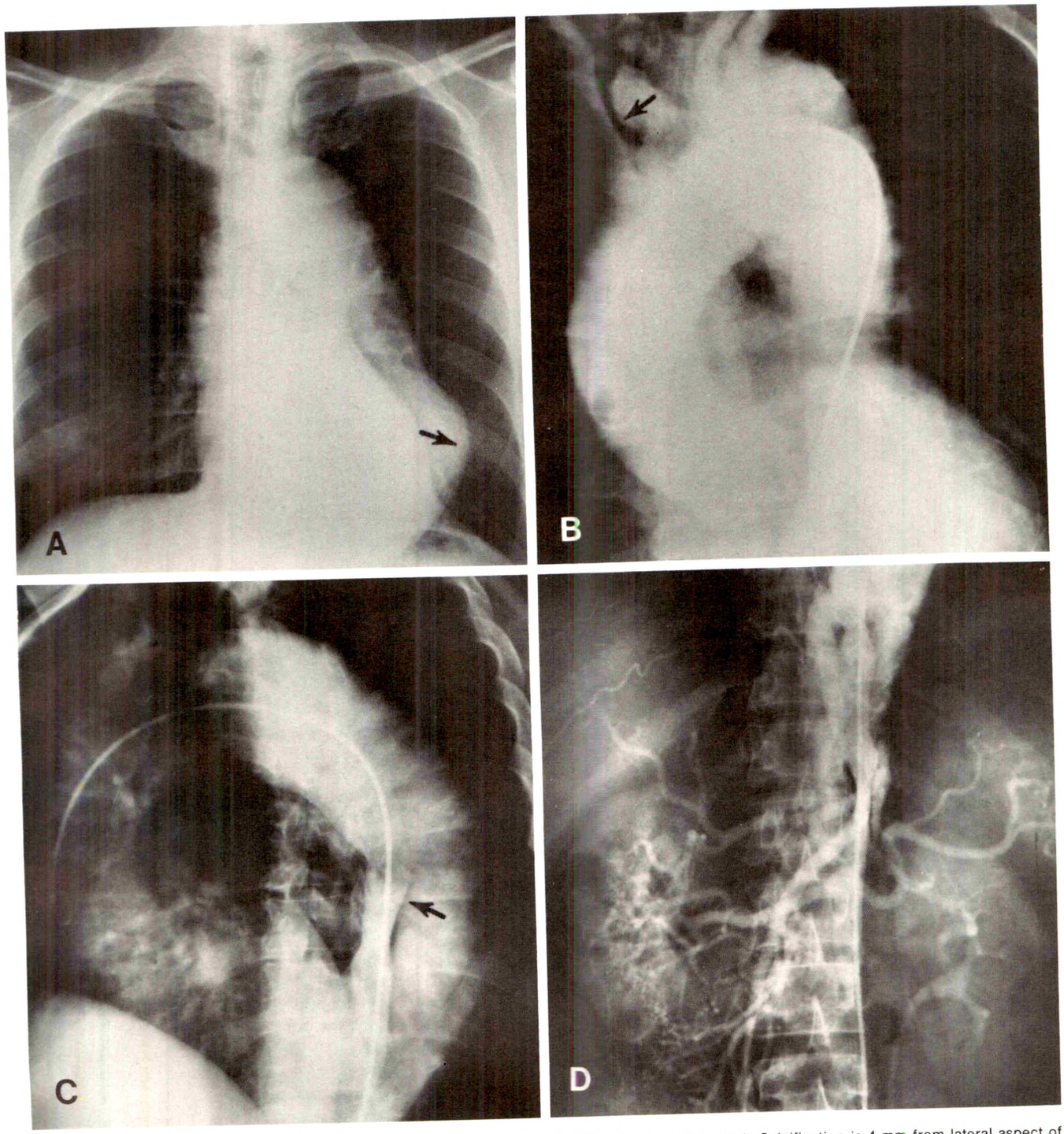


Fig. 3.—Case 3. **A,** Aneurysm of descending thoracic aorta. Faint linear calcification in wall (*arrow*). Calcification is 4 mm from lateral aspect of aorta. **B,** Ascending aorta is normal. Dissection which began distal to origin of left subclavian artery has advanced proximally into arch and extended into origin of innominate artery (*arrow*); however, there is good flow of contrast into all brachiocephalic vessels. **C,** Both true and false lumen fill well. Intimal flap (*arrow*); narrowing of true channel by false channel. **D,** True lumen remains narrowed in abdominal aorta. Celiac, superior mesenteric, and right renal arteries fill from true lumen. Left kidney functions well, although left renal artery presumably fills from false lumen.

who survive the acute dissection, death is often due to cardiac failure [8]. In a reported autopsy series of 30 dissections, 10% of the patients had presented with congestive failure [4].

Case 4

A 58-year-old man was followed for 6 years for an asymptomatic abdominal aortic aneurysm first discovered on routine physical examination. An increase in the size of the aneurysm was noted 3 weeks before admission. There was no history of chest or abdominal pain, but the patient had been moderately hypertensive for 6 years. Physical examination revealed a 7 cm pulsatile mass in the lower abdomen. Blood pressure was 146/90 and pulses were equal. Chest radiography demonstrated a diffuse aneurysm of the descending thoracic aorta and left

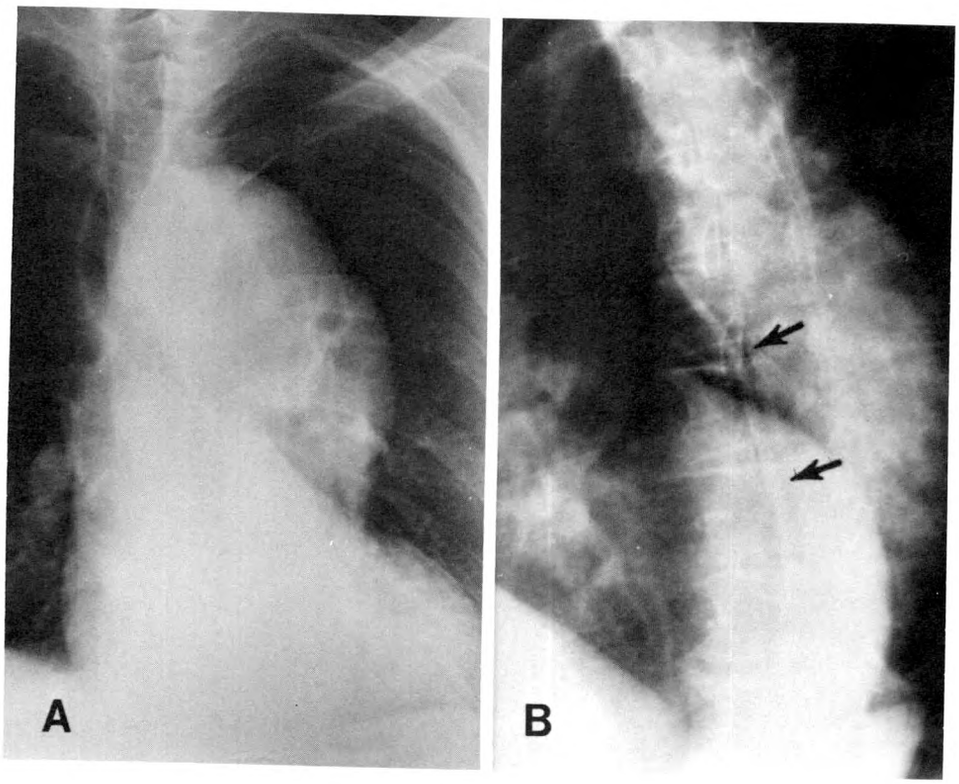


Fig. 4.—Case 4. **A,** Fusiform aneurysm of descending thoracic aorta and left ventricular enlargement. **B,** Very large false lumen markedly compresses true aorta lumen. Intimal flap between two channels (*arrows*).

ventricular prominence (fig. 4A). Ultrasound confirmed the presence of an abdominal aortic aneurysm 7 cm in diameter. Angiography, done to determine the extent of the aneurysm, revealed a DeBakey type III dissection extending into the abdominal aorta (fig. 4B). Since the aneurysm was enlarging, it was resected.

Discussion

Aortic dissections generally present as acute and rapidly fatal events. However, about 10% of dissections survive more than 6 weeks and are then classified as chronic. Chronic dissections have specific characteristics not commonly seen in acute (survival of less than 2 weeks) or subacute (survival of 2–6 weeks) dissections [2, 9]. The most frequently used classification of aortic dissections is DeBakey's, according to location and extent. Type I dissections start in the ascending aorta and progress into the descending aorta. They may extend into the abdominal aorta and lower extremity vessels. Type II dissections are limited to the ascending aorta. Type III dissections begin past the origin of the left subclavian artery and extend for varying distances.

While about two-thirds of aortic dissections are types I or II, chronic dissections are overwhelmingly type III [3, 10, 11]. All type III dissections have a greater chance of long-term survival, since they do not involve the brachiocephalic vessels and also are less likely to rupture into the pericardium [3]. Another aspect of chronic dissections important for longer survival is that they have a reentry point(s) back into the true aortic lumen [12, 13]. The true aortic lumen is the original aortic channel, and the false lumen is the new channel formed by the dissection of blood between intima and adventitia, usually through the media [14].

In 1843, Peacock (cited in [1]) referred to the phenomenon of reentry in aortic dissections as an "imperfect natural cure." It is because of the process of reentry that chronic dissections are referred to as "healed." Although the dissection still exists, the patient often becomes asymptomatic with reentry into the true lumen [6]. In a series of 73 patients with dissections surviving more than 5 weeks, 90% had reentry points [8]. Wyman [9] found that 96% of patients without a reentry point died in less than 5 weeks, whereas only 28% with a reentry point died in that time.

Chronic dissections may be painless, well tolerated, and found incidentally [15, 16] with no history of an acute episode elicited, even retrospectively. Wood et al. [13] postulated that, in patients who have no pain, the dissection may have progressed slowly. Not infrequently in cases where an episode of chest pain did occur, a diagnosis of myocardial infarction was made [1, 2]. When chronic dissections do become symptomatic, it is usually due to cardiac failure. Hirst et al. [2], in a review of 505 cases of aortic dissection, of which 10% were chronic, listed congestive heart failures as the most common presentation of chronic dissection and stated that these patients with chronic dissections have a 40% incidence of the murmur of aortic insufficiency. The occurrence of these findings in chronic dissections is puzzling, since most of these cases are type III and do not involve the ascending aorta. The etiology of the aortic murmur in types I and II also remains controversial [17]. It is important to stress that chronic dissections can

rupture, and cases of death from rupture as long as 19 years after the dissections first occurred have been reported [7, 8, 18, 19].

Absent or unequal pulses are common in acute dissections, but uncommon in chronic ones for two reasons. First, the chronic dissections are usually type III, and since they begin after the take-off of the brachiocephalic vessels there is no decrease in blood flow to the head or arms. Second, chronic dissections have reentry points distally and this allows sufficient blood to the lower extremities to equalize pulses [10]. Common points shared by acute and chronic dissections are that the major predisposing factor for both is primary systemic hypertension and that the dissection usually occurs in the fifth to seventh decade [1, 15, 20].

Chronic dissections may sometimes have distinctive radiographic characteristics. One sign of an acute dissection is displacement of intimal calcification more than 5–6 mm from the outer wall of the aorta [5, 21]. This is especially significant if a prior chest film shows the calcification more peripherally. However, in chronic dissections there may be calcification quite peripherally. Case 3 had a thin linear calcification only 4 mm from the most lateral portion of the aortic wall. It is presumed that with chronicity there is endothelialization of the false lumen with occasional calcification of the wall of this channel [22]. As with acute dissections, differentiation between the true and false lumen may be difficult; however, as with acute dissections, the channel that has slow flow of contrast, a posterolateral position in the descending and abdominal aorta and lack of filling of intercostal and lumbar arteries is usually the false lumen [14].

Another radiographic distinction between acute and chronic dissections is related to the relation of aneurysmal disease to the dissection. Although dissections are frequently referred to as dissecting aneurysms, in fact an aneurysm is usually not present. The true aortic channel is actually narrowed by the blood dissecting through the media [5, 14]. For this reason, although there may be widening of the mediastinum, the typical appearance of an atherosclerotic thoracic aneurysm is often not present in acute dissections. However, chronic aortic dissections often appear on the chest film as fusiform, atherosclerotic aneurysms associated with a tortuous aorta. This was true in cases 2–4. In a series of 12 chronic dissections, one-third were in typical atherosclerotic aneurysms [7, 22].

The incidental discovery of aortic dissections at autopsy and surgery supports the concept that prolonged survival in the disease is more common than previously appreciated [15, 23]. In a classic paper on aortic dissections, Shennan [1] found that 79 of 300 cases were chronic; more recently, Slater and De Sanctis [23] reported four cases discovered during surgery for aortic valve disease. The increased use of angiography has also led to the incidental discovery of aortic dissections [15]. It is therefore important for radiologists to remember that not all dissections present as acute episodes, and that chronic aortic dissections do occur, may be asymptomatic, and may be found by chance during angiography done for other problems.

REFERENCES

1. Shennan T: *Dissecting Aneurysms*. Medical Research Council. Special Report Series, no. 193, London, His Majesty's Stationary Office, 1934
2. Hirst AE Jr, Johns VJ Jr, Kime SW Jr: Dissecting aneurysms of the aorta: a review of 505 cases. *Medicine* 37:217–279, 1958
3. Lindsay J Jr, Hurst JW: Clinical features and prognosis in dissecting aneurysm of the aorta. *Circulation* 35:880–888, 1967
4. Erb BD, Tullis F: Dissecting aneurysms of the aorta. The clinical features of 30 autopsied cases. *Circulation* 22:315–325, 1960
5. Eyler WR, Clark MD: Dissecting aneurysms of the aorta: roentgen manifestations including a comparison with other types of aneurysms. *Radiology* 85:1047–1057, 1965
6. Spicknall CG, Binford CH: Healed dissecting aneurysm of the aorta with signs of aortic insufficiency. *Milit Surg* 102: 47–49, 1948
7. Flaxman N: Dissecting aneurysm of the aorta. *Am Heart J* 24: 654–664, 1942
8. Prior JT, Buran RT, Perl T: Chronic (healed) dissecting aneurysms. *J Thorac Surg* 33:213–228, 1957
9. Wyman SM: Dissecting aneurysm of the thoracic aorta: its roentgen recognition. *AJR* 78:247–255, 1957
10. Drury RAD: Healed dissecting aneurysm of the aorta. *Br Med J* 2:1114–1116, 1955
11. DeBakey ME, Henly WB, Cooley DA, Morris GC Jr, Crawford ES, Beall AC Jr: Surgical management of dissecting aneurysms of the aorta. *J Thorac Cardiovas Surg* 49:130–149, 1965
12. Hemley SD, Kanick V, Kittredge R, Finby N: Dissecting aneurysms of the thoracic aorta. *AJR* 91:1263–1282, 1964
13. Wood FC, Pendergrass FP, Ostrum HW: Dissecting aneurysm of the aorta. *AJR* 28:437–465, 1932
14. Hayashi K, Meaney TF, Zelch JV, Tarar R: Aortographic analysis of aortic dissection. *AJR* 122:769–782, 1974
15. Verstraete M, Collen D: Dissecting aneurysm at the descending aorta: a frequently unrecognized condition with overrated fatality. *Angiologia* 7:28–38, 1970
16. Steinberg I, Stein HL: Painless chronic dissecting aneurysm of the aorta. Report of a case. *AJR* 97:416–421, 1966
17. Levinson DC, Edmeades DT, Griffeth GC: Dissecting aneurysm of the aorta: its clinical, electrocardiographic and laboratory features. *Circulation* 1:360–387, 1950
18. Rineberg BA, Forlire JW, Orgain ES: Long-term survival after dissecting aneurysm of the aorta. *JAMA* 173:785–788, 1960
19. Rota AN, Fransman SL: Dissecting aneurysm of the aorta. *Can Med Assoc J* 82:529–533, 1960
20. Brast AN: Dissecting aorta aneurysm. *Cardiovasc Clin* 3: 151–157, 1971
21. Baron MG: Dissecting aneurysm of the aorta. *Circulation* 43:933–943, 1971
22. Nusbacher N, Bockel R, Bryk D: Chronic calcified aortic dissection. *Chest* 69:235–237, 1976
23. Slater EE, De Sanctis RW: The clinical recognition of dissecting aortic aneurysm. *Am J Med* 60:625–633, 1976

Observer Variation in the Interpretation of Lower Limb Venograms

M. S. F. McLACHLAN,[1] J. G. THOMSON,[2] D. W. TAYLOR,[3] MARY E. KELLY,[3] AND D. L. SACKETT[3]

After agreeing on diagnostic criteria and after a pilot study, two experienced radiologists twice independently reviewed 40 lower limb venograms performed by a standard technique in patients suspected or known to have venous thrombosis. The observers reviewed 20 examinations at a time, their analysis requiring separate identification of 11 major veins. At each site observers stated whether thrombus was "absent," "doubtful," "presumed," or "definite," or declared "no opinion possible." They then rediscussed criteria of diagnosis and, using the same experimental design, examined another 40 venograms. To correct for agreement expected by chance, data were analyzed by using the kappa statistic. In general, levels of agreement were higher than those reported for many other clinical and radiologic investigations, probably because of refinement of criteria after the pilot study. Nonetheless, observers disagreed about the probable presence or absence of thrombus at some site in the limb in about 10% of examinations. Observer variation should be considered when venography is used as a reference standard to evaluate other methods of diagnosing thrombi.

The value of lower limb venography in the diagnosis of thrombi is well recognized [1, 2]. It forms the standard with which other methods of investigating suspected venous thrombosis are compared [3, 4]. However, interpretation of venograms, as in other clinical investigations [5], is subject to observer variation. This study examines the magnitude of variation between the interpretation of venograms by experienced observers, applying uniform criteria, and assesses the effect of further discussion of diagnostic criteria during the course of the study.

The simple calculation of percentage agreement can overestimate the extent of agreement, since some agreement will occur by chance. To correct for agreement expected by chance and also to permit statistical tests of the significance of observed differences in agreement, the data were analyzed by using the kappa statistic [5–9].

Materials and Methods

The venograms used in this study were those of patients aged 20–67 years (mean, 43) suspected or known to have lower limb venous thrombosis, by a modification of the technique of Rabinov and Paulin [1] and Thomas [2]. Water-soluble contrast agent was injected into a vein on the dorsum of the foot with the patient semiupright on a tilting fluoroscopic table. A tourniquet was applied to the ankle of the limb being examined which was not weight-bearing. Each examination was assigned a unique random number and all patient identifying data were masked.

Radiographs were presented in random order to two radiologists experienced in vascular radiology with particular interest and expertise in the interpretation of lower limb venograms. Each limb was assessed independently for the presence or absence of deep vein thrombosis without reference to appearances in the contralateral limb. Observers recorded their opinions with separate entries for the common and external iliac veins, the common and superficial femoral veins, the popliteal vein (defined as extending from the junction of peroneal and posterior tibial veins to 10 cm above the knee joint), and each trunk of the anterior and posterior tibial veins and of the peroneal vein. Since deep femoral and soleal veins frequently were not opacified, thrombosis in these veins was recorded only if it was confined to them. For each of these veins, observers stated whether deep vein thrombi were "definite," "presumed," "doubtful," or "absent," and expressed "no opinion possible" when the film was technically inadequate. These categories were defined as follows:

Definite: One or more well defined filling defects in an otherwise well opacified vein, seen on more than one radiograph.

Presumed: Nonopacification of a vein, despite an adequately performed venogram, with definite thrombus at other sites. Anterior tibial veins, which a technically satisfactory venogram performed by this technique may fail to opacify [1], were excepted.

Doubtful: Less well defined filling defects, believed to be due to turbulence, but which could not with certainty be distinguished from thrombi.

Absent: Absence of any of the above findings.

No opinion possible: Inadequate study, usually because of incomplete filling with contrast medium or because veins were obscured.

These diagnostic criteria, methods of assessment, and the following study protocol were developed in a pilot study in which 53 venograms were independently assessed and then discussed by the two observers. The pilot study was undertaken to minimize differences of approach between the two observers, who worked in different institutions. The most important differences of opinion that it uncovered concerned the adequacy of the exmainations and the degree of certainty with which abnormality could be excluded in the presence of small filling defects resulting from turbulence or admixture of unopacified blood. Recognition of the extent of these differences led to changes in the definition of categories; these changes were aimed at encouraging greater uniformity.

None of the 53 venograms was used for the subsequent definitive study, which documented both intraobserver and interobserver variation as follows. The venograms of 40 limbs (20 right, 20 left) were randomly grouped in batches of 10 and systematic combinations of two batches were distributed to the observers in a fashion which presented each limb for assess-

Received July 11, 1978; accepted after revision November 9, 1978.

[1] Department of Radiology, McMaster University Medical Centre, Hamilton, L8S 4J9, Ontario, Canada. Present address: Department of Radiology, Strong Memorial Hospital, Rochester, New York 14642. Address reprint requests to M. S. F. McLachlan.

[2] Department of Radiology, Henderson General Hospital, Hamilton, L8V 1C3, Ontario, Canada.

[3] Department of Clinical Epidemiology and Biostatistics, McMaster University Medical Centre, Hamilton, L8S 4J9, Ontario, Canada.

0361-803X/79/1322-0227 $0.00

AJR 132:227–229, February 1979

© 1979 American Roentgen Ray Society

ment twice, without the observers knowing that this had occurred (series 1). First and second assessments were made at least 4 weeks apart to minimize the possibility that observers would remember their earlier assessments. All opinions were independently recorded, coded and analyzed, and the results presented to the observers. The diagnostic criteria were discussed a second time and a second set of 40 venograms was examined according to the same protocol (series 2).

Observer variation was analyzed in two ways for (1) calf veins, (2) proximal veins (including popliteal veins), and (3) the whole limb. First, to evaluate agreement over the full range of five possible interpretations, each venogram was coded according to the most serious opinion expressed at each of these three major anatomic sites. Opinions, in descending order of seriousness, were: definite, presumed, doubtful, and absent deep vein thrombosis, and no opinion possible. For example, if both observers considered that definite thrombosis was present in the calf, this was regarded as agreement even when they differed about which vein was affected. Second, to reflect the treatment decisions made on the basis of venography, the range of possible interpretations was condensed into two categories, thrombosis present (combining the "definite" and "presumed" interpretations) and absent (combining the "doubtful" and "absent" interpretations), for the calf, the proximal limb, and the limb as a whole.

Agreement between observers (interobserver agreement) and between two observations by the same observer (intraobserver agreement) was calculated. The proportion of opinions that coincided was calculated and expressed as a percentage. Since this can overestimate the extent of agreement by failing to take account of agreement due to chance, data were also analyzed by using the kappa statistic. This analysis effectively excludes agreement attributable to chance alone. Kappa (k) is calculated from the equation, $k = p_o - p_c / 1 - p_c$, where p_o is the proportion of agreement actually observed and p_c is the proportion of agreement expected by chance, calculated according to simple probability theory [7, 8]. Kappa may be considered to resemble a correlation coefficient; by placing a numeric value on agreement, it allows tests of statistical significance [5] of observed differences to be performed. A kappa value of +1 indicates perfect agreement; a value of 0 indicates that agreement is entirely due to chance.

Results

Kappa values for intraobserver and interobserver variation are summarized in table 1. For comparison, percentage agreement is indicated.

In the first series of venograms, intraobserver agreement was generally higher for observer B than for observer A, and in two instances (over all five categories for proximal veins and over two categories for calf veins) the differences were statistically significant ($Z > 1.96$; $P < 0.05$). In the second series, intraobserver agreement tended to rise for observer A and to fall slightly for observer B; no statistically significant differences between observers were found in this series.

With rare exceptions, interobserver agreement was, as expected, lower than intraobserver agreement. Furthermore, there was a trend toward greater interobserver agreement after a review of diagnostic criteria between the two series of films.

With a single exception, intraobserver agreement was higher when only two categories of interpretation (deep vein thrombosis present or absent), rather than five, were considered.

Agreement according to calf veins vs. proximal veins was not consistently greater at one site than at the other. Although intraobserver agreement about proximal veins was consistently greater in series 1, the opposite was noted in series 2.

When chance-expected agreement was *not* excluded, percentage interobserver agreement on the presence or absence of deep vein thrombosis was 78%–90% (mean,

TABLE 1

Kappa Values for Intraobserver and Interobserver Variation

Anatomic Site	Intraobserver Agreement		Interobserver Agreement	
	Observer A	Observer B	1st Reading	2d Reading
Series 1:				
All five categories:				
Calf	0.47 (75)	0.74 (85)	0.47 (70)	0.46 (73)
Proximal	0.58* (78)	0.87* (93)	0.58 (78)	0.52 (73)
Whole Limb	0.61 (83)	0.83 (90)	0.59 (78)	0.54 (78)
Two categories:†				
Calf	0.56* (83)	0.90* (95)	0.68 (85)	0.47 (78)
Proximal	0.68 (88)	0.93 (98)	0.57 (85)	0.47 (80)
Whole Limb	0.66 (88)	0.95 (98)	0.78 (90)	0.51 (80)
Series 2:				
All five categories:				
Calf	0.74 (88)	0.81 (90)	0.64 (83)	0.62 (80)
Proximal	0.57 (88)	0.51 (83)	0.63 (90)	0.46 (80)
Whole Limb	0.75 (88)	0.63 (78)	0.59 (80)	0.47 (68)
Two categories:†				
Calf	0.75 (90)	0.85 (95)	0.60 (85)	0.73 (90)
Proximal	0.55 (90)	0.84 (97)	0.77 (95)	0.84 (97)
Whole Limb	0.82 (93)	0.93 (97)	0.68 (88)	0.81 (93)

Note.—Numbers in parentheses indicate percentage agreement.
* Difference between observers statistically significant ($Z > 1.96$; $P < 0.05$).
† Deep vein thrombosis "present" or "absent."

85%) for calf veins, 80%–97% (mean, 88%) for proximal veins, and 80%–93% (mean, 88%) for the whole limb.

Discussion

Lower limb venography constitutes the standard on which the accuracy of other methods of diagnosing lower limb venous thrombosis has been judged [3, 4]. Nonetheless the reliability of interpretation of venograms cannot be accepted without question; considerable observer variation has been documented for many clinical and radiologic judgments [5]. However, comparison with other studies is often made difficult by differences in methods of analyzing and presenting data.

The arguments for using the kappa statistic are discussed at length elsewhere [5–9] and will be only briefly reviewed here. The kappa method allows statistical tests of the significance of observer differences to be performed. By examining the proportion of agreement above and beyond chance, it provides a more accurate assessment of agreement. Several times in the present study, when levels of agreement were compared, kappa values differed though values for percentage agreement were similar. This was particularly true for the proximal veins, the frequency with which they were considered to be free from thrombus giving rise to a large proportion of agreement attributable to chance. For example, a decline in intraobserver agreement for proximal veins for observer B between the first and second series was apparent only when kappa values (0.87 and 0.51) were compared; values for percentage agreement (93% and 83%) resembled one another much more closely. The differences in intraobserver agreement which existed between the two observers provide many other examples; on two occasions the differences could be demonstrated to be statistically significant.

Variation due to differences in anatomic interpretation, which were most likely to occur in the calf due to overlapping veins, was diminished by consolidating data from proximal and distal sites in the limb for the purposes of analysis. Ranking of judgments effectively set aside agreement which might have resulted when "no opinion possible" was expressed in incompletely demonstrated areas. In series 1, observers consistently (on at least three of the four occasions) declared no opinion possible when examining one-third of anterior tibial veins and one fifth of external iliac veins, which, for technical reasons [1, 2], may opacify incompletely. In series 2, this judgment was made in no more than 5% of cases, observers being more likely to classify partially filled veins under one of the other categories. Since the venograms were performed by a number of radiologists, albeit by a standard technique, variation in quality was considered inevitable. The observers felt that a modification in technique would have been appropriate in some patients.

Despite the greater complexity of calf veins, differences in observer variation between them and proximal veins were inconsistent and not statistically significant. When the two observers were compared, significant differences in intraobserver agreement were apparent in series 1. Observer B was more consistent than observer A, whose approach changed in a systematic way between readings, his judgment tending to alter in the direction of greater certainty. This tendency was much less obvious in series 2, after further discussion of the diagnostic criteria. As a result, agreement between observers on the probable presence or absence of thrombus tended to improve.

As in other investigations [10, 11], observer variation was reduced by practice and discussion of criteria. The refinement of diagnostic definitions after the pilot study may explain why the levels of agreement between observers reported here, even for series 1, are higher than those reported for many other forms of investigation [5]. Nonetheless, the interobserver agreement rates documented in this study, even when chance agreement is *not* excluded, suggest that independent observers, though experienced and applying uniform definitions, will disagree about the presence of thrombus at some point in the examined limb in about one-tenth of cases. Observer variation must be borne in mind when venography is used as the standard for validating other methods of diagnosing lower limb venous thrombosis.

ACKNOWLEDGMENT

Most patients studied were under the care of Dr. J. Hirsh.

REFERENCES

1. Rabinov, K, Paulin S: Roentgen diagnosis of venous thrombosis in the leg. *Arch Surg* 104:134–144, 1972
2. Thomas ML: Phelbography. *Arch Surg* 104:145–151, 1972
3. Harris WH, Salzman EW, Athanasoulis C, Waltman A, Baum S, DeSanctis RW, Potsaid MS, Sise H: Comparison of ^{125}I fibrinogen count scanning with phlebography for detection of venous thrombi after elective hip surgery. *N Engl J Med* 292:665–667, 1975
4. Hull R, VanAken WG, Hirsh J, Gallus AS, Hoicka G, Turpie AGG, Walker I, Gent M: Impedance plethysmography using the occlusive cuff technique in the diagnosis of venous thrombosis. *Circulation* 53:696–700, 1976
5. Koran LM: The reliability of clinical methods, data and judgments. *N Engl J Med* 293:642–646, 695–701, 1975
6. Fleiss JL: *Statistical Methods for Rates and Proportions*. New York, Wiley, 1973
7. Cohen J: Weighted kappa: nominal scale agreement with provision for scaled disagreement or partial credit. *Psychol Bull* 70:213–220, 1968
8. Spitzer RL, Cohen J, Fleiss JL, Endicott J: Quantification of agreement in psychiatric diagnosis: a new approach. *Arch Gen Psychiatry* 17:83–87, 1967
9. McLachlan MSF, Banna M: Observer variation in interpreting radiographs of the pituitary fossa. *Invest Radiol*. In press, 1979
10. Baron JH, Connell AM, Lennard-Jones JE: Variation between observers in describing mucosal appearances in proctocolitis. *Br Med J* 1:89–92, 1964
11. Godfrey S, Edwards RHT, Campbell EJM, Armitage P, Oppenheimer EA: Repeatability of physical signs in airways obstruction. *Thorax* 24:4–9, 1969

Computed Tomography in the Diagnosis of Adrenal Disease

MELVYN KOROBKIN,[1,2] ERIC A. WHITE,[1] HERBERT Y. KRESSEL,[1,3] ALBERT A. MOSS,[1] AND JEAN-PHILLIPE MONTAGNE[1,4]

A series of 63 patients with suspected adrenal disease was evaluated by computed tomography (CT). In 15 additional patients CT diagnosed unsuspected adrenal disease. The CT results were correlated with surgical, postmortem, or compelling clinical data. In those patients with adequate visualization of both adrenals, CT correctly identified all adrenal masses subsequently proven at surgery or postmortem examination. CT accurately predicted the presence or absence of a unilateral adrenal neoplasm in patients with Cushing's syndrome and primary aldosteronism. Unsuspected primary or metastatic neoplasms of the adrenals were occasionally detected in patients scanned for other reasons. CT is a safe and accurate method of evaluating patients with suspected adrenal disease.

Initial reports describing application of computed tomography (CT) in extracranial portions of the body did not emphasize its major role in evaluating adrenal disease. Subsequent reports [1, 2] described the CT findings in a small number of patients with adrenal masses, but a comprehensive report of the CT findings in patients with known or suspected adrenal disease is not yet available.

We [3] and others [4] recently described the CT appearance of the normal adrenal glands (fig. 1). Reported here are CT findings in 78 consecutive patients being evaluated for known or suspected adrenal disease, or in whom unsuspected adrenal abnormalities were discovered while being scanned for other reasons.

Materials and Methods

From June 1976 to June 1978, 63 patients were referred for CT scanning of the adrenal glands because clinical evidence suggested adrenal disease. The suspected clinical disorder, the results of CT evaluation, and the final clinical diagnosis for each patient are reported. An additional 15 patients are included in whom an abnormality was discovered in one or both adrenal glands, although the CT examination had been requested for suspected disease in other organs. We made no attempt to determine how many patients with suspected or subsequently proven adrenal disease during the same period were not referred for CT evaluation. Moreover, we did not systematically evaluate how many patients undergoing upper abdominal CT evaluation for other reasons had adrenal disease that was not detected by CT.

All CT scans were performed on either a prototype model of the EMI 5000 or a production model of the EMI 5005 (both with an 18 sec scan time, 13 mm slice thickness, and 160 × 160 matrix) or a prototype or production model of the GE CT/T body scanner (4.8 sec scan time, 10 mm slice thickness, and 320 × 320 matrix). In patients scanned for suspected adrenal disease, contiguous slices were obtained at 1 cm intervals through the expected region of both adrenals [3]. Patients studied for suspected disease in other organs had scans obtained at 1 or 2 cm intervals.

An adrenal gland was interpreted as normal if it met the previously described size and shape criteria [3]. An occasional gland was interpreted as abnormally enlarged if it appeared disproportionately thickened relative to the surrounding organs and tissues, even if it did not clearly exceed the upper size limit sometimes seen in normal patients. The size of an adrenal mass was determined by measuring its major and minor axes on the slice in which it appeared largest, and estimating its cephalocaudal dimension by observing the number of contiguous slices on which it was visible. However, in tabulating the results for this report, we have listed only the maximum diameter for each adrenal mass. Size of the normal and abnormal gland was determined by correcting measurements made on the hard copy recording medium routinely used to true size by multiplying by the minification factor determined for each scanner and its recording device.

Most patients ingested 480–720 ml of a 2%–3% solution of sodium diatrizoate to allow identification of bowel loops. Most patients were scanned without intravenous contrast material. Occasionally, the scan was repeated after contrast injection, especially if a paucity of retroperitoneal fat made it difficult to identify the inferior vena cava or if the adrenal glands were difficult to distinguish from the adjacent vessels or upper pole of the kidneys.

Results

Most patients referred for CT evaluation of the adrenal glands had strong clinical suspicion of Cushing's syndrome, pheochromocytoma, or primary aldosteronism (table 1). A small number were scanned for several other adrenal diseases (grouped here under miscellaneous adrenal disorders).

Because some patients were scanned only with and others only without intravenous injection of contrast material, we did not attempt to define the spectrum of attenuation values for each type of adrenal lesion. Without intravenous contrast material, adrenal masses varied from values similar to adjacent liver to values similar to

Received July 14, 1978.; accepted after revision November 9, 1978.
M. Korobkin was recipient of National Institutes of Health Research Career Development Award GM 00055 from the National Institute of General Medical Sciences. Work by E. A. White was supported in part by National Institutes of Health Training Grant GM 01272 from the National Institute of General Medical Sciences.

[1] Department of Radiology, M-380, University of California School of Medicine, San Francisco, California 94143. Address reprint requests to A. A. Moss.
[2] Present address: Department of Radiology, Duke University Medical Center, Durham, North Carolina 27710.
[3] Present address: Department of Radiology, University Hospital, University of Pennsylvania, Philadelphia, Pennsylvania 19174.
[4] Present address: Radiologie, Hôpital Rousseau, 75012, Paris, France.

AJR 132:231–238, February 1979
© 1979 American Roentgen Ray Society
0361-803X/79/1322-0231 $0.00

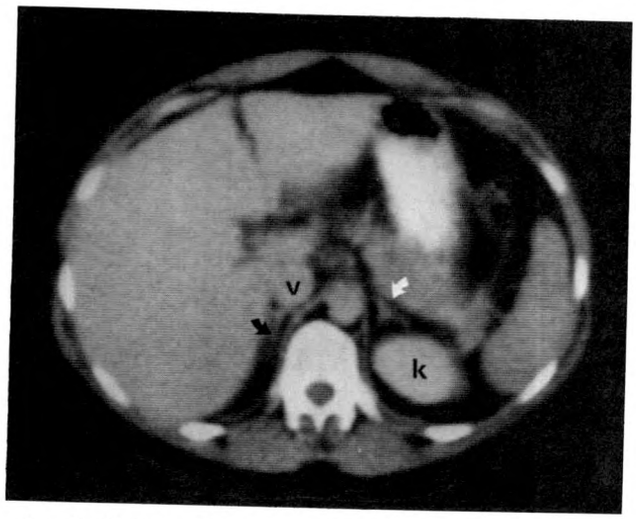


Fig. 1.—Normal adrenal glands in patient with ACTH-dependent Cushing's syndrome. Curvilinear right adrenal (*black arrow*) posterior to inferior vena cava (v) between right lobe of liver and right crus of diaphragm. Left adrenal (*white arrow*) has inverted "Y" appearance anteromedial to upper pole of left kidney (k).

TABLE 1

Indications for CT

Indication	No. Patients
Suspected adrenal disease:	
Cushing's syndrome	19
Pheochromocytoma	10
Primary aldosteronism	24
Miscellaneous adrenal disorders	10
Other indications	15
Total	78

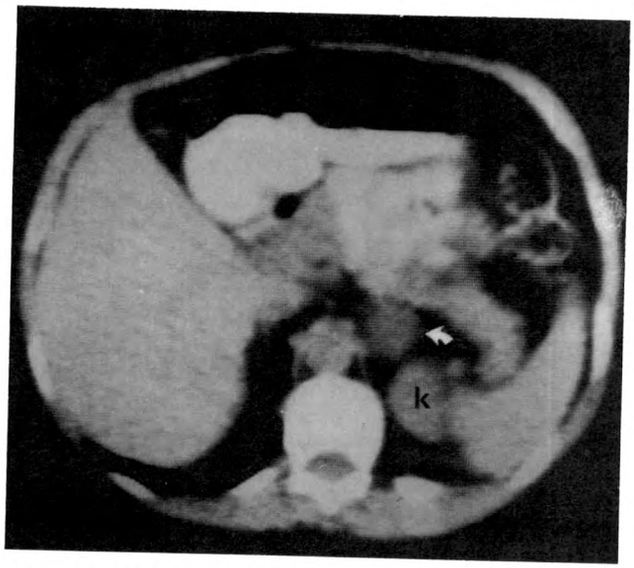


Fig. 2.—Cushing's syndrome with adenoma of left adrenal gland; 3 cm left adrenal mass (*arrow*) anteromedial to left kidney (k).

TABLE 2

Final Diagnoses

Final Diagnoses and No. Grouped by Referring Diagnosis	CT Findings		
	Unilateral Mass	Normal Glands	Other
Cushing's syndrome (19):			
Adrenal adenoma (2)	2	...	...
Adrenal carcinoma (1)	1	...	...
Bilateral hyperplasia* (3)	...	...	3*
Pituitary adenoma* (10)	...	6	4†
After bilateral adrenalectomy (2)	1‡	...	1§
Indeterminate (1)	...	1	...
Suspected pheochromocytoma (10):			
Adrenal pheochromocytoma (4)	4	...	...
Bilateral adrenal pheochromocytoma (1)	1‖	...	...
Extra-adrenal pheochromocytoma (1)	...	1#	...
No pheochromocytoma (4)	...	4	...
Suspected primary hyperaldosteronism (24):			
Proven adrenal adenoma (5)	4	...	1**
Suspected adrenal adenoma (6)	4	...	2‖,**
Adrenal hyperplasia (7)	...	7	...
Essential hypertension (2)	...	2	...
Indeterminate (4)	1	1	2
Unsuspected adrenal disease (15):			
Unilateral metastasis (4)	4	...	...
Bilateral metastasis (7)	2‖	...	5††
Adrenal adenoma (1)	1	...	...
Adrenal pheochromocytoma (1)	1	...	...
Pancreatic tail neoplasm (1)	1	...	...
Indeterminate (1)	1‡‡	...	...

* Bilateral diffuse enlargement.
† Bilateral diffuse enlargement (3); diffuse bilateral enlargement with single nodule in each gland (1).
‡ In expected position of adrenal.
§ Neither gland identified.
‖ Only one gland identified.
Tumor site correctly identified in bladder dome.
** Neither gland visualized.
†† Bilateral masses.
‡‡ Suspected myelolipoma.

or less than water. Pheochromocytomas and adrenal metastases, especially after intravenous contrast material, often had a mottled appearance apparently representing zones of hemorrhage or necrosis.

Cushing's Syndrome

A unilateral adrenal mass (fig. 2) was identified by CT in three patients from this group (table 2). At surgery two had an adrenal adenoma and the other an adrenal carcinoma. Two of the patients had a normal-appearing contralateral adrenal gland; in the other, the contralateral gland could not be identified.

Six patients had diffuse enlargement of both adrenal glands, but the normal shape and configuration of the adrenals were preserved (fig. 3). In an additional patient with bilaterally enlarged adrenals, a single nodule smaller than 1 cm was superimposed on each gland.



Fig. 3.—Cushing's syndrome with bilateral adrenal hyperplasia. Left adrenal gland (*arrow*) thicker than normal; more cephalad scans revealed thickened right adrenal gland. Bilateral adrenalectomy showed both glands twice normal size.

Four of the six patients had surgical, autopsy, or compelling clinical evidence of bilateral adrenal hyperplasia secondary to a pituitary adenoma; one had a final clinical diagnosis of adrenogenital syndrome with bilateral adrenal hyperplasia. Length, width, and thickness of each resected adrenal gland in the patient undergoing bilateral adrenalectomy were virtually identical to those predicted from the CT scan.

In seven of the patients both adrenal glands appeared normal on CT examination. In six of these a final clinical diagnosis of bilateral adrenal hyperplasia secondary to tumor or other abnormality of the pituitary gland was made; one had surgical resection of a pituitary adenoma, three underwent pituitary irradiation, and the other two had compelling clinical evidence of a pituitary lesion but have not yet received therapy. The four patients who underwent pituirary ablation had clinical evidence of regression of their Cushing's syndrome after therapy. Final clinical diagnosis for the seventh patient was virilizing syndrome secondary to bilateral adrenal hyperplasia.

Two patients had recurrent Cushing's syndrome after bilateral adrenalectomy. In one, neither adrenal was visualized by CT. In the other, CT showed absence of the left adrenal gland, but a 1 cm mass was found in the expected position of the right adrenal; this patient refused further surgery.

Pheochromocytoma

In five patients, CT identified a unilateral adrenal mass (fig. 4) with normal contralateral gland; in each case, an adrenal pheochromocytoma was surgically removed, with complete resolution of the patient's hypertension. In the patient with bilateral adrenal pheochromocytomas, a right adrenal mass was seen on CT, but the left gland was not clearly identified. One patient with normal adrenal glands had an oval mass abutting the bladder wall on CT scans of the pelvis; a pheochromocytoma was surgically removed, with subsequent resolution of the hypertension. In four patients, CT showed both adrenals to be normal; angiography and/or repeat biochemical studies failed to substantiate a diagnosis of pheochromocytoma in any of these patients.

Primary Aldosteronism

In nine patients, CT interpretation was a mass in one adrenal (fig. 5). An adrenal adenoma was surgically resected in four of these patients; surgical exploration is planned in three others. Advanced age and associated medical diseases preclude surgery in the other two patients.

Both adrenal glands were interpreted as normal in 10 of the patients with suspected aldosteronism. Seven of these had compelling biochemical and clinical evidence of bilateral adrenal hyperplasia and are being treated with spironolactone. Surgery is not planned for this

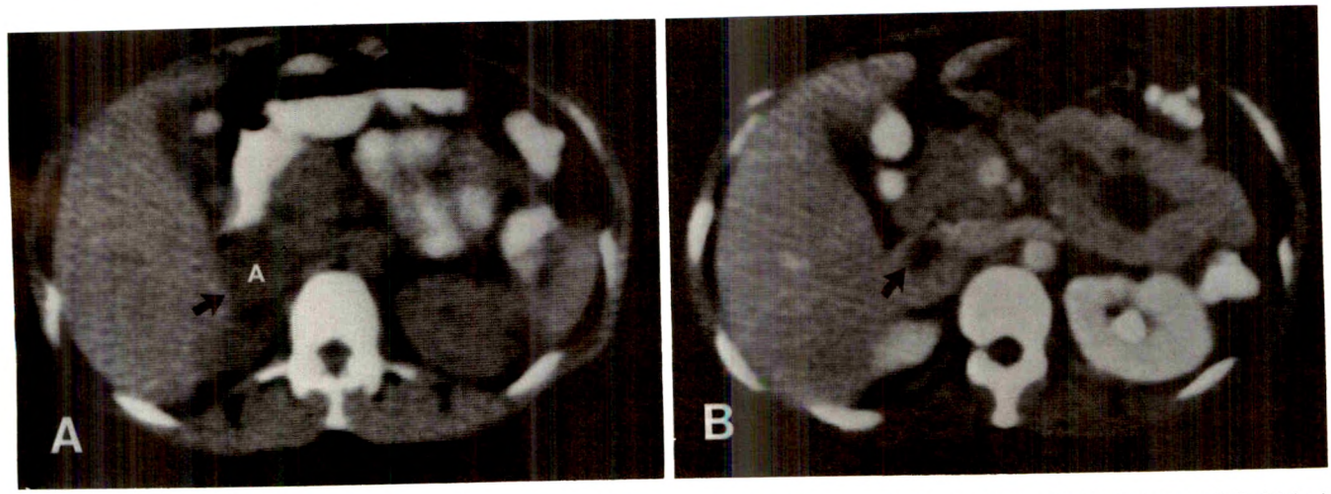


Fig. 4.—Right adrenal pheochromocytoma. **A,** Mass involving right adrenal gland (*arrow*) has uniform density. **B,** Central zone of diminished perfusion (*arrow*) evident after intravenous contrast material. Cystic and hemorrhagic zones within tumor found at pathologic examination of surgical specimen.

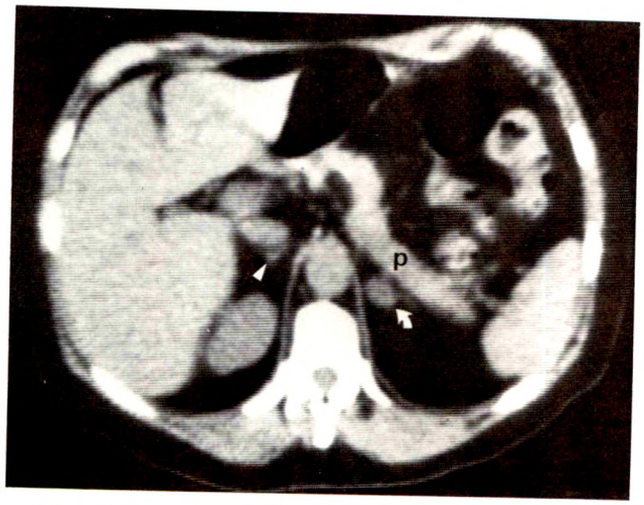


Fig. 5.—Primary aldosteronism with adrenal adenoma (surgery pending); 1.5 cm left adrenal mass (*arrow*) between pancreatic tail (p) and left diaphragmatic crus. Normal right adrenal (*arrowhead*) posterior to inferior vena cava.

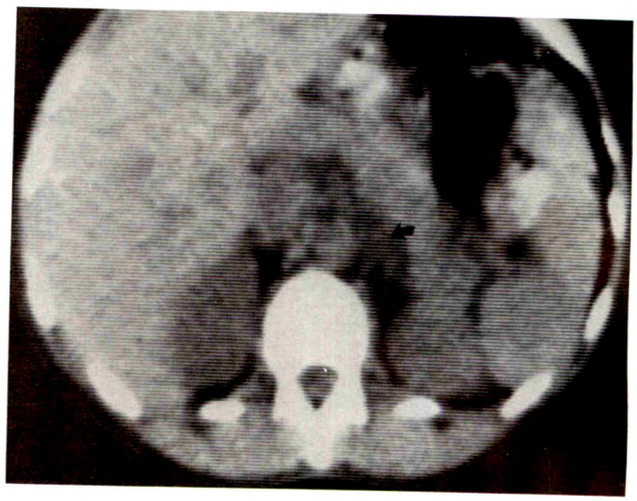


Fig. 6.—Primary aldosteronism with left adrenal adenoma. Paucity of retroperitoneal fat prevented clear delineation of either adrenal gland; possible site of 2 cm adenoma found at surgery (*arrow*).

group. Two had repeat biochemical studies that excluded the initial impression of primary aldosteronism. Final clinical diagnosis is uncertain in the tenth patient.

In three patients, either one or both adrenals were not identified because of a marked paucity of retroperitoneal fat. In one of these patients, a 2 cm adenoma was found at surgery (fig. 6); surgery is pending in one and is not planned in the other. In two patients, previous unilateral adrenalectomy for a presumed adenoma did not cure the hypertension or reduce the elevated urinary aldosterone levels to normal. Results of biochemical studies after surgery were more consistent with bilateral hyperplasia rather than adenoma. A normal adrenal, contralateral to the resected gland, was identified on CT in both cases.

Miscellaneous Adrenal Disorders

Three patients had biochemical evidence of hypoadrenalism or had suspected adrenal atrophy (table 3). Both adrenal glands appeared normal by CT in two of these patients, one on long-term steroid therapy after renal transplantation and the other with clinical evidence of hypoadrenalism after pituitary irradiation. CT in a patient with intravascular coagulation and acute hypoadrenalism showed bilateral adrenal masses (fig. 7), thought to represent adrenal hemorrhage.

Three patients had CT evaluation of a suspected adrenal mass diagnosed by excretory urography. An adrenal mass, subsequently proven to be a pheochromocytoma, was seen in one of these patients, but a normal adrenal adjacent to an upper pole renal cyst was diagnosed by CT in the other two. A normal adrenal gland was seen in one patient with a previous venographic diagnosis of an enlarged gland.

In one patient, CT confirmed a previously diagnosed adrenal carcinoma. In another, angiographic evidence suggested recurrence of a previously resected carcinoma of the right adrenal gland. CT showed a mass in the posterior segment of the right lobe of the liver, but no evidence of a tumor recurrence in the bed of the right adrenal. Postmortem examination confirmed both findings. In the final patient, a 2 cm left adrenal mass was seen on CT after biopsy diagnosis of neuroblastoma metastatic to the orbit.

Unsuspected Adrenal Disease

Either one or both adrenal glands were interpreted as abnormal by CT in 15 patients not specifically examined for adrenal abnormalities. Most of these patients had metastatic carcinoma, and CT was used to search for possible primary neoplasm in the pancreas. In two patients, CT was requested to search for abdominal metastases; in one to evaluate a retrogastric mass found on upper gastrointestinal series; in one to evaluate lateral displacement of the left kidney at urography; and in two to evaluate unexplained abdominal pain.

In five patients, CT showed both adrenal glands were enlarged by a spherical or irregular mass (fig. 8). One had bilateral adrenal metastases documented at autopsy and the other four died with widespread metastatic disease but had no postmortem examination.

In eight patients, CT showed a unilateral adrenal mass with a normal-appearing contralateral gland: a unilateral adenoma was surgically resected in one and a unilateral pheochromocytoma in another. In one patient, a unilateral adrenal metastasis was found at postmortem examination. In one there was clinical evidence of widespread metastatic disease from a lung carcinoma. One patient with metastatic disease from an unknown primary was lost to clinical follow-up. One had a bladder carcinoma with liver metastases. One had CT evidence of an adrenal myelolipoma, but was lost to follow-up. One patient had surgical evidence of a neoplasm of the pancreatic tail rather than a left adrenal mass.

In two patients, the gland contralateral to an adrenal mass was not identified by CT due to technical factors or a paucity of retroperitoneal fat: one had bilateral adrenal

TABLE 3

Results of CT Scans in 10 Patients with Miscellaneous Adrenal Disorders

Case No.	Suspected Adrenal Disease	CT Findings	Final Diagnosis
1	Hypoadrenalism	Both adrenals normal	Hypoadrenalism*
2	Adrenal atrophy	Both adrenals normal	Long-term steroid therapy; normal-sized adrenals
3	Acute hypoadrenalism	Bilaterally enlarged adrenals with low density centers	Acute adrenal hemorrhage*
4	? Right adrenal mass on excretory urography	Right adrenal mass (8 cm)	Right adrenal pheochromocytoma (8 cm)†
5	? Right adrenal mass on excretory urography	Cyst upper pole right kidney; right adrenal normal	Right renal cyst†; right adrenal normal†
6	? Right adrenal mass on excretory urography	Cyst upper pole right kidney; right adrenal normal	Cyst right kidney*; right adrenal normal*
7	? Enlarged left adrenal at venography	Both adrenals normal	Normal left adrenal*
8	Known right adrenal carcinoma	Right adrenal mass (9 cm); left adrenal normal	Right adrenal carcinoma†
9	Prior resection right adrenal carcinoma; suspected recurrence	Sequential enlargement of liver mass; posterior segment right lobe	Large hepatic metastasis; no recurrent adrenal neoplasm‡
10	Neuroblastoma, metastatic to orbit	Left adrenal mass (2 cm); right adrenal normal	Left adrenal neuroblastoma*; patient died with metastatic neuroblastoma

* Compelling clinical evidence.
† Surgery.
‡ Autopsy.

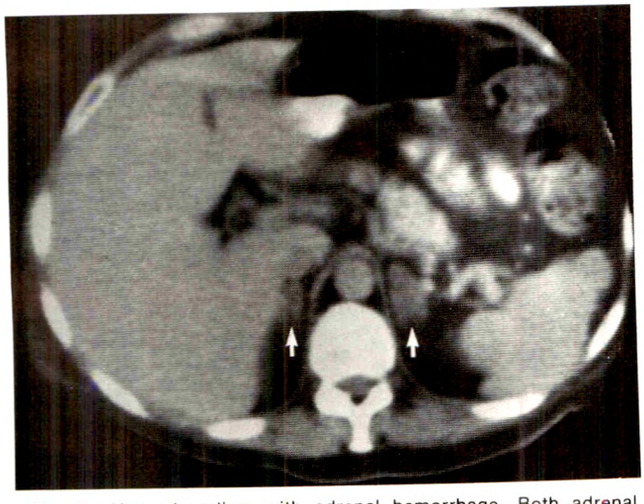


Fig. 7.—Hypoadrenalism with adrenal hemorrhage. Both adrenal glands (*arrows*) diffusely enlarged.

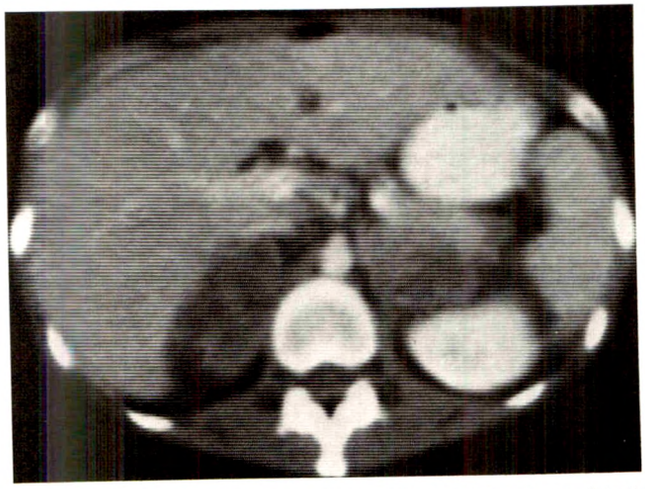


Fig. 8.—Bilateral adrenal metastases. Mottled appearance of both enlarged adrenals probably represents zones of necrosis or hemorrhage.

metastases identified at autopsy and the other had clinical evidence of metastatic osteogenic sarcoma.

Discussion

The large number of imaging techniques advocated for diagnosing suspected adrenal disorders reflects the limitations of each method. Adrenal calcification may be seen on plain abdominal radiographs in patients with carcinoma or neuroblastoma, but is unusual in pheochromocytoma, rare in adenoma, and not seen with hyperplasia [5]. Conventional urography will show downward displacement of the ipsilateral kidney only if a large adrenal mass is present. The use of large doses of intravenous contrast material, combined with linear tomography, greatly increases accuracy of urography in detecting adrenal tumors, but lesions less than 2 cm will still not be identified [6].

Angiography is useful in detecting adrenal masses [7–10], but the well known risks of arteriography, in addition to the technical difficulties and potential risk of adrenal infarction using adrenal venography [11], are significant limitations. Adrenal scintigraphy, using isotopically labeled iodocholesterol [12], can be useful in lateralizing adrenal adenomas, but a delay of 4–15 days

after injection of the isotope is usually required. Recent reports suggest that gray scale ultrasonography may be useful in detecting adrenal masses [13–15], especially those larger than 2–3 cm. The major limitation of ultrasonography is the high degree of technical expertise needed to both obtain and interpret the images.

CT offers several important advantages in evaluating suspected adrenal disorders. Most patients do not require a vascular injection of contrast media, so the risks of angiography, and even urography, can be avoided. The resolution available on scanners capable of recording data during suspended patient respiration allows identification of normal sized adrenal glands in at least 75% of patients [3]. The scans depend on anatomic, rather than functional, adrenal properties, and the large amount of retroperitoneal fat present in many patients, especially those with Cushing's syndrome, makes imaging diagnosis of bilateral adrenal hyperplasia a real possibility for the first time. Additional technical improvements, such as 5 mm collimators, should improve the already promising application of CT in imaging small organs, such as the adrenal glands.

It is essential to differentiate those patients with Cushing's syndrome due to an adrenal neoplasm from those with bilateral adrenocortical hyperplasia dependent on ACTH production. This distinction can often be made by measuring plasma ACTH levels and the effect of suppression tests with high doses of dexamethasone [16]. However, occasionally these biochemical studies yielded inconclusive or anomalous results, and in these patients a simple and accurate method of imaging the adrenal glands can be vital. Even in patients with unequivocal biochemical evidence of Cushing's syndrome due to an adrenal neoplasm, adrenal imaging is essential to localize the side of the tumor before surgery.

Our study suggests that CT can accurately differentiate ACTH-dependent Cushing's syndrome from that due to a unilateral neoplasm. The three patients with a unilateral neoplasm were easily identified, and all 13 patients with clinical and therapeutic evidence of bilateral adrenocortical hyperplasia had CT evidence of bilaterally normal adrenals or bilaterally enlarged adrenals that maintained their normal shape. One of the latter patients had a solitary nodule superimposed on each enlarged gland, probably representing the "nodular" form of bilateral adrenocortical hyperplasia [17]. Pathologic studies of the adrenal glands in patients with ACTH-dependent Cushing's syndrome show that some patients have adrenals that are grossly and histologically normal [18]. Therefore, it is not surprising that many of our patients had a CT appearance of bilaterally normal adrenal glands. Although there may be some uncertainty in any individual case about the borderland between normal and hyperplastic adrenal glands in patients with Cushing's syndrome, our study indicates that CT can accurately differentiate tumorous and nontumorous forms of this disease.

Pheochromocytoma is a tumor that secretes abnormal amounts of catecholamines, and is associated with a seldom seen, but dramatic, syndrome of variable hypertension and episodic attacks of tachycardia, diaphoresis, and anxiety [19]. Urography, and especially arteriography, have proven useful in confirming the diagnosis and detecting the site or sites of a pheochromocytoma. The tendency for patients to undergo a marked increase in blood pressure after injection of contrast material into a blood vessel feeding the tumor can be considered either a deleterious effect of the procedure or a valuable provocative test [20]. In our study, CT proved to be highly accurate in the assessment of 10 patients with known or clinically suspected pheochromocytoma. All five patients with adrenal tumors were identified, although one with bilateral adrenal tumors had insufficient visualization of the left adrenal gland to identify or exclude a neoplasm on that side. The role of angiography with respect to CT is unclear from this small group of patients because all the adrenal tumors were large (4–8 cm) and only one had an ectopic origin. It is unknown whether angiography can detect an abdominal pheochromocytoma that is not visualized by CT. However, it is clear that potential complications of an iatrogenic hypertensive crisis can be avoided with CT.

Primary aldosteronism is a rare syndrome characterized by hypertension, hypokalemia, increased aldosterone production, and absent or subnormal plasma renin activity [21, 22]. Between 65% and 75% of cases are associated with a unilateral adrenal adenoma, while most of the remaining patients have "idiopathic" aldosteronism, often called "bilateral adrenocortical hyperplasia" [21], and glands of normal size [17].

For unknown reasons, adrenal surgery, even total adrenalectomy, is unlikely to cure patients with bilateral hyperplasia [21], but unilateral adrenalectomy usually cures the hypertensive patient with a solitary adenoma. An absolute distinction between bilateral hyperplasia and unilateral adenoma cannot be made on biochemical features alone [23].

Bilateral adrenal venography and adrenal venous sampling [24–26] have been reported to successfully identify unilateral adenomas and bilateral hyperplasia. However, difficulty in routinely catheterizing the right adrenal vein and reports of adrenal infarction after adrenal venography have prevented widespread use of these techniques.

Adrenal imaging with ^{131}I-19-iodocholesterol [27], especially when used after dexamethasone suppression [28], may localize a unilateral adenoma in about 80% of patients. The necessity of repeating scintiscans from 4–19 days after injection of the isotope is a drawback not present with a newer agent, ^{131}I-6B-iodomethyl-19-norcholesterol [29]. Unfortunately, these drugs remain available only as investigational agents and have been limited to a few medical centers.

The results of our study suggest that CT is an easy and accurate method of differentiating unilateral adenoma from bilateral hyperplasia in patients with primary aldosteronism. A unilateral adrenal mass was demonstrated in all nine patients having biochemical evidence favoring a unilateral adenoma in whom both adrenal glands were

visible on the CT scan. Four have been confirmed at surgery, and an additional three patients will be operated on in the near future. All seven patients with biochemical evidence favoring diagnosis of idiopathic aldosteronism in whom both adrenals were visualized had CT appearance of bilaterally normal glands. Confirmation of the absence of a unilateral adenoma has led to a medical rather than surgical approach in these patients. The limitation of CT in patients with a sparsity of retroperitoneal fat is illustrated by the patient in our series in whom a unilateral adenoma was found surgically in a gland not delineated by CT. Isotopic adrenal scanning was performed in some of these patients with primary aldosteronism as part of prospective study, and a complete description and analysis of that study will be part of a separate report.

Three factors limit firm conclusions regarding CT scanning in primary aldosteronism: (1) surgical results in the four patients to be operated on are necessary to confirm the accuracy of a CT diagnosis of a small aldosterone producing adenoma; (2) the clinical evidence against diagnosis of a unilateral adenoma in those patients whose CT examinations showed normal adrenals bilaterally means that surgical confirmation of idiopathic aldosteronism will not be available; and (3) it is unknown whether CT will be able to identify adenomas smaller than 1 cm because none of the tumors in our series were as small as some described in previous reports.

When a mass was seen in the region of the adrenal gland during excretory urography, CT was useful in determining whether the lesion was renal or adrenal in origin. This distinction should be easy in patients with an upper pole renal cyst, where a normal adrenal gland is usually well seen, but may be difficult if a solid renal mass invades the adrenal compartment.

It was somewhat surprising to see normal-appearing adrenal glands in CT evaluations of patients with hypoadrenalism from pituitary irradiation or long-term steroid therapy. Factors that may account for this finding are the continued presence of functioning adrenal medullary tissue and the unknown relation between functional and structural cortical atrophy. The presence of bilateral adrenal masses in one patient with acute hypoadrenalism and intravascular coagulation suggests that adrenal hemorrhage may be easily identified by CT.

Our study indicates that CT may be useful in evaluating the adrenal glands for metastatic disease, which could have important implications in staging. In patients with breast or lung carcinoma, the presence of unilateral or bilateral adrenal masses is most likely due to metastatic disease. Most of the patients with proven or likely metastases to the adrenal glands in our study were being scanned to search for a primary neoplasm. Unfortunately, our study suggests that unilateral adrenal metastasis is indistinguishable from a primary adrenal neoplasm, both showing a spherical replacement of all, or part, of the involved gland.

A nonfunctioning adrenal adenoma was found in one patient scanned for abdominal pain, while a 3 cm adrenal mass was seen in another patient evaluated for a displaced contralateral kidney seen at urography. It is clear that the capacity of CT to image both adrenal glands will lead to occasional discovery of asymptomatic adrenal disease.

Because of the inconsistent use or availability of other imaging procedures in the patients described in our study, we were unable to systematically compare CT with other methods. However, our study clearly suggests an important role for CT in the evaluation of adrenal disease. The vast majority of adrenal masses proven by surgery were detected by CT, and none were missed in those glands clearly delineated. CT was able to differentiate tumorous from nontumorous forms of adrenal disease in patients with Cushing's syndrome and primary aldosteronism. Unsuspected primary and metastatic neoplasms of the adrenals were occasionally detected in patients scanned for other reasons. CT seems to be a simple and accurate method to assess the adrenal glands in patients suspected of adrenal disease.

REFERENCES

1. Behan M, Martin EE, Muecke EC, Kazam E: Myelolipoma of the adrenal: two cases with ultrasound and CT findings. *AJR* 129:993–996, 1977
2. Schaner EG, Dunnick NR, Doppman JL, Strott CA, Gill Jr JR, Javadpour N: Adrenal cortical tumors with low attenuation coefficients: a pitfall in computed tomography diagnosis. *J Comput Assist Tomogr* 2:11–15, 1978
3. Montagne JP, Kressel HY, Korobkin M, Moss AA: Computed tomography of the normal adrenal glands. *AJR* 130:963–966, 1978
4. Brownlie K, Kreel L: Computer assisted tomography of normal suprarenal glands. *J Comput Assist Tomogr* 2:1–10, 1978
5. Kahn PC: The radiologic identification of functioning adrenal tumors. *Radiol Clin North Am* 5:221–230, 1967
6. Pickering RS, Hartman GW, Weeks RE, Sheps SG, Hattery RR: Excretory urographic localization of adrenal cortical tumors and pheochromocytomas. *Radiology* 114:345–349, 1975
7. Alfidi RJ, Gill Jr WM, Klein HJ: Arteriography of adrenal neoplasms. *AJR* 106:635–641, 1969
8. Colapinto RF, Steed BL: Arteriography of adrenal tumors. *Radiology* 100:343–350, 1971
9. Reuter SR, Blair AJ, Schteingart DE, Bookstein JJ: Adrenal venography. *Radiology* 89:805–814, 1967
10. Mitty HA, Nicolis GL, Gabrilove JL: Adrenal venography: clinical-roentgenographic correlation in 80 patients. *AJR* 119:564–574, 1973
11. Bookstein JJ, Conn J, Reuter SR: Intra-adrenal hemorrhage as a complication of adrenal venography in primary aldosteronism. *Radiology* 90:778–779, 1968
12. Lieberman LM, Beierwaltes WH, Conn JW, Ansari AN, Nishiyama H: Diagnosis of adrenal disease by visualization of human adrenal glands with ^{131}I-19-iodocholesterol. *N Engl J Med* 285:1387–1393, 1971
13. Bernardino ME, Goldstein HM, Green B: Gray scale ultrasonography of adrenal neoplasms. *AJR* 130:741–744, 1978
14. Yeh HC, Mitty HA, Rose J, Wolf BS, Gabrilove JL: Ultrasonography of adrenal masses: usual features. *Radiology* 127:467–474, 1978

15. Sample WF: Adrenal ultrasonography. *Radiology* 127:461–466, 1978
16. Besser GM, Edwards CRW: Cushing's syndrome. *Clin Endocrinol Metab* 1:451–490, 1972
17. Neville AM, Mackay AM: The structure of the human adrenal cortex in health and disease. *Clin Endocrinol Metab* 1:361–395, 1972
18. Mitty HA, Gabrilove JL, Nicolis GL: Non-tumorous adrenal hyperfunction: problems in angiographic-clinical correlation. *Radiology* 122:89–94, 1977
19. Engelman K: Phaeochromocytoma. *Clin Endocrinol Metab* 6:769–797, 1977
20. Zelch JV, Meaney TF, Belhobek GH: Radiologic approach to the patient with suspected pheochromocytoma. *Radiology* 111:279–284, 1974
21. Biglieri EG: Review article: a perspective on aldosterone abnormalities. *Clin Endocrinol Metab* 5:399–410, 1976
22. Melby JC: Solving the adrenal lesion(s) of primary aldosteronism. *N Engl J Med* 294:441–442, 1976
23. Biglieri EG, Schambelan M, Brust N, Chang B, Hogan M: Plasma aldosterone concentration: further characterization of aldosterone-producing adenomas. *Circ Res* 34 (suppl 1): 183–191, 1974
24. Melby JC, Spark RF, Dale SL, Egdahl RH, Kahn PC: Diagnosis and localization of aldosterone-producing adenomas by adrenal-vein catheterization. *N Engl J Med* 277:1050–1056, 1967
25. Horton R, Finck E: Diagnosis and localization in primary aldosteronism. *Ann Intern Med* 76:885–890, 1972
26. Bookstein JJ, Walter JF: The role of abdominal radiography in hypertension secondary to renal or adrenal disease. *Med Clin North Am* 59:169–200, 1975
27. Hogan MJ, McRae J, Schambelan M, Biglieri EG: Location of aldosterone-producing ^{131}I-19-Iodocholesterol. *N Engl J Med* 294:410–414, 1976
28. Conn JW, Morita R, Cohen EL, Beierwaltes WH, McDonald WJ, Herwig KR: Primary aldosteronism: photoscanning of tumors after administration of ^{131}I-19-Iodocholesterol. *Arch Intern Med* 129:417–425, 1972
29. Sarkar SD, Beierwaltes WH, Ice RD, Basmadjian GP, Hetzel KR, Kennedy WP, Mason MM: A new and superior adrenal scanning agent, NP-59. *J Nucl Med* 16:1038–1042, 1975

Scapular Defects: A Normal Variation

OLCAY S. CIGTAY[1] AND VINCENT J MASCATELLO[1]

Sharply marginated defects were observed in the scapulae of five patients. In all cases the defects were benign in appearance and unrelated to symptoms. These patients have been observed up to 5 years without change in the radiographic appearance. Recognition of the benign nature of these defects is important to avoid confusion with pathologic conditions.

Defects in the scapulae are unusual. A literature search, including the standard texts by Kohler and Zimmer [1] and Keats [2] failed to reveal mention of similar defects. In five patients we have incidentally identified sharply marginated defects which did not alter in radiographic appearance during intervals up to 5 years.

Case Reports

Case 1

J. B., a 26-year-old male physician, after cervical spine fracture with quadriplegia, underwent a chest radiography as part of a routine trauma series. History did not include previous trauma. The chest film revealed two (30 × 30 mm and 25 × 20 mm) defects in the body of the left scapula (fig. 1). On serial chest radiography the defects remained unchanged during a 4-year period.

Case 2

R. A., a 54-year-old man, was referred for radiography of the left shoulder because of pain related to spondylosis of the cervical spine. A 40 × 9 mm lucency was demonstrated in the body of the scapula (fig. 2). The margins of the defect were well demarcated and sclerotic. A similar lesion (1–2 mm) was lateral to the first. Follow-up chest radiography over a 3-year period showed no change in the defect.

Case 3

S. J., a 44-year-old woman, underwent chest radiography as part of a routine preemployment physical. The film (fig. 3) showed a 36 × 6 mm defect situated in the body of the scapula. The patient's history was unremarkable.

Case 4

C. J., a 51-year-old black man with a history of glaucoma, had a routine chest film which revealed a 20 × 7 mm defect in the body of the left scapula (fig. 4). There was no history of trauma or symptoms referrable to the shoulder.

Case 5

R. H., a 69-year-old black man with carcinoma of lung, had shoulder radiography as part of a metastatic survey. The film demonstrated two defects measuring 30 × 20 mm and 35 × 10 mm, respectively (fig. 5). The lucencies appeared almost identical to the defects in cases 1–4. A bone survey showed multiple metastases in the pelvis which differed from the scapular defects in that the margins of the metastases were not sharply demarcated or sclerotic.

Discussion

The scapula begins to ossify by the eighth postovulatory week. In microscopic sections of the 12 mm embryo, the body of the scapula consists mainly of precartilage; the acromion and the coracoid processes are recognizable as areas of condense mesenchyme [3]. At birth a large part of the scapula is osseous. The adult scapula is formed by the subsequent addition of seven or more nuclei of ossification. At about 15 years, the first of two or more secondary centers at the inferior angle and at the medial border begin to ossify.

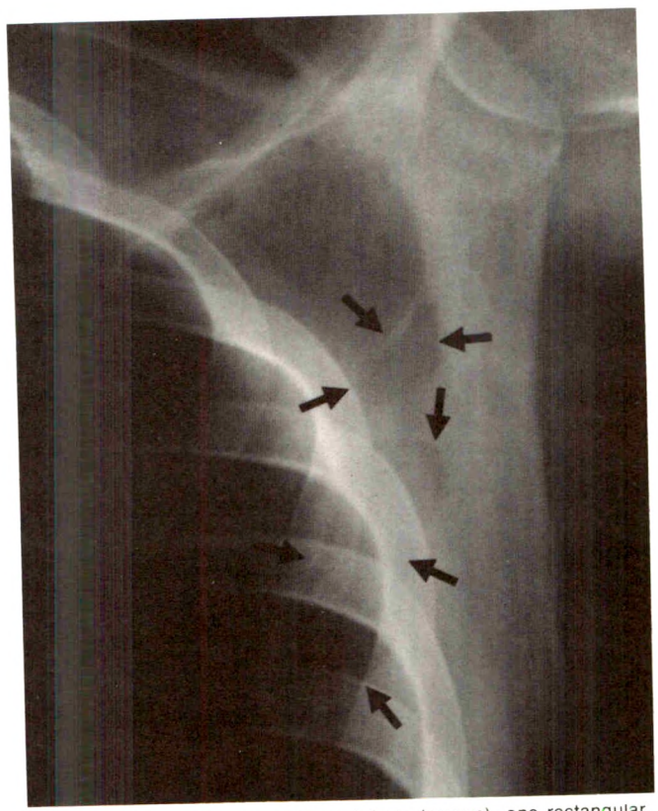


Fig. 1.—Case 1. Two large bony defects (*arrows*), one rectangular, one triangular, involve entire thickness of body of scapula.

Received June 30, 1978; accepted after revision October 25, 1978.

[1] Department of Radiology, Georgetown University Medical Center, 3800 Reservoir Road, N.W., Washington, D.C. 20007. Address reprint requests to O. S. Cigtay.

0361-803X/79/1322-0239 $0.00

AJR 132:239–241, February 1979

© 1979 American Roentgen Ray Society

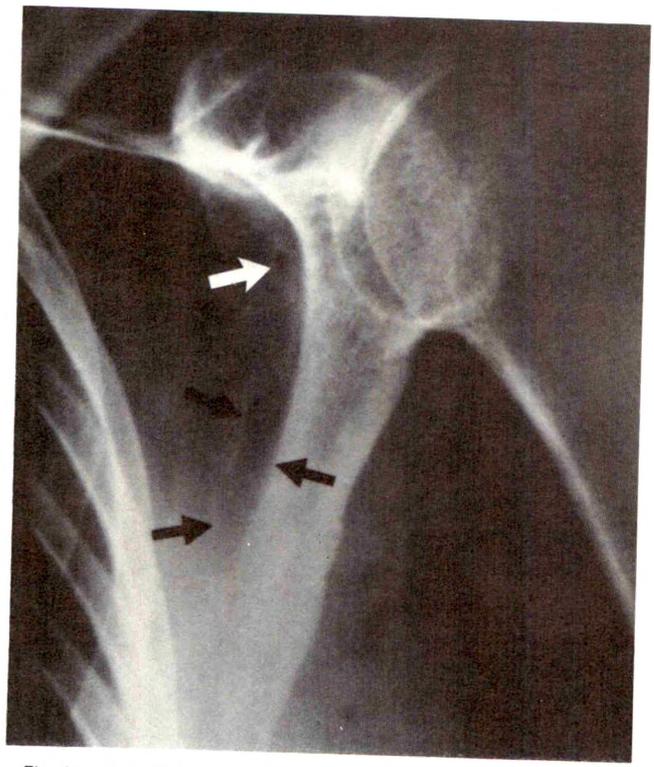


Fig. 2.—Case 2. Narrow vertically oriented bony defect lies parallel to lateral margin of scapula (*arrows*). Note large nutrient foramen at base of collum scapulae (*white arrow*).

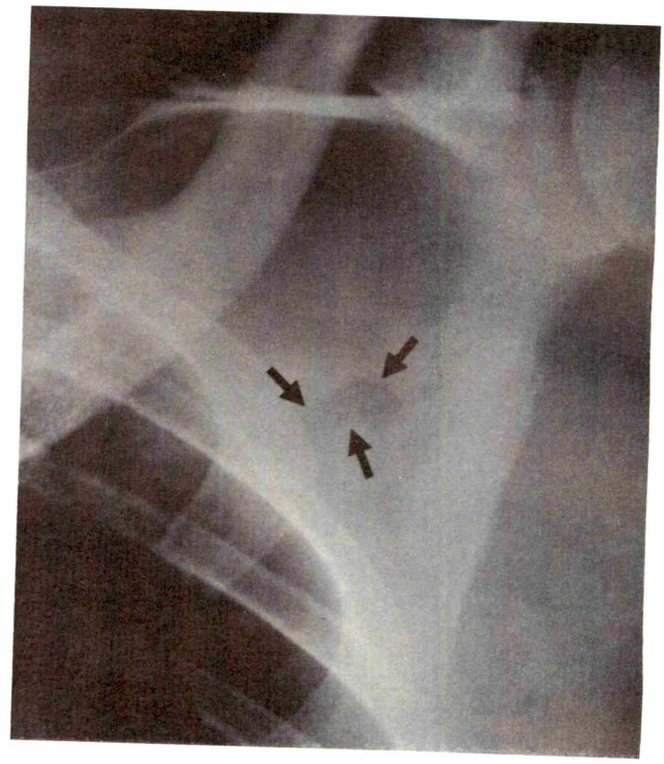


Fig. 4.—Case 4. Ovoid defect in midbody of scapula (*arrows*) with horizontal long axis.

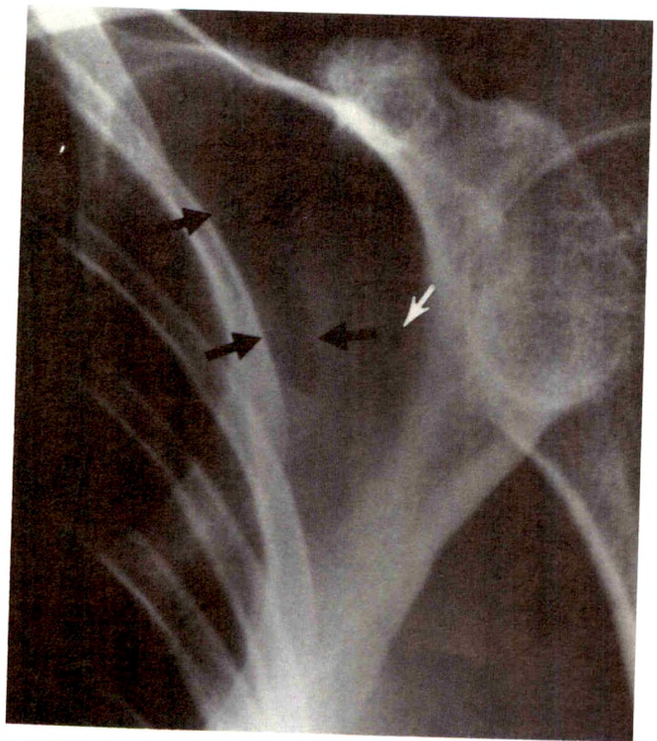


Fig. 3.—Case 3. Bony defect in midportion of scapula is similar to defect in case 2 (*arrows*). Note nutrient foramen (*white arrow*).

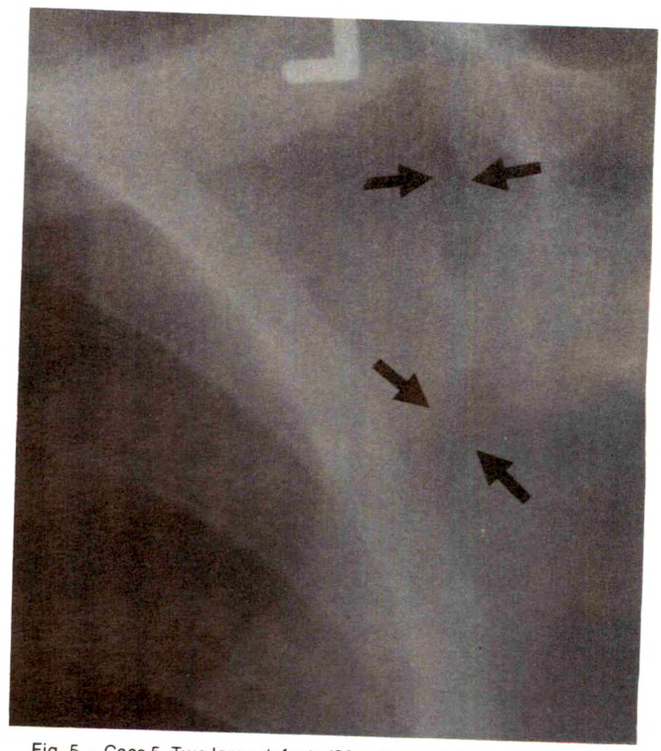


Fig. 5.—Case 5. Two large defects (30 × 20 and 35 × 10 mm) parallel to lateral margin of scapula and at base of collum scapulae (*arrows*).

The defects in the five patients described are strikingly similar. In all, the defects were asymptomatic and the lucencies were usually multiple and sharply demarcated with sclerotic borders. In addition, all of these defects were identified within the body of the scapula.

A search of the literature [3–6] and a review of the standard reference texts by Kohler and Zimmer [1] and Keats [2] failed to show similar anomalies. McClure and Raney [3] observed that the thinner areas of the scapular body are sometimes absent, but failed to show such a case, nor did they include a reference.

The defect most probably represents an area in which bone did not develop. We have not identified the defect in children, possibly because the scapula is incompletely ossified. The recognition of the benign nature of these defects is important, since they could be confused with primary or secondary malignancy.

REFERENCES

1. Kohler A, Zimmer EA: *Borderlands of the Normal and Early Pathologic in Skeletal Roentgenology*, New York, Grune & Stratton, 1968
2. Keats T: *An Atlas of Normal Roentgen Variants that May Simulate Disease*. Chicago, Year Book Medical Publishers, 1973
3. McClure JG, Raney RB: Anomalies of the scapula. *Clin Orthop* 110:22–31, 1975
4. Chung SM, Nissenbaum MM: Congenital and developmental defects of the shoulder. *Orthop Clin North Am* 6:381–392, 1975
5. Bell JF, Kuhlmann RE, Molloy MK: Congenital defects of shoulder girdle, sternum, spine and pelvis. *Pediatr Clin North Am* 14:397–418, 1967
6. Tachdjian MO: Diagnosis and treatment of congenital deformities of the musculoskeletal system in the newborn and the infant. *Pediatr Clin North Am* 14:307–358, 1967

Ultrasonic Demonstration of Myometrial Contractions in Intrauterine Pregnancy

ROBERT L. WILSON[1] AND NANCY J. WORTHEN[1]

An incidental finding associated with ultrasound examination of early intrauterine pregnancy is transient thickening of a limited region of the myometrium, which we interpret as a localized contraction. Contractions were demonstrated in nearly all 881 patients examined and were shown to significantly change in configuration within a 30 min period. In all except one patient, the contractions were completely asymptomatic, and they seem to be of no discernible clinical significance.

Diagnostic ultrasound in the examination and assessment of the obstetrical patients has been well established and readily accepted by the medical community [1–5]. Ultrasound offers the physician a unique opportunity to image the entire gravid uterus and its contents in a relatively undisturbed physiologic state. Ultrasonic demonstration of one physiologic phenomenon, localized myometrial thickening, is reported here.

Some researchers [6] believe local myometrial thickening is due to an unsoftened portion of the uterus, implying a time span of considerable length (e.g., several weeks). We found that this phenomenon lasts from minutes to hours, which suggests a more transient event that we believe to be an asynchronous myometrial contraction.

Materials and Methods

All patients were referred for ultrasonic examination for reasons unrelated to suspected uterine contractions. Clinical indications included possible fetal demise, possible multiple gestation, medical genetics workup, possible hydatidiform mole, large for dates, and possible uterine tumor. A large majority of the patients examined were outpatients; all patients were ambulatory and in good clinical condition. All patients were examined before any invasive procedures, such as amniocentesis.

Although 960 patients were examined, 79 patients of 8–14 week gestations were not included in the study because of the confusing effects of the decidua basalis reaction in the region of placental implantation. Therefore, focal uterine contractions were analyzed in 881 patients.

The age range for the entire group of 881 patients was 14–43 years (table 1). Three peaks occurred in the age distribution: 15–17, 22–25, and 35–40 years. The last category was impacted by medical genetics referrals (table 2).

The patients in the medical genetics group (table 2) were being counseled and analyzed for reasons such as advanced maternal age, previous genetic defect, exposure to toxin or teratogen, and possible familial trait. All but two patients over 35 were in this category; the youngest patient in this group was 23 years old. All patients in this category had an amniocentesis.

The patients were examined in the ultrasound laboratory with one of several types of gray scale B-scan units (Rohnar 5550, Litton, or Toshiba Picker EDC). Recently, certain patients were also examined with a linear array real time unit operating at 3.5 MHz. The B-scan results were obtained primarily with a 2.25 MHz transducer having a 19-mm-diameter housing and long internal focus. Occasionally a patient would be examined on the B-scan unit using a 19-mm-diameter, long internal focus 3.5 MHz transducer.

The scanning instruments, both B-scan and real time, were adjusted to display the optimum range of soft tissue gray scale. Each patient required a slightly different setting of the various controls. The overall gain and attenuation compensation curve were positioned to allow for differentiation between placental and myometrial echo patterns. The fact that these tissues have different acoustic properties has been documented [7, 8] and should be used to advantage in the imaging process. All of the major tissue regions were adequately differentiated from each

TABLE 1

Patient Age and Incidence of Contractions

Age	No. Patients	No. Contractions	%
14–16	81	56	69
16–18	97	69	71
18–20	61	37	61
20–22	59	39	66
22–24	101	71	70
24–26	47	36	76
26–28	68	47	69
28–30	47	32	68
30–35	90	66	73
35–40	201	152	76
40–45	29	20	69
Total	881	625	71

TABLE 2

Clinical History

Reason for Examination	No. Patients	%
Medical genetics	467	53.0
Dates vs. size disparity	253	29.0
Possible multiple gestation	38	4.3
Suspected fetal demise	26	2.9
Possible hydatidiform mole	21	2.4
Suspected uterine tumor	11	1.2
Possible pregnancy	10	1.1
Other	55	6.1
Total	881	100.0

Received April 18, 1978; accepted after revision October 30, 1978.

[1] Diagnostic Ultrasound Section, Department of Radiology, Harbor General Hospital, 1000 West Carson Street, Torrance, California 90509. Address reprint requests to R. L. Wilson.

0361-803X/79/1322-0243 $0.00

AJR 132:243–247, February 1979

© 1979 American Roentgen Ray Society

TABLE 3

Distribution of Contractions

Location	No. Patients	% (N = 625)	% of Total (N = 881)
Single anterior corpus	289	46.2	32.8
Single posterior corpus	301	48.2	34.2
Fundus	8	1.3	0.9
Lower segment	21	3.4	2.4
Multiple simultaneous areas	6	0.9	0.7
Total	625	100.0	71.0

other; specifically, myometrium, placenta, fetal structures, amniotic fluid, maternal bladder, cervix, and vaginal vault.

The patient was supine during scanning, and multiple transverse and longitudinal views of the pelvis were obtained. The urinary bladder was filled to varying degrees of distension. The results of each study were recorded on Polaroid film or multiformat camera radiograph film.

If an area of suspected uterine contraction was demonstrated during routine obstetrical ultrasound, it became standard practice to repeat that same view later in the examination to determine the constancy of the phenomenon. The vast majority of these examinations required 30 min or less. It was not uncommon to reexamine an area of contraction only to find that the first contraction had relaxed and a second contraction had appeared in another area of the uterus. These contractions were routinely noted and recorded. Analysis of these findings forms the basis of this report.The complete examination record was available to inspect the actual photos for clarification of confusing notations.

Results

All 79 patients in the first trimester demonstrated an area of increased echogenicity and an apparent resistance to deformity in the region of the placental implantation. It was believed, but not proved, that this was attributable to the decidua basalis reaction and was not a true myometrial contraction.

It was far more difficult to appreciate and characterize the contractions that seemed to occur in the lateral wall without appreciable anterior or posterior projections. Perhaps if all possible uterine sites could be accurately examined, the total number of contractions noted would be closer to 100% rather than 71%. Since we must assume that the patients are being examined at completely random times between 14 and 30 weeks gestational age, it follows that during this period the gravid uterus must nearly always be in a state of localized contraction and relaxation. If one then normalizes the distribution of contractions (table 3) as a general function of segment volume, the location of each contraction will also be random. In other words, the sections of the uterus with a larger volume of tissue will have more contractions.

A comparison of gestational age to incidence of contractions (table 4) suggests that it may be somewhat easier to demonstrate or recognize random uterine contractions at a gestational age greater than 20 weeks, but the sampling in each category may not be comparable. Other factors that may have exerted a significant influence are not evident on a retrospective study, such as patients' clinical and psychologic condition at the time of the ultrasound examination, a requested abbreviated study for amniocentesis site only, drug history, or previous cesarean deliveries. As with other obstetrical phenomena, the patient's age could be expected to be influential but this was not appreciated (table 1).

TABLE 4

Gestational Age and Incidence of Contractions

Gestation (weeks)	No. Patients	Noted Contractions	
		No.	%
14–16	133	97	73
16–18	297	195	66
18–20	181	136	75
20–22	127	92	72
22–24	38	23	69
24–26	29	24	83
26–28	31	22	71
28–30	45	36	80
Total	881	625	71

When similar segments of the uterus are compared, it seems that about 60% of observed contractions occur opposite the site of placental implantation versus about 40% for ipsilateral contractions. This may be due to a combination of the following: (1) the placental implantation site physically resists the formation of myometrial contractions; (2) the myometrial irritability is slightly greater in those areas distant from placental implantation; and (3) the contralateral contractions are more easily demonstrated or visualized.

Another interesting finding was that 23 patients in the group of 881 patients had clinically evident uterine leiomyomata. These tumors were all easily distinguishable because they were slightly less echogenic than usual contractions, were seen to distort the boundary or periphery of the gravid uterus and not the endometrium, and did not change in size or shape over a 30 min period.

An illustrative contraction from this series that represents a typical change in configuration over a rather typical time span is shown in figure 1. This patient demonstrated the contraction in the first week of the third trimester in a location more easily recognized (opposite to the placental implantation site). Contractions in other portions of the uterus in other patients behaved similarly. Three patients were noted to have two distinctly different areas of the uterine myometrium contract simultaneously (fig. 2A).

Discussion

John Braxton Hicks [10–13] described the clinical findings of uterine contractions throughout pregnancy, and actually postulated their usefulness in pregnancy diagnosis. He did not elaborate on whether all of these contractions were subclinical as far as the patients were concerned, but he did state that he could detect them from the first trimester onward and that they seemed to occur intermittently. The type of contractions named after Hicks are those sporadic, painless, nonrhythmic

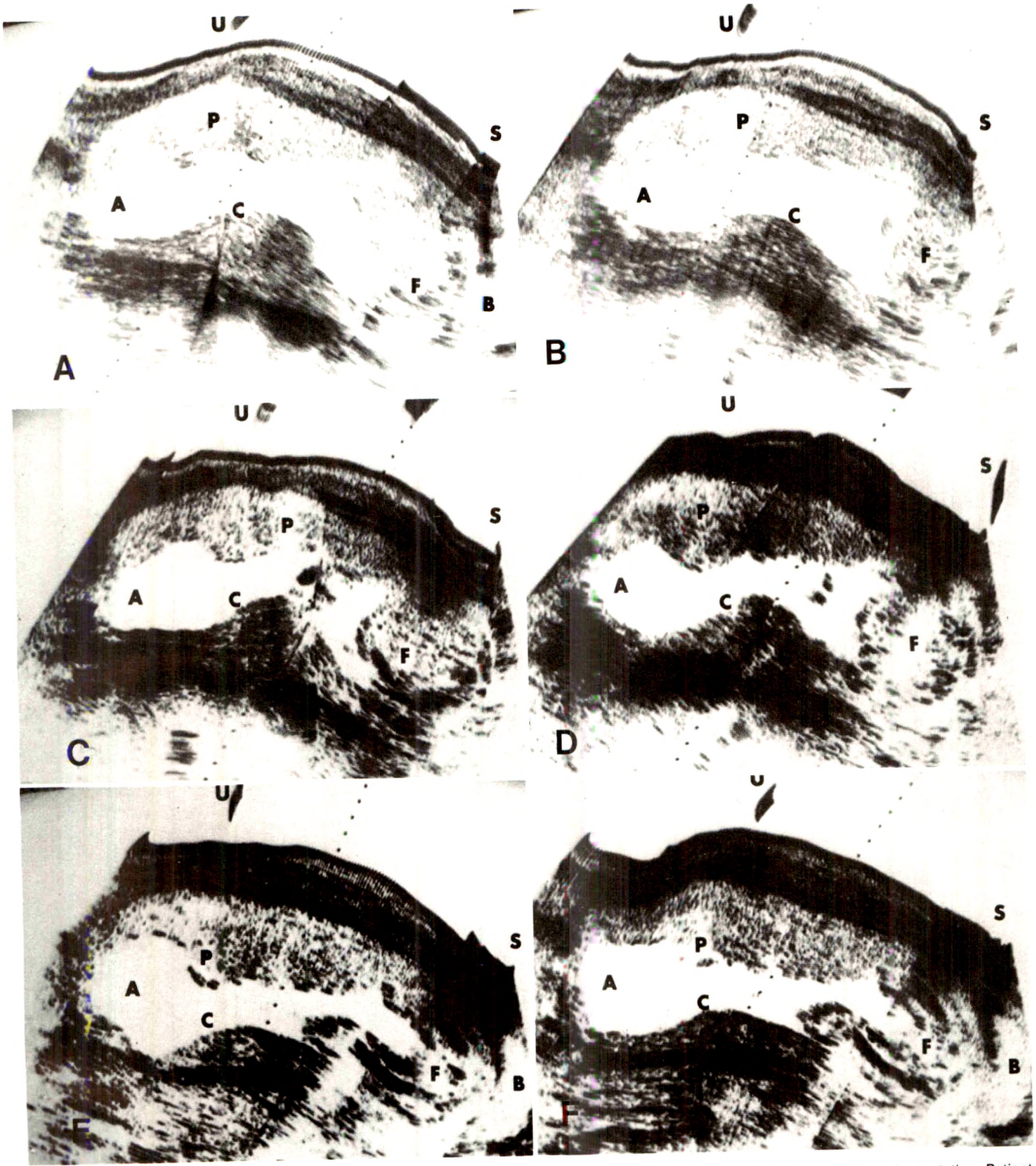


Fig. 1.—Longitudinal scans slightly left of midline at 2–3 min intervals of 32-year-old gravida 3, parity 2 patient at about 27 weeks gestation. Patient is supine. Fetus was constantly moving. Slight alteration in placental configuration seems inconstant result of some of these contractions. (A = amniotic fluid; P = placental tissue in anterior corpus; U = level of umbilicus; C = contraction of posterior myometrium; F = fetus; S = level of pubic symphysis; B = maternal bladder.)

contractions sensed by the patient and occurring later in the third trimester. These contractions are probably more intense versions of the same phenomena that Hicks noticed in the first trimester.

Early in the bistable storage scope era, one of us (R. L. W.) occasionally made the diagnosis of either a strange type of intrauterine tumor or an extremely odd placental configuration. This usually occurred in a sec-

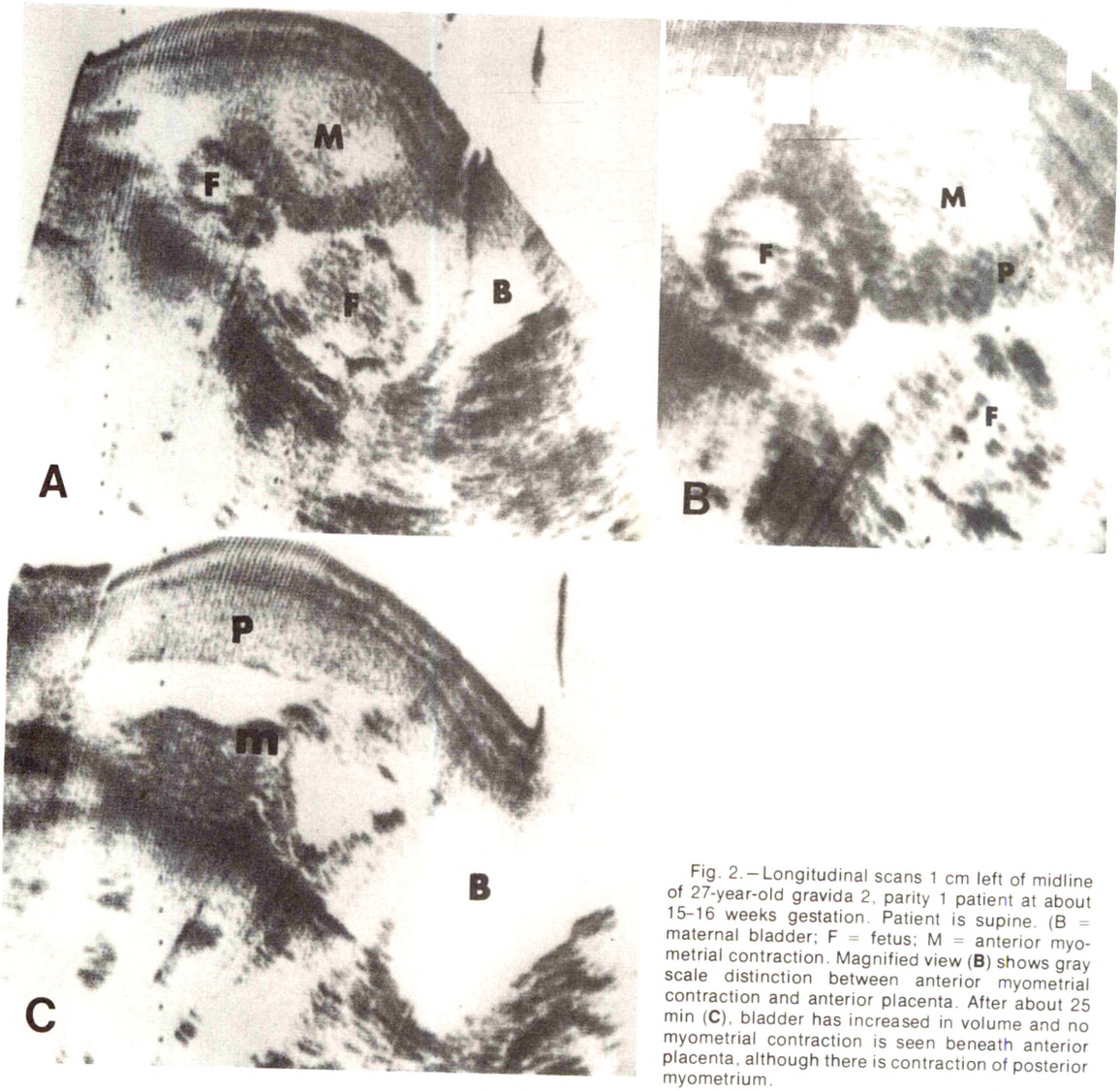


Fig. 2.—Longitudinal scans 1 cm left of midline of 27-year-old gravida 2, parity 1 patient at about 15–16 weeks gestation. Patient is supine. (B = maternal bladder; F = fetus; M = anterior myometrial contraction. Magnified view (**B**) shows gray scale distinction between anterior myometrial contraction and anterior placenta. After about 25 min (**C**), bladder has increased in volume and no myometrial contraction is seen beneath anterior placenta, although there is contraction of posterior myometrium.

ond trimester patient; her physician was then alerted and the patient scheduled for a second examination within 2 weeks, at which time the "tumor" would invariably be absent or the placenta would have a more understandable configuration. Subsequent deliveries were uneventful and no pathology could be detected in the gestational components. The time delay for reexamination was gradually decreased, and it soon became evident that these represented a transient phenomenon and were probably uterine contractions. However, the bistable image, prevented simultaneous differentiation between placental and myometrial echoes. The newer gray scale imaging techniques allow a display of tissue dynamic range unavailable in 1973 when the contractions were first demonstrated.

The question of a placental extension confusing the image is easily eliminated by using all the parameters available, namely tissue dynamic range in the display and time. Placental tissue just does not generate the same type of echoes as does the myometrium [7, 8], nor can the placenta change its location within the hour [14]. The tissue differentiation may not be quite so obvious in the case of possible leiomyoma, but the time factors should be diagnostic.

The submucous variety of leiomyomata could initially be a diagnostic dilemma, since it is entirely capable of distorting a localized area of endometrium, but serial scans in that same region over a 30 min period should resolve the difference. It was also not apparent that the presence of the leiomyoma stimulated an increased incidence of uterine contractions; of 23 patients with documented leiomyomata, only 17 (74%) manifested a demonstrable contraction.

There were five sets of twins in the group of 881

patients and two of their mothers were noted to have myometrial contractions. One of these contractions occurred in a set of dizygotic twins with a demonstrable membrane. The contraction occurred in the posterior uterine corpus and both placentas were implanted anteriorly. The other contraction with twins had similar features, except that a membrane was not demonstrated. The twin series was not large enough to determine any differences from the singleton group. If uterine irritability is a causative factor in the generation of myometrial contractions, then any differences should manifest themselves late in the third trimester with twins. These patients are known to become more irritable at an earlier stage of gestation when compared to singleton pregnancies [9], but this should not be a factor up to 30 weeks gestation.

The advent of ultrasound has resulted in the imaging of processes that previously elicited mixed responses in the professional community. Although this report does not explain the etiology of uterine contractions or their clinical significance, it does firmly establish their presence in the second and third trimester of pregnancy. It could be speculated that these same contractions exist throughout pregnancy, as Hicks believed.

The results of our experience and the data presented above compel us to modify our examination techniques for all obstetrical patients. If one of these myometrial contractions is observed in a patient scheduled for amniocentesis or suspected of having a placenta previa, the examination is continued until the myometrium relaxes. Also, it is usually beneficial for the patient to void a majority of the bladder volume, especially when obviously over distended. The apparent change in placental localization can be quite remarkable and may constitute an acceptable and plausible explanation for the so-called "migrating placenta."

REFERENCES

1. Kohorn EI, Morrison J, Ashford C: Ultrasound scanning in obstetrics and gynecology. *Obstet Gynecol* 34:515–522, 1969
2. Stocker J, Desjardius P, Deleon A: Ultrasonography: its usefulness and reliability in early pregnancy. *Am J Obstet Gynecol* 121:1084–1092, 1975
3. Kohorn EI, Kaufman M: Sonar in the first trimester of pregnancy. *Obstet Gynecol* 44:473–483, 1974
4. Robinson HP: Sonar measurements in the evaluation of the normal early pregnancy, in *Ultrasonography in Obstetrics and Gynecology*, edited by Sanders RC, James AE, New York, Appleton Century Crofts, 1977, pp 97–112
5. Sanders RC, Conrad MR: Sonography in Obstetrics, *Radiol Clin North Am* 13:435–455, 1975
6. Sample WF: The unsoftened portion of the uterus. *Radiology* 126:227–230, 1978
7. Wells PNT: Ultrasonics in medicine and biology. *Phys Med Biol* 22:629–669, 1977
8. Kossoff G, Garrett WJ, Radovanovich G: Grey scale echography in obstetrics and gynaecology. *Australas Radiol* 18: 62–111, 1974
9. Hellman LM, Pritchard JA: Maternal physiology in pregnancy, chapter 8 in *Williams' Obstetrics*, 14th ed, New York, Appleton Century Crofts, 1971, pp 236–277
10. Hicks JB: On the contractions of the uterus throughout pregnancy, their physiological effects and their value in the diagnosis of pregnancy. *Trans Obstet Soc London* 13:216–231, 1871
11. Hicks JB: Further remarks on the use of the intermittent contractions of the pregnant uterus as a means of diagnosis. *Trans Intern Med Congress London* 4:271, 1881
12. Hicks JB: Why does the uterus contract during pregnancy? *Lancet* 1:765, 1889
13. Hicks JB: On intermittent contractions of uterine fibromata, and in pregnancy, in relation to diagnosis. *Med Press Circular*, May 9, 1894, p 481
14. Buttery B, Davidson G: The dynamic uterus revealed by time-lapse echography. *JCU* 6:19–23, 1978

Simple, Rapid Thyroid Function Testing with ^{99m}Tc-Pertechnetate Thyroid Uptake Ratio and Neck/Thigh Ratio

PETER B. SCHNEIDER[1]

To avoid the technical difficulties and errors inherent in the measurement of early thyroid uptake of $^{99m}TcO_4^-$, techniques which are independent of absolute uptake, neck extrathyroidal background and dose standards were evaluated in a series of 108 patients. After intravenous injection of 2 mCi $^{99m}TcO_4^-$, radioactivity was recorded over the neck and thigh. Thyroid uptake ratios were calculated as the ratios of activity over the neck at two times. A neck/thigh ratio was calculated from the recorded activities at 15 min after injection. Examination of these parameters showed that a combination of the 15 min neck/thigh ratio and the 10′/2′ thyroid uptake ratio best served to discriminate thyroid function: 92% of hyperthyroid cases were correctly identified by a neck/thigh ratio above 4.7 and 95% of hypothyroid cases were identified by the combination of a neck/thigh ratio below 3 and a 10′/2′ thyroid uptake ratio below 1. Correct classification of euthyroidism was 84% but with the exclusion of patients previously treated with ^{131}I, this rose to 91%. The accuracy of the ^{99m}Tc procedure is comparable to that of the standard 24 hr ^{131}I uptake run concurrently in this series and duplicates the accuracy of computer assisted determinations of absolute thyroid $^{99m}TcO_4^-$ uptakes. The procedure provides a convenient method for the evaluation of thyroid function as an accompaniment to $^{99m}TcO_4^-$ thyroid imaging.

Introduction

Although the diagnosis of thyroid function is now made primarily by assay of serum hormone levels, radionuclide uptake tests retain a confirmatory or clarifying role when other tests are ambiguous or contradictory and are useful adjuncts in the interpretation of thyroid scans. The classical 24 hr thyroid radioiodine uptake test has a major disadvantage of requiring a return visit by the patient. Earlier uptake tests have been used to some extent for many years [1–5] and although they are successful screening tests for hyperthyroidism, they do not serve well to discriminate hypothyroidism.

Since ^{99m}Tc first became available, its use in a 20 min uptake test has also been studied [6–15]. Such tests have the advantage of being rapid. They are also convenient since $^{99m}TcO_4^-$ is widely used for thyroid imaging thus allowing concurrent evaluation of structure and function. However, the absolute uptake of $^{99m}TcO_4^-$ by the thyroid is low and its measurement is complicated by the necessity of accurately measuring and subtracting the background extrathyroidal radioactivity in the neck. Neck background activity has been measured by counting dots in areas adjacent to the thyroid on rectilinear scans [6–9], by using regions of interest around the thyroid on gamma camera studies [10–12], and by using a computer linked to a gamma camera to subtract background activity determined from flagged areas around the thyroid [13, 14]. These procedures are either tedious or require relatively expensive equipment. They all serve to discriminate hyperthyroid patients from euthyroid patients but, except for the computer aided technique [13], they cannot satisfactorily discriminate hypothyroidism.

The measurement of the rate of uptake of ^{131}I by the thyroid has been suggested as a rapid function test which is independent of the necessity of determining absolute uptake and background activity [4]. Another test in use for evaluating thyroid radioiodide uptake has been the "neck-thigh ratio" proposed first in the early 1950s [1, 3]. This procedure merely requires the calculation of the ratio of activity recorded over the neck to that recorded over the thigh at about 1 hr after oral administration of $^{131}I^-$. More recently, the neck/thigh ratio method has been used with $^{99m}TcO_4^-$ to study thyroid function [15]. These simpler tests serve as well as the more complicated procedures to diagnose hyperthyroidism but are not satisfactory for hypothyroidism.

We examined the utility of ^{99m}Tc uptake techniques which are independent of absolute uptake values and background corrections and have compared them to the classical radioiodine uptake. The results of this investigation have validated a combination consisting of the measurement of the neck/thigh ratio and rates of thyroid uptake as a technique for the rapid evaluation of thyroid function which permits discrimination of hyper- and hypothyroidism.

Materials and Methods

Radioactivity over the neck and thigh was recorded continuously for 15 min after injection of 2 mCi of ^{99m}Tc-pertechnetate into an antecubital vein. (This dose allowed concomitant thyroid imaging and served to provide good statistics in the uptake measurements. Without imaging, a dose of about 0.5 mCi would suffice.) Two probes with 5-cm-diameter crystals and flat field collimators were used. The collimators extended 20 cm from the crystal surface with the bore tapering from 5 to 11 cm. One probe was centered over the thyroid area and the other over the thigh about 10 cm proximal to the patella, with both collimators at skin contact. Activity was measured in 10 sec intervals with scalers coupled to digital to analog converters and a two-channel strip chart recorder to provide a hard copy of the time-activity curves (figs. 1 and 2). For analysis, thyroid uptake rates were quantitated in terms of the ratio of recorded neck activity at one time to that at a previous time. Such thyroid uptake ratios were calculated for 5′/1′, 10′/1′, 15′/1′, 10′/2′, 10′/5′, and 15′/

Received August 4, 1978; accepted after revision October 30, 1978

[1] Nuclear Medicine Service, Division of Medicine, Memorial Hospital, 119 Belmont Street, Worcester, Massachusetts 01605, and Department of Medicine, University of Massachusetts Medical School, Worcester, Massachusetts.

AJR 132:249–253, February 1979

© 1979 American Roentgen Ray Society

0361–803X/79/1322–0249 $0.00

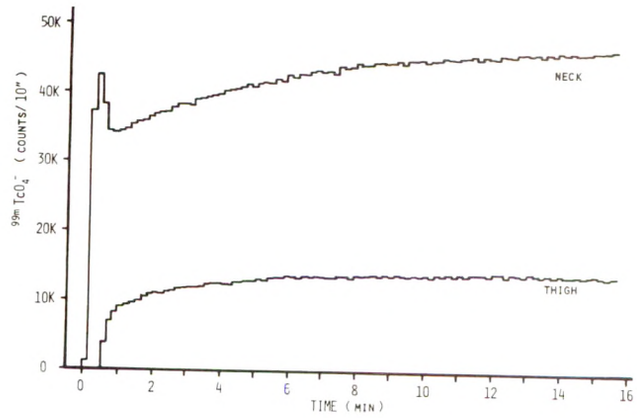


Fig. 1.—$^{99m}TcO_4^-$ uptake curves over neck and thigh in normal individual.

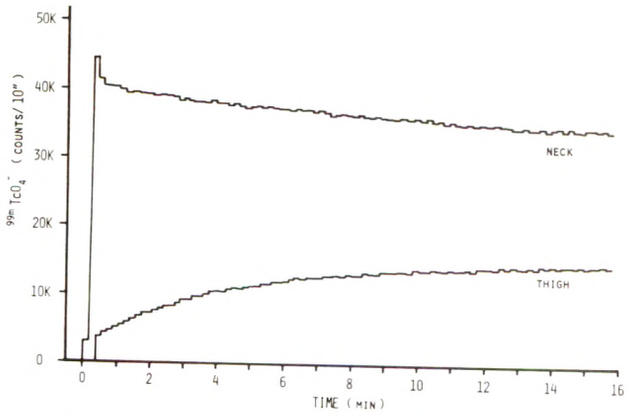


Fig. 2.—$^{99m}TcO_4^-$ uptake curves over neck and thigh in hypothyroid patient.

5′. At 15 min the neck/thigh activity ratio was also calculated. The initial appearance of radioactivity on the neck recording rather than the time of injection was considered "zero time" for the analysis although in the final procedure, this distinction proved unimportant. A standard 24 hr $^{131}I^-$ thyroid uptake was measured for comparison within 24 hr of the ^{99m}Tc studies.

Subjects included a variety of patients from eastern Massachusetts referred to the Nuclear Medicine Unit for thyroid function and imaging studies. Diagnoses are indicated in figures 3 and 4. The diagnoses were determined by clinical and laboratory examinations which included serum T4 and T3 resin uptake determinations plus serum T3, TSH, and TRH stimulation tests where appropriate. Euthyroid individuals included patients suspected of thyroid dysfunction but who proved to be euthyroid, patients screened because of childhood x-irradiation to the neck, and those tested prior to a planned hypophysectomy for the palliation of cancer or diabetic retinopathy.

Results

The typical normal $^{99m}TcO_4^-$ uptake curve over the neck (fig. 1) shows a continuing slow rise of activity following an initial spike as the injected bolus passes through the neck. An occasional normal curve may have a broad peak at about 5–10 min with a subsequent decline. In contrast, the typical hypothyroid curve (fig. 2) shows a monotonic decrease of activity following the initial spike. Hyperthyroid curves characteristically show an exaggerated rise of activity extending beyond the 15 min mark although occasionally, an earlier peak (5–10 min) with a subsequent decrease is seen.

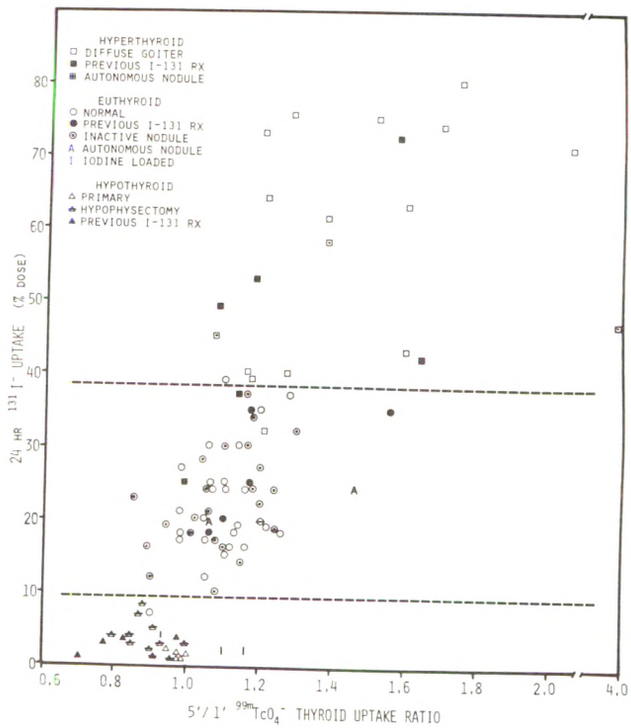


Fig. 3.—Relation of 24 hr radioiodine thyroid uptake to 5′/1′ $^{99m}TcO_4^-$ thyroid uptake ratio for 102 patients with variety of diagnoses. Horizontal lines (38% and 9%) indicate ^{131}I uptake which best discriminates hyperthyroid, euthyroid, and hypothyroid cases. No reasonable discrimination can be achieved with uptake ratio. (Open circle with horizontal line indicates euthyroid patient with incomplete hypophysectomy.

Thyroid $^{99m}TcO_4^-$ uptake ratios were compared to the 24 hr radioiodine uptake for 102 patients. Such a comparison for the 5′/1′ uptake ratio (ratio of neck activity at 5 min to that at 1 min) is illustrated in figure 3. The ^{131}I test, using the indicated upper and lower limits (38% and 9%) for the 24 hr uptake, served as an accurate indicator of thyroid function, correctly identifying 20/23 hyperthyroid, 54/56 euthyroid (three iodide-loaded patients excluded), and 20/20 hypothyroid patients. The ^{99m}Tc thyroid uptake ratio was mildly correlated with the ^{131}I uptake ($r = 0.5$) but was useless as a discriminator of thyroid function. Similar analysis was performed with the 10′/1′, 10′/2′, 10′/5′, 15′/1′, and 15′/5′ uptake ratios. The correlation of these ratios with radioiodine uptake ranged from $r = 0.40$–0.62 with the best correlation shown by the 10′/2′ ratio. None of these ratios could reliably classify thyroid function.

An examination of the neck/thigh ratio at 15 min disclosed a correlation of 0.72 with the ^{131}I uptake and proved able to distinguish hyperthyroid patients although it did not serve for hypothyroidism. However, the combination of the neck/thigh ratio with thyroid uptake ratios extended the test into the hypothyroid range. Of

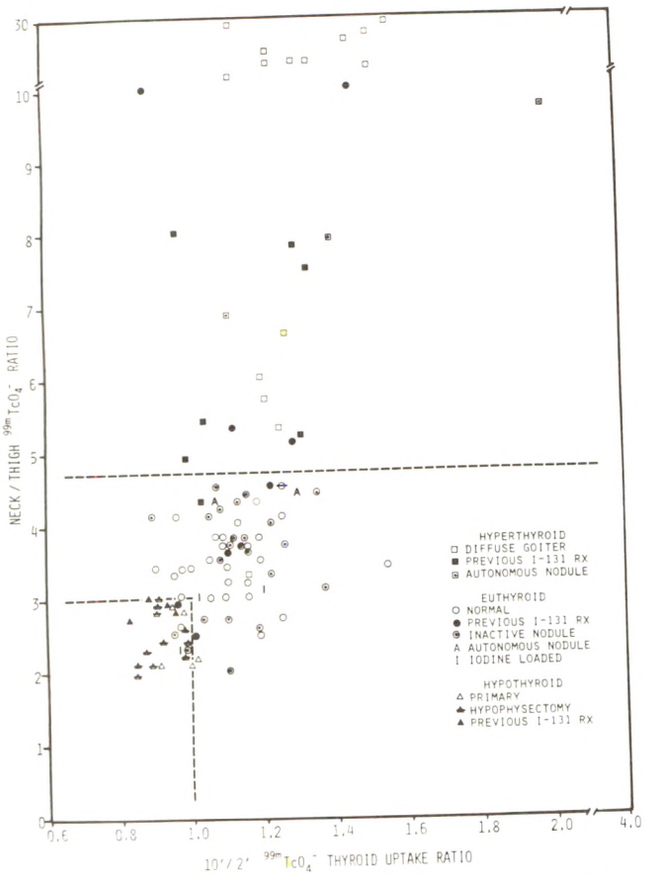


Fig. 4.—Diagnosis of thyroid function with combination of 15 min neck/thigh ratio and 10'/2' $^{99m}TcO_4^-$ thyroid uptake ratio in 108 patients. Neck/thigh ratio above 4.7 identifies hyperthyroid cases while hypothyroidism is identified by both neck/thigh ratio of 3.0 or less and uptake ratio of 1.0 or less.

the various uptake ratios tested, the 10'/2' ratio was the most useful (fig. 4). The diagnosis of hyperthyroidism is dependent on the neck/thigh ratio alone with a nominal cutoff value of 4.7. This finding confirms the experience of Selby et al. [15] who reported a cutoff value of 5.0. The diagnosis of hypothyroidism, on the other hand, is dependent on two criteria: a 15' neck/thigh ratio of 3.0 or less and a 10'/2' thyroid uptake ratio of 1.0 or below. Using these criteria the proportion of correctly identified patients is listed in table 1 for both the ^{131}I and ^{99m}Tc studies. It should be emphasized that the criteria for classification are relatively arbitrary in some cases where there are no major discrete separations between groups. Thus, lowering the upper limit for the radioiodine uptake from 38% to 36% improves the diagnosis of hyperthyroidism to the same level as listed for $^{99m}TcO_4^-$ tests while the correct identification of euthyroidism decreases to approach that found with the $^{99m}TcO_4^-$.

TABLE 1

Proportion of Patients Who Were Correctly Identified

Diagnosis	^{131}I 24 hr Uptake		$^{99m}TcO_4^-$ 15' Neck/Thigh and 10'/2' Uptake Ratios	
	No. Patients	(%)	No. Patients	(%)
Hyperthyroid	20/23	(87)	23/25	(92)
Euthyroid	54/59	(92)	53/63	(84)
Previous ^{131}I therapy	5/5		3/8	
Iocine loaded	0/3		2/3	
Hypothyroid	20/20	(100)	19/20	(95)
Total	94/102	(92)	95/108	(88)

Discussion

Although two probes and a dual channel recorder were used for this study and though continuous recording is convenient, this instrumentation is not necessary for the test as finally validated. A single probe and scaler are sufficient. Radioactivity over the thyroid is measured at 2 and 10 min after intravenous injection of the nuclide. Counting intervals of 10–30 sec are adequate when 2 mCi of $^{99m}TcO_4^-$ are used. At 15 min radioactivity over the neck and then over the thigh is measured. Classification of the patient's thyroid function is accomplished by comparing the 15 min neck/thigh ratio and the 10'/2' thyroid uptake ratio with the numerical criteria described. Plotting the results of a test on a chart (fig. 2) and noting their location with respect to the criteria is helpful in judging the degree of confidence with which the diagnosis of thyroid function can be made.

The combination of the thyroid $^{99m}TcO_4^-$ uptake ratio and the neck/thigh ratio provides a technique for functional evaluation that does not require the generally difficult determinations of neck background and absolute thyroid uptake nor measurements of dose standards. The technique is relatively insensitive to geometry with no significant change in the neck/thigh ratio if the probe is moved ±5 cm along the thigh and the thyroid is included with the "flat" response portion of the neck collimator. It is possible that with a different geometry (e.g., different collimator design) the absolute value of the neck/thigh ratio may change and a normal value may have to be redetermined for a particular laboratory. Timing is noncritical for the neck/thigh ratio since these curves are relatively flat at 15 min except for some patients with severe hyperthyroidism in which case this ratio is so elevated that even several minutes of timing error will not change the diagnostic significance of the result.

Since the discriminatory value for the thyroid uptake ratio (i.e., 1.0) indicates merely the difference between a rising curve and a level or falling one, this parameter also is independent of geometry as long as the relative position of the thyroid and probe is the same during the two measurements. Similarly, timing need not be highly precise for the thyroid uptake ratio. Although the numerical values of the 10'/2' and 15'/5' ratios were usually different, the diagnostic significance was the same. That is, the 15'/5' ratio was never above 1.0 when the 10'/2' ratio was 1.0 or less and in several cases where the curves had an early peak resulting in a potentially misleading 15'/5' value below 1.0, the neck/thigh ratio clearly excluded these cases from the hypothyroid area.

Though it was not our primary aim to examine the utility of the radioiodine uptake, it is of interest that this

study shows that the 24 hr ^{131}I uptake remains a very reliable test of thyroid function in our population (eastern Massachusetts) as opposed to other geographic areas [16–18] where dietary iodine may be much higher. A major contributor to dietary iodine has been white bread [18] but at least in this area, the use of iodate as an additive in the baking process had been discontinued by major bakeries several years ago (personal communication, Wonder Bread bakery). A similar decrease in the use of iodides may be in progress in other sections of the country. It is noteworthy that the pertechnetate test correctly identified two of three euthyroid iodine-loaded (recent angiography) patients, all of whom gave low radioiodine uptake values. This suggests that the pertechnetate tests may be less sensitive to an iodine load and may be useful in those geographic areas where high dietary iodine intake continues to diminish the utility of the radioiodine uptake test.

The ^{99m}Tc-pertechnetate procedure described is not as accurate as the radioiodine uptake, particularly because of the misclassification of Grave's disease patients who have previously been treated with ^{131}I. This discrepancy between the two tests is understandable since the phenomena measured (ion trapping for the $^{99m}TcO_4^-$ and trapping plus hormone production for the $^{131}I^-$) though closely related are not identical. It has been shown that in some patients ^{131}I therapy may have a more pronounced effect on iodide organification than on ion transport [19, 20] and our results reflect this. Thus, in our series the ^{131}I-treated patients who are misclassified are euthyroid presumably because radiation has damaged the organification and hormone synthesizing systems while the ion transport system remains hyperactive and is reflected in the elevated $^{99m}TcO_4^-$ tests. In this limited series there appears to be no clear relation between test results and the time after therapy. The patients misclassified as hyperthyroid had been treated 4–9 months previously while for the rest of the euthyroid patients, it was 2–13 months since therapy. Similarly, it was 4–12 and 4–17 months since therapy for the hyperthyroid and hypothyroid patients, respectively.

As in the previously mentioned cases, patients with Hashimoto's thyroiditis may exhibit a dissociation between their iodide trapping and organification processes in the early or intermediate stages of the disease. Although no cases of Hashimoto's thyroiditis were included in this series, it may be supposed that if they were studied at the appropriate stage, their ^{99m}Tc-pertechnetate studies might show a euthyroid result when the patient, in fact, was hypothyroid. At a later stage of the disease when further thyroid damage ensues, the tests should be concordant.

It has been similarly reported that an occasional thyroid nodule which is "cold" on the conventional radioiodine scan may nevertheless retain its ability to concentrate pertechnetate. If such a nodule represents a sizable proportion of the gland, it also might result in a falsely elevated value of the ^{99m}Tc-pertechnetate test.

Maisey et al. [13] in a study of the computer-assisted thyroid ^{99m}Tc uptake reported an accuracy of 91.5% for their technique. If our results are adjusted by the exclusion of iodine loaded and ^{131}I treated patients, which are not included in the population of Maisey et al., then the accuracy of our technique (93%) coincides with that of the computer method.

Although nuclide uptake tests as indicators of thyroid function have been largely superceded by assays of serum hormone levels, they are still useful as confirmatory procedures or when ambiguity surrounds the other tests. In these cases the ^{99m}Tc test has the main advantage of speed over the classical 24 hr iodine uptake. Moreover, scans are being increasingly performed with $^{99m}TcO_4^-$ for a variety of reasons (lower radiation dose and a more suitable emission for the gamma camera than ^{131}I, lower cost than ^{123}I) and it is as an accompaniment to imaging that the utility of the pertechnetate function tests should be most apparent. The state of thyroid function is an important point in the interpretation of thyroid scans (e.g., a goiter has different significance if it has increased, normal, or decreased activity) and the procedure reported here permits the routine determination of thyroid function at the time of $^{99m}TcO_4^-$ imaging with only simple instrumentation and without the necessity of administering a second nuclide.

REFERENCES

1. Pochin EE: Investigation of thyroid function and disease with radioactive iodine. *Lancet* 2:41–46, 1950
2. Kohler PO, Wynn J: One hour thyroid uptake of radioactive iodine. *Arch Intern Med* 116:177–182, 1965
3. Foote JB, MacLagan NF: The neck-thigh clearance: a simplified radioactive test of thyroid function. *Lancet* 1:868–871, 1951
4. Rosenthall L: A fifteen minute test of the rate of thyroid trapping of radioactive iodine. *J Nucl Med* 5:657–663, 1964
5. Higgins HP: The 10 minute uptake of ^{131}I: a clinical study and comparison with other tests of thyroid function. *J Clin Endocrinol Metab* 19:557–566, 1959
6. Andros G, Harper PV, Lahtrop KA, McCardle RJ: Pertechnetate-99m localization in man with applications to thyroid scanning and the study of thyroid physiology. *J Clin Endocrinol Metab* 25:1067–1076, 1965
7. deGarreta AC, Glass HI, Goolden AWG: Measurement of uptake of ^{99m}Tc by the thyroid. *Br J Radiol* 41:896–898, 1968
8. Goolden AWG, Glass HI, Williams ED: Use of ^{99m}Tc for routine assessment of thyroid function. *Br Med J* 4:396–399, 1971
9. Shimmins J, Hilditch T, Harden R McG, Alexander WD: Thyroidal uptake and turnover of the pertechnetate ion in normal and hyperthyroid subjects. *J Clin Endocrinol Metab* 28:575–581, 1968
10. Sokole EB, van der Schoot JB, Alberts C: ^{99m}Tc-pertechnetate uptake in the thyroid measured with a scintillation camera. *Radiol Clin North Am* 44:35–44, 1975
11. Burke G, Halko A, Silverstein GE, Milligoss M: Comparative thyroid uptake studies with ^{131}I and $^{99m}TcO_4^-$. *J Clin Endocrinol Metab* 34:630–637, 1972
12. Higgins HP, Ball D, Eastham S: 20 minute ^{99m}Tc thyroid uptake: a simplified method using the gamma camera. *J Nucl Med* 14:907–911, 1973

13. Maisey MN, Natarajan TK, Hurley PJ, Wagner HN Jr: Validation of a rapid computerized method of measuring ^{99m}Tc-pertechnetate uptake for routine assessment of thyroid structure and function. *J Clin Endocrinol Metab* 36:317–322, 1973
14. Armstrong DI, Rogers TGH, Brownlie BEW: Computer assisted thyroidal technetium uptake measurement using a short pinhole to surface distance. *AJR* 123:60–66, 1975
15. Selby JB, Caldwell JG, Magoun SE, Beihn RM: The use of the ^{99m}Tc-pertechnetate neck/thigh ratio as a test of thyroid function. *Radiology* 114:107–110, 1975
16. Caplan RH, Kujak R: Thyroid uptake of radioactive iodine: A reevaluation. *JAMA* 215:916–918, 1971
17. Robertson JS, Nolan NG, Wahner HW, McCohahey WM: Thyroid radioiodine uptakes and scans in euthyroid patients. *Mayo Clin Proc* 50:79–84, 1975
18. Pittman JA, Dailey GE, Beschi RJ: Changing normal values for thyroidal radioiodine uptake. *N Engl J Med* 280:1431–1434, 1969
19. Kirkland RH: Impaired organic binding of radioiodine by the thyroid following radioiodine treatment of hyperthyroidism. *J Clin Endocrinol Metab* 14:565–571, 1954
20. Kieffer J, Medeiros-Neto GA, Rueda RR, Peironi RR, Neto AC, Campusano LL, Cintra ABU: Perchlorate test in hyperthyroid patients treated with radioactive iodine. *N Engl J Med* 273:1326–1327, 1965

Carcinoma of the Supraglottic Larynx

JAMES E. MARKS,[1] RICHARD B. FREEMAN,[2] FRANSISKA LEE,[1] AND JOSEPH H. OGURA,[2]

Retrospective review of 160 patients with carcinoma of the supraglottic larynx was accomplished for the period 1964 to 1974. The majority were treated by low dose preoperative radiation and conservation surgery and the rest by preoperative radiation and total laryngectomy or radiation alone. Relapse-free and actuarial 5 year survival for all patients was 71% and 45%, respectively. Of primary and neck failures, 85% occurred within 2 years. Primary, nodal, and distant failures occurred in 11%, 21%, and 14% of all patients, respectively. Of 40 T and/or N failures, 33 (83%) occurred in the neck and three T and six N failures (23%) were surgically salvaged. Voice was preserved in 71% of the patients. Major complications were noted in 16% and minor complications in 26% of surgically managed patients; operative mortality was 4%. The presence of microscopic lymph node metastases best predicted those who would later develop T and/or N failure and distant metastases. Second primary tumors occurred in 26% and the leading cause of death was tumor.

The major goal in the treatment of carcinoma of the supraglottic larynx is control of the primary tumor and regional lymph nodes with preservation of voice. Radiation alone with surgical salvage of radiation failures [1–5] and surgery with ipsilateral neck dissection and adjuvant pre- or postoperative radiation [6–9] are the two major approaches that have been used in the treatment of carcinoma of the supraglottic larynx. In our institution, conservation surgery in conjunction with ipsilateral neck dissection and low dose preoperative radiation has been used routinely for 15 years. This approach has yielded high rates of voice preservation and control of the primary tumor, but major problems still exist in the control of lymphatic metastases. The purposes of this report are to document treatment results, complications, and patterns of failure after low dose preoperative radiation and conservation surgery; to determine which clinical characteristics of supraglottic cancer best predict relapse; and to record second primary tumors and cause of death.

Subjects and Methods

From 1964 to 1974, 160 patients with carcinoma of the supraglottic larynx were referred to the Division of Radiation Oncology, Mallinckrodt Institute of Radiology, Washington University School of Medicine. There were 132 male and 28 female patients, 147 white and 13 black. Of the 160 patients, 139 were private patients; five were ward; the other 16 came from Veterans and City Hospitals. Age range was 34–83 years (mean, 58).

Treatment for the majority (74%) consisted of low dose preoperative irradiation and conservation surgery. Subtotal supraglottic laryngectomy was the most common operation used. It was selected for patients whose lesions were centrally located without spread beyond the margins of the supraglottic larynx. Intraoperative conversion to total laryngectomy was necessary in some because there was invasion of thyroid cartilage or inferior spread, usually at the anterior commissure with involvement of true vocal cords. Extended subtotal supraglottic laryngectomy was done for lesions which extended superiorly to involve the valleculae and base of tongue. Partial laryngopharyngectomy was done for marginal lesions which involved the free margin of the epiglottis, aryepiglottic fold, and arytenoid with or without slight involvement of the medial wall of the pyriform sinus. Among the 140 surgically managed patients, 125 had ipsilateral and 10 had bilateral neck dissection; only five patients did not have neck dissection. There were four patients in the radiation-alone group who had palliative neck dissection; in these patients the primary lesion or neck nodes proved unresectable. These four patients were not included in the prognostic analysis of radical neck specimens because gross tumor was left behind in either the neck or the primary site. Hence, these patients differed from those who underwent radical neck dissection with removal of all disease and weren't analyzed with the latter patients because of the higher risk of tumor recurrence.

Low dose preoperative radiation was given to 129 patients at the rate of 200 rad per day and 1,000 rad per week; 11 surgically treated patients did not receive preoperative radiation. Radiation portals encompassed the larynx and neck and were unilateral for 76 (59%) patients with delivery of about 3,750 rad to depth of electronic build-up and 3,000 rad to the midplane of the neck. The remaining 53 patients were treated with opposed portals. Preoperative radiation doses were 200–5,000 rad with delivery of 3,000 rad ± 500 rad to 88 (68%) patients; 26 patients received less than 2,500 rad; 15 received more than 3,999 rad. A few patients received postoperative radiation and a few had surgery only, without adjuvant radiation. Twenty patients received radiation alone because they were poor operative risks, had fixed unresectable lymph nodes, unresectable primary tumor, or refused surgery. The radiation doses for these patients were 800–8,400 rad; seven received palliative doses less than 5,000 rad. Treatment for all patients is summarized in table 1.

Hospital charts, otolaryngology office notes, and radiation oncology treatment records were retrospectively reviewed to determine staging, results of treatment, and complications. Using diagrams and direct laryngoscopy reports, each lesion was clinically staged according to the criteria proposed by the American Joint Committee in 1977 [10]. Lymph nodes were examined pathologically for the presence of microscopic metastases in clinically positive and negative necks. Endpoints for this study included local control of the primary tumor and regional nodes, actuarial survival, sites of failure, distant metastases, voice preservation, complications, cause of death, and second primaries. Primary and neck failures were recorded

Received May 25, 1978; accepted after revision October 23, 1978.

[1] Division of Radiation Oncology, Mallinckrodt Institute of Radiology, Washington University School of Medicine, 510 South Kingshighway, St. Louis, Missouri 63110. Address reprint requests to J. E. Marks.

[2] Department of Otolaryngology, Washington University School of Medicine, St. Louis, Missouri 63110.

0361-803X/79/1322-0255 $0.00

AJR 132:255–260, February 1979

© 1979 American Roentgen Ray Society

TABLE 1

Treatment for patients

Treatment	No. Patients
Subtotal supraglottic laryngectomy:	
Preoperative irradiation	92
Postoperative irradiation	1
No irradiation	7
Subtotal	100 (89; 7)*
Partial laryngopharyngectomy:	
Preoperative irradiation	11 (11)
Extended subtotal supraglottic laryngectomy:	
Preoperative irradiation	7
Postoperative irradiation	1
Subtotal	8 (8)
Total laryngectomy:	
Preoperative irradiation	19
No irradiation	2
Subtotal	21 (17; 3)
Radiation alone	20 (4)
Total	160

* The first number in parentheses is patients who had an ipsilateral neck dissection and the second is the number of patients who had bilateral neck dissection.

whenever tumor was documented in these sites by physical examination or biopsy. In seven patients the status of the lymph nodes and primary tumor could not be determined during the follow-up period; these patients were enumerated separately and not classified as local control or failure. Distant metastases to lungs, bone, liver, and brain were documented by radiography and radionuclide scanning. Voice was categorized as lost for patients who died as the result of the operation, those who had persistent or recurrent primary tumor, and those who underwent conservation surgery but subsequently required tracheostomy for edema, bilaterally fixated true vocal cords, or cartilage necrosis. Using the method of Cutler and Ederer [11], actuarial survival was calculated from the initial date of treatment, usually the first day of radiation since workup and staging were complete by that time. Patients who died within 60 days of surgery were classified as operative deaths. All patients were followed until death or for a minimum of 3 years from the date of diagnosis; eight were lost to follow-up and were categorized as dead for the analysis of absolute survival. No patients were excluded in the analysis of results.

Results

Staging (table 2)

Of the primary tumors, about 75% were compartmentalized or confined to the larynx (T1–T3) while about 25% were noncompartmentalized with spread beyond the confines of the larynx (T4). Careful categorization showed that 67 tumors (42%) were centrally located involving epiglottis and/or false vocal cords; 62 (39%) were marginal involving free margin of epiglottis, aryepiglottic fold, or arytenoid; 28 (17%) involved valleculae or base of tongue; and 3 (2%) penetrated the soft tissues of the neck. Eleven patients (7%) required tracheostomy for airway obstruction. Type of treatment correlated with T stage: subtotal supraglottic laryngectomy was done for 87% of patients with T1–T2 lesions, while other operations or radiation alone were used to treat 65% of patients with T3–T4 lesions. Lymph nodes were palpable in 39% of all patients. Nodes were bilateral in 15 patients (9%) and fixed in 11 (7%). Palpable lymph nodes were more common with advancing T stage and varied according to the location and invasive characteristics of the primary tumor; nodes were palpated in 67% of penetrating, 50% of valleculae/base of tongue, 48% of marginal, and 24% of central tumors.

Control of Primary Tumor and Regional Nodes (table 2)

Control of tumor and nodes was significantly better for patients without (N0) than patients with (N+) palpable nodes ($\chi^2 = 25.50$, $P < 0.001$). Control of tumor and nodes did not differ significantly for patients with different size tumors (T1–T4) ($\chi^2 = 1.5$, not significant) or patients with palpable nodes in various degrees of advancement (N1–N3) ($\chi^2 = 1.14$, not significant). Control of primary tumor and nodes was less for valleculae/base of tongue lesions, but did not vary for other anatomic locations; T and N control was achieved for 76% of central tumors, 74% of marginal tumors, 64% of valleculae/base of tongue tumors, and 100% of penetrating tumors. Control of primary tumor and nodes did not vary significantly for surgically treated patients, but was less for those who received radiation only; T and N control was achieved for 88% of extended subtotal supraglottic laryngectomy patients, 73% of subtotal supraglottic laryngectomy patients, 73% of partial laryngopharyngectomy patients, 67% of total laryngectomy patients, and 55% of radiation-alone patients. No primary tumor was found in the specimen of 22 (17%) of the 129 patients who received preoperative radiation; 14 of these had control of their primary tumor and nodes. Five patients had positive margins and only one had T and N control.

Survival

Five year relapse-free and actuarial survival for all patients was 71% and 45%, respectively (fig. 1). After 3 years minimum follow-up, 90 patients were alive, 8 were lost, and 62 dead, for an absolute 3 year survival of 56%; after 5 years minimum follow-up, 53 patients were alive, 7 were lost, 69 were dead, and 31 were not at risk for a 5 year absolute survival of 41%. Survival, like control of the primary tumor and lymph nodes, correlated with compartmentalization of the primary tumor (T1, T2, T3, vs. T4), the presence or absence of palpable lymph nodes (N+ vs. N0), the location and invasive characteristics of the primary tumor, and type of treatment. Three year actuarial survival was 46%, 69%, and 63% for compartmentalized T1, T2, and T3 tumors, respectively, and it was 43% for noncompartmentalized T4 tumors. It was 68% for patients without palpable nodes (N0) and 48% for those with palpable nodes (N+); it was 70% for central, 67% for penetrating, 53% for marginal, and 46% for valleculae/base of tongue lesions. Actuarial survival (3 year) was 66% for subtotal supraglottic laryngectomy and extended subtotal supraglottic laryngectomy, 70% for partial laryngopharyngectomy, 43% for total laryngectomy, and 30% for radiation-alone patients.

TABLE 2

Control of Primary Tumor and Lymph Nodes by Stage Before Surgical Salvage

	T1	T2	T3	T4	Total
N0	9/11	40/46 [1]	17/21	15/20	81/98 (83)
N1	0/2	5/12 [1]	5/8	5/7	15/29 (52)
N2*	. . .	3/5	0/1	3/3	6/9 (67)
N3*	. . .	5/8 [2]	3/5 [1]	3/11 [2]	11/24 (46)
Total	9/13 (69)	53/71 (75)	25/35 (71)	26/41 (63)	113/160 (71)

Note.—After surgical salvage of three T and six N failures, ultimate rate of control of tumor and nodes was 122/160 (76%). Data reported as number of patients with control/total patients in group. Numbers in parentheses are percentages. Numbers in brackets are patients for whom status of primary tumor and lymph nodes was unknown during follow-up period.

* Subcategories N2a, N2b, N3a, and N3b as defined by American Joint Committee [1] were grouped together as N2 and N3.

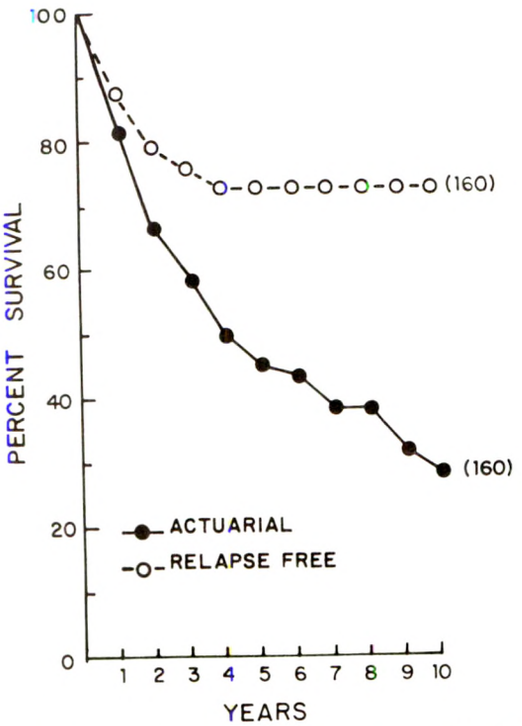


Fig. 1.—Relapse-free and actuarial survival for 160 patients with carcinoma of supraglottic larynx. Patients who were lost or died of causes other than cancer were withdrawn alive for relapse-free curve; this curve therefore depicts only deaths from cancer.

Interval from End of Treatment to Relapse (table 3)

Of primary and neck recurrences, 85% occurred within 2 years. The interval from treatment until the appearance of distant metastases was slightly longer than the interval from treatment until T and/or N recurrence.

Site of Failure (fig. 2)

The major site of failure for surgically treated patients was the neck with involvement of the ipsilateral neck in 7, both necks in 8, and the contralateral neck in 14 patients; there was one stomal recurrence which was classified as a neck failure; altogether 30 (21%) of surgically treated patients experienced a neck failure. Failure at the primary site occurred in 12 (9%) and distant metastases in 29 (14%) of surgically treated patients. Site of failure for radiation-alone patients was analyzed separately, since the distribution of TNM failures usually differs from the distribution after surgery; of the 20 patients who received radiation alone, six (30%) had either persistent or recurrent tumor at the primary site, three (15%) had a neck recurrence, and two (10%) developed distant metastases.

Surgical Salvage

Of 40 T and/or N failures, nine (23%) were salvaged by additional surgery: six patients had neck dissection and three had completion laryngectomy with ultimate control of nodal and primary disease. One patient who underwent completion laryngectomy had cancer in the resected margins and received high dose postoperative radiation which may have contributed to ultimate control of the tumor.

Voice Preservation (table 4)

Voice preservation was excellent for patients subjected to conservation surgery, worse for patients who received radiation alone, and absent for patients who underwent total laryngectomy; altogether voice was preserved in 71% of all patients. Voice loss was caused most often by advanced, persistent, or recurrent tumor and less often by treatment complications that required tracheostomy.

Complications

Of the 140 patients who were treated surgically, 23 (16%) developed major complications, five of which resulted in death within 60 days after operation. Deaths were due to myocardial infarction in three and pneumonia in two patients. The most common major complication was pharyngocutaneous fistula which occurred in 12 patients; airway obstruction occurred in three patients and carotid rupture, stroke, and tracheoesophageal fistula in three others.

Minor complications occurred in 36 (26%) of the patients treated surgically. Aspiration due to glottic incompetence was the most common minor complication (11 patients). Treatment of aspiration required feeding gastrostomy or Teflon injection of vocal cords to improve glottic closure. Vocal cord paralysis occurred in seven patients, four of whom had bilateral and three of whom had unilateral paralysis. The other complications con-

TABLE 3

Interval from End of Treatment to Development of Primary and/or Neck Recurrence and Distant Metastases

Type of Relapse	No.	Interval in Months							
		0	0–6	6–12	12–18	18–24	24–30	30–36	>36
T and/or N	40	3	10	12 (63)	5	4 (85)	2	1 (93)	3
M	22	2	5	5 (55)	4	0 (73)	1	2 (86)	3

Note.—Numbers in parentheses are percentages of patients who developed relapse before designated interval. Data on 51 patients.

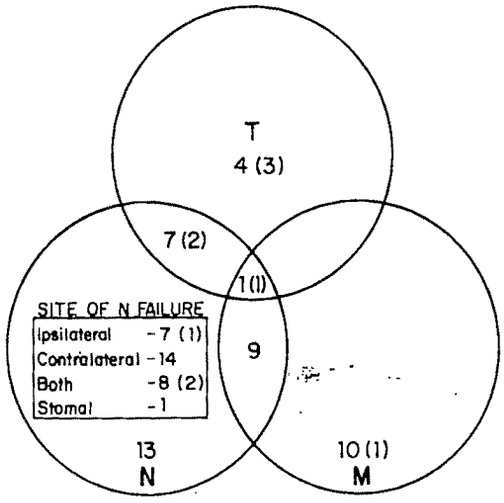


Fig. 2.—Distribution of 51 TNM failures for 160 patients with carcinoma of supraglottic larynx before surgical salvage of nine failures. Numbers in parentheses are patients who failed after radiation alone.

TABLE 4

Relation Between Type of Treatment and Voice Preservation

Treatment	No.	Voice Loss		Voice Preserved
		Tumor	Effects of Treatment*	
Subtotal supraglottic laryngectomy	100	9	8	83 (83)
Extended subtotal supraglottic laryngectomy ..	8	0	1	7 (88)
Partial laryngopharyngectomy	11	1	0	10 (91)
Total laryngectomy	21	21†	0	0
Radiation alone	20	6	0	14 (70)
Total				114 (71)

Note.—Numbers in parentheses are percentages with voice preservation for particular treatment category. Minimum follow-up is 3 years. Data on 160 patients.

* Voice loss due to effects of treatment include: operative deaths (three) plus tracheostomy for edema (three), bilateral true vocal cord paralysis (two), and cartilage necrosis (one).

† Two T failures occurred in the pharynx of patients who had total laryngectomy and two operative deaths resulted.

sisted of wound infection in six patients, dysphagia in four, flap necrosis in four, supraglottic stenosis in two, esophageal stenosis in one, and hypoglossal nerve palsy in one. There were no complications among the 20 patients treated by radiation alone.

Second Primary Tumors

Among the total population of patients with supraglottic cancer, 41 second primary tumors were diagnosed (26%); of these second tumors, 12 were diagnosed before the diagnosis of laryngeal cancer, four at the same time, and 25 after. The median time from diagnosis of a nonlaryngeal to diagnosis of a laryngeal tumor was 5 years; from diagnosis of a laryngeal to a nonlaryngeal tumor was 4 years. Second tumors originated in other head and neck sites in 14 patients, lung in 14, skin in 7, and other sites (such as esophagus, breast, and colon) in 6. Three primary tumors were noted for 5 patients. The original primary tumor and regional lymphatic metastases were controlled and distant metastases absent in 35 of the 41 patients who had more than one primary tumor.

Predictors of TNM Relapse (table 5)

Microscopic lymph node metastases predicted best those patients who would later develop TNM relapse. For patients with microscopic lymph node metastases, the rates of primary and/or nodal failure and distant metastases were significantly higher than rates for patients without microscopic lymphatic metastases. The rates of TNM relapse did not vary significantly by size of primary tumor (T1–T4), by nodal status (N1–N3), by location and invasive characteristics of the primary tumor, or by age or sex.

Cause of Death

Among the 94 patients known to be dead at the time of analysis, 37 (39%) of deaths could be attributed to tumor, 19 (20%) to intercurrent disease, 19 (20%) to unknown causes, 12 (13%) to second cancers, and 7 (8%) to complications of treatment. Within 60 days of operation, five of 140 patients who underwent surgery died, an operative mortality of 4%.

Discussion

Patients with carcinoma of the supraglottic larynx who have been treated by low dose preoperative radiation and surgery have a relatively favorable prognosis. The primary tumor and lymph nodes were controlled and voice preserved in 71%. Those patients who remain tumor-free live more than 3 years and are subject to other factors that result in mortality such as age, cardiovascular disease, and second primary tumors (fig. 1). Second primary tumors occurred in 26% of our patients,

TABLE 5

Relation Between Palpable and Microscopic Lymph Node Metastases and Primary and/or Nodal Failures, Distant Metastases and Actuarial Survival

Lymph Node Metastases Palpable/Microscopic	No.	T and/or N Failure		Distant Metastases		3-Year Actuarial Survival
		No.	%	No.	%	(%)
Yes/Positive	32	17	74	12	84	38
No/positive	18	6		4		49
Yes/negative	20	3		1		66
No/negative	62	5		2		81

Note.—Data on 132 patients. Excluded from analysis were 20 patients who received radiation alone, five without neck dissection and three whose pathology reports were not located. Microscopic positive vs. microscopic negative, TNM relapse vs. no relapse. $\chi^2 = 55.56$, $P < 0.001$.

an incidence also reported by others [2, 3]. The incidence of second primary cancers after conservation surgery for supraglottic cancers is greater than after laryngectomy for transglottic cancers [3] because patients who have had laryngectomy are generally forced to stop smoking and risk of second aerodigestive cancers decreases with time after cessation of smoking [12]. Those patients who relapse usually do so within 2 years; tumor-related deaths resulted for about 75% of those with primary and/or nodal recurrence and all of those with distant metastases.

Several facts about the selection of treatment for patients with carcinoma of the supraglottic larynx are notable. Only a few received palliative treatment because distant metastases were present, the primary cancer or regional nodes were unresectable, or the patient's medical status was too poor to withstand the insult of surgery. The majority of patients had tumors and nodes that were resectable and most of these had primary tumors amenable to conservation surgery. Overall, about 75% of the patients in our population were subjected to conservation surgery which supports the findings of dye injection [13] and whole-organ serial section studies [14, 15], showing that most supraglottic cancers are confined to the supraglottic compartment and removable with preservation of the anatomy responsible for phonation. A few patients in our series had tumors more extensive than originally expected by preoperative assessment and these required total laryngectomy. Other patients had total laryngectomy because patient reliability was judged too poor for adequate follow-up to deal with potential complications. In contrast to others who fear complications after conservation surgery and more often do total laryngectomy with loss of voice [7], we feel that mortality and complication rates are low enough after conservation surgery to justify the increased rates of voice preservation that result.

The current staging system [10] has limited prognostic value whether the treatment be radiation alone followed by surgical salvage or preoperative radiation and conservation surgery. In the case of radiation alone where size of tumor is important for local control [1], the two-dimensional size of the lesion is not recorded in the current staging system and the third dimension of the tumor, its depth of penetration, is difficult to assess. Tumor size does not always correlate well with T stage in the current staging system; for instance, a small diameter tumor at the junction of the false vocal cord and epiglottis and a larger bulky tumor involving the same sites are both classified as T2; radiocurability of the small lesion is undoubtedly greater than for the larger one and yet both are given the same T stage. In the case of surgical management of cancer of the supraglottic larynx, it is compartmentalization and not size that predicts ability to control the tumor; the local control rates are similar for T1–T3 lesions since these are confined to the supraglottic compartment and removable. It is only when the tumor spreads beyond the confines of the supraglottic compartment or becomes T4 that a decrease in local control results [9]. In our patients the highest rate of local failure occurred in valleculae/base of tongue lesions which had escaped the anatomic barriers of the supraglottic compartment and were, therefore, more difficult to remove with adequate margins. Others have also noted the lack of correlation between two-dimensional T staging in the supraglottic larynx and prognosis in surgically treated patients [9, 16]. Norris et al. [16], in a whole-organ serial section study of a group of patients who underwent laryngectomy, were unable to correlate T stage and involvement of the preepiglottic space with survival; however, they correlated depth of tumor penetration with survival. Therefore, it might be recommended that a different staging system be developed that provides a two-dimensional surface measurement of the lesion and assesses its compartmentalization.

In this series of patients treated predominantly by low dose preoperative radiation and conservation surgery, local control of the primary tumor and lymph nodes and voice preservation were achieved in 71% of all patients which compares favorably with results achieved by radiation alone followed by surgical salvage of radiation failures [1–5]. A number of radiation series report ultimate local control rates of 46%–84% and voice preservation rates of 43%–68% [1–5] (table 6). After radiation alone for carcinoma of the supraglottic larynx, roughly half of the patients develop local failure and half of these failures are then salvaged by laryngectomy which gives the same local control rate reported in our series. However, the rate of voice preservation in most radiation-alone series is less than that reported here for conservation surgery since surgical salvage is generally achieved by total laryngectomy which results in loss of voice [17, 18]. Consequently, only about 50% of the patients after radiation alone, compared with about 75% after conservation surgery, are left with a functioning larynx.

The major site of failure after low dose preoperative radiation and conservation surgery for carcinoma of the supraglottic larynx is the neck. Study of the distribution of failures within the neck shows that about 25% occur in the ipsilateral neck, about 25% in both sides of the neck, and about 50% in the contralateral neck. The

TABLE 6
Ultimate Local Failure and Voice Preservation after Radiation Alone

Reference	No.	Radiation Failures	Salvage	Ultimate Failure	Voice Preservation
[1]	115	37 (32)	19	18 (16)	78 (68)
[4]	163	79 (48)	25	54 (33)	84 (52)
[3]	52	28 (54)	16	12 (23)	25 (48)
[2]	92	48 (52)	?	?	44 (48)
[5]	184	105 (57)	6–10, few N	99 (54)	79 (43)

Note.—Numbers in parentheses are percentages of total patients.

appearance of tumor in the clinically negative contralateral neck in 75% of those who developed neck failure demonstrates that low dose preoperative radiation is inadequate to sterilize microscopic disease in lymph nodes.

The presence of microscopic cancer in lymph nodes best predicted those patients who would develop primary and/or nodal recurrence and distant metastases. As expected, these patients also had significantly lower survival rates than those without recurrent tumor or distant metastases. It would therefore seem logical to deliver more aggressive local treatment to patients with microscopic lymph node metastases, since they are the ones more likely to develop local recurrence. Higher doses of radiation than used in our series are probably necessary, since tumor at the primary site and in lymph nodes was eliminated in only a small percentage of patients and neck recurrences subsequently developed in a significant proportion of patients. We were unable to compare patients treated by low dose preoperative radiation with those treated by 5,000 rad or more since there were too few of the latter. The impact of low dose preoperative radiation on local recurrence and survival is uncertain since objective comparisons with no radiation and higher doses of pre- and post operative radiation are lacking. Post operative radiation in doses of 5,000–6,000 rad has been compared to surgery alone and shown to effectively reduce primary and neck recurrences [1].

Selection of primary treatment can probably be based on the morphology and size of the supraglottic tumor. Radiation alone is recommended for small exophytic lesions of the supraglottis since rates of local control and voice preservation are high and surgical complications nonexistent [1, 19, 20]. Conservation surgery, when applicable, is recommended for ulcerating lesions and those with significant bulk since rates of local control and voice preservation are higher than those achieved by radiation alone followed by surgical salvage.

ACKNOWLEDGMENTS

We thank Mary Ann Hederman who obtained follow-up for patients, Sherry Breaux and Dr. Jeannette Lee, who assisted with the statistical analysis, Gregory Merrick and Helen Pares who did the illustrations, Barbara Wollberg who typed the manuscript, and Dr. Carlos A. Perez for his helpful critique.

REFERENCES

1. Fletcher GH, Jesse RH, Lindberg RD, Koons CR: The place of radiotherapy in the management of squamous cell carcinoma of the supraglottic larynx. *AJR* 108:19–26, 1970
2. Fu KK, Eisenberg L, Dedo HH, Phillips TL: Results of integrated management of supraglottic carcinoma. *Cancer* 40:2814–2881, 1977
3. Goffinet DR, Eltringham JR, Glatstein E, Bagshaw MA: Carcinoma of the larynx: results of radiation therapy in 213 patients. *AJR* 117:553–564, 1973
4. Hendrickson FR, Kline TC, Hibbs GG: Primary squamous cell carcinoma of the larynx. *Laryngoscope* 85:1650–1666, 1975
5. Wang CC: Megavoltage radiation therapy for supraglottic carcinoma. *Radiology* 109:183–186, 1973
6. Bocca E: Supraglottic cancer. *Laryngoscope* 85:1318–1326, 1975
7. Coates HL, DeSanto LW, Devine KD, Elveback LR: Carcinoma of the supraglottic larynx. *Arch Otolaryngol* 102:686–689, 1976
8. Ogura JH, Sessions DG, Spector GJ: Conservation surgery for epidermoid carcinoma of the supraglottic larynx. *Laryngoscope* 85:1808–1815, 1975
9. Shah JP, Tollefsen HR: Epidermoid carcinoma of the supraglottic larynx. *Am J Surg* 128:494–499, 1974
10. *Manual for Staging of Cancer, 1977*. Chicago, American Joint Committee, 1977
11. Cutler SJ, Ederer F: Maximum utilization of the life table method in analyzing survival. *J Chronic Dis* 8:699–712, 1958
12. Wynder EL, Covey LS, Mabuchi K, Muskinski MH: Environmental factors in cancer of the larynx—a second look. *Cancer* 38:1591–1601, 1976
13. Pressman JJ, Simon MB, Monell C: Anatomical studies related to the dissemination of cancer of the larynx. *Trans Am Acad Ophthalmol Otolaryngol* 64:628–638, 1960
14. Kirchner JA, Som ML: Clinical and histological observations on supraglottic cancer. *Ann Otolaryngol* 80:638–645, 1971
15. Tucker GF, Smith HR: A histological demonstration of the development of laryngeal connective tissue compartments. *Trans Am Acad Ophthalmol Otolaryngol* 66:308–318, 1962
16. Norris CH, Kuo BF, Tucker GF, Pitser WF: A correlation of clinical staging, pathological findings and five year end results in surgically treated cancer of the larynx. *Ann Otolaryngol* 79:1033–1048, 1970
17. DeSanto LQ, Lillie JG, Devine KD: Surgical salvage after radiation for laryngeal cancer. *Laryngoscope* 86:649–657, 1976
18. Skolnik EM, Martin L, Yee KF, Wheatley MA: Radiation failures in cancer of the larynx. *Ann Otolaryngol* 84:804–811, 1975
19. Ghossein A, Bataini JP, Ennuyer A, Stacey P, Kirshnaswamy V: Local control and site of failure in radically irradiated supraglottic cancer. *Radiology* 112:187–192, 1974
20. Shukovsky LJ: Dose, time, volume relationships in squamous cell carcinoma of the supraglottic larynx. *AJR* 108:27–29, 1970

Dose Considerations in Total Skin Electron Irradiation for Mycosis Fungoides

THEODORE C. M. LO,[1] FERDINAND A. SALZMAN,[1] AND KENNETH A. WRIGHT[2]

Two hundred patients with generalized cutaneous mycosis fungoides were treated with total skin electron irradiation (TSEI) in the Lahey Clinic Radiotherapy Department–MIT High Voltage Research Laboratory between 1964 and 1973. None of the patients had any clinical evidence of extracutaneous disease at presentation. The 3-year absolute survival rate was 54% (107 patients). Analysis of these 107 long-term survivors evaluated the relation between incidence of generalized cutaneous recurrence and total treatment dose given during the initial course of TSEI.

Results indicated that in patients with erythroderma, the need for a second course of TSEI was inversely related to the total dose given during the first course. However, the curve seemed to flatten at about 1,500 cGy (rad). In plaque disease, the percentage of patients who received repeated courses of TSEI seemed to be relatively constant independent of total dose given during the initial course (65%–80%). In patients with tumor lesions, the incidence of generalized cutaneous recurrence was directly proportional to total dose.

The optimal dose of TSEI for patients with mycosis fungoides may vary depending on types of skin lesions. Total dose during the initial course of TSEI should be kept relatively conservative, particularly in patients with generalized plaques where relapse rate is high allowing reserve of normal tissue tolerance for further TSEI when indicated.

Total skin electron irradiation (TSEI) remains one of the most effective modes of treatment for generalized mycosis fungoides confined to the skin today [1–6]. Although cure rates are still low, its palliative value is definitely irrefutable [1, 2, 5, 6]. However, once disease has progressed beyond the cutaneous system, prognosis becomes ominous, and survival is measured in terms of months [4]. Unfortunately, systemic chemotherapy, either single agent or combination drugs, has not been found significantly effective in control of the disease to date [4]. Thus, meaningful assessment of the value of total skin electron irradiation would pertain only to the group of patients with clinical disease confined to the skin who survived for a substantial length of time. A study was carried out to evaluate such a group of patients with respect to local control with TSEI.

Subjects and Methods

Two hundred new patients with generalized cutaneous mycosis fungoides were treated with total skin electron irradiation (TSEI) in the Lahey Clinic Radiotherapy Department–MIT High Voltage Research Laboratory between 1964 and 1973. The constant potential electrostatic generator used was of the Van de Graaff type with the capacity of producing electrons with energies up to 3.5 MeV. We believe this energy is adequate for lesions not more than 1 cm thick. Both the physical aspects and the dosimetry of the apparatus have been described in detail [7].

The total treatment dose reported throughout this paper is the specified maximum entry dose computed with the formula

$$SMD = \Sigma^{c}\left(\frac{d \times f}{2}\right)_{c}$$

where SMD is the total specified maximum entry dose, c is the number of cycles per treatment course, d is the daily entry dose per field, f is the number of fields per cycle, and the subscript designates the technique used. The advantages of the use of the SMD concept have been discussed [5]. It standardizes the method of reporting doses among various institutions when different techniques are employed, and it guides the therapist to limit total dose within acute and chronic normal tissue tolerance. Obviously, during each treatment session all fields used must be complementary to one another.

All 200 patients presented with generalized multiple or confluent skin lesions covering at least 50% of the total skin area, and none had clinical evidence of nodal or systemic disease on the first day of TSEI. Pathology was reviewed and confirmed by our pathologists.

Before January 1972, the six-field cycle technique was used, and since then, an eight-field cycle technique has been used. The details of these techniques have been discussed [5]. All patients were treated on a 5 day per week basis.

Results

Table 1 shows the absolute overall survival at 3 years after initiation of TSEI for all 200 patients. Patients were categorized into three subgroups by primary lesion type as presented on the first day of TSEI. Of the 200 patients, 107 (54%) survived for 3 years or longer; 32 patients had erythroderma, 56 patients had plaque lesions, and 19 patients had tumors. The poor prognosis of patients with tumors was commonly due to rapid onset of metastatic visceral disease [5].

Among all 200 patients, 81 received only a single course of TSEI without further electron irradiation, and 35 of them survived for 3 years or longer. These patients are listed by primary lesion type shown in table 1.

Table 2 shows the current status of this group of 35 patients. Fourteen patients were considered "cured." All of these patients have now been studied for at least 5 years (table 3) and none of them needed further treatment since the initial course of TSEI. As expected, the highest cure rate was demonstrated in the group of

Received July 17, 1978; accepted after revision October 30, 1978.
Presented at the annual meeting of the American Radium Society, New Orleans, April 1978.
[1] Department of Radiotherapy, Lahey Clinic Foundation, Boston, Massachusetts 02215. Address reprint requests to T. C. M. Lo.
[2] High Voltage Research Laboratory, Massachusetts Institute of Technology, Cambridge, Massachusetts 02139.

AJR 132:261–263, February 1979
© 1979 American Roentgen Ray Society
0361–803X/79/1322–0261 $0.00

TABLE 1
Survival

	Erythroderma	Plaque	Tumor	Total
Total patients	57	89	54	200
Overall 3-year survival	32 (56)	56 (63)	19 (35)	107 (54)
One course of TSEI:				
Patients studied	36 (63)	25 (28)	20 (37)	81 (41)
Survived 3 years	19 (53)	13 (52)	3 (15)	35 (43)

Note.—Numbers in parentheses are percentages.

TABLE 2
Status of 3-Year Survivors Who Had Only One Course of TSEI

	Erythro-derma	Plaque	Tumor
Cured	11*	2	1
Living with disease	6†	9	2
Died from disease	2	2	0
Total	19	13	3

* One patient died of intercurrent disease at 5 years (NED).
† One patient is now NED after a course of chlorambucil.

TABLE 3
"Cure" after One Course of TSEI

Case	Dose* (rad)	Tech-nique (no. fields)	Survival (years)
Erythroderma:			
1	900	6	12
2	1,200	6	6
3	1,050	6	5
4	1,300	6	7
5	1,125	6	5
6	1,125	6	5
7	3,000	6	6
8	1,800	8	5
9	1,800	8	5
10	900	8	5
11	1,200	8	5
Plaque:			
12	900	6	11
13	1,000	6	5
Tumor:			
14	1,200	6	12

* Specified maximum entry dose.

patients with erythroderma. Of these 14 patients, 13 received a total dose of less than 2,000 rad.

Unfortunately, once cutaneous disease recurred after the initial course of TSEI, the chance of "cure" appeared to be extremely remote. Table 4 shows the outcome of the 72 3-year survivors who required further electron irradiation, either local spot treatment or TSEI or both, after the initial course of TSEI; only two patients could be considered "cured." One patient with tumor died from an automobile accident 8 years after two courses of TSEI and one course of local "spot" irradiation, and another patient with tumor survived 5 years free of disease after one course of TSEI and seven courses of local spot treatments.

We were interested in the relation between the treatment dose during the first course of TSEI and subsequent generalized cutaneous recurrence when a second course of TSEI was required among this group of 107 long-term survivors. In patients with erythroderma, the need for a second course of TSEI was inversely proportional to the total dose given during the initial course (table 5). Clinically this implies that for this type of lesion, high-dose irradiation would perhaps be indicated if tolerance allowed.

However, for plaque disease, the percentage of patients who received repeated courses of TSEI seemed to be relatively constant, ranging from 65% to 80% regardless of total dose given during the first course of TSEI (table 5), suggesting a universally high relapse rate for this particular type of lesion even with an aggressive initial approach. In patients with tumors the incidence of generalized cutaneous recurrence was directly related to total dose (table 5). Unfortunately, among the six patients with tumor who received high-dose irradiation (more than 1,500 rad), only one survived longer than 3 years for this analysis. This patient received a second course of TSEI at 3 years and is now living with disease at 5 years.

TABLE 4
All 3-Year Survivors Who Had More Electron Therapy Than One Course of TSEI

	Erythro-derma	Plaque	Tumor
No	13	43	16
%	41	78	84
Spots only	1	5	4
Dead	6	15	6*
Living with disease	7	28	10†

* One patient died of intercurrent disease (NED) 8 years after last spot irradiation (had two TSEI and one spot treatment).
† One patient is NED 5 years after last spot irradiation (had one TSEI and seven spot treatments).

Discussion

Mycosis fungoides is a rare and chronic form of lymphomatous malignancy arising from the cutaneous system. The optimal treatment for this disease remains undetermined today. However, the distinct value of total skin electron irradiation, as one of the most successful means for local control of this disease, is well known.

TABLE 5

Incidence of Generalized Recurrence: All 3-Year Survivors

SMD (rad)	No. Patients	Recurrence Rate (%)
Erythroderma (N = 32):		
≤1,100	17	9 (53)
1,100–1,500	9	2 (22)
1,500–2,500	3	0
2,500–3,500	3	1 (33)
Plaque (N = 56):		
≤1,100	28	19 (68)
1,100–1,500	17	11 (65)
1,500–2,500	5	4 (80)
2,500–3,000	3	2 (67)
3,000–4,000	3	2 (67)
Tumor (N = 19):		
≤1,100	11	6 (55)
1,100–1,500	7	5 (71)
>1,500 (1,687)	1	1 (100)

Unfortunately, the prognosis becomes ominous as soon as the disease has spread beyond the cutaneous system, since response to chemotherapy has been poor [4]. Thus, we believe that meaningful assessment of the value of TSEI would pertain only to the group of long-term survivors with disease still confined to skin.

Our results are similar to those reported by others [2, 8]. In patients with generalized skin lesions, the cure rate after one single course of TSEI is less than 10%, even when higher doses were given. Apparently TSEI alone is not expected to be the curative mode of treatment for this disease. Many centers including ours have embarked on a program to give patients adjuvant topical nitrogen mustard after completion of TSEI. No significant improvement in long-term disease-free survival has been seen so far [9]. Others are also using a multidisciplinary approach with TSEI, total nodal photon irradiation, topical nitrogen mustard, and systemic chemotherapy. The results remain pending at present [8].

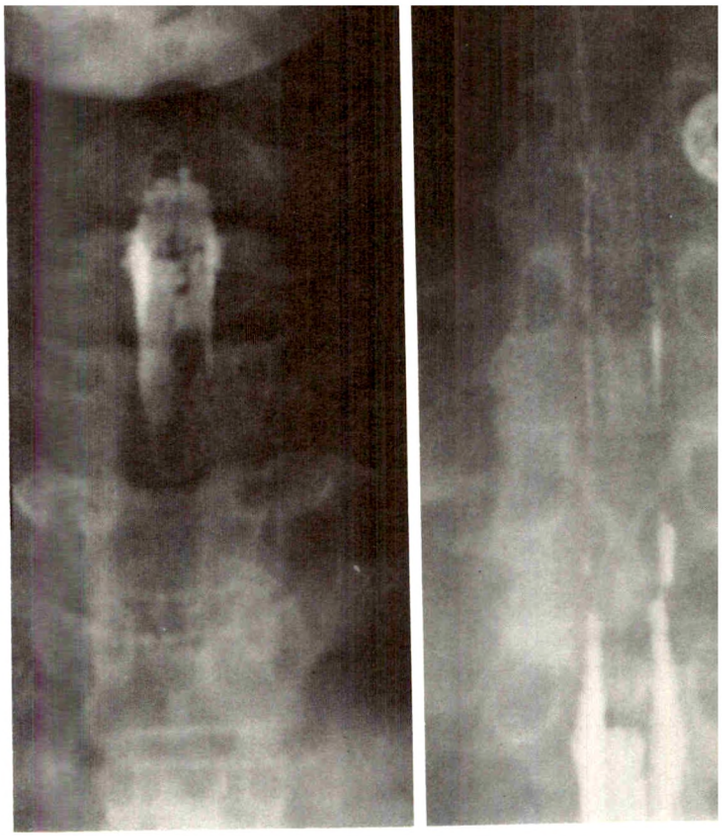
Our results suggest that in patients with erythroderma, total dose during the initial course of TSEI is inversely related to generalized recurrence rate. However, in patients with plaques or tumors, this relationship seems to be much less obvious. The Stanford group also found that while the incidence of complete regression was directly related to treatment dose during the first course of TSEI in their group of patients with erythroderma, there was an inverse relationship in their group of patients with tumor lesions [2].

We conclude that the optimal dose of TSEI for patients with mycosis fungoides may vary depending on type of skin lesions. We believe that total dose during the initial course of TSEI should be kept relatively conservative, particularly in patients with generalized plaques where relapse rate is high, allowing reserve of normal tissue tolerance for further TSEI when indicated.

REFERENCES

1. Fromer JL, Johnston DO, Salzman FA, Trump JG, Wright KA: Management of lymphoma cutis with low megavolt electron beam therapy; nine year follow-up in 200 cases. *South Med J* 54:769–776, 1961
2. Fuks ZY, Bagshaw MA, Farber EM: Prognostic signs and the management of the mycosis fungoides. *Cancer* 32: 1385–1395, 1973
3. Hare HF, Fromer JL, Trump JG, Wright KA, Anson JH: Cathode ray treatment for lymphomas involving the skin. *Arch Dermatol* 68:635–642, 1953
4. Levi JA, Wiernik PH: Management of mycosis fungoides—current status and future prospects. *Medicine* 54:73–88, 1975
5. Lo TCM, Salzman FA, Moschella SL, Tolman EL, Wright KA: Whole body surface electron irradiation in the treatment of mycosis fungoides: an evaluation of 200 patients. *Radiology*. In press, 1979
6. Smedal MI, Johnston DO, Salzman FA, Trump JG, Wright KA: Ten year experience with low megavolt electron therapy. *AJR* 88:215–228, 1962
7. Trump JG, Wright KA, Evans WE, Anson JH: High energy electrons for treatment of extensive superficial malignant lesions. *AJR* 69:623–629, 1953
8. Wallner PE, Brady LW, Vonderheid E, Van Scott EJ: Technical considerations for a program of remission induction and maintenance of mycosis fungoides utilizing total body electrons, total nodal photons, topical nitrogen mustard and systemic chemotherapy. Presented at the annual meeting of the American Society of Therapeutic Radiologists, Denver, November 1977
9. Price NM, Hoppe RT, Constantine VS, Fuks ZY, Farber EM: The treatment of mycosis fungoides: adjuvant topical mechlorethamine after electron beam therapy. *Cancer* 40:2851–2853, 1977

Diagnostic Oncology Case Studies



Treated Stage IIB Hodgkin's Disease Complicated by Late Paraplegia

In 1969, a 17-year-old black boy with Stage IIB Hodgkin's disease (mixed cellularity type) was studied. There was radiologic involvement of the mediastinum and bilateral cervical lymphadenopathy. A full staging laparotomy was negative. Subsequently he received 4,000 rad to the central axis of a "mantle" field in 53 days.

The patient began to develop progressive lower extremity weakness with muscle wasting 4 years later. A muscle biopsy indicated polymyositis, and subsequent trial of high-dose cortisone was ineffective. Nine months later the patient complained of back pain and increasing difficulty in walking upstairs, associated with hypesthesia of the feet. Neurologic examination revealed a sensory level at T2 with bilateral hyperreflexia of the knees and ankles. Plain films of the spine were normal. Myelography showed a high-grade extradural block from T2 to T9 (lead picture). Chest radiography, complete blood count, alkaline phosphatase, bone marrow examination, and liver-spleen scan were normal.

The presumptive clinical diagnosis was recurrent (intraspinal) Hodgkin's disease, occurring nearly 40 months after initial diagnosis and radiation therapy. The patient received a combination of Vincristine and irradiation of the entire thoracic cord. After 1600 rad, he became totally paraplegic. An emergency thoracic laminectomy revealed a poorly defined, friable mass in the epidural space. The histopathologic diagnosis was intraspinal lipoma (fig. 1). There was little postoperative neurologic improvement; 5 years after his first examination, the patient has developed recurrence of Hodgkin's disease in the periaortic nodes.

Discussion

Hodgkin's disease in the mediastinum usually appears as an anterior (pretracheal) mass [1]; nevertheless, opposing radiation fields are usually recommended rather than a single anterior field, because of the possibility of "silent" disease in the middle and/or posterior mediastinum (i.e., a paraspinous mass) [2]. Hodgkin's disease may also extend into the extradural space directly from involved prevertebral lymph nodes, or via the intercostal and epidural veins. This patient was treated initially with opposing fields; at the time of the extradural block 4½ years later, the thoracic paraspinous region appeared normal on chest films. Close scrutiny of the vertebral bodies, pedicles, and ribs also revealed no bony abnormality.

Radiographic involvement of the vertebral bodies or the pedicles with Hodgkin's disease is not, as with the majority of other cancers metastatic to the spinal column [3], a common antecedent or concommitant of clinical extradural involvement. However, late extradural Hodgkin's disease often will occur *in conjunction* with a recurrence of tumor elsewhere in the body. Furthermore,

This is another in a bimonthly series of case reports prepared by A. Robert Kagan and Richard J. Steckel (Southern California Permanente Medical Group, 1510 North Edgemont, Los Angeles, California 90027, and UCLA Jonsson Comprehensive Cancer Center, 924 Westwood Boulevard, Suite 650, Los Angeles, California 90024, respectively) to present and discuss contemporary problems and procedures in the identification and staging of neoplasms. Case contributed by Hussein M. Abdel-Dayem and Young S. Oh (both, Department of Radiology, State University of New York at Buffalo and Erie County Medical Center, 462 Grider Street, Buffalo, New York 14215) and Ranajit Sil (Department of Pathology, State University of New York at Buffalo and Erie County Medical Center, Buffalo, New York 14215). Address reprint requests to H. M. Abdel-Dayem.

AJR 132:265–266, February 1979
© 1979 American Roentgen Ray Society
0361–803X/79/1322–0265 $0.00

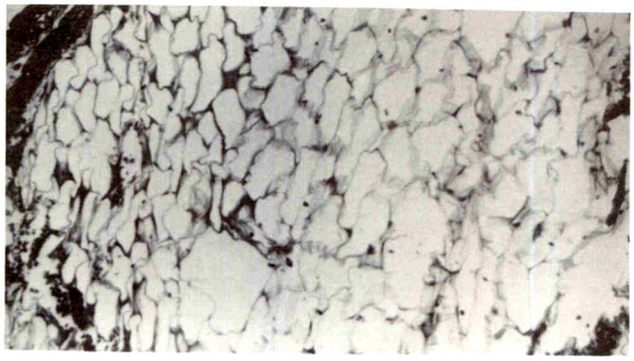


Fig. 1.—Histopathologic examination of excised extradural mass. Mature, fat-containing cells compatible with intraspinal lipoma.

intraspinal involvement as a manifestation of recurrent Hodgkin's disease is commonly accompanied or preceded by an exacerbation of systemic ("B") symptoms [4]. This patient had neither clinical evidence of tumor recurrence elsewhere nor systemic symptoms.

Furthermore, reirradiation of the spinal cord should always be approached with caution because of the risk of myelitis. Radiation myelitis, while a rare complication of treatment, may become manifest usually within 6 months to 1 year after spinal irradiation. In this patient, laminectomy to determine the etiology of the extradural block was indicated before irradiation of this suspected "solitary" recurrence (of Hodgkin's disease), especially in an area of the thoracic cord which had earlier received over 4,000 rad.

Intraspinal lipomas are indeed rare [5–8]; while the interpedicular spaces were not widened in this patient, a lipoma may erode or separate the pedicles like any other slowly growing tumor [9–12]. Meningiomas, ependymomas, and neurofibromas are more common. An extradural abscess can simulate a tumor; however, in addition to severe local pain (which this patient had) there usually is narrowing of the disc interspaces, with or without adjacent vertebral destruction. The presence of a block on the myelogram makes an anterior spinal artery thrombosis, transverse myelitis secondary to radiation [13], or other demyelinating disorder unlikely.

In a patient already treated for cancer, focal symptoms may result from recurrent tumor or as a complication of treatment, but it is important to recognize an entirely *new* condition when it occurs. In this patient the absence of "B" symptoms, the lack of evidence of late nodal or visceral recurrence, and tte negative spine and soft tissue radiographs in the area of a demonstrated myelographic block indicated a lower probability of recurrent Hodgkin's disease and should have raised the suspicion of a new neurologic disorder.

REFERENCES

1. Steckel RJ, Kagan AR: Hodgkin's disease in *Diagnosis and Staging of Cancer: A Radiologic Approach,* edited by Steckel RJ, Kagan AR, Philadelphia, Saunders, 1976, pp 1–8
2. Fayos JV: Extrapulmonary intrathoracic manifestations of Hodgkin's disease. *Radiol Clin North Am* 6:131–141, 1968
3. Segall HD: Spinal cord, in *Diagnosis and Staging of Cancer: A Radiologic Approach,* edited by Steckel RJ, Kagan AR, Philadelphia, Saunders, 1976, pp 334–342
4. Williams HM, Diamond HD, Graver LF, Parsons H: *Neurological Complications of Lymphomas and Leukemias.* Springfield, Ill., Thomas, 1959
5. Giuffre R: Intradural spinal lipomas. Review of the literature (99 cases) and report of an additional case. *Acta Neurochir* (Wien) 14:69–95, 1966
6. Van Dellan JR, Van Den Heever CM: Intraspinal lipoma. A case report. *S. Afr Med J* 50:49–50, 1976
7. Caram PC, Scarcella G, Carton CA: Intradural spinal lipomas of the spinal cord with particular emphasis on intramedullary lipomas. *J Neurosurg* 14:28–42, 1957
8. Thomas JE, Miller RH: Lipomatous tumors of the spinal cord. *Mayo Clinic Proc* 48:393–400, 1973
9. Anderson RE, Shealy CN: Cervical pedicle erosion and rootlet compression cased by a tortuous vertebral artery. *Radiology* 95:537–538, 1970
10. Fagan CJ, Swischuk LE: Dumbbell neuroblastoma or ganglioneuroma of the spinal canal. *AJR* 120:453–460, 1974
11. Halaby HM, Long PM, Chou SN, French LA: Intraspinal lipomas. *AJR* 92:1293–1297, 1964
12. Zimmerman HB, Farrell WJ: Cervical vertebral erosion caused by vertebral artery tortuosity. *AJR* 108:767–770, 1970
13. Marty R, Minckler DS: Radiation myelitis simulating tumor. *Arch Neurol* 29:352–354, 1973

Case Reports

Esophageal Obturator Airway: Radiographic Appearance

M. JOYCE PAIS[1] AND HOWARD B. SEGAL[1]

The esophageal obturator airway, developed by Don Michael et al. [1], is a simple tool to improve ventilation during cardiopulmonary resuscitation (CPR). Paramedic and other CPR support personnel can be easily trained to effectively use the esophageal obturator airway to maintain breathing and circulation until the patient can be transported to a hospital for other life support systems, such as endotracheal intubation. A laryngoscope is not needed for insertion and the danger of aspiration is reduced.

A modified device, designed by Gordon in 1970 (cited in [2]), has been used by the Los Angeles Fire Department paramedic and other CPR teams [2–5]. In May 1973 it was accepted at the National Conference on Standards for CPR in emergency cardiac care as "a recent innovation in the management of cardiac arrest patient" [5], and it has been designated one of the basic life support systems by the American Heart Association [6].

A face mask is attached to a cuffed tube that is passed blindly into the esophagus. A soft plastic obturator blocking the distal end of the tube is inflated once the cuff is passed. At the upper end of the tube (near the hypopharynx) are 3 mm holes (fig. 1). The face mask is placed tightly over the mouth and nose and ventilation using air (mouth–mouth) or oxygen (which prevents air leakage through the nose or mouth) is begun. Sealing the distal end precludes air from entering the stomach, as well as vomiting and aspiration. If the facilities and personnel are available, endotracheal intubation is instituted. Since vomiting often accompanies tube removal, it is not removed until after the endotracheal tube has been inserted.

Contraindications for using the esophageal obturator airway are a conscious patient, any patient under age 15, and those with known esophageal cancer or other esophageal lesions. Complications include unrecognized endotracheal intubation; in the conscious patient, vomiting against the inflated balloon that results in esophageal injury; traumatic laceration of the airway including the hypopharynx; vomiting after removal; and inflation of the stomach if the balloon is not adequately inflated [7].

Since the esophageal obturator airway is removed immediately after insertion of the endotracheal tube, it is usually not seen on initial radiography in the emergency room. However, if it has not been removed before initial radiography, recognition by the radiologist will avoid possible confusion.

Case Report

A 58-year-old American Indian woman had many past medical problems, including diabetes and a cerebro vascular accident sustained 1 year before admission that left her with a spastic left hemiparesis and expressive aphasia. About 1 week before admission, she was seen as an outpatient for a left lower lobe pneumonia. Later, she developed respiratory arrest, and a paramedic introduced an esophageal obturator airway while she was still at home. In the emergency room, an endotracheal tube was inserted and radiography demonstrated both the

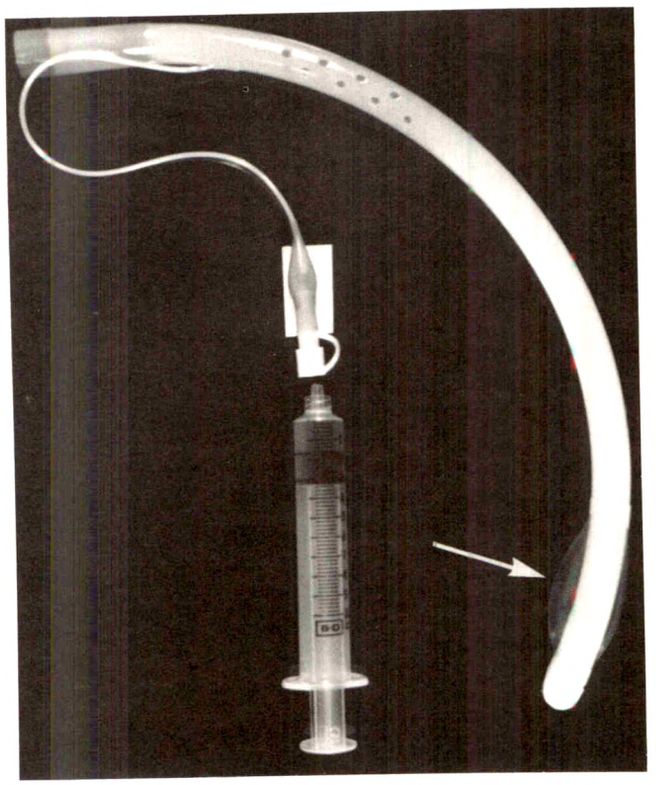


Fig. 1.—Esophageal obturator airway. Air or oxygen enters proximal end through small holes and is forced into trachea. Balloon at distal end (*arrow*) occludes esophagus to prevent vomiting.

Received September 1, 1978; accepted after revision October 17, 1978.
[1] Department of Diagnostic Radiology, Yale University School of Medicine, 333 Cedar Street, New Haven, Connecticut 06510. Address reprint requests to M. J. Pais.

© 1979 American Roentgen Ray Society

0361-803X/79/1322-0267 $0.00

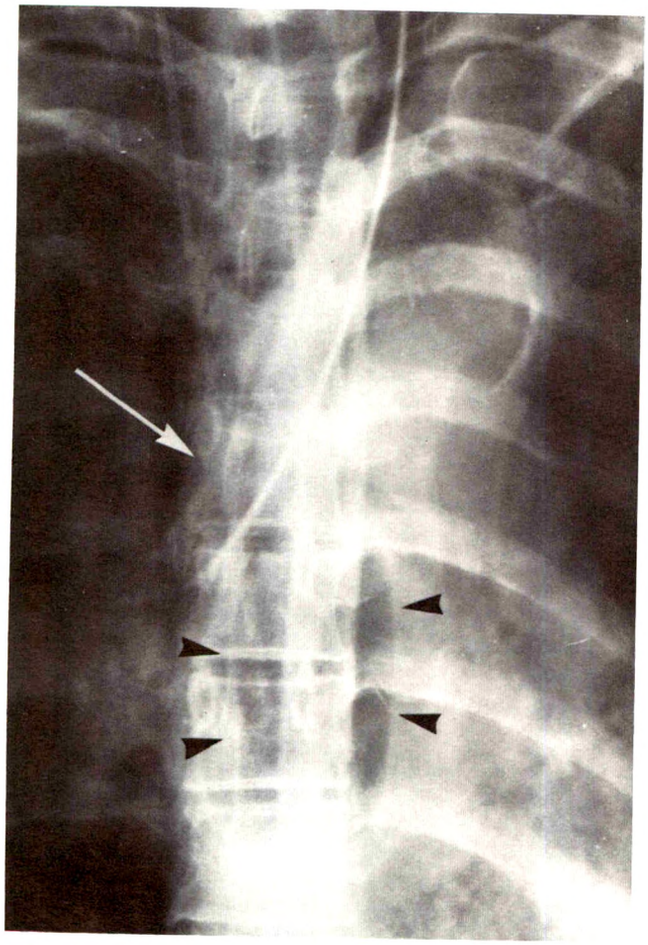


Fig. 2.—Esophageal obturator airway with inflated balloon in esophagus (*arrowheads*). Endotracheal tube is in right main stem bronchus (*arrow*).

tracheal airway in the right main stem bronchus and the esophageal obturator airway (fig. 2). The tracheal tube was relocated and the esophageal obturator airway removed. Blood gases were satisfactory. However, because of her numerous systemic problems, the patient died 3 days later.

Discussion

Since esophageal obturator airways are being used widely throughout the country by paramedics, those interpreting radiographs should be able to recognize the appearance of a ballooned tube in the esophagus. They should also be aware that complications, such as unrecognized endotracheal intubation, traumatic laceration of the airway with or without associated pneumomediastinum, vomiting after withdrawal, and aspiration pneumonia, though rare, may occur.

REFERENCES

1. Don Michael TA, Lambert EH, Mehran A: Mouth-to-lung airway for cardiac resuscitation. *Lancet* 2:1329, 1968
2. Farley M: The esophageal obturator airway. *Respir Ther* 3: 95, 1973
3. Greenbaum DM, Poggi J, Grace WJ: Esophageal obstruction during oxygen administration: a new method for use in resuscitation. *Chest* 65:188–191, 1974
4. Smock SN: Esophageal obturator airway: preferred CPR technique. *JACEP* 4:232–233, 1975
5. Schofferman J, Oill P, Lewis AJ: The esophageal obturator airway—a clinical evaluation. *Chest* 69:67–71, 1976
6. Standards for cardiopulmonary resuscitation (CPR) and emergency cardiac care (ECC). *JAMA* [Suppl] 227:833–868, 1974
7. Johnson KR, Genovesi MG, Lassar KH: Esophageal obturator airway; use and complications. *JACEP* 5:36–39, 1976

Hairy Esophagus: A Complication of Pharyngoesophageal Reconstructive Surgery in Two Cases

GORDON K. McLEAN[1] AND IGOR LAUFER[1]

Carcinomas of the head and neck account for 5% of all malignancies occurring annually in the United States [1]. Current therapy for invasive lesions generally consists of a combination of radiation and surgery. Attempts at a truly curative procedure may require radical resection with loss of major portions of the hypopharynx and esophagus. This, in turn, necessitates extensive secondary reconstruction in order to maintain a degree of normal oropharyngeal function. In some of these operations, a full thickness skin graft is mobilized to reconstruct the pharynx and esophagus [2, 3]. Since the epithelial surface becomes the inner surface of the reconstructed tube, these flaps may continue to bear hair. This may give rise to dysphagia and, in addition, give rise to a characteristic radiographic appearance in postsurgical esophagrams. We describe the problems encountered in two patients who developed endopharyngoesophageal hair after reconstructive surgery for neck carcinoma. We also point out the characteristic radiographic appearance of this postsurgical state.

Case Reports

Case 1

A 72-year-old man was seen in 1974 with a complaint of dysphagia. Examination disclosed a 2 × 4 cm mass on the left lateral hypopharyngeal wall with extension to the aryepiglottic fold. Biopsy showed a well differentiated squamous carcinoma and the lesion was classed T2N0M0. A total laryngectomy and left radical neck dissection were then performed. A pharyngocutaneous fistula developed postoperatively but closed spontaneously within 2 months. Increasing dysphagia developed and was treated with bougienage; however, passage of dilators became increasingly difficult and, 6 months after initial surgery, a revision of the pharyngeal stricture was performed using a deltopectoral skin flap.

At 3 months after the reconstruction, the patient again experienced dysphagia. Examination revealed "exuberant" hair growth in the hypopharynx. Endoscopic removal of the hair produced relief. Recurrence of dysphagia secondary to regrowth of the hair necessitated return visits for endoscopic "haircuts" every 4–6 months for the next 2½ years.

In June 1977, persistent left neck pain associated with hemoptysis prompted a complete endoscopic examination which revealed a superficial epidermoid carcinoma of the esophagus as well as endoesophageal hair. A barium swallow showed an unusual filling defect due to a mass of hair along the right lateral wall of the cervical esophagus. The surface was irregular with small rounded filling defects due to hair follicles. Just distal to this area, minimal mucosal abnormality corresponded to the superficial esophageal carcinoma (fig. 1). Although radiation therapy was instituted, the endoesophageal hair growth persists at this time.

Case 2

A 60-year-old man complained of a neck mass. Biopsy of a large left tonsillar mass extending into the oropharynx showed squamous cell carcinoma. A "composite procedure" (left radical tonsillectomy, left hemimandibulectomy, partial left hemiglossectomy, partial resection of the left oropharynx and hypopharynx, and left radical neck dissection) was performed followed by use of a deltopectoral skin flap. The postoperative course was marked by persistent dysphagia; endoscopic examination disclosed extensive hair growth in the reconstructed pharynx as well as a stricture at its juncture with the cervical esophagus. Removal of the hair with forceps and bougienage of the esophageal introitus produced relief.

Over the next 6 years the patient returned for removal of endopharyngeal hair and bougienage. Initially this produced relief for only 3 to 4 months before dysphagia recurred. The amount of hair was noted to decrease over the years with a corresponding decrease in dysphagia. An esophagram in September 1976 showed marked distortion of the pharynx due to the skin flap. There was a stricture at the junction of skin flap with the cervical esophagus. The surface of the skin flap was coarse and irregular with numerous small, rounded filling defects. This appearance was due to the residual hair follicles (fig. 2). Since the last hair removal in September 1976, hair growth has not recurred. The esophageal introitus remains stenotic but produces only mild dysphagia.

Discussion

Since wide excision of these tumors frequently requires the sacrifice of substantial parts of the hypopharynx and cervical esophagus, a variety of reconstructive procedures involving the mobilization of full thickness deltopectoral or laterally based neck flaps are used. These provide the reconstructed tube with a squamous epithelium which desquamates and resists abrasion and ulceration. Since these flaps are frequently hair-bearing in males, they may result in a "hairy esophagus," an endopharyngeal or endoesophageal mass of hair. Since the growth may be exuberant and produce considerable dysphagia, periodic endoscopic hair removal is advised. Although the hair growth has been reported to cease spontaneously within 1 year of surgery, our patients required periodic hair removal for 3 and 6 years, respectively. Although standard otorhinolaryngology texts mention this complication [2, 3], there have been no illustrations of its endoscopic or radiographic appearance and we have found no references to it in the radiologic literature.

Received March 24, 1978; accepted after revision October 9, 1978.

[1]Department of Radiology, Hospital of the University of Pennsylvania, 3400 Spruce Street, Philadelphia, Pennsylvania 19104. Address reprint requests to I. Laufer.

AJR 132:269–270, February 1979
0361–803X/79/1322–0269 $0.00

© 1979 American Roentgen Ray Society

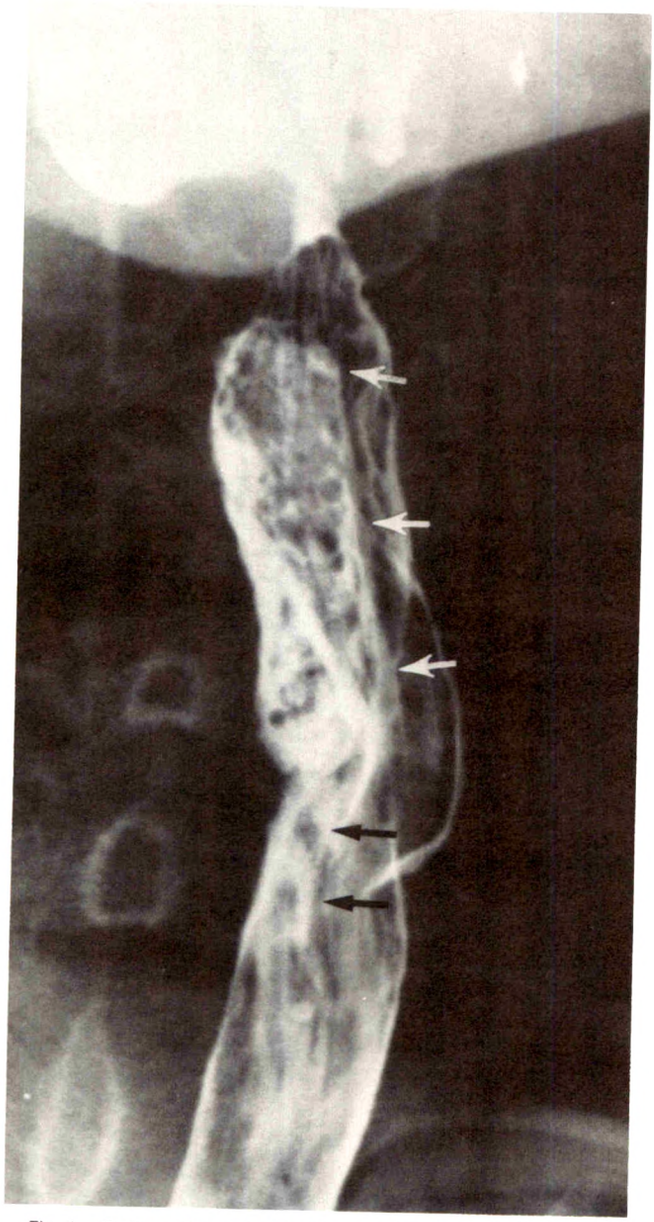


Fig. 1.—Endoesophageal hair after reconstruction of cervical esophagus. Filling defect along right lateral wall of cervical esophagus (*white arrows*). Surface of mass is irregular with multiple small rounded filling defects due to hair follicles. Distally, there is minimal mucosal abnormality due to superficial squamous carcinoma of esophagus (*arrows*).

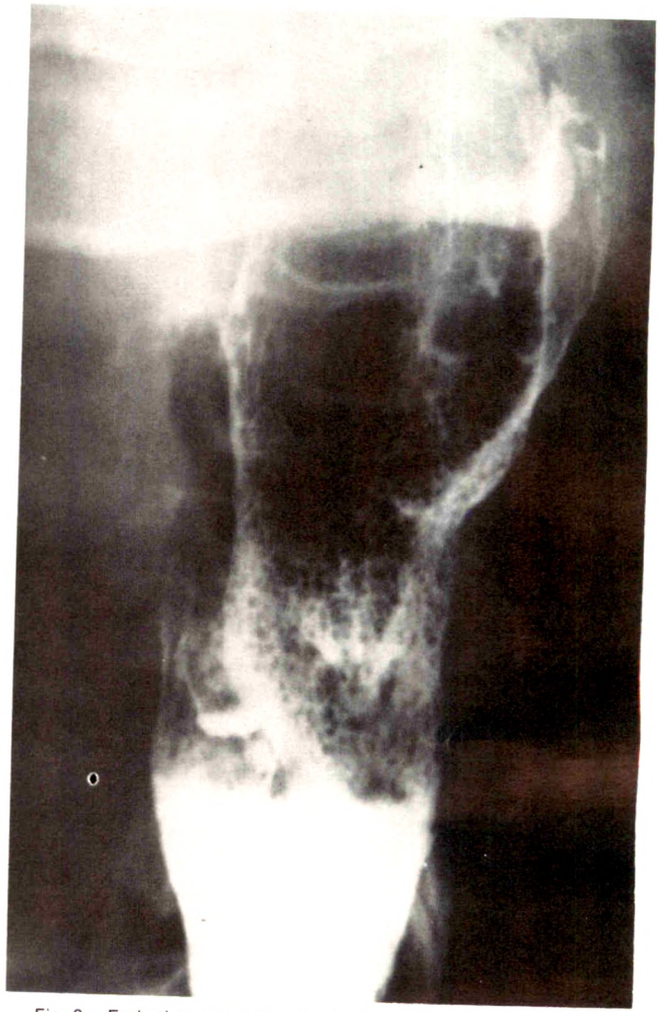


Fig. 2.—Endopharyngeal hair due to reconstruction of pharynx. Frontal view shows multiple small rounded filling defects due to hair follicles growing on skin flap.

The radiologic appearance of the reconstructed pharynx and esophagus will vary depending on the extent of surgical resection, the size of the skin flap, and the presence of postoperative complications. Nevertheless, the presence of endopharyngeal or endoesophageal hair on the skin flap does have a characteristic radiographic appearance. It will depend to some extent on whether the esophagram is performed before or after hair removal. Before hair removal, there may be a mass of hair with an irregular surface, suggestive of a bezoar. After hair removal, one may see a coarse surface with multiple, small rounded filling defects representing the hair follicles. This characteristic appearance should not be mistaken for a foreign body, recurrent tumor, moniliasis, or herpes esophagitis.

ACKNOWLEDGMENT

We thank Drs. Richard Scipion and Melvyn Richter for referring case 1 for study.

REFERENCES

1. Bales HW: Head and neck tumors, in *Clinical Oncology for Medical Students and Physicians. A Multidisciplinary Approach*, edited by Rubin P, New York, American Cancer Society, 1971, pp 228–261
2. Montgomery W: *Surgery of the Upper Respiratory System*. Philadelphia, Lea & Febiger, 1973
3. Mullen RW: Reconstruction of the hypopharynx and cervical esophagus, in *Otolaryngology, Head and Neck*, Vol 3, edited by Paparella M, Shumrick D, Philadelphia, Saunders, 1973, pp 784–792

Spontaneous Aortic Rupture Associated with Chronic Steroid Therapy for Rheumatoid Arthritis in Two Cases

DOUGLAS C. SMITH[1] AND ALBERT E. HIRST[2]

We recently encountered spontaneous rupture of the descending thoracic aorta in two patients who had received long term steroid therapy for rheumatoid arthritis. The striking similarity of their symptoms and angiographic and surgical findings suggested chronic steroid therapy may have been causally related to the spontaneous rupture of the aorta.

Case Reports

Case 1

A 55-year-old white woman awakened with severe pain in the left side of her chest that lessened somewhat by hospital admission. Physical examination revealed some tenderness over the left side of the anterior chest wall. The heart showed a regular sinus rhythm; lungs were clear. The blood pressure was 120/70 mm Hg. The fingers displayed severe rheumatoid arthritic deformity with ulnar deviation. She had had rheumatoid arthritis for 30 years and had been taking prednisone 10 mg daily for the past 11 years. Blood pressures recorded 10 and 3 years earlier were 112/80 and 128/90 mm Hg, respectively. A VDRL test for syphilis was nonreactive. Chest radiography the same day revealed a left hilar mass (fig. 1A) that was not present 2 years earlier. Because there were no pulsations in the mass on fluoroscopy, a presumptive diagnosis of bronchogenic carcinoma was made.

Bronchoscopy on hospital day 4 revealed no lesions. Mediastinoscopy revealed a large nonpulsatile mass. Incisional biopsy resulted in pulsatile arterial bleeding that was quickly controlled with sutures. A rapid frozen section from the biopsy site revealed only necrotic tissue. Aortography (fig. 1B) on hospital day 6 revealed partial opacification of an irregular cavity within an 8 × 10 cm smoothly contoured mass originating from the inner curvature of the distal arch of the aorta and projecting into the left hemithorax. Comparison with initial radiograph showed the mass had enlarged in the 6 days since admission (fig. 1).

A 12 cm saccular-type false aneurysm arising from the distal aortic arch was resected and repaired on day 7. The aneurysm originated from the aorta by a 2 cm wide orifice and was filled with thrombus. Mattress sutures, including Teflon felt pledgets, were used because of the paper-thin aortic wall. Respiratory insufficiency gradually developed and a tracheostomy was performed 8 days after surgery. She suddenly became cyanotic and hypotensive 2 days later and died. Autopsy was refused.

Case 2

A 68-year-old white woman suddenly developed steady, sharp, precordial chest pain radiating into the back and was hospitalized with a presumptive diagnosis of myocardial infarction. Chest radiography revealed a parenchymal density at the base of the left lung that gradually enlarged on repeat films. On hospital day 3 the mediastinum was widened and a left pleural effusion was present. The patient was transferred to the university hospital with presumptive diagnosis of acute dissecting aneurysm of the aorta.

Physical examination revealed no acute distress. There were decreased breath sounds at the base of the left lung. The blood pressure was 110/60 mm Hg. The fingers were severely deformed with pronounced ulnar deviation. She had a 28 year history of rheumatoid arthritis and had taken prednisone (5 mg 3 times a day) for many years. The VDRL test was nonreactive. Aortography shortly after admission revealed a 1.5 × 3 cm smoothly contoured collection of contrast material projecting from the inner aspect of the distal aortic arch (fig. 2A). At surgery a 2 cm transmural laceration in the distal arch was surrounded by a large hematoma extending down the descending thoracic aorta. Aspiration of the left pleural cavity produced 200 ml blood. A 26-mm-long Dacron graft was interposed to restore aortic continuity. Teflon felt pledgets were used because the consistency of the aortic wall resembled "wet tissue paper." Histologic studies of the resected segment revealed extensive smooth muscle depletion in the outer media. Verhoeff stain revealed fragmentation of elastica in the outer media and clumping of elastic tissue in the inner media (fig. 2B). Intimal atherosclerosis was minimal. The postoperative course was complicated by recurrent episodes of left hemothorax. Bleeding gradually ceased and she was apparently well when discharged 8 weeks after surgery.

Discussion

Spontaneous rupture of the thoracic aorta is most commonly a complication of dissecting aneurysm [1], syphilis [2], cystic medionecrosis [3], coarctation [4], atherosclerosis [5], or mycotic process [6]. Atherosclerosis has recently displaced syphilis as the most frequent cause of thoracic aortic aneurysm [7, 8]. Since the initial report of Rodriquez and Rivera [9], in which rupture was associated with extensive aortic atherosclerosis, a number of similar cases have been reported by other authors [10–14].

However, atherosclerosis seems to have played little or no part in aortic rupture in our cases. In the first case the normal caliber and smooth contour of the aortic wall, as well as the absence of intimal calcification, suggest that atheromatous changes were minimal; in the second case histologic sections of the aortic wall failed to reveal significant atheromatous change.

Neither patient had a clinical picture of inflammation or sepsis. There were no signs of inflammation on gross or microscopic tissue examinations of the rupture site.

Received May 5, 1978; accepted after revision October 5, 1978.
[1] Department of Radiology, Loma Linda University Medical Center, Loma Linda, California 92354. Address reprint requests to D. C. Smith.
[2] Department of Pathology, Loma Linda University Medical Center, Loma Linda, California 92354.

AJR 132:271–273, February 1979
0361–803X/79/1322–0271 $0.00
© 1979 American Roentgen Ray Society

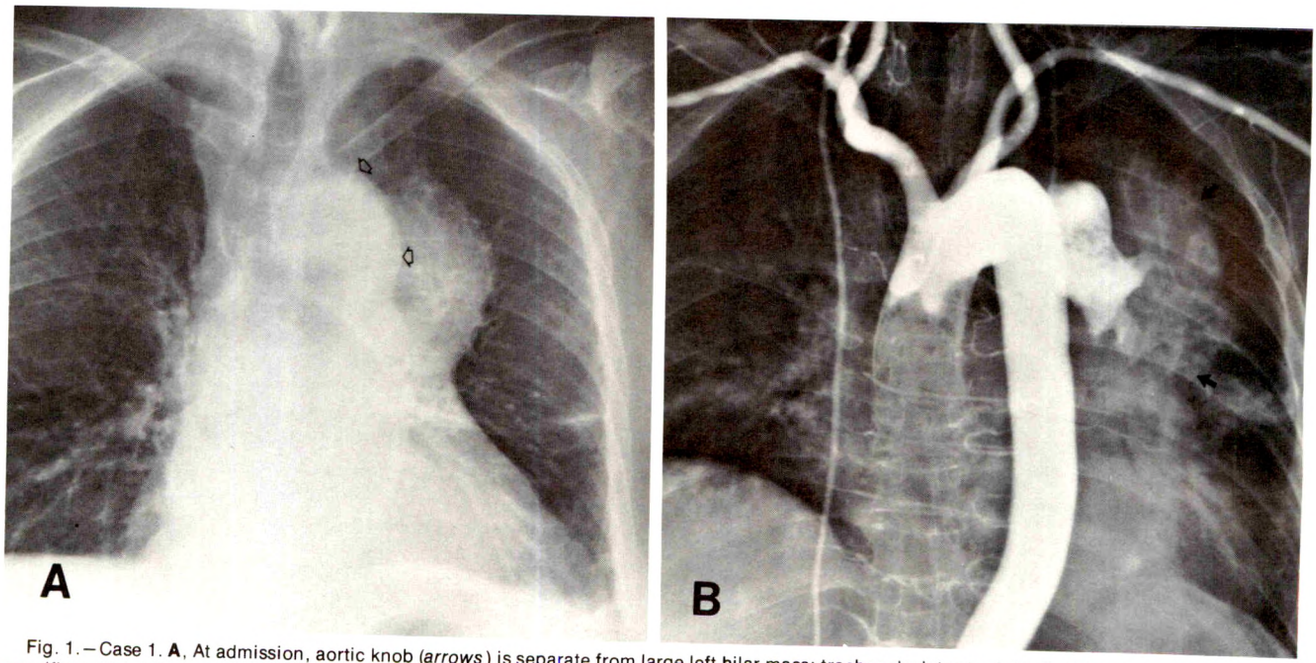


Fig. 1.—Case 1. **A**, At admission, aortic knob (*arrows*) is separate from large left hilar mass; trachea deviates to right. **B**, 6 days later. Irregular cavity opacifies within hilar mass (oblique projections revealed that cavity communicated with inner curvature of distal aortic arch). Hilar mass (*arrows*) larger than at admission.

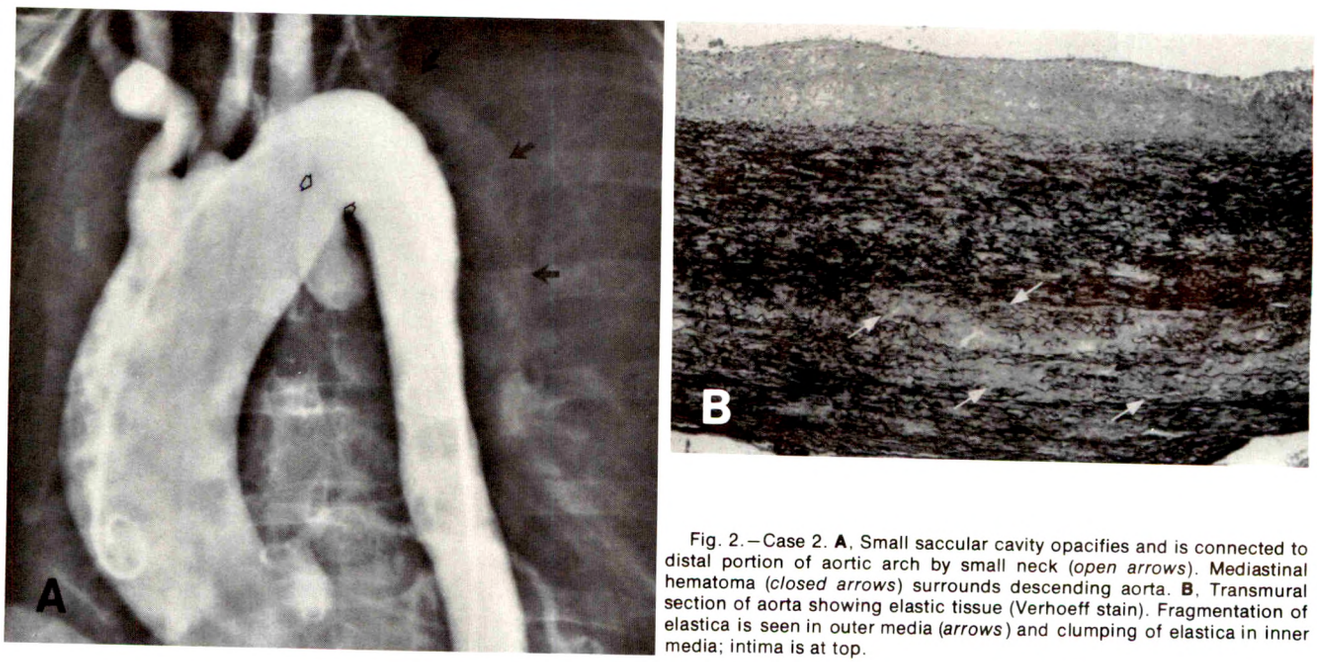


Fig. 2.—Case 2. **A**, Small saccular cavity opacifies and is connected to distal portion of aortic arch by small neck (*open arrows*). Mediastinal hematoma (*closed arrows*) surrounds descending aorta. **B**, Transmural section of aorta showing elastic tissue (Verhoeff stain). Fragmentation of elastica is seen in outer media (*arrows*) and clumping of elastica in inner media; intima is at top.

Case 2 has tolerated a Dacron aortic prosthesis for 18 months without evidence of infection. Thus, we do not believe these patients had spontaneously rupturing mycotic aneurysms.

Patients with rheumatoid arthritis not on corticosteroid therapy seldom develop vascular lesions [15]. Aortic lesions encountered in rheumatoid arthritis usually remain localized to the region of the aortic valve and include aortic insufficiency due to scarring and retraction of the aortic valve cusps and focal calcification and destruction of elastic tissue in the aortic ring [16]. Such changes may be responsible for congestive heart failure.

Lesions in small peripheral arteries have been attributed to rheumatoid arthritis [17] and range from perivascular inflammation without evident involvement of the vessel wall to severe panarteritis with destructive changes resembling polyarteritis nodosa. Such lesions have not involved the aorta and do not resemble the changes seen in case 2.

We have not found aortic rupture reported as a com-

plication of chronic steroid therapy in humans [18, 19]. Corticosteroids administered to hamsters and rats have frequently produced spontaneous rupture of the aorta [20–23]. Histologic lesions in steroid-induced rupture included metaplastic transformation and necrosis of smooth muscle cells in the media in some [20, 21], while in others dissecting aneurysm of the aorta developed [22, 23]. Cortisone administered to rats has been shown to impair the integrity of the aortic wall producing loss of elastin [24]. Corticosteroid administration to rabbits and rats resulted in inhibition of synthesis of collagen, chondroitin sulfate, and hyaluronic acid, as well as accelerated degradation of collagen [24–26]. Degeneration of the aortic media has occurred in mice with subcutaneous transplants of functioning adrenocortical carcinoma [23]. Rabbits receiving corticosteroids showed depressed reparative capability after mechanical aortic injury [25]. Such animal experiments indicate that the integrity of the aortic wall may be compromised by excess corticosteroids.

In each of the cases presented here, the surgeon was impressed by the extreme thinness and friability of the aortic wall. Suturing proved a difficult problem, because the aortic wall had the strength of "wet tissue paper." Since the aortic changes in these two cases resemble those found in laboratory animals on corticosteroid administration, but lack the characteristic features of advanced atherosclerosis or rheumatoid aortitis, a relation to steroid therapy is suggested.

REFERENCES

1. Hirst AE, Johns VJ, Kime SW: Dissecting aneurysm of the aorta: a review of 505 cases. *Medicine* (Baltimore) 37:217–279, 1958
2. Sopher IM, Spitz WU: Exsanguinating hemoptysis due to a ruptured syphilitic aneurysm. *J Forensic Sci* 18:118–121, 1971
3. Hirst AE, Gore I: Editorial—Is cystic medionecrosis the cause of dissecting acrtic aneurysm? *Circulation* 53:915–916, 1976
4. Nakaidoh H, Idriss FS, Riker WL: Aortic rupture in children as a complication of coarctation of the aorta. *Arch Surg* 107:838–841, 1973
5. DeBakey ME, Noon GP: Aneurysm of the thoracic aorta. *Mod Concepts Cardiovasc Dis* 44:53–58, 1975
6. Anderson CB, Butcher HR, Ballinger WF: Mycotic aneurysms. *Arch Surg* 109:712–717, 1974
7. Higgins CB, Silverman NR, Harris RD, Albertson KW: Localized aneurysms of the descending thoracic aorta. *Clin Radiol* 26:475–482, 1975
8. Hardy JD, Suzuki A: Thoracic aortic aneurysms. *J Miss S ate Med Assoc* 15:507–511, 1974
9. Rodriquez HF, Rivera E: Spontaneous rupture of the thoracic aorta through an atheromatous plaque. *Ann Intern Med* 54:307–313, 1961
10. Case records of the Massachusetts General Hospital (case 43—1970). *N Engl J Med* 283:862–870, 1970
11. Calick A, Vance ZB, Berger SA: Spontaneous aortic rupture through atheromatous plaque. *NY State J Med* 73:2068–2070, 1973
12. Legaay MB: Spontaneous rupture of non-aneurysmatic abdominal aorta. *J Cardiovasc Surg* (Torino) 15:490–493, 1974
13. Case records of the Massachusetts General Hospital (case 24—1977). *N Engl J Med* 297:996–1003, 1977
14. Cosio-Pascal M, Cardoso M: Rupture of the aorta into the left lung (aortopulmonary fistula with lung hematoma formation): report of a case of successful treatment by operation. *J Thorac Cardiovasc Surg* 51:834–838, 1966
15. Pirani CL, Bennett GA: Rheumatoid arthritis: a report of three cases progressing from childhood and emphasizing certain systemic manifestations. *Bull Hosp Joint Dis* 12:335–367, 1951
16. Clark WS, Kulka JP, Bauer W: Rheumatoid aortitis with aortic regurgitation. *Am J Med* 22:580–592, 1957
17. Johnson RL, Smyth CJ, Holt GW, Lubchenco A, Valentine E: Steroid therapy and vascular lesions in rheumatoid arthritis. *Arthritis Rheum* 2:224–249, 1959
18. Dujovne CA, Azarnoff DL: Clinical complications of corticosteroid therapy: a selected review. *Med Clin North Am* 57:1331–1342, 1973
19. Diethelm AG: Surgical management of complications of steroid therapy. *Ann Surg* 185:251–263, 1977
20. Frenkel JK: Dissecting aneurysms of the aorta, and pancreatic islet cell hyperplasia with diabetes in corticosteroid- and chlorothiazid-treated hamsters. *Prog Exp Tumor Res* 16:300–324, 1972
21. Valigorsky JM: Metaplastic transformation of aortic smooth muscle cells in cortisone-induced dissecting aneurysms in hamsters. *Fed Proc* 28:802, 1969
22. Selye H, Bois P: Effect of corticoids upon experimental lathyrism. *Endocrinology* 60:507–513, 1957
24. Steffee CH, Snell KC: Dissecting aortic aneurysm in hamsters treated with cortisone acetate. *Proc Soc Exp Biol Med* 90:712–714, 1955
24 Bartos F, Ledvina M: The effect of glycocorticoids on the formation and cross-linking of elastin in aortas of adult and new-born rats. *Sb Ved Pr Lek Fak Karlovy Univ* 13:323–330, 1970
25 Manthorpe R, Garbarsch C, Lorenzen I: Glucocorticoid effect on repair processes in vascular connective tissue. *Acta Endocrinol* (Kbh) 80:380–397, 1975
26. Manthorpe R, Helin G, Kofod B, Lorenzen I: Effects of glucocorticoid on connective tissue of aorta and skin in rabbits. *Acta Endocrinol* (Kbh) 77:310–324, 1974

Occlusion of the Right Pulmonary Artery by Acute Dissecting Aortic Aneurysm

CHUSILP CHARNSANGAVEJ[1]

Aneurysm of the thoracic aorta is known to cause obstruction of the right and left pulmonary arteries on a chronic basis [1, 2]. Occlusion of the right pulmonary artery by an acute dissecting aneurysm of the ascending aorta is rare. Only two cases have been reported in the literature. This report describes such a phenomenon along with angiographic findings in a patient who had a clinical presentation suggesting a massive pulmonary embolism.

Case Report

H. W., a 66-year-old black man, was seen in the emergency room with sudden onset of chest pain, jaw pain, shortness of breath, and hemoptysis. Eight months earlier, he had undergone valve replacement for severe aortic regurgitation, with postoperative improvement of symptoms of congestive heart failure.

Physical examination revealed a blood pressure of 170/90 mm Hg. Pulse and temperature were normal. The right lung was clear to auscultation; a few rales and rhonchi were present at the left base. The heart was enlarged with a grade 2/6 systolic murmur at the apex and the left sternal border. No diastolic murmur was heard. The abdominal examination was not remarkable. Peripheral pulses were intact.

Laboratory data revealed a hemoglobin of 17.4 g/100 ml, hematocrit of 50%, and white cell count of 9,500 with a normal differential. Blood chemistries were normal. Arterial blood gas study demonstrated a pO_2 of 51, pCO_2 of 26, pH of 7.44, and 81% O_2 saturation.

Chest radiography showed an enlarged cardiac silhouette with Shiley valve prosthesis, a widened mediastinum (when compared with a chest film made 6 months earlier), and a patchy infiltrate in the right upper lobe (fig. 1A). A ^{99m}Tc macroaggregated albumin lung scan revealed absent perfusion of the right lung and a few patchy defects on the left.

After a preliminary diagnosis of massive pulmonary embolism of the right lung, heparinization was started. A follow-up lung scan 9 days later again revealed no perfusion of the right lung. During this period, the patient had occasional hemoptysis but was in no acute distress. Pulmonary angiography (injection of contrast material into the main pulmonary artery) revealed displacement of the pulmonary artery trunk to the left, with complete obstruction of the right pulmonary artery 2 cm beyond the bifurcation. There were no filling defects in the pulmonary arteries (fig. 1B). The aortogram phase showed a collection of contrast material in the wall of the dilated ascending aorta.

Thoracic aortography was then performed via a right femoral arterial approach, demonstrating a dissection of the ascending aorta posteriorly and downward towards the prosthetic valve (fig. 1C). There was also dissection posteriorly and laterally, with compression obstruction of the right pulmonary artery (fig. 1D).

Operation disclosed a massive dissecting aneurysm of the ascending aorta with extension posteriorly and toward the aortic arch. The large dissecting hematoma compressed and occluded the right pulmonary artery. The aortic valve prosthesis was intact. The patient died at surgery after an attempt was made to replace the aneurysm with a graft. Autopsy was not performed.

Discussion

Demonstration of the absence of pulmonary artery perfusion by lung scan is infrequent, with an incidence of 2% in one series [3]. The common causes are bronchogenic carcinoma, hyperlucent lung syndrome, massive pulmonary embolism, and extensive parenchymal disease of the lung.

In massive pulmonary embolism, angiography usually shows a filling defect with convex border, commonly found at the branching of the right or left pulmonary artery [4]. Wormlike filling defects may be seen in some of the small vessels.

In carcinoma of the lung, the pulmonary artery is usually compressed in the hilar region [5], but usually it is not completely obstructed [6].

Mediastinal fibrosis due to various inflammatory processes such as histoplasmosis, tuberculosis, and sclerosing mediastinitis, can cause obstruction of the mediastinal structures including the superior vena cava, pulmonary artery, pulmonary vein, esophagus, and bronchus [7–9].

Buja et al. [10] reported an autopsy case of acute dissection of the ascending aorta with hematoma compressing the right pulmonary artery. They demonstrated the anatomic relation of the ascending aorta and the pulmonary outflow tract, which share the same adventitia layer, as well as the relation of the ascending aorta and the right pulmonary artery. When dissection occurs at the posterior wall of the ascending aorta, the hematoma can compress the right pulmonary artery which lies posterior to the ascending aorta. Nasrallah et al. [11] demonstrated by angiography the compression of the pulmonary outflow tract and occlusion of the right pulmonary artery by a dissecting aneurysm of the ascending aorta, confirmed at surgery.

Although rare, obstruction of the right pulmonary artery by dissecting aneurysm of the ascending aorta can mimic pulmonary embolism. The distinction between these entities is important; anticoagulation therapy for suspected embolism is contraindicated if the patient has aortic dissection. Evidence on the chest radiograph of acute widening of the mediastinum, most reliable with the availability of a previous chest study, favors the diagnosis of dissection of the aorta. Pulmo-

Received June 20, 1978; accepted after revision October 19, 1978.

[1] Department of Radiology, Albert Einstein College of Medicine, 1300 Morris Park Avenue, Bronx, New York 10461.

© 1979 American Roentgen Ray Society

0361-803X/79/1322-0274 $0.00

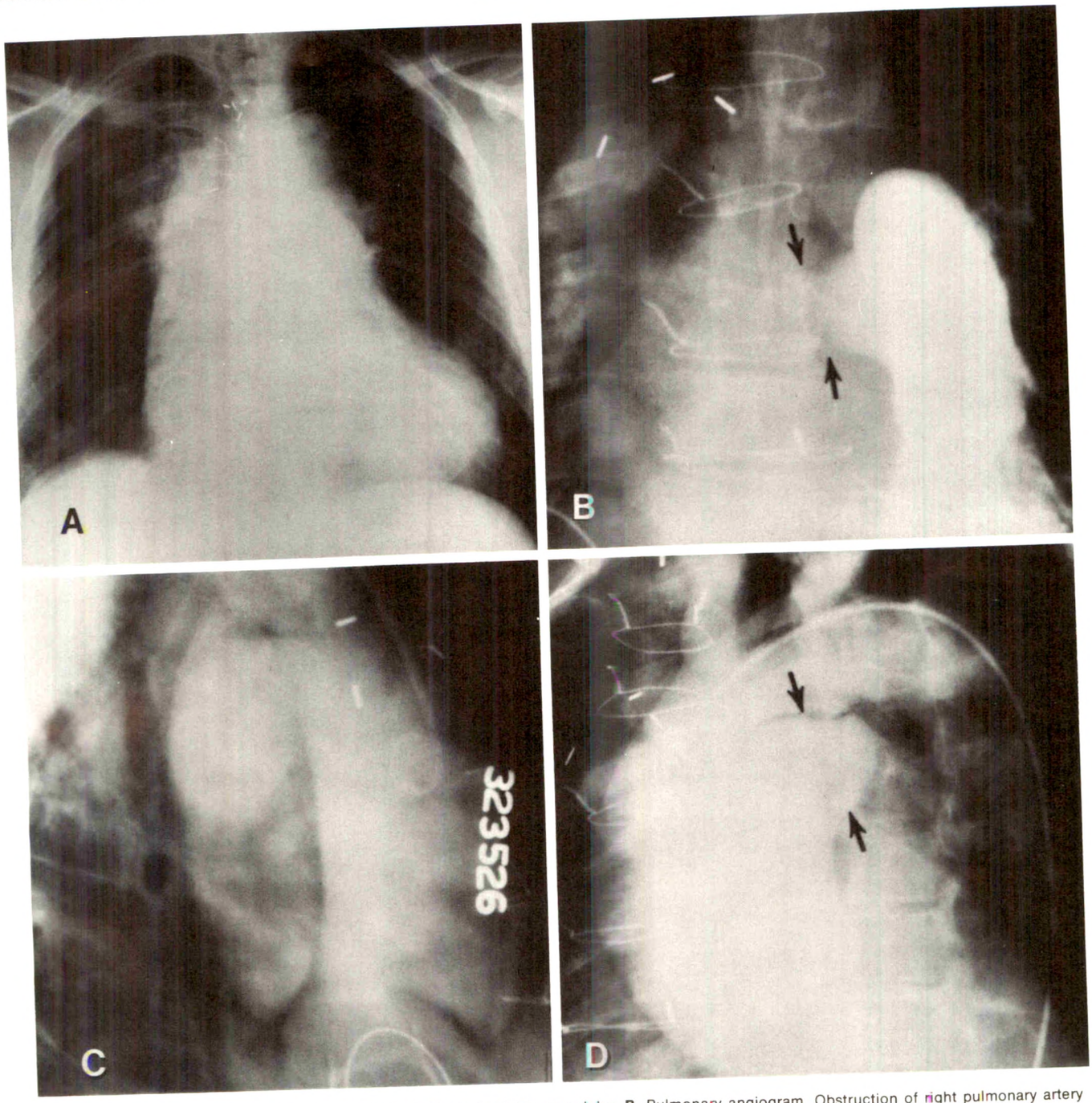


Fig. 1.—**A**, Widening of mediastinum with patchy infiltrate in right upper lobe. **B**, Pulmonary angiogram. Obstruction of right pulmonary artery (*arrows*). **C and D,** Injection of contrast material into lumen of ascending aorta. **C,** Steep right anterior oblique projection. Dissection extending to root of aorta. **D**, Simultaneous right posterior oblique projection. Hematoma of dissection (*arrows*) compresses right pulmonary artery.

nary angiography and aortography will provide the definite diagnosis.

REFERENCES

1. Drachler DH, Willis PW III: Acquired right ventricular outflow tract obstruction. *Am Heart J* 82:536–540, 1971
2. Varkey B, Tristani FE: Compression of pulmonary artery and bronchus by descending thoracic aortic aneurysm. *Am J Cardiol* 34:610–614, 1974
3. White RI Jr, James AE Jr, Wagner HN Jr: The significance of unilateral abscence of pulmonary artery perfusion by lung scanning. *AJR* 111:501–509, 1971
4. Miller GAH, Sutton GC: Acute massive pulmonary embolism. *Br Heart J* 32:518–523, 1970
5. Vasallo CL, Gee JBL, Wholey MH, Vester JW: Lung scanning in hilar bronchogenic carcinoma. *Am Rev Respir Dis* 97:851–858, 1968
6. Moloney JV Jr, Bennett LR, Longmire WP, Madden SC, Rigler LG, Simmons DH, Steele JD, Stein JJ, Troup GM,

Weber AP: The UCLA interdepartmental conference: carcinoma of the lung. *Ann Intern Med* 64:165–188, 1966

7. Goodwin RA, Nickell JA, Des Prez RM: Mediastinal fibrosis complicating healed primary histoplasmosis and tuberculosis. *Medicine* 51:227–246, 1972
8. Marshall RJ, Edmundowicz AC, Andrews CE: Chronic obstruction of the superior vena cava due to histoplasmosis: a hemodynamic and angiographic correlation. *Circulation* 29:604–609, 1964
9. Dye TE, Saab SB, Almond CH, Watson L: Sclerosing mediastinitis with occlusion of pulmonary vein: manifestation and management. *J Thorac Cardiovasc Surg* 74:137–141, 1977
10. Buja LM, Ali N, Fletcher RD, Roberts WC: Stenosis of the right pulmonary artery: a complication of acute dissecting aneurysm of the ascending aorta. *Am Heart J* 83:89–92, 1972
11. Nasrallah A, Goussous Y, El-Said G, Garcia E, Hall RJ: Pulmonary artery compression due to acute dissecting aortic aneurysm: clinical and angiographic diagnosis. *Chest* 67:228–230, 1975

Radiographic Features of the Linear Nevus Sebaceous Syndrome

JOHN C. LEONIDAS,[1] SAMUEL M. WOLPERT,[1] MURRAY FEINGOLD,[2] AND ROY G. K. McCAULEY[1]

A rare neurocutaneous syndrome recognized recently is characterized by an epidermal nevus (linear nevus sebaceous of Jadassohn), seizures, and mental retardation [1–6]. In many cases the syndrome is associated with gross anatomic malformations of the central nervous system, eye, and tissues of mesenchymal origin, including the cardiovascular system and skeleton [2–10]. A great variety of radiographic manifestations have been reported, mostly in isolated case reports. However, none of the radiographic findings is characteristic for this syndrome; only correlation with clinical features, notably the skin lesion, can lead to the correct diagnosis.

We recently examined two children with clinical features of the linear nevus sebaceous syndrome, one of whom had no evidence of any detectable anatomic cerebral, visceral, or skeletal anomaly and no abnormal radiographic findings. The second child had craniocerebral anomalies associated with significant radiographic manifestations of uncertain nature until the skin lesion was identified as a linear sebaceous nevus. (fig. 1). This case is briefly described below.

Case Report

A 3-day-old boy was admitted because of a left-side facial lesion at birth. Family history, gestation, labor, and delivery were all unremarkable. The infant was born at term weighing 3,750 g.

The skin lesion consisted of a crop of soft, slightly yellowish papules extending from the left lateral canthus down the left cheek, passing lateral to the left angle of the mouth, and continuing to the middle of the chin in a linear arrangement (fig. 1). The left palpebral fissure was enlarged. There were medial and lateral limbal epibulbar dermoids of the conjunctiva of the left eye. Fundoscopic examination revealed a pale left optic disc with a deep central cup and decreased pigment of the pigmented layer of the retina on the left. There was also anisocoria with a large left pupil that had a slightly decreased response to light.

Histologic examination of a skin biopsy on day 8 showed the characteristic features of nevus sebaceous of Jadassohn [5]. Skull radiography revealed cranial asymmetry with a prominent left hemicranium and elevation of the left lesser wing of the sphenoid bone. The left parietal bone was thicker than the right. The orbits were also asymmetric, the left being larger, and there was definite asymmetry of the optic foramina (3 mm right, 5 mm left). Hypocycloidal tomography 4 days later showed a normal right optic foramen. On the left the canal was difficult to evaluate, but it appeared enlarged. There was hypoplasia of the left greater sphenoid wing (fig. 2A). Mild developmental retardation with delayed psychomotor function became evident in the next few months. At age 17 months, episodes of generalized seizures developed and were treated with phenobarbital. Electroencephalography showed occipital slowing. Skull radiography revealed no change from previous findings, except for the addition of hypoplasia of the left maxillary sinus. Skeletal survey was within normal limits.

Computed tomography (CT) of the skull revealed dilatation of the left lateral ventricle. In the left middle cranial fossa, just anterior to the petrous bone, an area with very low absorption values extended from the bony table to the basal cisterns (fig. 2B). Bilateral carotid angiography showed normal vasculature on the right. On the left, the siphon of the left carotid artery was opened and displaced anteriorly. The sylvian point was elevated and the sylvian branches were displaced anteriorly. These findings were believed caused by an avascular intraaxial mass of the left posterior temporal lobe corresponding to the lesion shown on CT (fig. 2C). In view of the absorption values found on CT and the clinical diagnosis of the linear nevus sebaceous syndrome, the mass was considered most likely to represent a fatty tumor, probably a hamartoma, but there was no pathologic proof of this assumption. Pneumoencephalography showed the left lateral ventricle to be dilated. Both ventricles were shifted from right to left, as was the third ventricle. The aqueduct and fourth ventricle were normal. Tomography revealed asymmetry of the temporal horns, with the left dilated and elevated. There was also slight elevation of the petrous bone. Combined radiologic studies indicated no space-occupying lesion on the left,



Fig. 1.—Characteristic linear distribution of soft yellowish papules of sebaceous nevus; left eye and orbit larger than right.

Received June 27, 1978; accepted after revision October 26, 1978.

[1] Department of Radiology, Boston Floating Hospital, Tufts–New England Medical Center Hospital, 171 Harrison Avenue, Boston, Massachusetts 02111. Address reprint requests to J. C. Leonidas.

[2] Department of Pediatrics, Division of Birth Defects, Tufts–New England Medical Center Hospital, Boston, Massachusetts 02111.

© 1979 American Roentgen Ray Society

0361-803X/79/1322-0277 $0.00

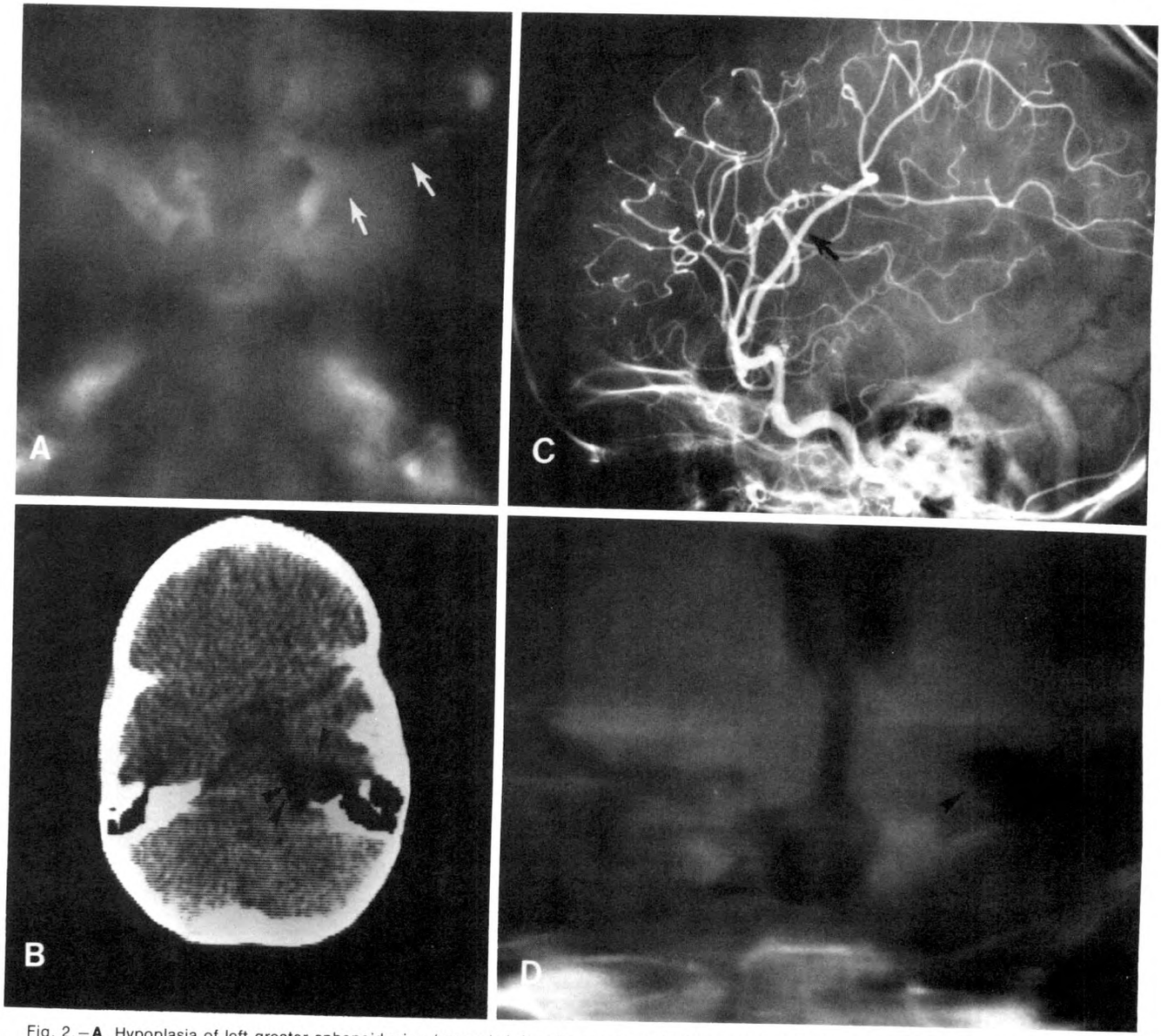


Fig. 2.—**A**, Hypoplasia of left greater sphenoid wing (*arrows*); left optic canal poorly demonstrated. **B**, Low absorption area consistent with fatty tumor adjacent to left petrous tip (*arrowheads*). **C**, Anterior displacement of left carotid siphon and elevation of sylvian branches (*arrow*) and point. **D**, Dilatation of left lateral ventricle after pneumoencephalography. Midline structures displaced from right to left; left temporal horn (*arrow*) and left petrous ridge elevated. (Findings consistent with atrophy of left cerebral hemisphere.)

but cerebral hemiatrophy with a left posterior temporal en plaque hamartomatous lesion (fig. 2 D).

At age 2 years the patient continues to have mild mental retardation, left esotropia, optic atrophy, and a conjunctival dermoid. Seizures are essentially under control.

Discussion

There is considerable disagreement and confusion regarding the classification of organoid nevi [11, 12], and discussion of the subject is beyond the scope of this report. Linear sebaceous nevus is a form of organoid nevus, in most instances unassociated with any other malformations. First described by Jadassohn in 1895 as a clinically and histopathologically distinct entity considered a hamartoma, the lesion is generally noted at birth and usually involves the scalp and face, although occasionally it occurs elsewhere [5].

Sebaceous nevus with a linear facial distribution, present at birth and associated with seizures and mental retardation, was first described by Schimmelpenning [13], and subsequently by Feuerstein and Mims [1], as a distinct neurocutaneous syndrome. The syndrome may involve a variety of tissues of ectodermal and mesenchymal origin and resembles other entities such as neurofibromatosis, tuberous sclerosis, the Sturge-Weber syndrome, von Hippel–Lindau disease, incontinentia pigmenti, and others.

The nevus sebaceous of Jadassohn is a relatively common cutaneous lesion, but its association with central nervous system and other malformations (the linear

nevus sebaceous syndrome) is rare, having been reported in only about 35 cases [10]. About half of these report eye changes [10, 14], as in our case. There may be cutaneous lesions of a different nature [2, 6–8]. Seizures of various types develop in almost all cases [6, 10]; however, there are reports of normal intelligence [6].

Associated gross malformations of the brain, viscera, and skeleton produce a variety of radiographic findings, most of them described in isolated case reports, but rarely illustrated. Radiographic changes have been reported in about half of the reported cases of the linear nevus sebaceous syndrome.

The most common radiographic manifestations of the linear nevus sebaceous syndrome involve the skull and brain. There is frequently cranial asymmetry with or without asymmetry of the facial bones and orbits [2–4, 9]. Premature closure of the sphenofrontal suture, sphenoid bone malformation, and abnormalities of the sella turcica have also been reported [2, 3]. Our patient had asymmetry of the optic foramina as part of the abnormal development of the left sphenoid bone.

Cerebral atrophy or hemiatrophy associated with ventricular dilatation, midline shift, and asymmetric thickening of the cranial vault are relatively common [2, 3, 7, 9]. Hydrocephalus, porencephaly, and intracranial hamartomas have also been described [7, 9, 15].

Changes of the axial and appendicular skeleton are uncommon, reported in only a few cases. They have no specific appearance or distribution. Such changes include deformities of spine (scoliosis, kyphoscoliosis), pelvis, and long bones (malformed clavicles, lytic defect of ribs, bowing of ulna, fragmentation, and sclerosis of distal radius in isolated cases) [4, 7, 8, 15]. Occasionally there are cardiac and renal malformations of nonspecific nature, as well as hypoplasia of major arteries (celiac, renal) [2, 8].

Because the distribution of radiographic abnormalities parallels other cutaneous dysplasias, the skin lesion distinguishes the linear nevus sebaceous syndrome from other neurocutaneous syndromes. Differential diagnosis may be especially difficult from tuberous sclerosis. Adenoma sebaceum very rarely appears at birth and presents a distinctly different histologic picture [6]. In addition, no intracranial calcifications have been reported in the linear nevus sebaceous syndrome [10].

There is a higher tendency for patients with the linear nevus sebaceous syndrome to develop hemartomatous tumors (nephroblastomatosis, ameloblastoma, subarachnoid cyst, etc.) [6, 8, 15]. Our patient had a left temporal en plaque mass with a high fat content, most likely a hamartoma, although there has been no tissue confirmation.

Linear nevus sebaceous syndrome should be considered when a variety of craniocerebral abnormalities, and occasionally other radiographic manifestations, is seen in a child who has seizures and is mentally retarded. The skin lesion is usually characteristic of the diagnosis.

REFERENCES

1. Feuerstein RC, Mims LC: Linear nevus sebaceous with convulsions and mental retardation. *Am J Dis Child* 104: 675–679, 1962
2. Marden PM, Venters HD: A new neurocutaneous syndrome. *Am J Dis Child* 112:79–81, 1966
3. Moynahan EJ, Wolff OH: A new neurocutaneous syndrome (skin, eye and brain) consisting of linear naevus, bilateral lipodermoid of the conjunctivae, cranial thickening, cerebral cortical atrophy and mental retardation. *Br J Dermatol* 79:651–652, 1967
4. Solomon LM, Fretzin DF, Dewald RL: The epidermal nevus syndrome. *Arch Dermatol* 97:273–285, 1968
5. Bianchine JW: The nevus sebaceous of Jadassohn. *Am J Dis Child* 120:223–228, 1970
6. Lovejoy FH, Boyle WE Jr: Linear nevus sebaceous syndrome. Report of two cases and a review of the literature. *Pediatrics* 52:382–387, 1973
7. Sugarman GI, Reed WB: Two unusual neurocutaneous disorders with facial cutaneous signs. *Arch Neurol* 21:242–247, 1969
8. Lansky LL, Funderburk S, Cuppage FE, Schimke N, Diehl AM: Linear sebaceous nevus syndrome. *Am J Dis Child* 123: 587–590, 1972
9. Chalhub EG, Volpe JJ, Gado MH: Linear nevus sebaceous syndrome associated with porencephaly and nonfunctioning major cerebral venous sinuses. *Neurology* (Minneap) 25:857–860, 1975
10. Deschamps P, Leroy D, Vabret J: Naevus sébacé linéaire et comitialité. *Sem Hop Paris* 52:2427–2430, 1976
11. Solomon LM, Esterly NB: Epidermal and other congenital organoid nevi. *Curr Probl Pediatr* 6:3–56, 1975
12. Mehregan AH, Pinkus H: Life history of organoid nevi. Special reference to nevus sebaceous of Jadassohn. *Arch Dermatol* 91:574–587, 1965
13. Schimmelpenning GW: Klinischer Beitrag zur Symptomatologie der Phakomatosen. *ROEFO* 87:716–720, 1957
14. Monahan RH, Hill CW, Venters HD: Multiple choristomas, convulsions and mental retardation as a new neurocutaneous syndrome. *Am J Ophthalmol* 64:529–532, 1967
15. Holden KR, DeKaban AS: Neurological involvement in nevus unis lateralis and nevus linearis sebaceus. *Neurology* (Minneap) 22:879–887, 1972

Fatal Intrathoracic Hemorrhage After Percutaneous Aspiration Lung Biopsy

LEE B. MILNER,[1] KEVIN RYAN,[2] AND JOHN GULLO[3]

Because of a lower incidence of complications, aspiration lung biopsy is performed in preference to other closed-lung biopsy techniques. Norenberg et al. [1] noted the increased risk of a cutting type or Vim-Silverman needle in performing closed-lung biopsies. This has been confirmed by Herman and Hessel [2]. The mechanisms of death after aspiration lung biopsy are tension pneumothorax, air embolism, and pulmonary hemorrhage with or without aspiration [3]. Of 1,562 patients undergoing aspiration lung biopsy, the fatality rate was 0.1% [2]. Four documented fatalities from aspiration lung biopsy are recorded in the literature [3–6]. This case reemphasizes the potential hazard of this increasingly common procedure.

Case Report

A 61-year-old white man had multiple pulmonary nodules. History included a nephrectomy for a hypernephroma about 1½ years prior to admission. About 2 months before admission several pulmonary nodules were discovered. The largest were in the posterior basal segment of the left lower lobe and were best seen at 4 cm by tomography. These were suspected to represent metastases from the known hypernephroma; however, more obscure causes could not be excluded, and a lung biopsy was suggested. Coagulation studies, including complete blood count, prothrombin time, partial thromboplastin time, and bleeding time, were normal. Preoperative electrocardiography was also normal. The lesion at the left base was selected for biopsy.

The technique used was that described originally by Dahlgren and modified by Meyer et al. [7]. This procedure had been successfully performed in 50 patients by one of us (L. B. Milner) either alone or with another radiologist. A 15.2 cm 20 gauge needle with a radial bevel tip was utilized, marked off to a depth of 4.5 cm. Superficial anesthesia with a 25-gauge needle was carefully placed to a depth of 1 cm. The lesion was localized under fluoroscopy and a single pass was performed with no patient motion or respiration. Fluoroscopy immediately after the procedure demonstrated no pneumothorax. About 5 min after the procedure, the patient complained that he had to cough and expectorated about 20 ml bright red blood. He also complained of some heaviness in his chest. He was placed with the left chest down and rapidly became unresponsive. Extensive attempts at cardiac resuscitation were unsuccessful. A left chest tube was placed during the resuscitation and 500 ml bright red blood was removed.

At autopsy, the posterolateral aspect of the thoracic wall demonstrated a small puncture at the percutaneous biopsy site. About 900 ml blood was present in the left thoracic cavity. The left lung weighed 850 g and was the site of acute massive intraparenchymal hemorrhage and congestion. There were five pleural-parenchymal tears in the posterolateral aspect of the left lower lobe within a 1 cm radius (fig. 1). Within one tear a small muscular artery appeared to have been severed. The position of all five tears was anatomically juxtaposed to the closed biopsy site. About 3.9 cm distal to the five tears and obliquely in line with them was a 2.3 cm nodule of metastatic renal cell carcinoma. There was no gastric aspiration or blood within the tracheobronchial tree and no evidence of thrombotic or air embolism. The coronary vasculature, cerebral vasculature, and central nervous system were unremarkable.

Discussion

Despite careful patient selection, aspiration needle biopsy remains a potentially fatal procedure. The usually accepted contraindications include a known bleeding diathesis or abnormal coagulation studies, emphysematous blebs or bullae in the biopsy area, pulmonary hypertension, central or suspected vascular lesions, pulmonary function studies indicating inability to tolerate a significant pneumothorax, and inability of the patient to cooperate. This patient fell into none of these categories, and the exact reason for his death remains obscure. Slight respiratory motion may have caused the superficial tears, resulting in laceration of the small muscular artery, and causing acute massive exsanguination. Considerable pulmonary edema, hemorrhage, and massive hemothorax compromised the patient's cardiopulmo-



Fig. 1.—Left lower lobe. Largest pleural-parenchymal tear with lacerated small muscular artery (*open arrow*), smaller superficial tears (*arrows*), and severe intraparenchymal hemorrhage (*arrowhead*).

Received July 28, 1978; accepted after revision October 5, 1978.

[1] Department of Radiology, Georgetown University Hospital, 3800 Reservoir Road, N.W., Washington, D.C. 20007. Address reprint requests to L. B. Milner.

[2] Department of Pathology, Georgetown University Hospital, Washington, D.C. 20007.

[3] Department of Medicine, Division of Medical Oncology, Georgetown University Hospital, Washington, D.C. 20007.

© 1979 American Roentgen Ray Society

0361-803X/79/1322-0280 $0.00

nary status. A previous syncopal episode suggests a possible underlying cardiac abnormality. However, this was not confirmed at autopsy.

Despite meticulous attention to detail the patient succumbed to a fatal complication. Short of standby facilities of a shock trauma unit, at present nothing can prevent similar complications. The extreme rarity of this situation mitigates against the use of such extensive precautions. In evaluating the benefit-to-risk ratio in the individual patient, the radiologist should continue to be aware of the potential mortality of aspiration lung biopsy.

REFERENCES

1. Norenberg R, Claxton CP Jr, Takaro T: Percutaneous needle biopsy of the lung: report of two fatal complications. *Chest* 66:216–218, 1974
2. Herman PG, Hessel SJ: The diagnostic accuracy and complications of closed lung biopsies. *Radiology* 125:11–14, 1977
3. Westcott JL: Air embolism complicating percutaneous needle biopsy of the lung. *Chest* 63:108–110, 1973
4. Lauby VW, Burnett WE, Rosemond GP, Tyson RR: Value and risk of biopsy of pulmonary lesions by needle aspiration. *J Thorac Cardiovasc Surg* 49:159–172, 1965
5. Pearce JG, Patt NL: Fatal pulmonary hemorrhage after percutaneous aspiration lung biopsy. *Am Rev Respir Dis* 110:346–349, 1974
6. Woolf CR: Applications of aspiration lung biopsy with review of literature. *Dis Chest* 25:286–300, 1954
7. Meyer JE, Gandbhir LH, Milner LB, McLaughlin MM: Percutaneous aspiration biopsy of nodular lung lesions. *J Thorac Cardiovasc Surg* 73:787–791, 1977

Percutaneous Drainage of Lung Abscess

DIXIE J. ARONBERG,[1] STUART S. SAGEL, R. GILBERT JOST, AND JONG I. LEE

Since entering the antibiotic era, pulmonary abscess has generally not been a therapeutic problem. When medical therapy fails, surgical drainage or resection of the cavity is usually curative [1]. However, surgery may subject some patients to substantial hazard and in the poor operative risk patient, percutaneous drainage of the abscess may be an effective alternate treatment. This case report describes a patient, refractory to the usual treatment methods, who responded to percutaneous drainage of a complicated lung abscess.

Case Report

W. S., a 63-year-old man, suffered weight loss, chest pain, and hemoptysis. Chest radiography disclosed a left hilar mass, an infiltrate in the superior segment of the left lower lobe, and a left pleural effusion. Adenocarcinoma was found by bronchoscopic biopsy. Fluid from a thoracentesis also revealed malignant cells. For 2 months, radiation therapy to 6,000 rad was delivered to opposing 8 × 9 cm portals.

Late in the course of irradiation the patient developed chills, fever, and a large cavitary mass with an air-fluid level in the superior segment of the left lower lobe (fig. 1). Antibiotics were administered intravenously for 2 weeks but there was no change in clinical status or chest radiographs. Complete obstruction of the superior segmental orifice precluded drainage of the cavity by fiberoptic bronchoscopy. Percutaneous needle aspiration of the cavity with an 18-gauge needle was performed to try to establish the infecting organism, and 150 ml of purulent material was obtained; culture yielded a mixed growth of diphtheroids, *Staphylococcus aureus*, and beta-hemolytic streptococcus. Additional antibiotics administered for several days had no effect.

At this time the patient was not considered a surgical candidate due to the poor prognosis of his underlying disease, his severely compromised pulmonary function status, and the prior high-dose radiation therapy. Using percutaneous Seldinger technique, a fluoroscopically guided no. 8 French pigtail angiographic catheter was placed into the abscess cavity (fig. 2) to establish drainage. This method is modified from the percutaneous nephrostomy placement procedure [2]. The catheter was secured to the skin with sutures, and the skin-catheter interface was sealed with vaseline-impregnated gauze. The catheter clogged with necrotic debris, necessitating intermittent irrigation.

The patient improved clinically and the fluid within the cavity resolved. He was discharged 5 days later on oral penicillin therapy with the catheter in place, and it was removed after 2 weeks. Repeat radiography showed a residual cystic structure

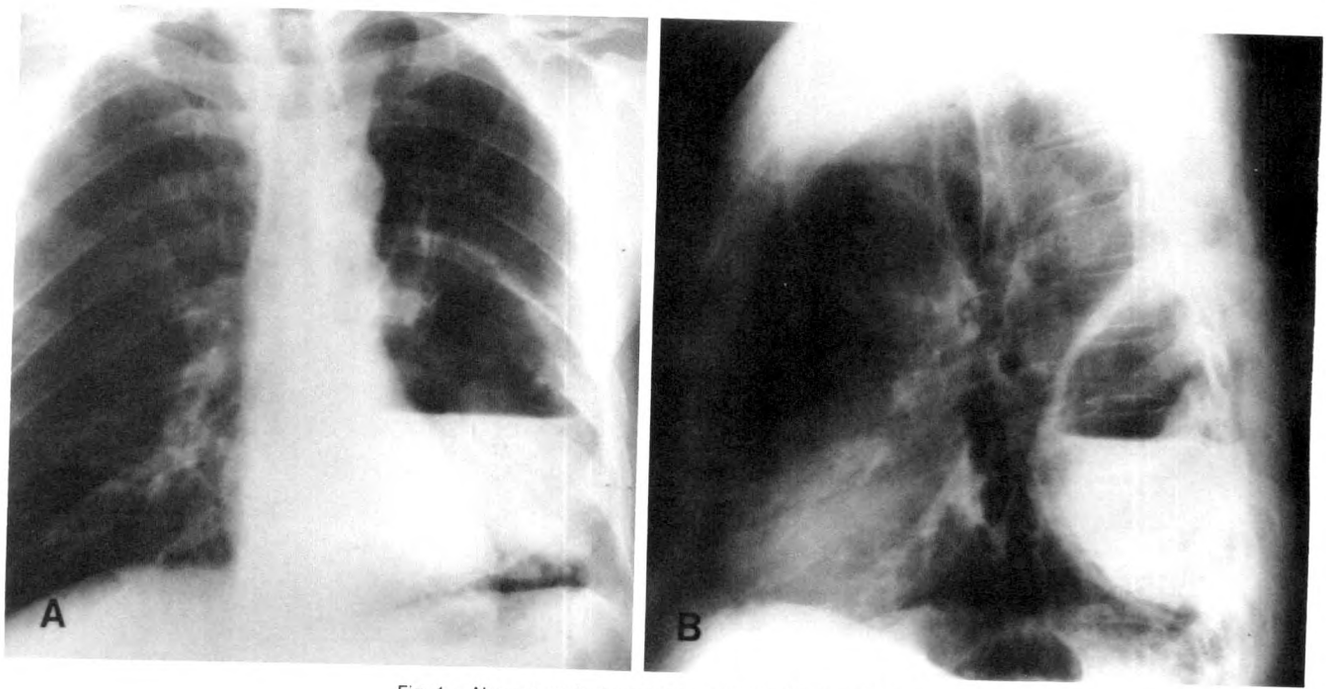


Fig. 1.—Abscess cavity in superior segment of left lower lobe.

Received August 28, 1978; accepted after revision October 17, 1978.

[1] All authors: Mallinckrodt Institute of Radiology, Washington University School of Medicine, 510 South Kingshighway Boulevard, St. Louis, Missouri 63110. Address reprint requests to D. J. Aronberg.

© 1979 American Roentgen Ray Society

0361-803X/79/1322-0282 $0.00

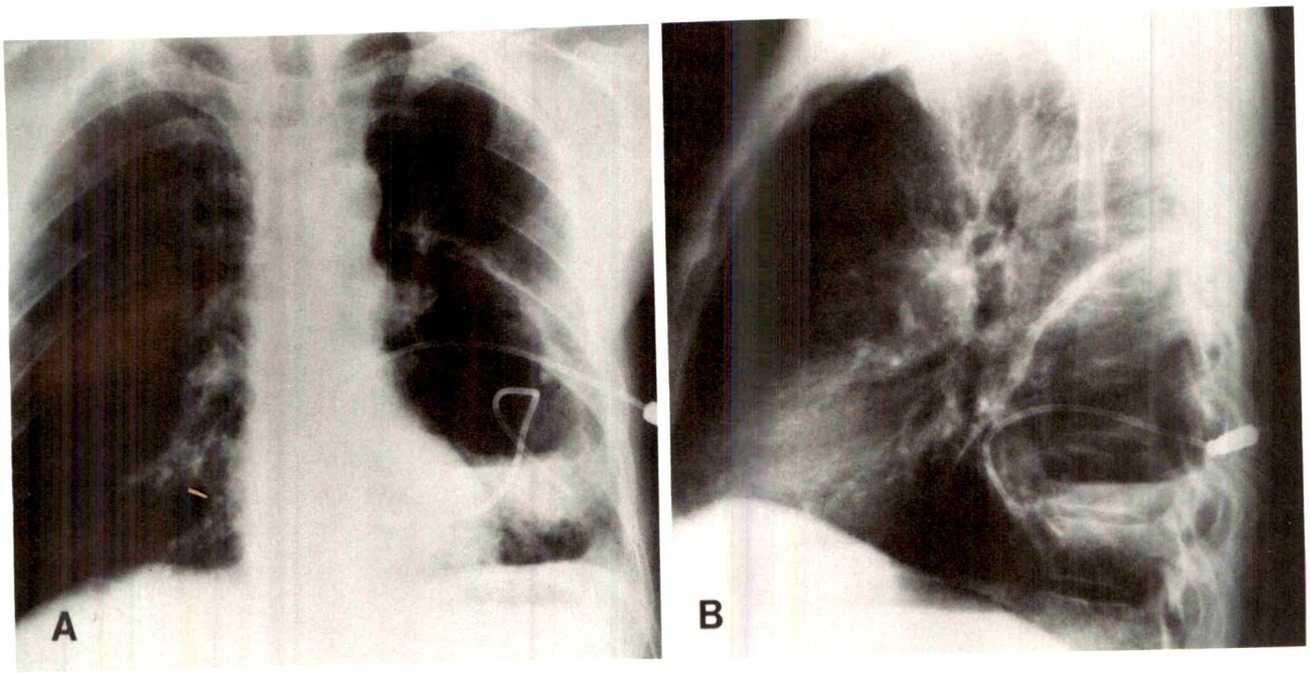


Fig. 2.—**A**, After placement of drainage catheter. **B**, Catheter well within abscess cavity.

without fluid content. The patient is alive without pulmonary symptoms 6 months after percutaneous catheter drainage.

Discussion

Lung abscess today is largely a medical disease [1]. In our case, the presence of a proximal obstructing lesion inhibiting drainage was primarily responsible for development of this refractory abscess. Resecting the abscess (lobectomy) has been the recommended treatment for patients unresponsive to medical therapy; however, surgical mortality is high in patients with associated debilitating disease [1]. The risk for this patient seemed prohibitive. Alternate drainage methods include both transbronchial [3] (which was precluded in this case by bronchial obstruction) and percutaneous catheter techniques. Percutaneous tube drainage of cavitary lesions, first used to treat tuberculous lesions and more recently pyogenic lung abscesses [4–6], has not been emphasized in the radiologic literature.

The potential complications of percutaneous catheter drainage, primarily pneumothorax [7], probably parallel needle aspiration biopsy. The risk of pneumothorax is undoubtedly greatly diminished in subacute or chronic abscesses because of the development of pleurodesis. There is a theoretical potential for causing an empyema, although this may occur spontaneously as well. This risk should also be reduced when preexisting pleural adhesions are present. In this patient the possibility of developing a persistent sinus tract was considered, especially because of the preceding high-dose radiation therapy; fortunately this did not occur.

REFERENCES

1. Chidi CC, Mendelsohn HJ: Lung abscess: results of 90 consecutive cases. *J Thorac Cardiovasc Surg* 69:168–172, 1974
2. Barbaric JL, Wood B: Emergency percutaneous nephropyelostomy: a series and review. *AJR* 128:453–458, 1977
3. Marquis J: Treatment of lung abscess by transbronchial catheter drainage. *Radiology* 107:61–62, 1973
4. Monaldi V: Endocavitary aspiration in the treatment of lung abscess. *Chest* 29:193–201, 1956
5. Morris JF, Okies JE: Enterococcal lung abscess: medical and surgical therapy. *Chest* 65:688–691, 1974
6. Vainrub B, Musher DM, Guinn GA, Young EJ, Septimus EJ, Travis LL: Percutaneous drainage of lung abscess. *Am Rev Respir Dis* 117:153–160, 1978
7. Sagel SS, Fergusson TB, Forrest JV, Roper CL, Weldon CS, Clark RE: Percutaneous transthoracic aspiration needle biopsy. *Ann Thorac Surg*. In press, 1978

Severe Radiation Pneumonitis Precipitated by Withdrawal of Corticosteroids: A Diagnostic and Therapeutic Dilemma

TED M. PARRIS,[1] JAMES G. KNIGHT[1] CHARLES E. HESS,[1] AND WILLIAM C. CONSTABLE[2]

Pulmonary injury secondary to radiation (radiation pneumonitis) is a well recognized syndrome [1]. The occurrence and extent of damage are related, in part, to the total dose and degree of fractionation of radiation and the volume of lung irradiated. The concomitant use of various cancer chemotherapeutic agents is thought to exacerbate this radiation effect [1]. Recently, Kaplan [2] and Castellino et al. [3] described a group of patients who appeared to develop radiation pneumonitis when corticosteroids were abruptly discontinued or tapered rapidly. Our case is notable in view of the severity of the radiation pneumonitis which occurred after the abrupt cessation of corticosteroids and the confirmation of the diagnosis by lung biopsy prior to the reinstitution of corticosteroids.

Case Report

About 1 month after a nonproductive cough and fever, a 17-year-old white boy noted a painless swelling in the left supraclavicular area. Left prescalene node biopsy was performed and interpreted as non-Hodgkin's lymphoma. He was then referred to our institution. Clinical findings included bilateral supraclavicular and axillary lymphadenopathy and splenomegaly. Bilateral iliac crest bone marrow biopsies revealed no evidence of lymphoma. Chest radiography showed massive mediastinal lymphadenopathy (fig. 1A). Chest radiography performed 4 months earlier was reviewed and interpreted as normal. Review of the left prescalene node biopsy was consistent with diffuse histiocytic lymphoma, but interpretation was difficult because of distortion of the tissue, and a repeat biopsy was suggested.

Under general anesthesia, a left supraclavicular node biopsy was performed. When extubation was attempted, the patient was unable to ventilate. Bronchoscopy showed severe extrinsic compression of the trachea at the level of the carina requiring continued intubation and positive pressure ventilatory assistance. As an emergency measure, radiotherapy was started to the mediastinal mass. A total dose of 1,100 rad was given to the midplane in three fractions over 3 days using an 8 MV linear accelerator. By postoperative day 4, the patient was extubated and was able to ventilate without difficulty. Repeat chest radiography 6 days after biopsy revealed marked regression in the size of the mediastinal mass (fig. 1B). The biopsy confirmed the diagnosis of diffuse histiocytic lymphoma. Eight days after biopsy, C-MOPP chemotherapy was begun (1,000 mg cyclophosphamide and 2 mg vincristine intravenously on days 1 and 8, 200 mg procarbazine and 100 mg prednisone orally days 1–14) [4].

After 14 days of C-MOPP therapy, the oral prednisone and procarbazine were stopped; 6 days later the patient was seen because of a 2-day history of a cough productive of minimal amounts of mucoid sputum and a low grade fever (oral temperature, 37.7°C). Chest radiography revealed only minimal residual lymphadenopathy in the right paratracheal region. Sputum and throat cultures were negative. Treatment with oral ampicillin resulted in some improvement, but the symptoms persisted until the second course of C-MOPP (48 days after the start of the first) when all symptoms subsided within 24 hr.

The oral prednisone and procarbazine was stopped after 15 days. The next day the patient again developed malaise, fever, headache, and a nonproductive cough. Within 5 days, he had developed dyspnea and was readmitted for evaluation. Physical examination revealed a rectal temperature of 38.4°C and respirations of 22/min. Lungs were clear to auscultation and percussion. No lymphadenopathy was noted and the spleen was not palpable. Chest radiography revealed mixed interstitial and alveolar infiltrates in both lungs in a distribution that corresponded to the radiation field used 2 months earlier (fig. 1C). The radiation dosage schedule used is believed to be acceptable for lung tolerance when compared on an equivalent dose basis [5].

A transbronchial lung biopsy revealed thickened alveolar septae with a predominantly mononuclear cell infiltration consistent with the diagnosis of acute radiation pneumonitis; no organisms were seen on special stain and subsequent bacterial, viral, fungal, and mycobacterial cultures were negative.

Because of increasing dyspnea and the probable diagnosis of radiation pneumonitis secondary to corticosteroid withdrawal, prednisone (100 mg/day orally) was instituted on day 3 of this admission. Within 12 hr, the patient was symptomatically much improved. Repeat chest radiography 6 days later showed almost complete resolution of the infiltrates (fig. 1D). The prednisone dose was slowly tapered over a period of 6 weeks and stopped. The patient subsequently received four additional courses of C-MOPP (prednisone eliminated) without difficulty. After completion of chemotherapy, an additional 1,600 rad was given to the midplane of the mediastinum in eight fractions over 8 days using a 6 MV linear accelerator. Restaging after completion of therapy confirmed the achievement of a complete remission, and the patient remains relapse-free at 1 year.

Discussion

The occurrence and severity of radiation pneumonitis depends on several factors such as radiation dosage, volume of lung irradiated, and the rate of delivery of the radiotherapy [1]. Other factors thought to potentiate radiation injury to the lung and other tissues include the concomitant administration of antineoplastic drugs, previous radiotherapy, and corticosteroid withdrawal [1–3]. Radiation pneumonitis precipitated by corticosteroid

Received August 17, 1978; accepted after revision October 25, 1978.
This work was supported by the Research and Development Fund, grant 4-66672, University of Virginia School of Medicine.
[1] Department of Internal Medicine, Hematology Division, University of Virginia School of Medicine, Box 180, Charlottesville, Virginia 22908. Address reprint requests to C. E. Hess.
[2] Department of Radiology, Radiation Oncology Division, University of Virginia School of Medicine, Charlottesville, Virginia 22908.

© 1979 American Roentgen Ray Society

0361-803X/79/1322-0284 $0.00

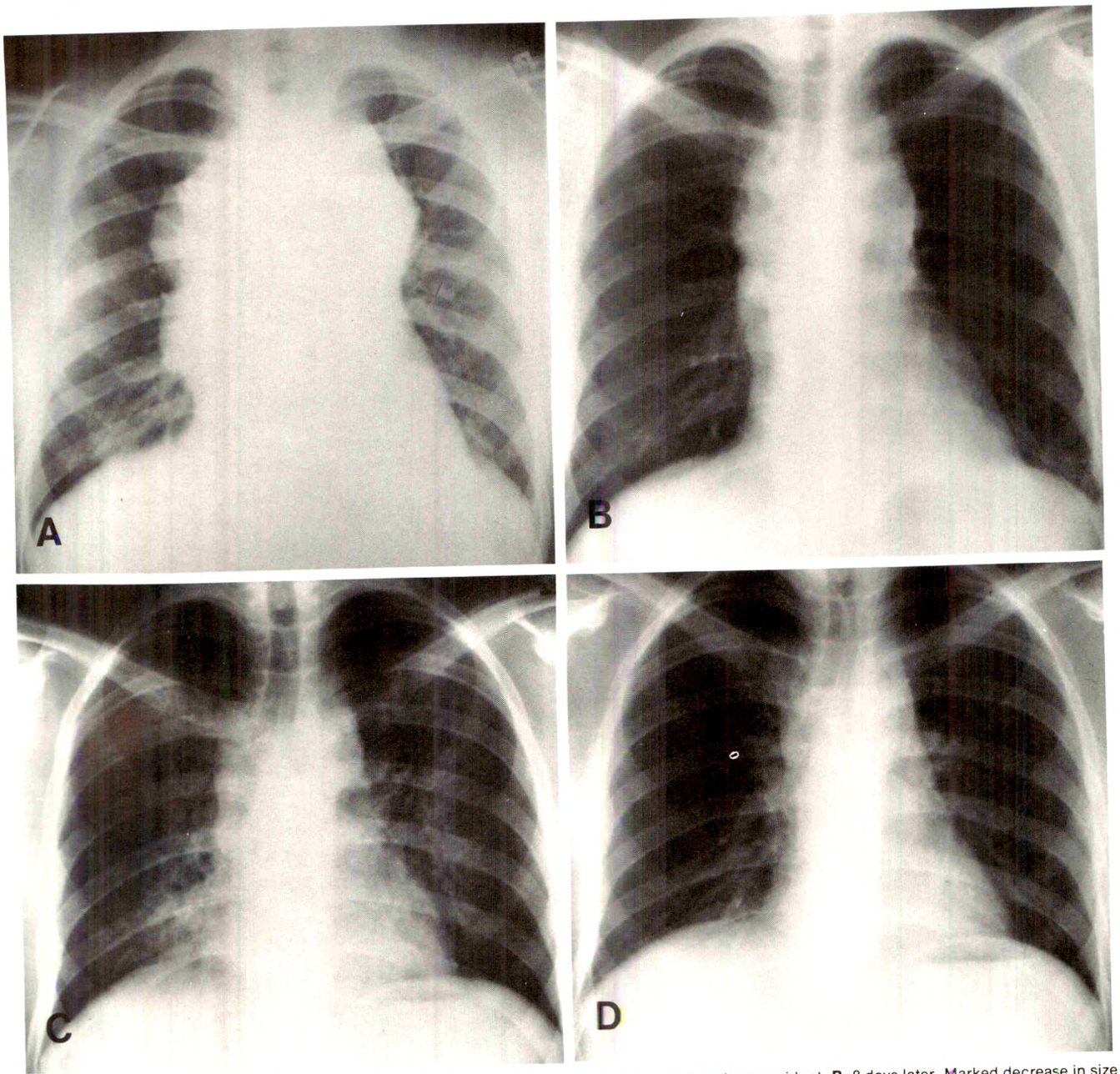


Fig. 1.—**A**, Original chest film. Extent of mediastinal and hilar involvement by histiocytic lymphoma evident. **B**, 8 days later. Marked decrease in size of tumor mass after only 1,100 rad of radiotherapy. **C**, 55 days after **B**. Extensive bilateral mixed alveolar and interstitial pulmonary infiltrates; pattern of distribution of pneumonitis corresponds to radiation field. **D**, 6 days after reinstituting prednisone (8 days after **C**). Note almost complete resolution of pneumonitis.

withdrawal is not a common complication of radiotherapy. Castellino et al. [3] reported only seven such occurrences among 150 patients with Hodgkin's disease who received chest irradiation followed by combination chemotherapy which included corticosteroids.

The development of rapidly progressive pulmonary infiltrates in the compromised host is a difficult diagnostic and therapeutic problem. Since a variety of opportunistic organisms, including gram-negative bacteria, is usually the etiologic agent, the need to establish a definitive diagnosis and begin appropriate therapy is extremely important. In our case, the extent of the pneumonitis and the associated progressive respiratory distress prompted an early decision to perform a lung biopsy. The pathologic findings were consistent with radiation pneumonitis. The fact that the distribution of the pulmonary infiltrates corresponded to the radiation field (fig. 1C) strongly supported this diagnosis. The rapid symptomatic improvement and the subsequent complete resolution of the infiltrates after reinstitution of the prednisone established the diagnosis.

The decision to give such patients a trial of cortico-

steroids, especially without a lung biopsy, is obviously difficult. Several factors may prove helpful in making such a decision and avoiding the need for a lung biopsy. These include: (1) the temporal relationship between the corticosteroid withdrawal and the onset of symptoms; (2) the findings that the distribution of the pneumonitis corresponds to the radiation field; and (3) the prompt symptomatic improvement, usually within 12–24 hr, after reinstitution of the corticosteroids. Close follow-up for the first 24 hr for symptomatic improvement and serial chest films for 4–6 days to document resolution of the pneumonitis should confirm the diagnosis. Complete radiographic resolution of the pulmonary infiltrates usually occurs within 4–6 days. The prednisone should then be slowly tapered over a period of 4–6 weeks, and preferably not used again. If the continued use of prednisone is thought to be necessary, the drug should be slowly tapered each time it is discontinued.

REFERENCES

1. Gross NJ: Pulmonary effects of radiation therapy. *Ann Intern Med* 86:81–92, 1977
2. Kaplan HS: *Hodgkin's Disease*. Cambridge, Harvard University Press, 1972
3. Castellino RA, Glatstein E, Rurbow MM, Rosenberg S, Kaplan HS: Latent radiation injury of lungs or heart activated by steroid withdrawal. *Ann Intern Med* 80:593–599, 1974
4. DeVita VT, Canellos GP, Chabner BA, Schein P, Hubbard SP, Young RC: Advanced diffuse histiocytic lymphoma, a potentially curable disease. *Lancet* 1:248–250, 1975
5. Ware WM, Phillips TL, Margolis LW, Smith V: Radiation pneumonitis: a new approach to the derivation of time-dose factors. *Cancer* 32:547–552, 1973

Emphysematous Pyelonephritis Demonstrated by Computed Tomography

DANIEL S. KIM,[1] MERLIN E. WOESNER, THORA F. HOWARD, AND LINDA K. OLSON

From 1898 to 1975, 39 cases of emphysematous pyelonephritis have been reported [1, 2]. The first case documented by abdominal CT in which the disease process extended to the lesser sac is reported here. To our knowledge, involvement of the lesser sac has not been previously reported.

Case Report

A 67-year-old Mexican American man with known but poorly treated diabetes mellitus for 8 years had fever and chills for 18 hr. Physical examination revealed minimal left costovertebral angle tenderness; however, no abdominal mass was palpated and the abdomen was negative for rigidity or rebound tenderness. No diabetic retinopathy was noted. Urinalysis showed 70 leukocytes, one erythrocyte, and minimal glucose. Initial blood sugar was 746 mg/100 ml. Medical history included a suprapubic prostatectomy performed in Mexico 5 months before admission. The patient's condition deteriorated rapidly after admission requiring endotracheal intubation with respiratory assistance and cardiac monitoring. Blood and urine cultures grew *E. coli*. Abdominal radiography on day 3 revealed left emphysematous pyelonephritis (fig. 1A). High dose excretory urography with tomograms showed no opacification of the renal parenchyma or collecting systems bilaterally (fig. 1B). CT scan later the same day revealed extension of the emphysematous process to the splenic capsule, lesser sac, and posterior portion of the costodiaphragmatic recess (fig. 2). Because of the patient's moribund condition and the extent of the emphysematous process shown by CT, surgical drainage of the left kidney was performed rather than nephrectomy. Additional drainage was used deep to the renal and perirenal area, guided by the CT findings. Repeat CT scan 3 weeks later showed significant improvement of the emphysematous process and no gas was noted in the lesser sac. The patient underwent left nephrectomy 3 weeks later and was discharged in fair condition 82 days after admission.

Discussion

Emphysematous pyelonephritis is a rare entity most often seen in diabetics [1–3]. One-third to one-half of the patients with this condition have associated urinary tract obstruction. Organisms cultured from the surgical or drainage specimens include those of the gastrointestinal tract, most commonly *E. coli*; however, *Pseudomonas, Aerobacter aeruginosa*, and *Klebsiella aerobacter* have all been reported [1, 7]. Treatment generally consists of antibiotic therapy, surgical drainage, and/or nephrectomy [4, 5]. Overall prognosis is poor regardless of therapy, with a 50%–55% mortality rate generally reported [2, 6].

Correct diagnosis can be made by plain abdominal radiography and excretory urography. In our case, CT scan documented more extensive emphysematous involvement than plain radiography or traditional tomographic examination. Tomography demonstrated emphysema of the renal parenchyma and pelviocalyceal system with extension through the renal capsule to Gerota's fascia. There was also tomographic evidence of contiguous involvement of the paravertebral space. The CT scan added the information that the process extended to the posterior portion of the diaphragmatic

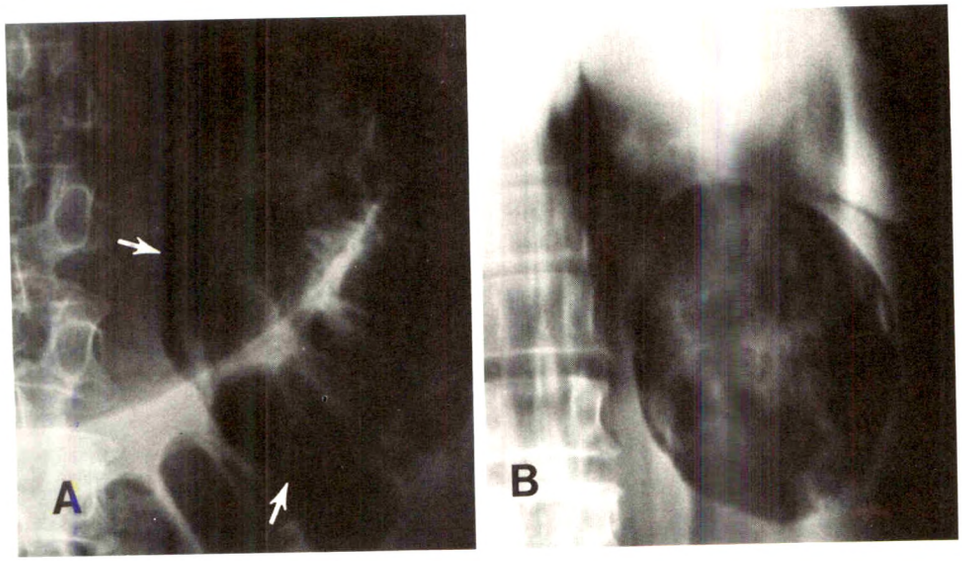


Fig. 1.—**A**, Abnormal gas collection (*arrows*) in left upper quadrant in region of left kidney. **B**, Gas surrounds emphysematous left kidney and upper ureter and has dissected into paravertebral space and toward splenic capsule. No opacification of renal collecting systems.

Received March 14, 1978; accepted after revision October 26, 1978.
[1] All authors: Department of Radiology, White Memorial Medical Center, 1720 Brooklyn Avenue, Los Angeles, California 90033. Address reprint requests to D. S. Kim.

AJR 132:287–288, February 1979
0361–803X/79/1322–0287 $0.00
© 1979 American Roentgen Ray Society

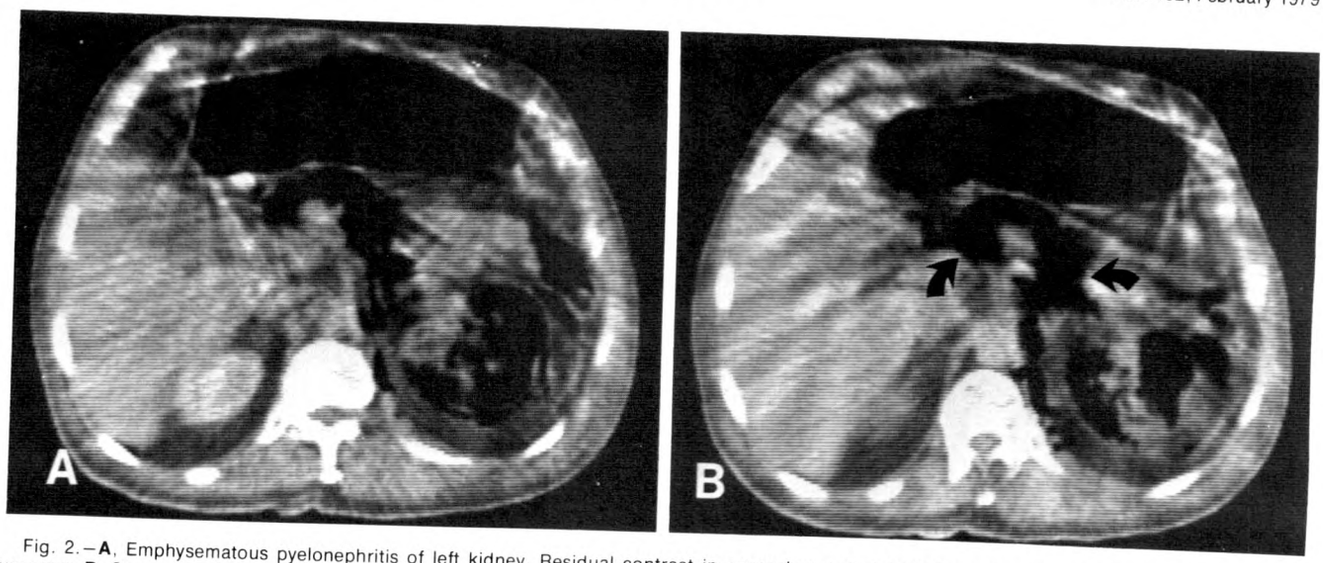


Fig. 2.—**A**, Emphysematous pyelonephritis of left kidney. Residual contrast in parenchyma of right kidney was not seen on previous excretory urogram. **B**, Gas extends through paravertebral space into lesser sac (*arrows*).

recess, splenic capsule, and lesser sac. On this basis, we feel that CT scanning provides more precise anatomic information to guide surgical planning.

REFERENCES

1. Langston CS, Pfister RC: Renal emphysema: a case report and review of the literature. *AJR* 110:778–786, 1970
2. Dunn SR, DeWolf WC, Gonzalez R: Emphysematous pyelonephritis: report of 3 cases treated by nephrectomy. *J Urol* 114:348–350, 1975
3. Goergen TG: Unusual abdominal gas collection. *JAMA* 239:347–348, 1978
4. Murphy JF, Fred HL, Carlson J: Renal and perirenal gas in a diabetic man. *JAMA* 237:801–802, 1977
5. Rosenberg JW, Quader A, Brown JS: Renal emphysema. *Urology* 1:237–239, 1973
6. Schainuck LI, Fouty R, Cutler RE: Emphysematous pyelonephritis: a new case and review of previous observations. *Am J Med* 44:134–139, 1968
7. Bliznak J, Ramsey J: Emphysematous pyelonephritis. *Clin Radiol* 23:61–64, 1972

A Benign Cause of Increased Radiocolloid Accumulation on a Liver Scan

HARRY G. GREDITZER, III[1, 2] JUDITH E. HO,[1] MICHAEL WOLVERSON,[3] AND PATRICK JOYCE[3]

Increased focal radiotracer accumulation in the ^{99m}Tc sulfur colloid liver scan was initially described in 1972 [1]. Subsequently, this finding has been reported most commonly in association with superior vena caval obstruction [2, 3]. Other less common causes of this abnormality include the Budd-Chiari syndrome [4], hepatic hemangioma [5], hamartomas [6], solitary hepatic abscesses [7], and inferior vena caval obstruction [2].

The location and intensity of the liver scan abnormality apparently correlates well with certain types of pathologic processes. The demonstration of a focal increase in radioactivity along the inferior edge of the liver between the right and left lobes has been suggested as indicative of superior vena caval obstruction [3]. It has been postulated that obstruction to flow in the superior vena cava leads to systemic-portal shunting via superficial thoracic and abdominal venous collaterals with resultant increased delivery and phagocytosis of radiocolloid in the liver overlying the portal vein [3].

Our case had a static liver scan consistent with superior vena caval obstruction. A normal superior vena cava was subsequently demonstrated. The etiology of the focal increase in radioactivity seen on the scan was found to be a benign alteration in hepatic morphology.

Case Report

A 68-year-old white man was referred to our institution after a laryngeal tumor was demonstrated by indirect laryngoscopy. Some 12 months before admission, he noticed a gradual onset of shortness of breath accompanied by increasing hoarseness. Two weeks before admission, he experienced marked increase in shortness of breath with respiratory stridor. Medical history and review of systems were essentially noncontributory. On admission, he was noted to be tachypnic with marked inspiratory stridor. Other than a midline abdominal ventral hernia, the physical examination was within normal limits. Admission laboratory values were within normal limits with the exception of arterial blood gases which revealed a pH of 7.33, pCO_2 of 50, and pO_2 of 83 mm Hg while receiving 6 l of O_2/min. Admission chest radiography showed normal lungs and a prominent superior mediastinum with paratracheal mass. Because of the patient's marked respiratory distress, an emergency tracheostomy was performed without complication. Direct laryngoscopy demonstrated a large mass which involved the pyriform sinuses and supraglottic, and subglottic areas. Biopsy of this mass revealed an invasive, well differentiated squamous cell carcinoma.

As part of the evaluation for metastatic disease, a ^{99m}Tc sulfur colloid liver scan was obtained including views in the anterior, posterior, and right lateral projections. A focal area of increased tracer accumulation was identified along the inferior edge of the liver medial to the gallbladder fossa (fig. 1A). A dynamic liver study demonstrated early visualization of the same area of the liver with no evidence of abnormal venous collaterals. Radionuclide superior venacavography was normal. The liver, when reexamined with radiocolloid and the patient in the standing right lateral position, demonstrated herniation and molding of the anterior portion into a large ventral hernia (fig. 1B). Abdominal CT showed that, even in the supine position, a portion of the liver protruded anteriorly into the hernia (fig. 1C). The remaining workup failed to demonstrate evidence of metastatic disease. A total laryngectomy was subsequently performed without complication.

Discussion

It has been well documented that the demonstration of an isolated increase in uptake of radiolabeled sulfur colloid in static liver images, in conjunction with the finding of abnormal collateral venous circulation, is quite specific for superior vena caval obstruction [2, 3]. Even in the absence of an accompanying flow study, previous workers have associated the liver "hot spot" with significant vascular or parenchymal pathology. No prior reports of the association of increased hepatic focal accumulation of sulfur colloid with benign changes in liver morphology were found.

The pathophysiology of the liver hot spot in various disorders has been previously discussed. However, the etiology of focal increase in radioactivity in the present case is less certain. It is possible that because of the molding of the liver into the patient's ventral hernia, the gamma camera "saw" a relatively greater depth of liver tissue in the anterior position, with a subsequent increase in amount of radioactivity. Enhancement of the hot spot may also have occured because the anterior pseudopod of liver tissue was actually 5–6 cm closer to the crystal than the remainder of the liver. Alternatively, the relative lack of tissue attenuation from the anterior wall of the hernia in comparison with the remainder of the abdominal wall, which allowed more counts to be accumulated over that area, may explain the hot spot seen in the liver. It would also explain the findings in the liver flow study.

Because of the characteristic vascular findings, the use of dynamic imaging in the investigation of a liver hot spot is quite useful and revealing. However, without that mode of imaging, the findings of such a typically located "hot spot" may lead directly to contrast venacavography, a more invasive procedure with greater risk. Our case demonstrates a relatively benign cause of increased focal radioactivity which should be excluded before more invasive procedures are instituted.

Received June 8, 1978; accepted after revision October 26, 1978.

[1] Division of Nuclear Medicine, Department of Internal Medicine, St. Louis University School of Medicine, 1325 South Grand Boulevard, St. Louis, Missouri 63104. Address reprint requests to J. E. Ho.

[2] Present address: Department of Diagnostic Radiology, Mayo Clinic, 200 First Street S.W., Rochester, Minnesota 55901.

[3] Department of Diagnostic Radiology, St. Louis University School of Medicine, St. Louis, Missouri 63104.

© 1979 American Roentgen Ray Society

0361-803X/79/1322-0289 $0.00

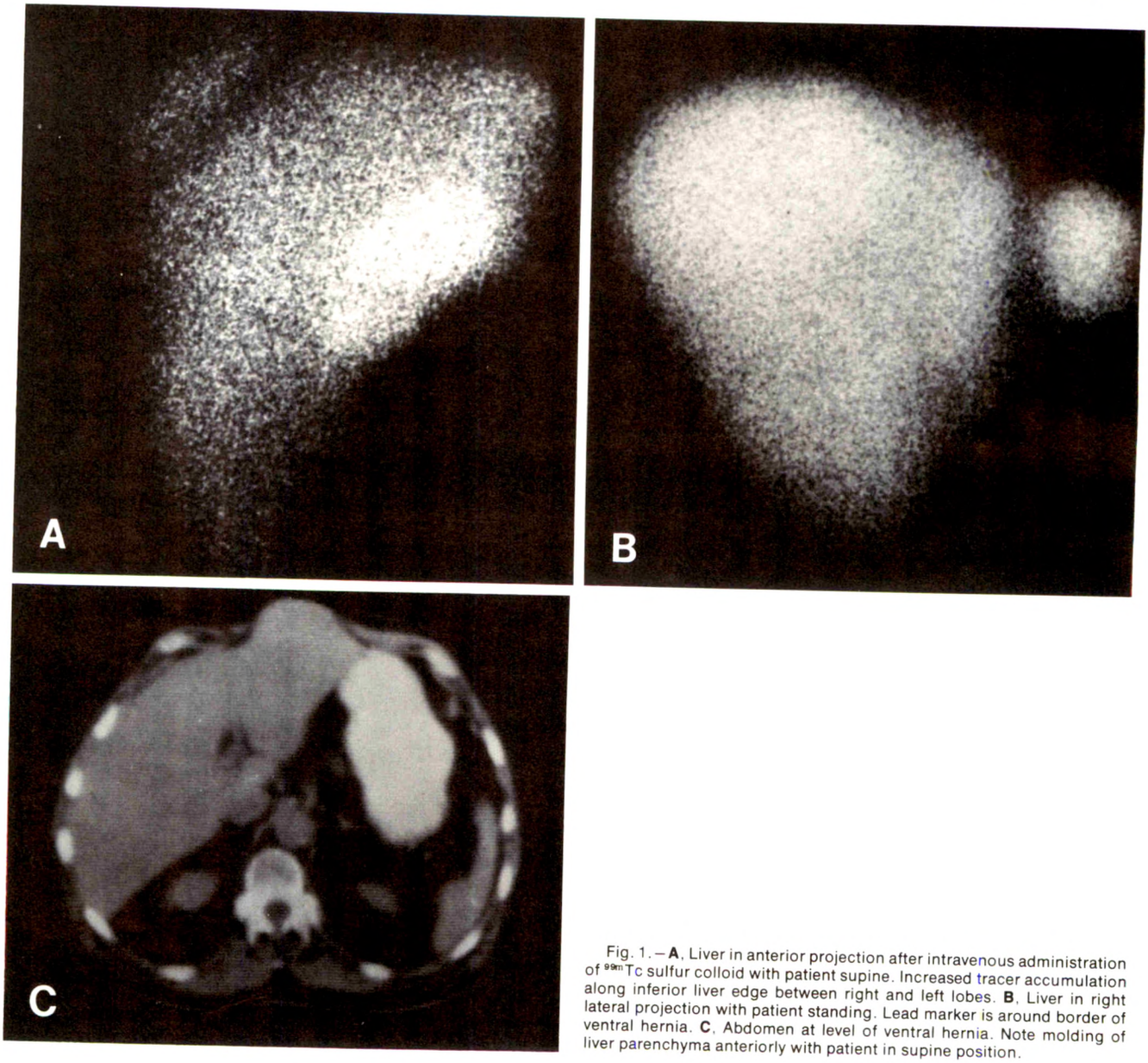


Fig. 1.—**A**, Liver in anterior projection after intravenous administration of ^{99m}Tc sulfur colloid with patient supine. Increased tracer accumulation along inferior liver edge between right and left lobes. **B**, Liver in right lateral projection with patient standing. Lead marker is around border of ventral hernia. **C**, Abdomen at level of ventral hernia. Note molding of liver parenchyma anteriorly with patient in supine position.

REFERENCES

1. Coel M, Halpern S, Alazraki N, Ashburn W, Leopold G: Intrahepatic lesion presenting as an area of increased radiocolloid uptake on a liver scan. *J Nucl Med* 13:221–222, 1972
2. Gooneratne N, Buse M, Quinn J, Selby J: "Hot spot" on hepatic scintigraphy and radionuclide venacavography. *AJR* 129:447–450, 1977
3. Tetalman M, Kusumi R, Gaughran G, Baba N: Radionuclide liver spots: indicator of liver disease or a blood flow phenomenon. *AJR* 130:291–296, 1978
4. Meindok H, Langer B: Liver scan in Budd-Chiari syndrome. *J Nucl Med* 17:365–368, 1976
5. Volpe J, Johnston G: "Hot" hepatic hemangioma: a unique radiocolloid-concentrating liver scan lesion. *J Surg Oncol* 2:373–377, 1970
6. Pasquier J, Dorta T: Hyperfixation of radiocolloid by the liver. *J Nucl Med* 15:725, 1974
7. Chayes Z, Koenigsberg M, Freeman L: The "hot" hepatic abscess. *J Nucl Med* 15:305–307, 1974

Protrusio Acetabuli Following Pelvic Irradiation

FERRIS M. HALL,[1] PETER M. MAUCH,[2] MARTIN B. LEVENE,[2] AND MICHAEL A. GOLDSTEIN[3]

This report documents extensive symmetric bony changes with acetabular protustion and femoral head deformities after relatively small amounts (3,800 rad of therapeutic pelvic radiation. Literature review revealed only one other case report of bilateral protrusio acetabuli secondary to irradiation, and this followed large doses of 7,000 rad [1].

Case Report

A 69-year-old woman had a left-side pelvic mass; laparotomy revealed a large unresectable poorly differentiated adenocarcinoma of probable ovarian origin. Three small metastatic liver foci were identified. Excretory urography showed partial obstruction of the distal left ureter.

The patient was treated with cyclophosphamide (50 mg three times a day) for 7 weeks after surgery, but this medication was discontinued after repeat excretory urography showed no improvement of the left hydronephrosis. No other cytotoxic or steroid medications were administered. The patient was then given 3,000 rad whole abdominal irradiation extending to the level of T12, followed by another 800 rad to the pelvis. This was delivered over 4 weeks at 175 rad per fraction, 5 fractions per week, with anterior and posterior fields using a 4 MeV linear accelerator. Posterior kidney blocks were added after the first 1,000 rad had been delivered. Nausea and bone marrow depression occurred during treatment. The patient remained asymptomatic for 18 months after treatment—she was ambulatory and had no musculoskeletal symptoms.

Radiography of the pelvis and spine at initial diagnosis and inception of radiation therapy was normal. Pelvic radiography 20 months after radiation therapy because of bilateral hip pain showed only slight interval demineralization (fig. 1A). Pain progressed to involve the lower back, and further radiography after another 8 months (a total of 28 months after irradiation) revealed the interval appearance of symmetric deformities of both femoral heads and further demineralization (fig. 1B), as well as compression fractures of T12–L5. No thoracic fractures were present above the level of T12 at this time. The patient's symptoms progressed, and 46 months after irradiation she was ambulatory only with a walker. Radiography at that time showed still further demineralization and symmetric progression of the abnormalities of the hips and lower spine (figs. 1C and 2).

Initial bone scan 12 months after start of radiation therapy and before onset of skeletal symptoms was normal except for focal increased radioactivity over the second lumbar vertebral body consistent with fracture. Repeat bone scan 46 months after irradiation (at the time of radiography in figs. 1C and 2) showed marked symmetric increase in radioactivity over both hips and the entire lumbar spine with normal uptake in the rest of the pelvis. In addition, there was increased activity in several ribs and thoracic vertebral bodies, outside the radiation field, compatible with recent fracture and/or metastatic disease. Radiography of the thoracic spine confirmed vertebral compression fractures at T7 and T9, but pedicles were intact.

The patient currently, almost 6 years (70 months) after irradiation, has no definite evidence of recurrent tumor. She continues to have hip pain and difficulty in ambulation. The pelvic mass persists and recent barium enema examination and sigmoidoscopy show an area of sigmoid narrowing, little changed over 4 years, suggesting radiation stricture or possibly neoplasm. The patient has never experienced joint pain outside of the hip and low back areas and repeatedly denies an early morning component to these symptoms. Hand films show no evidence of rheumatoid arthritis and the latex fixation test has been negative on three occasions. Radiologic bone surveys reveal no evidence of Paget's disease. The creatinine and alkaline phosphatase levels have been normal on repeated measurements throughout the patient's course. On admission for urinary tract infection 1 month after completion of irradiation, serum calcium was 7.7 and phosphorus 2.1. The serum albumin was 2.0 at that time with an otherwise unremarkable serum electrophoresis. Serum calcium and phosphorus measurements were normal 2, 4, and 5½ years after the initial low levels.

Discussion

Bilateral symmetric acetabular protusion with accompanying "necrosis" of the femoral heads is highly characteristic of rheumatoid arthritis, particularly after high dose steroid treatment [2], and is occasionally seen after other granulomatous types of arthritis secondary to rheumatoid variants. Bilateral protusio acetabuli is also classically seen in Paget's disease with severe osteomalacia and in an idiopathic childhood form that is occasionally familial. Unilateral protrusion occurs in tuberculosis or after acetabular fracture. Murray and Jacobson [3] described unusual instances of this abnormality secondary to gout, ochronosis, and osteogenesis imperfecta. Slaughter [4] and Dalinka et al. [5] each illustrated a case of unilateral acetabular protrusion believed secondary to pathologic postirradiation fractures. A single previous case of bilateral protusio acetabuli following pelvic radiation was recently reported by Hasselbacher and Schumacher [1].

Howland et al. [6] described the radiologic appearances of postirradiation bone abnormalities consisting of (in approximate order of severity) a coursened trabecular pattern, diffuse demineralization, and focal lytic and/or sclerotic changes. Postirradiation osseous complications include fractures and, to a lesser extent, true bone necrosis, osteomyelitis, and sarcoma [5–8]. The incidence of complications varies with dosage. Howland

Received March 28, 1978; accepted after revision September 12, 1978.

[1]Department of Diagnostic Radiology, Beth Israel Hospital, Harvard Medical School, 330 Brookline Avenue, Boston, Massachusetts 02215. Address reprint requests to F. M. Hall.

[2] Joint Center for Radiation Therapy, Beth Israel Hospital, Harvard Medical School, Boston, Massachusetts 02215.

[3] Department of Medicine, Beth Israel Hospital, Harvard Medical School, Boston, Massachusetts 02215.

© 1979 American Roentgen Ray Society

0361–803X/79/1322–0291 $0.00

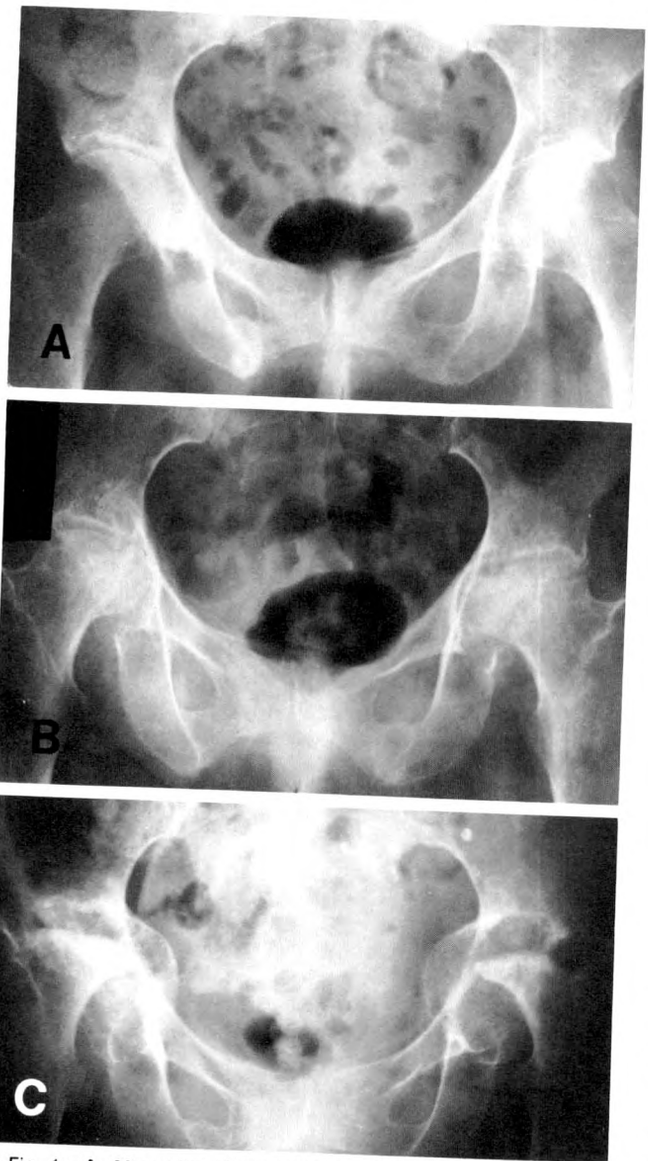


Fig. 1.—**A,** 20 months after irradiation. Slight demineralization (not seen on preirradiation film). **B**, 28 months after irradiation. Femoral heads show symmetric "avascular necrosis" with subcapital fractures and flattening and minimal acetabular protrusion. **C**, 46 months after irradiation. Gross dissolution and deformity of femoral heads with symmetric acetabular protrusion and interval demineralization of entire pelvis.

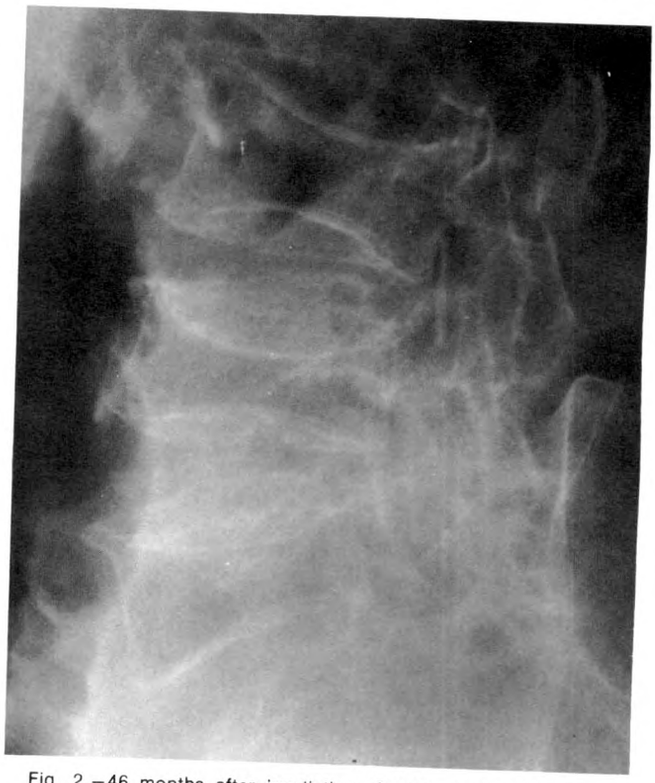


Fig. 2.—46 months after irradiation. Severe demineralization and central compression fractures involving all irradiated vertebral bodies including T12 (not shown). Preirradiation films of this area were normal.

et al. [6] found no demonstrable postirradiation bone abnormalities in the first year after treatment, but when changes occurred they were always present by the end of the third year. This time sequence is in keeping with that of our patient, whose pelvic radiographs were normal 20 months, but positive 28 months, after treatment, and with the case reported by Hasselbacher and Schumacher [1], in which the earliest radiologic evidence of acetabular protusion was seen 22 months after irradiation and rapidly progressed in the following 3 months.

The predisposition of proximal femoral heads to develop "aseptic or avascular necrosis" from a variety of etiologies, and of the femoral necks to fracture after radiation therapy [8], may relate to weight-bearing stresses, as well as to the unique vascular supply of these areas. Postirradiation osteocytic injury may result predominantly from damage to microvasculature with intimal fibrosis and narrowing and/or obliteration of arterioles, rather than from a direct radiation effect upon osteocytes [9–10]. Parodi et al. [11] demonstrated in studies of rat jaws that bone resorption, and presumably a predisposition to complications such as fracture, are enhanced when stress is applied to irradiated areas. The lytic/sclerotic changes and deformities in our patient may reflect the inability, or compromised ability, of damaged but possibly still viable bone cells to repair normally occurring micro-stress fractures. The viability of some cells would explain the relatively normal uptake of the bone scanning agent in our patient 1 year after irradiation at a time when cell damage had probably occurred but no radiologically demonstrable deformities were seen. The actual mechanism of radiation-induced protrusio is unclear, but undoubtedly relates to the weight-bearing forces operative in the hip, and possibly multiple insufficiency type stress fractures superimposed upon the diminished structural strength occurring during bone revascularization and remodeling.

Although our patient's osseous changes in the hips and lumbar spine very likely relate to the radiation delivered to these areas, the uniquely severe abnormalities are disproportionate to the relatively small and well documented dose of 3,800 rad. The patient of Hasselbacher and Schumacher [1] received 7,000 rad. Bone is

relatively resistant to radiation and the minimal tolerance dose (defined as that amount of radiation given under standard conditions which results in no more than a 5% severe complication rate) is estimated to be 6,000 rad for mature bone [10, 12]. In the jaw, where more clinical and experimental data are available, doses under 6,000–7,000 rad produce an acceptable small complication rate [8]. In the shoulder girdle in patients undergoing supraclavicular radiation for breast carcinoma, Howland et al. [6] observed mild atrophic changes at doses of 4,200–5,200 rad, but more severe lytic-sclerotic changes and complications were rarely seen except with higher doses.

We found no data to suggest that the preirradiation course of chemotherapy might explain the severity of the osseous changes in our patient. It would be extremely unusual for adult onset osteomalacia to produce this degree of acetabular protrusions and only one of four serum calcium levels obtained over a 5 year interval on this patient was low, which can be attributed to a very low albumin level at that time. Alkaline phosphatase levels have never been elevated. A very unusual presentation of seronegative rheumatoid arthritis superimposed on the osseous radiation damage cannot be entirely excluded as an explanation for the protrusio in this patient. However, the severe focal changes in the lower spine (T12–L5) corresponding exactly to the field of radiation make a primary systemic or metabolic cause appear unlikely. The chronologic association of bone changes after irradiation further suggests the latter treatment as the primary etiologic factor. The reasons for this patient's presumedly increased sensitivity to irradiation remains unexplained.

REFERENCES

1. Hasselbacher P, Schumacher HR: Bilateral protrusio acetabuli following pelvic irradiation. *J Rheumatol* 4:189–196, 1977
2. Hastings DE, Parker SM: Protrusio acetabuli in rheumatoid arthritis. *Clin Orthop* 108:76–83, 1975
3. Murray RO, Jacobson HG: *The Radiology of Skeletal Disorders*. Baltimore, Williams & Wilkins, 1972
4. Slaughter DP: Radiation osteitis and fractures following irradiation. *AJR* 48:201–212, 1942
5. Dalinka MK, Edeiken J, Finkelstein JB: Complications of radiation therapy: adult bone. *Semin Roentgenol* 9:29–40, 1974
6. Howland WJ, Loeffler RK, Starchman DE, Johnson RG: Post-irradiation atrophic changes of bone and related complications. *Radiology* 117:677–685, 1975
7. Bragg DG, Shidnia H, Chu FCH, Higinbotham NL: The clinical and radiological aspects of radiation osteitis. *Radiology* 97:103–111, 1970
8. Parker RG: Tolerance of mature bone and cartilage in clinical radiation therapy. *Front Rad Ther Oncol* 6:312–331, 1972
9. Kim JH, Chu FCH, Pope RA, Woodard HQ, Bragg DB, Schidnia H: Time dose factors in radiation induced osteitis. *AJR* 120:684–690, 1974
10. Rubin P, Casarett GW: Concepts of clinical radiation pathology, in *Medical Radiation Biology*, edited by Dalrymple GV, Gaulden ME, Kollmorgen GM, Vogel HH, Philadelphia, Saunders, 1973, pp 160–189
11. Parodi RJ, Ubios AM, May J, Cabrini RL: Total body irradiation effects on the bone resorption mechanism in rats subjected to orthodontic movements. *J Oral Pathol* 2:1–6, 1973
12. Rubin P: The radiographic expression of radiotherapeutic injury, an overview. *Semin Roentgenol* 9:5–13, 1974

Popliteal Pseudoaneurysm as a Complication of an Adjacent Osteochondroma: Angiographic Diagnosis

GUERDON GREENWAY,[1] DONALD RESNICK,[2] AND JOSEPH J. BOOKSTEIN[1]

Complications of single and multiple osteochondromata are well established, consisting most frequently of skeletal deformity, growth abnormality, limitation of joint movement, malignant degeneration, and vascular and nerve compression. Less common complications include spinal cord compression, dystocia, and hemothorax. We describe a case of pseudoaneurysm of the popliteal artery secondary to an adjacent femoral osteochondroma. The initial clinical diagnosis was malignant degeneration of an exostosis. Angiography provided the correct diagnosis, permitting appropriate surgical management.

Case Report

A 16-year-old white woman with multiple hereditary exostoses had a 1-week history of pain in the posterior aspect of her right knee which first occurred as she exited a car. Shortly thereafter, she noted swelling and tenderness along the posteromedial aspect of the distal right thigh. There was no history of trauma. Physical examination revealed a short adolescent female with the stigmata of multiple exostoses. There was swelling, tenderness, and increased warmth along the posteromedial aspect of the right thigh. The overlying skin was mildly ecchymotic and the right popliteal pulse was absent. The dorsalis pedis pulses were faintly palpable bilaterally, although the posterior tibial pulses were normal. Laboratory evaluation revealed an erythrocyte sedimentation rate of 23 mm/hr, and an alkaline phosphatase of 13.5 IU/dl (normal, 2.6–11.1 IU/dl). Hematocrit, white blood count, SGOT, and lactic dehydrogenase were normal. A skeletal survey demonstrated multiple osteochondromata.

Two exostoses arose from the distal medial femoral metaphysis, a thin pedunculated lesion anteriorly, and a broad sessile osteochondroma posteriorly. The cortical margin of the posterior osteochondroma was discontinuous both on tomography and on magnification radiography (fig. 1A). No old films were available for evaluation of interval change.

Scintigraphy revealed increased uptake of radionuclide in the distal right femur. The clinical impression, after this initial evaluation, was malignant degeneration of the posterior right femoral osteochondroma. Angiography was requested to delineate the relation of the distal femoral and popliteal arteries to the osteochondroma, and to evaluate neovascularity and soft tissue extension. A selective right femoral artery injection demonstrated posterior displacement and partial compression of the proximal popliteal artery with stretching of branches adjacent to the posterior osteochondroma (fig. 1B). Contrast medium extravasated into a defined periarterial space through a small anterior defect in the popliteal artery. Magnification angiography, with and without angiotensin, demonstrated mass effect adjacent to the osteochondroma, but no pathologic vessels. The radiologic diagnosis was popliteal artery pseudoaneurysm with no angiographic evidence of malignancy.

Surgical exploration revealed a 3 mm erosion of the anterior aspect of the popliteal artery adjacent to the osteochondroma. A large amount of old, organized hematoma surrounded the popliteal artery and the osteochondroma. The entire osteochondroma and a 1 cm segment of the popliteal artery containing the erosion were excised with end-to-end anastomosis of the vessel. Pathologic examination of the osseous specimen demonstrated a benign osteochondroma without evidence of malignancy. The postoperative course was uneventful, and 4 months later the patient had resumed normal activity.

Discussion

Pseudoaneurysms secondary to adjacent osteochondromata are unusual lesions. Review of the English literature reveals 25 previously reported cases [1–22]; several additional cases have been documented in foreign language publications [23–25]. These 25 cases were analyzed for age and sex incidence, laterality, type of trauma, and clinical characteristics.

Of 25 patients with this lesion, 22 (88%) were male. This striking male predominance may be related to the propensity for more vigorous physical activity in that gender. The lesions occurred with almost equal frequency on both sides and were evenly divided between those with solitary and multiple exostoses. Although the age range was wide (9–55 years), the average age at onset of symptoms was 19 years. The appearance of this lesion in late adolescence is most probably related to the growth characteristics of the osteochondroma. An osteocartilaginous exostosis grows by enchondral ossification, similar to the growth of an epiphyseal cartilage plate. According to Jaffe [26], the cartilaginous cap on the surface of the osteochondroma generally ceases to proliferate by the time the patient stops growing. At this time, the cartilaginous surface becomes closed off by a thin osseous plate and the residual cartilage may undergo regressive changes.

These growth characteristics may well explain the mechanical basis for the formation of pseudoaneurysms around the time of skeletal maturity. The loss of a smooth protective cartilaginous cap places the adjacent popliteal artery in contact with the osseous surface of the exostosis. Arterial pulsation or movements of the knee joint result in repetitive trauma to the popliteal artery, producing abrasion and, eventually, laceration of the vascular wall. Pseudoaneurysm formation results.

Almost all of the pseudoaneurysms complicating osteochondromata have arisen in the proximal portion of

Received August 8, 1978; accepted after revision October 19, 1978.

[1]Department of Radiology, University of California Hospital, 225 West Dickinson Street, San Diego, California 92103. Address reprint requests to G. Greenway.

[2]Department of Radiology, University of California, San Diego, and Veterans Administration Hospital, La Jolla, California 92037.

© 1979 American Roentgen Ray Society

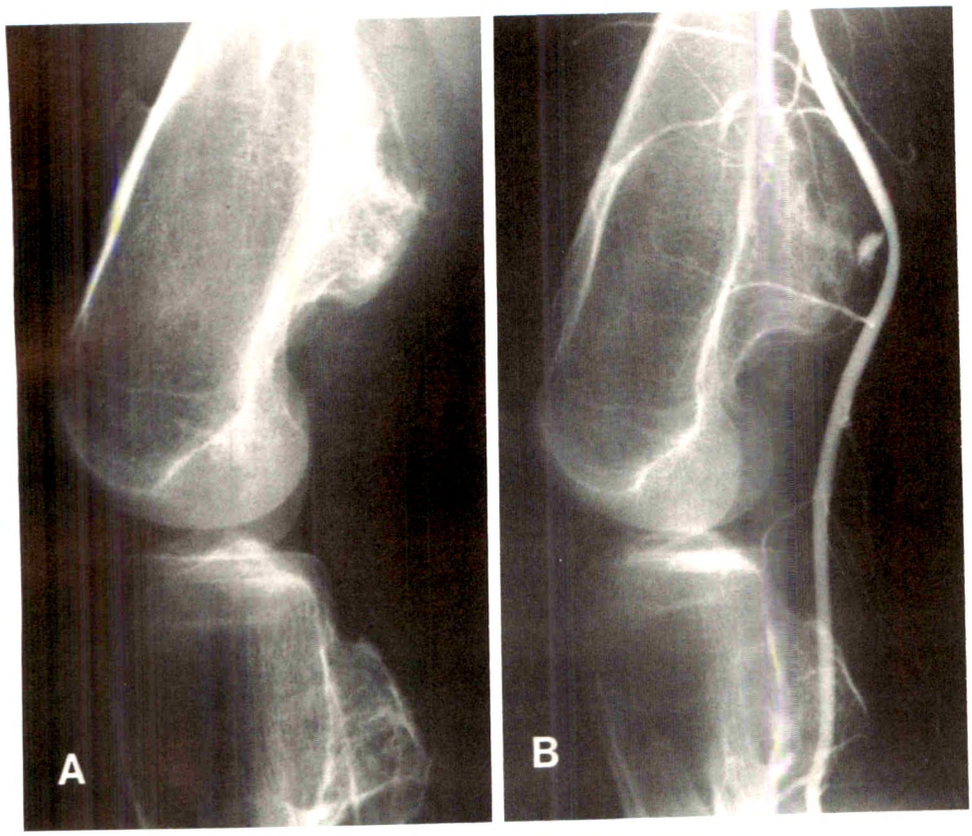


Fig. 1.—**A**, Distal femur. Irregularity and cortical discontinuity of posterior osteochondroma. **B**, Compression of popliteal artery with extravasation of contrast into pseudoaneurysm. Branches of popliteal artery, although stretched, show no evidence of encasement or neovascularity.

the popliteal artery, although Chalstrey [8] and Lemaire and Beaujean [23] reported pseudoaneurysms of the posterior tibial artery associated with osteochondromata of the proximal end of the tibia, and Cachera et al. [27] documented a case of laceration of the brachial artery by an exostosis of the proximal humerus. Pseudoaneurysms tend to occur in the popliteal region for two reasons: (1) the most common locations for osteochondromata are the lower metaphysis of the femur and upper metaphysis of the tibia [26]; and (2) the proximal end of the popliteal artery is fixed as it passes through the opening in the adductor magnus muscle. Similarly, the popliteal artery is tethered distally by its divisions into the anterior and posterior tibial arteries. Thus, both the proximal and distal portions of the popliteal artery have little mobility and tend to be "bow-stringed" over adjacent osteochondromata.

The clinical manifestations of these lesions vary. Of 22 patients in whom an appropriate history was available, 13 (59%) had no trauma; five developed symptoms after dancing, bicycle riding, or vigorous exercise, and four had direct trauma. Furthermore, in 12 of 22 patients, the posterior thigh mass was nonpulsatile. Similarly, 55% of patients had no changes in the distal pulses. Thus, in many cases, including ours, the clinical findings simulated malignant degeneration of an osteochondroma rather than indicating a primary vascular problem.

The implication of these findings is clear. Patients with single or multiple exostoses who develop posterior thigh masses should undergo femoral angiography to exclude pseudoaneurysm formation. Preoperative diagnosis permits appropriate orthopedic management and ensures participation of a vascular surgeon so that definitive therapy can be provided.

ACKNOWLEDGMENT

We thank the authors of references 3, 4, and 12 for additional clinical information.

REFERENCES

1. Manner R, Makinen E: Angiographic findings in a false popliteal aneurysm due to osteochondroma of the femur. *Pediatr Radiol* 3:244–246, 1975
2. Solhaugh JH, Olerud SE: Pseudoaneurysm of the femoral artery caused by osteochondroma of the femur. *J Bone Joint Surg [Am]* 57:867–868, 1975
3. Cassie GF, Dawson AS, Sheville E: False aneurysm of femoral artery from cancellous exostosis of the femur. *J Bone Joint Surg [Br]* 57:379, 1975
4. Hovelius L: Aneurysm of popliteal artery caused by cartilaginous exostosis. *Acta Orthop Scand* 46:836–838, 1975
5. Schoene HR, Berthelsen S, Ahn C: Aneurysm of femoral artery secondary to osteochondroma. *J Bone Joint Surg [Am]* 55:847–849, 1973
6. Hershey SL, Landsen FT: Osteochondromas as a cause of false popliteal aneurysms. *J Bone Joint Surg [Am]* 54:1765–1768, 1972
7. Kover JH, Schwalbe N, Levowitz BS: Popliteal aneurysm due to osteochondroma in athletic injury. *NY State J Med* 70:3001–3003, 1970
8. Chalstrey LJ: Aneurysm of the posterior tibial artery due to a tibial osteochondroma. *Br J Surg* 57:151–154, 1970

9. Mukerjea SK: Traumatic aneurysm of the popliteal artery due to osteochondroma. *Br J Surg* 54:810–811, 1967
10. Heilman RS, Topuzlu C, Molloy M: Femoral artery injury secondary to osteochondroma of the distal femur. *AJR* 100:533–537, 1967
11. Masson AF, Pullan JM: Aneurysm complicating exostosis. *Br J Surg* 53:929–932, 1966
12. Clark PM, Keokarn T: Popliteal aneurysm complicating benign osteocartilaginous exostosis. *J Bone Joint Surg [Am]* 47:1386–1388, 1965
13. Fischer KA, Jackson BB: Traumatic aneurysm of the popliteal artery from perforation by an osteochondroma. *J Trauma* 4:339–343, 1964
14. Anastasi GW, Wertheimer HM, Brown JR: Popliteal aneurysm with osteochondroma of the femur. *Arch Surg* 87:636–639, 1963
15. Denman FR, Shindler TO, Hampton J, Hanson L: Aneurysm of the popliteal artery caused by osteochondroma of the femur. *J Bone Joint Surg [Am]* 41:1526–1528, 1959
16. Desmond AM: Traumatic aneurysm of the popliteal artery in a boy aged 11 years, associated with an osteoma of the lower femur. Treatment by aneurysmectomy and repair of vessel wall. *Proc R Soc Med* 51:179–180, 1957
17. Lesser AJ, Greeley, CE: Femoropopliteal arteriovenous aneurysm caused by fractured osteochondroma of the femur. *JAMA* 167:1830–1833, 1958
18. Stevenson CA, Zuska JJ: Aneurysm of the popliteal artery from perforation by a solitary exostosis of the femur. *J Bone Joint Surg [Am]* 39:431–434, 1957
19. Hudson OC: Traumatic aneurysm of the popliteal artery due to osteochondroma. *Am J Surg* 90:528–530, 1955
20. Paul M: Aneurysm of the popliteal artery from perforation by a cancellous exostosis of the femur. *J Bone Joint Surg [Br]* 35:270–271, 1953
21. Cohn R, Mathewson C: Conservative operation in the treatment of false aneurysm of the popliteal artery. *West J Surg Obstet Gynecol* 61:74–78, 1953
22. Brailsford JF: *The Radiology of Bones and Joints*, 4th ed. Baltimore, Williams and Wilkins, 1948
23. Lemaire R, Beaujean M: Popliteal aneurysm complicating an osteogenic exostosis of the tibia. *Acta Orthop Belg* 41:625–635, 1975
24. Rouanet JP, Chalut J, Bacourt F, Gruner M, Goldlust D: Rare cause of arterial aneurysm: exostosis. *J Radiol Electrol Med Nucl* 57:171–174, 1976
25. Rocek V, Vyslouzil F, Konecna H, Tomsu M, Procek J, Wagner K: Vascular complications in multiple cartilaginous exostoses. *Cesk Radiol* 30:392–397, 1976
26. Jaffe JJ: *Tumors and Tumorous Conditions of the Bones and Joints*, Philadelphia, Lea and Febiger, 1958
27. Cachera JP, Letournel E, Kieffer E: A case of arterial aneurysm complicating an osteogenic exostosis of the upper extremity or the humerus. *J Chir* (Paris) 99:39–44, 1970

Radiographic Appearance of Laparoscopic Tubal Ring

MARY LEE McJUNKIN[1] AND JOHN A. CURTIS[1]

Many types of pelvic calcifications and densities encountered during excretory urography are well known [1]. However, less familiar are opaque medications [2, 3], ingesta [4], and certain devices. The laparoscopic tubal ring [5] used for sterilization is a relatively recent innovation of which radiologists should be aware.

Case Report

A 24-year-old woman with lower abdominal pain was evaluated by excretory urography. The scout radiograph showed two small (0.5 × 0.3 cm) oblong densities on each side of the pelvis (fig. 1A). Subsequent radiography showed these to be outside of the urinary tract, and to change in shape from rectangular to circular densities with a central lucency (fig. 1B). The sharp margins and geometric shape suggested they were iatrogenic. Further history confirmed the patient had had laparoscopic sterilization 1 year earlier and the densities represented silicone rubber rings used in the Falope ring sterilization procedure (fig. 2).

Discussion

In recent years several laparoscopic procedures for female sterilization have been developed, including tubal electrocoagulation and HemoClip occlusion. The former may be complicated by intestinal burns and hemorrhage, and the latter by significant pregnancy rates and ectopic pregnancies [5]. To develop a safer and more reliable method of laparoscopic sterilization, and to retain the potential for successful future recanalization procedures, a new laparoscopic sterilization approach using silicone rubber rings has been developed [6].

The silicone rubber rings are composed of dimethylopolysiloxane impregnated with 5% barium sulfate. They are 2.2 mm thick, with an inner diameter of 1 mm and an outer diameter of 3.6 mm (fig. 2). These rings are placed around the fallopian tubes by means of a laparoscope and ring applicator. The ring applicator consists of grasping forceps contained within two concentric cylinders (fig. 3A). The silicone rubber ring (which has a 90%–100% memory) is stretched to an inner diameter of 6 mm when placed over the end of the inner cylinder. After carbon dioxide insufflation of the pelvis, the loaded applicator is inserted through a trocar sleeve that has been introduced through an umbilical incision. The grasping forceps are extended out of the inner cylinder about 5 cm from the cornu of the uterus and a segment of fallopian tube is lifted up. The forceps, along with the grasped segment of fallopian tube, are then drawn into the inner cylinder. The outer cylinder is moved forward, displacing the silicone ring from the inner cylinder and onto the segment of fallopian tube. After the application

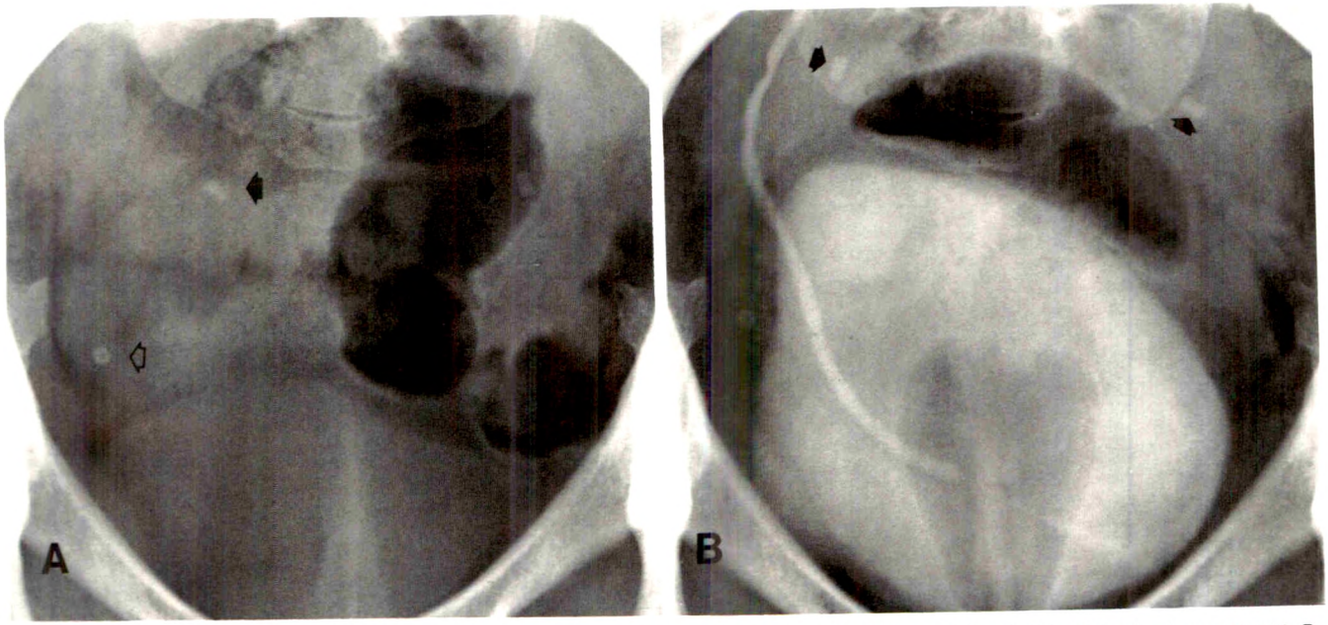


Fig. 1.—**A**, Opaque laparoscopic tubal rings (*solid arrows*) have density quite similar to phlebolith medial to right ischial spine (*open arrows*). **B**, Laparoscopic tubal rings clearly outside urinary tract.

Received July 25, 1978; accepted after revision October 20, 1978.
[1] Department of Radiology, Thomas Jefferson University Hospital, Philadelphia, Pennsylvania 19107. Address reprint requests to M. L. McJunkin.

© 1979 American Roentgen Ray Society

0361-803X/79/1322-0297 $0.00

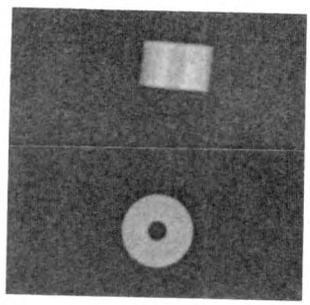


Fig. 2.—Magnified radiograph shows characteristic round (ovoid) or rectangular shape of laparoscopic tubal ring with central lucency.

of the ring(s), the forceps are moved forward out of the inner cylinder to release the occluded segment of fallopian tube (fig. 3B) [7].

This procedure limits tubal damage to the small easily identifiable segment of fallopian tube encircled by the silicone ring. Recanalization is easier to achieve after this procedure than after cauterization, because in cauterization thermal damage cannot be so precisely limited to the fallopian tube.

Radiographically, the silicone rings may be identified as sharply outlined rectangular, ovoid, or circular densities located in the region of the ovaries. The density of the rings is about the same as calcium or bone; however, their geometric shape and central lucency are characteristic features of manmade objects.

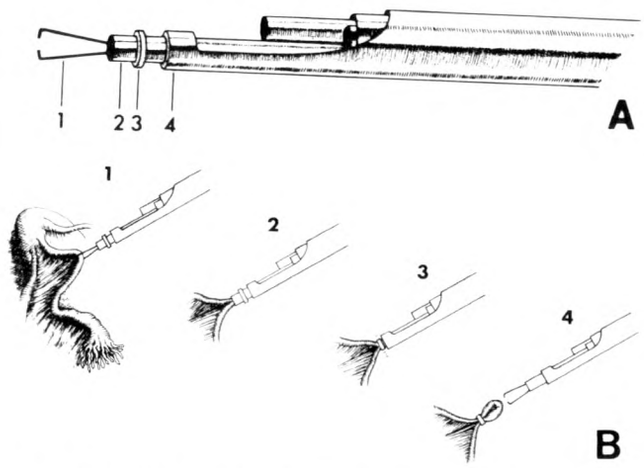


Fig. 3.—**A**, Ring applicator: forceps (1), inner cylinder (2), silicone rubber band (3), and outer cylinder used in conjunction with a standard laparoscopic lens system (4). **B**, Segment of fallopian tube grasped by forceps (1), drawn into inner cylinder (2) where ring is applied (3), and is released by forceps after completion of procedure (4).

REFERENCES

1. McAfee JG, Donner MW: Differential diagnosis of calcifications encountered in abdominal radiographs. *Am J Med Sci* 243:609–650, 1962
2. Spitzer A, Caruthers SB, Stables DP: Radiopaque suppositories. *Radiology* 121:71–73, 1976
3. Handy CA: Radiopacity of oral nonliquid medications. *Radiology* 98:523–533, 1971
4. Schabel SI, Rogers CI: Opaque artifacts in a health food faddist simulating ovarian neoplasm. *AJR* 130:789–790, 1978
5. Yoon IB, Wheeless CR, King TM: A preliminary report on a new laparoscopic sterilization approach: the silicone rubberband technique. *Am J Obstet Gynecol* 120:132–136, 1974
6. Yoon IB, King TM, Parmley TH: A two year experience with Falope ring sterilization procedure. *Am J Obstet Gynecol* 127:109–112, 1977
7. Yoon IB, King TM: A preliminary and intermediate report on a new laparoscopic tubal ring procedure. *J Reprod Med* 15:54–56, 1975

Technical Notes

Gelfoam Embolization: A Simplified Technique

WILLIAM O. BANK[1] AND CHARLES W. KERBER[2]

Therapeutic embolization of the blood supply to neoplasms and vascular malformations has evolved significantly since introduced in the late 1960s [1–4]. With improvements in radiographic equipment and refinements in the techniques of selective and, later, hyperselective catheterization [5–8], occlusive techniques have progressed beyond the stage of occasional or experimental use.

Although particulate Gelfoam (Upjohn) gained widespread use for embolization, vascular occlusion was seldom permanent [9]. Consequently, Gelfoam is being replaced by the more fashionable and permanent balloons, tissue adhesives, and polymers [8, 10–14]. However, when extensive preoperative embolization must be performed (as in juvenile nasopharyngeal angiofibroma), Gelfoam is most effective for postoperative resorption of emboli lodged in normal vessels.

An analysis of the Gelfoam embolization procedure revealed several areas of high cost in time and energy: (1) preparation of emboli during the case; (2) handling and delivery of the particles once prepared; and (3) frequent angiography to assess runoff. To minimize these impediments, we have used readily available disposable hospital supplies for preprocedural preparation of emboli and for facilitating handling and delivery.

Technique

Preprocedural Preparation of Emboli

At some point before intended embolization, a gelatin sponge (Gelfoam sponge size 12–7 mm) is removed from its package and flattened between thumb and fingers. A surgically clean work area and sterile gloves help prevent introduction of pyrogens. The flattened sponge is first inserted into the barrel of a 20 ml glass syringe and pushed in and out several times to reduce the normally present electrostatic charge.

The flattened sponge is then cut lengthwise into 1–2 mm strips with fine scissors. These strips will repel each other due to the modified electrostatic charge. Holding the strips together while crosscutting over the upended syringe barrel allows the dry particles to fall and/or be repelled from the sponge and attracted into the syringe (fig. 1).

The plunger is carefully replaced within the syringe barrel so that most of the air is excluded but the particles are not compressed. This prevents clumping during sterilization.

Each 20 ml syringe contains the particles from one Gelfoam sponge (size 12–7 mm) and is usually adequate for an extensive embolization (e.g., a large nasopharyngeal angiofibroma supplied by both external carotid arteries). Each glass syringe with emboli is packaged individually and steam sterilized. A sealed packaging system as opposed to cloth or porous paper wrapping, (Bard Blue Film Steri-Peel Packaging System, C. R. Bard, Murray Hill, N. J. 07974), has a 6 month shelf life.

Rapid Delivery System

A 3-way plastic stopcock joins two 51 cm intravenous connecting tubings, one of which is attached to a 5 ml disposable syringe (fig. 2). When assembled, this unit is packaged for gas sterilization.

The prepackaged 20 ml syringe and emboli attach to the free connecting tubing and constitute the reservoir portion of the system. The 5 ml syringe delivers the emboli into the angiographic catheter with precise control. The section of tubing from the 5 ml delivery syringe to the stopcock serves as a transparent chamber where the emboli can be counted and controlled.

Particle Preparation

Preparing the particles for delivery into the patient first involves drawing 15 ml of 60% contrast agent into one of the presterilized 20 ml syringes. Next, all of the air is expressed, and the index finger of one hand is held over the syringe orifice while the plunger is pulled up vigorously. This creates a partial vacuum within the syringe, displacing air from the particles and replacing it with contrast agent that penetrates the interstices of the gelatin foam. This maneuver is repeated until all of the air has been exchanged for contrast agent and the particles are evenly suspended within the fluid.

The 20 ml reservoir syringe is then connected to its end of the delivery system. Air is cleared from the entire system and the 3-way stopcock is placed onto the end of the angiographic catheter (fig. 2).

Received June 6, 1978; accepted after revision October 31, 1978.

[1]Department of Radiology, University of California School of Medicine, San Francisco, California and Neuroradiology Section, Radiology Service, Veterans Administration Hospital, 4150 Clement Street, San Francisco 94121. Address reprint requests to W. O. Bank.

[2]Department of Radiology, Division of Neuroradiology, University of Pittsburgh School of Medicine, Presbyterian-University Hospital, Pittsburgh, Pennsylvania 15261.

© 1979 American Roentgen Ray Society

0361-803X/79/1322-0299 $0.00



Fig. 1.—Preparation of emboli: gelatin sponge is cut into 1–2 mm strips and then crosscut over upended barrel of glass syringe to produce supply of emboli for subsequent heat sterilization.

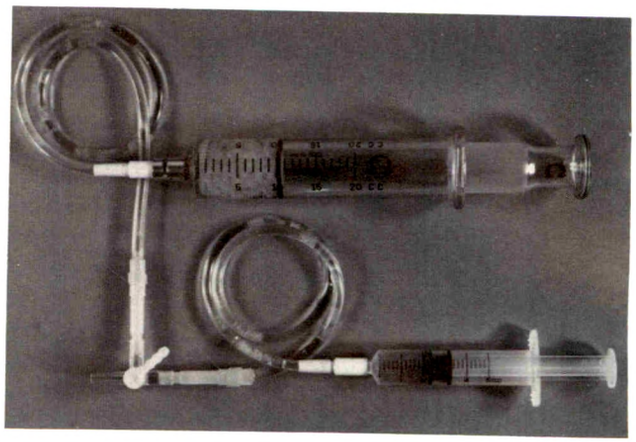


Fig. 2.—Delivery system: two 51 cm intravenous connecting tubings (coiled) are joined by 3-way stopcock, which is then attached to angiographic catheter. Emboli in 20 ml syringe (top) are suspended in contrast agent and system is cleared of air. Note particles in tubing. Bottom coil serves as counting chamber for controlling number of particles injected by 5 ml syringe.

By appropriately positioning the stopcock, Gelfoam particles suspended in contrast agent pass into the tubing connected to the small syringe where they can readily be counted and their proximity to one another checked. Turning the stopcock allows emboli to be introduced into the angiographic catheter and then into the patient with precise control.

Discussion

Sterilization

Two considerations have led us to heat sterilize and store Gelfoam emboli in glass syringes: (1) qualitative analysis of Gelfoam after gas sterilization has revealed trace amounts of ethylene oxide, ethylene chlorhidrin, and ethylene glycol (Upjohn, personal communication) and (2) there is some question in the literature regarding the diffusion of plasticizers from polyvinyl chloride into organic substances stored in this material for long times [16, 17]. Consequently, the plastic components of our system are gas sterilized in one package, while the emboli are heat sterilized in glass syringes. A side benefit of this arrangement is that the rapidity of resorption of the Gelfoam is slightly decreased by heat sterilization (Upjohn, personal communication).

Opaque Propellant

Suspension of the emboli in 60% contrast agent at the time of use results in uniform viscosity of all the emboli. Conventional techniques may result in too short a suspension time and emboli that are too rigid to pass through the constrictions of the delivery system. However, too long a suspension time will cause the Gelfoam particles to dissolve, and this must be monitored in long procedures. Less than 60% contrast agent frequently is inadequate for the necessary monitoring of vessel runoff during the occlusion.

Delivery System

To preserve a closed system, we connect two plastic extension tubings to a 3-way stopcock. The 20 ml reservoir syringe attaches to a free end of one of these tubings, while a small syringe is attached to the other end to serve as the ultimate deliverer of the contrast agent and emboli. Larger syringes give poor hydraulic control, and we have found that careful fluoroscopic monitoring of the ever decreasing vessel runoff is crucial to prevent inadvertent embolization with subsequent neurologic deficit [18].

We emphasize that at no time should contrast agent or emboli introduced into the vessel be occluded at a rate faster than its acceptance or runoff. We do not use balloon occlusion of the vessel to be embolized while particles are being delivered for three reasons: (1) it deprives the operator of a safe end point; (2) particles can reflux from the occluded vessel at the time of balloon deflation and spill into adjacent normal arteries; and (3) it permits forcing of particles through small collateral channels into other vascular territories (e.g., from external carotid into internal carotid or vertebrobasilar systems).

Each element of the system separately contributes to a reduction in patient morbidity, while the system in toto additionally frees the operator to concentrate on the patient's well-being and to make more refined assessments about the progress of the case.

REFERENCES

1. Djindjian R, Houdart R, Cophignon J, Hurth M, Comoy J: Premiers essais d'embolisation par voie fémorale de fragments de muscle dans un cas d'angiome medullarie et dans un cas d'angiome alimente par le carotide externe. *Rev Neurolog* (Paris) 125:119–130, 1971
2. Djindjian R, Cophignon J, Theron J, Merland JJ, Houdart R: L'embolisation en neuro-radiologie vasculaire. Technique et indications a propos de 30 cas. *Nouv Presse Med* (Paris) 1:2153–2158, 1972
3. Doppman JL, DiChiro G, Ommaya A: Obliteration of spinal cord arteriovenous malformation by percutaneous embolization. *Lancet* 1:477, 1968

4. Newton TH, Adams JE: Angiographic demonstration and non-surgical embolization of spinal cord angioma. *Radiology* 91:873–876, 1968
5. Djindjian R, Cophignon J, Theron J, Merland JJ, Houdart R: Embolization by superselective arteriography from the femoral route in neuroradiology. Review of 60 cases. I. Technique, indications, complications. *Neuroradiology* 6: 20–26, 1973
6. Djindjian R, Cophignon J, Rey A, Theron J, Merland JJ, Houdart R: Superselective arteriographic embolization by the femoral route in neuroradiology. Study of 50 cases. II. Embolization in vertebromedullary pathology. *Neuroradiology* 6:132–142, 1973
7. Djindjian R, Cophignon J, Rey A, Theron J, Merland JJ, Houdart R: Superselective arteriographic embolization by the femoral route in neuroradiology. Study of 50 cases. III. Embolization in craniocerebral pathology. *Neuroradiology* 6:143–152, 1973
8. Djindjian R: Superselective internal carotid arteriography and embolization. *Neuroradiology* 9:145–156, 1975
9. Barth KH, Strandberg JD, White RI: Long-term follow-up of transcatheter embolization with autologous clot, oxycel, and Gelfoam in domestic swine. *Invest Radiol* 12:273–280, 1977
10. Hilal SK, Michelsen JW: Therapeutic percutaneous embolization for extra-axial vascular lesions of the head, neck, and spine. *J Neurosurg* 43:275–287, 1975
11. Serbinenko FA: Balloon catheterization and occlusion of major cerebral vessels. *J Neurosurg* 41:125–145, 1974
12. Kerber CW, Bank WO: Polyvinyl alcohol foam: prepackaged emboli for therapeutic embolization. *AJR* 130:1193–1194, 1978
13. Kerber CW: Intracranial cyanoacrylate: a new catheter therapy for arteriovenous malformation. *Invest Radiol* 10:536–538, 1975
14. Kerber CW, Bank WO, Cromwell LD: Cyanoacrylate occlusion of carotid cavernous fistula with preservation of carotid artery flow. Submitted for publication.
15. Kerber CW, Cromwell LD: Presurgical embolization of neurogenic hamartoma in an infant. *Radiology* 117:397–398, 1975
16. Jaeger RJ, Rubin RJ: Plasticizers from P.V.C. *Lancet* 2:778, 1970
17. Jaeger RJ, Rubin RJ: Plasticizers from plastic devices: extraction, metabolism, and accumulation by biological systems. *Science* 170:460–462, 1970
18. Kerber CW: Catheter therapy: fluoroscopic monitoring of deliberate embolic occlusion. *Radiology* 125:538–540, 1977

Identifying Dorsal Pedal Lymph Vessels without Blue Dye

HEUN Y. YUNE,[1] EUGENE C. KLATTE,[1] AND SOLOMON BATNITZKY[1, 2]

The original lymphography technique introduced by Kinmonth et al. [1] has been used for over 20 years without any major modification. To help identify a subcutaneous lymph vessel, a number of vital blue or green dyes have been used. After a trial period, some of these dyes were eliminated from the clinical use for various reasons. A current literature survey indicates that the agent most frequently used outside of the United States is "patent blue." This agent is not available for clinical use in the U.S. although some investigators have found methylene blue to be a satisfactory substitute. However, a number of reports [2–4] concern hypersensitivity reactions to vital dyes, some of which have been serious and anaphylactoid.

With careful attention to anatomic detail [5, 6], a subcutaneous lymph vessel can be identified consistently without using vital dyes. During the past 3 years, we successfully performed bipedal lymphography on 162 consecutive patients without using vital dyes. In seven other instances during the same period, methylene blue was used to confirm the presence of obliterated peripheral lymph vessels. This report describes the anatomic details of subcutaneous lymph vessels for their identification without the use of a vital dye.

Site, Anesthesia, and Incision

The site chosen is on the dorsum of the foot about 2 cm proximal to the tarsometatarsal junction. This site is preferred because many dorsal pedal lymphatics converge and a number of large lymphatics can be found in a relatively short incision. In infiltrating the skin with local anesthetic both intradermal and subcutaneous injections are made. This aids subsequent isolation of blood and lymph vessels from surrounding connective tissue.

A transverse incision 2–2½ cm long is made in the anesthetized skin. A transverse incision is preferred because more lymphatics are identified than in a longitudinal incision, and the incision parallels the skin crease. The cutting edge of the blade should not extend below the layer of dermis on initial incision. Many subcutaneous lymph vessels are located immediately below the superficial subcutaneous fascia and may be injured by an incision deeper than dermis.

A hole through the full thickness of the dermis is made on one margin of the dermal incision and a thin tip (but not sharp and pointed) mosquito clamp is slipped immediately beneath the dermis; blunt dissection of the dermis away from the subdermal tissues is carried out, exercising extreme care to avoid inclusion of superficial layers of subcutaneous connective tissue on the side of the dermis. The blade can be placed under the dermis between the open tips of the mosquito clamp with its cutting edge pointing upward. In this way, incision of the full thickness of the dermis can be extended safely and quickly without jeopardizing subcutaneous vessels.

Isolation and Identification of Vessels

After the full thickness of dermis is incised, a thin but tough meshlike subcutaneous fascia will be found. When this fascia is incised in the same manner as the incision of the dermis, strands of fatty tissue and vessels that hide most of the lymph vessels will be exposed. Blunt and very gentle dissection in a longitudinal direction parallel to the vessels will strip fatty tissue from the surface of these vessels. Numerous small blood and lymph vessels about 1 mm or less in diameter will then be found (fig. 1A). To differentiate small blood vessels from lymphatics, a mosquito clamp is placed behind the isolated vessel; when it is withdrawn, a blood vessel will return to a taut straight position and appear nontransparent. In contrast, the lymph vessel will remain tortuous and flabby when the dissecting clamp is withdrawn from behind it and will appear semitransparent, pinkish, and slightly milky.

At this stage the lymph vessel is collapsed. A temporary occlusion of the lymph vessel is applied and the lymph vessel can be distended by stroking the tissues distal to the incision in a proximal direction. By this method a lymph vessel may become distended 3 times or more its original diameter (fig. 1A). The increased transparency of the distended vessel is the ultimate clue that this is indeed a lymph vessel. Frequently a network of tiny vasa vasorum may be seen on the wall of the distended and transparent lymph vessel. In contradistinction to this, arteries will collapse with proximal occlusion. Also, a miniscule pulsation that is usually visible on careful observation will be obliterated. A small vein of similar size can seldom be distended to the degree of a lymph vessel, and they will appear to contain pink blood and be nontransparent.

Once the lymphatic is confidently identified, cannulation is performed according to previously described standard techniques (fig 1B). Injection of 1 ml of 1% Xylocaine confirms proper needle placement and also prevents the cramping pain that sometimes develops during Ethiodol infusion.

Identification and cannulation of a subcutaneous lymph vessel on the dorsum of the foot without using

Received June 13, 1978; accepted after revision October 3, 1978.

Presented in part at the annual meeting of the American Roentgen Ray Society, Boston, Massachusetts, September 1977, and at the scientific assembly of the Radiological Society of North America, Chicago, Illinois, November 1978.

[1] Department of Radiology, Indiana University Medical Center, 1100 West Michigan Street, Indianapolis, Indiana 46202. Address reprint requests to H. Y. Yune.

[2] Present address: Department of Radiology, University of Kansas Medical Center, Rainbow Boulevard at 39th Street, Kansas City, Kansas 66103.

© 1979 American Roentgen Ray Society

0361-803X/79/1322-0302 $0.00

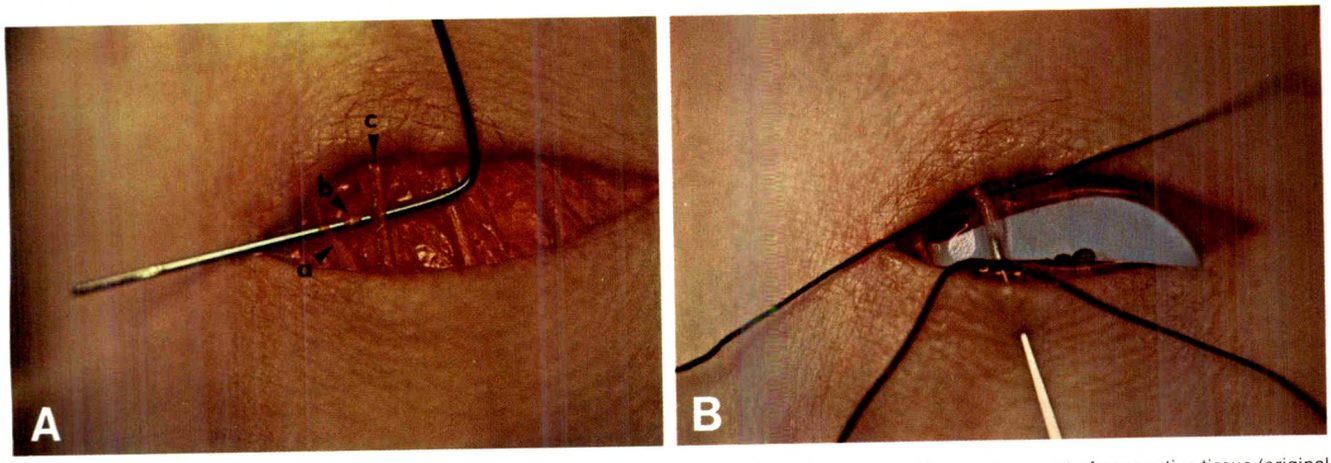


Fig. 1.—**A**, Bent round needle placed behind lymph vessels (a and b) and small artery (c) surrounded by small amount of connective tissue (original sizes of a, b, and c were 0.5, 0.6, and 0.3 mm, respectively). Miniscule pulsation was visible on c; flaccid posture and transparency of lymph vessels against needle seen in background; larger lateral vessel under angle of bent needle is vein (original size, 1.2 mm). **B**, Needle is in lymph vessel (b, fig. 1**A**); foil behind vessel obscures background. Proximal ligature temporarily applied to distend vessel has been released; distal ligature is tied around vessel over needle. About 1 ml 1% Xylocaine has been injected intralymphatically. Lymph vessel exhibits characteristic transparency.

vital dyes did not prolong the procedures and was accomplished in the 162 consecutive patients (324 limbs) without a single instance of failure; 15 of these patients were less than 16 years old. We believe that the use of vital dyes may now be limited to a small minority of cases to confirm the presence of acquired or congenital lymphatic hypoplasia or obstruction where a patent subcutaneous lymph vessel is unavailable.

REFERENCES

1. Kinmonth JB, Taylor GW, Harper RK: Lymphography: a technique for its clinical use in the lower limb. *Br Med J* 1:940–942, 1955
2. Koehler PR: Complications of lymphography. *Lymphology* 1:117–120, 1968
3. Mortazavi SH, Burrows BD: Allergic reactions to patent blue dye in lymphangiography. *Clin Radiol* 22:389–390, 1971
4. Platzbecker H, Kohler K, Lucas D: Bedrohliche Zwischenfalle nach Injektion von Patentblau Violett als Komplikation bei der Lymphographie. *Zarztl Fortbild* 64:1224–1225, 1970
5. Rusznyak I, Foldi M, Szabo G: *Lymphatics and Lymph Circulation—Physiology and Pathology*, 2nd edition, New York, Pergamon, 1967
6. Segurjonsson K: Lymphography without the aid of vital dyes. *Lymphology* 7:121–123, 1974

Society for Pediatric Radiology Abstracts: 1978 Meeting

The Society for Pediatric Radiology met in Denver, Colorado, September 22-24, 1978, and was invited to submit abstracts from its formal scientific program for publication. Thorne Griscom, secretary-treasurer of the society, edited the abstracts in conjunction with the authors. Abstracts are arranged in the order of presentation.

CONTENTS

Maturation as a Factor in Pulmonary Oxygen Toxicity. Northway W, Petriceks R, Canty E

Unilateral Pulmonary Hypoplasia Following Pulmonary Artery Banding. Fletcher BD, Garcia EJ, Fink R, Borkat G

Pleural Telangiectasia and Pulmonary Agenesis. Kleinman PK

Membranous Laryngotracheobronchitis (Membranous Croup). Han B, Dunbar JS, Striker TW

Appendiceal Abscess and the Pediatric Cul-de-sac. Barnes JC, Kirks, DR, Currarino G

Veno-occlusive Hepatic Disease in Acute Myelocytic Leukemia (AML): Evaluation by Serial Liver Imaging. Harcke HT, Naiman JL, Huff DS

Chemotherapy-Induced Inhibition of Compensatory Renal Growth in the Immature Mouse. Moskowitz PS, Donaldson SS

The Whitaker Test: Differentiation of Obstructive from Nonobstructive Uropathy. Jaffe RB

The Uroradiographic Evaluation of the Enuretic Child. Seibert J, Redman J

The So-Called "Megaureter-Megacystis Syndrome". Lebowitz RL, Willi U

Comparison of Radiologic Methods for Measuring Femoral Anteversion in Infancy and Childhood. O'Connor JF, Mital MA, Ruby L, Spira J

Arthrographic Evaluation of the Joint Cartilage in Avascular Necrosis of the Femoral Head. Ozonoff MB

Coracoclavicular Fracture Separation - The Pediatric Equivalent of Acromioclavicular Separation. Reed MH

An Efficacy Study for the Value of Comparison Views in Extremity Injuries in Children. McCauley RGK, Schwartz AM, Leonidas JL, Darling DB

Relative Efficacy of Radiographs and Bone Scans in the Detection of the Skeletal Lesions of Histiocytosis-X. Parker BR, Pinckney LE, Etcubanas E, Goris ML

The Radiographic Features of Eosinophilic Gastroenteritis (Allergic Gastroenteropathy) of Childhood. Teele RL, Katz AJ, Goldman H

The Diagnosis of Hiatus Hernia, Reflux and Esophagitis. Knapp K, Del Hoyo ML, Diez-Pardo J, Martinez A

Radiology and Manometry in the Selection of Patients for Antireflux Surgery. Cumming WA

The Diagnosis and Management of Gastro-esophageal Reflux in the Pediatric Patient. Smith LE, Byrne WJ, Fonkalsrud EW, Kangarloo H

Maturation as a Factor in Pulmonary Oxygen Toxicity

Northway W, Petriceks R, Canty E (Stanford Univ., Stanford, CA 94305)

Previous investigation suggests that newborn animals are less susceptible to pulmonary oxygen toxicity than the adult of the same species. Sixty percent of newborn C57BL mice survive continuous exposure to 100 percent oxygen for one week, and 18 percent survive continuous exposure for six weeks. All adult C57BL mice exposed continuously to 100 percent oxygen die by six days of exposure.

The time for the newborn mouse to become "adult" in its mortality response to continuous exposure to 100 percent oxygen was investigated by allowing newborn C57BL mice to live in room air a predetermined period before exposure. The age at which the newborn mouse becomes "adult" in its mortality response was gauged by using death by six days of exposure to define "adultness". The littermate mixing and assignment to a "standard litter" were done in a standard fashion.

Preliminary results indicate that the change to "adult" mortality response with continuous exposure to 100 percent oxygen occurs between 14 and 28 days of life, approximately the age of weaning. Identification of this interval of change from the newborn to the adult pattern of mortality will allow correlation with nutritional, hormonal, biochemical, and morphological events and may lead to further insight into means of protection against pulmonary oxygen toxicity.

Unilateral Pulmonary Hypoplasia Following Pulmonary Artery Banding

Fletcher BD, Garcia EJ, Fink R, Borkat G (Rainbow Babies and Childrens Hospital, Cleveland, OH 44106)

Two patients, one with truncus arteriosus type I, the other with coarctation of the aorta with ventricular septal defect, underwent pulmonary artery banding during early infancy because of intractable congestive heart failure. In both cases, the right pulmonary artery was inadvertently completely occluded. Subsequent chest radiographs showed diminished pulmonary vasculature on the right, and follow-up examinations over 2 years showed a relative lack of lung growth on that side. Fluoroscopic studies and lung scans demonstrated normal ventilation. Plastic repair of the right pulmonary artery and insertion of a right ventricular-pulmonary artery conduit resulted in partial restoration of lung volume in one of the patients. The other patient died a few years later, and autopsy confirmed ipsilateral pulmonary hypoplasia.

A third patient, with pulmonary atresia and a surgical shunt between the ascending aorta and right pulmonary artery, developed surgical obstruction of the left pulmonary artery. Post-operative radiographs over many years also showed hypoplasia of the underperfused left lung.

The radiographic findings in these patients must be differentiated from "unilateral hyperlucent lung syndrome" and congenital interruption of a pulmonary artery. They suggest that pulmonary arterial perfusion exerts a major influence on postnatal lung growth. Pulmonary artery obstructions should be corrected as early as possible in order to minimize interference with alveolar multiplication.

Pleural Telangiectasia and Pulmonary Agenesis

Kleinman PK (Univ. of Massachusetts Medical Center, Worcester, MA 01605)

The radiologic features of unilateral pulmonary artery agenesis are often sufficiently characteristic to allow a plain film diagnosis. They include a small hemithorax, ipsilateral displacement of the mediastinum, and an absent corresponding pulmonary artery. A source of collateral blood supply is the bronchial circulation, which produces a branching reticulated appearance in the lung fields. Larger confluent shadows are also encountered in pulmonary artery agenesis, and their presence is often ascribed to bronchial collateral circulation.

An examination of six cases of unilateral pulmonary agenesis (5 right, 1 left) revealed peripheral hazy confluent densities in association with pleural thickening in 3 cases. Aortography disclosed extensive intercostal and subdiaphragmatic transpleural collaterals which formed telangiectatic networks within the pleura of the oligemic lungs. The telangiectasia corresponded to the peripheral areas of increased density noted on the plain film. In two instances, rib notching was present. Others have described similar densities, but restricted to the apices, in patients with cyanotic congenital heart disease.

Thus, the development of pleural telangiectasia appears to be a non-specific response to profound, long-standing pulmonary oligemia. An assessment of collateral blood supply in such conditions should include examination of the intercostal circulation as well as any contribution from transdiaphragmatic collaterals. The appearance of these pleural collaterals is sufficiently characteristic to serve as a helpful clue in the radiologic diagnosis of

AJR 132:305-308, February 1979

© 1979 American Roentgen Ray Society

0361-803X/79/1322-0305 $00.00

pulmonary artery agenesis. Pleural telangiectasis in association with any cause of prolonged pulmonary oligemia indicates the presence of significant transpleural collaterals.

Membranous Laryngotracheobronchitis (Membranous Croup): Han B, Dunbar JS, Striker TW (Children's Hospital Medical Center, Cincinnati, OH 45229)

The clinical and roentgen findings of ordinary laryngotracheobronchitis (croup) are well known. We have studied twenty-eight cases of membranous laryngotracheobronchitis (membranous croup). It differs in the following respects from ordinary croup:

1. The clinical findings are more severe.
2. It tends to affect a slightly older age group.
3. The subglottic obstruction shown radiologically may be more severe.
4. The mucosa of the upper trachea may be thickened and irregular.
5. The detached or semi-detached membranes, formed of mucus, inflammatory cells, and fibrin, may be visible in the upper trachea and are diagnostic of the disease. If their nature is not recognized, they may be mistaken for foreign bodies.
6. Probably membranous croup is due to bacterial infection, alone or superimposed on viral croup, since pathogenic bacteria were usually cultured from tracheal secretions or membranes. Furthermore, most patients did not respond to racemic epinephrine but did respond to antibiotic therapy.

Appendiceal Abscess and the Pediatric Cul-de-sac: Barnes JC, Kirks DR, Currarino G (Children's Medical Center, Univ. of Texas Southwestern Med. School, Dallas, TX 75235)

Appendicitis in children is sometimes complicated by a large mass of purulent material in the cul-de-sac, the peritoneal recess found between the bladder and the rectum in the male and between the uterus and the rectum in the female. The symptoms and physical findings usually point to an abdominal process but may be too vague to permit exact diagnosis. Other entities are often mimicked. For this reason, radiographic procedures are requested, especially urographic and gastrointestinal studies. Once diagnosis is suspected, confirmation can be obtained by simultaneous cystography and barium enema with the patient in the lateral projection. Sonography and computed tomography also help.

We present 17 such cases, 4 representing abscesses forming after appendectomy, the other 13 developing before operation was undertaken.

Veno-occlusive Hepatic Disease in Acute Myelocytic Leukemia (AML): Evaluation by Serial Liver Imaging: Harcke HT, Naiman JL, Huff DS (St. Christopher's Hospital for Children, Philadelphia, PA 19133)

Veno-occlusive disease of the liver is a recently identified complication of chemotherapy in patients with AML. Serial liver imaging with Technetium-99m sulfur colloid was performed on 3 children with AML (total of 12 studies) who developed hepatomegaly and abdominal distention following chemotherapy with daunorubicin, ara-c, and thioguanine. All had a marked increase in liver size and decreased reticuloendothelial activity in a patchy, non-homogeneous distribution. Splenomegaly and increased marrow uptake were present. Biopsies revealed intense congestion around the central veins, thickened venous walls, and hemorrhage but no significant leukemic infiltration.

The acute effects occurred 2 to 4 weeks after institution of therapy. Follow-up studies over 6 to 8 months remained abnormal, but in all 3 patients the liver size diminished and the colloid distribution within the liver became more homogeneous. Reintroduction of chemotherapy in one patient produced an exacerbation of toxicity in that the liver enlarged and the colloid uptake diminished.

Veno-occlusive disease must not be mistaken for leukemic infiltration. The diagnosis is suggested by the acute onset, the drug history, and the image pattern. Serial radionuclide imaging with sulfur colloid appears useful in documenting recovery.

Chemotherapy-Induced Inhibition of Compensatory Renal Growth in the Immature Mouse: Moskowitz PS, Donaldson SS (Stanford Univ., Stanford, CA 94305)

Recent reports have drawn attention to adverse long-term effects of radiation and chemotherapy on renal function in children. Little is known of the effects of chemotherapy on renal growth. Our observation of two children treated for Wilms' tumor in whom normal renal compensatory hypertrophy failed to develop following nephrectomy, whole-abdominal radiation and chemotherapy with Actinomycin-D (AMD), Vincristine (VCR), and Adriamycin (ADR) prompted us to study the effect of AMD, VCR, and ADR on compensatory growth in the immature mouse kidney.

Weanling BLcF1 female mice underwent left nephrectomy. Left kidney and initial body weights were recorded. Minimal lethal doses of (LD_1) of AMD, VCR, or ADR were given intraperitoneally for five consecutive days starting immediately after nephrectomy. Control animals followed an identical protocol but received intraperitoneal saline. Animals were sacrificed 3, 5, 8, 14, 21 and 28 days after nephrectomy. At sacrifice, right kidney and final body weights were compared to left kidney and initial body weights, and measurements of kidney ^{3}H-thymidine uptake, DNA and protein concentration were obtained.

AMD inhibited early kidney and body growth, with recovery by 8 days; body growth inhibition proportionately exceeded kidney growth inhibition. VCR inhibited early kidney growth without affecting body growth; recovery occurred by 8 days. ADR inhibited kidney growth for 21 days; body growth inhibition persisted at 28 days and was proportionate to kidney growth inhibition. ^{3}H-thymidine uptake was decreased at 5 days and increased at 14 days with AMD, VCR, and ADR. DNA concentration was diminished at 8 days with AMD and VCR and increased at 8 and 14 days with ADR. Protein concentration was increased at 3 days with AMD, decreased with VCR from 3 to 14 days, and unchanged with ADR.

Thus, AMD and ADR inhibit compensatory renal growth and body growth in the immature mouse. VCR selectively inhibits renal growth. Renal growth inhibition with AMD and ADR is related to generalized body growth suppression, and with AMD, VCR, and ADR to a delay in the mitotic response to contralateral nephrectomy.

(Supported by the James Picker Foundation, Grant No. 830, from the American Cancer Society, California Division, and Adria Laboratories)

The Whitaker Test: Differentiation of Obstructive from Nonobstructive Uropathy: Jaffe RB (Primary Children's Medical Center, Salt Lake City, UT 84103)

The Whitaker test, a urodynamic and radiographic study, has been utilized recently to evaluate persistent upper urinary tract dilatation after operative correction of obstruction. This test helps to differentiate patients with residual or recurrent obstruction from those with dilatation secondary to permanent changes in the musculature. It is also useful in evaluating patients with questionable ureteropelvic junction obstruction or primary defects in the ureteral musculature, as in the prune belly syndrome.

Percutaneous puncture of the renal pelvis is performed, or an indwelling nephrostomy tube is used. The upper urinary tract is then perfused at a constant rate of 5 to 10 cc/min with saline or dilute contrast material, and serial pressure recording is made in the renal pelvis and bladder.

The high flow rate utilized will be tolerated easily in a nonobstructed system without a progressive rise in renal pelvic pressure. In obstructed systems abnormally high pressure (above 12 cm of water) or a constant rise in pressure will be recorded. Videotaping of ureteral peristalsis and spot films of the upper urinary tract complete the evaluation.

The utility of this study has been shown by a series of 10 examinations in 7 patients. No complications have occurred.

The Uroradiographic Evaluation of the Enuretic Child: Seibert J, Redman J (Arkansas Children's Hospital, Little Rock, AR 72201)

In an effort to decrease the number of enuretic children undergoing radiologic examination without diminishing the chances of uncovering important anatomic abnormalities, we have standardized our approach. Over a five-year period, 138 children were

evaluated uroradiographically. Twenty-one children had a significant anatomic abnormality. These abnormalities were found only in children with 1) a history of a urinary tract infection, 2) infected urine at the time of examination, or 3) obstructive signs or symptoms. A simple algorithm allows separation of those few enuretic children likely to have organic problems from the many with virtually no probability of structural disease.

The So-Called "Megaureter-Megacystis Syndrome": Lebowitz RL, Willi U (Children's Hospital Medical Center, Boston, MA 02115)

The "megaureter-megacystis syndrome" is not a syndrome. However, this term has been used for at least 25 years to describe a group of children with severe refluxing hydronephrosis and a very large bladder without obstructive uropathy. It was thought that the large bladder was responsible for the reflux, but this cause-and-effect relationship is an illusion. These children simply have massive vesico-ureteric reflux and its sequelae.

21 children will be presented with the so-called "megaureter-megacystis syndrome". All were boys. They ranged in age from 1 day to 13 years. They presented in various ways including urinary tract infection, abdominal mass, increasing abdominal girth, abdominal pain, dysuria, hematuria, and failure to thrive. The diagnosis could have been made in each case by means of intravenous urography and fluoroscopically monitored voiding cystourethrography. In all, the underlying problem was massive vesico-ureteric reflux, either unilateral, bilateral, or into the lower moiety of a duplex collecting system. The reflux often mimicked function at urography. The function of the bladder, the bladder neck, and the urethra were normal in all. Apparent poor emptying of the bladder and the belief that there must be some underlying obstruction were common diagnostic misconceptions and led to many unnecessary operations. Anti-reflux surgery alone would presumably have resolved the underlying problem.

Comparison of Radiologic Methods for Measuring Femoral Anteversion in Infancy and Childhood: O'Connor JF, Mital MA, Ruby L, Spira J (Boston City Hospital, Boston, MA 02118)

The presence of excessive anteversion is a common clinical problem complicating the measurement of patients with congenital dislocation of the hip, Legg-Perthes disease and in-toeing. Several techniques for measuring femoral anteversion in living subjects have been described and are in use. We measured the accuracy and reproducibility of the fluoroscopic method, the bi-plane radiographic method, and the axial roentgenographic method with an experimental model and have also measured the clinical reproducibility of these methods in 64 patients.

All three methods are reasonably accurate, the fluoroscopic method being slightly more accurate than the others in experienced hands. The bi-plane radiographic method carries the least radiation hazard.

Arthrographic Evaluation of the Joint Cartilage in Avascular Necrosis of the Femoral Head: Ozonoff MB (Newington Children's Hospital, Newington, CT 06111)

Since plain roentgenography of the hip fails to delineate the critical femoral head and acetabular cartilage interfaces, these relationships were studied by positive contrast arthrography in 185 patients with idiopathic avascular necrosis of the femoral head (Legg-Perthes disease).

Measurement of the depth and diameter of the involved (as compared with the contralateral normal) cartilage reveals that overgrowth of both femoral head and acetabular cartilages occurs very early in the course of the disease, even before symptoms occur, and continues for many months or several years. In most instances, this cartilage overgrowth explains the apparent subluxation of the ossification center seen early in the disease; in other cases, actual lateral displacement was present.

In the earlier phases, minimal but definite cartilage flattening over the ossification center fracture occurs. With time, this localized incongruence becomes larger, and the normal femoral head sphericity changes to a more ovoid configuration.

In intermediate stages, the cartilaginous femoral head outline usually retains its surface regularity despite extensive resorption of the ossific epiphysis. In later stages, lateral growth and extrusion of the cartilage beyond the acetabular labrum may occur. Repeat arthrography in selected cases has shown cartilage remodelling as a confirmation of the biological plasticity of the growing chondroepiphysis.

Coracoclavicular Fracture Separation - The Pediatric Equivalent of Acromioclavicular Separation: Reed MH (Health Sciences Children's Centre, Winnipeg, Manitoba-CAN R3E 0W1)

Shoulder dislocations, including acromioclavicular separations, are rare in children. However, one injury in older children is quite similar to an acromioclavicular separation. The injury comprises a fracture, sometimes through bone, sometimes merely through the cartilaginous tip, of the lateral end of the clavicle. Radiologically the acromion and clavicular tip are depressed with respect to the shaft of the clavicle. The lateral fragment of the clavicle remains with the acromion because the acromioclavicular joint is essentially intact. The coracoid is displaced downward from the clavicle, and the coracoclavicular ligament is torn or its periosteal attachment to the clavicle is stripped off.

Since 1965 we have seen 12 children with this injury ranging in age from 7 to 15 years. Eleven were boys. In all seven patients where the information was available, the injury resulted from a direct blow to the shoulder. In 4 cases the injury was severe enough to require open reduction and internal fixation. In the same period we have seen only 5 children with true acromioclavicular separations.

A coracoclavicular fracture-separation seems, therefore, to be the pediatric equivalent of the acromioclavicular separation of adult life.

An Efficacy Study for the Value of Comparison Views in Extremity Injuries in Children: McCauley RGK, Schwartz AM, Leonidas JL, Darling DB (Tufts Univ., Boston, MA 02111)

The radiographs of 300 children referred because of extremity trauma were reviewed prospectively by staff pediatric radiologists. Comparison radiographs (which heretofore were routinely taken in our department) were not viewed before diagnosis, which was based on the films of the involved side only. The need, if any, to view comparison radiographs before establishing a diagnosis was recorded, as well as any change in diagnosis caused by information gained from the contralateral side. These cases were read later by two radiology residents in a simulated clinical setting; the comparison views were withheld unless requested. The medical record of each case was subsequently reviewed and the ultimate accuracy of the initial radiologic diagnosis verified.

In 23 cases comparison views were considered necessary by the pediatric radiologists (8%). In some of these 23 cases, the comparison views changed an equivocal report to a firm report. Usually they were of little value. Similarly, the main value of comparison views for residents was to change the initial reading from equivocal to confident.

Therefore, when radiographs for peripheral trauma in children are interpreted by pediatric radiologists, comparison views are seldom necessary. In the few cases when they are needed, they may be obtained after the injured side has been examined. This approach, which we are adopting, is efficient in cost and radiation.

Relative Efficacy of Radiographs and Bone Scans in the Detection of the Skeletal Lesions of Histiocytosis-X: Parker BR, Pinckney LE, Etcubanas E, Goris ML (Stanford Univ., Stanford, CA 94305)

Recent reports have suggested that radioisotopic bone scans provide a screening mechanism for the

detection of the skeletal lesions of histiocytosis-X and, in fact, may be more sensitive than skeletal radiographs for this purpose.

We have reviewed the records of 19 consecutive, previously-untreated patients with histiocytosis-X seen over a five year period. Bone scans were not performed in five patients and only after therapy in another five patients. Scans and skeletal radiographs were performed prior to therapy, and within ten days of one another, in the remaining nine patients. One of these patients had no lesions identified by either modality. The scans and radiographs of three patients correlated precisely with one another. One patient with a solitary eosinophilic granuloma by radiography had a completely negative scan, while four patients in whom both radiographs and scans were positive had more lesions detected radiographically than by scan. Of the 34 lesions identified radiographically in these eight patients, only 12 were detected by the bone scan. All isotopically demonstrable lesions were detected on the radiographs. Factors such as age of patient, presence and duration of symptoms, number of lesions, anatomic location, and radiographic appearance did not correlate with the lack of bone scan accuracy.

Our data suggest that the radiographic skeletal survey is a more sensitive detector of the bony lesions of histiocytosis-X than is the radioisotopic bone scan.

The Radiographic Features of Eosinophilic Gastroenteritis (Allergic Gastroenteropathy) of Childhood: Teele RL, Katz AJ, Goldman H (The Children's Hospital Medical Center, Boston, MA 02115)

The child with eosinophilic gastroenteritis has failure to thrive, a history of allergy or asthma, iron deficiency anemia, and peripheral eosinophilia. This report presents the radiographs of six such children. Pathologic change in the gastric antrum, present in all patients by biopsy, correlated with an abnormal air-contrast examination of the antrum; the affected children had an irregular, lacy antral surface rather than the smooth, bald surface seen in normal children. The small bowel in eosinophilic gastroenteritis is usually abnormal, though the mucosal thickening shown is non-specific. Much more specific is the combination of small bowel and gastric antral abnormalities. As a result of our findings, we encourage air contrast radiographs of the antrum in children suspected of having eosinophilic gastroenteritis.

The Diagnosis of Hiatus Hernia, Reflux and Esophagitis: Knapp K, Del Hoyo ML, Diez-Pardo J, Martinez A (Clinica Infantil "La Paz" - Universidad Autonoma - Madrid, SPAIN)

In the last twelve years, we have seen 1371 infants and children with hiatus hernia, 92 cases of esophagitis, and 89 esophageal stenoses caused by gastro-esophageal reflux. Since the radiologic diagnosis of hiatus hernia and gastro-esophageal reflux is reasonably standard, there is clearly a higher incidence of these conditions in Spain than in North America. Many of these children have required surgery. "Chalasia" is rarely diagnosed; most cases of "chalasia" actually have hiatus hernias.

Radiology and Manometry in the Selection of Patients for Anti-reflux Surgery: Cumming WA (Hospital for Sick Children, Toronto, Ontario, CAN M5G 1X8)

We reviewed the 42 patients who had anti-reflux surgery at our hospital in the past five years. All 42 had barium examinations, and 31 showed gastro-esophageal reflux. 21 had manometric examinations, done with fluoroscopic monitoring, and 15 had low-pressure lower esophageal sphincters. All patients with low-pressure lower esophageal sphincters showed reflux with barium. 3 patients showed reflux with barium but had normal pressures. This suggests that barium may be better than manometry at detecting reflux.

In our opinion, the patients with symptoms suggesting reflux fall into three groups. Some have normal-pressure sphincters and no reflux by barium swallow; surgery is not necessary. Some have normal-pressure sphincters but reflux with barium; these probably require non-operative therapy only. The last group have low-pressure sphincters and also reflux with barium; these probably need operation, especially if complications are severe.

The Diagnosis and Management of Gastro-esophageal Reflux in the Pediatric Patient: Smith LE, Byrne WJ, Fonkalsrud EW, Kangarloo H (UCLA Sch. of Med., Los Angeles, CA 90024)

Between May, 1977 and May 1978 105 pediatric patients presented with symptoms suggesting gastro-esophageal reflux. Of these patients, 51 had recurrent pneumonia; 34 were subsequently shown to have gastro-esophageal reflux, as is described below. 53 patients were seen because of vomiting, and 27 were demonstrated to have gastro-esophageal reflux.

Investigation for gastro-esophageal reflux was done using a combination of barium esophagram, Tuttle (pH) test, and esophageal manometry. The diagnosis of gastro-esophageal reflux was considered established in 48 patients by demonstrating that two of these studies were positive. In 32 of the 48, both the Tuttle test and barium swallow were positive, in 12 patients the Tuttle test and manometry study were positive, and in 4 patients the barium swallow and manometry study were positive. In a further 17 patients the barium swallow was the only positive examination, and in 7 patients the Tuttle test was the only positive study.

20 of our patients were medically managed. Of these, 11 patients are asymptomatic and 9 patients continue to have symptoms. 28 patients were surgically treated, and 25 of these remain symptom free, while 3 patients continue to have symptoms.

We prefer to use the Tuttle test and barium swallow examination as complementary tools in diagnosis. Esophageal manometry seems less reliable and is in less routine use. We are concerned that there may be false positive findings from the Tuttle test and false negative findings from the barium esophagram.

Editorial

The Complex World of Adverse Reactions

Most adverse reactions to drugs are toxic. These reactions are predictable, may occur in anyone if the dose is high enough, and, fortunately, usually can be anticipated from animal testing. Clinical reactions may occur with (1) overdose, (2) impaired metabolism or excretion, (3) drug interaction, or (4) intolerance. The last is defined as the condition of some individuals who experience the usual toxic symptoms and signs at unusually low doses [1].

Allergic reactions are not predictable from animal testing and theoretically do not occur on first exposure. Clinical manifestations of acute reactions are limited to a few characteristic symptoms and signs, such as flushing, urticaria, angioedema, nasal congestion, bronchospasm, and hypovolemic shock. Whereas a toxic reaction may be prevented by modest reduction in the dose or rate of administration, even minute doses can produce reactions in allergic patients. Acute allergic reactions are caused by one or more chemical mediators that are activated when an antigen reacts with a specific antibody. Thus histamine, anaphylactic slow-reacting substance, and perhaps bradykinin, among others, are released from mast cells and basophils sensitized with antibodies of the immunoglobulin E (IgE) class. Reactions involving IgG and IgM antibodies activate complement, and products of the third and fifth components of complement (C3a and C5a, the anaphylatoxins) can also release histamine.

Vascular endothelial injury produced by antigen-antibody complexes and complement activates Hageman factor (factor XII), the starting point for three parallel series of reactions leading to blood coagulation, fibrinolysis, and plasma kinin (bradykinin) generation. Products of the first two, thrombin and plasmin, can also activate the complement system with anaphylatoxin production as a result [2]. All these systems include a series of enzymatic reactions that are associated with specific inhibitors that normally keep these reactions under control. One example is the inhibitor of the activated form of C1. This esterase inhibitor is also involved in the regulation of coagulation, fibrinolysis, and kinin generation. Its absence in man is associated with a potentially fatal form of angioedema.

Iodinated contrast media have the same potential for causing adverse reactions as do drugs. Most reactions, with nausea and vomiting heading the list, are clearly not allergic [3]. The allergic-type symptoms mentioned above occur with sufficient frequency, though, to be of concern to allergists and radiologists alike. These symptoms may be explosive and, if shock and/or airway angioedema develop, can be fatal. Despite the typical symptoms, most of these reactions may not be truly allergic—that is, antibody-mediated. Brasch and Caldwell [4] did find significantly more antibodylike activity (globulin binding of diatrizoate) in the sera of patients after severe reactions, compared with controls, but acknowledged that there was no proof that this had anything to do with the production of symptoms. Among other things, the occurrence of acute reactions in patients with no prior exposure and the development of a reaction on one occasion but not the next in the same patient argue against allergic sensitization being responsible for these reactions. There are reasonable alternative explanations.

Several drugs, including the opiates, release histamine from mast cells without antibody mediation in a predictable, dose-related fashion [1]—so do contrast agents, both in vitro and in vivo. However, a problem with the histamine release concept as an explanation for clinical reactions is that the plasma histamine has been found to increase just as much after injection of the contrast medium in patients who did not have a reaction as in those who did [5].

Contrast agents also activate complement via the alternative pathway (bypassing the first three reacting components, C1, C4, and C2) according to some reports, while others have implicated both the classical (C1 activation) and alternative pathways [6]. As with histamine release, though, complement activation is insufficient to explain clinical reactions, for it also seems to occur to the same degree in patients who don't react as in those who do [5].

It is possible that contrast agents affect complement indirectly, via Hageman factor (factor XII) activation. If this is so, then such activation may be important in other ways. In this issue of the Journal is a report by Lasser et al. on the effect of intravenous meglumine iodipamide on blood coagulation in rabbits. They observed a reduction in factor XII levels and evidence for activation of the intrinsic and even the extrinsic coagulation systems. They again observed the reduction in complement activity that they had reported earlier. Mortality was not changed by prior depletion of the later reacting components of complement by cobra venom. This is not surprising; if complement activation had contributed to mortality, then cobra venom administration itself should produce more serious reactions than it does. The most significant observations were that mortality could be greatly reduced by either fibrinogen depletion or heparin treatment. This may have a clinical counterpart; a few human cases of disseminated intravascular coagulation have been recognized after injection of a contrast agent.

Since the effect on the clotting mechanism appears to be universal in rabbits, could it also be a common and predictable finding in man? The answer seems to be "yes." In the same study in which histamine and complement levels were compared, fibrinogen split products were found in the serum of almost half of the patients after a contrast study. Again, there was no difference between those who had reactions and those who did not [5].

Obviously the answers are not all in. The kinin generating system that is triggered by factor XII activation certainly deserves more consideration. The chemical actions of contrast media do seem to affect all patients more or less equally. Rather than reacting to excessive mediator activation, those who experience allergylike (anaphylactoid) reactions may have an unusual degree of reactivity to a usually innocuous level of one or more mediators. This could be tested. Lasser et al. have raised another interesting possibility in their paper. They suggested that those who have clinical reactions are deficient in some inhibitor, and they have taken the logical step of looking at the C1 esterase inhibitor. However, it should be kept in mind that subjects who have a proven deficiency of this inhibitor suffer only from edema, so such a suggestion might not be adequate to explain the urticarial, bronchospastic, and other anaphylactoid reactions to iodinated contrast media.

Paul P. VanArsdel, Jr.
University of Washington School of Medicine
Seattle, Washington 98195

REFERENCES

1. VanArsdel PP Jr: Adverse drug reactions, in *Allergy Principles and Practice*, vol 2, chapter 61, edited by Middleton E Jr, Reed CE, Ellis EF, St. Louis, Mosby, 1978
2. Wells JV: Immune mechanisms in tissue damage, in *Basic and Clinical Immunology*, 2d ed, chapter 23, edited by Fudenberg HH, Stites DP, Caldwell JL, Wells JV, Los Altos, Calif., Lange, 1978
3. Witten DM: Reactions to urographic contrast media. *JAMA* 231:974–977, 1975
4. Brasch RC, Caldwell JL: The allergic theory of radiocontrast agent toxicity: demonstration of antibody activity in sera of patients suffering major radiocontrast agent reactions. *Invest Radiol* 11:347–356, 1976
5. Simon RA, Schatz M, Stevenson DD, Curry N, Yamamoto F, Plow E, Ring H, Arroyave CM: Radiographic contrast media infusions: measurement of mediators and correlation with clinical parameters. *J Allergy Clin Immunol* 61:145, 1978
6. Lieberman P, Siegle RL, Taylor WW Jr: Anaphylactoid reactions to iodinated contrast material. *J Allergy Clin Immunol* 62:174–180, 1978

ARRS 79th Annual Meeting: Condensed Schedule

March 26–30, 1979 at the Sheraton Centre, Toronto, Canada

Friday, March 23

8 a.m.–5 p.m. Society for Pediatric Radiology (SPR) Board of Directors meeting
4–7 p.m. SPR registration

Saturday, March 24

7:30 a.m.–12:30 p.m. SPR registration
8:30 a.m.–5:30 p.m. SPR Scientific meeting (members only)
9 a.m.–noon. ARRS Editorial Policy Committee
Noon–2 p.m. SPR luncheon business meeting (members only)
1–5 p.m. ARRS Publications Committee

Sunday, March 25

8 a.m.–noon. SPR meeting (members only)
8:30 a.m.–5 p.m. ARRS executive council
10 a.m.–5 p.m. On site registration
8:30 a.m.–noon. ARRS Categorical Course on Neuroradiology
11 a.m.–9 p.m. Society of Photo-Optical Instrumentation Engineers (SPIE) registration
12:30 p.m. SPR luncheon (members only)
1–5 p.m. SPIE session I
1:30–6 p.m. SPR and Neuhauser Lecture (open to ARRS members)
2–4:30 p.m. Categorical Course on Neuroradiology
5–6:30 p.m. SPIE dinner
6:30–9:30 p.m. SPIE session II
7–11 p.m. Scientific exhibits
9:30 p.m. SPIE wine and cheese reception

Monday, March 26

7–8 a.m. ARRS instructional course faculty breakfast
7 a.m.–11 p.m. Scientific exhibits
8 a.m.–4:30 p.m. On site registration
8 a.m.–noon. SPIE session III
8–9:30 a.m. Categorical Course on Neuroradiology
8:30 a.m.–1 p.m. Spouses' hospitality room
9 a.m.–5:30 p.m. Technical exhibits
9:30–10 a.m. Opening ceremonies
10 a.m.–12:30 p.m. Scientific program
10:30 a.m.–2 p.m. Spouses' program tour
Noon–1:30 p.m. SPIE luncheon
1:30–5 p.m. SPIE session IV
1:30–6 p.m. SPR Board of Directors Meeting
2–5 p.m. Categorical Course on Neuroradiology
3:30–5 p.m. Instruction Courses

Tuesday, March 27

7–8 a.m. ARRS instructional course faculty breakfast
7 a.m.–11 p.m. Scientific exhibits
8 a.m.–4:30 p.m. On site registration
8–9:30 a.m. SPIE breakout sessions (Hotel Toronto)
8–9:30 a.m. Instruction courses
8–10 a.m. Categorical Course on Neuroradiology
8:30 a.m.–1 p.m. Spouses' hospitality room
9 a.m.–5:30 p.m. Technical exhibits
9:30 a.m.–4 p.m. Spouses' program tour
10 a.m.–12:30 p.m. Scientific program (joint ARRS/SPIE session)
12:30–2 p.m. AJR luncheon
2–4 p.m. Scientific program
4:30–5:30 p.m. ARRS business meeting (members only)
6:30–8 p.m. Reception at technical exhibit area (admission by badge)

Wednesday, March 28

7–8 a.m. ARRS instructional course faculty breakfast
7 a.m.–11 p.m. Scientific exhibits
8 a.m.–4:30 p.m. On site registration
9–10:15 a.m. Scientific program
9 a.m.–5:30 p.m. Technical exhibits
9:30 a.m.–4:30 p.m. Spouses' program tour
10:30 a.m.–12:30 p.m. Announcements of awards and Caldwell Lecture
12:30–2 p.m. ARRS past presidents' luncheon
1 p.m.–about 7 p.m. Tennis tournament
2–3:30 p.m. Instruction courses
3:30 p.m. ACR panel presentation
7–11 p.m. Executive Council reception and dinner

Thursday, March 29

7–8 a.m. ARRS instructional course faculty breakfast
7 a.m.–11 p.m. Scientific exhibits
8 a.m.–4:30 p.m. On site registration
8–9:30 a.m. Instruction courses
8–10 a.m. Categorical Course on Neuroradiology
8:30 a.m.–1 p.m. Spouses' hospitality room
9 a.m.–5:30 p.m. Technical exhibits
10 a.m.–noon. Spouses' program brunch
10 a.m.–12:30 p.m. Scientific program
2–4 p.m. Scientific program
4:30–5:30 p.m. ARRS business meeting (members only)
6:30–10 p.m. Social evening at Ontario Place
American Thermographic Society meeting

Friday, March 30

7–8 a.m. ARRS instructional course faculty breakfast
7 a.m.–1 p.m. Scientific exhibits
8 a.m.–noon. On site registration
8–9:30 a.m. Instruction courses
8–10 a.m. Categorical Course on Neuroradiology
8:30–11 a.m. Spouses' hospitality room
10 a.m.–12:30 p.m. Scientific program
American Thermographic Society meeting

Saturday, April 1

American Thermographic Society meeting

© 1979 American Roentgen Ray Society

0361–803X/79/1322–0311 $0.00

U.S. Internal Revenue Service Rules on Deduction of Expenses Incurred while Attending Foreign Conventions

The U.S. Tax Reform Act of 1976 provides that no deduction is allowed for the expense of any individual attending more than two foreign conventions, seminars, or similar meetings during his taxable year. Foreign means Canada and Mexico as well as overseas.

In addition, strict limits are imposed on the amount of the allowable deductions for expenses of attending any two foreign conventions, as follows:

1. No deduction is allowed for expense of transportation outside the U.S. to and from the site of the convention in an amount which exceeds the lowest coach or economy rate charged by commercial airline during the calendar month in which the convention begins. If there is no coach or economy rate, then a deduction of the first class rate is allowed. This rule applies only to transportation outside the U.S., which for air travel purposes means from the last point of a scheduled stop. Thus, if a person flies from Los Angeles nonstop to Toronto, his entire fare is subject to these rules, but if his flight from Los Angeles stops in Detroit before going to Toronto, only the Detroit to Toronto portion is subject to the rules.

2. The full amount of the transportation expense for travel outside the U.S. referred to in item 1 is allowed only if more than one-half the total days of the trip, excluding the days of transportation to and from the site of the convention, are devoted to business related activities, as determined under the rules described in item 4. If fewer than one-half of these days are devoted to business related activities, the deduction of transportation expenses is allowed only in the same percentage as the percentage of days devoted to business activities.

3. Expenses for lodging, meals, tips, local transportation, and other necessary expenses (subsistence expenses) are not deductible to the extent they exceed the dollar per diem rate in effect for U.S. government employees or civilians working in the area of the site of the convention. The rate for Toronto in March 1979 is expected to be $50/day.

4. A deduction for a full day of subsistence expenses described in item 3 is allowed only if there are at least 6 hr of scheduled business activities during the day, and the individual attends at least two-thirds of these activities (i.e. two-thirds of the actual number of hours scheduled, not just 6 if more than 6 hr are scheduled) and a deduction for a half-day of subsistence expenses is allowed only if there are at least 3 hr of scheduled business activities during the day (but less than 6 hr) and the individual attends two-thirds of these activities. However, if 6 hr are scheduled, an individual cannot attend for 2 hr and be entitled to a half day of subsistence expenses. Banquet time is taken into account only for the time devoted to a business related speech or lecture. (These rules are also used to determine days devoted to business related activities for purposes of the deduction of transportation expenses under item 2.) A deduction for subsistence expenses for all of the days and half days is allowed if the individual has attended at least two-thirds of the scheduled business activities in the aggregate and each full day consists of at least 6 hr of scheduled business activities and each half day consists of at least 3 hr.

In addition no deduction is allowed for any transportation or subsistence expenses unless the individual attaches to his tax return a written statement signed by him containing information describing the total days of the trip, excluding transportation days to and from the convention site, the number of hours of each day that were devoted to scheduled business activities, and a program of those activities. At registration in Toronto, ARRS will supply forms that comply with Internal Revenue Service regulations.

American College of Radiology
Legal Council Report

Scientific Program

Monday, March 26

9:30 a.m. Opening ceremonies. Call to order of seventy-ninth annual meeting of American Roentgen Ray Society by President Harry Z. Mellins, Boston, Massachusetts. Installation of President-elect Paul A. Riemenschneider, Santa Barbara, California, by H. Z. Mellins and John L. Gwinn, Los Angeles, California, chairman of Executive Council. **Presidential Address:** Paul A. Riemenschneider

I. Pediatric Radiology (Joint program with Society for Pediatric Radiology)

10 a.m. 1. John Caffey Award Paper to be selected by Society for Pediatric Radiology

10:15 a.m. 2. The radiographic manifestations of bone marrow transplant complications in children. The spectrum of pulmonary disease. JJ Pagani, MT Gyepes, SA Feig, PM Falk, Los Angeles, California

10:30 a.m. 3. B-mode gray scale ultrasonography of the head in the newborn and young infant. DS Babcock, BK Han, GW LeQuesne, Cincinnati, Ohio

10:45 a.m. 4. The teardrop sign: plain film recognition of ankle effusions. RB Towbin, R. Clark, JS Dunbar, Cincinnati, Ohio

11 a.m. 5. The Ask-Upmark kidney: congenital or acquired? CJ Hodson, New Haven, Connecticut

11:15 a.m. 6. Necrosis of Wilms' tumors. GF Gates, JH Miller, P Stanley, Los Angeles, California

11:30 a.m. 7. Pancuronium bromide effect on the neonatal abdomen. PH Winchester, PW Brill, RJ Katz, New York, New York

11:45 a.m. 8. Atypical infantile pyloric stenosis (Incomplete muscle hypertrophy and a new nonhypertrophic form). LE Swischuk, CK Hayden Jr, Galveston, Texas

Noon. 9. Megacystis-microcolon-intestinal hypoperistalsis syndrome: four neonatal cases of functional intestinal obstruction. LW Young, BR Girdany, WK Sieber, EJ Yunis, Pittsburgh, Pennsylvania

12:15 p.m. 10. Cholestatic syndromes in infancy and childhood. GF Gates, FR Sinatra, DW Thomas, Portland, Oregon (GF Gates) and Los Angeles, California

II. Head and Neck Radiology

10 a.m. 11. American Society of Neuroradiology Award Paper, Xenon Enhanced Cranial Computed Tomography. BP Drayer, S. Wolfson Jr, M Boehnke, M Dujovny, E Cook, AE Rosenbaum, Pittsburgh, Pennsylvania

10:15 a.m. 12. Preliminary observation on the clinical value of emission computed tomography. TC Hill, P Costello, HF Gramm, BJ McNeil, RD Lovett, Boston, Massachusetts

10:30 a.m. 13. Selecting surgical candidates with normal pressure hydrocephalus using new CT and radionuclide imaging criteria. LR Altemus, RC Briggs, W Leschey, Portland, Maine

10:45 a.m. 14. Computed tomography in brainstem injury. FY Tsai, JE Huprich, MF Quinn, J Ahmadi, HD Segall, JS Teal, San Marino, California

11 a.m. 15. CT guided brain biopsy. MA Weinstein, J Hahn, PM Duchesneau, Cleveland, Ohio

11:15 a.m. 16. Pitfalls and limitations of computerized tomography in intracranial disorders. KY Chynn, N Finby, I Altman, WI Shaw, New York, New York

11:30 a.m. 17. Efficacy of plain skull x-rays in routine evaluation of head trauma. SJ Masters, Pittsfield, Massachusetts

11:45 a.m. 18. Malignant external otitis: a radiographic clinical correlation. G Mendez Jr, R Quencer, MJD Post, NA Stokes, Miami, Florida

Noon. 19. Neuroradiological features of juxtasellar sarcoidosis with special emphasis on enlargement of the optic canal and sella turcica. A report of five cases. KF Lee, YE Lee, Philadelphia, Pennsylvania

12:15 p.m. 20. Epidurography: selective catheter technique and review of 53 cases. GH Roberson, HP Hatten Jr, JR Hesselink, Charlotte, North Carolina

Tuesday, March 27

III. Physics, Instrumentation, Technique (Joint program with Society for Photo-Optical Instrumentation Engineers)

10 a.m. 21. Exposure from diagnostic radiologic studies—fetal vs. parenteral radiosensitivity. GV Dalrymple, ML Baker, Little Rock, Arkansas

10:15 a.m. 22. Nuclear magnetic resonance zeugmatographic imaging. PC Lauterbur, Stony Brook, New York

10:40 a.m. 23. How to apply case series review results to evaluation of individual cases in diagnostic radiology. JR Thornbury, DG Fryback, LR Kuhns, Ann Arbor, Michigan

IV. Gastrointestinal Radiology

10 a.m. 30. The Society of Gastro-intestinal Radiologists Award Paper. Reactions to intravascular contrast media: apparent relationship to increased complement consumption. EC Lasser, JH Lang, AE Hamblin, SG Lyon, San Diego, California

10:15 a.m. 31. Double contrast esophagography in esophagitis. HY Kressel, I Laufer, MP Banner, Philadelphia, Pennsylvania

10:30 a.m. 32. Antral mucosal diaphragm—a roentgen anatomic correlation. JL Clements Jr, WE Torres, JR Jinkins, J Thomas, B Thomas, RA Elmer, Atlanta, Georgia

(III cont.)

10:55 a.m. 24. Microwave thermography applied to the detection of breast cancer. AH Barrett, PC Myers, NL Sadowsky, Cambridge and Boston (NL Sadowsky), Massachusetts

11:10 a.m. 25. Microdose radiography: the physics of a radiographic system. DJ Curtis, P Bjorkholm, RM Quillin, E Frederick, RJ Ayella, JH Jackson, Bethesda, Maryland

11:25 a.m. 26. The use of a multiformat camera for recording television images during fluoroscopic examinations. DM Hynes, E Edmonds, C Krametz, D Baranoski, Toronto, Ontario, Canada

11:40 a.m. 27. Progress in ultrasonic CT of the breast and initial pulse echo comparisons. PL Carson, AL Scherzinger, TV Oughton, JE Kubitschek, PA Lambert, GE Moore, MG Dunn, Denver, Colorado

11:55 a.m. 28. Limits of detectability by computed tomography as a function of diameter and attenuation differential. DB Plewes, PB Dean, Rochester, New York

12:10 p.m. 29. CT imaging of cardiopulmonary structure and function with DSR—a progress report. EL Ritman, RA Robb, PA Chevalier, BK Gilbert, JH Kinsey, EH Wood, Rochester, Minnesota

(IV cont.)

10:45 a.m. 33. The gastric cardia and its variations on double contrast study. R. Grossman, H Herlinger, I Laufer, HY Kressel, RH Ochs, Philadelphia, Pennsylvania

11 a.m. 34. Villous tumors of the upper gastrointestinal tract. JH Miller, LH Weiland, JJ Gisvold, DC McIlrath, Los Angeles, California

11:15 a.m. 35. Fifteen years' experience with selective hypotonic duodenography: rare duodenal lesions. LB Costopoulos, Edmonton, Alberta, Canada

11:30 a.m. 36. Ischemic colitis mimicking chronic ulcerative colitis and Crohn's disease. RL Eisenberg, CK Montgomery, AR Margulis, HY Kressel, San Francisco, California

11:45 a.m. 37. Iatrogenic intubation injuries of the gastrointestinal tract. GG Ghahremani, MA Turner, RB Port, Evanston, Illinois

Noon. 38. Clinical classification of abnormalities of small bowel mucosal patterns. SW Nelson, Seattle, Washington

12:15 p.m. 39. Ceruletide-assisted examination of the small bowel. AH Robbins, SM Wetzner, MD Landy, Boston, Massachusetts

Tuesday Afternoon

V. Gastrointestinal Radiology

2 p.m. 40. The abnormal rectal contour demonstrated on the air contrast enema. TE Herman, RE Koehler, JKT Lee, St. Louis, Missouri

2:15 p.m. 41. Lymphoid hyperplasia of the colon: an unappreciated entity in adults. FM Kelvin, RJ Max, TA Oddson, WM Thompson, RP Rice, JT Garbutt, Durham, North Carolina

2:30 p.m. 42. Angiodysplasia of the colon: incidence and coexistence with other bowel lesions in nonbleeding patients. S Kadir, CA Athanasoulis, AC Waltman, W Cutcliff, Nashville, Tennessee

2:45 p.m. 43. Intraarterial vasopressin infusion for treatment of Mallory-Weiss tears of the esophagogastric junction. RA Clark, Cincinnati, Ohio

3 p.m. 44. Computerized tomography of the esophagus: normal and carcinoma. RH Daffner, MD Halber, WM Thompson, RW Postlethwait, Durham, North Carolina

3:15 p.m. 45. Computed tomography of the pelvis following abdomino-perineal resection for carcinoma of the rectum. B Williamson Jr, RR Hattery, DH Stephens, PF Sheedy II, Rochester, Minnesota

3:30 p.m. 46. Upper abdominal abscess—a continuing and deadly problem. TR Connell, DH Stephens, HC Carlson, ML Brown, Rochester, Minnesota

3:45 p.m. 47. Guided percutaneous catheter drainage for nonoperative treatment of abdominal abscesses. SG Gerzof, AH Robbins, D Birkett, WC Johnson, Boston, Massachusetts

VI. Genitourinary Radiology

2 p.m. 48. Renal duplication with a diminutive low pole: the nubbin sign. JA Curtis, HM Pollack, Philadelphia, Pennsylvania

2:15 p.m. 49. The hypernephroma halo: a reliable tumor sign in excretory urography. HP Jander, CA Pereira Centola, Birmingham, Alabama

2:30 p.m. 50. Calcified renal cell carcinoma: a biologically distinct subgroup of renal parenchymal tumors. KW Sniderman, TA Sos, GR Seligson, JN Krieger, New York, New York

2:45 p.m. 51. Multilocular cyst of the kidney: a lesion in search of a name. MP Banner, HM Pollack, Philadelphia, Pennsylvania

3 p.m. 52. Radiologic studies in the patient with multiple endocrine neoplasia, type II syndrome and suspected pheochromocytoma. KJ Cho, DT Freier, TL McCormick, ME Forrest, A Kaufman, Ann Arbor, Michigan

3:15 p.m. 53. Outpatient renal vein renin sampling. TA Sos, KW Sniderman, DB Case, New York, New York

3:30 p.m. 54. Von Hippel Lindau's disease: the role of renal arteriography in its management. S Kadir, AC Waltman, WS Kerr JR, CA Athanasoulis, Nashville, Tennessee

3:45 p.m. 55. Transcatheter occlusive therapy of genitourinary abnormalities using isobutyl 2-cyanoacrylate (Bucrylate). PC Freeny, WH Bush, CR Kidd, R Mennemeyer, Seattle, Washington

Wednesday, March 28

VII. Bone Radiology

9 a.m. 56. Determination of bone mass by computed tomography. PS Jensen, SC Orphanoudakis, EN Rauschkolb, R Baron, R Lang, H Rasmussen, New Haven, Connecticut

9:15 a.m. 57. Arthrographic abnormalities and normal variations of the popliteus tendon sheath. H Pavlov, AB Goldman, New York, New York

9:30 a.m. 58. Computed tomography of the lumbar spine: applications of reconstructed sagittal and coronal images. CG Ullrich, SA Kieffer, EF Binet, Syracuse, New York

9:45 a.m. 59. Improved imaging of the spinal canal and its contents with the A.S. and E. CT scanner. MC Chiu, C Fong, KG Terbrugge, Toronto, Ontario, Canada

10 a.m. 60. Computed tomography and angiography of tumors of the lower extremity: critical evaluation and clinical significance. RT Heelan, RC Watson, J Smith, New York, New York

VIII. Chest Radiology

9 a.m. 61. Round atelectasis of the lung mimicking tumor. HJ Schneider, B Felson, L Gonzalez, Cincinnati, Ohio

9:15 a.m. 62. Positive and expiratory pressure (PEEP) and the chest x-ray: radiologic-physiologic correlations. JE Zimmerman, LR Goodman, MBG Shahvari, Philadelphia, Pennsylvania

9:30 a.m. 63. What becomes of pulmonary infarcts? PJ McGoldrick, MM Figley, T Rudd, J Wilhelm, Seattle, Washington

9:45 a.m. 64. The effect of emphasizing patient care upon chest x-ray interpretation. P Lahaie, PA Lazar, JW Gard, EJ Potchen, East Lansing, Michigan

10 a.m. 65. Sequential chest radiologic findings in Legionnaire's disease. LC Chiu, RL Schapiro, CM Helms, JP Viner, Iowa City, Iowa

Awards Session

10:30 a.m. President's Award Paper

10:45 a.m. Scientific exhibit awards. Announcement by BG Brogdon, chairman, Scienfific Exhibits Committee

11 a.m. The Caldwell Lecture. Radiology of the abdomen: impact of the new modalities. Joseph P. Whalen, New York, New York

3:30 p.m. ACR panel presentation. Update from the American College of Radiology: Legal update, P Gebhard; Coping with the regulatory process, RE Wise; Activities of the Commission on Diagnostic Radiology, JF Wiot; College communications, SH Madell

Thursday, March 29

IX. Genitourinary Radiology

10 a.m. 66. The integrated operation of computed radiography (CR) and CT scanning in intravenous urography. WD Foley, TJ Imray, TL Lawson, TA Quiroz, JE Youker, Milwaukee, Wisconsin

10:15 a.m. 67. Computed tomography of the perineum. J Tisnado, MA Amendola, MA Turner Richmond, Virginia

10:30 a.m. 68. Computerized tomography in the diagnosis and management of urinary extravasation. HA Mitty, HC Yeh, New York, New York

10:45 a.m. 69. Ultrasound of the renal sinus: new observations. AT Rosenfield, KJW Taylor, AG Dembner, M Crade, GN Viscomi, P Jacobson, New Haven, Connecticut

11 a.m. 70. Ultrasound evaluation of bladder and perivesical abnormalities which affect the urinary tract. RL Bree, TM Silver, Ann Arbor, Michigan

11:15 a.m. 71. Gray scale ultrasound evaluation of bladder tumors. S Edell, J Pahira, Philadelphia, Pennsylvania

11:30 a.m. 72. Evaluation and treatment of fluid-filled renal structures in children—combined use of ultrasound and renal puncture. JC Anderson, GH Bickers, MJ Mazer, HA Baltaxe, FF Bartone, Omaha Nebraska

11:45 a.m. 73. Amniography: an adjunct to obstetrical sonography. L Calenoff, RE Sabbagha, BA Sakowicz, Chicago, Illinois

X. Chest Radiology

10 a.m. 76. The chest roentgenogram in desquamative interstitial pneumonitis (DIP). DS Feigin, PJ Friedman, San Diego, California

10:15 a.m. 77. Conglomerate pulmonary disease due to foreign particle emboli in narcotic patients. DJ Sieniewicz, A Nidecker, Toronto, Ontario, Canada

10:30 a.m. 78. TTNA: complications with respect to location and type of lesion. PB Bailey, TH Berquist, DA Cortese, JK Crowe, WE Miller, Rochester, Minnesota

10:45 a.m. 79. The efficacy of full lung tomography in the detection of early metastatic disease from carcinoma of the breast. AM Curtis, CE Ravin, P Collier, CE Putman, TC McLoud, RH Greenspan, New Haven, Connecticut

11 a.m. 80. Linear versus pluridirectional tomography of the chest—a correlative roentgen-anatomical study. JT Littleton, ML Durizch, Mobile, Alabama

11:15 a.m. 81. Diagnosis of thymoma at the Mayo Clinic—a 10 year review. LR Brown, JR Muhm, JK Crowe, Rochester, Minnesota

11:30 a.m. 82. CT-pathologic correlation of pulmonary abnormalities. PG Herman, J Goldstein, SJ Hessel, JM Drummey, JP Balikian, Boston, Massachusetts

(IX cont.)

Noon. 74. Comparisons of renal ultrasound and renal radionuclide scanning in the diagnosis of hydronephrosis. G Adamo, HL Neiman, S Malave, SJ Cisternino, Chicago, Illinois

12:15 p.m. 75. Computerized radionuclide urogram in the assessment of acute renal disease. EK Lang, JU Schlegel, New Orleans, Louisiana

(X cont.)

11:45 a.m. 83. Computed tomographic evaluation of the breast: a significantly improved diagnostic tool. CHJ Chang, JL Sibala, SL Fritz, SJ Dwyer III, AW Templeton, Kansas City, Kansas

Noon. 84. Computerized tomographic mamography. JJ Gisvold, DF Reese, Rochester, Minnesota

12:15 p.m. 85. Value of microfocal spot magnification mammography in differentiating benign from malignant clustered breast microcalcifications. EA Sickles, San Francisco, California

Thursday afternoon

XI. Cardiovascular Radiology

2 p.m. 86. Epidural anesthesia in aortoiliofemoral arteriography. DG Spigos, SR Akkineni, WS Tan, GE Espinosa, AR Vasireddy, AP Winnie, Chicago, Illinois

2:15 p.m. 87. The use of anesthesia in arteriography of the extremities. Y Ben-Menachem, BM Rigor, JH Duke Jr, Houston, Texas

2:30 p.m. 88. Angiographic pitfalls in Prinzmetal's variant angina (PVA): differentiating PVA spasm from catheter-induced spasm and refractory PVA spasm from "fixed" lesions. AC Friedman, H Spindola-Franco, T Nivatpumin, Bronx, New York

2:45 p.m. 89. The right superior septal perforator artery: its angiographic description and clinical significance. PR Bream, AS Souza Jr, GC Curry, B Soto, Birmingham, Alabama

3 p.m. 90. Percutaneous transluminal angioplasty: modifications of the Gruntzig technique. TA Sos, KW Sniderman, RK Baxi, S Saddekni, TG Pickering, DB Case, New York, New York

3:15 p.m. 91. The use of an ECG-gated interlaced radiographic system for evaluation of patients with aortic regurgitation. RE Dinsmore, SW Miller, R Wernikoff, MS Potsaid, Boston, Massachusetts

3:30 p.m. 92. Single photon transaxial emission computed tomography of the heart with thallium-201. BL Holman, TC Hill, J Wynne, RD Lovett, Boston, Massachusetts

3:45 p.m. 93. Using gated nuclear cardiac scans to investigate cardiomegaly—the practical approach. BP Sherman, ML Friedman, BJ Ostrum, Philadelphia, Pennsylvania

XII. Bone Radiology

2 p.m. 94. Gout: a radiologic evaluation based upon over 2,000 patients. C Bloch, G Herman, TF Yu, New York, New York

2:15 p.m. 95. A comparison of the radiologic features of erosive osteoarthritis and psoriatic arthritis in the hand, wrist, and foot. W Martel, AW Dworin, K Stuck, Ann Arbor, Michigan

2:30 p.m. 96. Arthrotomography of the temporomandibular joint: preliminary observations. RW Katzberg, MF Dolwick, DJ Bales, CA Helms, Lackland Air Force Base, Texas

2:45 p.m. 97. Evaluation of fractures using radionuclide scanning and radiographic examination. Y Wang, Pittsburgh, Pennsylvania

3 p.m. 98. The role of radionuclide bone scanning in the detection of loosening of the total knee arthroplasty. JC Hunter, RS Hattner, HK Genant, WR Murray, San Francisco, California

3:15 p.m. 99. Radiographic detection of the Hill-Sachs lesion: a cadaveric study. G Greenway, LA Danzig, D Resnick, San Diego, California

3:30 p.m. 100. The osseous manifestations of stress at the elbow associated with sports activities. LF Rogers, R Gore, J Bowerman, J Suker, CE Compere, Baltimore, Maryland

3:45 p.m. 101. Arthrography and arthroscopy of the knee: complementary diagnostic procedures. EM Levinsohn, BE Bamer, Syracuse, New York

Friday, March 30

XIII. Cardiovascular Radiology

10 a.m. 102. An experimental study of the morphological changes in the renal transplant using ultrasound. MR Conrad, RM Dickerman, RA Bridges, BC Carlson, HJ Helderman, RC May, EB Morrison, Dallas, Texas

10:15 a.m. 103. Reducing venous thrombosis as a complication of contrast phlebography. MA Bettman, D Rosenthal, K Rabinov, R Nebesar, GP Clagett, J Skillman, G Davies, J Ploetz, E Salzman, Boston, Massachusetts

XIV. Gastrointestinal Radiology

10 a.m. 112. The significance of intrapancreatic gas demonstrated by CT: a review of nine cases. G Mendez Jr, MB Isikoff, Miami, Florida

10:15 a.m. 113. Inflammatory complications of acute pancreatitis monitoring by computing tomography. SS Siegelman, BE Copeland, GP Saba, JL Cameron, RC Sanders, Baltimore, Maryland

(XIII cont.)

10:30 a.m. 104. The incidence and significance of left circumaortic venous rings. CF Beckman, HL Abrams, Boston, Massachusetts

10:45 a.m. 105. The calcified aortic plug syndrome—a new manifestation of atherosclerosis. JF Walter, C Olcott IV, JT Mehigan, L Gonzalez-Lavin, Palo Alto, California

11 a.m. 106. Balloon occlusion superior mesenteric arteriography for demonstration of the mesenteric and portal venous anatomy. DA Phillips, DF Adams, CF Beckmann, HL Abrams, Boston, Massachusetts

11:15 a.m. 107. Hepatic artery catheter position verification by radionuclide imaging. BG McConnell, RW McConnell, Houston, Texas

11:30 a.m. 108. Radiologic follow-up of vena cava filter devices. LL Berland, FE Maddison, VM Bernhard, Milwaukee, Wisconsin

11:45 a.m. 109. Gray scale ultrasound evaluation of arterial grafts. AH Wolson, HA Kaupp, KM McDonald, Allentown, Pennsylvania

Noon. 110. Ultrasound evaluation of pseudoaneurysms complicating peripheral by-pass surgery. SA Hausserman, AB Crummy, HA Berkoff, Madison, Wisconsin

12:15 p.m. 111. Ultrasonic evaluation of vascular abnormalities. TL Lawson, F Quiroz, WD Foley, FE Maddison, Milwaukee, Wisconsin

(XIV cont.)

10:30 a.m. 114. A comparative study of CT and ultrasonography in carcinoma of the pancreas. PD Kamin, ME Bernardino, S Wallace, Houston, Texas

10:45 a.m. 115. The changing role of pancreatic angiography: the impact of newer diagnostic modalities. PC Freeny, TJ Ball, J Ryan, Seattle, Washington

11 a.m. 116. Visualization of normal biliary ductules and diagnosis of preicteric obstruction by ultrasound. KJW Taylor, M Crade, RK Zeman, J Gold, AT Rosenfield, New Haven, Connecticut

11:15 a.m. 117. Biliary pseudocalculus effect in the ultrasonic examination of the postcholecystectomy patient. V Raptopoulos, Worcester, Massachusetts

11:30 a.m. 118. Biliary tract exploration via the T-tube tract—an improved technique. JG Whelan Jr, JP Moss, Louisville, Kentucky

11:45 a.m. 119. The significance of the nonopacified gallbladder in the differential diagnosis of the abnormal endoscopic retrograde cholangiogram. CA Rohrmann, Jr, HJ Ansel, RL Protell, FE Silverstein, SE Silvis, JA Vennes, Seattle, Washington

Noon. 120. Transhepatic cholangiography today—does the "skinny" needle help? EA Stewart, HC Carlson, PF Sheedy, DH Stephens, RR Hattery, Rochester, Minnesota

12:15 p.m. 121. Comparison of success and risk in percutaneous transhepatic cholangiography using 19- versus 22-gauge needle. CR Irish, TF Meaney, Cleveland, Ohio

Spouses' Program

The Spouses' Committee has arranged three tours in the Toronto area. The first, Monday, March 26, will be backstage at the St. Lawrence Centre for the Arts to see an aspect of the theater that few people have an opportunity to appreciate. The centre houses a summer and winter repertory theater and provides space for numerous public events. Luncheon will be served at the end of the tour in the theater lobby.

On Tuesday, March 27, tour participants have a choice of a walk through a maple woods to see the production of maple syrup, or a bus ride through downtown Toronto. Both groups will meet for lunch at the Board of Trade Country Club. The afternoon will be spent at the "most Canadian gallery in the country," McMichael Canadian Collection in Kleinburg. The gallery, housed in log buildings, is a clear representation of the Group of Seven, the only internationally recognized school of Canadian art. There is also a fine collection of Indian and Eskimo art.

Niagara Falls and Niagara-on-the-Lake are the sites of a day-long tour on Wednesday, March 28. Lunch will be served at a country inn at Niagara-on-the-Lake. Ample time will be provided for photography at the American Falls and the Canadian Horseshoe Falls. After lunch, time will be provided for shopping and a drive around the former colonial capital, now home of the renowned Shaw Festival.

In addition to the three tours, a fashion show and brunch will provide entertainment on Thursday, March 29, in the Aloha Lagoon, Sheraton Centre. The creations of well known Canadian designer Claire Haddad will be shown as well as the best in fur designs by Norman Rogul. Top Canadian models will show the designs.

Schedule of Courses

Sunday, March 25, through Friday, March 30
Categorical Course on Neuroradiology, five sessions, 15 hr. Fee is $25 and must be paid by society members as well as guests. **Registration in this course precludes registration in any other courses.**

Monday, March 26, 3:30–5 p.m.
101. Parkey, Lewis. Nuclear Cardiology Review
102. Greenspan. Intrathoracic Air Trapping
103. Alfidi. Computed Tomography of the Human Body
104. Berk. Radiology of the Gallbladder and Bile Ducts
105. Egan, McSweeney. Correlated Clinical, Radiographic, and Pathologic Approach to Detect Early Breast Cancer
106. Gardiner, Stevenson. Inflammatory Bowel Disease
107. Gehweiler, Charlton. Radiology of Facial Fractures
108. Gilula. Radiology of the Wrist, Part I
109. Meyers. Dynamic Radiology of the Abdomen: Normal and Pathologic Anatomy
110. Hattery. Computed Tomography of the Genitourinary Tract, Retroperitoneum, and Pelvis
111. Carey. CT Scanning—Abdomen and Thorax: Fundamental Considerations

Tuesday, March 27, 8–9:30 a.m.
201. Alazraki, Resnick. Bone and Joint Scanning
202. L'Heureux. The Child with a Flank Mass
203. Chase, Kricheff. Computed Tomography: Noneoplastic Lesions of the Brain
204. Felson. Some interesing patterns of Pulmonary Neoplasms
205. Gehweiler. Cervical Spine Trauma—A Practical Guide to Diagnosis
206. Ackerman. Noninvasive Diagnosis of Carotid Artery Disease
207. Harris. The Radiographic Diagnosis of Acute injuries of the Lower Cervical Spine
208. Gilula. Radiology of the Wrist, Part II
209. Knight. CT of the Body and Thorax
210. Martel. The Alimentary Tract. Radiologic Vignettes
211. Potter. What Every Radiologist Should Know about the Ear
212. Reilly. Problems of the Immature Infant

Wednesday, March 28, 2–3:30 p.m.
301. Siegel, Koehler, Melson. Comparison of Radionuclide Ultrasound and CT Imaging of the Abdomen
302. Freeny. Algorithmic Approach to Radiologic Diagnosis of Suspected Pancreatic Disease
303. Chase, Kricheff. Computed Tomography: Nonneoplastic Lesions of the Brain
304. Felson. Some Interesting Patterns of Pulmonary Neoplasms
305. Gold. Computed Tomography of the Brain
306. Harwood-Nash. Hydrocephalus in Children: Old Principles, New Philosophies
307. McLelland, Thompson. Inflammatory Diseases of the Colon
308. McLeod. Computed Tomography of the Skeletal System and Soft Tissues
309. Thornbury. Radiologic Diagnosis: A Horse-Sense Approach
310. Kazam, Whalen. Anatomic Approach to Radiology of the Thorax, Part I
311. Wolfe. Mammography, Part I
312. Simon. The Pulmonary Circulation and the Radiologist

Thursday, March 29, 8–9:30 a.m.
401. Christie, Chiu. A Comparison of CT and Radionuclide Imaging in Central Nervous System Disease
402. Goldberg, Cole-Beuglet. An Introduction to Diagnostic Ultrasound
403. Goldman. Interventional Angiography
404. Gray, Muhm, Brown. Radiation Exposure and Risks—In Perspective
405. Heitzman. Computed Tomography of the Thorax
406. Jacobson, Siegelman. Skeletal Radiology—New Concepts and Provocative Challenges, Part I
407. McCallum. Current Concepts in the Anatomy, Pathology, and Radiology of the Male Lower Urinary Tract
408. Payne, McCullough. Basic Principles of Computed Tomography
409. Rosenfield. Renal Ultrasound: Current Concepts
410. Kazam, Whalen. Anatomic Approach to Radiology of the Abdomen, Part II
411. Wolfe. Mammography, Part II
412. Wilkinson. Skeletal Trauma in Infants and Children

Friday, March 30, 8–9:30 a.m.
501. Maynard, Cowan. Radionuclides and the Thyroid Gland
502. MacEwan. Balanced Radiology Services on a Tight Budget
503. Janower. Everything You Ever Wanted to Know About Running a Radiology Department but Were Afraid to Ask
504. Kattan. Tricks and Treats in Tomography
505. King. Cardiac Ultrasound
506. Jacobson, Siegelman. Skeletal Radiology—New Concepts and Provocative Challenges, Part II
507. Marshak. Radiologic-Pathologic Correlation of Interesting Lesions of the Gastrointestinal Tract
508. Singleton. Obstructive Lesions of the Alimentary Tract in the Newborn and Young Infant
509. Stephens. Gastrointestinal Applications of Computed Tomography
510. Swischuk. Neonatal Chest Problems
511. Theros. Exercises in the Analysis of the Unknown Lesion in Bone

Hugh M. Wilson, 1902–1978



The death of Hugh M. Wilson on April 21, 1978, after a lingering illness, culminated the career of one of the great teachers of radiology. Born in Jacksonville, Illinois on October 21, 1902, he received his M.D. from Washington University School of Medicine in St. Louis, Missouri in 1927 and remained to train in surgery under Dr. Evarts Graham. His switch from surgery to radiology was prompted by a severe dermatitis of his hands and the persuasive influence of Dr. Sherwood Moore, then chairman of the Radiology Department at the Mallinckrodt Institute of Radiology.

In 1934 he was called to the Yale School of Medicine to be the director of radiology which was then a division in the Department of Surgery. Under his energetic leadership the importance of radiology as a clinical and educational discipline was recognized and elevated to departmental status. He became the first chairman of radiology at Yale and was awarded an honorary degree. He was regarded by many of his Yale students as the best teacher on the entire faculty. He stimulated students to correlate the clinical and pathologic aspects of disease with what they could see on the x-ray.

In 1949 he returned to St. Louis to succeed his former chief, Sherwood Moore and become the second professor and chairman of the Department of Radiology at Washington University and the second director of the Mallinckrodt Institute of Radiology.

Hugh Wilson was an unassuming man who disliked public speaking. He was singularly dedicated to teaching, particularly medical students and house staff, and preached the importance of a radiologist being a clinical consultant, rather than a film reader. He developed the preview system of radiologic education for medical students and residents during his early years at Yale, a method which has been adopted at many university departments throughout the country. In 1960 he received the Distinguished Alumni Award from Washington University in recognition of his inspiration to students.

He refused to have his portrait painted for Washington University but agreed instead to the establishment of an endowment to encourage and recognize excellence in radiology among medical students. The Hugh M. Wilson Award for meritorious work in radiology is presented annually to a member of the graduating class of Washington University.

More than any other single person, he was the founder of the Association of University Radiologists, stimulated by a desire to encourage young radiologists in academic careers and give them a forum to present their original investigations. He was to receive its first gold medal but died just prior to the meeting. The award was made posthumously.

Hugh Wilson had a dynamic personality which endeared him to many. His scrupulous honesty and at times brutally frank evaluation of himself as well as others was sometimes difficult to accept even though his motives were always unimpeachable. He was always motivated by a deep concern for the welfare of the patient and a profound sense of integrity.

He is survived by two daughters, Sarah and Martha, a brother, William T. Wilson, and a sister, Mrs. Edward Bullard. For those who had the privilege of being his student, resident, or colleague, his influence will always remain a guiding principle. He was truly an extraordinary man.

William B. Seaman
New York, New York

© 1979 American Roentgen Ray Society

0361-803X/79/1322-0319 $0.00

Alexander S. Macmillan, Jr.



The subspecialty of head and neck radiology has attracted a small but distinguished group of radiologists. Alexander S. Macmillan, Jr. was a prominent member in this select group of physicians. A Bostonian by birth and education, he attended Harvard University for undergraduate and medical education. After graduating from the Harvard Medical School in 1946 he served surgical and medical internships at Boston City Hospital. His training was interrupted from 1947–1949 when he served as a captain in the medical service of the United States Air Force.

After his military service, Sandy followed in the footsteps of his illustrious father who had established an international reputation as a head and neck radiologist. His residency in radiology at Massachusetts General Hospital was followed by staff appointments at Peter Bent Brigham Hospital and the Massachusetts Eye and Ear Infirmary where he succeeded his father as chairman in 1966. In addition to being recognized as our local scholar in head and neck radiology, Sandy had the unique honor of being invited to present annual lectures in head and neck radiology at the refresher courses of the American Roentgen Ray Society from 1966 to 1977. My own personal contact with Sandy occurred in his role as staff radiologist for the Harvard teaching service at Boston City Hospital, a position he held from 1957–1973. He was a regular lecturer for residents and staff and it was always a delight to attend his presentations. He not only managed to enlighten and instruct us all with reference to a small and difficult anatomic area but was so willing to share with his colleagues and students his knowledge and experience. In later years when many hospitals acquired complex and sophisticated radiologic equipment to study the head and neck, Sandy felt frustrated in his own attempts to persuade his prestigous institution to follow the lead set by others. Nevertheless he maintained his skills in using the most basic equipment and competed successfully with his clinical colleagues—a tribute to his unique intelligence, knowledge, and perseverance. Sandy Macmillan held positions as consulting radiologist to the Peter Bent Brigham Hospital and assistant clinical professor of radiology at Harvard Medical School. He was a fellow in the American College of Radiology and a member of all the major national scientific radiologic societies.

Alexander S. Macmillan, Jr. died unexpectedly on March 15, 1978. He was an individual of unusual charm, warmth, and sensitivity. Only those who had the privilege of working with him could appreciate his sense of humor, coupled with a respect for his exceptional professional competence. He is survived by his mother, his wife, Jeanne, and their six children, Alec, Cameron, Alison, James, Anne, and Lucy.

Jerome H. Shapiro
Boston, Massachusetts

Letters

Radiography of Fast-Food Stomach

We recently became aware of an unusual appearance of the stomachs of some of our scoliosis clinic patients. These were frequently distended with frothy appearing material, and we initially wondered if this indicated some type of diminished motility related to the use of bracing devices.

It finally became apparent that our observation was the result of an early afternoon clinic in a hospital with its own fast-food restaurant. Patients would present themselves to the main-lobby radiographic suite and, if a 10 or 15 min wait were anticipated, run across the hall for a quick lunch. Figure 1A

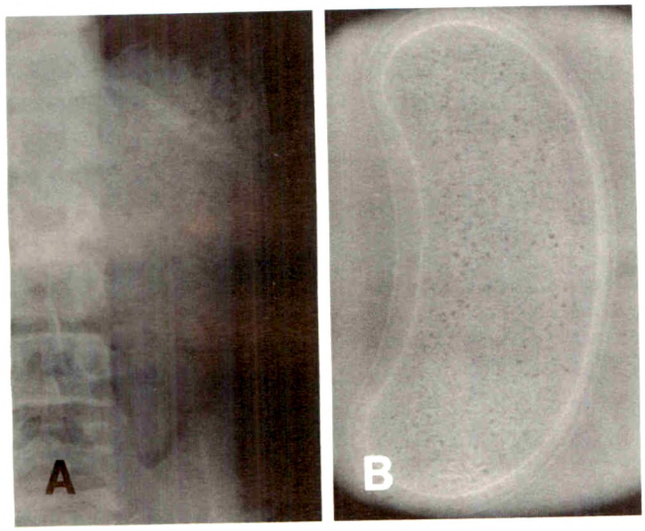


Fig. 1.—Fast-food lunch. **A,** In vivo. **B,** In vitro.

shows a radiograph made 15 min after ingestion of a large cheeseburger, a small order of fries, and a vanilla shake.

For confirmation of our hypothesis, a quarter-pound hamburger and a carbonated beverage were mixed in the blender. The resulting mush was poured into a plastic basin which was in turn placed in a plastic pan containing a small amount of water to mimic surrounding soft tissues. A radiograph of this experimental preparation (fig. 1B) provided a remarkably good match for the stomach contents seen in our clinic patients.

We offer this experience as a radiologic challenge which was fun to solve and as a curiosity which may amuse or interest the readers of our letter. The soft consistency of the meal and the rapidity with which fast foods are often ingested no doubt contribute to their appearance.

Thomas J. Spackman
Suzanne E. Betsch
Children's Hospital of Philadelphia
Philadelphia, Pennsylvania 19104

Furosemide-Augmented Intravenous Urography

In their article on furosemide-augmented intravenous urography Talner et al. [1] claim that this radiographic method is not a satisfactory test of renovascular hypertension. This test is, in fact, based on measurement of renal surface variations, which does not exactly explain the concomitant volume variation, in view of the particular geometry of the kidney. However, these nonsignificant variations in surface observed by Talner et al. probably correspond to important variations in volume, in view of the shape of the kidney, which might be called a prolate spheroid.

Under these conditions, the renal volume is calculated by the formula: $v = 4/3\ \pi\ ab^2$, where a and b are, respectively, half the large axis and half the small axis of the prolate spheroid [2]. This formula bears witness to the great importance of the small axis, or width of the kidney at the hile, since this parameter is used to the second power. This formula is used at my institution [3] in renal scintigraphy for calculating an extraction per unit of hippuran volume. My colleagues and I find that different extractions per surface unit can correspond to identical extractions per volume unit and vice versa; this proves the primordial role of the width of the kidney in variation of volume.

Therefore, I believe that despite difficulties both theoretical (assimilation of the normal and pathologic kidney to a prolate spheroid) and experimental (measurement of the axes when kidneys are often deformed by diseases), the calculation of renal volume provides a useful parameter whose variation can show normal or induced functional variations better than the surface parameter. The renal volume parameter can also serve as reference in renal physiopathology.

Michel Collard
Hôpital Ed. Herriot
69374 Lyon
France

REFERENCES

1. Talner LB, Stone RA, Coel MN, Levy SB, Emarine CW: Furosemide-augmented intravenous urography: results in essential hypertension. *AJR* 130:257–260, 1978
2. Kartz MA, Blantz RC, Rector FC Jr, Seldin DW: Measurement of intrarenal blood flow. I. Analysis of microsphere method. *Am J Physiol* 220:1903–1913, 1971
3. Collard M, Guey A, Claveyrolas P, Mendoza M, Traeger J, Lyonnett D, Pinet A: Effet d'une artériographie sur la fonction tubulaire rénale mesurée à l'aide de la scintigraphie à l'hippuran. *J Radiol Electrol* 59:23–28, 1978

Reply

Dr. Collard correctly points out that estimation of renal volume is better than measurement of surface area when one is interested in renal size changes from a stimulus such as furosemide injection. However, I am afraid that the application of renal volume measurement to intravenous urography is so fraught with dangers, both theoretical and practical, that it

© 1979 American Roentgen Ray Society

0361-803X/79/1322-0321 $0.00

would not be productive. Not the least of the problems is Dr. Collard's statement about the short axis of the kidney, that is the width of the kidney measured from the hilar surface to the lateral margin. As we indicated in our article, this measurement is done by drawing a medial tangent line, which itself introduces inaccuracy. Nevertheless, it is the best we can do on many of these urograms. When that error is compounded by squaring, I believe the calculated volume would be untrustworthy at best.

Our main point was that patients with essential hypertension showed such a wide variation in renal area change that it was not likely to be useful in culling out those patients with renal artery stenosis. I see nothing in Dr. Collard's letter to indicate that this aspect of the problem would be obviated by attempting to measure volume changes.

Lee B. Talner
University Hospital
University of California, San Diego
San Diego, California 92103

Systemic Air Embolism in Necrotizing Enterocolitis

I have recently seen a neonate with necrotizing enterocolitis and pneumoperitoneum with portal venous gas who, in a premortem film, showed gas in the femoral vessels. Previously, I thought this might justify a case report; however, since an article in September 1978 *AJR*, a letter seemed more appropriate.

In a recent article, Kogutt [1] states that systemic air embolus is a documented complication of hyaline membrane disease and its treatment. While the mechanism for intravascular air is not well understood, it is attributed to a pressure phenomenon with dissection of air into pulmonary veins and from there into the systemic circulation. As stated, systemic air embolism can also be seen in other clinical situations as "following surgical procedures, trauma, in submarine personnel and in asthmatics." To this list, I would like to add necrotizing enterocolitis.

A 20-day-old premature male infant was hospitalized since birth for prematurity and sepsis. The child had done well clinically and was expected to be discharged soon. The infant had never shown clinical or radiographic evidence of hyaline membrane disease and had never been placed on a respirator. At 20 days of life, abdominal distension and bloody diarrhea were noted. A plain film of the abdomen showed marked distension of multiple bowel loops and portal venous gas. A film 4 hr later showed a large pneumoperitoneum and extensive pneumatosis intestinalis (fig. 1). Air was present in femoral

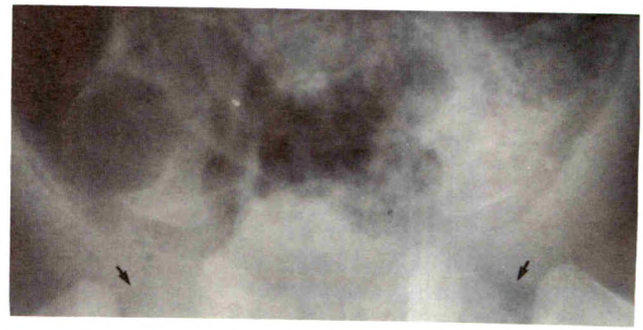


Fig. 1

vessels (probably veins) bilaterally (*arrows*) and also in portal veins. The chest was normal and gas was not observed in other vessels nor the heart. The infant died and permission for autopsy was refused.

The etiology of systemic air embolism in the chest is somewhat obscure, but generally felt to be related to alveolar rupture and dissection of air into the perivascular spaces. Air embolism is probably secondary to air-block phenomenon with interstitial air, pneumothorax, pneumomediastinum, or pneumopericardium usually present. In short, air under pressure and outside of its normal spaces must be present for systemic air embolism. Such a condition exists in pneumoperitoneum secondary to necrotizing enterocolitis. There is a large collection of free air under tension in the peritoneal cavity which should be capable of dissecting along the vascular sheaths and into the systemic circulation.

While I suspect that the air in this case is probably venous, I cannot be certain. The amount of pressure necessary to overcome venous pressure would be somewhat less than arterial and air should preferentially fill the venous system. The caliber of the air column of the vessels in this case seems larger than the collapsed arteries one would expect to find in a neonate in extremis.

Theodore Miller
Martin Luther King, Jr. General Hospital
Los Angeles, California 90059

REFERENCE

1. Kogutt MS: Systemic air embolism secondary to respiratory therapy in the neonate: six cases including one survivor. *AJR* 131:425–429, 1978

Abstracts of Current Literature

Cardiovascular

Chromosome Damage in Infants and Children after Cardiac Catheterization and Angiocardiography. Adams FH et al. (Division of Cardiology, Department of Pediatrics, University of California Los Angeles School of Medicine, Los Angeles, California). *Pediatrics* 62:312–316, Sept 1978

Current diagnostic cardiac studies in infants and children result in longer x-ray exposure times and in more angiocardiograms per patient. Blood samples removed before and immediately after such studies in 20 infants and children have shown chromosome damage in all. The damage was equal to in vitro absorbed dose in the range of 20 to 50 rads. Since the effect was considerably greater than that calculated from the x-ray exposure dose to the patient, it is concluded that the damage is mainly due to the contrast agent used in angiocardiography. Long-term follow-up studies on such patients are indicated.

Author Abstract

Transcatheter thromboembolectomy of acute renal artery occlusion. Millan VG, Sher MH, Deterling RA, Packard A, Morton JR, Harrington JT (Tufts University Medical School, Boston, Massachusetts). *Arch Surg* 113:1086–1092, Sept 1978

The authors have developed an angiographic technique for relief of acute thrombotic or embolic occlusion of the renal artery as an alternative to surgical intervention in poor risk patients, and report their experience with four cases. After the diagnosis of acute renal artery occlusion is established angiographically, a catheter is advanced in the renal artery to the point of obstruction, and strong suction is applied in an attempt to aspirate the thrombus. If this fails, the catheter is positioned at the origin of the renal artery, and a no. 3 Fogarty catheter is advanced in coaxial fashion through the angiographic catheter beyond the occlusion. With fluoroscopic control the balloon is cautiously inflated with contrast material to indicate its size and location. The clot is removed by withdrawing the inflated balloon into the aorta. After each passage of the balloon, a small amount of contrast medium is injected into the renal artery to determine the amount and position of remaining clot. When maximal patency is achieved, a final selective renal arteriogram is performed.

In each of their cases, renal function was restored promptly. Embolization of extruded thrombus down the aorta produced no clinical problems in any of the four patients.

Reiley Kidd

Takayasu Arteritis and Renovascular Hypertension in Childhood. Wiggelinkhuizen J, Cremin BJ (Department of Pediatrics, Red Cross War Memorial Children's Hospital, University of Cape Town, South Africa). *Pediatrics* 62:209 Aug 1978

Takayasu arteritis with renal artery involvement was the cause of severe persistent hypertension in eight children under 12 years of age. Features of severe hypertension dominated the clinical picture. Unequal or absent pulses were found in three patients. An irregular contour of the descending thoracic aorta on the chest roentgenogram was an early clue to the diagnosis. On aortography both renal arteries were affected in five patients, although a discrepancy in kidney size on excretory urography had suggested a unilateral lesion. Total aortography is mandatory to outline the full extent of the vascular abnormalities. All the patients had strongly positive tuberculin skin tests, and, although myobacteria were not isolated, all patients received antituberculous as well as antihypertensive therapy. Nephrectomy of the worse kidney is contraindicated if the renal arteries are asymmetrically involved, for fear of later extension of the arteritis. Takayasu arteritis is an important cause of severe persistent hypertension in nonwhite children.

Author Abstract

Extramural or intraluminal inferior vena cava occlusion in pulmonary embolism. Popovsky J, Edelstein J, Walzer L, Vlastou C, Ryan C (Mount Sinai Hospital of Cleveland, University Circle, Cleveland, Ohio 44106). *Ann Thorac Surg* 26:50–53, July 1978

Anticoagulant therapy is the treatment of choice for pulmonary embolism but is successful in only 80% of patients. In the remaining 20%, such therapy is ineffective or unadvisable, leaving operative interruption of the inferior vena cava as the most effective procedure. This procedure is preferred in patients with (1) recurrent pulmonary emboli despite satisfactory anticoagulation; (2) a contraindication to anticoagulation (i.e., bleeding); 3) massive embolism with shock; and (4) a high risk of embolism following surgery. Interruption of the inferior vena cava can be accomplished in two ways. The first, extramural occlusion by suture or staple plication or clipping, is associated with a 40%–53% incidence of complications, an incidence of recurrent embolism of 0%–18%, and an operative mortality of 5%–27%. The second method of inferior vena cava interruption, the percutaneous insertion of a Mobin-Uddin umbrella filter, is considered by the authors as the procedure of choice because of its simplicity and comparable or superior performance. The complication rate reported for umbrella filters is only 13%, while recurrent pulmonary emboli occur in 2%, and operative mortality in only 1%.

W. Richard Webb

Echocardiography of left ventricular masses. Ports TA, Cogan J, Schiller NB, Rapaport E (Division of Cardiology, Department of Medicine, Room 1186-Moffitt Hospital, University of California, San Francisco, California 94143). *Circulation* 58:528–536, Sept 1978

The M-mode and two-dimensional real-time echocardiographic findings in 10 patients with left ventricular masses are discussed. Two patients had left ventricular tumors which were recognized in both cases by both M-mode and two-dimensional echocardiography. One tumor was intracavitary producing dense echoes within the left ventricular chamber in both modalities, while in the other patient a large hemangioma could be seen infiltrating the posterior left ventricular wall on both M-mode and real-time study.

Eight patients had left ventricular thrombi. The M-mode echocardiogram failed to detect the left ventricular thrombus in all cases, although in two patients fine nonspecific "dust-like" echoes suggestive of a thrombus were noted on retrospective examination. However, two-dimensional echocardiographic examination using the apex views demonstrated large and inhomogeneous left ventricular clots in all four patients. There were no false positive echocardiograms. The left ventricular clots were not seen by two-dimensional echocardiography using the long and short axis views.

Four patients had mural thrombi. M-mode echocardiography failed to reveal thrombi in each case while two-dimensional echocardiography in both the apex and long axis views identified the left ventricular aneurysm when present but did not detect the associated mural thrombus.

In summary, while M-mode and two-dimensional real-time echocardiography both prove useful in the evaluation of left ventricular tumors, M-mode echocardiography was not able to detect left ventricular thrombus in all instances. Two-dimensional echocardiography was able to identify large and inhomogeneous left ventricular thrombi but did not clearly identify four cases of smaller mural thrombi.

Richard B. Jaffe

Intravenous arteriography with xerography: a noninvasive method for the demonstration of peripheral vessels. Kramann

© 1979 American Roentgen Ray Society

0361–803X/79/1322–0323 $0.00

B, Christen N (Institut fuer Roentgendiagnostik der Technischen Universitaet Muenchen, 8 Muenchen 80, Germany). *Fortschr Geb Roentgenstr Nuklearmed* 128:319–323, 1978

Peripheral arteriography of the upper or lower extremity was performed in 59 patients using a xerographic recording technique of the extremity to be examined 4–10 sec following rapid manual intravenous injection of contrast medium into the cubital vein. Acceptable arteriograms of the examined extremity could be obtained in all but two patients. In the authors' opinion, this technique constitutes a noninvasive arteriographic examination suitable for demonstrating vascular lesions in the extremities.

Peter F. Winter

Two-dimensional echocardiographic assessment of Ebstein's anomaly. Ports TA, Silverman NH, Schiller NB (Cardiology, 1186-Moffitt Hospital, University of California, San Francisco, California 94143). *Circulation* 58:336–343, Aug 1978 (by permission American Heart Association)

Nine patients with Ebstein's anomaly of the tricuspid valve were studied by two-dimensional echocardiography, using the standard long and short axis views as well as the apex four chamber view. With this latter view, the displacement of the tricuspid valve into the right ventricle was clearly seen in all nine cases of Ebstein's anomaly and was not noted in a control population. The severity of the tricuspid displacement was assessed by comparing the position of the mitral and tricuspid valves relative to the cardiac apex. The apex four chamber view allowed visualization of the atrioventricular ring simultaneously with the displaced tricuspid valve, and therefore the size of the "atrialized" right ventricle, true right ventricle, and right atrium could be determined. These dimensions compared favorably with angiography.

Author Abstract

Use of contrast echocardiography for evaluation of right ventricular hemodynamics in the presence of ventricular septal defects. Serwer GA, Armstrong BE, Anderson AW et al. (P.O. Box 3090, Duke University Medical Center, Durham, North Carolina 27710). *Circulation* 58:327–336, Aug 1978 (by permission American Heart Association)

Intracardiac blood flow is altered in the presence of a ventricular septal defect (VSD), with different sizes of defects producing different flow patterns that can be visualized by peripheral injection contrast echocardiography. The utility of these patterns in allowing estimation of right ventricular pressure and resistance to ejection of blood from the right ventricle (RV) was investigated. Forty-four patients underwent 46 contrast echocardiographic procedures, all within 24 hr before cardiac catheterization. All patients were placed in one of four groups based on catheterization findings. Group I, which consisted of patients with no VSD, or a small VSD with a pulmonary-to-systemic flow ratio (Qp/Qs $<1.5:1$ and right ventricular pressure $<$one third systemic) had echo-dense material appear in the RV only. Group II consisted of those with moderate-sized VSD with Qp/Qs $\geq 2.5:1$ and right ventricular pressure 60%–80% systemic; in these patients echo-dense material appeared in the RV and in the left ventricle (LV) anterior to the mitral valve. The contrast appeared in the LV in early diastole and cleared from the LV in systole, with none appearing in the aorta or left atrium. Time from the preceding QRS to appearance of echo-dense material in the LV divided by the R-R interval (appearance time to R-R interval ratio) was 0.62–0.69. Group III consisted of those with large VSDs, Qp/Qs $>3:1$ and systemic right ventricular pressure with low pulmonary vascular resistance and no pulmonary stenosis. These patients had appearance of echo-dense material in LV during early diastole anterior to the mitral valve as in group II, but the material remained in the LV to be ejected into the aorta. Appearance time to R-R interval ratio was the same as in group II. Group IV consisted of patients with tetralogy of Fallot and one patient with a large VSD and increased pulmonary vascular resistance. Echo-dense material again appeared in the LV early in diastole and was ejected into the aorta during systole. The appearance time/R-R ratio was significantly less than in groups II or III, allowing a clear separation between those patients in group III from group IV. Contrast echocardiography allows estimation of the right ventricular pressure and evaluation of increased resistance to pulmonary flow due to either pulmonary stenosis (PS) or increased pulmonary vascular resistance in the presence of VSDs. This technique also provides a minimally invasive method which may be useful for serial evaluation of such patients, and will permit early detection of developing PS, or possibly increasing pulmonary vascular resistance. Decreasing right ventricular pressure due to spontaneous closure of the VSD may also be detected by this technique.

Author Abstract

Diagnosis of ventricular septal defect by pulsed Doppler echocardiography, sensitivity, specificity, and limitations. Stevenson JG, Kawabori I, Dooley T, Guntheroth WG (Division of Pediatric Cardiology, Department of Pediatrics, RD-20, University of Washington School of Medicine, Seattle, Washington 98195). *Circulation* 58:322–326, Aug 1978 (by permission American Heart Association)

The M-mode echocardiographic findings of ventricular septal defect (VSD) are nonspecific. A specific pulsed Doppler echocardiographic (PDE) diagnosis of VSD can be made by following the turbulent VSD jet through the septum. To assess the sensitivity, specificity, and limitations of PDE diagnosis of VSD, 105 children undergoing cardiac catheterization were examined by PDE. These children had a variety of cardiac defects, and a PDE diagnosis of VSD was made in 46/51 (90%) who had VSD proven at catheterization. There was one false positive PDE diagnosis of VSD, for a specificity of 98%. Factors influencing the ability to diagnose VSD by PDE include the location of the defect, level of pulmonary vascular resistance, and direction of blood flow through the VSD. The presence of additional defects did not interfere with PDE diagnosis of VSD. The PDE detection of additional defects may identify situations where M-mode echocardiographic estimation of dimensions may not be indicative of the size of the VSD shunt.

Author Abstract

Real-time cross sectional echocardiographic imaging and measurement of the patent ductus arteriosus in infants and children. Sahn DJ, Allen HD (Department of Pediatrics, University of Arizona Health Sciences Center, Tucson, Arizona 85724). *Circulation* 58:343–354, Aug 1978 (by permission American Heart Association)

While echocardiography has been used to noninvasively document indirect effects on the heart of left-to-right shunting through a patent ductus arteriosus, no noninvasive technique has been developed to image the duct itself. In this study, 35 sequential studies were performed on 28 patients with a mechanical sector scanner to image the distal pulmonary artery and its bifurcation by scanning along the axis of the right ventricular outflow tract. Cross-sectional imaging, just superior to the take-off of the right pulmonary artery, provided visualization of the patent ductus as a distal continuation of the pulmonary artery connecting to the descending aorta. Ductal visualization by cross-sectional echo was validated by saline echo contrast observations of right-to-left and left-to-right shunting through the duct in 14 patients, by surgical observations in 11, angiographic observations in 13, and autopsy observation in three. Angiographic size of the ductus arteriosus, whether constricted or widely patent, tortuous or straight, was predicted correctly and echo/angiographic correlations for smallest inner ductal dimension were excellent ($r = 0.97$). This study provides a method for and validates the direct imaging of the ductus arteriosus and suggests that cross-sectional echocardiography can accurately predict ductal contour and quantitative ductal cross-sectional size noninvasively.

Author Abstract

Gastrointestinal

Anatomy and pathology of the kidney by gray scale ultrasound. Rosenfield AT, Taylor KJW, Crade M, DeGraaf CS (Yale University School of Medicine, New Haven, Connecticut 06510). *Radiology* 128:737–744, Sept 1978

Gray scale ultrasound can define intrarenal structures which could not previously be visualized. The normal calyces and infundibula within the renal sinus can be evaluated for abnormalities. Parenchymal anatomy (cortex, medulla, and arcuate vessels) of the right kidney is best demonstrated with the patient supine, using the liver as a window; anatomy of the left kidney is best appreciated using coronal scans in the right lateral decubitus position. Criteria and differential diagnosis of "Type I" parenchymal changes, in which the echo intensity within the cortex is increased, and "Type II" changes, in which there is a focal or diffuse disruption of normal renal parenchymal anatomy, are presented.

Author Abstract

Crohn's disease in Barrett's esophagus. Lee CS, Mangla J, Lee S (University of Rochester School of Medicine, Rochester, New York). *Am J Gastroenterol* 69:646–654, June 1978

Crohn's disease involving the esophagus is extremely rare and only 15 cases have been reported in the English literature. The authors describe a patient with histologically proven Crohn's disease of the distal ileum who developed a benign esophageal stricture. Biopsy of this lesion showed only granulation tissue. He was treated with antacids and Maloney bougie dilatation and because of a gradual deterioration of his condition, he was admitted for further evaluation 16 months after the onset. A long tubular stricture was demonstrated by barium studies and endoscopy showed almost complete obliteration of esophageal lumen 30 cm from the incisor teeth. A biopsy revealed granulation tissue with a cluster of atypical mucosal cells, suggestive of squamous cell carcinoma. Because of this, the esopahgus was resected and followed by gastroesophagostomy, pyloroplasty, and feeding jejunostomy. A week after operation, he developed an esophageal-mediastinal fistula, which took 3 months to close. The resected esophagus showed transmural inflammation, muscular hypertrophy, neuromatous lesions with hypertrophied nerves, and areas of granuloma formation. Barrett's mucosa was also found in the resected specimen. The authors suggest that Crohn's disease has a predilection for columnar epithelium and indicate that this is the only case in which the two conditions have occurred simultaneously.

James M. Halls

Adrenergic influences on the gallbladder emptying. Lechin F, Van Der Dijs B, Bentolila A, Pena F (Instituto de Vias Digestivas de Caracas, Facultad de Medicina, Universidad Central de Venezuela, Caracas, Venezuela). *Am J Gastroenterol* 69:662–668, June 1978

Hormonal control of the extrahepatic biliary system appears to be mediated by cholecystokinin released by the proximal small bowel. It contracts the gallbladder and relaxes the sphincter of Oddi. There are also contracting mediating cholinoreceptors and alpha receptors in the gallbladder and sphincter, as well as relaxation mediating beta receptors. There is no consensus concerning the relationship between hormonal and neural controls. It seems likely that the latter is of minor importance. Cholecystograms were performed on 70 volunteer subjects and gallbladder contraction was provoked by a test meal in 35 and 0.5 U/kg of CCK injected intravenously in 35 subjects. Ten days later, a cholecystogram was performed on these patients and 1 mg of dihydroergotamine was injected intramuscularly 45 min before the cholecystokinetic stimulus. DHE counteracted gallbladder contraction by both endogenous and exogenous CCK, the effect being pronounced in those patients given a test meal. The authors' results suggest that the decreased contraction was due to the relaxation of the gallbladder, in addition to duodenal spasticity induced by DHE.

James M. Halls

Intestinal obstruction due to a wandering spleen. Keidar S, Freud M, Rosenschein S, Meir J, Rothfeld H (Department of Medicine, Carmel Hospital, Carmel, California). *Am J Gastroenterol* 69:701–704, June 1978

Intestinal obstruction due to a wandering spleen is quite rare and the pathogenesis of the condition is controversial. In some series, the occurrence is rare in childhood, suggesting an acquired etiology. Other authors have described cases with persistent mesentery of the descending colon and hypermobility of the cecum and ascending colon, supporting a congenital etiology. There is also evidence in the literature to support the contention that the condition is due to an incomplete fusion of the mesogastrium posteriorly. This might also lead to an intraperitoneal pancreas. The authors describe a 25-year-old male who presented with recurrent sigmoid volvulus and who had a second obstruction in the ascending colon caused by the pedicle of a wandering spleen.

James M. Halls

Microangiographic study of the normal and pathological gallbladder (in Italian). Ruffato C, Liessi G, Valente R, Roma R (Ospedale Civile, via Ospedale, I-31033 Castelfranco Venetto, Italy). *Radiol Med* 63:1059–1072, 1977

The authors have examined 30 surgically removed gallbladders anatomically and with microangiography in order to improve in vivo angiographic evaluation. In five cases the gallbladder was normal, in 23 the pathologic diagnosis was of cholecystitis and/or cholelithiasis and in two, porcelain gallbladder was diagnosed.

The procedure was as follows. As soon as the gallbladder was removed, a thin Rabinov catheter was introduced into the cystic artery, and in a few cases into the veins, and a very dilute solution of Microtrast (10%–15%) was injected slowly under image amplifier control. Photographs of the specimen were taken and the gallbladder was then immersed in a solution of formalin. After 72 hr the specimen was opened and radiographed on Kodak Type M film. Later transverse sections of different thicknesses were radiographed on Kodak HRP films, for a more detailed microangiographic evaluation.

The microangiographic patterns of a normal gallbladder are described, the cystic artery, its branches to the adventitial and subserosal arteriolar plexus and the venous mucosal plexus.

The pathologic patterns are divided into chronic atrophic cholecystitis, hypertrophic cholecystitis, and porcelain gallbladder. In the first type, arterioles are quite tortuous and irregular with incomplete or absent filling of the venous bed. The abnormal findings are noted in particular in the muscular and mucosal plexuses. The second type is less frequent. The gallbladder is small with thick walls, the muscular and mucosal plexuses show abundance of circulation with trabecular network and distorted various branches grouped together. In the subserosal arteriolar and venous plexuses, the vessels have a spiral or corkscrew appearance, while in the mucosal and muscular plexus the pattern was similar to atrophic cholecystitis.

Antonio F. Govoni

Double contrast hypotonic duodenography. Blain F, Le Guyader J, Dutel JL, Boscq M, Bellet M (Service de Radiologie, C.H.U. Hopital Morvan, 5 Avenue Foch, F 29200 Brest, France). *J Radiol Electro Med Nuc* 59:183–190, 1978

Double contrast hypotonic duodenography is a simple procedure, easily adapted to routine studies of the upper digestive tract. While intended primarily for examination of the duodenum, double contrast studies of the stomach and esophagus can be readily performed during the same procedure. Following routine radioscopy of the chest and abdomen, barium is administered by mouth and routine films are obtained in the upright and horizontal position. The patient is then placed in the right lateral decubitus position to insure adequate filling of the

duodenum with barium. This position is maintained while an antispasmodic is injected followed by oral administration of an effervescent salt. Films of the duodenum are obtained without changing the position of the patient. The patient is then turned to the left decubitus position allowing air to rise into the duodenum. Under radioscopic control several films are obtained in the right anterioobliique position, followed by double contrast studies of the stomach and esophagus.

The outline of the duodenum, contour of the mucosal folds, region of the papilla, and pancreatic and common bile ducts are clearly visualized. Based on the authors' experience, the following pathologic conditions are presented, with excellent illustrative radiographs: duodenal ulcer; duodenitis with and without ulcer crater; chronic pancreatitis with compression and narrowing of the descending duodenum; pancreatic cysts with marked widening of the duodenal loop; carcinoma of the pancreas with irregular infiltration into the descending and/or horizontal duodenum; compression and/or infiltration into the duodenal papilla with accompanying jaundice; impacted biliary calculus with marked dilatation of the ampulla; dilatation of the common bile duct with compression of the duodenum.

The duodenum is a fertile site for both intrinsic and extrinsic lesions which may not always be readily demonstrated on routine studies. Double contrast hypotonic duodenography brings about clear and accurate demonstration of lesions ordinarily missed on routine studies and is particularly helpful in the detection of very early lesions.

William H. Shehadi

Extension of infiltrating carcinoma of the stomach into the transverse colon. L'Herminé C, Froment T, Lescut J, Roger J, Lemaitre G (Service de Radiologie Est, C.H.U. F 59000 Lille, France). *J Radiol Electrol Med Nucl* 59:261–266, 1978

The most common route of extension of infiltrating carcinoma of the stomach to the colon is through the gastrocolic ligament. The segment most frequently involved is the superior aspect of the transverse colon. The appearance and location of the lesion in the transverse colon is considered to be typical of extrinsic involvement from a primary carcinoma of the stomach. In the presence of a negative gastric endoscopic biopsy of a gastric lesion a typical appearance and location of an infiltrating lesion of the colon may suggest a gastric origin.

The radiologic appearance is that of effaced haustration with progressive rigidity and infiltration into the superior aspect of the colon. The mucosa is fixed at the site of contact presenting a serrated or saw tooth pattern. By contrast the apposing or inferior segment of the colon is soft and pliable. At times it may present a compensatory pseudodiverticular configuration. While initially the infiltrating lesion may be localized, it may extend laterally in either direction along the superior border of the colon.

By comparison, extension of malignant disease from a primary ovarian or pancreatic carcinoma through the mesocolon will infiltrate into the *inferior* aspect of the transverse colon.

William H. Shehadi

Musculoskeletal

Giant-cell containing "fibrous" lesion of the sacrum. Dehner LP, Risdall RJ, L'Heureux P (Departments of Laboratory Medicine and Pathology, University of Minnesota Medical School, Minneapolis, Minnesota). *Am J Surg Pathol* 2:55–70, March 1978

Three similar and unique, predominantly osteolytic lesions are reported in young patients between the ages of 4 and 19 years. Progressive low back or leg pain and neurologic deficits were the principal clinical features. The initial radiographic impression was that of a malignant tumor, either primary or metastatic. Osteolytic destruction, varying only in the extent of involvement, was a constant finding and no residual bone remained in the osteolytic area. In two cases extrinsic displacement of the lower dural sac without evidence of dural invasion was seen on myelograms. A characteristic feature, however, was a sclerotic rim which sharply demarcated the lesion from the surrounding bone. At surgery replacement of bone by a firm, grey-white gritty mass was found; it did not invade the epidura and sacral nerves.

The consistent histologic finding was a spindle-cell stroma containing a variable number of giant cells, usually occurring in aggregates; but histologic and ultramicroscopic features which would be diagnostic for giant cell tumor were not present. The possible relationship of this tumor to nodular fasciitis and desmoplastic fibroma, i.e. as intraosseous equivalents, is hypothesized on the basis of ultrastructural studies. Despite incomplete resection in each case, healing has occurred during the follow-up interval (up to 8 years) with one interim exception, where recurrence of symptoms necessitated repeat excision. Radiographs taken 1 year or more after surgery showed progressive sclerosis in all three cases.

Louise M. Wiegenstein
Department of Pathology
University of Washington

Xeroradiography of soft tissue (in Italian). Nessi R (Istituto Nazionale Tumori, via G. Venezian 1, I-20133 Milano, Italy). *Radiol Med* 63:1083–1092, 1977

This is a report on 39 patients examined by xeroradiography who had primary malignant bone tumors (17 cases), metastases to the skeletal system (3 cases), or benign neoplastic or inflammatory lesions (19 cases). Twenty-five cases were also examined by conventional radiographic studies. In 24 of these, the radiographic diagnosis was confirmed at surgery and/or by histologic examination. A critical review of the data obtained showed that the value of xeroradiography is in better demonstration of the cutaneous, subcutaneous, and musculo-tendinous structures than shown by standard radiographic techniques. Using this to delineate soft tissue extension of the lesion is helpful in treatment planning.

Antonio F. Govoni

Nervous System

Computerized tomography in neurological evaluations. Naidich TP, Solomon S, Leeds NE (Mallinckrodt Institute of Radiology, 510 South Kingshighway, St. Louis, Missouri 63110). *JAMA* 240:565–568, Aug 11, 1978

The authors report their diagnostic approach to CT brain scanning after 10,000 CT brain scans during the last 2 years. They recommend that patients with severe head trauma be examined immediately without contrast to localize and differentiate a high density acute hematoma from low density edema or contusion. They feel that virtually all patients requiring emergency surgery may go directly from the CT suite to the operating room. Angiography was performed when arterial dissection, pseudoaneurysm or thrombosis of a major vessel was suspected. All patients with suspected subacute or chronic subdural hematomas were studied first by CT with and without contrast enhancement. If the CT scan was diagnostic, therapy was initiated without further examination. If the CT scan was normal or equivocal, a radionuclide scan was performed. If the radionuclide scan was abnormal but the CT scan was normal, arteriography was then performed. If both CT and radionuclide scans were normal, a subdural hematoma was excluded.

CT was of help in evaluating tumors in the sella region. If CT demonstrated a pituitary adenoma arteriography was performed to exclude aneurysm or encasement of major vessels and to define the site of origin of the posterior cerebral artery. Suprasellar and parasellar extension was well defined by CT. Pituitary microadenoma were usually not seen on CT and were best defined by tomography and hormonal studies. The empty sella

syndrome was easily defined by CT as an enlarged sella turcica filled with cerebrospinal fluid density material. Pneumography was still recommended to confirm the diagnosis and exclude the possibility of coexistent microadenoma.

CT was very useful in evaluating masses in the cerebellopontine angle. Arteriography was still required to rule out an aneurysm or arteriovenous malformation prior to surgery. When the CT scan was negative, tomography and posterior fossa myelography were employed to rule out an intracanalicular acoustic neuroma or other small lesion.

CT was useful in diagnosing gliomas and meningiomas. Arteriography was usually employed to define the exact location and vascular pedicle. In dealing with possible metastatic brain tumors a combination of a normal CT scan, normal radionuclide scan, and a nonfocal EEG was considered sufficient to exclude a metastatic lesion. The authors recommend that a CT brain scan be performed routinely prior to resection of any primary tumor known to metastasize frequently to the central nervous system even in patients without neurologic findings. Either radiation necrosis or recurrent tumor can be identified as a mass lesion which contrast enhances.

In dealing with infections of the central nervous system, CT was best used to evaluate patients suspected of having a brain abscess. In evaluating cerebrovascular disease arteriography is still the study of choice but should be employed only in those patients whose therapy might be altered by demonstrating a remediable vascular lesion. In patients with suspected subarachnoid hemorrhage the authors recommend CT prior to a lumbar puncture to identify unsuspected hematoma or mass. The authors feel that CT has almost completely replaced emergency angiography in the initial evaluation of patient with subarachnoid hemorrhage. Demonstration of ischemia by CT suggests the presence of severe vasospasm which may contraindicate arteriography. In dealing with arteriovenous malformations, radionuclide brain scans will occasionally demonstrate a malformation not seen on CT. Arteriography is still necessary to plan therapy.

The authors do not recommend CT if the patient has typical tension headaches or uncomplicated migraine. In evaluating a demented patient, the CT findings of disproportionate enlargement of the temporal horns and fourth ventricle, periventricular edema, and the absence of prominent parasagittal sulci suggest the diagnosis of normal pressure hydrocephalus. The authors feel that computed tomography is superior to all other methods in the detection and localization of intracranial lesions, but radionuclide scans continue to have a place in the neurologic work up particularly in the evaluation of arteriovenous malformations, subacute subdural hematomas, and herpes encephalitis. They also feel that in many situations, CT and radionuclide brain scanning are complementary modalities.

Paul M. Chikos

Computed tomography of the optic nerve: Part I normal results. Salvolini U, Cabanis E, Rodalec A, Menichelli F, Pasquini U, IBA-Zezen MT (Ospedale Civile Umberto I Ancona, Italy). *J Computer Assisted Tomography* 2:141–149, April 1978

A total of 97 normal CT studies of the orbit done on an EMI Mark I brain scanner (160 × 160 matrix and 8 mm collimation) are examined. High quality color photos of gross sections through the orbit and appropriate CT scans are presented, as are attenuation measurements of the optic nerve, retroglobar intraorbital fat, rectus musculature, and structures within the optic globe. No significant modification of density of any of these structures has been noted after intravenous contrast enhancement.

Michael J. Meagher

Computed tomography of the optic nerve: Part II size and shape modifications in papilledema. Cabanis E, Salvolini U, Rodalec A, Menichelli F, Pasquini U, Bonnin P (X-ray Department, National Center of Ophthalmology, 28 Rue De Charenton 75571 Paris Sedex 12, France). *J Computer Assisted Tomography* 2:150–156, April 1978

Some 8,000 CT examinations of the brain and orbits were examined retrospectively; an increase in the diameter of the optic nerve was noted in 197 cases. In 103 of these cases, the increased diameter of the optic nerve was associated with papilledema. Multiple cases of papilledema such as intracranial tumors, hydrocephalus, and pseudotumor cerebri were found. Enlargement of the optic nerve may also be demonstrated by CT scanning of patients with papilledema secondary to optic neuritis.

Michael J. Meagher

Dynamic aspect of brain edema in cases of acute carbon monoxide poisoning (in Japanese). Kondo T, Ikeda T, Mogami H, Miura T, Mitomo M, Shimazaki S, Sumimoto T (Osaka University, Osaka, Japan). *Brain and Nerve* 30:525–531, May 1978

Eleven cases of acute carbon monoxide poisoning in various stages were evaluated by 17 computed tomography examinations. In the early stage of acute carbon monoxide poisoning, CT revealed diffuse subcortical low density without ventricular dilatation. The basis of this finding was presumed to be edema related to hypoxic increase in permeability of blood vessels. This diffuse edema of white matter subsided in about 2 weeks after which progressive cerebral atrophy and ventricular dilatation supervened. Generally the intensity of brain edema observed on CT correlated with a poor prognosis although two vegetative patients had normal CT scans. Pathogenesis of brain edema and the effect of hyperbaric therapy in the cases of acute carbon monoxide poisoning were also discussed.

Hozumi Arii

Juvenile primary pontine hemorrhage (in Japanese). Kobayashi K, Toyama M, Kurita I, Nakai O, Sato S (Brain Research Institute, Niigata University, Niigata, Yamagata University, Yamagata and Yamagata Prefectural Central Hospital, Yamagata, Japan). *Brain and Nerve* 30:749–756, July 1978

Juvenile primary pontine hemorrhage is a rare disease and the diagnosis of this entity was not easy before the introduction of computed tomography. Four cases of primary pontine hemorrhage of children and young adults were reported and diagnostic efficacy of computed tomography was stressed. Cases 1 and 2 had been diagnosed as pontine glioma and irradiated before the introduction of computed tomography. Since these patients had recurrent attacks, they underwent computed tomography and the diagnosis of pontine hemorrhage was made. Cases 3 and 4 were confirmed by operation and autopsy, but both were before the introduction of CT. Since pathogenesis of this entity has been said to be small angiomatous malformation, the value of angiography is also stressed. Only in case 2 was an abnormally enlarged vein found.

Hozumi Arii

Extra-axial posterior fossa lesions simulating intra-axial lesions on computed tomography. Miller EM, Newton TH (University of California School of Medicine, San Francisco, California). *Radiology* 127:675–679, June 1978

Previously reported signs of an extraaxial mass as seen on computed tomography were: (1) bony destruction; (2) extrinsic displacement of brain from the calvarium with apparent widening of subarachnoid space; (3) continuity of the lesion with either the tentorium or calvarium; and (4) sharp definition of the lesion margin. These signs are often not present.

The authors report six cases of what appeared to be intraaxial lesions on computed tomography which were clearly shown to be extraaxial by angiography. These included a large aneurysm arising proximal to the PICA, partially thrombosed vertebral artery aneurysm, posteroinferior cerebellar artery aneurysm, an aneurysm arising from the posteroinferior cerebellar artery, clivus meningioma, and a right ninth cranial nerve neurinoma. False localization is attributed to a slowly growing mass which burrows into the brain. Angiography is essential with further

evaluation necessary at times by means of pneumoencephalography.

Asher Nov

Enlarged cisternae magnae and posterior fossa cysts simulating Dandy-Walker syndrome on computed tomography. Archer CR, Darwish H, Smith Jr K (St. Louis University Hospitals, St. Louis Missouri). *Radiology* 127:681–686, June 1978

The authors use Ford's definition of the Dandy-Walker syndrome: "obliteration of the outflow of CSF from the fourth ventricle." Two conditions exist. In the first, the roof is thin and transparent but does not contain openings, in the second there is thickening of the meninges and obliteration of the cisterna magna. In addition to these findings there are instances in which the middle and posterior parts of the vermis are missing. The Dandy-Walker variant is described and shown to be hypoplasia of the vermis at its inferior portion; in addition an extraaxial posterior fossa cyst situated posterior or lateral to the fourth ventricle may either be separated or communicate with the ventricle and the subarachnoid space. The cisterna magna on the other hand lies posteriorly and laterally and always communicates through the midline. The article describes five patients in whom CT alone could not determine the specific nature of a posterior fossa cystic lesion. Correlated studies were necessary which either entailed pneumoencephalography or sagittal reconstruction of axial tomography.

Asher Nov

Computed tomography in craniopharyngiomas. Fitz CR, Wortzman G, Harwood-Nash DC, Holgate RC, Barry JF, Boldt DW (Hospital for Sick Children, Toronto, Canada). *Radiology* 127:687–691, June 1978

CT examination of 28 children and 12 adults with proved craniopharyngiomas were analyzed to determine characteristics of this tumor type. Three characteristics noted were contrast enhancement, calcification, and cyst formation. Individual characteristics of either of these were nonspecific. The combination of either two in a centrally located suprasellar tumor were indicative of a craniopharyngioma. Contrast enhancement was more frequent in preoperative pediatric patients and more frequent in postoperative adult patients. Cystic changes of the tumor were again more frequently seen in pediatric patients.

Atypical appearances included a 59-year-old patient showing a nonenhancing increased density in the right thalamus and a second patient showing a suprasellar enhancing noncalcified mass which was totally within the third ventricle. Differential diagnosis in adult patients would include meningioma as well as pituitary adenomas. Other suggested radiographic studies include angiography when total removal is planned. When the third ventricle is identified on CT there is no further need of pneumoencephalography or ventriculography. Follow-up CT examinations are of extreme importance in assessing residual tumor, regrowth, or residual tumor expansion.

Asher Nov

Neurodiagnostic tests in children with brain tumors: changing patterns of use and impact on cost. Winston KR (Department of Neurosurgery, Children's Hospital Medical Center, 300 Longwood Avenue, Boston, Massachusetts 02115). *Pediatrics* 61:847–852, 1978

The utilization of neurodiagnostic tests in the initial work up in children with brain tumors was relatively stable during the 3 years before computed tomography (CT) became available. After this test became available there was a significant ($P < .05$) reduction in the utilization of cerebral angiography, echoencephalography, electroencephalography, and ventriculography in children with tumors below the tentorium. In children with tumors above the tentorium, only a reduction in the use of cerebral angiography and radioisotopic scanning was demonstrated. These changes have resulted in a significant ($P < .05$) reduction in cost to the patient (or third party) for the initial neurodiagnostic work up. Since CT became available, children with brain tumors undergo fewer tests, and the greatest reduction has been in tests that have the greatest cost.

Author Abstract

Radiologic findings of hamartomas of the tuber cinereum and hypothalamus. Lin SR, Bryson MM, Goblen RP, Fitz CR, Lee YY (University of Rochester School of Medicine, Rochester, New York). *Radiology* 127:697–703, June 1978

Approximately 46 cases have been reported in literature with the present article describing a series of five patients. Hamartoma is a congenital malformation with a tumor-like collection of nerve cells which resemble those of the tuber cinereum. It is commonly anatomically connected with the tuber cinereum by a stalk. Lesions measure from several millimeters to 1 cm in size.

Clinical manifestations are precocious puberty, seizure disorder, and mental changes. Recent studies suggest the appearance of a hamartoma either stimulates the median eminence directly or autonomously produced gonadotropin releasing factors. Seizures are of both petit mal and subcortical toxic types. Mental changes manifest as behavior disorders, abnormal effective responses, and intellectual deterioration.

CT radiographic findings are nonspecific. Signs commonly seen are distortion or obliteration of the posterior suprasellar cistern and anterior third ventricle. There is usually no contrast enhancement. Pneumoencephalography is indicated whether CT is negative or positive. Typical findings are a well circumscribed soft tissue mass in the postchiasmatic, interpeduncular, and prepontine cisterns. Further evaluation by means of angiography will depend on the individual case. The usual angiographic findings are posterior displacement of the basilar artery and anterior pontomesencephalic vein.

Differential diagnosis of suprasellar mass lesion in children includes several entities. Craniopharyngiomas generally cause eniargement of the sellar turcica and suprasellar calcification. Optic chiasm gliomas often spread bilaterally causing J-shaped deformity of the sellar turcica and enlargement of the optic canals. They can often manifest as avascular masses either displacing the third ventricle or causing lateral ventricular enlargement. Their location is generally more anterior than those of the tuber cinereum hamartomas.

Other considerations include: Infundibulomas, pituitary adenoma, ectopic pinealoma, suprasellar teratoid tumors, and chordomas.

Arachnoid cysts will generally cause more erosion and enlargement of the sellar turcica and seldom cause precocious puberty. Pinealomas generally have a very distinct tumor blush. Teratoid tumors are more commonly calcified than are tumor cinereum hamartomas. Chordomas will frequently show retrosellar calcification and destruction of the clivus.

Asher Nov

Neuroradiological manifestations of intracranial sarcoidosis. Bahr AL, Krumholz A, Kristt D, Hodges FJ III (study from Johns Hopkins Hospital and Sinai Hospital of Baltimore, Maryland. A. L. Bahr present address, LDS Hospital, 325 Eighth Avenue, Salt Lake City, Utah 84143). *Radiology* 127:713–717, June 1978

The reported incidence of central nervous system sarcoid has been 1–16% with an average of 3.5%. Six cases of neurosarcoidosis are discussed including three patients in whom the initial manifestations of sarcoid were related to the central nervous system. The most common radiographic finding is hydrocephalus. This was of the communicating type but less frequently related to obstruction in the region of the fourth ventricle foramina. Other manifestations are an intracerebral mass seen on CT as a dense focus of abnormality with enhancement following contrast injection. Angiography and radionuclide brain scans will demonstrate an avascular mass and region of increased uptake. Central nervous system sarcoid may be manifested as multiple small granulomata in the meninges. Most patients show improvement following steroid treatment. CT scan is found to be the most useful means of assessing both the

presence of intracranial lesions and hydrocephalus. It is also useful in following progress after initiation of treatment.

Asher Nov

Absence of the corpus callosum: computed tomographic evaluation in infants and children. Byrd S, Harwood DC, Fitz CR (Hospital for Sick Children, 555 University Avenue, Toronto, Ontario, Canada M5G1X8). *J Can Assoc Radiol* 29:108–112, June 1978

The authors discuss their experience over a 5 month period with 10 children with absence of the corpus callosum. The CT criteria for making a diagnosis of absence of the corpus callosum is: (1) marked separation of the lateral ventricles; (2) narrow frontal horns in the absence of hydrocephalus; (3) sharply angled lateral peaks of the frontal horns and bodies of the lateral ventricles, and a concave inner border to the lateral ventricles due to a long callosal bundle; (4) dilation of the occipital horns with a convex medial border of the ventricle; and (5) dilation of the third ventricle with varying degrees of interposition between the lateral ventricles.

Eight of the ten patients also had other associated craniocerebral lesions, such as lipoma of the corpus callosum, microcephaly, and aqueductal sclerosis. The authors state that the chief importance of computed tomography is the accurate demonstration of absence of the corpus callosum and its commonly associated intracranial lesions, some of which are amenable to surgery. Also, a diagnosis of this entity indicates a greater degree of cellular brain maldevelopment.

Jack M.A. Tishler

The radiology of intracranial tuberculosis in children. Reed MH, Ferguson CA (Health Sciences Children's Centre, Winnipeg, Manitoba, Canada). *J. Can Assoc Radiol* 29:113–119, June 1978

The authors report their experience with 23 patients with documented intracranial tuberculosis, 15 with tuberculous meningitis, and eight with tuberculomas. In the 15 with meningitis, 12 had abnormal chest radiographs. Common neuroradiologic findings were minor suture separation, mild ventricular dilation, and vasculitis. The brain scans showed abnormal activity in the region of the Sylvian fissure. In the eight patients with tuberculomas, only half had abnormal chest radiographs. Radiographs of the skull showed evidence of increased intracranial pressure with hydrocephalus and mass lesions demonstrated on air studies. The brain scan showed deep focal lesions. The tuberculomas tended to calcify within 1 year.

Jack M.A. Tishler

Clinical testing of Amipaque for cerebral angiography. Amundsen P, Dugstad G, Slettebo M (Ulleval Hospital, Oslo, 1 Norway) *Neuroradiology* 15:89–93, April 1978

The authors compare the nonionic contrast medium, metrizamide (Amipaque) and the ionic contrast medium, meglumine metrizoate (Isopaque cerebral) as agents for cerebral angiography in 20 patients using a double blind format. In both contrast agents the concentration of iodine was 280 mg iodine/ml. This study differs from an earlier report in *Neuroradiology* because each patient served as his own control and two injections were made in the common carotid artery using 10 ml of each contrast agent. In an additional 13 patients the effects of these two contrast agents were compared during external carotid injections using 3–5 ml of contrast. Qualitative assessment of patient discomfort and quantitative measurement of blood pressure and heart rate were compared as well as film quality. The patients reported significantly less discomfort in both common and external carotid injections with metrizamide. The authors also commented that metrizamide has been used in 54 other selective external carotid angiograms and patient discomfort was graded as mild to none without late effects. No serious side effects were noted with either contrast agent. The authors conclude that metrizamide is better tolerated for cerebral angiography than the ionic contrast agent meglumine metrizoate. The authors do, however, caution that small pieces of the rubber cap may be introduced into the metrizamide bottle when the solvent is introduced by perforating the rubber cap with a needle. They recommend that the contrast agent be withdrawn from the bottle into the injection syringe via a microfilter to prevent foreign body embolization during angiography.

Paul M. Chikos

A randomized trial of aspirin and sulfinpyrazone in threatened stroke. The Canadian Cooperative Study Group (Barnett HJM, University Hospital, London, Ontario N6A 5A5, Canada.) *N Engl J Med* 299:53–59, July 13, 1978

A total of 585 patients who had experienced at least one cerebral or retinal ischemic attack in the preceding 3 months were assigned to one of four treatment groups; placebo, aspirin, sulfinpyrazone, and both drugs. The patients were followed for an average of 26 months during which time there were 85 strokes and 42 deaths. Aspirin (325 mg taken four times daily) reduced the risk of continuing ischemic episodes, stroke, or death by 19% and when restricted to stroke or death by 31%. Aspirin was of no benefit in reducing stroke or death in women and in men with prior myocardial infarction. The greatest response was found among men without prior myocardial infarction where a risk reduction of 62% for stroke or death was observed. Although sulfinpyrazone alone was of no benefit a trend favoring therapy with both drugs was observed among men.

P. M. Chikos

Large decompressive craniotomy in the treatment of acute subdural hematoma. Britt RH, Hamilton RD (Stanford University School of Medicine, Stanford, California 94305). *Neurosurgery* 2:195–200, May/June 1978

A series of 42 patients who had large decompressive craniotomies for acute subdural hematoma has been reviewed with regard to long term results. Postoperative mortality (within 30 days of surgery) was 36%. Delayed but related deaths accounted for an additional 19% mortality, for a total mortality of 55%. Fourteen patients (33%) were able to return home, but there was a significant morbidity in terms of intellectual impairment, hemiparesis, and dysphasia. Recommended management includes establishment of an adequate airway, intravenous administration of mannitol, and performance of an emergency computed tomography scan before operation. A large decompressive craniotomy is performed, with removal of the blood clot, establishment of hemostasis, patch-grafting of the dura, and removal of the bone flap to allow the edematous, swollen brain to expand away from the brain stem. The mortality and morbidity will probably always remain high because in the majority of the cases significant structural damage to the cortical and brain stem structures occurs at the time of the injury.

Author Abstract

Pediatric Radiology

Ultrasonic diagnosis of gynecologic disorders in children. Haller JO, et al. (State University of New York, Downstate Medical Center, Brooklyn, New York). *Pediatrics* 62:339–342 Sept 1978

A study of 350 females under 15 years of age by ultrasound revealed several applications in the pediatric patient. Pregnancy was the most common condition diagnosed, occurring in 60% of the cases, one in a 9 year old child. The study was helpful in the assessment of pelvic masses, or in the exclusion of pelvic masses. Useful information was obtained about the internal genitalia in girls with abnormalities of the vagina or with labial fusion. Infantile genital structures could not be visualized.

B. J. Wood

Choledochal cyst: delayed diagnosis in a jaundiced infant. Harris VJ, Kahler J (Cook County Children's Hospital, University of Illinois, Chicago, Illinois). *Pediatrics* 62:235, Aug 1978

A 5½ month old infant with jaundice at 2 days of age was found at postmortem to have a choledochal cyst. Exploratory surgery had been refused at 4 weeks of age. An upper gastrointestinal series examination showed compression and anteroinferior displacement of the second and third portions of the duodenum. The cyst wall was not visualized by excretory urography with total body opacification. Early diagnosis is essential in infants with prolonged jaundice due to the early development of irreversible liver damage. Ultrasound and angiography may assist in diagnosis.

B. J. Wood

Ventricular tahcyarrhythmia due to cardiac sarcoidosis in a child. Serwer CA, et al. (Duke University Medical Center, Durham, North Carolina). *Pediatrics* 62:322–325 Sept 1978

Involvement of the heart in sarcoidosis occurs in less than 10% of pediatric patients with the disease and the usual mode of presentation in these is heart block. A 12-year-old black female is described who presented with exercise intolerance, paroxysmal nocturnal dyspnea, and palpitations with exercise. Physical examination revealed a rapid irregular heart rate, an apical systolic murmur, and peripheral edema. The E.C.G. showed multiple premature ventricular beats. The chest radiograph showed generalized cardiomegaly with evidence of congestive heart failure but no lymphadenopathy. The diagnosis of sarcoid was made on biopsy of the supraclavicular lymph nodes. She subsequently developed cervical and inguinal lymphadenopathy, small nodules on the forearms, uveitis, and pituitary involvement. The case is unique in the presentation with ventricular tachyarrhythmia in this age group.

B. J. Wood

Early-onset haemophilus sepsis in newborn infants: Clinical, roentgenographic, and pathologic features. Lillien LD, et al (Cook County Hospital, Hektoen Institute for Medical Research, Chicago, Illinois). *Pediatrics* 62:299–303 Sept 1978

Early onset hemophilus sepsis is reported in nine premature infants. Eight of the infants were less than 1,500 g and all died. A patient of 1,700 grams survived. Respiratory distress was present in all and radiographs in six of the eight cases were available and showed changes of hyaline membrane disease. One patient had diffuse interstitial and alveolar infiltration, and one had right lower lobe alveolar process. Pleural effusion was not seen. Pure cultures of hemophilus were obtained from blood and/or cerebrospinal fluid. Only one of these was Type B.

B. J. Wood

Computed tomography in child abuse and cerebral contusion. Ellison PH, Tsai FY, Largent JA (Albany Medical College, Albany, New York). *Pediatrics* 62:151–154 Aug 1978

The advent of computed tomography has allowed the demonstration of cerebral edema and of contusional hemorrhage and the differentiation between them. Cerebral contusion is believed to be the cause of mental retardation and of cerebral palsy in children who have been abused. This may occur in the absence of subdural hematoma and without visible external injury. Four infants are presented who demonstrate this.

B. J. Wood

Miscellaneous

Lymphographic investigations of lower extremity edema following reconstructive vascular surgery in the femoro-popliteal region. Schmidt KR, Welter H, Pfeifer KJ, Becker HM (Roentgenabteilung der Chirurgischen Klinik der Universitaet Muenchen, 8 Muenchen 2, West Germany). *Fortschr Geb Roentgenstr Nuklearmed* 128:194–202,1978

In 37 patients with lower extremity edema following reconstructive surgery of the femoro-popliteal arterial system, lymphography was performed between the third and ninth postoperative days. Partial to total disruption of the lymphatic vessels was found in 27 patients, whereby the degree of the swelling correlated with the number of intact lymphatic vessels (with more than three intact lymphatic vessels the leg circumference was increased by 1–2 cm and with all lymphatic vessels interrupted, the circumferential increase amounted up to 7 cm). The preoperative condition of the arteries, the presence of venous disease and the postoperative blood flow had no influence on the postoperative edema.

Peter F. Winter

Multiple primary malignant tumors (in Italian). De Marzi S, Bernini P (Spedali Riuniti, Viale Alfieri, I-57100, Livorno, Italy). *Radiol Med* 64:135–146, 1978

The authors report on 54 patients presenting with a primary malignant tumor and in whom a metachronous malignancy developed. The primary solitary lesion was a carcinoma of the breast in 11 cases, of the cervix in four, of the skin in 11, of sigmoid in four, of larynx in five, bladder in one and nasopharynx, tongue, and lips in 16. In two cases the primary process was leukemia. All cases had histologic confirmation of the lesion.

The highest incidence of multiple primary malignant tumors was noted between the breast and uterus or cervix (seven cases) and between cancer of the cervix and breast (three cases). Two cases of sigmoid carcinoma later developed carcinoma of the breast. In 12 cases the two neoplastic lesions were synchronous, the metachronous ones developed between 2 months and 25 years, in each case cervix followed by breast malignancy.

Antonio F. Govoni

Ultrasonics

Gray scale ultrasonography of the jaundiced patient. Sample FW, Sarti DA, Goldstein LI, Weiner M, Kadell BM (University of California School of Medicine, Los Angeles, California 90024). *Radiology* 128:719–725, Sept 1978

In 143 jaundiced patients, ultrasound demonstrated the extrahepatic biliary system in 38% of those with medical and 74% of those with surgical jaundice. The size of the extrahepatic biliary system indicated that surgical was best differentiated from medical jaundice when 5 mm served as the upper normal limit for the common hepatic or common bile duct in patients without prior biliary surgery. Half of those patients with prior biliary bypass surgery had nondiagnostic sonograms. In 22% of the jaundiced patients, no additional imaging procedures were performed before definitive therapy. The role of ultrasound in evaluating jaundiced patients is discussed.

Author Abstract

The use of ultrasound to enhance the diagnostic utility of the equivocal liver scintigraph. Sullivan DC, Taylor KJW, Gottschalk A (Yale University School of Medicine, New Haven, Connecticut 06510). *Radiology* 128:727–732, Sept 1978

Using state-of-the-art technology in nuclear medicine and ultrasound, directed ultrasound examinations were performed with attention to equivocal areas identified on hepatic isotope studies. In 100 patients studied prospectively, 110 equivocal radionuclide findings were identified. Proven diagnoses were obtained in 99 cases. Overall accuracy figures were 74% for scintigraphy and 93% for ultrasound. Scintigraphy in general showed high sensitivity, but ultrasound showed greater specificity and accuracy. It was concluded that a directed ultrasound examination is accurate and useful when the hepatic scintigraph is equivocal for any reason.

Author Abstract

Sensitivity of pancreatic ultrasonography in the detection of pancreatic disease. Lawson TL (George Washington University Medical Center, Washington, D.C. 20037). *Radiology* 128:733–736, Sept 1978

In a large series of patients an abnormal pancreatic ultrasonogram was found to be significant with only a 3% false positive rate. It is recommended that patients with an abnormal ultrasonogram undergo further diagnostic procedures to establish a diagnosis. Only 81% of patients with a normal pancreas by ultrasonography were ultimately found to be normal. The greatest false negative rate was in patients with chronic pancreatitis. The overall accuracy in separating patients with a normal pancreas from those with an abnormality is 87%. It is concluded that an abnormal pancreatic ultrasonogram is significant and usually indicates disease while a normal pancreatic ultrasonogram does not exclude disease and does not have the significance of an abnormal ultrasonogram.

Stephen J. Carter

Lipomatous tumors of the kidney and adrenal: apparent echographic specificity. Scheible W, Ellenbogen PH, Leopold GR, Siao NT (San Diego Medical Center, 4647 Zion Avenue, San Diego, California 92120). *Radiology* 129:153–156, Oct 1978

Several fatty tumors of the kidney and adrenal gland were evaluated by gray scale ultrasound. An extremely dense echogenic pattern was common to all lesions. There were three solitary angiomyolipomata (renal hamartoma), a presumed diffuse hamartomatous involvement of the kidney in a patient with tuberous sclerosis, and one myelolipoma of the adrenal gland. This marked echogenicity is thought to be a feature of fatty tumors and enables relatively specific preoperative diagnosis of these lesions, all of which are benign. With regard to renal angiomyolipoma, this assessment may allow conservative treatment and preservation of functioning renal tissue.

Author Abstract

Nephrosonography during pregnancy. Schmoller H, Mentel C (Roentgendiagnostisches Zentralinstitut der Landeskrankenanstalten Salzburg, A-5020 Salzburg, Austria). *Fortschr Geb Roentgenstr Nuklearmed* 129:98–103, 1978

In a series of 128 pregnant women without evidence of renal disease, macromorphologic changes of the renal collecting systems were investigated ultrasonographically and the degree of dilatation correlated with primiparity and multiparity as well as with the gestational age. Dilatation of the collecting systems was found during the first trimester in nine of 27 nulliparas and in 10 of 17 multiparas, during the second trimester in 19 of 27 nulliparas and 12 of 17 multiparas, and during the third trimester in 16 of 17 nulliparas and 17 of 23 multiparas. Of the entire patient group studied, 65.6% of the pregnant women had a sonographically detectable dilatation of the collecting systems; of these pregnant women with dilatation, the finding was only on the right in 58.3%, bilateral or more pronounced on the right in 34.5%, and only on the left in 7.2%.

Peter F. Winter

The value of ultrasound examination in tumors and hyperplasia of the adrenal glands. Scherer K, Mischke W (Abteilung Radiodiagnostik der Radiologischen Klinik des Universitaets-Krankenhauses Eppendorf, 2 Hamburg-Eppendorf, Germany). *Fortschr Geb Roentgenstr Nuklearmed* 128:609–615, 1978

The results of sonographic examinations of the adrenal glands are reported in 76 patients with hypertension (75%), obesity (20%), or hirsutism (5%). Enlargement of one adrenal gland due to tumor was found in 10 patients (including pheochromocytomas, aldosterone-producing adenoma, recurrent primary carcinoma and metastasis to the adrenal gland. Bilateral hyperplasia relating to Cushing's syndrome was found in five patients. These findings were confirmed at surgery or by autopsy or angiography. Two false positive and two false negative sonographic results were detected at surgery. Both false negative results were encountered in patients with Conn's syndrome and small adrenal tumors; one of the false positive findings was probably caused by a prominent gastric fundus. The true false negative results in the remaining 57 patients were confirmed by the subsequent clinical course.

Peter F. Winter

Book Reviews

The Diagnostic Limitations of Computerised Axial Tomography. Edited by J. Bories. Berlin: Springer, 1978, 220 pp. $27

The Sixth Congress of the European Society of Neuroradiology took place in Dijon in September 1976. The theme of that meeting was the place of computed tomography in the present and near future with emphasis on the diagnostic limitations of CT. Papers from that meeting constitute the essence of this book.

This work is composed of five chapters and they discuss in order: (1) the diagnostic limitation of computed tomography and cerebral tumors; (2) the limitations of CT in the diagnosis of diseases of the orbital region and of the skull, base, and face; (3) the limitations of CT in the diagnosis of cerebral infarcts, cerebral edema, and subdural hematomas; (4) a comparison of CT and other neuroradiologic techniques; and (5) the accuracy of computed tomography and future prospects. A total of 24 papers is included in this work.

The quality of the papers varies greatly. Those with little information are presented in a form resembling an abstract, while those with more valuable information are presented as full manuscripts. The most interesting and sobering portion of this compendium is the section dedicated to a comparison between CT and conventional neuroradiologic techniques. Drs. Ruggiero and Sabattini offer a beautifully illustrated paper in which CT scans and air encephalography are compared. This paper truly was presented in the spirit of the symposium, a claim which other manuscripts cannot make. Drs. Szikla and Talairch demonstrate the difficulty of localizing intraparenchymal lesions and indicate the necessity of angiography to obtain a three-dimensional pattern of vascular abnormality as a superior method of localization.

The comments on the new developments in computed tomography and the use of a body scanner for neurodiagnostic purposes are somewhat outdated. Similarly, much of the information offered in the section on the limitations of CT in the diagnosis of tumors is a rehash of information offered elsewhere. The section on the diagnosis of orbital disease is weak as is the part devoted to the perisellar region and base of the skull.

The image quality is reproduced faithfully; however, many of the images were acquired from the early EMI console rather than the diagnostic display console and reflect the inherent problems with this type of display. Some of the scans are presented in the 80 × 80 matrix format and others are from an early ACTA scanner. There are scattered typographic mistakes, but for the most part the manuscripts are lucid and are presented in a reasonable format.

I would recommend this book for individuals with an interest in cranial CT. Those who are concerned about the future of the conventional neuroradiologic studies will be pleased by several of the articles. Also, those starting out in CT would gain from this book, since not only would much of the basic material be of value but they would at the same time realize that computed tomography is not a panacea for all radiologic dilemmas.

Charles M. Citrin
The Neurology Center
Chevy Chase, Maryland 20015

Very Early Recognition of Coronary Heart Disease. Edited by Lawson McDonald, John Goodwin, and Leon Resnekov. Amsterdam: Excerpta Medica, 1978, 194 pp. $32.75

This volume is based on a symposium arranged by the Cardiothoracic Institute associated with the National Heart and Chest Hospitals, and held at the Royal College of Physicians, London, in May 1977. Most of the papers were presented by investigators from the United States and Great Britain. The main theme of the conference concerned various means of detecting coronary heart disease in the preclinical or latent stage.

There were comprehensive discussions of risk factors, the importance of a detailed history and physical examination, the metabolic basis of atherogenesis, the role of Doppler imaging of carotid arteries in the detection of stenotic lesions, and M-mode echocardiography in the evaluation of dysfunctional left ventricular contraction and septal motion. Excellent presentations were made on computer processing of radiographic images obtained during femoral angiography in evaluating atherosclerotic plaques; the criteria for, and interpretation of, data derived from stress exercise testing, as viewed by investigators at various centers; indications, complications, and limitations of coronary angiography, accompanied by an excellent discussion of recent technologic improvement which has served to increase diagnostic yield; and a very understandable discussion of definitions regarding the statistical assessment of data. Radioisotopic evaluation of heart disease included myocardial infarct imaging, myocardial imaging with thallium-201, and gated cardiac blood pool imaging. Surprisingly, one of the discussions did not include illustrations. The role of cyclotron produced positron imaging was discussed in depth by Dr. Resnekov.

This book has an attractive cover and a fair binding. The bibliographies are extensive and current. The type face is rather light and the occasional nonsyllabic division of words can be distracting. General internists and family practitioners will find this book useful as a review. Radiologists involved in nuclear medicine and nuclear physicians will be disappointed by the less than detailed discussions of patterns of abnormal scintiphotos. However, the radiologists will gain valuable insights into the current thought process of cardiologists who sometimes appear to split metabolic and physiologic hairs.

Edwin G. Goldstein
550 West Thomas Road
Phoenix, Arizona 85013

© 1979 American Roentgen Ray Society

0361-803X/79/1322-0332 $0.00

Principles of Chest X-ray Diagnosis, 4th ed. By George Simon. Boston: Butterworths, 1978, 296 pp. $32.75

The fourth edition of this well known book follows the pattern of its predecessors in arranging material under headings that are descriptive of the radiographic shadows rather than of clinical diseases. Appropriately, Chapter 1 leads off with succinct definitions of the terms used throughout the book, most of which possess the same connotation to radiologists on both sides of the Atlantic. The remaining 12 chapters deal with the following topics: anatomic landmarks and variations; homogeneous shadows grouped according to shape, size, or distribution; linear shadows; high density shadows and hypertransradiancies; the pulmonary vessels in lung disease; cardiovascular abnormalities; the mediastinal and diaphragmatic shadows; bones and soft tissues of the thorax; combinations of different shadows; bronchography; tomography; and the time factor in x-ray diagnosis.

Much of the text has been rewritten from previous editions and certain changes of order have been made. New material is included on pulmonary angiography and vascular anomalies, and a number of charts, tables, and diagrams have been added to supplement the text. An appendix at the end includes some useful hints on x-ray technique, although the author persists in the belief that low kVp chest radiographs provide information equivalent to that obtained with high kVp, a view with which most North American radiologists will disagree.

The text is easy to read, and the multitude of headings and subheadings makes it relatively simple to locate descriptions of specific radiographic patterns. Unfortunately, despite the statement of the publishers that the quality of the illustrations has been improved, the contrary is true: comparison of illustrations in this edition with identical figures from the third edition reveals a distinct deterioration, although in most instances it is possible to identify the points made in the legends.

As in previous editions, the bibliography is rather sparse, containing only 67 citations. However, it was never the intent of the author to be exhaustive in his review of the literature; rather, he depended on his own powers of observation and on a meticulous correlation with physiologic and pathologic material to derive from a chest radiograph the maximum amount of information possible. It should be emphasized that the first edition of this book, published in 1956, was the first successful attempt by anyone to organize all opacities seen on chest radiographs in terms of their morphologic nature, and it is very much to the author's credit that this approach to radiographic interpretation has stood the test of time and has constituted a source of stimulation to all those who have had an opportunity to read his books or to hear his lectures.

This book is aimed primarily at the trainee in diagnostic radiology, although it should prove of considerable value to all physicians and surgeons interested in the interpretation of chest radiographs, and even to senior medical students. It contains a wealth of information presented in a clear manner by a keen and fastidious observer. Some readers may object to the relative lack of emphasis on disease entities, but to this reviewer this aspect does not detract significantly from the value of the book as an objective analysis of radiographic opacities.

George Simon died in 1977 before this edition was published. He would have been proud of it. It is a great pity that the medical community will not see further editions from Dr. Simon's fertile mind. It is a greater pity that we won't see more of the man himself.

Robert G. Fraser
University of Alabama in Birmingham
Birmingham, Alabama 35233

Encyclopedia of Medical Radiology, vol. 5. Diseases of the Skeletal System (Roentgen Diagnosis). Part 6. Bone Tumors. Edited by K. Ranniger. Berlin: Springer, 1977, 825 pp. $170.20

This volume is an encyclopedia of radiology with major emphasis on tumors of the bone. These bone lesions are classified according to the system of the World Health Organization. The volume includes introductory sections on the diagnosis, classification, and nomenclature of bone tumors, as well as a discussion of the radiologic approach to these tumors. A short section on the pathology of bone is presented in a somewhat abbreviated form.

The bulk of the volume systematically presents tumorous and nontumorous conditions of bone. The content varies from section to section according to each author's inclination. For example, some sections include extensive pathologic material and histologic micrographs, while others include none. Most of these sections discuss the radiologic features of the lesions and give numerous examples.

Three sections at the end of the volume discuss the study of bone tumors with radionuclides, angiography of bone tumors, and high-resolution radiographic techniques for detection and study of skeletal neoplasms.

In general, the organization of the book is quite satisfactory. The three sections involving specialized radiographic techniques might have been better placed after the introductory sections to facilitate reading all sections in sequence. This is a minor criticism, however, since the volume will serve primarily as a reference book, and the reader can refer to the specialized sections if questions arise during reading of the earlier sections.

Although the content of the sections is somewhat uneven, the volume meets its goal of presenting the radiologic appearance of bone tumors. Since the book is very well referenced and well indexed, readers wishing specific information on areas not well covered, such as the histology of a particular process, could locate this information with relative ease.

A significant drawback is the omission of a discussion of new techniques in radiology, such as body scanning. Body scanning is a rapidly expanding field of endeavor which may make significant changes in the interpretation of lesions of bones as well as of other body parts. However, a volume of this type cannot be expected to include up-to-date information on all the rapidly developing areas of radiology, some of which may quickly become obsolete. The volume's major strength is its classic representation of multiple images of bone lesions using standard radiographic techniques. This technology will certainly not change appreciably in coming years, and thus the book will have lasting value. The excellent quality of the reproductions of the radiographs is one of the best features.

This book will be of greatest value to individuals whose primary function is the interpretation of radiographs. The clinical and pathologic material in the volume is quite adequate and provides a useful background. The volume obviously does not replace any of the in-depth works on pathology of bone tumors.

I feel this is a useful volume which would be a desirable addition to a radiologist's library. It should also be useful to orthopaedic surgeons, surgeons, or oncologists who deal with tumors of bone.

Theodore K. Greenlee, Jr.
Department of Orthopedics
University of Washington
Seattle, Washington 98195

1978 Yearbook of Diagnostic Radiology. Edited by W. M. Whitehouse. Chicago: Year Book Medical, 1978, 470 pp. $27.50

The *Yearbook of Diagnostic Radiology 1978* covers appropriate current articles from May 1976 to May 1977 that are significant to medical imaging, although nuclear medicine is not included specifically. The synopses of articles are concise and accurate and provide the reader with a valuable overview. The 470 pages include 331 articles, 406 illustrations, and 194 editorial comments. Individual chapters are: Technical Developments by W. M. Whitehouse; Angiography by J. J. Bookstein; Neuroradiology by T. O. Gabrielson; The Spine and Extremities by W. Martel; The Chest by W. M. Whitehouse; The Gastro-Intestinal Tract by W. Martel; The Genito-urinary Tract by J. R. Thornbury; Pediatric Radiology by J. F. Holt; and Ultrasound by T. M. Silver.

The organization is well done and the quality of the illustrations is quite good. Most articles are easy to understand; in fact, most of the pertinent data and conclusions can be derived from the synopses. In a few cases there is some confusion, but one can always refer to the original article. The editorial comments are generally appropriate and informative.

There are a few typographical errors, but these must be expected since rapid publication of a book of this type is essential. The articles are derived from about 100 different journals. Computed tomography articles are scattered throughout the different chapters; unfortunately, some have the patient's right side on the viewers left, and others vice versa. But this inconsistency is due to lack of agreement from the different journals and is not the fault of this book.

The book will be of value to general diagnostic radiologists as well as subspecialists. Although many articles originally appeared in journals that a radiologist would routinely read, the additional review is still helpful.

Harris Newmark III
Century City Hospital
Los Angeles, California 90067

Ultrasound in Gynecology and Obstetrics. By N. Hassani. New York: Springer, 1978, 182 pp. $22.80

This concise and easy-to-read summary of ultrasound in gynecology and obstetrics is divided under four broad headings: principles of ultrasound, gynecologic ultrasound, ultrasonography in obstetrics, and ultrasonography of gynecologically and obstetrically related medical and surgical disorders.

The more than 300 figures are well labeled and generally of high caliber. Illustrations occupy about half the book. Two of the figures are erroneously numbered on page 117, and there is one glaring spelling error in the caption of the figure on page 59: intervenous (I hope not) pyelogram.

The section on the principles of ultrasound is both well organized and illustrated and is a good introduction to the basic fundamentals and terminology of ultrasound. The chapter on gynecology is adequately illustrated and is a thorough exploration of the field.

The obstetrical section, about twice the size of any other section, is disappointing. Dogmatic statements are made without qualification such as on page 87, "A mature fetus with weight greater than 2500 g may be diagnosed when the biparietal measurement is at least 8.7 cm." Admittedly, this statement is true most of the time, but by no means all of the time. Similarly the statement on page 101, "The average increase in the BPD is approximately 1 to 2 mm. per week" is misleading. The author emphasizes the "gray zone" between the tenth and thirteenth fetal week in at least four places in the book, and although this was a problem with the old bistable equipment, it does not exist with current gray scale imaging or with modern real time scanners. No mention is made of crown-rump measurement for early gestational dating, nor is there adequate discussion of the ultrasound management of a patient with suspected intrauterine growth retardation.

This book contains a good selection of references, with most of the landmark articles cited. Unfortunately, a paragraph alluding to radiation effects on the fetus (p. 171) has only one reference and that is incorrect.

This book could serve as an introduction for technicians doing ultrasound in these areas, but I did not feel that the obstetrical section had the depth to make it useful for the consulting physician.

Edward B. Grantmyre
Dalhousie University
Halifax, Nova Scotia
Canada

The Pacemaker and Valve Identification Guide. By Dryden Morse and Roberg M. Steiner. Garden City, N. Y.: Medical Examining, 1978, 395 pp. $40

The authors state that the purpose of the book is to incorporate the fine details of valves and pacemakers in a single volume together with some explanatory material to guide the reader. The result is a volume which includes an enormous amount of detail about these devices which would only interest those intimately involved with partients who have prosthetic valves or implanted pacemakers. On the other hand, the explanatory material is very brief and terse, unnecessary for the sophisticated cardiovascular radiologist and insufficient for the uninitiated. The quality of the cardiac films is generally poor. In the chapter "The Radiographic Diagnosis of a Pacemaker Failure and Complications" all of the illustrations have been previously published.

The volume makes technical data on these widely used devices readily available and the ring binding allows for easy updating. I believe the book will be of considerable value to a very small group of physicians, but do not recommend it to most radiologists.

Andrew B. Crummy
University of Wisconsin Medical Center
Madison, Wisconsin 53706

News

Abdominal Radiology Course

A postgraduate course in abdominal radiology will be May 14–17 in Boston. Program directors are R. C. Pfister and J. T. Ferrucci, Jr. A total of 24 hr AMA Category I credit will be available. The course will be divided into two sections: gastrointestinal radiology on May 14 and 15 and genitourinary radiology on May 16 and 17. Fees are $250 for the entire course or $150 for half the course. For information, write: Associate Dean, Department of Continuing Education, Harvard Medical School, 25 Shattuck St., Boston, MA 02115.

Practical Advances in Diagnostic Radiology and Nuclear Medicine

The Johns Hopkins Medical Institutions is sponsoring its seventh annual symposium, "Practical Advances in Diagnostic Radiology and Nuclear Medicine", April 17–20. This symposium will offer a review of current advances with emphasis on modern techniques, recently developed procedures, new clinical concepts, and diagnostic equipment. Presentations will be designed for the practicing radiologist. The course will consist of formal lectures and informal sessions. Other highlights will be a series of workshops in which registrants will meet in small groups with the faculty. Workshops will be offered in pediatrics, urinary, gastrointestinal, orthopedics, computerized reporting, cardiovascular, chest, ultrasound, nuclear medicine, ear, nose and throat, and computed tomography. The program carries 32 hr AMA Category I credit. Fee is $300; $150 for residents and fellows. Additional information is available from: Program Coordinator, Turner Auditorium Room 22, 720 Rutland Ave., Baltimore, MD 21205; phone (301) 955-5880.

University of Pennsylvania Diagnostic Radiology Seminar

The Department of Radiology, University of Pennsylvania, will present its Annual Diagnostic Radiology Seminar, June 4–8. Directors are R. H. Troupin and H. Y. Kressel. The program will combine lectures, workshops, and syllabus to provide a state of the art review of imaging modalities in clinical radiology. Chest, gastrointestinal, urinary, skeletal, neuro, and vascular systems will be explored utilizing radiography, ultrasound, computed tomography, and radionuclide imaging. The outstanding guest faculty will include G. Potter, M. Bosniak, D. Forrester, R. Koehler, P. Herman, A. Greenfield, A Bonakdarpour, R. Schapiro, and S. Goldsmith. Participating from the University of Pennsylvania will be: S. Baum, P. H. Arger, S. Borden IV, M. K. Dalinka, H. I. Goldberg, I. Laufer, H. M. Pollack, W. T. Miller, E. Ring, A. Alavi, M. P. Banner, L. T. Bilaniuk, J. Bonavita, B. G. Coleman, M. J. Eymontt, D. Freiman, V. Gohel, J. A. Horton, H. Y. Kressel, C. B. Mulhern, R. H. Troupin, and R. A. Zimmerman.

The seminar is approved for 34 Category I credit hr. The registration fee is $275 for staff; $150 for physicians in residency training.

For further information contact: Department of Radiology, Mrs. Carol Reynolds, Hospital of the University of Pennsyvania, 3400 Spruce Street, Philadelphia, PA 19104; telephone (215) 662-3049.

Angiography: Current Methods and Basic Problems

The departments of Continuing Education, Harvard Medical School, and of Radiology, Massachusetts General Hospital, announce a course on Angiography: Current Methods and Basic Problems. The course will be April 19–21 in Boston. The practical aspects of therapeutic angiography will be emphasized. Lengthy theoretical discussions and descriptions of standard angiographic findings will be purposely omitted. Emphasis will be on methodology, especially transluminal angioplasty, transcatheter embolizations, balloon catheters, and therapeutic drug infusions. The basic problems of renovascular hypertension and peripheral vascular occlusive disease will be discussed with input from medical and surgical experts in these fields. Special instruction features will be "hands on" small group workshops and panel discussions with audience participation. A syllabus will be provided. The course should prove useful to radiologists and nonradiologists involved in therapeutic angiographic procedures, radiology residents and fellows in training and special procedure-radiologic technologists. A total of 16 hr AMA Category I credit is offered. Attendance is limited.

For further information write: Associate Dean, Department of Continuing Education, Harvard Medical School, 25 Shattuck St., Boston, MA 02115.

Clinical Nuclear Medicine: 1979

Clinical Nuclear Medicine: 1979 is a continuing medical education seminar scheduled for March 30–April 1 in Dallas. Sponsor is the Nuclear Medicine Division, Department of Radiology, Southwestern Medical School. Program chairmen are R. W. Parkey and S. E. Lewis. Guest faculty will include: B. A. Siegel, Mallinckrodt Institute; H. N. Wagner, Jr., Johns Hopkins; and D. L. Gilday, Hospital for Sick Children, Toronto. Participating from Southwestern Medical School will be: R. W. Parkey, S. E. Lewis, W. Gray, and others to be announced. The seminar meets the criteria for 15 hr AMA Category I credit. Fee is $250. For information and the program brochure, contact L. W. Kiker, Administrative Coordinator, Department of Radiology, Southwestern Medical School, 5323 Harry Hines Blvd., Dallas, TX 75235; phone (214) 688-2502.

AAPM Summer School

The American Association of Physicists in Medicine will hold its 1979 summer school, July 22–28, at Chapel Hill, North Carolina. This course, The Physics of Imaging: Recording System Measurements and Techniques, will provide information on image recording systems in terms of their basic characteristics, proper measurements, and selection and use for various medical imaging procedures and techniques. Topics will include: photographic process (latent image formation); recording systems and their physical characteristics; film processing; image evaluation; image quality factors and recording systems in chest, tomography, mammography, angiography, abdomen, CT scanning, ultrasound, nuclear medicine, intensified fluoroscopy, electron radiography, and xeroradiography. The recording system measurements section will be devoted to sensitometry (characteristic curve), line spread function, edge gra-

© 1979 American Roentgen Ray Society

0361-803X/79/1322-0335 $0.00

dient, modulation transfer function, square wave response, granularity, Wiener spectra, perceptibility curve, and receiver operating characteristics curve.

For information, contact: A. G. Haus, Director, 1979 AAPM Summer School, Department of Physics, M. D. Anderson Hospital, Houston, TX 77030.

New Perspectives in Evaluating Hepatobiliary and Renal Function

The Imaging Systems Division of Union Carbide will host a seminar, New Perspectives in Evaluating Hepatobiliary and Renal Function, March 16–19, in Nassau. Faculty members will include: Z. D. Grossman, R. A. Holmes, G. S. Johnston, P. T. Kirchner, R. C. Reba, L. Rosenthall, E. M. Smith, and E. V. Staab. The course carries 16 hr AMA Category I credit. Fees are $175 for physicians; $100 for technologists and residents. For information, contact: Mrs. L. Bolliger, Union Carbide Imaging Systems, Inc., 333 Providence Highway, Norwood, MA 02062; telephone (617) 769-5400.

Austrian Nuclear Medicine Meeting

The seventeenth International Annual Meeting of the Society of Nuclear Medicine will be September 11–14 in Innsbruck, Austria. For information write: Prof. Dr. George Riccabona Universitätsklinik für Nuklearmedizin, Anischstr. 35, A-6020 Innsbruck, Austria.

Percutaneous Biopsy and Therapeutic Vascular Occlusion

An International Symposium on Percutaneous Biopsy and Therapeutic Vascular Occlusion will be May 7–9 in Munich. Sponsor is the Institute of Diagnostic Radiology of the Technical University of Munich, Klinikum rechts der Isar. The symposium will address the percutaneous biopsy of bone, lung, mediastinum, pancreas, kidney, liver, lymphnodes, and mammary gland, as well as therapeutic vascular occlusion in traumatic or other pathologic bleedings of the gastrointestinal tract, lung, liver, kidneys, and cervicalfacial, cerebromedullary, and gynecologic areas. Simultaneous translation will be provided in German, English, and French.

Information is available from the Secretary of Professor Dr. H. Anacker, Institut für Röntgendiagnostik, Klinikum rechts der Isar, Ismaningerstrasse 22, 8000 München 80, West Germany.

Leo Rigler Lecture and Convention on Pediatric Radiology

The eighteenth annual Leo G. Rigler Lecture and Convention on Pediatric Radiology will be May 8–10 in Herzlia-on-Sea, Israel. The lecture and tour will follow the meeting of the European Society for Pediatric Radiology in Cologne, West Germany, May 3–5. Sponsors are the Tel-Aviv University Sackler School of Medicine, Section of Diagnostic Radiology, and the Municipal Government Medical Center Tel-Aviv/Yaffo. The 1979 Rigler Lecturer will be John A. Kirkpatrick, Jr., Children's Hospital Medical Center of Boston. Guest faculty will include: W. E. Berdon, N. Cremer, J. S. Dunbar, K. D. Ebel, S. G. Gerzoff, B. A. Girdany, C. A. Gooding, H. Grossman, J. L. Gwinn, M. T. Gyepes, H. J. Kaufmann, R. S. Lachman, J. C. Leonidas, A. E. Oestreich, F. N. Silverman, E. B. Singleton, and J. Spranger. Other faculty members will be drawn from the academic staff of the four medical schools in Israel.

Registration fee is $150; $100 for residents. Additional information may be obtained from Professor S. Schorr, Ichilov Hospital, Tel-Aviv, Israel. Hotel reservations and postconvention tour information is available from Kenes Tours, 7, Leteris Street, Tel-Aviv, Israel.

Humanities Seminars for Medical School Teachers

The National Endowment for the Humanities has announced a new program of summer humanities seminars for teachers and administrators at American academic health science centers. Its purpose is to bring medical and health care teachers together for 4–6 weeks of full-time study with distinguished scholars who bring disciplines of the humanities to bear on questions involving biomedical ethics, medical education, health care delivery, and the roles of health care professionals. Four seminars will be held during the summer of 1979.

Seminar location, dates, and topics are as follows: (1) University of California, San Francisco, Aug. 6–31, The Role of the Medical Profession in American Society: Historical Evolution of Issues in Health Care, G. H. Brieger, director; (2) University of Virginia, Charlottesville, July 2–27, Ethics and Health Care, J. F. Childress, director; (3) Georgetown University, Washington, D.C., June 11–July 20, The Philosophical Roots of Bioethics, H. T. Engelhardt, Jr., director; (4) Williams College, Williamstown, Massachusetts, July 9–August 3, Human Nature and the Healer, W. F. May, director.

From 12 to 15 persons attend each seminar tuition-free, receiving stipends of $1,250 for 4 weeks and $1,875 for six. Application deadline is March 1. For applications and further information, write: Professions Program, Division of Fellowships, MS 101, National Endowment for the Humanities, Washington, D.C. 20506.

Summer Humanities Seminars for Physicians

The National Endowment for the Humanities, a federal agency, will support eight humanities seminars for physicians and other health care professionals in 1979. The seminars, which meet during the summer at selected colleges and universities, will bring health care professionals together for a month of full-time study under the direction of distinguished philosophers, ethicists, scientists, historians, and other scholars. The program's purpose is to advance public understanding and use of the humanities as a resource for helping to clarify American values and goals by giving men and women with practical responsibilities the opportunity to stand back from their work and explore its humanistic dimensions. Seminar topics cover a wide range of public policy and other questions which underlie present day concerns about the quality of life.

Three seminars are open to physicians and other health care professionals, including public health officials, nurses, and hospital administrators. They deal with such topics as the evolution of the American medical profession, ethical questions facing medical practitioners, and the relationship between individual and public rights in health care. Five other seminars are intended for members of various professions, including health care professionals.

From 12 to 15 persons will attend each seminar tuition-free, receiving a stipend of up to $1,200 to cover expenses, plus reimbursement for travel. Application deadline is April 16. For applications and further information write: Professions Program, Division of Fellowships, MS 101, National Endowment for the Humanities, Washington, D.C. 20506.

Symposium: Fundamentals in Technical Progress

An International Symposium: Fundamentals in Technical Progress will be May 11 and 12 in Liège, Belgium. Featured

papers will be in the areas of ultrasound, dose planning, and data processing in nuclear medicine. Official languages are French and English. For information, write: J. Garsou, Dr. Sc., Service de Radiothérapie de l'Université de Liège, Hôpital de Bavière, B-4020 Liège, Belgium.

Meeting and Course Review

For reader convenience, a summary of upcoming meetings and courses is provided. Detailed listings of these events appeared in journal issues indicated in parentheses.

CT in Radiotherapy, workshop, March 28–30, Geneva, Switzerland (June).

Courses in Ultrasound, 8-week postgraduate course beginning April 2, Winston-Salem, N.C. (July).

Body CT Course, February 26–March 1, San Diego (September).

Two Courses: Snowbird and Park City, February 24–March 3, Park City Ski Resort, Utah (September).

XII Interamerican Congress of Radiology, July–August 1979, Quito, Ecuador (October).

Sixth Congress of Radiation Research, May 13–19, Tokyo (October).

Noninvasive Imaging in Medicine, symposium, June 6–9, Lund, Sweden (October).

Conferences on Medical and Biological Engineering and Medical Physics, August 19–24, Jerusalem (October).

L. H. Gray Conference, September 10–14, Cambridge, England (October).

Asian Oceanian Congress of Radiology, October 28–November 3, Singapore (October).

Diagnostic and Therapeutic Angiography, course, March 21–25, Puerto Rico (October).

Diagnostic Ultrasound Preceptor Training Programs, San Diego, one month programs (October).

Double Contrast Techniques in GI Radiology, seminar, March 8–10, Philadelphia (November).

Diagnostic Ultrasound Course, series, Philadelphia (November).

Abdominal Real Time Sonography Courses, March 12–16, June 11–15, July 16–20, August 6–10, December 9–13, 1979, Winston-Salem, North Carolina (November).

LSU Diagnostic Radiology Seminar, March 25–17, New Orleans (November).

Fleischner Society Ninth Symposium (and course), June 11–13, Stockholm, (November).

Musculoskeletal Course and Cruise, April 28–May 5, Caribbean (November).

Diagnostic Radiology Course, March 12–16, San Francisco (November).

International Symposium and Course on CT, April 16–20, Las Vegas (November).

Gastrointestinal Radiology, Update '79, seminar, March 9–11, San Diego (November).

European Cardiovascular Radiology Congress, May 3–5, Nuremberg, West Germany (November).

LA Bone and Joint Conference, continuing once monthly course, Los Angeles, (November).

Diagnostic Ultrasound Seminar, April 21 and 22, New York City (November).

San Diego Postgraduate Course, 1 and 2-week programs (November).

San Francisco Cancer Symposium, March 23 and 24 (November).

American Board of Radiology, oral and written examination dates and locations for 1979 and 1980 (December).

AFIP Diagnostic Radiology Seminars, series, May 7–11, August 27–31, November 12–16, Washington, D.C. (December).

Radiation Biology in Cancer Research, symposium, February 27–March 2, Houston (December).

AFIP Alumni Course, March 1–4, Deerfield Beach, Florida (December).

Clinical Advances in CT, seminar, March 10 and 11, Washington, D.C. (December).

Canadian Radiologists Annual Meeting, June 24–28, Vancouver (December).

Multidisciplinary Aspects of Brain Tumor Therapy, June 8–10, Lake Garda, Italy (December).

Radiology of Bone and Chest Diseases, course, April 23–27, San Diego (December).

Radiology of the Chest, course, April 2–6, Durham, North Carolina (December).

Skeletal Radiology Course, May 14–18, New York City (December).

Controversies in Radiology and Medicine, course, March 4–9, Vermont (December).

Spring Physics Seminar, April 23–25, Las Vegas (December).

Nuclear Radiology Workshop, May 4 and 5, Ann Arbor, Michigan (December).

National Breast Cancer Conference, March 5–8, Atlanta (January).

Radiation Therapy Seminar, April 26–28, Gainesville, Florida (January).

Conference on CT, Ultrasound, Nuclear Medicine, Feb. 23–25, Albuquerque (January).

Symposium: Computerized Tomography of the Brain, Sept. 20–22, Bordeaux, France (January).

Gastrointestinal Radiology, postgraduate course, April 5–7, New York City (January).

Bone Radiology Course, March 4–8, Williamsburg, Virginia (January).

Aspen (Colorado) Radiology Conference, Feb. 25–March 3 (January).

Diagnostic Imaging Seminar, March 6 and 7, Philadelphia (January).

Abdominal Ultrasound and CT of the Trunk, May 24–26, Dallas (January).

Nuclear Medicine: Spring Meeting, Feb. 22–24, Chicago (January).

Diagnostic Ultrasound Training Programs, continuing weekly series, New York City (January).

National Conference on Urologic Cancer, April 4–6, Los Angeles (January).

Aspen (Colorado) Seminar: Chest and Abdominal Radiology, March 5–9 (January).

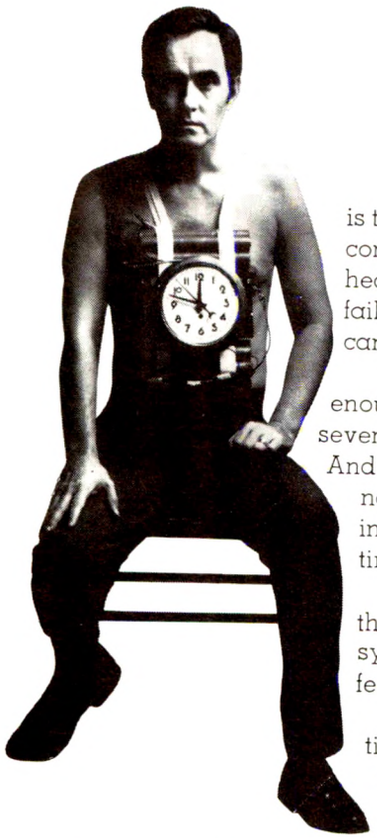
Diagnostic Ultrasound Workshop, weekly postgraduate sessions through December 14, Houston (January).

Cardiac Imaging Refresher Course, April 23–26, Hilton Head, South Carolina (January).

Eighth Congress, European Society of Neuroradiology, Sept. 7 and 8, Strasbourg, France (January).

Tahiti Diagnostic Radiology Seminar, March 16–24 (January).

ONE-SEVENTH OF YOUR EMPLOYEES MAY BE DYING. HELP SAVE THEIR LIVES.



High Blood Pressure is the country's leading contributor to stroke, heart disease and kidney failure. Any of which can kill.

And, frighteningly enough, one out of every seven of your workers has it. And half of them have no idea they're walking around with this time bomb inside them.

That's because there are usually no symptoms. The victim feels fine.

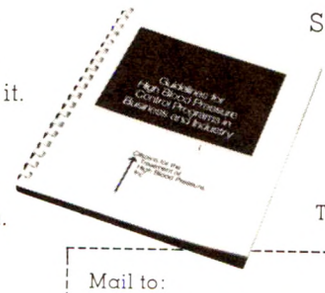
But all the while, the time bomb is ticking away.

Until, suddenly, it explodes.

But you can help. By giving your employees a chance to check their blood pressure. It takes only seconds to measure a person's blood pressure. And it's painless. Best of all, your own medical or nursing personnel can do the job, simply.

When a case of High Blood Pressure is detected, the employee is then referred to a doctor for treatment. And treatment is usually as simple as taking a pill every day.

To help you implement this life-saving program, we have a special kit, "Guidelines for High Blood Pressure Control Programs in Business and Industry." The kit includes complete instructions on screening, publicity, referral, follow-up, education. And more.



Send for your kit today. It may be the best thing you've ever done for your employees. And your company.

A Public Service of this Magazine & The Advertising Council

Mail to:

National High Blood Pressure Education Program
120/80, National Institutes of Health
Room 1012—Landow Bldg.
Bethesda, Md. 20014

Please send me _____ copy(ies) of "Guidelines for High Blood Pressure Control Programs in Business and Industry."

Name _____

Title _____

Company _____

Address _____

City _____ State _____ Zip _____

HIGH BLOOD PRESSURE
Treat it...and live.

The National High Blood Pressure Education Program, U.S. Department of Health, Education, and Welfare.

"Productivity is up 10% to 20%"

"Lower absenteeism"

"You can tell by their attitude—the workers who participate are happier, more cooperative, much sharper"

"We can identify direct savings of $2,000,000 per year"

"The program has had a distinct bearing on staff performance. Our engineering people now have a camaraderie with their counterparts in other departments"

"It started in headquarters. By next year we hope to have it in all our factories and research facilities"

These are actual quotes from executives of large and small companies and organizations in Denver, Omaha, Birmingham, and Greenwich. They're talking about company fitness programs. That's right, many employers now provide facilities or opportunities for exercise for their employees. They are glad they did.

Most began with a concern for employee health and well being. What they have found is a variety of additional benefits. These benefits add up to *increased productivity*—so much so that several companies can demonstrate that the fitness program pays for itself. Add to this improved morale, better internal communications, and employee health. How can you lose? Write us now for more information:

The President's Council on Physical Fitness and Sports
Department B
Washington, D.C. 20201

Employee Fitness: In the long run you will be the winner.

A Public Service of this magazine & The Advertising Council Ad Council



Your Business can be one, too.

Red Cross needs individual volunteers, and donors of blood and money, by the millions.

But we need even more help. We need the solid support of American Business. And we never needed it more.

If your business is already helping, by organizing blood drives, and by supporting payroll deductions—either directly for the Red Cross, or through the local combined fund drive—the whole community owes you thanks. And we thank you, too.

Last year, with help from our friends, we offered major aid at over 30,000 disasters—from typhoons, to local (but just as devastating) house fires.

We were able to help the elderly with practical programs, we helped veterans by the hundreds of thousands, we taught people by the millions to swim or swim better. And that's just the tip of the iceberg.

Think of America without The American Red Cross.

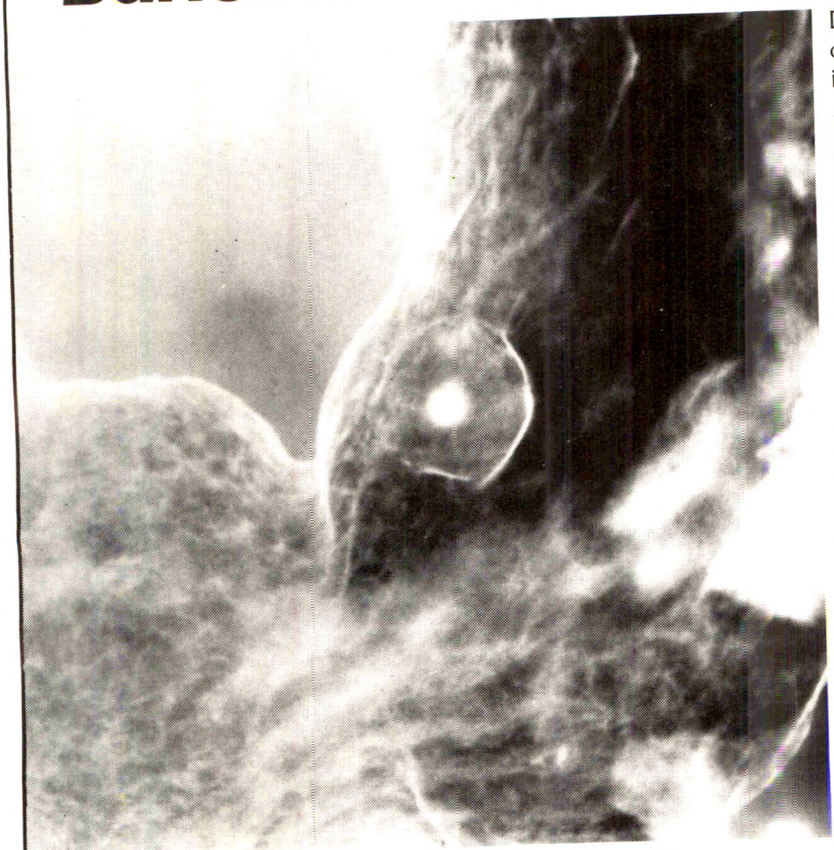
And you'll know why we need your business as a Red Cross Volunteer. In your community. And all across America. Contact your local Red Cross Chapter to see how your company can become a volunteer.

Red Cross. The Good Neighbor.

For Double Contrast Stomachs, Use

NEW! E-Z-HD™

High Density with High Fluidity Barium Sulfate for Suspension USP



ANTERIOR WALL LEIOMYOMA WITH CENTRAL STALACTITE (HANGING DROPLET)
Film courtesy of Igor Laufer, M.D. Hospital of the Univ. of Pennsylvania

Double contrast radiography appears to offer the potential for significant improvements in diagnostic accuracy.

Double contrast studies of the stomach best demonstrate the surface pattern of the stomach (areae gastricae). This leads to improved detection of superfical erosions and ulcers, malignancies, polyps and other benign tumors, and ulcer scars.

E-Z-HD barium sulfate provides the basic ingredient necessary for good double contrast of the stomach.

The higher the density of the barium suspension, the better the coating. E-Z-HD allows for the highest density suspension of any commercial product on the market today: 85% w/w, 250% w/v. E-Z-HD achieves this density while remaining fluid for ease of administration.

- High density
- High fluidity
- Palatable
- Unit dose convenience.

E-Z-HD — The barium for the double contrast examination of the stomach and duodenum.

Optimal Density & Fluidity for the Modern Double Contrast Examination of the Stomach and Duodenum

Refrences:

David W. Gelfand: The Japanese-Style Double Contrast, Examination of the Stomach. Gastrointest Radiol. 1, 7-17 (1976)

Igor Laufer: The Diagnostic Accuracy of Barium Studies of the Stomach and Duodenum — Correlation with Endoscopy. Radiology 115: 569-573. June 1975

Roscoe E. Miller: The Air Contrast Stomach Examination: an overview. Radiology 117: 743-744 Dec. 1975

Order from your local X-ray supplier.

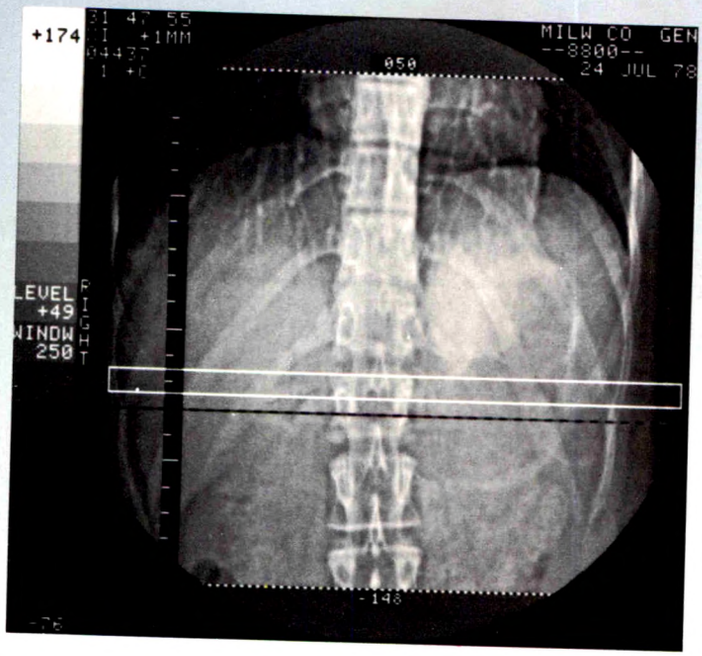
E-Z-EM

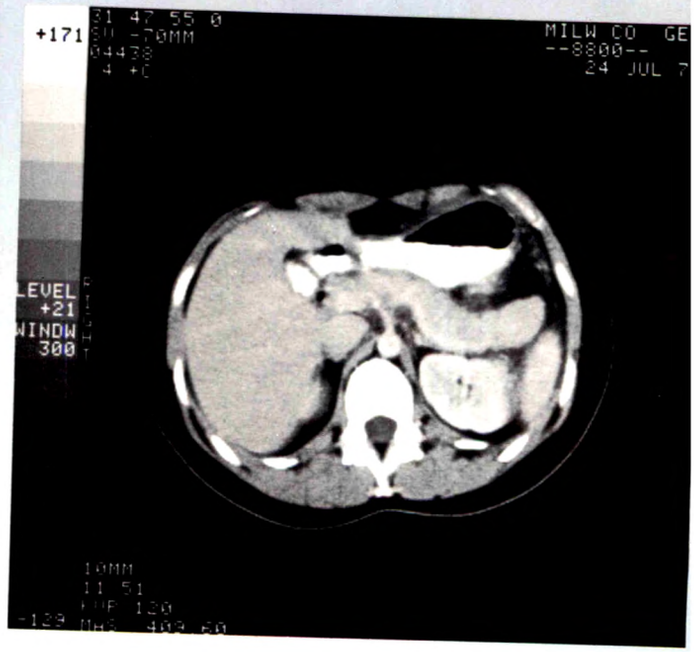
7 Portland Ave.
Westbury, New York 11590
(516) 333-8230

© 1/79

International Affiliates: E-Z-EM Rooster B. V., Infirmeriestraat 6-8, Rotterdam 16, Netherlands
E-Z-EM De Mexico, S. A. de C. V. Calz. Azcapotzalco La Villa No. 882, Zona Industrial Vallejo, Mexico 16 D. F.

New imaging versatility.





These images demonstrate how ScoutView imaging simplifies pancreatic localization. An axial slice taken at the mid to lower L-1 vertebral level is almost invariably at the takeoff of the superior mesenteric artery from the abdominal aorta, and the body of the pancreas will be included in the same slice.The scan sequence can then be monitored both above and below this level to ensure that the complete pancreas has been studied. Unnecessary slices resulting from attempts to define the level of the pancreas from external landmarks are thus avoided.

The image at the right was taken at the level indicated by the box on the ScoutView image. In this case, the patient has a horizontally oriented pancreas, and the slice taken at this level, following an intravenous bolus injection of 25 cc of Renographin 60, clearly demonstrates the splenic vein and superior mesenteric vein, in addition to the superior mesenteric artery on the posterior surface of the pancreas. Note the obliteration of the spleno-renal angle due to pancreatitis. Gas is present within the distal common bile duct secondary to a previous sphincteroplasty on the ampulla of Vater.

Clinical documentation of ScoutView's usefulness in diagnostic procedures is provided in a new 4-page Medical Systems Report. It's yours for the asking from your GE Medical Systems representative, or write ScoutView, P.O. Box 414 (W-512), Milwaukee, WI 53201.

New operator's console, one part of the ODC package, lets you initiate ScoutView imaging, then position a cursor on the image to select scan locations and plan gantry angulation. The new console also allows set up and control of axial scans, plus viewing of the last slice. When the physician's console is not in use, image analysis can be controlled at the operator's console.



SDC physician's console (far right), standard with CT/T systems, provides complete axial, sagittal and coronal scan image manipulation and analysis capability. With the optional ODC package, this console also displays ScoutView images, which can be analyzed with magnification, angle measure and grid/annotate.

You'd expect it from GE.

GE's new Optional Diagnostic Capability package (ODC) offers these key features:

- **New operator's console with image viewing, manipulation and recording capability**
- **Improved, coordinated anatomical reference system utilizing new table electronics**
- **1.5 mm contiguous axial slice capability**
- **ScoutView™ localization imaging—AP/PA, lateral and oblique**
- **Easily installed on existing CT/T 7800 and 8800 systems**

ScoutView localization provides important new benefits for the CT/T operator. The scanner actually generates a radiograph-like image that is used to accurately plan first and last slice locations, plus the exact gantry angulation needed. Each axial scanning procedure is thus tailored precisely to the anatomy of the individual patient, since the ScoutView image and the axial scans share a coordinated anatomical reference system.

A ScoutView procedure is performed in just 5 to 10 seconds, and the image is reconstructed in less than 40 seconds. Dosage is low, varying from 6 mR to 600 mR depending on technic and patient size.

At the operator's console, ScoutView images and the last slice may be viewed without interrupting diagnostic activity at the physician's console. And when the physician's console is not in use, the operator can perform virtually all image manipulation and recording functions at the operator's console.

ScoutView images can also be displayed, manipulated and analyzed at the physician's console. Because of the coordinated reference system, axial scans can be selected for viewing according to their locations on the ScoutView image.

This new package is further evidence of GE's Continuum concept: to provide important options without major systems changes. This cost-saving concept has brought you GE's fast-reconstruct option, X-2 ultra-high resolution detector, and the Independent Diagnostic Console. And now the ODC with ScoutView imaging.

That's just what you'd expect from GE. The best images and best value... now and in the future.

General Electric Medical Systems,
Milwaukee, Toronto, Madrid.



GENERAL ELECTRIC



Research & development

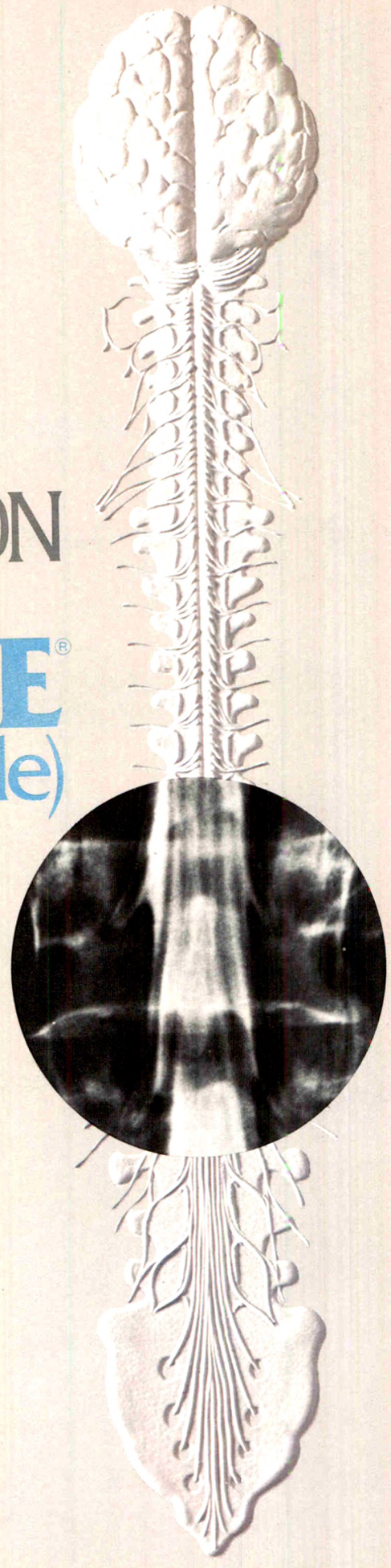
GUERBET

Better contrast media through research

Laboratoire GUERBET
16-24, rue Jean Chaptal - 93609 Aulnay-sous-Bois - Cedex FRANCE
Tél. : 929.78.37 - Télex : 212382 F.

DISCOVER MORE WITH CLEAR DEFINITION

new AMIPAQUE® (metrizamide)

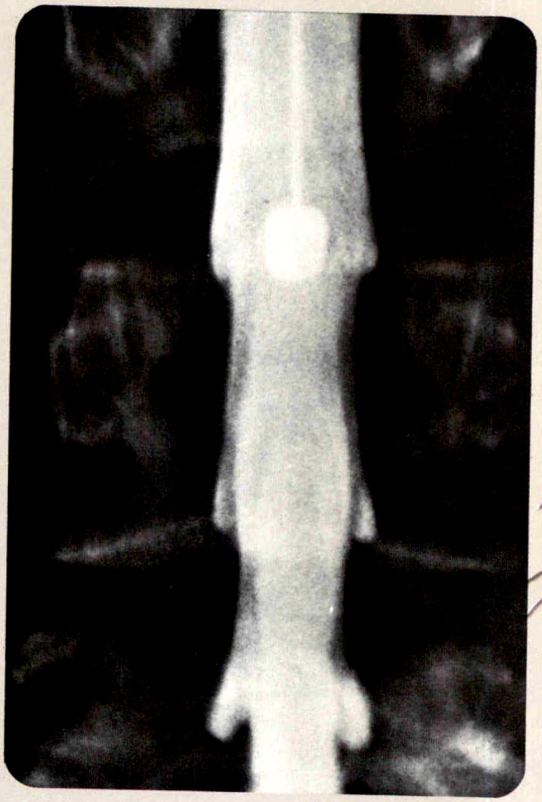


See last page for important product information including warnings, adverse reactions, and prescribing and precautionary recommendations.

COMPARE RADIOGRAPHS

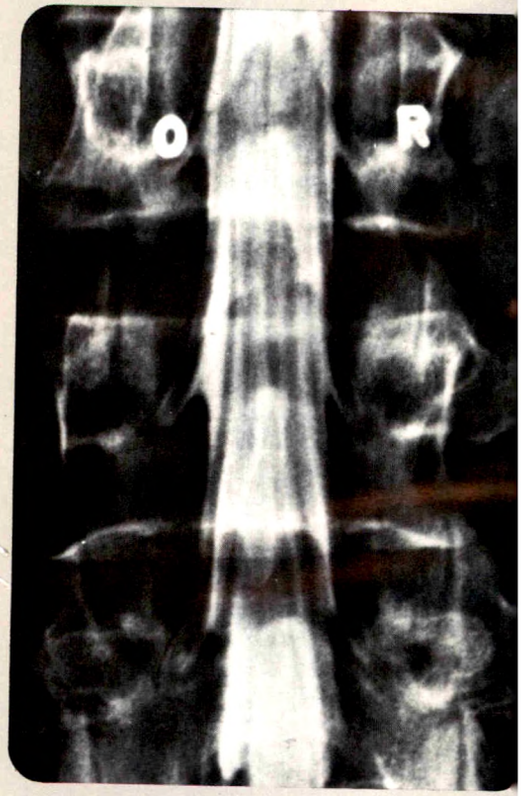
iophendylate

Lumbar myelogram of 27-year-old female (anteroposterior view): Note high-density shadows and failure of contrast medium to adequately fill nerve-root sheaths.



AMIPAQUE (metrizamide)

Lumbar myelogram of 20-year-old male (anteroposterior view): Note graded density of shadows and filling of nerve-r sheaths by the low-viscosity, water-solub contrast medium.



See last page for important product information including warnings, adverse reactions, and prescribing and precautionary recommendations.

CLEARER VISUALIZATION

Water-soluble, low viscosity

- ☐ Miscible with CSF for more uniform distribution around structures in subarachnoid space.[1,2]
- ☐ Flows into and through narrow subarachnoid spaces, fills slender cavities of nerve-root sheaths.[1,3]
- ☐ Usually diffuses around all except total obstructions with a single injection.
- ☐ Radiographic contrast provides nonobscured view of fine details.

Slightly hyperbaric

- ☐ Allows control of contrast distribution during initial phase of radiologic study, if desired.[1,3]

SIMPLIFIED MYELOGRAPHY

Nonionic...does not dissociate in solution

Isotonic with CSF at concentrations most frequently used (170 mgI/ml).

Low viscosity

- ☐ Allows use of narrow-bore needle (22-gauge).
- ☐ Less chance of CSF leakage...less chance of trauma to dura.

Resorbed and excreted mainly via kidneys in 48 hours

- ☐ No need for aspiration or second puncture...lessens potential for neurologic damage.
- ☐ No needle left in place during procedure...facilitates patient manipulation.

PATIENT TOLERANCE

- ☐ In general, the types of adverse reactions following subarachnoid injection of AMIPAQUE are not substantially different from those seen after lumbar puncture alone.
- ☐ The most frequently occurring reactions are headache, nausea, and vomiting.
- ☐ Rarely have reactions been severe or persistent beyond 24 hours.
- ☐ Although metrizamide is relatively safe and, in comparative studies, less toxic than other compounds for these indications, side effects ranging from headache and nausea to epileptic fits, convulsions, slow wave patterns on EEGs, petit mal states, paralysis, and arachnoiditis have occurred with the use of such compounds. Neurologic examinations were performed before and at intervals after the procedures in 1,495 of 1,850 cases. No clinically significant changes were found.

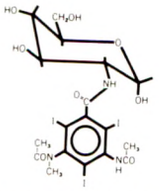
INDICATIONS: lumbar, thoracic, cervical, and total columnar myelography; and for use in computerized tomography of the intracranial subarachnoid spaces following spinal subarachnoid injection.

new **AMIPAQUE**® (metrizamide)

More fully investigated before introduction than any other subarachnoid contrast agent

☐ 158 published reports ☐ 5 years in clinical research ☐ 2 years in U.S. medical centers

Description: Metrizamide, 2-[3-Acetamido-2,4,6-triiodo-5-(N-methylacetamido) benzamido]-2-deoxy-D-glucopyranose, is a compound derived from metrizoic acid and glucosamine. It is a nonionic water-soluble contrast medium with a molecular weight of 789 (iodine content: 48.25%). The chemical structure is as follows:



AMIPAQUE (metrizamide) is provided as a sterile, white lyophilized powder. Each 3.75 g/20 ml vial contains 3.75 g metrizamide (1.81 g organically-bound iodine) and 1.2 mg edetate calcium disodium. Each 6.75 g/50 ml vial contains 6.75 g metrizamide (3.26 g organically-bound iodine) and 2.16 mg edetate calcium disodium.

Each 20 ml vial of sterile aqueous diluent contains 0.05 mg/ml sodium bicarbonate in water for injection. pH is adjusted with carbon dioxide, USP, if necessary.

When AMIPAQUE is reconstituted to the lowest recommended concentration (170 mgI/ml) it has a specific gravity of 1.184 at 37°C, is hyperbaric to cerebrospinal fluid, is isotonic with CSF, and has a pH of approximately 7.4.

Clinical Pharmacology: AMIPAQUE is absorbed from cerebrospinal fluid into the bloodstream. Approximately 60 percent of the administered dose is excreted unchanged through the kidneys within 48 hours.

The initial concentration and volume of the medium, in conjunction with appropriate patient manipulation, will determine the extent of the diagnostic contrast that can be achieved. This can be monitored by fluoroscopy.

Following spinal subarachnoid injection, conventional radiography will continue to provide diagnostic contrast for approximately an hour. At 4 to 5 hours contrast is hazy and none is detectable at 24 hours.

Following subarachnoid placement, irrespective of the position the patient has maintained, upward diffusion of AMIPAQUE takes place through the CSF.

After introduction into the lumbar subarachnoid space, computerized tomography (CT) shows CSF contrast enhancement in the thoracic region in about one hour, in the cervical region in about 2 hours, and in the basal cisterns in 3 to 4 hours.

When low doses of AMIPAQUE (see DOSAGE AND ADMINISTRATION) are introduced into the lumbar CSF and moved cephalad under gravity control and examined by CT scanning, they will provide immediate CSF contrast in the basal cisterns. Depending on the specific technique used, the lateral, third, and fourth ventricles may also be visualized. The contrast in this area will markedly diminish at 6 hours and disappear by 24 hours. CSF enhancement will be evident at the cortical sulci and interhemispheric fissures at 6 hours. Between 12 and 24 hours the surfaces of the cerebrum and cerebellum, in contact with the subarachnoid spaces, will develop a "blush" effect on the scan which will normally disappear in 36 to 48 hours. The rate, time, extent of diffusion, and the disappearance or stasis of AMIPAQUE as demonstrated with CT scanning, can be used to detect or infer the presence of CNS abnormalities.

Indications and Usage: AMIPAQUE is indicated for lumbar, thoracic, cervical, and total columnar myelography and for use in computerized tomography of the intracranial subarachnoid spaces following spinal subarachnoid injection.

Contraindications: AMIPAQUE should not be administered to patients with a known hypersensitivity to metrizamide.

Warnings: If grossly bloody CSF is encountered, the possible benefits of a myelographic procedure should be considered in terms of the risk to the patient.

Usage in pregnancy. No teratogenic effects attributable to AMIPAQUE have been observed in reproduction studies in animals. However, before administration of AMIPAQUE to women during pregnancy, the benefit to the patient should be carefully weighed against the possible risk to the fetus.

Until further experience is gained in children younger than 12 years, administration of AMIPAQUE in this age group is not recommended.

Fatal reactions have been associated with the administration of water-soluble contrast media. Although no fatal reactions have been associated with AMIPAQUE, it is of utmost importance that a course of action be carefully planned in advance for the immediate treatment of serious reactions, and that adequate and appropriate facilities and personnel be readily available in case of a severe reaction.

Precautions: Caution is advised in patients with a history of epilepsy, severe cardiovascular disease, chronic alcoholism, multiple sclerosis, or with a history of bronchial asthma or other allergic manifestations.

Before a contrast medium is injected, the patient should be questioned for a history of allergy. Although a history of allergy, including asthma, may imply a greater than usual risk, it does not arbitrarily contraindicate the use of the medium. Premedication with antihistamines to avoid or minimize possible allergic reactions may be considered. No conclusive relationship between severe reactions and antigen-antibody reactions or other manifestations of allergy has been established.

Patients who are receiving anticonvulsants should be maintained on this therapy. Should a seizure occur, intravenous diazepam or sodium phenobarbital is recommended.

Prophylactic anticonvulsant treatment with barbiturates or diazepam orally for 24 to 48 hours should be considered in patients with evidence of inadvertent intracranial entry of a large or concentrated bolus of the contrast medium since there is an increased risk of seizures in such cases.

Any drugs, such as neuroleptics, including phenothiazine derivatives, which lower the seizure threshold should be avoided. These drugs should not be used as premedications. If possible, they should be withdrawn at least 48 hours before the examination and not used for at least 12 hours postprocedure.

In patients with severe renal insufficiency or failure, the drug is excreted by the liver into the bile at a much slower rate. Patients with hepatorenal insufficiency should not be examined unless the possibility of benefit clearly outweighs the additional risk. Reexamination should be delayed for five to seven days.

Adverse Reactions: In general, the adverse reactions following subarachnoid injection of AMIPAQUE are not substantially different from those seen after lumbar puncture alone. The most frequently occurring adverse reactions are headache, nausea, and vomiting. These reactions occur 3 to 8 hours postinjection, almost all occurring within 24 hours. They are usually mild to moderate in degree lasting for a few hours and disappearing within 24 hours. Rarely have the headaches been severe or persisted beyond 24 hours.

Backache, neck stiffness, numbness and paresthesias, leg or sciatic-type pain occurred less frequently, often in the form of a transient exacerbation of preexisting symptomatology. Temperature elevations and dizziness have also been reported.

Rarely, muscle spasm or generalized convulsions have occurred 4 to 8 hours following injection and in some cases were attributed to a history of epilepsy, medication with neuroleptic drugs, or inadvertent overdose. In all cases, treatment with intravenous diazepam or sodium phenobarbital has provided rapid control.

Transient alterations in vital signs may occur, the significance of which is difficult to assess since these parameters may be affected by the procedure or the patient's physical or emotional state.

Other rarely occurring adverse reactions include the following:
Allergy or Idiosyncrasy: chills, pruritus, urticaria, nasal congestion, and dyspnea.
CNS: mild and transitory perceptual aberrations such as hallucinations, depersonalization, anxiety, depression, hyperesthesia, visual and speech disturbances, confusion and disorientation. In addition, malaise, weakness, EEG changes, and meningismus have occurred.
Cardiovascular: chest pain, tachycardia, bradycardia, and arrhythmia.
Other: diarrhea.

Dosage and Administration: The dosage and concentration of AMIPAQUE will depend on the degree and extent of contrast required in the area(s) under examination and on the equipment and technique employed. Concentrations which are approximately isotonic (170 to 190 mgI/ml) are recommended for examination in the lumbar region. For movement of the medium to distant target areas, higher concentrations are recommended to compensate for dilution of AMIPAQUE with CSF.

A total dose of 3000 mg of iodine should not be exceeded.

The recommended usual and maximum doses of AMIPAQUE are summarized in the following table:

DOSAGE TABLE

Procedure	Conc. of Solution (mgI/ml)	Usual Recommended Dose* (ml)	Max. Dose Total (mgI)
Lumbar myelogram	170-190	10-15	2850
Thoracic myelogram	220	12	2640
Cervical myelogram (via lumbar injection)	250-300	10	3000
Cervical myelogram (via lat. cervical inj.)	220	10	2200
Total columnar myelography	250-280	10	2800
CT cisternography (via lumbar inj.)	170-190	4-6	1140

*Refer to RECONSTITUTION TABLE for preparation of Solution.

PATIENT MANAGEMENT

PREPROCEDURE: Anesthesia is not necessary. Premedication sedatives or tranquilizers are usually not needed. The use of neuroleptic drugs, including phenothiazine derivatives, should be avoided and such medication should be discontinued, when possible, 48 hours before the procedure (see PRECAUTIONS). Epileptic patients should be maintained on their anticonvulsant medication.

INSTRUCTIONS FOR PREPARATION OF THE SOLUTION: Contents under vacuum. Use only if vacuum is present as evidenced by diluent being drawn into vial when stopper is punctured.

1. Fill a sterile syringe with the exact volume of diluent as indicated in the following RECONSTITUTION TABLE to obtain the desired iodine concentration. *Examples: a.* For vials containing 3.75 g AMIPAQUE: To obtain 170 mgI/ml, use 8.9 ml of diluent; to obtain 190 mgI/ml, use 7.8 ml of diluent. *b.* For vials containing 6.75 g AMIPAQUE: To obtain 170 mgI/ml, use 16.1 ml of diluent; to obtain 190 mgI/ml, use 14.0 ml of diluent.

RECONSTITUTION TABLE

Conc. of Solution (mgI/ml)	Volume of Diluent to be Added 3.75 g Vial (ml)	6.75 g Vial (ml)
170	8.9	16.1
180	8.3	15.0
190	7.8	14.0
220	6.5	11.7
250	5.5	10.0
260	5.2	9.4
270	5.0	9.0
280	4.7	8.5
290	4.5	8.1
300	4.3	7.8
	The volume of the final solution will equal the volume of the diluent + 1.7 ml	The volume of the final solution will equal the volume of the diluent + 3.1 ml

The volume of the final solution will exceed the amount required to achieve the recommended dosage. For precise volume for injection refer to DOSAGE TABLE.

2. Inject the diluent into the vial, and leave the syringe and needle in place.
3. Gently swirl the vial (without shaking) until its contents are dissolved (approximately 3 to 10 minutes). The solution should be clear and colorless to slightly yellow.

Use immediately after reconstitution (see DOSAGE AND ADMINISTRATION). Discard any unused portion.

As with any lumbar puncture, sterile technique must be employed. The lumbar puncture is usually made between L3 and L4, but if pathology is suspected at this level the interspace immediately above or below may be selected. A lateral cervical puncture may also be used.

POSTPROCEDURE: The lumbar puncture needle may be removed immediately following injection since it is not necessary to remove AMIPAQUE after injection into subarachnoid spaces.

Management of the patient is similar to that used following simple lumbar puncture. Maintaining the patient recumbent in bed with the head raised 15° to 30° for 8 hours may reduce the rate of upward dispersion of the medium. The patient may then remain horizontal for a further 16 hours at the discretion of the physician.

How Supplied: *Kits, each containing:* one-3.75 g/20 ml single-dose vial of AMIPAQUE with 1 vial of diluent (NDC 0024-0044-01); or one-6.75 g/50 ml single-dose vial of AMIPAQUE with 1 vial of diluent (NDC 0024-0046-01).
Combination packs, each containing: five-3.75 g/20 ml single-dose vials of AMIPAQUE with 5 vials of diluent (NDC 0024-0044-12); or five-6.75 g/50 ml single-dose vials of AMIPAQUE with 5 vials of diluent (NDC 0024-0046-12).

Protect vials of AMIPAQUE from light.

References: 1. Grainger RG, Kendall BE, Wylie IG: Lumbar myelography with metrizamide—a new non-ionic contrast medium. *Br J Radiol* 49:996-1003, 1976. **2.** Peeters FLM: Myelography with metrizamide. *Radiol Clin* 46:203-213, 1977. **3.** Hindmarsh T: Myelography with the non-ionic water-soluble contrast medium metrizamide. *Acta Radiol [Diagn] (Stockh)* 16:417-435, 1975.

new AMIPAQUE® (metrizamide)

from the originators of the broad line of contrast media

Winthrop

Winthrop Laboratories
New York, N.Y. 10016

Most computer tomograph scanners have excessive lag-time between machine scanning and image reconstruction.

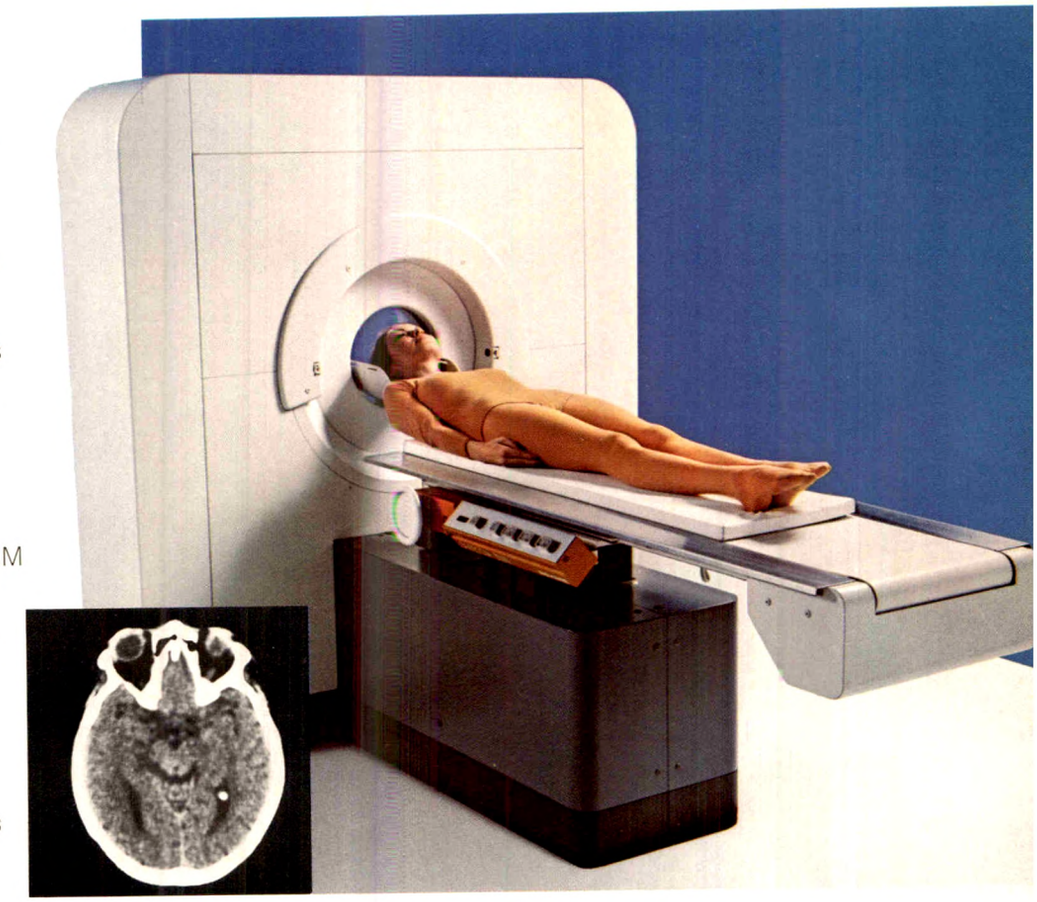
The Siemens Difference: Instantaneous image reconstruction

Immediate clinical evaluation

Delayed processing time is a thing of the past with Siemens computer tomographs, SIRETOM and SOMATOM. A specially designed high-speed computer reconstructs scanned images instantaneously. This permits immediate decisions as to diagnosis and course of treatment while providing for faster and smoother patient processing.

Reduced scan time

Scanning for both SIRETOM (head scanner) and SOMATOM (whole body scanner) is governed by the SCINTILLARC fan-beam solid-state detector array system. The result of this advanced engineering is evidenced by a dramatic reduction in setup and scan time along with unsurpassed quality tomograms achieved under clinical conditions.



Concepts... engineered to radiologic excellence

SIEMENS

Most high-energy linear accelerators continue to use thick target and thick scattering foil techniques to produce X-ray and electron beams.

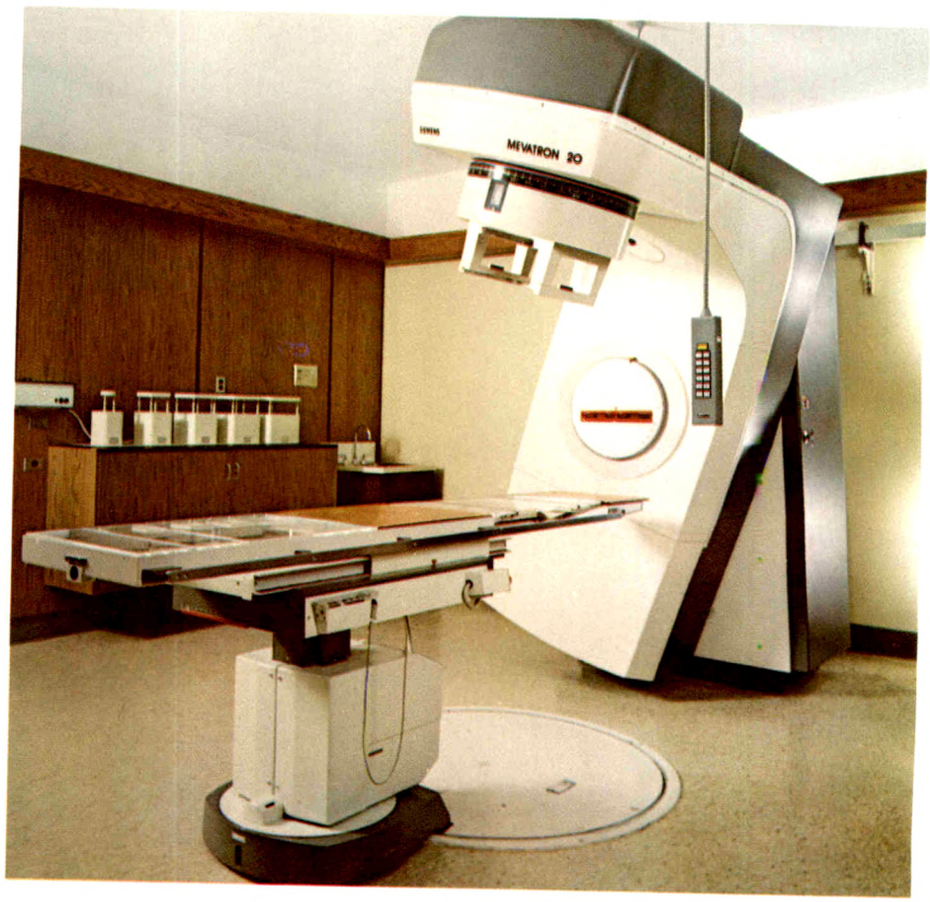
The Siemens Difference: Advanced X-ray target and electron scattering foil systems

The MEVATRON-20

Siemens' newest accelerator, the MEVATRON-20, utilizes a multiple element X-ray target and a unique double-foil electron scattering system to produce outstanding beam quality. Additionally, it features an integral verification capability for error-free machine setup. And with the highly flexible "Z" patient table, it forms a truly integrated installation ideally suited for modern radiation therapy technique.

The MEVATRON series

Siemens' product selection also includes the MEVATRON-6 and MEVATRON-12 which, together with MEVATRON-20, cover the full spectrum of energy and modality requirements.



Most remote-controlled examination units are products of alterations to standard radiographic and fluoroscopic units.

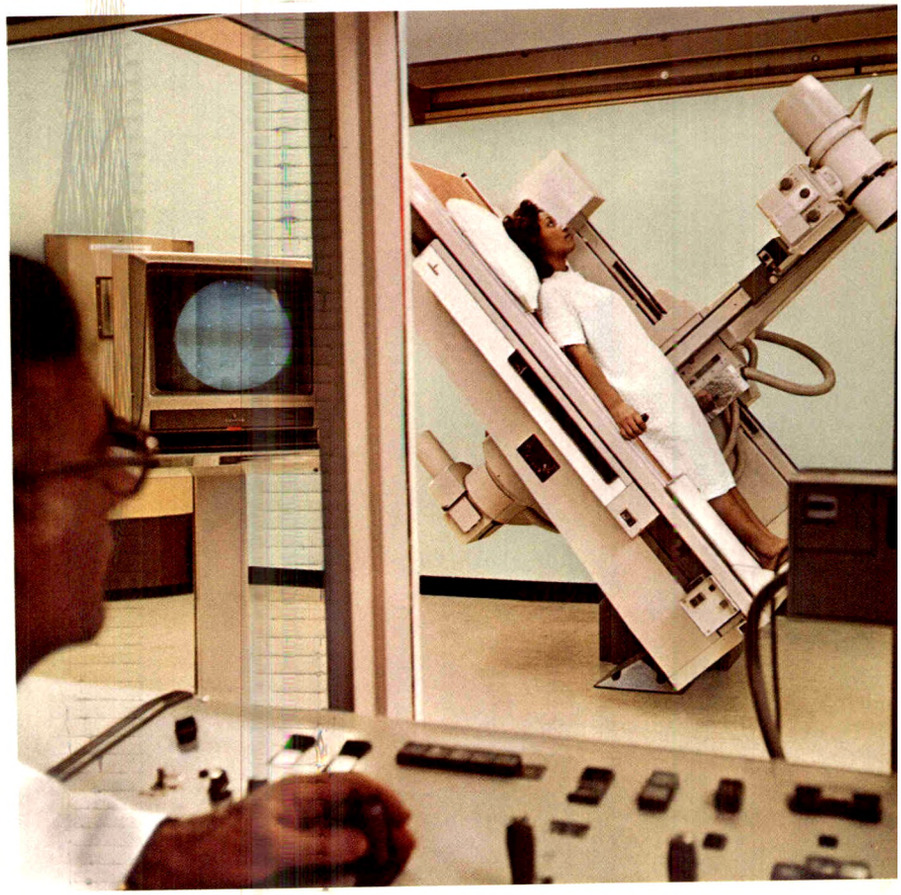
The Siemens Difference: Specific systems for specific needs

Versatile applications

Siemens responds to the varying needs of the radiologist with a full line of remote-controlled examination units – SIREGRAPH A, SIREGRAPH B, and SIREGRAPH II. Virtually every radiographic or fluoroscopic examination may be performed on a system from our wide selection of universal procedure or dedicated-purpose remote-controlled diagnostic products.

Individualized systems

Our systems were developed to meet the growing preference for remote examination tables and to meet the need for individual, custom-designed units that would satisfy different levels of requirements for versatility and application.



Concepts... engineered to radiologic excellence

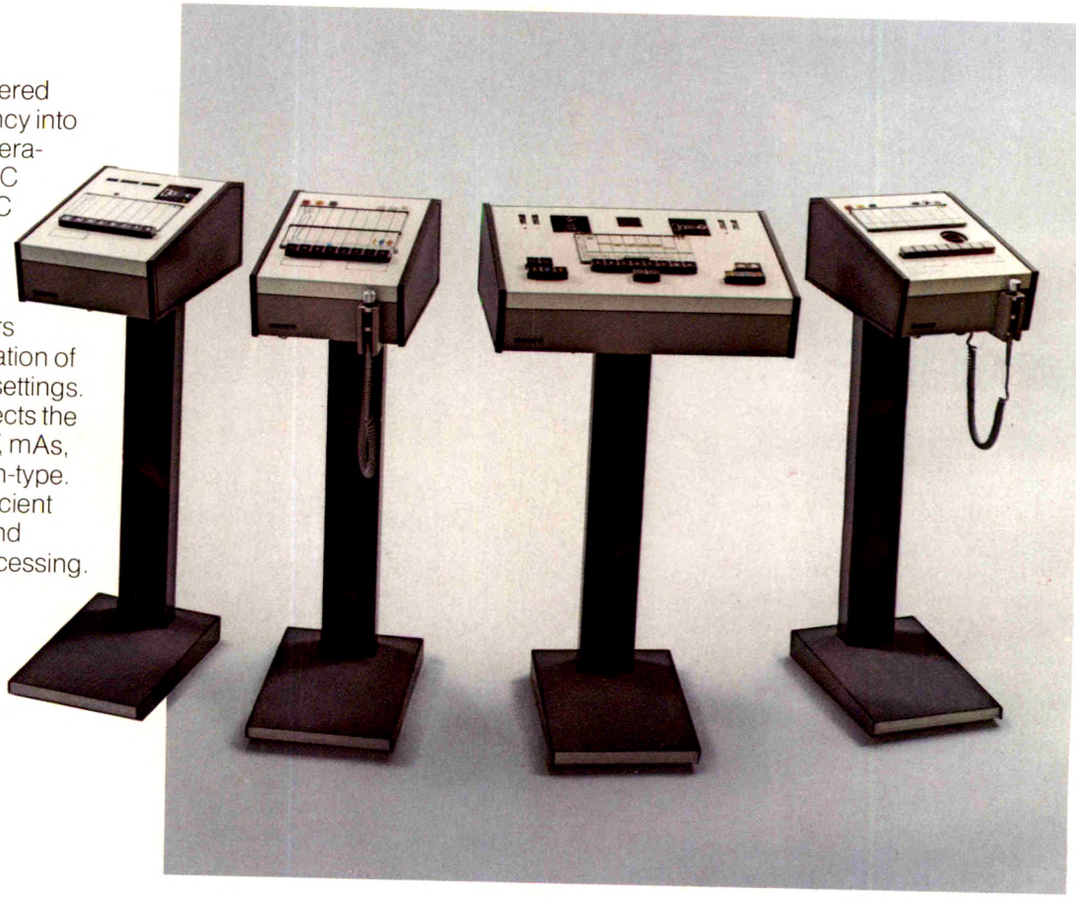
SIEMENS

Most of today's diagnostic X-ray generators still require lengthy programming of routines—individual selection of exposure time, focal spot, milliampere, and major and minor kilovoltage settings.

The Siemens Difference: Organ-related push-button programming

Simplicity of operation

Siemens has engineered operator time efficiency into diagnostic X-ray generators. Both OPTIMATIC and ORGANOMATIC generator series feature organ-related techniques which eliminate errors caused by miscalculation of exposure times and settings. One push button selects the examination units, kV, mAs, focal spot, and screen-type. The result is more efficient operational control and improved patient processing.



What the most demanding radiology departments in America can expect from the second largest film maker in the world.

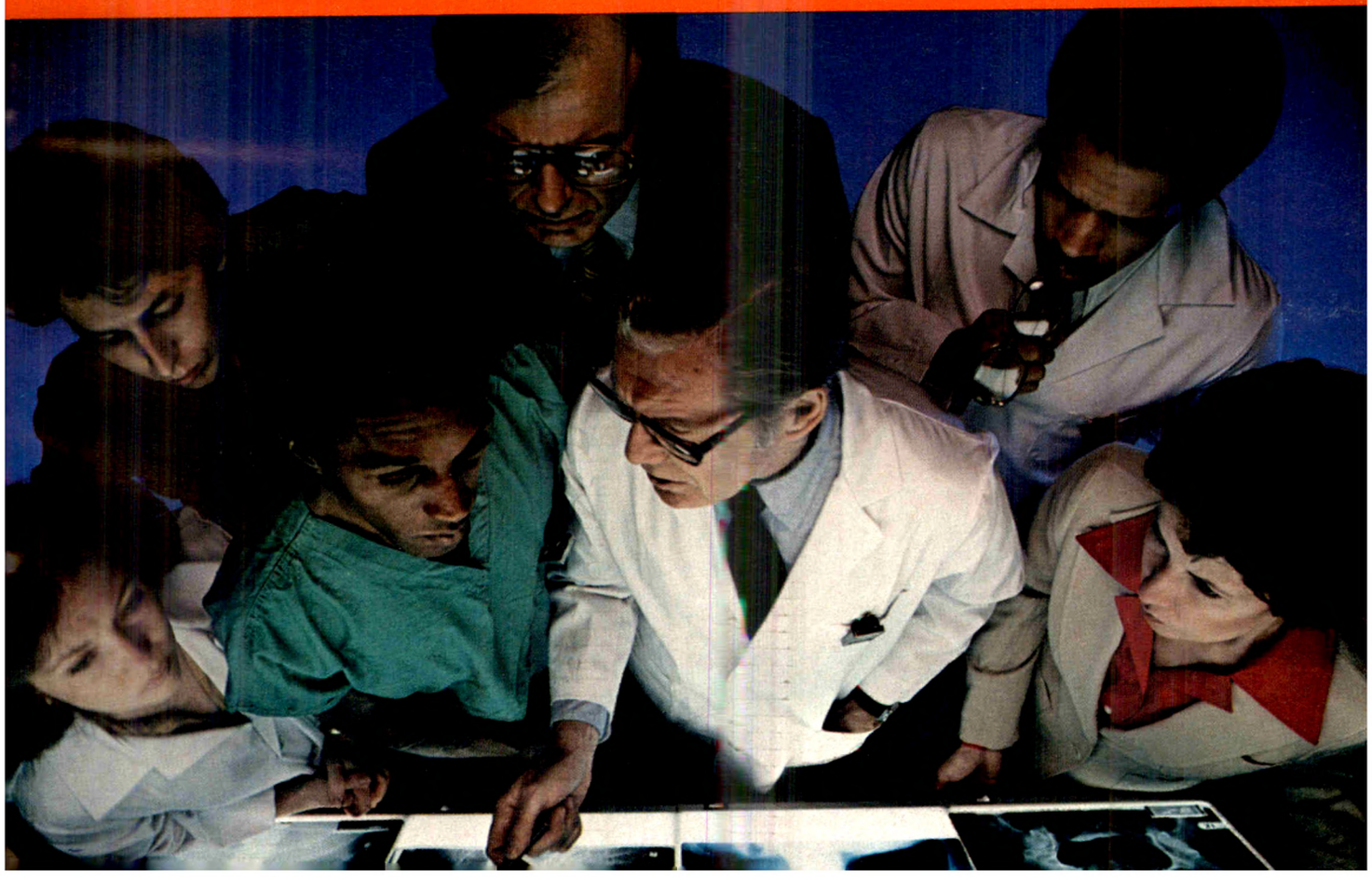
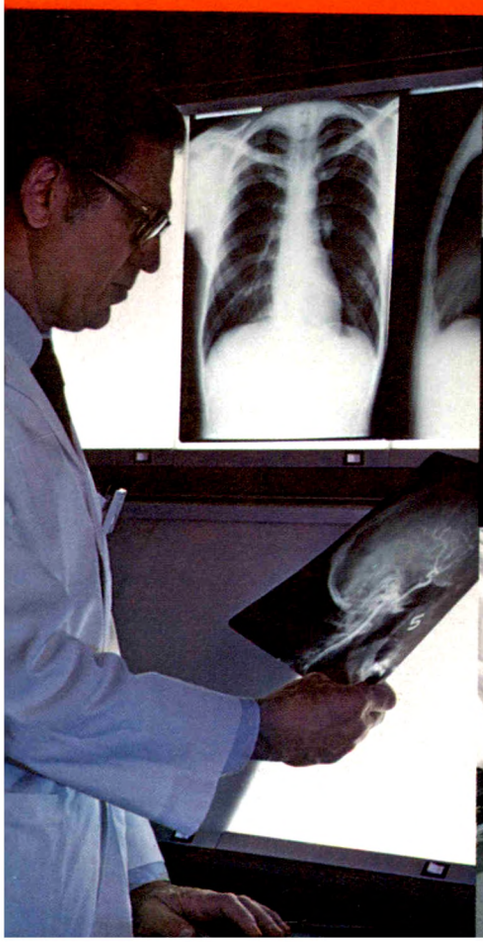


Image quality and service second to none.

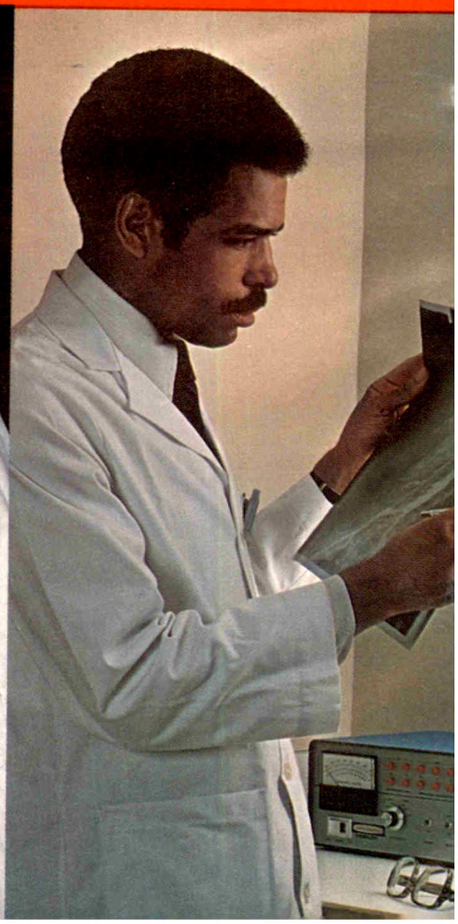
A complete line of superior, sensitometrically dependable X-ray films.
All have the finest definition and image quality to help make precise diagnoses. And all offer appropriate speed for the desired technique. Whether it's general purpose radiology, or special procedures, such as cine-fluorography, angiography, or mammography, Agfa-Gevaert Rex has the film to meet your diagnostic needs.

An extensive line of blue-emitting rare earth screens.
Agfa-Gevaert Rex has a full line of rare earth screens that provide for virtually all possible film/screen combinations. Our screens permit reduced patient exposure and increased tube life . . . without sacrificing image quality.

Quality assurance and technical support.
To complement our products and services, Agfa-Gevaert Rex offers innovative support systems designed to save time and labor. Systems like CHEMALERT, our Automatic Processor Monitor and CHEMATIC II Automatic Solution Mixer have demonstrated ability to reduce operating cost and improve overall efficiency.







AGFA-GEVAERT REX INC.

A subsidiary of Agfa-Gevaert Group, the second largest film maker in the world. White Plains, N.Y. Tel. 914 682-5650

Quality with economy
Because Agfa-Gevaert is a prime manufacturer and world-wide distributor of base films and emulsions, our film selling price is very competitive. You get the same high quality images to which you are accustomed . . . at a very economical price.

A commitment to education.
In addition to sponsoring hospital training programs, Agfa-Gevaert Rex is opening new Technical Training Centers throughout the country. These Radiological and Technological Education Seminars provide hands-on experience with the latest equipment and imaging technology. You'll have the opportunity to see and hear recognized experts. And many of these seminars will be designed to meet requirements for accredited Continuing Education Programs.

Complementary services
Agfa-Gevaert Rex is committed to the concept that customer service starts with quality film. Experts in X-ray technique, processing, chemistry, and sensitometry, our technical representatives provide the support you need to achieve and maintain maximum efficiency in your department. Once our system is initiated, these specialists will provide the required service on a continuing basis.



LIQUID POLIBAR™...

THE SECOND GENERATION FOR DOUBLE CONTRAST COLON.

And now dramatically improved to give even better results in the entire GI tract.



THE BARIUM

- Thicker, smoother enface coating
- Optimized viscosity
- New, creamier appearance
- Can be diluted
- Maintains opacity even in severely hydrated colons
- Better tasting—better than ever for routine upper GI's and esophageal studies.

Liquid Polibar is a micronized barium in a bubble free, non-precipitating suspension. A 100% w/v (55% w/w) suspension results in the optimum balance between density and viscosity. The nominal viscosity is 65 seconds as measured in a number 4 Ford cup. Liquid Polibar can now be used for routine B.E.'s and routine upper G.I.'s, where the convenience of a liquid is desired. Variable contrast and conventional esophageal studies are outstanding with the new Liquid Polibar.*

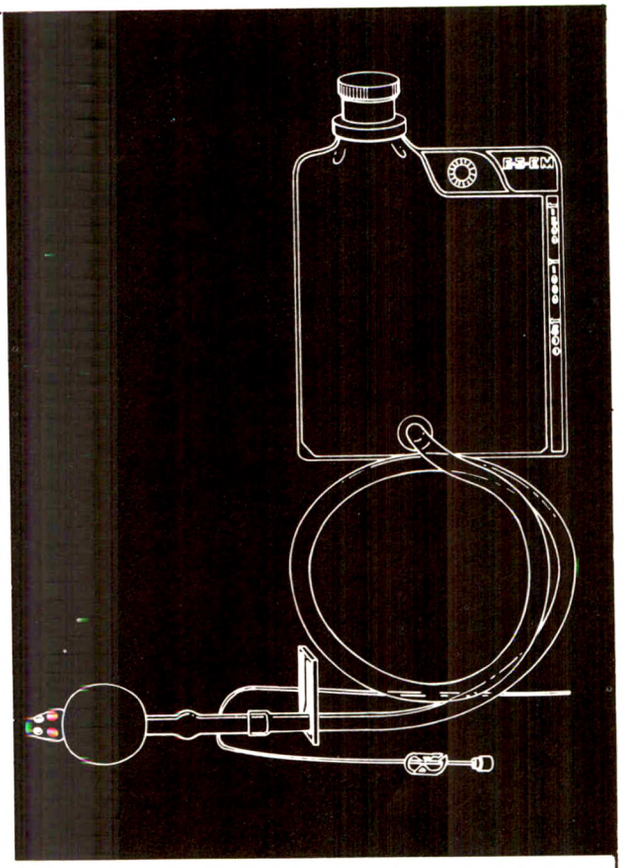
*Harvey Goldstein, M.D., Methodist Hospital, San Antonio, Texas.

THE SYSTEM

New Improved Super XL™ Air Contrast System.

It's the best system for double contrast procedures...and we've just improved it.

A new rectal tip with extra delivery holes, coupled to one half inch lumen tubing results in a faster flow of the Liquid Polibar. The new rigid spout bag is supplied with the Miller Air Retention Tip (with or without cuff). The system is designed to meet your every professional standard.





Multiple pseudo filiform polyps in the splenic flexure in longstanding ulcerative colitis. Film courtesy of Richard Palmer Gold M.D. Columbia Presb. Medical Center N.Y.

THE RESULTS

If you want your double contrast examinations to routinely look like the X-ray presented here, why not try the new Polibar system? Our trial order, catalog number 199, makes it easier than ever for you to try it. Just ask your dealer for E-Z-EM catalog number 199 and we will do the rest.

We know that all advertisers put out the best X-ray to show in their ads. But we firmly believe that your X-rays can routinely look like this one, and we back it with a money back guarantee. If you don't like the results, just let us and your dealer know that you are dissatisfied. Immediate and full credit will be given.

E-Z-EM®

7 Portland Avenue, Westbury, New York 11590 (516) 333-8230

International Affiliates: E-Z-EM Rooster B. V., Infirmeriestraat 6-8, Rotterdam 16, Netherlands
E-Z-EM De Mexico. S. A. de C. V., Calz. Azcapotzalco La Villa No. 882. Zona Industrial Vallejo. Mexico 16 D. F.

©12/78

PULMORAPID™



CGR's new fast vertical chest system for radiography

Pulmorapid is an advanced approach to chest radiography. The system consists of a film exposure cabinet and an integrated tubestand—both floor mounted. So your ambulatory patient always remains standing at the floor level during the examination.



Exposure cabinet and tubestand are electronically interlinked to provide automatic centering of x-ray tube to film. No mechanical linkage. Patient-to-film distance is only 20mm (.787") grid and phototimer pick up chamber included. And there's excellent film-to-screen contact via pneumatic pressure. Two systems are available depending on your choice of film formats—14 x 17" (35cm x 43cm) or 16 x 16" (40cm x 40cm). And both models have a 12 x 12" (30cm x 30cm) image size reduction instantly available for pediatrics.

Pulmorapid is offered with an integrated automatic film processor or with a removable film receiving magazine. With the film processor, you achieve exposed film to dry processed film in only 136 seconds.

The new systems are designed for fast, easy technologist operation. Convenient 100 sheet film packs load quickly in daylight. Film is advanced and keyed automatically by simply inserting the patient's IBM type ID card. A digital film counter, of course, with warning light when film supply reaches five sheets. And there's easy access to intensifying screens for routine cleaning.

Other features include a removable grid—110 line, 10:1 ratio, 72" focus and a U80 three field integrated phototiming pick up chamber.

Pulmorapid. A clean, fast, cost effective system for chest radiography.

Your CGR representative has all the details.





CGR MEDICAL CORPORATION
2519 Wilkens Avenue
Baltimore, Maryland 21223
(301) 233-2300

CGR CANADA LTÉE-LTD.
500 Boulevard de l'Aéroparc
Lachute, Québec, Canada
(514) 562-8806

CGR
13 Square Max Hymans
75741 Paris, France
273-8200

HARVARD MEDICAL SCHOOL,
DEPARTMENT OF CONTINUING EDUCATION
AND DEPARTMENT OF RADIOLOGY,
MASSACHUSETTS GENERAL HOSPITAL

ANNOUNCE

ANGIOGRAPHY:

CURRENT METHODS AND BASIC PROBLEMS

A practical course on therapeutic applications of Angiography, including "hands on" workshops on transluminal angioplasty and transcatheter embolizations.

APRIL 19–21, 1979

AT THE PARKER HOUSE, BOSTON

Under the direction of

C.A. Athanasoulis, M.D. and
A.C. Waltman, M.D.

For information contact: Department of Continuing Education, Harvard Medical School, 25 Shattuck St., Boston, MA 02115

Mental retardation can happen to anyone.

It can happen to you!

But you can prevent mental retardation.

To find out how, write:
National Association for Retarded Citizens,
Civitan Inquiry Program,
P. O. Box 6109, Arlington, Texas 76011.

AJR Index to Advertisers

(In Order of Appearance)

Agfa-Gevaert Rex, Inc.
Atomic Energy of Canada
CGR Medical Corporation
Dunn Instruments, Inc.
Eastman Kodak Company
Elema-Schonander, Inc.
E-Z-EM Company
General Electric Company
Guerbet Laboratories
Harvard Medical School
Machlett Laboratories
Medi-Tech Division
Nuclear Associates
Ortho Pharmaceutical
Precise Optics/Photo Medic Equipment, Inc.
Pfizer, Inc.
Philips Medical Systems, Inc.
Picker Corporation
Purdue Frederick Company
Pyne X-Ray Corporation
Radiologic Sciences, Inc.
Siemens Corporation
Smith Kline & French Laboratories
E.R. Squibb & Sons ,Inc.
Winthrop Laboratories



Protect your patient's eyes from over-exposure and potential cataractogenic doses during special x-ray procedures

RADILENS® Eye Lens Shield

• *Lead-glass shield reduces eye lens dose approximately 90%**

Inadequate protection of a patient's eye lens during diagnostic x-ray exams in the cranial region can lead to cataracts or other eye damage. Therefore, the eyes should be covered with a Radilens Shield. Its cup-shaped, lead-glass lenses have x-ray absorption characteristics equivalent to 1 mm lead. Each lens is contoured to fit the outer eye orbits snugly and protect the eyes, even in the lateral projection. The lenses are held by a cord which stretches to fit any patient. Since the shields are transparent, the subject's pupils can be observed when necessary.

When the Radilens is used in carotid angiography in projections that do not obscure the vascular regions to be evaluated, such as in lateral and A.P. I projections, the dose rate to the eye lens is reduced to about 10%. The Radilens is also used widely to reduce radiation exposure during tomographic exams of the temporal bone.*

56-500CR Radilens Eye Lens Shield **$125.00**

VICTOREEN

NUCLEAR ASSOCIATES
Division of VICTOREEN, INC.
100 Voice Road • Carle Place, N.Y. 11514 • (516) 741-6360

**Copies of references and dosimetry data are available on request. Ask for Bulletin 144-C.*

X-RAY IMAGE INTENSIFYING SYSTEMS

precise optics

IT MAY SURPRISE YOU.....

. . . to know that the people at Precise Optics have been supplying X-Ray Image Intensifying Systems since 1954. Precise specializes in Imaging, and offers a complete line of systems to meet requirements ranging from the private office to the special procedures room, at a cost savings over comparable units, without sacrificing quality.

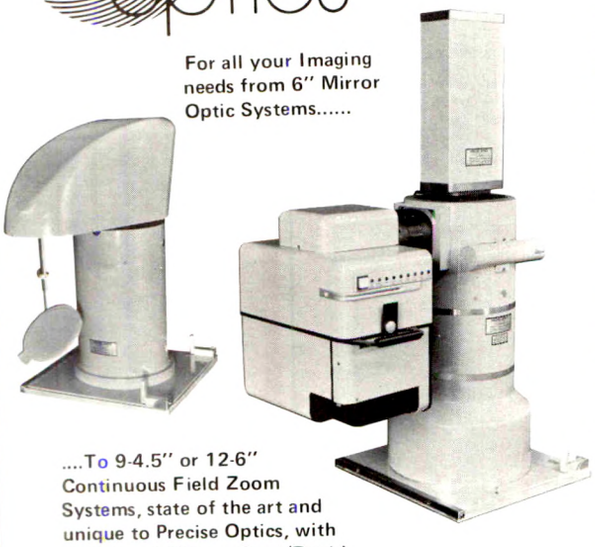
EVERY SYSTEM CONTAINS a guaranteed optimal performance cesium iodide image tube and field-proven solid-state power supply, covered by a two-year warranty.

THE PRECISE CCTV SYSTEM uses x-ray rated separate mesh vidicons, selected for high resolution and low-lag characteristics. Brightness compensation is an excellent 10,000:1, assuring the correct light level despite large variations in body densities.

THE NEW 105mm SPOT/RAPID SEQUENCE CAMERA (roll film, 6 frames per second maximum) utilizes the same digital electronics package and many of the mechanical sections of our other reliable 105mm cameras, while incorporating a rapid-load film transport and daylight receiving cassettes.

ACCESSORIES AVAILABLE INCLUDE: TWO-AND THREE-PORT LIGHT DISTRIBUTORS for spot and cine filming capabilities, ABS SYSTEM with automatically variable kV and selectable mA, SPOT FILM ADAPTERS compatible with any spot film device, CEILING SUSPENSION UNITS with smooth vertical and horizontal movements, CCTV MONITOR CARTS that are lightweight and easily mobile.

For all your Imaging needs from 6" Mirror Optic Systems.....



....To 9-4.5" or 12-6" Continuous Field Zoom Systems, state of the art and unique to Precise Optics, with CCTV and 105mm Spot/Rapid Sequence Cameras.

PRECISE OPTICS/PHOTO MEDIC EQUIPMENT, INC.
239 SO. FEHR WAY
BAYSHORE, N.Y. 11706
TEL. (516) 242-6600
TWX 510-227-9837

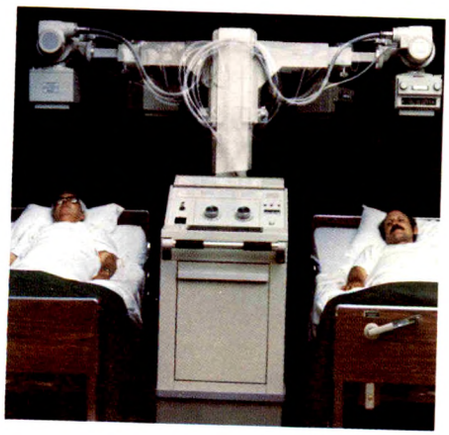
Tech-Mobile: new concepts



Designing a mobile, battery-operated X-ray unit that would be significantly better than any other unit presently available was our goal. We succeeded with Tech-Mobile.

From its simplified controls to its recessed wheels, the sturdy Tech-Mobile was created to give easy maneuverability, reliable operation and consistent high-quality radiographs.

Pushing, pulling and tugging are a thing of the past. Variable-speed, hand-grip controls let you maneuver easily on tile, carpeting or almost anywhere. Simply drive the cordless Tech-Mobile to the patient's bedside. And if Tech-Mobile's safety bumper contacts a door, wall or any other stationary object when traveling forward, it stops immediately and gently reverses to disengage the object. You'll never be stuck in a corner.





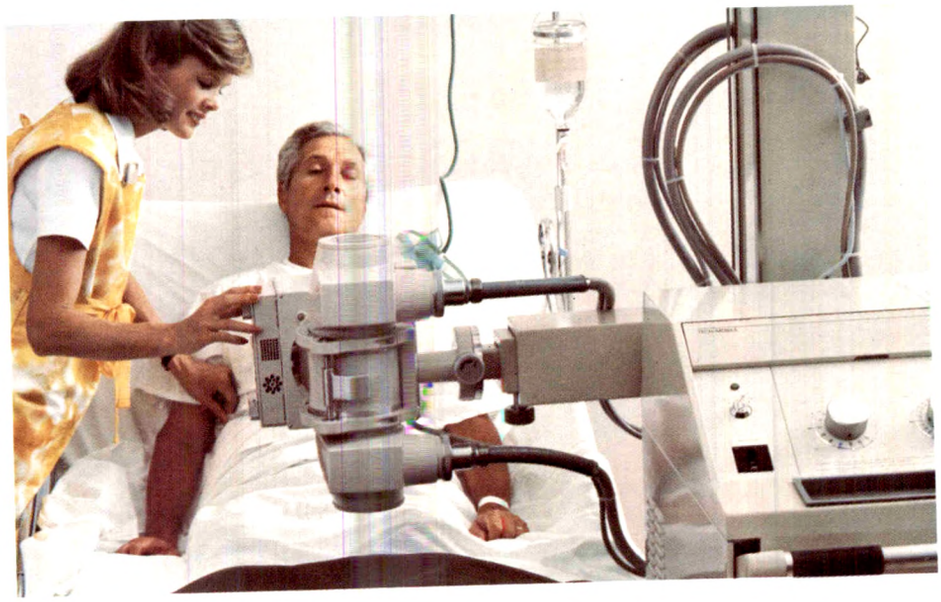
And because Tech-Mobile is only 23 inches (590 mm) wide, it fits easily between beds, doorways and crowded corridors.

Powered completely by a strong nickel-cadmium battery pack, the Tech-Mobile has a 12,000 mAs exposure capacity on hand for a full day's caseload. Then, a standard electrical outlet is all that's needed to recharge the unit to full capacity in a matter of hours.

Minimal effort is required to position the unit. Setting exposure parameters and making the exposure are simplified. And the battery-

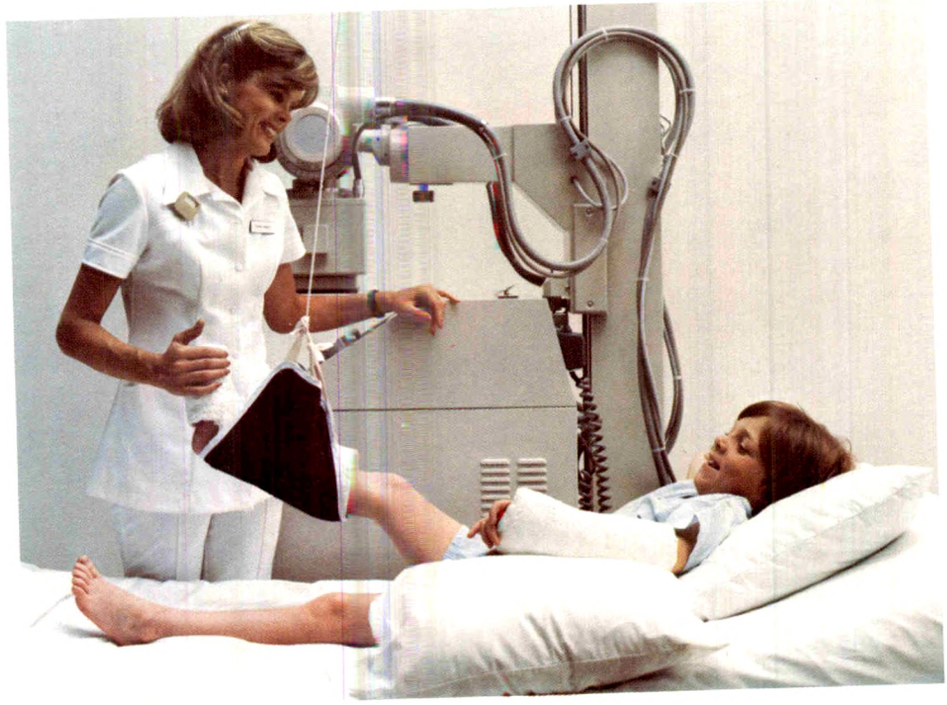
n coruless radiography.





erated Tech-Mobile has no cord
grounding wire, simplifying its
e in CCU and ICU. This means
ending less time in preparing each
ocedure.

We even included some convenient
tras: an accessory tray to store
n markers, a requisition clip, remote
llimator field light switch, a large
ld-out exposure guide and a
nvenient apron hook.





Tech-Mobile is backed by our worldwide service organization. And it can be leased, if you wish, with assistance from our parent, CIT Financial Corporation. For more information about the newest concepts in mobile radiography, contact your local Picker representative, or write Picker Corporation or Picker International, 595 Miner Road, Cleveland, OH 44143.

PICKER®
ONE OF THE CIT COMPANIES

new Section 4: Golden's Diagnostic Radiology Series RADIOLOGY OF THE HEART AND GREAT VESSELS, 3rd edition

By **Robert N. Cooley, MD,** Professor of Radiology; and **Melvyn H. Schreiber, MD,** Professor and Chairman, Department of Radiology; both of University of Texas Medical Branch, Galveston.

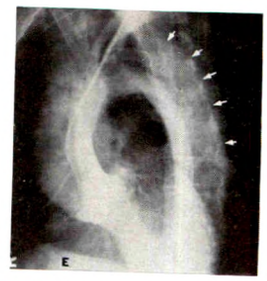


Fig. 517. Type I dissecting aneurysm (hematoma) with origin in the ascending aorta. (E) Injection into lumen. A large hematoma is seen in aortic wall (arrowhead) and the lumen of the aorta is narrowed.

Completely rewritten and updated, RADIOLOGY OF THE HEART AND GREAT VESSELS will soon be the cornerstone of the radiologist's working library as well as the one book heart and chest specialists will turn to for method, technique, and interpretation in the roentgenologic study of the heart and great vessels.

- the authors cover every facet of both acquired and congenital heart disease from clinical, anatomical, and radiologic points of view.
- the style is succinct and to the point.
- the 734 illustrations, nearly all radiographs, have been chosen as much for their interpretive value as for their outstanding precision and clarity.
- the illustrations are carefully labeled with clear, helpful legends.
- the excellent bibliography allows quick and easy reference and has been updated to include the latest work in the specialty.
- the rigid standards of the world-renowned reputation of the Golden's Diagnostic Radiology Series have been met with both radiologic expertise and excellence.

This new third edition, with its complete revision reflects the very latest developments in cardiac radiology, including the newest techniques of cardiography and nuclear imaging. RADIOLOGY OF THE HEART AND GREAT VESSELS is virtually the definition of the field.

CONTENTS

PROCEDURES: Fluoroscopy. Chest Films. Body Section Radiography. Cardiac Catheterization. ANGIOCARDIOGRAPHY: History. Patient Preparation. Venous Angiocardiography. Selective Angiocardiography. Thoracic Aortography. CONTRAST SUBSTANCES: Toxicity. Factors Governing Injection. Injectors. Dosage. Reactions. EQUIPMENT: Conefluorographic. Film Changers. EMBRYOLOGY OF HEART AND GREAT VESSELS: Interior of Heart. Blood Vessels. ROENTGENOLOGIC APPEARANCE: Contours and Topography of Normal Heart. Pulsations of Normal Heart & Great Vessels. Relation of Esophagus to Cardiovascular Contours. Normal Angiocardiogram. Cardiac Catheterization. Normal Ventriculogram. MEASUREMENT OF HEART AND GREAT VESSELS. GENERAL SYMMETRICAL AND ASYMMETRICAL CARDIAC ENLARGEMENT—CHANGE IN SIZE OF SPECIFIC CHAMBERS—ABNORMAL PULSATIONS. DISEASES OF PULMONARY VASCULAR SYSTEM: Anatomy & Physiology. Obstructions. Dilatation. Alterations in Vascular Permeability. Intralobar Sequestration. RHEUMATIC HEART DISEASE: Acute Rheumatic Carditis and Valvulitis. Chronic Rheumatic Heart Disease. Mitral Valvular Disease. Aortic Stenosis and Calcific Aortic Stenosis. Combined or Multiple Valvular Disease. Radiologic Changes after Surgery. CONGENITAL ANOMALIES: Classification. Obstructions. Abnormal or Persistent Openings Between Right & Left Sides of Circulation. Congenital Malpositions of Heart or Cardiac Chambers. Anomalies of Great Vessels without Significant Circulation Changes. HYPERTENSIVE HEART DISEASE: Cardiac Compensation. Isolated Left Ventricular Failure, Combined Left and Right Heart Failure. Drug Effects. Hypertension with Nephritis. Bernheim's Syndrome. ATHEROSCLEROTIC CHANGES: CORONARY ARTERIOSCLEROSIS: MYOCARDIAL INFARCTION: Valves. Cardiac Aneurysm. Heart Rupture. CORONARY ARTERIOGRAPHY. CARDIOMYOPATHIES. SYPHILITIC HEART DISEASE. MUCOID OR MYXOMATOUS CHANGES IN CARDIAC VALVES. TUMORS OF THE HEART. THE HEART IN SYSTEMIC DISEASE: Endocrine Disorders. Anemia. Nutritional Deficiency States. Rhythm Abnormalities. IMPLANTABLE CARDIAC PACEMAKERS. CALCIFICATION WITHIN HEART AND PERICARDIUM. TRAUMA TO HEART AND GREAT VESSELS. HEART DISPLACEMENT. DISEASES OF THE PERICARDIUM. DISEASES OF THORACIC AORTA AND ITS BRANCHES. VALVE REPLACEMENTS. Index.

December, 1978/676 pages/734 illustrations/$65.00

Yes, please send me _____ copy(ies) of RADIOLOGY OF THE HEART AND GREAT VESSELS, 3rd edition, (#2103-6) at $65.00 each, on 20-day approval.

name

address

city state zip code

All orders sent on 20-day approval. Maryland residents please add 5% sales tax. Prices subject to change without notice.
TOLL-FREE TELEPHONE ORDERING
(9am to 4pm), call: 1-800-638-0672; Maryland residents call collect: 528-4221.

☐ Check enclosed ☐ VISA ☐ MasterCharge ☐ Bill me

card# expiration date

Williams & Wilkins P.O. Box 1496 Baltimore, Md. 21203

CHANGEX

Handle more chest studies without handling film.



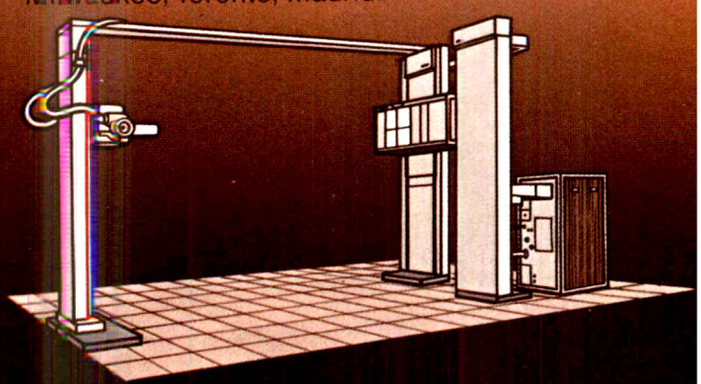
If your department's chest film volume is heavy, Changex system can lighten your load. This compact system—including chest changer, tube support, film transport and Kodak automatic processor—lets the technologist take up to 100 14 x 17 exposures without touching the film or handling individual cassettes.

Inexperienced operators handle Changex with ease. After inserting a loading magazine, the tech just pushes a button to adjust the changer to the patient's height. The x-ray tube moves automatically, maintaining alignment. Inserting the patient's I.D. card advances the film and provides positive patient identification.

Exposed film is transported automatically to the processor, eliminating trips to the darkroom. The technologist is free to concentrate on radiography and to handle more patients.

Film quality is excellent. And the Kodak X-Omat M6A-N processor delivers reliable performance with minimum maintenance. So let Changex increase throughput and reduce film handling. Talk to your GE representative.

General Electric Medical Systems, Milwaukee, Toronto, Madrid.



GE: leading the way in diagnostic imaging.

GENERAL ELECTRIC

American Journal of Roentgenology

Vol. 132 February 1979 No. 2

DIAGNOSTIC IMAGING

171 **Complement and Coagulation: Causative Considerations in Contrast Catastrophies.** *Lasser EC, Slivka J, Lang JH, Kolb WP, Lyon SG, Hamblin AE, Nazareno G*

177 **Percutaneous Transhepatic Portography. I. Technique and Application.** *Burcharth F*

183 **Percutaneous Transhepatic Portography. II. Comparison with Splenoportography in Portal Hypertension.** *Burcharth F, Nielbo N, Andersen B*

187 **Infusion Hepatotomography for Evaluation of Obstructive Jaundice.** *Cynn WS, Levin BL, Gureghian PA, Chait A*

191 **Significance of the Nonopacified Gallbladder in Endoscopic Retrograde Cholangiography.** *Rohrmann CA Jr, Ansel HJ, Protell RL, Silverstein FE, Silvis SE, Vennes JA*

197 **Predictability of Rectal Incontinence on Barium Enema Examination.** *Stewart ET, Dodds WJ*

201 **Ultrasonographic Evaluation of Pericholecystic Abscesses.** *Bergman AB, Neiman HL, Kraut B*

205 **Ultrasonic Appearance of the Falciform Ligament.** *Hillman BJ, D'Orsi CJ, Smith EH, Bartrum RJ*

207 **Calibrated Leak Balloon Microcatheter: A Device for Arterial Exploration and Occlusive Therapy.** *Kerber CW, Bank WO, Cromwell LD*

213 **CT Detection of Demyelinated Plaques in Multiple Sclerosis.** *Haughton VM, Ho KC, Williams AL, Eldevik OP*

217 **Computed Tomography of Intracerebral Leukemic Masses.** *Wendling LR, Cromwell LD, Latchaw RE*

221 **Unsuspected Aortic Dissection: The Chronic "Healed" Dissection.** *Ambos MA, Rothberg M, Lefleur RS, Weiner S, McCauley DI*

227 **Observer Variation in the Interpretation of Lower Limb Venograms.** *McLachlan MSF, Thomson JG, Taylor DW, Kelly ME, Sackett DL*

231 **Computed Tomography in the Diagnosis of Adrenal Disease.** *Korobkin M, White EA, Kressel HY, Moss AA, Montagne JP*

239 **Scapular Defects: A Normal Variation.** *Cigtay OS, Mascatello VJ*

243 **Ultrasonic Demonstration of Myometrial Contractions In Intrauterine Pregnancy.** *Wilson RL, Worthen NJ*

NUCLEAR MEDICINE

249 **Simple, Rapid Thyroid Function Testing with ^{99m}Tc-Pertechnetate Thyroid Uptake Ratio and Neck/Thigh Ratio.** *Schneider PB*

RADIATION ONCOLOGY

255 **Carcinoma of the Supraglottic Larynx.** *Marks JE, Freeman RB, Lee F, Ogura JH*

261 **Dose Considerations in Total Skin Electron Irradiation for Mycosis Fungoides.** *Lo TCM, Salzman FA, Wright KA*

265 **Diagnostic Oncology Case Studies: Treated Stage IIB Hodgkin's Disease Complicated by Late Paraplegia.** *Contributed by Abdel-Dayem HM, Oh YS, Sil R*

CASE REPORTS

267 **Esophageal Obturator Airway: Radiographic Appearance.** *Pais MJ, Segal HB*

269 **Hairy Esophagus: A Complication of Pharyngoesophageal Reconstructive Surgery in Two Cases.** *McLean GK, Laufer I*

271 **Spontaneous Aortic Rupture Associated with Chronic Steroid Therapy for Rheumatoid Arthritis in Two Cases.** *Smith DC, Hirst AE*

274 **Occlusion of the Right Pulmonary Artery by Acute Dissecting Aortic Aneurysm.** *Charnsangavej C*

277 **Radiographic Features of the Linear Nevus Sebaceous Syndrome.** *Leonidas JC, Wolpert SM, Feingold M, McCauley RGK*

280 **Fatal Intrathoracic Hemorrhage After Percutaneous Aspiration Lung Biopsy.** *Milner LB, Ryan K, Gullo J*

282 **Percutaneous Drainage of Lung Abscess.** *Aronberg DJ, Sagel SS, Jost RG, Lee JI*

284 **Severe Radiation Pneumonitis Precipitated by Withdrawal of Corticosteroids: A Diagnostic and Therapeutic Dilemma.** *Parris TM, Knight JG, Hess CE, Constable WC*

287 **Emphysematous Pyelonephritis Demonstrated by Computed Tomography.** *Kim DS, Woesner ME, Howard TF, Olson LK*

289 **A Benign Cause of Increased Radiocolloid Accumulation on a Liver Scan.** *Greditzer HG III, Ho JE, Wolverson M, Joyce P*

291 **Protrusio Acetabuli Following Pelvic Irradiation.** *Hall FM, Mauch PM, Levene MB, Goldstein MA*

294 **Popliteal Pseudoaneurysm as a Complication of an Adjacent Osteochondroma: Angiographic Diagnosis.** *Greenway G, Resnick D, Bookstein JJ*

297 **Radiographic Appearance of Laparoscopic Tubal Ring.** *McJunkin ML, Curtis JA*

TECHNICAL NOTES

299 **Gelfoam Embolization: A Simplified Technique.** *Bank WO, Kerber CW*

302 **Identifying Dorsal Pedal Lymph Vessels without Blue Dye.** *Yune HY, Klatte EC, Batnitzky S*

305 **Society for Pediatric Radiology Abstracts: 1978 Meeting.**

309 **Editorial: The Complex World of Adverse Reactions.** *VanArsdel PP Jr*

311 **ARRS Meeting Information**

319 **Memorials**

321 **Letters**

323 **Abstracts of Current Literature**

332 **Book Reviews**

335 **News**

186 **Guidelines for Authors**

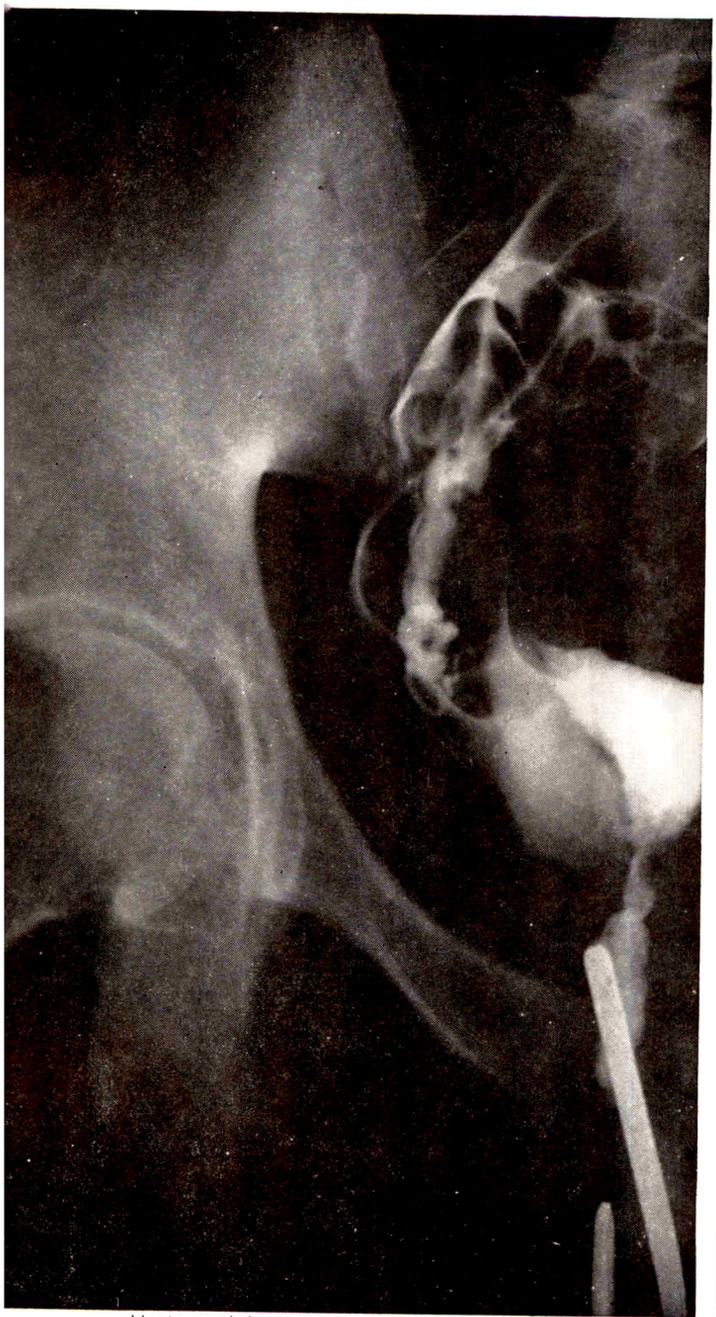
Acc.
8.879

AJR

American
Journal of
Roentgenology

UNIVERSITY

March 1979



Hysterosalpingogram with Salpix Contrast Medium.



24-hour postinjection x-ray of same patient.

now you see it

now you don't

With Salpix as your contrast medium, your gynecologic patient needn't undergo the 24-hour postinjection x-ray usually required with iodized oils. Water-soluble Salpix leaves virtually no irritating radiopaque residue to produce foreign-body reactions, yet it provides the viscosity needed for adequate visualization.

Contraindications: Contraindications to hysterosalpingography include the presence of severe vaginal or cervical infections, existing or recent pelvic infection, marked cervical erosion or endocervicitis, and pregnancy. The procedure is contraindicated during the immediate pre- or post-menstrual phase.

Sensitivity Test: If indicated in the patient's history, an intracutaneous skin test or sublingual absorption observation may be done with 0.1 cc Salpix.

Warning: Not for intravenous use.

© ORTHO PHARMACEUTICAL CORPORATION 1970

CONTRAST MEDIUM

Salpix

TRADEMARK

EACH CC CONTAINS:
sodium acetrizoate 0.53 g and
polyvinylpyrrolidone 0.23 g

Ortho

ORTHO PHARMACEUTICAL CORPORATION • RARITAN, NEW JERSEY 08869

Official Journal
American Roentgen Ray Society
American Radium Society

AJR

American Journal of Roentgenology

Diagnostic Imaging • Radiation Oncology
Related Sciences

Editor Melvin M. Figley

Associate Editor Rosalind H. Troupin

Assistant Editor John D. Harley

Contributing Editor E. Frederick Lang

Consulting Editorial Board Luther W. Brady • Kent Ellis
E. Robert Heitzman • Donald L. King • N. Thorne Griscom
Eugene C. Klatte • Kenneth Krabbenhoft • John G. McAfee
Russell H. Morgan • Thomas H. Newton • Robert G. Parker
Stewart R. Reuter • William B. Seaman • Robert J. Shalek
John Storer • Michel M. Ter-Pogossian • Joseph P. Whalen
David M. Witten

Editorial Staff K. A. Murray, manager • M. J. Leonard, manuscript editor • J. Anderson, assistant manuscript editor • A. C. Van Dyck, secretary

Published monthly by The Williams & Wilkins Co., 428 East Preston St., Baltimore, Maryland 21202. All correspondence, except editorial office business, should be addressed to the publisher. Annual subscription rates: $40 ($20 for residents with letter of verification) plus appropriate mailing surcharge (see note next page). Single copies, $5. Undelivered or damaged copies replaced within 60 days of publication; 90 days for foreign subscribers. Allow 90 days for address changes. © 1979 by American Roentgen Ray Society. Second-class postage paid at Baltimore, Maryland, and at additional mailing offices. Printed in U.S.A. ISSN 0361-803X



American Roentgen Ray Society

President: Harry Z. Mellins
President Elect: Paul A. Riemenschneider
1st Vice-president: Joseph D. Calhoun
2nd Vice-president: Charles E. Bickham, Jr.
Secretary: James F. Martin
Treasurer: Harley C. Carlson

COMMITTEES 1977–1978

Executive Council: H. Z. Mellins, P. A. Riemenschneider, J. D. Calhoun, C. E. Bickham, Jr., J. F. Martin, H. C. Carlson, M. M. Figley, R. G. Evens, B. G. Brogdon, R. A. Gagliardi, E. Gedgaudas, G. A. Kling, T. F. Leigh, S. F. Ochsner, J. F. Wiot, R. E. Buenger, E. C. Klatte, J. P. Tampas, J. L. Gwinn, chairman

Finance and Budget: A. E. James, E. C. Klatte, R. McLeeland, J. P. Tampas, R. G. Evens, chairman

Publications: M. P. Capp, K. Ellis, F. F. Ruzicka, Jr., E. R. Heitzman, R. A. Gagliardi, chairman

Editorial Policy: M. M. Figley, E. F. Lang, R. H. Troupin, E. R. Heitzman, K. Ellis, F. F. Ruzicka, Jr., M. P. Capp, R. A. Gagliardi, chairman

Advisory Committee on Education and Research: J. E. Youker, G. Wilson, G. W. Hartman, L. F. Rogers, E. Gedgaudas, chairman

Scientific Exhibits: T. C. Beneventano, G. Dodd, B. G. Brogdon, chairman

Constitution and Bylaws: J. H. Walker, W. M. Whitehouse, J. P. Tampas, chairman

American Board of Radiology Representatives: J. F. Roach, R. W. McConnell, S. W. Nelson

Program Committee: H. Z. Mellins, J. F. Martin, J. L. Gwinn, M. M. Figley, R. A. Gagliardi, B. G. Brogdon, E. Gedgaudas, G. A. Kling, P. Riemenschneider, chairman

Instruction Courses: E. Gedgaudas, director; G. W. Hartman, associate director

American College of Radiology Board of Chancellors Representative: W. B. Seaman

Annual Meeting: March 25–30, 1979, Sheraton Centre, Toronto, Canada

Scientific Program: P. A. Riemenschneider, president elect, Cottage Hospital, Santa Barbara, California 93105

Manager Annual Meeting: George A. Kling, Harper Hospital, Detroit, Michigan 48201

Membership: John L. Gwinn, 4650 Sunset Blvd., Los Angeles, California 90027

Business Office: Keith W. Gundlach, comptroller, American College of Radiology, 20 North Wacker Drive, Chicago, Illinois 60606

American Radium Society

President: Frederick W. George, III
President Elect: Alfred S. Ketcham
1st Vice-president: Julian P. Smith
2d Vice-president: Edwin M. Jacobs
Secretary: Norah duV. Tapley
Treasurer: Simon Kramer

COMMITTEES 1978–1979

Executive: A. S. Ketcham, J. P. Smith, E. M. Jacobs, N. duV. Tapley, S. Kramer, L. W. Brady, R. H. Jesse, F. W. George, F. Rutledge, chairman

Public Relations: V. Marcial, J. Vaeth, C. Honaker, ex-officio, and F. George, chairman

Publication: K. L. Krabbenhoft, D. Hussey, A. Raventos, I. Fix, L. W. Brady, chairman

Scientific Program: R. Parker, J. Durant, A. S. Ketcham, M. S. Mitchell, G. Murphy, F. Rutledge, M. Griem, W. E. Powers, M. Apuzzo, F. George, chairman

Local Arrangements: L. Davis, J. Vaeth, J. Nolan, R. McKenna, J. Slater, J. Stein, J. Scallon, S. Kramer, J. Helsper, chairman

Constitution and Bylaws: A. S. Glicksman, P. J. DiSaia, K. L. Krabbenhoft, chairman

Audiovisual: C. R. Bogardus, J. Helsper, R. Schweitzer, R. H. Jesse, C. Perez, J. Glassburn, A. M. Nisar Syed, R. Young, B. Herrington, F. George, chairman

American Board of Radiology Representatives: J. J. Stein, R. E. King, N. duV. Tapley

American College of Radiology Board of Chancellors Representative: L. W. Brady

American College of Radiology Council Representative: J. del Regato

Editorial Board of AFCOS Newsletter Representative: J. Vaeth

National Council on Radiation Protection and Measurements Liaison Representative: L. W. Davis

Annual Meeting: March 4–8, Los Angeles, California

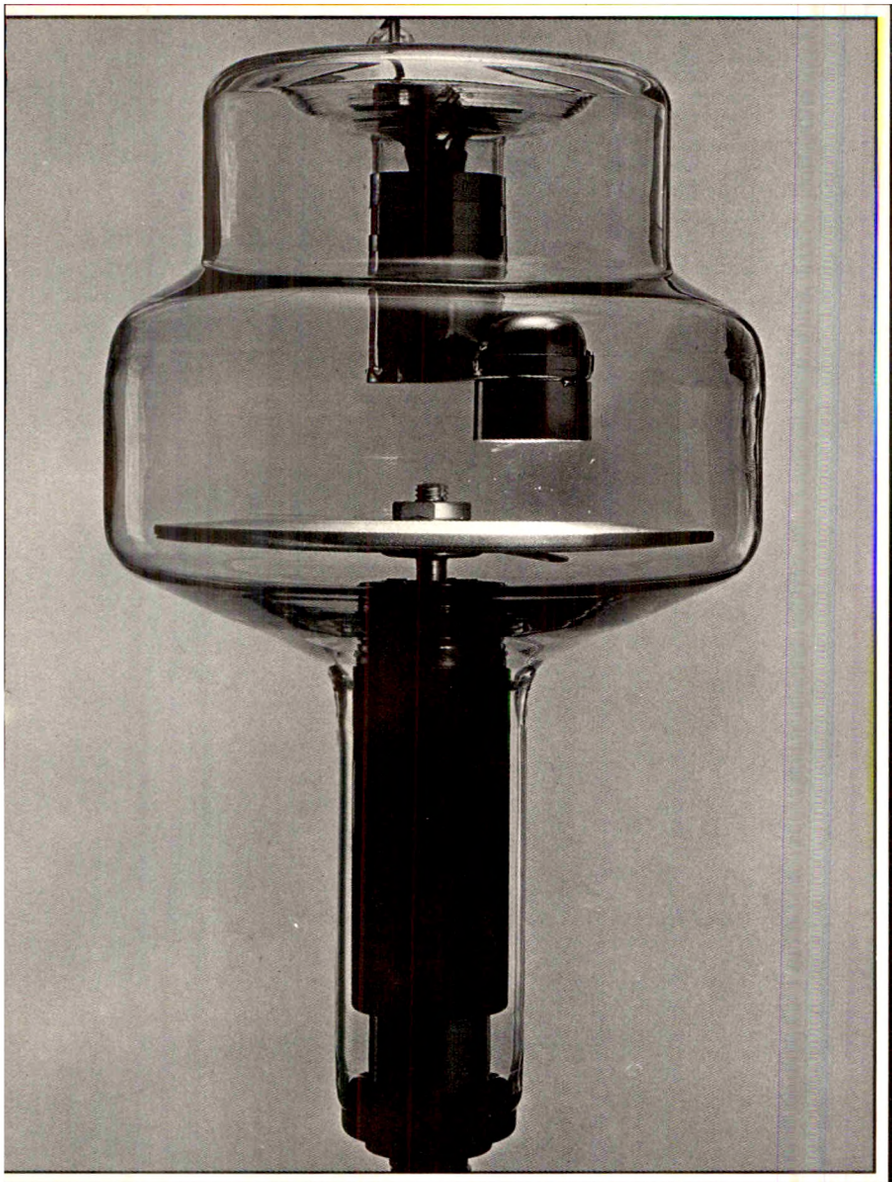
Scientific Program: F. W. George, III, University of Southern California School of Medicine, Los Angeles, California 90033

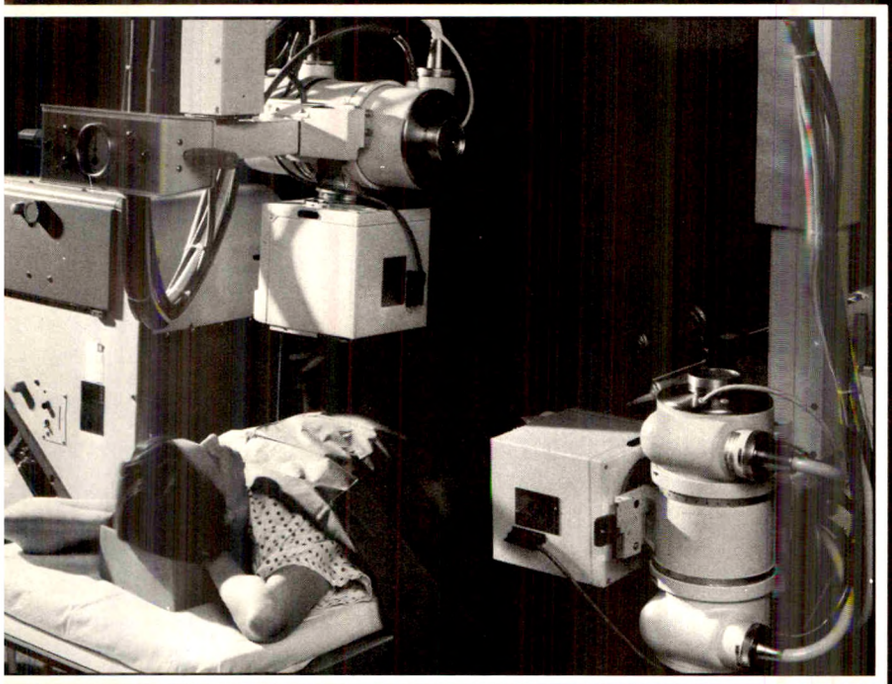
Local Arrangements: James Helsper, Pasadena, California

Membership: Norah duV. Tapley, secretary, M. D. Anderson Hospital, 6723 Bertner Avenue, Houston, Texas 77030

Business Office: N. V. Jordan, c/o R. H. Jesse, M. D. Anderson Hospital and Tumor Institute, 6723 Bertner Avenue, Houston, Texas 77030

Mailing note.—Mailing surcharges: U.S. and possessions, none; European countries, $25; Japan, $45; other, $10. European rates apply to Algeria, Austria, Belgium, Czechoslovakia, Denmark, Finland, France, Germany, Great Britain, Greece, Hungary, India, Iran, Ireland, Israel, Italy, Kenya, Luxembourg, Netherlands, Nigeria, Norway, Portugal, Romania, South Africa, Spain, Sweden, Switzerland, Turkey, Uganda, Yugoslavia. All subscriptions to Japan and European countries are delivered by air freight; there is no option for surface mail.





Machlett for high-power angiography

procedure-designed dynamax 78E 15/10 x-ray tube

Designed for the exacting techniques of high-power cardiac and abdominal angiography, the Dynamax 78E 15/100 is rated at 100 KW, with the large focus allowing for heavy-duty angiographic factors within the functional range of conventional films and screens.

With the small focus biased, the Dynamax 78E 15/100 will resolve 5.9 line pairs per millimeter at 2-power magnification at 150 mA and 80 kVp.

The Dynamax 78E's high thermal capacity (400kHU) makes it ideally suited for rapid film techniques, providing for high patient volumes and repetitive studies without lengthy cooling periods.

For complete technical information on the Dynamax 78E 15/100, or for consultation relative to its application, contact your x-ray dealer or

MACHLETT

The Machlett Laboratories, Incorporated
1063 Hope St.
Stamford, Connecticut 06907
(203) 348-7511

A Raytheon Company

NEURORADIOLOGY AND RADIOLOGY OF THE HEAD, NECK AND SPINE

New York Hilton, Rockefeller Center,
April 30–May 4, 1979

A postgraduate course sponsored by the Department of Radiology of the *Neurological Institute of the Columbia-Presbyterian Medical Center* in New York. The course is intended to review for radiologists, neurologists, neurosurgeons and ophthalmologists, as thoroughly as possible most of the topics of neuroradiology. Special topics of interest will include a symposium on the sella turcica and the pituitary gland, a symposium on the spine and spinal cord and its study by high resolution CT, as well as water soluble myelographic agents. Imaging of the eye, orbit, and petrous bone with conventional tomography and with high resolution CT will be an important feature of this course. A great emphasis will be made throughout the presentation on the results obtained with the new CT scanners with *resolution reaching the submillimeter range.*

A review symposium will be carried out on the most recent developments in interventional techniques in neuroradiology. A discussion of particulate and liquid emboli will be presented.

The course will feature a discussion and preliminary clinical results of emission positron tomography and nuclear magnetic resonance imaging.

The course is valid for 33 Category I credits. The registration fee is $330 for the entire course, with a reduced fee of $250 for residents and fellows. This fee covers tuition, educational materials, coffee breaks and lunches for registrants Monday through Friday. Requests should be made directly to Dr. Sadek K. Hilal at the Neurological Institute, Box 63, 710 W. 168th St., N.Y., N.Y. 10032.

The course faculty includes:

Robert Ackerman
George Ascherl
Walter E. Berdon
R. Thomas Bergeron
R. Nick Bryan
Kyo-York Chynn
Kenneth R. Davis
Giovanni DiChiro
Romeo Ethier
Mokhtar H. Gado
S. Ramaiah Ganti
William Glenn
Derek Harwood-Nash
Sadek K. Hilal
O. Wayne Houser
Michael S. Huckman
Peter M. Joseph
Charles Kerber
Stephen A. Kieffer
Irvin I. Kricheff
Paul Lauterbur
Norman E. Leeds
W. Jost Michelsen
Paul F. J. New
Guy D. Potter
D. Gordon Potts
Arthur Rosenbaum
Paul Sane
Mannie M. Schechter
William B. Seaman
John Silver
Juan M. Taveras
Stephen L. Trokel
Margaret A. Whelan
Earl Zimmerman
Robert Zimmerman

clear, clean colon

X-Prep® Liquid

(standardized extract of senna fruit)

versatile bowel evacuant for diagnostic procedures



Versatile in indications

May be used prior to:

G.I. radiography
Urologic radiography
Colonoscopy
Sigmoidoscopy
Other diagnostic bowel procedures

Versatile in administration

May be used:

Alone, in a single dose
Alone, in divided doses, particularly in elderly or debilitated patients
With adjunctive use of citrate of magnesia, laxative suppositories and enemas, as required
As part of other regimens, such as hydration

X-PREP Liquid is formulated specifically for effective bowel evacuation prior to diagnostic procedures. It induces peristalsis through virtually colon-specific action. X-PREP Liquid has been found effective in cleansing the colon for diagnostic evaluation in 95% of 749 patients prepared for barium enemas, intravenous pyelography, or colonoscopy.* Its pleasant taste meets with high patient acceptance, and its ease of administration is appreciated by the patient and nursing staff.

Supplied: X-PREP Liquid (standardized extract of senna fruit) in 2½ fl. oz. bottles (alcohol 7% by volume). X-PREP Powder (standardized senna concentrate) in ¾ oz. containers. **Now Available:** X-PREP™ Bowel Evacuant Kit. Each kit contains: two SENOKOT® S Tablets (standardized senna concentrate and dioctyl sodium sulfosuccinate), one bottle of X-PREP® Liquid 2½ fl. oz., and one RECTOLAX™ Suppository (bisacodyl 10 mg), plus easy-to-follow patient instructions for hydration, clear liquid diet, and the correct time sequence of administering the above laxatives.

*Bibliography available upon request.

Colonoscope, courtesy of Olympus

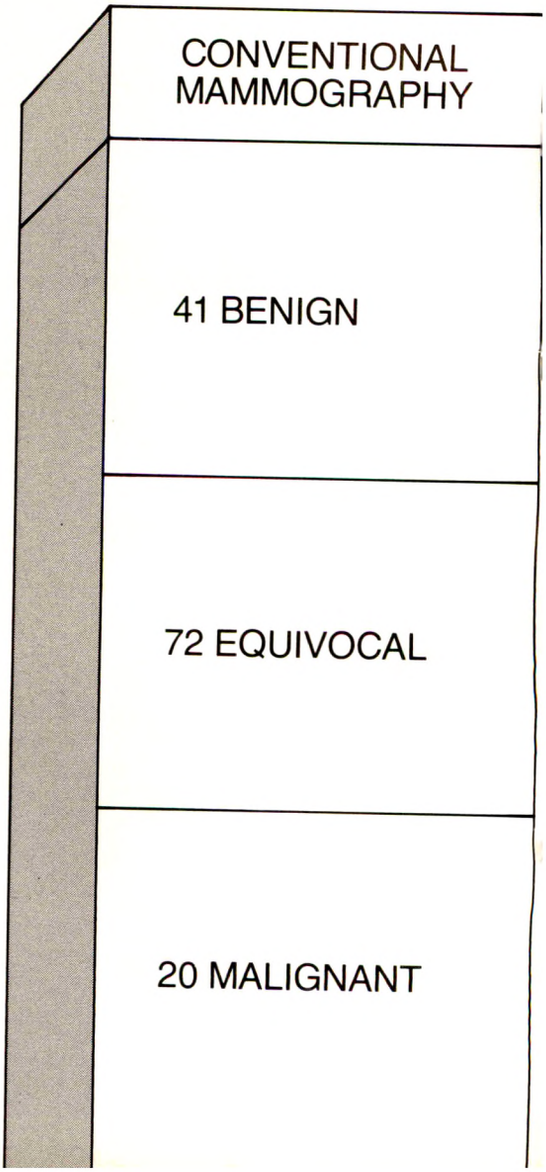
Gray Pharmaceutical Co., Affiliate
The Purdue Frederick Company

© Copyright 1978, Gray Pharmaceutical Co. Norwalk, CT 06856

A9047 194578

A New Study Confirms...

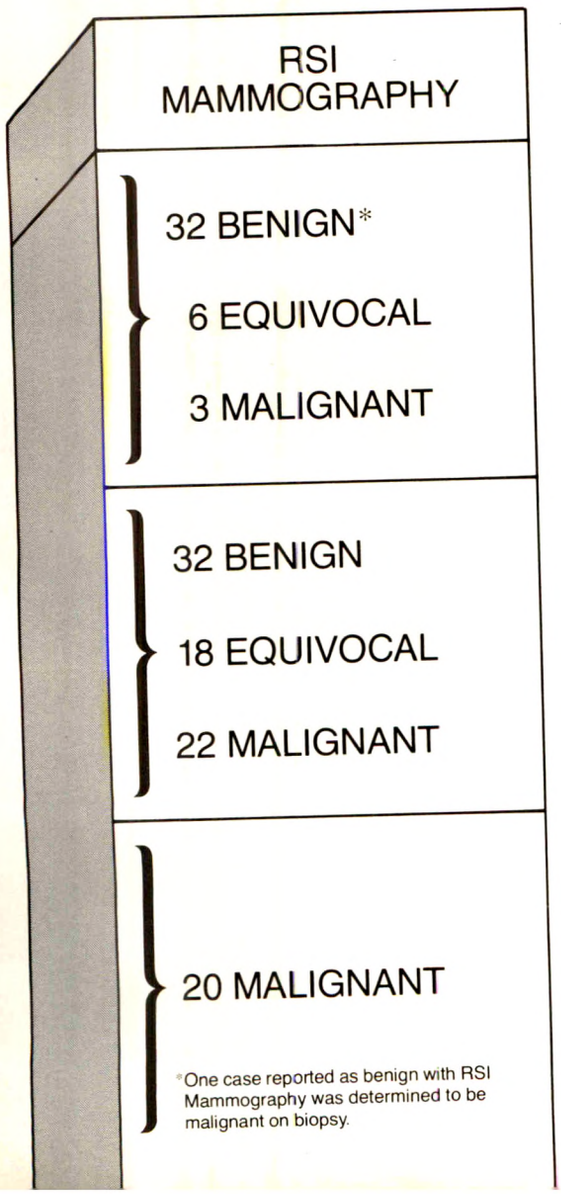
THE RSI MAMMOGRAPHIC SYSTEM **INCREASES DIAGNOSTIC ACCURACY**



Take a good look at the chart. You'll see the remarkable results of a study published by Dr. Edward A. Sickles, making a clinical comparison of 133 patients who received both conventional mammography and RSI Magnification Mammography. The results were confirmed with pathological diagnosis.*

This new study confirms just how accurate RSI Mammography really is. In fact, Dr. Sickles wrote in 1977, that magnification mammograms are "...clearly superior both quantitatively and qualitatively to conventional contact mammograms."[1]

Diagnostic Accuracy in Mammographic Examinations[2]
Clinical Data of Edward A. Sickles, M.D.
Assistant Professor of Radiology, University of California, San Francisco
Clinical Comparison of 133 Cases



Out of 41 cases diagnosed as benign with conventional mammography, RSI Mammography determined that 3 of these cases were, in fact, malignant. In addition, with conventional mammography alone, 72 cases were diagnosed as equivocal and direct magnification mammography (RSI System) was able to differentiate these as: 22 malignant, 32 benign, and only 18 remained equivocal. This revealing clinical comparison clearly shows that RSI Magnification Mammography increases the certainty in diagnosis, decreases the time between examination and confirmation, and may even reduce the need for biopsy.

In a radiologic symposium presented in New York City, Dr. Sickles remarked, "...in dealing with difficult cases, we considerably improved our diagnostic accuracy [with RSI Magnification Mammography]."[2]

These more accurate diagnoses are the direct result of the capability of the RSI Mammography's System to give you—

- Clearer definition of mass borders
- Improved image sharpness and resolution
- Resolution of malignant microcalcifications often not discernible by conventional mammography
- Delineation of trabecular patterns

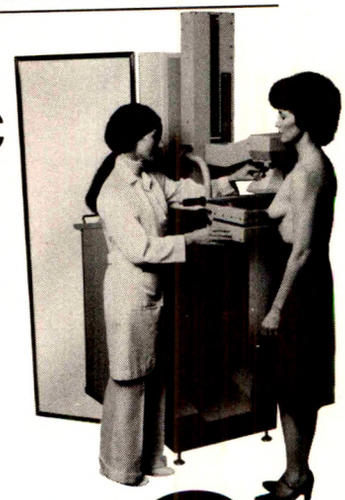
The RSI Mammography System offers high-detail resolution in the magnification mode as well as the conventional contact mode. The superior image which results from the exceptionally uniform focal spot provides a new level of confidence in the detection of breast cancer.

For more detailed information on the RSI Mammographic System and a reprint of the study published by Sickles *et al* in 1977, please write or call, Radiologic Sciences Inc., a subsidiary of Pfizer Inc., 235 East 42nd St., New York, N.Y. 10017 (212) 573-7941.

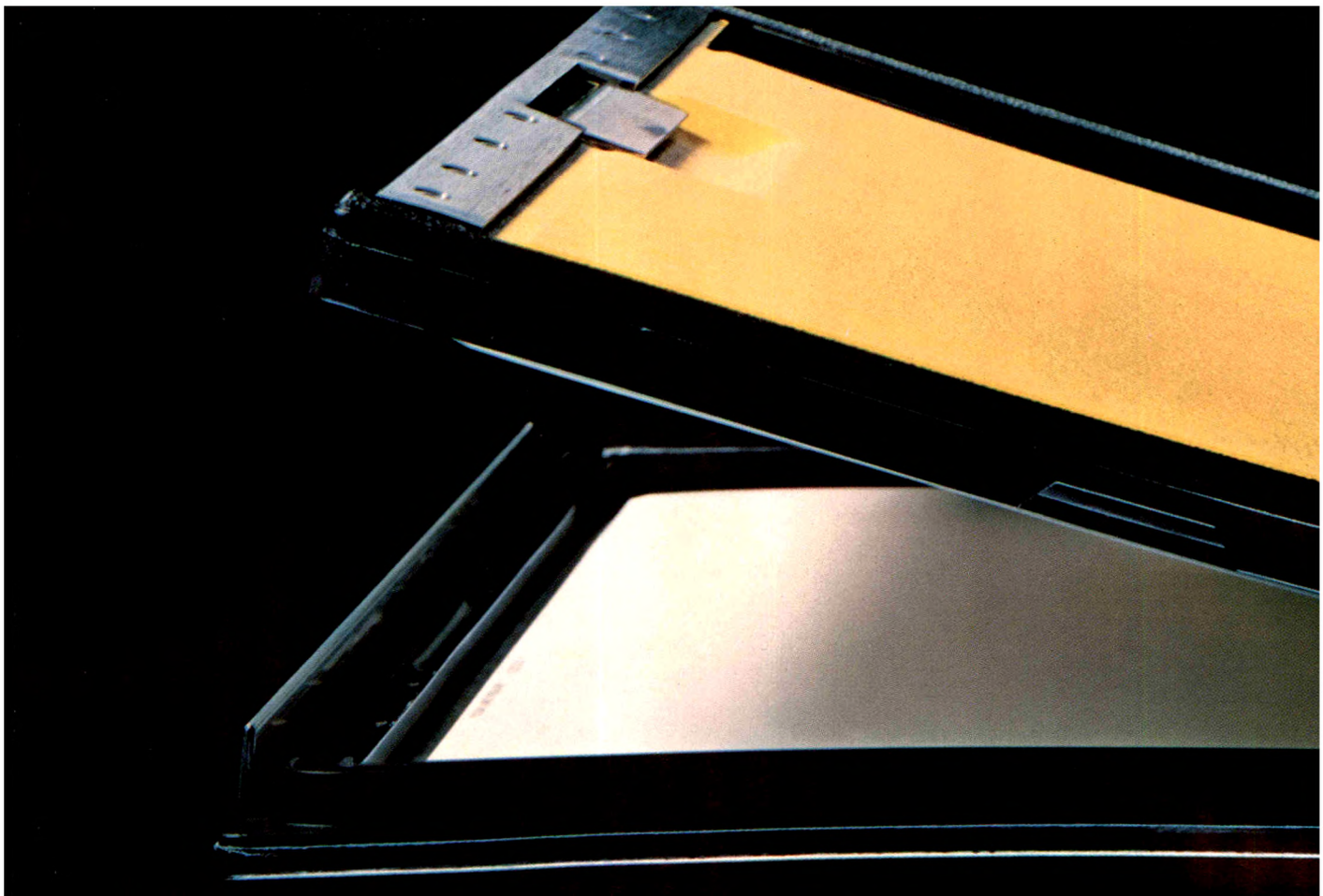
References: 1. Sickles, E.A.; Doi, K.; Genant, H.K.: *Radiology* 125:69-76, October 1977. **2.** Sickles, E.A.: *Microfocal Spot Magnification Mammography.* Presented at a Symposium, New York City, June 1, 1978.

THE RSI MAMMOGRAPHIC SYSTEM

INCREASES DIAGNOSTIC ACCURACY



RADIOLOGIC SCIENCES INC. Pfizer
A subsidiary of Pfizer Inc., New York, N.Y. 10017



TWO KODAK DESIGNS

KODAK INTENSIFYING SCREENS

Kodak expertise in turning energy into images provides you useful options.

KODAK X-OMATIC Intensifying Screens were designed for improved sharpness, compared to high-speed calcium tungstate screens. We eliminated the reflector layer, resulting in improved sharpness. And, the ultraviolet emission reduced crossover, which also improved sharpness. KODAK X-OMATIC Screens are available in two types—regular intensifying screens for general-purpose examinations, and fine intensifying screens for examinations where fine bone detail is required.

KODAK LANEX Screens, on the other hand, can provide you with exceptional *speed*. With phosphors that em primarily in the green portion of the spectrum and absorb a higher percentage of the x-ray energy than the high-speed calcium tungstate screens, KODAK LANEX Screen and KODAK Ortho Films can record images at speeds up to four times that of high-speed calcium tungstate screen when used with KODAK X-OMAT RP Film.

Whatever your imaging needs, investigate KODAK Intensifying Screens. Your Kodak Representative will be happy to help with your evaluation.

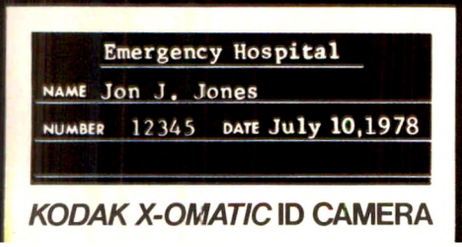


FOR EFFICIENT IMAGING

KODAK X-OMATIC CASSETTES

KODAK X-OMATIC Cassettes feature a double-curve design that provides intimate film/screen contact. Extremely durable. Single latch permits one-hand loading.

The KODAK X-OMATIC Cassette's design permits close contact between film and screen. Both cassette panels are curved; so, the act of closing the cassette actually expels air, reducing the possibility of trapped air between screens and film.



KODAK X-OMATIC ID CAMERA

The KODAK X-OMATIC Cassette is extremely rugged, highly resistant to scratches, abrasions, and distortion from dropping. And because the single latch is located in the center, it may be opened with one hand.

For convenient and positive identification, we recommend the KODAK X-OMATIC Cassette C-1 which contains a window to provide patient identification as shown at left. The cassette can be used in the KODAK X-OMATIC Identification Camera. If you prefer lead letters for patient identification, order the KODAK X-OMATIC Cassette C-2, which is windowless.

For more information about Kodak screens and cassettes, consult your Kodak Technical Sales Representative and ask for a demonstration. Or contact your medical x-ray products dealer. Or write: Eastman Kodak Company, Dept. 740-B, Rochester, New York 14650.

TURNING ENERGY INTO IMAGES

Kodak

COMPUTED TOMOGRAPHY • NUCLEAR MEDICINE

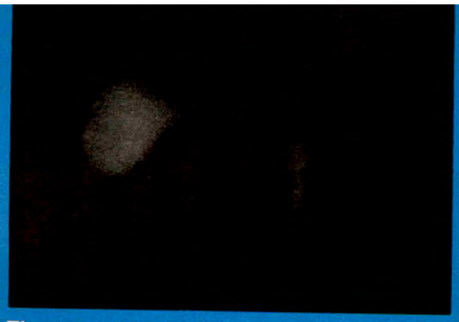


Figure 3. Nuclear liver scan: negative.

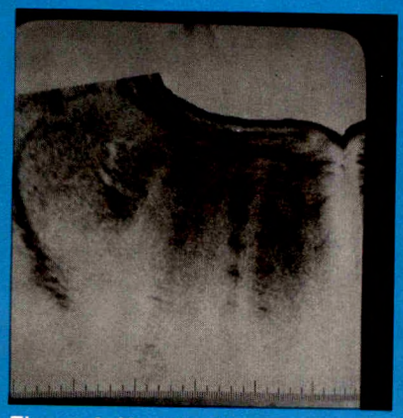


Figure 4. Hepatic Ultrasound: negative.

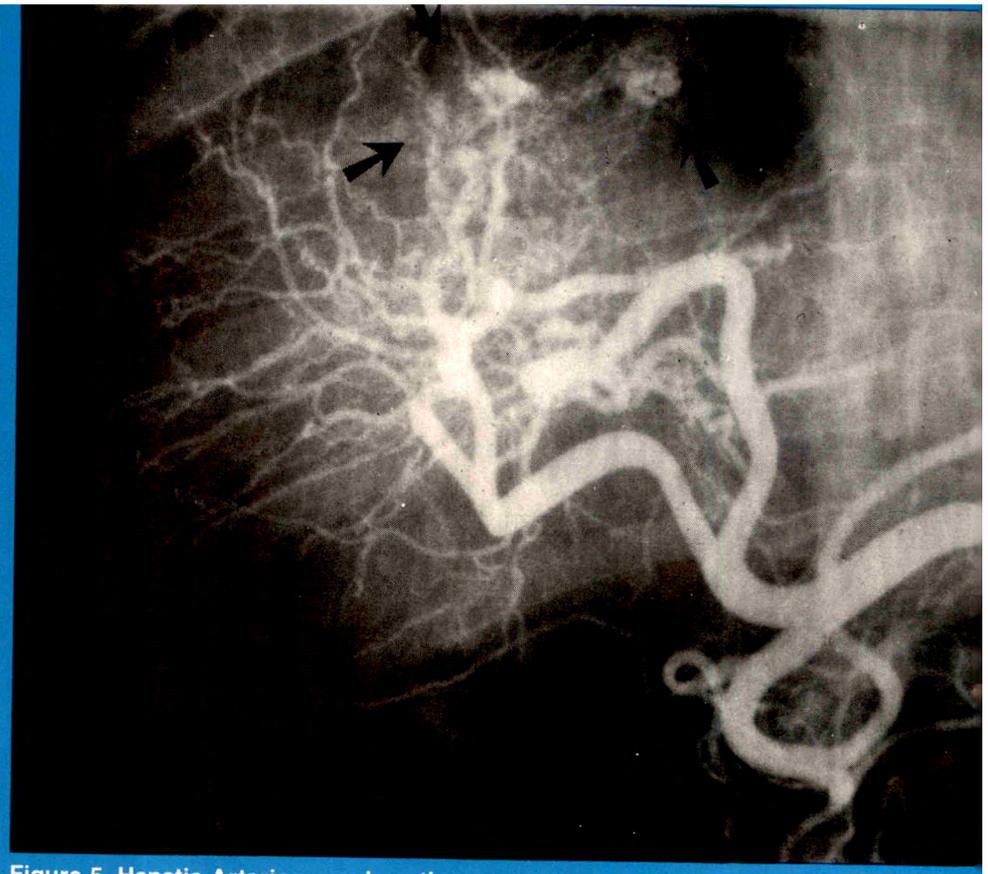


Figure 5. Hepatic Arteriogram: hepatic metastases.

History:
65 year old male with a history of multiple pulmonary emboli who, on the most recent admission, was discovered to have microhematuria. An intravenous pyelogram revealed a mass in the right kidney. The patient was then referred for imaging consultation.

Imaging Evaluation:
Renal and hepatic arteriography (Fig. 1,5) demonstrated an extensive renal cell carcinoma with thrombosis of the renal vein and metastatic extension to the liver. Although the renal carcinoma was visible in all imaging modes, only the hepatic arteriography confirmed the liver metastases.

When strong clinical suspicions exist, then multiple imaging modalities are mandatory. Although all modes have satisfactory sensitivity, angiography remains "high on the the list" for diagnostic specificity.

Study courtesy of Department of Radiology, Shadyside Hospital, Pittsburgh, Pennsylvania.

While CT, ultrasound and nuclear imaging have all proved to be highly sensitive diagnostic techniques, in many cases angiography is necessary to make a specific diagnosis. And Elema-Schonander has two types of sheet-film changers to meet your requirements for any angiographic application.

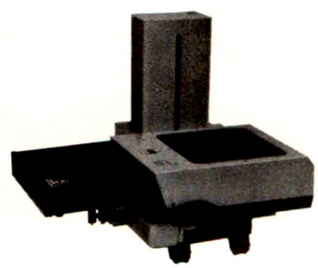
Both AOT-S and PUCK models are equipped with Elema-Schonander's recently developed Carbon-Fiber Reinforced Plastic (CFRP) front plate. Other materials, like aluminum and bakelite, generally used in front plates compromise either x-ray transparency or screen/film contact. However, Elema-Schonander's uncompromising CFRP front plate combines very low x-ray attenuation with superior screen/film contact, year after year. The result is excellent image contrast, optimum resolution at all exposure rates, less patient radiation, less scatter, and greater optimization of exposure technique.

Call or write for more information about the many other advantages of Elema-Schonander AOT-S and PUCK Sheet-Film Changers. Elema-Schonander, Inc., 699 Lively Blvd., Elk Grove Village, IL 60007. (312) 593-6770.

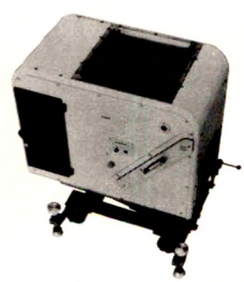


CFRP Aluminum

Experimental exposure using split front plate of CFRP and aluminum for demonstration purposes.



PUCK Sheet-Film Changer.



AOT-S Sheet-Film Changer.

elema·schonander

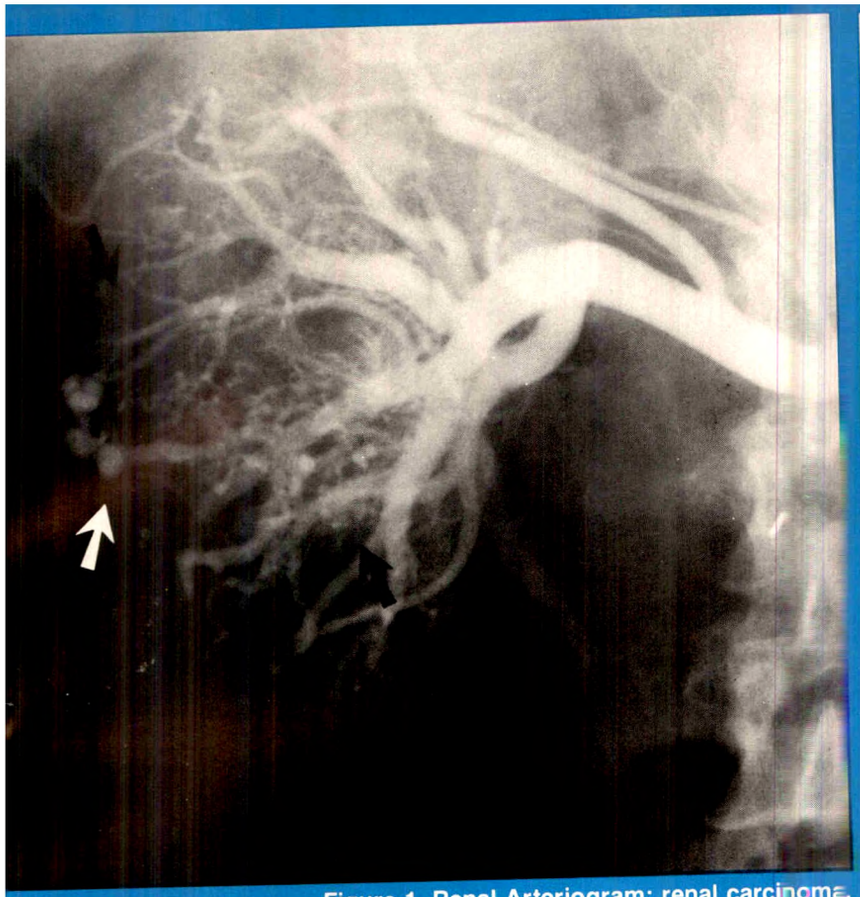


Figure 1. Renal Arteriogram: renal carcinoma.

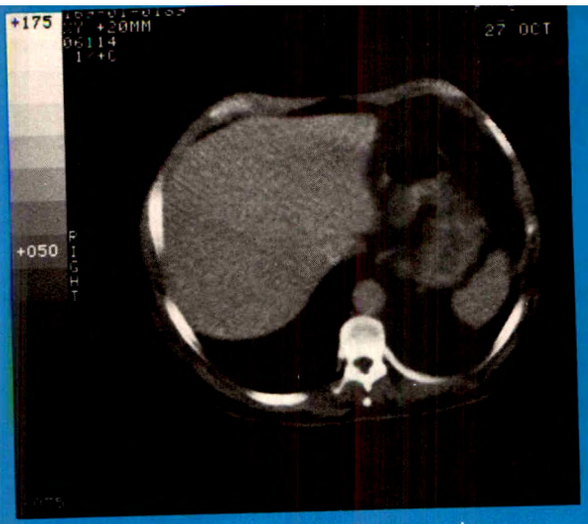


Figure 2. Computed Hepatic Tomography: negative.

All images are reproduced at 71% of their original size.

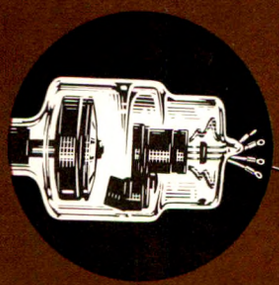
Angiography... CT, nuclear, and ultrasound scanning.

Each has its own special diagnostic advantages in this era of expanding imaging technology.

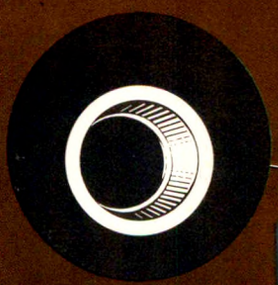
Angiography and Elema-Schonander.

For diagnostic specificity.

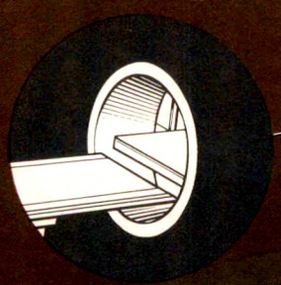
SIEMENS



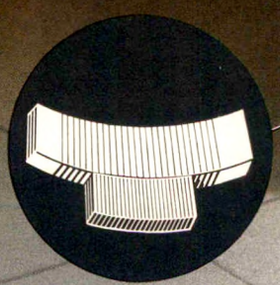
The custom application OPTI-150 CT X-ray tube permits continuous patient scanning at a rate of up to 125 scans/hour.



Wide gantry aperture and scan field (both 54 cm. in diameter) facilitate patient handling and positioning.



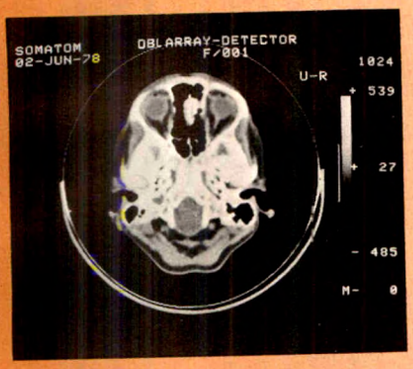
Exclusive dual-section, flat-top table system with motorized patient conveyor.



SCINTILLARC-DUAL detector system provides maximized detector utilization with optimized clinical results.

Visit Siemens Booth "A"
Fifth Annual CT International Symposium and Course
Las Vegas Hilton, April 16-20, 1979

The only CT scanners with instantaneous image reconstruction



Instantaneous image reconstruction makes the SOMATOM (whole body scanner) and the SIRETOM (head/neck scanner) the most sophisticated computed tomographic systems available today. Upon completion of each scan, the image is immediately available for clinical evaluation. The SOMATOM offers selectable scan times of four and eight seconds while the SIRETOM scan time options are 60, 120, and 180 seconds.



The EVALUSKOP, an independent evaluation console, extends the capability for CT image manipulation and analysis. Programmable and available at the push of a button are window variation, multiple region of interest selection, distance and angle measurement, histogram, magnification, saggital/coronal reconstruction, multiple tomogram displays, tomogram addition and subtraction, and filter manipulation.

Siemens' full line of computed tomographic equipment is designed to fulfill the exacting requirements of CT application. Behind each system definition—X-ray tubes, tables, generators, radiation measurement, and signal processing—is more than 100 years of engineering excellence.



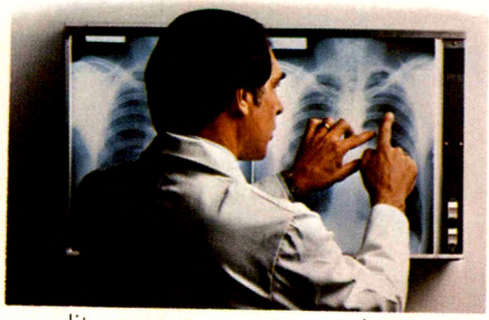
Siemens' world-wide reputation for product support and service is unsurpassed. In the United States alone, Siemens has a technical staff of over 500 trained professionals ready to serve you—should the need arise.

For further information
Please contact your local Siemens Representative or Siemens Corporation, Medical Systems Division, 186 Wood Avenue South, Iselin, New Jersey (201) 494-1000.
In Canada: Siemens Electric Limited, Medical Systems. P.O. Box 7300, Pointe Claire, Quebec H9R 4R6.

Concepts... engineered to radiologic excellence

SIR-408

Isn't it time you asked their first name?



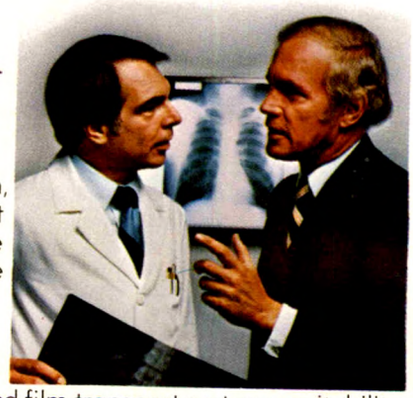
Get familiar with GAFMED.®

GAF® makes it easy to be the first name you think of when ordering quality x-ray films, chemicals, screens and cassettes. We call all our medical x-ray products GAFMED.® Our first-name, only name basis of identity.

It's called GAFMED for one good reason. It's one consistent x-ray system with the confidence to meet a variety of your radiographic needs.

GAF's solid experience and foresight are behind its contemporary x-ray products. This enables GAFMED to respond to any radiographic requirement—be it consistency in your x-ray film, fail-safe chemicals or quality screens, cassettes and accessories. We know you develop favorites in this business and GAF wants to be one of them by measuring up to your toughest standards.

GAFMED®Film and Chemicals: Quality through consistency. To help you manage x-ray imaging, such as getting excellent radiographic contrast and detail, GAF offers a superb line of film that gives you the kind of stability you need in whatever mode you work.



GAFMED®SR/1 When you need an expanded useful density range, wide-latitude SR/1 is your diagnostic radiographic film. It provides high contrast in those low density areas where most radiographic detail is visualized. In addition, SR/1 simultaneously delivers low contrast in high density regions to increase soft tissue detail with maximum exposure latitude. GAFMED SR/1 is designed for use with all blue and blue-green emitting intensifying screens and is fully compatible with all conventional processing methods.

GAFMED®SR/2 SR/2 is a general-purpose medical radiographic film with medium speed, low fog, high contrast and blue spectral sensitivity. Features that make this widely accepted film outstanding are its ideal performance in automated film transport systems, suitability for all automatic and manual processing modes and its high definition image quality. SR/2 renders a wide variety of system speeds when used in combination with GAFMED calcium tungstate and Rarex® rare earth intensifying screens.

GAFMED®SR/S GAFMED SR/S Photofluorography film is designed for use with image intensifiers employing 70mm and 105mm roll film cameras. SR/S features high speed, high contrast and a low base fog for superb optical clarity. GAFMED SR/S is also designed for all 90-second short cycle and extended cycle automatic processing systems.

GAFMED®SC/90 You'd expect the company responsible for the first color-coded chemistry to be equally as innovative with the new GAFMED SC/90 chemical system. **SC/90 DEVELOPER,** color coded red requires no starter solution and cannot be over-replenished. The red pH sensitive quality control feature enables you to quickly determine chemical processing energy through visual check. **SC/90 FIXER,** color-coded blue for easy identity and fail-safe mixing, is designed for use in all short cycle automatic processors and provides excellent archival activity.



formed x-ray products



SC/90 chemistry is also a clean-working solution for consistent quality assurance that's part of the GAFMED system.

GAFMED® Screens and Cassettes. The right film and chemicals is just the start.

For optimum radiographic performance the winning GAFMED combination is: a high quality film, superior screens and dependable cassettes.

GAF manufactures two premium GAFMED cassettes to meet your specific requirements: the lightweight Comp-I-Sette™ and the durable Titan.™

The Comp-I-Sette design insures superior screen-film contact for optimum definition. Its lightweight metal construction and special epoxy coating are geared to provide long cassette wear.

The Titan cassette, known for its excellent screen-film contact, is ruggedly constructed to guarantee long lasting service. Its positive-locking feature makes it resistant to sudden jars and jolts. Well recognized as a standard of the industry, Titan cassettes are available in regular and phototiming models.

The GAFMED system also features a wide variety of intensifying screens to meet your particular imaging needs. Our GAFMED Calcium Tungstate screens have an abrasion resistant surface making them ideal for automated film transport systems. Of the four types available, TF-3 with a fast exposure rating, is the most popular for general radiographic applications.

GAFMED Rare Earth Intensifying Screens allow you to significantly reduce the exposure without requiring a special film or a change in safe-light illumination. Our popular BG High Speed screens allow a 4 time exposure reduction compared to a typical par speed calcium tungstate system.

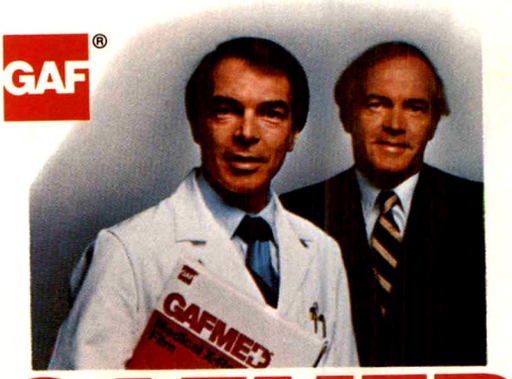
All GAFMED screens minimize static related artifacts by incorporating an aluminized backing.

GAFMED Product Service: You can't beat the system.

GAFMED is more than a name for our quality line of medical x-ray products. It stands for the GAF people who safeguard your operations with a comprehensive field support program called Radiographic Engineering Services.

Our skilled GAF technical representatives and x-ray engineering consultants will help you get the most efficiency from your radiology department. They provide expert product consultation and high impact training programs to assure consistent radiographic image quality while reinforcing your expertise.

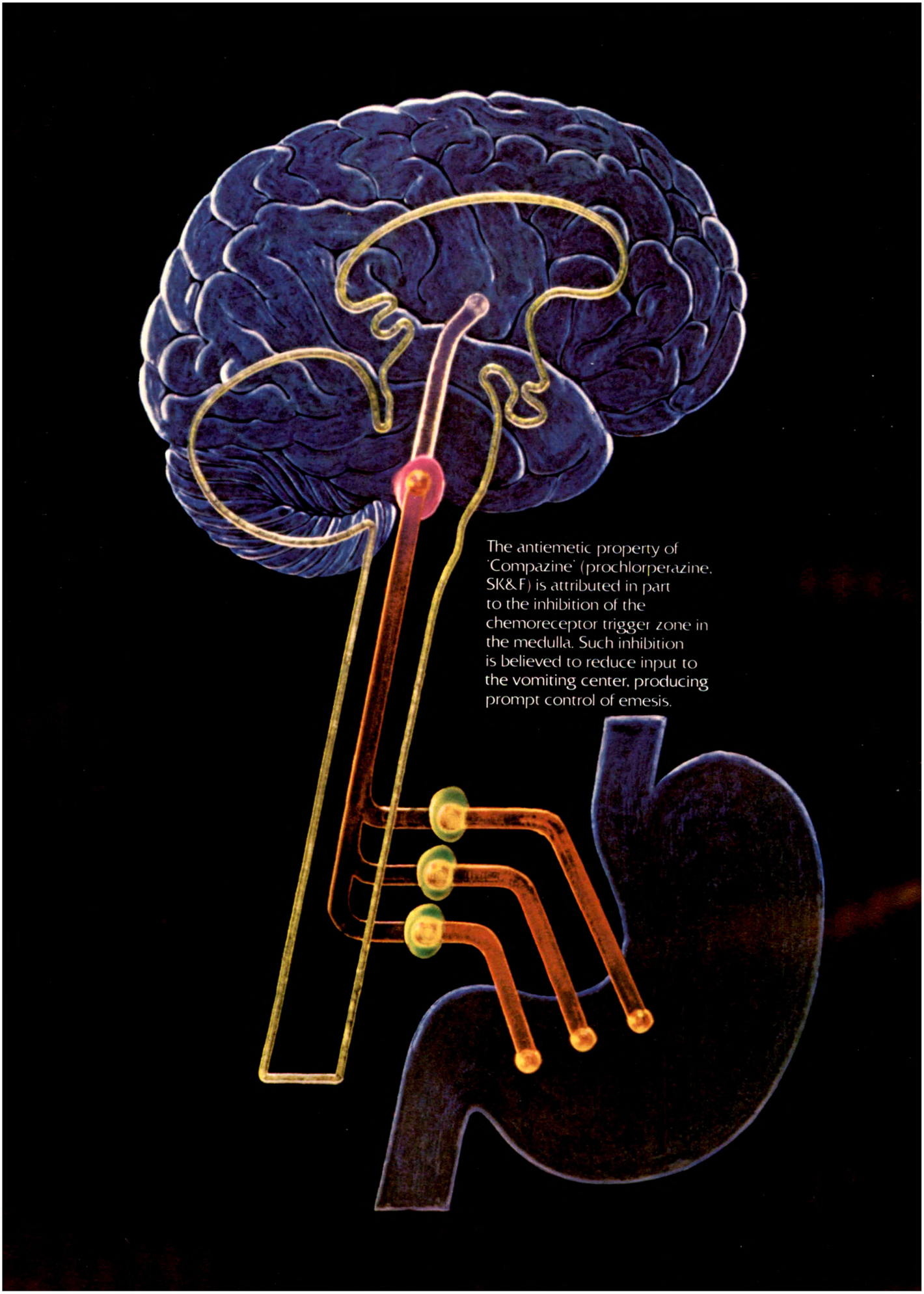
Now is the time to get familiar with GAFMED by contacting your local GAF technical sales representative...GAF x-ray dealer... or GAF Corporation, Medical X-Ray Products, 140 West 51st Street, New York, N.Y. 10020.



GAFMED®

Medical X-Ray Products.
The image of confidence.




The antiemetic property of
'Compazine' (prochlorperazine,
SK&F) is attributed in part
to the inhibition of the
chemoreceptor trigger zone in
the medulla. Such inhibition
is believed to reduce input to
the vomiting center, producing
prompt control of emesis.

Compazine®

Injection 5 mg./ml.
disposable syringe

brand of
prochlorperazine

Shouldn't it be your first choice for severe nausea and vomiting that often accompany cancer therapy?

- **Unsurpassed antiemetic action**
- **12 dosage forms and strengths**

Before prescribing, see complete prescribing information in SK&F literature or PDR. The following is a brief summary.

Indications: Management of the manifestations of psychotic disorders; management of psychoneurotic patients displaying primarily symptoms of moderate to severe anxiety and tension; and for control of severe nausea and vomiting.

'Compazine' has not been shown effective in the management of behavioral complications in patients with mental retardation.

Contraindications: Comatose or greatly depressed states due to C.N.S. depressants; bone marrow depression; pediatric surgery.

Warnings: The extrapyramidal symptoms which can occur secondary to 'Compazine' may be confused with the central nervous system signs of an undiagnosed primary disease responsible for the vomiting, e.g., Reye's syndrome or other encephalopathy. The use of 'Compazine' and other potential hepatotoxins should be avoided in children and adolescents whose signs and symptoms suggest Reye's syndrome.

Avoid using in patients hypersensitive (e.g., blood dyscrasias or jaundice) to any phenothiazine. Caution patients about activities requiring alertness (e.g., operating vehicles or machinery) especially during the first few days' therapy. Prochlorperazine may intensify or prolong the action of other C.N.S. depressants. Not recommended for children under 20 pounds or 2 years of age.

Use in pregnancy only when potential benefits outweigh hazards.

Precautions: The antiemetic action of 'Compazine' may mask the signs and symptoms of overdosage of other drugs and may obscure the diagnosis and treatment of other conditions such as intestinal obstruction, brain tumor and Reye's syndrome (See WARNINGS). Postoperative aspiration of vomitus has occurred in a few surgical patients who received prochlorperazine as an antiemetic. Deep sleep and coma have been reported, usually with overdosage. Patients on long-term therapy, especially high doses, should be evaluated periodically for possible adjustment or discontinuance of drug therapy. **In children with acute illnesses or dehydration, use only under close supervision.**

Adverse Reactions: Drowsiness, dizziness, amenorrhea, blurred vision, skin reactions. Hypotension. Cholestatic jaundice, leukopenia, agranulocytosis. Fatty changes in the liver have been observed in a few patients who died while receiving the drug (no causal relationship has been established). Neuromuscular (extrapyramidal) reactions: motor restlessness, dystonias, pseudo-parkinsonism, persistent tardive dyskinesia. Contact dermatitis is a possibility with concentrate and injectable forms.

Other adverse reactions reported with Compazine (prochlorperazine, SK&F) or other phenothiazines: Some adverse effects are more frequent or intense in specific disorders (e.g., severe hypotension in mitral insufficiency or pheochromocytoma).

Grand mal convulsions; altered cerebrospinal fluid proteins; cerebral edema; prolongation and intensification of the action of C.N.S. depressants, atropine, heat and organophosphorus insecticides; dryness of mouth, nasal congestion, headache, nausea, constipation, obstipation, adynamic ileus, inhibition of ejaculation; reactivation of psychotic processes, catatonic-like states; hypotension (sometimes fatal); cardiac arrest; pancytopenia, thrombocytopenic purpura, eosinophilia; biliary stasis; lactation, galactorrhea, gynecomastia, menstrual irregularities, false-positive pregnancy tests; photosensitivity, itching, erythema, urticaria, eczema up to exfoliative dermatitis; asthma, laryngeal edema; angioneurotic edema, anaphylactoid reactions; peripheral edema; reversed epinephrine effect; hyperpyrexia; a systemic lupus erythematosus-like syndrome; pigmentary retinopathy with prolonged administration of substantial doses, skin pigmentation, epithelial keratopathy, and lenticular and corneal deposits.

EKG changes have been reported, but relationship to myocardial damage is not confirmed. Discontinue long-term, high-dose therapy gradually.

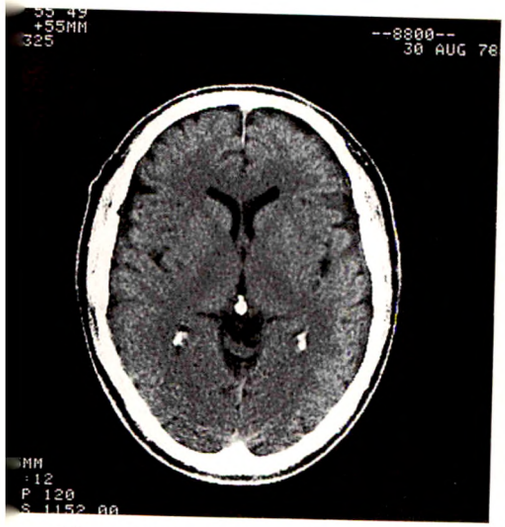
NOTE: Sudden death in patients taking phenothiazines (apparently due to cardiac arrest or asphyxia due to failure of cough reflex) has been reported, but no causal relationship has been established.

Supplied: Tablets – 5, 10 and 25 mg., in bottles of 100; Spansule® capsules – 10, 15, 30 and 75 mg., in bottles of 50; Injection – 5 mg./ml. in 2 ml. ampuls, 10 ml. vials, and 2 ml. disposable syringes; Suppositories – 2-1/2, 5 and 25 mg.; Syrup – 5 mg./5 ml.; Concentrate (intended for institutional use only) – 10 mg./ml.; Single Unit Packages of 100 (intended for institutional use only) – 5 and 10 mg. tablets; 10, 15 and 30 mg. 'Spansule' capsules.

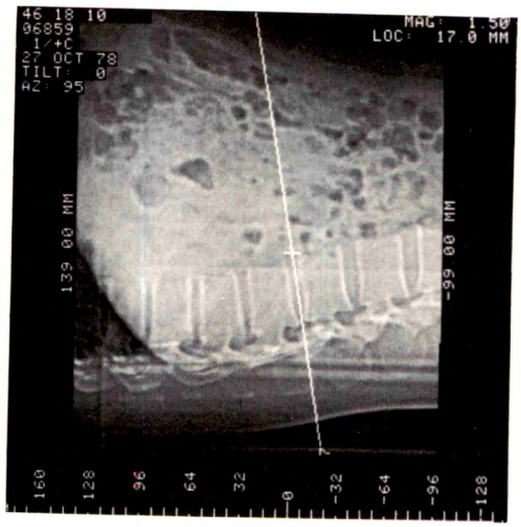
SK&F
a SmithKline company

Smith Kline & French Laboratories
Philadelphia, PA

Simple addition.



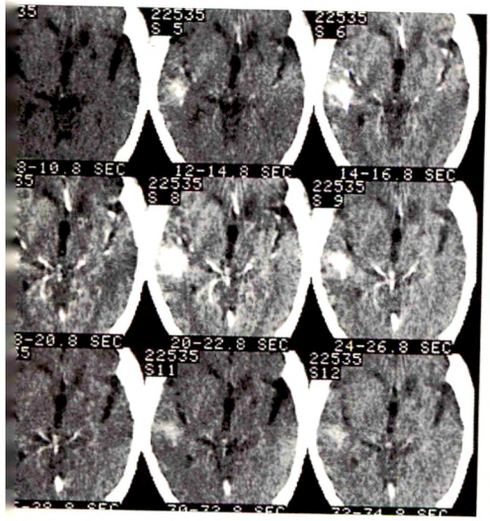
Ultra-high resolution X-2 detector
Optional on CT/T 7800, standard on CT/T 8800.



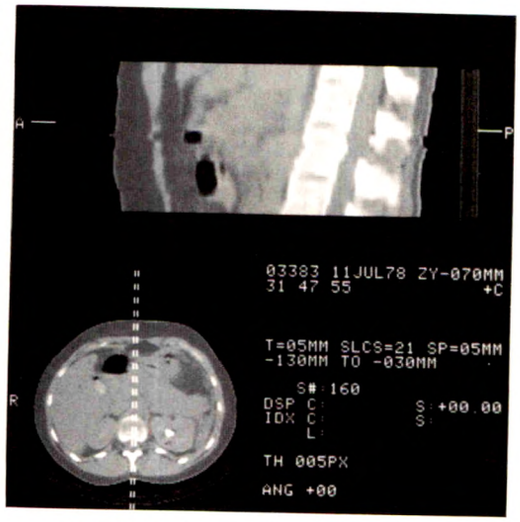
ScoutView localization
Included in Optional Diagnostic Capability package.



1.5 mm axial slice capability
Included in Optional Diagnostic Capability pa

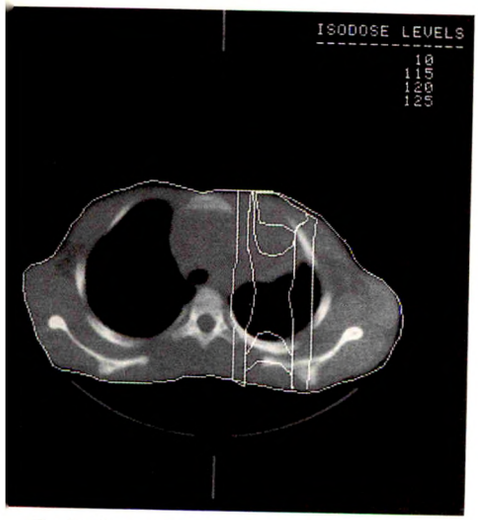


Dynamic scanning
Optional.



Sagittal and coronal transformations
No added cost.





Radiotherapy Treatment Planning
No added cost.

These advanced capabilities can be added to any CT/T system, even the first one installed in 1976.

You'd expect it from GE

How would you like a CT system that resists obsolescence? One that lets you choose the capabilities that match your department... now and in the future?

That's the objective of General Electric's CT/T Continuum.

We've designed our scanner so that new functions can be added at minimum cost to any new or existing CT/T system. For example:

Ultra-high resolution X-2 detector (optional). Unprecedented image quality. Resolving power of 1.0 mm (AAPM pin phantom) and 4.0 mm resolution at 0.4% contrast (GE Mod I gray/white phantom) in one reconstruction. Standard on CT/T 8800 systems.

Optional Diagnostic Capability (ODC) with ScoutView localization. Improves throughput. ScoutView images are digitized radiographs in AP, PA, lateral or oblique planes. They allow the physician to develop a scan prescription for first and last slice locations and gantry angulation. Subsequent axial scans can visualize extremely small anatomy, with 1.5 mm contiguous slice capability to minimize partial volume effect.

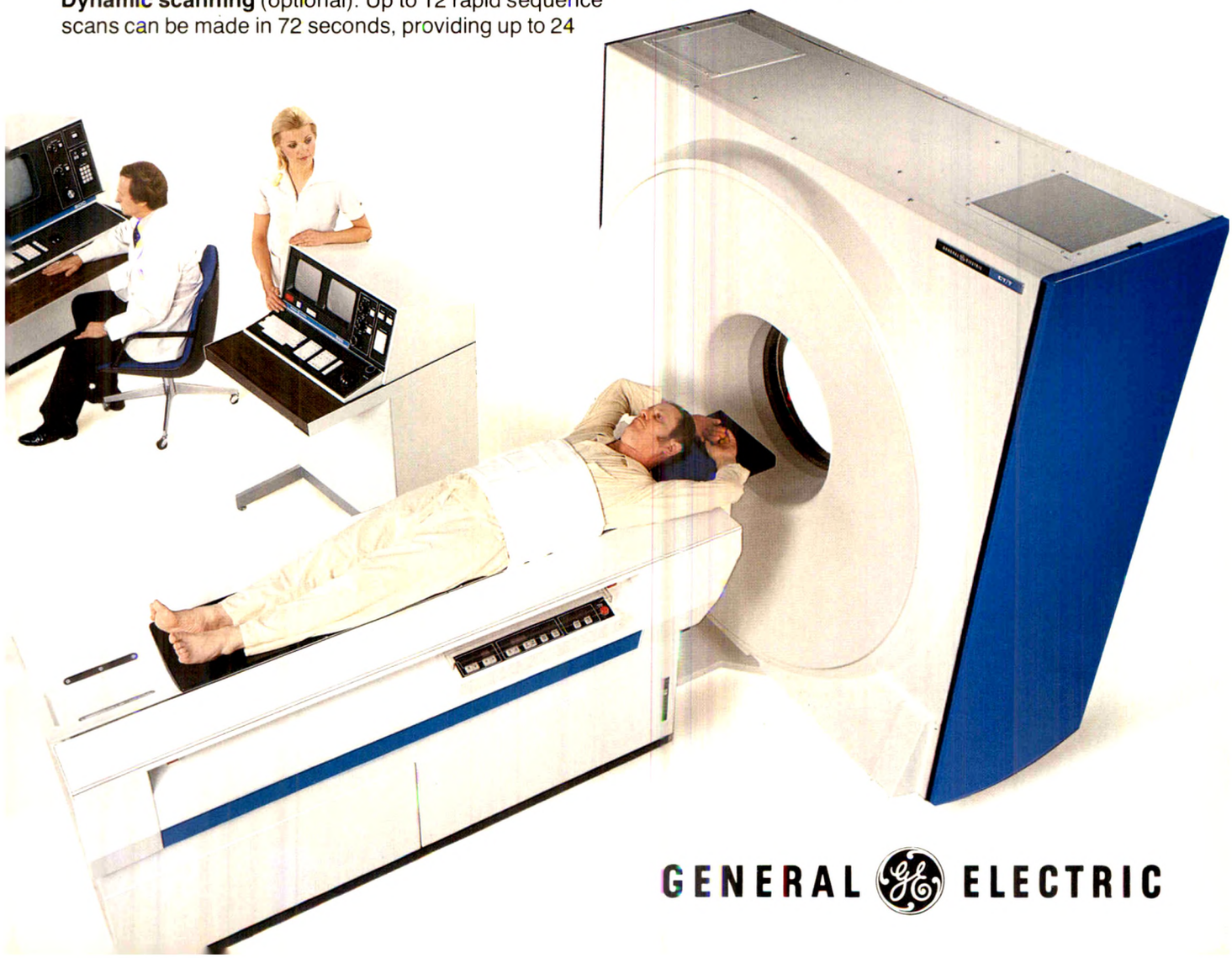
Dynamic scanning (optional). Up to 12 rapid sequence scans can be made in 72 seconds, providing up to 24 images. These allow visualization of a contrast bolus passing through a designated anatomical slice (CT transit study).

Sagittal and coronal transformations (no added cost). Use axial scan data to reconstruct either sagittal or coronal images, which are ready for display in less than 15 seconds per axial slice. Selectable thickness from 1 to 320 pixels. Allows three-dimensional image analysis.

Radiotherapy Treatment Planning (no added cost). Lets the operator establish external outlines, target outline and internal inhomogeneity outlines; assign densities; plan beam positions; calculate depth dose; and display isodose contours, dose, beam or patient data. A complete plan in a few minutes.

And General Electric is now developing even more CT/T capabilities for you in the future. So when you're choosing a CT system, total up GE's advantages: best images, best value, best service and protection against obsolescence. It all adds up.

General Electric Medical Systems,
Milwaukee, Toronto, Madrid.



GENERAL ELECTRIC

Fourth Annual International Body Imaging Conference



Royal Lahaina Hotel · Maui, Hawaii

OCTOBER 13–21, 1979 • CATEGORY I AMA-CMA CREDITS

The Fourth Annual International Body Imaging Conference will be held at the Royal Lahaina Hotel, Maui, Hawaii, October 13 through 21, 1979. Formal sessions Oct. 14–18

The Conference offers approximately 30 Category I AMA-CMA credits and will present to the participant a correlated approach to the principles, indications, uses, interpretation, and results obtained with computed tomography, ultrasonography, and nuclear imaging. Course participation by practicing imaging physicians, residents, technologists, and corporate personnel is encouraged.

COURSE FACULTY:

George Leopold, UC San Diego, California
Michael Johnson, M.D., University of Colorado Medical Center, Denver, Colorado
Leonard Rosenthall, M.D., Montreal General Hospital, Montreal, Quebec
John Haaga, M.D., Cleveland Clinic, Cleveland, Ohio
Pat Sheedy, M.D., Mayo Clinic, Rochester, Minnesota
W. F. Sample, M.D., UCLA Medical Center, Los Angeles, California
Stephen Fierstien, M.D., University of California at Irvine, Irvine, California

Enrollment limited. Registration fee $295. Residents and Technologists $225 (with letter)

W. FREDERICK SAMPLE, M.D. — Faculty Coordinator
RONALD J. FRIEDMAN, M.D. — Conference Coordinator
MICHAEL R. TERK, M.D. — Conference Co-Coordinator

For enrollment or further information write: Conference Secretary
Fourth Annual International Body Imaging Conference
Department of Radiology, West Park Hospital
22141 Roscoe Boulevard, Canoga Park, California 91304
213 340-0580 ext. 248

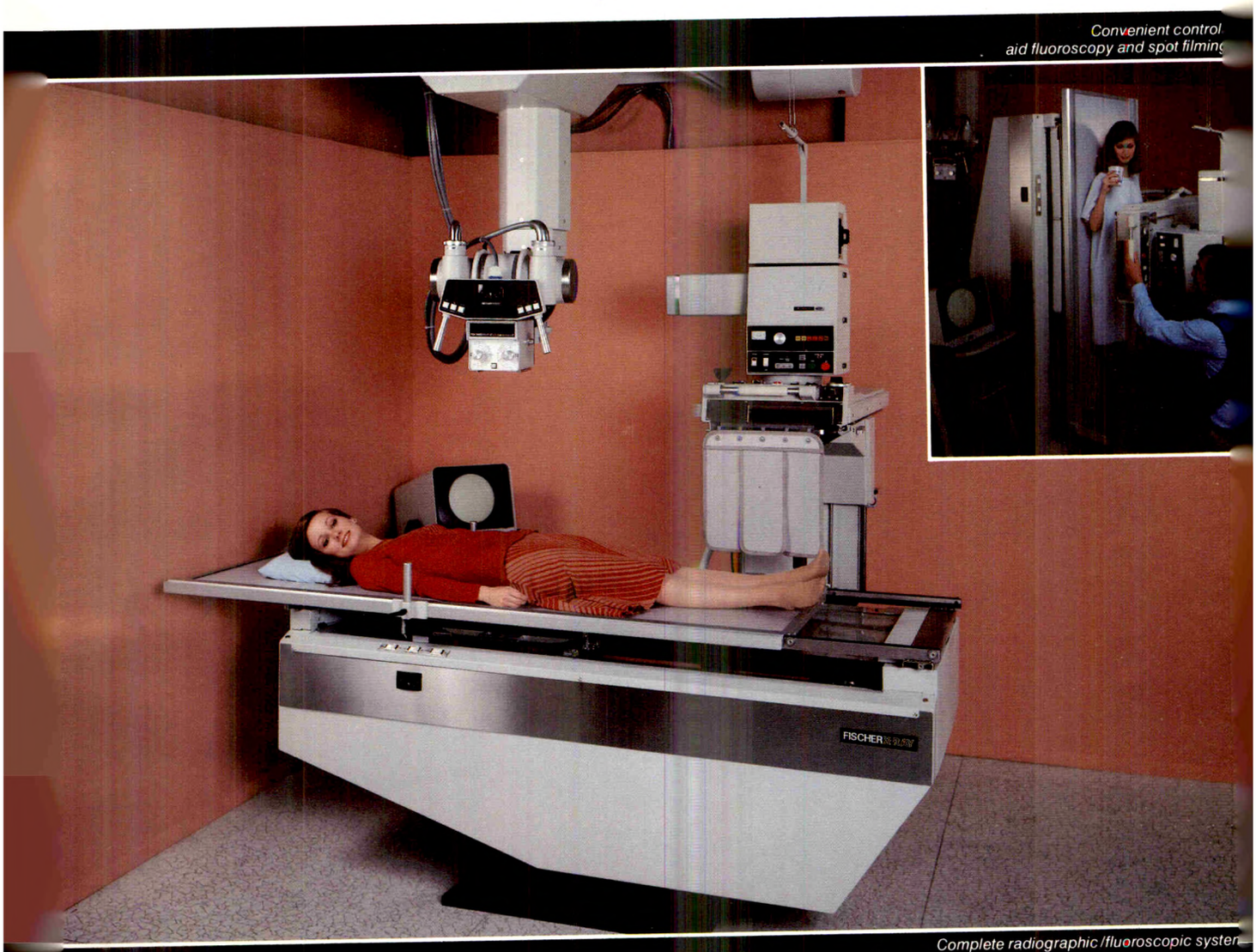
NAME _____

ADDRESS _____

CITY _____ STATE _____ ZIP _____

PHONE (Home) _____ (Business) _____

FISCHER X-RAY
introduces...new systems for Radiography/Fluoroscopy



Convenient control aid fluoroscopy and spot filming

Complete radiographic/fluoroscopic system

- FX650 or FX525 generator
- 90°/15° Concept 90 table
- 100mm fluoro spot film system

Modular design, economy and exceptional convenience characterize these new R/F systems. The motor driven Concept 90 table has automatic stops at 15° Trendelenburg, horizontal and vertical. Its 4-way top has a unique, 2¼" tabletop-to-film distance for superior image sharpness. Generators include 600mA/150kVp and 500mA/125kVp, both with ionization phototiming for consistent exposures at minimum patient dosage. Fischer's Cascade I Ceiling Tubemount provides 59" of vertical travel; digital display indicates focal distance. The superb optics of the Old Delft "Anodica" camera ensure excellent overall film detail. A unique optical distributor permits shock-free switching from fluoroscopy to film and back within one second.

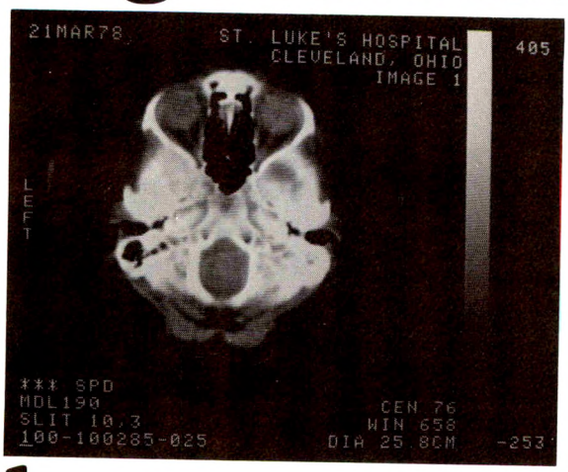
Write or call for detailed information, or the name of your local Fischer X-Ray Representative.

FISCHER® X-RAY

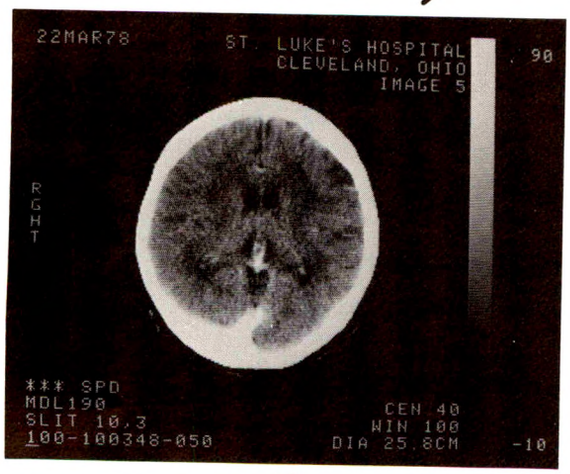
An established manufacturer of radiographic equipment, serving the medical profession since 1910.

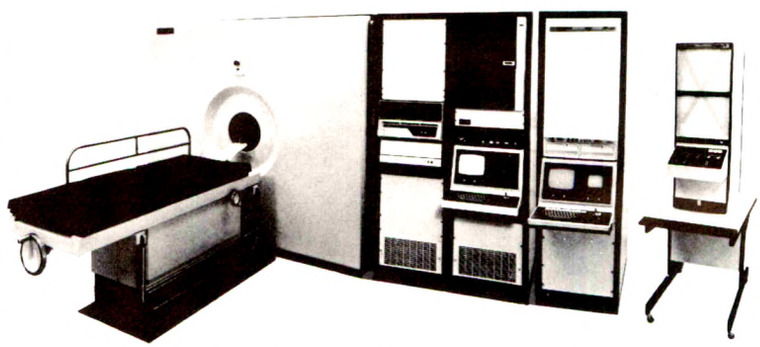
H.G. FISCHER, INC. 3816 N. Carnation Street, Franklin Park, Illinois 60131 • 312/671-5275

High-resolution,



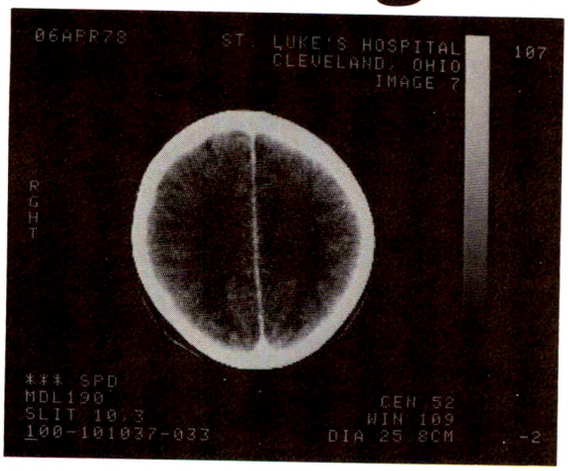
low-cost,





DeltaScan™ 100 Series.

neurological CT scanners



Computerized Tomography of the Brain, unquestionably the preferred modality in neurologic diagnosis, is now available at an economically feasible price.

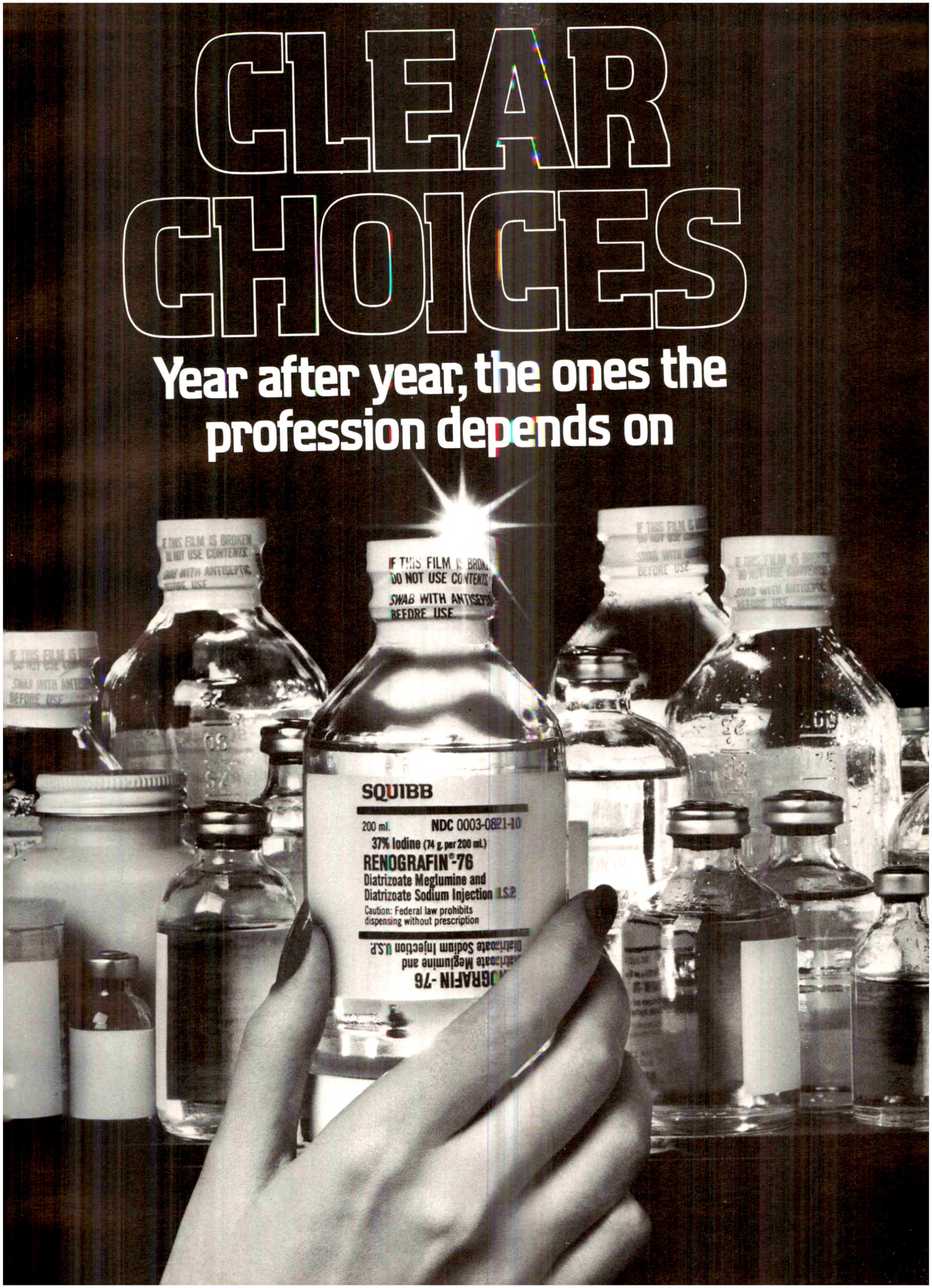
The DeltaScan 100 Series scanners, starting at $96,500, combine uncompromised resolution with a uniquely compact, new design, resulting in affordable, clinically proven CT scanners which are ideally suited for smaller institutions with moderate patient throughput needs.

For additional information concerning cost and performance of the DeltaScan 100 Series scanners, contact Ohio-Nuclear, Inc.

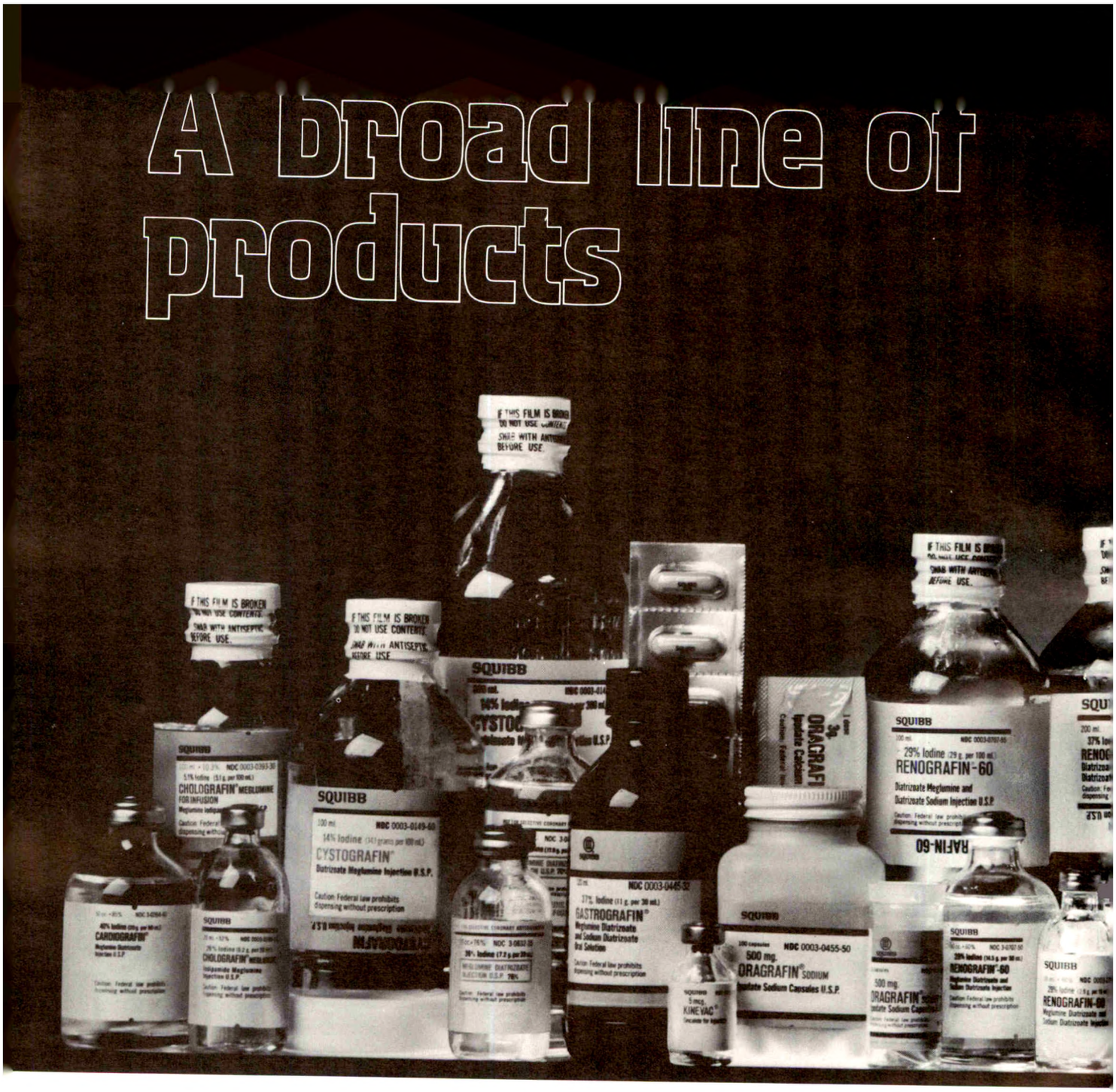
from Ohio-Nuclear, Inc.

A subsidiary of Technicare Corporation

29100 Aurora Road, Solon, Ohio 44139
Phone: (216) 248-1800
TWX No. 810-427-2696


CLEAR
CHOICES
Year after year, the ones the profession depends on
SQUIBB
200 ml.
NDC 0003-0821-10
37% Iodine (74 g per 200 mL)
RENOGRAFIN®-76
Diatrizoate Meglumine and
Diatrizoate Sodium Injection U.S.P.
Caution: Federal law prohibits
dispensing without prescription

A broad line of products



Cardiografin®
Diatrizoate Meglumine
Injection USP (85%)
50 ml

Cholografin® Meglumine
Iodipamide Meglumine
Injection USP (52%)
20 ml

Cholografin® Meglumine for Infusion
Iodipamide Meglumine
Injection USP (10.3%) 100 ml

Cystografin®
Diatrizoate Meglumine
Injection USP (30%)
100 ml, 300 ml

Diatrizoate Meglumine Injection USP 76%
20 ml, 50 ml

Gastrografin®
Diatrizoate Meglumine and
Diatrizoate Sodium Solution USP
(66%/10%)
120 ml

Kinevac®
Sincalide for Injection
5 mcg

Oragrafin® Calcium Granules
Ipodate Calcium for
Oral Suspension USP
3 g ipodate calcium per 8 g packet

Oragrafin® Sodium Capsules
Ipodate Sodium Capsules USP
0.5 g per capsule
Vials of 6 capsules, bottles of 100,
Unimatic® packages of 100

A wide range of sizes



Renografin®-60
Diatrizoate Meglumine and Diatrizoate Sodium Injection USP (52%/8%)
10 ml, 30 ml, 50 ml, 100 ml

Renografin®-76
Diatrizoate Meglumine and Diatrizoate Sodium Injection USP (66%/10%)
20 ml, 50 ml, 100 ml, 200 ml

Reno-M-60®
Diatrizoate Meglumine Injection USP (60%)
10 ml, 30 ml, 50 ml, 100 ml

Reno-M-30®
Diatrizoate Meglumine Injection USP (30%)
50 ml, 100 ml

Reno-M-DIP®
Diatrizoate Meglumine Injection USP (30%)
300 ml

Renovist®
Diatrizoate Meglumine and Diatrizoate Sodium Injection USP (34.3%/35%) 50 ml

Renovist® II
Diatrizoate Meglumine and Diatrizoate Sodium Injection USP (28.5%/29.1%)
30 ml, 60 ml

Renovue®-65
Iodamide Meglumine Injection 50 ml

Renovue®-DIP
Iodamide Meglumine Injection 24%
300 ml

Sinografin®
Diatrizoate Meglumine and Iodipamide Meglumine Injection (52.7%/26.8%)
10 ml

SQUIBB®
E. R. Squibb & Sons, Inc.

Professional service



Squibb Representatives are always happy to discuss Squibb's well-known, extensive line of products. However, they also like to talk about educational materials and to be of service in ways which will help radiologists in their professional activities. For example, there's "Clinical Radiology." It's a CME audio-visual program for use as a teaching aid for radiology residents, or as an in-service review for staff physicians, or just as a personal refresher course.

Current service materials are listed below. Check your interests and mail the form. Your Squibb Representative will soon be at your service.

© 1978 E. R. Squibb & Sons, Inc. 659-501

Radiology Product Manager,
E. R. Squibb & Sons, Inc., Box 4000,
Princeton, N.J. 08540

The leader in radiologic diagnostics

SQUIBB™ contrast media

I am interested in:

- ☐ Clinical Radiology (audio/visual program)
- ☐ *X-Ray Atlas* (review of diagnostic procedures)
- ☐ Motion pictures on radiology
- ☐ Squibb Radiology Education Program (slide/tape presentations)
- ☐ *Selected Radiologic Emergencies* (wall chart)
- ☐ *The Challenge...Radiography, Nuclear Medicine, Radiotherapy* (brochure on career opportunities in technology)
- ☐ Patient dose/instruction envelopes for cholecystography (English and Spanish)

Name _____ Position _____

Hospital _____ Address _____ Phone _____

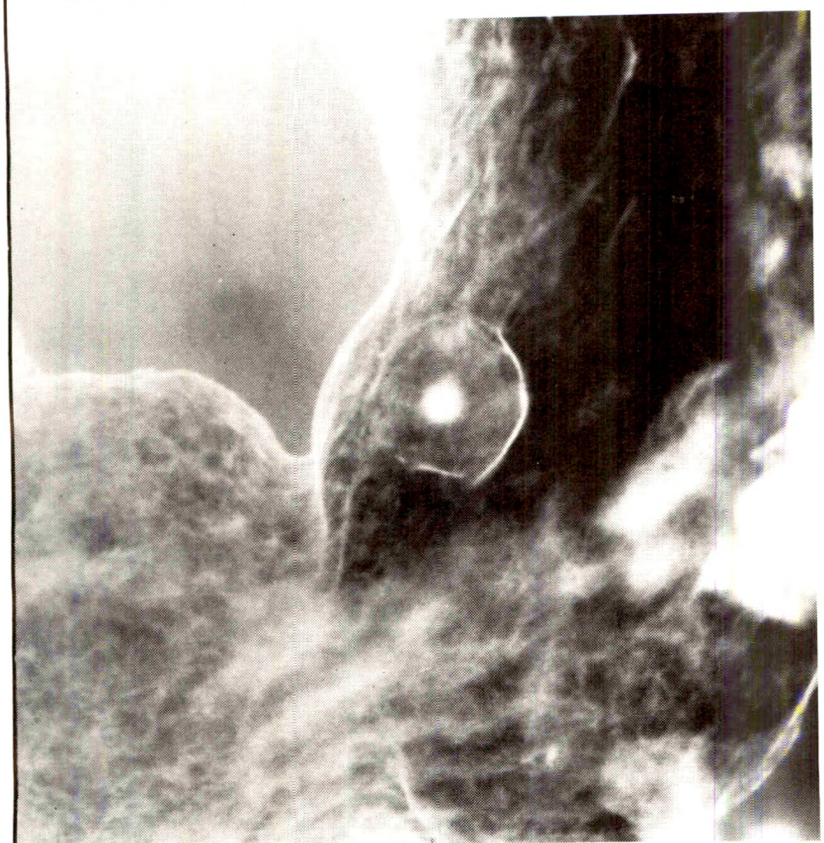
City _____ State _____ Zip _____

AB

For Double Contrast Stomachs, Use

NEW! E-Z-HD™

High Density with High Fluidity Barium Sulfate for Suspension USP



ANTERIOR WALL LEIOMYOMA WITH CENTRAL STALACTITE (HANGING DROPLET).
Film courtesy of Igor Laufer, M.D. Hospital of the Univ. of Pennsylvania

Double contrast radiography appears to offer the potential for significant improvements in diagnostic accuracy.

Double contrast studies of the stomach best demonstrate the surface pattern of the stomach (areae gastricae). This leads to improved detection of superfical erosions and ulcers, malignancies, polyps and other benign tumors, and ulcer scars.

E-Z-HD barium sulfate provides the basic ingredient necessary for good double contrast of the stomach.

The higher the density of the barium suspension, the better the coating. E-Z-HD allows for the highest density suspension of any commercial product on the market today: 85% w/w, 250% w/v. E-Z-HD achieves this density while remaining fluid for ease of administration.

- High density
- High fluidity
- Palatable
- Unit dose convenience.

E-Z-HD – The barium for the double contrast examination of the stomach and duodenum.

Optimal Density & Fluidity for the Modern Double Contrast Examination of the Stomach and Duodenum

Refrences:

David W. Gelfand: The Japanese-Style Double Contrast, Examination of the Stomach, Gastrointest Radiol. 1, 7-17 (1976)

Igor Laufer: The Diagnostic Accuracy of Barium Studies of the Stomach and Duodenum – Correlation with Endoscopy. Radiology 115: 569-573, June 1975

Roscoe E. Miller: The Air Contrast Stomach Examination: an overview. Radiology 117: 743-744 Dec. 1975

Order from your local X-ray supplier.

E-Z-EM 7 Portland Ave.
Westbury, New York 11590
(516) 333-8230

© 1/79

International Affiliates: E-Z-EM Rooster B. V., Infirmeriestraat 6-8, Rotterdam 16, Netherlands
E-Z-EM De Mexico, S. A. de C. V., Calz. Azcapotzalco La Villa No 882, Zona Industrial Vallejo, Mexico 16 D. F.

better

The 600 Beta Series Camera



Nice looking. The camera, we mean.

No need to pout. This camera won't let you make any careless mistakes, like forgetting to pull the dark slide.

Easy access. Takes the pain out of installation and service.

How do you name the heir to a classic?

We needed a way to tell the world that our new generation of 600 Series cameras was part of the original family of multi-format, video display cameras. But different. Totally redesigned for improved performance. But recognizably the same. So we picked the second letter of a classic alphabet – the Greek – and called it the Beta camera. It's second, but not second best. In fact, it's better.

Better than the camera that established the concept of multiple image hard copy on 8"×10" x-ray film? (And has the patent to prove it.) That has sold more units in this country and abroad than any of its numerous imitators? Hard to believe . . . hard to achieve. But true.

Better operating, for one thing. Single-handed front loading. Film cassette and dark slide interlocks that keep you from taking a picture when you shouldn't. Automatic Reset when a new film is loaded so you operate the camera almost without thinking.

We still offer the proven formats. And all the proven features, like flash card data entry, spot meter exposure system and footswitch remote operation. Our components will always be the finest available, including a new, high performance video monitor, Schneider lens and CMOS electronics.

This all pays off where it counts – in image quality. And when you see our images, you'll know for sure that Beta's not only better. It's best.

For more information, call collect or write: Dunn Instruments, Inc., 544 Second Street, San Francisco, CA 94107, (415) 957-1600

Dunn Instruments

The 600 Beta Series Camera



Single-handed front loading. Lets you install the Beta anywhere you like and load it on the run.

Ho hum. Simplified front panel controls make picture-taking a breeze.

Where Beta's best – superb clinical images in any format, positive or negative.

AJR Guidelines for Authors

Address manuscripts and correspondence to the Editorial Office, American Journal of Roentgenology, 403 Pacific National Bank Building, 4545 15th Avenue N.E., Seattle, Washington 98105; telephone (206)633-2754.

Publication Policy

The Journal publishes original and timely contributions to the advancement of radiologic diagnosis and treatment. Although the content is predominantly clinical, laboratory investigations are accepted when their relevance to clinical practice is demonstrable. In prospective clinical investigations, authors should indicate if informed consent from patients was obtained. Decisions on manuscripts are based on the opinions of at least two outside reviewers. Reviewers receive manuscripts without title pages to protect the identity of authors and to ensure an unbiased review; names of reviewers, in turn, are not revealed to authors. Statements within an article are the responsibility of the authors and not the Journal or its publisher.

It is understood that material submitted has not been published and is not currently submitted elsewhere. Portions of the data or illustrations from previously published works may be included if permission release forms accompany the manuscript and such material is clearly credited in the text. Prior publication of abstracts will not prejudice publication of the complete study.

Copyright Information

In accordance with Journal implementation of the 1976 U.S. Copyright Law, authors must release first and subsidiary rights to their manuscript at submission. A dated cover letter, containing signatures of all authors, should state: "We, the authors, assign first and subsidiary rights to the American Roentgen Ray Society in the event that our manuscript (title) is published by AJR." The Journal, in turn, grants authors the right to use portions of their manuscript, without charge, in books or articles of which they are authors or editors.

Manuscript Form

Manuscripts should be typed double-spaced throughout, including references, tables, and figure legends. Tables, footnotes, and figure legends should be on separate sheets, and a separate title page should be provided. In addition to the original typewritten copy, a duplicate copy complete with figures, tables, and references is required. Authors' names should be on title page only and should not be on figures so that author anonymity can be maintained during the review process.

Figures should be submitted as 13 × 18 cm glossy prints, untrimmed and unmounted. Labels and arrows must be of professional quality and should be removable from the prints. Each figure should be numbered to correspond with figure legends, and the top should be indicated. Specific permission for publication of facial photographs of patients is required. Line illustrations and graphs should be drawn in black ink on white background.

References should be cited in the text by number (e.g., [3, 4]). The bibliography should be arranged in the numerical order that references are cited in the text and typed double-spaced throughout. Data for each reference should be arranged according to the uniform style on bibliographic citations adopted by many biomedical journals. Provide all authors' names and inclusive pages. Abbreviations for titles of medical periodicals should conform to those published in *Index Medicus* Examples:

1. Miller RE, Chernish SM, Skucas J, Rosenak BD, Rodda BE: Hypotonic roentgenography with glucagon. *AJR* 121:264–274, 1974
2. Boijsen E: Superior mesenteric angiography, in *Angiography*, edited by Abrams H, Boston, Little, Brown, 1971, pp 1091–1119

Organization

Title page. Titles should be brief and specific. Include addresses for each author and acknowledgment of grant support when appropriate.

Abstract. A description of the purpose, methods, results and conclusions of the study is required.

Introduction. Clearly state the purpose of the investigation including necessary background facts.

Materials and methods. Decribe the protocol clearly. Use standard abbreviations as presented in the *Council of Biology Editors Style Manual*, 3d ed. Metric measurements should be used throughout.

Results. Present results in logical sequence.

Discussion. Interpret the results to lend meaning and importance to the observations. Hypotheses and speculation based on the results are encouraged. When results differ from those of previous investigators, an attempt should be made to explain the discrepancy.

References. Only include references which provide adequate background and present fairly any opposing evidence and concepts. Accuracy of reference data is the responsibility of the author.

Legends. Legends should be brief but should provide sufficient description to interpret the figure.

Special Communications

Case Reports. Concise case reports are accepted if they present unusual experiences that are medically important and educational. Clarity and brevity are essential. After preliminary screening by an editor to determine whether the requirement of medical significance has been met, qualifying papers will undergo the same peer review as major papers.

Technical notes. Brief descriptions of new techniques or significant modifications of older ones which are directly applicable to clinical practice will be accepted.

Letters to the Editor. Letters are subject to editing and condensation. Criticism of published articles should be objective and constructive. Letters may also discuss matters of general interest to radiologists.

Diagnostic Radiology: Geography of a High Technology

W. PETER COCKSHOTT[1]

A survey was made of the manpower employed, facilities available and utilization of radiology in countries in tropical Africa and Southeast Asia. The data obtained are compared with those from industrialized societies in temperate climates. The level of use of radiographic services varied by a factor as high as 40. The differences between the level of radiology manpower available could be over a hundredfold and for x-ray tehnologists, many hundred times. The concentration of services in capital cities is characteristic of many tropical societies. Measures to improve radiologic health care in tropical countries, with particular emphasis on rural areas, are discussed. The main need is for availability of radiodiagnosis close to the primary care level in rural areas to deal with the important clinical problems of trauma, chest infections, and obstetrics. Simplification of equipment and employment of technicians with short training can help relieve maldistribution of services.

Little information is available concerning the manpower situation in radiology and radiography, the facilities and resources deployed, and the degree of utilization of radiology in the tropical world. Several countries in Africa and the Far East were visited during the 1977–78 academic year to study the provision of radiologic health care.

The data gathered are presented and contrasted with figures from industrialized nations. Though the needs of communities differ and there is no absolute index of an ideal radiologic service, the quantitative differences revealed raise questions as to the role of this high technology discipline in different settings of health care. The existing economic constraints in developing areas raise issues in health priorities and resource allocations of a sort that are becoming more apparent in more affluent societies. No easy solutions are seen; various responses are discussed. There is a need to make radiology available outside large towns. The provision of simple facilities can meet most needs at a certain stage development.

Methods

The countries studied were Senegal, Liberia, Ivory Coast, Nigeria, Congo Republic, Kenya, Tahiti, New Zealand, New Guinea, Singapore, and Malaysia. Recent data from the Philippines [1], Brunei [2], and New Zealand were also included. For comparison, information pertaining to industrialized states was abstracted from the literature [3, 4].

In most countries I had access to official and unofficial data through contacts made during previous stays. In Africa, the local office of the World Health Organization frequently provided invaluable demographic information. This was supplemented by informants from Ministries of Health and University Departments of Radiology, Epidemiology, Social Medicine, and Public Health.

Much of the needed information was not directly available. Data were obtained by abstracting material from health and manpower reports, inspecting hospital returns and records, the files of professional organizations, and so on. Figures obtained from informants in radiology, radiography, and the local agents of the film and x-ray industry provided a useful cross reference on the reliability of the data.

The difficulty of obtaining valid statistics on medical manpower and the utilization of services is well known. To do this on a multinational scale and single handed may seem foolhardy. However, previous residence in the tropics suggested that the task was feasible since in most of the countries visited considerable centralization of radiologic services and records existed under the aegis of government. There were few agencies providing health care. The private sector was small and directly approachable. Thus information gathering was not unduly complex except in Nigeria where, because of recent decentralization into many federal states, it was not possible to obtain complete information on the population of 80 million in the time available. I did not attempt to study other large countries, such as India and Indonesia, since each would have been a formidable undertaking. I estimate the reliability of figures gathered to within ±10%. Since the order of differences is many times that figure, errors do not substantially affect interpretations of the statistics.

Utilization of Radiology

For comparison, there are several indices that indicate the relative use of radiology. Measurement of the number of examinations per thousand population in a year is an established criterion. It is imperfect in that it is purely quantitative and not qualitative, since it equates a complex procedure with the simplest. However, since the major work load of any department consists of simple procedures (especially in the tropics), no weighting factor for complexity has been introduced. The quantitative differences of utilization between countries are of sufficient size that a more refined calculation would not alter the inferences that may be made.

The data gathered apply to either the year 1976 or 1977 unless stated otherwise. It is evident from the histogram (fig. 1) that in many developing areas radiology is used about 30 times less often per capita in the tropics than in temperate states. There are some anomalies. Liberian utilization is relatively high because of a network of plantation and mining concession hospitals providing an excellent service to small defined segments of the community. Tahiti holds an anomalous situation throughout this review due to circumstances that will be detailed later.

The consumption of film serves as another indicator of

Received October 2, 1978; accepted after revision November 21, 1978.

[1] Department of Radiology, McMaster University Medical Centre, 1200 Main Street West, Hamilton, Ontario L8S 4J9, Canada.

© 1979 American Roentgen Ray Society

0361–803X/79/1323–0339 $0.00

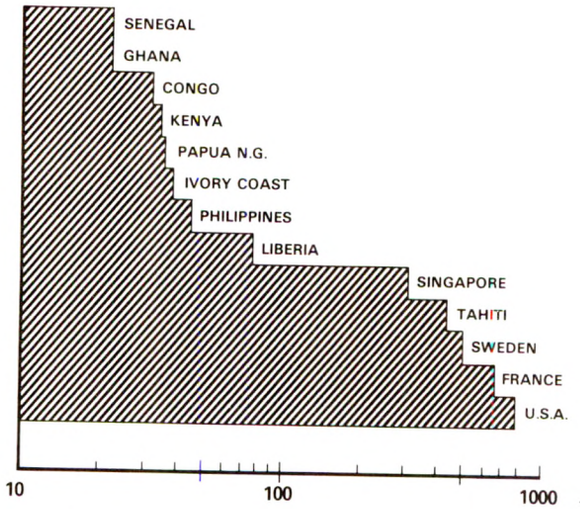


Fig. 1.—Radiographic examinations per 1,000 population per year.

TABLE 1
Film Consumption

1976 or 1977		1972	
Ghana	2.7	Australia	125*
Papua, New Guinea	4	Sweden	131*
Kenya	4.8	Belgium	139*
Brunei	18.5		
Malaysia	27.8		
Tahiti	113		

Note.—Data reported in square meters per 1,000 population per annum.
* Derived from Dutch commercial source.

the use of radiography. Unfortunately this is difficult to determine for most nations; comprehensive government statistics do not exist. Competing film companies are usually reluctant to disclose their market information. I was only able to determine the square meters of films used per 1,000 population each year in countries where films were largely purchased or distributed centrally, where importation was suitably recorded, or in Malaysia where the film suppliers were helpful. For 1972 comparable figures for Europe were available from a Dutch commercial source providing a bench reference. Once again, the least developed areas consume (including wastage) about 25 times less film than parts of Europe 4 years earlier (table 1).

An approximation of the complexity of studies may be gained by dividing the number of radiographic examinations per annum into the area of film used (assuming the same rate of wastage everywhere). One can argue more legitimately that the film area usage reflects the radiation dose delivered to the population. Such a calculation can be fallacious in communities where a great deal of mass miniature radiography is carried out. However, my impression is that this radiographic activity world wide has diminished considerably in recent years. Such calculations indicate that, as expected, the complexity of studies and the radiation delivered to the population in the tropics, with the exception of Tahiti, was well below the level obtaining in industrialized countries.

TABLE 2
World Barium Use

	Barium Used	
	tons	%
U.S. and Canada	6000	50
Japan	2000	17
Europe	2600	22
Rest of world	1400	11

Note.—Derived from market research by Herskovitz 1975.

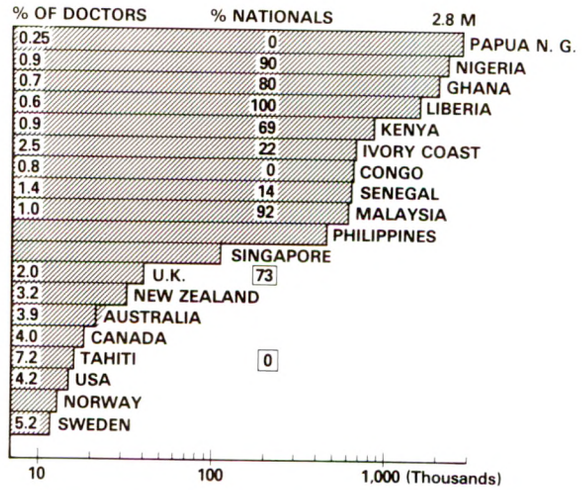


Fig. 2.—Population per radiologist. % of doctors = percentage of all doctors who are radiologists; % nationals = percentage of radiologists who are nationals.

Crude figures of world barium sulphate consumption (excluding China and the Soviet bloc) compellingly indicate utilization discrepancies with two-thirds of the world's medicinal barium being used in the U.S., Canada, and Japan (table 2). Barium studies require trained staff and sophisticated equipment for their performance, so that they are only carried out extensively where adequate staffing facilities exist.

Manpower and Facilities in Radiology

For effective use of facilities, individuals trained to an appropriate level must be available. Scarcity and maldistribution of both radiologists and radiographers (x-ray technicians) is apparent from the survey.

Radiologists

The country most poorly endowed with radiologists in the survey had 230 times fewer per capita than Sweden (fig. 2). This figure is extreme; nevertheless many tropical areas have about 40 times fewer radiologists per capita than Sweden.

In the United States, radiologists represent 4% of all physicians [3] and in Sweden, 5.2%; whereas, with the notable exception of Tahiti (7.2%), in most of the tropical world, less than 1% of doctors practice radiodiagnosis. A consequence of this absolute shortage, which is further exacerbated by maldistribution, is that most radio-

graphic studies are never seen by radiologists. Examinations requiring a radiologist such as barium investigations and special procedures are rarely done.

The proportion of radiologists who are nationals or citizens was indicated for those countries where this could be calculated. In English-speaking countries, the majority of radiologists are citizens; whereas in former French territories, expatriate military medical officers provided under technical assistance programs are the main cadre of the radiology work force.

Countries with a shortage of physicians rely on foreign technical assistance, short term contracts, or immigration to attract radiologists. There is still a shortage of radiologists world wide. Foreign medical graduates can command a salary that is difficult for most developing countries to meet unless they produce oil or have other attractive natural advantages such as climate. Tahiti is an example of the latter. Its seductive scenery becomes known to French military radiologists, some of whom after retirement settle there and establish a private practice. Consequently this island with no Polynesian radiologists has, by military presence, the highest ratio of radiologists to other physicians in the world. This has naturally led to a high utilization of radiology and presumably to a high per capita radiation dose. This is unfortunate given the world wide concern over the exposure of that particular population to fallout from atomic tests [5].

The mobility of radiologists is toward a more prosperous environment, rather than a traffic from developed areas to the tropics. Inadequate economic rewards and poor professional facilities naturally lead to emigration.

There are more Philippine radiologists in the U.S. than in their homeland. Australia and New Zealand have attracted many Southeast Asian radiologists. North America and the Antipodes have drawn British, Indian, and South African radiologists for many years. Many of these countries now have adequate radiology manpower and have developed immigration barriers that have curtailed the "brain drain." Holland and oil rich countries still attract foreign radiologists.

Dissatisfaction with monetary rewards cannot be readily quantitated due to differences in living standards, cost of living, exchange fluctuations, and other variables. For a crude measure of local purchasing power, I determined what the before-tax estimating earnings of a radiologist 5 years in practice would purchase locally of such commodities as chickens, local beer, local cigarettes, and Bic pens. This crude form of consumer price index makes clear that some radiologists in the tropics received emoluments which have 30 times less purchasing power than radiologists practicing in North America.

In the countries surveyed, private practice accounted for a small proportion of the radiology done. I realize this is not true for all the tropics, because in parts of Latin America the private sector is important in radiology. In the newer nations of Africa, the high capital investment required and the competition of adjacent government facilities discourage private radiology. Potential patients are few. The affluent elite who wish to pay for the luxury of personal uncrowded service, those covered by company medical schemes, and expatriates ineligible for government medical care constitute a small segment of the community on which to establish a viable practice.

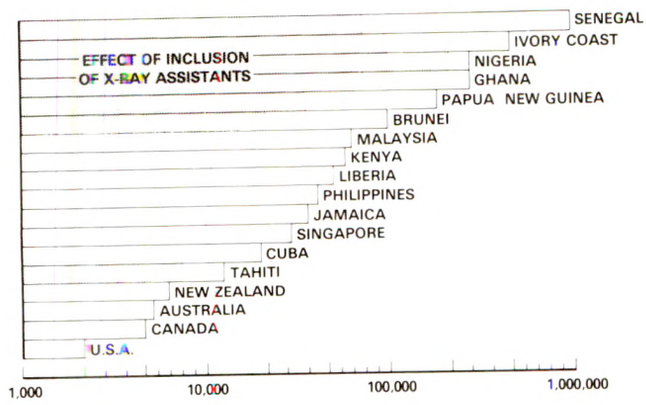


Fig. 3.—Population per x-ray technologist.

Though radiologists may not provide much private radiology, other categories of physicians not infrequently own simple low-output x-ray equipment. In rural areas where no other facilities exist this can be useful service. In urban areas, the small-capacity portable machines allied to an ineffective darkroom and unskilled operator produce films that may defy even skilled interpretation. Their value is then minimal. The existence of an x-ray set is sometimes more of a status symbol attracting patients to generate income rather than provide information.

Radiographers (X-ray Technologists)

International comparisons of technician manpower are hindered by varying definitions, terminology, and levels of training. Most English-speaking countries have some equivalence of grade which may be acknowledged by reciprocity in the recognition of qualifications permitting individuals to exercise their profession in many states. Countries of Latin culture often do not have such a tradition of high level training in this field. A less well educated and trained group who have received brief on-the-job training forms the majority of x-ray technicians in many areas.

Variations in policy between English-speaking areas and others is reflected in the training arrangements. In most English-speaking countries, there are well developed formal schools of radiography with a 2 to 3 year course combining theory and practical experience. Sometimes these may be supplemented by schools with less rigorous entry requirements and perhaps only 6 months to a year of training. These produce staff variously termed technicians, assistant radiographers, or "operateurs." It is some form of this category who predominate numerically in French-speaking areas and in much of Central and South America [4].

Radiography is globally a multitiered service including individuals of differing levels of expertise and training. The relative workload contribution made by the less trained technicians can be significant. In the histogram on comparative radiography manpower (fig. 3), Senegal

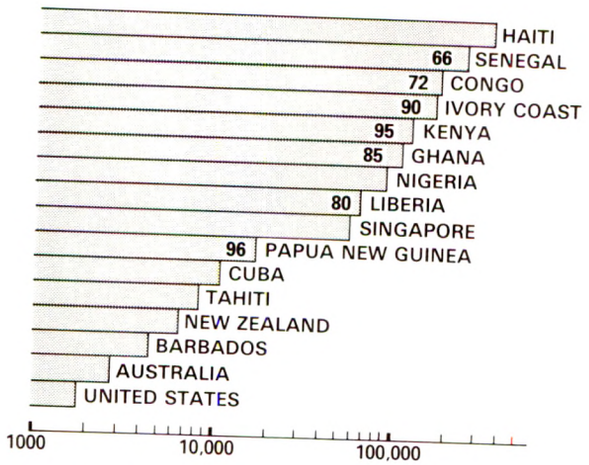


Fig. 4.—Population per x-ray unit. Numbers indicate percentage of functioning equipment.

is shown to have only one radiographer for about one million population but, by the inclusion of technicians (operateur), the level of service to the public is raised tenfold. Similar observations apply to the Ivory Coast, Ghana, and Papua, New Guinea.

Equipment

The relative distribution of x-ray installations (excluding dental sets) is depicted in the bar graph (fig. 4). The pattern of variation is by now familiar. The calculations are based on the actual total number of units, irrespective of whether they were capable of working or not. The true picture increases the disparities, since tropical countries have a high and at times prolonged breakdown rate of x-ray equipment. I have indicated the percentage of functioning equipment in those countries where this was possible (fig. 4). It is a liberal figure based on considering a machine as unserviceable only when it was completely devoid of function. In most countries at least 20% of apparatus had significant faults.

Many factors are responsible for lack of proper equipment and all are basically related to the market place and economics. The budget for spares and maintenance is often inadequate. Spares are no longer available for obsolete equipment. Service engineers are few and have too large a territory to serve. Donated equipment may be unsuitable by being obsolete or too sophisticated for the application. Equipment aid and gifts often provide no commission to the local agent who later may show disinterest when breakdowns occur.

Three quarters of the expensive complex remote-control units that I saw were inoperative in the tropics—in one case for over 2 years. This is a tragic waste of resources. In any case, I can see little justification for remote-control units that render an examination even more impersonal. The equipment further separates the patient from the radiologist who often, even if a citizen, has to battle with dialect and language problems to communicate with a patient. A voice close at hand—even an interpreter's—is better than a disembodied microphone command made from behind a lead glass enclosure.

TABLE 3

Capital City Syndrome

	Radiologist (%)	Population (%)	Exams (%)
Congo	100	29	84
Papua, New Guinea	100	6	25
Liberia	100	20	35
Ivory Coast	89	15	79
Senegal	86	30	84
Ghana	86	7	35
Kenya	75	5	29
Malaysia	44	7	25
Nigeria	38	5	. . .

Capital City Syndrome

The concentration of facilities in large urban areas results in considerable maldistribution of services. Some examples of this are shown in table 3, which indicates how a small segment of the population in the capital city receives most of the available service. The presence of tertiary hospitals and the needs of a medical school in the capital are bound to distort the natural distribution of service. It is the degree by which this process deprives rural areas of skilled radiology service that is alarming.

Discussion

Initially radiology came to the tropics during colonial wars. Even the primitive equipment of the late 1890s was capable of detecting major fractures and metallic foreign bodies of combatants in such diverse areas as the northwest frontier of India [6], the Sudan [7], Cuba [8], and South Africa. These early ventures exemplify the requirements of a successful radiology program: defined objectives capable of realization with the means available.

Radiology services are viewed by health planners as a high technology that imposes heavy demands on available capital and operating funds and skilled manpower. Health authorities fear radiology because it can make large demands on the budget and yet apparently only produce poorly defined intangible benefits. When there are few dollars to spend per capita on health, officials favour preventive public health measures, perhaps benefiting the many, to the funding of curative and diagnostic services directed at few individuals [9]. Radiology is competing for funds and may have a low priority [10] compared with say a scheme to provide a piped water supply to control endemic bacterial and parasitic waterborne diseases.

What are the objectives and needs of a radiodiagnostic program? How much radiology is needed? Where should facilities be located? What are the manpower requirements? Such questions are not usually posed nor answered, in the tropics any more than elsewhere, since

radiology develops in an ad hoc fashion responding to demands and pressures as well as needs. In some countries the civil service is strong—a colonial legacy—so that it exerts more influence than the weak private sector. In many countries the increasing numbers of city dwellers and influential patients are creating pressures for greater availability of diagnostic services in the cities. Tertiary care hospitals and medical schools require sophisticated hospital radiographic facilities. Gradually a much higher level of radiology develops in the towns than in rural areas with the major share of costs in the towns. The capital city syndrome (see above) is the result. This is not a critical comment—the phenomenon is universal and few if any societies have effectively provided similar standards of care to rural and urban people. The task is probably impossible.

How much radiology and what kind?

There is no abstract standard of ideal utilization of radiology or of resource and manpower allocation. The level of service provided in North America may seem needlessly high to some, whereas that available in the tropics is inadequate. One or both of these views may be valid, but such statements are only matters of judgment. The level found in a community depends on priorities accorded, market place factors, political systems and doctrines, history, and economic considerations. Each situation is unique. The comparative statistics gathered in the first part of this paper merely document existing differences.

Cost benefits and effectiveness are fashionable concepts to mention in discussions concerned with the role of radiology as a health maneuver. Methodologies have been developed to study these ideas, but none have been applied yet in the tropics [11]. However, even without such tools to evaluate radiologic needs, certain policies seem to have advantages.

The role of radiology in the initial diagnosis of many common tropical diseases is low in comparison with the value of clinical examinations and, particularly, laboratory studies. This is so in malaria, trypanosomiasis, schistosomiasis, leishmaniasis, filariasis, and hookworm. There are many clinical tropical endemic diseases where radiology is of value in diagnosis and management, but these conditions are often not quantitatively important.

Many health problems of the tropics are cosmopolitan: trauma, chest infections in children and adults, and obstetric problems. Road accidents are major problems in most developing countries. Radiology is invaluable for diagnosis and management of limb, chest, abdominal, and head injuries.

Pulmonary disorders are a major contribution to childhood mortality, particularly in malnourished children. Primary pulmonary tuberculosis and skeletal tuberculosis rely extensively on radiographic services for diagnosis and management. Industrial and mining dustborne diseases exist only in small foci in the tropics and do not pose general problems.

While most of the world eschews obstetric radiology in favour of ultrasound studies, this is not so in the tropics. Ultrasound machines are expensive, complex, and require expert electronic care. As such they are unsuitable except in sophisticated hospitals in large cities. Most births occur in rural areas. Detection of cephalopelvic disproportion, fetal age and malposition, and even placental localization can still be effectively done with simple x-ray apparatus.

One can find many other problems in which radiology can be of help, but those related to trauma, chest infection, and obstetrics dominate at the district level where the people live.

As Schumaker [12] said in another context:

> In the dual economy of a typical developing country we may find fifteen percent of the population in the modern sector mainly confined to one or two big cities. The other eighty-five percent exists in the rural areas and small towns . . . the heart of the matter . . . is the stark fact that world poverty is primarily a problem of two thousand million villagers.

What equipment and where?

The closer radiographic facilities can operate to the primary care level, the greater their availability; at the same time, the number of units required obviously increases with the degree of dispersion. Unless an area is exceptionally remote, a unit will be underutilized if there are not at least one or preferably two physicians to refer cases and study the films.

There is a need for equipment to carry out chest, extremity, abdominal, and spine films as close to the primary care level as possible. The degree of dispersion in a rural area must match that of physicians to ensure adequate use, since a radiographic examination will not only be ordered but also interpreted by the same doctor or doctors.

The equipment should be simple for many reasons. Reliability is related to complexity; the possibility of a malfunction increases according to the product of the number of components and not their sum. A simple machine is cheaper to buy and easier to operate. Yet simplicity need not impose significant operational limitations. Practical experience in a teaching hospital indicates a mobile unit can carry out about 80% of all radiographic procedures. At the health care unit levels, it can meet virtually all demands. There is no need for fluoroscopy there. Indeed elimination of fluoroscopy removes radiation hazards to patients and operators. It also avoids the use of fluoroscopy to spare the cost of films.

The World Health Organization has developed guidelines on suitable basic x-ray equipment [12, 13]. Technologic advances have now made it possible for manufacturers to provide battery operated units that do not require sophisticated stable high-capacity line supplies—an advantage in the tropics. Some are powered by nickel-cadmium and others by lead-acid batteries. I fa-

vour the latter because they are better understood due to the universal presence of cars.

Bulk purchasing of such units with standardization would result in a lowering of unit price. A further advantage would be in the improved availability of spares. Repairs would be facilitated once locally trained personnel became familiar with a locally prevalent model. Diversity of equipment was an important factor in many service problems I saw in the tropics.

In more sophisticated hospitals, fluoroscopy units do not generally require television. Mirror optics or direct-viewing intensifying panels eliminate the weakest link in the video chain.

Modern industry can provide simple reliable x-ray equipment. Bulk purchase offers great advantages. It is to be hoped that such a policy will develop not only in a country, but perhaps even among adjacent territories with low population density.

Manpower Needs

Simple equipment dispersed out of the main towns does not need operators trained for 2 years who can do a full range of radiography. Their skills will be unused and they will not have career satisfaction in doing simple tasks. In any case, skilled manpower is difficult to attract out of cities. It is far more realistic and cheaper to train a paratechnician or assistant radiographer for perhaps 3 months. Such an individual will function effectively and be willing to remain at the local level.

In large countries schools of radiography will meet the needs of the larger hospitals where more sophisticated techniques are required. Experienced radiographers can be trained to carry out an extended clinical role in circumstances where radiologists are scarce. It has long been shown that they can do fluoroscopic procedures effectively [14].

Scarcity of radiologists is more difficult to overcome. Technical aid programs can assist by financing foreign graduates. This is a short term solution. Sending local graduates overseas for training is often necessary but also has disadvantages. Trained radiologists may not return to their homeland. They will be trained to face diseases abroad that may not be frequent in their home environment. They will have become used to elaborate equipment and support services that are unlikely to be duplicated in their country. Instead, if the country is large enough and has a medical school, as much local training as possible should be done locally. Here an established foreign school can help by sending staff to work locally to assist in training programs and to provide training overseas for a segment of the course. Such a dual program avoids loss of contact with local clinical problems and exposes the training radiologist to an established learning environment. To keep radiologists in a training institution, it is necessary to ensure that the level of remuneration does not differ greatly from that in the private sector. Otherwise the objective of establishing a local training cadre will be defeated.

Only a few of the problems raised by the findings of the radiology survey have been discussed. Generalizations can provide a false impression of realities. External controls and regulations are historically relatively new to health services. Alone they often fail. For health plans to succeed, there must be a sense of commitment, understanding, and will to implement policies both by government and health workers. This is the most difficult phase of action. To meet the rising health expectations of the people in the tropics some nontraditional approaches show promise and need to be extended.

I do not advocate barefoot radiographers and radiologists, but there is no need for all to wear city shoes. Sandals and boots are not amiss if a comprehensive service is to be provided.

ACKNOWLEDGMENTS

This study was carried out during a sabbatical year supported by McMaster University, McMaster University Medical Centre, the James Picker Foundation, and the assistance of the World Health Organization. Numerous informants and sources generously provided their data and knowledge in 16 different countries.

REFERENCES

1. Bretland PM: *W.H.O. Report, Regional Office For The Western Pacific*, ICP/RAD/003, 1978
2. Jones A: *Report of State Radiologist Specialist*, State of Brunei, 1978
3. Riemenschneider PA: Radiology manpower update, 1976: shortage or surfeit. *AJR* 129:575–582, 1977
4. Organizacion Panamericana de la Salud/Organizacion Mundial de la Salud: Reunion de Directores de Escuelas de Technologos en Radiodiagnostico de America Latina. Caracas, October 1976
5. Danielsson B, Danielsson MT: *Moruroa Mon Amour. The French Nuclear Tests In The Pacific*. Victoria, Penguin (Australia), 1977
6. Beevor WC: The working of the roentgen ray in warfare. *J Roy United Service Institution* 42:1152–1170, 1898
7. Battersby J: The present position of the roentgen rays in military surgery. *Arch Roentgen Ray* 3:74–80, 1899
8. Borden WC: *The Use of The Roentgen Ray By The Medical Department of The United States Army In The War With Spain, 1898*. Washington, D.C. Government Printing Office, 1900
9. Lambeth JT, Chamberlain RH: The radiologist and health care in "the developing world." *Radiology* 116:231–232, 1975
10. Yudkin JS: Provision of medicines in a developing country. *Lancet* 2:810–812, 1978
11. *The Efficacy and Efficiency of the Diagnostic Application of Radiation and Radionuclides. Report of a WHO Meeting of Investigators, Brussels, November 1977*. Geneva, WHO, 1978
12. *Report of a WHO Seminar on the Use of Medical Radiological Apparatus and Facilities, Singapore, November 1970*. Geneva, WHO, 1971
13. *A Primary Care Radiological System, Report on a Meeting, Washington, D.C., March 1975*. Washington, D.C., PAHO, 1975
14. Campbell JA, Lieberman M, Miller RE, Dreesen RG, Hoover C: Experience with "test" performance of gastrointestinal examination. *Radiology* 92:65–73, 1969

Performance Evaluation of Computed Tomography Scanners Using a Phantom Model

ERROL M. BELLON,[1] FLORO D. MIRALDI, AND ERNEST J. WIESEN

A phantom was designed to test computed tomography (CT) scanner performance relative to spatial resolution, contrast resolution, field uniformity, spatial linearity, artifact resistance, and radiation dose. Translate/rotate, stationary detector with rotating x-ray tube, and rotate-only scanners were tested under conditions that produced the best possible results for each machine within the dose ranges used in clinical practice. Machines can be ranked according to results for each parameter tested. The range of performance exhibited on machines tested was unrelated to class of scanner. Further, machine dedication to a particular body region did not necessarily secure superior results for that region. Spatial resolution at low contrast levels (poor on most machines) seems to be the most sensitive test of performance.

Many factors must be considered in the selection of a computed tomography (CT) scanner for clinical use: purchase and maintenance costs, scan time per slice, radiation dose, ease and efficiency of operation, and image quality. Of these, image quality is not easily evaluated by simple observation because of the many factors which influence image presentation. Nonstandard images on a display monitor (or their hard copy versions) are unreliable for experimental analysis since substantial manipulation of the image is possible. Although many investigators have considered this problem from both theoretical and experimental perspectives [1–4], interscanner parallel comparison is difficult since images are not presented under controlled conditions. Furthermore, as Brasch et al. [5] observed in testing radiation dose and resolution capacity on several CT scanners, the validity of results is questionable and subject to error unless the model used is designed to test those variables integral to image reconstruction under control conditions as closely parallel to the clinical situation as possible. As yet, this has not been attempted by other researchers.

It is with these considerations in mind that we devised a phantom model which (1) provides objective data on the overall performance of a CT scanner system; (2) allows characterization of image quality produced by an individual scanner under test; and (3) permits unbiased, parallel interscanner comparison based on objective data.

Experimental Design

The phantom was designed in two parts (A and B) to evaluate the following parameters: (1) field uniformity, (2) spatial linearity, (3) resistance to artifact, (4) spatial resolution, (5) contrast resolution, and (6) radiation dose per single scan slice and per adjacent scan slice. Phantom A tested spatial resolution at various contrast levels. Phantom B tested each parameter in a composite structure consisting of six sections.

We selected Plexiglas as the most appropriate material because it has uniform density, is easily machined, is readily available, and possesses a suitable difference in absorption coefficient relative to air, water, Lexan, and calcium chloride encompassing the dynamic ranges seen clinically.

Phantom A

Phantom A (fig. 1) consists of a support about 20 cm in diameter capable of holding five Plexiglas block inserts, each 9.8 × 7.6 × 1.9 cm. It was designed to demonstrate CT scanner performance relative to spatial resolution at different contrast levels. The contrast level was adjusted by changing the medium used to fill series of drill holes 5, 3, 2, and 1 mm in diameter in a Plexiglas block (the center-to-center distance between holes is twice the diameter). The depth of the drill holes was varied for ease in manufacture.

Sucrose/water solutions, calcium chloride solutions, and air were used to provide attenuation coefficient differences with the Plexiglas. Material attenuation coefficients are shown on table 1. The values for sugar and calcium chloride were calculated from their atomic composition for 70 kV effective. The values for Plexiglas,

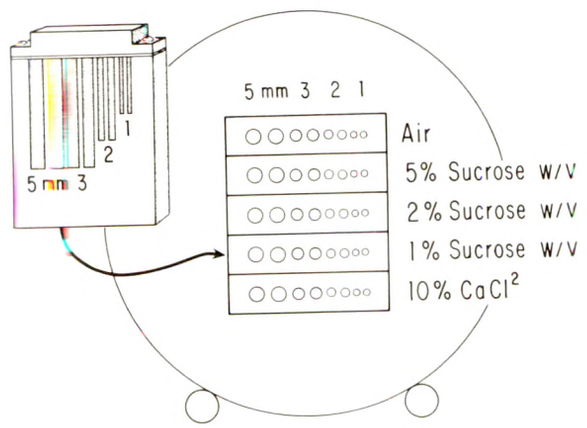


Fig. 1.—Construction of phantom A.

Received September 5, 1978; accepted after revision December 5, 1978.
[1] All authors: Department of Radiology, Case Western Reserve University and Cleveland Metropolitan General Hospital, 3395 Scranton Road, Cleveland, Ohio 44109. Address reprint requests to E. M. Bellon.

AJR 132:345–352, March 1979
© 1979 American Roentgen Ray Society
0361–803X/79/1323–0345 $0.00

TABLE 1

Material Attenuation Coefficients and Contrast Relative to Plexiglas

Material	Attenuation Coefficient (μ (cm^{-1}))	Contrast (%) Relative to Plexiglas ($\Delta\mu/\mu$)
Plexiglas	0.218	0
Sugar:		
0.45%	.225	+3.2
1%	.224	+2.7
2	.221	+1.3
5%	.215	−1.3
Water	.195	−11.0
Lexan	.213	−2.3
Calcium chloride (10% solution)	.293	+34.0
Aluminum	.645	+195
Iron	6.62	+ very large
Air	.0002	− very large
Bone	.423	+94

water, and Lexan are by McCullough et al. [1]; for aluminum, air, and bone by Johns and Cunningham [6]; and for iron by Grodstein [7]. Attenuation coefficients were extrapolated to 70 kV effective according to Zatz and Alvarez [8].

The sucrose/water solutions were used to provide a small contrast level difference with the Plexiglas to simulate soft tissue differences in the clinical situation. Calcium chloride solutions provided a greater contrast difference comparable to bone/soft tissue contrast. The ultimate high contrast level differences were provided with the air-filled holes in the Plexiglas. Slots were milled in the phantom holder to provide locations for thermoluminescent dosimeters used to measure single-slice dose.

Phantom B

Phantom B (fig. 2) is 20 cm in diameter and 1.5 cm thick. It holds six individual test sections, each 1 cm

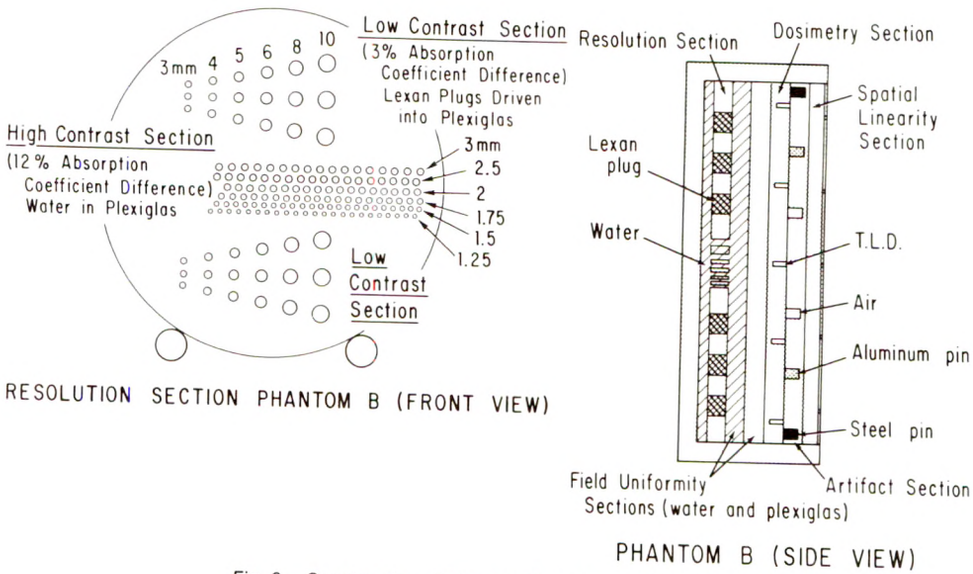


Fig. 2.—Construction of phantom B: front and side views.

TABLE 2

CT Scanner Characteristics

Scanner Class	Scan Time (sec)	Machine	Type	Manufacturer and Model
Class I: Translate/rotate	20–240	G	Head	EMI 1010
		E	Body	EMI 5005
		F	Body	EMI 5005
Class II: Stationary detector with rotating x-ray tube	4–20	C	Body	Ohio Nuclear 2020
		D	Body	A. S. E.
Class III: Rotate only	3–96	A	Body	GE 7800
		B	Body	Varian
		H	Body	GE 8800

TABLE 3

Results of CT Scanner Performance

Machine	Field Uniformity*	Spatial Linearity*	Resistance to Artifact*	Spatial Resolution (mm), Substance Relative to Plexiglas				Radiation Dose/ Slice (rad)
				Calcium Chloride	Air	Lexan	1% Sugar Water	
A	+++	++++	++++	<3	2	<3	5	3.2
B	++	++++	++	3	2	<4	5	3.5
C	+++	++++	+++	2	2	<4	5	1.9
D	++++	++++	+++	2	2	<4	<5	3.6
E	+++	++++	+++	. . .	>1	<3	3	4.0
F	+++	++++	+++	. . .	1	<<3	. . .	12.0
G	+++	++++	+++	. . .	<2	<<3	. . .	2.5
H	+++	++++	+++	>1	1	<<3	<3	6.1

* The following grading system was used: ++++ = excellent; +++ = Good; ++ = Fair; + = Poor.

thick, and each designed to demonstrate a single aspect of scanner performance.

Section 1 evaluated high contrast spatial resolution using water-filled holes drilled in Plexiglas. This provided a contrast difference of about 12%. The rows of holes were 3, 2.5, 2, 1.75, 1.5, and 1.25 mm in diameter with a center-to-center distance between holes of twice the diameter. The high contrast section was designed to test the ultimate resolution capability of the scanner independent of dose. This section was also used to show spatial resolution at low contrast levels using Lexan pins driven into Plexiglas (about 3% absorption coefficient difference, table 1). The pins were 2, 3, 4, 5, 7, and 10 mm in diameter with the distance between holes equal to the diameter of each hole. This was used to show spatial resolution at normal dose levels.

Section 2 was a uniform water bath that measured field uniformity across the water bath.

Section 3 was essentially similar to section 2, except that Plexiglas was used as the absorbing material.

Section 4 contained nine thermoluminescent dosimeters in the Plexiglas to measure the single-slice dose.

Section 5 contained two steel pins, two aluminum pins, and two air holes. The air holes and aluminum pins simulate the air-bone contrast ranges seen clinically. The two steel pins serve as small, high contrast objects to provoke artifacts.

Section 6 tested spatial linearity by imaging two sets of equally spaced orthogonal lines milled into the surface.

Methods

A team of three investigators tested seven clinical models (table 2) when the manufacturer in each case had determined that the scanner was operating at optimal performance. All tests were performed by the same group of investigators who followed identical experimental procedure.

Parallel conditions of test were not always possible since the operating factors were sometimes limited by equipment design. For example, when we were unable to vary kilovoltage, slice thickness, amperage, or scan time per slice, we used those recommended by the manufacturer. When these factors were variable, we performed the tests at several settings and used the best result in evaluation of that particular scanner.

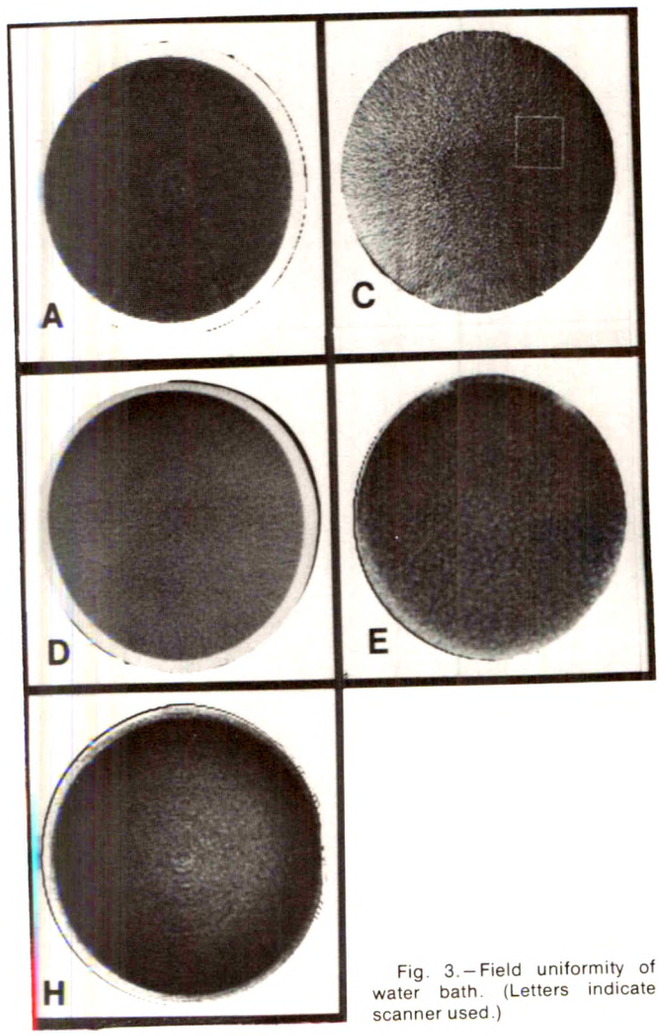


Fig. 3.—Field uniformity of water bath. (Letters indicate scanner used.)

Results

The comprehensive results of our tests are given in table 3, and are illustrated selectively in figures 3 through 12. Comments and interpretations of actual results are offered in this section only where they are not self-evident from the figures.

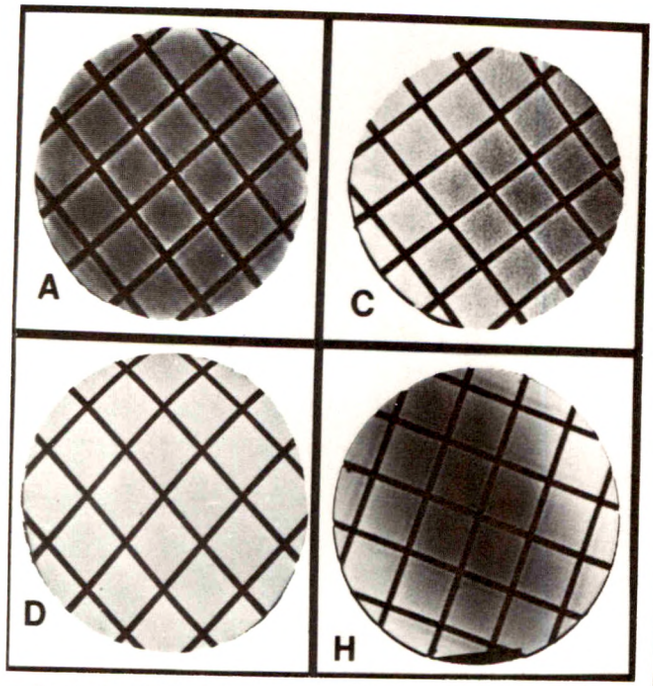


Fig. 4.—Spatial linearity of orthogonal lines (air) in Plexiglas. (Letters indicate scanner used.)

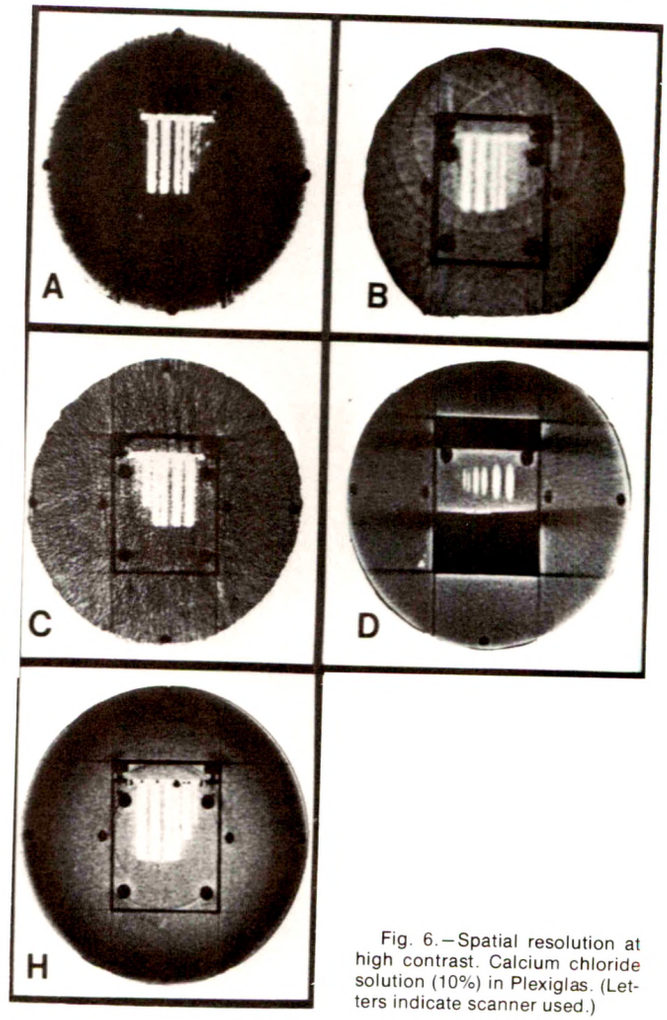


Fig. 6.—Spatial resolution at high contrast. Calcium chloride solution (10%) in Plexiglas. (Letters indicate scanner used.)

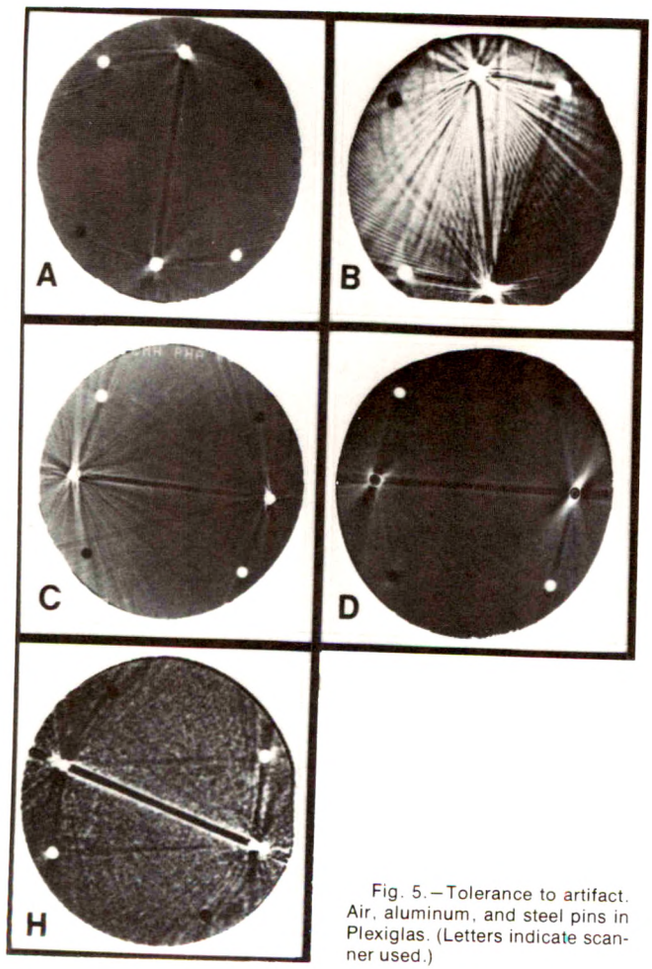


Fig. 5.—Tolerance to artifact. Air, aluminum, and steel pins in Plexiglas. (Letters indicate scanner used.)

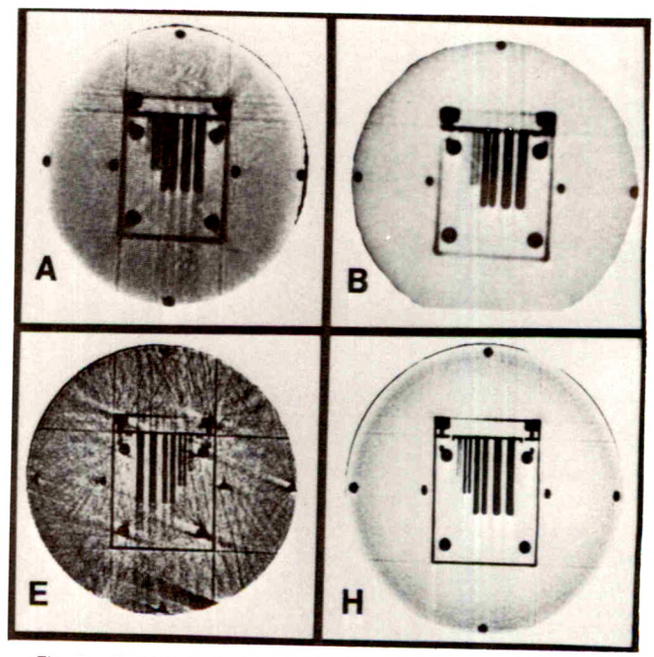


Fig. 7.—Spatial resolution at high contrast. Air in Plexiglas. (Letters indicate scanner used.)

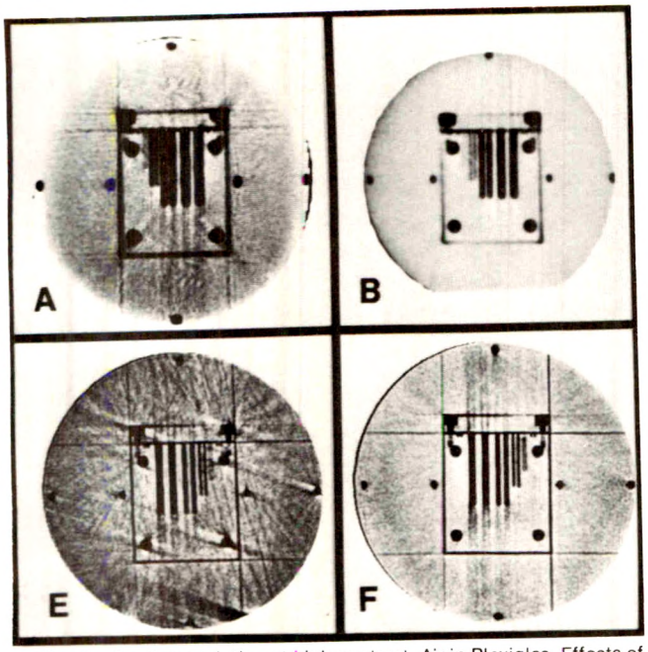


Fig. 8.—Spatial resolution at high contrast. Air in Plexiglas. Effects of dose dependence with machines E and F.

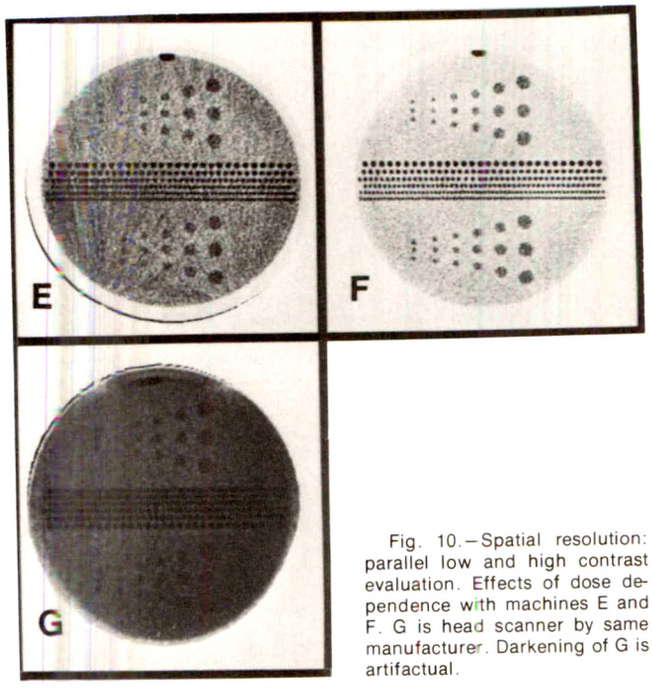


Fig. 10.—Spatial resolution: parallel low and high contrast evaluation. Effects of dose dependence with machines E and F. G is head scanner by same manufacturer. Darkening of G is artifactual.

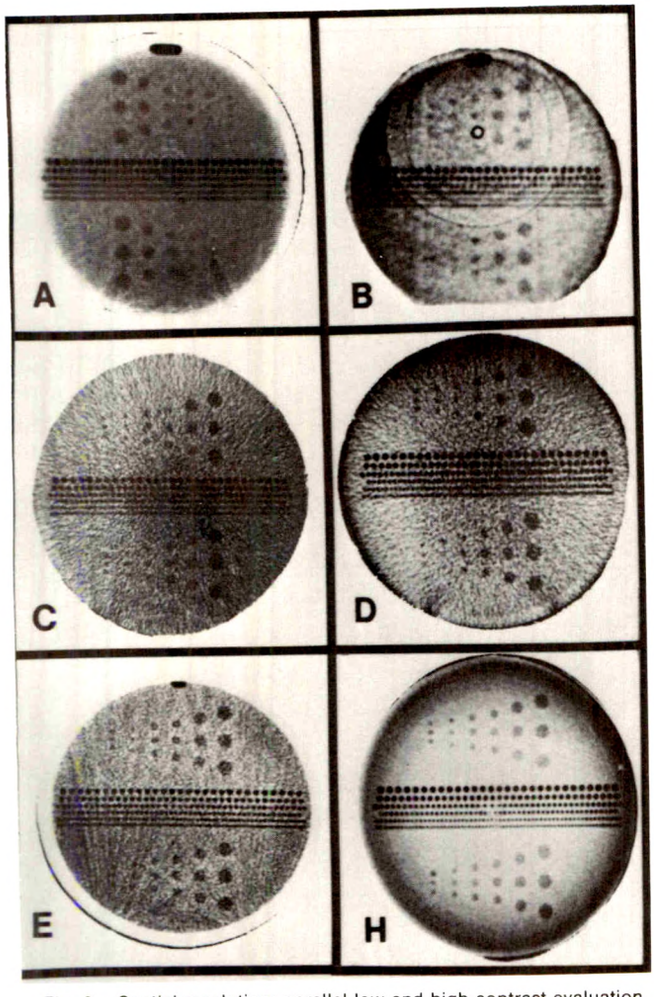


Fig. 9.—Spatial resolution: parallel low and high contrast evaluation. Air and Lexan in Plexiglas. (Letters indicate scanner used.)

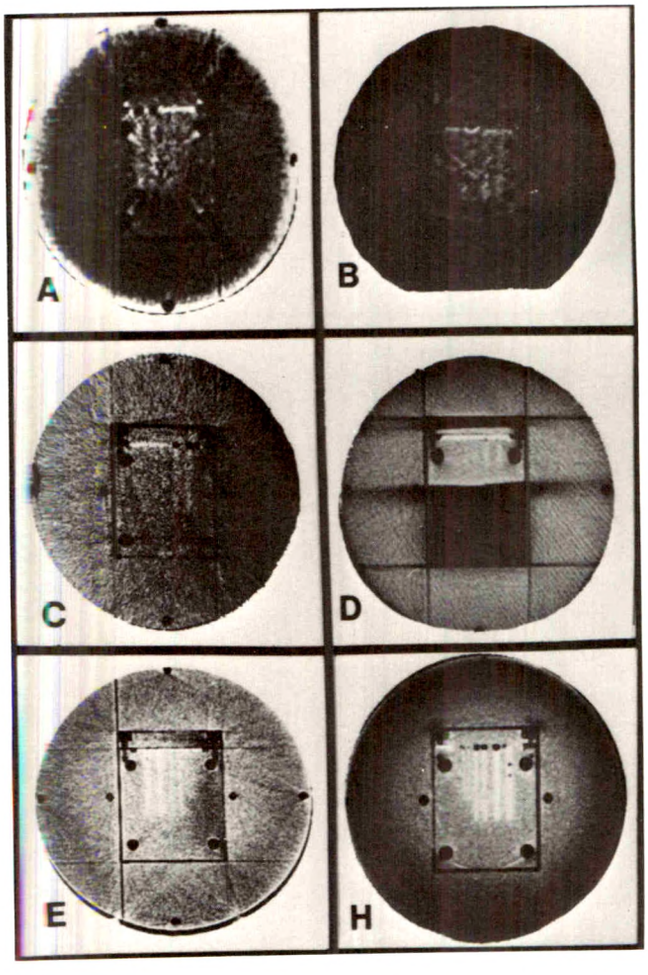


Fig. 11.—Spatial resolution at low contrast. Sucrose solution (1%) in Plexiglas ($\Delta \mu \approx 2\%$). (Letters indicate scanner used.)

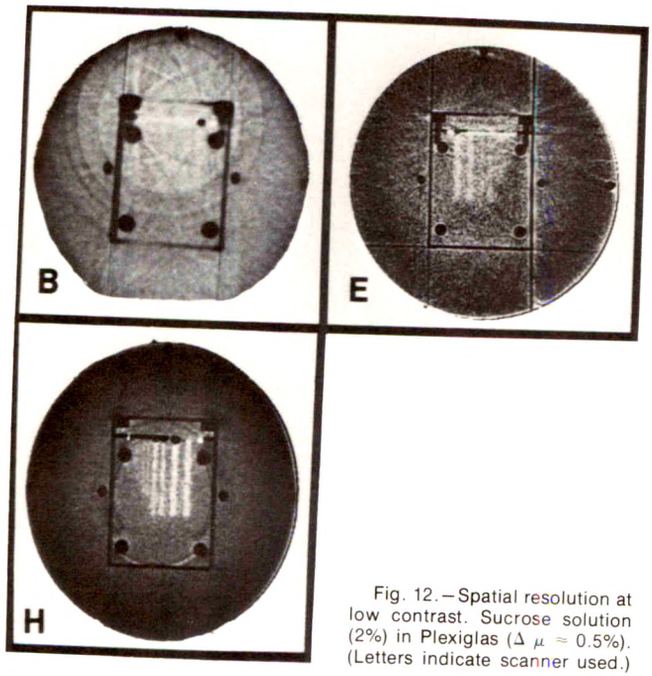


Fig. 12.—Spatial resolution at low contrast. Sucrose solution (2%) in Plexiglas ($\Delta \mu \approx 0.5\%$). (Letters indicate scanner used.)

Field Uniformity

Machine A (fig. 3) demonstrated a relatively uniform field but showed moderate ring artifact close to the center. Two linear artifacts at the base of Machine A were reflections of the feet of the phantom which resulted from slight misalignment during the test.

Machine C demonstrated a relatively grainy uniform field biased to the left and showed a general increased intensity in the center relative to the periphery.

Machine D showed a relatively uniform field with a slight gradation at the upper part of the picture, caused by a misalignment of the phantom.

Machine E demonstrated linear artifacts, and had a slight bias in the upper half of the picture.

Machine H demonstrated a halo effect with slight ring artifact in the center of the picture as well.

Comment. All machines tested showed some degree of nonuniformity. The extent of nonuniformity is probably not severe enough to limit diagnostic ability. This is further borne out where the test results superimposed on the slight field imperfections caused the latter to be barely noticeable (figs. 9 and 11). Ring artifact, in contrast, is visually disturbing and even small amounts interfere with diagnostic ability.

Spatial Linearity

Four representative images are shown (fig. 4). In all cases the linearity was very good and there was little distortion. The greatest distortion was noted in machine D, but even this was minimal and was caused by a television monitor maladjustment, not by poor image reconstruction.

Comment. We felt it important to demonstrate that the reconstruction alogrithms did not distort the image significantly.

Resistance to Artifact

It is obvious (fig. 5) that machine A showed the least disturbance from large contrast changes and that Machine B showed the most. Machines C, D, and H were also very good in resisting strong perturbations from these large contrast changes.

Comment. All machines may show artifacts from large changes in attenuation coefficient, but good engineering design can reduce these to a minimum, particularly as seen in machines A and D.

Spatial Resolution at High Contrast

In the calcium chloride/Plexiglas experiment (fig. 6), machine A demonstrated a capability of resolving 3 mm lines and began to resolve 2 mm. Machine B did not demonstrate resolution beyond 3 mm. Machine C clearly demonstrated 2 mm and hinted at the 1 mm resolution. Machine D also demonstrated 2 mm lines clearly, but did not show any capability below this level. Machine H just began resolution at the 1 mm level and hinted at separation between the pair.

At the higher levels of contrast demonstrated with air/Plexiglas interfaces (figs. 7 and 8), the spatial resolution increased in all machines. All instruments resolved the 2 mm lines. Machines F and H definitely resolved the 1 mm line pair and machine E almost approached this. Machines A and B did not resolve at the 1 mm level.

Comment. Most machines have excellent spatial resolution at high contrast levels. Machines F and H seemed to have the best spatial resolution in this series.

An example of the care required in obtaining this study is demonstrated by comparing machines E and F; the resolution capabilities show F to be distinctly superior to E. However, this is the same machine tested under identical conditions, except that different scan times were used resulting in a dose about three times greater in F as compared to E (12 vs. 4 rad). Performance showed great dependence on dose; therefore, dose levels are included in table 3. This effect has been noted by others [1].

Although the attenuation coefficient was negative in figure 6 and positive in figures 7 and 8, the same general machine ranking obtains.

Spatial Resolution at High and Medium Contrast

The horizontal line of holes in figures 9 and 10 represents an air/Plexiglas interface. The symmetrically placed series of lines represents Lexan in Plexiglas (fig. 2).

The results of the high contrast tests are similar to those discussed in figures 6–8. Machines F, G, and H demonstrated the best results. Spatial resolution in machines A, B, C, D, and E was comparable. In this study the field nonuniformities compromise results as is partic-

ularly notable in B. Although the spatial resolution of B is similar to that of A or C, the ring artifacts in B are confusing because they blur the image. Similar effects, though not as pronounced, are seen in the lower half of D, in the left half of C, and in the lower portion of E. Machines F, G, and H demonstrate clean images.

Comment. Again, machine F is machine E operated at about three times the dose level. There is noticeable improvement in both spatial resolution and in decrease in noise and artifact.

Spatial Resolution at Low Contrast Differences

This is a severe test of any instrument (figs. 11 and 12). There is little question that machine H had a superior ability to resolve at low contrast levels: 3 mm lines were definitely seen and 2 mm lines were barely seen. Machine E almost approached machine H in this study with 3 mm line resolution. The other machines attained visualization of no less than 5 mm. Ring artifacts and high noise levels in these machines destroyed even the 5 mm lines in some cases.

Comment. These results show that spatial resolution cannot be specified independently of contrast level, and suffers drastically at low contrast levels. Although some of these machines are capable of resolving 2 mm lines at high contrast, they are barely able to resolve 5 mm lines at low contrast levels.

Radiation Dose Per Single Scan-Slice

Table 3 gives the radiation dose per single scan slice for all machines tested, and represents in each case one scan slice from a series of six adjacent scan slices.

Summary of Results

Spatial resolution at high contrast is excellent and approaches the 1 mm range on several machines. Spatial resolution at low contrast is significantly poorer in most machines and constitutes a limiting factor in performance.

Field uniformity and spatial linearity seem adequate for all machines tested. We felt it important to demonstrate preservation of uniformity and linearity during the reconstruction process.

There are modest differences among various scanners in their tolerance to large contrast differences and resistance to artifact, but these are reduced to a minimum in several machines. However, ring artifact is very disturbing, even at minimal levels.

Discussion

We are confident that our results represent the best possible performance for each machine since we emphasized parallel experimental technique for each test and multiple testing under various operating conditions for each machine. We feel that this approach is valid because it accords with actual use in a clinical setting. Performing all tests under the same operating conditions would have created an artificial situation representing a departure from actual clinical practice.

Experimental results for any parameter must be seen within the constellation of all the other operating parameters at the time of testing in order to make valid comparisons. In this way performance can be ranked by each parameter. We believe this ranking of machine capability is directly translatable to clinical performance. For example, the scanner showing the best experimental low-contrast resolution at a given dose can also be expected to have the best clinical low-contrast resolution at the same dose. However, because of numerous clinical variables, it does not follow that a machine that resolves a 2 mm line-pair in a phantom will be able to resolve a 2 mm structure in a 115 kg patient.

We emphasize that we do not believe our phantom model is in any way unique (it was designed and implemented prior to publication of the model of the American Association of Physicists in Medicine [9]). While many phantom designs may be used to test one or more parameters, it is of primary importance that the study design be consistent in execution and meet the experimental objectives of providing valid, unforced comparisons. As noted previously, we chose to obtain the best results for each test on each instrument, rather than force all the instruments to operate under arbitrary conditions.

Conclusions

Results for individual machines tested ranged in quality from excellent to fair (table 3), either for overall performance or for a particular parameter. This was unrelated to class since we observed widely varying results on scanners within the same class (class II scanners A, B, and H). Therefore, we conclude that although there may be a theoretical advantage of one class over another, it seems that attention to engineering detail and manufacturing tolerance provides the functional limitation on performance at present. Furthermore, machine dedication to a particular body region does not necessarily ensure superior results for that region. Specifically, our study does not support the claims for superiority of dedicated head scanners.

In clinical terms, the inability of most machines studied to resolve at low contrast conditions means that identification of lesions may not be possible unless they are of considerable size. Thus, for clinical application, spatial resolution under low contrast conditions is probably the most important single parameter in comparing machines. It is in this area also that the greatest dose dependence is demonstrated. Overall then, spatial resolution under low contrast conditions seems to be the most sensitive test of machine performance.

Our experiments demonstrate that phantom models provide an inexpensive and practical means by which to compare CT scanner performance, thus facilitating decisions regarding selection for clinical use. Phantoms also permit ongoing monitoring of optimal performance

of an in-house scanner after a baseline reference has been established. Further, the effect of varying one aspect of performance on a given CT system can be assessed in terms of the performance of the overall system.

REFERENCES

1. McCullough EC, Payne JT, Baker HL, Hatley RR, Sheedy PF, Stephens DH, Gedgaudus E: Performance evaluation and quality assurance of computed tomography scanners, with illustrations from the EMI, ACTA, and Delta Scanners. *Radiology* 120:173–188, 1976
2. Goodenough DJ, Weaver KE, Davis PO: Development of a phantom for evaluation and assurance of image quality in CT scanning. *Optical Eng* 16:52–65, 1977
3. MacIntyre WJ, Alfidi RJ, Haaga J, Chernak E, Meany TF: Comparative modulation transfer functions of the EMI and Delta scanners. *Radiology* 120:189–191, 1976
4. Cohen G, Bassano D, Payne J: Protocol for CT scanning performance repository. Paper presented at the annual meeting of the Radiological Society of North America, Chicago, November 1977
5. Brasch RC, Boyd DP, Gooding CA: Computed tomographic scanning in children: comparison of radiation dose and resolving power of commercial CT scanners. *AJR* 131:95–101, 1978
6. Johns HE, Cunningham JR: *Physics of Radiology.* Springfield, Ill., Thomas, 1971
7. Grodstein GW: *X-Ray Attenuation Coefficients From 10 KeV to 100 MeV.* U.S. National Bureau of Standards no. 583, 1957 (McGinnies RT: Supplement to no. 583, 1959)
8. Zatz LM, Alvarez RE: An inaccuracy in computed tomography: the energy dependence of CT values. *Radiology* 124: 91–97, 1977
9. Task Force on CT Scanner Phantoms: *Phantoms for Performance Evaluation and Quality Assurance of CT Scanners.* Chicago, American Association of Physicists in Medicine, 1977

CT Resolution and Diagnostic Accuracy

ALAN L. WILLIAMS[1] AND VICTOR M. HAUGHTON[1]

To justify CT purchases and document certificates of need, the clinical effectiveness of CT scanners with different cost and resolution must be compared. The diagnostic accuracy and anatomic detail in three scanners with different resolution were studied. Seventeen patients were studied with both a first or a second generation CT scanner and a third generation scanner. Appearance of normal and pathologic structures was compared. Cerebral sulci, corticomedullary discrimination, basal cistern vessels, and some pathologic lesions were seen in third generation images that were not seen in the others. Higher resolution scans provide significantly better anatomic detail and accuracy in detecting pathologic processes.

Higher spatial and contrast resolution in general requires more expensive CT scanners and higher radiation dose. Although higher resolution in CT scanning may be assumed to permit greater diagnostic accuracy, a study of resolution and diagnostic accuracy has not yet been reported. Without such published data, the purchase of the more expensive CT scanners may be difficult to justify to a health regulatory agency. We compared cerebral CT anatomic detail and diagnostic accuracy in scanners with different resolution capabilities.

Materials and Methods

The scans of 17 patients who had been scanned with both a first (scanner A, EMI CT 1005) or second (scanner B, Ohio Nuclear Delta 50) generation scanner and a third generation scanner (scanner C, General Electric CT/T 8800) were reviewed. We compared the appearance of cerebral sulci, cerebral cortex and medulla, basal cisterns, and pathologic lesions in the two studies. Resolution of scanners A, B, and C was measured with phantoms.

Patients were selected for examination in scanner C because a higher resolution scan was desired. Since scanner C was a prototype instrument installed in a factory, patients who required sedation, intravenous contrast material, or nursing care were excluded. Scanner C was operated at maximal radiographic factors to produce the highest resolution (dose 4–6 rad/examination) [1]. Scanners A and B were operated with customary radiographic factors within a hospital (dose 1–2 rad/examination) [2–4]. Sedation and contrast media were given as necessary. Official reports were used as the diagnostic impression of images from scanners A and B. However, only the unenhanced scans from scanners A and B were used for comparison with scanner C images.

The time interval between scanning in the different scanners ranged from 1 day to 5 months, but was several days in most patients. With one exception, none of the patients received treatment between scans.

Spatial resolution was measured in each of the 3 scanners using an AAPM high-contrast hole-pattern phantom. Measurements and calculations were made by the departmental radiation physicist.

Results

Contrast Resolution

High-contrast resolution of scanners A, B, and C was determined to be 2.0, 1.8, and 1.0 mm, respectively. These measurements correlate well with previously reported results [1].

Cerebral Sulci

In six patients, images through the centrum semiovale were obtained on both scanner A or B and scanner C.

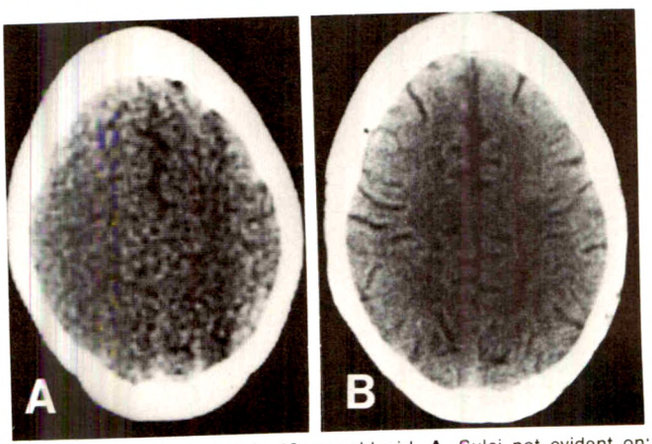


Fig. 1.—Cerebral sulci in 13-year-old girl. **A**, Sulci not evident on initial scan. **B**, 2 weeks later. Sulci clearly demonstrated.

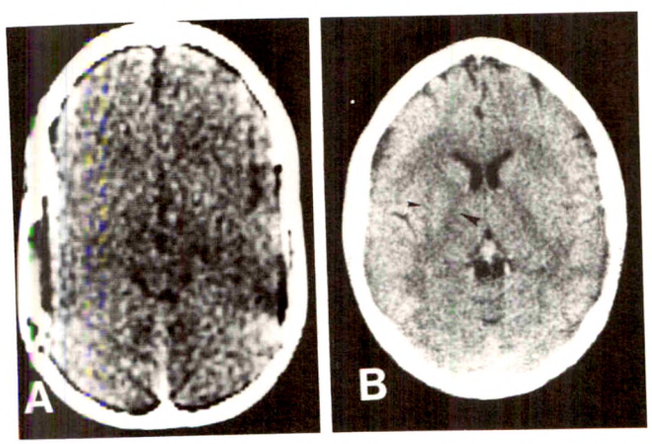


Fig. 2.—Corticomedullary differentiation in 19-year-old girl with optic atrophy. Scanner C image (**B**) revealed discrimination of cortex and medulla not apparent on initial scan (**A**). Internal capsule (*large arrowhead*); external capsule (*small arrowhead*).

Received July 6, 1978; accepted after revision November 21, 1978.
[1] Department of Radiology, Milwaukee County Medical Complex, 8700 West Wisconsin Avenue, Milwaukee, Wisconsin 53226. Address reprint requests to A. L. Williams.

AJR 132:353–355, March 1979
© 1979 American Roentgen Ray Society
0361–803X/79/1323–0353 $0.00

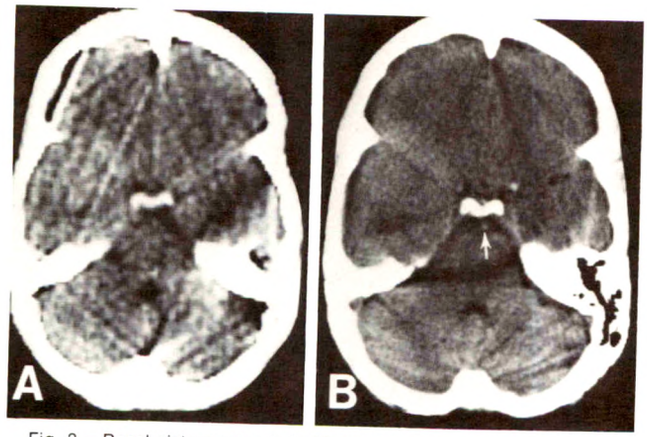


Fig. 3.—Basal cistern vessels in 56-year-old woman. **A**, Basilar artery not evident in initial scan. **B**, Basilar artery (*arrow*) demonstrated without contrast material in scanner C image.

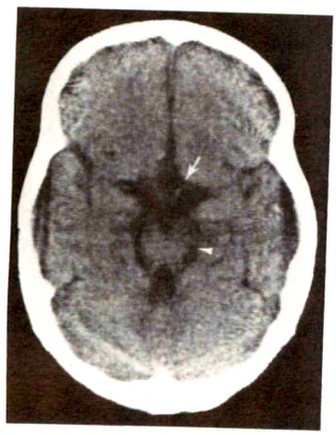


Fig. 4.—Basal cistern vessels in 13-year-old girl (same patient as fig. 1). Middle cerebral (*arrow*) and posterior cerebral (*arrowhead*) arteries visualized without contrast medium in scanner C image.

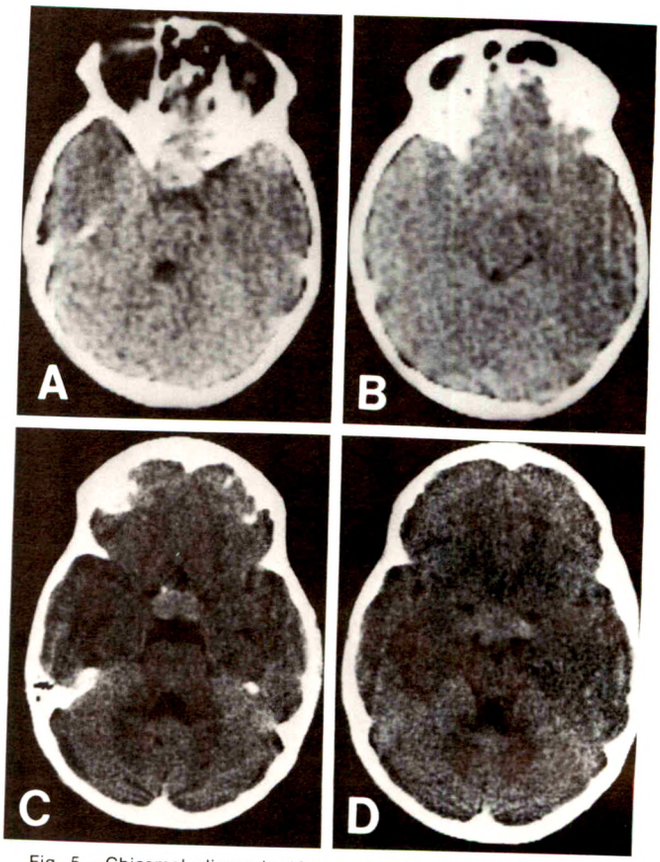


Fig. 5.—Chiasmal glioma in 10-year-old girl with neurofibromatosis and decreased visual acuity. **A** and **B**, Initial scans interpreted as normal. **C** and **D**, Images from scanner C demonstrate large mass within chiasmatic cistern. Chiasmal glioma confirmed surgically.

TABLE 1

CT Diagnosis

Patient	Scanner A or B	Scanner C
S. M.	Normal	Brainstem glioma
J. R.	Hydrocephalus	Brainstem glioma
J. S.	Normal	Optic chiasm glioma
M. B.	? Pseudotumor cerebri	Pseudotumor cerebri
R. J.	Thalamic glioma	Thalamic glioma
V. K.	Thalamic mass	No brainstem lesion
C. L.	Aqueductal stenosis	Aqueductal stenosis
D. S.	Pituitary adenoma	No suprasellar extension

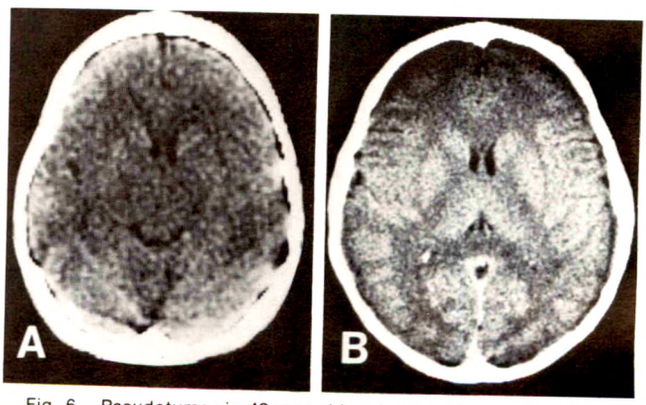


Fig. 6.—Pseudotumor in 42-year-old male physician with headaches and memory loss. **A**, Initial scan shows small lateral ventricles consistent with pseudotumor cerebri. **B**, Abnormally low attenuation of white matter on scanner C image further supported diagnosis of pseudotumor.

Cerebral sulci were demonstrated in the scanner C images in all six patients, but were not visualized in any of these patients with scanners A or B (fig. 1).

Cortex-Medulla Discrimination

In the six patients with studies on scanner A or B and scanner C through the centrum semiovale, cortex and medulla were differentiated in all patients with scanner C scans and in only one patient with scanner A or B scans. Corticomedullary discrimination in scans from scanners C and A is illustrated in figure 2.

Basal Cistern Vessels

Seven patients had CT scans on scanner C and scanner A or B that included the basal cisterns. In the scanner C images the basilar artery was visualized without intravenous contrast media in all seven patients. In two patients the basilar artery was identified on scans from scanners A or B (figs. 3 and 4).

Diagnostic Accuracy

In eight patients who were scanned with both scanner A or B and scanner C, a clinical diagnosis was confirmed by conventional diagnostic studies, by follow-up course, and, in some cases, by surgery or autopsy. Interpretations of the two CT studies were compared (table 1). In four patients more specific interpretation was made on scans from scanner C than on those from A or B. For example, a glioma of the optic chiasm was detected in one patient with scans from scanner C but not from the other scanner (fig. 5). In two other patients, findings of pontine glioma were identified on the scanner C images but not on the scans from the other scanners. One case of pseudotumor was demonstrated better with scanner C than scanner A (fig. 6). In four patients interpretation of the scanner C and other (A or B) scans were the same.

Discussion

A rigorous study of CT diagnostic accuracy is difficult to design. Weaknesses of the present study are (1) elapsed time between scans; (2) variable scanner quality control and factory maintenance; (3) lack of randomization of patient selection; (4) small patient sample; and (5) lack of double-blinding. However, these weaknesses do not invalidate the basic conclusion.

Higher CT resolution improves discrimination of anatomic detail and accuracy of radiologic diagnosis. Appearance of cerebral sulci, cortex and medulla, basal cisterns, and some pathologic lesions vary from one scanner to another. For example, in the recognition of cerebral sulci, images from one scanner may disclose atrophy but from another scanner may appear normal. Improved diagnostic accuracy documented in this study may justify purchasing more expensive CT scanners with greater resolution capabilities.

ACKNOWLEDGMENT

We thank Dr. Charles R. Wilson for assistance with the scanner resolution measurements.

REFERENCES

1. Payne JT: CT scanner performance and radiation dose. Paper presented at the International Symposium and Course on Computed Tomography, Miami Beach, March 1978
2. McCullough EC, Payne JT, Baker HL, Hattery RR, Sheedy PF, Stephens DH, Gedgaudus E: Performance evaluation and cuality assurance of computed tomography scanners, with illustrations from the EMI, ACTA, and Delta scanners. *Radiology* 120:173–188, 1976
3. Shrivastava PN, Lynn SL, Ting JY: Exposures to patient and personnel in computed axial tomography. *Radiology* 125: 411–415, 1977
4. Ter-Fogossian MM: Computerized cranial tomography: equipment and physics. *Semin Roentgenol* 12:13–25, 1977

AJR Guidelines for Authors

Address manuscripts and correspondence to the Editorial Office, American Journal of Roentgenology, 403 Pacific National Bank Building, 4545 15th Avenue N.E., Seattle, Washington 98105; telephone (206)633-2754.

Publication Policy

The Journal publishes original and timely contributions to the advancement of radiologic diagnosis and treatment. Although the content is predominantly clinical, laboratory investigations are accepted when their relevance to clinical practice is demonstrable. In prospective clinical investigations, authors should indicate if informed consent from patients was obtained. Decisions on manuscripts are based on the opinions of at least two outside reviewers. Reviewers receive manuscripts without title pages to protect the identity of authors and to ensure an unbiased review; names of reviewers, in turn, are not revealed to authors. Statements within an article are the responsibility of the authors and not the Journal or its publisher.

It is understood that material submitted has not been published and is not currently submitted elsewhere. Portions of the data or illustrations from previously published works may be included if permission release forms accompany the manuscript and such material is clearly credited in the text. Prior publication of abstracts will not prejudice publication of the complete study.

Copyright Information

In accordance with Journal implementation of the 1976 U.S. Copyright Law, authors must release first and subsidiary rights to their manuscript at submission. A dated cover letter, containing signatures of all authors, should state: "We, the authors, assign first and subsidiary rights to the American Roentgen Ray Society in the event that our manuscript (title) is published by AJR." The Journal, in turn, grants authors the right to use portions of their manuscript, without charge, in books or articles of which they are authors or editors.

Manuscript Form

Manuscripts should be typed double-spaced throughout, including references, tables, and figure legends. Tables, footnotes, and figure legends should be on separate sheets, and a separate title page should be provided. In addition to the original typewritten copy, a duplicate copy complete with figures, tables, and references is required. Authors' names should be on title page only and should not be on figures so that author anonymity can be maintained during the review process.

Figures should be submitted as 13 × 18 cm glossy prints, untrimmed and unmounted. Labels and arrows must be of professional quality and should be removable from the prints. Each figure should be numbered to correspond with figure legends, and the top should be indicated. Specific permission for publication of facial photographs of patients is required. Line illustrations and graphs should be drawn in black ink on white background.

References should be cited in the text by number (e.g., [3, 4]). The bibliography should be arranged in the numerical order that references are cited in the text and typed double-spaced throughout. Data for each reference should be arranged according to the uniform style on bibliographic citations adopted by many biomedical journals. Provide all authors' names and inclusive pages. Abbreviations for titles of medical periodicals should conform to those published in *Index Medicus*. Examples:

1. Miller RE, Chernish SM, Skucas J, Rosenak BD, Rodda BE: Hypotonic roentgenography with glucagon. *AJR* 121:264–274, 1974
2. Boijsen E: Superior mesenteric angiography, in *Angiography*, edited by Abrams H, Boston, Little, Brown, 1971, pp 1091–1119

Organization

Title page. Titles should be brief and specific. Include addresses for each author and acknowledgment of grant support when appropriate.

Abstract. A description of the purpose, methods, results and conclusions of the study is required.

Introduction. Clearly state the purpose of the investigation including necessary background facts.

Materials and methods. Decribe the protocol clearly. Use standard abbreviations as presented in the *Council of Biology Editors Style Manual*, 3d ed. Metric measurements should be used throughout.

Results. Present results in logical sequence.

Discussion. Interpret the results to lend meaning and importance to the observations. Hypotheses and speculation based on the results are encouraged. When results differ from those of previous investigators, an attempt should be made to explain the discrepancy.

References. Only include references which provide adequate background and present fairly any opposing evidence and concepts. Accuracy of reference data is the responsibility of the author.

Legends. Legends should be brief but should provide sufficient description to interpret the figure.

Special Communications

Case Reports. Concise case reports are accepted if they present unusual experiences that are medically important and educational. Clarity and brevity are essential. After preliminary screening by an editor to determine whether the requirement of medical significance has been met, qualifying papers will undergo the same peer review as major papers.

Technical notes. Brief descriptions of new techniques or significant modifications of older ones which are directly applicable to clinical practice will be accepted.

Letters to the Editor. Letters are subject to editing and condensation. Criticism of published articles should be objective and constructive. Letters may also discuss matters of general interest to radiologists.

High Dose Preoperative Irradiation of the Lower Neck and Supraclavicular Fossae

R. H. SAGERMAN,[1] C. T. CHUNG, G. A. KING, P. DALAL, AND W. S. YU

Preoperative irradiation of 5,000 rad in 5 weeks before total laryngectomy with radical neck dissection was compared for two groups of patients: (1) those treated to a smaller volume through lateral opposed fields (37 patients) and (2) those treated to a larger volume by adding a third field directed to the lower neck and supraclavicular fossae (46 patients). There were no significant differences in tolerance to irradiation or in postoperative complications. However, locoregional tumor control improved significantly from 63% to 90% ($P < 0.02$) with the three-field technique, and all four stomal recurrences were in the two-field group. Deaths from intercurrent disease and from distant metastases without local recurrence account for the failure to improve the overall survival rate.

In 1968, a high dose (5,000 rad/5 weeks) preoperative irradiation program for advanced head and neck cancer was initiated at the State University of New York, Upstate Medical Center [1]. Although philosophy and surgical technique have remained constant, a third radiation field has been added to the original right and left lateral pair for better coverage of the lower cervical and supraclavicular nodes. This has provided interesting data different from that originally obtained.

This report analyzes the differences in reactions, complication rates, survival results, and local tumor control rates between the groups treated either with or without lower neck irradiation.

Subjects and Methods

From 1968 to 1976, 83 patients with advanced (stage III-IV) cancer of the laryngopharynx entered a high dose preoperative irradiation protocol. All patients had histologically proven invasive squamous cell carcinoma. The 74 men and nine women ranged from 40 to 76 years in age (mean, 60). There were no significant differences in the age and sex characteristics of patients in the two groups.

Irradiation was accomplished with either a 4 MV linear accelerator or a cobalt-60 teletherapy unit. A 5,000 rad tumor dose was delivered in 5 weeks. Before 1973, 37 patients were treated through equally weighted opposing right and left lateral ports (fig. 1A) encompassing the primary lesion and a major portion of the cervical chain (two-field group). Since experience demonstrated good patient tolerance to the program, a matching lower anterior neck field (fig. 1B) was added to electively irradiate the lower neck and supraclavicular fossae in the next 46 patients (three-field group). Each field was treated daily at 200 rad midplane for the lateral fields and 200 rad at 3 cm depth for the anterior neck field. Wide field total laryngectomy with unilateral or staged bilateral radical neck dissection was performed after a 4–6 week postirradiation rest period.

The American Joint Committee Classification of 1977 [2] was used to reclassify each of the 83 patients (table 1). Comparison between the groups shows a greater percentage with a negative neck in the two-field group (46% vs. 25%) and a greater percentage with an N2–N3 neck in the three-field group (52% vs. 30%).

Of the 83 patients, 72 completed the planned irradiation and surgery (table 2). Six of the 19 patients with a pyriform sinus primary did not complete treatment. In contrast, only one or two patients in each of the other categories were unable to finish. Of the patients in the two- and three-field groups, 84% (31/37) and 89% (41/46), respectively, completed the program. Of the six in the two-field group not completing treatment, one refused surgery, two died of intercurrent disease during the course of irradiation, and distant metastases were preoperatively detected in the three other patients. Five patients in the three-field group did not complete the program; two refused to undergo the planned surgery after completing irradiation, one died of a massive myocardial infarction after 1,200 rad, and distant metastases were discovered in two.

Results

Skin and mucosa, body weight, and systemic reactions were studied during irradiation. Mucosal and skin reac-

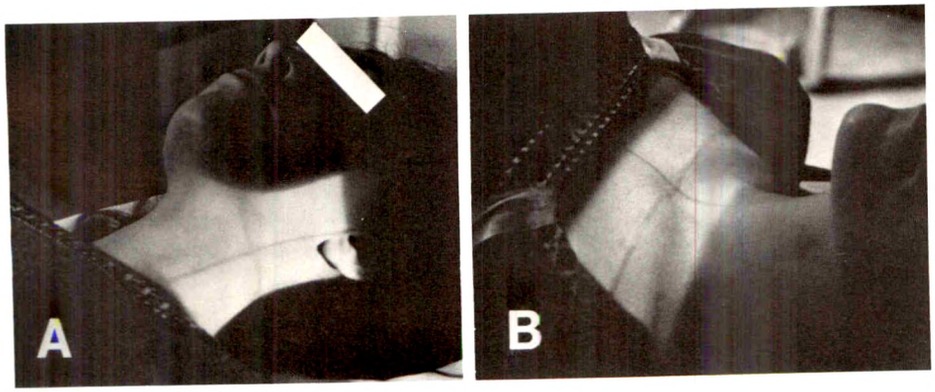


Fig. 1.—**A,** Primary site and most anterior cervical nodes included in opposing right and left lateral fields. **B,** Lower cervical and supraclavicular nodes treated through anterior field including stomal area; central shield not used. Field can be lengthened to include more mediastinum.

Received May 25, 1978; accepted after revision November 21, 1978.
Presented at the annual meeting of the American Radium Society, New Orleans, April 1978.
[1] All authors: Radiation Oncology Division, Department of Radiology, State University of New York, Upstate Medical Center, Syracuse, New York 13210. Address reprint requests to R. H. Sagerman.

© 1979 American Roentgen Ray Society

0361-803X/79/1323-0357 $0.00

TABLE 1
Stage at Program Entry

	2 Field				3 Field				Total
	T1	T2	T3	T4	T1	T2	T3	T4	
N0	0	0	5	12	0	0	2	10	29
N1	0	2	4	3	0	1	3	6	19
N2	0	1	0	3	1	4	1	4	14
N3	0	1	0	6	0	2	4	8	21
Total	0	4	9	24	1	7	10	28	83

TABLE 2
Site of Primary Cancer

Primary Site	2 Field		3 Field		Total	
	Entered	Completed	Entered	Completed	Entered	Completed
Glottic	11	10	9	8	20	18
Supraglottic	15	14	29	27	44	41
Pyriform sinus	11	7	8	6	19	13
Total	37	31	46	41	83	72

tions were classified as mild in 26% (eight patients) vs. 17% (seven), as moderate in 65% (20) vs. 66% (27), and as severe in 9% (three) vs. 17% (seven) for the two- and three-field groups, respectively. Weight loss averaged 2.68 kg vs. 2.72 kg for the two groups throughout the course of irradiation; only one patient (from the three-field group) lost more than 10% of body weight. No unusual local or systemic reactions were encountered, and all patients completed radiation therapy on schedule.

The major surgical complication rate was 19.3% (six) for the two-field group and 14.6% (six) for the three-field group (table 3). Complications included one postoperative death, four fistulae, and a large hematoma in the two-field group, and one postoperative death and five fistulae in the three-field group. Minor complication rates were 16.1% (five) and 12.2% (five) for the two- and three-field groups, respectively. None of these differences is statistically significant.

Of the 72 patients completing the program, 69 have been followed for more than two years or until death. Sixteen of 31 patients in the two-field group and 21 of 41 in the three-field group are alive without evidence of recurrence or cancer extension (table 4). In the two-field group, 10 died with local recurrence; three of these also had distant metastases (table 4). One patient died of distant metastases with local tumor control. The remaining three patients died of intercurrent disease without detectable cancer.

In the three-field group, only four patients died with local recurrence, and none of these had distant metastases; seven patients with local tumor control died of distant metastases. Two of these seven patients developed extension in the mediastinum just below the lower anterior neck field. Eight died of intercurrent disease.

TABLE 3
Surgical Complication Rates

Complication	2 Field (N=31)		3 Field (N=41)	
	No.	%	No.	%
Major:				
Postoperative death	1	3.2	1	2.4
Fistula	4	12.9	5	12.2
Other	1	3.2	0	0
Total	6	19.3	6	14.6
Minor	5	16.1	5	12.2

TABLE 4
Survival Rates

Status	2 Field		3 Field	
	No.	%	No.	%
No evidence disease	16*	52	21†	51
Postoperative death	1	3	1	2
Deaths:				
Recurrence only	7	22	4	10
Recurrence plus metastases	3	10	0	0
Distant metastases only	1	3	7	17
Intercurrent disease	3	10	8	20
Total	31	100	41	100

* One salvaged by additional radiation therapy after recurrence.
† All 2 year survival except three patients at 22 months.

Accordingly, local tumor control rates were 63% (19/30) for the two-field group and 90% (36/40) for the three-field group ($P < 0.02$), if postoperative deaths are excluded. In fact, tracheal stomal recurrence was the first

evidence of recurrent cancer in four patients (all in the two-field group).

Discussion

This review evaluates the role of lower neck and supraclavicular fossae irradiation for treatment of patients with advanced laryngopharyngeal cancer. Although the literature is replete with reports of combinations of radiotherapy and surgery for management of head and neck cancer, with each report advocating a particular irradiation dose range and volume, a host of variables has frustrated meaningful comparisons of results. Fletcher [3] reported use of postoperative irradiation for advanced laryngopharyngeal cancer at M. D. Anderson Hospital. Different volumes are treated according to the primary site, the histology, and the nodal status. In general, the entire neck is irradiated. For those patients with a high risk of stomal recurrence, Schneider et al. [4] and Tong et al. [5] discuss the effectiveness of postoperative irradiation to the stoma in preventing such recurrence.

In our series, irradiation and surgery were done by an interdisciplinary team with a unified philosophy. On the basis of careful observation and analysis of data gathered in the first years, the lower cervical-supraclavicular field was added in 1973. Surgical techniques and perioperative care (1968–1976) were accomplished by the same group of surgeons.

The additional volume irradiated did not engender unusual or marked reactions or require special nutritional programs. An almost equal proportion of the patients entered in the two- and three-field groups completed the entire program. Major surgical complication rates were 19% vs. 15% in the two- and three-field groups, respectively (table 3). These results suggest that the additional lower neck irradiation is well tolerated, without increased morbidity and mortality, in a preoperative program at a level of 5,000 rad over 5 weeks.

It was disappointing to find the survival rates equal in the two groups (table 4). However, local tumor control rate and eventual cause of death are noteworthy. The local tumor control rate improved from 63% (19/30) in the two-field group to 90% (36/40) in the three-field group, a statistically significant improvement ($P < 0.02$). Conversely, local failure occurred in 37% (11/30) in the two-field group in contrast to 10% (4/40) in the three-field group. All four stomal recurrences occurred in the two-field group and confirm other reports of the value of lower neck irradiation in patients at high risk of stomal recurrence [4, 5].

At 2 years, intercurrent disease without clinically demonstrable cancer caused twice as many deaths in the three-field group (20% vs. 10%). Also, death due to distant metastases was 6 times more common in the three-field group (17% vs. 3%). However, the overall incidence of distant metastasis was nearly the same for the two groups among those completing the program (13% vs. 17%) as well as those entering the program (19% vs. 20%). These figures support the effectiveness of combined irradiation-surgery programs in controlling locoregional cancer.

This study may also be valuable in considering the addition of chemotherapy to irradiation-surgery programs. Chemotherapy may aid in (1) prevention and control of distant metastases; (2) increase of the locoregional disease control rate; or (3) decrease of the dose of irradiation or the extent of surgery required to achieve the currently available local tumor control rate. Our data suggest a metastatic disease incidence of about 20%, similar to that reported by Wang [6] and others [3, 7]. If the 10% local failure rate is added to this figure, we can look for improvement in only 30% of the patients seen. Unfortunately, no available evidence suggests that less radical surgery or irradiation can yet be considered. Given the relatively small number of patients seen at any one institution and the fewer available for protocol studies, it is likely that the benefits of adding currently available chemotherapeutic regimes can be determined only by a multinstitutional cooperative venture.

ACKNOWLEDGMENT

We thank our colleagues in the Department of Otorhinolaryngology for helping to care for these patients and providing the surgical data, and Maureen Knopp for assistance in preparing the manuscript.

REFERENCES

1. Sagerman RH, Chung CT, King GA, Yu WS, Cummings CW, Johnson JT: High dose preoperative irradiation for advanced laryngeal-hypopharyngeal cancer. *Ann Otol Rhinol Laryngol*. In press, 1979
2. *Manual for Staging of Cancer 1977*. Chicago, American Joint Committee for Cancer Staging and End Results Reporting, 1977
3. Fletcher, GH: *Textbook of Radiotherapy*, 2d ed. Philadelphia, Lea & Febiger, 1973, pp 255–287
4. Schneider JJ, Lindberg RD, Jesse RH: Prevention of tracheal stoma recurrences after total laryngectomy by postoperative irradiation. *J Surg Oncol* 7:187–190, 1975
5. Tong D, Moss WT, Stevens RS Jr: Elective irradiation of the lower cervical region in patients at high risk for recurrent cancer at the tracheal stoma. *Radiology* 124:809–811, 1977
6. Wang CC: Megavoltage radiation therapy for supraglottic carcinoma. Results of treatment. *Radiology* 109:183–186, 1973
7. Jesse RH, Lindberg RD: The efficacy of combining radiation therapy with a surgical procedure in patients with cervical metastasis from squamous cancer of the oropharynx and hypopharynx. *Cancer* 35:1163–1166, 1975

Sequential CT Observations of Irradiated Intracranial Germinomas

YUICHI INOUE,[1] TETSUICHI TAKEUCHI,[1] MASAO TAMAKI,[1] KIYOSHI NIN,[2] AKIRA HAKUBA,[2] AND SHURO NISHIMURA[2]

Computed tomography (CT) has improved the accuracy of preoperative diagnosis of intracranial tumors. CT findings of germinoma are a mass of isodensity or of slightly increased density with significant, homogeneous enhancement after intravenous contrast injection. These findings are characteristic but not pathognomonic, and differential diagnosis from other solid tumors is not easy. Cerebrospinal fluid cytology and response to irradiation aid in this differential diagnosis. The nine cases of germinoma reported showed rapid response to irradiation even at small doses (600 rad), and complete disappearance of the mass on CT at 1,600–3,300 rad. Other radiosensitive masses to be differentiated in the pineal region are pinealocytoma or pinealoblastoma.

Objective evaluation of the effectiveness of radiation therapy in cerebral tumors is difficult. Computed tomography (CT) has proved to be accurate in evaluating change in tumor extent and the presence or absence of edema or necrosis during and after radiation treatment [1].

Subjects and Methods

During a 13 month period, nine cases of intracranial germinomas were studied with CT before, during, and after radiation therapy (table 1). The seven male and two female patients were 12–36 years old (average, 19 years). The tumors were localized as midline masses either in the pineal region (seven cases) or in the suprasellar region (two cases). The only exception was case 7, which showed a transtentorial mass extending from the pineal region to the midbrain, vermis, and fourth ventricle.

Headache was an initial complaint in eight cases. Ocular manifestations, such as dip opia, paralysis of upward gaze, and papilledema, were common. Precocious puberty was seen in one patient. Two cases had the classic features of "ectopic pinealoma" consisting of visual disturbances and diabetes insipidus. Pituitary dwarfism was seen in one of these two patients. Cytologic study of cerebrospinal fluid in all nine patients showed the combination of large tumor cells and small lymphoid cells characteristic of germinoma [2].

All nine patients received daily radiation treatments 5 days a week with 15 MeV X-rays from a betatron or a linear accelerator through bilateral opposite portals. Total radiation dose to tumor was 4,200–5,500 rad with daily doses of 150–200 rad. As a rule, a dose of 2,500 rad was delivered locally with a small field; the remainder was delivered tc a large field that included a volume larger than the ventricular system. Two patients had additional spinal axis irradiation of 1,300–2,000 rad.

CT scanning was performed before, during (after 2,000–2,500 rad), and at completion of radiation therapy. Follow-up CT scanning was done 1, 3, 6, 9, and 12 months after the end of the radiation therapy. CT was performed with an EMI-1000 scanner at 120 kV and 33 mA with 13 mm collimation. Contrast enhanced scanning was done in all cases using rapid intravenous drip infusion of 220 ml of 30% meglumine iothalamate (Conray) in adults or intravenous injection of 2 ml/kg of 60% meglumine iothalamate (Conray) in smaller patients.

Representative Case Reports

Case 6

A 19-year-old man had a 5 month history of diplopia and occipital headache. Upward gaze and bilateral papilledema were impaired, but there was no endocrine abnormality. Skull radiography showed destruction of the dorsum sellae. No calcification was seen in the pineal region.

Plain CT showed a mass of slightly increased density in the pineal region and marked dilatation of the third and lateral ventricles (fig. 1A). No peritumoral low density was seen. The tumor enhanced homogeneously on contrast CT (EMI nos. 35–45) (fig. 1A). Ventriculoperitoneal shunt was performed and cerebrospinal fluid cytology demonstrated the combination of large tumor cells and small lymphoid cells suggesting a germinoma. The patient received 3,000 rad of 15 MeV betatron x-rays to the third ventricle and pineal region via opposing lateral 6 × 6 cm portals, and 2,100 rad of 15 MeV linear accelerator x-rays were added via opposing lateral 18 × 14 cm portals.

CT scan at the 600 rad midline dose demonstrated significant reduction in tumor size (fig. 1B), and it disappeared completely on CT image at 2,400 rad (fig. 1C). Diplopia and upward gaze improved. The patient was doing well 4 months after radiation therapy. Cases 1–5 showed findings similar to those in this case.

Case 7

A 35-year-old man, seen with vomiting, had had diplopia and a broad based gait for 4 months. Trunkal ataxia, nystagmus, and bilateral abducent palsy were noted, and fundoscopic study showed atrophic discs. Emergency ventriculoperitoneal shunt was performed after carotid arteriography at another hospital. Cerebrospinal fluid cytology identified the combination of large tumor cells and small lymphoid cells indicative of a germinoma.

Plain CT (figs. 2A and 2B) showed an isodense mass in the pineal region. The ambient cistern was asymmetric and the quadrigeminal cistern and the fourth ventricle were poorly seen. Contrast CT (figs. 2A and 2B) demonstrated an enhanced tumor (EMI nos. 20–40 or 45) in the posterior third ventricle extending into midbrain, vermis of the cerebellum, and the fourth ventricle. No peritumoral low density was shown. An unusual calcification anterior to the pineal gland was not believed to be habenular calcification, but may have represented a teratoid nest in the tumor, as mentioned by Russell [3].

Initially 3000 rad of 15 MeV betatron x-rays were given to the third and fourth ventricular area via opposing lateral 7 × 5 cm portals, followed by 2,500 rad of 15 MeV linear accelerator x-rays via opposing lateral 16 × 12 cm portals. The tumor

Received June 6, 1978; accepted after revision November 29, 1978.

[1] Department of Radiology, Osaka City University Medical School, 1-5-7 Asahi-machi, Abeno-ku, Osaka City, Japan 545. Address reprint requests to Y. Inoue.

[2] Department of Neurosurgery, Osaka City University Medical School, Osaka, Japan.

© 1979 American Roentgen Ray Society

0361–803X/79/1323–0361 $0.00

TABLE 1
Case Summaries

Case No.	Age and Sex	Symptoms	CT Findings; Tumor Size (cm)	Portal Size (cm)	Dose (rad/fraction/days)	Dose at Tumor Disappearance (rad)
1	25, M	Diplopia, inability to gaze upward, papilledema, nystagmus	Slightly high dense mass in pineal region (2.4 × 1.8)	12 × 20 12 × 9	2,500 whole brain 3,000 cone down 5,500/33/46	2,500
2	16, M	Headache, diplopia, papilledema, inability to gaze upward	Same as case 1 (2.4 × 2.5)	5 × 5 14 × 18	2,500 cone down 3,000 whole brain 5,500/41/54	1,600
3	14, M	Headache, vomiting, ataxia, mental confusion, papilledema, left hemiplegia	Same as case 1 (3.0 × 2.4)	12 × 20	4,200/24/92	2,000
4	14, M	Headache, diplopia, papilledema, inability to gaze upward	Same as case 1 (3.0 × 1.8)	7 × 7 13 × 10	2,600 cone down 2,900 whole brain 5,500/45/59	2,700
5	13, M	Headache, diplopia, papilledema, inability to gaze upward, precocious puberty	Same as case 1 (1.2 × 1.8)	5 × 5 13 × 10	2,800 cone down 2,700 whole brain 5,500/44/64	2,000
6	18, M	Headache, visual disturbance, inability to gaze upward, papilledema	Same as case 1 (3.5 × 2.1)	6 × 6 18 × 14	3,000 cone down 2,100 whole brain 5,100/44/74	2,400
7	35, M	Diplopia, difficulty walking, nystagmus, trunkal ataxia, atrophic disc	Isodense mass in pineal region (3.0 × 1.5 cm) to fourth ventricle (3.0 × 3.0), abnormal calcification in tumor anterior to pineal calcification	7 × 5 16 × 12	3,000 cone down 2,500 whole brain 5,500/43/64	3,300
8	12, F	Headache, diabetes insipidus, impaired visual acuity, right hemianopsia	Slightly high dense mass in suprasellar area (2.6 × 2.6)	5 × 5 12 × 8	2,200 cone down 2,300 whole brain 4,500/37/51	1,800
9	13, F	Pituitary dwarfism, headache, vomiting, papilledema, decreased vision, diabetes insipidus	Slightly high dense mass in third ventricular area (2.9 × 2.6)	5 × 5 18 × 10	2,800 cone down 2,000 whole brain 4,800/39/61	2,000

Note.—Only case 8 had no decompression; all others had ventriculoperitoneal shunt. All masses enhanced on CT.

disappeared completely on plain and contrast CT at 3,300 rad (fig. 2C). Nystagmus, trunkal ataxia, and bilateral abducent palsy improved, but slight diplopia remained. The patient was doing well 4 months after radiation therapy.

Case 8

A 12-year-old girl had mild frontal headache, polydipsia, and polyuria for 1 month. No neurologic abnormality was found and optic fundi were normal. Skull radiography and plain and contrast CT with 8 mm collimation showed no abnormality (figs. 3A and 3B). The patient was discharged with diagnosis of idiopathic diabetes insipidus. Excessive urine volume was controlled with Diabenese.

After 6 months, she noted decreased vision and right hemianopsia, although she had no headache, nausea, vomiting, or choked disc. Plain CT (figs. 4A and 4B) demonstrated a suprasellar mass of slightly increased density that was markedly enhanced on contrast CT (EMI nos. 23–40 or 45) (figs. 4A and 4B). The mass in the suprasellar cistern was confirmed by pneumoencephalography. Cerebrospinal fluid cytology showed the combination of large tumor cells and small lymphoid cells suggestive of a germinoma.

The suprasellar region was irradiated with 2,200 rad of 15 MeV betatron x-rays via opposing lateral 5 × 5 cm portals and 2,300 rad via opposing lateral 12 × 8 cm portals. Impaired visual acuity improved rapidly. There was marked decrease in tumor size on CT scan at the 600 rad dose (fig. 4C). Plain and contrast CT at 1,800 rad no longer showed the tumor, and the suprasellar cistern was seen normally (fig. 4D).

Urine volume decreased somewhat; but diabetes insipidus persisted. The patient has done well after radiation therapy, and her urine volume is being controlled with oral Diabenese.

Results

In all cases, tumors appeared on plain CT scan as midline masses of normodensity or slightly increased density (EMI nos. 20–25) without peritumoral low density. With contrast, all tumors showed significant enhance-

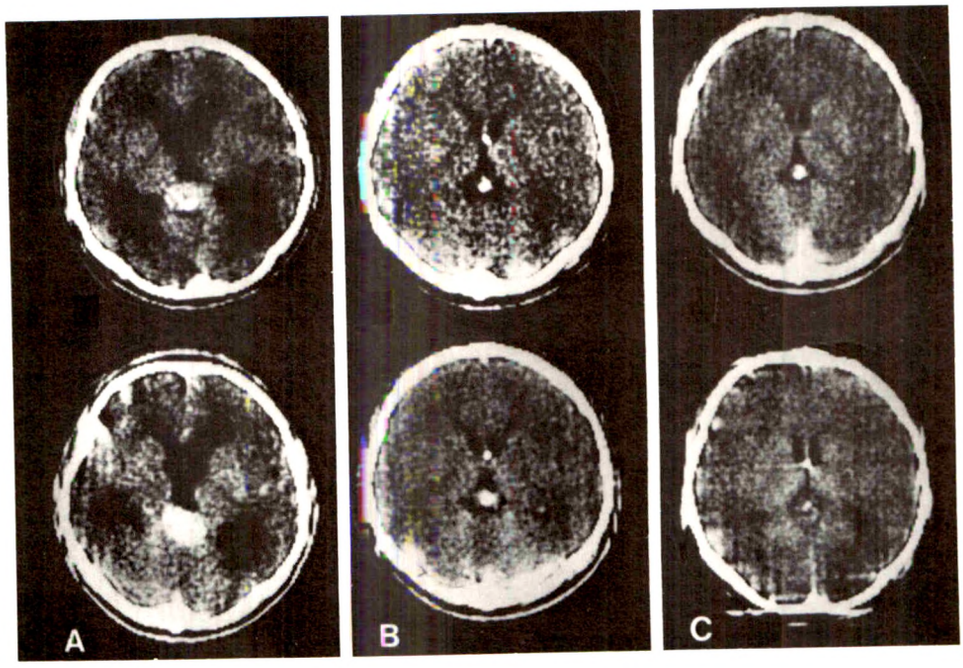


Fig. 1.—Case 6, germinoma in pineal region. CT without (top row) and with (bottom row) contrast enhancement. **A,** Before radiation therapy, tumor is well defined area of slightly increased density, markedly enhanced by contrast material. Moderate dilatation of third and lateral ventricles. **B,** At 600 rad, tumor has significantly diminished; ventricles almost normal. Tip of shunt tube in area of right foramen of Monro. **C,** At 2,400 rad, tumor no longer seen.

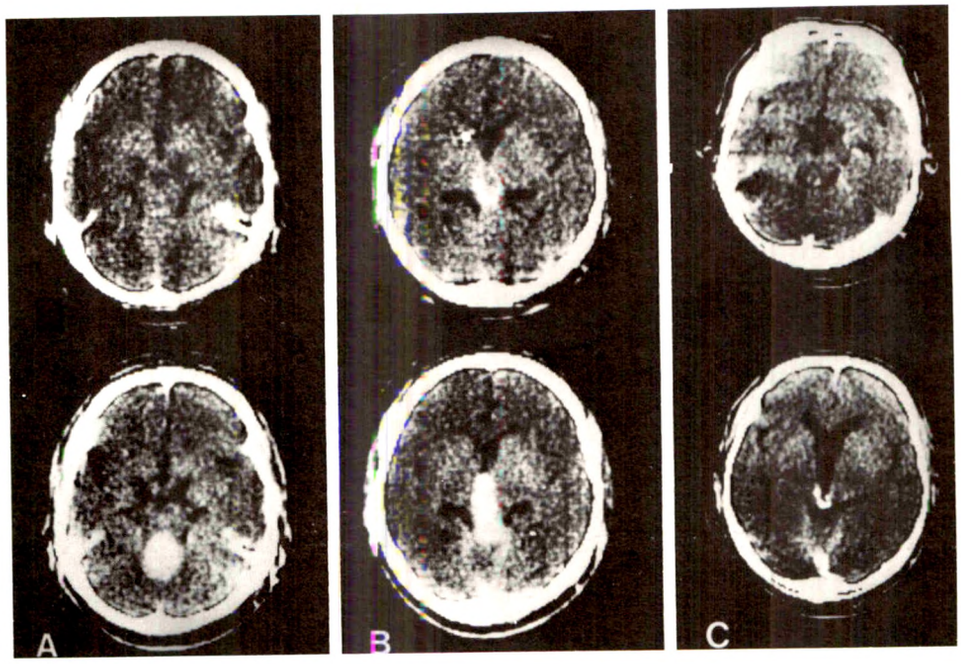


Fig. 2.—Case 7, germinoma in pineal region, vermis of cerebellum, and fourth ventricle. CT without (top row) and with (bottom row) contrast enhancement. **A** and **B,** Before radiation therapy, tumor not well seen. Left ambient, quadrigeminal cistern, and fourth ventricle not visualized. Tumor markedly enhanced in pineal region down to fourth ventricle. Abnormal calcification in posterior third ventricular area. **C,** At 3,300 rad, large tumor no longer seen.

ment (EMI nos. 35–45) of almost homogeneous density, with a less dense zone at the margin probably due to partial volume effect.

All tumors became markedly smaller on serial CT scans, even at small irradiation doses, and disappeared entirely after 1,600–3,300 rad. Clinical improvement was dramatic during radiation therapy in all patients, but diabetes insipidus has not improved in cases 8 and 9, and two of nine patients still complain of slight diplopia at lateral gaze. Precocious puberty did not change on physical examination in one patient. No sign or symptom of spinal or meningeal metastasis has been noted so far in our patients.

Although germinomas are known to be notoriously malignant, some seem to smolder for years and then show striking acceleration [4]. To our knowledge, case 8 is the first CT demonstration of the sudden increase in size of a germinoma in the literature. In a similar reported case, no contrast CT was performed on the initial study [5].

Discussion

In 1972, adopting Friedman's proposal [6], Rubinstein [7] classified all midline central nervous system tumors in one group, using the term "germinoma" regardless of whether they arose in the pineal region or the suprasellar region. The intracranial germinomas are the most common form of growth in the region of pineal body, accounting for over 50% of all neoplasms in this area. DeGirolami and Schmidek [8] reported 53 tumors of the pineal region, of which 35 were pathologically verified: 14 germinomas, three teratomas, three pinealocytomas, five pinealoblastomas, and 10 gliomas.

Since germinomas are radiosensitive and often radiocurable, and surgical resection is hazardous and frequently incomplete [8, 9], surgical decompression followed by radiotherapy is the acceptable primary treatment regardless of whether there is pathologic verification [8, 10–15]. The 5 year survival rate after irradiation to these tumors is reported to be 50%–80% [8, 9, 13, 16]. These figures include not only germinoma but also teratoma, choriocarcinoma, pinealocytoma, pinealoblastoma, gliomas, and metastatic tumor. When germinoma alone is adequately selected and irradiated, the 5 year survival rate may be higher than 80% [13].

The CT findings in our series consisted of a midline (pineal or suprasellar) solid mass that was isodense or of slightly increased density on plain CT and that enhanced in a homogeneous manner with contrast. We believe these findings combined with a rapid response to radiation therapy are virtually diagnostic of germinoma. The radiosensitive tumors to be differentiated are pinealocytoma and pinealoblastoma in the pineal region and the rare lymphoma or reticulum cell sarcoma in the suprasellar region [7]. Cerebrospinal fluid cytology may aid differential diagnosis. Takeuchi et al. [2] described a characteristic cerebrospinal fluid cytologic finding in suprasellar germinomas consisting of the combination of large tumor cells and small lymphoid cells. These authors conclude that cerebrospinal fluid cytologic examination should be performed whenever a germinoma is suspected on clinical or radiologic grounds. When the cerebrospinal fluid cytology shows the characteristic pattern, the patient should be irradiated without surgery [2].

In children, suprasellar germinomas exhibit a distinct clinical triad of diabetes insipidus, hemianopsia, and hypopituitarism. Rapid response to radiation therapy

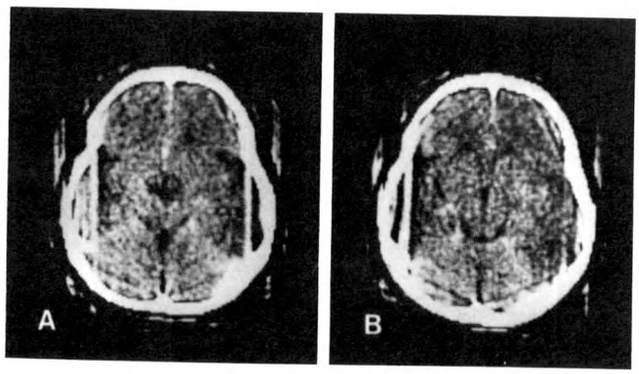


Fig. 3.—Case 8, suprasellar germinoma. CT with contrast enhancement. No abnormality seen.

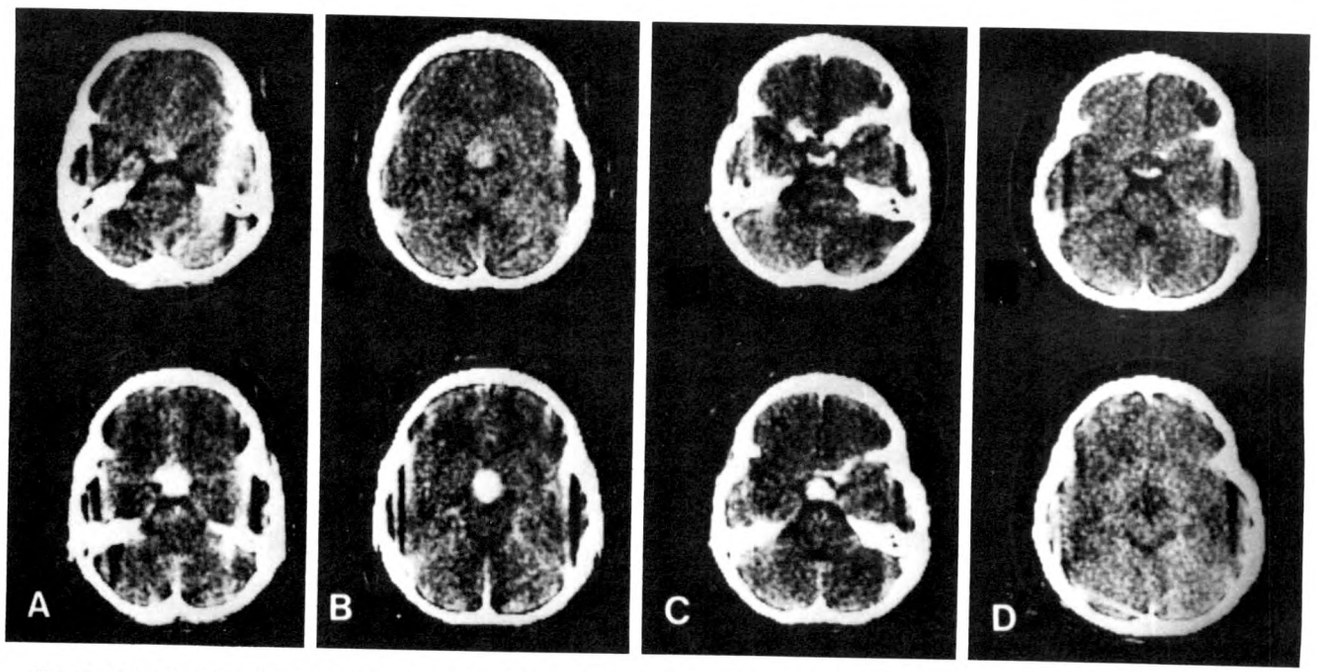


Fig. 4.—Case 8, suprasellar germinoma 6 months after fig. 3. CT without (top row) and with (bottom row) contrast enhancement. **A** and **B**, Suprasellar cistern filled by mass of slightly increased density impinging into floor of third ventricle. Mass homogeneously enhanced. **C**, During radiation therapy at 600 rad, tumor significantly diminished. **D**, During radiation therapy at 1,800 rad, suprasellar mass disappeared and suprasellar cistern clearly visualized.

documented by serial CT scanning and positive cerebrospinal fluid cytology reasonably establishes the diagnosis of germinoma. The most difficult diagnostic differentiation is between germinoma and lymphoma or reticulum cell sarcoma because (1) the latter are very rare but can selectively involve the hypothalamus and the neurohypophysis [7]; (2), the latter are not clearly separated from a germinoma by cerebrospinal fluid cytology (J. Yamashita, neurosurgery, Kyoto University, personal communication); and (3) the latter are radiosensitive.

Germinomas in our series disappeared on follow-up CT scans at the 1,600–3,300 rad dose. If the serial CT scans had been at closer intervals, such as each 500 rad, we assume that the tumor might have become invisible at less than 2,000–2,500 rads.

We emphasize that traditionally recommended doses of 4,500–5,500 rad to this kind of tumor [8, 11, 12, 14, 15, 17, 18] should not be changed on the basis of our study, because complete disappearance of a tumor shadow on CT scans does not necessarily indicate the complete disappearance of microscopic tumor cells. There are reports of recurrent germinomas after apparently adequate irradiation [13, 16, 17].

REFERENCES

1. Carella RJ, Pay N, Newall J, Farina AT, Kricheff II, Cooper JS: Computerized (axial) tomography in the serial study of cerebral tumors treated by radiation. *Cancer* 37:2719–2728, 1976
2. Takeuchi J, Handa H, Nagata I: Suprasellar germinoma. *J Neurosurg* 49:41–48, 1978
3. Russell DS: The pinealoma; its relationship to teratoma. *J Pathol Bacteriol* 56:145–150, 1944
4. Russell D, Rubinstein L: Pineal neoplasms, in *Pathology of Tumors of the Nervous System*, edited by Russell D, Rubinstein L, London, Arnold, 1971, pp 208–220
5. Case records of the Massachusetts General Hospital (case 38–1975). *N Engl J Med* 293:653–660, 1975
6. Friedman NB: Germinoma of the pineal. Its identity with germinoma ("seminoma") of the testis. *Cancer Res* 7:363–368, 1947
7. Rubinstein LJ: Tumors of the central nervous system, in *Atlas of Tumor Pathology*, series 2, fascicle 6, Washington, D.C., Armed Forces Institute of Pathology, 1972, pp 268–284
8. DeGirolami U, Schmidek H: Clinicopathological study of 53 tumors of the pineal region. *J Neurosurg* 39:455–462, 1973
9. Obrador S, Soto M, Gutierrez-Diaz JA: Surgical management of tumours of the pineal region. *Acta Neurochir* (Wien) 34:159–171, 1976
10. Bouchard J: Central nervous system, in *Textbook of Radiotherapy*, edited by Fletcher G, Philadelphia, Lea & Febiger, 1973, p 401
11. Mincer F, Meltzer J, Botstein C: Pinealoma. A report of twelve irradiated cases. *Cancer* 37:2713–2718, 1976
12. Bradfield JS, Perez CA: Pineal tumors and ectopic pinealomas. Analysis of treatment and failures. *Radiology* 103:399–406, 1972
13. Jenkin RDT, Simpson JK, Keen CW: Pineal and suprasellar germinomas. *J Neurosurg* 48:99–107, 1978
14. Maier JG, DeJong D: Pineal body tumors. *AJR* 99:826–832, 1967
15. El-Mahdi AM, Philips E, Lott S: The role of radiation therapy in pinealoma. *Radiology* 103:407–412, 1972
16. Smith NJ, El-Mahdi AM, Constable WC: Results of irradiation of tumors in the region of the pineal body. *Acta Radiol [Ther]* (Stockh) 15:17–22, 1976
17. Wara WM, Fellows CF, Sheline GE, Wilson CB, Townsend JJ: Radiation therapy for pineal and suprasellar germinomas. *Radiology* 124:221–223, 1977
18. Rubin P, Kramer S: Ectopic pinealoma: a radiocurable neuroendocrinologic entity. *Radiology* 85:512–523, 1965

Erratum

In the January issue of the *AJR*, the article by Dunnick et al. (*AJR* 132:1–6, 1979) contains an error. In the first paragraph of the Discussion (p. 5), Ebstein-Barr should be Epstein-Barr.

CT Metrizamide Myelography for Intraspinal and Paraspinal Neoplasms in Infants and Children

I. MARGARETA RESJÖ,[1, 2] DEREK C. HARWOOD-NASH,[1] CHARLES R. FITZ,[1] AND SYLVESTER CHUANG[1]

Computed tomographic (CT) metrizamide myelography is an accurate and satisfactory method for examining the spinal cord in infants and children with suspected intraspinal neoplasms. It was performed in 13 infants and children and in one adult with intra- and paraspinal neoplasms. CT metrizamide myelography in paraspinal masses provides the total geography of the mass; that is, possible intraspinal extension, as well as the paraspinal portion itself. As such, it is superior to conventional myelography.

Until recently, radiologic diagnosis of intraspinal neoplasms and intraspinal extension of paraspinal neoplasms was always made by conventional myelography, tomography, and plain radiography. However, in the past few years several authors [1–5] have reported on the use of CT in diagnosing lesions of the spinal cord and spinal canal. With CT it has been possible to outline intra- and paraspinal lesions before and after enhancement with intravenous contrast material [6–8]. Both the normal and abnormal cord is exquisitely outlined by intrathecal metrizamide [9–13], as is its relationship to paraspinal masses and vertebral bony abnormalities.

During the past 2 years, we performed CT metrizamide myelography on 84 patients to diagnose possible paraspinal and intraspinal abnormalities, including intra- and paraspinal neoplasms.

Subjects and Methods

All scans were performed with an Ohio-Nuclear Delta Scanner with a matrix of 256 × 256 124 kV, 34 mA, 2–2.5 min scanning time, and 20–40 cm circle size.

The level of the scanning area was chosen from a preliminary plain film with a radiopaque ruler (fig. 1). The ruler was then placed beside the patient on the scanning table and the starting level marked on the patient. Each level of the CT images was calculated from the plain film. The patients were positioned either supine or prone. A detailed description of the CT metrizamide myelography technique was reported earlier [12].

Traditionally, metrizamide myelography under general anesthesia precedes CT, but recently we have been performing CT myelography alone. Myelography was performed as described by Barry et al. [14]. When CT myelography is the only examination, a small amount of 170 mg/100 ml metrizamide is injected into the subarachnoid space through a lumbar puncture under local anesthesia. The smaller children are sedated with Nembutal [15], while older, more cooperative children are examined without sedation or general anesthesia.

Of the 14 patients with intra- and/or paraspinal neoplasms we examined, one was less than 6 months old, two were between 6 months and 1 year, three were 1–2 years, seven were 6–14 years, and one was adult. Half the patients were male and half female. The types of neoplasms in the 14 patients were three primarily intramedullary or filum neoplasms, seven neuroblastomas, one ganglioneuroma, one sarcoma, and metastases from a medulloblastoma in one and from a pterygoid fossa sarcoma in another.

Results

Three patients had a primary intramedullary/filum neoplasm. In the first of these, with back pain and meningismus, lumbar puncture revealed subarachnoid hemorrhage. Both metrizamide myelography (fig. 2A) and CT metrizamide myelography (fig. 2B) showed a large mass lesion at the tip of the conus. CT myelography enabled us to separate two compartments of the mass (fig. 2C): the smaller one above and going partly alongside the



Fig. 1.—Marker technique. Preliminary plain film with radiopaque centimeter ruler; also paraspinal mass.

Received June 6, 1978; accepted after revision December 1, 1978.

[1] Department of Radiology, Hospital for Sick Children, 555 University Avenue, Toronto, Ontario M5G 1X8, Canada. Address reprint requests to D. Harwood-Nash.

[2] Present address: Röntgenavd, Regionsjukhuset, S-58185 Linkoping, Sweden.

© 1979 American Roentgen Ray Society

0361–803X/79/1323–0367 $0.00

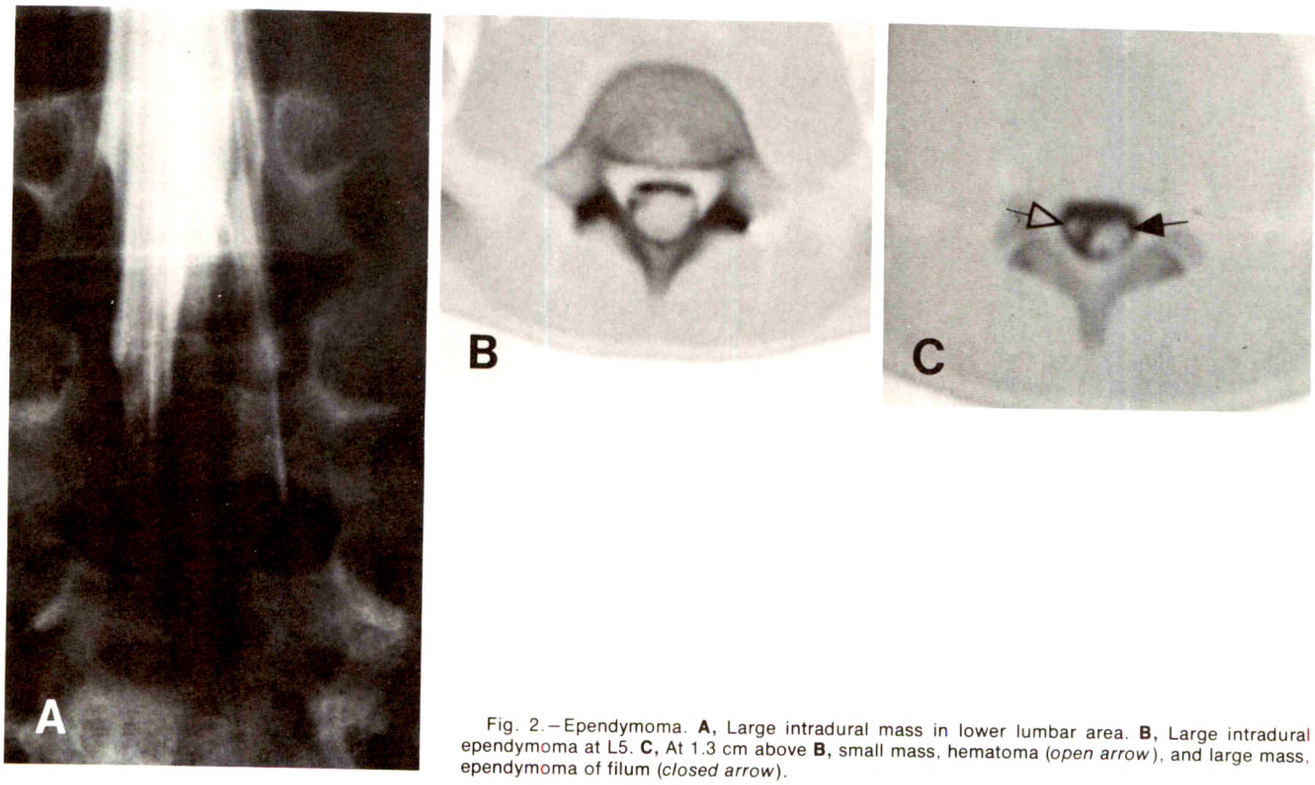


Fig. 2.—Ependymoma. **A,** Large intradural mass in lower lumbar area. **B,** Large intradural ependymoma at L5. **C,** At 1.3 cm above **B,** small mass, hematoma (*open arrow*), and large mass, ependymoma of filum (*closed arrow*).

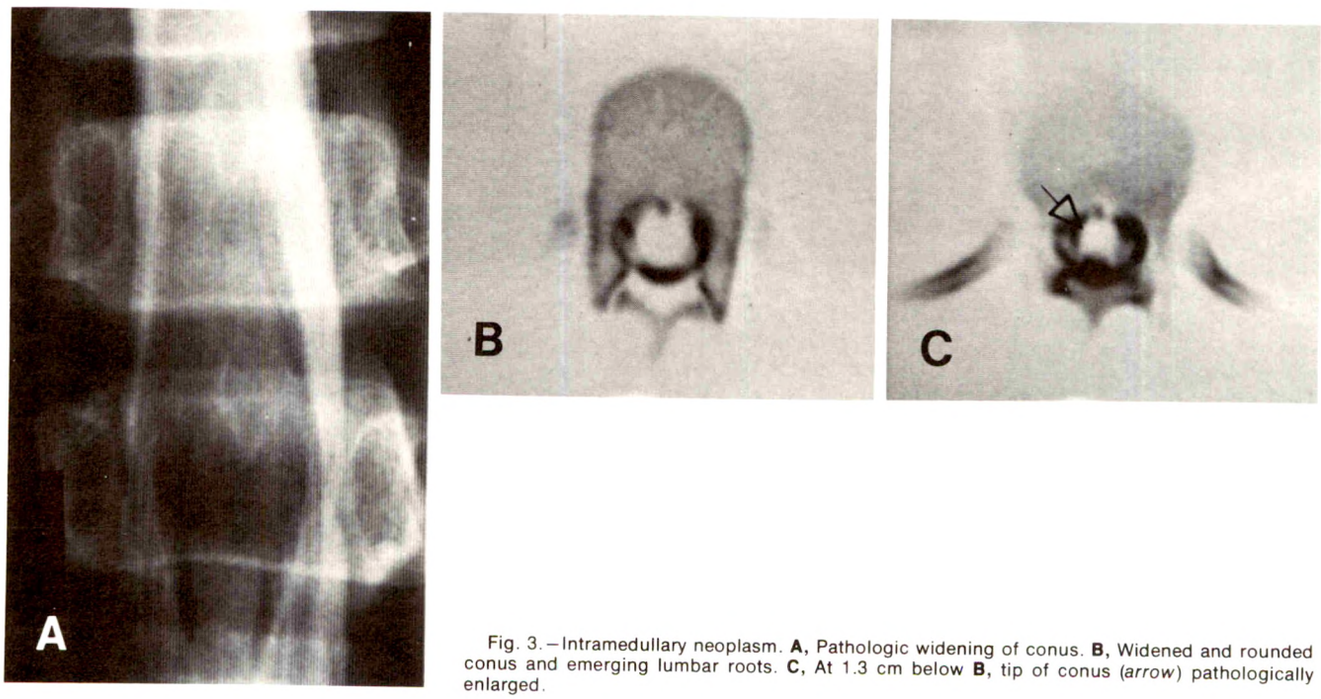


Fig. 3.—Intramedullary neoplasm. **A,** Pathologic widening of conus. **B,** Widened and rounded conus and emerging lumbar roots. **C,** At 1.3 cm below **B,** tip of conus (*arrow*) pathologically enlarged.

main mass. The Hounsfield numbers of the smaller part were almost twice as high as for the main mass, suggesting it might be a hematoma. Operation confirmed a hematoma at the upper part of the mass; histology proved ependymoma of the filum.

In another patient, a 14-year-old boy with both motor and sensory deficits of the right foot, metrizamide myelography (fig. 3A) and CT myelography (figs. 3B and 3C) revealed a mass in the conus. There was no dysraphism, and radiographic diagnosis was a true neoplasm of the conus. No operative proof is available because his parents refused operation, but his clinical status has deteriorated since examination.

In the third patient, an adult with a cervical astrocy-

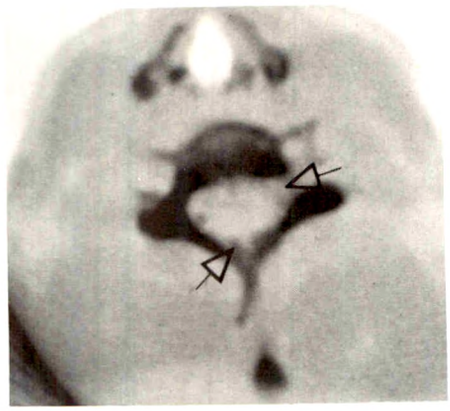


Fig. 4.—Intramedullary astrocytoma. At C4, irregular, markedly compressed subarachnoid space containing metrizamide (*arrows*) due to nodular intramedullary neoplasm.

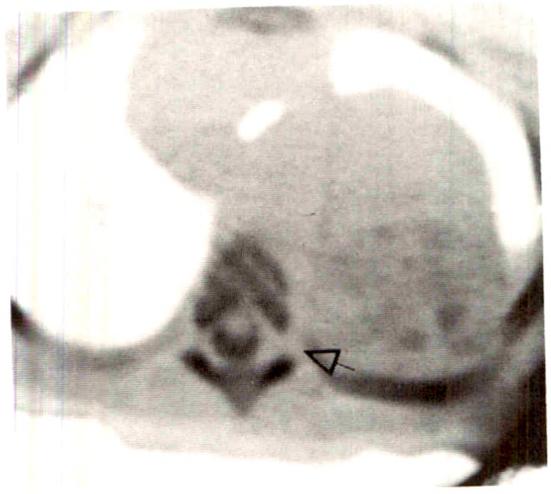


Fig. 5.—Neuroblastoma in mediastinum. Cord and dural sac displaced to right, left intervertebral foramen widened (*arrow*), and large mediastinal mass with mottled calcifications.

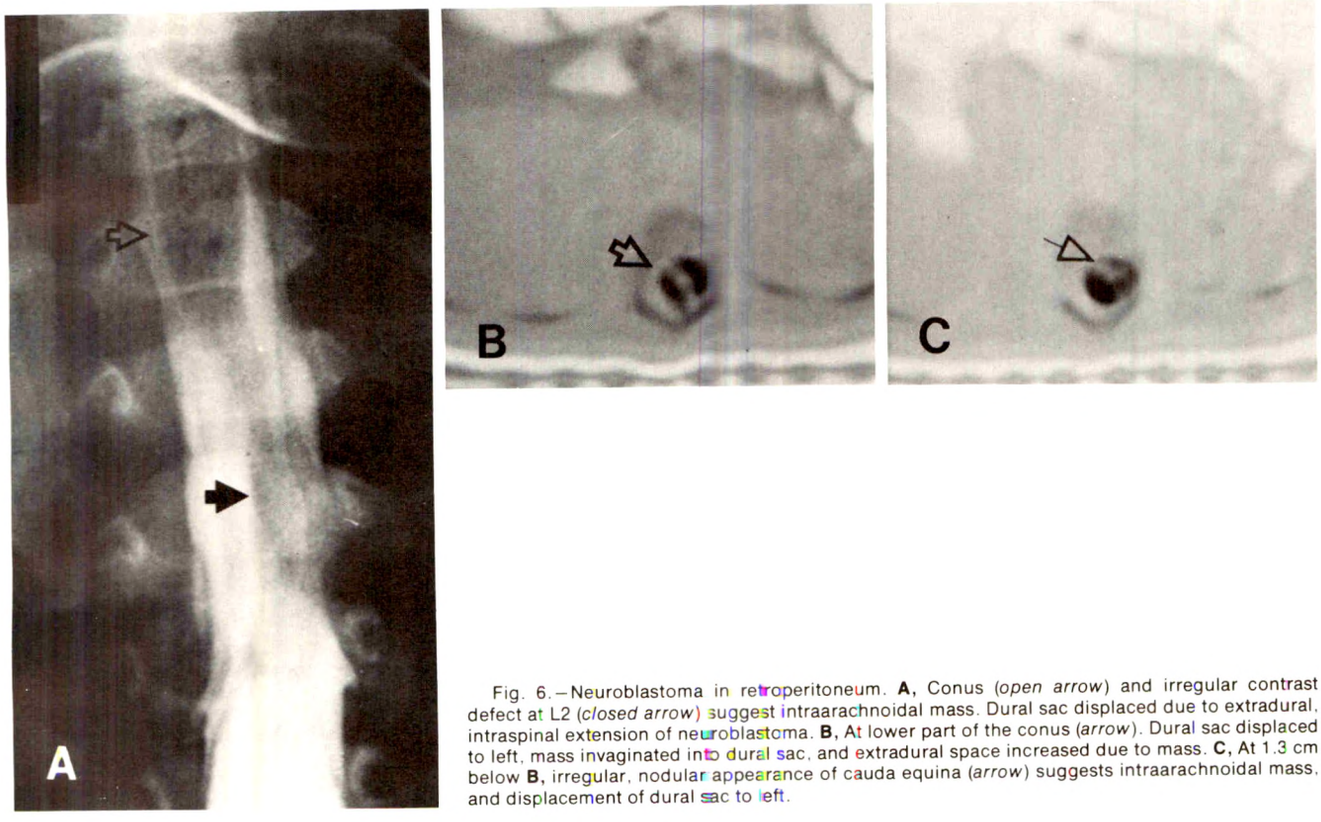


Fig. 6.—Neuroblastoma in retroperitoneum. **A,** Conus (*open arrow*) and irregular contrast defect at L2 (*closed arrow*) suggest intraarachnoidal mass. Dural sac displaced due to extradural, intraspinal extension of neuroblastoma. **B,** At lower part of the conus (*arrow*). Dural sac displaced to left, mass invaginated into dural sac, and extradural space increased due to mass. **C,** At 1.3 cm below **B,** irregular, nodular appearance of cauda equina (*arrow*) suggests intraarachnoidal mass, and displacement of dural sac to left.

toma, pantopaque myelography in another hospital showed total block at T3, suggesting an intramedullary lesion. Metrizamide myelography showed a similar block, but at CT myelography a very low concentration of contrast material in the cervical area outlined a nodular mass in an enlarged cervical cord (fig. 4). The Hounsfield numbers within this part of the cord varied from 16 to 60 or 70. No intravenous enhancement was performed. However, the varying Hounsfield numbers and the irregular outlining suggested a partly necrotic intramedullary neoplasm, which was proved at operation to be a partly necrotic astrocytoma.

Seven patients had a neuroblastoma and one had a ganglioneuroma in the mediastinum. In four patients, the neuroblastoma was in the posterior mediastinum, and in three, in the retroperitoneal space in the abdomen/pelvis. The tumor was new in seven patients and a recurrence in one.

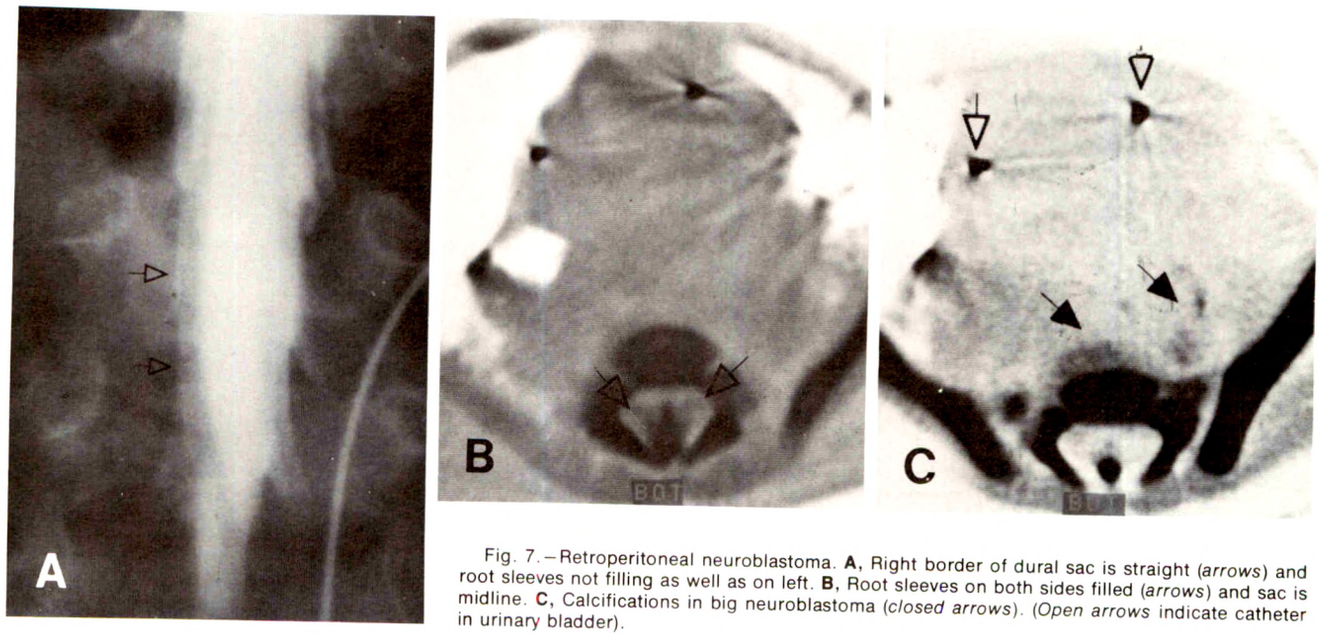


Fig. 7.—Retroperitoneal neuroblastoma. **A,** Right border of dural sac is straight (*arrows*) and root sleeves not filling as well as on left. **B,** Root sleeves on both sides filled (*arrows*) and sac is midline. **C,** Calcifications in big neuroblastoma (*closed arrows*). (*Open arrows* indicate catheter in urinary bladder).

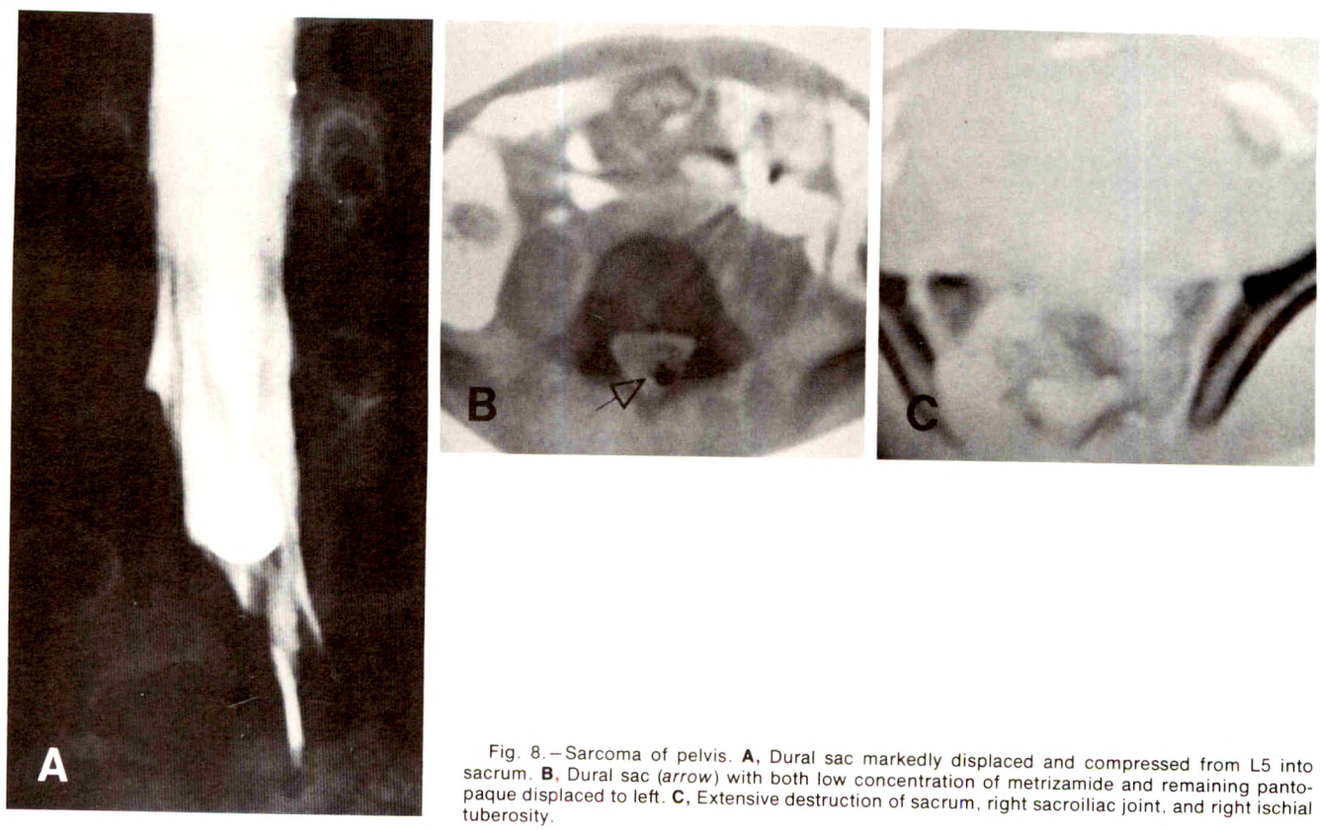


Fig. 8.—Sarcoma of pelvis. **A,** Dural sac markedly displaced and compressed from L5 into sacrum. **B,** Dural sac (*arrow*) with both low concentration of metrizamide and remaining pantopaque displaced to left. **C,** Extensive destruction of sacrum, right sacroiliac joint, and right ischial tuberosity.

In two of the patients, CT myelography showed extension into the spinal canal, one in the thoracic (fig. 5) and the other in the lumbar area. In both, this extension was proven at operation. In the patient with extension into the lumbar spinal canal, myelography (fig. 6A) and CT myelography (figs. 6B and 6C) suggested both extra- and intradural involvement, but at operation only extradural extension was found. The intradural defect is believed to be edema of the filum and lumbar sacral roots related to the extradural mass. In five of these eight patients, no involvement of the spinal canal was seen. However, in one myelography was equivocal with an unusual straight right border of the lower part of the dural sac and poor filling of the sacral root sleeves (fig. 7A). CT myelography

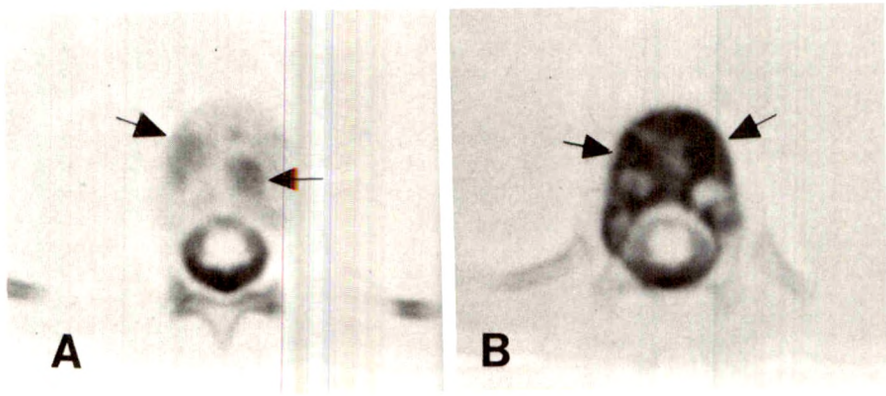


Fig. 9.—Metastases. Cord and dural sac normal. Extensive sclerotic and lytic metastases (*arrows*) to vertebrae.

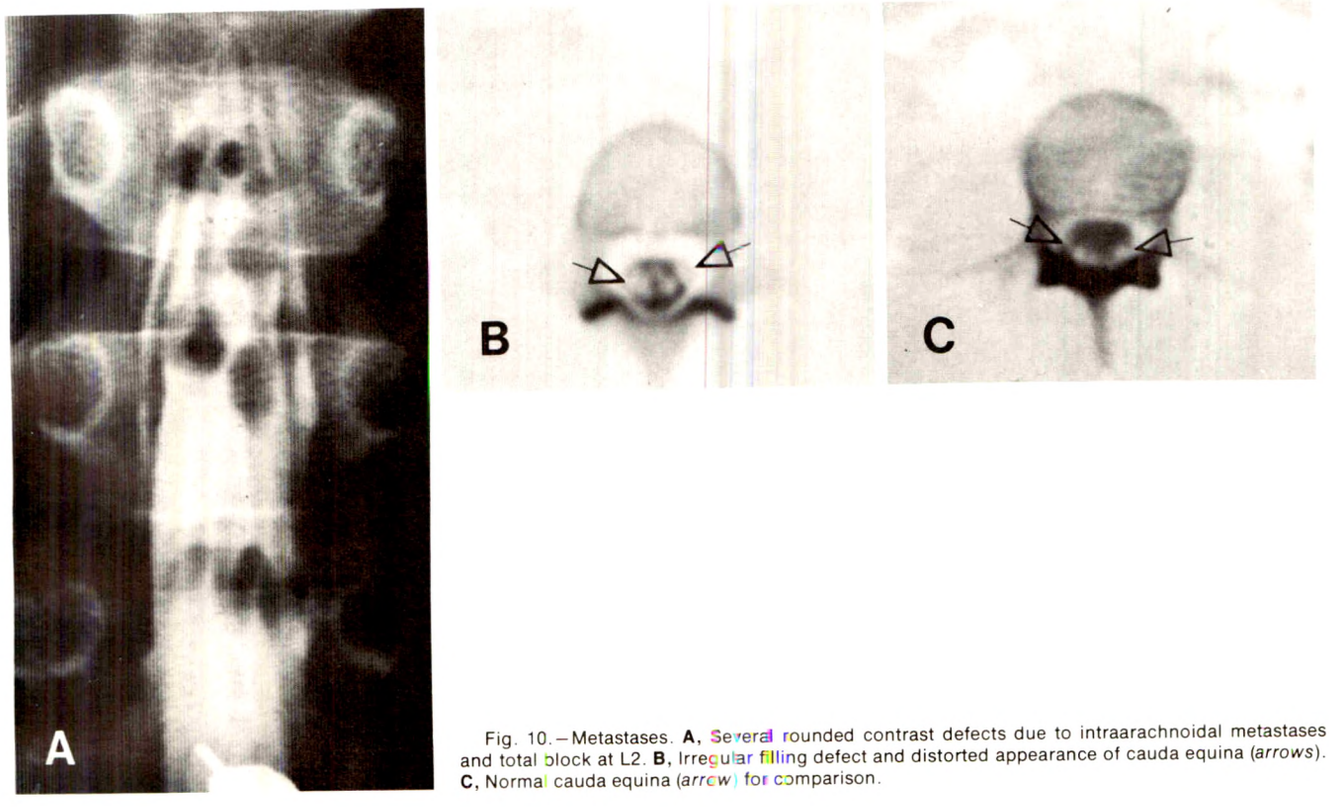


Fig. 10.—Metastases. **A,** Several rounded contrast defects due to intraarachnoidal metastases and total block at L2. **B,** Irregular filling defect and distorted appearance of cauda equina (*arrows*). **C,** Normal cauda equina (*arrow*) for comparison.

showed a normal dural sac even in the lower part (figs. 7B and 7C).

In the remaining child with previous operative removal of an intraspinal, extradural part of the neuroblastoma from the lumbar area, subsequent myelography and CT myelography showed irregularities of the dural sac. It was impossible to differentiate between tumor recurrence into the spinal canal and postoperative changes. At operation no extension into the spinal canal was found.

One patient had an undifferentiated sarcoma of the sacrum. Plain radiography of the pelvis and lumbosacral spine was normal and initial myelography showed only minor displacement of the lower part of the dural sac, mistakenly considered normal. Myelography 2 months later revealed a more marked displacement of the dural sac and increased width of the extradural space (fig. 8A). CT myelography showed displacement of the sac (fig. 8B), but also a massive destruction of the sacrum and right sacroiliac joint (fig. 8C), findings that were impossible to see on plain films, but distinguishable on conventional tomography of the pelvis. If routine myelography is performed (as in figs. 7A and 8A) decubitus views are an essential addition to prone and supine views.

Two children had metastases, one from a medulloblastoma and the other from a pterygoid fossa sarcoma. The patient treated for postfossa medulloblastoma had extensive metastases to all vertebrae and other bones.

Some weakness in the right leg and sensory loss with the level at L2 were the indications for myelography. Both myelography and CT myelography (fig. 9) showed a normal cord and dural sac.

The other patient with sarcoma had a total block to the metrizamide at L2, both on myelography and CT myelography. There were irregular filling defects inside the lower lumbar dural sac due to metastases, obvious on myelography (fig. 10A) and CT myelography (fig. 10B), that appeared quite different from normal cauda equina (fig. 10C).

Discussion

We believe diagnostic accuracy of CT metrizamide myelography for intraspinal neoplasms is equal to conventional myelography. CT myelography more accurately demonstrates the total extension of the paraspinal neoplasm inside and outside the spinal canal, and bony destruction and eventual calcifications within the tumor, than do other diagnostic methods. While CT itself adds little to the histologic diagnosis of neuroblastomas and ganglioneuromas [16], CT metrizamide myelography gives information on the possible intraspinal extension and the total geography of the tumor on the same examination. For any paraspinal mass lesion, it is our policy to perform a preliminary myelography prior to thoracotomy or laparotomy in order to detect possible intraspinal extension [17]. This is performed even after a negative neurologic examination. If intraspinal extension is detected, decompressive laminectomy must be performed before thoracotomy, laparotomy, or even irradiation to prevent inadvertent bleeding or increasing mass effect within an intact spinal canal.

As reported by Reilly [16], unique information regarding pelvic neoplasms, such as osteogenic sarcomas, can be provided by CT, and we believe that any patient with suspected bony neoplasms of the spine or pelvis and peripheral neurologic signs should have plain radiography and CT metrizamide myelography as the primary examinations to detect possible intraspinal extension. We now perform CT myelography on all bony neoplasms of the spine or pelvis regardless of the presence or absence of peripheral and neurologic signs. We believe CT myelography is as good as standard myelography in investigating metastatic neoplasms with suspected intraspinal involvement, and it also gives more complete information concerning associated bony and paraspinal lesions at the same examination.

CT myelography can be performed without general anesthesia in most children; it requires only a small dose of intrathecal metrizamide, and thereby probably reduces the potential side effects of this contrast agent. The need for other radiographic diagnostic procedures, such as tomography and conventional myelography, is virtually eliminated thus the total diagnostic procedure is more efficient, economical, and subjects the patient to less radiation exposure.

REFERENCES

1. Hammerschlag SB, Wolpert SM, Carter BL: Computed tomography of the spinal canal. *Radiology* 121:361–367, 1976
2. James HE, Oliff M: Computed tomography in spinal dysraphism. *J Comput Assist Tomogr* 1:391–397, 1977
3. Lohkamp F, Claussen C, Schuhmacher G: Changes of the spinal cord accompanying spina bifida and diastematomyelia, in *Progress in Pediatric Radiology, Skull, Spine and Contents*, part II, vol 6, edited by Kaufmann HJ, Basel, Karger, 1978, pp 200–227
4. Weinstein MA, Rothner AD, Duchesneau P, Dohn DF: Computed tomography in diastematomyelia. *Radiology* 117: 609–611, 1975
5. Wolpert SM, Scott RM, Carter BL: Computed tomography in spinal dysraphism. *Surg Neurol* 8:199–206, 1977
6. Di Chiro G, Doppman JL, Wener L: Computed tomography of spinal cord arteriovenous malformations. *Radiology* 123: 351–354, 1977
7. Handel S, Grossman R, Sarwar M: Computed tomography in the diagnosis of spinal cord astrocytoma. *J Comput Assist Tomogr* 2:226–228, 1978
8. Isherwood I, Fawcitt RA, Nettle JRL, Spencer JW, Pullan BR: Computer tomography of the spine. A preliminary report, in *Computerized Axial Tomography in Clinical Practice*, edited by du Boulay GH, Moseley IF, Berlin, Springer, 1977, pp 322–335
9. Nakagawa H, Huang YP, Malis LI, Wolf BS: Computed tomography of intraspinal and paraspinal neoplasms. *J Comput Assist Tomogr* 1:377–390, 1977
10. Di Chiro G, Schellinger D: Computed tomography of spinal cord after lumbar intrathecal introduction of metrizamide (computer assisted myelography). *Radiology* 120:101–104, 1976
11. Harwood-Nash DC: Computed tomography of the spine, in *Computed Tomography*, edited by Norman D, Knobin M, Newton TH, San Francisco, University of California, 1977, pp 343–352
12. Resjö IM, Harwood-Nash DC, Fitz CR, Chuang S: Normal cord in infants and children examined with computed tomographic metrizamide myelogram. *Radiology*. In press, 1979
13. Resjö IM, Harwood-Nash DC, Fitz CR, Chuang S: Computed tomographic metrizamide myelography (CTMM) in spinal dysraphism in infants and children. *J Comput Assist Tomogr* 2:549–558, 1979
14. Barry JF, Harwood-Nash DC, Fitz CR, Byrd SE, Boldt DW: Metrizamide in pediatric myelography. *Radiology* 124:409–418, 1977
15. Byrd SE, Harwood-Nash DC, Fitz CR, Barry JF, Boldt DW: Coronal cranial computed tomography in infants and children. Part I. *Radiology* 124:705–709, 1977
16. Reilly BJ: Extracranial computerized tomography in children. *Comput Axial Tomogr* 1:257–270, 1977
17. Kirks DR, Berger PE, Fitz CR, Harwood-Nash DC: Myelography in the evaluation of paravertebral mass lesions in infants and children. *Radiology* 119:603–608, 1976

Radiographic Changes of the Skull in Sickle Cell Anemia

JENO I. SEBES[1] AND L. W. DIGGS[2]

Skull radiographs of 194 patients from 4 months to 55 years old with sickle cell anemia revealed porous decreased bone density in 25%, widening of diploë associated with a relative decrease in the width of the outer table in 22%, and vertical "hair-on-end" striations in 5%. The youngest patient with vertical striations was 5 years old and the oldest was 39. Serial examinations in 60 patients revealed no decrease of the skull width nor disappearance of the striations with age.

Interest in skull and other bone lesions associated with severe anemia was stimulated in 1925 when Cooley and Lee [1] described striking radiographic abnormalities in the bones of children with the disease then known as "Mediterranean anemia" and later identified as "Cooley's anemia" and "thalassemia major." The calvarial lesions described included widened diploë, thinning of external table, increased radiolucency, and vertical trabecular striations.

Cooley et al. [2, 3] later reported similar but less striking lesions in patients with sickle cell anemia. Since that time, there have been numerous reports of radiographic abnormalities and anatomic lesions in the skulls of patients with sickle cell hemoglobinopathies (table 1). Many of these are reports of a few interesting cases or small series of cases. They usually depict the more striking and unusual manifestations without furnishing information concerning the incidence of the various types of lesions, the age of the patient when the lesion was first manifest, or the changes that occur in the appearance of the lesions with age.

The most noteworthy coverage of the radiographic features of sickle cell anemia and related hemoglobinopathies is found in a monograph by Reynolds [4]. Other selected reports of radiographic abnormalities in bones are listed [5–11]. Anatomic lesions in the skull and other bones were reported by Diggs [12, 13].

Reported here are information about the skull afforded by a study of 194 patients with classical sickle cell anemia, the incidence of various abnormalities, and the evolution and progression of lesions with advancing age.

Subjects and Methods

Radiographic manifestations in bones and in other organs were studied as part of a long-term investigation of the natural history of sickle cell hemoglobinopathies. Patients seen at University of Tennessee Sickle Cell Center for any symptoms had a bone survey that was repeated at 5 year intervals, if possible. Before 1954, diagnosis of sickle cell anemia was established by classic clinical manifestations of a chronic, regenerative hemolytic anemia and recurrent painful crises together with sickle erythrocytes in air-exposed blood smears and in sealed moist preparations of blood. In later years, diagnosis of sickle cell anemia was confirmed by additional tests, including sodium metabisulfite moist preparation, tube solubility tests, electrophoretic mobility of hemoglobin, and concentrations of fetal hemoglobin, hemoglobin F, and hemoglobin A_2.

Hemoglobin SS patients studied totaled 194 (101 male and 93 female) and ranged from 4 months to 55 years old. Of the 194 patients, 134 had a single skull examination, 40 had two, 12 had three, and eight had four or more. The follow-up period of the 60 patients with more than one skull examination was 9 months to 13 years, (mean follow-up, 9.2 years). Routine skull examination included anteroposterior and lateral views.

Patients with the sickle cell trait (Hb AS), hemoglobin SC disease, sickle cell thalassemia, and other heterozygous S hemoglobinopathies were excluded from this study.

Results

Lateral views of the skull were evaluated for alterations in density and texture, expansion of the diploë, and the "hair-on-end" sign. The most frequent finding was a subtle change in texture of the frontal and parietal bones. Descriptively, it was a nonhomogenous, or "granular," decrease in bone density, and was present in 48 (25%) patients with sickle cell anemia. Because of the variable criteria for radiographically diagnosing osteoporosis, only the most severe changes of granularity were interpreted as positive for this study (fig. 1). The granular porous appearance of the skull was observed before expansion of the diploë occurred. Even with severe increased overall lucency, the inner table was distinct in all patients, the diploë revealed variable extents of granularity, and the outer table became progressively less distinct. Granularity was not observed in patients younger than 1 year.

Measurement of diploetic expansion was by the procedure used by Reynolds [4]. Total calvarial thickness, as well as the expansion of the diploë and the inner and outer tables, was measured on the lateral view of the skull with a caliper in the frontal and parietal bones at points of greatest diameter. The diploë was considered abnormally expanded when the diploetic width was at least 2.5 times greater than the combined measurement of the inner and outer tables. The width of the diploë in normal patients is considered less than 2.3 times the width of the bony tables [4]. Diploetic expansion was noted in 42 (22%) sickle cell disease patients. In 28 of 60

Received June 27, 1977; accepted after revision December 5, 1978.
This work was supported in part by U.S. Public Health Service grant HL 15169.
[1]Department of Diagnostic Radiology, University of Tennessee Center for the Health Sciences, 865 Jefferson Avenue, Memphis, Tennessee 38163. Address reprint requests to J. I. Sebes.
[2]Department of Medicine and Comprehensive Sickle Cell Center, University of Tennessee Center for the Health Sciences, Memphis, Tennessee 38163.

AJR 132:373–377, March 1979
0361–803X/79/1323–0373 $0.00
© 1979 American Roentgen Ray Society

TABLE 1
Literature Summary

Reference	No. Cases	Prominent Diploë Thickening of Calvarium		Radial Striations ("hair-on-end")	
		No.	%	No.	%
[4]	32	16	50	...	...
[7]	30	4	12	1	3.3
[8]	30	7	23.3	2	6.7
[9]	26	...	...	...	...
[10]	49	...	...	4	8.1
[11]	58	27	46.6	1	1.7
[15]	124	20	16.0	7	6
[19]	180	...	...	5	2.7
[20]	21	13	61.9	...	...

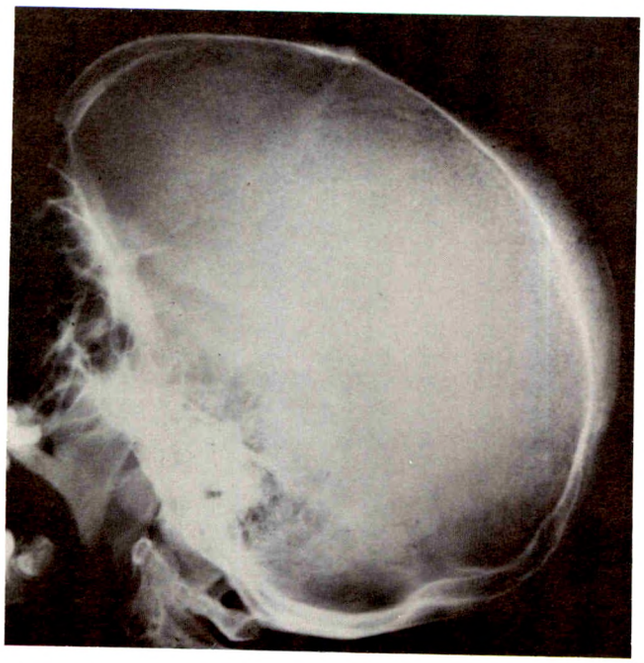


Fig. 1.—Coarsely granular appearance and diploeic widening of frontal and parietal bones in 10-year-old patient with sickle cell disease.

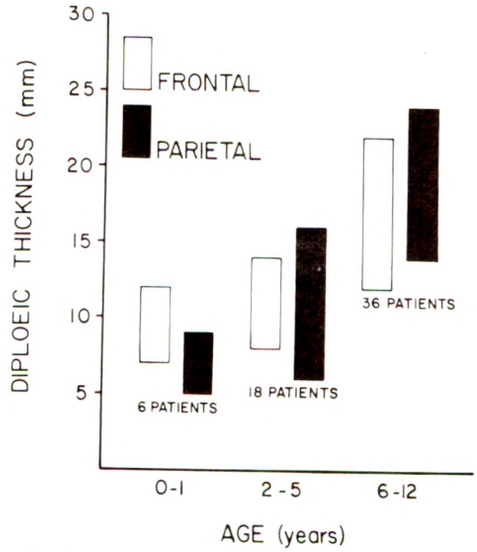


Fig. 2.—Progression of diploetic widening with age in frontal and parietal bones.

patients with multiple skull films, diploetic expansion occurred initially in the frontal area, followed later by expansion in the parietal area. Moreover, frontal expansion occurred first in all of the four patients who had more than one skull film before age 50. In the six patients 1 year old or less, frontal diploetic width was 7–12 mm compared to 5–9 mm for the greatest parietal diploetic width. In the 2–5 year age group, expansion of the parietal diploë became more prominent, and in the 6–12 year age group, parietal expansion surpassed the width of the diploë in the frontal bone (fig. 2). Parietal widening became progressively more prominent during the patients' second and third decades of life (fig. 3). In contrast to a previous report [14], the occipital diploë was not expanded in any of our 194 patients and no regression of the diploetic expansion was observed.

The classical "hair-on-end" sign was diagnosed only when definite long thin spicules were observed (fig. 4). It was present in 10 (5%) patients. Once present, this lesion persisted without regression in any patients observed from 2½ months to 22 years. There was no correlation between the prominence of this finding and the clinical course of the disease, nor was there a consistent relationship connecting onset, progression, and the severity of the anemia. Previously reported regression of calvarial changes with regression of sclerosis and widening were not observed in any patients in this study.

One patient with homozygous disease showed multiple discreet radiolucent lesions with distinct margins (fig. 5) resembling those seen in multiple myeloma. Repeated medical evaluations did not demonstrate any clinical or laboratory evidence of myeloma or metastatic disease. At autopsy, the multiple lytic areas proved to be islands of hyperplastic red marrow surrounded by fibrosis.

Discussion

Pathologic changes leading to abnormal radiographic appearance of bones in sickle cell anemia have been studied and are well described [4, 15–22]. Like the changes in axial and appendicular skeletons, skull abnormalities are produced by cellular hyperplasia, circulatory factors, or a combination of the two. The lesions, caused by red marrow hyperplasia, such as expansion of diploë, thinning of the outer table, progressive increase in the granular appearance of the skull, and vertical trabeculations ("hair-on-end"), are nonspecific and have been described by early investigators in thalassemia major, hereditary spherocytosis, and in iron deficiency anemia [23–26]. Circulatory factors, such as stasis and small vessel occlusions, result in patchy or diffuse opacity with gradual vault widening. The rare findings of distinct multiple radiolucent lesions amid diffusely scle-

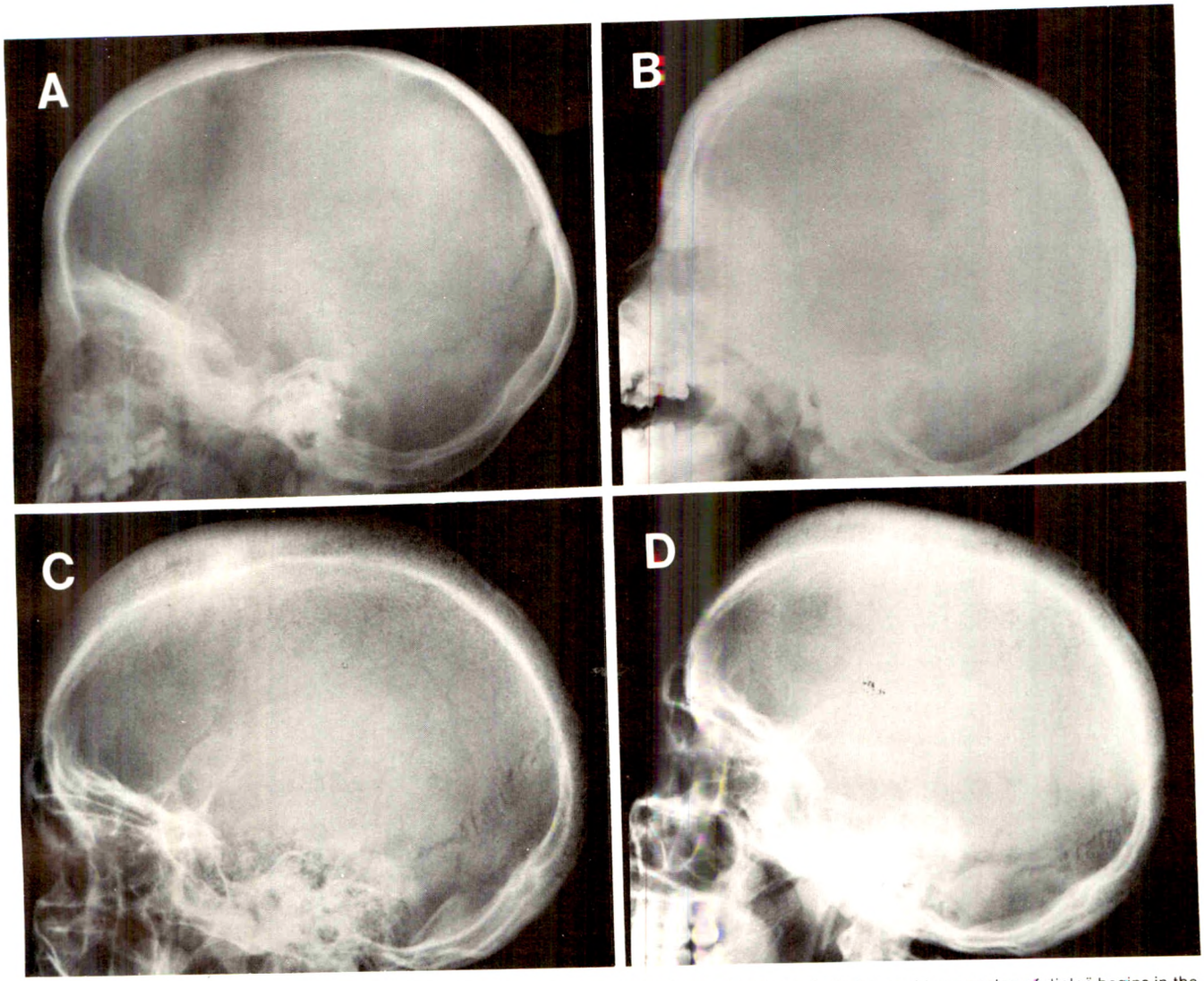


Fig. 3.—30 year progression of calvarial changes in male homozygous sickle cell anemia patient. **A**, At 1 year old, expansion of diploë begins in the posterior frontal area and is definitely identifiable. **B**, At age 2 expansion is prominent. At ages 23 (**C**) and 30 (**D**), false "hair-on-end" sign appears.

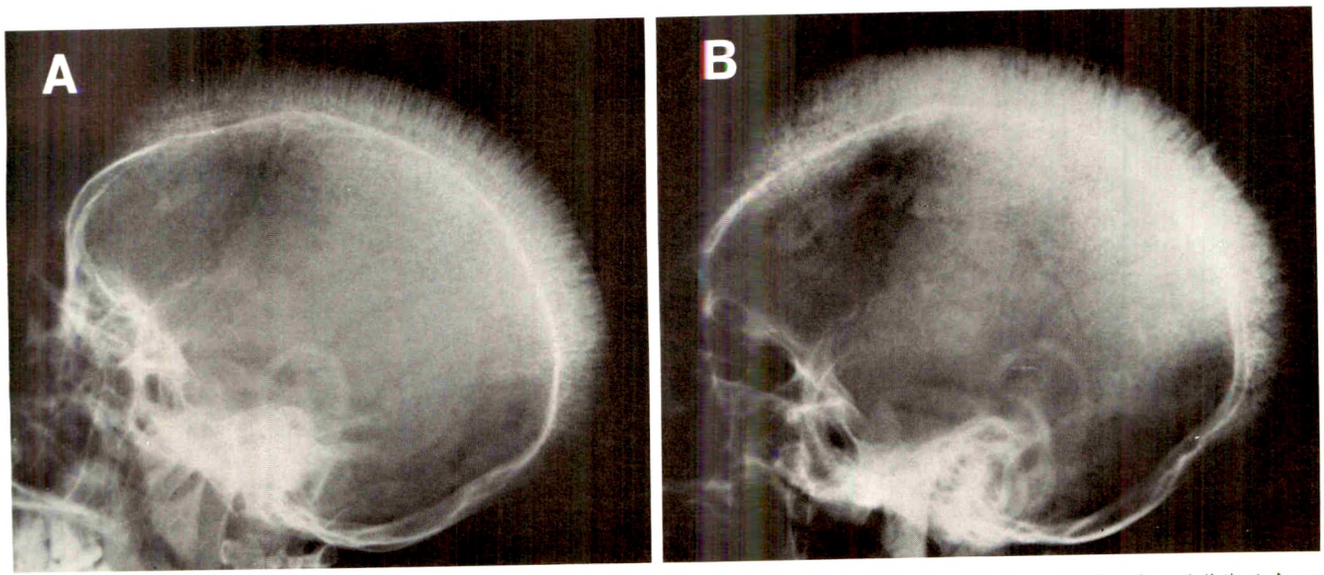


Fig. 4.—Classical "hair-on-end" effect. **A**, At age 15, long, thin vertical spicules. **B**, At age 31, they become wide, more sclerotic and distinct. Areas of sclerosis in frontal and anterior parietal areas have distinct lucent central component resembling "doughnut" lesions. Occipital bone is not expanded.

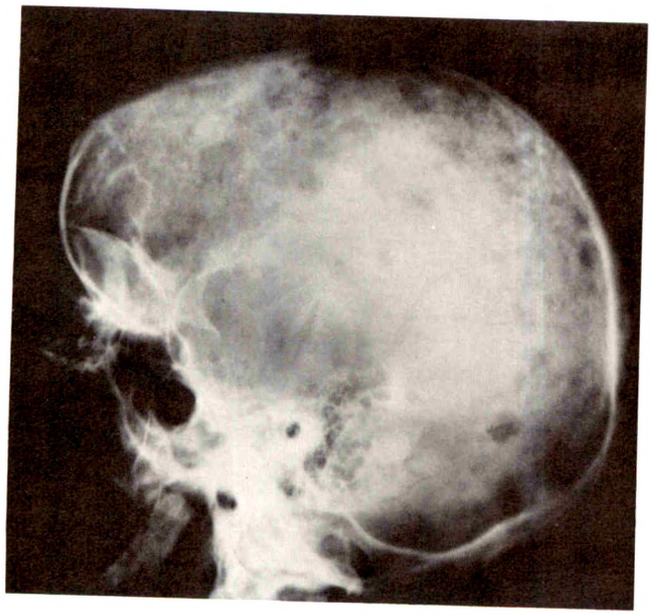


Fig. 5.—Multiple lytic lesions in 41-year-old sickle cell anemia patient with no clinical or laboratory evidence of myeloma.

rotic bone represent residual islands of hyperplastic red marrow rather than areas of calvarial infarction.

The granular appearance of the skull, which is usually misinterpreted as osteoporosis, results from increased red marrow volume, rather than removal of already present mineral. Granularity appears in the skull before widening of the diploë and vertical striations occur.

Our findings indicate that definite diploetic expansion can be seen before age 2 years. Four of the six patients having skull films at or before age 1 year showed definite expansion. Furthermore, in four of the six skulls, frontal rather than parietal expansion occurred first. Our findings do not support previous reports [6, 11, 27] indicating that expansion of the skull occurs most often after age 5 and usually involves the parietal region. In the 2–5-year-old group, seven of 18 skulls showed distinct calvarial expansion first in the frontal bone. Between ages 6 and 12, expansion of the diploë progressed posteriorly to involve the parietal areas but sparing the occipital bone.

The previously reported wide range incidences of diploetic expansion, 12% to 61.9%, result from the variable criteria used for evaluation. Objective measurement of calvarial thickness had not been carried out by most investigators. In our study, diploetic expansion was established only if the width of the diploë was greater than 2.5 times the combined thickness of the inner and outer tables.

The "hair-on-end" effect seen in 5% of our patients corresponds to the incidence in previous studies, reconfirming the rarity and nonspecificity of this finding. This has been exaggerated in the early literature on sickle cell disease, mostly because of its rather spectacular radiographic appearance. The true "hair-on-end" sign (figs. 3A and 3B) demonstrates thin long spicules extending through the entire width of the cranial vault, while in the false "hair-on-end" sign (figs. 2C and 2D), the vertical striations are not distinct and do not extend to the inner table.

While much has been written about long bone infarction, little is known about calvarial infarction [28]. No anatomic or pathologic studies concerning calvarial infarction are available in the literature. Areas of sclerosis, as well as marginated lucencies, are referred to as infarction.

Other reports of single [29] and multiple [30] calvarial lesions with a ringlike appearance have been referred to as "doughnut lesions." These lucent areas with a sclerotic rim were not associated with anemia or skeletal abnormalities, and were presumed to be areas of fibrosis. However, even on the basis of the histologic pattern of the biopsied lesion, no definite diagnosis of calvarial infarction could be made. In patients with sickle cell anemia, the areas of lucencies in the skull probably represent residual sites of active red marrow rather than infarction, as demonstrated by the autopsy findings in the last case described in this report.

REFERENCES

1. Cooley TB, Lee P: Series of cases of splenomegaly in children with anemia and peculiar bone changes. *Am Pediatr Soc Trans* 37:29–30, 1925
2. Cooley TB, Lee P: Observation on the sickle cell phenomenon. *Am Pediatr Soc Trans* 38:58–59, 1926
3. Cooley TB, Witwer ER, Lee P: Anemia in children with splenomegaly and peculiar changes in the bones. Report of cases. *Am J Dis Child* 34:347–363, 1927
4. Reynolds J: *The Roentgenological Features of Sickle Cell Disease and Related Hemoglobinopathies*. Springfield, Ill., Thomas, 1965
5. Grinnan A: Roentgenologic bone changes in sickle cell and erythroblastic anemia. *AJR* 34:297–309, 1935
6. Caffey J: The skeletal changes in the chronic hemolytic anemias (erythroblastic anemia, sickle cell anemia and chronic hemolytic icterus). *AJR* 37:293–324, 1937
7. Diggs LW, Pulliam HN, King JC: Bone changes in sickle cell anemia. *South Med J* 30:249–259, 1937
8. Macht SH, Roman PW: The radiologic changes in sickle cell anemia. *Radiology* 51:697–707, 1948
9. Legant O, Ball RP: Sickle cell anemia in adults, roentgenographic findings. *Radiology* 51:665–675, 1948
10. Carroll DS, Evans JW: Roentgen findings in sickle cell anemia. *Radiology* 53:834–845, 1949
11. Ehrenpreis B, Schwinger HN: Sickle cell anemia. *AJR* 68: 28–36, 1952
12. Diggs LW: Anatomic lesions in sickle cell disease, in *Sickle Cell Disease*, edited by Abramson H, Bertles JF, Wethers DL, St. Louis, Mosby, 1973, pp 189–229
13. Diggs LW: Bone and joint lesions in sickle cell disease. *Clin Orthop* 52:119–143, 1967
14. Tori G: Clinical radiological observations on 102 cases of sickle cell anemia. *Clin Radiol* 23:87–108, 1954
15. Carroll DS: Roentgen manifestations of sickle cell disease. *South Med J* 50:1486–1490, 1957
16. Middlemiss JH: Sickle cell anemia. *J Faculty Radiol* 9:16–24, 1958

17. Moseley JE: Patterns of bone change in the sickle cell states. *Mt Sinai J Med NY* 26:424–439, 1959
18. Golding JSR, MacIver JE, Went LN: The bone changes in sickle cell anemia and its genetic variants. *J Bone Joint Surg [Br]* 41:711–718, 1959
19. Cockshott WB: *Hemoglobin Diseases in Tropical Radiology*. London, Heinemen Medical Books, 1961, pp 79–97
20. Hewett BV, Nice CM: Radiographic manifestations of sickle cell anemia. *Radiol Clin North Am* 2:249–259, 1964
21. Middlemiss JH, Raper AB: Skeletal changes in hemoglobinopathies. *J Bone Joint Surg [Br]* 48:693–702, 1966
22. Argen RJ, Sullivan MA: Bone changes in sickle cell disease. *NY State J Med* 66:1238–1243, 1966
23. Eng LIL: Chronic iron deficiency with bone changes resembling Cooley's anemia. *Acta Haematol* (Basel) 19:263–268, 1958
24. Sax B: Roentgen manifestations of iron deficient anemia in the skull of infants and children simulating those seen in Cooley's and sickle cell hemolytic anemia. *J Germantown Hosp* 4:72–75, 1963
25. Moore S: The bone changes in sickle cell anemia with note on similar changes observed in skulls of ancient Mayan Indians. *J Missouri State Med Assoc* 26:561–564, 1929
26. Bohrer SP, Graham EC: Pathology in 700-year-old Nigerian bones. *Radiology* 98:581–584, 1971
27. Robinson IB, Sarnat BG: Roentgen studies of the maxillae and mandible in sickle cell anemia. *Radiology* 58:517–523, 1952
28. Bohrer SP: Bone infarcts in sickle cell anemia. *Tropenmed Parasitol* 22:299–312, 1971
29. Keats TE, Holt JF: The calvarial "doughnut lesion": a previously undescribed entity. *AJR* 105:314–318, 1969
30. Royen PM, Ozonoff MB: Multiple calvarial "doughnut lesions." A case report. *AJR* 121:121–123, 1974

Radiography of Glycogen Storage Diseases

JOHN H. MILLER,[1] PHILIP STANLEY, AND GARY F. GATES

Sixty-three patients with glycogen storage disease were evaluated. Findings on plain film examinations, excretory urography, barium gastrointestinal studies, ultrasonography, and angiography were categorized by type of glycogen storage disease. In type I findings include hepatomegaly with hepatic dysfunction, renomegaly with an increased incidence of renal calculi, and osteopenia with various associated osseous abnormalities. These changes were less pronounced in types III, IV, and VI. Type II displayed either cardiac or skeletal muscle glycogen deposition. Correlation with postmortem examination in 14 individuals is given.

Glycogen storage diseases are autosomally recessive genetic disorders of carbohydrate metabolism categorized into six groups on the basis of the specific enzymatic defect (table 1). Glucose absorption is normal in all types and its storage as glycogen is normal in all but types III and VI. However, the various enzymatic defects in all types of glycogen storage disease result in faulty glycogenolysis. Anerobic pathways of carbohydrate metabolism are used, resulting in chronic ketoacidosis. These diseases, present at birth, may not be detected until late childhood [1, 2].

Glycogen storage disease I, the most frequent type, is seen in early infancy as a "failure to thrive," as repeated episodes of hypoglycemia with seizures, or as severe metabolic acidosis. Hepatomegaly, present at birth, is due to glycogen accumulation within hepatocytes, plus fatty metamorphosis that is often qualitatively greater in magnitude than the former. Glycogen deposition within the proximal convoluted tubules results in a progressive nephromegaly [1–3].

Patients with type II glycogen storage disease usually have marked cardiomegaly and cardiac failure within their first year of life that often result in death. Occasionally, a patient with type II has only skeletal muscle hypotonia without cardiac disease, for which prognosis is much better [1, 4].

Patients with type III have many features of type I, but have a less severe clinical course that may regress at puberty. The liver may be enlarged or may return toward normal size. Splenomegaly is seen, but renal enlargement is not [1]. Type IV is very rare, with death occurring in early childhood due to hepatic cirrhosis, which may result from a "foreign body reaction" to the abnormal liver glycogen (table 1) [1]. Type V is limited exclusively to skeletal muscle and restricts physical activity. Type VI disease shares many features with type I, but seems to be milder [1].

The purpose of this study was to categorize and define radiographic findings in glycogen storage diseases and to determine if the specific enzymatic defect could be identified by radiographic findings.

Subjects and Methods

Since 1950, 63 patients with glycogen storage disease have been examined in the Childrens Hospital of Los Angeles radiology department. On the basis of specific enzymatic defect, 33 were categorized as glycogen storage disease type I, six as type II, six as type III, two as type IV, five as type VI, and 11 were unspecified. Ages ranged from less than 1 year to 31 years old. The longest follow-up has been 26 years. There were 40 male and 23 female patients. Initial diagnoses were based on typical clinical features, plus either identification of a sibling with proven glycogen storage disease or a liver enzyme assay. Histopathologic diagnoses were established in 50 patients; postmortem correlations obtained in 14. Films were available in 50 cases. The data on the remaining 13 were from microfilmed records. The majority of these cases were not specified as to type of disease.

Nearly all patients had chest and abdominal radiography. Bone age determinations were performed on 47 patients using the standards of Greulich and Pyle [5]. Radiographic skeletal survey was performed in 24 individuals; excretory urography in 38. Upper gastrointestinal barium examinations were performed in 22 patients, while eight had barium enemas. Dynamic and static hepatic scintigraphy were performed in 22 patients and ultrasonography in seven. Angiocardiography was performed in three patients and selective celiac angiography in one.

Results

Hepatomegaly (fig. 1), assessed by extension of the liver well below the costal margins, was almost uniformly evident in every type of glycogen storage disease (table 2). Frequently, the liver extended to the iliac crest. Hepatic scintigraphy with ^{99m}Tc sulfur colloid (fig. 2A) revealed hepatomegaly in all types (table 3). All were well outside 2 standard deviations, and the majority were outside 4 standard deviations for the mean for overall liver height established by Holder et al. [6]. All patients had diminished hepatic uptake of radiocolloid. Focal defects were observed in seven patients with type I. Dynamic scintigraphy was abnormal in five cases (table 3) and showed hypervascularity of regions later represented as focal defects on static scintigrams. All patients had an increased splenic accumulation of radiocolloid compared with the liver uptake. Bone marrow accumulation of the tracer occurred in six patients with type I. An enlarged right renal impression was observed on the posterior view of the hepatic scintigram in 11 individuals.

Ultrasonic examination revealed hepatomegaly in all individuals. Maximum height and width measurements of liver size at the right midclavicular line at the costal

Received January 10, 1978; accepted after revision November 28, 1978.
Presented at the annual meeting of the Society for Pediatric Radiology, Boston, September, 1977.
[1] All authors: Department of Radiology, Childrens Hospital of Los Angeles, P. O. Box 54700, Los Angeles, California 90054. Address reprint requests to J. H. Miller.

0361-803X/79/1323-0379 $0.00

AJR 132:379–387, March 1979
© 1979 American Roentgen Ray Society

TABLE 1
Glycogen Storage Diseases

Type	Enzyme Defect	Target Organ	Glycogen Structure	Eponymic Name	Suggested Clinical Name
I	Glucose 6-phosphatase	Liver, kidney, small intestine	Normal	Gierke's disease	Glucose 6-phosphatase deficiency hepatorenal glycogenosis
II	Alpha-1, 4-glucosidase (acid maltase)	Generalized; includes central nervous system, leukocytes, heart	Normal	Pompe's disease	Alpha-1, 4-glucosidase deficiency generalized glycogenosis
III	Amylo-1, 6-glucosidase (debrancher)	Liver, heart, muscle, leukocytes	Abnormal; outer chains missing or very short	Cori's (Forbes') disease	Debrancher deficiency limit dextrinosis
IV	Amylo-1,4–1,6-transglucosidase (brancher)	Liver, probably other organs	Abnormal; very long inner and outer unbranched chains	Andersen's disease	Brancher deficiency amylopectinosis
V	Muscle glycogen phosphorylase	Skeletal muscle	Normal	McArdle's disease	Myophosphorylase deficiency glycogenosis
VI	Liver glycogen phosphorylase	Liver, leukocytes	Normal	Hers' disease	Hepatophosphorylase deficiency glycogenosis

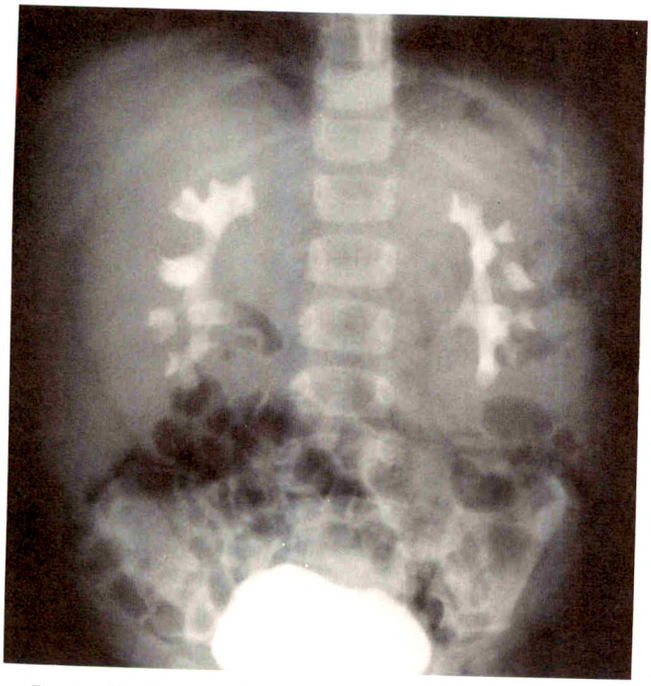


Fig. 1.—3½-year-old girl with type I disease. Renomegaly and hepatosplenomegaly.

margin were compared to measurements obtained in similar planes by scintigraphy; in all individuals the values from both procedures corresponded to within 1 cm. Characteristically, the liver showed a densely reflective parenchyma (fig. 2B). In three of four individuals, additional ultrasonography confirmed scintigraphic voids.

One patient with type I disease had a large hepatic mass on hepatic scintigraphy and ultrasonography.

TABLE 2
Nonosseous Radiographic Abnormalities in Glycogen Storage Disease

Abnormality	Disease Type			
	I	III	IV	VI
Hepatomegaly	27/28	5/6	2/2	5/5
Splenomegaly	8/28	2/6	1/2	2/5
Renomegaly	17/25	0/6	0/1	0/5
Renal calculi	5/25	0/6	0/2	0/5
Ca ++ urate	4	0	0	0
Uric acid	1	0	0	0
Secondary obstructive uropathy	2	0	0	0
Hiatal hernia	3/10	0/2	0/2	0/2
Reflux esophagitis	1	0	0	0
Gastrostomy	2/10	0/2	0/2	0/2

Note.—Ratios represent numbers of individuals with positive findings to number of individuals examined. Types II and V do not affect abdominal viscera.

Percutaneous selective celiac angiography revealed a circumferential vascular supply with centrally penetrating parallel vessels and delayed dense tumor blush suggesting a hepatic cell adenoma, which was later confirmed by open biopsy [7].

Splenomegaly, though less frequently observed, was present in types I, III, IV, and VI (table 2). In all types examined by scintigraphy (table 3), the spleen was increased in overall size.

Nephromegaly, assessed when renal size was demonstrated to be equal to or greater than the height of five lumbar vertebral bodies (fig. 3) was seen exclusively in type I (table 2). Radiopaque renal calculi were discovered in four individuals with type I disease. One additional individual with type I was found to have a radiolucent uric acid stone at the time of retrograde pyelography (table 2). Obstructive uropathies secondary to these calculi were seen in two of these patients.

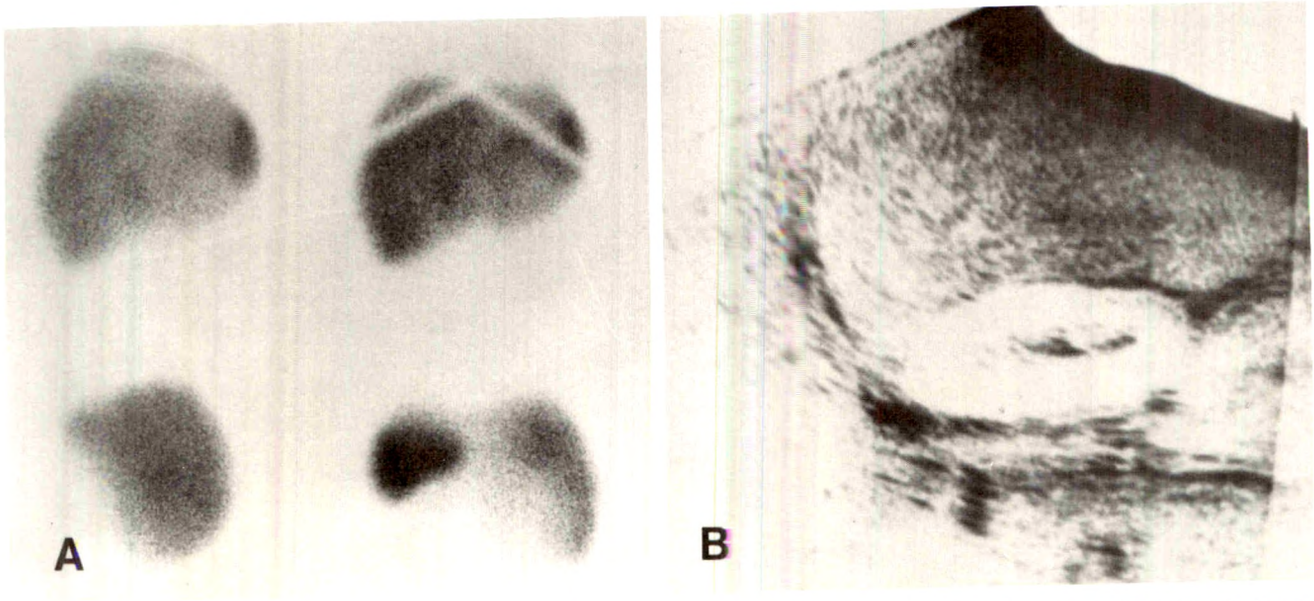


Fig. 2.—6-year-old boy with type I disease. **A,** ^{99m}Tc sulfur colloid scans. Markedly enlarged liver with reduced traced accumulation and enlarged spleen. (Top row, anterior view with costal markers (left); bottom row, right lateral (left) and posterior (right) scans.) **B,** Right longitudinal ultrasound scan. Densely reflective hepatic parenchyma and nephromegaly. Hepatic reflective pattern probably due to both increased fat and glycogen content.

TABLE 3

Scintigraphic Abnormalities in Glycogen Storage Disease

Abnormality	Disease Type		
	I	III	VI
Liver:			
Hepatomegaly	15/15	4/4	2/2
Diminished uptake	15/15	4/4	2/2
Voids	7/15	0/4	0/2
Perfusion abnormality	4/15	1/3	0/1
Spleen:			
Splenomegaly	11/15	4/4	2/2
Increased uptake	15/15	4/4	2/2
Vertebral body activity	6/15	0/4	0/2
Pronounced right renal fossa	10/15	1/4	0/2
Abnormal isotope renogram	3/3	0/1	0

Note.—Ratios represent numbers of individuals with positive findings to numbers of individuals examined. Type II and IV not examined by scintigraphy.



Fig. 3.—20-year-old man with type I disease. Enormous kidneys.

Radionuclide renography (fig. 4) showed abnormal renal tubular function in three of four individuals. There was slow renal clearance and a delay in tubular drainage of the radiohippuran (fig. 5A).

Ultrasound confirmed nephromegaly; the kidneys displayed a very rounded, almost plump and relatively anechoic appearance compared with the overlying densely reflective liver parenchyma (fig. 6).

Esophageal hiatal hernia was demonstrated by upper gastrointestinal examination in three patients with glycogen storage disease I, and one had asociated reflux esophagitis. In two patients, feeding gastrostomy tubes allowed continuous nocturnal glucose alimentation in place with concomitant deformity of the gastric wall at the time of upper gastrointestinal examination. Barium enema study was normal in all eight patients.

Skeletal radiography demonstrated osteopenia (osseous undermineralization), as evidenced by loss of primary and/or secondary trabeculation, thinned cortices, and apparent expansion of medullary cavities in types I, III, and VI (table 4). Multiple growth arrest lines associated with osteopenia were observed in types I and VI, but also were seen in types I and VI in the absence of osteopenia (table 4). Scalloping of the anterior surface of the thoracolumbar vertebral bodies (T11, T12, L1, and L2) was seen in types I, III, IV, and VI (fig. 7). Multiple

fractures were seen in eight individuals with type I disease who also experienced hypoglycemic seizures. Accentuation and increased diameter of the nurtrient foramina to the middle phalanx of the finger (fig. 8) occurred in 10 patients (table 4). Tubulation errors of the long bones were observed in nine patients with type 1; eight of these consisted of overconstriction (fig. 9A) and one of failure of constriction in the metaphyseal region (fig. 9B). Spiculation of the physeal plate (fig. 10) was seen in six patients younger than 3 years with all types except II. Subchondral erosions similar to those seen in tophaceous gout were seen in two individuals with type I disease. As a group, the number and variety of osseous abnormalities were diverse (table 4).

Marked biventricular cardiomegaly (fig. 11A) was seen in five individuals with type II glycogen storage disease. Pulmonary vascular congestion was seen in three of these individuals, but was not observed until late in the course of the disease when congestive heart failure supervened. No cardiac abnormality was observed in a patient whose type II disease was limited to skeletal muscle.

Angiocardiography (figs. 11B and 11C) in three patients revealed hypertrophied ventricular walls associated with chamber dilatation. Excess trabeculation of the myocardium was observed in one individual. In another, diminished ventricular contractility was suggested.

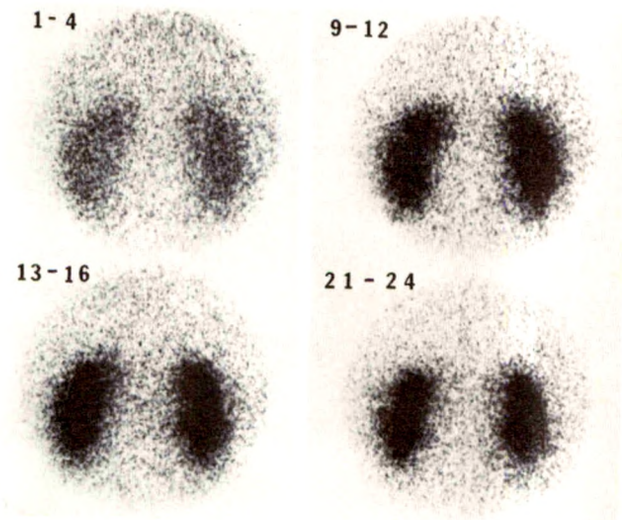


Fig. 4.—^{131}I orthoidohippurate renography, posterior scans. Progressive accumulation of activity within kidneys. Poor migration from cortex to pelvic area. (Numbers indicate time in minutes after tracer injection.)

Discussion

Specific Organ Involvement

Glycogen storage diseases, except types II and V, were characterized by radiographically identified hepatomegaly in 39 of 41 individuals. Liver enlargement can reach enormous proportions, completely filling the abdomen and extending into the pelvis (fig. 1). The hepatic weight of ten individuals with type I disease at autopsy was 1.3–6.2 times anticipated normal weight.

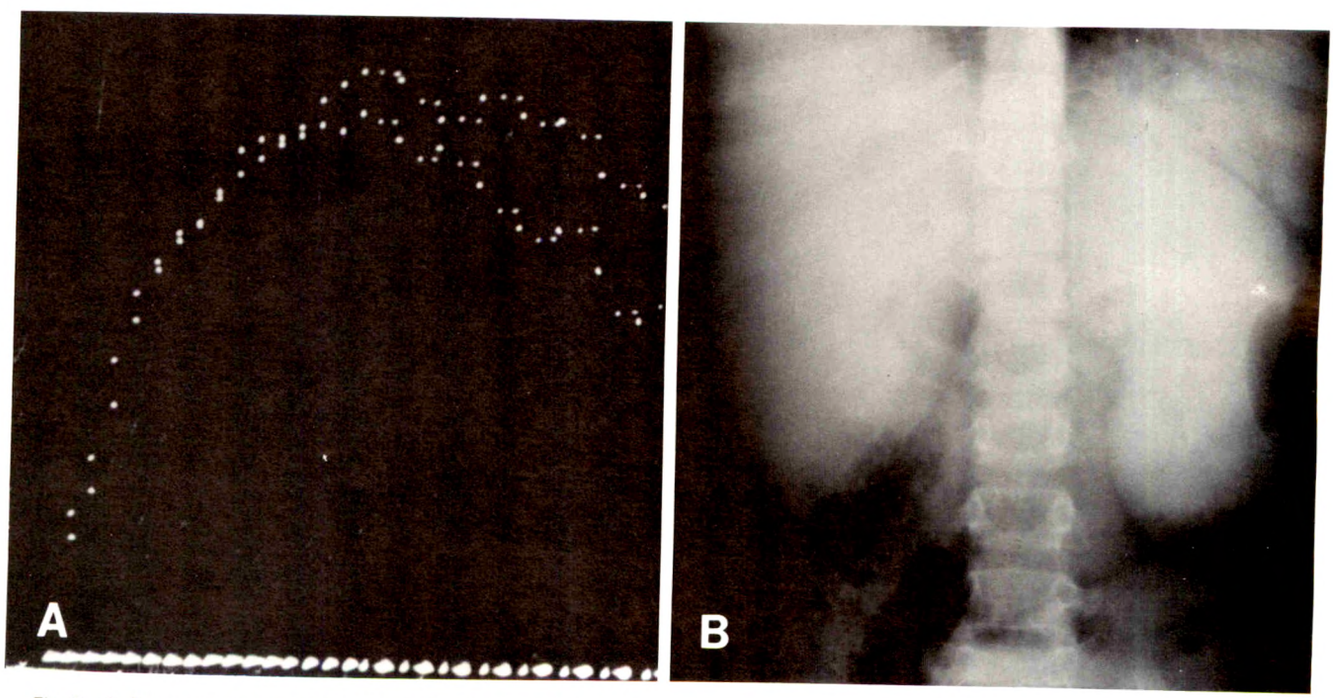


Fig. 5.—**A**, Renogram curves. Slow drainage of radiohippuran from kidneys (30 min study; each baseline point represents 1 min). **B**, 18-year-old man with type I disease. 7 hr nephrogram, probably indicating poor tubular clearance of contrast agent.

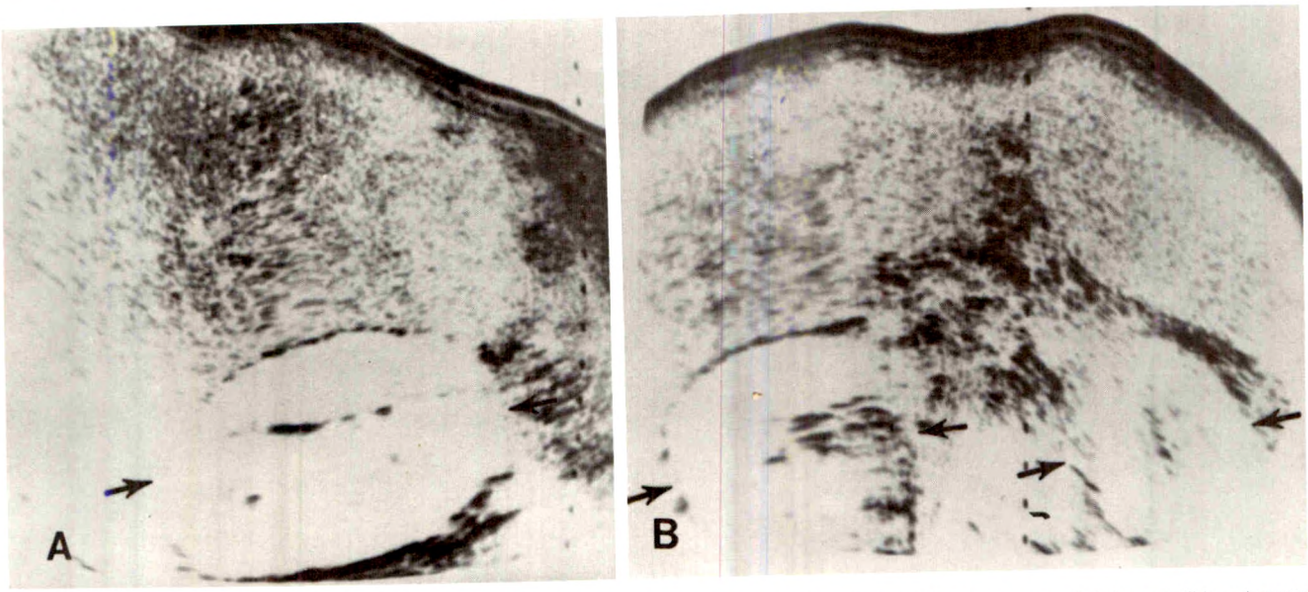


Fig. 6.—18-year-old man with type I disease (same patient as fig. 5B). Longitudinal (A) and transverse (B) supine scans of abdomen. Kidney (*arrows*) display very rounded appearance and are markedly anechoic compared with overlying echogenic liver. Discomfort secondary to massive hepatomegaly prohibited prone examination.

TABLE 4

Osseous Abnormalities in Glycogen Storage Disease

Abnormality	Disease Type			
	I	III	IV	VI
Osteopenia	20/30	3/6	0/2	5/5
Retarded maturity	18/29	4/6	1/2	2/5
Multiple growth lines:				
With osteopenia	13/30	0/6	0/2	3/5
Without osteopenia	2/30	0/6	2/2	0/5
Scalloped vertebral bodies	9/30	2/4	1/2	4/5
Multiple fractures	8/30	0/6	0/2	0/5
Prominent nutrient foramina	8/30	1/6	0/2	1/5
Overconstriction of long bones	8/30	0/6	0/2	0/5
Spiculation of the physeal plate	3/30	1/6	1/2	1/5
Subchondral erosions	2/30	0/6	0/2	0/5
Other osseous abnormalities*	14/30	0/6	2/2	0/5

Note.—Ratio represents numbers of individuals with positive findings to number of individuals examined. Types II and V do not affect the skeleton.

* Kirner's deformity (dystelphalangy), overexpansion of ribs and sternum, multiple growth centers for metacarpal heads, osteochondroma C5, large fibrous cortical defects of ilium, tibiofibular synostosis, slow healing of fractures, double center for greater multangular, Schmorl's node, constriction of base of metacarpals, cystic changes in proximal femoral ossification centers, narrowed proximal interphalangeal joints, and radioulnar joint erosions.



Fig. 7.—34-year-old man with type I disease. Abnormal scalloping of anterior margin of several thoracic and lumbar vertebral bodies, presumably secondary to pressure of massive liver.

The hepatocytes showed marked glycogen infiltration and fatty metamorphosis. Cirrhosis did not occur in types I and VI but was present in both individuals with type IV. Cirrhosis has been reported in type III disease, but did not occur in our six cases [1].

Liver scintigraphy (fig. 2) has revealed hepatomegaly with diminished uptake of radiocolloid, increased splenic activity, and vertebral body imaging [8]. In addition, focal hepatic defects detected by hepatic scintigraphy were believed to represent hepatic cell adenomata [8, 9]. These lesions are likely to undergo malignant change [10]. Three individuals with type I disease were found to have carcinomatous change at autopsy. Only one of these individuals had hepatic scintigraphy, that revealed scintigraphic voids in which hepatic cell carcinoma was found at autopsy. We and others believe that hepatic cell carcinoma may be a potential end result of type I glycogen storage disease [8–10]. It did not occur in any other type.

Ultrasonic evaluation revealed a characteristic pattern of hepatomegaly with densely reflective hepatic parenchyma (fig. 2B) that shares many features with the ultrasonographic pattern seen in fatty metamorphosis [11]. The dense echographic pattern may hinder detection of scintigraphic voids, although they were identifiable as focal defects in three of four individuals examined.

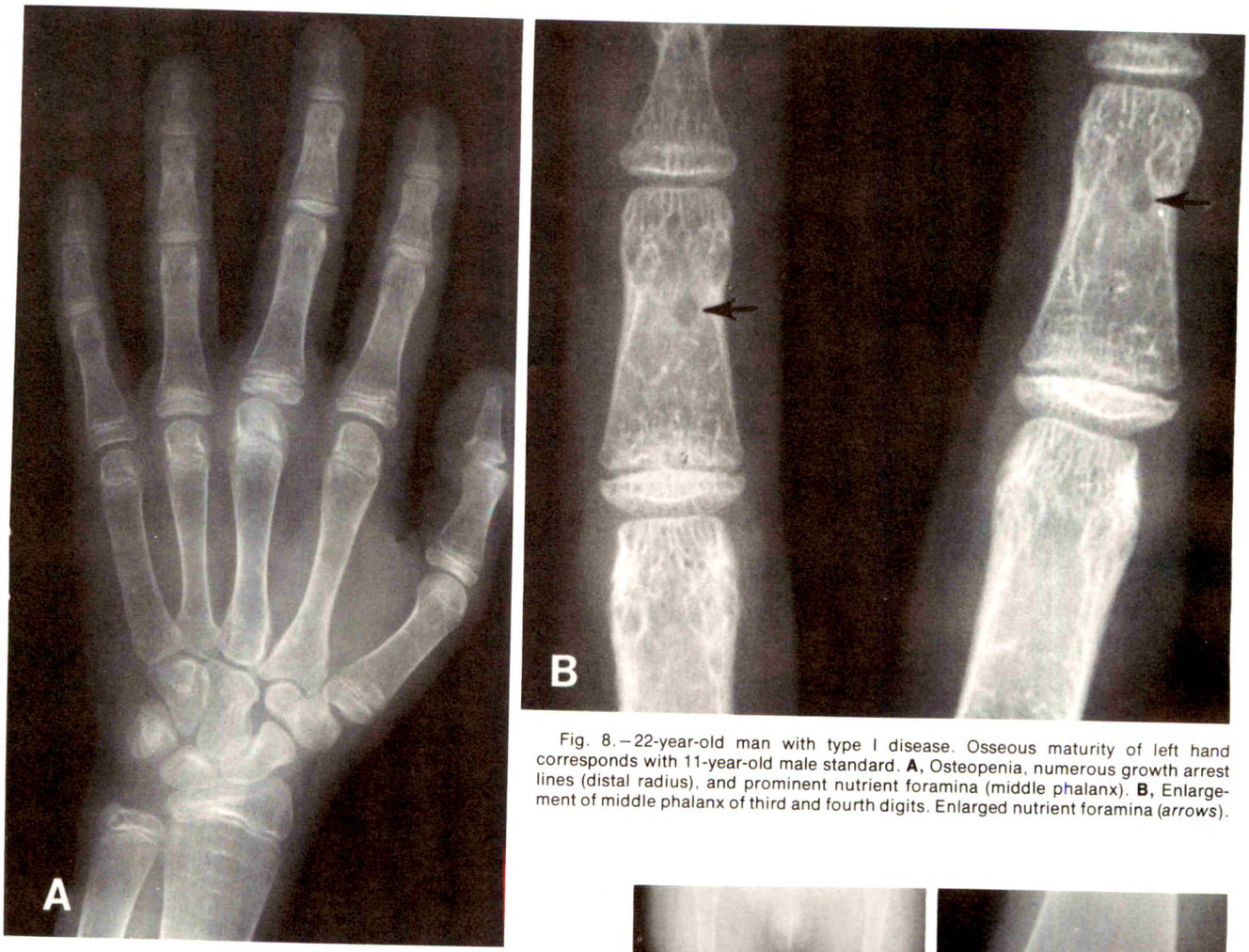


Fig. 8.—22-year-old man with type I disease. Osseous maturity of left hand corresponds with 11-year-old male standard. **A**, Osteopenia, numerous growth arrest lines (distal radius), and prominent nutrient foramina (middle phalanx). **B**, Enlargement of middle phalanx of third and fourth digits. Enlarged nutrient foramina (*arrows*).

Splenomegaly was radiographically demonstrated in 13 of 41 individuals and was noted in 17 of 21 patients on scintigraphic examination. There has been no evidence of hypersplenism despite increased uptake of radionuclide by the spleen. This may suggest hepatic dysfunction, portal hypertension due to compression of hepatic sinusoids by swollen liver cells, or infiltration of the spleen by lipid histiocytes (xanthoma response of the reticuloendothelial system secondary to the marked hyperlipidemia typical of glycogen storage diseases) [8]. Postmortem review revealed splenomegaly in five of 10 individuals with type I. Spleen weight was 1.2–2.3 times anticipated normal weight.

Renomegaly was limited to type I disease and increased in size with age (fig. 2A)[3]. Autopsy data confirmed renomegaly in seven of 10 individuals with type I. Renal weight was 1.2–2 times anticipated normal weight. Histochemical studies of these cases revealed marked glycogen deposition in proximal convoluted tubules, which accounts for the increase in size and possibly for the apparent ultrasonographic sonolucency of these kidneys. These children provide an interesting comparison of the increased echogenicity of a liver undergoing

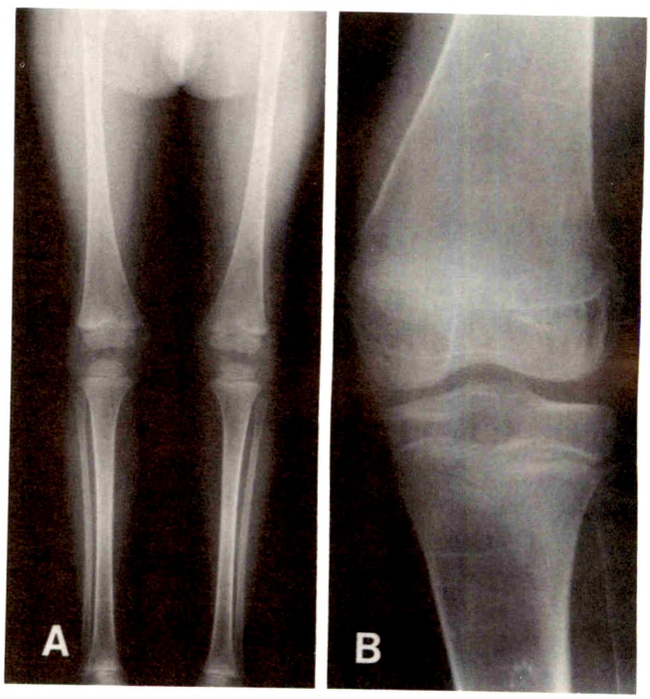


Fig. 9.—**A**, 7-year-old boy with type I disease. Overconstriction of shafts, osteopenic bones with numerous growth arrest lines, and loss of muscle mass. **B**, 22-year-old man with type I disease. Metaphyseal constriction failure, delayed maturation, osteopenia, and numerous growth arrest lines in left knee.

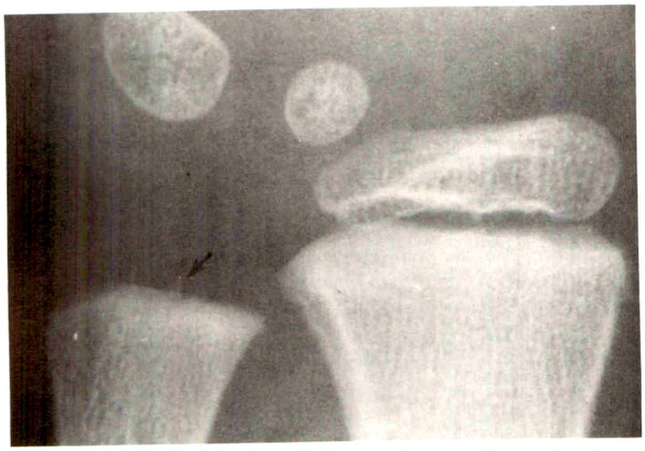


Fig. 10.—7-year-old with type I disease. Spiculation of the physeal plate in wrist (*arrow*) initially seen at age 2. Osseous maturity 4 years.

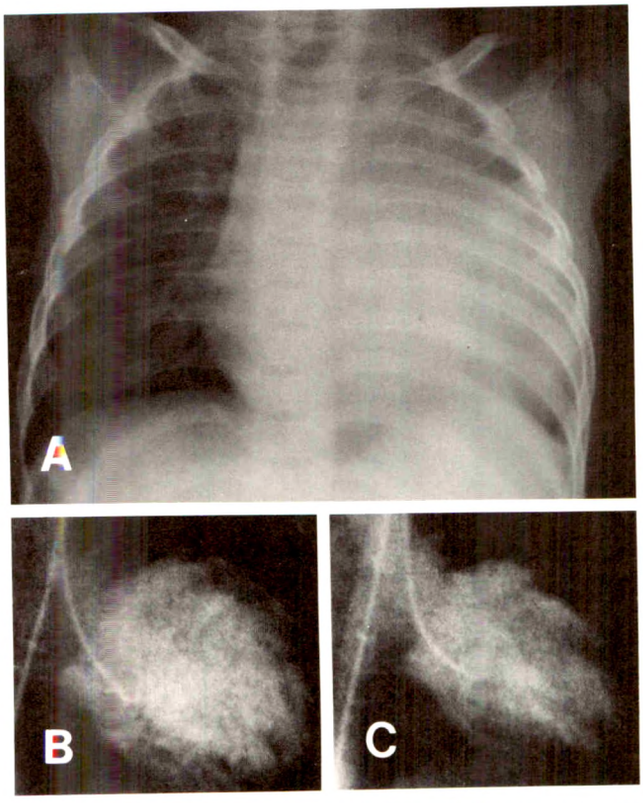


Fig. 11.—6-month-old boy with type II disease. **A,** Massive cardiomegaly. **B,** Diastolic. Marked left ventricular dilatation with coarsened endocardial trabecular pattern. **C,** Systolic. Diminished ventricular contractility with reduced volume of ejected blood. (Angiocardiogram courtesy of Dr. Masato Takashahi.)

fatty metamorphosis and the decreased echogenicity of kidneys involved by glycogen infiltration.

To our knowledge, an increased occurrence of radiopaque renal calculi in glycogen storage disease has not been previously reported. Four individuals with type I had radiopaque renal calculi. In one of these the calculus was shown to be calcium urate. An additional patient was shown to have a radiolucent uric acid stone by retrograde pyelography. Obstructive uropathy secondary to these calculi was encountered in two of these five individuals; the remaining calculi were passed spontaneously. Chronic acidosis may alter normal calcium metabolism and influence formation of renal calculi. Evidence substantiating some degree of tubular dysfunction was demonstrated by radionuclide renography (fig. 4) in three individuals by slow extraction and slow tubular passage of ^{131}I orthoidohippurate on perfusion curves (fig. 5A). Slow excretion of radiographic contrast material was observed in one patient with delayed film examination (fig. 5B).

Glycogen storage disease in three patients with type I disease was manifested as esophageal hiatal hernia, which may be related to abnormal biomechanics secondary to a massively enlarged liver. In one individual, reflux esophagitis was radiographically demonstrated, while changes in the distal esophagus in three more patients were compatible with chronic esophagitis at autopsy. Barium enema studies were normal in these cases. Previous reports have indicated a loss of haustral markings [12].

The mechanism of interference in normal osseous development in these individuals in speculative. Chronic acidosis promotes a negative calcium balance [1]. There is possibly increased calcium loss in the urine as well, secondary to some interference with tubular reabsorption. This is further suggested by the increased incidence of calcium-containing calculi in these patients.

Osteopenia and retarded osseous maturity in type I glycogen storage disease was reported by Preger et al. [13], who speculated that chronic acidosis, cellular starvation, abnormal insulin levels, or even hypogonadism may play a role. The actual mechanism of this defect remains unknown at this time; the bone marrow at postmortem examination of our patients showed no increased glycogen deposition or other cellular change to account for this radiographic appearance. We found osteopenia in all disease types except IV. Retarded osseous maturity (fig. 3) was seen in all types except II. Multiple growth lines occurred in all types, but in types II and III these lines were not always associated with osteopenia. Scalloping of the anterior margin of the thoracolumbar vertebral bodies (fig. 7) occurred in older individuals with massive hepatomegaly. Multiple fractures were seen in eight patients with type I disease who had both hypoglycemic seizures and osteopenic bones. These fractures seemed to display somewhat retarded healing.

Prominent nutrient foramina (fig. 8B) observed in the middle phalanx of the digits of the hands in types I, III, and VI, may be secondary to lifelong osteopenia and pressure from a pulsatile nutrient vessel. Metaphyseal overconstriction was seen only in type . This was associated with loss of muscle mass and may represent a failure of stress modeling (fig. 9A). Metaphyseal overexpansion of the long bones occurred in one patient with type I disease. This appearance was reminiscent of

Gaucher's disease (fig. 9B). There was no correlation between bone marrow appearance at autopsy and over- or underconstriction of the long bones. Spiculation of the physeal growth plate (fig. 10) was seen in types I, III, IV, and VI prior to 3 years of age. These changes can be seen in phenylketonuria, homocystinuria, and rarely in normal individuals [14–16]. This spiculation was seen at an early age in the wrists of individuals with glycogen storage disease and retarded osseous maturity.

Hyperuricemia was present in some patients either as the result of increased breakdown of nucleic acids or from renal tubular dysfunction [17]. Two persons with type I disease had radiographic evidence of subchondral erosive changes at the bases of the proximal phalanges of the hands. However, they did not have clinical gout.

Glycogen storage disease type II, with its generalized involvement, was radiographically different from type I. It was usually associated with congestive cardiac failure and a massively enlarged heart resulting from massive deposition of stored glycogen in all cardiac fibers, which causes a biventricular enlargement (fig. 11A) [18]. Radiographic evidence of pulmonary vascular congestion, a manifestation of congestive failure secondary to a failing myocardium, usually occurred late in the disease process, which helped differentiate this cardiac lesion from those with anatomic cardiac abnormalities. Differential diagnosis of this radiographic picture includes anomalous origin of the left coronary artery and idiopathic endocardial fibroelastosis. Consequently, angiocardiography performed in three cases showed dilated cardiac chambers with ventricular wall hypertrophy and excess trabeculation of the endocardium (fig. 11C).

Ventricular outflow obstruction secondary to marked glycogen infiltration of the myocardium in the ventricular outflow tract can occur, but was not seen in this series [18]. Diminished contractility of the ventricular wall (fig. 11D) can be associated with development of endocardial sclerosis and was present in three of four individuals with type II disease at postmortem examination [19]. At autopsy, average heart weight for the four patients with type II was 4.1 times that of the anticipated normal weight. One individual in this series, the brother of a deceased patient with type II disease, was found to have the unusual form of type II that is limited to skeletal muscle. This individual had no cardiomegaly and he appeared clinically well except for some skeletal muscle weakness.

Type of Glycogen Storage Disease

Initial presentation of patients with glycogen storage disease may be failure to thrive with hepatomegaly. Characteristic radiographic findings may suggest the correct diagnosis and full appreciation of the subtle differences between types permits even more specific diagnosis.

A child with type I disease displays the most characteristic patterns of organ system involvement with massive hepatomegaly, renomegaly, and varying degrees of splenomegaly. Renal calculi were seen only in this type, as was hiatal hernia. Osseous structures show osteopenia and retarded maturation. Overconstriction of long bones was seen only in type I disease, as were the majority of the minor osseous abnormalities.

Glycogen storage disease II involvement so profoundly affects the cardiovascular system that it overshadows any other aspect of this type.

Type III shares many features with type I, but its effects appear somewhat less profound, being characterized by a lesser extent of hepatomegaly and a not unusual diminution in liver size with increasing age. Although common, splenomegaly is also present to a lesser degree than in type I. Renomegaly is not seen. Osseous manifestations are less frequent in type III as well. The frequency of osteopenia is decreased and multiple growth lines were not observed in this category. Gastrointestinal manifestations are not likely to occur.

Type IV disease is so uniformly fatal that beyond midchildhood it should not enter the differential diagnosis, and in early childhood it cannot be differentiated from types I, III, or VI. The only significant distinguishing feature is lack of osteopenia, which may in fact relate to the early mortality of these children.

Type V has no radiographic features and is clinically diagnosed.

Type VI, like types I, III, and IV, shows hepatomegaly and splenomegaly. As in type III, renomegaly does not occur. However, osseous involvement more closely parallels type I with more frequent osteopenia and retarded maturation. Growth arrest lines were frequently seen, and perhaps the differences in osseous manifestations could permit differentiation between types III and VI, which are otherwise very similar. Type VI is not known to show the regression in organ involvement of type III.

Glycogen storage diseases offer an interesting and varied spectrum of radiographic abnormalities, and accurate recognition of patients with this disease requires examination by all disciplines of radiology.

REFERENCES

1. Howell RR: The glycogen storage diseases, in *The Metabolic Basis of Inherited Disease*, 3d ed, edited by Stanbury JB, Wyngaarden JB, Fredrickson DS, New York, McGraw-Hill, 1972, pp 149–173
2. Spencer-Peet J, Norman ME, Lake BD, McNamara J, Patrick AD: Hepatic glycogen storage disease. *Q J Med* 40:95–113, 1971
3. Lee FA, Gwinn JL: Four uncommon pediatric conditions associated with bilateral nephromegaly. *Ann Radiol* (Paris) 12:285–292, 1969
4. John AR, Lambert EC: Glycogen storage diseases of the heart, in *Paediatric Cardiology*, edited by Watson H, St. Louis, Mosby, 1968, pp 758–675
5. Greulich WW, Pyle SI: *Radiographic Atlas of Skeletal Development of the Hand and Wrist*, 2d ed. Stanford, Stanford University Press, 1959
6. Holder LE, Strife J, Padikal TN, Perkins PJ, Kereiakes JG: Liver size determination in pediatrics using sonographic and scintigraphic techniques. *Radiology* 117:349–353, 1975
7. Goldstein HM, Neiman HL, Mena E, Bookstein JJ, Apple-

man HD: Angiographic findings in benign liver cell tumors. *Radiology* 110:339–343, 1974
8. Miller JH, Gates GF, Landing BH, Kogut MD, Roe TF: Scintigraphic abnormalities in glycogen storage disease. *J Nucl Med* 19:354–358, 1978
9. Howell RR, Stevenson RE, Ben-Menachem Y, Phyliky RL, Berry DH: Hepatic adenoma with type I glycogen storage disease. *JAMA* 236:1481–1484, 1976
10. Landing BH: Tumors of the liver in childhood, in *Hepatocellular Carcinoma,* edited by Okuda K, Peter RL, New York, Wiley, 1976, pp 205–226
11. Taylor KJW, Carpenter DA, Hill CR, McCready VR: Gray scale ultrasound imaging: the anatomy and pathology of the liver. *Radiology* 119:415–423, 1976
12. Fellows RA, Berdon WE, Baker DH, Harris R: Barium enema findings in type I hepatorenal glycogen storage disease. *Pediatr Radiol* 3:75–77, 1975
13. Preger L, Saunders GW, Gold RH, Steinbach HL, Pitman P: Roentgenographic skeletal changes in the glycogen storage diseases. *AJR* 107:840–487, 1969
14. Feinberg SB, Fisch RO: Roentgenologic findings in growing long bones in phenylketonuria. *Radiology* 78:394–398, 1962
15. Morrees CL, Fletcher BD, Weilbaecher RG, Dorst JP: The roentgenographic features of homocystinuria. *Radiology* 90:1150–1158, 1968
16. Holt JF, Allen RJ: Radiologic signs in the primary aminoaciduria. *Ann Radiol* (Paris) 10:317–321, 1967
17. Roe TF, Kogut MD: The pathogenesis of hyperuricemia in glycogen storage disease type I. *Pediatr Res* 11:664–669, 1977
18. Hernandez A, Marchesi V, Goldring D, Kissave J, Hartmann AF: Cardiac glycogenosis. *J Pediatr* 68:400–412, 1966
19. Dincsoy MY, Dincsoy HP, Kessler AD, Jackson MA, Sidbury JB: Generalized glycogenosis and associated endocardial fibroelastosis. *J Pediatr* 67:728–740, 1965

Radiology of the Pterygoid Plates and Pterygopalatine Fossa

ANNE G. OSBORN[1]

The pterygopalatine fossa is a major distribution center for the parasympathetic innervation and vascular supply of deep facial structures. Through eight bony canals or foramina, this fossa communicates with the nasal and oral cavities, infratemporal fossa, orbit, pharynx, and middle cranial fossa. Therefore this important structure provides a natural pathway for dissemination or spread of disease processes to contiguous structures. The normal gross and radiographic anatomy of the pterygopalatine fossa and the adjacent pterygoid plates are considered in detail. Variation in these structures as well as their alterations in a variety of pathologic entities are described.

The advent of sophisticated diagnostic procedures such as multiplanar computed tomography [1–3] and superselective magnification angiography [4–6] has made precise radiographic analysis of deep facial lesions possible. Detailed knowledge of facial osseous and soft tissue anatomy has become a prerequisite for the correct interpretation of these complex examinations.

The pterygopalatine or sphenomaxillary fossa is a major distribution center for the parasympathetic innervation and vascular supply of deep facial structures. While the radiology of the pterygopalatine fossa has been described briefly [7, 8], a thorough consideration of this important structure and its contiguous pterygoid plates has been lacking. This report describes in detail the normal gross and radiographic anatomy of the pterygopalatine fossa and pterygoid plates. Normal variations are discussed as well as the alterations in these structures that occur with a variety of traumatic, inflammatory, and neoplastic lesions.

Materials and Methods

Anteroposterior, lateral, and submentovertex hypocycloidal tomograms (1 mm slices) were obtained through the pterygoid plates and pterygopalatine fossae in 10 dried skulls. These were compared to comparable routine facial tomograms in 20 normal patients. The contours of the pterygoid plates and pterygopalatine fossae were mapped on tracing paper. The contours, maximum width, and length of the pterygopalatine fossae were noted on each lateral view.

Normal Gross Anatomy

The pterygopalatine fossa is a somewhat elongated, funnel-shaped compartment lying just behind the posterior wall of the maxillary sinus (fig. 1A). Its posterior border is formed by the fused anterior mass of the medial and lateral pterygoid plates (fig. 1B), and it is bordered anteriorly by the corpus maxillae. Bounded superiorly by the body of the sphenoid bone, the fossa narrows inferiorly to become the pterygopalatine canal. Its most important contents are the maxillary artery and nerve and the pterygopalatine (sphenopalatine) ganglion.

Through a variety of fissures and foramina, the pterygopalatine fossa communicates with the nasal and oral cavities, infratemporal fossa, orbit, pharynx, and middle cranial fossa. Eight passageways lead directly to or from the pterygopalatine fossa itself [5, 9]. It is through these bony canals that branches of the pterygopalatine ganglion and terminal maxillary artery are distributed (fig. 2). In most instances, both the vessels and accompanying nerves are named for the canal through which they are transmitted.

Laterally, the pterygopalatine fossa is continuous with the infratemporal fossa via the pterygomaxillary fissure. The third or pterygopalatine portion of the maxillary artery enters via the pterygomaxillary fissure, loops within the pterygopalatine fossa, and gives rise to its terminal branches which leave the fossa by passing into a bony canal or foramen (fig. 2).

The perpendicular lamina of the palatine bone forms the medial border of the pterygopalatine fossa, separating it from the nasal cavity. The pterygopalatine and nasal fossae communicate via the sphenopalatine foramen. Anterosuperiorly, the pterygopalatine fossa is connected to the orbital apex through the posteromedial aspect of the infraorbital fissure. Inferiorly, the lesser and greater palatine canals communicate with the oral cavity, transmitting their respective nerves and arteries.

Three posteriorly directed foramina exit from the pterygopalatine fossa in an obliquely oriented line within the root of the sphenoid bone. From lateral to medial they are: (1) the foramen rotundum; (2) the pterygoid or vidian canal; and (3) the pharyngeal or palatinovaginal canal.

The foramen rotundum lies above and lateral to the pterygoid canal, connecting the pterygopalatine and middle cranial fossae. It runs laterally as it courses anteriorly. The pterygoid or vidian canal lies within the body of the sphenoid between the roots of the medial and lateral pterygoid plates. The vidian canal connects the pterygopalatine fossa with the foramen lacerum. In contrast to the foramen rotundum, the vidian canal runs medially as it courses anteriorly. The palatinovaginal or pharyngeal canal is formed by the junction of the processus vaginalis of the sphenoid bone and sphenoidal process of the nasopharynx with the pterygopalatine fossa [10] and transmits the pharyngeal nerve.

The pterygoid process arises from the base of the sphenoid bone at the junction of the body and greater ala and forms the posterior border of the pterygopalatine fossa. Fused anterosuperiorly, the pterygoid process

Received July 25, 1978; accepted after revision December 1, 1978.

[1] Department of Radiology, University of Utah College of Medicine, Salt Lake City, Utah 84132.

AJR 132:389–394, March 1979
0361–803X/79/1323–0389 $0.00

© 1979 American Roentgen Ray Society

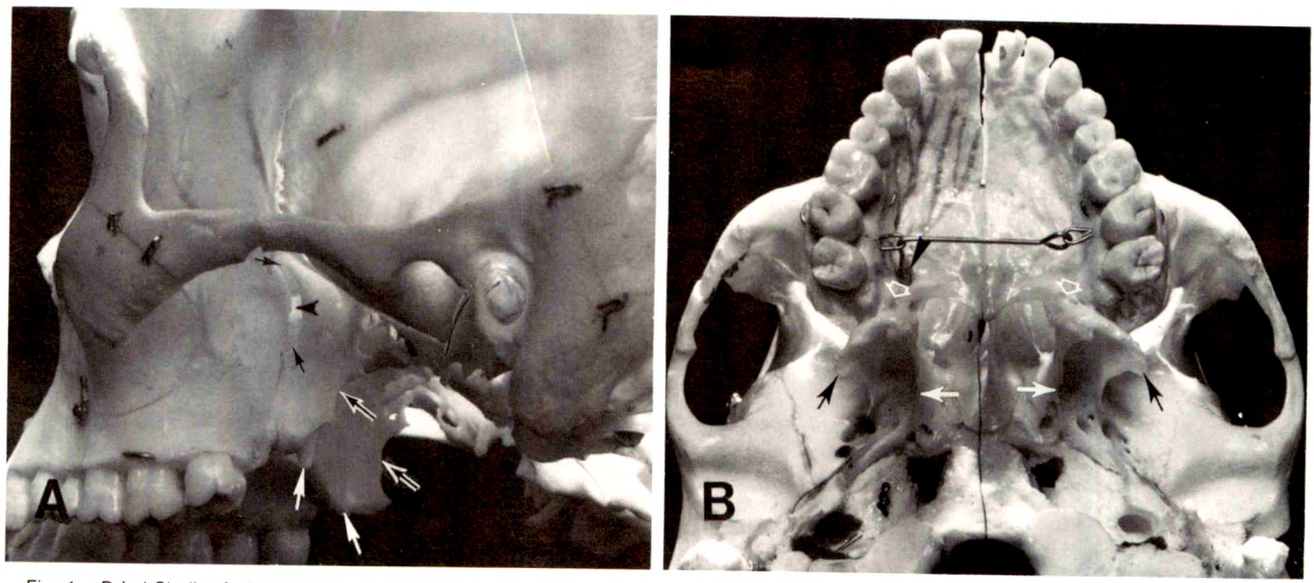


Fig. 1.—Dried Skulls. **A**, Lateral view. Sphenopalatine foramen (*arrowhead*) is within pterygopalatine fossa (*arrows*). Note lateral pterygoid plates (*outlined arrows*) and pterygoid hamuli (*white arrows*). Fusion is seen between posterior maxillary sinus wall and inferior aspects of pterygoid plates. **B**, Submentovertex view. Pterygoid fossae are between lateral (*arrow*) and medial pterygoid plates (*white arrows*). Greater (*arrowhead*) and lesser (*open arrows*) palatine foramina also seen.

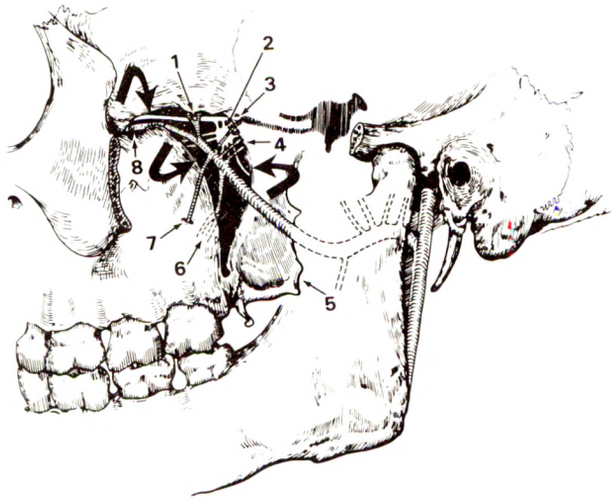


Fig. 2.—Pterygopalatine fossa and major contents. Zygomatic arch and part of mandible were removed to show fossa (area indicated by *curved arrows*) which narrows inferiorly to become pterygopalatine canal. Maxillary artery enters fossa through pterygomaxillary fissure. 1 = Sphenopalatine foramen, with sphenopalatine branches of maxillary artery exiting to supply nasal cavity. 2 = Sphenopalatine (pterygopalatine) ganglion. 3 = Foramen rotundum. Maxillary nerve exits through foramen and passes through superior part of fossa. Note also artery of foramen rotundum. 4 = Pterygoid or vidian (upper branch) and pharyngeal (lower branch) arteries. Vidian and pharyngeal canals are not visible. 5 = Lateral pterygoid plate. 6 = Greater and lesser palatine arteries. 7 = Posterior superior alveolar artery. 8 = Inferior orbital fissure. Infraorbital artery and nerve pass through fissure to enter orbit.



Fig. 3.—Variations in configuration of pterygopalatine fossa. Drawn from actual radiographs.

consists of medial and lateral lamellae that diverge posteriorly to form a V-shaped fossa, the pterygoid fossa (fig. 1B) which contains the medial pterygoid muscle and tensor veli palatini. The outer surface of the lateral pterygoid plate forms the medial wall of the infratemporal fossa and gives attachment to the lateral pterygoid muscle [11]. The medial pterygoid lamina curves laterally at its inferior margins into a hooklike process, the pterygoid hamulus, and forms the lateral boundary of the posterior nasal fossa.

Normal Radiographic Anatomy

The pterygopalatine fossa itself is surprisingly variable in size and shape (fig. 3). The transverse diameter as well as overall length of the fossa vary considerably from side to side and from patient to patient. The configurations range from an elongated, slitlike fissure to a somewhat more triangular teardrop-shaped opening (fig. 3). In all normal instances, the surrounding cortical margins of the fossa are well delineated.

Plain film radiographs and lateral hypocycloidal tomograms through the pterygopalatine fossa and medial pterygoid plate show the broader superior portion of the fossa as it narrows inferiorly to become the pterygopalatine canal (fig. 4A). Tomograms through the medial pterygoid plate show a somewhat bulbous inferior prominence, the pterygoid hamulus. The lateral pterygoid plate is rarely seen in its entirety on a single lateral tomographic section because of its more oblique orientation. The lateral pterygoid lamina is scimitar-shaped, with a posteriorly directed, slightly concave surface (fig. 2).

The base of the pterygoid plates and the pterygoid fossa, the V-shaped space contained between the two pterygoid plates, are both best appreciated on either anteroposterior (fig. 4B) or submentovertex (fig. 4C) tomograms. The foramen rotundum and pterygoid canal

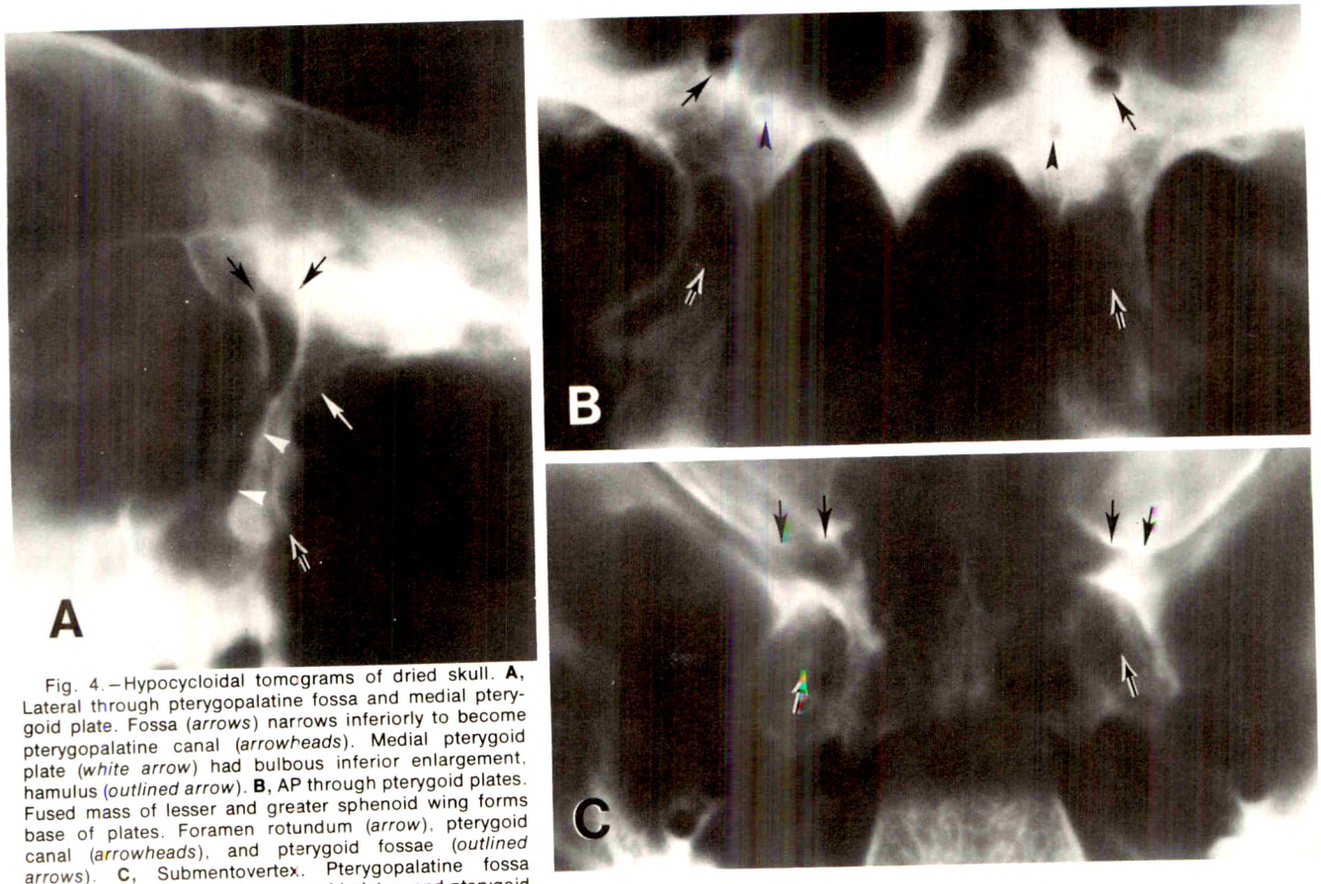


Fig. 4.—Hypocycloidal tomograms of dried skull. **A**, Lateral through pterygopalatine fossa and medial pterygoid plate. Fossa (*arrows*) narrows inferiorly to become pterygopalatine canal (*arrowheads*). Medial pterygoid plate (*white arrow*) had bulbous inferior enlargement, hamulus (*outlined arrow*). **B**, AP through pterygoid plates. Fused mass of lesser and greater sphenoid wing forms base of plates. Foramen rotundum (*arrow*), pterygoid canal (*arrowheads*), and pterygoid fossae (*outlined arrows*). **C**, Submentovertex. Pterygopalatine fossa (*arrows*), lateral and medial pterygoid plates, and pterygoid fossa (*outlined arrows*).

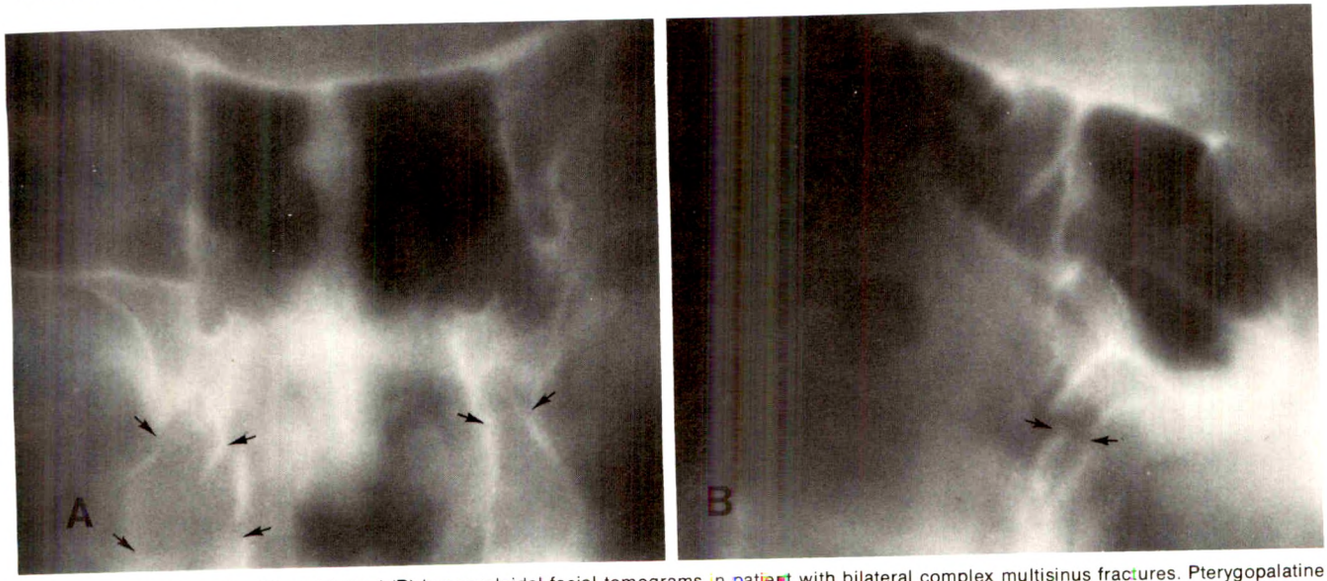


Fig. 5.—Anteroposterior (**A**) and lateral (**B**) hypocycloidal facial tomograms in patient with bilateral complex multisinus fractures. Pterygopalatine fossa and pterygoid plates have been fractured (*arrows*).

can also be identified on these views. The palatinovaginal or pharyngeal canal is anatomically insignificant and is rarely visualized.

Pathologic Radiographic Anatomy

Severe facial trauma often involves the pterygoid plates. Complex zygomaticomaxillary [12–14] and LeFort or bilateral multisinus fractures may involve these structures. Because the middle and inferior portions of the pterygoid processes are fused to the posterior maxillary wall (fig. 1A), the application of lateral or frontal force to the maxilla may result in pterygoid plate interruption [7, 12]. LeFort I and II (pyramidal) fractures usually extend through the pterygomaxillary fissure, often widening the

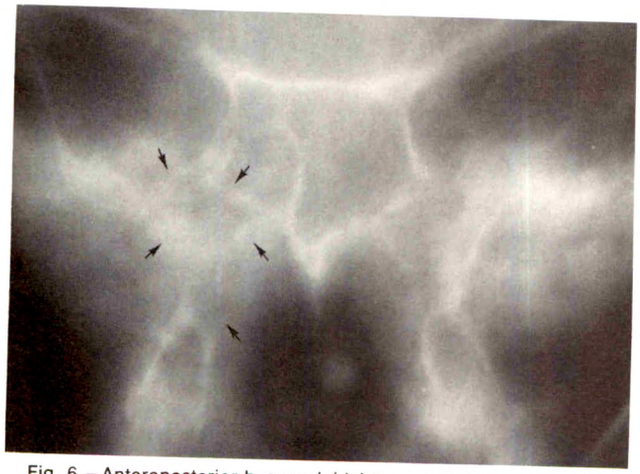


Fig. 6.—Anteroposterior hypocycloidal tomogram in patient with histologically proven rhinocerebral mucormycosis which involved nasal cavity and right maxillary sinus. Extension into base of right pterygoid plates, orbit, and pterygopalatine fossa is indicated by patchy bone destruction (*arrows*). Ethmoid sinuses are opacified. Lateral tomograms demonstrated involvement of foramen rotundum.

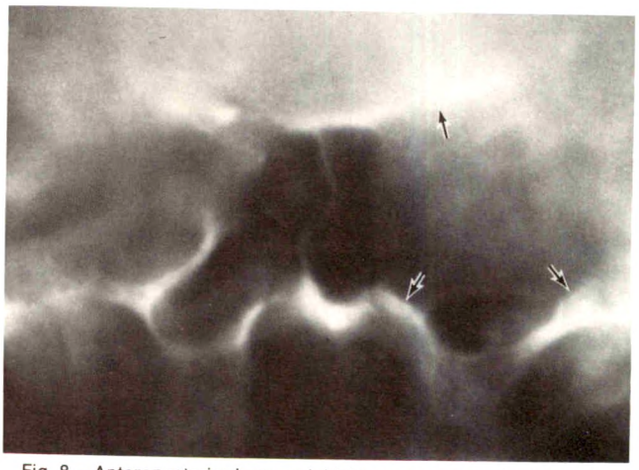


Fig. 8.—Anteroposterior hypocycloidal tomogram in patient with giant aneurysm of cavernous internal carotid artery (*arrows*) that has eroded sphenoid sinus wall and roof of left pterygoid plates.



Fig. 7.—Lateral hypocycloidal facial tomogram in patient with giant sphenoethmoidal mucocele (*arrow*) that has almost destroyed sella turcica, roof of pterygoid plates, and pterygopalatine fossa.



Fig. 9.—Anteroposterior tomogram in patient with severe fibrous dysplasia (*arrows*) involving lesser and greater sphenoid alae, body, sphenoid sinus, pterygoid plates, and pterygopalatine fossa.

pterygopalatine fossa and involving the inferior or midportion of the pterygoid plates. LeFort III injuries (craniofacial disjunction) interrupt the pterygoid plates near the apex of the pterygopalatine fossa at the junction of the plates with the body of the sphenoid. Multiple pterygoid plate fractures are common in patients with severe facial injury (fig. 5), although fractures of the medial pterygoid lamina have been described as an isolated but unusual abnormality [14]. Both anteroposterior and lateral tomograms are usually necessary for complete delineation of the extent of severe facial trauma.

Uncomplicated inflammatory lesions of the nose and paranasal sinuses do not involve the pterygopalatine fossa [15]. Chronic hypertrophic polypoid rhinosinusitis (a condition characterized by marked polypoid mucosal hypertrophy of the nasal fossa and paranasal sinuses) may be distinguished by extensive bony erosion or sclerosis [16, 17]. In such instances the marked bone destruction may suggest a more ominous diagnosis such as neoplasm, necrotizing granuloma, or fungal infection. The presence of associated bone expansion plus a clinical history of vasomotor rhinitis, chronic sinusitis, and nasal polyps should be helpful in the radiographic differential diagnosis [17, 18].

Necrotizing granulomas and fungal infections can and often do involve the pterygopalatine fossa. Focal bone destruction without expansion is present in the nasal cavity (fig. 6). Several paranasal sinuses are usually

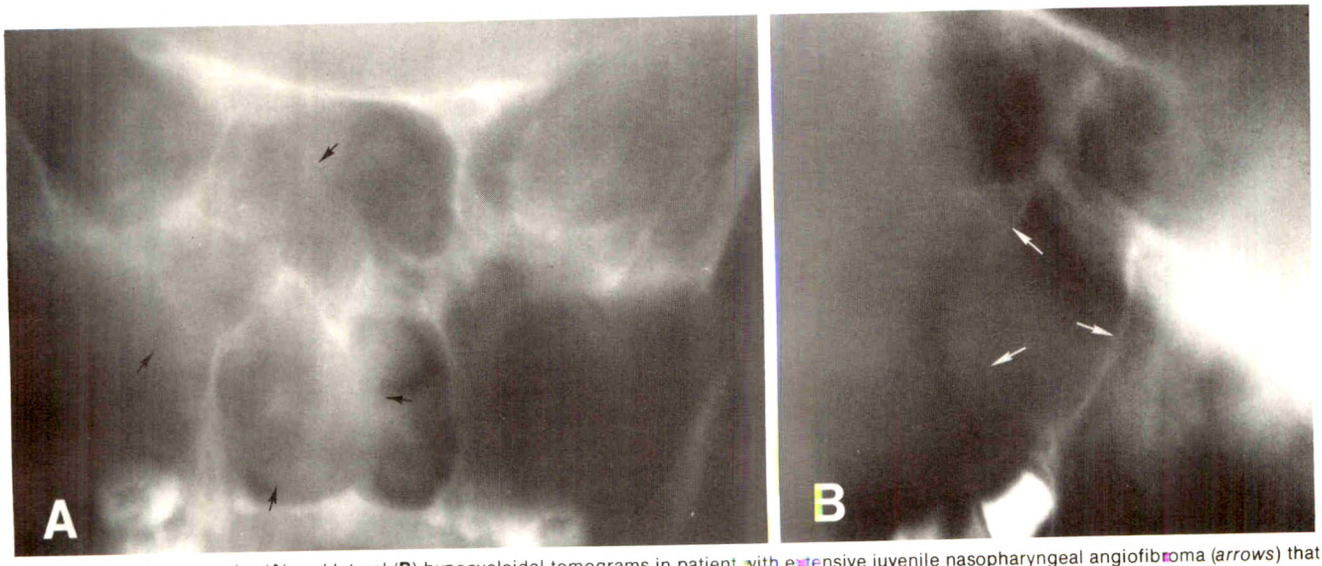


Fig. 10.—Anteroposterior (**A**) and lateral (**B**) hypocycloidal tomograms in patient with extensive juvenile nasopharyngeal angiofibroma (*arrows*) that has expanded and partially destroyed right pterygopalatine fossa, roof of pterygoid plates, and extended superiorly into sphenoid sinus.

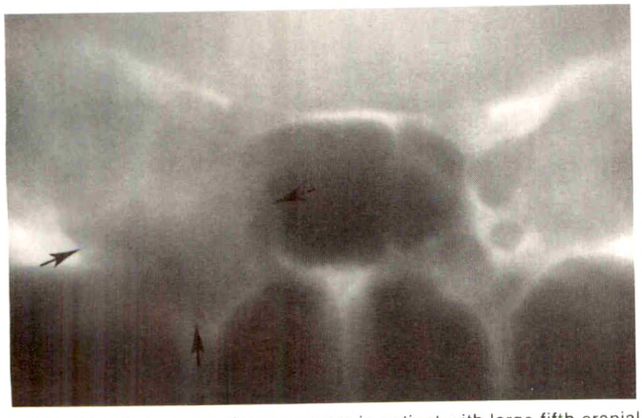


Fig. 11.—Anteroposterior tomogram in patient with large fifth cranial nerve neurinoma. Lesion (*arrows*) has produced pressure erosion of sphenoid wing, and extended into base of right pterygoid plates and sphenoid sinus.

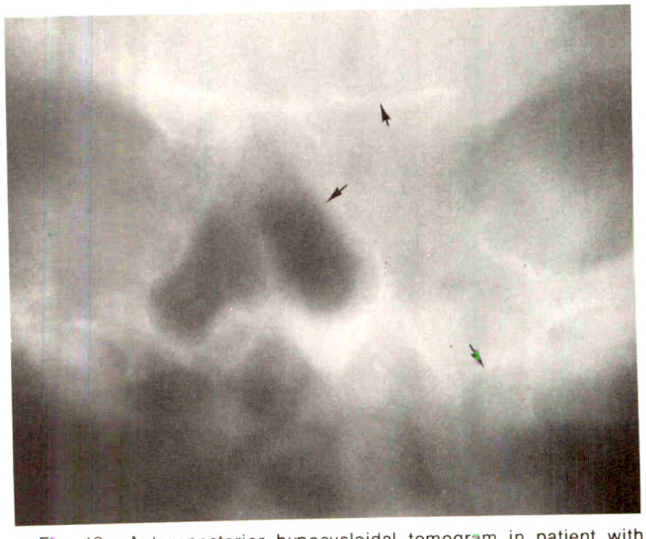


Fig. 12.—Anteroposterior hypocycloidal tomogram in patient with squamous cell carcinoma of ethmoid sinuses. Tumor has eroded base of sphenoid and extends into pterygoid plates (*arrows*).

involved [19] and the bone destruction initially tends to follow natural foramina and fissures.

The rare but unusually extensive sphenoethmoidal mucocele may involve the pterygopalatine fossa (fig. 7). Multiple curvilinear expansile deformities of the adjacent sinus walls (suggesting a benign, long-standing process), opacification, and focal areas of bone thinning or destruction suggest the diagnosis [20–22].

Benign, nontumorous lesions like giant carotid cavernous sinus or paraclinoid aneurysms may produce pressure erosion of the sphenoid sinus [23]. If the aneurysm is of sufficient size, the bone destruction may extend into the base of the pterygoid process (fig. 8).

Other nonneoplastic lesions may involve the pterygopalatine fossa and pterygoid plates. Localized or regional fibrous dysplasia may involve several adjacent bones of the facial skeleton and anterior cranial fossa (leontiasis ossea). Bone replacement by dense osteoid and fibrous tissue results in varying degrees of bone thickening and encroachment (fig. 9). The differential diagnosis includes Paget's disease, meningioma, osteoblastic metastasis, epidermoid carcinoma, and chronic osteomyelitis [24].

A variety of benign tumors may involve the pterygopalatine fossa and pterygoid plates. The epithelial or inverting papilloma usually presents as a unilateral soft tissue mass accompanied by simultaneous bone expansion and focal destruction. Juvenile nasopharyngeal angiofibromas demonstrate a nasopharyngeal soft tissue mass and expansion of the pterygopalatine fossa (fig. 10).

Since these lesions tend to spread locally by extension along natural foramina and fissures, enlargement and/or destruction of these openings into the fossa may be demonstrated by careful tomography [25]. Other benign tumors such as large pituitary adenomas or neurinomas of the trigeminal ganglion may erode the sphenoid alae, extending into the base of the pterygoid plates and apex of the fossa (fig. 11).

The rare primary meningioma of the nasal fossa, as well as the more common sphenoid wing meningioma, may extend predominately extracranially, producing striking sclerosis involving the pterygopalatine fossa and pterygoid plates. Angiography is helpful in delineating these lesions. The differential diagnosis includes Paget's disease, fibrous dysplasia, and osteoblstic metastases.

Primary malignant tumors of the paranasal sinuses usually produce opacification and bone destruction without evidence for focal expansion of the sinus walls [18]. Squamous cell carcinoma (fig. 12), adenocarcinoma, melanoma, rhabdomyosarcoma, and the uncommon esthesioneuroblastoma may all involve the pterygopalatina fossa and adjacent pterygoid plates by direct extension.

Metastatic lesions to the pterygoid plates and pterygopalatine fossa are uncommon. Osteoblastic metastases from prostate carcinoma may simulate meningioma, fibrous dysplasia, or Paget's disease. Other common metastases are from hypernephroma, carcinoma of the breast, multiple myeloma, or melanoma.

Because of its many interconnections between the nasal and oral cavities, infratemporal and middle cranial fossae, and orbit, the pterygopalatine fossa provides a natural pathway for contiguous spread of those many disease processes that initially tend to follow natural foramina and fissures. Therefore, careful radiographic examination of this important structure should be performed in patients presenting with any of these deep facial lesions.

REFERENCES

1. Byrd SE, Harwood-Nash DC, Barry JF, Fitz CR, Boldt DW: Coronal computed tomography of the skull and brain in infants and children. I. Technique and results. *Radiology* 124:705–709, 1977
2. Claussen CD, Wohkamp FW, Krastel A: Computed tomography of trauma involving brain and facial skull (craniofacial injuries). *J Comput Assist Tomogr* 1:472–481, 1977
3. Osborn AG, Anderson RE: Direct sagittal CT scans of the face and paranasal sinuses. *Radiology* 129:81–87, 1978
4. Allen WE, Kier EL, Rothman SLG: The maxillary artery: normal arteriographic anatomy. *AJR* 118:517–527, 1973
5. Allen WE, Kier EL, Rothman SLG: The maxillary artery in craniofacial pathology. *AJR* 121:124–138, 1974
6. Osborn AG: The nasal arteries. *AJR* 130:89–97, 1978
7. Potter GD: The pterygopalatine fossa and canal. *AJR* 107: 520–525, 1969
8. Bryc S: Roentgen diagnosis of pterygopalatine fossa and canal. *Polski Przegl Radiol* 36:633–636, 1972
9. Pfaff GH: *Anatomy of the Head and Neck*. Philadelphia, Saunders, 1973, pp 141–146
10. Sondheimer FK: Basal foramina and canals, in *Radiology of the Skull and Brain*, vol 1, edited by Newton TH, Potts DG, St. Louis, Mosby, 1971, pp 289–347
11. Gray H: *Anatomy of the Human Body*. Edited by Goss CM, Philadelphia, Lea & Febiger, 1973, pp 178–179
12. Dolan KD, Jacoby CG: Facial fractures. *Semin Roentgenol* 13:37–51, 1978
13. Zizmor J, Noyek AM: Fractures of the paranasal sinuses. *Otolaryngol Clin North Am* 6:473–485, 1973
14. Archer CR, Sundarain M: Uncommon sphenoidal fractures and their sequelae. *Radiology* 122:157–161, 1977
15. Zizmor J, Noyek AM: Inflammatory diseases of the paranasal sinuses. *Otolaryngol Clin North Am* 6:459–472, 1973
16. Wilson M: Chronic hypertrophic polypoid rhinosinusitis. *Radiology* 120:609–613, 1976
17. Winestock DP, Bartlett PC, Sondheimer FK: Benign nasal polyps causing bone destruction in the nasal cavity and paranasal sinuses. *Laryngoscope* 88:675–679, 1978
18. Dubois PJ, Schultz JC, Perrin RL, Dastur KJ: Tomography in expansile lesions of the nasal and paranasal sinuses. *Radiology* 125:149–158, 1977
19. Addlestone RB, Baylis GJ: Rhinocerebral mucormycosis. *Radiology* 115:1137–1170, 1975
20. Diaz F, Latchow R, Ruball AJ III, Quick CA, Erickson DL: Mucoceles with intracranial and extracranial extensions. *J Neurosurg* 48:284–288, 1978
21. Roberson GH, Patterson AK, Deeb ME, Maisel RH, Bone RC: Sphenoethmoidal mucocele: radiographic diagnosis. *AJR* 127:595–599, 1976
22. Takahasi M, Jingu K, Nakayania T: Roentgenologic appearances of sphenoethmoidal mucocele. *Neuroradiology* 6: 45–49, 1973
23. Nutik SN: Carotid paraclinoid aneurysms with intradural origin and intracavernous location. *J Neurosurg* 48:526–533, 1978
24. Zizmor J, Noyek AM: Cysts, benign tumors, and malignant tumors of the paranasal sinuses. *Otolaryngol Clin North Am* 6:487–508, 1973
25. Wilson GH, Hanafee WN: Angiographic findings in 16 patients with juvenile nasopharyngeal angiofibroma. *Radiology* 92:279–284, 1969

Ultrasonic Recognition of Parenchymal Gas

M. R. CONRAD,[1] R. BREGMAN AND W. J. KILMAN

Abdominal sonography in six febrile patients was suspicious for parenchymal gas. In five, immediate radiographic confirmation was obtained. Four patients had gas-containing abscesses, one had gas sequestered in a hepatic hematoma, and in the other subcapsular hepatic gas probably originated by mesenteric dissection from pneumatosis cystoides intestinals.

Sonography, well established for detecting fluid-filled abscesses [1], may also disclose parenchymal gas. Careful attention to such gas is important in the febrile patient since: (1) it is highly probable that a gas-containing abscess is present; (2) the fluid-filled portion of the abscess may be concealed from ultrasound imaging by the gas; and (3) the gas may be obscured or confused with normal bowel gas on plain abdominal films.

Kressel and Filly [2] recently reported sonographic diagnosis of abdominal abscesses containing gas in six patients by imaging a characteristic dense echo collection with or without acoustic shadowing. We report six patients in whom parenchymal gas was suspected by sonography and confirmed by radiography. The importance of obtaining immediate confirmatory radiographic studies is emphasized.

Case Material

About 800 abdominal sonographic examinations are done each year at University of Texas Health Science Center at Dallas and Parkland Memorial Hospital to find abdominal abscesses. During a 1 year period, parenchyma gas was suspected in six patients. Gas within a solid organ suggests a gas-forming abscess. A focal echo collection of moderate intensity or greater was present on transverse and longitudinal sections. Acoustic shadowing was present in five cases. Radiography immediately after sonography confirmed parenchymal gas.

Case Reports

Case 1

A 51-year-old Latin American man with adult onset diabetes mellitus had fever to 38.9°C, chills, low back pain, marked right costovertebral tenderness, and pyuria. Initial plain film showed a gas-filled hepatic flexure, but no abnormality. One day after admission creatine was 5.5 mg/100 ml, and sonography, performed to exclude hydronephrosis, imaged an enlarged right kidney containing diffuse increased sonolucency. A focal echo collection with acoustic shadowing was present within the upper pole (fig. 1A). Anteroposterior and oblique radiography

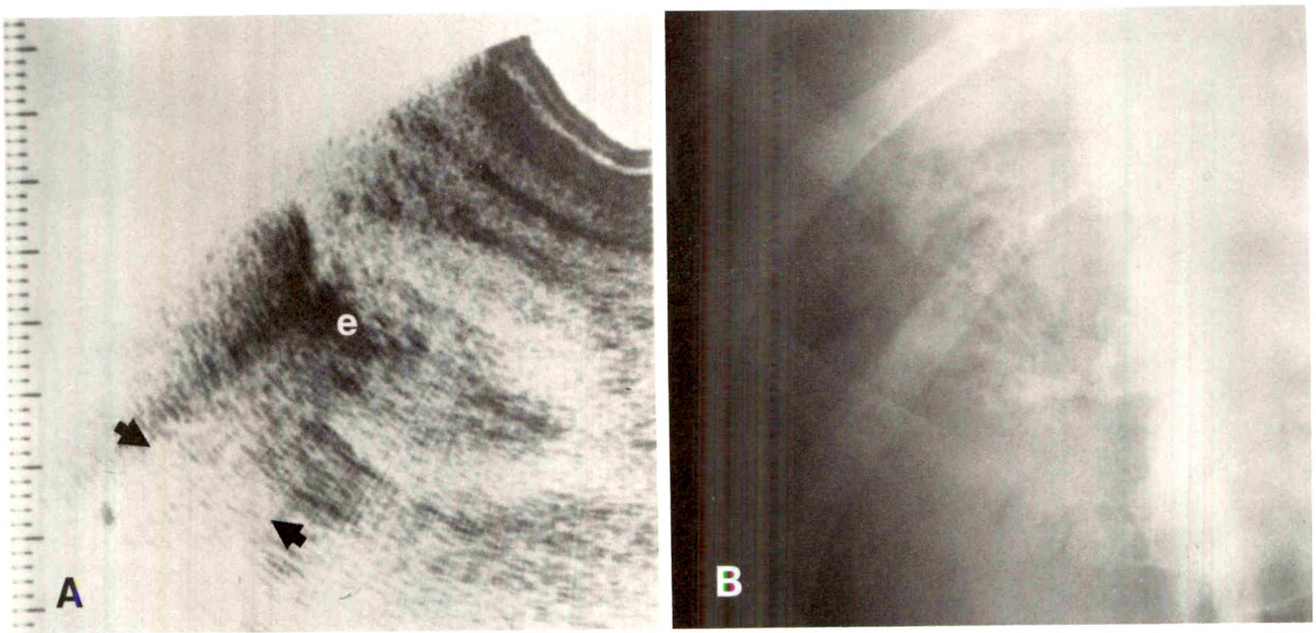


Fig. 1.—Case 1. **A,** Longitudinal scan, patient prone. Broad, strong focal echo collection (e) with acoustic shadowing (*arrows*) within upper pole of enlarged right kidney. **B,** Retroperitoneal extraluminal gas demonstrated by posterior position of gas bubbles on opposite oblique view of right kidney.

Received July 25, 1978; accepted after revision November 16, 1978.

[1]Department of Radiology, University of Texas Health Science Center at Dallas and Parkland Memorial Hospital, 5323 Harry Hines Boulevard, Dallas, Texas 75235. Address reprint requests to M. R. Conrad.

© 1979 American Roentgen Ray Society

0361–803X/79/1323–0395 $0.00

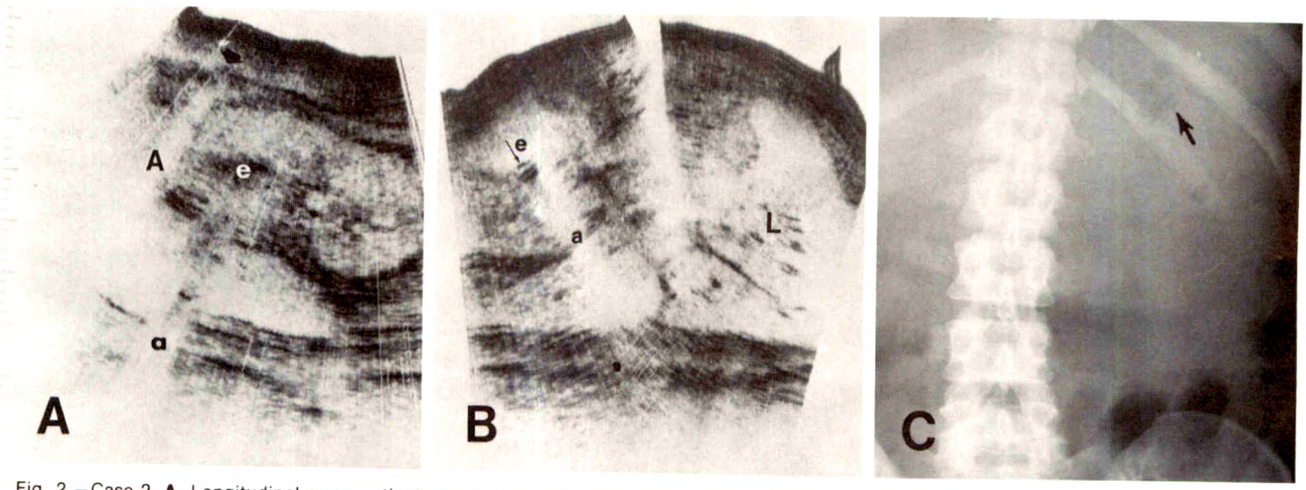


Fig. 2.—Case 2. **A,** Longitudinal scan, patient prone. Intense focal echoes (e) with acoustic shadowing (a) within upper pole parenchyma of left kidney. Focal echo with acoustic shadow (A) due to reverberation artifact from overlying rib (*arrow*). **B,** Transverse scan, patient prone. Renal parenchymal origin of focal echoes (e, *arrow*) and acoustic shadowing (a) confirmed (L = right lobe of liver). **C,** Gas collection (*arrow*) in region of upper pole of left kidney (oblique view confirmed extraintestinal and retroperitoneal location).

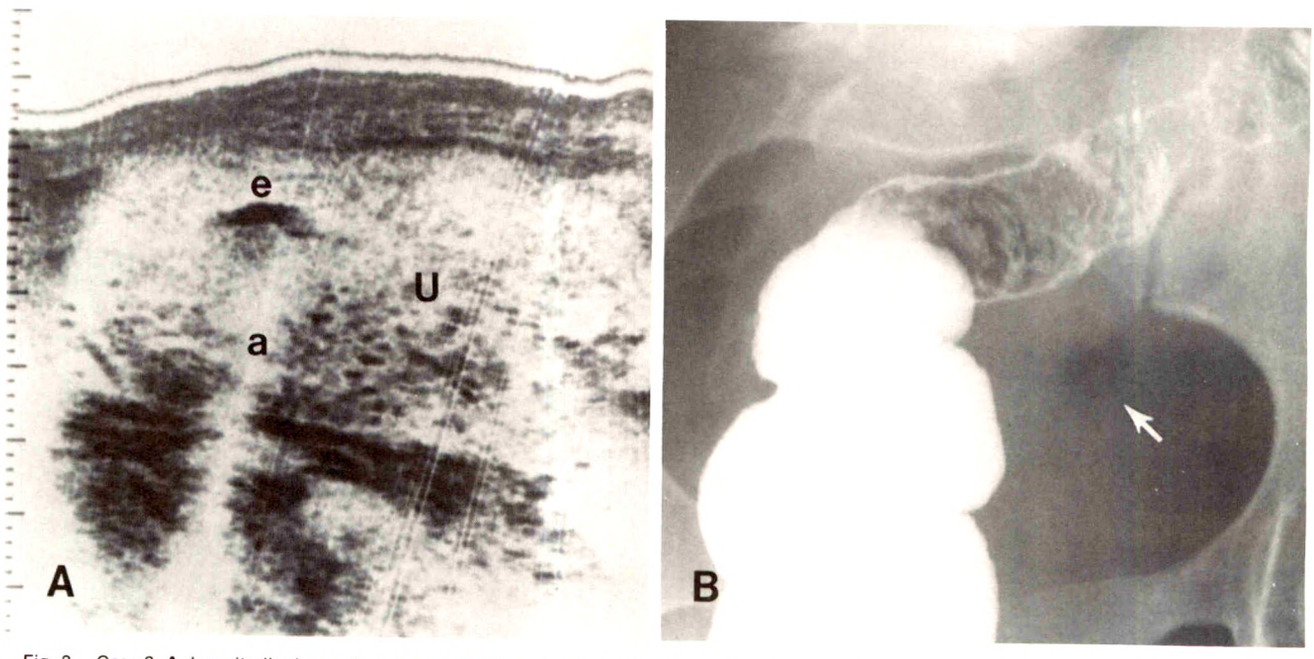


Fig. 3.—Case 3. **A,** Longitudinal scan 2 cm left of midline. Intense focal echo (e) with acoustic shadowing (a) within enlarged postpartum uterus (U). **B,** Extraintestinal gas collection (*arrow*).

showed numerous small gas bubbles (fig. 1B). At surgery, emphysematous pyelonephritis with an upper pole abscess cavity due to *Klebsiella* was found. The rest of the kidney was markedly edematous and contained numerous micro- and macroabscesses (3–4 mm). Nephrectomy was done.

Comment. In this case, sonography differentiated renal abscess from perinephric abscess. Decreased renal echoes and enlargement was due to diffuse acute inflammatory reaction. The numerous small macroabscesses (3–4 mm) were not imaged.

Case 2

A 44-year-old black woman with adult onset diabetes mellitus had chills and left flank pain for 2 weeks and fever of 38.3°C at hospitalization. Initial plain film was interpreted as normal. A small gas collection in the left upper quadrant was thought to be in the stomach. Acute pyelonephritis was diagnosed, but the patient did not respond to antibiotic therapy. Sonography, performed to search for a renal inflammatory lesion, imaged a focal echo with acoustic shadowing in the left upper pole (figs. 2A and 2B) that was shown to be retroperitoneal gas on anteroposterior and oblique radiography (fig. 2C). Severe acute pyelonephritis with diffuse edema and a confluent abscess cavity in the upper pole was found at surgery. Nephrectomy was done.

Comment. Although the focal echo with acoustic shadowing of this renal abscess appeared within the parenchyma on the longitudinal section, confirmation was provided by the transverse section that excluded a rib reverberation artifact. Sonography may reveal a perinephric or renal abscess when acute pyelonephritis fails to respond to antibiotic therapy.

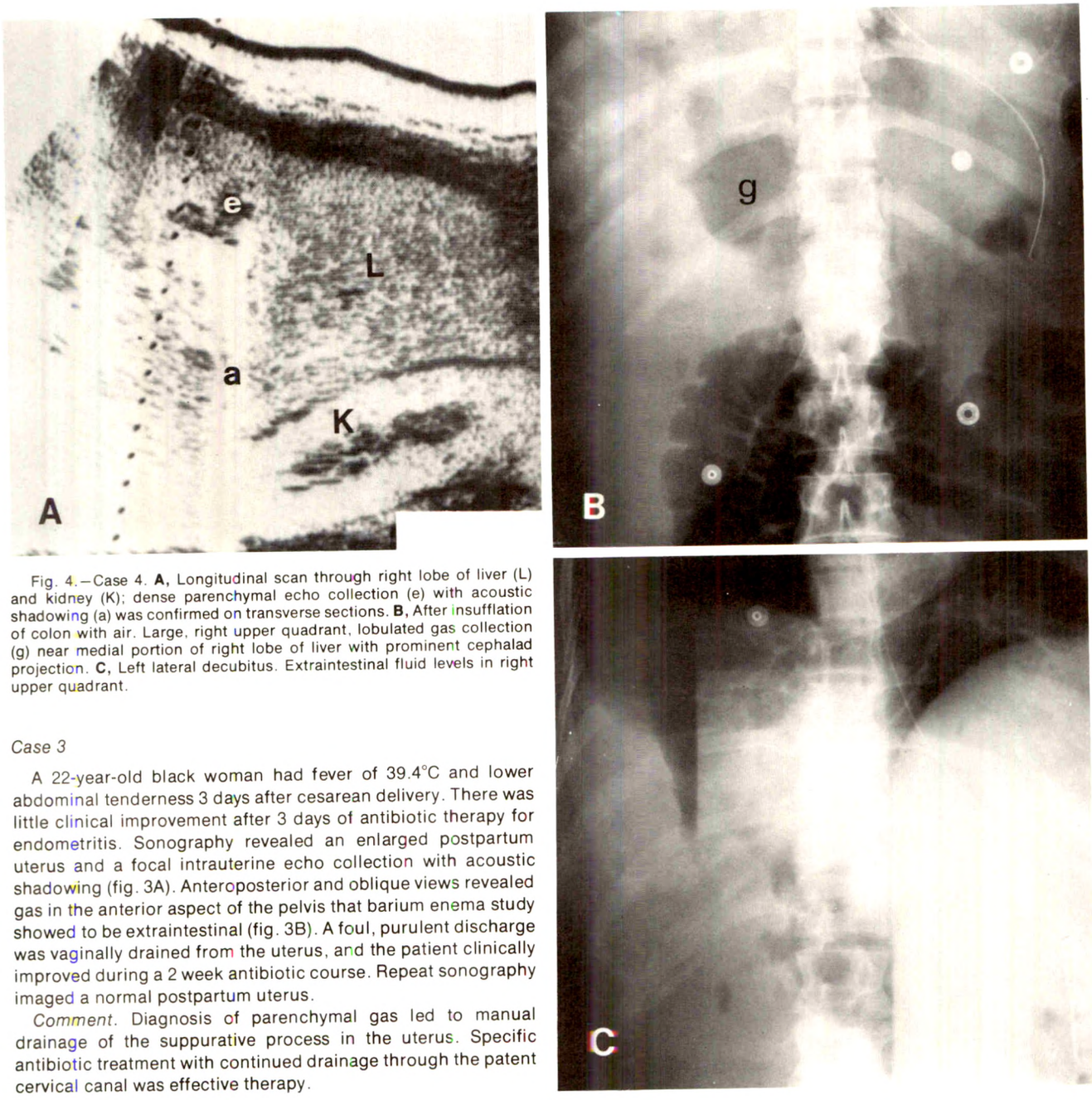


Fig. 4.—Case 4. **A,** Longitudinal scan through right lobe of liver (L) and kidney (K); dense parenchymal echo collection (e) with acoustic shadowing (a) was confirmed on transverse sections. **B,** After insufflation of colon with air. Large, right upper quadrant, lobulated gas collection (g) near medial portion of right lobe of liver with prominent cephalad projection. **C,** Left lateral decubitus. Extraintestinal fluid levels in right upper quadrant.

Case 3

A 22-year-old black woman had fever of 39.4°C and lower abdominal tenderness 3 days after cesarean delivery. There was little clinical improvement after 3 days of antibiotic therapy for endometritis. Sonography revealed an enlarged postpartum uterus and a focal intrauterine echo collection with acoustic shadowing (fig. 3A). Anteroposterior and oblique views revealed gas in the anterior aspect of the pelvis that barium enema study showed to be extraintestinal (fig. 3B). A foul, purulent discharge was vaginally drained from the uterus, and the patient clinically improved during a 2 week antibiotic course. Repeat sonography imaged a normal postpartum uterus.

Comment. Diagnosis of parenchymal gas led to manual drainage of the suppurative process in the uterus. Specific antibiotic treatment with continued drainage through the patent cervical canal was effective therapy.

Case 4

A 37-year-old febrile American Indian woman had upper right quadrant pain and anorexia for 1 month. Sonography, performed to exclude cholelithiasis, imaged a focal echo collection with acoustic shadowing within the hepatic parenchyma (fig. 4A). Anteroposterior film of the abdomen showed a large lobulated gas collection in the right upper quadrant. Its extraintestinal location was demonstrated by air insufflation of the colon and stomach (fig. 4B). Air-fluid levels were seen on the decubitus view (fig. 4C). At surgery, a large multiloculated abscess in the right lobe of the liver extending into the subhepatic space was drained. The fluid grew anaerobic streptococcus. The postoperative course was uneventful.

Comment. Although a large air-fluid level was demonstrated radiographically in the hepatic abscess, the fluid-filled portion of the liver abscess was effectively obscured to ultrasound imaging by the gas component.

Case 5

A 30-year-old Latin American woman with known ulcerative colitis was admitted with fever and bloody diarrhea. Total colectomy was performed 8 days later for toxic megacolon. Liver sonography (in the coronal plane) after 2 more weeks showed multiple strong focal echoes within the liver substance (fig. 5). Anteroposterior film showed a huge pneumoperitoneum but no radiographic evidence of gas in the liver. At laparotomy, diffuse anaerobic peritonitis due to *Clostridia* sepsis was found along with extensive pneumatosis of the small bowel and liver capsule. Subcapsular hepatic gas pockets averaged 2–4 mm.

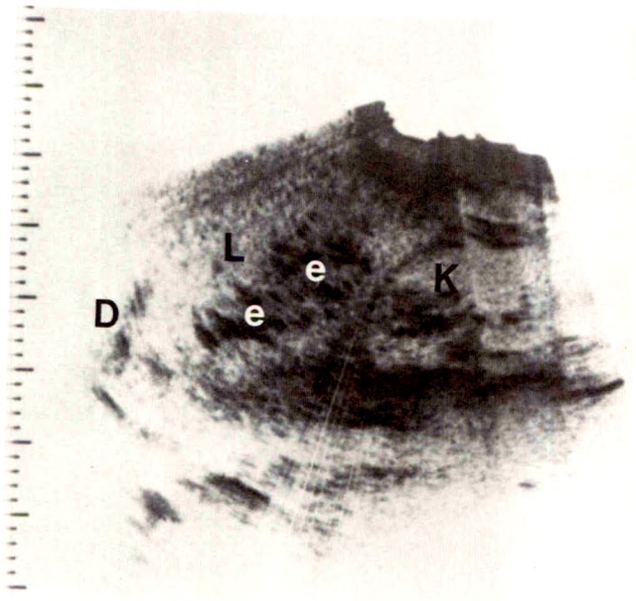


Fig. 5.—Case 5. Coronal scan. Right kidney (K), liver (L), and multiple strong focal echoes (e) without acoustic shadowing within liver D = diaphragm).

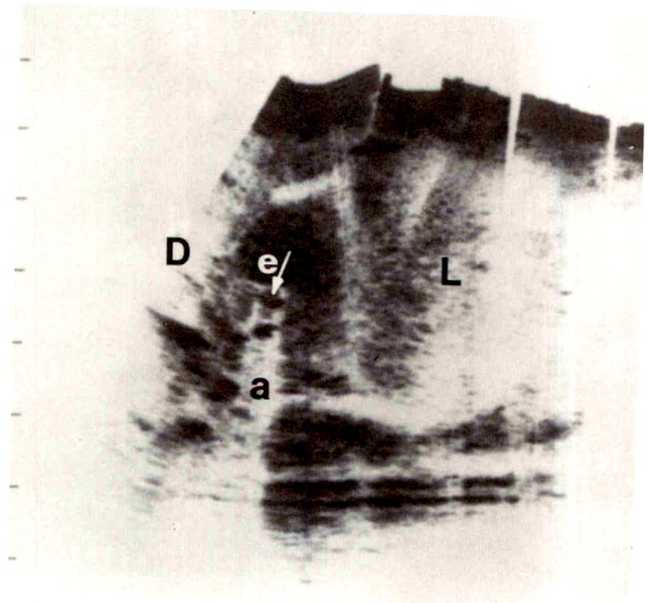


Fig. 6.—Case 6. Longitudinal scan. Focal echoes (e, *arrow*) with acoustic shadow (a) in region of dome of right lobe of liver (L). Region of diaphragm (D) not imaged well because of hematoma.

The patient died 3 days later, and at autopsy the subcapsular pneumatosis had disappeared. There was no evidence of clostridial infection involving the liver, portal vein and branches, or porta hepatis.

Comment. Absence of hepatic clostridial infection at autopsy suggests the subcapsular hepatic gas probably originated from the pneumatosis intestinalis. The centrally located echoes on the sonogram probably represented gas within the perivascular fibrous capsule of the porta hepatis due to mesenteric dissection of gas from the proven pneumatosis intestinalis.

Case 6

A 33-year-old black man underwent exploratory laparotomy and repair a lacerated diaphragm for a gunshot wound 3 weeks before current admission. Fever, chills, and pain in the right arm and flank developed 5 days before this admission. Chest radiography showed a right pleural effusion. Sonography revealed a focal echo with acoustic shadowing in the dome of the right liver lobe (fig. 6), confirmed to be a small gas pocket on anteroposterior and oblique radiography. A loculated empyema was drained from the chest, and a grossly noninfected, nonpurulent, subphrenic hematoma was found at the dome of the liver. *Staphylococcus aureus* was cultured from the hematoma and empyema. Recovery was uneventful.

Comment. Although a gas collection in the dome of the liver was documented by sonography and radiography, a gas-forming abscess was not present. Most likely the gas was "trapped" (sequestered) in the liver hematoma after the bullet wound and initial surgery.

Discussion

Early recognition of a gas-forming parenchymal abscess is imperative because of associated high mortality and morbidity [3–8]. Plain film findings may not be diagnostic since the patients are quite ill and uncooperative, may have ileus obscuring gas in the abscess (case 1), or the extraintestinal gas may be confused with normal bowel gas (case 2). Moreover, in severe inflammatory kidney disease, excretory urography often shows nonvisualization, leaving the differential diagnosis unresolved among hydronephrosis, renal abscess, or perinephric abscess.

Although gas generally creates difficulty in ultrasound imaging, parenchymal gas may be helpful. Strong focal echoes within the parenchyma of an organ with or without acoustic shadowing are suspicious, but not necessarily evidence of a gas-forming abscess. Confirming the intraparenchymal origin of the echo complex should be obtained on both longitudinal and transverse sonographic sections to avoid confusion with a reverberation artifact (fig. 2). High quality radiographs should be examined immediately to differentiate gas from calcification, a strong reflective process that can create similar ultrasound findings. Radiographic documentation of the extraintestinal location of the gas may be more certain with decubitus views and/or contrast studies appropriate to the suspicious organ.

In the series of Kressel and Filly [2] of both abdominal and parenchymal gas-containing abscesses, radiography did not identify gas in two of six cases. In five of our six cases of parenchymal gas, radiographic documentation was possible with properly exposed and collimated films. In contrast to their series [2], two abscesses were erroneously diagnosed in our series (cases 5 and 6). In both of these patients, clinical findings made exploration mandatory. In case 6, sequestration of air in a hepatic hematoma was the apparent explanation. In case 5, mesenteric dissection of gas originating from pneumatosis intestinalis presumably produced hepatic gas that was not radiographically visible and lacked acoustic shadowing. The absence of acoustic shadowing when

microscopic or small pockets of gas ("microbubbles") are present is probably a partial volume effect due to the small size of the gas bubbles. The resulting acoustic shadow of narrow diameter is not imaged due to statistical averaging over the significantly larger beam width.

ACKNOWLEDGMENTS

We thank Gayle Blust for manuscript preparation and Nancy Schreiber for photographic assistance.

REFERENCES

1. Doust BD, Quiroz F, Stewart JM: Ultrasonic distinction of abscesses from other intra-abdominal fluid collections. *Radiology* 125:213–218, 1977
2. Kressel HY, Filly RA: Ultrasonographic appearance of gas-containing abscesses in the abdomen. *AJR* 130:71–73, 1978
3. Costas S: Renal and perirenal emphysema. *Br J Urol* 44: 311–318, 1972
4. Whiteley PF, Hamlett D: Pyometra—a reappraisal. *Am J Obstet Gynecol* 109:108–112, 1971
5. Joseph WL, Kahn AM, Longmire WP Jr: Pyogenic liver abscess. *Am J Surg* 115:63–68, 1968
6. Banks DE, Persky L, Mahoney SA: Renal emphysema. *J Urol* 102:390–392, 1969
7. Foster SC, Schneider B, Seaman WB: Gas-containing pyogenic intrahepatic abscesses. *Radiology* 94:613–618, 1970
8. Schainuck LI, Fouty R, Cutler RE: Emphysematous pyelonephritis. *Am J Med* 44:134–139, 1968

Ultrasound Diagnosis of Masses Elevating the Inferior Vena Cava

ALFRED B. KURTZ,[1] CARL RUBIN, AND BARRY B. GOLDBERG

The inferior vena cava is frequently involved in diseases of the abdomen and retroperitoneum. Critical evaluation of this vessel's course can greatly help in determining the origin of an adjacent mass. Ultrasound was used to divide the inferior vena cava into three parts. A vector type principle was applied to masses anteriorly displacing the vena cava, and the location of the mass was compared to the particular portion of the cava most affected. With this approach, it was often possible to determine what structures a mass may have originated from.

The first radiographic attempt to visualize the inferior vena cava was by Dos Santos in 1935 [1] and modified in 1947 by O'Loughlin [2] and Fariñas [3]. Subsequent technical refinements, including visualization of the vena cava in two projections (such as an anteroposterior and a lateral or oblique), have made the inferior vena cavogram an important study in evaluating abdominal and retroperitoneal disease [4–6]. Since the incidence of congenital abnormality of the inferior vena cava is low, the vena cava is angiographically identified in normal anatomic position in more than 98% of patients [7].

With ultrasound, the superior portion of the inferior vena cava can be successfully visualized in almost every patient [8, 9]. However, the distal portion may occasionally be obscured by overlying bowel gas. With longitudinal and transverse images, both the anteroposterior and lateral positions of the inferior vena cava can be accurately defined, as well as its relation to adjacent organs and vessels. In a longitudinal projection, the distal and midportion of the vena cava are horizontal in course, while more proximally it is hammock shaped (concave anteriorly) [10].

The walls of the inferior vena cava are thin and thus prone to deformity by adjacent masses [6]. Any displacement or change in the shape of the vena cava can be easily evaluated by either contrast or sonocavogram. Specific organs and blood vessels are situated posterior to the inferior vena cava. We examined masses that elevated the vena cava anteriorly and attempted to locate their origins.

Subjects and Methods

From June 1977 to June 1978, 2,850 abdominal and retroperitoneal examinations were performed at Thomas Jefferson University Hospital in Philadelphia. In 21 of these, masses caused anterior displacement of the inferior vena cava. There were 11 female and 10 male patients aged 3–78 years.

Patients were initially examined supine using high-resolution contact gray scale B-scan equipment with a 3.5 MHz transducer. A 2.25 MHz transducer was substituted for large body types to image the inferior vena cava. Other positions used for more complete imaging of the vena cava included a left oblique or decubitus view with scanning performed through the right flank. The patient's arms and legs were given adequate support for maximum relaxation of the anterior abdominal musculature. Since swallowed air or ingested barium can obscure large parts of the inferior vena cava, the patient was instructed to fast prior to the examination and was not scanned after a recent barium meal.

Ultrasonography was performed in both longitudinal and transverse planes. Usually, the full extent of the inferior vena cava was best visualized in the longitudinal axis 1–2 cm right of the midline beginning at the xiphoid process with a single sweep from under the costal margin caudally toward the umbilicus. Transverse scans were then obtained at 1–2 cm intervals from the xiphoid to the umbilicus. The patient was instructed to breathe deeply to displace the liver downward, which often provides a more complete visualization of the vena cava. A Valsalva maneuver frequently improves visualization, but sometimes abdomen expansion during the procedure actually hinders adequate imaging.

Results

The first eight of the 21 cases, composed of seven tumors and one blood vessel abnormality, included: one liver mass (hepatoma), one right renal mass (polycystic kidney disease), one right adrenal tumor (pheochromocytoma), four lymph node enlargements (three metastases and one lymphoma), and one tortuous abdominal aorta.

On the basis of these initial cases, it became apparent

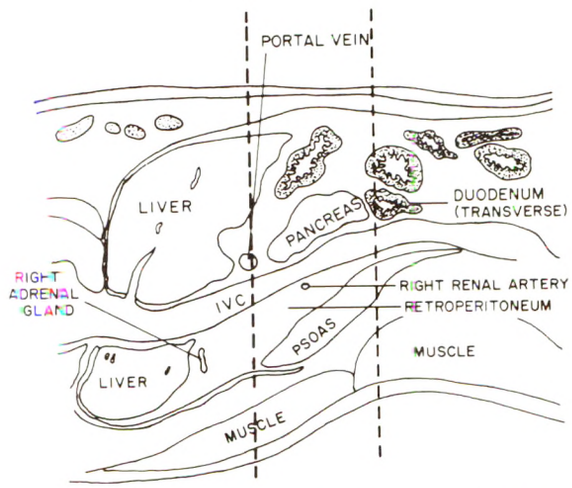


Fig. 1.—Longitudinal diagram of inferior vena cava. Dashed lines divide vena cava into three segments: upper (hepatic), middle (pancreatic), and lower (small bowel).

Received August 1, 1978; accepted after revision November 1, 1978.

[1]All authors: Division of Diagnostic Ultrasound, Thomas Jefferson University Hospital Curtis Building, Fifth Floor, 1015 Walnut Street, Philadelphia, Pennsylvania 19107. Address reprint requests to A. B. Kurtz.

AJR 132:401–406, March 1979

© 1979 American Roentgen Ray Society

0361-803X/79/1323-0401 $0.00

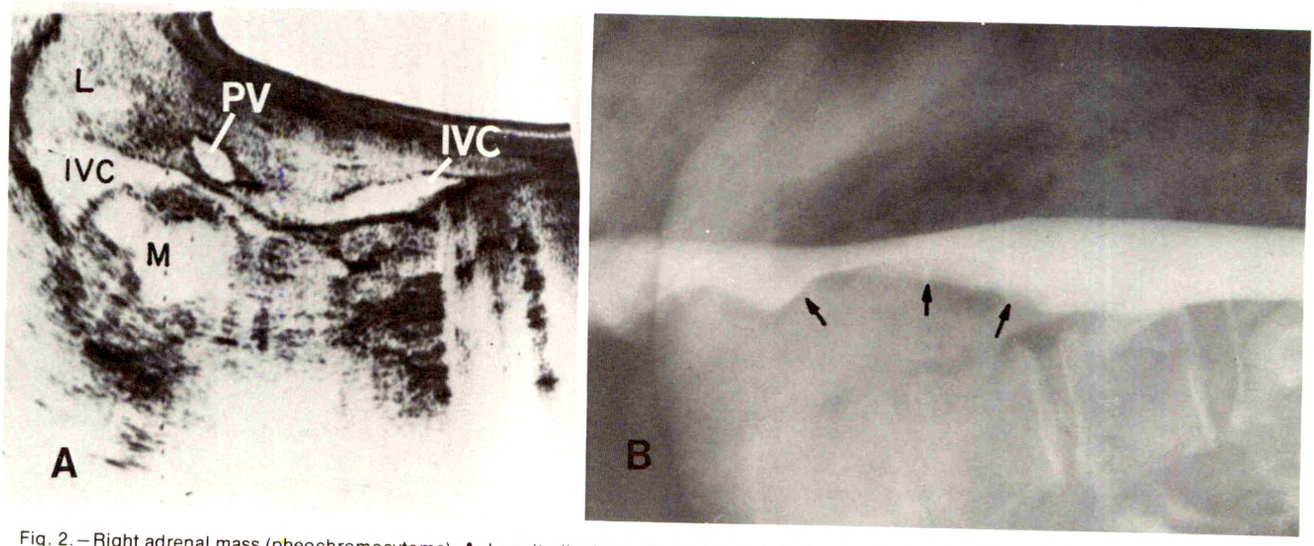


Fig. 2.—Right adrenal mass (pheochromocytoma). **A**, Longitudinal scan 2 cm right of midline. Primarily solid mass with anechoic areas (M) of right adrenal gland. Predominant anterior displacement in upper division of inferior vena cava (IVC). L = liver; PV = portal vein. **B**, Anterior displacement of vena cava (*arrows*).

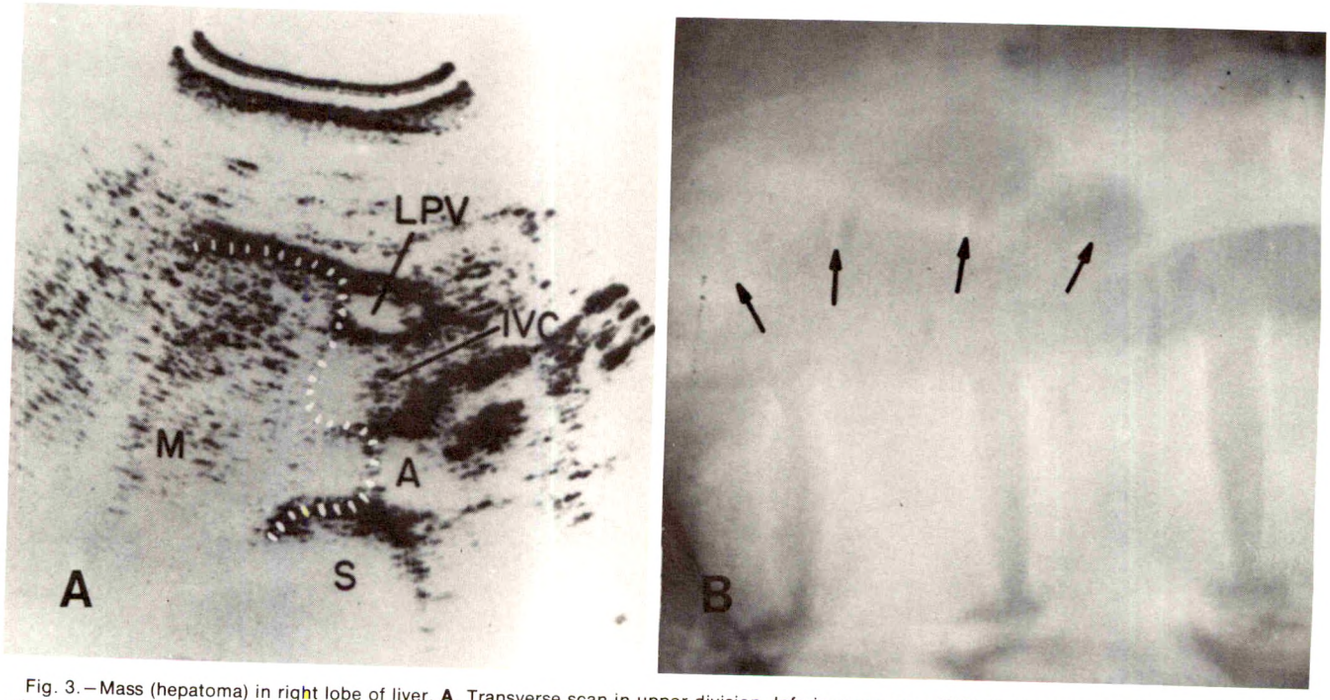
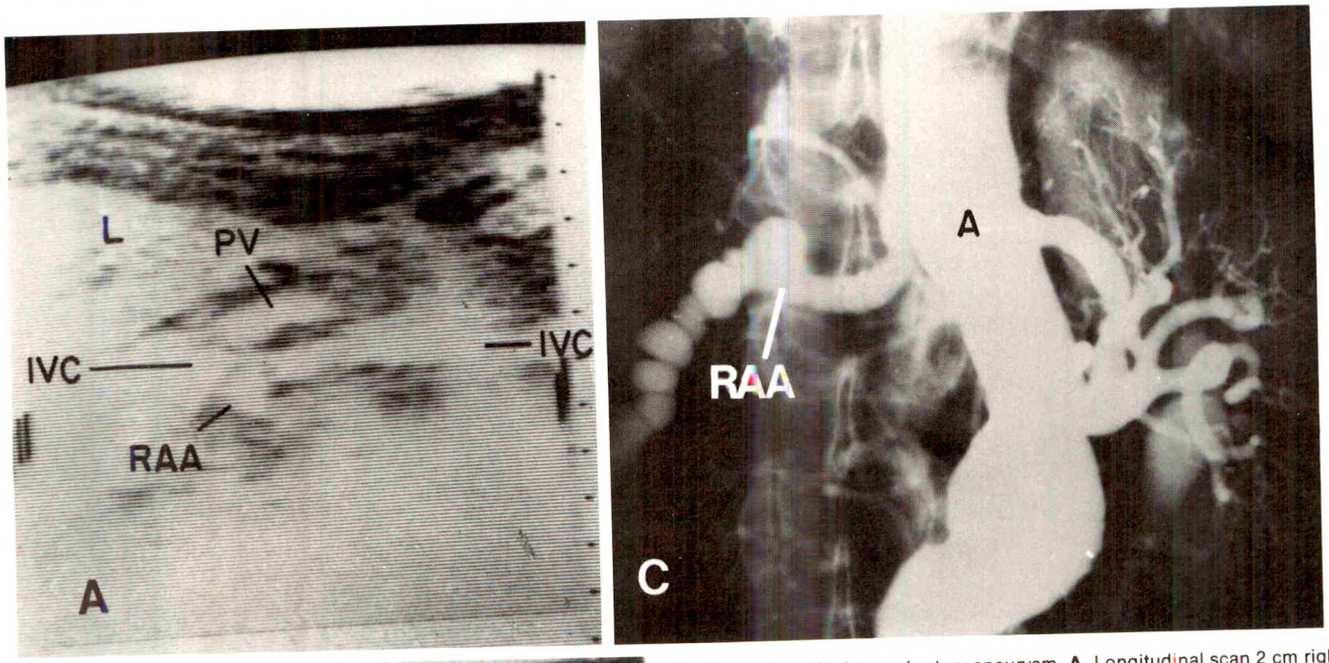


Fig. 3.—Mass (hepatoma) in right lobe of liver. **A**, Transverse scan in upper division. Inferior vena cava (IVC) displaced anteriorly and medially by echogenic liver mass (M). Echoes within vena cava consistent with tumor thrombus. A = aorta; S = spine; LPV = left portal vein. **B**, Anterior displacement (*arrows*) with filling defects (clot) within opacified vena cava.

that masses originating from specific organs usually elevate specific parts of the inferior vena cava. Therefore, a better determination of the origin of a mass can be made by: (1) defining the mass' ultrasound pattern and (2) determining the part of the inferior vena cava most anteriorly displaced by the expanding mass. This approach was used in the next 13 cases of vena caval elevation in 11 tumors and two blood vessel abnormalities, which included: one liver mass (polycystic liver disease), one right adrenal tumor (pheochromocytoma), one neurogenic tumor (neuroblastoma), one muscle mass (rhabdomyosarcoma), seven lymph node enlargements (four metastases and three lymphomas), one tortuous abdominal aorta, and one right renal artery aneurysm.

Discussion

Angiographically, the inferior vena cava was initially divided into two parts: (1) superior to and (2) inferior to the renal veins [11]. Later, it was proposed that the



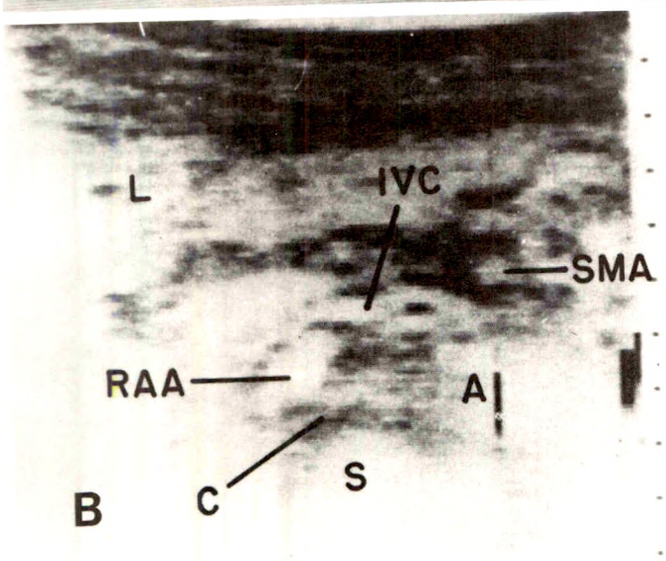


Fig. 4.—Right renal artery aneurysm. **A**, Longitudinal scan 2 cm right of midline. Inferior vena cava (IVC) elevated by renal artery aneurysm (RAA) immediately posterior to portal vein (PV). **B**, Transverse scan 3 cm below xiphoid with similar findings. L = liver; A = aorta; S = spine; SMA = superior mesenteric artery; C = right crux of diaphragm. **C**, Right renal artery aneurysm (RAA) secondary to fibromuscular dysplasia. Arteriosclerotic changes and aneurysmal dilatation of abdominal aorta (A).

inferior vena cava be divided into three parts: (1) the lower part below the entrance of the renal veins, (2) the middle portion between the renal veins and the hepatic veins, and (3) the upper part above the hepatic veins [5, 12].

Since the renal veins are not imaged on longitudinal scans of the inferior vena cava and are occasionally not seen even by transverse scanning, a new three-part division was proposed for ultrasound imaging of the inferior vena cava (fig. 1). The upper division, the hepatic part, courses through the liver extending cranially from the hemidiaphragm to the portal vein caudally. Both the liver and portal vein are easily identifiable structures. Since there is no bowel gas to obscure caval imaging, this part is almost always seen. The middle division, the pancreatic part, is limited to the region posterior to the pancreas extending from the portal vein cephalad to the caudalmost extent of the pancreatic head. The lower division is termed the small bowel part because segments of the duodenum and jejunum lie anteriorly. It extends from the caudalmost extent to the pancreatic head caudally to the bifurcation of the inferior vena cava into the common iliac veins. Since the bowel may be gas filled, this part is the most difficult to visualize of the three divisions.

Ideally, if a mass has a characteristic sonographic pattern, its site of origin can be determined. In general, this is not the case and additional information is needed. When a mass is detected, the midpoint of the mass can be defined in relation to the division of the cava most affected by this expansion. Knowing the anatomic relation of normal structures to specific parts of the inferior vena cava, a differential diagnostic approach to the anterior displacement of the cava can be made. This is a modification of the vector principle [13]. The following sections discuss the three ultrasound divisions and the organs or vessels most commonly associated with these parts. In addition, a fourth generalized category is used for diffuse processes that cannot be confined to a specific segment.

Upper or Hepatic Part

Expanding masses immediately posterior to this segment are most likely to be of right adrenal, neurogenic, or hepatic origin.

Our two right adrenal masses produced anterior displacement of the upper portion of the inferior vena cava

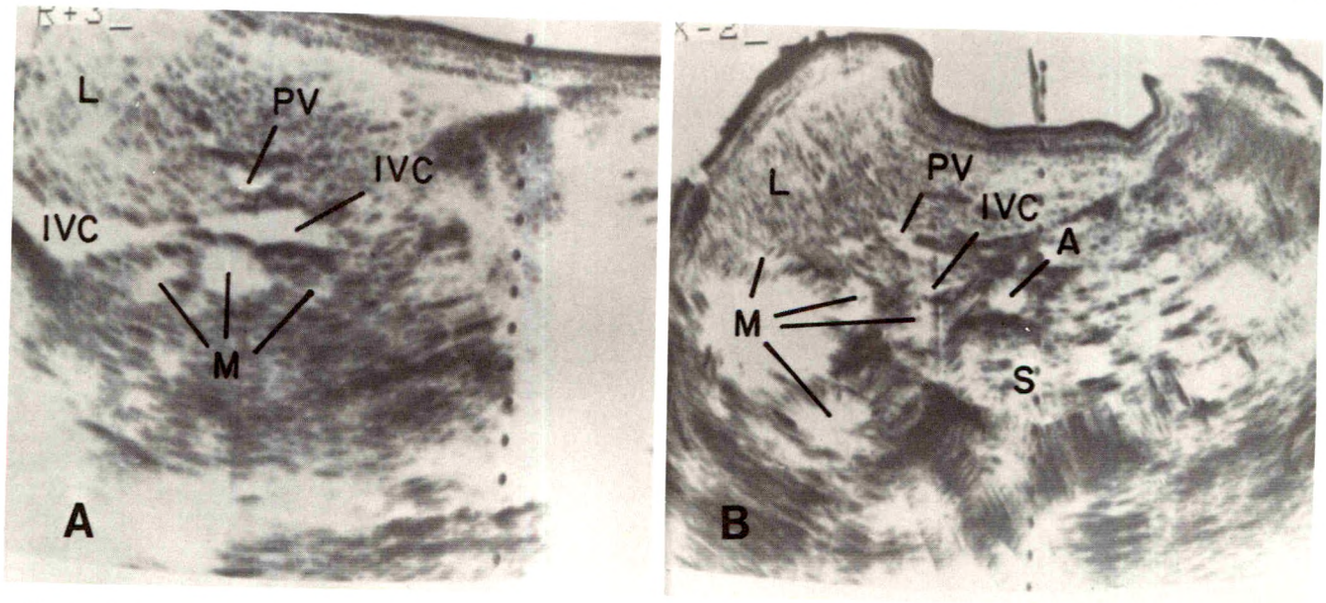


Fig. 5.—Right renal mass (polycystic kidney disease). **A**, Longitudinal scan 3 cm right of midline. Elevation of both upper and middle portions of inferior vena cava (IVC) by cystic renal masses (M). **B**, Transverse scan 2 cm below xiphoid demonstrates similar displacement. L = liver; PV = portal vein; A = aorta; S = spine.

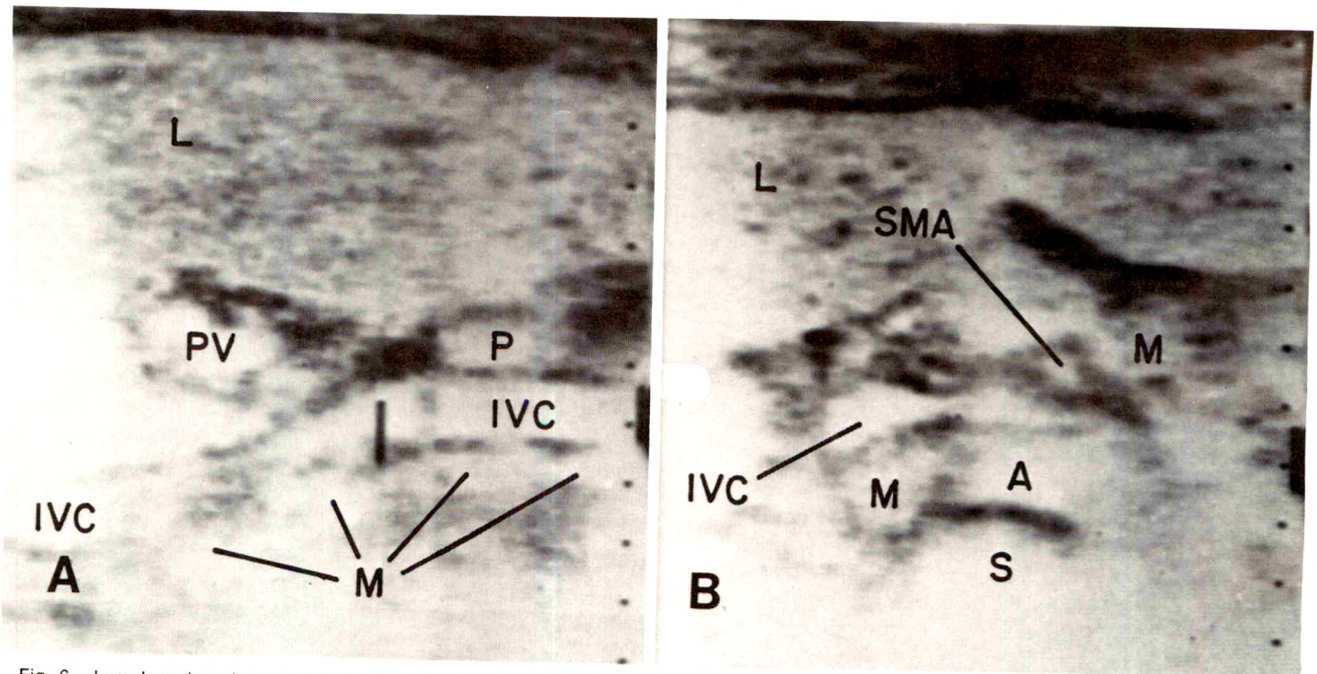


Fig. 6.—Lymph node enlargement in Hodgkin's disease. **A**, Longitudinal scan 2 cm right of midline. Solid masses (M) anteriorly displace upper, middle, and lower divisions of inferior vena cava (IVC). **B**, Transverse scan 4 cm below xiphoid. Liver (L) enlarged by lymphomatous infiltrate. PV = portal vein; P = pancreas; A = aorta; S = spine.

(fig. 2). From an anatomic standpoint, this is consistent with the position of the right adrenal gland. It is usually situated at the superior aspect of the renal fascia and immediately posterior to the inferior vena cava (especially the medial limb of the right adrenal gland). Therefore, expanding tumors will usually elevate this portion of the vena cava [5, 14, 15].

A neuroblastoma also elevated the hepatic part of the inferior vena cava [6, 16]. In the retroperitoneum, neural tumors most commonly originate from the adrenal medulla, or, less commonly, from the sympathetic nerve chain, particularly the celiac (semilunar) ganglion [4]. While any division of the vena cava may be affected, the upper part is most commonly elevated by enlarging neurogenic masses.

The two liver masses that displaced the upper part of

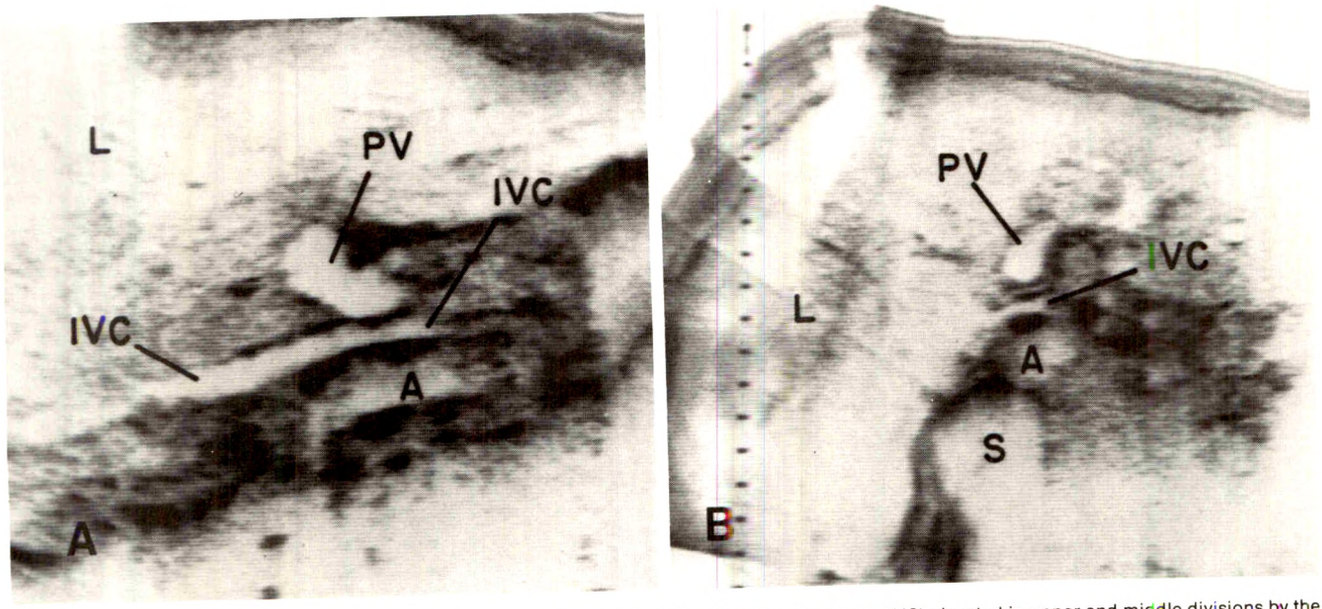


Fig. 7.—Tortuous abdominal aorta. **A**, Longitudinal scan 3 cm right of midline. Inferior vena cava (IVC) elevated in upper and middle divisions by the tortuous aorta. **B**, Transverse scan 4 cm below xiphoid. L = liver; PV = portal vein; A = aorta; IVC = inferior vena cava; S = spine.

the vena cava anteriorly were a generalized hepatic enlargement (polycystic liver disease) and a localized posterior right lobe mass (hepatoma). Normally, posterior impression of the inferior vena cava may be caused by the caudate lobe [4]. When overall hepatic enlargement occurs, the vena cava is generally compressed rather than displaced [5], except when one area of the liver is preferentially involved. When localized masses produce displacement of the inferior vena cava, it is usually in a posterior, lateral, or medial direction, since little of the liver parenchyma is posterior to the cava. However, masses of the posterior aspect of the caudate and right lobes may cause elevation of the inferior vena cava (fig. 3). A mass in the right lobe of the liver may also enlarge the liver and extend caudad to affect the cava distal to the portal vein, thus involving both the upper and middle divisions.

Middle or Pancreatic Part

Abnormalities of the right renal artery, right kidney, lumbar spine, and lymph nodes will most commonly elevate this segment.

A right renal artery aneurysm may anteriorly displace the inferior vena cava (fig. 4). Although there is variability in the relation of this artery to the portal vein, it generally arises at the interspace between the first and second lumbar vertebrae or caudad to the portal vein within the middle division [17]. The right renal artery is frequently noted by its impression of the posterior surface of the vena cava on contrast cavogram [4–6, 8, 18, 19] and is visualized in both transverse and longitudinal planes on sonocavogram [20]. On arteriography, a normal renal artery does not exceed 1 cm in diameter and shows gradual tapering from its origin [21].

Although the position of the right kidney is also variable in relation to the portal vein, the majority of the kidney is usually situated in the middle division, but may affect the upper and occasionally even the lower segment. Since the right kidney is predominantly lateral to the inferior vena cava, only masses that extend medially will impinge upon and elevate the vena cava [4, 5]. The one right renal mass, polycystic disease of the kidney, caused anterior displacement of the inferior vena cava primarily in the middle but also in the upper division (fig. 5).

Anterior changes in the lumbar vertebrae or interposed disc spaces may elevate the inferior vena cava, although no cases were detected in this series. The most common causes are anterior osteophytes and exaggeration of the normal lordotic curve [4, 5, 19].

Lower or Small Bowel Part

There are usually no major organs or blood vessels posterior to this segment, and, in general, only abnormalities in the lumbar spine and lymph nodes may elevate this portion of the vena cava.

Generalized

Lymph node enlargement constitutes most of the abnormalities in this group. Retroperitoneal tumors, tortuous abdominal aortas, and rarer causes are also discussed below.

Lymph node enlargement is the most common cause of anterior displacement of the inferior vena cava. Of our 11 cases, seven were metastatic disease and four were lymphoma, with little difference between the two, except that lymphoma tended to be more widespread than the metastatic disease [4]. Although any of the divisions can be elevated by enlarged lymph nodes, the middle and lower segments are more likely to be affected [18] (fig.

6). Lymphadenopathy as a cause of anterior displacement of the inferior vena cava has been extensively documented on both contrast cavogram [4, 6–8, 18, 22–24] and sonocavogram [9, 25].

The literature states that 20% of tortuous abdominal aortas curve convexly to the right impinging on the left side of the cava [26, 27]. In our two cases of tortuous abdominal aortas, the aorta extended posterior to the inferior vena cava causing elevation of the upper and cephalad parts of the middle divisions (fig. 7). The left renal vein originates from the inferior vena cava and courses anterior to the aorta. It is postulated that when a tortuous abdominal aorta curves to the right in this region, it should extend posterior to the vena cava.

A rhabdomyosarcoma of the right psoas and crux was found to elevate the inferior vena cava. Other causes not found in this series are primary retroperitoneal tumors, especially sarcoma [4, 5], retroperitoneal fibrosis [28], and hematoma [8]. Although not reported, retroperitoneal abscess may similarly elevate the vena cava. To date, no reported cases of anterior displacement of the inferior vena cava by pelvic lipomatosis or retrocaval ureter have been found.

Anterior elevation of the inferior vena cava is not a common occurrence, although at times an abnormality in this structure is the only pathologic indication in the abdomen or retroperitoneum. Ultrasound division of the inferior vena cava combined with the vector principle has proven useful in differentiating masses.

REFERENCES

1. Dos Santos R: Phlebographie d'une veine cave inférieure suture. *J Urol Med Chir* 39:586–593, 1935
2. O'Loughlin BJ: Roentgen visualization of the inferior vena cava. *AJR* 58:617–619, 1947
3. Fariñas PL: Abdominal venography. *AJR* 58:599–602, 1947
4. Ferris EJ, Hipona FA, Kahn PC, Phillips E, Shapiro JH: *Venography of the Inferior Vena Cava and its Branches*. Baltimore, Williams & Wilkins, 1969
5. Harris RD: The etiology of inferior vena cava obstruction and compression. *CRC Crit Rev Diagn Imaging* 8:57–86, 1976
6. Helander CG, Lindbom Å: Roentgen examination of the inferior vena cava in retroperitoneal expanding processes. *Acta Radiol [Diagn]* (Stockh) 45:289–296, 1956
7. Bolooki H, Margulies M, Yermakov M, Gliedman M: Portal hypertension with anomalies of inferior vena cava and hepatic veins. *Arch Surg* 94:267–270, 1967
8. Taylor KJW: Ultrasonic investigation of inferior vena caval obstruction. *Br J Radiol* 48:1024–1026, 1975
9. Gosink BB: The inferior vena cava: mass effects. *AJR* 130: 533–536, 1978
10. Filly RA, Goldberg BB: Normal vessels, in *Abdominal Gray Scale Ultrasonography*, edited by Goldberg BB, New York, Wiley, 1977, pp 26–31
11. Helander CG, Lindbom Å: Venography of the inferior vena cava. *Acta Radiol [Diagn]* (Stockh) 52:257–268, 1959
12. Missal ME, Robinson JA, Tatum RW: Inferior vena cava obstruction—clinical manifestations, diagnostic methods, and related problems. *Ann Intern Med* 62:133–161, 1965
13. Whalen JP, Evans JA, Shanser J: Vector principle in the differential diagnosis of abdominal masses: the left upper quadrant. *AJR* 113:104–118, 1971
14. Sample WF: Adrenal ultrasonography. *Radiology* 127:461–466, 1978
15. Yeh HC, Mitty HA, Rose J, Wolf BS, Gabrilove JL: Ultrasonography of adrenal masses: unusual manifestations. *Radiology* 127:475–483, 1978
16. Tucker AS: The roentgen diagnosis of abdominal masses in children—intravenous urography vs. inferior venacavagram. *AJR* 95:76–90, 1965
17. Taniguchi T: Beitrag zur topographic der grossen Äste der Bauchaorta. *Folia Anat Jpn* 9:201–214, 1931
18. Holtz S, Powers WE: Inferior vena cavagrams. *Radiology* 78:583–590, 1962
19. Lien HH, Kolbenstvedt A: Nonmalignant venography abnormalities of the inferior vena cava. *Radiology* 122:105–110, 1977
20. Leopold GR: Gray scale ultrasonic angiography of the upper abdomen. *Radiology* 117:665–671, 1975
21. Olsson O: Anatomic and physiologic consideration, in *Angiography*, edited by Abrams HL, Boston, Little, Brown, 1971, pp 779–782
22. Brower AC, Seale DL: A critical appraisal of radiographic studies employed in staging of patients with Hodgkin's disease. *Radiology* 110:97–101, 1974
23. Lee BJ, Nelson JH, Schwartz G: Evaluation of lymphangiography, inferior venacavography, and intravenous pyelography in the clinical staging and management of Hodgkin's disease and lymphosarcoma. *N Engl J Med* 271:327–337, 1964
24. Mahaffy RG: A comparison of the diagnostic accuracy of lymphography, cavography, and pelvic venography. *Br J Radiol* 37:422–429, 1964
25. Albertson KW, Leopold GR: Liver, in *Abdominal Gray Scale Ultrasonography*, edited by Goldberg BG, New York, Wiley 1977, pp 131–132
26. Crummy AB, Hipona FA: The aortic impression in inferior vena cavography. *Clin Radiol* 15:130–131, 1964
27. Gabriele OF, Bell D, Martineau R: Pitfalls in inferior vena cavography. *AJR* 100:417–423, 1967
28. Chew CK, Jarzylo SV, Valberg LS: Idiopathic retroperitoneal fibrosis with protein-losing enteropathy and duodenal obstruction successfully treated with corticosteroids. *Can Med Assoc J* 95:1183–1188, 1966

Ultrasonic Assessment of Renal Transitional Cell Carcinoma: Preliminary Report

PETER H. ARGER,[1] CHARLES B. MULHERN,[1] HOWARD M. POLLACK,[1] MARC P. BANNER,[1] AND ALAN J. WEIN[2]

The value of ultrasound in determining the etiology of nonopaque filling defects seen in the renal pelvis at intravenous urography is under study. The ultrasound findings in three patients with proven transitional cell carcinoma of the kidney were similar and consisted of separation of the central renal echo complex by a region of low-intensity echoes. This pattern is distinct from characteristically echogenic nonopaque renal calculi and anechoic hydronephrosis. Renal collecting system blood clots may have an echo pattern similar to collecting system tumors, but can usually be distinguished by their mobility and transitory nature. Further investigation into the specificity and sensitivity of the ultrasonic diagnosis of renal collecting system masses is underway.

Nonopaque filling defects in the renal pelvocalyceal system present a diagnostic problem. A noninvasive diagnostic method which could help distinguish urothelial transitional cell or squamous cell tumors from clot or nonopaque stones would be of significant value.

To assess the value of ultrasound in this clinical situation, we scan all patients with nonopaque filling defects in the renal pelvocalyceal system. This report details our initial experience with three patients with proven transitional cell carcinoma of the renal pelvis. The ultrasonic findings differ from our experience with nine proven cases of nonopaque stones [1]. Comparison with two cases of pelvocalyceal system blood clots was also done.

Materials and Methods

All ultrasonic examinations were done on a Unirad Sonograf 3 commercially available gray scale machine. Both 3.5 MHz and 5 MHz 13 mm- medium-focused transducers were used. Images were recorded on x-ray film. Single, linear, noncompounded scans and, where necessary, compounded scans of the kidney were obtained in both the longitudinal and transverse planes with the patients prone. In right-side lesions, the liver was scanned with the patient supine.

Case Reports

Case 1

A. L., a 73-year-old white man, was found to have microscopic hematuria on a routine physical examination. Intravenous urography showed a nonopaque filling defect in the left pelvocalyceal system. Renal ultrasound evaluation showed separation of the central dense echo complex with low-intensity echoes between (fig. 1A). Intravenous urography suggested the presence of a papillary mucosal lesion which was confirmed by retrograde pyelography (fig. 1B).

Pathologic examination of the resected left kidney and ureter revealed transitional cell carcinoma of the renal pelvis with superficial invasion. Ultrasound water-bath scanning of the kidney specimen showed separation of the central echo complex with low-intensity echoes between the separation (fig. 1C). The intensity of these echoes was similar to that of the corticomedullary portion of the kidney and did not represent electronic noise. No acoustic enhancement distal to the separated central echo complex was seen.

Case 2

H. R., a 65-year-old white woman had painless gross hematuria for 3 weeks. She had had numerous episodes of cystitis in the previous 5 years, but no hematuria. Intravenous urography revealed a right renal mass of uncertain origin which involved the renal pelvis. Retrograde pyeloureterography showed an irregular papillary mass strongly suggestive of a urothelial neoplasm filling the upper part of the right pelvocalyceal systems. The upper calyx did not fill with contrast material (fig. 2A).

Renal ultrasound examination showed separation of the dense central echo complex with low-intensity echoes between (figs. 2B and 2C). Pathologic examination (gross and microscopic) of the resected right kidney and ureter demonstrated transitional cell carcinoma which was largely confined to the renal pelvis, although in one small area there was a suggestion of superficial parenchymal invasion.

Case 3

P. H., a 58-year-old asymptomatic white man, was found to have a filling defect in the right renal pelvis on routine follow-up intravenous urography 2 years after cystectomy for transitional cell carcinoma of the bladder. Retrograde injection of the ileal loop confirmed the filling defect (fig. 3A). Repeat intravenous urography 2 months later showed a persistent defect with mild hydronephrosis. Urine cytology was class V × 2. Surgery has been deferred.

Renal ultrasound examination showed separation of the central echo complex in the region of the renal pelvis with low-intensity echoes between. The echo intensity was similar to that of the corticomedullary area of the kidney (fig. 3B).

Discussion

Tumors originating from the renal pelvocalyceal mucosa constitute about 7% of all malignant renal neoplasms [2]. The vast majority of these lesions are transitional cell, although squamous cell carcinoma and, rarely, adenocarcinoma may also occur. Most collecting system tumors are malignant with a poor prognosis. The outlook is determined by both tumor stage and grade.

The presence of a urothelial renal tumor is usually first

Received May 2, 1978; accepted after revision November 30, 1978.

[1] Department of Radiology, Hospital of the University of Pennsylvania, 3400 Spruce Street, Philadelphia, Pennsylvania 19104. Address reprint requests to P. H. Arger.

[2] Department of Urology, Hospital of the University of Pennsylvania, Philadelphia, Pennsylvania 19104.

© 1979 American Roentgen Ray Society

0361–803X/79/1323–0407 $0.00

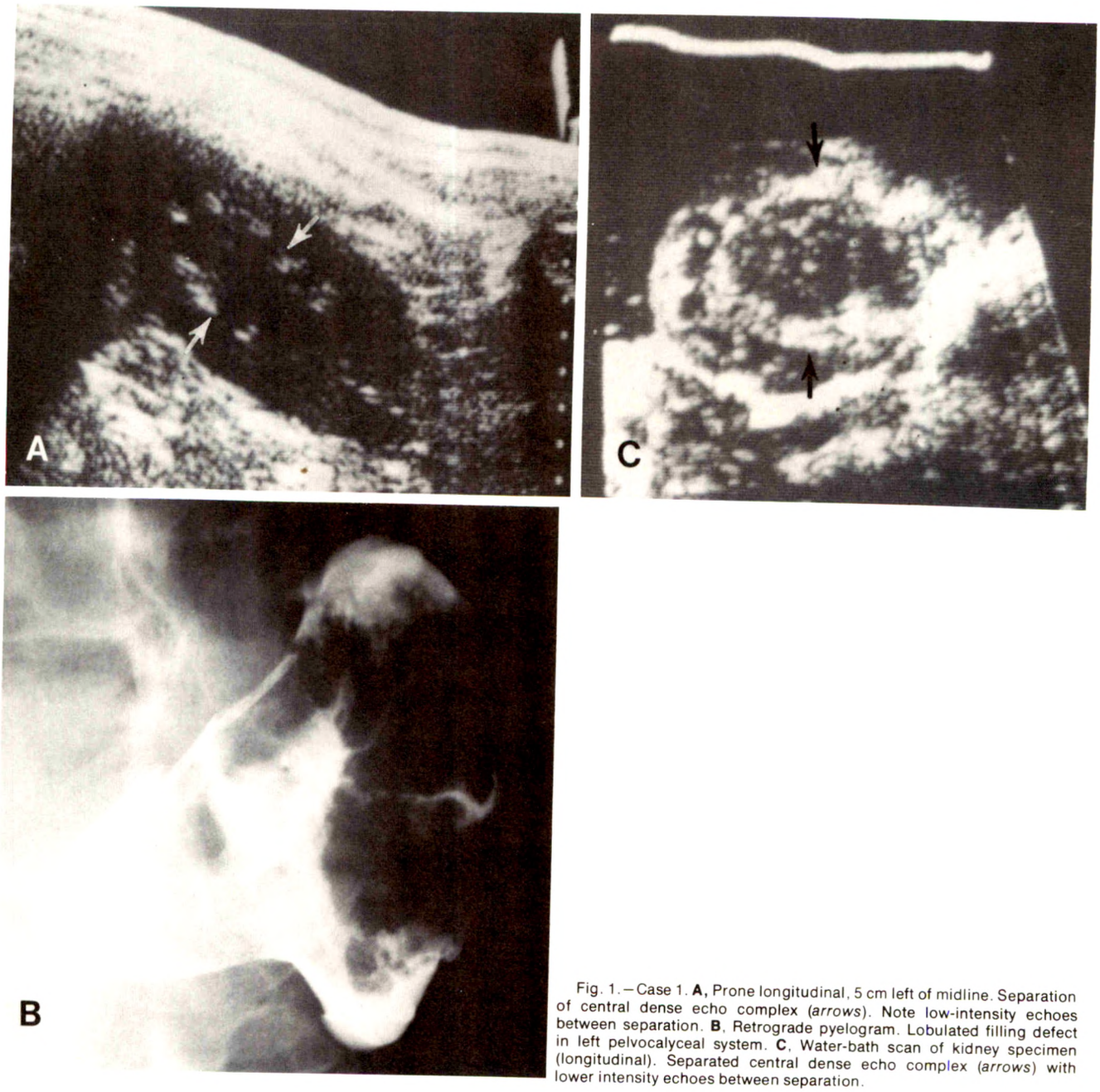


Fig. 1.—Case 1. **A**, Prone longitudinal, 5 cm left of midline. Separation of central dense echo complex (*arrows*). Note low-intensity echoes between separation. **B**, Retrograde pyelogram. Lobulated filling defect in left pelvocalyceal system. **C**, Water-bath scan of kidney specimen (longitudinal). Separated central dense echo complex (*arrows*) with lower intensity echoes between separation.

suspected because of a pelvocalyceal system filling defect seen on intravenous urography. Unfortunately, appearances of such defects are often nonspecific. Blood clots, nonopaque stones, and invading renal cell lesions, as well as a number of other less common entities such as fibromas, hemangiomas, or leiomyomas, may have a similar appearance.

Unlike calculi and blood clots, urothelial lesions tend to have irregular outlines reflecting their papillary or polypoid nature. While such an appearance may suggest the presence of a urothelial tumor, more substantial proof is usually required before surgery is done.

Inflammatory reactive changes are not easily distinguished from neoplasia by urinary cytology. Reported cytology sensitivity is 60%–90% [3].

Since collecting system tumors are usually very hypovascular, angiography tends to be of limited value [4], although renal phlebography may show vascular encasement [5]. Endoscopic brush biopsy has been used, but is somewhat cumbersome and not well suited for lesions in the middle and lower calyces [6]. Ultrasonic investigation of urothelial tumors was undertaken in the hope that it would add another significant dimension to the preoperative assessment of these lesions.

We have examined five patients with suspected transitional cell carcinomas of the renal pelvis, three of whom

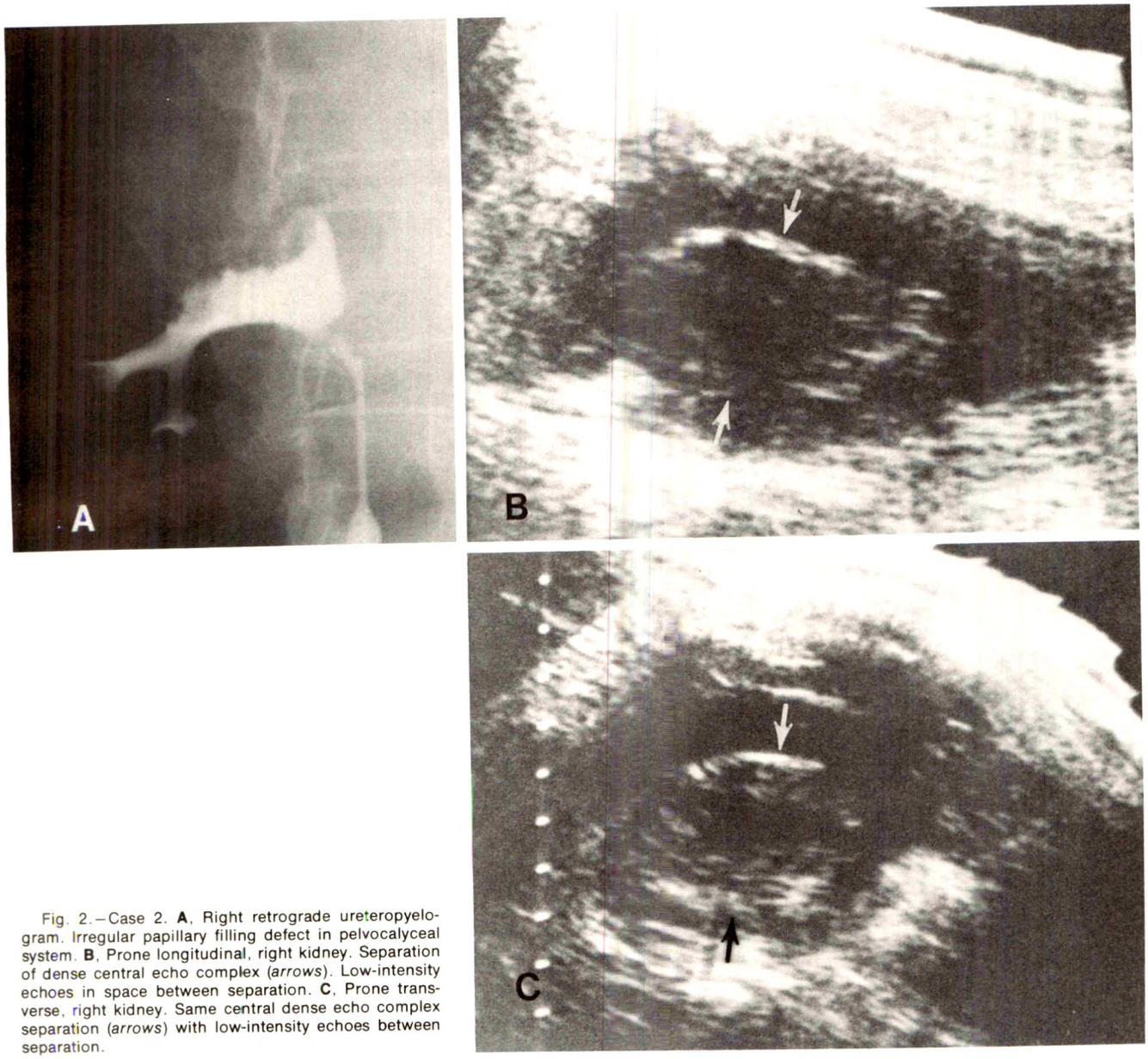


Fig. 2.—Case 2. **A**, Right retrograde ureteropyelogram. Irregular papillary filling defect in pelvocalyceal system. **B**, Prone longitudinal, right kidney. Separation of dense central echo complex (*arrows*). Low-intensity echoes in space between separation. **C**, Prone transverse, right kidney. Same central dense echo complex separation (*arrows*) with low-intensity echoes between separation.

have had subsequent confirmation of the diagnosis. Our experience with these three patients indicates that the ultrasonic characteristics of the lesion were similar in each case. The normally compact dense echoes in the renal hilus (central echo complex) were separated and the space between contained a low-intensity echo. This appearance is somewhat similar to that seen in hydronephrosis, except that the central low-intensity echoes indicate the presence of echogenic material within the pelvocalyceal system and acoustic enhancement seen with hydronephrosis is not present. These findings also differ markedly from those seen in nonopaque renal stones where dense echoes with acoustic shadowing are encountered [1].

This pattern is also different from the ultrasonic pattern of hypernephroma. Both the densely and the poorly echo-producing hypernephromas can be expected to have their primary manifestations in the renal substance rather than the collecting systems, while the situation is reversed with urothelial tumors. Though extensive growth of either hypernephromas or of transitional cell tumors could mimic each other, this would be unusual.

The ultrasonic appearance of intrapelvic blood clots is not unlike that of pelvic tumors, although clots may be more strongly echogenic. The mobility of blood clots as the patient's position is changed, as well as their transitory nature, will usually differentiate them from pelvic tumors (fig. 4). The lack of acoustic shadowing helps distinguish small clots from radiolucent stones (fig. 5).

The smallest lesion imaged was 1.0–1.5 cm (fig. 3).

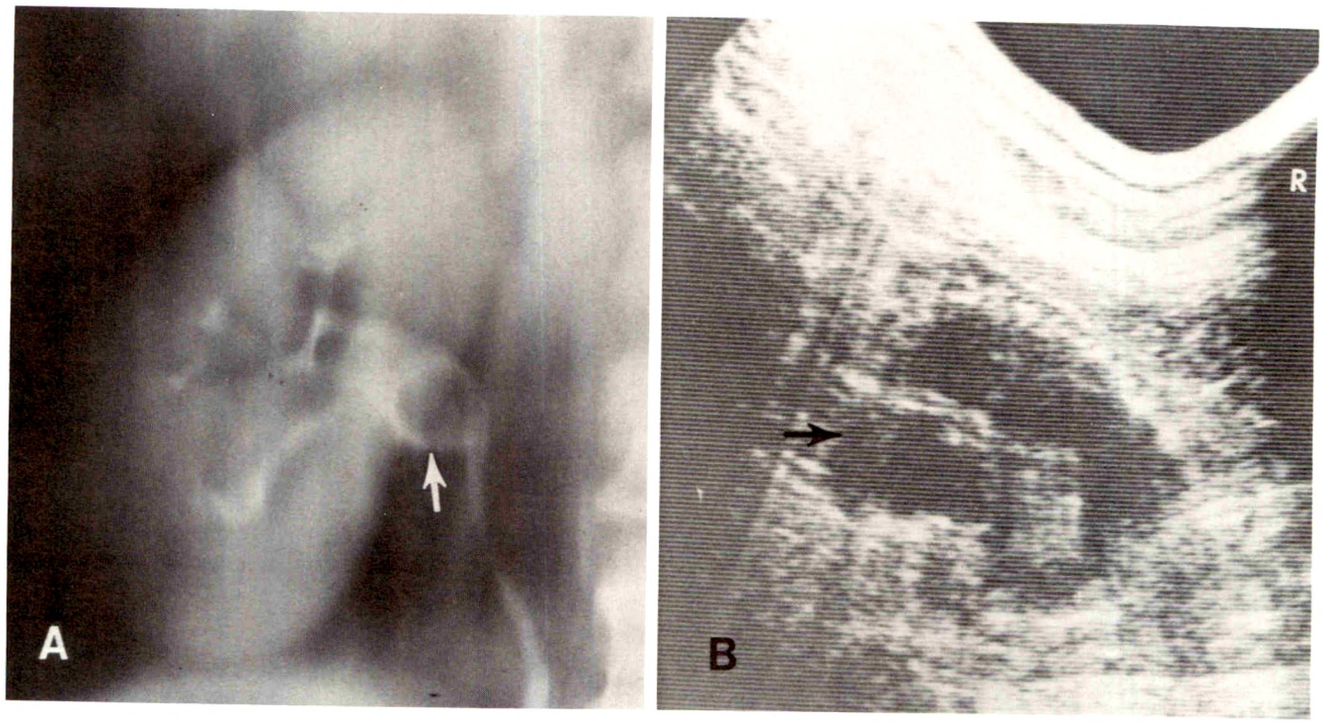


Fig. 3.—Case 3. **A**, Intravenous urogram. Filling defect (*arrow*) in medial pelvis. **B**, Prone transverse, 7 cm above iliac crest. Separation of medial central echo complex due to hydronephrosis. In medial aspect of hydronephrotic pelvis, there are persistent low-intensity echoes (*arrow*).

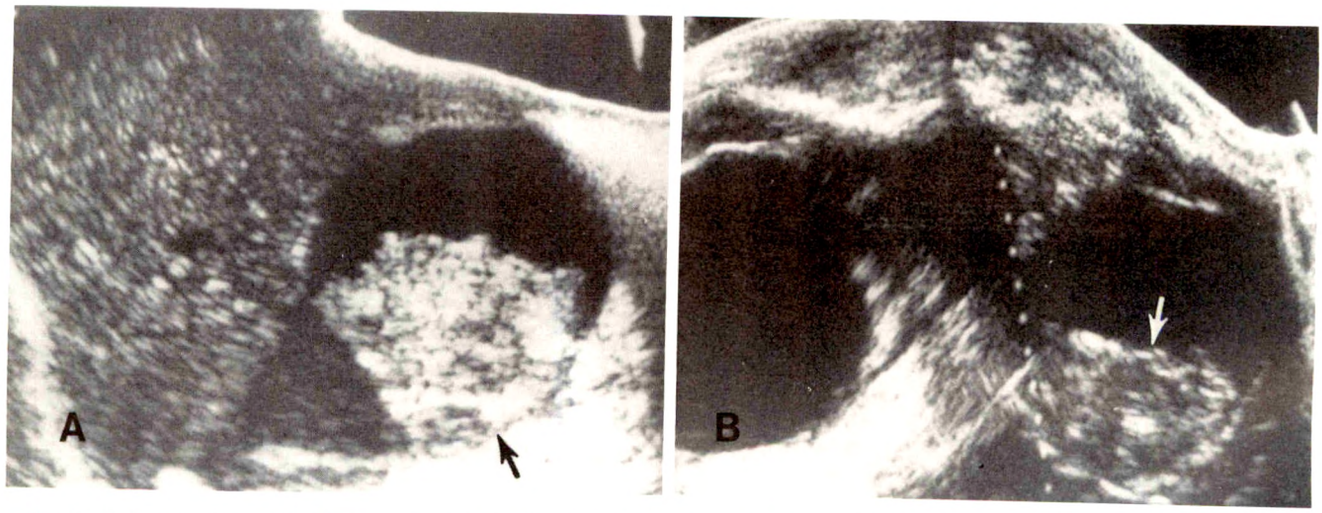


Fig. 4.—**A**, Supine longitudinal. Densely echogenic blood clots in posterior aspect of markedly hydronephrotic right renal pelvis (*arrow*). **B**, Prone transverse. Marked bilateral hydronephrosis. Right intrapelvic echogenic blood clots have moved anteriorly in dilated right renal pelvis (*arrow*).

Noncalculous filling defects which do not separate the central echo complex are not likely to be imaged because of the lack of acoustic shadowing (fig. 5B).

These preliminary results suggest that ultrasound can aid in determining the etiology of renal pelvis nonopaque filling defects. The pattern observed for renal transitional cell carcinoma is distinctly different from that of nonopaque calculi. Renal pelvocalyceal system blood clots pose a problem because their sonographic appearance may mimic transitional cell tumors. However, their mobility and transitory nature aid in distinguishing them from tumors. Further investigation is needed and is

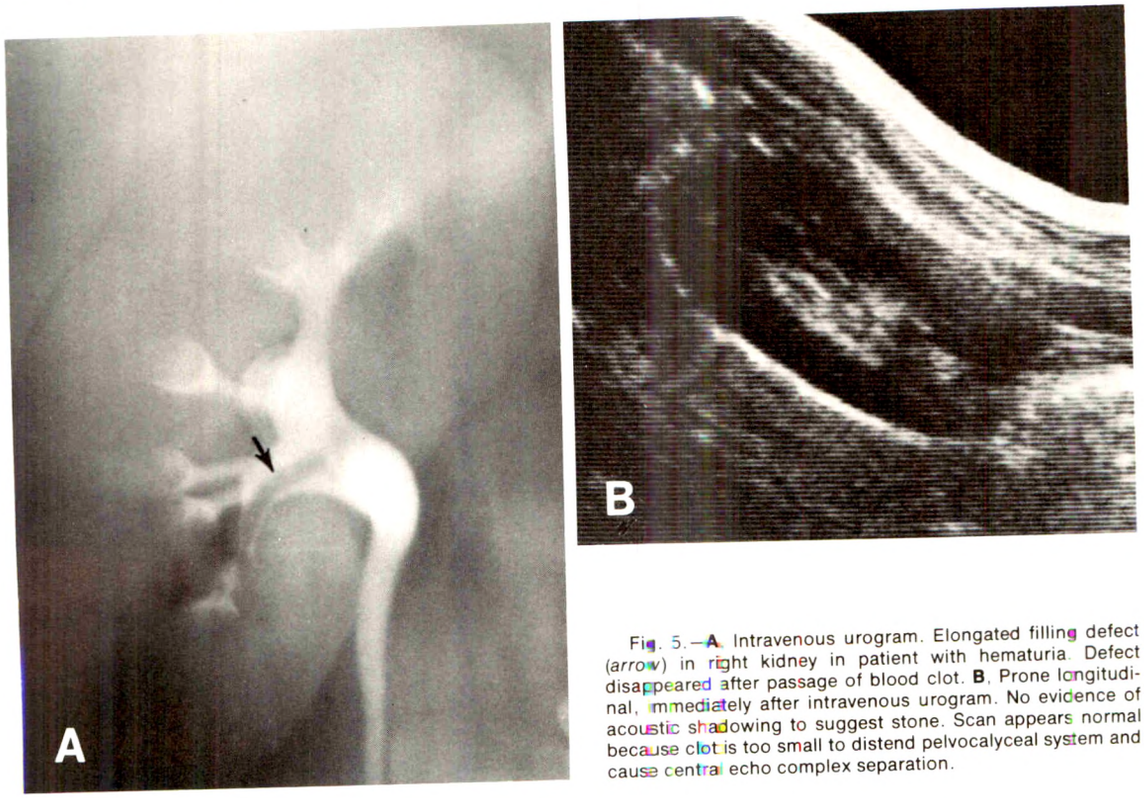


Fig. 5.—**A**, Intravenous urogram. Elongated filling defect (*arrow*) in right kidney in patient with hematuria. Defect disappeared after passage of blood clot. **B**, Prone longitudinal, immediately after intravenous urogram. No evidence of acoustic shadowing to suggest stone. Scan appears normal because clot is too small to distend pelvocalyceal system and cause central echo complex separation.

proceeding to determine the specificity and sensivitity of ultrasound in nonopaque renal pelvocalyceal system filling defects.

ACKNOWLEDGMENTS

We thank Dr. Vijay Gohel, Veterans Administration Hospital, Philadelphia, Pennsylvania, for the use of the case illustrated in figure 4.

REFERENCES

1. Pollack HM, Arger PH, Goldberg BB, Mulholland SG: Ultrasonic detection of non-opaque renal calculi. *Radiology* 127: 223–237, 1978
2. Deming CL, Harvard BM: Tumors of the kidney, chap 24, in *Urology*, vol 2, edited by Campbell MF, Philadelphia, Saunders, 1970, pp 930–936
3. Tweeddale DN: *Urinary Cytology*. Boston, Little, Brown, 1977
4. Goldman SM, Meng C, White RI, Naraval RC, Siegelman SS, Diamond AB, Kaufman SL, Harrington DP: Transitional cell tumors of the kidney: how accurate is the angiogram? *AJR* 129:99–105, 1977
5. Smith JC, Rösch J, Athanasoulis CA, Baum S, Waltman AC, Goldman M: Renal venography in the evaluation of poorly vascularized neoplasms of the kidney. *AJR* 123:552–556, 1975
6. Gill WB, Lu CT, Thomsen S: Retrograde brushing: a new technique for obtaining histologic and cytologic material from ureteral, renal pelvic and renal calyceal lesions. *J Urol* 109:573–578, 1973

Medial Deviation of the Pelvic Ureters after Abdominoperineal Resection of the Rectum

GEORGE YOUNG,[1] MARVIN E. GOLDBERG,[1] AND FREDERIC D. NEMER[2]

Pre- and postoperative urograms of 47 patients undergoing abdominoperineal resection were reviewed for ureteral deviation and obstruction. Postoperative medial deviation occurred in 11 patients (23.4%). Both ureters were involved in six of these patients. Ureteral deviation was identified as early as 3 days after surgery. Obstruction of the ureters occurred in four patients and was due to tumor in three of these.

Urinary tract complications after abdominoperineal resection of the rectum have been well documented [1–6]. The urographic finding of medial deviation of the ureters following such resection of the rectum is generally well known. However, the frequency of occurrence has not been documented [3, 5] and is the subject of this investigation.

Materials and Methods

We reviewed records of 54 consecutive patients who underwent abdominoperineal resections at the University of Minnesota Hospitals during a 7½ year period ending in May 1977. We identified 47 cases in which pre- and postoperative excretory urograms were obtained. The urograms were reviewed for development of postoperative deviation of the ureters or obstruction (fig. 1). The presence of deviation of the ureters was determined independently by two observers (M. E. G., G. Y.). Initial attempts to measure the displacement of the ureters from a nearby bony landmark were abandoned because radiographs were not always available at the same phase of ureteral peristalsis from both pre- and postoperative studies. As a result, a judgment as to ureteral deviation was made by viewing films from each study. The elapsed time from date of surgery to date of the urogram varied from 3 days to 3 years (table 1).

Results

During the period studied, 54 patients underwent abdominoperineal resection. Of these, 44 had resection for carcinoma of the rectosigmoid and 10 for ulcerative colitis. In the group undergoing resection for carcinoma, 38 patients had urograms. Medial deviation of the ureters was found in 10 patients in this group. In the group with ulcerative colitis, urograms were reviewed in nine cases. Medial deviation of the ureters occurred once (11.1%). A total of 11 of 47 (23.4%) patients had medial deviation of the pelvic ureters postoperatively (table 1). Deviation of the ureters was found to be bilateral in six of 11 instances.

Four patients had ureteral obstruction. In two of these (E. C. and S. S.), the obstructive findings were associated with tumor recurrence. One patient (V. K.) had ureteral obstruction on a study obtained 3 days after surgery (obstruction thought due to postoperative edema, since 2 years later this patient was free of tumor recurrence). Another (E. P.) had obstruction at 13 days due to persistent tumor.

Discussion

Alteration in the normal position, size, and course of the ureters is not uncommon after pelvic surgical procedures. When major colon and rectal resections are performed transabdominally, care is taken to identify both ureters. During the mobilization of the rectosigmoid for a low anterior resection or proctectomy, the ureters are swept laterally by blunt sweeping movements in hand dissection. In the resection for carcinoma of the rectum, an extensive lymph node dissection is performed unlike ulcerative colitis where lymph node dissection is not done. While a lymph node dissection may contribute to the later deviation of the ureters, the difference in frequency of medial deviation between the carcinoma group and the colitis group (26.3% vs. 11.1%) is not statistically significant. In the abdominoperineal resection, the anterior abdominal aspect is completed and the proctectomy is performed either synchronously or as a second stage when the abdomen has been closed and the patient turned over in the prone jackknife position. In either event, after anterior resection of the rectum or abdominoperineal resection, the residual peritoneum that formed the floor of the pelvis is reconstructed [7]. It is believed that during the reconstruction of the pelvic floor by suturing the peritoneum and drawing the lateral margins medially, the major deviation of the ureter occurs. Other factors contributing to medial deviation include metastatic spread of neoplasm to the retroperitoneal lymph nodes or local tumor extension [3].

In previous studies [3, 5, 6], obstruction of the ureters was usually due to tumor recurrence. Our series confirms that ureteral obstruction is suggestive but not conclusive evidence of tumor recurrence. While the appearance of medial displacement of the pelvic ureters ranged from 3 days to 3 years, no attempt was made to obtain serial studies of the urinary tract.

As mentioned by Friedenberg et. al. [3], the following additional conditions should be considered in the differential diagnosis of medial ureteral deviation: idiopathic

Received April 18, 1978; accepted after revision November 30, 1978.

[1] Department of Radiology, University of Minnesota Hospitals, Box 292 Mayo Memorial Health Science Center, 420 Delaware Street S.E., Minneapolis, Minnesota 55455. Address reprint requests to M. E. Goldberg.

[2] Department of Surgery, Division of Colon and Rectal Surgery, University of Minnesota Hospitals, Minneapolis, Minnesota 55455.

© 1979 American Roentgen Ray Society

0361-803X/79/1323-0413 $0.00

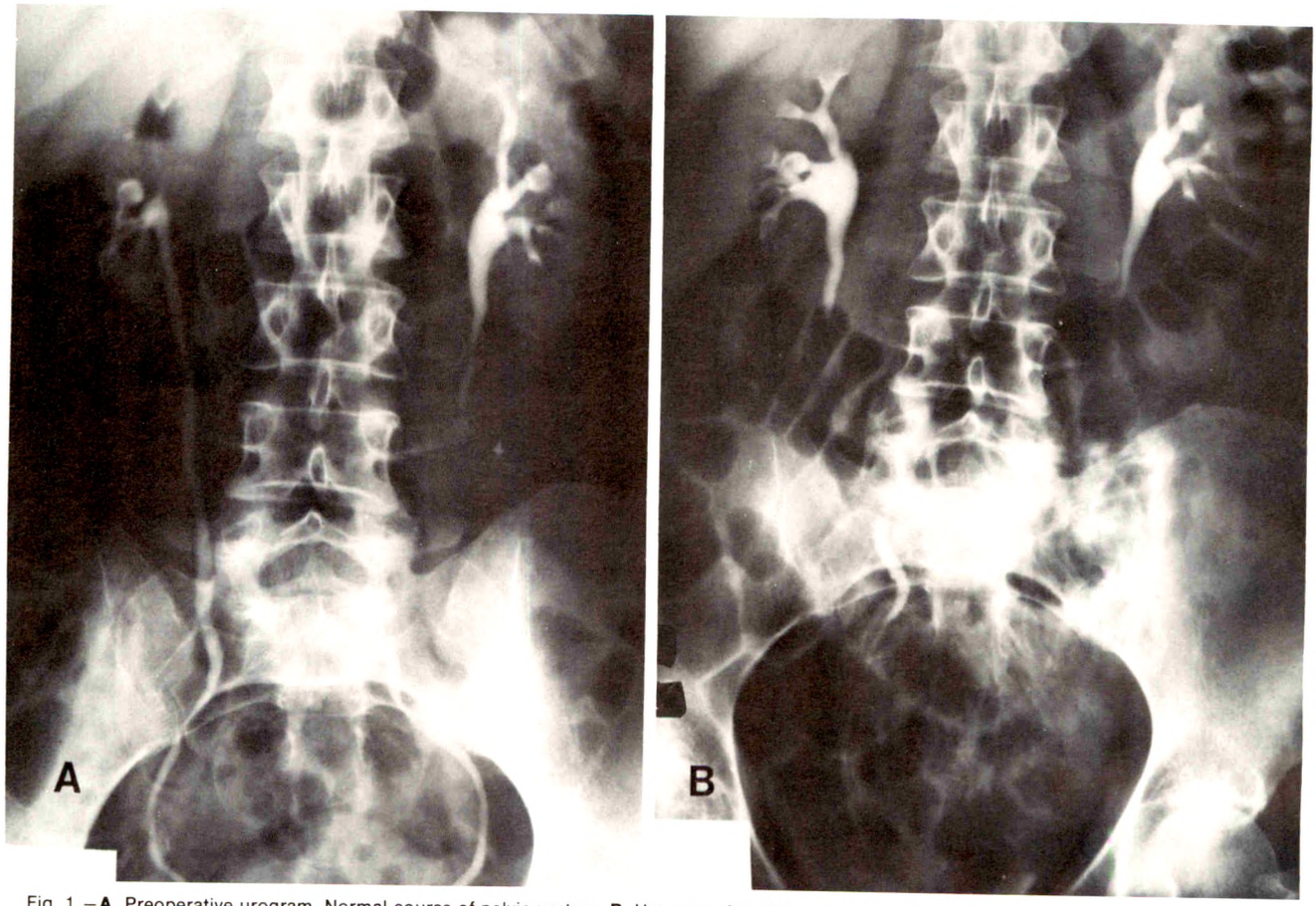


Fig. 1.—**A**, Preoperative urogram. Normal course of pelvic ureters. **B**, Urogram after abdominoperineal resection of rectal carcinoma. Both ureters retracted medially and left ureter is not filled to same extent as right.

TABLE 1

Abdominoperineal Resection and Ureteral Deviation: Clinical and Radiographic Data

Patient	Age and Sex	Medial Deviation or Ureter	Time of Urogram After Surgery (months)	Obstructed
V. K. . .	77, F	Bilateral	0.1	+
E. P. . .	72, M	Right	0.4	+
F. K. . .	64, M	Bilateral	6	–
W. L. . .	70, M	Bilateral	6	–
L. W. . .	66, M	Right	12	–
E. C. . .	70, M	Bilateral	18	+
D. B. . .	66, F	Right	18	–
S. S. . .	72, M	Bilateral	24	+
F. W. . .	58, F	Bilateral	36	–
J. H. . .	38, M	Right	2	–
B. B. . .	62, F	Right	14	–

Note.—All patients underwent resection for carcinoma of the rectosigmoid except J. H. who had ulcerative colitis and B. B. who had cloacal carcinoma. Tumors recurred only in E. C., S. S., and E. P. who had persistent tumor.

retroperitoneal fibrosis; retroperitoneal tumor such as lymphoma, sarcoma, or metastasis from the bladder, prostate, or ureter; inflammatory lymphadenopathy; or aneurysmal dilatation of the iliac arteries. Distal obstructive uropathy may also produce medial deviation as a result of tortuosity and dilatation of the ureters.

ACKNOWLEDGMENT

We thank Dr. Lawrence Williams for statistical evaluation and Susan Marthaler for assistance in manuscript preparation.

REFERENCES

1. Andersson A, Bergdahl L: Urologic complications following abdominoperineal resections of the rectum. *Arch Surg* 111: 969–971, 1976
2. Baumrucker GO, Shaw JW: Urologic complications following abdominoperineal resections of the rectum. *Arch Surg* 67:502–513, 1953
3. Friedenberg RM, Ney C, Lopez FA, Stachenfeld RA: Clinical significance of deviations of the pelvic ureter. *J Urol* 96: 146–151, 1966
4. Sankey ME, Heller E: The urologic complications of abdominoperineal resection. *J Urol* 97:367–370, 1967
5. Spillane RJ, Kaiser TF, Prather GC: Medial deviation of the ureters complicating carcinoma of the rectum and sigmoid and proctosigmoidectomy. *Surg Gynecol Obstet* 93:273–282, 1951
6. Ward JN, Nay HR: Immediate and delayed urologic complications associated with abdominoperineal resection. *Am J Surg* 123:642–648, 1972
7. Child CG, III, Donovan AJ: Abdominoperineal resection of the rectum, in *Diseases of the Colon and Anorectum*, edited by Turell R, Philadelphia, Saunders, 1969, pp 501–532

Ureteral Obstruction Resulting from Vascular Prosthetic Graft Surgery

DONALD A. TRACY,[1] RONALD L. EISENBERG, AND MARCUS W. HEDGCOCK

Four cases of ureteral obstruction are described which were primarily due to compression from an overlying vascular graft and retroperitoneal fibrosis. Infection may also be causal. Excretory urography should be performed routinely after vascular prosthetic surgery to permit early diagnosis of this complication. Ultrasonography may also be helpful in certain cases.

Ureteral obstruction can produce the serious complications of hydronephrosis, infection, urine extravasation, and fistulas. Important but not previously well recognized causes of such obstruction after vascular bypass surgery are mechanical compression, retroperitoneal fibrosis, and infection. Only 17 cases of ureteral obstruction after vascular bypass surgery have been described [1–8]. We report four additional cases.

Surgical Technique

Standard technique for aortofemoral or aortoiliac bypass surgery involves a midline abdominal incision from the xiphoid process to the symphysis pubis, retraction of the intestines, and incision of the retroperitoneal tissues to expose the distal aorta. If the distal end of the graft is to be anastomosed to the femoral artery, a separate groin incision is made to expose the intended site of anastomosis. For an aortoiliac graft, the original incision is extended to expose the site for iliac anastomosis. Using blunt dissection of the retroperitoneal soft tissues anterior and parallel to the iliac artery, a tunnel is created into which the graft prosthesis is placed. The ureter normally crosses anteriorly to the distal common iliac artery before entering the bladder. Unless care is taken to make the tunnel for the graft posterior to the ureter by dissecting beneath the posterior parietal peritoneum and cleanly along the anterior surface of the iliac artery, the graft may be positioned anterior rather than posterior to the ureter. In this situation ureteral compression may be anticipated.

Case Reports

Case 1

A 52-year-old man experienced left leg claudication 9 months after placement of a bilateral aortofemoral graft. Aortography demonstrated occlusion of the left limb of the graft. The patient underwent further surgery, in which another bilateral prosthetic aortofemoral graft was inserted. The patient was readmitted 6 months later because of right flank pain and right leg claudication. Excretory and retrograde urography (figs. 1A and 1B) disclosed partial ureteral obstruction bilaterally at the level of the iliac vessels; aortography showed occlusion of the right limb of the graft.

At surgery the left ureter was trapped between the remnant of the original graft and the left limb of the replacement graft. The ureter was dissected free, and the remnant of the original graft removed. The left ureter was then slung in a retroperitoneal tunnel by suturing the psoas fascia laterally. The tunnel was extended from the pelvic brim to the lower pole of the left kidney. On the right side, exploration revealed the right ureter to be obstructed not by compression from the grafts, but rather by constricting adhesions from surrounding dense retroperitoneal fibrosis. After lysis of the adhesions, the right ureter was slung in the same type of retroperitoneal tunnel as the left. Retrograde excretory urography during postoperative removal of stent catheters demonstrated bilateral clearing of ureteral obstruction and reduced hydronephrosis (fig. 1C).

Comment. This unique case demonstrates two different causes of postgraft ureteral obstruction—entrapment with resulting mechanical obstruction of the left ureter between original and replacement grafts, and obstruction of the right ureter secondary to postsurgical retroperitoneal fibrosis. The surgical technique was designed to prevent recurrence of ureteral obstruction from the retroperitoneal fibrosis.

Case 2

A 67-year-old man had a ruptured abdominal aortic aneurysm resected and replaced with a bilateral aortoexternal iliac graft. Postoperative complications included acute renal failure, attributed to acute tubular necrosis secondary to both intraoperative hypotension and suprarenal cross-clamping of the aorta for 8 min. The patient was maintained on hemodialysis for 3 weeks and had serum creatinine levels reaching 6.0 mg/dl. When the patient was discharged, serum creatinine had dropped to 3.0 mg/dl, and 2 months later to 2.6 mg/dl. During the next 4 months, renal function became worse, and a urinary tract infection developed. Excretory urography demonstrated left ureteral obstruction with hydronephrosis and cortical atrophy of the left kidney. Tomography of the ureter clearly demonstrated the exact site of obstruction (fig. 2), which was thought to be caused by compression from the overlying graft and/or retroperitoneal fibrosis. However, corrective surgery was not undertaken because of the patient's frail condition. Ten months later, renal function had worsened, serum creatinine levels had risen to 4.9 mg/dl, and the ureteral obstruction had not diminished.

Comment. This patient's ureteral obstruction resulted from either mechanical compression by the graft or retroperitoneal fibrosis.

Case 3

A 60-year-old man underwent resection of a thoracoabdominal aortic aneurysm and placement of an aorta–to–common iliac artery bypass graft. Postoperative excretory urography, performed to evaluate renal function, demonstrated hydronephrosis of the left kidney due to ureteral obstruction at the level of S1. The patient did well clinically, although follow-up retrograde excretory urography disclosed persistence of the ureteral

Received April 7, 1978; accepted after revision December 11, 1978.

[1] All authors: Departments of Radiology, University of California School of Medicine, and Veterans Administration Hospital, San Francisco, California 94143. Address reprint requests to R. L. Eisenberg, Department of Radiology, University of California, San Francisco, California 94143.

AJR 132:415–418, March 1979

© 1979 American Roentgen Ray Society

0361–803X/79/1323–0415 $0.00

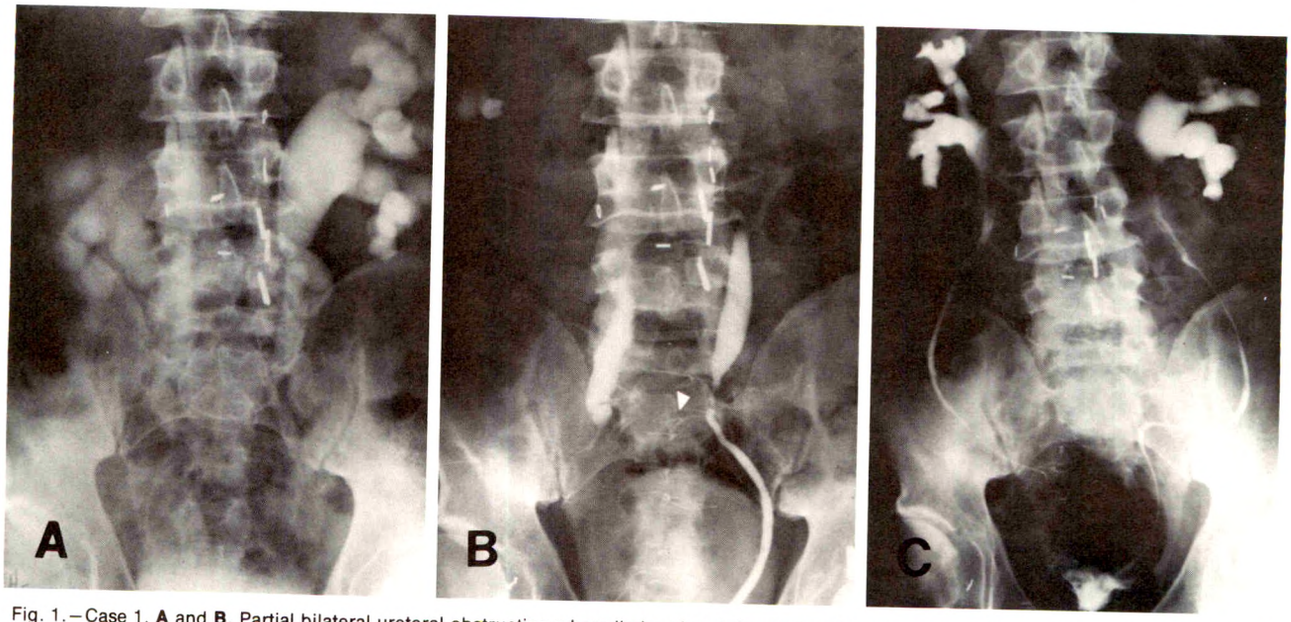


Fig. 1.—Case 1. **A** and **B**, Partial bilateral ureteral obstruction where limbs of aortofemoral graft cross and resulting ureterectasis, caliectasis, and hydronephrosis. **C**, Postoperative during removal of stent catheters. Ureters in lateral retroperitoneal tunnels. Previous bilateral ureteral obstruction is diminished.



Fig. 2.—Case 2. Ureteral obstruction where prosthetic graft crosses ureter.

narrowing. The patient was readmitted 4 years later for painless gross hematuria. Results of renal function tests were normal, but excretory urography (fig. 3A) showed left renal cortical thinning with the persistent partial ureteral obstruction. During the next 18 months, the patient had no further urinary tract symptoms, although excretory urography showed no improvement in renal function. Aortography demonstrated adequate blood flow to both kidneys, indicating that the loss of left renal cortical substance was most likely due to the chronic partial ureteral obstruction. The ureter was found to be compressed by the graft and by the patient's native left common iliac artery (fig. 3B).

Comment. Decreasing renal function in this asymptomatic patient seems to have resulted mainly from direct mechanical compression of the ureter by the overlying graft, although reactive retroperitoneal fibrosis may also have contributed.

Case 4

A 68-year-old man underwent resection of an abdominal aortic aneurysm and placement of an aortofemoral prosthetic graft. Two weeks after discharge, he returned with flank pain. Excretory urography demonstrated hydronephrosis on the left caused by ureteral obstruction at the level of L5. Follow-up excretory urography 1 month later showed no ureteral obstruction and decreased hydronephrosis. Follow-up excretory urography 3 years later showed the left urinary tract to be within normal limits. Five years after the graft surgery, the patient was hospitalized after 3 months of fatigue and pain in the region of the left femoral artery. Excretory urography demonstrated recurrence of the ureteral obstruction at the level of L5 and hydronephrosis of the left kidney. Aortography disclosed the ureteral obstruction at the point where the graft crossed the left ureter. At that time, the patient's serum creatinine level was 1.9 mg/dl, and no surgical correction of the ureteral obstruction was attempted. Over the next 5 years, excretory urography continued to show left ureteral obstruction with hydrone-

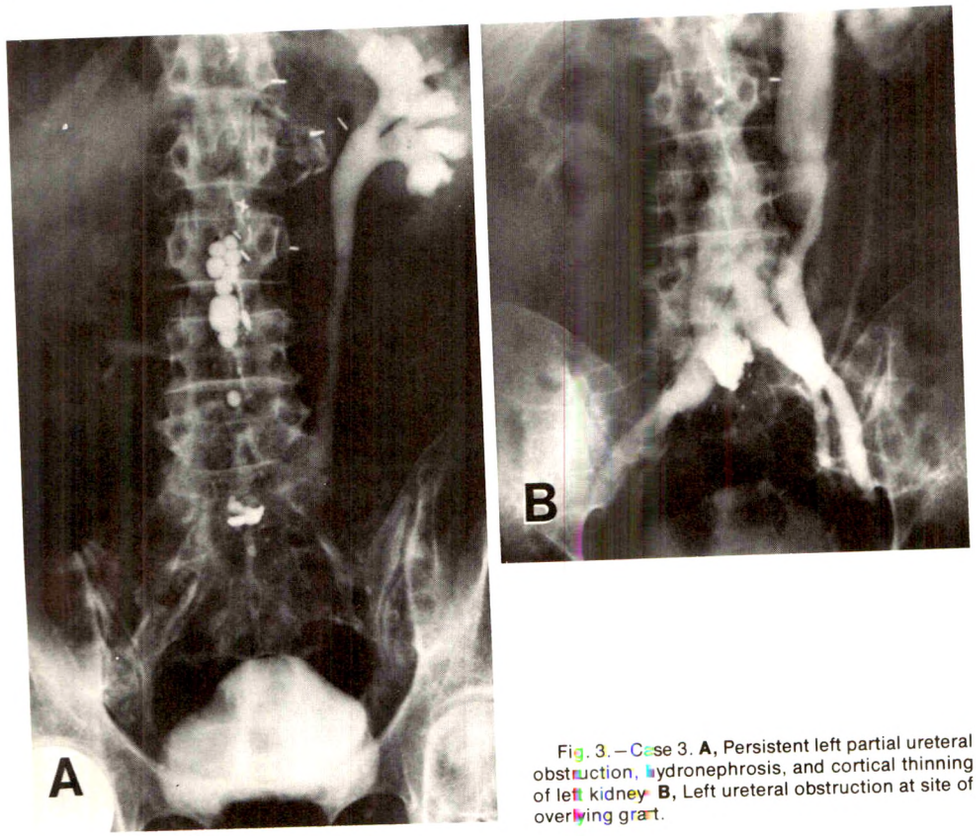


Fig. 3.—Case 3. **A,** Persistent left partial ureteral obstruction, hydronephrosis, and cortical thinning of left kidney. **B,** Left ureteral obstruction at site of overlying graft.

phrosis, and the patient experienced chronic renal failure with the serum creatinine levels rising to 3.1 mg/dl.

Comment. The delayed onset of ureteral obstruction in this patient suggests that the cause was reactive retroperitoneal fibrosis.

Discussion

Ureteral obstruction occurring after aortofemoral or aortoiliac bypass surgery can have several causes. The most common is compression of the ureter by an overlying graft limb. In 73% (11 of 15) of the reported episodes of ureteral obstruction [1–8], including ours, in which the site was known, the obstruction developed about where the graft crossed a posteriorly positioned ureter. In one of our patients, the ureter was trapped between the remnant of an old graft posteriorly and a newer graft anteriorly, a type of compression not previously reported.

Retroperitoneal fibrosis can also produce ureteral obstruction after graft surgery [9]. Retroperitoneal fibrosis always occurs after aortic bypass surgery, the extent varying with the amount of surgically induced tissue damage, residual hematoma, and surrounding inflammatory reaction to the prosthetic graft [4, 7]. In 27% (4 of 15) of the episodes of ureteral obstruction in which the position of the graft was reported, the grafts had been placed posterior to the ureters, and the obstruction was caused by periureteric fibrosis alone. Even in cases in which compression of the ureter is the primary cause of obstruction, retroperitoneal fibrosis may contribute to the obstruction by not permitting the ureter to move free of the graft.

Although graft infection did not occur among our four patients, it can also cause ureteral obstruction. In five (24%) of the 21 cases, graft infection, either from concomitant periureteric fibrosis or from abscess expanding against the ureter, produced obstruction of the ureter. Ureteral intramural fibrosis resulting from constant pounding of the ureter between a pulsatile graft and a stenosed artery has also been postulated as a cause of ureteral obstruction [3]. However, it should be noted that ureteral obstruction has diminished in all cases in which surgical intervention to reposition the ureters and lyse adhesions was undertaken.

The most common clinical signs of ureteral obstruction due to prosthetic bypass graft surgery have been pain (flank, lower back, or abdominal), sepsis, and signs of urinary tract obstruction and chronic renal failure. Hypertension [7], hematuria [3], and chyluria [10] have also been symptoms. In only one instance (case 3) has the ureteral obstruction been demonstrated in an asymptomatic patient.

Symptoms referable to ureteral obstruction in the 21 reported cases have occurred as early as 2 weeks and as late as 5 years after surgery. All but four cases were diagnosed within a year of surgery. Those cases diagnosed early were mainly due to direct mechanical obstruction of the ureter by the prosthetic graft. Delays in the development of symptoms have been associated with the complication of retroperitoneal fibrosis. All of the

four reported cases of abscess formation about the graft causing ureteral obstruction were diagnosed 3–5 months after surgery.

Of the 21 reported patients, 14 were treated surgically, most by graft revision or a ureteral-freeing procedure, although two required nephrectomy. Of the seven who were medically treated, all have had persistent ureteral obstruction and chronic renal failure.

The incidence of ureteral obstruction after graft surgery has not been assessed because the unilateral hydronephrosis it produces may not cause symptoms [10]. However, in graft patients who have had ureteral obstruction diagnosed, frequent and serious associated morbidity has occurred, including chronic renal failure and sepsis. Such serious sequelae underscore the need for awareness of ureteral obstruction as a complication of reconstructive vascular surgery.

Preservation of the normal anatomic relation of the ureter to the common iliac artery may decrease the incidence of postgraft ureteral obstruction [2–7]. Therefore, during vascular surgery, the ureter should be placed anterior to the prosthetic graft. This maneuver is especially important since the correction of ureteral obstruction involves either reanastomosis of the graft, with the attendant risk of graft occlusion, or division and repositioning of the ureter, with the possibility of graft sepsis produced by extravasation of infected urine. Case 1 had ureteral obstruction due to entrapment between old and new grafts; this indicates, we believe, that an old graft should be completely resected when a new one is inserted. In patients with obstruction due to retroperitoneal fibrosis alone who are undergoing lysis of constricting adhesions, we concur with Ross and Goldsmith [11] that, as was done in case 1, an attempt be made to avoid recurrence of ureteral obstruction by placing the ureter laterally. Theoretically, in patients whose physical condition precludes further surgery, steroid therapy might reduce the incidence of obstructing adhesions by limiting the periureteric inflammatory reaction induced by the prosthetic graft. However, this mode of therapy needs further evaluation.

Excretory urography is the most sensitive procedure for detecting ureteral obstruction and should be performed routinely after reconstructive aortic bypass surgery. Two of our patients had symptoms of ureteral obstruction within 6 weeks of surgery; thus, excretory urography soon after surgery seems advisable. In 81% (17 of 21) of the reported cases, including ours, the ureteral obstruction occurred within 1 year of surgery; in 48% (10 of 21) of these patients obstruction developed within the first 4 months. Therefore, a second postoperative excretory urogram probably should be obtained within 4 months of surgery to detect silent unilateral obstruction before serious complications occur. Excretory urography should be performed without significant delay if the postgraft patient has any lower urinary tract symptoms or develops urinary tract infection.

In all reported cases, ureteral obstruction occurred most commonly at the level of L4–S1. When excretory urography fails to show the ureters in patients with previous graft surgery, tomography may be necessary at the level of L4–S1 to demonstrate the site of obstruction (case 2, fig. 2). Impressions by overlying graft limbs can sometimes be identified radiographically and may exclude other causes of obstruction such as nonopaque calculus. Hydronephrosis is also commonly seen on excretory urograms in patients with postgraft ureteral obstruction; this occurred in all four of our patients. In patients with sepsis, an adjacent abscess can cause a mass effect on the ureters [1]. Extravasation of contrast material from the obstructed ureter into fistulous tracts has also occurred [1, 5]. In patients hypersensitive to contrast material, ultrasonography can be used to evaluate for hydronephrosis.

REFERENCES

1. Shaw RS, Baue AE: Management of sepsis complicating arterial reconstructive surgery. *Surgery* 53:75–85, 1963
2. Veith FJ, Hartsuck JM, Crain C: Management of aortoiliac reconstruction complicated by sepsis and hemorrhage. *N Engl J Med* 270:1389–1391, 1964
3. Lytton B: Ureteral obstruction following aortofemoral bypass grafts. *Surgery* 59:918–922, 1966
4. Dorfman LE, Thomford NR: Unusual ureteral injury following aorto-iliac by-pass graft: case report. *J Urol* 101:25–27, 1969
5. Ehrlich RM, Hecht HL, Veenema RJ: Chyluria following aorto-iliac bypass graft: a unique method of radiologic diagnosis and review of the literature. *J Urol* 107:302–303, 1972
6. Petrone AF, Dudzinski PJ, Maniatis W: Ureteral obstruction secondary to aortic femoral bypass. *Ann Surg* 179:192–196, 1974
7. Wallijn E, Renders G, Vereecken L: Urological complications following aortofemoral bypass graft. *Br J Urol* 47:617–621, 1975
8. Jacobsen ME, Mastio GJ, Berkas EM: Ureteral obstruction as a late complication of abdominal aneurysm resection. *J Kans Med Soc* 63:516–518, 1962
9. Wotley RG: Anatomy and physiology of the ureter, in *Urology*, edited by Blandy J, London, Blackwell Scientific Publications, 1976, pp 568–598
10. Lytton B, Epstein FH: Obstructive uropathy, in *Harrison's Principles of Internal Medicine*, 7th ed, New York, McGraw-Hill, 1974, pp 1409–1411
11. Ross JC, Goldsmith HJ: The combined surgical and medical treatment of retroperitoneal fibrosis. *Br J Surg* 58:422–427, 1971

Metastatic Transitional Cell Carcinoma from the Bladder: Radiographic Manifestions

STANFORD M. GOLDMAN,[1, 2] ARTURO A. FAJARDO,[1] ROGELIO C. NARAVAL,[3] AND JOHN E. MADEWELL[4]

Metastases from transitional cell carcinoma of the bladder are not widely appreciated radiographically, although they are commonly found at autopsy. Radiographic evidence of metastatic disease was reviewed in 51 patients. Sites included lung, 28; bone, 24; mediastinum, eight; liver, eight; brain, three; urethra, one; abdominal nodes, one; and extradural space, two. The patterns of lung metastases consisted of solitary nodules, multiple nodules, segmental infiltrates, pulmonary edema, and a Pancoast tumor. A sarcoidlike pattern with hilar and interstitial disease was also seen. One patient had a malignant pleural effusion. Mediastinal lymph node enlargement was isolated or associated with lung involvement. Bone metastases demonstrated either an osteoblastic or a mixed osteolytic-osteoblastic pattern in 47% of the instances. Ivory vertebrae were identified in three patients. Because of the significance of identifying metastatic disease before any extensive curative bladder surgery, we recommend at least a preoperative chest radiograph, a bone scan, and a liver scan.

Metastases from transitional cell carcinoma of the bladder are commonly identified by the pathologist. In an autopsy series of untreated patients, the incidence of distant metastases was 65% [1]. Among 107 autopsies performed at Johns Hopkins Hospital, distant metastases in treated patients varied from 70% for stage C tumors to 58% for stage B lesions [2]. Despite the apparently high incidence of metastases reported in the pathologic literature [1–4], most radiologists are unfamiliar with the radiographic manifestations of metastatic bladder cancer.

No review of the subject exists in either general or subspecialty radiologic textbooks, and the little information they do contain is contradictory. In the past 50 years, every journal report but one describes the radiographic manifestations in fewer than 12 patients [5–32]. In the one exception [21], the authors describe only bone involvement. Furthermore, of the 37 sites reviewed in their 24 patients, 20 were in the pelvis and sacrum. We believe most of these were direct extensions of tumor and not hematogenous or lymphatic metastases.

An extensive review of the spectrum of radiographic manifestations from bladder carcinoma should be of particular value in this age of radical surgery and aggressive chemotherapy. Our experience in 51 patients with radiographic evidence of metastatic bladder disease is reported here. In 25 of these, autopsy or biopsy proof of metastases was available. In all patients, the bladder lesion was biopsied and proven to be a transitional cell carcinoma of the bladder, and metastases to the lung, mediastinum, bone, liver, brain, urethra, abdominal lymph nodes, and extradural space were demonstrated. We believe that metastatic bladder carcinoma is much more frequent than currently recognized.

Materials and Methods

The case material was obtained from: (1) Sinai Hospital of Baltimore, (2) Greater Baltimore Medical Center, and (3) Armed Forces Institute of Pathology. Metastases were identified in 32 (9.5%) of 335 patients with pathologically proven transitional cell carcinoma of the bladder from records at Sinai Hospital over a 10 year period, 1967–1977. Metastases in 13 (29%) of 45 patients were recognized in a similar manner from files of the Greater Baltimore Medical Center over a 5 year period, 1972–1977. Also included are six patients whose radiographs were from the Armed Forces Institute of Pathology.

Metastases were confirmed in 12 patients by autopsy and in 13 others by biopsy (six, bone; two, mediastinum; two, lung; one, liver; one, urethra; and one, extradural space). The other patients in this series at no time showed evidence of a second primary. On the basis of both clinical and radiologic evaluation, we are convinced that we were dealing with lymphatic and/or hematogenous spread in these patients. Abnormalities that could possibly be attributed to direct extension of tumor were excluded.

Types of radiographic examinations evaluated were chest radiographs, lung and mediastinal tomograms, central and appendicular skeletal films, urethrograms, myelograms, bone scans, liver scans, and brain scans. One positive lymphangiogram was also available. Not all of the above studies were performed on every patient; only studies clinically indicated were obtained. All patients from Sinai Hospital and the Greater Baltimore Medical Center had at least a chest radiograph. In addition, 25 lung and mediastinal tomograms, 61 bone surveys, 68 bone scans, 62 liver scans, 10 brain scans, three urethrograms, four lymphangiograms, and two myelograms were obtained for these patients. A total of 86 patients had either bone scan, bone survey, or both. For statistical purposes, repeat or follow-up examinations of any single body part were considered as one study. Thus, two or more bone surveys in an individual were considered a single examination in order to compute the biologic frequency of metastases.

Received July 18, 1978; accepted after revision November 17, 1978.
Presented at the annual meeting of the Society of Uroradiology, New York, September 1978.
[1]Department of Radiology, Sinai Hospital of Baltimore, Inc., Belvedere at Greenspring Avenues, Baltimore, Maryland 21215. Address reprint requests to S. M. Goldman.
[2]Department of Radiology, University of Maryland School of Medicine, Baltimore, Maryland 21201 and Johns Hopkins University School of Medicine, Baltimore, Maryland 21205.
[3]Department of Radiology, Greater Baltimore Medical Center, 6701 North Charles Street, Towson, Maryland 21204.
[4]Department of Radiological Pathology, Room M115, Armed Forces Institute of Pathology, Washington, D. C. 20306.

© 1979 American Roentgen Ray Society

0361-803X/79/1323-0419 $0.00

Results

Metastases from transitional cell carcinoma of the bladder was identified in 51 patients. Average age was 58 years (range, 43–87) with a 4:1 male to female ratio (39:12). We could not identify a relation between age or sex and sites of metastases.

Metastases were radiographically identified in 75 sites (table 1). The skeletal system was considered a single metastatic site, no matter how many bones were involved. The frequencies of metastases radiographically identified were: chest and/or mediastinum, 23/380 (6%); bone, 24/86 (28%); liver, 8/62 (13%); and brain, 3/10 (30%). Isolated instances of metastases to the urethra (one of three positive urethrograms), abdominal lymph nodes (one of four positive lymphangiograms), and extradural space (two of two myelograms) were also seen. The six patients from the Armed Forces Institute of Pathology (five with lung metastases and one with bone involvement) were not included in these percentages. In all patients where metastases were identified, biopsy of the primary tumor revealed grade II or III transitional cell carcinoma.

TABLE 1

Radiographic Identification of Metastases

Location of Metastasis	No.	Positive Radiographs (no., %)
Lung*:		23/380, 6
Multiple nodules	13	
Solitary nodule	7	
Infiltrate	5	
Pulmonary edema	2	
Pancoast tumor	1	
Subtotal	28	
Bone:		23/81, 28
Osteolytic	11	
Osteoblastic	6	
Mixed	4	
Scan only	3	
Subtotal	24	
Mediastinum	8	
Liver:		8/62, 13
Solitary nodule	5	
Multiple or diffuse nodules	3	
Subtotal	8	
Brain (all solitary)	3	3/10, 30
Urethra (multiple)	1	1/3, 33
Abdominal lymph nodes with punched out lesions	1	1/4, 25
Extradural metastases via myelography	2	2/2, 100
Total	75	

* Recurrent pleural effusions and interstitial disease (one case) were seen but not included in series.

Lung and/or Mediastinal Involvement

Lung metastases (fig. 1) appeared as multiple nodules (13 patients), a single nodule or mass (seven), a pulmonary infiltrate (five), pulmonary edema (two), and a Pancoast tumor (one). One documented case of recurrent metastatic pleural effusions was also seen; however, this patient is not included in our series.

In general, the nodules were well circumscribed, rounded lesions without calcifications or cavitation. Only a few of the lesions had poorly defined borders. There was no predilection to any specific lobe or location. Sizes varied from small (2–3 mm) nodules best seen on tomography to large (10 cm or more) "cannonball" lesions. Follow-up studies of some patients were available, and we saw some decrease in tumor size with chemotherapy in a few cases. In at least one patient (fig. 1A), four small (3–4 mm) nodules progressed to huge masses and death in 10 months despite aggressive chemotherapy.

The pulmonary infiltrates were segmentally distributed in four patients (fig. 1B). The disease was always interstitial, although initial impression in two cases was of alveolar disease, since the nodules were small and tended to coalesce. However, there were no air bronchograms. One patient had a sarcoidlike pattern with lymph node enlargement and thickening of the interstitium (fig. 1C). Although purely interstitial metastases reported with prostate was not seen, we believe it can occur (on the basis of fig. 1C).

Both patients with a pulmonary edema pattern were autopsied. In one (fig. 1D), the lungs were studded with tumor emboli in the pulmonary vessels and no pulmonary alveolar filling by fluid edema was found. In the second there was interstitial metastatic carcinoma that led to congestive heart failure and pulmonary edema. One patient supposedly had a primary Pancoast tumor; biopsy proved the apical mass to be metastatic bladder carcinoma (fig. 1E).

Mediastinal lymph node enlargement was identified in eight patients (fig. 1G). In three of these, only mediastinal involvement was present. The other five had metastases to the lungs and bones. The lymphadenopathy was in the middle mediastinum, usually bilateral, and fairly symmetrical. Bilateral hilar enlargement was identified in three patients and unilateral in two.

Full lung tomography was performed in 23 patients with bladder cancers admitted for total cystectomies. No metastases were identified on pulmonary tomograms in patients with normal chest radiographs. In three patients with at least one nodule on chest radiography, lung tomography showed several nodules. In one of these, chest radiography demonstrated only a single 3 mm nodule; tomography showed four additional lesions, altering radiographic impression from "small granuloma" to metastatic disease. The patient died 10 months later with disseminated metastatic bladder cancer (fig. 1A).

Bone Metastases

Bone metastases were radiographically identified in 21 of 24 patients. In the remaining three, only bone scans were performed. Of the metastatic lesions, 11 were osteolytic, six were osteoblastic, and four were a combination of both (fig. 2) (table 2). Spine films in three cases initially demonstrated a single "ivory" vertebra. All of

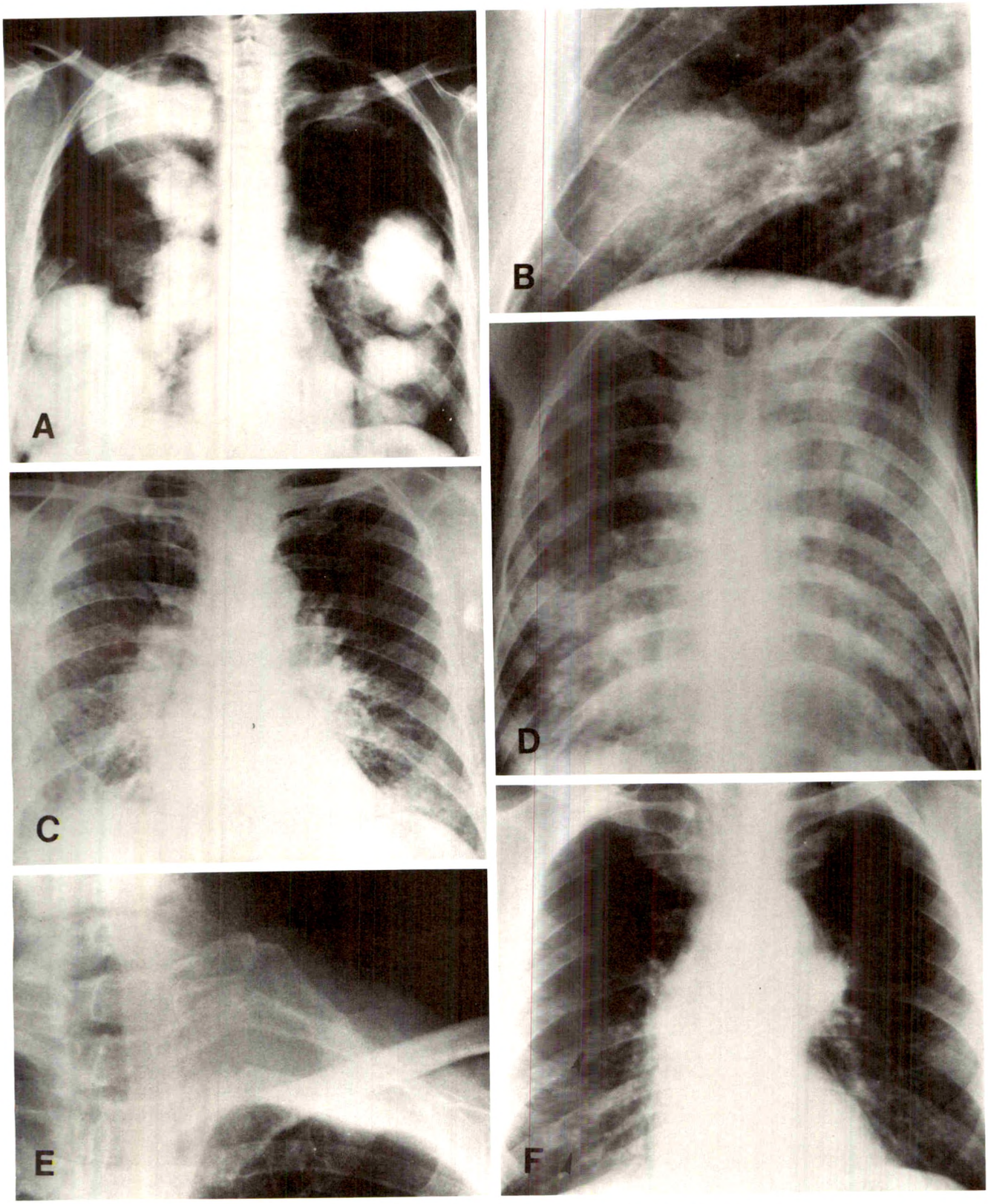


Fig. 1.—Lung and mediastinal metastases. **A**, Multiple nodules in 58-year-old woman (autopsy). **B**, "Pneumonia" pattern in 76-year-old man with progression in bone and lungs over months (autopsy). **C**, Sarcoidlike pattern with hilar and interstitial disease in 55-year-old patient (biopsy). **D**, Pulmonary edema in a 62-year-old woman. Pattern due to tumor emboli and infarction (autopsy). **E**, Pancoast tumor; classic symptoms include Horner's syndrome in 49-year-old woman (biopsy). **F**, Extensive mediastinal involvement with only a few small nodules (*arrowheads*) in lung of 57-year-old man (biopsy).

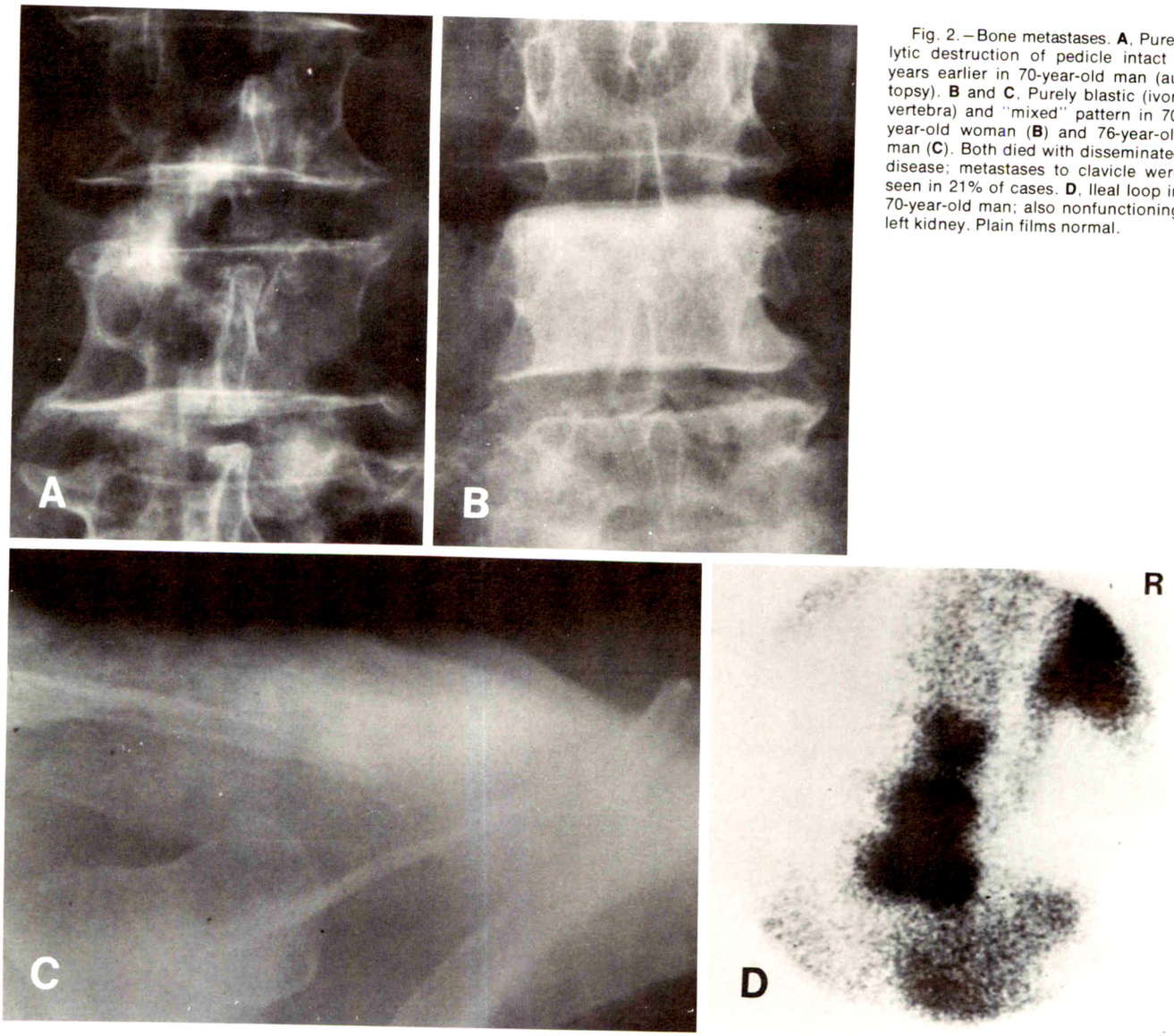


Fig. 2.—Bone metastases. **A**, Purely lytic destruction of pedicle intact 4 years earlier in 70-year-old man (autopsy). **B** and **C**, Purely blastic (ivory vertebra) and "mixed" pattern in 70-year-old woman (**B**) and 76-year-old man (**C**). Both died with disseminated disease; metastases to clavicle were seen in 21% of cases. **D**, Ileal loop in 70-year-old man; also nonfunctioning left kidney. Plain films normal.

these patients subsequently developed disseminated disease. Five of the 24 patients with bone metastases had clavicular involvement, six had proximal femoral involvement, and six had proximal humerus involvement.

Of the four autopsies performed in this group of patients, three had either an osteoblastic or a mixed osteolytic-osteoblastic pattern. In all three, the prostate was invaded with transitional cell carcinoma of the bladder. Autopsy of the fourth patient demonstrated purely osteolytic metastases with no evidence of prostatic involvement.

There were 17 positive bone scans which, in general, showed more metastatic lesions than evident on companion plain film bone surveys.

Liver Metastases

Of the eight positive liver scans, five showed single metastases and three showed either multiple defects or diffuse involvement (fig. 3). In two, these were the only known sites of metastatic disease.

TABLE 2

Bone Metastases

Site	No.
Lumbar spine	12
Thoracic spine	10
Pelvis	9
Ribs	8
Femur, proximal	6
Humerus, proximal	6
Clavicle	5
Skull	4
Scapula	3
Total	63

Other Sites Of Metastases

The three patients with positive brain scans demonstrated metastases elsewhere. All the brain lesions were solitary; two were autopsy proven. The one patient with biopsy-proven metastases to the urethra showed multiple shaggy nodules on urethrography (fig. 4A).

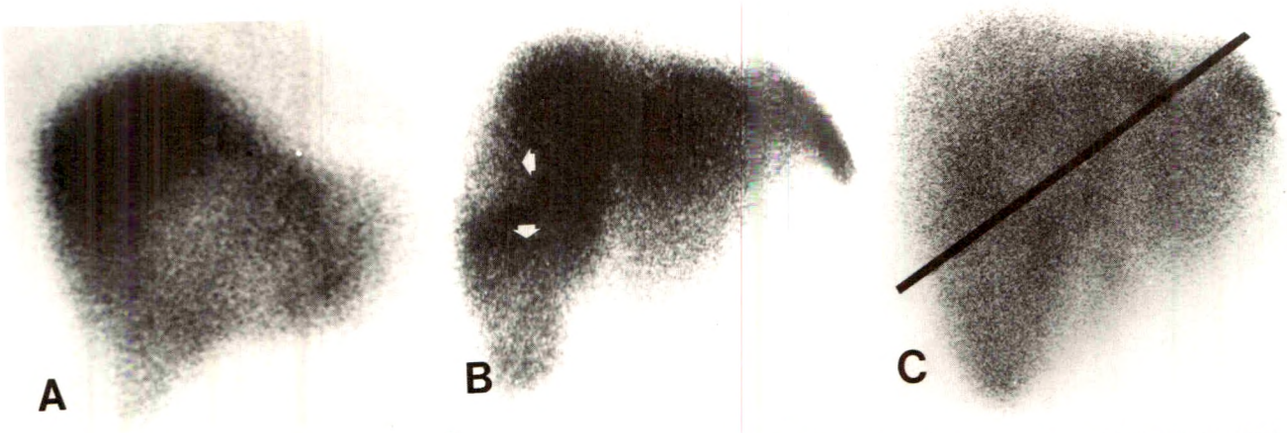


Fig. 3.—Liver metastases. **A**, Large solitary lesion in 83-year-old woman (autopsy). **B**, Multiple nodules (*arrows*) in 70-year-old woman also with bone lesions (autopsy). **C**, Diffuse involvement in 62-year-old man (autopsy).

The one positive lymphangiogram (fig. 4B) showed abnormal iliac and paraaortic nodes with filling defects characteristic of metastatic disease. This patient also had multiple lung metastases on chest radiography. There were three negative lymphangiograms in the series. Two cases of extradural metastases were identified on myelography (fig. 4C).

Discussion

Although the radiographic pattern for metastases from most neoplasms is well known, the radiographic findings of metastases from transitional cell carcinoma of the bladder are not. McCallum and Colapinto [33] state that of the 10% with bone or lung metastases "only a small number will be detected radiologically." Our study shows that radiographically identifiable metastases are more common than is generally appreciated, with incidences of 9.5% (32/335) and 29% (13/45). If anything, the total frequency reported here may be low, since not every individual in this study had every radiographic examination.

To appreciate potential metastatic sites from the bladder, normal and abnormal drainage pathways must be understood [34–36]. Local lymphatic spread occurs via lymph nodes into the superior and inferior gluteal, the obturator, and the external and common iliac nodes. From there, the metastases flow into the paraaortic chain to the thoracic duct and the general circulation. Lymphohematogenous spread occurs when the local nodes become obstructed and tumor cells are shunted into the vascular compartment. Hematogenous metastases spread either via the pelvic plexuses into the inferior vena cava and general circulation or via the perivertebral veins into the azygos, hemiazygos, intercostal, and other systemic veins.

In reviewing the sites of metastases in the 51 patients in this series, we found lung involvement most common; 6% of the chest films were abnormal. In a small series of patients with normal posteroanterior chest radiographs [22], no evidence of metastases was identified by full-lung chest tomography. However, in the three patients where at least one nodule was identified on plain chest film, tomography identified other unrecognized lesions. This helped distinguish metastatic disease from a single granuloma. Although some of our urologists still routinely request tomography on patients with bladder carcinomas before cystectomy, we are not convinced of its value.

We are also unable to make specific recommendations about the value of CT in identifying metastases in patients with normal posteroanterior chest radiographs. A prospective study of patients slated for total cystectomy would probably identify at least a few unsuspected metastases. Where CT is available, it is possible that it will supplant routine chest tomography.

Some uroradiologists believe that transitional cell metastases to the lung cavitate [32]. None of the cases reported here nor any subsequent cases seen at our hospitals showed any radiographic evidence of cavitation.

The second most common site of metastases was the skeletal system. Although most of the metastases were to the vertebral column, lesions were also identified in the clavicle (5/24), femur (6/24), humerus (6/24), pelvis, ribs, skull, and scapula.

As recently as June 1978 [28], bone metastases from bladder carcinoma were described as lytic. Similarly, McCallum and Colapinto [33] state that they "are usually lytic" and Murray and Jacobson [37] report that they are "predominately lytic, bone forming if prostate involved."

Our study and that of Sutton [38] show that osteoblastic and mixed osteolytic-osteoblastic patterns are extremely common. Purely osteoblastic metastases were found in 28% (6/21) and 19% (4/21) had a mixed osteolytic-osteoblastic pattern. Three patients had "ivory" vertebrae.

Four of the patients with metastatic bone lesions were autopsied. The three patients who had either an osteoblastic or a mixed radiographic pattern demonstrated prostatic involvement with bladder carcinoma. The other autopsied case was purely osteolytic without prostatic involvement. Prostatic involvement may well be related to development of osteosclerotic metastases [37]. In one case, metastases to the vertebra caused a complete

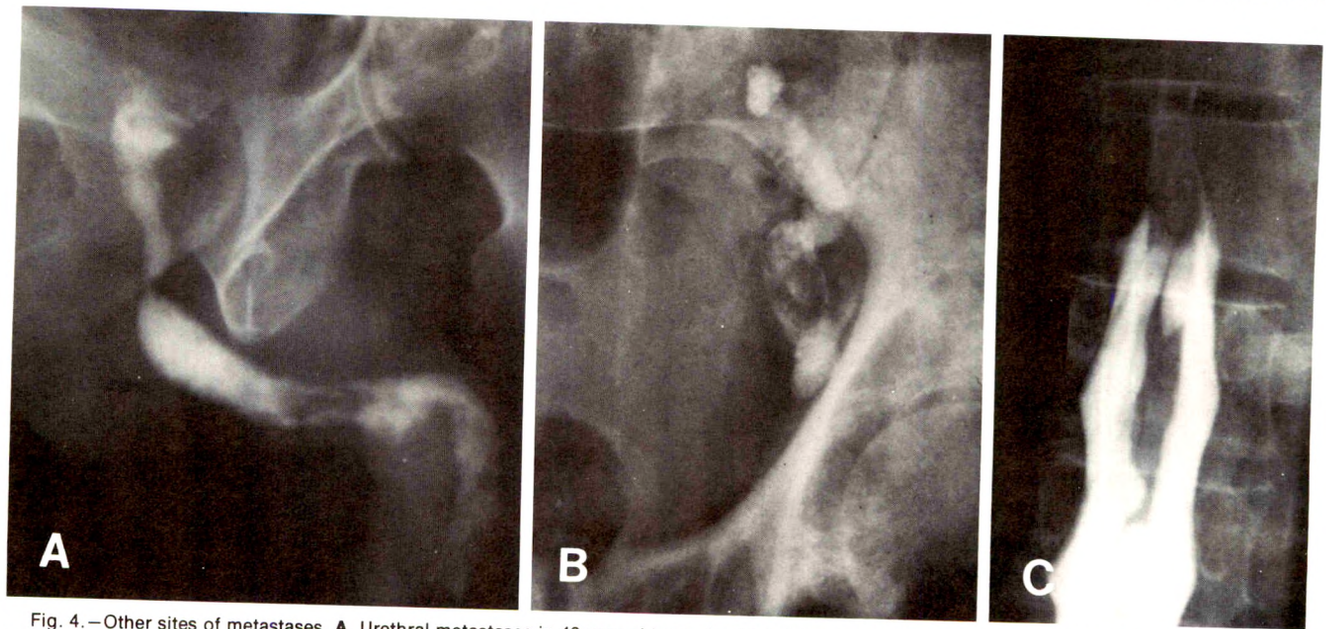


Fig. 4.—Other sites of metastases. **A**, Urethral metastases in 43-year-old man (multiple biopsies). **B**, Lymphatic metastases in 77-year-old man with lung metastases also (surgery). (Paget's disease of pelvis also seen.) **C**, Complete extradural block in 53-year-old man (biopsy).

epidural block. We found no case of heterotopic bone formation, although it has been reported [11].

Other sites of metastases in this study included the liver (eight cases), brain (three), urethra (one), abdominal lymph nodes (one) and epidural space (two). Lymphangiography was infrequently performed and we are unable to evaluate its efficacy. It did identify metastases in one case. Some investigators feel it has a very limited applicability because of the significant number of false positives and negatives [39]. CT may prove to be an alternative noninvasive method for identifying lymph node metastases. However, false positives and negatives may be a problem with this method as well.

In evaluating the radiographic frequency of metastases to any specific organ system reported here it should be remembered that not every patient had every study. For example, bone scans, bone surveys, and liver scans were obtained only in symptomatic patients or in those with advanced local disease. Thus, the frequency reported here is probably fairly high. On the other hand, the incidence of chest and mediastinal metastases may be somewhat low since CT was not performed.

Jewett and Strong [2] showed a direct relation between the depth of bladder tumor penetration and incidence of local and distal metastases. In our study, only patients with advanced grades of primary tumors (II and III) were identified as having metastases. In view of the high incidence of bone metastases (28%) and lung metastases (6%) reported here, chest radiography and bone scan are the minimal studies required to properly evaluate patients with advanced local disease. Since the bone scan seemed to identify more lesions, bone survey might possibly be reserved for confirming the etiology of a positive isotopic study. We believe liver scans (13% positive) should be performed as well. Future studies are needed to assess the value of CT in identifying lung and lymph node metastases in this disease. We believe that extensive curative surgery should not be contemplated without these minimal preoperative studies.

However, on the basis of a brief review of clinical follow-ups of early stage bladder cancer by our tumor board and the clinical or pathologic incidence of metastases reported [2–4], extensive radiographic workup is probably neither indicated nor cost effective in these patients. Unfortunately, an actual prospective radiographic study of the incidence of metastases in early transitional cell carcinomas of the bladder does not exist.

REFERENCES

1. Friedell GH, Mcauley RL: Untreated bladder cancer: 31 autopsy cases. *J. Urol* 100:293–296, 1978
2. Jewett HJ, Strong GH: Infiltrating carcinoma of the bladder, relation of depth of penetration of the bladder wall to incidence of local extension and metastases. *J Urol* 55:366–372, 1946
3. Fetter TR, Bogrev JH, McCuskey B, Seres JJ: Carcinoma of the bladder: sites of metastasis. *J Urol* 81:746–748, 1959
4. Melicow MM: Tumors of the bladder: a multifaceted problem. *J Urol* 112:467–478, 1974
5. Mullin EM, Glenn JF, Paulson DF: Lesions of bone and bladder cancer. *J Urol* 113:45–46, 1975
6. Fegetter JGW: An osteolytic lesion as a presentation of bladder carcinoma. *Br J Urol* 48:254, 1976
7. Treggiden R: Mandibular metastasis from carcinoma of the bladder. *J Oral Surg* 34:1016–1018, 1976
8. Resnick MI, O'Connor VJ Jr, Grayhack JT: Metastasis to the eye from transitional cell carcinoma of the bladder. *J Urol* 114:722–724, 1975
9. Seymour JE, Malin JM, Pierce JM Jr: Late metastasis of a superficial transitional cell carcinoma of the bladder. Report of a case. *J Urol* 108:277–278, 1972

10. Sternberg JJ, Bracken RB, Handel PB, Johnson DE: Combined chemotherapy (CISCA) for advanced urinary tract carcinoma. *JAMA* 238:2282–2287, 1977
11. Chinn D, Genant HK, Quivey JM, Carlsson A: Heterotopic-bone formation in metastatic tumor from transitional cell carcinoma of the urinary bladder. *J Bone Joint Surg* [*Am*] 58:881–883, 1976
12. Lunia S, Parthasarathy KL, Bakshi S, Bender MA: An evaluation of ^{99m}Tc-Sulfur colloid liver scintiscans and their usefulness in metastatic workup: a review of 1,424 studies. *J Nucl Med* 16:62–65, 1975
13. Lome LG, Navani S, Aral IM: Spontaneous regression of pulmonary metastasis from transitional cell carcinoma of the bladder. *Cancer* 26:415–418, 1970
14. Fletcher DE: Skeletal involvement in carcinoma of the urinary bladder. *J Fac Radiol* 6:109–119, 1954
15. Livingston SK: Osteoblastic metastases in papillary carcinoma of the bladder. *AJR* 36:312–313, 1936
16. Kretschmer HL, McDonald JK: Carcinoma of the bladder with bone metastasis report of eight cases. *Surg Gynecol Obstet* 87:328–337, 1948
17. Greenfield H: Distant metastases from carcinoma of the urinary bladder. *Radiology* 37:181–185, 1941
18. Wills HG: Bone metastasis from primary carcinoma of the urinary bladder. *J Urol* 7:383–396, 1922
19. Jenkinson EL, Hunter A, Roberts EW: Bone carcinoma secondary to carcinoma of the urinary bladder. *Radiology* 28:89–92, 1937
20. Sauerbrunn BJL, Andrews GA, Hubner KF: Ga-67 citrate in tumors of the genitourinary tract: report of a cooperative study. *J Nucl Med* 19:470–475, 1978
21. Graves RC, Militzer RE: Bone metastasis from carcinoma of the urinary bladder. *J Urol* 31:769–789, 1934
22. Kinne AS: Metastases to bone from bladder tumors. *IMJ* 109:323–325, 1953
23. Miln DC: Phalangeal metastasis from urinary tract carcinoma. *Scott Med J* 33:131–132, 1952
24. Huang C: Bone metastasis in carcinoma of the urinary bladder. *Chin Med J* [*Engl*] 54:57–65, 1938
25. Herger CC, Sauer HR: Large bone metastases from carcinoma of the bladder. *Am J Surg* 57:29–37, 1942
26. Burkland CE, Leadbetter WF: The importance of early study for metastasis in tumors of the bladder. *Surgery* 6:98–111, 1939
27. Wheelock MC, O'Conner VJ: Metastasis in tibia from carcinoma of the urinary bladder. *Q Bull Northwestern Univ Med Sch* 27:111–113, 1953
28. Grant TT, de Kernion JB: Treatment of skeletal metastases from urologic malignancies. *Urology* 11:563–567, 1978
29. Ross JA, Newall J: Unusual metastases in bladder carcinoma. *J R Coll Surg Edinb* 6:51–58, 1960
30. Fletcher JW, Solaric-George JW, Henry RE, Donati RM: Radioisotopic detection of osseous metastases. *Arch Intern Med* 135:553–557, 1975
31. Orteza AM, Kandzara SJ, Milam DR: Transitional cell carcinoma of the bladder with pulmonary metastasis: case report on 5 year survival following resection of metastasis. *J Urol* 105:232–235, 1971
32. Weintraub RA: Roentgenogram of the month: excavating pulmonary metastases from a transitional cell carcinoma of the bladder. *Dis Chest* 44:633, 1963
33. McCallum RW, Colapinto V: *Urologic Radiology of the Adult Male Lower Urinary Tract*. Springfield, Ill., Thomas, 1976, pp 298–299
34. Wirtanen GW, Miller RC: Bladder lymphatics and tumor dissemination. *J Urol* 109:58–59, 1973
35. Goss CM (ed): *Gray's Anatomy of the Human Body*, 29th ed. Philadelphia, Lea & Febiger, 1973, pp 709–715, 738–740, 755–757
36. Cole WH: The mechanisms of the spread of cancer. *Surg Gynecol Obstet* 137:853–871, 1973
37. Murray RO, Jacobson HG: *The Radiology of Skeletal Disorders*, 2d ed. Edinburgh, Churchill Livingstone, 1977, pp 584, 1090
38. Sutton D: *Textbook of Radiology*. London, Livingston, 1969, p 83
39. Rarah RN, Cerny JC: Lymphangiography in staging patients with carcinoma of the bladder. *J Urol* 119:40–41, 1978

Risk Factors and Occult Breast Cancer in Young Women

GLORIA FRANKL[1] AND MONA ACKERMAN[1]

The National Cancer Institute guidelines for mammography in women 35–49 years old are challenged. Forty-nine occult breast cancer patients under 50 years of age were analyzed regarding risk factors and compared with an age-matched control group. Of the cancers, 86% would have been missed had NCI recommendations been followed. Results refuted the NCI guidelines and showed that late parity (over 28 years) and history of breast cancer in the extended family are statistically significant risk factors. Negative mode low-dose xeromammographic examinations permitted detection of 49 occult breast cancers, usually without axillary node metastases. Patients were screened because of risk factors enumerated in the article.

Working in diagnostic radiology and mammography, we are often asked, "Which asymptomatic women, if any, under 50 years should be sent for mammographies?" The National Cancer Institute recommends routine mammographic screening of women aged 35–49 only if there is a history of breast cancer or if there is a history of breast cancer in the immediate family (mother, sister) [1]. Two questions must be answered: (1) Are the National Cancer Institute guidelines appropriate? (2) Is the benefit or efficacy of mammography in young women demonstrated?

Subjects and Methods

In the last 6½ years, 20,805 patients have been studied by xeromammography at the Kaiser-Permanente Medical Center, Los Angeles. There were 740 pathologically verified breast cancers among these patients. Of these xeromammography studies, 34% were in women under 50 years of age. Of the 740 breast cancers, 214 (29%) were in women under 50.

We analyzed the 49 occult (nonpalpable) cancers in the younger age group, because all would agree that mammography was warranted in the 165 symptomatic cancer patients under 50 years; but what were the indications for study in the occult group? All of the 49 occult breast cancer patients under age 50 were studied because they had one of the risk factors listed in table 1. We recommended that those women between 35 and 49 years of age be studied because the listed high risk factors had been reported [2] and because our own preliminary data seemed to indicate that these women were indeed at an increased risk of developing breast cancer.

A control group of 100 women under age 50 all had recent normal breast examinations by a physician, and these women all denied any breast symptoms. Obviously, none of the control patients had a personal history of breast cancer.

Patients were examined with negative mode xeromammography, with 2.8 mm aluminium filtration, tungsten target, and craniocaudal and mediolateral projections delivering a total 0.22 rad to the mid-breast on a standard two-view study. On occasion, if the standard two views did not delineate a clinically described finding or at the discretion of the examining technologist, additional views were obtained.

Results

Three (6%) of the young, occult cancer patients had a history of breast cancer in the immediate family; four (8%) of the young occult cancer patients had a personal history of breast cancer (table 1). Thus only 14% of the breast cancer patients met the National Cancer Institute guideline recommendations for mammography.

History risk factors were tabulated (table 1) comparing the 100 women in the control group and the 49 young, occult cancer patients. Late parity and history of breast cancer in the extended family are significantly associated with occult breast cancer in women under 50. We did not establish this relationship for the other risk factors.

Axillary node status was compared in the young, occult breast cancer patients and the young, palpable cancer patients. Of 165 patients with palpable cancer, 76 (46%) had node involvement; of 49 patients with occult cancer, 13 (25%) had node involvement. This difference was statistically significant ($\chi^2 = 5.93, P < 0.05$).

Three (6%) of the young, occult cancer patients and 19 (12%) of the young, palpable cancer patients died in this rather short-term follow-up period. All of the patients who expired had metastases to axillary nodes at the time of breast cancer discovery, and all died as a consequence of breast cancer.

Breast parenchymal patterns were assessed in the young, occult breast cancer population. Of these patients, 80% had coalescent, dense dysplasia or more than one-fourth of the volume of their breasts occupied

TABLE 1

Risk Factors and Breast Cancer

Risk Factor	Occult Cancer Patients under 50 (%)	Normal Control Patients under 50 (%)
Late parity* (28 yrs or later)	29	8
Nulliparity	23	14
History of breast cancer in immediate family	6	4
History of breast cancer in extended family*	20	5
Personal history of breast cancer	8	. . .
Prior benign breast surgery	14	6

* Significant association by Chi squared test.

Received September 25, 1978; accepted November 16, 1978.

[1] Department of Diagnostic Radiology, Southern California Permanente Medical Center, 1505 North Edgemont Street, Los Angeles, California 90027. Address reprint requests to G. Frankl.

© 1979 American Roentgen Ray Society

0361–803X/79/1323–0427 $0.00

TABLE 2
Parenchymal Patterns in 49 Young Occult Cancer Patients

	No.	%
N1	0	0
P1	10	20
P2	24	50
Dy	15	30
Total	49	100

by prominent ducts, placing them in a high risk pattern group [3] (table 2).

Discussion

Of the occult breast cancers we studied, 86% would have been missed had we used the National Cancer Institute guideline recommendations for performing mammography. Late first parity and history of breast cancer in the extended family show a significant association with breast cancer. The role of personal history of breast cancer could not be tested, since women with a personal history of breast cancer were omitted from the control group. Patients who had prior benign breast biopsies did have more breast cancers, but the difference is not considered statistically significant. Nulliparity and cancer in the immediate family may be important risk factors in postmenopausal women, but the statistical significance of these factors in women under 50 was not established in our series of young women.

It would seem valid to determine benefits by examining mortality rates, survival rates, and the rates of axillary node metastases, since the prognosis in breast cancer is so closely linked with the absence or presence of axillary node metastases at the time of breast cancer surgery. We have no long-term (10 years or greater) survival or mortality rates; therefore, we have assessed benefit on: (1) the absence or presence of axillary node metastases at the time of breast cancer surgery, and (2) the preliminary comparison in mortality rates between the young, palpable and young, occult cancer patients. Haagensen [4] reports that 74% of breast cancer patients will survive 10 years if there are no axillary node metastases, but only 39% of breast cancer patients with node involvement will survive 10 years.

Our data show: (1) a significant decrease in the number of cancer patients with node involvement when comparing the palpable (46%) and occult (25%) groups, and (2) preliminary (less than 10 years) mortality figures show a decrease in mortality when comparing the palpable (12%) and occult (6%) groups. Our data on parenchymal pattern tend to corroborate Dr. John Wolfe's work on the predictive value of parenchymal pattern assignment, although his study was based on screening an asymptomatic population while our population is mixed and includes symptomatic and high-risk patients.

Since we purport benefit, it is a corollary to analyze any potential risk. Bailar [5], in an analysis of the Health Insurance Plan Study, assumed that 2 rad was absorbed by the midportion of the breast. But what is the validity of comparing a previous rather high dose to our current low dose technique?

Also there is some evidence that when adverse effects of radiation were noted, they were usually confined to women who received the ionizing irradiation before age 30 [6]. No one advocates screening women under 30; only 3% of our patients and 2% of the cancers were in women under 30. Any risk-benefit rates should be based on modern technique and current data, not on the results of obsolete data from the Health Insurance Plan Study, performed in New York in the early 1960s [7].

Conclusions

Our data refute the NCI guidelines which recommend that mammographic screening for women between 35 and 49 be restricted to those with a personal or close family history of breast cancer. Late first parity and a history of breast cancer in the extended family are shown to be statistically significant risk factors in a young, occult breast cancer population.

Prior benign breast biopsy, nulliparity, and history of breast cancer in the immediate family showed an associated tendency, but not a statistically significant increased risk in our young women. A personal history of breast cancer was not tested as a risk factor, but is assumed to be associated with increased risk based on literature review [8].

Negative mode xeromammography is an excellent low-dose system of radiographic breast examination. The appropriate interval for follow-up examination can be based on breast parenchymal pattern, coupled with important history risk factors. The risk of excluding mammography in a young, high-risk group exceeds any possible hazard of the small amount of irradiation necessary for detection.

ACKNOWLEDGMENT

Dr. Alan Forsythe reviewed the manuscript and provided the statistical analyses.

REFERENCES

1. Panel Report: NIH/NCI consensus development meeting on breast cancer screening, Bethesda, September 14–16, 1977. *AJR* 130:194–197, 1978
2. Frank G: Xeromammography for the detection of breast cancer. *Obstet Gynecol Digest* 19:17–21, 1977
3. Wolfe J: Breast patterns as an index of risk for developing breast cancer. *AJR* 126:1130–1139, 1976
4. Haagensen CD: *Diseases of the Breast*. Philadelphia, Saunders, 1971
5. Bailar JC III: Mammography: a contrary view. *Ann Intern Med* 84:77–84, 1976
6. Treves N, Holleb AL: A report of 549 cases of breast cancer in women 35 years of age or younger. *Surg Gynecol Obstet* 107:271–283, 1958
7. Shapiro S, Strax P, Venet I: Changes in five-year breast cancer mortality in a breast screening program, in *Seventh National Cancer Conference Proceedings*, New York, American Cancer Society, 1973
8. Seidman HMBA: Screening for breast cancer in younger women: life expectancy gains and losses. *CA* 27:66–87, 1977

Influence of Contrast Material on Renal Venous Renin Activity

S. O. HIETALA,[1] J. J. ZELENAK, M. C. BEACHLEY, AND J. TISNADO

The influence of contrast material on renal venous renin activity was evaluated in a prospective study of 20 hypertensive patients. It is concluded that the absolute values of renal venous renin activity are either unchanged or unpredictably changed after injection of contrast material. The renal venous renin activity ratios seem to be less valid than the absolute values in predicting the significance of renal vascular or parenchymal disease.

An abnormal ratio of plasma renin activity between the two main renal veins is now an accepted criterion for predicting surgical improvement on the ischemic kidney in renal artery stenosis [1, 2]. The different components in the renin-angiotensin system are affected by many physiologic and pharmacologic variables. Renin is synthesized and stored in the juxtaglomerular apparatus of the kidney. The precise mechanisms governing renin release are still speculative. However, it seems that changes in renal perfusion pressure, as well as changes in the concentration or amount of sodium in the distal tubules, have regulatory effects. The effects of blood pressure, blood volume, posture, and sodium intake on renin release are probably mediated by one of these variables. The biochemistry and physiology of the renin-angiotensin system and the methods of measuring each component have been thoroughly reviewed and discussed by Oparil and Haber [3].

Whether or not administration of contrast material influences renin activity is important because often venous sampling for renin is done during the same procedure as renal arteriography. We would like to be sure the arteriography does not significantly alter the validity of the renal vein renin analysis. Since results from the few previous reports dealing with this subject are controversial [4, 5], we designed a prospective study to evaluate whether injection of contrast material during the sampling procedures might significantly alter renal vein renin activity. A similar study of the techniques and methods of renal venous renin sampling was recently reported [6].

Subjects and Methods

All 20 patients in this study were evaluated for hypertension by arteriography and selective renal vein sampling for renin. The patients received the usual hospital diet, and antihypertensive drug therapy was withheld only on the morning of the study. Single blood samples were collected after overnight fasting and recumbency with the patient supine. A single thin-walled catheter (polyethylene Kifa, 2.2 mm OD, 1.2 mm ID) with one end hole and two side holes was introduced via the femoral vein to the main renal veins by the Seldinger technique. The catheter was shaped so that the length of the curved portion was about 5 cm and its position was identified by fluoroscopy without using any contrast material. The catheter tip was advanced into the venous hilus of the kidney as far as possible and a spot film was taken.

No difficulties were encountered in the procedure of catheterization or sampling. Additional samples were taken from the vena cava above and below the entrance of the renal vein for assessing the peripheral renin levels. Blood samples were collected in nonheparinized syringes and immediately placed in test tubes containing ethylenediamine-tetra-acetic acid. The tubes were kept on ice and centrifuged within 30 min after samples were obtained.

Subsequently, arterial catheterization and selective renal arteriography was performed using 8 ml of contrast material. Renal veins were catheterized within 15 min of arteriography and single blood samples obtained. Catheter position was checked by injection of small amounts of Renografin-76 contrast material (diatrizoate meglumine and diatrizoate sodium, Squibb), and repeat spot film to assure catheter position was identical to that before arteriography. The exact position of the catheter was then checked by superimposition of the before and after radiographs. The time between the first and second sampling procedures was usually within 30 min. If the angiographic procedure was prolonged, additional vena cava samples were obtained to ensure steady state conditions.

Plasma renin activity was determined by duplicate analysis of the samples by radioimmunoassay for angiotensin I. The ratio of renin concentration in the main renal vein of the affected kidney (RA) to that in the main renal vein of the opposite kidney (RO) was calculated (RA/RO). In cases with normal renal arteriograms or with bilateral disease, ratios were given as the relation between the kidney with the highest renin value to that with the lowest (RH/RL) (table 1).

Results

On the basis of the arteriographic studies, three patient categories were defined: (1) normal arteriographic findings, (2) unilateral or bilateral stenosis of a main renal artery, and (3) renal parenchymal disease. Renin values and ratios are given for patients with normal angiographic findings (figs. 1 and 2) and unilateral disease (figs. 3 and 4). The normal range of renin values for patients with a general diet (0.4–2.7 ng/ml/hr supine) is indicated, as well as the significant renin ratio used in our laboratory (1.5). It appears that renin values from both kidneys in four patients with normal angiographic findings (fig. 1) were within normal range before and after administration of contrast material. In two other patients, renin activity in one kidney changed from normal to borderline abnormal.

In one patient renin ratios (fig. 2) were abnormal both before and after contrast injection. In another, it was

Received June 27, 1978; accepted after revision November 16, 1978.

[1] All authors: Department of Radiology, Virginia Commonwealth University, Medical College of Virginia, Box 2, Richmond, Virginia 23298. Address reprint requests to M. C. Beachley.

© 1979 American Roentgen Ray Society

0361-803X/79/1323-0429 $0.00

TABLE 1
Results Before and After Contrast Injection

Case No.	Renin Values (ng/ml/hr)				Renin Ratios		Angiographic Findings
	Before		After		Before	After	
	Right	Left	Right	Left			
1	2.15	1.90	2.85	1.75	1.13	1.62	Normal
2	1.71	3.52	2.94	2.53	2.06	1.16	Cyst, left kidney
3	1.00	0.95	0.75	0.90	1.05	1.20	Cyst, left kidney
4	3.15	3.70	>6.00	2.55	1.17	2.35	Renal artery stenosis, right kidney
5	2.52	0.64	0.35	0.28	3.94	1.29	Fibromuscular hyperplasia, right renal artery
6	1.64	1.46	2.58	2.95	1.12	1.14	Normal
7	5.30	4.70	6.00	6.20	1.13	1.03	Bilateral chronic glomerulonephritis
8	0.10	0.09	0.10	0.22	1.11	2.20	Renal artery stenosis, right kidney
9	3.30	1.40	4.50	2.20	2.36	2.05	Renal artery stenosis, right kidney
10	>22.00	7.80	>22.00	12.80	2.80	1.72	Occluded right renal artery
11	0.92	1.98	1.31	0.91	2.15	1.44	Normal kidney, ? adrenal mass
12	2.60	1.00	1.60	0.92	2.60	1.74	Normal
13	2.20	1.70	1.00	1.40	1.29	1.40	Normal
14	0.45	0.45	0.55	0.35	1.00	1.57	Renal cell carcinoma, right kidney
15	0.60	7.00	4.65	0.75	11.67	6.20	Fibromuscular hyperplasia, left renal artery
16	1.80	1.22	0.82	0.63	1.48	1.30	Hydronephrosis, right kidney
17	9.99	6.09	6.04	3.12	1.64	1.94	Renal artery stenosis, right kidney
18	1.20	1.30	0.70	0.55	1.08	1.27	Cyst, left kidney
19	1.00	0.90	0.70	0.70	1.11	1.00	Normal
20	0.10	0.40	0.00	0.00	4.00	1.00	Renal artery stenosis, right kidney

Note.—All but case 1 were hypertensive.

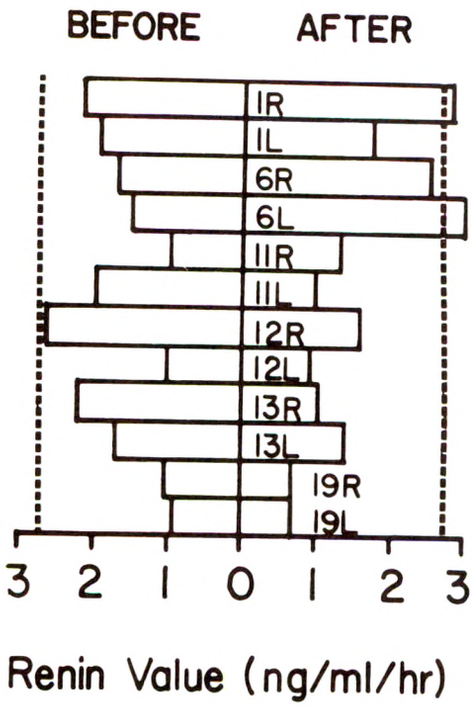


Fig. 1.—Renin values for six patients with normal arteriograms before and after contrast injection. (R = right kidney; L = left kidney; normal renin value = 2.7 ng/ml/hr, *dotted line*; numbers on bar graph = case nos. from table 1.)

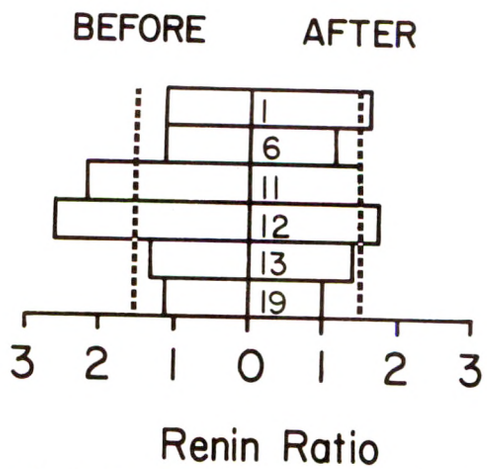


Fig. 2.—Renin ratios for six patients with normal angiograms before and after contrast injection. (Normal renin ratio = 1.5, *dotted line*; numbers on bar graph = case nos. from table 1.)

abnormal before, but normal after contrast injection. In a third patient, the renin ratio was normal before and abnormal after contrast injection. Renin ratios for the remaining three patients were normal both before and after contrast injection.

Renin values in patients with renal disease, including arterial stenosis, are illustrated in figure 3. The absolute renin values after administration of contrast material were considerably different from the corresponding values before contrast material injection, although in most patients the values before and after injection were either both within the normal range or within the abnormal range. In one patient with high abnormal renin activity before contrast material injection, there was a change to borderline normal activity. Renin ratios in patients with unilateral disease showed a pattern of variation similar to the patients with normal angiographic findings (fig. 4). A change from normal to abnormal ratios was seen in

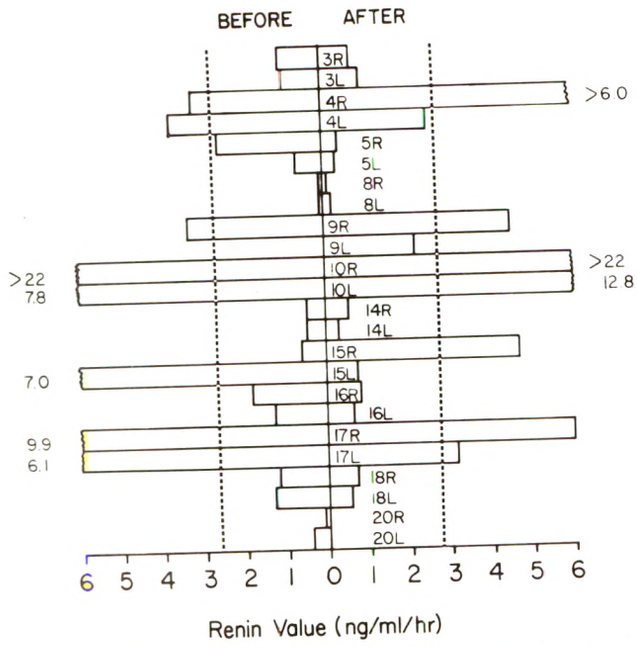


Fig. 3.—Renin values for 12 hypertensive patients with unilateral renal disease before and after contrast injection. (R = right kidney; L = left kidney; normal renin value = 2.7 ng/ml/hr, *dotted line*; numbers on bar graph = case nos. from table 1.)

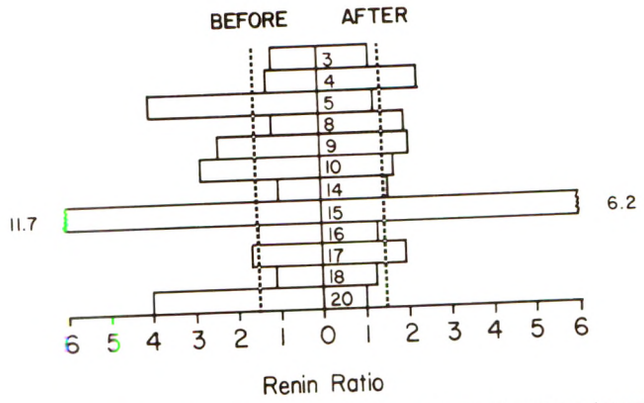


Fig. 4.—Renin ratios of 12 hypertensive patients with unilateral renal disease before and after contrast injection. (Normal renin ratio = 1.5, *dotted line*; numbers on bar graph = case nos. from table 1.)

two patients, and from abnormal to normal in two patients.

Discussion

It seems that numerous factors influence plasma renin values. Therefore, blood collected for renin determination must be rigorously controlled, and each laboratory should have strict rules for patient preparation and sampling procedures and should establish the normal range of renin values, accordingly. Technical artifacts can easily alter renin values. Thus, if the catheter is not placed into the venous hilus of the kidney, falsely lowered renin values may be received due to dilution from other veins, especially on the left side. It has been shown that segmental venous sampling [1] will give more specific results than sampling in the main renal vein [5]. This is especially true in patients with segmental lesions of the parenchyma or renal vasculature, such as renal infarct or stenosis of a segmental renal artery.

Commonly used contrast materials contain sodium. A larger sodium load in the distal tubules has been shown to be accompanied by an increase in distal tubular volume and increased contact with arteriolar cells resulting initially in decreased renin release [3]. An increased area of contact between the elements of the juxtaglomerular apparatus and the afferent arteriole may also be mediated by vasodilation. Injection of contrast materials, which are vasodilators, would consequently give an initial decrease in renin release. According to these theories, administration of a contrast medium would give a decrease and later a feedback-regulated increase in renal venous renin activity, whatever the mechanisms of its action.

Whelton et al. [6] found that simultaneous renal vein sampling was not essential, and recommended using a single catheter to sequentially obtain renal venous blood samples. We agree with their conclusions in that (1) renal venous renin activity is either unchanged or unpredictably changed by injection of contrast material and (2) renal venous renin activity ratios seem to be less valid than the difference in absolute values in predicting the significance of renal vascular disease.

Our results indicate the changes in renin levels could be ascribed to sampling and testing variations. Whatever the mechanism of contrast material influence on renin release, the measured renin values from before to after contrast material administration were, in most cases, both normal or both abnormal.

Renin values from individual kidneys were seen to increase or decrease after injection of contrast material in both normal and abnormal kidneys. Therefore, we conclude that no consistent change in renin activity can be ascribed to the injection of contrast material.

ACKNOWLEDGMENT

We thank Wanda Cunningham for secretarial and editorial assistance.

REFERENCES

1. Korobkin M, Glickman MG, Schambelan M: Segmental renal vein sampling for renin. *Radiology* 118:307–313, 1976
2. Stockgit JR, Collins RD, Noakes CA, Schambelan M, Biglieri EG: Renal-vein renin in various forms of renal hypertension. *Lancet* 1:1194–1198, 1972
3. Oparil S, Harber E: The renin-angiotensin system (first of two parts). *N Engl J Med* 291:389–401, 1974
4. Amplatz K: Angiography in assessing renovascular hypertension. Past and present. *Geriatrics* 29:52–57, 1974
5. Mallinckrodt, Nuclear: R/A-Mat® Angiotensin 11125 Kit 250 tests. For the in vitro determination of plasma renin activity by radioimmunoassay of angiotensin I. Mallinckrodt Inc., St. Louis, 1975
6. Whelton K, Harrington DP, Russell RP, White RI, Walker WG: Renal vein renin activity: a prospective study of sampling techniques and methods of interpretation. *Johns Hopkins Med J* 141:112–118, 1977

Minimum Blood Vessel Diameter Measured by Magnification Angiography

TAMAS SANDOR[1] AND DOUGLASS F. ADAMS[1]

Visibility of small blood vessels was improved by magnification angiography of biologic specimens. Blood vessel diameter was determined for increasing magnifications by various screen-film combinations. Significantly smaller vessels were recognized with the magnification technique in all screen-film combinations. Noisy screen-film combinations with better square wave transfer functions did not allow visualization of blood vessels as small as those screen-film combinations with poorer square wave transfer functions but less noise.

Radiographic magnification affects the modulation transfer function or square wave transfer function of the imaging system primarily by increasing both image contrast and resolution [1, 2]. In angiography, an increase in image contrast and resolution should allow visualization of blood vessels of smaller diameter. Documented benefits of magnification angiography should quantitatively compare angiograms taken at various magnifications. An in vivo animal model is not ideal for such comparisons, because the number of injections an animal can tolerate is limited and, after several injections, contrast agent accumulates heterogeneously within some organs and is retained for relatively long periods of time. Moreover, it is difficult to determine the true blood vessel diameter with precision because of inaccurate information concerning its depth within the organ. Finally, the effect of scattered radiation is not constant with varying magnification.

We used biologic specimens to eliminate these difficulties and to isolate the effect of magnification on blood vessel image quality. We measured improvement in subjective visibility of small blood vessels in magnification angiograms. The effects of magnification were assessed with two types of high-speed rare-earth intensifying screens that have high potential for clinical application and with a par-speed screen that has comparable resolution properties (square wave transfer function). The par-speed screen provided high quality measurements for comparison purposes.

Materials and Methods

Blood vessels from human brains and rabbit kidneys were injected with radiopaque Microfil. After fixation, 0.5–2.5 mm sections of these specimens were placed on thin glass plates. Films of uniform density (1.10 ± 0.05 optical density units) were made with a biasable Siemens Bi 125/3/50 RG microfocal spot x-ray tube (measured focal spot size = 0.15 × 0.18 mm²) at 50 kV. The tube had a fixed current of 30 mA. Films of the specimens were obtained at ×1.2–7 magnification on the following screen-film combinations: U.S. Radium experimental screens (a mixture of 75% yttrium and 25% gadolinium) with Dupont Cronex 4 and Kodak RPR films; Trimax Alpha 8 screens with XD films; and Radelin T-2 screens with Cronex 4 films. No scattering material was added. The ratio of exposure times to achieve equal optical densities at 50 kV were: US Rad/RPR:US Rad/Cr 4: ALPHA 8/XD: Radelin T-2/Cr 4 = 1:1.8:2:8.

The specimens were also exposed in contact with Kodak high resolution plates at 25 kV with a beryllium window tube to measure blood vessel diameter. Blood vessel diameters on these plates were then measured with a microscope to a precision of 1 μm. A rabbit kidney specimen taken with Alpha 8/XD combination at ×3 magnification is shown in figure 1A. For comparison, figure 1B shows a radiograph of the same specimen taken with a Kodak high resolution plate.

The radiographs were viewed by two observers in order of increasing magnification. The observers' task was to identify as many blood vessels within designated areas of the radiograph as they could. Each visible vessel in each section was specifically identified by the observers and tabulated against that particular vessel in the control radiograph. Since the specimens were thin, some vessels may have coursed in and out of the specimen. Each visible vessel section was counted as an independent vessel in the experiment. The length of the observation periods was restricted to a maximum of 1½ hr. Shorter periods were used when an observer appeared fatigued. Use of both magnifying and minifying lenses was permitted.

The number of blood vessels found on a designated area of the high resolution plate was plotted as a function of diameter in a control histogram. On another histogram, the number of vessels recognized by the observer was plotted for each magnification and screen-film combination. This histogram could be superimposed on the control histogram to produce a combined histogram such as the one for the Alpha 8/XD screen-film combination for observer 1 at ×3 magnification (fig. 2), in which the total bar height indicates the number of vessels of this diameter present on the high resolution plate.

From this combined histogram the percentage of total vessels of a particular diameter in the designated area that were perceived by the observer is determined. These percentages were replotted as a function of blood vessel diameter (fig. 3). The ascending part of the resultant data set is fitted with an exponential function. The 50% value of this function identifies the blood vessel diameter with a 50% probability of being perceived by the observer under the given filming specifications, which is termed the "threshold diameter." Plotting the threshold diameter as a function of magnification, an independent curve is obtained for each observer and each screen-film combination. These data are combined for the two observers to produce a single curve for each screen-film combination.

To determine the resolution properties of each screen-film combination, square wave transfer function was measured.

Received October 8, 1976; accepted after revision December 11, 1978.
This work was supported in part by U.S. Public Health Service grants HL 20895, HL 05832, GM 01910, and CA 23246.
[1] Department of Radiology, Harvard Medical School and Peter Bent Brigham Hospital, 25 Shattuck Street, Boston, Massachusetts 02115. Address reprint requests to T. Sandor.

© 1979 American Roentgen Ray Society

0361–803X/79/1323–0433 $0.00

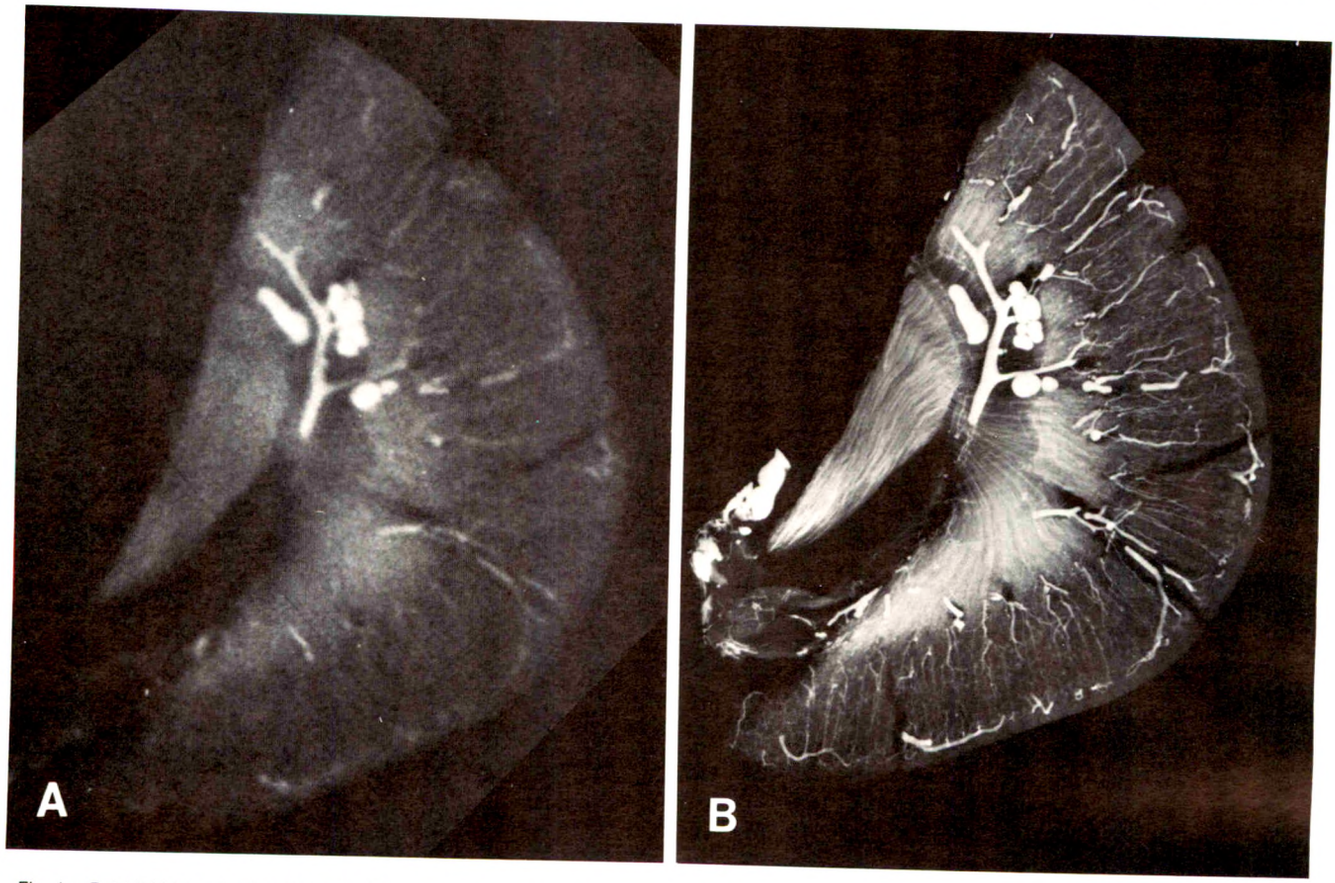


Fig. 1.—Rabbit kidney. **A**, With Alpha 8/XD combination at magnification ×3 and 50 kV. **B**, With Kodak high resolution plate, direct contact, at 25 kV.

(Square wave transfer functions have to be distinguished from the sine wave or modulation transfer function. The mathematic relation between the two is described in detail by Coltman [3].) This was obtained by exposing a screen-film combination in contact with a multiple bar line test pattern. The pattern was made of 0.05-mm-thick lead and contained rectangular bars in groups of four with increasing resolution up to 10 line pairs/mm. A densitometer was used to examine the resultant images. The ideal densitometric response of such a rectangular pattern should result in rectangular waves, commonly known from optics as square waves. From the diminishing amplitudes of the square wave groups toward higher frequencies, as obtained from computer analysis of densitometric tracings, the values of the square wave transfer function were determined for each bar group of given line pair/mm value. Square wave transfer functions obtained in this way are less accurate than modulation transfer functions measured by high precision slits, but they are adequate for the comparisons made here.

To obtain a measure of radiographic noise, the density fluctuations were determined for each screen-film combination. The root mean square density fluctuation can be written as

$$\sigma_D = [\overline{D(x, y)^2} - (\bar{D})^2]^{1/2},$$

where $D(x, y)$ is the point-by-point density on film and the bar denotes the respective means. It is known that the variance of the measured density fluctuation (σ_D^2) is the volume under the two-dimensional Wiener or noise-power spectrum [4]. The values of $D(x, y)$ were obtained by scanning 2,560 × 256 matrices on the films with an electrooptical scanner, which had a scanning aperture of 25 × 25 μm and a gray level resolution of 256 within the optical density range of 0–2. Therefore, the dimensions of an area strip were 64 × 6.4 mm².

Results

For all screen-film combinations, increasing the degree of magnification improved the visibility of small blood vessels. However, going beyond ×7 generated fuzziness or blurring. When magnification was increased to 7 times, the threshold diameter was reduced by 40%–60% (fig. 4).

The observers could see smaller vessels on the films obtained with the Radelin T-2/Cr 4 screen-film combination than on the Alpha 8/XD, the US Rad/RPR, or the US Rad/Cr 4 screen-film combinations.

The measurements of the square wave transfer function showed no major difference between the Radelin T-2/Cr 4 and the US Rad/RPR or US Rad/Cr 4 screen-film combinations (fig. 5). The Alpha 8/XD screen-film combination exhibited a significantly poorer square wave transfer function.

The fluctuations measured in the optical density values were: US Rad/RPR, 5.03; US Rad/Cr 4, 3.79; Alpha 8/XD, 3.64; and Radelin T-2/Cr 4, 3.19. The statistical error of the data was negligible due to the large number of

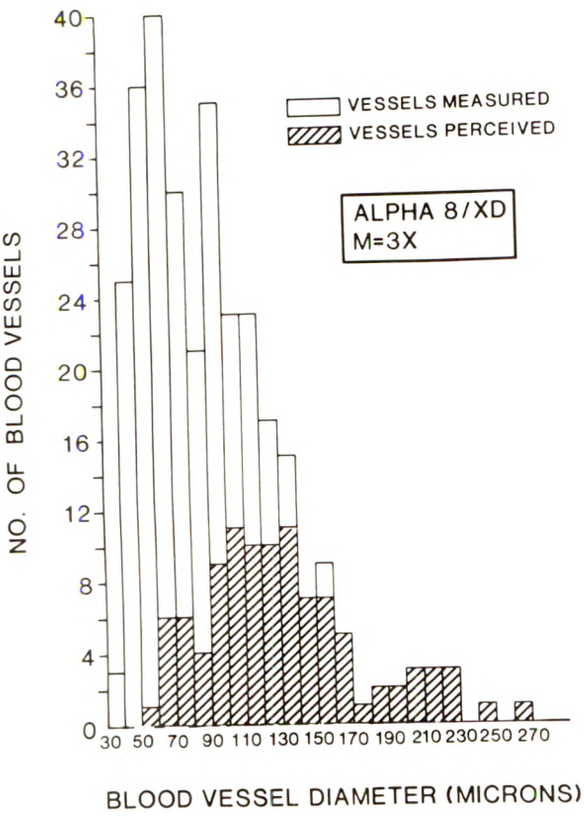


Fig. 2.—Histogram of vessels recognized by observer 1 on radiographs taken with Alpha 8/XD combination at ×3 magnification superimposed on histogram of all vessels measured on the high resolution plates.

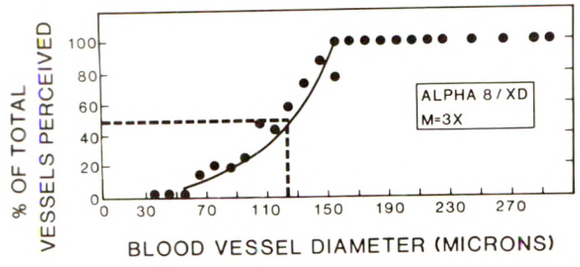


Fig. 3.—Percentage of total vessels perceived as a function of diameter for Alpha 8/XD combination at magnification ×3. Solid line indicates exponential curve fitted to ascending part of data. Threshold diameter corresponding to 50% amplitude indicates blood vessel diameter with 50% probability of being perceived.

points used in calculation. Systematic errors in σ_D associated with the data, such as film artifacts, scratches, and processing performance, are greater than the statistical error and estimated to be about 5%. Therefore, the results indicate a marked reduction in noise between the US Rad/RPR and the Radelin T-2/Cr 4, while no significant difference was found between US Rad/Cr 4 and Alpha 8/XD. The performance of the screen-film combinations can be judged more easily by ranking according to function (table 1).

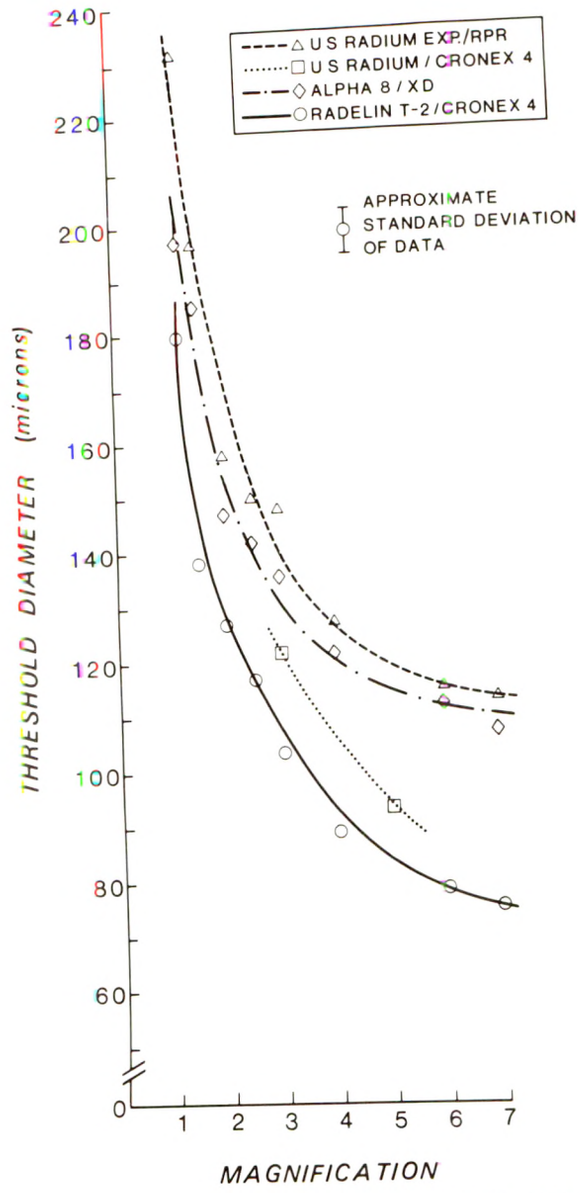


Fig. 4.—Threshold diameter as a function of magnification for various screen-film combinations. Data combined for both observers.

Discussion

This work confirms the usefulness of magnification radiography in displaying small blood vessels when magnification in excess of ×2 is used with focal spots of less than 0.2 mm. The disparity between the actual measured observer performance and that which might have been expected using the square wave transfer functions measured in a series of screen-film combinations is significant. On film examination, this disparity seemed due to radiographic mottle. This assumption is supported by observer performance on the US Radium screens when the slower Cronex 4 film was used: observer perform-

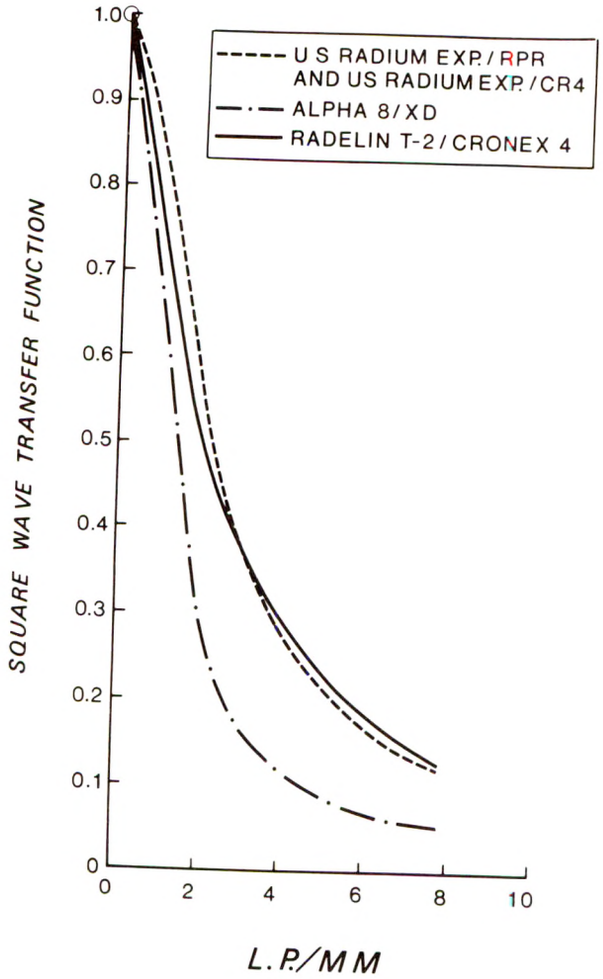


Fig. 5.—Square wave transfer functions of screen-film combinations used in study. L.P./MM = line pairs per millimeter.

ance improved along with reduction of the mottle. We believe this indicates that observer performance limitation in the model used is the photon flux rather than resolution properties of the screen-film combination.

The measured data on density fluctuation somewhat support this assumption, although they did not reveal a delineation in σ_D for US Rad/Cr 4 and Alpha 8/XD similar to the one found between the respective curves (fig. 4). These results also indicate the need for further in-depth study of radiographic noise, including the Wiener spectrum and possibly the quantitative assessment of image texture. They also suggest that a test of observer performance, such as outlined in this report, is an important adjunct to physical tests, such as the square wave (or modulation) transfer function measurements, in predicting the clinical performance of new components of imaging systems.

TABLE 1

Performance Results

Screen/Film	Visibility	Square Wave	Noise	Exposure
US Rad Exp/RPR	4	1	3	1
Alpha 8/XD	3	2	2	2
US Rad Exp/CR 4	2	1	2	1.8
Rad T-2/CR 4	1	1	1	8

Note.—1 = best exposure; 4 = poorest.

This study examines an ideal situation in which neither scattered radiation nor motion was involved. The data reflect the psychophysical effects of magnification per se on the amount of visualized anatomy for an imaging system of a given focal spot size, kilovoltage, contrast medium, mean optical density, and screen-film combination. Although it does not specify the diameter of the smallest blood vessel visible in a clinical setting with currently available equipment, the results do approximate the limits of relative improvement in threshold visibility of small blood vessels under such conditions. Our results can be extrapolated to clinical situations in which motion is not relevant and where the scattered radiation can be efficiently reduced (e.g., angiography of extremities).

REFERENCES

1. Sandor T, Adams DF, Herman PG, Eisenberg H, Abrams HL: The potential of magnification angiography. *AJR* 120: 916–921, 1974
2. Doi K, Rossman K: Computer simulation of small blood vessel imaging in magnification radiography, in *Small Vessel Angiography, Imaging, Morphology, Physiology, and Clinical Applications*, edited by Hilal SK, St. Louis, Mosby, 1973, pp 6–12
3. Coltman JW: The specification of imaging properties by response to a sine wave input. *J Opt Soc Am* 44:468–471, 1954
4. Dainty JC, Shaw R: *Image Science*. New York, Academic Press, 1974

Presacral Space Revisited

KENNETH R. KATTAN[1] AND ATHENA Y. KING[2]

Increase in the width of presacral space measurements is considered indicative of disease of the rectum and/or other structures in the pelvis. The traditionally accepted normal width of presacral space is not more than 15 mm. In some normal patients older than 45 years, the presacral space is wider than 15 mm and may even exceed 20 mm.

Increase in the width of presacral space measurements is considered indicative of disease of the rectum and/or other structures in the pelvis. The presacral space widens in ulcerative colitis [1, 2], granulomatous colitis [3], lymphogranuloma venereum, and in postirradiation changes [1]. It has been described in thrombosis of the inferior vena cava and tuberculous proctitis [4], and tumor of the sacrum or posterior wall of the rectum [5]. Carcinomatous deposits in the pelvis can also cause presacral space widening.

A presacral space of 7.5 mm is considered the average in the normal adults according to Chrispin and Fry [4]. However, the maximal normal varies among different authors. Edling and Eklof [2] consider 10 mm as the maximum normal and any increase as pathologic. Chrispin and Fry [4] suggest any value above 15 mm should be regarded with suspicion and above 20 mm should be considered abnormal. Although this is is generally true, we studied films of some patients in whom the presacral space was wider than 20 mm, with no pathology in the colon or pelvis. All of these patients were over 45 years old.

Materials and Methods

Study materials were barium enema studies from Batesville Hospital, Batesville, Indiana; Holmes and Drake Hospitals, Cincinnati, Ohio; Springboro Clinic, Ohio; and the Veterans Administration Hospital, Dayton, Ohio. The patients had no colonic pathology and no previous abdominal or pelvic surgery. Patients with colonic diverticulosis or with history of uncomplicated appendectomy were included in the study as normals. Of 252 patients studied, only 187 fulfilled the criteria for our study. The patients were 100 white men and 87 white women; age range was 17–89 years.

Measurements were done on the Bucky lateral view of the barium-filled rectum. The shortest distance between the posterior edge of the barium column and the anterior edge of the fifth sacral vertebra was measured in millimeters (fig. 1). No correction was made for magnification. The fifth sacral segment was chosen because the rectum lies in the midline at this level [4]; second, measurements as low as S3 are variable, since the sigmoid may extend as low as S3 [6].

Findings

Our findings are summarized in table 1 and figure 2. In 143 (76.47%) of 187 patients, the presacral space was 10 mm or less. In another 28 patients (14.97%) the presacral

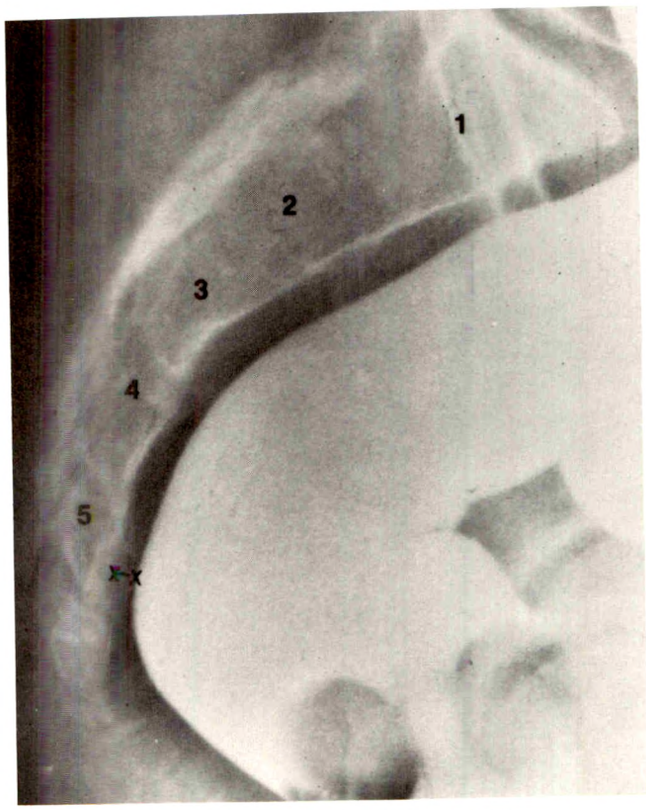


Fig. 1.—Lateral view barium-filled rectum.

TABLE 1

Distribution According to Age Group and Width of Presacral Space

Age (years)	Width (mm)			
	More than 20	16–20	10–15	1–10
Female:				
To 45	0	0	1	21
45–60	0	1	1	19
Over 60	2	2	4	36
Male:				
To 45	0	0	8	19
45–60	2	3	5	24
Over 60	3	3	9	24

Received February 24, 1978; accepted after revision November 16, 1978

[1] Department of Radiological Sciences, Wright State University Medical School, and Department of Radiology, Veterans Administration Medical Center, 4100 West Third Street, Dayton, Ohio 45428. Address reprint requests to K. R. Kattan.

[2] Department of Radiology, Christian Holmes Hospital, and University of Cincinnati College of Medicine, Cincinnati, Ohio 45219.

© 1979 American Roentgen Ray Society

0361–803X/79/1323–0437 $0.00

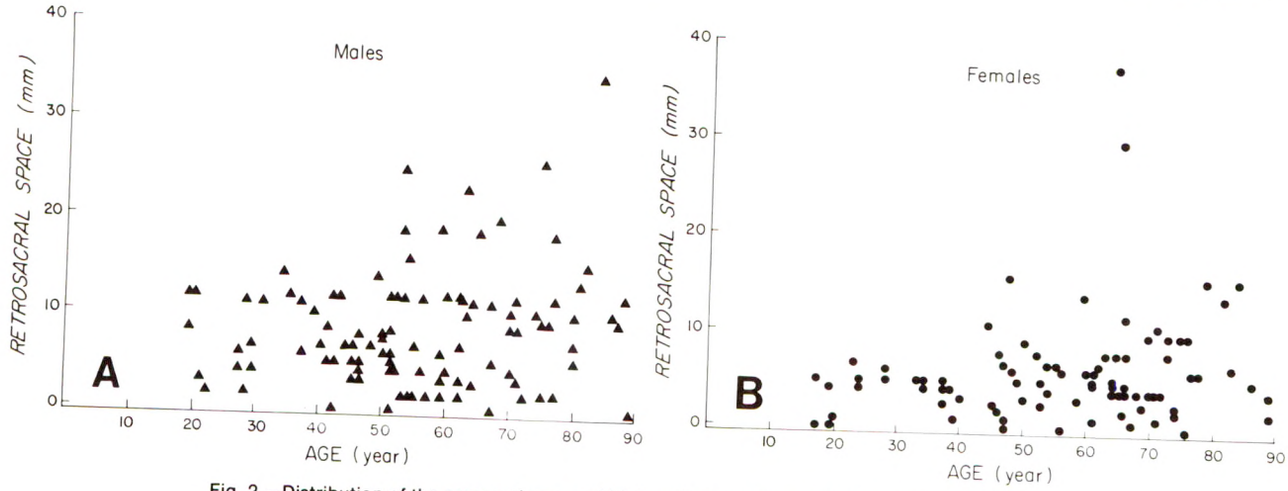


Fig. 2.—Distribution of the presacral space width in patients according to age. **A**, Male. **B**, Female.

TABLE 2

Measurement of Presacral Space

Age (years)	No. Patients	Mean (mm)	Standard Deviation (mm)
Female:			
To 45	22	4.5	3.2
46–60	21	5.7	4.1
Over 60	44	7.6	7.1
Male:			
To 45	28	7.4	3.8
46–60	34	8.1	6.6
Over 60	38	9.9	7.4

space was 11–15 mm. The presacral space of the other 16 patients (8.56%) was 16 mm or more. The patients in this last group were 46 years or older. That is, 16 (11.59%) of 138 patients over 45 had presacral space greater than 15 mm. On the average, men had predominance in this category (men, 11/73; women, 5/65).

In seven (5.01%) of the 138 patients who were 46 years and older, the presacral space was more than 20 mm. Five were men (two 46–60 years and three older than 60 years); only two women showed a presacral space wider than 20 mm (all over 60 years, none 46–60).

Statistical Analysis

The 100 male patients and 87 female patients were divided into three groups by age; up to 45 years, 46–60 years, and over 60 years. The means and standard deviations of the presacral space of those groups are shown in table 2.

For both men and women there was no significant difference at the 0.05 level among the means of the three age groups using the analysis of variance technique. For female patients the F-ratio was 2.3 and the associated probability that the groups have the same mean is 0.103. For male patients the F-ratio is 1.4 with associated probability of 0.243.

However, it cannot be assumed that the groups come from populations with the same standard deviation. For women the standard deviation of the oldest group is more than twice the standard deviation of the youngest group; for men the standard deviation of the oldest group is almost twice that of the youngest group. It seems that there is more dispersion in the oldest groups than in the youngest groups. Therefore, it may not be valid to assume a maximum normal presacral space for patients in all age groups.

Discussion

These findings show that the measurement of the presacral space in some patients exceeds the accepted "upper limits of normal" for no apparent reason. While in most patients, the normal presacral space measurement is 15 mm or less, there are some patients who have a higher value without any abdominal or pelvic pathology or surgery. It is interesting that all of these patients are over 45 years of age. In this study we found that individuals up to age 45 had presacral space whose upper limits of normal was 15 mm. Only one of 22 women in this age group had a measurement above 10 mm; the men had a higher number, namely eight of 25 (table 1).

This picture changes in patients over 45 (fig. 2). Between ages 46–60, five of 34 men showed measurements over 15 mm; two of these were more than 20 mm. In six of 39 men over 60, measurements were over 15 mm (three over 20 mm). The picture is less dramatic in women aged 46–60. In this group only one of 21 patients had values over 15 mm and none over 20 mm. Of 44 women older than 60, four had values over 15 mm (two over 20). We assume the lower measurements in women are attributable to the difference in body build. This assumption was not proven since we did not measure the patients' build and we do not have their weights for evaluation.

Conclusions

The upper limits of normal width of presacral space is 15 mm in patients not older than 45 years. Above this age, most patients still conform to this criterion. However, some patients have measurements over 15 mm with no apparent reason. Fewer still have measurements above 20 mm. This possibility increases with increased age. In the evaluation of the presacral space, factors

such as age, sex, and the weight of the patient should be taken into consideration.

ACKNOWLEDGMENT

We thank Diane Spurlock, Murray, Kentucky and James G. Kereiakes, Cincinnati, Ohio for the statistical analysis of the figures.

REFERENCES

1. Fennessy JJ, Sparberg M, Kirsner JB: Early roentgen manifestations of mild ulcerative colitis and proctitis. *Radiology* 87:848–858, 1966
2. Edling NPG, Eklof O: The retrorectal soft tissue space in ulcerative colitis. *Radiology* 80:949–953, 1963
3. Eklof O, Gierup J: The retrorectal soft tissue space in children: normal variations and appearances in granulomatous colitis. *AJR* 108:624–627, 1970
4. Chrispin AR, Fry IK: The presacral space shown by barium enema. *Br J Radiol* 36:319–322, 1963
5. Forrester HC, Soule AB: Profile lateral projection in the diagnosis of lesions of the rectum. *AJR* 84:332–338, 1960
6. Gardiner GA: Routine lateral view of the barium-filled colon. Is it worthwhile? A review of 2500 consecutive examinations. *AJR* 104:571–579, 1968

Foley Catheter Method of Esophageal Foreign Body Removal: Extension of Applications

GEORGE W. MIXON[1]

The fluoroscopically controlled Foley catheter technique can be used to remove nonopaque esophageal foreign bodies that are smooth or soft and foreign bodies in patients with esophageal strictures or after esophageal atresia repair. These situations have previously been felt to be contraindications for this procedure. Successful treatment was accomplished in 21 of 25 patients.

Removal of smooth, opaque esophageal foreign bodies by radiologists using Foley catheters under fluoroscopic control is a recognized procedure [1–4]. This method precludes hospitalization, general anesthesia, and the minimal risks of endoscopy. Previously, it was assumed that this technique could not be used for nonopaque esophageal foreign bodies or in patients with esophageal stricture or prior esophageal atresia repair. My experience indicates this procedure can be successfully used in these three situations.

Materials and Methods

During a 26-month period ending in August 1977, 14 children with 25 esophageal foreign bodies were seen at Primary Children's Medical Center. Ten children were under 4 years of age; the others ranged from 8–13 years. The foreign bodies were either nonopaque or occurred in patients with an esophageal stricture or a history of surgical repair for esophageal atresia. Three children were seen more than once; in one child more than one foreign body was found.

If opaque objects were not identified on conventional films or fluoroscopy, barium esophagograms were performed to determine the presence of nonopaque objects. When such bodies were identified, an attempt was made to identify the nature of the object by evaluating its radiographic characteristics and by questioning both the patient and his parents. When the body was defined as being smooth, removal was attempted.

After immobilization, the patient is placed in the right anterior oblique position. A Foley catheter with a 3 or 5 ml balloon is then passed transnasally into the esophagus. Barium is intermittently injected through the catheter into the esophagus as needed to outline the foreign body to facilitate catheter manipulation. After the catheter passes beyond the obstruction, the balloon is distended with barium (fig. 1) and traction is applied until the object is retracted into the hypopharynx. The child is then encouraged to spit out the foreign object and the balloon is deflated. After foreign body removal, an esophagogram is performed to demonstrate the status of the esophagus.

Results

In only four of the 14 patients studied was there no underlying esophageal abnormality; seven had esophageal atresia repair, two had strictures secondary to gastroesophageal reflux, and one had undergone an antireflux operation. Two of the patients with esophageal atresia repair had associated congenital distal esophageal stricture and each had repeated episodes of esophageal foreign bodies. In both individuals the anastomotic site was widely patent and the foreign bodies always lodged at the level of the congenital strictures.

Most of the foreign bodies consisted of gristle or a portion of a weiner, some surprisingly large. Other objects included a penny, pea, wad of masking tape, and various rubber or plastic items. Only two were opaque; the other 23 were nonapaque.

The catheter technique was successful in 21 of the 25 cases. In 16 instances the foreign body was removed, while in three it was pushed into the stomach by manipulation of the Foley catheter. In two others, vomiting induced by the procedure resulted in the foreign body being disgorged.

In four instances attempts to remove the objects were not successful; on two occasions a catheter could not be advanced beyond the gristle which was lodged at the site of an esophageal stricture and in one case the foreign body was successfully retracted into the oropharynx repeatedly but reswallowed each time. In these three instances endoscopic extraction was necessary. Another patient had no underlying esophageal abnormality but had a very large piece of gristle which was pushed into the stomach under fluoroscopic control with a mercury-filled rubber esophageal dilator. There were no complications in any of the cases.

Discussion

The technique of removing esophageal foreign bodies with the Foley catheter has been thought to be potentially dangerous in several situations: the removal of nonopaque objects that cannot be visualized during fluoroscopically controlled manipulations; in children with esophageal strictures because of the risk of perforation; and in postoperative esophageal atresia patients because they often have an anastomotic stricture and/or dilatation proximal to the anastomosis which makes retraction of objects difficult. My experience with the Foley catheter suggests that foreign object removal can be used safely in these situations.

Barium, rather than water-soluble contrast material, is used to opacify both the esophagus and balloon. This precludes the possible aspiration of a water-soluble

Received January 5, 1978; accepted after revision December 11, 1978.
[1] Departments of Radiology, Primary Children's Medical Center and University of Utah Medical Center, Salt Lake City, Utah 84103.

© 1979 American Roentgen Ray Society

0361–803X/79/1323–0441 $0.00

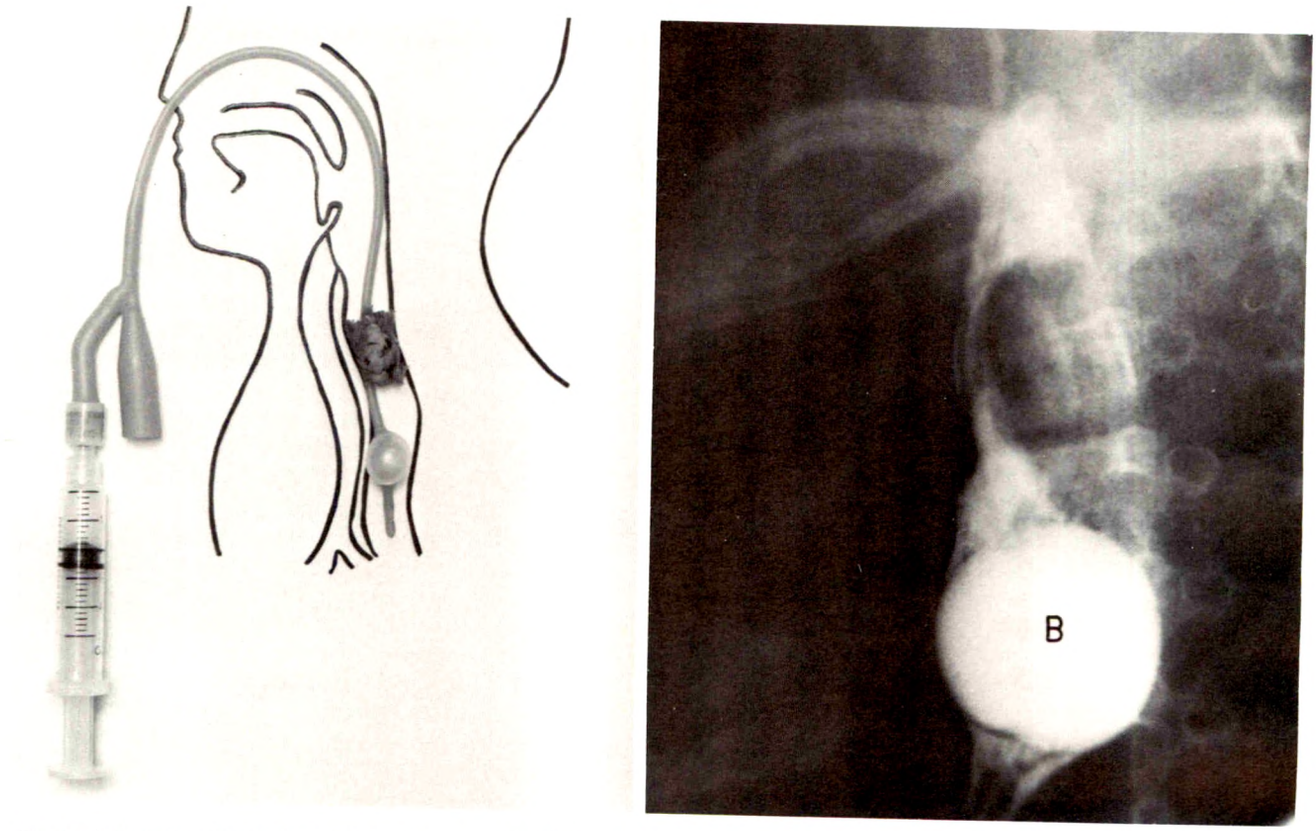


Fig. 1.—Left, method of esophageal foreign body removal. Right, Nonopaque esophageal foreign body removal. Barium outlines piece of gristle. Distended Foley balloon (B) is distal to foreign body.

agent into the upper respiratory tract structures. In children with an esophageal stricture, care should be taken to distend the balloon only a small amount initially. After the foreign body has been retracted above the narrowed area, further balloon distension can be done as required.

In four instances in which gristle had been lodged at the site of a stricture for several hours or days, a Foley catheter could not be advanced beyond the esophageal foreign body. In these cases a smaller vascular-type balloon catheter (such as Swan-Ganz, Berman, Rashkind) was used to retract the foreign body above the stricture site and the procedure was then completed with a Foley catheter.

I have found the right anterior oblique position to be best suited to this technique. While a Trendelenburg position has been recommended [1, 2], I have not found this maneuver helpful.

Although I believe the new technique to be safe, as a caution, I recommend that it be attempted only by radiologists who are experienced in removing opaque esophageal foreign bodies under the described conditions.

Successful treatment of esophageal food impaction in adults using intravenous glucagon has been reported [5]. This method was not used in this series and its usefulness in children has not been reported. In instances where there is no underlying esophageal abnormality its trial seems warranted.

REFERENCES

1. Shackelford GD, McAlister WH, Robertson CL: The use of a Foley catheter for removal of blunt esophageal foreign bodies from children. *Radiology* 105: 455–456, 1972
2. Campbell JB, Davis WS: Catheter technique for extraction of blunt esophageal foreign bodies. *Radiology* 108:438–440, 1973
3. Henry LN, Chamberlain JW: Removal of foreign bodies from esophagus and nose with the use of a Foley catheter. *Surgery* 71:918–921, 1972
4. Growe JE: Removal of blunt esophageal foreign bodies: Foley catheter technique. *NC Med J* 37:431–432, 1976
5. Ferrucci JT, Long JA: Radiologic treatment of esophageal food impaction using intravenous glucagon. *Radiology* 125: 25–28, 1977

Case Reports

Ultrasound Diagnosis of Neonatal Adrenal Hemorrhage

D. EDWARD MINEAU[1] AND P. RUBEN KOEHLER[1]

Ultrasound is a noninvasive means of evaluating abdominal and flank masses in the neonate. The case of a neonate whose abdominal mass first manifested as a solid-appearing lesion, suggesting a neuroblastoma, is reported here. Follow-up examinations at 3 and 7 days showed development of the anechoic appearance typical of hematoma. Correct diagnosis of adrenal hemorrhage was then made.

Case Report

S. A. weighed 3,260 g when delivered at full term from a frank breech presentation. Physical examination revealed ambiguous genitalia and a questionable right renal mass. Ultrasound (Picker EDC, 3.5 mHz transducer) performed at age 48 hr identified a large suprarenal mass with dense internal echoes (fig. 1A). Aortography performed because of the ultrasonic characteristics of a solid mass and the ambiguous genitalia, showed a large avascular suprarenal mass. Since the baby's hematocrit was only 39, a diagnosis of adrenal hemorrhage was entertained. Repeat ultrasound 72 hr later showed a more cystic appearance of the mass, and by age 10 days the mass had become almost completely anechoic (fig. 1B). The mass progressively diminished and the child was discharged after 19 days with diagnosis of adrenogenital syndrome and right adrenal hemorrhage secondary to birth trauma.

Discussion

Neonatal adrenal hemorrhage is an infrequent complication of birth trauma in breech presentations, large infants, and forceps deliveries. It may also be related to neonatal asphyxia [1]. Presentation ranges from asymptomatic flank mass to clinical symptoms resulting from acute adrenal failure. Shock due to blood loss may require transfusions [2]. Diagnosis often is not made until characteristic calcifications are found on abdominal films taken for other reasons later in childhood [3].

The differential diagnosis of a flank mass in the neonate includes neuroblastoma, fetal-renal hamartoma, multicystic kidney, hydronephrosis, and adrenal hemorrhage. Ultrasound can easily distinguish hydronephrosis and multicystic kidneys from solid masses. Neuroblastomas and fetal-renal hamartomas will appear as solid masses. Unfortunately, as in this patient, adrenal hemorrhage may initially appear on ultrasound examination

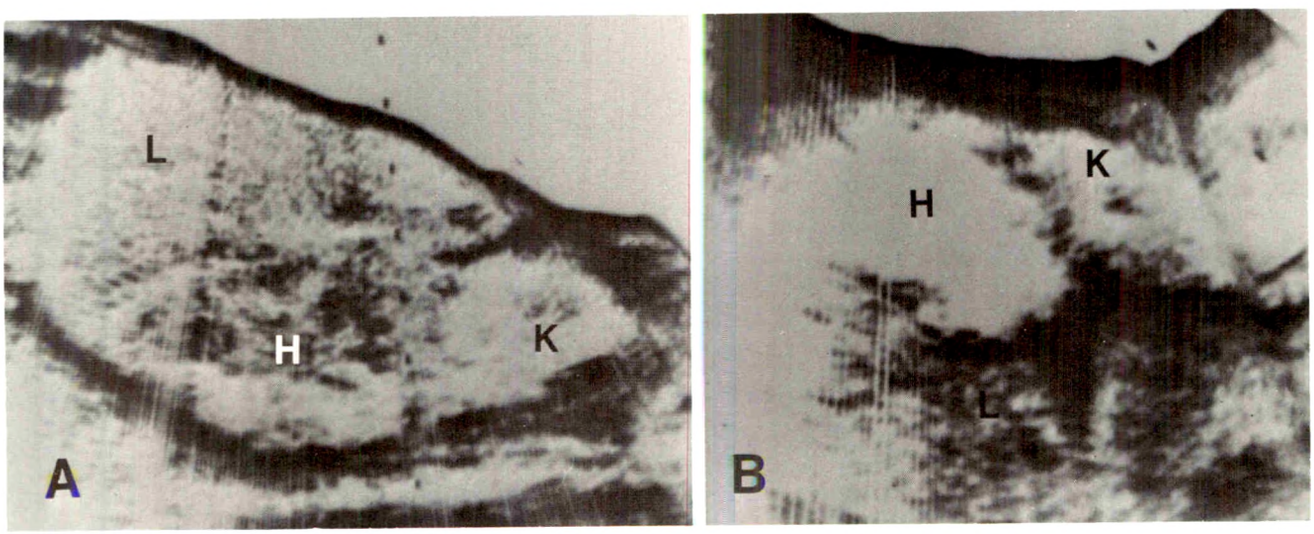


Fig. 1.—**A**, At 48 hr old, kidney (K), liver (L), and solid-appearing suprarenal mass (H). **B**, Sonolucent appearance of hematoma (H) 8 days later (prone scan).

Received July 28, 1978; accepted after revision November 9, 1978.
[1] Department of Radiology, University of Utah Medical Center, Salt Lake City, Utah 84132. Address reprint requests to D. E. Mineau.

© 1979 American Roentgen Ray Society

0361–803X/79/1323–0443 $0.00

as a solid lesion, only later to liquefy and acquire the more typical anechoic appearance of a hematoma.

Angiography will confirm the presence of a mass, but is of limited value in differentiating solid from cystic masses in this age group [4, 5]. Only half of neuroblastomas are vascular, and a solid but poorly vascularized tumor can easily be mistaken for a cyst.

If an adrenal mass is detected, and the possibility of adrenal hemorrhage is suspected, unnecessary surgery can be avoided if ultrasound is repeated at 3–5 day intervals. Change of the appearance of the mass from solid to cystic will establish diagnosis of adrenal hemorrhage.

Most ultrasound reports on abdominal hemorrhage refer to rectus sheath or retroperitoneal hematomas [6–10]. Hamilton [7] reported a 1-day-old hematoma which appeared solid. In the other cases in the literature, freshly clotted blood was found to be anechoic until the clot was fragmented, at which time it developed internal echoes [9]. In our case, the mass was initially solid and progressed through a complex to an anechoic pattern. The initial solid appearance may relate to either clot fragmentation or distribution of clotted blood throughout the adrenal tissue. The progressively anechoic change of the clot presumably relates to its degeneration and lysis.

REFERENCES

1. Vaughan VC, McKay RJ, Nelson WE: *Nelson Textbook of Pediatrics,* 10th ed, Philadelphia, Saunders, 1975
2. Hill EE, Williams JA: Massive adrenal hemorrhage in the newborn. *Arch Dis Child* 34:178–182, 1959
3. Jarvis JL, Seaman WB: Idiopathic adrenal calcification in infants and children. *AJR* 82:510–519, 1959
4. McDonald P, Hiller HG: Angiography in abdominal tumours in childhood with particular reference to neuroblastoma and Wilms' tumour. *Clin Radiol* 10:1–18, 1968
5. Moes CA, Burrington JD: Use of aortography in diagnosis of abdominal masses in children. *Radiology* 98:59–67, 1971
6. Hamilton JV, Flinn G, Haynie CC, Cefalo RC: Diagnosis of rectus sheath hematoma by B-mode ultrasound: a case report. *Am J Obstet Gynecol* 125:562–565, 1976
7. Hamilton WM: Clinical and ultrasonographic findings in the diagnosis and evaluation of abdominal wall hematoma, in *Ultrasound in Medicine,* vol 3A, edited by White D, Brown RE, New York, Plenum, 1977, pp 295–302
8. Kaftori JK, Rosenberger A, Pollack S, Rish JH: Rectus sheath hematoma: ultrasonographic diagnosis. *AJR* 128: 283–285, 1977
9. Kaplan GN, Sanders RC: B-scan ultrasound in the management of patients with occult abdominal hematomas. *JCU* 1: 5–13, 1973
10. Nowotny C, Niessner H, Thaler E, Lechner K: Sonography: a method for localization of hematomas in hemophiliacs. *Haemostasis* 5:129–135, 1976

Hypoglycemia and Extrapancreatic Tumors: a Report of Two Cases

PHILIP COSTELLO,[1] MELVIN E. CLOUSE,[1] AND ARTURO R. ROLLA[2]

The clinical syndrome of hypoglycemia is defined by symptoms of epinephrine release in the presence of a blood sugar level below 50 mg/100 ml rapidly reversible by carbohydrate administration. Three types of hypoglycemia are recognized: fasting, reactive, and intermittent. Fasting hypoglycemia is characterized by an abnormally low fasting blood glucose, poor tolerance of exercise, and symptoms of cerebral dysfunction. The important causes of fasting hypoglycemia are functioning islet cell tumors and extrapancreatic tumors. Liver disease, and hypofunction of the pituitary, thyroid, adrenal, or alpha cells of the pancreas are less common causes.

Reactive hypoglycemia is more commonly seen and occurs in response to ingestion of food. These patients have a normal fasting blood glucose and good exercise tolerance. The causes of reactive hypoglycemia include: functional emotional hypoglycemia; early diabetes mellitus; and dumping syndrome. Intermittent hypoglycemia may be seen one day but not the next. Causes are excessive alcohol ingestion after fasting and the administration of insulin or oral hypoglycemics.

This paper focuses attention on the group of nonpancreatic tumors associated with hypoglycemia. The radiographic findings are described in two patients with large retroperitoneal sarcomas presenting with fasting hypoglycemia, and the mechanisms by which these tumors may produce hypoglycemia are discussed. Reference is made to newer immunologic tests not described in the radiologic literature which, because of their specificity, may alert the clinician to the presence of such tumors.

Case Reports

Case 1

A 57-year-old man had progressive abdominal distension and swelling of the left leg for 3 months. One month before admission, he was found unconscious with a blood sugar of 40 mg/100 ml. A glucose tolerance test obtained several days later revealed a fasting blood sugar of 59 mg/100 ml, peak at 1 hr of 219 mg/100 ml, and a level at 5 hr of 42 mg/100 ml. He was discharged on a low carbohydrate, high protein diet, but symptoms rapidly worsened. He woke early in the morning confused and sweaty, but learned to avoid this by small feedings at 3 a.m. and 5 a.m.

Physical examination revealed a hard mass in the lower abdomen and swelling of the left leg. Glucose tolerance tests showed a fasting blood glucose of 36 mg/100 ml, 128 mg/100 ml at 30 min, and 66 mg/100 ml at 2½. The serum immunoreactive insulin was low at 2 μU/ml (normal 1–13 μU/ml). Levels of the serum immunoreactive nonsuppressible insulinlike peptide were markedly elevated at 21–26 mg/ml (normal, 1–4 mg/ml).

Barium enema study (fig. 1) revealed a huge soft tissue mass arising out of the pelvis displacing the sigmoid colon. Intravenous urography revealed a pelvic mass extrinsic to the bladder causing bilateral partial ureteric obstruction. Abdominal gray scale ultrasonography showed the mass was extrinsic to the bladder and contained multiple internal echos indicating solidity. Angiography, performed to outline the blood supply of the tumor, revealed it to be moderately vascular with the major supply from a large inferior mesenteric artery.

Surgical removal of a 3.6 kg retroperitoneal tumor was successful. Pathology revealed a fibrosarcoma with an unusually abundant proliferation of intracellular endoplasmic reticulum. The tumor tissue contained a high content of the insulinlike peptide (0.5 mg/g of tumor). Blood sugar was 141 mg/100 ml 5 min after surgery. At 5 months follow-up, the patient remained symptom free with a return of immunoreactive insulin to 11 μU/ml and a normal level of nonsuppressible insulinlike peptide.

Case 2

A 58-year-old woman developed diffuse abdominal pain associated with increased swelling of the abdomen over a 4-month period. Because of pain, nausea, and vomiting, a laparotomy was performed. At surgery a large retroperitoneal mass was biopsied with the pathology of undifferentiated sarcoma. The patient was treated by Adriamycin, Cytoxan, and dimethyl triazeno imidazole carboxamide and discharged. One month later she experienced early morning disorientation and memory loss and was found unconscious with a blood glucose level of 32 mg/100 ml. Hypertonic glucose relieved her symptoms. She underwent a second operation with removal of 50% of tumor bulk. Postoperatively, blood sugar remained low, requiring continuous infusions. She was admitted to our institution for further management.

The immunoreactive insulin level was 1 μU/ml and the serum immunoreactive nonsuppressible insulinlike peptide was markedly elevated at 33 mg/ml. Intravenous urography (fig. 2) and plain films outlined the extent of the soft tissue mass which displaced the ureters laterally with partial obstruction. Angiography was performed to assess tumor blood supply with a view to transcatheter occlusion, but numerous blood supplies from the superior and inferior mesenteric arteries as well as several lumbar vessels precluded such treatment. No further therapy was given other than continuous 20% glucose infusions and small feedings hourly. She died at home 3 weeks after discharge.

Discussion

Numerous nonpancreatic tumors producing hypoglycemia have been described [1]. The most important are: (1) mesenchymal (42%)—retroperitoneal fibrosarcomas or pleural mesotheliomas; (2) hepatoma (22%); (3) gas-

Received August 28, 1978; accepted after revision November 28, 1978.

[1] Department of Radiology, New England Deaconess Hospital, 185 Pilgrim Road, Boston, Massachusetts 02215. Address reprint requests to P. Costello.

[2] Department of Medicine, New England Deaconess Hospital, Boston, Massachusetts 02215.

© 1979 American Roentgen Ray Society

0361-803X/79/1323-0445 $0.00



Fig. 1.—Postevacuation film from barium enema study. Huge soft tissue mass arising from pelvis displaces sigmoid colon superiorly and to right. No mucosal invasion was noted, only extrinsic compression.

trointestinal carcinoma (10%); (4) adrenal cortical tumors (9%); (5) lymphoma (5%); and (6) miscellaneous (8%), including carcinomas of the lung and ovary, neuroblastoma, Wilms' tumor, and hemangiopericytoma.

A common characteristic of these tumors, particularly the fibrosarcomas, are their slow growth and massive size (2–10 kg). Hypoglycemia disappears after resection (as in case 1) or occasionally after irradiation of the tumor.

Proposed mechanisms by which these tumors induce hypoglycemia include: excessive glucose consumption by tumor tissue; decreased glucose output from the liver; and decreased lipolysis.

When a single large tumor mass is present, there may be increased use of glucose [2]. The half-life of glucose is reduced and glucose turnover rate may be up to four times normal. Some workers [3] suggest the possibility of decreased output of glucose from the liver. A hormone that reduces hepatic gluconeogenesis and lipolysis is postulated.

Islet cell tumors produce hypoglycemia by excess production of immunoreactive insulin; however, the serum immunoreactive insulin levels in patients with extrapancreatic tumors are decreased. A hormone with insulinlike activity is thought to be secreted by some tumors. The polypeptide secreted is probably closely related to insulin but not recognized immunologically as insulin. Recently, by the use of a new radioreceptor assay, elevation of the circulating concentration of the insulinlike peptide (nonsuppressible insulinlike activity) has been demonstrated in the serum of hypoglycemia patients. This serum peptide (dubbed NSILA-S) with a

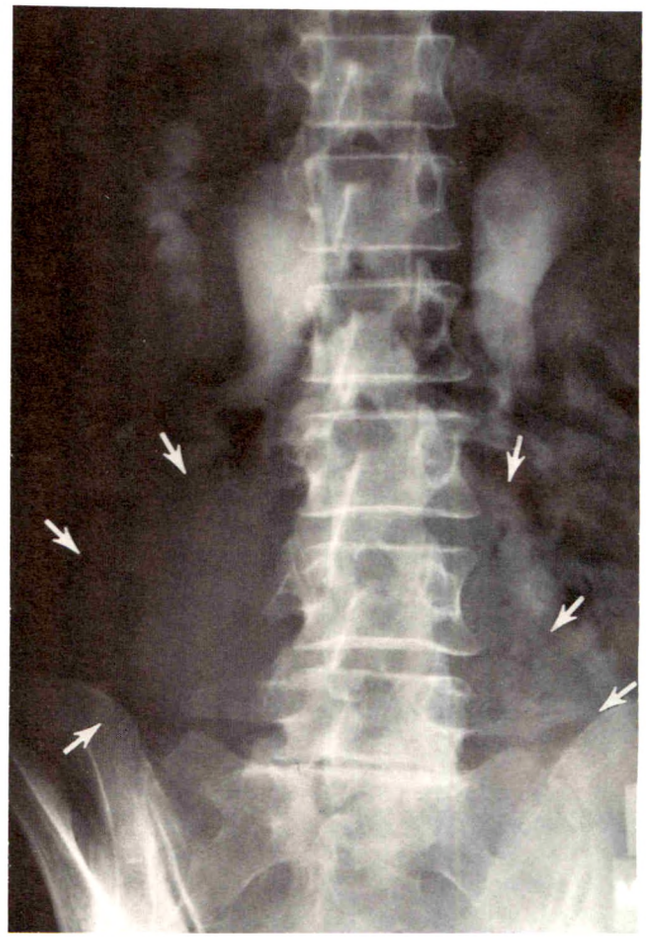


Fig. 2.—20 min intravenous urogram. Large soft tissue mass displaces bowel superiorly (*arrows*) with partial obstruction and lateral deviation of ureters.

molecular weight of about 6,000, has insulinlike activity in vitro and in vivo and cannot be suppressed by antiinsulin antibodies.

In the clinical evaluation of fasting hypoglycemia, differentiation of patients with functional islet cell tumors from those with extrapancreatic tumors can be made by measurements of serum immunoreactive insulin and of the serum peptite. Functional islet cell tumors produce elevated levels of insulin with normal nonsuppressible insulinlike activity levels. Extrapancreatic tumors lead to reduced insulin levels but the serum peptide levels may be increased in 30% of individuals [4].

A knowledge of these laboratory levels is important to the radiologist consulted at this stage. If an islet cell tumor is suspect, selective angiography of the pancreas will accurately localize the majority of the insulinomas [5]. Extrapancreatic tumors may be clinically obvious by their large size by the time the patient has hypoglycemic attacks, but their diverse origins may require radiographic evaluation [6]. Chest radiography may reveal parenchymal or pleural masses (mesotheliomas). Plain abdominal radiography followed by pyelography and barium studies of the gastrointestinal tract will define the

extent and nature of the intraabdominal masses [7]. Ultrasound and computed tomography provide unique information regarding the size, extent, composition, and nature of intrahepatic and retroperitoneal tumors. Arteriography is important prior to resection of retroperitoneal tumors since they may have a mesenteric blood supply. The lumbar arteries play an important role in the supply of retroperitoneal masses [8]. If a mass is surgically unresectable, transcatheter occlusion of the blood supply to the tumor may produce symptomatic relief by infarction and reduction in tumor hormone production [9].

REFERENCES

1. Steinke, J: Hypoglycemia, in *Joslin's Diabetes Mellitus*, edited by Marble A, Philadelphia, Lea & Febiger, 1971, pp 806–808
2. Unger RH: The riddle of tumor hypoglycemia. *Am J Med* 40: 325–330, 1966
3. Jakob A, Meyer VS, Flury R, Ziegler WH, Labhart A, Froesch ER: The pathogenesis of tumor hypoglycemia, block of hepatic glucose release and of adipose tissue lipocysis. *Diabetologia* 3:506–514, 1967
4. Hyodo T, Megyesi K, Kahn CR, McLean JP, Friesen HG: Adrenocortical carcinoma and hypoglycemia: evidence for production of nonsuppressive insulin-like activity by the tumor. *J Clin Endocrinol Metab* 44:1175–1184, 1977
5. Clouse ME, Costello P, Legg MA, Soeldner SJ, Cady B: Subselective angiography in localizing insulionomas of the pancreas. *AJR* 128:741–746, 1977
6. Rhys Davis E: The radiological and scintigraphic investigation of spontaneous hypoglycemia. *Clin Radiol* 24:177–184, 1973
7. Stevens DM, Sheedy PF, Mattery RR, Williamson B: Diagnosis and evaluation of retroperitoneal tumors by computed tomography. *AJR* 129:395–402, 1977
8. Levin DC, Watson RC, Baltaxe MA: Arteriography of retroperitoneal masses. *Radiology* 108:543–551, 1973
9. Goldstein MM, Wallace S, Anderson JM, Brel RL, Gianturco C: Transcatheter occlusion of abdominal tumors. *Radiology* 120:539–545, 1976

Extraadrenal Paraganglioma, Pulmonary Chondroma, and Gastric Leiomyoblastoma: Triad in Young Females

JAMES E. KNAKE[1] AND MILTON D. GROSS[2]

The unusual concurrence of extraadrenal paraganglioma, pulmonary chondroma, and gastric smooth muscle tumor (leiomyosarcoma or leiomyoblastoma) was reported once before in English literature [1] as two complete and two incomplete presentations of the triad, with reference to three other incomplete presentations from world literature [2–4]. Carney et al. [1] learned from personal communication that the patient described in the Italian literature [3] had subsequently manifested the complete triad.

Another of the incomplete cases [2] has now become complete and is presented here as the fourth known occurrence. Our encounter with this patient led to a review of the known syndromal and multitumoral associations of extraadrenal paragangliomas, but that study does not seem to clarify the relationships among these three uncommon neoplasms.

We followed the suggestion of Glenner and Grimley [5] by using the term "extraadrenal paraganglioma" to encompass all of the hormonally active or inactive tumors of the extraadrenal paraganglion system (including chemoreceptors) and in discarding terms such as "glomus tumor," "carotid body tumor," and "chemodectoma," which tend to make artificial distinctions among histologically identical neoplasms. In this nomenclature, the familiar name "pheochromocytoma" is strictly reserved for the tumor of the chromaffin cell of the adrenal medulla, though it also is histologically the same.

Case Report

At age 16 an otherwise healthy white girl was evaluated for chronic anemia and a nontender upper abdominal mass. Upper gastrointestinal radiography revealed a bulky tumor in the antrum and lower body of the stomach (fig. 1), and abdominal angiography was consistent with a smooth muscle tumor. At celiotomy one large (15 x 8 cm) and several smaller gastric tumor masses were found, and a 90% gastrectomy was done. Histologically, the lesions proved to be leiomyoblastomas, and this occurrence in an adolescent was sufficiently unusual to have been reported in surgical literature [2].

A solitary, minimally calcified pulmonary nodule was noted on preoperative chest radiography (fig. 2). This lesion was excised 3 months after gastric surgery and was described histologically as a chondromatous hamartoma.

At follow-up examinations over the next several years upper gastrointestinal and chest radiography showed no changes, and endoscopy was normal for the postoperative state. She was treated with parenteral iron for iron-deficiency anemia 4 years after surgery and responded well, with routine hematologic values returning to normal. She was normotensive.

The patient moved from the area and was not seen at this institution for several years. At age 26, she returned complaining of spells of weakness, tremulousness, and palpitations. She had been given hydrochlorothiazide for recently discovered hypertension, but had noted essentially no change in symptoms. Most recently, she had noted weakness and decreased size in the right side of her tongue. Physical examination revealed blood pressure ranging from 130 to 160 over 85 to 100 mm Hg and a right XII cranial nerve paresis. A firm 2 cm mass was palpated adjacent to the midcervical portion of the right carotid artery. Chest radiography, electrocardiography, and routine hematologic and blood chemistry values were normal except for elevated serum uric acid secondary to diuretic therapy. Urinary catecholamines were elevated.

Blood samples from the inferior and superior vena cava; innominate, right, and left internal jugular; and right and left adrenal veins all contained markedly elevated levels of norepinephrine. These were highest in the right internal jugular and right adrenal veins, which also showed the most striking elevations of epinephrine and dopamine. Selective carotid and vertebral angiography showed intensely vascular lesions characteristic of paragangliomas at the right jugular fossa, the right common carotid artery bifurcation, and posterior to the proximal portion of the right internal carotid artery (fig. 3). An additional faint vascular stain was superimposed on the left internal carotid artery at the level of the auditory canal in the lateral views, but could not be reliably identified in the corresponding frontal views and was not classified as a definite lesion.

Treatment with phenoxybenzamine resulted in a decrease in the patient's blood pressure and amelioration of her symptoms. This response and the angiographic appearance strongly suggest these tumors are extraadrenal paragangliomas. No surgery has been performed.

Discussion

The medical literature is replete with reports of paragangliomas occurring singly or multiply at locations including the common carotid artery bifurcation, jugulotympanic region, cervical distribution of vagus nerve, orbit, tongue, mandible, larynx, trachea, nasal sinus, nasal cavity, pineal gland, aortic arch branches, pulmonary artery bifurcation, lung, interatrial septum, aorticosympathetic segmental and collateral ganglia, stomach, duodenum, gallbladder, ileal mesentery, urinary bladder, and groin [5, 6], as well as in the kidney [7], soft palate [8], pancreas [9], and sella [10]. Some of these lesions have probably represented hemangiopericytoma,

Received August 17, 1978; accepted after revision November 2, 1978.

[1] Department of Radiology, Section of Neuroradiology, University of Michigan Medical Center, Ann Arbor, Michigan 48109. Address reprint requests to J. E. Knake.

[2] Department of Internal Medicine, Division of Nuclear Medicine, University of Michigan Medical Center, Ann Arbor, Michigan 48109.

© 1979 American Roentgen Ray Society

0361-803X/79/1323-0448 $0.00

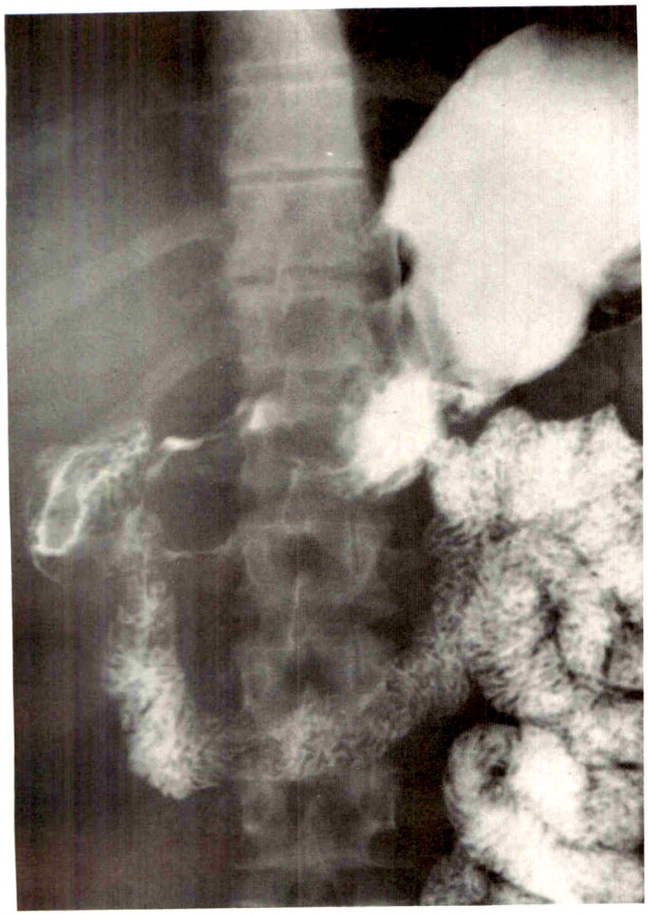


Fig. 1.—Antrum and lower body of stomach occupied by multilobular mass. At surgery, tumor nodules extended to within 2 cm of gastroesophageal junction.

alveolar soft part sarcoma, and other tumors of similar histologic appearance [5], but most are acceptably documented. A tendency toward multiplicity, especially in children [11] and in familial series [12], has long been noted. Associations have been reported with chronic obstructive pulmonary disease [12], living at high altitude [13], and hereditary deficiency of clotting factors VII and X [14]. Definite malignancy with metastasis is unusual but well established [5].

The concurrence of extraadrenal paraganglioma with other tumors necessarily involves consideration of the apudoma (amine precursor uptake and decarboxylation) concept as most prominently expounded by Pearse [15], which holds that totipotential cells of neuroectodermal origin migrate widely in early embryogenesis and retain potential for both amine and peptide hormone production. The neuroectodermal origin of neurons and Schwann cells has long been known. More recently, elaborate cytochemical, immunofluorescent, and ultrastructural studies [15, 16] have established the origin from neural crest, ventral neural ridge, and neural tube of such diverse mature cells as those of the adenohypophysis, pineal gland, hypothalamus, adrenal medulla, thymus, and paraganglion system, as well as thyroid "C"



Fig. 2.—Left upper lung. Faintly calcified 3 cm nodule shown more clearly than on plain posterioanterior chest radiographs.

cells, bronchial Kulchitsky cells, melanocytes, and the endocrine cells of the lung and intestinal tract including pancreatic islets. Thus, peptide hormone endocrinology and neuroendocrinology have been merged.

This unifying embryologic concept makes plausible the previously puzzling associations of extraadrenal paragangliomas with the tumors of neurofibromatosis [17, 18] and with pheochromocytoma [19–21], as well as further clinical associations of the latter entities with medullary thyroid carcinoma, pituitary adenoma, islet cell adenoma, intestinal and bronchial carcinoid, oat cell carcinoma, melanoma, pinealoma, neuroblastoma, and thymoma [16, 22–25]. The array of biogenic amines and peptides reported as products of these tumors is impressive; indeed, production of any of them by any of the tumor cell types is acknowledged to be possible and most have been demonstrated [15, 16].

Therefore, the apudoma concept encompasses the so-called "multiple endocrine adenomatoses," carcinoid syndromes, Zollinger-Ellison syndrome, Cushing's syndrome, Verner-Morrison (watery diarrhea–hypokalemia–achlorhydria) syndrome, and the more recently reported instances of mixed endocrinopathy [26–28] in which, for example, the concurrence of extraadrenal paraganglioma, pituitary adenoma, bronchial carcinoid, and hyperplasia of antral and duodenal gastrin cells was reported in a single patient. The reported association of extraadrenal paragangliomas with papillary and follicular thyroid carcinomas [29] remains unexplained by the current apudoma concept, since only the parafollicular cells ("C" cells) of the thyroid have been shown to have a neural crest origin.

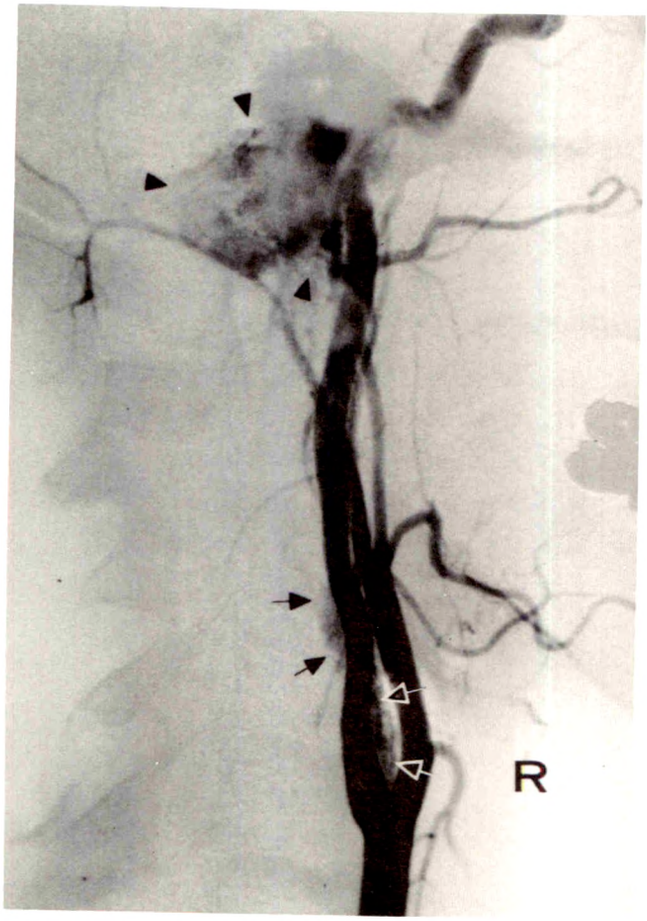


Fig. 3.—Paraganglioma jugulotympanicum (*arrowheads*) caused XII cranial nerve palsy and invaded right internal jugular vein. Tumors at carotid bifurcation (*open arrows*) and posterior to proximal internal carotid (*closed arrows*) may be ramifications of same mass or paragangliomas intercaroticum and intravagale of separate origin.

Similarly, the triad of tumors in the subject of this report and those previously cited [1, 3, 4] cannot presently be explained by invoking common cytogenesis, since chondromas in any location are considered to be of mesenchymal origin, as are gastric smooth muscle tumors. Nevertheless, the patients have all been young females, 12–24 years of age at first tumor recognition; in all cases the gastric tumors have been multiple. The improbability of this coincidence strongly suggests an etiologic syndrome. We agree with Carney et al. [1] that when one component of the triad appears in a young patient, a careful watch should be maintained for the others. Any of the three neoplasms will often be first identified by the radiologist, who, as consultant, should be aware of this recently recognized association.

ACKNOWLEDGMENTS

We thank Angela Hubbell and Donna Eder for preparing this manuscript.

REFERENCES

1. Carney JA, Sheps SG, Go VLW, Gordon H: The triad of gastric leiomyosarcoma, functioning extra-adrenal paraganglioma and pulmonary chondroma. *N Engl J Med* 296: 1517–1518, 1977
2. de Castro FJ, Olsen WR, Littler ER: Gastric leiomyoblastoma in an adolescent. *Am J Surg* 123:614–616, 1972
3. Vio A, Abate L, Leogrande G: Considerazioni su un singolare caso di tumore gastrico a nodi multipli (leiomioma bizarro di Stout) associato ad amartocondroma polmonare in una giovinetta di 12 anni. *Ann Ital Chir* 45:750–768, 1969
4. Mueller M, Ryncki PV, Saegesser F, Gardiol D: Hamartomes pulmonaires multiples bilatéraux: a propos d'une jeune femme préalablement opérée d'une tumeur musculaire de l'estomac. *Schweiz Med Wochenschr* 104:511–514, 1974
5. Glenner GG, Grimley PM: Tumors of the extra-adrenal paraganglion system (including chemoreceptors), in *Atlas of Tumor Pathology*, 2d series, fascicle 9, Washington, D.C., Armed Forces Institute of Pathology, 1974
6. Olson JR, Abell MR: Nonfunctional, nonchromaffin paragangliomas of the retroperitoneum. *Cancer* 23:1358–1367, 1969
7. Legace R, Tremblany M: Non-chromaffin paraganglioma of the kidney with distant metastases. *Can Med Assoc J* 99: 1095–1098, 1968
8. Dasgupta G, Deodhare SG: Chemodectoma of the soft palate. *Int Surg* 62:366–367, 1977
9. Goodof II, Lischer CE: Tumor of the carotid body and the pancreas. *Arch Pathol* 35:906–911, 1943
10. Bilbao JM, Horvath E, Kovacs K, Singer W, Hudson AR: Intrasellar paraganglioma associated with hypopituitarism. *Arch Pathol Lab Med* 102:95–98, 1978
11. Stackpole RH, Melicow MM, Uson AC: Phaeochromocytoma in children. *J Pediatr* 63:315–330, 1963
12. Chedid A, Jao W: Hereditary tumors of the carotid bodies and chronic obstructive pulmonary disease. *Cancer* 33: 1635–1641, 1974
13. Saldana MJ, Salem LE, Travezan R: High altitude hypoxia and chemodectomas. *Hum Pathol* 4:251–263, 1973
14. Kroll AJ, Alexander B, Cochios F, Pechet L: Hereditary deficiencies of clotting factors VII and X associated with carotid-body tumors. *N Engl J Med* 270:6–13, 1964
15. Pearse AGE: Neurochristopathy, neuroendocrine pathology and the APUD concept. *Z Krebsforsch* 84:1–18, 1975
16. Tischler AS, Dichter MA, Biales B, Greene LA: Neuroendocrine neoplasms and their cells of origin. *N Engl J Med* 296: 919–925, 1977
17. Harkin JC, Reed RJ: Tumors of the peripheral nervous system, in *Atlas of Tumor Pathology*, 2d series, fascicle 3, Washington, D.C., Armed Forces Institute of Pathology, 1974
18. Lee SP, Nicholson GI, Hitchcock G: Familial abdominal chemodectomas with associated cutaneous angiolipomas. *Pathology* 9:173–177, 1977
19. Revak CS, Morris SE, Alexander GH: Pheochromocytoma and recurrent chemodectomas over a twenty-five-year period. *Radiology* 100:53–54, 1971
20. Gibbs MK, Carney JA, Hayles AB, Telander RL: Simultaneous adrenal and cervical pheochromocytomas in childhood. *Ann Surg* 185:273–278, 1977
21. Sato T, Saito H, Yoshinaga K, Shibota Y, Sasano N: Concurrence of carotid body tumor and pheochromocytoma. *Cancer* 34:1787–1795, 1974
22. Bader LV, Lykke AWJ, Hinterberger H: Multiple biogenic amine-secreting "carcinoid" tumour of the stomach: a case report. *Pathology* 9:353–358, 1977
23. Mason GA, Millar EJ, Strang LB, Wynne NA: Adrenaline secreting neuroblastoma in an infant. *Lancet* 2:322–325, 1957

24. Friesen SR, Hermreck AS, Mantz FA: Glucagon, gastrin, and carcinoid tumours of the duodenum, pancreas and stomach: polypeptide "Apudomas" of the foregut. *Am J Surg* 127:90–101, 1974
25. Keiser HR, Beavan MA, Doppman J, Wells S, Buja M: Sipple's syndrome: medullary thyroid carcinoma, pheochromocytoma, and parathyroid disease. *Ann Intern Med* 78:561–579, 1973
26. Hansen OP, Hansen M, Hansen HH, Rose B: Multiple endocrine adenomatosis of mixed type. *Acta Med Scand* 200:327–331, 1976
27. Berg B, Björklund A, Grimelius L, Ingemansson S, Larsson L, Stenram U, Åkerman M: A new pattern of multiple endocrine adenomatosis. *Acta Med Scand* 200:321–326, 1976
28. Zawirska VB, Rabczynski J: Metachrone und synchrone Geschwülste mit Metastasen bei einer 47 jährigen Frau. *Zentralbl Allg Pathol* 118:226–231, 1974
29. Albores-Saavedra J, Durán ME: Association of thyroid carcinoma and chemodectoma. *Am J Surg* 116:887–890, 1968

Contraceptive-Associated Hepatic Tumor

KARL T. BENEDICT, JR.,[1] PETER S. CHEN,[1] MURRAY L. JANOWER,[1] MELVIN H. FARMELANT,[2] JOHN T. HOWARD,[3] AND WILLIAM McDERMOTT[4]

Since the report of Baum et al. [1], numerous other reports [2–4] have associated oral contraceptive use and increased incidence of benign hepatic tumors in young women. These tumors can usually be classified as either benign hepatic cell adenoma (liver cell adenoma, hepatic adenoma) or focal nodular hyperplasia (hamartoma). Most lesions have been totally resected. Occasionally a lesion has only been biopsied, which allows its natural history to be observed. Spontaneous regression after withdrawal of oral contraceptives has occurred and has been documented by follow-up clinical examination and/or isotopic liver scanning [3, 5–8]. A patient in whom regression of a benign hepatic tumor is documented by angiographic as well as isotopic follow-up is reported here.

Case Report

D. G., a 26-year-old woman, entered St. Vincent Hospital complaining of the sudden onset of left shoulder and left upper quadrant pain. One day earlier, she was accidentally kicked in the abdomen by her 6-year-old son. She had been using a mestranol-containing oral contraceptive for 5 years, but took no other medications and had been well. Her temperature was 38.3°C. She had tachycardia (140 beats/min) and was normoten-

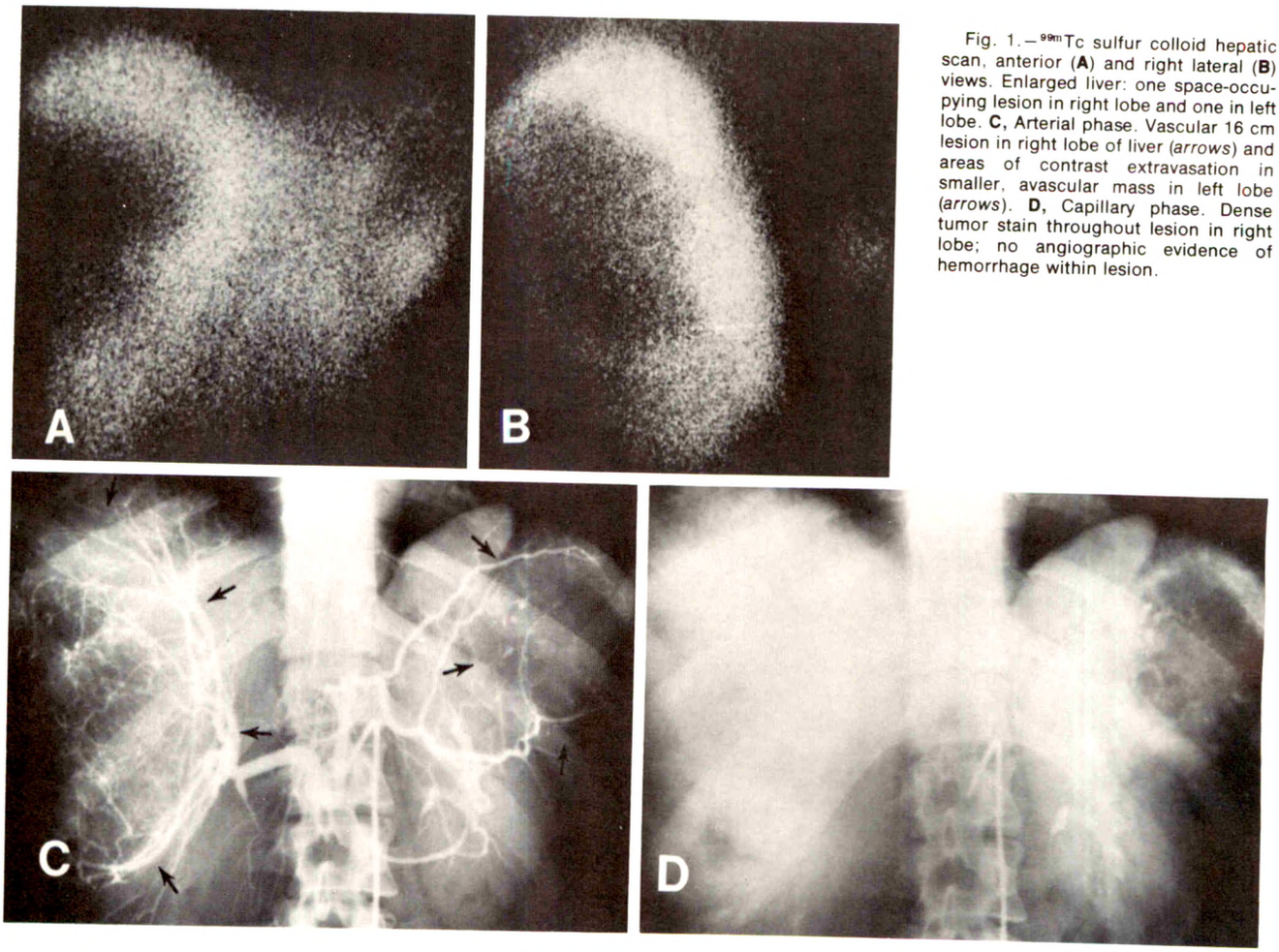


Fig. 1.—^{99m}Tc sulfur colloid hepatic scan, anterior (**A**) and right lateral (**B**) views. Enlarged liver: one space-occupying lesion in right lobe and one in left lobe. **C**, Arterial phase. Vascular 16 cm lesion in right lobe of liver (*arrows*) and areas of contrast extravasation in smaller, avascular mass in left lobe (*arrows*). **D**, Capillary phase. Dense tumor stain throughout lesion in right lobe; no angiographic evidence of hemorrhage within lesion.

Received June 30, 1978; accepted after revision November 21, 1978.
[1] Department of Radiology, St. Vincent Hospital, Worcester, Massachusetts 01610. Address reprint requests to K. T. Benedict.
[2] Department of Radiology, Division of Nuclear Medicine, St. Vincent Hospital, Worcester, Massachusetts 01610.
[3] Department of Surgery, St. Vincent Hospital, Worcester, Massachusetts 01610.
[4] Department of Surgery, New England Deaconess Hospital, Boston, Massachusetts 02215.

© 1979 American Roentgen Ray Society

0361–803X/79/1323–0452 $0.00

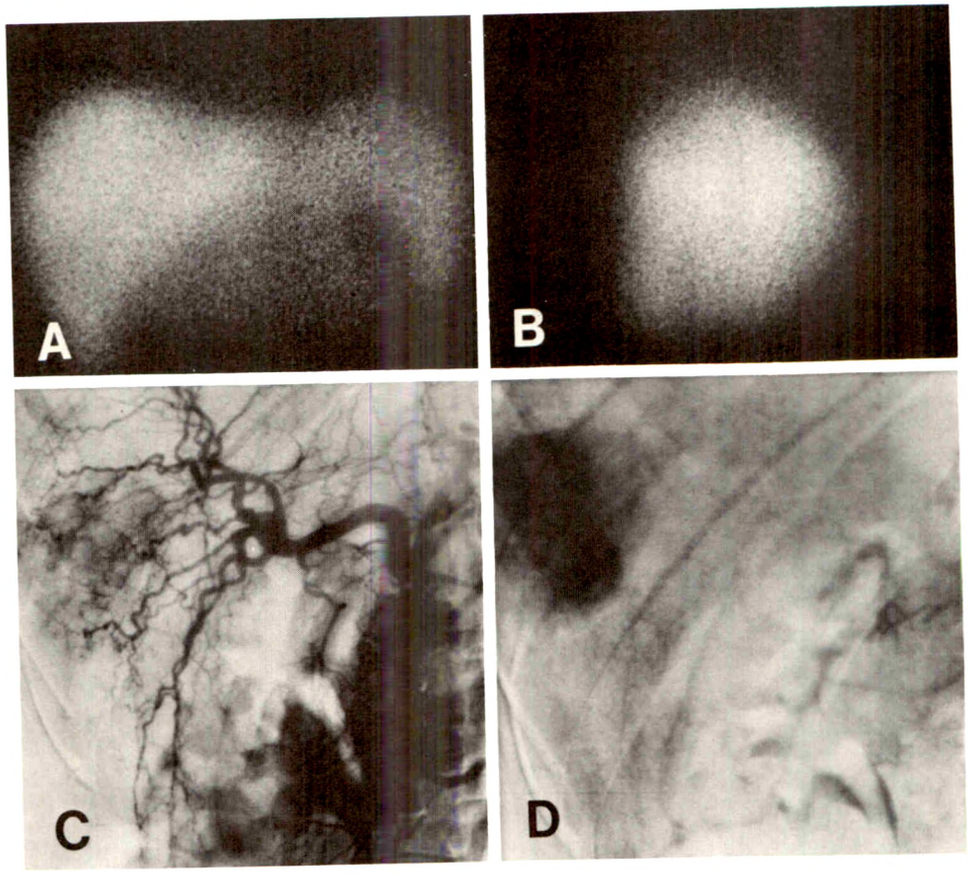


Fig. 2.—One year after figure 1. ^{99m}Tc sulfur colloid hepatic scan, anterior (**A**) and right lateral (**B**) views. Scans essentially normal. Marked decrease in size of right lobe; no evidence of residual mass. **C,** Arterial phase. Marked reduction in size of tumor mass in right lobe; some residual neovascularity. **D,** Hepatogram phase. Extent of tumor better shown. Persisting tumor stain.

sive. Abdominal examination revealed tenderness and guarding in the epigastrium and left upper quadrant. Laboratory data included normal hemoglobin and hematocrit, white blood cell count of 16,000/mm^3, alkaline phosphatase of 112 U (normal, 30–85), and SGOT of 90 (normal, 5–40). Emergency ^{99m}Tc sulfur colloid liver scan showed hepatomegaly, a large defect in the right lobe, and a smaller defect in the left lobe. The spleen was normal (figs. 1A and 1B). Selective common hepatic arteriography revealed a very vascular 16 cm mass in the right lobe of the liver. The feeding arteries were stretched around the mass, and branches penetrated the tumor from the periphery. A tumor stain was present. A second 6 cm mass in the left lobe was avascular, but contained numerous pools of extravasated contrast material due to active bleeding within it (figs. 1C and 1D).

After the patient's condition stabilized, she was transferred to New England Deaconess Hospital where surgery revealed a tumor mass with central hemorrhage and hematoma formation in the left lobe of the liver. A larger, solid mass in the right lobe had no evidence of internal hemorrhage. Both lesions were biopsied and a wedge resection of the tumor of the left lobe was performed.

On pathologic examination, the lesion in the left lobe was described as "a hepatic cell mass with marked hematoma formation." Biopsy from the right lobe was interpreted as "a hepatic cell nodule consistent with nodular hyperplasia." The lesions were identical histologically and were described as being "more uniformly homogeneous and cellular than usually found in nodular hyperplasia, but not as active as hepatocellular carcinoma." The lesion had features that "some pathologists would call benign hepatic adenoma."

The patient was readmitted 1 year later with right upper quadrant pain and light-headedness. Vital signs and laboratory examinations were normal. Some tenderness was noted on deep palpation of the right upper abdomen. Follow-up liver scan was normal (figs. 2A and 2B). Repeat common hepatic arteriography revealed no evidence of residual tumor in the remaining left lobe of the liver. The vascular tumor in the right lobe had diminished markedly. Little mass effect was seen, but residual neovascularity and tumor stain were noted in a 5 cm area (figs. 2C and 2D).

Discussion

Hemorrhage, sometimes fatal, has been the most dire complication of benign hepatic tumors, particularly benign hepatic cell adenomas. Malignant transformation probably does not occur, although a malignant hepatoma within a benign liver cell adenoma has been reported [9]. Total resection of these lesions has been the treatment of choice. After resection, recurrence has been noted in at least two patients in whom birth control pills were not withdrawn postoperatively [3]. The tumors regressed in both patients when oral contraceptives were subsequently discontinued. Regression of nonresected or partially resected lesions after cessation of oral contraceptives has been reported in eight other patients [5–8, 10]. Regression was documented by follow-up hepatic scintiscan in five cases and by abdominal palpation in one other. Autopsy proof was available for an additional patient who died of another disease. Galloway et al. [10] reported angiographic follow-up in a patient taking oral contraceptives who had a hepatic lesion they

termed "minimal deviation hepatoma." However, this patient was treated with 5-fluorouracil, as well as with discontinuance of oral contraceptives. To our knowledge, no other case with angiographic follow-up has been reported.

Not all benign hepatic tumors will be detected on isotopic liver scan [11]. Some will be missed because they take up ^{99m}Tc sulfur colloid to the same degree as the adjacent normal liver, and others because of their small size. Size becomes a factor as lesions regress, since it can be anticipated that at some point the residual tumor will be too small to be detected on liver scintiscan. In our case, the scintiscan returned to normal when the residual tumor was readily detected by angiography. Since the vast majority of these benign hepatic tumors are vascular, angiography should be a more sensitive method of detecting residual lesions. This may be of prognostic importance as there are reports of hemorrhage occurring within residual lesions months after stopping oral contraceptives [12].

ACKNOWLEDGMENT

We thank Lorraine Bolduc and Joan Raymond for help in preparing and typing the manuscript, Jane Griesback for preparing the photographs and Steven Garney for technical assistance.

REFERENCES

1. Baum JK, Holtz F, Bookstein JJ, Klein EW: Possible association between benign hepatoma and oral contraceptives. *Lancet* 2:926–929, 1973
2. Edmondson HA, Henderson B, Benton B: Liver-cell adenomas associated with the use of oral contraceptives. *N Engl J Med* 294:470–472, 1976
3. Klatskin G: Hepatic tumors: possible relationship to use of oral contraceptives. *Gastroenterology* 73:386–394, 1977
4. Vana J, Murphy GP, Armoff BL, Baker HW: Primary liver tumor and oral contraceptives—results of a survey. *JAMA* 238:2154–2158, 1977
5. Stauffer JQ, Lapinski MW, Honold DJ, Myers JK: Focal nodular hyperplasia of the liver and intrahepatic hemorrhage in young women on oral contraceptives. *Ann Intern Med* 83:301–306, 1975
6. Ross D, Pina J, Mirza M, Galvan A, Lucas P: Regression of focal nodular hyperplasia after discontinuance of oral contraceptives. *Ann Intern Med* 85:203–204, 1976
7. Hillard JL, Grahan DY, Spjut HS: Hepatic adenoma: a possible complication of oral contraceptive therapy. *South Med J* 69:683–687, 1976
8. Edmondson HA, Reynolds TB, Henderson B, Benton B: Regression of liver cell adenomas associated with oral contraceptives. *Ann Intern Med* 86:108–182, 1977
9. Davis M, Portmann B, Searle M, Wright R, Williams R: Histological evidence of carcinoma in a hepatic tumor associated with oral contraceptives. *Br Med J* 4:496–498, 1975
10. Galloway SJ, Cararella WJ, Lattes R, Seaman WB: Minimal deviation hepatoma: a new entity. *AJR* 125:184–192, 1975
11. Salvo AF, Schiller A, Athanasoulis C, Goldabiri J, McKusick KA: Hepatoadenoma and focal nodular hyperplasia: pitfalls in radiocolloid imaging. *Radiology* 125:451–455, 1977
12. Fechner RE: Benign hepatic lesions and orally administered contraceptives. *Hum Pathol* 8:255–268, 1977

Hepatic Rupture with Toxemia of Pregnancy: Angiographic Diagnosis

DANIEL G. SOMMER,[1,2] GUERDON D. GREENWAY,[1] JOSEPH J. BOOKSTEIN,[1] AND MARSHALL J. ORLOFF[3]

Hepatic rupture is a rare but serious complication of toxemia in pregnancy. The mortality rate is high, and survival usually depends on prompt surgical therapy. Preoperative diagnosis is infrequent and has usually been based on radioisotopic liver scans. This paper describes the features and role of angiography in diagnosing a patient with bilobar hepatic rupture and subcapsular hematoma secondary to toxemia. We were unable to find another case of preoperative angiographic diagnosis in the radiologic literature.

Case Report

L. R. (UCSD no. 697-411), a 35-year-old white woman (gravida 3, para 3) was in her twenty-fourth week of pregnancy. Medical history included hypertension, intermittently treated with thiazides, and use of oral contraceptives for several years before this pregnancy. Her antenatal course had been complicated by exacerbation of her hypertension and intermittent right upper quadrant pain. There was no history of trauma during the pregnancy; she did admit to a moderately heavy alcohol intake. On the day of admission, the patient had gone to an outside hospital with severe right upper quadrant pain, hypotension (systolic blood pressure 80 mm Hg), and hematocrit of 25%. After receiving 2 units of whole blood, she was transferred to University Hospital.

On arrival, her blood pressure was 100/60 mm Hg and her pulse was 100/min. Her abdomen was diffusely tender, especially in the right upper quadrant. The uterus was palpable at the level of the umbilicus; no fetal movements or heart tones were noted. Laboratory values included hematocrit, 33%; white blood cell count, 10,700 mm^3; prothrombin time, 11.8/11.0 sec; partial thromboplastin time, 37.6/32.4 sec; platelets, 150,000 mm^3; blood urea nitrogen, 26 mg/100 ml; creatinine, 0.8 mg/100 ml; bilirubin, 0.4 mg/dl direct with 1.3 mg/dl total; SGOT, 148 IU; and alkaline phosphatase, 62 IU. Urinalysis revealed 3+ proteinuria with no cells on microscopic examination.

Because of the previous use of oral contraceptives, bleeding hepatic adenoma was the initial clinical impression. After stabilization in the emergency room, emergent angiography was requested.

Celiac and selective hepatic angiography demonstrated a large right subcapsular hematoma and a small area of contrast extravasation at the tip of the right lobe of the liver (fig. 1). A second and more brisk bleeding site was identified in the left lobe of the liver (fig. 2), as well as stretching of the branches of the left hepatic artery indicating intrahepatic hematoma (fig. 1). Prominent arterioportal shunting with apparent retrograde portal flow was also evident (fig. 2). There was no evidence of hepatic adenoma. The spleen was normal. Ultrasonography confirmed an intrauterine pregnancy and demonstrated sonolucent areas within both lobes of the liver consistent with intrahepatic hematomata.

Laparotomy revealed about 2 l of nonclotted blood within the peritoneum, as well as a large subcapsular hematoma extending across the anterior and superior aspects of both the right and left hepatic lobes. The capsule had ruptured along the superior surface of both lobes, although the dissection and rupture in the left lobe appeared to be slightly older than that on the right. The right subcapsular hematoma was evacuated and a left hepatic lobectomy performed. The patient also underwent a hysterotomy and termination of pregnancy. She recovered well postoperatively, with only mild persistent hypertension controlled with diuretics.

Histologic review of the placenta revealed hyalinized partially necrotic vessels typical of preeclampsia. Liver tissue examination demonstrated evidence of both recent hemorrhage and underlying liver disease characterized by a periportal infiltrate of lymphocytes, plasma cells, and histiocytes. Bile duct proliferation was present, as well as scattered areas of fibrosis. These findings were interpreted as evidence of a chronic hepatitis, compatible with the patient's history of increased alcohol consumption. Superimposed on these findings were areas of hemorrhagic necrosis, as well as deposition of fibrin in hepatic sinusoids, consistent with toxemia.

Discussion

Toxemia in pregnancy is associated with abnormal liver function (elevated alkaline phosphatase and SGOT levels) in about 50% of patients; jaundice is uncommon [1]. Histologic examination of the liver in toxemia may demonstrate fibrin thrombi obstructing hepatic sinusoids with contiguous areas of hemorrhagic hepatic necrosis. Necrosis may become confluent and extensive; when this occurs in the periphery of the liver, a subcapsular hematoma results. Rupture of the hematoma produces intraperitoneal bleeding.

The hepatic lesions in toxemia of pregnancy have been attributed to disseminated intravascular coagulation [2-4]. McKay [3] believes eclampsia itself is a form of disseminated intravascular coagulation and that areas of hemorrhagic necrosis and sinusoidal fibrin deposition are present in all patients with this disease. In hepatic rupture, a complete coagulation profile is infrequently obtained because of the urgency of the situation; however, several reports [2, 3] document abnormal coagulation parameters indicating disseminated intravascular coagulation in patients with hepatic rupture and toxemia. Spontaneous subarachnoid and intracerebral hemorrhages, subcapsular splenic hematomata, and spontaneous retroperitoneal and rectus muscle hematomata have been reported with eclamptic patients, and are also possibly related to disseminated intravascular coagulation.

Our patient did not have the typical coagulation profile of disseminated intravascular coagulation, although only an incomplete coagulation series was obtained. However, she did have the hepatic histologic picture of

Received August 24, 1978; accepted October 26, 1978.

[1] Department of Radiology, University of California Medical Center, 225 Dickinson Street, San Diego, California 92103. Address reprint requests to G. D. Greenway.

[2] Present address: Department of Radiology, Ventura Memorial Hospital, Ventura, California 93003.

[3] Department of Surgery, University of California Medical Center, San Diego, California 92103.

0361-803X/79/1323-0455 $0.00

AJR 132:455-456, March 1979

© 1979 American Roentgen Ray Society

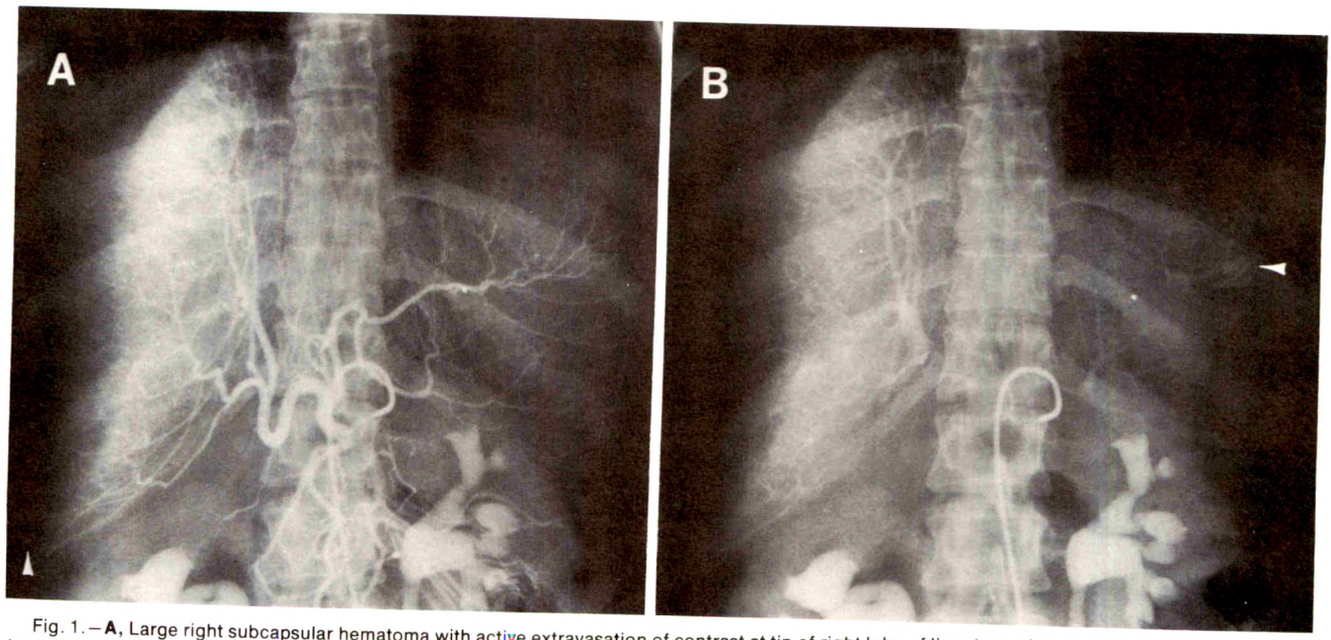


Fig. 1.—**A**, Large right subcapsular hematoma with active extravasation of contrast at tip of right lobe of liver (*arrowhead*); stretched branches of left hepatic artery indicate intrahepatic hematoma. **B**, Contrast extravasation within left lobe (*arrowhead*) and prominent arterioportal shunting.

toxemia and probable disseminated intravascular coagulation.

Although hepatic rupture has been reported in uncomplicated pregnancies [5], it is far more commonly associated with eclampsia. In this situation hepatic rupture may occur before, after, or at delivery. Associated fetal mortality is high secondary to toxemia and shock. These patients are usually multiparous and have a sudden onset of severe abdominal pain, frequently localized to the right upper quadrant, and signs of hypovolemia secondary to blood loss. However, the pain may be chronic, secondary to small areas of necrosis and hemorrhage or distention of the liver from sinusoidal obstruction. With rupture of Glisson's capsule, major intraperitoneal hemorrhage occurs. In this situation mortality approaches 100% without surgical intervention [6, 7]. Prompt surgical exploration has been reported to reduce the mortality rate to 30% [6]. Because of the acute nature of the bleeding, as well as the sudden hypotension, early diagnosis is essential [8].

In the past, preoperative diagnosis has been largely based on clinical grounds, although radionuclide scanning has provided the correct diagnosis in a few cases [9]. In our patient, angiography permitted accurate diagnosis of the bleeding sites, as well as preoperative delineation of the extent of the process. Hemorrhage from a clinically suspected hepatic adenoma was excluded. Preoperative demonstration of bleeding from both lobes of the liver helped the surgeon correctly manage this case.

The prominent arterioportal shunting demonstrated in this case is a nonspecific finding, probably related to the patient's shock or increased intracapsular pressure (J. Bookstein, D. Dail, unpublished data).

Because of the urgency of this situation, many of these patients will undergo immediate surgery without benefit of preoperative radiologic studies. However, if vital signs are stable, angiography can provide a more complete diagnosis enabling optimal surgical planning.

ACKNOWLEDGMENTS

We thank Dr. Kurt Benirschke, Department of Pathology, University of California, San Diego, for reviewing the microscopic slides on this case.

REFERENCES

1. Burrow G, Ferris T: *Medical Complications During Pregnancy*. Philadelphia, Saunders, 1975, pp 351–381
2. Mokotoff R, Weiss L, Brandon L, Camillo M: Liver rupture complicating toxemia of pregnancy. *Arch Intern Med* 119: 375–380, 1967
3. McKay D: Hematologic evidence of disseminated intravascular coagulation in eclampsia. *Obstet Gynecol Surv* 27: 399–417, 1972
4. Beller F, Schmidt E: Local and systemic coagulation properties in hypertensive disorders in pregnancy. *Clin Obstet Gynecol* 4:563–571, 1977
5. Hibbard L: Spontaneous rupture of the liver in pregnancy: a report of eight cases. *Am J Obstet Gynecol* 126:334–338, 1976
6. Bis K, Waxman B: Rupture of the liver associated with pregnancy: a review of the literature and report of two cases. *Obstet Gynecol Surv* 31:763–773, 1976
7. Nelson E, Archibald L, Albo D: Spontaneous hepatic rupture in pregnancy. *Am J Surg* 134:817–820, 1977
8. Jewett J: Eclampsia and rupture of the liver. *N Engl J Med* 297:1009–1011, 1977
9. Castañeda H, Garcia-Romero H, Canto M: Hepatic hemorrhage in toxemia of pregnancy. *Am J Obstet Gynecol* 107: 578–584, 1970

Radiographic Findings of Lymphoma Involving the Larynx: A Report of Two Cases

MICHAEL A. NOON,[1] MICHAEL BRANT-ZAWADZKI, STUART W. YOUNG, AND RONALD A. CASTELLINO

The protean manifestations of malignant lymphoma have been well documented and include unusual presentations in extranodal, nonlymphoid organs. Although the lung and gastrointestinal tract of the extranodal organs have been more commonly associated with lymphomatous involvement [1], the larynx may also be subject to isolated involvement as well as involvement associated with systemic disease [2, 3]. This report describes a patient with an isolated lymphomatous pedunculated polyp of the left aryepiglottic fold and another patient with a laryngeal lymphomatous mass producing acute airway obstruction in association with systemic disease.

Case Reports

Case 1

A 90-year-old Japanese man had a 6 month history of persistent cough and a 9 month history of voice change and hoarseness. His medical history included a 60 pack/year history of smoking, hypertension, and prostatism. Indirect laryngoscopy revealed a 2 cm polypoid mass arising from the left aryepiglottic fold. A 1 cm firm, mobile, right midjugular lymph node was also noted. The rest of the physical examination was unremarkable. Laryngeal tomography demonstrated a 2.5 × 1.5 cm polyp on a stalk, attached to the left aryepiglottic fold (fig. 1). A 2.3 × 1.2 × 1.0 cm polyp, covered by intact mucosa and attached to the left aryepiglottic fold by a thin stalk, was removed at surgery. The histologic diagnosis was malignant lymphoma, diffuse well differentiated lymphocytic type with plasmacytoid features.

Chest radiography revealed no evidence of adenopathy or intrathoracic involvement. A bone marrow biopsy was normal. Further staging procedures were not performed because of the patient's advanced age. Screening laboratory tests were normal except for an IgG monoclonal gammopathy. The patient was treated with 5,000 rad to the larynx and 4,000 rad to the posterior cervical nodes and has no evidence of disease 10 months after diagnosis.

Case 2

A 20-year-old male Kenyan college student, who had recently developed lymphadenopathy, was seen with acute stridor. He described progressive dyspnea over several months, recent hoarseness, dysphagia, and a 9 kg weight loss. Generalized palpable lymphadenopathy was noted as well as respiratory distress with audible stridor. Laboratory studies were normal, although blood gas analysis showed a pH of 7.36, pCO_2 of 48 mm HG, and pO_2 of 79 mm HG. Chest radiography was normal. Soft tissue radiography of the neck (fig. 2) demonstrated masses involving the uvula, epiglottis, and lingual tonsils, as well as a large mass involving the larynx from the base of the epiglottis to just below the vocal cords.

An emergency tracheostomy was performed, and a concurrent biopsy of the laryngeal mass showed a lymphoblastic lymphoma. The patient was started immediately on corticosteroid therapy, and a prompt reduction in the size of the neck masses occurred. He was subsequently placed on a chemotherapy regimen and is alive with disease 3 months later.

Discussion

About 50 cases in the otolaryngology literature document the larynx as a site of involvement by malignant lymphoma. Lymphoma involving the larynx as the first manifestation of disease and without evidence of involvement elsewhere is very rare. Of 5,319 patients with Hodgkin's disease and non-Hodgkin's lymphomas, nine had disease confined to the larynx [3]. In a review of the world literature, Anderson et al. [2] found 14 cases of laryngeal lymphoma without peripheral manifestations and added one of their own. All 15 patients in their review complained of hoarseness at the time of diagnosis, three had frank dyspnea, and one had sufficient airway obstruction to warrant a tracheostomy. Ten of these 15 lesions were described as being smooth, supraglottic masses usually involving the epiglottis and aryepiglottic



Fig. 1.—Laryngeal tomogram during phonation. Large polypoid mass in laryngeal vestibule, protruding medially from left aryepiglottic fold.

Received October 11, 1978; accepted December 4, 1978.
This work was supported in part by National Cancer Institute grant CAO-5838.
[1] All authors: Division of Diagnostic Radiology, Stanford University School of Medicine, Stanford, California 94305. Address reprint requests to R. A. Castellino.

© 1979 American Roentgen Ray Society

0361–803X/79/1323–0457 $0.00

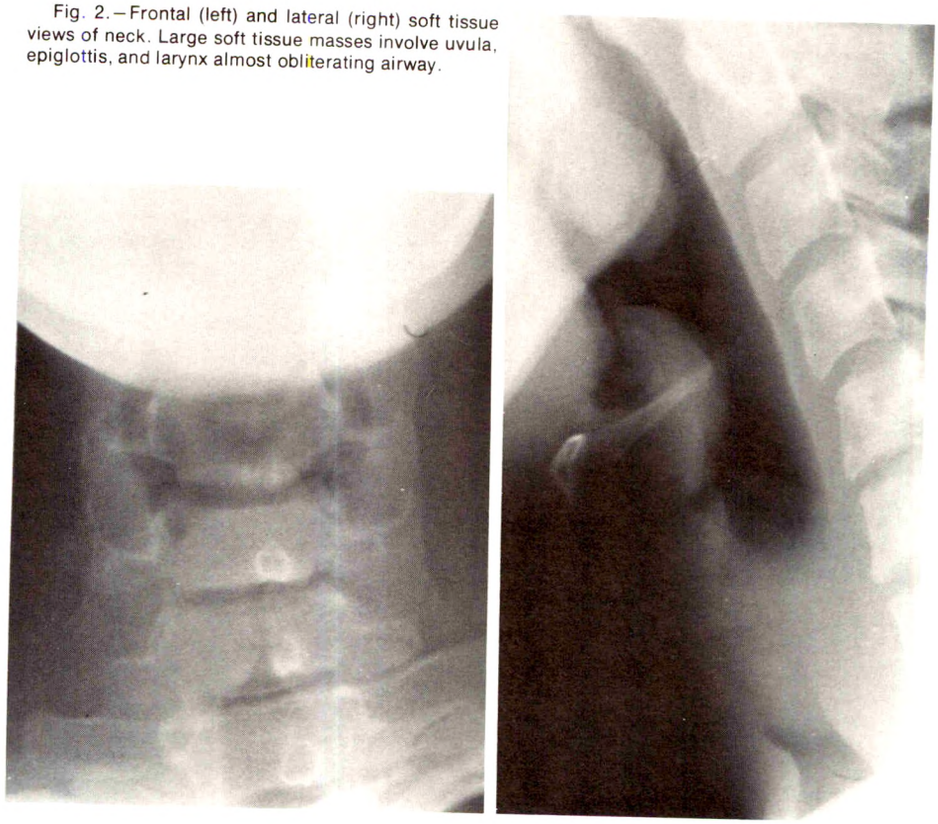


Fig. 2.—Frontal (left) and lateral (right) soft tissue views of neck. Large soft tissue masses involve uvula, epiglottis, and larynx almost obliterating airway.

folds. Although these clinical features were seen in case 1, lymphoma of the larynx as a pedunculated polypoid mass has not been previously reported.

Long term survivals of more than 10 years have been recorded for patients with laryngeal involvement by malignant lymphoma [4–6]. However, in rare cases subsequent pulmonary, orbital, occipital, and gastric involvement with lymphoma have been discovered 2½–6 years after the initial presentation [3, 7]. Since most of these patients did not undergo a complete staging workup, such cases may represent a slow progression of previously unrecognized and untreated disease.

The plain film radiographic features of lymphoma involving the larynx appear to be nonspecific. A mass lesion may be seen in other types of malignant tumors as well as in benign lesions. The polypoid feature of case 1 suggested a benign process on the radiographs and at the time of excision a lymphoma was not suspected. Case 2 was associated with systemic disease and the characteristics of the mass were nonspecific.

REFERENCES

1. Freeman C, Berg JW, Cutler SJ: Occurrence and prognosis of extranodal lymphomas. *Cancer* 29:252–260, 1972
2. Anderson HA, Maisel RH, Cantrell RW: Isolated laryngeal lymphoma. *Laryngoscope* 86:1251–1257, 1976
3. DeSanto LW, Weiland LH: Malignant lymphoma of the larynx. *Laryngoscope* 80:966–978, 1970
4. Clerf LH: Sarcoma of the larynx. *Arch Otolaryngol* 44:327–337, 1934
5. Holmes GW, Schulz MD: Radiation treatment of lymphoma. *N Engl J Med* 235:789–791, 1946
6. Wang CC: Malignant lymphoma of the larynx. *Laryngoscope* 82:97–100, 1972
7. Dickson R: Lymphoma of the larynx. *Laryngoscope* 81:578–585, 1971

Mucoid Pseudotumors of the Tracheobronchial Tree in Two Cases

DAVID KARASICK,[1, 2] STEPHEN KARASICK,[1, 2] AND JAMES F. LALLY[1, 3]

Mucus collections in the tracheobronchial tree have been termed "mucus plug," "inspissated mucus," and "mucoid impaction of the bronchi." We suggest the term "mucoid pseudotumor" when the mucus collection simulates a neoplastic mass on chest radiography or tomographic section. Two patients in whom coughing and expectoration differentiated these "mucoid pseudotumors" from true neoplasms are reported here.

Case Reports

Case 1

E. V., a 78-year-old white man, had progressive dyspnea on exertion, ankle swelling, and occasional retrosternal pain for 1 month. He had no history of chronic cough, expectoration, hemoptysis, or cyanosis at admission. He had a smoking history, but had abstained for the last 13 years.

The lungs were clear to auscultation. Arterial blood gases showed a respiratory alkalosis with hypoxemia on room air. Perfusion lung scans revealed multiple bilateral pulmonary defects. Xenon lung scan confirmed that the perfusion defects were probably due to pulmonary emboli. Sputum analysis was negative for malignant cells.

Chest radiography 1 week before admission showed abnormal right midlung density and a soft tissue density in the lower trachea on the left anterior oblique view (fig. 1A). Tomograms provided better detail of the peripheral lung nodule, but also confirmed the presence of the soft tissue density at the carina bulging from the right tracheobronchial wall (fig. 1B). There was thickening of the tracheobronchial wall in this region. After repeated forceful and productive coughing efforts, follow-up tomograms were obtained. Disappearance of the soft tissue density confirmed that a mucus plug had been expelled after vigorous coughing (fig. 1C).

The patient died 1 week later. Autopsy revealed a right pulmonary artery thrombus, normal tracheobronchial tree, and granulomatous nodule in the right lung.

Case 2

E. L., a 73-year-old white man, complained of weakness in both legs and ptosis of the right eye. He had had myasthenia gravis for 12 years and had smoked seven to eight cigars daily until 4 months before admission. No history of shortness of breath or dyspnea on exertion was discovered. Physical exami-

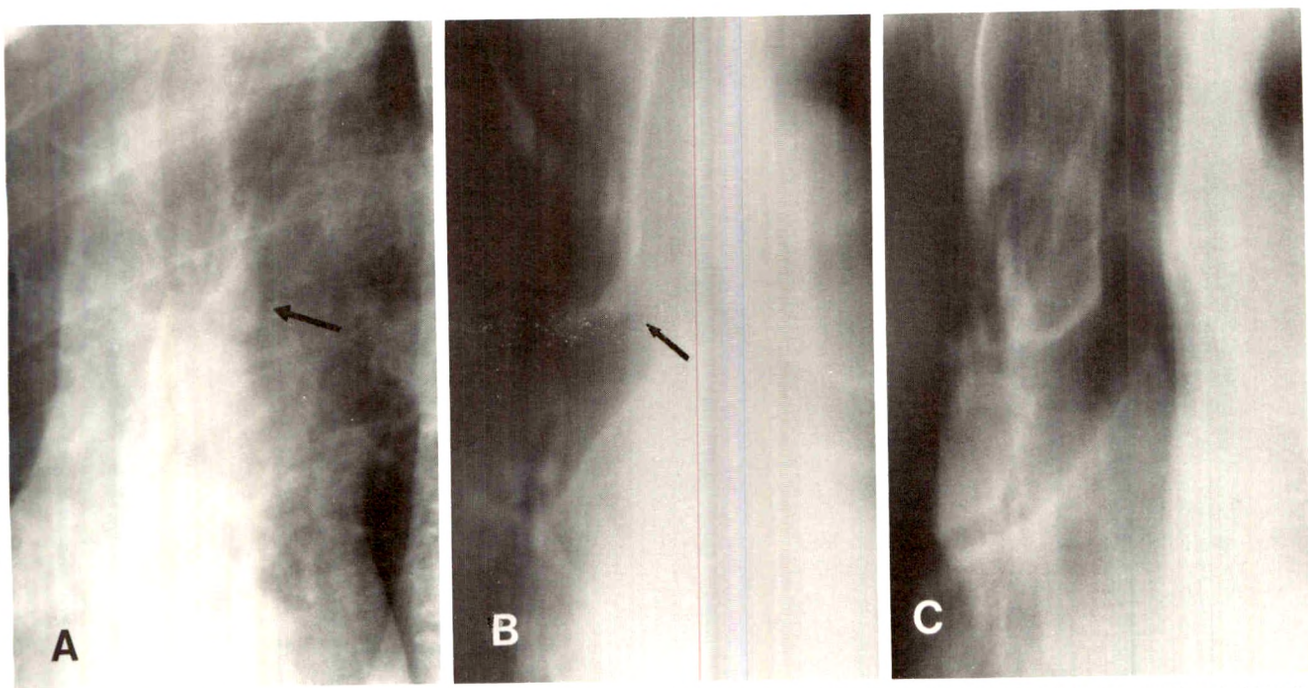


Fig. 1.—Case 1. **A,** Soft tissue density intraluminally at right tracheobronchial angle (*arrow*). **B,** Sessile tracheobronchial mass associated with wall thickening (*arrow*) (incidental azygos lobe of right lung). **C,** Pseudotumor has disappeared; mucus plug was expelled.

Received July 5, 1978; accepted after revision November 6, 1978.

[1] Department of Radiology, Thomas Jefferson University Hospital, 10th and Walnut, Philadelphia, Pennsylvania 19107.

[2] Present address: Department of Radiology, Episcopal Hospital, Front Street and Lehigh Avenue, Philadelphia, Pennsylvania 19125. Address reprint requests to D. Karasick.

[3] Present address: Department of Radiology, Wilmington Medical Center, Delaware Division, Wilmington, Delaware 19899.

© 1979 American Roentgen Ray Society

0361-803X/79/1323-0459 $0.00

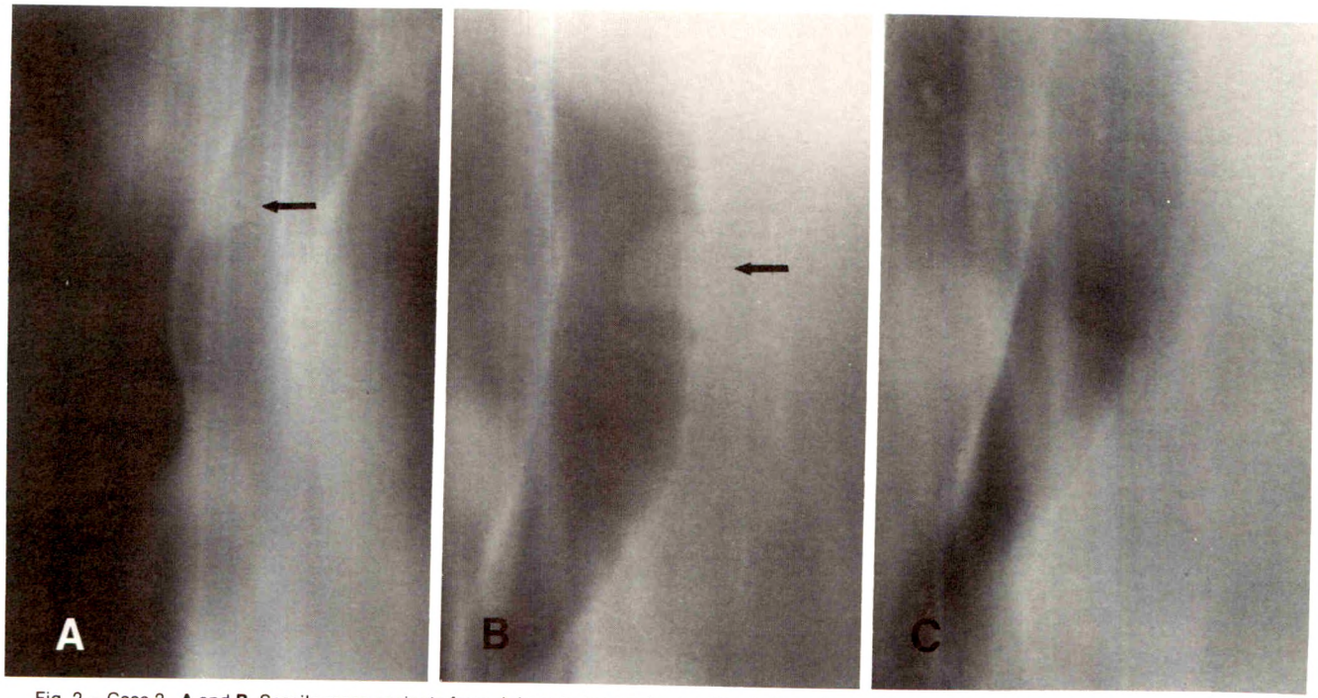


Fig. 2.—Case 2. **A** and **B**, Sessile mass projects from right anterior tracheal wall just above level of aortic arch (*arrows*); bronchoscopy was negative. **C**, After 4 months, pseudotumor has disappeared.

nation revealed no cardiopulmonary abnormality. Laboratory studies showed no abnormality except for an elevated serum lactic dehydrogenase.

Admission chest radiography revealed some fullness to the anterior mediastinum and a soft tissue density overlying the anterior trachea on lateral view. Tomography showed a sessile soft-tissue nodular density within the trachea attached to the anterior and right lateral walls about 7 cm from the carina (figs. 2A and 2B) and measuring about 1.5 × 1.8 cm in greatest dimensions. No calcifications were noted. No anterior mediastinal mass was seen. The fullness seen in the chest radiograph was believed due to uncoiling of the aorta in its ascending portion.

Bronchoscopy, performed because of possible primary tracheal neoplasm, revealed a normal trachea without evidence of any intraluminal mass. The larynx, bronchi, and carina also appeared normal.

The patient was discharged, but was readmitted 4 months later for anal fistulectomy and perirectal abscess drainage. Admission chest radiography again showed fullness of the anterior mediastinum, but no definite mass lesion. Repeat tomography revealed no evidence of the tracheal soft-tissue mass previously seen (fig. 2C). The disappearance of the mass and normal bronchoscopic examination is best explained by expectoration of a mucus plug by the patient.

Discussion

Abnormal mucus formation, composition, or transport, which can be precipitated by smoking, can result in formation of a mucus plug or inspissated mucus and precede abnormal respiratory function in the lungs. Once a smoker develops chronic bronchitis, mucus transport seems to be irreversibly damaged. Impairment has been shown even in patients who have abstained from cigarette smoking for many years. In addition, increased quantities of intraluminal mucus have been demonstrated in smokers [1]

These cases exemplify the difficulty in interpreting nonobstructive sessile lesions in the trachea or main stem bronchi. Inspissated mucus adherent to the tracheobronchial wall may simulate a neoplastic mass on routine radiography and tomography. Repeat tomography in the area of the suspected mass is recommended after forceful and vigorous coughing, as in case 1. In this way, these "mucoid pseudotumors" can be differentiated from true neoplasms. Repeat tomography after respiratory treatment or after an appropriate interval of time may likewise aid in identifying such pseudotumors, as in case 2 [2, 3].

REFERENCES

1. Wanner A: Clinical aspects of mucociliary transport. *Am Rev Respir Dis* 116:73–125, 1977
2. Littleton JT: *Tomography: Physical Principles and Clinical Applications*. Baltimore, William & Wilkins, 1976, pp 601–604
3. Westra D: Mucus plugs. Phantom tumours of the major air passages. The tomographic appearances. *ROEFO* 112:428–434, 1975

Intraluminal Diverticula of the Stomach

KONG-MENG TAN[1]

Intraluminal diverticula of the duodenum are not uncommon [1–4]. Schreiber and Davis [5] recently described the first two cases of intraluminal diverticula of the esophagus. To my knowledge, this is the first reported case of gastric intraluminal diverticula. Unlike previously reported solitary esophageal and duodenal diverticula, this case had two adjacent intraluminal diverticula.

Case Report

A 50-year-old white man had nausea and vomiting accompanied by epigastric pains for 3 days. An upper gastrointestinal series with the patient upright showed immediate filling of a large diverticulum in the proximal portion of the lumen of the stomach with an adjacent diverticulum just superior to the first (figs. 1A and 1B). The diverticula were sharply separated from the remainder of the barium in the stomach by a thin radiolucent line. All projections indicated the diverticula to be within the stomach lumen. Radiography with the patient supine showed immediate loss of barium from the diverticula (fig. 1C). The lesions were not recognized at endoscopy a few days later. A repeat barium study several months later failed to demonstrate the diverticula.

Discussion

An intraluminal duodenal diverticulum has been described as a solitary saclike structure lined with duodenal mucosa on both its inner and outer surfaces and lying entirely within the confines of the duodenal lumen [4]. Its characteristic radiographic appearance is of a large, smooth ovoid collection of barium surrounded by a thin, smooth radiolucent line. This barium mass is always seen distinctly and entirely within the duodenal lumen.

Since intraluminal diverticula have been described in the esophagus and duodenum, the occurrence of a diverticulum in the stomach is not surprising. However, in previous reports, such diverticula have only been solitary. In this case, a second diverticulum appeared just proximal to the first. As in the case of an esophageal intraluminal diverticulum reported by Schreiber and Davis [5], this diverticulum could not be demonstrated a second time; it may not have been sufficiently distended for visualization at endoscopy. The orifice leading into the diverticulum may also have been too small and not continuously patent [5].

The pathophysiology is uncertain; the most probable cause seems related to intermittently or chronically increased intraluminal pressure associated with an area of congenital or acquired weakness of the mucosa. A small pulsion diverticulum could eventually grow, carrying a layer of mucosa before it. The wall of the diverticulum covered with mucosa on both sides would account for the thin radiolucent line separating barium in the diverticulum from barium in the remainder of the stomach. Another cause might be a congenital web undergoing the same pulsion forces.

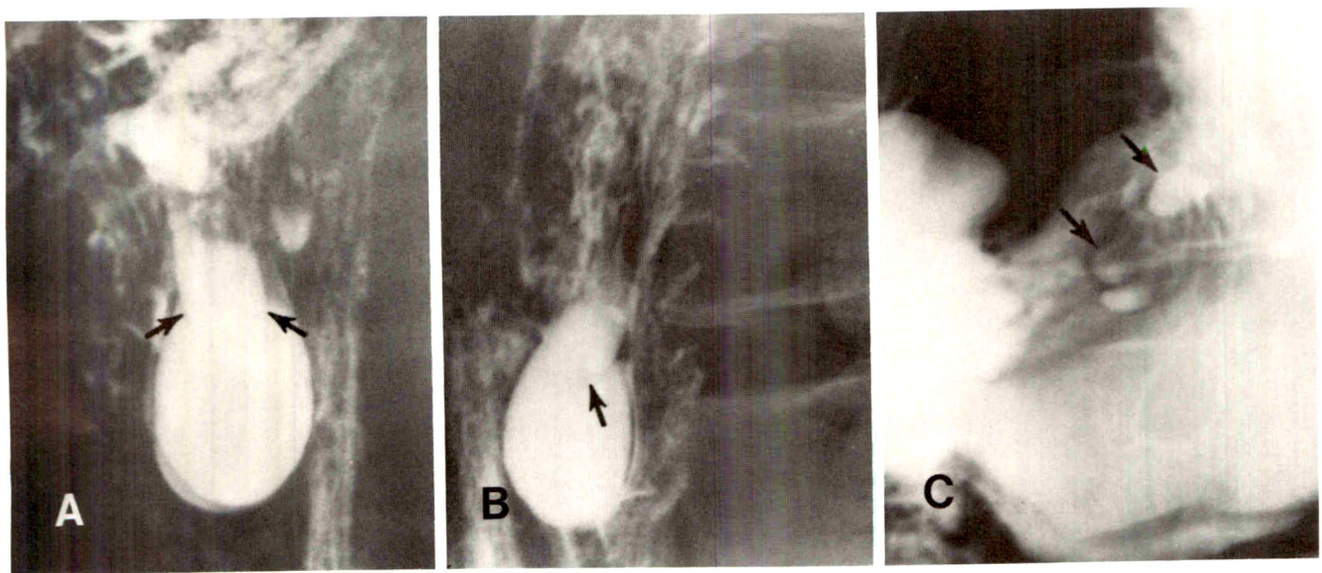


Fig. 1.—**A** and **B**, Large intraluminal diverticulum with second smaller diverticulum superiorly (*arrows*). **C**, Residual barium (*arrows*) within same two diverticula.

Received June 27, 1978; accepted after revision November 9, 1978.
[1] Department of Radiology, Kaiser-Permanente Medical Center, 14th and Cutting Boulevard, Richmond, California 94804.

AJR 132:461–462, March 1979
0361–803X/79/1323–0461 $0.00
© 1979 American Roentgen Ray Society

REFERENCES

1. Nelson WI: Congenital diaphragm of the duodenum: case report with preoperative x-ray studies. *Minn Med* 30:745–752, 1947
2. Kinzer RE: Intraluminal diverticulum and other lesions producing intermittent duodenal obstruction or stasis. *AJR* 61: 212–218, 1949
3. Wiot JF, Spiro E: Intraluminal diverticulum: a form of duplication. *Radiology* 80:46–49, 1963
4. Zatzkin HR, Macy JJ, Kveton FW: Intraluminal duodenal diverticulum: report of a case. *AJR* 82:1036–1037, 1959
5. Schreiber MH, Davis M: Intraluminal diverticulum of the esophagus. *AJR* 129:595–597, 1977

Splenic Flexure Volvulus: Two Case Reports and Review

ROBERT LANTIERI,[1,2] STEVEN K. TEPLICK,[1] AND MALCOLM J. LABELL[3]

The first two cases of splenic flexure volvulus in radiologic literature were reported by Buenger [1]. Since then, 12 more cases have been cited [2–11]. Volvulus of the colon accounts for 3% of all intestinal obstructions and 10% of colonic obstructions [10]. About 96% of cases occur in the sigmoid colon or cecal regions and about 4% occur in the transverse colon [11]. Volvulus at the splenic flexure is rare because this part of the colon is usually rigidly immobilized by ligamentous attachments and the retroperitoneal location of the descending colon. The following cases illustrate typical acute and chronic intermittent types of splenic flexure volvulus.

Case Reports

Case 1

A 56-year-old man, transferred from a mental institution after 3 days of vomitting, had a history of multiple episodes of abdominal distention and three laparotomies for lysis of bowel adhesions. On examination, the abdomen was mildly distended but soft with normal bowel sounds. Abdominal radiography revealed a large air collection in the left upper quadrant (fig. 1A). Small bowel study showed delayed passage of barium at the splenic flexure (fig. 1B). Barium enema study demonstrated findings of chronic recurrent splenic flexure volvulus with incomplete obstruction and adhesive bands involving descending colon (fig. 1C).

At laparotomy, the splenic flexure was freely movable (probably from previous surgery), but not acutely obstructed. Adhesive bands narrowed the lumen at the splenic flexure–descending colon junction. The adhesions were lysed and the splenic flexure immobilized. Subsequent hospitalization was uneventful.

Case 2

A 52-year-old man, recovering from right inguinal hernia surgery, developed acute abdominal distention with hyperactive

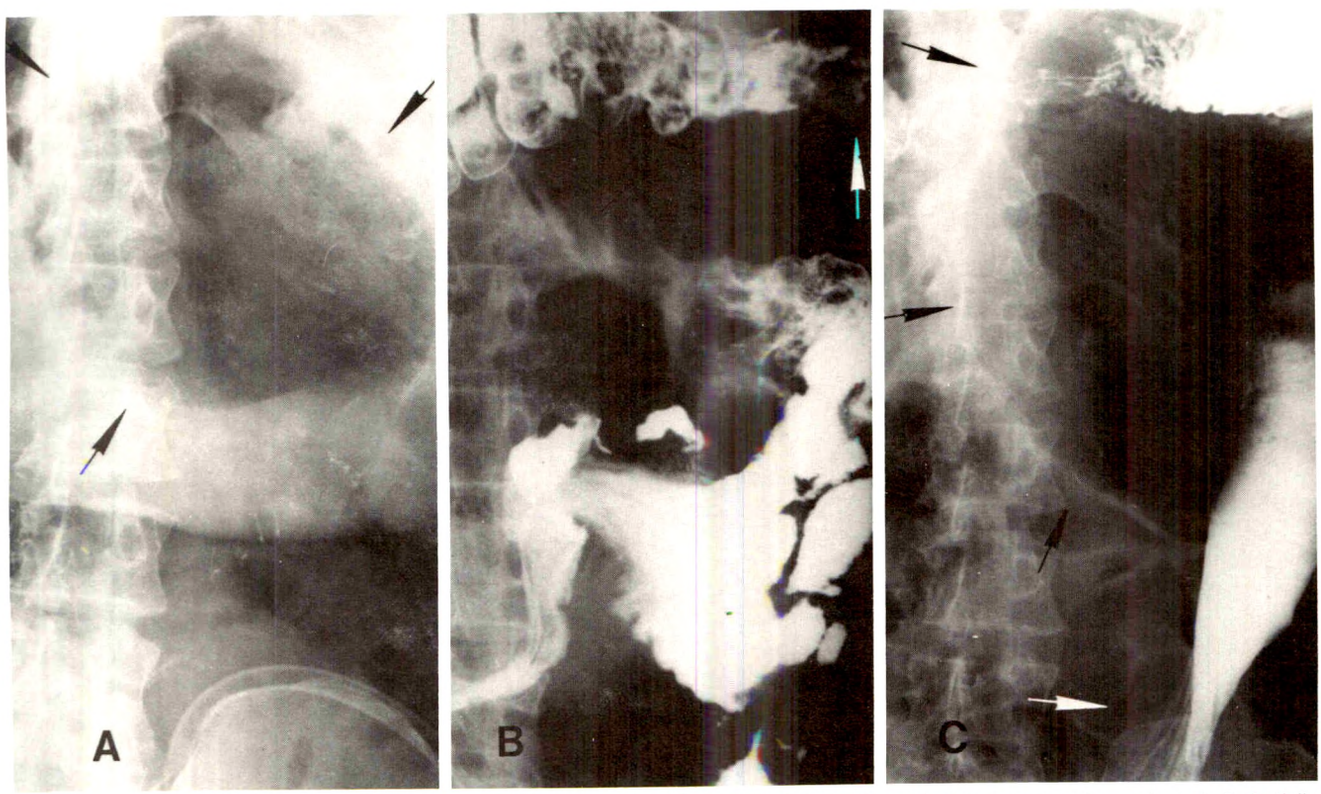


Fig. 1.—Case 1, 56-year-old man. **A,** Large left upper quadrant gas collection (*arrows*). **B,** Holdup of barium at splenic flexure (*arrow*). **C,** Partially reduced splenic flexure volvulus (*black arrows*) and adhesive bands involving descending colon (*white arrow*).

Received June 8, 1978; accepted after revision November 21, 1978.
[1] Department of Diagnostic Radiology, Hahnemann Medical College and Hospital, 230 North Broad Street, Philadelphia, Pennsylvania 19102.
[2] Present address: Department of Radiology, Division of Nuclear Medicine, Stanford University Medical Center, Stanford, California 94305. Address reprint requests to R. Lantieri.
[3] Department of Radiology, Sturdy Memorial Hospital, Attleboro, Massachusetts 02703.

© 1979 American Roentgen Ray Society

0361-803X/79/1323-0463 $0.00

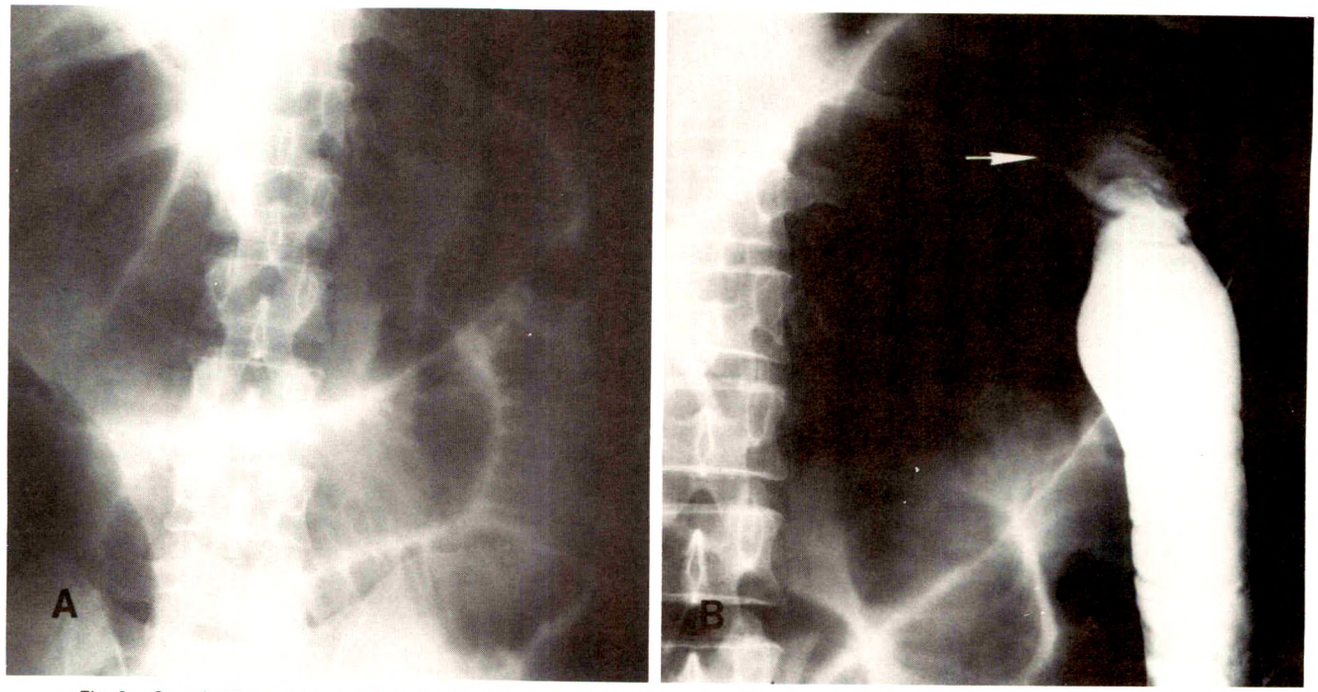


Fig. 2.—Case 2, 52-year-old man. **A,** Large bowel obstruction in region of splenic flexure. **B,** Site of volvulus at splenic flexure (*arrow*).

bowel sounds. Abdominal radiography revealed findings of obstruction in the region of the splenic flexure (fig. 2A). Barium enema study showed obstruction at the splenic flexure with evidence of volvulus (fig. 2B), which was partially reduced by the barium enema. Splenic flexure volvulus was confirmed at surgery. There was no ischemia and no mention of unusual mobility of splenic flexure. The segment of colon was resected and the patient recovered well.

Discussion

Sixteen cases of splenic flexure volvulus, including the two here, have been reported. Age range is 19–78 years, (average, 51); there are nine women and seven men. Of the 16 patients, 11 had previous abdominal surgery. In all cases except one, diagnosis was made by barium enema study. Usual symptoms are crampy abdominal pain, distention, constipation, and vomiting. In most instances, the symptoms are those of chronic recurrent volvulus. Less frequently, the patient has a surgical emergency.

Predisposing factors permit mobility of the splenic flexure. The supporting ligaments (phrenocolic, splenocolic, and gastrocolic) are either congenitally absent or have been surgically removed. Sometimes the splenic flexure is redundant and on a long mesentery [2, 3, 5, 8]. Adhesive bands were noted in a few cases [1, 9, 11], and in one here. Detorsion of the volvulus may occur spontaneously or during barium enema or a passage of a rectal tube [1, 5, 7, 8]. However, to prevent recurrence preferred treatment is primary resection with end-to-end anastomosis. A decompression colostomy may be necessary as a first stage operation [10].

Awareness of the entity by radiologists may lead to more frequent recognition. The condition should be suspected when evaluating patients with recurrent abdominal pain and distention, especially those with a history of previous abdominal surgery and evidence of obstruction near the splenic flexure.

REFERENCES

1. Buenger RE: Volvulus of the splenic flexure of the colon. *AJR* 71:81–83, 1954
2. Blumberg NA: Volvulus of the splenic flexure: report of a case with a review of the literature. *Br J Surg* 46:292–295, 1958
3. McGarity WC, Bobo WE, Haynes CD: Volvulus of the splenic flexure of the colon: report of two cases and literature review. *Am Surg* 32:425–430, 1966
4. Ponka JL: Volvulus of the colon. *Dis Colon Rectum* 12:430–437, 1969
5. Poppel MH, Zeitel BE, Abrams RM: Volvulus of the splenic flexure. *Am J Dig Dis* 1:380–386, 1956
6. Todd JS: Volvulus of the splenic flexure and tension pneumoperitoneum complicating routine caesarean section. *NY State J Med* 62:3634–3640, 1962
7. Wolf BS, Guglielmo J: Case of volvulus of the splenic flexure. *J Mt Sinai Hosp* 23:741–745, 1956
8. Wray RC Jr, Wangensteen SL: Volvulus of the splenic flexure and cecum. *Surgery* 27:351–352, 1971
9. Young MO: Coexistent volvulus of the splenic flexure and cecum. *Surgery* 37:983–990, 1955
10. Sachidananthan CK, Soehner B: Volvulus of the splenic flexure of the colon: report of a case and review of the literature. *Dis Colon Rectum* 15:466–469, 1972
11. Ghahremani GG, Bowie JD: Volvulus of the splenic flexure: report of a case. *Dis Colon Rectum* 17:100–102, 1974

Splenic Abscess: Comparison of Four Imaging Methods

E. GRANT,[1] M. A. MERTENS, AND V. J. MASCATELLO

This report compares the relative usefulness of four imaging studies in recognizing a splenic abscess, a clinical rarity most often encountered in patients with preexisting hematologic disorder, primary infection elsewhere, or local trauma. A recent review [1] reported a 60% mortality rate in patients with splenic abscess. In about half of these patients, the abscess contributed directly to the fatal outcome. In this series only 40% of

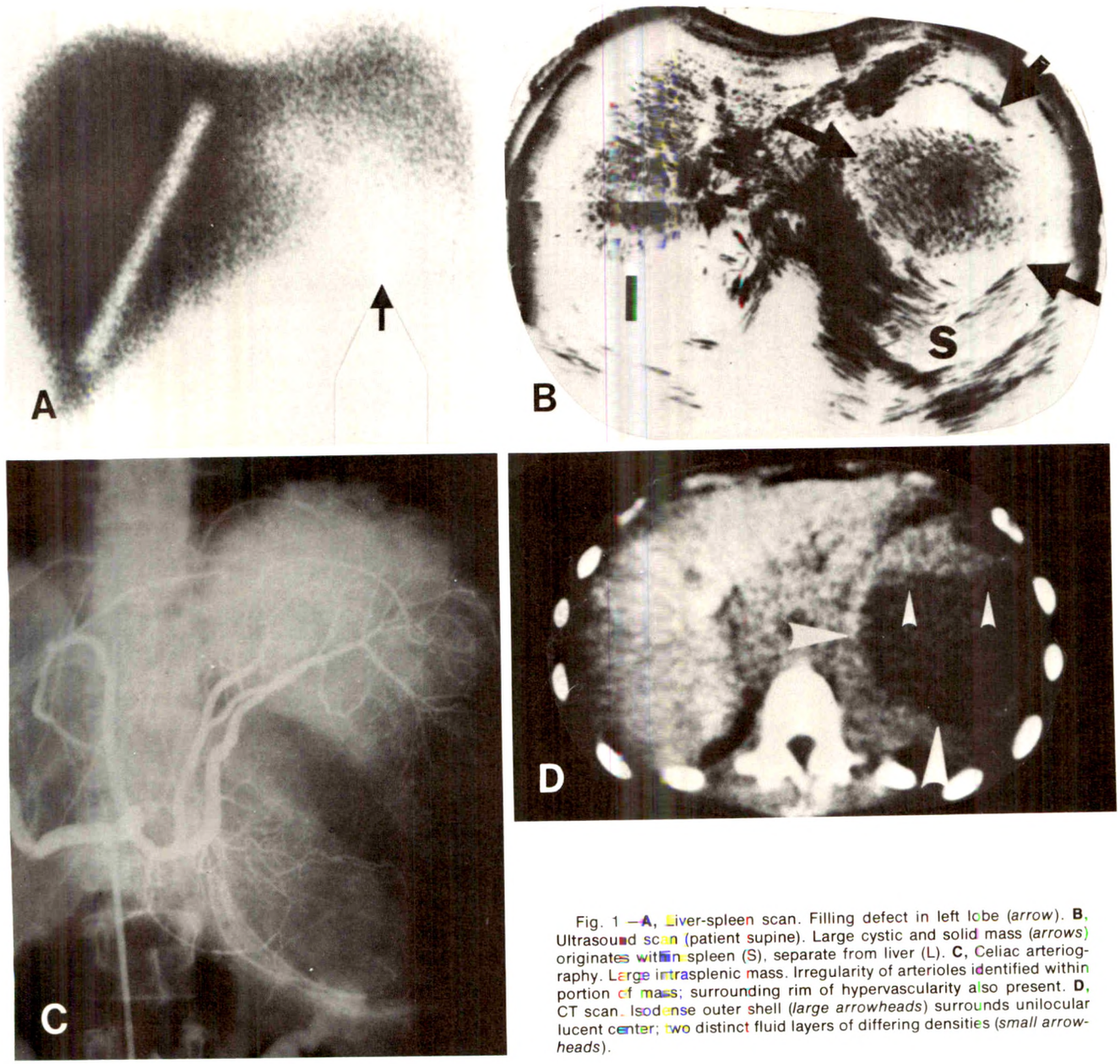


Fig. 1.—**A**, Liver-spleen scan. Filling defect in left lobe (*arrow*). **B**, Ultrasound scan (patient supine). Large cystic and solid mass (*arrows*) originates within spleen (S), separate from liver (L). **C**, Celiac arteriography. Large intrasplenic mass. Irregularity of arterioles identified within portion of mass; surrounding rim of hypervascularity also present. **D**, CT scan. Isodense outer shell (*large arrowheads*) surrounds unilocular lucent center; two distinct fluid layers of differing densities (*small arrowheads*).

Received April 25, 1978; accepted after revision November 13, 1978.

[1] All authors: Department of Radiology, Georgetown University Hospital, 3800 Reservoir Road, Northwest, Washington, D. C. 20007. Address reprint requests to M. A. Mertens.

0361-803X/79/1323-0465 $0.00

AJR 132:465–466, March 1979

© 1979 American Roentgen Ray Society

the cases were diagnosed prior to surgery or autopsy. No fatalities occurred in the group of patients where definitive surgical treatment followed correct diagnosis.

Case Report

A 25-year-old white woman was admitted with a 1 week history of left upper quadrant, intermittent, crampy abdominal pain. She also had associated shaking chills, nausea, diaphoresis, and spiking fevers to 40°C. Her previous health had been excellent with no similar episodes.

On physical examination, a left upper quadrant mass was tender to palpation. There were no signs of peritoneal irritation; bowel sounds were decreased. Hematocrit was 30% and white blood cell count 18,000/mm^3, with 68% segmented polymorphonuclear leukocytes and 17% bands. Platelets were normal, as were routine chemistry and electrolyte values. Urinalysis (during menstruation) revealed 5–10 white blood cells/high-power field, numerous bacteria, and epithelial cells.

Salmonella enteritidis group C1 was isolated in stool cultures. Several blood cultures yielded no growth. Chest radiography demonstrated a small left pleural effusion, while abdominal films indicated splenomegaly. A ^{99m}Tc sulphur colloid liver-spleen scan was interpreted as demonstrating a mass extrinsic to, but compressing, the spleen, arising in the left lobe of the liver (fig. 1A). A ^{67}Ga citrate scan showed a rim of activity surrounding a central region of diminished activity (not illustrated).

Ultrasound study demonstrated a normal liver and a large compound mass (mixed cystic and solid) within the body of the spleen consistent with necrotic tumor or abscess (fig. 1B). Abdominal arteriography revealed an intrasplenic mass that displaced and stretched normal vessels. In addition, there were irregular vessels within one portion of the mass, and a surrounding rim of increased vascularity demonstrated in the capillary phase (fig. 1C). Computed tomography (CT) demonstrated an isodense outer shell surrounding a unilocular lucent center, containing two fluid layers of different densities (fig. 1D).

Surgery revealed a large intrasplenic abscess that contained more than 1,000 ml of brownish fluid. Cultures of this fluid grew *Salmonella enteritidis* group C1 identical to the previous stool culture. After splenectomy there was prompt and complete recovery.

Discussion

Splenic abscess was first reported in the surgical literature in 1954 [2]. Zatzkin et al. [3] reviewed the radiographic findings of splenic abscess, but did not include any of the newer diagnostic methods. Baltaxe et al. [4] described the angiographic findings in a single case. Jacobs et al. [5] reported four cases of splenic abscess, all of which developed in patients with predisposing abnormalities.

The most recent review of splenic abscess emphasized the difficulty of clinical diagnosis [1]. In that report, Chulay and Lankerani suggested that the most useful radiographic information was contributed by the ^{99m}Tc liver-spleen scan. In our patient, the nuclear scan was misleading, since it suggested a mass originating in the liver. Other authors have also reported the nonspecificity of nuclear scans [6].

In our case arteriography was performed the next day, when the clinical impression favored a malignant mass in the liver and its resection was contemplated. This study did demonstrate an intrasplenic mass with stretched vessels and a hypervascular rim, findings previously described for splenic abscess by Reuter and Redman [7]. Its extent, encapsulation, and internal structure seemed optimally defined by subsequent ultrasound and CT studies, undertaken to substantiate the arteriographic impression. CT further showed fluid levels of differing densities within the mass. While an abscess was anticipated preoperatively on the basis of the combined imaging studies, in retrospect, the least invasive and least expensive ultrasound study alone might have sufficed.

REFERENCES

1. Chulay JD, Lankerani MR: Splenic abscess. *Am J Med* 61: 513–522, 1976
2. Reid SE, Lang SJ: Abscess of the spleen. *AJR* 88:912–917, 1954
3. Zatzkin HR, Drazan AD, Irwin GA: Roentgenographic diagnosis of splenic abscess. *AJR* 91:896–899, 1964
4. Baltaxe HA, Watson RC, Levin DC: The angiographic appearance of splenic masses. *Angiology* 23:316–328, 1972
5. Jacobs RP, Shanser JD, Lawson DL, Palubinskas AJ: Angiography of splenic abscesses. *AJR* 122:419–424, 1974
6. LePage JR, Pratt AD Jr, Miale A, Calvert WP: Diagnosis of splenic abscess by radionuclide scanning and selective arteriography. *J Nucl Med* 13:331–332, 1972
7. Reuter SR, Redman HC: *Gastrointestinal Angiography*. Philadelphia, Saunders, 1972

Abdominal Wall Endometrioma

WILLIAM B. MILLER, JR.[1] AND G. LELAND MELSON[1]

Endometriosis in the superficial soft tissues is a rare and comparatively unknown occurrence that most commonly occurs in surgical incisions and scars. An unusual example of an endometrioma to an unscarred upper abdomen is reported here. To our knowledge, this is the first such lesion examined by diagnostic ultrasound.

Case Report

A 32-year-old black woman, gravida 3, para 1, abortion 2, was admitted to Barnes Hospital, St. Louis with recurrent right upper quadrant pain associated with a mass of 5 years. The onset of symptoms was related to minor trauma to the right upper quadrant and the pain and swelling exacerbated at menses. Upper gastrointestinal series and oral cholecystography at another hospital were reportedly normal, and no abnormal findings were reported after laparascopic tubal ligation in 1973.

Physical examination revealed a small firm mass in the right upper quadrant just caudal to the costal margin. The mass was fixed to the subcutaneous tissue but not to overlying skin, which was normal.

Gray scale ultrasound using 5 MHz transducers demonstrated a sharply defined 4.0 × 3.0 × 0.8 cm solid mass in the posterior sheath of the rectus abdominus muscle having an echo texture very similar to the adjacent muscle. The line of demarcation between the muscle and its posterior sheath was indistinct. There was no indication of extension of a primary intraabdominal process (fig. 1).

A raised nodular firm mass adherent to the sheat was excised at surgery. Pathologic examination revealed endometriosis with large areas of fibrosis within the adjacent rectus muscle. No other evidence of endometriosis was found.

Discussion

Although endometriosis outside the pelvis is most common in surgical scars, it may also develop spontaneously, most frequently in the umbilicus as a bluish black tumor [1]. Less commonly, it spontaneously arises in the peritoneum and vulva, and rarely in remote locations such as lung and extremities [2]. In a series of 82 patients with ectopic endometriosis reported by Steck and Helwig [3], 77 endometriomas appeared in preexisting scars, either at the site of previous surgery or in the physiologic scar of the umbilicus. Most were after gynecologic surgery. The remaining five were considered spontaneous and occurred in the inguinal region. All of their patients were affected at or below the umbilical level.

Most extrapelvic lesions respond cyclically to endogenecus hormonal stimulation. Intermittent swelling and pain associated with menses is common, and in the more superficial lesions cyclic bleeding can be seen [1].

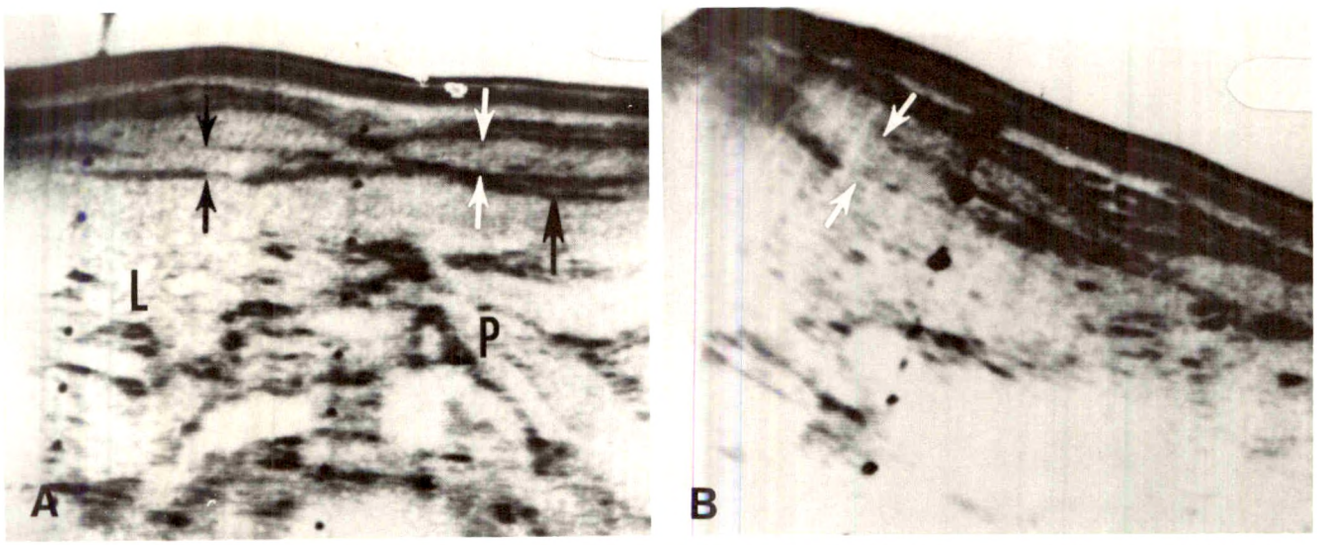


Fig. 1.—**A**, At 6 cm below xiphoid, normal left posterior rectus sheath (*large black arrow*), rectus abdominus muscle (*white arrows*). Right posterior rectus sheath (*small black arrows*) is thickened and similar in echo texture to right rectus abdominus muscle, from which it is poorly demarcated. Intraperitoneal structures are normal. (L = liver, P = pancreas.) **B**, At 3 cm to right, thickening of posterior rectus sheath (*arrows*) is poorly separable from overlying rectus abdominus.

Received September 11, 1978; accepted November 14, 1978.

[1] Mallinckrodt Institute of Radiology, Washington University School of Medicine, 510 South Kingshighway, St. Louis, Missouri 63110. Address reprint requests to G. L. Melson.

© 1979 American Roentgen Ray Society

0361-803X/79/1323-0467 $0.00

Symptoms of pelvic endometriosis are usually absent and pelvic involvement is characteristically confirmed in only one-half of patients at exploratory operation [3].

The pathogenesis of cutaneous endometriosis has not been clarified [3–6]. Mechanical transportation by iatrogenic or surgical transport and spontaneous implantation or seeding via lymphatic channels or blood vessels have been implicated. Another major theory based on mutation is the metaplasia of mesothelium into endometriumlike tissue. A third suggests activation of embryonic rests by cyclic female hormonal stimuli. At present, no theory is preeminent and none satisfactorily explains the variety of clinical presentations observed.

The histologic features are essentially those of endometriosis elsewhere [1, 3]. Endometrial stroma surrounding glandular structures lined with columnar epithelium of variable height is present. A decidual reaction is observed with apparent cyclic changes normally seen in uterine mucosa [3, 4].

Few reports concern ultrasound in evaluating superficial abdominal masses [7, 8]. Ultrasonography has proven most useful in determining whether a mass is cystic, mixed, or solid. The most commonly reported of these superficial masses are rectus sheath hematomas, which characteristically conform to the shape of the rectus and may display either a cystic or complex ultrasonic pattern depending on their age [7–9].

In our patient, ultrasonic examination confirmed the solidity of the mass, provided accurate localization, and excluded underlying ventral extension of intraabdominal pathology. Differential diagnosis of a sonographically complex or solid mass in the anterior abdominal wall is broad and includes abscess, hernia, sebaceous cyst, lipoma, hemangioma, and malignancy such as lymphoma and sarcoma [7]. However, if such a lesion occurs in a reproductive female and is associated with exacerbation of symptoms with menses and, most particularly, if it is at the site of surgical scar, an endometrioma should be considered.

REFERENCES

1. Williams HE, Barsby S, Storing W: Umbilical endometrioma (silent type). *Arch Dermatol* 112:1435–1436, 1976
2. Haines M, Taylor C: *Gynecological Pathology*. London, Longman, 1975
3. Steck WD, Helwig EB: Cutaneous endometriosis. *Clin Obstet Gynecol* 9:373–383, 1966
4. Popoff L, Raitchev R, Andreev VC: Endometriosis of the skin. *Arch Dermatol* 85:66–69, 1962
5. Kistner RW, Marik JJ: Endometriosis etiology. *J Reprod Med* 19:301–302, 1977
6. Ferrari B, Shollenbarger DR: Abdominal wall endometriosis following hypertonic saline abortion. *JAMA* 238:56–57, 1977
7. Goldberg B: Ultrasonic evaluation of superficial masses. *J Clin Ultrasound* 3:91–94, 1975
8. Kaftori JK, Rosenbarger A, Pollack S, Fish J: Rectus sheath hematoma: ultrasonic diagnosis. *AJR* 128:283–285, 1977
9. Hamilton JV, Flinn G, Haynie C, Cefalo RC: Diagnosis of rectus sheath hematoma by B-mode ultrasound. *Am J Obstet Gynecol* 125:562–565, 1976

Distant Metastases to Bone from Bladder Carcinoma: Report of Three Cases

N. REED DUNNICK[1] AND TOM ANDERSON[2]

Bone involvement by transitional cell carcinoma of the bladder is uncommon. When it occurs, it usually affects the adjacent pelvic bones as a result of direct extension [1]. Involvement of distant bones, a result of hematogenous dissemination, is rare. Three cases of distant bone metastases from transitional cell carcinoma of the bladder are reported.

Case Reports

Case 1

K. A., a 58-year-old woman, had dyspareunia and vague lower abdominal pain for 10 months. Excretory urography demonstrated a nonfunctioning right kidney and cystoscopy revealed a mass at the right ureteral orifice. Biopsy showed grade 3 transitional cell carcinoma of the bladder. Surgery proved the tumor to be unresectable because of extension into the broad ligament, invasion of the musculature of the right lateral pelvic wall, and involvement of the distal right ureter.

The patient did well for 2 months after radiation therapy but then developed pain in her right ankle and swelling and tenderness in her right lower leg. Initial ankle films and leg venography were negative. Bone scan revealed an area of increased radionuclide uptake in the right ankle. Aspiration of the ankle joint was sterile and cytology revealed only reactive cells. Repeat ankle films 3 weeks later showed a suspicious lucency in the right talus. Tomography demonstrated a 2 cm lytic lesion in the lateral aspect of the talus (fig. 1). Open biopsy of the talus demonstrated transitional cell tumor identical to the primary. Local irradiation controlled the bone disease. Subsequent soft tissue recurrence in the pelvis 7 months later responded to chemotherapy.

Case 2

H. S., a 66-year-old woman, underwent cystoscopy for persistent hematuria. Carcinoma of the bladder was diagnosed, and surgical excision of the tumor was followed by fulguration.

Recurrent local tumor 18 months later required ureteral ileostomy and pelvic irradiation. Right mandibular pain after 3 more months was not relieved by removing three teeth. A lytic lesion seen in the right mandible 2 months later (fig. 2) was confirmed at biopsy as a metastasis from transitional cell carcinoma of the bladder. Local irradiation was begun. The patient developed a pathologic fracture of the mandible and had persistent local bleeding. Despite hospitalization, the patient continued to deteriorate and died 2 months later in marked uremia.

Case 3

J. L., a 79-year-old man found to have transitional cell carcinoma of the bladder after 8 months of hematuria, underwent urinary diversion to relieve bilateral hydronephrosis and had postoperative irradiation to the bladder. Evidence of bone metastases developed after 3 months. The right pedicle of T6 was destroyed and two lytic lesions developed in the parietal region of the skull. He received local radiation therapy to the spine, but continued to deteriorate and died within 3 weeks. No postmortem examination was performed.

Discussion

Carcinoma of the bladder is locally invasive; it may spread laterally along or penetrate through the bladder wall. Even early tumors may metastasize through lymphatic channels to involve retroperitoneal lymph nodes [2]. However, bone involvement is uncommon. Pelvic bones, particularly the ischium and pubis, may be involved by local extension. Involvement of the lumbosacral spine may represent tumor extension via lymphatic pathways to retroperitoneal lymph nodes or via Batson's venous plexus. Involvement of distant bones, presumably as a result of hematogenous spread, has not been clinically significant due to the high incidence of local disease recurrence. However, results from trials involving preoperative radiotherapy and radical cystectomy demonstrate a decreased incidence of local recurrence. Miller [3] reports a reduction in local tumor recurrence to 16% with preoperative radiation therapy and radical cystectomy, compared with 33% with postoperative irradiation or 45% with definitive radiation therapy alone. Despite this significant improvement in local tumor control the incidence of distant metastases remained constant. Prout [4] reported on the location of metastases in 38 patients who previously underwent cystectomy. Distant metastases developed in 27 (71%) of these patients and local metastases in only 11. Thus the ability to more effectively control disease locally and the demonstrated ability of chemotherapy to produce tumor regression [5] make early recognition of disseminated disease more important.

Cases 1 and 2 represent rare sites of bone metastases. In both cases etiologies other than metastatic bladder carcinoma were suspected. In case 1, leg venography was performed for suspected deep vein thrombosis. Indeed, peripheral bone metastases are usually secondary to bronchogenic carcinoma [6]. In case 2, three teeth were extracted and antibiotics prescribed for a suspected dental abcess. Distant bone metastases should now be considered more common in patients with bladder carcinoma.

REFERENCES

1. Mullin EM, Glenn JF, Paulson DF: Lesions of bone and bladder cancer. *J Urol* 113:45–46, 1975.

Received June 20, 1978; accepted after revision November 9, 1978.

[1] Department of Diagnostic Radiology, National Institutes of Health, Clinical Center, Building 10, Room 6S211, Bethesda, Maryland 20014. Address reprint requests to N. R. Dunnick.

[2] Medicine Branch, Division of Cancer Treatment, National Cancer Institute, Bethesda, Maryland 20014.

0361–803X/79/1323–0469 $0.00

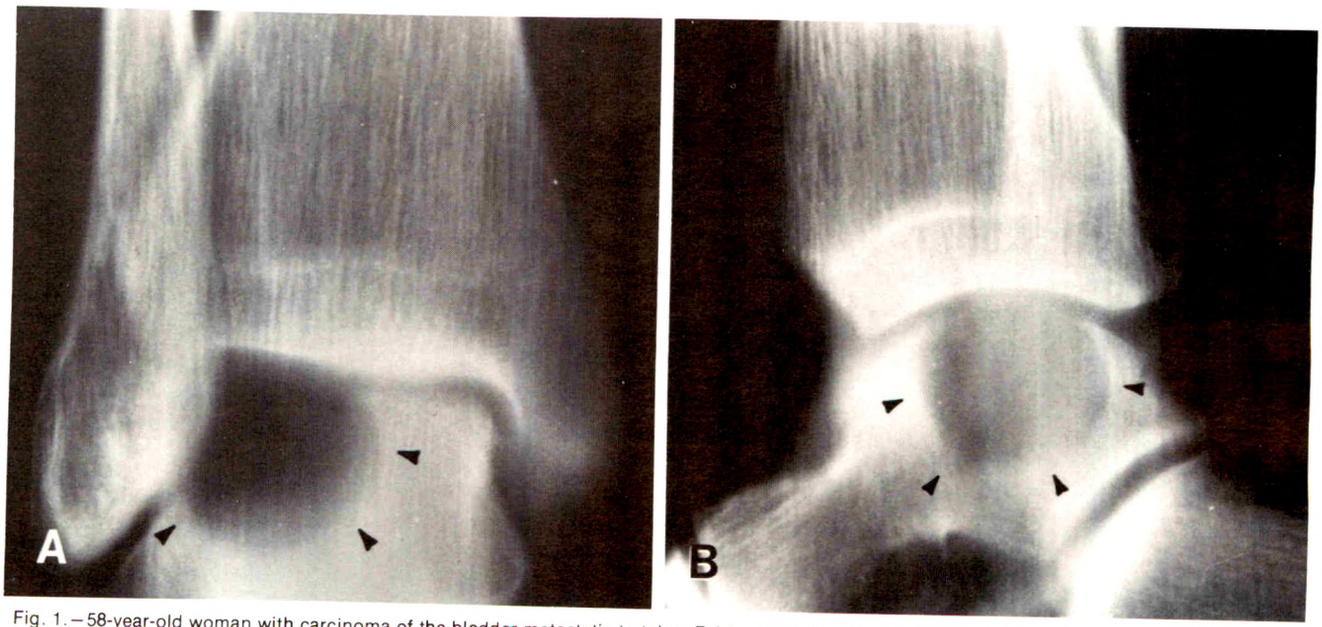


Fig. 1.—58-year-old woman with carcinoma of the bladder metastatic to talus. Fairly well defined lytic lesion (*arrowheads*) in lateral aspect of talus.

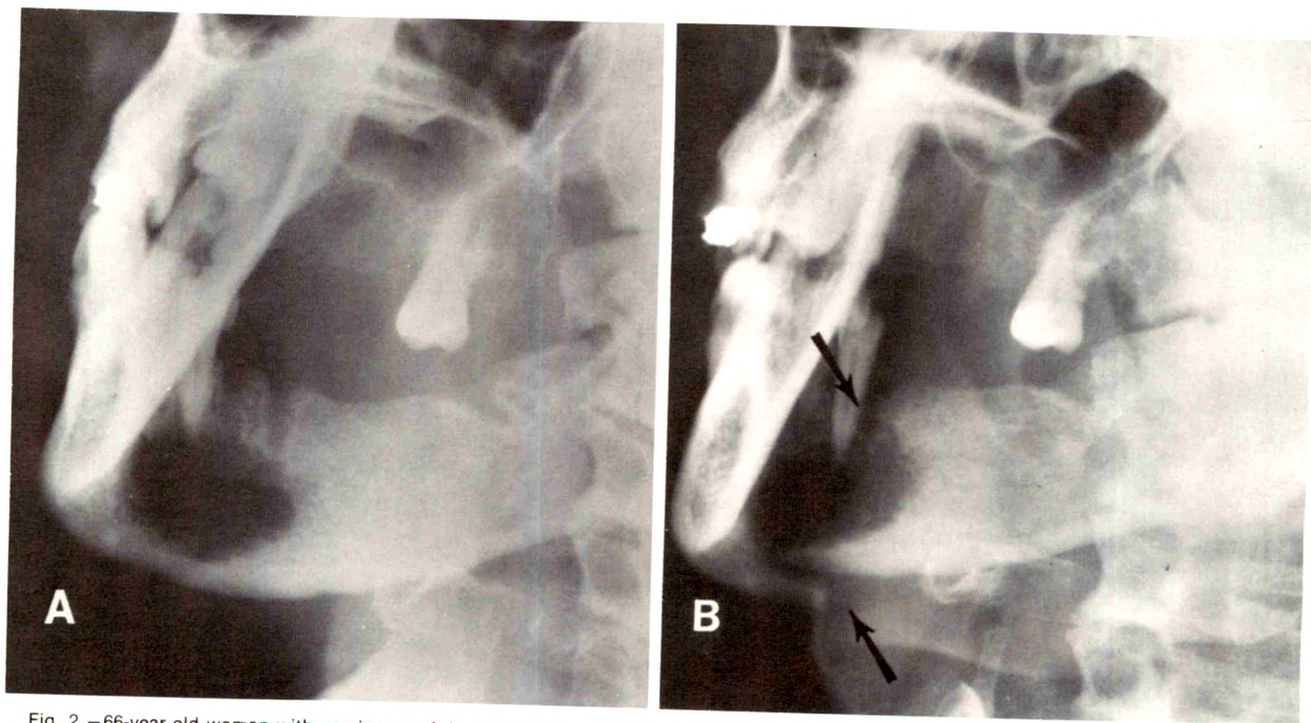


Fig. 2.—66-year-old woman with carcinoma of the bladder metastatic to mandible. **A,** 2 cm lytic lesion in right mandibular ramus. **B,** Pathologic fracture through lesion 2 months later (*arrows*).

2. Wirtanen GW, Miller RC: Bladder lymphatics and tumor dissemination. *J Urol* 109:58–59, 1973
3. Miller LS: Bladder cancer: superiority of pre-operative irradiation therapy and cystectomy in clinical stages B_2 and C. *Cancer* 39:973–980, 1977
4. Prout GR: The role of surgery in the potentially curative treatment of bladder carcinoma. *Cancer Res* 37:2764–2770, 1977
5. Sternberg JJ, Bracken RB, Handel PB, Johnson DE: Combination chemotherapy (CISVA) for advanced urinary tract carcinoma. *JAMA* 238:2282–2287, 1977
6. Mulvey RB: Peripheral bone metastases. *AJR* 91:155–160, 1964

Intraarticular Lipoma with Osseous Metaplasia: Radiographic-Pathologic Correlation

ROCHELLE M. PUDLOWSKI,[1] LOUIS A. GILULA,[1] AND MICHAEL KYRIAKOS[2]

Although lipomas are common soft tissue tumors, their location within a joint space is extremely rare [1, 2]. To our knowledge, only three such cases have been reported [3–5], none of which contained either calcification or ossification. We report the features of a partially ossified, true lipoma of the knee joint and the first such case with radiologic and histopathologic correlation.

Case Report

A 53-year-old black man was admitted to Barnes Hospital with pain, swelling, and instability of the left knee 5 months after injuring both knees in a fall. Physical examination was normal except for some distention of the left suprapatellar bursa. Routine laboratory examinations were normal.

Radiography of the left knee showed osteoarthritis (fig. 1). In addition, a 3 × 4 cm ossified mass projected over a distended suprapatellar space. No lucency could be seen in the bursa on the plain films.

Clear yellow fluid (8 ml) was aspirated from the knee joint. Double contrast arthrography demonstrated a 4 × 6 cm, round, soft tissue mass with a focus of trabecular bone along its anterior margin that arose from a broad base along the posterior wall of the suprapatellar bursa. The mass filled the posterior one-third of the bursa and changed shape with motion of the knee joint. A torn medial meniscus, femoral and patellar cartilage erosions, and a small joint body in the suprapatellar bursa were also seen (fig. 2).

At operation, an encapsulated intraarticular mass was excised from the posterior wall of the suprapatellar bursa. It was distinct and separate from the subsynovial fat pad. The small osteocartilaginous joint body was resected from its separate

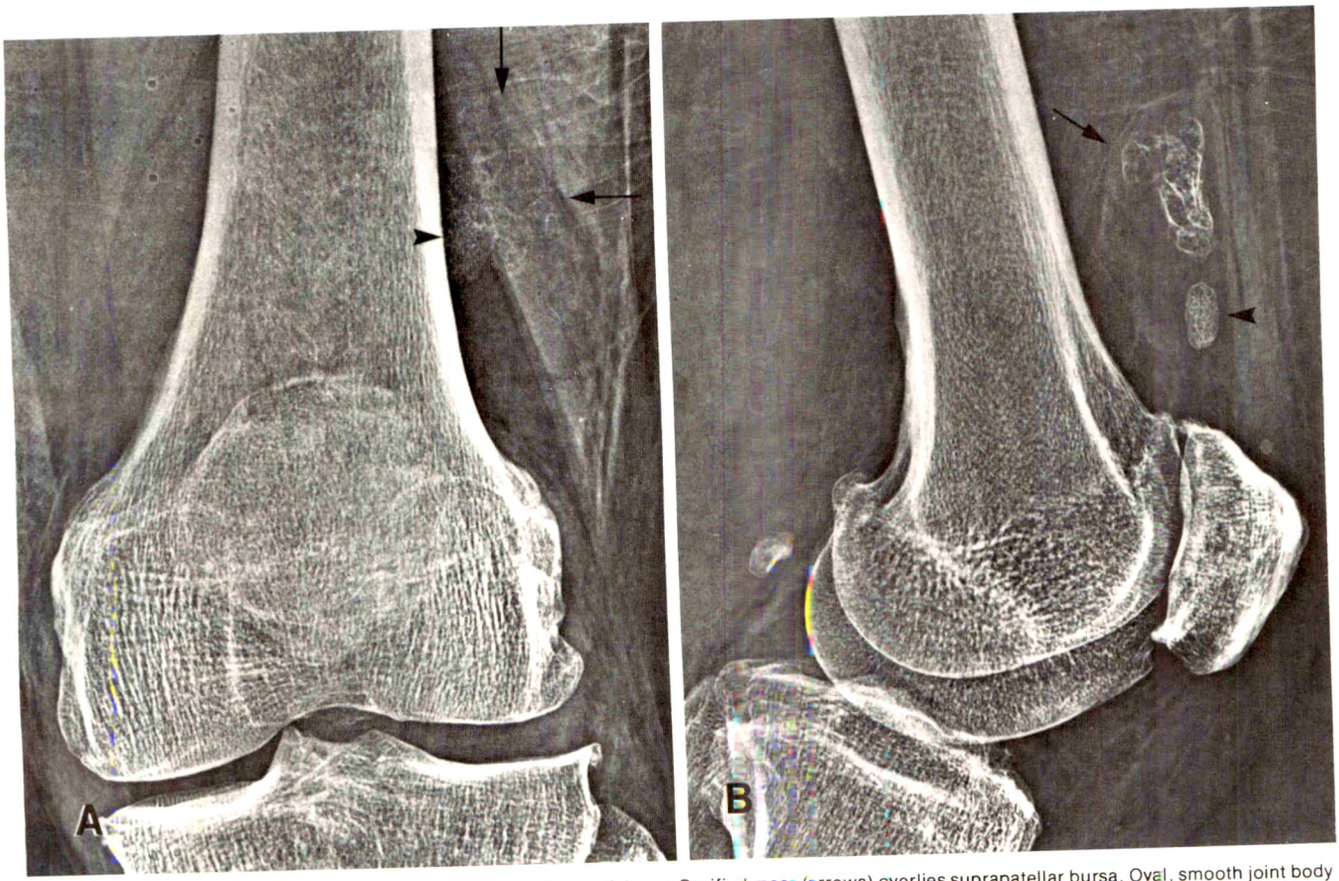


Fig. 1.—Anteroposterior (**A**) and lateral (**B**) xeroradiographs of left knee. Ossified mass (*arrows*) overlies suprapatellar bursa. Oval, smooth joint body (*arrowhead*) lies along anterior bursal wall beneath mass, and projects over mass in anteroposterior projection.

Received July 6, 1978; accepted after revision November 29, 1978.

[1] Musculoskeletal Section, Mallinckrodt Institute of Radiology, Washington University School of Medicine, 510 South Kingshighway Boulevard, St. Louis, Missouri 63110. Address reprint requests to R. M. Pudlowski.

[2] Department of Pathology, Washington University School of Medicine, St. Louis, Missouri 63110.

0361-803X/79/1323-0471 $0.00

AJR 132:471–473, March 1979

© 1979 American Roentgen Ray Society

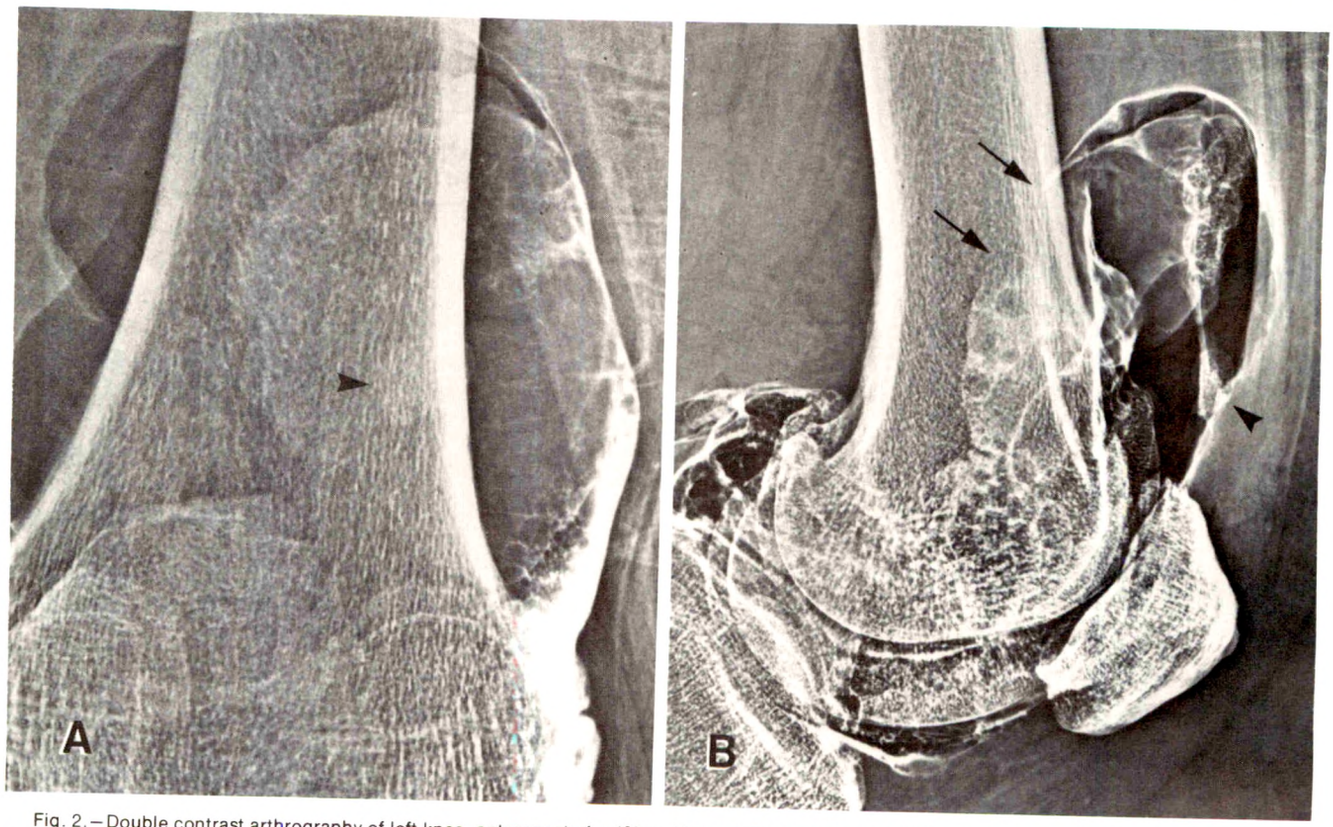


Fig. 2.—Double contrast arthrography of left knee, anteroposterior (**A**) and lateral (**B**) xeroradiographs. Large, smoothly lobulated, partially ossified intraarticular mass arises from posterior wall of suprapatellar bursa (*between arrows*). Small joint body attaches to anterior wall of bursa (*arrowhead*) and on **B** is clearly separate from main tumor mass.

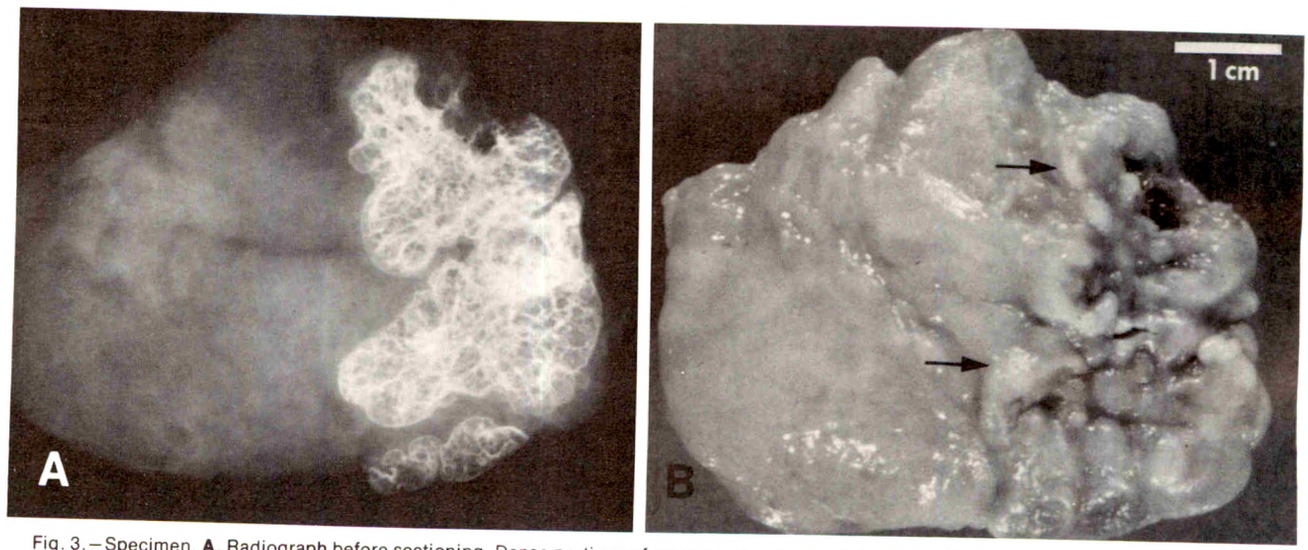


Fig. 3.—Specimen. **A,** Radiograph before sectioning. Dense portions of mass are composed of trabecular bone. **B,** Islands of bone (*arrows*) in direct continuity with surrounding adipose tissue.

attachment beneath the mass, and a medial meniscectomy was performed.

The specimen (fig. 3) consisted of a 5.5 × 4.5 × 2.5 cm mass of soft, yellow, adipose tissue covered by a thin glistening white capsule. There was a 3 × 4 cm nodular zone of ossification at one pole, entirely covered by the tumor capsule and in direct continuity with the remainder of the fatty tissue. The bone was divided into lobules by white fibrous septae.

Microscopic examination of the mass showed mature adipose tissue traversed by delicate fibrous septae and covered by a fibrous capsule of varying thickness, on which rested a layer of flat mesotheliumlike cells. In focal areas, these cells were

rounded and formed layers two to three cells deep resembling synovium. The osseous component consisted of a rim of lamellar bone which surrounded a central core of fat, blood vessels, hematopoietic cells, and bony trabeculae. The bone contained osteocytes and was lined by plump osteoblasts and occasional osteoclasts. No cartilage was seen. The pathology was consistent with an intraarticular lipoma with focal osseous metaplasia.

Discussion

The true intraarticular lipoma is a solitary, round to oval mass of mature adipose tissue encased by a thin fibrous capsule just like its soft tissue counterpart. It may be covered by synovium and may possess a vascular pedicle. It apparently arises *de novo*, unrelated to other joint pathology [3–5].

This lesion must be distinguished from the more common lipoma arborescens, which is characterized grossly by numerous villous projections of fatty synovial tissue [3, 5–10]. It is usually associated with posttraumatic or inflammatory joint conditions, but may also arise *de novo* [6–10].

True intraarticular lipomas are extremly rare, since a search of the literature uncovered only three acceptable examples [3–5]. As in our patient, the lipomas were located within the knee joint. The previous patients were all women, aged 38, 52, and 56 years. All three had joint swelling and pain of varying duration related to interposition of the tumor mass between the articular surfaces and strangulation of the tumor secondary to volvulus about its stalk. No descriptions of the radiologic appearance of the lesions were included in these reports.

A questionable case of an intraarticular lipoma of the subdeltoid bursa in a patient with rheumatoid arthritis has been reported [11]. Arthrography showed multiple, radiolucent masses within the shoulder joint and the communicating subdeltoid bursa. The description and the radiologic appearance of this lesion is more consistent with a lipoma arborescens than with a true lipoma.

In our case, the area of ossification within the lipoma allowed its identification on the plain films. The changing shape of the mass with joint movement noted during arthrography strongly suggested intraarticular lipoma; this was confirmed at operation.

While it cannot be proved, we suspect that the osseous metaplasia was a result of the trauma suffered by the patient in his fall 5 months earlier, which was severe enough to have torn the medial meniscus. However, there have been reports of ossified lipomas of the soft tissue unassociated with known trauma [12, 13].

As to the origin of these tumors, Jaffe [3] felt that they could arise from the subsynovial fat near the patellar ligament, the fat pad anterior to the surface of the femur, the synovium near the anterior horn of the medial meniscus, or, as in our patient, from the posterior wall of the suprapatellar bursa.

ACKNOWLEDGMENT

We thank Dr. Barry Paull for his valuable assistance in the translation of several foreign language references.

REFERENCES

1. Stout AP, Lattes R: Tumors of the soft tissues in *Atlas of Tumor Pathology*, 2d series, fascicle 5, Washington, D.C., Armed Forces Institute of Pathology, 1967, pp 52–58
2. Hass A: Uber Gefasstumoren der Kniegelenkkapsel. *Dtsch Z Chir* 173:130–141, 1922
3. Jaffe H: *Tumors and Tumorous Conditions of the Bones and Joints*. Philadelphia, Lea & Febiger, 1974, pp 574–575
4. Diamant-Berger ML: Un cas de volvulus d'un lipome pédiculé intra-articulaire du genou. *Bull Memoires Soc Natl Chir* 56:744–745, 1930
5. Smillie IS: *Diseases of the Knee Joint*. Edinburgh, Churchill Livingstone, 1974, p 411
6. Hoffa A. Zur Bedeutung des Fettgewebes für die Pathologie des Kniegelenks. *Dtsch Med Wochenschr* 30:337–338, 1904
7. Burgan DWL: Lipoma arborescens of the knee: another cause of filling defects on a knee arthrogram. *Radiology* 101:583–584, 1971
8. Arzimanoglu A: Bilateral arborescent lipoma of the knee—a case report. *J Bone Joint Surg [Am]* 39:976–979, 1957
9. Weitzman G: Lipoma arborescens of the knee—report of a case. *J Bone Joint Surg [Am]* 47:1030–1033, 1965
10. Placeo F, Tassi D: Considerazioni cliniche su 62 osservazioni di lipoma arborescente postraumatico del ginocchio come entita pathologica a se sante ed associated a lesione meniscale. *Minerva Chir* 8:316–322, 1953
11. Weston WJ: The intra-synovial fatty masses in chronic rheumatoid arthritis. *Br J Radiol* 46:213–216, 1973
12. Murphy NB: Ossifying lipoma. *Br J Radiol* 47:97–98, 1974
13. Plaut GS, Salm R, Truscott DE: Three cases of ossifying lipoma. *J Pathol* 78:292–295, 1959

Neurofibromatosis: Unusual Lymphangiographic Findings

JACK M. PRESTON,[1] ROBERT J. STARSHAK,[2] AND HERBERT W. OECHLER[3]

Neurofibromatosis (Recklinghausen's disease) is a relatively uncommon disorder resulting from a mesodermal and neuroectodermal dysplasia; it is transmitted as an autosomal dominant, although one-half of the cases are spontaneous mutants. Virtually any organ system may become involved, producing various radiologic findings that have recently been summarized [1–3]. However, lymphatic system involvement has received scant attention. A bizarre lymphangiographic appearance in a patient with neurofibromatosis is reported.

Case Report

A 15-year-old black girl was admitted to Milwaukee Children's Hospital with increasing swelling and pain of her left leg for 1 month (fig. 1). She was first seen at age 14 months because of an upper respiratory tract infection. Physical examination at that time revealed a markedly enlarged left lower extremity with associated hyperpigmentation present since birth. There were café-au-lait spots on the back and left leg. Diagnosis of neurofibromatosis was histologically confirmed 2 years later. Her parents had no stigmata of neurofibromatosis.

The patient was readmitted to Milwaukee Children's Hospital numerous times for cosmetic and orthopedic surgery related to her left leg, including two leg shortening procedures, a wedge osteotomy for genu valgum deformity, and an epiphysiodesis of the knee. Infection of the surgical sites was not a clinical problem.

Radiography demonstrated the classic findings of neurofibromatosis, including scoliosis and posterior scalloping of the lumbar vertebrae. However, focal gigantism of the left lower extremity was the most striking. Maximum leg length discrepancy was 8 cm. There was overgrowth and abnormal modeling of the ilium, as well as of the bones of the left leg.

Cannulation of a lymphatic in the right foot was unsuccessful. Lymphatics visualized in the left leg during lymphangiography were markedly dilated; the valves were preserved (fig. 2A). The anteromedial aspect of the leg just distal to the knee had an irregular collection of lymph vessels, some of which looked like dermal lymphatics, corresponding to a localized area of soft tissue prominence. There was partial lymphatic obstruction at groin level (fig. 2B). On nodal phase, several moderately enlarged popliteal lymph nodes were noted. The opacified nodes in the left groin and pelvis demonstrated massive enlargement with filling defects (fig. 2C).

Lymph node biopsy was recommended to exclude neoplastic involvement, but the patient's family refused surgery, and she was lost to follow-up until 18 months later when she was seen with progressive swelling and a "burning" sensation in the left leg. There was a large mass on the lateral aspect of the distal thigh just above the knee. Inguinal lymphadenopathy remained unchanged.



Fig. 1.—Massive overgrowth of soft tissue and café-au-lait spots on patient's legs.

Several of these palpable inguinal lymph nodes were excised. The mass in the thigh was a large neurofibroma. Histologic examination of the lymph nodes revealed that the neurofibromatous tissue encased the nodes and permeated them by extension through their hila (fig. 3). There was no evidence of blood or lymphatic vessel invasion, and malignant degeneration and mitotic figures were not identified.

Since then, the patient has been treated for recurrent dislocation of her left hip and evaluated for abdominal neurofibromas. There has been no evidence of malignancy.

Discussion

Most radiographic findings in neurofibromatosis are related to the skeletal system, especially the vertebral column. Osseous changes other than those of the vertebrae occur frequently, and Holt [3] encountered four patients with pelvic configuration identical to that seen in this case. Included in this category is bone overgrowth usually associated with hypertrophy of the adjacent soft tissues, consisting in part of large plexiform neurofibroma. When massive enlargement exists, the condition is referred to as elephantiasis neuromatosa [4, 5]. Caffey [6] states that the bone overgrowth is secondary to chronic hyperemia due to the adjacent hemangiomatous

Received June 27, 1978; accepted after revision November 16, 1978.

[1] Department of Radiology, University of Wisconsin, Madison, Wisconsin 53706.

[2] Department of Radiology, Milwaukee Children's Hospital, 1700 West Wisconsin Avenue, P. O. Box 1997, Milwaukee, Wisconsin 53201. Address reprint requests to R. J. Starshak.

[3] Department of Pathology, Milwaukee Children's Hospital, Milwaukee, Wisconsin 53201.

© 1979 American Roentgen Ray Society

0361–803X/79/1323–0474 $0.00

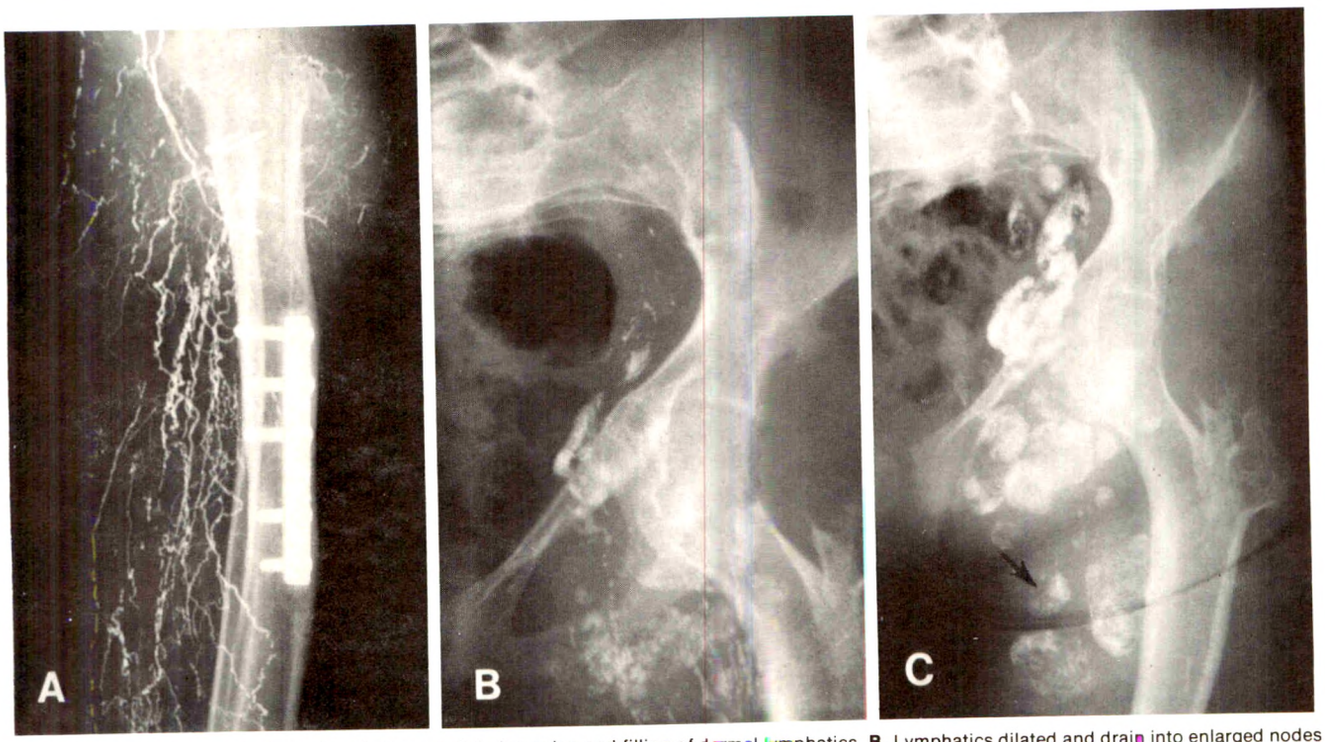


Fig. 2.—**A**, Dilated and tortuous lymphatic vessels in lower leg and filling of dermal lymphatics. **B**, Lymphatics dilated and drain into enlarged nodes in left half of pelvis. **C**, In nodal phase, enlarged nodes contain numerous filling defects, most prominently at hila (*arrow*).

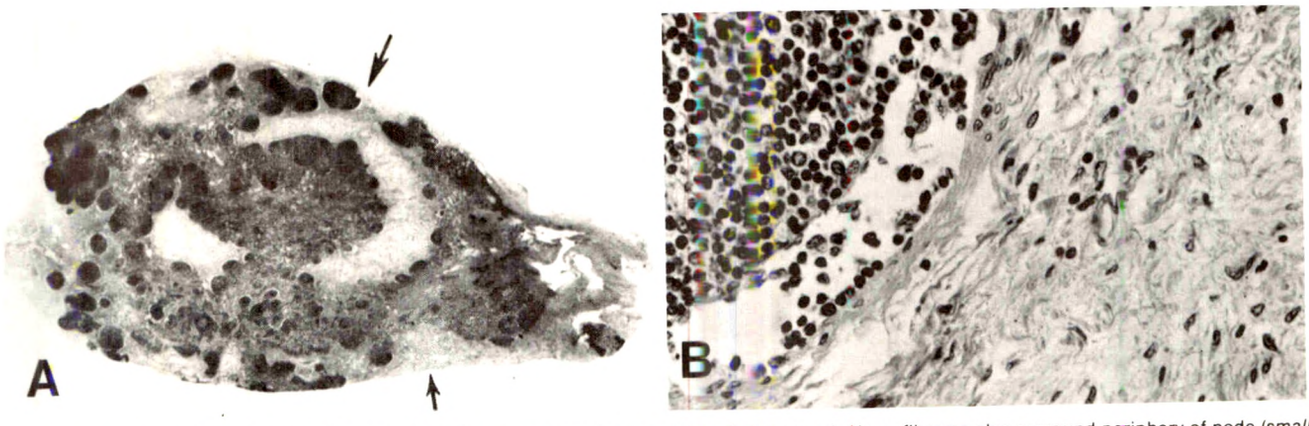


Fig. 3.—Resected lymph node. **A**, Strands of neurofibroma enter node at hilum (*large arrow*). Neurofibroma also surround periphery of node (*small arrow*). **B**, Neurofibromatous tissue with wavy collagen bands abuts on lymph node.

and lymphangiomatous tissue. Others feel that mesodermal dysplasia contributes to the overgrowth [3, 7]. Elephantiasis neuromatosa must be differentiated from congenital hemihypertrophy; the two conditions have been reported to coexist [8].

Although skeletal manifestations are generally well known, lymphatic changes have received little emphasis. In a recent case report [9], upper extremity lymphangiography in a patient with neurofibromatosis associated with gross enlargement of the arm since birth revealed marked dilatation of the lymph vessels; in this case, the valves were not discernible. Anomalous flow from the superficial to deep lymphatics was also described but the status of the nodes was not demonstrated [9].

Neurofibromatosis is associated with an increased incidence of certain malignancies (e.g., central nervous system tumors, pheochromocytoma, and leukemia) [3]; recently a possible association with Burkitt's lymphoma has been questioned [10]. Of greater importance is the sarcomatous degeneration of the neurofibromas reported in 2%–16% of patients [1, 11]. However, neurofibrosarcomas in patients with or without Recklinghausen's disease have not been found to metastasize to regional lymph nodes [12–14]. Involvement of the lymph nodes in neurofibromatosis is not surprising in view of the protean manifestations of this disease with tendency for neurofibromas to produce bulky regional masses. It is possible that plexiform neurofibromas can extend

along the nerves that enter the medullary portions of lymph nodes at the hilum. Such extension could account for the enlargement of the nodes as well as the filling defects.

Abnormal lymphographic appearance of nodes in a patient with neurofibromatosis does not necessarily indicate malignancy. Additional studies in such patients will be required to determine the frequency of this finding.

ACKNOWLEDGMENT

We thank Dr. John F. Holt for encouragement and assistance in preparing this manuscript.

REFERENCES

1. Klatte EC, Franken EA, Smith JA: The radiographic spectrum in neurofibromatosis. *Semin Roentgenol* 11:17–33, 1976
2. Casselman ES, Miller WT, Lin SR, Mandell GA: Von Recklinghausen's disease: incidence of roentgenographic findings with a clinical review of the literature. *CRT Crit Rev Diagn Imaging* 9:387–419, 1977
3. Holt JF: Neurofibromatosis in children. *AJR* 130:615–639, 1978
4. Moore BH: Some orthopaedic relationships of neurofibromatosis. *J Bone Joint Surg* [Am] 23:109–140, 1941
5. Wescott RJ, Ackerman LV: Elephantiasis neuromatosa. *Arch Dermatol Syphiol* 55:233–241, 1947
6. Caffey J: *Pediatric X-ray Diagnosis,* 6th ed. Chicago, Year Book Medical Publishers, 1972, pp 1268–1271
7. Pitt MJ, Mosher JF, Edeiken J: Abnormal periosteum and bone in neurofibromatosis. *Radiology* 103:143–146, 1972
8. Praharaj KC, Mohanta KD, Nanda BK, Nanca CN: Congenital hemihypertrophy with neurofibromatosa. *Indian J Med Sci* 23:146–150, 1969
9. Lantsov VP, Kramorev VA: State of the lymphatic system in neurofibromatosis (according to roentgenolymphographic data). *Vestn Rentgenol Radiol* 2:99–101, 1976
10. Berman BW, Binder RA, Cornfield DB: Burkitt lymphoma in a patient with neurofibromatosis and pheochromocytoma. *JAMA* 237:993–994, 1977
11. Crowe FW, Schull WJ, Neel JV: A clinical pathological and genetic study of multiple neurofibromatosis. Springfield Ill. Thomas, 1976, pp 32–33
12. Ghosh BC, Ghosh L, Huvos AG, Fortner JG: Malignant schwannoma: a clinicopathologic study. *Cancer* 31:184–190, 1973
13. D'Agostino AN, Soule EH, Miller RH: Sarcomas of the peripheral nerves and somatic soft tissues associated with multiple neurofibromatosis (von Recklinghausen's disease). *Cancer* 16:1015–1027, 1963
14. D'Agostino AN, Soule EH, Miller RH: Primary malignant neoplasms of nerves (malignant neurilemomas) in patients without manifestations of multiple neurofibromatosis (von Recklinghausen's disease). *Cancer* 16:1003–1014, 1963

Technical Notes

Precision Technique for Positioning the Head During Tomography

GREGORIO FAIVOVICH,[1,2] KARL-ÅKE OMNELL,[1] AND ALVAR SVENSSON[1]

Slight deviations in head orientation during axial tomography can be troublesome. Due to the thinness of the layers depicted when hypocycloidal movement is used, it may be impossible to compare the anatomic structures on one side with the corresponding structures on the opposite side of the midsagittal plane. In a recent paper [1], we described a simple technique for patient positioning during axial tomography of the head using a device designed for the Philips-Massiot Universal Polytome.

Positioning

The patient is placed prone on the table, with his head and neck superextended and his chin resting on a chin support. The orbitomeatal line is parallel to the table top. The sagittal midline of the face is placed to coincide with a fixed narrow vertical beam of light projected from a source mounted on a vertical rod. The head is then fixed in the proper position by a forehead support.

A lateral light source, also mounted on a vertical rod, yields a narrow horizontal beam projected simultaneously on the patient's face and on a height indicator placed on the table top close to the face. The beam of light is adjusted vertically to the desired tomography level. The distance between this level and the table top is read from the height indicator and the level of the table top is regulated accordingly.

Although this positioning method is satisfactory in many situations, small deviations in alignment can still occur that may not be detected by the naked eye. Moreover, the exterior of the face does not always reflect the asymmetries of the skull.

Device

We tried to increase the accuracy of tomographic examination of the fine structures of the skull and facial skeleton with a sensitive positioning device (fig. 1) that permits detection of very slight lateral head tilting. Accuracy should be increased using this technique: (1) during primary positioning of the head; (2) for fine corrections of the head position during examination; and (3) in situations requiring equivalent projections for repeat examinations.

Light emitted from source (A) is collected by an optical lens (B) and transmitted via optical fibers (C) to two small aluminum tubes (D). Each tube holds a mirror (E) placed at a 45° angle to the direction of the light beam, a screen cut with a central cross (F), and an object lens (G). The light from the optical fibers is reflected by the mirror projecting the cross on the screen via the object lens onto 2 mm sectioned vertical transparent scales. The scales are attached symmetrically to each side of the tomographic table (figs. 2 and 3). Metal bars housed by guide bushings (H) and joined by a thin steel bow (J) are used to connect the tubes (D) to ear rods (K). The ear rods can be moved on a common axis coinciding with the axes of the two light beams, the movement being guided by the bushings. A spring mechanism (L) is activated when the ear rods are moved in opposite directions, forcing the rods toward each other. The spring is also designed to prevent rotation of the bars in the guide bushings.

Procedure

With the patient prone, his head is oriented according to the procedure described above [1]. After the spring mechanism is activated, the ear rods are introduced into the external auditory canals with the steel bow resting on the back of the patient (figs. 2 and 3). Head position is adjusted so that both scales on the tomographic table give the same reading. The axes of the two light beams are now parallel to the plane of the film and to the tomographic level.

When a tomographic series is required, the readings on the scales are checked before each exposure and, if necessary, adjustments made to ensure identical position of the head throughout the examination. Identical readings on the two scales will result in axial tomograms in which the structures on both sides of the midsagittal plane are comparable when the external auditory canals are symmetrically positioned and the skeleton of the head exhibits symmetry.

Axial tomograms that do not depict comparable structures on each side of the midsagittal plane may be caused by asymmetrical positioning of the external auditory canals and/or the other parts of the head skeleton, despite identical readings on the scales. Such asymmetries can be compensated for by a slight tilt, that is, rotating the frontal plane of the head with respect to the horizontal tomographic level. It should be understood that the patient is positioned with the axis of rotation located above the midline of the tomographic table.

Received September 15, 1977; accepted after revision November 16, 1978.
[1] School of Dentistry, University of Lund, S-214 21 Malmo, Sweden. Address reprint requests to K. A. Omnell.
[2] Present address: School of Dentistry, University of Chile, Santiago, Chile.

AJR 132:477–479, March 1979
0361–803X/79/1323–0477 $0.00
© 1979 American Roentgen Ray Society

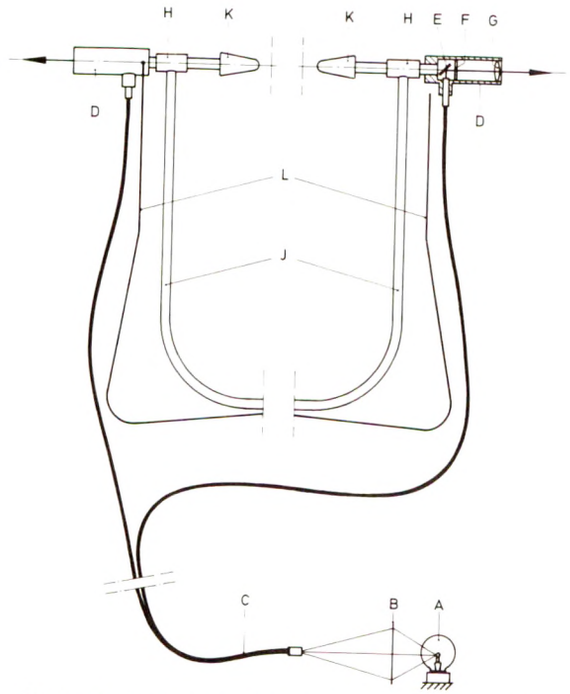


Fig. 1.—Device for accurate positioning of patient during axial head tomography. A, light source; B, optical lens; C, optical fibers; D, aluminum tubes; E, mirror; F, screen with cross; G, object lens; H, guide bushings; J, steel bow; K, ear rods; L, spring mechanism.

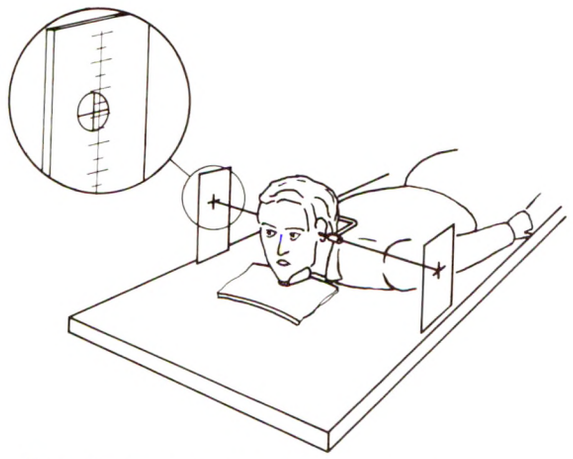


Fig. 2.—Patient prone for axial head tomography. Positioning aided by narrow beams of light projected from patient on transparent scales attached to each side of table.

Adjustments

Figure 4 explains the geometry involved: A = distance between the midline of the table (sagittal midline of the face) and one of the scales; B = difference between the readings taken from the two scales before and after tilting of the head; C = horizontal distance between a vertical plane through the midline of the table and the location of a given landmark of the head; and D = distance traveled in vertical direction by the given landmark. If B/D = A/C, then B = AD/C.

For a given tomographic table, A is a constant. In our case, using the Polytome, A = 360 mm. It is obvious that if the anatomic landmark is moved in a superior or inferior direction over a given distance (D), the difference between the two readings (B) will depend on the distance (C) between the landmark and the vertical plane through the midline of the table.

Figure 5 indicates the variances in the ratio B/D with the distance, C, when using the Polytome. If the landmark travels 1 mm, then D = 1 mm and the vertical axis of the diagram is read in millimeters. The dependence of the difference, B, on the distance, C, is clear. Therefore, the more distant a given structure (landmark) is located from the vertical plane through the midline of the table, the smaller the magnification of its movement when the head is tilted in the frontal plane.

Movement of a structure located in the most lateral parts of the head, about 70 mm from the midsagittal plane, will cause magnification of about 5 times on the scales; movement of a structure located only 10 mm from the midsagittal plane will be magnified 36 times.

If an asymmetry is found during examination, it can be compensated for by tilting the head in the frontal plane as follows. Allowing for the degree of magnification on the tomogram, the radiographic distance between the midsagittal plane and the area under investigation is measured. The corrected distance equals C (fig. 4).

On the basis of radiographic anatomy, the examiner can estimate distance, D, and determine the direction in which the head must be tilted to bring the required structure into the tomographic level. The graph (fig. 5) is used to guide repositioning. The number of B/D corresponding to the known distance, C, is located on the graph. To find the correct readings on the two scales, B/D is multiplied by the estimated distance, D. The resulting number, B, is then used to correct the original readings on the scales. This whole operation takes only a few seconds.

Discussion

The device described here has been used on 100 patients. Mostly the temporomandibular joints have been examined; however, the procedure has also been applied to other parts of the middle third of the facial skeleton and to the base of the skull.

This device is remarkably accurate for positioning of the head during axial tomography. The position of the ear rods in the external auditory canals has proven to be very stable, partly due to the resilience of the system and partly due to the small amount of weight from the steel bow that rests on the back of the patient. The probability of patient movement is far greater than movement of the device relative to the patient. In this context, it should be pointed out that the magnification of movements of the patient is such that the light dots on the scales travel short distances up and down due to patient breathing.

Costs of manufacturing, purchasing, and assembling the necessary parts of the device are about $3,000. Time required to set up the device on the tomograph before examination should be 5–10 min.

Patients with cervical spinal column stiffness might have difficulty with the prone position. However, it seems

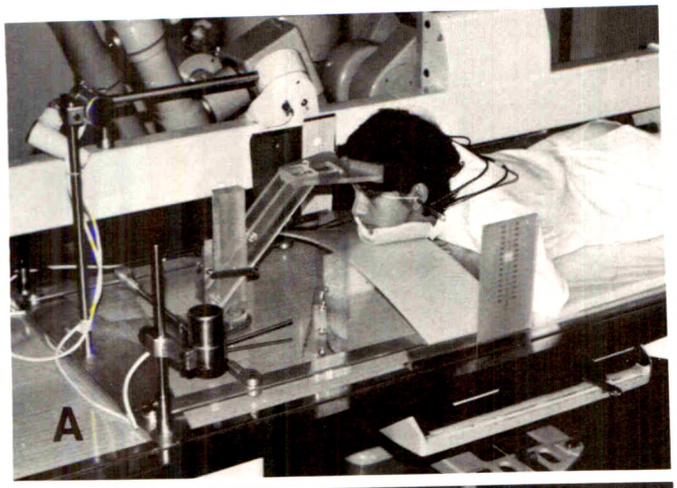
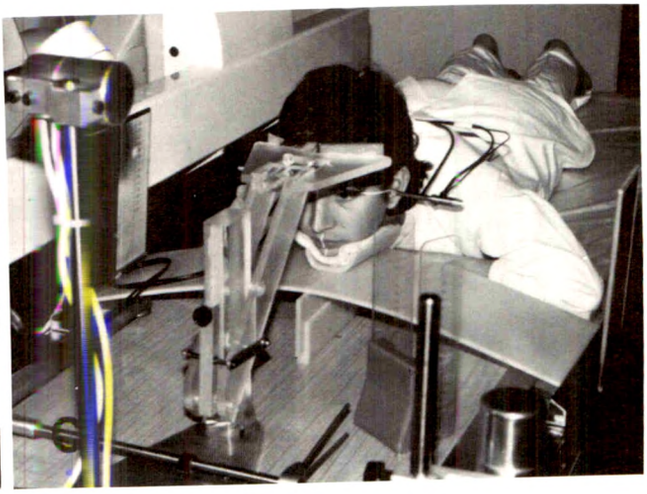


Fig. 3.—Prone position during axial head tomography. Primary positioning achieved by narrow beams of light casting vertical and horizontal planes on face. Head rests against adjustable forehead and chin support. Device attached to patient by ear rods projects light beams on scales mounted on each side of table. Accurate positioning aided by magnified registration of head deviations.





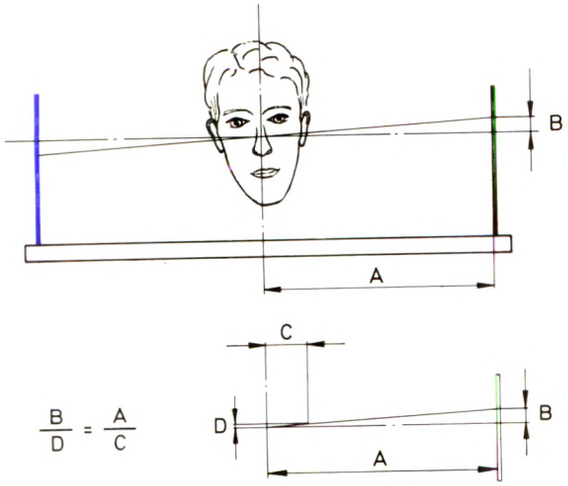


Fig. 4.—Adjustments. A, distance between midline of tomographic table and scale; B, difference between two readings obtained before and after rotating head in frontal plane; C, distance between vertical plane through midline of tomographic table and anatomical landmark; D, distance traveled in vertical direction by landmark.

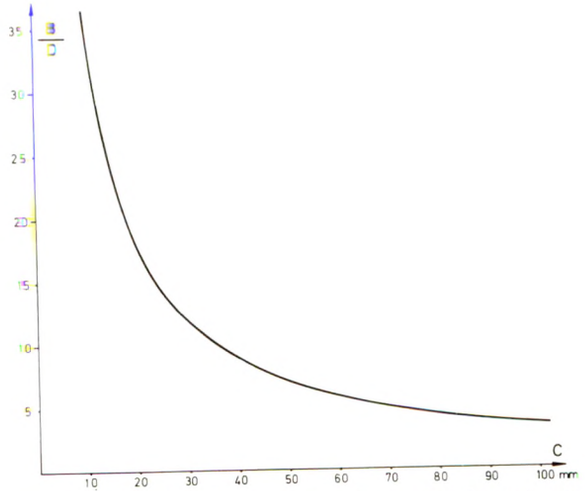


Fig. 5.—Variation of ratio B/D with distance C; applies to Polytome where constant A = 360 mm.

the prone position is more easily endured during axial tomography than the more common supine position.

Finally, the systematic positioning and repositioning possible with our device will reduce the number of retakes that easily result from a nonsystematic trial-and-error procedure.

REFERENCE

1. Falvovich G, Omnell KÅ, Svensson A: A modified technique for axial tomography of the skull. *Medicamundi* 22:6–10, 1977

Liver Localization by Percussion for CT Scanning

GORDON GOODMAN,[1] LAWRENCE R. KUHNS, WILLIAM G. NOVAK, AND HIDEO ONITSUKA

Most of the various methods for localizing the liver for CT scanning use radiographic or fluoroscopic techniques [1–4]. Since percussion of the liver has proven reliable in assessing its size [5], we attempted to define the upper liver border by percussion for more convenient localization.

The upper border of the liver was localized by percussion in the right midclavicular line during the respiration phase in which CT was to be performed. We found that dullness to percussion of the upper liver margin was more easily and reproducibly defined in deep inspiration. CT scanning with an EMI 5005 scanner was begun at this level in 20 randomly selected patients who could hold their breath for 18 sec. In 18 of the 20, localization of the upper liver and right hemidiaphragm by percussion was at the same level as on subsequent CT scans (fig. 1). In two patients, localization by percussion was too low by 3 and 4 cm, perhaps due to more than usual interposition of lung between the liver and chest wall.

When using the xiphoid as an external landmark for localizing the upper liver border prior to this study, many unnecessary scans were obtained. On a random sample of 40 CT body scans, the range of the upper liver border was from 6 cm above to 4 cm below the xiphoid. One-third of the upper liver borders were within 0.5 cm of the xiphoid, but only 16% were below the xiphoid.

A significant reduction in patient exposure and time of liver CT scanning was achieved by the simple method of percussion of the upper liver border in the right midclavicular line for CT localization in most (90%) patients. We now routinely use this method for CT assessment of the liver.

REFERENCES

1. Kuhns LR, Borlaza GS, Seigel R, Thornbury JR: External anatomic landmarks of the abdomen related to vertebral segments: applications in cross-sectional imaging. *AJR* 131:115–117, 1978
2. Lamarque JL, Bruel JM, Dondelinger R, Vendrell B: Liver and pancreas, in *Clinical Computer Tomography, Head and Trunk*, edited by Baert A, Jeanmart L, Wackenheim A, New York, Springer, 1978
3. Harell GS, Marshall WH Jr, Breiman RS, Seppi EJ: Early experience with the Varian six second body scanner in the diagnosis of hepatobiliary tract disease. *Radiology* 123: 355–360, 1977
4. Stephens DH, Sheedy PF II, Hattery RR, MacCarty RL: Computed tomography of the liver. *AJR* 128:579–590, 1977
5. Lawson EE, Grand RJ, Neff RK, Cohen LF: Clinical estimation of liver span in infants and children. *Am J Dis Child* 132:474–476, 1978

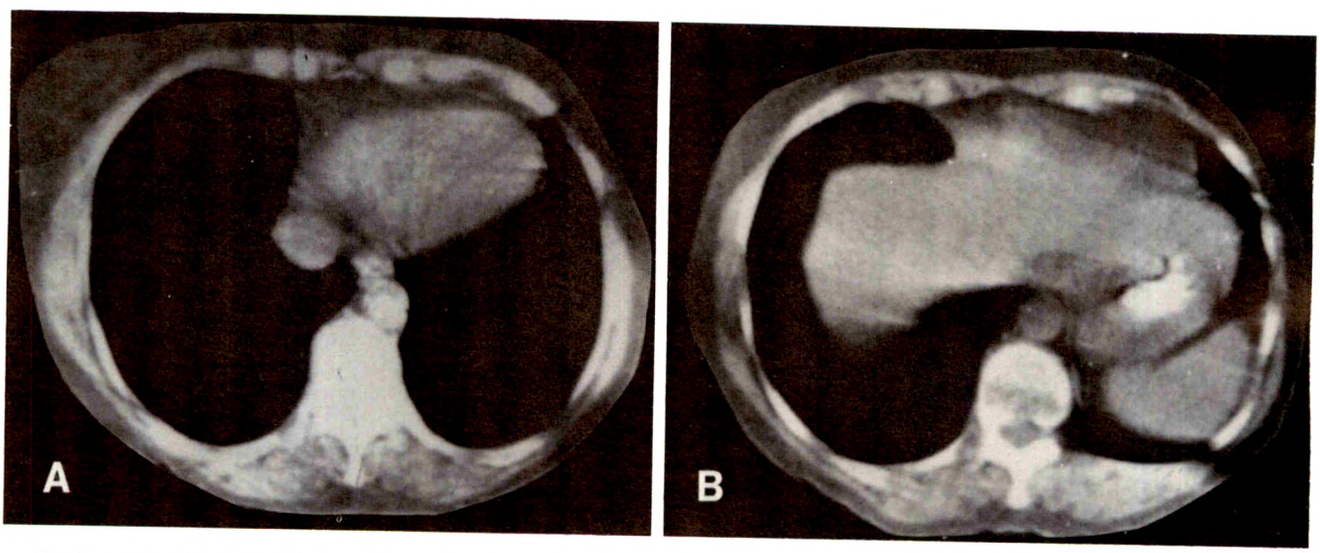


Fig. 1.—**A**, At level of xiphoid. **B**, 2 cm below, inclusion of upper liver border, which was upper level of percussed dullness in midclavicular line.

Received November 20, 1978; accepted December 5, 1978.
[1]All authors: Department of Radiology, University of Michigan Medical Center, Ann Arbor, Michigan. Address reprint requests to G. Goodman.

© 1979 American Roentgen Ray Society

0361-803X/79/1323-0480 $0.00

Versatile Ceiling Tube Mount for Direct Magnification Radiography

MURALI SUNDARAM,[1] JOHN SHIELDS, ARMAND BRODEUR, AND E. RICHARD POLING

A microfocus tube with a focal spot of 90 μm and a stationary anode for direct magnification radiography (RSI MFT I) has been availabe as a wall-mounted system. More recently these have been available as mobile units. We acquired a microfocus tube and transformed it into a ceiling mounted system for greater flexibility and versatility in carrying out direct macro radiography (fig. 1).

The features of the ceiling-mounted flexible microfocus system are:

1. Tube/object distance is not fixed and can be varied to produce optimal anode/object distances.

2. The x-ray tube is independent of the film-holding device [1] and the two can be moved independently of one another, a feature not afforded by the wall-mounted system or the portable system.

3. The x-ray tube can be angulated 360° in both vertical and horizontal planes.

4. Horizontal beams can be obtained with this system like any other conventional radiographic tube and are of particular value in cervical trauma.

5. The system permits macroradiographs to be obtained of patients on a stretcher or in a bed with no more effort or time than contact radiographs under similar circumstances.

6. The system is conveniently situated in a room allocated for routine and emergency radiography.

A patient's inability to cooperate and assume an optimal position is circumvented by the flexibility of the system. Those patients with facial or cervical trauma unable by their condition to have tomography or orthopantomography can have the benefits of macroradiography using this system. This applies to those patients in traction, unable to be transferred from their beds on to an x-ray table.

A drawback with our present system is the lack of adjustable collimation; diaphragms are used instead. When our system was installed, the available microfocus tubes did not have light collimation, but this is now available and would only add to the practicalities of a solid ceiling mount. The versatility of this ceiling-mounted microfocus system lends itself to several clinical settings, some having already been evaluated [2]. The microfocus tube can also be used for contact (unmagnified) peripheral bone and joint radiography.

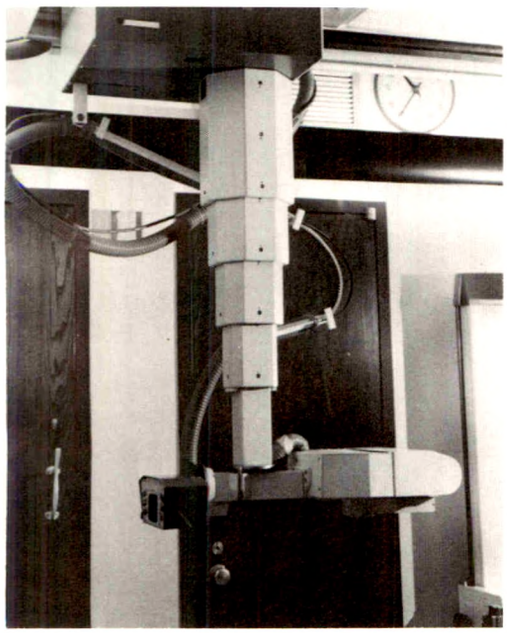


Fig. 1.—Unobtrusively placed ceiling mounted system for direct magnification radiography.

REFERENCES

1. Poling ER, Sundaram M: Versatile film holding device for direct magnification radiography. *AJR* 132:482–483, 1979
2. Sundaram M, Brodeur AE, Burdge RE, Joyce PF, Riaz MA, Poling ER: The clinical value of direct magnification radiography in orthopedics. *Skeletal Radiol* 3:85–90, 1978

Received November 20, 1978; accepted December 5, 1978.

[1]All authors: Department of Radiology, St. Louis University Hospitals, 1325 South Grand Boulevard, St. Louis, Missouri 63104. Address reprint requests to M. Sundaram.

© 1979 American Roentgen Ray Society

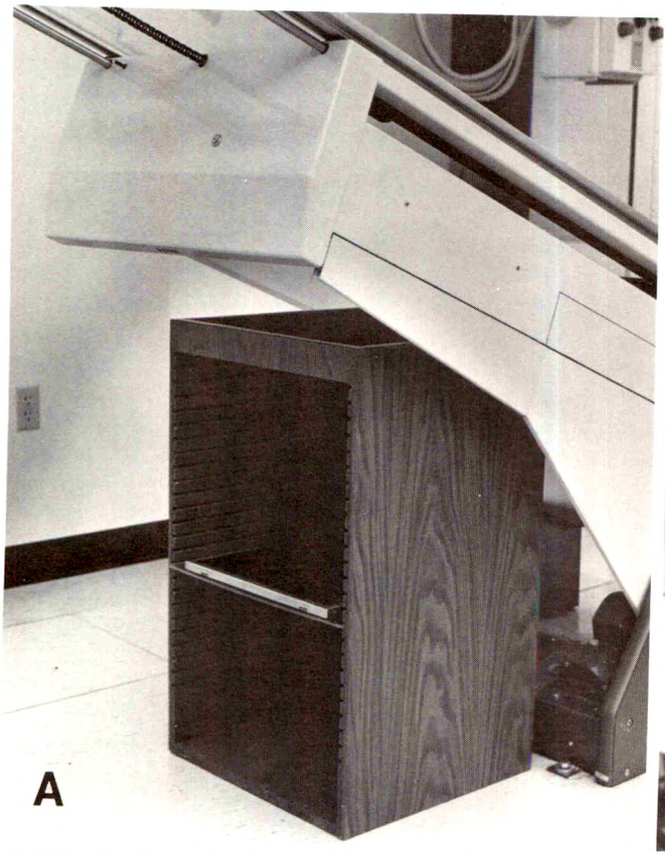
0361-803X/79/1323-0481 $0.00

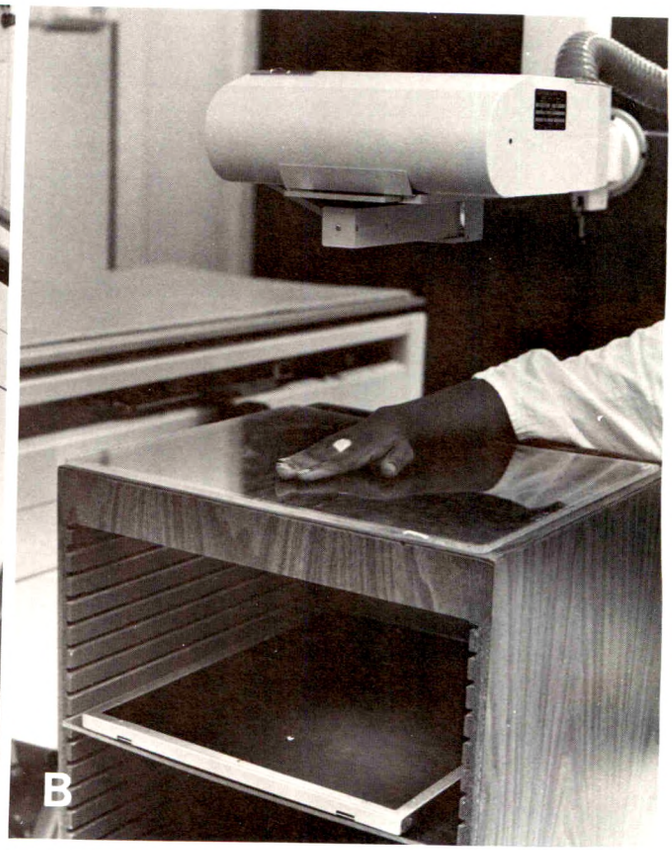
Versatile Film Holding Device for Direct Magnification Radiography

E. RICHARD POLING[1] AND MURALI SUNDARAM[1]

A wooden box with slots spaced at about 2.5 cm intervals has been constructed as a film-holding device for direct magnification radiography. This can be used as an independent unit or in conjunction with a radiographic table. It has been used with our ceiling-mounted magnification tube [1] for over 2 years, providing versatile and convenient film positioning.

The box measures 80 × 50 × 47 cm. It has a removable





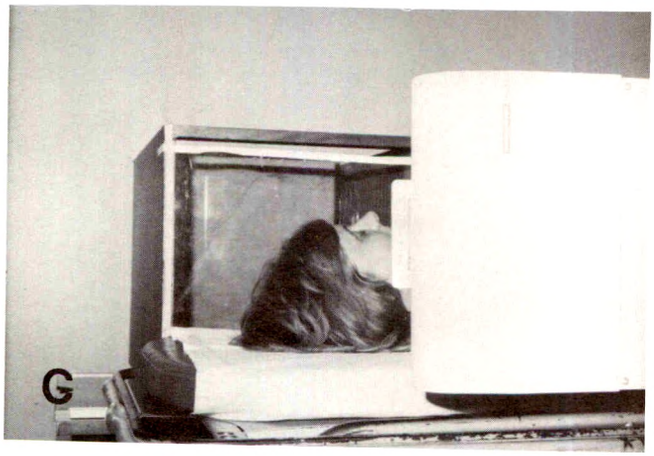


Fig. 1.—**A**, Box placed under transparent table top before table is tilted level. (Plexiglass top has been removed.) **B**, Box used independent of table. **C**, Box used in horizontal beam mode for cross-table cervical spine lateral projection.

Received November 20, 1978; accepted December 5, 1978.

[1]Department of Radiology, St. Louis University Hospitals, 1325 South Grand Boulevard, St. Louis, Missouri 69104. Address reprint requests to M. Sundaram.

© 1979 American Roentgen Ray Society

0361–803X/79/1323–0482 $0.00

0.6 cm plexiglass top and an adjustable plexiglass sheet for cassette support at variable object/film distances (fig. 1). There are 25 slots spaced about 2.5 cm apart. The desired magnification is achieved by determining the anode/object distance and varying the object/film distance by placing the cassette-supporting plexiglass sheet at the proportional distance in the proper slot. This design will accommodate any commercially available cassette up to 43 × 43 cm.

The film holder has been so designed that it can be used for direct magnification radiography in conjunction with the table (fig. 1A), independently of the table (fig. 1B), and for patients on beds and stretchers (fig. 1C). The unit can also be used as an extension to the table at either end or either side, since with the plexiglass top in place it is level with the table top. This helps in examining the skull, neck, and peripheral body parts while the patient is firmly supported on the radiographic table. The device can be used with the horizontal radiographic beam (fig. 1C) and is of considerable value in the radiography of patients on traction and in bed.

Department of Health, Education and Welfare approval, as necessary for radiographic equipment, has been received. This film holder with the ceiling-mounted microfocus tube [1] has proved to be adaptable to many body parts, radiographic examinations, and patients, irrespective of the patient's limited ability to cooperate. It is an integral part of a versatile system designed for the clinical application of direct magnification radiography.

REFERENCE

1. Sundaram M, Shields J, Brodeur A, Poling ER: Versatile ceiling tube mount for direct magnification radiography. *AJR* 132:481, 1979

The Second International Symposium on Radiopharmaceuticals
March 19–22, 1979, Olympic Hotel, Seattle, Washington

Presented by
THE RADIOPHARMACEUTICAL SCIENCE COUNCIL
The Society of Nuclear Medicine

Program Committee

VINCE J. SODD, Ph.D.
Food and Drug Administration
Nuclear Medicine Laboratory
Cincinnati, Ohio

DAVID R. ALLEN, Ph.D.
University of Washington
Seattle, Washington

RODNEY D. ICE, Ph.D.
University of Oklahoma
Oklahoma City, Oklahoma

DENNIS R. HOOGLAND, Ph.D.
University of Minnesota
Minneapolis, Minnesota

ABSTRACTS (LISTED IN ORDER OF PRESENTATION)

1. Technetium-99m Sulfur Colloid - Evaluation of Preparation Parameters for Kits from Four Commercial Manufacturers
2. Comparison of the Rat and Mouse Model for Monitoring the Radiochemical Purity of Tc-99m Human Serum Albumin
3. Labeled Proteins: Criteria for Quality
4. Acceptance Testing of I-123
5. Effect of Solubility on the Biodistribution and Evaluation of 16-[^{123}I]-9-Hexadecenoic Acid as a Myocardial Imaging Agent
6. Reevaluation of the Contaminants in the Mo-99 Tc-99m Generator Eluants
7. Design and Development of Te-123m Labelled Radiopharmaceuticals
8. Te-123m-Labeled Isosteres of Palmitoleic and Oleic Acids Show High Myocardial Uptake
9. Selenaproline-Se-75: A Radiolabeled Imino Acid
10. Synthesis of 6-Radioiodo-6-Deoxygalactose, and Its Tissue Distribution and Excretion in Rats
11. An Efficient Microscale Preparation of Sn-117m-Tin Tetra-Chloride--A Pivotal Intermediate for the Synthesis of Sn-117m-Labeled Radiopharmaceuticals
12. Preparation of a New Oxotechnetium (V)-Sulfur Complex
13. Ion Exchange Methods for the Determination of Net Charge on Some Radiopharmaceuticals
14. Microscale Synthesis and Biodistribution Studies of PT-195m-Labeled Cis-Dichlorodiammineplantinum(II), Cis-DDP
15. The Synthesis of F-18-5-Fluorouridine (F-18-5-FUR) as a Probe for Measuring RNA Synthesis and Tumor Growth Rates in Vivo
16. Evaluation of Radiolabeled Ruthenium Compounds as Tumor-Localizing Agents
17. Conjugates of Bleomycin with Bifunctional Chelating Agents for Stable Tumor Localizing Radiopharmaceuticals
18. Compartmental Studies of a Mouse Brain Tumor
19. The Kinetics of Uptake and Macromolecular Binding of Ga-67 and Fe-59 by the EMT-6 Sarcoma-like Tumor of BALB/C Mice
20. Differential Uptake of ^{67}Ga in Canine Tumors and Abscesses
21. Development of a Lymphscintigraphy Agent: Tc-99m-Sn-PO_4
22. Relative Stability of In-111 and Ga-67 Desferrioxamine (DFF) and Transferrin (TF) Complexes
23. Noninvasive Radioisotopic Technique for Detection of Platelet Deposition in Coronary Artery Bypass Grafts in Dogs and Its Prevention with Platelet-Inhibitors
24. An in Vitro Study of the Mechanism of the in Vivo Red Blood Cell Labeling Technique
25. Studies on the Accumulation of Radiopharmaceuticals in Injured Tissues
26. Nuclear Pharmacology/Radiopharmacokinetics, a New Dimension of Radiopharmacy/Nuclear Medicine
27. Pharmacodynamics of Tin(II)-Chelates Administered with Technetium-99m Chelates for Radionuclide Imaging
28. Affinity Constants of Technetium-99m Pertechnetate and Tc-Chelates with Human Serum Albumin
29. Transport Properties of ^{99m}Tc Compounds through the Blood Barrier
30. Uptake of Radiopharmaceuticals in Developing Myocardial Lesions
31. Potential Myocardial Imaging Agents: Synthesis and Biologic Distribution of ^{99m}Tc Labeled Palmitic Acid Derivatives
32. Improved Form of Technetium-99m Heparin for the Scintigraphic Detection of Experimental Infarcts
33. Potassium-38, a 7.6 Minute Half-lived Radionuclide for Assessment of Myocardial Blood Flow
34. Development and Results of Routine Quality Control Procedures for Tc-99m Iminodiacetate Hepatobiliary Agents
35. In Vivo Kinetics of Hepatobiliary Agents in Jaundiced Animals
36. Radioligands that Bind to Cell-Specific Receptors: Asialo-Proteins for Hepatic Scintigraphy
37. Mechanism of Biliary Excretion of Tc-99m N,N-(2,6-Diethylacetanilide)-Iminodicarboxylate (Diethyl-IDA).
38. Benzimidazolyl Methyliminodiacetic Acids - New Bifunctional Chelators of Technetium for Hepatobiliary Scintigraphy
39. A Comparison of Colloidal Preparations for Bone Marrow Imaging
40. An Improved Model for Calcium-HEDP Solution Equilibria
41. Oxidation State of Technetium in Bone Scanning Agents
42. Antioxidant Stabilization of Bone Agents
43. Tc-99m Hydroxymethane Diphosphonate (HMDP): A Skeletal Imaging Agent with High Uptake in Bone and Infarcted Myocardium and Rapid Clearance from Blood and Muscle
44. Design of Radiopharmaceuticals for Adrenal Imaging: Effect of Structure and Metabolism on the Distribution of H-3 and F-18 Labeled Pregnenolones
45. I-125 7-Iododiazoxide: Potential Radiopharmaceutical for Pancreatic Tumor Imaging
46. Radiolabeled Enzyme Inhibitors as Potential Pancreatic Scanning Agents
47. Use of Technetium-99m Labeled Spermatozoa for Monitoring Sperm Transport in the Female Reproductive Tract
48. Mini-p Production of Fe-52 and the Mn-52m Generator
49. Cyclotron Production and Use of Inorganic Radionuclides for Positron Emission Tomography
50. High-Level Production of C-11-Carboxyl-Labeled Amino Acids
51. Cyclotron Production of Thallium-201 via the ^{205}Tl(p,5n) ^{201}Pb$\rightarrow$^{201}Tl Reaction
52. Development of a Chromatographic ^{68}Ge-^{68}Ga Generator Yielding Ionic Gallium
53. Tantalum-178 Radiopharmaceuticals for Lung and Liver Imaging

1. TECHNETIUM-99m-SULFUR COLLOID - EVALUATION OF PREPARATION PARAMETERS FOR KITS FROM FOUR COMMERCIAL MANUFACTURERS. D.L. Fortman and V.J. Sodd. FDA, Nuclear Medicine Laboratory, Cincinnati, Ohio.

Preparation of Tc-99m-sulfur colloid via the reaction of an acid on sodium thiosulfate requires more chemical and physical manipulation than other commercially available "kits" to produce radiopharmaceuticals for routine use in diagnostic nuclear medicine. Multiple injection of reagents, heating, and cooling are required before it is ready for use. This study investigated the adequacy of the preparation instructions found in the package inserts of four commercial suppliers of sulfur colloid "kits." Labeling efficiency vs. time of reaction, temperature of reaction, concentration of Tc-99m, and effect of stabilizers and other additives were studied. It was found that in most cases the package inserts were adequate, and should be rigidly followed. For example, if the temperature of the hot water bath is at 90°C instead of 95-98°C, the labeling efficiency becomes erratic, ranging from 70% to 95%. Also, it was found that the amount of Tc-99m added to the kits was critical, in that with kits from two manufacturers, the addition of Tc-99m below ≈30 mCi resulted in labeling efficiency below the 92% U.S.P. specifications. Conversely the other two manufacturers' kits did not fail until the Tc-99m level was ≈10 mCi. The time required for the reaction vial to be in the boiling water bath to reach quantitative yields was found to be between 3 to 4 minutes for all four manufacturers.

2. COMPARISON OF THE RAT AND MOUSE MODEL FOR MONITORING THE RADIOCHEMICAL PURITY OF Tc-99m HUMAN SERUM ALBUMIN. J.R. McLean, L.J. Rockwell, and W.J. Welsh. Dep't. of National Health and Welfare, Ottawa, Canada.

Our regulatory activities include an ongoing sampling and analysis program for in vivo radiodiagnostic (i.e. cold) kits. Recently we have noted what appeared to be a consistent difference between our biodistribution results for Tc-99m labeled human serum albumin using mice and the kit manufacturers' results obtained using rats.

Kits from 4 manufacturers were reconstituted according to package insert instructions. The radiochemical purity of each preparation was assessed by in vitro techniques prior to injection. Six mice and 6 rats were used for each product. The animals were sacrificed at 30 minutes post-injection. Blood samples were taken from the heart (for mice) and vena cava (for rats). Mouse livers were excised, washed with phosphate buffered saline, cut into small pieces and treated with 0.83% ammonium chloride solution. Rat livers were perfused through the portal vein with phosphate buffered saline.

Analysis of variance (at p=0.05) indicates that there is a significant difference between the tissue distribution results for rats and mice. Also there is a statistically significant difference at p=0.05 between companies with respect to blood results but not liver results. Hence it may not be acceptable to assess products on the basis of liver values.

3. LABELED PROTEINS: CRITERIA FOR QUALITY. W.A. Pettit, F.H. DeLand, L. Blanton. Veterans Administration Hospital Lexington, KY.

Proteins labeled with several different radionuclides have been evaluated in regard to (1) radioactive contaminants, (2) stability of the label, and (3) retention of biological activity. Radioactive contaminants in labeled protein preparations were readily detected by Sephacryl S-200 gel filtration. Stability was evaluated by incubation of the labeled protein with another protein of different molecular weight prior to the gel filtration assay. Retention or loss of biological activity is best examined by radioimmunoassay procedures. Following labeling the reaction mixture was placed over a short (6.0 cm) column of G-25 or S-200 in order to remove radioactive salt contaminants. The labeled protein obtained demonstrated variability in regard to high molecular weight contaminants and stability depending on the radionuclide and labeling procedure used. Iodination by lactoperoxidase or chloramine-T provided the most satisfactory products. Labeling with Tc-99m provided acceptable products if stannous tartrate was used as the reductant. Stannous chloride and electrolytic procedures produced high molecular weight artifacts. When IgG labeled with Hg-203 was incubated with albumin, the activity was almost quantitatively transferred to albumin.

4. ACCEPTANCE TESTING OF I-123, J. Barnes, K. Breslow, and B.A. Rhodes, University of New Mexico Radiopharmacy, Albuquerque, New Mexico.

Iodine 123 produced by the $^{127}I(p,5n)^{123}Xe \rightarrow {}^{123}I$ has only one significant radionuclidic impurity, Iodine 125. The usual test for radionuclidic purity, gamma ray spectrometry is not directly applicable for this analysis because the two spectra are not resolved by NaI(Tl) detectors. In order to dispense I-123 solutions of acceptable radionuclidic purity, a rapid method is needed for the evaluation of the level of I-125 contamination. The purpose of this study was to develop a rapid acceptance test of Iodine 123 solutions for clinical use. The determination is based on an analysis of the decay curve of the X-ray peak and on the ratio of the X-ray peak (I-123 plus I-125) to the gamma-ray peak (I-123 only). Duplicate samples of I-123 produced by Crocker Nuclear Laboratories were analyzed by this method and by the National Bureau of Standards. In each case, the result obtained by this method was comparable to that determined by the NBS.

% I-125 Contamination of I-123

Sample	UNM Method	NBS
1	1.41 ± .04	1.35
2	2.86 ± .32	2.77
3	3.26 ± .43	3.28

It is concluded that this method provides a means of rapidly assessing the radionuclidic purity of I-123 contained by I-125.

5. EFFECT OF SOLUBILITY ON THE BIODISTRIBUTION AND EVALUATION OF 16-[^{123}I]-9-HEXADECENOIC ACID AS A MYOCARDIAL IMAGING AGENT. J.P. Weichert, S.A. Sirr, D.R. Hoogland, M.P. Frick, and M.K. Loken, University of Minnesota, Minneapolis, MN.

The use of 16-[^{123}I]-9-hexadecenoic acid (IHDA) for potential application in measuring myocardial metabolism, and methods for synthesis have been reported. However, IHDA distribution in non-cardiac organs has not been described. Preliminary biodistribution studies in mice indicated very high uptake in the lungs, which could be related to particulates in the final product. Procedures for producing a particulate-free solution were evaluated, and the resultant effects on biodistribution of IHDA were studied.

The reaction is light sensitive, and 70% yields of IHDA were obtained by refluxing the reactants in small volumes of acetone in a dark environment. Mild heating of the 6% HSA, ultrasounding for 30 minutes, and filtering through 0.45 and 0.22 micron filters producted a particulate-free solution with minimal loss of IHDA.

With any IHDA solution, maximum myocardial uptake occurred 2-3 minutes after intravenous administration. With the particulate-free solution, IHDA concentration in the lungs was decreased from 21 to 7.7 %d/gm, while heart activity increased from 4.5 to a peak of 22 %d/gm. Initial myocardial images in the dog have been very encouraging.

These studies demonstrate that evaluation of IHDA as a myocardial imaging agent can be misleading if a particulate-free solution is not administered and biodistribution in non-cardiac organs is not examined.

6. REEVALUATION OF THE CONTAMINANTS IN THE Mo-99 Tc-99m GENERATOR ELUANTS. I.L. Preiss, A.S. Frank, Rensselaer Polytechnic Institute, Troy, N.Y. and R. Kishore, Veterans Administration Medical Center, Albany, N.Y.

There have been many studies to determine the level of contamination in generator produced Tc-99m. Such studies are required so that reasonably accurate dose calculations, which include all radiation from a sample, can be made. We have conducted a set of experiments designed to establish the origin of the as yet unassigned 320 KeV gamma-ray often observed as the major contaminant in generator produced Tc-99m eluant fractions. Classical radiochemical milking of daughter from parent and grandparent was employed along with high resolution gamma-ray spectroscopy. These experiments in which energy and half-life were determined verifying the conclusion of Jones

and Griffin that the 320 KeV gamma-ray is the result of the beta decay of Tc-99m itself decaying to its daughter Ru-99. This β-decay branch leads to an increased dose of about 250 mRad per mCi per gram of tissue. Our results to date do not preclude a beta decay to the first excited state of Ru-99 at 89 KeV nor is a second gamma decay between 320 KeV and 89 KeV levels of Ru-99 ruled out. Thus, the 250 mRad value must be considered a lower limit of increased dose.

7. DESIGN AND DEVELOPMENT OF Te-123m LABELLED RADIOPHARMACEUTICALS. G.P.Basmadjian, R.D.Ice, R.A.Magarian, G.R.Parker, S.L.Mills, and A.S.Kirschner. College of Pharmacy, University of Oklahoma HSC, Oklahoma City, OK.

Tellurium-123m has favorable physical characteristics (159 keV isomeric transition photons, 84% abundance; $t_{1/2}$ 119 d) and forms stable C-Te bonds, allowing the radiochemist to synthesize hundreds of compounds containing a γ-emitting radionuclide without affecting the parent molecule's physiological characteristics.

The development of a quick method for solubilizing Te-123m metal using the following reaction facilities the handling of Te-123m:

$$\text{Te-123m} + NaBH_4 \text{ -------} \rightarrow Na_2Te^* \xrightarrow{\text{Te-123m}} Na_2Te_2{}^*$$

The reaction incorporates 100% of the radioactivity with no volatile by-products (e.g. H_2Te) into a useful reagent for producing Te-123m labelled organotellurides.

Nucleophiles with the structure $R\text{-}Te^-Na^+$ were easily prepared by the reaction of alkyl halides with Na_2Te_2 and reduction of the resulting colored ditellurides with $NaBH_4$ in a basic medium. The Te-123m nucleophiles were then reacted with a second alkyl halide or alkyl sulfonate ester to form the required telluride. Unstable tellurides can be stabilized by the formation of telluronium salts. Primary C-Te bonds are more stable than secondary and hindered C-Te bonds. Branched chain R-groups in the above nucleophiles are more stable than methyl analogs.

The labelling method has been used to synthesize Te-123m cholesterol analogs, fatty acids and hydrocarbons.

8. Te-123m-LABELED ISOSTERES OF PALMITOLEIC AND OLEIC ACIDS SHOW HIGH MYOCARDIAL UPTAKE. F. F. Knapp, Jr., K. R. Ambrose, and A. P. Callahan, Nuclear Medicine Technology Group, Health and Safety Research Division, Oak Ridge National Laboratory, Oak Ridge, Tennessee, and R. A. Grigsby and K. J. Irgolic, Chemistry Department, Texas A & M University, College Station, Texas.

Fatty acids labeled with γ-emitting nuclides are important myocardial imaging agents. The biological properties of many compounds are maintained by the isosteric replacement of the $>C=C<$ moiety with S, Se or Te. We wished to determine if myocardial uptake was affected when the 9(10)olefinic linkages of palmitoleic acid and oleic acid were replaced with the Te heteroatom. The synthetic scheme involved the following steps: RX + NaTeTeNa → RTeTeR → R-Te-Na + X-heptyl-COOMe → R-Te-heptyl-COOH. In this manner 9-tellurapentadecanoic acid (R=n-hexyl) and 9-telluraheptadecanoic acid (R=n-octyl) were prepared as "isosteres" of palmitoleic and oleic acids, respectively. The structures were confirmed by chromatographic, infrared, ultraviolet, mass spectral, and nuclear magnetic resonance studies. The Te-123m- labeled agents were prepared in the same manner and tissue distribution studies in rats showed pronounced heart uptake after five minutes (2-3% dose/gram of tissue). These distribution results closely parallel similar data reported in the literature for labeled oleic acid. (Research sponsored by the Division of Biomedical and Environmental Research, U.S. Department of Energy, under contract W-7405-eng-26 with the Union Carbide Corporation).

9. SELENAPROLINE-Se-75: A RADIOLABELED IMINO ACID. S.H. Wong, R.P. Spencer, A. Weaver. Department of Nuclear Medicine, University of Connecticut Health Center, Farmington, CT.

While the distribution of amino acids, labeled with gamma ray emitting radionuclides, has been studied in vivo, there are almost no data on the fate of imino acids. Hence we have synthesized a radiolabeled imino acid, selenaproline-Se-75, and followed its in vivo fate and excretion. The synthesis is based on the method used by DeMarco and coworkers for production of the nonlabeled compound. Selenocystine-Se-75 was brought to an alkaline pH and reduced by addition of sodium borohydride, to produce the intermediate compound, selenocysteine-Se-75. Added formaldehyde accomplished ring cyclization to yield the selenaproline-Se-75. Over a period of time there is slight cleavage of selenaproline-Se-75 to the starting compound. Whole body retention in mice showed initially greater retention of radioactivity when selenaproline-Se-75 was injected as compared with the starting amino acid; at 4 hours and later, these differences were not apparent. There was a striking difference in the distribution of radioactivity when introduced as the imino acid. In rats for example, there was a 5 fold higher concentration of radioactivity in the brain after use of selenaproline-Se-75 as compared with the amino acid. There appear to be 2 initial uses of the radiolabeled imino acid. 1. As a model compound for following imino acid entry into brain and other tissues. 2. As in vitro probe of collagen synthesis, up to the point of 4-hydroxylation.

(Supported by USPHS Grant CA-17802 from NCI)

10. SYNTHESIS OF 6-RADIOIODO-6-DEOXYGALACTOSE, AND ITS TISSUE DISTRIBUTION AND EXCRETION IN RATS. R. Flanagan, B.C. Lentle, L.I. Wiebe, F. Helus and W. Maier-Borst. Division of Bionucleonics and Radiopharmacy, U. of A., and Cross Cancer Institute, Edmonton, Canada; and German Cancer Research Center, Heidelberg, FRG.

The erythrocyte glucose carrier mechanism is known to bind 6-iodogalactose(I). The transport inhibition constants for this binding are relatively high, but molar transport of I is low. This investigation was undertaken to prepare radiolabeled I, and to determine its potential as a non-invasive diagnostic tool for in vivo studies of glucose transport systems.

Radioiodo I has now been prepared by exchange iodination of 1,2:3,4-diisopropylidine-6-iodo-6-deoxygalactose with I-123, I-125 and I-131, followed by acid hydrolysis. 6-[I-128]-Iodo-6-deoxygalactose was prepared by neutron irradiation of I in the U. of A. Slowpoke Reactor.

Radioiodo-I was injected intravenously into rats. Rapid uptake of radioactivity by hepatic and renal tissue, and subsequent excretion in the bile and urine, were observed. Non-invasive studies showed little differential uptake. These findings were supported by quantitative data from dissected tissues.

Metabolic investigations indicated that the unchanged iodogalactose is secreted into bile and urine. The minimal accumulation of radioiodine by the thyroid gland was taken as evidence for the in vivo stability of the carbon-iodine bond.

11. AN EFFICIENT MICROSCALE PREPARATION OF Sn-117m-TIN TETRACHLORIDE--A PIVOTAL INTERMEDIATE FOR THE SYNTHESIS OF Sn-117m-LABELED RADIOPHARMACEUTICALS. D. V. Woo, F. F. Knapp, Jr., A. P. Callahan and T. A. Butler, Nuclear Medicine Technology Group, Health and Safety Research Division, Oak Ridge National Laboratory, Oak Ridge, Tenn.

The Sn-117m nuclide decays with the emission of a single γ-photon with an optimal energy of 158 keV (half-life = 14 days). Organotin chemistry is very versatile, and tin can replace carbon to form stable organometallic compounds. The combination of favorable radionuclidic properties, well defined chemistry and synthetic versatility suggest that the synthesis of Sn-117m-labeled radiopharmaceuticals should be explored. A crucial step is the initial conversion of metallic Sn-117m into a versatile intermediate such as tin tetrachloride. Our goal was to develop a high-yield microscale synthesis of tin tetrachloride by chlorination of metallic tin. A unique inert atmosphere, flow-through system in which tin tetrachloride is cryogenically distilled directly into a special reaction vessel has been developed. Yields of tin tetrachloride are consistently greater than 90%. Reagents can be added directly to this vessel, eliminating the unnecessary transfer and manipulation of the highly reactive tin tetrachloride. Alkyl lithium and Grignard reagents have been used to prepare a variety of useful intermediates by reaction with tin tetrachloride prepared by this method. (Research sponsored by the Division of Biomedical and Environmental Research, U.S. Department of Energy, under contract W-7405-eng-26 with the Union Carbide Corporation).

12. PREPARATION OF A NEW OXOTECHNETIUM (V)-SULFUR COMPLEX. B.V. DePamphilis, A. Davison, A.G. Jones, and M.A. Davis. Joint Program in Nuclear Medicine, Harvard Medical School and Peter Bent Brigham Hospital, Boston, MA., and Department of Chemistry, Massachusetts Institute of Technology, Cambridge, MA.

The reaction of chelating dithiols with Tc-99 pertechnetate in a variety of reducing media has previously been shown to produce stable, soluble complexes of Tc(V). X-ray crystal structural analyses of two members of this class have shown them to be monoanions of square pyramidally coordinated technetium with an oxygen atom at the apex, and four sulfur atoms defining the basal plane. Infrared spectra of these compounds have a strong band between 925 and 950 cm^{-1}, characteristic of the technetium-oxygen bond.

We have been exploring the possibility of forming oxotechnetium complexes with other bis-chelating ligands. Reaction of 3,4-toluenedithiol(tdt) with ammonium pertechnetate and sodium dithionite in alkaline solution yields a complex that can be isolated as its tetrabutylammonium salt and crystallized from acetone-water mixture. The compound exhibits a maximum in its electronic spectrum at 360 nm, and a strong band in its infrared spectrum at 930 cm^{-1}. The compound is formulated as $(Bu_4N)[TcO(tdt)_2]$, and this is supported by a technetium microanalysis (% Tc calc. 14.9; found 14.5). Like $[TcO(SCH_2COS)_2]^-$ and $[TcO(SCH_2CH_2S)_2]^-$, $[TcO(tdt)_2]^-$ is air-stable in solution and is not subject to coordination by a donor solvent in its sixth position.

13. ION EXCHANGE METHODS FOR THE DETERMINATION OF NET CHARGE ON SOME RADIOPHARMACEUTICALS. A. Owunwanne, R.E. O'Mara and M. Blau. University of Rochester, Rochester, NY and SUNY, Buffalo, NY

The ion exchange distribution method was used to determine the charge on the radioactive species in Ga-67 citrate, Tl-201 chloride, Yb-169DTPA , Tc-99m-HEDP, -pertechnetate, -glucoheptonate (GH) and the reactive species produced when pertechnetate is reduced by Sn(2+). To study the charge on an unknown ion, its equilibrium distribution between the resin and a solution containing competing ions of known charge is measured as a function of solute concentration.

For TlCl and Ga citrate the cation resin was in the Na(+) form, and the solute was sodium perchlorate. For the reactive Tc species the cation resin was in the Sn(2+) form and the solute was stannous perchlorate. The displacement slope for Tl-201 chloride was 0.95, confirming the charge of +1.0. Ga citrate at pH 6.8 had a displacement curve with changing slopes of 0.52 and 1.1 indicating charges of +0.5 and +1.0. The slope for the reactive Tc species following Sn(2+) reduction at pH ≤2.0 was 0.98 indicating a charge equal to that of the displacing ion, +2.

For Yb-169DTPA, Tc-99mHEDP, pertechnetate and Tc-99mGH the anion resin was in perchlorate form and the solute was sodium perchlorate. The slopes of Yb-169DTPA, pertechnetate and Tc-99mGH were 2.3, 0.98 and 1.0, indicating charges of -2.0, -1.0 and -1.0 respectively. Tc-99mHEDP had a curve with changing slopes of 0.5 and 2.0 indicating species with charges of -5.0 and -2.0. The advantage of the ion exchange method is that studies are done with carrier-free amounts.

14. MICROSCALE SYNTHESIS AND BIODISTRIBUTION STUDIES OF PT-195m-LABELED *CIS*-DICHLORODIAMMINEPLANTINUM(II), *CIS*-DDP. J. D. Hoeschele and T. A. Butler. Nuclear Medicine Technology Group, Health and Safety Research Division, Oak Ridge National Laboratory, Oak Ridge, TN.

Cis-DDP is a unique metal-based antitumor drug which exhibits potent activity toward cancers of genitourinary origin. The major dose-limiting side-effect of *cis*-DDP is nephrotoxicity, which limits broader clinical use. We have initiated studies using Pt-195m-labeled *cis*-DDP to elucidate the critical pharmacological parameters affecting nephrotoxicity. The results of these studies will hopefully suggest how the retention of *cis*-DDP and presumably, kidney impairment can be reduced. The general details of the optimized microscale synthesis (50 μmole scale) and the effects of varying the dose and concentration of *cis*-DDP, and the use of a diuretic on the biodistribution of Pt-195m-labeled *cis*-DDP are as follows: (1) yields of *cis*-DDP, average 75%, (2) the product meets the well-defined purity criteria established for *cis*-DDP, (3) the % dose retained / gm. tissue is independent of both dose and concentration (at a fixed dose) of *cis*-DDP, and (4) injection of the diuretic furosemide at 2 and 4 mg/kg leads to enhanced retention of Pt-195m in most organs at 24 hrs. The potential clinical implications of these results will be discussed. (Research sponsored by the Division of Biomedical and Environmental Research, U. S. Department of Energy, under contract W-7405-eng-26 with the Union Carbide Corporation).

15. THE SYNTHESIS OF F-18-5-FLUOROURIDINE (F-18-5-FUR) AS A PROBE FOR MEASURING RNA SYNTHESIS AND TUMOR GROWTH RATES IN VIVO. C. Y. Shiue, J. S. Fowler, R. R. MacGregor and A. P. Wolf. Brookhaven National Laboratory, Upton, N.Y.

5-Fluorouracil (5-FU) is known to be converted to 5-fluorouridine (5-FUR) or 5-fluorouridylate (5-FUMP) and then incorporated into RNA. However, it is well documented that 5-FUR is incorporated into RNA more efficiently than 5-FU and that 5-FUMP is dephosphorylated in vivo to give 5-FUR. We have therefore explored the possibility of labeling 5-FUR with fluorine-18 by chemical methods for use as a probe for measuring RNA synthesis and tumor growth rates in vivo.

F-18-5-FUR is synthesized by direct fluorination of 2',3',5'-tri-O-acetyluridine (1) with fluorine-18 in glacial acetic acid followed by hydrolysis with sodium methoxide in methanol. Fluorination of 1 with a 8-fold excess of fluorine-18 gives 2',3',5'-tri-O-acetyl-5,6-dihydro-F-18-5,6-difluorouridine (2) in quantitative yield. Hydrolysis of 2 with NaOMe/MeOH followed by neutralization on an ion exchange column gives F-18-5 FUR (3) which is purified by silica gel chromatography. Current production procedures give radiochemical yield of 3.1% (based on theoretical F-18) in a synthesis time of 90 minutes from EOB providing 1.2 mg (65%) of 3. Thus, this procedure allows the preparation of F-18-5-FUR with specific activities of 800 μCi (EOB)/μAhr irradiation time/mg.

16. EVALUATION OF RADIOLABELED RUTHENIUM COMPOUNDS AS TUMOR-LOCALIZING AGENTS.† S. Srivastava, P. Richards, G. Meinken, P. Som, H. Atkins, Brookhaven National Laboratory, Upton, NY; S. Larson, Z. Grunbaum, J. Rasey, VA Hosp, Seattle, WA; M. Clarke, M. Dowling, Boston College, MA.

Ru-97($t_{½}$ 2.9d, 216 keV γ, 86%) is a potential nuclide for application in nuclear oncology because of: (i) the excellent physical properties of Ru-97; (ii)the high chemical reactivity of Ru; (iii)the chemotherapeutic promise shown by a number of Ru coordination compounds; and (iv) BLIP production of Ru-97 that appears feasible. Preliminary studies using Ru tracer on the synthesis and animal screening for tumor localization of a variety of Ru compounds have been carried out. A number of labeled compounds were synthesized, characterized and evaluated in normal and tumor-bearing(EMT-6 sarcoma, Balb/c mice, and squamous-cell carcinoma, Fisher CDF female rats)animals. The compounds studied included ionic Ru, O,O;O,N and N,N chelates, and various ammine compounds, with Ru in II,III and IV oxidation states. At 24 hr, tumor uptake(% dose g^{-1})of a number of compounds(3.1-7.0)is close to that of Ga-67 citrate(7.0) as well as tumor-to-blood(T/B)and tumor-to-muscle(T/M)ratios. The tumor concentration index(TCI),defined as the ratio of % dose g^{-1} in tumor to % dose g^{-1} in whole body, at 24 hr, for nine most active compounds(1.33-2.33)is comparable to that of Ga-67 citrate(2.01). In the EMT-6 sarcoma, cis-dichlorotetraammineruthenium(III)chloride looks particularly promising(T/B 2.4;T/M 6.9;TCI 2.33) when compared to Ga-67 citrate(T/B 3.7;T/M 9.5;TCI 2.01). Efforts are in progress to improve tumor uptake and reduce blood and normal tissue uptake by using various approaches. Results to date demonstrate considerable promise for several Ru-labeled agents.

† Work done under Contract EY-76-C-02-0016 U.S.D.O.E.

17. CONJUGATES OF BLEOMYCIN WITH BIFUNCTIONAL CHELATING AGENTS FOR STABLE TUMOR LOCALIZING RADIOPHARMACEUTICALS. D.A. Goodwin, C.F. Meares, L.H. DeRiemer, and C.I. Diamanti, Veterans Administration Hospital and Stanford University School of Medicine, Palo Alto, CA.,& U.C. Davis, CA

In this study we show bifunctional chelating agents may be attached to bleomycin without greatly modifying its transport properties in vivo.

The bleomycin demethyl-A2 conjugate of EDTA (BLEDTA) was rapidly and specifically labeled with In-111 citrate (0.1M) in 5 min. at 23°C. Whole body retention, organ distribution and tumor uptake was studied at 18 hours in BALB/c mice bearing "KHJJ" adenocarcinoma in the flank. Whole body scanning of rabbits bearing VX 2 adenocarcinomas implanted in the right hind leg, was done following I.V. injection. Control experiments included In-111 Cl_3, In-111 Bleo (directly chelated), In-111 phenyl-EDTA and Co-57 Bleo. Whole body retention at 24 hours in mice correlated

well with stability: In-111 Cl_3; 90%, In-111 Bleo (directly chelated); 20%, In-111 BLEDTA; 4.4%, Co-57 Bleo; 2.7%. Tumor uptake (% dose/gm) was; In-111 Cl_3; 5.0%, and In-111 Bleo (directly chelated); 2.0%, but high background reduced tumor to organ ratios. In-111 BLEDTA tumor uptake; 0.40%, was lower than Co-57 Bleo; 1.10% but low background with both these agents produced tumor/organ ratios > 1 in all organs except the kidney. Rabbit scans using 0.7 mCi In-111 BLEDTA showed significant tumor uptake at 2 and 24 hrs over the control In-111 phenyl-EDTA scans. Studies are in progress with the non-radioactive cobalt bleomycin-demethyl A_2 EDTA derivative labeled with In-111 and Tc-99m.

18. COMPARTMENTAL STUDIES OF A MOUSE BRAIN TUMOR. H.J. Glenn, M. Atallah, T.P. Haynie, and G.L. Raulston. M. D. Anderson Hospital and Tumor Institute, Houston, TX.

The purpose of this study was to determine the hematologic compartments, vascular, plasma, and extracellular fluid volumes of a brain tumor, normal brain, muscle, skin, liver and kidney in a well established mouse brain tumor model. Tumor, tissue, blood and plasma contents of selected tracers were determined from 10 min. to 48 hr. and the compartmental spaces calculated by dividing tissue content by the appropriate blood or plasma content. Tumor vascular volume, determined using Cr-51 labeled red blood cells, was found to be 0.019 ml/g tumor over the first hour. Higher or "apparent" vascular volumes for longer time periods are probably the result of RBC sludging, metabolic activity, or of capillary permeability within the tumor. Plasma volumes of these tissues were estimated using I-131 labeled albumin. Only the 10 min. value (when corrected by the plasmacrit) of 0.019 ml/g tumor agreed with the vascular volume. The regular increase in "apparent" plasma volume with time can possibly be used to estimate tracer perfusion and capillary permeability. Extracellular fluid space, measured using S-35 sulfate, was found to be 0.51 ml/g tumor after an equilibration time of 6 hours. Relatively constant compartmental space values were obtained for other tissues except liver, probably indicating for liver a blood storage and release function. Where comparisons could be made, compartmental space values obtained agreed well with limited data reported in literature for other tumors and species.

19. THE KINETICS OF UPTAKE AND MACROMOLECULAR BINDING OF GA-67 AND FE-59 BY THE EMT-6 SARCOMA-LIKE TUMOR OF BALB/C MICE. Steven M. Larson, Janet S. Rasey, Norma J. Nelson, Zdenka Grunbaum, David R. Allen, George D. Harp and David L. Williams. V.A. Hospital and University Hospital, Seattle, WA.

In previous communications, we reported the presence of a transferrin receptor on nonhematopoietic experimental neoplasm EMT-6 sarcoma-like tumor of BALB/c mice. This receptor is important to tumor uptake of Ga-67 citrate and Fe-59 citrate. The present study was to further compare the kinetics of uptake and binding of Fe-59 and Ga-67. Tumor and liver tissue was homogenized and homogenates extracted with distilled water, followed by concentration using an Amicon concentration cell and passed over a Sephacryl 200 S column in 0.2 molar Tris + HCl at pH 7. Ga-67 was bound to macromolecules with molecular weight of 180,000, 82-100,000, 40,000, and a small component of less than 10,000. The same basic profile was seen for both liver and tumor tissue. For Fe-59, activity was predominately associated with > 180,000 molecular weight component and the 84,000 molecular weight component. Similar profiles were observed for both liver and tumor. The kinetics of Ga-67 and Fe-59 uptake was compared to 125-I labeled transferrin in tumor cells growing in tissue culture. Exponentially growing cells were harvested and uptake studied at intervals during a 48 hour period after addition of radioactivity. There was an initial rapid increase in uptake of iodinated transferrin with a plateau in 1 hour. Fe-59 and Ga-67 showed progressive uptake.

20. DIFFERENTIAL UPTAKE OF ^{67}Ga IN CANINE TUMORS AND ABSCESSES. U. Terner, H. Wong, A. Noujaim, B.C. Lentle, and J.R. Hill. Faculty of Pharmacy, University of Alberta and Cross Cancer Institute, Edmonton, Alberta Canada.

Radiogallium as ^{67}Ga - ^{125}I double labelled transferrin as well as ^{68}Ga-citrate were used to investigate the mechanism of differential uptake of gallium into inflammatory lesions and tumors induced in dogs. A multiprobe system connected to a 4-input MCS was used to dynamically record radioactivities in the blood, tumor, abscess and muscle. The ratio of ^{125}I to ^{67}Ga uptake by the sterile abscess remained constant following the I.V. administration of labelled transferrin. The behaviour of ^{68}Ga-citrate was identical to that of ^{67}Ga-transferrin. On the other hand, the ratio of $^{67}Ga/^{125}I$ in tumors appeared to increase immediately after injection, whereas the level of ^{125}I associated with the tumor remained constant throughout the period of the experiment. ^{68}Ga-citrate exhibited a delayed uptake in tumors becoming evident two hours after administration.

From these results it appears that since the uptake of Ga preparations is non-specific in the case of abscesses while being selectively incorporated by transferrin-mediated transport in tumors, it is now possible to differentiate between Ga uptake in tumors and abscess by the measurement of the Ga/I ratio.

(Supported by the National Cancer Institute of Canada.)

21. DEVELOPMENT OF A LYMPHSCINTIGRAPHY AGENT: Tc-99m-Sn-PO_4 D.L.Gilliland, G.P.Basmadjian, A.S.Kirschner, J.C.Leonard, R.D.Ice and H.T.Kurkjian. College of Pharmacy, University of Oklahoma HSC, Oklahoma City, OK.

Stannous chloride when dissolved in a solution of Na_2HPO_4, pH 9.0 gives a stable solution of Sn(II) ions. When Pertechnetate-99m or -99 is added to such a solution, a stable, soluble complex of Tc-Sn-PO_4 results. This is a mixed metal complex, in which the Tc is present in the (III)+ oxidation state and the Sn is an integral part of the complex.

This complex localizes in the RES when injected I.V. due to the formation of an in-vivo colloid with Ca(II) ions in the blood. When injected subcutaneously, the Tc-99m complex travels through the lymphatic channels and precipitates in the lymph nodes, also presumeably due to Ca(II) ions.

In rabbits, axillary and popliteal nodes can be seen by injecting SC into the dorsum of the hind and fore paws. Fore paw SC injection, also results in uptake in the liver kidneys and bone marrow. Hind paw SC injection in addition to the popliteal nodes, results in the prominent uptake in the kidneys, bladder and at later times bone marrow. Intratesticular injection in dogs, visualizes para-aortic lymph nodes within 30 min.

Lymphangiography is not reliable in the diagnosis of metastatic disease from mammary, testicular and prostatic malignancies. The possibility of using such a radiopharmaceutical as a substitute is entertained.

22. RELATIVE STABILITY OF In-111 AND Ga-67 DESFERRIOXAMINE(DEF) AND TRANSFERRIN (TF) COMPLEXES. R.E. Weiner, M.L. Thakur, M. Goodman and P.B. Hoffer. Yale University, New Haven, CT.

DEF is an iron chelating agent used in the treatment of acute and chronic iron overload. We have previously shown the relative stability of DEF complexes as: Ga DEF > Fe DEF > In DEF > Cu DEF. DEF administered I.M. binds Ga-67 in vivo and reduces tissue concentration of this radionuclide. To elucidate these in vivo events we have studied the relative stability of In-111 and Ga-67 DEF and TF complexes using equilibrium dialysis (ED) and paper chromatography (solvent: n-butanol:n-propanol:H_2O, 9:6:5).

To one compartment of the ED apparatus a solution of either Ga-67 or In-111 was added. A second solution containing 13 μM TF with sufficient bicarbonate and nitrilotriacetic acid to yield 1.2 mM and 10 μM respectively, was placed in the other compartment. The complexes were then challenged with 26 μM DEF at a suitable time.

The results from both techniques revealed the stability of Ga DEF > Ga TF and In DEF < In TF. Ga-67 bound to DEF could not be removed by addition of TF and Ga-67 TF complex readily dissociates in the presence of DEF. By comparison, DEF could not remove the In-111 already bound to TF. When DEF and In-111 were added simultaneously with the TF, the In-111 was taken up slowly by the TF and not retained by the DEF.

These findings help explain the rapid in vivo clearance of Ga-67 induced by DEF. They also suggest that DEF will not be an effective clearance agent for In bound to TF.

23. NONINVASIVE RADIOISOTOPIC TECHNIQUE FOR DETECTION OF PLATELET DEPOSITION IN CORONARY ARTERY BYPASS GRAFTS IN DOGS AND ITS PREVENTION WITH PLATELET-INHIBITORS.
M. K. Dewanjee, V. D. Fuster, M. P. Kaye, and M. Josa, Mayo Clinic and Mayo Foundation, Rochester, MN.

At 8 and 24 hours after saphenous vein bypass graft surgery in 4 dogs, in vivo images of the graft were obtained with a gamma camera after I.V. injection, 2 hours postoperatively of autologous Indium-111 labeled platelets (0.25 - 0.50 mCi). Autologous canine platelets were labeled with Indium-11 oxine. Platelet deposition in the grafts could be accurately estimated from the scintiphotos. Under idential conditions, in 6 dogs treated with Dipyridamole (2.5 mg/kg/day) plus Aspirin (15 mg/kg/day) (D + ASA), the grafts had significantly less platelet deposition as estimated by imaging ($p<0.01$). The in vitro radioactivity ratios (mean + S.E.) of isolated graft sections to non-target tissues of blood and lung in control and treated animals are as follows:

	Sections	Graft/Blood	Graft/Lung
Control	Proximal	23.2 ± 17.9	22.9 ± 15.0
	Distal	13.6 ± 4.2	16.4 ± 3.9
Treated	Proximal	3.7 ± 1.7	7.3 ± 4.4
	Distal	4.9 ± 2.1	9.6 ± 6.0

This noninvasive technique may be a promising tool for a better understanding of the role played by platelets in the process of occlusion of saphenous vein bypass grafts and arteriosclerosis and its prevention with platelet inhibitors.

24. AN IN VITRO STUDY OF THE MECHANISM OF THE IN VIVO RED BLOOD CELL LABELING TECHNIQUE.
M.W. Billinghurst, E.A. Somers. Health Sciences Centre, Winnipeg, Manitoba, CANADA.

This study was undertaken to establish the mechanism by which a preinjection of stannous pyrophosphate results in the tagging of Tc-99m to red cells upon injection of Tc-99m pertechnetate. The study showed that the labeling of the red blood cells is primarily dependent on the concentration of stannous ion with efficient labeling occurring when the stannous ion concentration is between 0.08 and 0.04 ugm per ml of blood. When the stannous ion concentration was below 0.04 ugm per ml of blood the Tc-99m was found to be present in plasma as free pertechnetate while if the stannous ion concentration was over 0.08 ugm per ml the Tc-99m was increasingly present in the plasma as Tc-99m labeled compounds. When the red blood cells and plasma were separated prior to the addition of Tc-99m pertechnetate it was observed that red cell labeling occurred whenever the original stannous content exceeded 0.04 ugm per ml of initial blood while the percentage labeling of compounds in the plasma at concentrations above this value was found to be the complement of the red cell labeling in the whole blood.

Thus we postulate that the red cell labeling will occur only when there is insufficient stannous ion to produce in vivo labeling to the components in the plasma but adequate to cause reduction of the pertechnetate for the binding to the red cells.

25. STUDIES ON THE ACCUMULATION OF RADIOPHARMACEUTICALS IN INJURED TISSUES.
E. Robbins, L.R. Chervu, and M.D.Blaufox. Albert Einstein College of Medicine, Bronx, NY.

Although many theories have been proposed to explain the accumulation of Ga-67 in tumors and abscesses, none has been verified. The main purpose of this study is to determine if tissue injury is a significant factor in this accumulation. Localization of Ga-67 and Tc-99m in various rat tissues was studied following diverse insults. These included: infarction, purulent abscess induction, pressure clamping and thermal injury. In all cases, Ga-67 accumulation was markedly enhanced provided blood flow to the injured area was maintained. The ratio of radioactivity in the injured area reached 5:1 within one hour. The rapid time course and minimal injury required for the enhanced uptake to occur ruled against inflammation per se as the mechanism. Tc-99m-glucoheptonate and Tc-99m-pyrophosphate also accumulated rapidly in abscesses and otherwise injured tissues. When compared to Ga-67, these radiopharmaceuticals provided equally diagnostic information. This lack of specificity of radiopharmaceutical uptake in injured tissue lends additional support to the probable importance of local tissue injury and/or changes in blood vessel permeability in the localization of radiopharmaceuticals.

(This work has been supported in part through funding from American Cancer Society Grant No. VC-172.)

26. NUCLEAR PHARMACOLOGY/RADIOPHARMACOKINETICS, A NEW DIMENSION OF RADIOPHARMACY/NUCLEAR MEDICINE.
W. Wolf, R.C. Manaka, D. Young, A. Schumitzky, J.K. Siemsen and J. Shani. Radiopharmacy Program, University of Southern California, Los Angeles, CA.

Previous work had shown that F-18-5-fluorouracil concentrates more in an L1210 murine tumor responsive to 5-FU treatment, than in the non-responsive variant. Because this drug, like most other drugs, undergoes rapid metabolism, and because of the hypothesis (C. Heidelberger) that F-dUMP levels are closely related to chemotherapeutic response, it is possible that the radioactivity in the tumor at later times consists mainly of F-dUMP. Blood level determinations of drugs followed by their kinetic analysis ("pharmacokinetics") can now be extended to all organs by the use of γ-labeled drugs. These radiopharmacokinetic studies of F-18-5-FU correlate the non-invasively observed radioactivity with the specific metabolites present at a given site (e.g., tumor) and hopefully will predict responsiveness. In a parallel study we have analyzed the blood radiopharmacokinetics of cis-dichlorodiammine platinum as a 3-entity model. By monitoring renal levels of Pt-195m, we expect to decrease nephrotoxicity while increasing the effectiveness of high dose cis-Platin treatment. These studies, for which we propose the term "Nuclear Pharmacology," utilize a combination of methods, such as determinations of the kinetics of distribution and localization of γ-labeled drugs, analysis of their metabolites, some minimal invasive measurements in selected fluids, all combined with a novel mathematical treatment of the above data.

27. PHARMACODYNAMICS OF TIN(II)-CHELATES ADMINISTERED WITH TECHNETIUM-99m CHELATES FOR RADIONUCLIDE IMAGING.
Mrinal K. Dewanjee, Gregory Anderson, and Heinz W. Wahner, Mayo Clinic and Mayo Foundation, Rochester, MN.

Considerable amounts of stannous-chelates are administered with ^{99m}Tc-labeled chelates to patients undergoing nuclear medicine imaging procedures. The pharmacodynamics of stannous chelates given as tin-human serum albumin (Sn-HSA), tin-glucoheptonate (Sn-GH), tin-dimercaptosuccinate (Sn-DMSA), and tin-pyrophosphate (Sn-PP), all labeled with ^{113}Sn, was studied in 30 rabbits. Tin(II)-chelates were prepared by adding $^{113}SnCl_2$ (12-16 mCi/mg) to 15-25 mg of the ligands in 3-4 ml of nitrogen purged saline solution. The final pH was adjusted to 5.5. The solution was membrane filtered for removal of residual colloid. The results show that (1) Sn-PP and Sn-GH are unstable in vivo and give rise to free Sn(II) ion; (2) (35-45)% of Sn(II) ion localizes mainly in bone, and most of the rest is excreted in the urine; (3) Sn-DMSA is a more stable chelate and its biodistribution is similar to that of ^{99m}Tc-DMSA; (4) like ^{99m}Tc-PP, Sn(II) ion localizes in the infarcted myocardium; and (5) in the myocardium, (20-27)% of ^{113}Sn(II) ion is found in the mitochondria; the subcellular distribution resembles that of calcium ion; (6) the affinity of stannous ion for hemoglobin is 40-50 times higher than that of HSA. The study shows that tin(II) chelates show pharmacodynamics different from those of ^{99m}Tc-chelates.

28. AFFINITY CONSTANTS OF TECHNETIUM-99m PERTECHNETATE AND Tc-CHELATES WITH HUMAN SERUM ALBUMIN.
Mrinal K. Dewanjee, Paul Brueggemann and Heinz W. Wahner, Mayo Clinic and Mayo Foundation, Rochester, MN.

Using Tc-99m and Tc-99-carrier we have determined the affinity constants of pertechnetate and Tc-chelates by equilibrium dialysis technique. Tc-Hydroxyethylene diphosphonate (Tc-HEDP), Tc-pyrophosphate (Tc-PP), Tc-glucoheptonate (Tc-GH), Tc-dimercaptosuccinate (Tc-DMSA), and Tc-HIDA were prepared by stannous chloride reduction in nitrogen purged saline. Equilibrium dialysis in cellulose tubing was performed for 24 hours in triplicate and samples in presence of Tc-99m chelates (90-100μCi) and Tc-99m chelates (5-100μg) with 50 and 100 mg of human serum albumin. Scatchard plots of all Tc-compounds except pertechnetate and Tc-HEDP show two values of (high and low) affinity constants (HAC and LAC) as shown below:

$ACx10^4$	TcO_4^-	Tc-HIDA	Tc-HEDP	Tc-PP	Tc-GH	Tc-DMSA
HAC	-	2.25	4.81	7.50	11.7	11.91
LAC	1.13	-	-	0.45	1.4	2.42

The two affinity constant values of some Tc-chelates may represent either two binding sites on the albumin molecule, Tc in two predominant oxidation states or two Tc-complexes with two different molar ratios of Tc vs. ligand. Affinity constants of comparable magnitudes have been reported for other metal chelates with human serum albumin.

29. TRANSPORT PROPERTIES OF ^{99m}Tc COMPOUNDS THROUGH THE BLOOD BARRIER. M.D. Loberg, E.S. Hedlund, A.T. Fields and P.S. Callery. University of Maryland, Baltimore, Md.

The development of new ^{99m}Tc radiopharmaceuticals has been hindered by the inability of polar ^{99m}Tc compounds to penetrate lipophilic cell membranes. This work reports the development of diffusable ^{99m}Tc compounds which have access into the intracellular space. Twelve chelating agents were prepared by adding substituents to either IDA, EDTA, DTPA, or oxine so as to alter the lipophilicity of the final complex. Radiochemical purity was determined. Lipophilicity was measured by octanol/buffer partitioning, and extent of protein binding was determined by equilibrium dialysis. The ability of the ^{99m}Tc complexes to transport through a lipophilic barrier was compared to that of the diffusable tracer ^3H_2O using the brain uptake index (BUI) technique developed by Oldendorf.

Pure ^{99m}Tc complexes were found to be capable of crossing the blood-brain barrier in proportion to their lipophilicity. The IDA chelates have a BUI of up to 22.2% requiring long (C_{18}) alkyl chain substituents in order to overcome the permanent anionic charge associated with the complexes. Substituted oxines forming neutral complexes with ^{99m}Tc have BUI of up to 68.6% and offer promise for the development of new intracellular tracers. ^{99m}Tc-5-alanyl-oxine is of particular interest since it demonstrated excellent membrane penetrability despite very low lipophilicity. Comparing the finding of this study with those of Oldendorf strongly suggests that this complex undergoes an amino acid specific, carrier-mediated uptake into the brain.

30. UPTAKE OF RADIOPHARMACEUTICALS IN DEVELOPING MYOCARDIAL LESIONS. H.F. Kung, M. Blau and R. Ackerhalt. Dept. of Nuclear Medicine, SUNY at Buffalo, Buffalo, NY.

There is a need for agents which localize in myocardial infarcts within the first few hours after lesion onset. We used a convenient model, isoproterenol (iso-P) induced myocardial necrosis in rats, to evaluate the uptake of various radiopharmaceuticals in developing lesions.

Tc-99m PPi, MDP, glucoheptonate (GH), gluconate (GA) or F-18 NaF was injected (iv) 0-24 hr after the onset of a myocardial lesion induced by a single injection of iso-P (30 mg/kg, subcut.). The rats were dissected 1 hr after radiopharmaceutical injection. The damaged-heart to normal-heart ratio (DH/N) was calculated by comparing the uptake in the whole damaged heart to that in the heart of a normal rat. For every agent, a time curve (DH/N vs time after iso-P injection) was obtained.

All of the time curves showed a biphasic pattern; an early peak at 1 hr after lesion induction and a late uptake peak at 6 hr. For the bone localizing agents, the DN/N ratios at 6 hours were always 2 or 3 times higher than the corresponding values at 1 hr. This late peak parallels the maximum influx of Ca into the injured myocardium.

On the other hand, Tc-99m GH and GA have a major peak at 1 hr and there was only a small increase at 6-8 hr. This confirms reports of localization of these two agents in early myocardial lesions.

The animal model reflects the clinical behavior of these known agents and should be useful for the development of new compounds which have high uptake in early infarcts.

31. POTENTIAL MYOCARDIAL IMAGING AGENTS: SYNTHESIS AND BIOLOGIC DISTRIBUTION OF ^{99m}Tc LABELED PALMITIC ACID DERIVATIVES. E. Livni, M.A. Davis, and V.D. Warner. Children's Hospital Medical Center and Northeastern University, Boston, MA.

Based on the hypothesis that ^{99m}Tc labeled palmitic acid derivatives would behave biologically like palmitic acid and thus serve as myocardial imaging agents, three palmitic acid derivatives have been prepared. The compounds synthesized were 2-mercaptopalmitic acid (I), 16-mercaptopalmitic acid (II), 2-mercapto-1,16-hexadecanedioic (III), and their ^{35}S analogs (IV-VI). Synthesis of I-VI was accomplished by reaction of the corresponding bromo compounds with thiourea or ^{35}S-thiourea. Compounds I-III were radiolabeled with ^{99m}Tc by dissolution of the palmitic acid derivative in glacial acetic acid, addition of $^{99m}TcO_4^-$ and incubation at room temperature for 30 minutes. The resultant solution was evaporated to dryness and the residue dissolved in propylene glycol. The biologic distribution of 16-^{14}C-palmitic acid, and the ^{99m}Tc and ^{35}S palmitic acid derivatives was carried out in rats with a heat inflicted myocardial infarction. The ^{99m}Tc derivatives of I-III do not have the same biologic distribution as 16-^{14}C-palmitic acid. The ^{99m}Tc derivatives of I and III localize primarily in the liver while that of II is found in both liver and lung. All of the ^{99m}Tc labeled material showed greater uptake in the infarcted myocardium than in normal. This difference in myocardial specificity compared to native fatty acids is most likely ascribed to changes in polarity and solubility.

32. IMPROVED FORM OF TECHNETIUM-99m HEPARIN FOR THE SCINTIGRAPHIC DETECTION OF EXPERIMENTAL MYOCARDIAL INFARCTS. P.V. Kulkarni, R.W. Parkey, L.M. Buja, J.E. Wilson, F.J. Bonte, J.T. Willerson. Univ. Texas Hlth. Sci. Center at Dallas, TX

We have previously reported that technetium-99m heparin (TcH) accumulates in and allows scintigraphic identification of damaged canine myocardium occurring with temporary left anterior descending (LAD) occlusion (occl) and reperfusion. A recent modification of TcH now allows in vivo scintigraphic detection of irreversibly damaged canine myocardium with permanent (P) LAD occl. The modification consists of using heparin from sheep lung and stannous phosphate as the reducing agent. In 13 dogs with P LAD occl, 7 (group 1) were injected IV with TcH (3-6 mCi) 24 hrs postoccl and 6 (group 2) 48 hrs postoccl. Scintigrams and blood samples were obtained serially for 3 hrs; the dogs were then sacrificed. Each experimental animal demonstrated increased TcH uptake in the LV infarct region as compared to normal myocardium. A ratio (R) of the activity (cpm/gm) of blood, bone, and damaged myocardium compared to cpm/gm of normal LV was calculated. The R (mean ± SD) for damaged myocardium in group 1 was: peripheral infarct epicardium (PIEP) 7.0 ± 3.61; peripheral endocardium (PE) 8.3 ± 6.25, infarct epicardium (IEP) 7.4 ± 3.65, and endocardium (E) 4.1 ± 2.83. In group 2: PIEP 11.9 ± 4.16, PE 9.3 ± 6.12, IEP 12.1 ± 2.36, E 7.0 ± 6.53. R of blood and bone were 1.9 and 3.7 respectively. The in vivo scintigrams in all animals with histologically documented infarcts were positive. The results suggest that this modified TcH has value for identifying experimental myocardial infarcts; the reduced bone uptake compared to Tc-phosphates may be an advantage.

33. POTASSIUM-38, A 7.6 MINUTE HALF-LIVED RADIONUCLIDE FOR ASSESSMENT OF MYOCARDIAL BLOOD FLOW. R. Chandra*, J.M. McDonald, R.E. Reiman, and R.S. Tilbury. Memorial Sloan-Kettering Cancer Center and *New York University Medical Center, New York, New York.

Potassium-38, a positron emitting radionuclide, has been produced in amounts of up to 30 mCi by 14.7 MeV He-4 ion irradiation of sodium chloride. The product is sterile, pyrogen-free in isotonic saline, with no added potassium carrier. Sapirstein (1958) and others have shown that radiopotassium may be used as an indicator of blood flow to the heart.

Potassium-38 was administered i.v. and its uptake in the myocardium of anesthetized dogs was measured before and at about 15, 70 and 130 minutes after injection of various drugs. The uptake of K-38 was measured by scanning with a rectilinear scanner using the 511 keV photons, and a correction applied for Compton scatter from the 2.17 MeV photon. Scans were started at 5 minutes after injection and took about 10 minutes to scan the heart. Dipyridimole caused a 49% increase in K-38 uptake at 19 minutes after injection, a 36% increase at 70 minutes and within the normal range at 130 minutes. Digoxin and propranolol caused different effects.

We have shown that K-38 can be readily produced in a compact medical cyclotron in a form and dosage suitable for measurement of in vivo myocardial uptake at about hourly intervals.

34. DEVELOPMENT AND RESULTS OF ROUTINE QUALITY CONTROL PROCEDURES FOR Tc-99m IMINODIACETATE HEPATOBILIARY AGENTS. A.R. Fritzberg and D. Huckaby, University of Colorado Medical Center, Denver, CO.

Several Tc-99m labeled hepatobiliary scanning agents based on iminodiacetate analogs of lidocaine are becoming available for routine use. The objective of this study was the development and evaluation of rapid, convenient quality control methods for their analysis. Various solvent systems were evaluated on paper and silica gel. Tc-99m complexes studies were 2,6-dimethyl, 2,6-diethyl and p-isopropyl derivatives of N,α-acetanilide-iminodiacetic acid (HIDA, Diethyl-IDA and PIPIDA).

The lipophilicity of these complexes allows them to have Rf values between 0 and 1 in a number of convenient systems on both paper and silica gel. They include saline on silica gel (glass fiber) for Tc-99m PIPIDA and acetonitrile: water (3:1) on both 3M paper and silica gel (plastic backed), 1-butanol on silica gel (glass fiber) and 1-butanol:acetic acid:water (4:1:1) on silica gel (plastic backed) for all agents. Several peaks were observed in these systems for all three agents. The relative size of these peaks was also found to reproducibly change for all agents during the first 30 min post preparation. Increasing the volume of preparation from 3 to 8 ml did not appreciably alter the initial pattern of changes, but did increase the amount of insoluble radioactivity. It is suggested that preparation volumes be limited and that use of these agents be delayed 30 min post preparation in order to maximize reproducibility of biological parameters.

35. IN VIVO KINETICS OF HEPATOBILIARY AGENTS IN JAUNDICED ANIMALS. A.-L. Jansholt, D.R. Vera, K.A. Krohn, and R.C. Stadalnik*. Radiology Dept., Univ. of Calif., Davis, CA.

Several Tc-99m-labeled hepatobiliary imaging agents have been reported which offer significant improvements over the oral cholecystogram; however elevated serum bilirubin is a limiting factor in their usefulness. We developed an animal model to study the effect of bilirubin on the in vivo kinetics of these compounds. Elevated bilirubin (up to 15 mg%) is produced in rabbits by infusion of unconjugated bilirubin into a leg vein of an animal positioned under a camera. The radiopharmaceutical is injected into an ear vein and total body images are collected with a computer to obtain uptake/clearance curves over heart, liver, gallbladder, kidneys and bladder. Blood and urine samples are also obtained to convert the computer curves to units of %ID and to measure bilirubin levels. These results have been compared to data in normal rabbits for rose bengal (RB), pyridoxylideneglutamate (PyG) and the diethyl and dimethyl derivatives of acetanilidoiminodiacetic acid (IDA). Biliary tract and duodenum were seen 10 min post injection with all radiopharmaceuticals. The degree of urinary excretion of PyG and dimethyl-IDA was increased at elevated bilirubin levels, and the blood clearance rate was decreased, but there was no significant change in the liver uptake rate. With RB and diethyl-IDA neither urinary excretion nor the rate of liver uptake were significantly changed. Poor biliary tract visualization in jaundiced patients is not explained by high serum bilirubin per se, but is probably secondary to underlying hepatocellular dysfunction.
*Picker Scholar, James Picker Foundation.

36. RADIOLIGANDS THAT BIND TO CELL-SPECIFIC RECEPTORS: ASIALOPROTEINS FOR HEPATIC SCINTIGRAPHY. D.R. Vera, K.A. Krohn and R. C. Stadalnik, Department of Radiology, University of California, Davis, CA.

Our interest in radiopharmaceuticals which bind to cell-specific receptors has led us to study asialoproteins, a family of compounds that bind to receptors found only on the hepatocyte membrane. This property gives exceptional liver specificity and the molecular biology of hepatic binding protein (HBP) and its ligands (asialoproteins) is well characterized. The function of HBP is catabolism of plasma proteins after their *in vivo* desialylation. This intimate involvement in a major liver function led us to postulate that uptake of HBP ligands would be moderated by liver pathology. We have labeled asialoceruloplasmin (AsCp) with I-123 by the ICl method and Tc-99m by electrolysis and purified the products by polyacrylamide GPC. *In vitro* hydrolysis of the iodinated compound detected no I^- by 24 hrs, whereas the Tc-99m hydrolyzed at 0.27%/hr. AsCp uptake by HBP is an irreversible process which peaks at about 10 min in normal rabbits, and its duration in the liver allows for multiple scintigraphic views. We have tested HBP ligands in rabbits with elevated bilirubin (7 mg%) and found no changes in the liver uptake kinetics or the biodistribution. Further development of HBP ligands for imaging will involve Tc-99m-neogalactoalbumin and AsCp in cirrhotic and hepatomatous animals and in human liver metastases. Our preliminary results suggest that labeled HBP ligands represent a superior class of new hepatocyte imaging agents. (Supported in part by BRS and the Picker Foundation.)

37. MECHANISM OF BILIARY EXCRETION OF Tc-99m-N,α-(2,6-DIETHYLACETANILIDE)-IMINODICARBOXYLATE (DIETHYL-IDA). A.R. Fritzberg, W.H. Whitney, and W.C. Klingensmith III. University of Colorado Medical Center and Denver Veterans Administration Hospital, Denver, CO.

Recent clinical studies have shown several Tc-99m complexes of iminodiacetic acid analogs of lidocaine to be superior to I-131-Rose Bengal for hepatobiliary imaging. Interpretations of studies under various pathological and genetic conditions require knowledge of the mechanism by which these complexes are excreted by the liver. In order to discern if and which of the possible anion dye, bile acid or quarternary amine pathways is followed, saturating doses of competitive members of each pathway were administered to rats using constant infusion techniques. The effect on biliary excretion was monitored by 10 min period collections of bile from the common bile duct.

After reaching steady state, infusion of bromsulfophthalein (BSP) at 2.5 μmol/min/kg reduced bile output of Tc-99m-diethyl-IDA from 78% to 41% and I-131-Rose Bengal from 53% to 11%. Administration of taurocholate at 13 μmol/min/kg caused an increase in output of both agents with a return to steady state values after 20 min. Procaine amide ethobromide, which required 20 mg/kg for saturation, resulted in no effect on either agent. Finally increasing the Rose Bengal carrier dose to 0.035 μmol/min/kg markedly decreased the rate of appearance in the bile of both agents and decreased the steady state output of Tc-99m-diethyl-IDA by 55%. These results indicate that Tc-99m-diethyl-IDA shares a common pathway with BSP and Rose Bengal.

38. BENZIMIDAZOLYL METHYLIMINODIACETIC ACIDS - NEW BIFUNCTIONAL CHELATORS OF TECHNETIUM FOR HEPATOBILIARY SCINTIGRAPHY. F.C. Hunt, J.G. Wilson, D.J. Maddalena. AAEC Research Establishment, Lucas Heights, N.S.W. Australia.

There are many benzimidazole compounds used as anthelmintic drugs. Benzimidazolyl methyliminodiacetic acid (BIMIDA), a known complexone, forms complexes with a number of metals. The investigation of BIMIDA compounds with alkyl and halogen substituents as chelators for Tc-99m was therefore investigated. The benzimidazolyl methyliminodiacetic acid compounds were synthesised by literature methods. [J. Chem. Soc., 2296 (1959)].

The BIMIDA derivatives were labelled by the stannous chloride reduction method. Radiochromatography using silica-gel TLC and saline solvent revealed almost quantitative labelling efficiencies.

Biodistribution studies of Tc-99m dimethyl BIMIDA were performed in rats and rabbits. At 60 minutes post I.V. injection in rabbits, the liver, intestinal and urinary activities were 7.2%, 68.5% and 6.7% of injected dose respectively. For rats, the 60 minute percentages of injected activities were 1.73%, 84.0% and 6.0%. Scintigraphic studies of dimethyl- and chloro-BIMIDA in rabbits revealed a pattern of rapid hepatobiliary clearance and low urinary excretion. The gallbladder was visualised at 10 minutes post injection and most of the liver activity had cleared by 60 minutes. The BIMIDA compounds revealed similar excretion dynamics to the Tc-99m HIDA compounds described by Loberg. These BIMIDA compounds may be useful as hepatobiliary radiopharmaceuticals.

39. A COMPARISON OF COLLOIDAL PREPARATIONS FOR BONE MARROW IMAGING. S. Heyman, M.A. Davis, P. Shulkin, and S. Treves. Children's Hospital Medical Center, Boston, MA.

Normal bone scans and roentgenograms do not exclude bone marrow involvement by lymphomas, leukemia or metastases. ^{99m}Tc-sulfur colloid and ^{111}In-chloride are used clinically for marrow imaging but neither is ideal. In order to find a preparation showing a more favorable bone marrow uptake, the distribution of various technetium-99m labeled colloids was compared to sulfur colloid in two adult female baboons. The agents, which were injected in a

dose of 80μCi/Kg, included sulfur colloid (0·1-1·0μ), filtered sulfur colloid (<0·1μ), antimony sulfur colloid (0·003-0·012μ), calcium phytate microaggregated albumin (0·1-1·0μ) and minimicroaggregated albumin (0·05-0·20μ). Imaging commenced 20 minutes after injection. Anterior and posterior views of the liver, spleen and lower spine were obtained, with simultaneous computer acquisition. Additional images were obtained at 1 hour and 3 hours, or later. The peak activity per cell was obtained, and allowing for background the ratios of liver/marrow, spleen/marrow and liver/spleen activity were determined. The total activity in the liver, spleen and fixed area of bone marrow was also determined, and expressed as a percentage of the injected activity. At 20 minutes after injection the minimicroaggregated albumin showed the most favorable organ ratios with about twice the bone marrow uptake of the sulfur colloid. This was followed by the antimony sulfur colloid, and the filtered sulfur colloid. The calcium phytate showed the poorest ratios and bone marrow uptake.

40. AN IMPROVED MODEL FOR CALCIUM-HEDP SOLUTION EQUILIBRIA. M.L. Lamson, J.L. Fox and W.I. Higuchi. College of Pharmacy, The University of Michigan, Ann Arbor, MI.

HEDP has been used for (1) bone scanning, (2) dental research, (3) radiotherapy, and (4) Paget's disease therapy. The formation of Ca-HEDP mono- and polynuclear species is relevant in each case due to the presence of Ca++ in vivo. This work was undertaken to refine the solution model presented earlier by Grabenstetter and Cilley (J.Phys.Chem., 75, 676-682, 1971). Several sets of data were analyzed using specialized FORTRAN programs, as well as a more general non-linear least squares parameter fitting routine. The equilibria were studied using standard pH titration methods: mixtures of HEDP and calcium were titrated with TMAOH at constant T (25°C) in 0.1M TMACL. Also, published formation curve data were used both separately, and together with the pH titration data, to determine best-fitting values of constants describing the equilibria. Simultaneous fitting provided a model which agrees closely with both types of experimental results. Computer experiments varying sets of complexes and individual constants, and simultaneous fitting, yielded several useful predictions: (1) plots of formation number vs Ca++ may be a useful method for determining polynuclear complex equilibria at physiological pH; (2) for equal molar ratios of total Ca and total HEDP the largest average complex size occurs around pH 7: (3) species concentration-pH profiles indicate that polynuclear complexes become important at about pH 6 and have an extreme pH dependency in this region. This study is important in the understanding of HEDP adsorption or localization.

41. OXIDATION STATE OF TECHNETIUM IN BONE SCANNING AGENTS. C.D. Russell and A.G. Cash. VA and University Medical Centers, Birmingham, AL

Though technetium complexes are in wide use for bone and myocardial scanning, their chemical composition has not yet been established. We have identified the oxidation state of technetium by polarography after electrolytic reduction of pertechnetate in complexing media of pyrophosphate, methylene diphosphonate (MDP), and ethane-1,hydroxy-1,1-diphosphonate (EHDP). In the same media we have identified the oxidation state resulting from reduction with Sn(II) by means of amperometric titration. The stable states resulting from electrolytic reduction were found to be Tc(III) and Tc(IV) below pH 6, and Tc(IV) and Tc(V) above pH 10, for all three ligands. Between pH 6 and 10 the results depended on the ligand present. Tc(III) and Tc(IV) were identified in pyrophosphate and MDP, while in EHDP Tc(III) and Tc(V) were identified with certainty, Tc(IV) questionably. Though two stable products thus resulted from electrolytic reduction at each pH, tin reduction gave only a single product, which was always Tc(IV) except in EHDP, where Tc(V) was formed in neutral or alkaline solution. Even though these methods indicated single oxidation states, column chromatography shows the products are often heterogeneous, presumably representing multiple complexes of the same oxidation state.

42. ANTIOXIDANT STABILIZATION OF BONE AGENTS. A. J. Tofe, J. A. Bevan, M. B. Fawzi, H. S. Whitehouse and M. D. Francis. Miami Valley Laboratories, The Procter & Gamble Company, Cincinnati, OH.

Instability associated with Tc-99m stannous radiopharmaceuticals is a direct result of oxidants, either radiolytically induced or through chemical contamination. While maintenance of a nitrogen atmosphere or increased concentrations of Sn(II) decrease instability, the addition of an antioxidant is a more efficacious stabilizer.

In-vitro stabilization for low tin bone imaging agents has been demonstrated with ascorbic acid and in this paper gentisic acid is shown to be an equally effective antioxidant. In-vitro studies in the presence of oxygen show less than 2% free or hydrolyzed-reduced pertechnetate-99m at 24 hours with the gentisic acid stabilizer. Studies in rats at 3 hours show no effect upon biodistribution by addition of either antioxidant to HEDP bone agent.

	%Tc-99m-HEDP Dose/Gram (n=3)		
	Gentisic Acid	Ascorbic Acid	No Stabilizer
Bone	2.0±0.1	1.9±0.3	2.0±0.1
Blood	0.032±0.005	0.029±0.002	0.026±0.003

Gentisic acid is a safe and effective stabilizer and clinical studies have shown equivalency with ascorbic acid.

43. Tc-99m HYDROXYMETHANE DIPHOSPHONATE (HMDP): A SKELETAL IMAGING AGENT WITH HIGH UPTAKE IN BONE AND INFARCTED MYOCARDIUM AND RAPID CLEARANCE FROM BLOOD AND MUSCLE. J. A. Bevan, A. J. Tofe, M. D. Francis, B. L. Barnett and J. J. Benedict. Miami Valley Laboratories, The Procter & Gamble Company, Cincinnati, OH.

The hydroxymethane diphosphonate ligand (HMDP) is a homolog of hydroxyethane diphosphonate (HEDP). Crystallographic studies with HEDP suggest the importance of the hydroxyl group in binding of the ligand to the growing surface of hydroxyapatite. Tc-99m HMDP has been investigated for use as a skeletal imaging agent.

In Sprague-Dawley rats (195±7g) the bone-to-blood and bone-to-femur ratios averaged 169 and 638 respectively 3 hours after IV administration. In normal beagle dogs (n=6) the 3-hour total blood retention averaged 1.2±0.4 percent of dose and the cumulative 24-hour urinary excretion averaged 58.6±11.2 percent of dose. In an acute myocardial infarct dog model (n=8) the infarct-to-normal myocardium and infarct-to-rib ratios averaged 35.7 and 1.0 respectively. The animal studies show that Tc-99m HMDP has higher uptake in bone and infarct than any current skeletal imaging agent. In addition, the rate of clearance from blood and soft tissue is at least as rapid as with Tc-99m MDP. Clinically, the HMDP bone agent should provide significantly better resolution of target compared to non-target tissues.

44. DESIGN OF RADIOPHARMACEUTICALS FOR ADRENAL IMAGING: EFFECT OF STRUCTURE AND METABOLISM ON THE DISTRIBUTION OF H-3 AND F-18 LABELED PREGNENOLONES. L.A. Spitznagle, R.R. Eng, and C.A. Marino. Univ. Conn. Health Center, Farmington, CT.

Previous work in this laboratory indicated that 21-F-18-fluoropregnenolone-3-acetate (I) reaches high concentrations in the rat adrenal glands. Therefore, the kinetics of the tissue distribution of 21-F-18-fluoropregnenolone (II) were studied in the rat to evaluate the effect of the 3-acetate group on the biological fate of the molecule. Since degradation of the pregnane side chain is known to occur during the metabolism of pregnenolone, we compared the tissue distribution of both I and II labeled with F-18 on the pregnane side chain and with H-3 on the steroid nucleus.

The maximum tissue concentration was 4.1±0.5 %ID/g in the adrenal glands, obtained 5 min. after administration of II labeled with F-18. The presence of the 3-acetate group in I reduced the maximum adrenal gland concentration to 2.4 ±0.4 %ID/g. However, the ratio of the F-18 activities in adrenal/blood were not significantly different. The ratios of F-18/H-3 concentrations were high in the adrenal glands (4.4-6.8), between 1.0 and 2.0 for most other tissues and significantly less than 1.0 in the liver at 1 and 2 hours after administration.

The data indicates that the adrenal glands contain a high concentration of F-18 activity not associated with the steroid nucleus. Both F-18 labeled pregnenolones are potentially useful radiopharmaceuticals for imaging the adrenal glands and measuring adrenal metabolism rates.

45. I-125 7-IODODIAZOXIDE: POTENTIAL RADIOPHARMACEUTICAL FOR PANCREATIC TUMOR IMAGING. N. D. Heindel, H. D. Burns, E. Corley, E. Michener, T. Honda, & V. Risch, Hahnemann Medical College, Phila., Pa.

Diazoxide has achieved clinical utility in treatment of hyperinsulinism accompanying islet cell malignancy. Its effects may be indirect but are believed to involve the islet cells. In search of a pancreatic tumor delineator we have prepared I-125 7-iodo-3-methylbenzo-1,2,4-thiadiazine 1,1-dioxide ("iododiazoxide"). Direct iodination by displacement of the 7-Cl of diazoxide (NaI/glycol) or by electrophilic substitution (ICl) onto the unsubstituted parent, was not successful. Thallation-iodination methods gave multiple products. Nitration/reduction of diazoxide at C #5 was successful but attempted diazotization/iodination yielded peri-fused triazoles.

The title compound was obtained in two ways. Cyclization of 2-amino-5-iodobenzenesulfonamide with acetic anhydride gave the non-labeled target in 43% yield. Radioiodination (NaI/glycol) gave a less than 5% isotopic incorporation. Better radiochemical yield was obtained by reduction, diazotization, and treatment with I-125 NaI of the 7-nitro-3-methylbenzo-1,2,4-thiadiazine 1,1-dioxide. Tissue distribution studies in hamsters bearing beta-cell tumor transplants showed a tumor/pancreas ratio of approximately 6 at 1 hr post-dosing but tumor levels never exceeded blood levels.

46. RADIOLABELED ENZYME INHIBITORS AS POTENTIAL PANCREATIC SCANNING AGENTS. S.T. Mosley, P.V. Kulkarni, R.W. Parkey. Univeristy of Texas Health Science Center at Dallas, Texas.

We have studied the tissue distribution of 3 radiolabeled inhibitors of the pancreatic protease enzymes trypsin and chymotrypsin: I-125-soybean inhibitor (SBI), I-125-human antitrypsin, 3H-diisopropylfluorophosphate. SBI was tested for proteolytic inhibition before and after labeling and found not to be altered by ICl iodination. Assay of tissue radioactivity at 5,15,30,60 min and 24 hr after iv injection in 200 gm rats showed pancreas:liver (P:L) ratios of < 1.4 and pancreas:blood (P:B) ratios of < 1 at all time intervals for each compound. However, ip injection of I-125 SBI gave the following results [$\bar{x}$ (range) of 3-15 rats]:

	5 min	15 min	30 min	60 min
P:L	5.9(4.6-9.3)	5.5(4.8-7.2)	6.2(1.8-5.9)	6.3(5.3-7.8)
P:B	3.4(1.7-8.3)	3.0(2.1-3.5)	1.8(1.1-2.3)	2.1(1.7-3.1)

These ratios resemble those of Se-75-Selenomethionine (SEM) except that kidney values are higher. As a control, we gave nonspecific I-131-IgG ip and found similar results at 15 min: P:L=6.2, P:B=2.0. Most amino acid analogs given iv can pass relatively intact through the liver to the pancreas with good P:L ratios based on the higher metabolic rate of the pancreas. Our data suggest that proteins can show similarly good early pancreas uptake by escaping immediate liver metabolism when given ip. We are now studying potentials of Tc-99m and I-131 (to simulate I-123) compounds that promise to perform as well as Se-75-SEM or better, without the associated high radiation dose or other drawbacks but with better imaging properties.

47. USE OF TECHNETIUM-99m LABELED SPERMATOZOA FOR MONITORING SPERM TRANSPORT IN THE FEMALE REPRODUCTIVE TRACT. S.P. Lorton, S.J. Gatley, L.M. Lieberman, and N.L. First. Endocrinology-Reproductive Physiology Program and the Department of Radiology (Nuclear Medicine), University of Wisconsin, Madison, WI.

We have inseminated sheep with Tc-99m labeled ram sperm prepared with stannous chloride as previously described. (Biol. Reprod. 18 supp. 1 p51A (1978)). Ovariectomised sheep were brought into heat by sequential administration of progesterone and estradiol cyprionate. The animals were killed up to six hours after insemination and their reproductive tracts resected and examined with a gamma camera or rectilinear scanner. Radioactivity was clearly observed in the Fallopian tubes of most of the animals, with larger amounts in the vagina, cervix and uterus. When Tc-99m labeled sperm was replaced with Tc-99m pertechnetate, much less radioactivity remained in the tract and this was evenly distributed. The thyroid was visualized in animals given pertechnetate and was not visualized in those given labeled sperm, although some radioactivity did appear in the blood of the latter animals.

Electrophoretic examination showed that Tc-99m leaving the sperm cells was not in the form of pertechnetate. When labeled sperm were allowed to migrate for 2 cm through cervical mucus, half the bound radioactivity was washed off. However, radioactivity remains on the cells long enough to consider attempting to monitor sperm transport in vivo in species where the reproductive tract has a suitable anatomy.

48. BLIP PRODUCTION OF Fe-52 AND THE Mn-52m GENERATOR.† T.H. Ku, P. Richards, L.G. Stang, Jr., and T. Prach. Brookhaven National Laboratory, Upton, NY.

Fe-52 ($t_{1/2}$=8.3 h) is the only radioisotope of iron with decay properties suitable for imaging applications (100% 169-keV and 112% annihilation gammas). It can also be used in a Fe-52/Mn-52m generator system as a source of short-lived Mn-52m ($t_{1/2}$=21.1m) which is well suited for positron-emission tomography (192.5% annihilation gammas). This study was initiated to explore the possibility of producing substantial quantities at the Brookhaven Linac Isotope Producer (BLIP) by bombarding a manganese or nickel target. The results have successfully demonstrated the feasibility of the production of clinically useful quantities of Fe-52. The total yields achievable are 120 mCi with a manganese target and several hundred millicuries with a nickel target. After irradiation, Fe-52 is isolated from both targets by an anion exchange method and then loaded onto the generator column consisting of 0.6 ml AG 1X8 resin. The generator is eluted with 2 ml of 8N HCl, which recovers approximately 90% of the generated Mn-52m. The eluate is evaporated to dryness and Mn-52m is redissolved in acetate buffer (pH=5.6). Mn-52m and the generator are being evaluated at Brookhaven. Preliminary studies with the PETT III tomographic instrument have shown promising results for myocardial imaging.

† This work was done under Contract No. EY-76-C-02-0016 with the U.S. Department of Energy.

49. CYCLOTRON PRODUCTION AND USE OF INORGANIC RADIONUCLIDES FOR POSITRON EMISSION TOMOGRAPHY. R. M. Lambrecht and A. P. Wolf, Chemistry Department, Brookhaven National Laboratory, Upton, New York 11973, U.S.A.

A combination of recent events has resulted in a significant movement towards short-lived cyclotron produced radionuclides, and chemistry to design radiopharmaceuticals to be used in combination with positron emission tomography for the quantitative in vivo determination of metabolic function and disease state. Short-lived radionuclides present radiochemical challenges in production and processing to assure rapid manipulation into radiopharmaceuticals; and in design of automated, remotely operated equipment to assure minimal radiation exposure to users. Several simple inorganic species of positron emitting radionuclides have physiological properties which permit their near-direct clinical use. For example ^{38}K ($T_{1/2}$ = 7.62 m), ^{15}OO ($T_{1/2}$ = 122 s), $^{13}NH_4^+$ ($T_{1/2}$ = 10 m) and ^{19}Ne ($T_{1/2}$ = 17.2 s). Other inorganic species, e.g. ^{18}F-F_2, are more conveniently used as a synthetic intermediate for the preparation of organic radiopharmaceuticals. We have tabulated the physical characteristics of more than 200 positron emitting radionuclides. Consideration is given to half life, the positron energy spectra and effective positron range with reference to the absorbed radiation dose, and instrumental resolution. Recent progress in the accelerator production and development of 24 selected radionuclides will be reviewed. Special emphasis will be placed on $^{38}K^+$ for myocardial perfusion studies. (Research supported by U.S. Department of Energy)

50. HIGH-LEVEL PRODUCTION OF C-11-CARBOXYL-LABELED AMINO ACIDS, L. C. Washburn, T.T. Sun, B. L. Byrd, R. L. Hayes, T. A. Butler, and A. P. Callahan. Oak Ridge Associated Universities (ORAU) and Oak Ridge National Laboratory (ORNL), Oak Ridge, TN.

C-11-Labeled amino acids have significant potential as agents for positron tomographic functional imaging. We have developed a rapid, high-temperature, high-pressure modification of the Bücherer-Strecker amino acid synthesis (Int J Appl Radiat Isot 29:186-187, 1978) and found it to

be quite general for the production of C-11-carboxyl-labeled neutral amino acids. Production of C-11-carboxyl-labeled DL-tryptophan requires certain modifications in the procedure. A total of 12 different amino acids have been produced to date by this technique. Synthesis and chromatographic purification require approximately 40-45 min.

Improved C-11 targetry and refinements in the techniques for amino acid synthesis have greatly increased our C-11-labeled amino acid production capabilities. Yields as high as 420 mCi of C-11-labeled 1-aminocyclobutanecarboxylic acid (C-11-ACBC), 375 mCi of C-11-labeled DL-phenylalanine, 360 mCi of C-11-labeled DL-valine, 325 mCi of C-11-labeled DL-tryptophan, and 300 mCi of C-11-labeled 1-aminocyclopentanecarboxylic acid (C-11-ACPC) have been obtained. No radiation decomposition of the amino acids has been observed. (ORAU operates under contract number EY-76-C-05-0033 with the U.S. Government, Department of Energy. ORNL is operated by Union Carbide Corp. for US DOE)

51. CYCLOTRON PRODUCTION OF THALLIUM-201 VIA THE $^{205}Tl(p,5n)^{201}Pb \rightarrow {}^{201}Tl$ REACTION. Manuel C.Lagunas-Solar, John A. Jungerman, and David W. Paulson. Crocker Nuclear Laboratory University of California, Davis, California 95616 U.S.A.

The production of the clinically usefull ^{201}Tl radioisotope was investigated based upon the utilization of 99.5% enriched ^{205}Tl targets. ^{201}Tl yields and the excitation functions for the Tl(p,xn)Pb reactions were measured in the 34-to-60-MeV energy range. Results for the formation of ^{201}Pb, ^{200}Pb, and ^{202m}Pb are shown in Figures 1,2,and 3, respectively. ^{201}Tl, ^{200}Tl and ^{202}Tl yields were then calculated for a 8-hour irradiation (Figure 5). The results of this work demonstrated the feasibility of utilizing the p,5n reaction to produce ^{201}Tl of similar characteristics (patient dose and image quality) than the p,3n product.

With a 44-MeV incident H^+ beam on a 6.5 MeV thick ^{205}Tl metallic target, a yield of 1.6 mCi/μA-hr can be obtained (see figure 5). However, this preparation will contain 2% ^{200}Tl and 0.5% ^{202}Tl at 32 hours post bombardment. This level of contamination will produce a 15% increase in WB-dose but no measurable effect in imaging characteristics (H.Hines and M.C.Lagunas-Solar, work in progress). Higher energy H+ beams can also be used if a waiting period is allowed to reduce the ^{200}Tl to an adequate level (Figure 4).

If a variable energy cyclotron is available, this reaction can be used to produce ^{201}Tl with a less expensive target, with variable production schedules , and similar yields to the p,3n method. Because the exit beam is sufficiently energetic, tandem targetry is also possible. This targetry is presently being developed at U.C. Davis.

52. DEVELOPMENT OF A CHROMATOGRAPHIC ^{68}Ge-^{68}Ga GENERATOR YIELDING IONIC GALLIUM. R.D.Neirinckx and M.A. Davis. Joint Program in Nuclear Medicine, Harvard Medical School and Children's Hospital Medical Center, Boston, MA.

The behavior of germanium and gallium on various inorganic and organic chromatographic supports, some of them made in this laboratory, was investigated. The aim was to develop a simple high-yield chromatographic system that could be made available for the routine production of ionic gallium-68 from a ^{68}Ge-^{68}Ga generator in a typical hospital setting. The requirement for simplicity precludes the use of extraction and distillation, techniques which are normally the methods of choice in germanium separation chemistry.

The most attractive systems developed are based on adsorption of germanium-68 on a commercially available anion-exchange resin (Bio-Rad AG 1x8) or on a new synthetic resin, developed specifically for adsorption of germanium.

The generator based on Bio-Rad AG 1x8 with 0.01N HF as the eluent yields 95% of the available gallium-68, in ionic form, in a 3 ml volume. Up to 600 elutions were performed before germanium breakthrough rose over 0.01%. Preliminary toxicity studies indicate the eluent to be injectable by simple neutralization and adjustment of the ionic strength. The system based on the new synthetic resin collected more than 60% of available Ga-68 in 1 ml of 0.3N HCl. More than 600 collections were performed from the same generator, all of them displayed germanium-68 breakthrough levels of less than 10^{-3} percent.

53. TANTALUM-178 RADIOPHARMACEUTICALS FOR LUNG AND LIVER IMAGING. R.D.Neirinckx, B.L.Holman, and M.A. Davis. Joint Program in Nuclear Medicine, Harvard Medical School, Children's Hospital Medical Center and Peter Bent Brigham Hospital, Boston, MA.

A ^{178}W-^{178}Ta generator system, which has been developed in our laboratory, is presently being used for the development of ^{178}Ta-labeled radiopharmaceuticals.

The study has centered around the incorporation of tantalum-178 into particulate matter of discrete size range for imaging of the lungs and liver. ^{178}Ta-ferrous hydroxide, ^{178}Ta-macroaggregated albumin and ^{178}Ta-human albumin microspheres for lung scanning as well as ^{178}Ta-tantalum hydroxide, ^{178}Ta-mini microspheres and ^{178}Ta-mini aggregated albumin for liver scanning were developed and the labeling parameters studied.

Animal distribution results suggest that the distribution characteristics of the new agents are comparable to those of the corresponding ^{99m}Tc compounds. The tantalum-178 compounds have the advantage that the radiation dose administered to the target organ and to the whole body is considerably lower than with ^{99m}Tc, due to the much shorter half-life of the ^{178}Ta ($T_{½}$ = 9.3 min). This is an important consideration, especially in the pediatric population. Furthermore, since the activity of the ^{178}Ta agents decreases rapidly, a repeat injection of the pharmaceutical or the scanning of a different organ can be undertaken within an hour after a previous injection.

Editorial

The Primary Radiologic Consultant

Primary care in medicine has recently enjoyed a resurgence of interest and support; a similar resurgence in the primary role of the radiologist as consultant is indicated. As radiology continues to differentiate into subspecialties, dictated by the increasing complexity of radiologic techniques and rising expectations of professional competence [1], a corresponding development of new problems in the delivery of radiologic services is inevitable. These problems are already acute in university medical centers and in larger community hospitals where radiologic subspecialization has been carried the furthest. Staff clinicians and house officers in these institutions are now faced with a welter of different radiologic consultants in various subspecialty areas; there may be no "primary radiologic consultant" to whom the clinician can turn for advice to plan a logical series of radiologic diagnostic tests in the context of the patient's total needs [2]. Similarly, there may be no designated person in the radiology department with whom the clinician can collate all of the complex data from several radiologic subspecialty areas that might impinge on his patient's problem.

Since we are "physicians first and radiologists second" [3], and since the welfare of the patients is our ultimate concern, we must look at the burgeoning subspecialization in diagnostic radiology and ask two questions:

1. Does increasing subspecialization in radiology indeed constitute a problem to the clinician who is seeking radiologic consultation for the *total* workup of his patient?

2. If increasing radiologic subspecialization does bring problems (as well as advantages) to a close interactive relation between clinician and radiologist, what can we do now to mitigate these problems?

The Radiologic "Supermarket"

Today many larger radiology departments can be compared to supermarkets, with well stocked shelves filled with "goods" (i.e., the numerous available radiologic procedures), a system of organization which displays these goods in separate subsections or areas, and a generous turnover of merchandise that is governed by clinical supply and demand. However, when the large subspecialized radiology department is opened-up to the "shopper" (the patient's physician) some problems may surface. Physicians, like consumers faced with an abundance of opportunities to buy, may become "compulsive shoppers." Furthermore, it may be difficult to find a "store manager" who knows the location of all the desired items on the shelves. Moreover the physician-shopper himself may not know precisely what radiologic procedures to order for his patient. He may or may not already have a "shopping-list," and when he does, it may not adequately meet the needs of his patient. On the other hand, he may be referred (or self-referred) to various sections in the radiologic supermarket for specific items, and each subspecialist may afford him an excellent view of the studies available in his particular area. However, it is a far cry from the abundance of the supermarket and the pressure and excitement of making multiple "purchases," to preparing a well planned "meal" for the individual patient!

While modern radiology departments are often divided organizationally as well as geographically into many sections or subsections, in some departments the films may be further segregated into various subfiles (e.g., chest, gastrointestinal, urography, CT/ultrasound, and so on) and are removed periodically from the master folder for review by individual sections. The clinicians or trainees on each clinical service are expected to seek out the appropriate radiologic subspecialists for advice in planning a series of studies appropriate to each patient. Although there may no longer be a consultant radiologist managing the examination sequence, what a panoply of new radiologic studies there is to choose from! The managers of subspecialty areas are highly trained and enthusiastic about their own radiologic procedures [2]. Trainees (residents or fellows) assigned to each section of a large radiology department get an excellent exposure to the complexities of each subspecialty. As each radiologic study on a patient is interpreted and signed out, the clinician adds the result to the entire series.

Eventually, the time will come to assemble a management plan from all of the radiologic studies chosen, and the clinician may or may not have a knowledgeable radiologic consultant close at hand to assist him. Certain necessary radiologic procedures may have been omitted. Other radiologic procedures might have been made without proper consideration of their cost or actual consequence for the patient's management. Unnecessary expense and discomfort may result; at the least, time is wasted and diagnostic as well as therapeutic opportunites may be lost.

Proposal: Primary Radiologic Consultant

There should be no misunderstanding about the analogy just offered: subspecialization in diagnostic radiology is inevitable and highly desirable. A variety of informative imaging procedures results, and improved quality of service and training may be facilitated by subdividing the radiology department with highly trained "managers" in each area. However, the patient's physician should not be expected to "shop" alone. Clinicians require consultative guidance not only in the use and appropriate sequencing of radiologic procedures, but

AJR 132:497–499, March 1979
© 1979 American Roentgen Ray Society
0361–803X/79/1323–0497 $0.00

also in the final synthesis of complex information from radiologic studies that have been performed. Just as the clinician should not be forced to select procedures without first discussing the total workup of the patient with a consultant radiologist, he also should hesitate to draw final conclusions from a profusion of studies without reviewing them with a radiologic consultant conversant with the specialty of the clinician.

In some instances subspecialization has *facilitated* consultation between the clinician and the radiologist: for example, there is no doubt that the neuroradiologist may work more closely with his neurologic and neurosurgical clinical colleagues than the general radiologist. Similarly, the GU radiologist may develop a close daily working relationship with the genitourinary surgeons and their trainees, and in fact the GU radiology unit may be located in close proximity to the GU clinic area. While under these circumstances it becomes increasingly difficult for the separated parts of a subspecialized radiology department to "hold together" (when radiologic subspecialists communicate more frequently with their corresponding clinical colleagues than with other radiologists), the advantages of radiologic subspecialization for facilitating closer consultative relations with clinicians are clear in several instances.

Nevertheless, large radiology departments with numerous subspecialty areas would serve physicians and patients better if one or more primary radiologic consultants corresponding to each major clinical service (e.g., general medicine, general surgery, oncology) met daily with clinicians and trainees from these services to plan detailed radiologic workups on each patient, to "refer" physicians to appropriate radiologic subspecialties and to assist the clinicians' final collation of the results of radiologic examinations from diverse subspecialty areas. Physicians, institutions, and training programs have been responsive to the need for identifying and training *primary care physicians* dedicated to treating the "whole patient" and seeking specialty referrals when appropriate; the complexities of modern diagnostic radiology also dictate that we identify primary radiologic consultants within larger radiology departments, to serve our clinical colleagues and patients in an analogous way in the face of growing radiologic subspecialization. With our radiologic tools more powerful and expensive than ever before, this need is all the greater!

Practical Role of the Primary Radiologic Consultant

Primary radiologic consultants will be most useful for those clinical areas where a large clinical service group exists without a counterpart subspecialty section in the radiology department. For example, individual primary radiologic consultants should be designated to meet regularly with the general medical and general surgical services, with the thoracic surgeons, and possibly with the clinical oncology services [4] particularly with medical oncology and radiation oncology, and with gynecologic oncology and surgical oncology if they operate as separate services. In many general hospitals, these clinical services will in fact embrace the majority of patients seen within the institution. The primary radiologic consultant for each major clinical service should meet with the members of the service daily to review *all* radiologic studies performed in the past day on patients that are of current interest (table 1). In addition, the consultant should remain with the clinical group while new patients are presented briefly to determine, *together* with the clinicians, the type and the sequence of radiologic studies required as part of the workup. Patients currently progressing through an already planned series of radiologic examinations and with special interim problems requiring consultation with the primary radiologic consultant, will also be discussed at this time. Specific arrangements might be made by the consultant with individual clinicians, to meet later during the day to consider the results of certain examinations as they are performed. It may also be advisable to review briefly the radiologic studies planned during the current workday and/or for the next day. Appropriate cancellations and other changes in the radiologic schedule can be arranged with the consultant at this time.

TABLE 1

Illustrative Schedule of Primary Radiologic Consultant for General Medical Services in Large Teaching Hospital

Hour	Activity
Morning:	
8–10	Direct medical/x-ray consultation rounds (four services, meeting about 30 min each).
10–10:30	Consult with selected clinicians and ultrasound subspecialist concerning CT/ultrasound findings on selected patients.
10:30–11	Attend pathology conference on a medical service patient with the patient's clinicians and pathologist (bring films to discussion).
11–noon	Lecture to medical students on general radiologic diagnosis topic.
Afternoon:	
Noon–1	Attend daily x-ray conference for all radiology staff and residents.
1:30	Meet clinicians and angiographer in angiography suite to discuss findings from the morning angiogram on an acutely ill medical service patient.
2:30–3:15	Give talk and film seminar to five medical service residents on the clinical-radiologic workup of "fever of unknown origin."
4–5:30	Review the day's x-ray examinations on medical service patients with radiology residents (and radiology subspecialists, as appropriate) for tomorrow's early morning medical x-ray rounds.

It is important to emphasize that *all* radiologic studies planned or already performed should be discussed by the clinicians with their primary radiologic consultant. This does not preclude the desirability of their meeting also with the radiologic subspecialist who is scheduled to perform a particular study, or from whom there has been a report of a significant abnormality on a given patient. The primary radiologic consultant is also responsible for discussing with the subspecialists in his

own department, the plans for and the results of specialized examinations performed on his clinical service patients. In addition, when specific problems arise concerning the choice of a specialized examination or the results thereof (see table), the primary radiologic consultant should accompany the clinician for a direct discussion between the radiologic subspecialist and the clinician immediately after the daily "x-ray rounds." In this way the consultant assists effectively, not only the clinicians with whom he has a special ongoing relationship, but also the subspecialists in his own department. However, to conceive of the consultant as a go-between for the clinician and the radiologic subspecialist would be to understate his purpose. The consultant should be an active *facilitator,* whose role is to plan the radiologic studies that are needed for each patient on his assigned clinical service and to bring the clinicians and their patients into contact with the appropriate radiologic subspecialists; he must also assist the clinician in synthesizing the final results from numerous radiologic studies, together with other clinical and diagnostic findings on each patient, to reach appropriate prognostic and treatment decisions.

Ideally, the consultant assigned to a large clinical service should have special interests, training, and/or experience that are relevant to his assigned clinical area. For example, the consultant assigned to the oncology services should have special training or experience in oncology diagnosis and management,* the primary radiologic consultant for the general medicine service should have a background in internal medicine, and so on. An obvious underlying requirement is that the consultant, a certified radiologist, also possess sound fundamental training in, and a contemporary appreciation of, all areas of diagnostic radiology.

It might reasonably be asked how the added expense of designating specific positions for primary radiologic consultants can be justified when the focus of current efforts is toward reducing health care costs and increasing efficiency. While reasonable, this question assumes that clinical decision-making is efficient today. Could it be, as we subspecialize further in radiology, that certain radiologic studies of marginal utility may tend to persist or even to proliferate? Could it be that as radiologists continue to subspecialize, we may further lose control over the optimal choice and sequence of the radiologic examinations that are ordered? Is it conceivable, in turn, that with careful attention to designating qualified primary radiologic consultants for each major clinical service, we could guide the clinician more efficiently in the choice and sequencing of radiologic studies and in the use of the resultant diagnostic information, leading to shortened hospital stays, diminished costs, and improved overall service to patients? In short, whose definition of "efficiency" will be determinative?

While current experience in large radiology departments suggests the advantage of designated primary radiologic consultants for the major clinical services, the answers to all of these questions are not available and should be sought. More efficient use of increasing technology in the various subspecialties of radiology can be anticipated with immediate benefits to the patient and his physician. Already today, and even more in the future, clinicians need this kind of guidance; fortunately, everyone (patients, clinicians, *and* radiologists) will benefit.

Richard J. Steckel
UCLA School of Medicine
and Jonsson Comprehensive Cancer Center
Los Angeles, California 90024

* The primary radiologic consultant for the clinical oncology services, for example, could have spent 1–2 years as a radiology trainee or fellow in a major cancer center or institute.

REFERENCES

1. Rigler LG, Steckel RJ: Future of graduate education in roentgen diagnosis. *Proceedings XIII International Congress of Radiology in Madrid V.I.*, October 1973, pp 188–192
2. Hessel SJ, Abrams HL: Diagnostic radiology: beyond mere technology. *Radiology* 129:249–250, 1978
3. Goin LS: Radiology and the future. *Radiology* 48:284–288, 1947
4. Steckel RJ: Oncologic diagnosis: an emerging subspecialty in diagnostic radiology. *Invest Radiol* 8:425–426, 1973

Letters

Subglottic Edema in Acute Epiglottitis in Children

I would like to compliment Drs. Shackelford, Siegel, and McAlister [1] on their fine article, "Subglottic Edema in Acute Epiglottitis in Children." We have had a similar experience.

In a single year, seven of our 25 patients with epiglottitis had subglottic narrowing on the frontal plain film prior to intubation. I feel that the authors' point, "the presence of subglottic edema in our patients had no effect on their management," is one of the essential aspects of this paper. It is interesting that two of the patients in their hospitals had tracheostomies for epiglottitis. In our institution, this is very rarely, if ever, done. All seven of our patients were intubated, as were the other 18 patients who did not have subglottic narrowing. The mean duration of intubation in the seven patients with subglottic narrowing and epiglottitis was 30 hr, the longest 48 hr, and the shortest 18 hr. This was exactly the same interval of intubation as the 18 patients without subglottic narrowing. All of our patients had normal frontal and lateral films 1–2 wk after their acute episode.

At the recent meeting of the American College of Otolaryngology in a course on pediatric airway disease, a prominent otolaryngologist emphasized that those children with subglottic narrowing who have epiglottitis need to have a tracheostomy. In all of our patients, and three of the reported cases, endotracheal intubation was a successful mode of therapy. In the Shackelford et al. report, two patients were managed with tracheostomies. In discussing these cases with Dr. Shackelford, he noted that this was the current mode for all patients with epiglottitis at that time. I think Dr. Shackelford's experience and our experience would begin to mitigate against mandatory tracheostomy in those children with epiglottitis and subglottic narrowing.

Since it is the radiologist who will make the diagnosis of subglottic narrowing in frontal films, I feel we have an important role in clearly defining the natural history of these children with subglottic narrowing and epiglottitis. This experience will help our otolaryngological colleagues in their treatment plan.

Congratulations to Dr. Shackelford and his group for bringing this little known change to the attention of all.

Thomas L. Slovis
Edgardo Arcinue
Children's Hospital of Michigan
Wayne State University School of Medicine
Detroit, Michigan 48201

REFERENCE

1. Shackelford GD, Siegel MJ, McAlister WH: Subglottic edema in acute epiglottitis in children. *AJR* 131:603–605, 1978

Fracture of the Occipital Condyle

The recent article by Bolender et al. [1] describes two cases of head trauma with interesting correlation between cranial nerve dysfunction and site of the fracture line. However, to enhance the educational value of these cases, I feel that two additional points should be stressed. First, the occipital condyle per se is not fractured. Rather, the fracture line runs lateral to the dense bony mass of the occipital condyle–jugular tubercle and interrupts the jugular foramen. Second, the visualized bony interruptions and displacement most likely represent more extensive fractures of the posterior fossa–skull base extending onto the squamous portion of the occipital bone and very probably onto the clivus [2].

These cases demonstrate the usefulness of multiple method investigation in patients whose symptoms suggest an abnormality of the skull base.

Charles G. Jacoby
University of Iowa
Iowa City, Iowa 52242

REFERENCES

1. Bolender N, Cromwell LD, Wendling L: Fracture of the occipital condyle. *AJR* 131:729–731, 1978
2. Gurdjian ES: *Impact Head Injury.* Springfield, Ill., Thomas, 1975, p 32

On the Inadequacies of Translumbar Aortography

"These pipes and these conveyances of our blood. . . ."
Shakespeare: *Coriolanus* V, 1, 54

In his emotional appeal for translumbar aortography, Dr. Reuter [1] neglected to consider one crucial point: does translumbar aortography provide data comparable to that obtainable with the transfemoral catheter approach?

Diagnostic radiologic studies should be designed to provide maximum information at minimal risk and patient discomfort. The same is true for aortography. In this context, the various approaches to aortography should be viewed not as to the rapidity with which the study can be performed nor the convenience of the radiologist, but rather as to the wealth of "essential information" that each approach can provide.

More "essential information" can be obtained with a catheter that can be moved to various positions in a blood vessel than with a translumbar needle placed in the patient's aorta. The question, of course, is who needs this information? Information that a surgeon cannot use in his decision making process is superfluous. However, I would venture to say that in the 1970s vascular surgeons wish to have more diagnostic data than those provided by translumbar aortography.

Specifically, the editorial leaves unanswered the following questions:

1. *Does Dr. Reuter direct the needle below or above the renal arteries?* If below, crucial information would be missed about the status of the aorta at the level of the renal arteries and about stenotic lesions of the renal arteries themselves. If above, the opacification of the runoff vessels cannot be optimal.

2. *Does he take oblique views of the pelvis in order to evaluate the origins of the deep femoral arteries?* If so, is it safe

© 1979 American Roentgen Ray Society

0361–803X/79/1323–0500 $0.00

to move the patient to various oblique positions with a needle in the aorta?

3. *Does Dr. Reuter obtain pressures to evaluate the hemodynamic significance of inflow lesions?* If so, femoral arterial punctures would be necessary to complement translumbar aortography for pressure determinations. In that case why not a femoral artery puncture to begin with?

4. *Has Dr. Reuter recently visited the operating room to realize how difficult it is to dissect the retroperitoneal vessels if surgery is performed within 24–48 hr after translumbar aortography?* Small retroperitoneal bleeding occurring with every translumbar puncture is not considered a major complication. However, dissection becomes difficult and more risky for the patient.

5. *Which is more comfortable, the prone or the supine position?* Californians are perhaps more stoic than New Englanders, but patients in our hospital have assured me that they are more comfortable when supine.

Dr. Reuter admits that the translumbar approach is not as versatile as the transfemoral. I concur. I further add that this versatility is important. The arteries are not just "pipes" but also "conveyances of our blood." Hence, the demonstration of altered anatomy needs to be complemented with data about the hemodynamic significance of atherosclerotic lesions.

My response to Dr. Reuter's closing remark is: I have tried the translumbar approach and found it inadequate. Try the transfemoral approach. It will be more beneficial to your patients.

Christos A. Athanasoulis
Harvard Medical School
Boston, Massachusetts 02114

REFERENCE

1. Reuter SR: On behalf of translumbar aortography. *AJR* 131: 733, 1978

Reply

Dr. Athanasoulis's letter advocates the valid position that all necessary information should be obtained from angiographic examinations. However, what is necessary varies from patient to patient and is determined by the needs of the clinician. If the surgeon wants or needs to know the pressure gradient across a stenotic lesion, the transfemoral approach to aortography is clearly superior to the translumbar. I have had the opportunity to be associated with several excellent vascular surgeons; none wanted this information. They have used the angiogram to determine the location and degree of stenosis and have relied upon their noninvasive flow studies and clinical judgment to assess the significance of the stenoses.

My editorial omitted several technical details in the interest of conserving space. However, Dr. Athanasoulis's questions are important and easily answered. The ideal position of the needle tip is about 1 cm below the origins of the renal arteries. This allows the renal arteries to be visualized during diastolic reflux of the contrast medium up the aorta and still prevents excessive loss of contrast medium into the visceral branches. However, insignificant renal artery stenoses are of academic interest; if the patient has a significant stenosis, the resulting hypertension is a contraindication to the translumbar approach. Oblique views of the femoral bifurcation area can be obtained by gently rolling the patient into the proper position with the needle in the aorta. I have had no complications from doing this to date. I frequently, but not routinely, obtain oblique views after a review of the posteroanterior examination and discussions with the surgeon.

I have done several hundred translumbar aortograms over the past 10 years and have yet to hear a surgeon complain that the periaortic hematoma caused a problem at subsequent bypass surgery. On the other hand, several have told me that the periarterial hematoma resulting from a transfemoral catheterization has made a subsequent femoral-popliteal bypass operation more difficult. Finally, it is true that patients are more comfortable supine than prone. However, the average translumbar aortogram takes only about 15 min to perform and most patients tolerate the prone position for this length of time.

I apologize if the editorial sounded emotional. It was certainly not meant to be. There are many things in this life about which I still become emotional; peripheral angiography is not one. The purpose was simply to advocate translumbar aortography as a safe, rapid, and effective method of demonstrating occlusions in the conveyances of our blood. As noted by the sage, Anon.: "There are many ways to skin a cat." A person in the cat skinning business should be well versed in all the techniques. The one chosen in any given situation depends on the reason the cat was to be skinned in the first place and the technique with which the skinner feels most secure.

Stewart R. Reuter
University of California
Davis and San Francisco, California 98143

Complication Rate with Supine Phlebography

Coel and Dodge [1] report a reduction in the complication rate following lower extremity phlebography that they attribute primarily to patient supine positioning during the procedure. It is widely accepted that the contact time between venous endothelium and contrast medium is a major determinant in postphlebographic side effects, and all current literature emphasizes the importance of emptying the veins of contrast agent immediately after diagnostic films have been obtained. The supine position would be expected to reduce such side effects by allowing a more rapid central runoff of the peripherally injected contrast agent. A similar benefit can be accomplished by decreasing the concentration [2] or the quantity of the contrast media. Recent reports from European centers suggest that nonionic contrast agents may virtually eliminate postphlebographic discomfort (Paulin, personal communication, 1978).

A major shortcoming of the Coel and Dodge report is their failure to document, or even comment upon, the diagnostic accuracy of their method denoted as "machine injected supine peripheral venography." A single reference to this technique refers the interested reader to an article from the same department entitled "Ascending Lumbar Venography in Lumbar Disc Disease" [3], but this paper does not include any description of this technique in lower leg phlebography. The lack of documentation of accuracy is unfortunate in light of the tacit assumption made by the authors that their modified technique is diagnostically equivalent to similar examinations in the predominantly upright position.

The introduction of semierect positioning for lower extremity phlebography was a major factor in establishing this examination as a reliable diagnostic procedure. As early as 1943, Kjellberg [4] pointed out the potential errors in interpreting filling defects due to relatively dense contrast media layering in the low flow venous system. Rabinov and Paulin [5], in summarizing these problems, state " . . . the general accepted opinion that in order to obtain a proper diagnostic phlebogram it is

necessary to examine the patient in a predominantly upright position" [5]. Readers should be reluctant to change these accepted methods without evidence of comparable, or near comparable, accuracy.

Ferris M. Hall
Beth Israel Hospital
Boston, Massachusetts 02215

REFERENCES

1. Coel MN, Dodge W: Complication rate with supine phlebography. *AJR* 131:821–822, 1978
2. Bettman MA, Paulin S: Leg phlebography: the incidence, nature and modification of undesirable side effects. *Radiology* 122:101–104, 1977
3. O'Dell CW, Coel MN, Ignelzi RJ: Ascending lumbar venography in lumbar-disc disease. *J Bone Joint Surg* [*Am*] 59: 159–163, 1977
4. Kjellberg SR: Die Mischungs- und Strömungsverhältnisse von wasserlöslichen Kontrastmittel bei Gefäss- und Herzuntersuchunger. *Acta Radiol* (Stockh) 24:433, 1943
5. Rabinov K, Paulin S: Roentgen diagnosis of venous thrombosis in the leg. *Arch Surg* 104:134–144, 1972

Reply

We appreciate Dr. Hall pointing out an error in our references. Instead of referring to the article on supine phlebography we mistakenly interchanged another of our articles on lumbar venography. The correct reference should have been: O'Dell CW, Coel MN: Continuous injection supine phlebography. *J Can Assoc Radiol* September 1976, pp 186–192.

In that article, which fully describes our technique, there were several additional points. For one, cross-table lateral films taken during injection of contrast medium revealed excellent mixing of contrast media and blood; thus, no layering. In addition, every other film is taken with the patient's leg in lateral position, then anteroposterior, then lateral, and so forth. There is never any layering seen.

As for the ability of this technique to visualize the various venous channels, we found that we had to do central venograms in 11% of cases in order to see the common iliac veins and inferior vena cava. This is well below other reported incidences. Thomas [1] state that "Peripheral phlebograms gave an adequate demonstration of the major veins from ankle to inferior vena cava in 37 (*7 per cent*) [italics mine] of the patients in the trial group. . . . " We are in the midst of completing a comparison of 100 normal venograms, 50 supine and 50 upright. The comparison, as yet incomplete, seems to bear out our findings that the techniques are equal in the calves and thighs, but the supine technique is superior in the pelvis. There also appears to be greater visualization of the soleal and gastrocnemius veins and the deep femoral veins on the supine studies.

Finally, although admittedly unscientific, several radiologists who have tried this technique have switched to it almost exclusively. They confirm the ease of performance, the improved venous opacification, the lowered side effects, and the patient comfort when using this technique. The patients themselves also find lying down during this examination more tolerable. The technique is especially suited to the patient undergoing simultaneous (bilateral) examinations, as well as the elderly, the infirm, the paraplegic-hemiplegic, and the postoperative patient.

We apologize for the incorrect reference, and hope that those who are interested will refer to the original article.

Marc N. Coel
University of California, San Diego
San Diego, California 92161

REFERENCE

1. Thomas ML, Andress MR, Browse NL, Fletcher EWL, Phillips JD, Pim HP, McAllister V, Stephenson RH, Tonge K: Phlebography in the prevention of recurrent pulmonary embolism—techniques and value. *AJR* 110:725–733, 1970

Urographic Sign of Ureteral Calculus

I wish to comment on the paper by Korobkin et al. [1] in the November issue of the Journal.

After using this sign for several years, I, too, find that it can be helpful in the diagnosis of stone, but with one caveat: if a ureteral compression device is used, especially one that compresses each ureter individually, the device may be applied more efficiently on one side than on the other, causing diminished radiopacity of the contrast in the side with the more efficiently compressed ureter.

Christian V. Cimmino
Mary Washington Hospital
Fredericksburg, Virginia 22401

REFERENCE

1. Korobkin M, Jacobs RP, Clark RE, Minagi H: Diminished radiopacity of contrast material: a urographic sign of ureteral calculus. *AJR* 131:847–850, 1978

Standardization of Imaging Films

With the development of the many new imaging modes, there is an obvious confusion to the uninitiated about the method by which the images are presented. Traditionally, radiographic films have been presented with the viewer looking at the films in the anatomic position. Until relatively recently, when the manufacturers removed the image orientation switch from equipment, nuclear images were also presented in this manner. However, nuclear medicine images are now presented in the manner obtained: the anterior views are presented in the anatomic image and the posterior views are presented as if the patient were prone, which reverses the right and left sides to the viewer. To add to the confusion, cranial CT images are presented as if you are looking from the head of the patient down with the patient's back to the viewer. Thus, the patient's left is on the viewer's left. But in ultrasound images (and CT body scans), presented as if you are looking from the bottom of the patient upward with the patient supine, the right side of the image is usually to the viewers left (the anatomic position).

I write this to encourage the *AJR* to take a stand on this confusing array of presentations and to develop a standard of presentation in the scientific community for the various images that will be carried over into publications.

Joseph L. Izenstark
E. C. "Gene" Nuclear Medical Center
Bakersfield, California 93301

Sidney Rubenfeld, 1907–1978



Sidney Rubenfeld, who died on October 15, 1978 at the age of 71, was a radiologist whose hallmarks were honesty, loyalty, integrity, and a high professional competence. He was ever helpful, never expedient, and gave of himself freely with a warm, friendly, generous, and kind manner. He instilled hope in many patients when hope was difficult to come by and he had a great capacity for compassion.

He was born May 10, 1907 in New York City. He received his B.S. in 1927 and his M.D. in 1930 from New York University. After an internship at St. Vincent's Hospital in Portland, Oregon, he returned to NYU's Bellevue Medical Center to begin a relationship which was to last for the rest of his life, ending as director of the Radiation-Therapy-Radioisotopes Service and finally as consultant. On the teaching side, he began as an assistant and ended as professor emeritus. At New York University Hospital and at the New York Eye and Ear Hospital he was an attending radiation therapist. In addition he was visiting professor to the Hadassah Medical School, Jerusalem, Israel, and was a consultant to the Veterans' Administration Hospitals in Manhattan and the Bronx, the Naval Hospital at St. Albans, and other hospitals.

During World War II, he served in the Army in New Guinea, Australia, and the Philippines, returning as a Lt. Colonel.

Dr. Rubenfeld was the author or coauthor of more than 65 publications. From 1946–1948, he was a coeditor of the therapeutic section of the Year Book of Radiology.

He was a fellow of the American College of Radiology and the New York Academy of Medicine; a member of the American Radium Society, the New York Roentgen Society, the Radiological Society of North America, the American Society for Nuclear Medicine, the American Association for the Advancement of Science, and the Society of Sigma Xi.

His honors included: past president, New York University Medical School Alumni (1958), New York Roentgen Society (1957), Society of Nuclear Medicine, Greater New York Chapter (1955), and the New York Cancer Society (1962). He served as vice president of the New York University Alumni Federation (1965). In 1959 he received the highest award of his alma mater, the Alumni Meritorius Award. In addition, he was a member of the Alpha Omega Alpha honorary medical society, and an honorary police surgeon, New York City Police Department.

He is survived by his wife, Marie, two daughters, Maxine and Beth, and four granddaughters.

M. H. Poppel
Southbury, Connecticut 06488

Asa Elmore Seeds, 1905–1978



Asa Elmore Seeds died unexpectedly at his home on Mercer Island, Washington, September 4, 1978. Seeds had returned to his adopted state of Washington to be near his family after living in Tucson, Arizona after his retirement from active practice.

Asa Seeds was born in Columbus, Ohio, November 29, 1905. His education was at William and Mary College and the University of Virginia where he received his M.D. degree in 1931. His radiologic training was at the Johns Hopkins Medical School from 1932–1936, where he subsequently served as an instructor. Later, he was professor and chairman of the Department of Radiology of Baylor University Medical School in Dallas and director of the Tumor Clinic.

Following overseas military service in Africa, he returned to Dallas briefly and then moved his family to Vancouver, Washington, where he spent the major portion of his radiologic career. He was director of radiology and chief of nuclear medicine at the Memorial Hospital in Vancouver until he retired in 1970. One of his great enthusiasms was nuclear medicine and the Society of Nuclear Medicine. He was a founder of this society and served as its second president. He participated faithfully in its activities while watching it grow from its first meeting of 125 members in Seattle in 1954 to close to 10,000 members at his death in 1978. He served as its historian until his retirement.

Dr. Seeds was also interested in cancer detection and control. He was director of the Clark County Detection Center and Tumor Registry from 1955–1960. He was on the board and executive committee of the Washington division of the American Cancer Society and vice chairman of its research committee.

He also served as president of the Clark County Medical Society; was a member of the Board of Trustees for the Washington State Medical Association; and was a member of the American Roentgen Ray Society.

After his retirement from private practice in Vancouver,

© 1979 American Roentgen Ray Society

0361–803X/79/1323–0503 $0.00

he became associated with the Veterans Administration, serving as radiologist in several hospitals until 1975.

Dr. Seeds is survived by two sons and two daughters. Dr. Asa Elmore Seeds, Jr. is professor of Obstetrics and Gynecology at the University of Cincinnati Medical School; Lt. Commander John William Seeds, U.S. Navy, is also in obstetrics and gynecology and is now serving in Rota, Spain; a daughter, Barbara Engel, lives on Mercer Island; a second daughter, Suzee Merryman, lives in Los Angeles.

Thomas Carlile
Seattle, Washington 98104

Jacob H. Vastine, II, 1897–1976

Jacob Hursh Vastine, II, died in March 1976 at the age of 78. He was born April 3, 1897 at Catawissa, Pennsylvania into a medical family. His father was a physician and his maternal grandfather and Dr. George L. Pfahler were cousins. There were almost 40 physicians in his family and that of his wife, Frances B. Anderson Vastine.

A graduate of Bloomsburg State Normal School in 1914, Dr. Vastine studied engineering for the next 3 years at Cornell, before entering the service and later studying medicine at the University of Pennsylvania. He received his M.D. degree in 1923. He interned at Easton Hospital and did general practice for a year prior to becoming a resident in radiology at Peter Bent Brigham Hospital under Merrill C. Sossman. Perhaps it was natural that he went into radiology, the field of his illustrious relative, George Pfahler, and with his own engineering background.

He was a diplomate of the American Board of Radiology and became lecturer in radiology at Woman's Medical College in 1926 and professor of radiology in 1929, a post in which he served with distinction and charm until he became professor emeritus in 1962.

He was an excellent teacher and clinician. He loved people and he loved radiology, setting a great example for students. He also was a prolific writer, publishing 36 articles over the years.

From 1932–1960, Dr. Vastine was associate professor of radiology at the Graduate School of Medicine of the University of Pennsylvania. He was chief of radiology at Woman's Medical College Hospital, at Presbyterian Hospital from 1938–1948, at Eastern Pennsylvania Psychiatric Hospital from 1956–1974; he practiced his specialty until 2 years before his death.

He was a Fellow of the American College of Radiology and of the College of Physicians of Philadelphia. He also served as president of the Philadelphia Roentgen Ray Society, the Medical Club of Philadelphia, and the West Branch of the Philadelphia County Medical Society. In addition, he was a member of many organizations including the American Roentgen Ray Society and the Radiological Society of North America. In 1973, he received a Distinguished Senior Alumnus Award from the University of Pennsylvania School of Medicine.

Jacob and Frances Vastine had three children and 11 grandchildren, one of whom recently received his M.D. degree.

Katharine R. Sturgis
Wynnewood, Pennsylvania 19096

Abstracts of Current Literature

Chest

The efficacy of chest physiotherapy and intermittant positive-pressure breathing in the resolution of pneumonia. Graham WGB, Bradley DA (Department of Medicine, Medical Center Hospital of Vermont, Burlington, Vermont 05401). *N Engl J Med* 299:624, Sept 21, 1978

This interesting paper describes a randomized control study using physiotherapy and positive-pressure breathing in treating patients with pneumonia. Some 170 patients were considered for the study; 98 were specifically excluded prior to the randomization because of complicating factors such as lung abscess, bronchiectasis, tuberculosis or severe respiratory failure or because they were severely compromised hosts. A few others were excluded for technical reasons. The patient group randomized consisted of 54 individuals, half men and half women, with an average age of 62 years. More than half were smokers. The proportions of gram-positive and gram-negative infections were similar in both groups and the antibiotic treatment was standardized on the basis of initial gram stains. The number of lobes of the lungs involved radiologically was also similar for the two groups. The chest physiotherapy was administered according to routine techniques and positive-pressure breathing was given every 4 hr by a standard technique. When the results were analyzed, there was no difference in the duration of fever or the rate of improvement of the patients as determined by chest radiographs or by clinical evaluations. The patients receiving chest physiotherapy and positive-pressure breathing had equivalent durations of their hospital stays to the patients in the control group. This study therefore, suggests that the routine use of these procedures is of little help to most patients with pneumonia. It would also appear that the benefits of these procedures in other patients deserve further study.

David C. Dale
Department of Medicine
University of Washington

Legionnaires' disease: clinical features of 24 cases. Kirby ED, Snyder KM, Meyer RD, Finegold SM (Infectious Disease Section 691/111F, Building 550, Room 3658, Wadsworth Veterans Administration Hospital, Los Angeles, California 90073). *Ann Intern Med* 89:297–309, Sept 1978

This report details the clinical course and treatment of 24 patients with Legionnaires' disease seen at Wadsworth Hospital between July and December 1977. All but one were men. Diagnosis was based upon serological criteria in 20 cases, on postmortem tissue examination in two patients, and on both studies in two others. The serological tests were performed by the Center for Disease Control in Atlanta. The histologic diagnoses were based upon a silver staining method or a direct fluorescent antibody staining method. All patients in this study and all the patients with suspected Legionnaires' disease were treated with erythromycin.

In this population, Legionnaires' disease was seen most frequently as a complication of immunosuppressive therapy. Eleven of the patients were receiving corticosteroids. Seven others had severe cardiorespiratory disease. In general, their illnesses were characterized by weakness, malaise, fever, and a dry cough. General laboratory data (white blood cell counts, chemistry batteries, etc.) showed nonspecific changes and the patients' chest x-rays most often showed patchy infiltrates most often in the lower lobes. Pleural effusions were common, being seen in 13 of 22 patients, but none of the patients developed lung cavities. The clinical course of the patients was quite variable; four died, but several others had very mild illnesses. As indicated in the editorial accompanying this article (*Ann Intern Med* 89:413, 1978), the spectrum of Legionnaires' disease is undoubtedly quite broad and pneumonia is only one feature of this multifaceted infectious problem.

David C. Dale
Department of Medicine
University of Washington

55° posterior oblique tomography of the pulmonary hilum. Janower MI (St. Vincent Hospital, Worcester, Massachusetts 01604). *J Can Assoc Radiol* 29:158–164, Sept 1978

The author suggests that 55° ipsilateral posterior oblique tomograms should be included as part of the conventional radiographic investigations of the hilum. These films are obtained with the patient in a 55° ipsilateral posterior position, using linear tomography and a through filter with a 20° angle. The radiographic factors used were 125 kV, 30–40–200 mA, and 0.3 sec: 3.4 mm sections were obtained from 7 to 14 cm, with additional levels added if necessary. The author nicely describes and demonstrates both the normal anatomy and various mass lesions. He also states that this projection has its limitations as it does not adequately demonstrate the paratracheal and subcarinal nodes, but these are well seen on the accompanying anteroposterior tomograms.

Jack M.A. Tishler

Experimental evaluation of reexpansion pulmonary edema. Sewell RW, Fewel JG, Grover FL, Arom KV (Division of Cardiothoracic Surgery, University of Texas Health Science Center, San Antonio, Texas 98284). *Ann Thorac Surg* 26:126–132, Aug 1978

Reexpansion pulmonary edema results when a large pleural effusion or pneumothorax is rapidly evacuated, and can result in severe respiratory distress or death. Three mechanisms suggested as causes for reexpansion edema are: (1) use of excessive suction; (2) decreased surfactant activity resulting in increased surface tension and more negative intrapleural pressure; and (3) extended duration of collapse with hypoxic damage to capillary endothelium allowing leakage of fluid.

This study was designed to evaluate the mechanisms and to correlate reexpansion pulmonary edema. The authors created right pneumothorax in 30 goats. The animals were divided into three groups by duration of pneumothorax (1, 2, or 3 days), and technique of reexpansion (waterseal versus 10 cm H_2O suction). Following reexpansion, chest radiographs were obtained and both lungs were removed for study. Results seem to support each of the three above mechanisms. Important decreases in surfactant activity occurred in all, and electron microscopy revealed grossly thickened capillary basement membranes likely due to anoxia. Further, both increased time of collapse and suction reexpansion tended to correlate with increased pulmonary extravascular water volume, decreased surfactant and arterial PO_2, and increased alveolar-arterial O_2 gradient. In general, radiographs revealed minimal findings of edema while gross examination of lungs showed fluid in bronchi and alveoli.

W. Richard Webb

Visualization of the pulmonary arteries in pseudotruncus by pulmonary vein wedge angiography. Nihill MR, Mullins CE,

© 1979 American Roentgen Ray Society

0361–803X/79/1323–0505 $0.00

McNamara DG (Texas Children's Hospital, Houston, Texas 77030). *Circulation* 58:140–147, July 1978 (by permission American Heart Association)

Pulmonary venous wedge angiography revealed the anatomy of the mediastinal and parenchymal pulmonary arteries in 22 patients with obstruction of the right ventricular outflow tract, proximal pulmonary arteries, or branch pulmonary arteries when conventional angiographic methods had failed. Retrograde pulmonary wedge angiograms were obtained by wedging an endhole catheter in the pulmonary vein and slowly injecting by hand 0.2–0.45 ml/kg of contrast material followed by a flush of dextrose solution (1–2 ml/kg).

Author Abstract

Cardiovascular

Improved plainfilm diagnosis of right aortic arch anomalies with high kilovoltage-selective filtration-magnification technique. Wolf EL, Berdon WE, Baker DH (Babies Hospital, Children's Medical and Surgical Center, Columbia-Presbyterian Hospital, New York, New York). *Pediatr Radiol* 7:141–146 Sept 1978

Recognition of a right aortic arch is important in diagnosis of compressive and noncompressive vascular rings, and of congenital heart disease, and is important in patients with esophageal atresia were the surgical approach will be modified. High kilovoltage technique with air-gap magnification and selective filtration allows excellent visualization of the airway and facilitates recognition of right aortic arch abnormalities.

B. J. Wood

Echocardiographic estimation of aortic-valve gradient in aortic stenosis. Schwartz A, Vignola PA, Walker HJ, King ME, Goldblatt A (Cardiac Ultrasound Laboratory, Massachusetts General Hospital, Boston, Massachusetts 02114). *Ann Intern Med* 89: 329–335, Sept 1978

A series of 45 consecutive patients with suspected aortic stenosis underwent both cardiac catheterization and echocardiographic evaluation to determine if the echocardiographic method would detect significant aortic stenosis in some or all of these patients. It was found that the echocardiogram accurately predicted the severity of the stenosis in patients with normal left ventricular function, but that it was not satisfactory for patients with congestive heart failure, previous valve surgery or those with presumed or proven subaortic stenosis. These conclusions suggest that the echocardiogram may be a useful screening technique for the early evaluation of patients with possible aortic stenosis, but indicates that cardiac catheterization is still necessary most of the time to quantitatively evaluate gradients across the aortic valve.

David C. Dale
Department of Medicine
University of Washington

Isolated drainage of the superior vena cava into the left atrium in a 52-year-old man. A rare congenital malformation in the adult presenting with cyanosis, polycythemia, and an unsuccessful lung scan. Ezekowitz MD, Alderson PO, Bulkley BH, Dwyer PN, Watkins L, Lappe DL, Greene HL, Becker LC (Department of Medicine, University of Oklahoma Health Science Center, Cardiology Section P. O. Box 26901, Oklahoma City, Oklahoma 73190). *Circulation* 58:751–756, Oct 1978 (by permission American Heart Association)

This report describes a 52-year-old black male with the isolated finding of an anomalous superior vena cava draining into the left atrium. The patient presented with dizziness, mild cyanosis, polycythemia and normal cardiac and pulmonary findings. The first major diagnostic clue in this confusing clinical presentation was an unsuccessful lung perfusion scan in which intravenous tracer consistently bypassed the lungs. This appears to be the first adult presenting with this rare anomaly. This condition should be suspected if cyanosis, clubbing, and a "normal" cardiac examination coexist and if the more common pulmonary and hematological causes of this triad have been excluded.

Author Abstract

Primate mesenteric blood flow: effects of vasopressin and its route of delivery. Freedman AR, et al. (K. G. Swan, Department of Surgery, CMDNJ-New Jersey Medical School, 100 Bergen Street, G510, Newark, New Jersey 07103). *Gastroenterology* 74: 875–878, May 1978

Vasopressin was injected in seven monkeys as a bolus, or by infusion intravenously and intraarterially, to assess the influence of the route and method of administration on hemodynamics in the superior mesenteric artery and on mean arterial pressure and portal venous pressure. Dose dependent decreases in superior mesenteric arterial flow were observed during both intraarterial and intravenous injections of vasopressin. No statistically significant differences in blood flow and/or in pressure were observed between the two routes of administration decreases. Based on their observations, the authors conclude that intravenously administered vasopressin would be as effective as intraarterially administered vasopressin in reducing mesenteric blood flow and consequently reducing portal venous pressure. The authors include three figures which demonstrate the results of their experiments.

Charles A. Rohrmann, Jr.

Changes in left ventricular segmental wall motion following randomization to medicine or surgery in patients with unstable angina. Priest MF, Curry GC, Smith LR, Rogers WJ, Mantle JA, Rackley CE, Kouchoukos NT, Russell RO Jr (R. O. Russell, Jr., Division of Cardiology, Department of Medicine, University of Alabama, University Station, Birmingham, Alabama 35294). *Circulation* 58:162–168, Sept 1978 (by permission American Heart Association)

Twenty-six patients with unstable angina pectoris had biplane left ventricular angiograms and coronary arteriograms initially and at a median of 1 year following randomization to medical or surgical therapy. Left ventricular segmental wall motion was more frequently improved in surgical patients than in medical patients. In surgical patients, there was a significant correlation between changes in left ventricular segmental wall motion and perfusion to left ventricular segments supplied by the left anterior descending coronary artery.

Abbreviated Author Abstract

Anomalous aortic origin of coronary arteries. Kimbiris D, Iskandrian AS, Segal BL, Bemis CE (Likoff Cardiovascular Institute, Hahnemann Medical College and Hospital, 230 North Broad Street, Philadelphia, Pennsylvania 19102). *Circulation* 58:606–614, Oct 1978 (by permission American Heart Association)

Among 7,000 patients who underwent diagnostic coronary arteriography at Hahnemann Medical College and Hospital, we found 45 patients (0.64%) with anomalous aortic origin of one or more coronary arteries. The patients were classified into the following groups: (1) anomalous origin of the circumflex coronary artery (26 patients, 57.8%); (2) both coronary arteries arising from the left sinus of Valsalva (12 patients, 26.7%); (3) both coronary arteries arising from the right sinus of Valsalva (four patients, 8.9%); (4) anomalous origin of the left anterior descending coronary artery from the right sinus of Valsalva (two patients); and (5) anomalous origin of the first septal perforator from the right sinus of Valsalva (three patients). In certain patients with anomalous origin of the left main coronary artery from the right sinus of Valsalva, myocardial perfusion is probably impaired and may be associated with serious cardiac events whether the initial course of the left main coronary artery is

posterior to the aorta, between the aorta and the pulmonary artery, and/or anterior to the pulmonary artery. Sudden death occurs in young individuals with anomalous origin of the left main coronary artery.

Abbreviated Author Abstract

Comparison of single-dose and double-dose thallium-201 myocardial perfusion scintigraphy for the detection of coronary artery disease and prior myocardial infarction. Blood DK, McCarthy DM, Sciacca RR, Cannon PJ (P. J. Cannon, Department of Medicine, College of Physicians and Surgeons, Columbia University, 630 West 168th Street, New York, New York 10032). *Circulation* 58:777–787, Nov 1978 (by permission American Heart Association)

Thallium-201 myocardial perfusion scintigraphy was performed after exercise, 4 hours after exercise (redistribution) and after a separate rest injection in 87 patients undergoing coronary arteriography. Significant coronary lesions were present in 62 of the patients.

Interpretation of the rest and redistribution scintiscans was the same in 69 patients, 45 of whom had coronary artery disease (CAD). In 16 of the 17 patients with CAD and differing interpretations, defects were present on redistribution scintiscans but not on rest scintiscans; 11 of these patients had evidence of prior transmural myocardial infarction and the other five had an occluded coronary artery supplying the region of the defect.

Redistribution scintiscans were more sensitive than rest scintiscans for the detection of prior myocardial infarction (93% vs 54%; $P < 0.01$). The increased sensitivity was confined to the detection of prior inferior myocardial infarctions. In 36 of 38 patients with persistent perfusion defects on 4-hour redistribution scintiscans, either a prior infarction or an occluded coronary vessel was present.

Exercise scintiscans were compared with rest scintiscans or with redistribution scintiscans for the detection of CAD. The sensitivity was not significantly different with either technique (90% and 89%, respectively), but both scintigraphic techniques were more sensitive than exercise electrocardiography (66%, $P < 0.01$).

These data demonstrate that redistribution thallium-201 scintiscans may be substituted for conventional rest scintiscans, resulting in reduced cost and radiation exposure to the patient.

Author Abstract

Gastrointestinal

Celiac axis compression syndrome; a critical review. Brandt L, Boley S (Montefiore Hospital, 111 East 210 Street, Bronx, New York 10467). *Dig Dis Sci* 23:633, July 1978

The authors critically review the available clinical and experimental data to determine whether the celiac axis compression syndrome exists as a cause of abdominal pain, and if so, whether the pain is a result of gastrointestinal ischemia. Historical, anatomic, and clinical information from the literature is reviewed. Angiographic information and its significance is evaluated. The authors summarize by agreeing that there are a small number of patients with abdominal pain whose symptoms are relieved by some aspect of the operations performed for celiac axis compression. They do not view the entity as well defined and have found the pathophysiologic basis for the celiac axis compression syndrome poorly understood. They do not support the concept that ischemia plays a pathogenetic role in the syndrome, and propose that the pain is most likely neurogenic in origin, resulting from pressure in the celiac axis. They advocate detailed preoperative and postoperative angiographic, hemodynamic, and metabolic evaluations to provide the ultimate answers to the questions surrounding the celiac axis compression syndrome.

Charles A. Rohrmann, Jr.

The normal cholangiogram. Lasser RB, Silvis SE, Vennes JA (S. E. Silvis, VA Hospital, 54th Street and 48th Avenue South, Minneapolis, Minnesota 55417). *Dig Dis Sci* 23:586, July 1978

Utilizing endoscopic retrograde cholangiography, two groups of patients were studied to determine the normal measurements of the extrahepatic biliary system. The endoscope in place in the duodenum was utilized as a known measure for magnification correction. Forty-nine patients without known history of biliary tract or liver disease and no history of biliary tract surgery were studied. In addition, 25 patients with known liver disease and abnormal liver function tests were evaluated.

Three basic measurements were obtained: (1) the common hepatic duct; (2) the prepancreatic portion of the common bile duct; and (3) the intrapancreatic portion of the common bile duct. The mean maximal duct width found for the normal patients were intrapancreatic common bile duct, 4.3 mm (range 2.3–6.9 mm); prepancreatic common bile duct, 4.9 mm (range 2.3–8.5 mm); common hepatic duct, 4.6 mm (range 2.1–9.2 mm). Patients with liver disease showed no significant difference in the diameter of the intrapancreatic and prepancreatic common bile ducts. The common hepatic duct with a mean diameter of 5.4 mm, was significantly larger than the common hepatic duct in patients without liver disease (4.6 mm).

To determine whether age had any influence on the extrahepatic biliary system, data was separated into three age groups. In the first group (18–39 years old), there were 11 patients. The second group (40–59 years old) consisted of 24 patients. In the last group (over 60 years old), there were 14 patients. There was no significant difference in the diameter of the intrahepatic portion of the common bile duct among these groups. For the prepancreatic common bile duct and for the common hepatic duct, an increase with age was noted to be significant.

This study implies that the mean maximum diameters of the main extrahepatic bile ducts are slightly smaller than what had previously been reported in the literature but agrees with the maximum normal diameter of 8 mm for the extrahepatic biliary system. The finding of increased ductal diameter with age also agrees with prior autopsy information. It differs, however, with a prior study of operative cholangiography.

Charles A. Rohrmann, Jr.

Yeast overgrowth in operated stomachs. Strom BG, Beaudry R, Morin F (Centre Hospitalier Universitaire, Sherbrooke, Quebec, Canada). *J Can Assoc Radiol* 29:161–164, Sept 1978

The authors describe their experience with 17 cases of yeast overgrowth in the stomach of patients who have undergone gastric surgery. These patients had either Bilroth I or Bilroth II surgical procedures for duodenal ulcer disease and generally presented several months later with complaints of vague epigastric pain, a feeling of fullness in the epigastrium, and vomiting; the vomitus often being a thick white fluid.

The fungus overgrowth is generally *C. albicans*, but *T. glabrata*, *C. pseudotrop*, and *C. catenulata* have also been isolated in a few patients. These bezoars are generally more friable than the more common phytobezoar and may mimic retained food particles. Radiographically they present as large floating bezoars, multiple small filling defects or both in an otherwise normal postoperative stomach.

Jack M. A. Tishler

Prolonged gallbladder opacification after oral cholecystography. Koehler RE, Stanley RJ, DiCroce J (Mallinckrodt Institute of Radiology, Washington University School of Medicine, St. Louis, Missouri). *Radiology* 128:601–603, Sept 1978

A total of 122 patients undergoing oral cholecystography were randomly selected. Oral cholecystography was performed by giving 3 g of iocetamic acid (Cholebrine) 3 hr after a light, low fat meal. Radiographs were obtained 10–14 hr following administration of contrast. Insufficient opacification in 13 patients was followed by a second dose of 3 g of iocetamic acid

and repeated filming the following day. A 25.4 × 30.5 cm radiograph was made the day of examination, 24 hr following examination, and 48 hr later. Radiographs were obtained at 75 kVp with phototiming (or as near to 75 kVp as possible). Each patient was interviewed at 24 hr or 48 hr for dietary history.

Persistant opacification 24 hr following oral cholecystogram was noted in 75% of the patients studied with opacification persistent at 48 hr in 27%. Percentages were similar in patients with cholecystitis with calculi, acalculous cholecystitis, and normals.

Two factors are proposed as being a partial explanation for prolonged opacification. The first is low oral intake of fatty foods with prolonged opacification due to stasis. In addition, it has been shown that conjugated iopanoic acid is excreted into the bile and is reabsorbed by going into hepatic portal recirculation. The authors propose that this same mechanism may occur with iocetamic acid.

This prospective study with a randomly selected patient population disagrees with studies of Adams and Foxley which contend that prolonged gallbladder opacification may indicate acalculous cholecystitis.

Asher Nov

The inflammatory esophagogastric polyp and fold. Bleshman MH, Banner MP, Johnson RC, DeFord JW (Wilford Hall USAF Medical Center, Lackland Air Force Base, Texas 78236). *Radiology* 128:589–593, Sept 1978

The radiographic findings in nine patients with a clinical history of gastroesophageal reflux or esophagitis are correlated with endoscopy and pathology. Findings of chronic reflux esophagitis include abnormal motility, incomplete distensibility, and lack of good coating of the mucosal wall by barium. Long standing esophagitis will show deformity alteration and scarring. Areas of focal narrowing may represent either stricture or spasm. The authors described a finding of a single thickened gastric mucosal fold coursing toward the esophageal gastric junction with polypoid filling defect at the proximal end. Both the fold and polypoid defect could not be effaced and did not show any change during contraction. This finding was best seen in the prone oblique position. Endoscopic findings correlated with the radiographic findings. Insufflation of the esophagus could not efface either the fold or polypoid lesion. Brush cytology and biopsies showed squamous and/or gastric epithelium with inflammatory changes. The findings were at or just under the squamocolumnar junction. All cytologic specimens were interpreted as benign. Sentinal fold was previously described as an endoscopic finding of early esophagitis. A pseudotumor at the esophagogastric junction caused by gastric mucosal prolapse aids in the differential diagnosis. This entity is seen to change and can be effaced as opposed to inflammatory changes of esophagitis. The authors conclude that the thickened gastric fold and inflammatory polyp are findings of early esophagitis with the polypoid defect representing thickening at the proximal end of the sentinal fold.

Asher Nov

Frequency of intrahepatic arteriovenous fistula as a sequela to percutaneous needle puncture of the liver. Okuda K et al. (Chiba University Hospital, Chiba (208), Japan) *Gastroenterology* 74:1204–1207, June 1978

Hepatic arteriograms obtained 1 month following needle biopsy of the liver, percutaneous transhepatic cholangiography, or transhepatic catheterization of an intrahepatic bile duct or portal vein, were analyzed to determine the presence of arterial abnormalities, especially fistulae between the arterial and portal systems.

Of 93 patients having percutaneous liver biopsy utilizing either a Silverman needle (2 mm in caliber), or the Menghini needle (1.9 mm in diameter), 5.4% demonstrated intrahepatic arteriovenous fistulae when studied by hepatic arteriography within 1 month following the biopsy. Of 79 patients having percutaneous transhepatic cholangiography utilizing the Chiba needle with a 0.7 mm. diameter, 3.8% demonstrated arteriovenous shunting. Of 26 patients having percutaneous transhepatic catheterization of either biliary or portal venous systems utilizing a polyethylene catheter 1.3 mm in diameter, 26.2% demonstrated arteriovenous fistulae when studied by hepatic arteriography within 1 month of the procedure. Clinical followup was limited to five patients being seen 6 months to 3 years after arteriography. There was no sign of increased spleen size or development of esophageal varices. Angiography was repeated in only one patient with no evidence of fistula but with an advancing hepatocellular carcinoma.

Charles A. Rohrmann, Jr.

Clofibrate therapy and gallstone induction. Bateson MC, et al. (Department of Medicine, Ninewells Hospital and Medical School, Dundee, DDI 9S Y, Scotland). *Dig Dis Sci* 23:623, July 1978

Two hundred consecutive patients referred to a clinic for the management of serum lipid disorders were studied to determine the presence of gallstones. It was found that of these patients, those undergoing clofibrate therapy for hyperlipidemia had a fourfold increase in the presence of gallstones. The overall mean duration of treatment was 3.6 years but no relationship to duration of therapy was established. The tendency for gallstones to appear was found to be greater in women than men.

Charles A. Rohrmann, Jr.

Genetics of gastrointestinal polyposis. Bussey HJR, et al. (Pathology Department, St. Mark's Hospital, City Road, London ECIV 2PS, England). *Gastroenterology* 74:1325, June 1978

This is a review of the types of gastrointestinal polyposis in which genetic factors play a part such as the hamartomatous lesions: Peutz-Jeghers syndrome, juvenile polyposis, and the neoplastic type: familial polyposis coli, and multiple adenomas. These conditions are discussed in their mode of inheritance, associated lesions, malignant potential, and possible interrelationships between the other various types of polyposis syndromes. Their clinical presentations as well as the use of the knowledge of their familial incidence with application to genetic counseling and treatment is described.

Charles A. Rohrmann, Jr.

Clinical conference: intestinal pseudoobstruction. Anuras S, et al. (Internal Medicine, University of Iowa College of Medicine, Iowa City, Iowa 52242). *Gastroenterology* 74:1318, June 1978

This clinical conference presents the case of a 59-year-old woman with a long history of abdominal complaints suggesting intestinal obstruction. The conference participants present an approach to patients with intestinal pseudoobstruction including the radiologic studies of esophagography, upper gastrointestinal series, small bowel follow through, and barium enema. It is emphasized that complete diagnostic evaluation of this type of patient is indicated since the signs of pseudoobstruction may predate the clinical manifestation of the underlying disease in nonidiopathic cases of pseudoobstruction such as scleroderma, myxedema, myotonic dystrophy, pheochromocytoma, diabetes, or porphyria.

The pathophysiologic basis of idiopathic intestinal pseudoobstruction is incompletely defined but factors of etiologic importance include abnormalities in the intestinal smooth muscle itself, in the nervous system, or disturbances of secretion or action of gastrointestinal hormones. The syndrome is summarized as being heterogeneous, with extremely variable symptoms, and a pathophysiology that is diverse and as yet imprecisely defined. The treatment is correspondingly empirical.

Charles A. Rohrmann, Jr.

Colonic varices (a complication of pancreatitis with splenic vein thrombosis). Burbige EJ, et al. (Veterans Administration

Hospital, 150 Muir Road, Martinez, California 94553). *Dig Dis Sci* 23:752, Aug 1978

This is a case report of a 50-year-old male who was hospitalized with recurrent gastrointestinal bleeding. He had a history of prior pancreatitis. The barium enema demonstrated a filling defect in the proximal descending colon. This was followed by colonoscopic observation of large varices in the distal transverse and proximal descending colon. An angiogram was performed which revealed complete occlusion of the splenic vein with markedly enlarged venous collaterals. Following splenectomy, colonoscopy showed regression of the varices. This is a unique report, colonic varices not having been previously described as a complication of splenic vein thrombosis. This case emphasizes the need for combined radiographic and endoscopic approach to patients with gastrointestinal bleeding.

Charles A. Rohrmann, Jr.

Cholangiographic abnormalities in ulcerative colitis associated pericholangitis which resemble sclerosing cholangitis. Blackstone MO, Nemchausky BA (Department of Medicine, University of Chicago, Chicago, Illinois 60637). *Dig Dis Sci* 23: 579, July 1978

Endoscopic retrograde cholangiography was done in eight asymptomatic patients who had long standing ulcerative colitis. In seven of these patients, endoscopic retrograde cholangiography demonstrated abnormalities which resemble those previously attributed to sclerosing cholangitis. The findings are those of intrahepatic ductal beading and strictures. In two of the eight, the common bile duct was similarly involved. In one patient, a histologic progression to cirrhosis from a histologic appearance 2½ years previously of pericholangitis was documented. It is concluded therefore that patients with ulcerative colitis who present with the clinical picture of pericholangitis may have biliary abnormalities which radiographically resemble those described in what is known as sclerosing cholangitis.

Charles A. Rohrmann, Jr.

Genitourinary

Pneumopericystography in the diagnosis of infiltrating carcinoma of the bladder (in German). Frank T, Hintze A (Albers-Schönberg-Institut am Allgemeinen Krankenhaus St. Georg, Hamburg, Lohmuehlenstr. 5, 2 Hamburg 1, Germany). *ROEFO* 129:202–204, 1978

Pneumopericystography, as employed by the authors, consists of suprapubic injection of 400–800 ml of air into the perivesical tissue and the intravesical instillation of 50–250 ml of air via an indwelling bladder catheter, followed by rapidly obtained tomographic sections with the patient supine and prone. To define the extent of the infiltrating growth of known bladder carcinomas, this procedure was performed in 35 patients. The radiologic findings could be correlated with findings at autopsy (2), cystoscopy (16), partial bladder resection (6), and cystectomy (2). In 25 of these 27 patients with correlation, there was agreement between the pneumopericystographic and clinical-pathological findings.

Peter F. Winter

Renal abscess in children. Moenne-Loccoz JP, Bomsel F, Gatti JM, Prot D (Service de Radiologie, Hopital de Montmorency, Montmorency and Service de Radiologie, Hopital Bretonneau, Paris, France). *Pediatr Radiol* 7:150–154 Sept 1978

Four children, 18 months to 15 years of age, presented with clinical evidence of infection, back or abdominal pain, elevated white blood count and sedimentation rate. Excretory urograms showed increased volume of the lower pole and displacement and blurring of the calyces. A clear rim delineated the affected pole and appears specific for abscess. The authors feel that angiography is unnecessary in this clinical setting. The patients recovered rapidly on antibiotics and the excretory urograms returned to normal.

B. J. Wood

The effect of iodine containing contrast media on the renal function in patients with multiple myeloma. A retrospective study (in German). Baltzer G, Jacob H, Esselborn H, Gassel WD (Medizinische Universitätsklinik der Universität Marburg/Lahn, Marnkopfstr. 1, D-3550 Marburg/Lahn, Germany). *ROEFO* 129: 208–211, 1978

In a retrospective study, the records were reviewed of 89 patients with multiple myeloma from 1959 to 1974. Thirty-one patients underwent an intravenous pyelogram and in none of these patients was a reduction of renal function observed. The authors conclude that a known multiple myeloma alone is not a contraindication for the application of iodine containing contrast material as long as dehydration of the patient can be avoided.

Peter F. Winter

Musculoskeletal

The Jones fracture revisited. Kavanaugh JH, Brower TD, Mann RV (Division of Orthopedic Surgery, University of Kentucky Medical School, Lexington, Kentucky 40506). *J Bone Joint Surg [Am]* 60:776–782, Sept 1978

An intriguing new dimension to the normally mundane topic of 5th metatarsal fractures is added by this excellent article. The Jones fracture is a fracture of the proximal portion of the 5th metatarsal which differs very significantly from the typical fracture of the most proximal portion of the 5th metatarsal. The Jones fracture is normally seen 3 cm from the proximal end of the 5th metatarsal and represents an unusual stress fracture. Occasionally only a small lucent line or small defect is noted at this site on the original films but if this fracture exists, it tends to widen upon weight bearing.

This injury can be far more disabling than might be expected, in fact, this injury can simply disable an active athlete for a prolonged period. The authors stress that although these fractures can be treated conservatively with lack of weight bearing and a plaster cast, if this injury is noted in an active athlete they recommendation immediate screw fixation. They believe that the procedure is safe and simple and will allow early mobilization. Lack of prompt fixation of this injury in an active athlete may impair future athletic development and may cause disabling for an entire season from pain. For the nonathlete or the recreational athlete nonoperative treatment is advised.

Gerald R. Smith

Arthroscopy of the knee. McGinty JB, Matza RA (Newton-Wellesley Orthopedic Associates, Inc., 2000 Washington Street, Newton Lower Falls, Massachusetts 02162). *J Bone Joint Surg [Am]* 60:787–789, Sept 1978

For the radiologist who is inundated with knee arthrograms, this article represents an excellent discussion. In nearly 300 arthroscopic knee examinations performed under local anesthesia alone, no complications were encountered. In a similar series of nearly 300 knees examined under general or spinal anesthesia, numerous complications occurred including a pulmonary embolus. As the acceptability of outpatient arthroscopy improves and the experience of the orthopedic specialist widens, this procedure may ultimately play a much greater role in the primary evaluation of the menisci and ligaments and cause a decreasing number of requests for the admittedly cumbersome and occasionally confusing arthrogram.

Gerald R. Smith

Results of reduction and stabilization of the severely fractured thoracic and lumbar spine. Dickson JH, Harrington PR, Erwin

WD (6535 Fannin, Houston, Texas 77030). *J Bone Joint Surg [Am]* 60:799–805, Sept 1978

The role of instrumentation of the severely injured thoracic and lumbar spine versus conservative management of the same injury has been controversial and often a subject of heated discussions even by members of the same speciality. This article is directed towards that conflict. A series of 95 patients with fracture-dislocations of the spine were treated with Harrington instrumentation and fusion relatively soon after injury. The results of this treatment are reviewed.

The authors found no greater return of neural function in the patients treated with instrumentation than for patients treated with postural reduction and bed rest. The authors believe, however, that immediate operative stabilization of the spine in their patients shortened the total hospital stay and allowed quicker mobilization of the patients, thereby avoiding complications associated with prolonged recumbency and bed rest. These benefits must be weighed against the 25% complication rate associated with the operations.

Gerald R. Smith

Parosteal (juxtacortical) osteogenic sarcoma. A roentgenological study of 30 patients. Smith J, Ahuja SC, Huvos AG, Bullough PG (Memorial Sloan-Ketterling Cancer Center, 1275 York Avenue, New York, New York 10021.) *J Can Assoc Radiol* 29:167–174, Sept 1978

The authors present a rather detailed analysis of the radiographic findings in 30 documented cases of parosteal osteogenic sarcoma seen at their institution from 1934 to 1975. Patients ranged in age from 12 to 45 years, with a peak incidence in the third decade. Sex distribution was approximately equal. The most common presenting symptom was a dull aching pain or a mass. More than half the cases involved the lower half of the femur, (17) the next most common site was the proximal humerus (five). Most lesions were relatively large when first seen (3–25 cm in diameter) and tended to present as bulky oval or spherical masses with a sessile base. Once the lesion encircled the whole bone shaft, it often resembled a smooth collar. The lesions tended to be densely ossified but most contained lucent areas. The margins of the tumor were most often irregular, with linear extensions into adjacent soft tissue seen in two-thirds of the cases reviewed. The lesions were denser at the base than at the periphery. The supposedly characteristic periosteal lucency (cleavage plane) was found in only 30% of patients and cortical and medullary destruction was uncommon, except in long standing cases.

Periosteal elevation prior to biopsy was extremely uncommon. Four patients had femoral angiograms which demonstrated vessels that were displaced by tumor but no abnormal vessels or tumor encasement. No correlation could be made between radiographic findings and histologic grade.

Jack M. A. Tishler

Post-injection calcification of the deltoid muscle. Keats TE (University of Virginia School of Medicine, Charlottesville, Virginia 22901). *J Can Assoc Radiol* 29:165–166, Sept 1978

The author describes a discrete solitary calcification in the deltoid muscle, secondary to previous intramuscular injection of a variety of agents. These calcifications are generally on the left, as this is the preferred site for injections in most patients. Unlike tendinous and bursal calcifications, the postinjection calcifications bear a constant relationship to the humerus with movement of the shoulder, indicating that they lie within the deltoid muscle; they also may lie more laterally from humerus.

Jack M. A. Tishler

Further pitfalls in knee arthrography. Hall FM (Beth Israel Hospital and Harvard Medical School, 330 Brookline Avenue, Boston, Massachusetts 02215). *J Can Assoc Radiol* 29:179–184, Sept 1978

This is a follow-up paper to the one which appeared in 1976 in *Radiology* (118:55–62) entitled "Pitfalls in Knee Arthrography". The author describes some additional problems and pitfalls in interpretation encountered based on his experience with 550 knee arthrograms. He states that on occasion, peripheral separations of the posterior medical meniscus demonstrated at arthrography may not be apparent at arthroscopy. In several patients the abnormality was not even apparent at arthrotomy or even on examination of the resected specimen. The author therefore urges that the decision to undergo meniscectomy in this category of patient should be based primarily on clinical disability.

Arthrographic recognition of an oblique bucket-handle meniscal tear may be difficult when the visualized outer fragment maintains a triangular appearance. The tunnel projection may be helpful in these cases. The author also states that normal synovial folds may mimic the anterior cruciate ligament and that there is an increased incidence of chondromalacia in symptomatic postmeniscectomy knees.

Jack M. A. Tishler

Lipohemarthrosis of the elbow joint. Yousefzadeah DK, Jackson JH Jr (University of Iowa Hospitals, Iowa City, Iowa). *Radiology* 128:643–645, Sept 1978

Radiographic demonstration of three cases of lipohemarthrosis of the elbow is discussed. Lipohemarthrosis is superior to posterior fat pad as a more specific sign of elbow trauma because posterior fat pad merely indicates increased intraarticular pressure while lipohemarthrosis is due only to intracapsular fracture or cartilage and/or ligament injury. Little fat accumulated in the anterior compartment of the joint can be demonstrated by horizontal-beam technique and lipohemarthrosis may conceivably be observed before posterior fat pad is displaced dorsally. With horizontal-beam technique, the patient is more comfortable and it seems unnecessary to irradiate the other elbow.

Author Abstract

Nervous System

Ventricular opacification after intravascular injections of contrast material. Lee BCP, Zimmer J (New York Hospital-Cornell Medical Center, New York, New York). *Radiology* 128:647–649, Sept 1978

Two cases are reported in which the ventricles of neonates were demonstrated on CT and radiographs following intraarterial injection of contrast material. Contrast material reaches the cerebrospinal fluid through: (1) choroid plexuses; (2) pia-arachnoid arterioles and venules; (3) through the brain parenchyma. The tight junctions of cerebral vessels open to excessive intravascular osmolality. The second factor in passage through the blood-brain barrier is the lipid solubility of the contrast material. The authors conclude that visualization of cerebral ventricles in neonates following intraarterial injection of contrast material may occur in the normal state. Contrast material in the ventricles following intravenous injection was believed to indicate damage to the blood-brain barrier. Such damage is caused by severe and prolonged anoxia as indicated by the fact that cerebral vessels are more resistant to anoxia than neuronal tissues.

Asher Nov

Computer assisted tomography in primary malignant lymphomas of the brain. Kazner E, Wilske J, Steinhoff H, Stochdorph O (Ludwig-Maximilians-Universitat Munchen, Marchioninistrasse 15,8000 Munchen 70, Federal Republic of Germany). *J Computer Assisted Tomography* 2:125–134, April 1978

The authors report their CT experience in 10 patients with primary malignant lymphomas of brain of the non-Hodgkin's type. The patients, six females and four males, ranged in age from 39 to 69 years. The CT scanning was performed on EMI

Mark I scanner with a 160 × 160 matrix and a bolus of 60% contrast (1 ml/kg) was used for enhancement. In most instances the CT appearance was that of either single or multiple nodules of increased density on plain scan (mean 18.9 EMI units) with an area of surrounding edema. In the nine cases in which contrast enhancement was employed all the lesions enhanced (mean of 26.7 EMI units). In one instance, the tumor was localized as a single decreased attenuation focus in the right basal ganglia. No contrast was given. Depending on location and number of these nodules, they were interpreted as being infarction, multiple metastases, meningioma, pituitary adenoma, butterfly glioma, multifocal glioblastoma. Medulloblastomas and melanomas were also considered in the differential diagnosis. In their experience, the difficult differential was between malignant lymphomas and meningiomas. They found that blurred margins of the tumor nodules were an important clue to the diagnosis of malignant lymphoma and were seen in four cases.

Paul M. Chikos

Computed tomography in primary malignant lymphoma of the brain. Tadmor R, Davis KR, Roberson GH, Kleinman GM (Massachusetts General Hospital, Boston, Massachusetts 02114). *J Computer Assisted Tomography* 2:135–140, April 1978

The authors report four cases of primary lymphoma of brain which occured in the course of 14,000 CT scans (0.3%). All four cases were men ranging in age from 43 to 55. These cases presented with a rapidly progressive clinical course suggesting a malignant brain tumor. In two cases, the area of lymphomatous involvement had abnormally low attenuation values and contrast enhancement occurred in one. In the other two cases, there was a focus of heterogeneous high attenuation which contrast enhanced surrounded by an area of low attenuation. In two cases, the tumor spread across midline through the corpus callosum. In two of three cases, the radionuclide brain scan showed areas of increased activity which correlated with the CT scan. Angiography was performed in two and showed in one, an avascular mass; and in the other abnormal medullary veins in the area of lymphomatous involvement without mass effect. The authors include in the differential diagnosis gliomas and progressive multifocal leukoencephalopathy.

Primary malignant lymphomas of brain are characterized histologically by perivascular and parenchymal infiltrates of pleomorphic round cells. The cell of origin is currently felt to be a lymphocyte. Primary lymphoma of brain, while rare (0.2%–2% incidence), is more frequent than metastatic lymphomatous brain involvement. If untreated these patients typically have a progressive rapidly fatal course with death occurring within a few months after onset of symptoms. These tumors are radiosensitive and prolonged survival times have been achieved with early radiotherapy.

Paul M. Chikos

Computed tomography in the diagnosis of spinal cord astrocytoma. Handel S, Grossman R, Sarwar M (University of Texas Medical School at Houston, 1203 Ross Sterling, Houston, Texas 77030). *J Computer Assisted Tomography* 2:226–228, April 1978

The authors report a case of a 55-year-old woman who developed right upper arm weakness with myelographic evidence of severe cervical spondylosis who responded to upper cervical laminectomy. Six months later, the patient noted decreasing strength in the right hand, and paresthesias in the right shoulder. Pantopaque and gas myelography defined enlargement of the midcervical spinal cord. The differential diagnosis was between intramedullary tumor and syringomyelia. The patient was scanned on an Ohio Nuclear Delta 50 scanner with a scan time of 2½ min before and after the bolus injection of 150 ml of Renografin 60. On the precontrast CT scan, the spinal cord could not be seen as a distinctive structure. However, after contrast an enhancing nodule occupying much of the right side of the spinal canal was seen in the midcervical region with a mean attenuation value after contrast enhancement of 93 Hounsfield units. At surgery an astrocytoma of the cervical cord was found.

Paul M. Chikos

Subependymal and leptomeningeal spread of systemic malignant lymphoma demonstrated by cranial computed tomography. Dubois PH, Martinez AJ, Myerowitz RL, Rosenbaum AE (Presbyterian-University Hospital, University of Pittsburgh School of Medicine, Pittsburgh, Pennsylvania 15261). *J Computer Assisted Tomography* 2:218–221, April 1978

The authors report a 73-year-old female who presented with a 2 week history of lethargy and diplopia. Two years previously she was treated for systemic histiocytic lymphoma with multiple drug chemotherapy and irradiation to the spine. Computed tomography showed slight increased attenuation in the periventricular regions with a subtle adjacent area of decreased attenuation. Following contrast administration, there was marked enhancement throughout the ventricular system including the subependymal area and choroid plexus, surface of the brain, sylvian fissures, and basilar cisterns. At autopsy a yellow-gray membrane resembling a purulent exudate covered the external surface of the brain. On sectioning, soft gray white gelatinous friable material lined the ventricular system, invaded the adjacent subependymal tissues, and encompassed the choroid plexus. On microscopy the entire leptomeninges were infiltrated by a poorly differentiated neoplasm with abnormal histocytes. Sub-ependymal spread was noted with involvement of the entire choroid plexus. Similar CT appearances have been described with bacterial meningitis, meningoencephalitis, and meningeal seeding of metastatic medulloblastoma and ependymoma. Increased attenuation with contrast enhancement has also been described in the basal cisterns and sylvian fissures with coccidioidal and tuberculous meningitis.

Paul M. Chikos

Computed tomography with use of metrizamide. Arii H, Takahashi M, Tamakawa Y, Odani R, Nakano Y, Suzuki M, Shindo M, Okazaki M, Ohkubo K (Akita University School of Medicine, Akita, Japan). *Nippon Igaku Hoshasen Gakkai Zasshi* 38:528–538, 1978

Computed tomography was performed after intrathecal injection of metrizamide in a group of patients with normal pressure hydrocephalus, pituitary tumor, cerebellopontine angle tumor, clivus tumor, and other conditions occurring near the base of the skull. About 10 ml of isotonic metrizamide was injected via lumbar route. Computed tomography was performed after 2–6 hr in cases with tumors and after 2, 6 and 24 hr for evaluation of normal pressure hydrocephalus. In tumor cases, extension to the cisterns was well demonstrated. In nine cases, radionuclide cisternograms were obtained and compared with metrizamide CT and correlated closely.

Author Abstract

Computed tomography of acoustic neurinoma. Robbins B, Marshal WH Jr (Stanford University School of Medicine, Stanford, California). *Radiology* 128:367–370, Aug 1978

The authors present a retrospective study in which CT scans of 37 patients were analyzed with a clinical question of acoustic neurinoma. A 160 × 160 matrix was used, scans were performed with a 25° inclined to Reid's baseline. Slice thickness was 10 mm with 5 mm between slices. Scans were performed both pre- and postinfusion of contrast material. Analysis was done at both the usual window width and level as well as at a bone level of 400 and 300–450. In the 37 patients analyzed, 39 acoustic neurinomas were present. Six tumors (15%) were detected prior to infusion of contrast material, four of these were of increased density and two were of decreased density. Of the 39 tumors, 23 were seen only following contrast infusion. Ten tumor masses (26%) were not identified either pre- or postcontrast infusion.

The authors analyzed ventricular position, subarachnoid and cisternal anatomy, as well as any bony or soft tissue abnormali-

ties. They reaffirm previous reports stressing the importance of overlapping cuts and motion-free scanning. Of interest is their analysis of the bony component which has not been previously stressed. Using a window width of 400 and level of 300–450, 21 of the 39 (54%) internal auditory canals showed widening or erosion. In improving diagnostic accuracy, the authors identified 17 (43%) additional abnormalities when a bone window was used. In the 10 tumors which did not show enhancement following intravenous injection, four were seen to have bone erosion or flaring and were the only CT finding suggestive of neurinoma. The authors reconfirm that tumors approximately 2 cm in diameter are the usual threshold for detection. Their series confirms a 15%–20% false negative rate.

Asher Nov

An angiographic study of the temporal horn. Salamon G, Lecaque GL, Strother CM (Hôpital de la Timone, Marseille, France). *Radiology* 128:387–392, Aug 1978

The anatomy of the posterior cerebral artery and its branches is described. Evaluation of the temporal horn, inferior and posterior temporal masses, and thalamic masses as they affect this artery and its branches are described. The posterior cerebral artery is divided into three sections for descriptive purposes: (1) peduncular; (2) ambient; and (3) quadrigeminal. Generally the ambient segment will give rise to the anteromedial artery which divides into calcarine, occipital, and occipitoparietal branches and to the posterolateral which divides into temporal and temporooccipital branches. Medial and lateral posterior choroidal branches arise from the cisternal segment. The lateral choroidal arteries originate as single or multiple trunks. The lateral choroid artery courses through the choroidal fissure which defines the medial aspect of the temporal horn. Temporal branches course and often will terminate within the collateral sulcus at the collateral eminence defining the inferior surface of the temporal horn. Masses arising within the temporal lobe or within the temporal horn will deviate the lateral choroidal artery medially whereas the thalamic mass will deviate the artery laterally.

The authors stress that on the vertebral angiogram the position of the temporal horn can be assessed indirectly by: (1) position of the lateral choroidal artery as it courses in the choroidal fissure; (2) temporal branches of the posterior cerebral artery as they pass and terminate within the collateral sulcus; and (3) position and course of crural and ambient segments of the posterior cerebral artery as they pass around the midbrain. The first two are of more importance due to normal anatomic variation.

Asher Nov

Angiographic diagnosis of fourth ventricle tumors. Numaguchi Y, Kishikawa T, Fukui M, Komaki S, Russel WJ, Ikeda J, Okudera T, Matsuura K, Kitamura K (Kyushu University Hospital, Fukuoka, Japan). *Radiology* 128:393–403, Aug 1978

The authors analyze angiograms of 34 patients with tumors involving the fourth ventricle. Primary neoplasms included eight ependymomas, one epidermoid, one choroid plexus papilloma, one hemangioblastoma, and one meningioma. There were 22 medulloblastomas. In the pediatric age group tumors of the fourth ventricle include ependymomas constituting 53%, astrocytomas which comprise 20%, and medulloblastomas, 14%. In overall population, medulloblastomas comprise 38%, ependymomas 25%, astrocytomas 23%. Less common tumors include epidermoid, choroid plexus papillomas, hemangioblastomas, meningiomas, teratomas, oligodendrogliomas, and myxochondrosarcomas.

Angiographic features of primary fourth ventricle tumors include: (1) lateral displacement of the posterior medullary and supratonsillar segments of the posteroinferior cerebellar artery (PICA); (2) anterior displacement of the posterior medullary segment of the PICA; (3) elongation of the supratonsillar segment of the PICA without much inferior displacement; (4) posterior displacement of the copular point and the retrotonsillar tributaries of the inferior vermian vein; (5) posterior angulation of the fissural portion of the precentral cerebellar vein; and (6) lateral displacement of the vein of the lateral recess of the fourth ventricle.

Manifestations of medulloblastomas are: (1) diffuse inferior and anteroposterior elongations of the supratonsillar segment of the PICA without lateral displacement; (2) superior displacement of the supraculminate vein and superior displacement of the anterior culminate and superior vermian branches of the superior cerebellar artery; (3) posterior displacement of the nodular branches of the PICA; (4) inferior displacement of the inferior vermian vein; (5) poor visualization of the fissural portion of the precentral cerebellar vein and the vein of the lateral recess of the fourth ventricle. Authors stress the importance of angiotomography.

Asher Nov

A randomized trial of aspirin and sulfinpyrazone in threatened stroke. The Canadian Cooperative Study Group (Barnett HJM, principal investigator, Neurological Sciences, University Hospital, London, Ontario, Canada). *N Engl J Med* 299:53–59, July 13, 1978

This report concerns a multicenter, double-blind randomized clinical trial of the use of aspirin (325 mg), sulfinpyrazone (200 mg), or placebo, taken singly or in several combinations, four times a day, to try to prevent strokes in patients with transient ischemic attacks. The study was carefully conducted to try to avoid many of the pitfalls of a multicenter study. The results clearly indicated that aspirin alone or in combination with sulfinpyrazone reduced the frequency of strokes or death in the study population. Sulfinpyrazone did not show similar benefit. The results of this study are impressive and the study will undoubtedly be a model for other investigations on the benefits of these agents in other diseases.

David C. Dale
Department of Medicine
University of Washington

Pediatric Radiology

Diskitis: a prospective diagnostic analysis. Fisher GW, Popich GA, Sullivan DE, Mayfield G, Mazat BA, Patterson PH (Tripler Army Medical Center, Honolulu, Hawaii). *Pediatrics* 62:543–547, Oct 1978

Seven children with proven disk space infection were seen over a 3-year period. Routine lumbar spine radiographs were negative for 3–8 weeks before the characteristic disk space narrowing and irregularity of the adjacent vertebral margin was seen. Tc 99m diphosphonate scans were positive within 7 days, and gallium citrate Ga 67 within 2 weeks. Back symptoms were present in only two cases. Hip or leg symptoms were the most common mode of presentation. The etiology of the disk space infection remains obscure.

B. J. Wood

Vertebral osteomyelitis in children: report of four cases. Bolivar R, Kohl S, Pickering LK (University of Texas Medical School at Houston, Houston, Texas). *Pediatrics* 62:549–553, Oct 1978

Osteomyelitis of the vertebrae is unusual in children. The authors present four cases due to *Staphylococcus aureus*. Radiographic changes were seen in all, and the agent recovered from the blood in three cases, and from bone in one patient. Back pain was not a prominent feature. Abdominal symptoms were the presenting symptoms in all cases. The lower thoracic and lumbar spine were involved.

B. J. Wood

Pulmonary and hepatic echinococcosis in children. Thumler J, Munoz A (Department of Radiology, Exequiel Gonzalez Cortes

Hospital for Children, Santiago de Chile, Chile). *Pediatr Radiol* 7:164–171, Sept 1978

Hydatid disease due to *Echinococcus granulosus* is endemic in Chile, and the authors present 57 pulmonary cases and 23 involving the liver. Hydatid cyst is the larval stage of the tapeworm, and occurs in man by ingestion of eggs from the feces of canine, or by ingestion of contaminated food or water. The embryos leave the human gastrointestinal tract and enter the portal circulation. Most are filtered out either in the liver or in the lung, and if not destroyed by phagocytes, develop into a cyst.

Pulmonary involvement is more common than hepatic and presents two types: the simple closed cyst and the ruptured cyst. In the former, a homogeneous, dense, sharply outlined mass is seen in the pulmonary parenchyma. It is usually round, but may be oval or irregular depending on its location. As it grows, it may produce a pleural reaction or local atelectasis. At fluoroscopy, it is possible to see change in shape between inspiration and expiration which aids in the differential diagnosis. The ruptured cyst shows first a crescent of lucency around the periphery due to erosion of a bronchus and dissection of air between the ectocyst and the endocyst. As dissection progresses, an air-fluid level is seen. Later the membrane collapses and floats on the remaining fluid to produce the "water lily" sign. If the membrane is expelled with coughing, an empty cavity results. With hepatic involvement there may be a local prominence of the upper or lower liver margin. Calcification around the periphery of the cyst is the most important sign.

B. J. Wood

Radiologic evaluation of the thymus in juvenile myasthenia gravis. Thurmond AS, Brasch RC (University of California Medical Center, San Francisco, California 94143). *Pediatr Radiol* 7: 136–140, Sept 1978

Myasthenia gravis, an autoimmune disease which affects the acetylcholine receptors at neuromuscular junctions occurs in three forms. The newborn form is seen in 10%–15% of infants of mothers with myasthenia gravis and is transient. The juvenile form is progressive and occurs under the age of 21 years. It is rarely associated with thymoma. The adult variety begins over 21 years of age and is associated with thymomas in 15% of cases. Thymectomy by some unknown mechanism frequently ameliorates symptoms in patients with myasthenia gravis.

Nineteen patients with juvenile myasthenia gravis were reviewed; 84% were female. Thymectomy had been performed in all by 24 years of age. Chest radiographs were considered normal in 17 patients and an anterior mediastinal mass was suggested in two. Lateral tomograms were done in 10 cases, and these were normal in eight, and suggested mass in two. Computed tomography, done in only one patient, was negative. At surgery, there were no thymomas; two showed normal histology, and 17 revealed hyperplasia and/or abnormal germinal centers. Due to the low incidence of thymomas in the juvenile variety of myasthenia gravis, the authors suggest that computed tomography and tomography of the mediastinum be reserved for cases showing abnormal plain chest films.

B. J. Wood

Urinary tract infection in high-risk newborn infants. Maherzi M, Guignard JP, Torrado A (Department of Pediatrics, Centre Hospitalier Universitaire Vaudois, Lausanne, Switzerland). *Pediatrics* 62:521–523, Oct 1978

The prevalence of neonatal urinary tract infection was studied in 1,762 high risk neonates. Symptomatic bacteriuria was found in 1.9% and asymptomatic bacteriuria in 0.5%. Male preponderance was 5:1. Clinical manifestations were extremely variable: vomiting, weight loss, and diarrhea being the prominent symptoms. Bacteremia was associated with urinary tract infection in six infants. The organisms identified in the urine obtained by suprapubic aspiration were *Escherichia coli, Klebsiella,* and *Proteus.* A mixed infection was found in four patients. Roentgenographic examination of the urinary tract showed abnormalities in 44% of the symptomatic patients. It is concluded that symptomatic high risk newborn infants should be screened for bacteriuria, and that radiologic investigations be performed in those with proven infection.

Author Abstract

Neonatal osteomyelitis. Fox L, Sprunt K (Department of Pediatrics, College of Physicians and Surgeons, Columbia University, New York, New York). *Pediatrics* 62:535–542, Oct 1978

The author has reviewed 45 cases of osteomyelitis occurring in infants within the first 10 weeks of life. The majority had clinical evidence of osteomyelitis by 2 weeks of age; 39 had some associated abnormality in the pregnancy, delivery, or in early postnatal life. Multiple sites of osteomyelitis were seen in 47%, with long bone involvement being most common. Septic arthritis was commonly associated with infection of the long bones. Facial bone involvement was seen in 10 cases. The mode of onset in most infants was relatively mild such as swelling or decreased movement of an extremity. A recent shift in causative organism was seen with staphycoccus being the agent isolated in 24 of 25 cases before 1965 but present in only five of 16 organisms since 1965. Streptococci were isolated in nine of the later cases.

B. J. Wood

Computed tomography and ultrasound in the diagnosis and management of neuroblastoma. Berger PE, Kuhn JP, Munschauer RW (Children's Hospital of Buffalo, New York). *Radiology* 128:663–667, Sept 1978

Gray-scale ultrasound and computed tomography were found to be diagnostically and clinically valuable in the study of 13 of 17 children with neuroblastoma. Use of ultrasound and computed tomography: (a) resulted in diagnoses not possible with conventional techniques, such as plain radiographs and excretory urograms; (b) defined more clearly the normal and pathologic anatomy in a three-dimensional perspective; (c) was an aid in evaluating extra-abdominal manifestations; and (d) permitted follow-up after surgery, radiation, and chemotherapy.

Author Abstract

Congenital rectal stenosis: a sign of a presacral pathologic condition. Malangoni MA, Grosfeld JL, Ballantine TVN, Kleiman M (Indiana University School of Medicine, Indianapolis, Indiana). *Pediatrics* 62:584–587, Oct 1978

Congenital rectal stenosis may be detected in the newborn during the initial physical examination. Failure of conservative therapy (dilatation) should alert the physician to the presence of an associated pathologic condition in the presacral space. Presacral teratoma, anterior sacral meningocele, or bony anomalies may be the underlying extrinsic causes of congenital rectal stenosis. Prompt recognition and appropriate operative management directed at the presacral lesion will relieve obstructive symptoms and minimize morbidity.

Author Abstract

Cervical metrizamide myelography by lumbar puncture. Sty JR, Babbitt DP (Milwaukee Children's Hospital, Milwaukee, Wisconsin). *Pediatr Radiol* 7:133–135, Sept 1978

In eight children with suspected cervical pathology, metrizamide introduced through the lumbar route produced good to excellent visualization of the cervical region. The examination was done with intramuscular sedation. The added safety of the lumbar route was emphasized.

B. J. Wood

Book Reviews

The Radiology of Skeletal Disorders, 2d ed. By Ronald O. Murray and Harold G. Jacobson. Edinburgh: Churchill Livingstone, 2,036 pp. in 4 volumes, 1977. $195

Two acknowledged authorities in bone radiology have written a monumental atlas, *The Radiology of Skeletal Disorders.* For reference purposes the second edition of Murray and Jacobson's text should be present in radiology departmental libraries.

This four volume edition is more than just a reference. By means of a unique organization, the understanding of bone radiology is enhanced. By grouping a series of related cases into a quiz format the learning process is not only enlivened, but is facilitated. In particular a set of different anatomic, pathologic, and radiologic appearances can be simultaneously assessed. In the ensuing discussion the authors improve overall comprehension by utilizing the set of case examples to compare and contrast. This format also allows progression from simple to more difficult problem cases. Admittedly, not everyone will be attracted to this format.

Those familiar with the first edition will appreciate that this new edition has nearly double the information content. Furthermore, some specific additions such as sections on arthrography, myelography, and isotope bone scanning now make this new edition a comprehensive bone imaging text.

Another helpful added feature is the separate, small Volume IV that contains a reprinting of the Appendix and the Index. The Appendix is an extensive series of lists and tables that summarizes key features of many aspects of bone radiology. The addition of this separate volume improves utilization of the book as a reference text, particularly in the retrieval and correlation of information located in diverse sections of the book. In practice this is quite a workable arrangement.

The quality of radiographic reproductions is adequate, especially considering the many cases retrieved from film archives across the world. In some instances it is disappointing to be unable to distinguish on the reproductions some subtle detail that apparently was present on the original radiograph. This is especially noticeable when participating in the quiz format that challenges the observer to carefully scrutinize the images.

Despite an inflationary price tag, this new edition represents a bargain for those interested in bone radiology whatever their level of expertise or particular discipline.

Curtis Northrop
University of Washington
Seattle, Washington 98195

Radiology of the Skull and Brain: Anatomy and Pathology, vol. 3. Edited by T. H. Newton and D. G. Potts. St. Louis: Mosby, 434 pp., 1977. $47.50

This latest addition to the series contains nine chapters with contributions from 16 of the world's leading neuroscientists. Much of the information contained in this book is not readily available in standard textbooks of neuropathology. The editors state at the outset that they believe an emphasis on anatomy and pathology which are the foundations of neuroradiology will hopefully be of value in the years ahead especially as the present diagnostic techniques are refined and new ones such as CT are developed. There are relatively new radiographs in this volume and indeed the information content transcends specific imaging techniques.

The first chapter by Leon Kier is a phylogenetic and ontogenetic study of the cerebral ventricles. The material, though fascinating, is not directly applicable to the everyday practice of neuroradiology.

The chapter devoted to cerebrospinal fluid (by Gordon Potts and Daniel Gomez) examines mechanisms of formation and absorption as well as factors that cause ventricular enlargement.

Topographic anatomy of the brain is superbly detailed in a chapter by Charles Strother and Georges Salamon.

There are three chapters on pathology: congenital anomalies (Samuel Ludwin and Nathan Malamud); intracranial tumors (Charles Wilson, John Moossy, Edwin Boldrey, and Nathan Malamud); and of cranial cerebral injuries (Richard Lindenberg).

The next chapter by Ellsworth Alvord and Cheng-Mei Shaw is a very scholarly dissertation on the infectious, allergic, and demyelinating diseases of the central nervous system. The last two chapters deal with pathology of cerebral vascular insufficiency (Helga Einsiedel-Lechtape and Paul Kleihues) and pathology of hydrocephalous and brain atrophy (Charles Hughes and Mokhtar Gado).

The illustrations are of excellent quality. The beginning of each chapter has an outline which is followed very well throughout the text. The end of each chapter contains an excellent bibliography.

This book is a must for anyone interested in the neurosciences and is recommended as an addition to every major library. The editors are once again to be congratulated for assembling another valuable volume in their series.

Lawrence Cromwell
University of Washington Hospital
Seattle, Washington 98195

Cerebral Computed Tomography. A Text-Atlas. By Leon A. Weisberg, Charles Nice, and Myron Katz. Philadelphia: Saunders, 337 pp., 1978. $22.50

The initial published studies of CT emphasized technical aspects, including description of the apparatus, physical principles of operation and image reconstruction, computer systems specific normal brain tissue sections, and abnormal scan findings in pathologic conditions. These early studies investigated diagnostic accuracy in many specific pathologic conditions. This book was conceived and developed to serve as an introduction to CT scanning in evaluating neurologic disorders as well as to place CT scanning in the appropriate diagnostic perspective relative to other currently available diagnostic studies (both invasive and noninvasive). As such, it is directed towards the neurologist, neurosurgeon, psychiatrist, internist, pediatrician, and other physicians who will be ordering this study.

© 1979 American Roentgen Ray Society

0361–803X/79/1323–0514 $0.00

Part one provides an overview of CT scanning and briefly reviews techniques of image reconstruction, normal anatomy, performance, and interpretation of CT scans. It lists directions for use of contrast infusion stating it should not be considered as a "routine" procedure. I do not agree with this. We use contrast infusion as a routine procedure except within the first week of trauma. We have found it rewarding as well as easier and less confusing for the technical staff. Likewise, a review of the authors' criteria leaves very few "noncontrast cases."

Part two deals with the evaluation of specific neurologic symptoms and signs. It consists of multiple chapters with the headings: Neurological Deficit of Rapid Onset; Progressive Neurological Deficit; Studies in Patients with Suspected Metastatic Disease; Juxtasellar Region (Visual, Endocrine or Radiographic Abnormalities); Increased Intracranial Pressure; Progressive Mental Deterioration and Impaired Consciousness; Dizziness and Hearing Impairment; Intracranial Inflammatory Diseases; Head Trauma; Gait and Movement Disorders; Headache; Seizure Disorders and Correlation with Specific EEG Pattern; Visual Symptoms; Calcifications; Children with Increasing Head Circumference; and ending with CT Evaluation of Various Treatment Modalities.

The book throughout each chapter discusses the potential yield and accuracy of CT as compared to other diagnostic procedures as well as its appropriate role in specific clinical situations and in the broad field of diagnostic evaluation. It is called a text-atlas, and is more of a text than an atlas. I found this book very well organized, well written, and easy to read. The illustrations, for the most part, are good (many, however, may be difficult to understand for those inexperienced in interpreting CT scans). It was primarily written for the nonradiologist and, as such, is excellent. I feel, because of its clinical approach, style and organization, it is a valuable addition to the radiologist's library.

Melvyn L. Weiner
949 Central Avenue
Woodmere, New York 11598

Human Brainstem Vessels. By Henri M. Duvernoy. (Translated by M. L. Clay.) New York: Springer-Verlag, 188 pp., 1978, $128

This book is an extensively-illustrated description of the small-vessel anatomy of the human brainstem. Some 150 fresh cadaver specimens were injected, dissected, and the superficial vessel dissections were photographed. Ten brainstems were studied in thick section and a description of the internal brainstem vasculature was formulated. Forty-three brainstems were thin-sectioned, and the capillary networks illustrated.

The book is organized into two parts. The text and references occupy 29 pages. There are 148 pages of illustrations and a brief index. The illustrations are highlighted by 13 color drawings which summarize the information contained in the photographs of the sections. Large color fold-out drawings of anterior and posterior views of the vessels of the brainstem complete the work.

The quality of the illustrations is excellent. The photographs of superficial vessel dissections are magnified, allowing easy identification of small branches, and each is accompanied by a line drawing for orientation.

This could be a source book for neuroradiologists interested in high-magnification angiography of the brainstem. The section on the capillary network (100 pages) will be of little use to radiologists. Unfortunately, the excessive cost of the volume will probably limit its distribution to university research libraries.

Frank W. Farrell, Jr.
Forsyth Memorial Hospital
Winston-Salem, North Carolina 27104

Modern Concepts in Brain Tumor Therapy: Laboratory and Clinical Investigations. NCI Monography 46. Edited by Audrey E. Evans. Washington DC: U.S. Government Printing Office, 250 pp., 1977. $8

As described in the title, this National Cancer Institute monograph is a collection of the laboratory and clinical investigations presented at the National Cancer Institute-sponsored Brain Tumor Conference held in Atlanta, Georgia, in February 1976. The volume is well organized and the illustrations are generally of high quality. The format is a collection of relevant scientific papers with discussions by the conference participants. Subjects include animal tumor modeling, tumor nomenclature, methods of diagnosis, effects of various treatment regimes on normal brain tissue, and treatment results and recommendations for various brain tumors. A review of ongoing clinical trials is also presented.

The first section, which deals with animal tumor models of brain tumors, presents a well-selected overview of this subject. The advantages and disadvantages of various animal tumor models are discussed. A particularly interesting paper is on the therapeutic implications of brain tumor cell kinetics.

The second section is devoted to the diagnostic workup and evaluation of patients with brain tumors. Conventional methods such as CT scanning, nuclear scanning, and cerebrospinal fluid evaluation, as well as experimental diagnostic tools such as cerebrospinal fluid sterols, polyamines, astrocytin, and malignin are evaluated.

The third section discusses various treatment methods including surgery, radiation therapy, and chemotherapy as well as prognostic indicators and criteria of response. The last section outlines the various ongoing research by various cooperative groups.

This monograph should serve as a valuable reference for both physicians and laboratory researchers interested in current directions in brain tumor research.

Thomas W. Griffin
University of Washington Hospital
Seattle, Washington 98195

Pediatric Radiology. Edited by Jack G. Rabinowitz. Philadelphia: Lippincott, 513 pp., 1978. $50

This book is of moderate length, well illustrated, and covers diseases of both the infant and young child. Six of our residents who were rotating through pediatric radiology read and enjoyed it. One senior resident, Joel Swartz, read the entire book twice and commented, "The original organization on the basis of gamuts was very appealing. There is a substantial amount of clinical information in the discussion segments. I have read no book which 'reads' as easily. A few major topics (congenital hip dislocation, congenital foot deformity, slipped capital femoral epiphysis, juvenile rheumatoid arthritis) were not given appro-

priate discussion, probably because they did not fit under any particular gamut." Probably the most appealing aspect of the book for our residents has been its organization. For each radiographic sign, a list of differential diagnoses is given, and this is followed by a discussion of each possible diagnosis. The list of differential diagnoses is often surprisingly complete; for example, in the section on narrowed bowel, tuberculous enteritis, Salmonella colitis, and hemolytic-uremic colitis are listed and illustrated. In the discussion of gamuts, the embryology and pathophysiology of disease states and potential benefits of angiography and ultrasonography are mentioned. Surgical specimens are illustrated along with preoperative radiographs in some instances. Computed tomograms and ultrasonograms are not illustrated.

There are certain rather categorical statements which are of questionable validity. For example: "Ganglioneuroma usually occurs in the posterior mediastinum, just as neuroblastoma" (page 30); "The association of meconium ileus with cystic fibrosis is almost 100 percent . . . " (page 65); "Meconium plug syndrome is due to a basic functional disturbance of the colon that causes excessive water resorption . . . " (page 72); "Installation of a few drops of contrast material into the esophagus adequately defines the level of the atresia. However, this procedure is not necessary . . . " (page 202); "The detection of a right aortic arch on the chest radiograph frequently indicates the existence of a vascular ring" (page 209); "The most common pulmonary disease in children with kyphosis is cystic fibrosis" (page 324).

So what is the place for this book in radiology residency? It will be a very popular book among radiology residents because of its outstanding organization and excellent illustrations. A few of the statements may have to be taken with a "grain of salt". Practicing general radiologists should find the gamuts for roentgen signs helpful. Pediatric radiologists will probably not benefit much from reading this book themselves.

Lawrence R. Kuhns
R. Hernandez
University of Michigan Medical Center
Ann Arbor, Michigan 48109

Gynecologic Oncology. By Larry McGowan. New York: Appleton-Century-Crofts, 435 pp., 1978. $35

This is the third new book on the subject of gynecologic oncology to appear within 4 years. Gynecologic oncology has become a distinct subspecialty, separate from traditional gynecology and, in the process, the field has become increasingly complex. The stated purpose of Dr. McGowan's volume is to create a text of "sufficient scope to meet the needs of medical students, residents and fellows in gynecology, practicing obstetricians and gynecologists, physicians in closely allied fields, and gynecologic oncologists". This ambitious effort has been achieved in a general sense, but in an effort to encompass all things, certain areas have necessarily suffered by abbreviation.

The material is contained in 25 chapters and reflects contributions from 20 different authors, each well recognized in his particular field. The book is particularly well illustrated and in many of the summary chapters, such as that on gynecologic chemotherapy, the diagrams and outlines well supplement the text.

The book will serve as an excellent resource text for basic information in gynecologic cancer chemotherapy, radiation physics, and tumor immunology. Moreover, it is a very satisfactory compendium of current and standard approaches to the various gynecologic cancers. In succeeding chapters, each type of malignancy is approached in a methodical fashion by the different authors and for the major cancers of the genital tract, a separate chapter on radiation therapy has been appended. While acknowledging the excellent material on radiation therapy, this has often created a fragmented approach to the disease in question, and is particularly true in the section on vulvar carcinoma. Such criticism is probably unavoidable in the multiple author approach employed.

If only one criticism were allowed, it might be that the authors were unduly conservative and preferred to stay safely within established dogmas and conventional approaches. Many of the more challenging problems in gynecologic oncology are approached rather hesitantly. Except in the very excellent section on pathology, there is little reference to borderline tumors of the ovary. The problem of gestational trophoblastic disease resistant to established chemotherapy is avoided. The relationship of exogenous estrogens and endometrial cancer is treated rather casually. Some of the chapters with provocative titles fall short of the mark in substance. The final chapter, dealing with "The Dying Gynecologic Cancer Patient and Society" was a bit disappointing in the coverage of an important area often neglected in our literature.

Invariably, no book can promise all things to all readers. This book is an excellent resource text for the student, resident, and practicing physician. It offers few exciting or innovative suggestions and little speculation on the newer thoughts in gynecologic oncology. In the balance, however, it emerges as a comprehensive volume meeting many needs and containing a great deal of accurate information. It should certainly be in the library of those involved in the practice of gynecologic oncology.

David C. Figge
Department of Obstetrics and Gynecology
University of Washington Hospital
Seattle, Washington 98195

Radiographic Positioning and Related Anatomy, 2d ed. By Isadore Meschan. Philadelphia: Saunders, 590 pp., 1978. $21.75

The first edition of this book was published in 1968 as a companion volume to the *Atlas of Normal Radiographic Anatomy*. The present edition is considerably larger than the first and its content has been taken from two much larger companion volumes which are much more detailed. This smaller volume has been designed for "the average radiographer, technologist, or even medical student".

Compared with the first edition, this new volume includes many new positions and more specific directions addressed to the technologist. It also includes a smattering of computed radiology, angiography, and basic anatomy.

The diagrams and photographic illustrations are generally of good quality. The computed tomographic reproductions do not show the detail that one can achieve with more recent equipment. A glossary of medical terms pertinent to radiology is included.

The book achieves its purpose in providing the average technologist with somewhat detailed instructions in radiographic positioning and providing the technologist with an overview of some of the newer techniques in radiology. The more experienced technolcgist or technician specialist would most likely refer to the considerably larger and more detailed companion volumes.

Arthur Lieber
University of Kentucky Medical Center
Lexington, Kentucky 40506

Atlas of Radiologic Anatomy. By Lothar Wicke. Baltimore: Urban and Schwarzenberg, 234 pp., 1978. $15

The author has apparently worked with care and good intent to produce a volume to "afford the student an opportunity to check and expand his knowledge of the anatomic details that are observable by radiology". The result is a collection of 118 positive mode radiographs matched on the opposite page with a labeled line drawing of the radiograph.

Unfortunately the author has failed in several ways to achieve the desired results. The radiologic anatomy demonstrated, runs the gamut from spine to extremity to cerebral angiography and even fetography. No one area is, however, really covered in any depth. The terminology used is the Wiesbaden anatomic nomenclature adopted in 1965. Such terms may be well known in Europe but are not in common usage in North America. (The gallbladder, for example, is called the vesical felleae.) Finally, the illustrations are in the positive mode, by the author's choice, to "maximize picture quality and detail" even though it is acknowledged that this is not the common way of presenting x-rays. Unfortunately, the reproductions are of poor quality and cannot compare with those commonly seen in radiology texts or journals in this country and thus do not serve the intended purpose.

Overall, I do not feel there is a need for this atlas in our medical school libraries, anatomy departments, or radiology residency programs. There are many far superior radiologic-anatomy texts already available.

Gerald A. L. Irwin
Yale University School of Medicine
Norwalk Hospital
Norwalk, Connecticut 08556

Books Received

Receipt of books is acknowledged as a courtesy to the sender. Books that appear of sufficient interest will be reviewed as space permits.

A Radiographic Index, 6th ed. By M. Goldman, D. Cope. Chicago: Year Book Medical Publishers, 98 pp., 1978. $8.95

Radiobiological Research and Radiotherapy. Proceedings of a Symposium, Vienna, 22–26 November 1976. Vol I—Fractionation of doses—radiomodifiers—hyperthermia—combined radio and chemotherapy. Vol II—Effects of High-LET radiation—cellular models—radiobiological effects in vivo—late effects. Vienna: International Atomic Energy Agency, 457 pp., 304 pp., respectively, 1977. $34 and $23, respectively (available U.S. from UNIPUB, Box 433, Murray Hill Station, New York, NY 10016)

Health Implications of Nuclear Power Production. Report on a Working Group, Brussels, 1–5 December 1975. Copenhagen: WHO Regional Office for Europe, 75 pp., 1978. $4 (available U.S. from WHO Publications Centre, 49 Sheridan Ave., Albany, NY 12210; ISBN 92 9020 103 7)

Handbook of Chemistry and Physics, 59th ed. Edited by R. C. Weast, West Palm Beach, Fla.: CRC Press, 2,512 pp., 1978. $459

Telescreen and Radiographic Examination of Urinary Transport (in English). By E. Hajós. Budapest: Akadémiai Kiadó, 115 pp., 1978. $10.50

Radioimmunoassay and Related Procedures in Medicine 1977, vol I and vol II. Proceedings of a Symposium, Berlin, 31 October–4 November 1977. Vienna: International Atomic Energy Agency, 539 pp., 541 pp., respectively, 1978. vol I, $43; vol II, $40 (available U.S. from UNIPUB, Box 433, Murray Hill Station, New York, NY 10016)

Textbook of Nuclear Medicine: Basic Science. Edited by A. F. Gonçalves Rocha, J. C. Harbert. Philadelphia: Lea & Febiger, 412 pp., 1978. $27.50

Experimental Radiological Health Physics. By D. A. Gollnick. New York: Pergamon Press, 257 pp., 1978. $9.75 (soft cover); $20 (hard cover)

Introduction to Clinical Radiology: A Correlative Approach to Diagnostic Imaging. By R. H. Daffner. St. Louis: Mosby, 410 pp., 1978. $14.95

The Radiobiology of Human Cancer Radiotherapy, 2d ed. By J. R. Andrews. Baltimore: University Park Press, 591 pp., 1978. $39.50

Noninvasive Cardiovascular Diagnosis: Current Concepts. Edited by E. B. Diethrich. Baltimore: University Park Press, 524 pp., 1978. $39.50

Reflux and Renal Scarring. By P. G. Ransley, R. A. Risdon. London: British Journal of Radiology, supplement 14, 35 pp., 1978. £3.60

Radiologic Management of the Massively Traumatized Patient. Edited by R. J. Ayella. Baltimore: Williams & Wilkins, 312 pp., 1978. $50

Introduction to the Physics of Diagnostic Radiology, 2d ed. By E. E. Christensen, T. S. Curry, III, J. E. Dowdey. Philadelphia: Lea & Febiger, 428 pp., 1978. $18

Radiobiology for the Radiologist, 2d ed. By E. J. Hall. Hagerstown, Md.: Harper & Row, 460 pp., 1978. $25

Radiology of the Skull and Brain, vol. 4. **Ventricles and Cisterns.** Edited by T. H. Newton, D. G. Potts, St. Louis: Mosby, pages 3223–3834, 1978. $59.50

Atlas of Roentgenographic Measurement, 4th ed. By L. B. Lusted, T. E. Keats. Chicago: Year Book Medical Publishers, 354 pp., 1978. $39.85

The Cranium of the Newborn Infant. An Atlas of Tomography and Anatomical Features. By R. H. Pierce, M. W. Mainen, J. F. Bosma. Bethesda: U.S. Department of Health, Education and Welfare (no. NIH 78-788), 148 pp., 1978. $13.25 (Available, U.S. Government Printing Office)

Textbook of Diagnostic Ultrasonography. By S. L. Hagen-Ansert. St. Louis: Mosby, 493 pp., 1978. $44.50

Anatomical Exercises in Computerized Tomography Body Scanning. By F. C. Shipps. Springfield, Ill.: Thomas, 67 pp., 1978. $22.75

Atlas of Abdominal Ultrasonography in Children. By G. F. Gates. New York: Churchill Livingstone, 283 pp., 1978. $27.50

Roentgenology of Fractures and Dislocations. A *Seminars in Roentgenology* reprint. Edited by B. Felson. New York: Grune & Stratton, 179 pp., 1978.

Acetabular Dysplasia. Skeletal Dysplasia in Childhood. Progress in Orthopaedic Surgery, vol. 2. Edited by U. H. Weil. Berlin: Springer-Verlag, 199 pp., 1978. $20

The Radiology of Acute Cervical Spine Trauma. By J. H. Harris, Jr., Baltimore: Williams & Wilkins, 136 pp., 1978. $18.95

Clinical Sialography. By G. B. Manashil. Springfield, Ill.: Thomas, 99 pp., 1978. $16.75

Real Time Ophthalmic Ultrasonography. By S. N. Hassani. New York: Springer-Verlag, 214 pp., 1978. $34.50

L'Angiographie Digestive. Chez L'Adulte et L'Enfant (in French). By D. Doyon, A. Roche, P. Chaumont. Pairs: Masson, 204 pp., 1978. 192 F

Radiculosaccography with Water-soluble Contrast Media. By P. Capesius. E. Babin, Berlin: Springer-Verlag, 166 pp., 1978. $49

Asbestos Related Disease. Edited by L. Preger. New York: Grune & Stratton, 271 pp., 1978. $24

A Study Guide for Radiologic Technologists. By J. P. Baron. Springfield, Ill.: Thomas, 540 pp., 1978. $17.50

Clinical and Experimental Applications of Krypton 81 m. Edited by P. J. Lavender. London: British Journal of Radiology, special report no. 15, 193 pp., 1978. £12

MGH Textbook of Emergency Medicine. Edited by E. W. Wilkins, Jr. Baltimore: Williams & Wilkins, 829 pp., 1978. $59.95

Undergraduate Medical Education and the Elective System. Experience with the Duke Curriculum, 1966–1975. Edited by J. F. Gifford, Jr. Durham, N.C.: Duke University Press, 243 pp., 1978.

Policy Implications of the Computed Tomography (CT) Scanner. Office of Technology Assessment. DC: U.S. Government Printing Office, 195 pp., 1978. $4

Renaissance of Interstitial Brachytherapy. Frontiers of Radiation Therapy and Oncology, vol. 12. 12th Annual San Francisco Cancer Symposium, March 4–5, 1977. Edited by J. M. Vaeth. Basel: Karger, 178 pp., 1978. $64.25

The Image and the Reality. A Case-Study of the Impacts of Medical Technology. By B. Stocking, S. L. Morrison. Oxford: Oxford University Press, 80 pp., 1978. $7.95

Basic Science of Nuclear Medicine. By R. P. Parker, P.H.S. Smith, D. M. Taylor. Edinburgh: Churchill Livingstone, 374 pp., 1978. $19.50

News

Irish-American Radiology Symposium

An Irish-American Radiology Symposium, covering recent advances in the field including computed tomography and ultrasound, will be Sept. 15–21 in Killarney, Ireland. The course is sponsored by the University of Connecticut Health Center and the Faculty of Radiologists, Ireland.

Guest faculty will include: B. Felson, A Lalli, E. McIlrath, J. G. McNulty, R. O. Murray, R. Taylor and J. P. Whalen. Participating University of Connecticut faculty will include: D. B. Crawford, F. U. Conard, G. R. Ramsby, R. Spencer and T. J. Spackman.

Further information is available from: Dr. D. B. Crawford, Department of Radiology, University of Connecticut Health Center, Farmington, CT 06032.

Beth Israel Courses

Beth Israel Medical Center in New York City will host three courses during March and April. Recent Advances in Diagnostic Modalities and Therapy for Breast Cancer will be March 14 while Controversy in Diabetes Mellitus is slated for March 20. On April 27, Rehabilitation in Arthritis and Related Disorders will be presented.

The course on diagnostic modalities and breast cancer therapy is cosponsored by the American Cancer Society and will feature a discussion of the basics of mammography and xeroradiography, basics of thermography, breast cancer screening, conservative versus radical surgery, and psychiatric aspects. The respective roles of radiation therapy, chemotherapy, and immunotherapy will be discussed. Dr. L. Venet is program chairman.

Controversy in Diabetes Mellitus will review several of the problems faced by physicians dealing with the condition. Each will be discussed by a protagonist and an antagonist. Discussion will focus on glucagon and its importance in diabetic ketoacidosis; preventable microvascular complications; and insulin receptors and juvenile and adult onset diabetes. Dr. G. J. Friedman is program chairman.

The course, Rehabilitation in Arthritis and Related Disorders, will present the clinical aspects and recent immunologic developments in rheumatoid arthritis and the sero-negative arthritides. Indication, techniques, and results of the surgical management of the arthritic lower limb will be discussed, including the most recent experience with knee, ankle, and toe placement of joints and supporting structures.

For information on these courses, contact: B. R. Lawrence, Post-Graduate Education Office, Beth Israel Medical Center, 10 Nathan D. Perlman Place, New York, NY 10003; telephone (212) 420-2000.

Diagnostic Ultrasound Courses

A series of 2-week courses in diagnostic ultrasound have been announced by the Health Sciences Center in Winnipeg, Manitoba. Courses will be given in September and November, 1979, and January, March, and June, 1980. Each is designed to provide a basic introduction to all aspects of diagnostic ultrasound, and will consist of formal lectures, film reading sessions, teaching files, video tapes, and clinical practice. A total of 68 hr of continuing education credit is available. Tuition is $600; enrollment is limited to 15 participants per program. For information, contact: Dr. E. A. Lyons, Section of Diagnostic Ultrasound, 700 William Ave., Winnipeg, Manitoba, Canada R3E OZ3; telephone (204) 787-3701.

Update on Ultrasonography

Update on Ultrasonography, a course for radiologists, sonographers, and other interested medical personnel will be April 7 and 8 in New Haven, Connecticut. Sponsor is the Section of Diagnostic Ultrasound of Yale-New Haven Hospital. Proceeds will go to the Hospice Home Care program for terminally ill patients.

The program will include recent advances in abdominal, pelvic, and obstetrical scanning, current developments in physics and instrumentation including real time and Doppler as well as scanning of the chest, breast, prostate, and other superficial organs. Sessions will be given on advanced scanning techniques. Emphasis will be "what's new in ultrasound".

There are no prerequisites. Tuition is $150; $75 for sonographers and residents. For further information and registration forms contact: Dr. K. J. W. Taylor, Section of Diagnostic Ultrasound, Department of Diagnostic Radiology, Yale-New Haven Hospital, 789 Howard Ave., New Haven, CT 06504; telephone (203) 436-0683.

New Orleans Spring Roentgen Conference

The New Orleans Radiology Society will host its seventh annual Spring Roentgen Conference, April 19–21. April 19 will be devoted to thoracic imaging including nuclear techniques, CT, and special procedures, while general diagnostic radiology is the topic for the following days.

Guest faculty will be: P. L. Cooperberg, Vancouver (Canada) General Hospital, ultrasound; D. Resnick, Veterans Administration Hospital, San Diego, bone and joint; J. F. Wiot, University of Cincinnati Medical Center, gastrointestinal; T. H. Newton, University of California, San Francisco, neuroradiology; W. E. Berdon, Columbia-Presbyterian Hospital, New York City, pediatric; and B. G. Brogdon, University of South Alabama Medical Center, Mobile, American College of Radiology activities. Guest faculty presenting the thoracic program will include: A. Gottschalk, Yale, nuclear imaging; S. S. Sagel, Mallinckrodt Institute, St. Louis, computed tomography; and E. R. Heitzman, State University of New York, Syracuse, chest.

Registration fee is $195; $110 for residents. The program meets the criteria for 20 hr AMA Category I credit. Information is available from Dr. A. M. Landry, New Orleans Radiology Society, P.O. Box 19024, New Orleans, LA 70179.

Physics of Radiology and Nuclear Medicine

A refresher course for radiology residents in the Physics of Radiology and Nuclear Medicine will be May 7–10 in New York City. Sponsor is the Beth Israel Medical Center. The course is intended to prepare residents for the American Board of Radiology examination. For information, contact: B. Lawrence, Medical Education Office, Beth Israel Medical Center, 10 Nathan D. Perlman Place, New York, NY 10003; phone (212) 420-2000.

Gastrointestinal Refresher Course

The Society of Gastro-Intestinal Radiologists will present its annual refresher course and scientific program, Oct. 11–14 in Williamsburg, Virginia. Additional information is available from Dr. M. Donner, Dept. of Radiology, Johns Hopkins Hospital, 601 North Broadway, Baltimore, MD 21205.

March Nuclear Medicine Meeting

The Greater New York Chapter of the Society of Nuclear Medicine will host a spring meeting on March 24 in Atlantic City, N.J. The day-long program will feature a number of topics including: Bone imaging in staging malignant disease; bone imaging of benign disease; the nitty-gritty of gallium imaging—equipment, methodology, and normal variants; new clinical applications of gallium imaging; fool the experts—a gallium sandbag session; and submitted papers. For information contact Dr. G. W. Moskowitz, Division of Nuclear Medicine, Long Island Jewish-Hillside Medical Center, New Hyde Park, NY 11040; phone (212) 470-2476.

Clinical Nuclear Medicine: 1979

The Departments of Radiology and Continuing Education of Harvard Medical School will present a third annual postgraduate course in nuclear medicine, April 4–7, in Boston. Four morning sessions of didactic material will address: bone imaging, practical cardiac examinations, evaluation of comparative modalities in the study of the brain and hepatobiliary system, assessment of myocardial perfusion, right and left ventricular function, and acute infarct imaging. Afternoons will be devoted to workshops. A total of 26 hr AMA Category I credit is available. Fee is $260; $175 for residents and fellows. For information contact: Dr. W. D. Kaplan, Program Director, Department of Radiology, Harvard Medical School, 25 Shattuck St., Boston, MA 02115; telephone (617) 732-6265.

Update on Ultrasonography

Update on Ultrasonography, a course for radiologists and sonographers will be April 7 and 8 in New Haven. Sponsors are the Section of Diagnostic Ultrasound and Department of Diagnostic Radiology, both Yale-New Haven Hospital. Course emphasis will be on "what's new in ultrasound." Tuition is $150 for physicians; $75 for sonographers and residents. For information and registration forms, write: Dr. K. J. W. Taylor, Diagnostic Ultrasound, Yale-New Haven Hospital, 789 Howard Ave., New Haven, CT 06504.

Gastrointestinal Radiology

A postgraduate course in gastrointestinal radiology will be April 5–7 at Mount Sinai Medical Center, New York City. The course carries 16¾ hr AMA Category I credit. Faculty from Mount Sinai will be joined by the following guest faculty: S. Baum, T. C. Beneventano,, J. Farman, H. G. Jacobson, E. Kazam, W. B. Seaman, and S. C. Sommers. For information, contact: Director, Page and William Black Post-Graduate School of Medicine, Mount Sinai School of Medicine, 1 Gustave L. Levy Place, New York, NY 10029; phone (212) 650-6737.

Diagnostic Course in Switzerland

The eleventh International Diagnostic Course will be in Davos, Switzerland, April 1–7. Sponsor is the European Association of Radiology. The seminar is based on radiologic analyses of radiographs of the abdomen, including barium studies, nuclear medicine, computed tomography, and echocardiography. Information is available from: IDKD 11, P. O. Box 2132, 8028 Zurich, Switzerland.

Meeting and Course Review

For reader convenience, a summary of upcoming meetings and courses is provided. Detailed listings of these events appeared in journal issues indicated in parentheses.

XIII Interamerican Congress of Radiology, July–August 1979, Quito, Ecuador (October).

Sixth Congress of Radiation Research, May 13–19, Tokyo (October).

Noninvasive Imaging in Medicine, symposium, June 6–9, Lund, Sweden (October).

Conferences on Medical and Biological Engineering and Medical Physics, Aug. 19–24, Jerusalem (October).

L. H. Gray Conference, Sept. 10–14, Cambridge, England (October).

Asian Oceanian Congress of Radiology, Oct. 28–Nov. 3, Singapore (October).

Diagnostic Ultrasound Courses, series, Philadelphia (November).

Abdominal Real Time Sonography Courses, June 11–15, July 16–20, Aug. 6–10, Dec. 9–13, 1979, Winston-Salem, N.C. (November).

Fleischner Society Ninth Symposium (and course), June 11–13, Stockholm (November).

Musculoskeletal Course and Cruise, April 28–May 5, Carribean (November).

European Cardiovascular Radiology Congress, May 3–5, Nuremberg, West Germany (November).

LA Bone and Joint Conference, continuing once monthly course, Los Angeles (November).

Diagnostic Ultrasound Seminar, April 21 and 22, New York City (November).

San Diego Postgraduate Courses, 1 and 2-week programs (November).

American Board of Radiology, oral and written examination dates and locations for 1979 and 1980 (December).

AFIP Diagnostic Radiology Seminars, series, May 7–11, August 27–31, November 12–16, Washington, D.C. (December).

Canadian Radiologists Annual Meeting, June 24–28, Vancouver (December).

Multidisciplinary Aspects of Brain Tumor Therapy, June 8–10, Lake Garda, Italy (December).

Radiology of Bone and Chest Diseases, course, April 23–27, San Diego (December).

Radiology of the Chest, course, April 2–6, Durham, North Carolina (December).

Skeletal Radiology Course, May 14–18, New York City (December).

Spring Physics Seminar, April 23–25, Las Vegas (December).

Nuclear Radiology Workshop, May 4 and 5, Ann Arbor, Michigan (December).

Radiation Therapy Seminar, April 26–28, Gainesville, Florida (January).

Symposium: Computerized Tomography of the Brain, Sept. 20–22, Bordeaux, France (January).

Gastrointestinal Radiology, postgraduate course, April 5–7, New York City (January).

Abdominal Ultrasound and CT of the Trunk, May 24–26, Dallas (January).

Diagnostic Ultrasound Training Programs, continuing weekly series, New York City (January).

National Conference on Urologic Cancer, April 4–6, Los Angeles (January).

Diagnostic Ultrasound Workshop, weekly postgraduate sessions through December 14, Houston (January).

Cardiac Imaging Refresher Course, April 23–26, Hilton Head, South Carolina (January).

Eighth Congress, European Society of Neuroradiology, Sept. 7 and 8, Strasbourg, France (January).

Abdominal Radiology Course, May 14–17, Boston (February).

Practical Advances in Diagnostic Radiology and Nuclear Medicine, symposium, April 17–20, Baltimore (February).

University of Pennsylvania Diagnostic Radiology Seminar, June 4–8, Philadelphia (February).

Angiography: Current Methods and Basic Problems, course, April 19–21, Boston (February).

Clinical Nuclear Medicine: 1979, seminar, March 30–April 1, Dallas (February).

AAPM Summer School, July 22–28, Chapel Hill, N.C. (February).

Austrian Nuclear Medicine Meeting, Sept. 11–14, Innsbruck (February).

Percutaneous Biopsy and Therapeutic Vascular Occlusion, symposium, May 7–9, Munich (February).

Leo Rigler Lecture and Convention on Pediatric Radiology, May 8–10, Herzlia-on-Sea, Israel (February).

Summer Humanities Seminars for Physicians, eight locations, application deadline April 16 (February).

Symposium: Fundamentals in Technical Progress, May 11 and 12, Liège, Belgium (February).

American Journal of Roentgenology

Please enter my subscription as follows:

Beginning with _____, _____.
month *year*

Name _____

Address _____

City and State _____ Zip Code _____

Specialty _____

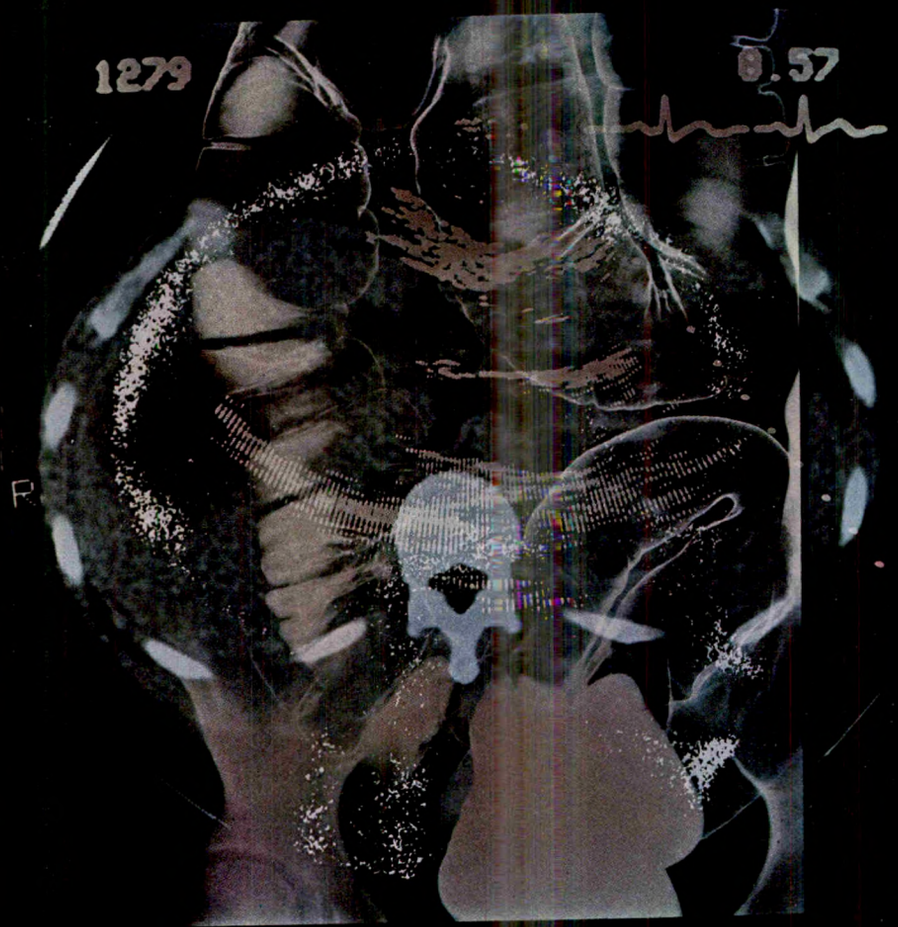
Amount enclosed $ _____

Annual subscription rates: $40 ($20 for residents with letter of verification) plus appropriate mailing surcharge. Mailing surcharges: U.S. and possessions, none; European countries,* $25; Japan, $45; other, $10. Subscriptions to Japan and European countries are delivered by air freight. There is no option for surface mail.

Send this form and remittance to Charles C Thomas, Publisher, 301-327 East Lawrence Avenue, Springfield, Illinois 62717.

* The European mailing surcharge applies to the following countries. All receive Journal delivery via air freight to Europe. Algeria, Austria, Belgium, Czechoslovakia, Denmark, Finland, France, Germany, Great Britain, Greece, Hungary, India, Iran, Ireland, Israel, Italy, Kenya, Luxembourg, Netherlands, Nigeria, Norway, Portugal, Romania, South Africa, Spain, Sweden, Switzerland, Turkey, Uganda, Yugoslavia.

For Total Imaging



TOSHIBA
MEDICAL SYSTEMS

At Toshiba, the concept has always been total imaging. It is the reason the world looks to us for all four types of imaging systems in use today.

From modular radiology and fluoroscopy systems, to the world's first super high resolution large field gamma camera, six decades as medicine's international imaging leader goes into every system we make.

Two things make Toshiba Medical Systems the image to look for, resolution and human engineering.

As an example, both have contributed equally to making Toshiba's Ultrasound Sonolayergraph series the finest available to modern clinical medicine.

Backing Toshiba Medical System's 60 years of medical imaging experience, is Toshiba Corporation's position as a leader in electronics and computer integrated systems of all types.

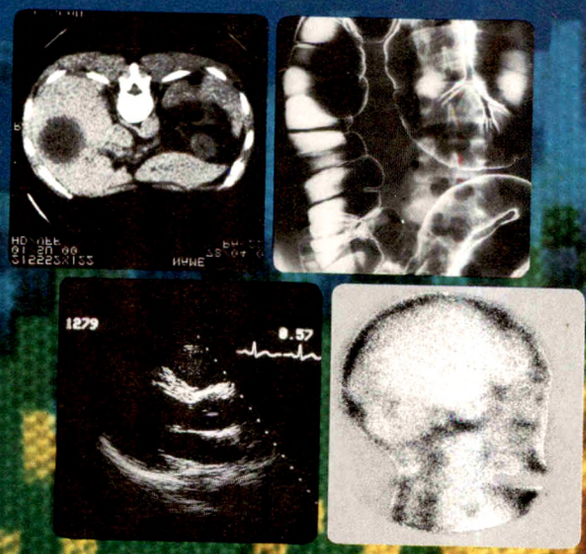
This kind of technical capability enabled Toshiba to incorporate the latest advances from a wide range of fields, to produce a new level of computer tomography with Toshiba's whole body CT scanner.

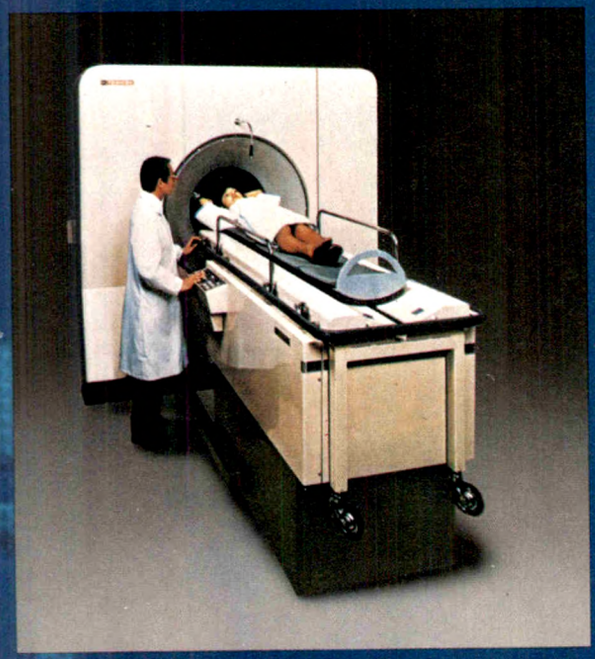
As medicine goes forward, you can be assured Toshiba Medical Systems will be there to give you the most useful diagnostic image you can get. That's because our commitment to giving you the finest imaging is as deep as your commitment to the good health of your patients.

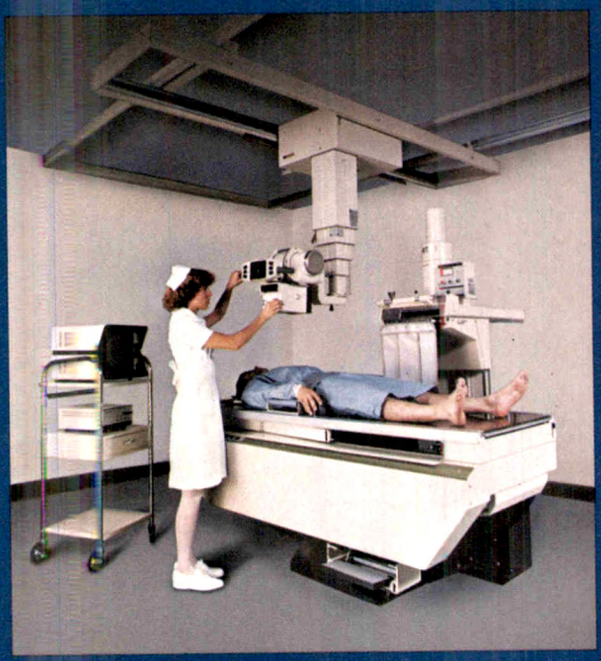
Look to us, we are your total imaging company.

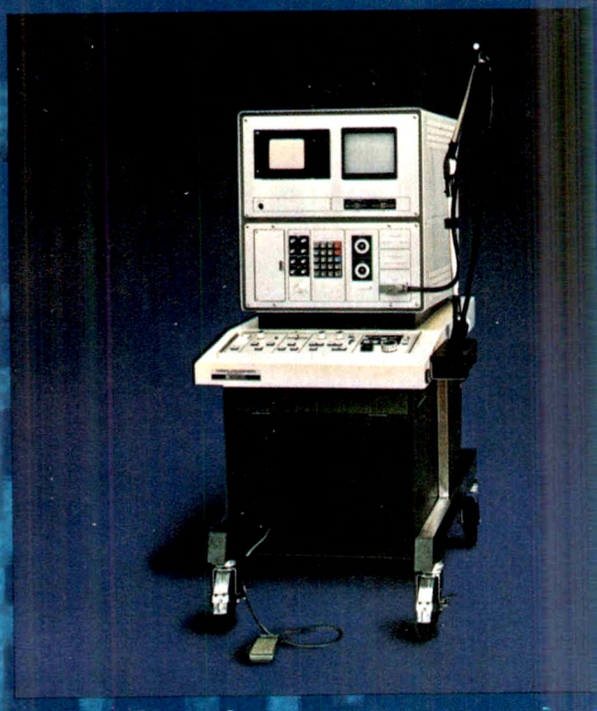
Toshiba is Your Total Image,

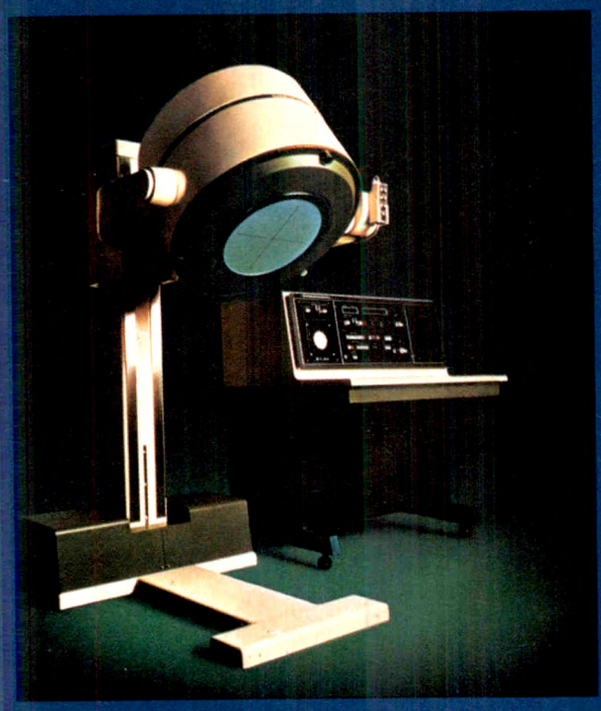
manufacturing the total gamut of imaging systems.











The ultimate in image clarity and human engineering for Radiology and Fluoroscopy, Ultrasound, Computer Tomography and Nuclear Medicine.

EXTENDED SERVICE PLANNING

Toshiba Medical Systems is also your total service company. With engineering personnel and logistics support that span the globe, Toshiba is committed to provide around the clock service and support anywhere in the world.

Toshiba Medical Systems sales and service headquarters around the world:

Argentina, Buenos Aires
Australia, Sydney
England, London
Hong Kong, Hong Kong
Iran, Teheran
Mexico, Mexico City
The Netherlands, Amsterdam
New Zealand, Wellington
Philippines, Manila
Republic of South Africa, Johannesburg
Taiwan, Taipei
Thailand, Bangkok
Venezuela, Caracas

Toshiba Medical Systems
Division of Toshiba International, Corporation, U.S.A. — Los Angeles, California

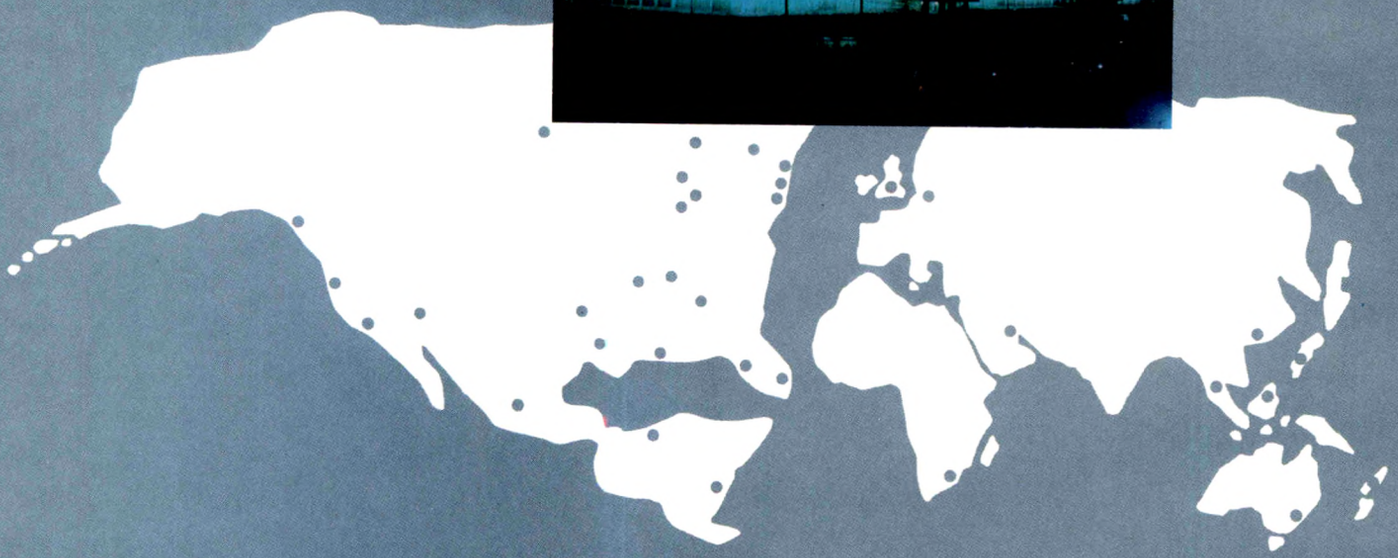
Atlanta, Georgia
Boston, Massachusetts
Chicago, Illinois
Cincinnati, Ohio
Cleveland, Ohio
Dallas, Texas
Detroit, Michigan
Houston, Texas
Kansas City, Missouri
Los Angeles, California
Memphis, Tennessee
Miami, Florida
New Orleans, Louisiana
New York, New York
Philadelphia, Pennsylvania
Phoenix, Arizona
San Francisco, California
Seattle, Washington
Tampa, Florida
Washington, D.C.
Ontario, Canada

Toshiba Medical do Brasil, Ltda. — Sao Paulo, Brazil









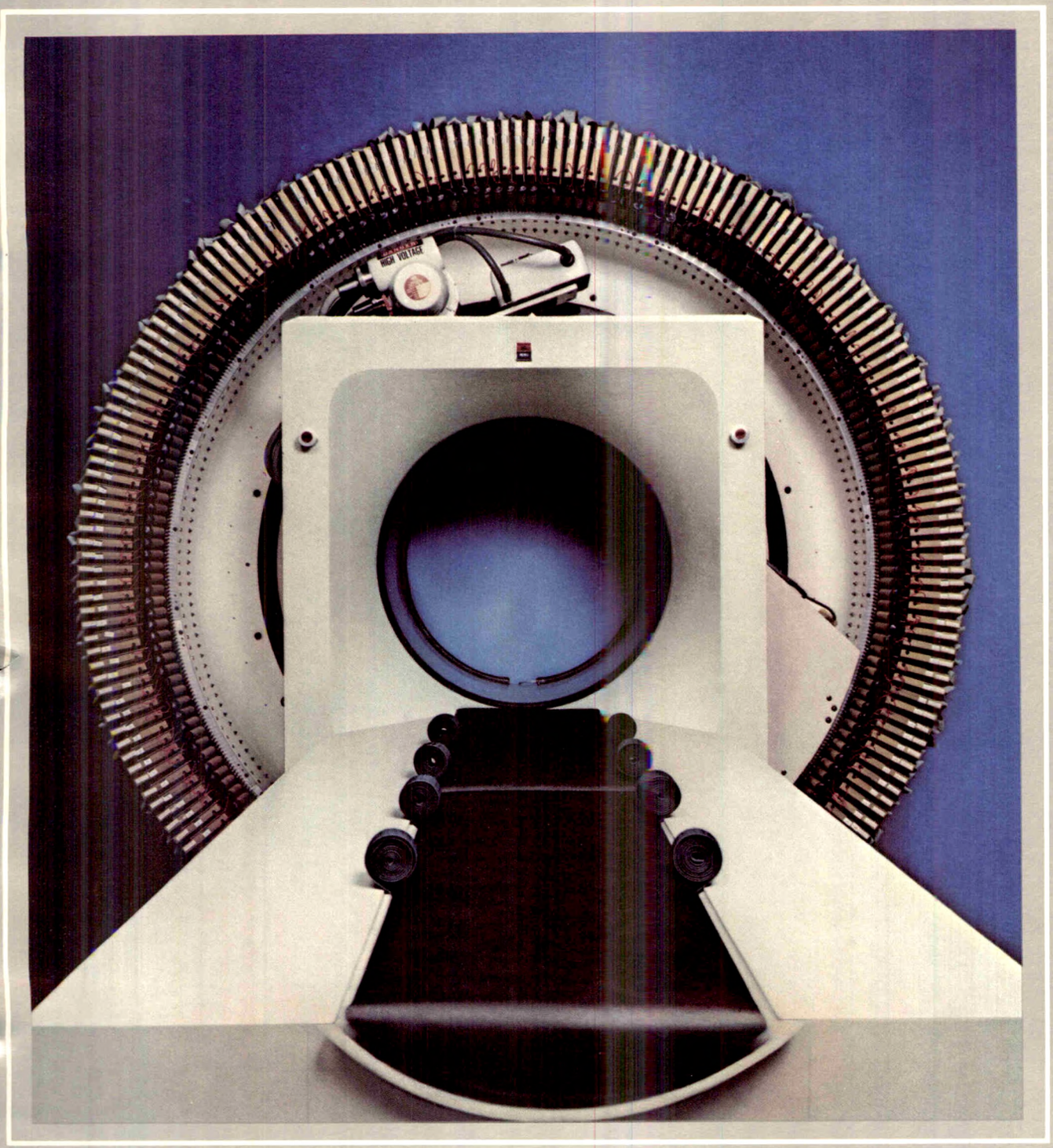
Toshiba

TOSHIBA

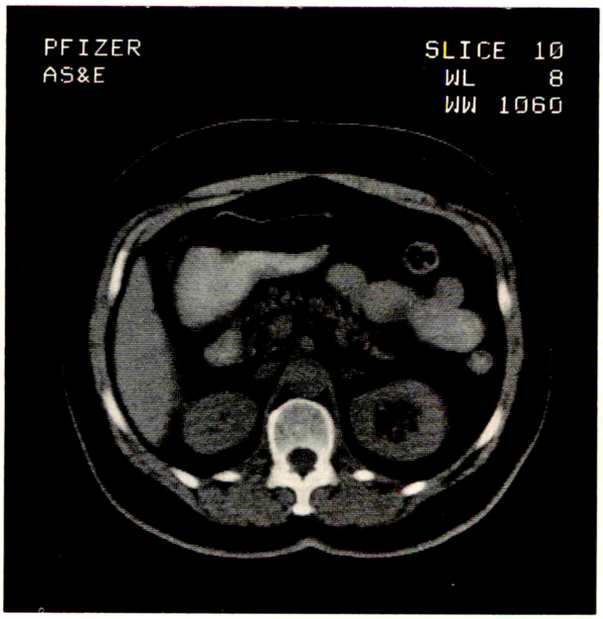
Toshiba Corporation, Tokyo, Japan

A new standard of accuracy in CT imaging

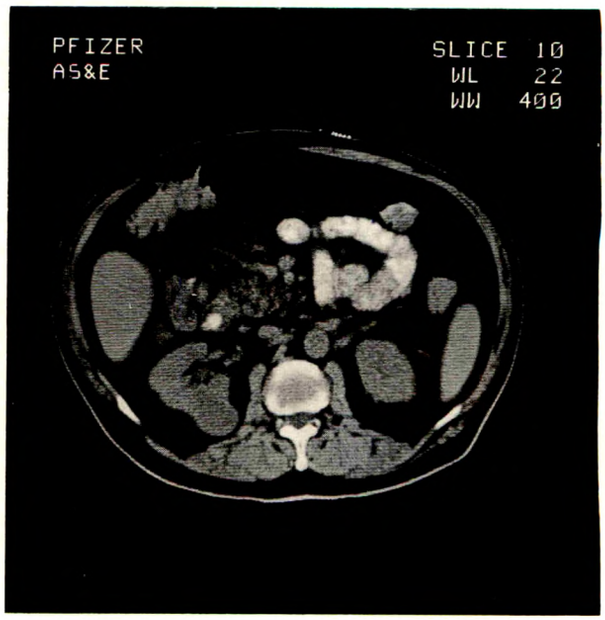
Pfizer/AS&E Generation IV



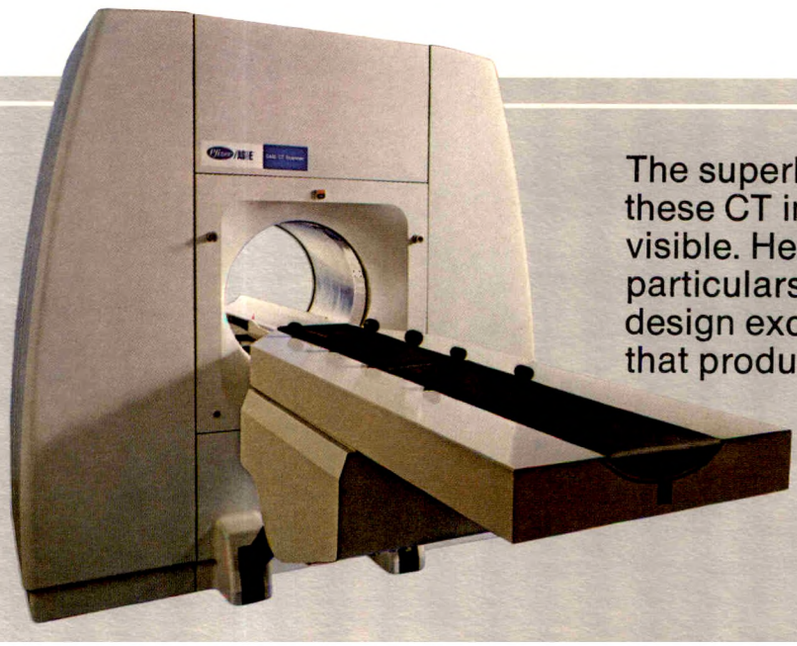
Superior scans from stationary detectors



CT scan of the abdomen. The inferior portion of the left adrenal gland is well visualized as is the vertical portion of the superior mesenteric artery anterior to the aorta.



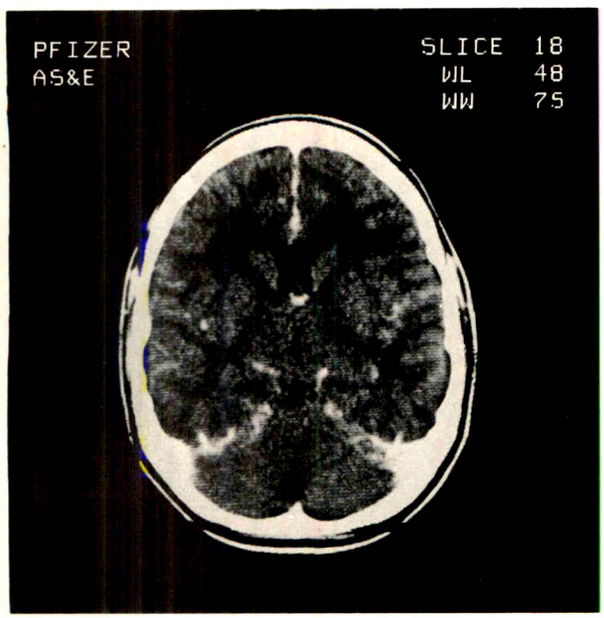
CT scan of the abdomen. The spinal cord and nerve roots are well demonstrated. Note the mass at the posterior medial aspect of the right kidney.



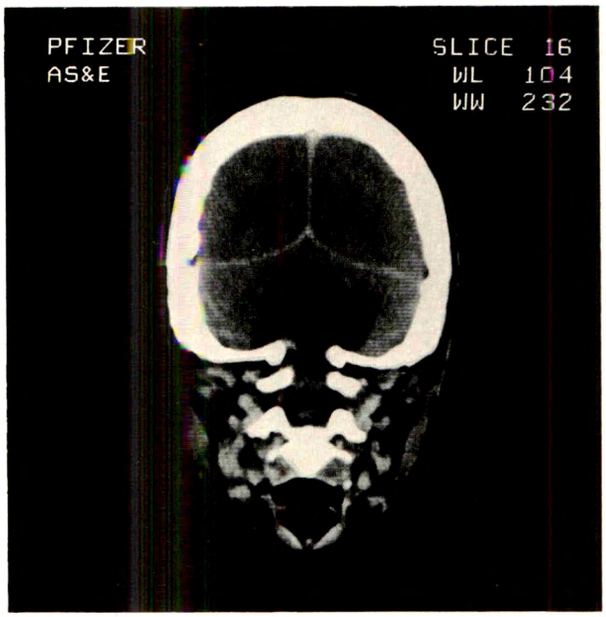
The superb quality of these CT images is clearly visible. Here are some particulars of the design excellence that produced them:

Pfizer/AS&E

0450



CT scan of the head. There is excellent separation of central white and gray matter. The caudate nucleus and basal ganglia are clearly seen.



CT scan of the head. Coronal view. Contrast enhanced tentorium demonstrated. There is a midline posterior fossa arachnoid cyst. Note the absence of artifacts.

Continuous detector calibration for the most accurate CT numbers and images available...

Pfizer/AS&E 0450. Generation IV. Only the x-ray tube rotates; the full circle of photon detectors is stationary. All attenuation data are continuously referenced to objects of known attenuation within, and immediately outside, the patient scan field. And each detector is calibrated on every scan—making possible DENSET, the precise CT number stabilization system which eliminates even potential errors in data acquisition. DENSET clearly provides a new dimension in CT diagnosis—reliable, repeatable imaging across the entire scan field.

...And freedom from artifacts

Pfizer/AS&E Generation IV. Where every detector reviews the entire scan field, not just a small portion. The classic image-degrading circular artifact caused by detectors viewing individual circles within the scan field simply cannot occur. 0450 Generation IV CT images are, by design, free from geometric defects.

Superior scans from advanced technology

More efficient detection—better dose utilization

The scintillation crystal/photomultiplier detectors used in the Pfizer/AS&E 0450 provide you and your patient with optimum dose utilization. Because we start with solid crystals, having twice the detector efficiency of comparable Xenon chambers at high pressures, over 98% of all x-ray photons striking the crystal are detected and contribute to the final image.

Less noise—better contrast resolution

Of all x-ray detectors, the solid scintillation photomultiplier tube combination provides the highest signal-to-noise ratio and widest dynamic range. Readings are not degraded by noise introduced with less sensitive detectors. Contrast resolution and range of dose utilization are superior by design.

Faster detector response—better spatial resolution

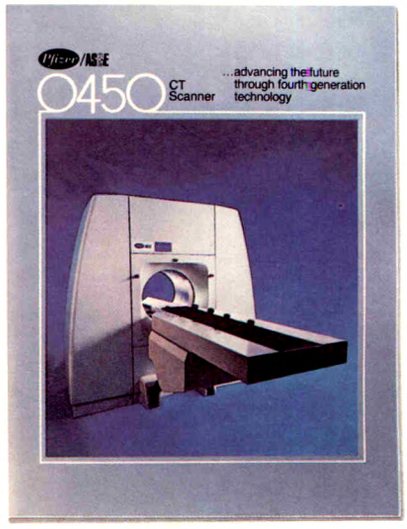
0450 detectors are sensitive, exhibit fast response, and do not become saturated. These properties allow data to be collected continuously instead of at the rate with which the x-ray source can be pulsed. The results: more data, faster scans and superb spatial resolution.

Full field resolution—image integrity

Tiny anatomical structures (1-1.5 mm) varying only slightly in density are faithfully resolved and displayed uniformly over the entire scan field even at *lowest dose settings.* This ultra-high fidelity is achieved by using a 640 x 512 matrix which is reconstructed from more than 700,000 data measurements—requiring no extensive "smoothing" software.

Pfizer/AS&E 0450

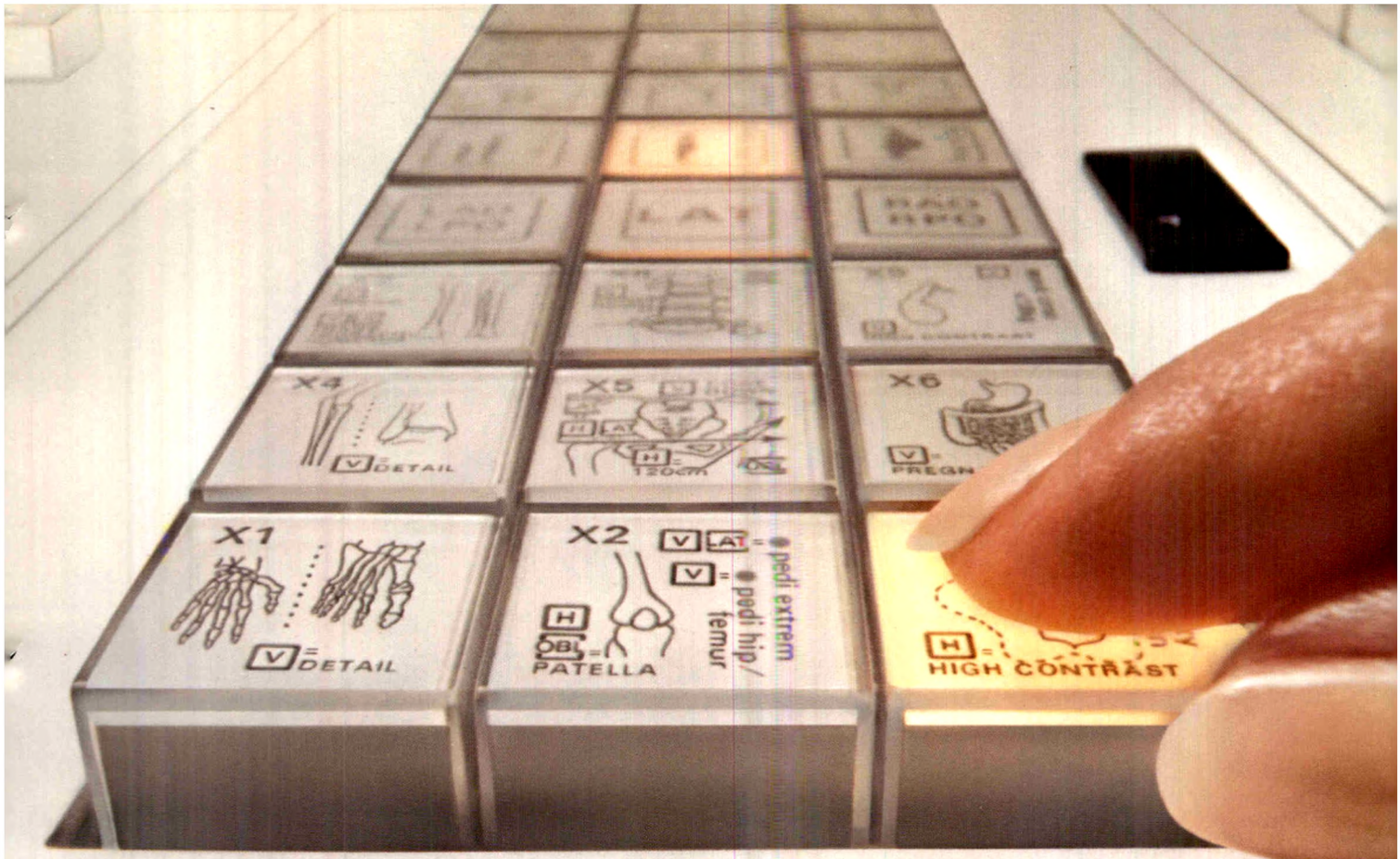
The superior CT scanning system you'll want to know more about



Write us for a detailed brochure:
Pfizer Medical Systems, Inc.
235 East 42nd Street, New York, N.Y. 10017

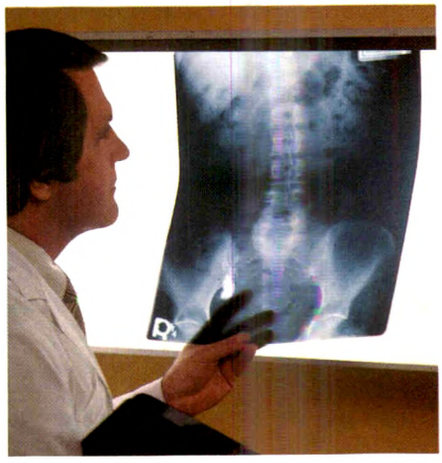
PFIZER MEDICAL SYSTEMS, INC.
A subsidiary of Pfizer Inc.
235 East 42nd Street, New York, N.Y. 10017
Telephone: (212) 573-2323
Telex: 234088 (RCA) 62422 (WUI) 420440 (ITT)

PRINTED IN U.S.A.



On the button, every time.

MPX computerized generators give you high quality films, time after time.



That's because Quantamatic™ tx technic management consistently provides the right settings for each procedure, with microprocessor speed and precision.

You can store all your technics in the tx memory for instant access. Just press the appropriate selection buttons and the microprocessor instantly calculates and displays all technic parameters. Any setting may be overriden on command.

With over 200 programmed AEC and fixed time technics (on or off table) available, you can handle virtually every patient size. From infant to obese adult. And any body part, including extremities. You'll get standardized film quality, from exam to exam, room to room.

Fast, consistent technic selection means more time for patient positioning. And elimination of costly retakes. With MPX, you're right on the button every time.

You'd expect it from GE.

General Electric Medical Systems, Milwaukee, · Toronto, Madrid.

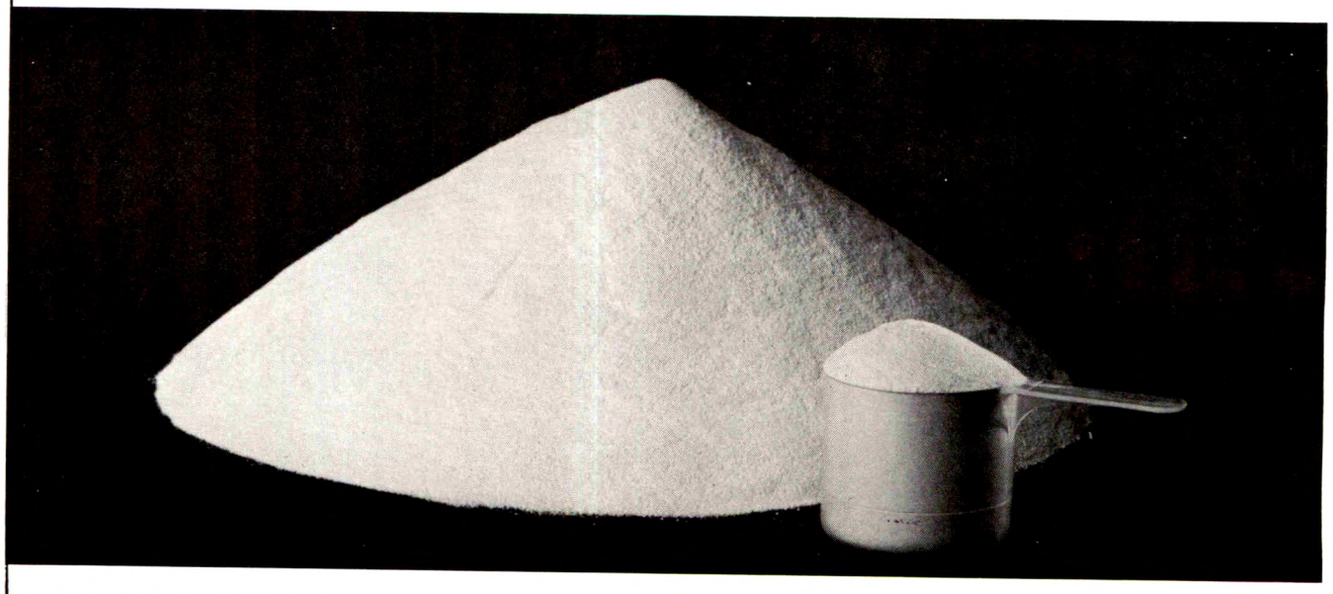
GENERAL ELECTRIC

ROUTINE BARIUM

NOT JUST WHAT YOU WANT... BUT EXACTLY WHAT YOU WANT!

If you are not using an E-Z-EM Barium Enema System you are not using the best.

We know that as a professional, your requirements are very specific. And that's why we make available barium enema systems in virtually any configuration you specify. Our extensive range of barium sulfate formulations, bags, tips, and tubing lets you select exactly what you need. We then combine them into the customized system that's best for you. If you would like further details or assistance in creating your own particular "package," call an E-Z-EM distributor or contact us directly.

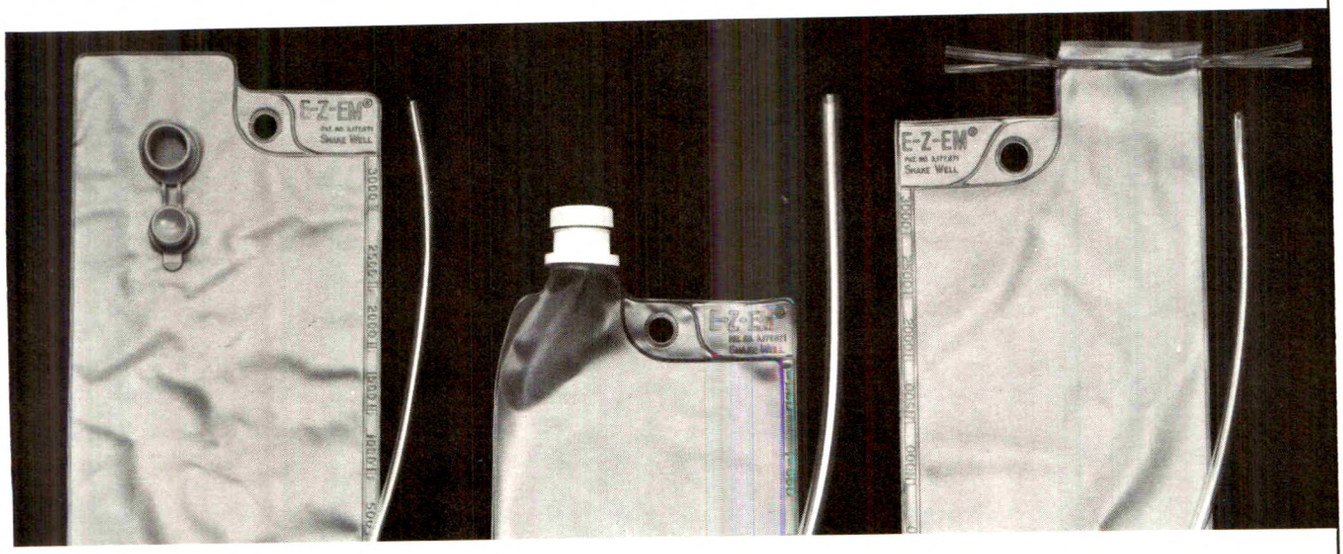


BARIUM

While most suppliers offer you a choice of only one barium sulfate formulation... we give you four distinct formulations... to fit your budgetary needs and give you greater working flexibility: Sol-o-Pake,™ Polibar™ Powder, E-Z-Paque,® and new ACB.™ Whichever you select, you can be sure of the highest quality radiographs... because they're all from E-Z-EM.

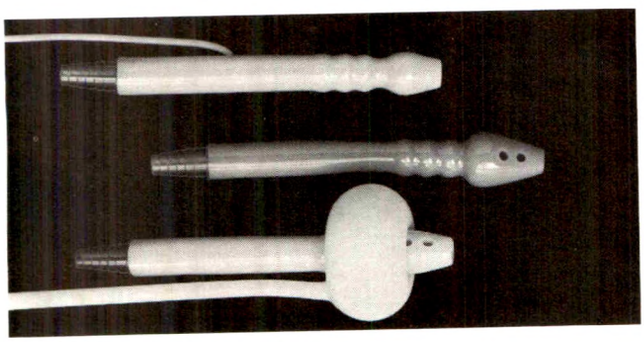
All E-Z-EM Barium systems offer density versatility from the lightest (12% w/w) for see through effect to 60% w/w for single stage air contrast.

ENEMA SYSTEMS.



BAGS

There's one to meet every preference . . . all made of durable, non-crack, heavyweight vinyl. Our selection includes snap cap models . . . 1 and 2–piece rigid spout . . . retrograde fill . . . double tie wrap . . . and others, each crafted to our highest standards, and every enema bag is completely inspected to assure compliance with our rigorous quality control standards.

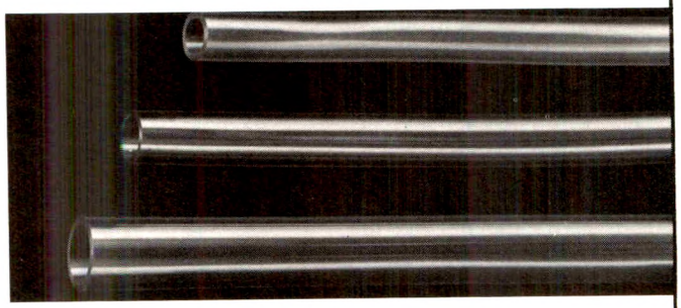


TIPS

Perhaps the largest selection anywhere. Choose from flexible tips . . . Miller air tips for double contrast, with and without cuffs . . . colostomy air contrast tips . . . pediatric tips and over 30 other specialized designs that make your work easier.

TUBING

We use only the finest grade of flexible vinyl . . . to be a perfect component of any E-Z-EM barium enema system you create. Available in either standard 5/16" lumen, 3/8" XL, and 1/2" Super XL.



Call today . . . we have the knowledge and the products!

E-Z-EM® 7 Portland Avenue, Westbury, New York 11590 (516) 333-8230

International Affiliates: E-Z-EM Rooster B. V., Infirmeriestraat 6-8, Rotterdam 16, Netherlands
E-Z-EM De Mexico, S. A. de C. V., Calz. Azcapotzalco La Villa No 882, Zona Industrial Vallejo, Mexico 16 D. F.

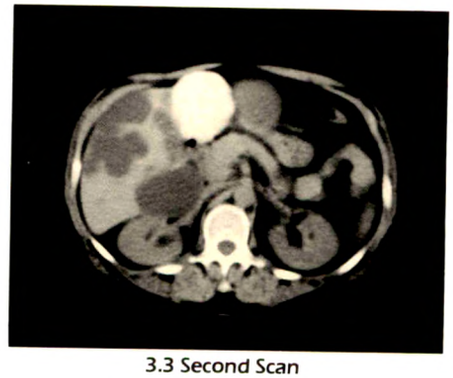
©1/79

...r high-qu...lity ...Ti...y sc...ns,



1 Second Scan

The advantages of speed in body scanning are evident in the absence of artifacts due to physiological motion. Note the well-defined loops of bowel in the above scan. Other structures seen are the kidneys and the renal arteries.



3.3 Second Scan

The above image demonstrates polycystic disease of the liver. Note the clear delineation of the pancreas, superior mesenteric artery and renal arteries. In addition, the left colic or splenic flexure can be seen.



f ster is bett-r.

To achieve high-quality body scans, faster is better. Synerview is the fastest scanning CT system presently available. It can routinely perform high-quality scans, as fast as 1 second.

Because of the natural involuntary motions that occur within the human body, fast-scanning capabilities are necessary for clear images in body scans. The faster your CT scanning capabilities, the more you can minimize motion artifacts caused by peristaltic, muscular, respiratory, and cardiovascular actions.

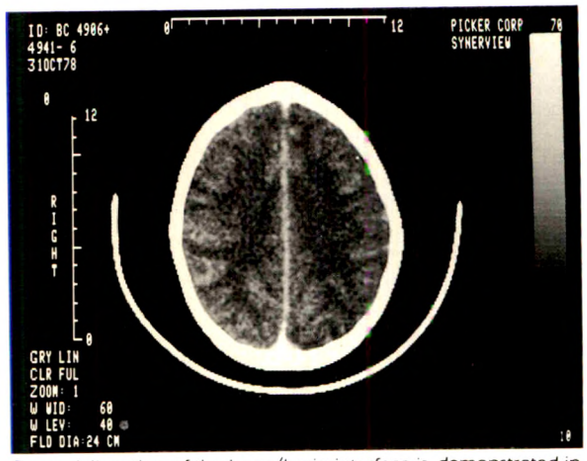
And for CT diagnosis to be effective for uncooperative, unconscious, pediatric or geriatric patients, you need 1-second scanning.

Ready to advance the state-of-the-art for CT. An investment in Synerview is the best way to obtain a high-quality CT scanner and minimize the obsolescence factor. Other manufacturers have reached the limit of their CT capabilities with the technology employed in their present systems. But Synerview, based on the proven Stationary Detector principle, has the potential to advance state-of-the-art for CT. Synerview is ready to expand its capabilities when new technology becomes available.

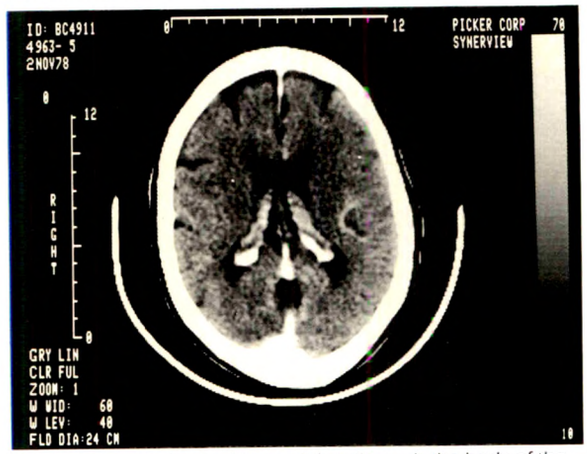
Synerview performance features. Synerview has features that help make CT operation fast and convenient. Our unique patient transport is one example. It lets you prepare a patient for scanning almost anywhere in the hospital. And to maximize your patient throughput, Synerview combines fast patient-data entry and scanning selection protocol with processing as fast as 25 seconds.

Superb software capabilities bring added dimensions to your CT operations. Synerview can display sagittal and coronal reconstructions in less than 5 seconds. Our bone correction software provides better visualization of the bone/brain interface. In addition, Synerview's optional therapy treatment planning feature can be supplied either for economical shared use, or for more versatile independent use.

And a field size of 48 cm means Synerview can perform body scans with even your larger patients.



Sharp delineation of the bone/brain interface is demonstrated in the above image. Note the white and gray matter separation.



In this contrast-enhanced image taken through the body of the lateral ventricles we see enhanced choroid plexus, torcula, and vein of galen. Note the white and gray matter differentiation as well as cortical sulci.

Head to head, there's no one better. We have the latest technology and the images to prove it.

A large portion of any CT caseload involves head scans. It's of particular significance to know that Synerview brings you high-quality head scans in addition to high-quality body scans. It's also important that you can position your patient's head easily with Synerview. You can get the right scan — the first time. And, for accurate Towne's projections, Synerview's ultra-stable gantry can tilt ±20 degrees.

For a free portfolio of Synerview head and body scans, contact your local Picker representative, or call collect 216/461-9100, CT Marketing, extension 332. Picker Corporation, 595 Miner Road, Cleveland, OH 44143.

PICKER®

ONE OF THE CIT COMPANIES

X-RAY IMAGE INTENSIFYING SYSTEMS

precise optics

IT MAY SURPRISE YOU.....

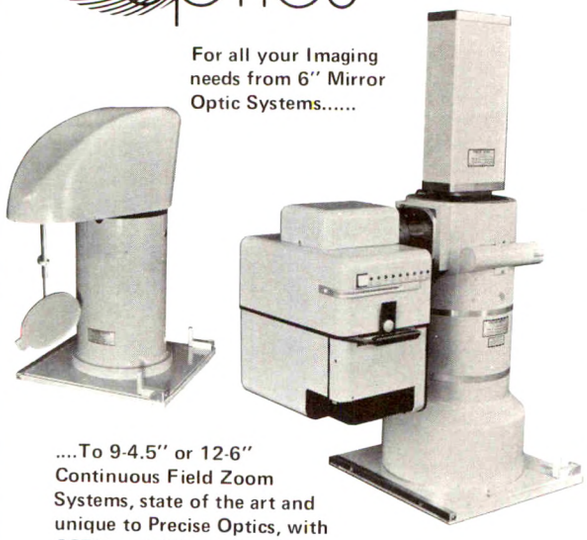
. . . to know that the people at Precise Optics have been supplying X-Ray Image Intensifying Systems since 1954. Precise specializes in Imaging, and offers a complete line of systems to meet requirements ranging from the private office to the special procedures room, at a cost savings over comparable units, without sacrificing quality.

EVERY SYSTEM CONTAINS a guaranteed optimal performance cesium iodide image tube and field-proven solid-state power supply, covered by a two-year warranty.

THE PRECISE CCTV SYSTEM uses x-ray rated separate mesh vidicons, selected for high resolution and low-lag characteristics. Brightness compensation is an excellent 10,000:1, assuring the correct light level despite large variations in body densities.

THE NEW 105mm SPOT/RAPID SEQUENCE CAMERA (roll film, 6 frames per second maximum) utilizes the same digital electronics package and many of the mechanical sections of our other reliable 105mm cameras, while incorporating a rapid-load film transport and daylight receiving cassettes.

ACCESSORIES AVAILABLE INCLUDE: TWO-AND THREE-PORT LIGHT DISTRIBUTORS for spot and cine filming capabilities, ABS SYSTEM with automatically variable kV and selectable mA, SPOT FILM ADAPTERS compatible with any spot film device, CEILING SUSPENSION UNITS with smooth vertical and horizontal movements, CCTV MONITOR CARTS that are lightweight and easily mobile.



For all your Imaging needs from 6" Mirror Optic Systems.....

....To 9-4.5" or 12-6" Continuous Field Zoom Systems, state of the art and unique to Precise Optics, with CCTV and 105mm Spot/Rapid Sequence Cameras.

PRECISE OPTICS/PHOTO MEDIC EQUIPMENT, INC.
239 SO. FEHR WAY
BAYSHORE, N.Y. 11706
TEL. (516) 242-6600
TWX 510-227-9837

Everything we know about money-saving, time-saving, energy-saving ride sharing programs is yours for the asking.

Free. Our Double Up kit contains facts, figures, ideas, promotional help and other good things you and your company should know about.

I want to know it all. Please send your Double Up kit right away.

Name _____ Title _____

Company _____

Address _____

City _____ State _____ Zip _____

Ad Council

A public service of this magazine, the U.S. Department of Transportation and The Advertising Council.

PHILIPS TOMOSCAN 300

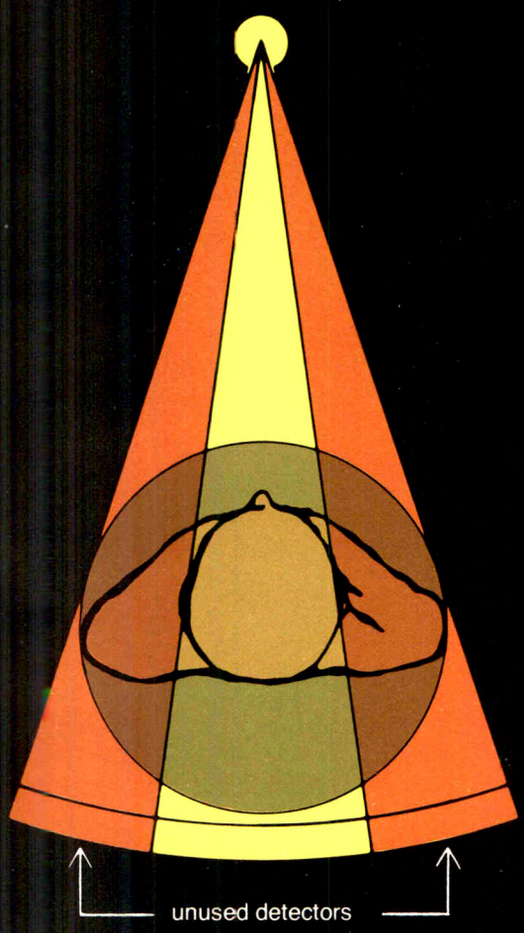
Philips Tomoscan 300

the only fast
scanner with variable
geometrical enlargement
–and full use of every
Xenon detector.

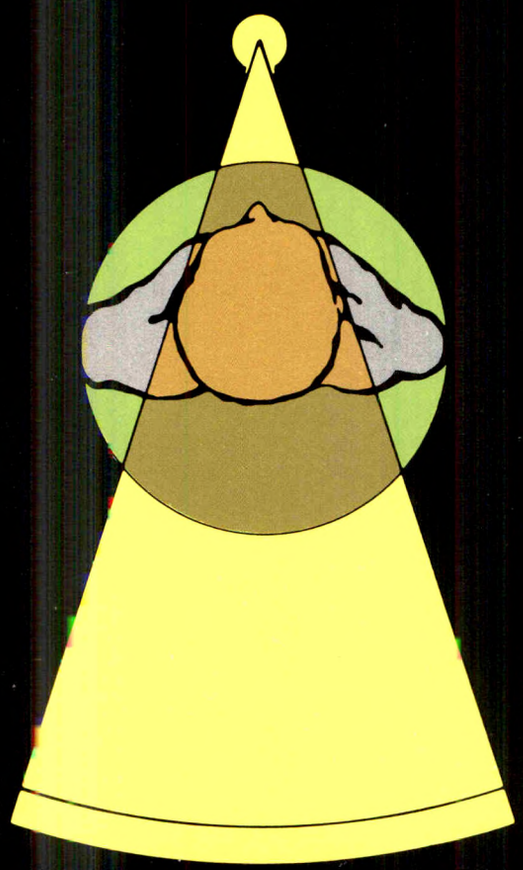
You're entitled to your points of view... all 172,800 of them.

Today's scanners are missing the points, especially for cerebral and pediatric studies. Philips isn't. Judge for yourself.

The problem: unused detectors



Philips' solution: geometrical enlargement



Only Philips makes full use of all detectors all the time. Why? Because the number of detector channels used and the number of pulses per scan create a data profile of image points which the computer reconstructs into an image. The more detectors used, the more image points. And the more "points of view," the closer the image comes to maximum spatial resolution and a better diagnostic result.

Philips Tomoscan 300 produces a superb image every time.

Actually, it's good old fashioned logic: waste not, want not.

While everyone else built scanners frantically, Philips built the best—on medical basics, not medical gimmickry.

Turn the page. We've got more of the best to offer.

PHILIPS®
TOMOSCAN 300

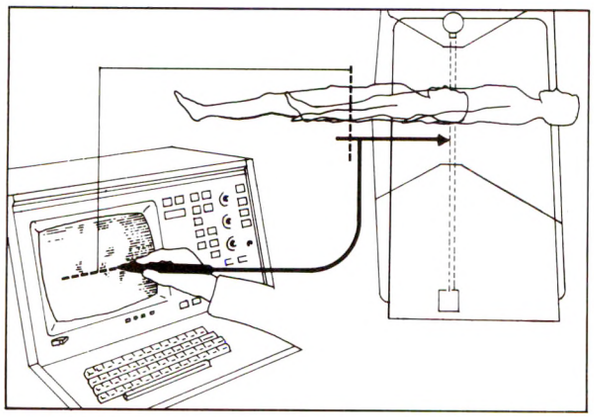
A 4.2 second whole body CT scanner

The concept was developed slowly and methodically—right in the middle of an industry-wide frenzy to sell systems that, in many cases, were outdated before installation was complete.

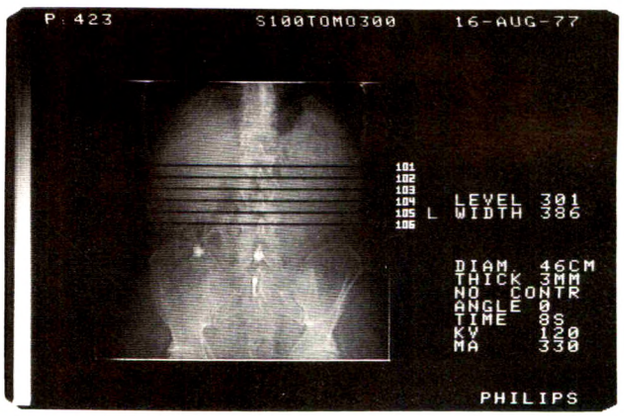
Philips did it differently. In close consultation with medical professionals worldwide, we evaluated *real* clinical needs. We said "No" to the unnecessary gadgetry that gives scanners a futuristic look. Instead, we returned to basics and developed a scanner with a future.

The result is our TOMOSCAN 300, a truly universal fast-scanner designed first and foremost as a medical instrument. Its features, like its specifications, stem from an appraisal of the system's medical application. Consider just some of the key reasons why you'll want to select TOMOSCAN 300.

THE SCANOGRAM



AN ACTUAL SCANOGRAM



- Computerized patient positioning for survey studies at very low dose exposures. The Scanogram provides lines that identify each slice by number and location of the body for lightpen selection of the exact scan location. The touch of a button brings the area of interest into the scan plane. The Scanogram eliminates trial scans and unnecessary radiation. Automatic patient positioning can also be done with a lightbeam.
- Rapid image reconstruction time (15 seconds)
- Wide choice of scanning parameters for precise adaptation to applicational requirements. For example:

——variable scanning speed—from 2.6s to 4.2s
——variable slice diameters—from 25cm (10″) to 48cm (19″)
——variable slice thickness—3, 6, 9 or 12mm

- Outstanding image quality
- Extraordinary range of viewing facilities, including:

——slow and fast window level control
——11-step window width control
——calculation capability for average attentuation, standard deviation and number of pixels for three regions of interest of both irregular and circular regions
——enlargement, image reversal and distance measurement between any two pixels
——Stand-alone physician's viewing console with lightpen

There's more, much more . . . because Philips considers *your* point of view.

PHILIPS MEDICAL SYSTEMS, INC.
710 Bridgeport Avenue, Shelton, Conn. 06484

® TM N.V. Philips of Holland

Our references incorporate the latest research and the most precise techniques to help you get the best results.

COMPUTED TOMOGRAPHY OF ABDOMINAL ABNORMALITIES. By John Haaga, M.D.; and Norbert F. Reich, D.O.; with 4 contributors. Increase your understanding and more effectively interpret the results of abdominal CT scanning with this excellent atlas. Based on the authors' extensive experience, it clearly describes and beautifully illustrates CT examinations of the abdomen; methods of examination; pathologic abdominal abnormalities; and proper interpretation methods. A particularly interesting chapter includes up-to-date CT images from 4th generation instrumentation, or the 2-second body scanner. 1978. 442 pp., 516 illus. **Price, $47.50.**

NUCLEAR MEDICINE PHYSICS, INSTRUMENTATION, AND AGENTS. Edited by F. David Rollo, Ph.D., M.D.; with 12 contributors. Keep pace with the instruments and agents you currently use with this fine book. It examines both the physics upon which instrumentation is based and the materials you use daily. Throughout, the emphasis is on quality control — to evaluate and improve both equipment performance and quality of results. Initial chapters help you review basic and applied electronics. Succeeding chapters explore such subjects as special imaging devices — tomographic scanners, positron cameras, three-dimensional reconstruction techniques — and statistical therapy. 1977. 712 pp., 626 illus. **Price, $54.50.**

A New Book. **ATLAS OF PEDIATRIC NUCLEAR MEDICINE.** By Philip O. Alderson, M.D.; David L. Gilday, M.D., B.Eng., F.R.C.P.; Henry N. Wagner, M.D.; with the assistance of Judith Buchanan and Wendy A. North, B.A., M.I.R., N.M.T. Gain new insights into the latest diagnostic techniques in pediatric nuclear medicine with the help of this unique graphic atlas. Discussions explore technical considerations and skeletal, soft tissue, pulmonary, cardiovascular, liver, spleen, genitourinary, gastrointestinal, thyroid, and central nervous systems. More than 170 cases accompany the superb illustrations, and provide you with concise descriptions and interpretations. December, 1978. 314 pp., 789 illus. **Price, $44.50.**

A New Book. **CARDIOVASCULAR ANGIOGRAPHY FOR TECHNOLOGISTS.** By David Garrison, Ph.D.; and Anne Donnell, R.T. (ASRT). Heart catheterization lab personnel can now receive standardized training with this new manual. It summarizes the necessary knowledge and skills required of heart cath lab personnel. Coverage includes organization of the laboratory and staff, the basic laboratory equipment, lab examinations, contrast media, anatomy and physiology of the cardiovascular system, invasive techniques, and neuroradiography. January, 1980. Approx. 225 pp., 86 illus. **About $13.95.**

A New Book. **MATHEMATICS FOR TECHNOLOGISTS IN RADIOLOGY, NUCLEAR MEDICINE, AND THERAPEUTIC RADIOLOGY.** By Stefano S. Stefani, M.D.; and Lincoln B. Hubbard, Ph.D. Review essential computations with this handy reference. Emphasizing practical application, the book provides problems and worked examples that illustrate fundamental mathematic principles — scientific figures and notations, basic algebra, geometry, graphical display, logarithms, probability and statistics, and computational methods. Helpful tables are provided for selected conversion factors and constants. Answers are listed for all questions and problems posed. May, 1979. Approx. 256 pp., 117 illus. **About $10.95.**

A New Book. **MEDICINE — AN ILLUSTRATED HISTORY.** By Albert S. Lyons, M.D.; and R. Joseph Petrucelli, II, M.D. All of the fascination, pride, inspiration and traditions of medicine are graphically described in this well documented and superbly illustrated atlas. Two distinguished physicians trace the historical record of human achievement in the healing arts with impressive documents, drawings, statuettes and wall paintings. Written for interested professionals and laymen alike, this singular pictorial survey will give you a new understanding and appreciation of medicine. See it for yourself. December, 1978. 618 pp., 1,020 illus., including 250 in color. **Price, $75.00.**

Prices subject to change.

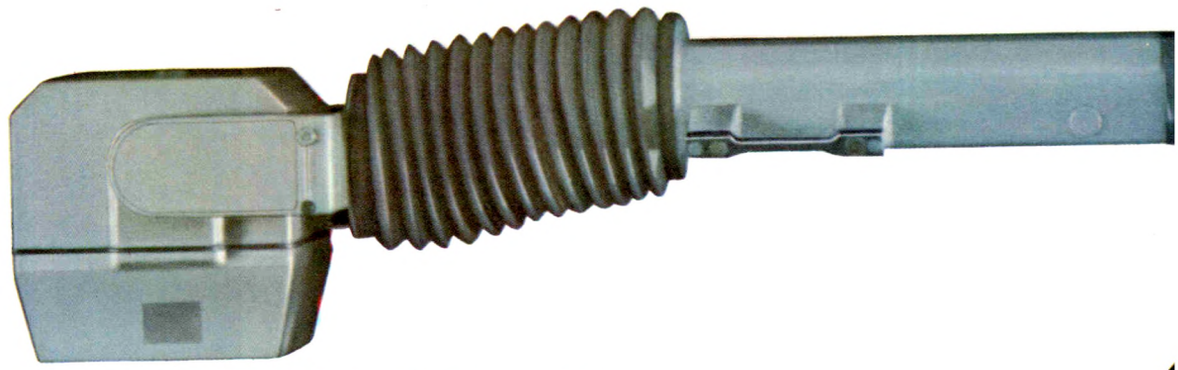
ORDER BY PHONE! Simply call toll free (800) 325-4177 ext. 10; in Missouri, call collect (314) 872-8370 ext. 10 during normal business hours.

MOSBY

TIMES MIRROR

THE C. V. MOSBY COMPANY
11830 WESTLINE INDUSTRIAL DRIVE
ST. LOUIS, MISSOURI 63141

SIEMENS



Introducing the MOBIL XR: A revolutionary concept in X-ray systems

Siemens has taken the concept of mobile X-ray systems and redesigned it from top to bottom. The result is total freedom of positioning, exceptional maneuverability, and ease of operation seen only in the MOBIL XR.

Only the MOBIL XR simplifies positioning.
Its innovative flexible extender arm provides a height and distance capability over and above any other mobile X-ray system. Without moving the unit from the foot of the patient's bed, the operator can easily maneuver the X-ray tube housing into any position, including lateral. Typically, at a bed height of 32 inches, the MOBIL XR will allow a 60-inch source-image distance. No other mobile unit can offer this capability.

Only the MOBIL XR has complete computerized organ programming.
By simply activating the push-button controls, the operator can select specific organ programs, reprogram the unit for specialized application techniques, or switch to manual settings. And for functional security, a digital readout displays the Kv, mAs, and battery condition of the unit.





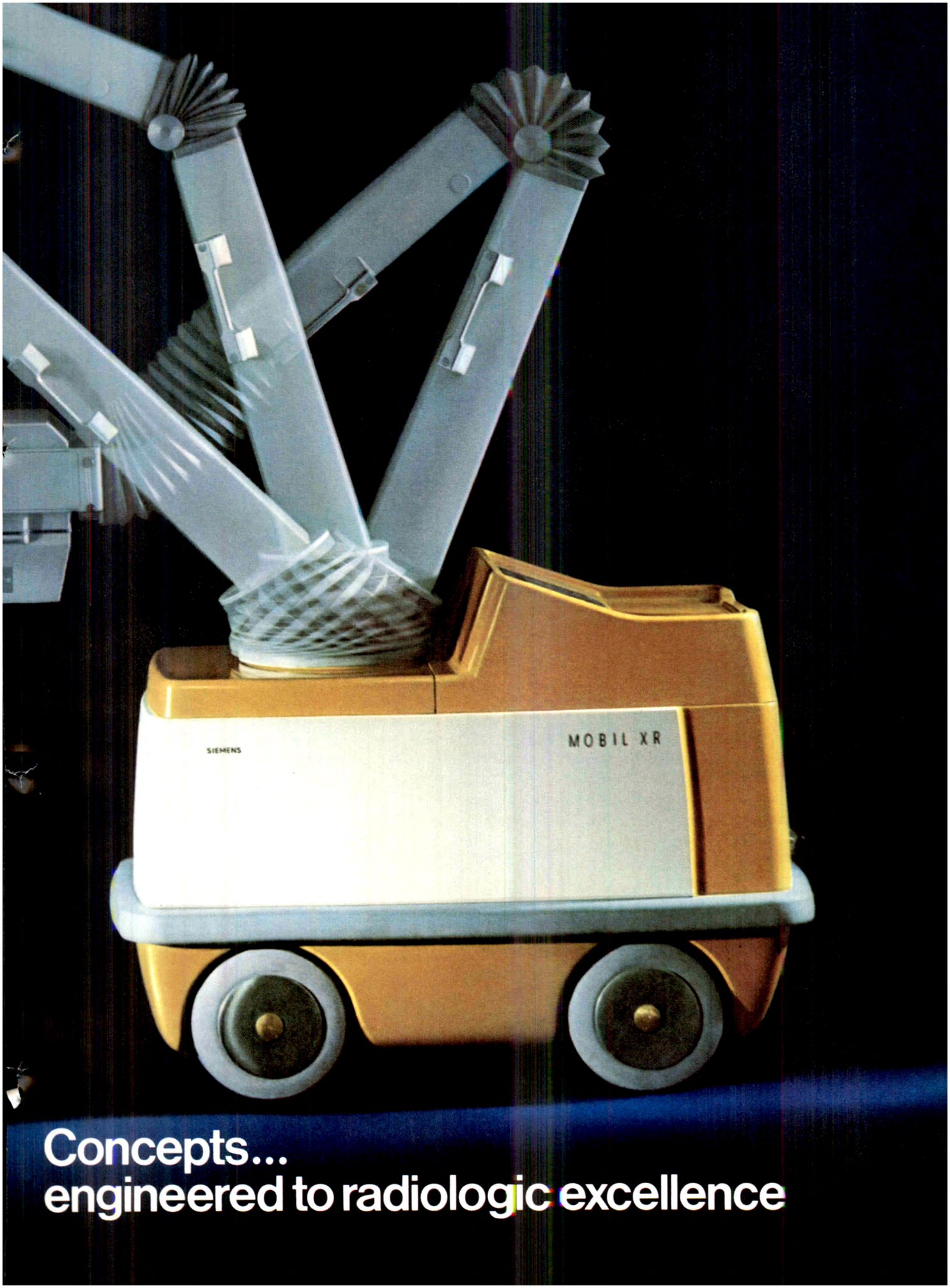
Only the MOBIL XR has a custom-designed cassette tunnel.
It establishes and maintains the proper perpendicular relationship between X-ray tube and film cassette to provide optimum geometric positioning accuracy.

Only the MOBIL XR is easy to clean and keep aseptic.
That's because its design is free of corners, ridges, and hidden surfaces. Bacteria has no place to hide on the smooth fiberglass body of the MOBIL XR.

The Siemens family of mobile X-ray units extends beyond the MOBIL XR to include the KONDIAMOBIL 125 and the SIREMOBIL 2U. All are products of the quality engineering that reflect Siemens' standard of excellence in the field of radiological equipment.

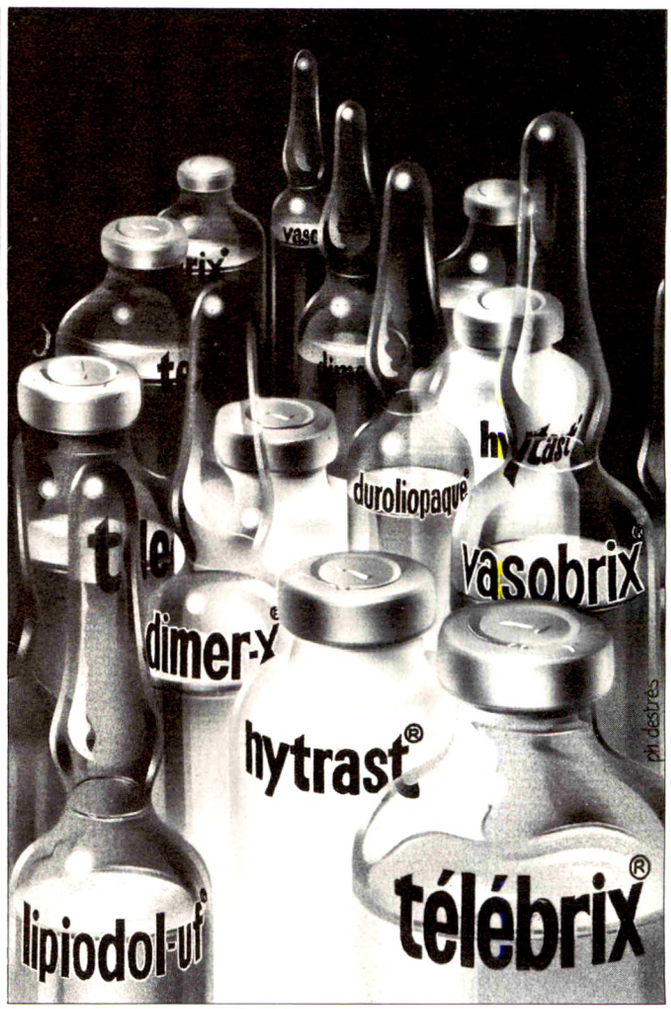
For further information, please contact your local Siemens Representative or Siemens Corporation, Medical Systems Division, 186 Wood Avenue South, Iselin, New Jersey (201) 494-1000. In Canada: Siemens Canada Limited, P.O. Box 7300, Pointe Claire 730-P.Q.

SIR-409



Concepts...
engineered to radiologic excellence





Research & development

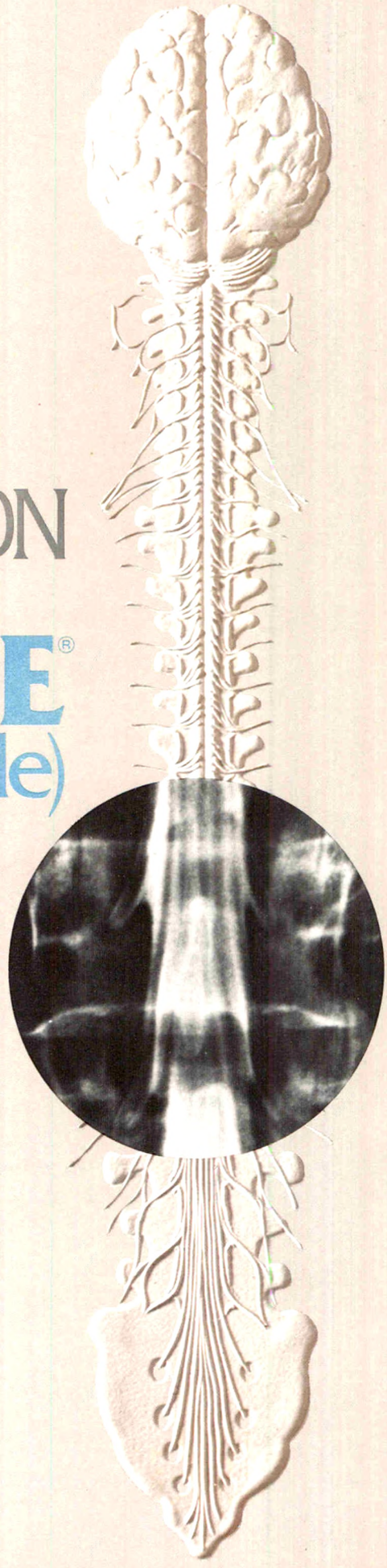
GUERBET

Better contrast media through research

Laboratoire GUERBET
16-24, rue Jean Chaptal - 93609 Aulnay-sous-Bois - Cedex FRANCE
Tél. : 929.78.37 - Télex : 212382 F.

DISCOVER MORE WITH CLEAR DEFINITION

new AMIPAQUE® (metrizamide)

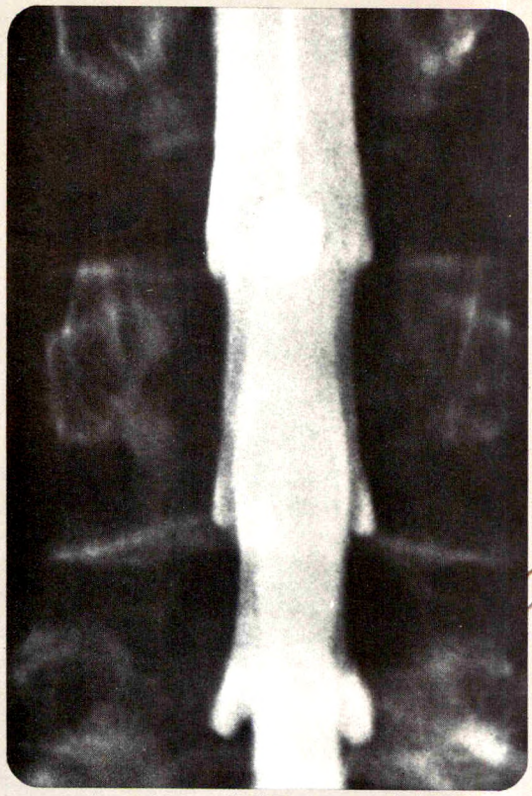


See last page for important product information including warnings, adverse reactions, and prescribing and precautionary recommendations.

COMPARE RADIOGRAPHS

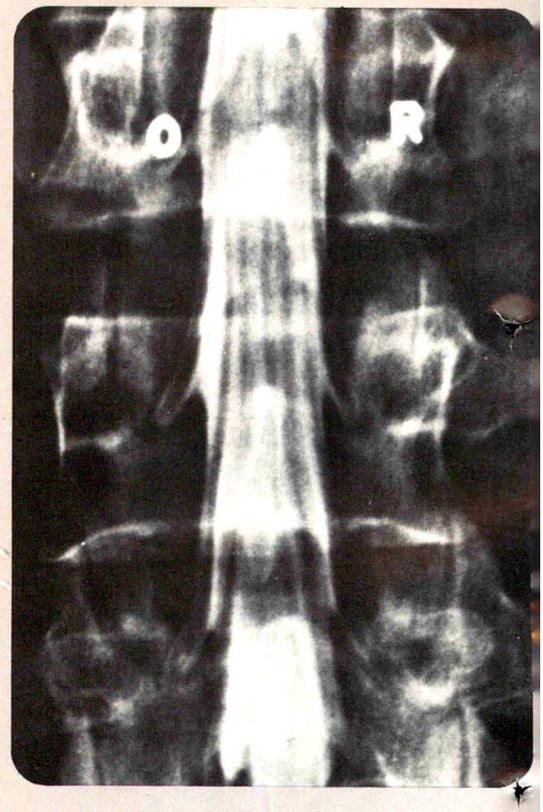
iophendylate

Lumbar myelogram of 27-year-old female (anteroposterior view): Note high-density shadows and failure of contrast medium to adequately fill nerve-root sheaths.



AMIPAQUE (metrizamide)

Lumbar myelogram of 20-year-old male (anteroposterior view): Note graded density of shadows and filling of nerve-roo sheaths by the low-viscosity, water-soluble contrast medium.



See last page for important product information including warnings, adverse reactions, and prescribing and precautionary recommendations.

CLEARER VISUALIZATION

Water-soluble, low viscosity

- ☐ Miscible with CSF for more uniform distribution around structures in subarachnoid space.[1,2]
- ☐ Flows into and through narrow subarachnoid spaces, fills slender cavities of nerve-root sheaths.[1,3]
- ☐ Usually diffuses around all except total obstructions with a single injection.
- ☐ Radiographic contrast provides nonobscured view of fine details.

Slightly hyperbaric

- ☐ Allows control of contrast distribution during initial phase of radiologic study, if desired.[1,3]

SIMPLIFIED MYELOGRAPHY

Nonionic... does not dissociate in solution

Isotonic with CSF at concentrations most frequently used (170 mgI/ml).

Low viscosity

- ☐ Allows use of narrow-bore needle (22-gauge).
- ☐ Less chance of CSF leakage... less chance of trauma to dura.

Resorbed and excreted mainly via kidneys in 48 hours

- ☐ No need for aspiration or second puncture... lessens potential for neurologic damage.
- ☐ No needle left in place during procedure... facilitates patient manipulation.

PATIENT TOLERANCE

- ☐ In general, the types of adverse reactions following subarachnoid injection of AMIPAQUE are not substantially different from those seen after lumbar puncture alone.
- ☐ The most frequently occurring reactions are headache, nausea, and vomiting.
- ☐ Rarely have reactions been severe or persistent beyond 24 hours.
- ☐ Although metrizamide is relatively safe and, in comparative studies, less toxic than other compounds for these indications, side effects ranging from headache and nausea to epileptic fits, convulsions, slow wave patterns on EEGs, petit mal states, paralysis, and arachnoiditis have occurred with the use of such compounds. Neurologic examinations were performed before and at intervals after the procedures in 1,495 of 1,850 cases. No clinically significant changes were found.

INDICATIONS:

lumbar, thoracic, cervical, and total columnar myelography; and for use in computerized tomography of the intracranial subarachnoid spaces following spinal subarachnoid injection.

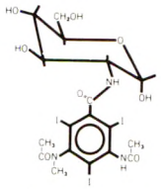
new **AMIPAQUE**®

(metrizamide)

More fully investigated before introduction than any other subarachnoid contrast agent

☐ 158 published reports ☐ 5 years in clinical research ☐ 2 years in U.S. medical centers

Description: Metrizamide, 2-[3-Acetamido-2,4,6-triiodo-5-(N-methylacetamido) benzamido]-2-deoxy-D-glucopyranose, is a compound derived from metrizoic acid and glucosamine. It is a nonionic water-soluble contrast medium with a molecular weight of 789 (iodine content: 48.25%). The chemical structure is as follows:



AMIPAQUE (metrizamide) is provided as a sterile, white lyophilized powder. Each 3.75 g/20 ml vial contains 3.75 g metrizamide (1.81 g organically-bound iodine) and 1.2 mg edetate calcium disodium. Each 6.75 g/50 ml vial contains 6.75 g metrizamide (3.26 g organically-bound iodine) and 2.16 mg edetate calcium disodium.

Each 20 ml vial of sterile aqueous diluent contains 0.05 mg/ml sodium bicarbonate in water for injection. pH is adjusted with carbon dioxide, USP, if necessary.

When AMIPAQUE is reconstituted to the lowest recommended concentration (170 mgI/ml) it has a specific gravity of 1.184 at 37°C, is hyperbaric to cerebrospinal fluid, is isotonic with CSF, and has a pH of approximately 7.4.

Clinical Pharmacology: AMIPAQUE is absorbed from cerebrospinal fluid into the bloodstream. Approximately 60 percent of the administered dose is excreted unchanged through the kidneys within 48 hours.

The initial concentration and volume of the medium, in conjunction with appropriate patient manipulation, will determine the extent of the diagnostic contrast that can be achieved. This can be monitored by fluoroscopy.

Following spinal subarachnoid injection, conventional radiography will continue to provide diagnostic contrast for approximately an hour. At 4 to 5 hours contrast is hazy and none is detectable at 24 hours.

Following subarachnoid placement, irrespective of the position the patient has maintained, upward diffusion of AMIPAQUE takes place through the CSF.

After introduction into the lumbar subarachnoid space, computerized tomography (CT) shows CSF contrast enhancement in the thoracic region in about one hour, in the cervical region in about 2 hours, and in the basal cisterns in 3 to 4 hours.

When low doses of AMIPAQUE (see DOSAGE AND ADMINISTRATION) are introduced into the lumbar CSF and moved cephalad under gravity control and examined by CT scanning, they will provide immediate CSF contrast in the basal cisterns. Depending on the specific technique used, the lateral, third, and fourth ventricles may also be visualized. The contrast in this area will markedly diminish at 6 hours and disappear by 24 hours. CSF enhancement will be evident at the cortical sulci and interhemispheric fissures at 6 hours. Between 12 and 24 hours the surfaces of the cerebrum and cerebellum, in contact with the subarachnoid spaces, will develop a "blush" effect on the scan which will normally disappear in 36 to 48 hours. The rate, time, extent of diffusion, and the disappearance or stasis of AMIPAQUE as demonstrated with CT scanning, can be used to detect or infer the presence of CNS abnormalities.

Indications and Usage: AMIPAQUE is indicated for lumbar, thoracic, cervical, and total columnar myelography and for use in computerized tomography of the intracranial subarachnoid spaces following spinal subarachnoid injection.

Contraindications: AMIPAQUE should not be administered to patients with a known hypersensitivity to metrizamide.

Warnings: If grossly bloody CSF is encountered, the possible benefits of a myelographic procedure should be considered in terms of the risk to the patient.

Usage in pregnancy. No teratogenic effects attributable to AMIPAQUE have been observed in reproduction studies in animals. However, before administration of AMIPAQUE to women during pregnancy, the benefit to the patient should be carefully weighed against the possible risk to the fetus.

Until further experience is gained in children younger than 12 years, administration of AMIPAQUE in this age group is not recommended.

Fatal reactions have been associated with the administration of water-soluble contrast media. Although no fatal reactions have been associated with AMIPAQUE, it is of utmost importance that a course of action be carefully planned in advance for the immediate treatment of serious reactions, and that adequate and appropriate facilities and personnel be readily available in case of a severe reaction.

Precautions: Caution is advised in patients with a history of epilepsy, severe cardiovascular disease, chronic alcoholism, multiple sclerosis, or with a history of bronchial asthma or other allergic manifestations.

Before a contrast medium is injected, the patient should be questioned for a history of allergy. Although a history of allergy, including asthma, may imply a greater than usual risk, it does not arbitrarily contraindicate the use of the medium. Premedication with antihistamines to avoid or minimize possible allergic reactions may be considered. No conclusive relationship between severe reactions and antigen-antibody reactions or other manifestations of allergy has been established.

Patients who are receiving anticonvulsants should be maintained on this therapy. Should a seizure occur, intravenous diazepam or sodium phenobarbital is recommended.

Prophylactic anticonvulsant treatment with barbiturates or diazepam orally for 24 to 48 hours should be considered in patients with evidence of inadvertent intracranial entry of a large or concentrated bolus of the contrast medium since there is an increased risk of seizures in such cases.

Any drugs, such as neuroleptics, including phenothiazine derivatives, which lower the seizure threshold should be avoided. These drugs should not be used as premedications. If possible, they should be withdrawn at least 48 hours before the examination and not used for at least 12 hours postprocedure.

In patients with severe renal insufficiency or failure, the drug is excreted by the liver into the bile at a much slower rate. Patients with hepatorenal insufficiency should not be examined unless the possibility of benefit clearly outweighs the additional risk. Reexamination should be delayed for five to seven days.

Adverse Reactions: In general, the adverse reactions following subarachnoid injection of AMIPAQUE are not substantially different from those seen after lumbar puncture alone. The most frequently occurring adverse reactions are headache, nausea, and vomiting. These reactions occur 3 to 8 hours postinjection, almost all occurring within 24 hours. They are usually mild to moderate in degree lasting for a few hours and disappearing within 24 hours. Rarely have the headaches been severe or persisted beyond 24 hours.

Backache, neck stiffness, numbness and paresthesias, leg or sciatic-type pain occurred less frequently, often in the form of a transient exacerbation of preexisting symptomatology. Temperature elevations and dizziness have also been reported.

Rarely, muscle spasm or generalized convulsions have occurred 4 to 8 hours following injection and in some cases were attributed to a history of epilepsy, medication with neuroleptic drugs, or inadvertent overdose. In all cases, treatment with intravenous diazepam or sodium phenobarbital has provided rapid control.

Transient alterations in vital signs may occur, the significance of which is difficult to assess since these parameters may be affected by the procedure or the patient's physical or emotional state.

Other rarely occurring adverse reactions include the following:

Allergy or Idiosyncrasy: chills, pruritus, urticaria, nasal congestion, and dyspnea.

CNS: mild and transitory perceptual aberrations such as hallucinations, depersonalization, anxiety, depression, hyperesthesia, visual and speech disturbances, confusion and disorientation. In addition, malaise, weakness, EEG changes, and meningismus have occurred.

Cardiovascular: chest pain, tachycardia, bradycardia, and arrhythmia.

Other: diarrhea.

Dosage and Administration: The dosage and concentration of AMIPAQUE will depend on the degree and extent of contrast required in the area(s) under examination and on the equipment and technique employed. Concentrations which are approximately isotonic (170 to 190 mgI/ml) are recommended for examination in the lumbar region. For movement of the medium to distant target areas, higher concentrations are recommended to compensate for dilution of AMIPAQUE with CSF.

A total dose of 3000 mg of iodine should not be exceeded.

The recommended usual and maximum doses of AMIPAQUE are summarized in the following table:

DOSAGE TABLE

Procedure	Conc. of Solution (mgI/ml)	Usual Recommended Dose* (ml)	Max. Dose Total (mgI)
Lumbar myelogram	170-190	10-15	2850
Thoracic myelogram	220	12	2640
Cervical myelogram (via lumbar injection)	250-300	10	3000
Cervical myelogram (via lat. cervical inj.)	220	10	2200
Total columnar myelography	250-280	10	2800
CT cisternography (via lumbar inj.)	170-190	4-6	1140

*Refer to RECONSTITUTION TABLE for preparation of Solution.

PATIENT MANAGEMENT

PREPROCEDURE: Anesthesia is not necessary. Premedication sedatives or tranquilizers are usually not needed. The use of neuroleptic drugs, including phenothiazine derivatives, should be avoided and such medication should be discontinued, when possible, 48 hours before the procedure (see PRECAUTIONS). Epileptic patients should be maintained on their anticonvulsant medication.

INSTRUCTIONS FOR PREPARATION OF THE SOLUTION: Contents under vacuum. Use only if vacuum is present as evidenced by diluent being drawn into vial when stopper is punctured.

1. Fill a sterile syringe with the exact volume of diluent as indicated in the following RECONSTITUTION TABLE to obtain the desired iodine concentration. *Examples: a.* For vials containing 3.75 g AMIPAQUE: To obtain 170 mgI/ml, use 8.9 ml of diluent; to obtain 190 mgI/ml, use 7.8 ml of diluent. *b.* For vials containing 6.75 g AMIPAQUE: To obtain 170 mgI/ml, use 16.1 ml of diluent; to obtain 190 mgI/ml, use 14.0 ml of diluent.

RECONSTITUTION TABLE

Conc. of Solution (mgI/ml)	Volume of Diluent to be Added 3.75 g Vial (ml)	6.75 g Vial (ml)
170	8.9	16.1
180	8.3	15.0
190	7.8	14.0
220	6.5	11.7
250	5.5	10.0
260	5.2	9.4
270	5.0	9.0
280	4.7	8.5
290	4.5	8.1
300	4.3	7.8
	The volume of the final solution will equal the volume of the diluent + 1.7 ml	The volume of the final solution will equal the volume of the diluent + 3.1 ml

The volume of the final solution will exceed the amount required to achieve the recommended dosage. For precise volume for injection refer to DOSAGE TABLE.

2. Inject the diluent into the vial, and leave the syringe and needle in place.
3. Gently swirl the vial (without shaking) until its contents are dissolved (approximately 3 to 10 minutes). The solution should be clear and colorless to slightly yellow.

Use immediately after reconstitution (see DOSAGE AND ADMINISTRATION). Discard any unused portion.

As with any lumbar puncture, sterile technique must be employed. The lumbar puncture is usually made between L3 and L4, but if pathology is suspected at this level the interspace immediately above or below may be selected. A lateral cervical puncture may also be used.

POSTPROCEDURE: The lumbar puncture needle may be removed immediately following injection since it is not necessary to remove AMIPAQUE after injection into subarachnoid spaces.

Management of the patient is similar to that used following simple lumbar puncture. Maintaining the patient recumbent in bed with the head raised 15° to 30° for 8 hours may reduce the rate of upward dispersion of the medium. The patient may then remain horizontal for a further 16 hours at the discretion of the physician.

How Supplied: *Kits, each containing:* one-3.75 g/20 ml single-dose vial of AMIPAQUE with 1 vial of diluent (NDC 0024-0044-01); or one-6.75 g/50 ml single-dose vial of AMIPAQUE with 1 vial of diluent (NDC 0024-0046-01).

Combination packs, each containing: five-3.75 g/20 ml single-dose vials of AMIPAQUE with 5 vials of diluent (NDC 0024-0044-12); or five-6.75 g/50 ml single-dose vials of AMIPAQUE with 5 vials of diluent (NDC 0024-0046-12).

Protect vials of AMIPAQUE from light.

References: 1. Grainger RG, Kendall BE, Wylie IG: Lumbar myelography with metrizamide—a new non-ionic contrast medium. *Br J Radiol* 49:996-1003, 1976. **2.** Peeters FLM: Myelography with metrizamide. *Radiol Clin* 46:203-213, 1977. **3.** Hindmarsh T: Myelography with the non-ionic water-soluble contrast medium metrizamide. *Acta Radiol [Diagn] (Stockh)* 16:417-435, 1975.

new **AMIPAQUE**® (metrizamide)

from the originators of the broad line of contrast media

Winthrop Winthrop Laboratories New York, N.Y. 10016

The Second Announces A First

Advanced regional learning seminars on radiographic imaging. From the second largest producer of photographic products in the world the Agfa-Gevaert Group.



Introducing

The Image Center

Advanced learning seminars on radiographic imaging.

A unique Resource Center.
Now, Radiology Departments throughout the country will have regional facilities to provide the most up-to-date information available on radiographic imaging: The Image Center. An educational resource where ideas can be exchanged. A resource that offers the opportunity to discuss new systems and techniques with recognized experts. A resource that provides continuing education credits in selected subject areas.

Located throughout the country.
These state-of-the-art centers, located in major cities in the U.S. including Los Angeles, Atlanta, San Francisco, Chicago, Dallas and metropolitan New York, contain classrooms, conference rooms and fully equipped radiographic rooms. Designed specifically for study and practice of new radiographic techniques, The Image Center provides hands-on experience with the latest equipment and imaging technology.

For the Radiologist.
The Image Center is a forum for bringing physicians together to exchange the latest ideas, procedures and information. Speakers who are experts in their field will conduct seminars on relevant topics in medical imaging. Business, government and legal aspects of radiology will be discussed . . . topics not readily available from other sources.



Demonstration of radiographic techniques in one of The Image Center classrooms

AGFA-GEVAERT REX INC.

A subsidiary of Agfa-Gevaert Group, the second largest film maker in the world. White Plains, N.Y. Tel. 914 682-5650

For the Radiologic Technologist.
The Image Center is an educational resource for teaching and keeping technologists up-to-date on current techniques and trends in medical radiography. It is a technical, in-service, educational program with emphasis on key factors affecting diagnostic quality of the finished radiographs. Laboratory sessions will provide the opportunity to use a variety of imaging and processing systems and to discuss related technical problems.

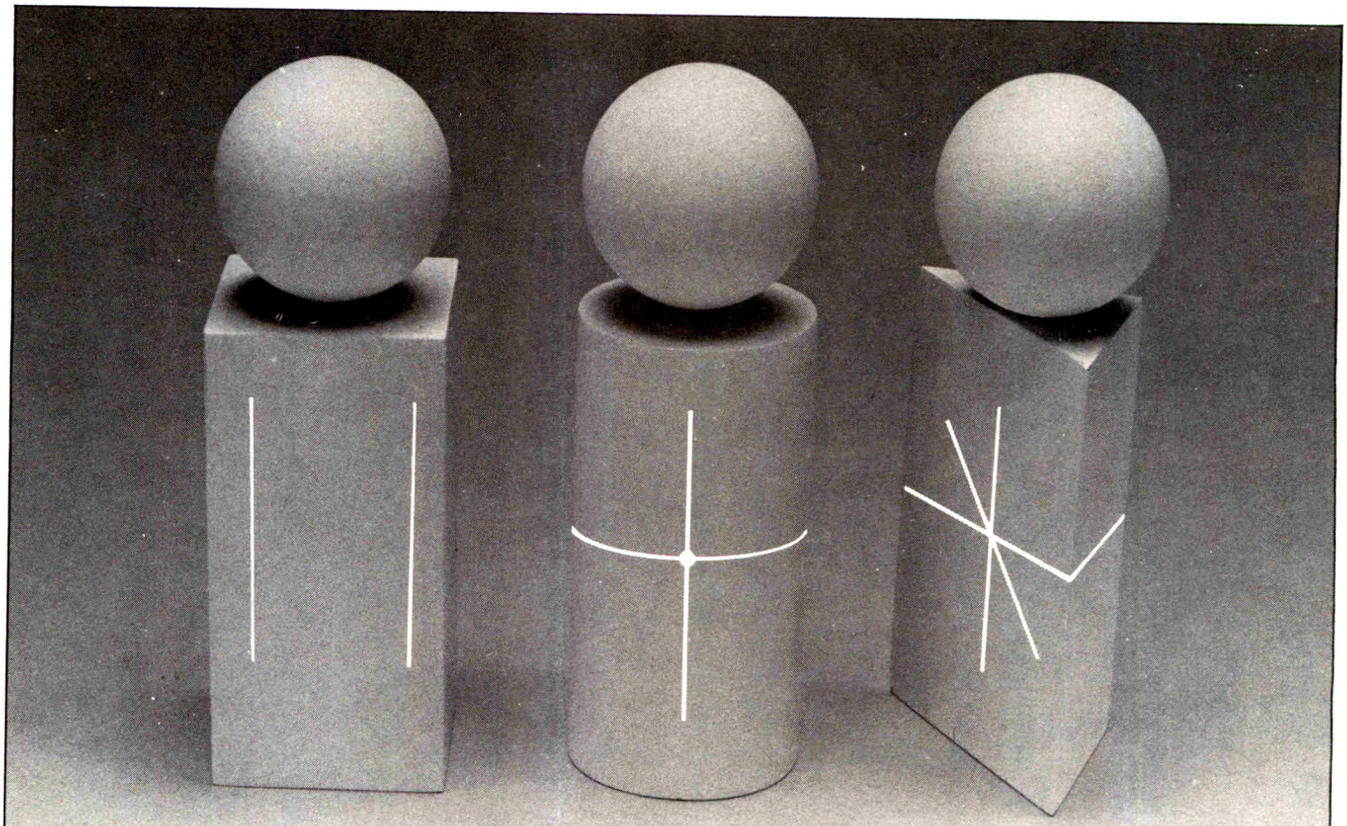
For the Resident.
Whether it's sensitometry, conventional radiography, CRT imaging or ultra-sound, The Image Center offers a broad range of educational seminars. Latest advances in radiographic imaging will be covered and many seminars qualify for Continuing Education credits.

For the Department Administrator.
Special seminars on cost effectiveness, business and financial management workshops are all available at The Image Center.

For the Physicist.
Physicists will receive information directly related to basic aspects of X-ray film and chemistry. Technical seminars will cover relevant R & D subjects and new products under development.

Contact your Agfa-Gevaert Rex representative for more information about scheduled seminars and programs being offered at The Image Center servicing your area.





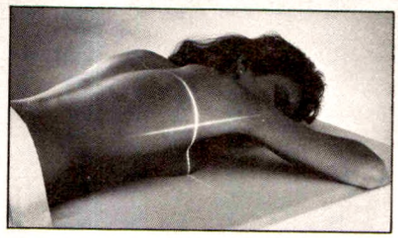
BECAUSE EVERY BODY IS DIFFERENT . . .

Regardless of patient size or shape, Gammex Laser Positioning Systems assure faster set-ups and greater throughput for your entire radiology department.

Employing low energy lasers, these systems provide a new dimension in precision for routine and complex positioning requirements in diagnostic radiology.

A system of laser lines and crosses, projected on the patient's body, enables the radiologist or technologist to accurately visualize the three axes of the area being treated or imaged.

Laser positioning significantly reduces unnecessary radiation exposure due to patient misalignment. Reproducibility time after time, even with patient weight gain or loss, is assured.



GAMMEX LASER PRECISION!

REAL COST EFFICIENCIES

In hospitals, medical centers and clinics, Gammex systems pay for themselves by immediately saving time and money . . . . . for the hospital and patient . . . . . through faster and more accurate set-ups . . . . . fewer retakes . . . . . and quicker, more repeatable relocations for future examinations. Gammex has laser positioning systems for specific applications, such as CT scanning, routine chest x-ray, pluridirectional tomography and dose compensation contouring in therapy.

Gammex, inc.
6685 North Sidney Place
Milwaukee, Wisconsin 53209
414/228-7400

CHAIRMAN
DEPARTMENT OF
RADIOTHERAPY

The Albert Einstein College of Medicine is seeking a Chairman of the Dept. of Radiotherapy. Candidates should be individuals with credentials reflecting considerable clinical accomplishment as well as academic achievement and potential.

Please address correspondence to
Boyce Bennet, MD
Dept. of Pathology.

**ALBERT EINSTEIN
COLLEGE OF MEDICINE**
1300 Morris Park Ave., Bronx, N.Y. 10461

an equal opportunity employer

Mental retardation can happen to anyone.

It can happen to you!

But you can prevent mental retardation.

To find out how, write:
National Association for Retarded Citizens,
Civitan Inquiry Program,
P. O. Box 6109, Arlington, Texas 76011.

Index to Advertisers

In Alphabetical Order

Agfa-Gevaert Rex, Inc.
AMRAD, a Raytheon Company
Body Imaging Conference
Dunn Instruments, Inc.
Eastman Kodak Company
Elema-Schonander, Inc.
E-Z-EM Company
H. G. Fischer, Inc.
GAF Corporation
General Electric Company
Gammex, Inc.
Guerbet Laboratories
Machlett Laboratories
C. V. Mosby Company
Ohio Nuclear
Ortho Pharmaceuticals
Pfizer, Inc.
Philips Medical Systems, Inc.
Picker Corporation
Precise Optics
Presbyterian Hospital
Purdue Frederick Company
Radiologic Sciences, Inc.
Siemens Corporation
Smith Kline & French Laboratories
E. R. Squibb & Sons, Inc.
Toshiba Medical Systems
Winthrop Laboratories


MPX
120
500
400
125
90
0.0
GENERAL ELECTRIC
RSX Mercury



A classic breakthrough.

GE's new R&F system saves you time, space, money and dose. And gives you excellent images.

Here's a totally new R&F system that offers you many advantages over existing units—it's a major breakthrough in classical R&F. Let's take a closer look at each component.

Fluoricon® L300 suspensionless intensifier gives you 9″ triple field performance, high frame rate photospot capability and improved imaging in a new lightweight package.

Diagnostic detail is exceptional—with advanced video camera technology and high resolution, high contrast ratio image tubes.

User-selectable dose rate and video gain let you add video gain for imaging obese patients, and provide the lowest dosage for young or thin patients.

When you choose the computerized technic management option at the spotfilmer, unique values of kVp, mA and focus are stored for each spotfilm and photospot procedure. Patient size selection includes pediatrics down to the neonate range.

And the new suspensionless design allows ample clearance for an overhead tube, facilitating radiography and attachment of an optional tomograph. The compact design fits into smaller, problem-sized rooms, giving you large room R&F capability.

RFX™ table and spotfilmer, with user-selectable grids, combines lower dose fluoro and high kVp spotfilms in one easy-to-use system.

The spotfilmer's unique, effort-sensing power assist simulates the feel of an unpowered fluoroscopic screen.

Two-per-second spotfilming with sequence anticipation allows two to four manually sequenced spotfilms without cassette return. Load from the front or rear, with pushbutton changeover.

Diagnostic advantages include automatic masking to format with full field, 2-on-1 vertical or transverse, or 4-on-1 formats. Masking is internal, allowing full field fluoro with the cone in place.

Additional RFX features include: (1) cone lockout for myelography; (2) automatic cassette return; (3) rapid access spotfilming (.75 sec.); (4) arthrographic collimation and ion chamber compensation for 9-on-1 or 6-on-1 formats; and (5) improved radiation protection at all routine angulations.

MPX computerized generator, with Quantamatic™ tx technic management, stores all of your department's standard radiographic settings.

The operator simply presses the appropriate anatomical selection buttons. The microprocessor instantly displays all technic parameters, including kVp, mA, mAs, time, focal spot size and AEC status. And the operator may raise or lower factors to suit special patient situations.

With over 200 programmed AEC and fixed-time technics (on or off the table) available, you can handle virtually every patient size. From infant to obese adult. And any body part, including extremities.

Quantamatic tx technic management gives you consistent, high-quality films. Throughput increases. Costly retakes due to technic error are virtually eliminated. And programmed constant load design extends tube life by optimizing tube loading.

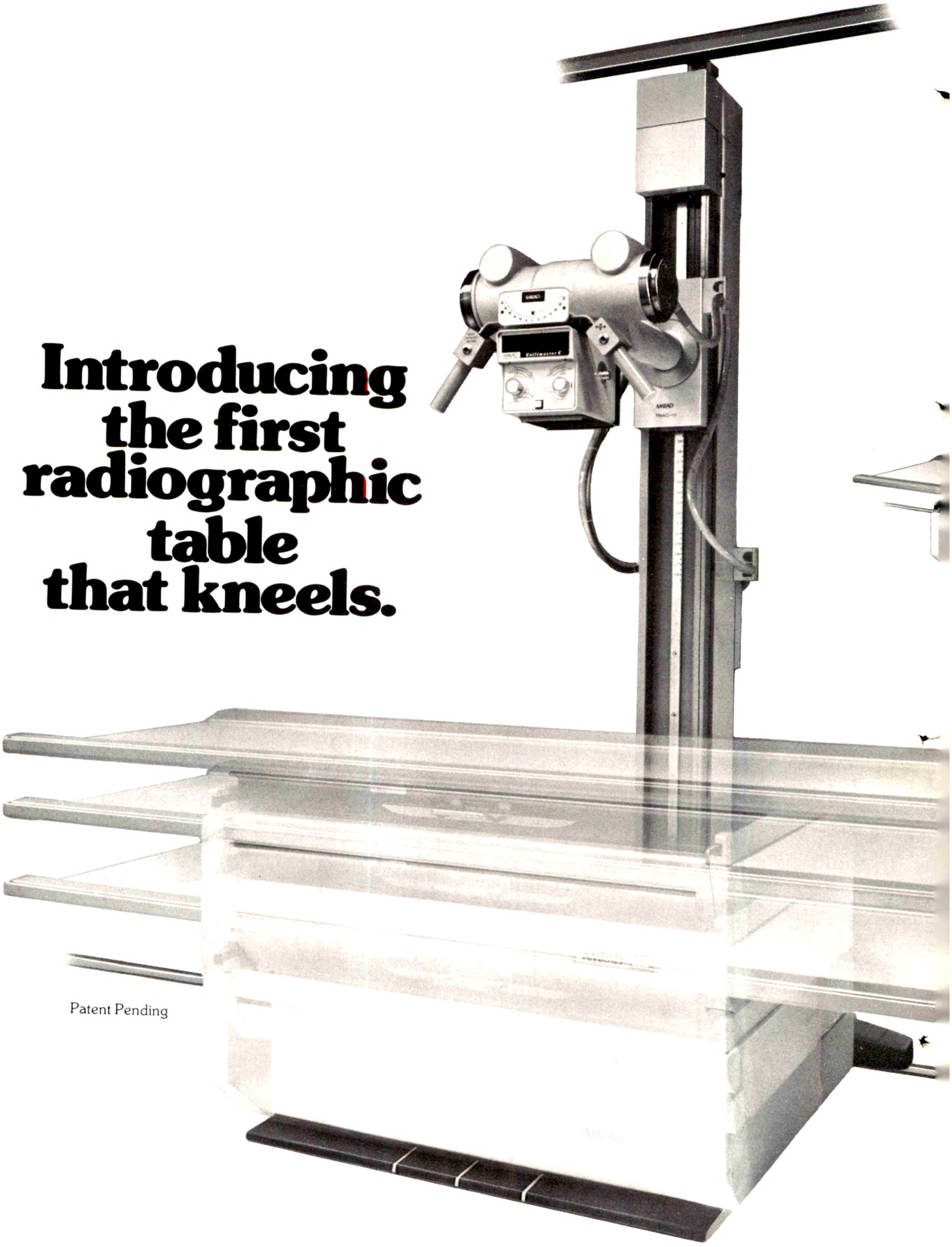
You'd expect it from GE.

Contact your GE representative to get all the facts on this important R&F breakthrough. Fluoricon L300/RFX/MPX....it's a classic.

General Electric Medical Systems, Milwaukee, Toronto, Madrid.

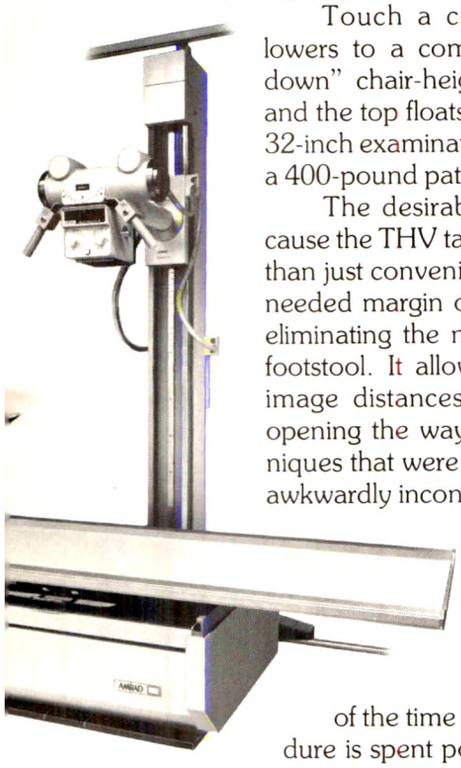
GENERAL ELECTRIC

Introducing the first radiographic table that kneels.



Patent Pending

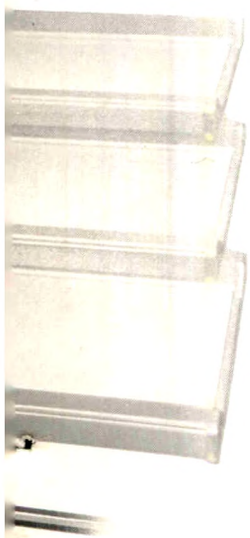
Amrad's new THV table literally obsoletes every horizontal radiographic table on the market—including, unfortunately, some of our own. "THV," you see, stands for *Top Height Variable*.



Touch a control and the top lowers to a comfortable, "please-sit-down" chair-height. Touch it again, and the top floats effortlessly back to a 32-inch examination height, even with a 400-pound patient aboard.

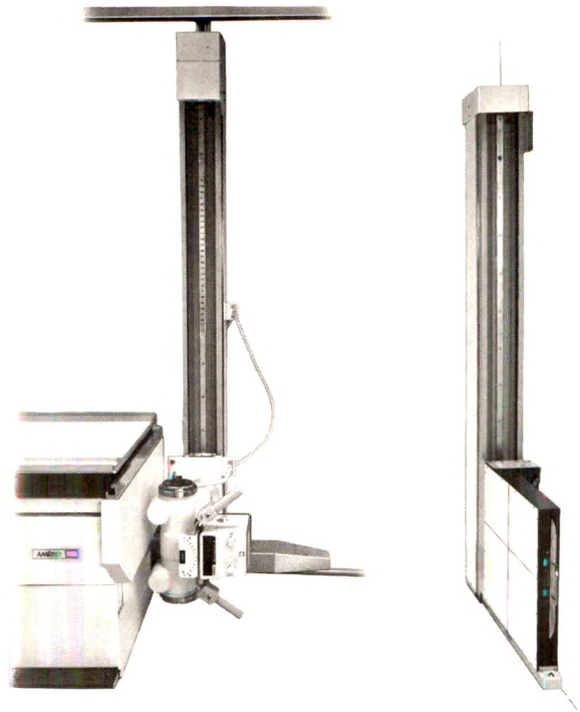
The desirability is obvious. Because the THV table offers much more than just convenience. It adds a much needed margin of safety—completely eliminating the need for a hazardous footstool. It allows extended source-image distances of 55″ or more—opening the way to many new techniques that were either not possible or awkwardly inconvenient before.

And with today's spiraling costs, the Amrad THV table offers an important *savings of time*. After all, most of the time for an average procedure is spent positioning the patient. Procedures are often complicated by patient feebleness or incapacity—certainly a common problem in every radiographic facility. Throughout the day, extra people must be available to help the technologist with those instances.



But not with the Amrad THV table. An Amrad THV room allows fewer people to perform more examinations in less time.

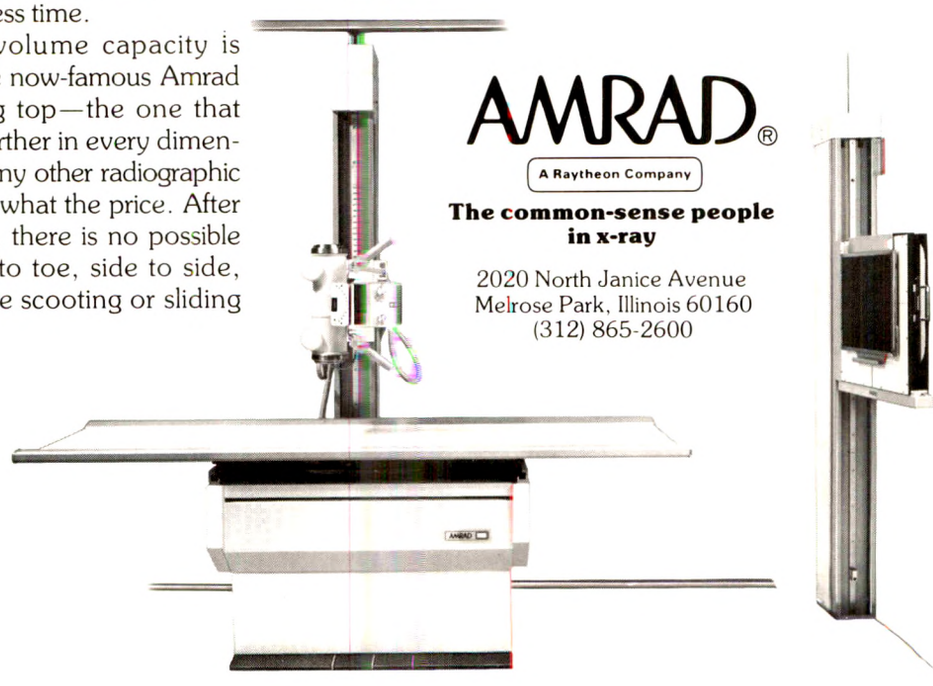
That high-volume capacity is augmented by the now-famous Amrad four-way floating top—the one that travels as far or farther in every dimension than that of any other radiographic table—no matter what the price. After initial positioning, there is no possible coverage, head to toe, side to side, that could require scooting or sliding the patient.



The table is augmented by the Amrad tubestands—the ones where the tube and vertical bucky combination *goes all the way to the floor*—allowing weight-bearing procedures to be handled with a minimum of dangerous and bulky platform accessories. And by the superb Craig-series of 600 MA generators—the ones with the small, remote-control console connected with low-voltage telephone cable. The ones that have earned a near-perfect record of reliability.

And so Amrad's new THV table makes possible the first radiographic room that is designed around people, instead of machines. Surprisingly, it's not expensive—costing little or no more than obsolete tables. Phone collect for the name of your local Amrad dealer.

And go sit down on the first radiographic table that kneels.



AMRAD®

A Raytheon Company

The common-sense people in x-ray

2020 North Janice Avenue
Melrose Park, Illinois 60160
(312) 865-2600

American Journal of Roentgenology

Vol. 132 March 1979 No. 3

DIAGNOSTIC IMAGING

339 **Diagnostic Radiology: Geography of a High Technology.** *Cockshott WP*
345 **Performance Evaluation of Computed Tomography Scanners Using a Phantom Model.** *Bellon EM, Miraldi FD, Wiesen EJ*
353 **CT Resolution and Diagnostic Accuracy.** *Williams AL, Haughton VM*
357 **High Dose Preoperative Irradiation of the Lower Neck and Supraclavicular Fossae.** *Sagerman RH, Chung CT, King GA, Dalal P, Yu WS*
361 **Sequential CT Observations of Irradiated Intracranial Germinomas.** *Inoue Y, Takeuchi T, Tamaki M, Nin K, Hakuba A, Nishimura S*
367 **CT Metrizamide Myelography for Intraspinal and Paraspinal Neoplasms in Infants and Children.** *Resjö IM, Harwood-Nash DC, Fitz CR, Chuang S*
373 **Radiographic Changes of the Skull in Sickle Cell Anemia.** *Sebes JI, Diggs LW*
379 **Radiography of Glycogen Storage Diseases.** *Miller JH, Stanley P, Gates GF*
389 **Radiology of the Pterygoid Plates and Pterygopalatine Fossa.** *Osborn AG*
395 **Ultrasonic Recognition of Parenchymal Gas.** *Conrad MR, Bregman R, Kilman WJ*
401 **Ultrasound Diagnosis of Masses Elevating the Inferior Vena Cava.** *Kurtz AB, Rubin C, Goldberg BB*
407 **Ultrasonic Assessment of Renal Transitional Cell Carcinoma: Preliminary Report.** *Arger PH, Mulhern CB, Pollack HM, Banner MP, Wein AJ*
413 **Medial Deviation of the Pelvic Ureters after Abdominoperineal Resection of the Rectum.** *Young G. Goldberg ME, Nemer FD*
415 **Ureteral Obstruction Resulting from Vascular Prosthetic Graft Surgery.** *Tracy DA, Eisenberg RL, Hedgcock MW*
419 **Metastatic Transitional Cell Carcinoma from the Bladder: Radiographic Manifestations.** *Goldman SM, Fajardo AA, Naraval RC, Madewell JE*
427 **Risk Factors and Occult Breast Cancer in Young Women.** *Frankl G, Ackerman M*
429 **Influence of Contrast Material on Renal Venous Renin Activity.** *Hietala SO, Zelenak JJ, Beachley MC, Tisnado J*
433 **Minimum Blood Vessel Diameter Measured by Magnification Angiography.** *Sandor T, Adams DF*
437 **Presacral Space Revisited.** *Kattan KR, King AY*
441 **Foley Catheter Method of Esophageal Foreign Body Removal: Extension of Applications.** *Nixon GW*

CASE REPORTS

443 **Ultrasound Diagnosis of Neonatal Adrenal Hemorrhage.** *Mineau DE, Koehler PR*
445 **Hypoglycemia and Extrapancreatic Tumors: Report of Two Cases.** *Costello P, Clouse ME, Rolla AR*
448 **Extraadrenal Paraganglioma, Pulmonary Chondroma, and Gastric Leiomyoblastoma: Triad in Young Females.** *Knake JE, Gross MD*
452 **Contraceptive-Associated Hepatic Tumor.** *Benedict KT Jr, Chen PS, Janower ML, Farmelant MH, Howard JT, McDermott W*
455 **Hepatic Rupture with Toxemia of Pregnancy: Angiographic Diagnosis.** *Sommer DG, Greenway GD, Bookstein JJ, Orloff MJ*
457 **Radiographic Findings of Lymphoma Involving the Larynx: Report of Two Cases.** *Noon MA, Brant-Zawadzki M, Young SW, Castellino RA*
459 **Mucoid Pseudotumors of the Tracheobronchial Tree in Two Cases.** *Karasick D, Karasick S, Lally JF*
461 **Intraluminal Diverticula of the Stomach.** *Tan KM*
463 **Splenic Flexures Volvulus: Two Case Reports and Review.** *Lantieri R, Teplick SK, Labell MJ*
465 **Splenic Abscess: Comparison of Four Imaging Methods.** *Grant E, Mertens MA, Mascatello VJ*
467 **Abdominal Wall Endometrioma.** *Miller WB Jr, Melson GL*
469 **Distant Metastases to Bone from Bladder Carcinoma: Report of Three Cases.** *Dunnick NR, Anderson T*
471 **Intraarticular Lipoma with Osseous Metaplasia: Radiographic-Pathologic Correlation.** *Pudlowski RM, Gilula LA, Kyriakos M*
474 **Neurofibromatosis: Unusual Lymphangiographic Findings.** *Preston JM, Starshak RJ, Oechler HW*

TECHNICAL NOTES

477 **Precision Technique for Positioning the Head During Tomography.** *Faivovich G, Omnell KA, Svensson A*
480 **Liver Localization by Percussion for CT Scanning.** *Goodman G, Kuhns LR, Novak WG, Onitsuka H*
481 **Versatile Ceiling Tube Mount for Direct Magnification Radiography.** *Sundaram M, Shields J, Brodeur A, Poling ER*
482 **Versatile Film Holding Device for Direct Magnification Radiography.** *Poling ER, Sundaram M*

485 **Second International Symposium on Radiopharmaceuticals**

497 **Editorial: The Primary Radiologic Consultant.** *Steckel RJ*
500 **Letters**
503 **Memorials**

505 **Abstracts**
514 **Book Reviews**
519 **News**
356 **Guidelines for Authors**
366 **Erratum**

Rec.
13.9.79

AJR

American
Journal of
Roentgenology

April 1979

Fleet® Barium Enema Prep Kits: Make us your first choice for fewer retakes.

The greatest defect in colon examinations is in the preparation of the colon.[1]

Fleet® Barium Enema Prep Kits systematize and improve colon prepping because they conform to the recommended method which provides a combination of diet, hydration and proven laxation which stimulates the large and small intestines.[2] The result? Cleaner colons, clearer x-rays and fewer retakes.

All Fleet Prep Kits offer three laxative steps: 1½ oz. of Fleet® Phospho-Soda® followed by four Fleet® Bisacodyl tablets, plus a final cleansing step. Prep Kit 1 offers Fleet® Bisacodyl suppository. Prep Kit 2 offers a large-volume disposable Fleet® Bagenema. And Prep Kit 3 offers our new Fleet® Bisacodyl enema. And all three Prep Kits have easy-to-follow instructions with a choice of flexible time-tables to fit your schedule.

With Fleet Barium Enema Prep Kits, you'll be sure of convenient, dependable, effective colon prepping every time. And that's reason enough to make Fleet Prep Kits your first choice for fewer retakes.



Fleet Barium Enema Prep Kits
for cleaner colons, clearer x-rays and fewer retakes.

Fleet pharmaceuticals
C.B. Fleet Co., Inc.
Lynchburg, Va. 24505

[1]Dr. R.E. Miller, Ad Hoc Committee on Detection of Cancer of the Colon, Detection of Colon Lesions, American College of Radiology, (Chicago, Ill., 1973) p. 76.
[2]Dr. W.R. Eyler, Ibid. pp. 203, 204.

Official Journal
American Roentgen Ray Society
American Radium Society

AJR

American Journal of Roentgenology

Diagnostic Imaging • Radiation Oncology
Related Sciences

Editor Melvin M. Figley

Associate Editor Rosalind H. Troupin

Assistant Editor John D. Harley

Contributing Editor E. Frederick Lang

Consulting Editorial Board Luther W. Brady • Kent Ellis
E. Robert Heitzman • Donald L. King • N. Thorne Griscom
Eugene C. Klatte • Kenneth Krabbenhoft • John G. McAfee
Russell H. Morgan • Thomas H. Newton • Robert G. Parker
Stewart R. Reuter • William B. Seaman • Robert J. Shalek
John Storer • Michel M. Ter-Pogossian • Joseph P. Whalen
David M. Witten

Editorial Staff K. A. Murray, manager • M. J. Leonard, manuscript editor • J. Anderson, assistant manuscript editor • A. C. Van Dyck, secretary

Published monthly by The Williams & Wilkins Co., 428 East Preston St., Baltimore, Maryland 21202. All correspondence, except editorial office business, should be addressed to the publisher. Annual subscription rates: $40 ($20 for residents with letter of verification) plus appropriate mailing surcharge (see note last page). Single copies, $5. Undelivered or damaged copies replaced within 60 days of publication; 90 days for foreign subscribers. Allow 90 days for address changes. © 1979 by American Roentgen Ray Society. Second-class postage paid at Baltimore, Maryland, and at additional mailing offices. Printed in U.S.A. ISSN 0361-803X



"Productivity is up 10% to 20%"

"Lower absenteeism"

"You can tell by their attitude—the workers who participate are happier, more cooperative, much sharper"

"We can identify direct savings of $2,000,000 per year"

"The program has had a distinct bearing on staff performance. Our engineering people now have a camaraderie with their counterparts in other departments"

"It started in headquarters. By next year we hope to have it in all our factories and research facilities"

These are actual quotes from executives of large and small companies and organizations in Denver, Omaha, Birmingham, and Greenwich. They're talking about company fitness programs. That's right, many employers now provide facilities or opportunities for exercise for their employees. They are glad they did.

Most began with a concern for employee health and well being. What they have found is a variety of additional benefits. These benefits add up to *increased productivity*—so much so that several companies can demonstrate that the fitness program pays for itself. Add to this improved morale, better internal communications, and employee health. How can you lose? Write us now for more information:

The President's Council on Physical Fitness and Sports
Department B
Washington, D.C. 20201

Employee Fitness: In the long run you will be the winner.

We designed our new high-capacity processor and chemical mixer to help control imaging costs and improve X-ray department efficiency.



Imaging Management

DUPONT

REG U.S. PAT. & TM. OFF.


The CRONEX® Chemical Mixer
The CRONEX® QC-1 Film Processor

DuPont's new processing equipment can save time and money in your department...plus improve the consistency of your radiographs.

We designed our new CRONEX* Processor and Chemical Mixer to provide the three things you want most from your processing system: image quality, operating efficiency and economy in use.

Result: several brand new engineering features, plus important improvements in many areas of construction.

Our new tabletop CRONEX® QC-1 Processor offers these innovations:

100% solid-state electronic controls to assure long-term reliability and processing consistency. (And give you more uniform radiographs.)

Two major energy-saving features— (1) an automatic standby circuit that shuts down the processor during periods of non-use; (2) a cold-water wash that uses less water than conventional processors.

Other improvements in processor design make operation faster and easier. All control switches and utility hookups are grouped together near the feed tray, where they're easy to get at. Electronic controls are modular for faster service. Separate drains are provided on developer and fixer tanks to help you comply with EPA regulations.

And there's much more. (See next page.)

The CRONEX® QC-1 Processor is the product of DuPont's 10 years' experience in marketing film processors for radiography and the graphic arts. It may be used in room light with a DuPont Daylight Processor Loader (shown here) and other components of the DuPont Daylight Film Handling System. Or you can use it in conventional through-the-wall darkroom service.



Loading the QC-1 Processor in room light.

You'll find our new CRONEX Chemical Mixer equally advanced in design.

This remarkably attractive unit offers:

A completely automated cycle for uniform, spill-free mixing. All your operator has to do is install two boxed containers of concentrate; the machine does the rest. It automatically punctures, drains and rinses the containers, and mixes 38 liters (10 gal.) each of developer and fixer...accurately, consistently, and without splash or spill.

Double its initial capacity. If reserve containers of concentrate are installed when solution tanks are full, the mixer will automatically make up new developer and fixer when needed. That means its total capacity is really 76 liters of each chemical! Which explains why one CRONEX Chemical Mixer can serve two full-size processors.

See the next page for more details.

When combined with the DuPont Daylight System, the new QC-1 Processor and CRONEX Chemical Mixer offer systems that let you handle film all the way from automatic dispensing through final processing...**in room light without a darkroom.** Your radiology department benefits from lower costs, higher efficiency and better quality radiographs.

But even more important, the patient benefits, too.

Your technologist can complete an exam without leaving the patient unattended. Radiographs can be viewed before the patient leaves the examining suite, eliminating callbacks and reducing waiting time. This is why DuPont's Daylight Film Handling System is considered a major advance in patient care.

Ask your DuPont Technical Representative how the new CRONEX® QC-1 Processor, the CRONEX Chemical Mixer, and other parts of DuPont's Daylight Film Handling System can help control quality, contain costs and improve patient care in your department.

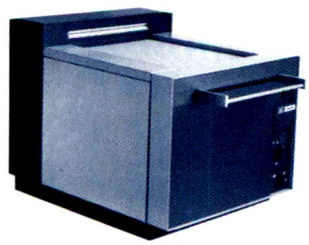
Or write to DuPont at our address on the next page.

*CRONEX is a trademark of the DuPont Company for its X-ray films, screens, and equipment. Reg. U.S. Pat. & Tm. Off.

Specification and Performance Data

CRONEX® QC-1 Tabletop Processor

- size: 28" wide x 35" long x 27" high (71 cm x 89 cm x 69 cm)
- capacity: 175 films/hour (14" x 17" or 35 cm x 43 cm)
- cycle: 2 minutes, dry to drop
- solid-state electronic controls
- energy-saving standby circuit
- cold-water wash (3/4 gpm or 2.9 liters per min.) with automatic recirculation
- 5-gallon (19-liter) plastic tanks
- developer temperature controlled to ± 0.3°F (±0.17°C)
- external controls; centralized utilities hookup
- optional stand available
- use with Daylight Equipment or in conventional darkroom installation



CRONEX® Chemical Mixer

- size: 24" wide x 22" long x 40" high (61 cm x 56 cm x 102 cm)
- capacity:

	developer	fixer
initial	38 liters	38 liters (10 gal.)
reserve	38 liters	38 liters (10 gal.)
total	76 liters	76 liters (20 gal.)

- solid-state electronic controls
- automatic mix and remix cycles
- solutions mix independently
- minimizes chemical handling, spills, splashes
- display lights show mixing sequence
- alarm sounds when solution is low
- can serve two full-size processors
- optional pumping station available



Quality Imaging Products for Improved Imaging Management

Cost-efficient equipment, such as DuPont's new processor and mixer, is one of three keys to effective management of the hospital radiology department.

The skilled administrator recognizes that imaging products must be integrated with two other critical management tools—people and services—to meet the specific needs and goals of his department.

Imaging Management is a practical, results-proven managerial process, pioneered by DuPont. It can help administrators utilize these tools to achieve measurable improvement in the areas of image quality, department costs and patient care.

Ask your DuPont Technical Representative for more information about this new management concept and how you can put it to work in your X-ray department.

For complete details on DuPont's new CRONEX® QC-1 Processor and Chemical Mixer write: DuPont Company, Room 36329, Wilmington, DE 19898.

Imaging Management.
It puts you in control of image quality, costs and patient care.

DUPONT
REG. U.S. PAT. & TM. OFF.

DuPont's new processing equipment can save time and money in your department...plus improve the consistency of your radiographs.

We designed our new CRONEX* Processor and Chemical Mixer to provide the three things you want most from your processing system: image quality, operating efficiency and economy in use.

Result: several brand new engineering features, plus important improvements in many areas of construction.

Our new tabletop CRONEX® QC-1 Processor offers these innovations:

100% solid-state electronic controls to assure long-term reliability and processing consistency. (And give you more uniform radiographs.)

Two major energy-saving features— (1) an automatic standby circuit that shuts down the processor during periods of non-use; (2) a cold-water wash that uses less water than conventional processors.

Other improvements in processor design make operation faster and easier. All control switches and utility hookups are grouped together near the feed tray, where they're easy to get at. Electronic controls are modular for faster service. Separate drains are provided on developer and fixer tanks to help you comply with EPA regulations.

And there's much more. (See next page.)

The CRONEX® QC-1 Processor is the product of DuPont's 10 years' experience in marketing film processors for radiography and the graphic arts. It may be used in room light with a DuPont Daylight Processor Loader (shown here) and other components of the DuPont Daylight Film Handling System. Or you can use it in conventional through-the-wall darkroom service.



Loading the QC-1 Processor in room light.

You'll find our new CRONEX Chemical Mixer equally advanced in design.

This remarkably attractive unit offers:

A completely automated cycle for uniform, spill-free mixing. All your operator has to do is install two boxed containers of concentrate; the machine does the rest. It automatically punctures, drains and rinses the containers, and mixes 38 liters (10 gal.) each of developer and fixer...accurately, consistently, and without splash or spill.

Double its initial capacity. If reserve containers of concentrate are installed when solution tanks are full, the mixer will automatically make up new developer and fixer when needed. That means its total capacity is really 76 liters of each chemical! Which explains why one CRONEX Chemical Mixer can serve two full-size processors.

See the next page for more details.

When combined with the DuPont Daylight System, the new QC-1 Processor and CRONEX Chemical Mixer offer systems that let you handle film all the way from automatic dispensing through final processing...**in room light without a darkroom.** Your radiology department benefits from lower costs, higher efficiency and better quality radiographs.

But even more important, the patient benefits, too.

Your technologist can complete an exam without leaving the patient unattended. Radiographs can be viewed before the patient leaves the examining suite, eliminating callbacks and reducing waiting time. This is why DuPont's Daylight Film Handling System is considered a major advance in patient care.

Ask your DuPont Technical Representative how the new CRONEX® QC-1 Processor, the CRONEX Chemical Mixer, and other parts of DuPont's Daylight Film Handling System can help control quality, contain costs and improve patient care in your department.

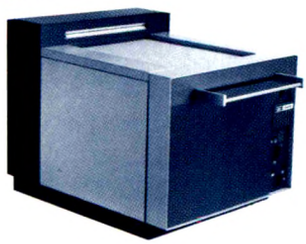
Or write to DuPont at our address on the next page.

*CRONEX is a trademark of the DuPont Company for its X-ray films, screens, and equipment. Reg. U.S. Pat. & Tm. Off.

Specification and Performance Data

CRONEX® QC-1 Tabletop Processor

- size: 28" wide x 35" long x 27" high (71 cm x 89 cm x 69 cm)
- capacity: 175 films/hour (14" x 17"or 35 cm x 43 cm)
- cycle: 2 minutes, dry to drop
- solid-state electronic controls
- energy-saving standby circuit
- cold-water wash (3/4 gpm or 2.9 liters per min.) with automatic recirculation
- 5-gallon (19-liter) plastic tanks
- developer temperature controlled to ± 0.3°F (±0.17°C)
- external controls; centralized utilities hookup
- optional stand available
- use with Daylight Equipment or in conventional darkroom installation



CRONEX® Chemical Mixer

- size: 24" wide x 22" long x 40" high (61 cm x 56 cm x 102 cm)
- capacity:

	developer	fixer
initial	38 liters	38 liters (10 gal.)
reserve	38 liters	38 liters (10 gal.)
total	76 liters	76 liters (20 gal.)

- solid-state electronic controls
- automatic mix and remix cycles
- solutions mix independently
- minimizes chemical handling, spills, splashes
- display lights show mixing sequence
- alarm sounds when solution is low
- can serve two full-size processors
- optional pumping station available



Quality Imaging Products for Improved Imaging Management

Cost-efficient equipment, such as DuPont's new processor and mixer, is one of three keys to effective management of the hospital radiology department.

The skilled administrator recognizes that imaging products must be integrated with two other critical management tools—people and services—to meet the specific needs and goals of his department.

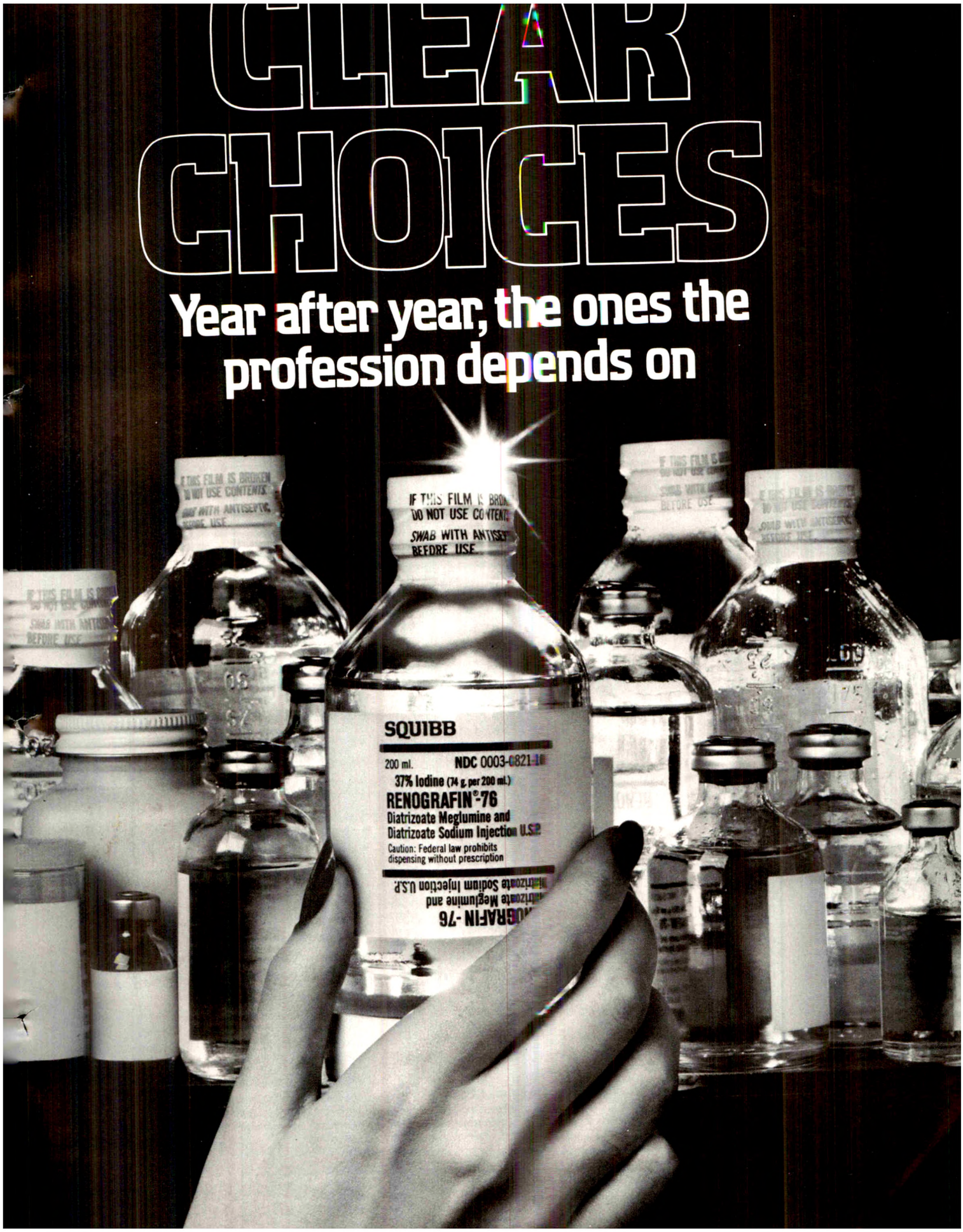
Imaging Management is a practical, results-proven managerial process, pioneered by DuPont. It can help administrators utilize these tools to achieve measurable improvement in the areas of image quality, department costs and patient care.

Ask your DuPont Technical Representative for more information about this new management concept and how you can put it to work in your X-ray department.

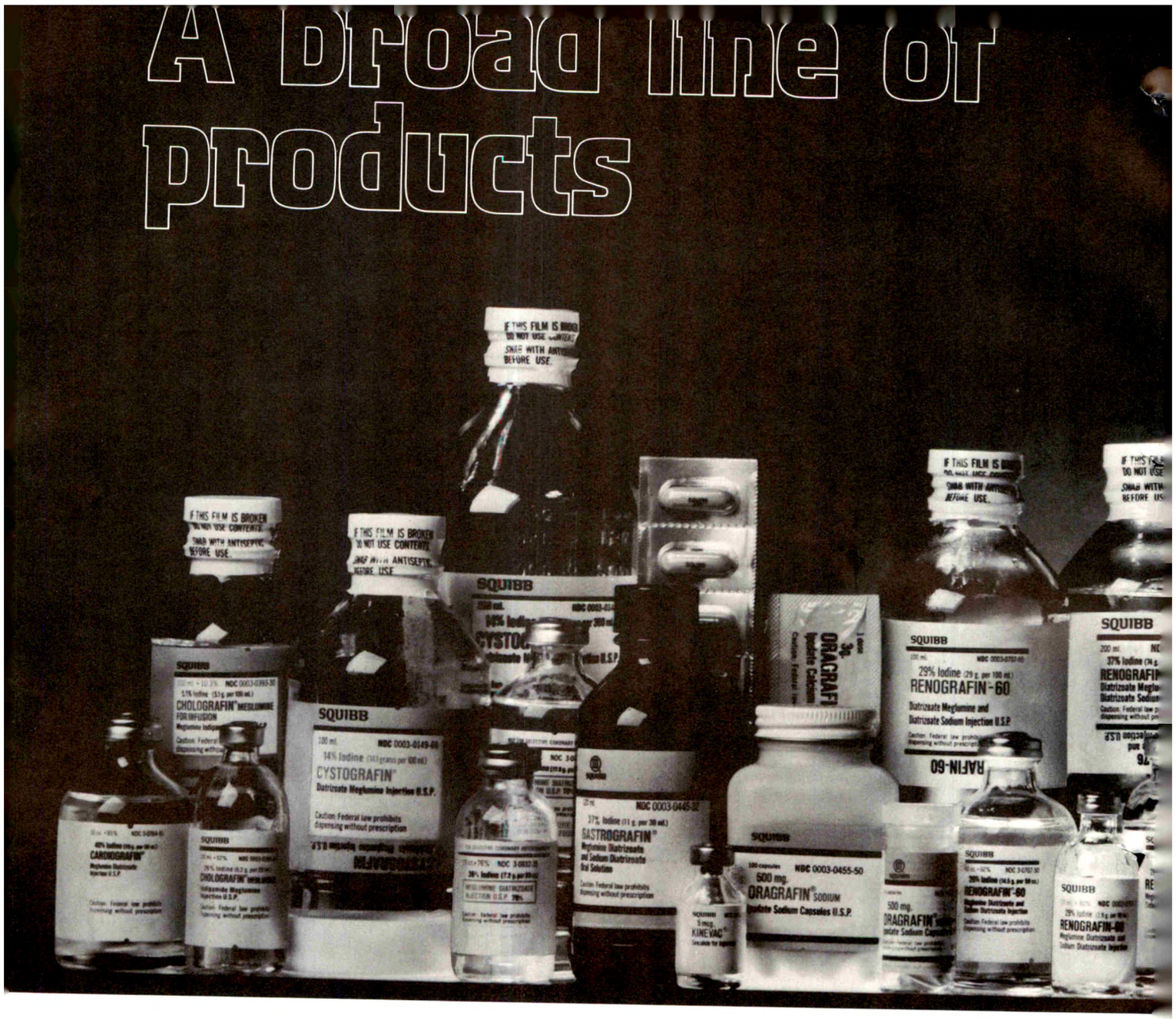
For complete details on DuPont's new CRONEX® QC-1 Processor and Chemical Mixer write: DuPont Company, Room 36329, Wilmington, DE 19898.

Imaging Management.
It puts you in control of image quality, costs and patient care.

DUPONT
REG. U.S. PAT. & TM. OFF.


CLEAR
CHOICES
Year after year, the ones the profession depends on
IF THIS FILM IS BROKEN
DO NOT USE CONTENTS
SWAB WITH ANTISEPTIC
BEFORE USE
SQUIBB
200 ml.
NDC 0003-0821-10
37% Iodine (74 g per 200 ml.)
RENOGRAFIN®-76
Diatrizoate Meglumine and
Diatrizoate Sodium Injection U.S.P.
Caution: Federal law prohibits
dispensing without prescription

A broad line of products



Cardiografin®
Diatrizoate Meglumine
Injection USP (85%)
50 ml

Cholografin® Meglumine
Iodipamide Meglumine
Injection USP (52%)
20 ml

Cholografin® Meglumine for Infusion
Iodipamide Meglumine
Injection USP (10.3%) 100 ml

Cystografin®
Diatrizoate Meglumine
Injection USP (30%)
100 ml, 300 ml

Diatrizoate Meglumine Injection USP 76%
20 ml, 50 ml

Gastrografin®
Diatrizoate Meglumine and
Diatrizoate Sodium Solution USP
(66%/10%)
120 ml

Kinevac®
Sincalide for Injection
5 mcg

Oragrafin® Calcium Granules
Ipodate Calcium for
Oral Suspension USP
3 g ipodate calcium per 8 g packet

Oragrafin® Sodium Capsules
Ipodate Sodium Capsules USP
0.5 g per capsule
Vials of 6 capsules, bottles of 100,
Unimatic® packages of 100

A wide range of sizes



Renografin®-60
Diatrizoate Meglumine and Diatrizoate Sodium Injection USP (52%/8%)
10 ml, 30 ml, 50 ml, 100 ml

Renografin®-76
Diatrizoate Meglumine and Diatrizoate Sodium Injection USP (66%/10%)
20 ml, 50 ml, 100 ml, 200 ml

Reno-M-60®
Diatrizoate Meglumine Injection USP (60%)
10 ml, 30 ml, 50 ml, 100 ml

Reno-M-30®
Diatrizoate Meglumine Injection USP (30%)
50 ml, 100 ml

Reno-M-DIP®
Diatrizoate Meglumine Injection USP (30%)
300 ml

Renovist®
Diatrizoate Meglumine and Diatrizoate Sodium Injection USP (34.3%/35%) 50 ml

Renovist® II
Diatrizoate Meglumine and Diatrizoate Sodium Injection USP (28.5%/29.1%)
30 ml, 60 ml

Renovue®-65
Iodamide Meglumine Injection 50 ml

Renovue®-DIP
Iodamide Meglumine Injection 24%
300 ml

Sinografin®
Diatrizoate Meglumine and Iodipamide Meglumine Injection (52.7%/25.8%)
10 ml

SQUIBB®
E. R. Squibb & Sons, Inc.

Professional service



Squibb Representatives are always happy to discuss Squibb's well-known, extensive line of products. However, they also like to talk about educational materials and to be of service in ways which will help radiologists in their professional activities. For example, there's "Clinical Radiology." It's a CME audio-visual program for use as a teaching aid for radiology residents, or as an in-service review for staff physicians, or just as a personal refresher course.

Current service materials are listed below. Check your interests and mail the form. Your Squibb Representative will soon be at your service.

© 1978 E. R. Squibb & Sons, Inc. 659-501

Radiology Product Manager,
E. R. Squibb & Sons, Inc., Box 4000,
Princeton, N.J. 08540

The leader in radiologic diagnostics

SQUIBB™ contrast media

I am interested in:

- ☐ Clinical Radiology (audio/visual program)
- ☐ *X-Ray Atlas* (review of diagnostic procedures)
- ☐ Motion pictures on radiology
- ☐ Squibb Radiology Education Program (slide/tape presentations)
- ☐ *Selected Radiologic Emergencies* (wall chart)
- ☐ *The Challenge...Radiography, Nuclear Medicine, Radiotherapy* (brochure on career opportunities in technology)
- ☐ Patient dose/instruction envelopes for cholecystography (English and Spanish)

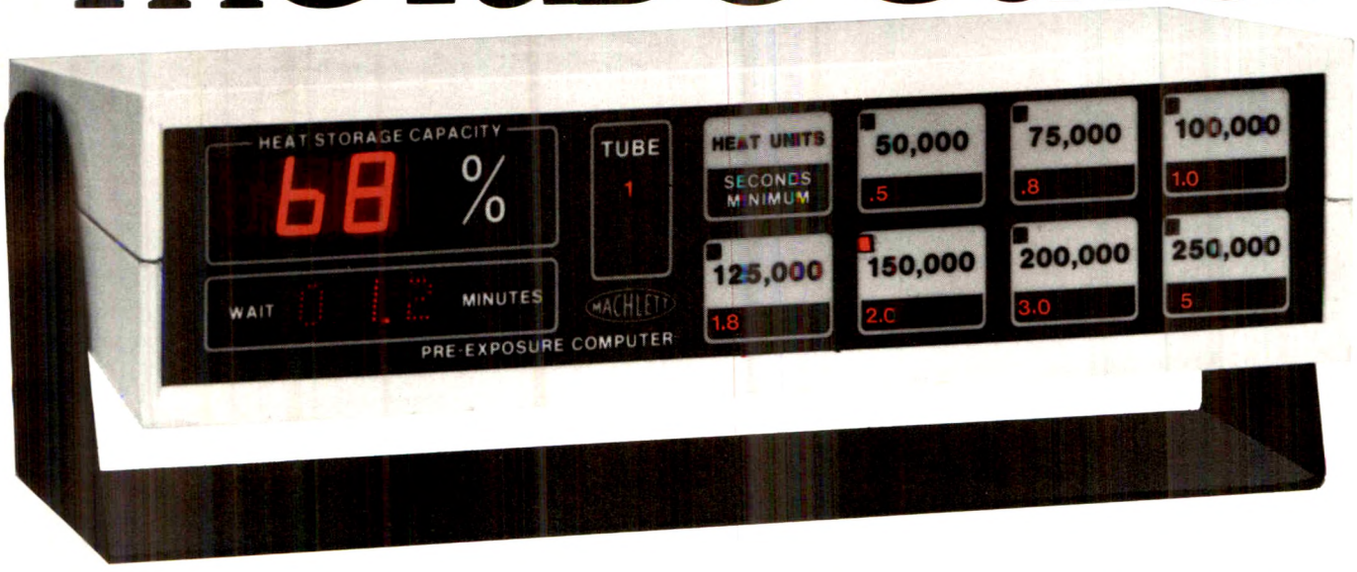
Name _____ Position _____

Hospital _____ Address _____ Phone _____

City _____ State _____ Zip _____

AB

"The Tube-Saver"



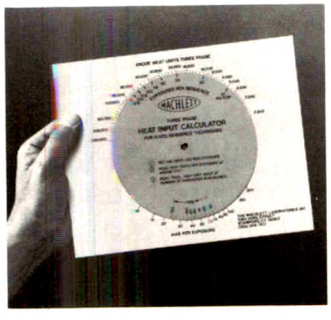
Machlett's Pre-Exposure Computer

Minimize the expense of downtime and tube failure
Know when it's safe to make the next exposure

Machlett's Pre-Exposure Computer is a lot more than just an anode heat monitor.

It also:

- Tells if the tube can handle the next exposure series immediately.
- Indicates necessary waiting time if the next series cannot be safely conducted immediately.
- Warns of tube overloads.
- Can be used with **any** x-ray tube and **any** generator.



Easy to install and simple to operate, the Pre-Exposure Computer is particularly valuable in angiography and cinefluorography.

One unit can selectively serve any of three x-ray tubes connected to a single generator.

The Pre-Exposure Computer comes complete with all cables and with this slide chart Heat Input Calculator to permit easy prediction of Heat Units resulting from planned procedures.

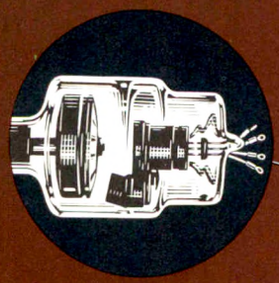
MACHLETT

For complete information, contact:

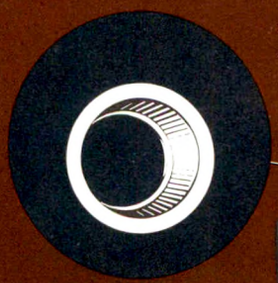
The Machlett Laboratories, Incorporated
1063 Hope Street
Stamford, Connecticut 06907 U.S.A.
(203) 348-7511
TWX: 710-474-1744

A Raytheon Company

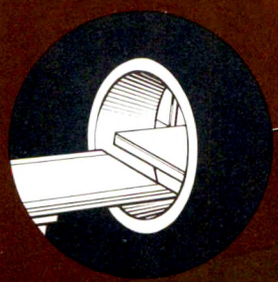
SIEMENS



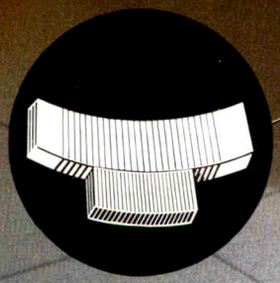
The custom application OPTI-150 CT X-ray tube permits continuous patient scanning at a rate of up to 125 scans/hour.



Wide gantry aperture and scan field (both 54 cm. in diameter) facilitate patient handling and positioning.



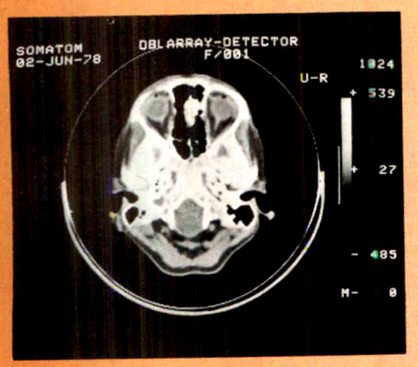
Exclusive dual-section, flat-top table system with motorized patient conveyor.



SCINTILLARC-DUAL detector system provides maximized detector utilization with optimized clinical results.

Visit Siemens Booth "A"
Fifth Annual CT International Symposium and Course
Las Vegas Hilton, April 16-20, 1979

The only CT scanners with instantaneous image reconstruction



Instantaneous image reconstruction makes the SOMATOM (whole body scanner) and the SIRETOM (head/neck scanner) the most sophisticated computed tomographic systems available today. Upon completion of each scan, the image is immediately available for clinical evaluation. The SOMATOM offers selectable scan times of four and eight seconds while the SIRETOM scan time options are 60, 120, and 180 seconds.



The EVALUSKOP, an independent evaluation console, extends the capability for CT image manipulation and analysis. Programmable and available at the push of a button are window variation, multiple region of interest selection, distance and angle measurement, histogram, magnification, saggital/coronal reconstruction, multiple tomogram displays, tomogram addition and subtraction, and filter manipulation.

Siemens' full line of computed tomographic equipment is designed to fulfill the exacting requirements of CT application. Behind each system definition—X-ray tubes, tables, generators, radiation measurement, and signal processing—is more than 100 years of engineering excellence.

Siemens' world-wide reputation for product support and service is unsurpassed. In the United States alone, Siemens has a technical staff of over 500 trained professionals ready to serve you—should the need arise.

For further information
Please contact your local Siemens Representative or Siemens Corporation, Medical Systems Division, 186 Wood Avenue South, Iselin, New Jersey (201) 494-1000.
In Canada: Siemens Electric Limited, Medical Systems. P.O. Box 7300, Pointe Claire, Quebec H9R 4R6.

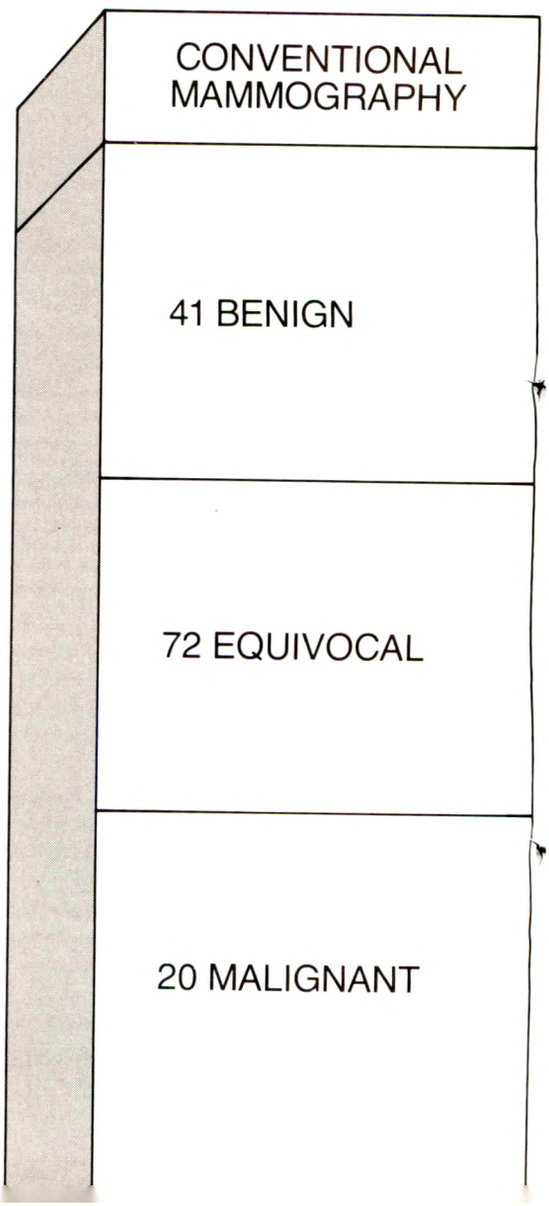


Concepts... engineered to radiologic excellence

SIR-40B

A New Study Confirms...

THE RSI MAMMOGRAPHIC SYSTEM **INCREASES DIAGNOSTIC ACCURACY**



Take a good look at the chart. You'll see the remarkable results of a study published by Dr. Edward A. Sickles, making a clinical comparison of 133 patients who received both conventional mammography and RSI Magnification Mammography. The results were confirmed with pathological diagnosis.*

This new study confirms just how accurate RSI Mammography really is. In fact, Dr. Sickles wrote in 1977, that magnification mammograms are "...clearly superior both quantitatively and qualitatively to conventional contact mammograms."[1]

Diagnostic Accuracy in Mammographic Examinations[2]
Clinical Data of Edward A. Sickles, M.D.
Assistant Professor of Radiology, University of California, San Francisco
Clinical Comparison of 133 Cases

Out of 41 cases diagnosed as benign with conventional mammography, RSI Mammography determined that 3 of these cases were, in fact, malignant. In addition, with conventional mammography alone, 72 cases were diagnosed as equivocal and direct magnification mammography (RSI System) was able to differentiate these as: 22 malignant, 32 benign, and only 18 remained equivocal. This revealing clinical comparison clearly shows that RSI Magnification Mammography increases the certainty in diagnosis, decreases the time between examination and confirmation, and may even reduce the need for biopsy.

In a radiologic symposium presented in New York City, Dr. Sickles remarked, "...in dealing with difficult cases, we considerably improved our diagnostic accuracy [with RSI Magnification Mammography]."[2]

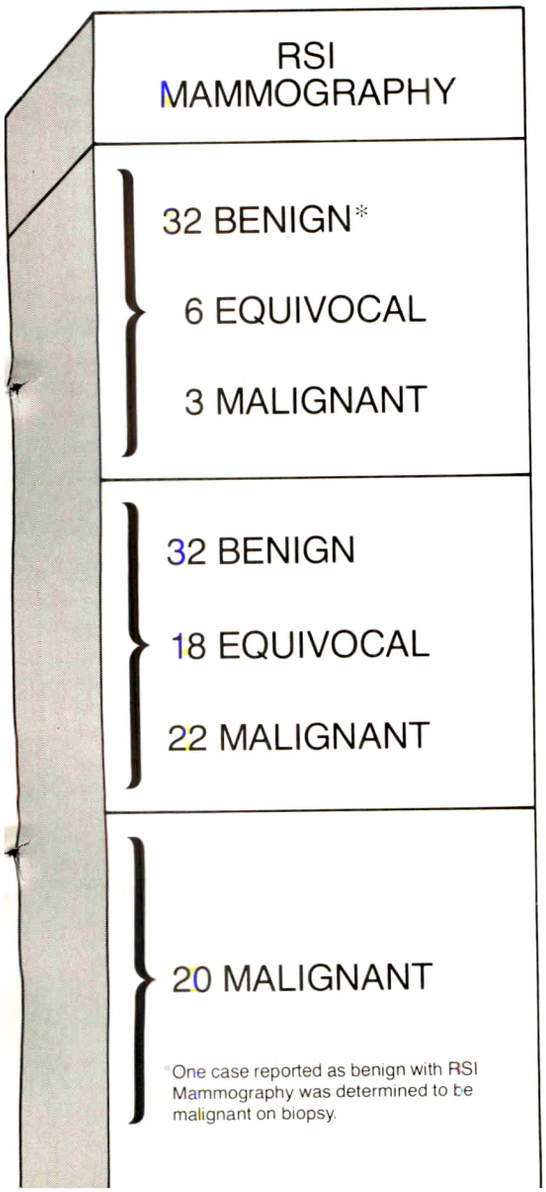
These more accurate diagnoses are the direct result of the capability of the RSI Mammography's System to give you—

- Clearer definition of mass borders
- Improved image sharpness and resolution
- Resolution of malignant microcalcifications often not discernible by conventional mammography
- Delineation of trabecular patterns

The RSI Mammography System offers high-detail resolution in the magnification mode as well as the conventional contact mode. The superior image which results from the exceptionally uniform focal spot provides a new level of confidence in the detection of breast cancer.

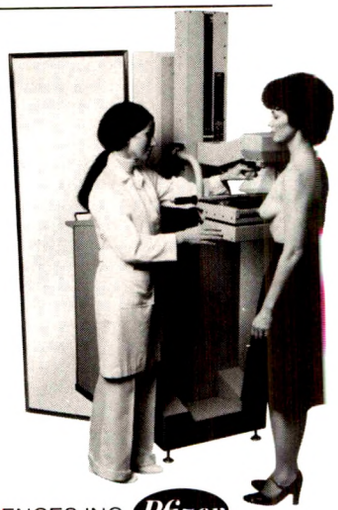
For more detailed information on the RSI Mammographic System and a reprint of the study published by Sickles *et al* in 1977, please write or call, Radiologic Sciences Inc., a subsidiary of Pfizer Inc., 235 East 42nd St., New York, N.Y. 10017 (212) 573-7941.

References: 1. Sickles, E.A.; Doi, K.; Genant, H.K.: *Radiology* 125:69-76, October 1977. **2.** Sickles, E.A.: *Microfocal Spot Magnification Mammography.* Presented at a Symposium, New York City, June 1, 1978.



THE RSI MAMMOGRAPHIC SYSTEM

INCREASES DIAGNOSTIC ACCURACY



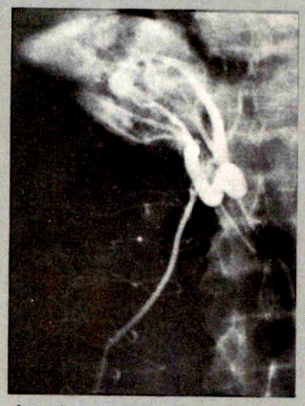
RADIOLOGIC SCIENCES INC.
A subsidiary of Pfizer Inc., New York, N.Y. 10017

Pfizer

PROBLEM: Reflux and Migration of Embolic Agents

SOLUTION: MEDI-TECH Occlusion Balloon Catheters

REF: Greenfield, A.J.; Transcatheter Embolization: Complications and Prevention With Balloon Catheters. PROGRAM OF THE AMERICAN ROENTGEN RAY SOCIETY: Seventy-eighth Annual Meeting, September 26-30, 1977, Boston, Mass.



Arteriogram performed with balloon inflated prior to embolization



Medi-Tech Occlusion Balloon Catheter OB/7/2/65 (also used in X-Ray at left)

When carrying out therapeutic embolization, the risk that embolic agents will be carried to non-intended locations should be considered.

REF: Woodside, J.; Schwarz, H.; Bergreen, P.: Peripheral Embolization Complicating Bilateral Renal Infarction With Gelfoam. American Journal of Roentgenology: Vol. 126: 1033-1034, 1976.

Gang, D.L.; Dole, K.R.; Adelman, L.S.: Spinal Cord Infarction Following Therapeutic Renal Artery Embolization. JAMA: VOL. 237, No. 26, June, 1977.

Bradley, E.L.; Goldman, M.L.: Gastric Infarction After Therapeutic Embolization. SURGERY: Vol. 79, No. 4, April, 1976.

With the development of the MEDI-TECH Occlusion Balloon Catheters this risk has been significantly reduced.

MEDI-TECH offers the only balloon catheter available today with a polyethylene catheter body. Unlike polyvinyl chloride (PVC) which softens at body temperature, polyethylene retains its torque and holds pre-set curves. This enables selective placement of the balloon either with or against the blood flow.

The smooth tip profile and large I.D. (.038" in the 7F) allow percutaneous introduction by Seldinger Technique over a .035" guide wire.

(For more information fill out the coupon below and mail, or call Toll Free 800-225-3238).
In Massachusetts 617-923-1720.

CATHETERS AVAILABLE

Catalog Number	French	Lumens	Balloon Dia. (mm)	Tip I.D. (.000")	Usable Length (cm)
OB/7/2/65	7	2	12	38	65
OB/7/2/100	7	2	12	38	100
OB/5/2/65	5	2	8.5	27	65
OB/5/2/100	5	2	8.5	27	100

MEDI-TECH
Div. of Cooper Scientific Corporation
372 Main Street • Watertown, Massachusetts 02172

☐ I'd like more information sent
☐ I'd like a representative to call

Name_____ Dept. _____
Hosp. _____
Address _____
City_____ State _____ Zip _____
Phone_____ ( ) Area Code

Lower-cost, Higher-resolution, Neurological CT scanners: $119,500 from Omnimedical.

THE MODEL 4001

WITH THESE FEATURES FOUND ONLY ON MUCH MORE EXPENSIVE SYSTEMS...

- ☐ Tilting gantry, +10° −15°
- ☐ Auto-indexing patient table
- ☐ Auto power-up of X-Ray source
- ☐ Elapse time indicator for contrast injection
- ☐ Cursor for mean CT numbers and standard deviation
- ☐ Laser for patient alignment
- ☐ Dual Floppy discs
- ☐ Patient intercom
- ☐ Digital display of K.V., M.A., and table position in M.M.
- ☐ Compact installation in 216 sq. ft.
- ☐ Optional dual slice
- ☐ Variable height patient table
- ☐ Simultaneous scan and view
- ☐ Minified image directory



High quality images...
operator simplicity...
integrated servicing aids...
THE OMNIMEDICAL 4001 HEAD SCANNER IS THE COST- EFFECTIVE ANSWER TO YOUR CT NEEDS.

Omnimedical 16312 GARFIELD AVE., PARAMOUNT, CA 90723

☐ Send me more information ☐ Current need
☐ Have a sales representative contact me ☐ Future need

Name _____

Institution _____

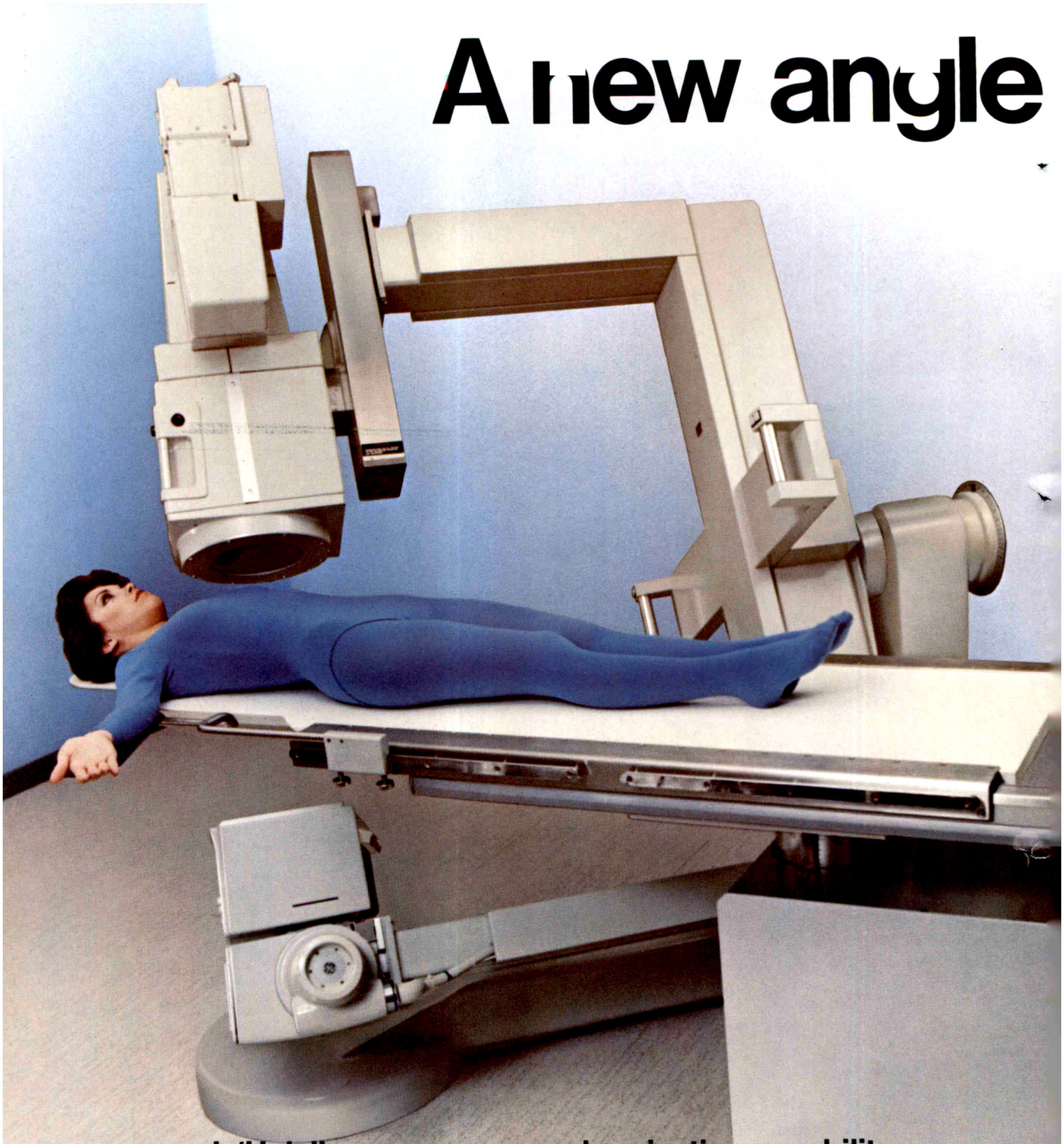
Address _____

City, State, Zip _____

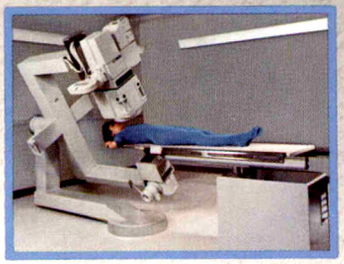
Telephone (_____) _____

Omnimedical
16312 GARFIELD AVE., PARAMOUNT, CALIFORNIA 90723
213-633-5660

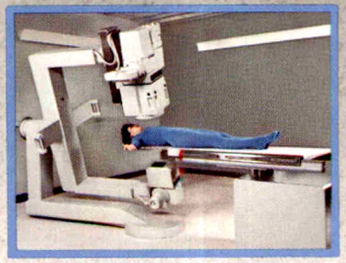
A new angle



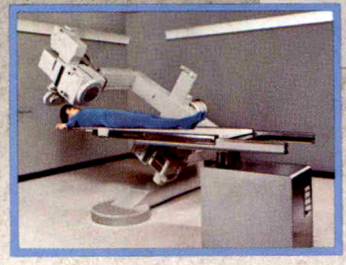
L/U delivers unsurpassed projection capability.



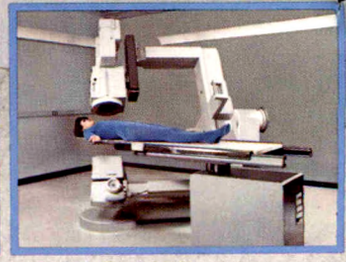
30° RAO



20° RAO, 15° Caudal

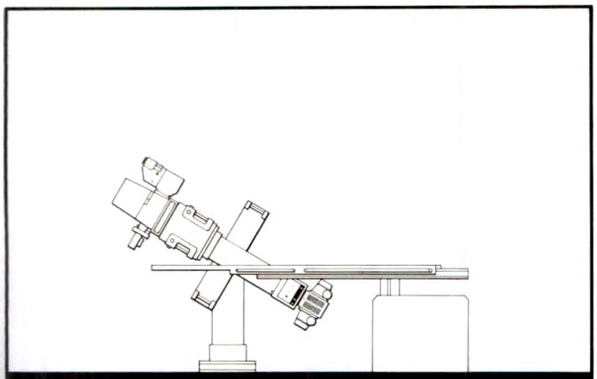


60° Cranial



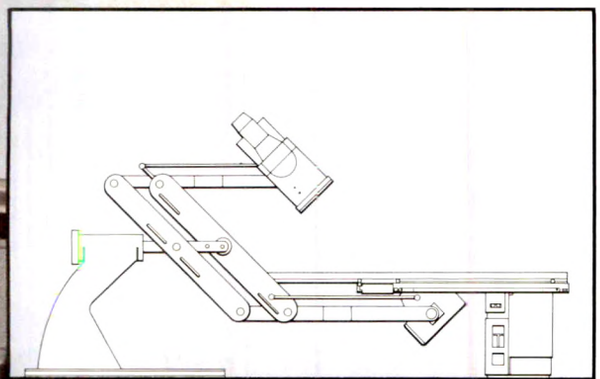
45° LAO, 30° Cranial

for saving space.



60° Cranial

Space-saving design of the new GE system (above) is compared to a conventional unit (below).



45° Cranial

GE's new L/U system gives you compact design and motorized positioning.

Here's a new vascular system that provides the full range of imaging positions for cardiac, neuro, abdominal and peripheral angiography without patient rotation or movement. It requires one-third less floor space than a conventional system . . . and costs less too.

It's the new L/U system from General Electric.

Either motorized or manual positioning can be used to rapidly obtain AP, PA, lateral, oblique or compound views.

The unique stand allows universal positioning of the tube and intensifier anywhere in the transverse, vertical and longitudinal axes. The table provides triaxial movement plus rotary positioning to cover the entire anatomical range. And the low absorption carbon fiber reinforced top facilitates high contrast studies.

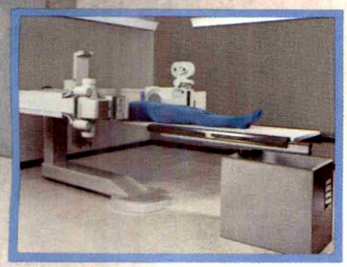
You'll also get the proven performance of the Fluoricon® 300 intensifier. With 9″ triple field capability. And superior 14.5 megahertz bandwidth video imaging with high mA cine and photospot recording. Resolution, contrast ratios and quantum detection efficiency are optimized for vascular procedures.

Ask your GE representative about the new L/U system. It gives you all the angles and all the room you'll ever need.

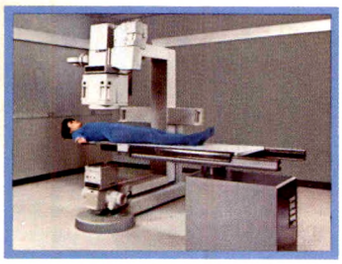
General Electric Medical Systems,
Milwaukee, Toronto, Madrid.

You'd expect it from GE.

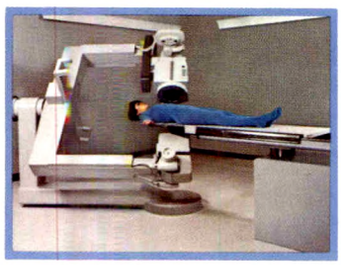
GENERAL ELECTRIC



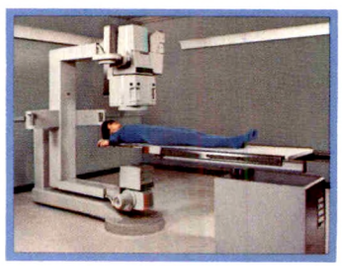
Lateral



PA



45° LAO, 40° Cranial



PA

ULTRASOUND IN PEDIATRICS

Edited by

MURRAY MISKIN, M.D.

Diagnostic ultrasound has been in clinical use for over a decade, yet only in recent years has it been extensively applied in pediatrics. *Ultrasound In Pediatrics* is the first comprehensive text of its kind to illustrate and analyse the usefulness of diagnostic ultrasound in pediatric practice. The book confines itself to the major areas of current ultrasound investigation in children. It presents a wealth of vital information which has not been generally available heretofore. *Ultrasound In Pediatrics* will show readers just what can be accomplished at present and will stimulate them to broaden the scope of this field. In addition to thorough chapters on echoencephalography and echocardiography, there is an extensive discussion of the role of ultrasound in pediatric gynecology. The chapters on the abdomen and urinary tract contain a great deal of relevant material on these aspects of ultrasonography. The text is amply illustrated with 549 photographs and diagrams.

1979, 352 pp., illus., $29.50 ISBN: 0-8089-1117-1

Send payment with order and save postage and handling charge.

Prices are subject to change without notice.

GRUNE & STRATTON

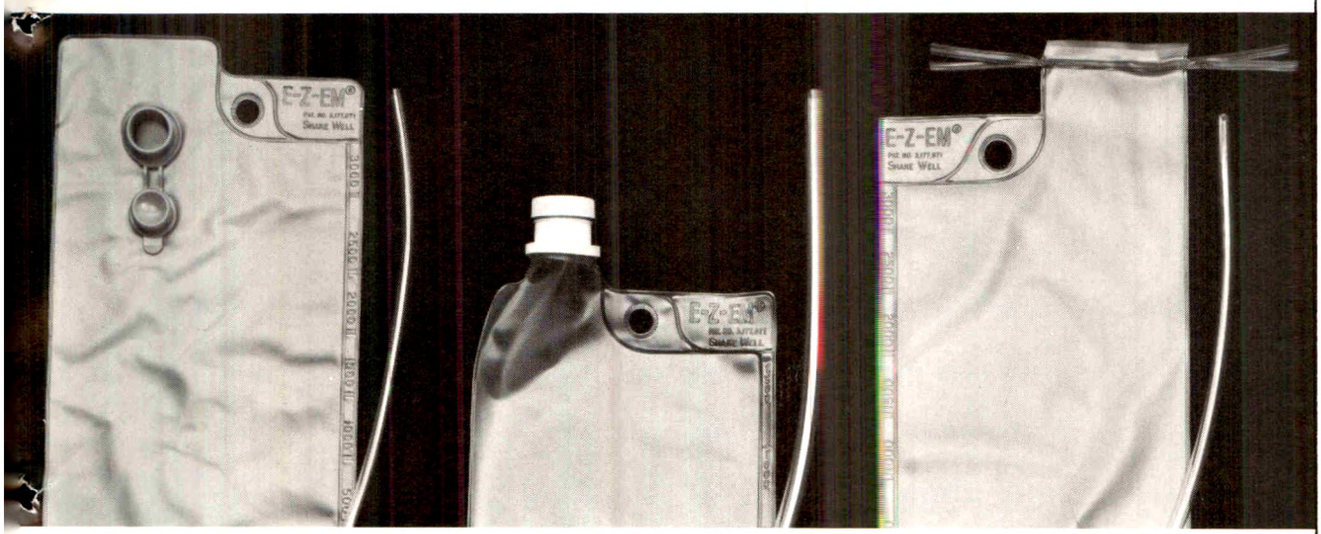
A Subsidiary of
Harcourt Brace Jovanovich, Publishers
111 FIFTH AVENUE, NEW YORK, N.Y. 10003
24-28 OVAL ROAD, LONDON NW1 7DX

Index to Advertisers

In Alphabetical Order

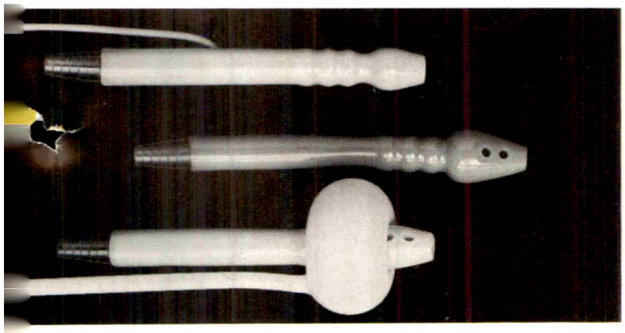
Agfa-Gevaert Rex, Inc.
Atomic Energy of Canada
CGR Medical Corporation
Dunn Instruments, Inc.
DuPont CRONEX® Processor and Chemical Mixer
Eastman Kodak Company
E-ZEM Company
Elema-Schonander, Inc.
C. B. Fleet Co.
General Electric Company
Grune & Stratton, Inc.
Imaging Systems
Machlett Laboratories
Medi-Tech Division
Ohio Nuclear
Omnimedical
Pfizer Medical Systems, Inc.
Philips Medical Systems, Inc.
Picker Corporation
Precise Optics
Purdue Frederick Company
Pyne X-Ray Corporation
Radiologic Sciences, Inc.
Siemens Corporation
E. R. Squibb & Sons, Inc.

ENEMA SYSTEMS.



BAGS

There's one to meet every preference...all made of durable, non-crack, heavyweight vinyl. Our selection includes snap cap models...1 and 2–piece rigid spout...retrograde fill...double tie wrap...and others, each crafted to our highest standards, and every enema bag is completely inspected to assure compliance with our rigorous quality control standards.

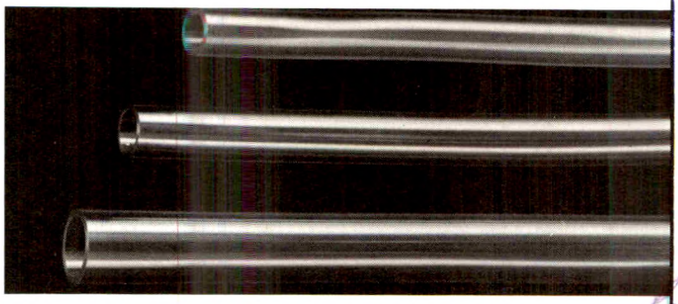


TIPS

Perhaps the largest selection anywhere. Choose from flexible tips...Miller air tips for double contrast, with and without cuffs... colostomy air contrast tips...pediatric tips and over 30 other specialized designs that make your work easier.

TUBING

We use only the finest grade of flexible vinyl...to be a perfect component of any E-Z-EM barium enema system you create. Available in either standard 5/16" lumen, 3/8" XL, and 1/2" Super XL.



Call today...we have the knowledge and the products!

E-Z-EM® 7 Portland Avenue, Westbury, New York 11590 (516) 333-8230

International Affiliates: E-Z-EM Rooster B. V., Infirmeriestraat 6-8, Rotterdam 16, Netherlands
E-Z-EM De Mexico, S. A. de C. V., Calz. Azcapotzalco La Villa No 882, Zona Industrial Vallejo, Mexico 16 D. F.

©1/79

LIBRARY



NEW *KODAK* AUTOMIXER PUTS *KODAK* CHEMICALS TO WORK FOR YOU.

FAST. EASY. EFFICIENTLY.

There are at least seven important reasons to use this new mixer with your automatic processors. You may discover others.

To be sure of consistent processing results, your chemicals should be fresh and accurately mixed. The new KODAK Automixer handles this chore for you with astonishing ease. One automixer will feed two processors.

1. Easy to load. The convenient batch size (5 gallons each for developer and fixer replenishers) makes it easy for the operator—no heavy chemical containers to lift. Dispenser automatically breaks seals, meters in the correct amount of water, while uniformly mixing the fresh replenisher.

2. Safe. The plastic openers are permanently mounted. They do not move. Dispenser shapes are such that they will accept only the correct chemical containers.

3. Fast. Mix takes from 2 to 3½ minutes, depending on local water pressure. Far faster than manual operation.

4. Fresher chemicals. With a total 10-gallon capacity, chemical oxidation is reduced, keeping chemicals at full potency.

5. Easy to teach. Because operation is so simple, personnel training time is minimal. And because handling is neat, simple, and quick, department personnel can easily attend to it.

6. Automatic. The automixer protects against accidental refills with water alone. An automatic signal tells you when levels are low.

7. Accessible. Outlets on the tanks will accept standard replenisher hoses from any processors.

Ask your Kodak Technical Sales Representative to tell you more about the new KODAK Automixer. It's the fast, easy, efficient way to put KODAK Chemicals to work. Or write: Eastman Kodak Company, Dept. 740-B, Rochester, New York 14650.

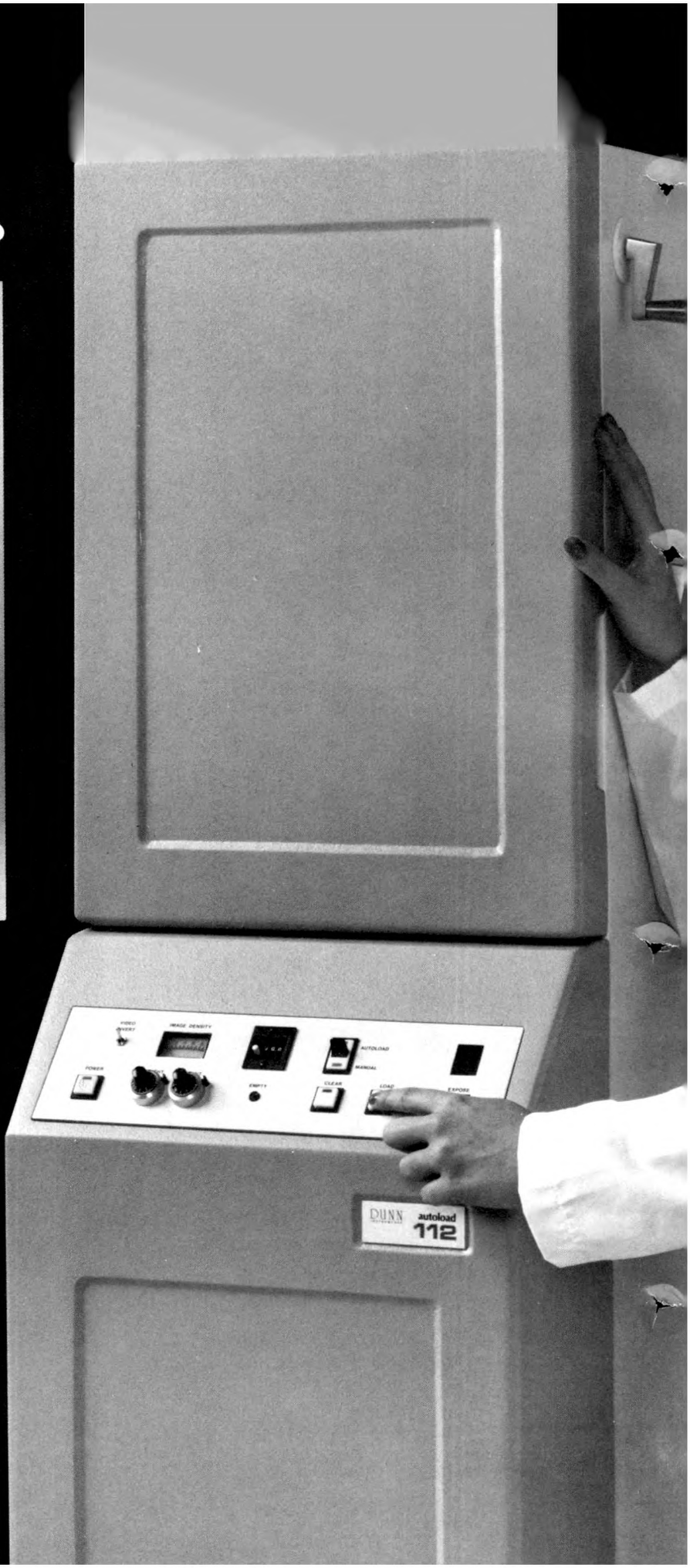
TURNING ENERGY INTO IMAGES

Kodak

COMPUTED TOMOGRAPHY • NUCLEAR MEDICINE
ULTRASOUND • RADIOGRAPHY • THERMOGRAPHY

Film handling overload?







Handle it with Auto Load

Autoload 112 is the natural development of an idea whose time is still with us. Four years ago, Dunn Instruments introduced the multi-image camera with X-ray film to serve the growing revolution in video-based diagnostic imaging. Economy, convenience and superior image quality brought instant acceptance. Since then, in the familiar pattern, progress itself has created new challenges. Like film handling, which in some applications can be a hassle: where the caseload or the imaging requirements per patient are great. Or in any institution where heavy demand produces a bottleneck at the darkroom. Then dealing with manually loaded film cassettes can waste valuable time and space, and multiply the chances for error.

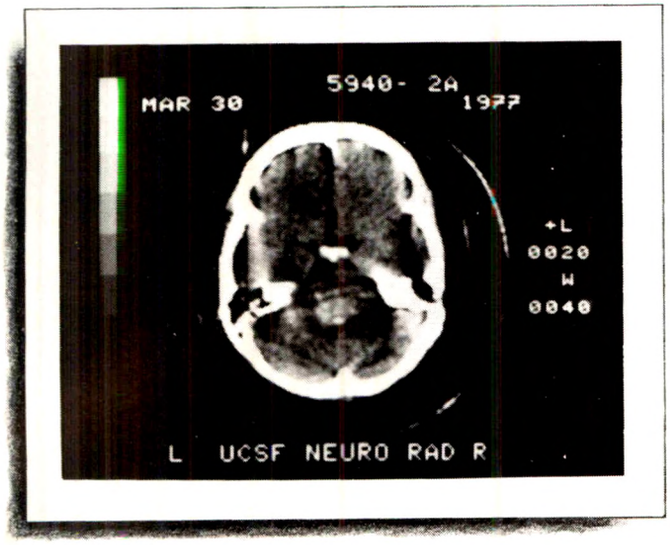
With Autoload you bulk load 100 sheets of film at a time, in a matter of seconds, directly into the camera in full daylight. Then expose as many sheets as you want and take them in the film transport drawer to the darkroom. Or better yet, get Autoload with optional direct feed into its own companion film processor, and have developed film in 90 seconds right in the imaging lab!

Automated film handling is only part of what makes Autoload 112 the most advanced multi-image camera ever. The uncompromising quality of its components is exemplified by the Tektronix 634 flat-faced video monitor, with 1400 lines resolution and backporch-clamped black level stability. Other standard features include on-axis Schneider optics, microprocessor control electronics, remote operation and video inversion. You can order Autoload in your choice of film sizes (up to 14″ x 17″) and image formats (including switch-selectable multi-format models).

If film hassling is holding you up, you should look into Autoload. For further information, call us collect or write Dunn Instruments, 544 Second Street, P.O. Box 77172, San Francisco, California 94107. Telephone (415) 957-1600.

Autoload 112
by Dunn Instruments





Diagnosis:
Posterior Inferior Cerebellar Artery Aneurysm

Clinical Data:
55 year old woman with diplopia, increasing right-sided weakness and hyperacousis in the left ear of 18 months duration

CT Scan:
A midline mass is noted in the posterior fossa. The mass is partially calcified and enhanced slightly after contrast infusion. On the basis of this scan it is impossible to determine if this lesion is intra or extra-axial in location.

Left Vertebral Arteriogram:
A large aneurysm arising from the proximal posterior inferior cerebellar artery is shown.

The arteriogram and the CT scan reproductions are both reduced to 79% of their original size.

Angiography and CT scanning.

Each has its own special diagnostic advantages in this era of expanding imaging technology.

Angiography and Elema-Schonander.

For diagnostic specificity.

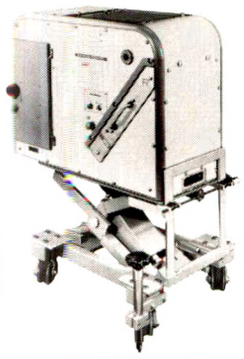
While CT has proved to be a highly sensitive diagnostic technique, in many cases angiography is necessary to make a specific diagnosis. And, no matter what your angiographic applications are, Elema-Schonander has a sheet-film changer to meet your requirements.

AOT-S Models: Six exp/sec, 30-film capacity AOT-S Models are available to accommodate either 35cm x 35cm (14″ x 14″) or 24cm x 30cm sheet-film sizes.

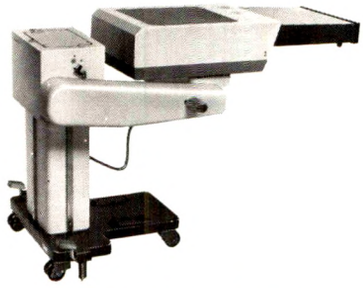
PUCK Models: Three exp/sec, 20-film capacity PUCK Models, which handle the same sheet-film sizes, are available for applications in which increased mobility, compactness and magnification are important considerations.

Both AOT-S and PUCK sheet-film changers have Elema-Schonander's CFRP (carbon-fiber reinforced plastic) front compression plate for low x-ray attenuation with intimate screen/film contact. Both are punch card controlled for accuracy and convenience. Both can be used for single plane, or biplane simultaneous or alternating sequences.

Call or write for brochures describing the AOT-S and PUCK sheet-film changers. Elema-Schonander, Inc., 699 Lively Blvd., Elk Grove Village, IL 60007. (312) 593-6770.



AOT-S Sheet-film Changer



PUCK Sheet-film Changer

elema-schonander

78216

What's new in contrast media for excretion urography?

Renovue®
Iodamide Meglumine
is new!



Fast opacification

Maximal opacification of renal passages may begin as early as one minute following injection of Renovue-65 (Iodamide Meglumine Injection) and within five minutes after start of infusion of Renovue-DIP (Iodamide Meglumine Injection 24%).

High contrast density

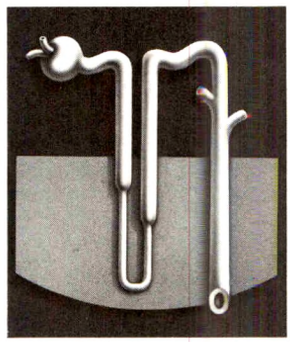
Iodamide meglumine produces dense opacification of calyces, renal pelves and ureters.

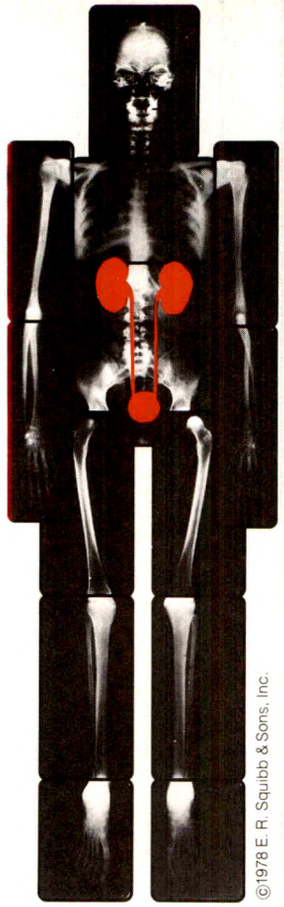
Rapid urinary excretion

Contrast medium is excreted essentially unchanged in the urine, principally by glomerular filtration, but *at least one-third is secreted by renal tubules.*









©1978 E. R. Squibb & Sons, Inc.

Renovue®-65
Iodamide Meglumine Injection

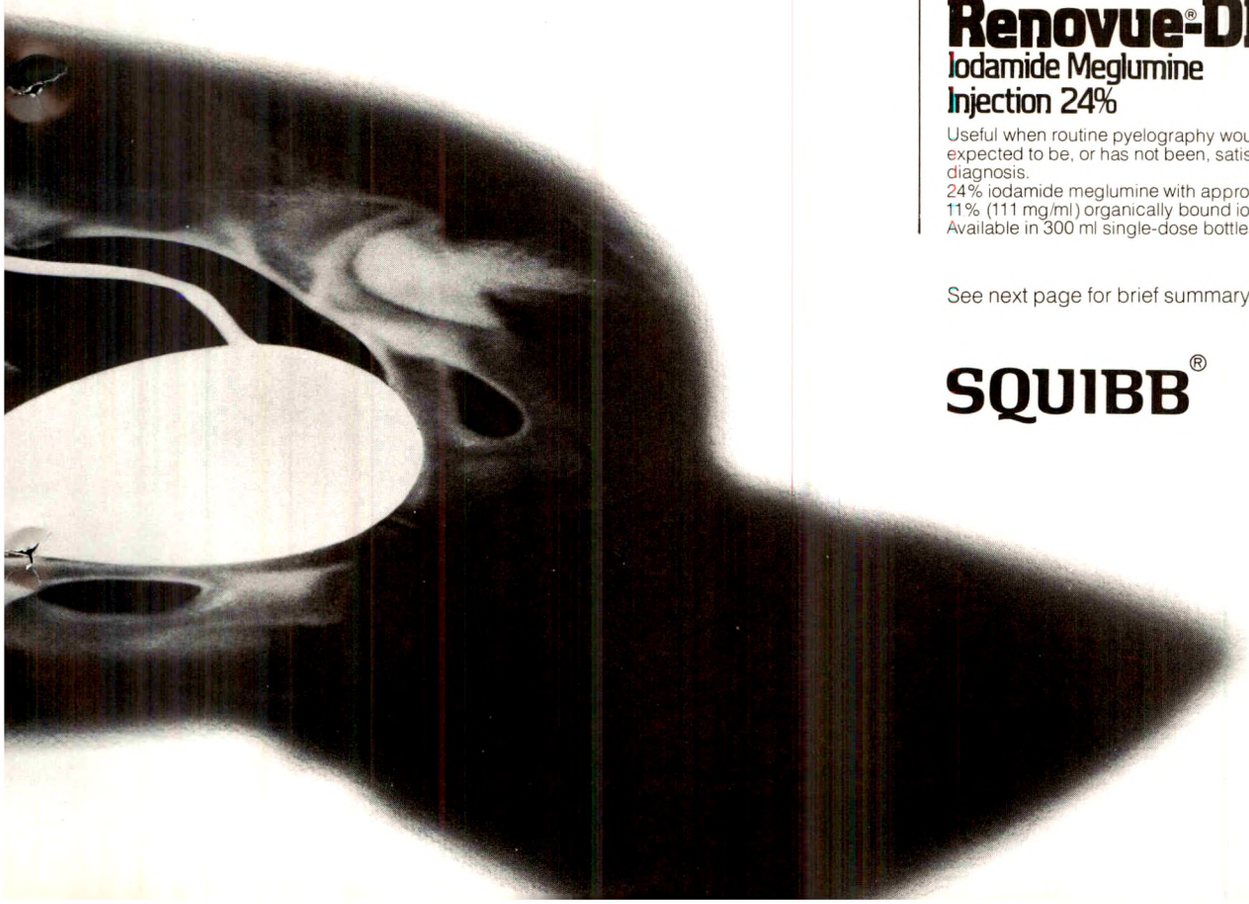
65% iodamide meglumine with approximately 30% (300 mg/ml) organically bound iodine.
Available in 50 ml single-dose vials.

Renovue®-DIP
Iodamide Meglumine Injection 24%

Useful when routine pyelography would not be expected to be, or has not been, satisfactory for diagnosis.
24% iodamide meglumine with approximately 11% (111 mg/ml) organically bound iodine.
Available in 300 ml single-dose bottles.

See next page for brief summary.

SQUIBB®



RENOVUE®-65
Iodamide Meglumine Injection
Renovue®-DIP
Iodamide Meglumine Injection 24%

DESCRIPTION: Renovue-65 (Iodamide Meglumine Injection) and Renovue-DIP (Iodamide Meglumine Injection 24%) are radiopaque urographic contrast agents supplied as sterile, nonpyrogenic, aqueous intravenous solutions. Renovue-65 provides 65% iodamide meglumine with approximately 30% (300 mg/ml) organically bound iodine with 0.01% edetate disodium as a sequestering stabilizing agent. *Renovue-65 contains approximately 0.0124 mg (0.0005 mEq) sodium per ml.* Renovue-DIP provides 24% iodamide meglumine with approximately 11.1% (111 mg/ml) organically bound iodine with 0.00368% edetate disodium as a sequestering stabilizing agent. *Renovue-DIP contains approximately 0.0046 mg (0.0002 mEq) sodium per ml.*

CONTRAINDICATIONS: No absolute contraindications; however, see WARNINGS.

WARNINGS: Because of the great possibility of producing transient to fatal renal failure, a definite risk exists with excretion urography in patients with multiple myeloma. The risk in these patients is not a contraindication to the procedure; however, avoid dehydration in preparing these patients since this may predispose to precipitation of protein in the renal tubules.

Administer radiopaque materials to patients known or suspected to have pheochromocytoma only if the physician deems that the possible benefits outweigh the considered risks and then only with extreme caution while keeping the volume of drug at an absolute minimum. Assess blood pressure throughout the procedure and have measures for treatment of a hypertensive crisis available.

Intravenous contrast media have been shown to promote sickling in persons homozygous for sickle cell disease. Perform urography with extreme caution in presence of anuria or severe concomitant hepatic and renal disease. Although not an absolute contraindication to use of iodamide meglumine, a history of sensitivity to iodine *per se* or to any contrast agent calls for extreme caution in administration.

PRECAUTIONS: *General*—Since all procedures utilizing contrast media carry a definite risk of producing side effects, carefully evaluate the risk-benefit factor before undertaking a procedure because life-threatening and fatal reactions may occur without warning. Constantly have available a fully equipped emergency cart (or equivalent supplies and equipment) and personnel competent in recognizing and treating all degrees of adverse reactions to the drug or to the procedure. Immediately discontinue administration of the contrast agent if a serious reaction occurs. Keep competent personnel and emergency facilities available for at least 30 to 60 minutes after administration to cope with severe delayed reactions.

Renal toxicity has been reported in a few patients with liver dysfunction who were given oral cholecystographic agents followed by urographic agents; therefore, if known or suspected hepatic or biliary disorder exists, administration of iodamide meglumine preparations should be postponed following the recent ingestion of cholecystographic agents. Exercise caution with use of contrast media in severely debilitated patients and in those with marked hypertension. Consider the functional ability of the kidneys before injecting iodamide meglumine preparations. Bear in mind the possibility of thrombosis or other complications due to mechanical trauma of the intravenous procedure. Collect urine before or two or more days after administration of the drug since contrast agents interfere with some chemical determinations made on urine specimens. Perform PBI and radioactive iodine uptake studies, if such are indicated, prior to administration of the drug since iodine-containing contrast agents may alter thyroid function test results. If use of an antihistamine for premedication or treatment of an adverse reaction is considered, recognize that admixture of an antihistamine with a contrast agent may result in a precipitate; because of this, different sites should be used to administer the antihistamine and the contrast agent. Use of a diuretic prior to the examination in order to increase the urinary concentration of the contrast agent is not desirable; dehydration may predispose to a greater incidence of, or more severe, reactions. Consider the increased osmotic load associated with drip infusion pyelography in patients with congestive heart failure; the diuretic effect of drip infusion pyelography may hinder assessment of residual urine in the bladder. Do not exceed recommended rate of infusion (appropriate volume infused in approximately 10 minutes) of Renovue-DIP (Iodamide Meglumine Injection 24%).

Sensitivity Testing—Severe, life-threatening reactions often resemble hypersensitivity phenomena. A personal or family history of asthma or allergy or a history of a previous reaction to a contrast agent warrants special attention and may predict more accurately than pretesting the likelihood of a reaction although not the type nor severity of the reaction in the individual. The value of any pretest is questionable. The pretest most performed is the slow I.V. injection of 0.5 to 1.0 ml of the preparation prior to injection of the full dose; however, the absence of a reaction to the test dose does not preclude the possibility of a reaction to the full diagnostic dose. Should the test dose produce an untoward response, the necessity for continuing the examination should be carefully re-evaluated; if deemed essential, the examination should proceed with all possible caution. In rare instances, reaction to the test dose may be extremely severe; therefore, close observation and facilities for emergency treatment are essential.

Usage in Pregnancy—No teratogenic effects attributable to iodamide meglumine preparations have been observed in mouse, rat, and rabbit reproduction studies. Safety for use during pregnancy in humans has not been established. Although there is no clearly defined risk, the possibility of infrequent or subtle fetal damage cannot be excluded. Iodamide meglumine should be used in pregnant women only when clearly needed.

Pediatric Use—Safety and effectiveness for pediatric use have not been established.

ADVERSE REACTIONS: In clinical studies, adverse reactions occurred in approximately 9.5 to 13% of patients. Nausea and/or vomiting, urticaria, pruritus, a rise or fall in blood pressure, sneezing, and sensation of warmth occur most frequently (individually occurring at a frequency of approximately 1 to 5% and usually mild). The following occur less frequently: generalized flushing, lacrimation, headache, edema of the eyelids, coughing, retching, bitter or metallic taste, pharyngeal burning sensation, nasal congestion, hoarseness, sweating and weakness, malaise, perianal burning sensation, pain and erythema at injection site due to faulty technique, bradycardia, hyperpnea, flank tenderness, chills, syncope, pulse rate increase, shortness of breath, chest pain, tachycardia, hemiparesis, and shock. Other reactions to iodinated contrast media include fever, dizziness, restlessness, lightheadedness, pallor, choking, laryngeal or pulmonary edema, dysphagia, facial or conjunctival petechiae, rash and other eruptions, wheezing, asthmatic reaction, cramps, tremors, anxiety, hematomas and ecchymoses around injection site due to faulty technique, vein cramp, partial collapse of injected vein, thrombophlebitis and cellulitis following injection, neutropenia, transient proteinuria, hysterical reaction and numbness of head and neck, and convulsions. "*Iodism*" (salivary gland swelling) has been reported infrequently; immediate or delayed rigors sometimes with hyperpyrexia has occurred rarely. Antihistaminic agents may be of benefit in event of adverse reactions. Adverse reactions may be severe enough to require discontinuation of injection of Renovue-65 (Iodamide Meglumine Injection) or infusion of Renovue-DIP (Iodamide Meglumine Injection 24%).

Severe reactions, which may require emergency measures, may take the form of a cardiovascular reaction characterized by peripheral vasodilatation with resultant hypotension and reflex tachycardia, dyspnea, agitation, confusion, and cyanosis progressing to unconsciousness. Cardiac arrest, ventricular fibrillation, cardiac arrhythmias, hypertension, temporary renal shutdown or other nephropathy may occur rarely. The histamine-liberating effect of an iodinated contrast agent may induce a reaction ranging in severity from rhinitis or angioneurotic edema to laryngeal or bronchial spasm and, rarely, anaphylactoid shock.

For full prescribing information, consult package inserts.

HOW SUPPLIED: Renovue-65 (Iodamide Meglumine Injection) is available in 50 ml single-dose vials. Renovue-DIP (Iodamide Meglumine Injection 24%) is available in 300 ml single-dose infusion bottles (designed to be suspended from an I.V. stand).

SQUIBB® 'The Priceless Ingredient of every product is the honor and integrity of its maker.'™

©1978 E. R. Squibb & Sons, Inc. 658-501

The UNION CARBIDE Bedside X-Ray System:

Reproducibility... Every Place, Every Time.



The 510 Bedside X-Ray System is a lightweight, low cost, mobile x-ray unit designed to achieve consistent reproducibility with routine bedside radiographic procedures.

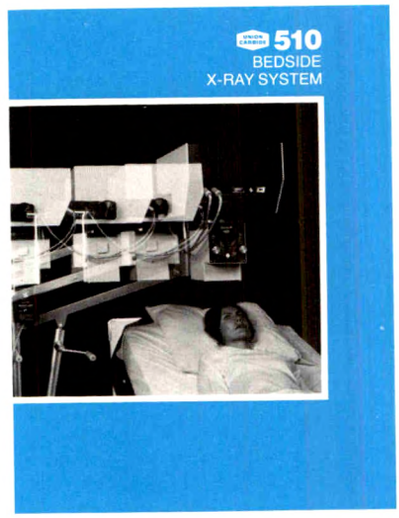
All exposure settings and operating controls are located on a convenient hand control module. Automatically computed and displayed mAs outputs up to 31mA at 100kVp or up to 35 mA at 60kVp reduce technique errors.

Diagnostic image quality is achieved by a combination of system power and speed. The 510 Bedside X-Ray System produces more power from a fixed anode tube allowing adult chest exposures with 100 kVp at 1/20 to 1/60 of a second; neonate studies at 1/40 to 1/120 of a second. Precise digital timing at speeds as fast as 1/120 of a second permits rapid exposures that effectively stop patient motion. This precision makes the unit effective with both traditional film/screen combinations and with newer "rare earth" systems.









Because the system is light in weight and small in size, it can be described as the most portable unit available. No bulky transport battery and motor. And because its price is so low, the 510 Bedside X-Ray System brings full diagnostic power *on a dedicated basis* to within economic feasibility for most potential users.

Ask Union Carbide for the Facts

Imaging Systems products from Union Carbide are designed to enhance diagnosis and research, produce a return on investment, and create better health care at lower patient cost.

If you feel you should know more about this new diagnostic tool, send today for descriptive literature. Or call for a personal presentation.



Touching your life through medicine . . .

UNION CARBIDE

Imaging Systems, Inc.
Medical Products Division
333 Providence Highway
Norwood, Massachusetts 02062
Within area 617, call 769-5400.
Outside, call 1-800-225-9887.
TELEX 924-494

clear, clean colon

X-Prep® Liquid

(standardized extract of senna fruit)

versatile bowel evacuant for diagnostic procedures



Versatile in indications

May be used prior to:

G.I. radiography
Urologic radiography
Colonoscopy
Sigmoidoscopy
Other diagnostic bowel procedures

Versatile in administration

May be used:

Alone, in a single dose
Alone, in divided doses, particularly in elderly or debilitated patients
With adjunctive use of citrate of magnesia, laxative suppositories and enemas, as required
As part of other regimens, such as hydration

X-PREP Liquid is formulated specifically for effective bowel evacuation prior to diagnostic procedures. It induces peristalsis through virtually colon-specific action. X-PREP Liquid has been found effective in cleansing the colon for diagnostic evaluation in 95% of 749 patients prepared for barium enemas, intravenous pyelography, or colonoscopy.* Its pleasant taste meets with high patient acceptance, and its ease of administration is appreciated by the patient and nursing staff.

Supplied: X-PREP Liquid (standardized extract of senna fruit) in 2½ fl. oz. bottles (alcohol 7% by volume). X-PREP Powder (standardized senna concentrate) in ¾ oz. containers. **Now Available:** X-PREP™ Bowel Evacuant Kit. Each kit contains: two SENOKOT® S Tablets (standardized senna concentrate and dioctyl sodium sulfosuccinate), one bottle of X-PREP® Liquid 2½ fl. oz., and one RECTOLAX™ Suppository (bisacodyl 10 mg), plus easy-to-follow patient instructions for hydration, clear liquid diet, and the correct time sequence of administering the above laxatives.

Colonoscope, courtesy of Olympus

Gray Pharmaceutical Co., Affiliate
The Purdue Frederick Company

*Bibliography available upon request.

© Copyright 1978, Gray Pharmaceutical Co. Norwalk, CT 06856

A9047 194578

Rapid and Accurate Diagnosis of Acute Cholecystitis with ^{99m}Tc-HIDA Cholescintigraphy

HEIDI S. WEISSMANN,[1] MICHAEL S. FRANK,[2] LESLIE H. BERNSTEIN,[2] AND LEONARD M. FREEMAN[1]

Technetium-99m dimethyl acetanilide iminodiacetic acid (HIDA) cholescintigraphy was performed on 90 patients with suspected acute cholecystitis. Visualization of the gallbladder established patency of the cystic duct and excluded the diagnosis of acute cholecystitis in 50 of 52 patients. Nonvisualization of the gallbladder with visualization of the common bile duct was diagnostic of acute cholecystitis in 38 patients, all subsequently proven at surgery. The observed accuracy of this procedure is 98% and specificity is 100%. The false negative rate is 5% and false positive rate is zero.

Technetium-99m-HIDA has many advantages which make it the procedure of choice in evaluating a patient for suspected acute cholecystitis. It is a rapid, simple, safe examination which provides functional as well as anatomic information about the hepatobiliary system in individuals with a serum bilirubin level up to 8 mg/100 ml.

The rapid and accurate assessment of the patient with suspected acute cholecystitis remains an extremely important and sometimes difficult problem. Cholelithiasis and its complications are the most common indications for abdominal surgery and the fourth most common cause for surgical hospitalization in adults. More than 500,000 operations are performed annually in the U.S.A. for gallbladder disease, a significant percentage of which are related to acute inflammatory disease of the gallbladder [1].

For many years, radiographic evaluation of suspected cholecystitis has depended on the use of iodinated contrast material, such as in oral cholecystography [2] and intravenous cholangiography [3]. More recently ultrasonography [4] and, to a lesser extent, computed tomography [5] have proved to be of value in this diagnostic area. While each method may contribute useful information in the workup of suspected cholecystitis, each has shortcomings.

A new noninvasive radionuclide imaging procedure, technetium-99m dimethyl acetanilide iminodiacetic acid (HIDA) cholescintigraphy, was introduced in 1975 by Harvey et al. [6]. This examination offers excellent visualization of the biliary system and, in particular, supplies functional information with regard to patency or obstruction of the cystic duct in patients with acute right upper quadrant abdominal pain. Our study was based on the results of ^{99m}Tc-HIDA cholescintigraphy in 90 patients with suspected acute cholecystitis. This technique proved to be more accurate and reliable than the previously reported methods currently in use. It seems to be the procedure of choice for this diagnostic problem.

Subjects and Methods

Ninety adult patients were studied for suspected acute cholecystitis. Their bilirubin levels ranged from 0.2 to 8.0 mg/100 ml (table 1). All patients were kept in a fasting state for at least 2 hr before the examination. Informed consent was obtained.

Patients were supine under an Anger scintillation camera (Elscint, Haifa, Israel) and 5–10 mCi of ^{99m}Tc-HIDA prepared from a commercial kit (Merck-Frosst Labs., Dorval, Quebec, Canada) was injected intravenously. This work was performed under an investigational new drug application of Merck-Frosst. The availability of several iminodiacetic acid compounds is anticipated in the latter part of 1979 and the cost will likely be comparable to other liver imaging agent kits. Five hundred thousand counts were accumulated for each scintiphoto. The field of view included the liver, gallbladder, duodenum, and jejunum (fig. 1). An image was obtained 1 min after injection to visualize the blood pool phase, followed by serial scintiscans every 5 min for the first 30 min and at 45 and 60 min. Delayed scans were obtained when necessary depending on the individual case. Most studies were completed within 1–1½ hr. If the gallbladder was visualized, the study was continued until activity was noted in the duodenum. An oral fatty meal (Liposperse, Summit Medical Products, New York) was then administered and poststimulation scans were obtained between 30 and 60 min. If no significant gallbladder contraction was observed, 40 Ivy dog units of cholecystokinin (CCK-PZ, GIH Research Unit, Karolinska Institute, Stockholm, Sweden) or 0.2 μg/kg of Sincalide (Kinevac, Squibb) was administered intravenously. In the latter part of this investigation, cholecystokinin was used as the sole gallbladder stimulant (see Discussion). Serial scans were obtained every minute for the first 15 min, then every 3 min for the remaining 15 min. In selected cases, this information was recorded in digital form on a computer (Dycomette, Elscint Corp., Haifa, Israel) for subsequent playback and quantitative evaluation of the degree of contraction after stimulation.

Results

Of the 90 patients studied for suspected acute cholecystitis, 52 showed filling of the gallbladder within the first hour, thereby demonstrating patency of the cystic duct (table 2) (see Discussion for pharmacokinetics). Of these 52 cholescintigrams, 50 exhibited a normal hepatobiliary-to-bowel transit time with identifiable intestinal activity in less than 1 hr, and gallbladder contraction after fatty meal or cholecystokinin stimulation. These

Received September 19, 1978; accepted after revision January 2, 1979.

[1]Department of Radiology, Division of Nuclear Medicine, Montefiore Hospital and Medical Center, Albert Einstein College of Medicine, 111 East 210th Street, Bronx, New York 10467. Address reprint requests to H. S. Weissmann.

[2]Department of Medicine, Division of Gastroenterology, Montefiore Hospital and Medical Center, Albert Einstein College of Medicine, Bronx, New York 10467.

© 1979 American Roentgen Ray Society

0361–803X/79/1324–0523 $0.00

TABLE 1

Bilirubin Levels at Time of ^{99m}Tc-HIDA Cholescintigraphy

Bilirubin (mg/100 ml)	No. patients
0.1–1.0	54
1.1–2.0	18
2.1–3.0	8
3.1–4.0	2
4.1–5.0	3
5.1–6.0	3
6.1–7.0	1
7.1–8.0	1

studies were interpreted as normal. In these 50 patients, the biliary tract was subsequently proven not to be the cause of the acute problem. Confirmatory data included 21 normal oral cholecystograms, four normal intravenous cholangiograms, 25 normal ultrasound gallbladder examinations, four normal gallbladders examined at surgery performed for other indications, and three normal postmortem specimens. In the 43 patients who had acute cholecystitis excluded by radiographic methods, the subsequent clinical course also was confirmatory.

In two of the 52 cholescintigrams that demonstrated visualization of the gallbladder, the hepatobiliary-to-bowel transit time was markedly delayed, exceeding 2 hr. One patient exhibited normal contraction after oral fat ingestion. The gallbladder of the second patient did not contract in response to cholecystokinin stimulation and right upper quadrant pain was experienced after the intravenous injection. Both patients had chronic cholecystitis and nonobstructing stones at surgery.

Thirty-eight cholescintigrams showed nonvisualization of the gallbladder with visualization of the common bile duct and duodenum. Cholecystitis was subsequently confirmed at surgery in all 38 patients (table 2).

On the basis of a visualized or nonvisualized gallbladder in less than 1 hr, the accuracy of ^{99m}Tc-HIDA cholescintigraphy in this series was 98% (88 of 90) and the specificity was 100% (38 of 38). The false positive rate (gallbladder nonvisualization) was zero (0 of 50) and the false negative rate (gallbladder visualization) was 5% (2 of 40) (table 2).

Additional abnormalities incidentally discovered in 15 ^{99m}Tc-HIDA examinations included pericardial effusion, ascites, ureteral obstruction, malrotation, hepatic masses, mass lesions in the head of the pancreas, and mass lesions displacing bowel.

No allergic reactions or other side effects were observed as a result of this procedure. The total amount of HIDA in each kit was 10 mg. Since each kit generally supplies two to four patients, the actual amount of HIDA received by any given patient would be decreased accordingly.

Discussion

Limitations of Current Procedures

Oral cholecystography, intravenous cholangiography, ultrasonography, and computed tomography have definite limitations in the evaluation of patients with acute right upper quadrant pain. A radionuclide imaging procedure such as ^{99m}Tc-HIDA cholescintigraphy, capable of yielding functional and anatomic information, does not have the same limitations nor any apparent contraindications. As with any diagnostic examination associated with radiation exposure, the benefit-to-risk ratio must be considered when the study is proposed for pregnant women.

Visualization of the gallbladder on oral cholecystography is limited by the need for oral ingestion, intestinal absorption, and hepatic conjugation of iopanoic acid or related compounds [7]. This delays the possibility of diagnosis by at least 12 hr [8] and, in 25% of cases, contrast material administration must be repeated on a second day [9]. Considering that the incidence of complications, especially gallbladder perforation, peaks around the third day of symptomatology, acute cholecystitis should be diagnosed promptly in order to maintain the lowest possible morbidity and mortality [1, 10, 11]. This generally precludes the use of oral cholecystography in patients with suspected acute cholecystitis. In addition, nonvisualization of the gallbladder on an oral cholecystogram is not specific for cholecystitis. There are numerous causes of nonvisualization unrelated to hepatobiliary disease, including failure to take or retain the pills, esophageal or pyloric obstruction, malabsorption, and diarrhea [2, 9]. Furthermore, oral cholecystography is of limited value in cases with hyperbilirubinemia.

Intravenous cholangiography offers an alternative to oral cholecystography, but it has several significant limitations. Any procedure using iodinated contrast media must be performed with caution, if at all, in patients with renal or hepatic failure. The renal and hepatotoxicity of the iodipamide contrast agent have been well documented [12–15]. Intravenous cholangiography has a morbidity of 10%–20%, including numerous side effects ranging from nausea and vomiting to anaphylaxis and death. Reported mortality is 1 in 5,000, two to six times greater than that of excretory urography [10, 16]. The ability to visualize the biliary tree by intravenous cholangiography decreases appreciably when the serum bilirubin level is in the range of 2–4 mg/100 ml, and virtually no visualization occurs above the level of 4 mg/100 ml [17]. Furthermore, the accuracy of intravenous cholangiography in diagnosing acute cholecystitis is reportedly limited [9, 17]. In one series [18] where intravenous cholangiography was performed with tomography, 12% of cases with nonvisualized gallbladder and visualized common bile duct had normal gallbladders at surgery. In the same study, the gallbladder failed to visualize in 22% of cases where a normal functioning gallbladder was visualized on oral cholecystography. Thus, nonvisualization of the gallbladder on intravenous cholangiography is also not a sine qua non for cholecystitis. Furthermore, when the gallbladder does visualize, cholelithiasis is diagnosed accurately in only 55% and choledocholithiasis in only 45% of cases [18].

The strengths of ultrasound and computed tomography are related to their ability to demonstrate anatomic

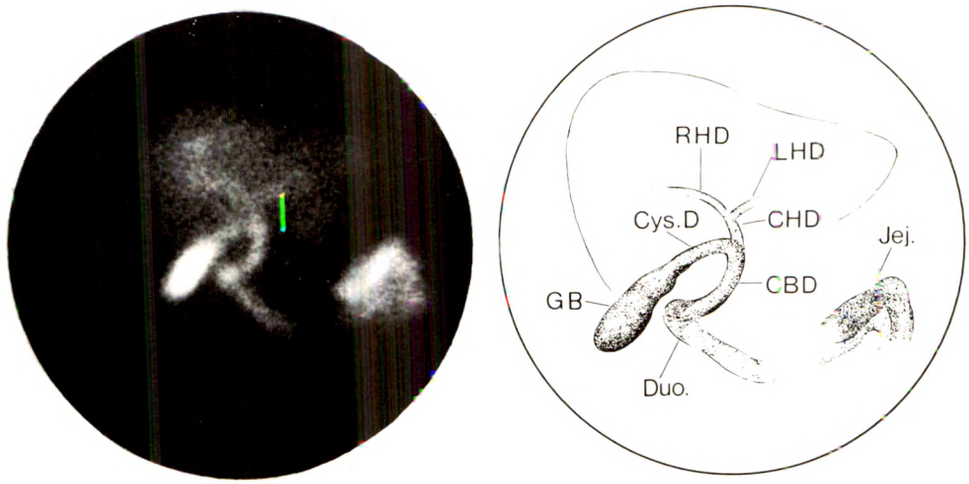


Fig. 1.—Normal ^{99m}Tc-HIDA cholescintigram at 20 min. RHD = right hepatic duct, LHD = left hepatic duct, CHD = common hepatic duct, Cys. D = cystic duct, GB = gallbladder, CBD = common bile duct, Duo. = duodenum, Jej. = jejunum.

TABLE 2

Clinical Results of ^{99m}Tc-HIDA Cholescintigraphy

Final Diagnosis	Nonvisible Gallbladder at 1 hr	Visible Gallbladder at 1 hr
Cholecystitis	38*	2†
Normal	0	50

* Cholecystitis confirmed at surgery.

† Chronic cholecystitis with numerous small stones and sludge in association with patent cystic ducts at surgery.

detail without contrast agents. This can be of particular value in patients with acute right upper quadrant pain if gallstones are seen in the region of the gallbladder neck, cystic duct, or common bile duct, or if there are other associated findings such as a thickened gallbladder wall [4]. The major weakness of ultrasonography and computed tomography is that they are purely anatomic methods of imaging and give limited information about function. Since 15 million Americans have gallstones, most of whom are asymptomatic [19], the documentation of their presence by either of these methods does not determine functional occlusion of the cystic duct and, therefore, cannot be unequivocally equated with acute cholecystitis.

Radiolabelled Compounds for Hepatobiliary Imaging

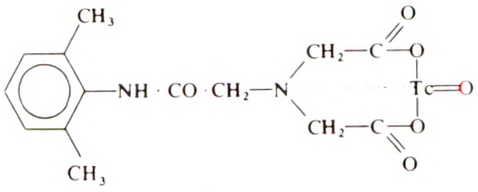
Until recently, radionuclide imaging in the workup of patients with acute cholecystitis was limited to iodine-131 rose bengal. While the biokinetics of liver uptake and excretion of rose bengal are acceptable, the usefulness of this agent is severely limited by the ^{131}I label. The long physical half-life of 8.1 days and the significant particulate (beta) emission associated with ^{131}I decay limits acceptable doses to the microcurie range. In addition, ^{131}I has a high primary photon energy peak of 364 keV which is suboptimal for Anger camera imaging. These factors do not allow adequate visualization of the biliary tree. A significant improvement was made by the introduction of ^{123}I rose bengal with a shorter physical half-life (13.1 hr), lower gamma photon peak of 159 keV, and lack of beta emission [20]. However, this relatively short-lived nuclide is cyclotron produced, which limits its availability.

Technetium-labeled agents have an ideal half-life of 6 hr and are pure gamma emitters. In view of these factors, multimillicurie doses, several orders of magnitude higher than the permissible dose of ^{131}I labeled agents, may be administered. The number of photon-emitting events capable of being detected are commensurately increased, resulting in a significant improvement in the statistics of nuclear imaging. Furthermore, the technetium photon peak of 140 keV is ideal for use with the thin 0.6 or 1.3 cm crystal of the Anger camera.

For these reasons, there has been a recent proliferation of technetium-labeled radiopharmaceuticals in an attempt to develop a hepatobiliary imaging agent of greater clinical usefulness than rose bengal [21, 22]. Experiments have been conducted with several potential hepatobiliary radiotracers such as ^{99m}Tc penicillamine [23], ^{99m}Tc pyridoxylideneglutamate [24], ^{99m}Tc dihydrothioctic acid [25], and the ^{99m}Tc-labeled iminodiacetic (IDA) derivatives, one of which is the subject of this study [26–29].

In 1975, Harvey and associates [6, 30] discovered that a small chelating group capable of binding technetium to iminodiacetic acid (IDA) was actively accumulated and excreted by the hepatobiliary system. They examined its potential usefulness by studying two specific N-substituted iminodiacetic acid derivatives, methyliminodiacetic acid (MIDA) and N-(2,6-dimethylphenylcarbamoylmethyl) iminodiacetic acid (HIDA), in vitro and in vivo in mice and dogs. They demonstrated that the biologic distribution of the radiopharmaceutical was governed almost exclusively by the N-substituted group.

The structural characteristics necessary for hepatobiliary uptake and excretion include a molecular weight of 300–1,000, a strong polar group, at least two ring systems in different planes, and strong binding to albumin [31]. Technetium-HIDA has a molecular weight of 387, a strong organic anion (COO−), two ring systems in different planes, and binds to albumin. Thus, it is structurally well suited for hepatobiliary imaging (fig. 2).



^{99m}Tc-HIDA

Fig. 2.—Chemical structure of ^{99m}Tc-HIDA: N-(2,6-dimethylphenylcarbamoylmethyl) iminodiacetic acid.

Normal ^{99m}Tc-HIDA Cholescintigram

Serial scintigrams after an intravenous injection of ^{99m}Tc-HIDA yield a dynamic representation of hepatobiliary function. Patients are fasted for at least 2 hr prior to examination to prevent the possibility of a false positive study (nonvisualization of the gallbladder), as has been observed with ^{99m}Tc Pyridoxylideneglutamate [32]. After eating, decreased visualization of the gallbladder is expected since the degree of postprandial gallbladder filling is small for at least 1 hr [32]. About 85% of ^{99m}Tc-HIDA is taken up by the hepatocytes and excreted unchanged into the biliary system and the bowel; the remaining 15% is excreted by the kidneys [27, 30]. In the normal individual, renal excretion is usually only observed within the first 10 min and then is no longer prominent. Activity peaks in the liver within 5–10 min; the common bile duct, gallbladder, and duodenum are usually visualized between 15 and 30 min. The upper limits of normal for visualization of these structures is 1 hr. Gallbladder contractility can be evaluated by stimulation with a fatty meal or intravenous cholecystokinin (fig. 3).

Advantages of ^{99m}Tc-labeled IDA Derivatives

Technetium iminodiacetic acid (IDA) derivative imaging seems to be a safe and simple procedure with no known contraindications or complications. In our series and all reported patients [26, 28, 33, 34], as with most radionuclide imaging procedures, no adverse reactions have been observed. The patient's habitus and the presence of bowel gas do not pose technical difficulties as they do in other radiographic procedures available.

Although most patients with suspected acute cholecystitis have normal or slightly elevated bilirubin levels, it should be noted that ^{99m}Tc-HIDA provides reasonably good visualization with bilirubin levels up to 7–8 mg/100 ml. Several other derivatives of IDA, such as the parabutyl analog, afford improved visualization with markedly elevated bilirubin levels [33]. The false negative rate of 5% and false positive rate of zero that we observed are considerably less than those associated with intravenous cholangiography [18].

In addition, technetium IDA imaging is capable of giving anatomic and functional information not obtainable from oral cholecystography and intravenous cholangiography. Hepatocyte function can be evaluated by the degree and rate of technetium uptake. During the first 15 min while the radiotracer is still in the hepatic parenchyma, space-occupying disease is detectable in a manner analagous to ^{99m}Tc sulfur colloid imaging. The intrahepatic ducts are frequently visualized, particularly in partially obstructed states. The visualization or exclusion of the gallbladder reliably implies patency or obstruction, respectively, of the cystic duct. This finding in suspected acute cholecystitis is considerably more important than the anatomic demonstration of gallstones by ultrasound or any other method.

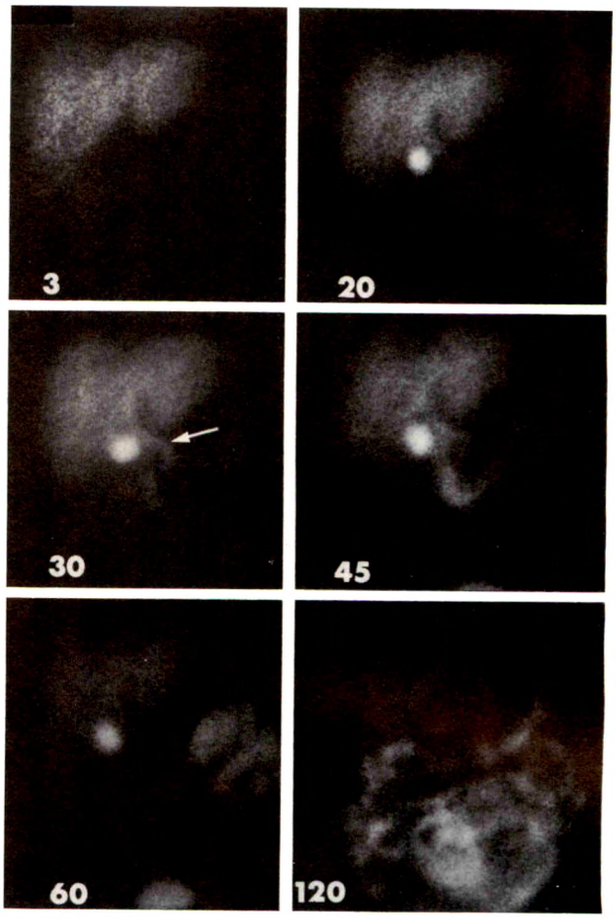


Fig. 3.—Normal ^{99m}Tc-HIDA cholescintigram. Serial scans. Hepatic uptake and excretion with sequential visualization of biliary tract and bowel. Common bile duct (*arrow*). Gallbladder well visualized from 20 min on; good contraction after fatty meal (lower right). Bladder activity in lower portion of 45 min and 1 hr scans.

Common bile duct obstruction can be readily determined by evaluating its size and observing the rate of excretion into the bowel. Furthermore, since the course of small and large intestine is clearly visualized, space-occupying masses in the abdomen may sometimes be inferred by the detection of bowel displacement.

Establishing the Diagnosis of Acute Cholecystitis

In our experience, when the gallbladder does not visualize in the face of normal hepatocyte uptake and common bile duct excretion in fasting patients with acute right upper quadrant pain, the diagnosis of cholecystitis can be made with certainty (fig. 4). Of the 38

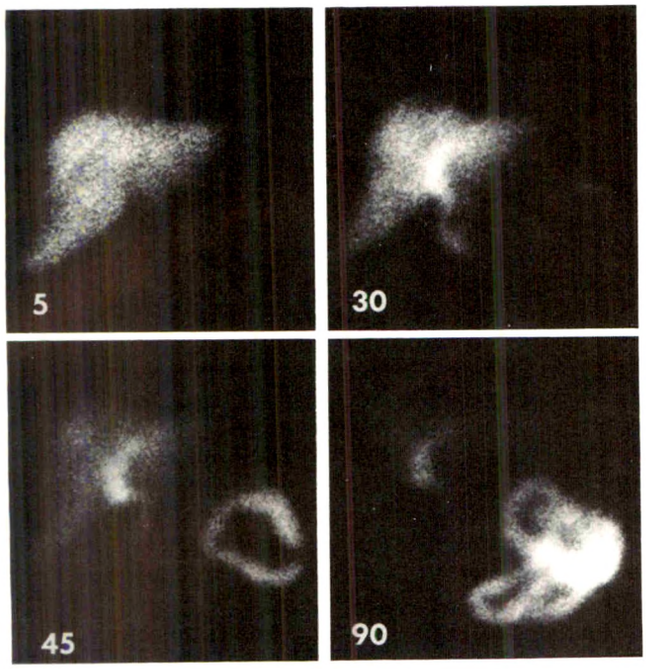


Fig. 4.—Acute cholecystitis. Serial scans. Normal hepatic uptake and excretion with visualization of common bile duct and small intestine. No gallbladder visualization throughout study. Acutely inflamed gallbladder with calculus obstructing cystic duct was found at surgery.

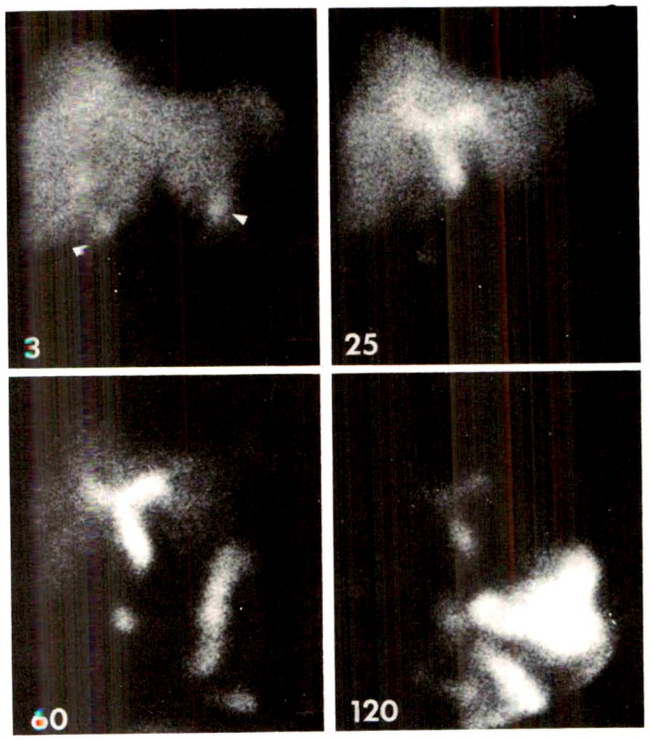


Fig. 5.—Acute cholecystitis associated with dilated common bile duct. Normal hepatic uptake and excretion with visualization of dilated intrahepatic and common bile ducts (seen best at 1 hr). Normal transit time to bowel. No gallbladder visualization. Right and left renal pelves (*arrowheads*). Cholecystitis with cholelithiasis found at surgery. Ducts were dilated, presumably due to previous passage of stones.

patients in our series who had this pattern, 100% were surgically proven to have cholecystitis. This is comparable to the findings recently reported [33] in a smaller series of patients where all those with acute cholecystitis had nonvisualized gallbladders. In addition, the caliber of the intrahepatic and common bile ducts can be evaluated (fig. 5).

While nonvisualization of the gallbladder seems to be diagnostic of cholecystitis, it does not necessarily differentiate between acute and chronic disease. It has been proposed that if the gallbladder fails to visualize within 2 hr, a repeat ^{99m}Tc-HIDA injection should be given 30 min after administration of cholecystokinin [34]. Persistent nonvisualization of the gallbladder confirms cystic duct obstruction and is diagnostic of acute cholecystitis; whereas, if the gallbladder visualizes after administration of cholecystokinin, the diagnosis of chronic cholecystitis with a patent cystic duct is made. In the clinical setting of acute right upper quadrant pain, in which we have used this test, the ability to distinguish between acute and chronic cholecystitis has not been a critical factor. We have not routinely administered cholecystokinin in cases of nonvisualization, and no diagnostic errors have resulted.

Excluding the Diagnosis of Acute Cholecystitis

If the gallbladder, common bile duct, and duodenum are visualized within 1 hr after injection, the diagnosis of acute cholecystitis can be virtually excluded, realizing, however, that acalculous cholecystitis remains a diagnostic possibility [35]. In view of this, a fatty meal or intravenous injection of cholecystokinin [36] or Sincalide [37] can be given and gallbladder contraction observed on serial scintiscans, as well as quantitated with the aid of a computer. As our study progressed, it became apparent that the necessary information regarding gallbladder contractility could be obtained most reliably by using intravenous cholecystokinin or Sincalide and omitting the fatty meal. We have not yet had the opportunity to study patients with acalculous cholecystitis. However, failure to respond to cholecystokinin stimulation was noted in one of the two false negative cholescintigrams where the gallbladder did visualize despite the presence of cholecystitis.

In the two false negative cases, ^{99m}Tc-HIDA cholescintigraphy revealed gallbladder and common bile duct visualization within 1 hr. The hepatobiliary-to-bowel transit time was markedly delayed in both cases, exceeding 2 hr. One patient did respond to fatty meal stimulation. The second patient was given intravenous cholecystokinin which provoked right upper quadrant pain. The gallbladder failed to contract on serial scans. Thus, despite gallbladder visualization, there were associated findings in both cases which suggested the presence of biliary disease. At surgery both patients had a patent cystic duct in the precence of chronic cholecystitis with multiple small stones and "sludge."

Visualization of the gallbladder in less than 1 hr essen-

tially excludes the diagnosis of acute obstructive cholecystitis; however, the possibility of chronic cholecystitis without cystic duct obstruction still exists. This was observed in three patients studied for reasons other than suspected acute cholecystitis, such as chronic abdominal pain or painless jaundice, who were not included in this series.

In individuals where chronic cholecystitis is being considered, oral cholecystography remains an excellent test of gallbladder function and can visualize gallstones. If the gallbladder does not visualize on oral cholecystography, ultrasonography and ^{99m}Tc-HIDA cholescintigraphy can be used to demonstrate the presence of calculi and cystic duct patency or obstruction, respectively. Our findings in 14 patients with chronic cholecystitis with cholelithiasis, not included in the 90 patients reported here, were quite variable depending on whether the gallbladder is filled with "sludge" and whether cystic duct and/or common bile duct obstruction exist. Thus, in cases of chronic cholecystitis, ^{99m}Tc-HIDA cholescintigraphy must be evaluated in conjunction with other radiographic methods, such as oral cholecystography, intravenous cholangiography, or ultrasonography.

REFERENCES

1. Schein CJ: *Acute Cholecystitis*. New York, Harper & Row, 1972
2. Ochsner SF: Performance and reliability of cholecystography. *South Med J* 63:1268–1271, 1970
3. Thorpe CD, Olsen WR, Fischer H, Doust VL, Joseph RR: Emergency intravenous cholangiography in patients with acute abdominal pain. *Am J Surg* 125:46–50, 1973
4. Wilson RL, Shaub M: The use of ultrasound in suspected cholecystitis. *Appl Radiol* 7:119–121, 1978
5. Stanley RJ, Sagel SS: Computed tomography of the liver and biliary tract, in *Radiology of the Biliary Tract*, edited by Berk RN, Clemett AR, Philadelphia, Saunders 1977, pp 352–375
6. Harvey E, Loberg M, Cooper M: Tc-99m-HIDA: a new radiopharmaceutical for hepatobiliary imaging (abstr). *J Nucl Med* 16:533, 1975
7. Berk RN, Loeb PM, Goldberger LE, Sokoloff J: Oral cholecystography with iopanoic acid. *N Engl J Med* 290:204–210, 1974
8. Whalen JP, Rizzuti RJ, Evans JA: Time of optimal gallbladder opacification with telepaque (iopanoic acid). *Radiology* 105:523–524, 1972
9. Mujahed Z, Evans JA, Whalen JP: The nonopacified gallbladder on oral cholecystography. *Radiology* 112:1–4, 1974
10. Danley RB, Love L, Pickelman JR: Rapid roentgenologic diagnosis of acute cholecystitis. *Surg Gynecol Obstet* 143:602–604, 1976
11. Barksdale JW, Johnston JH: Acute cholecystitis. *Ann Surg* 127:816–829, 1948
12. Stillman AE: Hepatotoxic reaction to iodipamide meglumine injection. *JAMA* 228:1420–1421, 1974
13. Craft IL, Swales JD: Renal failure after cholangiography. *Br Med J* 2:736–738, 1967
14. Canales CO, Smith GH, Robinson JC, Remmers AR, Sarles HE: Acute renal failure after the administration of iopanoic acid as a cholecystographic agent. *N Engl J Med* 281:89–91, 1969
15. Bergman LA, Ellison MR, Durea G: Acute renal failure after drip infusion pyelography. *N Engl J Med* 279:1277, 1968
16. Ansell G: Adverse reactions to contrast agents. Scope of the problem. *Invest Radiol* 5:374–384, 1970
17. Wise RE, Johnston DO, Salzman FA: The intravenous cholangiographic diagnosis of partial obstruction of the common bile duct. *Radiology* 68:507–525, 1957
18. Ekelberg ME, Carlson HC, McIlrath DC: Intravenous cholangiography with intact gallbladder. *AJR* 110:235–239, 1970
19. Ingelfinger FJ: Digestive disease as a national problem. V. Gallstones. *Gastroenterology* 55:102–104, 1968
20. Serafini AN, Smoak WM, Hupf HB: Iodine-123-rose bengal: an improved hepatobiliary imaging agent. J Nucl Med 17:36–39, 1976
21. Kubota H, Eckelman WC, Poulose P: Technetium-99m-pyridoxylideneglutamate, a new agent for gallbladder imaging: comparison with ^{131}I-rose bengal. *J Nucl Med* 17:36–39, 1976
22. Lin TH, Khentigen A, Winchell HS: A ^{99m}Tc-labelled replacement for ^{131}I-rose bengal in liver and biliary tract studies. *J Nucl Med* 15:613–615, 1974
23. Krishnamurthy GT, Tubis M, Endow JS, Bland WH: ^{99m}Tc-penicillamine. A new radiopharmaceutical for cholescintigraphy (abstr). *J Nucl Med* 13:447, 1972
24. Stadalnik RC, Matolo NM, Jansholt AL, Krohn KA, DeNardo GL, Wolfman EF: Technetium-99m pyridoxylideneglutamate (P.G.) cholescintigraphy. *Radiology* 121:657–661, 1976
25. Eikman EA, Cameron JL, Colman M, Natarajan TK, Dugal P, Wagner HN: A test for patency of the cystic duct in acute cholecystitis. *Ann Intern Med* 82:318–322, 1975
26. Chiotellis E, Sawas-Dimopoulou C, Koutoulidis C, Constantinides M: ^{99m}Tc-HIDA, a gallbladder imaging agent. Experimental aspects. Eur J Nucl Med 3:41–46, 1978
27. Wistow BW, Subramian G, Van Heertum RL, Henderson RW, Gagne GM, Hall RC, McAfee JG: An evaluation of ^{99m}Tc-labeled hepatobiliary agent. *J Nucl Med* 18:455–461, 1977
28. Tjen HS, van der Pompe WB, Cox PH: Technetium-99m-labelled diethyl-acetanilide-iminodiacetate: a new hepatobiliary agent. *Br J Radiol* 50:735–739, 1977
29. Subramian G, Chander J, Singh DN, Dham DN, Lakshmipathi N, Singh B: A new radiopharmaceutical for gallbladder studies: ^{99m}Tc-Sn-LIDA complex. *Nucl Med* 16:83–85, 1977
30. Loberg M, Cooper M, Harvey E, Callery P, Faith W: Development of new radiopharmaceuticals based on N-substitution of iminodiacetic acid. *J Nucl Med* 17:633–638, 1976
31. Firnau G: Why do Tc-99m chelates work for cholescintigraphy. *Eur J Nucl Med* 1:137–139, 1976
32. Baker RJ, Marion MA: Biliary scanning with Tc-99m pyridoxylideneglutamate—the effect of food in normal subjects: concise communication. *J Nucl Med* 18:793–795, 1977
33. Rosenthall L, Shaffer EA, Lisbona R, Paré P: Diagnosis of hepatobiliary disease by ^{99m}Tc-HIDA cholescintigraphy. *Radiology* 126:467–474, 1978
34. Paré P, Shaffer EA, Rosenthall L: Nonvisualization of the gallbladder by ^{99m}Tc-HIDA cholescintigraphy as evidence of cholecystitis. *Can Med Assoc J* 118:384–386, 1978
35. Camishion RC, Goldstein F: Partial, noncalculous cystic duct obstruction (cystic duct syndrome). *Surg Clin North Am* 47:1107–1114, 1967
36. Nathan MH, Newman A, Murray DJ, Camponovo R: Cholecystokinin cholecystography. A 4 year evaluation. *AJR* 110:240–251, 1970
37. Hedner P, Lundequist A: The use of the C-terminal octapeptide of CCK for gallbladder evacuation in cholecystography. *AJR* 116:320–326, 1972

Computed Tomography and ^{67}Ga Citrate Radionuclide Imaging for Evaluating Suspected Abdominal Abscess

ROBERT G. LEVITT,[1] DANIEL R. BIELLO, STUART S. SAGEL, ROBERT J. STANLEY, DIXIE J. ARONBERG, MARGARET L. ROBINSON, AND BARRY A. SIEGEL

A retrospective analysis of the results of ^{67}Ga citrate radionuclide imaging and computed tomography (CT) in 45 patients with suspected abdominal abscess was conducted to determine the merits of each method. Both techniques were highly sensitive in detecting abdominal abscesses, and often provided complementary and supplementary diagnostic information; their combined use many times offset the limitations of each method used alone. Guidelines are suggested that permit rapid evaluation, while limiting diagnostic errors, when using ^{67}Ga citrate radionuclide imaging and CT in the presence or absence of localizing symptoms and signs.

Both ^{67}Ga citrate radionuclide imaging and ultrasonography are known to be accurate, noninvasive methods of localizing inflammatory masses [1, 2]. The relative advantages and disadvantages of these two methods have been reported [3]. Computed tomography (CT) has recently been described as another accurate imaging method for the noninvasive diagnosis of abdominal abscess [4, 5] . We retrospectively analyzed the results of both ^{67}Ga radionuclide imaging, a whole body longitudinal imaging technique, and CT, a regional cross-sectional imaging technique, to ascertain the merits of each examination.

Subjects and Methods

From October 1975 to June 1978, 56 patients had both ^{67}Ga citrate radionuclide imaging and CT examinations as part of the diagnostic evaluation for a variety of clinical problems in which abdominal abscess was a significant consideration. Pathologic proof of diagnosis was obtained in 17 of the 56 patients (by surgery in 13, percutaneous biopsy in three, and autopsy in one). All nine abdominal abscesses in this series were proven pathologically. An additional 28 patients had strong clinical evidence supporting the final clinical diagnosis, including at least 6 months of clinical follow-up. The other 11 patients were deleted from the study for several reasons: six outpatients were lost to follow-up; two patients admitted with fever of unknown origin left the hospital before completion of diagnostic evaluations; and in three patients radionuclide and CT studies were separated by more than 3 weeks (23, 30, and 35 days). The 45 patients included in the study population had several clinical presentations: fever (18 patients), localized abdominal pain (two), fever and localized abdominal pain (seven), postoperative fever (five), bacterial septicemia (12), and acute change in mental status (one).

CT studies were performed on either the EMI CT 5000 prototype or an EMI CT 5005 body scanner. Both instruments complete a single 13-mm-thick scan in 18 sec. Oral contrast material, consisting of 0.28–0.56 g of 4% (V/V) solution of Gastrografin/water, was given 30–60 min before scanning to opacify intestinal loops. This was necessary to avoid mistaking fluid-filled intestinal loops for abnormal masses and to identify air collections and air-fluid levels outside the gastrointestinal tract. Peristaltic motion during scanning was limited by intravenous administration of 0.5 mg glucagon just before scanning. Iodinated urographic contrast medium was sometimes given intravenously to evaluate whether an abnormal mass identified on the initial CT scan enhanced with contrast material.

Gallium-67 citrate radionuclide imaging was routinely performed 24 and 48 hr after intravenous administration of 3 mCi of ^{67}Ga citrate. All patients in this study were injected in the afternoon, precluding 6 hr imaging. In some patients, 72 hr imaging was performed. Anterior and posterior whole body images were obtained on a large field scintillation camera fitted with a medium energy collimator on a whole body scanning table using triple spectrometer settings to detect the 93, 185, and 300 keV photons of ^{67}Ga. Total counts were 300,000–400,000 at 24 hr, 250,000–300,000 at 48 hr, and 150,000–200,000 at 72 hr. If abnormalities were noted, additional detailed images were often obtained. If the patient's condition permitted, oral cathartics were given the evening before each scan and cleansing enemas on the morning of the scan in order to eliminate ^{67}Ga activity in the bowel.

Each radionuclide and CT study was interpreted at the completion of the examination by one of several staff radiologists with knowledge of both the clinical history and the results of other diagnostic tests, including the radionuclide or CT study, but without knowledge of the final clinical diagnosis. The interpretation rendered at completion of each radionuclide or CT study was not reviewed for this investigation. In 35 cases, ^{67}Ga citrate radionuclide imaging was done first. Radionuclide and CT studies were performed within 7 days of one another in 41 cases (91%) and within 13 days in the other four cases.

Definitive CT diagnosis of abscess was made by identification of a low density mass (0–15 EMI units), containing air or an air-fluid level, clearly outside the gastrointestinal tract [5]. Occasionally, a higher density peripheral rim was seen surrounding the abscess. In contradistinction to the low density central area, this peripheral rim showed contrast enhancement after intravenous administration of iodinated urographic contrast medium. When a low density mass not containing air or an air-fluid level was identified, a specific diagnosis of abscess could not be made using CT. In these cases, diagnostic possibilities included abscess, tumor, and hemorrhage.

Gallium-67 citrate radionuclide imaging was considered abnormal when the images demonstrated an identical focal area of increased ^{67}Ga activity in two or more scans. Abnormal scan reports reflected a variety of possible diagnoses based on both clinical history and scan findings, but in this study ^{67}Ga citrate

Received September 5, 1978; accepted after revision December 13, 1978.
R. G. Levitt is a Picker Scholar.

[1] All authors: Mallinckrodt Institute of Radiology, Washington University School of Medicine, 510 South Kingshighway Boulevard, St. Louis, Missouri 63110. Address reprint requests to R. G. Levitt.

© 1979 American Roentgen Ray Society

0361–803X/79/1324–0529 $0.00

TABLE 1

Gallium-67 Citrate Radionuclide Imaging and Final Clinical Diagnosis

Radionuclide Imaging	No. Cases	Diagnosis				
		Abscess	Tumor	Inflam-mation	Infection	Fever of Unknown Origin
Persistent focus of increased activity	25	9	6*	4	7*,†	. . .
Normal	20	. . .	1	3	13	3

Note.—Focus of increased activity not related to primary final clinical diagnosis in one case of tumor, two cases of inflammation, and two cases of infection.

* Both liver metastases and ascending cholangitis were found at surgery in one case.

† Increased activity due to ^{67}Ga retained in bowel in one case.

TABLE 2

CT Scanning and Final Clinical Diagnosis

CT	No. Cases	Diagnosis			
		Abscess	Tumor	Infection	Fever of Unknown Origin
Abscess	6	6	. . .	. . .	. . .
Tumor	4	. . .	4*	1*	. . .
Low density mass: abscess vs. tumor	4	2	2	. . .	. . .
Other significant mass	2	. . .	. . .	1†	1‡
No significant mass	29	1	1	18§	2§

Note.—Seven cases of no significant mass on CT were diagnosed as inflammation.

* Liver metastases detected in one case by CT; liver metastases *and* ascending cholangitis found at surgery.

† Left upper quadrant phlegmon.

‡ ?Enlarged retroperitoneal lymph nodes.

§ Incidental renal cysts identified in one case of infection and one case of fever of unknown origin.

radionuclide imaging results were only classified as normal or abnormal.

Results

Gallium-67 Citrate Radionuclide Imaging

A persistent focus of increased activity was detected in 25 patients (table 1); the focus of increased activity was intraabdominal in 21 patients and extraabdominal in four patients. The increased activity corresponded to intra- or retroperitoneal abscess in nine patients, abdominal or retroperitoneal tumor in four, abdominal inflammatory process in two (radiation proctitis, lupus nephritis), abdominal infection in two (ascending cholangitis, left upper quadrant phlegmon), and aspiration pneumonia in one. The foci of increased activity in the seven other patients were not related to the primary final diagnoses, but represented retained ^{67}Ga activity in the colon in three patients, secondary sites of infection in three patients, and hyperplastic bone marrow in one patient.

Radionuclide studies were normal (i.e., no persistent focus of increased ^{67}Ga activity) in 20 patients. Final diagnosis was tumor in one patient (retroperitoneal lymphoma), inflammatory process in three (polyarteritis nodosa, Crohn's disease, myelofibrosis), infection in 13 (source identified in nine of these), and fever of unknown origin in three.

Computed Tomography

An abnormal low density abdominal mass was identified by CT in 16 patients (table 2). Specific CT diagnosis in 12 of these consisted of abscess in six, tumor in four, phlegmon in one, and questionably enlarged retroperitoneal lymph nodes in one. CT diagnosis corresponded to final clinical or pathologic diagnosis in all 12 patients in whom specific CT diagnosis was made (only diagnoses of phlegmon and questionably enlarged retroperitoneal lymph nodes lack pathologic proof). In one patient in whom CT showed liver metastases, ascending cholangitis was also found at surgery and was believed to account for his gram-negative bacterial septicemia. In four other patients, CT showed a low density abdominal mass, but abscess could not be differentiated from tumor or other low density mass by CT. At surgery, abscesses were found in two of these patients and neoplasms in the other two.

In 29 patients, no abnormal masses were identified on CT. Final clinical diagnoses were abscess in one patient, tumor in one, inflammatory process in seven, infection in 18, and fever of unknown origin in two. The abscess not identified on CT was a small pericecal abscess; the tumor was a 3 cm perforating jejunal carcinoma.

Correlation of Radionuclide and CT Studies

Gallium-67 citrate radionuclide imaging showed persistent foci of increased abdominal activity in 21 patients in this study and foci of extraabdominal increased activity in four. In 14 of the 21 patients with abdominal foci, CT identified abnormal abdominal masses corresponding to the foci and characterized ten of these 14 masses as abscess, phlegmon, or neoplasm. The intra- or extra-

peritoneal location, organ involvement, size, and extent of these lesions were all determined noninvasively because of the anatomic detail provided by CT.

CT did not demonstrate abnormal abdominal masses in the other seven patients with abdominal foci of increased activity on ^{67}Ga citrate radionuclide imaging. In one of these seven, a 20 ml pericecal abscess drained at surgery corresponded to the focus of increased activity on the radionuclide study. The location and configuration of the foci of increased activity in three of the seven suggested that they represented retained ^{67}Ga activity in the colon. In the other three patients, the localization of the increased ^{67}Ga activity on the radionuclide studies led to a specific diagnosis. Two patients had increased renal activity; chronic pyelonephritic changes were demonstrated in one of these by excretory urography, and lupus nephritis was diagnosed in the other by percutaneous renal biopsy. In the third, who had recently undergone radiation therapy for prostatic carcinoma, the finding of increased ^{67}Ga activity about the rectum and the absence of any pelvic mass on CT indicated radiation proctitis.

CT did not demonstrate an abnormal abdominal mass in the four patients with extraabdominal foci of increased ^{67}Ga activity. However, CT did identify enlarged retroperitoneal lymph nodes in two of the 20 patients with normal radionuclide studies.

Representative Case Reports

Case 1

A 27-year-old man had right lower quadrant pain and fever for 2 weeks. Gallium-67 citrate radionuclide imaging at 24 and 48 hr revealed a diffuse increase in activity within the pelvis (fig. 1A). A CT examination, obtained to differentiate abscess from inflammation (fig. 1B), demonstrated a moderate size presacral abscess that was subsequently surgically drained.

Case 2

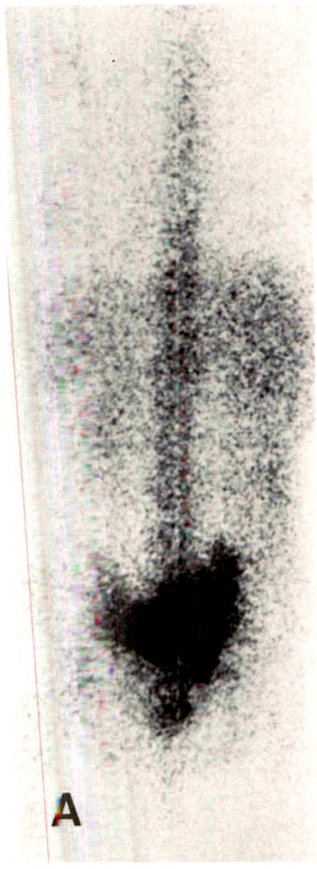
A 69-year-old woman, who had a cystectomy and ileal loop diversion for transitional cell carcinoma of the bladder with muscle invasion, developed fever 1 week after surgery. Urine and blood cultures grew *Proteus mirabilis*. The patient did not respond to antibiotic therapy.

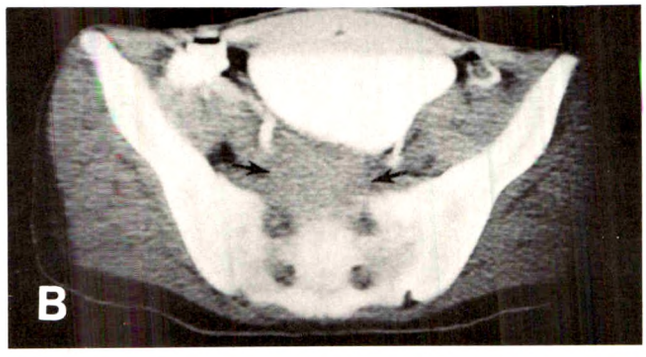
Gallium-67 citrate radionuclide imaging, performed to exclude a pelvic abscess, showed persistent increased activity in the left kidney, left and midpelvis, and left hip at 24 and 48 hr (fig. 2A). It was uncertain whether the cause was a large single abscess, multiple abscesses, or tumor. CT scans showed a somewhat low density, soft tissue mass involving the left psoas muscle at the pelvic brim extending caudally into the presacral and iliopsoas regions and anterior to the iliopsoas muscle in the thigh (figs. 2B–2D). A flank abscess with inferior dissection was believed most likely.

At operation, an infected urinoma secondary to disruption of the left ureteral anastomosis was found, with dissection inferiorly as suspected.

Case 3

A 69-year-old woman developed abdominal pain, fever, and leukocytosis after resection of a gangrenous left colon secondary to mesenteric artery thrombosis. The abdomen was diffusely tender.





Gallium-67 citrate radionuclide imaging showed increased left upper quadrant activity on the 24 and 48 hr images very suspicious for an abscess (fig. 3A). CT examination, performed to document the presence and extent of the presumed left upper quadrant abscess (fig. 3B), showed no abscess, but only linear soft tissue densities in the anterior pararenal space with thickening of the adjacent fascia consistent with a phlegmon. Planned recoperation was cancelled, and intensive antibiotic therapy given, with subsequent clinical improvement.

Case 4

A 66-year-old man with stage B carcinoma of the prostate, treated previously by radical prostectomy, pelvic lymphadenectomy, and postoperative radiation therapy, developed spiking fevers. A ^{67}Ga radionuclide imaging study, performed to determine if a pelvic abscess had developed, showed slightly increased activity over the left sacroiliac joint and a separate focus of activity about the rectum at 24 and 48 hr (fig. 4A).

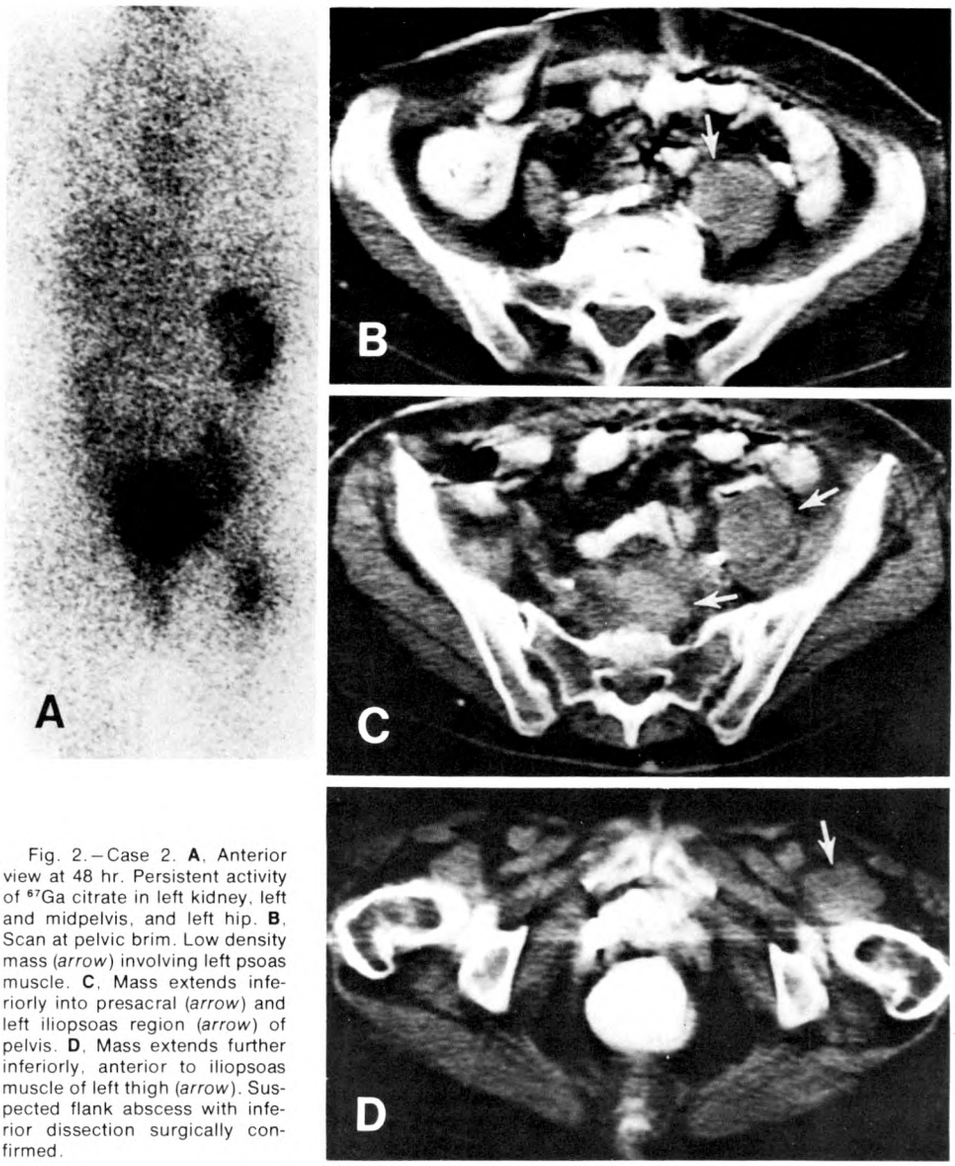


Fig. 2.—Case 2. **A**, Anterior view at 48 hr. Persistent activity of ^{67}Ga citrate in left kidney, left and midpelvis, and left hip. **B**, Scan at pelvic brim. Low density mass (*arrow*) involving left psoas muscle. **C**, Mass extends inferiorly into presacral (*arrow*) and left iliopsoas region (*arrow*) of pelvis. **D**, Mass extends further inferiorly, anterior to iliopsoas muscle of left thigh (*arrow*). Suspected flank abscess with inferior dissection surgically confirmed.

CT examination, performed primarily to differentiate perirectal abscess from recurrent tumor, showed no evidence of an abnormal mass within the pelvis (fig. 4B). Presumptive clinical diagnosis was changed to radiation proctitis, and the patient was treated symptomatically. The fevers abated, and a follow-up CT study 2 months later revealed no interval development of a pelvic mass.

Discussion

Diagnostic evaluation of patients with suspected intraabdominal abscess begins with a careful history and physical examination. Plain abdominal radiography may accurately localize an abdominal abscess, but has limited sensitivity as do contrast examinations of the gastrointestinal and genitourinary systems. The ^{99m}Tc sulfur colloid liver-spleen scan is quite sensitive for detecting intrahepatic and intrasplenic abscesses, but the sensitivity falls off dramatically for perihepatic and perisplenic abscesses. If these initial studies in the patient with a suspected abdominal abscess are unrevealing, ^{67}Ga citrate radionuclide imaging and/or CT imaging may benefit the patient.

The results of this retrospective analysis of 45 patients with clinically suspected abdominal abscess indicate that both radionuclide and CT studies are highly sensitive in detecting abdominal abscess. Gallium-67 citrate radionuclide imaging showed a focus of increased activity in nine of nine abscesses, while CT findings permitted the specific diagnosis of abscess in six of nine patients and a possible diagnosis of abscess in two of nine patients. These results concur with recent reports of larger numbers of patients studied by either ^{67}Ga citrate radionuclide imaging or CT scanning alone, in which both methods were found to have comparably high sensitivity in the detection of abscesses [3, 5]. The important finding in our study is that radionuclide and

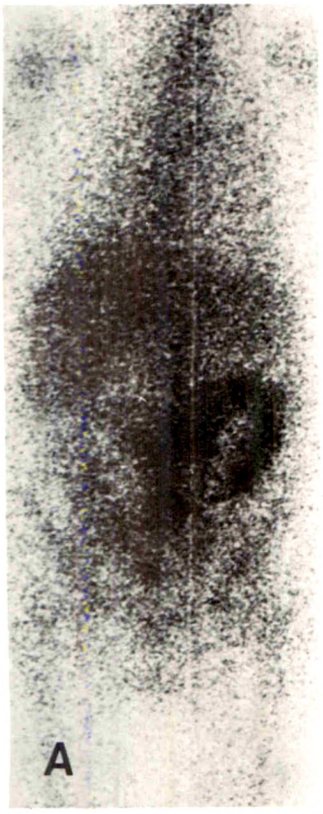
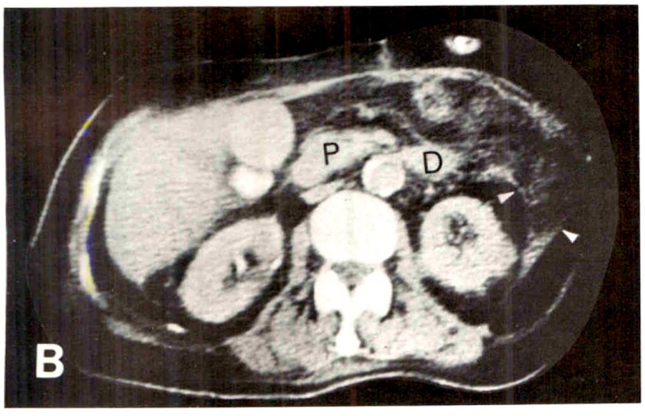


Fig. 3.—Case 3. **A**, Anterior view at 48 hr shows increased left upper quadrant activity of ^{67}Ga citrate. **B**, Linear soft tissue densities in anterior pararenal space with thickening of adjacent fascia (*arrowheads*) consistent with phlegmon. Head of pancreas (P) and unopacified third portion of the duodenum (D) adjacent to aorta.



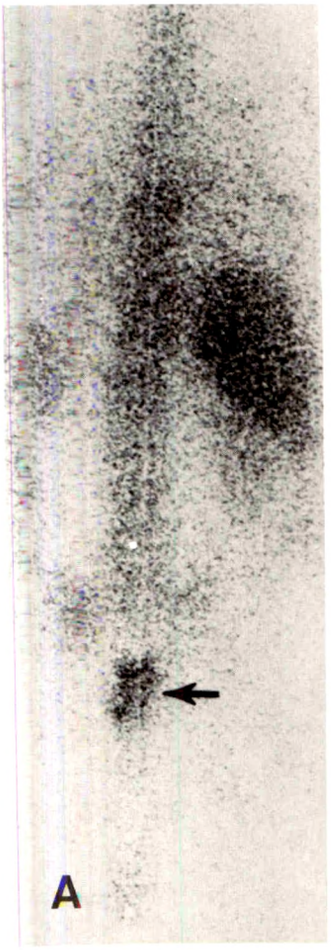
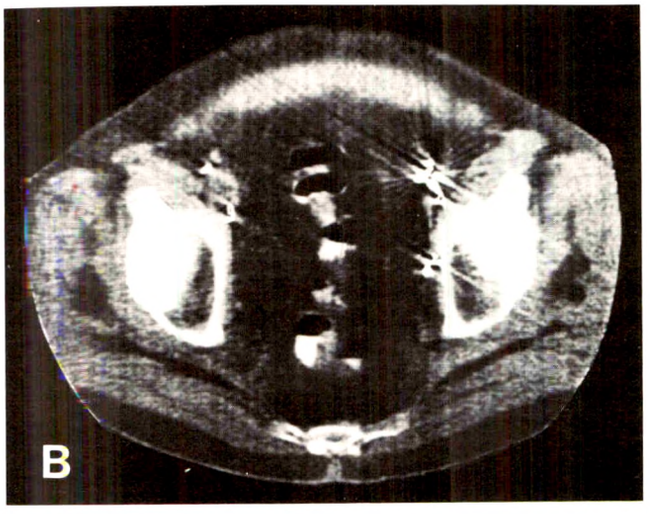


Fig. 4.—Case 4. **A**, Posterior view at 24 hr shows slightly increased activity of ^{67}Ga citrate over left sacroiliac joint and separate focus of activity about rectum (*arrow*). **B**, Scan through low pelvis. Abundant intrapelvic fat surrounding rectosigmoid colon, but no abnormal mass. Final clinical diagnosis was radiation proctitis.



CT studies often provide complementary results and thus overcome the limitations of each technique used alone.

While ^{67}Ga radionuclide imaging has the advantage of imaging the entire body, it has disadvantages as well. The delay between injection and scan interpretation may be 24–48 hr. If a persistent focus of increased activity is identified, the focus may represent any of several lesions other than localized abscess, such as phlegmon, infection, or vasculitis. When CT scanning is used to complement an abnormal radionuclide study, it can quickly determine whether the focus of increased ^{67}Ga activity corresponds to an abnormal mass or to inflammation/infection without mass formation. Often CT can be more specific and characterize an abnormal mass as abscess, phlegmon, or tumor. In this way, CT can provide a specific diagnosis, expedite surgery, or obviate exploratory laparotomy.

Gallium-67 citrate radionuclide imaging can also complement CT scanning. As demonstrated in this study and in others [4, 6], small abdominal abscesses may be missed by CT. The abscesses missed by CT in these recent reports have all shown foci of increased activity on ^{67}Ga citrate radionuclide imaging. Also, CT cannot

localize a site of inflammation not producing a mass, such as vasculitis, while ^{67}Ga citrate radionuclide imaging can. Respiratory motion in very ill patients and abdominal surgical clips may make a CT study uninterpretable, while technically acceptable ^{67}Ga citrate radionuclide imaging can usually be obtained in such patients.

Only two of the 45 patients in this retrospective analysis of radionuclide and CT studies also had ultrasound examinations. Thus, the role of ultrasound relative to CT in patients with suspected abdominal abscess cannot be determined from this study. As is true of CT, ultrasonography is a cross-sectional imaging technique with high sensitivity for detecting abdominal fluid collections. The technical advantages of ultrasonography compared with CT include its ability to display both longitudinal and transverse cross-sections of a region of interest and its freedom from respiratory motion degradation. Disadvantages of ultrasonography compared with CT in this clinical setting include interference from overlying gas, difficulty at times in distinguishing abscess from other fluid-filled structures, and its dependence on substantial technical expertise both in performing the examination and in interpreting the results.

We adopted the following approach to evaluate suspected abdominal abscess based on the merits and limitations of ^{67}Ga citrate radionuclide imaging, CT, and ultrasonography; the results of this study, and the results of a previous study [3] from our institution comparing ^{67}Ga citrate radionuclide imaging and ultrasonography in the evaluation of this clinical problem. This approach permits rapid evaluation while limiting diagnostic errors.

The patient is first evaluated clinically to determine the presence or absence of localizing symptoms or signs. If there is evidence of localized disease, either CT or ultrasonography should be performed initially since specific diagnosis of abscess can be most simply and rapidly confirmed or excluded with either of these methods. The choice between CT or ultrasonography should be based on clinical considerations, such as the patient's ability to suspend respiration, the presence or absence of ileus, the suspected location of the abscess, the presence of open wounds or surgical dressings, and local expertise. If the CT or ultrasonographic findings are characteristic of an abscess and they correlate with the clinical data, further radiologic investigation is not indicated. If an indeterminate low density mass is seen on CT or if a fluid-filled structure not typical of abscess is seen on ultrasonography, clinical correlation is needed. If diagnostic uncertainty persists, clinical experience at our institution (not reported here) has shown that the alternative cross-sectional imaging technique may demonstrate the mass to be an abscess by that technique's criteria for abscess. If the initial CT or ultrasound examination is negative in the patient with evidence of localized disease, then ^{67}Ga citrate radionuclide imaging should be performed. A normal radionuclide study ends the radiologic search for abscess. An abnormal study results in another CT or ultrasound study with attention drawn to the specific area of abnormality demonstrated by ^{67}Ga citrate radionuclide imaging to attempt to determine if the focus of increased ^{67}Ga activity is due to a mass (abscess, neoplasm, phlegmon) or due to inflammation not associated with a mass.

In the patient with nonlocalizing signs and symptoms, ^{67}Ga citrate radionuclide imaging should be performed first. CT and ultrasonography are initially less useful in this type of patient because they are regional scanning techniques, while ^{67}Ga citrate radionuclide imaging examines the entire body. If the radionuclide study is normal, no further radiologic evaluation is usually required. If an abnormality is present, CT or ultrasonography are used for further lesion characterization.

ACKNOWLEDGMENT

We thank Nancy M. Levitt for collating this data and Ann Marie Brock for editorial assistance.

REFERENCES

1. Harvey WC, Podoloff DA, Kopp DT: ^{67}Gallium in 68 consecutive infection searches. *J Nucl Med* 16:2-4, 1975
2. Taylor KJW, DeGraff C, Wasson JF, Rosenfield AT, Andirole VT: Accuracy of grey scale ultrasound diagnosis of abdominal and pelvic abscess in 220 patients. *Lancet* 1:83-84, 1978
3. Kumar B, Alderson PO, Geisse G: The role of Ga^{67} citrate imaging and diagnostic ultrasound in patients with suspected abdominal abscesses. *J Nucl Med* 18:534-537, 1977
4. Haaga JR, Alfidi RJ, Havrilla TR, Cooperman AM, Seidelmann FE, Reich NE, Weinstein AJ, Meaney TF: CT detection and aspiration of abdominal abscesses. *AJR* 128:465-474, 1977
5. Aronberg DJ, Stanley RJ, Levitt RG, Sagel SS: The evaluation of abdominal abscess with computed tomography. *J Comput Assist Tomogr* 2:384-387, 1978
6. Shimshak RS, Korobkin M, Hoffer PB, Schor R, Hill TC, Kressel HY: Complementary role of Ga^{67} imaging and CT in evaluation of suspected abdominal infection. *J Nucl Med* 19:262-269, 1978

Computed Tomography in the Evaluation of Osteosarcoma: Experience with 25 Cases

LUIS ALONSO deSANTOS,[1] MICHAEL E. BERNARDINO,[1] AND JOHN A. MURRAY[2]

Experience with computed tomography (CT) in 25 patients with histologically proven osteosarcoma is presented. CT was as accurate as conventional radiographic methods in determining the presence of a lesion, but it was definitely superior in defining the extent of disease, particularly intramedullary extension and soft tissue extraosseous tumor component. CT was capable of demonstrating skip metastases in one patient. CT plays a key role in the preoperative evaluation of osteosarcoma patients, particularly when less than radical surgery is planned as primary treatment and when postoperative recurrence is suspected. CT is also useful in assessing the response to therapy in nonsurgical cases. The technique involved in the performance of this examination is discussed.

With the rapid accumulation of a considerable amount of case material, the value of computed tomography (CT) in clinical diagnosis is being clearly established. In areas such as the brain, liver, and pancreas, comparative studies with other diagnostic methods have also been reported and others are in progress. Comparatively less attention has been paid to the use of CT in diagnosing musculoskeletal abnormalities [1-3].

At M. D. Anderson Hospital and Tumor Institute we have gained significant experience with the use of CT in the evaluation of musculoskeletal neoplasms and some definite guidelines are now apparent. This communication reports the value of CT in the clinical management of patients with osteosarcoma based on experience with 25 cases.

Subjects and Methods

Between March 1977 and May 1978, 136 cases of musculoskeletal neoplasms were evaluated by CT at M. D. Anderson Hospital and Tumor Institute. All the patients had additional radiographic studies including conventional radiography in four projections, hypocycloidal tomography in two planes, xeroradiography, and in selected cases arteriography. Among these 136 cases, 25 had a diagnosis of osteosarcoma that was histologically confirmed; three of the 25 cases had follow-up CT examinations. Therefore, 28 CT studies were available for evaluation.

All studies were performed with a commercially available EMI 5005 whole body scanner with a scanning time of 18 producing a 13 mm slice thickness. All cases were evaluated by adjacent sections. Occasionally, overlapping slices were obtained, particularly in small anatomic areas, such as hands and feet. In tumors involving an extremity bone, the study included the lesion itself and the remaining segments of the host bone to the nearest proximal joint space. The joint itself and the distal one-fourth of the other bone composing the joint were also included in the study.

In the axial skeleton the study was tailored, according to the clinical needs, to include the lesion and segments of the adjacent normal structures. Contrast material (300 ml drip, Renografin 30%) was administered intravenously in all cases. In those cases with involvement of the spine or pelvis, contrast material was administered orally in the form of diluted gastrografin and a bowel paralyzing agent, either 1 mg of glucagon (Lilly) or 15 mg propantheline bromide (Searle) was given intravenously before beginning the examination.

As part of this study tetracycline (250 mg four times a day) was administered orally to all patients undergoing surgical excision for 2 days prior to surgery. A fluorescent light study of the sectioned surgical specimen was also done in order to determine the extent of the osteoid tumor matrix. This was essential for adequate pathologic-radiologic correlation.

Results

CT was capable of accurately demonstrating the presence of tumor in all cases except one. This was an extremely obese female in whom only part of the lesion could be imaged because of limitations imposed by gantry size. The most common appearance of osteosarcoma was that of an area of destruction of the normal bony cortex with variable attenuation densities. The unequivocal presence of skip metastases was demonstrated in one patient with a distal femoral osteosarcoma; they were pathologically confirmed. These appeared as isolated areas of high density within the medullary cavity proximal to the tumor (fig. 1). Of the 17 lesions involving tubular bones, 14 demonstrated the presence of intramedullary tumor tissue by CT. Of these 14 lesions, 12 were central osteosarcomas and two were parosteal osteosarcomas with tumor extending into the medullary cavity. The three lesions without intramedullary extent consisted of two parosteal osteosarcomas and one periosteal. An extraosseous soft tissue mass component was seen in 15 lesions. Two tumors, one in the proximal femur and one in the midshaft of a femur, did not have soft tissue mass components. All eight lesions involving the axial skeleton had recognizable intramedullary and extraosseous tumor extension (fig. 2).

The attenuation coefficient of osteoid tissue was extremely variable and ranged from values of +20 EMI units to extremely high values as +200 EMI units, depending on the amount of calcification in the tumor.

Received August 3, 1978; accepted after revision December 11, 1978.

[1] Department of Diagnostic Radiology, University of Texas System Cancer Center, M. D. Anderson Hospital and Tumor Institute, Houston, Texas 77030. Address reprint requests to L. A. deSantos.

[2] Department of Surgery, Section of Orthopedics, University of Texas System Cancer Center, M. D. Anderson Hospital and Tumor Institute, Houston, Texas 77030.

© 1979 American Roentgen Ray Society

0361-803X/79/1324-0535 $0.00

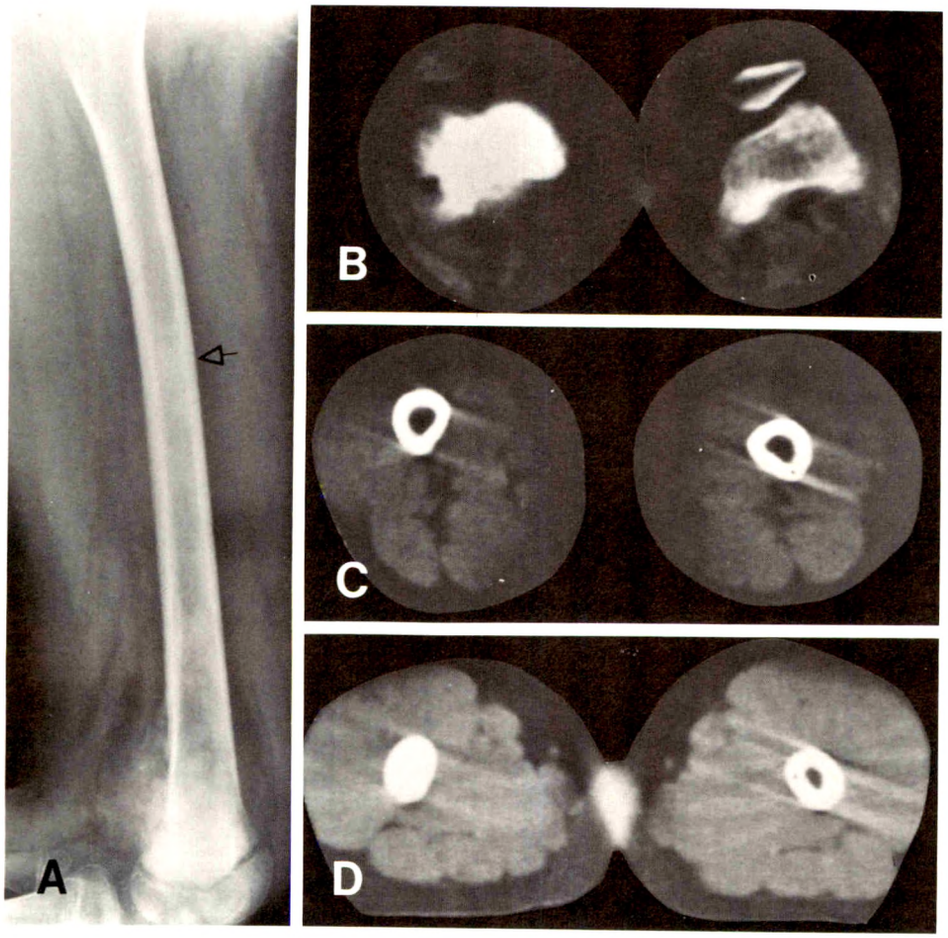


Fig. 1.—Osteosarcoma of distal femur with skip metastasis. **A,** Destructive dense lesion of distal femoral metaphysis with invasion of epiphysis. Vague area of density at junction of proximal and middle thirds of femur (*arrow*). **B,** CT scan through tumor. High density tissue outside medullary cavity. **C,** Scan several centimeters above **B.** Normal cortical bone and normal marrow cavity of low density. **D,** Scan above **C** through high density tissue in medullary cavity representing tumor osteoid matrix.

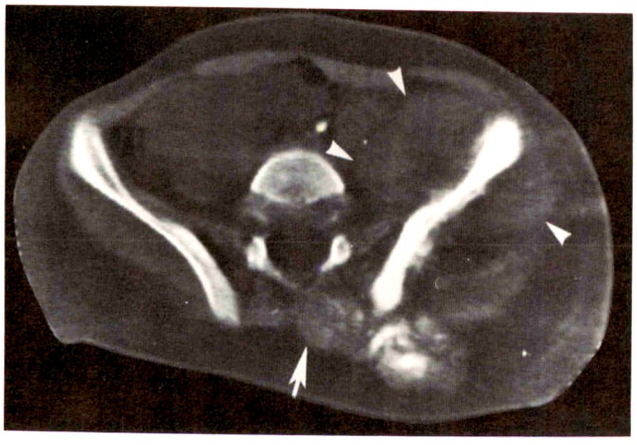


Fig. 2.—Extensive osteosarcoma of iliac bone. Scan through level of L5. High density within medullary cavity of left ileum when compared with opposite side. Large intra- and extrapelvic mass (*arrowheads*). Tumor mass extends to midline (*arrow*) (not demonstrated in the conventional radiographs).

Noncalcified osteoid tissue had density values ranging from +20 to +40 EMI units in both the intra- and extraosseous components. Intramedullary tumor osteoid matrix appeared as an area of higher density than the normal low density (fatty) medullary marrow tissue. The tumor extraosseous component appeared as a mass of variable density displacing and distorting the normal muscular groups in the area.

Comparison with Other Radiographic Methods

Presence and Character of a Lesion

CT demonstrated the presence of the lesion in *all* cases, but had no definite advantage over conventional radiographic methods in this respect. In one patient considerable obesity prevented depiction of the entirety of lesion in the CT scanning field. However, in another patient only subtle changes were seen on conventional radiography and tomography, but the lesion was clearly demonstrated by CT (fig. 3). The tumor itself had no characteristic specific features and appeared as an area of cortical rarefaction. The type and degree of bony permeation and subtle features of the periosteal reaction were at times not detectable by CT or not as well depicted as they were by conventional radiographic techniques. The cortical nature of parosteal and periosteal osteosarcomas was equally well defined by CT and conventional radiography. However, medullary invasion was definitely better delineated by CT.

Anatomic Relationships

CT was definitely superior to conventional radiographic techniques in demonstrating the anatomic rela-

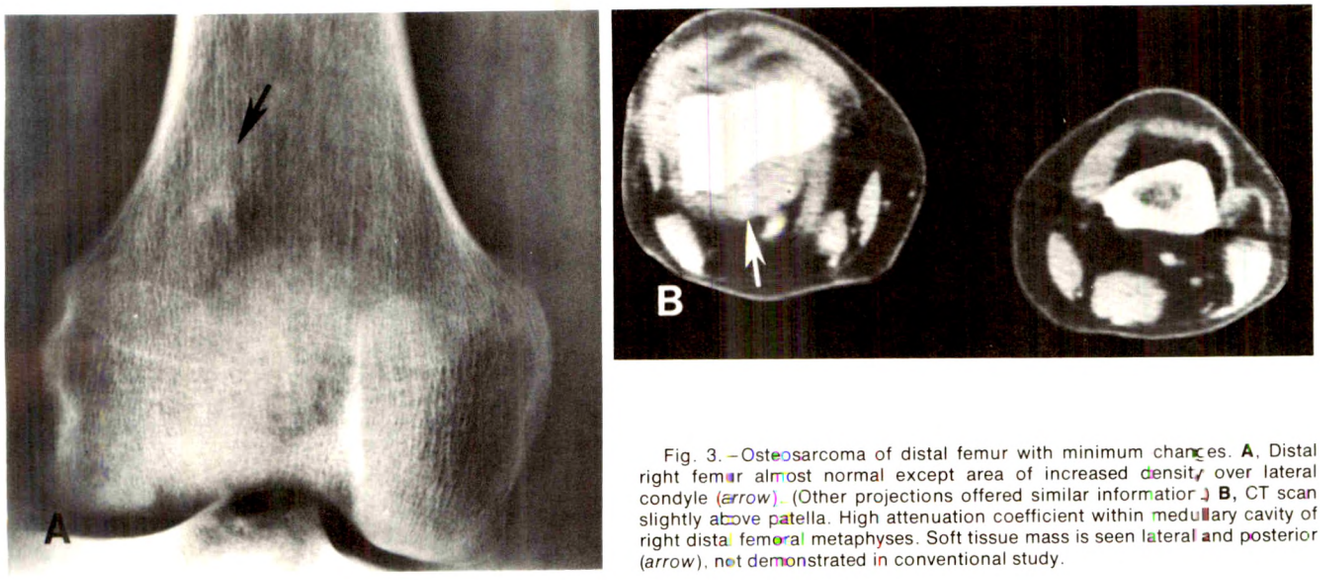


Fig. 3.—Osteosarcoma of distal femur with minimum changes. **A**, Distal right femur almost normal except area of increased density over lateral condyle (*arrow*). (Other projections offered similar information.) **B**, CT scan slightly above patella. High attenuation coefficient within medullary cavity of right distal femoral metaphyses. Soft tissue mass is seen lateral and posterior (*arrow*), not demonstrated in conventional study.

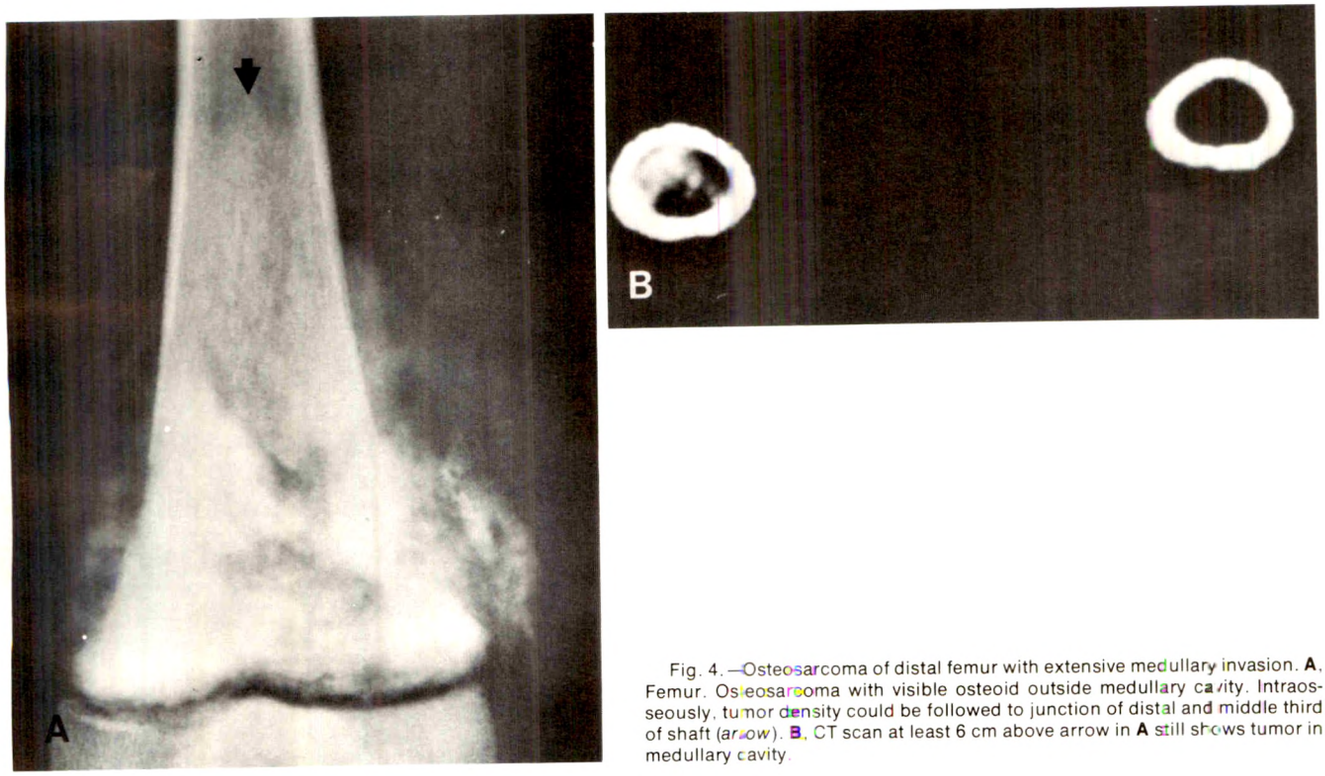


Fig. 4.—Osteosarcoma of distal femur with extensive medullary invasion. **A**, Femur. Osteosarcoma with visible osteoid outside medullary cavity. Intraosseously, tumor density could be followed to junction of distal and middle third of shaft (*arrow*). **B**, CT scan at least 6 cm above arrow in **A** still shows tumor in medullary cavity.

tionships of the tumor. Muscular groups and large neural structures, such as the sciatic nerve, were consistently demonstrated by CT and the relation of the tumor to them was clear in the majority of cases. This information was not obtainable by conventional radiographic methods, even arteriography. In the abdomen and pelvis, CT accurately demonstrated the relation of the tumor to structures of the gastrointestinal and genitourinary tracts in a single study with the added advantage of using another spatial perspective.

Extent of Disease

The nature and extent of the tumor was significantly better demonstrated by CT than by conventional radiography. Additional features were demonstrated by CT in 15 of the 25 cases that were not demonstrated by conventional radiologic techniques. These features were primarily the presence and extent of osteoid matrix in the medullary cavity, the presence of skip metastases, the presence and extent of extraosseous soft tissue mass component, and the presence of metastatic disease.

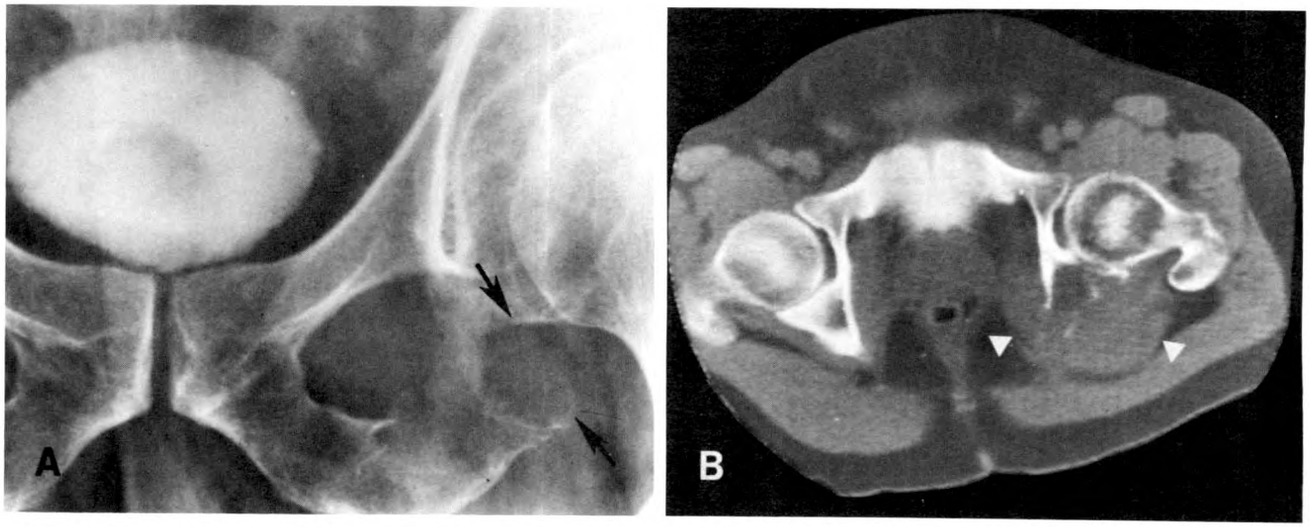


Fig. 5.—Osteosarcoma of left ischium. Occult soft tissue mass. **A**, Destruction of ischium (*arrows*). **B**, CT scan through level of femoral heads confirms destruction of left ischium. Fairly large soft tissue mass (*arrowheads*) is seen in area covered by gluteus maximus muscle and separated from rectum. Mass was not palpable.

CT did accurately determine the proximal extension of the tumor in the medullary cavity even when the osteoid matrix was not calcified. This was possible because tumor tissue has a higher attenuation coefficient than the marrow tissue in the medullary cavity (fig. 4). In the absence of calcification or ossification this cannot be demonstrated by conventional radiography or tomography. Angiography was performed in only one case, a parosteal osteosarcoma of the distal femur, and therefore, no definite comparison can be made with this method.

Skip metastases were demonstrated in one patient. They were obvious by CT. The initial radiographic examination demonstrated only the presence of a distal femoral osteosarcoma, but in retrospect areas of vague increased density could be recognized in the proximal femoral shaft that corresponded with the skip metastatic lesions demonstrated by CT (fig. 1). A radionuclide bone scan was not performed in this case.

The presence and extent of extraosseous soft tissue mass component was accurately demonstrated in all cases by CT, and this was confirmed in all cases by amputation or surgical exploration. The true extent of a soft tissue tumor mass component was always better demonstrated by CT. In six cases extraosseous component was markedly underestimated by conventional radiographic evaluation (fig. 5). In three patients, the presence of a soft tissue mass component could not be determined by conventional films and clinical examination but it was readily confirmed by CT. Unsuspected invasion of the inferior vena cava and adrenal glands by tumor was demonstrated in one patient with a previous disarticulation of the right lower extremity and recurrence in the iliac bone (fig. 6). Finally, pulmonary metastases were found in two patients not demonstrable by conventional radiography or hypocycloidal whole lung tomography.

Discussion

The treatment of osteosarcoma is aimed at two primary goals. First, the complete eradication of local disease; and second, the control and destruction of all metastatic foci, both macro- and microscopic. During the last 8 years, significant strides have been made in the development of chemotherapeutic combinations that have effective antitumor activity [4, 5]. As a result, the survival and tumor control in these patients has markedly improved and newer orthopedic approaches for less incapacitating local control of the tumor are currently being clinically investigated [6].

The pretherapy evaluation of osteosarcoma is highly dependent on diagnostic imaging procedures. At M. D. Anderson Hospital and Tumor Institute and within the Compadri V and Compadri VI protocols,* patients with suspected osteosarcoma are initially evaluated by percutaneous needle biopsy performed by the radiologist. An extensive battery of studies is also performed including conventional radiography of the lesion in several projections, hypocycloidal tomography of the lesion in two projections, xeroradiography, and computed tomography of the area involved. In some cases angiography and lymphangiography are also performed. In addition, all patients undergo whole lung hypocycloidal tomography in an attempt to determine the presence and extent of pulmonary metastases. The need for this extensive radiographic workup is based on the necessity for an extremely accurate assessment of the extent of disease. In addition, exact definition of the radiographic features is essential for proper diagnosis. Extensive experience

* Compadri V protocol consists of needle biopsy diagnoses followed by chemotherapy with high dose methotrexate. Surgical resection follows and additional chemotherapy with adriamycin, Cytoxan, and methotrexate is continued for a year. Compadri VI protocol has an identical chemotherapeutic regimen, but in addition includes whole chest preoperative irradiation.

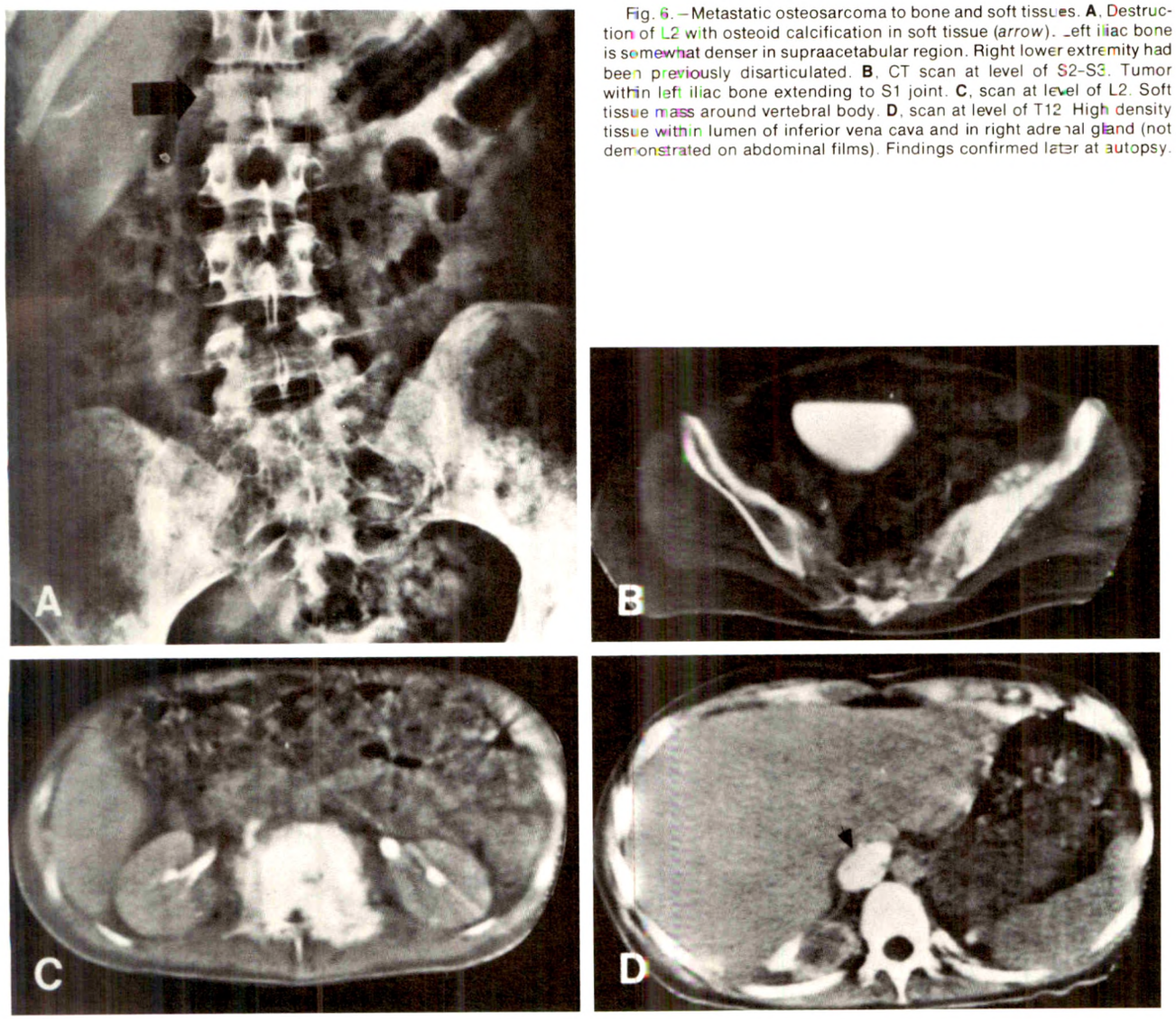


Fig. 6.—Metastatic osteosarcoma to bone and soft tissues. **A**, Destruction of L2 with osteoid calcification in soft tissue (*arrow*). Left iliac bone is somewhat denser in supraacetabular region. Right lower extremity had been previously disarticulated. **B**, CT scan at level of S2-S3. Tumor within left iliac bone extending to S1 joint. **C**, scan at level of L2. Soft tissue mass around vertebral body. **D**, scan at level of T12. High density tissue within lumen of inferior vena cava and in right adrenal gland (not demonstrated on abdominal films). Findings confirmed later at autopsy.

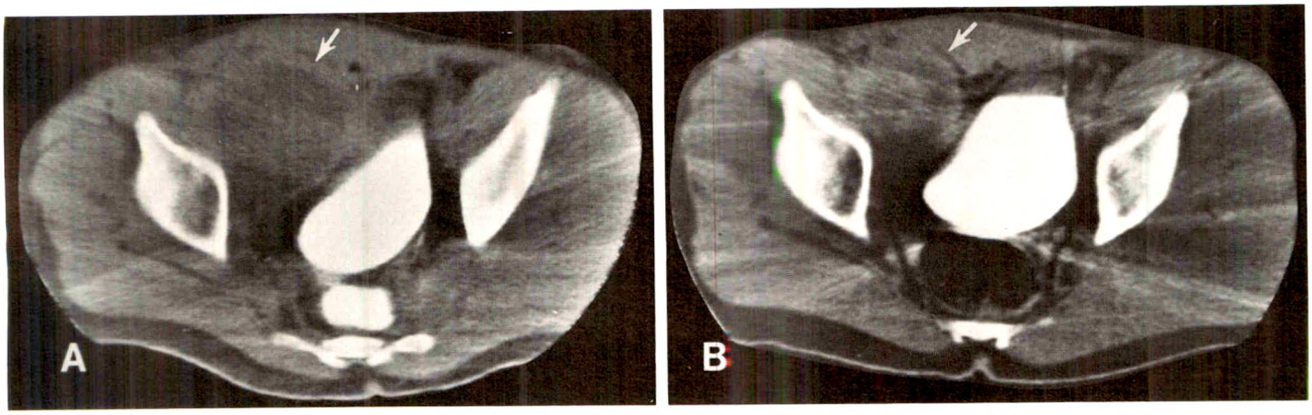


Fig. 7.—Pelvic osteosarcoma. Results of therapy. **A**, Before chemo- and radiotherapy. Large soft tissue mass of pelvic osteosarcoma (*arrow*) displaces urinary bladder and bowel. **B**, After chemotherapy, sections at similar level. Marked regression of mass (*arrow*).

with management of bone tumors at our institution has warranted adoption of this type of evaluation.

The presence of skip metastases or extensive medullary tumor extension are of critical value to the surgeon, since this extension contraindicates any type of local resective surgical procedure because of the certainty of local recurrence where tumor tissue is left behind [7]. With present techniques only 20% of skip metastatic foci are radiographically demonstrable and arteriography or radionuclide scanning have not been capable of demonstrating these small islands of tumor [7]. Although our experience is limited, we believe that CT can be of great help in detecting skip islands of tissue. Because of this we have been scanning the whole bone involved and the distal one-fourth of bone of the proximal joint in those lesions affecting the distal part of a long bone.

A large soft tissue extraosseous mass component is also a contraindication for local resection. These parameters are at best only fractionally determined by conventional radiography. The presence of a soft tissue mass component can be evaluated by arteriography, but it requires additional hospitalization and carries a small but definite risk as an invasive procedure. In addition to demonstrating the lesion itself, CT demonstrates adjacent muscular and soft tissue structures with great detail permitting the evaluation of the extent of disease with increased accuracy.

The presence of osteoid matrix in the medullary cavity is easily demonstrated by CT, since its attenuation coefficient is significantly higher than that of the normal marrow tissues even when it is not calcified (figs. 1 and 4). When local resection is chosen, CT is critical in determining the proper level of amputation.

In those lesions not amenable to surgical resection, CT can accurately determine the true extent of the tumor; therefore, the volume and critical anatomic relations of the lesion can be obtained for radiotherapy purposes. Also, CT can be used as a baseline to assess the response to therapy, particularly in the bony structures of the lower pelvic region where frequently masses of tumor tissue are not detectable by conventional radiographic methods or physical examination because of the large overlapping muscular structures of the gluteus and upper thigh muscles (figs. 5 and 7).

Computed tomography does not replace conventional radiographic techniques at this time, but rather complements its findings. CT is definitely inferior to conventional radiography in the evaluation of fine features of the tumor itself, such as the degree of lysis, type of bony margins, character of bony permeation, and the characteristics of periosteal reaction that are essential for radiographic differentiation of individual entities. CT, although extremely sensitive in detecting intramedullary tumor, is relatively nonspecific. Inflammation or nonosteoid tumor tissues can produce a similar increase in medullary density. Differentiation in those cases should rely on conventional radiographic data. The use of contrast enhancement has not proven very useful in defining the type and degree of vascularity of tumor tissue. However, it facilitates separation of extraosseous masses of tumor from normal muscular groups. Angiography remains a more useful technique than CT in the assessment of the type of tumor vascularity.

Our experience with CT in evaluating lung metastases in osteosarcoma is limited and we only have studied five cases. Of these five cases, two had metastatic nodules demonstrated by CT which were not seen on conventional radiographs of the chest and whole lung tomograms. Previous experience with CT in the chest has reported the superiority of CT over conventional tomography in demonstrating lung metastases [8, 9]. Although the demonstration of a few additional metastases is of little value in the patient with numerous tumor foci, the demonstration of isolated tumor deposits in patients with a normal conventional study is of obvious benefit since their removal is of value in the patient's survival [10].

REFERENCES

1. Wilson JS, Korobkin M, Genant HK, Bovill EG Jr: Computed tomography of musculoskeletal disorders. *AJR* 131:55–61, 1978
2. deSantos LA: Computed tomography in the evaluation of musculoskeletal neoplasms. *Radiology* 128:89–94, 1978
3. deSantos LA, Murray JA: Evaluation of giant cell tumor by computerized tomography. *Skeletal Radiol* 2:205–212, 1978
4. Sutow WW, Gehan EA, Vietti TJ, Frias AE, Dyment PG: Multidrug chemotherapy in primary treatment of osteosarcoma. *J Bone Joint Surg [Am]* 58:629–633, 1976
5. Jaffee N, Watts HG: Multidrug chemotherapy in primary treatment of osteosarcoma: an editorial commentary. *J Bone Joint Surg [Am]* 58:634–635, 1976
6. Rosen G, Murphy ML, Huvos AG, Guiterrez M, Marcove RC: Chemotherapy, enbloc resection and prosthetic bone replacement in the treatment of osteogenic sarcoma. *Cancer* 37:1–11, 1976
7. Enneking WF, Kagan A: Skip metastases in osteosarcoma. *Cancer* 36:2192–2205, 1975
8. Muhm JE, Brown LR, Crowe JR: Use of computed tomography in the detection of pulmonary nodules. *Mayo Clin Proc* 52:345–348, 1977
9. Schaner EG, Chang AE, Doppman JL, Conrle DM, Flye MW, Rosenberg SA: Comparison of computed and conventional whole lung tomography in detecting pulmonary nodules: a prospective radiologic-pathologic study. *AJR* 131:51–54, 1978
10. Spanos PK, Payne WS, Ivins JC, Pritchard DJ: Pulmonary resection for metastatic osteosarcoma. *J Bone Joint Surg [Am]* 58:624–628, 1976

Familial Hyperphosphatasemia: Diagnosis in Early Infancy and Response to Human Thyrocalcitonin Therapy

VAL DUNN,[1] VIRGIL R. CONDON,[1] AND MARVIN L. RALLISON[2]

Familial hyperphosphatasemia is an uncommon hereditary disorder of membranous bone with concurrent overproduction and overdestruction of bone and bone collagen by osteocytes. This process does not allow normal maturation into compact lamellar bone. Two cases of severely affected children are presented which demonstrate that the condition can be diagnosed in early infancy by abnormalities in the long bones. At this stage the skull may appear normal and the characteristic thickening of the calvarium appears later. The disease is treatable with human thyrocalcitonin; these and previously reported cases have responded favorably.

Familial hyperphosphatasemia is an uncommon hereditary disorder of membranous bone with concurrent overproduction and overdestruction of bone and bone collagen by osteocytes. Primitive fibrous bone fails to mature into compact lamellar bone. Affected children have severely limited motion and may never walk, crawl, or sit up. Radiographs are characterized by a generalized lack of discrete cortex and normal modeling. Long bones are bowed and, as the disease progresses, there is marked thickening in cortical regions of the skull and long bones. Recently, the inexorable progression of the disease seems to have been controlled by the administration of human thyrocalcitonin [1–3].

Two Navajo infants with this disorder have recently been studied. These cases are of particular interest because they demonstrate: (1) diagnostic radiographic changes at the earliest age reported; (2) absence of radiographic thickening of the skull at the time of diagnosis, previously reported as the common initial finding of all cases; and (3) evidence of response to human thyrocalcitonin therapy.

Case Reports

Case 1

L. H., the first child of Navajo parents from Shiprock, New Mexico, is the product of a normal pregnancy and delivery. She was believed to be normal at age 6 weeks when a "hip click" was discovered on routine physical examination. Because of abnormal radiographs, she was referred to Salt Lake City where the diagnosis of familial hyperphosphatasemia was made. Radiographic evaluation of the skeletal structures showed extensive subperiosteal new bone formation in most of the diaphyseal areas of the long bones, including some of the smaller bones of the hands and feet. Much of the cortical bone was completely absent, showing extreme osteopenia and apparent expansion of the medullary cavity (fig. 1A). There were some focal areas of radiolucency in the metaphyseal zones (fig. 1B). Bowing deformities were noted and microfractures had probably occurred in some of the poorly defined cortical areas. The epiphyses and epiphyseal plate areas were normal. The calvarium was adequately ossified and the bony tables were intact but not thickened (fig. 1C). The vertebral bodies showed no evidence of compression although osteopenia was evident. Alkaline phosphatase measured 3,600 IU. By age 16 months when the child returned for thyrocalcitonin therapy, clinical manifestations of the disease were obvious. She had never talked, walked, or sat alone, although she could roll over. She was extremely irritable and resisted motion. Her head was misshapened with flattening of the forehead and posterior skull. The phalanges were noticeably thickened. Other health problems included herpes stomatitis and recurrent ear infections, leading to the placement of myringotomy tubes. Radiographically, the extremities were not significantly changed. The skull films at 12 months (fig. 2) and 16 months showed severe calvarial thickening, narrowing of sutures, and absence of cortical margins. The diagnosis of hyperphosphatasemia was substantiated by cortical bone biopsy which showed woven trabecular bone with prominent osteoid seams and well defined osteoblastic membranes.

Human thyrocalcitonin therapy resulted in a prompt clinical and laboratory response. Almost immediately the child became more pleasant and less irritable. Her alkaline phosphatase fell from 3,188 to 1,199 IU over a 6 week period. After 9 months of therapy, with only partial compliance due to nausea and vomiting, she was able to sit without assistance. Comparison radiographs demonstrate formation of discrete cortex, most notably in the long bones (figs. 3 and 4). Subsequent radiography with continued therapy at age 30 months showed further development of cortical bone and more normal modeling (fig. 3C).

Case 2

M. H. is the only child of Indian parents from Shiprock Navajo Indian Reservation. The parents deny any kinship to the family of case 1. Family history, pregnancy, and delivery were unremarkable. At age 1 month, the mother noticed that the child was not "moving her arms." Clinical examination was normal. At age 6 weeks, after trauma to the left leg, radiography was performed. Because of multiple fractures and generalized bony abnormality, osteogenesis imperfecta was considered a likely diagnosis and she was referred to Salt Lake City. Skeletal radiographic changes were remarkably similar to case 1, except for more obvious fractures (fig. 5). Alkaline phosphatase measured 1,295 IU and the diagnosis of familial hyperphosphatasemia was made. At age 16 months, the child returned for initial thyrocalcitonin therapy. Before therapy she was hypoactive (having never rolled over), was extremely irritable, and had mild bowing of the extremities. She showed evidence of severe

Received October 20, 1978; accepted December 28, 1978.
This work was supported in part by Public Health Service grant no. RR-64 from the Division of Research Resources (M. L. Rallison).
[1] Department of Radiology, University of Utah Medical Center, Primary Children's Medical Center, 320 Twelfth Avenue, Salt Lake City, Utah 84103. Address reprint requests to V. R. Condon.
[2] Department of Pediatrics, University of Utah Medical Center, Primary Children's Medical Center, Salt Lake City, Utah 84103.

© 1979 American Roentgen Ray Society

0361–803X/79/1324–0541 $0.00

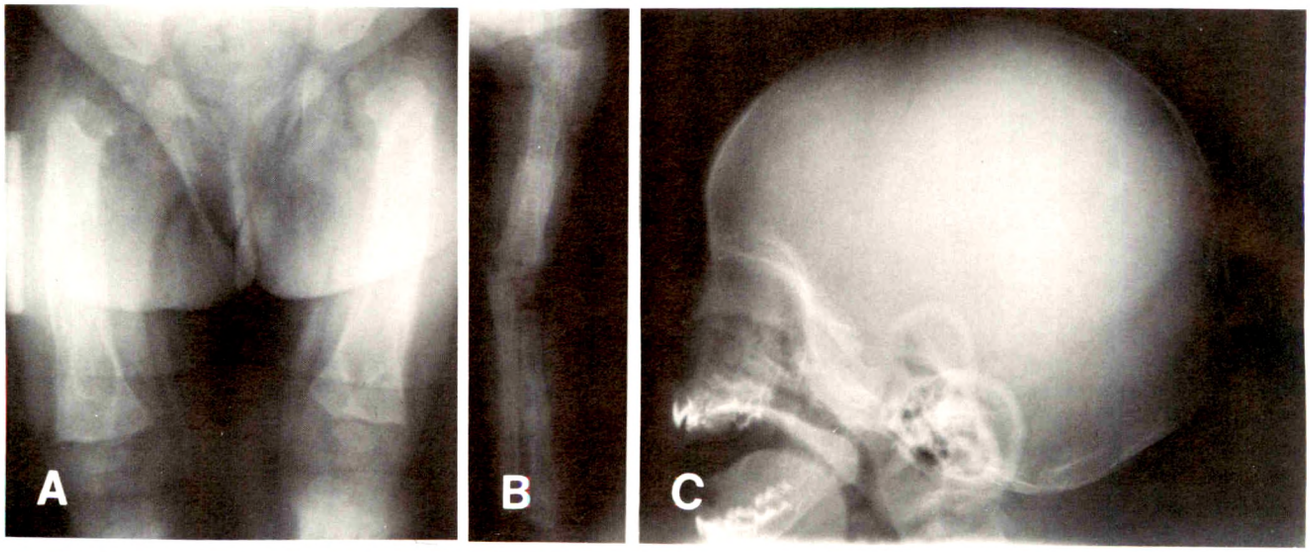


Fig. 1.—Case 1, age about 2 months. **A**, Lack of discrete cortex, medullary widening, severe osteopenia, coxa vara, and cystic areas of radiolucency. **B**, Similar findings in upper extremity. **C**, No diagnostic abnormality.

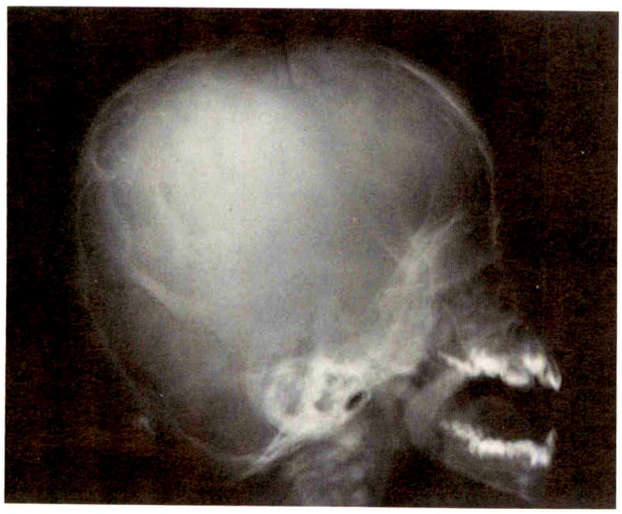


Fig. 2.—Case 1, age 12 months. Severe calvarial thickening has occurred in the first year of life. Cortical margins are indistinct and sutures are narrowed and closing.

deafness. Skull radiography demonstrated the interval development of calvarial thickening. On admission, serum alkaline phosphatase measured 3,600 IU and fell to 1,400 IU after 2 weeks of thyrocalcitonin therapy. Increased mobility has been noted on 1 month follow-up examination.

Discussion

In 1973 Caffey [4] reviewed 14 cases of familial hyperphosphatasemia including three sets of siblings and case reports as early as 1956 [4–10]. Various names have been applied to this disorder, including juvenile Paget's disease [2, 3], hyperostosis corticalis deformans infantalis [9], familial osteoectasia with macrocranium [5], and osteoectasia with hyperphosphatasia [11]. Familial hyperphosphatasemia is the preferred and most widely accepted term, especially since recent articles have pointed out significant differences from Paget's disease

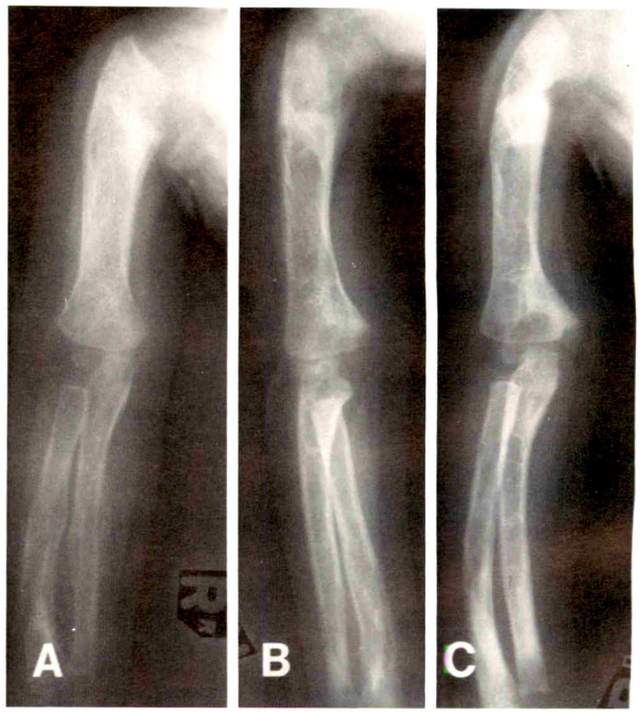


Fig. 3.—Case 1. Serial right arm films documenting effects of human thyrocalcitonin therapy. **A**, Age 18 months, shortly after onset of therapy. After 8 (**B**) and 12 (**C**) months of treatment, progressive development of compact cortical bone and differentiation of medullary cavity. More normal trabeculation and modeling.

[1]. Reported cases have come from a wide racial and geographic distribution, but Caffey [12] noted a high prevalence among Puerto Ricans and American Indians. Autosomal recessive heredity has been suggested.

Clinical Manifestations

Most authors report that clinical manifestations have their onset between 3 and 18 months of age, although

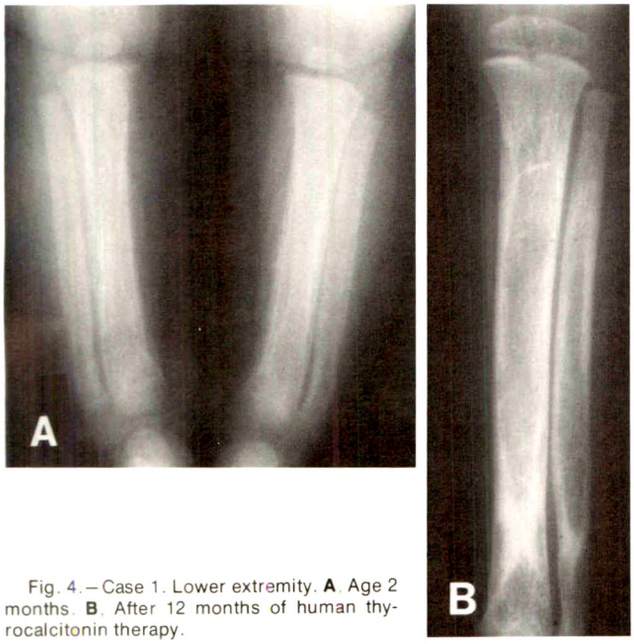


Fig. 4.—Case 1. Lower extremity. **A**, Age 2 months. **B**, After 12 months of human thyrocalcitonin therapy.

Swischuk [13] writes, "It is uncommon to present in the neonatal period and usually becomes manifest at the end of the first year or later. . . . " Our cases were first seen in early infancy and about half of those previously reported were seen initially in the first year of life. It seems that there is a fairly wide spectrum in the severity of the disease; the more severe disease is manifested at an earlier age with greater disability. Caffey [12] reported progressive enlargement of the head as the common initial clinical finding, although he alludes to an infant in whom bowing of the legs preceded enlargement of the head. Our experience has been that the abnormalities of the long bones precede those of the skull. Both of our patients had normal skulls at the time abnormalities were first noted in the extremities. Severe pain in the limbs, which are often swollen, accompanied by irritability and muscular weakness is crippling and severely affected children may never walk, crawl, or sit. Bowing and fractures of the long bones are common. Deficient visual and auditory acuity have frequently been noted. The clinical course prior to thyrocalcitonin therapy is progressive and frequently leads to death in childhood. Clinical experience with human thyrocalcitonin therapy is insufficient to predict eventual prognosis, although significant clinical improvement has resulted in every case [1–3].

Histology and Biochemistry

Whalen et al. [1] recently described the microscopic findings of familial hyperphosphatasemia in exquisite detail. They emphasized the role of hyperactive osteocytes in the accelerated absorption. Immature woven bone is rapidly laid down, but simultaneous rapid destruction prevents normal maturation and modeling in membranous bone. Haversion bone is absent and there is evidence of accelerated metabolic activity. Thick osteoid seams cover the trabeculae, which are devoid of a cartilagenous core. Intense osteocytic osteolysis in trabeculae is noted.

The biochemical diagnosis requires chronically and greatly elevated levels of osteogenic serum alkaline and acid phosphatase. All biochemical abnormalities reflect the significantly increased turnover of bone, collagen, and cellular elements. Serum lucine aminopeptidase and uric acids are elevated. Urinary excretion of uric acid, hydroxyproline, and other peptides are also increased.

Radiographic Findings

Radiographs are very characteristic and correlate well with the pathology described above. Epiphyses and endochondral bone are normal. There is no discrete cortex in membranous bone, presumably because accelerated osteolysis occurs before immature subperiosteal new bone matures and remodels. As our patients demonstrate, severe osteopenia and a lack of discrete cortex with medullary widening and bowing in long bones are detectable in early infancy while the skull may appear normal. All previously reported cases demonstrate thickening of the cortical regions of long bones and in the calvarium. We attribute lack of this finding in our two cases to the early age of diagnosis. Only later in the course of the disease did the classically described picture emerge with thickening of primitive woven bone in the cortical regions of the calvarium and prominent trabeculae in the widened medullary cavity (which may be the manifestation of microfracture). There is often evidence of obvious fracture, and bowing of the long bones is characteristic. Coxa vara is also a common finding. Late skull changes consist of excessive calvarial thickening (often having the "hair on end" appearance), irregular spots of increased density, and craniostenosis.

Differential diagnostic considerations are few because the radiographic, clinical, and biochemical data present a conclusive diagnostic picture that no other entity seriously mimics. Osteogenesis imperfecta shows some similarities. However, the skull manifestations of wormian bones and large fontanels is a significant differentiating feature. Paget's disease, which may show similar radiographic findings, begins later in life and is typically focal and symmetric with lesions developing in normal bone.

Human Thyrocalcitonin Therapy

In 1972, Woodhouse et al. [3] reported a rapid positive biochemical response to human thyrocalcitonin therapy in a 5-year-old boy with "juvenile Paget's disease." After 16 months of therapy, this boy demonstrated regression of the bony abnormalities of familial hyperphosphatasemia with development of compact cortical bone, diaphyseal tapering, and normal modeling. Investigators also noted an increased resistance to fracture. Subsequently, other patients with familial hyperphosphatasemia who have been treated with human thyrocalcitonin have all benefited from therapy and shown reversal of objective evidence of the disease. Significant clinical improvement including decreased pain and irritability have been noted almost immediately. With continued therapy, there is

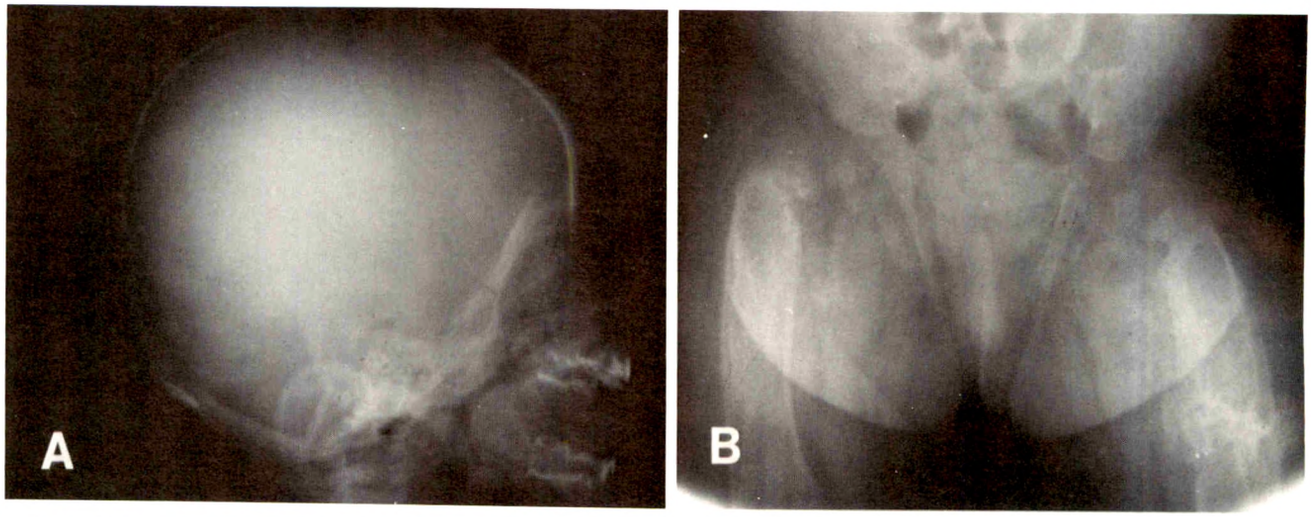


Fig. 5.—Case 2, age 10 weeks (cf. fig. 1). **A**, Normal lateral skull. **B**, Pelvis and femurs. Coxa vara, absence of corticomedullary differentiation, diaphyseal widening, and healing fracture.

resistance to fracture and increased mobility. Children who could previously assume only the supine position have been able to sit and even stand with support after months of treatment. Dramatic histologic evidence of improvement is seen as osteocytic osteolysis is inhibited and immature woven bone is replaced by normal lamellar bone. After the administration of thyrocalcitonin, alkaline phosphatase and urinary hydroxyproline levels significantly decrease but may not remain uniformly low [3]. Improvement is most notable radiographically in the diaphyseal regions of long bones. Discrete compact cortical bone is formed and improved modeling results in diaphyseal narrowing and more normal trabeculation. Although there is evidence of reversibility, there is as yet insufficient long-term experience with the disease and its treatment to modify long-term prognosis. However, the quality of life in treated patients has definitely improved.

Conclusions

Familial hyperphosphatasemia may manifest itself and be correctly diagnosed in infancy as our cases demonstrate. This is particularly true of severely affected patients. However, it should be noted that radiographic and clinical abnormalities found in later stages of the disease, particularly in the skull, were not present in our two patients on initial examination. Long bone findings must be relied upon for diagnosis at this early stage, since the skull may be normal. Our patients demonstrated severe osteopenia and a lack of discrete cortex with widening of tubular bones. "Cortical" thickening of the skull and long bones and craniostenosis seem to be later findings.

Success with human thyrocalcitonin has now been reported in five children treated for familial hyperphosphastasemia. In each case significant clinical benefit has resulted with decreased pain, increased mobility, and resistance to fracture. Biochemical evidence of healing is apparent almost immediately after onset of treatment, as evidenced by falling levels of alkaline phosphatase and urinary hydroxyproline. Normal cortical bone replaces abnormal woven bone and more normal modeling takes place as the accelerated osteocytic resorption decreases. Radiographic signs of improvement are obvious within a few months as discrete cortical bone forms in the long bones and normal modeling occurs with narrowing of the abnormal medullary canal. Successful treatment of familial hyperphosphatasemia with human thyrocalcitonin makes the accurate diagnosis and differentiation from other conditions mandatory.

ACKNOWLEDGMENT

We thank Dr. Melvin Horwith for his assistance with our two patients and for supplying the human thyrocalcitonin for therapy.

REFERENCES

1. Whalen JP, Horwith M, Krook L, MacIntyre I, Mena E, Viteri F, Torun B, Nunez EA: Calcitonin treatment in hereditary bone dysplasia with hyperphosphatasemia: a radiographic and histologic study of bone. *AJR* 129:29–35, 1977
2. Doyle FH, Woodhouse HJY, Glen ACA, Joplin GF, MacIntyre I: Healing of the bones in juvenile Paget's disease treated by human calcitonin. *Br J Radiol* 47:9–15, 1974
3. Woodhouse NJY, Fisher MT, Sigurdsson G, Joplin GF, MacIntyre I: Paget's disease in a 5-year old: acute response to human calcitonin. *Br Med J* 4:267–269, 1972
4. Caffey J: Familial hyperphosphatasemia with ateliosis and hypermetabolism of growing bone. *Prog Pediatr Radiol* 4: 438–468, 1973
5. Bakwin H, Eiger MS: Fragile bones and macrocranium. *J Pediatr* 49:558–564, 1956
6. Bakwin H, Golden A, Fox S: Familial osteoectasia with macrocranium. *AJR* 91:609–617, 1964
7. Desai MP: Chronic idiopathic hyperphosphatasia in the Indian child. *Am J Dis Child* 126:626–628, 1973
8. Fanconi G, Moreira G, Vehlinger E, Gigdion A: Osteochala-

sia desmalis familiaris. *Helv Paediatr Acta* 19:279–295, 1964
9. Swoboda W: Hyperostosis corticalis deformans juvenilis. *Helv Paediatr Acta* 13:292–312, 1958
10. Thompson RC Jr, Gaull GE, Horwitz S, Schenk RK: Hereditary hyperphosphatasia. Study of three siblings. *Am J Med* 47:209–219, 1969
11. International nomenclature of constitutional diseases of bone. *AJR* 131:352–354, 1978
12. Caffey J: Therapeutic value of thyrocalcitonin. *AJR* 129: 175–176, 1977
13. Swischuk LE: *Radiology of the Newborn and Young Infant.* Baltimore, Williams & Wilkins, 1973, p 430

AJR Guidelines for Authors

Address manuscripts and correspondence to the Editorial Office, American Journal of Roentgenology, 403 Pacific National Bank Building, 4545 15th Avenue N.E., Seattle, Washington 98105; telephone (206)633-2754.

Publication Policy

The Journal publishes original and timely contributions to the advancement of radiologic diagnosis and treatment. Although the content is predominantly clinical, laboratory investigations are accepted when their relevance to clinical practice is demonstrable. In prospective clinical investigations, authors should indicate if informed consent from patients was obtained. Decisions on manuscripts are based on the opinions of at least two outside reviewers. Reviewers receive manuscripts without title pages to protect the identity of authors and to ensure an unbiased review; names of reviewers, in turn, are not revealed to authors. Statements within an article are the responsibility of the authors and not the Journal or its publisher.

It is understood that material submitted has not been published and is not currently submitted elsewhere. Portions of the data or illustrations from previously published works may be included if permission release forms accompany the manuscript and such material is clearly credited in the text. Prior publication of abstracts will not prejudice publication of the complete study.

Copyright Information

In accordance with Journal implementation of the 1976 U.S. Copyright Law, authors must release first and subsidiary rights to their manuscript at submission. A dated cover letter, containing signatures of all authors, should state: "We, the authors, assign first and subsidiary rights to the American Roentgen Ray Society in the event that our manuscript (title) is published by AJR." The Journal, in turn, grants authors the right to use portions of their manuscript, without charge, in books or articles of which they are authors or editors.

Manuscript Form

Manuscripts should be typed double-spaced throughout, including references, tables, and figure legends. Tables, footnotes, and figure legends should be on separate sheets, and a separate title page should be provided. In addition to the original typewritten copy, a duplicate copy complete with figures, tables, and references is required. Authors' names should be on title page only and should not be on figures so that author anonymity can be maintained during the review process.

Figures should be submitted as 13 × 18 cm glossy prints, untrimmed and unmounted. Labels and arrows must be of professional quality and should be removable from the prints. Each figure should be numbered to correspond with figure legends, and the top should be indicated. Specific permission for publication of facial photographs of patients is required. Line illustrations and graphs should be drawn in black ink on white background.

References should be cited in the text by number (e.g., [3, 4]). The bibliography should be arranged in the numerical order that references are cited in the text and typed double-spaced throughout. Data for each reference should be arranged according to the uniform style on bibliographic citations adopted by many biomedical journals. Provide all authors' names and inclusive pages. Abbreviations for titles of medical periodicals should conform to those published in *Index Medicus*. Examples:

1. Miller RE, Chernish SM, Skucas J, Rosenak BD, Rodda BE: Hypotonic roentgenography with glucagon. *AJR* 121:264–274, 1974
2. Boijsen E: Superior mesenteric angiography, in *Angiography*, edited by Abrams H, Boston, Little, Brown, 1971, pp 1091–1119

Organization

Title page. Titles should be brief and specific. Include addresses for each author and acknowledgment of grant support when appropriate.

Abstract. A description of the purpose, methods, results and conclusions of the study is required.

Introduction. Clearly state the purpose of the investigation including necessary background facts.

Materials and methods. Decribe the protocol clearly. Use standard abbreviations as presented in the *Council of Biology Editors Style Manual*, 3d ed. Metric measurements should be used throughout.

Results. Present results in logical sequence.

Discussion. Interpret the results to lend meaning and importance to the observations. Hypotheses and speculation based on the results are encouraged. When results differ from those of previous investigators, an attempt should be made to explain the discrepancy.

References. Only include references which provide adequate background and present fairly any opposing evidence and concepts. Accuracy of reference data is the responsibility of the author.

Legends. Legends should be brief but should provide sufficient description to interpret the figure.

Special Communications

Case Reports. Concise case reports are accepted if they present unusual experiences that are medically important and educational. Clarity and brevity are essential. After preliminary screening by an editor to determine whether the requirement of medical significance has been met, qualifying papers will undergo the same peer review as major papers.

Technical notes. Brief descriptions of new techniques or significant modifications of older ones which are directly applicable to clinical practice will be accepted.

Letters to the Editor. Letters are subject to editing and condensation. Criticism of published articles should be objective and constructive. Letters may also discuss matters of general interest to radiologists.

Technique of Percutaneous Transluminal Angioplasty with the Grüntzig Balloon Catheter

ANDREAS GRÜNTZIG[1] AND DAVID A. KUMPE[2]

Recanalization of superficial femoral artery occlusions and of stenoses in the superficial femoral and pelvic arteries using the Grüntzig balloon catheter are described. Among patients successfully treated, 2 year patency rates of 72% and 87% for superficial femoral and iliac artery lesions, respectively, were achieved by this method. The catheter is now commercially available in the United States and Europe.

Since Dotter and Judkins [1] first reported percutaneous transluminal angioplasty as a technique for treating atherosclerotic vascular stenoses and occlusions, the method has received little attention or support in the United States. While Dotter et al. [2, 3] have continued to advocate the procedure, few are performed in the United States outside Dotter's own institution. This has not been true in Europe, where a number of investigators [4–12] have instituted the procedure and performed it on significant numbers of patients. At an international congress devoted exclusively to transluminal angioplasty in March 1977 [13], a total experience of about 1,800 cases of occlusions and stenoses in the femoropopliteal region alone treated by transluminal angioplasty was reported from twelve groups, to which Dotter contributed 322 cases.

Percutaneous transluminal angioplasty was introduced by one of us (A. G.) at the Kantonsspital Zürich in 1971. We used the original coaxial catheter technique of Dotter and Judkins [1] until February 1974, when clinical use of a new balloon catheter [14] was instituted. Porstmann [15] first reported use of a caged balloon catheter (Korsett-Katheter) in 1973. A modified version of this was introduced in the United States by Dotter (Cook Inc., Bloomington, Ind. 47401). Though effective, this caged balloon catheter is somewhat thrombogenic, and its use is confined to the iliac vessels.

We have now used the new balloon catheter for nearly 4 years. The catheter and its use are described here. The results of our patient series, which are reported more completely elsewhere [12], are briefly recounted as well.

Catheter Construction

The balloon catheter is a double-lumen, single end hole no. 8 French (2.8 mmOD) catheter. The outer lumen is composed of polyvinyl chloride and is smoothly tapered from catheter tip to hub, which accounts for its lower thrombogenicity. The balloon segment at the catheter tip is filled via a side channel at the proximal end of the catheter, which connects to a longitudinal groove cut along the outer surface of the inner catheter. The balloon segment can be manufactured in various lengths and maximal diameters, so that a balloon catheter can be tailored to individual obstructions and vessels. Balloon lengths of 4 cm for the superficial femoral artery and 2 cm for the iliac artery have proven best. Maximum expanded balloon diameters should never exceed the angiographic diameter of the vessels. In general, maximum diameters of 4–6 mm for the superficial femoral artery and 6–10 mm for the iliac artery are appropriate (fig. 1).

Using a 2 ml pressure syringe (fig. 2), 3–5 atm *P* can easily be generated to expand the balloon at its working pressure. This pressure is sufficient to compress the occluding material against the vessel wall in essentially all cases with noncalcified occlusions. During expansion of the balloon, dilating pressure is monitored with a pressure gauge (Fa. H. Schneider, Zürich, Switzerland) that attaches between the pressure syringe and balloon hub of the dilating catheter. As a safety feature, even if the working pressure is exceeded, the balloon expands only minimally beyond its predetermined diameter.

Before attempting any percutaneous transluminal dilatation using this technique, the operator should practice expanding balloons of various diameters to be thoroughly familiar with desired expansion pressures. Larger diameters require less pressure. Alternatively, a foot-operated pump (Fa. H. Schneider, Zürich, Switzerland), which uses compressed air or oxygen to compress and aspirate a pressure syringe, can be used to expand and collapse the balloon more rapidly while it lies within an obstructing lesion.

If the balloon ruptures in the vessel and the rupture line is perpendicular to the axis of the catheter, the rupture may snag at the puncture site on attempted withdrawal and require surgery to remove the catheter.

The catheter is now commercially available in both the United States (Cook, Inc., Bloomington, Inc. 47401) and Europe (Fa. H. Schneider, Zürich, Switzerland). The other equipment used is illustrated in figure 2.

Technique

Femoropopliteal Recanalization or Dilatation

Only occlusions less than 10 cm are treated because of low patency rates for longer recanalizations [16, 17]. After antegrade ipsilateral common femoral artery puncture, a no. 7 or 8 French Teflon catheter with a single

Received May 30, 1978; accepted after revision December 11, 1978.

[1] Department of Internal Medicine, Medical Polyclinic, Kantonsspital Zürich, Switzerland.

[2] Department of Radiology, University of Colorado Medical Center, 4200 East Ninth Avenue, Denver, Colorado 80262. Address reprint requests to D. A. Kumpe.

© 1979 American Roentgen Ray Society

0361–803X/79/1324–0547 $0.00

side hole near the tip is placed in the superficial femoral artery (fig. 3A). After injecting dilute contrast material under fluoroscopy, the proximal and distal ends of the occlusion are marked with towel clips on the drapes or by taping small lead markers to the skin overlying the ends of the obstruction. Angiography is performed (20 ml undiluted contrast) to document the preoperative appearance of the vessel, to assure that the limits of the occlusion are correctly demarcated, and to document the status of the distal calf vessels.



Fig. 1.—Balloon segments in collapsed and expanded states. Left: iliac artery catheter, maximum 8 mm diam. Right: superficial femoral artery catheter, maximum 4 mm diam.

The J guide wire is then carefully passed through the occluded segment (fig. 3B). If the wire will not pass through the occlusion in its J configuration, the tip is completely straightened using the movable core, and the hard wire tip is then carefully advanced about 1 cm into the occlusion. The J tip configuration is then reformed by retracting the movable core and an attempt is again made to advance the wire in its J configuration. If this fails again, the catheter is advanced over the wire to near the wire tip. The wire tip is withdrawn into the catheter and again straightened with the movable core. The stiffened wire is then advanced another 1–2 cm through the occlusion, and its J configuration reformed. This procedure is repeated until the wire lies in the patent distal segment (i.e., past the distal towel clip or skin marker). Wire manipulation is performed through the Y connector. Dilute contrast material is injected frequently through the other limb of the Y connector to assure the wire remains in the vessel lumen.

After the wire is through the occluded segment, the Teflon catheter is advanced over the wire (fig. 3C) to enlarge the tract for the dilatation catheter. If the Teflon catheter fails to pass through the occluding segment alone, it is reinforced by placing the stiffening cannula over the wire and inside the catheter. This is seldom necessary, however. After the catheter tip is distal to the occlusion, heparin (5,000 IU) and a vasodilator (e.g., Priscoline 25 mg or adenosine triphosphate 25 mg) are injected through the catheter into the distal calf arteries.

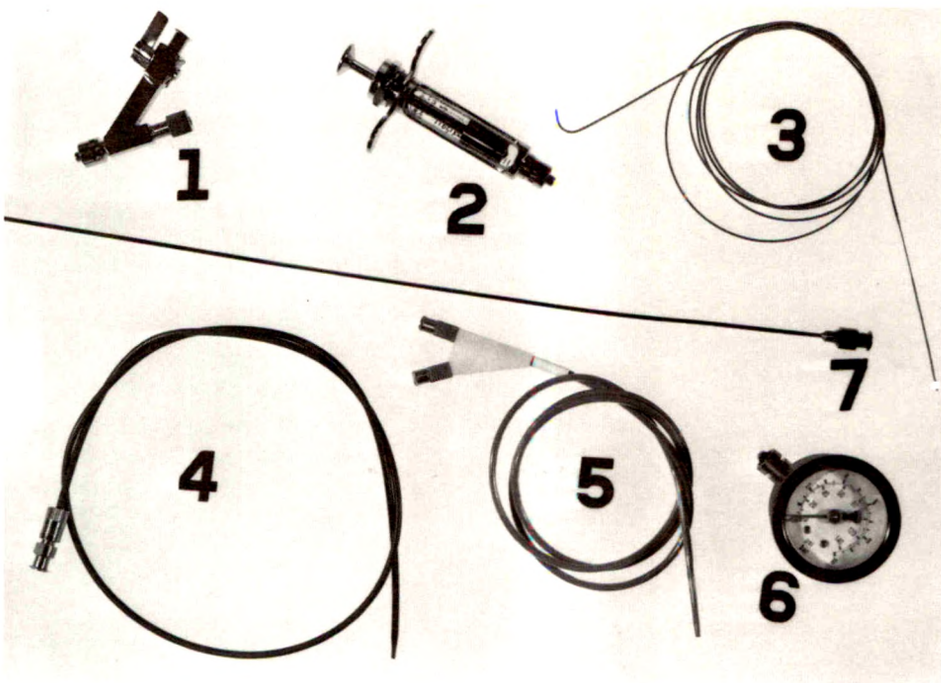


Fig. 2.—Transluminal recanalization equipment: (**1**) "Y" connector allows injection of contrast while wire is in catheter; (**2**) pressure syringe; (**3**) 0.097 cm 3 mm "J" guide wire with movable core; (**4**) relatively stiff no. 7–8 French Teflon catheter with single side hole for initial angiography and passage through occlusion; (**5**) balloon dilatation catheter; (**6**) pressure manometer to monitor balloon pressure during dilatation; and (**7**) stiffening cannula to support catheter when passage through occlusion is difficult.



Fig. 3.—Recanalization of superficial femoral artery: (**A**) catheter placed selectively in superficial femoral artery, extent of occlusion marked under fluoroscopy and angiography with runoff performed to document status of occlusion and runoff; (**B**) guide wire passed through occlusion; (**C**) angiographic catheter passed through occlusion; (**D**) exchange to balloon dilatation catheter; (**E**) balloon positioned into distal end of occlusion; (**F**) balloon expanded for 30–60 sec at 3.5–5 atm *P*; (**G**) balloon collapsed; (**H**) catheter withdrawn so collapsed balloon is repositioned in remaining occlusion; (**I**) balloon reexpanded (30–60 sec, 3.5–5 atm *P*); (**J**) balloon again collapsed; and (**K**) guide wire removed; angiography to document status of recanalization segment and of runoff.

Leaving the wire distal to the occlusion, the stiffer Teflon catheter is then exchanged for the balloon dilatation catheter (fig. 3D). Before the dilatation catheter is inserted at the groin, the balloon is evacuated and at the same time compressed manually and folded around the inner catheter, similar to folding a collapsed umbrella, so the puncture hole is not enlarged. The guide wire tip should be kept motionless during catheter exchange to avoid inducing spasm in the popliteal artery. The balloon is positioned in the distalmost end of the occlusion (fig. 3E). It is expanded with 3.5–5.0 atm *P* to its maximum diameter (4 mm is usually chosen) for 30–60 sec by injecting dilute contrast into the side channel of the catheter (fig. 3F). The balloon is then evacuated (fig. 3G), retracted into the adjacent untreated occlusion (fig. 3H), and reexpanded (fig. 3I). This process is repeated until the entire occlusive segment is recanalized. The foot-operated pump may be used to expand and collapse the balloon, rather than a pressure syringe. The wire is then removed and angiography of the thigh, calf, and foot performed to check for any residual stenoses and to assure that no distal embolization has occurred (fig. 3K). Any significant residual stenosis is redilated.

Distal ankle pressures should be monitored during the procedure; simple Doppler ultrasound measurements suffice if continuous recording plethysmography is not available. When measurements indicate that satisfactory hemodynamics have been established, the procedure should be terminated even if a small residual stenosis is present. Further dilatation for "vascular cosmetics" may result in distal embolization.

The same technique is applied to femoropopliteal stenoses. The wire is most easily passed through such stenoses if the movable core is advanced nearly to the wire's tip without straightening it completely.

The balloon segment should be aspirated completely before the dilatation catheter is removed from the artery.

Vascular laboratory determinations of leg pressures and pulse contours are recorded before and after dilatation for both femoral and iliac dilatations. Similar recordings are then made at each clinic follow-up visit.

Iliac Artery Stenoses

Only stenoses, not complete occlusions, are treated because of the uncertainty of determining the course of the common and external iliac arteries when obstructed.

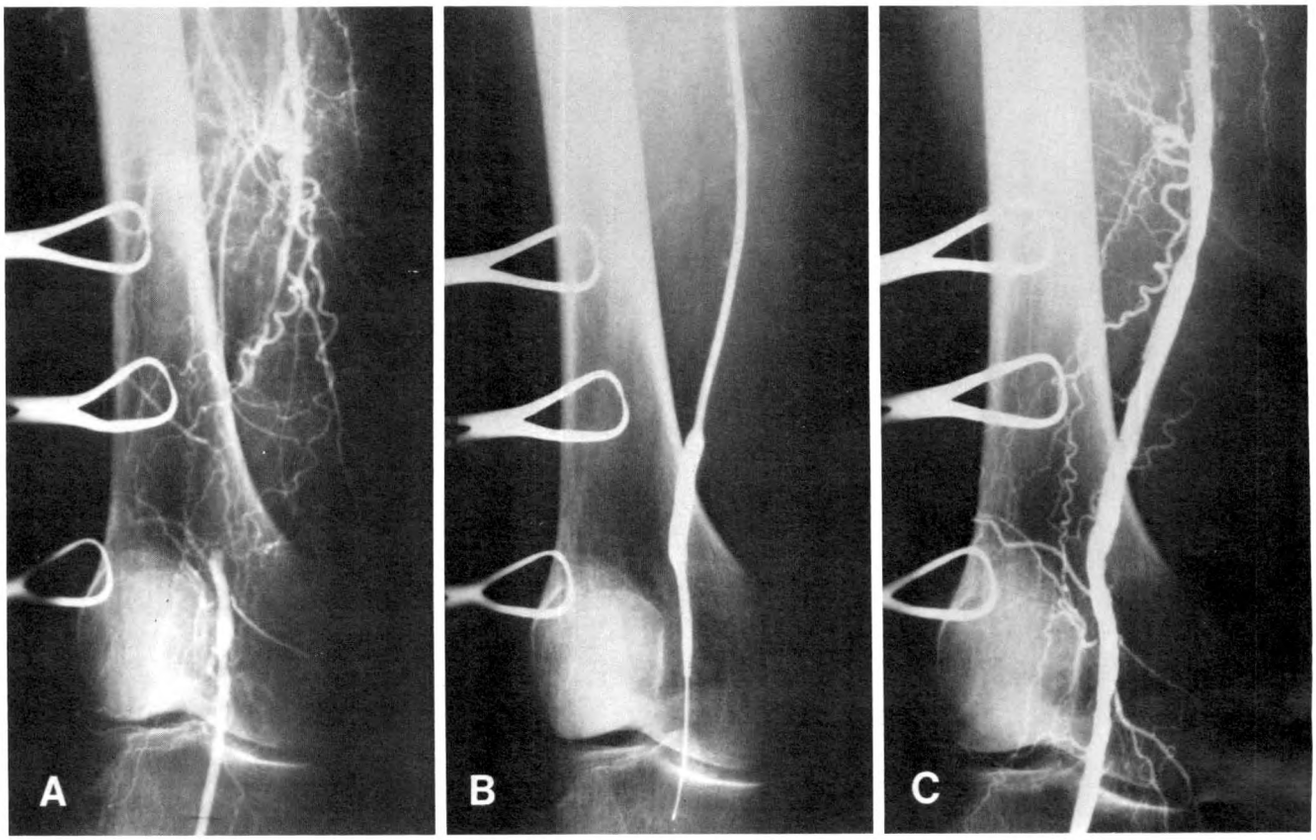


Fig. 4.—Case 1. **A,** Recanalization of 5.5 cm superficial femoral artery occlusion with another 6 cm of filiform stenosis proximally. **B,** Expanded balloon catheter in place. **C,** Immediately after recanalization.

We have been concerned about the possibility of perforating the artery and creating a hemorrhage difficult to control.

Before puncture of the affected side, a catheter is introduced (when possible) into the contralateral femoral artery and placed in the distal abdominal aorta or over the aortic bifurcation into the common iliac artery on the affected side. If the femoral pulse on the affected side is not palpable, the artery is punctured under fluoroscopy while contrast material is injected from this contralateral catheter. Pressures proximal and distal to the stenosis are recorded simultaneously via the two catheters.

The stenosis is marked and dilated as previously described, usually with an 8 mm diam balloon dilating catheter. Heparin (5,000 IU) and vasodilator are injected through the central lumen of the balloon catheter before dilatation. After dilatation, the tip of the dilating catheter is retracted distal to the stenosis and pressures again recorded. The procedure is ended when the pressure gradient across the stenosis is eliminated.

Representative Case Reports

Case 1

A 73-year-old man suffered bilateral calf claudication that was more severe on the right side. He had a history of hypertension, two myocardial infarctions, and bilateral renal surgery for nephrolithiasis. Translumbar aortography (not shown) demonstrated no hemodynamically significant lesion in the abdominal aorta or pelvic vessels. There was a 5.5 cm segmental occlusion of the distal right superficial femoral artery with another 6 cm of filiform stenosis proximally, and a 99% stenosis of the distal left superficial femoral artery. Both arteries were recanalized using balloon dilatation technique. The right side is shown before, during, and immediately after dilatation (fig. 4), and vascular laboratory data are given (table 1). The left side (not shown) was successfully treated in similar fashion 2 days later.

TABLE 1
Laboratory Results

Dilatation	Systolic Pressures (mm Hg)		
	Brachial Artery	Right Posterior Tibial Artery	Arm/Ankle Pressure Ratio
Case 1:			
Before	150/75	66	0.44
After 2 days	140/85	128	.91
After 1 year	130/85	120	.92
Case 2:			
Before	125/75	92	.74
Immediately after	125/75	128	1.02
After 1 year	120/90	126	1.05

Case 2

A 46-year-old man had left-side intermittent claudication for 9 months and a history of smoking, obesity, and hyperlipidemia. Abdominal aortography (not shown) revealed a tight stenosis of

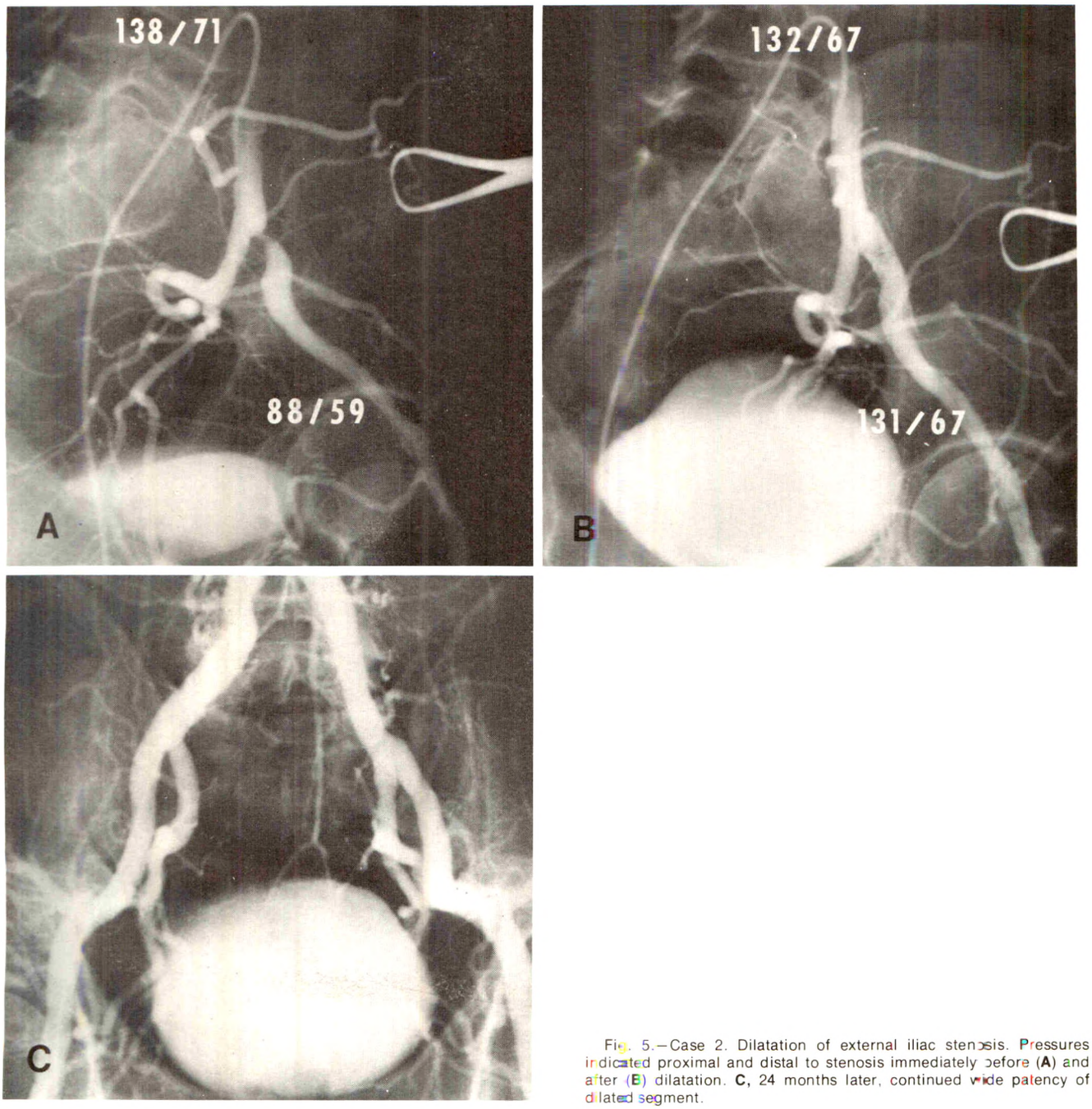


Fig. 5.—Case 2. Dilatation of external iliac stenosis. Pressures indicated proximal and distal to stenosis immediately before (**A**) and after (**B**) dilatation. **C,** 24 months later, continued wide patency of dilated segment.

the left external iliac artery. The lesion was dilated using the balloon catheter. Blood pressure status and angiographic appearance before and after dilatation are shown (figs. 5A and 5B). Two years later, angiography (fig. 5C) demonstrated continued wide patency of the dilated segment. Vascular laboratory studies (table 1) indicated normal hemodynamics immediately after the procedure and in follow-up.

Comment. Predisposing factors (hypertension, hyperlipidemia, and smoking) are treated before percutaneous transluminal angioplasty. It is particularly stressed that the patient stop smoking. The patient receives Anturane 200 mg 4 times daily for 4 days before percutaneous transluminal angioplasty for platelet inhibition. Heparin is given intraarterially during the procedure, and Coumadin is begun immediately after. The patient is kept on long-term Coumadin and Anturane unless contraindicated, since follow-up studies [5, 6, 17] have shown the reocclusion rate for femoropopliteal lesions is twice as high without long-term anticoagulation.

Results

We have treated over 300 patients with these methods since 1971, and our results have been comprehensively discussed [12]. Initial success rate is 84% for recanalizing femoropopliteal occlusions and 92% for iliac artery stenoses. Two year patency is 72% for successful femoropopliteal patients and 87% for successfully treated iliac artery stenoses. There were no operative deaths.

Distal embolization among our first 303 procedures was 5%. No embolus had a clinical sequela or required surgery. Our first 48 femoropopliteal patients were treated by Dotter's original coaxial technique, while subsequent patients (188 as of March 1978) have been treated with the balloon dilatation catheter. Two year patency rates with the dilatation technique are significantly higher than with the coaxial technique (86% vs. 64%), while a lower overall complication rate (8.5% vs. 20%) was obtained with the dilatation catheter. The dilatation group is less favorable clinically: older, with poorer calf outflow tracts, and more often (40% vs. 19%) in Fontaine's class III (rest pain) or IV (gangrene).

Discussion

Any treatment of an ischemic limb represents a local palliative measure in a relentless generalized disease. These patients have a worse prognosis than the general population. DeWeese and Rob [18] demonstrated 5 year mortality of 48% and 10 year mortality of 73% among patients who underwent femoropopliteal bypass reconstruction, with most deaths occuring from other cardiovascular events. In such a patient population, transluminal angioplasty has a definite role in management because of its relative simplicity and lack of morbidity and mortality.

The atheromatous lesions in this series were treated with a high degree of success using local anesthesia alone. Patients were ambulatory the day after treatment. Typical hospitalization time was 3 days. Dotter has even performed iliac dilatation on an outpatient basis (C. T. Dotter, personal communication). Advantages in both patient discomfort and hospitalization costs compared with reconstructive surgery are obvious. At the same time, reconstructive surgery or repeat angioplasty can be performed later, since neither established collaterals nor formation of new collateral channels are disturbed.

Two final points should be noted: (1) percutaneous transluminal angioplasty should only be performed by experienced angiographers who have observed the procedure in an institution where it is practiced and (2) close cooperation among the vascular radiologist, vascular surgeon, and attending clinician is mandatory so that optimal individualization and management of each case may result.

REFERENCES

1. Dotter CT, Judkins MP: Transluminal treatment of arteriosclerotic obstruction. Description of a new technique and a preliminary report of its application. *Circulation* 30:654–670, 1964
2. Dotter CT, Rösch J, Anderson JM, Antonovic R, Robinson M: Transluminal iliac artery dilatation. Nonsurgical catheter treatment of atheromatous narrowing. *JAMA* 230:117–124, 1974
3. Dotter CT: Catheter techniques in diagnosing and treating femoral artery atherosclerosis. *Geriatrics* 29:93–95, 1974
4. Zeitler E, Schoop W, Zahnow E: The treatment of occlusive arterial disease by transluminal catheter angioplasty. *Radiology* 99:19–26, 1971
5. Zeitler E, Schmidtke J, Schoop W: Die perkutane Behandlung von arteriellen Durchblutungsstörungen der Extremitäten mit Katheter. *Vasa* 2:401–408, 1973
6. Wierny L, Plass R, Porstmann W: Long-term results in 100 consecutive patients treated by transluminal angioplasty. *Radiology* 112:543–548, 1974
7. van Andel GJ: *Percutaneous Transluminal Angioplasty. The Dotter Procedure*. Amsterdam, Excerpta Medica, 1976
8. Sobbe A, Martin M, Zeitler E: Besondere Aspekte der transluminalen Katheterrekanalisation nach Dotter. *Fortschr Geb Roentgenstr Nuklearmed Suppl* 252–253, 1973
9. Palayew MJ, Sedlezky I, Sigman HH, Scheiner NM: Occlusive peripheral arteriosclerosis: treatment by percutaneous transluminal recanalization—"The Dotter procedure." *Can Med Assoc J* 101:66–72, 1969
10. Berglund G, Bodvall B, Eldh J, Ydén S: Nytt behandlingsalternative vid artiell insufficiens i benen. *Lakartidningen* 66: 129–138, 1969
11. Brahme F, Swedenborg J, Tibell B: Evaluation of transluminal recanalization of the femoral artery. *Acta Chir Scand* 135:679–684, 1969
12. Grüntzig A: Die perkutane transluminale Rekanalisation chronischer Arterienverschlüsse mit einer neuen Dilatationstechnik. Baden-Baden, Gerhard Witzstrock, 1977. English translation by Wipfelder R, Kumpe D, 1979
13. Zeitler E, Grüntzig A, Shoop W: *Percutaneous Vascular Recanalization*. New York, Springer, 1979
14. Grüntzig A, Hopff H: Perkutane Rekanalisation chronischer arterieller Verschlüsse mit einem neuen Dilatationskatheter. Modifikation der Dotter-Technik. *Dtsch Med Wochenschr* 99:2502–2505, 1974
15. Porstmann W: Ein neuer Korsett-Ballonkatheter zur transluminalen Rekanalisation nach Dotter unter besonderer Berücksichtigung von Obliterationen an der Beckenarterien. *Radiol Diagn* (Berl) 14:239–244, 1973
16. Zeitler E: Die perkutane Rekanalisation arterieller Obliterationen mit Katheter nach Dotter (Dotter-Technik). *Dtsch Med Wochenschr* 97:1392–1394, 1972
17. Schmidtke J, Zeitler E, Schoop W: Langzeitergebnisse der perkutanen Katheterbehandlung (Dotter-Technik) bei femoropoplitealen Arterienverschlüssen im Stadium II. *Vasa* 4:210–226, 1975
18. DeWeese JA, Rob CG: Autogenous venous grafts ten years later. *Surgery* 82:775–784, 1977

Aneurysm Rupture Secondary to Transcatheter Embolization

JOHN R. LINA,[1] PAUL JAQUES, AND VALERIE MANDELL

False aneurysms of the pancreatic and peripancreatic arteries are a well recognized complication of chronic pancreatitis due to proteolytic enzymatic digestion of the arterial wall. These false aneurysms can be a source of life-threatening hemorrhage. Three cases are reported in which attempted embolizations of these bleeding aneurysms resulted in rupture into the gastrointestinal tract. Special precautions should be taken in such a procedure because of the inherent weakness of the aneurysmal wall.

Various catheter techniques to induce vascular occlusion are becoming more and more widely practiced in a number of clinical circumstances [1–3]. The most common indication has been hemorrhage, particularly from chronic peptic ulceration, but more recently bleeding from vaginal, rectal, prostatic, and pelvic sources has also been controlled by transcatheter embolization. In addition, occlusion of a wide variety of aneurysms has been attempted. Three patients are reported in whom transcatheter embolization of peripancreatic pseudoaneurysms was attempted, and in whom the procedure was complicated by rupture of the aneurysms into the gastrointestinal tract.

Case Reports

Case 1

A 37-year-old black woman with recurrent episodes of upper gastrointestinal tract bleeding was admitted with a hemoglobin level of 9.5 g/100 ml. The patient continued to deteriorate despite transfusions, and subsequently developed right upper quadrant pain with rebound tenderness. Surgery disclosed a dilated biliary tree and gallbladder filled with blood. After cholecystectomy, blood continued to drain from the T tube. Subsequent angiography revealed a false aneurysm of the dorsal pancreatic artery and extravasation of contrast material into the second part of the duodenum. Selective celiac arterial vasopressin infusion for 2 days resulted in clinical cessation of bleeding. The patient was returned to the angiographic suite for embolization of the feeding vessel to the aneurysm and selective dorsal pancreatic arteriography (fig. 1A). With the catheter in a wedged position, small pieces of Gelfoam were used to embolize the artery. After about six pieces were injected, contrast material flowed promptly into the lower common bile duct and then into the duodenum (fig. 1B), indicating rupture of the false aneurysm. The catheter was left in a wedged position in the artery in the hope a thrombosis would develop. After 5 days of no clinical deterioration or evidence for active hemorrhage, repeat angiography demonstrated occlusion of the dorsal pancreatic artery and nonfilling of the aneurysm.

Case 2

A 34-year-old black man with a long history of alcoholism and chronic pancreatitis was admitted after 3 days of hematemesis and abdominal pain. Examination revealed a tender abdomen and a 4 cm pulsatile right upper quadrant mass. Angiography showed false aneurysms of the gastroduodenal and splenic arteries. Surgical obliteration was attempted, but neither aneurysm was accessible, and the patient was returned to the

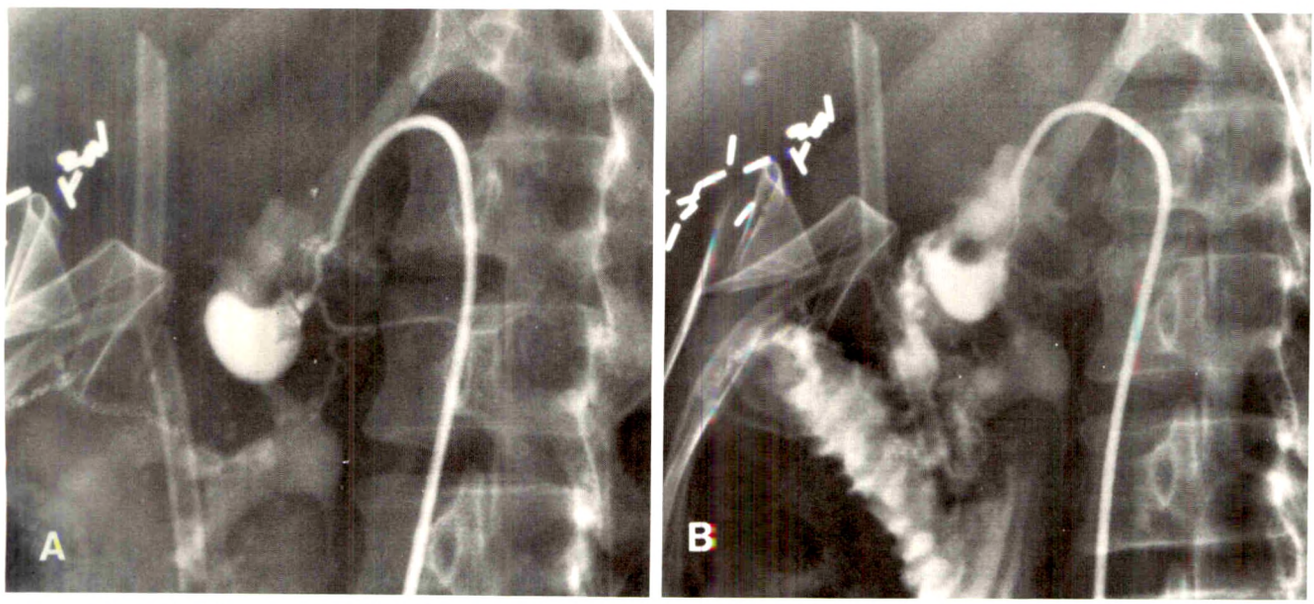


Fig. 1.—Case 1. **A**, False aneurysm of dorsal pancreatic artery. **B**, Immediately after embolization, aneurysm rupture and extravasation of contrast material into common bile duct and duodenum.

Received August 1, 1978; accepted after revision December 12, 1978.

[1] All authors: Department of Radiology, University of North Carolina, School of Medicine, Chapel Hill, North Carolina 27514. Address reprint requests to P. Jaques.

© 1979 American Roentgen Ray Society

0361-803X/79/1324-0553 $0.00

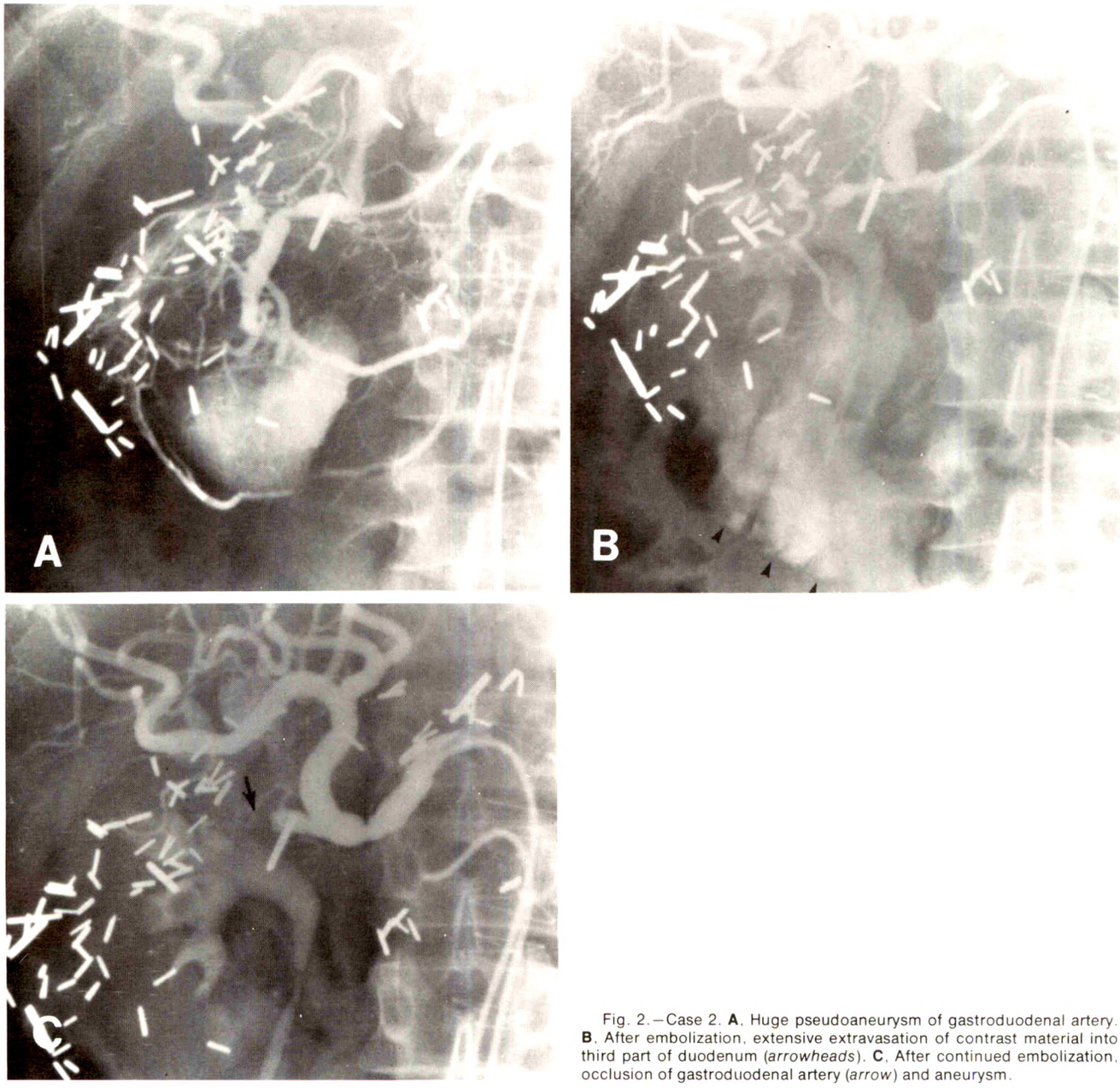


Fig. 2.—Case 2. **A**, Huge pseudoaneurysm of gastroduodenal artery. **B**, After embolization, extensive extravasation of contrast material into third part of duodenum (*arrowheads*). **C**, After continued embolization, occlusion of gastroduodenal artery (*arrow*) and aneurysm.

vascular suite for attempted occlusion of the gastroduodenal artery aneurysm (fig. 2A). During embolization, contrast material extravasated from the aneurysm into the third portion of the duodenum (fig. 2B), indicating rupture. Continued embolization resulted in occlusion of the gastroduodenal artery (fig. 2C). The patient recovered uneventfully.

Case 3

A 33 year-old chronic alcoholic with a long history of epigastric pain, recurrent pancreatitis, and peptic ulcer disease was evaluated for fluctuating jaundice and gastrointestinal blood loss. Exploratory celiotomy without prior angiography revealed an inflammatory mass in the head of the pancreas. In addition, the gallbladder was distended and contained numerous small black calculi. No active ulcer was found in the stomach or duodenum. Vagotomy, pyloroplasty, and T tube drainage of the common bile duct were performed. Postoperative intermittent bleeding from the common bile duct prompted angiography, which demonstrated a false aneurysm of an aberrant right hepatic artery arising from the superior mesenteric artery (fig. 3A). Embolization of the aneurysm with Gelfoam and autologous clot resulted in occlusion of the aberrant vessel and the aneurysm (fig. 3B). Follow-up angiography 1 week later demonstrated recanalization of the artery and reappearance of the aneurysm. A catheter was subselectively placed in a wedged position, and during attempts to reocclude the vessel the aneurysm ruptured into the biliary tree (fig. 3C). Hemobilia was noted through the T tube. Obliterative endoaneurysmorrhaphy and end-to-side choledochoduodenostomy were then performed to control hemorrhage. Surgery was successful and, after a stormy postoperative course complicated by septicemia, the patient was discharged.

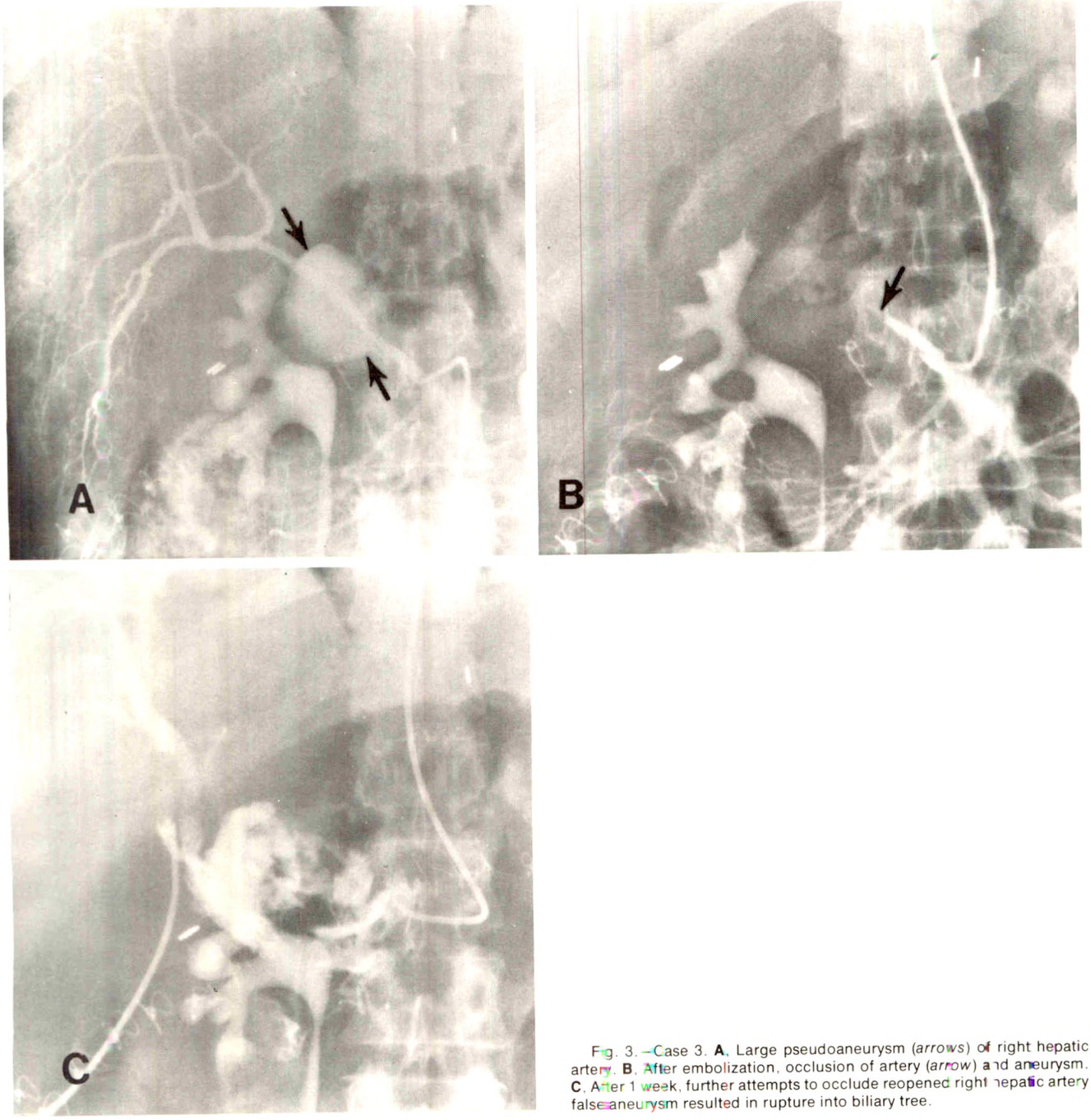


Fig. 3.—Case 3. **A**, Large pseudoaneurysm (*arrows*) of right hepatic artery. **B**, After embolization, occlusion of artery (*arrow*) and aneurysm. **C**, After 1 week, further attempts to occlude reopened right hepatic artery false aneurysm resulted in rupture into biliary tree.

Discussion

Arterial aneurysms in the peripancreatic vessels are often visualized during angiography in patients with a history of pancreatitis [3]. These aneurysms apparently evolve after pancreatitis with digestion of arterial walls by the pancreatic enzymes. Such aneurysms present strong evidence that the patient has had pancreatitis, and carcinoma can be virtually excluded [3–5]. Because walls of these pseudoaneurysms are thin and weak, they are prone to rupture with life-threatening hemorrhage [3, 6–9]. Since they are relatively inaccessible and are often associated with local inflammation secondary to continuing or previous pancreatitis, surgery is difficult and disappointing. Of our three cases, only one was ultimately surgically accessible.

Therefore, other methods, such as transcatheter arterial occlusion, may be attempted to prevent significant blood loss. However, these aneurysms are extremely fragile. In our three cases, this fragility was dramatically illustrated by their rupture into the gastrointestinal tract during embolization.

Routine embolic materials (Gelfoam, autologous clot, Ivalon sponge) used in these cases require a substantial

volume of fluid at a considerable pressure to facilitate their passage through the catheter. This exerts a very significant strain on the wall of the aneurysm, especially if the feeding vessel is small relative to catheter diameter. If the catheter is actually wedged in the vessel (cases 1 and 3), the whole of the injecting force is transmitted to the aneurysmal wall and rupture is likely. Therefore, on the basis of our experience and case material, we believe that these aneurysms require carefully controlled embolization, using minimal carrier fluid and only enough pressure to carry the embolus to the desired site. In this setting, other techniques of occlusion that do not require any carrier fluid may prove more appropriate. These include the Gianturco steel coil [10], transcatheter coagulation [11], detachable balloons [12], or polymerizing adhesives [13].

REFERENCES

1. Goldstein HM, Medellin H, Ben-Menachem Y, Wallace S: Transcatheter arterial embolization in the management of bleeding in the cancer patient. *Radiology* 115:603–608, 1975
2. Grace DM, Pitt DF, Gold RE: Vascular embolization and occlusion by angiographic techniques as an aid or alternative to operating. *Surg Gynecol Obstet* 143:469–481, 1976
3. White A, Baum S, Buranasiri S: Aneurysms secondary to pancreatitis. *AJR* 127:393–396, 1976
4. Boysen E, Tayler U: Vascular changes in chronic pancreatitis. *Acta Radiol [Diagn]* (Stockh) 12:34–48, 1972
5. Rentel SR, Redman HC, Joseph RR: Angiographic findings in pancreatitis. *AJR* 107:56–64, 1969
6. Schecter IM, Gordon HE, Passaro E: Massive hemorrhage of the celiac axis in pancreatitis. *Am J Surg* 128:301–305, 1974
7. Stanley JC, Freg CF, Miller TA, Lindenauer SM, Child CG: Major arterial hemorrhage. A complication of pancreatic pseudocysts and chronic pancreatitis. *Arch Surg* 111:435–440, 1976
8. Harris RD, Anderson JE, Coel MN: Aneurysms of the small pancreatic arteries. A cause of upper abdominal pain and intestinal bleeding. *Radiology* 15:17–20, 1975
9. Kadell BM, Riley FM: Major arterial involvement by pancreatic pseudocysts. *AJR* 99:632–636, 1967
10. Wallace S, Gianturco C, Anderson J, Goldstein HM, Davis JL, Bree RL: Therapeutic vascular occlusion using steel coil technique: clinical applications. *AJR* 127:381–387, 1976
11. Phillips JF, Robinson AE, Johnsrude IS, Jackson DC: Experimental closure of arteriovenous fistula by transcatheter electrocoagulation. *Radiology* 115:319–321, 1975
12. Kaufman SL, Strandberg JD, Barth KH, Gross GS, White RI: Therapeutic embolization with detachable silastic balloons. Long term effects in swine. Paper presented at the annual meeting of the Association of University Radiologists, San Antonio, May 1978
13. Goldman ML, Freeny PC, Tallman JM, Galambos JT, Bradley EL III, Salam A, Oen KT, Gordon IJ, Mennemeyer R: Transcatheter vascular occlusion therapy with isobutyl 2-cyanoacrylate (bucrylate) for control of massive upper-gastrointestinal bleeding. *Radiology* 129:41–49, 1978

Portal Vein Aneurysm

HUGH S. VINE,[1, 2] JOSEPH C. SEQUEIRA,[2] WARREN C. WIDRICH,[3] AND BARRY A. SACKS[1]

While there have been a few references to portal vein aneurysm in the world literature, this is the first report in United States radiologic literature. During a routine evaluation for fever in one patient, an ultrasound examination suggested this unusual entity at the junction of the splenic and superior mesenteric vein. It was later confirmed by angiography. Two other patients were being investigated angiographically for gastrointestinal bleeding when portal vein aneurysms were discovered. In contrast to the central location of the first patient's aneurysm, the latter two were more distal in the portal tree. The literature is reviewed and different etiologic hypotheses discussed.

Venous abnormalities of the portal system have been thoroughly investigated [1–4]. However, an aneurysm of the portal vein is uncommon. While investigating a patient (case 1) for a fever of unknown origin, abdominal ultrasound demonstrated a large anechoic area at the junction of the superior mesenteric and splenic veins. Subsequent angiography confirmed the initial impression that this represented a localized dilated venous structure. As this unusual entity was being researched, two similar cases were made known to us.

Barzilai and Kleckner [5] were apparently the first to report such an entity. They described a patient who developed postnecrotic cirrhosis, thrombosis of the right portal vein, and an aneurysm proximal to the thrombus with subsequent rupture into the biliary system. Seven other cases have been reported since, but none have used ultrasound evaluation [6–11]. Three more cases of portal vein aneurysm are reported here.

Case Reports

Case 1

A 50-year-old woman was admitted to the Peter Bent Brigham Hospital for evaluation of fever of unknown origin. Over the previous 10 years, several episodes of hemolytic anemia associated with elevated cold agglutinins had been successfully treated with steroids. Because of the fever and possible abdominal abscess, ultrasound was performed with both real-time phased-array scanning and a commercially available gray scale unit using a standard 2.25 MHz internally focused transducer. A 3.0 cm well circumscribed anechoic structure was noted at the junction of the splenic and portal veins. This was believed to most likely represent a portal vein dilatation or aneurysm (fig. 1A), and the phased array unit seemed to confirm this impression by demonstrating continuation of this structure with the intrahepatic portal venous radicles. Because this rare diagnosis was still uncertain, celiac arteriography was performed. During the arterial phase (fig. 1B), there was bowing and displacement of the gastroduodenal artery laterally, as well as minimal irregularity of the intrahepatic radicles. In the venous phase (fig. 1C), a large portal vein varix was seen at the confluence of the splenic and superior mesenteric veins. In addition, there was slight reflux of contrast material down the superior mesenteric vein. A ^{99m}Tc sulfur colloid liver scan demonstrated moderately heterogeneous uptake consistent with mild diffuse hepatic parenchymal disease. No liver biopsy was done.

Case 2

A 57-year-old man was admitted to the Boston Veterans Administration Hospital. He was a known chronic alcoholic with esophageal varices and several past episodes of upper gastrointestinal bleeding.

He first underwent a side-to-side splenorenal shunt and liver biopsy, which showed postnecrotic cirrhosis. Postoperatively, he did well for 12 days, when he developed massive upper gastrointestinal bleeding. Splenic arteriography and left renal venography demonstrated that the shunt had occluded. The venous phase of superior mesenteric arteriography showed a patent paraumbilical vein apparently draining from the right portal vein (fig. 2). A 3.5 cm venous aneurysmal dilatation was shown at the anastomosis of the portal vein branch and the paraumbilical vein. The bleeding was controlled with vasopressin (Pitressin) infusion. The venous hum of the Cruveilhier-Baumgarten syndrome was heard over the umbilicus. When the Pitressin was infused, the hum stopped, but when the Pitressin was discontinued, the hum returned.

Almost 7 weeks after initial surgery, he underwent an end-to-end portacaval shunt. No note was made of intraoperative visualization of the aneurysm. Postoperatively, he went into metabolic acidosis and died 11 days later. No autopsy was obtained.

Case 3

An 87-year-old white woman was transferred to Beth Israel Hospital with abdominal pain and hematemesis. She had a history of peptic ulcer disease (after vagotomy in 1962). During the night before admission, she developed sharp epigastric pain and vomited bright red blood. On admission, hematocrit was 29 and nasogastric lavage revealed bright red blood. Endoscopy showed an active bleeding site at the gastroesophageal region. Because of continued bleeding, the patient was referred for angiography. Celiac and superior mesenteric arteriography failed to demonstrate an active bleeding site. The parenchymal phase of hepatic arteriography showed an inhomogenous pattern consistent with diffuse hepatic disease (etiology unknown); the venous phase showed a large round intrahepatic collection of contrast believed to represent a portal vein aneurysm (fig. 3). Active bleeding stopped during arteriography, and hematocrit and metabolic status returned to normal. After several days of medical therapy, an upper gastrointestinal examination docu-

Received October 31, 1977; accepted after revision January 3, 1979.

[1]Department of Radiology, Beth Israel Hospital, Harvard Medical School, 330 Brookline Avenue, Boston, Massachusetts 02215. Address reprint requests to H. S. Vine.

[2]Department of Radiology, Peter Bent Brigham Hospital, Harvard Medical School, Boston, Massachusetts 02115.

[3]Department of Radiology, Veterans Administration Hospital, Tufts University School of Medicine, Boston, Massachusetts 02130.

© 1979 American Roentgen Ray Society

0361–803X/79/1324–0557 $0.00

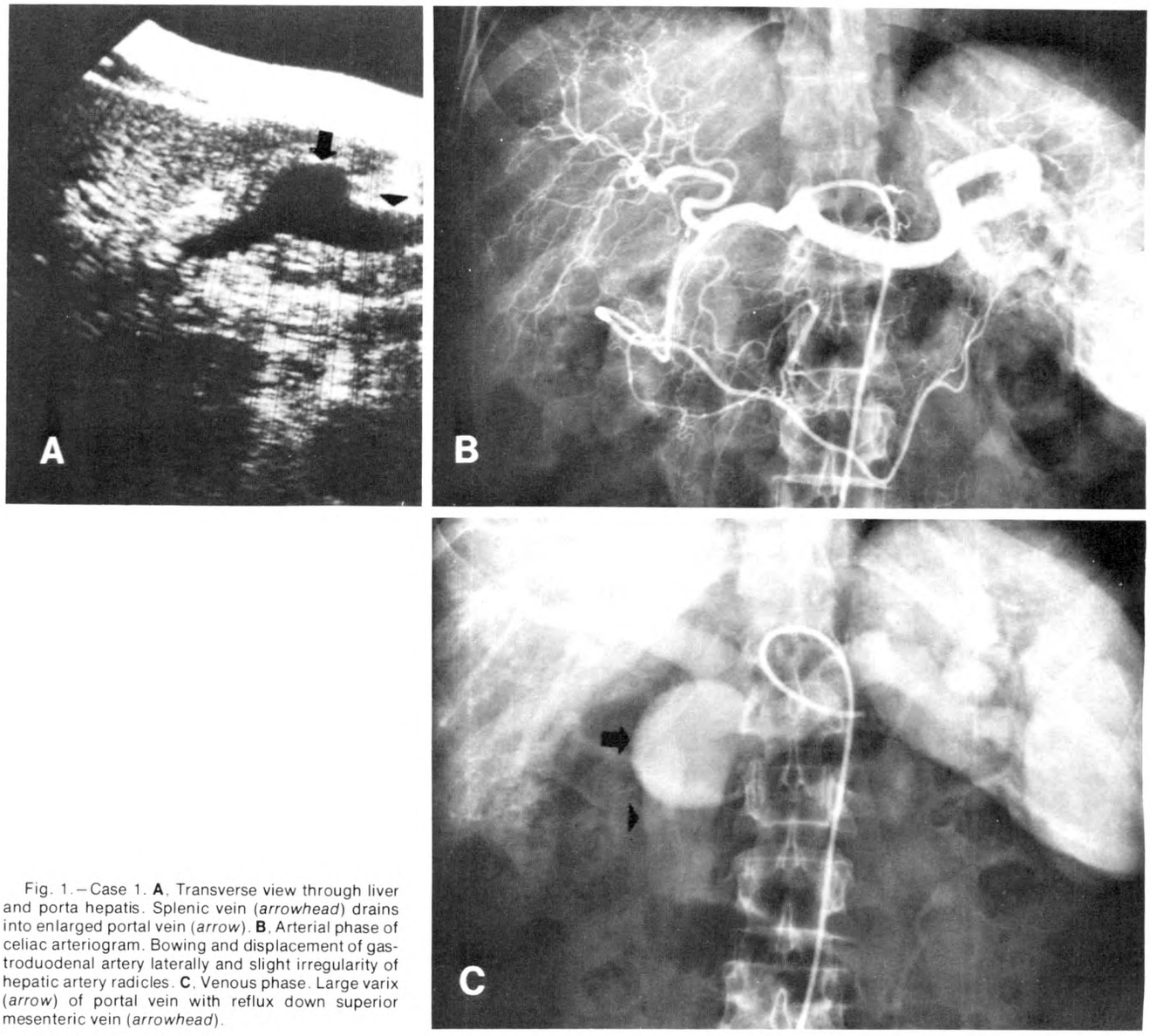


Fig. 1.—Case 1. **A**, Transverse view through liver and porta hepatis. Splenic vein (*arrowhead*) drains into enlarged portal vein (*arrow*). **B**, Arterial phase of celiac arteriogram. Bowing and displacement of gastroduodenal artery laterally and slight irregularity of hepatic artery radicles. **C**, Venous phase. Large varix (*arrow*) of portal vein with reflux down superior mesenteric vein (*arrowhead*).

mented a greater curvature gastric ulcer. She was discharged on a conservative regimen.

Discussion

The portal venous system develops from the vitelline and umbilical veins that drain the primitive intestine. Various congenital abnormalities of the portal vein have been described. The portal vein may be duplicate [2], receive anomalous pulmonary venous drainage [2, 3], become atretic [2], develop cavernous transformation [12], assume an abnormally ventral position [1], or manifest other anomalies of lesser radiographic importance.

The size of the portal vein is somewhat variable. In 92 dissections, Douglass et al. [13] found that the diameter of portal veins in patients without cirrhosis or portal hypertension was 0.64–1.21 cm (average, 0.89 cm). Purcell et al. [14] found the average diameter to be 1.09 cm. Reynolds [15] noted that although the average diameter is 1.2 cm, larger portal veins are found in cirrhotics. Doust and Pearce [16] ultrasonically studied both normal and cirrhotic patients, and the maximum anteroposterior diameter did not exceed 1.5 cm in normals and 1.9 cm in cirrhotics.

Aneurysms of the portal vein may occur either proximally at the junction of the superior mesenteric vein and splenic vein or more distally in the portal vein radicles. These aneurysms are thought to have two main etiologies: (1) congenital or (2) acquired secondary to portal hypertension. Liebowitz and Rousselot [9] reported a case of agnogenic myeloid metaplasia with a portal vein aneurysm, but without evidence for portal hypertension because of normal intrasplenic pulp pressure and absence of collateral venous circulation in the splenoportogram. Thomas [8] also believed that his two cases of

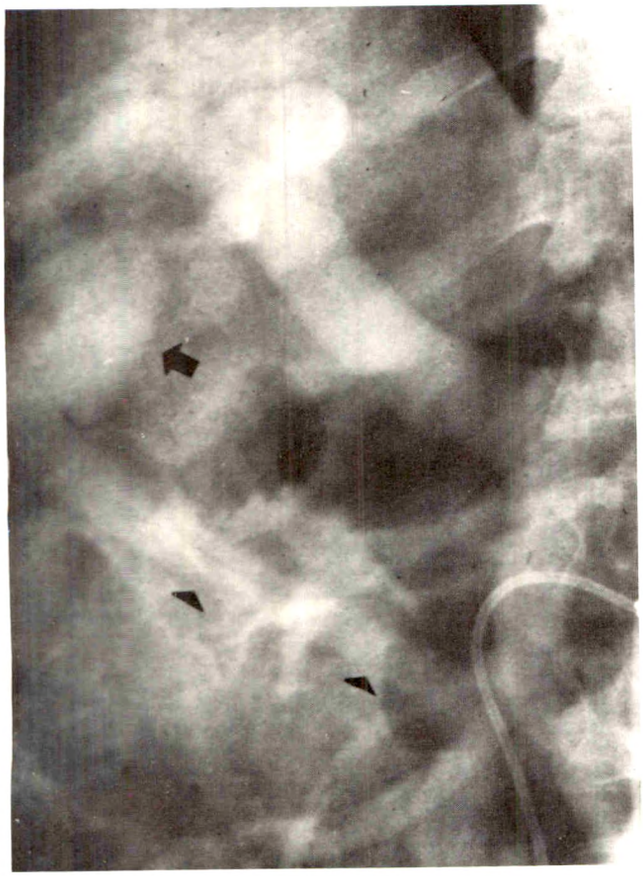


Fig. 2.—Case 2. Venous phase of superior mesenteric arteriogram. Portal vein aneurysm (*arrow*) in right lobe of liver at junction of portal vein branch and draining paraumbilical vein (*arrowheads*).

portal vein aneurysm were either hereditary or developmental because of the absence of gross intra- or extrahepatic obstruction. Thus, he postulated the portal hypertension was secondary to venous aneurysms. In contrast, Barzilai and Kleckner [5] believed that the hemocholecyst in their patient after rupture of a portal vein aneurysm resulted from portal hypertension secondary to postnecrotic cirrhosis. Leonsins and Siew [6] likewise believed that in their patient with Banti's syndrome and portal vein aneurysm, the most likely progression was cirrhosis causing portal hypertension, which led to esophageal variceal rupture, splenomegaly, and portal vein aneurysmal dilatation.

In our three cases, only one (case 2) had unequivocal evidence for hepatocellular disease. However, in the other two cases, the liver scintigram (case 1) and angiograms (cases 1 and 3) demonstrated evidence for hepatic parenchymal abnormality. Thus, as with all the cases in the literature, liver parenchymal abnormalities were associated with this unusual entity, but their sequence is difficult to ascertain. As discussed above, some authors believe that the portal vein aneurysm is secondary to portal hypertension. Wenz et al. [10] presented the most convincing evidence for a congenital or developmental abnormality. Their 6-year-old patient demonstrated portal hypertension, hepatofugal flow, and varices with biopsy-proven normal hepatic parenchyma. Unfortunately, our three cases do not clarify the etiologic issue.

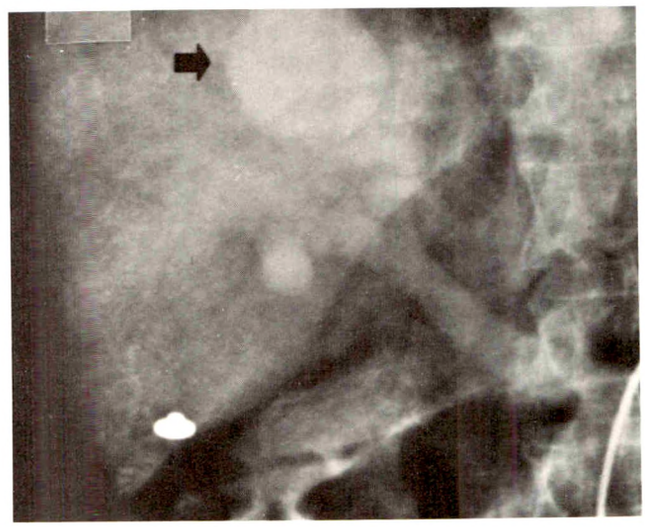


Fig. 3.—Case 3. Venous phase of superior mesenteric angiogram. Large portal vein aneurysm (*arrow*) lies directly beneath right hemidiaphragm.

Case 1 is unique because it is the only reported case with an ultrasonic image of the portal vein aneurysm. This well defined anechoic structure within the liver could be mistaken for a hepatic cyst if the connection with portal venous system were not appreciated. A high-speed scanner makes this characteristic more easily apparent. Once the vascular nature of this lesion is understood, the ultrasonic picture is essentially pathognomonic. Previously reported cases were evaluated angiographically. Most of the cases in the literature were discovered because of investigation for gastrointestinal bleeding. Several of these patients with both portal hypertension and portal vein aneurysms underwent portacaval shunts with excellent results [7, 8, 11]. Two other patients died from rupture of their aneurysm. One of Thomas's [8] patients bled into his lesser sac and retroperitoneum. The patient of Barzilai and Kleckner [5] ruptured into the biliary system with a resultant hemocholecyst. Thus, although the severity of these lesions seems apparent, these patients were all studied for acute gastrointestinal hemorrhage. It is not known what the significance is in patients (as in our case 1) who have neither bled nor have severe portal hypertension.

With the more frequent use of noninvasive studies such as ultrasound and computed tomography, both the incidence of portal vein aneurysms and their prognosis may become established. The etiology of these aneurysms is still unclear, but may be elucidated by serial studies.

ACKNOWLEDGMENT

We thank Deirdre Sullivan for help in preparing the manuscript.

REFERENCES

1. Harrell G: Ventral portal vein. *AJR* 121:369–373, 1974
2. Marks C: Surgical implications of portal system malformation. *Ann R Coll Surg Engl* 55:299–306, 1974
3. Olberg S, Olsson R: Congenital absence of portal venous system in a 50 year old woman. *Acta Med Scand* 196:343–345, 1974
4. Samanek M, Tuma S, Benesova D, Povysilova V, Prazsky F, Capova E: Atresia of right pulmonary veins and anomalous left pulmonary venous drainage into portal circulation. *Thorax* 29:446–450, 1974
5. Barzilai R, Kleckner MS: Hemocholecyst following ruptured aneurysm or portal vein. *Arch Surg* 72:725–727, 1956
6. Leonsins AJ, Siew S: Fusiform aneurysmal dilatation of the portal vein. *Postgrad Med J* 36:570–574, 1960
7. Hermann RE, Shafer WH: Aneurysm of the portal vein and portal hypertension. *Ann Surg* 162:1101–1104, 1965
8. Thomas TV: Aneurysm of the portal vein: report of two cases, one resulting in thrombosis and spontaneous rupture. *Surgery* 61:550–555, 1967
9. Liebowitz HR, Rousselot LM: Saccular aneurysm of portal vein with agnogenic myeloid metaplasia. *NY State J Med* 67:1443–1447, 1967
10. Wenz W, Beckenbach H, Daum R: Die kindliche Pfortader bei Erkankugen der Oberbauchorgane. *Eur J Pediatr* 9:354–362, 1971
11. Duhmke VE: Aneurysma der vena portae. *ROEFO* 125:474–475, 1975
12. Klemperer P: Cavernomatous transformation of the portal vein. *Arch Pathol Lab Med* 6:353–377, 1928
13. Douglass BE, Baggenstoss AA, Hollingshead WH: The anatomy of the portal vein and its tributaries. *Surg Gynecol Obstet* 91:562–576, 1950
14. Purcell HK, Connor JJ, Alexander WF, Scully NM: Observations on the extra-hepatic major radicles of the portal systems. *Arch Surg* 62:670–677, 1951
15. Reynolds TB: Portal hypertension, in *Diseases of the Liver*, edited by Schiff L, Philadelphia, Lippincott, 1975, p 330
16. Doust B, Pearce J: Gray-scale ultrasonic properties of the normal and inflamed pancreas. *Radiology* 120:653–657, 1976

Circumaortic Venous Ring: Incidence and Significance

CARL F. BECKMANN[1] AND HERBERT L. ABRAMS[1]

A left circumaortic renal vein was found in 11% of 74 left renal venograms, an incidence similar to that at autopsy. Cavography proved to be an unsatisfactory method of demonstrating the renal veins. Prior knowledge of a venous ring is important when blood samples from the adrenal or renal veins are to be collected. When caval interruption is planned, a circumaortic venous ring may provide a fully developed collateral pathway immediately after surgery if the procedure is planned without awareness of its presence.

The circumaortic left renal vein is a relatively common venous variation, with an incidence at autopsy of about 7% [1–3]. In this anomaly, one renal vein passes ventral to the aorta in the usual location and the other runs caudally and dorsal to the aorta to enter the inferior vena cava in the lower lumbar region. Although the size of the components varies, one study [1] has shown that the preaortic and retroaortic components of the ring are usually of equal size.

A venous ring is normally present in the 8 week embryo; later the retroaortic segment of the venous ring, together with the dorsal vein, becomes obliterated, leaving a single left preaortic renal vein as the normal anatomic arrangement [4].

Venous sampling of adrenal and renal veins for adrenal hormone and renin determinations are now routine and important diagnostic procedures; interruption of the inferior vena cava is widely used to prevent recurrent pulmonary embolism. Because a circumaortic venous ring may interfere with the successful completion of both of these procedures, an analysis of its incidence and characteristics as visualized during life was undertaken.

Materials and Methods

A series of 74 consecutive left renal venograms was analyzed. These did not include patients with occlusion of the renal vein by thrombus or with renal vein invasion by carcinoma. In all cases, precurved radiopaque renal vein catheters were inserted through the femoral vein into the inferior vena cava. In shaping the catheter, the tip was bent to about 130°, the length of the bent tip on the right being 5 cm and on the left, 10 cm. If both renal veins were catheterized, the right renal vein catheter was also used for the left side, with the aid of a guidance system. In some cases, a preshaped abdominal-visceral catheter combined with a controllable guide wire or a pigtail catheter with the aid of a Cook deflector was used. We found it useful to have two side-holes within 1 cm of the catheter tip. Under fluoroscopic guidance, the catheter tip was located in the peripheral segment of the main renal vein within the renal hilum, so as to prevent dislodgement during injection and to afford maximal opportunity for retrograde venous filling. In most examinations percutaneous renal artery catheterization was performed and the renal blood flow was deliberately slowed by injecting 6–10 μg epinephrine into the renal artery [5].

To determine how often a circumaortic venous ring can be diagnosed on cavography, 53 consecutive inferior vena cavograms were analyzed. A pigtail catheter was inserted through the femoral vein, and the catheter tip was placed either into the lower inferior vena cava just above the confluence of the iliac veins, or into a common iliac vein just below the origin of the vena cava. In rare instances, the patient was asked to perform a Valsalva maneuver during the examination.

Results

A circumaortic venous ring was found in eight of 74 renal venograms (11%). The preaortic limb, 11–22 mm in diameter (average, 16.25 mm), was always larger than the retroaortic vein and entered the inferior vena cava in the typical location in the region of L1–L2, most commonly at the level of the lower one-third of L1. When the adrenal veins were opacified, they were observed to have entered the preaortic portion (fig. 1). In two cases the

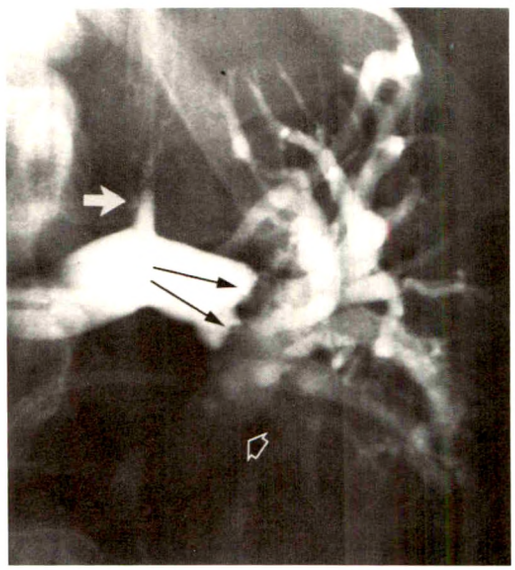


Fig. 1.—Patient with left circumaortic venous ring. Both preaortic and retroaortic renal veins (*open arrow*) arise in renal hilum. Latter seems to drain lower pole preferentially. Adrenal vein (*white arrow*) joins preaortic renal vein in typical location. Note valve of preaortic vein (*black arrows*).

Received September 15, 1978; accepted after revision December 28, 1978.

Presented at the annual meeting of the American Roentgen Ray Society, Toronto, March 1979.

This work was supported in part by Cine Training grant no. 5R01HL20895 and CV Training grant no. 5T01HL05832 from the National Institutes of Health.

[1]Department of Radiology, Harvard Medical School, Peter Bent Brigham Hospital, 25 Shattuck Street, Boston, Massachusetts 02115. Address reprint requests to C. F. Beckmann.

© 1979 American Roentgen Ray Society

0361–803X/79/1324–0561 $0.00

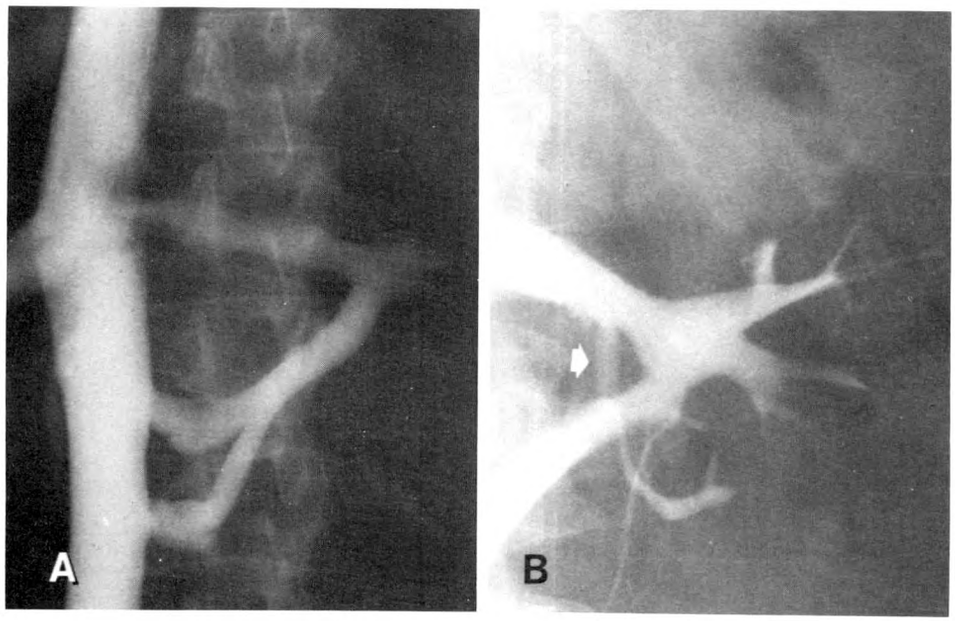


Fig. 2.—Patient examined for suspicion of renal vein thrombosis. **A**, Inferior vena cavogram. Circumaortic venous ring. Retroaortic vein splits before entering inferior vena cava. **B**, Renal venogram. Preaortic and retroaortic veins arise from main renal vein trunk. Left gonadal vein (*arrow*) drains into preaortic vein.

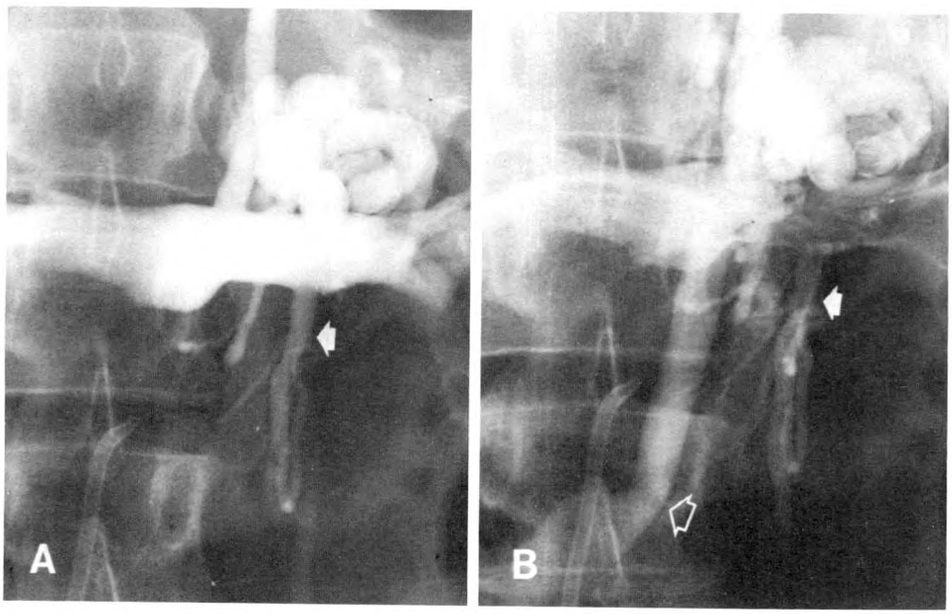


Fig. 3.—Asymptomatic patient underwent renal venography during workup as potential renal donor. **A**, Early phase. Filling of renal veins accompanied by opacification of hemiazygos vein and network of varicose veins adjacent to renal pelvis. Proximal ovarian vein (*arrow*) is visible. **B**, Late phase. Typical retroaortic vein (*open arrow*) now apparent. Ovarian vein (*closed arrow*) enters unsplit main renal vein trunk.

gonadal vein drained into the preaortic renal vein (fig. 2B) and in four into the undivided main renal vein trunk (fig. 3).

In six of the eight cases the retroaortic limb arose from an undivided main renal vein trunk within 2 cm of the renal hilum (figs. 2 and 3). The bifurcation occurred within the renal hilum (figs. 1, 4, and 5) or at the confluence of lobar renal veins on two occasions, and the retroaortic vein seemed to drain parts of the lower pole preferentially. The retroaortic vein, 4–13 mm in greatest diameter (average, 7.75 mm), entered the inferior vena cava at the level of L2 and L3 (average, middle one-third of L3). In one instance the retroaortic portion split before entering the vena cava (fig. 2A). In four instances retroperitoneal branches (lumbar veins, ascending lumbar vein) were seen entering the retroaortic vein (figs. 4 and 6).

In addition to the eight patients with a left circumaortic venous ring, one patient exhibited a single retroaortic renal vein entering the inferior vena cava in the region of L3 (fig. 7). This vein was 18 mm in greatest diameter.

Analysis of 53 inferior vena cavograms revealed partial opacification of the left main renal vein in only six patients (11%). In two of these a circumaortic venous ring was visible on cavography and subsequently confirmed on renal venography. The site of the caval orifices

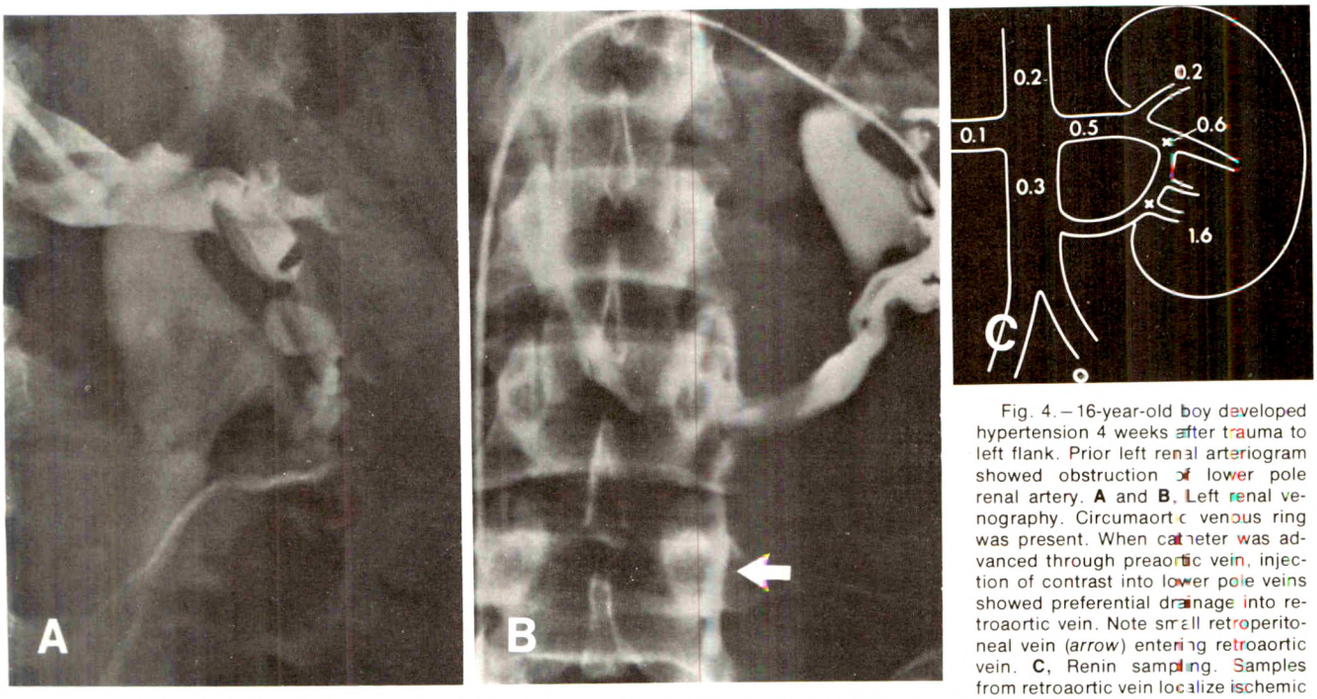


Fig. 4.—16-year-old boy developed hypertension 4 weeks after trauma to left flank. Prior left renal arteriogram showed obstruction of lower pole renal artery. **A** and **B**, Left renal venography. Circumaortic venous ring was present. When catheter was advanced through preaortic vein, injection of contrast into lower pole veins showed preferential drainage into retroaortic vein. Note small retroperitoneal vein (*arrow*) entering retroaortic vein. **C**, Renin sampling. Samples from retroaortic vein localize ischemic focus to lower pole, whereas those from preaortic vein are only mildly elevated. (Courtesy of Dr. Christos Athanasoulis.)

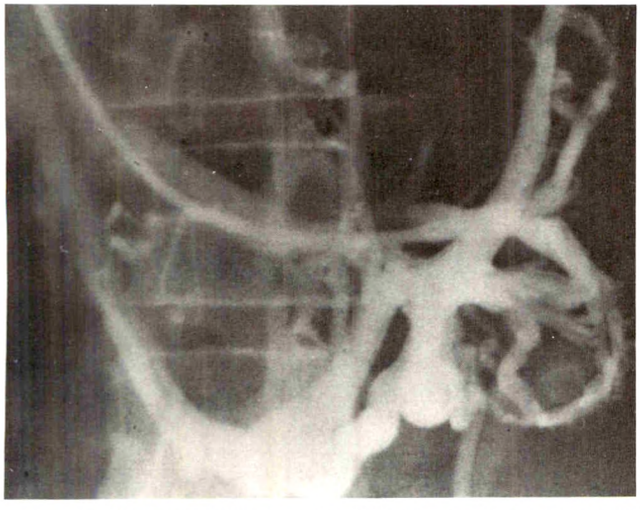


Fig. 5.—Circumaortic venous ring arising in renal hilum. Veins of lower pole drain preferentially into retroaortic vein.

of the renal veins usually was visualized mainly as reflected by the dilution defects of the inflow of nonopaque renal blood. A double inferior vena cava was seen in one patient.

In one patient whose vena cava had been ligated for recurrent pulmonary embolism, a circumaortic ring was found, illustrating its potential role as an alternate pathway for pulmonary embolism (fig. 7). Because of the potential importance of this variant of venous anatomy in pulmonary embolism, this case warrants a detailed report.

Case Report

A 41-year-old woman was admitted for evaluation of recurring episodes of dyspnea and chest pain. She had previously undergone caval ligation in an outside hospital for recurrent pulmonary embolism 2 months before her present admission. After operation, she had persistent thrombophlebitis in her left leg and persistent respiratory symptoms.

Physical examination was normal except for popliteal fossa and calf tenderness with a positive Homan's sign. Electrocardiography and chest radiography were unremarkable. A perfusion lung scan was highly suggestive of recurrent pulmonary embolism. Iliac vein injection demonstrated occlusion of both common iliac veins with collateral drainage via left ascending lumbar and paravertebral veins. The latter filled the lower inferior vena cava which appeared to be totally occluded in the region of L3 at the previous ligature site. Just distal to the vena cava ligature, there was filling of a 1-cm-thick vein which arose from the lower vena cava and after fusion with a dilated ascending lumbar vein in turn opacified the left renal vein (fig. 6). The venous anatomy was typical for a left circumaortic venous ring.

Because of the strong suspicion that the left circumaortic venous ring and the dilated ascending lumbar vein served as a collateral pathway for recurrent emboli from the lower extremity and inferior vena cava, it was felt advisable to ligate these veins, and surgery was therefore performed, which verified the venous ring. During 12 month follow-up the patient had no recurrent episodes of pulmonary embolism.

Discussion

Multiple renal veins are more common on the right than on the left side, occurring in 15% of autopsies [2]; typically there is one larger right renal vein and from one

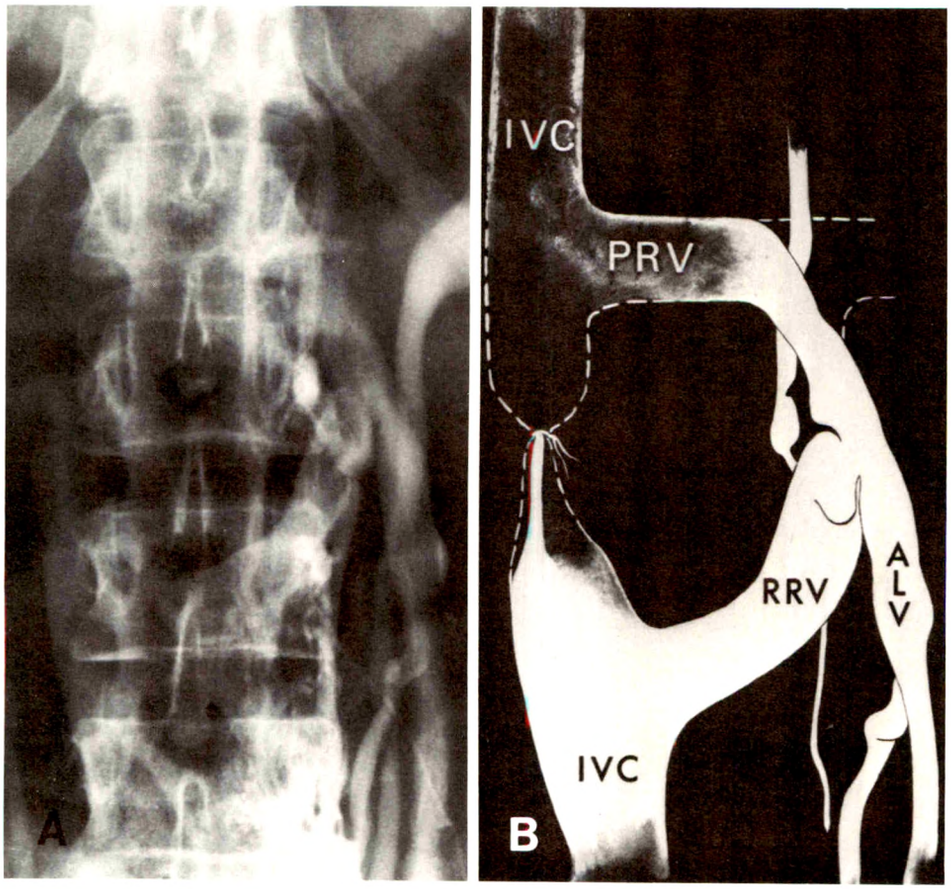


Fig. 6.—Caval ligation in patient with circumaortic venous ring. **A**, Inferior vena cavogram after injection of contrast material into both iliac veins. **B**, Explanation. Inferior vena cava (IVC) is occluded in region of L2. Opacified blood drains via retroaortic renal vein (RRV) into preaortic renal vein (PRV). ALV = ascending lumbar vein.

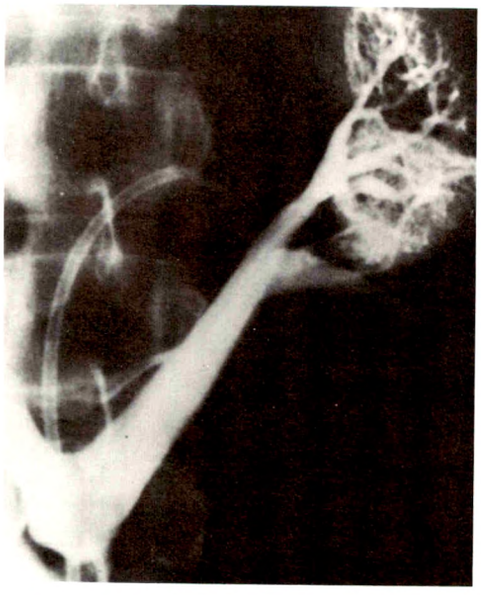


Fig. 7.—Solitary retroaortic renal vein entering inferior vena cava in region of L3. Prior knowledge of this variation is important if cava is to be ligated.

to three smaller accessory renal veins, which communicate in the renal hilum but leave it separately. In contrast, the two renal veins which constitute a circumaortic venous ring arise in most instances (75%) from a solitary main renal vein trunk close to the renal hilum. A circumaortic venous ring was readily diagnosed by selective renal venography in as high a percentage of cases as is found at autopsy. In contrast, cavography was an unsatisfactory method of demonstrating the renal veins. This is in agreement with the experience of other authors [6, 7].

Prior knowledge of a circumaortic venous ring is important when blood samples from the adrenal or renal veins are to be collected, or when caval interruption is planned. The adrenal vein always drains into the preaortic vein, and the gonadal vein can drain either into the preaortic vein or the undivided main renal vein trunk, rather than into the retroaortic vein. Therefore, in a patient with a circumaortic venous ring, the preaortic vein should be entered for venous sampling procedures. If a solitary retroaortic vein is present, the adrenal vein may drain either into the prehilar portion of this renal vein, or into the inferior vena cava directly [4].

The retroaortic vein may preferentially drain the lower pole of the kidney, a variation found in two of our eight patients. Therefore, if the ischemic focus is in the lower pole of the kidney, and renin samples are to be obtained, it is essential to catheterize this vein as well as the preaortic vein (fig. 4).

Of greatest importance is the circumaortic venous ring as a potential collateral pathway for recurrent pulmonary emboli from the lower extremity or pelvis after the cava has been interrupted (fig. 6). According to different authors [8, 9] there is a failure rate of up to 50%

associated with caval interruption. Common and well described important collaterals after caval interruption are the paravertebral, gonadal, and ascending lumbar veins [10], which dilate gradually until they are large enough to allow the passage of larger clots [11]. However, most of these collaterals either arise or terminate in a network of veins capable of filtering out a sizable clot. In contrast, the anatomic variation of a left circumaortic venous ring constitutes an instantaneous collateral pathway immediately after caval interruption. As our data show, the diameters of both the retroaortic and preaortic veins are large enough to allow the passage of even large emboli; in most instances (75%) the two veins communicate in a single main renal vein, rather than in a network of veins that would be capable of filtering out an embolus. Therefore, a careful search for this frequent anatomic variation must be made by renal venography before operation. If a circumaortic venous ring is found, the caval interruption should be performed at a level below the orifice of the retroaortic renal vein in the lower lumbar region.

REFERENCES

1. Davis CJ, Lundberg GD: Retroaortic left renal vein. *Am J Clin Pathol* 50:700–703, 1968
2. Pick JW, Anson FJ: The renal vascular pedicle. *J Urol* 44: 411–434, 1940
3. Reis RH, Esenther G: Variations in the pattern of renal vessels and their relation to the type of posterior vena cava in man. *Am J Anat* 104:295–318, 1959
4. Field S, Saxton H: Venous anomalies complicating left adrenal catheterization. *Br. J Radiol* 47:219–225, 1974
5. Olin TB, Reuter SR: A pharmakoangiographic method for improving nephrophlebography. *Radiology* 85:1036–1042, 1965
6. Abrams HL: Renal venography, in *Angiography*, 2d ed, edited by Abrams HL, Boston, Little, Brown, 1971, pp 915–925
7. Kahn PC: Selective venography of the branches, in *Venography of the Inferior Vena Cava and its Branches*, edited by Ferris EJ, Hipona FA, Kahn PC, Philips E, Shapiro JH, Baltimore, Williams & Wilkins, 1969, pp 154–224
8. Krause RJ, Cranley JJ, Hallaba MA, Strasser ES Hafner CD: Caval ligation in thromboembolic disease. *Arch Surg* 87: 184–192, 1963
9. Piccone VA, Vital E, Yarnoz M, Glass P, LeVeen HH: The late results of caval ligation. *Surgery* 68:980–998, 1970
10. Ferris EJ, Vittemberger FJ, Byrne JJ, Nabseth DC, Shapiro JH: The inferior vena cava after ligation and plication. *Radiology* 89:1–10, 1967
11. Gurewich V, Thomas DP, Robinov KR: Pulmonary embolism after ligation of the inferior vena cava. *N Engl J Med* 274: 1350–1354, 1966

Esophagitis Induced by Combined Radiation and Adriamycin

DANIELLE K. B. BOAL,[1] PETER E. NEWBURGER,[2] AND RITA LITTLEWOOD TEELE[1]

With the increasing use of combined chemotherapy and radiotherapy in the treatment of certain types of malignancy, a clinically distinct type of esophagitis has been recognized as an undesirable side effect. It occurs with low doses (less than 2,000 rad) of mediastinal radiation in patients who simultaneously or sequentially receive either adriamycin or actinomycin D. Characteristic of this entity is "recall": recurrent episodes of esophagitis with each course of chemotherapy. The radiographic findings are nonspecific, ranging from subtle alterations in motility to severe damage with irreversible stricture formation. The primary differential diagnostic considerations are infectious processes. The radiographic spectrum, clinical aspects, and differential diagnoses in five patients are discussed.

With increasing use of both chemotherapy and radiotherapy in the treatment of certain types of malignancy, a clinically distinct type of esophagitis has been recognized as an undesirable side effect of such treatment [1]. It occurs with low doses (less than 2,000 rad) of mediastinal radiation in patients who simultaneously or sequentially receive either adriamycin or actinomycin D [1–3]. Esophagitis occurring in the patient with a malignancy usually is attributed to opportunistic infection, particularly *Candida* and, rarely, *Herpesvirus hominis* (herpes simplex) [4–7]. This report describes the radiographic appearance of the esophagus in five patients with esophagitis due to radiotherapy in combination with adriamycin.

Newburger et al. [1] reviewed the records of patients undergoing combined radiotherapy and chemotherapy for non-Hodgkin's lymphoma, metastatic osteogenic sarcoma, and acute lymphocytic leukemia. Of the 21 patients treated with adriamycin and radiation during a 3 year period, seven developed esophagitis; 12 patients did not and two patients were not included because of oral mucositis so severe that esophageal disease could not be evaluated. The treatment and clinical course of the seven patients with esophagitis were discussed in detail in that report. The esophagitis in these seven patients was not of an infectious etiology as determined by currently available culture and serologic techniques.

We present the radiographic appearance of the esophagitis in five of those patients. The other two patients are excluded because one had no studies with barium and the other had received concurrent treatment with nystatin for oral moniliasis. Of the five patients, four were male and one was female; age range was 12–21 years. Two patients had non-Hodgkin's lymphoma, one, acute lymphocytic leukemia; and two, metastatic osteogenic sarcoma. Radiation to the esophagus (calculated for the midplane of the mediastinum) ranged from 500 to 2,500 rad. The dose of adriamycin varied between 30 and 86 mg/m^2 body surface area in the initial treatment of each patient with a 40%–50% reduction in dose for subsequent courses.

Case Reports

Case 1

F. F., a 21-year-old man with acute lymphocytic leukemia in relapse, developed three episodes of esophagitis during the course of chemotherapy for remission reinduction and radiation for sternal bone pain. All episodes were characterized by dysphagia and substernal chest pain. The first episode developed 10 days after treatment with adriamycin and 11 days after the initiation of radiation therapy. Symptoms lasted 28 days and necessitated hospitalization for total parenteral nutrition. Barium esophagography was performed four times during the first episode (fig. 1A). The findings at that time included a dilated esophagus with thickened folds and decreased peristalsis.

Two subsequent courses of adriamycin resulted in recall esophagitis. The first occurred 7 days after receiving one-half the previous dose of adriamycin; the symptoms lasted 7 days. The patient did not require hospitalization. One month later, the patient received the same (half) dose of adriamycin; symptoms of esophagitis developed 10 days later and persisted 35 days. Barium esophagography (fig. 1B) 16 days after the onset of symptoms revealed a narrow esophagus with stricture, irregular mucosal pattern, and absent peristalsis. Endoscopy the next day confirmed the radiographic findings. It is significant that *Candida* was not present in culture and biopsy material obtained at the time of endoscopy. The patient required a feeding gastrostomy.

Follow-up examination 2 months later (fig. 1C) revealed significant progression and stricture formation over the distal 9 cm of the esophagus. There had been no additional radiation or chemotherapy in the interval. At the time of his death 14 months later, the patient was just beginning to tolerate solid food by mouth. Postmortem examination revealed a stricture 8 mm in diameter replacing the epithelium and the inner muscular coats.

Case 2

J. P., a 13-year-old boy with thoracic epidural non-Hodgkin's lymphoma, developed dysphagia and substernal pain 7 days after the administration of adriamycin and 35 days after the initiation of radiation therapy. Symptoms persisted for 7 days and required hospitalization for parenteral hydration. A barium swallow 6 days after the onset of symptoms revealed thickened

Received July 25, 1978; accepted after revision December 13, 1978.
This work was supported in part by National Institutes of Health training grant no. HL-07146 (P. E. Newburger).
[1] Department of Radiology, Harvard Medical School, Children's Hospital Medical Center, 300 Longwood Avenue, Boston, Massachusetts 02115. Address reprint requests to R. L. Teele.
[2] Division of Pediatric Hematology–Oncology, Sidney Farber Cancer Institute and Children's Hospital Medical Center; Department of Pediatrics, Harvard Medical School, Boston, Massachusetts 02115.

© 1979 American Roentgen Ray Society

0361-803X/79/1324-0567 $0.00

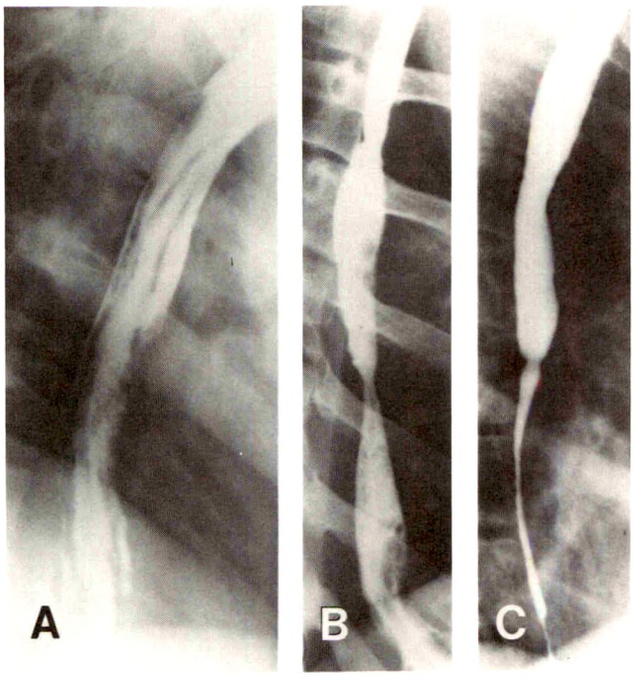


Fig. 1.—Case 1. **A**, Barium esophagram 10 days after onset of symptoms, first episode of esophagitis. Dilated esophagus with thickened mucosal folds. Peristaltic activity diminished at fluoroscopy. **B**, 16 days after onset of symptoms, third episode of esophagitis (second recall). Narrowed esophagus with markedly irregular mucosa and formation of stricture in distal one-half. No peristalsis. Barium study performed between **A** and **B** after second episode of esophagitis (first recall) demonstrated more normal mucosal pattern with slight narrowing of lumen. **C**, High grade stenosis involving about 9 cm of distal esophagus with significant obstruction. Lumen of the stricture is irregular. Transition between proximal esophagus, although abrupt, appears benign, characterized by concentric narrowing.

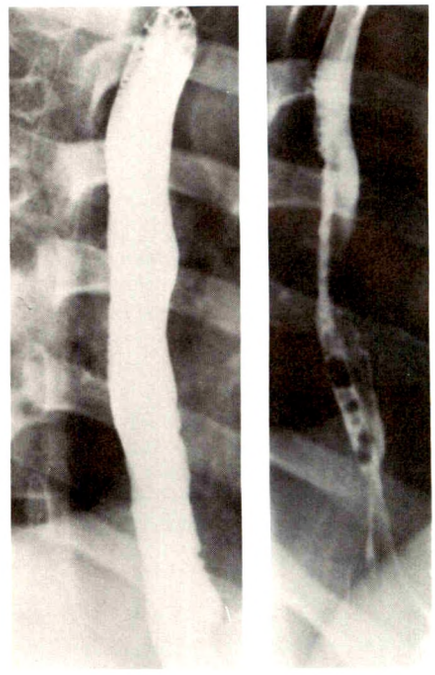


Fig. 2.—Case 2. Distal esophagus demonstrates thickened irregular mucosal folds. Decreased peristalsis noted at fluoroscopy.

irregular mucosal folds (fig. 2). A throat culture at this time was negative for *Candida*. The patient received subsequent courses of adriamycin which did not result in esophagitis.

Case 3

M. S., a 17-year-old boy with metastatic osteogenic sarcoma, developed esophagitis 50 days after receiving adriamycin and 14 days after the initiation of radiation therapy. Symptoms lasted 3 weeks necessitating hospitalization and treatment with intravenous hydration. Barium esophagography was performed three times during this period, revealing a localized mucosal irregularity (fig. 3). Throat cultures and serum precipitins for *Candida* were negative. The patient received no further adriamycin therapy.



Fig. 3.—Case 3. First barium swallow 4 days after onset of symptoms. Localized area of mucosal irregularity involving distal esophagus. Gastroesophageal reflux not elicited during study. Surgical clips in right hilum.

Case 4

J. G., a 12-year-old boy with mediastinal non-Hodgkin's lymphoma, developed his first episode of esophagitis 13 days after taking adriamycin and 16 days after initiation of radiation therapy. Symptoms lasted 7 days. The patient was hospitalized for parenteral hydration. Barium esophagography 3 days after the onset of symptoms was normal, as was a follow-up examination 5 days later. Recall esophagitis developed 7 days after a second course of therapy consisting of half the original dose of adriamycin. Symptoms were mild and lasted only 2 days. A barium swallow was not performed.

Case 5

K. G., a 12-year-old girl with metastatic osteogenic sarcoma, developed substernal chest pain and dysphagia 3 days after adriamycin therapy and 16 days after initiation of radiation therapy. Symptoms lasted about 2 weeks and she required intravenous hydration. Barium esophagography at the end of

her episode demonstrated mild mucosal irregularity of the distal esophagus with intermittent mild gastroesophageal reflux to the level of the midesophagus; a hiatus hernia was not demonstrated. Follow-up examination 1 year later, when the patient was asymptomatic, was totally normal. The patient received no further adriamycin after her first and only episode of esophagitis.

Radiographic Findings

As illustrated by these patients, a spectrum of radiographic findings, from normal to a severely damaged esophagus with strictures, has been found in patients with esophagitis due to adriamycin and radiation. The esophagitis involves only those areas within the field of radiation and predominantly affects the lower third of the esophagus. The reason for the preferential involvement of the distal esophagus is not clear. The radiographic appearance of the esophagus is not specific for any one etiology.

Motor dysfunction seems to be an early finding and may be missed on fluoroscopic study, because the patient with dysphagia is apt to swallow only small amounts of barium at a time. Motor dysfunction has been described as an early feature of esophagitis from several etiologies [8]. Mucosal irregularity, thickening of the folds and narrowing of the esophageal lumen (probably from spasm), occurs with severe esophagitis but is again nonspecific. Maximum distention of the esophagus during a barium study may mask subtle mucosal abnormalities. Barium coating without distention results in better delineation of mucosal abnormalities. Close attention to peristaltic activity often provides the first clue to esophageal disease.

At the other end of the spectrum of radiologic abnormality, case 1 developed esophageal stricture which appeared benign: smooth, concentric, tapered, without ulceration. His clinical course, the most stormy of all the patients, included several episodes of severe esophagitis. Angulation and ulceration which has been reported in radiation esophagitis was not noted [9].

Discussion

The radiographic findings in patients with esophagitis reflect the response of the esophagus to a toxic agent, be it radiation, infection, or caustic. The severity of the insult can be correlated directly with the severity of the response [10].

Radiation esophagitis occurring after doses of 2,000–4,500 rad is usually self limited and heals without sequellae [2]. Doses of radiation in the range of 4,500–6,500 rad and greater may lead to severe esophagitis with irreversible damage characterized by the formation of stricture or fistula [2, 9, 11]. Our patients with combined radiation and adriamycin therapy developed symptoms with doses as low as 500 rad, well below the level at which mild dysphagia has been reported with radiation alone.

Adriamycin is one of several drugs that interfere with a cell's ability to absorb or repair sublethal damage from radiation. These drugs augment the effects of radiation and produce the phenomenon of "recall." D'Angio [2] defined recall as reactivation of latent radiation changes in tissues previously irradiated but which have returned to normal appearance in the interval. He described reactivation of radiation dermatitis by actinomycin D. Cassady et al. [12] later reported augmentation of radiation reaction by adriamycin and the development of recall dermatitis in two patients. Horwich et al. [3] reported two cases of esophagitis and esophageal stricture after radiation (4,500–5,000 rad) concomitant with adriamycin. Greco et al. [13] reported a series of 10 patients treated with radiation therapy and adriamycin, in which eight patients developed recurrent esophagitis with each course of chemotherapy; two patients went on to develop esophageal stricture. In the series reported by Newburger et al. [1], from which our five patients are drawn, two of the three patients with recall esophagitis developed stricture. The implication of these series is that recurrent esophagitis predisposes the patient to increasingly severe esophagitis and formation of stricture.

As mentioned previously, monilial esophagitis cannot be differentiated from esophagitis caused by radiation and adriamycin by the radiographic findings alone [5, 6]. The clinical presentation of dysphagia and retrosternal pain is also nonspecific as to etiology. Cultures may be helpful; however, oral thrush does not necessarily mean the esophagus is infected; conversely a negative culture of the pharynx does not completely exclude monilial esophagitis [14]. To establish without doubt the diagnosis of monilial esophagitis, biopsy of the esophageal mucosa is necessary. The branching hyphae of *Candida* must be present in the tissue itself, not just on the surface (A. Goldman, personal communication). In actual practice, biopsy is performed infrequently. Usually the patients with suspected monilial esophagitis are treated empirically with oral nystatin or gentian violet, since both drugs are relatively innocuous. Esophagitis due to herpes simplex infection may assume a similar clinical and radiographic appearance [4]. Lesions are not always present elsewhere on the affected patient, so the diagnosis may depend on biopsy (or, more commonly, autopsy).

The diagnosis of esophagitis due to adriamycin and radiation therapy should be considered in the following situations: (1) when any patient receiving such therapy develops dysphagia at low doses of radiation therapy; (2) when symptoms of esophagitis develop after subsequent courses of adriamycin ("recall" esophagitis); and (3) when such a patient shows no evidence of oral or pharyngeal moniliasis by clinical examination, or there is no response to appropriate treatment for moniliasis. Because the esophagitis seems to increase in severity with repeated doses of adriamycin, early diagnosis may prevent development of strictures by signaling for a change in chemotherapeutic agents.

ACKNOWLEDGMENTS

We thank Eileen Walsh and Andrea Kelton for their excellent secretarial assistance and Drs. David Nathan, Norman Jaffe, and James Cassady for their suggestions.

REFERENCES

1. Newburger PE, Cassady JR, Jaffe N: Esophagitis due to adriamycin and radiation therapy for childhood malignancy. *Cancer* 42:417–423, 1978
2. D'Angio GJ: Clinical and biological studies of actinomycin D and roentgen irradiation. *AJR* 87:106–109, 1962
3. Horwich A, Lokich JJ, Bloomer WD: Doxorubicin, radiotherapy, and esophageal stricture. *Lancet* 2:561–562, 1975
4. Howiler W, Goldberg HI: Gastroesophageal involvement in herpes simplex. *Gastroenterology* 70:775–778, 1976
5. Kaufman HJ: *Candida* esophagitis in children with malignant disorders. *Ann Radiol* 13:157–162, 1970
6. Lewicki AM, Moore JP: Esophageal moniliasis—a review of common and less frequent characteristics. *AJR* 125:218–225, 1975
7. Meyers C, Durkin MG, Love L: Radiographic findings in herpetic esophagitis. *Radiology* 119:21–22, 1976
8. Simeone JF, Burrell M, Toffler R, Smith GJW: Aperistalsis and esophagitis. *Radiology* 123:9–14, 1977
9. Goldstein HM, Rogus LF, Fletcher GH, Dodd GD: Radiological manifestations of radiation induced injury to the normal upper gastrointestinal tract. *Radiology* 117:135–140, 1975
10. Dodds WJ: Current concepts of esophageal motor function: clinical implications for radiology. *AJR* 128:549–561, 1977
11. Boswit R, Malsky SJ, Reid CB: Radiation tolerance of the gastrointestinal tract. *Front Rad Ther Oncol* 6:160–181, 1972
12. Cassady JR, Richter MP, Piro AJ, Jaffe N: Radiation-adriamycin interactions: preliminary clinical observations. *Cancer* 36:946–949, 1975
13. Greco FA, Brereton HD, Kent H, Zimble H, Merrill J, Johnson RE: Adriamycin and enhanced radiation reaction in normal esophagus and skin. *Ann Intern Med* 85:294–298, 1976
14. Eras P, Goldstein MJ, Sherlock P: *Candida* infection of the gastrointestinal tract. *Medicine* (Baltimore) 51:367–379, 1972

Gallbladder: Common Cause of Antral Pad Sign

RENÉ SMEETS[1] AND J. ODO OP DEN ORTH[1]

An impression on the posteroinferior aspect of the gastric antrum is often caused by a mass lesion in the pancreas. However, the gallbladder more commonly causes such as indentation. In any case of this "antral pad sign," a gallbladder impression should first be excluded.

An indentation on the gastric antrum, especially on the posteroinferior aspect, is often said to represent a mass lesion in the head or body of the pancreas [1–8]. Such an indentation, commonly called the "antral pad sign," is not necessarily specific for pancreatic pathology. Mass lesions arising in other organs near the gastric antrum may produce identical findings [3, 4, 7, 9]. However, it is generally believed that, when finding an antral pad sign, a mass lesion in the head or in the body of the pancreas has to be primarily excluded.

Case Material

When performing an upper gastrointestinal series and a cholecystography in the same session, we regularly observed an antral pad sign caused by a normal or pathologic gallbladder (fig. 1). On other occasions, we observed impressions on the lesser curvature caused by the gallbladder (fig. 2).

To determine the frequency with which a gallbladder impression occurred, we reviewed a series of 222 consecutive combined examinations. In 18 cases (8.1%), a definite indentation on the posteroinferior aspect of the antrum was observed. In 27 cases (12.2%), we identified a gallbladder impression on the lesser curvature. During one examination, the gallbladder indentation was seen first on the greater curvature, then on the ventral aspect of the antrum, and finally on the lesser curvature (fig. 3).

Discussion

The gallbladder has only rarely been mentioned as a cause of a pad defect [4, 9]. The phenomenon can easily be explained when the normal anatomy of the right abdominal upper quadrant is considered.

The gallbladder is anterior in the abdomen and attached to the liver. It lies ventrolateral to the duodenal bulb. The gastric antrum is largely mobile [10]. Since the anterior abdominal wall is pliable, the liver and the gallbladder move to the left when a supine patient raises his right side [11]. The extent and nature of this movement depend on the patient's body type. Even the movement of the gallbladder from the greater curvature, ventral to the antrum, and then to the lesser curvature (fig. 3) can be explained in this way.

While we occasionally observed these antral impressions in single positive contrast studies with the patient prone or erect, it was far more commonly observed in the double contrast hypotonic phase of the biphasic



Fig. 1.—Hypotonic double contrast gastrography, patient supine, right side elevated. Normal gallbladder causes indentation on greater curvature side of antrum.

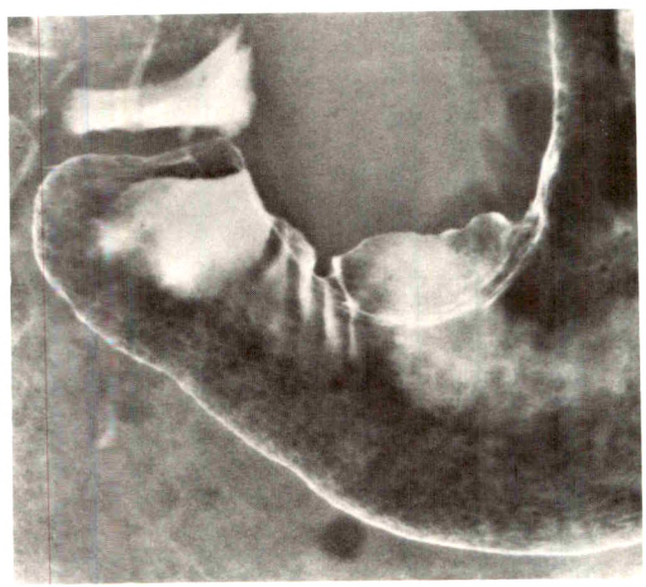


Fig. 2.—Hypotonic double contrast gastrography, patient supine, right side elevated. Indentation on lesser curvature side of antrum and angulus area caused by normal gallbladder.

Received July 28, 1978; accepted after revision December 12, 1978.

[1] Department of Radiology, St. Elisabeth's of Groote Gasthuis, Boerhaavelaan 22, Haarlem, Holland. Address reprint requests to J. O. Op den Orth.

© 1979 American Roentgen Ray Society

0361–803X/79/1324–0571 $0.00

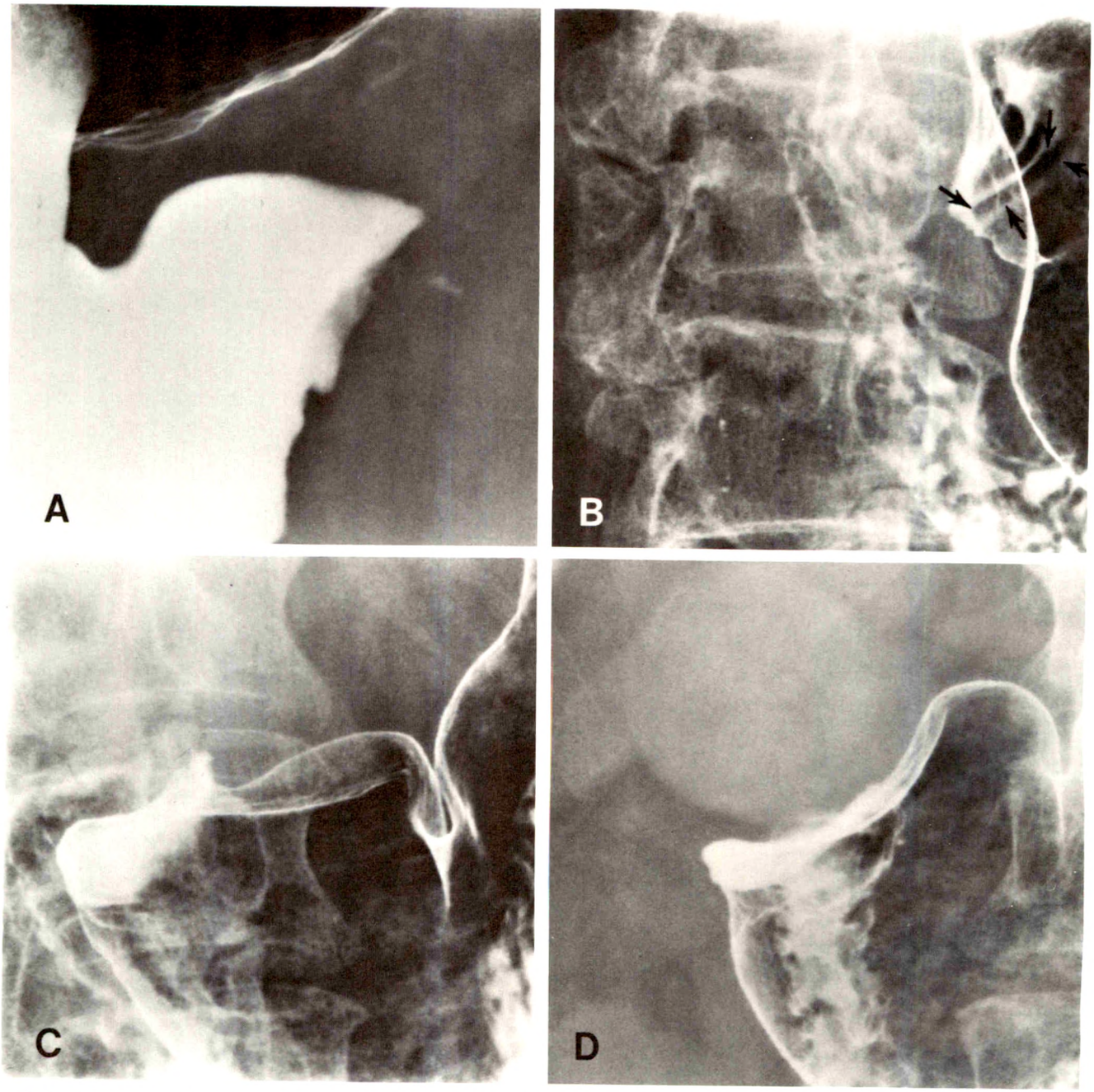


Fig. 3.—Indentations of distended gallbladder on different sides of antrum during single examination. **A**, Patient prone, left side elevated. Indentation on greater curvature side. **B**, Patient supine, right side elevated. Folds (*arrows*) identified as posterior wall folds because they appear as radiolucent belts dividing contrast pools along their course [13]. This establishes that gallbladder is partly ventral to antrum. **C** and **D**, Finally, gallbladder indents lesser curvature side of antrum. At surgery, normal attachment of gallbladder to liver was found; there was no mesentery causing "floating" gallbladder [9].

examination [12] performed in our department. During hypotonic studies, extrinsic impressions are more readily observed. The standard position for the double contrast film of the antrum is supine, right side elevated.

We believe that an antral pad sign does not necessarily imply a mass in the pancreas. When it is observed, oral cholecystography is recommended.

REFERENCES

1. Bockus HL: *Gastroenterology*, vol 3. Philadelphia, Saunders, 1976, p 981
2. Case JT: Roentgenology of pancreatic disease. *AJR* 44: 485–518, 1940
3. Eaton SB, Ferrucci JT: *Radiology of the Pancreas and Duodenum*. Philadelphia, Saunders, 1973, pp 10, 55–60, 341–342
4. Eyler WR, Clark MD, Rian RL: An evaluation of roentgen signs of pancreatic enlargement. *JAMA* 181:143–147, 1962
5. Hodes PJ, Pendergrass EP, Winston NJ: Pancreatic, ductal and Vaterian neoplasms: their roentgen manifestations. *Radiology* 62:1–15, 1954
6. Mani JR, Zboralske FF, Margulis AR: Carcinoma of the body and tail of the pancreas. *AJR* 96:429–446, 1966
7. Margulis AR, Burhenne HJ: *Alimentary Tract Roentgenology*. St. Louis, Mosby, 1973, p 1109
8. Paul LW, Juhl JH: *The Essentials of Roentgen Interpretation*. New York, Harper & Row, 1972, p 450
9. Hatfield PM, Wise RE: *Radiology of the Gallbladder and Bile Ducts*. Baltimore, Williams & Wilkins, 1976, pp 134, 147, 149
10. Hafferl A: *Lehrbuch der Topographischen Anatomie*. Berlin, Springer, 1957, pp 447–448
11. Whalen JP: *Radiology of the Abdomen: Anatomic Basis*. Philadelphia, Lea & Febiger, 1976, pp 93–101
12. Op den Orth JO, Ploem S: The standard biphasic-contrast gastric series. *Radiology* 122:530–532, 1977

Radiographic Features of Eosinophilic Gastroenteritis (Allergic Gastroenteropathy) of Childhood

RITA LITTLEWOOD TEELE,[1] AUBREY J. KATZ,[2] HARVEY GOLDMAN,[3] AND RACHEL M. KETTELL[1]

The child with eosinophilic gastroenteritis has failure to thrive, a history of allergy or asthma, iron deficiency anemia, and peripheral eosinophilia. This type of eosinophilic gastroenteritis has earned the designation "allergic gastroenteropathy." Pathologic change in the gastric antrum of six children with this disease correlated with an abnormal air-contrast examination of the antrum. The affected children had an irregular, lacy, antral surface rather than the smooth, bald surface seen in normal children. The small bowel in allergic gastroenteropathy is usually abnormal but nonspecific as to etiology. Much more specific is the *combination* of small bowel and gastric antral abnormalities. Findings encourage air-contrast radiography of the antrum in children with suspected allergic gastroenteropathy.

Eosinophilic gastroenteritis, a cluster of diseases of unknown etiology, is complex and confusing. However, one group of patients with eosinophilic gastroenteritis does appear to be distinct. This group comprises children who have strong histories of systemic allergy and whose initial symptoms usually include retardation of growth, abdominal pain, and diarrhea. On investigation they have peripheral eosinophilia, protein-losing enteropathy with hypogammaglobulinemia and hypoalbuminemia, iron deficiency anemia due to gastrointestinal loss of blood, and characteristic alterations of the mucosa of stomach and small bowel obtained by biopsy [1, 2]. In a study of six such patients, Waldmann et al. [1] coined the term "allergic gastroenteropathy."

We have followed six children who have allergic gastroenteropathy [2]. Their studies have included extensive clinical and laboratory investigation, radiographic examinations, and endoscopic gastric and duodenal biopsies. In all cases, the radiologic findings correlated well with pathologic material. We now describe the radiologic abnormalities in both small bowel and gastric antrum with special emphasis on the value of studying the gastric antrum with air contrast.

Subjects and Methods

Six children with known or suspected allergic gastroenteropathy each were evaluated with one or more upper gastrointestinal series over the last 3 years (table 1). An air-contrast view of

TABLE 1

Clinical, Radiographic, and Pathologic Correlation

Case No.	Age (years)		Symptoms	Radiology*	Biopsy†	
	Onset	Diagnosis			Small Bowel	Stomach
1	1/2	3	Growth retardation; chronic diarrhea; edema	Lacy antrum reverted to normal with treatment; mildly nodular small bowel	0–3+	3+
2	7	12	Growth retardation; abdominal pain; vomiting	Nodular antrum with lacy antral mucosa; coarsely nodular small bowel	0	3+
3	8	15	Abdominal pain	Lacy antrum; normal small bowel	1+	2+
4	3 1/2	12	Growth retardation; chronic diarrhea	Nodular antrum; no air contrast view; nodular small bowel	0–2+	2+
5	2	6 1/2	Growth retardation	Nodular antrum and small bowel reverted to normal with treatment	2+	2+
6	1/2	1/2	Anemia; cardiac failure; edema	No air contrast view of antrum; coarse folds in small bowel	2+	2+

Note.—Table adapted from [2]. All patients except case 3 were male. All patients had other allergies, except case 6 in whom there were none known.

* Done within several days of biopsy, while patients were symptomatic.

† Taken while patients were symptomatic. Cases 1 and 4 had multiple biopsies. Pathologic features (villous atrophy, epithelial necrosis, regeneration, eosinophils) are rated as absent (0) mild (1+) moderate (2+) severe (3+)

Received July 18, 1978; accepted after revision December 19, 1978.

Presented at the annual meeting of the Society for Pediatric Radiology, Denver, September 1978.

A. J. Katz is the recipient of Clinical Investigator Award from NIAMD #1K08AM00234-01A1 and Basil O'Connor Award from the National Foundation March of Dimes.

[1]Department of Radiology, Harvard Medical School, Children's Hospital Medical Center, 300 Longwood Avenue, Boston, Massachusetts 02115. Address reprint requests to R. L. Teele.

[2] Department of Medicine, Harvard Medical School, Children's Hospital Medical Center, Boston, Massachusetts 02115.

[3] Department of Pathology, Harvard Medical School, Children's Hospital Medical Center, Boston, Massachusetts 02115.

© 1979 American Roentgen Ray Society

0361–803X/79/1324–0575 $0.00

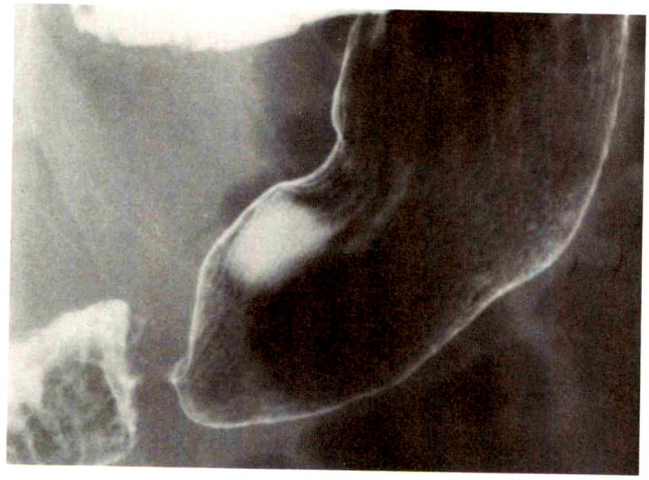


Fig. 1.—Case 3. Air-contrast view of antrum. Interlacing pattern similar to "areae gastricae" seen in adults. Gastric biopsy showed eosinophilic gastritis.

the gastric antrum is obtained routinely in children who have an upper gastrointestinal series. These are achieved by using barium of 60% W/W and swallowed air. It has been difficult to obtain a satisfactory study in babies. Their stomachs lie in a transverse position with the antrum diving posteriorly and barium does not coat the mucosa as well as in older children.

Results

In adults a lacy antral pattern, the areae gastricae, is commonly present [3, 4]. We have found that this pattern rarely occurs on air-contrast studies in normal children.

None of the symptomatic patients with allergic gastroenteropathy had the smooth, bald, antral surface seen on air-contrast examinations of normal children. The earliest change was replacement of the smooth surface by a lacy pattern, similar to the areae gastricae seen in adults (fig. 1). This was present in two patients. Two patients had nodular antra, and one child (case 2) had both the lacy pattern and nodularity. In one patient, the antral nodularity led to the diagnosis of an antral polyp (fig. 2A). With clinical remission, the "polyp" disappeared and the mucosal surface of the antrum became smooth (figs. 2B and 2C). Thus, in this patient and another (case 1), who had follow-up examinations, the antral changes were reversible with therapy. The sixth patient, a baby of 6 months, did not have an adequate air-contrast view of the antrum.

Our patients with allergic gastroenteropathy had the same radiographic appearance of the small bowel that has been reported under the broader term of eosinophilic gastroenteritis. The severity of the findings seems to correlate with the severity and chronicity of the disease. There is a wide range of normal small bowel patterns in children; those least affected with allergic gastroenteropathy may have a "normal" pattern [5] (fig. 3C). Usually, however, those with untreated disease have a definitely abnormal small bowel (fig. 4C). A combination of the infiltrative process and lower serum albumin results in mucosal nodularity, enlarged folds, and a thickened wall [6–8]. Nodularity of the mucosa has been attributed also to mesenteric lymphadenopathy associated with eosinophilic gastroenteritis [9]. Occasionally there is fragmentation of the column of barium indicating increased fluid within the lumen of the bowel.

Representative Case Reports

Case 1

A 6-year-old boy had been well until age 6 months when his growth slowed. At age 11 months, he was admitted to another hospital because of vomiting, diarrhea, and anasarca. Laboratory investigation (total protein, 3.05 mg/dl; albumin, 1.17 mg/dl; hematest positive stool) led to the diagnosis of protein-losing enteropathy. Because of recurrent vomiting, diarrhea, abdominal distention, edema, and failure to thrive, numerous admissions to the Children's Hospital Medical Center ensued over the next 4½ years. Concurrent with the onset of these gastrointestinal problems, the patient developed asthma.

Radiographic studies at ages 2 years 7 months, and 3 years, showed coarse folds throughout the small bowel; air-contrast views of the antrum were not performed. The diagnosis of eosinophilic gastroenteritis was made at age 3 by mucosal biopsy of the gastric antrum. There was necrosis of the epithelial surface and glands associated with eosinophilic and neutrophilic infiltration.

Biopsy of the mucosa of the small bowel was normal, but review of previous biopsies showed villous atrophy and eosinophilic infiltration. Initial therapy was dietary restriction of gluten, milk, eggs, and beef. When symptoms persisted, steroids were given and the patient improved.

At age 5, the patient was in clinical remission induced by therapy with steroids. Upper gastrointestinal series with small bowel follow through was normal (fig. 3A). Specifically, air contrast views of the gastric antrum were normal (fig. 3B). Dudodenal and gastric antral biopsies, done immediately after the radiographic studies, were normal.

A year later, the patient was reevaluated with radiographic studies and biopsy. His steroid therapy had been tapered and stopped and he was symptomatic. The radiographs of the small bowel were barely changed from the year before (fig. 3C) but there was a distinct difference in the appearance of the gastric antrum (fig. 3D). Gastric antral biopsy was also abnormal with marked eosinophilic infiltration of the mucosa and destruction of the epithelial cells. The patient was started again on prednisone; he had immediate symptomatic relief.

Case 2

A 12-year-old boy was referred to Children's Hospital Medical Center after his hospitalization elsewhere for abdominal pain and vomiting revealed low total protein and serum albumin, a hematocrit of 30, peripheral eosinophilia which ranged from 25% to 30%, and occult blood in the stool. He was at the third percentile for his height and weight and he had had asthma and eczema since early childhood. Episodes of abdominal pain and vomiting began at age 7 and seemed to be related to the ingestion of bread. He was thought to have gluten sensitive enteropathy (celiac disease), but did not respond to a gluten free diet and was referred to Children's Hospital Medical Center. On admission, total protein was 6 mg/dl; albumin, 2.21 mg/dl; hematocrit, 27; and there was a peripheral eosinophilia of 30%. Upper gastrointestinal series and small bowel follow through revealed nodular filling defects in the antrum and thickened nodular mucosa in the small bowel (figs. 4B and 4C). Review of previous biopsies from the gastric antrum showed the typical features of eosinophilic gastroenteritis with marked necrosis of

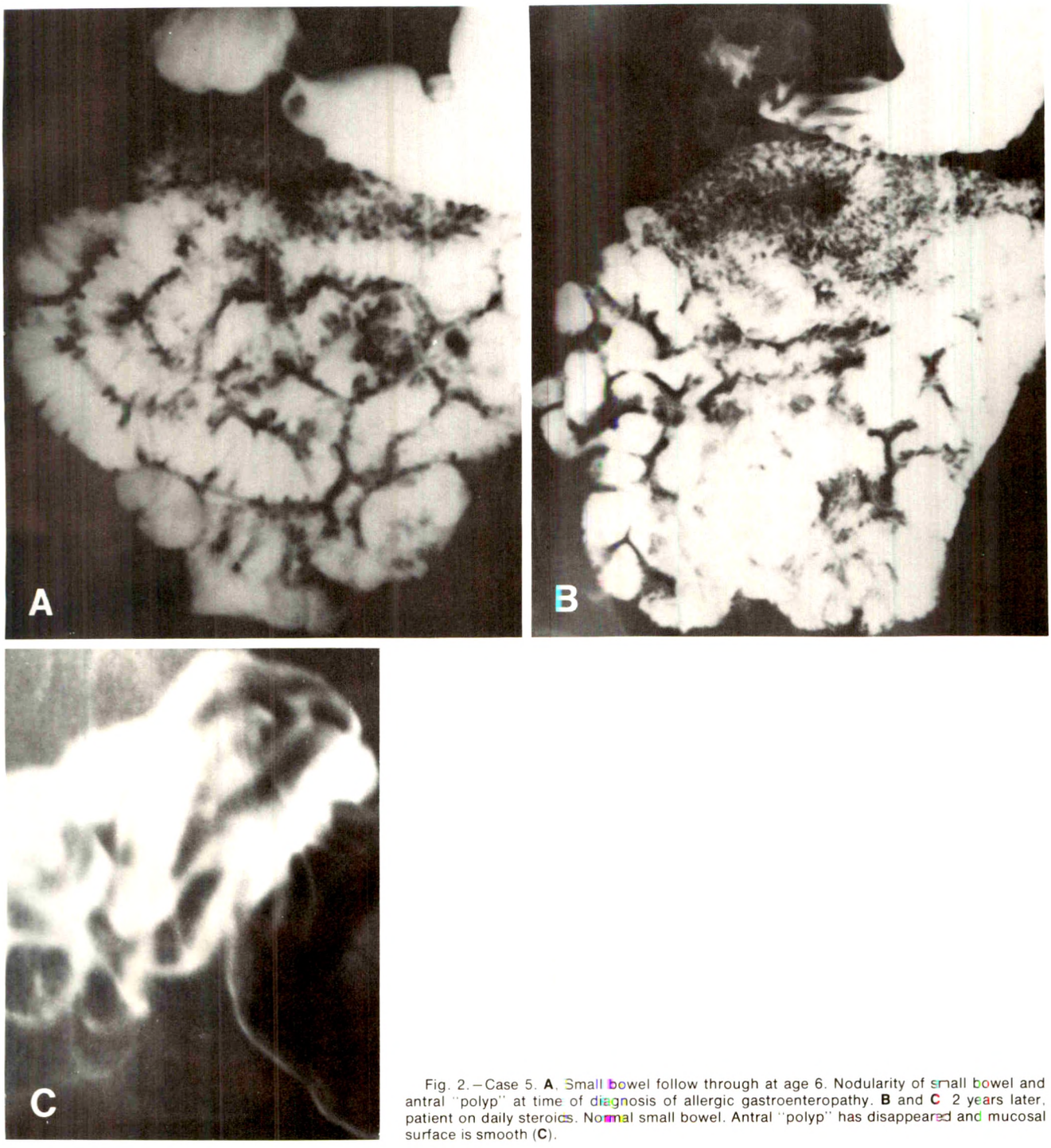


Fig. 2.—Case 5. **A**, Small bowel follow through at age 6. Nodularity of small bowel and antral "polyp" at time of diagnosis of allergic gastroenteropathy. **B** and **C** 2 years later, patient on daily steroids. Normal small bowel. Antral "polyp" has disappeared and mucosal surface is smooth (**C**).

epithelial cells and eosinophilic infiltration. The patient was begun on steroid therapy which resulted in marked symptomatic improvement. No further radiographic studies have been done.

Discussion

The particular type of eosinophilic gastroenteritis seen in children appears to have earned the designation "allergic gastroenteropathy." Affected children have a strong history of asthma and atopy, evidence for immediate hypersensitivity to many foods [10], elevated levels of serum IgE, peripheral eosinophilia, and good response to therapy with steroids. Although the lesion in the small bowel may be patchy in distribution [11, 12]—possibly accounting in part for some of the "normal" studies of the small bowel in such patients—the gastric antral lesion was diffuse and obvious in all of our

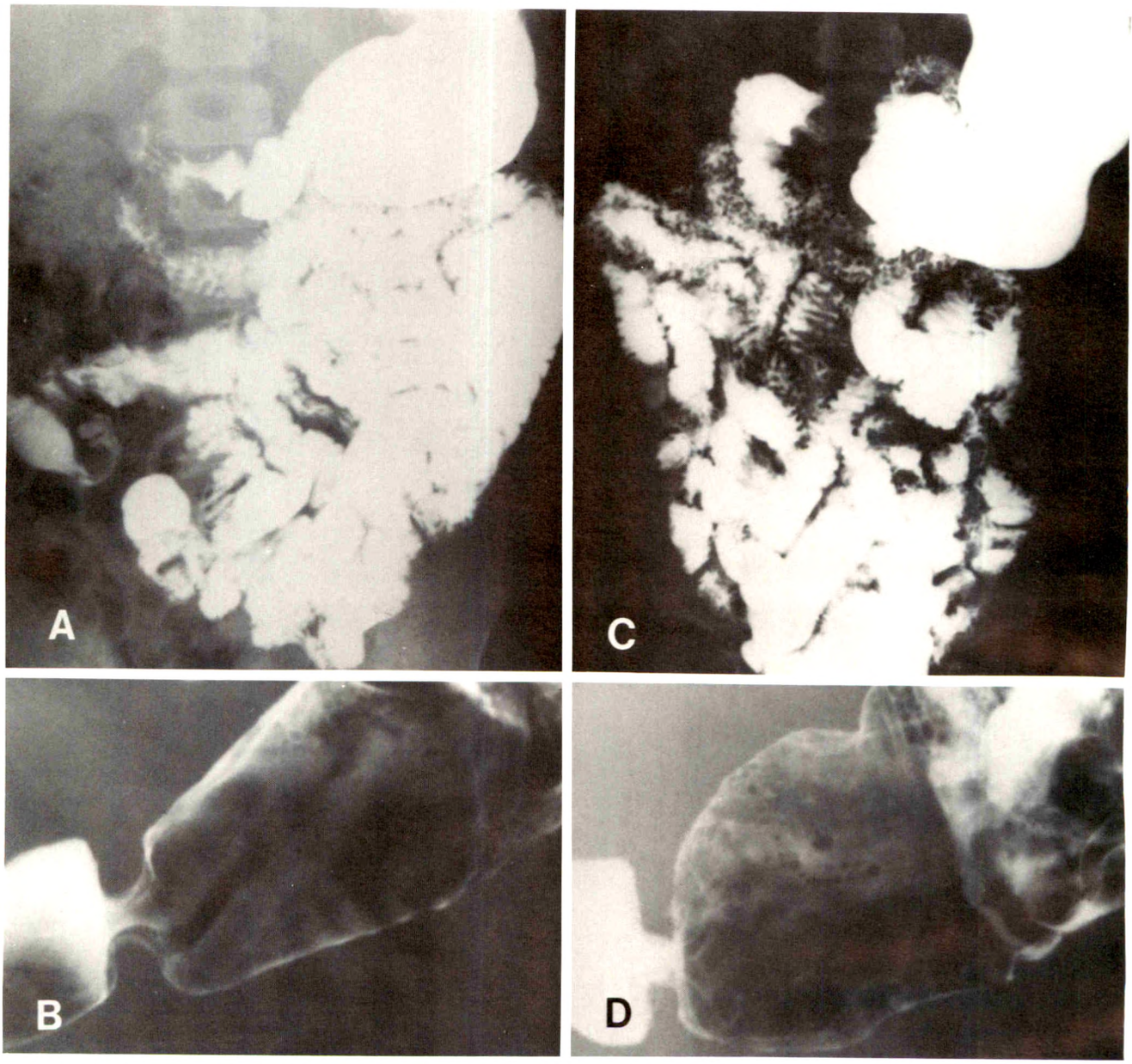


Fig. 3.—Case 1. **A** and **B**, Age 5. Normal small bowel. Patient in clinical remission from allergic gastroenteropathy. Note smooth, bald antral surface of stomach in air-contrast view (**B**). Gastric antral biopsy was normal. **C** and **D**, Age 6, patient symptomatic. **C**, minimal mucosal thickening of small bowel reappears. **D**, Air-contrast study of antrum (cf. fig. 2B). Mucosal surface is irregular; gastric wall, seen in profile, is finely spiculated. Gastric antral biopsy showed numerous eosinophils and focal areas of epithelial necrosis.

patients. When the correlation between pathologic and radiographic findings became evident, we were able to predict an abnormal biopsy on the basis of the radiographs.

Attempts have been made to separate eosinophilic gastroenteritis into three pathologic entities [12]: (1) mucosal disease leading to protein-losing enteropathy and malabsorption; (2) disease involving the muscular layers of the stomach and often presenting as pyloric obstruction; and (3) primary serosal disease which is rare and accompanied by eosinophilic ascites. The six patients discussed here obviously had mucosal disease as endoscopic biopsies were diagnostic. Deeper involvement may have been present; full thickness biopsies were not done.

When an antral abnormality is found in a child, a number of differential diagnoses must be considered. The "lacy" pattern in the antrum on radiographs with air contrast may be seen in any type of gastritis. We have seen it associated with the ingestion of aspirin, peptic ulcer disease, and early Crohn's disease. Nodularity and rigidity of the antrum adds to the list of differential diagnoses: corrosive gastritis, chronic granulomatous disease of childhood, and infections. The diagnosis of

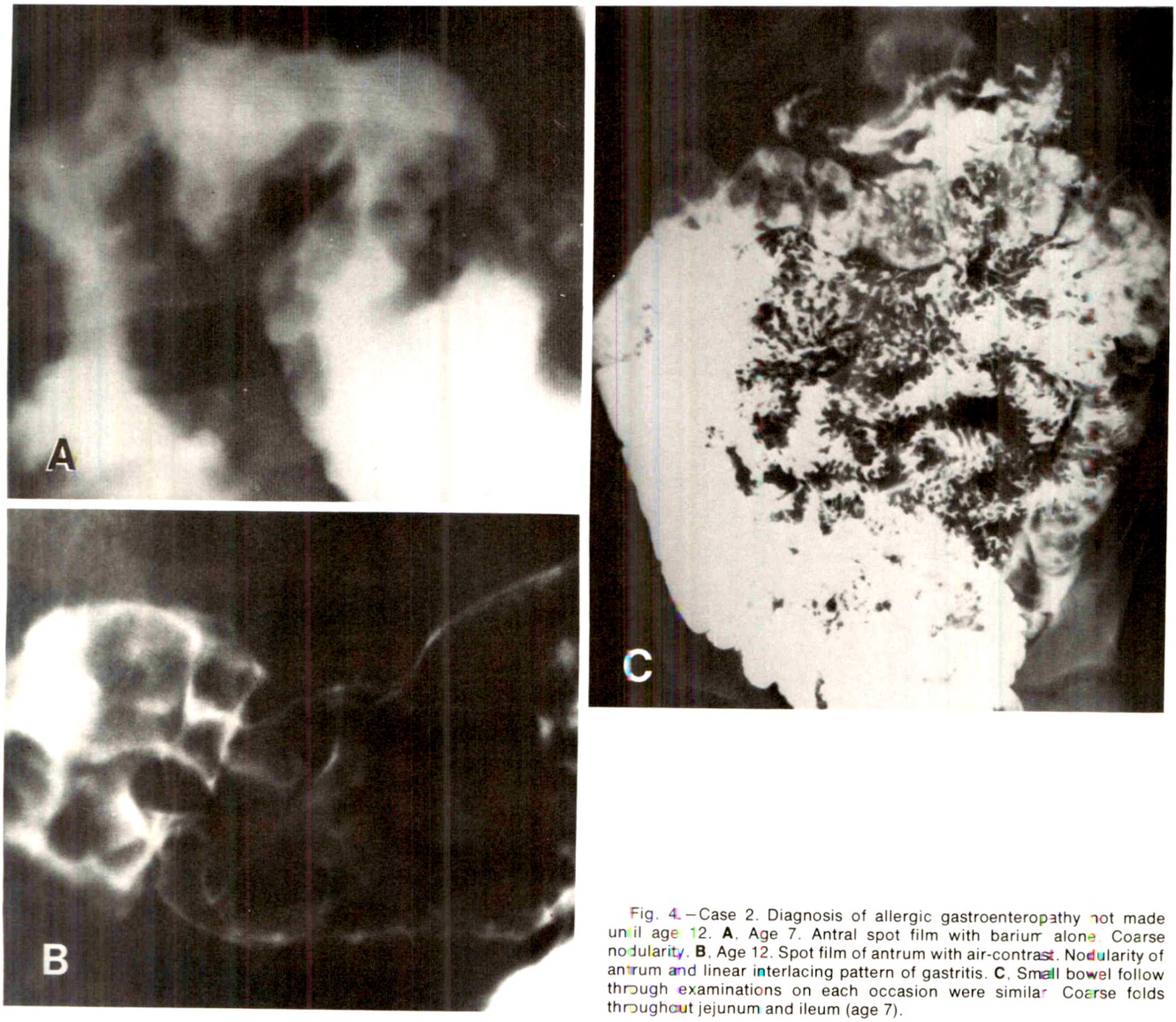


Fig. 4.—Case 2. Diagnosis of allergic gastroenteropathy not made until age 12. **A**, Age 7. Antral spot film with barium alone. Coarse nodularity. **B**, Age 12. Spot film of antrum with air-contrast. Nodularity of antrum and linear interlacing pattern of gastritis. **C**, Small bowel follow through examinations on each occasion were similar. Coarse folds throughout jejunum and ileum (age 7).

corrosive gastritis is usually obvious from the clinical history and associated esophageal lesions. Chronic granulomatous disease typically has a smooth rather than nodular tapering of the antrum [13]. Granulomatous infections of the gastrointestinal tract (e.g., tuberculosis, histoplasmosis) are encountered rarely in children in this country. Also rare are tumors of the gastric antrum; gastric carcinoma and lymphoma are almost unheard of in the pediatric age group [14]. Gastric leiomyoma or leiomyosarcoma, also rare in children, can present with localized nodularity in the antrum [15]; the mucosa of the small bowel is normal in such cases. The combination of the gastric lesion with the abnormality of the small bowel favors the diagnosis of eosinophilic gastroenteritis. Crohn's disease and granulomatous infections are the only other diseases to present with such a combination.

Patients with suspected eosinophilic gastroenteropathy should have careful air-contrast studies of the gastric antrum in order to detect early antral gastritis. Conversely, in patients with an abnormal small bowel pattern thought to be due to other causes (e.g., celiac disease, nonspecific enteritis), an abnormal gastric antrum should suggest allergic gastroenteropathy and encourage the clinician to pursue the diagnosis with gastric antral biopsy.

ACKNOWLEDGMENTS

We thank Eileen Walsh and Emily Andler for their secretarial help in preparation of this paper.

REFERENCES

1. Waldmann TA, Wochner RD, Laster L, Gordon RS: Allergic gastroenteropathy: a cause of excessive gastrointestinal protein loss. *N Engl J Med* 276:761–769, 1967

2. Katz AJ, Goldman H, Grand RJ: Gastric mucosal biopsy in eosinophilic (allergic) gastroenteritis. *Gastroenterology* 73: 705–709, 1977
3. Laufer I: A simple method for routine double-contrast study of the upper gastrointestinal tract. *Radiology* 117:513–518, 1975
4. Gelfand GW: The Japanese-style double-contrast examination of the stomach. *Gastrointest Radiol* 1:7–17, 1976
5. Gregg JA, Luna L: Eosinophilic gastroenteritis: report of a case with protein-losing enteropathy. *Am J Gastroenterol* 59:41–47, 1973
6. Goldberg HI, O'Kieffe D, Jenis EH, Boyce HW: Diffuse eosinophilic gastroenteritis. *AJR* 119:342–351, 1973
7. Wehunt WD, Olmsted WW, Neiman HL, Phillips JF: RPC from the AFIP. *Radiology* 120:85–89, 1976
8. Burhenne HJ, Carbone JV: Eosinophilic (allergic) gastroenteritis. *AJR* 96:332–338, 1966
9. Freundlich IM, Schaupp R, Lehman JS: Eosinophilic gastroenteritis: a case report with extensive jejunal involvement. *Radiology* 86:493–495, 1966
10. Ureles AL, Alschibaja T, Lodico D, Stabins SJ: Idiopathic eosinophilic infiltration of the gastrointestinal tract, diffuse and circumscribed. *Am J Med* 30:899–909, 1961
11. Leinbach GE, Rubin CE: Eosinophilic gastroenteritis: a simple reaction to food allergens? *Gastroenterology* 59: 874–889, 1970
12. Klein NC, Hargrove RL, Sleisenger MH, Jeffries GH: Eosinophilic gastroenteritis. *Medicine* 49:299–319, 1970
13. Griscom NT, Kirkpatrick JA, Girdany BR: Gastric antral narrowing in chronic granulomatous disease of childhood. *Pediatrics* 54:456–460, 1974
14. Humphrey HA: Some observations on gastric disease in pediatric roentgenology. *AJR* 84:518–531, 1960
15. Jakubowski A, Jakubowski K, Naumick A, Pietron K: Primary tumours of the stomach in children. *Ann Radiol* 13: 169–175, 1970

Ultrasound of Gallbladder Wall Thickening and its Relation to Cholecystitis

STEPHEN J. HANDLER[1]

A prospective ultrasound study of gallbladder wall thickness in patients with suspected gallbladder disease was performed over a 9 month period. Gallbladder walls thicker than 3 mm in fasting patients whose gallbladders were wider than 2 cm were considered abnormal. Gallstones were documented by ultrasound in 62 patients, a thickened gallbladder wall was demonstrated in 12 of these. Five patients without cholelithiasis had thick-walled gallbladders and were diagnosed as acalculous cholecystitis.

Within the past few years, gray scale ultrasonography has been widely used for detection and confirmation of gallbladder diseases [1–8]. The observation of a thickened gallbladder wall on ultrasound in both acute and chronic cholecystitis has occasionally been mentioned [9, 10], but its significance has not been fully documented. For this reason, a prospective study was undertaken to determine whether gallbladder wall thickening adds to the diagnostic accuracy and potential surgical significance of ultrasound examination of the gallbladder.

Subjects and Methods

Specific indications for the 117 adults with suspected gallbladder disease referred to the Ultrasound Laboratory of the Veterans Administration Hospital in Long Beach, California included possible acute or chronic cholecystitis, nonvisualization of the gallbladder after double-dose oral cholecystography, a palpable or suspected right upper quadrant mass, and jaundice of unknown etiology. The ultrasound observations were correlated with the surgical, pathologic, radiographic, and laboratory results as they became available.

A baseline of 1–2 mm was established for normal gallbladder thickness from measurements of 50 normal gallbaldder specimens from autopsies and surgery. The staff pathologist determined the normality of the gross specimens, and measured numerous sections of the individual gallbladders with the ultrasonographer. Our measurements correlated with the findings of others [11].

The examination was routinely performed with longitudinal and transverse scans in the supine and left lateral decubitus positions during suspended respiration. The patient remained in the left lateral decubitus position for 10–15 min before scanning to preclude the inclusion of inspissated bile in the measurement of the gallbladder wall. A 3.5 or 5.0 MHz transducer with a 7 cm focal length was used. Most patients followed the current practice of fasting at least 12 hr before examination. Patients with ascites were not included in this study because of technical difficulties in scanning and the uncertain boundaries of the gallbladder wall under these conditions.

For delineation of the gallbladder wall, the near-gain on the time gain compensation curve was increased and the transducer power was decreased as much as possible. Measurements of the gallbladder wall thickness were made on either Polaroid or x-ray film; a millimeter scale was placed on the left side of each image. The thickest portion of the gallbladder wall was measured independently by two physicians who were not aware of the clinical diagnosis. In anticipation of subjective measurement errors, 3 mm was considered the upper normal limit on the ultrasound images.

Results

Of the 117 patients, 40 were considered normal on the basis of cholecystography, lack of gallstones by ultrasound, and clinical observations. In 10 of the 40 normal patients, the 1–2 mm thick wall of the distended gallbladder was visualized. It appeared as a thin rim of medium light gray tone echoes within a rim of high-amplitude echoes (fig. 1).

Abnormal gallbladders were noted in 77 patients on the basis of ultrasound demonstration of gallstones, and clinical and surgical features. In 17 of these, gallbladder walls were 3–10 mm thick. The ultrasonic appearance of these gallbladder walls demonstrated a characteristic decrease in echogenicity [12, 13] compared with the normal medium light gray tones. Gallbladder walls were thickened in 12 of the 62 patients with gallstones.

The normal internal width of the gallbladder was 4–5 cm [11]. Contraction of the normal gallbladder can produce a "thickened" wall, presumably secondary to smooth muscle contraction (fig. 1B). To exclude this source of error, the patients with contracted gallbladders (less than 2 cm) were reexamined 24 hr later, after fasting for at least 12 hr. Patients whose gallbladders remained contracted with thickened walls were considered diseased.

Cholelithiasis was documented by ultrasound in 62 of the 117 patients. These patients were easily recognized by the discrete high-amplitude echoes within the gallbladder and characteristic posterior acoustic shadowing [1–8]. A thickened gallbladder wall was seen in 12 of the patients with cholelithiasis, and was surgically confirmed in seven. Five other patients with thickened gallbladder walls had no evidence of cholelithiasis, and were diagnosed as acalculous cholecystitis [14, 15]. Two of these had histologic confirmation after cholecystectomy.

All 10 patients in whom the gallbladder was not visualized had subsequent surgical proof of chronic chole-

Received March 22, 1978; accepted after revision January 2, 1979.
Presented in part at the annual meeting of the American Institute of Ultrasound in Medicine, San Diego, October 1978.
[1] Department of Radiology, University of California at Irvine, and Ultrasound Section, Radiology Service (114S), Veterans Administration Medicine Center, 5901 East Seventh Street, Long Beach, California 90822.

© 1979 American Roentgen Ray Society

0361–803X/79/1324–0581 $0.00

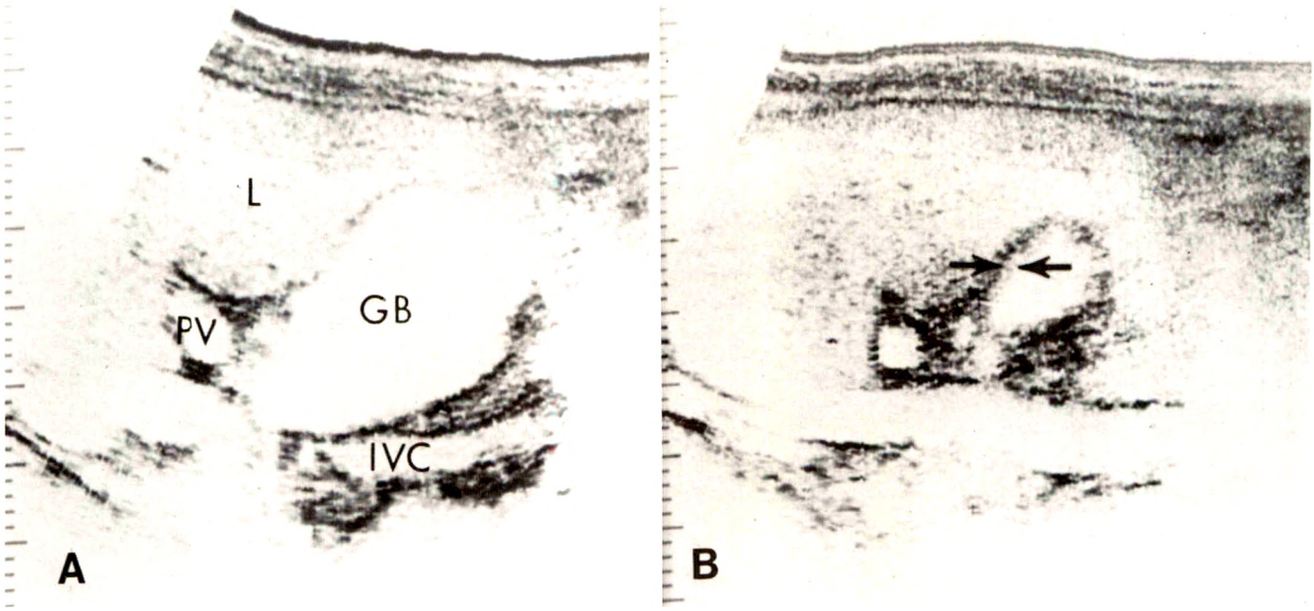


Fig. 1.—Normal gallbladder. **A,** Sagittal scan. Gallbladder wall not seen. GB = gallbladder, PV = portal vein, IVC = inferior vena cava, L = liver. **B,** After fatty meal, contracted gallbladder. Normal 2 mm gallbladder wall (*arrows*) surrounded by high-amplitude echoes.

cystitis. This experience correlated well with the findings of Weissberg and Gosink [12]. In one patient, a highly reflective echo in the lateral wall of the gallbladder did not become dependent in the left lateral decubitus position; it was assumed to represent a small polyp or possibly an adherent gallstone.

Representative Case Reports

Case 1

A 51-year-old Mexican-American man with a history of ethanol abuse came to the emergency room after 2 days of right upper quadrant pain. On physical examination he had an enlarged and tender liver. He developed spiking fever and chills 24 hr after admission, and an ultrasound examination revealed a thickened gallbladder wall of 10 mm (fig. 2). A large solitary stone with several small satellite stones was identified. Blood cultures were positive for *Klebsiella,* and after treatment with Keflin and ampicillin for 1 week, his fever subsequently defervesced. Double-dose oral cholecystography failed to visualize the gallbladder.

At operation, a grossly edematous gallbladder contained numerous small stones. The surrounding peritoneum was markedly inflamed. Pathologic diagnosis was cholelithiasis and subacute cholecystitis. The gallbladder wall measured 8 mm in the opened specimen.

Case 2

A 59-year-old white man complained of right upper quadrant tenderness without rigidity or rebound tenderness. At admission, he was febrile to 38.3°C; bed rest, intravenous fluids, and ampicillin were instituted.

Ultrasound on the first day demonstrated at least three gallstones of 3–6 mm. The gallbladder wall was thickened to 5 mm (fig. 3). The common bile duct and the head of the pancreas could not be seen because of overlying bowel gas. No intrahepatic biliary duct dilatation was detected.

At operation, several acute adhesions were seen and the right upper quadrant of the abdomen was hyperemic. The gallbladder was grossly inflamed and had numerous gallstones. Intraoperative cholangiography was negative for ductal stones. The pathology report described an edematous, ulcerated, necrotic gallbladder wall. Numerous 3 mm calculi were seen. Final diagnosis was acute gangrenous cholecystitis.

Case 3

A 45-year-old black man had upper abdominal pain for 1 week before admission. There was slight tenderness in the right upper quadrant of the abdomen. Ultrasound showed the gallbladder wall was markedly thickened at 6 mm (fig. 4). No gallbladder calculi were seen. The patient died within 1 month after admission.

At autopsy, the gallbladder was of normal size, but its wall was 4–5 mm thick. It contained 30 ml of viscous yellow-brown bile, but no gallstones. The histologic sections were consistent with the diagnosis of chronic acalculous cholecystitis.

Case 4

A 69-year-old white man had right upper quadrant abdominal pain for 3 weeks and jaundice and dark urine for 2 days. Ultrasound soon after admission showed chronic pancreatitis. The gallbladder wall was 3 mm thick and a solitary stone was identified (fig. 5). The patient was treated with conservative medical therapy. Final diagnosis was chronic pancreatitis and cholelithiasis.

Discussion

The clinical need for rapid gallbladder visualization independent of liver function has been met largely by the introduction of ultrasound [1–8]. Ultrasound can detect the presence of calculi, determine gallbladder size, and detect thickening of the gallbladder wall in some patients

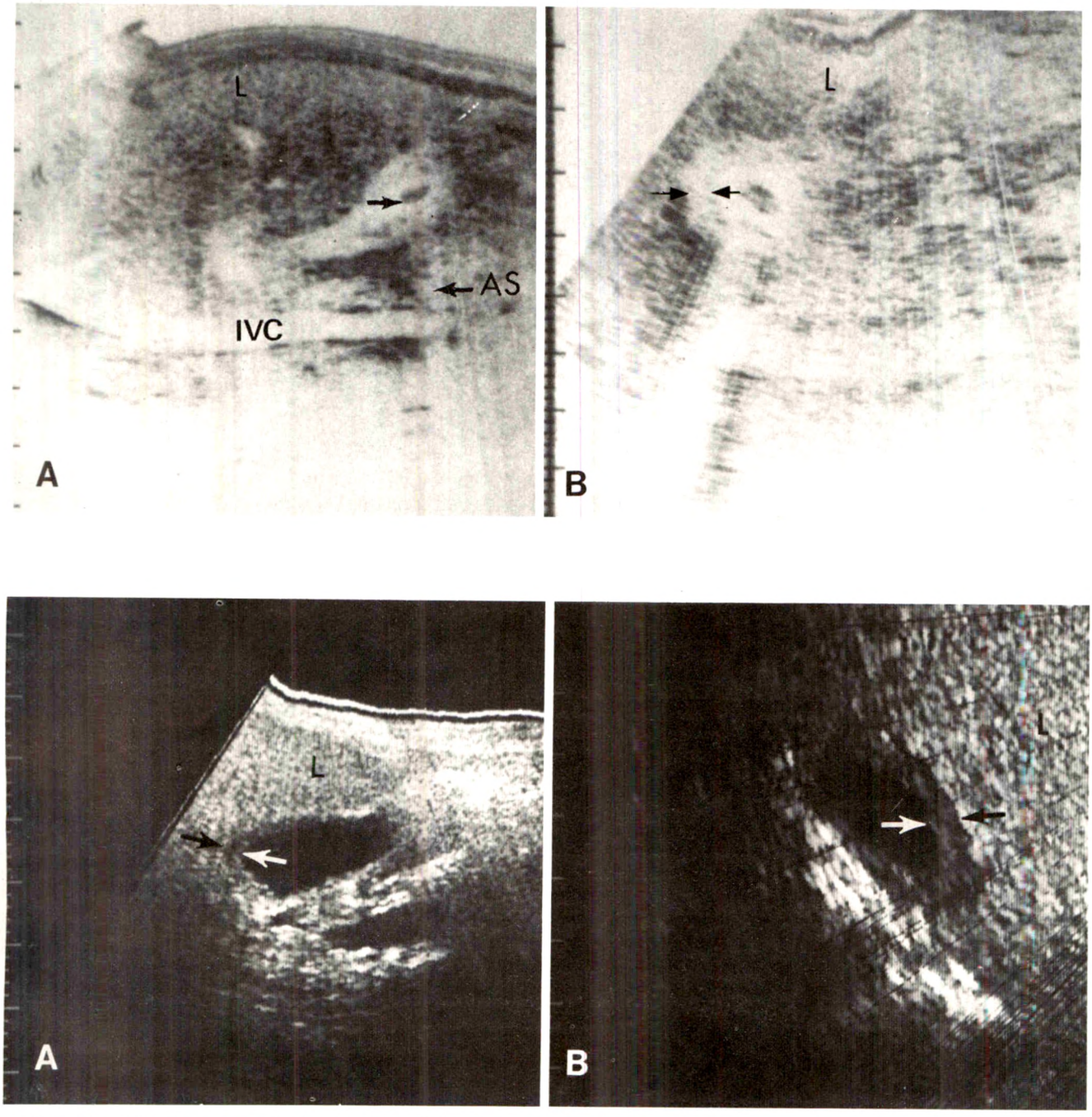


Fig. 3.—Case 2. Acute gangrenous cholecystitis. **A**, Sagittal section 5 cm right of midline. **B**, Transverse scan in left lateral decubitus position shows 5 mm gallbladder wall (*arrows*). Gallstones seen on other images. L = liver.

with cholecystopathy. Acute inflammation or chronic thickening produces a "halo" effect, and the discrete outline of the gallbladder is usually lost under these conditions [12, 13]. In this series, the incidence of gallbladder wall thickening in suspected cases of acute and chronic cholecystitis was 16%. Case 2 illustrates how positive ultrasound results may lead to early surgical intervention in acute cholecystitis, thus avoiding possibly imminent rupture of the gallbladder.

Difficulties in measuring the gallbladder wall include: (1) biliary sludge, which can interfere with demarcation of the wall; (2) beam width artifacts, which can lead to false positive results; and (3) a thickened wall after normal gallbladder contraction. Some of these problems may be overcome by maintaining the incident ultrasound beam perpendicular to the part of the wall being measured. Gallbladders less than 2 cm wide that have thick walls may represent a nonfasting state or possibly a pathologic condition. Repeat examination under carefully controlled conditions will increase diagnostic ac-

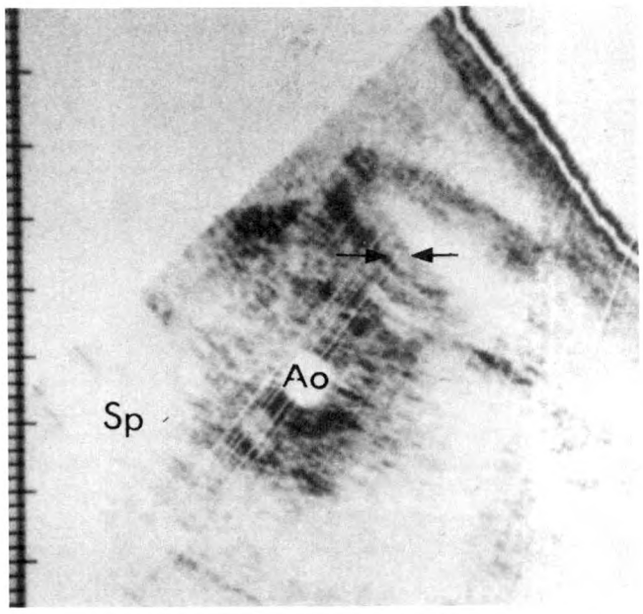


Fig. 4.—Case 3. Surgically proven acalculous cholecystitis. Transverse scan in left lateral decubitus position. No evidence of cholelithiasis, but thickened gallbladder wall (*arrows*). Sp = spine, Ao = aorta.

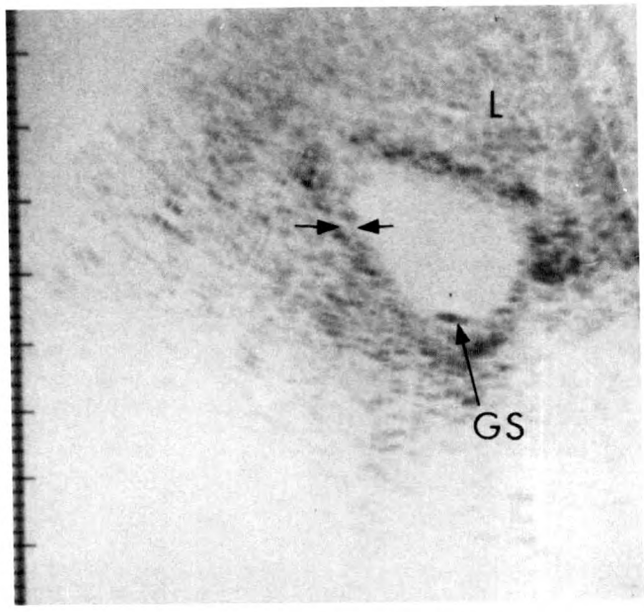


Fig. 5.—Case 4. Transverse scan with 3 mm gallbladder wall (*arrows*) and solitary 1 × 3 mm gallstone (GS). L = liver.

curacy by eliminating those patients who were not truly fasting.

The gallbladder wall was demonstrated in only 25% of the normal cases. With more sensitive equipment, it is expected that this percentage will increase.

The group of 10 patients whose gallbladders were not visualized by ultrasound were all proven diseased at surgery. These ultrasound and pathologic results provide significant correlation and agree with the experience of other investigators [12].

Ultrasound is valuable for diagnosing some cases of acute or chronic acalculous cholecystitis. As demonstrated here, gallbladder wall thickening can be determined even though there is no definite evidence of cholelithiasis. Although it is relatively uncommon, a localized area of thickening of the gallbladder wall with or without an adjacent mass should alert the ultrasonographer to the possibility of carcinoma [16, 17].

Infusion tomography has been suggested as a method of examining the gallbladder wall [18, 19]. There is evidence that this method may be subject to error and may not indicate the presence of disease. In a recent study by Morin et al. [19], visualization of the gallbladder wall by infusion tomography occurred in some normal cases. Therefore, the usefulness of infusion tomography in diagnosing cholecystitis may be limited.

Ultrasonic demonstration of a thickened gallbladder wall in suspected cases of acute or chronic cholecystitis is useful and may indicate early surgical intervention [20–23]. Thickening of the gallbladder wall may be more prevalent than this study indicates and should be explored in patients with clinical symptoms of acute or chronic gallbladder disease.

ACKNOWLEDGMENT

I thank David Toigo for technical assistance and Virginia Dobbs for typing and proofreading this manuscript.

REFERENCES

1. Hublitz UF, Kahn PC, Sell LA: Cholecystosonography: an approach to the non-visualized gallbladder. *Radiology* 103: 645–649, 1972
2. Goldberg BB, Harris K, Brooker W: Ultrasonic and radiographic cholecystography. *Radiology* 111:405–409, 1976
3. Doust BD, Muklad NF: Ultrasonic B-mode examination of the gallbladder. *Radiology* 110:643–647, 1974
4. Bartrum RJ, Crow HC, Foote SR: Ultrasonic and radiographic cholecystography. *N Engl J Med* 296:538–541, 1977
5. Anderson JC, Harned RK: Gray scale ultrasonography of the gallbladder: an evaluation of accuracy and report of additional ultrasound signs. *AJR* 129:975–977, 1976
6. Arnon S, Rosenquist CJ: Gray scale cholecystosonography: an evaluation of accuracy. *AJR* 127:817–818, 1976
7. Leopold GR, Amberg J, Gosink BB, Mittelstaedt C: Gray scale ultrasonic cholecystography: a companion with conventional radiographic techniques. *Radiology* 121:445–448, 1976
8. Lawson TL: Gray scale cholecystosonography: diagnostic criteria and accuracy. *Radiology* 122:247–251, 1977
9. Gosink BB, Leopold GR: Ultrasound and the gallbladder. *Semin Roentgenol* 11:185–189, 1976
10. Saunder RC, Conrad MR: Ultrasonic examination of the gallbladder, in *Radiology of the Gallbladder*, edited by Berk RN, Clemett AR, Philadelphia, 1977, Saunders, pp 37–48
11. Snyder WS, Cook MJ, Masset ES, Karhausen LR, Howells GP, Tipton IH: Report of the task group on reference man, in *International Commission on Radiological Protection, No. 23*, New York, Pergamon, 1975, p 148
12. Weissberg DK, Gosink B: Gray scale evaluation of the gallbladder. *Appl Radiol* 3:113–118, 1978
13. Marchul G, Crolla D, Baert AL, Fevery J, Kerremans R:

Gallbladder wall thickening: a new sign of gallbladder disease visualized by gray scale cholecystosonography. *JCU* 6:117–179, 1978

14. Howard RJ, Delany JP: Acute acalculous cholecystitis, in *Surgery of the Liver, Pancreas, and Biliary Tract*, edited by Najarian JS, Delaney JP, New York, Stratton Intercontinental Book, 1975, pp 159–164
15. Delaney JP: Chronic acalculous cholecystitis, in *Surgery of the Liver, Pancreas, and Biliary Tract*, edited by Najerian JS, Delaney JP, Stratton Intercontinental Book, 1975, pp 151–158
16. Petterson H: Carcinoma of the gallbladder: a review of 158 cases. *Acta Radiol [Diagn]* (Stockh) 15:225–236, 1974
17. Donaldson LA, Busuttid A: A clinicopathological review of 68 carcinomas of the gallbladder. *Br J Surg* 62:26–32, 1975
18. Love L: Infusion tomography of the gallbladder. *Semin Roentgenol* 11:181–184, 1975
19. Morin ME, Baker DA, Marsan RE: Visualization of the gallbladder wall at excretory urography: implication for infusion tomography of the gallbladder. *Radiology* 125:35–38, 1977
20. Klengensmith W, Watkins W, Oles P: Cholecystectomy in acute cholecystitis. *Arch Surg* 92:689–694, 1966
21. Van der Linden W, Sunzel H: Early versus delayed operation for acute cholecystitis: a controlled clinical trial. *Am J Surg* 120:7–13, 1970
22. Wright HK, Holden WD: The risks of emergency surgery for acute cholecystitis. *Arch Surg* 81:341–347, 1960
23. Hermann RE: Acute cholecystitis. *JAMA* 234:1251–1262, 1975

Erect Scanning of Pancreas Using a Gastric Window

HEBER MacMAHON,[1] JAMES D. BOWIE, AND CHRISTIAN BEEZHOLD

A technique that can offer improved ultrasonic visualization of the pancreas is reported and evaluated. One hundred subjects were scanned in an erect sitting position with fluid-filled stomachs ("erect gastric window" technique). Conventional supine scans were initially performed in all cases; oblique, semierect, decubitus, prone, and standing positions with and without fluid-filled stomach were also evaluated. Compared with supine scans, the "erect gastric window" technique, occasionally supplemented by semierect, oblique, or decubitus views, provided significantly improved visualization of the pancreas in 93% of subjects. The nonvisualization rate was reduced from 19% to 1%.

Although ultrasound is accurate for diagnosing pancreatic disease, inconsistent visualization of the gland has been a major limitation. It has resulted in a 17%–20% failure rate, largely due to overlying bowel gas [1, 2]. Dietary and pharmacologic measures designed to reduce the quantity of air in the bowel have produced only marginal benefits [3, 4]. In an attempt to improve the frequency and quality of pancreatic visualization, we scanned 100 subjects in both the conventional supine positions, and in various erect, semierect, and recumbent postures, with and without a fluid-filled stomach.

Subjects and Methods

The scanning arms on the commercially available gray scale units (Picker 80L with digital imager or Searle PhoSonic Digisonic; 3.5 MHz or 2.25 MHz, 19-mm-long internal focus transducers) [1] used for the examinations were tiltable to horizontal or near-horizontal positions, and enabled scanning of transverse sections with the subject erect. The subject could be converted to a sitting or semierect position by raising the back or lowering the foot of the adjustable table (Ritter 75, Ritter Co., Rochester, N.Y.). The table could also be rotated and raised or lowered during the examination, which greatly aided erect scanning.

Subjects fasted (except for clear liquids) on examination day. Supine scans were initially obtained, including transverse, sagittal, and oblique sections in the plane of the pancreas. When maximum information was gathered by this conventional technique, 75 ml of Lipomul-Oral (Upjohn Co., Kalamazoo, Mich.) was given followed by 540 ml of water. Tap water that had been allowed to stand for several minutes to allow bubbles to clear [5] was used in our study. Since bubbles are generated again on swallowing and also by gastric peristalsis, we waited about 5 min to allow initial gastric peristalsis to subside and for bubbles to clear. In seven subjects who were thought to have persistent gastric peristalsis, 1 mg of glucagon was given intravenously or subcutaneously. Transverse, sagittal, and oblique scans were then performed in the erect sitting position (fig. 1). In some cases, additional scans were also performed in one or several of the following positions: sitting erect without fluids; right decubitus, right posterior oblique semierect, and left posterior oblique semierect with fluid-filled stomach.

A total of 20 volunteers and 80 unselected patients who had been referred for pancreatic ultrasound were examined. Sections scanned in each position before and after ingestion of fluid were reviewed by two observers and compared with the conventional supine examination. Each image was graded for quality of visualization (excellent, adequate, poor, or nonvisualization) of the head, neck, body, and tail of the pancreas. Visibility of the pancreatic duct or splenic vein was also noted.

Results

The results are summarized in table 1. The "erect gastric window" technique (an erect sitting position with fluid-filled stomach) was the most useful single technique. It produced significantly improved visualization in 93 of the 100 subjects, compared with supine scans. There was usually enhanced visualization of the entire pancreas, especially the tail, which was often obscured by bowel gas in the supine position (figs. 2 and 3).

When the erect sitting position did not yield optimal results, placing the patient in a steep right posterior oblique (45°) semierect (20°) posture, or a complete right decubitus position, often improved visualization by throwing the fluid-filled stomach across the head and body of the pancreas (fig. 4). A left posterior oblique semierect position with fluid-filled stomach was occasionally helpful to visualize the pancreatic tail. The standing position showed no advantage over sitting and was technically more difficult. The supine position with fluid-filled stomach was predictably unhelpful in preliminary tests (due to swallowed air overlying the pancreas) and, therefore, was not used further.

If the patient was placed in an erect sitting position without administering fluids, there was still a significant improvement over supine scans in 48 (87%) of 55 cases. However, a second erect scan after ingestion of Lipomul-Oral and water showed further improvement in 45 (94%) of these 48 cases (fig. 2).

In the 100 subjects, there was no visualization of any part of the pancreas in 19% in the supine position. Of these 19, generally adequate or excellent visualization was obtained in 10 using the erect gastric window technique. However, in nine subjects visualization was generally less than adequate despite a gastric window and various postures. (In seven of these nine, the erect gastric window technique still provided improved visualization compared with supine scans.) Among these nine, three were grossly obese, one had an abdominal scar

Received October 2, 1978; accepted after revision January 3, 1979.

[1]All authors: Department of Radiology, University of Chicago, 950 East 59th Street, Chicago, Illinois 60637. Address reprint requests to H. MacMahon.

© 1979 American Roentgen Ray Society

0361–803X/79/1324–0587 $0.00

TABLE 1

Comparison of Scanning Techniques for Pancreatic Visualization

	Conventional Supine Technique (N = 100)		"Erect Gastric Window" Technique* (N = 100)	
	Adequate or Excellent	Poor or Non-visualization	Adequate or Excellent	Poor or Non-visualization
Area of pancreas:				
Head	49	51	84	16
Neck	59	41	92	8
Body	52	48	92	8
Tail	10	90	67	33
Pancreatic duct	6	94	23	77
Splenic vein	37	63	73	27

* Includes oblique and decubitus views, as required.



Fig. 1.—Erect pancreatic scan. Ritter table enables adjustment of posture, elevation, and axis.

that interfered with scanning, one was a heavyset man with an unusually muscular abdominal wall, and one had bowel obstruction and considerable ascites. This last subject represents the only instance where the upright scan completely failed to demonstrate the pancreas. In another case, the appropriate area had not been scanned completely in the erect position due to the examiner's initial lack of experience; this was the only time the upright scan was inferior to the supine scan.

The greatest improvement in visualization with the erect gastric window technique was in the region of the pancreatic tail. Using conventional supine technique, nonvisualization of the tail occurred in 75% and adequate or excellent visualization in only 10%. In contrast, with the erect gastric window technique, nonvisualization of the tail occurred in only 16% and adequate or excellent visualization occurred in 67%. In all 28 cases where preliminary prone scans were performed, the erect gastric window technique proved superior in visualizing the pancreatic tail.

An unexpected bonus in this study was the frequency with which we saw the normal pancreatic duct. Among the 20 healthy volunteers, portions of the pancreatic duct were identified in five cases on supine scans and in 12 cases with the erect gastric window technique. The duct was most frequently seen in the neck and body of the pancreas, appearing as either a single line of dense echoes or occasionally as two parallel lines (fig. 5). In the sagittal sections it appeared as a discrete echo, about in the center of the pancreas (fig. 6).

Discussion

The idea of scanning patients in the erect position with a fluid-filled stomach is not entirely new. It has been mentioned briefly by several authors [6], but results have generally been inconclusive or it has even been dismissed as unhelpful. We suspect that previous disen-

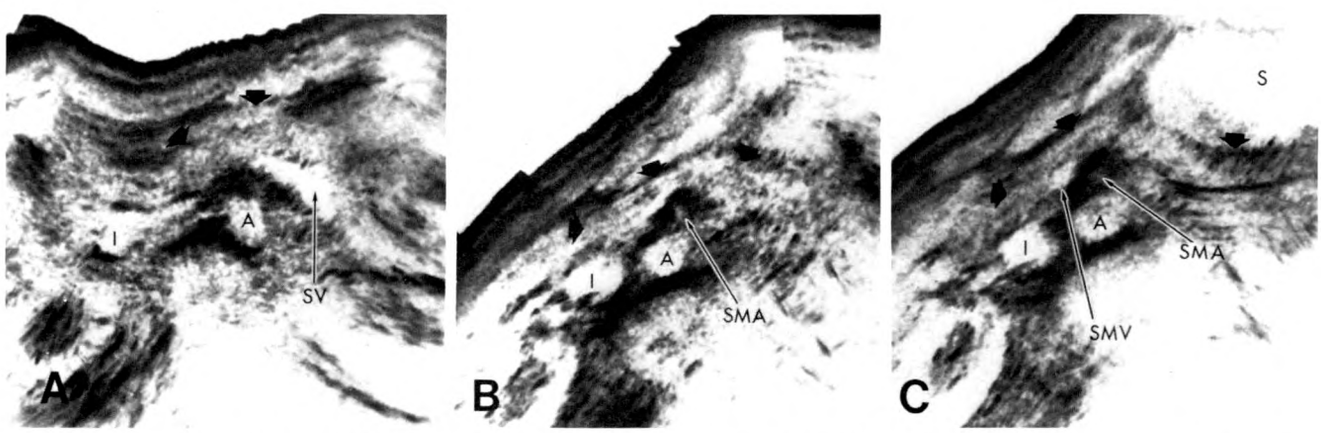


Fig. 2.—Male volunteer. **A**, Supine scan. Adequate visualization of head, neck, and body of pancreas (*arrows*). Tail obscured by bowel gas. I = inferior vena cava, A = aorta, SV = splenic vein. **B**, Erect sitting position. Improved delineation of head, neck, and body (*arrows*). Visualization of tail still poor. SMA = superior mesenteric artery. **C**, Repeat scan in erect position after ingestion of Lipomul-Oral and water. Excellent depiction of entire pancreas (*arrows*). Tail now seen through distended stomach. SMV = superior mesenteric vein, S = stomach.

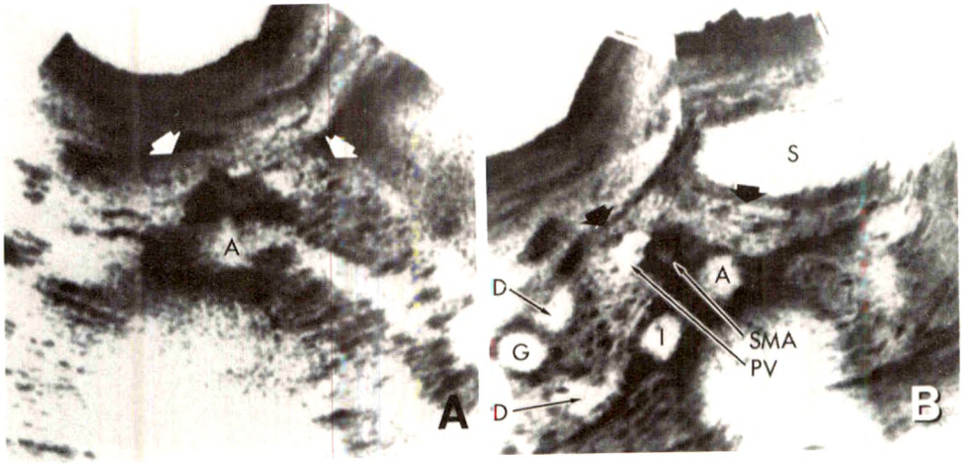


Fig. 3.—Male volunteer. **A**, Supine scan. Neck and body of pancreas (*arrows*). Partial obscuration of head and tail by bowel gas. A = aorta. **B**, Erect scan with fluid-filled stomach. Entire pancreas shown (*arrows*). Pancreatic head demarcated by fluid-filled duodenum. D = duodenum, G = gallbladder, PV = portal vein, I = inferior vena cava, SMA = superior mesenteric artery, S = stomach.

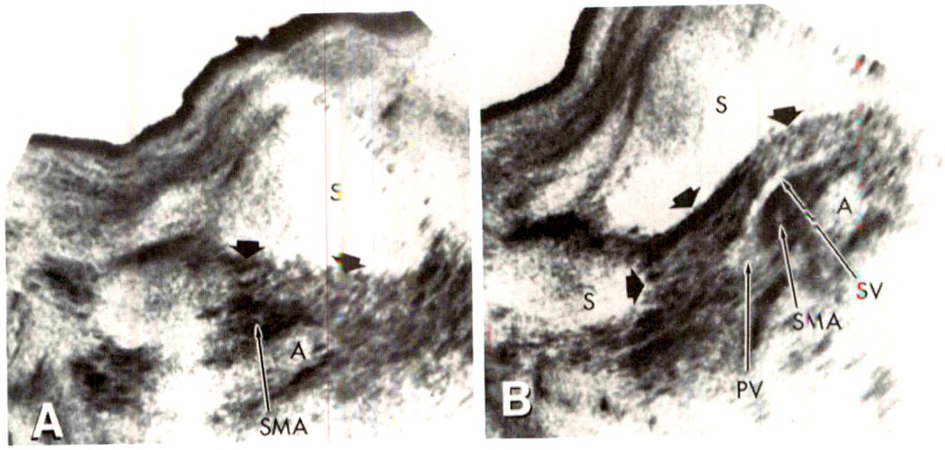


Fig. 4.—Pancreas had not been visualized on supine sections of 42-year-old woman patient. **A**, Upright section with fluid-filled stomach. Pancreatic tail (*arrows*). Head and neck obscured by bowel gas. SMA = superior mesenteric artery, A = aorta, S = stomach. **B**, Right posterior oblique semierect. Good visualization of head, neck, and body of pancreas (*arrows*) due to interposition of fluid-filled stomach, which provides sonic window. PV = portal vein, SV = splenic vein

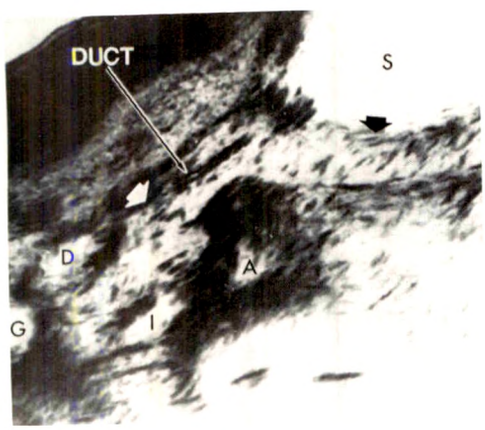


Fig. 5.—Erect scan of 28-year-old healthy male volunteer with filled stomach. Prominent duct (*arrows*) which is not uncommon in normals. G = gallbladder, D = duodenum, I = inferior vena cava, A = aorta, S = stomach.

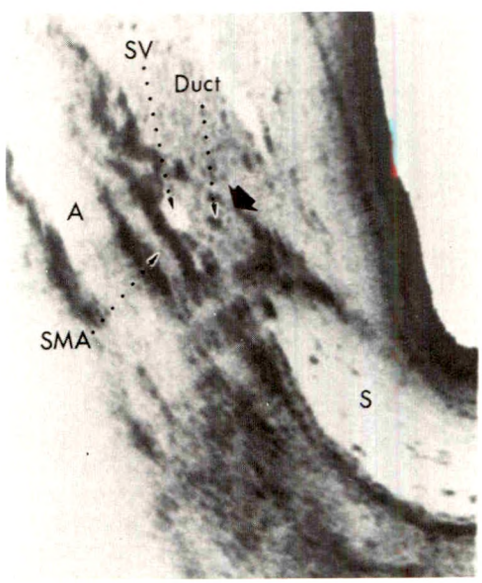


Fig. 6.—Upright sagittal section of 30-year-old healthy volunteer after ingestion of fluid. Body of pancreas (*arrow*) in cross section. Central echo represents main pancreatic duct. A = aorta, SMA = superior mesenteric artery, SV = splenic vein, S = stomach.

chantment with the technique mainly relates to failure to inhibit gastric peristalsis, which prevents clearing of the intragastric fluid and produces gastric emptying. Also, failure to adapt the method to variations in gastric

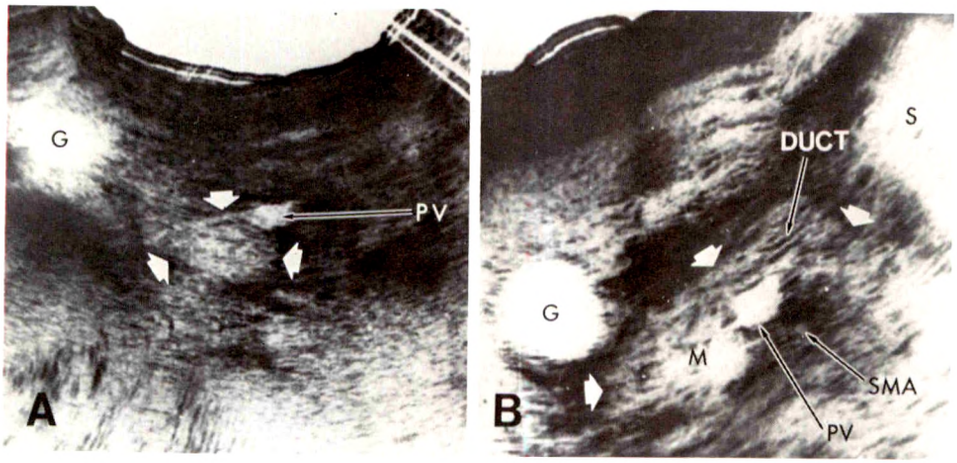


Fig. 7.—52-year-old man with painless jaundice. **A**, Supine scan. Poorly defined mass in area of head of pancreas (*arrows*). Gallbladder is distended. G = gallbladder, PV = portal vein. **B**, Erect. Sonolucent mass (M) in head of pancreas (*arrows*). Dilated pancreatic duct. SMA = superior mesenteric artery, S = stomach.

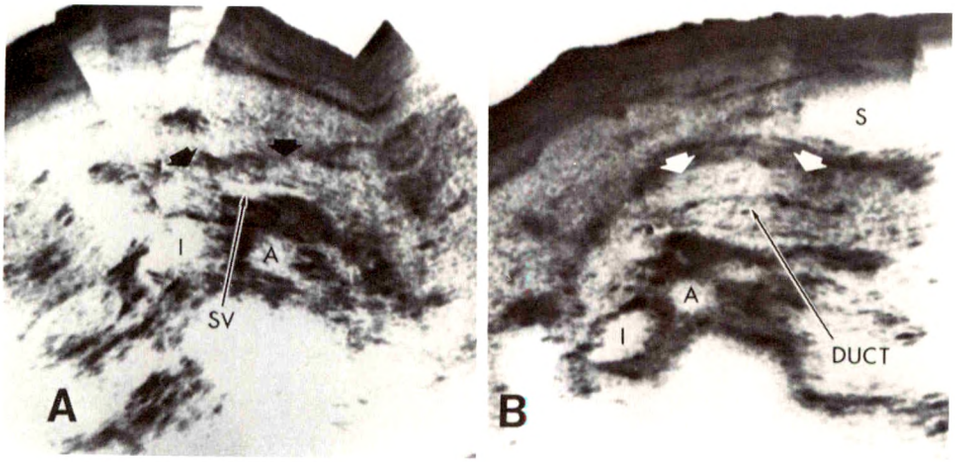


Fig. 8.—25-year-old alcoholic woman with epigastric pain. **A**, No definite abnormality in pancreas (*arrows*). Tail poorly shown. I = inferior vena cava, SV = splenic vein, A = aorta. **B**, Erect. Enlarged pancreatic tail with relatively anechoic area consistent with pancreatitis. Nondilated duct. S = stomach.

anatomy may account for some lack of success. To successfully apply this technique, the examiner must have an accurate conception of the positional changes of the stomach in various postures and the relative movements of air and fluid within it.

In the supine position, any air that is in the stomach will collect in the antrum, which usually overlies part of the pancreas. When the patient is erect, several changes beneficial to pancreatic scanning occur. First, air moves from the gastric antrum to the fundus where it does not overlie the pancreas. Second, the upper abdominal viscera move downward from under the ribs to a more accessible location. However, as the liver moves caudad rather more than the pancreas, an improved hepatic acoustic window is provided. Third, the major abdominal veins become relatively distended, which improves their visibility. These changes probably account for the improved visualization achieved in most patients who were scanned in the erect position prior to administration of fluids. When the patient drinks a large amount of fluid in the erect position, it accumulates in the body and antrum of the stomach, distending it and causing it to move more inferior. The small bowel and transverse colon are displaced downward by the distended stomach. Any swallowed air remains in the fundus. In this position, the gastric antrum is usually located immediately caudad to the body and neck of the pancreas.

When the head, neck, and body of the pancreas are poorly visualized in the erect position, the situation can usually be remedied by placing the patient in a right posterior oblique semierect or right decubitus posture, which tends to throw the fluid-filled stomach across the pancreas.

Failure to visualize the pancreas through the gastric window may result from persistent gastric motility. This difficulty is greatly aggravated by any solid food particles that may have remained in the stomach. In this series, we used a viscous fatty mixture (Lipomul-Oral), which is only mildly unpleasant and is well accepted by patients. Fat is a potent inhibitor of gastric emptying and has produced satisfactory results in the majority of patients. In seven cases where the stomach could not be visualized after ingestion of Lipomul-Oral and water, administration of glucagon resulted in a clear gastric window. We feel that failure to visualize the stomach in such cases is due to persistent peristalsis, which stirs up any residual food particles and possibly maintains microbubbles. Accordingly, we now administer intravenous glu-

cagon in any patient who does not show a clear gastric window within 5 min of swallowing the fluids.

Although the erect gastric window technique significantly improves pancreatic visualization compared with conventional technique, it is not always completely successful. Many of the partial failures that occurred in this series are understandable. The technique is not very useful in patients with ascites or previous gastric resection. The poor results in obese patients and those with heavily muscular abdomens are less readily explained. In many such cases, we were unable to inhibit gastric peristalsis with Lipomul-Oral, and visualization improved only when glucagon was given. In retrospect, we believe that glucagon should have been used more frequently for difficult cases.

Although we have used this technique mainly for the pancreas, it actually affords better delineation of the entire epigastric area. We have found good visualization of the left kidney in many patients using the erect gastric window technique, which is not common for conventional supine scans.

We believe the erect gastric window scanning technique generally provides a real improvement in the diagnostic quality of ultrasound examinations of the pancreas. The improved quality of visualization achieved in this series was not merely an aesthetic consideration, as was clearly shown in several abnormal cases (figs. 7 and 8). By obviating the necessity for special supine and prone sections, this method need not appreciably add to the time of the examination, and it is now routinely used in our department.

REFERENCES

1. Kressel HY, Margulis AR, Gooding GW, Filly RA, Moss AA, Korobkin M: CT scanning and ultrasound in the evaluation of pancreatic pseudocysts: a preliminary comparison. *Radiology* 126:153–157, 1978
2. Levitt RG, Geisse GG, Sagel SS, Stanley RJ, Evens RG, Koehler RE, Jost RG: Complementary use of ultrasound and computed tomography in studies of the pancreas and kidney. *Radiology* 126:149–152, 1978
3. Meire HB, Farrant P: Technical note: preparation of the patient for abdominal ultrasound scanning. *Br J Radiol* 51: 387–388, 1978
4. Somer G, Filly RA, Laing FC: Use of simeticone as a patient preparation for abdominal sonography. *Radiology* 125:219–221, 1977
5. Yeh HC, Wolf BS: Ultrasonic contrast study to identify stomach tap water microbubbles. *JCU* 5:170–174, 1977
6. Filly RA, Freimanis AK: Echographic diagnosis of pancreatic lesions. *Radiology* 96:575–582, 1970

Ultrasound of Epigastric Injuries After Blunt Trauma

L. CHRISTOPHER FOLEY[1] AND RITA LITTLEWOOD TEELE[1]

Blunt trauma to the epigastrium may result in a retroperitoneal hematoma involving the head of the pancreas and descending duodenum. Secondary effects include obstruction of the gastric outlet, obstruction of the biliary tree, and extrinsic compression of the inferior vena cava. Four patients with epigastric trauma were reviewed who had been examined by ultrasound of the abdomen. Ultrasound showed the extent of the retroperitoneal hematoma, its effect on contiguous organs, and was helpful in clinical management.

The radiographic features of injuries following blunt trauma to the epigastrium are well documented [1–4]. However, ultrasonic findings associated with closed injury to the upper gastrointestinal tract and retroperitoneum have not yet been described. Four patients who suffered blunt trauma to the epigastrium are reported and their ultrasonic examinations are discussed.

Case Reports

Case 1

T. M., a 12-year-old boy, was admitted to Children's Hospital Medical Center after 24 hr of epigastric pain, nausea, and vomiting. Physical examination disclosed a moderately distressed boy whose abdomen was silent to auscultation. On palpation, there was marked tenderness and guarding with spasm in the right upper quadrant and epigastrium. No mass was palpable. The only abnormal laboratory findings were a white blood cell count of 14,000/mm³ and an amylase of 247 caraway U/dl (normal, less than 150 U/dl).

Initial diagnostic examination of abdominal ultrasound demonstrated a 4 × 6 cm echogenic mass just right of the midline, anterior to the right kidney, and posterior to the liver. It extended inferiorly, parallel to the spine and psoas muscle (fig. 1A). The vena cava was compressed by the mass. The gallbladder was mildly dilated, but there was no dilatation of the common duct nor of the intrahepatic ducts. Diagnosis of a retroperitoneal hematoma extending along the tissue planes of the anterior pararenal space and involving the pancreas and duodenum was made after the patient recalled a blow to the epigastrium with a hockey stick 7 days earlier.

Upper gastrointestinal series showed the typical radiographic features of an intramural and extramural mass involving the second portion of the duodenum (fig. 1B). The patient slowly improved with conservative management. Resolution of the retroperitoneal mass over several months was documented by serial ultrasound examinations. No sequelae were recognized (fig. 1C).

Comment. In this patient, ultrasound findings prompted questions about the possibility of abdominal trauma and led to the diagnosis of a retroperitoneal hematoma with traumatic pancreatitis. Although not proven, the combination of appropriate trauma, radiographic findings, and clinical resolution supported this suspicion.

Case 2

K. B., a 12-year-old boy, was well until he had abdominal pain and dizziness, followed by nausea and vomiting, 24 hr before admission to Children's Hospital Medical Center. Physical examination disclosed diffuse abdominal tenderness, maximal in the right lower quadrant, with rebound tenderness. His temperature was 38°C. White blood cell count was 22,700/mm³ and hematocrit was 40. Tentative diagnosis was appendicitis, but at operation the appendix was normal. However, a large retroperitoneal hematoma surrounded the descending duodenum, extending inferiorly in the root of the mesentery to the level of the cecum. The retroperitoneum was not opened. No blood or fluid was found within the peritoneal cavity. When his history was reviewed, the patient recalled that 2 days before admission he had fallen onto the handle bars of his bicycle.

Upper gastrointestinal series the day after surgery showed complete obstruction of the gastric outlet. Abdominal ultrasound demonstrated a well defined mass of the hematoma in the epigastrium between the liver and right kidney. It extended from the inferomedial edge of the liver across the midline to the aorta, and inferiorly to the level of the iliac crest paralleling the right psoas muscle and the kidney (fig. 2A). It encompassed both the descending duodenum and the head of the pancreas. The common bile duct and gallbladder were dilated; a fluid/sludge level in the gallbladder from biliary stasis was present. The gastric antrum and duodenal bulb were dilated and filled with fluid (figs. 2B and 2C).

The patient gradually improved on conservative management with intravenous hydration and nasogastric suction. His serum amylase, 200 caraway U/dl in the immediate postoperative state, slowly decreased to normal. Serial examinations with ultrasound showed resolution of the hematoma.

Comment. The traumatic pancreatitis, retroperitoneal hematoma, and probable duodenal hematoma in this child are fairly typical of an injury to the epigastrium following a direct fall onto the handle bars of a bicycle. Ultrasound accurately confirmed the surgically discovered retroperitoneal hematoma. Secondary mild obstruction to the biliary tree was also documented.

Case 3

G. B., a 15-year-old boy, was well until he developed abdominal pain and pernicious vomiting 24 hr before admission. A blow to the epigastrium during a soccer match 3 days before admission was followed by development of a small bruise. Because of this trauma and the finding of a serum amylase level of 2,780 caraway U/dl, initial evaluation was abdominal ultrasound, which disclosed a mass anterior to the right kidney and posterior to the liver, but separate from these structures (fig. 3A). It extended along the psoas muscle to the level of the pelvis compressing the inferior vena cava. The gallbladder appeared normal. The gastric antrum and duodenal bulb were distended with fluid. Diagnosis was retroperitoneal hematoma in the anterior pararenal space involving the duodenum and pancreas with obstruction of the stomach and first part of the duodenum.

Received July 25, 1978; accepted after revision December 27, 1978.

[1] Department of Radiology, Children's Hospital Medical Center and Harvard Medical School, 300 Longwood Avenue, Boston, Massachusetts 02115. Address reprint requests to R. L. Teele.

© 1979 American Roentgen Ray Society

0361–803X/79/1324–0593 $0.00

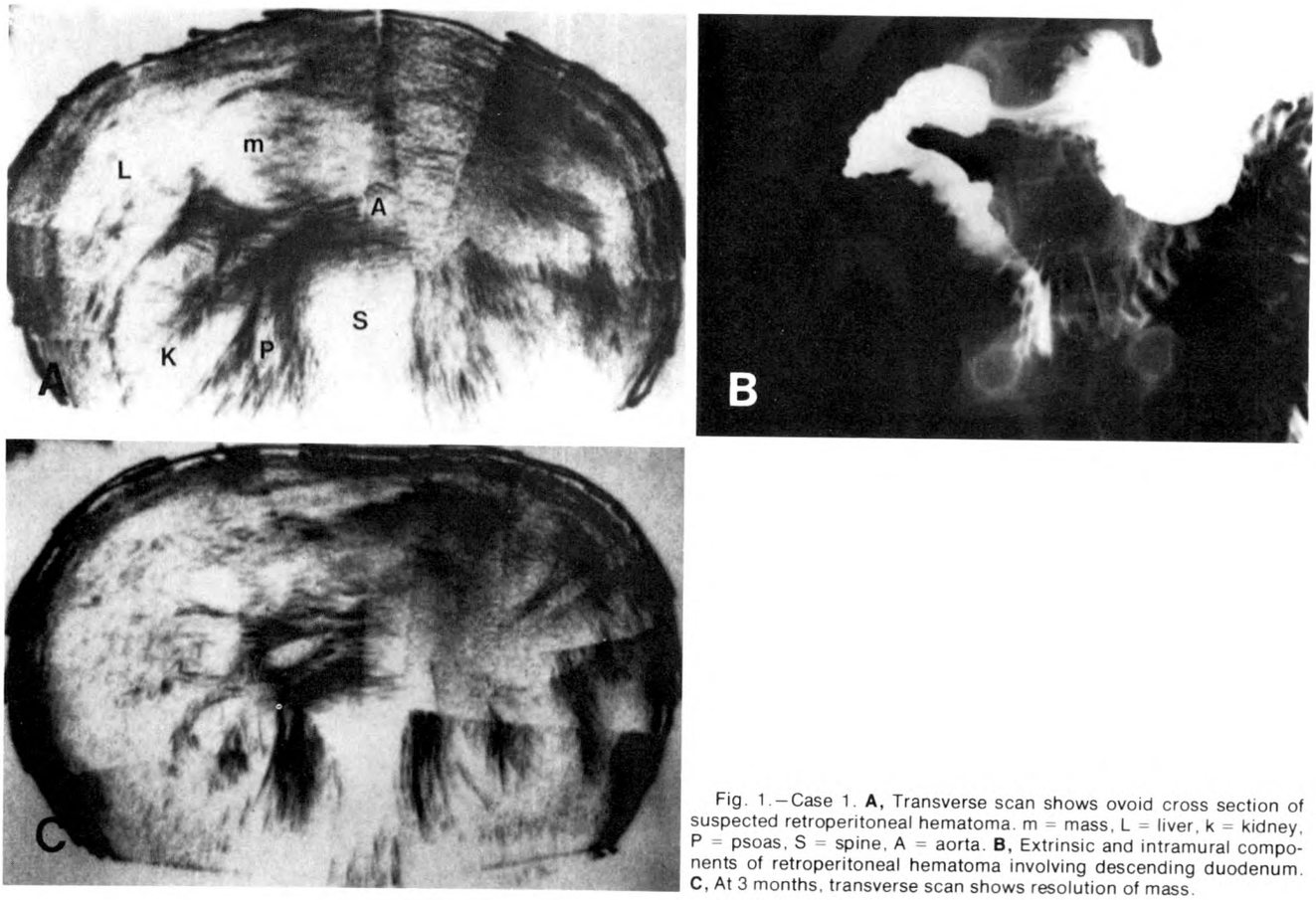


Fig. 1.—Case 1. **A,** Transverse scan shows ovoid cross section of suspected retroperitoneal hematoma. m = mass, L = liver, k = kidney, P = psoas, S = spine, A = aorta. **B,** Extrinsic and intramural components of retroperitoneal hematoma involving descending duodenum. **C,** At 3 months, transverse scan shows resolution of mass.

The patient slowly improved with conservative management. Upper gastrointestinal series 2 weeks after admission showed delayed gastric emptying and extrinsic compression, as well as submucosal "thumbprinting" of the second portion of the duodenum consistent with duodenal involvement by the retroperitoneal mass (fig. 3B). Serial ultrasound examinations showed slow resolution of the retroperitoneal mass and no evidence of development of a pancreatic pseudocyst.

Comment. Abdominal ultrasound delineated the location of the retroperitoneal injury in this patient, information not available by clinical or plain radiographic examination. Further, the dilatation of the gastric antrum and duodenal bulb, coupled with the patient's clinical picture, documented obstruction in the second portion of the duodenum.

Case 4

M. P., a 14-year-old girl, fell from a pony and suffered a concussion that made details of the accident vague. She developed left upper quadrant and left flank pain 6 months after the accident. Radiographic studies disclosed a "pancreatic abnormality" and medical management began. However, symptoms persisted, and the patient was referred to Children's Hospital Medical Center where, 18 months after injury, physical examination was normal. The only laboratory abnormality was a serum amylase of 220 caraway U/dl. Supine abdominal radiography showed several 2 mm to 1 cm calcific densities in the pancreas. Hypotonic duodenography demonstrated anterior displacement of the stomach and anterior, inferior displacement of the ligament of Treitz (fig 4A). Abdominal ultrasound showed enlargement of the body and tail of the pancreas with multiple echogenic foci representing calcification within the pancreas (figs. 4C and 4D). A pseudocyst was not identified. A small amount of ascitic fluid was present around the liver.

Endoscopic retrograde cannulation of the pancreatic duct revealed a normal proximal duct with a "pseudocyst" about 2 cm from the ampulla of Vater. There was a short stricture just distal to this collection; the rest of the pancreatic duct was dilated and contained several calcific stones (fig. 4B). At laparotomy, a markedly enlarged, inflamed, edematous pancreas was found. The pancreatic duct was quite dilated and contained numerous calcific concretions. A small pseudodiverticulum from the pancreatic duct was identified. A Peaustow pancreaticojejunostomy with Roux-en-Y anastomosis was constructed to drain the distal pancreas. Subsequently, the patient did well.

Comment. We assume that this child's fall resulted in a laceration of the pancreatic duct and the subsequent formation of the small pseudocyst and the stricture that caused distal obstruction.

Discussion

Blunt abdominal trauma is a common problem of the pediatric patient. Fortunately, significant intraabdominal sequellae are rare [6–8]. In one series of children admitted to the hospital for abdominal trauma, about 3%

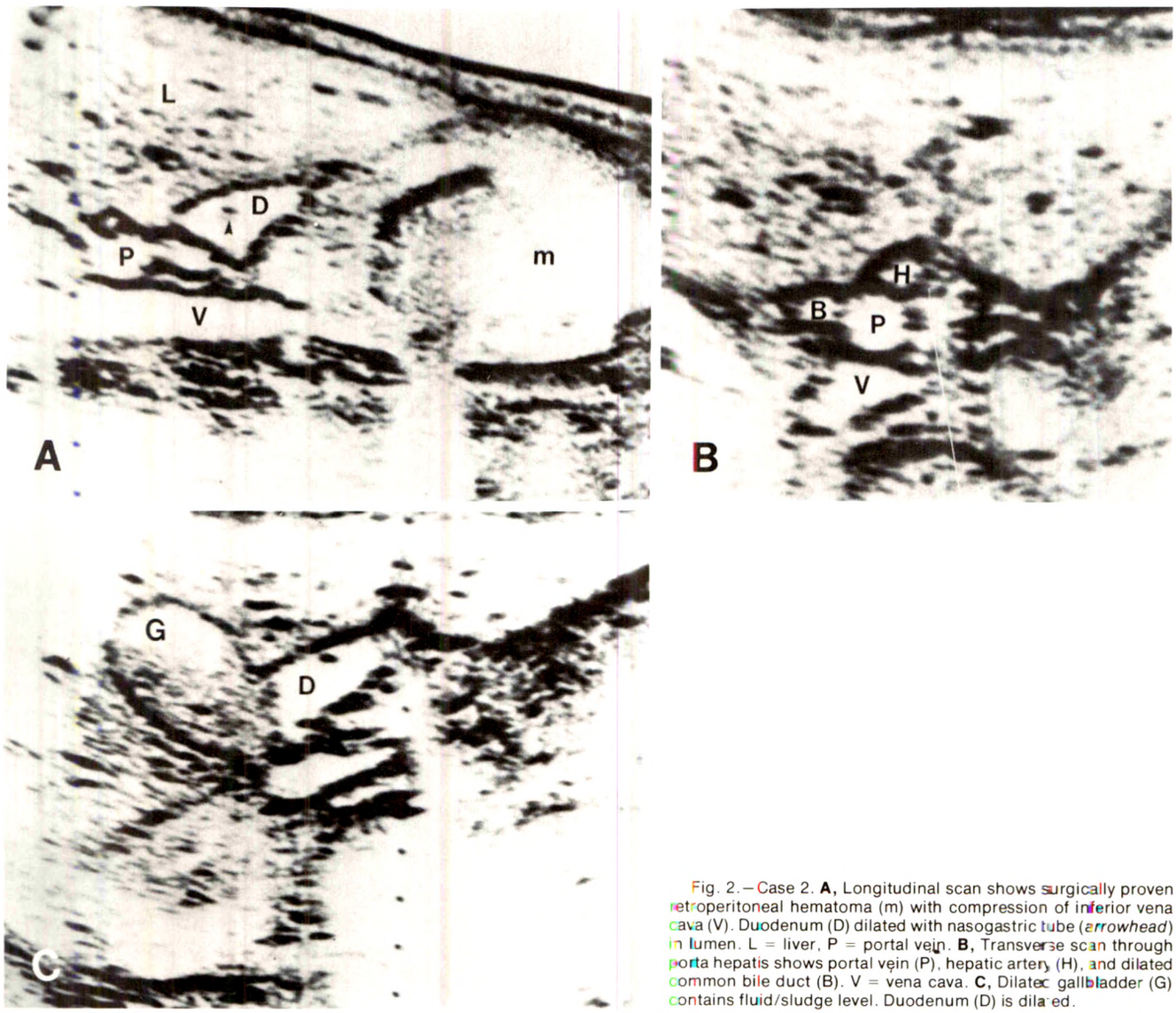


Fig. 2.—Case 2. **A,** Longitudinal scan shows surgically proven retroperitoneal hematoma (m) with compression of inferior vena cava (V). Duodenum (D) dilated with nasogastric tube (*arrowhead*) in lumen. L = liver, P = portal vein. **B,** Transverse scan through porta hepatis shows portal vein (P), hepatic artery (H), and dilated common bile duct (B). V = vena cava. **C,** Dilated gallbladder (G) contains fluid/sludge level. Duodenum (D) is dilated.

sustained isolated pancreatic injuries and 8% had isolated duodenal injuries [4].

Injury to the retroperitoneal structures in the epigastrium usually occurs after focal trauma with a force applied to a small area over the pancreas and duodenum. Because the pancreas and duodenum are fixed in position, they absorb the total force of such a blow. The relation of these soft organs to the spine and ribs makes damage in such a situation almost inevitable [8–11].

Clinically, these patients usually complain of epigastric abdominal pain, with or without radiation, nausea, and vomiting several hours to several days after the traumatic episode. Vital signs are usually normal. Physical examination reveals upper abdominal and, occasionally, rebound tenderness. Laboratory examination typically reveals a slightly elevated white blood cell count and, if there has been a large amount of retroperitoneal bleeding, a low hematocrit. If the pancreas has been injured, elevated levels of amylase and lipase are apt to be present in the serum and urine. It should be emphasized that the history of trauma may not be elicited early in the clinical course and only be recalled by the patient much later (cases 1, 2, and 4) [12–15].

With a knowledge of normal anatomy and its ultrasonic appearance [16–24], pathologic variation can be recognized. In three of our patients, a well circumscribed echogenic mass was the predominant finding. Its position anterior to the right kidney and posterior to the liver and its extension to, and even across, the midline indicated its location in the anterior pararenal compartment, thus involving the head of the pancreas and duodenal loop. In our one surgically proven case (case 3), the

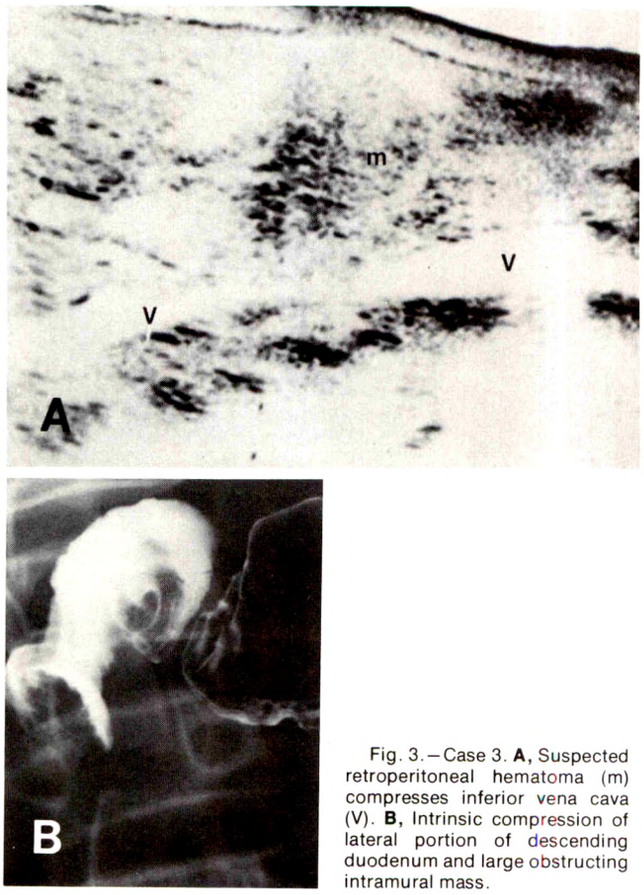


Fig. 3.—Case 3. **A,** Suspected retroperitoneal hematoma (m) compresses inferior vena cava (V). **B,** Intrinsic compression of lateral portion of descending duodenum and large obstructing intramural mass.

mass demonstrated by ultrasound was shown to be a large duodenal and retroperitoneal hematoma. Similar surgical findings in patients with duodenal and retroperitoneal hematomas following trauma have been documented [2, 8, 11, 12].

The three patients with retroperitoneal injury had both extramural and intramural involvement of the duodenum. Conceivably, isolated mural hematoma of the duodenum could occur, and appear on ultrasonic scans as a smaller, more circumscribed mass. Dilatation of the first portion of the duodenum, an intraperitoneal structure that usually escapes direct involvement by the hematoma, is evident on ultrasound. Some estimate of the degree of duodenal obstruction can be made on the basis of the size of a dilated duodenal bulb. Gastroduodenal examination with contrast material is necessary if duodenal perforation is suspected [4].

The biliary tree can be effected primarily or secondarily. Obstruction of the common duct by hematoma, edema, or pancreatitis can occur (case 2) [4, 25]. This obstruction leads to biliary stasis with dilatation of the common bile duct, gallbladder, and hepatic radicles. A fluid/sludge level in the gallbladder formed by layering of particulate matter in the static bile may be present. However, a fluid/sludge level in the gallbladder without dilated hepatic ducts is not a reliable sign of obstruction, since it may result from prolonged fasting or severe hepatic disease. Laceration of the common duct, a potential result of trauma to the epigastrium, cannot be diagnosed with ultrasound alone. Perhaps the presence of large amounts of intraperitoneal fluid would suggest this complication.

Injuries to the pancreas after trauma fall into three categories: (1) simple contusion with edema, (2) hematoma or hemorrhage, and (3) varying degrees of laceration [11]. Usually, the best view for showing the tail of the pancreas is prone. The head and body of the pancreas are seen best on the supine scans. The distortion of the vascular landmarks and visualization of an associated mass will permit diagnosis of pancreatic involvement [16, 19, 21]. In case 4, the small pseudocyst shown on endoscopic retrograde cannulation of the pancreatic duct was not seen because antral gas obscured the pancreas on supine scans. Decompression of the stomach by nasogastric suction or filling the antrum and duodenal bulb with water will allow ultrasonic visualization of abnormalities of the head of the pancreas. In addition, it has been shown that careful sector scanning of the pancreas will reveal dilatation (greater than 5 mm) of the pancreatic duct [25]. Most important are serial scans after the acute episode to search for pancreatic pseudocyst [27].

The inferior vena cava can be affected (cases 1–3), and it is best evaluated by longitudinal scans along its long axis. The potential exists for obstruction by anterior compression from the mass in the anterior pararenal space. In our patients, neither acute nor chronic sequelae resulted from compression of the inferior vena cava.

When examining the epigastrium, the liver, spleen, and kidneys should also be examined to detect traumatic alterations. In addition, there should be a search for peritoneal fluid (case 4).

Trauma to the epigastrium may result in a retroperitoneal hematoma in the anterior pararenal space. This hematoma typically involves the head of the pancreas and descending duodenum, with secondary effects on the biliary tree, inferior vena cava, and stomach. Ultrasonic examination can delineate the extent of the hematoma and can evaluate the organs affected by it. Ultrasound is also helpful in evaluating the delayed complications of abdominal trauma.

Since submitting this paper, we have seen two more patients with retroperitoneal hematoma after trauma. In one surgically proven case, the injury was complicated by a 1.5 cm pancreatic pseudocyst with pancreatic duct dilatation shown by ultrasound. Serial examinations documented resolution of the pseudocyst, the ductal abnormality, and the retroperitoneal mass. The second case was almost identical to the first three cases reported here. The patient had a large retroperitoneal mass that resolved after several months.

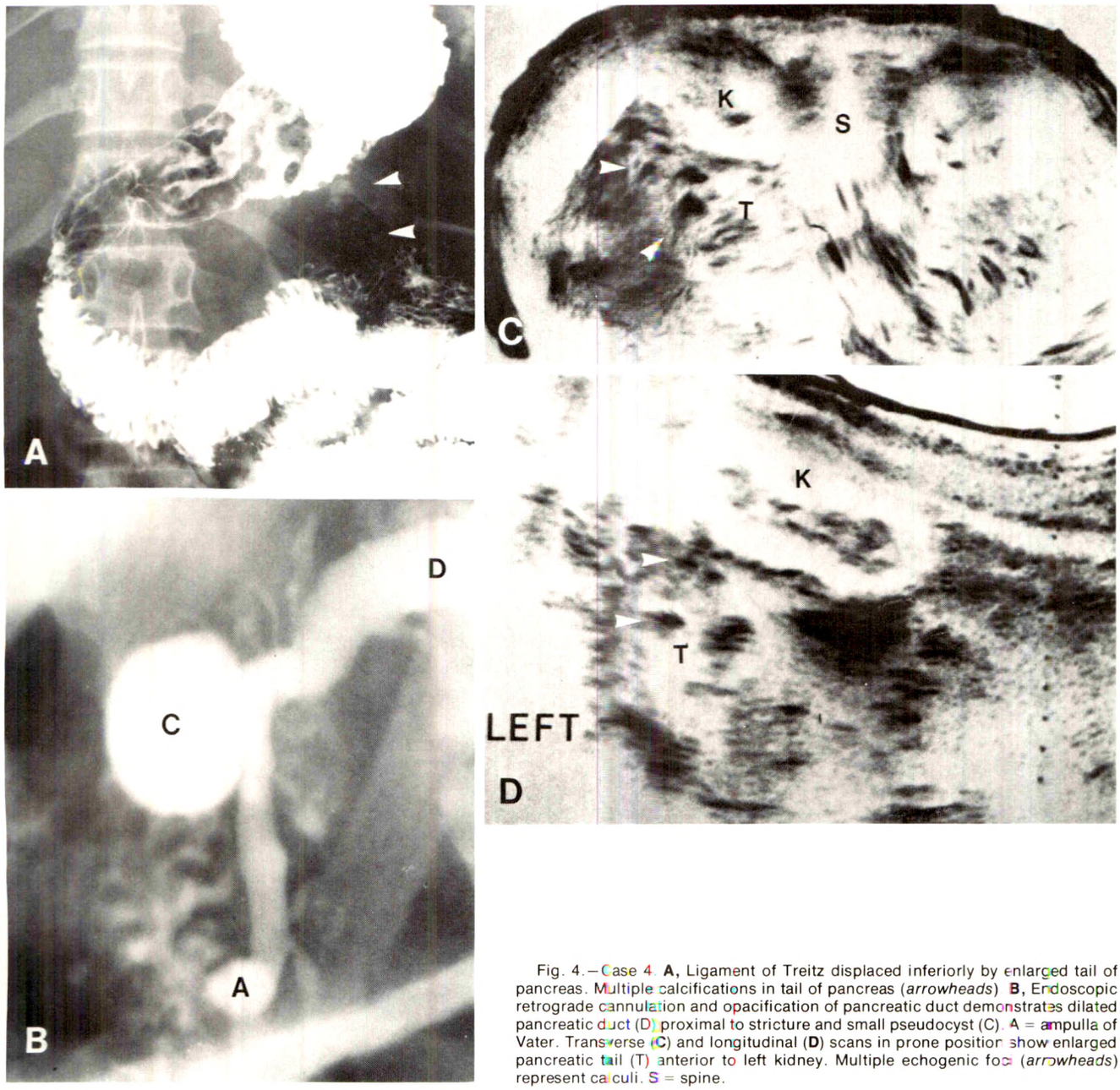


Fig. 4.—Case 4. **A,** Ligament of Treitz displaced inferiorly by enlarged tail of pancreas. Multiple calcifications in tail of pancreas (*arrowheads*). **B,** Endoscopic retrograde cannulation and opacification of pancreatic duct demonstrates dilated pancreatic duct (D) proximal to stricture and small pseudocyst (C). A = ampulla of Vater. Transverse (**C**) and longitudinal (**D**) scans in prone position show enlarged pancreatic tail (T) anterior to left kidney. Multiple echogenic foci (*arrowheads*) represent calculi. S = spine.

ACKNOWLEDGMENT

We thank Eileen Walsh and Andrea Kelton for assistance in preparing this manuscript.

REFERENCES

1. Ekgren K, Soderlund S: Radiological findings in traumatic lesions of the pancreas in childhood. *Ann Radiol* (Paris) 9: 279–285, 1966
2. Felson B, Levin EJ: Intramural hematoma of the duodenum: diagnostic roentgen sign. *Radiology* 63:823–830, 1954
3. Young LW, Adams JT: Roentgenographic findings in localized trauma to the pancreas in children. *AJR* 101:639–648, 1967
4. Young LW: Pancreatic and or duodenal injury from blunt trauma in childhood: radiopaque examinations and radiological review. *Ann Radiol* (Paris) 18:377–390, 1974
5. Adams JT, Elebute EA, Schwartz SI: Isolated injury to the pancreas from nonpenetrating trauma in children. *J Trauma* 6:86–98, 1966
6. Allen RB, Curry GJ: Abdominal trauma: a study of 297 consecutive cases. *Am J Surg* 93:398–404, 1957
7. Richardson JD, Belin RP, Griffen WL Jr: Blunt abdominal trauma in children. *Ann Surg* 176:213–216, 1972
8. Bailey WC, Akers DR: Traumatic intramural hematoma of

the duodenum in children. *Am J Surg* 110:695–703, 1965
9. Freeark RJ, Corley RD, Norcross WJ, Strohl EL: Intramural hematoma of the duodenum. *Arch Surg* 92:463–475, 1966
10. Andersson A, Bergdahl L: Intramural hematoma of the duodenum in children: review of literature and report of two cases. *Am Surg* 39:402–405, 1973
11. Kinnaird DW: Pancreatic injuries due to nonpenetrating abdominal trauma. *Am J Surg* 91:552–557, 1956
12. Resnicoff SA, Morton JH: Changing concepts concerning intramural duodenal hematomas. *J Trauma* 9:561–576, 1969
13. Mahour GH, Woolley MM, Gans SL, Payn VC Jr: Duodenal hematoma in infancy and childhood. *J Pediatr Surg* 6:153–160, 1971
14. Donovan AJ, Turrill F, Berne CJ: Injuries of the pancreas from blunt trauma: *Surg Clin North Am* 52:649–665, 1972
15. Judd DR, Taybi J, King H: Intramural hematoma of the small bowel. *Arch Surg* 89:527–535, 1964
16. Sample WF: Techniques for improved delineation of normal anatomy of the upper abdomen and high retroperitoneum with gray scale ultrasound. *Radiology* 124:197–202, 1977
17. Meyers MA: Radiological features of the spread and localization of extraperitoneal gas and their relationship to its source. *Radiology* 111:17–26, 1974
18. Gosink BB, Leopold GR: Ultrasound and the gallbladder. *Semin Roentgenol* 11:185–189, 1976
19. Leopold GR: Gray scale ultrasonic angiography of the upper abdomen. *Radiology* 117:665–671, 1975
20. Filly RA, Carlsen EN: Newer ultrasonographic anatomy in the upper abdomen. II. The major systemic veins and arteries with a special note on localization of the pancreas. *JCU* 4:91–96, 1975
21. Filly RA, Freimanis AK: Echographic diagnosis of pancreatic lesions: ultrasound scanning techniques and diagnostic findings. *Radiology* 96:575–582, 1970
22. Carlsen EN, Filly RA: Newer ultrasonographic anatomy in the upper abdomen. I. The portal and hepatic venous anatomy. *JCU* 4:85–90, 1975
23. Goss CM (ed): *Gray's Anatomy*, 29th ed. Philadelphia, Lea & Febiger, 1976
24. Meyers MA: *Dynamic Radiology of the Abdomen*. New York, Springer, 1976
25. Gosink BB, Leopold GR: The dilated pancreatic duct: ultrasound evaluation. Presented at the annual meeting of the American Institute of Ultrasound in Medicine, November 1977
26. Duncan JG, Imrie CW, Blumgart LH: Ultrasound in the management of acute pancreatitis. *Br J Radiol* 49:858–862, 1977
27. Gonzalez AC, Bradley EL, Clements JL Jr: Pseudocyst formation in acute pancreatitis: ultrasonographic evaluation of 99 cases. *AJR* 127:315–317, 1976

Dural and Direct Cavernous Sinus Fistulas

FRANS L. M. PEETERS[1] AND ROBERT KRÖGER[1]

Fistulas between the cavernous sinus and the carotid artery occur either after trauma or spontaneously. Unilateral exophthalmos is invariably the most conspicuous symptom. Until recently, treatment consisted of some method of occluding the carotid artery involved. Interventional catheter techniques have since been developed that use either Gelfoam embolization or released balloons. The results seem very promising, but long-term results of these new techniques are not yet available. Carotid–cavernous sinus fistulas may be dural or direct, each requiring a different interventional technique. Therefore, it is essential to determine the type involved by selective internal and external carotid angiography. This paper discusses 19 patients with carotid-cavernous fistulas, four of whom were successfully treated by catheter techniques. Gelfoam embolization was used in one case, and in three cases the fistula was closed with the aid of a balloon.

Cavernous sinus fistulas are abnormal communications between the carotid artery and the cavernous sinus. They can be divided into three groups: (1) those between meningeal branches of the internal carotid artery and the cavernous sinus; (2) those between meningeal branches of the external carotid artery and the cavernous sinus; and (3) those between the internal carotid artery and the cavernous sinus. Fistulas of the first two groups are also known as dural cavernous sinus fistulas (dural fistulas), while those of the third group are also known as direct cavernous sinus fistulas (direct fistulas).

Dural fistulas, regardless of whether meningeal branches of the internal or of the external carotid are involved, are based on arteriovenous malformation. Direct fistulas are usually posttraumatic. Until recently, treatment of cavernous sinus fistulas consisted of surgical ligation of the nutrient internal and external carotid artery. The severity of the symptoms determined the indication for this therapy.

The classic clinical features of cavernous sinus fistulas are pulsating exophthalmos, continuous murmur, arterialization of the orbital veins, headache, impaired eye movements, reduced visual acuity, and glaucoma. These symptoms can be posttraumatic or may occur spontaneously without a convincing history of trauma.

Reduced visual acuity can result from a direct traumatic lesion of the optic nerve or from an optic nerve lesion caused by disturbed blood supply. The glaucoma frequently observed in patients with a cavernous sinus fistula results from increased episcleral venous pressure. Disturbed eye movements, too, can be a direct result of a traumatic lesion of the trochlear, oculomotor, or abducens nerve, but may also be based on congestion of orbital veins and oedema. Pulsating exophthalmos is a conspicuous symptom, but it is not necessarily a consequence of arteriovenous communication in the cavernous sinus, and a carotid-cavernous communication does not necessarily produce pulsating exophthalmos [1].

Differentiation of the various types of cavernous sinus fistulas has not been essential for treatment by carotid ligation. However, recently developed methods use catheterization, closing the fistula itself but often leaving the nutrient artery intact. The artery is catheterized, and the fistula is closed by Gelfoam embolization or by depositing one or several balloons. Differentiation of the various cavernous sinus fistulas is essential for these therapeutic methods. Identification of each type is done by selective angiography of the internal and external carotid arteries.

Fistulas between meningeal branches of the external carotic and the cavernous sinus can be closed by Gelfoam embolization [2, 3]. Those between the internal carotic and the cavernous sinus can be closed with the aid of one or several balloons [4–6]. As yet, there are no reports on closure of fistulas between meningeal branches of the internal carotid and the cavernous sinus by catheterization techniques. Closure of these fistulas is perhaps only possible by deposition of a balloon at the site of origin of these meningeal branches.

This paper emphasizes the importance of differentiating the two dural types and the direct type with reference to our observations in the diagnosis and treatment of cavernous sinus fistulas.

Anatomic Features

Between the carotid canal and the anterior clinoid process, the internal carotid artery is lodged within the cavernous sinus. This sinus can be regarded as a venous network lying in the interstitial tissue of the local arteries and nerves [7].

The principal branches of the internal carotid artery extending through this area are the meningohypophyseal trunk and the inferior artery of the cavernous sinus. These are meningeal branches of the internal carotid, which anastomose with meningeal branches of the external carotid artery. The principal branches of the external carotid arise from the middle meningeal artery, the internal maxillary artery, and the ascending pharyngeal artery. Therefore, the venous network of the cavernous sinus lies between meningeal (dural) vessels arising both from the internal and external carotid arteries.

The oculomotor, trochlear, abducens, and branches of the trigeminal nerves are partly lodged in the venous network. The left and right cavernous sinuses communicate via a venous network localized on the clivus. Moreover, the cavernous sinus communicates anteriorly with

Received July 18, 1978; accepted after revision December 27, 1978.

[1] Department of Diagnostic Radiology, Wilhelmina Gasthuis, University of Amsterdam, The Netherlands. Address reprint requests to F. L. M. Peeters.

© 1979 American Roentgen Ray Society

0361–803X/79/1324–0599 $0.00

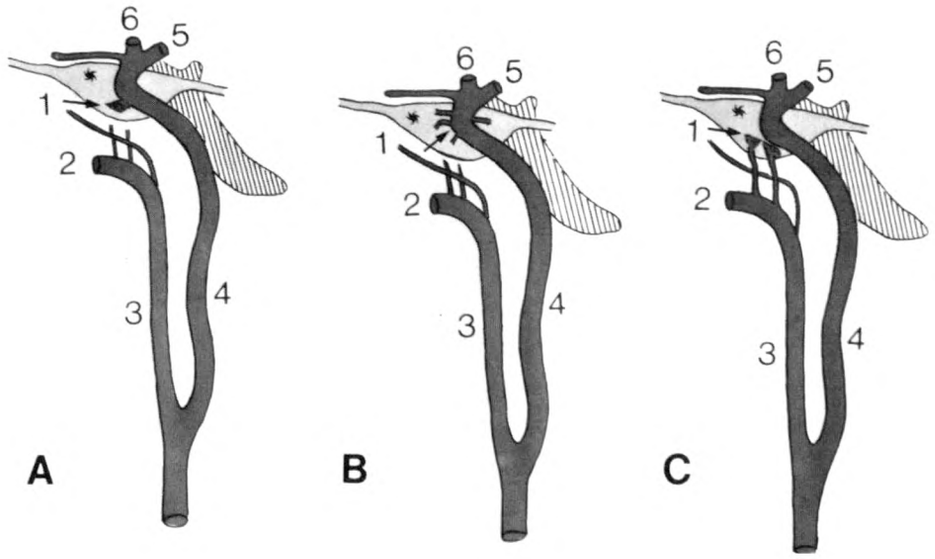


Fig. 1.—**A**, Direct internal carotid-cavernous sinus fistula (*arrow*). (1) middle meningeal artery; (2) internal maxillary artery; (3) external carotid artery; (4) internal carotid artery; (5) middle cerebral artery; (6) anterior cerebral artery; (*) cavernous sinus. **B**, Dural internal carotid-cavernous sinus fistula (*arrow*). **C**, Dural external carotid-cavernous sinus fistula (*arrow*).

the ophthalmic vein and the sphenoparietal sinus, posteriorly with the inferior and the superior petrosal sinus, and inferiorly with the veins to the pterygoid plexus and the plexus of the foramen ovale. Under normal conditions, the flow in the ophthalmic vein is toward the cavernous sinus, while that in the other veins is away from it.

On the basis of the anatomy, the following possibilities can be expected in the presence of pathologic communications with the cavernous sinus: (1) direct communication between the intracavernous part of the internal carotid artery and the cavernous sinus: direct internal carotid-cavernous sinus fistula (fig. 1A); (2) communication between meningeal branches of the internal carotid artery and the cavernous sinus: dural internal carotid-cavernous sinus fistula (fig. 1B); and (3) communication between meningeal branches of the external carotid artery and the cavernous sinus: dural external carotid-cavernous sinus fistula (fig. 1C). Combinations of these possibilities have also been described. In addition, a fistula between the basilar artery and the cavernous sinus has been reported [8]. How this fistula can be anatomically explained remains obscure.

Subjects and Methods

Cavernous sinus fistula was angiographically diagnosed in 19 patients within a 6 year period. Nine had dural fistula and 10 had a direct fistula. All patients with a dural fistula showed spontaneous exophthalmos. Actually, in all these cases the exophthalmos had been the indication for radiography or angiography. Only one of the dural fistula patients had a souffle. None had history of trauma in contrast to the direct fistula patients, who always had a serious head injury. With one exception, all these patients developed exophthalmos after head injury. The one patient without exophthalmos had a posttraumatic souffle, and sustained an arachnoidal hemorrhage a few weeks after the accident. A souffle was also found in all other direct fistula patients.

In patients with exophthalmos without souffle, orbital phlebography was the first radiologic examination until computed tomography (CT) was introduced in our institution; subsequently, CT became the first radiologic examination in these cases. Carotid angiography is the first radiologic examination when the clinical picture includes a souffle as well as exophthalmos. In all our patients, final diagnosis was established on the basis of carotid angiography.

The principal features of our patients are summarized in tables 1 and 2. It was often impossible to determine by angiography of the common carotid artery alone from which arteries the cavernous sinus was filled (table 1). Selective angiography of the internal and external carotid artery is required for accurate differentiation.

In eight of the dural fistula patients, no treatment was given. The other patient received Gelfoam embolization. Of the 10 direct fistula patients, seven were treated surgically by the Hamby method [9] and three were treated by the inflatable and released balloon technique of Debrun et al. [5, 6].

Findings

Increasingly, CT is the first radiologic examination in patients with unilateral spontaneous exophthalmos. Several authors [10, 11] have already pointed out that dilatation of the superior ophthalmic vein due to carotid-cavernous fistula (or from other causes) should be identifiable as such by CT. Such features were observed in five of our patients in whom CT was performed. However, CT cannot reveal the cause of dilatation.

For carotid-cavernous fistulas, the homolateral superior ophthalmic vein fails to fill at orbital phlebography [12], but no further information as to the cause is obtained. Therefore, carotid angiography remains the procedure of choice.

Given a direct communication between the intracavernous part of the internal carotid artery and the cavernous sinus, virtually the entire volume of the internal carotid artery flows into the cavernous sinus via the

TABLE 1

Patients with Spontaneous Onset of Fistula

Case No.	Age (years)	Dural Carotid-Cavernous Fistulas			Flow in Distal Branches of Internal Carotid
		Internal Carotid	External Carotid	Internal and/or External Carotid	
1	80	. . .	. . .	Left	+
2	52	Right	. . .	. . .	+
3	58	Right	. . .	. . .	+
4	64	Left	Left	Right	Left and right
5	68	. . .	. . .	Left	+
6	72	. . .	Right	. . .	+
7	19	. . .	Right	. . .	+
8	49	. . .	. . .	Left	+
9	70	. . .	Left and right	. . .	Left and right

TABLE 2

Patients with Fistula After Trauma

Case No.	Age (years)	Direct Internal Carotid-Cavernous Fistula	Flow in Distal Branches of Internal Carotid
10	20	Right	–
11	14	Left	+
12	38	Left	–
13	26	Left	–
14	45	Right	–
15	25	Right	–
16	20	Right	–
17	58	Right	–
18	25	Left	–
19	22	Right	+

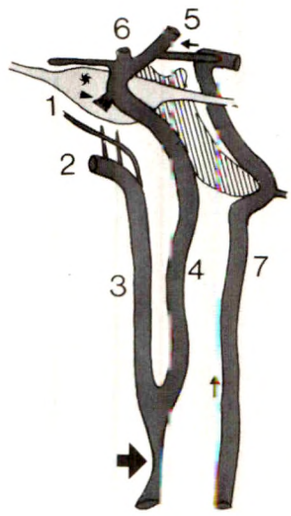


Fig. 2.—Injection into vertebral artery with compression of homolateral carotid artery. Direction of bloodflow (*small arrows*); fistula (*arrowhead*); compression site (*large arrow*); cavernous sinus (*).

fistula. Therefore, after contrast material is injected into the homolateral internal carotid artery, the cavernous sinus and the efferent veins are amply filled within a fraction of a second. The intracranial branches of the internal carotid artery are often no longer filled from the homolateral internal carotid artery, but from the contralateral internal carotid via the anterior communicating artery, and from the basilar artery via the posterior communicating artery. The homolateral ophthalmic vein generally shows marked dilatation.

Carotid angiography rarely allows determination of the exact fistula site even at an exposure rate of six frames per second. This failure is caused by superposition of the massively filled cavernous sinus and the efferent veins. The exact fistula site may be visualized by injection of contrast medium into the vertebral artery and simultaneous compression of the homolateral carotid artery in the cervical region [13]. Thus, the strong flow in the carotid artery is eliminated, and the contrast medium passes into the fistula via the posterior communicating artery and the reversed flow in the internal carotid artery (fig. 2). When the posterior communicating artery is not patent, a similar technique can be applied by injection into the contralateral carotid and simultaneous compression of the homolateral carotid artery. In that case the contrast medium passes into the contralateral carotid via the anterior communicating artery.

As already mentioned, differentiation of dural from direct shunts is important for planning therapy. The criteria for differentiation are found in the angiogram. In case of dural fistulas from the external carotid, the vessels afferent to the shunt are visible. The meningeal vessels from which the branches extend to the fistula, are dilated. These are the middle meningeal artery, meningeal branches from the internal maxillary artery (fig. 3A), and the ascending pharyngeal artery.

In dural fistulas from the internal carotid, the meningeal vascular network filling the fistula is likewise visible (fig. 3B), and the angiogram shows dilatation of the meningohypophyseal trunk and the inferior cavernous sinus artery [14]. Another indication of a dural shunt is

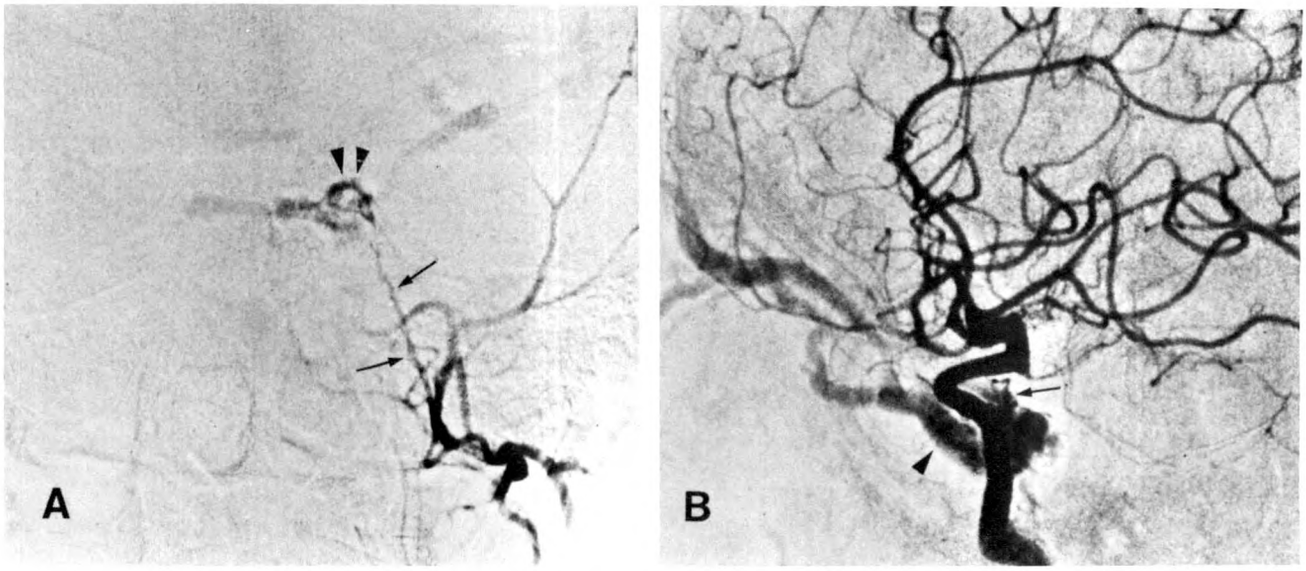


Fig. 3.—Case 4. Patient with dural external carotid- and dural internal carotid-sinus fistulas. **A**, Left external carotid artery. Small artery (*arrows*) runs from internal maxillary artery to cavernous sinus (*arrowheads*). **B**, Left internal carotid artery. Small meningeal vessels (*arrow*) run from carotid siphon to cavernous sinus (*arrowhead*).

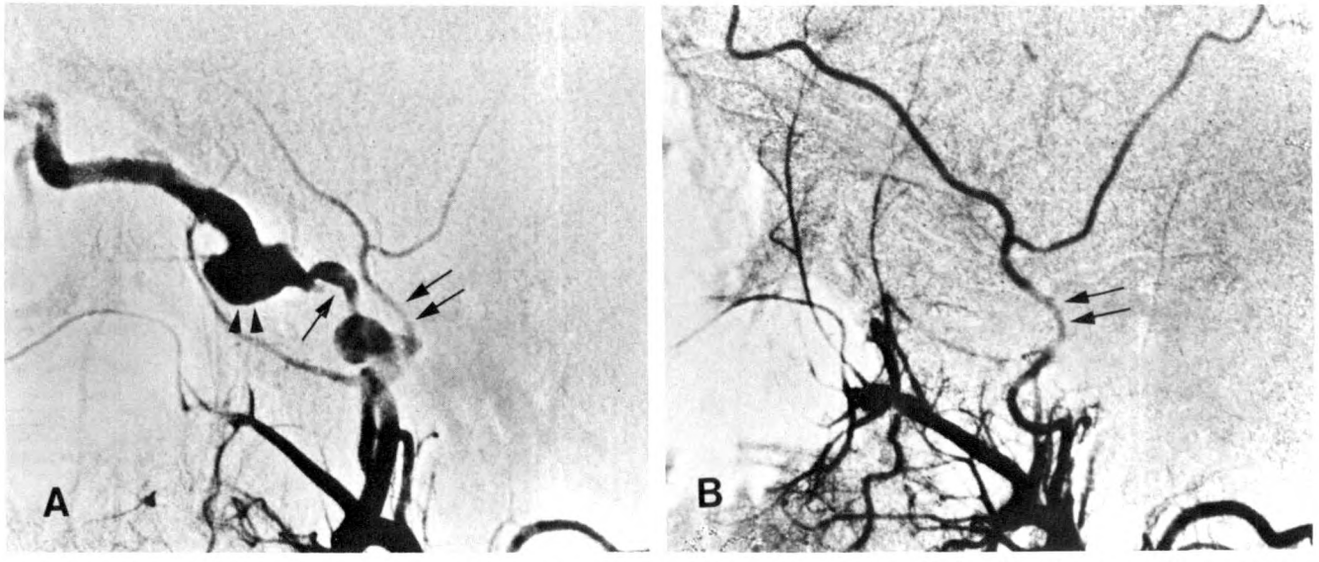


Fig. 4.—Case 7. Left external carotid artery in patient with dural external carotid-cavernous sinus fistula before (**A**) and after (**B**) embolization therapy. Meningeal vessel (*single arrow*) runs from internal maxillary artery to cavernous sinus (*arrowheads*). Superficial temporal artery (*double arrows*) better filled after treatment.

that, unlike a direct shunt, it allows filling of the intracranial branches via the homolateral internal carotid. This is indicative of a relatively low pressure, low flow shunt that differs from the direct type of fistula [15].

Treatment

Clinical symptoms of dural fistulas are often so insignificant that treatment is not necessary. If the symptoms require treatment, the method of choice for external carotid-cavernous sinus fistulas is embolization with Gelfoam, fibrin, silastic spheres, or muscle fragments [3, 16–19]. This technique uses selective catheterization of the external carotid or superselective catheterization of its branches. The emboli that finally occlude the fistula are injected via the catheter.

In eight of our nine patients (cases 1–6, 8, and 9), the sole clinical symptom of dural fistula was exophthalmos; treatment was considered unnecessary in these cases. Follow-up after 6 months showed that the clinical picture was unchanged in seven cases; in one (case 3), the exophthalmos had disappeared spontaneously and carotid angiography (repeated for another reason) revealed that the fistula had disappeared. One of the nine patients (case 7) had a troublesome murmur, as well as exophthalmos, and treatment was required.

This last patient (case 7) was treated by Gelfoam

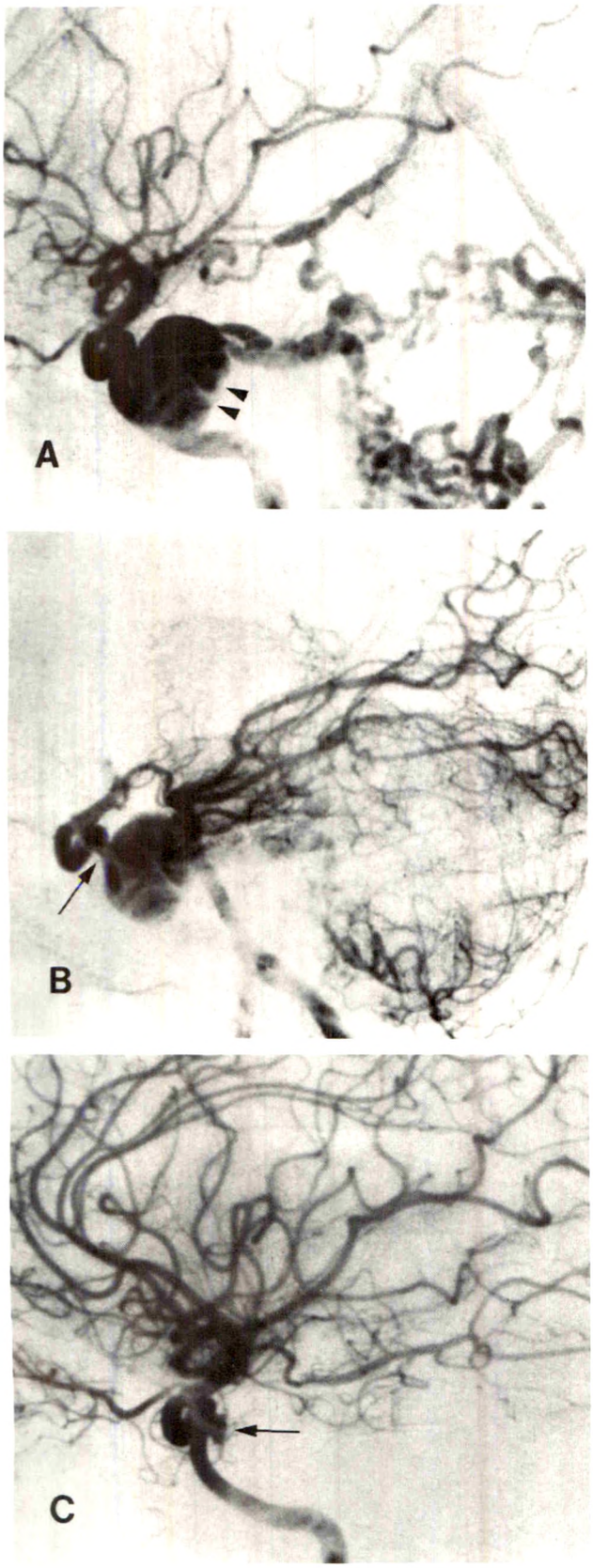


Fig. 5.—Case 18. **A**, Left internal carotid artery. Direct fistula between internal carotid artery and cavernous sinus (*arrowhead*). **B**, Left vertebral artery with compression of left common carotid artery in cervical region. Exact site of fistula now visible (*arrow*). **C**, Left internal carotid artery 1 month after closure of fistula. Small pseudoaneurysm resulting from diffusion of remnant of contrast medium from balloon (*arrow*).

embolization. The dural fistula in this patient was filled only from the right external carotid artery via a wide meningeal branch arising from the internal maxillary artery (fig. 4A). After selective catheterization of the right external carotid from the femoral artery, a single plug of Gelfoam closed the fistula (fig. 4B). At follow-up after more than 2 years, the patient was still asymptomatic; specifically, the preexisting exophthalmos and murmur were absent.

For the treatment of internal carotid-cavernous sinus (direct) fistulas, Hamby [9] developed a technique that consists of occlusion of the intracranial part of the internal carotid by surgical intervention, introduction of a fragment of muscle into the cervical part of the carotid artery (which travels with the flow toward the fistula), and, finally, occlusion of the cervical part of the internal carotid artery. An obvious disadvantage of this method is the arrest of the circulation in the carotid artery.

In order to avoid the disadvantages of the Hamby procedure, so-called balloon techniques have recently evolved. In the first balloon technique, a Fogarty catheter is introduced into the common carotid and passed into the internal carotid artery until it reaches the fistula. Both the internal carotid artery and the fistula are then occluded by filling the balloon with contrast medium. The catheter is left in situ [20, 21]. The advantage of this technique is that no intracranial intervention is required. However it does have the disadvantage that the internal carotid artery is occluded.

The most elegant solution is a recently evolved technique in which a balloon is introduced into the cavernous sinus via a catheter, leaving the circulation in the carotid artery intact. The balloon is inflated to occlude the fistula, it is released from the catheter, and the catheter is removed. This procedure is called the inflatable and released balloon technique [4–6]. Success, that is, continuous inflation of the balloon, is ensured by filling the balloon with a glue that becomes solid, and by attaching the balloon to the catheters so that premature release is prevented by adequate ligature around the neck of the balloon [22].

Our patients with a direct fistula (cases 10–16) were successfully treated by the Hamby method before the balloon technique was available. The inflatable and released balloon technique was successfully used in treating cases 17–19 with postraumatic carotid-cavernous sinus fistulas.

Unlike the other patients with a direct fistula in our series, case 18 showed no exophthalmos. Angiography was performed because an arachnoidal hemorrhage had occurred 4 weeks after the injury. The left oculomotor nerve had become totally dysfunctional immediately after the accident. Angiography of the left internal carotid artery revealed the cavernous sinus fistula, which drained mainly into the superior petrosal sinus (fig. 5A). After injection of contrast medium into the left vertebral artery and simultaneous compression of the left common

carotid in the cervical region, the exact site of the fistula became visible (fig. 5B). At our request, Dr. G. Debrun closed the fistula by his inflatable and released balloon technique [5, 6]. Follow-up 1 month after closure showed that the balloon had become slightly smaller due to diffusion of a remnant of contrast medium, resulting in a small pseudoaneurysm (fig. 5C).

In case 17, complete dysfunction of the right oculomotor nerve was noticed a few weeks after injury, and bilateral exophthalmos and chemosis developed within a few days. Angiography of the right common carotid (fig. 6A) revealed a carotid-cavernous sinus fistula with rapid perfusion and reduced filling of the intracranial branches. Vertebral arteriography with compression of the right carotid in the cervical region revealed that the posterior communicating artery was not patent. Angiography of the left carotid with compression of the right carotid revealed the exact site of the fistula: segment C4 of the internal carotid artery. We closed the fistula by the inflatable and released balloon technique. The balloon, filled with contrast medium, is seen in the cavernous sinus in figure 6B, which shows that the fistula has been closed and that the carotid artery is patent. Follow-up 1 month after closure of the fistula showed that the balloon had become slightly smaller (as in case 18), resulting in a small pseudoaneurysm (fig. 6C). The patient was entirely free from symptoms.

In case 19, right-side exophthalmos developed 1 week after an automobile accident. Angiography of the right internal carotid revealed a carotid-cavernous sinus fistula (fig. 7A). After injection of contrast medium into the left vertebral artery and simultaneous compression of the right common carotid in the cervical region, the exact fistula site became visible (fig. 7B). We closed the fistula by the inflatable and released balloon technique. Two balloons were needed in this case because, after inflation of one balloon with the maximum quantity of contrast medium (0.8 ml), the fistula still existed. After release of the first balloon, a second balloon was introduced and inflated with 0.6 ml contrast medium, which proved to close the fistula (fig. 7C). Follow-up 1 month after closure showed the patient was free from symptoms. Angiographic follow-up has not yet been performed.

Discussion

Three types of carotid-cavernous sinus fistula are anatomically distinguishable: (1) defects in the wall of the intracavernous part of the internal carotid artery; (2) dural arteriovenous malformations between meningeal branches of the internal carotid artery and the cavernous sinus; and (3) dural arteriovenous malformations between meningeal branches of the external carotid artery and the cavernous sinus. Differentiation among these three types of carotid-cavernous sinus fistulas is important for therapeutic indications. Treatment of carotid-cavernous sinus fistulas is primarily indicated by the clinical symptoms, but the fact that dural fistulas can close spontaneously must be considered also. In only one of our 10 patients with a dural fistula was therapy indicated.

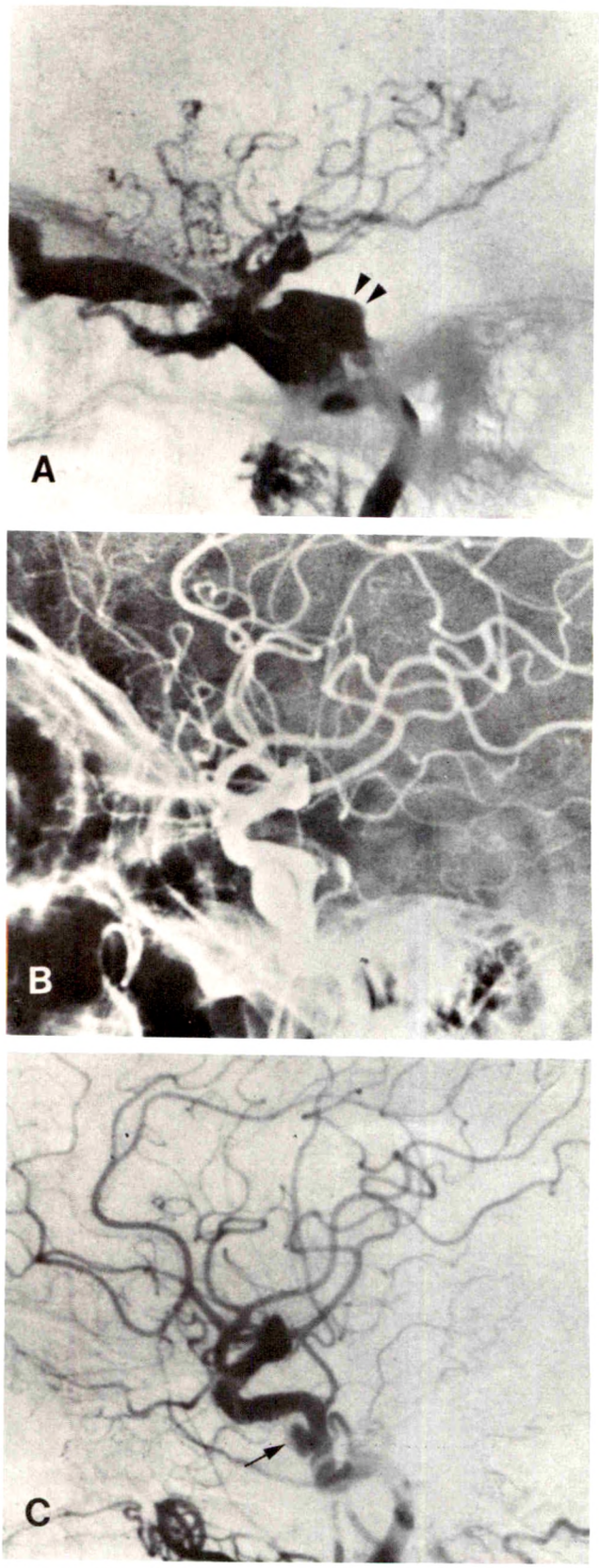


Fig. 6.—Case 17. Right common carotid artery. **A**, Direct internal carotid–cavernous sinus (*arrowheads*) fistula. **B**, After closure of fistula by balloon filled with contrast medium. **C**, 1 month after closure, small pseudoaneurysm resulting from diffusion of remnant of contrast medium from balloon (*arrow*).

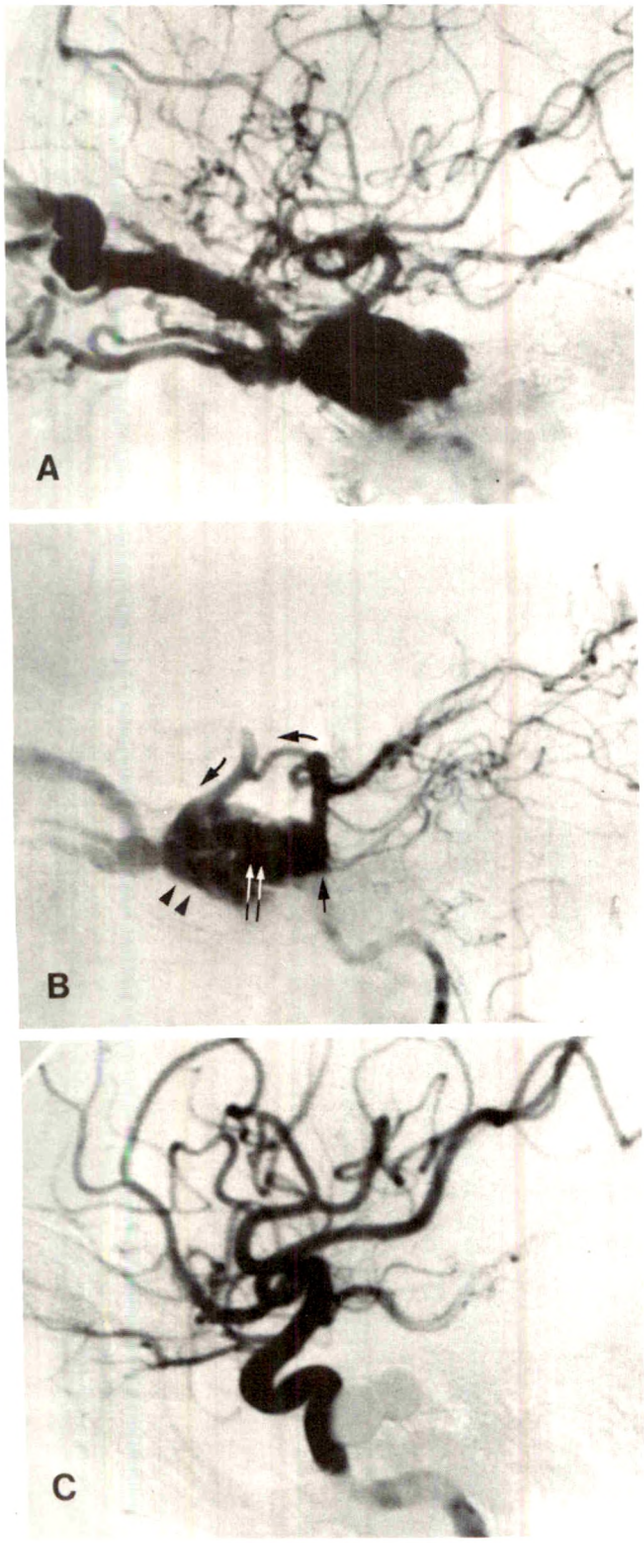


Fig. 7.—Case 19. **A**, Right internal carotid artery in patient with direct internal carotid-cavernous sinus fistula. **B**, Left vertebral artery with compression of right common carotid artery in cervical region. Direction of blood flow (*curved arrows*). Exact site of fistula (*double arrows*) with cavernous sinus (*arrowheads*) visible. **C**, Right internal carotid artery after closure of the fistula by two balloons.

Until recently, all carotid-cavernous sinus fistulas that required treatment were treated surgically by such means as ligation of the internal and external carotid artery alone or combined with the operative embolization of Hamby [9]. Ligation alone is successful in 30%–50% of cases; the Hamby procedure is successful in 50%–90% of cases [23].

Differentiation among the three types of carotid-cavernous sinus fistulas is not required for surgical treatment, but it is essential for choosing among the various catheterization methods. The fistula is identified by selective catheterization of the internal and external carotid artery.

Fistulas of the first type are either traumatic or develop spontaneously due to rupture of an aneurysm. In a direct internal carotid-cavernous sinus fistula, the so-called inflatable and released balloon technique makes it possible to close the fistula while leaving the circulation in the internal carotid artery intact. A prerequisite for this technique is that the exact fistula site be angiographically predetermined. Contrast medium is injected into the contralateral vertebral or carotid artery with simultaneous compression of the homolateral carotid artery, which delays the flow of contrast medium to the fistula via either the posterior or the anterior communicating artery. In this way the exact site of the fistula can be visualized.

Before the balloon technique was available, our patients with a traumatic direct internal carotid-cavernous sinus fistula (cases 10–16) were treated successfully by the Hamby method, in agreement with the forementioned reports in the literature. Three patients (cases 17–19) with direct fistulas were recently treated by the inflatable and released balloon technique, with good results in all cases. With this procedure, closure of the fistula was achieved, while the carotid patency was left intact.

For dural fistulas, closure by catheterization can be contemplated if clinical symptoms preclude awaiting possible spontaneous closure. For dural *external* carotid-cavernous sinus fistulas, Gelfoam embolization after selective catheterization should be regarded as the method of choice. Our series includes one patient with an external carotid-cavernous sinus fistula successfully treated by Gelfoam embolization. If treatment is indicated for a dural *internal* carotid-cavernous sinus fistula, occlusion of the internal carotid may be unavoidable.

Evidentally, Gelfoam embolization is impossible in cases of dural internal carotid-cavernous sinus fistula, nor is it possible to introduce a balloon into the cavernous sinus via the arteriovenous malformation. No case of dural *internal* carotid-cavernous sinus fistula treated by a catheterization technique has yet been described in the literature. Our series does not include such a case either. However, it is conceivable that the catheterization method can also be used to treat dural internal carotid-cavernous sinus fistulas. In such cases, the result will be closure of the fistula, but also occlusion of the internal carotid. The expected advantage over the Hamby procedure is that no intracranial intervention is required, and the ophthalmic artery remains patent. In these cases, the procedure should be carried out under local anesthesia

in order to verify whether the patient tolerates the occlusion without signs of dysfunction.

REFERENCES

1. Walsh FB, Hoyt WE: *Clinical Neuro-opthalmology*, vol 2. Baltimore, Williams & Wilkins, 1969, p 1714
2. Gilsbach J, Seeger W: Embolisation in der Neurochirurgie. *Radiologe* 17:514–520, 1977
3. Lins E, Wappenschmidt J: Transfemorale Embolisation einer Carotis-Externa-Sinus-Cavernosus-Fistel. *Roentgenblaetter* 30:621–625, 1977
4. Serbinenko FA: Balloon catheterization and occlusion of major cerebral vessels. *J Neurosurg* 41:125–145, 1974
5. Debrun G, Lacour P, Caron JP, Hurth M, Comoy J, Keravel Y: Inflatable and released balloon technique experimentation in dog-application in man. *Neuroradiology* 9:267–271, 1975
6. Debrun G, Lacour P, Caron JP: Balloon arterial catheter techniques in the treatment of arterial intracranial diseases, in *Advances and Technical Standards in Neurosurgery*, vol 4, edited by Krayenbühl H, New York, Springer, 1977, pp 131–145
7. Rabischong R, Vignaud J, Paleirac R, Clay C: Anatomie sérielle de la loge caverneuse. *Ann Radiol* (Paris) 17:215–224, 1974
8. Peeters F, Kröger R, Verbeeten B, Versteege C: The value of computer tomography, orbital venography and carotid angiography in the diagnosis of exophthalmos. *Radiol Clin* (Basel) 46:430–438, 1977
9. Hamby WB: *Carotid-Cavernous Fistula*. Springfield, Ill., Thomas, 1966
10. Bacon KT, Duchesneau PM, Weinstein MA: Demonstration of the superior ophthalmic vein by high resolution computed tomography. *Radiology* 124:129–131, 1977
11. Brismar J, Brismar G, Davis KR: Superior ophthalmic vein at computed tomography. *Acta Radiol [Diagn]* (Stockh) 18: 273–278, 1977
12. Vignaud J, Clay C, Bilianuk LT: Venography of the orbit. *Radiology* 110:373–382, 1974
13. Huber P: A technical contribution to the exact angiographic localization of carotid cavernous fistulas. *Neuroradiology* 10:239–241, 1976
14. Dilenge D: Angiography of spontaneous carotido-cavernous communications. *Mod Probl Ophthalmol* 14:110–119, 1975
15. Newton TH, Hoyt WF: Dural arteriovenous shunts in the region of the cavernous sinus. *Neuroradiology* 1:71–81, 1970
16. Cophignon J, Djindjian R, Rey A: Traitement des fistules carotido-caverneuses. *Ann Radiol* (Paris) 17:275–277, 1974
17. Théron J, Clay C, Djindjian R: Etude angiographique et embolisation d'un fistule artério-veineuse durale paracaverneuse d'un type anatomique particulier. *Ann Radiol* (Paris) 18:739–746, 1975
18. Hilal SK, Michelson JW: Therapeutic percutaneous embolization for extra-axial vascular lesions of the head, neck and spine. *J Neurosurg* 43:275–287, 1975
19. Djindjian R, Merland JJ: Super-selective arteriography of the external carotid artery, New York, Springer, 1978, pp 405–431
20. Prolo DJ, Hambery JW: Intraluminal occlusion of a carotid cavernous sinus fistula with a balloon catheter. Technical note. *J Neurosurg* 35:237–242, 1971
21. Picard L, Lepore J, Montant J, Hepner H, Roland J, Guyonnaud JC, Jacob F, André JM: Endoarterial occlusion of carotid-cavernous sinus fistulas *Neuroradiology* 8:5–10, 1974
22. Guillaume J, Roulleau J: Experimental embolization with inflatable and releasable balloons in dogs. *Neuroradiology* 14:85–88, 1977
23. Rey A, Cophignon J, Djindjian R, Houdart R: Traitement des fistules carotido caverneuses. *Neurochirurgie* 19:111–122, 1973

Contrast Enhanced CT Scan and Radionuclide Brain Scan in Supratentorial Gliomas

ALAN R. BUTLER,[1,2] ANTHONY M. PASSALAQUA,[1] ALEX BERENSTEIN,[1] AND IRVIN I. KRICHEFF[1]

The preoperative contrast enhanced CT and radionuclide brain scans of 60 patients with surgically verified supratentorial astrocytomas were evaluated and compared. Results indicated that the mechanisms of contrast enhancement and radionuclide uptake are identical in the detection of supratentorial gliomas. These diagnostic methods apparently mirror the integrity of the blood-brain barrier and therefore can be useful in assessing the degree of malignancy of supratentorial gliomas. However, lesions with an intact blood-brain barrier will be missed with radionuclide imaging. These parenchymal abnormalities and/or the associated mass effect will be detected with contrast enhanced computed tomography. These findings firmly establish contrast enhanced CT as the primary investigative tool in the suspected brain tumor.

The first description of the clinical results of computed tomography (CT) by Ambrose [1] included a brief discussion of the possibility of enhancing the density of brain lesions by intravenously injecting contrast material. He ascribed the accumulation of the contrast material to a breakdown in the blood-brain barrier. He also mentioned the retention of contrast enhancement at 2 hr in a meningioma. Ambrose and Paxton [2, 3] alluded to possible mechanisms in the extravascular accumulation of contrast material and emphasized that the extent of the abnormal vascularity was one of the major factors responsible for the degree of enhancement. New et al. [4] mentioned that contrast enhancement was dependent on the vascularization of the lesion. They suggested that delayed enhancement was secondary to the residual blood pool concentration of iodine. Ethier et al. [5] also assumed that contrast enhancement was secondary to iodinated contrast material in the vascular pool and referred to tissue density enhancement as computerized angiotomography.

Hatam et al. [6] presented the first thorough clinical investigation of contrast enhancement response with time. They concluded that, in part, contrast enhancement was secondary to the extravascular accumulation of contrast material through a defective blood-brain barrier. Gado et al. [7] determined the tissue-blood ratio of enhancement in pathologic conditions and concluded that there was an extravascular component in contrast enhancement. They emphasized the similarity in the mechanism of contrast enhancement and the abnormal accumulation of radioisotopes in brain lesions.

The positive radionuclide brain scan in brain tumors is in great measure secondary to the extravascular accumulation of the radioactive tracer via a local breakdown in the blood-brain barrier [8–13]. There is debate regarding the extent of the contribution of intravascular radioactive tracer in the positive static radionuclide scan, but vascularity does play some role if only to increase the capillary surface area for the extravasation of the diagnostic agent.

This investigation evaluates and compares the apparent parallel mechanisms of contrast enhancement and radionuclide uptake in a large group of homogeneous supratentorial gliomas and examines the roles of these diagnostic methods in assessing the degree of malignancy of these tumors.

Subjects and Methods

All patients with histologically confirmed supratentorial astrocytomas seen at the New York University Medical Center over 3 years were collected from the neuropathology files. Those patients who had high resolution preoperative pre- and postcontrast enhancement CT and radionuclide brain scans within a maximal interval of 4 weeks were included in the evaluation. Sixty patients met these criteria and formed the basis for this study.

Tumors were graded histologically according to the criteria of Kernohan et al. [14]. Grades I and II astrocytomas were designated low grade and grades III and IV were designated high grade. Grades III and IV correspond to the glioblastoma multiforme with a low and high degree of malignancy respectively [14].

The 60 cases included 46 high grade astrocytomas and 14 lesions of low grade malignancy (table 1). The median age of the patients with low grade gliomas was 38 years and those of high grade malignancy was 58 years. The patients' records were reviewed and particular note was made as to whether or not the patients were receiving steroids at the time of the CT or radionuclide brain scans.

CT scans were routinely performed with a 13 mm collimator and scan pairs were usually obtained from the base of the skull to the vertex. The contrast enhanced scan was performed immediately after the noncontrast study. Meglumine diatrizoate 30% (200 ml) was infused over a 5–7 min period. Scanning was started and an additional 100 ml was infused slowly throughout the scan series. Children received 4 ml/kg of body weight to a maximal dose of 200 ml.

The pre- and postcontrast CT scans were evaluated by direct viewing of the cathode ray tube, photographs, and the 160 × 160 digital print out. When contrast enhancement was observed, a central region of enhancement of at least 25 picture elements was identified and a mean of this region of interest was calculated. An attempt was made to locate the identical

Received January 24, 1978; accepted after revision December 12, 1978.
This work was supported in part by grant no. N01 CM 67059 from the National Brain Tumor Study Group.
[1] Department of Radiology, New York University Medical Center, New York, New York 10016.
[2] Present address: Department of Radiology, Hartford Hospital, Hartford, Connecticut 06115. Address reprint requests to A. R. Butler.

© 1979 American Roentgen Ray Society

0361–803X/79/1324–0607 $0.00

TABLE 1

Summary of Supratentorial Gliomas

	Astrocytomas (grades 1 and 2)	Astrocytomas (grades 3 and 4)
No. cases	14	46
Sex:		
Male	9	30
Female	5	16
Median age (range)	38 (3–60)	58 (31–78)
Location:		
Frontal	10	22
Parietal	1	10
Occipital	1	5
Temporal	2	9
Precontrast CT appearance:		
Hyperdense	1	4
Isodense	1	2
Hypodense	12	40

region of interest on the noncontrast scan, and this area was evaluated in a similar manner. The mean of the region of interest on the contrast scan was divided by the mean of the region of interest on the noncontrast scan. The resultant factor was designated the index of contrast enhancement. The intensity of contrast enhancement was evaluated according to the following scale: slight enhancement was equivalent to an index between 1.10 and 1.59; moderate enhancement represented an index factor of 1.60 to 2.49; marked enhancement indicated an index of 2.50 or greater.

Static radionuclide brain scans were obtained with the gamma camera 1 hr after intravenous administration of 15 mCi of ^{99m}Tc pertechnetate. All patients received 400 mg of $KCLO_4$ prior to the scans. Images were obtained in the anterior, posterior, Towne, and right and left lateral projections. On rare occasions, vertex views were obtained.

The radionuclide brain scans were evaluated by one of us (A. P.) without prior knowledge of the results of the CT scan or the histologic type or grade of the glioma. The intensity of the positive scans was graded from slight to marked by visually comparing the activity in the tumor with that of the superior sagittal sinus. Slight uptake was faintly seen; moderate uptake was well defined, but of less intensity than the superior sagittal sinus. Marked radionuclide uptake represented an intensity equal to or greater than the superior sagittal sinus.

Selective internal carotid cerebral angiograms were available in all 14 cases of the low grade astrocytomas and 40 of 46 cases of the high grade (Kernohan's III and IV) gliomas. The angiograms were divided into two groups: nonvascular and vascular. The criteria used for inclusion in the vascular category was the presence of either a capillary blush, neovascularity, or early filling veins.

Results

The results are summarized in tables 1–4. There were 14 astrocytomas of low grade malignancy. In nine of these cases there was no contrast enhancement and the radionuclide brain scans were falsely negative (table 2). The majority of nonenhancing low grade astrocytomas were seen as parenchymal lucencies on the pre- and postcontrast CT scan. In addition to the parenchymal abnormalities, the associated mass effect and ventricular size were clearly demonstrated. There was contrast enhancement in five low grade astrocytomas. In each case the intensity of uptake was slight. In four of these tumors the intensity of radionuclide uptake was moderate and in the other case the intensity of uptake was slight.

There was contrast enhancement in all 46 of the high grade gliomas (Kernohan's grade III and IV). The index of contrast enhancement was moderate in 25 cases and marked in 21 cases. Tumor mass was clearly separable from surrounding edema. The radionuclide brain scan was also positive in all of the high grade gliomas. The uptake of radionuclide was marked in 31 cases and moderate in 15 cases. Slight accumulation of iodine or radioactive tracer was not seen in any of the high grade

TABLE 2

Contrast Enhanced CT Compared with Radionuclide Brain Scanning

	Astrocytomas (grades 1 and 2)	Astrocytomas (grades 3 and 4)
Contrast enhancement:		
Positive	5	46
Negative	9	0
False negative	0	0
Total	14	46
Radionuclide scanning:		
Positive	5	46
Negative	9	0
False negative	9	0
Total	14	46

TABLE 3

Comparison of Intensity of Contrast Enhanced CT Scan and Radionuclide Brain Scan

	Astrocytomas (grades 1 and 2)	Astrocytomas (grades 3 and 4)
Contrast enhancement:		
Negative	9	0
Slight	5	0
Moderate	0	25
Marked	0	21
Total	14	46
Radionuclide scanning:		
Negative	9	0
Slight	1	0
Moderate	4	15
Marked	0	31
Total	14	46

TABLE 4

Angiographic Findings in the Series of Astrocytomas

	Astrocytomas (grades 1 and 2)		Astrocytomas (grades 3 and 4)	
	No.	%	No.	%
Vascular	2	14	31	78
Avascular	12	86	9	22
Lesion missed	0	0	0	0

gliomas. Moderate and marked accumulation of contrast material was uniformly seen in the high grade astrocytoma. Moderate accumulation of radioisotope was encountered in one-third of the high grade gliomas, but also in four low grade gliomas. Marked accumulation of radioisotope was uniformly seen in the high grade glioma.

Angiographic vascularity was demonstrated in 31 of 40 (78%) of the high grade gliomas and two of 14 (14%) of the low grade tumors (table 4). Those lesions which were not vascular were identified by vascular displacements.

Discussion

The extravascular accumulation of iodine and radioactive tracer is largely responsible for the detection of intracranial tumors with contrast enhancement CT and radionuclide brain scanning [8–13]. There is debate regarding the extent of the contribution of intravascular tracer, but tissue vascularity may play a role, particularly during the early phase of imaging [10–12].

The capillaries in normal brain are different from nonneural capillaries in that their junctions are fused and this prevents the free exchange of substances between the intravascular and extravascular compartments [11, 13]. These "tight junctions" form the structural basis for the concept of the blood-brain barrier. The lack of capillary junctional fenestrations normally prevents the extravascular accumulation of iodine and radioactive tracer. However in astrocytomas, these endothelial junctions are frequently patent and become progressively so as the malignancy of the tumor increases [15, 16]. This continuum in capillary abnormalities allows a progressive increase in the extravascular accumulation of these diagnostic agents [13].

In low grade gliomas the capillary endothelial cells are close to normal and junctional gaps are not present [15, 16]. These minor alterations in the blood-brain barrier may not allow or may significantly retard the extravascular accumulation of contrast media or radioisotope. The evaluation of 14 low grade gliomas with contrast enhancement CT and radionuclide brain scanning is consistent with these neuropathologic observations. There was no contrast enhancement and no radionuclide uptake in nine of the low grade gliomas. In all of these cases the radionuclide brain scan was normal. All of these nonenhancing lesions were seen with CT as unchanging parenchymal abnormalities on the pre- and postcontrast CT brain scans (fig. 1).

In the five enhancing low grade gliomas there was slight accumulation of iodine (figs. 2A and 2B). The minimal contrast enhancement probably reflected minor alterations in capillary permeability [13]. The radionuclide brain scan was positive in these lesions with an intensity evaluated as slight in one case (fig. 2C) and moderate in the other four. The most important point in these observations is the strong correlation between the presence of contrast enhancement and radionuclide uptake in these tumors. The criteria used for the evaluation of the intensity of accumulation of these tracers was different and one would not expect a definitive one to one correlation when comparing transmission CT and conventional emission radionuclide imaging. However, in relatively superficial lesions, there was a strong correlation between the intensity of uptake of iodine and radionuclide.

The parallel mechanisms of contrast enhancement and radionuclide uptake were clearly seen in this series of high grade gliomas. There was contrast enhancement in all of these tumors. The index of contrast enhancement

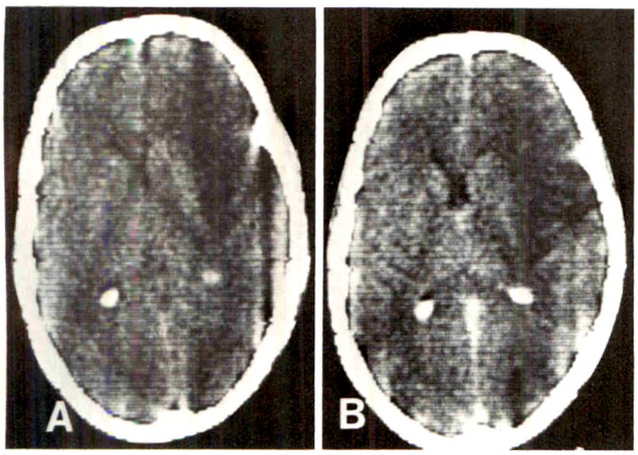


Fig. 1.—Low grade astrocytoma, right frontal area. **A**, Nonenhanced CT scan. Area of decreased absorption in right frontal area. Contralateral ventricular displacement. **B**, Enhanced CT scan. No contrast enhancement.

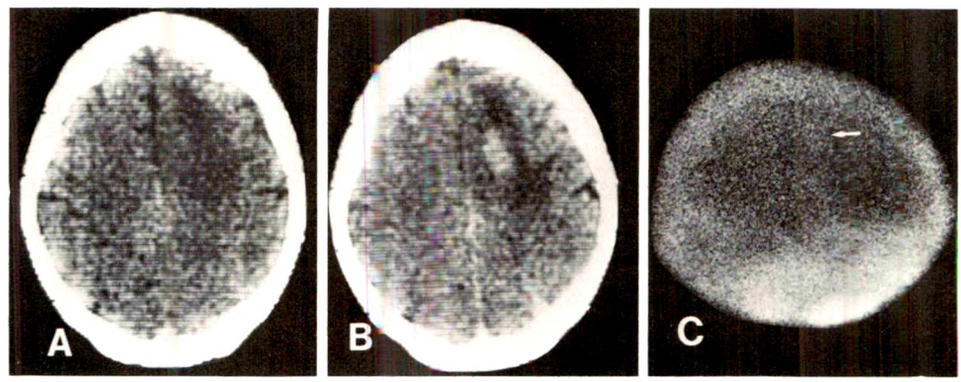


Fig. 2.—Low grade astrocytoma, right frontal area. **A**, Nonenhanced CT scan. Area of decreased absorption right frontal area. **B**, Enhanced CT scan. Slight central homogeneous enhancement. **C**, Right lateral radionuclide brain scan. Area of increased activity vaguely seen in right frontal area (*arrow*).

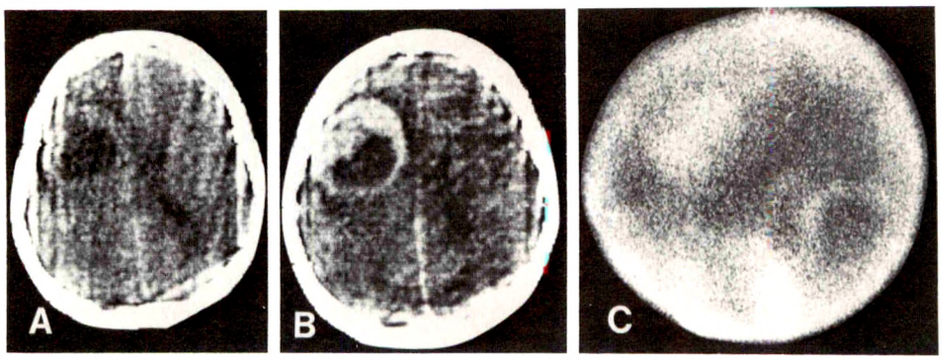


Fig. 3.—High grade astrocytoma, left frontal area. **A**, Nonenhanced CT scan. Discrete area of decreased absorption in left frontal area. **B**, Enhanced CT scan. Thick rimlike area of enhancement. **C**, Left lateral radionuclide brain scan. Intense region of increased activity in left frontal area.

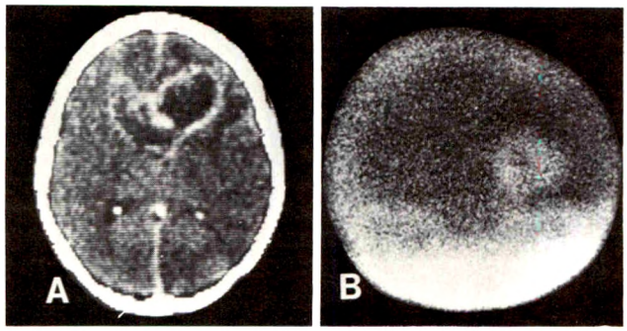


Fig. 4.—Bifrontal high grade astrocytoma. **A**, Enhanced CT scan. Bifrontal rimlike enhancement. **B**, Right lateral radionuclide brain scan. Marked uptake of radionuclide with central zone of decreased activity.

was moderate in 25 cases and marked in 21 cases. Radionuclide imaging was positive in all 46 of the high grade gliomas. The intensity of uptake in the radionuclide brain scans was moderate in 15 cases and marked in 31 cases. Marked accumulation of iodine and radiopharmaceutical was always encountered in the high grade astrocytoma (fig. 3). Despite the frequent occurrence of "ring" enhancement with CT, there was only one case in which decreased central activity was seen on the radionuclide brain scan (fig. 4). Moderate accumulation of radioisotope was seen in the high grade as well as the low grade glioma.

Our findings with contrast enhancement CT in low grade gliomas are similar to those of Tchang et al. [17]. However, these observers only included Kernohan's grade I gliomas in the low grade category, whereas we included Kernohan's grade I and II gliomas in the low grade group. These different neuropathologic groupings might explain any varying results.

Contrast enhancement in supratentorial astrocytomas is highly correlated with microscopic vascularity and necrosis [18]. Isolated increases in pleomorphism and cellularity are generally not associated with contrast enhancement [18]. This observation may explain why some so-called "anaplastic astrocytoma" may not accumulate iodine. Furthermore, in our experience, these tumors do not accumulate radioisotope.

The absence of contrast enhancement and radionuclide uptake in this series was singularly seen in the low grade astrocytoma. The contrast enhanced low grade gliomas clearly accumulated contrast media less intensely than the high grade gliomas. Although in a large series there may be some overlap, it seems that the intensity of contrast enhancement reflects qualitative abnormalities in the blood-brain barrier and can therefore be useful in assessing the degree of malignancy of these tumors. As experience accumulates, these findings may assume even greater significance because of the limited tissue sampling afforded by needle biopsy and subtotal resections. Contrast enhanced CT which samples the "entire tumor" may supply useful prognostic and therapeutic information.

Radionuclide imaging was falsely negative in nine low grade astrocytomas. The radionuclide brain scan is often normal in the low grade glioma [19–22]. In brain tumors the radionuclide brain scan evaluates the integrity of blood-brain barrier and possibly intrinsic vascularity. Contrast enhanced CT monitors these pathophysiologic parameters and, in addition, CT uniquely evaluates pathologic anatomy.

Steroid therapy has been associated with diminution in the intensity of radioisotope uptake and contrast enhancement in brain tumors [10, 23]. On occasion, the uptake of radioisotope may actually be prevented by steroid therapy [23]. None of the patients with low grade gliomas were on steroid therapy at the time of the CT or radionuclide brain scans. Nearly half of the patients with highly malignant gliomas were on therapeutic doses of steroids at the time of one or both of these diagnostic studies. One cannot speculate as to whether or not the intensity of the scans was diminished, since no serial scans were obtained with and without steroid medication.

High resolution cerebral angiography failed to demonstrate abnormal vascularity in 22% of the high grade gliomas (table 4). This finding is consistent with those of other observers [21]. The degree of malignancy of a glioma is more highly correlated with a positive radionuclide brain scan than it is with abnormal angiographic vascularity [21]. Furthermore, even magnification angiography with subtraction may fail to demonstrate very small abnormal vessels.

Angiographic vascularity was demonstrated in two of 14 cases (14%) of low grade gliomas in this series. This is consistent with the observations of others [21]. In each case there was no contrast enhancement and no uptake

of radioisotope. These two cases lend support to the concept that contrast enhancement and radionuclide uptake are in great measure secondary to the extravascular accumulation of these diagnostic agents.

This study was confined to gliomas of the supratentorial region because these tumors are of a different clinicopathologic entity than gliomas in the posterior fossa [24]. Therefore, the uptake of iodine and radioactive tracer have different histologic and biologic implications in the supra- and infratentorial regions. Intense contrast enhancement is often seen in low grade posterior fossa tumors [18].

Rarely a juvenile astrocytoma, which originates in the region of the third ventricle, or a "cerebellarlike" astrocytoma, which occurs in the cerebral hemispheres, may be encountered [24]. These are histologically benign tumors which often have increased vascularity and this could possibly be reflected in a positive contrast enhancement CT and radionuclide brain scan. We did not encounter such tumors in this series.

Conclusions

The strong correlation between the degree of contrast enhancement and radionuclide uptake demonstrated in this series of astrocytomas offers significant corroborative evidence that the mechanisms of contrast enhancement and radionuclide uptake are identical. Contrast enhanced CT and radionuclide brain imaging mirror the integrity of the blood-brain barrier and therefore can be useful in assessing the degree of malignancy of supratentorial astrocytomas. However, in the presence of an intact blood-brain barrier (low grade glioma), the radionuclide brain scan will be normal. In these cases there will be no accumulation of contrast media, but the parenchymal abnormality and/or the associated mass effect will be seen with CT. These findings establish contrast enhancement CT as the primary investigative tool in the diagnostic evaluation of the suspected brain tumor.

ACKNOWLEDGMENTS

We thank Christine M. Volzo and Linda Michaels for their help in the preparation of this manuscript.

REFERENCES

1. Ambrose J: Computerized transverse axial scanning (tomography). II. Clinical application. *Br J Radiol* 46:1023–1047, 1973
2. Ambrose J: Computerized x-ray scanning of the brain. *J Neurosurg* 40:679–695, 1974
3. Paxton R, Ambrose J: The EMI scanner. A brief review of the first 650 patients. *Br J Radiol* 47:530–565, 1974
4. New PFJ, Scott WR, Schnur JA, Davis KR, Taveras JM: Computerized axial tomography with the EMI scanner. *Radiology* 110:109–123, 1974
5. Ethier R, Sherwin A, Taylor S, et al.: Computerized angiotomography: the use of 100 cc. of Hypaque M-60%. Clinical and experimental results. Paper presented at the International Symposium of Computerized Axial Tomography, Montreal, May 1974
6. Hatam A, Bergvall R, Lewander S, Larsson S, Lind M: Contrast medium enhancement with time in computer tomography. Differential diagnosis of intracranial lesions, in *Computer Tomography of Brain Lesions*, edited by Lindgren E, *Acta Radiol [Suppl]* 346:63–81, 1975
7. Gado MH, Phelps ME, Coleman RE: An extravascular component of contrast enhancement in cranial computed tomography. I and II. *Radiology* 117:589–597, 1975
8. Bakay L: Basic aspects of brain tumor localization by radioactive substances. A review of current concepts. *J Neurosurg* 27:239–245, 1967
9. Baum S: The site of accumulation of ^{99M}Tc-sodium pertechnetate in brain tumors. *Radiology* 99:153–155, 1971
10. Crocker EF, Zimmerman RA, Phelps ME, Kuhl DE: The effect of steroids on the extravascular distribution of radiographic contrast material and technetium pertechnetate in brain tumors as determined by computed tomography. *Radiology* 119:471–474, 1976
11. Holman BL: The blood brain barrier: anatomy and physiology. *Prog Nucl Med* 1:236–248, 1972
12. Penning L, Front D, Bechar M, Go KG, Rodermond JM: Factors governing the uptake of the pertechnetate by human brain tumors. A sintigraphic study. *Brain* 96:225–234, 1973
13. Shuttleworth EC Jr: Barrier phenomena in brain tumors. *Prog Exp Tumor Res* 17:279–290, 1972
14. Kernohan JW, Mabon RF, Svien HJ, Adson AW: Symposium on new and simplified concept of gliomas: simplified classification of the gliomas *Mayo Clin Proc* 24:71–75, 1949
15. Long DM: Capillary ultrastructure and the blood-brain barrier in human malignant brain tumors. *J Neurosurg* 32:127–144, 1970
16. Long D: Capillary ultrastructure and the blood-brain barrier in human brain tumors, in *Proceedings of the Sixth International Congress of Neuropathology, Paris France, Aug 31–Sept. 4, 1970*. Paris, Masson, 1970, pp 994–996
17. Tchang S, Guiseppe S, Terbrugge K, Melançon D, Bélanger G, Milner C, Ethier R: Computerized tomography as a possible aid to histological grading of supratentorial gliomas. *J Neurosurg* 46:735–739, 1977
18. Butler AR, Horii SC, Kricheff II, Shannon MB, Budzilovich GN: Computed tomography in astrocytomas. A statistical analysis of the parameters of malignancy and the positive contrast enhancement CT scan. Paper presented at the annual meeting of the Radiological Society of North America, Chicago, November 1977
19. Bowallius M, Larsson A, Sköldborn H, Wickbom I: Brain scanning and conventional neuroradiologic methods in intracranial tumors. *Acta Radiol [Diagn]* 13:634–642, 1972
20. Cronqvist S, Efsing HO, Hughes R: Brain scanning in the differential diagnosis of supratentorial tumors. *Acta Radiol [Diagn]* 13:678–692, 1972
21. Fulghum JS III, Adcock DF, Faustino GC, Krigman MR, Radcliffe WB: Radionuclide imaging and tumor vascularity in supratentorial gliomas. *Invest Radiol* 6:388–391, 1971
22. Witcofski RL, Maynard CD, Roper TJ: A comparative analysis of the accuracy of the technetium-99M pertechnetate brain scan: follow-up of 1000 patients. *J Nucl Med* 8:187–196, 1967
23. Fletcher JW, George EA, Henry RE, Donati RM: Brain scans, dexamethasone therapy, and brain tumors. *JAMA* 232:1261–1263, 1975
24. Rubinstein LJ: Tumors of the central nervous system, in *Atlas of Tumor Pathology*, series 2, fascicle 6, Washington, D.C., Armed Forces Institute of Pathology, 1972, pp 1–104

CT Detection of Intracranial Aneurysms in Subarachnoid Hemorrhage

K. GHOSHHAJRA,[1] L. SCOTTI,[2] J. MARASCO,[2] AND P. BAGHAI-NAIINI[3]

Contrast enhanced computed tomography (CT) scans of 59 patients with subarachnoid hemorrhage were evaluated for intracranial aneurysms. After prospective study, the CT results were compared with angiography. Depending on the location, the CT detection rate varied from a low of 36% for the internal carotid artery complex to a high of 76% for anterior and middle cerebral artery aneurysms. It was concluded that angiography may be deferred if the causative aneurysm is demonstrated by CT.

Computed tomography (CT) has assumed preeminence for evaluation of subarachnoid hemorrhage and should be the first examination performed [1, 2]. The presence and extent of recent intracranial hemorrhage (subarachnoid, intraventricular, and intracerebral), ventricular size, displacements, and infarction are accurately defined by CT [3–5]. Detailed delineation of aneurysms and vascular spasm requires angiography. However, when more than one aneurysm is present, determination of the bleeding aneurysm is more accurate with CT, and CT provides a better size estimate when larger aneurysms are partially thrombosed.

CT has a high diagnostic accuracy in predicting the bleeding site when an intracerebral hematoma is present [5, 6]. While the pattern of cisternal blood may determine the bleeding site, difficulties in localization are greatly increased when a hematoma is not present. In such cases, identification of the aneurysm directly in the contrast-enhanced scan is of obvious value (fig. 1). Earlier reports [4, 7] identified large aneurysms (over 2 cm), but we are not aware of any study reporting the frequency of detection of aneurysms by CT. Therefore, a prospective study was undertaken to evaluate the ability of the contrast-enhanced scan to visualize the causative aneurysm in patients with subarachnoid hemorrhage.

Subjects and Methods

The study was composed of 59 patients with the clinical diagnosis of subarachnoid hemorrhage. Initial complaints of 80% of the patients were headache, stiff neck, lethargy, and cranial nerve palsies; the rest had major neurologic deficits. Patients were selected on the basis of clinical findings, spinal tap, and the presence of subarachnoid blood in the plain CT scan. Other causes of intracranial hemorrhage (trauma, tumor, and angioma) were excluded from the study.

Initially, EMI Mark I and ACTA 0100 scanners were used with 13 mm collimation; later, EMI 1010 S and ACTA 0200 FS scanners were used with 8 mm collimation. Plain and contrast-enhanced scans were obtained with multiple overlapping base sections and routine higher sections. A 10°–15° angle to orbitomeatal line was used; the base sections were obtained by moving the tomographic plane by 2–4 mm. The section through the "pentagon" of the suprasellar cistern usually incorporated the vascular structures (fig. 2). The anterior clinoid processes were used as reference points and the base arteries were usually visualized 3–5 cm above this plane. Individual anatomic variations required altered angulation and level so that monitoring was necessary to insure appropriate sections. The intravenous contrast agent was 300 ml of 30% iothalamate (42 g of iodine); the base sections were obtained after three-fourths of the contrast material had been injected. The scans were evaluated by at least three of us and correlated with the angiographic findings. Angiography was performed in all but two patients. These two patients had autopsy confirmation.

Results

Identification of intracranial aneurysms was greatly improved when second generation scanners were used. Anterior and middle cerebral artery aneurysms, as well

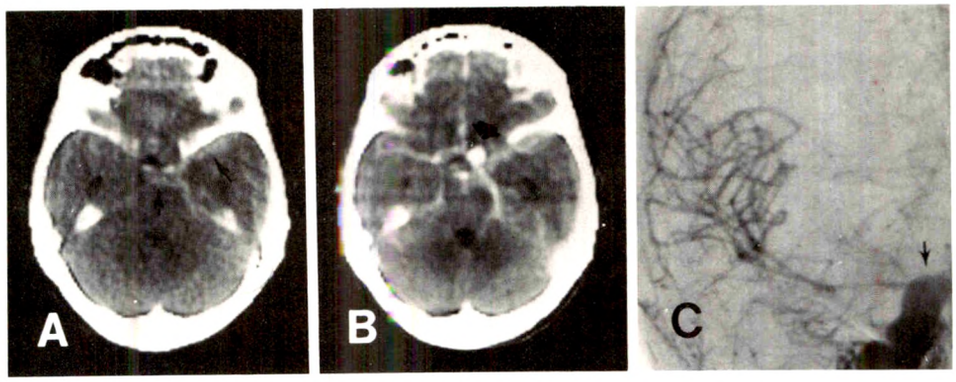


Fig. 1.—**A**, Plain scan. Subarachnoid blood (*arrows*) in basal cisterns. **B**, Enhanced scan. Well defined aneurysm of right internal carotid artery (*arrow*). **C**, Right carotid angiogram confirms aneurysm (*arrow*).

Received September 11, 1978; accepted after revision January 3, 1979.
Presented at the International Computed Tomography Symposium, Miami Beach, Florida, March 1978.
[1] Department of Radiology, Mercy Hospital, Pride and Locust Streets, Pittsburgh, Pennsylvania 15219. Address reprint requests to K. Ghoshhajra.
[2] Department of Radiology, St. Francis Hospital, Pittsburgh, Pennsylvania 15201.
[3] Department of Neuro-Surgery, Mercy Hospital, Pittsburgh, Pennsylvania 15219.

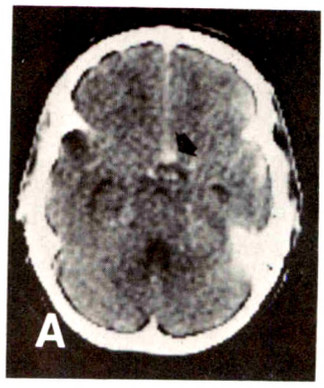
© 1979 American Roentgen Ray Society

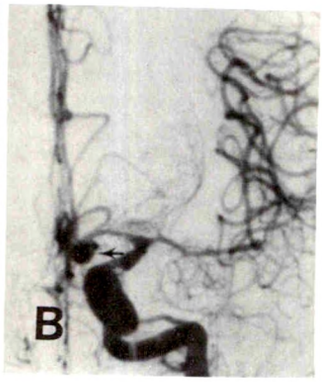
0361–803X/79/1324–0613 $0.00



Fig. 2.—Base section. Circle of Willis in normal contrast-enhanced scan.

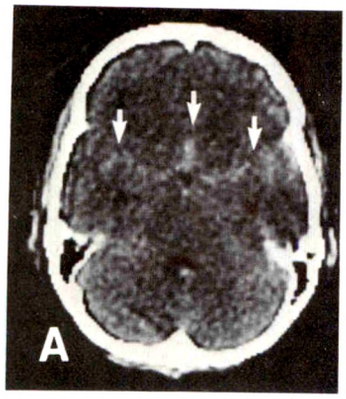
←





→

Fig. 3.—**A**, Enhanced scan of patient with acute subarachnoid hemorrhage. Aneurysm (*arrow*) of anterior communicating artery. **B**, Left carotid angiogram. 8 mm anterior communicating artery aneurysm (*arrow*).



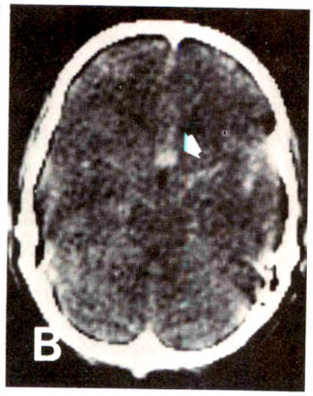
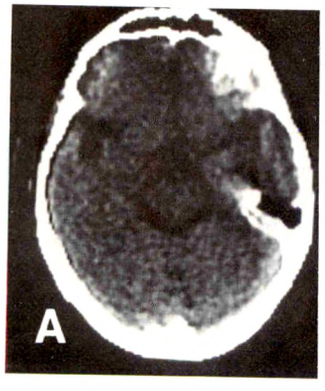
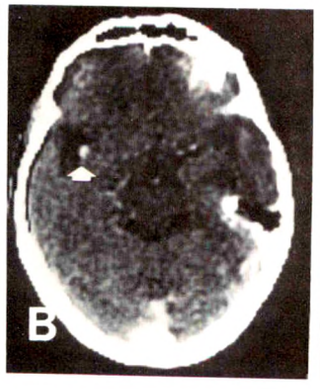




Fig. 4.—**A**, Plain scan. Subarachnoid blood (*arrows*). **B**, Enhanced 12 mm density (*arrow*) represents anterior communicating aneurysm. **C**, Left carotid angiogram confirmed aneurysm (*arrow*).





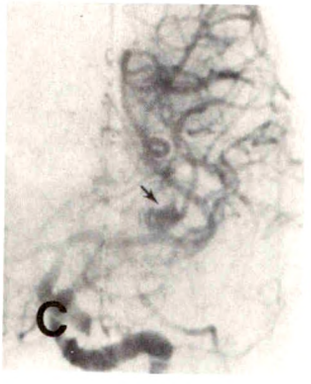


Fig. 5.—**A**, Plain scan 3 days after subarachnoid hemorrhage fails to demonstrate blood in subarachnoid space. **B**, Enhanced scan. Discrete aneurysm (*arrow*) in region of left middle cerebral artery. **C**, Left carotid angiogram. 8 mm aneurysm (*arrow*) of left middle cerebral artery.

as those arising from the fundus of the basilar artery, were easiest to detect (figs. 3–6, table 1). Internal carotid artery aneurysms, including those arising from the origin of the posterior communicating artery, were more difficult to detect, and none smaller than 12 mm were seen (figs. 7 and 8), which may be due to the proximity of bony structures.

Of the aneurysms successfully detected, 39 were 5–15 mm; four others were 16–25 mm. The smallest aneurysm visualized was 5 mm, although aneurysms as large as 15 mm were not detected due to motion, amount of cisternal blood, and location. The size of the aneurysm in the contrast-enhanced scan represented the diameter of its cross section. An obliquely projected aneurysm appeared larger when compared with angiography (fig. 7). The CT diameter of aneurysms correlated well with the angiographic diameter when an aneurysm measured 10 mm or more. There was no correlation between CT findings and vascular spasm. In five patients who had more than one aneurysm, only the causative aneurysm was detected. In one patient, the incidental aneurysm was seen retrospectively.

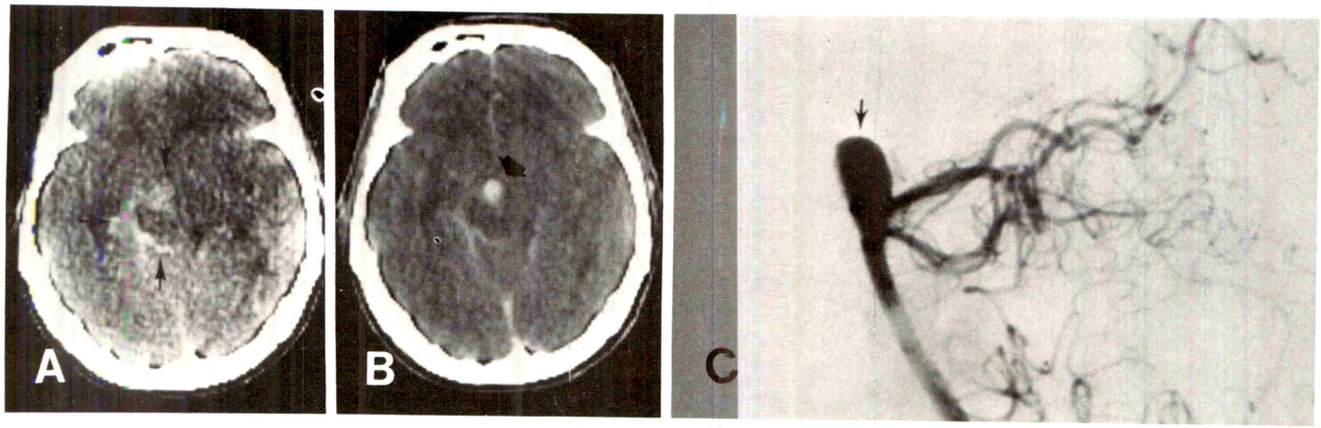


Fig. 6.—**A**, Plain scan. Blood (*arrows*) in left prepontine and ambient cisterns. **B**, Enhanced scan. Aneurysm of basilar artery (*arrow*). **C**, Angiogram confirms 12 mm aneurysm at tip of basilar artery (*arrow*).

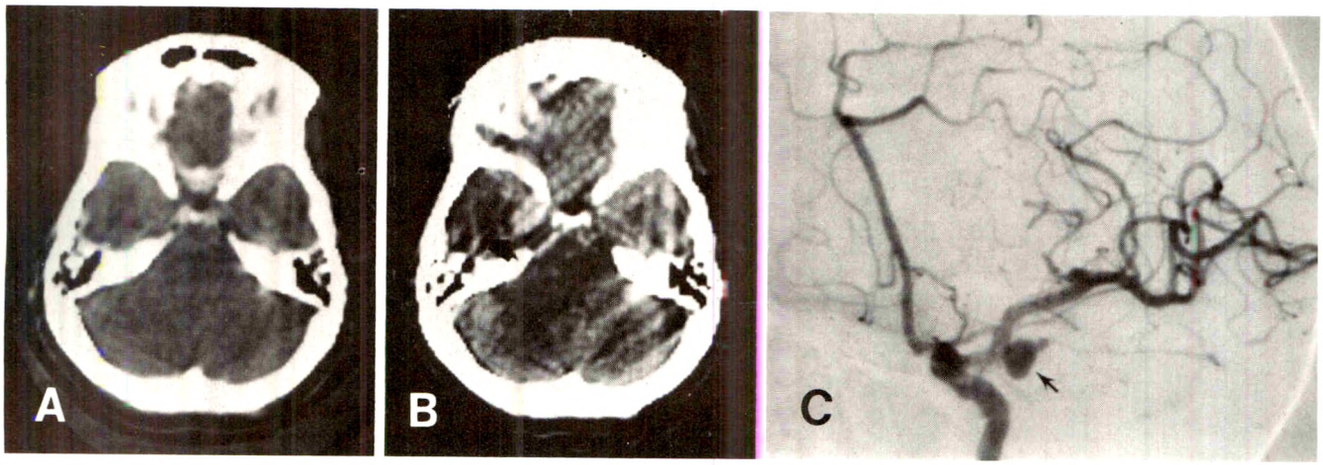


Fig. 7.—**A**, Plain scan. No blood was seen in subarachnoid space in patients with acute subarachnoid hemorrhage. **B**, Enhanced scan. Discrete oval aneurysm in region of left posterior communicating artery (*arrow*). **C**, Anteroposterior oblique view of left carotid arteriogram confirms CT diagnosis of posterior communicating artery aneurysm (arrow).

TABLE 1

Intracranial Aneurysms in Subarachnoid Hemorrhage

Aneurysm Location	No. Aneurysms	Detected After Enhancement	
		No.	%
Anterior communicating artery	23	17	74
Middle cerebral artery	17	13	76
Posterior communicating artery	11	4	36
Internal carotid artery	6	4	66
Basilar artery	6	5	83
Posterior inferior cerebellar artery	1	0	0
Total	64*	43	...

* Five of the 59 patients had two aneurysms.

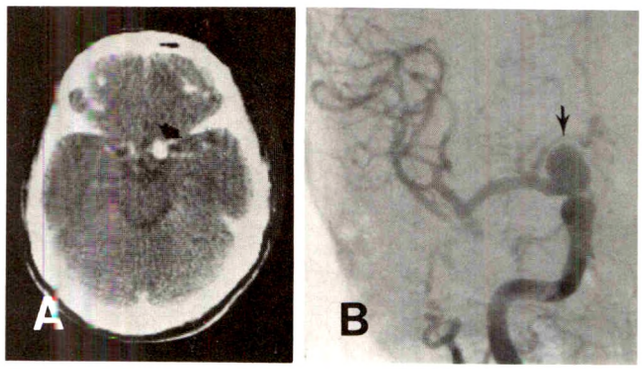


Fig. 8.—**A**, Enhanced scan. 15 mm supraclinoid internal carotid artery aneurysm (*arrow*). **B**, Internal carotid angiogram confirms size of aneurysm (*arrow*).

Discussion

Recognition of aneurysms by CT is improved with contrast enhancement and multiple scans through the base of the brain. While arterial contrast material has been used in conjunction with CT [8, 9], intravenous contrast material is easier to use. The routine six to eight

sections are insufficient for consistent visualization of the basal arteries [10]. By moving the tomographic plane 2 mm and adjusting the angulation, multiple overlapping sections will demonstrate the basal arteries and will also help avoid confusing bony densities produced by partial volume effect. Comparable views in both plain and enhanced scans may be helpful when a large amount of cisternal blood is present.

Depending on location, CT is moderately accurate in demonstrating cerebral aneurysms in patients with subarachnoid hemorrhage. Principal limiting factors are motion, amount of cisternal blood, and site. Size per se does not seem to restrict identification, although arteries less than 1.5 mm cannot be resolved by CT at present [11].

The CT demonstration of the causative aneurysm permits a specific diagnosis to be made. Angiography may be deferred until the patient's condition improves or until surgery is contemplated. In patients seen 5–7 days after onset of symptoms, there is frequently no discernible cisternal blood in the plain scan [2, 5]. In all of our six patients who had normal plain scans, the enhanced scan successfully identified the aneurysm (figs. 4 and 8). The enhanced scan was also helpful when there was symmetrical distribution of subarachnoid blood. While the pattern of cisternal blood in the plain scan may lateralize the cause to a specific side, CT visualization of the aneurysm will give a definitive anatomic location, such as anterior communicating or posterior communicating. This can shorten the angiographic procedure by limiting the study to the appropriate projections that best define the aneurysm arising from that particular site. The contrast-enhanced scan may also identify other causes of subarachnoid hemorrhage, such as arteriovenous malformation and angiomas, and areas of ischemia may be better defined.

It was disappointing that we were unable to find a correlation between the CT findings and the presence of vascular spasm. Even in patients with ischemic changes in their CT scans, spasm could not be reliably predicted.

With current technology, "computed angiotomography" cannot replace angiography in defining all vascular abnormalities. Nevertheless, in patients with subarachnoid hemorrhage, a surprisingly high percentage of the causative aneurysms can be identified on the contrast-enhanced CT scan. The highest detection rate occurred with aneurysms involving the anterior aspect of the circle of Willis. Specific diagnosis can be made and angiography may be deferred. When angiography is performed, it may be limited to the projections that best define the aneurysm.

REFERENCES

1. Liliequist B, Lindqvist M, Valdimarsson E: Computed tomography and subarachnoid hemorrhage. *Neuroradiology* 14:21–26, 1977
2. Scotti G, Ethier R, Melancon D, Terrbrugge D, Tchang S: Computed tomography in the evaluation of intracranial aneurysms and subarachnoid hemorrhage. *Radiology* 123: 85–90, 1977
3. Scott W, New P, Davis K, Schnur J: Computerized axial tomography of intracerebral and intraventricular hemorrhage. *Radiology* 112:73–80, 1974
4. Davis KR, New PFJ, Ojemann RG, Cromwell RM, Morawetz RB, Robertson GH: Computed tomographic evaluation of hemorrhage secondary to intracranial aneurysm. *AJR* 127: 143–153, 1976
5. Kendall BE, Lee BCP, Claveria E: Computerized tomography and angiography in subarachnoid hemorrhage. *Br J Radiol* 49:483–501, 1976
6. Hayward RD, O'Reilly GVA: Intracerebral hemorrhage: accuracy of computerized transverse axial scanning in predicting the underlying etiology. *Lancet* 1:1–4, 1976
7. Pressman BD, Gilbert GE, David OD: Computerized transverse tomography of vascular lesions of the brain. II. Aneurysms. *AJR* 124:215–219, 1975
8. Coin GC, Chan YS: Computed tomographic arteriography. *J Comput Assist Tomogr* 1:165–168, 1977
9. Weinstein MA, Duchesnew PM, Weinstein CE: Computed angiotomography. *AJR* 129:699–701, 1977
10. Naidich TP, Pudlowski RM, Leeds NE, Naidich JB, Chisolmn AJ, Rifkin MD: The normal contrast-enhanced computed axial tomogram of the brain. *J Comput Assist Tomogr* 1:16–29, 1977
11. Bergstrom M, Riding M, Greitz T: The limitations of definition of blood vessels with computer intravenous angiography. *Neuroradiology* 11:35–40, 1976

Lateral Decubitus Pneumoencephalography-Angiography for Localizing Atrial and Paraatrial Vascular Lesions

ROBERT M. QUENCER,[1] HUBERT L. ROSOMOFF,[2] AND BARTH A. GREEN[2]

In two cases where computed tomography (CT) and cerebral angiography failed to determine whether an arteriovenous malformation was within or directly adjacent to the atrium of a lateral ventricle, lateral decubitus pneumoencephalography combined with cerebral angiography successfully localized the lesions. This procedure may be necessary in the workup of angiographically vascular lesions in the atrial-paraatrial region if on CT the ventricular surface is poorly defined or surgical clips from a previous operation obscure the lesion or the adjacent ventricle. Interpretation of this study involves triangulation of the vascular lesions relative to the ventricle or observation of the movement of the lesion relative to the movement of the ventricle on differently angulated frontal projections. Since the surgical approach is influenced by the radiographic differentiation of an intraventricular from a paraventricular mass, this procedure is crucial in evaluating these vascular abnormalities.

Under certain conditions, it may be difficult for computed tomography (CT) to determine whether a lesion is within a ventricle or is directly adjacent to a ventricular surface. Distinguishing an intraventricular from a paraventricular mass is crucial from the surgical standpoint, since approach and operability may vary according to its exact location. When a vascular lesion exists in the atrial-paraatrial region, lateral decubitus pneumoencephalography-angiography may assist in identifying its exact location.

This technique, which to our knowledge has not been previously described, was used in the two cases reported here because CT did not localize the abnormality precisely enough. In both instances it was important in surgical planning.

Case Reports

Case 1

A 29-year-old woman was admitted with a right homonymous hemianopsia, mild right hemiparesis, and minimal aphasia. CT (fig. 1A) showed an area of decreased density in the left posterior temporal area with partial enhancement after intravenous contrast infusion. Cerebral arteriography showed a left intratemporal avascular mass and a small abnormal collection of contrast arising from the left posterior lateral choroidal artery that was associated with a venous aneurysm and an early draining vein (figs. 1B–1D). Angiographic diagnosis of a small arteriovenous malformation and a chronic intratemporal hematoma was made. It was not certain, even with CT and angiography, whether the malformation was in the pulvinar of the thalamus or in the choroidal fissure of the left atrium. After surgical removal of the intratemporal chronic hematoma, it was decided that the relation of the malformation to the ventricular surface could best be appreciated if combined pneumoencephalography-angiography were performed. With the patient's head in the right lateral decubitus position, air was trapped within the atrium and temporal horn of the left lateral ventricle just prior to repeat angiography. The lateral decubitus pneumoencephalogram-angiogram (fig. 2) showed the exact relation of the malformation and the abnormal draining vein to the anterior surface of the ventricle in the atrial region. A part of the vascular mass projected within the air-filled ventricle, while the rest of the mass and the venous aneurysm were just in front of the air-filled ventricular surface within the choroidal fissure. At a second craniotomy, an intraventricular malformation within the choroidal fissure and atrium of the left lateral ventricle was totally resected. Arteriography after the second operation demonstrated that the malformation had been completely removed.

Case 2

A 32-year-old woman experienced sudden headache associated with nausea and vomiting. Neurologic examination was normal except for meningismus. Lumbar puncture revealed bloody cerebrospinal fluid under increased pressure. CT scan (fig. 3) showed intraventricular blood, a small area of enhancement adjacent to the atrium of the right lateral ventricle, and an abnormal draining vein. Vertebral angiography (figs. 4A and 4B) showed a deep, right paramidline arteriovenous malformation fed mainly by small branches arising from the calcarine artery. During subsequent right parietooccipital craniotomy, the entire malformation was believed to have been removed. However, repeat angiography 1 week later (figs. 4C and 4D) showed a residual arteriovenous malformation that was receiving its blood supply from an enlarged right posterior lateral choroidal artery. Because of this choroidal blood supply, the possibility of this residual malformation being partially intraventricular was considered. On postoperative contrast enhanced CT scan, it could not be determined if the residual malformation was intra- or paraventricular because of the artifacts cast by the surgical clips. Therefore, lateral decubitus pneumoencephalography-cerebral angiography (fig. 5) was performed to best localize this residual malformation. With air situated in the atrium of the right lateral ventricle, vertebral angiography in varying frontal projections showed that the malformation did not move in synchrony with the movement of the ventricle, indicating extraventricular location of the malformation. At surgery, this anatomic topography was used to locate and remove the residual malformation. Intraoperative arteriography (right brachial arteriogram) confirmed successful resection of the malformation.

Technique

Routine pneumoencephalography is performed with the amount of air used dependent on the lateral ventricular size. The patient is placed in the lateral decubitus position which allows air to accumulate in the pertinent

Received September 22, 1978; accepted after revision December 12, 1978.

[1] Department of Radiology (R130), University of Miami School of Medicine, Jackson Memorial Medical Center, P. O. Box 016960, Miami, Florida 33101. Address reprint requests to R. M. Quencer.

[2] Department of Neurological Surgery, University of Miami School of Medicine, Jackson Memorial Medical Center, Miami, Florida 33101.

© 1979 American Roentgen Ray Society

0361–803X/79/1324–0617 $0.00

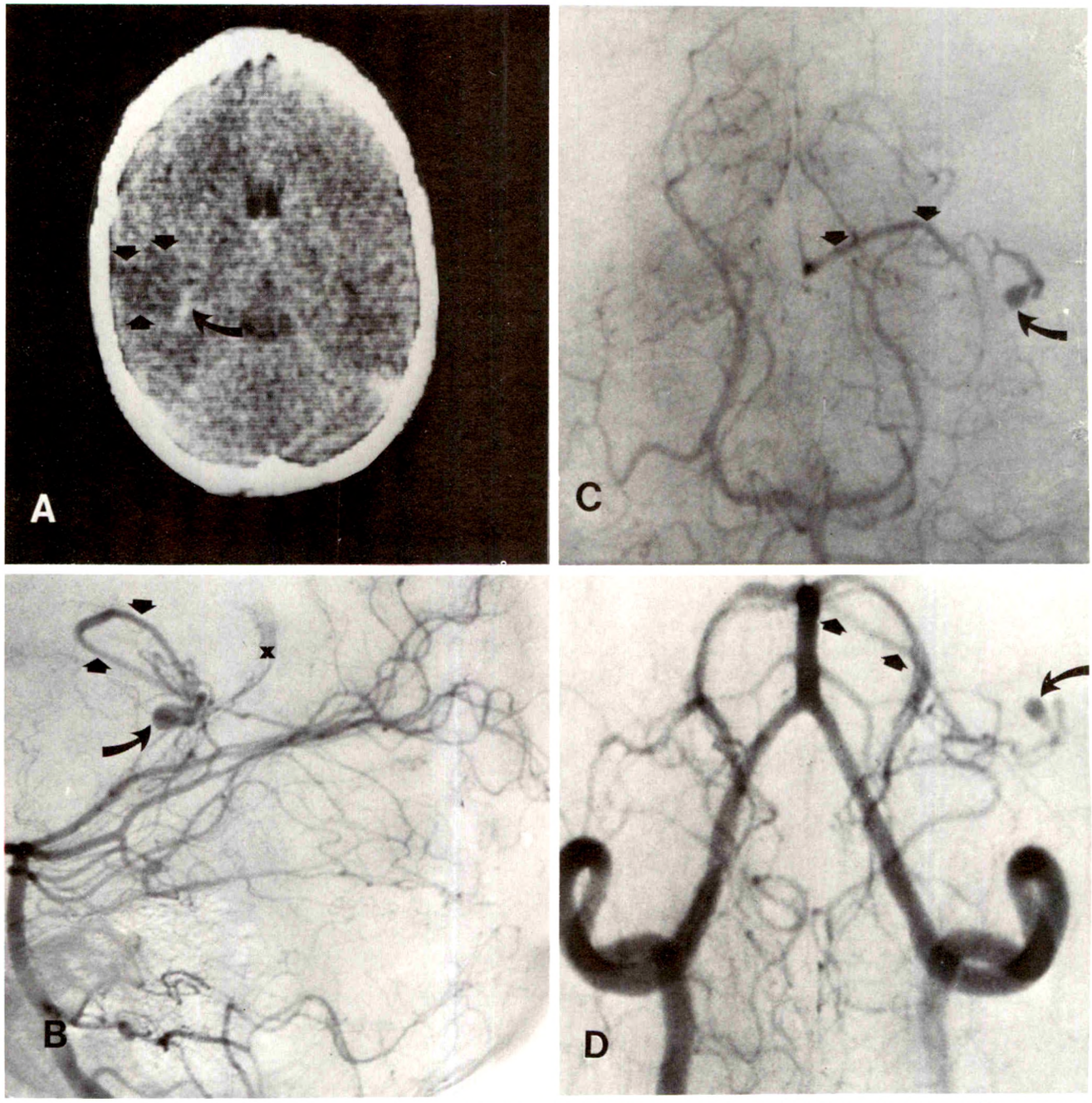


Fig. 1.—Case 1. **A**, Contrast enhanced CT scan. Diminished density in left temporal lobe (*arrowheads*) and, more deeply, area of linear contrast enhancement (*arrow*). Relation between increased density and atrium of left lateral ventricle not obvious. Area of decreased density surgically found to be chronic intracerebral hematoma. **B–D**, Vertebral angiogram, lateral (**B**), Towne (**C**), and base (**D**) projections. Venous aneurysm (*arrows*) associated with early vein (*arrowheads*) draining into vein of Galen (x). Small arteriovenous malformation supplied by left posterior lateral choroidal artery was primary diagnostic consideration, but it was uncertain whether malformation was in posterior lateral part of thalamus or in choroid plexus of atrium.

lateral ventricle (right lateral decubitus in case 1, left lateral decubitus in case 2). The patient is then transported to the angiography table with the head taped in the appropriate decubitus position. With the rest of the patient's body supine, transfemoral cerebral angiography is performed using the anteroposterior tube for the lateral angiographic series and the lateral tube for anteroposterior angiographic series. Routine angiographic equipment can be used in this procedure without the specialized equipment necessary for stereoscopic angiography or angiotomography [1]. A vascular intraventricular mass is diagnosed when the vessels or the tumor stain clearly project within the ventricle on the anteroposterior and lateral series (case 1) or superimpose on the air-filled ventricle in several angulated frontal projections. When the abnormality moves asynchronously rel-

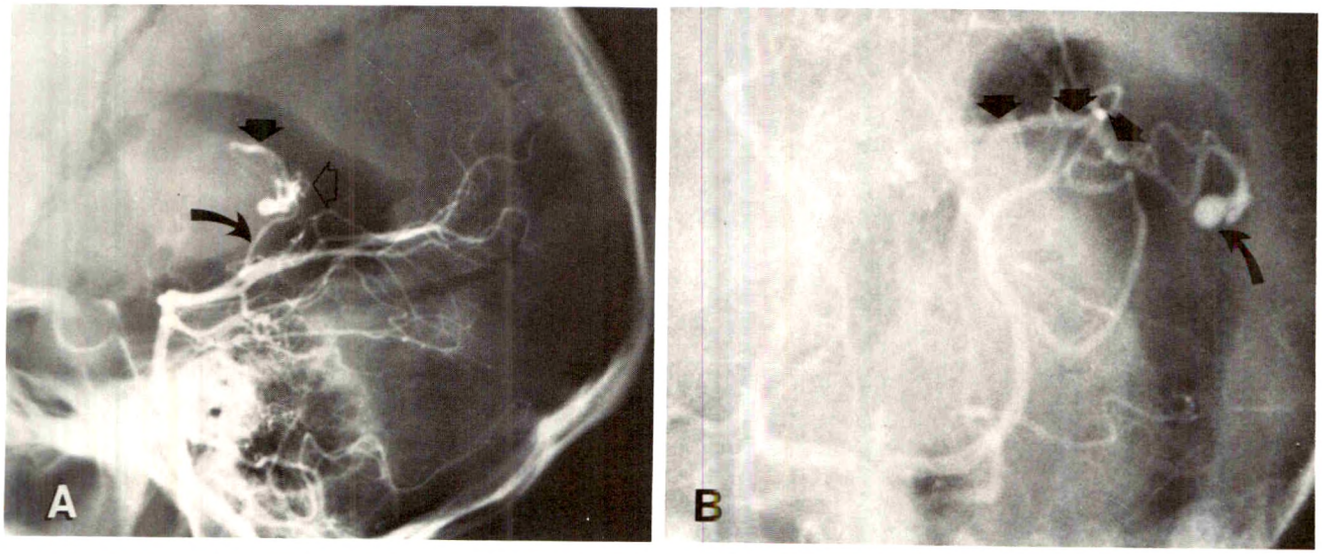


Fig. 2.—Case 1. Lateral decubitus pneumoencephalogram-angiogram. Small cluster of abnormal vessels (*open arrowhead*) project into air-filled lateral ventricle. Relation between venous aneurysm (*arrows*) and early draining vein (*arrowheads*) to anterior ventricular surface is clear.

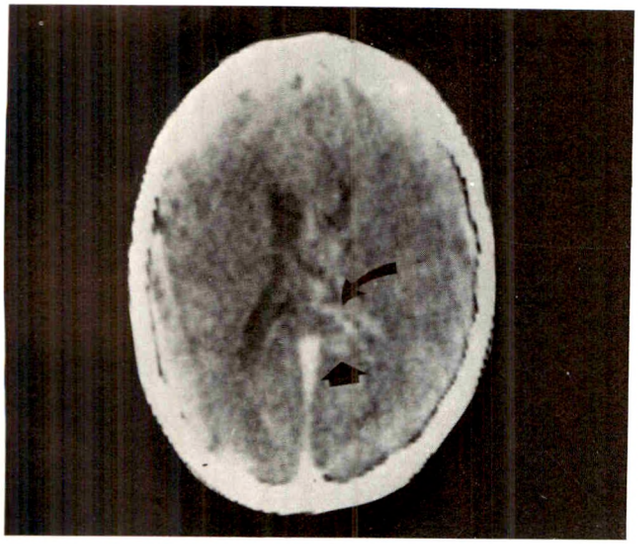


Fig. 3.—Case 2. Contrast enhanced CT scan. Intraventricular blood and small arteriovenous malformation (*arrowhead*) border on medial surface of right atrium. Associated enhancing linear structure (*arrow*) believed to represent abnormal draining vein. It was uncertain whether part of malformation extended into ventricle.

ative to the ventricle (case 2) an extraventricular position of the mass is assured.

If a ventricular shunt or external ventricular drainage tube is in place, it can be used for instillation of air into the ventricular system. The patient is then placed in the appropriate decubitus position and angiography is performed as described above. Although both of our cases had arteriovenous malformations, this technique could be used with any vascular mass in this region.

Discussion

Vascular lesions within the atrium of a lateral ventricle or directly adjacent to that ventricular surface include vascular malformations, aneurysms, ependymomas, choroid plexus papilomas, astrocytomas, meningiomas, metastases, and seeding from other primary central nervous system tumors [2, 3]. Determining whether the whole mass or any part of it lies within the lateral ventricle may influence the surgical approach to the lesion, since the ependymal surface, which serves as a well defined surgical landmark, should be violated only if there is proven intraventricular tumor. Unnecessary transgression of the ependymal wall may result in porencephaly, intraventricular hemorrhage with the possibility of subsequent communicating hydrocephalus, and/or cerebrospinal fluid contamination by potentially seeding tumors and infectious processes. Hodge and King [4] stress the importance of separating choroid plexus vascular lesions from periventricular malformations because, if it can be proven that there is only an intraventricular abnormality, less of a deficit should occur during surgery than during treatment of a periventricular lesion.

Although in the majority of cases, CT scanning can distinguish between an intraventricular and paraventricular mass, it may be limited when the ventricular surface is not well defined (case 1) or surgical clips obscure the mass (case 2). Coin et al. [5] reported the results of CT in three vascular tumors of the choroid plexus; however, in only two of these cases was the true intraventricular nature of these lesions demonstrated. Their third case had a vascular lesion at the level of the ventricular trigone, but since the ventricular surface was not well defined, a distinction between a totally intraventricular and a paraventricular lesion could not be made.

Cerebral angiography likewise may also fail to resolve this problem, since the choroidal arteries, which supply intra- and paraventricular structures in the trigone region, may be hypertrophied but not displaced in a sufficiently characteristic manner to determine whether the abnormality lies within or close to a ventricular

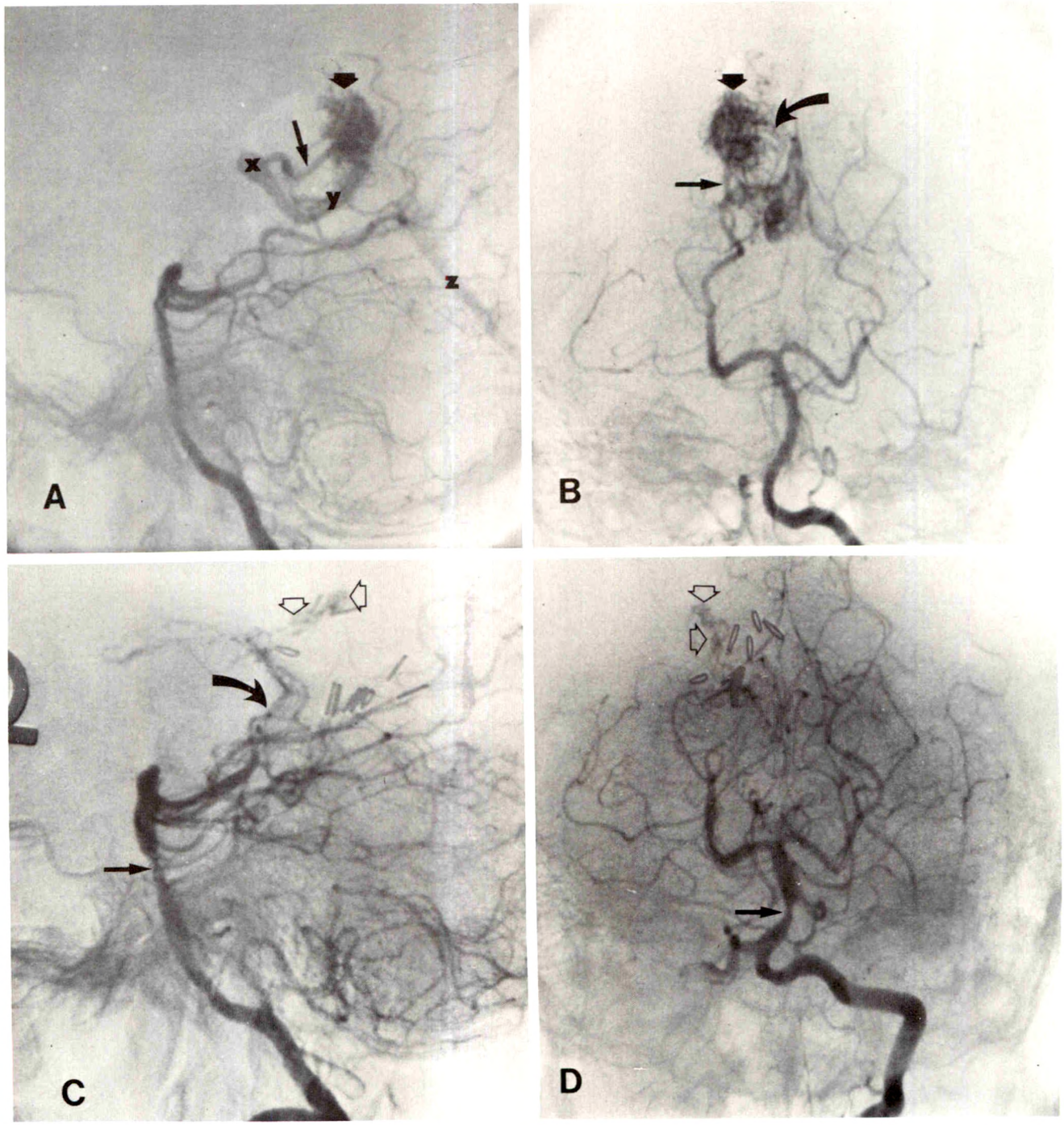


Fig. 4.—Case 2. Vertebral angiography. **A** and **B**, Preoperative. Arteriovenous malformation (*arrowheads*) supplied mainly by small branches (**B**, *curved arrow*) arising from right calcarine artery. Early vein (*straight arrows*) draining into posterior part of internal cerebral vein (x) with subsequent filling of vein of Galen (y) and straight sinus (z). **C** and **D**, 1 week after right parietooccipital craniotomy. Small residual arteriovenous malformation (*arrowheads*) supplied by enlarged right posterior lateral choroidal artery (**C**, *curved arrow*) suggesting possibility residual malformation is partly within ventricle. Segmental spasm of basilar artery (*straight arrow*) now present.

surface. This is particularly true in non-mass-producing vascular lesions, such as arteriovenous malformations. Therefore, under circumstances where angiography and CT do not properly localize the lesion, combined pneumoencephalography-angiography in the lateral decubitus position is the preferred radiographic technique.

Both fortuitous and planned pneumoencephalography-angiography have been reported [6–12], but in each case the patient was in a brow-up position. Fortuitous pneumoencephalographic-angiographic correlations made when cerebral angiography is performed within a day or two after an air study include: (1) the relation

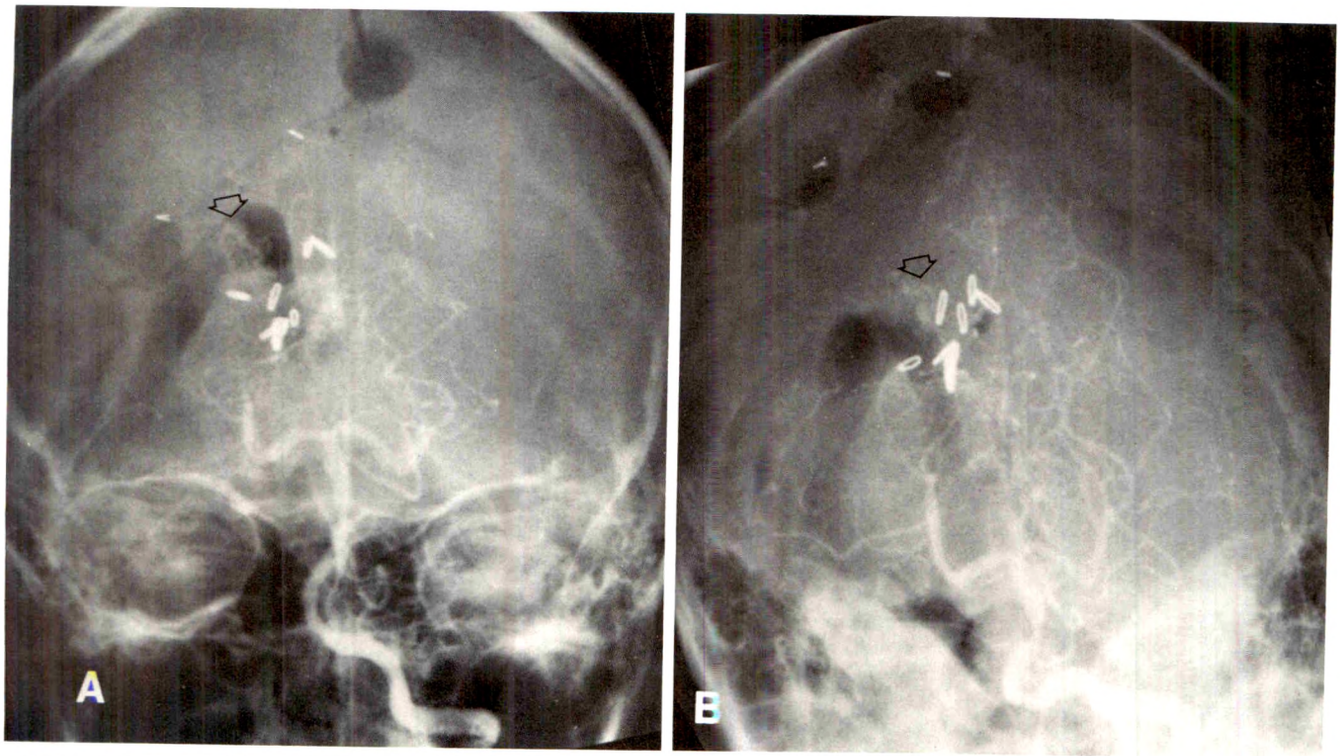


Fig. 5.—Case 2. Lateral decubitus pneumoencephalogram-angiogram. **A,** Initial series. Arteriovenous malformation (*arrowhead*) superimposed on air-filled ventricle. **B,** Towne view. Malformation (*arrowhead*) projects above atrium proving lesion is outside ventricular surface. On Caldwell view (not shown), malformation was seen below atrium indicating that it was posterior to ventricular wall.

between a small parietal arteriovenous malformation and focal cerebral atrophy [6]; (2) the abnormal course of branches of the anterior cerebral artery and the frontal horns of the lateral ventricles in a patient with agenesis of the corpus callosum [7]; and (3) the relation of the normal anterior cerebral artery complex and the frontal horns [8].

Deliberate combined pneumoencephalography-cerebral angiography has been reported in four cases. Use of the brow-up position in these cases only allowed evaluation of abnormalities that occur near or in the frontal or temporal horns of the lateral ventricles, since with commonly used air volumes, only anterior parts of the ventricular system are filled when the patient is in that position. Those cases showed the following: (1) a tortuous anterior cerebral artery as the cause of subependymal mass projecting into the base of the frontal horn near the septum pellucidum [9]; (2) the relation between an intrathalamic aneurysm supplied by the anterior choroidal artery and the adjacent ventricular system [10]; (3) the para- and intraventricular nature of an arteriovenous malformation of the caudate nucleus and the subependymal course of its draining veins [11]; and (4) an aneurysm of the anterior choroidal artery within the temporal horn [12]. In the last case [12], angiotomography in the anteroposterior and lateral projections was used in conjunction with brow-up pneumoencephalography.

Pooling air in an area other than the frontal horns immediately before cerebral angiography has been the subject of only one other article [13]. In that report, two cases of arteriovenous malformations (one intraventricular, the other in the thalamus) were studied with air ventriculography–stereoscopic angiography. In both cases, air was instilled into the frontal horns via ventricular cannulization through a right frontal burr hole. The head was placed in the proper lateral decubitus position and brachial arteriography was performed. There were no radiographs illustrating their findings. Burr holes and direct transcerebral puncture of the lateral ventricle would have not been necessary if routine pneumoencephalography via the lumbar route had been used and the head subsequently positioned, as we have described. The authors [13] admit that ventriculography in these cases carries the risk of direct trauma to the vascular lesion itself.

During pneumoencephalography, significant changes in systemic blood pressure, as well as changes in cerebrospinal fluid dynamics and shifts of parts of the brain in relation to fixed cranial and dural openings, may take place [6]. As a result, there is a potential hazard of subarachnoid hemorrhage from either an arterial aneurysm or an arteriovenous malformation. Despite this drawback, the information obtained in the selected cases we described is important enough to justify this extra risk.

The usefulness of lateral decubitus pneumoencephalography-angiography is demonstrated by our two cases. On the basis of our findings, a transependymal intraventricular approach was used to completely resect the

choroid plexus arteriovenous malformation in case 1; in case 2, total extraventricular surgery removed the paraatrial arteriovenous malformation. Therefore, this procedure is recommended in cases where CT cannot resolve the crucial question of whether a vascular lesion lies within or directly adjacent to the ventricle in the atrial region. Using the information from this study, proper surgical strategy can be planned.

ACKNOWLEDGMENT

We thank Shirley Moore for preparing the manuscript and Chris Fletcher for photographic work.

REFERENCES

1. Poole GJ, Potts DG, Newton TH: Angiotomography, in *Radiology of the Skull and Brain*, vol 2, book 1, edited by Newton TH, Potts DG, St. Louis, Mosby, 1974, pp 981–1001
2. Rubinstein LJ: *Tumors of the Central Nervous System*, 2d series, fascicle 6, Washington D.C., Armed Forces Institute of Pathology, 1972
3. Russell DS, Rubinstein LJ: *Pathology of Tumors of the Nervous System*, 14th ed. Baltimore, Williams & Wilkins, 1977
4. Hodge CJ, King RB: Arteriovenous malformation of choroid plexus, *J Neurosurg* 42:457–461, 1975
5. Coin CT, Coin JW, Glover MB: Vascular tumors of the choroid plexus: diagnosis by computed tomography. *J Comput Assist Tomogr* 1:146–148, 1977
6. Taveras JM, Wood EH: *Diagnostic Neuroradiology*, 2d ed, vol 1. Baltimore, Williams & Wilkins, 1976
7. Lin JP, Kricheff II: The anterior cerebral artery complex. III. Abnormal anterior cerebral artery, in *Radiology of the Skull and Brain*, vol 2, book 2, edited by Newton TH, Potts DG, St. Louis, Mosby, 1974, p 1436
8. Lin JP, Kricheff II: The anterior cerebral artery complex, in *Radiology of the Skull and Brain*, vol 2, book 2, edited by Newton TH, Potts DG, St. Louis, Mosby, 1974, p 1405
9. Anderson RE: Paraventricular "pseudotumor." A case report. *Radiology* 112:629–630, 1974
10. Caram PC, Sharkey PC, Alvord ED: Thalamic angioma and aneurysm of the anterior choroidal artery with intraventricular hematoma. *J Neurosurg* 17:347–352, 1960
11. Carton CA, Hickey WC: Arteriovenous malformation of the head of the caudate nucleus. Report of a case with total removal. *J Neurosurg* 112:414–418, 1955
12. Papo I, Salvolini V, Caruselli G: Aneurysm of the anterior choroidal artery with intraventricular hematoma and hydrocephalus. *J Neurosurg* 39:255–260, 1973
13. Gerber AM, Karkazis G, Mullen S: Localization of intraventricular arteriovenous malformations by ventriculography combined with stereoscopic arteriography. *J Neurosurg* 38: 249–250, 1973

Cranial CT Findings in Patients with Meningomyelocele

ROBERT D. ZIMMERMAN,[1] DAVID BRECKBILL,[2] MICHAEL W. DENNIS,[3] AND DAVID O. DAVIS[3]

The association between meningomyelocele and various cranial abnormalities, particularly Chiari II malformation is well established. Cranial CT scans in 47 patients with meningomyelocele proved to be a safe and effective method of elucidating the type and extent of anatomic abnormalities associated with this disorder, and evaluating and following the degree of hydrocephalus seen in these patients. Of the 47 patients, 43 (92%) showed CT findings indicative of an abnormally low fourth ventricle, the hallmark finding in Chiari II malformation. In 67% the fourth ventricle was not visualized, and in 25% it was directly visualized in an abnormally caudal position. Other findings included hydrocephalus (85%), a striking and possibly unique heart-shaped pseudomass in the posterior fossa (58%), and abnormal configuration of the lateral ventricles ("vampire bat" configuration). Calvarial abnormalities, in particular lacunar skull, were also noted at CT.

The association of meningomyelocele with multiple cranial defects, particularly Chiari type II malformation, is well established [1–7]. Computed tomography (CT) offers a noninvasive technique for studying patients with meningomyelocele. This communication discusses the CT findings in this group of patients and correlates these findings with those obtained from other radiographic procedures, in particular ventriculography and plain film radiography.

Subjects and Methods

The 75 CT scans in 47 patients with a clinical diagnosis of meningomyelocele were evaluated. The patients ranged in age from 6 days to 15 years at the time of the initial scans. There were 25 male and 22 female patients. All were referred from Children's National Medical Center of Washington, D.C. Scans were made on an EMI Mark I CT scanner with a 160 × 160 matrix. The patients were positioned with the head at 0°–20° with reference to the anthropologic baseline. In general, patients younger than 5 years were scanned at 0°–10°, whereas older children were scanned at 10°–20°. All patients were scanned without injection of contrast material. In one instance, a follow-up scan was obtained with contrast enhancement (100 ml 30% Hypaque). Medical records were reviewed for each patient. Previously obtained radiographs were also reviewed when available. In 43 of the 47 patients, ventriculography had been performed prior to the initial CT, and in one instance, a ventriculogram was obtained several months after the initial CT. Of these ventriculograms, 27 were available for review. They were evaluated independently without reference to the CT scan, and then the findings of the two methods were correlated (table 1). Twenty-five normal CT scans in children from 3 months to 5 years of age were reviewed and used as a control.

Results

Position of Fourth Ventricle

Chiari II malformation is always associated with meningomyelocele [1–7]. The ventriculographic hallmark of this disorder is elongation and caudal displacement of the fourth ventricle [4–8]. Ventriculograms were available for review in 25 of the 40 patients who had CT scans adequate for evaluation of the position of the fourth ventricle. In each case the ventriculograms were felt to be consistent with a diagnosis of Chiari II malformation. In 22 of these cases, the caudally placed fourth ventricle was not directly visualized and the diagnosis was based on the clinical picture and in some instances the characteristic deformities in the configuration of the third and lateral ventricles [8].

On CT, the level of normal fourth ventricular visualization varies and depends on scanning angle. At all routine angles (0°–20°), however, the fourth ventricle is visualized at or above the level of the superior third of the petrous bones (fig. 1). This was confirmed by study of the 25 normal CT scans. Therefore, if adequate scans are obtained from the midpetrous region upward, the fourth ventricle should be visualized. Nonvisualization under these circumstances must be due to either abnormal position or obliteration by mass.

CT scans in 24 of the 25 meningomyelocele patients with ventriculographic correlation showed evidence of an abnormal fourth ventricle. In 17 cases, the ventricle was not visualized due to abnormal position and small size (fig. 2). In seven cases, scans obtained low in the posterior fossa at the level of the inferior petrous bone directly visualized a small, caudally placed fourth ventricle (fig. 3). In one patient with ventriculographic evidence of Chiari II malformation (direct visualization of a caudally placed fourth ventricle), an elongated but not caudally placed fourth ventricle was noted.

TABLE 1

CT Evaluation of Fourth Ventricle

	With Ventriculographic Correlation (N = 25)	Without Ventriculographic Correlation (N = 15)	Total (N = 40)	
			No.	%
Nonvisualized fourth ventricle	17	10	27	67
Caudal and small fourth ventricle	7	3	10	25
Normal fourth ventricle	1	2	3	8

Received July 11, 1978; accepted after revision January 3, 1979.
Presented at the annual meeting of the American Society of Neuroradiology, Bermuda, March 1977.
[1]Department of Radiology, Montefiore Hospital and Medical Center, 111 East 210th Street, Bronx, New York 10467. Address reprint requests to R. D. Zimmerman.
[2] Department of Radiology, Children's National Medical Center, Washington, D.C. 20010
[3] Department of Radiology, George Washington University Hospital, Washington, D.C. 20052.

© 1979 American Roentgen Ray Society

0361–803X/79/1324–0623 $0.00

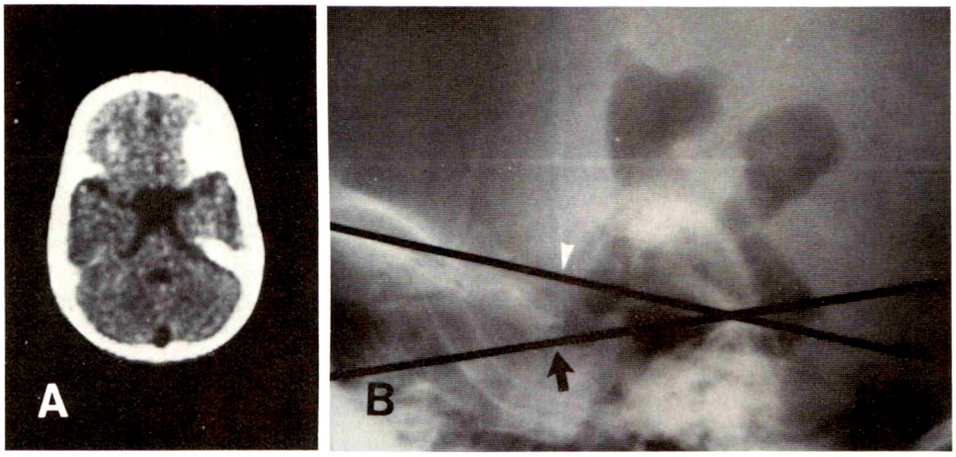


Fig. 1.—Normal position of fourth ventricle in early childhood. **A**, 8-month-old infant. Scan through superior aspect of frontal bones, superior aspect of petrous bone, and center of fourth ventricle. **B**, Ventriculogram in normal infant. Position of fourth ventricle. Lines drawn at 20° (*arrowhead*) and 0° (*arrow*) to Reid's baseline through tops of petrous bones. Scans in this series done between these angles. At either angle, scans through or above upper petrous bone pass through widest portion of fourth ventricle.

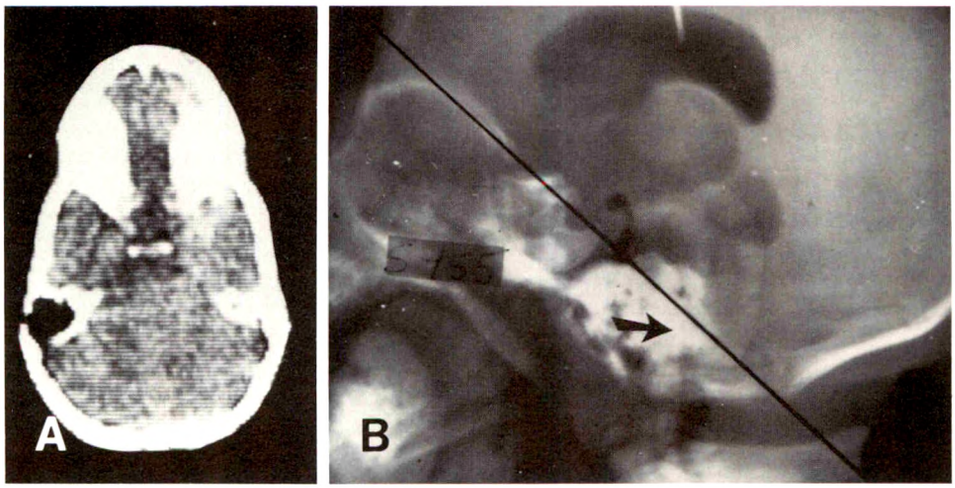


Fig. 2.—Nonvisualization of fourth ventricle in meningomyelocele. **A**, Scan through center of posterior fossa. No evidence of fourth ventricle. Posterior fossa has "blank" or featureless appearance. **B**, Ventriculogram demonstrates caudally placed fourth ventricle. Superior aspect of ventricle (*arrow*) is caudal to line drawn at angle and in plane of CT scan in **A**.

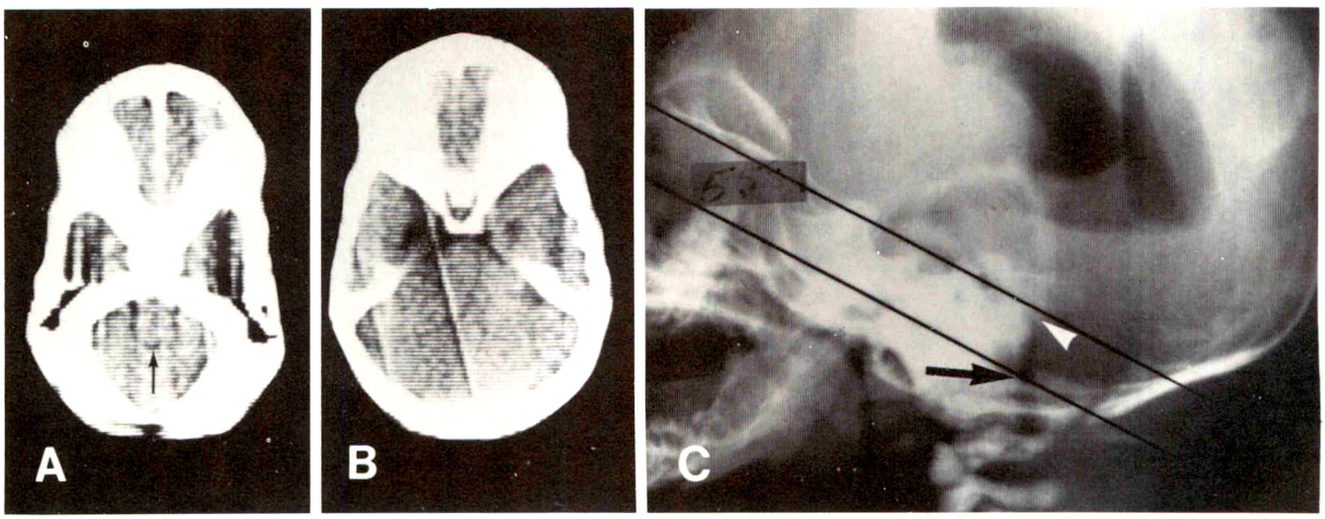


Fig. 3.—Direct visualization of caudally placed fourth ventricle. **A**, Scan low in posterior fossa. Small central lucency (*arrow*) represents caudally placed fourth ventricle. **B**, Scan at higher level. Featureless posterior fossa and no visualization of fourth ventricle in its normal position. **C**, Ventriculogram. Line drawn at level of lower scan passes through caudally placed fourth ventricle (*arrow*), whereas line drawn at level of upper scan passes above most cephalic portion of this structure (*arrowhead*).

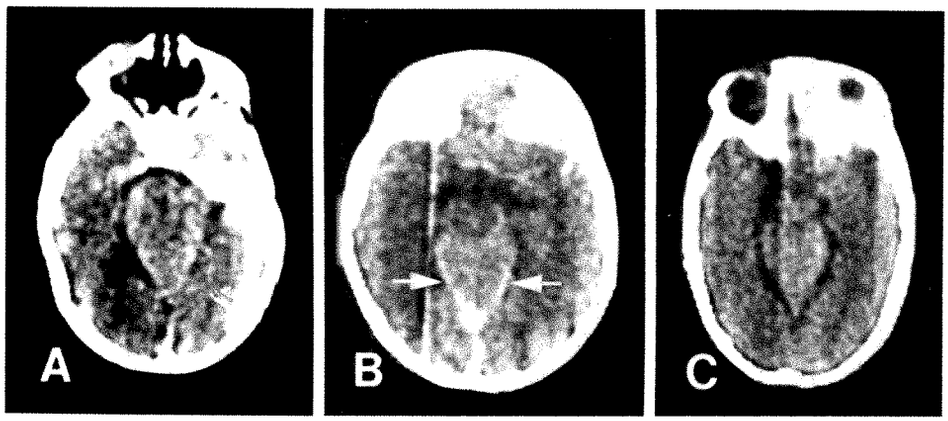


Fig. 4.—Tentorial-cerebellar pseudomass. **A**, Large central area of normal to slightly increased density surrounded by zone of cerebrospinal fluid density in middle of posterior fossa, represents brainstem and tentorial-cerebellar pseudomass. **B**, Contrast scan. Enhancement of tentorium (*arrows*) outlining same region seen as cerebrospinal fluid density on noncontrast scan. Low density areas lateral to enhancing leaves of tentorium may represent slightly dilatated subarachnoid space medial to occipital lobes or may be result of partial volume effect of enlarged infratentorial subarachnoid space. Central density is cerebellum. Leaves of tentorium converge to sharp angle producing V-shaped configuration. Junction of leaves of tentorium is more posterior than normal in this patient. **C**, Striking example of cerebellar-tentorial pseudomass noted in another case. Heart-shaped mass of normal or slightly increased density well visualized.

In the other 15 cases, all without ventriculographic correlation, 10 showed nonvisualization of the fourth ventricle and three showed visualization of a small and low fourth ventricle. Two patients had entirely normal CT scans and did not undergo ventriculography. A review of the clinical data revealed that these patients had meningoceles rather than meningomyeloceles and there was no clinical evidence of Chiari II malformation. In seven cases motion artifacts produced scans which were not of diagnostic quality.

Overall, there was nonvisualization of the fourth ventricle in 67% and visualization of a small, caudally placed fourth ventricle in 25% of patients. Therefore, 92% of the patients in this series showed evidence of abnormal placement of the fourth ventricle by CT. In contrast, in this series, only 12% of the ventriculograms available for review directly demonstrated the abnormal placement of this structure.

Ventricular Size and Configuration

At the time of the initial CT scan, 37 of 47 patients (79%) had already been shunted for hydrocephalus; therefore, the ability to evaluate the degree and distribution of hydrocephalic changes in these patients was limited. In the shunted patients, the ventricles tended to be moderately enlarged, and on serial studies their size seemed to correlate with variations in shunt function, rather than with the underlying disease process. In the 10 patients who had not been shunted prior to the initial scan, only three showed definite evidence of hydrocephalus, generally of mild to moderate degree.

In five cases, the ventricles were slightly enlarged, but showed an angular rather than rounded configuration and slight irregularity to the ventricular walls. The temporal horns were not enalrged. On the basis of these criteria, it was felt that the findings were secondary to cerebral dysgenesis rather than hydrocephalus (see discussion). There is no pathologic correlation in these five cases since these patients are still living. Both cerebral dysgenesis and hydrocephalus occur commonly in conjunction in patients with meningomyelocele, and it is often difficult to evaluate the contribution of each factor to ventricular enlargement. However, in these five cases, follow-up studies demonstrated a stable ventricular size and there was no clinical evidence of hydrocephalus.

Tentorial-Cerebellar Pseudomass

In 58% of the patients, an unusual configuration was noted in the posterior fossa directly behind the brainstem. A thin zone of cerebrospinal fluid density surrounded a heart-shaped central area of normal or slightly increased density (fig. 4). In one case a contrast-enhanced scan showed no enhancement of the heart-shaped pseudomass. However, the tentorium did enhance, and was parallel to the cerebrospinal fluid density line. The tentorial configuration itself was abnormal. The leaves of the tentorium came together in a straight line to form a sharp angle posteriorly, producing a V-shaped configuration, rather than the normal U shape. In addition, the leaves of the tentorium met more posteriorly than normal. Since none of the patients in this group had any clinical evidence of posterior fossa mass, this finding should be explainable as a manifestation of the underlying disease process. A combination of prominence of superior cerebellar cisterns, secondary to cerebellar hypoplasia [2, 3, 6, 7, 9] and inferior displacement of the cerebellum, plus an abnormal configuration of the tentorium [5, 7, 9] offers the best explanation for this finding (see discussion).

Configuration of Lateral Ventricles

The occipital horns were enlarged in 42 of the 47 patients. There was little correlation between the size of the occipital horn and that of the frontal and temporal horns. In those patients with follow-up studies, the occipital horns tended to remain constant in size, while

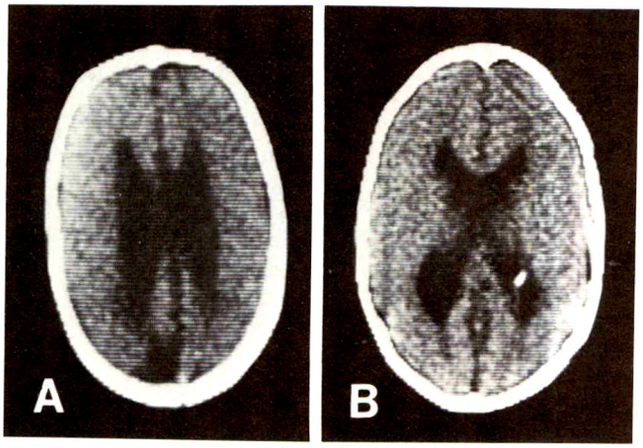


Fig. 5.—Configuration of lateral ventricle. Different patients after ventricular shunt procedures (shunt not visible in **A**). Note enlargement of occipital horns with pointed configuration. **A**, Medial concavity of frontal horns produces characteristic "vampire bat" configuration. **B**, Agenesis of corpus callosum.

TABLE 2

Summary of Findings in Meningomyelocele

Finding	%
Lacunar skull	62
Calvarial defects	4
Asymmetric skull	8
Nonvisualized or caudally displaced fourth ventricle (Chiari type II malformation)	92
Hydrocephalus	85
Anterior pointing and medical concavity of frontal horns	50
Enlarged occipital horns	89
Prominent interhemispheric fissure	85
Tentorial-cerebellar pseudomass	58
Absent septum pellucidum	50

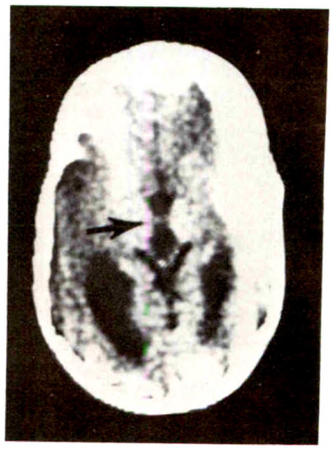
the size of the frontal and temporal horns varied with the degree of hydrocephalus and/or shunt function. The configuration of the enlarged occipital horns varied, but in 60% of the cases it was angular rather than rounded. The frontal horns also varied in size. A characteristic anterior pointing and medial concavity of the frontal horns was noted in 50% of the cases (fig. 5). This configuration could be obscured by hydrocephalus and in one case was seen only after the ventricle diminished after shunt revision.

A previously described ventriculographic feature of Chiari II malformation is inferior pointing of the frontal horns [8]. This was seen in 16 of 27 (60%) of the ventriculograms available for review in this series, but there was no correlation between this ventriculographic finding and anterior medial pointing of the frontal horns as seen on CT.

Evaluation of Septum Pellucidum

The septum pellucidum was completely or partially absent in 50% of our patients (fig. 5C). There was virtually 100% correlation between the ventriculographic and CT findings in this series with the exception of one case, in which partial absence of the septum could be identified only at CT.

Fig. 6.—Massa intermedia. Large massa intermedia in patient with meningomyelocele (*arrow*).



Intracranial Abnormalities Not Identifiable on CT

Abnormalities in the tectum, massa intermedia, and anterior third ventricle are often seen at ventriculography [4, 5, 8] in patients with Chiari II malformation. The frequency that these findings were noted in the ventriculograms available for review in this series was consistent with the literature. These abnormalities could not be identified with axial CT. (In one case, an unusually prominent massa intermedia was identified; fig. 6.) Aqueduct stenosis is commonly seen in patients with this disorder [4–6]. An attempt was made to determine if there were any findings indicative of this diagnosis on CT. Relative size of the fourth ventricle when compared with the third and lateral ventricles could not be used, since all patients had a small fourth ventricle secondary to the basic pathologic process, with or without aqueduct stenosis. The configuration of the third ventricle was carefully evaluated, but no characteristic feature that could accurately predict which patients would have ventriculographic evidence of aqueduct stenosis was discernible.

Calvarial Abnormalities Associated with Chiari II Malformation (table 2)

In five of eight patients scanned before age 4 months, marked thinning of the calvarium in multiple regions was identified (fig. 7). In all eight cases, the scans were evaluated retrospectively using bone window settings. In two cases with evidence of marked calvarial thinning on CT, skull radiographs within 2 weeks of the scan showed definite evidence or lacunar skull. In two cases one with evidence of calvarial thinning and one with normal bone on CT, the skull radiographs were not available for review. In the other four cases, two with evidence of calvarial thinning and two with normal CT, skull radio-

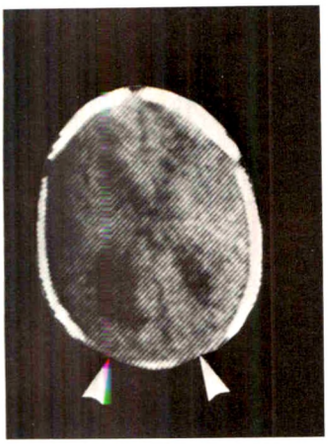


Fig. 7.—Lacunar skull. Several areas of thinning of calvaria in patient with meningomyelocele (*arrows*).

graphs were obtained, but two or more months before CT.

Patients with this disorder often have a small posterior fossa with flattening of the calvarium posterior to the foramen magnum [10]. The torcula is usually just above the foramen magnum [10]. This abnormality in configuration of the posterior fossa could not be consistently identified at CT. Changes in angulation of the head dramatically changed configuration of the posterior fossa on CT, and there was no correlation between apparent size of posterior fossa on CT and plain films in this series. Therefore, a small posterior fossa on CT is not believed to be a reliable sign of this disorder.

In two patients a large frontal bony defect was identified, both on CT and plain radiographs. In one a large frontal meningocele was identified on CT and ventriculography. In four patients there was marked asymmetry of the skull, seen on both CT and plain radiographs.

Discussion

The association between meningomyeloceles and intracranial abnormalities, particularly Chiari type II malformation is well known [1–7]. The etiology for this virtually constant association has been and remains controversial. Most recent theories view the abnormalities as various manifestations of a single congenital defect [2, 3, 6, 7]. The exact nature of this underlying abnormality is not fully understood, and a full discussion is beyond the limits of this presentation.

Evaluation of the position of the fourth ventricle proved to be a reliable method for establishing the diagnosis of Chiari II malformation (figs. 2 and 3). In only three cases was the fourth ventricle deemed to be normal in position. In two of these, reevaluation of clinical data and other tests indicated that the patient did not have Chiari II malformation; thus CT was instrumental in establishing the correct diagnosis. In most cases, of course, the diagnosis was not in doubt, since the presence of meningomyelocele virtually infers the presence of Chiari II malformation. As a method of confirmation, however, CT offers significant advantages over ventriculography. The first and most important advantage is the noninvasive nature of CT as compared with ventriculography with its attendant morbidity. Second, CT offers a method for directly establishing that the fourth ventricle is not in its normal position (92%), whereas ventriculography on the patients in this series directly demonstrated the fourth ventricle in only 12% of cases.

The reasons for the low percentage of fourth ventricle visualization on ventriculograms in this series are complex. The ventriculograms were performed over a several year period at another institution, and therefore technical adequacy cannot be evaluated. It is possible that many of the 18 ventriculograms not available for review were removed from the radiology file room precisely because they did demonstrate the major diagnostic features of this disorder. Of course, some of these patients did have aqueduct stenosis, accounting for the nonvisualization of the fourth ventricle. Pneumoencephalography was not performed, since information from ventriculography plus clinical data was felt to be sufficient to make the correct diagnosis and determine the degree of hydrocephalus.

In 67% of patients, the fourth ventricle was not visualized on CT. This is due to inability of the scanner used in this study to obtain adequate scans in the caudal posterior fossa. CT scanners which do not require the use of a water bag allow better visualization of anatomy in the region of the craniovertebral junction; use of such scanners should allow direct demonstration of the abnormally positioned fourth ventricle in more cases.

Many of these patients were initially seen prior to the advent of CT, and already had ventricular shunts inserted before their first scan. Since CT is demonstrated to be a safe and accurate tool for the measurement of ventricular size [11, 12], this method has been and will continue to be used to determine the degree of hydrocephalus in these patients, and in planning appropriate therapy. Because of its noninvasive nature, routine follow-up examinations to judge ventricular size and shunt function can be easily obtained.

However, difficulties do arise in determining the relative contributions of cerebral dysgenesis and hydrocephalus to increased ventricular size. On the basis of our study and in our experience in dealing with other patients with both dysgenesis and hydrocephalus, our clinical impression is that hydrocephalus produces enlargement of the temporal horns and a smooth rounded generalized enlargement of the lateral ventricles. In those patients with small temporal horns, a pointed configuration to the lateral ventricle and irregularities in the ventricular wall (heterotopic transmigration of grey matter?) [13, 14], a diagnosis of cerebral dysgenesis is more likely. However, pathologic correlation is not available on patients in this series.

Perhaps the most striking finding in this study was the unusual configuration of the posterior fossa seen in 58% of patients (fig. 4). This finding, which we call the tentorial-cerebellar pseudomass, is the product of two

abnormalities seen in patients with this disorder. The cerebellum is hypoplastic and placed low in the posterior fossa; thus the cisterns surrounding the cerebellum are more prominent than usual [2, 3, 6, 7, 9]. If a CT scan is obtained through these cisterns, they may be clearly visualized. This allows visualization of a centrally placed cerebellum and a peripherally placed supratentorial brain. The configuration of the cisterns depends on the configuration of the cerebellum and the tentorium, which is itself abnormal in patients with Chiari II malformation [5, 6, 9]. It attaches to the torcula which is low in the posterior fossa just above the foramen magnum [10]. Because of this low attachment, the slope of the tentorium in the midline is steeper than normal [5, 9]. Therefore, more cerebellum is shown on a given slice than is normally seen, and it is clearly outlined by the enlarged cisterns surrounding it. Thus the pseudomass configuration. The significance of this finding is twofold. First, it should not be mistaken for a true mass in patients with meningomyelocele. Second, it may be a specific finding of Chiari II malformation.

Evaluation of the lateral ventricles is somewhat limited because many of the patients had already been shunted prior to the initial scan, but several trends do appear. Evaluation of the size and configuration of the occipital horns could not be used to judge the degree of hydrocephalus or shunt function. The occipital horns were enlarged in virtually all patients; this probably represents either primary brain dysgenesis or changes secondary to shunting (fig. 5).

In contrast, the size of the temporal horns proved to be an extremely reliable method of evaluating the degree of hydrocephalus and, therefore, often shunt function. Although the frontal horns also tended to vary in size with the degree of obstruction and shunt function, the size of the temporal horns was a more reliable monitor of this in our experience. However, evaluation of the frontal horns did show a rather characteristic configuration in 50% of the cases (fig. 5) consisting of anterior pointing and medial concavity. When the frontal horns had this configuration and the occipital horns were also enlarged, the lateral ventricles took on a rather striking and characteristic "vampire bat" configuration on CT (fig. 5). This characteristic appearance of the frontal horns was obscured by ventricular dilatation, only to be demonstrated when the frontal horns diminished after decompression.

There was no correlation between the abnormal configuration of frontal horns as visualized at CT and a characteristic inferior pointing of the frontal horns as visualized in 60% of the patients with ventriculography in this series [8]. These two abnormalities undoubtedly represent separate manifestations of the underlying dysgenetic process present in these patients. Axial projections were not routinely obtained during ventriculograms and, therefore, the fact that this finding has not been previously reported is not surprising. Use of either direct coronal scanning or coronal reconstruction might clearly document the presence of inferior pointing on CT, but we have no direct experience with these techniques.

Ventriculography often demonstrates abnormalities in the tectum, massa intermedia, and anterior third ventricle [4–6, 8]. Aqueduct stenosis is also commonly seen in patients with Chiari II malformation. These abnormalities were noted at ventriculography in the patients in this series, but could not be documented by axial CT. Once again, use of either direct or reconstructed coronal images and reconstructed sagittal images might allow for direct identification of these various abnormalities. In particular, it may be possible in the future to directly diagnose aqueduct stenosis using sagittal reconstructions. However, the value of these additional views is problematic. We feel that the correct diagnosis can be made with a high degree of confidence using routine axial CT, and better delineation of the diffuse abnormalities in these patients will probably not affect the therapeutic regimen which is basically aimed at controlling hydrocephalus.

Changes in the calvarium are common in patients with Chiari II malformation and meningomyelocele [4–6, 10]. Virtually all patients are born with lacunar skull [6, 10], but this finding generally disappears by age 3–4 months. In five of eight patients scanned before age 4 months, there was marked thinning of the calvarium in several areas, a finding consistent with lacunar skull noted on skull radiographs obtained within 2 weeks of CT. In two of three patients who did not show evidence of lacunar skull on CT, with either routine or bone window technique, skull radiographs did demonstrate evidence of lacunar skull. However, these radiographs were obtained 2–3 months before CT; therefore, it is impossible to determine whether plain film changes were still present at the time CT was performed.

Large bony defects were also present in two patients. CT not only demonstrated these bony defects, but in one case showed evidence of an anterior meningocele confirmed at ventriculography. The posterior fossa has an abnormal configuration in patients with Chiari II malformation. It is smaller than normal, with the torcula close to the foramen magnum, and the region just posterior to the inion shows flattening and concavity. The configuration of the posterior fossa in these patients varied at CT and depended on head position and scanning angle. Thus, posterior fossa configuration cannot be used as a reliable sign of Chiari II malformation.

REFERENCES

1. Bloch S, Van Rensburg JM, Danziger J: The Arnold-Chiari malformation. *Clin Radiol* 25:335–341, 1974
2. Brocklehurst G: The pathogenesis of spina bifida: a study of the relationship between observation, hypothesis and surgical incentive. *Dev Med Child Neurol* 13:147–163, 1971
3. Carmel PW, Markesbery WR: Early descriptions of the Arnold-Chiari malformation. The contribution of John Cleland. *J Neurosurg* 37:543–547, 1972
4. Harwood-Nash DC, Fitz CR: *Neuroradiology in Infants and Children*. St. Louis, Mosby, 1976, pp 1000–1014

5. Newton TH, Potts DG: Angiography, in *Radiology of the Skull and Brain*, vol 2, St. Louis, Mosby, 1974, pp 2738–2740
6. Peach B: Arnold Chiari malformation: anatomic features of 20 cases. *Arch Neurol* 12:613–621, 1965
7. Padget DH: Development of so-called dysraphism: with embryologic evidence of clinical Arnold-Chiari and Dandy-Walker malformation. *John Hopkins Med J* 130:127–165, 1972
8. Gooding CA, Carter A, Hoare RD: New ventriculographic aspects of the Arnold-Chiari malformation. *Radiology* 89: 626–632, 1967
9. Wolpert SM: Dural sinus configuration: measure of congenital disease. *Radiology* 92:1511–1516, 1969
10. Kruyff E, Jeffs R: Skull abnormalities associated with the Arnold-Chiari malformation. *Acta Radiol [Diagn]* (Stockh) 5: 9–21, 1966
11. Berger PE, Kirks DR, Gilday DL, Fitz CR, Harwood-Nash DC: Computed tomography in infants and children: intracranial neoplasms. *AJR* 127:129–137, 1976
12. Harwood-Nash DC: Congenital craniocerebral abnormalities and computed tomography. *Semin Roentgenol* 12:39–51, 1977
13. Bergeron RT: Pneumographic demonstration of subependymal heteropic cortical grey matter in children. *AJR* 101: 168–177, 1967
14. Dodge E: Congenital malformations of the central nervous system, in *Neurological Pathophysiology*, edited by Eliason SG, Prensky AZ, Hardin WB, New York, Oxford University Press, 1974, pp 16–25

John Caffey Award:

Intraventricular Hemorrhage and Hydrocephalus in Premature Newborns: A Prospective Study with CT

JEROME BURSTEIN,[1] LU-ANN PAPILE,[2] AND ROCHELLE BURSTEIN[2]

In a prospective study, 100 premature infants were studied with computed tomography (CT) brain scans within the first week of life. In 44 of these, hemorrhages originated from the subependymal germinal matrix, and ranged in severity from isolated germinal matrix hemorrhages to blood-filled, dilated ventricles with extension of hemorrhage into the brain parenchyma. A system of grading the severity of hemorrhage was developed. Grades I and II hemorrhages resolved spontaneously and grades III and IV were associated with progressive hydrocephalus. Asymptomatic hemorrhages that would not have been diagnosed on clinical grounds were detected by CT. This study offers a clearer understanding of the true incidence and natural history of cerebroventricular hemorrhage and associated hydrocephalus in premature neonates and may clarify etiologic factors and identify children at risk for subsequent neurologic abnormalities.

Spontaneous hemorrhage into the cerebral ventricles is a phenomenon that occurs in premature neonates [1, 2]. It originates in the subependymal germinal matrix within the first 4 days of life [3, 4]. This study evolved from the observation that several premature neonates thought to have survived an intraventricular hemorrhage developed clinical hydrocephalus at 3–4 weeks of age. A second group of premature neonates who also developed hydrocephalus at 3–4 weeks old had no clinically apparent hemorrhage. This suggested that intraventricular hemorrhage might be clinically occult and still produce significant sequelae. In order to test this hypothesis, to determine the true incidence of intraventricular hemorrhage, and to study the relation between neonatal intraventricular hemorrhage and hydrocephalus, a prospective study using computed tomography (CT) brain scans of an at-risk population was performed. It is an extension of previous work in which we demonstrated that CT can be used to accurately diagnose germinal matrix hemorrhage and intraventricular hemorrhage in the living newborn [5].

Subjects and Methods

Computed tomography brain scans were performed before the seventh day of life on 100 consecutive premature neonates of birthweight less than 1,500 g admitted to the University of New Mexico Newborn Intensive Care Unit. Living infants were studied at 4–7 days of age. If the infant died before day 4, a postmortem CT scan was performed before brain fixation. None of the infants studied had congenital hydrocephalus at birth. The time of the initial scan was based on previous studies [3, 4] that indicated the majority of intraventricular hemorrhages in premature newborns occur before the fourth day of life. The infants were transported to the scanning suite in a transport isolette. Heart rate was monitored, heat lamps were used to prevent hypothermia, and a neonatologist was always in attendance. The scanner gantry was modified as previously described [5].

Serial CT scans were subsequently obtained on all surviving infants in whom the initial scan demonstrated a hemorrhage. Weekly scans were done until the hemorrhage was completely resolved and ventricular size was stable. There were no complications during transportation or scanning.

Results

Of the 100 neonates, 56 showed no evidence of hemorrhage on CT scan (table 1). Of these 56 infants, 13 died, most often of idiopathic respiratory distress syndrome or its complications. None of the 13 had evidence of hemorrhage or hydrocephalus at autopsy. The 43 remaining infants in this group survived and, although follow-up scans were not obtained, none of these infants had developed clinical hydrocephalus at 1-year follow-up.

Some degree of cerebroventricular hemorrhage was seen on CT scans in 44 of the 100 neonates. The mildest form (grade 1) was an isolated hemorrhage into one or both of the germinal matrices (fig. 1). Rupture of the germinal matrix hemorrhage into the ventricles was associated with either normal sized ventricles (grade II, fig. 2) or ventricular dilatation (grade III, fig. 3). The most extensive hemorrhages (grade IV, fig. 4) consisted of dilated blood-filled ventricles with extension of the germinal matrix hemorrhage into the adjacent brain parenchyma.

Weekly CT scans were performed on every infant with any grade of hemorrhage. Of the 44 neonates with hemorrhage, 22 survived at least 28 days, the length of time defined as the neonatal period. Serial scans were

Received September 8, 1978; accepted after revision January 16, 1979.
This work was supported in part by a James Picker Foundation pilot research grant and National Institutes of Health biomedical research support grant 5 S01 RR 05583.
Presented at the annual meetings of the Society for Pediatric Radiology and the American Roentgen Ray Society, Boston, September 1977.
[1] Department of Radiology, University of New Mexico, School of Medicine, Albuquerque, New Mexico 87131. Address reprint requests to J. Burstein.
[2] Department of Pediatrics, University of New Mexico, School of Medicine, Albuquerque, New Mexico 87131.

© 1979 American Roentgen Ray Society

0361–803X/79/1324–0631 $0.00

TABLE 1

Cerebroventricular Hemorrhage, Neonatal Deaths, and Progressive Ventricular Dilatation in Premature Infants

Initial Findings	Survivors		Deaths	Total
	Hydrocephalus	No Hydrocephalus		
Cerebroventricular hemorrhage:				
Grade I	0	7	3	10
Grade II	0	6	4	10
Grade III	5	1	8	14
Grade IV	3	0	7	10
Subtotal	8	14	22	44
No cerebroventricular hemorrhage	0	43	13	56
Total	8	57	35	100

Note—Grade of hemorrhage was assigned at initial CT scan. Grade I: isolated germinal matrix hemorrhage; grade II: intraventricular extension of hemorrhage with normal ventricular size; grade III: intraventricular hemorrhage with dilated ventricles; grade IV: grade III plus extension of germinal matrix hemorrhage into adjacent brain parenchyma. Survival period is first 28 days after birth.

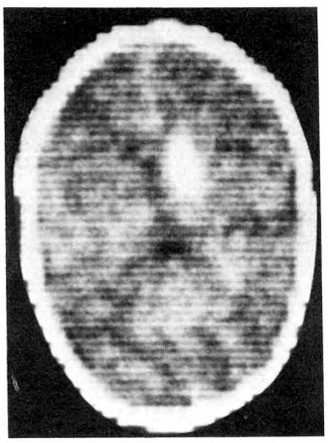


Fig. 1.—Grade 1 hemorrhage in 5-day-old, 28-week-gestation, 1021 g infant. Ovoid collection of blood on right side adjacent to third ventricle and frontal horn of lateral ventricle corresponds to location of largest concentration of germinal matrix tissue at junction of head of caudate nucleus and thalamus. Sections more cephalad and caudad did not show any hemorrhage.

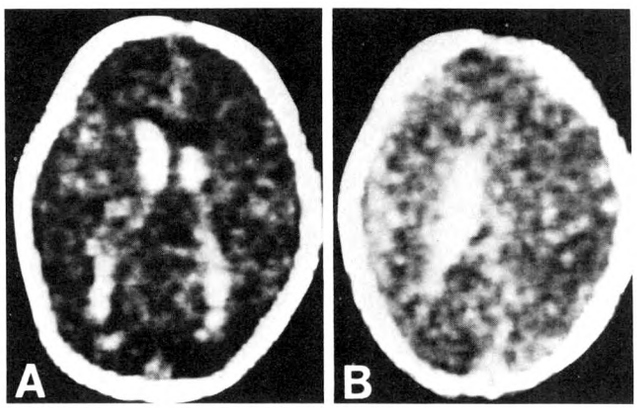


Fig. 2.—Grade II hemorrhage in 4-day-old, 30-week-gestation, 1,200 g infant. **A,** At level of germinal matrices and occipital horns of lateral ventricle. **B,** 8 mm higher. Bilateral germinal matrix hemorrhages larger at left than right. Hemorrhage extended into part of germinal matrix tissue adjacent to body of left lateral ventricle (**B**) and ventricles, settling into the occipital horns of the lateral ventricles. Normal ventricular size.

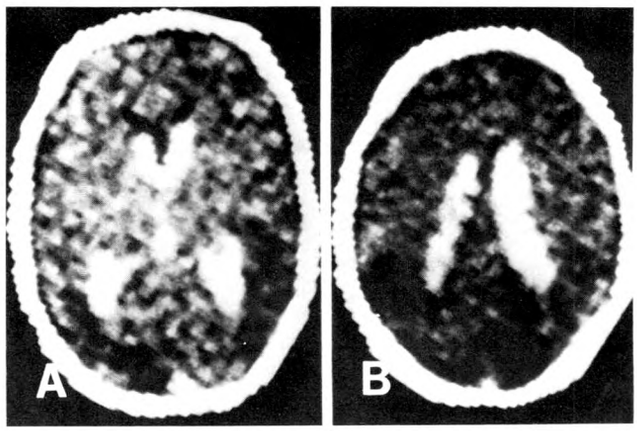


Fig. 3.—Grade III hemorrhage, 2-day-old, 32-week-gestation, 1,191 g infant (postmortem). Hemorrhage in germinal matrix at junction of head of caudate nucleus and thalamus, in third ventricle, in somewhat dilated occipital horns of lateral ventricles (**A**), and in germinal matrix tissue adjacent to bodies of lateral ventricles (**B**).

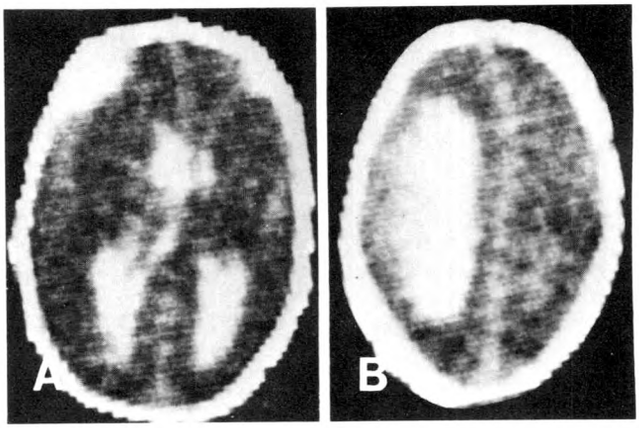


Fig. 4.—Grade IV hemorrhage, 5-day-old, 30-week-gestation, 936 g infant. **A,** Bilateral germinal matrix hemorrhage, larger on left than right, has broken into dilated ventricles. **B,** Left-side germinal matrix hemorrhage extends into left cerebral hemisphere almost to the cortex, exerting mass effect with shift of interhemispheric fissure from left to right. Reason for increased absorption coefficients interhemispheric fissure unclear. Several infants with this finding studied at autopsy had no evidence of subarachnoid hemorrhage.

continued in the subgroup of surviving infants with hemorrhage until the hemorrhages were resorbed and ventricular size stabilized.

None of the 13 infants with grade I or II hemorrhages who survived the neonatal period developed either CT or clinical hydrocephalus. One infant had an isolated germinal matrix hemorrhage without rupture into the ventricles or extension into the brain parenchyma (grade I). Serial scans showed resorption of the fresh blood with the final scan appearing normal. The child died at 28 days of age of a perforated duodenum. At autopsy, there was a thick-walled cystic lesion at the site of the germinal matrix hemorrhage (fig. 5). Therefore, even though a grade I or grade II hemorrhage was not associated with the development of hydrocephalus, structural damage to

the brain did occur in at least one case as a direct result of an isolated germinal matrix hemorrhage.

Weekly serial CT brain scans of the nine surviving infants with a grade III or grade IV hemorrhage demonstrated progressive ventricular dilatation (fig. 6) in eight (89%). Developing hydrocephalus was evident on CT scans before the development of an abnormal increase in head circumference. Early detection of ventricular dilatation by CT allowed early institution of appropriate therapy. In the three surviving infants in whom the initial germinal matrix hemorrhage extended into the brain parenchyma (grade IV), serial scans showed residual areas of paraventricular porencephaly, often of considerable size (fig. 7).

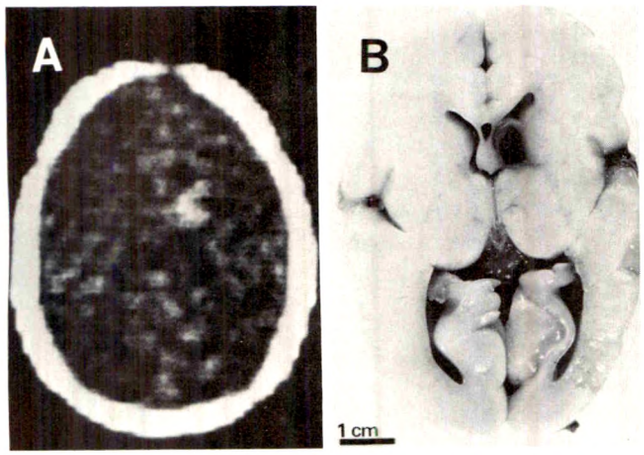


Fig. 5.—Grade I hemorrhage with residual paraventricular cyst in 5-day-old, 28-week-gestation, 721 g infant. **A,** Initial study at 5 days of age. Isolated right-side germinal matrix hemorrhage with no rupture into ventricles or extension into brain parenchyma. Follow-up sections were normal with no evidence of hydrocephalus or paraventricular cystic lesions. The child died of age 28 days of perforated duodenum. **B,** Autopsy section of the brain. Thick-walled cystic lesion at site of previous germinal matrix hemorrhage.

Discussion

Cerebroventricular hemorrhage originates in the germinal matrix [2], a structure located beneath the ependymal lining of the ventricles and largest in the groove between the head of the caudate nucleus and the thalamus. It is a highly vascular structure with little supporting tissue. It is a source of neuroblasts which migrate peripherally during development of the fetal brain. The germinal matrix is largest at 24–32 weeks gestation and then involutes so that it is much smaller in full term infants than prematures [6].

Our study demonstrated a broad spectrum of germinal matrix–related hemorrhage in the premature neonate, ranging from isolated germinal matrix hemorrhage to massive intraventricular hemorrhage with extension into the brain parenchyma. Cerebroventricular hemorrhage has been found at autopsy in 55%–75% of premature newborns who died from any cause [2, 4, 7]. The CT diagnosis of cerebroventricular hemorrhage in 22 of the 35 (63%) deaths in our series agrees with these figures. However, there has been no way to determine whether or not the rate found at autopsy could be extrapolated to the entire at-risk population. We found an incidence of 44% in all premature infants (survivors and nonsurvivors) weighing less than 1500 g studied by CT on one occasion between the fourth and seventh day of life.

Of the 44 infants with cerebroventricular hemorrhage, 22 survived the neonatal period. Before the advent of CT, such hemorrhage was diagnosed at autopsy or by the sudden development of hypotonia, hypotension, falling hematocrit, bulging fontaneles, acidosis, and seizures. We compared the accuracy of the clinical diagnosis of cerebroventricular hemorrhage in survivors to the CT diagnosis. Of the 22 infants who had CT-proven hemorrhages and survived the neonatal period, the diagnosis was not suspected clinically in 15 (68%). Therefore, since 15 of the 65 survivors of the neonatal period had sustained a clinically silent hemorrhage, there was a one

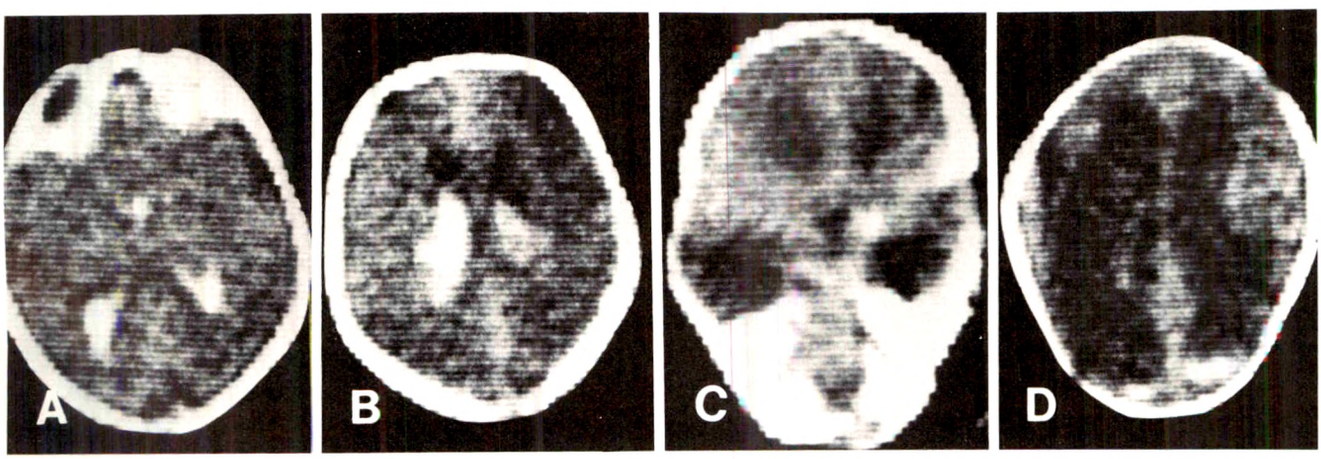


Fig. 6.—Hydrocephalus after grade III hemorrhage in 6-day-old, 30-week-gestation, 1,191 g infant. **A** and **B,** At 6 days of age. Grade III hemorrhage, greater on left than on right, and extravasation of blood into ventricles, which are only mildly dilated. **C** and **D,** At 13 days of age. Dilatation of lateral ventricles and third ventricle, with small amount of blood settled in most dependent portions of occipital horns of lateral ventricles.

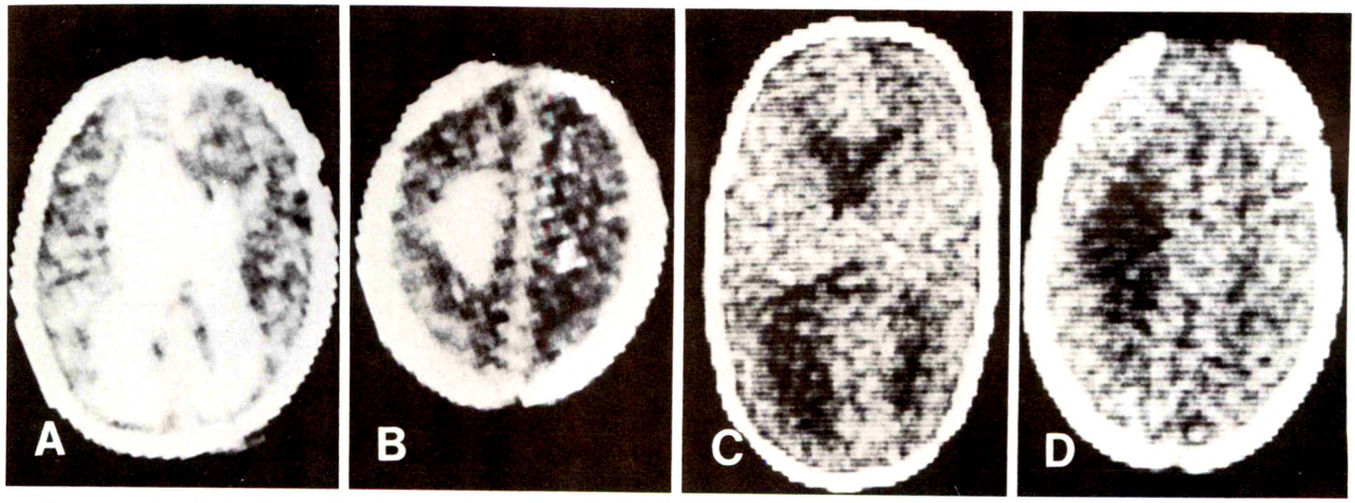


Fig. 7.—Grade IV hemorrhage with residual paraventricular porencephaly in 6-day-old, 28-week-gestation, 1,021 g infant. **A** and **B**, At 6 days of age. Grade IV hemorrhage with rupture into ventricles, dilated blood-filled ventricles, and extension of hemorrhage into left cerebral hemisphere. **C** and **D**, At 3 months of age. Slight dilatation of ventricular structures, but area of paraventricular porencephaly in left cerebral hemisphere at site of initial cerebral extension of left-side germinal matrix hemorrhage.

in four chance that a premature infant discharged from the Newborn Intensive Care Unit had experienced a clinically silent cerebroventricular hemorrhage.

The etiology of this hemorrhage is unknown. If it is due only to the fragility of the angioarchitecture of the germinal matrix [8], increasing the case findings with prospective CT studies will add little to the understanding of the disease process. However, since not all premature neonates have cerebroventricular hemorrhage, there must be other causative factors. These may include perinatal events such as asphyxia, method of delivery, development of idiopathic respiratory distress syndrome, and use of intravenous bicarbonate therapy [9]. Unfortunately, there are limitations to the use of the previously available autopsy data in evaluating these relationships [10], since cerebroventricular hemorrhage is survivable and often clinically occult. By identifying the hemorrhage in the entire population at risk, it should be possible to make a more accurate analysis of risk factors.

Hydrocephalus may develop after intraventricular hemorrhage as a result of inflammatory ependymitis, obstruction of the aqueduct or fourth ventricles by clot, or basilar arachnoiditis. Previous studies [11–14] reported the development of hydrocephalus in premature infants surviving intraventricular hemorrhage. However, diagnosis of such hemorrhage was made on clinical grounds without the use of CT. In this study, there were 15 surviving infants who had CT-documented intraventricular hemorrhage (grades II–IV). Eight (53%) of this group developed hydrocephalus, but seven did not. It seems that intraventricular hemorrhage is etiologic for hydrocephalus since there were no cases of hydrocephalus that were not associated with it. However, it is unclear why some premature newborns with intraventricular hemorrhage develop hydrocephalus and others do not. But since over one-half of the surviving infants with intraventricular hemorrhage develop hydrocephalus, we feel that once intraventricular hemorrhage has been documented with CT, serial scans should be performed until ventricular size has stabilized or until treatment is considered necessary. Serial scans were often useful in detecting the development of hydrocephalus before the onset of rapid head growth. This confirms previous reports [12, 15] that there is a lag between increasing ventricular size and increasing head circumference.

Accurate case findings with prospective CT scans have implications beyond the better understanding of incidence and etiology. Children born prematurely have a higher incidence of neurologic abnormalities than those born at term [16–18]. We have now identified a population of infants with clinically silent cerebral hemorrhages in the neonatal period. A long-term neurologic and psychometric follow-up of this group, using infants without hemorrhage as controls, has been instituted, which may help explain the higher rate of neurologic disability.

REFERENCES

1. Fredrick J, Butler NR: Certain causes of neonatal death. II. Intraventricular hemorrhage. *Biol Neonate* 15:247–290, 1970
2. Leech RW, Kohnen P: Subependymal and intraventricular hemorrhages in the newborn. *Am J Pathol* 77:465–476, 1974
3. Emerson P, Fujimura M, Howat P, Howes D, Keeling J, Robinson RO, Salisbury D, Tizard JPM: Timing of intraventricular haemorrhage. *Arch Dis Child* 52: 183–187, 1977
4. Tsiantos A, Victorin L, Reiler JP, Dyer N, Sundell H, Brill AB, Stahlman M: Intracranial hemorrhage in the prematurely born infant: timing of clots and evaluation of clinical signs and symptoms. *J Pediatr* 85:854–859, 1974
5. Burstein J, Papile L, Burstein R: Subependymal germinal matrix and intraventricular hemorrhage in premature in-

fants: diagnosis by CT. *AJR* 128:971–976, 1977
6. Friede RL: *Developmental Neuropathology*. New York, Springer, 1976, pp 1–37
7. Grunnet ML, Curless RG, Bray DF, Jung AL: Brain changes in newborns from an intensive care unit. *Dev Med Child Neurol* 16:320–328, 1974
8. De Reuck JL: The significance of the arterial angioarchitecture in perinatal cerebral damage. *Acta Neurol Belg* 77:65–94, 1977
9. Simmons MA, Adcock EW, Bard H, Battaglia FC: Hypernatremia and intracranial hemorrhage in neonates. *N Engl J Med* 291:6–10, 1974
10. Leviton A, Epidem SM, Gilles FH: Limitations of autopsy data in relating neonatal intracranial hemorrhage to buffer therapy. *Hum Pathol* 8:599–601, 1977
11. Deonna T, Payot M, Probst A, Prod'Hom L: Neonatal intracranial hemorrhage in premature infants. *Pediatrics* 56: 1056–1064, 1975
12. Korobkin R: The relationship between head circumference and the development of communicating hydrocephalus in infants following intraventricular hemorrhage. *Pediatrics* 56:74–77, 1975
13. Lorber J, Bhat US: Posthaemorrhagic hydrocephalus: diagnosis, differential diagnosis, treatment, and long-term results. *Arch Dis Child* 49:751–762, 1974
14. Wise BL, Ballard R: Hydrocephalus secondary to intracranial hemorrhage in premature infants. *Childs Brain* 2:234–241, 1976
15. Volpe JJ, Pasternak JF, Allan WC: Ventricular dilatation preceding rapid head growth following neonatal intracranial hemorrhage. *Am J Dis Child* 131:1212–1215, 1977
16. Bjerre I: Neurological investigation of 5-year old children with low birth-weight. *Acta Paediatr Scand* 64:859–864, 1975
17. Davies PA, Steward AL: Low-birth-weight infants: neurological sequelae and later intelligence. *Br Med Bull* 26:171–174, 1970
18. Teberg A, Hodgman JE, Wu PYK, Spears RL: Recent improvement in outcome for the small premature infant. *Clin Pediatr* (Phila) 16:307–313, 1977

Preliminary Report of the M. D. Anderson Hospital/Texas A & M Variable Energy Cyclotron Fast-Neutron Therapy Pilot Study

LESTER J. PETERS,[1] DAVID H. HUSSEY,[1] GILBERT H. FLETCHER,[1] PAUL A. BAUMANN,[2] AND MARVIN H. OLSON[3]

The records of 248 patients treated with fast neutrons and of 102 comparable but nonrandomized control patients treated conventionally with photons, surgery, or combined surgery and photon irradiation were reviewed. Fast neutron therapy included treatment with neutrons alone, a neutron boost after photon therapy, or a schedule of alternating neutron and photon treatments (mixed beam). The results with mixed beam irradiation were superior to those obtained with the other neutron therapy techniques, and compared favorably with the results of standard treatment methods. However, the lack of a conclusive advantage for neutron therapy in this pilot study illustrates the need for on-going randomized clinical trials.

Between October 1972 and July 1976, The University of Texas System Cancer Center, M. D. Anderson Hospital and Tumor Institute carried out a pilot study of fast neutron therapy using the Texas A & M variable energy cyclotron. Since January 1977, a randomized clinical trial of neutron therapy has been underway. The cyclotron was not available for clinical use during two periods: between July and December 1975 and between July and December 1976. During these times, patients who were candidates for the neutron therapy pilot study were registered in a "control group" and treated with surgery, photon therapy, or combined surgery and photon therapy.

This paper compares the preliminary results of the neutron therapy pilot study with those of the control group. The results obtained with the different fractionation schedules used in the neutron therapy pilot study are also discussed.

Materials and Methods

Energy and Dosage Conventions

The neutron beam energies quoted in this paper refer to the energies of the incident deuterons. The mean neutron energy is about 42% of this value. Initially, a neutron beam produced by bombarding beryllium with 16 MeV deuterons (16 $MeV_{d\rightarrow Be}$) was used, since there was clinical experience with this energy at Hammersmith Hospital. A 50 $MeV_{d\rightarrow Be}$ neutron beam has been used since March 1973. This beam has skin sparing and depth dose properties similar to 4 MeV photons.

Physical doses were determined by measurements with a tissue-equivalent ionization chamber immersed in tissue-equivalent liquid. They are expressed in rads including both the neutron and gamma components ($rad_{n\gamma}$).

Equivalent doses (rad_{eq}) were calculated by multiplying the physical dose delivered with neutrons by a factor of 3.1 and adding this to the dose delivered with photons. The equivalence factor of 3.1 was determined clinically by comparing the late effects obtained with neutrons delivered twice weekly with those of ^{60}Co delivered five times weekly. The complication rate seen with 2,080 $rad_{n\gamma}$/13 fractions/6½ weeks with 50 $MeV_{d\rightarrow Be}$ neutrons is similar to that seen with a dose of 6,500 rads/32 fractions/6½ weeks with ^{60}Co [1]. Radiobiology studies of rhesus monkey oral mucosa (J. H. Jardine, personal communication, 1977) and pig skin [2] have shown that the dose-response curves for late effects with neutrons are independent of weekly fractionation.

Clinical Material

The following tumor sites have been selected for analysis: (1) carcinoma of the head and neck, (2) gynecologic cancer, (3) squamous carcinoma of the esophagus, (4) adenocarcinoma of the breast, and (5) adenocarcinoma of the prostate. The analysis includes 248 patients treated in the neutron therapy pilot study and 102 patients in the control group. These are not randomized controls, but they do represent patients who would have been treated with neutrons had the facility been available for clinical use. The clinical material is compared by site and stage in table 1. Fifteen patients in the neutron therapy group and six in the control group who did not complete the planned course of treatment have been excluded from analysis.

Neutron Therapy Group Treatment

The standard photon treatment policies at M. D. Anderson Hospital were adapted for neutron therapy. The same total equivalent dose and overall treatment time as would be used with photon irradiation were used (table 2). For most tumor sites, the aim was to deliver 6,000 rad_{eq} in 6 weeks for moderately advanced tumors and 7,000 rad_{eq} in 7 weeks for massive tumors.

The number of fractions was determined by the availability of the cyclotron. The following fractionation schedules were used: (1) neutrons only, twice weekly; (2) neutrons only, four times weekly; (3) neutron boost after photon irradiation; and (4) combined neutrons and photons (mixed beam).

Neutrons only, twice weekly. This fractionation schedule was used in the initial phase of the study because the cyclotron was available for neutron therapy only twice weekly. The initial doses were based on pretherapeutic determinations of relative biologic effectiveness. The doses were subsequently modified on the basis of clinical observations [1]. For most tumor sites, the doses delivered with neutrons only, twice weekly, ranged from 1,920 $rad_{n\gamma}$ in 6 weeks to 2,560 $rad_{n\gamma}$ in 7 weeks (5,950 rad_{eq}/6 weeks to 7,900 rad_{eq}/7 weeks) (table 2).

Neutrons only, four times weekly. Between January and July 1976, the cyclotron was available for neutron radiotherapy four times weekly. During this period, patients with superficial and

Received July 20, 1978; accepted after revision December 11, 1978.
Presented at the annual meeting of the American Radium Society, New Orleans, April 1978.
This work was supported in part by grant no. CA 12542 from the National Cancer Institute.
[1]Department of Radiotherapy, University of Texas System Cancer Center, M. D. Anderson Hospital and Tumor Institute, 6723 Bertner Avenue, Houston, Texas 77030. Address reprint requests to D. H. Hussey.
[2]Department of Radiology, Wesley Medical Center, Wichita, Kansas 67214.
[3]Department of Radiology, Division of Radiation Oncology, University of Texas Medical Branch, Galveston, Texas 77550.

© 1979 American Roentgen Ray Society

TABLE 1

Clinical Material and Stage by Treatment Group

Cancer Site and Stage	Neutron Group*	Control Group†
Head and neck:		
T3N0–2 or T1–2N2	29	21
T4N0–3 or T0–3N3	83	25
Unstaged	4	3
Subtotal	116	49
Gynecologic:		
Late stage IIB	3	2
Stage IIIA	21	9
Stage IIIB	25	6
Stage IV	4	1
Miscellaneous	17	1
Subtotal	70	19
Esophageal:		
<5 cm long	2	4
5–9 cm long	9	4
>9 cm long	7	4
Subtotal	18	12
Breast:		
Primary ≤ 7½ cm and axillary nodes ≤ 5 cm	5	6
Primary >7½ cm; or axillary nodes >5 cm	21	9
Subtotal	26	15
Prostate:		
Not fixed	0	1
Fixed to one pelvic wall	8	3
Fixed to two pelvic walls	10	3
Subtotal	18	7
Total	248	102

* Exclusions: 12 patients who did not complete the planned course of treatment because of advancing local disease (three), deteriorating general condition (three), death (two), or distant metastasis (four); and three patients treated palliatively with abbreviated fractionation schedules.

† Exclusions: three patients who did not complete the planned course of treatment because of advancing local disease (two) or deteriorating general condition; and three patients treated palliatively with abbreviated fractionation schedules.

intermediately located tumors were treated with four-times-weekly fractionation. Fractions of 80 $rad_{n\gamma}$ were delivered four times weekly to a total dose of 1,920 $rad_{n\gamma}$ in 6 weeks to 2,240 $rad_{n\gamma}$ in 7 weeks (5,950 rad_{eq}/6 weeks to 6,950 rad_{eq}/7 weeks (table 2).

Neutron boost. The majority of patients treated with a neutron boost were initially selected for treatment with photons, but were referred for completion of treatment with neutrons because of persistent or progressive disease. These patients received 4,000–5,000 rad in 4–5 weeks with photons, followed by a neutron boost to the residual bulky disease (table 2). The neutron boost dose ranged from 640 $rad_{n\gamma}$ in 2 weeks to 960 $rad_{n\gamma}$ in 3 weeks (2,000 rad_{eq}/2 weeks to 3,000 rad_{eq}/3 weeks). beam schedule was adopted in September 1974 because twice-weekly fractionation with neutrons resulted in a relatively high local failure rate and a significant number of complications. The aim was to take advantage of five-times-weekly fractionation, but keep the same overall equivalent dose. Mixed beam treatments were given twice weekly with neutrons and three times weekly with photons. The neutron fraction size was 65 $rad_{n\gamma}$.This is equivalent to 200 rad with photons, assuming a relative biologic effectiveness of 3.1. For most sites, the equivalent doses ranged from 6,000 rad_{eq} in 6 weeks to 7,000 rad_{eq} in 7 weeks (table 2).

Control Group Treatment

The patients in the control group were treated with a variety of treatment methods depending on the tumor site and clinical presentation (table 3). About one half the patients with head and neck tumors and most of those with esophageal carcinomas were treated with combined surgery and radiotherapy. All of the patients with gynecologic or prostate tumors were treated with radiation therapy alone. Ultrafractionation techniques (twice-daily irradiation) were used for a significant number of head and neck and breast cancer patients.

Results

The data were analyzed in August 1977. The follow-up period for the control group is shorter than that for the neutron-irradiated group. The interval from the start of radiation therapy to the date of analysis ranged from 14 to 58 months (mean, 35.1) for the neutron therapy group and from 8 to 25 months (mean, 17.0) for the control group.

Disease-free and survival intervals were computed from the first day of treatment. Patients were scored as having their tumor locally controlled if they were alive with no evidence of disease at the time of analysis, or if they died of distant metastasis or intercurrent disease with no clinical evidence of local cancer. Patients lost to follow-up were considered to have died of local cancer Complications (e.g., mucosal ulceration or fistulae) developing in the area of residual or recurrent disease were attributed to persistent cancer and were not scored as complications of treatment.

Head and Neck Cancer

The clinical group with head and neck cancer included 116 patients in the neutron therapy group and 49 in the control group. The patients treated with neutrons had slightly more advanced tumors than those treated in the control group (table 1). This is because only massive tumors were treated during the first 18 months of the neutron pilot study when dosage schedules were poorly understood. The extent of disease treated with neutrons only, four times weekly, or the mixed beam was similar to that treated with conventional treatment methods in the control group.

The results for the control group are slightly better than the overall results of the neutron therapy pilot study, but the control group patients had slightly less advanced disease and have been followed for a shorter period. The overall local control rate for the neutron therapy group was 47.4% (55 of 116) and 13.8% (16 of 116) developed major complications (table 4). At the time of analysis, the local control rate for the control group was 57.1% (28 of 49), and the major complication rate was 24.5% (12 of 49).

The local control rate with mixed beam irradiation (57.9%, 11 of 19) is similar to that achieved with conventional treatment methods in the control group, and there have been no complications (table 4). The mixed beam results are superior to those obtained with neutrons only, twice weekly; neutrons only, four times weekly; or a neutron boost.

Gynecologic Cancer

The majority of gynecologic patients had stage III or IV squamous carcinomas of the uterine cervix (table 1).

TABLE 2

Treatment Methods for Neutron Group

	Head and Neck	Gynecologic	Esophagus	Breast	Prostate
Neutrons only, twice/week	49 (5,950–7,900)	16 (5,750–6,500)	8 (5,600–6,500)	16 (6,200–7,900)	1 (6,200)
Neutrons only, four times/week	19 (6,000–6,700)	. . .	3 (5,800–6,150)	. . .	1 (6,000)
Neutron boost	29 (6,000–7,900)	24 (5,900–7,000)	3 (5,100–6,100)	6 (7,200–7,350)	. . .
Mixed beam	19 (6,000–7,000)	30 (6,500–6,750)*	4 (5,000–6,000)	4 (7,000–7,150)	16 (5,900–6,600)
Total	116	70	18	26	18

Note.—Equivalent dose ranges in rad_{eq} listed in parentheses. Equivalent doses determined by multiplying the neutron physical dose (rad_{ny}) by 3.1, the equivalence factor for late effects, and adding this to the photon dose (see text).

* Or 4,700–5,000 rad_{eq} plus 3,000–5,500 mg hr Ra.

TABLE 3

Treatment Methods Used for Control Group

Treatment Method	Head and Neck	Gynecologic	Esophagus	Breast	Prostate
Surgery only	2	0	0	0	0
Combined surgery and photons	24 (5,000–6,250)	0	9* (3,000)	3 (5,000–6,000)	0
Photons only, once daily	5 (6,000–7,700)	19 (6,400–7,000)†	3 (5,500)	3 (7,000)	7 (6,000–6,600)
Photons only, twice daily	18 (6,500–8,000)	0	0	9 (6,600–7,600)	0
Total	49	19	12	15	7

Note.—Tumor dose ranges in rad_{eq} listed in parentheses.

* Planned preoperative radiotherapy and surgery; four of these patients did not complete treatment because of deteriorating general condition or distant metastases.

† Or 5,000–6,000 rad plus 4,000–6,000 mg hr Ra.

TABLE 4

Head and Neck Cancer

	Local Control		Complications		Control without Complications	
	No.	%	No.	%	No.	%
Neutron group:						
Neutrons only, twice/week (*N* = 49)	23	46.9	10	20.4	14	28.6
Neutrons only, four times/week (*N* = 19)	7	36.8	1	5.3	7	36.8
Neutron boost (*N* = 29)	14	48.3	5	17.2	9	31.0
Mixed beam (*N* = 19)	11	57.9	0	0	11	57.9
Total (*N* = 116)	55	47.4	16	13.8	41	35.3
Control group (*N* = 49)	28	57.1	12	24.5	23	46.9

TABLE 5

Gynecologic Cancer

	Local Control		Complications*		Control without Complications	
	No.	%	No.	%	No.	%
Neutron group:						
Neutrons only, twice/week (*N* = 16)	5	31.3	2	12.5	3	18.8
Neutrons boost (*N* = 24)	13	54.2	5	20.8	8	33.3
Mixed beam (*N* = 30)	19	63.3	4	13.3	15	50.0
Total (*N* = 70)	37		11	15.7	26	37.1
Control group (*N* = 19)	8	42.1	2	10.5	6	31.6

* 13 major complications (in six of 58) patients (8.9%) without node dissections; and seven of 31 patients (22.6%) with previous lymphadenectomy or recent pelvic surgery.

Seventy patients were treated with neutrons in the pilot study, and 19 were treated with photons in the control group.

The aim was to deliver 5,000 rad_{eq} to the whole pelvis in 5 weeks and reevaluate the patient for completion of treatment with intracavitary radium or an external beam boost. None of the patients treated with neutrons only or a neutron boost showed sufficient regression of parametrial disease to justify completion of treatment with intracavitary radium. However, 60.0% (18 of 30) patients treated with the mixed beam and 52.6% (10 of 19) patients in the control group showed enough tumor regression to allow the use of intracavitary radium.

The overall local control rate with fast neutrons was 52.9% (37 of 70); and 15.7% (11 of 70) developed major complications (table 5). This is slightly better than the results in the control group, where 42.1% (8 of 19) had local control of their disease and 10.5% (2 of 19) developed complications.

The best results were achieved with mixed beam irradiation. The local control rate with the mixed beam was 63.3% (19 of 30), and four patients (13.3%) experienced

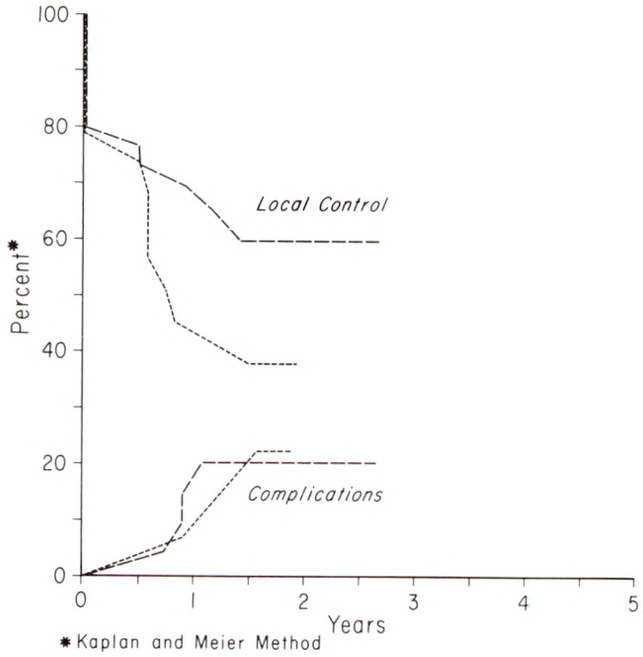


Fig. 1.—Actuarial local control and complication curves (Kaplan and Meier method [3]) for gynecologic cancers in 30 patients treated with mixed beam neutron irradiation (*long dashes*) and 19 treated with photon irradiation in control group (*short dashes*). Difference in local control in mixed beam group and control group not statistically significant (Wilcoxon test: $P = 0.27$).

TABLE 6

Squamous Carcinoma of the Esophagus

	Local Control		Complications		Control without Complications	
	No.	%	No.	%	No.	%
Neutron group:						
Neutrons only, twice/week ($N = 8$)	5		2		3	
Neutrons only, four times/week ($N = 3$)	0		1*		0	
Neutron boost ($N = 3$)	2		1		1	
Mixed beam ($N = 4$)	2		0		2	
Total ($N = 18$)	9	50.0	4	22.2	6	33.3
Control group ($N = 12$)	4	33.0	4†	33.0	4	33.0

* One patient had both local failure and complications.

† Four patients had both local failure and complications, including two surgical deaths.

major complications. However, three of those four had had a prior lymphadenectomy. Actuarial local control and complication curves (Kaplan and Meier method [3]) have been plotted to compare the results of mixed beam irradiation with those of conventional treatment, because the control group patients have been followed a shorter period (fig. 1). By this method of analysis, the local control rate with the mixed beam is better than that achieved with conventional treatment methods. The difference is not statistically significant ($P = 0.27$) because of the small sample size. The complication curves for the two groups are not appreciably different.

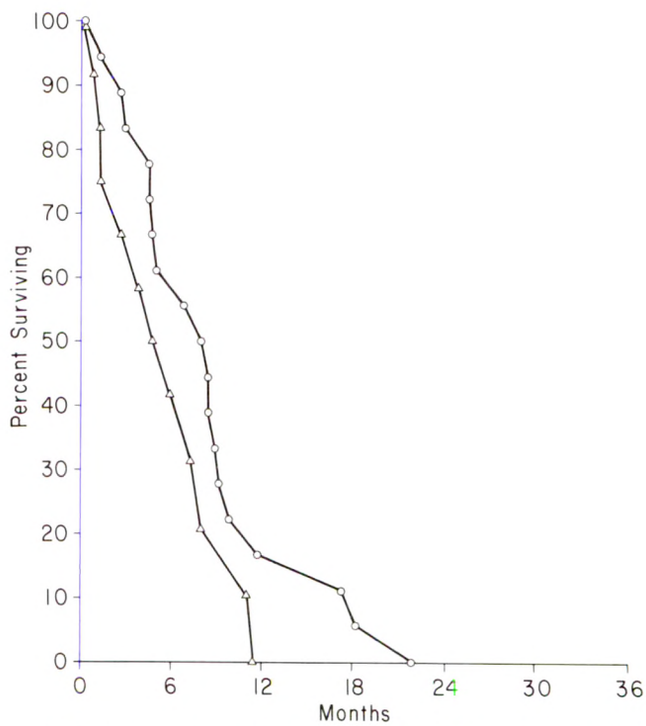


Fig. 2.—Actuarial survival curves (Kaplan and Meier method [3]) for squamous carcinoma of esophagus in 18 patients in neutron therapy pilot study (*circles*) and 12 patients (three received photons, nine received preoperative photons and surgery) in control group (*triangles*). Difference in survival not statistically significant (Wilcoxon test: $P = 0.17$).

Esophageal Carcinoma

Eighteen patients with squamous carcinoma of the esophagus were treated with fast neutrons. The majority received doses of 1,800–1,900 $rad_{n\gamma}$ in $5^1/_2$–6 weeks (5,600–5,900 rad_{eq}) with no correction for tissue inhomogeneity (table 2). Of the 18 patients, 16 were initially well palliated with radiographic evidence of significant tumor regression. Nine patients (50.0%) were scored as having local control (table 6). Three patients had autopsies showing no evidence of tumor locally.

Twelve patients were treated in the control group. Nine patients were scheduled for planned preoperative radiotherapy (3,000 rad/2–3 weeks) followed by esophagectomy. Four of these patients did not have surgery because distant metastases developed or their general condition deteriorated. Three patients were treated with definitive radiation therapy (5,000 rad/5–$5^1/_2$ weeks). Although the survival was uniformly poor regardless of the mode of treatment, the duration of survival was slightly longer for patients irradiated with neutrons than for patients in the control group (fig. 2).

Breast Carcinoma

Twenty-six patients with breast cancer were treated in the neutron therapy group and 12 in the control group. All patients had stage D disease by the criteria of Haagensen and Colley [4]. They were classified on the basis of the bulk of the disease at the primary site and in the axilla (table 1).

TABLE 7

Adenocarcinoma of the Breast

	Local Control		Complications		Control without Complications	
	No.	%	No.	%	No.	%
Neutron group:						
Neutrons only, twice/week (N = 16)	12	75.0	8	50.0	6	37.5
Neutron boost (N = 6)	3		1		2	
Mixed beam (N = 4) ...	3		0		3	
Total (N = 26)	18	69.2	9	34.6	11	42.3
Control group (N = 15) ..	9	60.0	1	6.7	8	53.3

TABLE 8

Adenocarcinoma of the Prostate

	Local Control		Complications		Control without Complications	
	No.	%	No.	%	No.	%
Neutron group:						
Neutrons only, twice/week (N = 1)	1		1*		1	
Neutron boost (N = 1)	1		0		1	
Mixed beam (N = 16)..	14	87.5	1	6.3†	14	87.5
Total (N = 18)	16	88.9	2	11.1	15	83.3
Control group (N = 7) ...	4		0		4	

* One complication, proctosigmoiditis.

† One complication, urethral stricture related to tumor invasion of penile urethra and multiple instrumentations (and biopsy-proven local recurrence).

A relatively high local control rate (69.2%, 18 of 26) was achieved with neutron therapy, but only at the expense of a high complication rate (34.6%, 9 of 26), particularly breast fibrosis (table 7). The high complication rate with neutrons is probably due to the limitations of treating the breast with a fixed horizontal beam, since it is difficult to irradiate both the breast and the peripheral lymphatics without overdosage at the junctions of the fields. However, the high fat content of the breast resulting in higher absorbed doses may have contributed to the severity of the fibrosis. Although only four patients were treated with mixed beam irradiation, no complications have been seen in this group of patients.

At the time of analysis, the results of photon therapy were slightly better than the results of neutron irradiation. Nine of 15 patients (60.0%) treated in the control group have had local control of their disease, and only 6.7% (1 of 15) have developed complications.

Prostatic Carcinoma

Eighteen patients with locally advanced adenocarcinomas of the prostate were treated with neutrons. These included eight patients with tumors fixed to one pelvic wall and 10 with bilateral pelvic wall involvement. Seven patients were treated in the control group—one without pelvic wall fixation, three with tumor extending to one pelvic wall, and three with bilateral pelvic wall fixation (table 1).

The preliminary results with neutron therapy are excellent, with an 88.9% (16 of 18) local control rate and an 11.1% (2 of 18) incidence of complications (table 8). Only four of seven patients treated in the control group were scored as having local control, but there have been no complications in this group.

Discussion

A comparison of the preliminary results of the neutron therapy pilot study with those of the control group illustrates the need for prospective randomized clinical trials. For most tumor sites, no distinct improvement in local control or morbidity was noted with either method. However, the patients treated with neutrons in the early phase of the pilot study had more extensive tumors and were treated at a time when dosage schedules were uncertain. Furthermore, the control group patients have been followed for a shorter period than those treated with fast neutrons. It is possible that an advantage of fast neutron therapy will become apparent in the pilot study with more time.

The results with the mixed beam fractionation are superior to those obtained with neutrons only or a neutron boost and compare favorably with the results obtained in the control group. The superiority of the mixed beam fractionation schedule may be partly due to differences in clinical material, since the patients treated with the mixed beam had slightly less advanced disease than those treated with neutrons only, twice weekly, or a neutron boost after photon irradiation. The extent of disease treated with the mixed beam fractionation schedule or neutrons only, four times weekly, was similar to that treated in the control group.

There are several technical reasons for the apparent superiority of the mixed beam fractionation schedule. The disadvantages of a fixed horizontal beam are reduced with the mixed beam schedule, and the volume distribution for deep-seated tumors is superior because the photon component is delivered with 25 MeV x-rays.

The superiority of the mixed beam fractionation schedule may be partly related to the five-times-weekly fractionation schedule. Fractionation is important with photons because dosage schedules using fewer fractions (i.e., large doses per fraction) produce more severe late effects for equal acute effects than more fractionated dosage schedules [5, 6]. The importance of fractionation with neutrons has not been established. The small group of patients treated with neutrons only, four times weekly, had a poor local control rate. However, there have been no complications in this group, indicating that these patients may have been underdosed.

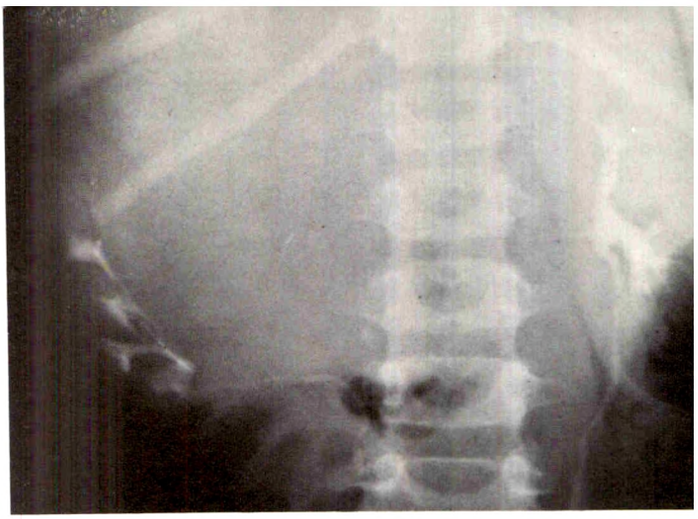
From these results, it would seem that the advantage of fast neutron therapy over conventional treatment methods will be modest. However, it should be emphasized that the results reported here are those of pilot studies and not of randomized clinical trials. In the randomized trial comparing fast neutrons with photons for treatment of head and neck cancer at Hammersmith Hospital, Catterall et al. [7] reported a significantly greater local control rate for patients receiving neutron

therapy, but at the expense of a higher complication rate. Randomized clinical trials are going on in the United States under the auspices of the Radiation Therapy Oncology Group, and in Great Britain, Europe, and Japan. It will be of considerable interest to see if these trials confirm the encouraging results reported from Hammersmith.

REFERENCES

1. Hussey DH, Parker RG, Rogers CC: Evolution of dosage schedules at the fast neutron therapy facilities in the United States. *Int J Radiat Oncol Biol Phys* 3:255–260, 1977
2. Withers HR, Flow BL, Huchton JI, Hussey DH, Jardine JH, Mason KA, Raulston GL, Smathers JB: Effect of dose fractionation on early and late skin responses to γ-rays and neutrons. *Int J Radiat Oncol Biol Phys* 3:227–233, 1977
3. Kaplan EL, Meier P: Nonparametric estimations from incomplete observation. *Am Statist Assoc J* 53:457–480, 1958
4. Haagensen CD, Colley E: Treatment of early mammary carcinoma. *Ann Surg* 157:157–169, 1963
5. Montague E: Experience with altered fractionation in radiation therapy of breast cancer. *Radiology* 90:962–966, 1968
6. Arcangeli G, Friedman M, Paoluzi R: A quantitative study of late radiation effect on normal skin and subcutaneous tissues in human beings. *Br J Radiol* 47:44–50, 1974
7. Catterall M, Bewley DK, Sutherland I: Second report on results of a randomised clinical trial of fast neutrons compared with x or gamma rays in treatment of advanced tumors of head and neck. *Br Med J* 1:1642, 1977

Diagnostic Oncology Case Studies



Abdominal Mass and Cervical Adenopathy in a Child

A 6-year-old white boy had a right upper quadrant abdominal mass (first noted by his mother) for 7 months. Physical examination revealed mild hypertension (140/90), hepatomegaly, and left cervical adenopathy. Excretory urography (above) showed a large right suprarenal mass and displacement of the proximal left ureter. Ultrasound (fig. 1) confirmed the findings of excretory urography, and a chest film (fig. 2A) revealed mediastinal abnormalities. Bone and liver scans (figs. 2B and 2C) were negative. A presumptive diagnosis of nephroblastoma was based on the patient's age and associated hypertension.

Exploratory surgery revealed an unresectable right suprarenal tumor invading the liver and the right diaphragm, with extensive paraaortic lymph node involvement. Subsequent biopsy of the enlarged cervical nodes revealed metastatic neuroblastoma. The patient was given a course of radiation therapy to the abdominal mass (3,000 rad over 4 weeks), along with intravenous cyclophosphamide and vincristine.

After 1 month, physical examination showed the abdominal mass had diminished (imaging studies were not repeated). Consequently, the right kidney and adrenal, a portion of the right diaphragm, and the enlarged retroperitoneal lymph nodes were resected. Large paraaortic lymph nodes extending through the diaphragm into the mediastinum were palpated and could not be resected. A 3 cm lymph node mass adherent to the inferior vena cava was also left unresected. Five units of blood, in addition to platelets and fresh frozen plasma, were required during surgery. The patient died 3 months later.

Discussion

Diagnostic workup for this patient should have begun with cervical node biopsy. With a clinical and pathologic diagnosis of metastatic neuroblastoma (stage IV), no radiologic procedures were necessary for staging purposes and surgery was contraindicated. Chemotherapy could have been initiated directly.

Survival in a patient 6 years old with stage IV neuroblastoma undergoing any form of treatment is negligible (2%–3%) [1]. Patients with stage IV tumors who have been salvaged have been under 1 year of age and have had small primary tumors with a defined pattern of metastatic spread, so-called stage IV S [2]. The S (special) means that metastases are confined to liver, skin, and/or bone marrow without radiographic evidence of bone metastases. Of great importance here is an awareness that occasional spontaneous tumor regression may play a large role in planning successful management of infants with stage IV neuroblastoma [3].

Exelby [4] summarized the situation with regard to surgical resection:

> Unfortunately less than 25 percent [of patients with adrenal neuroblastoma] fall into this category [e.g., resectability]. Many patients with localized disease are found to be unresectable at laparotomy. There has been considerable discussion in the past as to whether a grossly inoperable tumor should have a lengthy excisional procedure resulting in subtotal resection and considerable risk to the patient. At the present time the general consensus in this country is that an inoperable tumor should only be biopsied and the patient placed on radiation and chemotherapy, with a second-look procedure carried out at a later date with the hope that the tumor has shrunk sufficiently to be resectable.

This is another in a bimonthly series of case reports prepared by A. Robert Kagan and Richard J. Steckel (Southern California Permanente Medical Group, 1510 North Edgemont, Los Angeles, California 90027, and UCLA Jonsson Comprehensive Cancer Center, 924 Westwood Boulevard, Suite 650, Los Angeles, California 90024, respectively) to present and discuss contemporary problems and procedures in the identification and staging of neoplasms. Case contributed by Hooshang Kangarloo and William F. Sample (both, Department of Radiological Sciences, UCLA School of Medicine, Los Angeles, California 90024). Address reprint requests to R. J. Steckel.

© 1979 American Roentgen Ray Society

0361–803X/79/1324–0643 $0.00

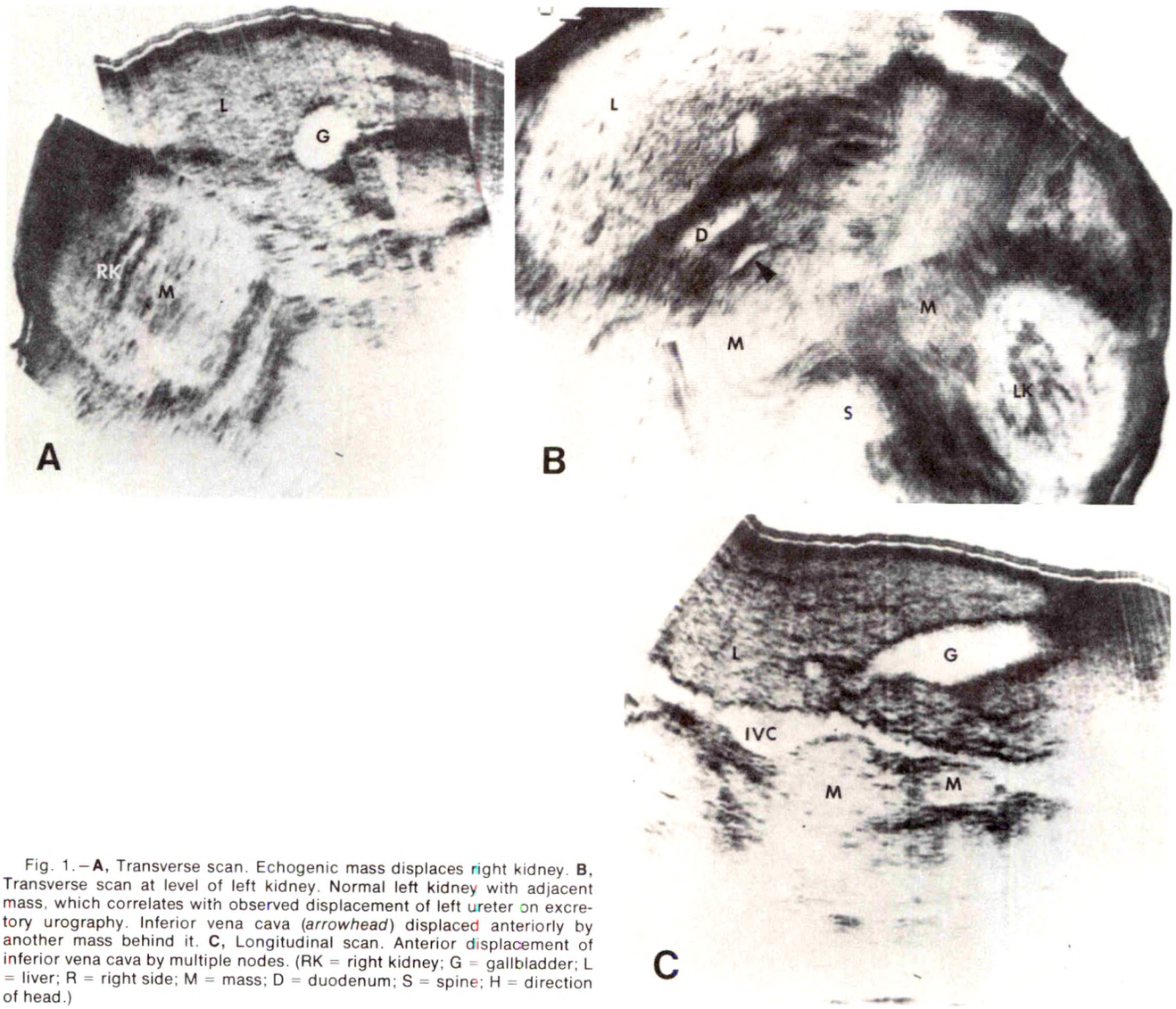


Fig. 1.—**A**, Transverse scan. Echogenic mass displaces right kidney. **B**, Transverse scan at level of left kidney. Normal left kidney with adjacent mass, which correlates with observed displacement of left ureter on excretory urography. Inferior vena cava (*arrowhead*) displaced anteriorly by another mass behind it. **C**, Longitudinal scan. Anterior displacement of inferior vena cava by multiple nodes. (RK = right kidney; G = gallbladder; L = liver; R = right side; M = mass; D = duodenum; S = spine; H = direction of head.)

These statements refer to stage III neuroblastomas (adrenal tumors large enough to cross the midline). Our patient's tumor was already stage IV (neuroblastoma with distant metastases).

Had it been determined immediately that this patient had metastatic neuroblastoma in cervical lymph nodes, no radiologic studies would have been necessary for staging. The palpable mass in the abdomen was sufficient to suggest the usual primary site for this tumor in an adrenal gland. Excretory urography and ultrasound both confirmed retroperitoneal metastases, but this was not crucial information for planning chemotherapy. The same is true for the chest film that demonstrated mediastinal metastases. The bone scan, too, was irrelevant for management. While it can be argued that "baseline" studies assist in subsequent evaluation of the effectiveness of chemotherapy, ultrasound examination might be preferred to excretory urography since it outlines the retroperitoneal metastases more discretely and is noninvasive.

This patient's tumor was somewhat unusual. Neuroblastomas tend to occur in younger children; the peak incidence is at age 2, and most are diagnosed before age 5. Indeed, nephroblastoma initially seemed a more appropriate diagnosis for a patient 6 years old. Lymphoma, embryonal sarcoma, or perhaps even a malignant hepatic tumor are also considerations in a youngster with a right abdominal mass and mediastinal masses combined with cervical adenopathy [5]. Unlike large Wilms' tumors that can remain encapsulated, large neuroblastomas tend to invade adjacent tissues; hence, few patients with adrenal neuroblastomas that cross the midline (stage III or higher) have been salvaged. Large midline neuroblastoma metastases in retroperitoneal lymph nodes almost always invade the inferior vena cava and by their nature are unresectable.

In summary, stage IV neuroblastoma in a 6-year-old child with a massive primary tumor cannot be treated curatively with present methods. Palliation is a reasonable treatment goal. In our patient, abdominal palpation,

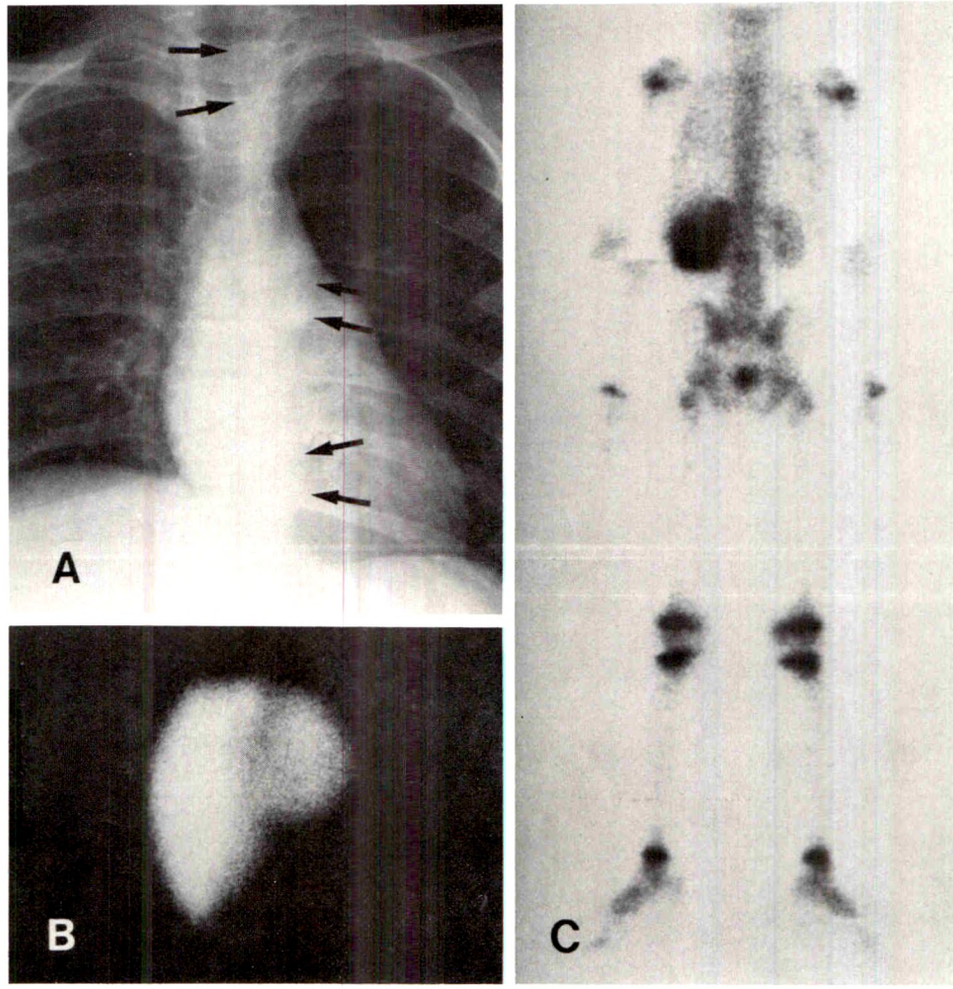


Fig. 2.—**A**, Neck and posterior mediastinal masses (*arrowheads*). **B** and **C**, Normal bone and liver scans.

cervical lymph node biopsy, and chemotherapy were all that were required absolutely to diagnose, stage, and treat this patient. Further radiologic procedures were superfluous and surgery was contraindicated.

REFERENCES

1. Evans AE, D'Angio JR: A proposed staging system for children with neuroblastoma. *Cancer* 27:374–378, 1971
2. D'Angio GJ, Evans AE, Koop CE: Special pattern of widespread neuroblastoma with a favorable prognosis. *Lancet* 1:1046–1049, 1971
3. Evans AE, Gerson J, Schnaufer: Spontaneous regression of neuroblastoma. *Natl Cancer Inst Monogr* 44:49–54, 1976
4. Exelby PR: Solid tumors in children: Wilms' tumor, neuroblastoma and soft tissue sarcomas. *CA* 28:146–163, 1978
5. Gyepes MT, Smith LE: Pediatric neoplasms in *Diagnosis and Staging of Cancer: A Radiologic Approach*, edited by Steckel RJ, Kagan AR, Philadelphia, Sauncers, 1976, pp 343–366

Case Reports

Balloon Catheter to Control Transhepatic Obliteration of Gastroesophageal Varices

ALAIN ROCHE,[1] FRANCIS KUNSTLINGER, PHILIPPE CURET, AND DOMINIQUE DOYON

Transhepatic obliteration of gastroesophageal varices is now well known [1–3]. Nevertheless, the procedure may still be unsafe, despite proper catheterization of the coronary vein and short gastric veins, if there is a double drainage from the catheterized vein toward both the liver and the varices. The danger is obliteration of the portal trunk. In 65 patients studied by transhepatic portography, we encountered two such instances of double

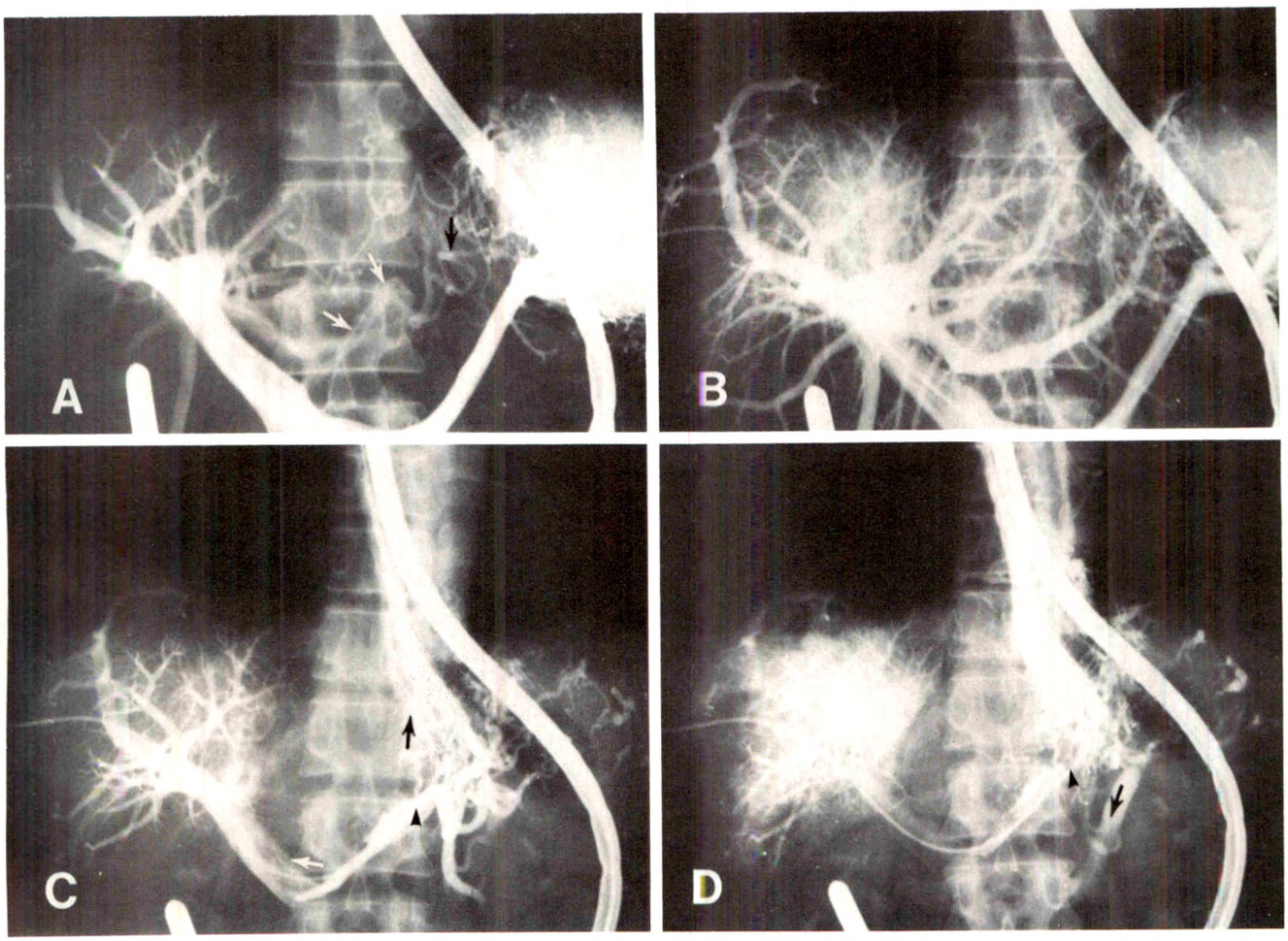


Fig. 1.—Before embolization. **A**, Early phase. Retrograde flow opacifies short gastric vein (*black arrow*) arising from superior polar splenic vein. Coronary vein (*white arrows*) then opacified with hepatopetal flow. **B**, Late phase. No opacification of coronary vein and esophageal varices. **C** and **D**, Selective catheterization of coronary vein. Early (**C**), bidirectional flow: hepatopetal toward portal trunk (*white arrow*) and hepatofugal toward esophageal varices (*black arrow*). Later (**D**), gastrorenal shunt opacified (*black arrow*). Catheter tip (*arrowhead*).

Received June 27, 1978; accepted after revision December 4, 1978.
This work was supported in part by research grants of Paris South University.
[1] All authors: Department of Radiology, Hôpital de Bicetre, 78, Rue du Général Leclerc, 94270, Kremlin Bicetre, France. Address reprint requests to A. Roche.

© 1979 American Roentgen Ray Society

0361–803X/79/1324–0647 $0.00

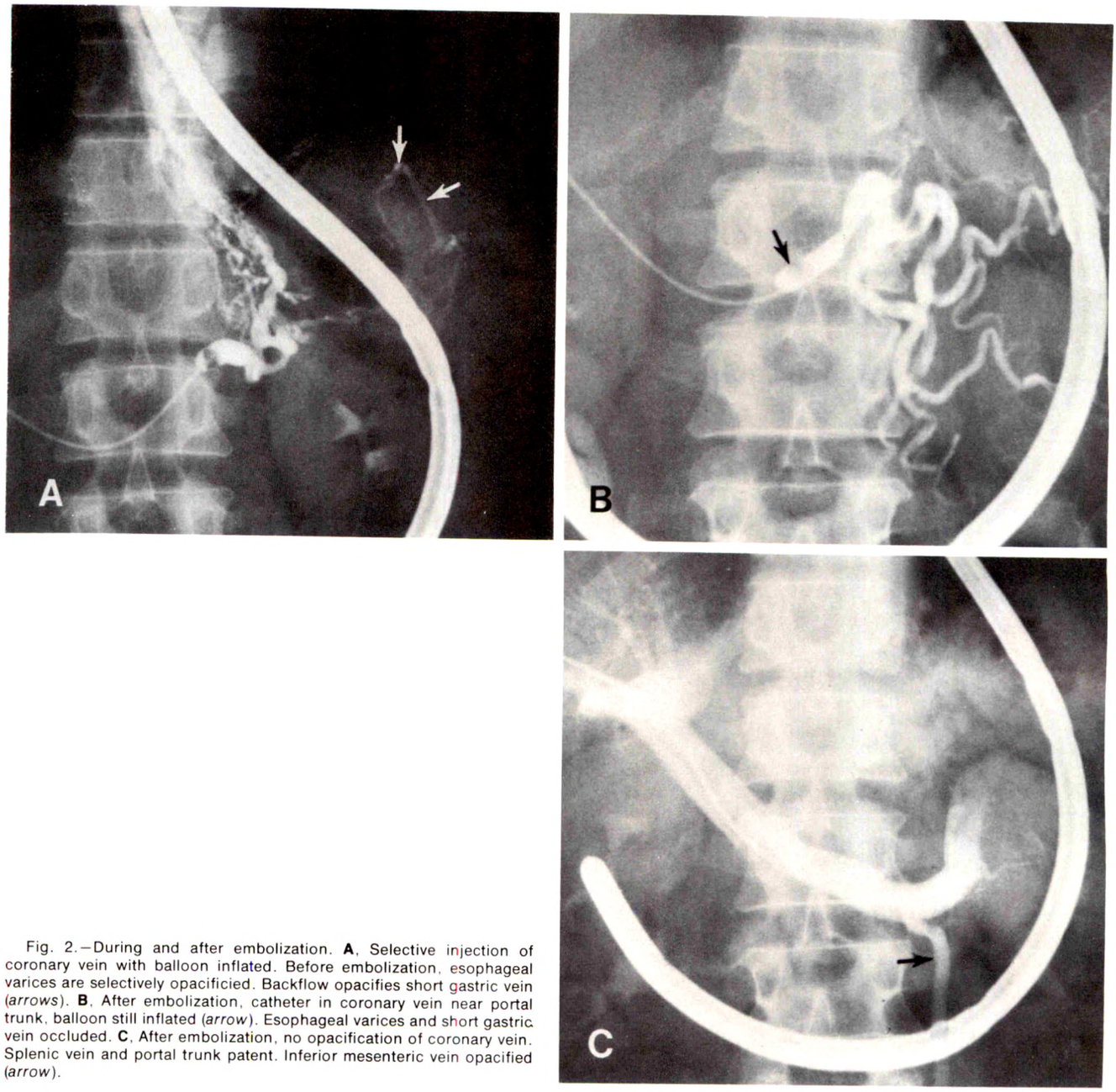


Fig. 2.—During and after embolization. **A**, Selective injection of coronary vein with balloon inflated. Before embolization, esophageal varices are selectively opacificied. Backflow opacifies short gastric vein (*arrows*). **B**, After embolization, catheter in coronary vein near portal trunk, balloon still inflated (*arrow*). Esophageal varices and short gastric vein occluded. **C**, After embolization, no opacification of coronary vein. Splenic vein and portal trunk patent. Inferior mesenteric vein opacified (*arrow*).

drainage. In one of them, the hepatopetal flow was controlled with a balloon inflated in the coronary vein near its junction with the portal trunk.

Case Report

A 57-year-old man with alcoholic cirrhosis had bleeding esophageal varices that could not be controlled with a Sengstaken-Blackemore tube. The extent of liver insufficiency was evaluated as Child's group B: negative ascites and encephalopathy; bilirubin, 6.7 mg/100 ml; serum albumin, 31 g/l; and prothrombin, 50%. Transhepatic obliteration of esophageal varices on an emergency basis was planned. Portal pressure was 26 cm saline.

On initial portography, with the catheter placed at the origin of the splenic vein, there was poor opacification of the esophageal varices. Serial films showed a very narrow short gastric vein originating from a superior polar splenic vein and opacification of the coronary vein with hepatopetal flow (figs. 1A and 1B). Selective injection of the coronary vein with a very low flow (so as not to modify the spontaneous circulatory conditions) showed three flow pathways: two away from the liver via the esophageal varices and the left adrenal vein and one toward the portal trunk (figs. 1C and 1D). In these hemodynamic conditions, the usual technique of obliteration was not considered safe.

Therefore, an end hole no. 5 French balloon catheter (OB 5.2/100, Ingenor, Paris) was selectively positioned within the coronary vein. Injection with the balloon inflated only opacified the esophageal varices and short gastric veins (fig. 2A). To

induce sclerosis of the veins, 160 ml of 66% glucose was injected. Thrombin (1,000 U) and small pieces of Gelfoam were then injected to complete the thrombosis.

Immediately after embolization, injection of the coronary vein while the balloon was still inflated showed complete variceal obliteration (figs. 2B and 2C). Portal pressure after embolization was 42 cm saline. The patient stopped bleeding immediately. However, he died 14 days later from severe hepatocellular insufficiency, without having bled again. Postmortem examination was not performed.

Discussion

In our case, the usual technique of thrombosis of esophageal varices was hazardous because of a spontaneous backflow in the coronary vein toward the liver. This backflow explains the failure to visualize the varices during initial portography.

To minimize potential complications from hemodynamic conditions, we used an end hole balloon catheter technique as follows: the coronary vein was selectively catheterized using the usual percutaneous transhepatic route; then a J-shaped guide wire (TA 3151, Ingenor, Paris) was positioned in the coronary vein, the first catheter was withdrawn, and a balloon catheter lubricated with sterile oil was advanced over the guide wire. Then the guide wire was withdrawn and the balloon, located within the coronary vein, was inflated with air and contrast material under fluoroscopic control.

This technique seems to have the following advantages: (1) better sclerosis than in the free flow state; (2) sclerosis and embolization without the risk of backflow in the portal trunk; and (3) a more durable obstruction than with the temporary balloon occlusion of other authors [4].

Besides the situation we describe, this balloon technique may be indicated in two other circumstances: (1) when the veins draining into varices are very wide and have a massive hepatofugal flow (two of 65 cases in our material) and (2) in case of complete thrombosis of the portal axis when the esophageal varices might be catheterized and occluded through an inferior vena cava route. In the first case, sclerosis is difficult and use of embolic material introduces the hazard of iatrogenic pulmonary embolism. Occlusion via the end hole balloon catheter seems less dangerous than the Ivalon or Isobutyl-cyanoacrylate obstruction suggested in this situation [5]. In the second case, after jugular puncture the catheter is passed successively into the inferior vena cava, the left renal vein, the left adrenal vein, and the left diaphragmatic crus vein (which communicates with a posterior gastric vein and the esophageal varices [6, 7]). We already catheterized the left diaphragmatic crus vein by this route with the balloon catheter; however, we have not yet attempted the occlusive balloon technique by this approach because the gastrorenal derivation was not large enough to allow subselective catheterization of varices.

REFERENCES

1. Doyon D, Mouzon A, Vadrot D, Franco D, Bismuth H: Embolisation trans-hépatique des varices oesophagiennes. *J Radiol Electrol Med Nucl* 56:917–921, 1975
2. Lunderquist A, Vang J: Transhepatic catheterization and obliteration of the coronary vein in patients with portal hypertension and oesophageal varices. *N Engl J Med* 291: 646–649, 1974
3. Viamonte M, LePage J, Lunderquist A, Pereiras R, Russell E: Selective catheterization of the portal vein and its tributaries. *Radiology* 114:457–460, 1975
4. Pereiras R, Viamonte M Jr, Russell E, LePage J, White P, Hutson D: New techniques for interpretation of gastro-oesophageal venous blood flow. *Radiology* 124:313–323, 1977
5. Viamonte M Jr, Pereiras R, Russell E, LePage J, Meier WL: Pitfalls in transhepatic portography. *Radiology* 124:325–329, 1977
6. Gillot C, Hureau J: Les anastomoses porto-caves et cavo-caves ce la loge sous-phrénique gauche. Etude anatomique et physio-pathologique. *J Chir* (Paris) 79:578–597, 1960
7. Nunez D Jr, Russell D, Yrizarry J, Pereiras R, Viamonte M Jr: Porto-systemic communications studied by transhepatic portography. *Radiology* 127:75–79, 1978

Cavitary Pulmonary Lesions Complicating Use of Flow-Directed Balloon-Tipped Catheters in Two Cases

MYUNG SOO SHIN[1] AND KANG-JEY HO[2]

The flow-directed balloon-tipped (Swan-Ganz) catheter for measurement of pulmonary capillary wedge pressures has been widely used for hemodynamic investigations of severely ill patients because of the simplicity of introduction and infrequent complications [1–4]. The major morbidity associated with its use is pulmonary infarction resulting from persistent wedging of the catheter tip in a peripheral artery, failure to deflate the balloon after use, and thromboembolism around the catheter [5]. The radiograph of the pulmonary infarction is usually classical in appearance and resolves in 2–3 weeks [6]. We encountered two cases of pulmonary complications directly related to the use of Swan-Ganz catheters which progressed from infarction to cavitary lesions. We believe no such cases have yet been reported.

Case Reports

Case 1

A 36-year-old white woman had suffered from seizure-disorder since age 2 and had been treated with Dilantin and phenobarbital. She was admitted to the University Hospital in status epilepticus with spontaneous respiration. She was comatose with hypotension, tachycardia, and bilateral ronchi. An endotracheal tube was inserted, and the blood pressure was supported with Isoprel drip.

The seizures were controlled by medications of Valium, Dilantin, and paraldehyde. However, the patient developed respiratory distress due to pulmonary edema and required mechanical respiratory support. A Swan-Ganz catheter was inserted into the right pulmonary artery for hemodynamic monitoring. Chest radiograph 2 days later revealed a homogeneous opacity, apparently pulmonary infarction, in the right lower lobe distal to the tip of the Swan-Ganz catheter (fig. 1A). The catheter was withdrawn immediately. Despite the improvement of respiratory function, a pulmonary cavitary lesion developed in the right lower lobe (fig. 1B), which doubled in size in 3 days (fig. 1C). Sputum culture at this time grew *Pseudomonas aeruginosa*, resistant to the antibiotics given. Her later course was complicated by septicemia, seizures, and hypotension. The patient expired 3 weeks after admission.

The pertinent autopsy findings included microcephaly (900 g) with severe hydrocephalus, acute bronchopneumonia, and a cavity 6 × 6 × 6 cm in the right lower lobe (fig. 1D). It had a thick fibrous wall and contained a greater deal of bloody, purulent, necrotic material. An organizing thromboembolus in the main branch of the pulmonary artery extended to the right lower lobe, partially occluding the lumen.

Case 2

An 8-year-old boy sustained extensive second and third degree flame burns involving 75% of the body surface; he responded well to the treatment of acute shock and topical therapy of the burn wounds. He improved steadily for about 2

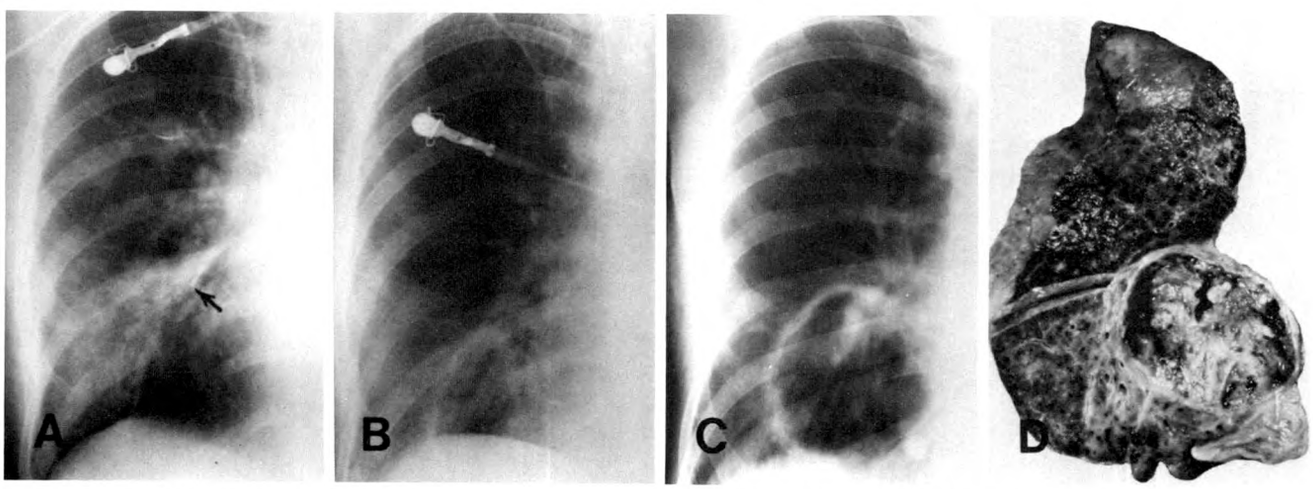


Fig. 1.—Case 1. **A,** Anteroposterior supine chest film. Triangular opacity in the right lower lobe distal to Swan-Ganz catheter tip (*arrow*) positioned in right main pulmonary artery. **B,** Anteroposterior supine chest film 5 days after removal of catheter. Relatively thick, poorly defined cavitary lesion in right lower lobe. **C,** Posteroanterior supine chest film 8 days after **B.** Persistent cavity in right lower lobe with irregular thick wall has enlarged to diameter of 6.0 cm. **D,** Cross-section of right lung. Abscess cavity with thick fibrous wall contains bloody, purulent, necrotic material. Bronchopneumonia involves other portions of lung.

Received September 29, 1978; accepted after revision December 27, 1978.

[1] Department of Diagnostic Radiology, University of Alabama School of Medicine, Birmingham, Alabama 35233. Address reprint requests to M. S. Shin.

[2] Department of Pathology, University of Alabama School of Medicine, Birmingham, Alabama 35233.

© 1979 American Roentgen Ray Society

0361-803X/79/1324-0650 $0.00

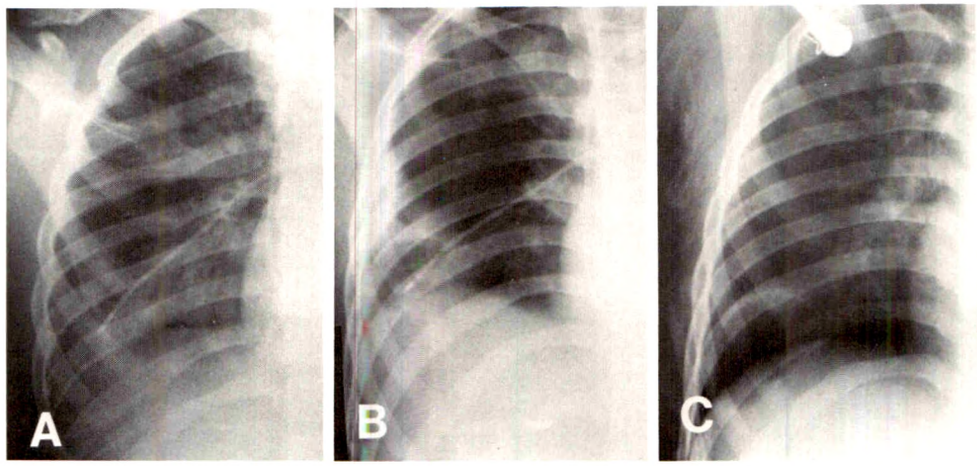


Fig. 2.—Case 2. Anteroposterior supine chest films. **A,** Lodging of Swan-Ganz catheter tip in peripheral branch of right pulmonary artery with poorly defined hazy opacity around tip. **B,** 1 day later. Cavitary lesion distal to Swan-Ganz catheter tip. **C,** 4 days after withdrawal of catheter. Persistent cavity (*arrows*) in right lower lobe.

months, but then developed respiratory insufficiency requiring endotracheal intubation and mechanical ventilatory assistance. A Swan-Ganz catheter was also inserted for hemodynamic monitoring.

Chest radiograph the day after insertion of the Swan-Ganz catheter showed the catheter tip in a peripheral branch of the right main pulmonary artery (fig. 2A). Follow-up chest radiograph the next day showed an area of consolidation with cavity formation in the right lower lobe (fig. 2B). The catheter was withdrawn, but the patient developed *Serratia* septicemia and acute renal failure requiring hemodialysis. A chest film shortly before his death showed enlargement of the cavitary lesion to 3 × 4 × 5 cm in the right lower lobe (fig. 2C). An autopsy was not performed; culture of the aspirated material in the lung cavity grew *Serratia marcescens*.

Discussion

The use of the Swan-Ganz catheter is generally considered safe [1–4]. The infrequent complications include pulmonary infarction [5–7], cardiac arrhythmias [1–4], rupture of the balloon [4], intracardiac knotting of the catheter [8], perforation of a pulmonary artery [9–11], and thrombosis around the catheter shaft [1]. Pulmonary infarction is by far the most common complication [5–6]. When the catheter was first introduced for clinical practice, Foote el al. [5] reported that pulmonary ischemic lesions occurred in nine of 125 patients (7.2%). Subsequently the frequency of the pulmonary complications has been reduced significantly [5].

The most common mechanism of pulmonary infarction is the persistent wedging of the catheter tip in a peripheral artery [5]. Scott et al. [12] noted a tendency for the Swan-Ganz catheter to slip distally into such a wedge position. This indeed occurred in case 2. Involvement of the right lower lobe is more common, since the catheter is often positioned in the interlobar branch of the right pulmonary artery. The ischemic lung lesion in case 1 was apparently related to the thrombus found at autopsy, which had presumably developed on injured intima caused by the catheter. The possibility of embolus from thrombus on the catheter cannot be ruled out. Thrombosis of an indwelling catheter has been repeatedly reported [13–16].

Pulmonary infarction associated with the Swan-Ganz catheter usually resolves within 2–3 weeks [5]. In our two cases, the infarcted lungs obviously were secondarily infected and progressed to cavitary lung abscesses. The continuous sloughing of the necrotic tissue and bleeding presumably led to expansion of the cavities. When a thick fibrous capsule was well developed the cavity ceased to grow.

In order to prevent such tragic pulmonary complications associated with the Swan-Ganz catheter, we recommend that the position of the catheter should be confirmed by chest radiograph as soon as possible after it is inserted. Follow-up chest films should be obtained at least once a day to assure the correct position of the catheter tip. At any time when the patient develops chest discomfort, the position of the catheter tip should be rechecked immediately because infarction and even cavitary lesions can develop within 24 hr. With such precautions, the pulmonary complications associated with the Swan-Ganz catheter should be minimized.

REFERENCES

1. Swan HJC, Ganz W, Forrester J, Marcus H, Diamond G, Chonette D: Catheterization of the heart in man with use of a flow-directed balloon-tipped catheter. *N Engl J Med* 283: 447–451, 1970
2. Swan HJC: Balloon flotation catheter—their use in hemodynamic monitoring in clinical practice. *JAMA* 233:865–867, 1975
3. Mond HG, Hunt D, Sloman G: Haemodynamic monitoring in the coronary care unit using the Swan-Ganz right heart catheter. *Br Heart J* 35:635–642, 1973
4. Cerra F, Milch R, Lajos TZ: Pulmonary catheterization in critically ill surgical patients. *Ann Surg* 177:37–39, 1973
5. Foote GA, Schabel SI, Hodges M: Pulmonary complications of the flow-directed balloon-tipped catheter. *N Engl J Med* 290:927–931, 1974
6. McLoud TC, Putman CE: Radiology of the Swan-Ganz catheter and associated pulmonary complications. *Radiology* 116:19–22, 1975
7. Lapin ES, Murray JA: Hemoptysis with flow-directed cardiac catheterization. *JAMA* 220:1246, 1972
8. Lipp H, O'Donoghue K, Resnekov L: Intracardiac knotting

of a flow-directed balloon catheter. *N Engl J Med* 284:220, 1971
9. Golden MS, Pinder T Jr, Anderson WT, Cheitlin MD: Fatal pulmonary hemorrhage complicating use of a flow-directed balloon-tipped catheter in a patient receiving anticoagulant therapy. *Am J Cardiol* 32:865–867, 1973
10. Chun GMH, Ellestad MH: Perforation of the pulmonary artery by a Swan-Ganz catheter. *N Engl J Med* 284:1041–1042, 1971
11. Bennett KR, Cibulski AA, Mublhill J, et al.: Perforation of the pulmonary artery by a Swan-Ganz catheter. *N Engl J Med* 284:1042–1043, 1971
12. Scott ML, Webre DR, Arens JF, Ochsner JL: Clinical application of a flow-directed balloon-tipped cardiac catheter. *Am Surg* 38:690–696, 1972
13. Becker AE, Becker MH, Martin FH, Edwards JE: Bland thrombosis and infection in relation to intracardiac catheter. *Circulation* 46:200–203, 1972
14. Henzel JH, DeWeese MS: Morbid and mortal complications associated with prolonged central venous cannulation: awareness, recognition and prevention. *Am J Surg* 121: 600–605, 1971
15. McDonough JJ, Altemeier WS: Subclavian venous thrombosis secondary to indwelling catheters. *Surg Gynecol Obstet* 133:397–400, 1971
16. Klein RL, Falor WH: Central venous thrombosis: A complication of catheterization and hyperalimentation. *Am Surg* 39:162–163, 1973

Ultrasonic Features of Acquired Renal Arteriovenous Fistula

JOHN L. THOMAS,[1,2] MARVIN E. B. LYMBERIS,[1] AND THOMAS H. HUNT[1]

The increasing frequency of renal biopsy, abdominal trauma, and certain types of urologic surgical procedures has resulted in a marked increase in the number of acquired renal arteriovenous fistulas reported in recent years [1]. Renal angiographic study has allowed definitive preoperative diagnosis of this condition. However, in many patients nonspecific clinical findings (e.g., abdominal pain, hematuria, hypertension, abdominal bruit) may prompt initial diagnostic study by excretory urography with referral for ultrasonic evaluation if a renal mass or nonfunctioning kidney is detected by excretory urography.

Ultrasonically, an acquired renal arteriovenous fistula may appear as an anechoic mass or, if located in the parapelvic region, may simulate hydronephrosis. Detection of associated dilatation of the renal vein and renal artery should suggest the proper ultrasonic diagnosis. We report the gray scale ultrasonic findings in a patient with a posttraumatic renal arteriovenous fistula.

Case Report

A 39-year-old man had epistaxis and a combined systolic and diastolic hypertension. The patient was treated 14 years earlier for a gunshot wound to the abdomen without known urologic sequelae. There was no subsequent history of abdominal pain, hematuria, or congestive heart failure. Physical examination revealed a left upper abdominal bruit, a left ventricular heave, and a systolic ejection murmur. Admission chest radiography demonstrated only left ventricular enlargement. Excretory urography revealed caliectasis and compression of the renal pelvis by a parapelvic mass.

Ultrasonography was performed with a Picker EDC scanner using a 2.25 MHz transducer. Scans in the prone position performed parallel to the long axis of the left kidney demonstrated a 3 cm oval anechoic area bordered by four quadrangular anechoic areas within the renal parenchyma; this pattern is compatible with hydronephrosis (fig. 1A). However, since excretory urography had demonstrated effacement of the renal pelvis, the oval mass in the region of the renal pelvis was interpreted as a parapelvic mass producing secondary caliectasis. A large channel extended from the anterior aspect of this parapelvic mass and expanded into a second anechoic area 9 cm in diameter.

Transverse supine scans again demonstrated the left parapelvic mass and the larger anterior anechoic area, which extended medially to the area of the inferior vena cava (figs. 1B and 1C). Several supine parasaggital scans over the left abdomen revealed an additional channel lying along the posterior superior aspect of the large anechoic mass and extending in the direction of the left renal hilus (fig. 1D). The presence of bowel gas made determination of the exact relation of these masses to the major abdominal vessels difficult. The detection of channels entering and exiting a parapelvic mass suggested that the mass was related to the major renal vessels. The parallel channels identified on the supine scans are compatible with enlargement of a left renal artery and varicoid dilatation of the left renal vein secondary to the increased flow associated with shunting of blood across a renal arteriovenous malformation.

Biplane aortography and selective left renal arteriography confirmed the left renal arteriovenous fistula, the left renal vein varices, and cephalad displacement of an enlarged tortuous renal artery (fig. 2). The patient subsequently had a left nephrectomy with en bloc removal of the left renal artery and vein. Inspection of the surgical specimen confirmed the anatomic findings demonstrated by gray scale sonographic examination.

Discussion

Over 200 cases of renal arteriovenous fistulas have been reported [1]. These may be classified as congenital, acquired, or idiopathic [2]. Congenital arteriovenous fistulas are diagnosed on the basis of their cirsoid or racemose appearance during angiography. Acquired ones, on the other hand, typically have a single arteriovenous communication and account for over three-fourths of all renal arteriovenous fistulas. The more common causes of the acquired form are percutaneous renal biopsy, tumors, nephrectomy, and trauma, either blunt or penetrating. Similarly, idiopathic renal arteriovenous fistulas have a noncirsoid appearance. These are presumably secondary to rupture of a renal artery aneurysm with renal venous perforation. The incidence of renal arteriovenous fistulas is increasing primarily because of widespread use of renal biopsy and a rise in abdominal trauma [1]. Indeed, the incidence of renal arteriovenous fistulas following biopsy may approach 15% [3].

The clinical diagnosis of a renal arteriovenous fistula is suggested if a patient has the classic findings of an abdominal bruit and hypertension, either systolic due to intrarenal shunting or diastolic secondary to associated renal ischemia, [2]. Other clinical findings include hematuria, abdominal pain, congestive heart failure, and cardiomegaly. Although suggestive, an abdominal bruit secondary to a renal arteriovenous fistula must be differentiated from a bruit caused by a renal artery stenosis or renal artery aneurysm. Clinical diagnosis is further complicated when the onset of symptoms is delayed by years following the traumatic incident. Moreover, idiopathic and neoplastic renal arteriovenous fistulas are unrelated to trauma.

Gray scale ultrasonography is a noninvasive imaging technique capable of high diagnostic accuracy in the

Received June 13, 1978; accepted after revision December 29, 1978.

[1] Department of Diagnostic Radiology, Bowman Gray School of Medicine, Winston-Salem, North Carolina 27103.

[2] Present address: Department of Radiology, Division of Diagnostic Ultrasound, Thomas Jefferson University, 11th and Walnut Streets, Philadelphia, Pennsylvania 19107. Address reprint requests to J. L. Thomas.

© 1979 American Roentgen Ray Society

0361–803X/79/1324–0653 $0.00

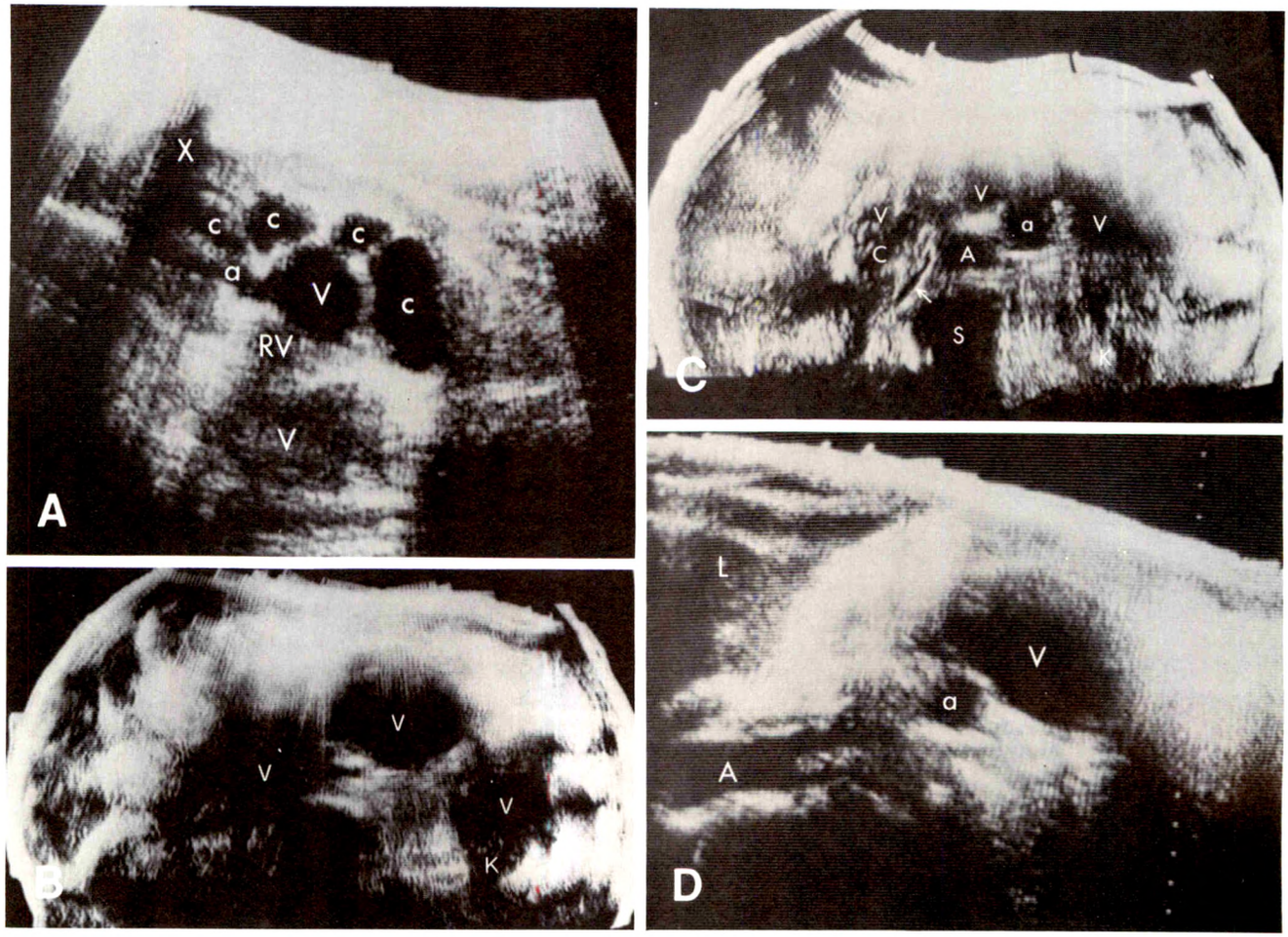


Fig. 1.—**A**, Prone longitudinal scan parallel to long axis of left kidney. Fistulous communication between superiorly displaced left renal artery (a) and renal vein (RV) with two areas of varicoid dilatation (V). Echoes in renal vein are secondary to beam width artifact. Compression of renal pelvis by enlarged renal vein varix has resulted in caliectasis (C). Rib artifact (X) overlies tip of upper pole of left kidney. **B** and **C**, Supine transverse abdominal scans. Large renal vein varices (V) arise on anterior surface of kidney (K), and extend toward area of inferior vena cava (C). Note enlarged left renal artery (a) adjacent to aorta (A). Right renal artery (*arrow*) courses between vena cava and spine (S). **D**, Supine longitudinal scan of abdomen 2 cm left of midline. Varicoid left renal vein (V) and dilated left renal artery (a) inferior to liver (L) and anterior to aorta (A).

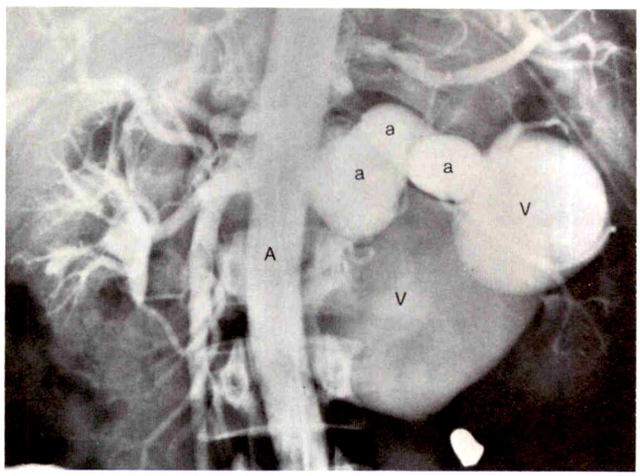


Fig. 2.—Abdominal aortogram. Cephalad displacement of enlarged tortuous renal artery (a) with arteriovenous fistula causing two areas of varicoid dilatation of renal vein (V); first overlies renal pelvis.

evaluation of renal masses detected by excretory urography [4]. A nonneoplastic, acquired renal arteriovenous fistula more than 2 cm in diameter should be detectable by gray scale sonographic examination as an anechoic mass. A parapelvic arteriovenous fistula may compress the renal pelvis producing caliectasis and ultrasonically simulate the findings of obstructive uropathy (fig. 1). Misdiagnosis of an acquired renal arteriovenous malformation as a parapelvic cyst or hydronephrotic kidney is a potential pitfall if the ultrasonic study is not preceded by excretory urography. Identification of one or more channels entering a parapelvic mass should suggest that the lesion is related to the renal vasculature. The vascular nature of a channel entering a parapelvic mass can be confirmed by tracing it into the aorta or inferior vena cava, or by use of real time or time motion scanning techniques to demonstrate pulsatile wall motion. If a dilated renal vein is detected, then a renal arteriovenous fistula may be distinguished from a renal artery aneu-

rysm. Recognition of these findings will allow the ultrasonographer to direct clinical management toward the treatment of the acquired renal arteriovenous fistula, rather than proceeding with a potentially hazardous percutaneous aspiration or percutaneous antegrade nephrostomy.

Conservative management of patients with renal arteriovenous fistulas after both trauma and renal biopsy has been emphasized recently since these lesions may close without surgical intervention [5, 6]. Gray scale ultrasonography is a noninvasive method for serial examination of such patients undergoing expectant treatment. Ultrasonic resolution of vascular dilatation produced by a renal arteriovenous fistula provides objective evidence of diminution of a lesion, but does not document absolute closure of an arteriovenous fistula, since a small arteriovenous shunt may not produce ultrasonically detectable renovascular enlargement. In contrast, progressive renovascular dilatation will alert the clinician to modify treatment.

REFERENCES

1. O'Brien DP, Parrott TS, Walton KN, Lewis EL: Renal arteriovenous fistulas. *Surg Gynecol Obstet* 139:739–743, 1974
2. Messing E, Kessler R, Kavaney PB: Renal arteriovenous fistulas. *Urology* 8: 101–107, 1976
3. Nelson BD, Brosman SA, Goodwin WE: Renal arteriovenous fistulas. *J Urol* 109:779–784, 1973
4. Goldberg BB, Pollack HM: Differentiation of renal masses using A-mode ultrasound. *J Urol* 105:765–771, 1971
5. Angorn IB: A conservative approach to traumatic intrarenal arteriovenous fistulae: experience with 13 cases. *Injury* 8: 290–297, 1977
6. Cosgrove MD, Mendez R, Morrow JW: Traumatic renal arteriovenous fistula: report of 12 cases. *J Urol* 110:627–631, 1973

Renal Emphysema of the Transplanted Kidney: Sonographic Appearance

A. NORMAN A. G. BRENBRIDGE,[1] ANTHONY J. BUSCHI,[1] J. ALAN COCHRANE,[1] AND RICHARD F. LEES[1,2]

The past several years have witnessed the refinement of renal transplantation and ultrasonography. Numerous reports detail the utility of sonography in following the medical course of the transplantation and evaluating the complications of the surgical procedure [1–3]. Besides monitoring changing renal size and finding a pararenal mass (such as lymphocoele and urinoma), work is underway to characterize changes in renal parenchymal texture as an index of disease (unpublished data). We describe the sonographic appearance of renal emphysema, resulting from gas-forming infections of the renal cortex, one of the most dreaded complications in immunosuppressed transplant recipients.

Case Report

A 33-year-old man, with an 11 year history of progressive renal failure consequent to poststreptococcal glomerulonephritis, received a cadaver transplant which was removed within 10 days due to acute rejection. He was maintained on renal dialysis. Two years after his first transplant, he received a second cadaver transplant and was immunosuppressed on a protocol of prednisone, solumedrol, azathioprine, and local irradiation to the transplanted kidney.

Initially the patient displayed good urine flow and diminished hypertension. However, after postoperative day 3 and over the next 2 weeks, function gradually deteriorated and was interpreted both clinically and by nuclear scintiscans as rejection. Serum glucose was initially normal, then rose intermittently to 125–141 mg/100 ml (with one value of 249 recorded). Glucosuria (1+) occurred; blood urea nitrogen rose steadily to 119, creatinine to 16.5. The patient became progressively anemic. Dialysis was resumed. On postoperative day 7 he began to have cyclic low-grade fevers to 37.8°C. The presence of *E. coli* was treated with antibiotics. Sonography on postoperative day 2 was considered normal baseline (fig. 1A). Sonography on days 15 and 23 was felt to be consistent with gas in the renal parenchyma (figs. 1B and 1C). Radiography of the abdomen on day 16 was initially misinterpreted as showing only bowel gas in the right lower quadrant but, on retrospective comparison with the sonograms, demonstrated collections of gas in a radial distribution through the transplant with a few possibly perinephric collections (fig. 1D). Biopsy of the transplant on day 17 demonstrated necrosis and bacteria. When the patient's objective signs (he had few subjective complaints) did not improve on appropriate medical therapy, the transplant was removed. The pathologic specimen demonstrated necrotic tissue and displayed numerous abscesses which grew *E. coli*. The patient was discharged in stable condition to await another transplant.

Discussion

The weakening of host defenses against invading microorganisms is one of the most dangerous sequelae of the immunosuppressive regimen necessary to avoid rejection of the transplanted kidney. Infections remain the most common cause of death of transplant recipients [4]; the urinary tract itself is cited as the most common site of primary infection in most reports [5]. The problem is compounded by the fact that not only is the patient's immune system suppressed, but signs and symptoms may also be masked for quite some time until sepsis is widespread. In our case, although the transplanted kidney was grossly infected, the patient felt well, had no subjective complaints of pain, experienced only mild tenderness over the transplant site, and exhibited only a low-grade intermittent fever and oliguria.

The single most frequent cause of renal failure in the immediate posttransplantation period, especially in recipients of cadaver kidneys, is acute tubular necrosis [6] which is associated with a high risk of infection [4]. The other principal graft complication, rejection, whether immediate or delayed, rapidly progresses to vasoocclusive processes and cortical necrosis. Steroid-induced diabetes elevates tissue glucose concentration and may result in glucosuria. It has been postulated that one cause of renal parenchymal emphysema might be impaired host response enabling organisms capable of fermenting glucose to utilize devitalized tissue as a substrate for carbon dioxide production [7].

Although renal emphysema, whether of native kidneys or of a renal transplant, can be recognized radiographically, pattern recognition can be quite difficult. Such gas collections can be mistaken, whether diffuse throughout the cortex or distributed radially along the planes of the columns of Bertini, as fecal-laden bowel unless the gas outlines the entire kidney [8, 9]. With careful technique, the distinction between colonic and renal gas is more easily made sonographically. Although one might be tempted to dismiss a gas collection in the area of the transplant as bowel obscuring the transplant, attention to detail obviates this difficulty. The value of a baseline sonogram performed shortly after transplantation to ascertain the texture, size, and lie of the transplant cannot be stressed too strongly. The transplant is placed poste-

Received August 21, 1978; accepted after revision December 29, 1978.

[1]Department of Radiology, Box 170, University of Virginia Medical Center, Charlottesville, Virginia 22908. Address reprint requests to A. N. A. G. Brenbridge.

[2]Present address: 13 Fergusson Square, Toorak Gardens, South Australia 5065, Australia.

© 1979 American Roentgen Ray Society

0361–803X/79/1324–0656 $0.00

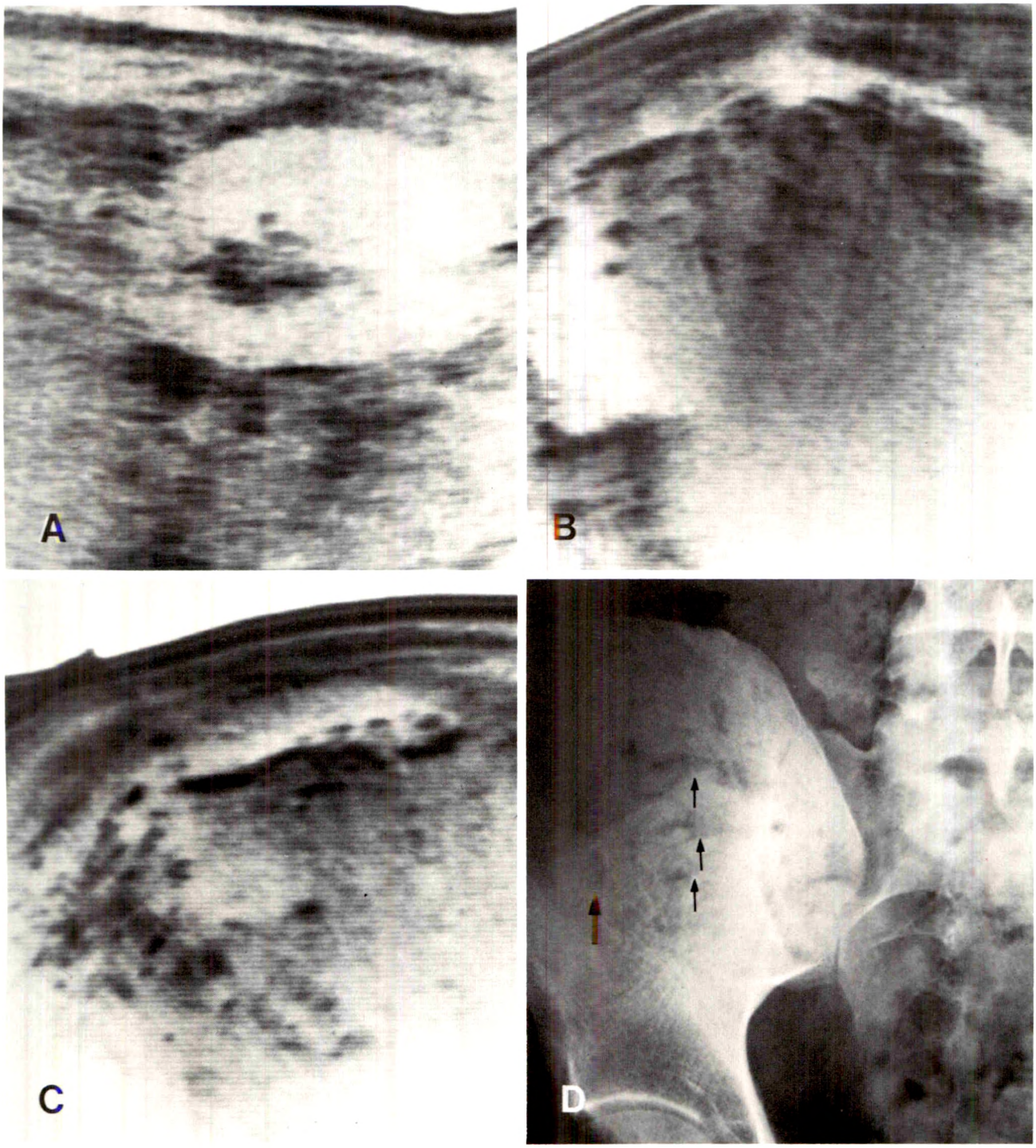


Fig. 1.—**A–C**, Sagittal scans parallel to long axis of kidney and oriented with head to reader's left. **A**, Normal baseline scan, 2 days after transplantation. Cortex of uniform echo texture surrounds dense echoes of renal collecting system. (Relative paucity of echoes at lower pole is artifact of single pass scanning, sonographic critical angle having been exceeded at curvature of lower pole.) **B**, Day 15. Dense echoes originating from within renal cortex represent gas. Acoustic shadowing and reverberations are deep to collections of gas. Some echoes, near upper pole, may originate in perinephric region. **C**, Day 23. Gas in the renal cortex. **D**, Right lower abdomen. Gas distributed radially through transplanted kidney (*small arrows*), along planes of columns of Bertini. Some gas may be perinephric (*large arrow*).

rior to the peritoneum, in the iliac fossa. Although theoretically bowel can lie anterior to the transplant, because of the oblique posture of the iliac fossa, the peritoneal space anterior to the transplant is fairly small when the patient is supine and bowel tends to fall into the more dependent part of the peritoneal cavity, leaving the transplant accessible to the transducer. Provided that large quantities of gas have not dissected into the

perinephric space, totally surrounding the kidney, the outer portion of the renal cortex should be recognizable. The marked acoustic impedance mismatch of gas and renal tissue results in dense echoes at the acoustic interface with total lack of penetration deep to this and typical reverberation artifacts.

Although theoretically calcium could produce a similar image, stone production would be unlikely in the early posttransplantation period, nor would it be so extensive. Even total calcification of the kidney, a late sequelae of rejection, would not be so diffuse as to obscure all underlying tissue [10]. Comparison with baseline studies permits determination that the gas is cortical rather than in the collecting system. The distinction is more than of just academic interest. Gas in the collecting system is secondary to ureteral obstruction and is associated with a much lower mortality than parenchymal emphysema [11].

If it is elected to attempt a course of medical therapy before resorting to nephrectomy, sonography can be used to monitor the distribution of renal gas. Carbon dioxide diffuses rapidly and is highly soluble. Were the bacteria to be irradicated, the gas would rapidly disappear [7]. Therefore, persistence of gas indicates viability of the bacteria, continued fermentation of glucose productive of CO_2, and ineffectiveness of medical treatment. Prompt nephrectomy is the procedure of choice once the diagnosis is established.

REFERENCES

1. Petrik J, Tilney NL, Smith EH, Williams JS, Vineyard GC: Ultrasound in renal transplantation. *Ann Surg* 185:441–447, 1977
2. Koehler PR, Kanemoto HH, Maxwell JG: Ultrasonic "B" scanning in the diagnosis of complications in renal transplant patients. *Radiology* 119:661–664, 1976
3. Bartrum RJ, Smith EH, D'Orsi CJ, Tilney NL, Dantono J: Evaluation of renal transplants with ultrasound. *Radiology* 118:405–410, 1976
4. Burgos-Calderon R, Pankey GA, Figueroa JE: Infection in kidney transplantation. *Surgery* 70:334–340, 1971
5. Boshiff HK, Hesse VE, Coetzee JN, Prozesky OW, Venter L, Van Wyk J: Infective complications in renal allograft recipients. *S Afr Med J* 52:1099–1100, 1977
6. Lee DBN, Prompt CA, Upham AT, Kleeman CR: Medical Complications of renal transplantation. *Urology (suppl)* 9: 7–31, 1977
7. Schainuck LI, Fouty R, Cutler RE: Emphysematous pyelonephritis: A new case and review of previous observations. *Am J Med* 44:134–139, 1968
8. Parameswaran R, Feest T: Gas nephrogram: an unusual complication of renal transplantation. *Br J Radiol* 50:438–440, 1977
9. Klein DE, Mohone SA, Youngen R, Schneider DH: Renal emphysema. *J Urol* 95:625–629, 1966
10. Harrison RB, Vaughan ED: Diffuse cortical calcification in rejected renal transplants. *Radiology* 126:635–636, 1978
11. Carris CK, Schmidt JD: Emphysematous pyelonephritis. *J Urol* 118:457–459, 1977

Ultrasound Demonstration of Diffuse Cortical Nephrocalcinosis in a Case of Primary Hyperoxaluria

DON A. WILSON,[1] JAMES E. WENZL,[2] AND GEOFFREY P. ALTSHULER[3]

Primary hyperoxaluria is a rare genetic disorder characterized by excessive formation and excretion of oxalate. Two forms of primary hyperoxaluria have been recognized, and both are transmitted as autosomal recessive traits. The clinical expression of these two forms is similar, and consists of oxalate crystalluria, nephrocalcinosis, and the production of oxalate calculi. Renal parenchymal injury, caused by the calcium oxalate deposits, leads to progressive renal failure. The finding of oxalate crystals in several tissues is referred to as oxalosis [1, 2]. A case of oxalosis in infancy is reported and the renal ultrasound findings are discussed.

Case Report

A. L., a female infant, the product of a term gestation, weighed 3.45 kg at birth. She was well until age 8 weeks when the mother noted periodic episodes of irritability with deviation of her eyes upward; these episodes lasted for about 30 sec but became increasingly frequent. At age 10 weeks, she was failing to thrive and was noted to have arching of the back with stiffening and flexion of the extremities. She was admitted to Oklahoma Children's Memorial Hospital with the diagnosis of seizure disorder.

Physical examination on admission revealed a well developed moderately pale infant who was having obvious seizures and carpopedal spasms. Her weight was 4.0 kg; length, 53 cm; pulse rate, 140/min; respirations, 40/min; and blood pressure, 90/40 mm/Hg.

Admission laboratory data revealed a white blood cell count of 15,300 mm^3; hemoglobin, 6.8 g/dl; and hematocrit, 20.6%. The serum sodium was 135; potassium, 4.3; chloride, 93; and CO_2, 8 meq/l. The serum urea nitrogen was 220 mg/dl; creatinine, 4.2 mg/dl; calcium, 4.9 mg/dl; and phosphorus, 9.5 mg/dl. A plain film of the abdomen showed the kidneys to be unusually dense but normal in size (fig. 1). Radionuclide scans of the kidneys revealed a generalized decrease in renal function. Abdominal ultrasound examination showed an exceptionally high echo content within the renal parenchyma (fig. 2).

An open biopsy showed marked deposition of calcium oxalate within the renal parenchyma (fig. 3). Urinary oxalate excretion was elevated at 127 mg of oxalate/24 hr/1.73^2. A bone marrow biopsy revealed calcium oxalate crystals within the bone marrow macrophages. These findings were consistent with the diagnosis of primary hyperoxaluria (oxalosis).

After histologic confirmation of the diagnosis, the infant was begun on treatment with pyridoxine in an attempt to decrease oxalate production. Treatment of her renal failure included

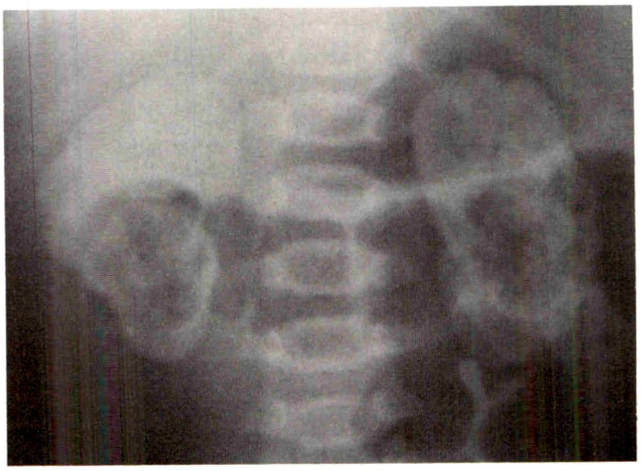


Fig. 1.—Plain film of abdomen. Diffuse variety of nephrocalcinosis.

aluminum hydroxide, calcium gluconate, and Vitamin D, which were administered to stabilize her serum phosphorus and calcium. At the time of this writing, she has slowly advancing renal failure but is not considered a candidate for renal dialysis or transplantation because of the probability of progression in other organs, and recurrence in the graft.

Discussion

Nephrocalcinosis refers to the pathologic deposition of calcium salts in the renal parenchyma. It occurs in two distinct radiographic patterns. The more common central or medullary type of calcification involves the renal pyramids. The diagnosis of this type of nephrocalcinosis by ultrasound has recently been reported [3]. The ultrasound appearance of the less common renal cortical variety of calcification is demonstrated in the present case.

The normal kidney, as imaged by B-mode gray scale techniques, is composed of renal parenchyma which is essentially anechoic and the pelvocalyceal system which appears as an echogenic central collection. The striking feature of our case of oxalosis is the diffusely increased echogenicity of the renal parenchyma at normal to low gain settings. This abnormal pattern is especially evident when comparing the kidneys with adjacent liver tissue

Received September 1, 1978; accepted after revision December 12, 1978.

[1] Department of Radiology, Oklahoma Children's Memorial Hospital, University of Oklahoma Health Sciences Center, 940 N. E. 13th Street, Oklahoma City, Oklahoma 73126. Address reprint requests to D. A. Wilson.

[2] Department of Pediatrics, Oklahoma Children's Memorial Hospital, University of Oklahoma Health Sciences Center, Oklahoma City, Oklahoma 73126.

[3] Department of Pathology, Oklahoma Children's Memorial Hospital, University of Oklahoma Health Sciences Center, Oklahoma City, Oklahoma 73126.

© 1979 American Roentgen Ray Society

0361–803X/79/1324–0659 $0.00

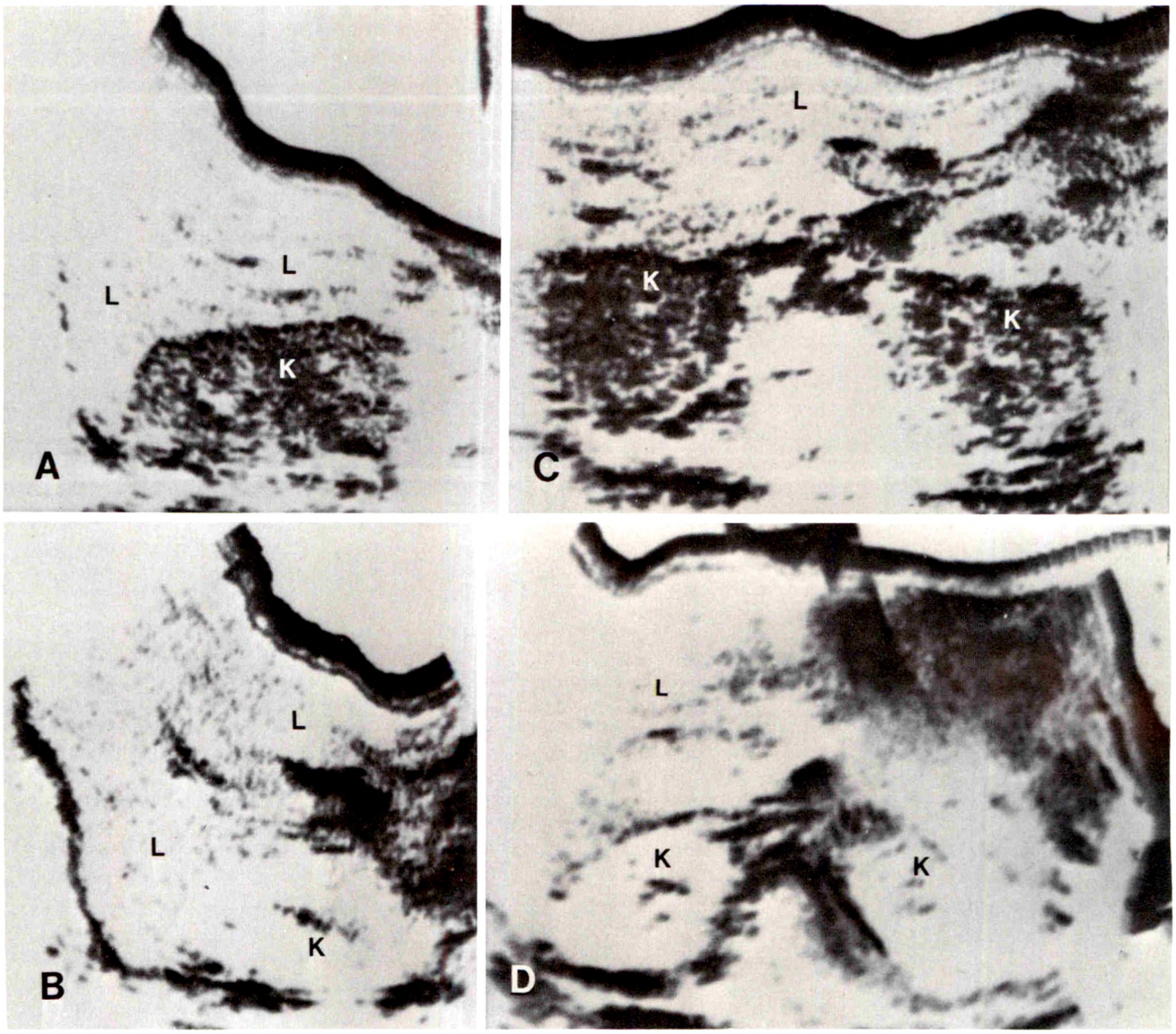


Fig. 2.—Supine longitudinal ultrasound of right kidney (**A**); normal kidney for comparison (**B**). Supine transverse scan of kidneys (**C**); with normal kidneys for comparison (**D**). Diffuse increase in echo content throughout renal parenchyma. K = kidneys, L = liver.

which usually contains more internal echoes than the renal parenchyma (fig. 2). The echogenic pattern of these kidneys is most probably related to the nonhomogeneous texture of the renal parenchyma caused by the diffuse infiltration of oxalate crystals.

The echogenic pattern seen in this case is not specific for oxalosis. A similar echo pattern has been observed by the authors in two cases of end-stage kidney disease; one, secondary to chronic glomerulonephritis, and the other caused by cystinosis. The cortical variety of nephrocalcinosis seen in this case of oxalosis has also been observed after acute renal cortical necrosis [4]. The kidneys in the present case of oxalosis and in most early cases of acute renal cortical necrosis are of normal size. The kidneys in most cases of end stage renal disease are smaller than normal. Oxalosis should be included in the differential diagnosis of normal-sized echogenic kidneys.

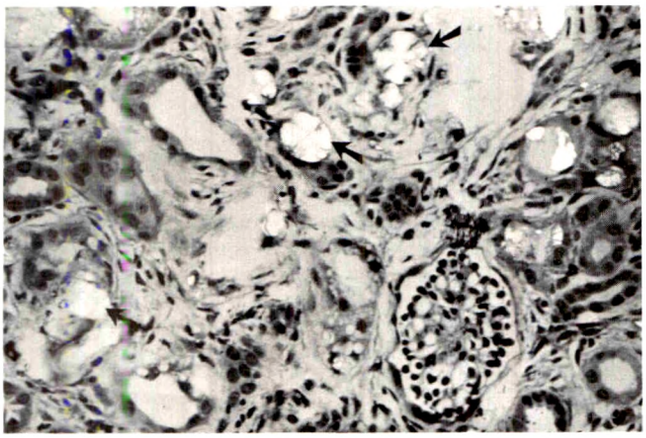


Fig. 3.—Photomicrograph of renal tissue under polarized light. Diffuse deposition of oxalate (*arrows*). H and E×475.

ACKNOWLEDGMENTS

We thank Ann Aldrich and Daisy Walker for their assistance in the preparation of this manuscript.

REFERENCES

1. Boquist L, Lindquist B, Östberg Y, Steen L: Primary oxalosis. *Am J Med* 54:673–681, 1973
2. Williams HE, Smith LH Jr: Disorders of oxalate metabolism. *Am J Med* 45:715–735, 1968
3. Cacciavell A, Young N, Levine A: Gray-scale ultrasonic demonstration of nephrocalcinosis. *Radiology* 128:459–460, 1978
4. Malek RS: Urolithiasis, in *Clinical Pediatric Urology*, edited by Kelalis PP, King LR, Philadelphia, Saunders, 1976, p 887

Ultrasonographically Guided Percutaneous Pancreatography: Report of Two Cases

P. L. COOPERBERG,[1] M. M. COHEN,[2] AND M. GRAHAM[1]

Until recently, direct pancreatography was possible only at the time of surgery on the pancreas [1]. Pancreatography can now be performed using the endoscopic retrograde approach [2], unless the duct is totally obstructed by a mass in the head of the pancreas. Dilated pancreatic ducts in association with carcinoma of the head of the pancreas have been demonstrated by ultrasound [3, 4]. This report documents two cases in which an ultrasound study performed to evaluate suspected cancer of the head of the pancreas demonstrated dilated pancreatic ducts. Under ultrasound guidance, the ducts were punctured percutaneously to obtain pancreatograms.

Case Reports

Case 1

A 63-year-old woman who had had a cholecystectomy 12 years earlier was seen at another hospital after 1 month of fatigue and sudden onset of jaundice. At laparotomy, it was believed she had a cancer in the head of the pancreas, but no biopsy was taken and a choledochoduodenostomy was performed. This procedure relieved her jaundice, but anorexia and fatigue persisted. She developed postprandial fullness and severe epigastric pain. An upper gastrointestinal series showed duodenal stricture.

On admission to Vancouver General Hospital 2 months later for further investigation and treatment, no mass was palpable on examination of her abdomen, but there was epigastric and right upper quadrant tenderness. Laboratory investigation showed mild anemia (hemoglobin 11.5 g/100 ml) and hypoproteinemia (total protein 4.9 g/100 ml), but no other abnormality. Plain films of the abdomen revealed pancreatic calcification. Ultrasonography of the pancreas confirmed a 3 cm mass in the head of the pancreas and an elongated sausage-shaped fluid-filled structure in the region of the pancreas believed to represent a dilated pancreatic duct or possibly a peculiar pseudocyst (figs. 1A–1C).

After 1 month, an ultrasound guided 22 gauge spinal needle was inserted into the fluid-filled structure and 15 ml of clear watery fluid was removed. This fluid was replaced by 10 ml of 30% and 5 ml of 60% sodium diatrizoate. Pancreatography (fig. 1D) confirmed a grossly dilated pancreatic duct. No cells were identified in the fluid withdrawn and its amylase content was only 25 IU/l. The transient episode of fever and chills that followed was treated with gentamicin and clindamycin. The next day, gastroenterostomy and pancreatogastrostomy were performed. Aspiration cytology of the mass in the head of the pancreas at operation was conclusive for adenocarcinoma.

Case 2

A 59-year-old woman with a long history of alcoholism and recurrent acute pancreatitis was seen at Vancouver General Hospital with abdominal pain and tenderness associated with elevation of the serum amylase. Ultrasonography showed a pseudocyst in the head of the pancreas that was confirmed by percutaneous fine needle aspiration of clear fluid with an amylase concentration greater than 10,000 IU/l. The pseudocyst rapidly recurred and another appeared in the region of the tail of the pancreas. Both pseudocysts were aspirated but again rapidly recurred. After 7 months, both pseudocysts were drained by cystogastrostomy. Despite complete resolution of the pseudocysts, the patient complained of nearly constant severe epigastric and back pain that required Demerol for control.

She was readmitted 3 months later for elective surgery for chronic pancreatitis. Laboratory investigation revealed iron deficiency anemia (hemoglobin 9.4 g/100 ml), but other values, including serum amylase, were normal. Plain abdominal films showed extensive calcification in the head of the pancreas. Ultrasonography 3 days after readmission showed an enlarged pancreas with dilatation of the pancreatic duct. An ultrasound guided 23 gauge spinal needle was inserted into the duct and 5 ml of clear watery fluid was removed and replaced by 15 ml of 60% sodium diatrizoate. Pancreatography (fig. 2) confirmed a multiloculated dilatation of the pancreatic ducts and the presence of pancreatic stones. No complications occurred and the procedure was not followed by any increase in pulse rate, temperature, or serum amylase concentration. The next day, a longitudinal pancreaticojejunostomy (Puestow) successfully relieved her abdominal pain.

Discussion

A good pancreatogram provides valuable information for planning pancreatic surgery. Preoperative pancreatography can usually be obtained only by endoscopic retrograde cannulation of the pancreatic duct. Ultrasound is usually the first investigation for suspected cancer of the pancreas. Our cases illustrate that if ultrasound demonstrates significant pancreatic duct dilatation, pancreatography can be obtained under ultrasound guidance using the fine needle technique. This technique is almost identical to that used for percutaneous aspiration biopsy of the pancreas [5, 6]. Needle puncture of an obstructed duct may cause pancreatitis and, as in transhepatic cholangiography of the obstructed biliary tree, should be followed by surgical decompression within 24–48 hr.

While it is not likely that this technique will find wide application, it was useful in our cases. Ultrasound or computed tomography can allow visualization of mild degrees of pancreatic duct dilatation resulting from neoplasm and chronic pancreatitis. A confident noninvasive diagnosis may eliminate the need for further proof of ductal dilatation. However, if the diagnosis is uncertain or if a pancreatic duct anastomosis is considered,

Received August 18, 1978; accepted after revision December 29, 1978.

[1] Section of Ultrasound, Department of Diagnostic Radiology, University of British Columbia and Vancouver General Hospital, 855 West 12th Avenue, Vancouver, British Columbia V5Z 1M9. Address reprint requests to P. L. Cooperberg.

[2] Department of Surgery, University of British Columbia and Vancouver General Hospital, Vancouver, British Columbia V5Z 1M9.

© 1979 American Roentgen Ray Society

0361–803X/79/1324–0662 $0.00

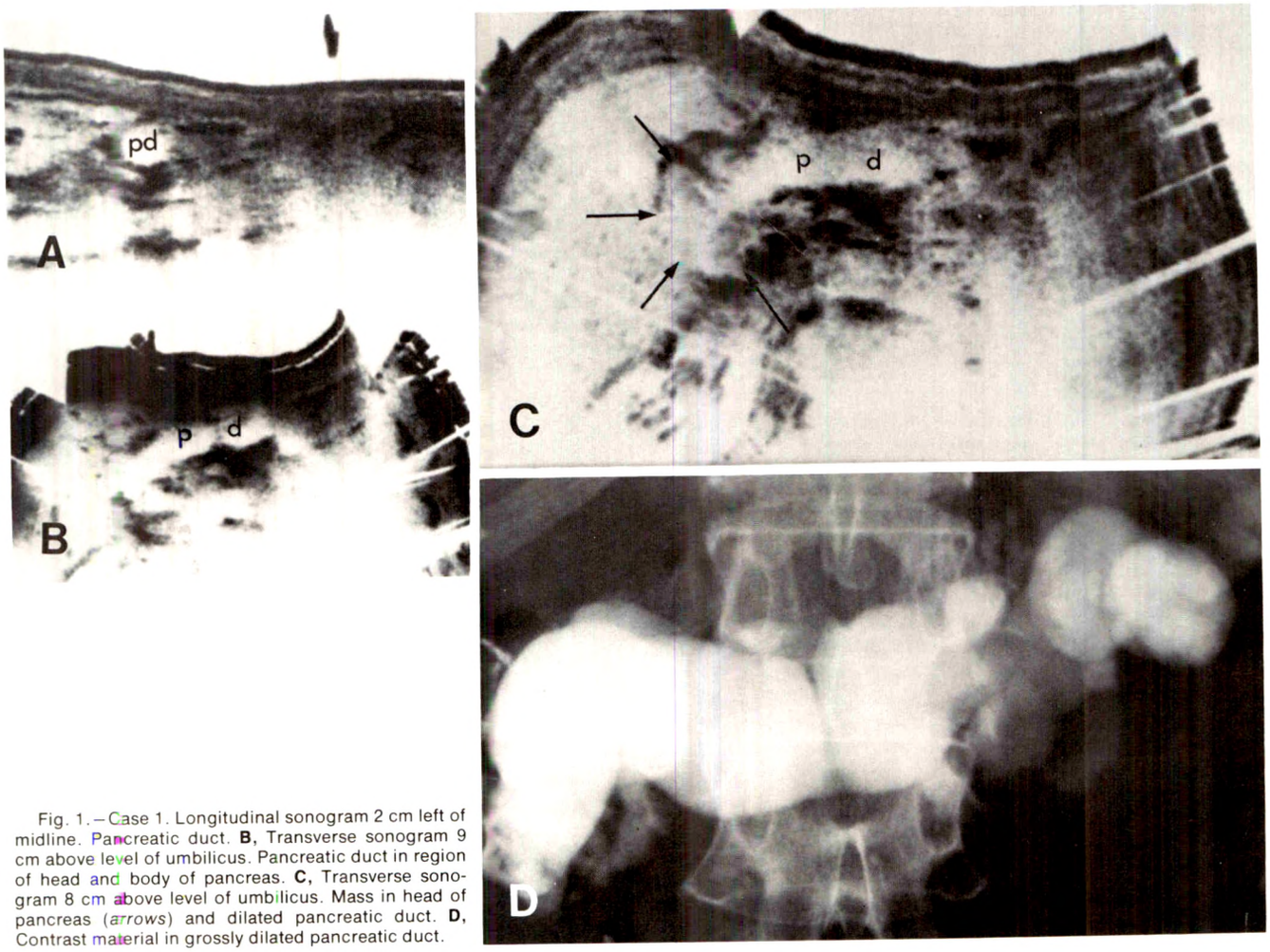


Fig. 1.—Case 1. Longitudinal sonogram 2 cm left of midline. Pancreatic duct. **B,** Transverse sonogram 9 cm above level of umbilicus. Pancreatic duct in region of head and body of pancreas. **C,** Transverse sonogram 8 cm above level of umbilicus. Mass in head of pancreas (*arrows*) and dilated pancreatic duct. **D,** Contrast material in grossly dilated pancreatic duct.

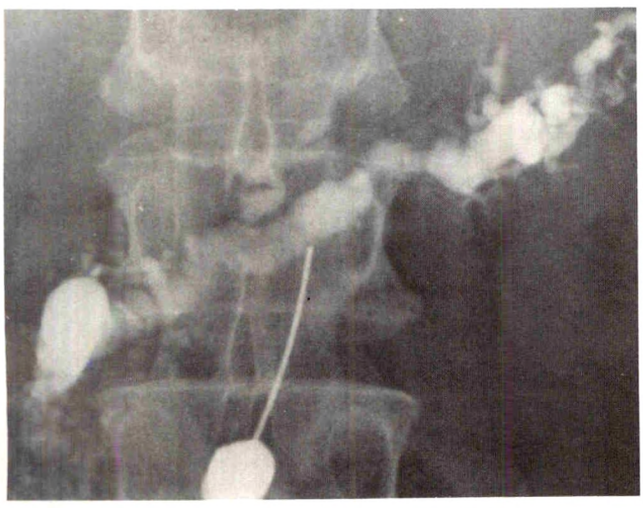


Fig. 2.—Case 2. Chronic complicated pancreatitis. Dilated main duct and secondary ducts, stenosis of proximal main duct, stones in main and accessory ducts, retention cysts in head of pancreas, and some contrast material in duodenum and jejunum.

percutaneous fine needle pancreatography may be very helpful.

REFERENCES

1. Howard JM, Short WF: An evaluation of pancreatography in suspected pancreatic disease. *Surg Gynecol Obstet* 129: 319–324, 1969
2. Varley PF, Rohrmann CA, Silvis SE, Vennes JA: The normal endoscopic evaluation. *Radiology* 118:295–300, 1976
3. Gosink B, Leopold G: The dilated pancreatic duct: ultrasonic evaluation. *Radiology* 126:475–576, 1973
4. Lee TG, Henderson SC, Berkman FE: Ultrasound visualization of the pancreatic duct and its clinical application, in *Ultrasound in Medicine*, vol. 4, edited by White D, Lyons EA, New York, Plennum, 1978, p 191
5. Smith ER, Bartrum RJ, Chang YC: Ultrasonically guided percutaneous aspiration biopsy of the pancreas. *Radiology* 112:737–738, 1974
6. Cohen MM, Cooperberg PL, Pontifex H: Percutaneous fine needle aspiration cytology of intra-abdominal masses. *Br Columbia Med J* 20:276–277, 1978

Metastatic Islet Cell Carcinoma to the Liver Visualized After Intraarterial Epinephrine

STEVEN R. MILLS,[1] JOHN L. DOPPMAN,[1] AND E. RONALD KAHN[2]

Pharmacoangiographic methods for evaluating primary and metastatic neoplasms of the liver using both vasoconstrictive and vasodilatory drugs have been reported [1–6]. The following case of metastatic islet cell carcinoma could only be documented by hepatic angiography after intraarterial epinephrine.

Case Report

A 48-year-old woman had jaundice. Radionuclide liver-spleen scan was negative; angiography revealed a hypervascular mass in the head of the pancreas with displacement of the superior mesenteric and portal veins to the left. She underwent total pancreaticoduodenectomy and splenectomy for a 5 cm nonfunctioning islet cell carcinoma of the head of the pancreas. No liver metastases were seen at operation, but unresectable tumor remained around the portal vein.

She was seen again 1 year later with weight loss, fever, anemia, and back pain. Barium enema and upper gastrointestinal series revealed a midabdominal mass with tethering of jejunal folds and displacement of the transverse colon. Ultrasound examination revealed upper abdominal masses to the left and right of midline with a mixed echo pattern, plus two well defined masses within the right lobe of the liver. These findings were believed to most likely represent recurrent islet cell carcinoma in the pancreatic bed and liver; however, a less likely possibility of an inflammatory process with liver abscesses was also considered. Abdominal arteriography revealed a hypervascular mass in the right upper quadrant of the abdomen obstructing the superior mesenteric vein. Selective right hepatic arteriography was normal (figs. 1A and 1B). Because liver masses had been demonstrated by ultrasonography, right hepatic artery injection was repeated after 20 μg of intraarterial epinephrine and revealed two well circumscribed hypervascular lesions in the right lobe of the liver (fig. 1c). Since both an inflammatory process and resectable tumor were excluded by the arteriographic findings, no further investigation or surgery was pursued.

Discussion

Several investigators have reported on the use of intraarterial epinephrine during hepatic angiography for evaluating suspected primary and metastatic neoplasms [1–4]. Visualization of metastases after epinephrine improved, worsened, or remained unchanged from control angiograms. Boijsen and Redman [1] and Kahn et al. [2] believe hypervascular liver metastases are better seen after epinephrine. This improved visualization of hypervascular metastases results from decreased contrast in the surrounding normal liver parenchyma combined with

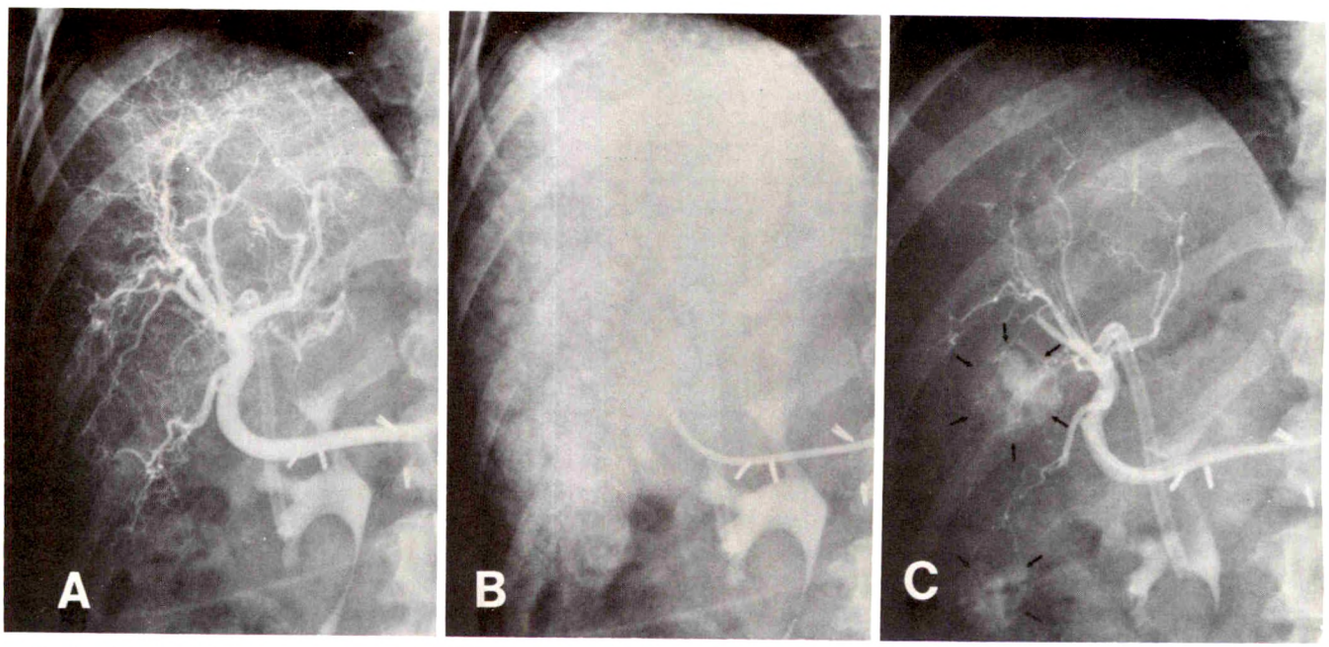


Fig. 1.—Selective right hepatic angiogram. **A,** Control angiogram, arterial phase. Biliary stent present. **B,** Control angiogram, parenchymal phase. **C,** After intraarterial epinephrine, two hypervascular metastases (*arrows*) appear. Gas in biliary ducts due to previous choledochojejunostomy.

Received June 23, 1978; accepted after revision December 8, 1978.

[1] Department of Diagnostic Radiology, National Institutes of Health, Clinical Center, Bldg. 10, Room 6S211, Bethesda, Maryland 20014. Address reprint requests to S. R. Mills.

[2] Diabetes Branch, National Institute of Arthritis, Metabolism, and Digestive Diseases, Bethesda, Maryland 20014.

0361-803X/79/1324-0664 $0.00

failure of tumor vasculature to react to the vasoconstrictive effects of epinephrine. Kahn et al. [2] believe hypovascular lesions probably are less well seen after epinephrine.

In Boijsen and Redman's series of 12 patients with liver metastases [1], all were seen on the control angiograms; however, in two, an increased number of metastases were appreciated after epinephrine. Goldstein and Miller [4] reported a case of liver metastases from carcinoid tumor of the small bowel visualized on celiac arteriography only after epinephrine.

Pharmacoangiography with drugs other than epinephrine has been described. Ekelund and Lunderquist [5] reported one patient in whom metastases from breast carcinoma to the liver could only be visualized during hepatic angiography after intraarterial angiotensin. Goldstein and Miller [6] reported the conversion of a negative to a positive hepatic angiogram for metastatic colonic carcinoma after intraarterial priscoline.

Thus, while many authors have reported the usefulness of vasoconstrictive or vasodilatory drugs in improving the visualization of liver metastases already apparent on controlled studies, conversion of a negative hepatic angiogram to a positive study is relatively rare and has not been reported in metastatic islet cell carcinoma. Vasoconstrictive angiography seems worthwhile whenever confirmation of hypervascular liver metastases is critical in managing the patient.

REFERENCES

1. Boijsen E, Redman H: Effect of epinephrine on celiac and superior mesenteric angiography. *Invest Radiol* 2:184–199, 1967
2. Kahn PC, Frates WS, Paul RE: The epinephrine effect in angiography of gastrointestinal tract tumors. *Radiology* 88: 686–690, 1967
3. Kaude JV, Wirtanen GW: Celiac epinephrine enhanced angiography. *AJR* 110:818–826, 1970
4. Goldstein HM, Miller M: Angiographic evaluation of carcinoid tumors of the small intestine: the value of epinephrine. *Radiology* 114:23–28, 1975
5. Ekelund L, Lunderquist A: Pharmacoangiography with angiotensin. *Radiology* 110:533–540, 1974
6. Goldstein HM, Thaggard A, Wallace S, Heiman HL: Priscoline augmented hepatic angiography. *Radiology* 119:275–279, 1976

Large Ulcerated Cecal Vascular Malformation: Unusual Gross and Histologic Features

GEORGE M. HOLLENBERG[1] AND ARNOLD J. SCHWARTZ[2]

Although their origin is disputed, cecal vascular malformations (also known as angiodysplasias or vascular ectasias) are now recognized as a cause of lower intestinal hemorrhage in the elderly [1–12]. Since gross anatomic findings in the resected colon are usually absent or minimal, these malformations are most often demonstrated by angiography [2–12]. Cecal erosions of undetermined etiology have also been described as causes of massive lower intestinal hemorrhage [13]. We describe a case of an angiographically proven cecal vascular malformation associated with a large, grossly obvious cecal ulcer over 3 cm in diameter.

Case Report

A 64-year-old Caucasian male was admitted because of recurrent rectal bleeding. He described seeing "wine colored blood," sometimes with clots, mixed with his stool. This bleeding was unaccompanied by diaphoresis, abdominal pain, or change in bowel habits. These bleeding episodes had started 18 months earlier and resulted in two previous hospitalizations. Exhaustive examination during these admissions, including upper and lower gastrointestinal series, disclosed only a few small diverticula in the sigmoid colon. However, no angiographic studies were done. As no source of bleeding was identified, he was given transfusions and released on a low residue diet and stool softeners. Neither the patient nor his family had a history of a bleeding diathesis, ulcer disease, or heart disease. His only medication was Hygroton (chlorthalidone) 50 mg/day orally which was taken for mild hypertension for a period of 7 months.

A physical examination revealed mild skin pallor and slight prostatic enlargement. On rectal examination, dark red blood was present on the examiner's finger. No organomegaly, cutaneous hemangiomas, or heart murmurs were noted.

Admission laboratory data included hemoglobin of 11.2 g/100 ml; hematocrit, 34.3 vol/100 ml; white blood cell count, 6,100/mm^3 with normal differential; platelets, 364,000/cm^3; prothrombin time, 11 sec with a control of 11 sec; partial thromboplastin time, 34 sec with a control of 32 sec. Blood urea nitrogen, total bilirubin, SGOT, SGPT, alkaline phosphatase, and urinalysis were normal.

The patient remained stable after admission with only slight rectal bleeding. Sigmoidoscopy and colonoscopy were performed on hospital day 5. Although blood was seen in the ascending colon, hepatic flexure, and right transverse colon, no bleeding site or ulceration could be identified. After random biopsies of the colon and ileocecal valve revealed edema and mild inflammation, visceral arteriography was performed. Injection of the distal superior mesenteric artery demonstrated a small collection of arterioles on the lateral margin of the proximal ascending colon in the area supplied by a branch of the right colic artery (fig. 1). Instantaneous filling of the vein draining this site occurred during the arterial phase. No other vascular anomalies were seen. The arteriographic findings in the lateral wall of the proximal ascending colon were interpreted as representing a localized arteriovenous communication. As a result of these findings, on hospital day 12, the patient underwent a right colectomy with ileotransverse colostomy. His postoperative course was uncomplicated and he was able to eat normally by postoperative day 5. He has continued stable for 6 months with no bleeding recurrence.

The surgical specimen was injected with 20 ml of Renografin 60 (diatrizoate meglumine and diatrizoate sodium injection) mixed with 2.5 ml of indigo carmine. The injection was carried out in the operating room with the specimen vessels isolated. The specimen radiograph was then compared with the previous angiographic findings and both radiographs were superimposed on the specimen to aid in the anatomic localization of the vascular anomaly.

The specimen consisted of a 30 cm portion of ascending colon including the cecum, vermiform appendix, and an attached 5 cm segment of the terminal ileum. Numerous petechial hemorrhages were present in the colonic mucosa. These were attributed to the intraoperative specimen isolation and resultant

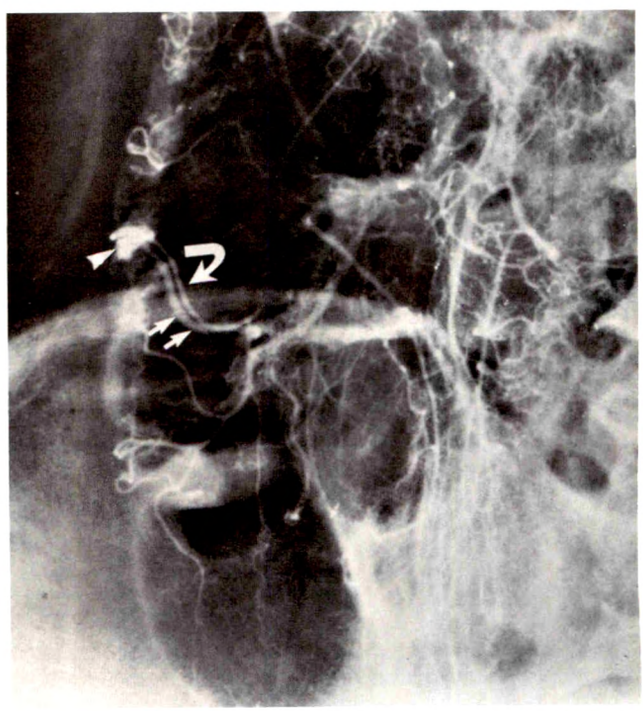


Fig. 1.—Arteriogram of ascending colon. *Arrowhead* indicates collection of arterioles; *curved arrow*, artery; *double arrows*, draining vein.

Received September 1, 1978; accepted after revision December 4, 1978.

[1] Department of Laboratories, Stamford Hospital, Shelburne Road and West Broad Street, Stamford, Connecticut 06902. Address reprint requests to G. M. Hollenberg.

[2] Department of Radiology, Stamford Hospital, Stamford, Connecticut 06902.

© 1979 American Roentgen Ray Society

0361–803X/79/1324–0666 $0.00

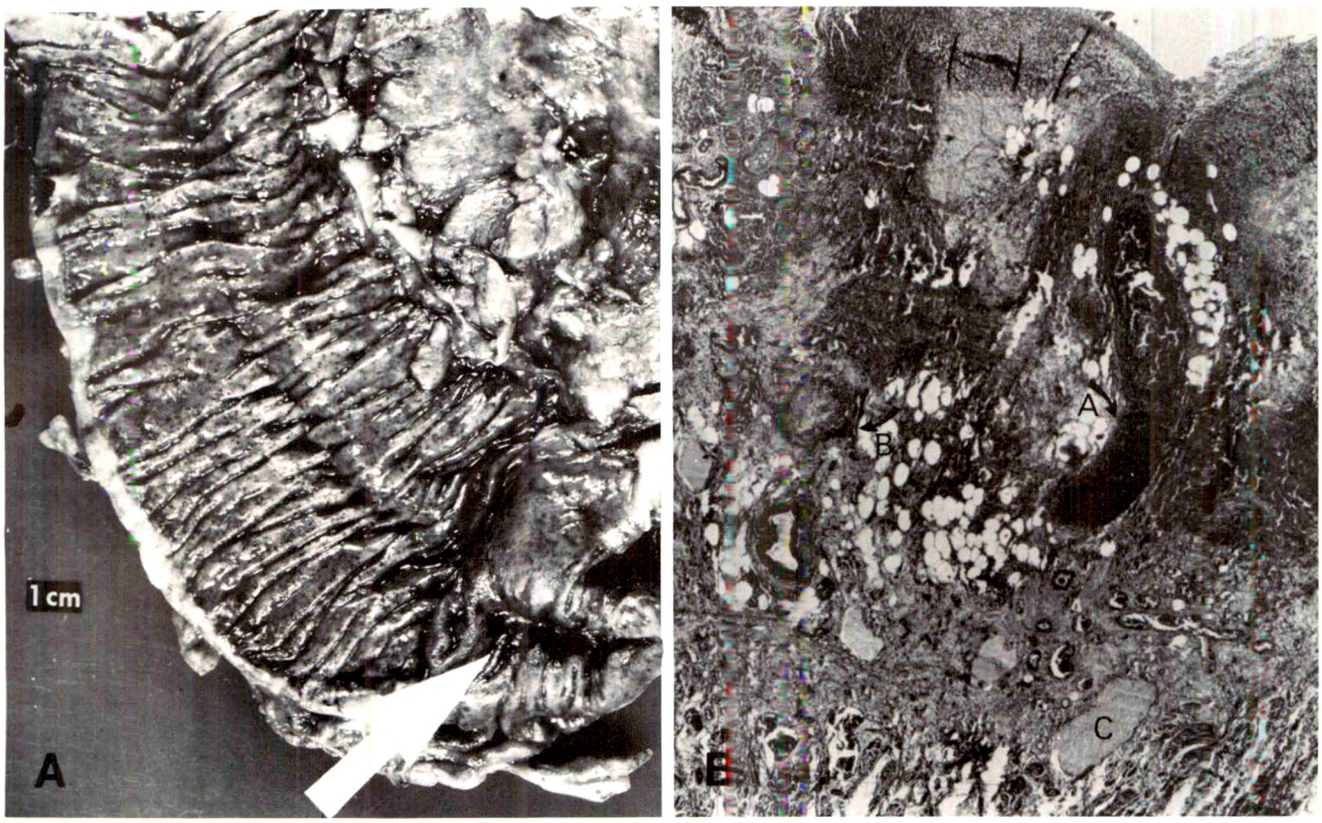


Fig. 2.—**A**, Resected ascending colon with cecal ulcer (*arrow*). **B**, Histology of ulcer showing thrombosed ectatic arteriole (A); arteriole with organizing thrombus (B); and dilated venule filled with contrast material (C). Elastic stain, ×20.

anoxia. In the area of the lateral proximal ascending colon overlying the site of the vascular malformation seen radiographically, a prominent mucosal ulcer was present. This ulcer was trenchlike, oriented longitudinally, and 3.1 cm long (fig. 2A). No other vascular malformations were found.

Sections of this ulcer showed an area of necrosis and hemorrhage involving the full thickness of the mucosa and submucosa to the level of the muscular wall of the colon (fig. 2B). The ulcer was permeated with polymorphonuclear leukocytes, lymphocytes, and red blood cells. Aside from vessels and some submucosal adipose tissue, few normal architectural features were retained. Arranged prominently within the ulcerated region were numerous large ectatic arterioles and veins. Some of the most ectatic arterioles were oriented with their long axes perpendicular to the ulcer's luminal surface. Thrombi ranging from acute to organizing were present in both dilated and nondilated arterioles. Some arterioles were filled either partially or completely with masses of red blood cells and fibrin while others contained occluding masses of organizing smooth muscle and connective tissue. An occasional arteriole revealed a completely organized subendothelial thickening. Dilated submucosal veins contained contrast material. The scattered petechial hemorrhages seen grossly were not associated with vascular malformations or direct arteriovenous communications. No cholesterol emboli were identified. The appendix and ileum were normal.

Discussion

Vascular malformations of the cecum and ascending colon are well known causes of lower intestinal hemorrhage in the elderly [1–12]. These lesions have been regarded as congenital [5], neoplastic [4], or acquired [8–12].

Although the origins are unknown, the vascular lesion and the gross and histologic findings are similar [2–12]. Gross anatomic findings are infrequent and often the absence of an obvious anatomic lesion presents a sampling problem to the pathologist. However, several reports have mentioned the presence of overlying mucosal erosions 0.1–1.0 cm in diameter [2, 5, 8–10, 12]. These erosions, if seen, may facilitate location of the underlying vascular lesion. Histologically the vascular malformations consist of ectatic veins, venules, capillaries, and occasionally arteries located in the colonic submucosa or mucosa and covered by a mucosal layer of variable thickness. Bleeding is thought to occur when this fragile system of vessels is somehow disrupted. In some of the reports associating vascular malformations with mucosal ulcerations, the presence of focal acute, organized intravascular, or partially extruded thrombi is also mentioned [2, 9, 10, 12]. Only one [9] comments on the etiologic relation between the mucosal ulcerations and the underlying, occasionally thrombosed, vascular malformations. These authors suggested that mucosal ischemia might result either from pressure created by large submucosal veins, thrombosis of submucosal arteries, or functional shunting of blood through mucosal capillaries. The actual arteriovenous communication seen angiographically

is rarely identified histiologically [2–12] and was not in our case.

Cholesterol emboli have occasionally been identified in arteries supplying the area of colonic vascular malformations [6–12]. The significance of these atheromatous emboli is in question; some believe them causative [6], others regard them as incidental [12]. None were identified in the present case.

Our case is believed to be the first of a large (greater than 3 cm) grossly obvious ulcer associated with an extensively thrombosed colonic vascular malformation. Whether trauma to the vascular malformation led to bleeding, ulceration, and secondary thrombosis or whether thrombosis itself in the intact vascular malformation was the primary event leading to ischemia and ulceration could not be determined. It may be that trauma as well as thrombosis and ischemia may be the final pathway in bleeding ulceration in some colonic vascular malformations.

Cecal erosions of undetermined etiology have been reported as causes of massive intestinal hemorrhage [13]. This case suggests that the existence of an underlying vascular malformation be sought in cases of otherwise unexplained colonic ulcerations. This may be facilitated by preoperative angiography or specimen angiography as well as exhaustive sectioning of the ulcer site.

The advisability of colonoscopy in the face of acute colonic bleeding is in question [13, 14]. In our case, no lesion was seen during colonoscopy and it is possible, although not proven, that trauma to the vascular malformation during the procedure (1 week prior to surgery) may have been an aggravating factor in ulceration.

ACKNOWLEDGMENT

We thank Drs. Walter J. Richar, Harvey L. Hecht, and Stuart A. King for assistance with preparation of this manuscript.

REFERENCES

1. Wholey MH, Bron KM, Haller JD: Selective angiography of the colon. *Surg Clin North Am* 45:1283–1291, 1965
2. Reuter SR, Bookstein JJ: Angiographic localization of gastrointestinal bleeding. *Gastroenterology* 54:876–883, 1968
3. Boss EG, Rosenbaum JM: Bleeding from the right colon associated with aortic stenosis. *Am J Dig Dis* 16:269–275, 1971
4. Upson JF, Bunnell I, Kokkinopoulis E: Hemangioma of the cecum: Diagnosis by angiography. *JAMA* 217:1104–1105, 1971
5. Whitehouse GH: Solitary angiodysplastic lesions in the ileocecal region diagnosed by angiography. *Gut* 14:977–982, 1973
6. Case records of the Massachusetts General Hospital (case 36, 1974). *N Engl. J Med* 291:569–575, 1974
7. Galloway SJ, Casarella WJ, Shinkin PM: Vascular malformation of the right colon as a cause of bleeding in patients with aortic stenosis. *Radiology* 113:11–15, 1974
8. Baum S, Athanasoulis CA, Waltman AC, Galdabini J, Shapiro R, Warshaw A, Ottinger LW: Angiodysplasia of the right colon as a cause of chronic gastrointestinal bleeding (abstr). *Gastroenterology* 68:862, 1975
9. Baer JW, Ryan S: Analysis of cecal vasculature in the search for vascular malformations. *AJR* 126:394–405, 1976
10. Moore JD, Thompson NW, Appelman HD, Foley D: Arteriovenous malformations of the gastrointestinal tract. *Arch Surg* 111:381–389, 1976
11. Skibba RM, Hartong WA, Mantz FA, Hinthorn DR, Rhodes JB: Angiodysplasia of the cecum: colonoscopic diagnosis. *Gastrointest Endosc* 22:177–179, 1976
12. Boley SJ, Sammartano BS, Adams A, DiBiase A, Kleinhaus S, Sprayregen S: On the nature and etiology of vascular ectasias of the colon. *Gastroenterology* 72:650–660, 1977
13. Corry RJ, Bartlett MK, Cohen RB: Erosions of the cecum a cause of massive hemorrhage. *Am J Surg* 119:106–110, 1970
14. Sugarbaker PH, Vineyard GC, Lewicki AM, Pinkus GS, Warhol MJ, Moore FD: Colonoscopy in the management of disease of the colon and rectum. *Surg Gynecol Obstet* 139:341–349, 1974

Third Ventricle Meningioma Mimicking a Colloid Cyst in a Child

YA-YEN LEE,[1] SHU-REN LIN,[1] AND FREDERICK A. HORNER[2]

Although meningiomas occur at any age, they are predominantly adult tumors. In a review of a 2,620 case series of intracranial tumors in childhood, the incidence of meningioma was estimated at 1.5% [1], in contrast to that of adults, which is around 10%–15% [2–5]. Intraventricular meningiomas are very rare. The major meningioma series, by Cushing and Eisenhardt [2], Olivecrona [3], and Simpson [4], with a total of 1,241 cases, showed that only 3% of the meningiomas arose within ventricles. In 1942, Abbott and Courville [6] reviewed 50 reported intraventricular meningiomas and found only four were in patients 10 years old or younger. Of the 50 meningiomas, 28 were in the left lateral ventricle, 15 were in the right lateral ventricle, and only two originated in the third ventricle. In these two third-ventricle meningiomas, one occurred in a 36-year-old woman, while the other occurred in an 11-year-old girl. Of particular interest is that most of these were either fibrous, fibroblastic, or psammomatous meningiomas.

In 1955, Heppner [7] reported two cases of third ventricle meningiomas in children, both located in the posterior third ventricle. Merten et al. [8] emphasized the increased frequency of calcification and higher incidence of location in the posterior fossa and within the ventricles of meningiomas in children and adolescents, but meningiomas originating in the third ventricle were not mentioned. A case of third ventricle meningioma with radiographic features of colloid cyst in a 10-year-old boy is reported here.

Case Report

M. G., a 10-year-old white boy, was in good health until 4½ months before admission when he began having occasional episodes of blurred vision with "black lines" after standing up quickly from a reclining position. One night in the month before admission, he was awakened by severe headache and abdominal pain, followed by nausea and vomiting. He was later awakened by severe stiffness and tenderness on the right side of the neck, and a private physician found bilateral papilledema without definite localizing signs. Later, he was transferred to Strong Memorial Hospital for further neurologic evaluation.

Neurologic examination revealed the patient was slightly ataxic. All the cranial nerves were intact. There was no definite motor or sensation deficit. The Romberg test was normal, but the patient had poor heel walking. Superficial and deep tendon reflexes were unremarkable. Babinski's sign was elicited on the right side. Thorough evaluation did not reveal evidence of neurofibromatosis.

Plain skull films showed separation of the sutures and increased digital markings, indicative of increased intracranial pressure. No definite intracranial calcifications were noted. CT demonstrated a 1.5 cm well circumscribed round mass in the region of the foramen of Monro associated with a marked degree of obstructive hydrocephalus (fig. 1A). A significant enhancement was noted after intravenous injection of contrast medium (fig. 1B). Calcification was noted in the choroid plexus of the lateral ventricles (fig. 1C). Cerebral angiography revealed a slightly hypertrophied distal posterior medial choroidal artery with a faint tumor blush in the region of the foramen of Monro (fig. 2). A colloid cyst was diagnosed preoperatively.

At right frontal craniotomy a tan-colored, 1.5 cm solid mass (fig. 3A), firmly attached to the anterior superior portion of the choroid plexus of the third ventricle, was found and completely removed. A meningioma of the meningothelial pattern with occasional psammoma bodies was verified histologically (fig. 3B). The postoperative course was essentially uneventful, except for an episode of questionable seizure.

Discussion

Although tumors arising from the anterior superior third ventricle are rare, they evoke interest both clinically and radiographically. Their symptoms result from obstructing the flow of the cerebrospinal fluid. Headache, vomiting, visual impairment, and acute intermittent papilledema are due to intermittent obstruction of the foramen of Monro. When the tumors become large, persistent obstructive hydrocephalus develops. Tumors considered in the differential diagnosis are: (1) colloid cyst, (2) meningioma, (3) ependymoma, and (4) choroid plexus papilloma.

Colloid cysts do not contain calcium; therefore, calcium in tumors in the region of the foramen of Monro virtually excludes the possibility of colloid cyst. Angiographically, the internal cerebral vein, as seen in the lateral view, may be flattened and displaced downward in its posterior third due to dilated lateral ventricles. The anterior third of the internal cerebral vein may be elevated, curving concavely downward around the cyst [9]. In our case, the anterior third of the internal cerebral vein was slightly elevated, but was not the typical humping described by others [9]. Although a faint choroid blush and the hypertrophied distal posterior choroidal arteries can be seen in the colloid cyst [10], it is probably more common in other third ventricle tumors, such as meningiomas (as in our case). A well defined oval or round mass of about 2.5 cm or less with a smooth margin, and associated with moderate to marked dilatation of the lateral ventricle, is always present on the air study [11–14]. CT will demonstrate a smooth mass with a density slightly greater than brain tissue. A significant enhancement of the lesion will be shown after contrast

Received October 13, 1978; accepted after revision December 27, 1978.

[1]Department of Radiology, University of Rochester Medical Center, 601 Elmwood Avenue, Rochester, New York 14642. Address reprint requests to S. R. Lin.

[2] Departments of Pediatrics and Neurology, University of Rochester Medical Center, Rochester, New York 14642.

© 1979 American Roentgen Ray Society

0361–803X/79/1304–0669 $0.00

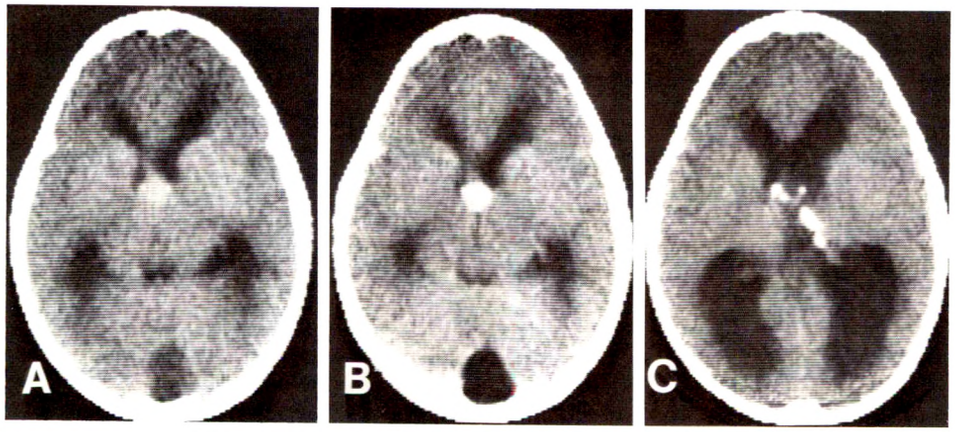


Fig. 1.—At level of foramen of Monro. **A**, Without contrast, mass with density slightly higher than normal brain tissue. **B**, With contrast enhancement, lesion is well circumscribed 1.5 cm mass. **C**, At 1 cm higher, calcification in lateral ventricles associated with marked obstructive hydrocephalus.

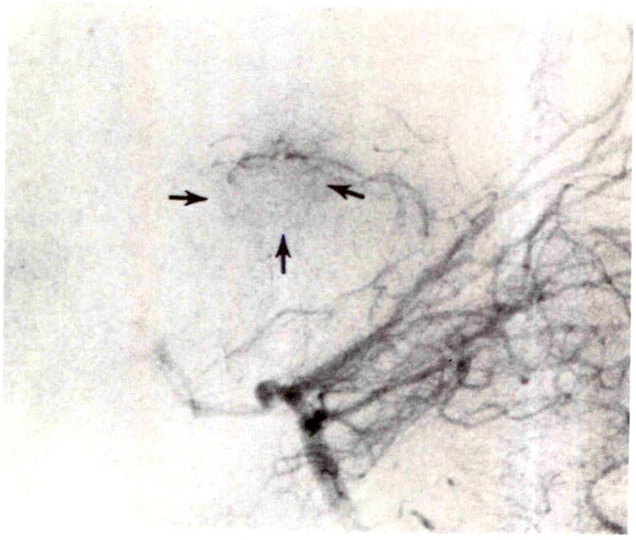


Fig. 2.—Lateral view, late arterial phase. Slightly hypertrophied distal medial posterior choroidal artery with faint tumor blush (*arrows*).

material is given [10, 11, 15, 16]. The combined findings in the air study and CT are virtually pathognomonic of a colloid cyst.

Ependymomas, common tumors in childhood, are distinguishable from colloid cysts. Most are located in the fourth and lateral ventricles and rarely in the third ventricle. The surface of these tumors is lobulated and tufted, resembling cauliflower [5]. CT often shows enhanced solid masses with a small central lucency [17].

Choroid plexus papillomas of the third ventricle are very rare [5, 18]. They are usually attached superiorly to the roof of the ventricle, as are colloid cysts. However, in contrast to the well circumscribed colloid cysts [18, 19], these tumors tend to be lobulated, and appear as irregular frondlike intraventricular masses with significant enhancement on CT [17]. In addition, calcification may be seen in both ependymomas and choroid plexus papilloma.

In our case, CT findings most resembled a colloid cyst. The calcification of choroid plexus of the lateral ventricles was believed to be unrelated to the tumor. Such calcification is very unusual in a patient this age, and its etiology remains unclear. Thorough evaluation failed to reveal evidence of neurofibromatosis. At surgery, a well circumscribed mass arising from the anterior roof of the third ventricle was found and a meningioma was verified.

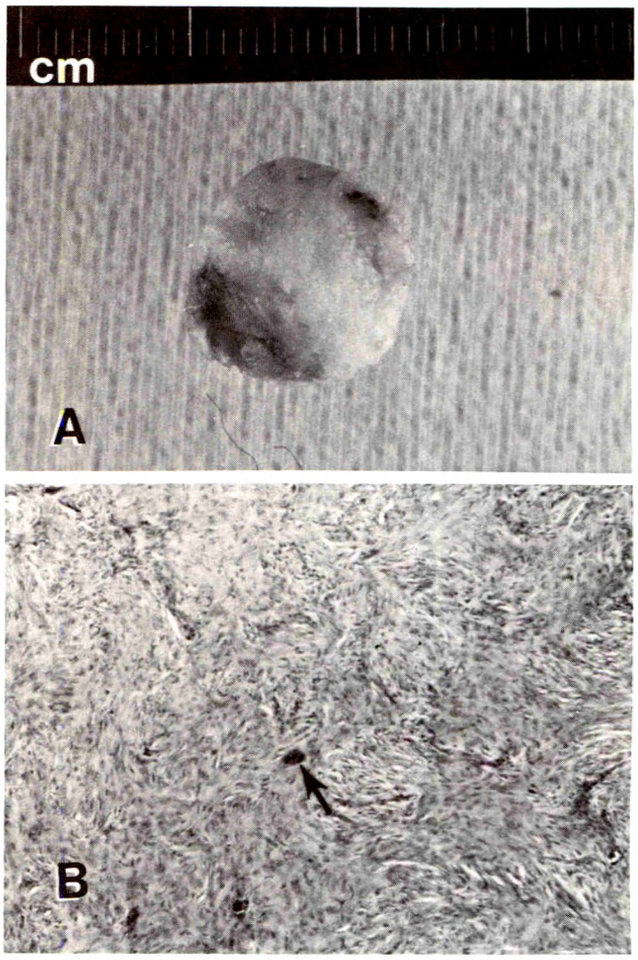


Fig. 3.—**A**, Solid mass. **B**, Meningioma of the meningothelial pattern. Psammoma body (*arrow*). (Low power magnification.)

REFERENCES

1. Jefferson G, Jackson H: Tumors of the lateral and of the third ventricles. *Proc R Soc Med* 32:1105–1137, 1939
2. Cushing H, Eisenhardt L: *Meningiomas. Their Classification, Regional Behavior, Life History, and Surgical End Results*. Springfield, Thomas, 1938
3. Olivecrona H: The parasagittal meningiomas. *J Neurosurg* 4:327–341, 1947
4. Simpson D: The recurrence of intracranial meningioma after surgical treatment. *J Neurol Neurosurg Psychiatry* 20: 22–39, 1957
5. Zülch KJ: *Brain Tumors: Their Biology and Pathology*. New York, Springer, 1965
6. Abbott KH, Courvzlle CB: Intraventricular meningiomas. Review of the literature and report of two cases. *Bull Los Angeles Neurol Soc* 7:12–28, 1942
7. Heppner F: Meningiomas of the third ventricle in children. Review of the literature and report of two cases with uneventful recovery after surgery. *Acta Neurol Psychiatr Belg* 30:472–481, 1955
8. Merten DF, Gooding CA, Newton TH: The radiologic features of meningiomas in childhood and adolescence. *Pediatr Radiol* 2:89–96, 1974
9. Batnitzky S, Sarwar M, Leeds NE, Schechter MM, Azar-Kia B: Colloid cysts of the third ventricle. *Radiology* 112:327–341, 1974
10. Sackett JF, Messina AV, Petito CK: Computed tomography and magnification vertebral angiotomography in the diagnosis of colloid cysts of the third ventricle. *Radiology* 116: 95–100, 1975
11. Lee KF, Lin SR: *Neuroradiology of Sellar and Juxtasellar Mass Lesions*. Springfield, Ill., Thomas, 1979
12. Little JK, MacCarty CS: Colloid cysts of the third ventricle. *J Neurosurg* 40:230–235, 1974
13. Sage MR, McAllister VL, Kendall BE, Bull JWD, Moseley IF: Radiology in the diagnosis of colloid cysts of the third ventricle. *Br J Radiol* 48:708–723, 1975
14. Taveras JM, Wood EH: *Diagnostic Neuroradiology*, 2d ed. Baltimore, Williams & Wilkins, 1976, pp 434–437
15. Davis DO: CT in the diagnosis of supratentorial tumors. *Semin Roentgenol* 12:97–100, 1977
16. Osborn AG, Wing SD: Thin-section computed tomography in the evaluation of third ventricular colloid cyst. *Radiology* 124:257–258, 1977
17. Naidich TP, Lin JP, Leeds NE, Pudlowski RM, Naidich JB: Primary tumors and other masses of the cerebellum and fourth ventricle. Differential diagnosis by computed tomography. *Neuroradiology* 14:153–174, 1977
18. Rovit RL, Schechter MM, Chodroff P: Choroid plexus papillomas: observation on radiographic diagnosis. *AJR* 110: 608–617, 1976
19. Thompson JR, Harwood-Nash DC, Fitz CR: The neuroradiology of childhood choroid plexus neoplasms. *AJR* 118: 116–133, 1973

CT Simulation of Cerebellopontine Tumor by Tortuous Vertebrobasilar Artery

KISHORE G. RAO[1] AND RAY M. WOODLIEF[1]

Cerebellopontine angle masses are usually due to tumors, most often acoustic neuromas. However, uncommonly the cause is an aneurysm or arteriovenous malformation. Rarely, an elongated vertebrobasilar artery may extend into the angle, causing cranial nerve symptoms. A case of a tortuous vertebrobasilar artery simulating a cerebellopontine angle tumor on computed tomography (CT) is reported here.

Case Report

A 55-year-old black man had right-side hearing loss for 6–7 years and low-pitched tinnitus for 3 months. There was no vertigo or facial spasm. Weber's test showed decreased hearing on the right and the Rinne's test was normal bilaterally. Neurologic examination was negative with no nystagmus and normal cerebellar functions. Audiologic evaluation showed very mild decreased sensorineural hearing loss and very poor speech discrimination in the right ear.

Tomography of the internal auditory canals showed widening of the porus acusticus on the right (fig. 1). CT showed a low density area in the right cerebellopontine angle with an adjacent discrete semicircular high density area seen only on enhanced CT (fig. 2). This was interpreted as a mass in the right cerebellopontine angle, probably representing a neoplasm with central and lateral necrosis allowing enhancement of the medial rim of the mass. Because of the possibility that this might be a vascular lesion, angiography was performed. Left vertebral arteriography showed a very tortuous vertebrobasilar artery extending into the right internal auditory canal (fig. 3).

Discussion

The differential diagnoses of cerebellopontine angle masses are wide ranging. According to Kieffer et al. [1], acoustic neuromas account for about 80% of the cerebellopontine angle masses. Another 10% are caused by meningiomas. The remaining 10% are accounted for by such diverse entities as epidermoid tumors, chondromas, arachnoid cysts, intraaxial tumors growing in an exophytic manner, arteriovenous malformations, aneurysms, or tortuous vertebral, basilar, or anterior inferior cerebellar arteries. Angiography is important in the diagnostic workup to exclude a vascular abnormality.

Involvement through direct pressure effect on cranial nerves has been caused either by an aneurysm or tortuous artery. Kramer and Eckman [2] reported three cases of hemifacial spasm associated with redundancy of the vertebral artery in 1972. That same year, three more cases of a tortuous vertebrobasilar system causing cranial nerve signs were reported by Kerber et al. [3]. In their three cases also, the main clinical feature was unilateral facial twitches. The facial twitches seem to be due to the medial location of the motor root of the facial nerve after it emerges from the pons. Consequently, lateral deviation of the vertebral or basilar arteries results in early involvement of the motor root of the facial nerve. Our patient's partial deafness is presumably due to vascular pressure on the eighth nerve.

CT has recently been emphasized as an extremely useful method in the diagnosis of cerebellopontine and internal auditory canal lesions. Several authors suggest it obviates the need for some or most of the traditional diagnostic examinations [4–6].

Positive contrast cerebellopontine angle cisternography is probably the most sensitive method of evaluating a suspected acoustic neuroma [4]. Contrast enhanced CT, though slightly less sensitive, has the advantage of being relatively noninvasive. However, information on vascular origin or supply of the mass can only be obtained by angiography. Thus, an enhancing cerebellopontine mass on CT, which is atypical for a tumor, requires angiography to exclude an aneurysm, arteriovenous malformation, or tortuous vessel, as evidenced by our case.

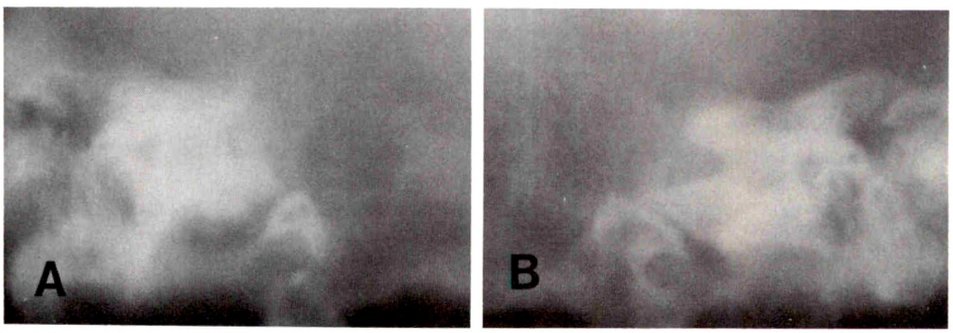


Fig. 1.—**A**, Right internal auditory canal. Widening of porus acusticus from erosion by adjacent tortuous vertebrobasilar artery. **B**, Normal left internal auditory canal.

Received August 28, 1978; accepted after revision December 4, 1978.

[1] Department of Radiology, Veterans Administration Hospital, 1201 Broad Rock Road, Richmond, Virginia 23249. Address reprint requests to K. G. Rao.

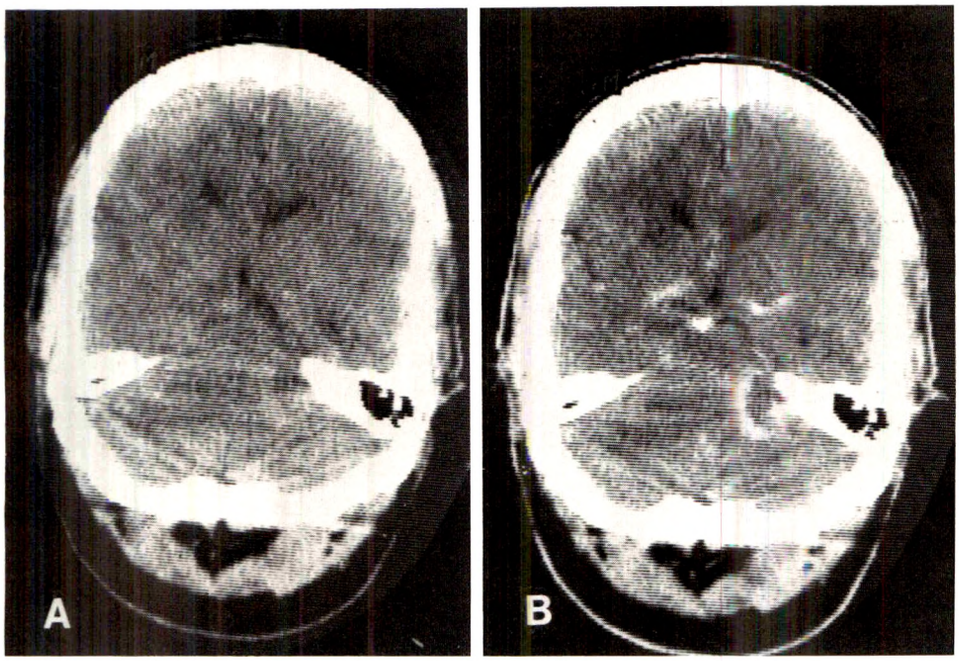


Fig. 2.—**A**, Unenhanced. Small low density area in right cerebellopontine angle. **B**, Enhanced. Sharp curvilinear high density zone just medial to low density area represents tortuous vertebrobasilar artery (not edge enhancement).

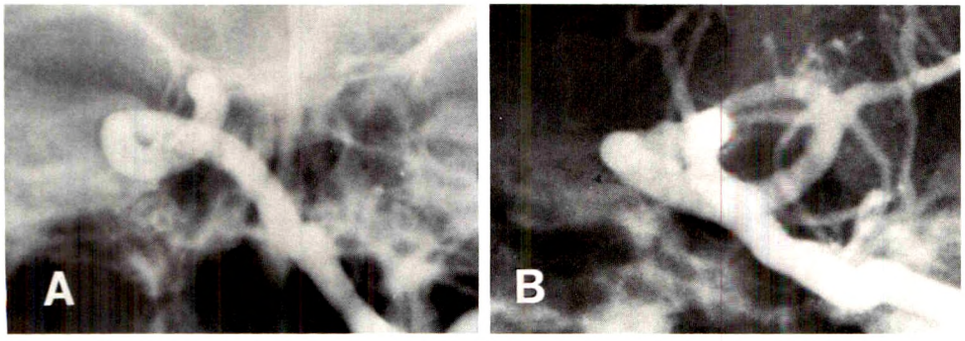


Fig. 3.—Tortuous artery extends into right internal auditory canal.

REFERENCES

1. Kieffer SA, Binet EF, Gold LHA: Angiographic diagnosis of intra- and extra-axial tumors in the cerebellopontine angle. *AJR* 124:297–309, 1975
2. Kramer RA, Eckman PB: Hemifacial spasm associated with redundancy of the vertebral artery. *AJR* 115:133–136, 1972
3. Kerber CW, Margolis MT, Newton TH: Tortuous vertebrobasilar system: a cause of cranial nerve signs. *Neuroradiology* 4:74–77, 1972
4. Dubois PJ, Drayer BP, Bank WO, Deeb ZL, Rosenbaum AE: An evaluation of current diagnostic radiologic modalities in the investigation of acoustic neurilemmomas. *Radiology* 126:173–179, 1978
5. Gyldensted C, Lester J, Thompsen J: Computer tomography in the diagnosis of cerebellopontine angle tumors. *Neuroradiology* 11:191–197, 1976
6. Messina AV: Computerized tomography of the head. *Arch Otolaryngol* 102:566–567, 1976

Anomalous Origin of Posterior Choroidal Artery from Basilar Artery

LINCOLN L. BERLAND[1] AND VICTOR M. HAUGHTON[1]

Anatomic variations of the circle of Willis are common. Posterior cerebral arteries develop late in embryologic life and have numerous variations [1]. We demonstrated an anomalous origin of the medial posterior choroidal artery by angiography. Its embryogenesis and significance are discussed.

Case Report

A 52-year-old woman was admitted to the Veteran's Administration Hospital, Wood, Wisconsin with trigeminal neuralgia on the left side. Selective left internal carotid and left vertebral angiography was performed. The left posterior cerebral artery originated from the internal carotid artery. The posterior cerebral arteries were not opacified from the basilar. One medial posterior choroidal artery was a branch of the basilar artery (fig. 1). Both vertebral arteries were small. There were no aneurysms and no other anomalous vessels.

Discussion

In the 40 mm embryo, the trunk of the mesencephalic and diencephalic vessels form the stem of the future posterior cerebral artery. The posterior choroidal arteries are branches of the diencephalic trunk. In the adult, the posterior cerebral artery (whether it arises from the internal carotid artery or the basilar artery) normally gives origin to the posterior choroidal arteries [1, 2]. In about 40% of cases, the origin of the medial posterior choroidal artery from the posterior cerebral artery is proximal to the posterior communicating artery [2, 3]. In the embryo, if the posterior choroidal artery origin is medial to the posterior communicating artery and the midposterior cerebral artery involutes, then the posterior choroidal artery will become a branch of the basilar artery (fig. 2). Bilateral origin of the posterior cerebral artery from the internal carotid artery with absent poste-

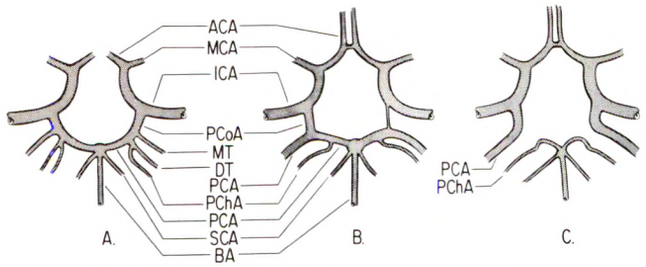


Fig. 2.—Development of anomalous posterior choroidal artery. **A**, 40 mm embryo. Lateral and medial posterior choroidal arteries (PChA) are branches of diencephalic trunk (DT). **B**, Adult. Posterior cerebral artery (PCA), which develops from diencephalic and mesencephalic (MT) trunks, may be branch of either internal carotid (ICA) or basilar artery (BA). Medial and lateral posterior choroidal arteries are branches of posterior cerebral artery unless (**C**) part of diencephalic trunk involutes after communication is developed between the diencephalic trunk and the basilar artery. (ACA = anterior cerebral artery; MCA = middle cerebral artery; PCoA = posterior communicating artery; SCA = superior cerebellar artery).

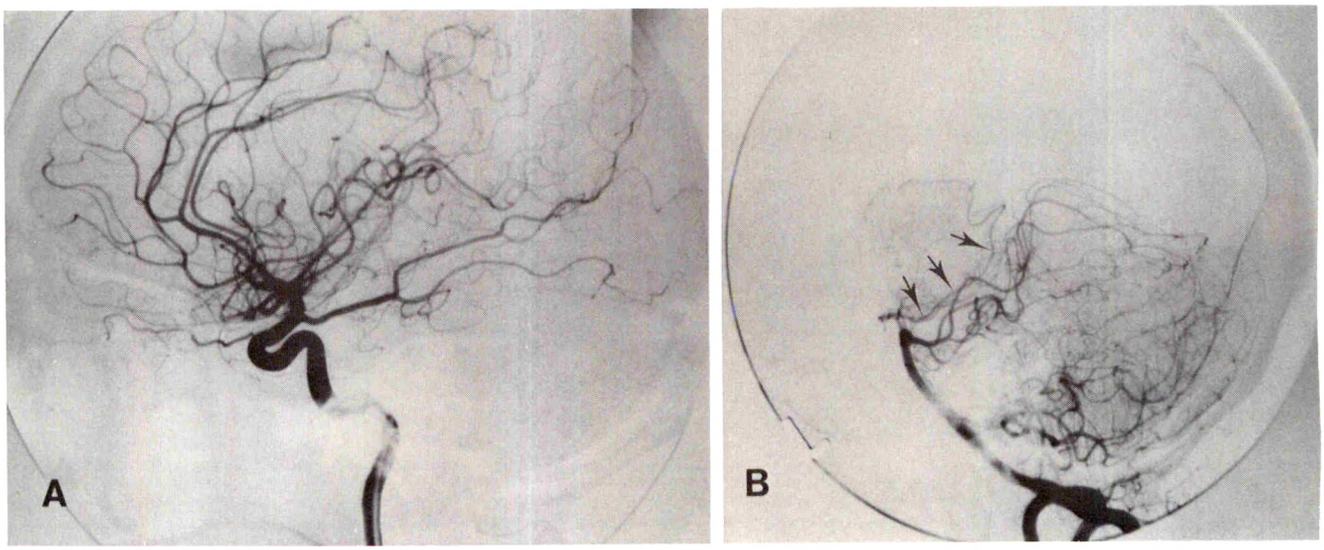


Fig. 1.—Anomalous posterior choroidal arteries. **A**, Left internal carotid artery injection. Posterior cerebral artery arises from internal carotid artery. **B**, Vertebral artery injection. Medial posterior choroidal artery (*arrows*) originates from basilar artery.

Received September 5, 1978; accepted December 4, 1978.

[1] Department of Radiology, Veterans Administration Hospital, Wood, Wisconsin and Medical College of Wisconsin, Milwaukee County General Hospital, 8700 West Wisconsin Avenue, Milwaukee, Wisconsin 53226. Address reprint requests to L. L. Berland.

© 1979 American Roentgen Ray Society

0361-803X/79/1324-0674 $0.00

rior communicating artery (fetal posterior cerebral artery) occurs in 0.25% of cases [2]. Therefore, anomalous origin of the posterior choroidal artery from the basilar artery occurs in less than 0.25%. In our case, the findings are incidental to the patient's clinical problem. Trigeminal neuralgia and hemifacial spasm may be associated with cranial nerve compression by various vessels [4]. However, to our knowledge, the anomalous posterior choroidal artery is not associated with trigeminal neuralgia.

In the presence of the anomalous posterior choroidal artery, a vertebral artery injection is necessary to demonstrate posterior choroidal circulation, despite good filling of the posterior cerebral artery from the carotid injection. Also, the anomalous posterior choroidal artery arising from the basilar artery might provide collateral circulation in cases of carotid or basilar artery occlusion.

REFERENCES

1. Lie TA: *Congenital Anomalies of the Carotid Arteries*. Amsterdam, Royal Van Gorcum, 1968, pp 4–15,
2. Newton T, Potts OG: Angiography, in *Radiology of the Skull and Brain*, vol 2, book 2, St. Louis, Mosby, 1974, pp 1542–1547, 1561–1564
3. Saeki N, Rhoton A: Microsurgical anatomy of the upper basilar artery and the posterior circle of Willis. *J Neurosurg* 36:563–578, 1977
4. Janetta EJ, Abbasy M, Maroon J, Ramos FN Albin MS: Etiology and definitive microsurgical treatment of hemifacial spasm. *J Neurosurg* 47:321–328, 1977

Xenon in the Gastric Fundus: Potential Pitfall in Ventilation Scan Interpretation

WILLIAM J. MARX,[1,2] JOHN V. COURTNEY,[1] HEBER MacMAHON,[1] AND KARIM REZAI-ZADEH[1,3]

Ventilation and perfusion scanning are well established diagnostic procedures used extensively for early detection of pulmonary embolism in adults [1, 2]. Lung scanning to demonstrate pulmonary emboli in children has been somewhat limited; however, it has been useful in assessing conditions such as unilateral hyperlucent lung, obstructive emphysema, bronchiectasis, and cystic fibrosis [3]. This report describes a potential pitfall of xenon-133 ventilation scan interpretation: a left lower lobe ventilation washout retention artifact caused by swallowed ^{133}Xe gas.

Case Report

A 2 1/2-year-old black boy was admitted to University of Chicago Hospitals and Clinics for evaluation of a chronic respiratory problem. He had numerous episodes of recurrent pneumonia and a few episodes of hemoptysis.

Chest radiography showed infiltrates and atelectasis of the right lower lobe. Despite this collapse consolidation, no overaeration of the left lung or shift of the mediastinum was seen. The rest of both lungs was normal. Bronchography revealed saccular and cylindrical bronchiectasis of the right lower lobe. The left lung was not studied.

A ^{133}Xe ventilation lung scan and ^{99m}Tc MAA perfusion lung scan showed a matched ventilation/perfusion defect in the right lung base posteriorly, corresponding with the findings on chest radiography and bronchography (fig. 1). However, delayed washout in the area of the left lower lobe was also seen, which was inconsistent with the patient's clinical presentation and other radiographic data. Swallowed ^{133}Xe gas in the fundus of the stomach was the most likely cause of this apparent abnormality, and an additional anterior abdominal scan in the 20° supine Trendelenburg position confirmed the presence of radionuclide within the stomach (fig 2).

Discussion

Lung scanning is an excellent method of delineating pulmonary ventilation and perfusion patterns. The procedures are relatively noninvasive and easy to perform in a cooperative patient. Crying during the examination and subsequent gas swallowing may be expected in infants and in young or uncooperative children. Single breath views may be virtually unobtainable, but equilibrium and washout scans can be made. If washout delays are seen in the area of the left lung base, swallowed ^{133}Xe gas within the stomach must be excluded before

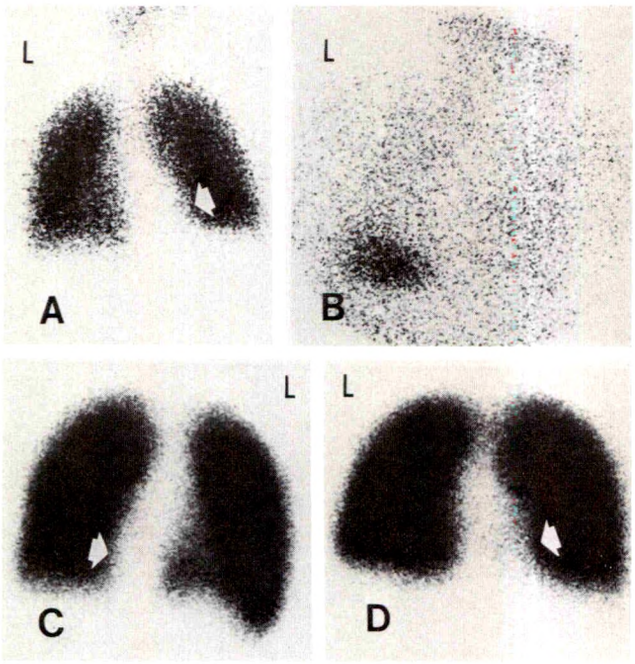


Fig. 1.—^{133}Xenon ventilation (**A** and **B**) and ^{99m}Tc MAA perfusion (**C** and **D**) lung scan images show matched ventilation and perfusion abnormality at right lung base (*arrows*). Swallowed gas in fundus of stomach simulates pulmonary Xenon retention.

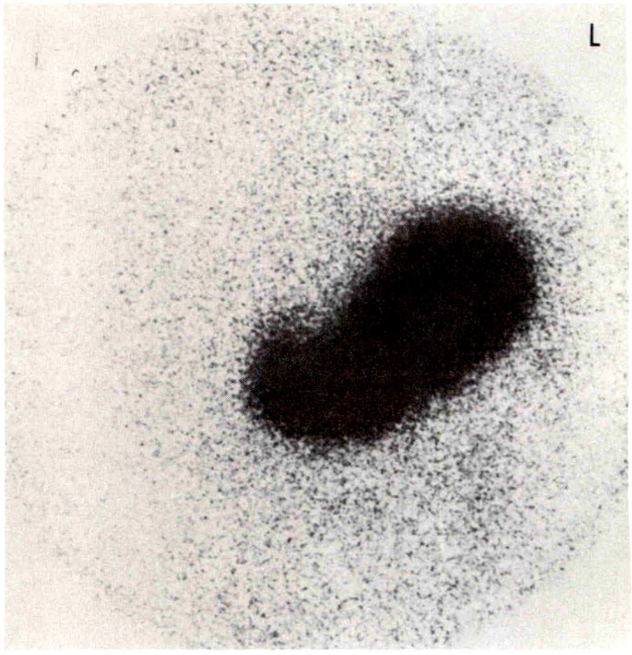


Fig. 2.—Supine anterior abdominal scan confirms ^{133}Xenon gas within stomach.

Received July 25, 1978; accepted after revision December 8, 1978.

[1] Department of Radiology, University of Chicago, 950 East 59th Street, Chicago, Illinois 60637.

[2] Department of Radiology, Swedish American Hospital, Rockford School of Medicine, University of Illinois, 1400 East Charles Street, Rockford, Illinois 61108. Address reprint requests to W. J. Marx.

[3] Present address: Section of Nuclear Medicine, Tehran Clinic, Shah Abbas Avenue, Tehran, Iran.

© 1979 American Roentgen Ray Society

0361–803X/79/1324–0676 $0.00

obstructive pulmonary disease can be diagnosed in either children or adults. In suspected ^{133}Xe swallowing during an erect scan, a supine anterior abdominal view will confirm the diagnosis. An artifact simulating right lower lobe washout retention caused by uptake of ^{133}Xe by a fatty liver has also been reported [4, 5].

REFERENCES

1. Secker-Walker RH, Siegel BA: The use of nuclear medicine in the diagnosis of lung disease. *Radiol Clin North Am* 11: 215–241, 1973
2. Farmelant M, Trainor JC: Evaluation of a ^{133}Xe ventilation technique for diagnosis of pulmonary disorders. *J Nucl Med* 12:586–590, 1971
3. Pendarvis BC, Swischuk LE: Lung scanning in the assessment of respiratory disease in children. *Radiology* 107:313–321, 1969
4. Bianco JA, Shafer RB: Implications of liver activity associated with ^{133}Xe ventilation lung scans. *Clin Nucl Med* 3: 176–178, 1978
5. Sutherland JB, McCarthy DS, Mark RJ, Thorlakson TK: ^{133}Xe uptake by fatty livers. *J Can Assoc Radiol* 29:82–84, 1978

Congenital Pseudarthrosis of the Clavicle: Report of Three Cases

GORDON MANASHIL[1] AND SAMUEL LAUFER[2]

Congenital pseudarthrosis of the clavicle is a rare benign condition with only one report in the radiologic literature [1]. There have been 107 case reports of this entity, although it is probably much more common than the literature suggests. Three additional cases are reported here, and the clinical, radiologic, and surgical spectrum of congenital pseudarthrosis is reviewed.

Case Reports

Case 1

A newborn boy, with no history of birth trauma and a product of a normal pregnancy and delivery, was referred to the x-ray department for chest examination because of a grade II out of VI systolic ejection murmur. Physical examination was normal except for the cardiac murmur and a palpable bump over the right clavicle. There was no evidence of tenderness, swelling, or restriction of motion in the right clavicle.

Chest radiography (fig. 1) revealed findings typical of congenital pseudarthrosis of the clavicle with overriding of clavicular fragments. The sternal segment was seen above the clavicular segment.

Case 2

A 2-year-old girl, product of a normal pregnancy and delivery, had a visible bump at the midportion of her right clavicle and a diagnosis of fracture was made. The parents stated that the child had never been uncomfortable on palpation over this bump, and there was full unrestricted range of motion of the right upper extremity. The child continued to have motion at the midportion of her clavicle, although the area was very prominent on abduction of the right shoulder. Right shoulder radiography revealed changes typical of congenital pseudarthrosis. Diagnosis of congenital pseudarthrosis of the clavicle was later made when the child was seen by her physician for a totally unrelated orthopedic problem (fig. 2). No treatment was necessary.

Case 3

A 10-day-old infant was seen for multiple tetramelic deformities consisting of syndactyly and clefts. Family history was negative for similar anomalies, and there was no history of teratogenic agents during pregnancy nor other abnormalities of pregnancy or delivery. The referring orthopedist's diagnosis of congenital pseudarthrosis of the right clavicle was based on a palpable mass at the midportion of the clavicle; the child was asymptomatic on shoulder motion. Subsequent radiography showed the characteristic findings (fig. 3).

Discussion

Congenital pseudarthrosis of the clavicle was first described and classified as an entity distinct from cleidocranial dysostosis by Fitzwilliams in 1910 [2]. Since then, most of the case reports have been in the orthopedic literature, with only one reference in the radiographic literature [3–5].

The entity is extremely interesting in that it almost always occurs on the right side of the patient. In 10%, involvement is bilateral [3]. There have been three cases of left-side congenital pseudarthrosis, but one of these

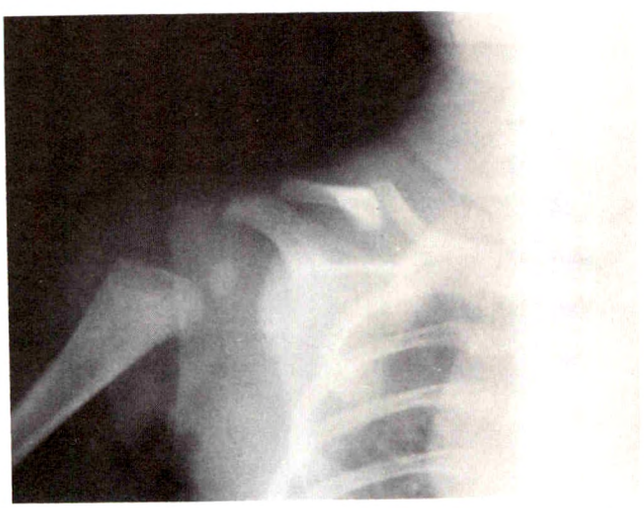


Fig. 1.—Case 1, newborn. Pseudarthrosis of right clavicle with sternal segment above clavicular segment.

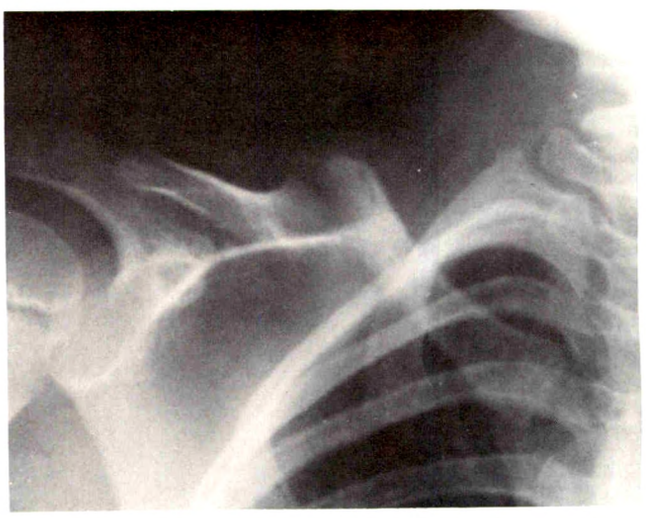


Fig. 2.—Case 2, 2-year-old. Ends of bone are bulbous in older patients, but no callus is present.

Received August 21, 1978; accepted after revision December 11, 1978.

[1] Department of Radiology, Monmouth Medical Center, Long Branch, New Jersey 07740. Present address: Department of Radiology, Desert Hospital, P. O. Box 1627, Palm Springs, California 92262. Address reprint requests to G. Manashil.

[2] Department of Orthopedics, Monmouth Medical Center, Long Branch, New Jersey 07740.

© 1979 American Roentgen Ray Society

0361-803X/79/1324-0678 $0.00

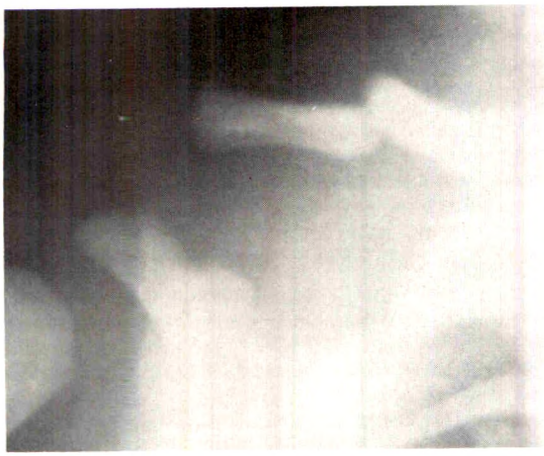


Fig. 3.—Case 3, newborn. Right clavicle has findings typical of congenital pseudarthrosis. Sternal segment overlies clavicular segment.

had associated dextrocardia [3]. The reason for the predominant right-side involvement is unclear, but several theories have been advanced. Lloyd-Roberts et al. [6] believe there is a relation between high right subclavian artery and pressure changes on the right side of the clavicle due to either cervical ribs on the right side or a high right subclavian artery itself.

The etiology of congenital pseudarthrosis of the clavicle is not clear. Fracture is an unlikely possibility because redness, tenderness, and a history of birth trauma are almost always absent. Usually there is no family history elicited, although one-third of Gibson's and Carroll's [5] 27 patients did have a family history. If in fact a family history can be elicited, the disorder is believed to be inherited as a Mendelian recessive gene.

In examining the embryology of the clavicle, some clues as to a possible etiology are found. The clavicle is the first bone to ossify in the human body at 5–6 weeks [7]. Some authors [8, 9] suggest that there are two centers of primary ossification of the clavicle, and that the failure of these two centers to coalesce gives rise to this condition. Other authors [5] claim that there is only one center of ossification of the clavicle, and the formation of pseudarthrosis is due to improper bony reabsorption of this center.

Regardless of the etiology of congenital pseudarthrosis of the clavicle, clinical diagnoses are usually quite similar. Diagnosis is usually made at birth or several months later. The patient's family notices a lump of increasing size, which is described as a prominent spike under the skin in the midportion of the clavicle. The most significant clinical feature is the absence of pain, which is critical to differentiation from traumatic nonunion. In traumatic nonunion, pain is the predominant feature [3]. Occasionally, there is some discomfort from activity, which is another reason the patient seeks medical help. A constant physical finding in congenital pseudarthrosis is that the sternal segment always overlies and is above the acromial segment. Café au lait spots are not a feature of congenital pseudarthrosis, although one case report indicated several spots with no other stigmata of neurofibromatosis. The absence of other congenital anomalies is also a constant finding in clinical evaluation of these patients. Case 3 in our series is quite atypical in that there were several teratogenic defects.

Radiographic diagnosis of pseudarthrosis of the clavicle is easy. The middle one-third of the clavicle is always involved, and the condition is usually close to the junction of the clavicle and the lateral third. The segments are not in continuity and the ends of the bone are enlarged. There is no callus present and no reactive bone. As mentioned before, the medial segment always overlies the lateral segment.

Differential diagnoses of congenital pseudarthrosis of the clavicle are primarily cleidocranial dysostosis and posttraumatic pseudarthrosis. Cleidocranial dysostosis usually affects other bones and midline structures. There are skull defects, bilateral clavicular defects, pelvic defects, and a very strong family history. Posttraumatic pseudarthrosis is a less distinct differential diagnosis. This entity is always painful; there is always tenderness on pressure and on motion of opposing fracture fragments [3]. Radiography of posttraumatic pseudarthrosis usually shows exuberant callus and the ends of the bone are quite bulbous.

The gross pathologic findings of congenital pseudarthrosis are constant. The ends of the two bone segments are covered by cartilage and often separated by fibrous tissue. There are no pathologic features of neurofibromatosis or fibrous dysplasia.

Surgical treatment of congenital pseudarthrosis is straightforward, consisting of excision of the cartilaginous cap, alignment of the fragments, and occasionally bone grafting or internal fixation. At least one-half of the cases of congenital pseudarthrosis of the clavicle are asymptomatic and need no further treatment.

REFERENCES

1. March HC: Congenital pseudarthrosis of the clavicle. *J Can Assoc Radiol* 19:167–169, 1968
2. Fitzwilliams DCL: Hereditary cranio-cleido-dysostosis. *Lancet* 2:1466–1475, 1910
3. Ahmadi B, Steel HH: Congenital pseudarthrosis of the clavicle. *Clin Orthop* 126:130–134, 1977
4. Chung SMK, Nissenboum MM: Congenital and developmental defects of the shoulder. *Orthop Clin North Am* 6: 381–392, 1975
5. Gibson DA, Carroll N: Congenital pseudarthrosis of the clavicle. *J Bone Joint Surg* [*Br*] 52:629–643, 1970
6. Lloyd-Roberts GC, Apley AG, Owen R: Reflection upon the etiology of congenital pseudarthrosis of the clavicle. *J Bone Joint Surg* [*Br*] 57:24–29, 1975
7. Hamilton WJ: *Human Embryology*, 2nd ed. Baltimore, Williams & Wilkins, 1952, p 349
8. Mall FP: On ossification centers in human embryos less than 100 days old. *Am J Anat* 5:433–458, 1906
9. Wall JJ: Congenital pseudarthrosis of the clavicle. *J Bone Joint Surg* [*Br*] 52:1003–1009, 1970

Mucocele of the Petrous Temporal Bone

ANNE G. OSBORN[1] AND JAMES L. PARKIN[2]

Mucoceles result from the accumulation of secretions in an obstructed sinus. Mucoceles of the frontal and ethmoidal sinuses are not uncommon, but are rarely located in the maxillary or sphenoidal sinuses [1–3]. While sphenoid sinus mucocele eroding the petrous temporal bone has been described [4, 5], mucocele originating within the petrous apex itself has not been reported. The case presented here adds mucocele to the extensive list of lesions that can cause a lytic defect in the petrous temporal bone.

Case Report

A 38-year-old woman had a 6 month history of roaring tinnitus and left-side hearing loss without otorrhea or vertigo. Otologic and neurologic examinations were normal except for markedly decreased left-side response to ice water calorics. Audiometry revealed a 50–60 dB left-side sensorineural hearing loss. Plain films and temporal bone tomography demonstrated a 2.5 cm lytic lesion with a surrounding sclerotic rim in the left petrous apex (fig. 1). CT scan showed no extension into the posterior fossa or cerebellopontine angle cistern. Magnification-subtraction left carotid and vertebral angiography and cerebellopontine angle cisternography were normal.

Repeat audiometry 6 months later demonstrated progressive sensorineural hearing loss. Calorics showed complete absence of left-side labyrinthine function.

A transcochlear petrous apetectomy, cochlear resection, and complete mastoidectomy were performed. At surgery, cloudy fluid was aspirated. Cultures were negative. Microscopic sections demonstrated a cyst wall lined by simple cuboidal epithelium. The final pathologic diagnosis was mucocele.

Discussion

To the extensive list of lesions that can cause lytic or cystic defects in or adjacent to the petrous apex, we add

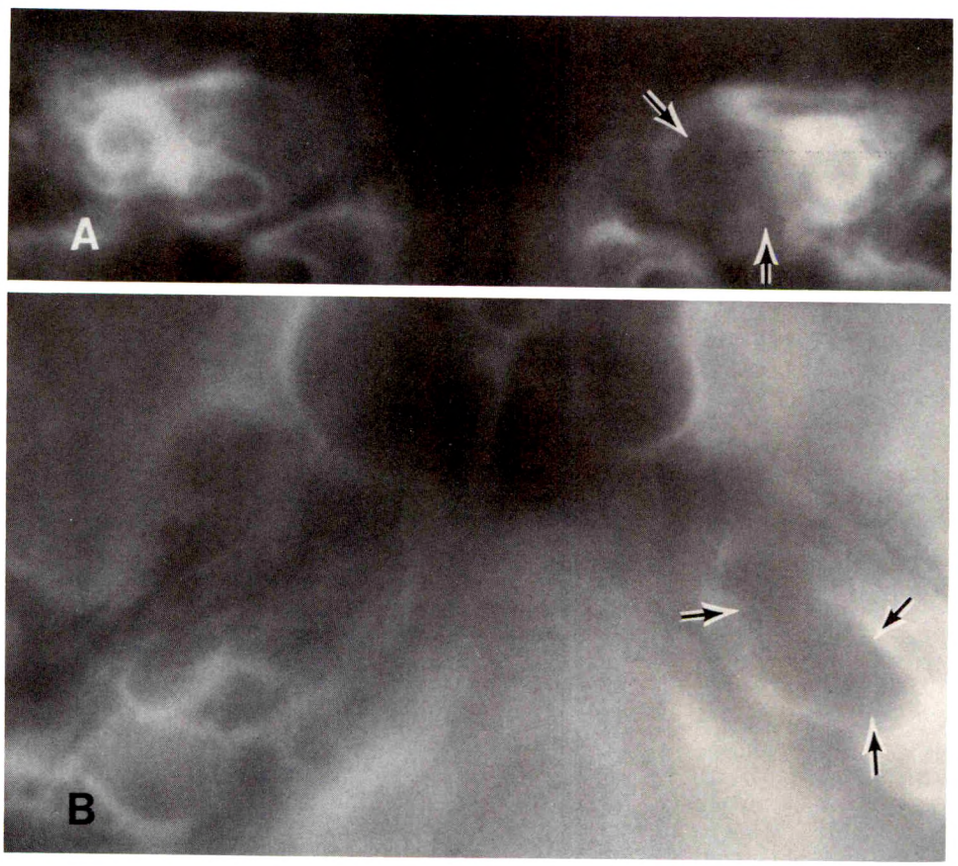


Fig. 1.—Surgically documented temporal bone mucocele. **A**, Anteroposterior hypocycloidal tomogram. Large lytic lesion (*arrows*) in petrous apex communicates with cochlea. More posterior sections also disclosed erosion of internal auditory canal and meatus. **B**, Submentovertex hypocycloidal tomogram. Scalloped zone of sclerosing osteitis surrounds margins of lytic lesion (*arrows*).

Received October 27, 1978; accepted December 28, 1978.

[1] Department of Radiology, University of Utah College of Medicine, 50 North Medical Drive, Salt Lake City, Utah 84132. Address reprint requests to A. G. Osborn.

[2] Department of Otolaryngology, University of Utah College of Medicine, Salt Lake City, Utah 84132.

© 1979 American Roentgen Ray Society

0361-803X/79/1324-0680 $0.00

temporal bone mucocele. The etiology of this unusual case is obscure, but likely involved inclusion of ectopic seromucinous tissue within the developing petrous ridge. The radiographic findings in mucocele of the petrous temporal bone are nonspecific. The destructive lesion may have scalloped, somewhat sclerotic borders. The major differential diagnostic considerations should include congenital epidermoid cyst, arachnoid cyst, petrous apex air cell, apical petrositis following otitis media, neurinoma, glomus tumor, aneurysm, systemic metabolic or metastatic disease, and secondary involvement of the temporal bone from lesions arising in the skull base or cranial fossae [6–9].

Large petrous apex air cells are usually an asymptomatic normal variant. Primary or congenital cholesteatomas in the petrous pyramid are developmental lesions. They occur behind an intact tympanic membrane and probably arise from embryonal inclusions of epithelial cell rests [10, 11]. Symptoms may include both profound sensorineural hearing loss and facial palsy of gradual onset and progression. Tomography usually discloses a lytic lesion with sclerotic, scalloped borders [12, 13]. The radiographic findings are indistinguishable from petrous apex mucocele.

Petrositis (Gradenigo's syndrome) results from an infection in the mastoid air cells surrounding the labyrinthine capsule and can occur only in the 30% of temporal bones where pneumatization extends to the petrous apex [6]. Otorrhea is a common feature and the symptoms frequently occur 10–50 days after an episode of acute otitis media or mastoiditis [14]. Radiographically this entity is characterized by patchy, irregular foci of bone destruction in the petrous pyramid [6].

Sarcomas, neurofibromas, giant cell tumors, chordomas, meningiomas, and a variety of metastatic lesions can all present as lytic defects in the petrous ridge [6, 15]. With the possible exception of neurofibroma, these lesions are usually poorly defined and do not show the marginal sclerosis often characteristic of mucocele or primary cholesteatoma. If of sufficient size, glomus tumors may also erode the petrous apex [15, 16].

Extracranial aneurysms of the internal carotid artery, particularly its petrous portion, are uncommon. True and false middle ear aneurysms have been reported [17–20]. The rare aberrant internal carotid artery [21, 22] as well as a high jugular bulb secondary to congenital bony dehiscence [23] appear radiographically as bony defects in the petrous ridge. However, these anomalies are usually limited to the middle ear cavity and their vascular nature is readily identified by cerebral angiography.

Systemic disease processes such as histiocytosis X and the various reticuloses may also cause destruction of the petrous apex. These can usually be distinguished by the presence of osseous lesions elsewhere.

REFERENCES

1. Bloom DL: Mucoceles of the maxillary and sphenoid sinuses. *AJR* 83:1103–1110, 1965
2. Robersón GH, Patterson AK, Deeb ME, Maisel RH, Bone RC: Sphenoethmoidal mucocele: radiographic diagnosis. *AJR* 127:595–599, 1976
3. Takahashi M, Jingu K, Nakayama T: Roentgenologic appearances of sphenoethmoidal mucocele. *Neuroradiology* 6:45–49, 1973
4. Phelps PD, Toland JA: Mucocele of the sphenoid sinus eroding the petrous temporal bone. *Br J Radiol* 42:845–847, 1969
5. Diaz F, Latchow R, Duvall AJ III, Quick CA, Erickson DL: Mucoceles with intracranial and extracranial extensions. *J Neurosurg* 48:284–288, 1978
6. Phelps PD, Toland JA, Sheldon PWE: Erosions of the petrous temporal bone. *J Laryngol Otol* 84:1205–1230, 1970
7. Gacek RR: Diagnosis and management of primary tumors of the petrous apex. *Ann Otol* 84 (suppl 18):1–20, 1975
8. Sumner TE, Benton C, Marshak G: Arachnoid cyst of the internal auditory canal producing facial paralysis in a three-year-old child. *Radiology* 114:425–425, 1975
9. Montgomery WW: Cystic lesions of the petrous apex: transsphenoid approach. *Ann Otol* 86:429–435, 1977
10. Derlacki EL: Congenital cholesteatoma of the middle ear and mastoid. *Arch Otolaryngol* 97:177–182, 1973
11. Derlacki EL, Clemis JD: Congenital cholesteatoma of the middle ear and mastoid. *Ann Otol* 74:706–727, 1965
12. Cawthorne T, Griffith A: Primary cholesteatoma of the temporal bone. *Arch Otolaryngol* 73:252–261, 1961
13. Brookler KH, Pulec JL, Hallberg OE: Congenital cholesteatoma of the temporal bone. *Arch Otolaryngol* 90:449–452, 1969
14. English GM: *Otolaryngology*. New York, Harper & Row, 1976, pp 224–225
15. Goldman AM, Martin JE: Tumors involving the temporal bone. *Radiol Clin North Am* 8:387–402, 1970
16. Rucker TN: Radiology of glomus jugulare tumors in the temporal bone. *AJR* 81:807–816, 1963
17. Margulis MT, Stein RL, Newton TH: Extracranial aneurysms of the internal carotid artery. *Neuroradiology* 4:78–89, 1972
18. Teal JS, Bergeron RT, Rumbaugh CL, Segall HS: Aneurysms of the petrous or cavernous portions of the internal artery associated with non-penetrating head trauma. *J Neurosurg* 38:568–574, 1973
19. Anderson RD, Liebeskind A, Achechter MM, Zergesser LH: Aneurysms of the internal carotid artery in the carotid canal of the petrous temporal bone. *Radiology* 102 639–642, 1972
20. Steffen TN: Vascular anomalies of the middle ear. *Laryngoscope* 78:171–197, 1968
21. Glasgold AI, Horrigan WD: The internal carotid artery presenting as middle ear tumor. *Laryngoscope* 82:2217–2221, 1972
22. Lapayowker MS, Liebman EP, Ronis ML, Safer JN: Presentation of the internal carotid artery as a tumor of the middle ear. *Radiology* 98:293–297, 1971
23. Overton SB, Ritter FN: A high placed jugular bulb in the middle ear: a clinical and temporal bone study. *Laryngoscope* 83:1986–1991, 1973

Editorial

Röntgen: Application Denied

Setting: The Town Hall of Würzburg in 1896. Enter a gentleman dressed in cape and top hat.

Official—May I help you?

Gentleman—My name is Wilhelm Conrad Röntgen. I am here to inquire about the status of my application for the new machine which I submitted to the Health Systems Agency of Greater Würzburg.

Official—Yes, Dr. Röntgen. We received your application, and we have examined it in great detail. There are, however, many questions left unanswered.

Dr. Röntgen—Yes, I found it was quite difficult for me to complete your application.

Official—Well, Dr. Röntgen, we anticipate that your new machine will cause many problems. You claim your new ray permits physicians to look inside the human body and to evaluate bones prior to surgery. We feel that there may be some slight merit to your invention; however, to consider this a medical necessity and to expend huge capital sums will raise the cost of medical care here in Würzburg. In addition to the equipment, think of the personnel needed to run each of these units. We would also have to purchase x-ray plates and record these images and then store this information.

Dr. Röntgen—But just think of what this x-ray means to patients; for the first time, we can diagnose fractures intelligently, and I am working on new applications of my ray that will permit a doctor to look inside the chest and abdomen and visualize the stomach, colon, and other areas of the body. Diseases may be found earlier when they can be corrected.

Official—Even if those procedures were possible, and they certainly have not been proven so, as yet, we can't do very much about most diseases, so why find them earlier. If we do find these diseases, we will only have a proliferation of surgical procedures and other ancillary medical tests. We must consider that our budget is limited, and we must put our health care dollars into more useful areas.

Dr. Röntgen—But think of. . . .

Official—If we don't limit the use of the new modality, each and every hospital will then want one of your units. What will happen to the cost of medical care then? If you are correct and your unit will allow physicians to see other parts of the body, not just bones, then, no doubt, there will be a third and fourth generation x-ray unit. How can we stop that proliferation? No, no, Dr. Röntgen, the Agency will only approve one of your units for the Greater Würzburg area. If we don't place these restraints on the unit, then the use of the x-ray will increase, and everyone with a headache or a stomachache will demand to have an x-ray.

Dr. Röntgen—Just think of the improved patient care my x-ray. . . .

Official—The Würzburg HSA has decided that x-ray is still an experimental modality. We will not have our third party payers reimburse any hospital for the use of x-ray on any part of the body but bones. Uses in the stomach, chest, etc. must be considered experimental and will not be reimbursed. I also would like to caution you to prevent your unit from falling into the hands of private practitioners. Who knows how many private x-ray offices would spring up if we did not include physicians' offices as part of our "certificate of need" legislation. Perhaps you could find some other use for your new ray—try shoe stores!

Harold Moskowitz
Mount Sinai Hospital
Hartford, Connecticut 06112

© 1979 American Roentgen Ray Society

0361-803X/79/1324-0682 $0.00

Letters

Accuracy of Lymphangiography

An article by Kademian and Wirtanen [1] in the December 1977 *AJR* misquoted work done by our group [2]. It incorrectly stated that our group reported the accuracy of positive lymphangiograms.

The work in question concerned 155 patients who underwent staging laparotomy, of whom 153 had negative or equivocal bipedial lymphangiograms. In 128 patients with negative lymphangiograms, four were found to have pathology in lymph nodes that also contained lymphangiogram reaction indicating they were visualized preoperatively. We consider the equivocal lymphangiograms in 25 patients to be negative; one of these patients was found to have Hodgkin's disease in the nodes seen on the lymphangiogram. Only two of the 155 patients had evidence of disease by lymphangiography. It was limited to inguinal and iliac areas and subsequently confirmed as such at surgery.

The incidence of false negative diagnoses in patients with negative or equivocal lymphangiograms is thus 5 in 153, or 3.3%. The accuracy of a negative lymphangiogram is therefore 96.7%.

Our study confirmed Kademian and Wirtanen's position that false negative lymphangiograms are infrequent, but it does not make any comment on the accuracy of positive lymphangiograms, as their reference to our work suggests.

Roger William Rodgers
Jess F. Gamble
James J. Butler
Lillian M. Fuller
University of Texas System Cancer Center
M. D. Anderson Hospital and Tumor Institute
Houston, Texas 77030

REFERENCES

1. Kademian TH, Wirtanen GW: Accuracy of bipedal lymphography in Hodgkin's disease. *AJR* 129:1041–1042, 1977
2. Gamble JF, Fuller LM, Martin RG, Sullivan MP, Jing BS, Butler JJ, Shullenberger CC: Influence of staging celiotomy in localized presentation of Hodgkin's disease. *Cancer* 35: 817–825, 1975

The Seurat Spleen

Radiologists often compare their arteriographic findings to works of art. In the case of the traumatized spleen, diffuse or localized nodular collections of contrast material in the late arterial and capillary phase have been likened to the stars in "Starry Night," a painting by Vincent van Gogh [1].

Mottling in a ruptured spleen has been attributed to several mechanisms. Brindle [2] suggests sinusoidal stasis, traumatic arteriovenous aneurysm, or contrast leakage from fragmented sinusoids. Scatliff et al. [1] postulate that stasis of blood and contrast material within marginal sinuses because of contusion, hematoma, or hypotension are responsible for this appearance. This pattern of opacification provides the angiographer with the most reliable sign of splenic injury. Other valuable findings include displacement and compression of splenic vessels and parenchyma by hematoma, radiolucent defects indicating laceration, and early venous filling [3].

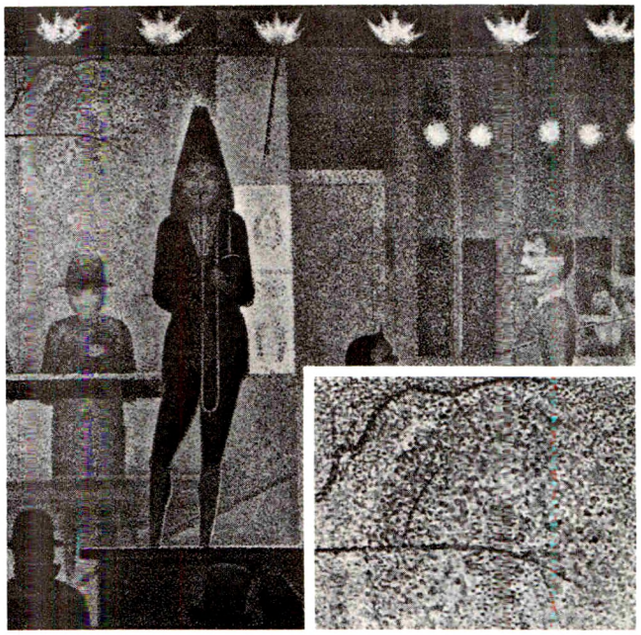


Fig. 1.—Section from "La Parade" by Georges Seurat illustrates pointillistic technique. Hundreds of tiny dots merge into single image. Dot patterns, clearly visible in magnified insert, are strikingly similar to arteriograms of traumatized spleen. (Reproduced with permission of the Metropolitan Museum of Art, New York.)



Fig. 2.—"Starry Night" by Vincent van Gogh has been compared to arteriographic findings in ruptured spleen. (Reproduced with permission of the Museum of Modern Art, New York.)

In our series of 45 patients with positive arteriograms and surgically proven ruptured spleens, 29 had some form of extravasation or mottling. In 16 of these cases, the pattern of extravasation was more reminiscent of the works of Georges Seurat than van Gogh, his contemporary.

© 1979 American Roentgen Ray Society

0361-803X/79/1324-0683 $0.00

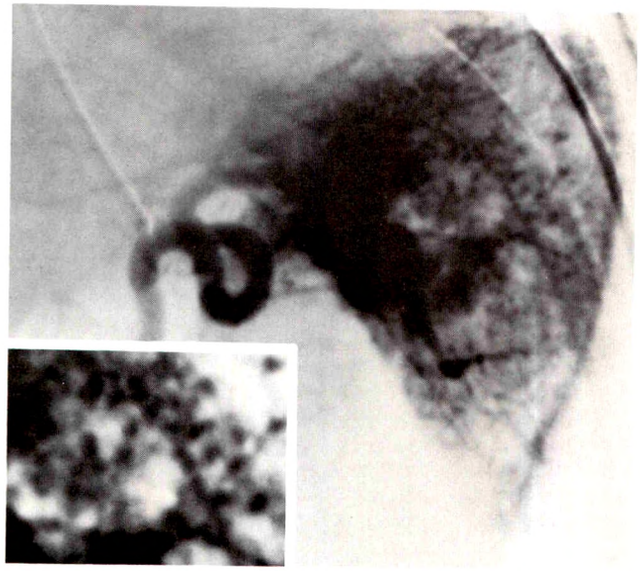


Fig. 3.—Ruptured spleen. Selective celiac arteriogram demonstrates multiple punctate areas most prominent at the midpole of the spleen similar to magnified insert of branching tree in fig. 1.

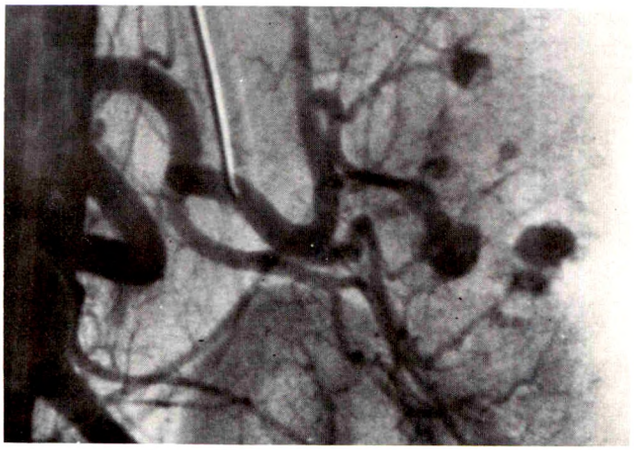


Fig. 4.—Ruptured spleen. Abdominal aortogram showing large globular areas of extravasation in the spleen is reminiscent of van Gogh's "Starry Night" (fig. 2).

Figure 1 typifies the work of Seurat (1859–1891), who, like van Gogh, was a late 19th century post-Impressionist period French artist [4]. The coarse swirling brush work of van Gogh (fig. 2) underscores the dissimilarity of the two artists' methods. While van Gogh relies on large globular images that exist independently of each other, Seurat delights in a pointillistic technique, composed of hundreds of tiny dots that merge almost imperceptibly at a distance. A celiac arteriogram on a patient with a proven ruptured spleen (fig. 3) nicely demonstrates the similarity to Seurat's technique. Seurat's subtlety of brush stroke is impossible with van Gogh, whose blaring blotches of color are more reminiscent of massive extravasation (fig. 4).

We propose the "Seurat spleen" as a more accurate artistic representation of splenic injury, lest the radiologist be accused of cultural ignorance.

Jeffrey B. Kass
Baylor College of Medicine
Richard G. Fisher
Baylor College of Medicine and
Ben Taub General Hospital
Texas Medical Center
Houston, Texas 77030

REFERENCES

1. Scatliff JH, Fisher ON, Guilford WB, McLendon WW: The starry night splenic angiogram. *AJR* 125:91–98, 1975
2. Brindle MJ: Arteriography and minor splenic injury. *Clin Radiol* 23:174–180, 1972
3. Gold RE, Redman HC: Splenic trauma: assessment of problems in diagnosis. *AJR* 116:413–418, 1972
4. Janson HW: *History of Art*. Englewood, N.J., Prentice-Hall, 1967, pp. 505–507

Antibiotic Therapy

In reference to Moss et al. [1], 2 years ago Dr. Moss presented his findings on the use of antibiotics in Crohn's disease at the annual meeting of the Society of Gastrointestinal Radiologists, Hilton Head, South Carolina. At that time, I commented that I have been using antibiotics for the last 10 years in selected cases of Crohn's disease with equivocal results. In those patients with sinus tracts and fistulae, antibiotics were useful prior to surgery.

In an occasional case without sinus tracts or fistulae, there was almost complete resolution of the radiographic findings with antibiotic treatment. Despite my equivocal results, I would recommend a trial of antibiotics in those patients with symptoms, especially since there is no specific therapy in Crohn's disease.

An unfortunate complication of antibiotic therapy is diarrhea, which necessitates discontinuation of the drug.

Richard H. Marshak
Mt. Sinai Hospital
New York, N.Y. 10028

REFERENCE

1. Moss AA, Carbone JV, Kressel HY: Radiologic and clinical assessment of broad-spectrum antibiotic therapy in Crohn's disease. *AJR* 131:787–790, 1978

Abstracts of Current Literature

Chest

Surgical management of malignant mesothelioma. DeLaria GA, Jensik R, Falser P, Kittle CF (Rush-Presbyterian-St. Luke's Medical Center, 1753 West Congress Parkway, Chicago, Illinois 60612). *Ann Thorac Surg* 26:375–381, Oct 1978

Malignant mesothelioma is a difficult disease to treat. This survey reviews the surgical management of 18 patients. Of this group, seven received limited treatment consisting only of pleurectomy or biopsy. Their survival was 10 months, and no patients were free of disease at the time of their death. The remaining 11 patients were treated by radical extrapleural pneumonectomy. There were two long-term, disease-free survivors at 2 and 4 years. Mean survival for this latter group was 15 months, and most patients experienced some relief of symptoms. The authors conclude that radical extrapleural pneumonectomy is safe, without major morbidity, offers good palliation, and an opportunity to achieve a cure.

W. Richard Webb

Mediastinal masses of vascular origin. A review. Kelley MJ, Mannes EJ, Ravin CE (University of California, San Diego School of Medicine, University Hospital, 225 West Dickinson Street, San Diego, California 92103). *J Thorac Cardiovasc Surg* 76:559–572, Oct 1978

Approximately 10% of mediastinal masses are of vascular origin, the majority of which are aortic aneurysms. This survey reviews numerous additional entities in which abnormal or dilated vessels produce a mediastinal mass lesion. Described conditions include abnormalities of the systemic and pulmonary arteries and veins.

W. Richard Webb

Pulmonary sequestration presenting as congestive heart failure. Rancom JM, Norton JB, Williams GD (Department of Surgery, University of Arkansas for Medical Sciences, 4301 West Markham, Little Rock, Arkansas 72201). *J Thorac Cardiovasc Surg* 76:378–380, Sept 1978

The authors report the case of a 6 month old infant with an intralobar sequestration in the left lower lobe producing a large aortic-to-pulmonary vein shunt and congestive heart failure. The anomalous systemic artery supplying the sequestration was equal in size to the aorta. Although such shunts are usually small and asymptomatic, they can increase in volume with age. Only one prior case of sequestration resulting in congestive heart failure has been reported.

W. Richard Webb

Pathogenesis of neurogenic pulmonary edema. Wray NP, Nicotra MB (Department of Medicine, Baylor College of Medicine and Veterans Administration Hospital, Houston, Texas). *Am Rev Respir Dis* 118:783–786, Oct 1978

The cause of pulmonary edema after severe injury of the central nervous system has been unclear. It has been suggested that the cause of pulmonary edema is massive alpha-adrenergic release from an irritative lesion in the central nervous system, resulting in marked but transient systemic and pulmonary hypertension. This presumably would produce a fluid shift from the systemic circulation to the more compliant pulmonary circulation with resulting fluid loss into the lung. The authors present a case supporting this hypothesis. A 64-year-old man suffered an intracranial hemorrhage. He had recurrent brief episodes of self-limited increased systemic arterial, pulmonary arterial, and pulmonary capillary wedge pressures, associated with worsening of his respiratory status and chest radiographs. Radiographs showed typical findings of pulmonary edema.

W. Richard Webb

Localized amyloidosis of the lower respiratory tract. Rubinow A, Celli BR, Cohen AS, Rigden BG, Brody JS (Thorndike 314, Boston City Hospital, 818 Harrison Avenue, Boston, Massachusetts 02118). *Am Rev Respir Dis* 118:603–611, Sept 1978

Amyloidosis limited to the lower respiratory tract is relatively rare, but can occur in three forms. Tracheobronchial deposition is the most frequent form of localized amyloidosis (41 reported cases), and often results in cough, dyspnea, and hemoptysis. In 56% of patients atelectasis distal to the site of obstruction is radiographically visible; 9% had hilar or mediastinal mass. Bronchoscopy is usually needed for diagnosis.

Nodular pulmonary amyloidosis (31 reported cases) can present with a solitary (16 cases) or multiple masses (15 cases) and both calcification and cavitation can be visible.

Diffuse parenchymal amyloidosis (four reported cases) with a radiographic pattern of interstitial densities has a poor prognosis with progression and respiratory failure.

W. Richard Webb

Subpulmonary pneumothorax. Schulman A, Dalrymple RB (Groote Schuur Hospital and University of Cape Town, South Africa). *Br J Radiol* 51:494–497, July 1978

Seven cases of subpulmonary pneumothorax are presented: four due to penetrating stab wounds, two to blunt trauma, and one to osteosarcoma metastasis, all on the left side. The typical and diagnostic appearance is a basal band of radiolucency bounded above by the thin hairline of visceral pleura paralleling the dome of the hemidiaphram. When partially clotted blood is also present, the appearance becomes less typical and must be differentiated from traumatic herniation of bowel and from traumatic pneumatocele by barium studies and by decubitus radiographs respectively.

The shape of the pleural cavity between the dome of the hemidiaphram and the concavity of the lung base is thought to allow the collection of a basal pneumothorax. Pneumothorax is rarely seen at this location, however, because blebs and bullae which are the most common causes of pneumothorax are most often located in the upper lobes. In six of these patients, there was no clinical or radiographic evidence of existing lung disease. Though this is an uncommon primary location, these authors stress the importance of scrutinizing the lung bases for evidence of a subpulmonary pneumothorax as well as the apices, particularly following basal trauma.

Noel K. Allan

Pulmonary complications in fulminant hepatic failure: analysis of serial radiographs from 100 consecutive patients. Warren R, Trewby PN, Laws JW, Williams R (King's College Hospital and Medical School, Denmark Hill, London SE5, England). *Clin Radiol* 29:363–369, July 1978

Serial chest radiographs of 100 consecutive patients with fulminant hepatic failure were analysed. In 48 patients, serial chest x-rays remained normal throughout their illness. Of the remaining 52 patients, 31 developed changes which could be

© 1979 American Roentgen Ray Society

0361–803X/79/1324–0685 $0.00

largely attributed to their unconscious state. The frequency was similar to that reported in patients unconscious following barbiturate and other sedative drug overdose. In this series, these included collapse of the right upper lobe after passage of an endotracheal tube (10%), collapse of other lobes or the whole lung as well as pneumothorax, lung abscesses, and pleural effusions. The frequency of pulmonary edema (37%) was much higher than that reported in other metabolic comas and may be related to accumulation of toxic compounds in the blood. These authors have previously demonstrated a high pulmonary extravascular water volume without evidence of heart failure to account for the edema. The degree of intrapulmonary shunting (25.3%) in 25 patients with normal chest x-rays was a further unexpected finding and unlike previous reports was not associated with any mottling on the chest x-ray. Direct arteriovenous communications were not found on wedge angiograms and the most likely cause of such shunting may be inappropriate dilatation throughout the pulmonary vascular tree. The early radiologic detection of these serial changes may explain why the mortality was no higher in those patients who developed pulmonary complications.

Noel K. Allan

Cardiovascular

Radiation exposure to the operator performing cardiac angiography with U-arm systems. Balter S, Sones FM Jr, Brancato R (Cleveland Clinic, 9500 Euclid Avenue, Cleveland, Ohio 44106). *Circulation* 58:925–932, 1978 (by permission American Heart Association)

We measured the radiation exposure received by a group of operators performing 700 coronary angiograms. All studies were performed using the brachial artery approach and the Philips Cardio Diagnost. Nineteen sites were monitored on each operator, using lithium fluoride thermoluminescent dosimeters. Four hundred examinations were performed with a table-mounted protective shield in place. Three hundred were performed without the shield. The average exposures (in mR per study) with and without the shield were 1.9/6 for the eyes and 1.4/8.3 for the thyroid.

The resulting operator exposure with the shield in place is low enough so that an operator performing 25 procedures per week on a continuous basis will not exceed the recommendations of the National Commission on Radiological Protection and Units. We therefore strongly recommend the use of a properly designed and appropriately positioned shield with all U-arm systems.

Author Abstract

The epinephrine effect in renal angiography revisited. Ekelund L, Gerlock J Jr, Goncharenko V (Vanderbilt University Hospital, Nashville, Tennessee 37232). *Clin Radiol* 29:387–392, July 1978

The effect of various doses of epinephrine on the renal vessels was studied angiographically in 15 kidneys including three renal tumours. Commonly used doses (10–25 μg) are often too high as demonstrated in this study. Our findings indicate that the optimal dose for pharmacoangiography of renal masses should be 2–5 μg of epinephrine. The time interval between drug administration and angiography should be less than 1 min and optimally in the range of 10–30 sec.

Author Abstract

Thymic venography in myasthenic and nonmyasthenic patients: report of 43 cases. Falappa PG, Bonomo L, Danza F, Quilici N, Renda F, Saracca L (Istituto di Radiologia dell'Università Cattolica del Sacro Cuore, via della Pineta Sacchetti 526, Roma, Italy). *Rays* 2:361–368, 1977

The authors have performed 43 thymic venographies of which 40 were carried out in patients with myasthenia. In 26 cases the pathologic process was of hyperplasia while in 14 the lesion was a thymoma. The three patients without myasthenia were also affected by thymomas.

A specially curved catheter of their own design, introduced using the Seldinger technique into a femoral vein was brought up to the level of the thymic vein. Six to 8 cc of a water soluble contrast medium were injected. The examination lasted 20–30 min. No significant complications were noted. If the pressure injection was too high, some extravasation of the contrast medium occurred in the thymus, resulting in minimal and transient retrosternal pain. Satisfactory results were obtained in 90% of the cases.

Lesions ranged in size from 2–12 cm. The presence of a very fine and irregular vascular pattern, or of an avascular area outlined by vessels surrounding it were the most common findings. The venographic patterns, however, did not allow a differential diagnosis between a benign or a malignant tumor.

Antonio F. Govoni

Isolated aneurysm of the iliac artery. Lowry SF, Kraft RO (St. Joseph Mercy Hospital, Ann Arbor, Michigan 48106). *Arch Surg* 113:1289–1293, 1978

Isolated atherosclerotic aneurysmal dilatation of the iliac artery (in the absence of aortic aneurysm) is rare and difficult to diagnose clinically for two reasons. First, symptoms of intact iliac artery aneurysms are unusual and when present often mimic urological or neurological disease; and secondly, because of its deep location, the isolated iliac artery aneurysm is rarely palpable on clinical examination. The detection of isolated iliac artery aneurysms prior to rupture is therefore frequently fortuitous, e.g., during aortography for peripheral vascular disease (and herein lies the significance of this entity to radiologists). The authors estimate that at least 50% of untreated iliac artery aneurysms will ultimately rupture, and urge elective surgical intervention, since operative mortality for ruptured iliac aneurysms was 52%.

Reiley Kidd

Angiography in the evaluation of traumatic lesions to the liver (in Italian). Rossi P, Passariello R, Simonetti G (Istituto di Radiologia, Policlinico Umberto I, I-00161 Roma, Italy). *Radiol Med* 64:283–286, 1978

This review of hepatic angiography in the setting of trauma is based on a large series of cases from which the authors draw conclusions regarding indications for the examination.

1. Posttraumatic preoperative evaluation for hemorrhage, hematoma, parenchymal damage or associated lesions of spleen, kidney, or bowel.
2. Hemorrhage from the digestive tract of undetermined origin, as in cases of hemobilia and of stress ulcer.
3. Possible intraperitoneal hemorrhage following surgery and as follow up after hepatic resection.
4. To follow progress of spontaneously resolving hematoma or pseudoaneurysms.
5. In cases of portal hypertension following hepatic trauma where thrombosis of the portal vein or an arterioportal fistula is suspected.
6. Instances where abdominal pain persists long after trauma and scintigraphic studies show abnormalities.

Antonio F. Govoni

Hepatic oil embolism following lymphography. Ngan H, James KW (Queen Mary's Hospital, Roehampton, London, SW 15, England). *Br J Radiol* 51:788–792, Oct 1978

Lymphograms of 1,000 patients were reviewed with special reference to the occurrence of hepatic oil embolism following the procedure. Oily contrast medium ("Lipidol" ultra-fluid) was found in the liver in seven cases, five of whom had carcinoma of

the cervix uteri. Hepatic oil embolism was not encountered in patients with lymphomas in this series. Complete or partial lymphatic obstruction was present in all seven cases and one patient had almost complete obstruction of the inferior vena cava. Malignant disease need not always be the predisposing factor since hepatic oil embolism occurred in one patient with retroperitoneal fibrosis. The routes through which the contrast medium may reach the liver are discussed and lymphaticoportal communications in the mesentery are thought to play an important role. Contrast was invariably seen in the liver within 2 hr of commencement of the injection and was still faintly visible in one case 3½ months later. The way in which the contrast pattern in the liver changes with time is described. An attempt is made to correlate the radiological appearances with the fate of the contrast medium in the liver.

Author Abstract

Gastrointestinal

Spatial distribution of colonic carcinoma. Morgenstern L, Lee SE, (Cedar-Sinai Medical Center, Los Angeles, California 90048). *Arch Surg* 113:1142–1143, Oct 1978

During the past several decades, there has been a shift in the distribution of colorectal cancer toward the right side, with an increase in colon lesions on the right side and a marked decrease in rectal lesions. The authors report 1,000 consecutive cases of colonic carcinoma resected at their institution in the decade between 1966 and 1977. Of these, 24% were located in the right colon, 16% in transverse colon, 7% in descending colon, 38% in sigmoid and rectosigmoid, and only 15% in the rectum. The older dogma that two-thirds or three-fourths of all colonic cancers discoverable by digital examination and proctosigmoidoscopy is no longer valid. Detection and screening methods must, therefore, be oriented toward the whole colon, rather than concentrating on its most distal segment. The stool guaiac test for occult blood (hemoccult test), the well-performed barium enema examination, and colonoscopy must play an increasingly prominent role in colonic detection and screening.

Reiley Kidd

Pseudopolyposis in Crohn's disease. Freeman AH, Berridge FR, Dick AP, Gleeson JA, Zeegen R (Addenbrooke's Hospital, Cambridge, England). *Br J Radiol* 51:782–787, Oct 1978

Eight cases of pseudopolyposis occurring in Crohn's colitis are described emphasizing the variability of these lesions. Four main types were found namely, localized multiple pseudopolyposis, localized giant pseudopolyposis, generalized pseudopolyposis, and long finger-like pseudopolyps.

Pseudopolyps in Crohn's disease are not an uncommon finding and their presence in itself does not help in the differentiation of ulcerative colitis from Crohn's colitis. Several previous authors have emphasized the importance of pseudopolyposis in ulcerative colitis as a distinguishing feature from Crohn's colitis. Multiple pseudopolyposis of the colon in Crohn's disease is a rare cause of obstructive symptoms and this report emphasizes that without clinical or other radiologic features, differentiation from a villous tumor may be difficult, except by colonoscopy or laparotomy. The two examples of localized giant pseudopolyposis in this series bring the total reported to eight.

Noel K. Allan

Changes in the detail mucosa pattern of the colon in early stages of ulcerative and granulomatous colitis (in German). Persighel M, Spieth W, Klose KC, Cen M (Abteilung Radiologie der Med. Fakultät an der Rhein.-Westf. Technischen Hochschule Aachen, Goethestr. 27–29, 5100 Aachen, Germany). *ROEFO* 129:177–178, 1978

The authors discuss the detailed relief pattern of the colonic mucosa as seen on the double contrast examination in relation to the early diagnosis of inflammatory bowel disease. The presence of a granular appearance suggests an early stage of ulcerative colitis, while multiple small flecks of contrast, sometimes surrounded by a clear area, indicate aphthous ulcers in an early stage of Crohn's disease. Since these findings are not seen on examinations using the full column technique, the double contrast examination should be considered the examination of choice in patients suspected of having inflammatory bowel disease.

Peter F. Winter

The effect of nonfractionated and fractionated administration of opanic acid on gallbladder visualization. Nehen AM, Kruse V (Aarhus Kommunehospital, University of Aarhus, Denmark). *Radiology* 128:605–607, Sept 1978

Visualization of the gallbladder after nonfractionated and fractionated administration of iopanoic acid was investigated in a blind experiment. The authors studied 168 patients; 73 were given 3 g iopanoic acid over a period of 6 hours (0.5 g/hour), and 95 received the same amount of contrast medium in a single dose. No differences in visualization were found for the two modes in both normal and pathological cases.

Author Abstract

Musculoskeletal

Radiology in low back pain and sciatica. An analysis of the relative efficacy of spinal venography, discography and epidurography in patients with a negative or equivocal myelogram. McCormick CC (Royal Perth Hospital, Perth, Western Australia). *Clin Radiol* 29:393–406, July 1978

Lumbar myelography with oily contrast media or lumbosacral radiculography with water-soluble contrast, is the mainstay of radiological diagnosis in the low back pain and sciatica syndrome. Though the introduction of relatively nontoxic aqueous materials has increased the accuracy of diagnosis, a few patients remain in whom the radiological examination fails to reveal the diagnosis before surgery. The development of discography, spinal venography, and epidurography is in part a consequence of radiologists' dissatisfaction with myelography. In this study, only patients with negative or equivocal myelographic findings have been subjected to one or more of these extra investigations in an attempt to improve the diagnostic yield before surgical exploration.

Analysis of the results indicates that spinal venography compares unfavorably with discography and epidurography because of its lower accuracy and higher incidence of complications. Discography and epidurography are equally precise, but the former is a painful experience for the patient and its use is now confined almost entirely to the assessment of patients who are to undergo anterior spinal fusion. Epidurography is technically easy to perform and may be combined with therapeutic epidural injection in some circumstances. Interpretation improves with experience and it is thought worthy of further evaluation both following negative myelography and as the procedure of first choice.

Author Abstract

Radiological aspects of posterior dislocation of the hip. Whitehouse GH (University of Liverpool, Liverpool, England). *Clin Radiol* 29:431–441, July 1978

Ninety-six cases of traumatic dislocation of the hip were admitted to one general hospital over a 10-year period. Eighty of these (83.3%) were posterior dislocations, usually with associated acetabular fractures (81.25%). The etiology and various complications of posterior hip dislocation are described and

discussed, together with the radiographic management. Radiologists should take special care to exclude associated femoral and pelvic fractures both within and beyond the acetabulum. Fractures of the ipsilateral femur associated with posterior hip dislocation usually involve the femoral head and the radiological appearances and assessment of this injury is important. Ipsilateral femoral shaft fractures are less frequent, but it may be the hip dislocation which is then overlooked unless there is an awareness of the combined injury.

Author Abstract

Idiopathic juvenile osteoporosis. Houang MTW, Brenton DP, Renton P, Shaw DG (University College Hospital, Gower Street, London WC1, England). *Skel Radiol* 3:17–23, 1978

The authors present the radiological and clinical findings in 14 patients with proven idiopathic juvenile osteoporosis. Clinically, previously healthy patients present about 2 years before puberty with spinal pain or pain in the ankles and knees due to metaphyseal infractions. These are often mistakenly diagnosed as some form of arthritis. Pathology of bone in these children reveals a quantitative rather than a qualitative change suggesting an increase in osteoclastic bone absorption. The only consistently abnormal metabolic finding has been a low positive to markedly negative calcium balance which usually correlates clinically well with the degree of clinical and radiological abnormality. The late form of osteogenesis imperfecta is the entity with which it may be confused. The authors divide patients with idiopathic juvenile osteoporosis into three groups, the mild, moderate and severe reflecting the mode of presentation, its course, prognosis and abnormal biochemical features. The axial skeleton was affected in all 14 patients presented. The dorsal and lumbar spines mainly reveal the abnormality with evidence of marked osteoporosis associated with collapse of one or several vertebral bodies. The degree of vertebral collapse and increase in the intervertebral spaces were directly proportional to the degree of involvement. In two patients the vertebral changes were associated with marked anterior displacement of the superior segment of the sacrum. With remission of the disease, the vertebral bodies tend to become more dense, oftimes attempting to reconstitute the shape of the normal.

In the pelvis osteoporosis, too, was commonly found. Several patients revealed associated protrusio acetabuli or slipping of femoral heads.

In contrast to osteogenesis imperfecta, skull changes were minimal in these patients. Careful observation revealed a degree of osteoporosis in the ribs sometimes associated with fractures.

The appendicular skeleton was almost universally affected being presented in 13 of the 14 patients described. The tubular bones showed marked loss of trabeculation and cortical thinning. Metaphyseal fractures were demonstrated in nine patients initially resembling fatigue fractures which later went on to involve the entire transverse diameter of the bone. The hands and feet showed marked osteoporosis often associated with fractures. Maturation of bone almost universally was within normal limits.

Of paramount importance is the recognition of the disease which commonly may be confused with other juvenile osteoporotic processes including leukemia, Cushing's disease and the juvenile form of rheumatoid arthritis.

Philip J. Hodes

Relation of vascular and osseous changes in leprosy. Johnson AC, James AE, Reddy ER, Johnson S (Vanderbilt University Hospital, Nashville, Tennessee 37232). *Skel Radiol* 3:36–41, 1978

Some 58 patients with leprosy were studied angiographically. Slowing of blood flow of the leg was seen in almost all patients (83%) with tapering of the column of contrast but no intrinsic irregularity or intraluminal occlusion. The distal arteries proceeded to fill very slowly with a dramatic delay in opacification at the level of the ankle, varying from 15–68 sec, the normal time being 8–11 sec. The posterior tibial artery showed this delayed phenomenon in over 60% of patients; the anterior tibial in approximately 35%. A peculiar intrinsic irregularity of the lumen was demonstrated which suggested a "ripple" effect rather than a constant abnormal configuration.

Despite the considerable slowing of circulation to the lower leg there was a striking absence of collaterals in patients with leprosy. As one might expect, patients with active chronic ulcers showed an abnormal vascular blush with early venous return at the site of the infection. A peculiar blushing of the thigh and calf muscles was also noted in the early arterial phase.

It was noteworthy that the sole of the foot the normal fibrofatty layer between bone, ligaments, and the stratum corneum was not seen in areas where trophic ulcers were present. Noteworthy, too, was the fact that in patients who eventually developed trophic ulcers they appeared in areas devoid of normal fibrofatty tissue layers.

It was not clear whether the primary neuropathology in leprosy affects the circulation or whether the circulatory insufficiency to nerve caused the nerve to undergo degeneration.

The bone changes seen in leprosy seem to be secondary to the vascular abnormalities commonly associated with chronic inflammation of the foot. With the chronic inflammation there appears increasing soft tissue tension in the perivascular and perineural portions of the lower extremity. This leads to ischemia with a paucity of collaterals. Trophic ulcers then occur in places of stress where normal tissue is replaced by granulomatous tissue; the bone changes apparently are secondary to the latter.

Philip J. Hodes

Disco-vertebral destructive lesions (so-called Andersson lesions) associated with ankylosing spondylitis. Dihlmann W, Delling G, (Allgemeines Krankenhaus Barmbek, Rübenkamp 148, D-2000 Hamburg 60, Federal Republic of Germany). *Skel Radiol* 3:10–16, 1978

Radiological examination of 31 patients with well established ankylosing spondylitis revealed disco-vertebral destructive lesions. Careful assessment of their radiographic features enabled differentiation between two types: (1) inflammatory, and (2) noninflammatory. Some 44 lesions were considered to be of the inflammatory type either active or a late sequel. The noninflammatory lesions appeared to reflect an attempt at repairing stress fractures in the diseased spinal column. The authors suggest that the term "Andersson lesion" be used to include all disco-vertebral destructive lesions related to ankylosing spondylitis as Andersson was the first to report these lesions.

Radiographically the inflammatory type shows a circumscribed defect in one or two neighboring vertebral bodies associated with varying degrees of narrowing of the intervening disc space usually associated with angular kyphosis of the affected spinal segment. A wide area of reactive sclerosis is evident in the vertebral body surrounding the defect.

The noninflammatory type is characterized either by extensive destruction of two neighboring vertebra or by an area of osteolysis which tends to be confined principally to a single vertebral body. Osteolytic destruction is its cardinal feature with narrowing of the adjacent disc space initially absent.

In the authors' experience, the inflammatory type occurs most commonly during the first 9 years after the onset of ankylosing spondylitis, whereas, the noninflammatory types were observed only after at least 12 years of the disease. The importance of radiologic differentiation between the two relates to their treatment. The inflammatory type usually heals spontaneously with fusion. The noninflammatory type, however, frequently requires surgical intervention.

Philip J. Hodes

Clinical application of bone mineral analysis. Griffiths HJ, Zimmerman RE (University of Rochester School of Medicine and Dentistry, Rochester, New York 14642). *Skel Radiol* 3:1–9, 1978

The authors call attention to the newer isotopic and phantom absorption techniques being used for measuring bone material and the latter technique in particular. The technique has been used in many clinical settings, the most common having been osteoporosis and renal failure. The ease of photon absorptiometric techniques has made possible the study of other conditions and some of these findings are presented.

In acromegaly although the bone may enlarge, the bone mineral remains within the normal range for the size of the bone. In alcoholics, the known decrease in bone mineral is shown to be the result of osteomalacia rather than osteoporosis, the osteomalacia being largely nutritional. Patients on long-standing anticonvulsant therapy show a significant decrease in bone mineral content. Insulin dependent diabetics under the age of 45 usually demonstrated decreased bone mineral, probably related to an associated acidosis.

Photon absorption studies in patients with hyperparathyroidism demonstrated a loss of bone mineral which antecedes the radiographic findings. Certain drugs such as steroids have long been known to lead to loss of bone mineral. More recently heparin and glutethimide have also been incriminated.

Other conditions studied included osteoarthritis, osteoporosis, renal bone disease, and thyrotoxicosis. The article is a good summary of the field.

Philip J. Hodes

Giant-cell tumour of bone. McInerney DP, Middlemiss JH (The Medical School, University Walk, Bristol BS8 ITD, United Kingdom). *Skel Radiol* 2:195–204, 1978

The authors report findings in 138 giant cell tumors in 135 patients with adequate clinical, radiological, and histological information. They reemphasize the subarticular location of most lesions, eccentric to the long axis of bone with ill-defined margins and eroded and expanded overlying bone cortex. Approximately half of the lesions exceeded 6 cm in length along the long axis with linear periosteal reactions and associated soft tissue masses. It is noteworthy that the authors found to individual radiological sign which proved to be helpful in distinguishing tumors which would recur following treatment. Recurrence in an apparently healed and consolidated treated tumor was not uncommon particularly in the first 3 years following treatment.

The rare occurrence of so-called "benign metastasizing giant cell tumors" from bone to lung merited particular attention. The authors call attention to common occurrence of giant cells in many bone neoplasms, both benign and malignant. Their presence was also noted in nonneoplastic lesions (posttraumatic cysts, villonodular synovitis).

Pain was the only or major presenting complaint in 97% of the cases, a mass being palpable in but 26%. Particularly noteworthy was the fact that of 120 tubular bone lesions, all but 14 were situated within 10 mm of the articular cortex. In 101 individuals the tumor involved the articular cortex.

The prognosis of giant cell tumor is influenced by the mode of treatment. The latter is subject to considerations of the site and size of the tumor, its growth rate and complications. The treatment of choice is complete excision or resection without consequent disability. In major long bones curretage with autogenous chip grafting revealed a significant recurrence rate. Generally speaking, small tumors in accessible sites with radiologic signs of slow growth have a better prognosis than larger and apparently more aggressive lesions. The high local recurrence rate in tumors associated with soft tissue extensions claimed by other authors was not confirmed in this study.

Philip J. Hodes

Stress fractures: current concepts. Daffner RH (Veterans Administration Hospital, Durham, NC 27705). *Skel Radiol* 2:221–229, 1978

Stress fractures result from repetitive prolonged muscular action on bones not accustomed to that action. Two synonyms have been used; fatigue fractures and insufficiency fractures.

The authors emphasize that these fractures are not "pathologic" in the sense of occurring in bones which are weakened by preexisting abnormalities. The classic history of stress fracture is that of pain following unusual activity relieved by rest. If the activity continues, pain increases until dramatic fractures of bone become obvious.

Two types of stress fractures occur, compression and distraction. The compression type occurs more frequently in children and elderly patients. They are most commonly located in the neck of the femur, the proximal tibial and calcaneus. Distraction fractures may be transverse, oblique or longitudinal.

Philip J. Hodes

Evaluation of giant cell tumor by computerized tomography. de Santos L, Murray JA (M. D. Anderson Hospital and Tumor Institute, Houston, Tex. 77030). *Skel Radiol* 2:205–212, 1978

The usefulness of computed tomography in the evaluation of giant cell tumor rests upon its ability to demonstrate the presence and extent of its soft tissue component as well as its intraosseous extent. Both appear to be more accurately demonstrated than by conventional radiographic methods.

The authors report findings in 62 patients suspected of having musculoskeletal tumors of which 10 were giant cell tumors. The article contains excellent reproductions of the various lesions thus studied. They concluded that the modality provided important information regarding the extent of the disease. Particularly useful was the combination of computed tomography with angiography. In addition to demonstrating the vascularity of the lesion, it enabled the more accurate assessment of the presence and extent of its extraosseous soft tissue components.

Philip J. Hodes

Nervous System

Computed tomography in olfactory neuroblastoma: one case of esthesioneuroepithelioma and four cases of esthesioneuroblastoma. Manelfe C, Bonafe A, Fabre P, Pessey JJ (Department of Neuroradiology, Centre Hospitalier Universitaire De Purpan 31052 Toulose, Cedex, France). *J Computer Assisted Tomography* 2:412–420, Sept 1978

Neurogenic tumors represent approximately 3% of all neoplasms of the nasal cavity and paranasal sinuses. There has been significant controversy concerning their pathogeneses and histopathology, but recent use of electron microscopic techniques has improved diagnostic specificity in this area. There are three types of tumor of the olfactory placode: esthesioneuroepithelioma, esthesioneurocytoma, and the esthesioneuroblastoma. These represent different degrees of maturation and differentiation of the same tumor yet there is no correlation between the degree of maturation of the tumor and clinical prognosis.

On CT, tumors of this type appear as homogeneous, well circumscribed masses that enhance after contrast infusion. The authors noted attenuation coefficients varying between 30 and 40 HU before and between 66 and 80 HU after contrast enhancement. Calcification was often demonstrated by computed tomography. The orbit was involved in 17% of cases and CT was capable of accurately delineating tumor extension into the orbit, extension into the orbit appearing to be restricted by the medial rectus muscle. In this study, computed tomography was more effective than angiography in estimating intracranial extension. Local recurrence of this tumor is frequent with recurrence occurring up to 13 years after initial treatment. The most

common sites of metastases are brain, lungs, bones, and liver, with a 5-year survival rate of approximately 50%.

Michael J. Meagher

Computed tomography in leptomeningeal spread of tumor. Enzmann D, Kirkorian J, York C, Hayward R (Stanford University School of Medicine, Stanford, California 94305). *J Computer Assisted Tomography*: 2:448–455, Sept 1978

Forty-five patients with documented spread of malignancy to the leptomeninges were examined. Twenty one of these patients had serial CT scans. Forty two patients were scanned after intravenous contrast enhancement, 3 without enhancement. Contrast enhancement of the subarachnoid space and/or loss of definition of the quadrigeminal plate cistern was the CT criterion for subarachnoid tumor.

In this series of forty-five patients, CT scan showed evidence of leptomeningeal tumor in only 10 patients (22%). The detection rate in patients with hematologic malignancy (lymphoma, histiocytosis, leukemia) was extremely low (3%) whereas other neoplasms in the subarachnoid space were detected with much greater frequency (54%).

The CT features of tumor extension to the meninges are not specific and may be shared by various types of meningitis.

Michael J. Meagher

Anterior pituitary function before and after trans-sphenoidal microsurgical resection of pituitary tumors. McLanaham CS, Christy JH, Tindal GT (Emory University School of Medicine, Atlanta, Georgia 30322). *Neurosurgery* 3:142–145, Sept/Oct 1978

The authors report the effect of transnasal transsphenoidal microsurgical resection of pituitary tumors on anterior pituitary function measured pre and postoperatively in 40 patients. This group consisted of 12 males and 28 females ranging in age from 16 to 76 years (mean 39 years). The pituitary-gonadal, thyroidal, and adrenal axes were evaluated. In the 23 patients with normal preoperative values, only two showed impaired function postoperatively. In 10 cases in which only one pituitary-target organ axis was impaired, six showed recovery and one had additional impairment. In the five patients with two major axes impaired, three were improved and two showed further impairment. In the two cases with all three pituitary-target organ axes impaired, no improvement occurred postoperatively.

The results of surgery were related to tumor size. Of 28 patients, 25 with tumors less than 2 cm in size, either retained or regained normal endocrine function after surgery, while only three of the 12 patients with tumors larger than 2 cm did so. Seventeen patients with the amenorrhea-galactorrhea syndrome and nine with acromegaly had good postoperative results with 23 of 26 showing normal endocrine function after surgery. In contrast, of the patients with hyperprolactinemia or nonsecreting tumors only four of 14 showed normal postoperative function.

Paul M. Chikos

Computed tomography on experimental canine hydrocephalus. Part I. Observations on changes of ventricular size and periventricular lucency (in Japanese). Murata T, Mori K, Handa H, Nakano Y (Kyoto University Medical School, Kyoto, Japan). *Brain and Nerve* 30:677–685, June 1978

Morphological changes of canine ventricles in experimental hydrocephalus were studied by sequential computed tomography. Hydrocephalus was induced by cisternal injection of kaolin suspension. CT was performed before and 1, 2, 4, 6, 8, 11 weeks after kaolin injection. Enlarging rate of ventricular size was the most marked in the first week and ventricles reached the maximum size in the fourth to sixth week. Periventricular lucency was noted on CT and was the most prominent around the frontal horns of lateral ventricles. Periventricular low density was distinct in the first week and gradually decreased in intensity thereafter. Pathogenesis of this low density was considered to be edema caused by absorption of cerebrospinal fluid at the ventricular wall.

Hozumi Arii

Significance of bilateral abnormalities on the CT scan in patients with severe head injury. Sweet RC, Miller JD, Lipper M, Kishore PRS, Becker DP (Medical College of Virginia, Richmond, Virginia 23298). *Neurosurgery* 3:16–21, July/Aug 1978

The authors report their experience with 140 severe head injury patients who were unconscious at presentation and had computed tomography within 1 hr. The authors noted that 23 patients with bilateral increased density lesions either at the initial CT scanning or developing contralaterally after surgical intervention had a very poor prognosis with 70% dying and only 26% making a good recovery or remaining moderately disabled. This group of patients also showed a significantly higher incidence (52%) of abnormal or absent motor activity in response to pain and in 12 of the 23 patients elevated intracranial pressure was a clinical problem. In 29 patients, a CT scan appearance showing symmetrical reduction of ventricular size to the point of disappearance with no change or slightly decreased density in brain parenchyma was defined as diffuse edema. These patients did not have a significantly worse outcome than patients with a normal CT scan and had a low incidence (two of 29) of developing increased intracranial pressure. In the 26 patients with normal CT scan, 21 (81%) had a good recovery or were moderately disabled, three (11%) were severely disabled or vegetative and two (8%) died. On the basis of the initial CT scanning, 58 of 140 cases (41%) were diagnosed as having lesions requiring surgical decompression.

Paul M. Chikos

Value of computed tomography in the diagnosis and management of subarachnoid hemorrhage. Modesti LM, Binet EF (Upstate Medical Center, 750 East Adams Street, Syracuse, New York 13210). *Neurosurgery* 3:151–156, Sept/Oct 1978

The authors report their experince with computed tomography with and without contrast enhancement in 31 patients with documented spontaneous subarachnoid hemorrhage: 18 were males and the mean age was 48 years. Subarachnoid hemorrhage was identified on CT scan in 15 of the 31 cases (50%). This figure was improved to 13 of 19 cases (68%), if the study was performed within the first 24 hr of ictus and did not contain gross motion artifacts. In 10 patients (30%), the vascular lesion responsible for subarachnoid hemorrhage was clearly identified on the enhanced CT scan (eight aneurysms and two arteriovenous malformations). In an additional nine cases (35%), the aneurysm itself was not identified on CT scan but the distribution of blood in the subarachnoid space suggested the correct location of the lesion which was confirmed by selective magnification angiography.

The presence of intracerebral hematomas and intraventricular hemorrhage on CT scan were associated with a poor prognosis. In the 11 patients with intracerebral hematomas on CT scan, six died and five remained disabled. In the 10 patients with intraventricular hemorrhage, four died and five remained disabled. In five cases, the CT scan demonstrated areas of decreased density consistent with infarction and in two of these the angiogram showed spasm of the supplying arteries. Ventricular dilatation was also a common finding and was present in 11 of 19 patients (63%) examined by CT scan during the first 24 hr after their ictus and four of these subsequently required shunting. The authors recommend that the CT scan be performed prior to selective angiography and that serial scanning should be used to evaluate ventricular enlargement.

Paul M. Chikos

The small ventricle in pseudotumor cerebri: demonstration of the small ventricle in benign intracranial hypertension by computed tomography. Hahn FJ, McWilliams FE (University of Iowa Hospitals and Clinics, Iowa City, Iowa 52242). *CT: J Computed Tomography* 2:249–253, Sept 1978

The authors report the CT appearance in 13 patients with the diagnosis of benign intracranial hypertension characterized as increased intracranial pressure without focal neurological signs, elevated cerebrospinal fluid pressure with normal cellular and chemical values, and no radiographic evidence of a discrete lesion. The 13 patients ranged in age from 12 to 49 and 11 were female. CT scans were performed with and without contrast enhancement and the size of the ventricles quantitated by using the ratio of the width of the lateral ventricle to the width of the brain at the anterior extent of the frontal horns, (bifrontal, normal 31% ± 4%), and at the level midcaudate nucleus (bicaudate, normal 15% ± 3%).

Using these indices of ventricular size, 11 of the 13 cases (85%) had abnormally small ventricles (10 using the bicaudate index, one using the bifrontal index). In most instances the third ventricle and sylvian fissure were not visualized and the frontal horns were compressed to the point of not being measurable. The differential diagnosis of small ventricles on CT scanning includes brain contusion with or without space occupying hemorrhage, intracranial metastases, viral encephalitis and seizure patients on Dilantin therapy. The authors conclude that a CT scan showing small ventricles and nonvisualization of the third ventricle and sylvian fissure associated with a normal radionuclide brain scan is sufficient for the diagnosis of pseudotumor cerebri without resorting to invasive radiographic methods.

Paul M. Chikos

Utilization and cost-effectiveness of cranial computed tomography at a university hospital. Knaus WA, Davis DO (George Washington University Medical Center, 2300 K Street, N.W., Washington, D.C. 20037). *J Computer Assisted Tomography* 2:209–214, April 1978

This study prospectively surveyed the utilization of cranial computed tomography (CCT) at George Washington University Hospital over a 12 month period. Of 3,070 scans studied, 1,098 (35%) resulted in a positive clinically important diagnosis for an overall case finding cost of $800. Within each of 25 individual indications for scanning, classified on the basis of the patient's most specific sign or symptom, case findings costs varied from a low of $411 for patients in coma to $35,000 for patients with headaches as their only indication for CT scanning. Within two diagnostic categories, malignant brain tumors and cerebral aneurysms, there was significant agreement ($P < 0.001$) between the prescanning diagnosis and the result on CCT. Overall there was also close agreement (correlation coefficient = 0.706) between the rank listing of the 25 indications for scanning compiled prior to CCT with that obtained after the scanning results were known.

Author Abstract

Miscellaneous

CT-assisted pelvic and abdominal aspiration biopsies in gynecological malignancy. Jaques PF, Staab E, Richey W, Photopulos G, Swanton M (North Carolina Memorial Hospital, Chapel Hill, North Carolina 27514). *Radiology* 128:651–655, Sept 1978

The results of 24 CT-directed biopsies performed in 17 women with gynecological malignancy are described by the authors. Eighteen of the 24 biopsies were from the pelvic wall or from a pelvic cyst. Eleven of the 17 patients had carcinomas of the cervix. Sixteen of the 24 biopsies (66%) were considered successful and eight (33%) unsuccessful. No patient developed any complication from the procedure. The authors stress that biopsies reported as suspicious for malignancy demand either a repeat biopsy or surgical exploration. Biopsies reported as "inflammatory tissue" raise the possibility that the clinical situation is not one of recurrent malignancy, but such reports do not exclude this diagnosis.

Herbert C. Berry

Galactography in the radiodiagnostics of the secreting breast. Alberti GP, Nicoli F, Soliani-Raschini C, Voltolini G, Margini F (Department of Radiology, Arcispedale S. Maria Nuova, Reggio Emilia, Italy). *Rays* 2:277–292, 1977

This is a report on galactography and the results obtained in a large series of cases. The technique is quite simple and consists of the introduction in a lactiferous duct of a curved needle of the type used to opacify the lacrimal duct, followed by the careful injection of a small amount of water soluble contrast medium. The authors review the various pathologic processes involving the mammary gland and their appearances, from benign to malignant processes. In the authors' opinion this procedure has proved valuable in improving the radiological evaluation of certain pathological processes and in allowing a definite roentgen diagnosis in false-negative cases.

Numerous illustrations accompany the article.

Antonio F. Govoni

Mammary angiography (in Italian). Ruffato C, Lessi G, Roma R, Valente R, Toson E (Istituto di Radiologia, Ospedale Civile, via Ospedale, I-31033 Castelfranco Veneto, Italy). *Radiol Med* 64:225–250, 1978

This reports on 97 angiograms of the mammary gland performed on 90 patients from 1969 to 1976. The series consisted of 87 females and three males between the ages of 18 and 76: average age 56 years. The localization of the lesions was unilateral and mostly in the left mammary gland (87 cases) and bilateral in three. The histologic diagnosis was mastitis in four cases, abscess in one, mammary dysplasia in 18, benign tumor in 10, Paget's disease in three, and carcinoma in the remaining cases. The technique consists of retrograde injection (under general anesthesia) of 40–50 cc of Conray 60% through the humeral or axillary artery into the subclavian artery. The injection is for 12–15 cc/sec with two radiographs/sec for the first 5 sec and 1/sec for 10 sec. General anesthesia permits a more detailed angiographic study and eliminates the burning sensation felt by the patient during the peripheral arterial stage. This sensation was associated with a brachio-thoracic erythema which was always looked for as a demonstration of satisfactory distal flow.

The angiographic findings are evaluated in the arterial stage, extramammary and mammary; the parenchymal, hyper- and hypovascularization; and, the venous stage, extramammary and mammary.

The various angiographic findings observed in the different pathological processes are described in detail. It is concluded that the procedure is: (1) easy to perform and free of any untoward complications; (2) provides useful information to the surgeon for planning of surgical intervention and also for possible chemotherapy, providing a vascular map of the mammary gland, thoracic wall, and shoulder; (3) is of particular value in those cases which remain doubtful even after the standard radiographic studies and telethermography of the mammary gland or in the cases in which it is not possible to obtain a satisfactory biopsy; and, (4) allows a definite evaluation of the results following surgery, chemotherapy, or irradiation.

A. F. Govoni

Computed tomography of the larynx. Archer C, Yeager V, Friedman W, Katsantonis G (St. Louis University School of

Medicine, St. Louis, Missouri 63104). *J Computer Assisted Tomography* 2:404–411, Sept 1978

The larynx is evaluated using computed tomographic techniques with sectioning in sagittal, transaxial, and coronal planes. High quality reproduction of scans and corresponding labeled photographs of tissue specimens are shown.

Michael J. Meagher

Evaluation of abdominal abscess with computed tomography. Aronberg D, Stanley R, Levitt R, Segal S (Mallinckrodt Institute of Radiology, Washington University School of Medicine, 510 South Kings Highway, St. Louis, Missouri 63110). *J Computer Assisted Tomography*: 2:384–387, Sept 1978

A retrospective study of 34 patients whose abdominal abscesses were investigated with computed tomography evaluated the efficacy of this technique in such a patient group. CT scans were done on an EMI 5005 body scanner. In 31 of the 34 patients with an abdominal abscess, computed tomography both suggested the correct diagnosis and assisted in defining its extent. The CT signs of intraabdominal abscesses were variable but, in general, included a low attenuation value and mass effect, often with a higher density peripheral rim after intravenous contrast enhancement. Additional CT findings in this pathologic process included the definition of abnormal (extraluminal) gas collections. A number of the patients in this study were also examined using radionuclide (gallium) techniques. However, rigorous comparison between the various modalities was not made.

Michael J. Meagher

Radiologic aspects of cancer of the breast in men. Dana A, Markovits P, Bergiron C, Contesso G, Gadenne C (Hôpital Necker, 151 rue de Sévres, F 75015, Paris, France). *J Radiol Electrol Med Nucl* 59:463–469, 1978

The value of mammography in the examination of the female breast has long been recognized and the practice is well established. In the male, however, cancer of the breast is much less frequent, thus the opportunity to study this tumor is limited. The published reports are very few. The authors stress the significant role of mammography in the diagnosis of cancer of the male breast, and the importance of correlating the clinical, radiological, and pathological (gross and microscopic) findings.

A series of 25 cases of cancer of the breast in the male was observed during a 16-year period. On each patient the clinical diagnosis, or suspicion, of a malignant breast tumor was confirmed by mammography and histologic examination of the biopsy specimen. There were 24 cases of adenocarcinoma of the breast and one case of sarcoma, most probably of muscular origin. The overall appearance and course of breast cancer in the male is not unlike that in the female. Physical examination reveals a hard nodular painless mass, often irregular. Central ulceration is present in long standing cases. Axillary metastasis was the rule rather than the exception. The macroscopic appearance of the tumor in the male is essentially the same as in the female, likewise the general histologic pattern. Microcalcification is strikingly absent. It was observed only in one case. The average size of the tumor as measured on the gross surgical specimen was 27 × 22 mm which is close to the tumor size of 25 × 21 mm as determined radiologically. Infiltration of the nipple was present in 20 cases: 17 massive and three less pronounced being intracanlicular. There were five cases of superficial Paget type cutaneous infiltration. Three patients had bilateral involvement of the breasts.

With the exception of two patients, aged 27 and 43, the average age was 63.7 years, with an age distribution of 50–80 years. The technique of the mammographic examination is essentially the same as in the female, usually consisting of a craniocaudal and lateral projection. In breasts which are very small, or reduced in size due to retractions, the projections were adjusted accordingly. The authors stress the importance of maintaining immaculate technique and of obtaining radiographs of the highest quality.

William H. Shehadi

Lymphography of the lower extremities in the presence of moderately altered dynamics of lymph flow. Bujar H, Bratan L, (Hopital-Clinique Colentine, Institut de Medecine Interne/Service de Radiologie, 19–21 Sos Stefan cel Mare, 72202 Bucarest 10, Rumania). *J Radiol Electrol Med Nucl* 59:478–492, 1978

Obstruction of the lymphatic circulation is not an uncommon manifestation of a variety of benign and malignant diseases. Advanced cases with pronounced chronic lymphedema are well known and readily recognized. However cases with early to moderately altered dynamics of the flow of lymph have not received the attention they deserve, both by the clinician and the radiologist. Early detection and appropriate treatment will prevent the development of more severe and disabling forms of this condition.

The authors report a series of 87 lymphangiographies of the lower extremities selected from a total of 211 lymphangiograms performed during a 3-year period. The lower extremities are particularly vulnerable to trauma and infection. The patients included in this study suffered from phlebitis, arthritis, chronic skin conditions, contusions, fractures, burns, arteritis, and the results of postirradiation changes after treatment of malignant disease.

The classical Kinmonth technique was used, injecting 0.1 ml ethiodol/min to a total of 10 ml in 10 min. Radiographs of the legs and thighs were made immediately after the injection and at 24 hr. The immediate films revealed one or more of the following: dilatation, retraction, tortuosity of the lymph vessels, localized cysts or pseudocysts, extravasation, and collateral circulation with the deeper vessels. The delayed films revealed prolonged stasis and more pronounced extravasation.

Based on the history and physical findings the patients in this series were divided into three groups: (1) those with previous as well as present symptoms, 53; (2) those without previous symptoms but with present symptoms, 11; (3) those with history of previous symptoms but no present symptoms, 23. The most frequent symptoms, and findings were pain, mild to moderate dependant edema in the late afternoon and evening, skin lesions (chronic inflammation), scars, pigmentation, and atrophy. Edema and pain occurred most frequently in patients with a history of phlebitis. Although some patients had no definite complaints and seemed to have adequately compensated, this was not the case with the majority. These latter run the risk of persistence and intensification of the symptoms, with accompanying increased suffering and disability. The authors voiced the need for a technique of microsurgery that will correct and reestablish proper circulation, alleviate the patients' symptoms and prevent worsening of the condition.

William H. Shehadi

Metopism in iron deficiency disease. A roentgenological study (in German). Reimann F, Gedikoglu G, Talasli U (Kinderklinik und Institut fuer Radiodiagnostik der Medizinischen Fakultaet Capa der Universitaet Istanbul, Saray Arkasi Sok. 20/4 Istanbul Ayaz Pasa, Turkey). *ROEFO* 129:246–249, 1978

In 166 patients, age 7–30 years, with severe chronic iron deficiency anemia since early childhood, a metopic suture was found in 40 (25.5%) and remnants of it in 41 (26.1%). In the remaining 76 (48.4%), a metopic suture was not visible. Another group of 13 patients (age 31 to 50 years) had an iron deficiency anemia which developed after childhood. In this group, an open metopic suture was found in two patients, remnants of it in two, and no evidence of a metopic suture in nine. In a third group of 48 patients with severe chronic anemia not caused by iron deficiency, these conditions were found: encompassing thalassemia major and intermedia (32); congenital hemolytic anemia (8); juvenile pernicious and nutritional megaloblastic anemia (6); and Fanconi anemia (2); a metopic suture could not be seen

in any case. The authors conclude that iron deficiency related growth disturbance rather than the anemia per se is responsible for the retarded occlusion of the metopic suture and the presence of a metopic suture in adults would indicate an iron deficiency in or since early childhood.

Peter F. Winter

Ultrasonics

Echocardiographic evaluation of the postoperative tetralogy of Fallot patient. Vick GW III, Serwer GA (Division of Pediatric Cardiology, P.O. Box 3090, Duke University Medical Center, Durham, North Carolina 27710). *Circulation* 58:842–849, Nov 1978 (by permission American Heart Association)

Echocardiographic and cardiac catheterization results were compared in 21 patients with tetralogy of Fallot. All patients had previously undergone total repair, and all except one were greater than 1 year postsurgery. Twenty of these patients were placed into one of the three groups based upon the degree of residual abnormalities present at cardiac catheterization. Group I ($n = 11$) had no residual intracardiac shunting and had right ventricular (RV) peak systolic pressures less than 45 mm Hg. All had mild pulmonic insufficiency and pulmonary stenosis with no tricuspid insufficiency. Echocardiographically, all except one had a larger-than normal RV diastolic dimension (RVDD) and all had smaller-than-normal-to-normal left ventricular diastolic dimension (LVDD). The RVDD/LVDD ratio was less than 0.65 in all. All had normal left ventricular (LV) function by echocardiographic and angiographic methods. Group 2 ($n = 6$) had no residual shunting but did have significant elevation of the RV pressure, with the peak systolic pressure > 75 mm Hg in all patients. Pulmonary artery pressure was normal in all. In addition, all had mild pulmonic insufficiency with no tricuspid insufficiency. Echocardiographically, all had a large RVDD, with a smaller-than-normal-to-normal LVDD. The RVDD/LVDD was $>$ 0.90 in all cases. The LV function was normal. Group 3($n = 3$) had either tricuspid insufficiency or severe pulmonic insufficiency. None had residual shunts. All had normal RV pressures. Echocardiographically, all had a large RVDD with a normal or smaller-than-normal LVDD and an RVDD/LVDD > 0.80. Additionally, all had classic paradoxical septal motion not found in either group I or group 2. The remaining patient, who was five months postsurgery, had a catheterization of a large left-to-right shunt through a residual ventricular septal defect. The RV and pulmonary artery pressure was systemic. Echocardiographically, the LVDD and RVDD were large, and the patient had a very large left atrial dimension. The RVDD/LVDD was 0.88. The echocardiographic findings accurately reflected the degree of residual defects in the long-term postoperative patient with tetralogy of Fallot, making them extremely useful in the postoperative management and follow-up of such patients.

Author Abstract

High-resolution real-time ultrasound in the evaluation of the normal and obstructed biliary tract. Cooperberg PL (Vancouver General Hospital, Vancouver, B.C.). *Radiology* 129:477–480, Nov 1978

The common hepatic duct was shown using a high-resolution real-time mechanical sector scanner as it passed anterior to the right portal vein. This was demonstrated in 98 out of 100 consecutive adult subjects without biliary tract disease. The internal diameter of the duct at this level ranged from 1–4 mm (average 3.2 mm). All patients with a duct diameter larger than 5 mm had either biliary obstruction or previous cholecystectomy.

Stephen J. Carter

Echocardiographic features of constrictive pericarditis. Voelkel AG, Pietro DA, Folland ED, et. al. (Veterans Administration Hospital, 1440 VFW Parkway, West Roxbury, Massachusetts 02132). *Circulation* 58:871–875, Nov 1978 (by permission American Heart Association)

The most characteristic echocardiographic features of 12 patients with constrictive pericarditis were compared with the findings in 10 normal volunteers. Left ventricular posterior wall (LVPW) "flatness" was quantified by measuring the diastolic change in distance from the crystal artifact to the LVPW endocardium. In 11 of 12 patients the net diastolic LVPW endocardial movement was > 1 mm. In 10 normal volunteers LVPW endocardium moved posteriorly in diastole from 1.5 to 4 mm (mean 2.2 ± 0.8).

Abnormal septal motion was present in five of 12 patients with constriction. Pericardial thickness measured using standard damping techniques for both constriction and normal populations did not distinguish the two groups.

The "flattening" of the left ventricular endocardium as quantified above verifies earlier qualitative observations and was the most consistent finding in this series of patients with constrictive pericarditis.

Author Abstract

Gray scale B scan characteristics of intra-abdominal cystic masses. Hill M, Sanders RC (University of Miami, P.O. Box 520875, Biscayne Annex, Miami, Florida 33152). *J Clin Ultrasound* 6:217–222, 1978

Hill and Sanders have described the sonographic characteristics of intraabdominal cystic masses in 119 cases. Internal echoes were a common finding and of little differentiating value, except in renal cysts where they were uncommon (2/25). Likewise, internal septa were nonspecific, being found in most types of lesions, but most commonly seen in mucinous cystadenomas (5/5), abscesses (9/24), and lymphoceles (5/12). Fluid/fluid levels were an uncommon finding and seen only in abscesses (2/24) and hematomas (3/20). Gross wall irregularity was most common in abscesses (6/24), lymphoceles (2/12) and malignant neoplasms (1/3), but also seen in 1/3 pancreatic pseudocysts, 1/20 hematomas, and 1/5 mucinous cystadenomas.

Conformity of the cystic mass to an adjacent organ was a relatively specific and common finding in hematoma (10/20) and seen in only 1/24 abscesses, 1/12 lymphoceles and 1/5 mucinous cystadenomas. The other cystic masses tended to displace and compress adjacent organs. Four of 24 abscesses and all three malignant neoplasms were the only lesions to produce adjacent soft tissue changes. The authors conclude that necrotic neoplasms and some abscesses and hematomas have gray scale characteristics that enable a specific diagnosis to be made from the echogram. In the other lesions, the list of likely possibilities can be narrowed significantly and, when indicated, aspiration can be performed under ultrasound control.

John D. Denney

The liquid-filled stomach—an ultrasonic window to the upper abdomen. Warren PS, Garrett WJ, Kossoff G (Royal Hospital for Women, Sydney 2021, Australia). *J Clin Ultrasound* 6:315–320, Oct 1978

An ultrasonic window to the upper abdomen is created by (1) filling the fasting stomach with methylcellulose suspension, (2) administering glucagon intravenously, and (3) examining the patient prone. Glucagon relaxes the gastric musculature and the prone position allows the stomach gas to rise to the fundus. This enables assessment of the relationships of the stomach to adjacent structures and permits display of structures forming the stomach bed. The equipment used was a commercially available water-delay system with wide-aperture focused transducers. The system gives good resolution and allows the gastric musculature to be distinguished from the mucosa and its overlying mucus.

Author Abstract

The upright position while giving water for the evaluation of the pancreas. Jacobson P, Crade M, Taylor K (Yale University School of Medicine, New Haven, Connecticut 06510). *J Clin Ultrasound* 6:353-354, Oct 1978

The authors recommend ultrasound examination of the patient while standing upright and drinking water through a straw for better visualization of the body and head of the pancreas in patients who would otherwise have to be rescheduled or examined by other means. Serial oblique and transverse scans are made with the patient remaining erect. This method supplements their previously published technique of having the patient drink water through a straw while being rotated from supine to a right-side down postion.

Stephen J. Carter

Nuclear Medicine

Extraosseous tumor uptake of 99m technetium phosphate compounds in children with abdominal neuroblastoma. Young G, L'Heureux P (University of Minnesota Hospitals, Minneapolis, Minnesota). *Pediatr Radiol* 7:159-163, Sept 1978

Sixteen patients with abdominal neuroblastoma had 99m technetium phosphate compounds (99m Tc-Pc) bone scans as a preoperative evaluation for metastatic disease. Ten patients (62%) had extraosseous tumor uptake while six patients (38%) did not. There was no difference in the incidence of tumor calcification, tumor necrosis or hydronephrosis in the two groups. However, VMA levels were significantly higher in the group with extraosseous tumor uptake. Various bone seeking radionuclides are compared to 99m Tc-Pc and possible mechanism for extraosseous uptake of such radionuclides are postulated. Awareness of the frequency of such uptake should reduce the possibility of errors in interpretation of bone scans in patients with neuroblastoma.

Author Abstract

The interpretation of phlebograms using fibrinogen labeled with ^{99m}Tc. Jonckheer MH, Abramovici J, Jeghers O, Dereume JP, Goldstein M (Department of Isotopes, A.Z. Vrije Universiteit Brussels, Bosstraat, B-1090 Brussels, Belgium). *Eur J Nucl Med* 3:233-238, 1978

This is a report on a new procedure for the detection of deep-vein thrombosis using antecubital injection of 20 mg of fibrinogen which has been labeled with 3-5 mCi of ^{99m}Tc. The optimal time for obtaining images was found to be 2 hr after injection. The patient voids before scintiscanning; 300,000-500,000 cps images are taken over the lower abdomen and thighs anteriorly, popliteal fossae and calves, posteriorly.

The results obtained in 14 consecutive radiologic and isotopic examinations done on 13 patients showed that four findings were important in the diagnosis of deep vein thrombosis in the scintiscans: (1) definite "hot-spots" produced by localization of TcFi into the thrombi; (2) nonvisualization of a large vein or a segment, representing an early deep vein thrombosis; (3) opacification of veins which are not usually visualized, such as the saphenous vein, indicating collateral circulation; (4) irregular, at times bead-like appearance of a vein, a finding which in most cases indicates thrombosis of vein in a stage of recanalization. Illustrations demonstrate findings.

Antonio F. Govoni

Internal mammary lymphoscintigraphy: a rational adjunct to the staging and management of breast carcinoma. Ege GN (Department of Nuclear Medicine, Princess Margaret Hospital, 500 Sherbourne Street, Totonto, Ontario M4X 1K9, Canada). *Clin Radiol* 29:453-456, July 1978

Radionuclide lymphoscintigraphy utilizing the bilateral subcostal introduction into the posterior rectus sheath of a small volume of radiocolloid of suitable particle size, ^{99m}Tc antimony colloid, has provided scintigraphic images of diagnostic quality of the parasternal nodes in 2,328 patients with malignant disease. An evaluation of the use of this technique in 1,072 patients with breast carcinoma underlines the value of a procedure which, utilized routinely, should alter conventional staging criteria and provide a more rational basis for the management of patients with breast carcinoma and assessment of end results.

Author Abstract

Computerized tomography and nuclear imaging of the liver: a comparative study of 83 cases. Scherer U, Büll U, Rothe R, Eisenburg J, Schildberg FW, Meister P, Lissner J (Radiologische Klinik der Universität, München, Klinikum Grosshadern, Marchioninistr. 15, D-8000 München 70, West Germany). *Eur J Nucl Med* 3:71-80, 1978

This study was performed to assess the relative diagnostic accuracy of computed tomography and nuclear liver scanning in detecting and defining circumscribed and diffuse liver diseases in 83 patients. Proof of liver status was based on invasive procedures such as biopsy, laparoscopy, laparotomy, and/or autopsy.

The percentage of true negative diagnoses was 94% for CT and 91% for static gamma imaging. With a rate of 94% true positive diagnoses, CT proved to be superior to radiocolloid gamma imaging (81% true positives) in diagnosing focal liver disease. CT was superior to nuclear imaging in discriminating the number and size of space occupying lesions. In contrast to nuclear screening, CT scans were pathognomonic in some focal liver disease such as cyst, metastasis, and echinococcus disease. Nuclear imaging was superior in cirrhosis.

Antonio Govoni

Serial bone scintigraphy for assessing the effectiveness of treatment of osseous metastases from prostatic cancer (in English). Langhammer H, Sintermann R, Hör G, Pabst HW (Nuklearmedizinische Klinik und Poliklinik rechts der Isar der Technischen Universität München, Ismaninger Str. 22, D-8000 München 80, West Germany). *Nuklearmedizin* 17:87-91, 1978

In 36 patients with skeletal metastases from prostatic cancer, serial bone scans were performed at intervals of 2-6 months to evaluate the response to therapy with estrogens and/or cytostatic drugs. Fourteen patients showed markedly decreased to normal uptake in the metastatic bone lesions following the initial scan, accompanied by a return of the elevated serum alkaline phosphatase levels to normal and signs of clinical improvement. In these patients, a transient rise in uptake by the bone lesions during the first months following commencement of therapy, as reported by others, was not observed.

Increased multifocal skeletal uptake was found in the remaining 16 patients, indicating progression of the disease. The authors conclude that skeletal scintigraphy is not only an important diagnostic tool for the early detection of osseous metastases but also of considerable value for assessing the response to therapy.

Peter F. Winter

^{67}Ga scanning in the evaluation of anaplastic carcinoma and malignant lymphoma of thyroid gland (in Japanese). Ito K, Mimura T, Ban Y, Hamada N, Nishikawa Y, Higashi T (Ito Hospital, Tokyo, Japan). *Jpn J Clin Radiol* 32:463-470, April 1978

Thirty cases with thyroid nodules were evaluated with ^{67}Ga citrate scanning to evaluate its use in preoperative diagnosis of anaplastic carcinoma and malignant lymphoma. Scanning was performed 48 hr after intravenous injection of ^{67}Ga-citrate in doses between 1.5 mCi to 3 mCi. In nine of 10 cases of anaplastic carcinoma, marked accumulation was observed. The other patient had undergone irradiation and chemotherapy and no accumulation was noted. Only slight accumulation of radio-

nuclide was seen in three of 13 cases with adenocarcinoma. There were three cases of malignant lymphoma and in these ^{67}Ga scans were strongly positive.

Marked uptake was observed also in three cases of chronic thyroiditis making it difficult therefore to differentiate chronic thyroiditis from malignant lesions. It was concluded, however, that ^{67}Ga scans could be useful in assessing the prognosis of cases with malignant thyroid tumors.

Hozumi Arii

Radiation Oncology

An acceptable rate of complications in combined doxorubicin-irradiation for small cell carcinoma of the lung: a Southwest Oncology Group study. Moore TN, Livingston R, Heilbrun L, Durrance FY, Tesh D, Hickman B, Bogardus C (Southwest Oncology Group, 3500 Rainbow Boulevard, Suite 100, Kansas City, Kansas 66103). *Int J Radiat Oncol Biol Phys* 4:675–680, Sept/Oct 1978

The authors present the combined Adriamycin-irradiation complications for patients with oat cell bronchogenic carcinoma (383) treated under the SWOG protocol from 1974–1976. Of these, 358 patients were evaluable. Chemotherapy consisted of Cytoxan (750 mg/m²) on weeks 0, 3, 12, 15, 18 etc., Adriamycin (50 mg/m²) on weeks 0, 3, 12, 15, 18, and Oncovin (1 mg) weekly for 12 weeks then discontinued. Irradiation consisted of 300 rad × 10 to brain and primary starting on week 6 plus an additional 380 rad × 5 at week 12 for patients with limited disease (2 HVL posteroanterior spinal cord block).

Of the 171 irradiation treated extensive disease patients, four developed significant esophagitis (two severe). Of the 89 limited disease patients irradiated under the protocol, nine developed significant esophagitis (seven severe). The overall incidence of significant esophageal symptoms was 5 (13/260). Seven patients developed significant radiation pneumonitis. Seven patients experienced cardiac reactions, two experienced epithelial reactions (4,500 rad), and two developed cerebral symptoms. The authors feel these represent an acceptable rate of complications.

Herbert C. Berry

Radiation-induced soft-tissue and bone sarcoma. Kim JH, Chu FC, Woodard HQ, Melamed MR, Huvos A, Cantin J (J. H. Kim, Memorial Sloan-Kettering Cancer Center, New York, New York 10021). *Radiology* 129:501–508, Nov 1978

The results of a retrospective analysis of patients receiving radiation therapy at Memorial Hospital over the past 50 years are presented with respect to radiation-induced sarcomas. Of the 47 patients with this established diagnosis, 20 had soft-tissue sarcoma arising in irradiated tissues and 27 had bone sarcoma arising from normal bones in the irradiated field. Latent periods were 12 and 11 years respectively. No radiation-induced bone sarcomas were seen at doses below 3,000 rads in 3 weeks. It appeared that children were more sensitive to cancer induction than adults. Sixteen of the 27 patients with radiation-induced bone sarcoma had received treatment with orthovoltage irradiation. No specific radiation therapy equipment data is presented for the radiation-induced soft-tissue sarcoma patients. A general discussion of the risk of radiation-induced sarcoma is presented.

Herbert C. Berry

Second neoplasms following megavoltage radiation in a pediatric population. Haselow RE, Nesbit M, Dehner LP, Khan FM, McHugh R, Levitt SH (R. E. Haselow, Box 494, University of Minnesota Hospitals, Minneapolis, Minnesota 55455). *Cancer* 42:1185–1191, 1978

The results of a retrospective analysis of 88 pediatric survivors of megavoltage irradiation for neoplasm treated at the University of Minnesota with an average follow-up period of 14 years are described. Seven second neoplasms were discovered, five of which were not associated with prior irradiation. Two of the seven neoplasms were malignant, one not being associated with the irradiation, the other associated with prolonged chemotherapy (chlorambucil). Both radiation-related neoplasms were associated with low doses (less than 1,500 rads). Based on these preliminary findings the authors suggest a low risk (1%) of induced malignancy following megavoltage irradiation.

Herbert C. Berry

Esophagitis due to Adriamycin and radiation therapy for childhood malignancy. Newburger PE, Cassady R, Jaffe N (Division of Hematology-Oncology, Children's Hospital Medical Center, 300 Longwood Avenue, Boston, Massachusetts 02115). *Cancer* 42:417–423, 1978

Esophagitis is described in seven patients receiving mediastinal irradiation and chemotherapy including Adriamycin for non-Hodgkin's lymphoma, osteogenic sarcoma, and acute lymphocytic leukemia. Doses of irradiation ranged from 500–2,500 rads, recall occurred in three patients including two episodes in one patient related to Adriamycin administration. Stricture occurred in this patient as well as one of the other recall patients but in none of the others. The patients were aged from 2½ to 21 years, strictures occurring in the 21-year-old patient with acute lymphocytic leukemia and the 2½-year-old patient with non-Hodgkin's lymphoma. This study confirms the observation of Adriamycin-enhanced radiation esophagitis in childhood, and extends the minimal radiation dose range to 500 rad, well below the level at which even mild dysphagia has been previously reported.

Herbert C. Berry

Non-Hodgkin's lymphoma. Involvement of Waldeyer's ring. Hoppe RT, Burke JS, Glatstein E, Kaplan HS (Division of Radiation Therapy, Stanford University Medical Center, Stanford, California 94305). *Cancer* 42:1096–1104, 1978

The authors review 59 patients with non-Hodgkin's lymphoma involving Waldeyer's ring evaluated at Stanford from 1953–1976. Most had less than stage IV disease. Of the patients with clinical stage III disease, 67% had bone marrow involvement. Ninety per cent of the biopsies were diffuse and in 55% the cell type was histiocytic. Most patients with stage I or II disease were treated with involved field or extended field irradiation, although some received total nodal irradiation along with the stage III patients. The stage I patients had a 50% 6-year relapse-free survival as opposed to 25% and 17% for stages II and III respectively. Most relapses occurred in untreated nodes. The bone marrow was the second most common site of relapse (10 patients).

Herbert C. Berry

Uterine sarcomas natural history, treatment and prognosis. Salazar OM, Bonfiglio TA, Patten SF, Keller BE, Feldstein M, Dunne ME, Rudolph J (Division of Radiation Oncology, P.O. Box 647, University of Rochester Cancer Center, 601 Elmwood Avenue, Rochester, New York 14642). *Cancer* 42:1152–1160, 1978

Seventy-three patients with uterine sarcoma are reviewed. All were seen at University of Rochester Strong Memorial Hospital from 1955 to 1975. There are three main histologic varieties: mixed mesodermal sarcoma (MMS), leiomyosarcoma (LMS), and endometrial stromal sarcoma (ESS). MMS was seen in 60% of the patients and LMS occurred in younger patients and tended to be stage I more often (80%) than the other cell types.

Of the patients, 45% were treated with surgery only, 43% with surgery and irradiation, and 12% with irradiation alone. Five-

year survival for MMS, LMS, and ESS was 22%, 38% and 39%, respectively. Overall 5-year survival for stage I patients was 54% versus 11% for stages II–IV. Five-year survival for stage I patients treated with surgery plus irradiation was 62% versus 53% in those treated by surgery only ($p > .05$). There were no significant differences for surgery versus surgery plus irradiation in more advanced tumors with 5-year survivals of 17% and 3% respectively.

The authors suggest surgical exploration for adequate staging and if resectable, TEH and BS&O should be performed. They then suggest adjuvant postoperative irradiation with 5,000 rads whole pelvis plus a 4,000 rad vaginal surface dose if the cervix is involved or if there is a high degree of suspicion of vaginal cuff residually.

Herbert C. Berry

Systematic restaging in patients with Hodgkin's disease. Herman TS, Jones SE (Section of Hematology and Oncology, University of Arizona College of Medicine, Tucson, Arizona 85724). *Cancer* 42:1976–1982, 1978

The authors report the results of systematic restaging according to the Southwestern Oncology Group protocol 7,406 for the treatment of patients with advanced Hodgkin's disease (Ann Arbor Stages III B, IV A, IV B). Treatment was randomized to MOPP + Bleomycin versus MOP – BAP #1 versus MOP – BAP #2 (Adriamycin day 8 or Adriamycin days 1 and 8 respectively). A total of 82 patients in complete clinical remission after 10 courses of chemotherapy were systematically restaged. No patient had received prior chemotherapy although about 25% had received prior irradiation. Ten patients had disease detected at restaging (12%) only one of whom had prior irradiation. Sites of residual disease were found almost entirely in lymph nodes (abdominal six, mediastinal three, and peripheral one) with only one of the 11 sites of persisting disease detected in an extranodal location. Chest radiography, gallium-67 tumor scanning, and lymphography were the most helpful procedures for detecting residual disease. Of the 72 patients felt to be free of disease after restaging, nine (13%) relapsed within 8 months.

The authors compare the results of this study with results of a previously published study regarding the use of systematic restaging in patients with non-Hodgkin's lymphoma and show significant differences in relapse rates at restaging (24% versus 12% for non-Hodgkin's lymphomas versus Hodgkin's disease, the use of chest radiography 1% versus 8% respectively, the use of bone marrow biopsy 13% versus 0% respectively, and the distribution of disease sites detected at restaging 41% versus 91% for nodal failure respectively and 59% versus 9% for extranodal failure respectively). The authors feel that systematic restaging of all patients who achieve apparent complete remission should be part of every future lymphoma treatment trial in order to more accurately assess the results of therapy.

Herbert C. Berry

Conservative management of operable breast cancer, 10 years experience at the Foundation Curie. Calle R, Pilleron JP, Schlienger P, Vilcoq JR (Foundation Curie, 26 Rue D'Ulm, 75231 Paris Cedex 05, France). *Cancer* 42:2045–2053, 1978

The authors have reviewed the results of 514 patients with surgically operable Stage T_1–T_3 and N_0–N_{1b}, infiltrating breast cancer referred to the foundation for conservative treatment with irradiation. Of these patients, 258 have a minimum follow-up of 10 years. To avoid deformity of the breast, the majority of patients who had lumpectomy had tumors which were 3 cm or less in diameter. For tumors greater than 3 cm in diameter (T_1, T_2, T_3) with or without clinically palpable nodes or smaller tumors with clinically suspicious axillary nodes, exclusive irradiation was performed. The former group received a tumor dose of 5,000 rads to breast and regional nodes with an additional 1,500 rads delivered to the lumpectomy area and an additional 1,000 rads to the lower axillary region. The latter group received 5,000–6,000 rads from 6 to 7 weeks to breast and nodal sites and with 50% or more regression was then boosted through reduced field to the primary mass for a dose of 2,000–2,500 rads plus an additional 1,000–1,500 rads to the lower axilla. Surgery was performed as additional treatment if there was no initial reduction in size after 5,000–6,000 rads or if there was persistent disease at 6 to 9 months in the case of small residual tumor remaining at the end of treatment.

Lumpectomy was performed on 120 patients and followed by irradiation with an 85% NED rate at 5 years and a 75% NED rate at 10 years (68 patients having a minimum follow-up of 10 years). Of the total group at 5 and 10 years, six patients had mastectomy and two had limited surgery for recurrence. Radiation sequelae in this group were minimal in 28%, moderate in 45%, and in 27% no severe radiation sequelae were noted.

Of the 394 patients treated exclusively by irradiation, 190 patients had a minimum follow-up of 10 years. The absolute survival NED at 5 and 10 years was 68% and 43% respectively. Of 394 patients, 234 (59%) required secondary surgery either for persistent or recurrent disease (81% persistent, 19% recurrent). Twenty per cent of this group had minimal radiation sequelae, 33% had moderate, and 1% severe (four patients).

The authors feel that lumpectomy followed by irradiation appears to be an adequate therapeutic method provided the tumor is unifocal, equal to or less than 3 cm, and without clinically suspicious axillary nodes. They point out that radical radiotherapy is the primary modality and is a more complex situation requiring meticulous techniques and close cooperation between the surgeon, radiation oncologist, and patient.

Herbert C. Berry

Book Reviews

Pain and Profit. The Politics of Malpractice. By Sylvia Law and Steven Polan. New York: Harper & Row, 305 pp., 1978. $12.95

Pain and Profit is a text which purports to be an objective, documented, and concerned analysis of the malpractice crisis. It alleges to examine the extent of chronic substandard medical practice in this country and to analyze the inadequate methods of professional self regulation and control. It also claims to evaluate equally the legal profession and its role in exploiting the crisis. No fault insurance and the supposed venality of contingency fees are to be analyzed. The authors then detail a number of proposed reforms, note some that have been enacted, and discuss potential for solving portions of the medical malpractice issue.

The book is interesting reading for all concerned with public health policy. It reflects the experience and bias of the authors to a much greater extent that may be recognized by introductory statements. If the reader accepts this bias, the text will be enjoyable, informative, and worthwhile.

In the introduction, the authors offer background on medical malpractice and the rise of the fault system. They correctly place medical malpractice into the law of torts and intelligently discuss the fiction of the reasonable man. They also note the legal standard applied to physician liability is that of the standard of the profession itself. The introduction concludes by emphasizing the difficulties that a patient has in providing evidence that a physician deviated from reasonable practices.

The second chapter, The Maldistribution of Malpractice, discusses the lack of appropriate distribution of physicians in the country and the trends toward subspecialization. Law and Polan emphasize that the laws of supply and demand do not assure that the supply of physicians will correspond to needs. This chapter also discusses how insurance programs, Medicare, and loan programs affect the distribution of physicians and the opportunity for certain population groups to receive compensation for injuries. The authors conclude that fault-based liability and variations in malpractice insurance rates do not directly influence physicians with regard to either the geographical location of their practice or their type of practice.

Chapter three concerns the problems of malpractice generated by physicians who engage in substandard delivery of health care. The major theme is that the present system is unreliable and not balanced. The groups that monitor physicians do not have enough regulatory control. In many states, professional incompetence is not grounds for disciplining a physician by the state medical board. The authors feel that the general powers of state medical boards need to be made explicit. The reporting system with regard to physicians, by hospitals, professional societies, and insurance companies, does not provide reasonable data upon which to judge the general practices of any individual. The authors term this a "conspiracy of silence" that is not acceptable to the public and should be unacceptable to physicians. The authors state that the overwhelming evidence is that professional ethics do not motivate physicians to take their peer review responsibility seriously. Unfortunately, no data are provided.

Chapter three also discusses the general practices of hospital staffing and suggests reasonable improvements. The authors conclude that there is inadequate effort to discover and to discipline physicians who regularly provide unacceptable care.

The activities of hospitals and their relation to malpractice is discussed in chapter four. Of reported malpractice, 75% occurs in hospitals, and 79% of all claims arise from hospital-incurred injuries. In addition, 83% of all settlement payments are for injuries suffered in hospitals. This chapter discusses the legal structure in which hospitals function and the activities of the Joint Commission on Accreditation of Hospitals, and describes the liability of hospitals for the negligent acts performed by physicians within the scope of their employment. Also considered is the response of the Joint Commission to the malpractice crisis. The authors discuss the effect and activities of the Professional Standards Review Organization which was mandated by Congress in 1972.

The chapter concludes by suggesting possible reforms. These include requiring hospitals to establish review mechanisms that collect information about individual physicians; reviewing physician activities on a systematic basis; and identifying those who falsify records and engage in unnecessary or incompetent practices. This review process should include those who do not have a vested interest in the welfare of the hospital or the physicians. Although the proposals may be implemented by the Joint Commission, the authors believe this organization's accreditation process fails to provide sufficient incentive for hospitals to take their institutional responsibilities seriously. They suggest that legislative and common law changes are necessary, and discuss the approach of channeling, which makes hospitals institutionally liable for all malpractice within their corporate entities. Law and Polan advocate that hospitals pay most physician malpractice insurance costs. The authors also believe need exists for a national publicly accountable agency to set and apply standards for hospitals.

Chapters five through eight consider the effect of the legal system on the malpractice issue. The initial discussion involves the effect of the contingent fee system on medicine. While this system is viewed by physicians as undesirable, the authors point to a number of positive features including providing lawyers with the incentive to accept only cases with a reasonable prospect of success. The American contigent fee system provides assurance that the ordinary citizen has access to legal services. The authors admit that this system encourages lawyers to argue for large awards. They conclude, however, that this is not undesirable and that there are other checks in the legal system. They believe the total amount of undercompensation from successful claims exceeds that paid in overcompensation.

Chapter six, The Rules of the Malpractice Game, discusses the changes in locality rule and in the doctrine of informed consent. The authors point out that the erosion of the locality rule has made it much easier to establish medical malpractice. The emphasis upon abolishing this rule seems unjustified as only a small percentage of malpractice cases involve this concept. Informed consent is a more complex issue. In this discussion, the authors take considerable license in their interpretation of data and show a lack of appreciation of the complexities of health care delivery. Their discussion of the Canterbury case is not only inappropriate but also inaccurate. Probably, the greatest criticism of this book by any reviewer would be in the discussion of this section. For the authors to recommend

© 1979 American Roentgen Ray Society

0361–803X/79/1324–0697 $0.00

physicians deal with informed consent by providing the patient with full information and allowing the patient to decide what is to be done represents a naive and unrealistic approach. Notwithstanding the moral issues, the simple task of doing this in the available time would reduce the number of patients a physician could see each day. To treat such a complex issue in a summary fashion shows the authors' lack of insight in this particular area.

Chapter seven deals with dispute resolution. It discusses the statute of limitations, the discovery rule, screening panels, and arbitration. The laws which force parties to arbitrate a medical malpractice dispute raise serious constitutional questions with regard to due process of law and the guarantee of trial by jury. The authors feel that laws are outrageous which restrict the amounts recoverable by seriously injured patients. They suggest an alternative of having both a primary and a secondary source of compensation. They suggest that if the purpose is to make the fault system of liability effective in deterring unnecessary injuries, the physicians liability insurance should be the primary source. If the objective is to spread the cost of injuries as widely as possible, then health insurance benefits, particularly those financed by the government, should be the primary source.

Chapter eight is an excellent discussion of the no fault alternative including limitations. I agree with the authors that there is a likelihood that no fault medical insurance would be more expensive than malpractice liability insurance. The authors conclude that the no fault system would eliminate the limited role which the law now plays in insuring quality health care and would deprive patients of a mechanism to initiate monitoring of substandard medical practice. This reviewer disagrees with the emphasis but agrees with the conclusion that the no fault alternative is not particularly attractive.

Chapters nine, 10, and 11 form part three of the text which is mainly concerned with the insurance industry. In these chapters, the authors provide a number of relevant facts that have not been widely reported and destroy some of the myths surrounding the insurance industry. They relate that data on profitability was available from the National Association of Insurance Commissioners during the period of greatest activity regarding malpractice insurance. These data were not released. Profitability for the 1976 policy year, without considering reserves for unreported claims, was 20.1%, in contrast to industry-wide profits on all lines of 4.3%. The authors discuss the territorial monopolies created through joint efforts of the insurance industry and the medical societies, and demonstrate how organized medicine assisted the insurance industry in creating an environment that set the stage for the medical malpractice insurance crisis of 1974–1975.

In Chapter 10, the authors discuss how insurance is underwritten and how the Joint Underwriting Association, a consortium of private insurance companies could be forced to write medical malpractice insurance without risk of loss or opportunity for profit. Physician-owned mutual companies are discussed under the context of captives. The authors relate (correctly) that these companies have direct authority to introduce incentives to reduce malpractice rates, but warn that captive companies may be setting their rates too low and that they may be undercapitalized.

Chapter 11, Conclusions, may prove the most stimulating. Some conclusions are directly related to the data provided in the first 10 chapters and others seem to result from the authors' logic and biases that lie outside the information provided in this book. The authors believe that many reforms and laws were postulated on inadequate data and misconception of legal doctrines. They believe that the economic limits to the legal profession mandated by law are not significantly different from the fees that lawyers commonly charge. They perceive that the heart of the malpractice problem is that many patients receive physician and hospital care that is below reasonable standards. The authors feel that the fee-for-service system and the major health insurance plans encourage over specialization, unnecessary hospitalizations, and excessive surgery. They also indicate that in advantaged situations, patients receive highly skilled, technical, and often, high-risk specialty care. They propose that more rational controls be exercised over who can practice medicine, where they can practice, and what specialty procedures they can perform, and their method of compensation.

Basic to the cause of medical malpractice, according to Law and Polan, is the absence of traditions of criticisms within and toward the practice of medicine. They suggest that the law be structured to encourage attitudes of criticisms and self-criticisms, especially within the hospital environment. The authors discuss in a summary fashion some of the activities of the legal profession but offer no substantial reforms. They conclude by recommending publicly controlled insurance because private malpractice insurance carriers have not had the ability or inclination to engage in serious risk control activities.

This text provides interesting reading, its major virtue is the data on the economics of risk for certain activities of physicians and the medical malpractice industry. Readers should not be dissuaded from personal analysis of the material by the biases of the authors. It is unfortunate that many of the statements are not specifically referenced as they would provide an excellent source and a very different use of this text had the authors chosen to document their facts in the usual scientific manner. The style is quite readable and if one is sufficiently inclined, the notes on the text are useful.

A. Everette James, Jr.
Vanderbilt University School of Medicine
Nashville, Tennessee 27232

Cross-Sectional Anatomy Computed Tomography and Ultrasound Correlation. By Barbara L. Carter, James Morehead, Samuel M. Wolpert, Steven B. Hammerschlag, Harry J. Griffiths and Paul C. Kahn. New York: Appleton-Century-Crofts, 140 pp., 1977. $42.50

This is a well-organized atlas of cross sectional anatomy: literally from head to toe. Comparison is made between anatomic drawings, specimen photographs and radiographs, computed tomography, and ultrasound images. The book is divided into four major sections: head and neck, body, pelvis, and extremities. A special section at the end correlates ultrasound with sagittal cadaver sections of the abdomen and pelvis.

In each division of the book, sagittal drawings index the level of cross sectional images. The anatomic drawings are taken from the atlas by Eycleshymer and Schoemaker and are oriented so that the reader views each section from above, placing the right side of the drawing on the reader's right. This conforms to convention for sections of the head, but is reversed for the abdomen. The authors compensate for this by including a small, difficult to read, reversed reproduction of the drawing for each section of the thorax and abdomen. Ultrasound images are included for the neck, abdomen, and extremities, but are not of the quality now achieveable with current ultrasound units. This is also true for the computed tomography images (2.5 min scans). The format is nicely arranged so that the CT

and ultrasound images face pages with the corresponding anatomic drawing; a short comment indicates the salient anatomic features at that level. At each level, the authors have attempted to use CT and ultrasound images most closely approximating those of the anatomic drawings. Radiographs of cadaver cross sections are included at some levels and are generally of less value because of postmortem distortion.

In general, the book is useful and logically organized and the format facilitates comparison of the diagnostic images and anatomic drawings. The authors made a difficult choice for the orientation of the anatomic drawings, and followed the convention of the anatomists. For a clinically oriented atlas, it would have been better to reverse these drawings. The quality of the CT images is acceptable, but not optimal by current standards. The ultrasound images, in general, are disappointingly suboptimal. The short section of sagittal ultrasound images compared with cadaver photographs is potentially very useful, but would be improved by better ultrasound images and more closely spaced anatomic sections. The CT images of the extremities lack sufficient detail for comparison with the excellent anatomic drawings.

Howard J. Ricketts
University of Washington Hospital
Seattle, Washington 98195

Radiology of Trauma: Textbook and Atlas. By Hermann Birzle, Rudolf Bergleiter, and Eugen H. Kuner. Translated by H. J. Kaufmann. Philadelphia: Saunders, 372 pp., 1978. $65

This is an introductory book on the radiology of trauma, and is primarily an atlas rather than a definitive tome on the subject. The authors have done a superb job of introducing the subject to radiology residents, traumatologists, orthopedic surgeons, neurosurgeons, and others "in whose hands the care of the injured patient truly lies".

The introduction has many excellent drawings showing common variations of the norm and possible sources for misinterpretation. There are brief pertinent remarks on indications for radiologic examinations after injury, the course of the x-ray investigation, analysis of radiographs, and the final report. Fifteen short chapters follow covering all aspects of trauma, including the axial and appendicular skeleton, thorax and abdomen, soft tissue injuries, and foreign bodies. There are also chapters on special problems in the pediatric patient, the sequelae of trauma, and CT examination of the skull and brain.

Because the text is well written and the 1,095 illustrations are exquisitely done, the book is very effective. I would like to see it expanded in the future.

The text is recommended to all physicians with an interest in traumatology.

John A. Gehweiler, Jr.
Duke University Medical Center
Durham, North Carolina 27710

The Cervical Spine in Trauma. By Amil J. Gerlock, Jr., Sandra G. Kirchner, Richard M. Heller, and Jeremy J. Kaye. Philadelphia: Saunders, 167 pp., 1978. $8.95.

This text is volume 11 in the series, *Exercises in Diagnostic Radiology*. The authors emphasize that this monograph is only intended as a basic guide to interpretation of lateral radiographs of the cervical spine in cases of trauma. No attempt has been made to make this a definitive treatise on the subject, rather the approach to evaluating a lateral radiograph is stressed. This is an important point since this reviewer has stressed in the literature that only two-thirds of fractures and dislocations may be diagnosed from a lateral radiograph of the cervical spine (Miller MD, Gehweiler JA, Martinez S, Charlton OP, Daffner RH: Significant new observations on cervical spine trauma. *AJR* 130: 659–663, 1978).

The book may be divided into two sections: (1) normal radiographic anatomy of the lateral view of the cervical spine; and (2) case studies. The anatomy section is excellent for medical students and first year residents with two exceptions. The illustrations, both radiographs and drawings are poor, and it is often difficult to observe exactly what the authors are referring to. Secondly, the anatomic terminology does not conform in all aspects to accepted anatomic notation. For example the term "posterior elements" is used without defining its meaning. That term is medical jargon and does not appear in any reference on medical lexicography. Similarly, the term "neural arch" is used incorrectly when referring to an adult spine. Standard anatomy texts clearly show a vast difference between a neural arch and a vertebral arch, and they cannot be interchanged, nor can the terms vertebral centrum and body. At birth, a vertebra is composed of three ossification centers joined by cartilage; the centrum and the neural arch halves. The neurocentral synchondrosis unites the centrum to the neural arch. During the first year of life, the neural arch halves unite dorsally. This union occurs first in the lumbar region and proceeds cranially through the thoracic and cervical regions. The neural arch fuses with the centrum in the cervical region at 3 years. This union proceeds caudally and is usually complete in the sacrum by age seven. The neural arch forms not only the vertebral arch but also contributes a tiny portion to the centrum on each side to form the vertebral body. Thus, on radiographs, the terms centrum and neural arch should only be used when there is still evidence that the neurocentral synchondroses are open. After closure of the synchondroses, the terms "vertebral body" and "vertebral arch" are appropriate.

The major portion of the book deals with case studies after cervical spine trauma. A lateral radiograph of the cervical spine is shown and on the opposite page four questions are asked. Space is provided for written answers. In each case, the questions are concerned with the anatomic structures involved and whether they are displaced, whether the injury is stable or unstable, and the common eponym or diagnostic term for each type of injury. Answers are supplied along with a brief discussion of the traumatic entity.

The book seems appropriate for medical students and first year residents in radiology rather than for those more advanced. While the illustrations are poor, the style of writing is clear but limited in scope.

John A. Gehweiler, Jr.
Duke University Medical Center
Durham, North Carolina 27710

An Atlas of Otolaryngologic Radiology. By Judah Zizmor and Arnold M. Noyek. Philadelphia: Saunders, 497 pp., 1978. $35

Zizmor and Noyek have assembled what amounts to a teaching file demonstrating the wide range of radiographically demonstrable diseases involving the temporal bone, orbit, nose, the paranasal sinuses, the nasopharynx, the oral cavity and hypopharynx, mandible, salivary glands, cervical soft tissues and cervical spine, larynx, trachea, bronchi, and esophagus.

The range of abnormalities extends from the more common findings to the frankly exotic and to those entities which (especially infectious processes) are rarely seen nowadays. Diagnostic pitfalls are presented including anatomic variants and entities, such as large petrous apex air cells, or unerupted teeth simulating air-fluid levels in the maxillary sinuses. Representative examples of many classic entities are shown.

Other imaging modalities besides radiography, such as thermography, computed tomography, orbital ultrasound, diagnostic ultrasound, xeroradiography, and nuclear medicine are shown where their utilization is appropriate and helpful. As might be expected, there is some emphasis on tomographic demonstration of many cases.

An excellent feature is the legends accompanying the figures. The book is an atlas and is not a text, yet the explanations accompanying the illustrations are highly informative and are probably one of the book's strongest points.

The reproductions are generally quite good and clearly labeled. There are a few illustrations where one would like to "bright light" the reproduction as one might a dark film, but this is a minor detraction.

The bibliography consists of 53 references, the most recent from 1977.

The book belongs in every basic library of radiology, and is strongly recommended for radiologists who are involved in head and neck work, as well as for all otolaryngologists.

Robert E. Schaefer
Wallace Radiology Group
Bellevue, Washington 98009

The Chemistry of Radiopharmaceuticals. Edited by Ned D. Heindel, H. Donald Burns, and Takashi Honda. New York: Masson, 294 pp., 1978. $27.50

The text is a composite of 17 contributions intended to present an overview of the development of radiopharmaceuticals utilizing both chemical and pharmacologic design parameters. Several chapters review the progress of localizing radionuclides in specific tissue on the basis of the organ's physiology and chemistry; several others discuss the chemistry of radiolabeled compounds as a prediction of biologic behavior. The chemistry of technetium is reviewed in one chapter, as are other metals (as one group), and positron emitters in other chapters.

The title, *The Chemistry of Radiopharmaceuticals* may be somewhat misleading, however, due to broad topic content. The following are discussed: the role of federal regulatory agencies in radiopharmaceutical development; Brookhaven's contribution to nuclear medicine; and a chapter on the rationale of color imaging. These topics may be pertinent to radiopharmaceutical development, but are somewhat outside the context of chemistry.

Each chapter is well referenced. For one interested in the topics covered, the references offer a good beginning for a literature search. The scope of the text makes it potentially appealing to the physician and the radiopharmaceutical scientist in nuclear medicine. Despite the apparent range of the topics discussed, the necessary brevity of the coverage makes the text possibly useful as either a starting point or as a quick review of parts of radiopharmaceutical science.

David Hartnett
University of Washington Hospital
Seattle, Washington 98195

Radiologic Diagnosis of Polyps and Carcinoma of the Large Bowel. By Masakazu Maruyama. New York: Igaku-Shoi, 262 pp., 1978. $52

Dr. Maruyama has accomplished the ultimate in producing an exquisite book detailing the radiologic and endoscopic diagnosis of colonic neoplasia. He begins with a historic review of the radiologic examination, detailing the evolution of the double contrast method. This is followed by a chapter which studies in detail the radiologic techniques for colon examination including both single and double contrast techniques. This chapter introduces the reader to the exquisite radiographic-pathologic correlations which is a characteristic of this work. The author also demonstrates the gyroscope, an apparatus permitting total controlled patient and radiographic tube position in all three planes.

Chapters are included which show the macroscopic and microscopic pathologic characteristics of colonic neoplasms and precisely correlate them with the radiologic appearances. These demonstrations are generously supported by double and single contrast radiographs of exquisite detail. Color prints of endoscopic appearances are also included. A chapter on endoscopic polypectomy details the technical approach and results. The Borrmann type classification is applied to the colonic neoplasms.

This book in atlas format describes multiple examples of colonic carcinomas and also less common entities such as familial polyposis, Peutz-Jeghers syndrome, and multiple colonic carcinomas. An extensive bibliography is included.

Charles A. Rohrmann, Jr.
University of Washington Hospital
Seattle, Washington 98195

Cancer: A Problem of Developmental Biology. By G. Barry Pierce, Robert Shikes, and Louis M. Fink. Englewood Cliffs, N. J.; Prentice-Hall, 242 pp., 1978. $15.95

This text reviews the general subject of cancer from several aspects including anatomy, biochemistry, immunology, physiology, etiology, genetics, and clinical presentation. These different aspects are discussed in some depth to provide the reader with an understanding of their importance in the development, diagnosis, and management of cancer. An example would be the various etiologies of cancer such as chemical, viral, and environmental. The biochemical aspects of tumors, such as ectopic ACTH syndrome, as related to the diagnosis of different malignancies are reviewed. In several chapters, the role of the cell membrane is described.

Other chapters concern the clinical presentations of cancer, including the initial features and metastases. The roles of surgery, radiotherapy, chemotherapy, and immunotherapy in the management of cancer are analyzed. An appendix details the natural history and treatment of well-known or frequently encountered tumors, e.g. breast cancer.

Illustrations are sparingly used and there is a bibliography at the end of the book. The index is well done.

This text is written for the graduate student in the basic medical sciences, e.g. anatomy, and freshmen and sophomore medical students. This text demonstrates the contributions that basic medical sciences have made to a better comprehension of cancer and how these affect the clinical evaluation and management of the cancer patient.

Larry D. Greenfield
City of Hope National Medical Center
Duarte, California 91010

Books Received

Receipt of books is acknowledged as a courtesy to the sender. Books that appear of sufficient interest will be reviewed as space permits.

The Veins of the Posterior Fossa. Normal and Pathologic Findings. By A. Wackenheim, J. P. Braun. Berlin: Springer-Verlag, 157 pp., 1978. $68

Diagnostic Radiology in Clinical Medicine, 2d ed. By R. H. Troupin. Chicago: Year Book Medical Publishers, 172 pp., 1978. $11.95

Radiological Physics. Examination Review Book, vol. 1, 2d ed. Edited by C. G. Orton, C.H. Marshall, J. B. Seibert. Garden City, N.Y.: Medical Examination Publishing, 200 pp., 1978. $12

Prevention and Detection of Cancer. Part II—Detection, vol. 1, High Risk Markers. Detection Methods and Management. Edited by H. E. Nieburgs. New York: Marcel Dekker, 1,328 pp., 1978. $62.50

International Directory of Specialized Cancer Research and Treatment Establishments, 2d ed. Published under auspices of Committee on International Collaborative Activities. Geneva: International Union Against Cancer, 724 pp., 1978.

Practical Aspects of Electron Beam Treatment Planning. Medical Physics Monograph No. 2. Edited by C. G. Orton, F. Bagne. New York: American Institute of Physics, 1978.

Atlas of Xeroradiographic Anatomy of Normal Skeletal Systems. By J. N. Wolfe, C. C. Kapdi, H. S. Murphy. Springfield, Ill.: Thomas, 193 pp., 1978. $29.50

Progress in Clinical Cancer, vol. 7. Edited by I. M. Ariel. New York: Grune & Stratton, 262 pp., 1978. $35

Progress in Nuclear Medicine, vol. 5. Newer Radiogases in Practice. Edited by M. Guter. Basel: Karger, 244 pp., 1978. $83.50

Therapy in Nuclear Medicine. Edited by R. P. Spencer. New York: Grune & Stratton, 404 pp., 1978. $34.50

Normal Radiologic Patterns and Variances of the Human Skeleton. An X-Ray Atlas of Adults and Children. By R. Birkner. Baltimore: Urban & Schwarzenberg, 564, pp., 1978. $74

The Radiology of Joint Disease, 2d ed. By D. M. Forrester, J. D. Brown, J. W. Nesson. Philadelphia: Saunders, 626 pp., 1978. $34.50

An Atlas of Radiological Anatomy. By J. Weir, P. Abrahams. Chicago: Year Book Medical Publishers, 287 pp., 1978. $29.95

A Color Atlas of Sectional Anatomy. Chest, Abdomen, and Pelvis. By E. A. Lyons. St. Louis: Mosby, 317 pp., 1978. $137.50

Clinical Radiology of the Ear, Nose and Throat, 2d ed. By E. Samuel, G. A. S. Lloyd. Philadelphia: Saunders, 252 pp., 1978. $30

Clinical Nuclear Cardiology. Edited by R. W. Parkey, F. J. Bonte, L. M. Buia, J. T. Willerson. New York: Appleton-Century-Crofts, 333 pp., 1979. $28.50

Atlas of Technetium Bone Scans. By D. L. Citrin, J. H. McKillop. Philadelphia: Saunders, 240 pp., 1978.

Handbook of Clinical Ultrasound. Edited by M. De Vlieger, J. H. Holmes, E. Kazner, G. Kossoff, A. Kratochwil, F. Kraus, J. Poujol, D. E. Strandness. New York: Wiley & Sons, 970 pp., 1978. $75

News

Clinical Problems in Radiology

Clinical Problems in Radiology—1979 is the title of a postgraduate course scheduled for May 18–20 in New York City. Sponsor is the Department of Radiology, Columbia-Presbyterian Medical Center. Course directors are D. H. Baker and W. J. Casarella.

The course will be organized into eight symposia which will deal with the use of computed tomography, ultrasound, nuclear medicine, angiography, and conventional radiography in the evaluation of jaundice, gastrointestinal hemorrhage, trauma, renal masses, mediastinal lesions, thromboembolism, pediatric emergencies, and central nervous system tumors.

Joining the faculty from Columbia-Presbyterian will be the following guest faculty members: M. A. Bosniak, New York University; J. O. Haller, State University of New York Downstate Medical Center; W. Green, Medical Center at Princeton; J. Rose, Mt. Sinai Medical School; R. Soulen, Temple University; and D. S. Zimmon, New York University.

Fee is $200 ($100 for residents and fellows). A total of 20 hr AMA Category I credit is available. For information, contact: H. J. Sauer, coordinator, Department of Radiology, Presbyterian Hospital, 622 W. 168th St., New York, NY 10032.

Radiation Therapy Clinical Research Conference

The University of Florida Division of Radiation Therapy will hold its ninth annual Clinical Research Conference, April 26–28, in Gainesville. This clinical oncology conference will emphasize multidisciplinary decision making and radiation therapy techniques. One day will be devoted to case presentations and two days to clinical research papers. Guest professor will be S. Hellman. The program is certified for 17 hr AMA Category I credit. Fee is $100. For information contact Dr. R. R. Million, program coordinator, Division of Radiation Therapy, Box J-385, J. Hillis Miller Health Center, Gainesville, FL 32610; telephone (904) 392-3161.

Virginia Postgraduate Course

The Department of Radiology, University of Virginia School of Medicine, is offering a diagnostic radiology postgraduate course April 22–26 in Charlottesville. Program director is T. E. Keats. Guest faculty will include M. A. Meyers, State University of New York at Stony Brook and A. F. Lalli, Cleveland Clinic Foundation. Faculty from the University of Virginia School of Medicine will be: B. A. Alford, N. A. G. Brenbridge, A. J. Buschi, R. W. Gandee, R. B. Harrison, T. E. Keats, H. O. Riddervold, C. B. Stelling, C. D. Teates, and C. J. Tegtmeyer. A total of 16 hr AMA Category I credit is available. Fee is $275. For information, contact Mr. E. E. Wolfe, President, Management Research Associates, 60 E. 42nd St., New York, NY 10017; telephone (212) 687-2560.

Baylor Annual Radiology Conference

Baylor University's Annual Radiology Conference will be May 6–12. The first two days will be in Houston while sessions May 8–12 will be in Acapulco, Mexico. Registration fee is $250. For information, contact: Office of Continuing Education, Baylor College of Medicine, Texas Medical Center, Houston, TX 77030; phone (713) 790-4941.

Diagnostic Ultrasound Course

The University of Michigan Medical School will offer a course in diagnostic ultrasound, Sept. 7–9 in Ann Arbor. T. M. Silver is course chairman. A total of 16 hr Category I credit is available. For information, contact Dr. F. C. Pennington, Office of Continuing Medical Education, University of Michigan Medical School, Towsley Center, Ann Arbor, MI 48109.

Diagnostic Ultrasound: 1979

The Departments of Radiology and Continuing Education of Harvard Medical School are sponsoring their fourth annual course in diagnostic ultrasound, April 30–May 2, in Boston.

The course surveys recent and advanced aspects of ultrasound imaging that have been established in clinical use. Emphasis is on practical methods. Topics include general areas of abdominal, hepatobiliary, genitourinary, pelvic, cardiac, and obstetric applications, as well as specialized uses including guided aspiration.

A total of 21 hr AMA Category I credit is available. Fee is $220 ($150 for residents and fellows). For information, contact Dr. E. H. Smith, program director, Department of Radiology, Harvard Medical School, 25 Shattuck St., Boston, MA 02115; phone (617) 732-6265.

Preceptor Training Programs in Diagnostic Ultrasound

The University of California, San Diego is offering 1-month programs to physicians interested in learning the basics of diagnostic ultrasound. The program is divided between the University Hospital and the Veteran's Administration Hospital in La Jolla, both major teaching hospitals. Lectures, videotapes, teaching files, and actual experience in scanning techniques are offered, with studies encompassing echoencephalography, echocardiography, B-scan imaging of the abdominal and pelvic organs, and obstetrics and gynecology. Approximately 15 to 20 cases are studied each day and reviewed with a member of the staff. A maximum of three trainees are accepted each month. Tuition is $1,500. The course is approved for 140 hrs CME Category I credit. For further information contact Ms. E. Novak, Division of Diagnostic Ultrasound, University Hospital, 225 Dickinson St., San Diego, CA 92103; telephone (714) 294-6657.

Radiology of Signs and Symptoms

This 4-day course provides a new approach to continuing medical education for the practicing radiologist. It reviews the diagnostic and interpretive process of applying a variety of radiographic procedures in a rational sequence to arrive at a pathophysiologic diagnosis when presented with a sign-and-symptom complex. Each day focuses on a different organ system—cardiopulmonary, gastrointestinal, bone, and genitourinary. The course will be May 30–June 2 in Cambridge and is sponsored by the Departments of Radiology and Continuing Education of Harvard Medical School.

This review of the modern approach to differential radiologic diagnosis should be useful also to those preparing for the specialty boards.

A total of 30 hr AMA Category I credit is available. Fees are $290; $195 for residents and fellows.

© 1979 American Roentgen Ray Society

0361–803X/79/1324–0702 $0.00

For further information, contact Dr. F. Adams, Program Director, Department of Radiology, Harvard Medical School, 25 Shattuck St., Boston, MA 02115; (617) 732-6265.

Cardiac Angiography

The Departments of Radiology and Continuing Education of Harvard Medical School will present an intensive 3½ day course for those who participate in or wish to remain abreast of coronary arteriography, ventriculography, cardiovascular radiology, certain noninvasive cardiac imaging techniques, and a variety of diagnostic and therapeutic problems relating to coronary artery disease. The program will be May 21–24 in Boston.

Fee is $260 ($175 for residents and fellows). A total of 28 hr AMA CAtegory I credit is available. For information, contact: D. C. Levin, Division of Cardiovascular Radiology, Peter Bent Brigham Hospital, 721 Huntington Ave., Boston, MA 02115; (617) 732-6265.

National Conference on Breast Cancer

The American Cancer Society will sponsor a conference on breast cancer, Sept. 6–8, in New York City.

The purpose of this conference is to improve the quality of care of the breast cancer patient by providing the primary physician with a greater understanding of the many factors which impact on the management of this disease. Experts in the various disciplines will present the latest information on the causation, pathology, detection and diagnosis, and the management of the patient at various stages of the disease. The social and psychological problems which concern the patient will be explored. Advance registration is requested; there is no registration fee. The conference has been approved for 16 hr Category 1 credit.

For further information write: Breast Cancer Conference, American Cancer Society, 777 Third Ave., New York, NY 10017.

Medical Imaging Meeting

The American College of Medical Imaging will host a meeting July 28–Aug 4 in Mauna Kea Beach, Hawaii. For information, contact the College at P. O. Box 27188, Los Angeles, CA 90027 or call (213) 275-1393.

Congress of Radiology in Otorhinolaryngology

The Seventh International Congress of Radiology in Otorhinolaryngology will be May 10–13 in New Orleans. Registration fee is $225. The course has been approved for 21 hr Category I credit. For information contact Dr. D. H. Johnson, Jr., 4317 Magnolia St., New Orleans, LA 70115.

IV European Congress of Radiology

The fourth European Congress of Radiology will be Sept. 4–8 in Hamburg, West Germany. The scientific program will touch on a number of topics including; diagnostic research of the upper abdomen including nuclear medicine; radiotherapy in genital tumors of males and females; combined therapy and risks of x-ray exposure; and radiophysics and techniques. Information is available from: Secretary, IV European Congress of Radiology, Postfach 10 64 07, D-2000 Hamburg 1, West Germany.

Arthrography Course

The Hospital for Special Surgery, New York City, will sponsor an arthrography course June 7–9. Registration is limited to 60. Fee is $225 and 16 hr AMA Category I credit is available. For information, contact: Dr. R. H. Freiberger, Director of Radiology, Hospital for Special Surgery, 535 East 70th St., New York, NY 10021; telephone (212) 535-5500, extension 424.

Uro-Radiology Seminar

The first annual Summer Uro-radiology Seminar, presented by Tulane Medical Center, is scheduled for Aug. 19–22 at Lake Chapala, Mexico. This program will provide urologists and radiologists with a comprehensive interdisciplinary review of new diagnostic modalities including: ultrasound, computed tomography, invasive radiologic studies and radionuclide imaging as used in the solution of urologic problems. The course is approved for AMA Category I credit. Fee is $ 200. For additional information contact: Tulane Medical Center, Office of Continuing Education, 1430 Tulane Ave., New Orleans, LA 70112 telephone (504) 588-5466.

Ultrasound Annual Meeting

The American Institute of Ultrasound in Medicine (AIUM) has scheduled its 24th annual meeting, Aug. 27–31, in Montreal. The group will meet with the American Society of Ultrasound Technical Specialists. Abstracts for formal presentations as well as for scientific exhibits must be received by April 15. Deadline for abstracts work-in-progress presentations is June 15. Information regarding the meeting and abstract submission is available from AIUM/ASUTS Montreal '79, 6161 N. May Ave., Suite 278, Oklahoma City, OK 73112; phone (405) 840-3721.

Diagnostic Radiology Refresher Course

The Radiology Department of the University of Cincinnati College of Medicine will sponsor its twenty-first annual Refresher Course in Diagnostic Roentgenology, June 4–8. Dr. B. Felson is director. The course will also cover radiation physics and nuclear medicine. Category I credit will be available. Fee is $250. Information may be obtained from Dr. H. B. Spitz, Department of Radiology, Cincinnati General Hospital, Cincinnati, OH 45267.

Uroradiology: Clinical Correlations

A postgraduate course, Uroradiology: Clinical Correlations, will be May 2–4 in New York City. Sponsors are the Department of Radiology and the Post-Graduate School of Medicine of the Mount Sinai School of Medicine (CUNY). Guest faculty will include: J. Becker, M. Bosniak, R. Friedenberg, and E. K. Lang. Participating from Mount Sinai will be: H. A. Mitty, J. G. Rabinowitz, H. Brendler, S. Efremidis, H. Goldman, S. Goldsmith, J. Krakoff, E. Leiter, M. Levitt, J. S. Rose, H. Weber, and H-C Yen. The course meets the criteria for 15 hr AMA Category I credit. For applications and information, contact: Page and William Black Post-Graduate School of Medicine, Mount Sinai School of Medicine, 1 Gustave L. Levy Place, New York, NY 10029; telephone (212) 650-6737.

Association of Radiation Oncologists of India Formed

The Association of Radiation Oncologists of India has been formed to promote the scientific specialty of radiation therapy and to elevate the status of the profession. The association also is promoting the development of radiotherapy centers. Information is available from Dr. T. K. Dutta, honorary general secretary, Department of Radiotherapy, Postgraduate Institute of Medical Education and Research, Chandigarh, India.

Asian Congress on Radiation Protection

The Second Asian Regional Congress on Radiation Protection of the International Radiation Protection Association will be Nov. 5–8, in Manila, the Philippines.

Theme will be Radiation Protection in the Developing Countries. Topics will include: environmental radiation hazards and protection; medical radiation hazards and protection; nuclear power and irradiation facilities; dosimetry; public education and acceptance; research and new developments in radiation protection; regulations, codes, and standards; nonionizing radiation; special topics on radiation protection; health physics training and manpower development.

Sponsoring societies are the Philippine Association for Radiation Protection and the Japan Health Physics Society. For further information, contact Dr. C. T. Anatalio, Congress Director, Radiation Health Office, Ministry of Health, San Lazaro Compound, Rizal Avenue, Station Cruz, Manila, Philippines.

Chest Radiography Symposium

A symposium on Optimization of Chest Radiography will be at the University of Wisconsin, Madison, April 30–May 2. Sponsors are the FDA's Bureau of Radiological Health and the University of Wisconsin. Attendance is limited to 200. Contributed papers are solicited on medical or physical methods to increase the information content of chest radiography and to assess and reduce radiation exposures. The proceedings will be published. Registration fee is $30. Category 1 credit has been applied for. For further information contact Dr. John Cameron, Department of Radiology, University Hospitals, Madison, WI 53706; (608) 262-2170.

Diagnostic Radiology Seminar

The Dayton (Ohio) Veterans Administration Hospital will present its ninth annual Radiological Seminar, May 11 and 12. Subjects will include bone, chest, cardiac, urologic, gastrointestinal, and biliary areas in additional to ultrasound and nuclear medicine. There is no registration fee and the seminar is approved for 12 hr AMA Category I credit. Admission is by advance registration only. For information, contact: Dr. E. Gutman, Veterans Administration Center 114, 4100 W. Third St., Dayton, OH 45428; phone (513) 268-6511 extension 337.

Advanced Cardiac Ultrasound Course

An advanced course in cardiac ultrasound will be April 23–27 at Harefield Hospital, England. The course is for physicians and technicians either working in the field or with some knowledge of the subject. R. Pridie and S. Hunter are course directors. Other speakers will be D. Gibson, G. Leach, R. Anderson, J. Gore, and D. Tunstall-Pedoe. Send applications to Mrs. L. Grieve, Ultrasound Department, Harefield Hospital, Harefield, Middlesex, England.

Pacific Northwest Radiological Society Meeting

The annual scientific meeting of the Pacific Northwest Radiological Society will be May 11–13 in Portland, Oregon. For information contact Dr. J. F. Sailer, 200 15th Ave. E., Seattle, WA 98112.

Radiation Therapy and Physics

A refresher course in Radiation Therapy and Physics will be April 23–27 at Queens Hospital Center, Jamaica, New York. Tuition is $200 for the week-long program which offers an intensive review for radiology board candidates. The course meets the criteria for 35 hr AMA Category I credit. Additional information is available from Dr. N. Akbiyik, Radiation Therapy Department, Long Island Jewish-Hillside Medical Center, 82–68 164th St., Jamaica, NY 11432; telephone (212) 990-2442.

International Symposium on Percutaneous Biopsy

The Institute of Diagnostic Radiology of the Technical University of Munich will host on May 7–9 an International Symposium on Percutaneous Biopsy of the bone, lung, mediastinum, pancreas, kidney, liver, lymphnodes, and mammary gland. The symposium will also feature therapeutic vascular occlusion in traumatic or other pathologic bleeding of the gastrointestinal tract, lung, liver, kidneys, cervicofacial, cerebromedullary, and gynecologic areas. Simultaneous translation will be into English, French, and German. Applications and information are available from: Secretary of Professor H. Anacker, Institute für Röntgendiagnostik, Klinikum rechts der Isar, Ismaninger Str. 22, 8000 Munich 80, West Germany.

Meeting and Course Review

For reader convenience, a summary of upcoming meetings and courses is provided. Detailed listings of these events appeared in journal issues indicated in parentheses.

XIII Interamerican Congress of Radiology, July–August 1979, Quito, Ecuador (October).

Sixth Congress of Radiation Research, May 13–19, Tokyo (October).

Noninvasive Imaging in Medicine, symposium, June 6–9, Lund, Sweden (October).

Conferences on Medical and Biological Engineering and Medical Physics, Aug. 19–24, Jerusalem (October).

L. H. Gray Conference, Sept. 10–14, Cambridge, England (October).

Asian Oceanian Congress of Radiology, Oct. 28–Nov. 3, Singapore (October).

Abdominal Real Time Sonography Courses, June 11–15, July 16–20, Aug. 6–10, Dec. 9–13, 1979, Winston-Salem, N.C. (November).

Fleischner Society Ninth Symposium (and course), June 11–13, Stockholm, (November).

European Cardiovascular Radiology Congress, May 3–5, Nuremberg, West Germany (November).

American Board of Radiology, oral and written examination dates and locations for 1979 and 1980 (December).

AFIP Diagnostic Radiology Seminars, series, May 7–11, August 27–31, November 12–16, Washington, D.C. (December).

Canadian Radiologists Annual Meeting, June 24–28, Vancouver (December).

Multidisciplinary Aspects of Brain Tumor Therapy, June 8–10, Lake Garda, Italy (December).

Skeletal Radiology Course, May 14–18, New York City (December).

Nuclear Radiology Workshop, May 4 and 5, Ann Arbor, Michigan (December).

Symposium: Computerized Tomography of the Brain, Sept. 20–22, Bordeaux, France (January).

Abdominal Ultrasound and CT of the Trunk, May 24–26, Dallas (January).

Diagnostic Ultrasound Training Programs, continuing weekly series, New York City (January).

Diagnostic Ultrasound Workshop, weekly postgraduate sessions through December 14, Houston (January).

Eighth Congress, European Society of Neuroradiology, Sept. 7 and 8, Strasbourg, France (January).

Abdominal Radiology Course, May 14–17, Boston (February).

Symposium: Fundamentals in Technical Progress, May 11 and 12, Liège, Belgium (February).

University of Pennsylvania Diagnostic Radiology Seminar, June 4–8, Philadelphia (February).

AAPM Summer School, July 22–28, Chapel Hill, N.C. (February).

Austrian Nuclear Medicine Meeting, Sept. 11–14, Innsbruck (February).

Percutaneous Biopsy and Therapeutic Vascular Occlusion, symposium, May 7–9, Munich (February).

Leo Rigler Lecture and Convention on Pediatric Radiology, May 8–10, Herzlia-on-Sea, Israel (February).

Irish-American Radiology Symposium, Sept. 15–21, Killarney, Ireland (March).

Beth Israel Courses, arthritis course, April 27, New York City (March).

Diagnostic Ultrasound Courses, series of 2-week courses, Winnipeg, Canada (March).

Physics of Radiology and Nuclear Medicine, refresher for residents, May 7–10, New York City (March).

Gastrointestinal Refresher Course, Oct 11–14, Williamsburg, Virginia (March).

Radiologic Societies

International Societies

Fleischner Society. Secretary K. Ellis, Columbia-Presbyterian Medical Center, 622 West 168th St, New York, NY 10032

Inter-American College of Radiology. Secretary, G. Morillo, Dept Radiology, Jackson Memorial Hospital, 1611 NW 12th Ave, Miami, FL 33136

International Commission on Radiological Protection. Secretariat, F. D. Sowby, Clifton Ave, Sutton, Surrey SM2 5PU, England

International Skeletal Society. Secretary-Treasurer, J. Edeiken, Radiology Dept, Thomas Jefferson University Hospital, 11th and Walnut Sts, Philadelphia, PA 19107

International Society of Radiology. Hon. Secretary-Treasurer, W. A. Fuchs, Dept of Diagnostic Radiology, University Hospital, Inselspital, CH-3010 Bern, Switzerland

U.S. National Societies

American Association of Physicists in Medicine. Secretary, J. Wright, Radiology Dept, Geisinger Medical Center, Danville, PA 17821

American Board of Radiology. Secretary, C. A. Good, Kahler East, Rochester, MN 55901

American College of Radiology. Executive Director, W. C. Stronach, 20 N Wacker Drive, Chicago, IL 60606. Annual meetings: 1979, Sept 16–20, Chicago, IL; 1980, Sept 21–25, New Orleans, LA

American Institute of Ultrasound in Medicine. Executive Secretary, D. LaMaster, PO Box 25065, Oklahoma City, OK 73125. Annual meetings: 1979, Aug 23–31, Montreal. Spring educational meetings: 1978, April 4–9, Puerto Rico; 1979, Feb 23–March 3, Lake Tahoe; 1980, March 1–6, Hilton Head

American Nuclear Society. Program Chairman, T. D. Tarr, U.S. Energy Research and Development Administration Mail Station A-436 Office of Assistant Administrator for Nuclear Energy, Washington, DC 20545

American Radium Society. Business office: N. V. Jordan, Office of the Secretariat, c/o M. D. Anderson Hospital, 6723 Bertner Drive, Houston, TX 77030. Annual meeting: 1980, April 27–May 1, Philadelphia

American Roentgen Ray Society. Secretary, J. F. Martin, 300 S Hawthorne Rd. Winston-Salem, NC 27103. Annual meetings: 1980, April 22–25, Las Vegas; 1981, March 24–27, San Francisco

American Society of Neuroradiology. Secretary, T. El Gammel, Medical College of Georgia, Augusta, GA 30902. Annual meeting: May 20–24, 1979, Toronto

American Society of Therapeutic Radiologists. Secretary, W. J. Taylor 1100 9th Ave, Seattle, WA 98101. Annual meeting: 1979, Oct 23–27, New Orleans

American Thermographic Society. Executive Director, N. M. Oldfield, PO Box 2055, Gaithersburg, MD 20760

Association of University Radiologists. Secretary-Treasurer, J. R. Thornbury, University of Michigan, Ann Arbor, MI 48109. Annual meeting: 1979, May 6–10, Rochester, NY

Health Physics Society. Executive Secretary, R. J. Burk Jr, 4720 Montgomery Lane, Bethesda, MD 20014

National Medical Association. Secretary, E. Mapp, Episcopal Hospital, Philadelphia, PA 19148

North American Society of Cardiac Radiology. Secretary-Treasurer, E. Carlsson, University of California, San Francisco, CA 94143

Radiation Research Society. Executive Director, R. J. Burk Jr. 4720 Montgomery Lane, Bethesda, MD 20014

Radiological Society of North America, Inc. Secretary, T. A. Tristan, Fifteenth Floor, One MONY Plaza, Syracuse, NY 13202. Annual meeting: 1979, Nov 25–30, Atlanta, GA; 1980, Nov 16–21, Dallas, TX; 1981, Nov 15–20, Chicago; 1982, Nov 28–Dec 3, Chicago

Section on Radiology, American Medical Association. Secretary, A. Raventos, Dept Radiology, School of Medicine, University of California, Davis

Society of Cardiovascular Radiology. Secretary-Treasurer, W. J. Casarella. Columbia-Presbyterian Medical Center, New York, NY 10032

Society of Chairmen of Academic Radiology Departments. Secretary-Treasurer, D. Bragg, University of Utah, Salt Lake City, UT 84132

Society of Gastrointestinal Radiologists. Secretary-Treasurer, J. F. Ferrucci, Jr., Massachusetts General Hospital, Boston, MA 02114

Society of Nuclear Medicine. President, 475 Park Avenue S, New York, NY 10016

Society for Pediatric Radiology. Secretary, B. P. Wood, University of Rochester Medical Center, 601 Elmwood Ave, Rochester, NY 14642

Society of Photooptical Instrumentation Engineers. Secretary, A. H. Gott, Aerospace Corp. PO Box 92957, Los Angeles, CA 90009.

Society of Uroradiology. Secretary-Treasurer, R. C. Pfister, Massachusetts General Hospital, Boston, MA 02114

U.S. State and Local Societies

ALABAMA

Alabama Academy of Radiology. Secretary-Treasurer, J. L. Wayland, 401 West College St, Florence, AL 35630

Section of Radiology, National Medical Association. Secretary, I. Brooks, Dept. Radiology, Veterans Administration Hospital, PO Box 511, Tuskegee, AL 36083

Southern Radiological Conference. Secretary-Treasurer, J. W. Maxwell, PO Box 2144, Mobile, AL 36601

ALASKA

Alaska Radiological Society. Chapter ACR. Secretary-Treasurer, J. J. Kottra, 3200 Providence Ave, Anchorage, AK 99504

ARKANSAS

Arkansas Chapter of ACR. Secretary-Treasurer, J. A. Gill, PO Box 1827, Fort Smith, AK 72902

ARIZONA

Arizona Radiological Society. Chapter of ACR. Secretary, A. Newman, PO Box 5099, Phoenix, AZ 85010

CALIFORNIA

California Radiological Society, California Chapter of ACR. Executive Secretary, J. M. Allen, 1225 8th St, Suite 590, Sacramento, CA 95814

East Bay Radiological Society. Secretary-Treasurer, J. J. Branscom, PO Box 175, Alamo, CA 94507

Los Angeles Radiological Society. Secretary J. E. Scallon, South Bay Hospital, 514 N, Prospect, Redondo Beach, CA 90277

Northern California Radiological Society. Secretary-Treasurer, V. C. Poirier, Mercy San Juan Hospital, 6501 Coyle Ave, Carmichael, CA 95608

Northern California Radiotherapy Association. Secretary-Treasurer, J. D. Earle, Stanford Medical Center, Stanford, CA 94305

Orange County Radiological Society. R. L. Argue, 100 E Valencia Mesa Dr, Fullerton, CA 93632

Radiological Society of Southern California. Secretary-Treasurer, D. E. Blickenstaff, La Jolla Radiology Medical Group, 7849 Fay Ave, La Jolla, CA 92037

Redwood Empire Radiological Society. Secretary, H. B. Peterson, 357 Perkins St, Sonoma, CA 95476

San Diego Radiological Society. President, D. J. Fleischli, 7849 Fay Ave, La Jolla, CA 92037

San Francisco Radiological Society. Secretary-Treasurer, P. A. Brodey, Dept Radiology, Mount Zion Hospital, San Francisco, CA 94115

South Bay Radiological Society. Secretary, R. Wirtz, Redwood Medical Clinic, 2900 Whipple Ave, Redwood City, CA 94062

South Coast Radiological Society Chapter of ACR. Secretary-Treasurer, B. R. Schnier, Dept of Radiology, Cottage Hospital, Pueblo at Bath, Santa Barbara, CA 93105

Southern California Radiation Therapy Society. Secretary-Treasurer, J. Stuhlborg, 514 N Prospect, Redondo Beach, CA 90277

Western Neuroradiological Society. Secretary-Treasurer, A. N. Hasso, Loma Linda University Medical Center, Loma Linda, CA 92354

COLORADO

Colorado Radiological Society. Secretary, P. Danner, St. Anthony Hospital, Denver, CO 80204

Rocky Mountain Radiological Society. Secretary-Treasurer. J. M. Grogan, 4200 E 9th Ave, Denver, CO 80206. Annual meeting: Aug 16–18, 1979, Denver

CONNECTICUT

Connecticut Valley Radiologic Society. Secretary-Treasurer, G. N. LaPierre, 759 Chestnut St, Springfield, MA 01107

Radiological Society of Connecticut, Inc. Secretary, E. F. Fox, 300 Main St, Briston, CT 06010

DELAWARE

Delaware Chapter of ACR. Secretary, E. S. Schubert, Wilmington Medical Center, PO Box 1951, Wilmington, DE 19899

DISTRICT OF COLUMBIA

Section on Radiology, Medical Society of the District of Columbia. Secretary-Treasurer, A. M. Zelna, 21 Masters St, Potomac, MD 20854

FLORIDA

The Florida Radiological Society, Chapter of ACR. Secretary, S. H. Sarasohn, PO Box, 610544, North Miami, FL 33161

The Florida West Coast Radiological Society, Inc. Secretary-Treasurer, M. Silbiger, 1 Davis Blvd, Suite 103, Tampa, FL 33606

Greater Miami Radiological Society. Secretary, J. A. Schneider, 1131 N 35 Ave, Hollywood, FL 33021

North Florida Radiological Society. Secretary, C. E. Bender, 1430 16th Ave S, Jacksonville Beach, FL 32250

Northeast Florida Radiological Society. Secretary, O. L. Jeter Jr, Orange Park Community Hospital, Orange Park, FL 32073

GEORGIA

Atlanta Radiological Society. Secretary-Treasurer, J. H. Larose, Dept Nuclear Medicine, South Fulton Hospital, East Point, GA 30344

Georgia Radiological Society. Chapter of ACR. Secretary, T. Vanderzalm, Medical College of Georgia, Augusta, GA 30902

HAWAII

Hawaii Radiological Society, Chapter of ACR. Secretary-Treasurer, M. Meagher, 1301 Punchbowl St, Honolulu, HI 96808

ILLINOIS

Chicago Radiological Society, Division of the Illinois Radiological Society, Chapter of Acr. Secretary-Treasurer, H. J. Lasky, 55 E Washington St. Suite 1735, Chicago, IL 60602

Illinois Radiological Society, Inc, Chapter of ACR. Secretary, R. D. Dooley, Hinsdale Medical Center, Hinsdale, IL 60521

INDIANA

Indiana Roentgen Society of ACR. Secretary, W. S. Tirman, 919 Jefferson Blvd, Sound Bend, IN 46617

Tri-State Radiological Society. Secretary, T. Harmon, St. Mary's Hospital, Evansville, IN 47750

IOWA

Iowa Radiological Society, Chapter of ACR. Secretary-Treasurer, D. L. Roberson, 1948 First Ave NE, Cedar Rapids, IA 52402

KANSAS

Kansas Radiological Society, Chapter of ACR. Secretary-Treasurer, R. H. Baehr, 310 Medical Arts Bldg, Topeka, KA 66604

KENTUCKY

Bluegrass Radiological Society. Secretary-Treasurer, J. King, 3313 Overbrook Dr, Lexington, KY 40504

Kentucky Chapter of ACR. Secretary-Treasurer, A. Lieber, University of Kentucky Medical Center, Lexington, KY 40506

LOUISIANA

Ark-La-Tex Radiological Society. Secretary, E. K. Lang, LSU School of Medicine, Shreveport, LA 71101

Louisiana Radiological Society, Chapter ACR. Secretary-Treasurer, S. L. Smith, 250 Vincent Ave, Metairie, LA 70005

Louisiana-Texas Gulf Coast Radiological Society. Secretary-Treasurer, J. Romero III, PO Box 3146, Lake Charles, LA 70602

Section on Radiology, Southern Medical Association. Secretary, M. Sullivan, 1514 Jefferson Highway, New Orleans, LA 70121

MAINE

Maine Radiological Society, Chapter of ACR. Secretary-Treasurer, P. E. Giustra. Penobsot Bay Medical Center, Rockland, ME 04841.

MARYLAND

Maryland Radiological Society, Chapter of ACR. Secretary, S. M. Goldman, Sinai Hospital of Baltimore, Belvedere at Greenspring Avenues, Baltimore, MD 21215

MASSACHUSETTS

Massachusetts Radiological Society, Chapter of ACR. Secretary, A. H. Robbins, 150 S Huntington Ave, Boston, MA 02130

New England Roentgen Ray Society. Secretary, H. F. Gramm, 185 Pilgrim Road, Boston, MA 02215.

New England Society for Radiation Oncology. Secretary, S. P. Kadish St. Vincent Hospital 25 Winthrop St, Worcester, MA 01604

Northeastern Society for Radiation Oncology. Secretary, C. C. Wang, Massachusetts General Hospital, Boston MA 02114

MICHIGAN

Michigan Radiological Society, Chapter of ACR. Secretary-Treasurer, F. P. Shea, Bon Secours Hospital, 468 Cadieux, Grosse Pointe, MI 48230

Michigan Society of Therapeutic Radiologists. Secretary, K. E. Murdock, 302 Kensington Ave, Flint, MI 48502

North Carolina Chapter of ACR. Secretary-Treasurer, M. A. Jones, Durham County Hospital, Durham, NC 27705

Southeastern Chapter Society of Nuclear Medicine. Secretary, V. J. Sodd, University of Cincinnati Medical Center, Cincinnati, OH 45267

NORTH DAKOTA

North Dakota Radiological Society, Chapter of ACR. Secretary, H. C. Walker Jr, PO Box 624, Devils Lake, ND 58301

OHIO

Cleveland Radiological Society. Secretary-Treasurer, C. M. Greenwald, Southwest General Hospital, 18697 E Bagley Rd, Middleburg Heights, OH 44130

Greater Cincinnati Radiological Society. Secretary-Treasurer, C. D. Eversole, 722 Scott St, Covington, KY 41011

Northwestern Ohio Radiological Society. Secretary, P. C. Chandnani, Medical College of Ohio, C. S. 10008, Toledo, OH 43699

MINNESOTA

Minnesota Radiological Society, Chapter of ACR. Secretary-Treasurer, J. B. Marta, 125 W College Ave, St. Paul, MN 55102

MISSOURI

Greater Kansas City Radiological Society. President-Secretary, G. D. Dixon, St Luke's Hospital, 44th & Wornall Road, Kansas City, MO 64111

Greater St. Louis Society of Radiologists. Secretary-Treasurer, D. G. Spalding, 621 S New Ballas Rd, St. Louis, MO 63141

Missouri Radiological Society, Chapter of ACR. Secretary-Treasurer, E. M. Herman, 701E 63rd St, Kansas City, MO 64110

MISSISSIPPI

Mississippi Radiological Society, Chapter of ACR. Secretary-Treasurer, J. B. Barlow, 514B E Woodrow Wilson, Jackson, MS 39216

MONTANA

Montana Radiological Society. Secretary-Treasurer, E. Drouillard, St. Patrick Hospital, Missoula, MT 59801

NEBRASKA

Nebraska Chapter of ACR. Secretary-Treasurer, W. H. Northwall. Good Samaritan Hospital, Kearney, NB 68847

NEW HAMPSHIRE

New Hampshire Chapter of ACR. Secretary-Treasurer, E. P. Kane, Claremont General Hospital, Claremont, NH 03743

NEW JERSEY

Radiological Society of New Jersey, Chapter of ACR. Secretary, A. J. Scher, 8 Lord William Penn Dr, Morristown, NJ 07083

NEW MEXICO

New Mexico Society of Radiologists, Chapter of ACR. Secretary, W. M. Jordan, 1100 Central Ave SE, Albuquerque, NM 87106

NEW YORK

Bronx Radiological Society, New York State, Chapter of ACR. Secretary-Treasurer, L. J. Corbin, 1369 Rosendale Ave, Bronx, NY 10472

The Brooklyn Radiological Society. Secretary-Treasurer, E. Arida, 450 4th Ave, Brooklyn, NY 11215

Buffalo Radiological Society. Secretary, A. Favorito, 166 Soldiers Pl, Buffalo, NY 14222

Central New York Radiological Society. Secretary-Treasurer, P. A. Randall, Upstate Medical Center, 750 E Adams St, Syracuse, NY 13210

Kings County Radiological Society. Secretary, M. Moore, 7315 Bay Parkway, Brooklyn, NY 11214

Long Island Radiological Society. Secretary, R. Meisell, 84 Beverly Road, Great Neck, NY 11021

Mid-Hudson Radiological Society. Secretary-Treasurer, W. D. Stiehm, 37 Flower Hill Rd, Poughkeepsie, NY 12603

New York Roentgen Society. Secretary-Treasurer, N. E. Leeds, Montefiore Hospital, 111 E 210th St, New York, NY 10467

New York State Chapter of ACR. Secretary-Treasurer, A. F. Keegan, 6 Secor Dr, Port Washington, NY 11050

Northeastern New York Radiological Society. Secretary, D. R. Morton, Dept Radiology, St. Claire's Hospital, Schenectady, NY 12304

Rochester Roentgen Ray Society. Secretary-Treasurer, R. E. Tobin, 135 Drumlin Vrew Dr, Mendon, NY 14506

Westchester County Radiological Society. Secretary, H. Kessler, Radiological Group, 45 Ludlow St, Yonkers, NY 10705

NEVADA

Nevada Radiological Society, Chapter of ACR. Secretary, R. Ellis, 828 Vegas Valley Dr, Las Vegas, NV 89109

NORTH CAROLINA

Catawba Valley Radiological Society. Secretary, J. N. Owsley, 18 13th Ave NE, Hickory, NC 28601

Miami Valley Radiological Society. President, G. W. Bretz, 520 IBM Bldg. 33 W 1st St. Dayton OH 45402
Ohio State Radiological Society, Chapter of ACR. Secretary, W. Howland, Aultman Hospital, 2600 Sixth St SW, Canton, OH 44710

OKLAHOMA
Northwestern Oklahoma Radiological Society. Secretary, W. L. Lavendusky, 100 Center Plaza Suite C, Tulsa, OK 74119
Oklahoma State Radiological Society, Chapter of ACR. Secretary, B. G. Eaton, 2508 Stillmeadow Rd, Edmond, OK 73034

OREGON
Oregon Radiological Society Chapter of ACR. Secretary-Treasurer, A. I. Kostiner, 8535 SW Bohmann Parkway, Portland, OR 97233

PENNSYLVANIA
Greater Delaware Valley Ultrasound Society. Secretary, W. G. M. Ritchie, Temple University School of Medicine, Philadelphia, PA 19140
Northeastern Pennsylvania Area Radiologists. Secretary-Treasurer, A. S. Haber, 181 Wilson Dr, Hazelton, PA 18201
Pennsylvania Radiological Society. Secretary R. Farrell, 201–6 Medical Arts Bldg, Scranton, PA
Philadelphia Roentgen Ray Society. Secretary, M. E. Haskin, 230 N Broad St, Philadelphia, PA 19102
Pittsburgh Roentgen Society. Secretary, R. J. Clearfield, Citizens General Hospital, 651 Fourth Ave, New Kensington, PA 15068

RHODE ISLAND
Radiological Society of Rhode Island, Chapter of ACR. Secretary, F. H. Scola, Rhode Island Hospital, Providence, RI 02902

SOUTH CAROLINA
South Carolina Radiological Society, Chapter of ACR. Secretary, G. W. Brunson, 4315 Woodleigh Rd, Columbia, SC 29206

TENNESSEE
Memphis Roentgen Society. Secretary-Treasurer, D. R. Ramey, Baptist Memorial Hospital, 899 Madison Ave, Memphis, TN 38140
Middle Tennessee Radiological Society. Secretary-Treasurer, H. P. Pendergrass. Vanderbilt University Hospital, Nashville, TN 37232
Tennessee Radiological Society, Chapter of ACR. Secretary-Treasurer, J. W. Grise, Methodist Hospital, 1265 Union Ave, Memphis TN 38104

TEXAS
Central Texas Radiology Society. Secretary-Treasurer, E. J. Schoolar, Scott and White Clinic, Temple, TX 76501
Dallas-Fort Worth Radiology Society. Secretary-Treasurer, J. T. Telle, 900 W Randol Mill Road, #120 Arlington, TX 76012
Houston Radiological Society. Secretary, T. S. Harle, 103 Jones Library Bldg, Texas Medical Center, Houston, TX 77030
San Antonio Civilian Military Radiological Society. Secretary, J. M. Chao, Diagnostic Clinic, San Antonio, TX
Texas Radiological Society, Chapter of ACR. Secretary-Treasurer, D. N. Dysart, Scott and White Clinic, Temple, TX 76501

UTAH
Utah State Radiological Society. Secretary-Treasurer, J. B. Rampton, Cottonwood Hospital, 5770 S Third E, Murray, UT 84107

VERMONT
Vermont Radiological Society, Chapter of ACR. Secretary, P. Dietrich, Medical Center Hospital of Vermont, Burlington, VT 05401

VIRGINIA
Mid-Shanandoah Valley Radiological Society. Secretary, K. L. Dwyer, King's Daughters Hospital, Stauton, VA 24401
Richmond Radiological Society. Secretary, M. Vinik, 9504 Carterwood Rd, Richmond, VA 23229
Virginia Chapter of ACR. Secretary-Treasurer, C. P. Winkler, 3500 Kensington Ave, Suite 2-A, Richmond, VA 23221

WASHINGTON
Pacific Northwest Radiological Society. Secretary-Treasurer, K. D. Moores, 1118 9th Ave, Seattle, WA 98101
Washingon State Radiological Society, Chapter of ACR. J. F. Sailer, 200 15th Ave E, Seattle, WA 98102

WEST VIRGINA
West Virginia Radiological Society, Chapter of ACR. Secretary-Treasurer, A. W. Goodwin II, 200 Medical Arts Bldg, Charleston, WV 25301

WISCONSIN
Milwaukee Roentgen Ray Society. Vice President, T. C. Lipscomb, 1004 N 10th St, Milwaukee, WI 53233
Society of Nuclear Medicine, Central Chapter. G. J. Weir Jr., Marshfield Clinic, Marshfield, WI 54449
Wisconsin Radiological Society. Chapter of ACR. Secretary-Treasurer, J. Unger, Wood VA Hospital, Wood, WI 53193
Wisconsin Society of Therapeutic Radiologists. Secretary, M. Greenberg, Milwaukee County General Hospital, 8700 W Wisconsin Ave, Milwaukee, WI 53222

WYOMING
Wyoming Radiological Society, Chapter of ACR. Secretary, T. E. Hettinger, 1609 E 19th ST, Cheyenne, WY

Canada

Canadian Association of Radiologists. Honorary Secretary, M. J. Palayew, Suite 806, 1440 St, Catherine St W, Montreal, Quebec, Canada H3G 1R8. Annual meetings: 1979, Sept 15–20, Vancouver; 1980, Oct 4–9, Montreal
Edmonton and District Radiological Society. Secretary, B. Caplan, 12320 103rd Ave, Edmonton, Alberta T5N ORZ, Canada
Toronto Radiological Society. Secretary, H. Shulman, Sunnybrook Hospital, 2075 Bayview Avenue, Toronto, Ontario, Canada

Central and South America

Asociacion Costarricense de Radiologia. Secretary, F. A. Arguedas Haug, Apartado 8-5340, San Jose, Costa Rica
Colegio Brasileiro de Radiologia. Secretary-General L. C. C. Teixeira, 01311 Avenida Paulista, 491, 13th Floor, cj. 132, São Paulo, Brazil
Sociedad Childena de Radiologia. Secretary, M. Neira, Casilla 13426, Santiago, Chile
Sociedad Colombiana de Radiologia. Secretary-General, G. Sanchez Sanchez, Bogota, Colombia
Sociedad Peruana De Radiologia. Secretary-General, E. de Olazaval Tejada, Colegio Médico del Perú, Casilla de Correo 20306, Lima Perú.
Sociedad de Radiologia del Atlantico. Secretary, R. Fernandez, Calle 40 #41–110, Baranquilla, Colombia
Sociedad de Radiologia. Radiotherapéutica y Medicine Nuclear de Rosario. Secretary-General, M. Muñoz, Santa Fe 1798, Rosario, Argentina

Europe

Bavarian-American Radiologic Society. Secretary, S. A. O'Byrne, Radiology Service, Stuttgart, West Germany, 5th General Hospital, APO NY 09154
British Institute of Radiology. Honorary Secretary, D. H. Trapnell, P. N. T. Wells, 32 Welbeck St, London, W1M/7PG, England
Čekoslovenská Radiologická Společnost. Secretary, J. Kolář, Clinic for Diagnostic Radiology ILF, 180 81 Praha 8, Budínova 2, Czechoslovakia
Danish Radiological Society. Secretary General, J. Praestholm, Radiological Dept I, Bispebjerg Hospital, DK-2400, Copenhagen NV, Denmark
Deutsch Rontgengesellschaft. President, W. Frik, Dept Radiology, Techn Univ Aachen, D-5100 Aachen, Goethestrasse 27/29, West Germany
European Society of Paediatric Radiology. Permanent Secretary, C. Fauré, Service de Radiologie, Hôpital Trousseau, 8–28, av du Dr. Arnold Netter, 75 571, Paris CEDEX 12, France. Annual meeting and postgraduate course: April 30–May 1, Köln.
Faculty of Radiologists (of Ireland). Honorary Secretary, M. Ryan, Faculty of Radiologists, Royal College of Surgeons in Ireland, Stephen's Green Dublin 2, Ireland
Finnish Radiological Society. Secretary, L. Laasonen, Box 963, SF-00101 Helsinki 10, Finland
The Hospital Physicists' Association. Honorary Secretary, R. F. Mould, Westminister Hospital, Physics Dept. Page St Wing, London SW1P2AR, England
Norsk Forening for Medicinsk Radiologi. General Secretary, A. Skjennald, Ullevål sykehus, Oslo, Norway
Netherlandse Vereniging voor Radiologie. Secretary, H. E. Schütte, Dept Radiology, Elizabeth Gasthuis, Haarlem, Netherlands
Royal College of Radiologists. Secretary, P. D. Thomson, 28 Portland Pl, London, W1N4DE, England
Scandinavian Radiological Society. Secretary-General, T. Drevvatne, Norwegian Radium Hospital, Montebello, Oslo 3, Norway
Schweizerische Gesellschaft für Radiologie und Nuklearmedizin. Soclete Suisse de Radiologie et de Medecine Nucleaire. Secretary, G. A. Schoch, 7 Gellerstrasse, CH—4052 Basal, Switzerland
Sociedad Española de Radiologia y Electrologia Médicas y de Medicina Nuclear. Secretary-General, P. G. Barberá, Villanueva, Madrid 1, Spain
Sociedade Portuguesa de Radiologia e Medicina Nuclear. General Secretary, J. Saldanha, 123, 1.°-Esq., Av. Elias Garcia, Lisbon, Portugal
Societá Itallana di Radiologia Medica e Medicina Nucleare. Administrative Secretary, R. Dall'Acqua, Ospedale Mauriziano, 10128, Torino, Italy
Societe Francaise de Radiologie Médicale, Nucléaire et Electrologie. Sec-

retary-General, J. Sauvegrain, Hôpital des Enfants-Malades, 149 Rue de Sèvres, 75730 Paris Cedex 15, France.

Société Française de Neuroradiologie. Secretary-General, R. Djindjian, 16, rue de l'Université 75, Paris 7°, France

Svensk Förening for Medicinsk Radiologi. Secretary, H. Ringertz, Dept Pediatric Radiology, Karolinska Sjukhuset, S—104 01 Stockholm, Sweden

Africa

Association of Radiologists of West Africa. Honorary Secretary, A. A. Obisen, Dept Radiology, University College Hospital, Ibadan, Nigeria

Radiological Society of South Africa. Secretary, A Visser, PO Box 8850, Johannesburg, South Africa

South African International Radiological Congress. Director, P. Sneider, PO Box 4878, Johannesburg, South Africa

Near East and Asia

Bengal Radiological Association. Honorary Secretary, B. Chatterji, 262 Rash Behari Ave, Calcutta 700019, India

Indian Radiological Association. Honorary General Secretary, S. P. Aggarwal, 1D–B Kasturba Ghandi Marg, New Delhi 110001, India

Indonesian Radiological Society. Secretary, G. Sasmitaatmadja, Radiology Dept, University of Indonesia, Salemba 6, Jakarta, Indonesia

Philippine College of Radiology. Secretary-Treasurer, A. Chavez, Box 1284, Commercial Center, Makati, Rizal, D-708, Philippines

Radiological Society of Thailand. Secretary, D. Prabbasawat, Dept Radiology, Siriraj Hospital Faculty of Medicine, Mahidol University, Bangkok 7, Thailand

Royal Australasian College of Radiologists. Honorary Secretary, B. Roberts, 37 Lower Fort St, Millers Point, NSW 2000, Australia

American Roentgen Ray Society

President: Harry Z. Mellins
President Elect: Paul A. Riemenschneider
1st Vice-president: Joseph D. Calhoun
2nd Vice-president: Charles E. Bickham, Jr.
Secretary: James F. Martin
Treasurer: Harley C. Carlson

COMMITTEES 1977–1978

Executive Council: H. Z. Mellins, P. A. Riemenschneider, J. D. Calhoun, C. E. Bickham, Jr., J. F. Martin, H. C. Carlson, M. M. Figley, R. G. Evens, B. G. Brogdon, R. A. Gagliardi, E. Gedgaudas, G. A. Kling, T. F. Leigh, S. F. Ochsner, J. F. Wiot, R. E. Buenger, E. C. Klatte, J. P. Tampas, J. L. Gwinn, chairman

Finance and Budget: A. E. James, E. C. Klatte, R. McLeeland, J. P. Tampas, R. G. Evens, chairman

Publications: M. P. Capp, K. Ellis, F. F. Ruzicka, Jr., E. R. Heitzman, R. A. Gagliardi, chairman

Editorial Policy: M. M. Figley, E. F. Lang, R. H. Troupin, E. R. Heitzman, K. Ellis, F. F. Ruzicka, Jr., M. P. Capp, R. A. Gagliardi, chairman

Advisory Committee on Education and Research: J. E. Youker, G. Wilson, G. W. Hartman, L. F. Rogers, E. Gedgaudas, chairman

Scientific Exhibits: T. C. Beneventano, G. Dodd, B. G. Brogdon, chairman

Constitution and Bylaws: J. H. Walker, W. M. Whitehouse, J. P. Tampas, chairman

American Board of Radiology Representatives: J. F. Roach, R. W. McConnell, S. W. Nelson

Program Committee: H. Z. Mellins, J. F. Martin, J. L. Gwinn, M. M. Figley, R. A. Gagliardi, B. G. Brogdon, E. Gedgaudas, G. A. Kling, P. Riemenschneider, chairman

Instruction Courses: E. Gedgaudas, director; G. W. Hartman, associate director

American College of Radiology Board of Chancellors Representative: W. B. Seaman

Annual Meeting: March 25–30, 1979, Sheraton Centre, Toronto, Canada

Scientific Program: P. A. Riemenschneider, president elect, Cottage Hospital, Santa Barbara, California 93105

Manager Annual Meeting: George A. Kling, Harper Hospital, Detroit, Michigan 48201

Membership: John L. Gwinn, 4650 Sunset Blvd., Los Angeles, California 90027

Business Office: Keith W. Gundlach, comptroller, American College of Radiology, 20 North Wacker Drive, Chicago, Illinois 60606

American Radium Society

President: Frederick W. George, III
President Elect: Alfred S. Ketcham
1st Vice-president: Julian P. Smith
2d Vice-president: Edwin M. Jacobs
Secretary: Norah duV. Tapley
Treasurer: Simon Kramer

COMMITTEES 1978–1979

Executive: A. S. Ketcham, J. P. Smith, E. M. Jacobs, N. duV. Tapley, S. Kramer, L. W. Brady, R. H. Jesse, F. W. George, F. Rutledge, chairman

Public Relations: V. Marcial, J. Vaeth, C. Honaker, ex-officio, and F. George, chairman

Publication: K. L. Krabbenhoft, D. Hussey, A. Raventos, I. Fix, L. W. Brady, chairman

Scientific Program: R. Parker, J. Durant, A. S. Ketcham, M. S. Mitchell, G. Murphy, F. Rutledge, M. Griem, W. E. Powers, M. Apuzzo, F. George, chairman

Local Arrangements: L. Davis, J. Vaeth, J. Nolan, R. McKenna, J. Slater, J. Stein, J. Scallon, S. Kramer, J. Helsper, chairman

Constitution and Bylaws: A. S. Glicksman, P. J. DiSaia, K. L. Krabbenhoft, chairman

Audiovisual: C. R. Bogardus, J. Helsper, R. Schweitzer, R. H. Jesse, C. Perez, J. Glassburn, A. M. Nisar Syed, R. Young, B. Herrington, F. George, chairman

American Board of Radiology Representatives: J. J. Stein, R. E. King, N. duV. Tapley

American College of Radiology Board of Chancellors Representative: L. W. Brady

American College of Radiology Council Representative: J. del Regato

Editorial Board of AFCOS Newsletter Representative: J. Vaeth

National Council on Radiation Protection and Measurements Liaison Representative: L. W. Davis

Annual Meeting: March 4–8, Los Angeles, California

Scientific Program: F. W. George, III, University of Southern California School of Medicine, Los Angeles, California 90033

Local Arrangements: James Helsper, Pasadena, California

Membership: Norah duV. Tapley, secretary, M. D. Anderson Hospital, 6723 Bertner Avenue, Houston, Texas 77030

Business Office: N. V. Jordan, c/o R. H. Jesse, M. D. Anderson Hospital and Tumor Institute, 6723 Bertner Avenue, Houston, Texas 77030

Mailing note.—Mailing surcharges: U.S. and possessions, none; European countries, $25; Japan, $45; other, $10. European rates apply to Algeria, Austria, Belgium, Czechoslovakia, Denmark, Finland, France, Germany, Great Britain, Greece, Hungary, India, Iran, Ireland, Israel, Italy, Kenya, Luxembourg, Netherlands, Nigeria, Norway, Portugal, Romania, South Africa, Spain, Sweden, Switzerland, Turkey, Uganda, Yugoslavia. All subscriptions to Japan and European countries are delivered by air freight; there is no option for surface mail.

CGR.

Four Major Systems for Superlative Tomography.

STRATOMATIC H.

The Stratomatic H is CGR's classic tomographic system. Completely integrated. Automatic. Solid state.

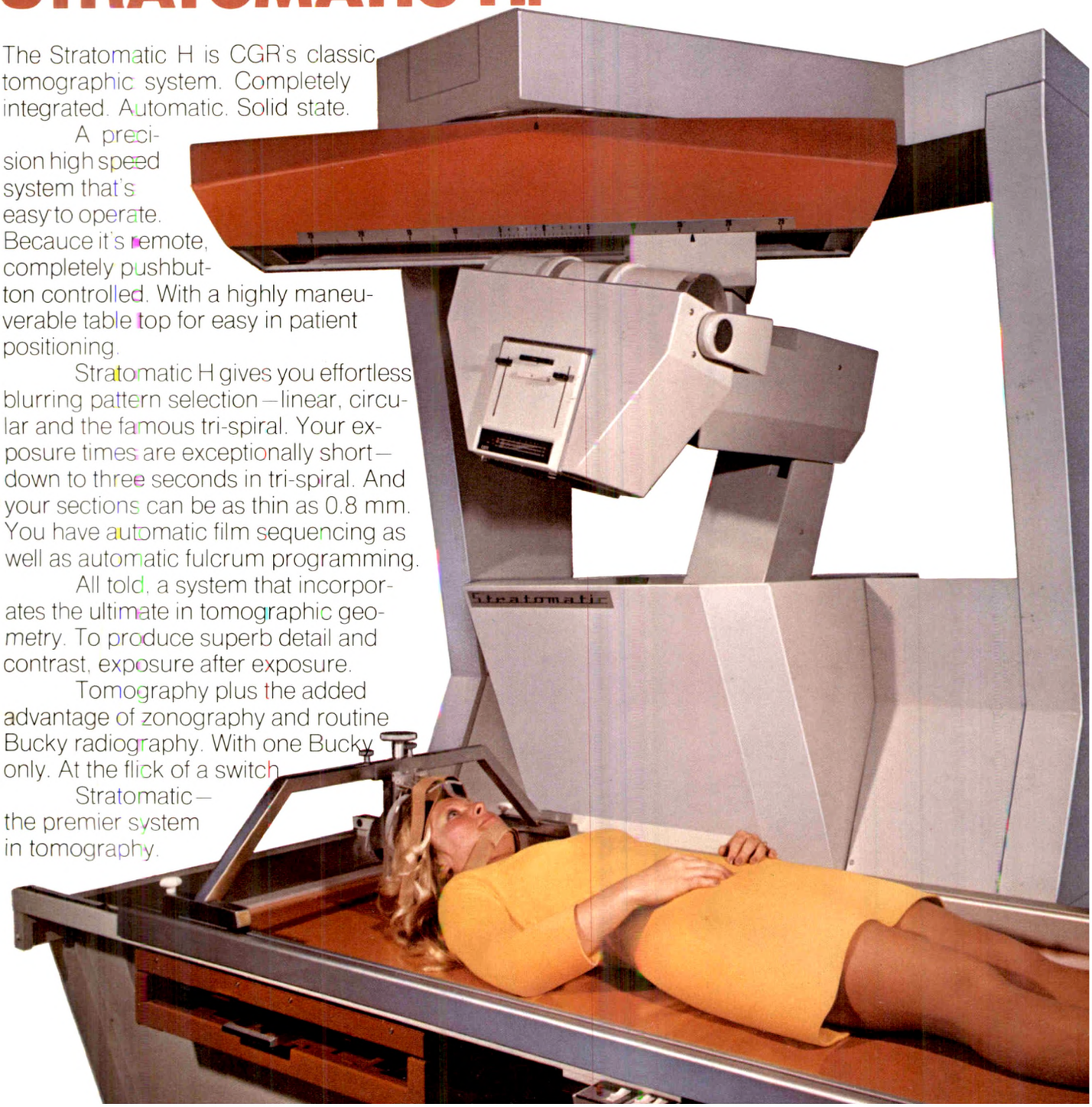
A precision high speed system that's easy to operate. Becauce it's remote, completely pushbutton controlled. With a highly maneuverable table top for easy in patient positioning.

Stratomatic H gives you effortless blurring pattern selection—linear, circular and the famous tri-spiral. Your exposure times are exceptionally short—down to three seconds in tri-spiral. And your sections can be as thin as 0.8 mm. You have automatic film sequencing as well as automatic fulcrum programming.

All told, a system that incorporates the ultimate in tomographic geometry. To produce superb detail and contrast, exposure after exposure.

Tomography plus the added advantage of zonography and routine Bucky radiography. With one Bucky only. At the flick of a switch.

Stratomatic—the premier system in tomography.



STRATOMATIC U.

Stratomatic U. The logical extension of CGR's classic Stratomatic H. The same integrated, remote, solid state approach.

Only now you have 240° tilting spectrum. To quickly and easily position patients for expanded technique opportunities. And a large table top for rapid, accurate longitudinal and transverse centering.

The classic three motions—linear, circular and tri-spiral. And short exposure times. A dramatic reduction over competitive units.

Stratomatic U also performs routine radiography, stereo-radiography and zonography. Magnification factor is the same for all modes. You have remarkably short film-to-patient distance.

Stratomatic U. Controlled tableside or remotely from the generator. For fast, accurate examinations. The logical extension in the Stratomatic family.



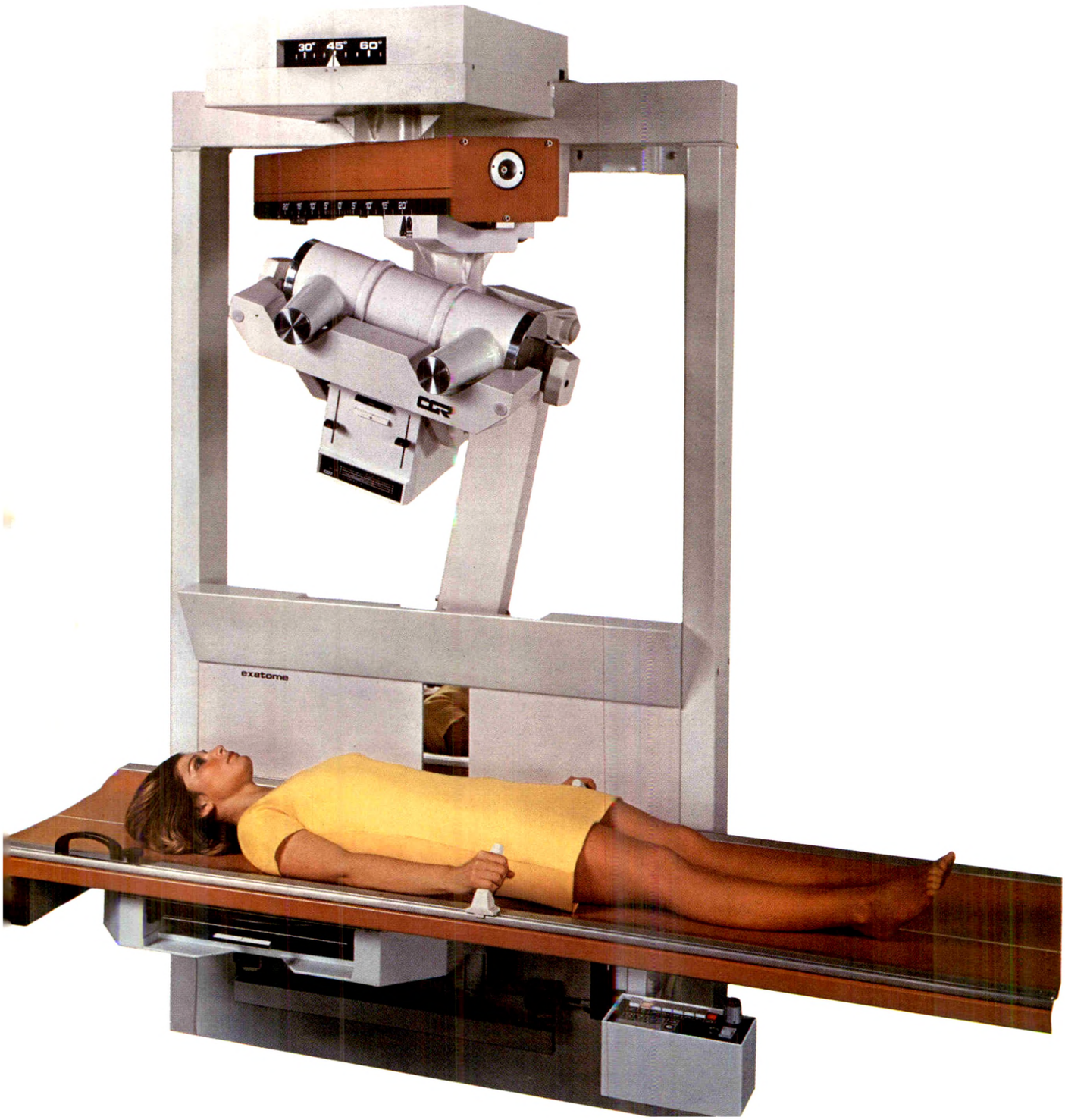
EXATOME.

The essence of the famous Stratomatics. Spartanly designed to be competitive with linear units. But featuring all three blurring motions—linear, circular *and* tri-spiral.

Exatome brings "real" tomography within the reach of every hospital and clinic. With a versatile system that permits routine Bucky examinations as well. At the flick of a switch.

The system is rugged. To give you stability for maximum film excellence. It's pushbutton operated tableside for fast, convenient positioning and operation. And the Exatome gives you a choice of single or three-phase generator systems.

Exatome—a great step forward in economical, multi-directional tomography.



COMPACT/ SYNCHROTOME.

Synchrotome is a unique breakthrough in radiography and linear tomography. A system that's completely "fulcrum arm free." There's no concealed mechanical linkage. It's all high precision electronics.

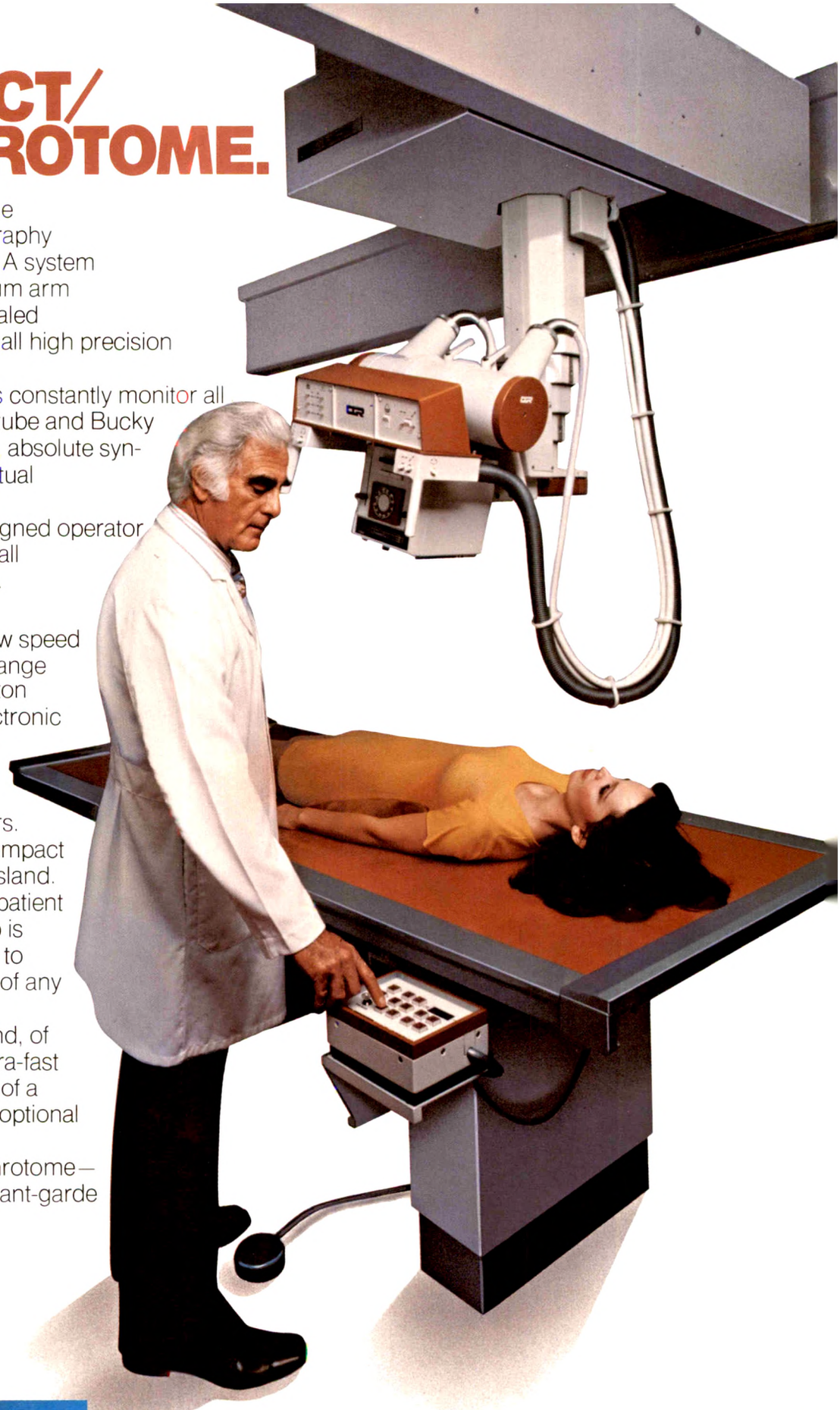
Microprocessors constantly monitor all tube suspension, x-ray tube and Bucky movements—complete, absolute synchronization about a virtual fulcrum point.

An advance designed operator programmer gives you all tomographic selections.

Three amplitude selections. Fast and slow speed options. Fulcrum level range of 0 to 27 cm, push button controlled. Even an electronic alarm clock to monitor those timed sequence examinations such as IVP's and IVC's or others.

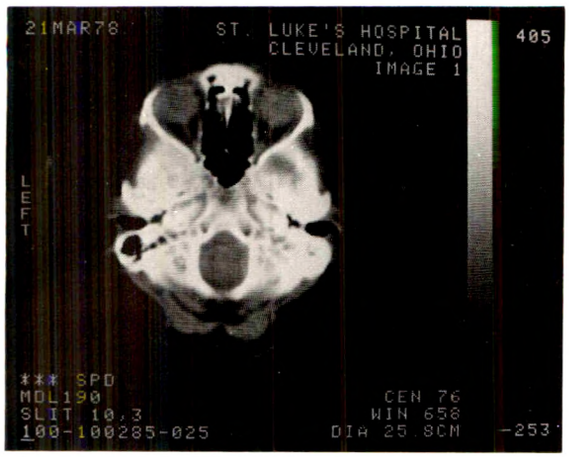
The system's Compact table is an easy-to-use island. Absolute access to the patient from all sides. Table top is four-way, floating, large to accommodate patients of any size. Your table-to-film distance is only 1.6". And, of course, you have an ultra-fast Bucky and your choice of a radiographic grid. With optional phototiming.

Compact/Synchrotome—a first in economical, avant-garde linear tomography.

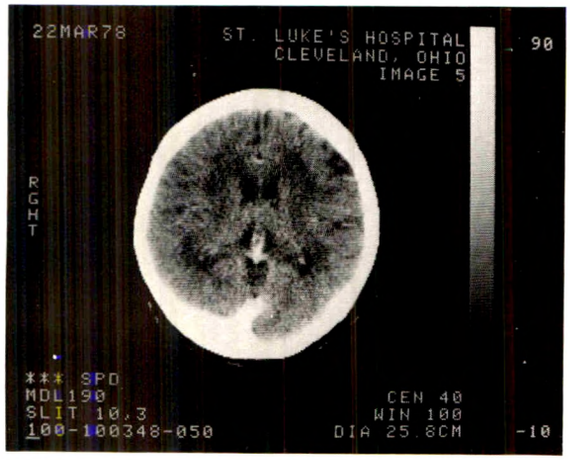


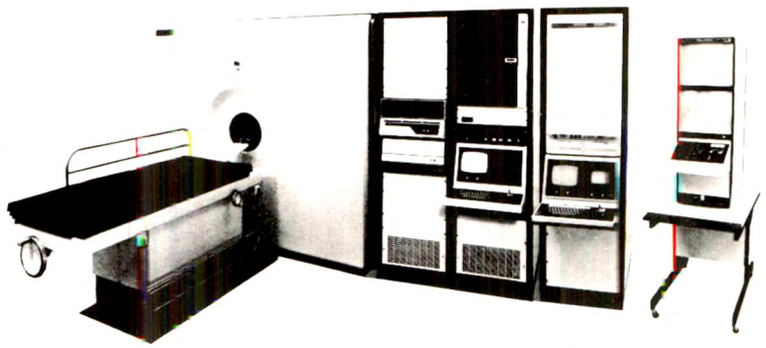
CGR MEDICAL CORPORATION, 2519 Wilkens Avenue, Baltimore, Maryland 21223 (301) 233-230
CGR CANADA LTÉE-LTD., 500 Boulevard de l'Aéroparc, Lachute, Québec, Canada, (514) 562-880
CGR, 13 Square Max Hymans, 75741 Paris, France, 273-8200

High-resolution,



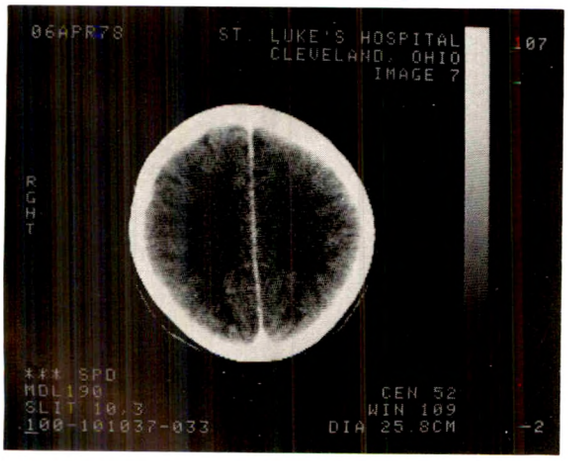
low-cost,





DeltaScan™ 100 Series.

neurological CT scanners



Computerized Tomography of the Brain, unquestionably the preferred modality in neurologic diagnosis, is now available at an economically feasible price.

The DeltaScan 100 Series scanners, starting at $96,500, combine uncompromised resolution with a uniquely compact, new design, resulting in affordable, clinically proven CT scanners which are ideally suited for smaller institutions with moderate patient throughput needs.

For additional information concerning cost and performance of the DeltaScan 100 Series scanners, contact Ohio-Nuclear, Inc.

from Ohio-Nuclear, Inc.

A subsidiary of Technicare Corporation

29100 Aurora Road, Solon, Ohio 44139
Phone: (216) 248-1800
TWX No. 810-427-2696


MFX
120
500
400
125
90
0.0
GENERAL ELECTRIC
RPX Nursery



A classic breakthrough.

GE's new R&F system saves you time, space, money and dose. And gives you excellent images.

Here's a totally new R&F system that offers you many advantages over existing units—it's a major breakthrough in classical R&F. Let's take a closer look at each component.

Fluoricon® L300 suspensionless intensifier gives you 9″ triple field performance, high frame rate photospot capability and improved imaging in a new lightweight package.

Diagnostic detail is exceptional—with advanced video camera technology and high resolution, high contrast ratio image tubes.

User-selectable dose rate and video gain let you add video gain for imaging obese patients, and provide the lowest dosage for young or thin patients.

When you choose the computerized technic management option at the spotfilmer, unique values of kVp, mA and focus are stored for each spotfilm and photospot procedure. Patient size selection includes pediatrics down to the neonate range.

And the new suspensionless design allows ample clearance for an overhead tube, facilitating radiography and attachment of an optional tomograph. The compact design fits into smaller, problem-sized rooms, giving you large room R&F capability.

RFX™ table and spotfilmer, with user-selectable grids, combines lower dose fluoro and high kVp spotfilms in one easy-to-use system.

The spotfilmer's unique, effort-sensing power assist simulates the feel of an unpowered fluoroscopic screen.

Two-per-second spotfilming with sequence anticipation allows two to four manually sequenced spotfilms without cassette return. Load from the front or rear, with pushbutton changeover.

Diagnostic advantages include automatic masking to format with full field, 2-on-1 vertical or transverse, or 4-on-1 formats. Masking is internal, allowing full field fluoro with the cone in place.

Additional RFX features include: (1) cone lockout for myelography; (2) automatic cassette return; (3) rapid access spotfilming (.75 sec.); (4) arthrographic collimation and ion chamber compensation for 9-on-1 or 6-on-1 formats; and (5) improved radiation protection at all routine angulations.

MPX computerized generator, with Quantamatic™ tx technic management, stores all of your department's standard radiographic settings.

The operator simply presses the appropriate anatomical selection buttons. The microprocessor instantly displays all technic parameters, including kVp, mA, mAs, time, focal spot size and AEC status. And the operator may raise or lower factors to suit special patient situations.

With over 200 programmed AEC and fixed-time technics (on or off the table) available, you can handle virtually every patient size. From infant to obese adult. And any body part, including extremities.

Quantamatic tx technic management gives you consistent, high-quality films. Throughput increases. Costly retakes due to technic error are virtually eliminated. And programmed constant load design extends tube life by optimizing tube loading.

You'd expect it from GE.

Contact your GE representative to get all the facts on this important R&F breakthrough. Fluoricon L300/RFX/MPX....it's a classic.

General Electric Medical Systems, Milwaukee, Toronto, Madrid.

GENERAL ELECTRIC



PYNE X-RAY CORPORATION

Proudly Announces

FUJI FILM

RX-M

Developed for use with multi-format imaging systems designed for CT Scanners, Nuclear Diagnostic Equipment, or Ultrasonic Diagnostic Equipment.

An orthochromatic, single-emulsion film, Fuji RX-M is also excellent for mammography, as it offers high speed plus superior contrast and resolution.

RX-M is available for immediate delivery. Please contact your nearest Pyne X-Ray office or your local authorized Fuji Film dealer.

Distributed throughout the U.S. by:

PYNE X-RAY CORPORATION

NEW YORK
20 North Avenue
Larchmont, New York 10538
(914) 834-4567

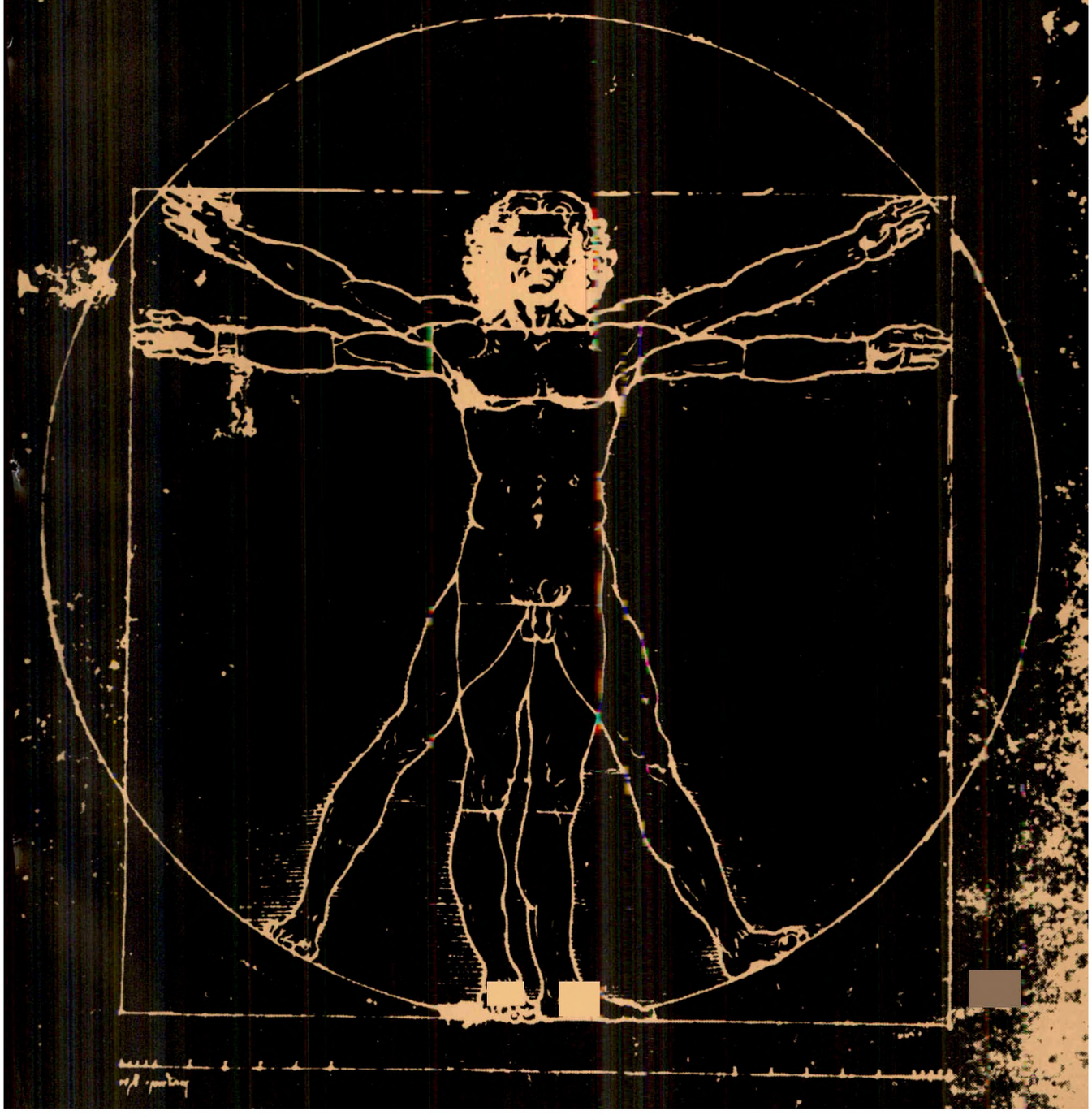
CHICAGO
1211 West Norwood Avenue
Itasca, Illinois 60143
(312) 773-3360

LOS ANGELES
1639 Gardena Avenue
Glendale, California 9
(213) 240-0280

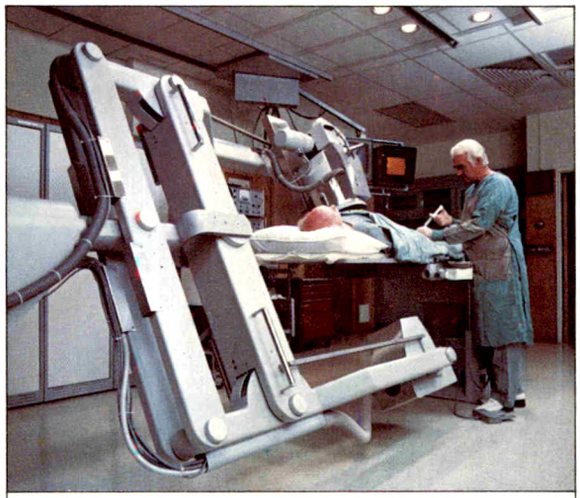
Philips Angiography Systems.

TOTAL BODY COVERAGE WITH THE BROADEST RANGE OF EQUIPMENT

. . . from the only company offering all the choices you need!



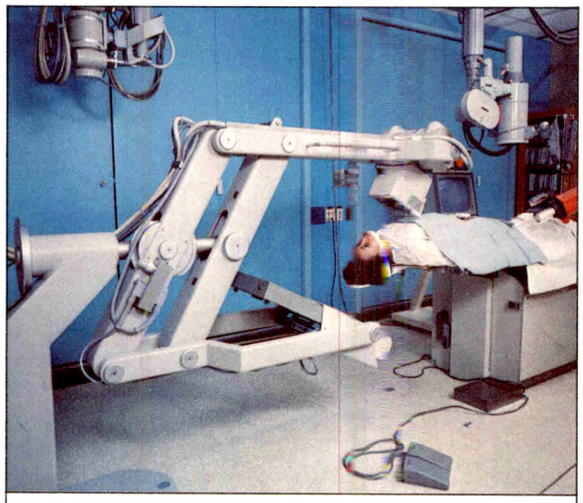
Poly Diagnost C



The parallelogram construction of the Poly Diagnost C permits the patient to remain stationary, leaving the physician more relaxed and able to concentrate fully on the procedure. Insuring maximum safety for both patient and operator, the Poly C provides both routine and cranio-caudal views that insure clear, unobstructed views of overlapping vessels. Stenoses which might have been obscured can be detected with a high degree of efficiency and operational ease.

Designed for both the brachial and femoral techniques of cardiac angiography, the Poly C is also successfully used in abdominal and thoracic studies.

Poly Diagnost N

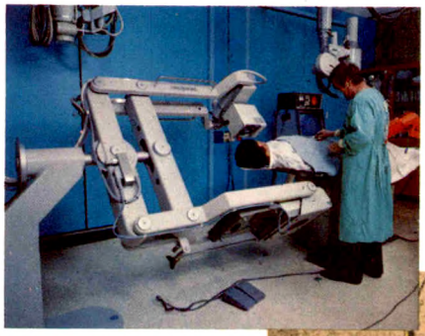


Designed specifically for cerebral angiography at 2:1 magnification, the Poly Diagnost N easily provides views of the patient previously difficult (or impossible) to achieve. The parallelogram construction allows full rotation around the long axis of the body *and* the maximum desirable head-to-foot angulation. The unique construction insures all motions are isocentric and all results are distortion free.

Designed for use in single or bi-plane operation with a Puck rapid film changer, the Poly N lends itself to extensions for more dedicated requirements, such as the latest configuration with a quickly interchangeable image intensifier and a rapid film changer.

PHILIPS MEDICAL SYSTEMS, INC.
710 Bridgeport Avenue, Shelton, Conn 06484

Philips Angiography Systems.



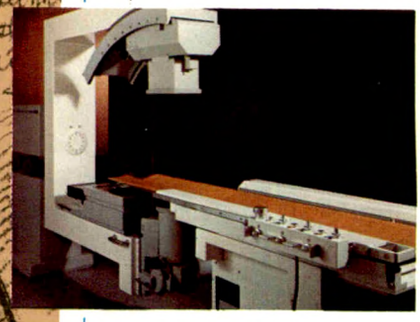
Poly Diagnost N

The first in Philips' family of dedicated cerebral angiography systems with parallelogram construction. For optimum results with isocentric patient positioning for all projections.



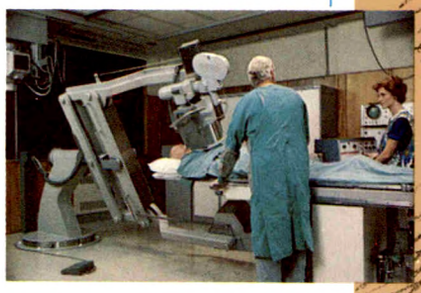
Poly Diagnost UPI

Philips' new universal angiography system for the most flexible filming of cerebral, thoracic, abdominal and peripheral angiography, with full provision for occasional cardiovascular examinations.

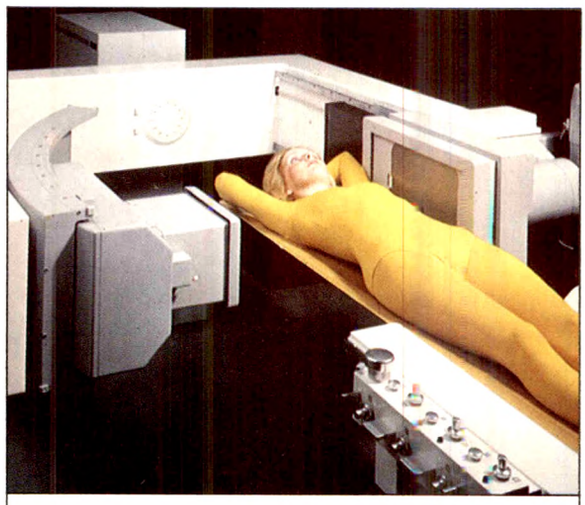


Poly Diagnost C

An extension of the U-arm principle first developed by Philips in the Cardio Diagnost, the Poly C is a dedicated cardiovascular system. Parallelogram construction provides routine and cranio-caudal views without moving the patient, making the Poly C widely used for imaging the thoracic and abdominal areas.



Poly Diagnost UPI



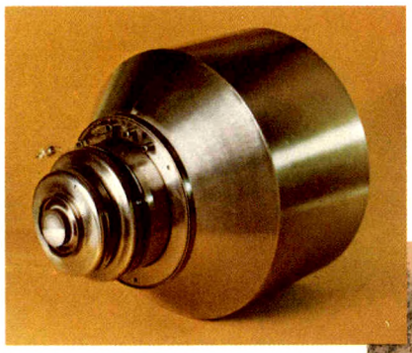
A universal system with revolutionary design, the Poly Diagnost UPI features a rotating U-arm that carries the X-ray tube and an image intensifier and rapid film changer which are quickly interchangeable.

A new experience in examination convenience, the Poly UPI is a masterful combination of system features: free choice of oblique, cranio-caudal and caudo-cranio projections; rapid changeover from fluoroscopy to film changer work; automatic control of object-film distance; motorized height adjustment of both table and U-arm, which provides contact and up to 2:1 geometric enlargement; and a unique boating movement that keeps the object centered in the beam while the object-film distance is automatically controlled in every projection. It's the ideal universal system for angiography!

PHILIPS®

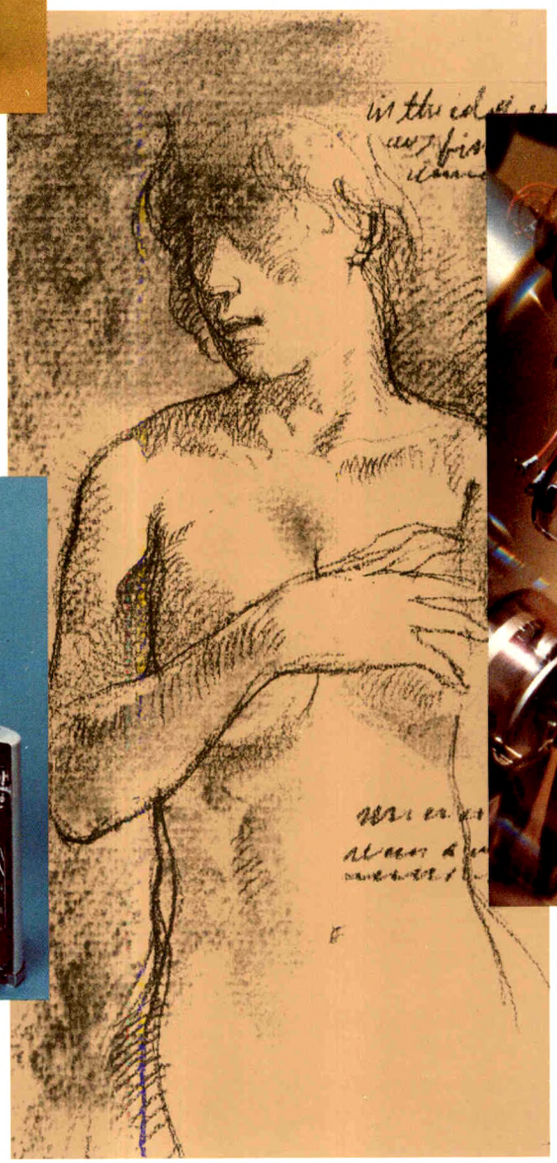
© TM N.V. Philips of Holland

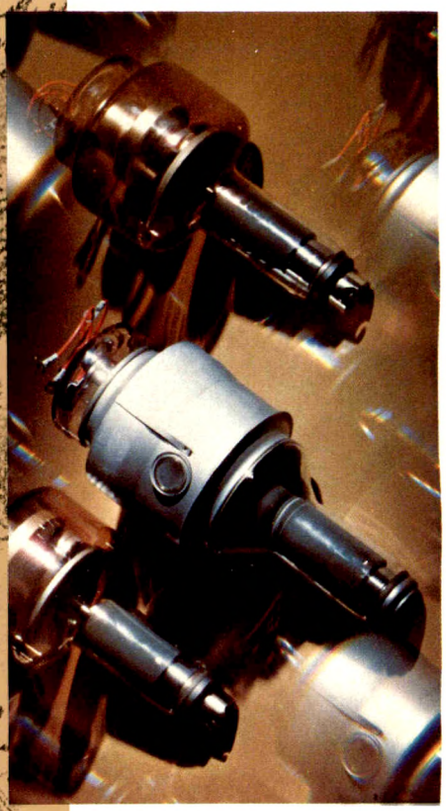
A COMPLETE FAMILY OF IMAGE INTENSIFICATION SYSTEMS, X-RAY TUBES AND GENERATORS FOR PHILIPS ANGIOGRAPHIC EQUIPMENT.

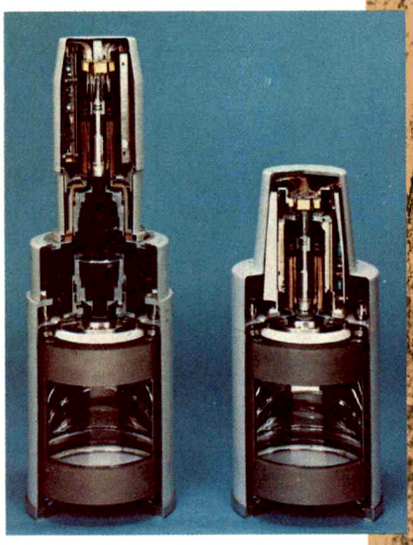


The 14″ Triple-Mode Image Intensifier
Another first from Philips! An amazingly lightweight 14″ image intensifier for highly detailed surveys with outstanding results.

Super Rotalix and Trinodex X-ray Tubes
Preferred for exceptional image quality and reliable performance in sustained operation, Philips' tubes are designed for high loadability and superbly efficient heat dissipation.







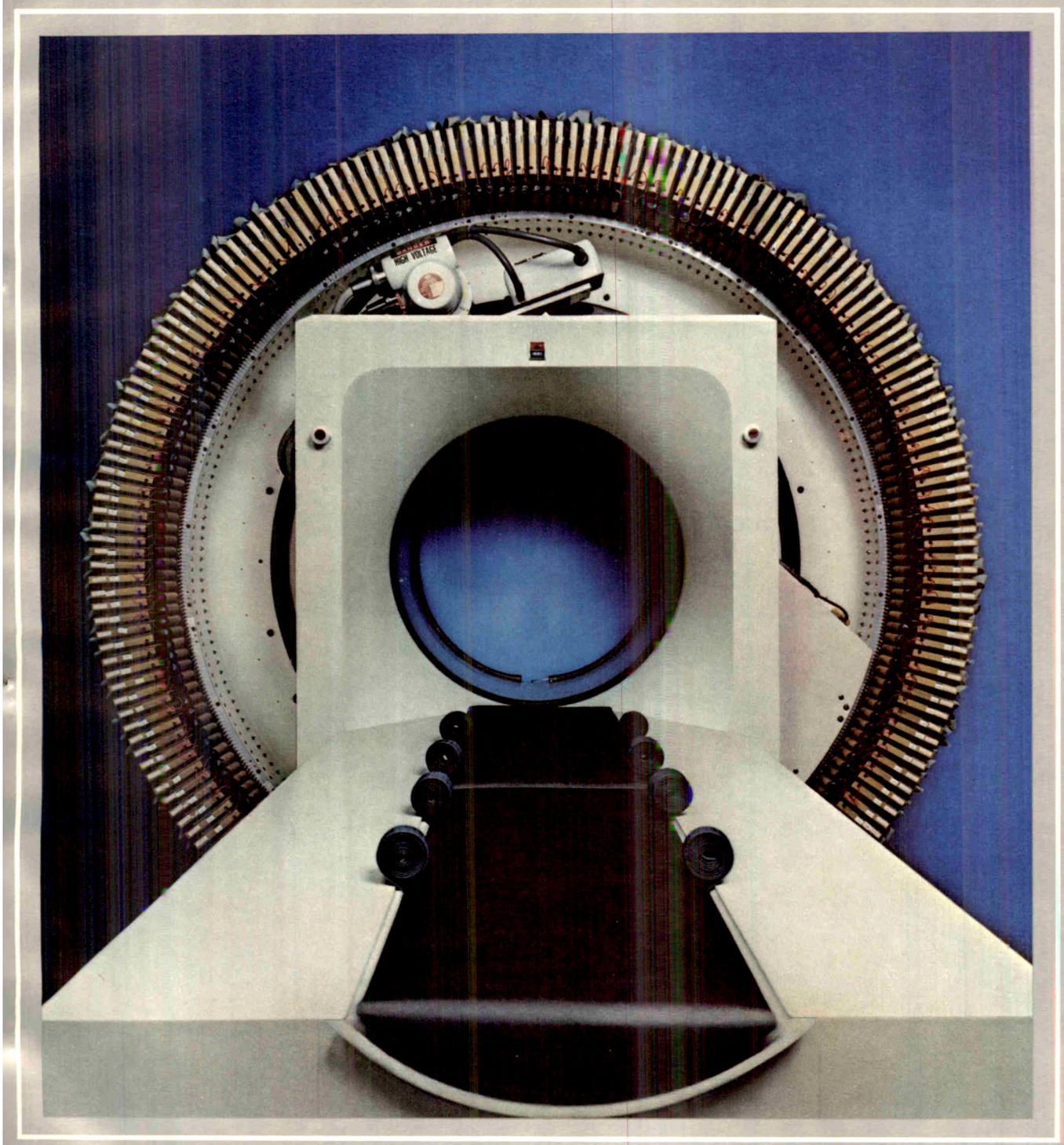
Conventional or Fiber Optic Image Intensifiers
Select from a full range of fields in conventional image intensifiers . . . or Philips' Exclusive Fiber Optic Image Intensification System. Fiber optics provides 30:1 contrast ratio for greater detail, uniform image quality over the entire screen, optimum image transfer and compactness for easy maneuverability.

PHILIPS®
the most reliable family of systems and people in the industry.

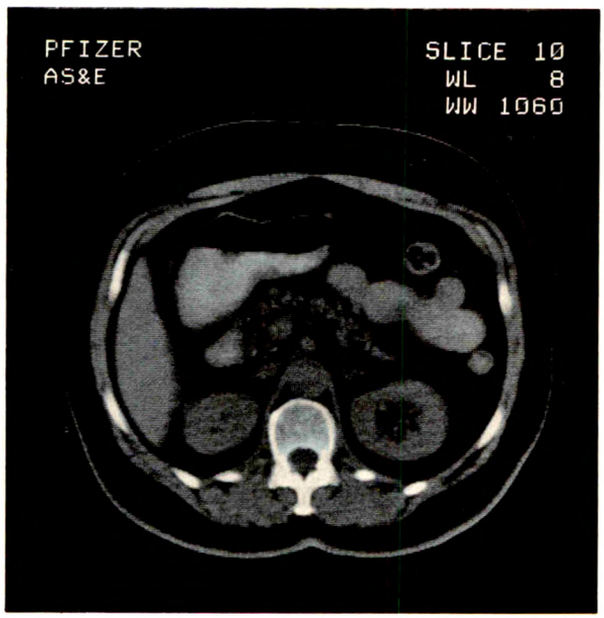
A Full Range of Generators
From the very affordable three-phase, high output Classic line, to a full range of Modular Generators, to the computerized Optimus M200, Philips' family of generators combines quality, performance and price for your every examination need.

A new standard of accuracy in CT imaging

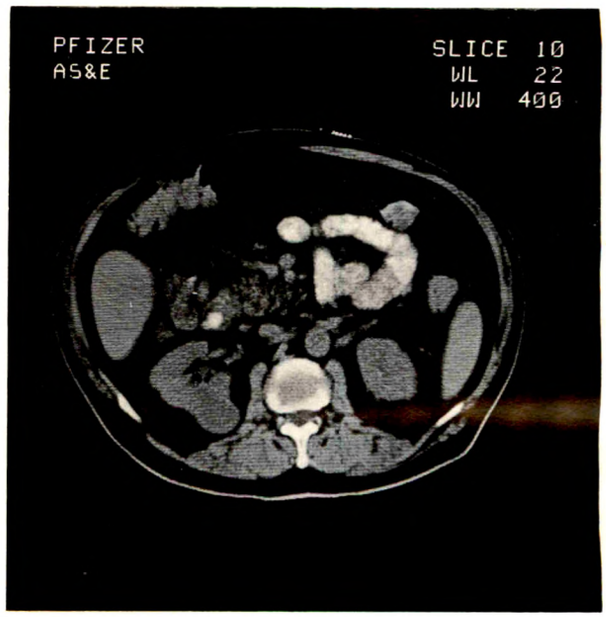
Pfizer/AS&E Generation IV



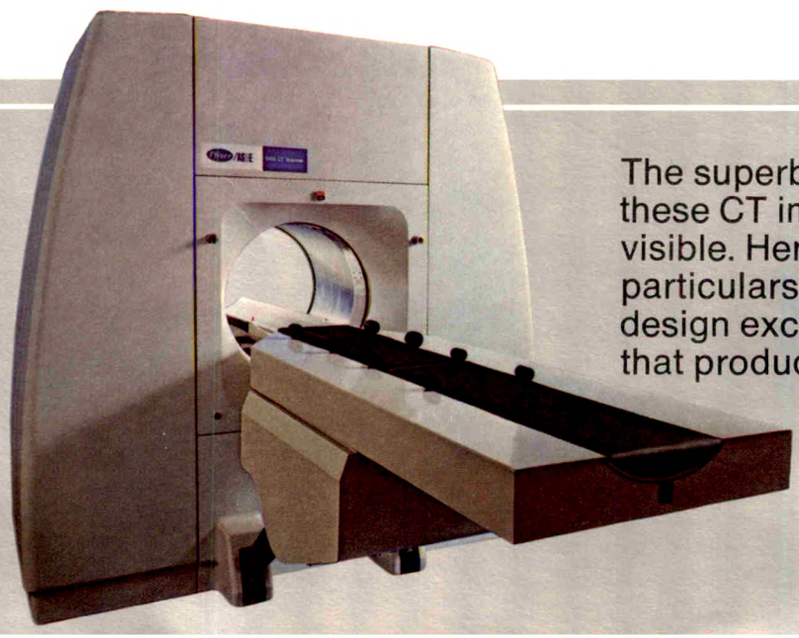
Superior scans from stationary detectors



CT scan of the abdomen. The inferior portion of the left adrenal gland is well visualized as is the vertical portion of the superior mesenteric artery anterior to the aorta.



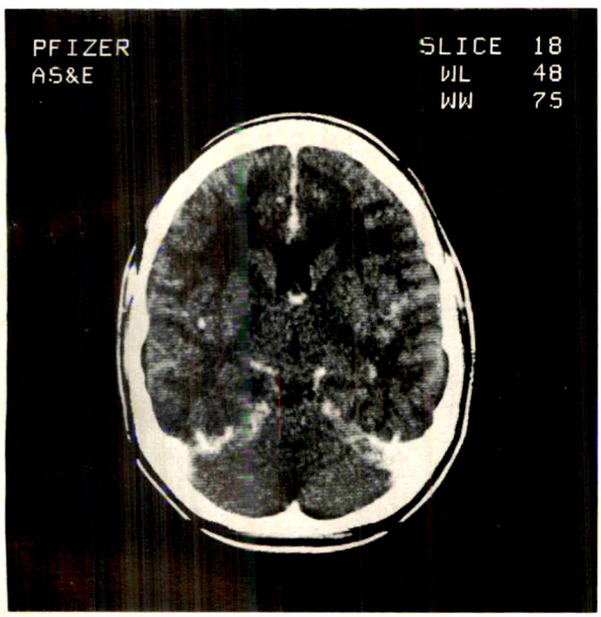
CT scan of the abdomen. The spinal cord and nerve roots are well demonstrated. Note the mass at the posterior medial aspect of the right kidney.



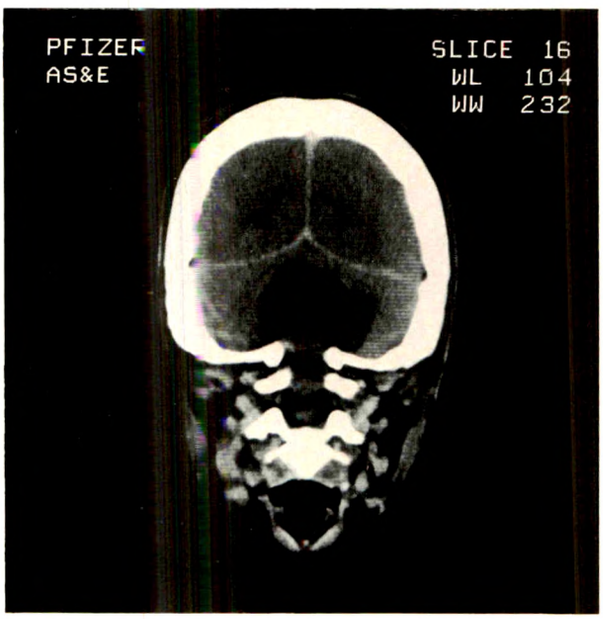
The superb quality of these CT images is clearly visible. Here are some particulars of the design excellence that produced them:

Pfizer/AS&E

0450



CT scan of the head. There is excellent separation of central white and gray matter. The caudate nucleus and basal ganglia are clearly seen.



CT scan of the head. Coronal view. Contrast enhanced tentorium demonstrated. There is a midline posterior fossa arachnoid cyst. Note the absence of artifacts.

Continuous detector calibration for the most accurate CT numbers and images available...

Pfizer/AS&E 0450. Generation IV. Only the x-ray tube rotates; the full circle of photon detectors is stationary. All attenuation data are continuously referenced to objects of known attenuation within, and immediately outside, the patient scan field. And each detector is calibrated on every scan—making possible DENSET, the precise CT number stabilization system which eliminates even potential errors in data acquisition. DENSET clearly provides a new dimension in CT diagnosis—reliable, repeatable imaging across the entire scan field.

...And freedom from artifacts

Pfizer/AS&E Generation IV. Where every detector reviews the entire scan field, not just a small portion. The classic image-degrading circular artifact caused by detectors viewing individual circles within the scan field simply cannot occur. 0450 Generation IV CT images are, by design, free from geometric defects.

Superior scans from advanced technology

More efficient detection—better dose utilization

The scintillation crystal/photomultiplier detectors used in the Pfizer/AS&E 0450 provide you and your patient with optimum dose utilization. Because we start with solid crystals, having twice the detector efficiency of comparable Xenon chambers at high pressures, over 98% of all x-ray photons striking the crystal are detected and contribute to the final image.

Less noise—better contrast resolution

Of all x-ray detectors, the solid scintillation photomultiplier tube combination provides the highest signal-to-noise ratio and widest dynamic range. Readings are not degraded by noise introduced with less sensitive detectors. Contrast resolution and range of dose utilization are superior by design.

Faster detector response—better spatial resolution

0450 detectors are sensitive, exhibit fast response, and do not become saturated. These properties allow data to be collected continuously instead of at the rate with which the x-ray source can be pulsed. The results: more data, faster scans and superb spatial resolution.

Full field resolution—image integrity

Tiny anatomical structures (1-1.5 mm) varying only slightly in density are faithfully resolved and displayed uniformly over the entire scan field even at *lowest dose settings.* This ultra-high fidelity is achieved by using a 640x512 matrix which is reconstructed from more than 700,000 data measurements—requiring no extensive "smoothing" software.

Pfizer/AS&E 0450

The superior CT scanning system you'll want to know more about

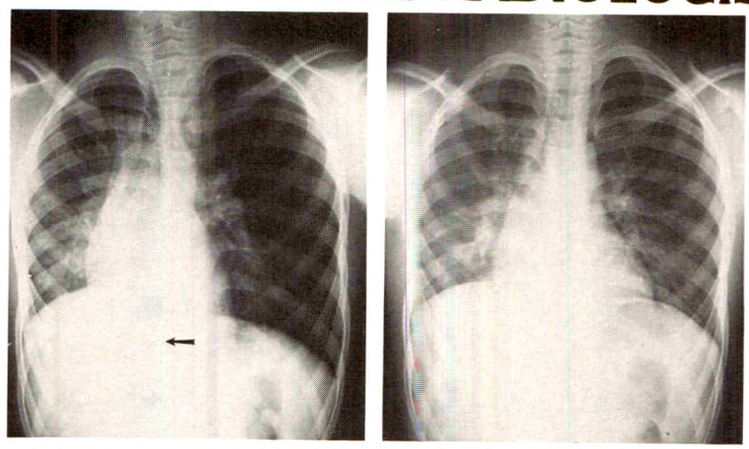


Write us for a detailed brochure:
Pfizer Medical Systems, Inc.
235 East 42nd Street, New York, N.Y. 10017

PFIZER MEDICAL SYSTEMS, INC.
A subsidiary of Pfizer Inc.
235 East 42nd Street, New York, N.Y. 10017
Telephone: (212) 573-2323
Telex: 234088 (RCA) 62422 (WUI) 420440 (ITT)

PRINTED IN U.S.A.

ALL NEW, ALL CLINICAL BOOKS FOR THE RADIOLOGIST



(From Swischuk, **Emergency Radiology of the Acutely Ill or Injured Child.**) **Mucous plug with distracting contralateral compensatory emphysema. A.** On this respiratory view, there is marked mediastinal shift to the right (arrow), and the left lung might be suspected as being the abnormal lung. However, as will be been in Fig. **B.** it is normal and on this view merely shows compensatory overaeration on inspiration. **B.** Expiratory films showing that the problem lies on the right. Note that the left lung has emptied but that the right lung has not changed in size on this view. A little mediastinal shift to the right persists, attesting to the fact that the problem is one of an obstructing mucous plug on the right. The thin radiolucent band outlining the left pericardial border represents a small medial pneumothorax.

Leonard E. Swischuk, MD
EMERGENCY RADIOLOGY OF THE ACUTELY ILL OR INJURED CHILD
Extremely practical and clinical, Swischuk's is the first book to focus exclusively on the interpretation of pediatric roentgenograms. With particular attention to initial (usually plain) films, the book outlines general approaches to diagnostic problems, helpful rules of thumb, and specific diagnostic signs as well as normal findings that mimic pathology in the pediatric age group. Many high quality illustrations allow comparison of significant findings with those of the patient at hand. A true "bread and butter" approach for the practicing radiologist.
1979/512 pp/576 figs/$45.00

Leonard E. Swischuk, MD
PLAIN FILM INTERPRETATION IN CONGENITAL HEART DISEASE
2nd ed. A precise, well-organized, and straight-to-the-point summary, again displaying that clarity of purpose that Swischuk has become famous for. All but the very rare conditions are covered and angiograms are used to emphasize plain film findings. Both positive and negative aspects of plain film interpretation are presented. This is a complex subject and there are very few places where one can get a valid summary in a nutshell. This is one of those places.
1979/about 278 pp/260 figs/ about $28.00

Elias H. Botvinick, MD, and David M. Shames, MD
NUCLEAR CARDIOLOGY: CLINICAL APPLICATIONS A core collection of case studies in nuclear cardiology, carefully chosen to illustrate high quality scintigrams from the authors' extensive files, is the basis for this clinical guide for the radiologist. An invaluable study that clearly sets forth when and why nuclear testing should be done, when and where **not** to do the tests, and how the tests compare with other noninvasive tests and with the findings of invasive techniques (such as echocardiography).
1979/264 pp/214 figs/$23.00

Please send me the following books on 20-day approval:

- ☐ Botvinick & Shames **NUCLEAR CARDIOLOGY** (0943-5) $23.00
- ☐ Swischuk **EMERGENCY RADIOLOGY** (8052-0) $45.00
- ☐ Swischuk **PLAIN FILM INTERPRETATION** (8041-5) about $28.00

Save postage and handling by enclosing payment with order. Maryland residents please add 5% sales tax; prices subject to change without notice.

name _____

address _____

city _____ state _____ zip _____

☐ Check enclosed ☐ Bill me ☐ VISA ☐ Master Charge

card # _____ expiration date _____

TOLL-FREE TELEPHONE ORDERING (9 am to 4 pm): for ordering with or without charge card, call 1-800-638-0672; Maryland residents call collect, 528-4221.

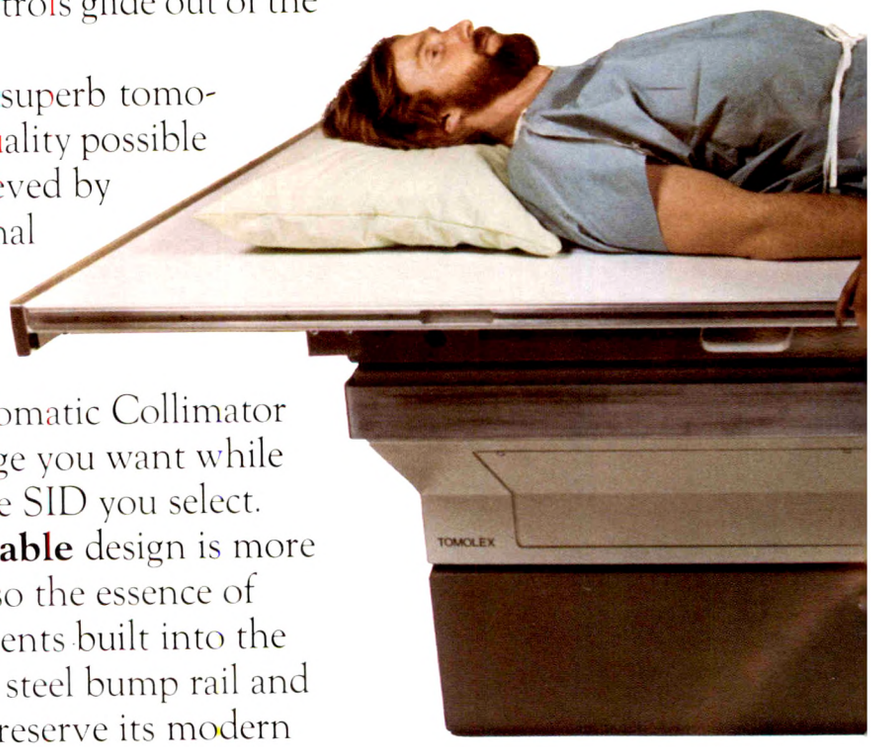
Williams & Wilkins
Dept. 257 P.O. Box 1496 Baltimore, Md. 21202

Still using fulcrum bar?



In Tomolex,™ there is no heavy, cumbersome fulcrum bar. With touch-button controls, just the finger tip is all that is required to set the Tomolex for tomography, erect-chest work or routine horizontal radiography. Being able to switch from tomography to radiography and back again within seconds assures maximum patient throughput.

Faster throughput isn't all that Tomolex offers. The four-way float-top table makes patient positioning faster and easier for the technologist, more comfortable for the patient. And the extra-wide tabletop gives your patient a greater feeling of security. Yet you can still position carts flush against the Tomolex top because tableside controls glide out of the way quickly and effortlessly.

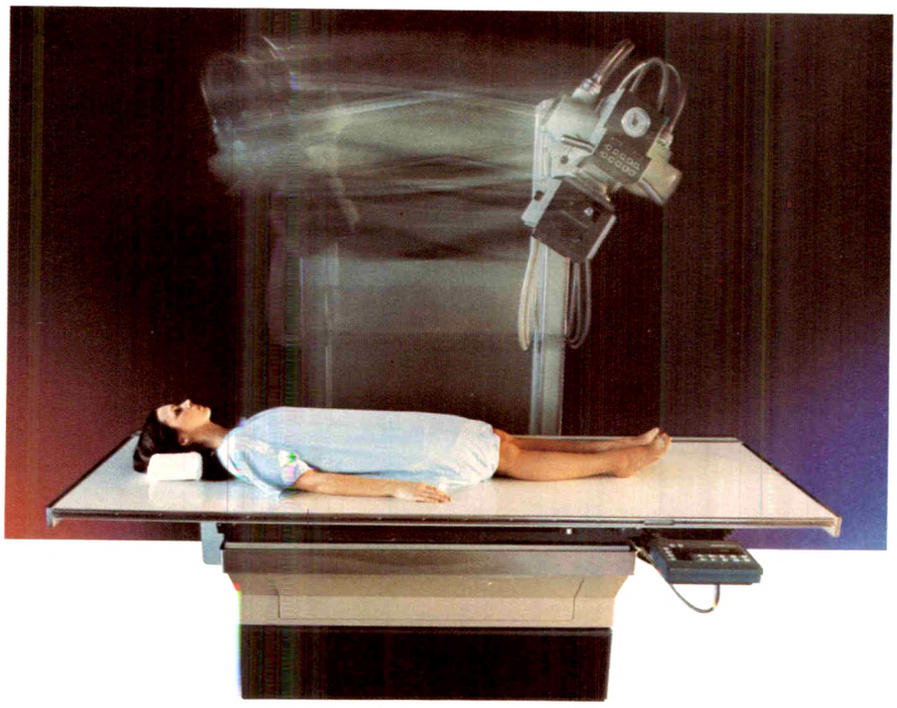


Radiologists appreciate the superb tomographic and radiographic image quality possible with Tomolex. Quality that's achieved by design from inception through final assembly. Further, automatic exposure control assures optimal radiologic film density — consistently. And the Collimatic Automatic Collimator provides the precise beam coverage you want while tracking film size, according to the SID you select.

Tomolex's award-winning table design is more than just visually attractive. It's also the essence of practicality with all table components built into the table base for servicing. Further, a steel bump rail and impact-resistant kick plate help preserve its modern good looks even in the busiest radiology suite.

Tomolex doesn't.





Customized acquisition plans, or leasing can be arranged through your channels or through Picker's parent CIT Financial Corporation.

For ease, speed and quality results, Tomolex is still the paragon in radiographic/linear tomography systems. And like all Picker equipment, it's backed by our worldwide service organization. Contact your local Picker representative, or write Picker Corporation or Picker International, 595 Miner Road, Cleveland, OH 44143.

PICKER®
ONE OF THE CIT COMPANIES

X-RAY IMAGE INTENSIFYING SYSTEMS

precise optics

IT MAY SURPRISE YOU.....

. . . to know that the people at Precise Optics have been supplying X-Ray Image Intensifying Systems since 1954. Precise specializes in Imaging, and offers a complete line of systems to meet requirements ranging from the private office to the special procedures room, at a cost savings over comparable units, without sacrificing quality.

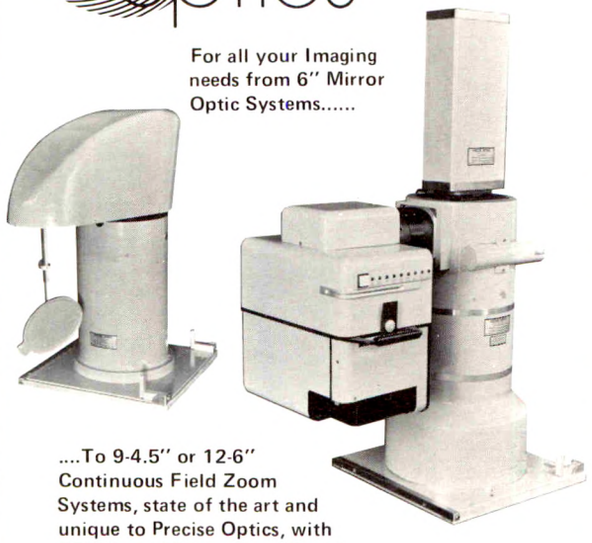
EVERY SYSTEM CONTAINS a guaranteed optimal performance cesium iodide image tube and field-proven solid-state power supply, covered by a two-year warranty.

THE PRECISE CCTV SYSTEM uses x-ray rated separate mesh vidicons, selected for high resolution and low-lag characteristics. Brightness compensation is an excellent 10,000:1, assuring the correct light level despite large variations in body densities.

THE NEW 105mm SPOT/RAPID SEQUENCE CAMERA (roll film, 6 frames per second maximum) utilizes the same digital electronics package and many of the mechanical sections of our other reliable 105mm cameras, while incorporating a rapid-load film transport and daylight receiving cassettes.

ACCESSORIES AVAILABLE INCLUDE: TWO-AND THREE-PORT LIGHT DISTRIBUTORS for spot and cine filming capabilities, ABS SYSTEM with automatically variable kV and selectable mA, SPOT FILM ADAPTERS compatible with any spot film device, CEILING SUSPENSION UNITS with smooth vertical and horizontal movements, CCTV MONITOR CARTS that are lightweight and easily mobile.

For all your Imaging needs from 6" Mirror Optic Systems.....



....To 9-4.5" or 12-6" Continuous Field Zoom Systems, state of the art and unique to Precise Optics, with CCTV and 105mm Spot/Rapid Sequence Cameras.

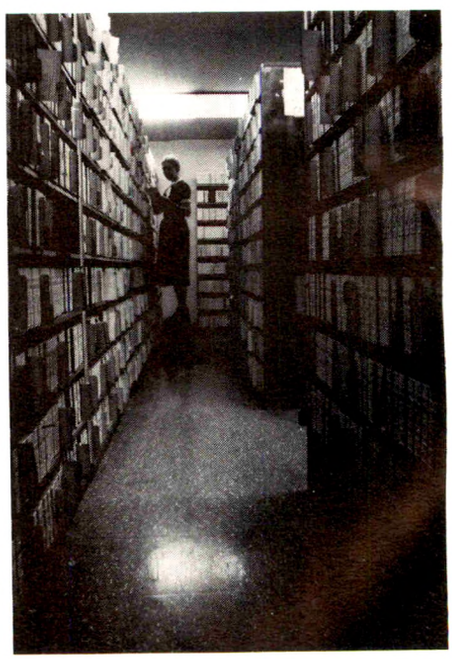
PRECISE OPTICS/PHOTO MEDIC EQUIPMENT, INC.
239 SO. FEHR WAY **BAYSHORE, N.Y. 11706**
TEL. (516) 242-6600 **TWX 510-227-9837**

We want you to talk in our library.

Ours is a living library of spoken words. A library of roughly 40,000 textbooks on tape, available free of charge to blind students. Eligible students also include the visually impaired, the learning disabled, and the physically handicapped who cannot handle printed material.

These students continually require new texts. And to fill this need, volunteer readers make tapes in our 29 recording studios across the country.

We urgently need readers with technical or professional backgrounds, and native speakers of foreign languages. If you can spare two hours a week, please volunteer. We are a non-profit organization supported by contributions from the public.

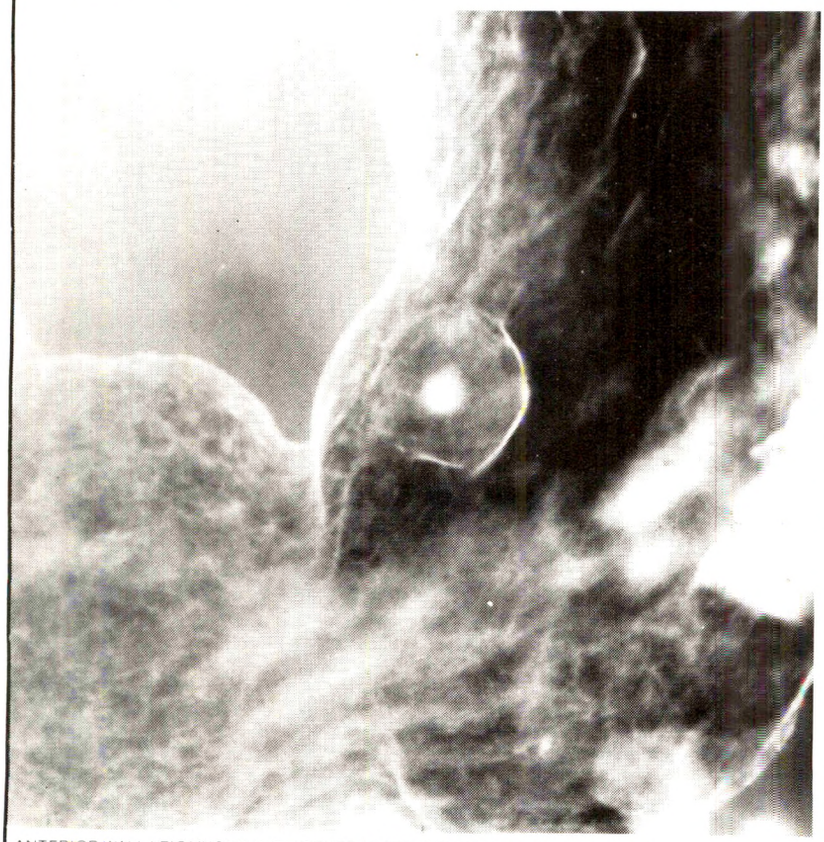


Recording for the Blind . . . . . *an educational lifeline*
215 East 58th St., New York, NY 10022.

For Double Contrast Stomachs, Use

NEW! E-Z-HD™

High Density with High Fluidity Barium Sulfate for Suspension USP



ANTERIOR WALL LEIOMYOMA WITH CENTRAL STALACTITE (HANGING DROPLET)
Film courtesy of Igor Laufer, M.D. Hospital of the Univ. of Pennsylvania

Double contrast radiography appears to offer the potential for significant improvements in diagnostic accuracy.

Double contrast studies of the stomach best demonstrate the surface pattern of the stomach (areae gastricae). This leads to improved detection of superfical erosions and ulcers, malignancies, polyps and other benign tumors, and ulcer scars.

E-Z-HD barium sulfate provides the basic ingredient necessary for good double contrast of the stomach.

The higher the density of the barium suspension, the better the coating, E-Z-HD allows for the highest density suspension of any commercial product on the market today: 85% w/w, 250% w/v. E-Z-HD achieves this density while remaining fluid for ease of administration.

- High density
- High fluidity
- Palatable
- Unit dose convenience.

E-Z-HD – The barium for the double contrast examination of the stomach and duodenum.

Optimal Density & Fluidity for the Modern Double Contrast Examination of the Stomach and Duodenum

Refrences:

David W. Gelfand: The Japanese-Style Double Contrast, Examination of the Stomach, Gastrointest Radiol. 1, 7-17 (1976)

Igor Laufer: The Diagnostic Accuracy of Barium Studies of the Stomach and Duodenum – Correlation with Endoscopy, Radiology 115: 569-573, June 1975

Roscoe E. Miller: The Air Contrast Stomach Examination: an overview: Radiology 117: 743-744 Dec. 1975

Order from your local X-ray supplier.

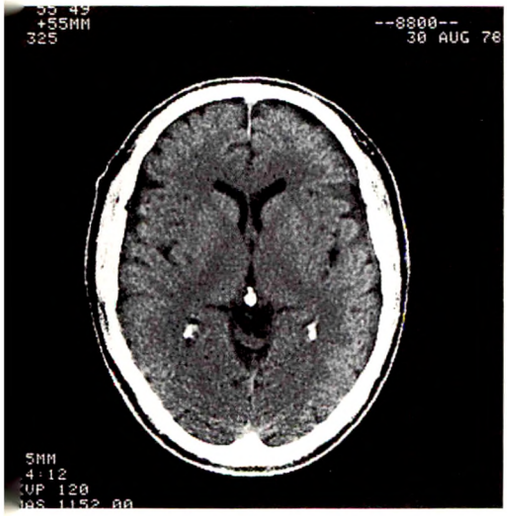
E-Z-EM

7 Portland Ave.
Westbury, New York 11590
(516) 333-8230

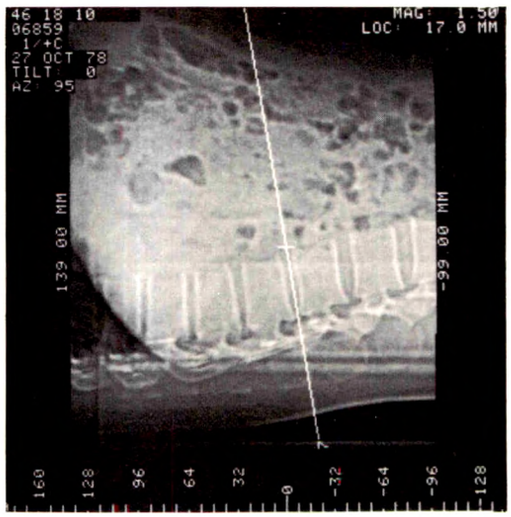
© 1/79

International Affiliates: E-Z-EM Rooster B. V., Infirmeriestraat 6-8, Rotterdam 16, Netherlands
E-Z-EM De Mexico S. A. de C. V. Calz. Azcapotzalco La Villa No 882, Zona Industrial Vallejo, Mexico 16 D. F.

Simple addition.



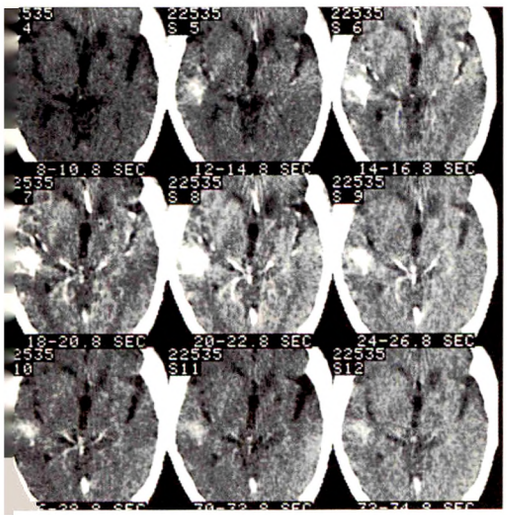
Ultra-high resolution X-2 detector
Optional on CT/T 7800, standard on CT/T 8800.



ScoutView localization
Included in Optional Diagnostic Capability package.



1.5 mm axial slice capability
Included in Optional Diagnostic Capability pa

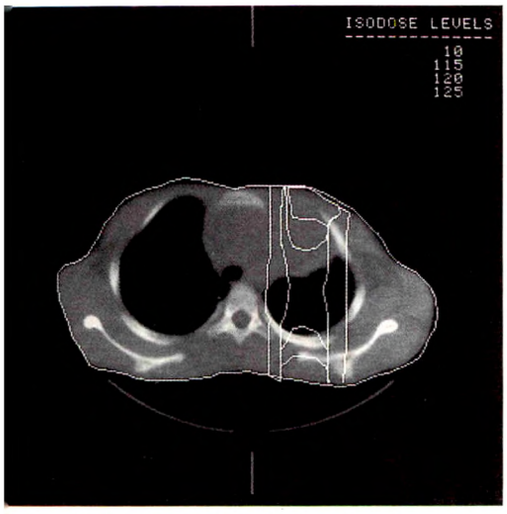


Dynamic scanning
Optional.



Sagittal and coronal transformations
No added cost.





Radiotherapy Treatment Planning
No added cost.

These advanced capabilities can be added to any CT/T system, even the first one installed in 1976.

You'd expect it from GE

How would you like a CT system that resists obsolescence? One that lets you choose the capabilities that match your department . . . now and in the future?

That's the objective of General Electric's CT/T Continuum.

We've designed our scanner so that new functions can be added at minimum cost to any new or existing CT/T system. For example:

Ultra-high resolution X-2 detector (optional). Unprecedented image quality. Resolving power of 1.0 mm (AAPM pin phantom) and 4.0 mm resolution at 0.4% contrast (GE Mod I gray/white phantom) in one reconstruction. Standard on CT/T 8800 systems.

Optional Diagnostic Capability (ODC) with ScoutView localization. Improves throughput. ScoutView images are digitized radiographs in AP, PA, lateral or oblique planes. They allow the physician to develop a scan prescription for first and last slice locations and gantry angulation. Subsequent axial scans can visualize extremely small anatomy, with 1.5 mm contiguous slice capability to minimize partial volume effect.

Dynamic scanning (optional). Up to 12 rapid sequence scans can be made in 72 seconds, providing up to 24 images. These allow visualization of a contrast bolus passing through a designated anatomical slice (CT transit study).

Sagittal and coronal transformations (no added cost). Use axial scan data to reconstruct either sagittal or coronal images, which are ready for display in less than 15 seconds per axial slice. Selectable thickness from 1 to 320 pixels. Allows three-dimensional image analysis.

Radiotherapy Treatment Planning (no added cost). Lets the operator establish external outlines, target outline and internal inhomogeneity outlines; assign densities; plan beam positions; calculate depth dose; and display isodose contours, dose, beam or patient data. A complete plan in a few minutes.

And General Electric is now developing even more CT/T capabilities for you in the future. So when you're choosing a CT system, total up GE's advantages: best images, best value, best service and protection against obsolescence. It all adds up.

General Electric Medical Systems,
Milwaukee, Toronto, Madrid.



GENERAL ELECTRIC

Maybe your business needs some new partners



We suggest that you form an alliance with the arts...that your company actively support now some form of the visual or performing arts.

There are vital humanistic reasons for this. All in life is not competition and striving for affluence. And there are sound business reasons for such support. For example: the design industry would be without vitality were there no modern art museums; the fashion industry uninspired without the great collections of textile artistry; and the advertising business very uncreative without the theater, art, and the world of music to draw upon. In fact, all business and industry need the arts.

Your support can be monetary, of course. You know of the financial crisis in the "labor intensive" field of the arts, and corporate gifts are essential. But there are many other kinds of gifts.

Your support can be the use of a display window to promote a local repertory company. Or the volunteering of interested employees' time, with their "time off" your contribution. There are many ways your company can help, and they're listed in a booklet which we hope you'll send for.

Start being a patron today! The arts deserve and need your support. And your new partnership will be a thoroughly enjoyable experience.

Support the Arts

Business Committee for the Arts, Inc.
1700 Broadway, New York, N.Y. 10019

Gentlemen:
Please send your booklet "126 Ways To Support the Arts."

Name _____

Address _____

City _____ State _____ Zip _____

PRESENTED AS A PUBLIC SERVICE BY WM. UNDERWOOD CO. IN COOPERATION WITH THE BUSINESS COMMITTEE FOR THE ARTS

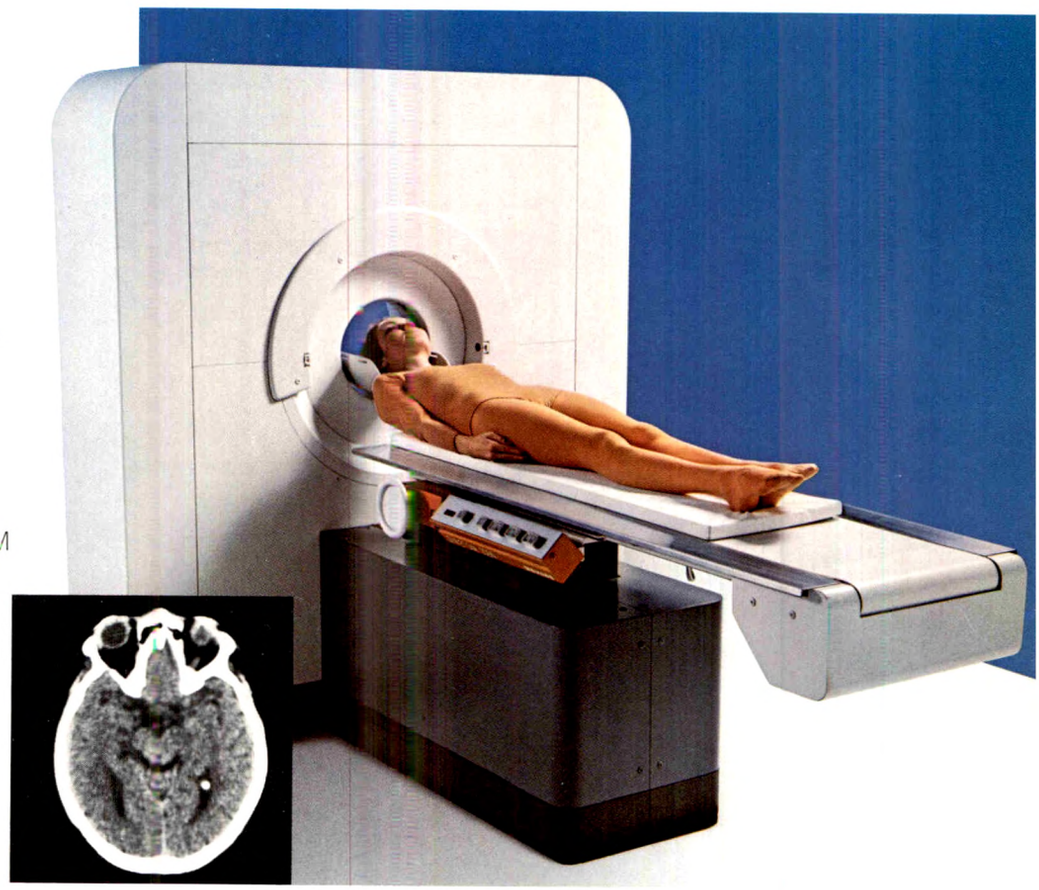
The Siemens Difference: Instantaneous image reconstruction

Immediate clinical evaluation

Delayed processing time is a thing of the past with Siemens computer tomographs, SIRETOM and SOMATOM. A specially designed high-speed computer reconstructs scanned images instantaneously. This permits immediate decisions as to diagnosis and course of treatment while providing for faster and smoother patient processing.

Reduced scan time

Scanning for both SIRETOM (head scanner) and SOMATOM (whole body scanner) is governed by the SCINTILLARC fan-beam solid-state detector array system. The result of this advanced engineering is evidenced by a dramatic reduction in setup and scan time along with unsurpassed quality tomograms achieved under clinical conditions.



Concepts... engineered to radiologic excellence

SIEMENS

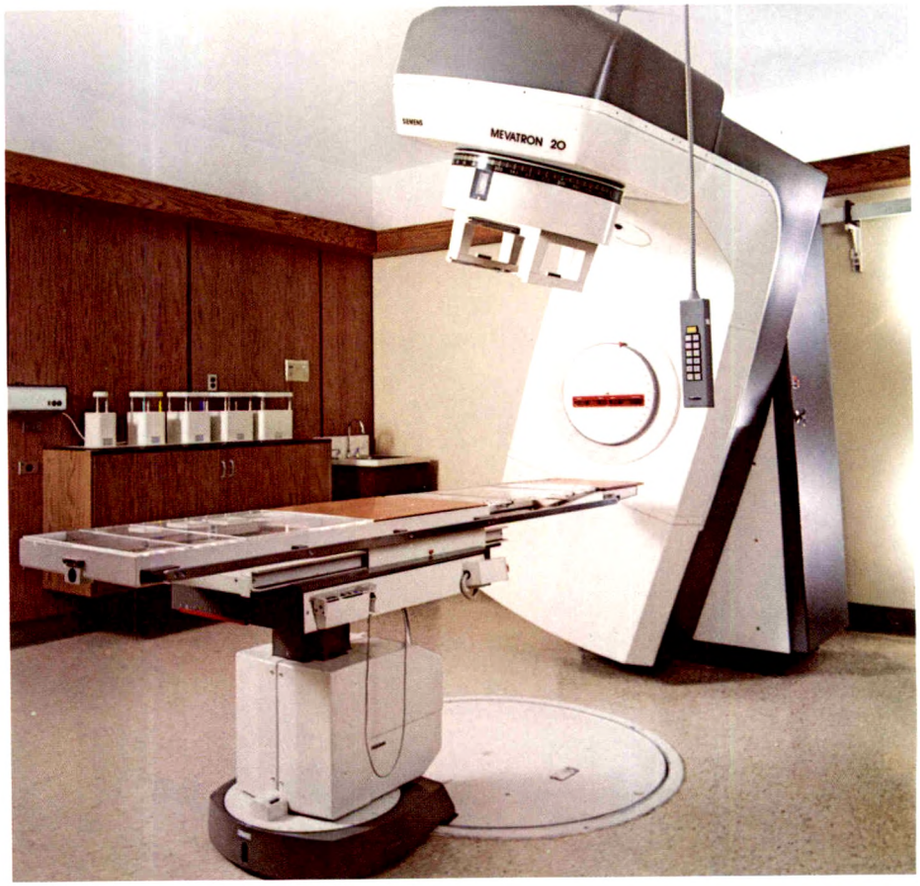
The Siemens Difference: Advanced X-ray target and electron scattering foil systems

The MEVATRON-20

Siemens' newest accelerator, the MEVATRON-20, utilizes a multiple element X-ray target and a unique double-foil electron scattering system to produce outstanding beam quality. Additionally, it features an integral verification capability for error-free machine setup. And with the highly flexible "Z" patient table, it forms a truly integrated installation ideally suited for modern radiation therapy technique.

The MEVATRON series

Siemens' product selection also includes the MEVATRON-6 and MEVATRON-12 which, together with MEVATRON-20, cover the full spectrum of energy and modality requirements.



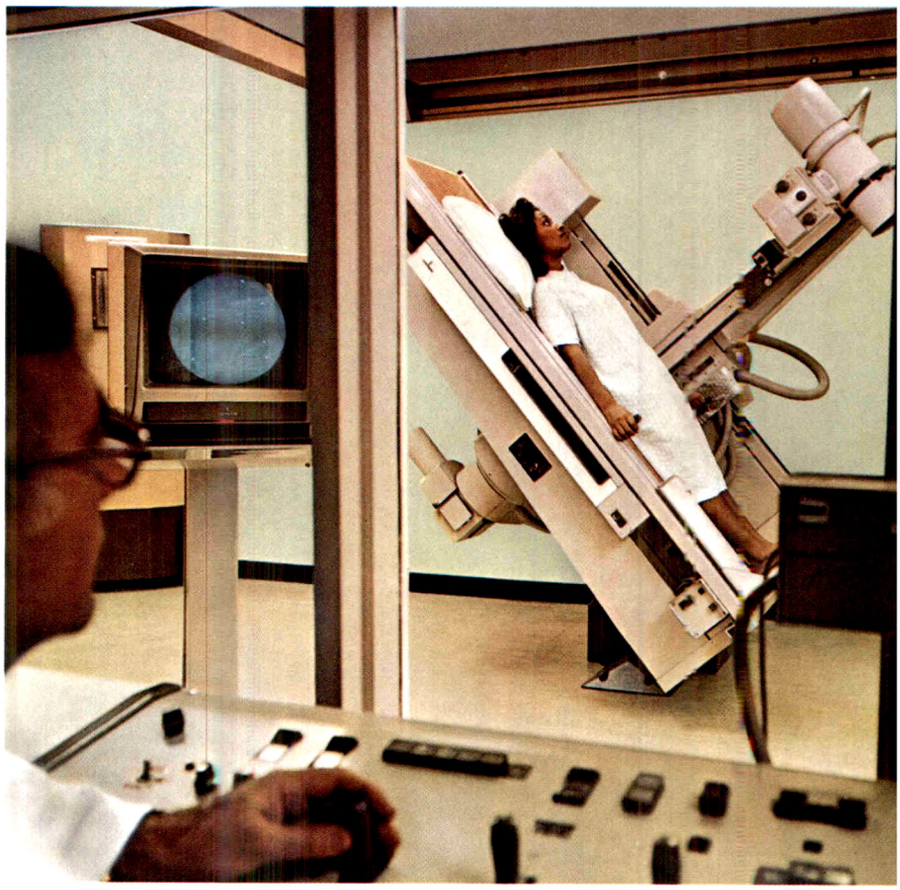
The Siemens Difference: Specific systems for specific needs

Versatile applications

Siemens responds to the varying needs of the radiologist with a full line of remote-controlled examination units – SIREGRAPH A, SIREGRAPH B, and SIREGRAPH II. Virtually every radiographic or fluoroscopic examination may be performed on a system from our wide selection of universal procedure or dedicated-purpose remote-controlled diagnostic products.

Individualized systems

Our systems were developed to meet the growing preference for remote examination tables and to meet the need for individual, custom-designed units that would satisfy different levels of requirements for versatility and application.



Concepts... engineered to radiologic excellence

SIEMENS

The Siemens Difference: Organ-related push-button programming

Simplicity of operation

Siemens has engineered operator time efficiency into diagnostic X-ray generators. Both OPTIMATIC and ORGANOMATIC generator series feature organ-related techniques which eliminate errors caused by miscalculation of exposure times and settings. One push button selects the examination units, kV, mAs, focal spot, and screen-type. The result is more efficient operational control and improved patient processing.



The Siemens Difference: Immediate automatic processing and printing of final reports

A new way of reporting

SIREP replaces the dictating machine and all other conventional methods of X-ray reporting with a computerized input terminal and a comprehensive radiological lexicon, RADLEX. Each RADLEX frame contains a vocabulary of diagnostic, anatomical, and radiologic terms from which the radiologist selects his findings. These are compiled in a logical manner by the radiologist to form a concise and accurate report emphasizing positive findings, degrees of certainty, statements of change, and advice for further study. Once the text has been completed and approved, the radiologist simply pushes a button to receive a perfectly typed copy of his final report.



Concepts... engineered to radiologic excellence

SIEMENS

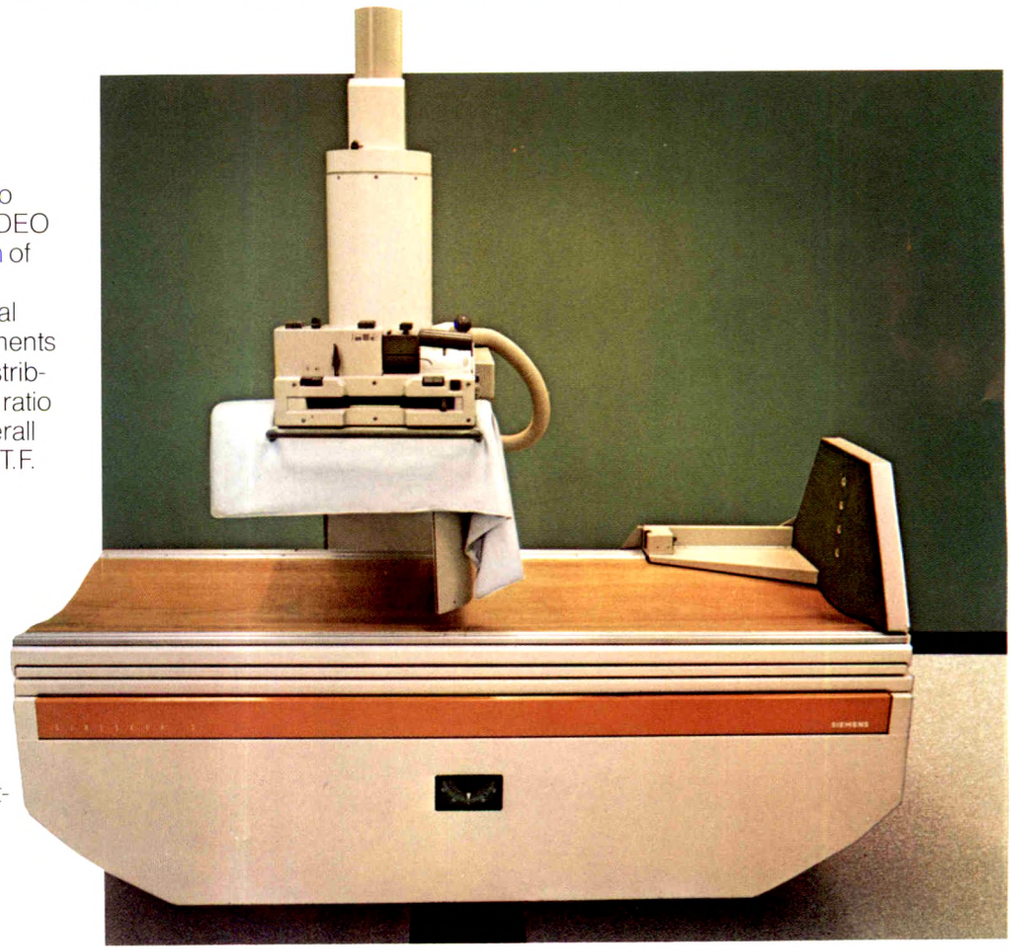
The Siemens Difference: Total electronic transfer of all available information

Improved image quality

Siemens has gone beyond doubling the line frequency to enhance the image of the VIDEO MED H. Electrical bandwidth of the video amplifier has been extended, resolution of optical and electron-optical components has been more uniformly distributed, and the signal-to-noise ratio has been increased. The overall result is improved system M.T.F.

Diagnose directly from the television display

The VIDEO MED H represents one of the truly great achievements in the use of X-ray television systems. Details of the fluoroscopic image maintain their sharpness, even with a high brightness level in the television display.



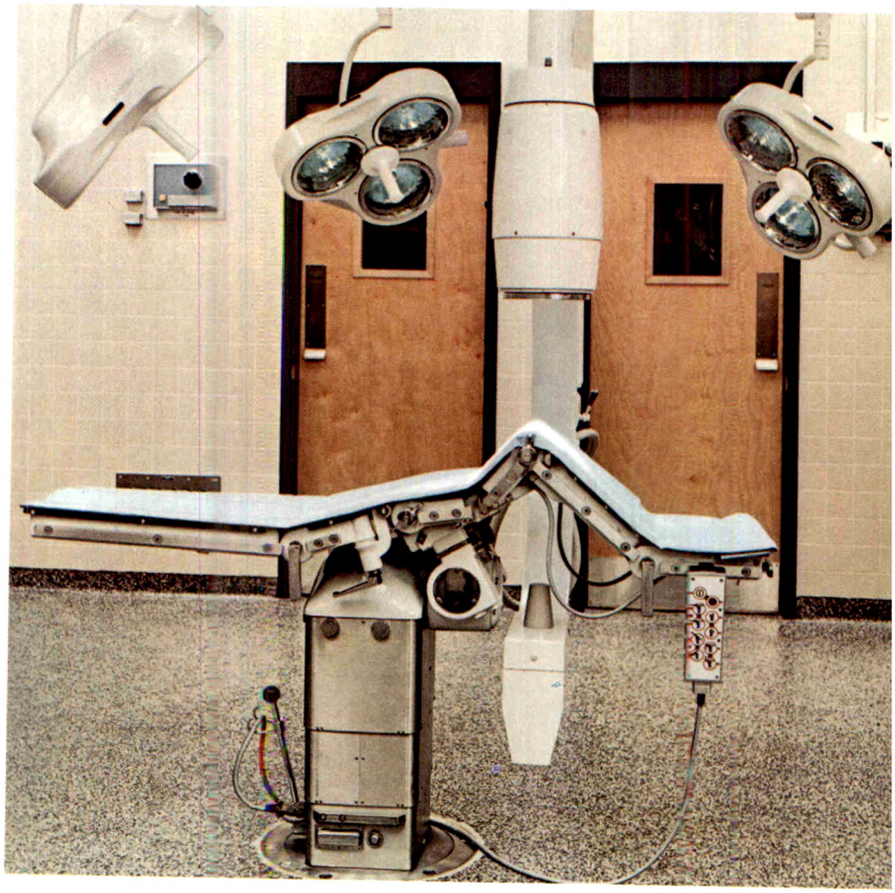
The Siemens Difference: Complete single-source O.R. systems

Total system planning

There is no room for error when it comes to planning something as complex and sophisticated as an operating room installation. Only Siemens offers an experienced approach that includes the designing, planning, installation, in-service training, financing, and servicing of a *total system* to meet your individual requirements.

Compatibility is engineered into the system

Because Siemens is a single-source supplier, system compatibility of all equipment is assured. Tables, lights, X-ray equipment, electrosurgical units, patient monitors, defibrillators—all are required to meet the high standard of Siemens' performance prior to system installation. Whenever you are planning an operating room, depend on Siemens.



Concepts... engineered to radiologic excellence

SIEMENS

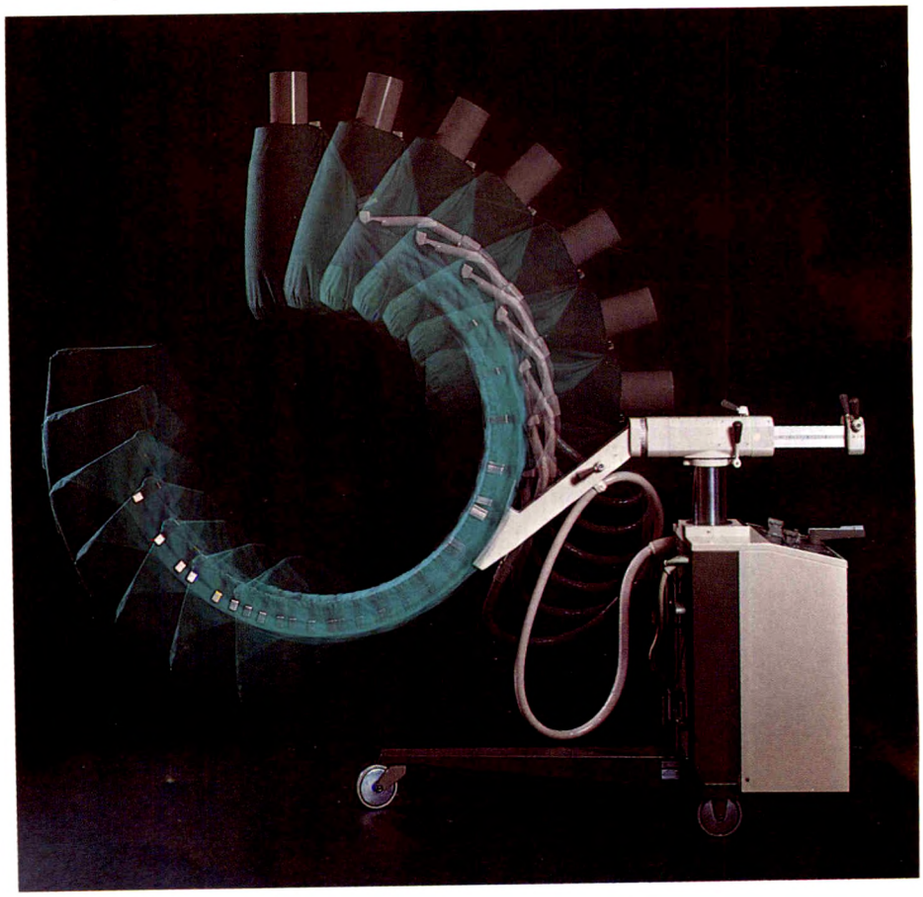
The Siemens Difference: Total maneuverability in aseptic procedures

No inhibition of mobility

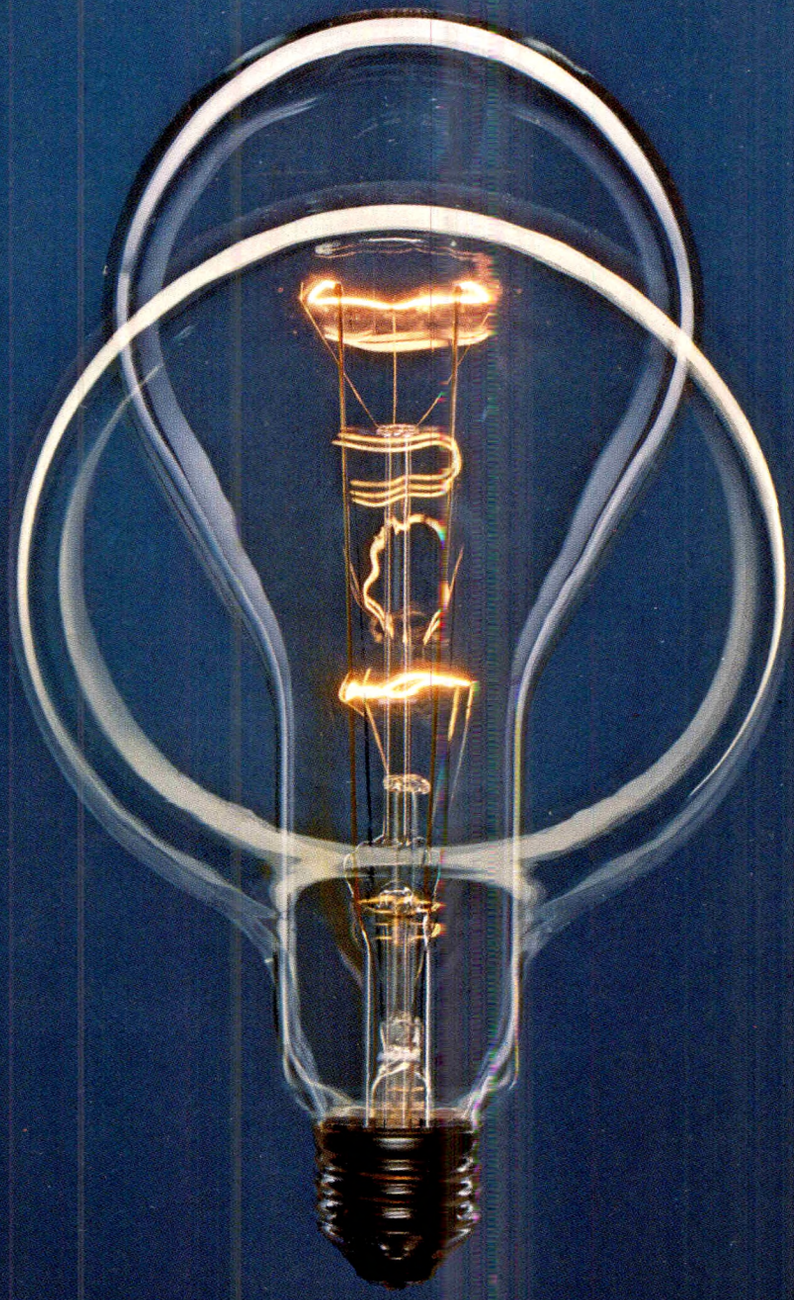
Siemens has designed the SIREMOBIL 2U with the special requirements of the operating environment in mind. The C-arm is uniquely assembled to the horizontal support with a recessed slide track mechanism. Because there are no external gears, maneuverability remains unobstructed during surgical procedures.

Other system benefits

The unique operating capability of the SIREMOBIL 2U is exceptionally enhanced with the IMAGE STORE disc recorder which allows alternating comparison of previously stored and live fluoroscopy images.



When two ideas are better as one.



TRIM

Simultaneous treatment planning and information management.

At AECL, we've taken two computer programming functions and made them work better as one. The result is TRIM—the Tumour Registry and Information Management system. It allows the user, for the first time, simultaneous treatment planning and information management. Designed for use with the AECL TP-11 system, TRIM can also operate independently.

Featuring a free format data base which allows the in-put of as much or as little patient data as necessary, TRIM is flexible enough to suit each individual user's specific needs. With built-in security control and three major rapid data retrieval functions, TRIM has economical modular expansion capability, permitting up to 16 terminals plus inter-user communication.

For complete information on the TRIM flexible data system and all its unique advantages, contact AECL.

Atomic Energy of Canada Limited
Commercial Products

P.O. Box 6300, Ottawa, Canada, K2A 3W3. Tel.: (613) 592-2790. Cable Nemota. Telex: 053-4162.

American Journal of Roentgenology

Vol. 132 April 1979 No. 4

DIAGNOSTIC IMAGING

523 **Rapid and Accurate Diagnosis of Acute Cholecystitis with ^{99m}Tc-HIDA Cholescintigraphy.** *Weissmann HS, Frank MS, Bernstein LH, Freeman LM*

529 **Computed Tomography and ^{67}Ga Citrate Radionuclide Imaging for Evaluating Suspected Abdominal Abscess.** *Levitt RG, Biello DR, Sagel SS, Stanley RJ, Aronberg DJ, Robinson ML, Siegel BA*

535 **Computed Tomography in the Evaluation of Osteosarcoma: Experience with 25 Cases.** *deSantos LA, Bernardino ME, Murray JA*

541 **Familial Hyperphosphatasemia: Diagnosis in Early Infancy and Response to Human Thyrocalcitonin Therapy.** *Dunn V, Condon VR, Rallison ML*

547 **Technique of Percutaneous Transluminal Angioplasty with the Grüntzig Balloon Catheter.** *Grüntzig A, Kumpe DA*

553 **Aneurysm Rupture Secondary to Transcatheter Embolization.** *Lina JR, Jaques P, Mandell V*

557 **Portal Vein Aneurysm.** *Vine HS, Sequeira JC, Widrich WC, Sacks BA*

561 **Circumaortic Venous Ring: Incidence and Significance.** *Beckmann CF, Abrams HL*

567 **Esophagitis Induced by Combined Radiation and Adriamycin.** *Boal DKB, Newburger PE, Teele RL*

571 **Gallbladder: Common Cause of Antral Pad Sign.** *Smeets R, Op Den Orth JO*

575 **Radiographic Features of Eosinophilic Gastroenteritis (Allergic Gastroenteropathy) of Childhood.** *Teele RL, Katz AJ, Goldman H, Kettell RM*

581 **Ultrasound of Gallbladder Wall Thickening and its Relation to Cholecystitis.** *Handler SJ*

587 **Erect Scanning of Pancreas Using a Gastric Window.** *MacMahon H, Bowie JD, Beezhold C*

593 **Ultrasound of Epigastric Injuries After Blunt Trauma.** *Foley LC, Teele RL*

599 **Dural and Direct Cavernous Sinus Fistulas.** *Peeters FLM, Kröger R*

607 **Contrast Enhanced CT Scan and Radionuclide Brain Scan in Supratentorial Gliomas.** *Butler AR, Passalaqua AM, Berenstein A, Kricheff II*

613 **CT Detection of Intracranial Aneurysms in Subarachnoid Hemorrhage.** *Ghoshhajra K, Scotti L, Marasco J, Baghai-Naiini P*

617 **Lateral Decubitus Pneumoencephalography-Angiography for Localizing Atrial and Paraatrial Vascular Lesions.** *Quencer RM, Rosomoff HL, Green BA*

623 **Cranial CT Findings in Patients with Meningomyelocele.** *Zimmerman RD, Breckbill D, Dennis MW, Davis DO*

631 **John Caffey Award: Intraventricular Hemorrhage and Hydrocephalus in Premature Newborns: A Prospective Study with CT.** *Burstein J, Papile LA, Burstein R*

RADIATION ONCOLOGY

637 **Preliminary Report of the M. D. Anderson Hospital/Texas A & M Variable Energy Cyclotron Fast-Neutron Therapy Pilot Study.** *Peters LJ, Hussey DH, Fletcher GH, Baumann PA, Olson MH*

643 **Diagnostic Oncology Case Study: Abdominal Mass and Cervical Adenopathy in a Child.** *Contributed by Kangarloo H, Sample WF*

CASE REPORTS

647 **Balloon Catheter to Control Transhepatic Obliteration of Gastroesophageal Varices.** *Roche A, Kunstlinger F, Curet P, Doyon D*

650 **Cavitary Pulmonary Lesions Complicating Use of Flow-Directed Balloon-Tipped Catheters in Two Cases.** *Shin MS, Ho KJ*

653 **Ultrasonic Features of Acquired Renal Arteriovenous Fistula.** *Thomas JL, Lymberis MEB, Hunt TH*

656 **Renal Emphysema of the Transplanted Kidney: Sonographic Appearance.** *Brenbridge ANAG, Buschi AJ, Cochrane JA, Lees RF*

659 **Ultrasound Demonstration of Diffuse Cortical Nephrocalcinosis in a Case of Primary Hyperoxaluria.** *Wilson DA, Wenzl JE, Altshuler GP*

662 **Ultrasonographically Guided Percutaneous Pancreatography: Report of Two Cases.** *Cooperberg PL, Cohen MM, Graham M*

664 **Metastatic Islet Cell Carcinoma to the Liver Visualized After Intraarterial Epinephrine.** *Mills SR, Doppman JL, Kahn ER*

666 **Large Ulcerated Cecal Vascular Malformation: Unusual Gross and Histologic Features.** *Hollenberg GM, Schwartz AJ*

669 **Third Ventricle Meningioma Mimicking a Colloid Cyst in a Child.** *Lee YY, Lin SR, Horner FA*

672 **CT Simulation of Cerebellopontine Tumor by Tortuous Vertebrobasilar Artery.** *Rao KG, Woodlief RM*

674 **Anomalous Origin of Posterior Choroidal Artery from Basilar Artery.** *Berland LL, Haughton VM*

676 **Xenon in the Gastric Fundus: Potential Pitfall in Ventilation Scan Interpretation.** *Marx WJ, Courtney JV, MacMahon H, Rezai-Zadeh K*

678 **Congenital Pseudarthrosis of the Clavicle: Report of Three Cases.** *Manashil G, Laufer S*

680 **Mucocele of the Petrous Temporal Bone.** *Osborn AG, Parkin JL*

682 **Editorial: Röntgen: Application Denied.** *Moskowitz H*

683 **Letters**

685 **Abstracts of Current Literature**

697 **Book Reviews**

702 **News**

706 **Radiologic Societies**

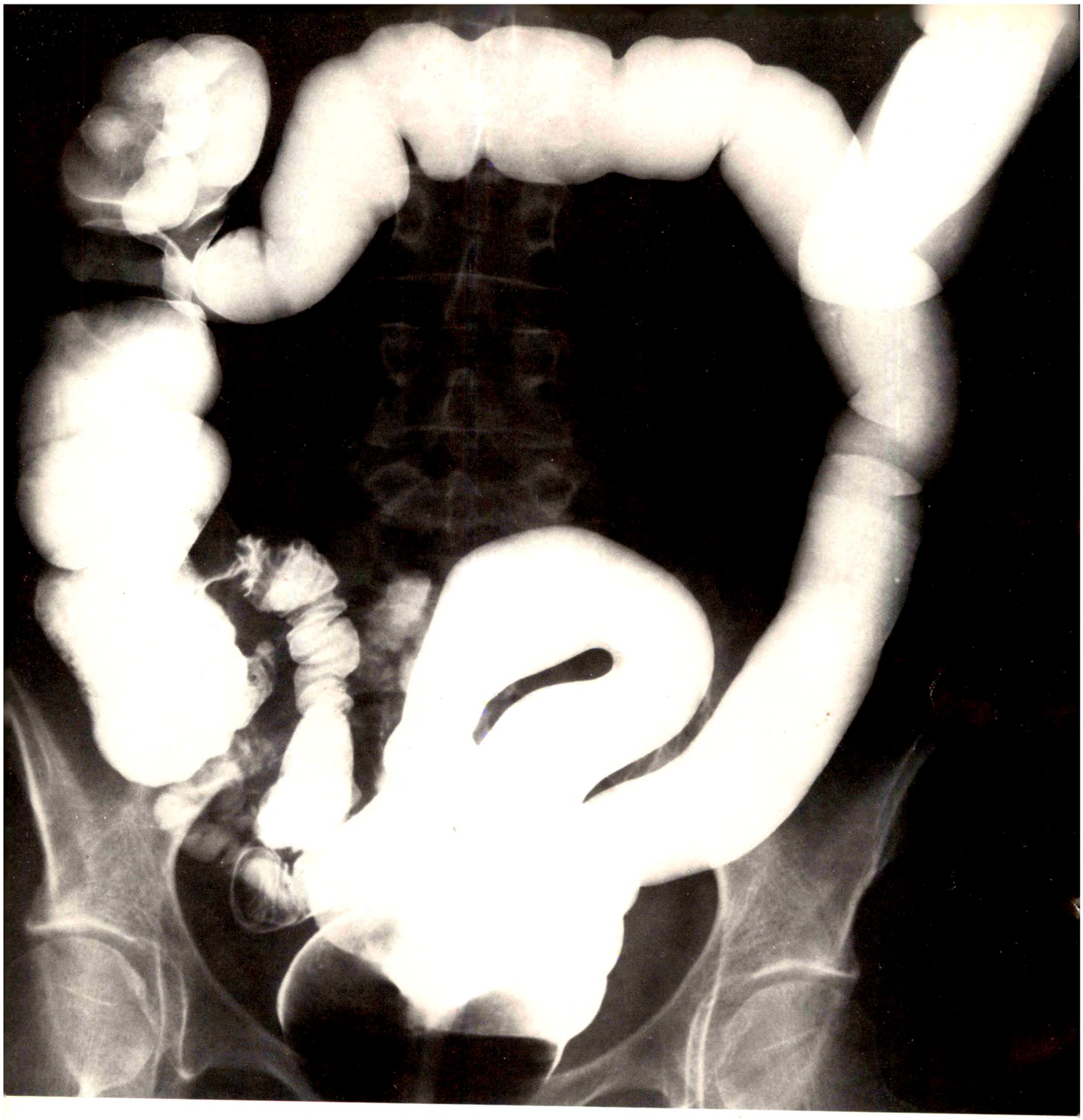
546 **Guidelines for Authors**

Acc.
23.7.79

AJR

American
Journal of
Roentgenology

May 1979



How to improve your reading speed... with increased comprehension

Complete evacuation is basic if a barium enema is to be interpreted quickly and accurately. That's why many radiologists specify bowel evacuation with Dulcolax as an integral part of the regimen. Whether used alone, or with magnesium citrate, Dulcolax can help you get clean films. The first time.

Dulcolax®
Tablets 5 mg
Suppositories 10 mg

Boehringer Ingelheim
Boehringer Ingelheim Ltd.
Ridgefield, CT 06877

Official Journal
American Roentgen Ray Society
American Radium Society

AJR

American Journal of Roentgenology

Diagnostic Imaging • Radiation Oncology
Related Sciences

Editor Melvin M. Figley

Associate Editor Rosalind H. Troupin

Assistant Editor John D. Harley

Contributing Editor E. Frederick Lang

Consulting Editorial Board Luther W. Brady • Kent Ellis
E. Robert Heitzman • Donald L. King • N. Thorne Griscom
Eugene C. Klatte • Kenneth Krabbenhoft • John G. McAfee
Russell H. Morgan • Thomas H. Newton • Robert G. Parker
Stewart R. Reuter • William B. Seaman • Robert J. Shalek
John Storer • Michel M. Ter-Pogossian • Joseph P. Whalen
David M. Witten

Editorial Staff K. A. Murray, manager • M. J. Leonard, manuscript editor • J. Anderson, assistant manuscript editor • A. C. Van Dyck, secretary

Published monthly by The Williams & Wilkins Co., 428 East Preston St., Baltimore, Maryland 21202. All correspondence, except editorial office business, should be addressed to the publisher. Annual subscription rates: $40 ($20 for residents with letter of verification) plus appropriate mailing surcharge (see note last page). Single copies, $5. Undelivered or damaged copies replaced within 60 days of publication; 90 days for foreign subscribers. Allow 90 days for address changes. © 1979 by American Roentgen Ray Society. Second-class postage paid at Baltimore, Maryland, and at additional mailing offices. Printed in U.S.A. ISSN 0361-803X

UNIVERSITY OF MEDICINE & DENTISTRY LIBRARY

KODAK LANEX SCREENS
KODAK ORTHO FILMS.

When tissue density would dim the image.

The speed* of Kodak Lanex regular screens with Kodak ortho G or H film gives you the flexibility to perform difficult exams with existing equipment, and usually with reduced exposure to patient and staff.

When obese patients or dense tissue structures are a concern, Lanex regular screens and ortho films enable you to select grid ratios and exposure technics to control scatter radiation and improve subject contrast. The result is an image that is crisp, clear, and informative.

If you've assumed that faster screen/film speeds must be "paid for" with reduced diagnostic information, we invite you to try Kodak Lanex regular screens and ortho films. The high x-ray absorption of Lanex regular screens permits you to perform exams that would otherwise be difficult or impractical with existing equipment. And, image quality is comparable to that achieved with conventional fast calcium tungstate screens.



Lanex regular screens/ortho films provide 2 to 4 times the speed of conventional fast calcium tungstate screens used with Kodak X-Omat RP film.

© Eastman Kodak Company, 1979

KODAK LANEX SCREENS
KODAK ORTHO FILMS.



When motion would blur the image.

The speed provided by Kodak Lanex regular screens with Kodak ortho G or H film is used to great advantage when voluntary or involuntary patient motion is a problem. In contrast studies, the reduced exposure possible with these Kodak products helps "freeze" the organ motion, thus providing more useful information.

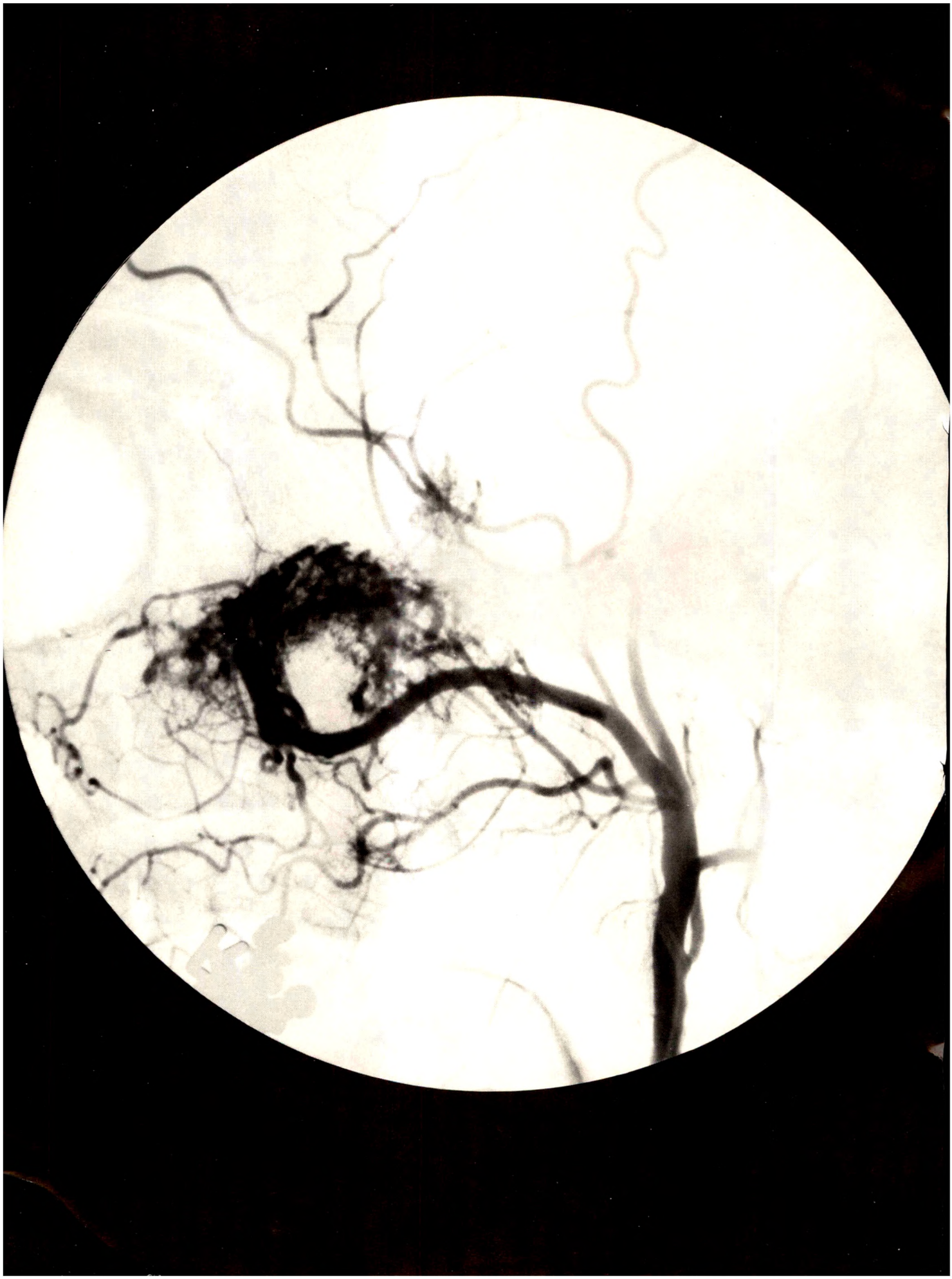
Similar benefits are available in other procedures where motion is a problem. Some blood vessels may move a distance equal to their diameter during normal exposures; but with Lanex regular screens/ortho films the motion is stopped, and the image is sharp and informative.

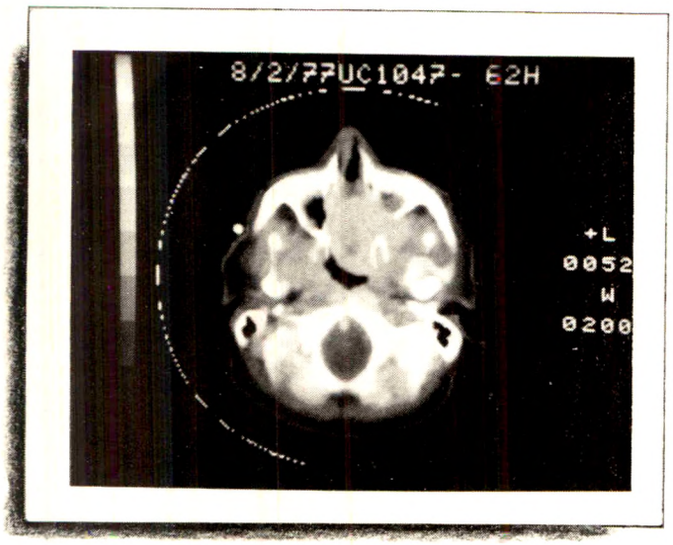
Also, use of a smaller focal spot for sharper images is now practical since the speed of Lanex regular screens/ortho films makes possible reduced mA settings.

To see Kodak Lanex regular screens and ortho film combinations firsthand, contact your Kodak Technical Sales Representative, or write Eastman Kodak Company, Health Sciences Markets Division, Dept. 740-B, Rochester, New York 14650.

TURNING ENERGY INTO IMAGES

RADIOGRAPHY · COMPUTED TOMOGRAPHY
ULTRASOUND · NUCLEAR MEDICINE · THERMOGRAPHY





Diagnosis:
Angiofibroma involving Ethmoid and Sphenoid Sinuses.

Clinical Data:
32 year old man with an eight month history of nasal congestion.

CT Scan:
A large soft tissue mass is noted in the nasopharynx extending upward into the sphenoid sinus and distorting the normal airway. Destruction of the medial and posterior walls of the left maxillary sinus is noted. Following intravenous contrast infusion, slight contrast enhancement is noted.

Selective Right External Carotid Arteriogram:
Study shows a highly vascular neoplasm in the nasopharynx extending upward into the sphenoid sinus. The angiographic appearance is typical for an angiofibroma.

The external carotid artery was embolized following which the angiofibroma was surgically excised.

The arteriogram and the CT scan reproductions are both reduced to 79% of their original size.

Angiography and CT scanning.

Each has its own special diagnostic advantages in this era of expanding imaging technology.

Angiography and Elema-Schonander.

For diagnostic specificity.

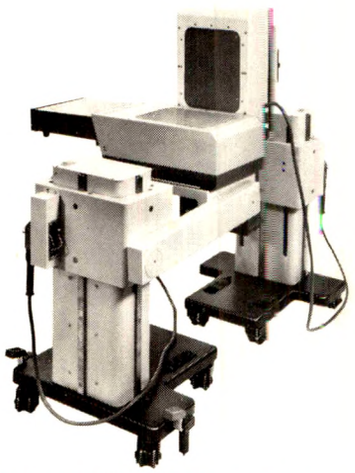
While CT has proved to be a highly sensitive diagnostic technique, angiography, in many cases, is necessary to make a specific diagnosis. And, no matter what your angiographic applications are, Elema-Schonander has a sheet-film changer to meet your requirements.

PUCK Models: Where increased magnification, mobility, and compactness are important considerations, 20-film capacity PUCK Model film changers are available to accommodate either 35cm x 35cm (14″ x 14″) or 24cm x 30cm sheet-film sizes. They operate at film exposure rates of up to 3 exp/sec in single plane or simultaneous biplane mode. When biplane alternating mode is chosen to eliminate cross-fogging, PUCK Models change film at 1.5 exp/sec. per plane.

AOT-S Models: Six exp/sec, 30-film capacity Model AOT-S film changers are available for the same sheet-film sizes. They also can be used for single plane, or biplane simultaneous or alternating sequences.

All Elema-Schonander sheet-film changers feature convenient, accurate punch card control (PDA), and are equipped with a newly developed carbon-fiber reinforced plastic (CFRP) compression plate that minimizes x-ray attenuation, while maintaining intimate film contact, year after year.

Call or write for brochures describing the PUCK and AOT-S sheet-film changers. Elema-Schonander, Inc., 699 Lively Blvd., Elk Grove Village, IL 60007. (312) 593-6770.



Biplane PUCK U24/30 installation
on PUCKWOP 24/35 Universal Stands

elema-schonander

78212

What you'd expect from RAYTHEON MEDICAL IMAGING



RFT-15
with the IRIS 100
Spot-Film System

FLUORO 1

A cost-effective x-ray system designed to let the radiologist concentrate on diagnosis

RFT-15
90/15 R/F Diagnostic X-Ray Table

Unencumbered by past practices and outmoded equipment, Raytheon Medical Imaging had but one goal in mind in developing its top-of-the-line RFT-15 diagnostic x-ray table —

To perfect a combination of motor-driven tilt table and spot-film console so easy to use that it would focus the skills of the radiologist by allowing him to concentrate on his patient, not his equipment.

The RFT-15 features:

Two-speed power tilt to 90-degree vertical and the full 15-degree Trendelenburg position with programmed stop at horizontal.

Two-way power-driven table top with an exceptional total movement of 61 inches (36 inches toward head, 25 inches toward feet), permitting great flexibility in patient positioning.

Desirable tabletop height of 31½ inches, comfortable for both patient and technologist.

One-handed operation of footrest latch.

Minimum table-top-to-film distance for excellent radiographs in conventional procedures.

Quiet, easily positioned power-driven spot-film tower.

Suspension-free television or mirror-viewing imaging systems. Also accommodates IRIS 100 intensified spot-filming systems.

Human-engineered pushbutton controls on spot-film console arranged for procedure-oriented operation. Patient positioning controls are duplicated on table side.

Available without fluoroscopic carriage for radiography-only rooms (RT-15).

Finally, easy installation is not the least of FLUORO 1's virtues. But this cost-effective system and its components offer so many other features, that you really should ask for our descriptive literature.

Contact your local Raytheon Medical Imaging representative, or

RAYTHEON

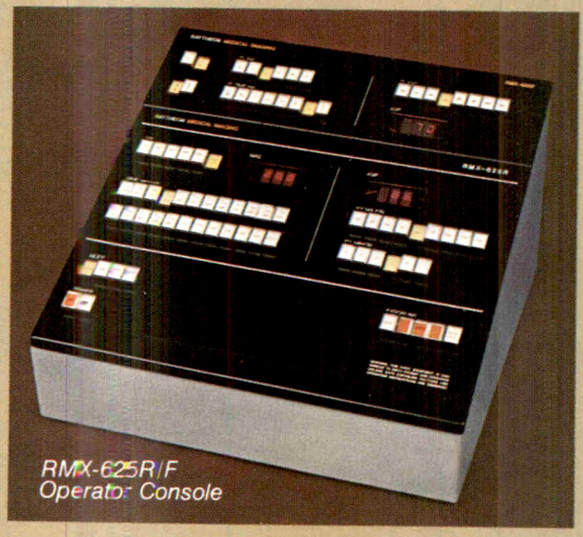
RAYTHEON MEDICAL IMAGING
Stamford, Connecticut 06907
(203) 348-2499

And a companion Generator
RMX-625R/F

Designed for heavy-duty service, the RMX 625R/F Radiographic/Fluoroscopic Generator is a fit companion for the RFT-15 Diagnostic Table in the FLUORO I System.

Its three-piece design — Remote Operator Console, Power Control Unit and High-Tension Transformer — permits total flexibility in location. Connected by low-voltage cables, the handsome Operator Console can be wall mounted, placed on a table or desk or equipped with its own free-standing pedestal, complete with writing surface.

Controls have been laid out to take advantage of both traditional operating sequences and the latest findings of human-factors engineering to provide the easiest operation available today.



RMX-625R/F Operator Console

Features include:

High power, 600 mA at 100 kVp, 500 mA at 125 kVp.

Digital pre-reading of mAs and kVp settings.

Pushbutton switches for all functions.

1/120-second solid-state timer/contactor, for long life and trouble-free accuracy.

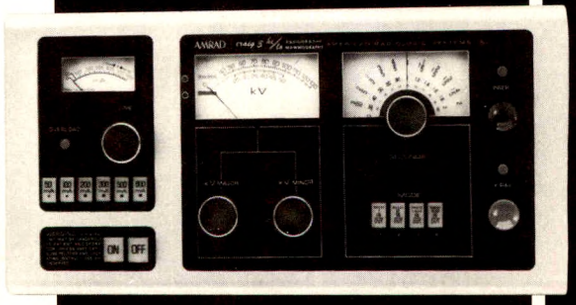
Automatic line compensation to eliminate the effects of changing power-line conditions.

When you put together a radiographic system,

Generators:

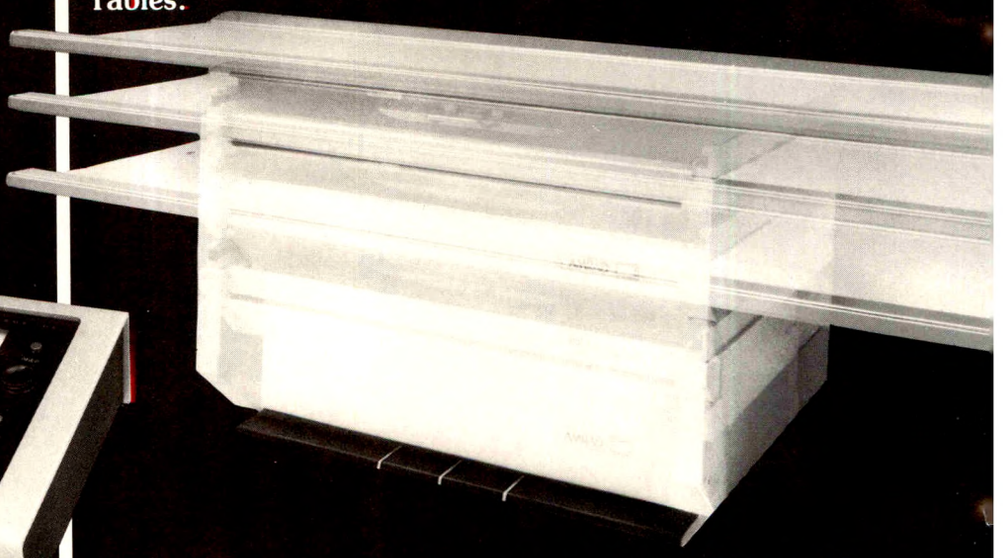


600 mA—125 kVp with proven track record for maximum reliability. The operator control connects remotely with a simple, low voltage cable. Automatic Exposure Control is available. What could be more sensible?

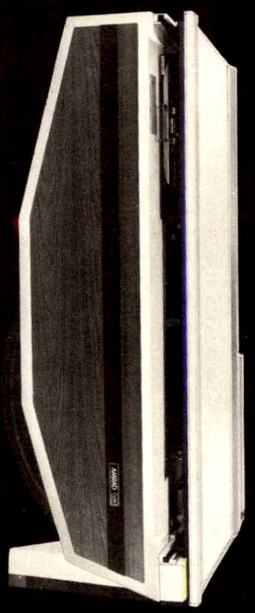


600 mA—150 kVp gives you more x-ray power—more than most. Same features, same reliability. Mammography, tomography and multiple-room options. Ultimate, state-of-the-art generators.

Tables:

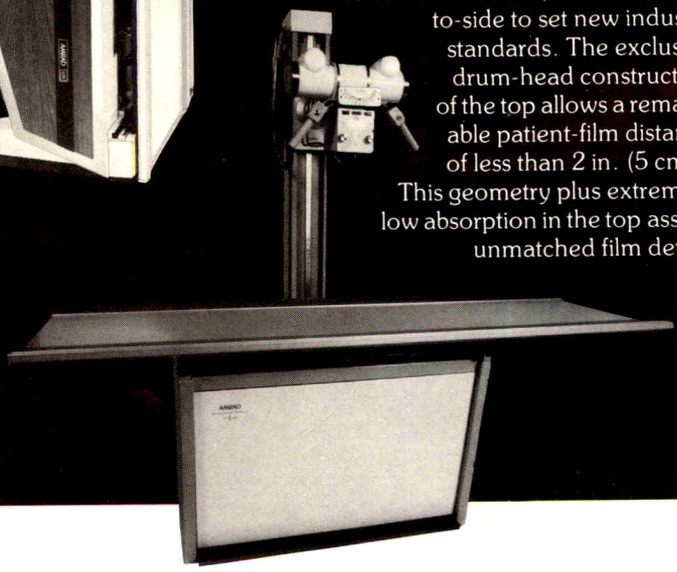


Here's our exclusive THV (top height variable) table. The superb floating top kneels to a comfortable, "Please-sit-down" height, then glides to an examination level with up to a 400-pound patient aboard. Patient safety, operator convenience, examination flexibility and through-put advantages are obvious. Only from AMRAD (patent pending).



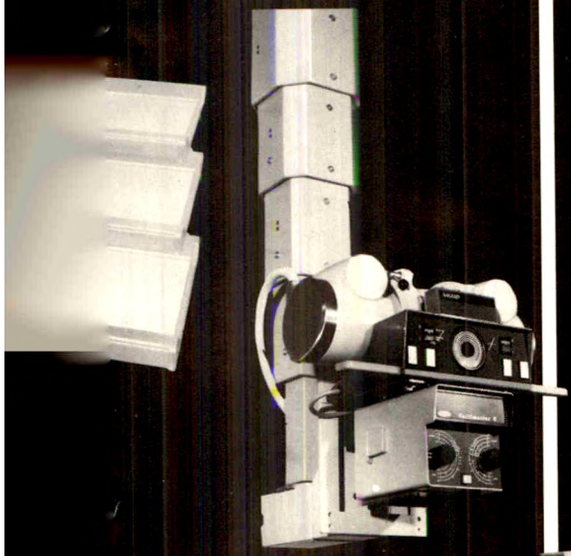
The AMRAD 105° table gives all the tilt capability required for general radiography without losing the precise feel of a manual four-way top preferred for exact patient positioning.

The 47/12 table with an integral tubestand is a "space saver" allowing a quick, plug-in installation. The operator control (about the size of your receptionist's telephone) goes anywhere you want it to by low voltage cable connection to the power pack *inside* the table. The table top floats 47 in. (119.4 cm.) head-to-foot and 12 in. (30.5 cm.) side-to-side to set new industry standards. The exclusive drum-head construction of the top allows a remarkable patient-film distance of less than 2 in. (5 cm.). This geometry plus extremely low absorption in the top assure unmatched film detail.



AMRAD offers you more.

Tubestands:



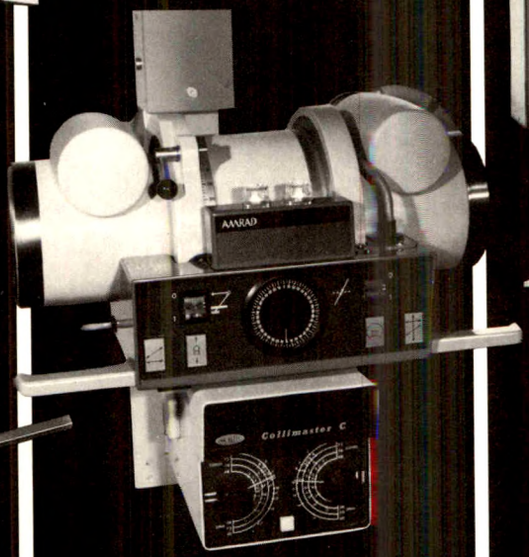
The new Trac 10 Overhead Tube Conveyor is the ultimate answer to the demands of a universal radiographic suite. With its longitudinal power assist, precision setups become a matter of touch, not jerks and tugs. And, rigidity, flexibility and positioning ease are yours to command with this deluxe tube conveyor.

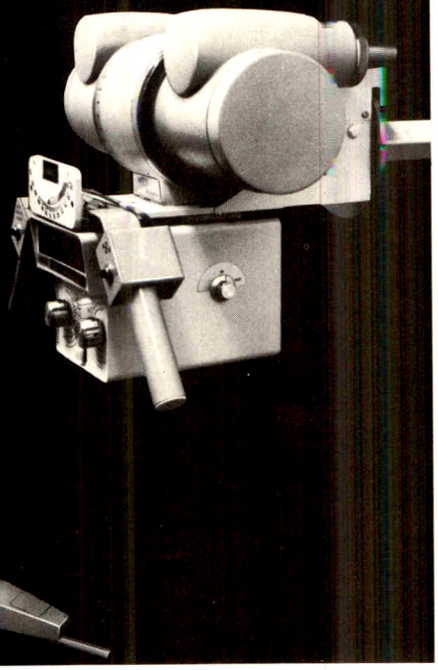


The Trac 4 Floor-to-Ceiling Tubestand uniquely lowers to permit weight-bearing procedures in combination with AMRAD's one-of-a-kind wall bucky. All this without compromising general radiographic or tomographic procedures.

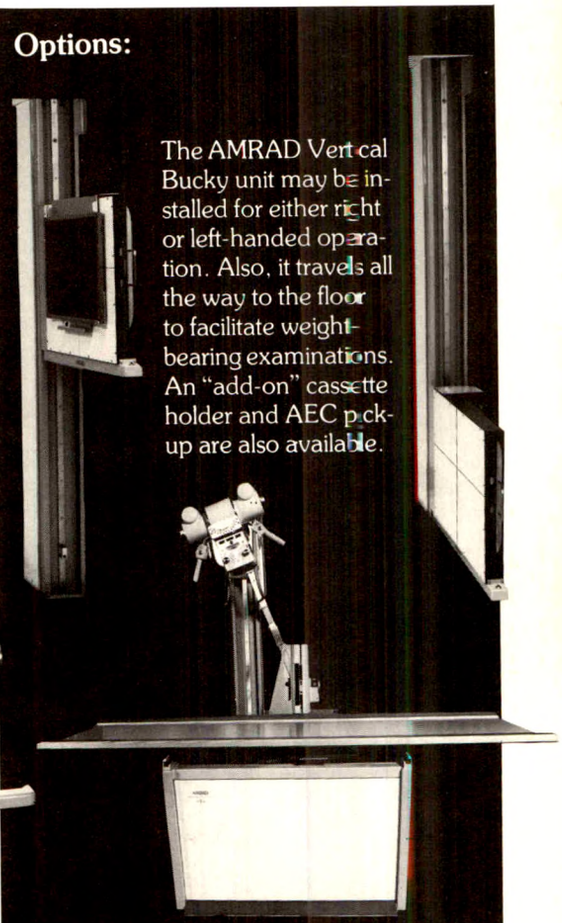
Tubes and Collimators:

What needs to be said? The well respected Machlett x-ray tubes, collimators, PBL systems and numerous options are all available.



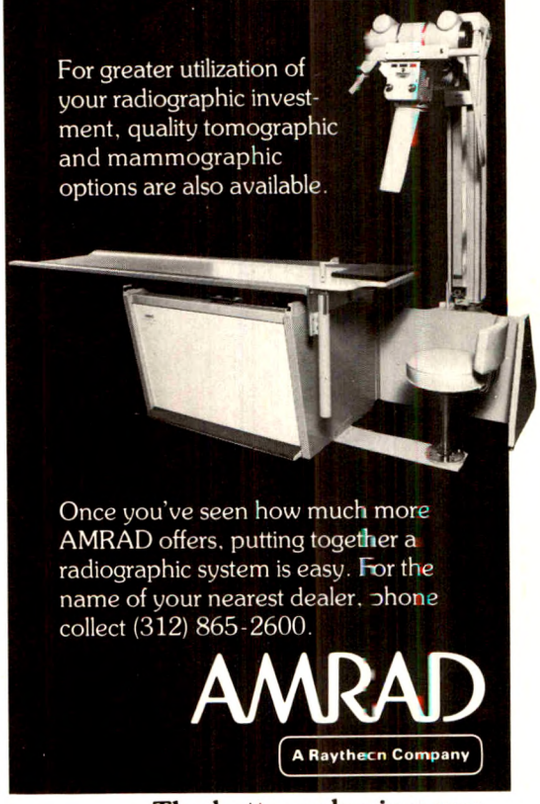


Options:



The AMRAD Vertical Bucky unit may be installed for either right or left-handed operation. Also, it travels all the way to the floor to facilitate weight-bearing examinations. An "add-on" cassette holder and AEC pick-up are also available.

For greater utilization of your radiographic investment, quality tomographic and mammographic options are also available.



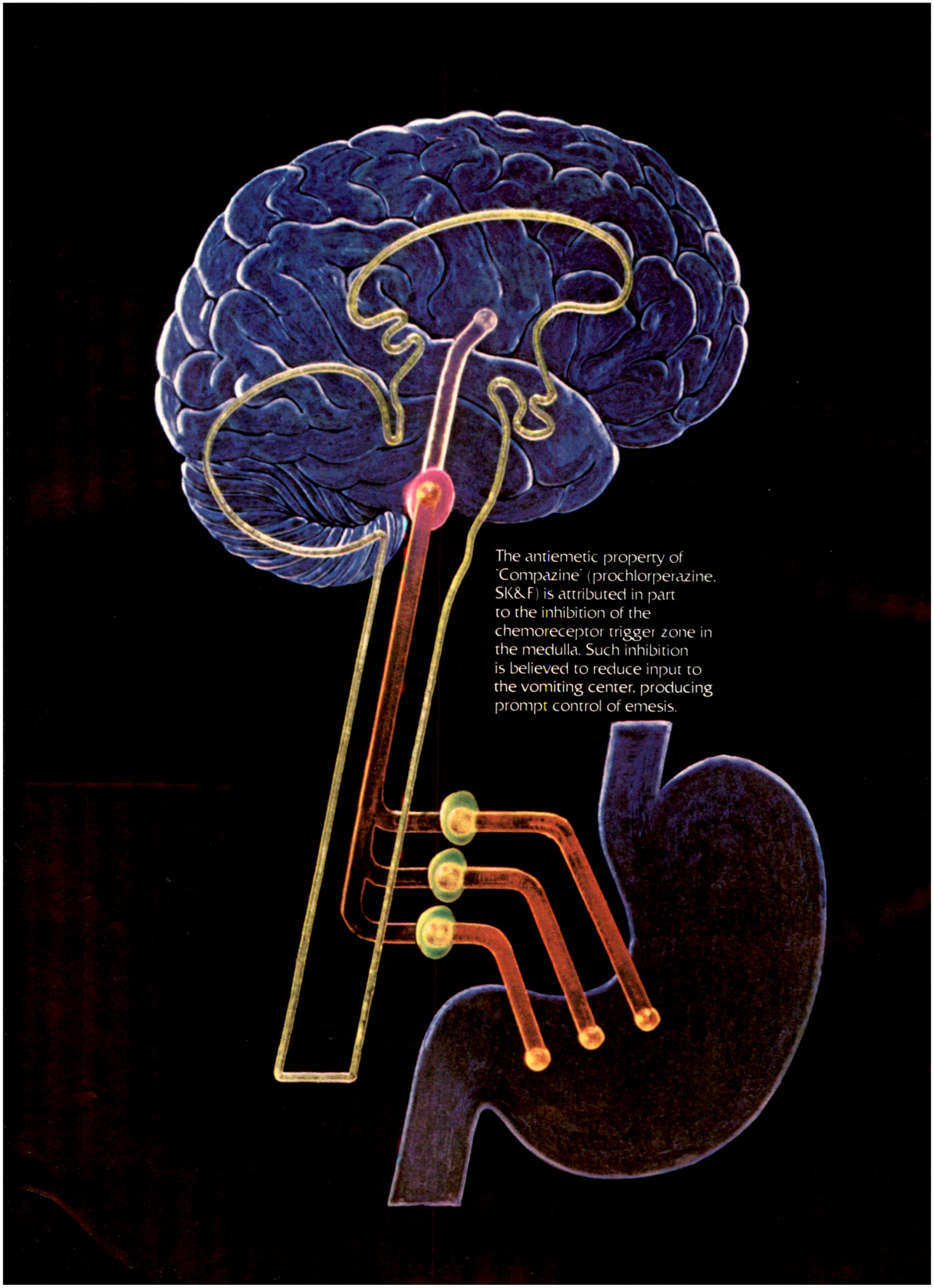
Once you've seen how much more AMRAD offers, putting together a radiographic system is easy. For the name of your nearest dealer, phone collect (312) 865-2600.

AMRAD

A Raytheon Company

The better value in x-ray

2020 North Janice Avenue, Melrose Park, IL 60160


The antiemetic property of 'Compazine' (prochlorperazine, SK&F) is attributed in part to the inhibition of the chemoreceptor trigger zone in the medulla. Such inhibition is believed to reduce input to the vomiting center, producing prompt control of emesis.

Compazine®

Injection 5 mg./ml.
disposable syringe

brand of
prochlorperazine

Shouldn't it be your first choice for severe nausea and vomiting that often accompany cancer therapy?

- **Unsurpassed antiemetic action**
- **12 dosage forms and strengths**

Before prescribing, see complete prescribing information in SK&F literature or PDR. The following is a brief summary.

Indications: Management of the manifestations of psychotic disorders; management of psychoneurotic patients displaying primarily symptoms of moderate to severe anxiety and tension; and for control of severe nausea and vomiting.

'Compazine' has not been shown effective in the management of behavioral complications in patients with mental retardation.

Contraindications: Comatose or greatly depressed states due to C.N.S. depressants; bone marrow depression; pediatric surgery.

Warnings: The extrapyramidal symptoms which can occur secondary to 'Compazine' may be confused with the central nervous system signs of an undiagnosed primary disease responsible for the vomiting, e.g., Reye's syndrome or other encephalopathy. The use of 'Compazine' and other potential hepatotoxins should be avoided in children and adolescents whose signs and symptoms suggest Reye's syndrome.

Avoid using in patients hypersensitive (e.g., blood dyscrasias or jaundice) to any phenothiazine. Caution patients about activities requiring alertness (e.g., operating vehicles or machinery) especially during the first few days' therapy. Prochlorperazine may intensify or prolong the action of other C.N.S. depressants. Not recommended for children under 20 pounds or 2 years of age.

Use in pregnancy only when potential benefits outweigh hazards.

Precautions: The antiemetic action of 'Compazine' may mask the signs and symptoms of overdosage of other drugs and may obscure the diagnosis and treatment of other conditions such as intestinal obstruction, brain tumor and Reye's syndrome (See WARNINGS). Postoperative aspiration of vomitus has occurred in a few surgical patients who received prochlorperazine as an antiemetic. Deep sleep and coma have been reported, usually with overdosage. Patients on long-term therapy, especially high doses, should be evaluated periodically for possible adjustment or discontinuance of drug therapy. **In children with acute illnesses or dehydration, use only under close supervision.**

Adverse Reactions: Drowsiness, dizziness, amenorrhea, blurred vision, skin reactions. Hypotension. Cholestatic jaundice, leukopenia, agranulocytosis. Fatty changes in the liver have been observed in a few patients who died while receiving the drug (no causal relationship has been established). Neuromuscular (extrapyramidal) reactions: motor restlessness, dystonias, pseudo-parkinsonism, persistent tardive dyskinesia. Contact dermatitis is a possibility with concentrate and injectable forms.

Other adverse reactions reported with Compazine (prochlorperazine, SK&F) or other phenothiazines: Some adverse effects are more frequent or intense in specific disorders (e.g., severe hypotension in mitral insufficiency or pheochromocytoma).

Grand mal convulsions; altered cerebrospinal fluid proteins; cerebral edema; prolongation and intensification of the action of C.N.S. depressants, atropine, heat and organophosphorus insecticides; dryness of mouth, nasal congestion, headache, nausea, constipation, obstipation, adynamic ileus, inhibition of ejaculation; reactivation of psychotic processes, catatonic-like states; hypotension (sometimes fatal); cardiac arrest; pancytopenia, thrombocytopenic purpura, eosinophilia; biliary stasis; lactation, galactorrhea, gynecomastia, menstrual irregularities, false-positive pregnancy tests; photosensitivity, itching, erythema, urticaria, eczema up to exfoliative dermatitis, asthma, laryngeal edema; angioneurotic edema, anaphylactoid reactions; peripheral edema; reversed epinephrine effect; hyperpyrexia; a systemic lupus erythematosus-like syndrome; pigmentary retinopathy; with prolonged administration of substantial doses, skin pigmentation, epithelial keratopathy, and lenticular and corneal deposits.

EKG changes have been reported, but relationship to myocardial damage is not confirmed. Discontinue long-term, high-dose therapy gradually.

NOTE: Sudden death in patients taking phenothiazines (apparently due to cardiac arrest or asphyxia due to failure of cough reflex) has been reported, but no causal relationship has been established.

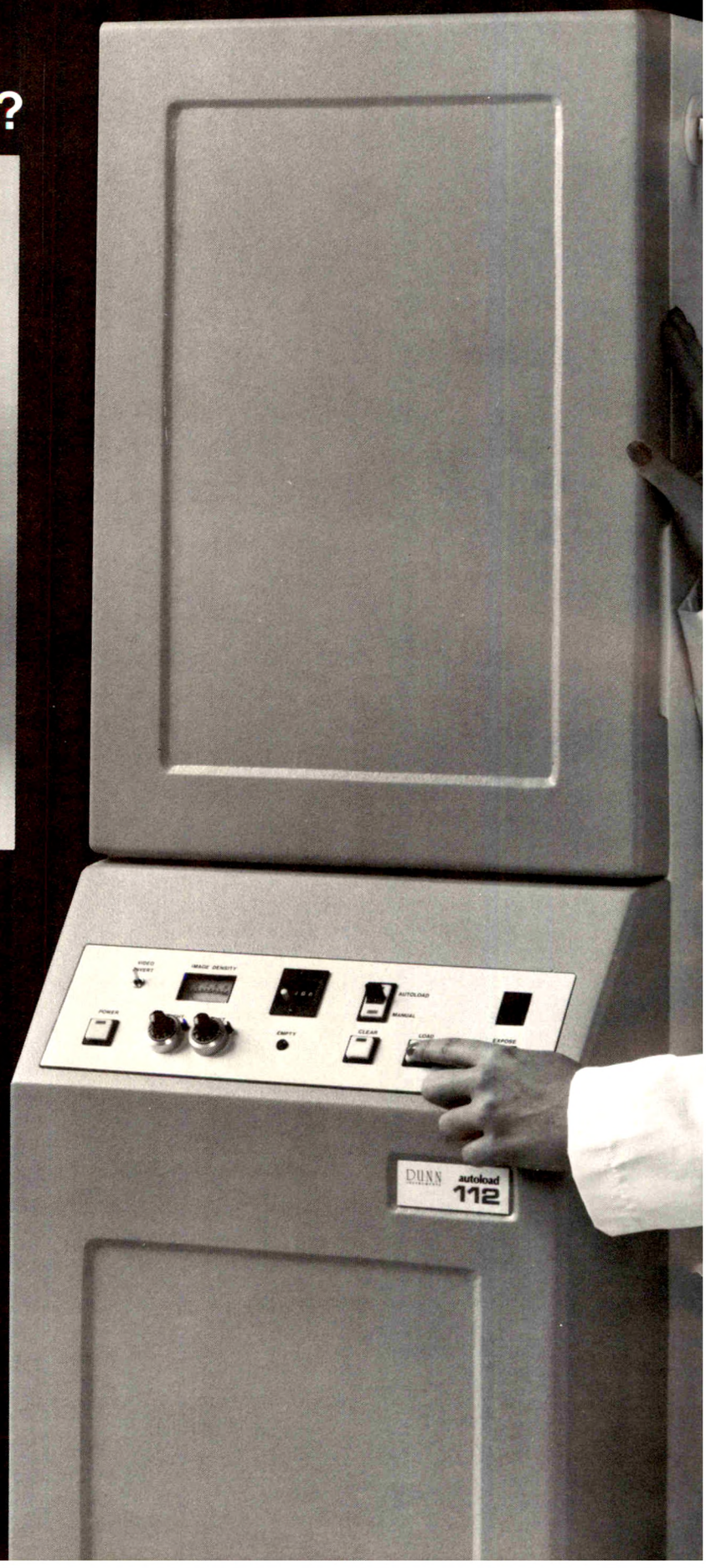
Supplied: Tablets – 5, 10 and 25 mg., in bottles of 100; Spansule® capsules – 10, 15, 30 and 75 mg., in bottles of 50; Injection – 5 mg./ml. in 2 ml. ampuls, 10 ml. vials, and 2 ml. disposable syringes; Suppositories – 2-1/2, 5 and 25 mg.; Syrup – 5 mg./5 ml.; Concentrate (intended for institutional use only) – 10 mg./ml.; Single Unit Packages of 100 (intended for institutional use only) – 5 and 10 mg. tablets; 10, 15 and 30 mg. 'Spansule' capsules.

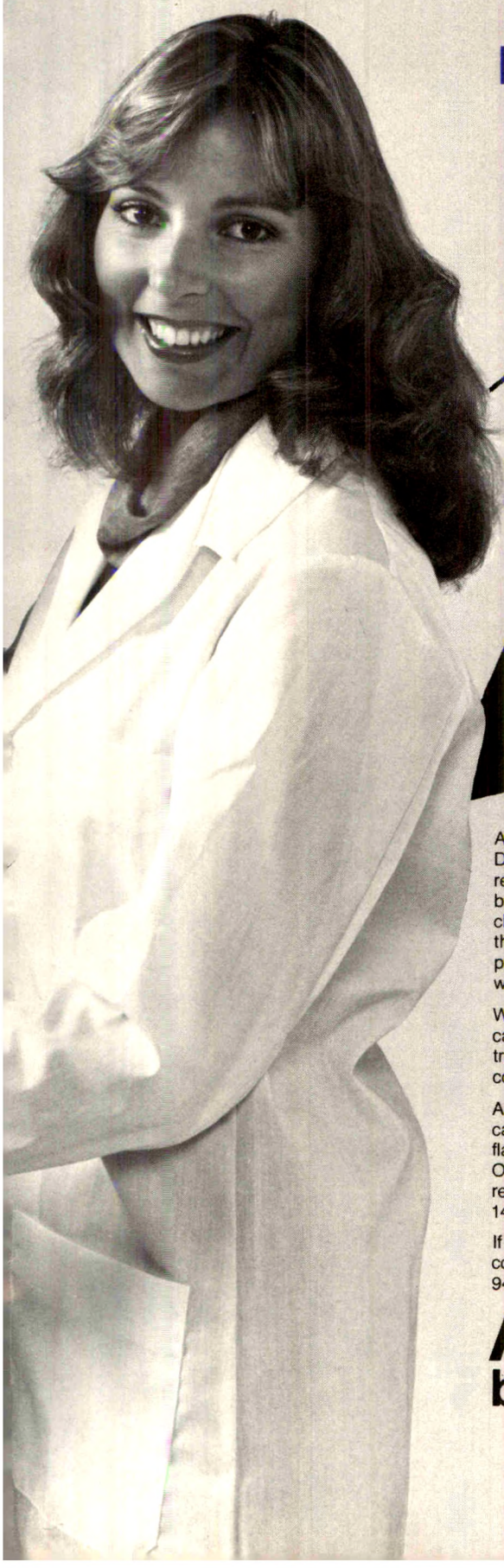
SK&F
a SmithKline company

Smith Kline &French Laboratories
Philadelphia, PA

Film handling overload?







Handle it with Autoload

Autoload 112 is the natural development of an idea whose time is still with us. Four years ago, Dunn Instruments introduced the multi-image camera with X-ray film to serve the growing revolution in video-based diagnostic imaging. Economy, convenience and superior image quality brought instant acceptance. Since then, in the familiar pattern, progress itself has created new challenges. Like film handling, which in some applications can be a hassle: where the caseload or the imaging requirements per patient are great. Or in any institution where heavy demand produces a bottleneck at the darkroom. Then dealing with manually loaded film cassettes can waste valuable time and space, and multiply the chances for error.

With Autoload you bulk load 100 sheets of film at a time, in a matter of seconds, directly into the camera in full daylight. Then expose as many sheets as you want and take them in the film transport drawer to the darkroom. Or better yet, get Autoload with optional direct feed into its own companion film processor, and have developed film in 90 seconds right in the imaging lab!

Automated film handling is only part of what makes Autoload 112 the most advanced multi-image camera ever. The uncompromising quality of its components is exemplified by the Tektronix 634 flat-faced video monitor, with 1400 lines resolution and backporch-clamped black level stability. Other standard features include on-axis Schneider optics, microprocessor control electronics, remote operation and video inversion. You can order Autoload in your choice of film sizes (up to 14″ x 17″) and image formats (including switch-selectable multi-format models).

If film hassling is holding you up, you should look into Autoload. For further information, call us collect or write Dunn Instruments, 544 Second Street, P.O. Box 77172, San Francisco, California 94107. Telephone (415) 957-1600.

Autoload 112
by Dunn Instruments

The UNION CARBIDE Bedside X-Ray System:

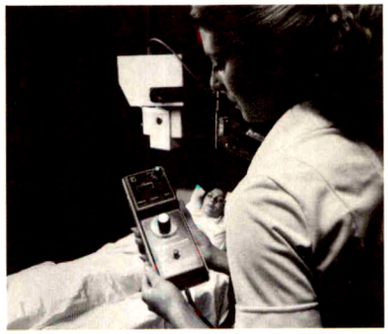
Reproducibility... Every Place, Every Time.



The 510 Bedside X-Ray System is a lightweight, low cost, mobile x-ray unit designed to achieve consistent reproducibility with routine bedside radiographic procedures.

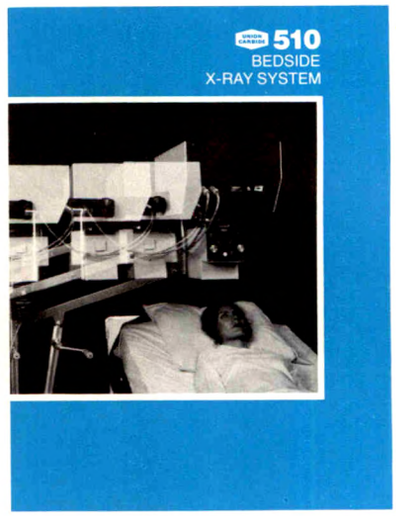
All exposure settings and operating controls are located on a convenient hand control module. Automatically computed and displayed mAs outputs up to 31mA at 100kVp or up to 35 mA at 60kVp reduce technique errors.

Diagnostic image quality is achieved by a combination of system power and speed. The 510 Bedside X-Ray System produces more power from a fixed anode tube allowing adult chest exposures with 100 kVp at 1/20 to 1/60 of a second; neonate studies at 1/40 to 1/120 of a second. Precise digital timing at speeds as fast as 1/120 of a second permits rapid exposures that effectively stop patient motion. This precision makes the unit effective with both traditional film/screen combinations and with newer "rare earth" systems.









Because the system is light in weight and small in size, it can be described as the most portable unit available. No bulky transport battery and motor. And because its price is so low, the 510 Bedside X-Ray System brings full diagnostic power *on a dedicated basis* to within economic feasibility for most potential users.

Ask Union Carbide for the Facts

Imaging Systems products from Union Carbide are designed to enhance diagnosis and research, produce a return on investment, and create better health care at lower patient cost.

If you feel you should know more about this new diagnostic tool, send today for descriptive literature. Or call for a personal presentation.



Touching your life through medicine . . .

UNION CARBIDE

Imaging Systems, Inc.
Medical Products Division
333 Providence Highway
Norwood, Massachusetts 02062
Within area 617, call 769-5400.
Outside, call 1-800-225-9887.
TELEX 924-494

The VAS array

Four memories for your image.

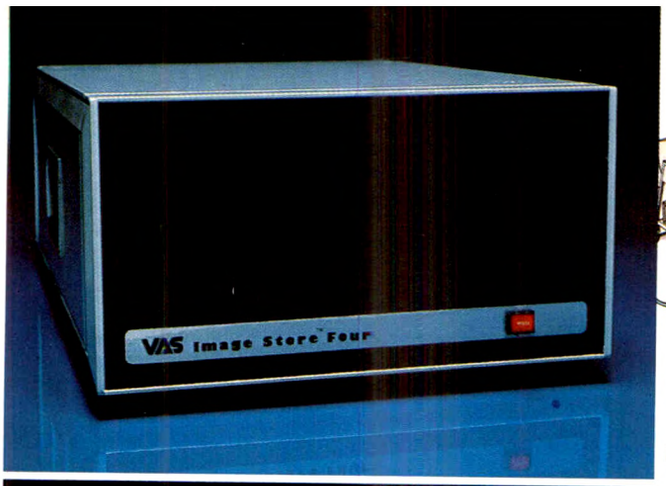
With shorter exposure times, Last Image Hold and instant replay, VAS Video Disc Recorders can mean up to a 95% dose reduction for staff and patients.

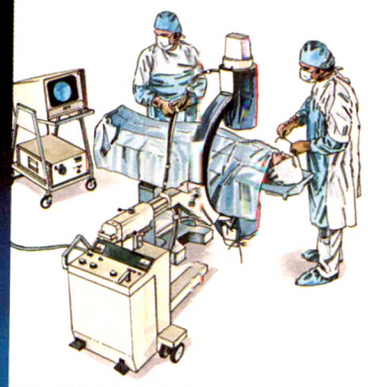
This, coupled with the ability to store from 100 to 500 successive images for reference and review, is the reason so many Radiology departments are specifying VAS Video Disc Recorders.

VAS makes Image Store™ Video Disc Recorders for every application — R and F rooms, surgery, special procedures, ultrasound and nuclear medicine.

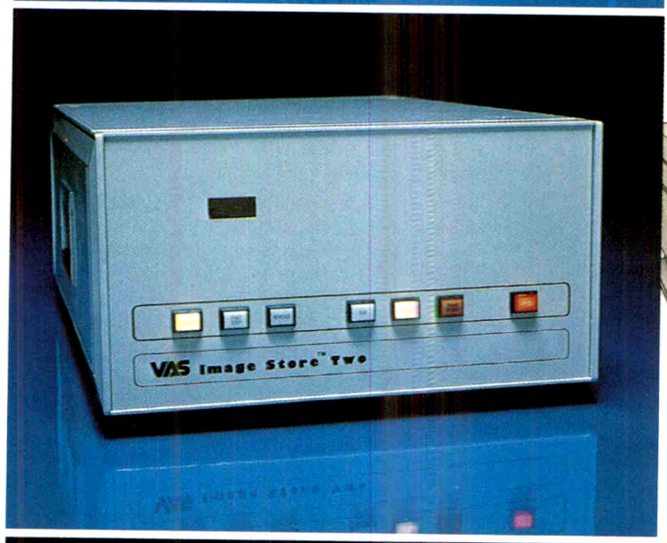
So remember us, we're your memory . . . VAS.

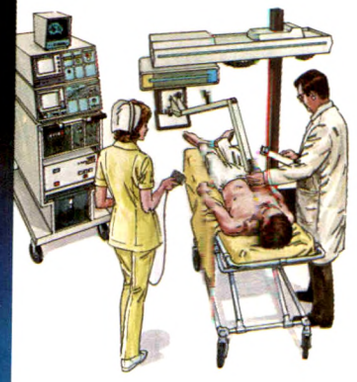
Detailed information can be supplied by your local X-Ray Dealer/Representative.





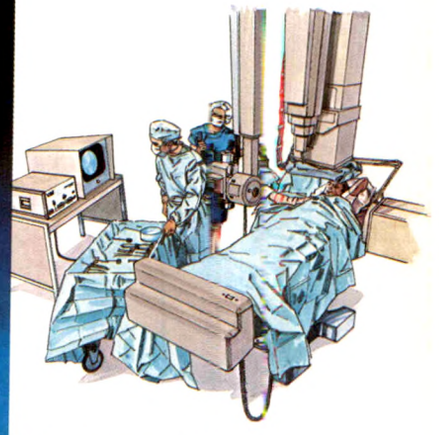
Surgical C-Arm



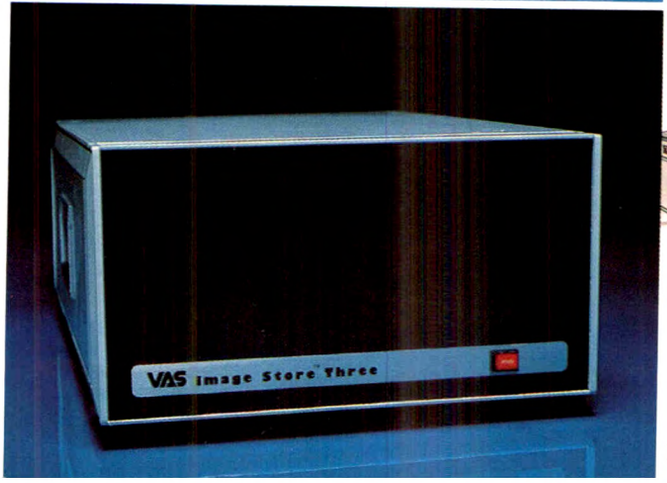


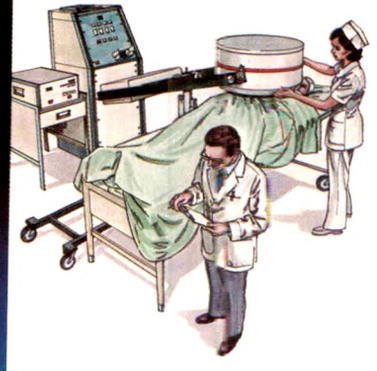
Ultrasound





Heart Catheterization





Nuclear Medicine

VAS

VAS Corporation
Medical Division
2525 Maricopa Street
Torrance, California 90503
(213) 320-8334

X-RAY IMAGE INTENSIFYING SYSTEMS

precise optics

IT MAY SURPRISE YOU.....

. . . to know that the people at Precise Optics have been supplying X-Ray Image Intensifying Systems since 1954. Precise specializes in Imaging, and offers a complete line of systems to meet requirements ranging from the private office to the special procedures room, at a cost savings over comparable units, without sacrificing quality.

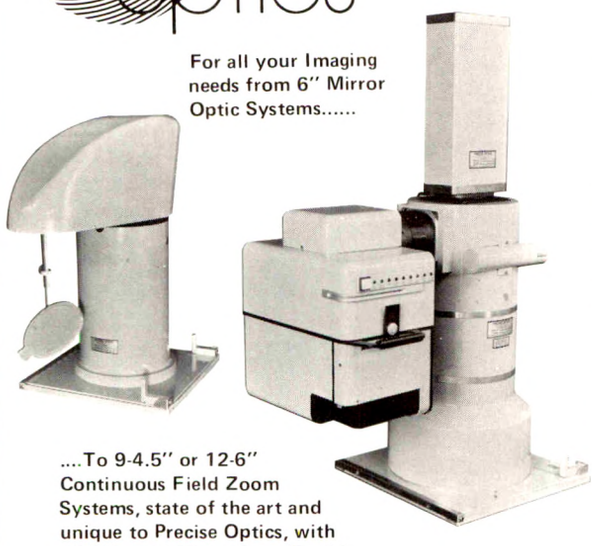
EVERY SYSTEM CONTAINS a guaranteed optimal performance cesium iodide image tube and field-proven solid-state power supply, covered by a two-year warranty.

THE PRECISE CCTV SYSTEM uses x-ray rated separate mesh vidicons, selected for high resolution and low-lag characteristics. Brightness compensation is an excellent 10,000:1, assuring the correct light level despite large variations in body densities.

THE NEW 105mm SPOT/RAPID SEQUENCE CAMERA (roll film, 6 frames per second maximum) utilizes the same digital electronics package and many of the mechanical sections of our other reliable 105mm cameras, while incorporating a rapid-load film transport and daylight receiving cassettes.

ACCESSORIES AVAILABLE INCLUDE: TWO-AND THREE-PORT LIGHT DISTRIBUTORS for spot and cine filming capabilities, ABS SYSTEM with automatically variable kV and selectable mA, SPOT FILM ADAPTERS compatible with any spot film device, CEILING SUSPENSION UNITS with smooth vertical and horizontal movements, CCTV MONITOR CARTS that are lightweight and easily mobile.

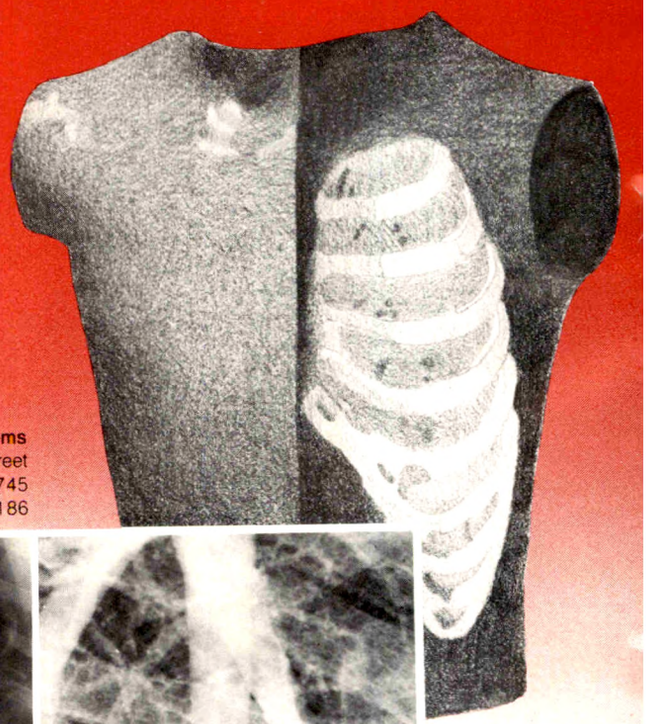
For all your Imaging needs from 6" Mirror Optic Systems.....



....To 9-4.5" or 12-6" Continuous Field Zoom Systems, state of the art and unique to Precise Optics, with CCTV and 105mm Spot/Rapid Sequence Cameras.

PRECISE OPTICS/PHOTO MEDIC EQUIPMENT, INC.
239 SO. FEHR WAY **BAYSHORE, N.Y. 11706**
TEL. (516) 242-6600 **TWX 510-227-9837**

The Lungs Are Real.



The Humanoid Lung-Chest Phantom.

Step wedges, lucite beads, steel wool and resolution charts just aren't the real thing. They never were.

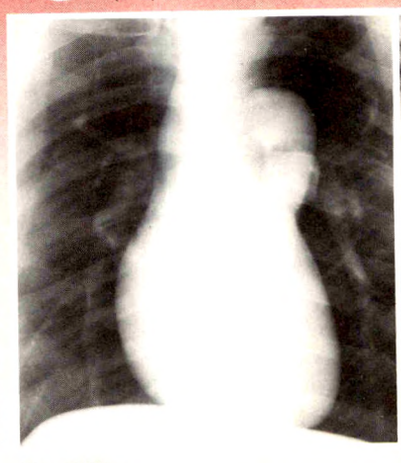
But our Lung-Chest Phantom is.

It's a **complete chest imaging system** featuring actual lungs. The only system of its kind in the world. A first.

Developed in conjunction with Department of Radiological Sciences at University of California/ Irvine, this remarkable "standard patient" provides the ideal method for maximizing quality control, teaching, researching, and producing consistent imaging. It permits development of the ideal set of factors for pathologies and patient histories. Optimizes magnification angiography. You can even add a variety of disease options.

The Lung-Chest Phantom eliminates unnecessary downtime by ensuring consistent, optimal results. Bottom line: maximum diagnostic effectiveness at lowest cost.

Humanoid Systems
747 East 223rd Street
Carson, California 90745
(213) 549-9631 Telex 69-1186



Normal View



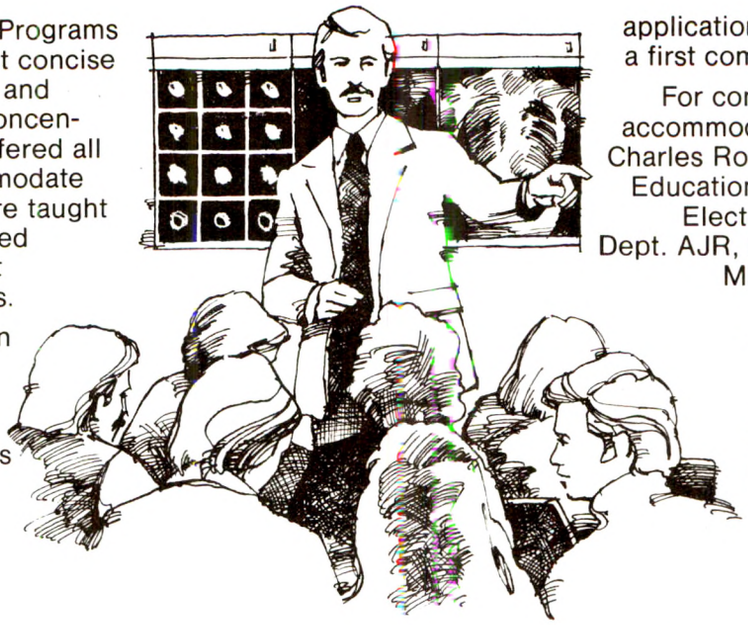
High Contrast View

Cutaway View

Send now for complete information.

GE Medical Education Programs are comprehensive, yet concise courses for physicians and technologists. These concentrated programs are offered all year around to accommodate busy schedules, and are taught by a skilled, experienced faculty, using the latest educational techniques.

Completed courses can be applied to meet accreditation and continuing education requirements. But class sizes are limited, so enroll today. All applications are processed on a first come, first served basis.



For complete details, dates, accommodations, etc., write to: Charles Rose, Director Medical Education Programs, General Electric Medical Systems, Dept. AJR, P.O. Box 414 TI 40, Milwaukee, Wisconsin 53201. Or call: 414-383-3211, ext. 2286, Dept. AJR.

Medical Education Programs

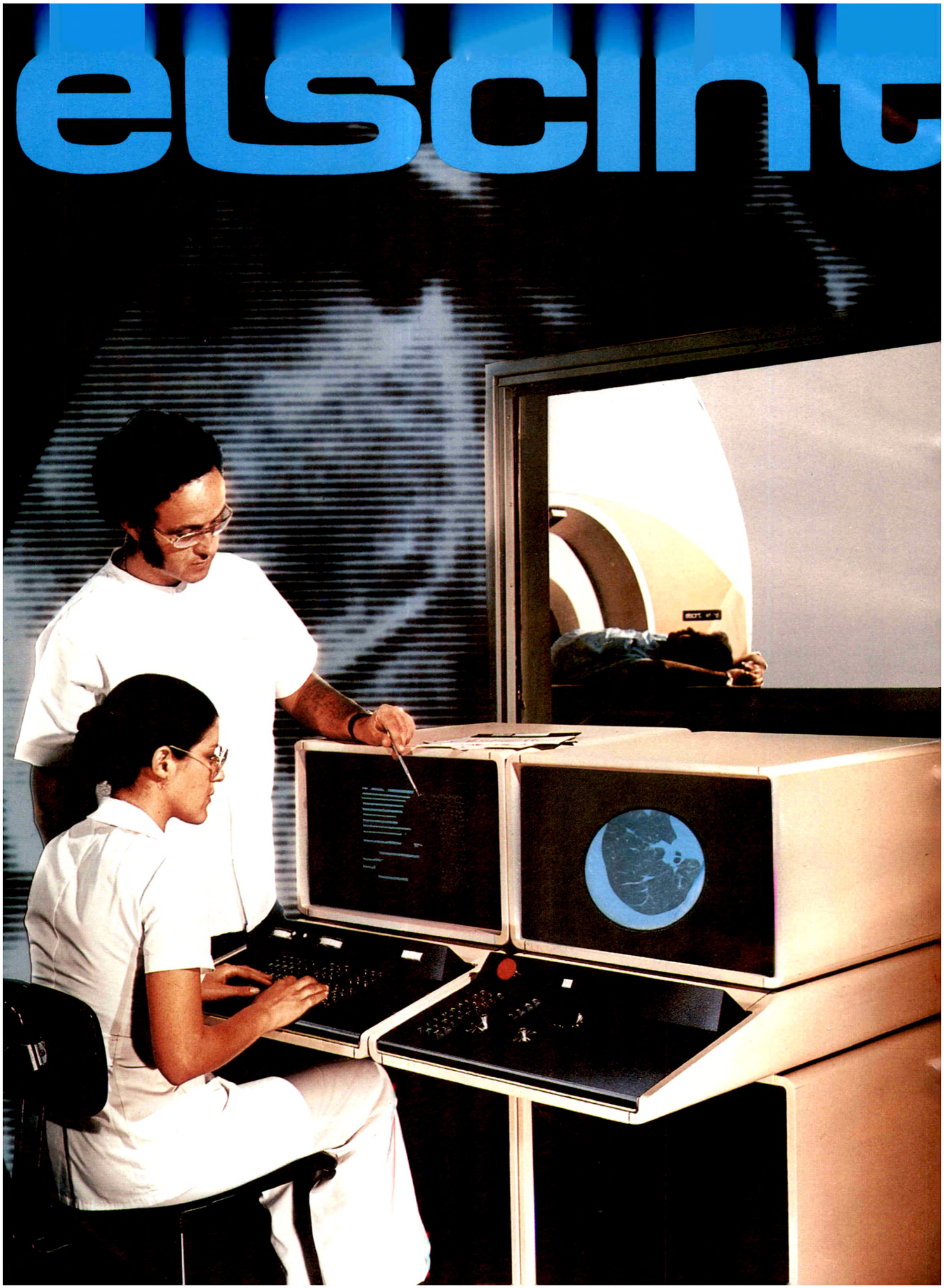
Announcing a 24 course, low-fat curriculum for healthcare professionals.

1979 GE MEDICAL EDUCATION PROGRAMS												
RADIOLOGY PROGRAMS	**JAN**	**FEB**	**MAR**	**APR**	**MAY**	**JUN**	**JUL**	**AUG**	**SEP**	**OCT**	**NOV**	**DEC**
Understanding X-ray Generation I		●						●				
Standardization of Radiologic Techniques II			●					●				
Quality Assurance in Radiology III			●					●				
Introduction to Radiologic Techniques						●						●
Radiology Registration & Certification				●						●		
Advanced Concepts in Diagnostic Imaging*											●	
COMPUTED TOMOGRAPHY PROGRAMS												
Principles of Computerized Tomography I			●						●			
Quality Control in Computerized Tomography II			●						●			
Quality Assurance in Computerized Tomography III			●						●			
Advanced Concepts in Diagnostic Imaging*											●	
NUCLEAR MEDICINE PROGRAMS												
Basics of Nuclear Medicine		●		●			●			●		
Quality Control & Compliance in Nuclear Medicine					●					●		
Advanced Concepts of Nuclear Medicine				●							●	
Dynamics in Nuclear Medicine					●				●			
Nuclear Cardiology	●						●				●	
Comprehensive Nuclear Medicine		●	●								●	
Nuclear Medicine Registration & Certification			●					●				
Radiopharmaceutical Techniques			●					●				
Advanced Concepts in Diagnostic Imaging*											●	
Radioisotope Handlers			●		●				●			●
MONITORING PROGRAM												
Principles of Cardiovascular Monitoring	●					●						
ULTRASOUND PROGRAMS												
Basics of Ultrasound I	●				●					●		
Quality Control & Compliance in Ultrasound II					●					●		
Advanced Concepts in Diagnostic Imaging*											●	
MANAGEMENT PROGRAMS												
Medical Management	●					●						●
Management Contract				●		●		●		●		
Medical Laboratory Management for Diagnostic Accuracy and Cost Containment							●					
DENTAL PROGRAM												
Radiological Techniques in Dentistry		●		●			●		●			●

*Includes Coverage of Radiology, CT, Ultrasound and Nuclear Medicine

GENERAL ELECTRIC

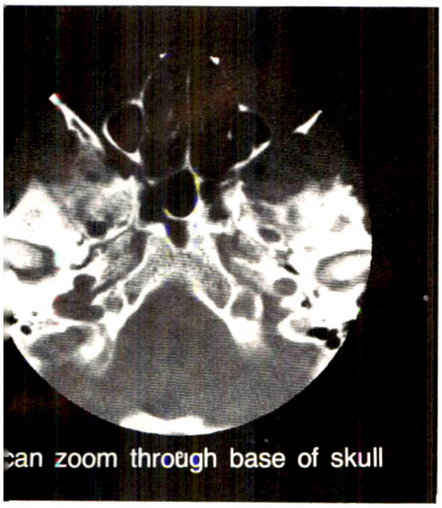
elsclnt



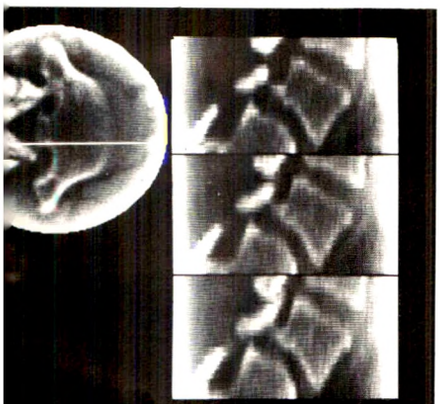
905 COMPUTERIZED TOMOGRAPH

KEL

The Total Commitment to Excellence The Ultimate in Cost-Effectiveness Now With 5-Second Scan Time



can zoom through base of skull



Scan zoom and sagittal reconstruction of vertebrae



Body planar densitograph

Excellence In Image Quality

Consistent high-quality brain scan with excellent gray and white differentiations

* Variable aperture cross - beam fine collimators
* Ultra high resolution images of vertebrae and skull base (13.5 line pairs/cm) obtained by scan - zoom of limited areas

Maximum photon utilization for superior density resolution

Exciting Operating Features

* Automatic patient positioning through built-in planar densitography

Up to 1000 scans per disk - 50 scans per diskette

* Reconstruction in any oblique plane

Compact, all-purpose diagnostic control console

Reconstructed image available 4.0 seconds after scan is completed

Extensive Versatility

Up to 15 pre-programmed scan protocols

Adaptive reconstruction processes to suit specific clinical situations

* Volumetric determination of organs or tumors
* Correction of metal clip artifacts

Specialized pediatric protocols

Radiotherapy planning programs

* ***Another Elscint first***

elscint inc.

Where quality counts . . . count on Elscint

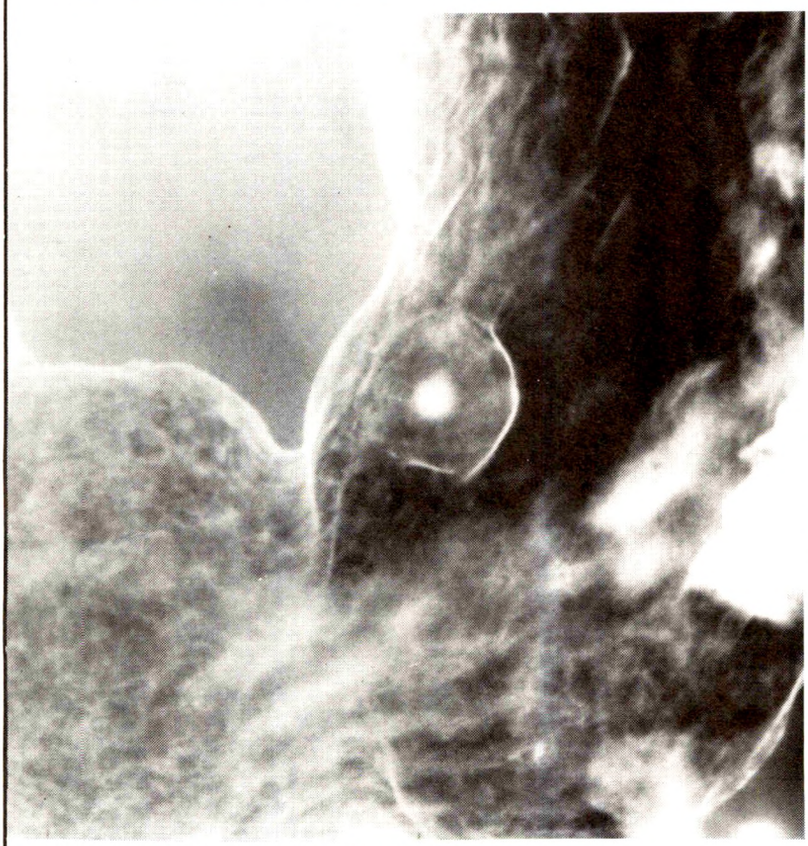
138-150 Johnson Ave. (P.O. Box 832), Hackensack, NJ. 07602,
Telephone (201) 487-5885

Elscint International, Annandale House North End Rd.,
London NW11 7QY Telephone: 01-4587323

For Double Contrast Stomachs, Use

NEW! E-Z-HD™

High Density with High Fluidity Barium Sulfate for Suspension USP



ANTERIOR WALL LEIOMYOMA WITH CENTRAL STALACTITE (HANGING DROPLET)
Film courtesy of Igor Laufer, M.D. Hospital of the Univ. of Pennsylvania

Double contrast radiography appears to offer the potential for significant improvements in diagnostic accuracy.

Double contrast studies of the stomach best demonstrate the surface pattern of the stomach (areae gastricae). This leads to improved detection of superfical erosions and ulcers, malignancies, polyps and other benign tumors, and ulcer scars.

E-Z-HD barium sulfate provides the basic ingredient necessary for good double contrast of the stomach.

The higher the density of the barium suspension, the better the coating, E-Z-HD allows for the highest density suspension of any commercial product on the market today: 85% w/w, 250% w/v. E-Z-HD achieves this density while remaining fluid for ease of administration.

- High density
- High fluidity
- Palatable
- Unit dose convenience.

E-Z-HD – The barium for the double contrast examination of the stomach and duodenum.

Optimal Density & Fluidity for the Modern Double Contrast Examination of the Stomach and Duodenum

Refrences:

David W. Gelfand: The Japanese-Style Double Contrast, Examination of the Stomach, Gastrointest Radiol. 1, 7-17 (1976)

Igor Laufer: The Diagnostic Accuracy of Barium Studies of the Stomach and Duodenum – Correlation with Endoscopy. Radiology 115: 569-573, June 1975

Roscoe E. Miller: The Air Contrast Stomach Examination: an overview. Radiology 117: 743-744 Dec. 1975

Order from your local X-ray supplier.

E-Z-EM

7 Portland Ave.
Westbury, New York 11590
(516) 333-8230

© 1/79

International Affiliates: E-Z-EM Rooster B. V., Infirmeriestraat 6-8, Rotterdam 16, Netherlands
E-Z-EM De Mexico, S. A. de C. V. Calz. Azcapotzalco La Villa No 882, Zona Industrial Vallejo, Mexico 16 D. F.



A cast of thousands

AMX mobile x-ray units. Thousands of proven performers. Producing high quality films every day in hospitals around the world.

When GE introduced battery-powered mobiles ten years ago, we solved a complex problem: how to combine fixed-base radiographic quality with mobility and self sufficiency.

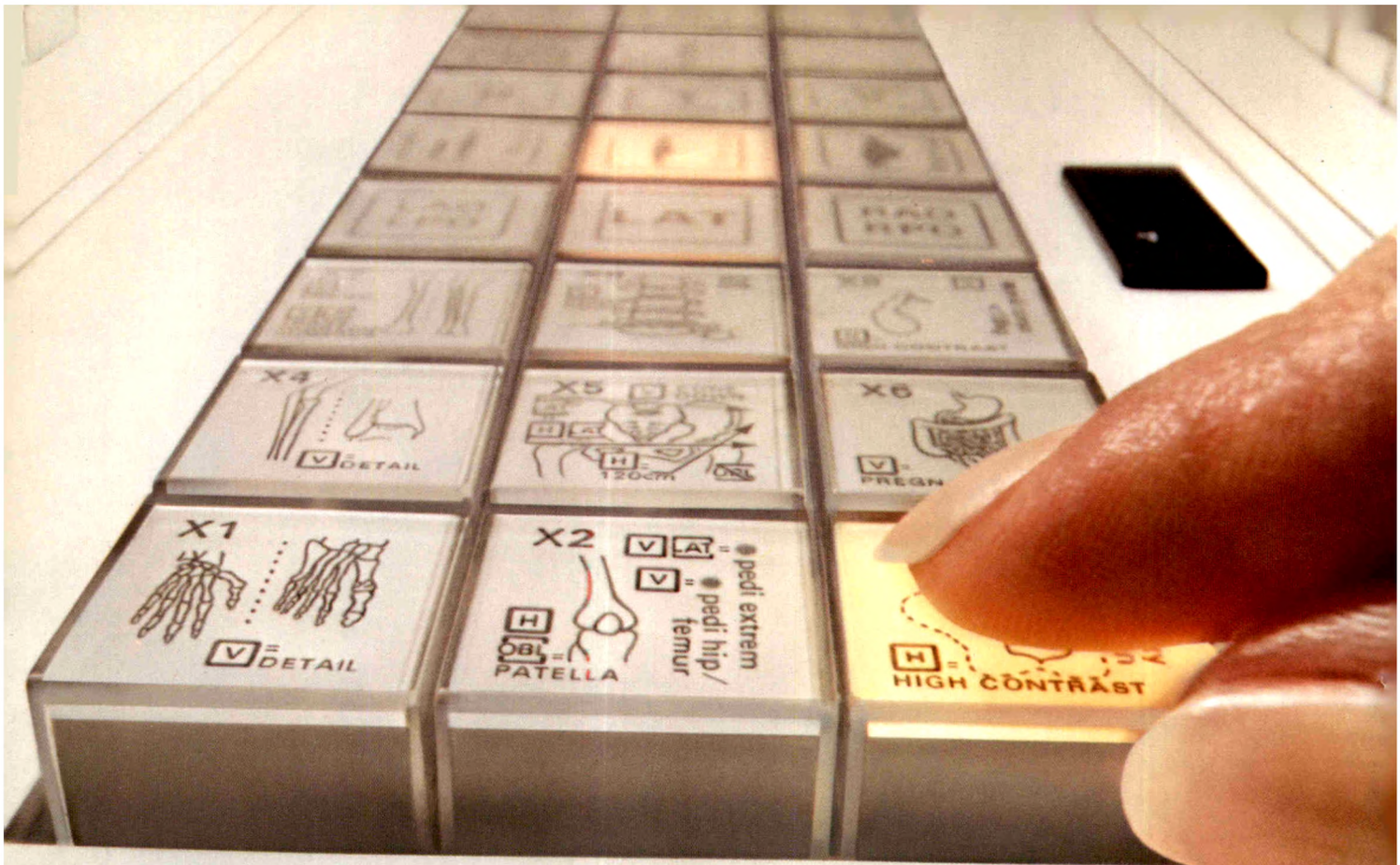
We made our system reliable, durable, easy-to-use and maintain. From the beginning, it outperformed plug-in mobiles; film quality was comparable to that of fixed systems.

In fact, AMX mobiles proved to be so practical that hospitals began to depend on them routinely, even for such studies as the lateral lumbar spine. And now it's not uncommon to find two, three—or more—AMX units in a single hospital.

One look at AMX film quality should convince you that this proven performer is right for your hospital too. Review the films from any of the thousands of AMX units in operation...at almost any hospital in your area. Then cast AMX in a supporting role. You'll get stellar performance. It's been proven by a cast of thousands.

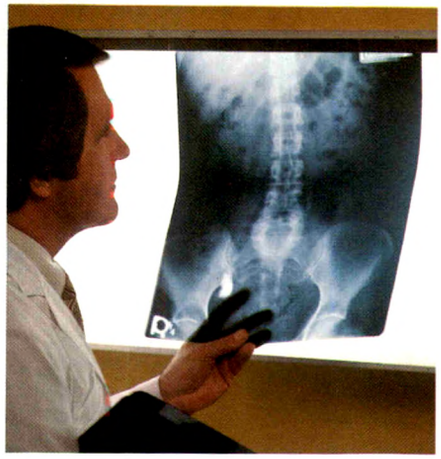
General Electric Medical Systems.

GENERAL ELECTRIC



On the button, every time.

MPX computerized generators give you high quality films, time after time.



That's because Quantamatic™ tx technic management consistently provides the right settings for each procedure, with microprocessor speed and precision.

You can store all your technics in the tx memory for instant access. Just press the appropriate selection buttons and the microprocessor instantly calculates and displays all technic parameters. Any setting may be overriden on command.

With over 200 programmed AEC and fixed time technics (on or off table) available, you can handle virtually every patient size. From infant to obese adult. And any body part, including extremities. You'll get standardized film quality, from exam to exam, room to room.

Fast, consistent technic selection means more time for patient positioning. And elimination of costly retakes. With MPX, you're right on the button every time.

You'd expect it from GE.

General Electric Medical Systems, Milwaukee, Toronto, Madrid.

GENERAL ELECTRIC

"Productivity is up 10% to 20%"

"Lower absenteeism"

"You can tell by their attitude—the workers who participate are happier, more cooperative, much sharper"

"We can identify direct savings of $2,000,000 per year"

"The program has had a distinct bearing on staff performance. Our engineering people now have a camaraderie with their counterparts in other departments"

"It started in headquarters. By next year we hope to have it in all our factories and research facilities"

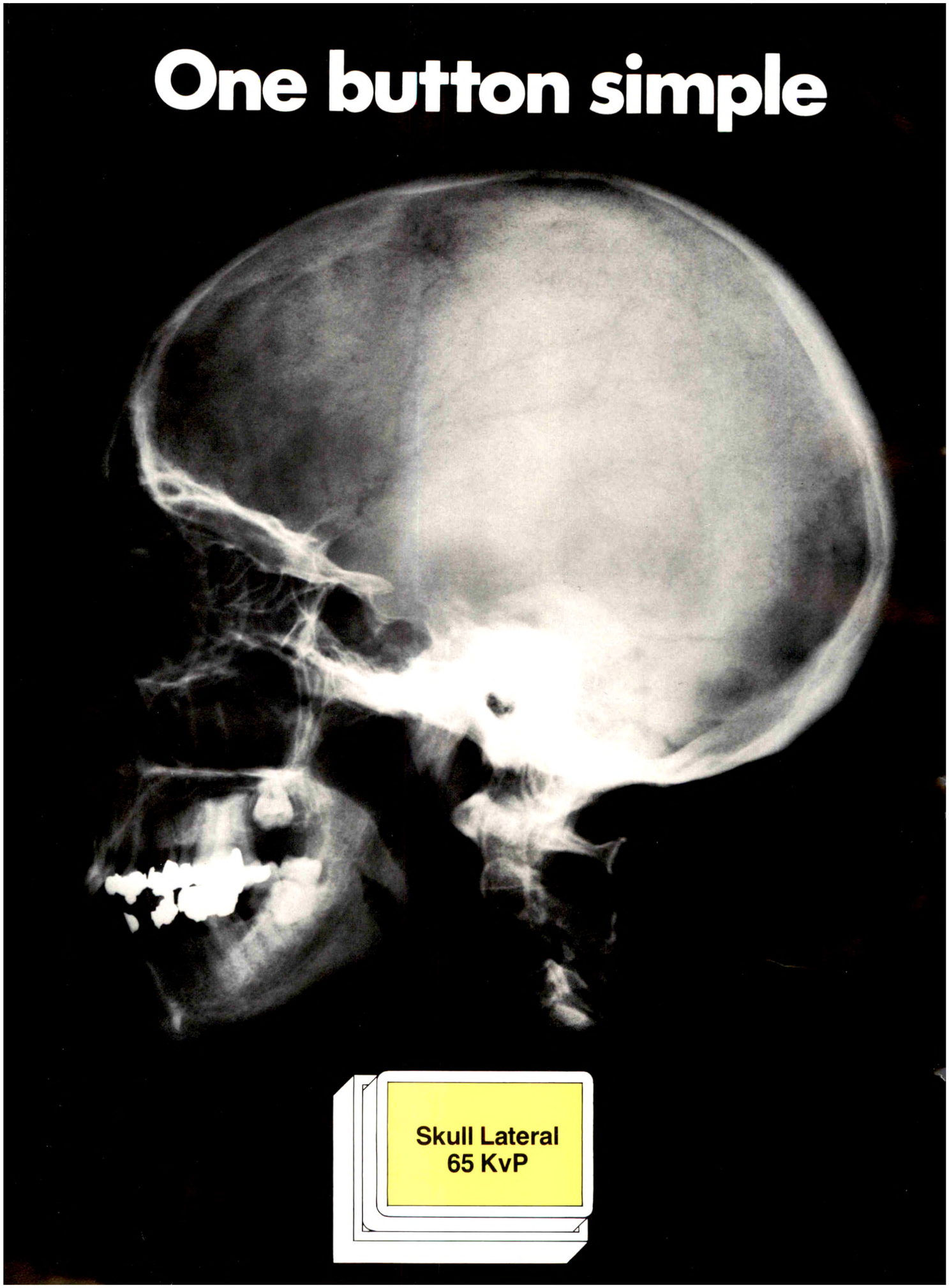
These are actual quotes from executives of large and small companies and organizations in Denver, Omaha, Birmingham, and Greenwich. They're talking about company fitness programs. That's right, many employers now provide facilities or opportunities for exercise for their employees. They are glad they did.

Most began with a concern for employee health and well being. What they have found is a variety of additional benefits. These benefits add up to *increased productivity*—so much so that several companies can demonstrate that the fitness program pays for itself. Add to this improved morale, better internal communications, and employee health. How can you lose? Write us now for more information:

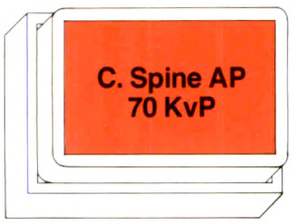
The President's Council on Physical Fitness and Sports
Department B
Washington, D.C. 20201

Employee Fitness: In the long run you will be the winner.

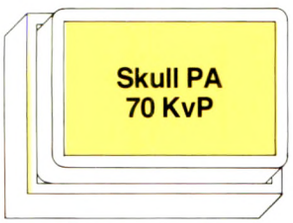
One button simple



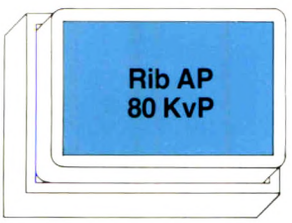
That's Philips APR (Anatomically Programmed Radiography) with Falling Load. It's made routine radiography one button simple for over two decades.



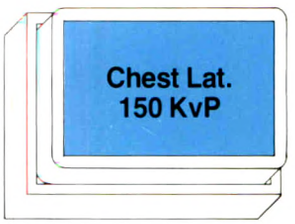
Philips APR pre-programs all *your* technic parameters for each body part into one button . . . with all the programs you need on the control desk *and* spot film device. Just press one simple button for a perfect exposure.



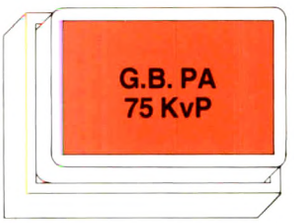
Fast, efficient and easy, APR returns the operator to his real purpose—professional *patient* management (instead of "technic management"). Time-consuming set-up tasks are eliminated. So are inadvertent operator errors.



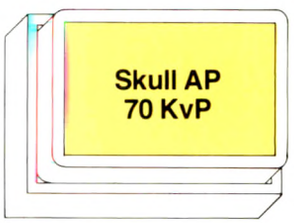
PHILIPS



Obviously, the shorter the exposure time the better because there's less blurring due to patient motion. So be wary of Constant Load, which requires advance knowledge of the exposure time (impossible) when using automatic exposure technic, and results in longer exposure times to cover the unknown. Falling Load *guarantees* the shortest possible exposure times for automatic operation.



In fact, Philips APR with Falling Load eliminates all the inefficiencies and risks of Constant Load. APR buttons are simple to read and operate. There are no button sequences to remember and none of the complexities of multiple programming. With APR, you can't overload the tube, you don't compromise tube specifications, and you don't have to play it safe with lower mA's and longer times to prevent running into the back-up time (with consequent underexposure and the need for a retake). With APR, each button has already managed the technic: you're free to provide professional *patient* management.



Philips APR with Falling Load: superior results and reproducibility you can count on. With just one button. If there *is* a simpler, more reliable way, we'll invent it.

PHILIPS®

PHILIPS MEDICAL SYSTEMS, INC.
710 Bridgeport Avenue, Shelton, Connecticut 06484

LEA & FEBIGER
Publishers Since 1785
WASHINGTON SQUARE
PHILADELPHIA, PA./19106

Radiation Protection In the Radiologic and Health Sciences

By MARILYN E. NOZ, Ph.D., *and* GERALD Q. MAGUIRE, JR., *both of New York University Medical School, New York, New York.* Taking a very practical approach, this book presents a readable source of radiation protection material for anyone working in the radiological and health sciences. It is the first suitable text on the subject for students preparing for careers as radiologic and nuclear medicine technologists, for residents, or for medical health physicists. It is an excellent reference guide for anyone using radiation in the health field, including the physician.

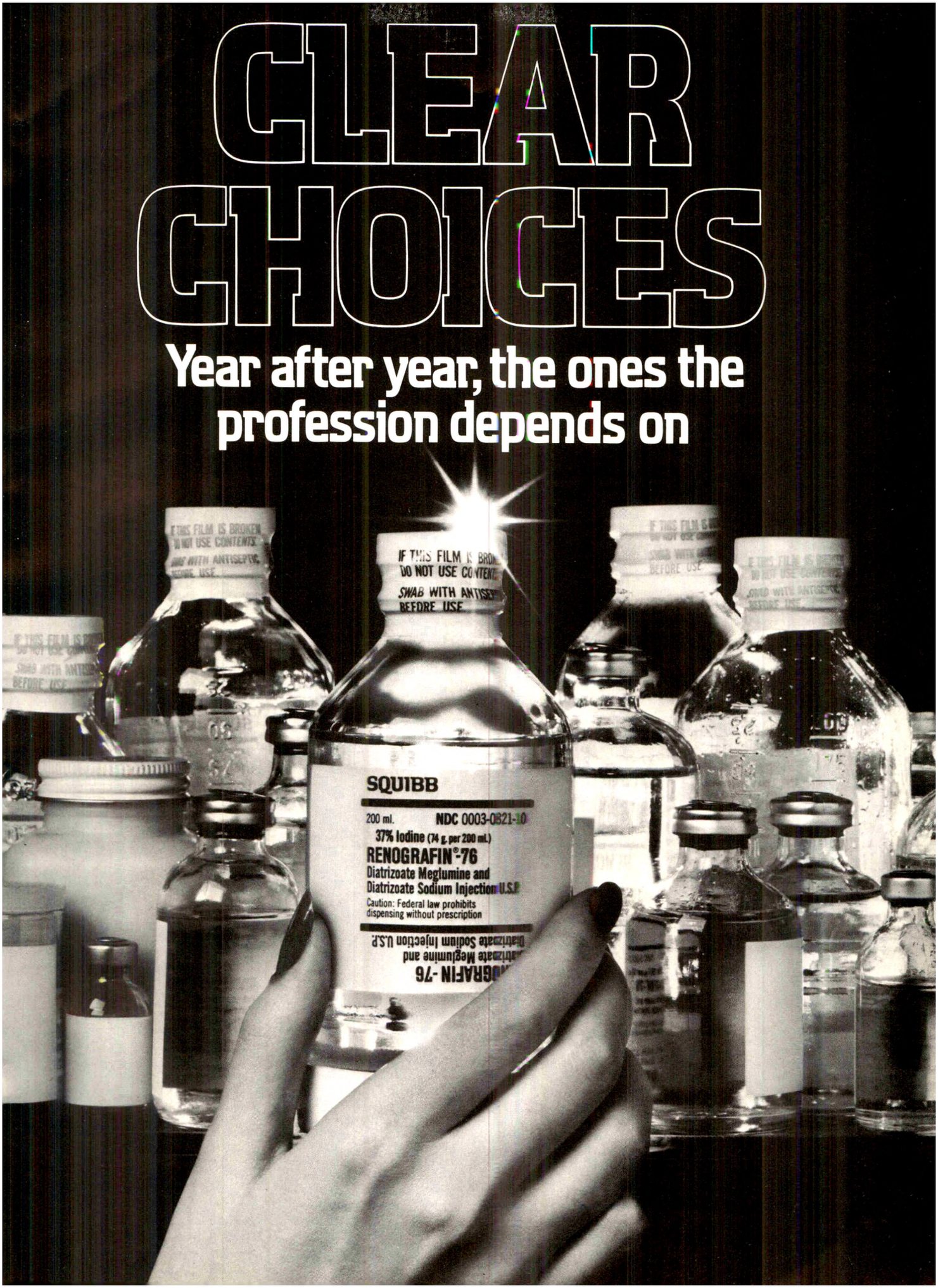
The first section, truly unique for the information presented, consists of radiation protection principles which have general application. It includes a discussion of instruments used in the field of radiation protection both for area and for personnel monitoring, as well as a description of SI units for radioactivity, exposure, and absorbed dose. The descriptions of the instrumentation used (survey and personnel monitors), are rarely found elsewhere. The sievert is used for dose equivalent and the maximum permissible dose (MPD) is expressed in those terms. The second section concerns itself with protection from sources of internal radiation. An outstanding chapter in this section includes a discussion of the absorbed dose calculation prepared by the Medical Internal Radiation Dose (MIRD) Committee of the Society of Nuclear Medicine. A chapter is also included on the licensing system for production, transportation, possession, and use of radionuclides as regulated by law. The third section is concerned with protection from sources of external radiation and includes both shielding requirements and absorbed dose calculations.

Contents: General Radiation Protection: Introduction; Gas-filled Detectors; Survey Meters; Personnel Monitors; The Units of Radiation Protection; Maximum Permissible Dose; Practical Means of Radiation Protection; Protection From Radionuclides: Good Working Habits; Radionuclides and the Law; Internal Dosimetry; Protection From External Radiation: Barriers; External Dose from Photons; Appendices; Glossary; Index. *218 pp., 37 illus., paperback, 1979, $12.50.*

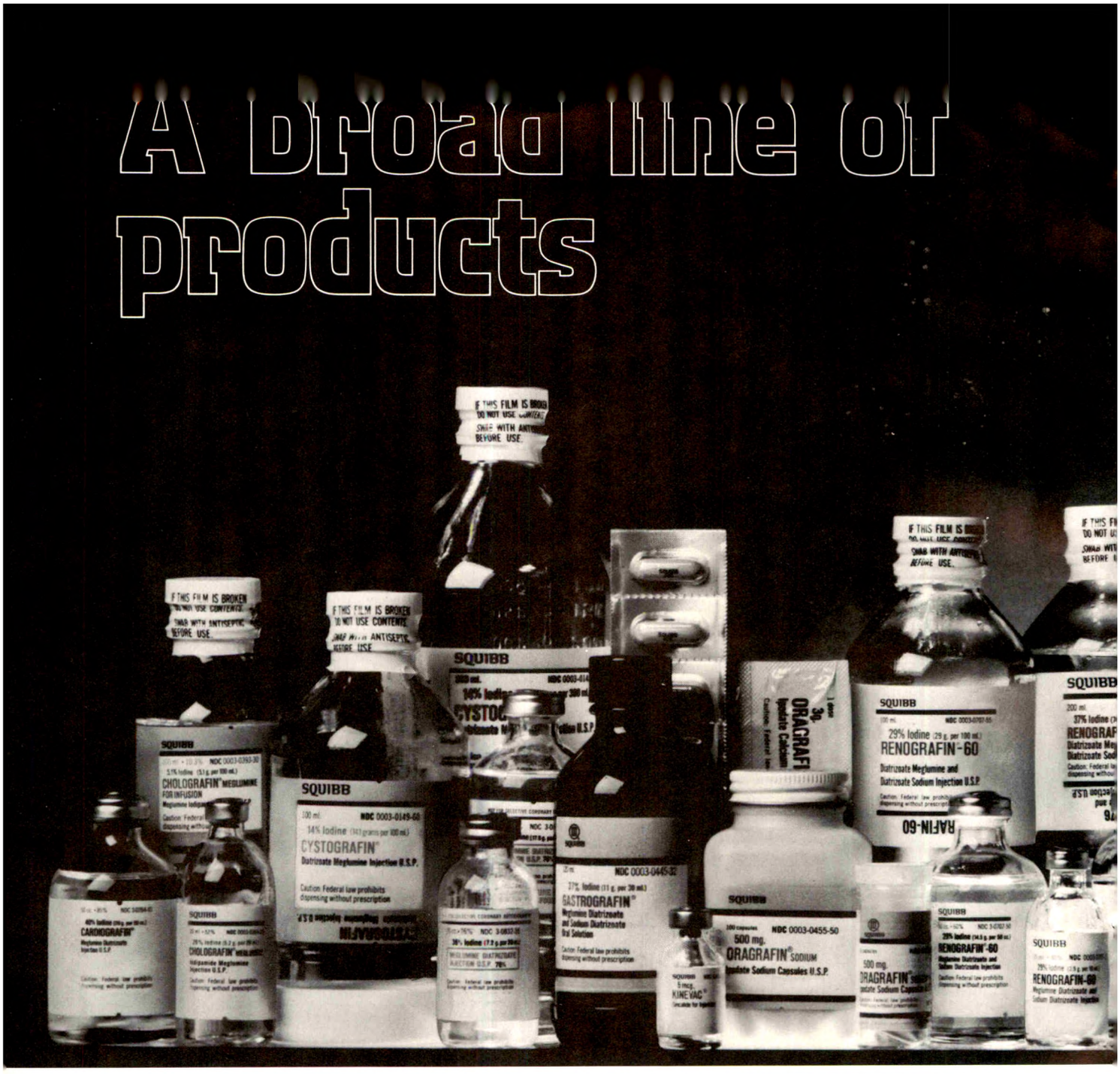
A New Edition! **AN INTRODUCTION TO THE PHYSICS OF DIAGNOSTIC RADIOLOGY, 2nd ed.** *By* EDWARD E. CHRISTENSEN, M.D., THOMAS S. CURRY, III, M.D., *and* JAMES E. DOWDEY, Ph.D., *all of the University of Texas Health Science Center, Dallas.* Extremely well written and easy to follow with carefully chosen illustrations, this new and up-dated Second Edition sets forth essential aspects of the physics of diagnostic radiology and incorporates recent advances in radiologic imaging. The authors introduce the important equipment advances and changes which confront radiologists. New chapters dealing with xeroradiography, computed tomography, ultrasound and radiologic protection have been added to this edition. Chapters on magnification and cinefluorography have been greatly expanded and completely revised. Major updating has been done on most chapters. *428 pp. (7 × 10), illus., 1978, $18.00.*

A New Book! **ULTRASOUND IN HIGH-RISK OBSTETRICS.** *By* RUDY E. SABBAGHA, M.D., *Prentice Women's Hospital, Chicago, Illinois.* Ultrasound has proven to be an excellent clinical tool in allowing the clinician to closely monitor the biophysical profile of the fetus; and because of its accuracy and non-invasive nature, indications for its use throughout gestation have greatly increased. This book concisely presents the present day applications of diagnostic ultrasound in high-risk pregnancy. Emphasis is placed on the means of formulating a correct clinical diagnosis by accurate definition of gestational age, distinction between normal and intrauterine growth retarded fetuses, detection of fetal congenital anomalies, diagnosis of placental abnormalities including placenta previa, delineation of the nature of pelvic masses associated with pregnancy. *About 150 pp., 94 illus., August 1979.*

A New Book! **TEXTBOOK OF NUCLEAR MEDICINE: Basic Science.** *Edited and with contributions by* ANTONIO FERNANDO GONCALVES ROCHA, M.D., *Centro de Medicina Nuclear, Guanabara, Brazil, and* JOHN CHARLES HARBERT, M.D., *Georgetown University Hospital, Washington, D. C. (32 Contributors).* Initially discussing the physical basis of matter and energy, radioactivity, decay processes, and interaction of radiation with matter, the text provides excellent coverage of radiation detector systems, radioactivity and statistical counting, compartmental analysis, biologic effects of radiation, radiation dosimetry and safety, production of radionuclides, radionuclide generator systems, radiopharmaceutical chemistry of technetium and iodine, radiopharmaceutical quality control, and discussion of rectilinear scanners, scintillation cameras, and computer systems. *412 pp. (7 × 10), illus., 1978, $27.50.*


CLEAR
CHOICES
Year after year, the ones the profession depends on
SQUIBB
200 ml.
37% Iodine (74 g. per 200 mL)
RENOGRAFIN®-76
Diatrizoate Meglumine and
Diatrizoate Sodium Injection U.S.P.
Caution: Federal law prohibits
dispensing without prescription

A broad line of products



Cardiografin®
Diatrizoate Meglumine
Injection USP (85%)
50 ml

Cholografin® Meglumine
Iodipamide Meglumine
Injection USP (52%)
20 ml

Cholografin® Meglumine
for Infusion
Iodipamide Meglumine
Injection USP (10.3%) 100 ml

Cystografin®
Diatrizoate Meglumine
Injection USP (30%)
100 ml, 300 ml

Diatrizoate Meglumine
Injection USP 76%
20 ml, 50 ml

Gastrografin®
Diatrizoate Meglumine and
Diatrizoate Sodium Solution USP
(66%/10%)
120 ml

Kinevac®
Sincalide for Injection
5 mcg

Oragrafin® Calcium Granules
Ipodate Calcium for
Oral Suspension USP
3 g ipodate calcium per 8 g packet

Oragrafin® Sodium Capsules
Ipodate Sodium Capsules USP
0.5 g per capsule
Vials of 6 capsules, bottles of 100,
Unimatic® packages of 100

A wide range of sizes



Renografin®-60
Diatrizoate Meglumine and Diatrizoate Sodium Injection USP (52%/8%)
10 ml, 30 ml, 50 ml, 100 ml

Renografin®-76
Diatrizoate Meglumine and Diatrizoate Sodium Injection USP (66%/10%)
20 ml, 50 ml, 100 ml, 200 ml

Reno-M-60®
Diatrizoate Meglumine Injection USP (60%)
10 ml, 30 ml, 50 ml, 100 ml

Reno-M-30®
Diatrizoate Meglumine Injection USP (30%)
50 ml, 100 ml

Reno-M-DIP®
Diatrizoate Meglumine Injection USP (30%)
300 ml

Renovist®
Diatrizoate Meglumine and Diatrizoate Sodium Injection USP (34.3%/35%) 50 ml

Renovist® II
Diatrizoate Meglumine and Diatrizoate Sodium Injection USP (28.5%/29.1%)
30 ml, 60 ml

Renovue®-65
Iodamide Meglumine Injection 50 ml

Renovue®-DIP
Iodamide Meglumine Injection 24%
300 ml

Sinografin®
Diatrizoate Meglumine and Iodipamide Meglumine Injection (52.7%/26.8%)
10 ml

COLLEGE OF MEDICINE
LIBRARY

SQUIBB®
E. R. Squibb & Sons, Inc.

Professional service



Squibb Representatives are always happy to discuss Squibb's well-known, extensive line of products. However, they also like to talk about educational materials and to be of service in ways which will help radiologists in their professional activities. For example, there's "Clinical Radiology." It's a CME audio-visual program for use as a teaching aid for radiology residents, or as an in-service review for staff physicians, or just as a personal refresher course.

Current service materials are listed below. Check your interests and mail the form. Your Squibb Representative will soon be at your service.

© 1978 E. R. Squibb & Sons, Inc. 659-501

Radiology Product Manager,
E. R. Squibb & Sons, Inc., Box 4000,
Princeton, N.J. 08540

The leader in radiologic diagnostics

SQUIBB™ contrast media

I am interested in:

- ☐ Clinical Radiology (audio/visual program)
- ☐ *X-Ray Atlas* (review of diagnostic procedures)
- ☐ Motion pictures on radiology
- ☐ Squibb Radiology Education Program (slide/tape presentations)
- ☐ *Selected Radiologic Emergencies* (wall chart)
- ☐ *The Challenge...Radiography, Nuclear Medicine, Radiotherapy* (brochure on career opportunities in technology)
- ☐ Patient dose/instruction envelopes for cholecystography (English and Spanish)

Name _____ Position _____

Hospital _____ Address _____ Phone _____

City _____ State _____ Zip _____

AB

Fleet® Barium Enema Prep Kits: Make us your first choice for fewer retakes.

The greatest defect in colon examinations is in the preparation of the colon.[1]

Fleet® Barium Enema Prep Kits systematize and improve colon prepping because they conform to the recommended method which provides a combination of diet, hydration and proven laxation which stimulates the large and small intestines.[2] The result? Cleaner colons, clearer x-rays and fewer retakes.

All Fleet Prep Kits offer three laxative steps: 1½ oz. of Fleet® Phospho-Soda® followed by four Fleet® Bisacodyl tablets, plus a final cleansing step. Prep Kit 1 offers Fleet® Bisacodyl suppository. Prep Kit 2 offers a large-volume disposable Fleet® Bagenema. And Prep Kit 3 offers our new Fleet® Bisacodyl enema. And all three Prep Kits have easy-to-follow instructions with a choice of flexible time-tables to fit your schedule.

With Fleet Barium Enema Prep Kits, you'll be sure of convenient, dependable, effective colon prepping every time. And that's reason enough to make Fleet Prep Kits your first choice for fewer retakes.



Fleet Barium Enema Prep Kits
for cleaner colons, clearer x-rays and fewer retakes.

Fleet pharmaceuticals
C.B. Fleet Co., Inc.
Lynchburg, Va. 24505

[1]Dr. R.E. Miller, Ad Hoc Committee on Detection of Cancer of the Colon, Detection of Colon Lesions, American College of Radiology, (Chicago, Ill., 1973) p. 76
[2]Dr. W.R. Eyler, Ibid. pp. 203, 204.

Cook County
Graduate School of Medicine

announces

CURRENT MANAGEMENT TECHNIQUES IN RADIOLOGY

For Radiologists,
Hospital Administrators
and
Radiology Department Managers.

August 17–18, 1979

Write or call for information and registration.

Registrar
707 South Wood Street
Chicago, Illinois 60612
(312) 733-2800

THE DEPARTMENT OF RADIOLOGY
UNIVERSITY OF MINNESOTA

announces

42nd Annual Course

CHEST RADIOLOGY

September 10–14, 1979

A five-day comprehensive review
for practicing radiologists
emphasizing

Fundamentals of Intrathoracic Anatomy
& Disease States Utilizing Conventional
Radiographs & CT Imaging

For further information contact:
Continuing Medical Education
c/o Chest Radiology Course
Box 293 Mayo Memorial Building
University of Minnesota
Minneapolis, Minnesota 55455
Telephone (612) 373-8012

"Equal Educational Opportunity"

Announcing a new series . . .

MULTIPLE IMAGING PROCEDURES

JEROME H. SHAPIRO, M.D. and
LEONARD M. FREEMAN, M.D., Editors

Volume 1, PULMONARY SYSTEM

Edited by STANLEY S. SIEGELMAN, M.D.,
FREDERICK P. STITIK, M.D., and
WARREN R. SUMMER, M.D.

CONTENTS: Chest Technique; Contrast Studies of the Airways; The Role of Radionuclide Studies in the Diagnosis of Pulmonary Disease; Pulmonary Arteriography; Computed Tomography; Cytopathology in the Diagnosis of Pulmonary Disease; Percutaneous Lung Biopsy; Mediastinoscopy; Efficacy of Various Techniques for Diagnosing Pulmonary Emboli; Diffuse Lung Disease; Pulmonary Disease in the Immunocompromised Host.

1979, about 416 pp., 181 illus., about $32.50
ISBN: 0-8089-1143-0

Volume 2, CENTRAL NERVOUS SYSTEM

Edited by SAMUEL M. WOLPERT, M.D.

CONTENTS: Subarachnoid Hemorrhage; Cerebrovascular Disease in the Adult; Cerebral Tumors; Intrasellar and Perisellar Lesions; Cerebellopontine Angle Masses; Cerebral Trauma; The Radiological Investigation of Dementia and Cerebral Atrophy; Degenerative Spinal Disorders; Congenital Spinal Disorders.

1979, about 208 pp., $18.50 ISBN: 0-8089-1155-4

FUNDAMENTALS OF ABDOMINAL SONOGRAPHY

A Teaching Approach

By HOWARD W. RAYMOND, M.D.

The book provides a guide to the utilization of sonographic procedures in the overall diagnostic workup, together with an approach to the interpretation of the various types of abdominal sonograms. A teaching format is employed in which the reader is advised to examine each case as it is presented and to make conclusions before proceeding to the discussion of the case which follows on the next page. An attempt is made to review and then build on the reader's knowledge. Whenever possible, abnormal sonograms are compared with both similar abnormal scans and normal studies. Separate chapters are devoted to: Basic Abdominal Sonogram; Gallstones; The Dilated Gallbladder; The Pancreas; The Liver; Renal Sonography; Abdominal Aortic Aneurysms and Miscellaneous Abdominal Conditions.

1979, about 196 pp., 301 illus., about $17.50
ISBN: 0-8089-1144-9

Send payment with order and save postage and handling charge. *Prices are subject to change without notice.*

GRUNE & STRATTON

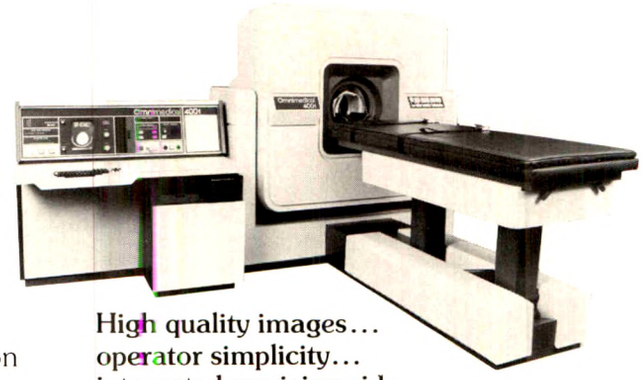
A Subsidiary of Harcourt Brace Jovanovich, Publishers
111 FIFTH AVENUE, NEW YORK, N.Y. 10003
24-28 OVAL ROAD, LONDON NW1 7DX

Lower-cost, Higher-resolution, Neurological CT scanners: $119,500 from Omnimedical.

THE MODEL 4001

WITH THESE FEATURES FOUND ONLY ON MUCH MORE EXPENSIVE SYSTEMS...

- ☐ Tilting gantry, +10° −15°
- ☐ Auto-indexing patient table
- ☐ Auto power-up of X-Ray source
- ☐ Elapse time indicator for contrast injection
- ☐ Cursor for mean CT numbers and standard deviation
- ☐ Laser for patient alignment
- ☐ Dual Floppy discs
- ☐ Patient intercom
- ☐ Digital display of K.V., M.A., and table position in M.M.
- ☐ Compact installation in 216 sq. ft.
- ☐ Optional dual slice
- ☐ Variable height patient table
- ☐ Simultaneous scan and view
- ☐ Minified image directory



High quality images...
operator simplicity...
integrated servicing aids...
THE OMNIMEDICAL 4001 HEAD SCANNER IS THE COST- EFFECTIVE ANSWER TO YOUR CT NEEDS.

Omnimedical 16312 GARFIELD AVE., PARAMOUNT, CA 90723

- ☐ Send me more information
- ☐ Have a sales representative contact me
- ☐ Current need
- ☐ Future need

Name_____

Institution_____

Address_____

City, State, Zip_____

Telephone(_____)_____

Omnimedical
16312 GARFIELD AVE., PARAMOUNT, CALIFORNIA 90723
213-633-6660

clear, clean colon

X-Prep® Liquid

(standardized extract of senna fruit)

versatile bowel evacuant for diagnostic procedures



Versatile in indications

May be used prior to:

G.I. radiography
Urologic radiography
Colonoscopy
Sigmoidoscopy
Other diagnostic bowel procedures

Versatile in administration

May be used:

Alone, in a single dose
Alone, in divided doses, particularly in elderly or debilitated patients
With adjunctive use of citrate of magnesia, laxative suppositories and enemas, as required
As part of other regimens, such as hydration

X-PREP Liquid is formulated specifically for effective bowel evacuation prior to diagnostic procedures. It induces peristalsis through virtually colon-specific action. X-PREP Liquid has been found effective in cleansing the colon for diagnostic evaluation in 95% of 749 patients prepared for barium enemas, intravenous pyelography, or colonoscopy.* Its pleasant taste meets with high patient acceptance, and its ease of administration is appreciated by the patient and nursing staff.

Supplied: X-PREP Liquid (standardized extract of senna fruit) in 2½ fl. oz. bottles (alcohol 7% by volume). X-PREP Powder (standardized senna concentrate) in ¾ oz. containers. **Now Available:** X-PREP™ Bowel Evacuant Kit. Each kit contains: two SENOKOT® S Tablets (standardized senna concentrate and dioctyl sodium sulfosuccinate), one bottle of X-PREP® Liquid 2½ fl. oz., and one RECTOLAX™ Suppository (bisacodyl 10 mg), plus easy-to-follow patient instructions for hydration, clear liquid diet, and the correct time sequence of administering the above laxatives.

Colonoscope, courtesy of Olympus

* Bibliography available upon request.

Gray Pharmaceutical Co., Affiliate
The Purdue Frederick Company

© Copyright 1978, Gray Pharmaceutical Co. Norwalk, CT 06856

A9047 194578

Primary and Metastatic Scirrhous Carcinoma of the Rectum

EMIL J. BALTHAZAR,[1] HOWARD D. ROSENBERG,[1] AND MARIANNA MOURADIAN DAVIDIAN[2]

Eight cases of scirrhous carcinoma of the rectum are described. Five patients had primary lesions and three had metastases from stomach and breast. Radiographic features were severe rectal narrowing, rigidity, and smooth contours or, more commonly, moderate narrowing, distorted nodular folds, and an irregular serrated contour mimicking inflammatory disease. Difficulties in the radiologic and histologic diagnosis and a short review of pertinent literature are reported.

Scirrhous carcinoma and linitis plastica are terms used to describe a type of gastrointestinal malignancy characterized by a diffusely infiltrating and usually mucogenic anaplastic carcinoma. It is commonly seen in the stomach, and involvement of the colon, although well documented [1–7], is distinctly unusual. The colonic lesions in the radiologic literature are either primary malignancies [8–10] or, in the majority, metastasis from other organs, such as stomach or breast [11–14]. The few published illustrations, mostly of sigmoid lesions, give no particular attention to the involvement of the rectum.

This report was triggered by the difficulties we encountered in establishing a correct preoperative diagnosis in cases of scirrhous carcinoma of the rectum. We report eight new proven cases of rectal involvement, describe radiographic patterns and pitfalls in the radiologic and histologic diagnosis, and briefly review the pertinent literature.

Subjects and Methods

Eight consecutive cases of diffusely infiltrating adenocarcinoma of the rectum detected at the Westchester County Medical Center during an 8 year period were studied. There were four men and four women, with average age of 61 years. Medical charts were reviewed and particular attention was given to the clinical presentation, endoscopic findings, pathologic features, and radiographic appearance. Table 1 provides a summary of the clinical and radiographic features. All cases were histologically proven by rectal biopsies, and in two cases specimens were available for pathologic examination.

Five cases were classified as primary tumors, and three as hematogenous metastases. The designation of primary tumor was made mainly by exclusion, on the basis of a negative clinical, radiologic, and/or surgical demonstration of primary tumors elsewhere. In the cases of metastatic involvement, subsequent radiologic and clinical investigation documented the presence of coexisting typical scirrhous carcinoma of the stomach in two cases and carcinoma of the breast in another case. Comparison of biopsy material demonstrated similar histologic features in the primary and metastatic lesions.

Findings

Clinical Features

Diarrhea, described as three to four soft to watery stools a day, was considered the main complaint in four of the patients. Diarrhea was intermittent and associated with periods of constipation in two patients. Constipa-

TABLE 1

Scirrhous Carcinoma of Rectum: Clinical and Radiographic Features

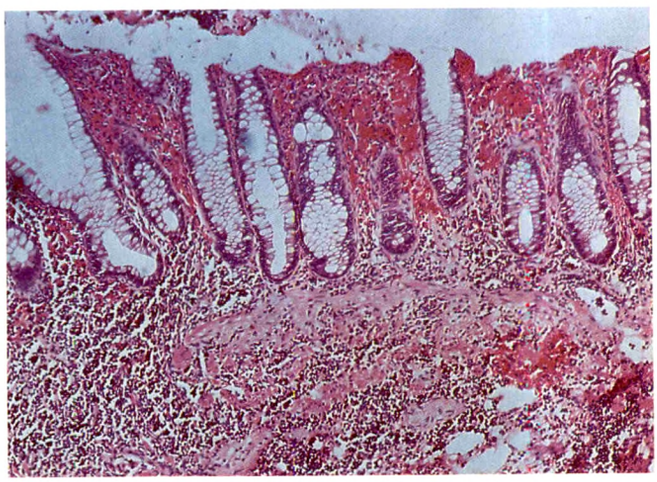
Tumor Origin and Case No.	Age and Sex	Clinical Features	Length of Involvement (cm)	Radiographic Pattern
Primary:				
1	60, M	Narrow stools, weight loss	8	Smooth contour, rigid, severe narrowing
2	84, M	Constipation, diarrhea, rectal bleeding	9	Serrated contour, thickened folds, moderate narrowing
3	48, F	Terminal ileitis, diarrhea, perianal fistulas	5	Irregular contour, nodularity, slight narrowing
4	64, M	Rectal bleeding, diarrhea, constipation	7	Serrated contour, distorted folds, moderate narrowing
5	34, F	Diarrhea, dysuria, narrow stools	12	Mixed pattern
Metastasis:				
6*	65, F	Distension, constipation, tenesmus	9	Smooth, rigid, severe narrowing
7†	72, F	Dysphagia, abdominal mass, weight loss	10	Irregular contour, nodular folds
8†	61, M	Constipation, rectal bleeding	7	Serrated contour, thickened folds

* Breast metastasis.
† Stomach metastasis.

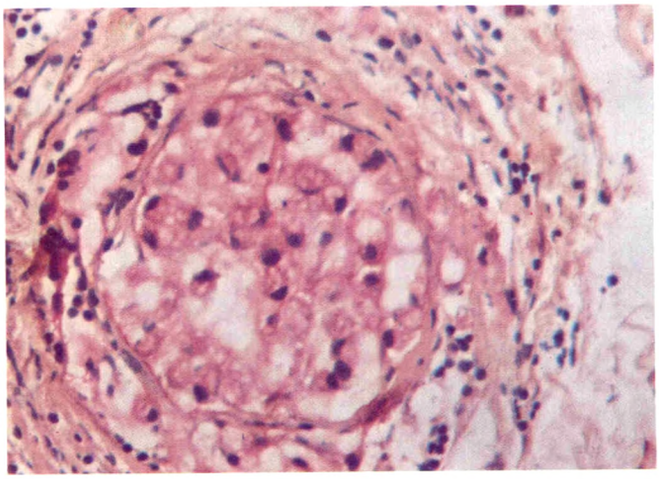
Received July 9, 1978; accepted after revision January 8, 1979.
[1]Department of Radiology, New York Medical College, Westchester County Medical Center, Valhalla, New York 10595. Address reprint requests to E. J. Balthazar.
[2]Department of Pathology, New York Medical College, Westchester County Medical Center, Valhalla, New York 10595.

© 1979 American Roentgen Ray Society

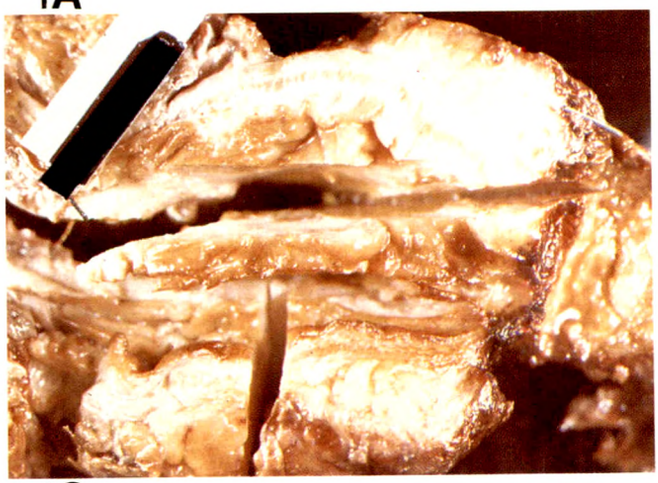
0361-803X/79/1325-0711 $0.00



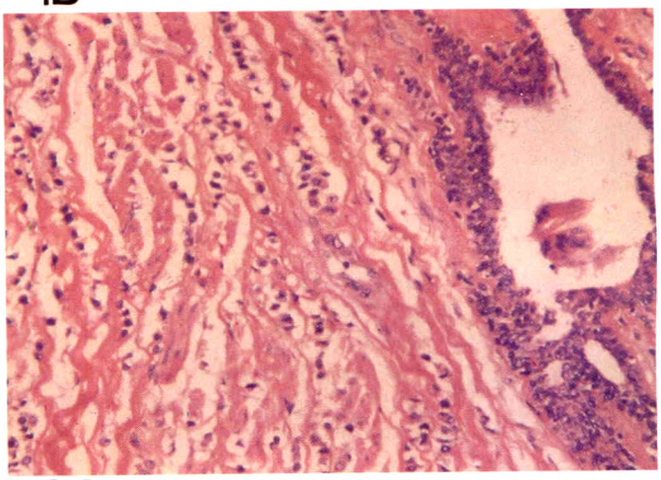
1A



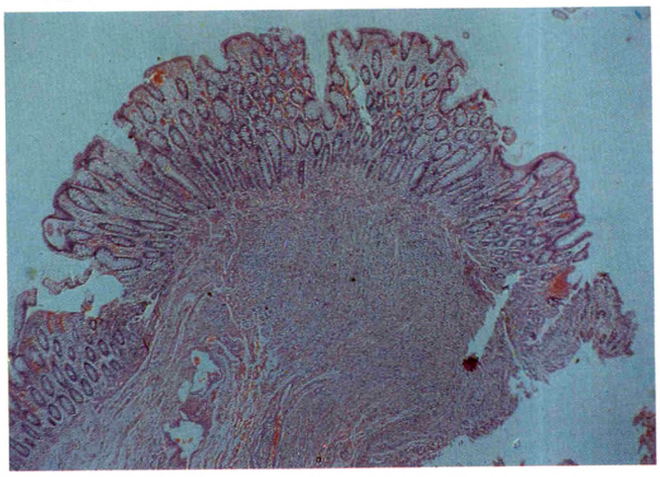
1B



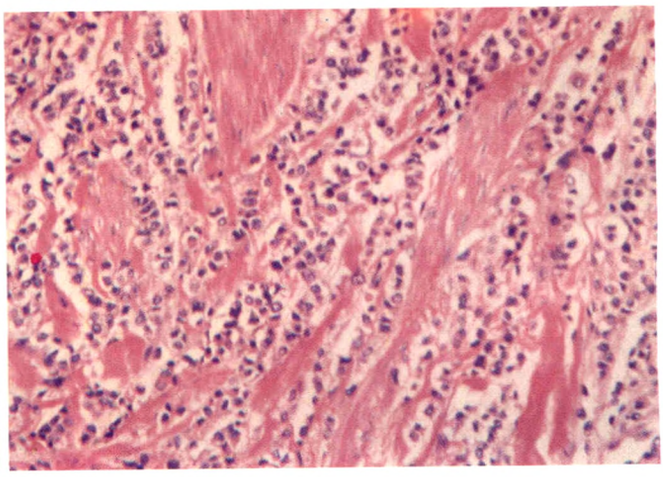
1C



2A



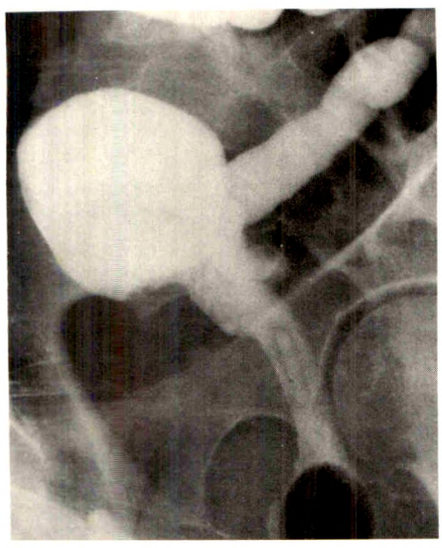
2B



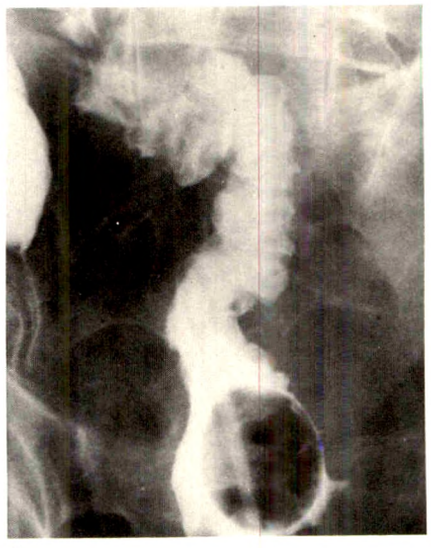
2C

Fig. 1.—Case 5. **A,** First rectal biopsy. Intact colonic mucosa with dense chronic inflammatory cell infiltration. (H and E ×25.) **B,** Deep rectal biopsy. Mucin secreting "signet ring" cells in lymphatic channel within submucosa. (Mucicarmine ×200.) **C,** Surgical specimen of rectosigmoid with intact mucosa. Rectal wall markedly thickened.

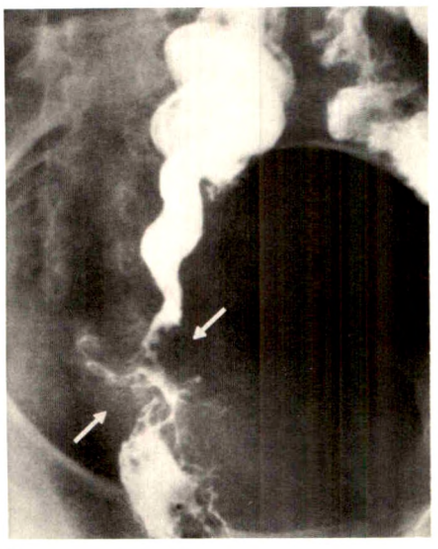
Fig. 2.—Case 6. **A,** Rectal biopsy. Columns and clusters of malignant cells infiltrating submucosa and muscularis of rectum. Mucosa is preserved. (H and E ×25.) **B,** Breast biopsy. Narrow columns of tumor cells infiltrating breast parenchyma. (H and E ×100.) **C,** Rectal biopsy. Columns and clusters of malignant cells similar to breast carcinoma. (H and E ×100.)



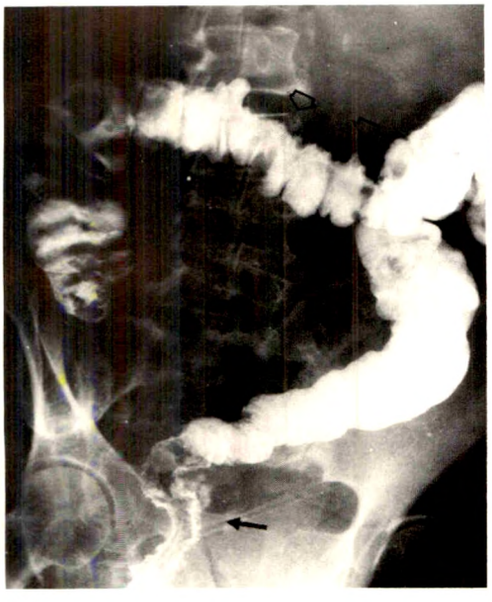
3



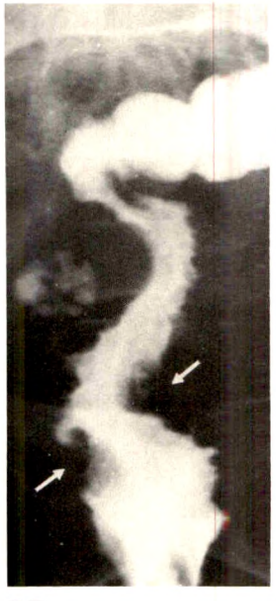
4



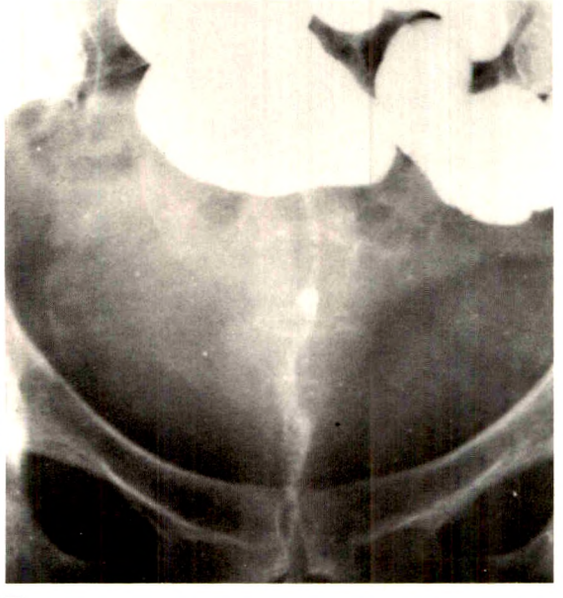
5



6A



6B



7

Fig. 3.—Case 1. Scirrhous carcinoma of rectum with narrowing, rigidity, smooth contours, and effacement of the mucosal folds. No ulcerations or filling defects. Abrupt transition at proximal edge of lesion.

Fig. 4.—Case 2. Moderate narrowing and thickened mucosal pattern with irregular serrated contour. At surgery, diffuse intramural infiltration from anal canal to peritoneal reflexion with massive pelvic lymphadenopathy and involvement of urinary bladder. Lesion considered unresectable.

Fig. 5.—Case 5. Scirrhous carcinoma of rectum. Mixed radiographic pattern. Distortion of mucosal folds (*arrows*) adjacent to segment of smooth narrowing. Ovarian metastases and pelvic lymphadenopathy at surgery.

Fig. 6.—Case 7. **A,** Narrowing of rectum and thickening of the mucosal folds with irregular contour (*closed arrows*). Tumor invasion of superior aspect of transverse colon from proven scirrhous carcinoma of stomach (*open arrow*). **B,** Close-up of rectum distended with barium. Diffuse thickening of mucosal folds and several intramural nodules (*arrows*).

Fig. 7.—Case 6. Metastatic scirrhous carcinoma of rectum from coexisting breast carcinoma. Significant colonic obstruction secondary to severe narrowing and rigidity of rectum.

tion was the major complaint in one patient and change in the caliber of the stool was observed by three other patients. Rectal bleeding, consisting of small amounts of bright red blood, was noticed by three patients only when defecating. Four of the patients were mildly anemic.

No other significant laboratory abnormalities or physical findings were documented. Although rectal digital examinations were generally reported as abnormal, they were entirely nonspecific.

One patient (case 3) had diarrhea associated with perianal fistulas, findings which were attributed to her long history of documented terminal ileitis. Another patient (case 7) experienced significant weight loss and dysphagia without lower intestinal symptomatology. The subsequent investigation documented the asymptomatic

rectal lesion and a scirrhous carcinoma of the stomach infiltrating the gastroesophageal junction.

Endoscopy

Rectosigmoidoscopies were performed in seven of the patients. In the eighth (case 6), the examination was attempted but could not be carried out because of the severity of the rectal narrowing. All patients showed narrowing and limited distensibility without intraluminal masses or localized large ulcerations. The visualized mucosa was described as pale, indurated, or nodular, and superficial mucosal erosions were observed in those patients with a history of rectal bleeding. There was no gross rectal bleeding documented at examination. Endoscopic findings were considered nonspecific, but the possibility of a malignant lesion was entertained in four of the patients in the differential diagnosis.

Pathology

Examination of biopsy material and available surgical specimens demonstrated several characteristic features that correlated well with the unusual clinical, endoscopic, and radiographic features of these patients. The rectal mucosa was maintained and generally intact, showing dense, chronic, and nonspecific inflammatory cell infiltration (fig. 1A). Initial rectal biopsies in three cases were nonspecific proctitis with subsequent deeper biopsies required to establish diagnosis. In one patient (case 5), two separate rectal biopsies were considered benign and proper diagnosis delayed until an open full thickness biopsy was obtained (fig. 1B).

The surgical specimens also demonstrated gross induration and circumferential thickening of the rectal wall. The rectal wall was about 2 cm thick and on gross inspection was covered by a smooth and apparently intact mucosa (fig. 1C). Histologically, the increased thickness was the result of fibrotic reaction, but mainly of a diffuse submucosal and intramuscular infiltration by malignant tumor cells. The type of cellular morphology varied slightly, with two cases considered well differentiated mucin-producing adenocarcinomas and the other six poorly differentiated or undifferentiated. Signet ring cells and mucin lakes were observed throughout the entire thickness of the rectal wall (fig. 1B).

Differentiation from metastatic scirrhous carcinoma was difficult since the metastatic lesions showed similar pathologic features. The mucosal layer was intact with columns and clusters of malignant cells infiltrating the submucosa and muscularis propria (fig. 2A). Comparison of the biopsy material from the primary lesion demonstrated histologic features similar to figures 2B and 2C.

Radiography

The radiographic feature common to all cases was the narrowing of the rectal ampulla, the length of involvement varying from 5 to 12 cm with no overhanging edges, intraluminal defects, or ulcerations. Two lesions demonstrated exquisitely smooth symmetrical contours, effacement of the mucosal folds, and marked rigidity (fig. 3). Five of the cases had a coarse, distorted, and somewhat nodular mucosal pattern with irregular, serrated contours and limited distensibility (fig. 4). The remaining case exhibited a mixed pattern with a segment of smooth narrowing adjacent to an area of marked distortion of the mucosal folds (fig. 5). In one case, large nodular defects were demonstrated with full distention of the constricted rectum.

The degree of rectal narrowing varied. The irregular, serrated contour was associated with only moderate narrowing and some distensibility (figs. 4 and 6), whereas the perfectly smooth contour was associated with marked rigidity and severe narrowing (figs. 3 and 7). All the colons had solitary rectal lesions except one (case 7), which showed a secondary malignant involvement of the superior aspect of the transverse colon (fig. 6).

Upper gastrointestinal examination in this case documented a typical scirrhous carcinoma of the stomach with spread, via gastrocolic ligament, to the colon. The only significant colonic obstruction was documented in the case of scirrhous carcinoma metastasizing from breast, with severe narrowing associated with marked rigidity (fig. 7). Radiographic diagnosis was correct only in the cases of smooth narrowing and marked rigidity and was erroneous in the lesions showing some distensibility, coarse folds, and serrated contours. These were considered inflammatory.

Discussion

Although specific microscopic features have been described, the terms linitis plastica and scirrhous carcinoma of the colon, as used today, designate a gross anatomic and radiologic configuration rather than a characteristic histologic pattern [1, 4]. The rapidly spreading malignant infiltration usually spares the superficial mucosal layers, invading the submucosa and often the muscularis propria and serosa. The colonic segment involved is thus converted into a narrow tube where the symmetry of involvement, tapered margins, lack of luminal defects or ulcerations, and a relatively preserved mucosal surface obscure the neoplasticity. Cellular infiltration and the desmoplastic reaction are responsible for the thickening and rigidity of the wall of the colon. However, these features vary greatly from case to case, explaining the different radiographic configurations.

The first four cases of primary linitis plastica of the colon were reported in 1951 [1]. Since then, only about 20 documented cases have been described [6, 7, 10]; most involved the left side of the colon. In one of the largest surgical series of carcinoma of the colon [2], the incidence of scirrhous lesions was less than one in 1,000, further documenting its rarity.

Secondary linitis plastica of the colon has been reported to be 5–10 times more common than the primary variety [9, 10]. It occurs as a consequence of local spread or, more often, as hematogenous metastasis from primary lesions, particularly in the stomach [8, 10], breast

[12, 14], gallbladder [10], and prostate [13, 15]. For this reason, discovery of a scirrhous carcinoma of the colon should trigger a prompt and thorough search for a primary lesion elsewhere.

About 20%–30% of cases of scirrhous carcinoma of the colon are found associated with ulcerative colitis [2, 9]. Although this association is well documented, only a minority of the malignant lesions discovered in these patients are scirrhous or are located in the rectum [16].

The prognosis has been generally very poor with mean survival after diagnosis established at only 4 months [10]. Perineural, vascular, and lymphatic permeation, as well as massive lymph node involvement and ovarian metastasis, are common findings. These invasive characteristics contrast to the benign looking radiographic appearance and often result in an unresectable lesion (fig. 2).

The literature contains only a few radiographic illustrations of scirrhous carcinoma of the rectum, which partially accounts for the diagnostic difficulties in the past and in our series. The more common specific and nonspecific inflammatory rectal lesions with similar radiographic features add to the radiographic error. In addition, endoscopic examination and rectal biopsies are often misleading, contributing to misinterpretations and delays in the diagnosis.

Therefore, several features should be emphasized regarding scirrhous carcinoma of the rectum: (1) the diagnosis should be considered not only in the cases with marked narrowing, rigidity, and smooth contours, but also in those exhibiting thickened, coarse, nodular folds, irregular serrated contours, moderate narrowing, and residual distensibility; (2) a benign histologic diagnosis should be regarded as only tentative, particularly if only superficial tissue is available for interpretation; and (3) there are no significant radiographic or histologic differences between primary and secondary scirrhous carcinoma of the rectum. Since rectal metastasis may occur as a solitary colonic lesion, primary tumor elsewhere must also be considered.

The differential diagnosis among scirrhous carcinoma of the rectum and a variety of specific and nonspecific inflammatory lesions may be very difficult. Marked narrowing with rigidity and effacement of the mucosal folds or nodularity suggests malignancy. Significant distensibility, spasticity, and sinus or fistulous tracts suggest inflammatory disease. With a high degree of suspicion and deep rectal biopsies, the correct diagnosis can be made expeditiously.

REFERENCES

1. Laufman H, Saphir O: Primary linitis plastica type of carcinoma of the colon. *Arch Surg* 62:79–91, 1951
2. Fahl JC, Dockerty MB, Judd ES: Scirrhous carcinoma of the colon and rectum. *Surg Gynecol Obstet* 111:759–756, 1960
3. Weintraub LB, Littman L: Primary linitis plastica of the rectum. Report of a case. *Dis Colon Rectum* 5:105–109, 1962
4. Sizer JS, Frederick PL, Osborne MP: Primary linitis plastica of the colon. Report of a case and review of the literature. *Dis Colon Rectum* 10:339–343, 1967
5. Dailey TH, Garret R: Primary linitis plastica of the rectum. Report of two cases. *Dis Colon Rectum* 14:218–221, 1971
6. Anderson JA, Hansen BF: Linitis plastica of colon and rectum. Report of two cases. *Dis Colon Rectum* 15:217–221, 1972
7. Tootla FS, Stein H, Bernacki E, Kiechle FL: Primary linitis plastica of the colon and rectum. *Am J Proctol* 28:29–34, 1977
8. Wolf BS, Marshak RH: Linitis plastica or diffusely infiltrating type of carcinoma of the colon. *Radiology* 81:502–507, 1963
9. McQueeney AJ, Olson RW, Medwid A: Primary scirrhous carcinoma of colon. Roentgenologic diagnosis. *AJR* 101:306–310, 1967
10. Raskin MM, Viamonte M, Viamonte M Jr: Primary linitis plastica carcinoma of the colon. *Radiology* 113:17–22, 1974
11. Wigh R, Tapley NduV: Metastatic lesions to the large intestine. *Radiology* 70:2 22–228, 1958
12. Melnick GS, Rosenholtz MJ: Metastatic breast carcinoma simulating ulcerative colitis. Report of a case. *AJR* 86:702–706, 1961
13. Khilnani MT, Marshak RH, Eliasoph J, Wolf ES: Roentgen features of metastases to the colon. *AJR* 96:302–310, 1966
14. Meyers MA, Oliphant M, Texidor H, Weiser P: Metastatic carcinoma simulating inflammatory colitis. *AJR* 123:74–83, 1975
15. Smith CJD: Difficulties with the diagnosis of linitis plastica carcinoma of the rectum and anal canal. *Med J Aust [Suppl]* 1:23–26, 1976
16. Fennessy JJ, Sparberg MB, Kirsner JB: Radiologic findings in carcinoma of the colon complicating chronic ulcerative colitis. *Gut* 9:388–397, 1968

AJR Guidelines for Authors

Address manuscripts and correspondence to the Editorial Office, American Journal of Roentgenology, 403 Pacific National Bank Building, 4545 15th Avenue N.E., Seattle, Washington 98105; telephone (206)633-2754.

Publication Policy

The Journal publishes original and timely contributions to the advancement of radiologic diagnosis and treatment. Although the content is predominantly clinical, laboratory investigations are accepted when their relevance to clinical practice is demonstrable. In prospective clinical investigations, authors should indicate if informed consent from patients was obtained. Decisions on manuscripts are based on the opinions of at least two outside reviewers. Reviewers receive manuscripts without title pages to protect the identity of authors and to ensure an unbiased review; names of reviewers, in turn, are not revealed to authors. Statements within an article are the responsibility of the authors and not the Journal or its publisher.

It is understood that material submitted has not been published and is not currently submitted elsewhere. Portions of the data or illustrations from previously published works may be included if permission release forms accompany the manuscript and such material is clearly credited in the text. Prior publication of abstracts will not prejudice publication of the complete study.

Copyright Information

In accordance with Journal implementation of the 1976 U.S. Copyright Law, authors must release first and subsidiary rights to their manuscript at submission. A dated cover letter, containing signatures of all authors, should state: "We, the authors, assign first and subsidiary rights to the American Roentgen Ray Society in the event that our manuscript (title) is published by AJR." The Journal, in turn, grants authors the right to use portions of their manuscript, without charge, in books or articles of which they are authors or editors.

Manuscript Form

Manuscripts should be typed double-spaced throughout, including references, tables, and figure legends. Tables, footnotes, and figure legends should be on separate sheets, and a separate title page should be provided. In addition to the original typewritten copy, a duplicate copy complete with figures, tables, and references is required. Authors' names should be on title page only and should not be on figures so that author anonymity can be maintained during the review process.

Figures should be submitted as 13 × 18 cm glossy prints, untrimmed and unmounted. Labels and arrows must be of professional quality and should be removable from the prints. Each figure should be numbered to correspond with figure legends, and the top should be indicated. Specific permission for publication of facial photographs of patients is required. Line illustrations and graphs should be drawn in black ink on white background.

References should be cited in the text by number (e.g., [3, 4]). The bibliography should be arranged in the numerical order that references are cited in the text and typed double-spaced throughout. Data for each reference should be arranged according to the uniform style on bibliographic citations adopted by many biomedical journals. Provide all authors' names and inclusive pages. Abbreviations for titles of medical periodicals should conform to those published in *Index Medicus*. Examples:

1. Miller RE, Chernish SM, Skucas J, Rosenak BD, Rodda BE: Hypotonic roentgenography with glucagon. *AJR* 121:264–274, 1974
2. Boijsen E: Superior mesenteric angiography, in *Angiography*, edited by Abrams H, Boston, Little, Brown, 1971, pp 1091–1119

Organization

Title page. Titles should be brief and specific. Include addresses for each author and acknowledgment of grant support when appropriate.

Abstract. A description of the purpose, methods, results and conclusions of the study is required.

Introduction. Clearly state the purpose of the investigation including necessary background facts.

Materials and methods. Decribe the protocol clearly. Use standard abbreviations as presented in the *Council of Biology Editors Style Manual*, 3d ed. Metric measurements should be used throughout.

Results. Present results in logical sequence.

Discussion. Interpret the results to lend meaning and importance to the observations. Hypotheses and speculation based on the results are encouraged. When results differ from those of previous investigators, an attempt should be made to explain the discrepancy.

References. Only include references which provide adequate background and present fairly any opposing evidence and concepts. Accuracy of reference data is the responsibility of the author.

Legends. Legends should be brief but should provide sufficient description to interpret the figure.

Special Communications

Case Reports. Concise case reports are accepted if they present unusual experiences that are medically important and educational. Clarity and brevity are essential. After preliminary screening by an editor to determine whether the requirement of medical significance has been met, qualifying papers will undergo the same peer review as major papers.

Technical notes. Brief descriptions of new techniques or significant modifications of older ones which are directly applicable to clinical practice will be accepted.

Letters to the Editor. Letters are subject to editing and condensation. Criticism of published articles should be objective and constructive. Letters may also discuss matters of general interest to radiologists.

Radiology of the Continent Ileostomy

DAVID H. STEPHENS,[1] BARRY E. MANTELL,[1] AND KEITH A. KELLY[2]

Construction of a continent ileostomy for selected patients who require total proctocolectomy is gaining wider use. The operation, introduced a decade ago, creates an internal ileal reservoir and, when successful, provides the patient with an ileostomy that remains completely continent between voluntary evacuations. Malfunction of the continent ileostomy usually results from a radiologically demonstrable architectural derangement of the ileal reservoir. This report, based on the findings of contrast examinations of ileal reservoirs in 86 patients, describes the method of examination and the radiologic anatomy of the continent ileostomy and its common late complications.

As construction of a continent ileostomy for patients who require total proctocolectomy becomes more widespread, radiologists will need to become familiar with the procedure and its complications. Developed by Kock [1, 2] in the late 1960s and early 1970s, the operation provides the patient with an internal reservoir, or pouch, that collects and stores ileal continent. The successfully functioning ileal reservoir remains completely continent of feces and gas between voluntary evacuations, which the patient accomplishes by inserting a catheter through the stoma. With the continent ileostomy, there is no need for the patient to wear a collecting applicance, and such problems as peristomal skin irritation and odor are avoided.

Although recent results with the continent ileostomy have been encouraging, a minority of patients has experienced complications [3–5]. Many of the complications, such as intestinal obstruction from adhesions and development of abdominal infections, are no different from those that may accompany other major abdominal operations. In our experience, malfunctions of the ileostomy that develop after the immediate postoperative period, incontinence, difficulty with intubation, or excessive output, are much more frequent. In investigating these delayed complications, we usually examined the ileal reservoir radiologically, since the common causes of malfunction are radiographically demonstrable and are usually surgically or medically correctable.

Despite the contributions of radiologic examination in assessing the continent ileostomy and its complications, it has received little attention in radiologic literature. To the recent report on the subject by Montagne et al. [6], we add further observations and emphasize the radiologic appearance of the architectural derangements of the ileostomy that are commonly responsible for its malfunction.

Subjects and Methods

During the first 7 years of the performance of continent ileostomies at the Mayo Clinic, 280 patients underwent the operation. Over 80% of the patients had ulcerative colitis, and the rest had some form of colonic polyposis or Crohn's colitis (the operation was abandoned in cases of Crohn's disease because of the high incidence of recurrent enteritis). Subsequent radiologic contrast examinations of the ileal reservoirs in 86 patients were usually performed to determine the cause of incontinence or difficulty with intubation. Of the patients who were examined, 63 underwent reoperation, which provided operative correlation with the radiologic findings.

Method of Examination

Although the ileal reservoirs can be examined with orally administered contrast material, a fluoroscopically controlled contrast ileal enema usually provides a better and more efficient examination. To reduce the inflow of ileal content, it is desirable for the patient to fast for several hours before examination. The contrast material can be administered through the patient's own drainage tube or other suitable nonballoon catheter. It is convenient to have the patient leave his catheter in place after draining the pouch immediately before the examination. The pouch is further evacuated by aspiration before contrast material is instilled. In cases of difficult intubation, it is sometimes helpful to manipulate the catheter gently under fluoroscopic control after opacifying the channel with a small amount of contrast material.

Either single or double contrast technique may be used. Double contrast examinations have the advantage of displaying internal architecture of the reservoir without the need for compression. For double contrast studies, a barium preparation designed for double contrast colon examination is used. After the pouch is filled with barium, the patient is rotated to ensure coating of the entire internal wall of the pouch. Air is instilled after

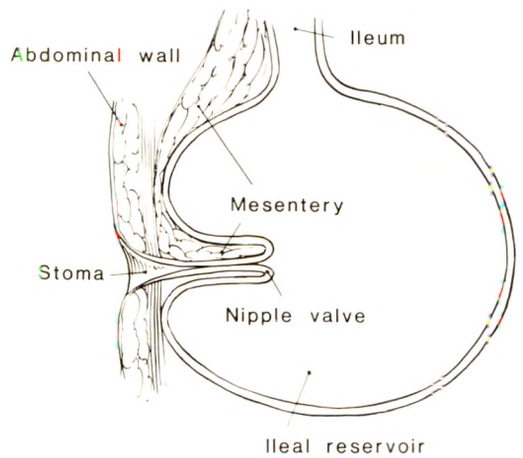


Fig. 1.—Continent ileostomy.

Received October 30, 1978; accepted after revision January 25, 1979.
[1] Department of Diagnostic Radiology, Mayo Clinic and Mayo Foundation, Rochester, Minnesota 55901. Address reprint requests to D. H. Stephens.
[2] Department of Surgery, Mayo Clinic and Mayo Foundation, Rochester, Minnesota 55901.

© 1979 American Roentgen Ray Society

0361-803X/79/0132-0717 $0.00

excess barium has been aspirated from the pouch. Spot radiographs, including profile projections of the nipple valve at the reservoir outlet (described below), are obtained. At least some of the films are made with the catheter in the pouch to demonstrate the position and orientation of the outflow conduit and its internal orifice. The barium and air are instilled gently under fluoroscopic observation.

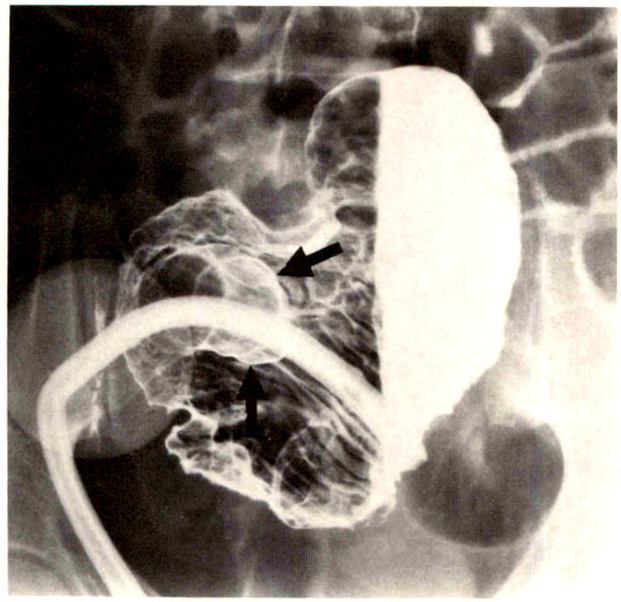


Fig. 2.—Double contrast radiograph in left lateral decubitus position of normal continent ileostomy. Nipple valve (*arrows*) protrudes into lumen of pouch.

Normal Continent Ileostomy

There are descriptions and illustrations of the surgical procedure for creation of the continent ileostomy in several recent publications [3, 4, 6, 7]. As currently constructed, the continent ileostomy has three components: (1) the ileal reservoir, (2) a valve to prevent leakage of ileal content, and (3) an efferent limb leading from the valve to the stoma (fig. 1). All three components are constructed from the terminal 40–45 cm of ileum. The reservoir is fashioned from the proximal 30 cm of this segment, which is looped upon itself, opened longitudinally, and folded over. The terminal 10–15 cm of ileum serves as a conduit to the skin. The valve is devised by reverse intussusception of the oral end of the outflow conduit to create a nipple that protrudes usually 4–6 cm into the pouch. The pouch capacity increases from 100 ml or less immediately after construction to 500–1,000 ml by the third to sixth postoperative month. A patient who has a satisfactorily functioning continent ileostomy

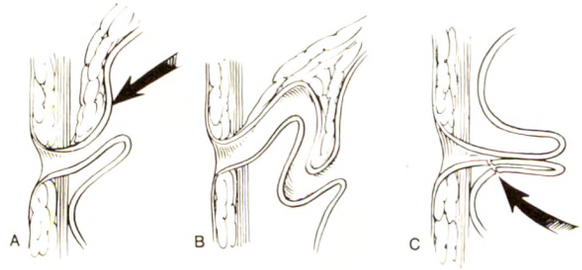
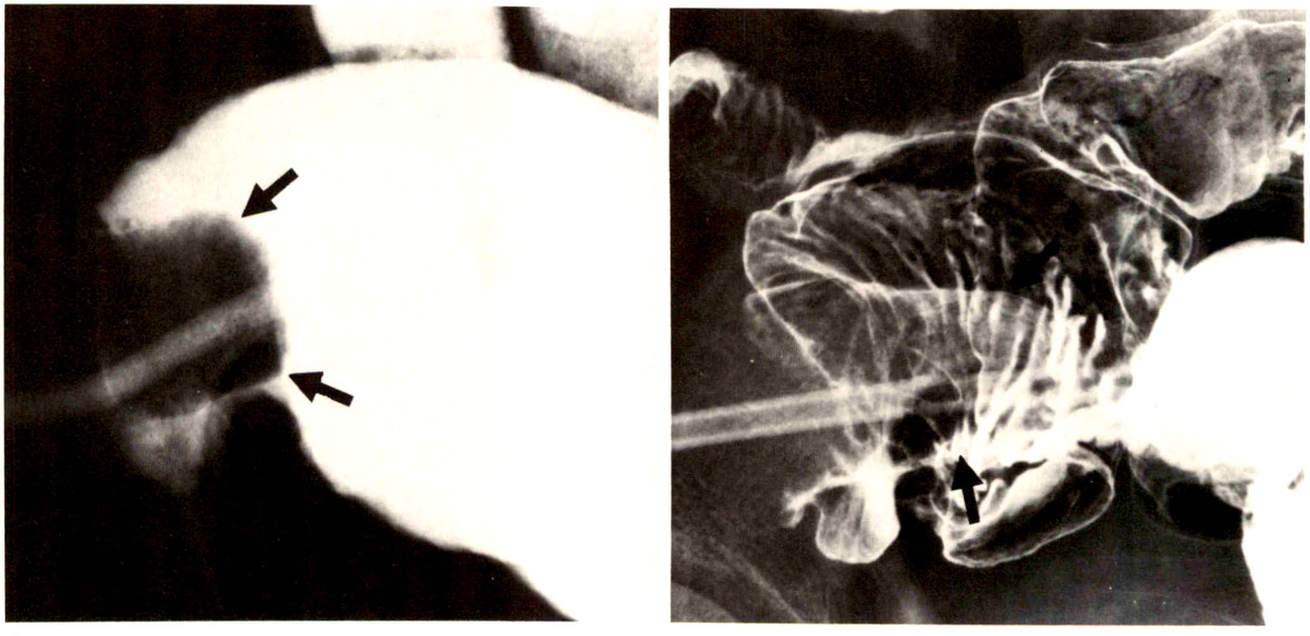


Fig. 4.—Complications involving nipple valve. **A**, partial reduction of nipple valve. Mesenteric wall (*arrow*) is reduced. **B**, Complete reduction of nipple valve. **C**, Internal fistula (*arrow*) through base of nipple.



A **B**

Fig. 3.—Normal configuration of nipple valve. **A**, Single contrast; **B**, double contrast. Nipple valve (*arrows*), about 6 cm long, symmetric except for slightly thicker mesenteric (upper) wall. Although ileostomy had been mildly incontinent, reoperation was avoided because of normal appearance of valve, and complete continence was subsequently acquired spontaneously.

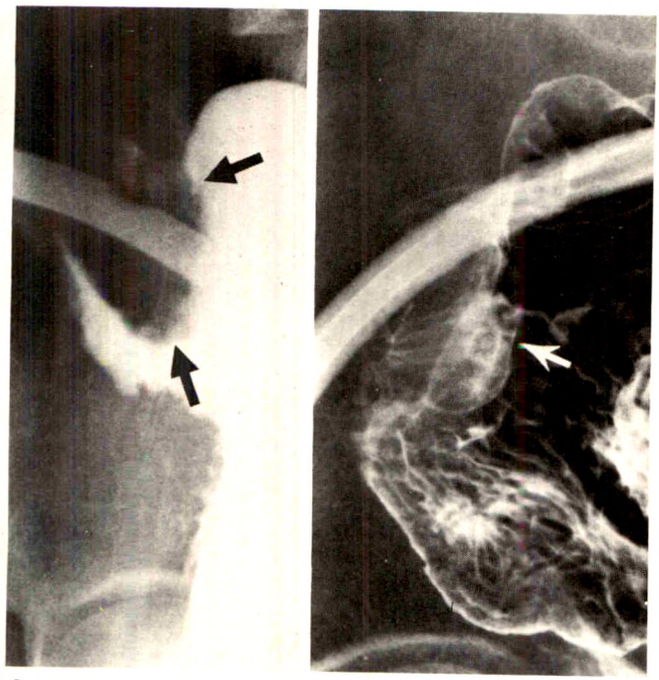


Fig. 5.—Asymmetric partial reduction of nipple valve. Different degrees of reduction of mesenteric wall (see fig. 4A). Upper side of valve diminished (more in **B** than **A**), and nipple (*arrows*) has lost symmetry. Presence of catheter helps locate position of channel and internal orifice of nipple.



Fig. 6.—Symmetric reduction of nipple valve. Valve abnormally shallow (about 2 cm) and blunted.

eventually needs to empty the reservoir only two to four times daily.

Radiographically, the distended ileal pouch is more or less spherical to oval and has an intact ileal mucosal pattern (fig. 2). The nipple valve, when projected in profile, protrudes into the pouch perpendicular to the adjacent wall of the reservoir at base of the nipple (fig. 3). The mesenteric (superior) wall of the nipple is usually slightly thicker than the opposite wall, but the nipple is otherwise symmetrical. Reflux of contrast material into the afferent (inflow) limb of ileum may or may not occur.

Malfunctioning Continent Ileostomy

Reduction of the nipple valve

In our experience, the most common problems that occur in patients with ileal pouches after the immediate postoperative period are caused by reduction of the nipple valve. This complication results in loss of continence and difficulty with intubation. The degree of reduction varies from partial sliding (fig. 4A) to complete extrusion of the nipple (fig. 4B). Reduction of the valve has been attributed to two mechanisms: (1) peristaltic activity within the nipple (the valve is created by *reverse* intussusception) [5] and (2) inability to anchor the valve firmly in the area where mesenteric fat and vessels are wedged between the intestinal walls of the nipple [3]. Surgical measures designed to prevent this complication include abrasion and cauterization of the serosal covering of the segment to be used as nipple valve [4, 5] and stripping of associated mesenteric peritoneum and fat [3].

Reduction of the nipple valve is readily demonstrated radiographically. Asymmetric partial reduction, which almost invariably involves the mesenteric aspect of the valve, causes shortening or disappearance of the mesenteric wall of the nipple (fig. 5). Symmetric partial reduction, in which the nipple is generally shortened but maintains its symmetry, occurs less commonly (fig. 6). In cases of total extrusion, the nipple completely disappears and the ileal conduit becomes elongated and tortuous (fig. 7).

Fistula

A less frequent cause of incontinence than reduction of the nipple valve is development of a fistula between the lumen of the pouch and the lumen of the conduit at the base of the valve (figs. 4C and 8). In this situation, incontinence occurs because the valve is bypassed. When a fistula is suspected, use of a water-soluble contrast agent may be preferable to a barium preparation.

Inflammation

Another radiologically demonstrable complication that affects the continent ileostomy is nonspecific ileitis. This condition, which develops in some patients whose ulcerative colitis prompted colectomy, causes abdominal discomfort and diarrhea. The inflammatory changes may be

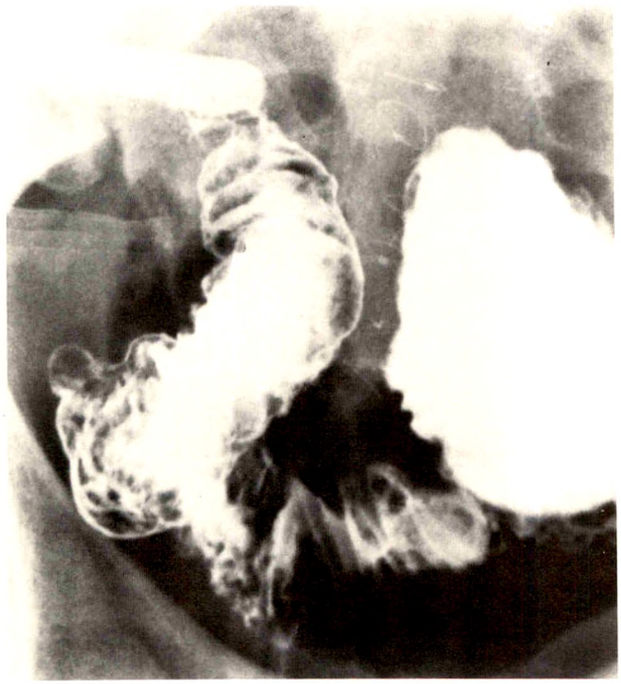


Fig. 7.–Complete reduction of nipple valve (see fig. 4B). Nipple completely extruded and conduit markedly elongated. Tortuosity of conduit prevents catheterization of pouch.

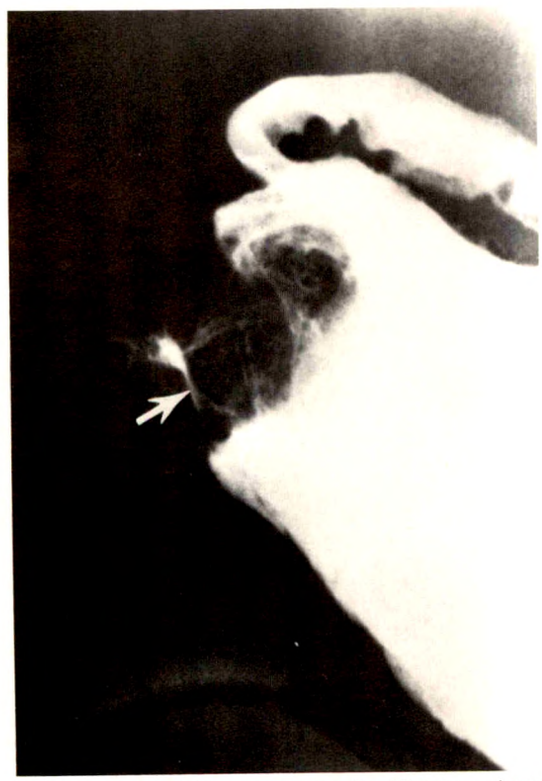


Fig. 8.—Internal fistula (*arrow*) (see fig. 4C) between lumen of pouch and outlet channel at base of nipple valve.

confined to the reservoir or may also involve the adjacent ileum for a variable distance proximal to the pouch. Usually the inflammation subsides with appropriate antibiotic therapy [3]. Radiologic examination in cases of



Fig. 9.—Nonspecific ileitis. Inflammatory changes, including superficial mucosal ulceration, involve entire pouch and adjacent segment of ileum. Inflammation appeared 2 years after colectomy of ulcerative colitis.

nonspecific ileitis shows thickened mucosal folds [6] and, in severe cases, ulceration (fig. 9).

The continent ileostomy is no longer recommended for patients with Crohn's colitis because of the likelihood of recurrent Crohn's disease in the small intestine [3, 4]. However, some patients with Crohn's disease did receive ileal reservoirs during the early years of the procedure, and the radiologist should be aware of the nature of the preexisting colonic disorder when evaluating the significance of inflammatory changes in the pouch or small intestine.

Discussion

A properly conducted radiologic examination is an accurate and easily accomplished means to depict the anatomy of the ileal reservoir and to determine the nature of its late complications. The indications for radiologic examination depend on the type of information desired. It seems reasonable that in most cases, a visual evaluation (either radiologic or endoscopic) of the pouch and valve should be made before subjecting the patient to surgical revision. As a result of the radiographic demonstration of a normally constructed pouch and nipple valve, reoperation has been avoided in some of our patients who eventually developed satisfactorily functioning continent ileostomies without further intervention (fig. 3).

Because creation of the continent ileostomy is a recent innovation, methods of construction are still being modified. For example, in some of the initial operations, a nipple valve was not created, and some of the earlier valves that were constructed were made shorter than the 4–6 cm nipples currently devised. Correct interpretation

of the radiologic appearance of an ileal pouch requires that the radiologist be familiar with the type of surgical construction used.

REFERENCES

1. Kock NG: Intra-abdominal "reservoir" in patients with permanent ileostomy. Preliminary observations on a procedure resulting in fecal "continence" in five ileostomy patients. *Arch Surg* 99:223–230, 1969
2. Kock NG: Ileostomy without external appliances: a survey of twenty-five patients provided with intra-abdominal intestinal reservoir. *Ann Surg* 173:545–550, 1971
3. Kock NG, Darle N, Hulten L, Kerventer J, Myrvold H, Philipson B: *Ileostomy*, vol 14 in *Current Problems in Surgery*, edited by Ravitch MM, Chicago, Year Book Medical, 1977
4. Gelernt IM, Bauer JJ, Kreel I: The continent ileostomy. *Practical Gastroenterol* 1:47–52, 1977
5. Beahrs OH: Present status of the continent ileostomy: ileal reservoir with ileostomy rather than ileostomy alone. *Dis Colon Rectum* 19:192–194, 1976
6. Montagne JP, Kressel HY, Moss AA, Schrock TR: Radiologic evaluation of the continent (Kock) ileostomy. *Radiology* 127:325–329, 1978
7. Beahrs OH, Kelly KA, Adson MA, Chong GC: Ileostomy with ileal reservoir rather than ileostomy alone. *Ann Surg* 179: 634–637, 1974

Neonatal Gastric Volvulus

JOHN B. CAMPBELL[1]

Three infants with acute gastric volvulus occurring during the first week of life are presented, bringing the total number of cases reported in the neonatal period to nine. Abdominal radiographs and contrast studies of the upper gastrointestinal tract were nearly identical in all three infants and showed a characteristic pattern that allowed unequivocal preoperative diagnosis. It is essential that the radiologist recognize the radiographic features of acute gastric volvulus, since prompt operative intervention is mandatory to prevent late complications, which include gastric perforation and death.

Acute volvulus of the stomach is an unusual but important cause of high intestinal obstruction. The vast majority of reported cases have been encountered in adults. In the pediatric age group, 51 cases have been described; however, it is rare to recognize this entity in the newborn period. This report describes the clinical and radiographic features of acute gastric volvulus observed in three neonates treated at Children's Hospital in Denver during a 3½ year period.

Case Reports

Case 1

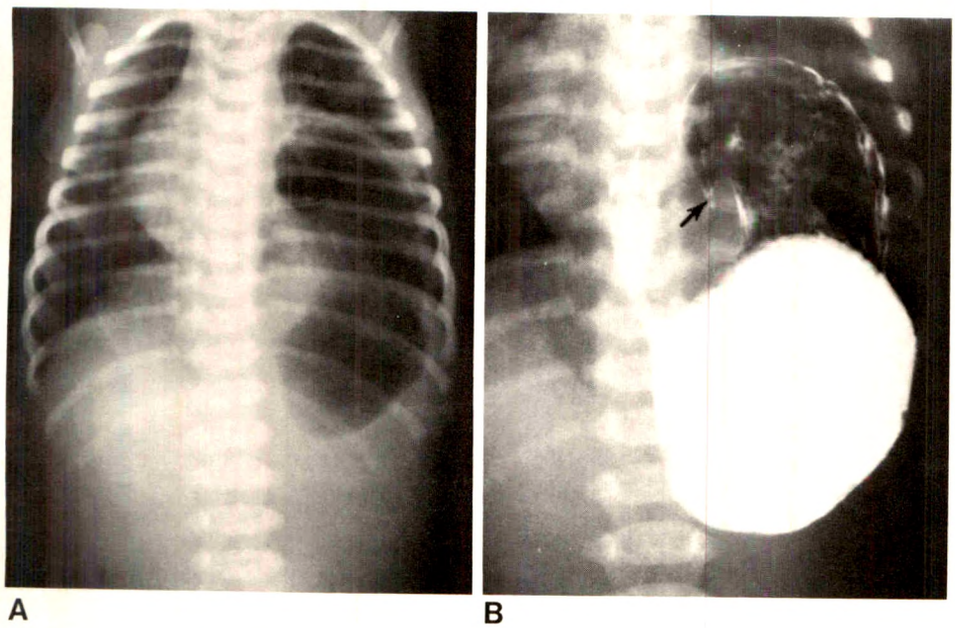
A 4-day-old infant was admitted with a history of poor feeding and intermittent mild vomiting. On physical examination, the abdomen was scaphoid and bowel sounds were absent. Supine radiography of the abdomen (fig. 1A) revealed a moderately large eventration of the left hemidiaphragm, immediately beneath which the stomach was distended with air. The rest of the abdomen was gasless except for a small amount of air in the rectosigmoid. Upper gastrointestinal series demonstrated volvulus of the stomach with complete obstruction of the distal antrum (fig. 1B).

At surgery, reduction of the gastric volvulus was accomplished without difficulty. Initially, the stomach appeared slightly discolored and grayish, suggesting that some degree of vascular compromise had occurred. This promptly cleared as the stomach was brought down and rotated into its normal anatomic position. No deficiencies in the gastric ligaments were noted. The eventration of the left hemidiaphragm was plicated and a feeding gastrostomy was performed. The postoperative course was uneventful.

Case 2

A 5-day-old boy was admitted with 3 days of inability to feed, persistent vomiting, and progressive mild abdominal distention. An upper gastrointestinal series performed elsewhere with a small amount of barium was reported as showing intestinal obstruction. On admission, physical examination confirmed upper abdominal distention. Bowel sounds were markedly decreased. A supine radiograph of the chest and abdomen showed eventration of the left hemidiaphragm and a distended stomach with no other gas in the alimentary tract (fig. 2A). Gastric volvulus accompanied by complete outlet obstruction was found on upper gastrointestinal series (fig. 2B).

Shortly after admission, volvulus of the stomach was reduced without difficulty. No impairment of gastric circulation was identified, and gastric ligaments appeared intact. The diaphragmatic eventration was treated with surgical plication. An ante-



A B

Fig. 1.—Case 1. **A**, Eventration of left hemidiaphragm with shift of mediastinum to right. Distended stomach beneath eventration with no air distally except in rectosigmoid. **B**, Cardioesophageal junction in normal position. Stomach has undergone volvulus and obstructed distal antrum forms "beak" (*arrow*) superiorly. (Reprinted from [7])

Received September 5, 1978; accepted after revision February 7, 1979.
[1]Department of Radiology, Children's Hospital, 1056 East 19th Avenue, Denver, Colorado 80218.

© 1979 American Roentgen Ray Society

0361-803X/79/1325-0723 $0.00

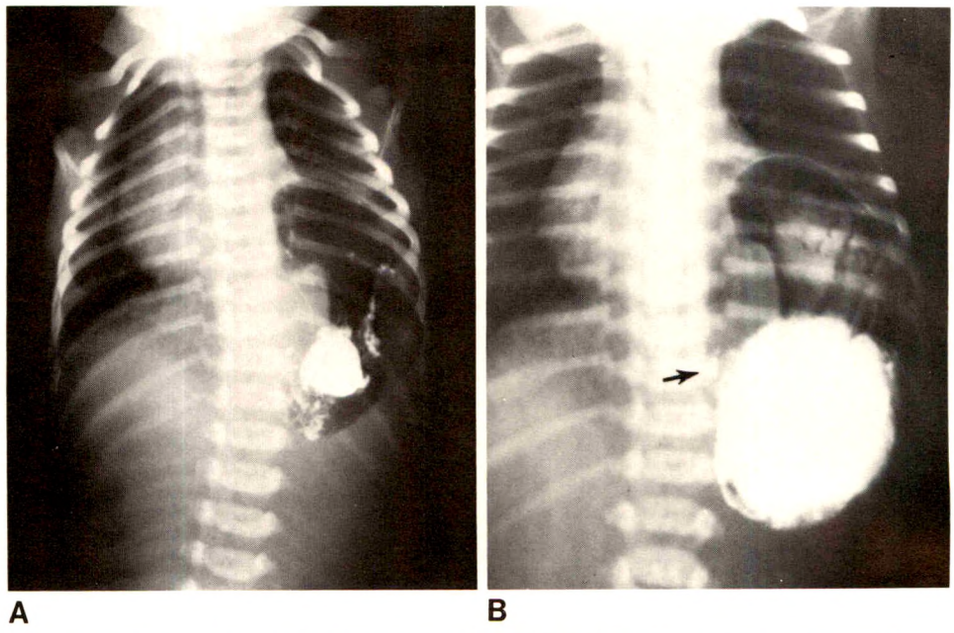


Fig. 2.—Case 2. **A**, Eventration of left hemidiaphragm. Barium in mildly distended stomach from barium swallow performed elsewhere. No gas in alimentary tract distal to stomach. **B**, Volvulus of stomach with obstructed distal antrum forming "beak" beneath hemidiaphragm. Cardioesophageal junction in normal position (*arrow*).

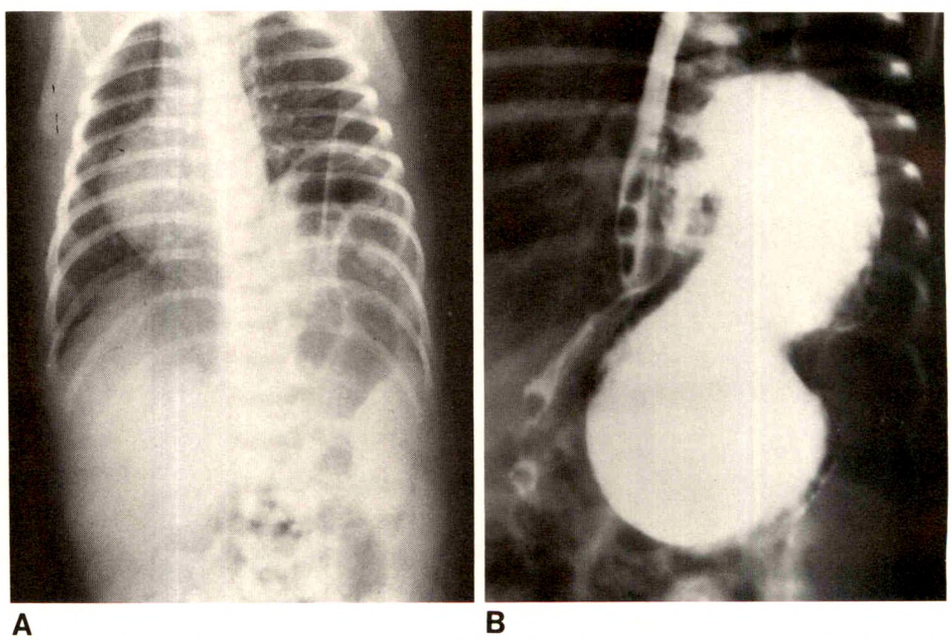


Fig. 3.—Case 3. Gas-filled loops of bowel beneath eventration of left hemidiaphragm. Mediastinal displacement toward right. **B**, Stomach has undergone volvulus. Antropyloric region twisted and narrow, but barium has passed into duodenum.

rior gastrostomy was performed. The patient did well after surgery.

Case 3

A 5-day-old girl was admitted because of continuous projectile, nonbilious vomiting from the first feedings at age 12 hr. At physical examination of the chest, heart sounds were best heard to the right of the midline. The abdomen was soft, nontender, and bowel sounds were normal. A radiographic study of the chest and abdomen (fig. 3A) demonstrated elevation of the left hemidiaphragm and mediastinal displacement to the right. Gas-containing bowel loops and stomach were observed just beneath the elevated hemidiaphragm. Upper gastrointestinal series showed that the cardioesophageal junction was in normal position and the stomach had undergone volvulus. The antropyloric area was narrowed and twisted but not completely obstructed (fig. 3B).

Shortly after admission, eventration of the diaphragm was repaired, the gastric volvulus was reduced, and a gastrostomy was performed. No ischemia of the stomach had occurred. Gastric fixation was anatomically normal. The patient did well postoperatively and has had no recurrence of symptoms.

Discussion

All three of these infants were found at surgery to have acute mesenteroaxial volvulus of the stomach. In this form of volvulus, the stomach rotates upon itself on an axis perpendicular to the long axis of the stomach. Obstruction usually develops in the antropyloric region, and occasionally obstruction of the cardioesophageal junction may occur. Over 275 cases of gastric volvulus have been reported in the medical literature. Including the three infants presented here, only nine cases of

acute gastric volvulus have been reported in the neonatal period [1–7]. Case 1 was previously included in a report from this institution on gastric volvulus in infancy and childhood [7]. The average age at diagnosis in this group of neonates was 7 days. Two-thirds of the cases were of the mesenteroaxial type of volvulus. Eight of the nine (88%) had some abnormality of the diaphragm, either diaphragmatic hernia or eventration.

The normal stomach is not likely to undergo volvulus because it is suspended relatively securely by the so-called gastric ligaments. These include the gastrohepatic ligament along the lesser curvature, the gastrocolic and gastrosplenic ligaments along the greater curvature, and the gastrophrenic ligament along the posterior aspect of the fundus. In addition, the esophagus holds the stomach in place superiorly and the fixed duodenum tends to hold the stomach inferiorly. If the gastric ligaments are absent or unusually lax, abnormal mobility of the stomach may result. The high incidence of congenital diaphragmatic abnormalities observed in the neonatal cases suggests that by allowing visceral rearrangement, diaphragmatic hernia and eventration create an anatomic situation that encourages gastric volvulus. An additional contributing factor may be that in some cases the cephalad displacement of the fetal stomach that occurs with diaphragmatic anomalies results in abnormal development of the gastric ligaments.

The clinical features of acute gastric volvulus are nonspecific but suggest a high obstruction of the gastrointestinal tract. The infants are first seen with acute onset of vomiting that usually occurs shortly after feedings and becomes progressively more severe. Distention of the upper abdomen is often observed, although in some instances the abdomen appears scaphoid. Bowel sounds may be decreased or absent. If the cardioesophageal junction becomes obstructed, abdominal distention and retching occur but the patient is unable to expel the vomitus. If nasogastric intubation is then attempted, obstruction to the tubal passage is encountered in the distal esophagus. These latter signs are diagnostic of gastric volvulus but were not seen in any of the nine neonatal cases.

The radiographic features of acute gastric volvulus in the neonate are similar from one case to another. Plain radiographs show a dilated stomach and a peculiar beak may be seen at the site of the distal gastric twist. Occasionally, erect films show a double fluid level, one in the body of the stomach and one in the antral beak. In cases of associated diaphragmatic eventration, elevation of the hemidiaphragm and displacement of the mediastinal structures will be observed. If diaphragmatic hernia is present, the dilated, twisted stomach will be seen above the contour of the hemidiaphragm.

Upper gastrointestinal series confirms the diagnosis of gastric volvulus. The cardioesophageal junction is in normal position and the stomach is seen to be rotated into an inverted position. There is usually complete obstruction of the antropyloric region. If the obstruction is not complete, the twisted, narrowed antropyloric canal is visualized as the contrast material passes distally into the duodenum and beyond.

The complications of acute gastric volvulus include perforation, peritonitis, shock, and death [1, 8, 9]. The mortality rate in this condition was 65% during the first 50 years of experience, but has dropped to 6.3% during the past 3 decades [1]. Eight of the nine neonatal cases survived.

Treatment of acute gastric volvulus is immediate surgery as soon as adequate resuscitation has been carried out. After the volvulus is reduced, predisposing causes should be sought. Diaphragmatic eventration or hernia should be surgically corrected. If one or more of gastric ligaments are absent or deficient, some attempt at gastropexy may be indicated. Anterior gastrostomy, uniformly recommended in the neonatal cases, serves the dual function of maintaining decompression and providing anterior gastric fixation.

REFERENCES

1. Cole BC, Dickinson SJ: Acute volvulus of the stomach in infants and children. *Surgery* 70:707–717, 1971
2. McDevitt JB: Intrathoracic volvulus of the stomach in a newborn infant. *Ir J Med Sci* 3:131–135, 1970
3. Moreno Torres E: Estenosis por hipertrofia di piloro con volvulo gastrico. *Boll Soc Valenciana Pediatr* 10:231–232, 1968
4. Helbig D: Dringliche abdominalchirurgie beim neugeborenen. *Med Welt* 15:791–793, 1966
5. Weiss F, Dwyer JC: Torsion of the stomach in the newborn. *Int Surg* 18:89–91, 1952
6. Kidd HA: Two cases of volvulus of the stomach in a diaphragmatic hernia. *Br J Surg* 36:58–60, 1948
7. Campbell JB, Rappaport LN, Skerker LB: Acute mesenteroaxial volvulus of the stomach. *Radiology* 103:153–156, 1972
8. Gharpure KC: Volvulus of the stomach ending in perforation. *Br J Surg* 26:630, 1939
9. Camblos JF: Acute volvulus of the stomach. *Am Surg* 35: 505–509, 1969

Nonvisualized Gallbladder by Cholecystosonography

WILLIAM P. HARBIN,[1] JOSEPH T. FERRUCCI, JR., JACK WITTENBERG, AND ROB H. KIRKPATRICK

To further define the significance of gallbladder nonvisualization by cholecystosonography, we studied follow-up data on 25 consecutive patients in whom the gallbladder could not be identified despite adequate fasting. In one patient, intravenous cholangiography demonstrated a large gallbladder but no gallstones. In the 24 cases for which a pathoanatomic diagnosis was established, all but two had diseased gallbladders with obliteration of the lumen. This 88% accuracy for positive prediction confirms results of previous sonographic studies and matches the diagnostic significance of nonvisualization at oral cholecystography. We recommend oral cholecystography for all ultrasonic nonvisualized gallbladders for greater diagnostic accuracy when surgery is contemplated.

Numerous reports have established the accuracy of gray scale cholecystosonography in the diagnosis of gallbladder disease. However, few studies have emphasized nonvisualization of the gallbladder by cholecystosonography as a sign of gallbladder disease. To further define the implication of gallbladder nonvisualization, we retrospectively reviewed the results of all cholecystosonographic examinations performed in our department over a 1½ year period.

Materials and Methods

Between January 1977 and June 1978, 361 patients underwent cholecystosonography at our institution. All ultrasonic examinations were performed on commercially available gray scale units (Rohé Rohnar, Searle PhoSonic). Routine longitudinal and transverse sector scans were obtained of the patients' upper abdomen in both the supine and left posterior oblique positions using a 2.25 or 3.5 mHz transducer. Receiver sensitivity and transducer output were optimized for each patient. All patients had fasted for at least 8 hr and many in whom the gallbladder was not visualized returned for second and third ultrasonic examinations on subsequent days. This was not possible in all cases because several patients underwent surgical exploration shortly after the first examination. A review of the results of 361 cholecystosonographic examinations revealed 44 (12%) patients in whom the gallbladder lumen was not imaged. Excluded from this group were seven patients in whom dense echogenic foci with acoustical shadowing were evident despite nonvisualization. Since these echogenic foci frequently represent gallstones, they constitute a subset of ultrasonic gallbladder nonvisualization which may have a different predictive accuracy of gallbladder disease and will be the subject of a future report. The medical records, radiographic reports, and pathologic results of the 44 selected patients were analyzed.

Results

Of the 44 patients with gallbladder nonvisualization, 22 came to surgical exploration and two to autopsy. Of these 24 patients, 23 had diseased gallbladders; 20 had both cholelithiasis and cholecystitis; one had mild chronic cholecystitis only; and two had carcinoma of the gallbladder with tumor obliterating the gallbladder lumen. In the 20 patients with both cholecystitis and cholelithiasis, the gallbladder lumen was either completely or nearly completely obliterated by a varying combination of numerous stones plus fibrotic scarring of the gallbladder. In the single case where only mild chronic cholecystitis was found, the gallbladder lumen was normal in size at surgery. One patient of this group of 24 was found to have a normal gallbladder at autopsy by gross inspection and palpation only; no histologic sections of this gallbladder were obtained.

Of the remaining 20 patients with gallbladder nonvisualization; 14 had no additional medical, surgical, or radiologic evaluation; five underwent oral cholecystography within 2 months of their ultrasonic examination and all five had abnormal results. In one patient, intravenous cholangiography demonstrated visualization of a large gallbladder but no gallstones.

When the documented presence or absence of the gallbladder lumen was used as the sole criterion for diagnostic accuracy, there were three cases of diagnostic error in which nonvisualization occurred despite a demonstrable lumen (the normal appearing gallbladder by intravenous cholangiography, the normal gallbladder by gross inspection at autopsy, and the cholecystectomy specimen with only mild chronic cholecystitis). Using decision matrix analysis, our calculated accuracy for positive prediction is 88% (22/25) with a diagnostic error rate of 12% (3/25). Of the 24 patients who came to either surgery or autopsy, 11 had also had an abnormal oral cholecystogram and all 11 had obliteration of the gallbladder lumen.

Discussion

Seven previous studies provide data concerning gallbladder nonvisualization by cholecystosonography [1–7], but only two of these attempted to determine the diagnostic accuracy of this finding in either a prospective or retrospective manner. In a prospective study, Leopold et al. [1] found six patients with gallbladder nonvisualization, all of whom proved to have gallstones (100% positive accuracy). Anderson and Harned [2] noted that 10 of 13 cases with gallbladder nonvisualization were found to have cholelithiasis (77% positive accuracy). Our positive accuracy of 88% correlates with these previous reports and establishes that sonographic nonvisualization of the gallbladder denotes gallbladder disease with

Received November 27, 1978; accepted February 6, 1979.

[1]All authors: Department of Radiology, Massachusetts General Hospital and Harvard Medical School, Boston, Massachusetts 02114. Address reprint requests to J. T. Ferrucci, Jr.

© 1979 American Roentgen Ray Society

0361–803X/79/1325–0727 $0.00

the same likelihood as does cholecystographic nonvisualization [8, 9].

Our study and the others mentioned suffer from a selection bias in that surgical results constitute the great majority of proven cases and only patients with a strong clinical suspicion of gallbladder disease (and often an abnormal oral cholecystogram) undergo surgical exploration. Unfortunately, there is no feasible alternative for obtaining definitive follow-up in the evaluation of cholecystosonography. In evaluating the accuracy of gallbladder nonvisualization by cholecystosonography, we considered surgical or autopsy evidence of actual lumen obliteration to be the only acceptable proof for a true positive case and not merely the demonstration of either cholelithiasis or cholecystitis. The previous reports on this subject failed to state whether their cases met this criterion.

The possible causes for gallbladder nonvisualization by cholecystosonography include: (1) diseased gallbladder with lumen obliteration; (2) physiologic contraction because the patient was not truly fasting or a longer fast was necessary; (3) obstruction of the biliary tree proximal to the cystic duct; (4) congenital absence of the gallbladder; (5) small volume gallbladder or one with an unusual shape or location; and (6) technical error. We attempted to eliminate the possibility of a broken fast by questioning all patients ourselves and by studying nonvisualized gallbladders a second and third time when clinically feasible. Obstruction of the biliary tree proximal to the cystic duct should be considered in any jaundiced patient with ultrasonographic findings of dilated intrahepatic bile ducts and a normal sized common duct. Congenital absence of the gallbladder is extremely rare.

The mechanism accounting for gallbladder nonvisualization in our three cases of diagnostic error is obscure. Doust and Maklad [3], using bistable B-mode scanning, noted that small volume gallbladders or those with an unusual shape or location accounted for gallbladder nonvisualization. Our follow-up data indicated that this was not the explanation for nonvisualization in our three cases. Similarly, technical error is unlikely since 1 cm serial scans would not fail to delineate a right upper quadrant gallbladder 8 cm in length (two of these three gallbladders were at least 8 cm in length). It is possible that these three patients were not truly fasting despite their claims to the contrary. It is also possible that the gallbladder lumen was obscured by adjacent gas pockets in the colon or small bowel, even though it has been our policy to declare abdominal sonograms incomplete when extensive intestinal gas was repeatedly encountered.

In order to decrease the diagnostic error rate of at least 12% when the gallbladder is not visualized by cholecystosonography, we feel that oral cholecystography should be performed in all such cases if surgical therapy is being considered. In our series of proven cases (surgery or autopsy), the positive accuracy for cases with both an abnormal oral cholecystogram and nonvisualization by cholecystosonography was 100% (11/11).

REFERENCES

1. Leopold GR, Amberg J, Gosink BB, Mittelstaedt C: Gray scale ultrasonic cholecystography: a comparison with conventional radiographic techniques. *Radiology* 121:445–448, 1976
2. Anderson JC, Harned RK: Gray scale ultrasonography of the gallbladder: an evaluation of accuracy and report of additional ultrasound signs. *AJR* 129:975–977, 1977
3. Doust BD, Maklad NF: Ultrasonic B-mode examination of the gallbladder. *Radiology* 110:643–647, 1974
4. Lawson TL: Gray scale cholecystosonography. Diagnostic criteria and accuracy. *Radiology* 122:247–251, 1977
5. Crade M, Taylor KJW, Rosenfield AT, de Graaff CS, Minihan P: Surgical and pathologic correlation of cholecystosonography and cholecystography. *AJR* 131:227–229, 1978
6. Thal ER, Weigelt J, Landay M, Conrad M: Evaluation of ultrasound in the diagnosis of acute and chronic biliary tract disese. *Arch Surg* 113:500–503, 1978
7. Laing FC, Gooding GAW, Herzog KA: Gallstones preventing ultrasonographic visualization of the gallbladder. *Gastrointest Radiol* 1:301–303, 1977
8. Burhenne HJ: Problem areas in the biliary tract. *Curr Probl Diagn Radiol* 5:1–40, 1975
9. Mujahed Z, Evans JA, Whalen JP: The nonopacified gallbladder on oral cholecystography. *Radiology* 112:1–3, 1974

Ultrasonography of Biliary Tract Dilatation Without Jaundice

DAVID P. WEINSTEIN,[1] BARBARA J. WEINSTEIN,[2] AND GEORGE J. BRODMERKEL[3]

The significance of intrahepatic biliary distension in the nonjaundiced patient was studied. Biochemical profiles and endoscopic and surgical findings were evaluated. Biliary tract disease was proven in 11 of 12 patients, with nine of the 11 having concurrent pancreatic disease. Ultrasound proved a more sensitive indicator of partial biliary obstruction than the serum bilirubin levels. The biliary tract of nonjaundiced patients with ultrasonographic evidence of biliary distension should be evaluated by additional studies regardless of the biochemical profile.

Ultrasound imaging permits noninvasive evaluation of the biliary tree. It has proved helpful in the differential diagnosis of jaundice since obstruction of the biliary tree can be reliably detected [1]. Recent reports have described the findings within the liver in obstructive jaundice. Simultaneous imaging of the portal vein branches and bile ducts is considered diagnostic of biliary tract dilatation. This appearance has been referred to as the "parallel channel" sign, "shotgun" sign, and "double barrel" sign [2–4]. The "double barrel" sign without jaundice was noted in 12 of our patients. The significance of biliary distension on the sonogram in the nonjaundiced patient was investigated.

Materials and Methods

During a 6 month period, 12 patients without jaundice demonstrated biliary distension on ultrasonography. The four men and eight women were 30–82 years old. Ultrasound examinations were performed to evaluate one or more of the following indications: epigastric pain, abdominal mass, elevated serum alkaline phosphatase, elevated serum γ-glutamyl transpeptidase, and elevated serum amylase. In addition to the biochemical tests, the status of the gallbladder and pancreas was analyzed and available endoscopic and surgical findings were reviewed. Each test was not performed in every case.

Ultrasound examinations were performed with commercially available analog scan converter gray scale equipment. A 13-mm-diam, medium focus, 3.5 MHz transducer was used. In addition to routine transverse and longitudinal scans, scans were obtained along the major axes of the pancreas and portal vein. Right subcostal oblique scans with cephalic tilting were also performed to evaluate the intrahepatic biliary tree.

Results

All 12 patients demonstrated intrahepatic biliary distension according to the recently established criteria (fig. 1). Five patients had intrahepatic biliary distension confirmed by percutaneous transhepatic cholangiography or endoscopic retrograde cholangiopancreatography.

Biochemical data are summarized in table 1. Eight patients had elevated serum alkaline phosphatase. Five patients, including patient 1, had serum γ-glutamyl transpeptidase determinations, and the results paralleled the serum alkaline phosphatase in each case. None of the 12 had elevated total or direct serum bilirubin levels. A morphine-secretin provocative test in patients 7 and 8 was positive, with serial determinations showing rises in serum alkaline phosphatase, serum γ-glutamyl transpeptidase, serum amylase, and serum lipase [5]. Patient 1 had a completely normal biochemical profile. Percutaneous transhepatic cholangiography revealed marked biliary distension (fig. 2).

Table 1 summarizes the status of the gallbladder and pancreas. Four patients (cases 6–8 and 10) had a previous cholecystectomy. Six (cases 1–3, 5, 9, and 11) had gallbladder distension with echoing bile dependently ("sludge") or stones [6]. The other two patients (cases 4 and 12) had thickened gallbladder walls [7].

In nine patients the pancreas was abnormal. Five (cases 1–5) had pancreatic masses; three of these had carcinomas, one had a tuberculoma, and one had a pseudocyst. The latter patient (case 5) and four others (cases 7–10) had chronic pancreatitis.

The final diagnosis for each patient is listed in table 1. Five patients had partial biliary obstruction due to a mass. Three had biliary stasis secondary to endoscopically proven papillary stenosis (cases 6–8, fig. 1). Patient 6 had concurrent surgically proven liver hilar nodal metastases from an unknown primary tumor (fig. 3).

Two additional patients (9 and 10) had concurrent pancreatitis and biliary tract disease (fig. 4). Endoscopic retrograde cholangiopancreatography was unsuccessful in patient 10 due to a gastrojejunostomy with antrectomy. Percutaneous transhepatic cholangiography in this patient revealed choledocholithiasis.

Patient 11 had chronic cholecystitis with cholelithiasis without pancreatic involvement. A serum alkaline phosphatase was mildly elevated in this patient.

Patient 12 had thick gallbladder walls on sonography. Endoscopic retrograde cholangiopancreatography revealed mild irregularities of the intrahepatic biliary tree; however, the biliary tree was incompletely filled. Liver biopsy revealed chronic active hepatitis.

All of the seven patients without a mass lesion, includ-

Received August 21, 1978; accepted after revision January 12, 1979.

[1] Division of Diagnostic Radiology, Allegheny General Hospital, Pittsburgh, Pennsylvania 15212. Current address: Department of Radiology, Citizens General Hospital, New Kensington, Pennsylvania 15068.

[2] Department of Radiology, Presbyterian-University Hospital, Pittsburgh, Pennsylvania 15261. Address reprint requests to B. J. Weinstein.

[3] Division of Gastroenterology, Allegheny General Hospital, Pittsburgh, Pennsylvania 15212.

© 1979 American Roentgen Ray Society

0361-803X/79/1325-0729 $0.00

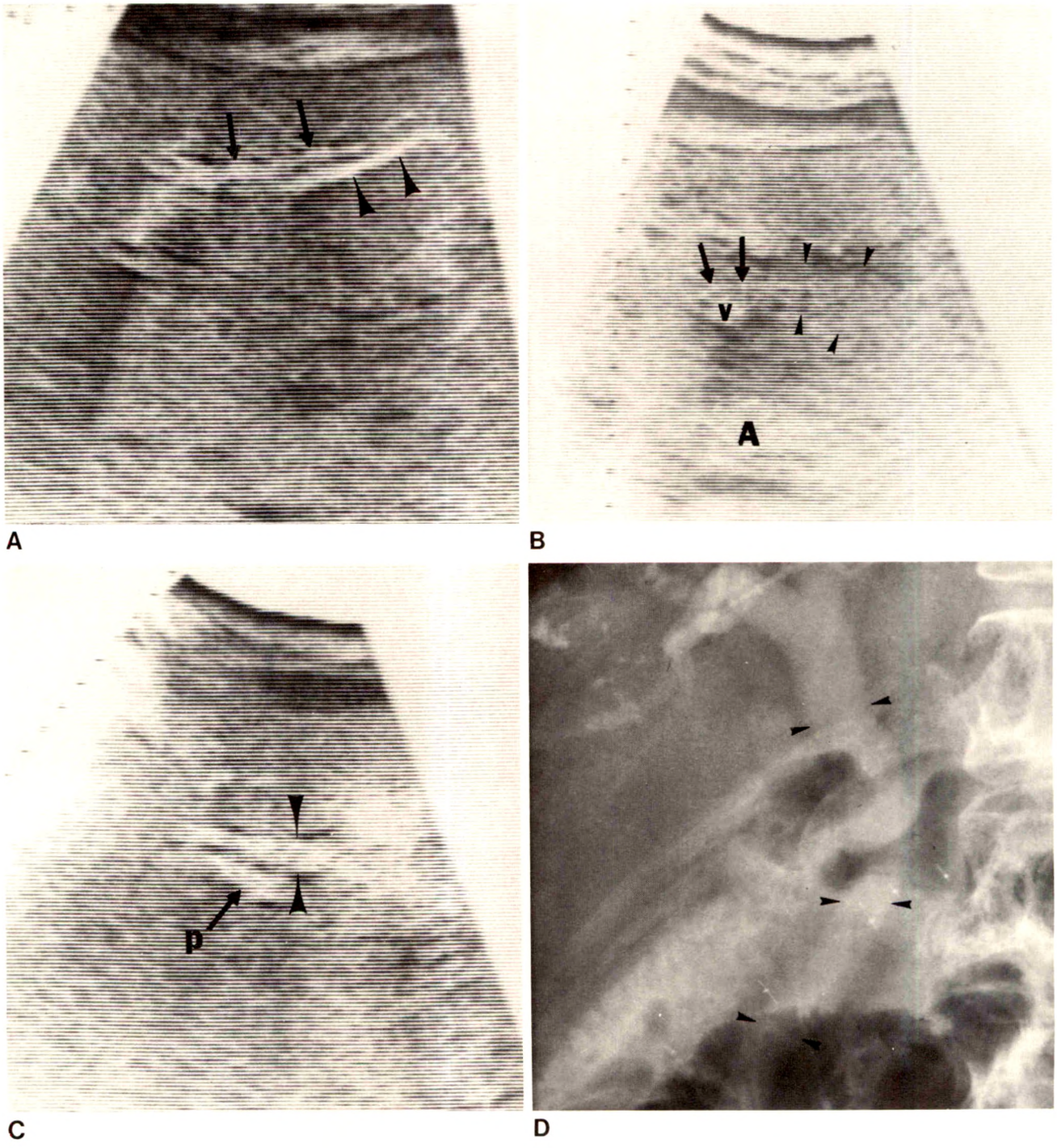


Fig. 1.—Case 8. **A,** Oblique subcostal scan of left lobe of liver. Simultaneous imaging of portal vein branch (*arrows*) and biliary duct (*arrowheads*). **B,** Oblique scan along axis of pancreatic body. Enlargement of gland (*arrowheads*) and ductal dilatation (*arrows*). A = aorta, V = superior mesenteric vein. **C,** Oblique scan along axis of portal vein (P). Dilatation of hepatic duct (*arrowheads*). **D,** Endoscopic retrograde cholangiogram confirms dilatation of biliary tree. Delayed emptying of common bile duct (*arrowheads*).

ing patient 6, were women. Eleven of the 12 patients were proven to have biliary tract disease.

Discussion

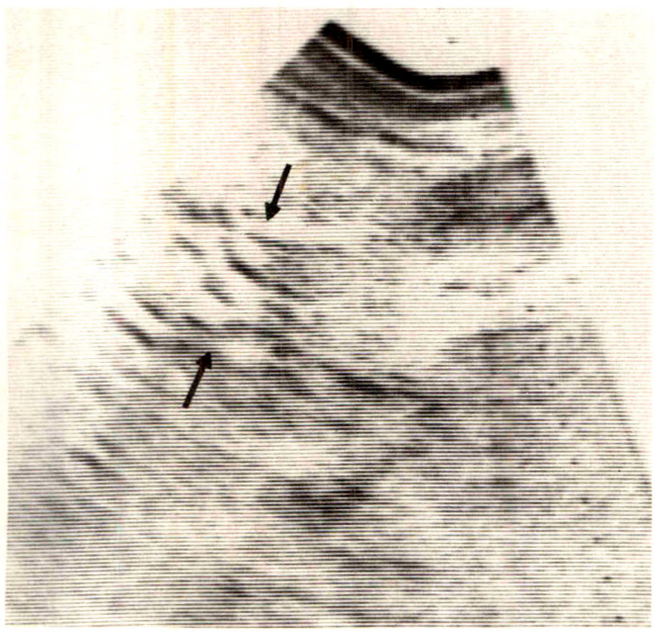
Ultrasound is a useful and reliable means of evaluating jaundiced patients [1]. Recent reports have cited criteria for the detection of intrahepatic biliary distension in the jaundiced patient [2–4]. Biliary tract distension can be detected by ultrasonography prior to development of jaundice using these same criteria. Intrahepatic biliary distension must be deliberately sought in multiple scanning planes. Exact scanning planes vary from individual

TABLE 1

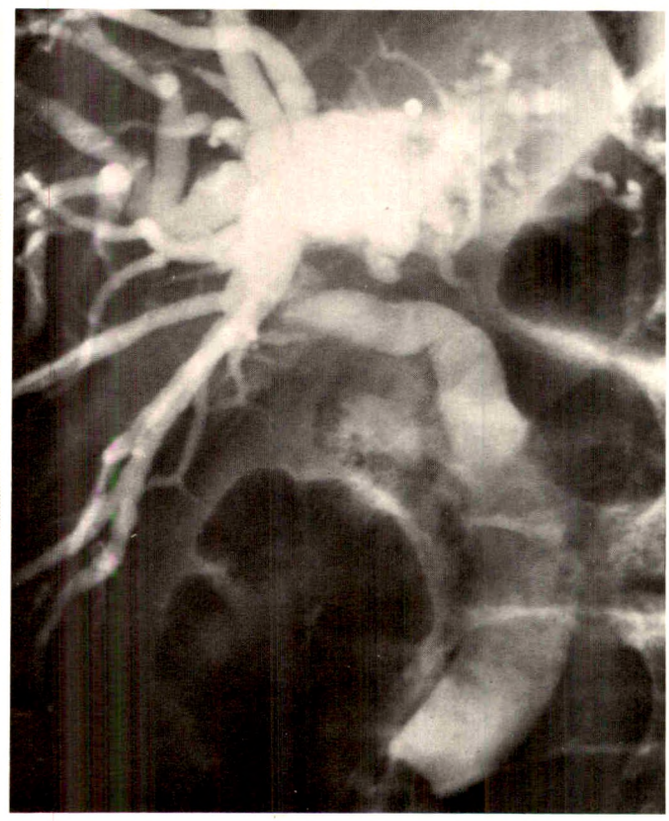
Laboratory and Ultrasound Findings and Final Diagnoses

Ultrasound of Gallbladder/Case No.	Laboratory Findings			Ultrasound of Pancreas	Final Diagnosis
	Bilirubin (1.7 g/dl*)	Alkaline Phospha-tase (98 IU/1*)	Amylase (79 U/dl*)		
Distension, sludge:					
1	0.4	76	30	Head invaded	Duodenal carcinoma
2	0.4	196	65	Carcinoma	Pancreatic carcinoma
3	0.6	333	. . .	Carcinoma	Pancreatic carcinoma
5	0.4	65	795	Chronic pancreatitis	Pseudocyst
9	0.1	198	249	Chronic pancreatitis	Chronic cholecystitis
11	0.7	120	72	Normal	Chronic cholecystitis with cholelithiasis
Thick walls:					
4	0.5	96	331	Granulomatous mass	Tuberculoma of pancreas and liver hilar nodes
12	1.3	778	25	Normal	Chronic active hepatitis
Removed:					
6	1.2	428	. . .	Normal	Carcinoma of liver hilar nodes, papillary stenosis
7	0.3	80	231	Chronic pancreatitis	Papillary stenosis
8	1.0	168	55	Chronic pancreatitis	Papillary stenosis
10	0.4	120	104	Chronic pancreatitis	Choledocholithiasis

* Normal values.



A

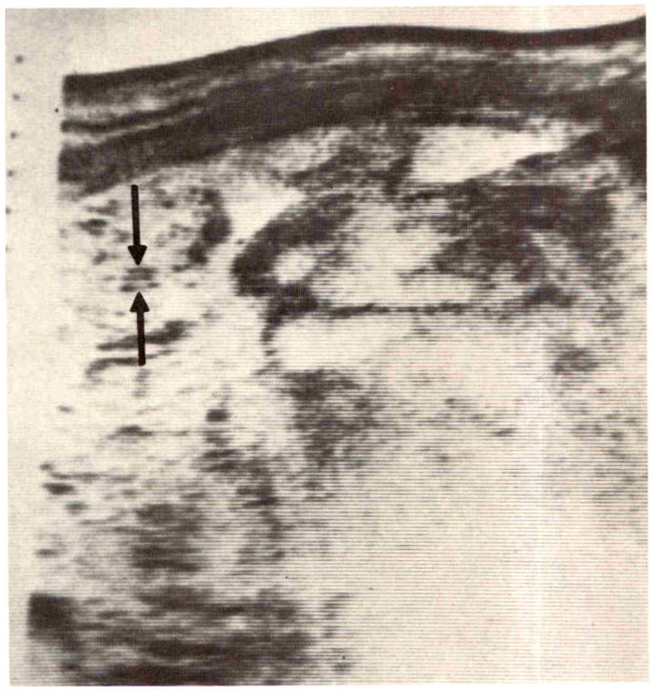


B

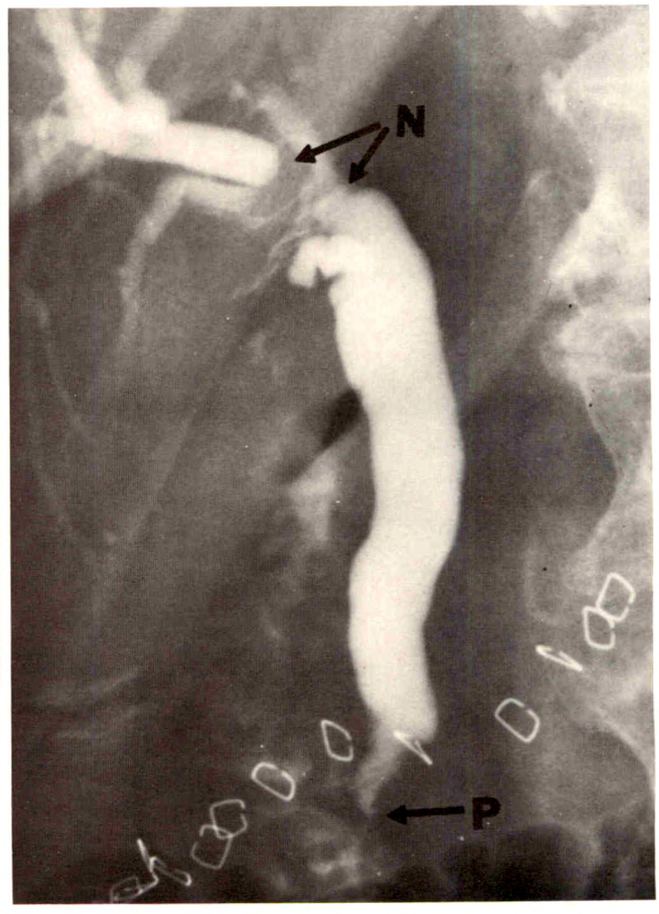
Fig. 2.—Case 1. **A,** Oblique scan through central portion of liver. Numerous dilated bile ducts (*between arrows*). **B.** Percutaneous transhepatic cholangiogram confirms marked biliary distension.

to individual. The purpose of scanning is to display as completely as possible the intrahepatic portal venous system. A cursory examination confined to routine longitudinal and transverse scanning planes would undoubtedly miss biliary distension in some cases.

Jaundice is an obvious indication for a comprehensive examination of the biliary tree. Nonjaundiced patients with more subtle evidence of biliary tract disease should also be examined comprehensively. In general, these patients have difficult diagnostic problems suggestive of



A



B

Fig. 3.—Case 6. **A,** Transverse scan of liver. Biliary duct adjacent to portal vein branch (*arrows*). **B.** Endoscopic retrograde cholangiogram. Partial obstruction at liver hilum due to hilar nodal metastasis (N). Narrowing of distal common bile duct due to concurrent papillary stenosis (**P**).

biliary tract disease, based on clinical or biochemical evidence.

Of the 12 patients in this study, 11 proved to have biliary tract disease. In the other patient (case 12), endoscopic retrograde cholangiopancreatography showed incomplete filling of the intrahepatic radicles. Ductular irregularities suggested pericholangitis or sclerosing cholangititis. Without indisputable evidence of biliary tract disease, we must consider that this case represents a false positive; that is, it is an example of intrahepatic biliary distension on the sonogram without biliary tract disease.

The most notable patient in this series (case 1) had considerable biliary distension secondary to an adenocarcinoma of the duodenum in the ampullary region. Despite the degree of biliary obstruction noted on the sonogram and the subsequent percutaneous transhepatic cholangiogram, his biochemical profile was entirely normal. The etiology of the partial biliary tract obstruction is obvious in this patient, as well as the other four cases with masses of the pancreatic head. The pathophysiology of biliary stasis is less obvious in the rest of the patients.

In three patients, papillary stenosis was demonstrated endoscopically, through difficulty in cannulation by an experienced endoscopist, dilatation of the biliary tree, and delayed emptying of the common bile duct [8]. Patient 7 had delayed emptying of the pancreatic duct as well. A morphine-secretin provocative test was positive in two of these cases, lending further support to the diagnosis of papillary stenosis with secondary biliary stasis [9].

The etiology of papillary stenosis is uncertain. It is most likely caused by a previous common duct exploration [10]. Scarring secondary to stone passage is another probable cause of papillary stenosis [11]. It may be congenital in some cases [12].

There has been considerable interest recently in the diagnosis and treatment of abnormalities at Oddi's sphincter [11, 13, 14]. The exact significance of these abnormalities, as well as the potential value of endoscopic sphincterotomy or surgical septectomy, remains controversial. Ultrasound affords a method of evaluating the biliary tree serially and may prove helpful in following these patients.

Patients 9 and 10 did not undergo endoscopic retrograde cholangiography. The association of biliary tract disease with pancreatitis is similar to the findings in the patients with papillary stenosis. Classically, these patients would be considered examples of pancreatitis

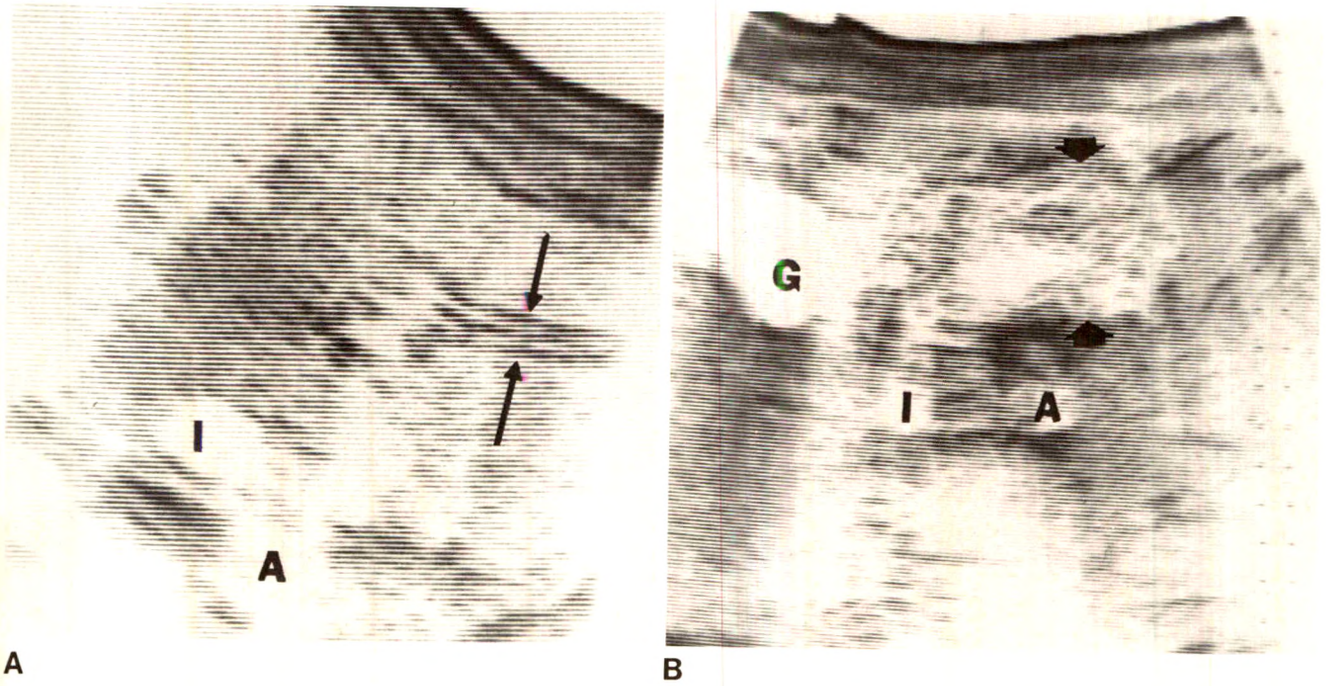


Fig. 4.—Case 9. **A,** Transverse scan of liver with patient in the left posterior oblique position. Bile duct adjacent to portal vein branch (*between arrows*). A = aorta, I = inferior vena cava. **B,** Transverse scan of pancreas. Enlargement and distortion of gland (*between arrows*). Distension of gallbladder (G). A = aorta, I = inferior vena cava.

secondary to biliary stones. Alternatively, the biliary stasis may be secondary to pancreatitis with narrowing of the common bile duct within an abnormal pancreatic head [15, 16].

It is well established that the serum bilirubin may remain normal in the presence of partial biliary obstruction. The serum alkaline phosphatase is more sensitive in biliary obstruction, becoming elevated with incomplete obstruction [10]. The serum γ-glutamyl transpeptidase is considered more sensitive than the serum alkaline phosphatase in biliary obstruction, and the serum γ-glutamyl transpeptidase does not rise in bone disease [17].

This study indicates that ultrasound can detect incomplete biliary obstruction in nonjaundiced patients, and even in some patients with normal biochemical profiles. A comprehensive multiplane ultrasonic investigation of the biliary tree should be performed in patients with elevated serum alkaline phosphatase, γ-glutamyl transpeptidase, or clinical evidence of biliary tract disease regardless of the bilirubin level. In addition, the presence of intrahepatic biliary distension on the sonogram warrants further evaluation of the biliary tree.

ACKNOWLEDGMENTS

We thank Margaret Hull for technical assistance, Janice French for manuscript preparation, and Joe Winstein for photographic support.

REFERENCES

1. Taylor KJW, Rosenfield AT: Grey scale ultrasonography in the differential diagnosis of jaundice. *Arch Surg* 112:820–825, 1977
2. Conrad MR, Landay MJ, Jones JO: Sonographic "parallel channel" sign of biliary tree enlargement in mild to moderate obstructive jaundice. *AJR* 130:279–286, 1978
3. Weill F, Eisencher A, Zeltner F: Ultrasonic study of the normal and dilated biliary tree. The "shotgun" sign. *Radiology* 127:221–224, 1978
4. Laing FC, London LA, Filly RA: Ultrasonographic identification of dilated intrahepatic bile ducts and their differentiation from portal venous structures. *JCU* 6:90–94, 1978
5. Gregg JA, Taddeo AE, Milano AF, McCartney AJ, Santoro BJ, Frager SH, Capobianco AG: Duodenoscopy and endoscopic pancreatography in patients with positive morphine prostigmine tests. *Am J Surg* 134:318–321, 1977
6. Crade M, Taylor KJW, Rosenfield AT, deGraaff CS, Minihan P: Surgical and pathological correlation of cholecystosonography and cholecystography. *AJR* 131:227–229, 1978
7. Marchal G, Crolla D, Baert AL, Fevery J, Kerremans R: Gallbladder wall thickening. A new sign of gallbladder disease visualized by gray scale cholecystosonography. *JCU* 6:177–179, 1978
8. Burrell M, Ball TJ, Cahow E, Dobbins J: The usefulness of ERCP in the diagnosis of stenosis of the sphincter of Oddi. *Gastroenterology* 74:1015, 1978
9. Gregg J, Clark G, Bair C, Volgak C, Milano A: The association of ampullary stenosis, pancreatitis, and retained common duct stones with the post cholecystectomy syndrome. Diagnosis by ERCP and morphine prostigmine test. *Gastrointest Endosc* 24:199, 1978
10. Spiro HM: *Clinical Gastroenterology*. New York, MacMillian, 1970
11. Moody FG, Berenson MM, McCloskey D: Transampullary septectomy for post-cholecystectomy pain. *Ann Surg* 186: 415–423, 1977
12. Malik SA, VanKley H, Knight WA: Inherited defect in hereditary pancreatitis. *Am J Dig Dis* 22:999–1004, 1977

Clinical Comparison of Iocetamic Acid (Cholebrine) and Ipodate Sodium (Oragrafin)

RUTH REID NEAL,[1] KEVIN G. HARVEY,[2] KATHLEEN G. CANTWELL,[2] AND HARRY C. PRESS, JR.[2]

Iocetamic acid (Cholebrine) and ipodate sodium (Oragrafin) were compared in a double blind study of 503 patients. The radiographs were evaluated for contrast density, visualization of common duct, gallstones, residual in the intestinal tract, and side effects. Cholebrine demonstrated better opacification, fewer repeat examinations, slightly greater common duct opacification, and more frequent visualization of gallstones. Oragrafin had less residue. Side effects were minimal with both contrast agents.

Cholecystography has been shown to be valuable for evaluating the gallbladder for evidence of disease [1–4]. Iocetamic acid (Cholebrine) is a cholecystographic agent now being used in the United States. Ipodate sodium (Oragrafin) was compared to iocetamic acid (Cholebrine) in weight dependent dosages and evaluated for efficacy and adverse side reactions.

Subjects and Methods

All hospital inpatients recommended for cholecystography were randomly included in a double blind study to receive either contrast agent. Of the 573 patients selected, 70 were excluded due to discharge from hospital, lack of sufficient laboratory data, pediatric age, or change to intravenous cholangiography.

With iocetamic acid, either a 3 g (four tablets) or 4.5 g (six tablets) dosage was recommended by the manufacturer, with no weight dependent breakdown. The four-tablet dose was assigned to patients weighing 67.5 kg or less, and the six-tablet dose to patients weighing more than 67.5 kg. With ipodate sodium, the manufacturer's specified weight-dependent dosage of 3–6 g (six to twelve 500 mg tablets) was administered (45–56 kg, six tablets; 56–67.5 kg, eight tablets; 67.5–90 kg, 10 tablets; and 90–101 kg, 12 tablets).

Iopdate sodium (500 mg/tablet) contains 61.7% organically bound iodine; iocetamic acid (700 mg/tablet) contains 62%. As administered in our study, iodine content was 1,850–3,700 mg for ipodate sodium and 1,730–2,600 mg for iocetamic acid.

The patients were given a fat-free meal the evening before administration of the contrast agent. After administration, nothing was permitted by mouth. The radiographic examination was performed by the technologist between 7:00 and 9:00 the next morning in the standard prone and oblique views with erect spot films. Patients were questioned by the technologist, who was unaware of the contrast material given to the patient, concerning the occurrence of nausea, vomiting, itching, diarrhea, or fainting.

The films were evaluated independently by two radiologists regarding contrast density and visualization of the common duct, gallstones, and residual contrast in the intestinal tract (table 1). The radiologists were unaware of the contrast material used. Contrast agents were administered randomly, without regard to age, sex, history of allergy, or clinical condition.

In cases of nonvisualization of the gallbladder (grade 0, table 1) the patient was given the same dosage of the same contrast agent in repeat examination the next morning. No dietary restrictions were imposed for the morning or midday meal, but a fat-free meal was again given the evening before examination.

Results

The findings of comparative evaluation of 503 patients are summarized in tables 1 and 2. Chi square analysis [5] provided a quantitative method of determining the significance of the results. Probability values less than 0.05 are significant. Probability values between 0.05 and 0.10 are probably significant.

The number of patients with excellent contrast (grade 3, table 1) in gallbladder visualization was significantly higher with iocetamic acid than with ipodate sodium ($P < 0.05$) (table 1). The number of patients in whom gallstones were demonstrated was significantly higher with iocetamic acid than with ipodate sodium (table 2). Common duct opacification was also significantly higher with iocetamic acid than with ipodate sodium.

Side effects, consisting of nausea and vomiting, were reported by two patients receiving iocetamic acid and by five patients receiving ipodate sodium. There were no reports of skin reactions, diarrhea, or fainting.

The number of patients who required repeat examinations due to nonvisualization of the gallbaldder (grade 0) on the first examination was 22 (8.9%) with iocetamic acid and 66 (25.8%) with ipodate sodium. Residual contrast material was found in the gastrointestinal tract in 22 (8.9%) patients with iocetamic acid and in four (1.6%) patients with ipodate sodium.

Discussion

Several investigators have considered the effectiveness of various cholecystographic agents, but no prior direct comparison has been made using iocetamic acid (Cholebrine) and ipodate sodium (Oragrafin). Juhl et al. [6] concluded that ipodate sodium was equal to iopanoic acid (Telepaque) in gallbladder opacification, but with fewer side effects. Stanley et al. [7] found iocetamic acid to give the densest shadows and highest diagnostic yield when compared with iopanoic acid or tyropanoate sodium (Bilopaque). Russell and Frederick [8] found iopanoic acid produced denser gallbladder shadows and higher frequency of stone demonstration compared with

Received April 12, 1977; accepted after revision January 30, 1979.
[1]Department of Radiology, Medical College of Georgia, Augusta, Georgia 30902.
[2]Department of Radiology, Howard University Hospital, Washington, D.C. 20060. Address reprint requests to H. C. Press, Jr.

© 1979 American Roentgen Ray Society

0361–803X/79/1325–0735 $0.00

TABLE 1

Density of Gallbladder Shadows, Single Dose

Grade	Criteria	Contrast Material: Iocetamic Acid (N = 247) No.	%	Ipodate Sodium (N = 256) No.	%
3, Excellent	Very bright, equal to density of vertebral body	55	22.3	41	16.0
2, Good	Bright, equal to ribs 11 or 12	136	55.0	128	50.0
1, Fair	Density adequate for stone visualization, but less than ribs 11 or 12	34	13.8	21	8.2
0, None	Nonvisualization	22	8.9	66	25.8

TABLE 2

Comparison of Results

Contrast Medium	Common Duct Opacification (SD = 1.31)	Demonstration of Stones (SD = 0.84)	Side Effects
Iocetamic acid (N = 247)	49 (19.8%)	31 (12.6%)	2 (0.8%)
Ipodate sodium (N = 256)	28 (10.9%)	18 (7.0%)	5 (2.0%)

Note.—With an observed difference of greater than twice the standard error, we conclude that its occurrence by chance is very unlikely [5].

ipodate sodium or tyropanoate sodium, but had a higher incidence of side effects. Parks [9] favored iocetamic acid in either of two dosage forms compared with tyropanoate sodium or iopanoic acid because of its better opacification of the gallbladder and lower incidence of repeat examinations.

Our study directly compared iocetamic acid and ipodate sodium for relative opacification of the gallbladder, repeat examinations, demonstration of gallstones, and side effects. Opacity of the common bile duct and residual contrast in the gastrointestinal tract were also considered.

According to our study, iocetamic acid gives better gallbladder opacity than ipodate sodium, as evidenced by a higher proportion of good and excellent grades of opacification. The proportion of patients demonstrating excellent contrast (grade 3) was significantly higher with iocetamic acid than with ipodate sodium at the 5% level of confidence. Demonstration of gallstones was better with iocetamic acid than with ipodate sodium. The number of repeat examinations required due to nonvisualization of the gallbladder was also statistically significant, with iocetamic acid requiring fewer repeats.

Reported side effects (nausea and vomiting) were minimal with both agents; the skin reactions reported with iocetamic acid by Janower and Hannon [10] and Zeit [11] were not seen.

Contrast residue was found more frequently in the gastrointestinal tract with iocetamic acid, but did not obscure visualization of the gallbladder [9]. The common bile duct was visualized in the studies with the greatest opacification of the gallbladder, consistent with the findings of Russell and Frederick [8].

Our study indicates that in routine cholecystographic examinations, iocetamic acid (Cholebrine) is as effective as, or better than, ipodate sodium (Oragrafin), gives a higher proportion of excellent grades of opacification of the gallbladder, requires fewer repeat examinations due to nonvisualization, and better demonstrates the common bile duct and gallstones. When side effects were evaluated, nausea and vomiting were minimal with both agents.

ACKNOWLEDGMENTS

We thank Jessie Hill and Denise Madison for their assistance.

REFERENCES

1. Bernstein C, Heilbrun N: Clinical trial of ipodate: a new oral cholangiographic agent. *JAMA* 181:1002–1003, 1962
2. Brinkbok GCF: The use of gallbladder media in practice and an objection method of assessment of the results of oral contrast media. *Ned Tijdschr Geneeskd* 112:2255–2256, 1968
3. Janbroers JM, Sanders JC, Til HP, Ferron VJ, DeGroot AP: Toxicologic and pharmacologic properties of iocetamic acid, a new oral cholecystographic agent. *Toxicol Appl Pharmacol* 14:232–241, 1969
4. Glenn JC Jr, O'Brien PS: Ipodate, a new medium for cholecystography and cholangiography. *South Med J* 56: 167–169, 1963
5. Hill AB: *Principles of Medical Statistics*, New York, Oxford University, 1956, pp 107–113
6. Juhl JH, Cooperman LR, Crummy AB: Oragrafin, a new cholecystographic medium. A double-blind comparison with Telepaque. *Radiology* 80:87–91, 1963
7. Stanley RJ, Melson GL, Cubillo E, Hesker AE: A comparison of three cholecystographic agents. A double-blind study with and without a prior fatty meal. *Radiology* 112:513–517, 1974
8. Russell JR, Frederick PR: Clinical comparison of tyropanoate sodium and iopanoic acid. *Radiology* 112:519–523, 1974
9. Parks RE: Double-blind study of four oral cholecystographic preparations. *Radiology* 112:525–528, 1974
10. Janower ML, Hannon MA: Skin reactions with iocetamic acid. *Radiology* 118:301, 1976
11. Zeit RM: Angioneurotic edema following ingestion of iocetamic acid. *Radiology* 123:590, 1977

Breast Cancer Missed by Mammography

JOHN E. MARTIN,[1] MYRON MOSKOWITZ,[2] AND JOHN R. MILBRATH[3]

Because a "negative" mammogram that is followed by a biopsy diagnostic of cancer is a matter of deep concern, a retrospective review was conducted of 48 such missed diagnoses at four Breast Cancer Detection Centers. The study group comprised 40,000 women participating in breast cancer screening examinations. From 3,271 biopsies during screening, 499 cancers had been found. Biopsies in the interval between screening examinations totaled 630 and yielded 48 malignancies. These 48 interval cancers were studied in an attempt to discover why they were not found on the preceding mammographic examination.

Three major categories of error were disclosed and each is discussed: (1) poor radiographic technique; (2) absence of radiographic criteria of cancer; (3a) obvious oversight by the radiologist; and (3b) lack of recognition of subtle radiographic signs. This last reason is discussed in detail in the belief that better recognition of these indirect radiographic signs will lead to more accurate diagnoses, particularly in early cancers.

The combination of mammography and physical examination has proved to be effective in detecting stage I breast cancers. Even with these diagnostic methods, however, some cancers are being missed. The dedicated mammographer has long been plagued by the "negative" mammogram which is followed by a surgical biopsy positive for breast cancer. We believe that a retrospective analysis of the objective data (i.e., serial mammograms) of patients with negative mammograms who were subsequently found to have interval cancers might be helpful in determining why these cancers had been overlooked originally.

In such an analysis, one must keep in mind that many in situ and intraductal lesions demonstrate no obvious radiographic patterns. Although the surgeon often assumes that what he palpated was the lesion found at biopsy, this is often not the case. The so-called "minimal" breast lesions are usually too small to be palpated and are more often found incidental to the biopsy of a benign process. On the other hand, there *are* subtle radiographic signs, not always recognized, that can lead to more accurate diagnosis of these earliest cancers, and these signs will be discussed.

For the purpose of this discussion, minimal breast cancer is defined as in the National Cancer Institute guidelines: a lesion no more than 1 cm in diameter. The more generally accepted definition of the term is that originally offered by Gallager and Martin in 1971 [1, 2]: a noninvasive intraductal carcinoma, a lobular carcinoma in situ, or an invasive carcinoma forming a mass with a volume no greater than a sphere 0.5 cm in diameter.

At this juncture, the question arises of whether the detection of minimal breast cancers by mammography is any less serendipitous than by physical examination. If so, one would expect a higher percentage of minimal cancers to be found in a screened population during the incidence years than in the prevalence years of the screening program. Statistics from two Breast Cancer Detection Centers (at Cincinnati and Milwaukee) revealed this to be the case. In the initial examinations of about 20,000 women (prevalence rate), 31% of the cancers found by physical examination were minimal lesions, compared with 38% of those found by mammography. However, in subsequent examinations of the same women (incidence rate), only 17% of the cancers found by physical examination were minimal, in contrast to 55% of those found by mammography. Thus it seems that finding minimal breast cancers by physical examination is largely serendipitous, but finding them by mammographic examination is not.

More puzzling, though, is the problem of a "negative" mammogram in a patient who has a true invasive lesion. One reason for missed diagnoses is poor mammographic technique. The importance of careful positioning cannot be overemphasized. It is difficult to image a lesion that is high on the chest wall or in the tail of the breast. Some masses are mobile and, in positioning the patient, the technician may allow the mass to slip out of the imaging field.

Even if the possibility of poor imaging technique is excluded, a disturbing number of clinically palpable lesions overlooked by the mammographer are noted. To determine the extent of the problem and the reasons for the missed diagnoses in these cases, we reviewed the statistics from four Breast Cancer Detection Centers (Houston, Cincinnati, Milwaukee, and Seattle).

Subjects and Methods

The study group consisted of slightly more than 40,000 women who had participated in the Breast Cancer Detection Program for 3–5 years. In this group, 3,271 biopsies had been performed as a result of the screening examinations and 499 cancers had been found (15.25%). This percentage of positive biopsies is less than the generally accepted figure of 25% in nonscreened hospital studies. It is not likely that the accuracy of biopsies in the screening program is less accurate than that of the community as a whole, leading to the question of whether an excess number of biopsies are being performed as a result of the screening examination. Another possibility would be that the screening program, in finding more *early* cancers than are generally biopsied in the community, requires a concomitant increase in the number of doubtful and negative biopsies.

Received July 25, 1978; accepted after revision January 15, 1979.

[1] Breast Cancer Detection Center, St. Joseph Hospital, Houston, Texas 77002. Address reprint requests to J. E. Martin.

[2] Department of Radiology, University of Cincinnati, and Breast Cancer Detection Center, Cincinnati General Hospital, Cincinnati, Ohio 45267.

[3] Breast Cancer Detection Center, Medical College of Wisconsin, Milwaukee, Wisconsin 53226.

© 1979 American Roentgen Ray Society

0361-803X/79/1325-0737 $0.00

Interval cancers are those whose signs or symptoms were first detected by the woman or her personal physician subsequent to a screening examination in which she had both a negative mammogram and a negative physical examination. There were 630 such biopsies performed and 48 cancers found (7.6%). It is important to note that the discovery rate of the screening program biopsies (15.25%) was twice that of the interval biopsies (7.6%). It is also rewarding to realize that 91.2% of the total cancers diagnosed were found as a direct result of the screening examinations.

Of the 48 cases in which cancer might have been overlooked in the preceding mammographic examination, some could have grown so rapidly as not to be present at the last examination; the intervals between screening and discovery of the interval cancers ranged from 1 to 23 months. However, 11 of these cancers were found within 6 months of the last screening examination, and all were found on retrospective review of the mammograms. Most of the remaining cancers were probably present, but were either not detected or were not detectable by current techniques.

All 48 patients with interval cancers were symptomatic at the time of diagnosis. Two had crusting of the nipple, two had bleeding from the nipple, one had pain in the breast, and 43 had palpable masses. Of the 43 palpated masses, 10 were found at surgery to be cysts, and the cancers were found incidentally; five were lobular in situ carcinoma and five intraductal carcinoma. These figures perhaps lend support to the hypothesis of Gallager and Martin [3] that some breast cancers cause excitation of surrounding tissues and an increase of periductal collagen or background stromal collagen, or even excitation of fibrocystic disease. This finding, although not yet fully confirmed, may have value in mammographic diagnosis of early breast cancers.

It is of considerable importance that 21% of these interval cancers (10 of 48) were classified as *minimal* cancers. This emphasizes the need for biopsy in any case involving thickening of breast tissue, nipple change, or nipple discharge. Detection of minimal cancers obviously cannot approach the accuracy rate of the larger, more invasive lesions, but progress can be made with more attention to the earliest signs.

The age distribution of the 48 patients with interval cancers is of some interest. Exactly half were 50 years old or younger. Five were 30–40 years old; 19 were 41–50; 17 were 51–60; and seven were 61–70. The right breast was the site of the lesion in 21 cases and the left breast in 27 cases.

Despite the fact that surgery was performed after symptoms and clinical signs were present, only 19 of these patients had positive axillary nodes. Roughly half the women in this study reported regular self-examination of their breast and virtually all reported some self-examination. Thus one would expect their cancers to be detected at an earlier stage than those found in a nonscreened population.

The 48 interval cancers were classified according to Wolfe's parenchymal patterns [4] (table 1). On pathologic examination, 41 of the lesions were invasive ductal carcinoma, three were medullary carcinoma, two were lobular invasive carcinoma, one was anaplastic carcinoma, and one was undifferentiated sarcoma. The anaplastic carcinoma and the sarcoma could fit the hypothesized category of rapidly growing neoplasm that does not show a diagnostic radiographic pattern. Medullary carcinomas are usually seen radiographically as a circumscribed mass which, especially in younger patients, may be misinterpreted as a cyst. Invasive ductal cancers are usually thought to have diagnostic patterns on mammography, and scrutiny of this group should yield important information about missed diagnoses.

TABLE 1

Cancers Missed on Mammography, Grouped by Wolfe's Classification [4]

	No.	%
N1	1	2.08
P1	11	22.92
P2	27	56.25
DY	9	18.75
Total	48	100

Results and Discussion

On the assumption that most of these 48 interval cancers had been present, although undetected, on the preceding screening examination, we reviewed the mammograms in each case. A blind reading of these mammograms mixed with a random day's screening would more accurately determine the true detectability of these lesions. However, we were more interested in determining *why* the interval cancers were overlooked, and for this reason the readings were done with prior knowledge of the diagnosis in each case.

In this retrospective examination, 14 cases (29%) were obvious oversights on the part of the original examiner (table 2); the cancers were readily apparent to the reviewer. Sixteen cases (33%) were still found to be lacking any radiographic evidence of cancer, despite the reviewer's knowledge of the diagnosis and site of the lesion.

The most interesting group was the 18 cases (38%) that were found on review to have subtle and indirect radiographic signs pointing to the diagnosis. Of these cases, 13 demonstrated asymmetry of breast tissue, with this being the only radiographic sign suggestive of a neoplastic process [5]. Two cases displayed the developing density sign [2, 5]; when compared with previous records, the mammograms displayed a progressive increase in density in a specific area without other signs. The other three cases displayed groups of calcifications that had been observed originally, but misinterpreted as benign. Later these calcifications were found to be associated with the malignant lesions [6].

In radiographic interpretation of mammograms, there are two major categories of diagnostic criteria: (1) direct signs: those provided by the cancer itself, which may be divided into primary signs and secondary signs, and (2) indirect signs: those not provided by the cancer itself but, rather, related to tissue reaction in the region of the cancer. Indirect signs may be shared by many benign proliferative disorders, but may also be vital to an early diagnosis of cancer.

Of the direct signs, the most important primary one is the presence of a mass, the characteristics of which have been thoroughly described. The direct signs that are secondary to the presence of a lesion are skin thickening, nipple retraction, diffuse lymphedema, spiculation, architectural deformity, and ulceration. These direct signs are rarely overlooked and require no elaboration here.

TABLE 2

Analysis of Mammography Errors

	No.	%
Inevitable error: no diagnostic radiographic signs found on review	16	33
Obvious oversight: diagnostic signs immediately apparent on review	14	29
Less obvious error: subtle radiographic signs noted by experienced examiner	18	38
Total	48	100

The indirect signs are more subtle and therefore go unrecognized more often. Five of these indirect signs are particularly important:

1. A solitary dilated duct under the areola or an unusual complex of dilated ducts that extends 3 cm or more within the breast. Either should invariably be considered suspicious of malignancy [3].

2. Intraductal and intralobular calcifications. Martin [6] reported that calcifications most likely to be associated with malignancy are those that are thin linear, thin curvilinear, or thin branching in pattern. Benign groupings usually appear as clusters of punctate calcifications. Whether or not the calcifications are characteristic of malignancy, it is better to biopsy, as any of these can be a subtle indication of an in situ or minimally invasive lesion.

3. A progressive density in a specific area is an important indicator which requires baseline mammograms for comparison. The breast is primarily an involuting organ, and when the mammogram demonstrates new or progressively increasing areas of density which were not present on previous studies, carcinoma should be suspected [2, 5].

4. Asymmetry of breast tissue. Any asymmetry noted in comparing two projections of the right and left breasts is an important sign [5], even with fibrocystic disease. This particular observation is overlooked more often than any other simple diagnostic criterion because many observers fail to compare the breasts. If the asymmetry is associated with any clinically palpable lesion, whether this is a mass or only an area of thickening, the yield for carcinoma is sufficiently high to warrant a recommendation for biopsy. In cases of asymmetry unaccompanied by other clinical signs, a multifocal intraductal carcinoma may be found, although the radiographic density is produced simply by the stimulation of secondary collagenosis in the breast [3].

5. A benign-appearing mass in a peri- or postmenopausal woman may be a valuable sign, as fibroadenomas can be associated with minimal lesions within or adjacent to the fibroadenoma. Thus while fibroadenomas in themselves are not considered preneoplastic lesions, they arise in the same background stroma of proliferative disorders, and it is probably wise to consider surgical excision of a solitary, dominant, noncalcified, benign-appearing fibroadenoma. In addition, a well circumscribed carcinoma may on occasion be misdiagnosed as a fibroadenoma.

ACKNOWLEDGMENT

We thank Dr. Thomas Carlile, Director, Breast Cancer Detection Center, Seattle, Washington for assistance.

REFERENCES

1. Gallager HS, Martin JE: An orientation to the concept of minimal breast cancer. *Cancer* 28:1505–1507, 1971
2. Martin JE, Gallager HS: Mammographic diagnosis of minimal breast cancer. *Cancer* 28:1519–1526, 1971
3. Gallager HS, Martin JE: The study of breast carcinoma by correlated mammography and subserial whole organ sectioning. Early observations. *Cancer* 23:855–873, 1969
4. Wolfe JN: Risk for breast cancer development determined by mammographic parenchymal pattern. *Cancer* 37:2486–2492, 1976
5. Gallager HS, Martin JE: Early phases in the development of breast cancer. *Cancer* 24:1170–1178, 1969
6. Martin JE: Breast calcifications—benign or malignant?, in *Diagnostic Radiology—1977*, University of California at San Francisco Press, 1978, pp 831–836

Pneumocystis carinii Infection of the Lung: Radiologic and Pathologic Correlation

PAUL DEE,[1] WASHINGTON WINN,[2,3] AND KELLY McKEE[2,4]

The incidence of *Pneumocystis carinii* infection of the lung was determined in 100 consecutive autopsies on patients with hematologic malignancies and in a control group of 50 patients with acute myocardial infarction and chronic obstructive pulmonary disease. Thirteen instances of infection were found in the study group and one instance in the control group. Of the 14 patients with *P. carinii* infection, five were classified as uncomplicated *P. carinii* pneumonia with typical host response and five had no evidence of any host response to the presence of the organisms. Four cases were impossible to assess because of complicating bacterial, viral, or fungal pneumonia.

The five patients with the typical histologic response to the presence of *P. carinii* organisms all showed diffuse pulmonary densities on the chest radiographs in accordance with the classic descriptions of *P. carinii* pneumonia. The five without any evidence of host response to the presence of *P. carinii* organisms showed no evidence of parenchymal disease on chest radiographs. The finding of *P. carinii* organisms in the lung is not necessarily an indication of clinically significant disease and, from this study, it seems that chest radiography is of considerable importance in determining the significance of such infestation.

Autopsy series on patients with hematologic malignancies have suggested a 4%–8% incidence of pneumonitis caused by *Pneumocystis carinii* [1, 2]. However, Perera et al. [3] suggested that the true incidence of infestation is higher because of the occasional finding of *P. carinii* organisms in lung tissue without any evidence of cellular reaction on the part of the host. This study attempted to determine the incidence of *P. carinii* infection in a series of patients who received immunosuppressive therapy for hematologic malignancies. The pathologic and radiologic findings were correlated in two groups of patients: a group with evidence of an inflammatory reaction to the organisms and a group in whom host reaction was minimal or absent.

Subjects and Methods

A series of 100 consecutive autopsies on patients with leukemia, lymphoma, and multiple myeloma was reviewed and compared with a control group in whom the major diagnosis was acute myocardial infarction (25 cases) or chronic obstructive pulmonary disease (25 cases). The hematologic malignancy patients were selected as a study group because the use of immunosuppressive therapy renders them at risk for *Pneumocystis carinii* infection. The analysis of the pathologic material (by W. W.) was carried out entirely independently of the review of the chest radiographs (by P. D.). A written description of the radiographs was made at the time of review for subsequent correlation with the pathologic findings, but no attempt was made to grade the severity of parenchymal disease. In the group of cases with *P. carinii* pneumonia, all radiographs reviewed were exposed within 24 hr of the patient's demise. In the group with *P. carinii* infestation but no histologic evidence of pneumonia, the time lag was longer and varied from 22 hr to 3 days. The difference in the time relationships can be explained by the differing respiratory status of the two groups. The patients with *P. carinii* pneumonia were manifestly in respiratory distress and therefore subject to frequent assessment with chest radiography.

An average of 3.4 lung tissue blocks per patient was available for study and a minimum of 5 sections was cut from each block. No attempt was made to systematically sample each lobe of the lung. The material was reviewed using hematoxylin and eosin stained sections and sections stained for the presence of cysts using the silver methenamine and Weigert-Gram techniques. In those areas with a suspicion of bacterial or fungal pneumonia, Brown and Hopp's stain for bacteria and Mayer's mucicarmine stain for fungi were used. Quantitation of the *P. carinii* organisms from 0 to 4+ was performed on the silver methenamine sections: 0 = no cysts found, 1+ = one cluster of cysts per section, 2+ = 2–10 clusters of cysts per section, 3+ = more than 10 clusters per section and less than one cluster per high power field, and 4+ = more than one cluster per high power field. In order to compare cases a *P. carinii* (PC) score was computed:

$$\frac{\text{Total quantitation of all sections (0–4+)}}{\text{Number of sections}}$$

The PC score reflects the average number of *P. carinii* organisms identified in the sections. The radiographs were reviewed without knowledge of the pathologic findings.

Results

Pathologic Findings

Cysts of *P. carinii* were demonstrated in 13 autopsies in the study group and in one autopsy in the control group. The pneumocystis cases were grouped according to histopathologic response in an attempt to simplify further analysis. Group 1 (five cases) comprised those patients in whom autopsy findings indicated a compatible inflammatory response to the *Pneumocystis* organisms. Group 2 (five cases) comprised those patients with either no evidence of any host response to the presence of the *P. carinii* organisms or presence of a noninfectious process such as pulmonary congestion. Group 3 (four cases) comprised those patients in whom the significance of the presence of *P. carinii* organisms

Received April 21, 1978; accepted after revision January 25, 1979.
[1]Department of Radiology, University of Virginia Medical Center, Charlottesville, North Carolina 22908. Address reprint requests to P. M. Dee.
[2]Department of Pathology, University of Virginia Medical Center, Charlottesville, North Carolina 22908.
[3]Department of Pathology, Medical Center Hospital of Vermont, Burlington, Vermont 05401.
[4]Present address: Department of Pediatrics, Vanderbilt University Medical Center, Nashville, Tennessee 37203.

© 1979 American Roentgen Ray Society

0361-803X/79/1325-0741 $0.00

could not be determined because of coincident bacterial or fungal pneumonia or pulmonary infarction.

The pathologic findings are summarized in (tables 1–3). The typical pathologic findings in *P. carinii* pneumonia are an interstitial round cell infiltrate, hyperplasia of the alveolar lining cells, and a foamy, relatively acellular intraalveolar exudate. On occasion the alveolar exudate may be modified by fibrin deposition and hyaline membrane formation. The *P. carinii* cysts can be identified by the silver methenamine and Weigert-Gram techniques. The cysts are predominantly located within the alveolar space and only uncommonly are observed within the interstitium of the lung.

Four of the five patients (cases 1–3 and 5) in group 1 were diagnosed during life as *P. carinii* pneumonia and received appropriate therapy. Case 3 died within 2 days of starting pentamidine therapy, but the other three had completed at least 10 days of pentamidine therapy before death. Cytomegalovirus inclusions were identified in three cases, but were plentiful in only one (case 1); a single *Aspergillus* microabscess was present in one case. No other infectious agents were found in the group 1 patients.

The histologic findings in group 2 were minimal or were related to the underlying disease. Acute and chronic congestion and focal hemorrhage were the most common findings. Case 6 showed some interstitial leukemic infiltrates, but there was no evidence of interstitial pneumonitis or alveolar exudation. Case 7 had slight proliferation of the alveolar lining cells but no other evidence of any other response. Conceivably the alveolar cell proliferation could have represented the earliest response to infection but was not regarded as diagnostic.

Acute bacterial or fungal penumonia and pulmonary infarction dominated the histology of group 3 patients. The presence of Gram-positive cocci in case 11 and *Cryptococci* and *Nocardia* in case 12 in association with focal pulmonary disease strongly suggested that the acute inflammatory response was not related to the coincidental presence of *P. carinii* organisms. Case 13 presented problems in grouping. The finding of an interstitial pneumonitis and an organizing alveolar exudate was certainly compatible with *P. carinii* pneumonia. However, *Staphylococcus aureus* organisms were isolated from the blood of this patient and the case was perforce relegated to group 3.

Radiologic Findings

If the pathologic findings in groups 1 and 2 in this study are clearly separable, then the radiologic findings are even more so. This is best illustrated by comparison of montages of the chest radiographs of the two groups. There is a uniformity of appearance in cases of group 1. *P carinii* pneumonia: all cases had extensive confluent parenchymal infiltrates with a normal sized heart and no secondary evidence of cardiac failure, such as the presence of pleural fluid (fig. 1). The infiltrates were perihilar and fairly symmetric. On some of the original films in the development of the infiltrates a vaguely nodular pattern was appreciated, but this tended to disappear as the infiltrates became confluent. Air bronchograms could frequently be seen. On the other hand the chest films in group 2 showed no suggestion of any diffuse parenchymal disease (fig. 2).

Discussion

Cysts of *Pneumocystis carinii* were demonstrated in 13 autopsies in the study group (13%) and in one autopsy in the control group (2%). The prevalence of cysts in hematologic patients with no inflammatory response (group 2, 4 of 100 or 4%) is not statistically different from that in cardiorespiratory patients (1 of 50 or 2%). There is thus no evidence that patients with hematologic malignancies have a higher incidence of infestation with *P. carinii* than patients in the control group. Infestation in this context is the presence of *P. carinii* organisms without any host response. It is possible that group 2 patients were too immunosuppressed to mount an inflammatory response. There is no means available to determine this. One can only say that those cases with hematologic malignancies did not differ in type of disease or therapy from the other patients in the study group. The autopsies indicated that the group 2 patients died from causes other than pulmonary disease.

Sheldon [4] introduced the concept of subclinical or latent infection with *P. carinii*, having observed the organisms in a number of patients without signs or symptoms referable to the respiratory tract. Cellular reaction was absent or minimal in his cases. Perera et al. [3] found 39 cases of latent *P. carinii* infection in an autopsy series in children with malignancies. The cases in group 2 in our series correspond well with the cases of Sheldon and Perera et al. A single case from the control group was similar. This patient was not debilitated and none of the risk factors associated with *Pneumocystis* infection were present. Nevertheless, *P. carinii* organisms were found in significant numbers. The lungs showed atelectasis and signs of chronic congestion but no inflammatory response or exudation.

The significance of the presence of *P. carinii* organisms without evidence of host reaction is unknown. There was no statistical difference in the quantity of organisms in the two groups of cases. In four of the five cases with established *P. carinii* pneumonia, however, pentamidine treatment may have reduced the total number of organisms. Furthermore, the number of sections available for review was smaller in group 2 than group 1 and sampling errors may have increased the count. In a clinical context, it is difficult to envisage such latent disease as life threatening. No cases showing intermediate features between groups 1 and 2 were found in this series. These subclinical infections may account for the presence of circulating *Pneumocystis* antigen in cancer patients without pneumonia [5].

Interstitial pneumonia is a response of the lung to a variety of insults. Atypical histologic responses in which the classic foamy exudate was not found have been

TABLE 1

Pathologic Findings in Group 1

Case No.	Diagnosis	Cause of Death	Honeycomb Exudate	Fibrous Exudate	Focal Interstitial Fibrosis	PC Score
1	Multiple myeloma	Pneumonia	+	–	–	3.0
2	Chronic lymphocytic leukemia	Pneumonia	–	+	–	3.5
3	Hodgkin's disease	Pneumonia	–	–	+	1.5
4	Chronic lymphocytic leukemia	Clinical: sepsis and myocardial infarction; pathologic: pneumonia	–	–	–	0.8
5	Acute lymphocytic leukemia	Pneumonia	–	+	+	1.75

Note.—All patients in group 1 had interstitial pneumonia, hyaline membranes, alveolar cell proliferation, and rare plasma cells.

TABLE 2

Pathologic Findings in Group 2

Case No.	Diagnosis	Cause of Death	Interstitial Pneumonia	Alveolar Cell Proliferation	PC Score
6	Chronic myelocytic leukemia	Sudden death, cause unknown	–	–	3.0
7	Multiple myeloma	Renal failure and acute myocardial infarction	–	Slight	1.0
8	Acute myocardial infarction	Acute myocardial infarction	Focal lymphocyte infiltrates	–	3.0
9	Lymphoma	Widespread lymphoma sepsis suspected but not documented	–	–	1.0
10	Lymphoma	Widespread lymphoma including central nervous system involvement	–	–	2.0

Note.—No patients in group 2 had hyaline membranes, honeycomb exudate, fibrous exudate, focal interstitial fibrosis, or plasma cells.

TABLE 3

Pathologic Findings in Group 3

Case No.	Underlying Disease	Chest Film	Lungs		PC Score
			Gross	Microscopic	
11	Carcinoma of rectum and multiple myeloma	Normal lungs	Focal consolidation with fibrinous pleurisy	Acute pneumonia with Gram-positive cocci	1.0
12	Acute monomyelocytic leukemia	Rapid development of right lower lobe infiltrate compatible with bacterial pneumonia	Pulmonary emboli and infarcts	Pulmonary emboli and infarction; focal thickening of alveolar septa	0.5
13	Acute lymphocytic leukemia	Rapid development of confluent infiltrates in the lungs	Uniform rubbery consistency; alveoli not totally obliterated	Interstitial lymphocytic infiltration, hyaline membranes, organizing fibrous exudate	1.0
14	Hodgkin's disease	Cavitary right lower lobe pneumonia	Congestion and edema; focal cavitary pneumonia	. . .	0.57

Note.—No patients in group 3 had plasma cells.

described in lung biopsies [6]. If cysts may be found in the lung without any cellular reaction, then cysts might be found incidentally in association with interstitial pneumonia of different etiology. It is impossible to absolutely exclude chemotherapy or even oxygen therapy as causes of the pulmonary lesions, but there was no circumstantial evidence that this was the case. The chemotherapeutic regimes were fairly standardized in the whole group of 100 patients and oxygen therapy was administered only in response to the effects of the developing pneumonia and not in advance. The nature of the study precluded the use of one important piece of evidence for the significance of the organisms—a satisfactory response to specific chemotherapy.

Chest radiography would seem of preeminent value in the diagnosis of *P. carinii* pneumonia. The patients with *P. carinii* pneumonia (group 1) had chest radiographs of remarkably uniform appearance with extensive confluent infiltrates distributed symmetrically in the lungs with no evidence of pleural reaction. The radiographic appearances conformed to the typical pattern described by others [7–9]. Variant appearances that have been described, such as localized nodular densities [10], unilateral or lobar predominance [11], pleural effusions, and

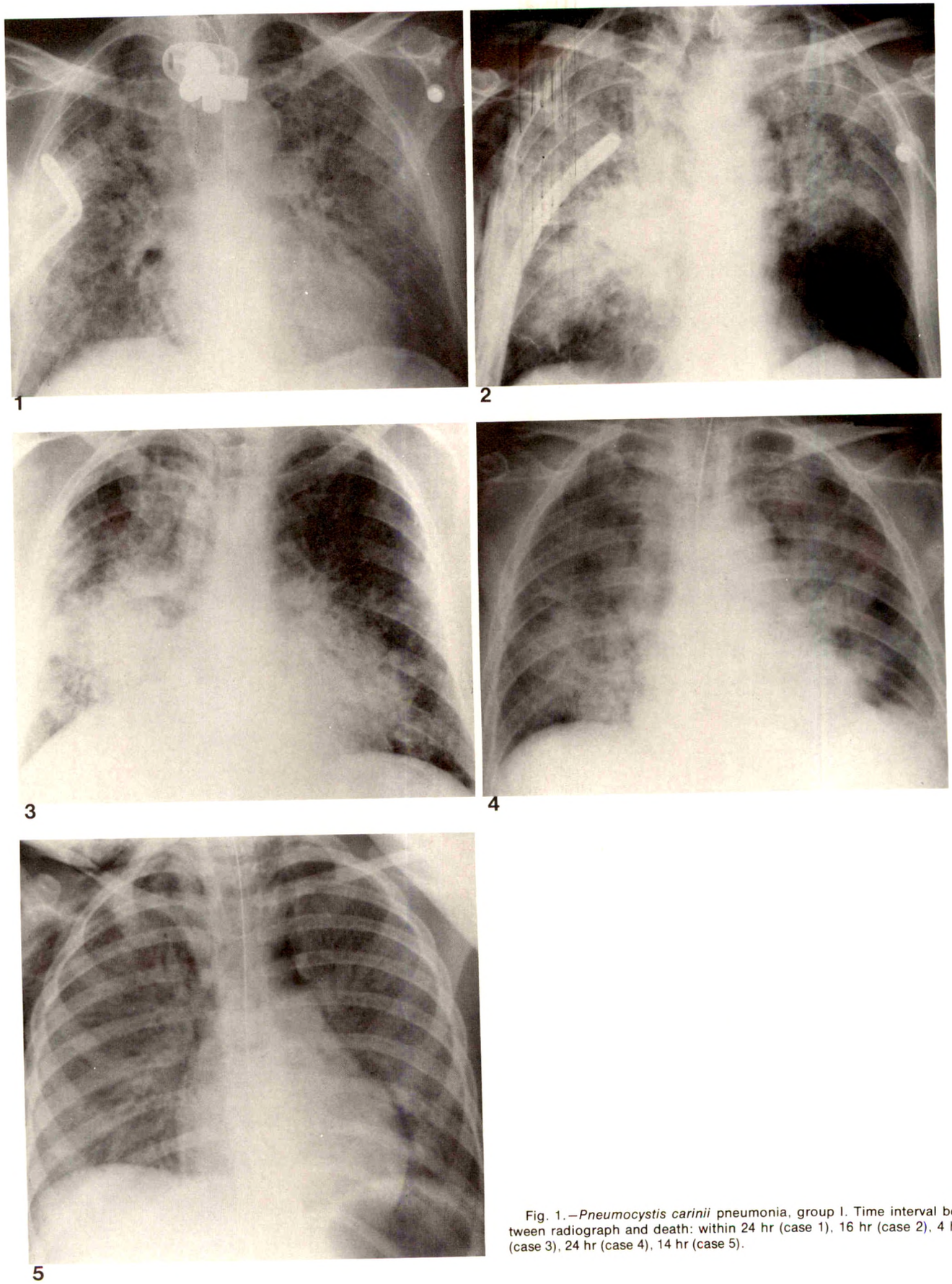
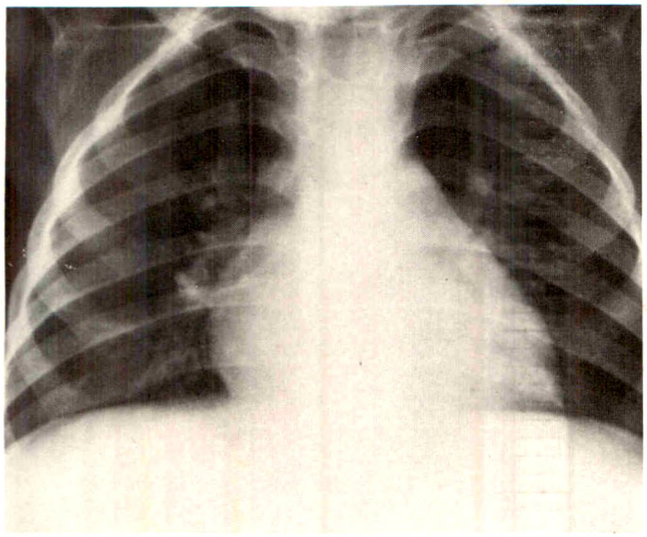
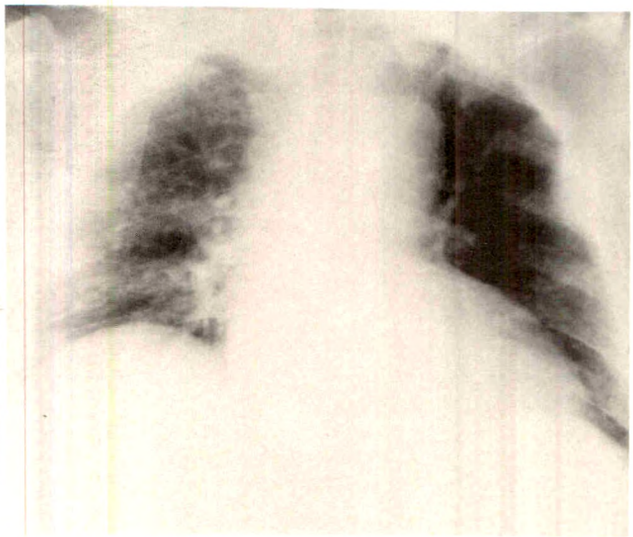


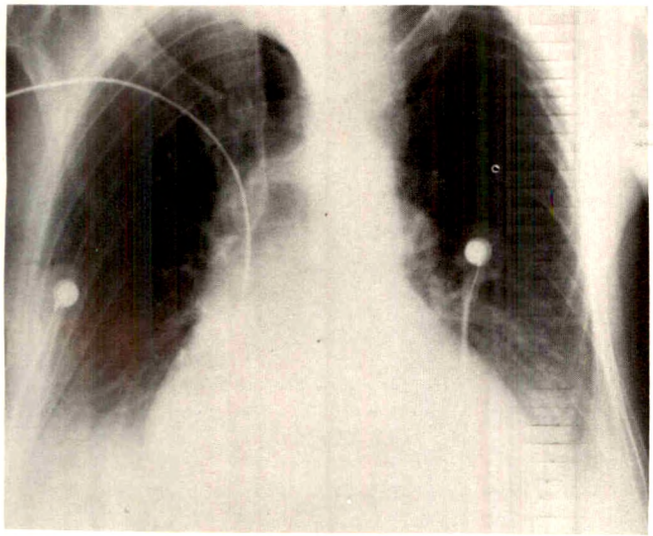
Fig. 1.—*Pneumocystis carinii* pneumonia, group I. Time interval between radiograph and death: within 24 hr (case 1), 16 hr (case 2), 4 hr (case 3), 24 hr (case 4), 14 hr (case 5).



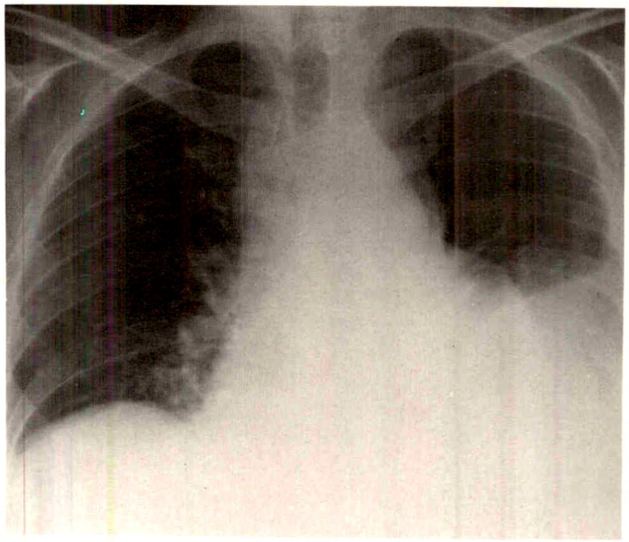
6



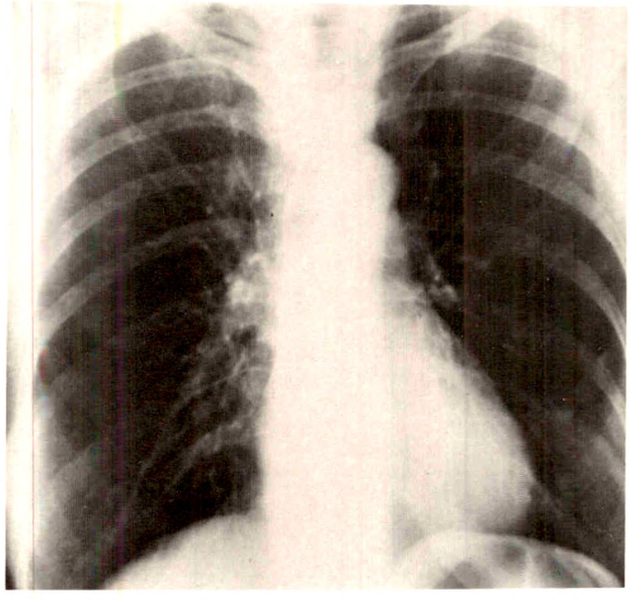
7



8



9



10

Fig. 1.—*Pneumocystis carinii* infestation, no pneumonia, group II. Time interval between radiograph and death: within 2 days (case 6), 3 days (case 7), 22 hr (case 8), and 24 hr (cases 9 and 10).

postirradiation sparing of lung [12], were not encountered. On the other hand, the group 2 patients showed no evidence of diffuse parenchymal lung disease. At most, pulmonary changes in this group indicated pulmonary venous congestion and heart failure. It should be noted that our study differs very radically from previous studies in that any suggestion of a coincident infective process, such as bacterial pneumonia, relegated the case to group 3. As far as was reasonably possible, the cases in group 1 were established as uncomplicated *P. carinii* pneumonia.

As there is no single reliable laboratory test for *P. carinii* pneumonia short of histologic examination, any information the chest films might offer would be useful. This study suggests that the chest radiograph is capable of sharply separating subclinical *P. carinii* infestation from manifest *P. carinii* pneumonia. In this small series, chest radiography accurately reflected the extent of the host response to the organism. It indicated the extent and severity of the cellular reaction and alveolar exudation.

However, as is well known, the radiographic findings in *P. carinii* pneumonia are not specific. The differential diagnosis of diffuse pulmonary opacities in an immunocompromised patient with an underlying hematologic malignancy would range from direct lymphomatous or leukemic involvement of the lung through adult respiratory distress syndrome from sepsis, pulmonary hemorrhage, and edema to the opportunistic viral, protozoal, bacterial, and fungal pneumonias. Lung biopsy is often necessary for differentiation. The finding of *P. carinii* organisms does not per se indicate that the infiltrates are a specific host response to these organisms, but certain histologic features described above are extremely valuable in this respect. Nevertheless in the appropriate clinical setting the development of extensive confluent opacities on the chest radiograph must make *P. carinii* pneumonia a very serious diagnostic consideration.

REFERENCES

1. Esterly JA, Warner NE: *Pneumocystis carinii* pneumonia. Twelve cases in patients with neoplastic lymphoreticular disease. *Arch Pathol* 80:433–441, 1965
2. Sedaghatian MR, Singer DB: *Pneumocystis carinii* pneumonia in children with malignant disease. *Cancer* 29:772–777, 1972
3. Perera DR, Western KA, Johnston HD, Johnson WW, Schultz MG, Akers PV: *Pneumocystis carinii* pneumonia in a hospital for children. Epidemiologic analysis. *JAMA* 214:1074–1078, 1970
4. Sheldon WH: Subclinical *Pneumocystis pneumonitis*. *Am J Dis Child* 97:287–297, 1959
5. Pifer LL, Hughes WT, Stagno S, Woods D: *Pneumocystis carinii* infection: evidence for high prevalence in normal and immunosuppressed children. *Pediatrics* 61:35–41, 1978
6. Weber WR, Askin FB, Dihner LP: Lung biopsy in *Pneumocystis carinii* pneumonia. A histopathologic study of typical and atypical features. *Am J Clin Pathol* 67:11–19, 1977
7. Capitanio MA, Kirkpatrick JA: *Pneumocystis carinii* pneumonia. *AJR* 97:174–180, 1966
8. Thomas SF, Dutz W, Khodadal EJ: *Pneumocystis carinii* pneumonia (plasma cell pneumonia). *AJR* 98:318–322, 1966
9. Falkenbach KH, Bachmann KD, O'Loughlin BJ: *Pneumocystis carinii* pneumonia. *AJR* 85:706–713, 1961
10. Cross AS, Steigbigel RT: *Pneumocystis carinii* pneumonia presenting as localized nodular densities. *N Engl J Med* 291:831–832, 1974
11. Doppman JL, Geelhoed GW, DeVita VT: Atypical radiographic features in *Pneumocystis carinii* pneumonia. *Radiology* 114:39–44, 1975
12. Forrest JV: Radiographic findings in *Pneumocystis carinii* pneumonia. *Radiology* 103:539–544, 1972

Endometriosis: Clinical and Ultrasonic Correlation

BEVERLY G. COLEMAN,[1] PETER H. ARGER, AND CHARLES B. MULHERN, JR.

Thirteen patients with surgically proven endometriosis underwent ultrasonography as part of their diagnostic evaluation. An attempt was made to assess the sonographic characteristics of endometriosis to determine if a characteristic pattern would emerge when the clinical presentations and physical findings were coupled with the ultrasonic picture. Ultrasound showed pelvic masses in all patients. Most masses appeared spherical and separate from the uterus and were cystic or predominantly cystic with scattered peripheral echoes. This retrospective study suggests a more useful role for ultrasound than previously recognized in the clinical management of patients with endometriosis.

Endometriosis results from the presence of actively functioning endometrial tissue in an aberrant location. Almost any organ of the body may be involved. The most common site is the cul-de-sac of the pelvis. Other frequently affected pelvic organs include the ovaries and fallopian tubes, uterus, rectosigmoid colon, and bladder. Remote disease has been described in the lungs and pleura, extremities, skin, umbilicus, appendix, kidney, and ureter [1].

Endometriosis is a clinical enigma because of its variable manifestation. The disease ranges from being totally asymptomatic to completely disabling. There is often a marked disparity between the extent of the disease and the symptomatology. Early diagnosis is crucial because endometriosis tends to be progressive and can result in complete loss of childbearing potential. Exploratory laporatomy is often performed when the diagnosis is still uncertain.

Gray scale image processing has resulted in enhancement of soft tissue detail in ultrasonic examination of the pelvis. This study attempted to assess the sonographic characteristics of endometriosis to determine if a characteristic pattern would emerge when the clinical presentations and physical findings were coupled with the ultrasonic picture.

Subjects and Methods

In the last 3 years, 13 patients with a histologically proven diagnosis of endometriosis underwent ultrasonic examination as part of their diagnostic evaluation. All examinations were performed prior to surgery with commercially available gray scale units, including a Picker EDC-6 and a Unirad Sonograf III. Either a 2.25 MHz or a 3.5 MHz transducer with the appropriate focus was used. Images were recorded on both Polaroid and x-ray film. Serial transverse and longitudinal scans at 1 cm intervals were performed on all patients. The ultrasound examinations were collected and subsequently reviewed for similarities. While all patients were known to have endometriosis, the extent of involvement and ultrasonic characteristics of the disease were not known. All cases were initially reviewed by one observer to evaluate both the extent of disease and its sonographic character. These observations were then reviewed and confirmed by two other observers.

Of 13 patients, 12 ranged in age from 21 to 32 years. The other patient was 66 years old. All patients were of low parity, none having experienced more than two term deliveries. The most frequent presenting complaints were pelvic pain and infertility.

In seven cases, clearly definable mass lesions were palpated on the initial physical examination. In two cases there was nonspecific nodularity, thickening, or tenderness in the cul-de-sac. In four cases, the pelvic examination was entirely normal. The disease was restricted to the pelvis in all cases except one (case 2) in which the endometrioma was at the incision site of a previous laparoscopy (fig. 1). The chronicity of the disease was evident in that most patients required two or more hospitilizations and underwent two or more surgical procedures because of recurrent disease. In two cases, surgery was delayed due to other clinical problems. Three cases are very recent and only one surgical procedure has been performed in each case thus far.

Results

Ultrasound was superior to the physical examination in indicating the presence of a mass lesion. Masses were seen on all ultrasound examinations even though there was no physical evidence of a mass in four of the 13 cases. Masses were 2–11 cm in their greatest dimension. In two cases, distinctly separate bilateral adnexal masses were seen (fig. 2). The overall shape of the mass was spherical in 10 cases (fig. 3). Eight masses had the acoustic properties of a cyst (fig. 4), two were solid, and three were complex with a predominently cystic component. In 10 cases, echoes occurred in the dependent or more peripheral portions of the mass (fig. 5). One cystic mass had a fluid level with echoes that dropped to the dependent portion of the mass when the patient was repositioned (fig. 6). In eight cases the masses were definable as structures separate from the uterus (fig. 7). Four cases lacked a distinct interface between the uterus and the adjacent mass. In one case there was an intervening pregnancy (fig. 8).

The surgical findings correlated well with the ultrasonic character of the lesions. In the mass with a fluid level, a chocolate cyst was found at surgery (case 4). No mass uterine interface was seen in four cases (cases 6, 9, 10, 13). In two of these four cases, the masses were very irregular in shape. Surgery revealed extensive pelvic endometriosis with uterine adhesions in three cases. In the fourth case (case 13), endometrial tissue had invaded the colon and bladder. Three cases required total abdominal hysterectomy and bilateral salpingo-oophorectomy thus demonstrating the serious nature of the dis-

Received August 3, 1978; accepted after revision February 9, 1979

[1]All authors: Department of Radiology, Hospital of the University of Pennsylvania, 3400 Spruce Street, Philadelphia, Pennsylvania 19104. Address reprint requests to B. G. Coleman.

© 1979 American Roentgen Ray Society

0361–803X/79/1325–0747 $0.00

ease. The results of the clinical and ultrasonic observations are summarized in table 1.

TABLE 1

Ultrasound Characteristics of Endometrial Masses

Acoustic Properties/ Case No.	Maximum Diameter (cm)	Mass/ Uterine Interface	Peripheral Echoes in Mass
Cystic:			
1	7	Yes	Yes
2	2	...	...
3	4	Yes	Yes
4	11	Yes	Yes
7	7	Yes	Yes
8	2R, 4L	Yes	Yes
11	8	Yes	Yes
12	5R, 3L	Yes	Yes
Complex:			
6	11	No	Yes
9	6	No	Yes
13	7	No	Yes
Solid:			
5	5	Yes	No
10	4	No	No

Note.—The masses in cases 6, 10, and 13 were of irregular shape; all others were spherical.

Discussion

Based on histologic studies, the incidence of endometriosis in all women undergoing gynecologic surgery, now varies from a low of 8% to as much as 30% [2]. Endometriosis is a difficult disease to manage clinically, and an optimal response to therapy is most likely if the disease is detected in its early stages prior to the development of an extensive inflammatory reaction. Therefore, it is important to recognize the disease as early as possible.

In our hospital, a large infertility clinic yields a considerable number of patients who are being managed for endometriosis. Since the clinical picture of endometriosis is often relatively specific, many of these patients are treated surgically with laparoscopy, commonly followed by laparotomy if indicated. Ultrasonography has not been performed as frequently as barium enemas and excretory urography.

The results of this study indicate that the ultrasonic appearance of endometriosis is more specific than previously appreciated. Pelvic masses are commonly visualized, though often not palpable on pelvic examination. Most of the masses encountered were either cystic or complex and the majority possessed a predominantly echo-free central core with scattered echoes confined to the periphery or dependent portion. Most masses were separate from the uterus. Contiguity with the uterus and/or an irregular shape indicated extensive disease with associated adhesions of the uterus. A very irregular mass also indicates the probability of involvement of adjacent organs such as the bladder and colon.

Other predominantly cystic masses that may pose a problem in the differential diagnosis include ovarian lesions such as cysts, abscesses or neoplasms, and ectopic pregnancy. Simple ovarian cysts differ from endometriosis in that these masses, although spherical, are usually sharply marginated and entirely echo free [3]. The masses are commonly discovered on routine physical examination in asymptomatic patients. Tuboovarian abscesses may be primarily cystic or complex. These are usually thick walled and irregular in shape with coarse internal echoes. The clinical setting is often the differentiating factor in that there is frequently moderate to severe tenderness on bimanual examination in patients with an elevated sedimentation rate, temperature, and white blood cell count [4]. On the other hand, patients with endometriosis seldom have signs of systemic infection.

Cystadenomas or cystadenocarcinomas are relatively uncommon ovarian neoplasms. Pseudomucinous cystadenomas tend to be multiloculated with a complex internal echo pattern because of the mucinous contents of the mass. Serous cystadenomas usually appear as smooth, thin-walled cysts. Two mucinous cystadenocarcinomas have been described as cystic masses with prominent septations like spokes of a wheel. Ascites may be associated with both serous and mucinous cystadenocarcinomas [5]. These lesions are usually discovered routinely in asymptomatic patients, or after metastatic spread of malignant disease.

With an ectopic gestation some uterine enlargement usually occurs with diffuse amorphous echoes secondary to the response of endometrial tissue to circulating hormones. A primarily cystic adnexal mass may be seen with an irregular margin. The clinical setting is often quite different from endometriosis. Patients may have a positive pregnancy test, irregular vaginal bleeding or passage of tissue fragments, and acute onset of severe abdominal pain or shock. An ectopic gestation can be diagnosed with certainty only if an adnexal mass is associated with an identifiable extrauterine gestational sac [6].

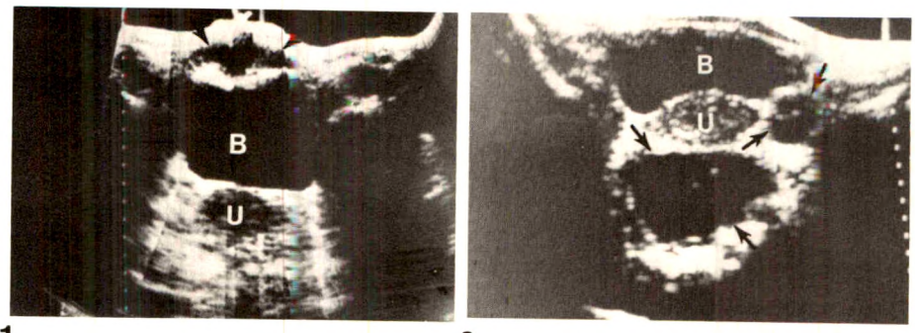
At the outset of this study, the diagnosis of endometriosis was seldom suggested to the clinician prior to surgery. However, after learning the histologic diagnosis and reviewing the echogenic characteristics of masses seen in the earlier cases, our ability to recognize the disease improved considerably. This enabled us to inform the surgeon of the most likely diagnosis of endometriosis prior to operation in our most recent cases.

Endometriosis should be suggested as the most likely diagnosis if the previously described clinical and ultrasonic criteria are met. We have found that the most important clinical findings are relatively young patients (21–32 years), nulliparous or of low parity, and with pelvic pain or infertility without laboratory data suggesting infection. The most important ultrasonic findings are cystic or predominantly cystic adnexal masses with peripheral echoes, spherical, and definable as separate structures from the uterus.

We believe ultrasound has a more useful role than usually ascribed to it in the diagnosis and clinical management of endometriosis. It provides a means of accurately assessing the presence, location, size, and echogenic characteristics of pelvic masses that may not be discernible clinically. In cases where surgery is contem-

Fig. 1.—Case 2. Transverse scan through pelvis. Small cystic endometrioma (*arrows*) in subcutaneous tissues just anterior to bladder (B). Endometrioma is in inferior portion of laparoscopy scar. U = uterus.

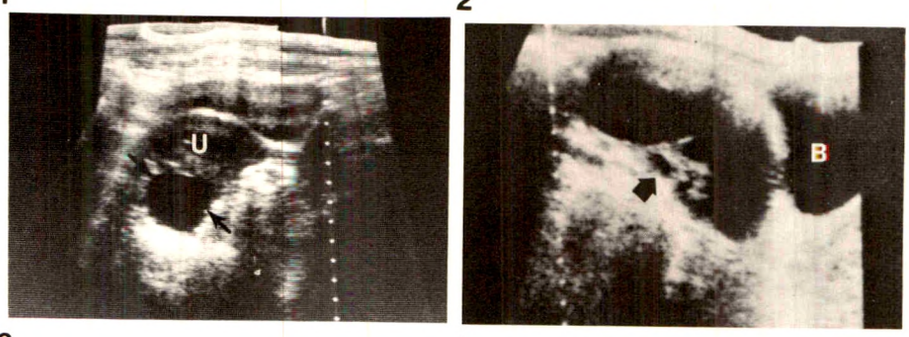
Fig. 2.—Case 12. Transverse scan through pelvis 10 cm below umbilicus. Bilateral endometriomas (*arrows*) clearly definable as separate structures from uterus (U). B = bladder.



1 2

Fig. 3.—Case 3. Transverse scan 12 cm from umbilicus. Spherical cystic mass (*arrows*) posterior to uterus (U).

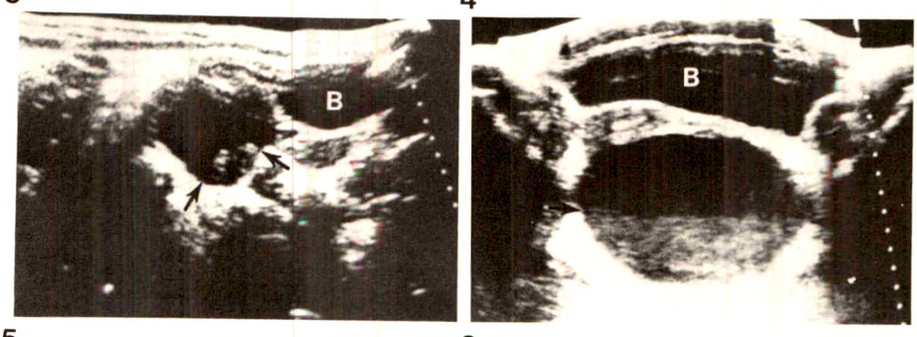
Fig. 4.—Case 6. Longitudinal scan 3 cm right of midline. Predominantly cystic mass with echoes confined to periphery of lesion (*arrow*). B = bladder.



3 4

Fig. 5.—Case 12. Longitudinal scan 4 cm left of midline. Echoes in dependent portion of endometrioma (*arrows*) of ovary.

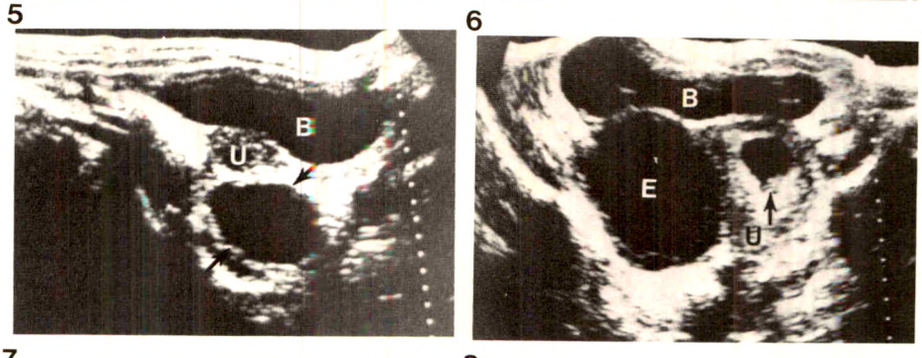
Fig. 6.—Case 4. Transverse scan of 11 cm endometrioma with apparent fluid level (*arrows*).



5 6

Fig. 7.—Case 7. Longitudinal scan in midline of pelvis. Bladder (B), uterus (U), and clearly separate cystic endometrioma (*arrows*).

Fig. 8.—Case 11. Transverse scan of pelvis. Intrauterine pregnancy with a gestational sac (*arrow*) within uterus (U) and large cystic endometrioma (E) in right adnexal region.



7 8

plated, valuable information may be obtained regarding the extent of disease and the likelihood of involvement of other organs. A specific histologic diagnosis of endometriosis can be suggested in conjunction with a strong supportive clinical history.

REFERENCES

1. William TJ, Pratt JH: Endometriosis in 1,000 consecutive celiotomies: incidence and management. *Am J Obstet Gynecol* 129:245–250, 1977
2. Ranney B: The prevention, inhibition, palliation and treatment of endometriosis. *Am J Obstet Gynecol* 123:778–784, 1975
3. Cochrane WJ: Ultrasound in gynecology. *Radiol Clin North Am* 13:457–66, 1975
4. Uhrich PC, Sanders RC: Ultrasonic characteristics of pelvic inflammatory masses. *JCU* 4:199–204, 1976
5. Lawson TL, Albarelli JN: Diagnosis of gynecologic pelvic masses by gray-scale ultrasonography: analysis of specificity and accuracy. *AJR* 128:1003–1006, 1977
6. Maklad NF, Wright CH: Gray-scale ultrasonography in the diagnosis of ectopic pregnancy. *Radiology* 123:221–225, 1978

Primary Renal Calculi: Anderson-Carr-Randall Progression?

ANDRÉ BRUWER[1]

Although numerous reports deal with the histology of renal medullary calcification, there has been only limited application of radiographic methods for its description. From routine autopsy material, findings on 61 kidneys studied by high resolution radiography are presented and related to those of Randall (1937), Anderson (1945), Carr (1954), and others. Histologically Anderson found microscopic plaques formed from coalesced calcific "droplets" in the pyramids of practically all of 168 kidneys, including some very young infants. Carr, using microradiographic techniques, also found calcific deposits in nearly all of 209 kidneys from patients over 9 years of age. Anderson and Carr separately concluded that the calcific deposits they demonstrated could, by migration, form the subepithelial plaques that Randall observed earlier. The present work illustrates some radiologic aspects of renal calcification which seem to support a hypothesis that primary renal calculi result, under certain circumstances, from the migration of calcific deposits from the substance to the surface of renal papillae. In order to emphasize the pathogenetic sequence of the work of the previously mentioned authors, it is proposed that the sequence of events be referred to as the Anderson-Carr-Randall morphologic progression of primary renal calculus formation. Proposals are made for additional experimental work.

Although much literature relates to the role of the kidney in the physiology and pathophysiology of calcium metablism [1, 2], the site of the formation of primary renal calculi is still uncertain. This is illustrated, for example, by some of the questions and answers given during discussions of the subject at a recent National Research Council Conference on the physical aspects of urolithiasis [3]. To the question whether a stone is formed in the renal substance or at the outlet of the tubules, the answer was that this is not known and that there are several points of view [3]. To a similar question another speaker replied that there was no certainty whether a stone formed in the renal papilla or in the calyces or perhaps even at a higher level than the papilla " . . . where stones actually originate constitutes a problem. . . . " [3].

Whereas some of the pieces of the puzzle of primary renal stone-formation seem to have been uncovered, a definitive study putting them together into a recognizable whole is still to be done. These include the observations of Randall [4, 5] suggesting an "initiating lesion" arising from a subepithelial calcium-containing plaque (Randall's plaque); the finding by Anderson and McDonald [6, 7] that microscopic calcareous deposits in the renal papilla are very common and may be normal; the work of Carr [8, 9] who showed that calcium could frequently be radiographically demonstrated in the kidney, and who theorized that the function of the renal lymphatic system plays a critical role in renal stone formation.

Building on an earlier proposal by Carr [3] and on more recent work by Haggitt and Pitcock [10] on the electron microscopic demonstration of renal parenchymal calcification, the following hypothesis is stated:

1. Histologically demonstrable calcium-containing structures are normally present in the human kidney.

2. Under abnormal conditions the normally present calcium accumulates in larger concretions which may either remain within the renal parenchyma or may migrate centrally, to the surface of one or more renal papillae and may then become clinically significant. Under these circumstances the calcium may be radiologically detectable, either by clinical or experimental radiographic methods, depending on the size of the accumulation. Such abnormal conditions would include one or more of many factors (e.g., biochemical, dietary, geographic, hormonal, immunologic, etc). The extent of the abnormal renal calcium deposition would depend on whether the entire environment of the kidney (renal macroenvironment) or only a small segment of the environment of the kidney (renal microenvironment) had been affected by such factors.

In the hope that an eponymous title will maintain a focus on the pathogenetic unity of the contributions of the original workers, the term *Anderson-Carr-Randall progression of renal calculus formation* is proposed.

There is a remarkable lack of radiographic literature dealing with the demonstration of renal calcific patterns in autopsy material. I present relatively limited radiographic findings from routine autopsy material, as they seem to lend support to the findings of those observers previously mentioned and to the hypothesis presented. Certain observations suggest further work that might define more clearly the pathogenesis of renal calculus formation.

Materials and Methods

The material presented in this report was derived from 61 grossly normal (except for postmortem congestion) kidneys removed at an equal number of autopsies. The 61 kidneys were from 27 female and 34 male patients aged 14–83 years. Most of the patients had died of conditions common to most busy community hospitals: chronic pulmonary diseases, diseases associated with arteriosclerosis, leukemia, and also following various types of surgery and subsequent complications. The state of hydration and nutrition and the biochemical composition of each patient's blood and urine prior to death unfortunately were not recorded and cannot be determined in retrospect. They might have provided interesting correlations with the radiographic studies of the autopsy tissue. Although many interrelated factors in the nutritional aspects of metabolic problems are associated with urolithiasis, the patient's fluid intake is by far the most important factor relating to the actual formation

Received July 6, 1978; accepted after revision January 29, 1979.
[1] Radiology, Ltd., no. 59, 601 North Wilmot, Tucson, Arizona 85711.

© 1979 American Roentgen Ray Society

0361–803X/79/1325–0751 $0.00

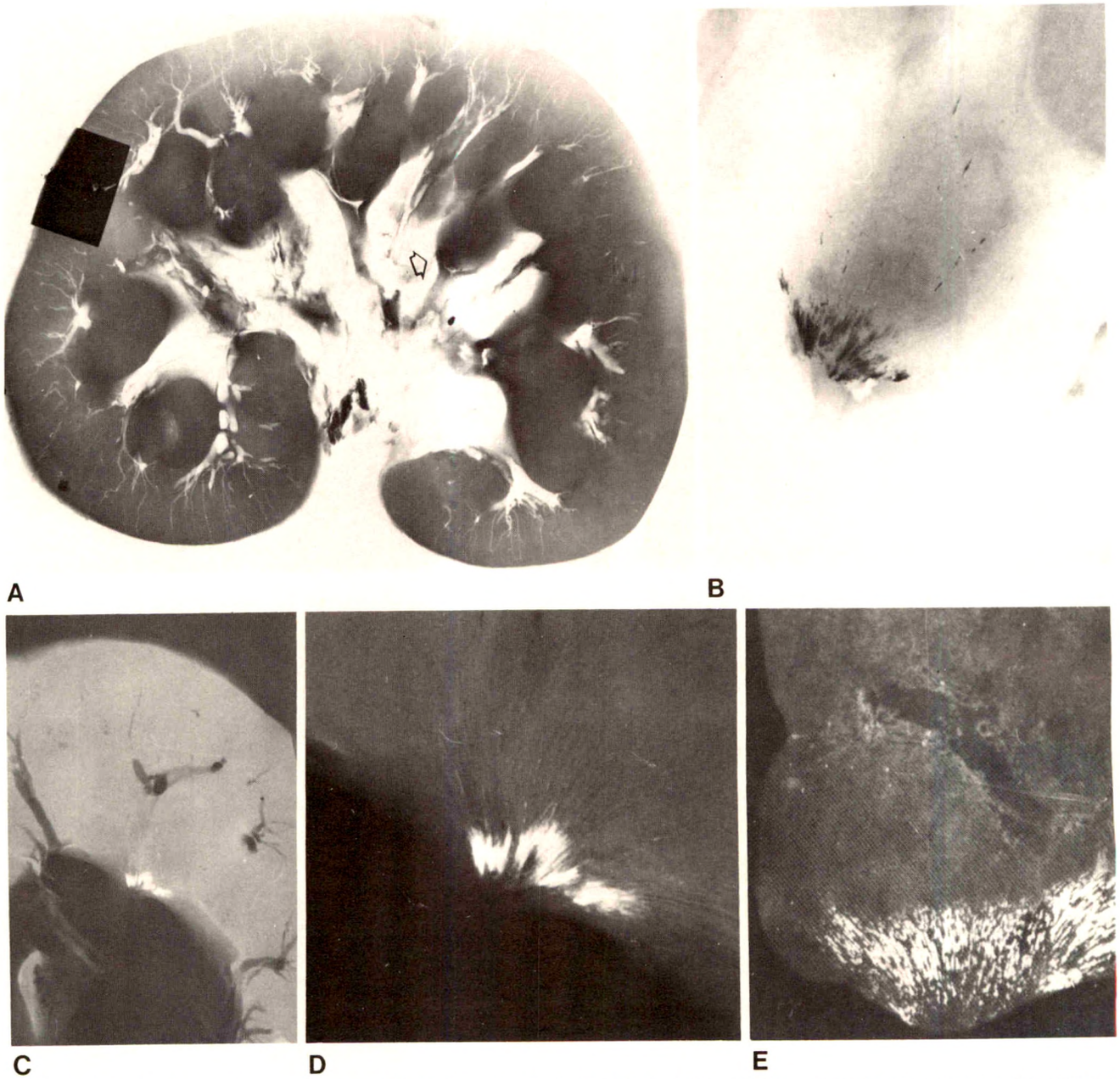


Fig. 1.—**A** and **B**, 51-year-old woman who died of multiple sclerosis. **A**, Radiograph of slice of kidney. Papilla (*arrow*) shows fan-shaped calcific pattern. **B**, Detail of **A**. **C** and **D**, 57-year-old woman who died of reticulum cell sarcoma. **C**, Radiograph of slice of tip of complex renal papilla demonstrating fan-shaped calcific pattern. **D**, Detail of **C**. **E**, Alizarin red-stained full-thickness section of histopathologic preparation of renal papilla (reprinted with permission from [11]).

or lack of formation of renal calculi according to Smith et al. [2].

The kidneys we examined were part of a larger group (160 kidneys) removed for the purpose of vascular anatomic injections. For various reasons the 61 cases used for this paper were found to be unsuitable for injection studies.

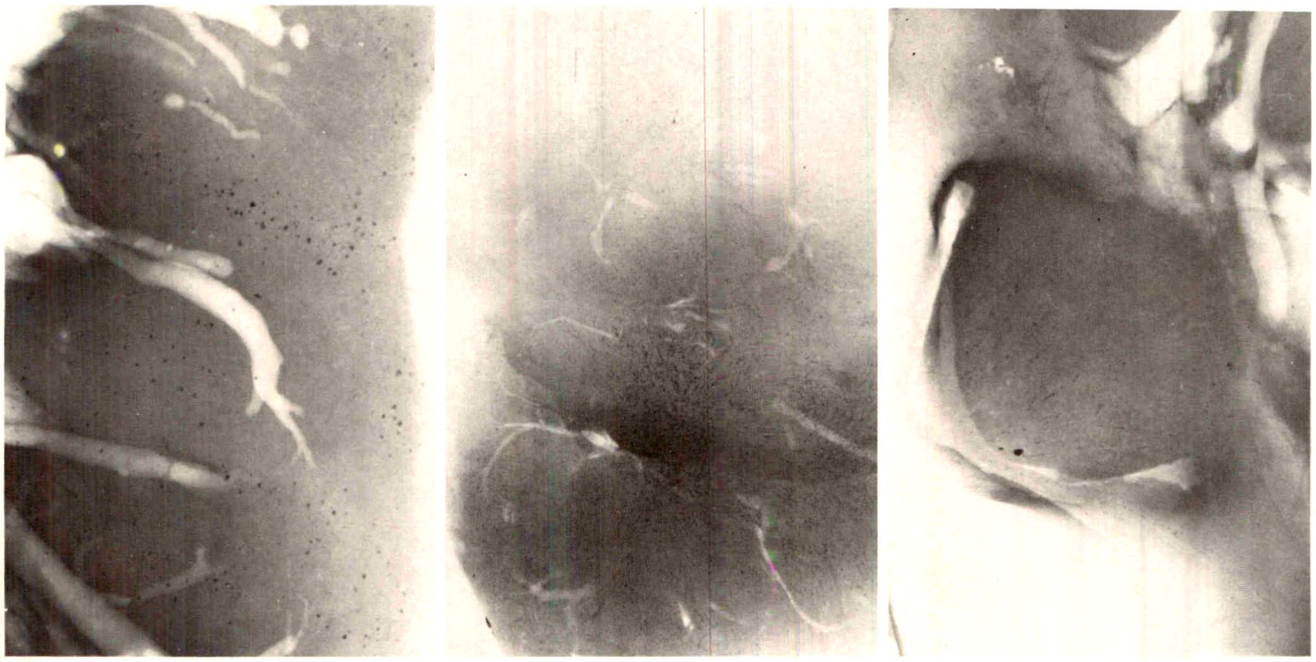
Radiography was first performed on the intact kidneys. Subsequently the kidneys were immersed in formalin for 2–3 days. Longitudinal coronal slices about 4 mm thick were then made, and the slices were radiographed.

All radiography was performed with Faxitron (Hewlett-Packard) equipment and Eastman Kodak industrial type film, either Type M or Type R, or both. The whole kidneys were exposed at 28 kVp and the slices at 16–18 kVp. Using a ×7 calibrated hand lens, we were able to see calcific particles of about 100 μm and perhaps even somewhat smaller.

In only 10% of these cases were radiographs that included the renal areas taken prior to death. In none of these could renal calcification be detected with any certainty.

Observations

Excluding calcification seen in arteriosclerotic vessels and in one tumor, we found evidence of varying degrees of parenchymal calcification in 39 of the 61 kidneys examined. This seemed to confirm radiologically a num-



A B C

Fig. 2.—**A**, 59-year-old woman who died of emphysema and cor pulmonale. Radiograph of slice of kidney, considerably enlarged. Cortical margin on right and pyramids at left. Numerous rounded 0.2 mm calcific densities throughout renal substance. **B**, 73-year-old woman who died with severe arteriosclerosis, active pyelonephritis, and arteriolar nephrosclerosis. Radiograph of slice near renal surface, considerably enlarged. Much of the calcification evident only under hand lens magnification. **C**, 66-year-old man who died with generalized arteriosclerosis. Radiograph of renal papilla. Note many tiny globular and streaky calcifications extending throughout pyramid. Several large calcifications near tip. Because of the thickness of the slice, some calcifications appear to lie outside contour of papilla. They are converging from bases of complex pyramid.

ber of calcific patterns previously described by others in histologic material. Thus, we demonstrated the following predominant patterns:

1. A fan-shaped pattern of calcific streaks, focusing on the tip of the renal papilla (figs. 1A–1D). This pattern conforms to the calcific pattern shown, for instance, in the full-thickness photomicrograph of a renal papilla illustrated by Cooke (fig. 1E) [11]. This pattern was found in 25 of the 61 kidneys, occurring in patients 28–83 years old.

2. A second pattern, composed of spherical stipples of calcification varying in size from being barely perceptible through a ×7 hand lens to about 0.2 mm, occurred in 23 kidneys of patients 14–77 years old. These calcific deposits varied widely in number, from a few scattered or clustered deposits to, in one case, a veritable cloud of particles. Such particles could be seen in any part of a kidney, but appeared to be more frequent in the medulla (fig. 2).

In 10 patients calcifications conforming to both patterns A and B were seen.

3. Another pattern, with the impression of calcific spherules clustered in a mulberry pattern, was seen in three middle-aged patients. One (fig. 3A) had an appearance similar to a case described by Randall in 1937 [4]. It was triangular, about 4 × 1.5 mm, and seemed plastered against the side of a complex papilla in the region of the fornix. An almost identical calcific density, identified as a "Randall's plaque," was illustrated in figure 4 of the article by Stewart [12], from a previously unpublished radiograph attributed to Carr.

Photographic magnification of the "plaque" in my case unexpectedly revealed that it was apparently composed of multiple tiny spherules (fig. 3B). It is obvious that this finding is identical to that of Carr in 1954 [8]. He found that "radiographs of thick sections through papillae with adherent stones confirm the view that in reality the 'plaque' is composed of multiple concretions aggregated together. . . ."

A kidney from another patient showed a semispherical calcific mass located along the lateral aspect of a papilla. This 4.5 × 3 mm density also had a mulberry appearance.

A kidney of a third patient showed a 4-mm-diam calcific deposit at the tip of a papilla (fig. 4A). Of interest is the fact that the main calcific mass appears to be "followed" by several smaller globular densities of the type described by Carr [8]. Of additional interest in the latter kidneys was the appearance of a striated calcific pattern in another papilla, which also contained a few tiny calcific spherules (fig. 4B). One can only speculate that the renal papilla of figure 4A at one time might have had the appearance seen in figure 4B.

Discussion

In 1937 Randall [4] first described his findings of a "milk patch" at or near the tip of one renal papilla in 12 kidneys from 104 routine autopsies. These plaques were visible by a hand lens and microscopically were seen to

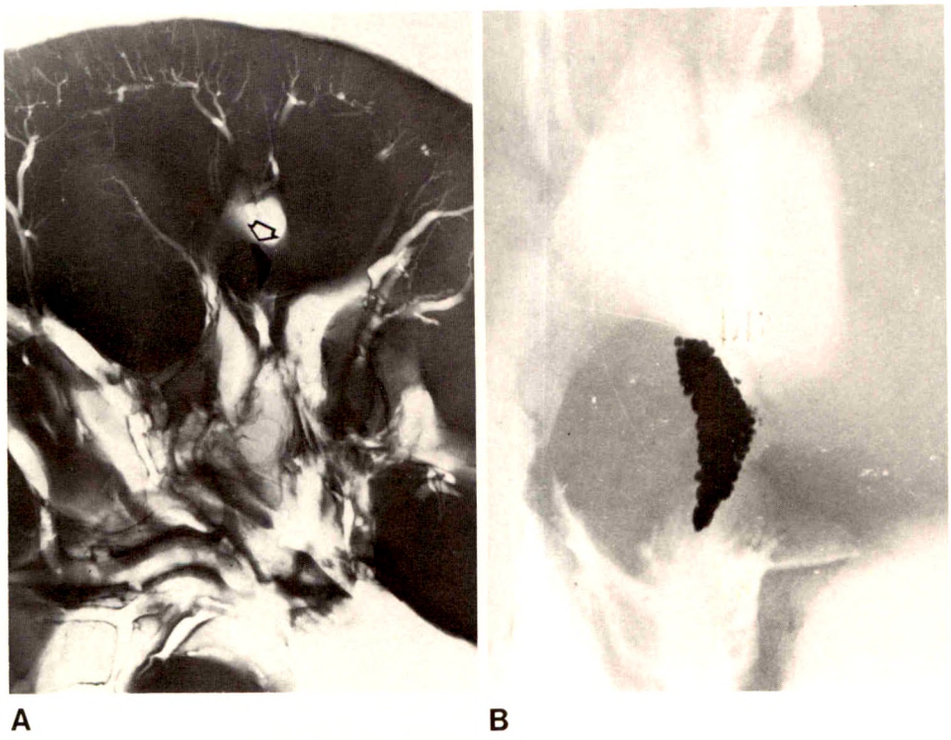


Fig. 3.—58-year-old man who died of bronchogenic carcinoma. **A**, Radiograph of slice of kidney. Calcification (*arrow*) near fornix of complex papilla. **B**, Detail of calcification. Actual size of calculus about 1.5 × 3 mm. Note mulberry contour.

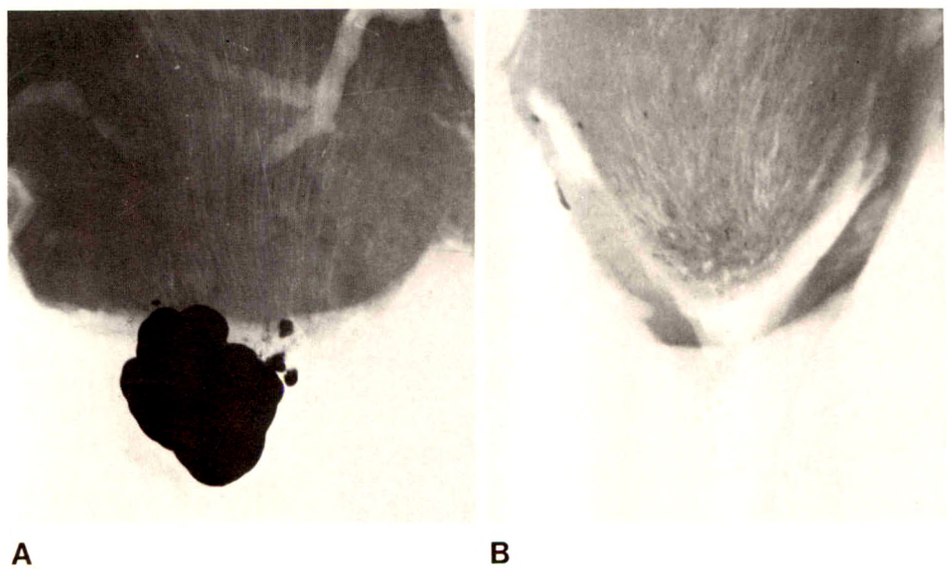


Fig. 4.—**A**, Radiograph of papillary tip and calyx. Calculus at tip of papilla. Note small, separate globular calcifications migrating (?) toward tip. Also fine calcific streaks in body of pyramid. **B**, Another papilla from same patient. Note striated pattern of calcific stipples and streaks in pyramid and calyceal wall.

be subepithelial. In one kidney such plaques had eroded through the papillary epithelium and had become the "initiating lesion" for the formation of a triangular mulberry calyceal calculus plastered against the side of its papilla.

Subsequently, Randall [5] reported such plaques as occurring in 19.6% of kidneys examined in 1,154 autopsies. He proposed that they developed in a small area of degenerated papillary tissue.

In a recent microscopic study of renal medullary calcifications involving 200 kidneys from 100 randomly selected autopsies, Haggitt and Pitcock [10] noted that the renal papillae of 23 of the patients contained grossly recognizable Randall's plaques. Figure 5 is reproduced from their article, a beautiful illustration of the entity known as a Randall's plaque.

The work of Anderson and McDonald [6, 7] gave a reasonable clue to the nature and origin of Randall's "initiating lesion." In studying 148 surgically removed, diseased kidneys and 20 apparently normal autopsy kidneys, Anderson found microscopic evidence of calcareous plaques or tiny stones in the parenchyma of renal pyramids in almost all specimens [6]. In only three grossly diseased kidneys, all from patients under age 2, he did not find such calcific deposits. Anderson pointed out that his determinations were made from an average

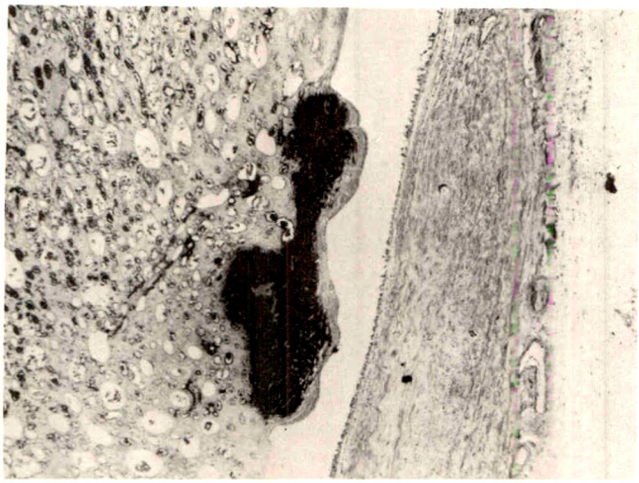


Fig. 5.—Subepithelial calcium deposit (Randall's plaque) at lateral margin of renal papilla reduced from ×35 (reprinted with permission from [10]).

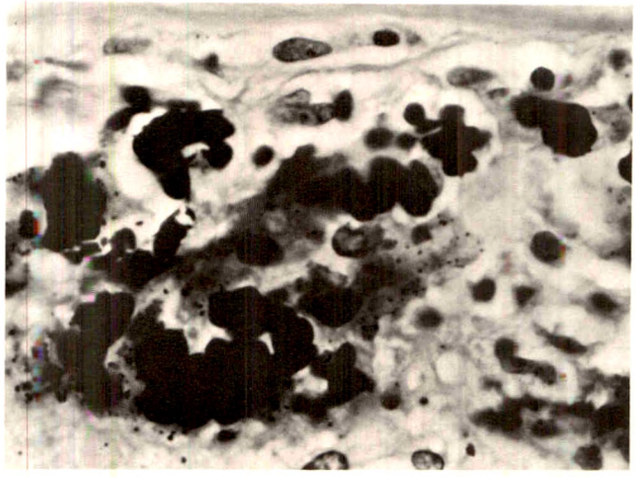


Fig. 6.—Photomicrograph from section of pyramid of pyelonephritic kidney (×700). Clearly apparent coalescence of microscopic "droplets" and of such droplets into calcific plaques. (Reprinted with permission from [7].)

of only three microscopic sections per kidney. He estimated that it would take 10,000 microscopic sections to completely examine a kidney with 10 pyramids.

Anderson [6] cited two "generally accepted postulates regarding kidney physiology" and correlated them with his microscopic findings, proposing as a result "a somewhat different interpretation of the etiology of kidney stones" from the one proposed by Randall. The postulates to which Anderson referred were: (1) the concentration of calcium and related ions is high in the tissue fluids about the renal tubules, and (2) phagocytic cells, probably macrophages, are abundant about renal tubules, and macrophages have an affinity for calcium.

The interstitial calcareous plaques (microplaques) demonstrated by Anderson seemed to be the result of coalescence of innumerable microspherules of calcareous material. Anderson referred to the microspherules as "droplets." These "droplets" were apparently formed as a result of calcareous material being absorbed by phagocytic cells, these cells subsequently dying and leaving calcareous "droplets" in the interstitial tissues (fig. 6).

Location of these "droplets" beneath the epithelial covering of the renal papilla might be followed by erosion of the epithelium. Anderson proposed that Randall's plaques were probably the result of aggregation of microcalculi which he had described and *not* due to primary degenerative changes in the papilla.

Carr's work [8] offers the best radiographic studies to date. Unfortunately Randall, Anderson, and Haggitt and Pitcock [10] did not use radiography in conjunction with histologic methods. Carr examined, by extremely sophisticated radiographic techniques, 98 partial nephrectomy specimens and 111 kidneys obtained at autopsies from patients dying of nonrenal causes. Intact kidneys and slices of kidneys were radiographed. Extremely thin slices were examined at voltages so low that a vacuum had to be used between the tube and the specimen, some exposures lasting 24 hr. Fine-grain film allowing magnification of 200–300 diameters was used. He found that, in practically all kidneys from patients over age 9, small concretions just visible to the naked eye could be demonstrated. Usually one or two could be seen, but some kidneys contained a dozen or more. The majority of these concretions, when they reached a diameter of about 0.2 mm, were spherical. Some were as large as 1–2 mm in diameter.

Carr's concretions were primarily located in three regions: (1) just outside the calyceal fornices or at the sides of the renal pyramids in line with the interlobar vessels; (2) in the corticomedullary junction zone; and (3) immediately beneath the renal capsule.

An aggregation of these concretions could in some kidneys be seen in the region of the fornix or adherent to the side of a papilla, and such "plaques" could be seen to be composed of numerous macroscopic round concretions, much as Anderson's microliths were composed of numerous microscopic "droplets." Even when a large stone formed at the tip of a papilla, smaller ones were seen behind its base. This would seem to match our figure 4A.

So consistently did Carr, radiologist, and Stewart, his surgical colleague, find small concretions in the region of the fornix (just extrinsic of the forniceal lumen) that they have used, respectively, the terms Stewart's nest [9] and Carr's pouch [12] in their publications.

Carr suggested that because the microliths demonstrated by Anderson are apparently a normal phenomenon, one must account for the way in which the body disposes of them. He proposed that this function is performed by the lymphatic system. Carr cites the work of Goodwin and Kaufman (cited [9]) and of Rawson [13] on the lymphatic system, and indicates that the renal lymphatic system undoubtedly plays an enormously vital "cleansing" role in the kidney. To quote Carr [9]:

> We know that in the lungs particulate matter inhaled gets into the alveoli, and then it is taken up in the lymphatics and transported to

> where it can do no more harm, as long as the mechanism is working properly. I believe that the kidney functions in the same way. I think that effete cells, debris of all sorts, calcium which has been re-absorbed and come out of solution in the interstitial fluid where there is always debris available to act as a nucleus to precipitation all get removed with the protein and interstitial fluid into the lymphatics.

Carr postulated that any abnormality that can result in overload of calcium in the kidney, or interference with lymphatic drainage, could result in overproduction of microliths and the development and accumulation of larger concretions. The rounded shape of the latter, he postulated, can be attributed to their being molded in lymphatic channels. Any of these concretions (macroliths formed from microliths) could eventually erode into the calyceal lumen. They may be washed out or, by being adherent, grow in size in a calyx. Because of microregional pathologic changes in the kidney, calculi would tend to re-form in the same region after having passed or having been removed without resection of the involved area.

Epstein [1] pointed out that the glomeruli of a healthy adult filter about 9–10 g of calcium per day and that 98% of this is reabsorbed by the renal tubules. Ullrich and Jarausch (cited in [1]) believed that the calcium content of the kidney manifests a gradient, the concentration being progressively higher toward the papillary tip. Such a chemical gradient was confirmed by the work of Cooke and Rosenzweig [14]. They found, by chemical analysis of calcium content in samples of kidney tissue, evidence of a calcium gradient in the human renal medulla, the highest values being in the region of the papilla.

Cooke [11], in a careful histologic examination of 62 apparently normal kidneys, found calcification in 43 cases (69 %). Calcium was seen in the papilla in all these cases, usually in substantial amounts, and occasional deposits were seen in the outer medulla in 20 cases. In nine cases calcification was seen in the cortex. Cooke's study showed that the location of papillary calcification was invariably in the basement membrane of the long loops of Henle, which descend for variable distances into the medulla, sometimes as far as the papilla. Although some showed evidence of calcium in all parts of the kidney, all showed calcium in the papilla. Cooke did not find calcium to lie free in the tubular lumens. Figure 1E, reproduced from Cooke's article, shows the fan-shaped calcific pattern, similar to that which we frequently encountered in our radiographs.

Anderson [6], too, concluded that the microscopic collections of calcium "seemed to occur anywhere except within the lumen of the tubule. A few specimens were found with the deposits within the tubules, but it seemed to me that they had eroded into the tubules from the surrounding parenchyma."

We should make reference to the work of Vermeulen et al. [15] on experimental calculogenesis. For example, by mixing oxamide in the diet of rats, they could rapidly produce spectacular oxamide deposits that extruded from the papillary tip. Streaks of oxamide crystals could be shown to involve the renal papillary substance extensively and these deposits were described as being "in the collecting ducts" [15], that is, quite unlike the findings of Anderson and Cooke in humans. Vermeulen et al. speculated that such accumulations usually "abort into the pelvis" and, being small enough, presumably usually wash out. But occasionally a small piece might be caught at the ostium of a duct of Bellini, thus providing an "embryo" upon which, under the right circumstances, crystallization would result in the development of a calculus.

Carr [9] does not believe that the work of Vermeulen et al. is relevant to the process of so-called primary renal calculus formation. He believes that their experimental results relate to nephrocalcinosis (i.e., "a totally different disease process to that of calculus formation").

Spheroidal morphology may have special significance. I was struck by the fact that many of the calculi demonstrated in the study material conformed to the spheroidal pattern described by Carr [8]. I also noted, as did Carr, that concretions might lie in a line or a chain. Another appearance that I noted was that spherules tend to cluster in the region of the papillary tip, sometimes seeming to follow a large calculus which appeared to be composed of multiple macrospherules in a mulberry or botryoidal pattern (figs. 3 and 4). Spheroidal geometry seems to play a basic role in the life cycle of primary renal calculi, from the microspheroidal stage to macrospheroidal agglomerations.

Haggitt and Pitcock [10] performed light and electron microscopic studies of renal medullary tissue obtained at necropsy from 100 patients aged 18–91 years. In all 100 pairs of kidneys examined, they were able to demonstrate minute laminated spherules which stained for calcium in the medullary interstitium and in the basement membranes of collecting ducts (fig. 7A). One of their illustrations of a typical spherule, enlarged ×54,000, demonstrates the lamination of these bodies beautifully (fig. 7B).

Doyle et al. [16] recently demonstrated concentric layering in concretions smaller than 50 μm obtained from mollusk kidneys (fig. 8).

Boyce [17] observed calcium and phosphate-containing microspherules and macrospherules by light, electron, and scanning electron microscopic analysis of calculi recovered from 28 patients classified as "idiopathic oxalate or phosphate stoneformers." Lamination was a common finding in their material.

Anderson and McDonald [6, 7] and Haggitt and Pitcock [10] found a strong tendency for aggregations of the concretions which they had described to migrate into a subepithelial location in the renal papillae, that is, for the formation of Randall's plaques, with a consequential proclivity to erode through the epithelium and initiate the development of a free calculus.

Conclusions

Hypothesis of Anderson-Carr-Randall progression of primary renal calculus pathogenesis. Anderson's histologic studies demonstrated the "normal" presence of

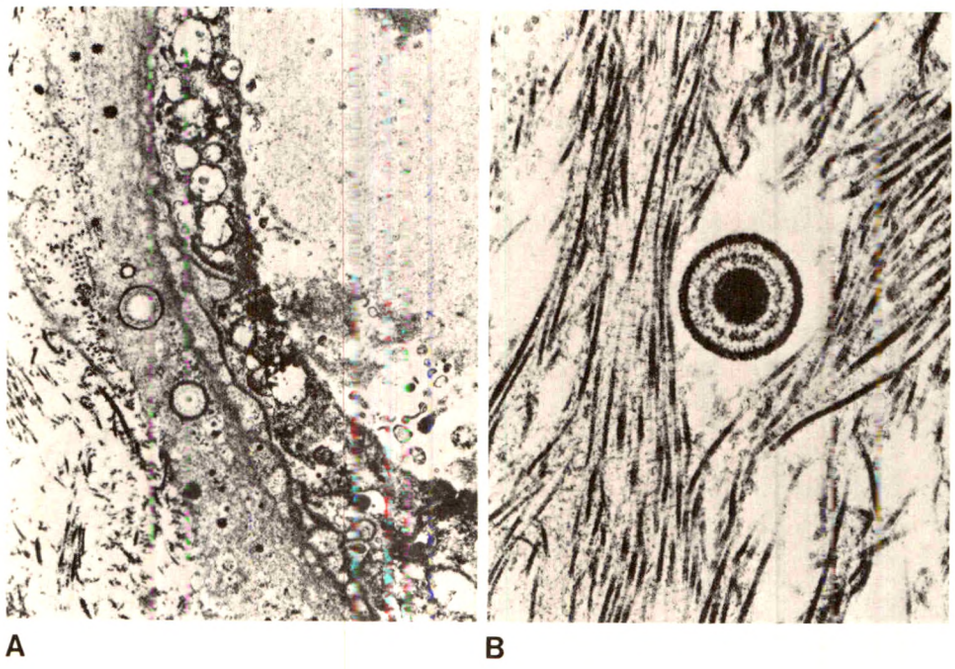


Fig. 7.—**A**, Reproduction of laminated electron-dense bodies in basement membrane of collecting duct. Duct epithelium shows postmortem degeneration. Reduced from ×21,000. (Reprinted with permission from [10].) **B**, Laminated electron-dense body in interstitium, surrounded by collagen fibrils. Reduced from ×54,000. (Reprinted with permission from [10].)

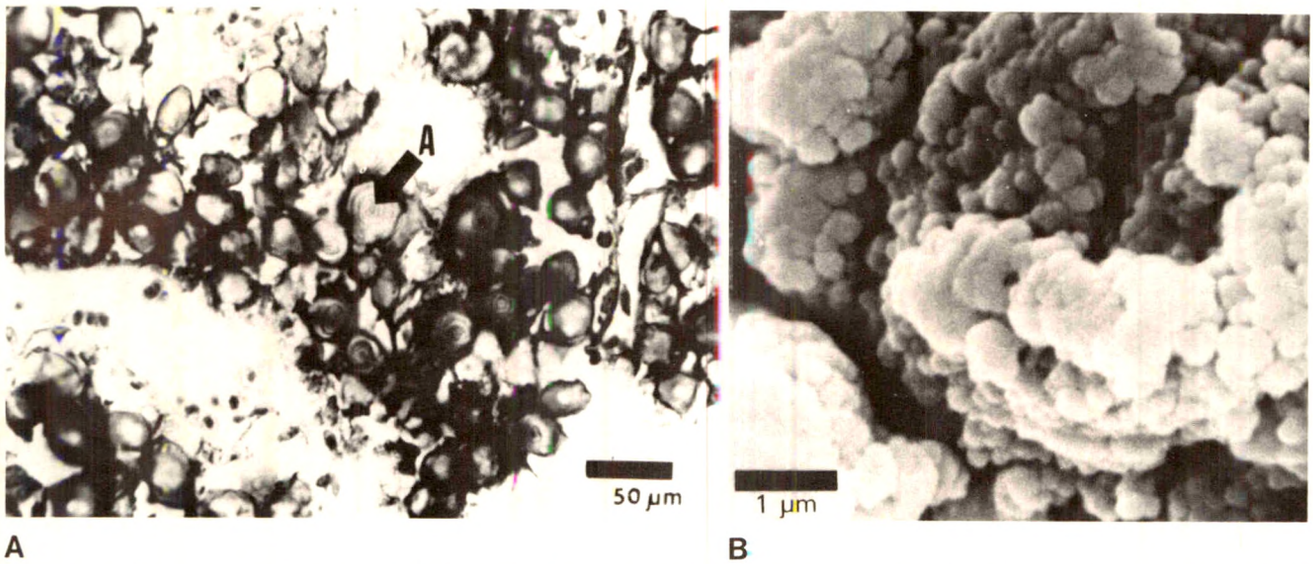


Fig. 8.—**A**, Tissue section (6 μm thick) of *Argopecten irradians* kidney choked with phosphorite concretions. Note concentric layering of concretion (A). H and E stain. (Reprinted with permission from [16]. **B**, Close-up of concretion from kidney of mollusk *Mercenaria mercenaria*, showing microbotryoidal texture (compare human "mulberry" texture). (Reprinted with permission from [16].)

calcium in the tissues of the renal papilla, work that has been confirmed by others [10, 11]. Carr's radiologic studies have substantiated, at the microradiographic level, Anderson's original work. Only the impossible—moving pictures of the drift of Anderson's and Carr's calcific deposits from a locus within the substance of a papilla to a subepithelial location near or at the surface of the papilla—could "prove" that Randall's subepithelial plaques and "initiating lesions" originate from deeper calcific deposits. I believe that the circumstantial evidence is overwhelming and there is useful logic in thinking of the formation of primary renal calculi as being initiated by a pathogenetic progression that I propose to call the Anderson-Carr-Randall progression of primary renal calculus formation.

Much more correlated information is needed concerning histopathologic and radiographic findings on much larger "normal" populations, under known conditions of hydration and nutrition. Investigations such as those being performed on the renal lymphatic system by Clark and Cuttino [18] are also of interest. For example, can methods of "sifting" the main renal lymphatics for calcareous microspherules under varying conditions of diet and hydration be developed? Or can the main renal lymphatics be obstructed with a view to subsequent radiologic and microscopic evaluations of the renal papillae for evidence of Carr's concretions and Randall's plaques?

Because of the common finding of calcific microspherules in the tissues of the renal papilla histologically and

radiographically, might one speculate, for example, that some or many cases of microhematuria might be due to erosion of these tiny plaques into the lumen of the urinary tract, and might electron microscopy of the urinary sediment from such patients be worthwhile? Furthermore, because the degree of physiologic hydration apparently affects the extent of the presence of calcium within the renal papilla and presumably, therefore, the chance of calculus formation [2], might electron microscopy of urinary sediment under various conditions of hydration perhaps be expected to yield, or not to yield, microcalculi?

We know that calcific "droplets" and microcalculi commonly exist in the renal pyramids. We also know that small, subepithelial calcific plaques composed of calcific microspherules are not uncommonly found in renal papillae, and that the epithelial cover of these plaques can erode to allow them to become "initiating lesions" for free primary calculi. Short of proving a central-to-surface drift of microcalculi by serial imaging, it is possible that additional pieces of circumstantial evidence in the form of investigation of the lymphatic system and urinary sediment under various conditions of controlled hydration and nutrition and other variables, might "prove" the Anderson-Carr-Randall progression hypothesis.

ACKNOWLEDGMENTS

I thank Dr. Mary-Ellen Shields for assistance with this project; and Richard Durbin, Dr. Richard Armstrong, and Dr. Gerd Schloss, Tucson Medical Center.

REFERENCES

1. Epstein FH: Calcium and the kidney. *Am J Med* 45:700–714, 1968
2. Smith LH, Van den Berg CJ, Wilson DM: Current concepts in nutrition. Nutrition and Urolithiasis. *N Engl J Med* 298: 87–89, 1978
3. Finalyson B, Hench LL, Smith LH (eds): Urolithiasis. Physical Aspects, in *Proceedings of the National Research Council Conference on Urolithiasis, Mayo Clinic, 1971*, National Academy of Sciences, Washington, D.C., 1972, pp 41, 61–62
4. Randall A: The initiating lesions of renal calculus. *Surg Gynecol Obstet* 64:201–208, 1937
5. Randall A: Papillary pathology as a precursor of primary renal calculus. *J Urol* 44:580–589, 1940
6. Anderson LE: *The Significance of Microscopic Calcareous Deposits in the Renal Pyramid*. Thesis (Master of Science in Surgery), University of Minnesota, 1945
7. Anderson L, McDonald JR: The origin, frequency, and significance of microscopic calculi in the kidney. *Surg Gynecol Obstet* 82:275–282, 1946
8. Carr RJ: A new theory on the formation of renal calculi. *Br J Urol* 26:105–117, 1954
9. Carr RJ: Etiology of renal calculi: Micro-radiographic studies, in *Proceedings of Renal Stone Research Symposium*, edited by Hodgkinson A, Nordin BEC, Churchill, London, 1969, pp 123–132
10. Haggitt RC, Pitcock JA: Renal medullary calcifications: a light and electron microscopic study. *J Urol* 106:342–347, 1971
11. Cooke SAR: The site of calcification in the human renal papilla. *Br J Surg* 57:890–896, 1970
12. Stewart HH: Calcifications and calculus formation in the upper urinary tract. *Br J Urol* 27:352–366, 1955
13. Rawson AJ: Distribution of the lymphatics of the human kidney as shown in a case of carcinomatous permeation. *Arch Pathol* 47:283–292, 1949
14. Cooke SAR, Rosenzweig D: The concentration of calcium in the human renal papilla and the tendency to form calcium containing stones. *Nephron* 8:528–539, 1971
15. Vermeulen CW, Lyon ES, Ellis JE, Borden TA: The renal papilla and calculogenesis. *J Urol* 97:573–582, 1967
16. Doyle LJ, Blake NJ, Woo CC, Yevich P: Recent biogenic phosphorite. Concretions in mollusk kidneys. *Science* 199: 1431–1433, 1978
17. Boyce WH: Some observations on the ultrastructure of "idiopathic" human renal calculi, in *Proceedings of the National Research Council Conference on Urolithiasis, Mayo Clinic 1971*, edited by Finlayson B, Hench LL, Smith LH, National Academy of Sciences, Washington, D.C., 1972, pp 97–114
18. Clark RL, Cuttino JT: Microradiographic studies of renal lymphatics. *Radiology* 124:307–311, 1977

CT Evaluation of Anomalies of the Inferior Vena Cava and Left Renal Vein

STUART A. ROYAL[1] AND PETER W. CALLEN[1]

Two patients with duplication of the inferior vena cava and two patients with a retroaortic left renal vein were examined by computed tomography (CT). The characteristic CT appearance of these two entities, as well as circumaortic left renal vein and transposition of the inferior vena cava, is discussed. A scheme by which these anomalies of the inferior vena cava and left renal vein may be distinguished from one another and from pathologic entities such as lymphadenopathy and a dilated gonadal vein is reported.

An understanding of the congenital abnormalities of the left renal vein and inferior vena cava is important to both surgeons [1, 2] and radiologists. [3, 4]. Although these anomalies are not common, their recognition is important before performing vascular procedures involving the renal pedicle and to avoid mistaking their unusual appearance on computed tomography (CT) scans as pathologic. We recently examined two patients with a retroaortic left renal vein and two patients with duplication of the inferior vena cava by CT. The CT appearance of these and related anomalies of the inferior vena cava and left renal vein is discussed.

Subjects and Methods

Four patients with anomalies related to the inferior vena cava were examined by CT on either an EMI 5005 or General Electric CT/T scanner. Patients were examined both before and after intravenous administration of urographic contrast material—infusion of 300 ml Conray 30%. When delineation of specific vessels was desired, a bolus injection of about 30–50 ml Conray 60% was administered via the saphenous vein. Scans were performed at 1–2 cm intervals. In three of the four cases, they were reconstructed in the sagittal and coronal planes, in addition to the conventional axial reconstruction.

Anatomic Considerations

The anatomy [5] and embryology [6, 7] of the normal inferior vena cava and left renal vein have been extensively reviewed in the surgical and radiologic literature and will not be discussed. The anomalies involving both the inferior vena cava and left renal vein can be divided into four major types: (1) transposition of the inferior vena cava (incidence, 0.2%–0.5%); (2) duplication of the inferior vena cava (incidence, 0.2%–3.0%); (3) circumaortic left renal vein (incidence, 1.5%–8.7%); and (4) retroaortic left renal vein (incidence, 1.8%–2.4%) [2]. Each of these conditions may have a retroaortic venous structure as part of its anomaly and thus they form a differential diagnostic gamut. Other congenital anomalies of the inferior vena cava, such as circumcaval ureter, interrupted inferior vena cava with azygous/hemiazygous continuation, and isolated left inferior vena cava, will not be discussed since retroaortic venous structures are not part of their anomaly. Transposition and duplication of the inferior vena cava are related embryologically since they are anomalies of persistence and/or regression of the left and right supracardinal veins [7].

Transposition of the Inferior Vena Cava

In transposition of the inferior vena cava, there is a single inferior vena cava that ascends on the left side of the spine and crosses either anterior or posterior to the aorta at the level of the renal veins to further ascend to the right atrium on the right side of the spine [2, 7, 8]. On CT, one would anticipate seeing a single right-side inferior vena cava at levels above the renal veins, a vascular structure crossing either anterior or posterior to the aorta at the level of the renal veins, and a large single venous structure (the transposed inferior vena cava) to the left of the spine at levels below the renal veins (fig. 1).

Duplication of the Inferior Vena Cava

In duplication of the inferior vena cava [2, 4, 7], there is a normal inferior vena cava along the right side of the spine. In addition, a left-side inferior vena cava ascends to the level of the renal veins to join the right-side inferior vena cava through a vascular structure that may pass either anterior or posterior to the aorta at the level of the renal veins. The characteristic CT appearance (fig. 1) is a single right-side inferior vena cava at levels above the renal veins, a vascular structure crossing either anterior or posterior to the aorta at the level of the renal veins, and a vascular structure to the left (i.e., the duplicated inferior vena cava) and right of the aorta below the level of the renal veins (figs. 1–3).

Duplication and transposition of the inferior vena cava may be differentiated by sections caudal to the level of the renal veins. In duplication, the right-side inferior vena cava will be seen as continuous to its bifurcation into the iliac veins, whereas the inferior vena cava will be absent on the right side in transposition of the inferior vena cava.

Circumaortic and retroaortic left renal veins compose a series of embryologic abnormalities of the left renal vein. Various combinations of persistence and regres-

Received October 2, 1978; accepted after revision January 23, 1979.
This work was supported in part by National Institutes of Health Training grant 01272.
[1]Department of Radiology, M-380, University of California School of Medicine, San Francisco, California 94143. Address reprint requests to P. W. Callen.

© 1979 American Roentgen Ray Society

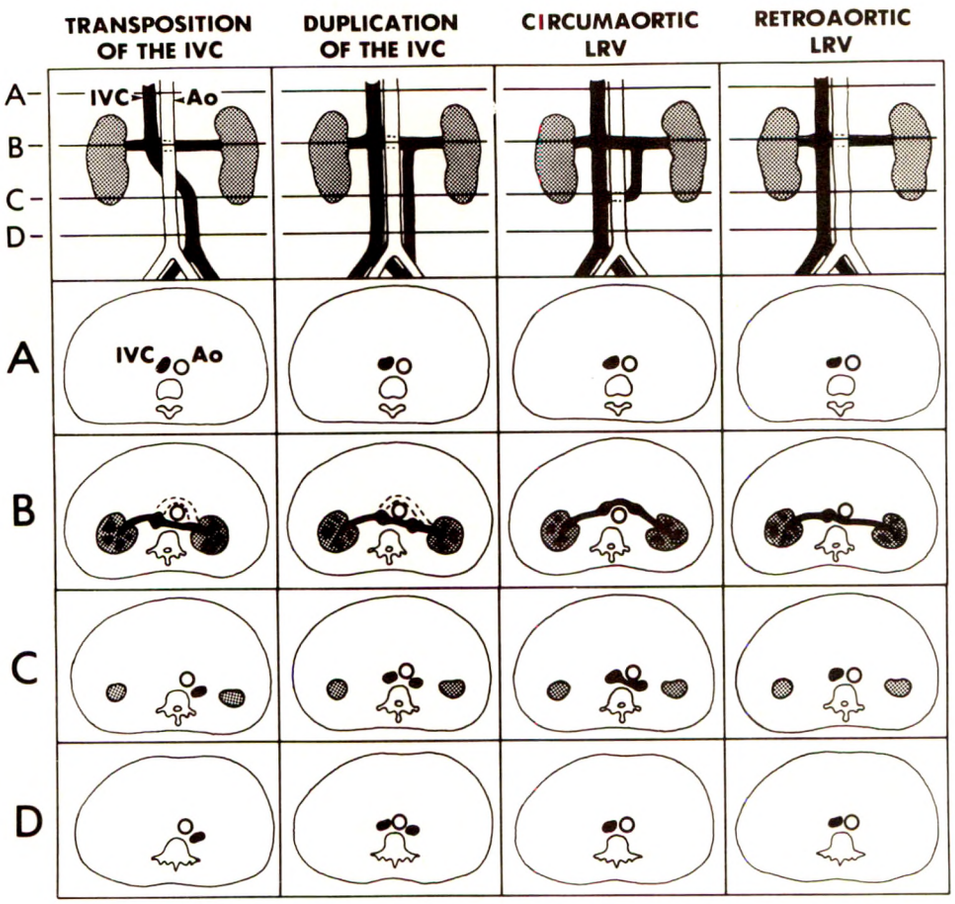
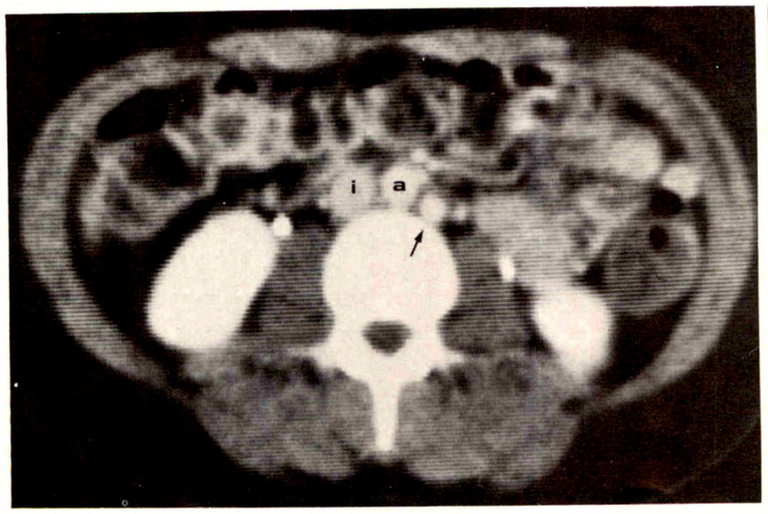
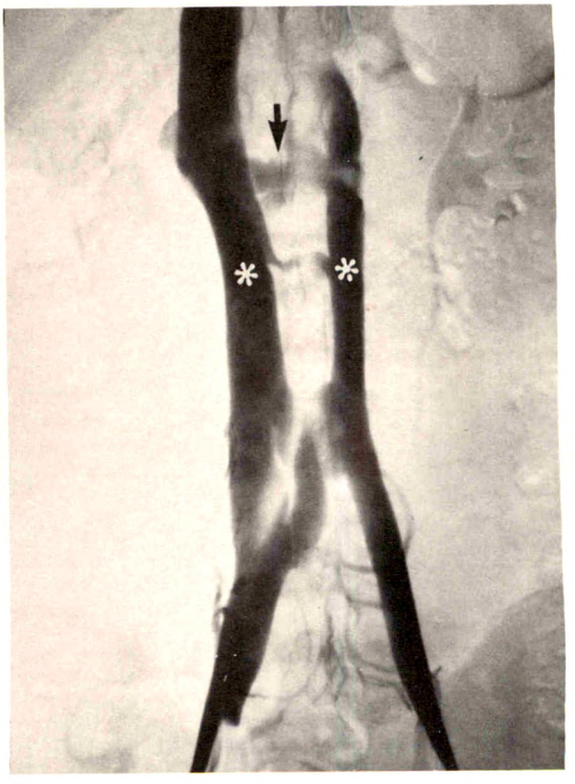


Fig. 1.—CT sections of aorta (Ao), inferior vena cava (IVC), and left renal vein in anomalies of inferior vena cava and left renal vein. In transposition and duplication of inferior vena cava venous structure may pass either anterior or posterior (*dashed lines*) to aorta at level of renal veins.

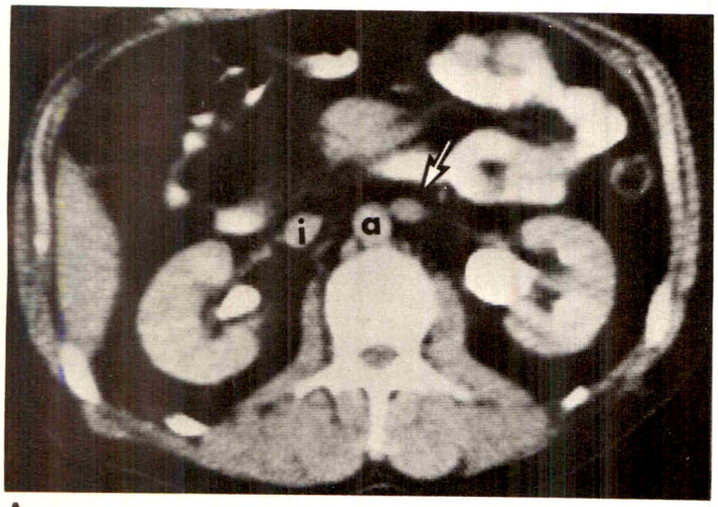


A

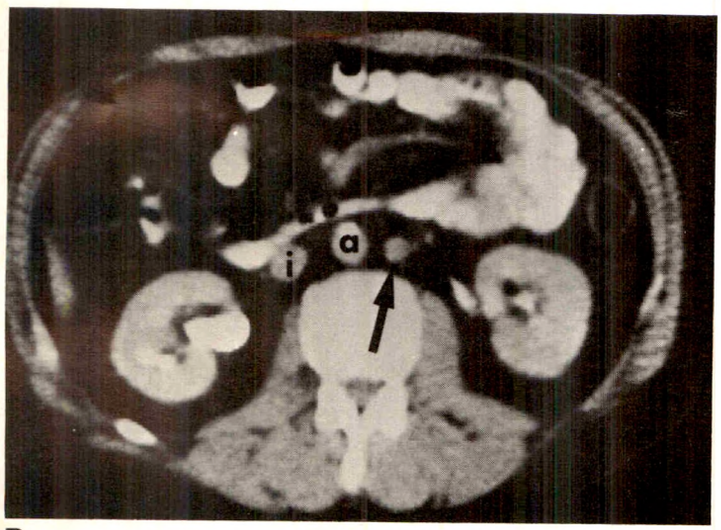


B

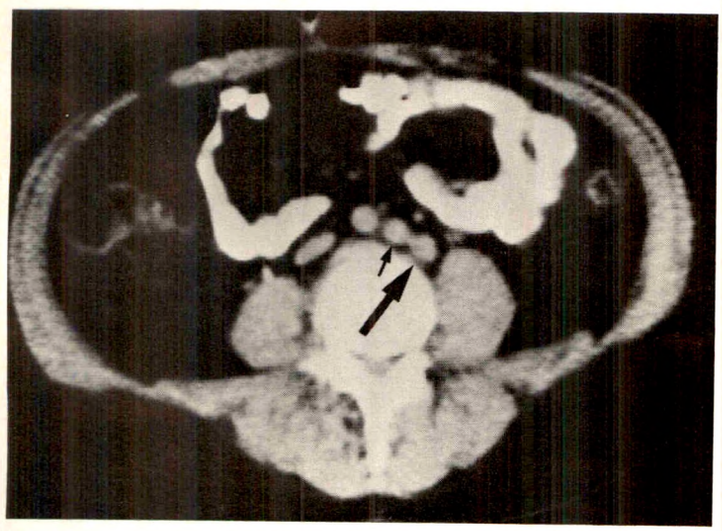
Fig. 2.—Patient with duplication of inferior vena cava. **A**, At level just caudad to renal veins. After bolus intravenous injection of contrast material, left inferior vena cava (*arrow*) appears as rounded enhanced structure prior to entrance into left renal vein. a = aorta, i = normal right-side inferior vena cava. **B**, Inferior vena cavogram. Both inferior vena cavas can be seen (*), as well as vascular connection (*arrow*) at level of kidneys.



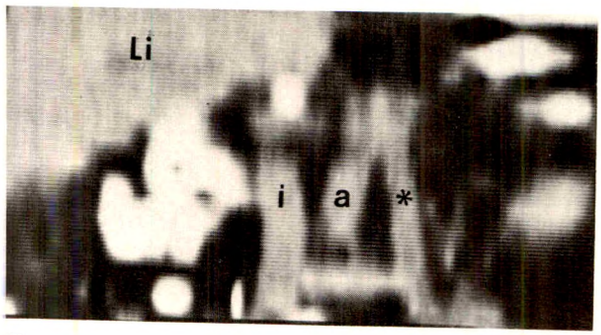
A



B



C



D

Fig. 3.—Patient with duplication of inferior vena cava. **A**, At level of renal veins. Entry of duplicated inferior vena cava unites into left renal vein seen as focal dilatation (*arrow*) of left renal vein. **B**, just caudad to renal veins. Duplicated inferior vena cava (*arrow*) continues as large vascular structure immediately left of aorta (a). **C**, Immediately cephalad to bifurcation of iliac veins. Duplicated inferior vena cava (*large arrow*) seen as prominent vascular structure left of common iliac artery (*small arrow*). **D**, Coronal reconstruction. Continuous nature of duplicated inferior vena cava (*) from level just cephalad iliac veins to entrance into left renal vein. Li = liver, a = aorta, i = normal right-side inferior vena cava.

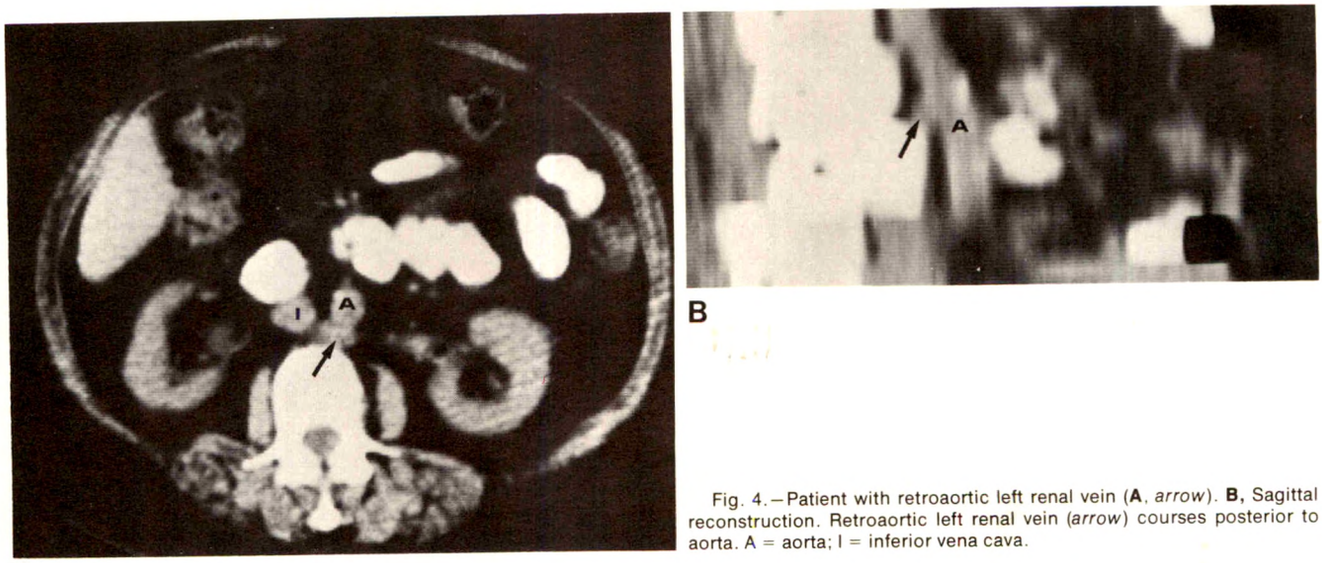


Fig. 4.—Patient with retroaortic left renal vein (**A**, *arrow*). **B**, Sagittal reconstruction. Retroaortic left renal vein (*arrow*) courses posterior to aorta. A = aorta; I = inferior vena cava.

sion of the left supracardinal (posterior to the aorta) and left subcardinal (anterior to the aorta) veins that occur during embryogenesis produce the anomalies [6].

Circumaortic Left Renal Vein

In circumaortic left renal vein, there is a true vascular ring about the aorta. The preaortic left renal vein crosses from the left kidney to the inferior vena cava at the expected level of the renal veins. The retroaortic vein connects the preaortic vein to the inferior vena cava by descending caudally and crossing the spine behind the aorta, usually one to two vertebral levels below the level of the preaortic left renal vein [3, 11–13]. In this situation, CT will demonstrate the preaortic left renal vein in the expected course of the normal left renal vein and the anomalous retroaortic left renal vein in a more caudal position (fig. 1).

Retroaortic Left Renal Vein

In retroaortic left renal vein, the anterior subcardinal veins regress completely and only the retroaortic supracardinal veins remain to connect the left kidney to the inferior vena cava. The course of the left renal vein can be either retroaortic at the level of the normal left renal vein or it may course obliquely caudad behind the aorta to enter the inferior vena cava as low as the confluence of the iliac veins (fig. 1) [2, 9, 10]. In both of our cases, the retroaortic left renal vein crossed at the level of the normal renal vein (figs. 4 and 5). An unopacified segment of the third part of the duodenum must not be mistaken as the normal left renal vein, thus suggesting the incorrect diagnosis of a circumaortic left renal vein in the presence of a retroaortic left renal vein.

Since both transposition and duplication of the inferior vena cava may have venous structures that pass posterior to the aorta at the level of the renal veins, they may be confused with simple circumaortic and retroaortic left renal veins. However, they should be easily distinguished on CT, since circumaortic and retroaortic left renal veins have no associated inferior vena cava anomaly. Thus, in the presence of a retroaortic vascular structure at the level of the renal veins on CT, the inferior vena cava anatomy below the level of the renal veins should help distinguish isolated left renal vein anomalies from transposition and duplication of the inferior vena cava.

Discussion

Other diagnostic considerations may be entertained when evaluating the patient with an infrarenal left inferior vena cava by CT. On a single tomographic section, the left inferior vena cava may look like an enlarged lymph node. The continuous nature of the inferior vena cava anomaly on consecutive sections, or as seen with sagittal or coronal reconstructions (fig. 3D), should be apparent and serve to distinguish this from an enlarged lymph node. In addition, intravenous contrast enhancement of the inferior vena cava should further help distinguish these two structures. A second differential consideration would be an enlarged left gonadal vein, since its distal portion can simulate a left inferior vena cava by joining the left renal vein and coursing along the left side of the spine.

However, these two can be distinguished anatomically since, proceeding caudally, the proximal left gonadal vein crosses the psoas muscle to enter the inguinal canal; whereas the left inferior vena cava will continue to run along the left side of the spine to join the left common iliac vein (fig. 2B). These two structures can be differentiated by observing the effect of intravenous contrast enhancement after a bolus injection into the left saphenous vein using sequential rapid scans. The left inferior vena cava should show immediate contrast enhancement as opposed to delayed enhancement (after the aorta) of the left gonadal vein.

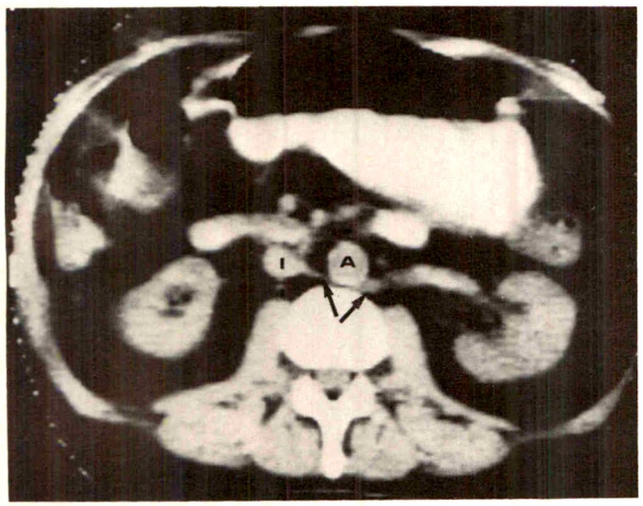


Fig. 5.—Patient with retroaortic left renal vein. Left renal vein (*arrows*) points posteriorly prior to course behind aorta (A). I = inferior vena cava.

The importance of diagnosing left renal vein and inferior vena cava anomalies has been documented. Surgically, these anomalies can affect decisions regarding shunt placement for portal hypertension, choosing prospective renal transplant donors, choosing the site for inferior vena cava ligation for thromboembolic disease, repairing aortic aneurysms, and performing other retroperitoneal surgery [1, 2, 9, 11]. Angiographically, awareness of this anomaly is important in performing adrenal venography, renal vein sampling, and in avoiding the false interpretation that a mass lesion is causing the inferior displacement of the retroaortic left renal vein [3, 6]. Using the framework presented here, these anomalies can be categorized by CT and can be differentiated from other pathologic entities.

REFERENCES

1. Thomas TV: Surgical implications of retroaortic left renal vein. *Arch Surg* 100:738–740, 1970
2. Brener BJ, Darling RC, Frederick PL, Linton RR: Major venous anomalies complicating abdominal aortic surgery. *Arch Surg* 108:159–165, 1974
3. Kottra JJ, Castellino RA: The circumaortic left renal vein: angiographic appearance. *Radiology* 95:141–143, 1970
4. Berkow AE, Henkin RE: Double inferior vena cava or iliac vein occlusion? A diagnostic problem in radionuclide venograms. *AJR* 130:529–531, 1978
5. Pick JW, Anson BJ: The renal vascular pedicle. An anatomical study of 430 body-halves. *J Urol* 44:411–434, 1940
6. Chuang VP, Mena CE, Hoskins PA: Congenital anomalies of the left renal vein: angiographic consideration. *Br J Radiol* 47:214–218, 1974
7. Chuang VP, Mera CE, Hoskins PA: Congenital anomalies of the inferior vena cava. Review of embryogenesis and presentation of a simplified classification. *Br J Radiol* 47:206–213, 1974
8. Pillari G, Wind ES, Wiener SL, Baron MG: Left inferior vena cava. *AJR* 130:366–367, 1978
9. Thomford NR: Abnormal left renal vein. No barrier to Warren shunt. *Am J Surg* 129:503–505, 1975
10. Davis CJ, Lundberg GD: Retroaortic left renal vein—a relatively frequent anomaly. *Am J Clin Pathol* 50:700–703, 1968
11. Bosniak MA, Madayag M: Angiographic appearance of the circumaortic left renal vein. *J Urol* 108:18–20, 1972
12. Mitty HA: Circumaortic renal collar: a potentially hazardous anomaly of the left renal vein. *AJR* 125:307–310, 1975
13. Lien HH, Kolbenstuedt A: Nonmalignant venographic abnormalities of the inferior vena cava. *Radiology* 122:105–110, 1977

Accessory Renal Hilus

THOMAS F. STEPHENSON[1] AND GEORGE J. PAUL[1]

A defect in the renal margin secondary to extrahilar entry of renal vessels was detected at urography in three patients. Extrahilar entry of renal vessels is not uncommon and is well known to anatomists and surgeons. It has not been previously reported as a radiographic finding. In the past these marginal defects may have been assumed to be persistent fetal lobulation or scarring from previous renal infarction or pyelonephritis. Arteriography may be necessary to distinguish between these possibilities and occasionally to exclude a renal tumor or cyst.

As noted by Older et al. [1], modern excretory urography and nephrotomography have made it possible to evaluate the anatomy of the urinary tract more precisely. This improved technology has resulted in reports of several new diagnostic signs [2, 3]. We recently observed three patients with a renal marginal defect secondary to extrahilar entry of renal vessels. This normal variation is to be distinguished from scarring due to renal infarction or pyelonephritis and occasionally from a renal cyst or tumor.)

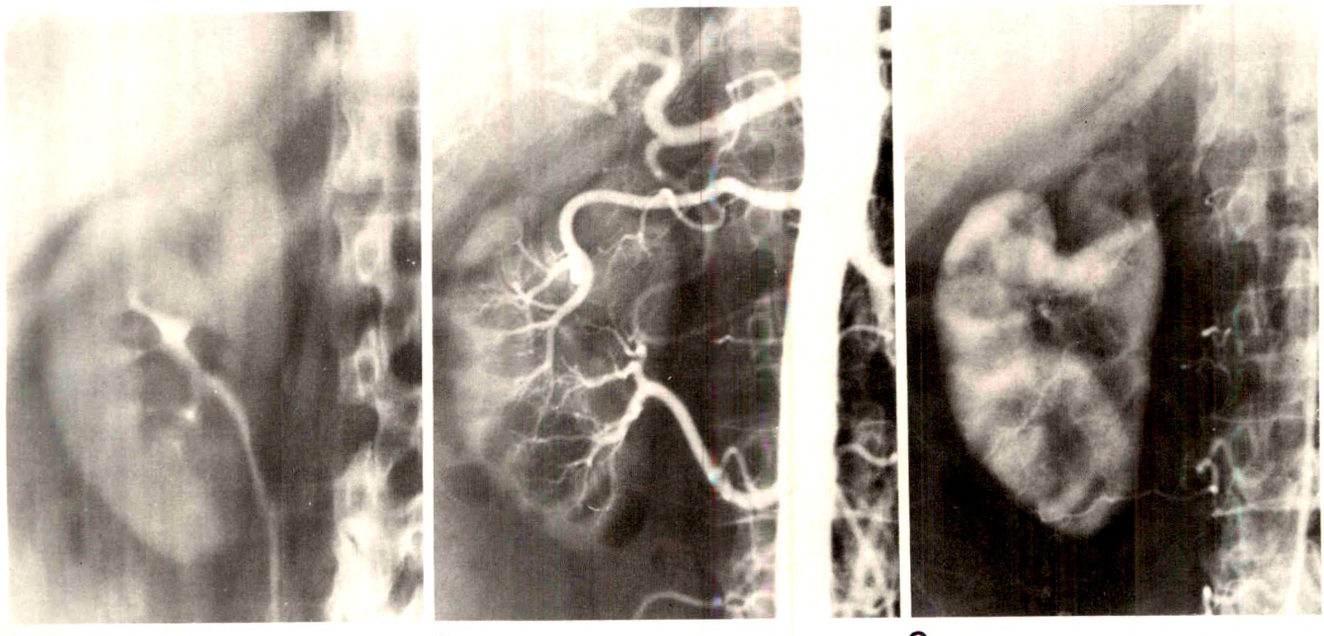
Case Reports

Case 1

A 62-year-old white woman was admitted with a perforated appendix. In the postoperative period, she had persistent low grade fever. Urinalysis revealed pyuria and excretory urography (fig. 1A) showed a questionable mass in the upper pole of the right kidney. Arteriography revealed a cleft in the upper pole of the right kidney corresponding to the site of entrance of one of two right renal arteries of about equal size (figs. 1B and 1C). On the nephrogram phase of arteriography (fig. 1C) there was an absence of a hilar indentation along the medial aspect of the right kidney. Renal venography suggested that the right renal vein also exited the kidney via this cortical defect. The subsequent hospital course was uneventful; the fever disappeared over several days.

Case 2

A 77-year-old white woman with a history of cholelithiasis and cholecystectomy was admitted because of abdominal pain and jaundice. On intravenous cholangiography, renal excretion of the contrast material suggested an abnormality in the upper pole of the right kidney. Excretory urography with nephrotomography (fig. 2A) showed a notch defect in the superior pole of the right kidney. Renal arteriography (figs. 2B and 2C) showed a single right renal artery entering the right kidney at the cleft in the upper pole. Fibromuscular hyperplasia and renal artery stenosis were noted. The patient was normotensive. Renal venography (fig. 2D) showed the renal vein also exiting via the upper pole notch in the right kidney. In addition, the right kidney had a flattened or pancake appearance compatible



A B C

Fig. 1.—Case 1. **A**, Nephrotomogram during excretory urography. Deformity with possible mass in upper pole of right kidney. **B**, Aortogram. Two renal arteries on right. Superior of these enters kidney through large apical defect. **C**, Nephrogram phase. Large right apical defect well delineated.

Received October 16, 1978; accepted after revision January 31, 1979.
[1]Department of Radiology, St. Mary's Hospital, 89 Genesee Street, Rochester, New York 14611. Address reprint requests to T. F. Stephenson.

© 1979 American Roentgen Ray Society

0361–803X/79/1325–0765 $0.00

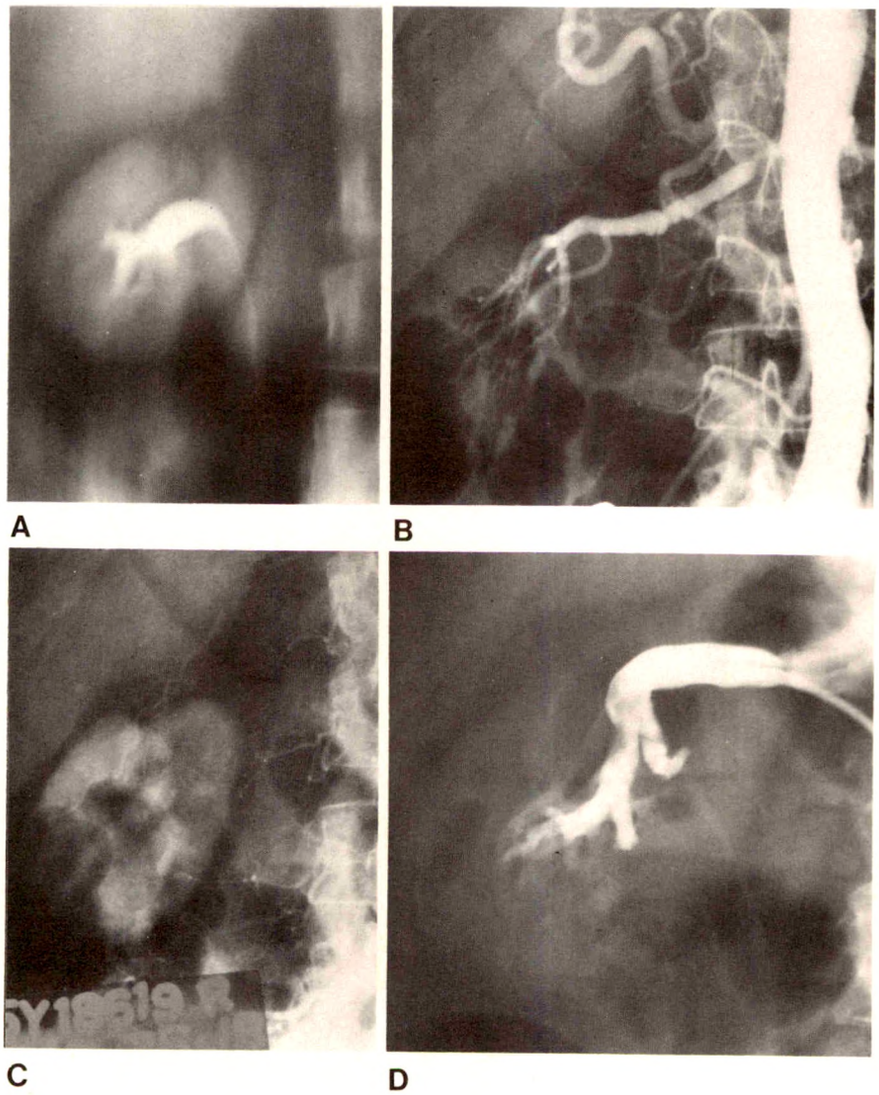


Fig. 2.—Case 2. **A**, Nephrotomogram during excretory urography. Right upper pole defect. **B**, Aortogram. Right renal artery enters kidney through apical defect. Fibromuscular hyperplasia and renal artery stenosis are present. **C**, Nephrogram phase. Apical defect on right. **D**, Right renal venogram. Renal vein exits kidney via defect.

with malrotation about the horizontal axis. This type of rotational anomaly may be associated with an anomalously located renal hilus and corresponding superior marginal defect, rather than a true accessory renal hilus.

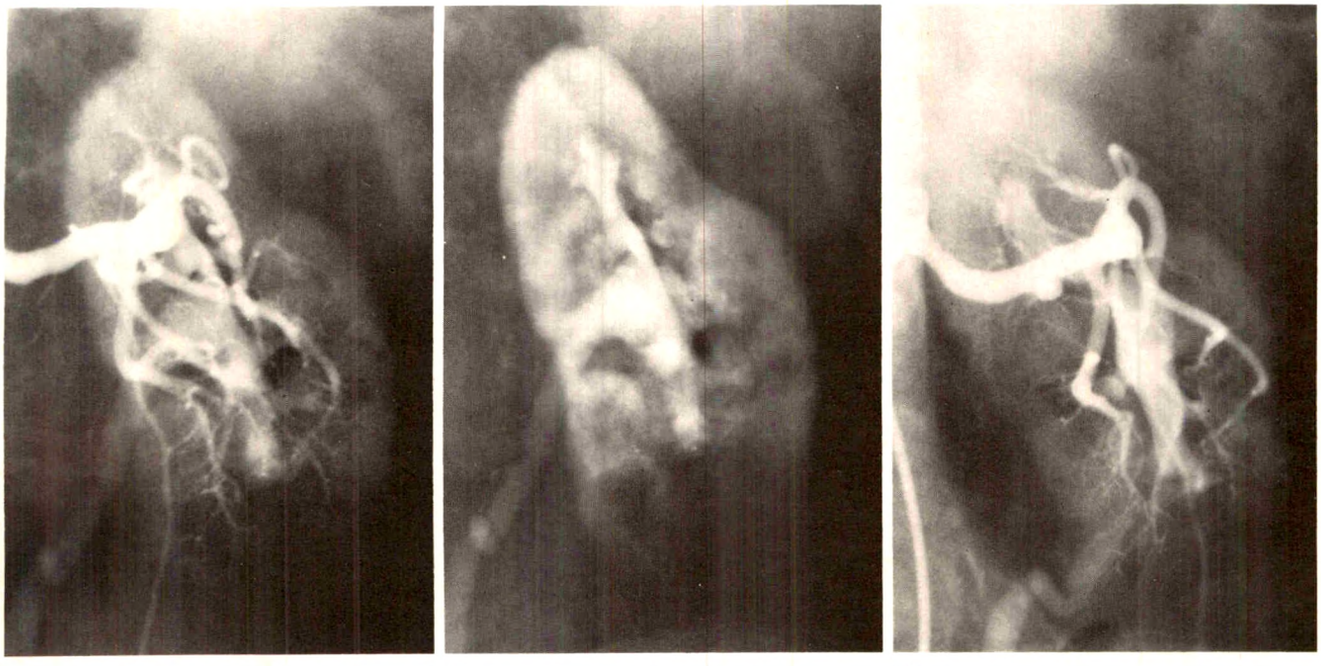
Case 3

A 72-year-old white man complained of intermittent abdominal pain. There was a palpable 8 × 6 cm mass in the left upper quadrant. Excretory urography revealed a large mass in the lower pole of the left kidney, which was cystic by ultrasound but also showed a branching linear pattern of internal echoes suggesting internal septation or multiloculation. Renal arteriography (figs. 3A and 3B) showed a 7 cm, largely avascular mass of the lower pole. A notch defect was incidentally noted along the lateral margin of the upper pole of the left kidney. Arteriography in the left posterior oblique projection (fig. 3C) showed a branch of the renal artery entering the kidney at this point. Because of the persistent possibility of tumor associated with the lower pole cyst, laparotomy and left nephrectomy were performed. Pathologic examination revealed a 7 cm renal cyst with changes of chronic inflammation. The specimen also showed a small depression over the anterior surface of the upper pole corresponding to the site of entry of a branch of the renal artery.

Discussion

The literature contains many detailed descriptions of renal artery anatomy and its variability [4–12]. Extrahilar entry of renal vessels is well documented in the surgical and anatomic literature [12–15]. However, we have found no previous reports of urographically demonstrated renal marginal defects due to renal vessels perforating the cortex outside the usual area of the renal hilus.

The embryonic urogenital ridge from which the kidneys develop is supplied by several paired vessels, the rete arteriosum urogenitale. The initial mesonephric kidneys are supplied by several paired arteries originating from the aorta and iliac arteries. The later developing metanephric kidneys persist in a more cephalad location and usually retain only a single pair of mesonephric arteries, however a variable number may persist. While some are contained in a common pedicle with the main



A B C

Fig. 3.—Case 3. **A**, Left renal arteriogram. Subtle defect on lateral margin of upper pole and lower pole cyst. **B**, Nephrogram phase. **C**, Left renal arteriogram in left posterior oblique position. Branch of renal artery perforates upper pole cortex anterolaterally. Marginal defect is seen in profile.

renal artery, others run independently to one of the poles of the kidney.

Merklin and Michels [9] in a study of 11,000 necropsy cases, noted that "aberrant" renal arteries may arise from the aorta anywhere between the T11 and L4 vertebrae. They emphasize that so called "aberrant" arteries are really persistent mesonephric vessels. As noted by Davis and Kincaid [5], the terms "auxiliary," "accessory," and "supplementary" are inappropriate since they connote an already adequate or complete vascularization of the kidney by the main renal artery when such is not the case. In fact, each of these additional arteries, like the main renal artery, is a terminal vessel and acts as the sole supply to a circumscribed segment of the renal parenchyma.

Graves' [6] description of renal segmental blood supply is most accepted. According to Graves [6], the main trunk of the renal artery divides at a variable point between the aorta and the hilum of the kidney into an anterior and posterior division. The anterior division gives rise to the upper, middle, and lower segmental arteries and the apical segment.

The *apical segment* is thus supplied by an artery which most frequently arises from the anterior division. However, it is a vessel whose origin is the most varied of all segmental arteries. In 23% of Graves' cases, the artery arose from the main renal artery or the aorta itself. The artery may run with its fellows to the hilum, or it may make an extrahilar entry into the side of its segment and in this respect may have the appearance of an aberrant artery. In Graves' series of specimens, about one-third of this type had an extrahilar entry, most of the vessels having arisen directly from the aorta.

Extrahilar veins on either side are much less common than extrahilar arteries (7% vs. 43% in Pick and Anson's series) [15]. Merklin and Michels [9] concluded that about 12% of kidneys have two or more arteries of aortic origin that enter at or close to the hilus of the kidney. They also noted about 12% more have two arteries of aortic origin, with one entering the hilus and the other entering one pole of the kidney. Supernumerary arteries are equally frequent on the two sides. Since polar arteries may originate from renal artery as well as aorta, they may or may not be supernumerary vessels, although they are aberrant. All of the supernumerary arteries of aortic origin that pierced the cortex of the upper pole of the kidney in Sykes' series [13] were apical segment arteries. All those that pierced the lower pole were lower pole segment arteries. Anson et al. [14], reported that about half of the supernumerary arteries they found entered at the hilus and about half entered at the poles. Pick and Anson [15], found extrahilar arteries in about 43% of kidneys.

Renal marginal defects due to extrahilar entry of renal vessels are a previously unreported radiographic finding which must be considered in the differential diagnosis of renal marginal defects. Detection of these normal variations and the pathologic changes from which they must be distinguished is facilitated by high dose urography and nephrotomography. However, arteriography may be necessary to discriminate between the two.

ACKNOWLEDGMENTS

We thank Sandy Johnson and Mary Daniels for assistance in preparation of the manuscript, and Joan Baker and Betty Gilligan for technical assistance.

REFERENCES

1. Older RA, Cleeve DM, McLelland R: The nonspecificity of some radiological signs in excretory urography. *Radiology* 127:553–554, 1978
2. Paul GJ, Stephenson TF: The cortical rim sign in renal infarction. *Radiology* 122:338, 1977
3. Barbaric ZL: Pelvocalyceal wall opacification—a new radiological sign. *Radiology* 123:587–589, 1977
4. Boijsen E: Angiographic studies of the anatomy of single and multiple renal arteries. *Acta Radiol [Suppl]* (Stockh) 183:1–135, 1959
5. Davis GD, Kincaid OW, Hunt JC: Roentgenological evaluation of multiple renal arteries. *AJR* 90:583–592, 1963
6. Graves FT: The anatomy of the intrarenal arteries and its application to segmental resection of the kidneys. *Br J Surg* 42:132–139, 1954
7. Graves FT: The aberrant renal artery. *J Anat* 90:553–558, 1956
8. Graves FT: The aberrant renal artery (synopsis). *Proc R Soc Med* 50:368–369, 1957
9. Merklin GM, Michels NA: The variant renal and suprarenal blood supply with data on the inferior phrenic, ureteral and gonadal arteries: a statistical analysis based on 185 dissections and review of literature. *J Int Coll Surgeons* 29:41–76, 1958
10. Olsson O: Anatomic and physiologic considerations, in *Angiography,* edited by Abrams H, Boston, Little, Brown, 1971, pp 779–782
11. Kincaid OW: Techniques and applications of renal arteriography, in *Clinical Urography,* edited by Emett JL, Witten DM, Philadelphia, Saunders, 1971, pp 97–137
12. Fine H, Keen EN: The arteries of the human kidney. *J Anat* 100:881–894, 1966
13. Sykes D: The arterial supply of the human kidney with special reference to accessory renal arteries. *Br J Surg* 50: 368–374, 1963
14. Anson BJ, Richardson GA, Minear WL: Variations in the number and arrangement of the renal vessels: a study of the blood supply of four hundred kidneys. *J Urol* 36:211–219, 1936
15. Pick JW, Anson BJ: The renal vascular pedicle: an anatomical study of 430 body halves. *J Urol* 44:411–434, 1940
16. Hollinshead WH: The thorax, abdomen and pelvis, in *Anatomy for Surgeons,* 2d ed, vol 2, New York, Harper & Row, 1971

Arterial Impressions on the Stomach

MICHAEL H. CHILDRESS,[1] KYUNG J. CHO, NANCY NEWLIN, AND WILLIAM MARTEL

The splenic artery frequently produces a contour defect on the posteromedial aspect of the stomach, particularly in elderly individuals. When the artery is tortuous or aneurysmal, the impression is prominent and may simulate a neoplasm. Similarly, the aorta can produce a gastric impression. Recognition of these impressions on the stomach wall avoids erroneous diagnosis and unnecessary exploratory surgery.

Gastric contour defects produced by a tortuous splenic artery are seldom recognized. Both clinical and anatomic studies have shown that the splenic artery is closely related to the stomach and often produces a subtle contour deformity of the posteromedial segment [1]. Such a lesion has previously been reported as a pseudotumor [2]. We recently observed a large pseudotumor caused by a tortuous splenic artery. This case prompted us to review the frequency and significance of arterial impressions on the stomach. These impressions are usually related to tortuous and aneurysmal vessels. Although radiologists are familiar with the mass effect produced by an abdominal aortic aneurysm, the deformity produced by the splenic artery has not been sufficiently described.

Case Material

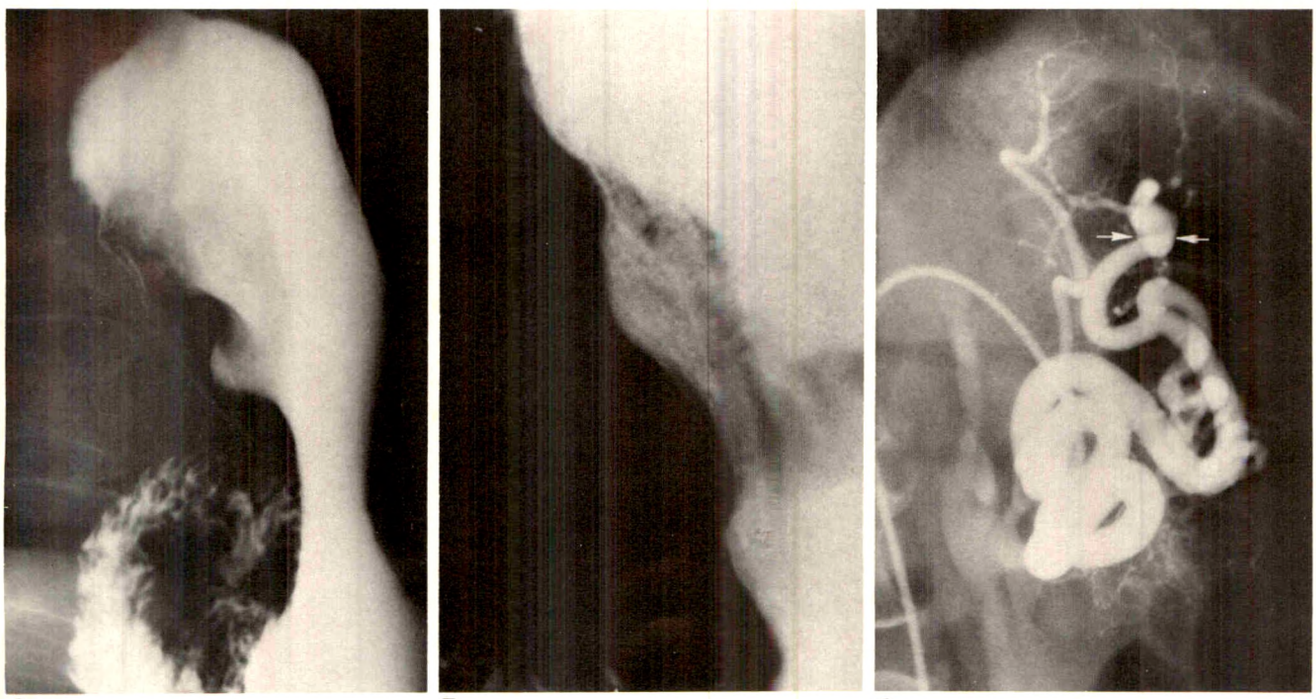
Retrospective review identified 25 cases in which angiograms showed the splenic artery to be significantly tortuous. The appearance of the stomach on examinations with barium was then reviewed in these cases and correlated with the position and course of the splenic artery.

The patients were 21–86 years old; there were 14 women and 11 men. Five patients had subtle impressions and eight had prominent ones. Prominent impressions tended to occur more frequently in the older individuals.

Representative Case Reports

Case 1

A 64-year-old woman had epigastric pain for 6 months. An upper gastrointestinal barium examination revealed an "ulcer-



A B C

Fig. 1.—Case 1. **A**, Lateral view of stomach, initial study. Broad multilobular defect on posterior wall. Barium between adjacent defects simulates ulcer. **B**, Spot film. Sinuous contour deformity. **C**, Left posterior view. Tortuous splenic artery indents contour of gas-filled stomach. Aneurysm (*arrows*).

Received March 14, 1978; accepted after revision January 12, 1979.

[1] All authors: Department of Radiology, University of Michigan Medical Center, Ann Arbor, Michigan 48109. Address reprint requests to M. H. Childress.

© 1979 American Roentgen Ray Society

0361-803X/79/1325-0769 $0.00

ating tumor" of the stomach (fig. 1A). Gastroscopy was inconclusive for a tumor. Barium examination (fig. 1B) at the University of Michigan Medical Center revealed an extrinsic impression on the stomach that differed from the previous study. Endoscopy revealed a broad intramural or extrinsic lesion without mucosal ulceration. Celiac angiography showed tortuosity of the splenic artery. After insufflation of the stomach, splenic angiography demonstrated that the defect was caused by a tortuous splenic artery (fig. 1C). Subsequently, cholecystectomy for cholelithiasis corroborated the normalcy of the stomach.

Case 2

A 74-year-old woman was admitted to the University of Michigan Medical Center after 4 months of anorexia and a weight loss of 18 kg. She also had epigastric pain for 3 months that radiated to the left breast. It was initially intermittent, but later became constant. Barium examination of the stomach revealed a broad impression on the posteromedial aspect of the stomach just distal to the cardia (fig. 2). Exploratory laparatomy revealed a tortuous aorta producing this mass effect. Autopsy 9 years later confirmed these findings.

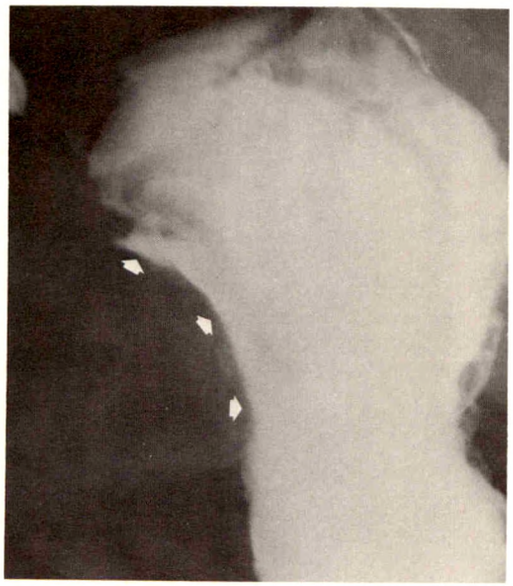


Fig. 2.—Case 2. Broad posterior wall contour defect (*arrows*) produced by tortuous aorta.

Case 3

A 68-year-old woman was admitted to the University of Michigan Medical Center after 6 days of left upper quadrant pain, which had disturbed her sleep. It was not related to eating or position. A bruit was audible over the upper abdomen. Barium study of the stomach revealed an extrinsic impression on its posteromedial aspect (figs. 3A and 3B). Angiography showed a large pseudoaneurysm of the splenic artery (fig. 3C) at the site of this impression. These findings were confined at laparotomy when the ruptured aneurysm was resected. Histologic examination revealed disruption of the internal elastic membrane of the splenic artery and normal adjacent pancreas.

Discussion

A mass effect on the stomach produced by an abdominal aortic aneurysm is well recognized, but tortuosity of the aorta seems to be an uncommon cause for such extrinsic impressions. The splenic artery often produces a gastric contour defect. The proximal segment of the artery approaches the stomach near the incisura where it may produce a defect; the more distal segment often produces a defect near the cardia. These defects vary from a small localized deformity to a rather long undulating impression (figs. 4–6). The extent of the defect may not be recognized initially, since only a part of it may be viewed in profile in a single projection (fig. 5). Furthermore, unless spot films are obtained with precise positioning designed to demonstrate such defects, they will usually be missed.

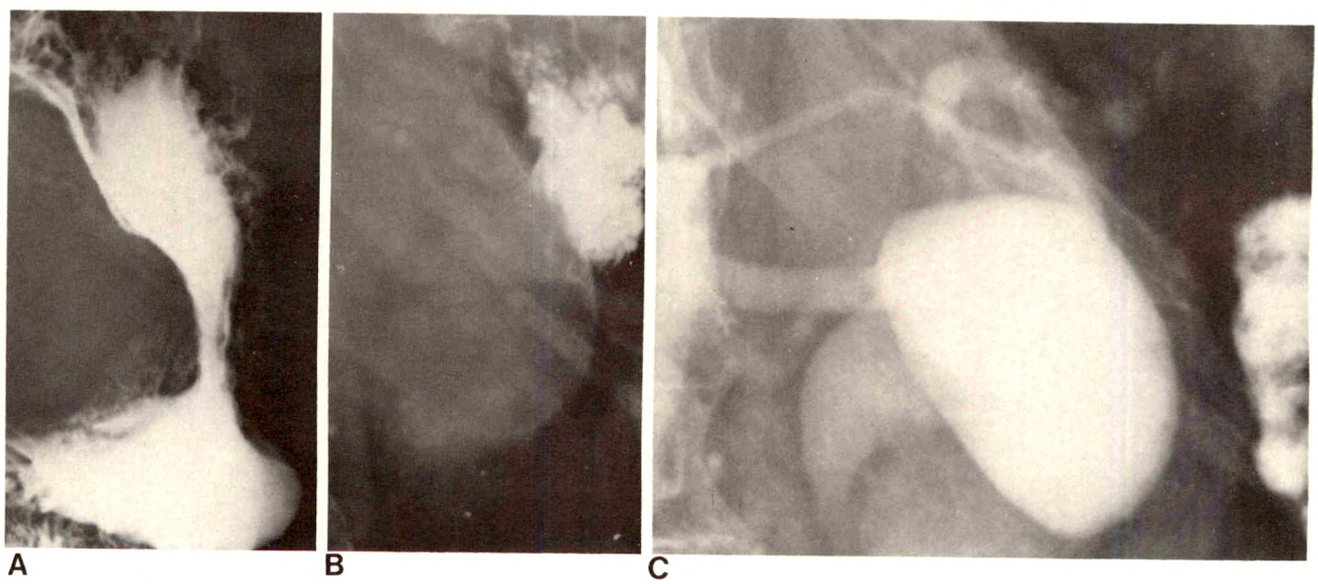


Fig. 3.—Case 3. **A** and **B**, Large extrinsic pressure defect on lesser curvature and posterior wall of stomach. **C**, Celiac angiogram. Impression on gas-filled stomach by splenic artery aneurysm.

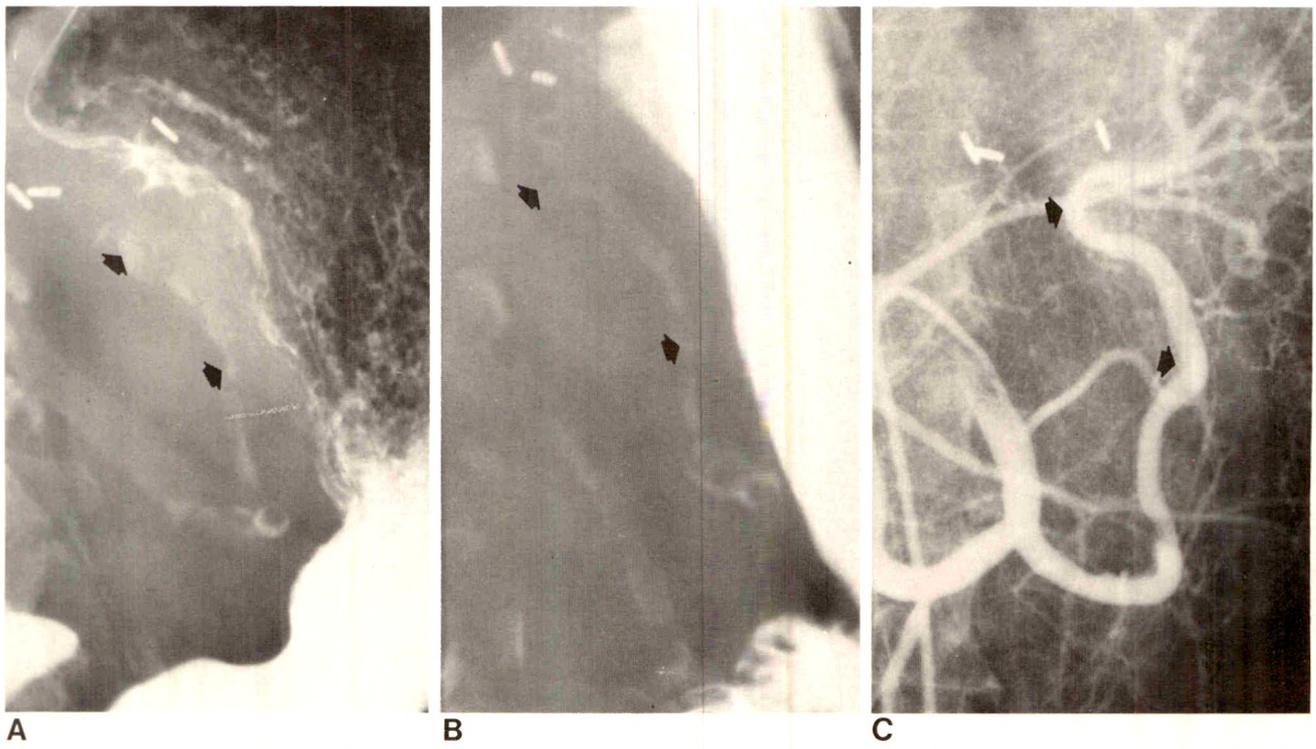


Fig. 4.—79-year-old woman. **A,** Posteroanterior film. Broad wavy defect caused by distal part of splenic artery (*between arrows*). Calcification also present in this location. **B,** Lateral film. Broad defect (*arrows*) (cf. **A**). **C,** Celiac angiogram supports interpretation that defect is due to segment of splenic artery (*between arrows*) near hilus of spleen.

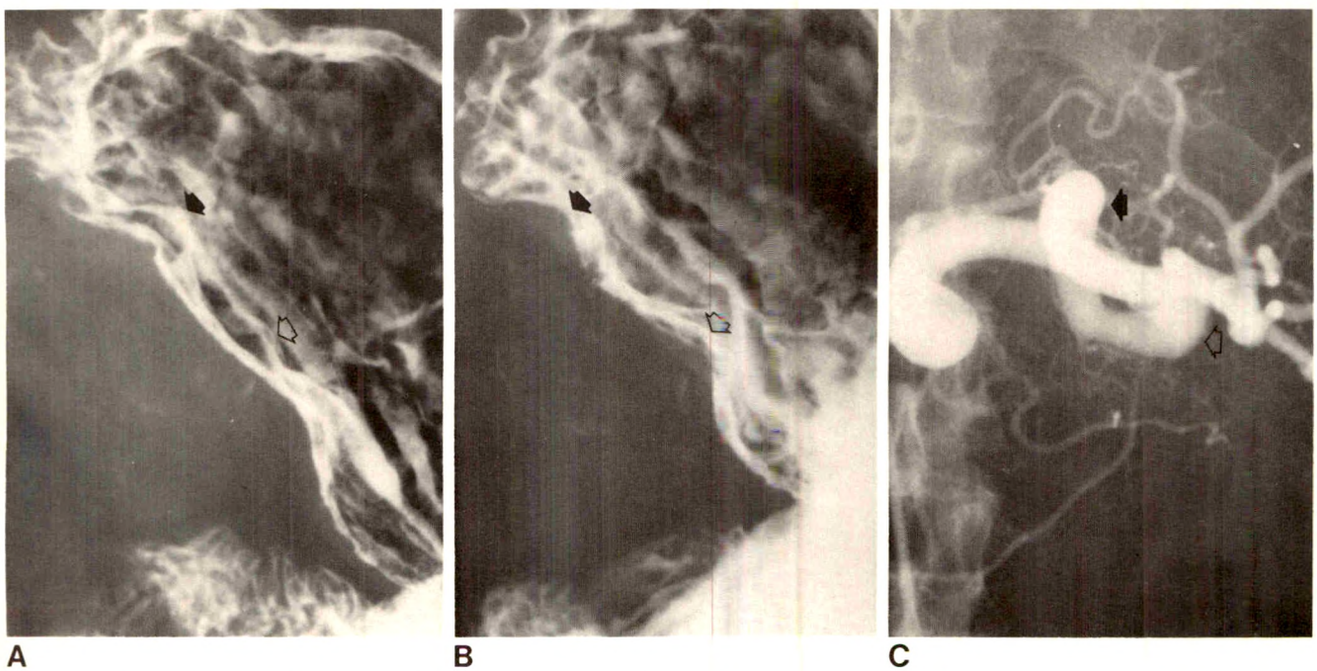


Fig. 5.—57-year-old woman. Oblique view. Several defects (*arrows*) not tangentially visualized in profile. **B,** Posteroanterior view. Defects are related and due to distal segment of splenic artery (*closed arrow*) and more proximal segment (*open arrow*). **C,** Celiac angiogram. More distal segment (*closed arrow*) higher than more proximal one (*open arrow*).

Certain features should suggest that an extrinsic gastric defect may be caused by the splenic artery. The defect itself has a characteristic location either near the incisura or the cardia (fig. 4A). Occasionally, it is identified as broad and undulating involving the posterior portion of the stomach between these two points (fig. 5). The defect is almost always broad and shallow, characteristic of extrinsic rather than intramural lesions. The

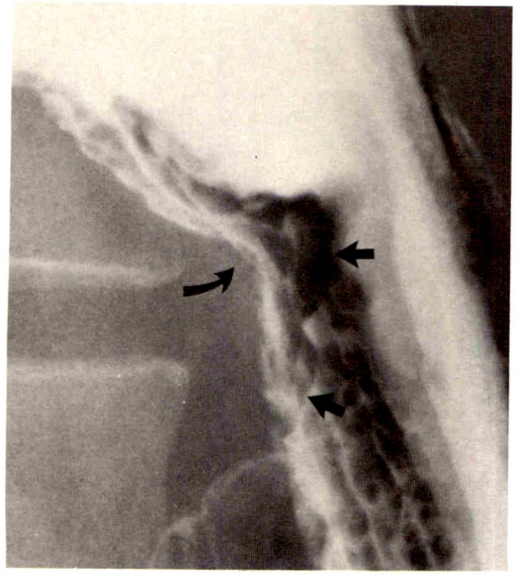


Fig. 6.—32-year-old man. Lateral film. Defects due to distal splenic artery (*arrows*) more anterior than those caused by proximal segment (*curved arrow*).

overlying gastric mucosa is invariably intact. Calcification of the splenic artery or focal pulsation of the gastric wall at fluoroscopy sometimes identifies the position of this vessel. It may be necessary to induce gastric hypotonia for better appreciation of transmitted pulsations. The possibility should always be considered that patients may have extrinsic or intramural lesions involving the stomach in addition to defects caused by tortuosity of aneurysmal change of the splenic artery.

REFERENCES

1. Whalen JP, Bader LM, Wolfman R: Evaluation of the retrogastric space. Normal appearance and variation. *AJR* 121:348–356, 1974
2. Simon M, Annes GP, Brenner SR, Seidenberg B: Pseudotumor of the stomach simulated by splenic artery tortuosity. A case report. *Am J Gastroenterol* 52:433–438, 1969

Suprarenal Aortic Occlusion

JOSEPH C. SEQUEIRA,[1, 2] CARL F. BECKMANN,[1] AND DAVID C. LEVIN[1]

Proximal propagation of an occlusive distal aortic thrombus to the suprarenal level is rare, probably resulting from diminished renal blood flow, and is invariably accompanied by renal failure. Three similar cases of total suprarenal aortic occlusion with renal failure are presented. In each, one kidney was significantly smaller than the other, probably caused by long-standing disease. The combination of bilaterally absent or markedly decreased femoral pulses with diminished renal function or a unilateral small kidney should therefore be considered dangerous. To prevent proximal propagation of thrombosis and death from renal failure, such patients should undergo arteriography and surgical repair promptly even though their clinical symptoms might be relatively mild and stable.

Total occlusion of the abdominal aorta usually begins at the bifurcation. Although it may be caused by an embolic lesion, more commonly it is due to thrombosis superimposed upon atherosclerotic disease. It is believed that in many such patients, propagation of clot occurs back to a point just below the renal arteries where the high flow through the renal arteries prevents the obstruction from extending any further proximally [1]. More proximal propagation of thrombosis to the suprarenal level is rare with only scattered reports in the surgical literature [2, 3] and none in the radiologic literature. We describe three cases of total suprarenal aortic occlusion with identical clinical findings and fatal outcome.

Case Reports

Case 1

An 80-year-old white male was referred for evaluation of anuria of 72 hr duration. He had been hypertensive for many years. Blood pressure was 220/160 mm Hg. Pulses were absent in and below both femoral arteries. Blood urea nitrogen was 125 mg/100 ml and creatinine, 11.3 mg/100 ml. A technetium scan showed no uptake in the kidneys. Intravenous urography showed nonopacification of kidneys up to 5½ hr. Retrograde pyelography and abdominal ultrasonography showed no evidence of obstruction; the left kidney was noted to be shrunken.

Abdominal aortography was then performed via the left axillary approach. The study (fig. 1) showed total occlusion of the aorta above both the renal arteries and the superior mesenteric artery. The superior mesenteric artery was opacified by collaterals from the celiac axis. There was no opacification of renal arteries in the delayed radiographs. The patient was then dialyzed and stabilized preoperatively.

At surgery the aorta was found to be thrombosed up to the celiac axis. Aortic endarterectomy, bilateral renal endarterectomies, and aorta-to-left profunda and right common femoral bypass grafts were performed. The patient died of cardiac

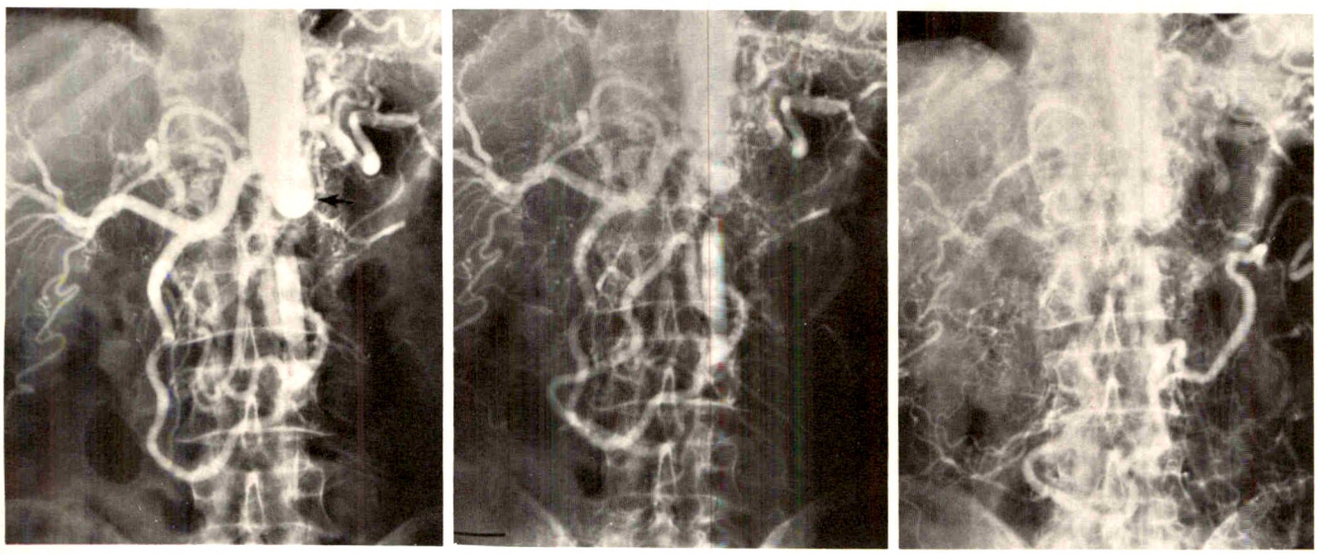


Fig. 1.—Case 1. Early, mid, and late phase films showing complete occlusion of aorta (*arrow*) above origin of superior mesenteric and both renal arteries. Both the superior and inferior mesenteric arteries fill via collateral circulation from celiac axis. Renal arteries never opacified and no nephrogram phase was observed.

Received November 14, 1978; accepted after revision February 2, 1979.
This work was supported in part by U.S. Public Health Service grants HL20895, HL05832, and GM18674.
[1]Department of Radiology, Peter Bent Brigham Hospital, Harvard Medical School, Boston, Massachusetts 02115.
[2]Present address: Department of Radiology, Beth Israel Hospital, Harvard Medical School, 330 Brookline Avenue, Boston, Massachusetts 02215. Address reprint requests to J. Sequeira.

© 1979 American Roentgen Ray Society

0361–803X/79/1325–0773 $0.00

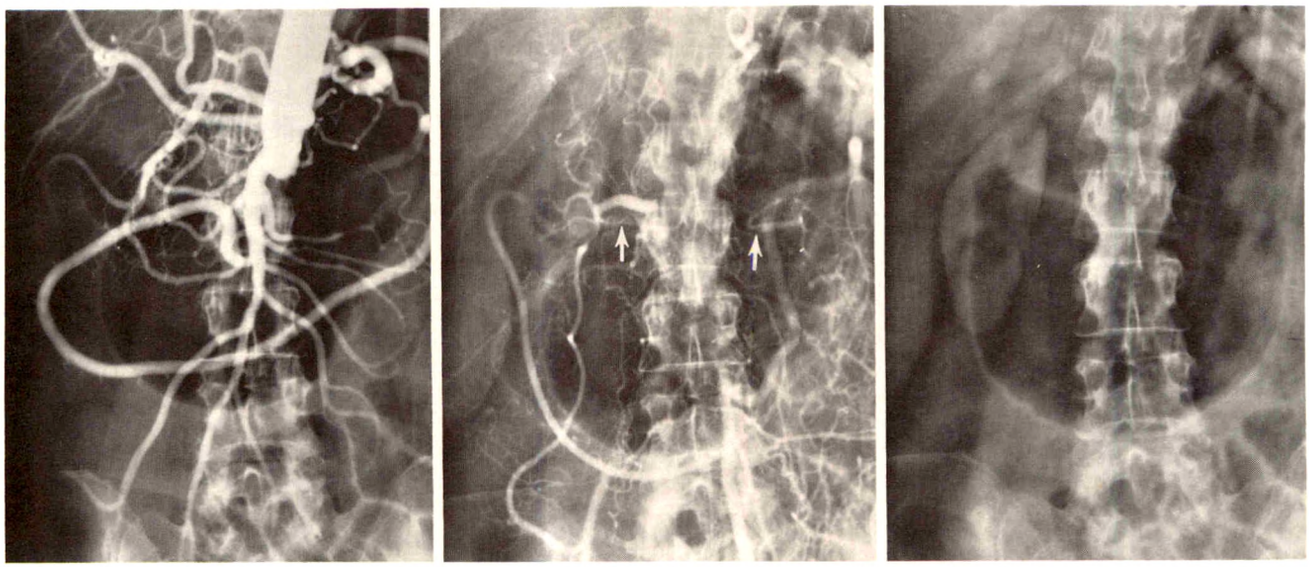


Fig. 2.—Case 2. Early, late, and capillary phase films show complete occlusion of aorta above both renal ateries but below celiac axis and superior mesenteric artery. Renal arteries opacify (*arrows*) via collateral circulation. During capillary phase, faint nephrogram was observed bilaterally and right kidney was noted to be small.

complications on the second postoperative day. No autopsy was performed.

Case 2

A 59-year-old hypertensive white female was admitted with anuria of 48 hr duration. She was obese with absent femoral pulses and no palpable distal pulses. Blood urea nitrogen was 51 mg/100 ml and creatinine was 5.3 mg/100 ml. A technetium renal scan showed visualization of the upper abdominal aorta and perfusion of liver and spleen with no perfusion below this level. Retrograde pyelography was normal. Abdominal ultrasound showed a left kidney measuring 11 × 12 cm and a shrunken right kidney.

The patient underwent abdominal angiography (fig. 2) via a left axillary approach which showed occlusion of the aorta above both renal arteries and extending to a point just below the origin of the superior mesenteric artery. In the delayed films, opacification of both renal arteries occurred via collaterals. Faint nephrograms were also identified.

Following surgery for aorto-femoral bypass grafting and bilateral renal and distal endarterectomies, the patient died on the fourteenth postoperative day of a massive left cerebral hemispheric infarct. There was no recovery of renal function on the left side. At autopsy, the distal aorta and the iliac arteries showed severe atherosclerotic disease. The right kidney was grossly shrunken with thrombosed renal artery. The aorto-bifemoral bypass grafts were patent and functional.

Case 3

A 61-year-old white male was admitted for evaluation of anuria of 48 hr duration. On admission to a local hospital a week earlier, he was oliguric with a blood urea nitrogen of 48 mg/100 ml. His past history included an aorto-femoral bypass graft 16 years earlier for peripheral vascular disease. His blood pressure was 170/90 mm Hg. Femoral and distal pulses were absent. An intravenous urogram with nephrotomography (fig. 3A) revealed a shrunken right kidney, a normal sized left kidney, and a poorly visualized delayed nephrogram bilaterally. Plain films of the abdomen showed a calcified dilated distal abdominal aorta (fig. 3B).

A left transaxillary abdominal aortogram (figs. 3C and 3D) showed total aortic occlusion extending above the renal arteries. The superior mesenteric artery was patent. The renal arteries did not opacify via collaterals and no nephrograms were seen. Surgery confirmed total occlusion extending above the renal arteries and aorto-femoral and left renal bypass grafts were placed. The patient died postoperatively of ventricular fibrillation and persistent anuria. No autopsy was obtained.

Discussion

The most frequently encountered form of aortic atherosclerosis is deposition of many irregular plaques in the aortic wall. Actual occlusion occurs secondary to superimposed thrombosis. When thrombosis occurs at the bifurcation, the associated clinical picture is referred to as the Leriche syndrome. Frequently the occlusion ascends to a level just below the renal arteries as a result of proximal progression of thrombosis from an occluded aortic aneurysm or, more commonly, from a terminal aortic occlusion [4]. Bergen and Trippel [4] suggested that aortic thrombosis ascended still further to involve one or both renal arteries in from 3%–15% of patients with distal aortic occlusion. As it ascends, it may gradually encroach upon a renal artery and produce increasingly severe hypertension. Wyatt and Felson [1] described three cases of distal abdominal aortic thrombosis in whom significant hypertension was initially absent. In each case a marked increase in blood pressure subsequently developed. Translumbar aortography before and after onset of hypertension showed retrograde propagation of thrombosis resulting in partial obliteration of circulation to a renal artery. The hypertension was then relieved by nephrectomy.

Various authors have recorded cases of proximal propagation of thrombosis in the aorta to obliterate the renal and more rarely the upper visceral arteries [2, 3, 5, 6]. While the syndrome of occlusion of the terminal aorta is frequently observed, the symptom complex caused by aortic obliteration at or above the renal artery level is

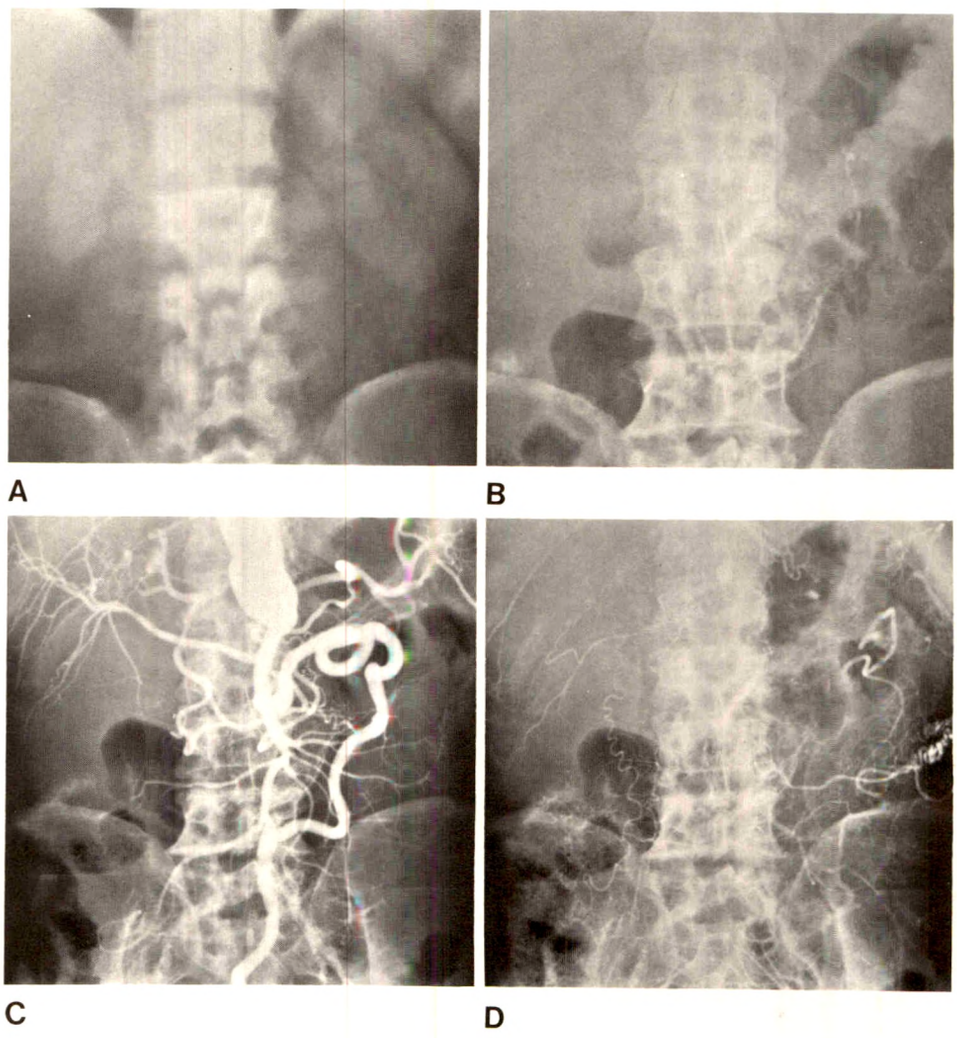


Fig. 3.—Case 3. **A**, Nephrotomogram showing shrunken right kidney. **B**, Supine abdominal film shows calcified abdominal aortic aneurysm. **C**, Aortic occlusion above origins of renal arteries. Celiac axis is also occluded at origin and its branches and those of inferior mesenteric artery fill via collaterals from superior mesenteric artery. **D**, Late phase failed to show collateral circulation to renal arteries.

seldom seen [4]. There have been occasional reports in the literature of high abdominal aortic occlusion with patent renal arteries in patients with coarctation of the aorta [7]. Throughout the arterial system an occlusion of an artery leads to the extension of thrombus distally from the point of occlusion to the level of entrance of inflow from a major collateral pathway. Thrombosis also extends proximally from the site of obstruction to or nearly to the exit of a major arterial branch. In most patients with distal abdominal aortic occlusion, high volume blood flow through the renal arteries limits proximal extension of thrombosis.

Fifty-five patients with juxtarenal atherosclerotic occlusion of the abdominal aorta were studied by Starrett and Stoney [6] over a 23-year-period. Of a group of 13 patients without surgery, 11 died and at autopsy, six (46%) had occlusion of one or both renal arteries. The mechanism in five was direct extension of aortic thrombosis; the mechanism in the sixth was not specified. Two of these also had occlusion of the superior mesenteric artery. All six died in complete or partial renal failure.

Although the Leriche syndrome is often a chronic condition which can be tolerated for a prolonged period, the presence of decreased function of one or both kidneys seems to add significant risk of retrograde propagation of thrombus to the suprarenal level. Presumably, in such cases, the superimposed renal disease reduces flow through one or both renal arteries to the point where it no longer deters the progression of thrombosis. This sets up a vicious cycle whereby thrombosis extends proximally, occludes both renal arteries, and leads to complete renal shutdown. In each of our three cases, one kidney was significantly smaller than the other, probably on the basis of long-standing disease. Combinations of bilaterally absent or markedly decreased femoral pulses with diminished renal function or a unilateral small kidney should therefore be considered dangerous. Such patients may be advised to undergo arteriography and surgical repair promptly to prevent renal failure, even though clinical symptoms might be relatively mild and stable.

ACKNOWLEDGMENT

We thank Ms. Cindy Clarke for secretarial assistance.

REFERENCES

1. Wyatt GM, Felson B: Aortic thrombosis as a cause of hypertension, an arteriographic study. *Radiology* 69:676–

682, 1957
2. Johnson JK: Ascending thrombosis of abdominal aorta as fatal complications of Leriche's syndrome. *Arch Surg* 69: 663–668, 1954
3. Potter DJ, Hopkins JG: Reversible paraplegia and acute renal failure due to occlusive disease of the abdominal aorta. *Ann Intern Med* 69:777–780, 1968
4. Bergan JJ, Trippel OH: Management of juxta-renal aortic occlusions. *Arch Surg* 87:60–68, 1963
5. Bron KM: Thrombotic occlusion of the abdominal aorta. *AJR* 96:887–895, 1966
6. Starrett RW, Stoney RJ: Juxta-renal aortic occlusion. *Surgery* 76:890–897, 1974
7. Lipchick E, Rob CG, Schwartzberg S: Obstruction of abdominal aorta above the level of renal arteries. *Radiology* 82:443–445, 1964

Partial Splenic Embolization in the Treatment of Hypersplenism

D. G. SPIGOS,[1] O. JONASSON,[2] M. MOZES,[2] AND V. CAPEK[1]

Transcatheter embolization of the spleen has been associated with serious complications, such as splenic abscess, rupture of the spleen, pneumonia, and septicemia. These complications, with their grave consequences, have prevented the use of this procedure as an alternative to operative splenectomy in selected cases. A detailed description of our method, which consists of partial splenic embolization, antibiotic prophylaxis, adequate pain control, and careful pre- and postembolization, is reported. Thirteen patients with hypersplenism were successfully treated with transcatheter partial embolization of their spleen.

Transcatheter arterial embolization has recently gained an increased acceptance in the treatment of various conditions. Arterial embolization has been successfully used in occlusion of vascular lesions of the brain [1–3], head and neck [4, 5], cardiovascular system [6] gastrointestinal tract [7–10], and genitourinary system [11–14]. Accompanying the impressive successes of this new therapeutic method, alarming complications have been reported [15–19], including an almost uniform occurrence of splenic abscesses after splenic embolization [20–23]. In addition to abscess formation, other grave complications, such as rupture of the spleen [22], septicemia, and pneumonia [23], have prevented the use of splenic embolization as an alternative to operative splenectomy in selected cases of hypersplenism. We modified the technique of splenic embolization and followed detailed protocols of asepsis, antibiotic use, and postembolization management. Partial splenic embolization was successfully performed on 13 consecutive patients with hypersplenism.

Methods and Results

All patients in this series were treated while on the renal transplant service, either before transplantation while on hemodialysis (six patients) or after transplantation while on immunosuppressive medications (seven patients). The indications for partial splenic embolization were persistent leukopenia (white blood cell count less than 6,000/mm^3) and splenic enlargement determined by a spleen scan. Workup included bone marrow aspiration and, in nine patients, a hydrocortisone stimulation test (as described by Dale et al. [24]). The presence of a hypoplastic bone marrow was not considered a contraindication to partial splenic embolization, since persistent leukopenia was assumed to represent the effect of hypersplenism due to splenomegaly, magnified by a failure of suppressed bone marrow to compensate.

The risks and potential benefits of splenic embolization were explained to each patient and informed consent was obtained. Preparatory measures included whole body povidone-iodine (Betadine) baths both the night before and the morning of embolization. All patients began antibiotic prophylaxis 6 hr before embolization, which consisted of 1,000,000 IU of penicillin G injected intramuscularly and gentamycin 3 mg/kg. Penicillin and gentamycin were continued for 5 days. Strict aseptic technique was observed in the angiography suite. The embolic material, absorbable gelatin sponge (Gelfoam) was cut into 2 × 2 mm pieces and suspended in an antibiotic solution of 1,000,000 U penicillin G and 80 mg gentamycin in 100 ml of normal saline immediately before the intraarterial injection. The same solution of antibiotics was used for the injection of embolic particles, instead of contrast medium.

Femoral or axillary artery approach was used for splenic artery catheterization with the tip of the catheter always well advanced selectively into the splenic artery. Depending on the spleen size, 20–40 pieces of Gelfoam were injected, and the extent of infarction was monitored fluoroscopically and radiographically. No attempt was made to infarct the total splenic mass and the embolization was stopped when about two-thirds of the splenic parenchyma was ablated. The overall results are summarized in table 1.

The patients received 25–50 mg of meperidine hydrochloride (Demerol) intravenously immediately before the embolization. The eliminated most of the pain, which can be quite severe if left unmodified (case 1). Potent analgesics were required for at least 3 days. In our last seven patients, epidural anesthesia using bupivacaine hydrochloride 0.5% completely eliminated pain during the embolization procedure and for the ensuing 72 hr, since an indwelling catheter is left in the epidural space. Because of the epidural anesthesia, postembolization pain and discomfort were effectively controlled.

Representative Case Reports

Case 1

A 17-year-old boy with Alport's syndrome received a cadaver renal transplant. An acute rejection that developed 10 days later responded to standard immunosuppressive treatment. He developed *Listeria monocytogens* meningitis, which was treated with large doses of intravenous penicillin, 20 days after transport. At the same time, severe leukopenia (white blood cell count of 1,200/mm^3) and thrombocytopenia (platelet count, 19,000/mm^3) occurred, despite cessation of immunosuppres-

Received August 21, 1978; accepted after revision January 16, 1979.

[1] Department of Medical Radiology, University of Illinois Hospital, 840 South Wood Street, Chicago, Illinois 60612. Address reprint requests to D. G. Spigos.

[2] Department of Surgery, University of Illinois Hospital, Chicago, Illinois 60612.

© 1979 American Roentgen Ray Society

0361–803X/79/1325–0777 $0.00

TABLE 1

Partial Splenic Embolization Results

Case No.	Embolization (%)	Adverse Effects
1	60	Severe postinfarction pain
2	80	Moderate pleural effusion
3	60	Minimal pleural effusion
4	80	Platelike atelectases
5	90	Pleural effusion for 5 weeks
6	60	Pancreatitis, bilateral pneumonia

Note.—Embolization was uneventful in cases 7–13. Hematology for all patients was normal after embolization.

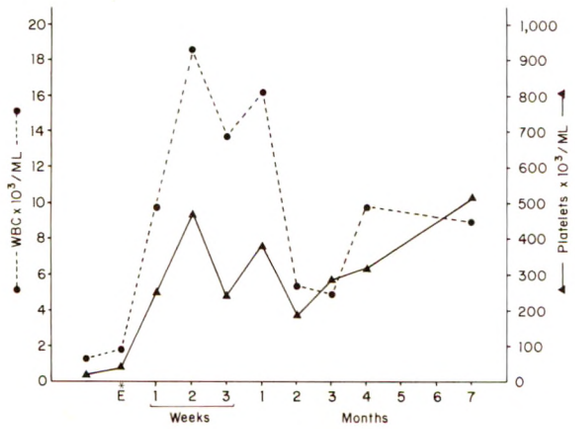


Fig. 1.—Case 1. After splenic embolization, sharp increase in both white blood cells and platelet series with eventual return to normal levels. Patterns were analogous in other patients.

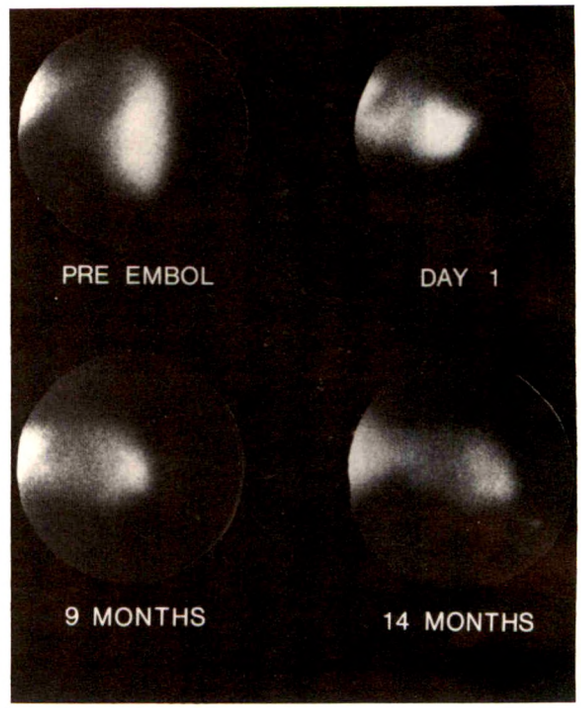


Fig. 2.—Case 1. ^{99m}Tc sulfur colloid scans of spleen over 14 months. Remaining uninfarcted portion of spleen did not hypertrophy to significant degree.

sive medications. A ^{99m}Tc sulfur colloid scan showed marked splenic enlargement. The bone marrow was hypoplastic. Subcutaneous injection of 0.5 mg epinephrine 1:1,000 increased both white blood cell and platelet counts, implicating the spleen as the likely source of white blood cell and platelet sequestration. About 60% splenic infarction was produced after injection of 40 Gelfoam pieces in the splenic artery. The patient's hematologic status improved rapidly (fig. 1), and the white blood cell count remained normal on maintenance doses of immunosuppression. The patient remained in good condition more than 2 years after embolization without any evidence of adverse effects from the procedure, although chronic rejection necessitated a nephrectomy 8 months after transplant. Periodic spleen scans show no evidence of significant hypertrophy of the uninfarcted part of the splenic parenchyma (fig. 2).

Case 2

A 40-year-old man received a cadaver renal transplant. Because of persistent leukopenia, a reduction of the azathioprine dosage to less than 1 mg/kg/day was necessary. An acute rejection episode that occurred 50 days after operation was reversed by standard immunosuppressive treatment. The liver-spleen scan demonstrated splenic enlargement, and a bone marrow aspiration revealed a hyperplastic marrow. About 80% infarction of the splenic parenchyma was produced by embolization. Thereafter, the white blood cell count rose to normal levels, permitting administration of routine doses of immunosuppression. Follow-up scans for 12 months did not show any significant regeneration of the splenic parenchyma (fig. 3). At 2 years after embolization, the patient had no side effects from the procedure. His white blood cell count was normal on maintenance azathioprine doses (2 mg/kg/day) and renal function was also normal.

Case 3

A 30-year-old man with a 12 year history of malignant hypertension had a bilateral nephrectomy. He was subsequently maintained on chronic renal dialysis, but had chronic leukopenia (white blood cell count , 3,000–4,000/mm^3) and thrombocytopenia (platelet count, 50,000/mm^3). The spleen scan demonstrated splenomegaly and the bone marrow was found to be hypocellular. Because of the leukopenia and thrombocytopenia, embolization of the spleen was performed before renal transplant. Splenic embolization 2 years after nephrectomy resulted in an ablation of about 60% of the splenic parenchyma. After embolization, the patient developed transient abdominal and chest pain, a pleural effusion, and a low grade fever. His white blood cell count was 12,600/mm^3 and his platelet count was 290,000/mm^3 the day after embolization. The pain, pleural effusion, and fever subsided within 72 hr. A renal transplant was performed 5 weeks later, at which time his hematologic status was normal. The posttransplant period was complicated with repeat episodes of hypertension, two acute rejections, a urine extravasation, a perineal abscess, and, finally, a cerebral hemorrhage that caused his death 5 months after transplant. Leukopenia did not recur.

Case 4

A 24-year-old man developed chronic renal failure at age 14. He had been on hemodialysis for 2 years. In the course of his pretransplant workup he was noted to have a persistent low white blood cell and platelet count. The liver-spleen scan

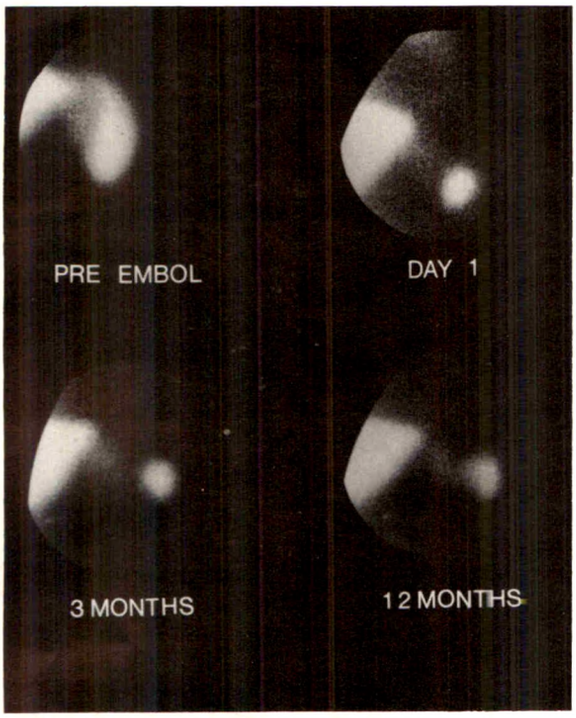


Fig. 3.—Case 2. ^{99m}Tc sulfur colloid spleen scans over 12 months. Uninfarcted part of spleen remained virtually unchanged.

demonstrated splenomegaly and the bone marrow showed a mild increase in cellularity. The hydrocortisone stimulation test was positive, indicating that hypersplenism was responsible for the leukopenia. Splenic embolization resulted in about 80% ablation of the splenic parenchyma. The patient had an uneventful postembolization course and was discharged 2 weeks after embolization without evidence of side effects from the procedure. At renal transplant 6 months later, hematologic values were normal and azathioprine tolerance was good (2 mg/kg/day).

Case 5

An 18-year-old man had been on chronic hemodialysis for 8 months when he received a cadaver renal transplant. The patient had an uneventful posttransplant course, except for a mild acute rejection that responded to treatment. Because of leukopenia (white blood cell count less than 3,000/mm^3), the azathioprine dose was reduced to less than 1 mg/kg/day. A bone marrow aspirate showed hypocellularity. The liver-spleen scan demonstrated splenomegaly. Splenic embolization was proposed to increase the tolerance to azathioprine. Splenic embolization 5 weeks after transplant resulted in about 90% splenic infarction (fig. 4). The patient experienced moderate left flank and epigastric pain for 48 hr and also developed a left pleural effusion. His white blood cell and platelet counts remained high after embolization, allowing reinstitution of an adequate maintenance dose of azathioprine. The patient was well with a normal white blood cell count and a normally functioning kidney transplant 4 months after partial splenic embolization.

Case 6

A 33-year-old woman candidate for a second renal transplant had persistent leukopenia (white blood cell count 3,000–5,000/mm^3) since rejection and removal of her first cadaver transplant. Immunosuppressive therapy had been stopped at transplant nephrectomy 6 months before. Her bone marrow showed hypocellularity, and a liver-spleen scan showed splenomegaly. Splenic embolization was proposed in preparation for retransplantation. This was performed using Gelfoam powder and resulted in about a 60% splenic ablation. It was necessary to use powder instead of sponge because of the small coaxial catheter required to enter the tortuous splenic artery. The patient's white blood cell and platelet counts increased after embolization. She developed pancreatitis (serum amylase, 2,000 Somogyi U), bilateral pleural effusions, and bilateral pneumonitis, all of which resolved with treatment within 9 days. Pancreatitis was assumed to be due to inadvertent embolization of pancreatic arterial branches by the Gelfoam powder. Her white blood cell count remained more than 6,000/mm^3 and she received a successful cadaver renal transplant 3 months after splenic embolization. Routine immunosuppressive therapy was instituted.

Discussion

In 1952, King and Shumacker [25] reported an increased incidence of serious infections in children after splenectomy. Their report focused on the significance of the spleen in overall defense. This observation was later verified in the larger series of Eraklis and Filler [26] and Singer [27], who found that asplenic children, especially those who underwent splenectomy because of thalassemia or idiopathic thrombocytopenic purpura, were at a higher risk to develop an overwhelming bacterial infection when compared with a nonsplenectomized population.

Recently, similar fulminant bacterial septicemias, with fatalities occurring within 18 hr after onset of symptoms, have also been reported in adult patients with Hodgkin's disease who underwent splenectomy for staging purposes [28, 29], in renal transplant recipients where splenectomy was performed in order to improve their tolerance to azathioprine [30], in patients with functional absence of splenic tissue, such as in sickle cell disease [31, 32], and in patients with congenital asplenia [33].

Although the physiology and functions of the spleen are poorly understood, it is known that the spleen, representing one-fourth of the total lymphatic mass, serves as a biological filter for the clearance of bacteria and also is essential for rapid antibody production after challenge with blood-borne particulate antigen in the absence of preexisting antibodies [34, 35]. In addition, the spleen appears to be the site of production of a nonspecific leukophilic immunoglobulin, tuftsin, that increases the phagocytic activity of polymorphonuclear leucocytes [36]. Thus, it is apparent that the spleen has important and, at times, critical functions and its removal is not to be taken lightly. Partial splenic embolization represents a potential alternative method to splenectomy when ablation of the splenic parenchyma is desired, particularly in compromised patients, where splenectomy carries significant morbidity and mortality rates [37].

Splenic embolization has been successfully used experimentally in the treatment of splenic trauma [38, 39]. Hematologic changes after embolization have been observed, especially in the white blood cell and platelet

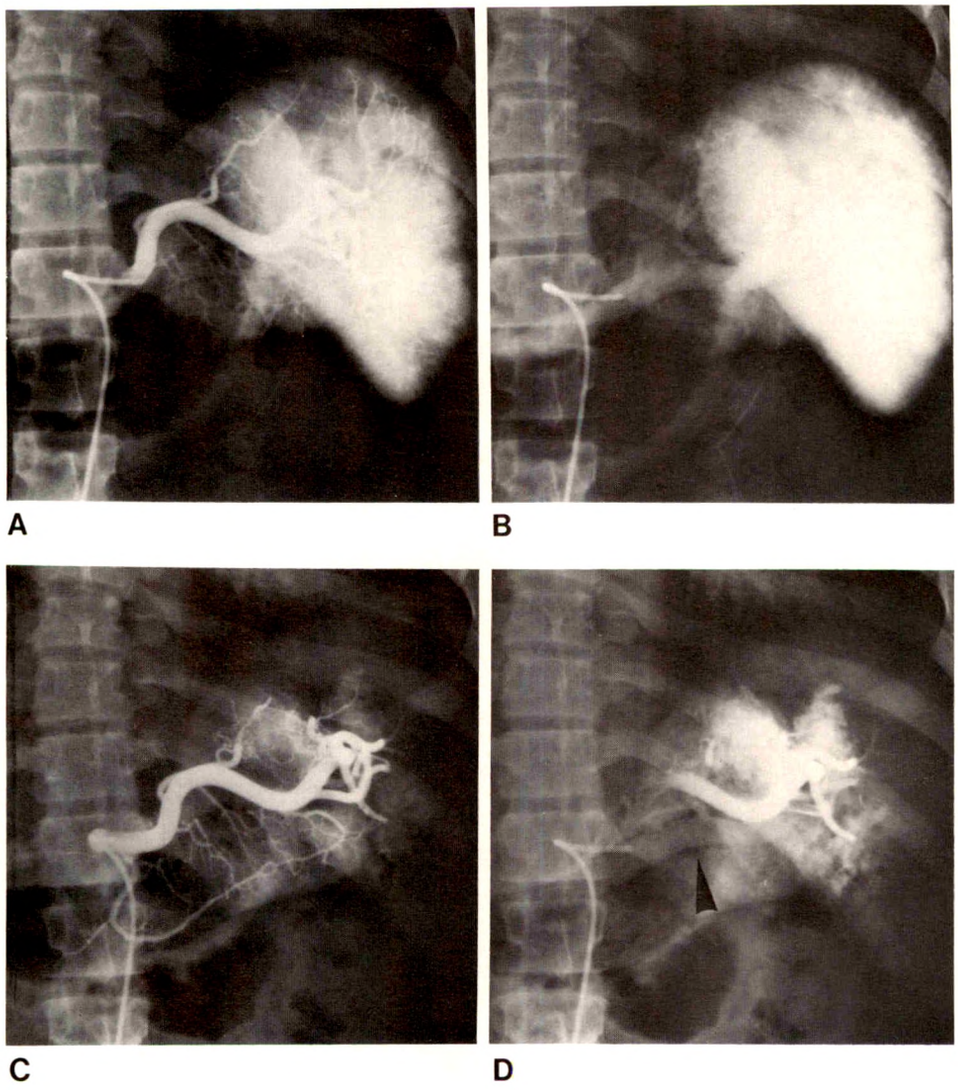


Fig. 4.—Case 5. Arterial (**A**) and venous (**B**) phases immediately before embolization. Catheter well advanced into splenic artery, prerequisite for safe embolization. Postembolization arteriograms show abrupt interruption of intrasplenic branches (**C**) and irregular uninfarcted splenic parenchyma (**D**). Splenic vein (*arrowhead*) remains patent after embolization.

series [40, 41]. There have also been sporadic reports of successful splenic embolization in humans with thrombocytopenia due to hypersplenism of portal hypertension [42–46]. With the exception of these few reports, where long-lasting improvement was observed, the overall experience with this procedure remained negative because of serious complications such as splenic abscesses [20–23, 44] (S. R. Reuter, J. Petasnick, and C. Athanasoulis, personal communications), septicemia and pneumonia [21, 23], and splenic rupture [22]. A number of authors have advocated that this procedure should be performed only as a prelude to operative splenectomy in patients with thrombocytopenia to improve hematologic status, so that the operative splenectomy can be performed more safely [21, 22].

Despite the fact that the patients in whom we performed splenic embolization represented a high risk population since they were uremic or on continuous immunosuppression, complications such as abscesses were not observed. We attribute this lack of significant complications to: (1) the differences between total and partial splenic embolization; (2) the strict aseptic technique and antibiotic prophylaxis; (3) the effective control of pain; and (4) careful postembolization care. Since we routinely perform only partial embolization, part of the splenic parenchyma remains intact. While the amount of functional capacity of remaining splenic tissue required to provide protection from overwhelming bacteria sepsis is not known, it is expected that the uninfarcted part may provide this protection.

In addition to the expected immunologic advantages, partial embolization might prevent development of splenic abscesses by preservation of the normal direction of the blood flow through the splenic circulation. In total splenic embolization, the arterial flow to the spleen is completely interrupted, and the direction of the flow in the splenic vein is reversed [47, 48]. This phenomenon might cause contamination of the infarcted splenic parenchyma with bacteria that are carried from the gastrointestinal tract through the portal circulation. Owman et al. [46] were successful when they performed 30% or sequential splenic embolization in patients with hyper-

splenism due to portal hypertension, but experienced abscesses in two patients when 90% of the spleen was infarcted. Castaneda et al. [21] similarly observed that dogs undergoing partial splenic embolization experienced minor complications in comparison with those with complete embolization, where complications such as rupture and pneumonia were common.

The data from these investigators and our own support the hypothesis that partial and/or sequential splenic embolization is well tolerated, with only minor adverse effects. Other potential causes of splenic abscesses might be the introduction of bacteria with catheters contaminated from the skin [22] or secondary to bacterial contamination of the embolic particles. Since the bacteria that have been isolated most commonly from splenic abscesses are *Staphylococcus epidermidis, Klebsiella pneumoniae,* and *Clostridium perfringens,* a combination of antibiotics, such as penicillin-gentamycin, given systemically, provides adequate prophylaxis. The suspension of embolic particles in the antibiotic solution may also eradicate possible bacterial contamination of the splenic parenchyma.

Adequate control of pain with epidural anesthesia or narcotics prevents, to some degree, splinting of thoracic wall and diaphragm and allows better lung expansion and bronchial toilet. Complications due to hypostatic pneumonia can thus be largely prevented.

Among the various embolic materials that have been used for "medical splenectomy," absorbable gelatin sponge was chosen for our patients. Its advantages include easy use, availability in a sterile form, and pieces can be cut as small as needed to occlude peripheral branches of the splenic artery, permitting partial splenic embolization. Because of the physiochemic structure of Gelfoam (protein matrix sponge), it may form a bond with the antibiotics, thus providing sustained antibiotic presence in the infarcted portion of the splenic parenchyma. Other materials, such as nonabsorbable polyvinyl alcohol and silastic spheres, have also been used successfully for splenic infarction [21, 39].

Autologous clot might be the chosen material in cases of splenic trauma, but since the clot usually lyses within 48 hr, it may not produce permanent results. Materials such as cyanoacrylate, metallic devices, or balloons cause occlusion of the main trunk of the splenic artery, but the changes in the splenic parenchyma are minimal since collateral circulation usually reconstitutes the splenic artery distal to the obstruction [49, 50]. Balloon catheter occlusion of the splenic artery does produce temporary improvement of the hematologic status in patients with thrombocytopenia, thus allowing a safe performance of splenectomy [22]. However, in addition to the reconstitution of the splenic artery distal to the occlusion, the catheter itself may become the source of bacteremia, a complication known to occur when catheters remain in arteries or veins for a prolonged period of time [51, 52].

Splenectomy is known to improve the hematologic status of a significant number of patients suffering from disorders such as hereditary spherocytosis, thalassemia, idiopathic thrombocytopenic purpura, and congestive splenomegaly and of renal transplant recipients who developed intolerance to azathioprine. Since partial splenic embolization causes permanent ablation of sufficient splenic parenchyma to allow subsequent improvement of hematologic status, we believe that it will become an alternative to splenectomy in selected patients with hypersplenism. Among other advantages, it is relatively easy to perform, has minimal morbidity, the splenic vein is preserved, and a portion of the splenic parenchyma remains intact to carry on the immunologic roles.

REFERENCES

1. Djindjian R, Cophignon J, Rey A, Theron J, Merland JJ, Houdart R: Superselective arteriographic embolization by the femoral route in neuroradiology; study of 50 cases. 111. Embolization in craniocerebral pathology. *Neuroradiology* 6:143–153, 1973
2. Kricheff JJ, Madayag M, Braunstein P: Transfemoral catheter embolization of cerebral and posterior fossa arteriovenous malformation. *Radiology* 103:107–111, 1972
3. Serbinenko FA: Balloon catheterization and occlusion of major cerebral vessels. *J Neurosurg* 41:125–145, 1974
4. Sokoloff J, Wickbom I, McDonald D, Brahme F, Goergen TG, Goldberger LE: Therapeutic percutaneous embolization in intractable epistaxis. *Radiology* 111:285–287, 1974
5. Roberson GH, Biller H, Sessions DG, Ogura JH: Presurgical internal maxillary artery embolization in juvenile angiofibroma. *Laryngoscope* 82:1524–1532, 1972
6. Porstmann W, Wierny L, Warneke H, Gerstberger G, Romaniuk PA: Catheter closure of patent ductus arteriosus; 62 cases treated without thoracotomy. *Radiol Clin North Am* 9:203–218, 1971
7. Rosch J, Dotter CT, Brown MJ: Selective arterial embolization; a new method for control of acute gastrointestinal bleeding. *Radiology* 102:303–306, 1972
8. Reuter SR, Chung VP, Bree RL: Selective arterial embolization for control of acute gastrointestinal bleeding. *Radiology* 102:303–306, 1972
9. Goldman ML, Land WC, Bradley EL, Anderson J: Transcatheter therapeutic embolization in the management of massive upper gastrointestinal bleeding. *Radiology* 120: 513–521, 1976
10. Bookstein JJ, Naderi MJ, Walter, JF: Transcatheter embolization for lower gastrointestinal bleeding. *Radiology* 127: 345–349, 1978
11. Bookstein JJ, Goldstein HM: Successful management of post-biopsy arteriovenous fistula with selective arterial embolization. *Radiology* 109:535–536, 1973
12. Almgard LE, Fernstrom L, Haverling M, Ljungqvist A: Treatment of renal adenocarcinoma by embolic occlusion of the renal circulation. *Brit J Urol* 45:474–479, 1973
13. Mariasoosai M, Wilson A, Gonick P: Selective renal artery embolization treatment for metastatic sarcoma with hematuria. *JAMA* 237:363–364, 1977
14. Miller FJ, Mortel R, Mann WJ, Jahshan AE: Selective arterial embolization for control of hemorrhage in pelvic malignancy: femoral and brachial catheter approaches. *AJR* 126: 1028–1032, 1976
15. Woodside J, Schwarz H, Bergreen P: Peripheral embolization complicating bilateral renal infarction with Gelfoam. *AJR* 126:1033–1034, 1976

16. Gang DL, Dole KB, Adelman LS: Spinal cord infarction following therapeutic renal artery embolization. *JAMA* 237: 2841–2842, 1977
17. Tegtmeyer CJ, Smith TH, Shaw A, Barwick KW, Kattwinkel J: Renal infarction: a complication of Gelfoam embolization of a hemangioendothelioma of the liver. *AJR* 128:305–307, 1977
18. Bradley EL, Goldman, ML: Gastric infarction after therapeutic embolization. *Surgery* 79:421–424, 1976
19. Braf ZF, Koontz WW: Gangrene of bladder. Complication of hypogastric artery embolization. *Urology* 9:670–671, 1977
20. Goldstein HM, Wallace S, Anderson JH, Bree RL, Giantruco C: Transcatheter occlusion of abdominal tumors. *Radiology* 120:539–545, 1976
21. Castaneda-Zuniga WR, Hammerschmidt DE, Sanchez R, Amplatz K: Non-surgical splenectomy. *AJR* 129:805–811, 1977
22. Wholey MH, Chamorro H, Rao G, Chapman W: Splenic infarction and spontaneous rupture of the spleen following therapeutic embolization. *Cardiovasc Radiol* 1:249–253, 1978
23. Witte CL, Ovitt TW, Van Wyck DB, Witte MH, O'Mara RE, Woolfenden JM: Ischemic therapy in thrombocytopenia from hypersplenism. *Arch Surg* 111:1115–1121, 1976
24. Dale DC, Fauci AS, Guerry D, Wolff SM: Comparison of agents producing neutrophilic leucocytosis in man. *J Clin Invest* 56:808–813, 1975
25. King H, Shumacker HB: Splenic Studies. 1. Susceptibility to infection after splenectomy performed in infancy. *Ann Surg* 136:239–242, 1952
26. Eraklis AJ, Filler RM: Splenectomy in childhood: a review of 1413 cases. *J Pediatr Surg* 7:382–388, 1972
27. Singer DB: Post-splenectomy sepsis, in *Perspectives in Pediatric Pathology*, vol 1, edited by Rosenberg HS, Bolandre RP, Chicago, Year Book Medical, 1973, pp 285–311
28. Chilcote RR, Baehner RL, Hammond D, investigators and special studies committee of the Childrens Cancer Study Group: Septicemia and meningitis in children splenectomized for Hodgkin's disease. *N Engl J Med* 15:798, 1976
29. Weitzman S, Aisenberg AC: Fulminant sepsis after successful treatment of Hodgkin's disease. *Am J Med* 62:47–50, 1977
30. Schroter GPJ, West JC, Weil R: Acute bacteremia in asplenic renal transplant patients. *JAMA* 237:2207–2208, 1977
31. Barret-Conner E: Bacterial Infection and Sickle Cell Anemia. *Medicine* (Baltimore) 50:97–112, 1971
32. Gaurilis P, Rothenberg SP, Guy R: Correlation of low serum IGM levels with absence of functional splenic tissue in sickle cell disease syndromes. *Am J Med* 57:542–545, 1974
33. Gopal V, Bisno AL: Fulminant pneumococcal infection in "normal asplenic hosts". *Arch Intern Med* 137:1526–1530, 1977
34. Ellis EF, Smith RT: The role of the spleen in immunity with special reference to the post-splenectomy problem in infants. *Pediatrics* 37:111–119, 1966
35. Likhite VV: Immunological impairment and susceptibility to infection after splenectomy. *JAMA* 236:1376–1377, 1976
36. Constantopoulos A, Najjar VA, Wish JB, Necheles TH, Stolbach LL: Defective phagocytosis due to tuftsin deficiency in splenectomized subjects. *Am J Dis Child* 126:663–665, 1973
37. Bergin JJ, Zuck TF, Miller RE: Compelling splenectomy in medically compromised patients. *Ann Surg* 178:761–768, 1973
38. Chuang VP, Reuter SR: Selective arterial embolization for the control of traumatic splenic bleeding. *Invest Radiol* 10: 18–24, 1975
39. Guilford WB, Scatliff JH: Transcatheter embolization of the spleen for control of splenic hemorrhage and in situ splenectomy. An experimental study using silicone spheres. *Radiology* 119:549–553, 1976
40. Chuang VP, Reuter SR: Experimental diminution of splenic function by selective embolization of the splenic artery. *Surg Gynecol Obstet* 140:715–720, 1975
41. Anderson JH, Buban A, Wallace S, Hester JP, Burke JS: Transcatheter splenic arterial occlusion: an experimental study in dogs. *Radiology* 125:95–102, 1977
42. Maddison F: Embolic therapy of hypersplenism. *Invest Radiol* 8:280–281, 1973
43. Papadimitriou J, Tritakis C, Karatzas G, Papaioannou A: Treatment of hypersplenism by embolus placement in the splenic artery. *Lancet* 2:1268–1269, 1976
44. Spigos DG, Jonasson O, Felix E, Capek V: Transcatheter therapeutic embolization of hypersplenism. *Invest Radiol* 12:418, 1977
45. Spigos DG, Jonasson O, Mozes M, Capek V: Partial splenic embolization. Presented at the annual meeting of the Association of University Radiologists, San Antonio, Texas, May 1978
46. Owman T, Lunderquist A, Alwmark A, Borjesson B: Embolization of the spleen-treatment for hypersplenism in the patient with portal hypertension. Presented at the World Congress of Gastroenterology, Madrid, June 1978
47. Witte CL, Witte MH, Renert W, O'Mara RE, Lilien DL: Splenic artery ligation in selected patients with hepatic cirrhosis and in sprague dawley rats. *Surg Gynecol Obstet* 142:1–12, 1976
48. Tsapogas MJ, Peabody RA, Karmody AM, Chuntrasakul C, Goussous H, Eckert C: Patho-physiological changes following ischemia of the spleen. *Ann Surg* 178:179–185, 1973
49. Probst P, Castaneda-Zuniga WR, Gomes AS, Yonehiro EG, Delaney JP, Amplatz K: Non-surgical treatment of splenic artery aneurysms. *Radiology* 128:619–623, 1978
50. Kaufman SL, Strandberg JD, Bart KH, Gross GS, White RI: Therapeutic embolization with detachable silastic balloons. Long term effects in swine. Presented at the annual meeting of the Association of University Radiologists, San Antonio, Texas, May 1978
51. Forsberg L, Hafstrom L, Lunderquist A, Sundqvist K: Arterial changes during treatment with intrahepatic arterial infusion of 5-fluorouracil. *Radiology* 126:49–52, 1978
52. Maki DG, Goldman DA, Rhame FS: Infection control in intravenous therapy. *Ann Intern Med* 79:867–887, 1973

Sinus Histiocytosis: Some Radiologic Observations

MARILYN J. SIEGEL,[1] GARY D. SHACKELFORD, AND WILLIAM H. McALISTER

Sinus histiocytosis with massive lymphadenopathy is an unusual disease characterized by prominent lymph node enlargement, especially in the cervical region. The clinical course is benign although prolonged, and no specific treatment is required. The etiology and pathogenesis are unknown. Four cases of sinus histiocytosis are reported, one in association with mediastinal lymph node enlargement and two in patients with orbital enlargement. One other patient had cervical masses. The radiologic features are reviewed to increase awareness of this entity as a cause of lymph node and orbital enlargement.

Sinus histiocytosis with massive lymphadenopathy is a benign condition characterized by painless lymph node enlargement. The cervical nodes are usually affected, although other lymph nodes may be involved. Pathologically, the lymph nodes show sinusoidal dilatation with numerous foamy histiocytes that often contain lymphocytes. There is no known etiology and no specific treatment. The clinical features are highly suggestive of lymphoma or malignant histiocytosis.

Four cases of sinus histiocytosis are presented. One patient had hilar and mediastinal lymph node enlargement. In two patients there were periorbital masses and orbital enlargement. One other patient had cervical masses. The pathologic and clinical features of cases 1, 2, and 4, have been mentioned elsewhere [1–3].

Case Reports

Case 1

A 3-year-old white male was in good health until 6 weeks prior to admission when he developed bilateral cervical masses that fluctuated in size. There were no associated symptoms. Physical examination revealed a well developed male with soft, nontender, mobile submandibular masses. There was no other adenopathy or hepatosplenomegaly. Laboratory data were negative. A chest radiograph revealed bilateral hilar and right paratracheal lymph node enlargement (fig. 1). Radiographs of the mandible showed submandibular soft tissue masses without bony involvement. A skeletal survey was unremarkable.

A submandibular lymph node was biopsied and histologic examination revealed capsular fibrosis and marked dilatation of the subcapsular and medullary sinuses which were filled with atypical histiocytes, many containing lymphocytes. The pathologic diagnosis was sinus histiocytosis. Bacterial, fungal, and viral cultures were negative.

Follow-up physical examinations over a 4-year period showed slight regression in the size of the cervical adenopathy. No further chest radiographs were obtained. The child continued to be asymptomatic.

Case 2

A 3-year-old black male presented with bilateral upper eyelid masses that had increased in size over several weeks. No symptoms were present. On physical examination there were firm masses in the upper eyelids and submandibular adenopathy. Ophthalmologic examination was normal. The differential diagnosis was lymphoma versus infectious granulomatous disease.

Laboratory data including an immunologic workup were normal. Paranasal sinus radiography revealed clouding of both maxillary sinuses and bilateral orbital enlargement (fig. 2). A chest radiograph was normal. Biopsies of a cervical node and an eyelid mass were compatible with sinus histiocytosis. Cultures were negative.

Follow-up radiographs 1 year after discharge again showed bilateral orbital enlargement. Subsequent examinations have revealed no change.

Case 3

A 16-year-old black female was referred for evaluation of a nontender mass in the left lower eyelid that had progressively enlarged over 3 months. There were no visual difficulties. Nine years previously the patient had undergone excisional biopsies of several large cervical nodes. On physical examination a firm, rubbery mass fixed to underlying tissues was palpable in the inferiomedial portion of the left orbit. The globes were asymmetric with the left eye showing 3 mm of proptosis and an increased height of 2 mm and width of 4 mm relative to the right eye.

Radiographs of the skull and orbits were normal except for opacification of the maxillary and ethmoid sinuses. Computed tomography of the orbits revealed a soft tissue mass in the inferomedial region of the left orbit extending 3 cm posteriorly behind the globe (fig. 3). The optic nerves were symmetrical. A chest radiograph was normal.

Surgical exploration revealed a 7 × 5 × 5 mm firm gray-white encapsulated mass anteriorly and inferomedially in the left orbit. This was attached by a small isthmus to a much larger mass in the posterior portion of the orbit. The orbital rim was intact.

Microscopic sections of the anterior portion of the bilobed mass showed diffuse infiltration by plasma cells and focal small areas of lymphophagocytosis. The infiltrate extended into the extraocular fat and skeletal muscles. The final pathologic diagnosis was sinus histiocytosis with massive lymphadenopathy.

The original cervical node biopsy was reviewed and felt to be consistent with sinus histiocytosis. Following discharge the patient was lost to follow-up.

Case 4

A 7-month-old white male was in good health until 5 months of age when he developed a painless firm swelling in the right parotid area, unresponsive to antibiotics. Physical examination was otherwise unremarkable. At operation a firm, tan colored mass involved the parotid gland. A definite diagnosis was not made microscopically but the differential diagnosis included malignant lymphoma, reticuloendotheliosis, and chronic inflammation. The patient was discharged with no further treatment.

At 13-months of age he was readmitted with a firm mass in

Received November 6, 1978; accepted after revision January 29, 1979.

[1] All authors: Mallinckrodt Institute of Radiology, Washington University School of Medicine, 510 South Kingshighway Boulevard, St. Louis, Missouri 63110. Address reprint requests to M. J. Siegel.

© 1979 American Roentgen Ray Society

0361–803X/79/1325–0783 $0.00

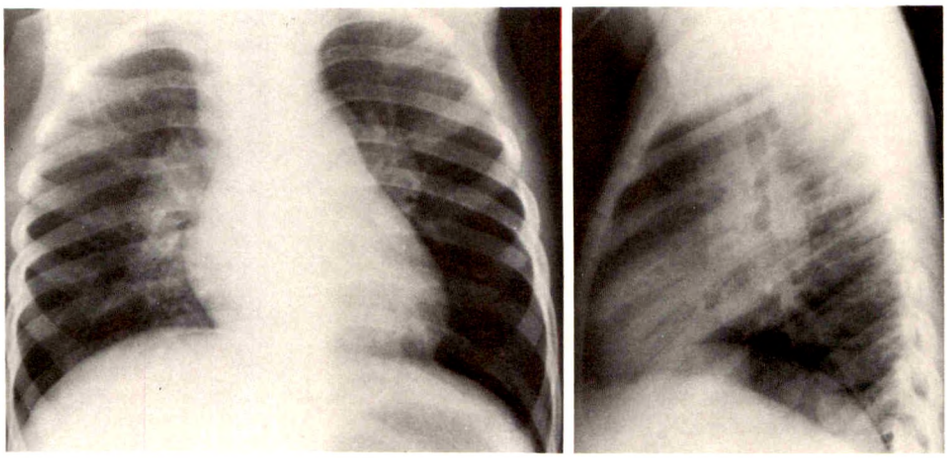


Fig. 1.—Case 1. Left, anteroposterior and, right, lateral chest radiographs showing enlargement of bilateral hilar and right paratracheal nodes.

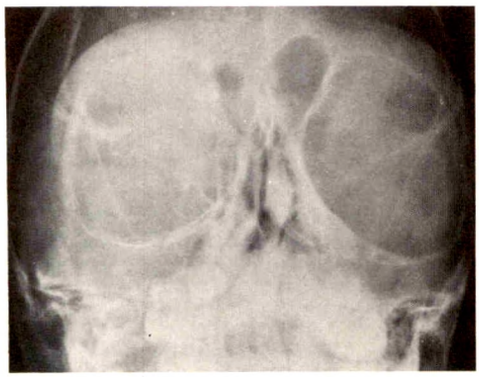


Fig. 2.—Case 2. Waters view of paranasal sinuses demonstrating bilateral orbital expansion and cloudy maxillary sinuses.



Fig. 3.—Case 3. CT scan through orbits showing soft tissue mass (*arrow*) in left orbit medial to globe.

the left occipital area and generalized enlargement of lymph nodes. Laboratory data were unrevealing except for white blood cell count of 14,700/mm^3 with 80% lymphocytes and hypergammaglobulinemia. A chest radiograph was normal. Excisional biopsy of the mass in the occipital area revealed matted lymph nodes. The microscopic diagnosis was Letterer-Siwe disease. The patient received a course of nitrogen mustard and was discharged. At two months after discharge, the adenopathy had regressed and the white blood count was normal.

Two years later the cervical nodes enlarged again and a repeat biopsy revealed "sinus histiocytosis." Fourteen years after the original diagnosis of Letterer-Siwe disease the patient was doing well. However, minor upper respiratory infections were associated with significant cervical lymph node enlargement that regressed when the infection resolved.

Discussion

Rosai and Dorfman [2] introduced the term sinus histiocytosis with massive lymphadenopathy in 1969 in a report of four cases; in 1972 30 additional cases were described [3]. Most patients are in the first two decades of life. The most common presenting feature is painless cervical lymph node enlargement (97% of cases) but enlarged lymph nodes at other sites have been described [4]. There is lack of significant hepatosplenomegaly. Extranodal deposits in the soft tissues of the tonsils, orbit, eyelids, testicle, and skin have been reported, as well as epidural infiltration [3, 5]. Microscopic changes of sinus histiocytosis have been seen in the mucosa of the small bowel and upper respiratory tract [3]. Fever, leucocytosis, an elevated erythrocyte sedimentation rate and hypergammaglobulinemia are not unusual. The clinical course is essentially benign but prolonged, and gradually the lymph node enlargement regresses, although it may take several years. Various modes of treatment have little effect on the course of this disease.

The exact etiology is unknown. The two most popular theories implicate an infectious etiology and an immunodeficiency state. The presence of lymphadenopathy, fever, leukocytosis, an elevated erythrocyte sedimentation rate, and hypergammaglobulinemia in a previously well patient is consistent with an infectious disorder. On the other hand, cultures and laboratory tests have been unsuccessful in documenting an organism. The second possibility of an immunologic abnormality is suggested by transient deficiencies in cellular immune functions found in some patients [6] and abnormalities of the thymus found on autopsy in two patients [3]. In both cases, dense fibrous tissue containing clusters of lymphocytes or plasma cells had replaced normal thymic tissue.

Occasional histiocytes were present in one of the specimens.

The most frequent finding on chest radiography is lymph node enlargement. Approximately 30%–43% of patients having chest radiographs show hilar or mediastinal lymph node enlargement [3, 4]. There is an equal frequency of unilateral and bilateral involvement. Occasionally focal pulmonary consolidation is seen and in one patient with a right upper lobe infiltrate, biopsy was consistent with either an infarct or necrotizing inflammation. Retroperitoneal lymphangiography reveals enlargement of the inguinal, iliac, and paraaortic lymph nodes with a reticular pattern or interruption in the marginal sinuses. The lymphographic findings suggest lymphoma.

Radiographically sinus histiocytosis is indistinguishable from many other conditions that cause lymphadenopathy in children. These primarily include malignant, inflammatory, and immune deficiency disorders. Orbital enlargement is a more unusual radiographic feature and the causes in children include neurofibromatosis, congenital glaucoma, tumors such as hemangioma, lymphoma, and rhabdomyosarcoma, orbital or retroorbital pseudotumors, and vascular anomalies, especially varices. The etiology of the orbital enlargement with sinus histiocytosis is uncertain. A long-standing intraorbital lesion can cause enlargement, and infiltration of the intraorbital fat and muscles was found in case 3. In case 2 the periorbital masses were clinically apparent only for "several weeks." However, intraorbital involvement could have preceded the appearance of the external masses. The diagnosis of sinus histiocytosis with massive lymphadenopathy is established by biopsy.

REFERENCES

1. Fickering LK, Phelan E: Sinus histiocytosis. *J Pediatr* 86: 745–748, 1975
2. Rosai J, Dorfman RF: Sinus histiocytosis with massive lymphadenopathy. A newly recognized benign clinico-pathological entity. *Arch Pathol Lab Med* 87:63–70, 1969
3. Rosai J, Dorfman RF: Sinus histiocytosis with massive adenopathy. A pseudolymphomatous benign disorder. Analysis of 34 cases. *Cancer* 30:1174–1188, 1972
4. Chener LP: Pediatric Surgical Pathology. St. Louis, Mosby, 1975
5. Kessler E, Srulijes C, Toledo E, Shalit M: Sinus histiocytosis with massive lymphadenopathy and spinal epidural involvement. A case report and review of the literature. *Cancer* 38: 1614–1618, 1976
6. Becroft DMO, Dix MR, Gillman JC, Macgregor BJL, Shaw RL: Benign sinus histiocytosis with massive lymphadenopathy: transient immunological defects in a child with mediastinal involvement. *J Clin Pathol* 26:463–469, 1973

Epidurography: Selective Catheter Technique and Review of 53 Cases

GLENN H. ROBERSON,[1, 2] H. PAUL HATTEN, JR.,[1, 3] AND JOHN H. HESSELINK[1]

Lumbar epidurography was performed in 53 patients at Massachusetts General Hospital, and the diagnostic efficacy of the procedure was documented. The anatomy of the epidural space and the techniques for epidurography are discussed. The procedure is advocated as an adjunct to lumbar myelography, particularly in patients with a prominent ventral epidural space and confusing or equivocal clinical examination.

Several of the terms applied to the radiographic technique for contrast examination of the epidural space include lumbar peridurography [1, 2], canalography [3], and epidurography [4, 5]. The descriptive anatomic term, epidurography, was chosen to describe the technique of selective catheterization with injection of water-soluble contrast material of the epidural space developed at Massachusetts General Hospital. Radiographic examination of the epidural space was first described in 1941 using both air-[4] and water-soluble contrast media [6]. Several large European series of epidurograms have been reported, including a series of 600 cases [7] and another of 102 cases [2].

Epidurography can add a much needed dimension to the diagnosis of difficult back problems. From December 1976 to June 1978, 53 epidurograms were performed at Massachusetts General Hospital with excellent results. We developed a modified Seldinger technique with selective catheterization of the epidural space. With this technique and positive injection of contrast material, epidurography augmented conventional myelography and aided in the diagnosis of difficult cases of disc disease during this period.

Anatomy

The epidural space (fig. 1) extends from the foramen magnum to the sacral notch. It is bounded cephalad by the attachment of the dura mater to the foramen mag-

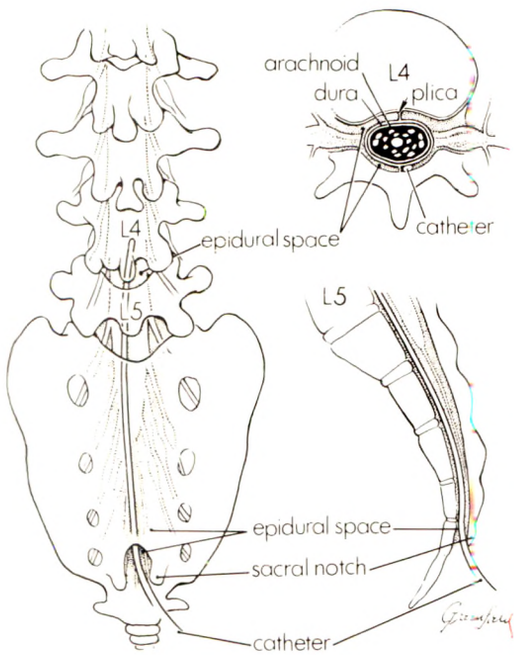


Fig. 1.—Catheter in place. Epidural space extends from foramen magnum to sacral notch; dural mater forms its central boundary, and periosteum of vertebral body its peripheral margin.

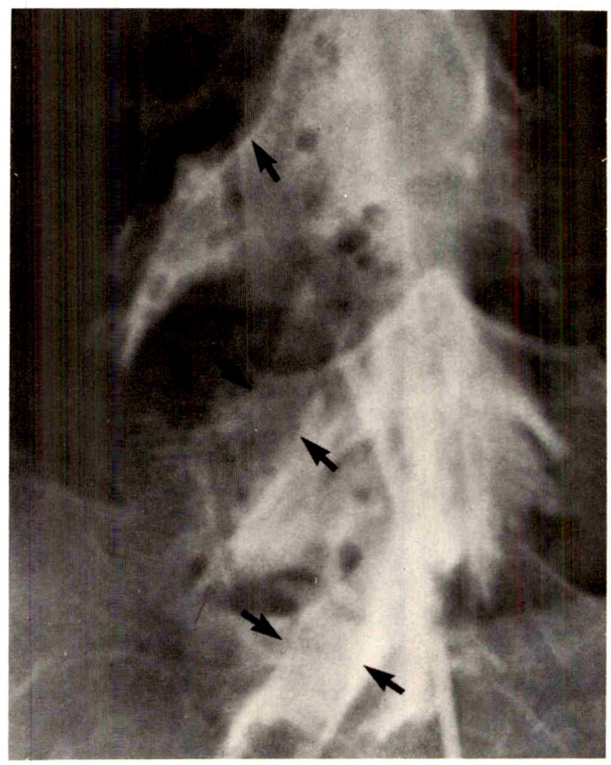


Fig. 2.—Normal filling of several lower nerve roots (*arrows*). Relation of nerve roots to pedicles of vertebral bodies evident.

Received August 14, 1978; accepted after revision January 15, 1979.
Presented at the annual meeting of the American Roentgen Ray Society, Toronto, Canada, March 1979.
[1]Department of Radiology, Section of Neuroradiology, Massachusetts General Hospital and Harvard Medical School, Boston, Massachusetts 02114.
[2]Present address: Department of Radiology, Albany Medical College, Albany, New York 12208.
[3]Present address: Department of Radiology, Presbyterian Hospital, P.O. Box 33549, Charlotte, North Carolina 28233. Address reprint requests to H. P. Hatten, Jr.

© 1979 American Roentgen Ray Society

0361-803X/79/1325-0787 $0.00

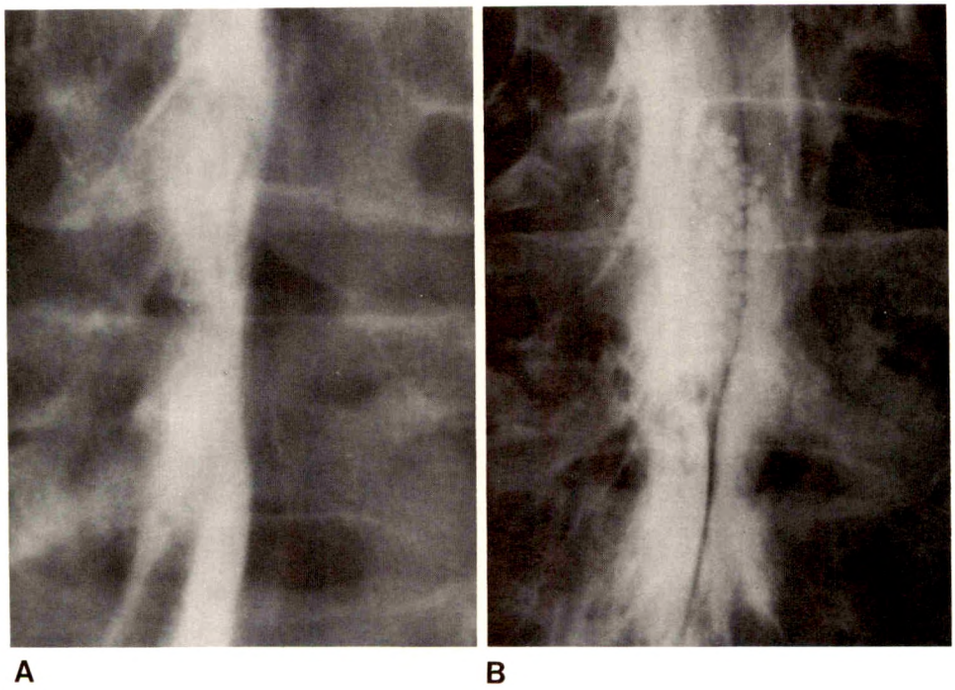


Fig. 3.—Plica mediana dorsalis in various normal anatomic configurations. **A,** Plica totally separating epidural space into right and left compartments. **B,** Plica as median translucency with filling of right and left sides of epidural space.

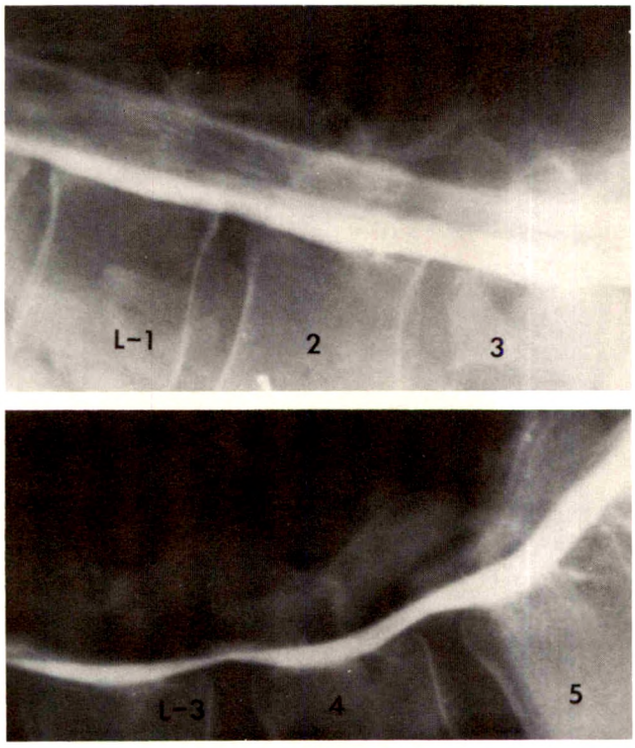


Fig. 4.—Normal filling of ventral and dorsal epidural space.

num and caudal by the membranous covering of the sacral notch. Dura mater forms the central boundary and the periosteum of the vertebral bodies the peripheral margin of the epidural space. Periosteum of the vertebral bodies is absent at the foramen of each spinal nerve allowing contrast in the epidural space to outline the dural investment of nerve sheaths (fig. 2). The epidural space contains areolar connective tissue, blood vessels, and transmits the spinal nerves with their investments.

The plica mediana dorsalis is seen as a median translucency (fig. 3) on epidurography and frequently is well enough formed to separate the epidural space into right and left compartments. The plica had been seen at surgery and demonstrated on cadavers [8], and its presence can represent a significant technical problem in trying to fill both right and left sides of the epidural space.

Technique

The initial description of epidurography was of a technique in which the epidural space was punctured with a needle and air was introduced [4]. The next refinement was the introduction of water-soluble contrast media into the epidural space [1, 3]. The positive contrast provided better definition of the epidural space, including dorsal and ventral components (fig. 4).

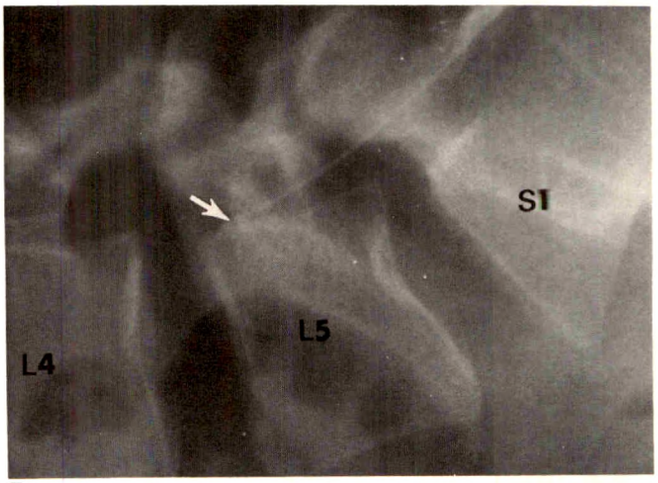
Our efforts at epidurography initially involved puncture of the epidural space at the sacral notch and passage of a 22 gauge catheter into the epidural space. The plica mediana dorsalis often prevents filling of one side of the epidural space (fig. 3). When this situation arose, direct intralaminar puncture of the epidural space was performed attempting to place the needle in the ventrolateral epidural space.

Dimer-X (which has since been removed from the market) was used for the initial 12 cases, and iothalamate meglumine (Conray-60, Mallinckrodt Pharmaceuticals, Inc., St. Louis, Mo.) was injected in the remaining 41 cases. Metrizamide has been used successfully in dogs [9, 10] and humans [10] with good results, and should be the contrast agent of choice in the future.

The technique that we developed consists of placement of an epidural catheter with a modified Seldinger



A



B

Fig. 5.—**A,** Initial film with epidural catheter low in sacrum. **B,** Catheter (*arrow*) in ventral epidural space higher in lumbar region before injection of contrast material.

technique. A prepackaged intravenous placement unit (Intracath, Desert Pharmaceutical Co., Sandy, Ut.) that includes a 14 gauge needle and a 60 cm, 16 gauge catheter is used in combination with a 0.063-cm-diam TSF heparin-coated guide wire (Amplatz Heparin Coated Wire Guide, Cook, Inc., Bloomington, Ind.). The guide wire is passed through the 14 gauge needle into the epidural space via puncture at the sacral notch. The 16 gauge catheter is then advanced through the needle over the guide wire, after which the needle is removed, with catheter extending cephalad in the sacral canal and epidural space (fig. 5).

Selective catheterization of either the right or left epidural space is thus possible. When it is necessary to study both sides and the plica prevents bilateral filling, the guide wire is reintroduced, the catheter is withdrawn, and the needle is again placed in the sacral hiatus. By manipulating and deflecting the needle, it is possible to selectively catheterize the desired side. The catheter tip is generally positioned at the level of the L5 vertebral body (fig. 6), and 15–20 ml of contrast material is slowly injected. Anteroposterior, lateral, and oblique films of the desired location are obtained. This modified Seldinger technique for selective catheterization of the epidural space is the factor that improved the failure rate in the last part of our series and eliminated the need for direct intralaminar puncture of the epidural space.

Lateral tomography is used to identify midline ventral defects and is useful when contrast material fills both sides of the epidural space and both right and left root sleeves (fig. 7). In this situation, midline defects are obscured by the lateral contrast and tomography has proven helpful in eliminating this source of error. Body computed tomography scans (EMI 5005) were performed in several patients after epidural contrast injection; however, present technology does not permit the necessary detailed resolution to identify disc herniation.

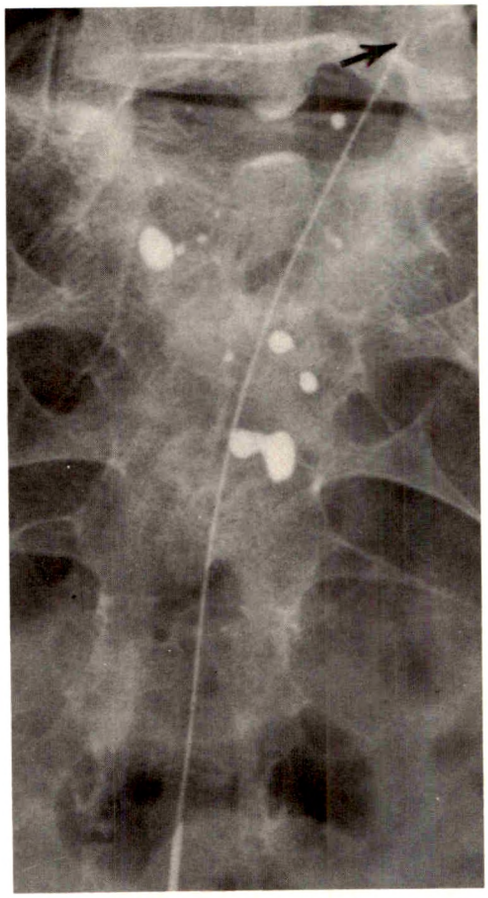


Fig. 6.—Epidural catheter position (*arrow*) before injection of contrast material. Anteroposterior projection shows how specific side and disc space can be selected for level of injection. Small amount of residual Pantopaque within subarachnoid space from previous myelography.

Results

The 53 epidurograms were divided into six groups (table 1) that correlate with the clinical and/or surgical results of these patients. The negative group, 29 of 53 patients (54.7%), includes all patients with negative epidurography who were judged negative on clinical grounds and received no further workup or surgery. A

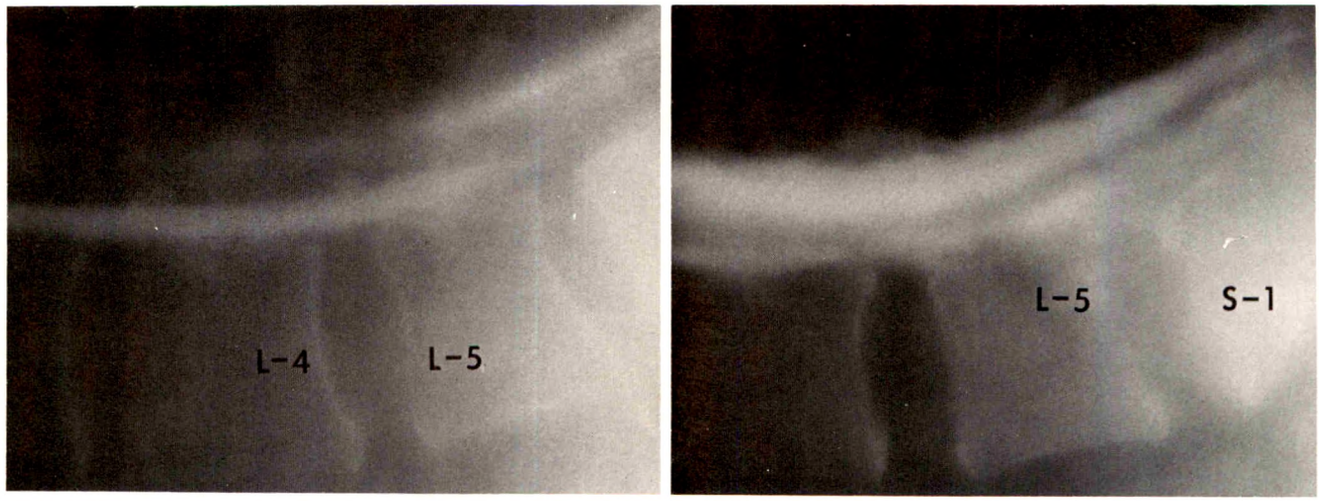


Fig. 7.—Lateral tomography helpful in eliminating lateral contrast and in evaluating ventral epidural space.

TABLE 1
Epidurography Results

Results	No. Patients (*N* = 53)	Incidence (%)
Negative	29	54.7
True positive	7	13.2
False positive	4	7.5
False negative	1	2.0
Surgically unconfirmed positive	4	7.5
Technical failures (nondiagnostic)	8	15.1

large number of patients in this group were individuals with a wide ventral epidural space, particularly at L5-S1, and confusing or equivocal physical examination. In these patients, negative epidurography helped avoid unnecessary surgery. This is the most important group in the series and validates epidurography as an important diagnostic procedure in evaluating and treating patients with confusing physical examinations and equivocal myelography.

In the true positive group of seven patients (13.2%), epidurographic diagnosis of pathology was confirmed by surgery (figs. 8 and 9). Four patients (7.5%) had epidurograms interpreted as abnormal, but surgical exploration was normal (false positive group). One patient (2%) had a negative epidurogram, but continued pain suggested a herniated disc to clinicians. A small disc herniation was found at surgery (false negative).

Four patients (7.5%) with abnormal epidurograms did not have surgical confirmation. Several cases had clinical improvement with conservative therapy. Surgery was avoided in another case because clinicians were not convinced there was a significant disc herniation despite the abnormal epidurogram.

The last group, technical failures (nondiagnostic epidurograms), includes eight patients (15.1%). In the series of Luyendijk and van Voorthuisen [7] of 600 epidurograms, a 7.5% failure rate was reported. Most of our failures occurred in the initial phase of the series and involved nonfilling of the one side of the epidural space because of the plica mediana dorsalis. As the selective catheter technique was refined, nonfilling of a symptomatic side was reduced. However, other situations present continued technical problems. In the obese patient with a large adipose covering of the sacral notch, the notch is not only difficult to locate, but, more importantly, if the covering is too thick, the 14 gauge needle is too short to puncture the ligamentum flavum. Another potential problem exists if the catheter is positioned in the dorsal epidural space. In this situation, injected contrast material may not fill the ventral epidural space and the root sleeves.

Discussion

Indications

Epidurography offers valuable information in several important clinical situations. In patients in whom previous lumbar myelography shows a large ventral epidural space between the intervertebral discs and the anterior margin of the thecal sac and clinical findings suggest a herniated disc, epidurography can opacify the space of interest to diagnose or exclude space-occupying lesions, notably disc herniations (fig. 10). Identification of a normal epidural space with a high degree of accuracy and precision is tremendously important. Patients with a wide ventral epidural space at lumbar myelography, negative epidurography, and equivocal clinical findings can be spared unnecessary disc surgery.

Patients with normal or equivocal lumbar myelography and clinical suspicion of a laterally herniated lumbar disc are also indicated for epidurography. In this group, nerve sleeves can be outlined to identify or exclude significant disc pathology by identifying displacement or deflection of specific nerve roots.

Another useful indication for epidurography is clearly documented arachnoiditis. Myelography in such patients may be difficult, painful, and hazardous. Epidurography is ideally suited for evaluating patients with arachnoiditis

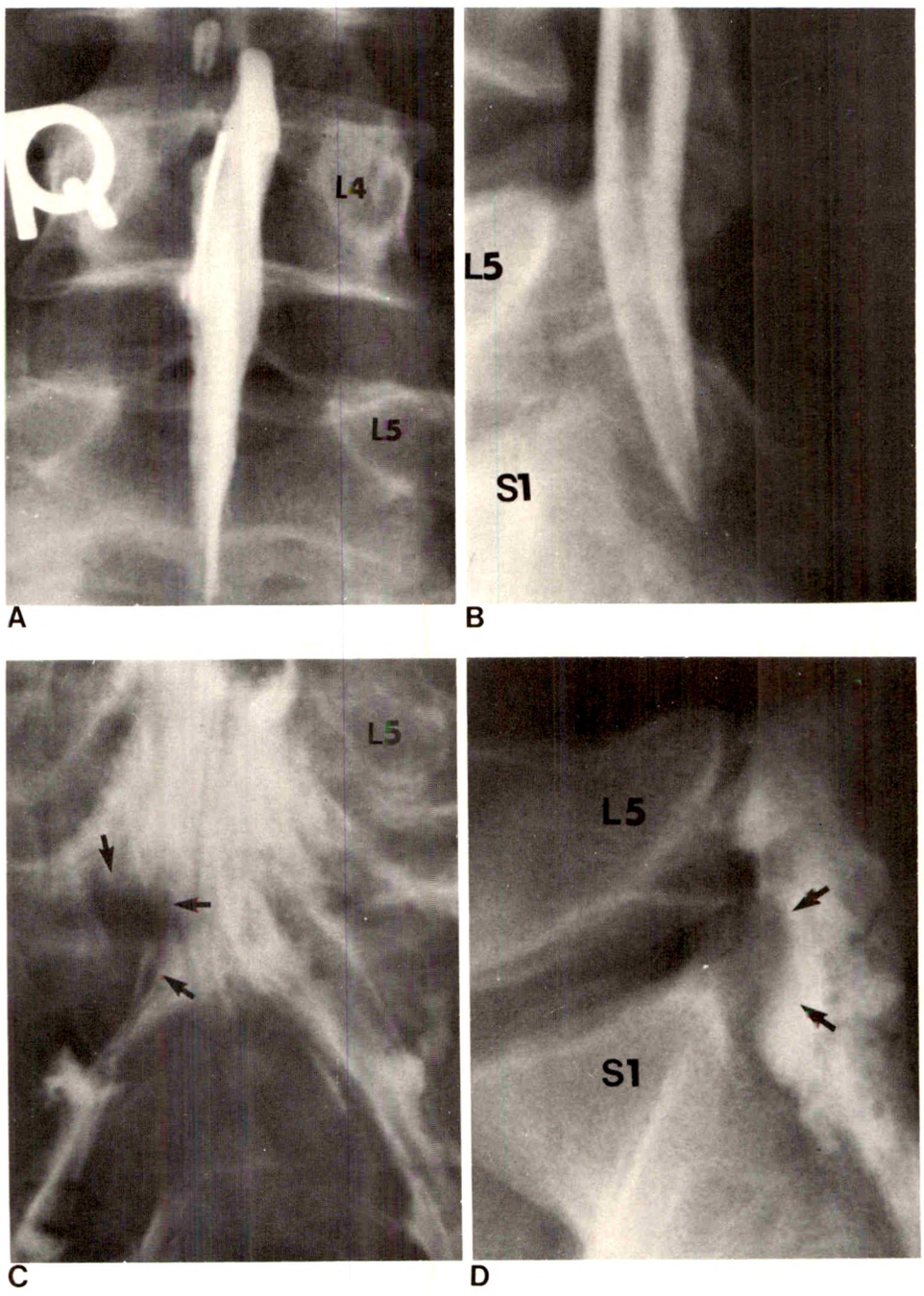


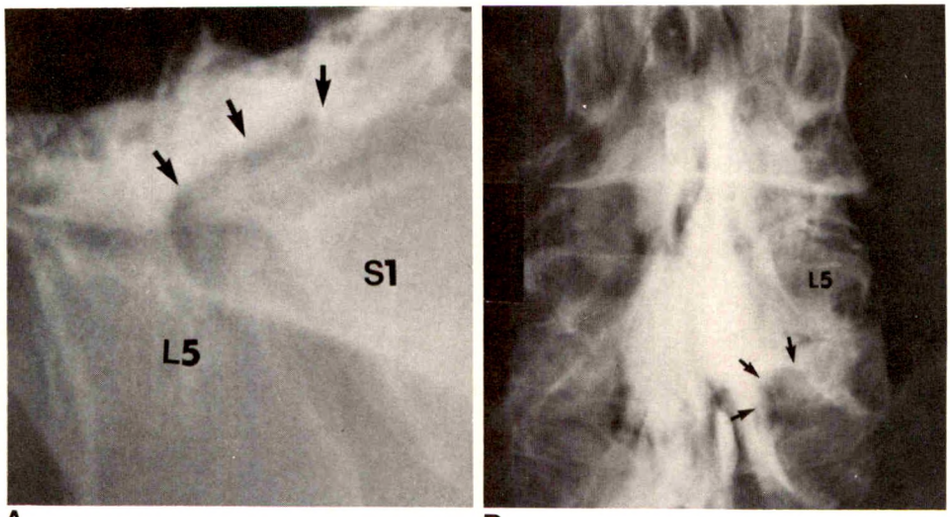
Fig. 8.—Surgically proven right L5–S1 herniated disc. **A** and **B,** Initial Pantopaque myelogram. Postsurgical scarring of thecal sac and widening of ventral epidural space. **C** and **D,** Epidurogram. Defect ventrally on the right at L5–S1 (*arrows*). No filling of right S1 nerve root.

and suspected disc herniation. Many patients, because of previous surgery, arachnoiditis, or anatomic variation, have short thecal sacs. In this situation, Pantopaque may not cover the lower lumbar region and epidurography can evaluate the epidural space.

Complications

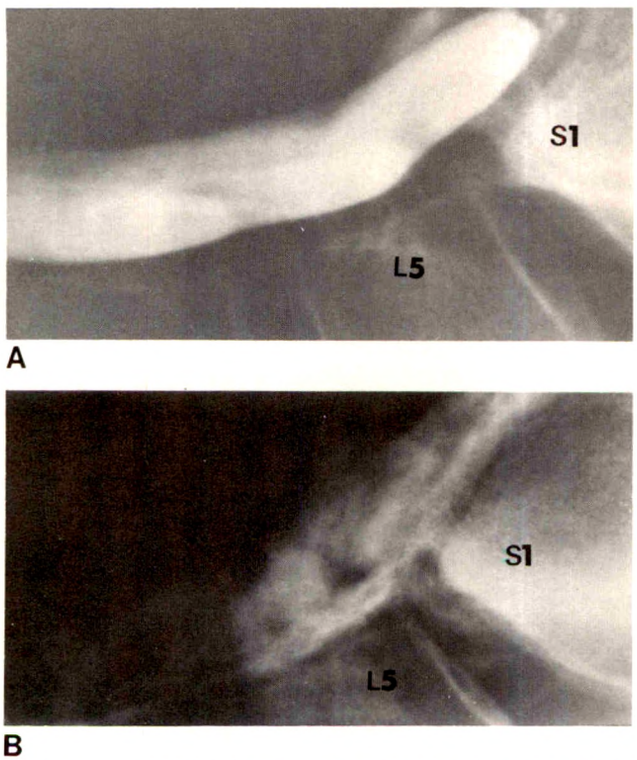
The two complications noted in our 53 cases related to the use of iothalamate meglumine (Conray-60). Dimer-X, used initially, was removed from the market in early 1977, and the decision to use Conray-60 was based on the experience of others with this agent in the subarachnoid space [11–13], and previous experience with Conray-60 and sodium diatrizoate [3, 5, 7] for epidurography.

In one patient, spasms that developed in both legs after epidurography were treated with Valium and intravenous steroids and resolved in 18 hr. The epidurography was performed 4 days after lumbar myelography. The second complication involved an aseptic meningitis. This patient developed a fever, nuchal rigidity, elevated cerebrospinal fluid protein, and white blood cells within the cerebrospinal fluid. Numerous blood and cerebrospinal fluid cultures failed to identify a bacterial pathogen, and the patient was treated with steroids and recovered



A B

Fig. 9.—Surgically proven L5–S1 herniated disc. Epidurogram. **A**, Large ventral defect (*arrows*) at L5–S1. **B**, Large defect (*arrows*) at left L5–S1 and nonfilling of left S1 root sleeve.



A B

Fig. 10.—Important Indication for epidurography. Congenitally wide epidural space (**A**) with Pantopaque not covering ventral epidural space at L5–S1 and (**B**) filling ventral epidural space.

with no sequelae. Her epidurography was performed 4 days after lumbar myelography and Conray-60 within the subarachnoid space was noted on examination, evidently due to leakage through the recent dural puncture.

Muscular spasm and meningitis have been reported with subarachnoid Conray-60 [13], and it is assumed that both complications were related to Conray-60 entering the subarachnoid space. It has been suggested that because of subarachnoid entry, 2–21 days should elapse between lumbar puncture or lumbar myelography and epidurography [7]. However, Conray-60 within the subarachnoid space during epidurography was noted in several patients in this series with no adverse effects (fig. 11A). Our policy is to wait as long as possible between lumbar puncture or lumbar myelography and epidurography.

The risk of serious complication secondary to contrast agents should be further reduced by using metrizamide for epidurography. The safety of metrizamide in the subarachnoid space makes it an ideal agent in the epidural space. With metrizamide epidurography, there is less contact of metrizamide with neural structures than with conventional metrizamide myelography, further reducing any hazard from the contrast media.

Several other minor complications occurred in our series. Contrast material injected into the soft tissues of the buttocks on one occasion (fig. 11B) produced pain but no other problems. Twice the epidural venous plexus within the lumbar epidural space was accidentally catheterized and injected with contrast material (fig. 11C), which produced a picture identical to epidural lumbar venography. In both cases, the catheter was withdrawn from the vein and technically satisfactory epidurography was performed.

Advantages of Epidurography

Compared with myelography, epidurography offers several important advantages. Since there is no lumbar puncture, patients experience no headache after the procedure. Epidurography can be performed on outpatients and patients can ambulate immediately after the study. An important benefit is that the subarachnoid space is not breached, reducing the risk of arachnoiditis.

Discography [14] and epidural venography [15–17] are two other alternatives used to augment conventional myelography. Despite multiple reports of success with these procedures for evaluating patients with equivocal or nondiagnostic myelograms, we believe that epidurography is easier to perform and interpret and involves less patient discomfort. While the current indication of epi-

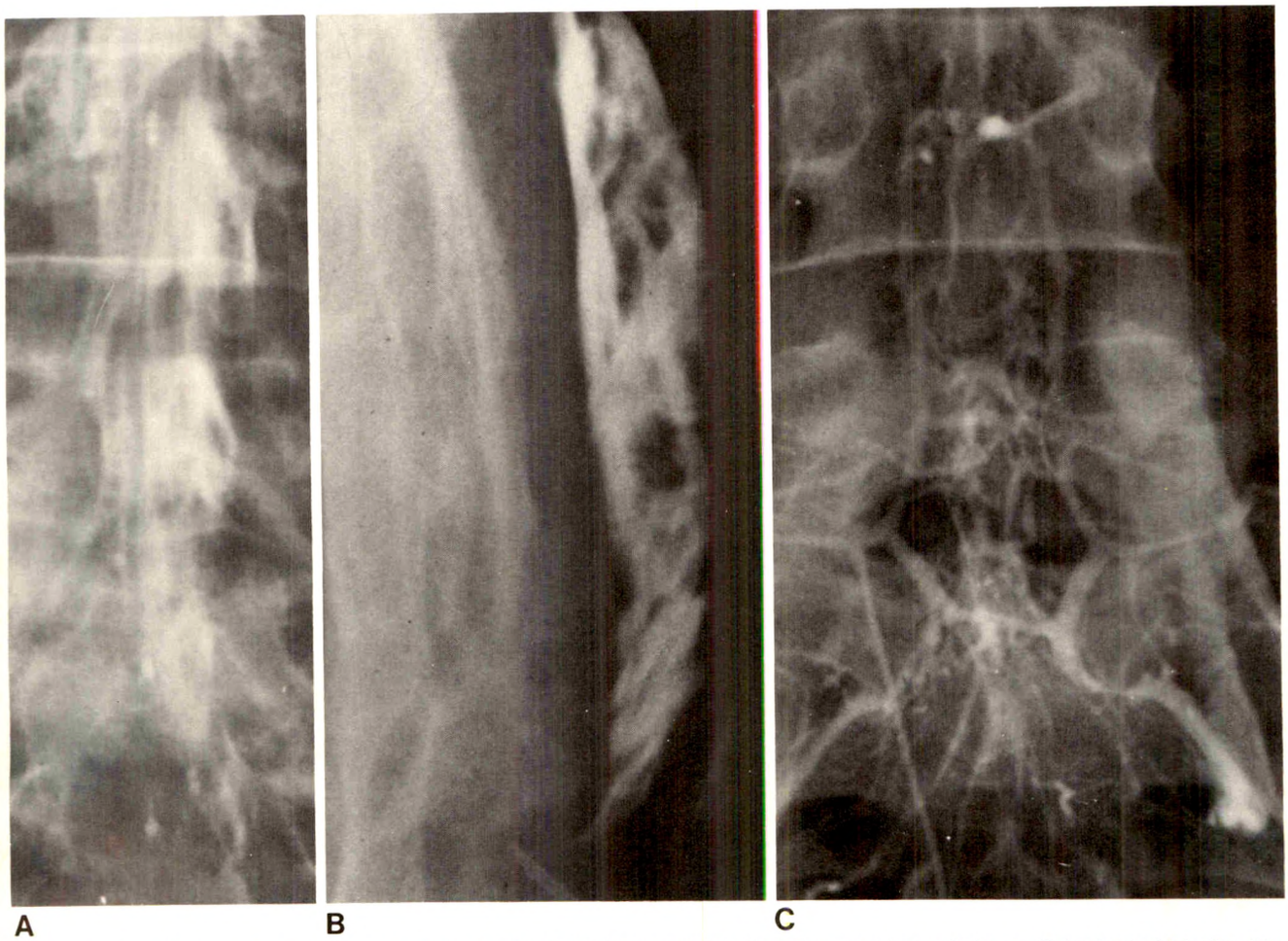


Fig. 11.—Complications. **A**, Subarachnoid entry of Conray-60. **B**, Inadvertent injection of contrast into soft tissues. **C**, Inadvertent injection into lumbar epidural venous plexus. After both **B** and **C**, needle and catheter were repositioned and technically satisfactory epidurograms obtained.

durography is as an adjunct to an equivocal myelogram, we would propose its usefulness as an initial diagnostic procedure.

REFERENCES

1. Lewit K, Sereghy T: Lumbar peridurography with special regard to the anatomy of the lumbar peridural space. *Neuroradiology* 8:233–240, 1975
2. Lewit K: The contribution of peridurography to the anatomy of the lumbosacral spinal canal. *Folia Morphol* (Praha) 24: 289–295, 1976
3. Luyendijk W: Canalography, roentgenological examination of the peridural space in the lumbosacral part of the vertebral canal. *J Belge Radiol* 46:236–253, 1963
4. Sanford H, Doub HP: Epidurography, a method of roentgenologic visualization of protruded intervertebral disks. *Radiology* 36:712–716, 1941
5. Matthews JA: Epidurography—a technique for diagnosis and research, in *The Lumbar Spine and Back Pain*, edited by Jayson M, London, Sector, 1976, pp 173–187
6. Knutsson F: Experiences with epidural contrast investigation of the lumbosacral canal in disc prolapse. *Acta Radiol* (Stockh) 22:694–703, 1941
7. Luyendijk W, van Voorthuisen AE: Contrast examination of the spinal and epidural space. *Acta Radiol* [*Diagn*] (Stockh) 5:1051–1066, 1966
8. Luyendijk W: The plica mediana dorsalis of the dura mater and its relation to lumbar peridurography (canalography). *Neuroradiology* 11:147–149, 1976
9. Kido DK, Schoene W, Baker RA, Rumbaugh C: Metrizamide epidurography in dogs. *Radiology* 128:119–122, 1978
10. Bromage PR, Bramwell RSB, Catchlove RFH, Belanger G, Pearce CGA: Peridurography with metrizamide: animal and human studies. *Radiology* 128:123–126, 1978
11. Campbell RL, Campbell JA, Heimburger RF, Kalsbeck JE, Mealey J: Ventriculography and myelography with absorbable radiopaque medium. *Radiology* 82:286–289, 1964
12. Davis FM, Llewellyn RC, Kirgis HD: Water-soluble myelography using meglumine iothalamate (Conray) with methylprednisolone acetate (Depo-medrol). *Radiology* 90:705–709, 1968
13. Praestholm J, Lester J: Water-soluble contrast lumbar myelography with meglumine iothalamate (Conray). *Br J Radiol* 43:303–308, 1970
14. Feinberg SB: The place of diskography in radiology as based on 2,320 cases. *AJR* 92:1275–1281, 1964
15. Gargano FP, Meyer JD, Sheldon JJ: Transfemoral ascending lumbar catheterization of the epidural veins in lumbar disk disease. *Radiology* 111:329–336, 1974
16. Gershater R, Holgate RC: Lumbar epidural venography in the diagnosis of disc herniations. *AJR* 126:992–1002, 1976
17. Miller MH, Handel SF, Coan JD: Transfemoral lumbar epidural venography. *AJR* 126:1003–1009, 1976

Nontraumatic Intravasation of Myelographic Contrast Medium

JOSEPH L. ZITO[1, 2] AND DIETER SCHELLINGER[1]

Venous intravasation of radiopaque contrast agents is a rare complication of myelography. Reports in the literature suggest needle trauma during myelography as the most plausible cause. The case reported here reinforces congenital fistulization between the subarachnoid space and the venous plexus as an alternative cause for intravasation.

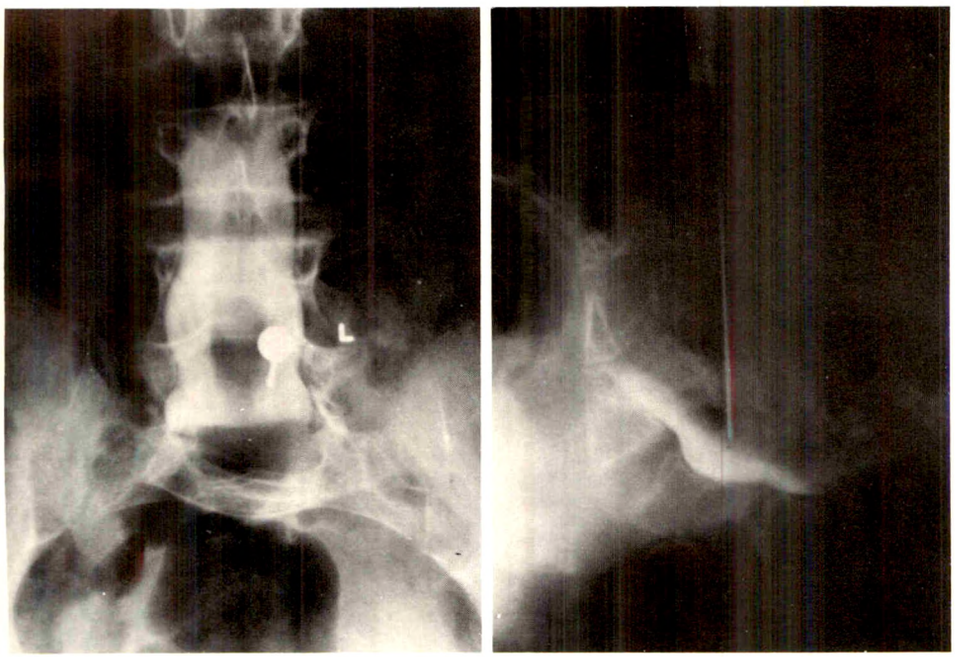
Intravasation of Pantopaque into the venous system during myelography is a rare myelographic complication. Its clinical significance has been discussed in several reports [1–10]. In all these reports, pulmonary Pantopaque embolization occurred. Most authors who have reported on Pantopaque intravasation feel it is related to inadvertent entry of the spinal needle into the epidural vertebral veins during the initial puncture. Trauma to the venous structures while reositioning the spinal needle or during repuncture for removal of contrast material represents another mechanism. In each of these circumstances, Pantopaque can find access to the venous system. We describe a case in which Pantopaque intravasation was not the result of needle trauma, but rather secondary to a preexisting connection between the arachnoid space and the epidural venous plexus.

Case Report

B. S., a 13-year-old white girl, had occult spinal dysraphism that left her paraplegic with minimal bladder and rectal tone from birth. She underwent multiple surgical procedures for treatment of lower extremity contractures. No surgical procedure involved the lumbosacral spine. She was stable, with a permanent indwelling Foley catheter and various medications for chronic urinary tract infections, when it was noted that a previous sacral sensory level had progressed to a low lumbar level. She was admitted for evaluation of possible surgical intervention to halt the progression of disease.

During lumbar myelography under general anesthesia, she was placed prone on the fluoroscopy table with a bolster beneath her abdomen. An 18 gauge needle was then introduced under fluoroscopic control. The subarachnoid space was punctured at the L4–L5 level left of midline to prevent potential cord trauma in case a tethered cord might be present. The first spinal puncture was successful with immediate return of clear spinal fluid. Injection of 10 ml metrizamide (Amipaque) contrast material confirmed the tethering of the spinal cord with its distal end anchored at the L5 level. Cross table lateral film demonstrated the needle within a rather large and expanded subarachnoid space, but posterior to the cord (fig. 1).

Because of the unexplainable rapid disappearance of metri-



A B

Fig. 1.—Pantopaque myelograms. **A**, anteroposterior, and **B**, lateral. Cord in abnormally low position (tethered cord). Spinal needle at L5–S1 level left of midline. Pantopaque leakage (not shown) from right L5–S1 nerve root sleeve was observed under fluoroscopy.

Received November 13, 1978; accepted after revision February 6, 1979.

[1]Department of Radiology, Georgetown University Medical Center, 3000 Reservoir Road Northwest, Washington, D.C. 20007. Address reprint requests to D. Schellinger.

[2]Present address: Department of Radiology, Massachusetts General Hospital, Boston, Massachusetts 02114.

© 1979 American Roentgen Ray Society

0361-803X/79/1325-0795 $0.00

TABLE 1

Summary of Reported Cases

Reference	Quality of Tap	Time of Intravasation	Site of Leak	Explanation of Intravasation
Hinkel [1]	Nontraumatic	During fluoroscopy, leak prompted by induced cough	Not described	Needle trauma while coughing
Fullenlove [2]	Traumatic	Initial phase of myelography	Along path of puncture hole	Needle trauma
Steinbach and Hill [3].	Nontraumatic first tap	No leak during fluoroscopy	Exact site not described	Needle trauma
	Traumatic second tap (for contrast removal)			
Ginsburg and Skorneck [4]	Traumatic needle anterior in spinal canal	Initial phase of myelography	Needle tip within vertebral body	Needle trauma
Keates [5]	Nontraumatic first tap	No leak		
	Traumatic second tap (for contrast removal)	Sudden cough; all contrast disappeared	Exact site not observed	Needle trauma implied
Todd and Gardner [6].	Nontraumatic needle anterior in spinal canal	Sudden cough during exam; contrast later found to have disappeared	Exact site not observed	Needle trauma implied
Schultz and Miller [7].	*Case 1*: nontraumatic	During fluoroscopy	Exact site not described	Needle trauma
	Case 2: quality of tap not described	During fluoroscopy	Needle in epidural vein	Needle trauma
	Case 3: clear cerebrospinal fluid when leak occurred; slightly bloody when contrast removed	During fluoroscopy	Exact site not seen	Needle trauma
Ruberti et al. [8]	*Cases 1–8*: traumatic	During dye removal	Site not observed	Needle trauma
	Case 9: nontraumatic first tap	No leak		
	Traumatic second tap (for contrast removal)	Leak during fluoroscopy; cough; mild signs of circulatory collapse	Exact site not seen	Needle trauma during contrast removal
Lin and Clarke [9]	*Case 1*: nontraumatic	During fluoroscopy	Left side of subarachnoid space and anteriorly	Needle trauma implied
Aspelin and Lester [10]	*Case 2*: traumatic			
	Nontraumatic first tap	During fluoroscopy	Exact site not described	Needle trauma
		No leak		
	Traumatic second tap for contrast removal after surgery	During phase of contrast	Exact site not seen	Needle trauma

zamide, it was decided to inject Pantopaque. Clear spinal fluid was again noted at stylet removal. After injection of 10 ml of Pantopaque, the large dural sac containing a tethered cord was easily identified. About 1 min after injection, globules of Pantopaque were seen rapidly passing out of a right lateral nerve root sleeve, then proceeding rapidly cephalad. Chest fluoroscopy revealed globules of Pantopaque swirling rapidly through the heart. It was assumed that the Pantopaque had entered the lumbar venous plexus and embolized to the lungs via the right ventricle. The patient was placed in the left decubitus position, thus keeping the contrast column away from the point of leakage. Except for minimal residuals, all the spinal Pantopaque was removed in this position.

Serial chest radiography revealed fine, punctate densities throughout both lungs that persisted for about 12 hr. These were believed to represent Pantopaque emboli. The patient was kept under close observation for 24 hr after myelography. She was asymptomatic during this period, and made an uneventful postanesthesia recovery with a few small discoid atelectases as the only residuals.

Discussion

Review of the literature has produced 10 reports (21 cases) on contrast intravasation during myelography (table 1). In most cases (17), a traumatic spinal puncture with return of bloody cerebrospinal fluid was reported. Therefore, the authors concluded that needle trauma to the neighboring venous structures prompted the escape of contrast material into the venous system. In the other four cases, the spinal puncture did not produce bloody cerebrospinal fluid; therefore, the initial tap was thought to be nontraumatic. Nonetheless, in each of these cases, the authors believed that needle trauma probably initiated the leak. In one of four patients, induced cough was thought to have caused needle trauma to a vein [1]. Trauma was proposed in the case of Steinbach and Hill [2] because the needle tip was shown to be placed too anteriorly. One patient in the case material of Schultz and Miller [7] and another in the report of Lin and Clarke [9] had nontraumatic taps, but the authors still suspected a traumatic cause.

Review of the literature and analysis of the individual cases supports trauma as the cause of Pantopaque intravasation in most cases. Actually, no alternative etiologic mechanism is suggested in the literature except for Hinkel [1], who proposed the presence of abnormal

veins in the cord or meninges as a possible but unlikely cause for Pantopaque intravasation. On reviewing the case material, further observations corroborate the primary role of trauma. In four cases [3, 4, 8, 10], intravasation did not occur during the initial phase of myelography, but was induced later either during the introduction of a second needle for contrast removal or during repeat myelography.

Our case suggests an alternative, nontraumatic cause. Needle trauma could not have caused the leakage of contrast material in our case. The needle was intentionally placed toward the left of midline, while the intravasation originated from the right nerve root sleeve. Only one needle pass had been made and the cerebrospinal fluid was clear at all times. Literature case reviews produce at least three patients [1, 7, 9] who would fit into this nontraumatic category. A preexisting anatomic connection between the subarachnoid space and the epidural venous plexus in the lumbar region is the proposed pathway by which Pantopaque intravasation occurred in our case. We advance this theory because there is considerable evidence to confirm normally existing anatomic connections between the arachnoid space and the epidural venous plexus via spinal arachnoid villi

Cerebrospinal fluid absorption through structures other than intracranial arachnoid villi was suggested as early as 1929 by Dandy [11], and later by Bedford [12], and Bering and Sato [13]. In 1923, Elman [14] first described structures resembling arachnoid villi of cerebral meninges in the dura mater of the spine. The structures extend through the dura mater and project into the vascular lumen of veins associated with spinal nerves. Welch and Pollay [15] made similar observations and concluded that these structures closely resemble arachnoid villi of the cerebral meninges. Lorenzo et al. [16] conducted cerebrospinal fluid perfusion studies in cats and concluded that a detectable amount of absorption does indeed occur in the spinal subarachnoid compartment. Since carbon particles were found accumulated in the arachnoid villi of the spinal roots, they postulated that cerebrospinal fluid absorption does occur through these structures. Evaluation of the pharmacokinetics of intrathecal metrizamide absorption from the subarachnoid space by Golman [17] demonstrated the absorption to follow first order kinetics. Golman concluded that after lumbar intrathecal injection, most of the absorption probably occurs in the lumbar spinal canal. This finding was supported by Enzmann et al. [18], who noted early high plasma iodine concentration after lumbar intrathecal metrizamide injection without computed tomographic evidence of iodine in the basal cisterns.

Human spinal arachnoid villi and granulations were studied by Kido et al. [19]. They found that these structures were distributed throughout the nerve roots of the thoracic and lumbar spine. These arachnoid villi and granulations were divided into three types, based on anatomic locations. The first is located internal to the nerve root dura mater, the second extends into the dura mater, and the third completely penetrates the dura mater. As in Elman's study [14], particles of blue dye that were infused into the subarachnoid space were seen in the arachnoid proliferations and in the venous sinuses. Kido et al. [19] showed endothelial lined tubules opening directly into venous tributaries. The pore size of these tubules was not mentioned.

We suggest that in our case and in reported cases where no traumatic tap had occurred, Pantopaque reached the venous plexus via arachnoid granulations. It remains impossible to determine whether intravasation is a result of a pathologic state of these physiologic connections or a localized, momentary alteration in normal physiology. The fact that this spontaneous fistulization occurred in a patient suffering from a congenital spinal anomaly supports the theory that these connections might be congenital and represent the pathologic caricature of a normally existing connection between those two spaces.

REFERENCES

1. Hinkel CL: The entrance of Pantopaque into the venous system during myelography. *AJR* 54:230–233, 1945
2. Fullenlove TM: Venous intravasation during myelography. *Radiology* 53:410–412, 1949
3. Steinbach HL, Hill WB: Pantopaque pulmonary embolism during myelography. *Radiology* 56:735–738, 1951
4. Ginsburg LB, Skorneck AB: Pantopaque pulmonary embolism, a complication of myelography. *AJR* 73:27–31, 1955
5. Keats TE: Pantopaque pulmonary embolism. *Radiology* 67: 748–750, 1956
6. Todd EM, Gardner WJ: Pantopaque intravasation (embolization) during myelography. *J Neurosurg* 14:230–234, 1957
7. Schultz EC, Miller JH: Intravasation of opaque media during myelography: a report of three cases. *J Neurosurg* 18:610–613, 1961
8. Ruberti R, Galligioni R, Iraci G, Nori A: Venous intravasation of iodized oil during myelography. *AJR* 98:720–722, 1966
9. Lin PM, Clarke J: Spinal fluid venous fistula: a mechanism for intravascular Pantopaque infusion during myelography. *J Neurosurg* 41:773–776, 1974
10. Aspelin P, Lester J: Pantopaque pulmonary embolism following myelography. *Neuroradiology* 14:43–44, 1977
11. Dandy WE: Where is cerebrospinal fluid absorbed? JAMA 92:2012–2014, 1929
12. Bedford THB: The movement of cerebrospinal fluid over cerebral hemispheres of the dog. *J Physiol* (Lond) 128:51–52, 1955
13. Bering E, Sato O: Hydrocephalus changes in formation and absorption of cerebrospinal fluid within the cerebral ventricles. *J Neurosurg* 20:1050–1063, 1963
14. Elman R: Spinal arachnoid granulations with special reference to the cerebrospinal fluid. *Bull Johns Hopkins Hosp* 34:99–104, 1923
15. Welch K, Pollay M: The spinal arachnoid villi of the monkeys cercopithecus aethiops sabaeus and macaca irus. *Anat Rec* 145:43–48, 1963
16. Lorenzo AV, Hammerstad JP, Cutler RWP: Cerebrospinal fluid formation and absorption and transport of iodide and sulfate through the spinal subarachnoid space. *J Neurol Sci* 10:247–258, 1970
17. Golman K: Absorption of metrizamide from cerebrospinal fluid to blood: pharmicokinetics in humans. *J Pharm Sci* 64: 405–407, 1974
18. Enzmann D, Norman D, Newton T: Computer tomography in cisternography with metrizamide. *Acta Radiol* [*Suppl*] (Stockh) 355:294–298, 1977
19. Kido DK, Gomez, DG, Pavese AM, Potts DG: Human spinal arachnoid villi and granulations. *Neuroradiology* 11, 221–228, 1976

Modification of Cyanoacrylate for Therapeutic Embolization: Preliminary Experience

LAURENCE D. CROMWELL[1] AND CHARLES W. KERBER[2]

Cyanoacrylate is a satisfactory material for therapeutic embolization, but it has the disadvantage of not being radiopaque and polymerizing within 1 sec after contact with ionic materials. Its behavior was modified with varying concentrations of iophendylate and were able to satisfactorily control its polymerization from 1 to 30 sec. This control should allow penetration of arteriovenous malformations, which is necessary if cure is to result. The iophendylate adds radiopacity and seems to enhance the suspension of tantalum, another opacifying agent. Preliminary experience in dogs is encouraging, but too few humans have been treated with this method to recommend it as more than an experimental procedure at this time.

The cyanoacrylates are powerful adhesives that have been used for therapeutic embolization to obliterate blood vessels and form intravascular casts [1, 2]. They polymerize on contact with ionic materials, such as blood or endothelium, using excess electrons to initiate polymerization [3]. As currently available, these tissue adhesives have two major disadvantages: (1) they polymerize so rapidly that the physician has but 1–2 sec to make the injection and (2) they are not radiopaque.

Others have recognized and attempted to correct these deficiencies. Zanetti and Sherman [3], used dextrose 5% and water to wash out all ionic materials before injecting the cyanoacrylate. Thelan et al. [4] suggested that 50% dextrose would render the cyanoacrylate more suitable for use as embolic material. We conceived of the possible advantages of mixing cyanoacrylate with iophendylate (Pantopaque, Lafayette Pharmacol Inc., Lafayette, Ind.) and attempted to find a mixture that would allow us more control and that would also give the desired radiopacity needed for monitoring the injection fluoroscopically. We report a successful effort.

Materials and Methods

Because of the work of Zanetti and Sherman [3] and Thelan et al. [4], we initially compared the polymerization time of various concentrations of isobutyl-2-cyanoacrylate (Ethicon, Somerville, N.J.) and dextrose and water. Duration of polymerization was determined by dropping the mixture on citrated human blood. Various concentrations of iophendylate and cyanoacrylate were prepared and tested in a similar manner (table 1, fig. 1). The effect of lowering the temperature of the mixtures was also studied (table 2). Radiopacity of the 50% mixture of cyanoacrylate and iophendylate was compared with the standard opacification obtained with tantalum (1.0 ml cyanoacrylate and 2 g tantalum). Kerber balloon catheters (Cook, Inc., Bloomington, Ind.) were inflated with either a 50% mixture of cyanoacrylate and iophendylate, or a standard cyanoacrylate and tantalum preparation. These were superimposed over a patient's head while a lateral film was obtained.

Results

Varying amounts of dextrose 5% added to cyanoacrylate do not alter the polymerization time of the mixture. None of the various concentrations are miscible and, furthermore, they form a white emulsion within a few minutes. Mixing 50% dextrose with cyanoacrylate in various concentrations also yielded an unstable white emulsion, although the time for formation of the emulsion was longer than with the 5% dextrose. No consistent results were obtained, and the mixture was difficult to use.

However, iophendylate gave reproducible and consistent changes in the polymerization time of the cyanoacrylate and formed a stable and completely miscible solution (table 1, fig. 1). The iophendylate slightly increased the viscosity of the cyanoacrylate, but the mixture could still be passed with ease through microcatheters. No exact measurements of the viscosity were undertaken, although iophendylate was chosen rather than Ethiodol, inasmuch as the iophendylate is known to be less viscous.

Lowering the temperature of the mixture was found to increase the polymerization time (table 2). However, this advantage may not be applicable in intraarterial situations.

Radiopacity of the 50% cyanoacrylate-iophendylate mixture was satisfactory and could be seen with average fluoroscopes. The opacity was similar to that obtained with the tantalum mixtures (fig. 2).

Discussion

Isobutyl-2-cyanoacrylate is a powerful and rapidly polymerizing adhesive. We have had difficulty in the past when too rapid polymerization has on occasion trapped our microcatheters and has not allowed us to penetrate the central parts of arteriovenous malformations as much as we wished. We agree with Doppman et al. [5] that to effect a cure, material must pass into the substance of the malformation itself and not merely plug the feeding vessels. A second disadvantage to unaltered cyanoacrylate is that it is not radiopaque. We have used tantalum mixed with the cyanoacrylate, but tantalum is

Received September 20, 1978; accepted after revision January 12, 1979.
This work was supported by American Cancer Society institutional cancer grant IN-26.
[1]Department of Radiology, University of Washington School of Medicine, Seattle, Washington 98195. Address reprint requests to L. D. Cromwell.
[2]Department of Radiology, University of Pittsburgh, Pittsburgh, Pennsylvania 15261.

© 1979 American Roentgen Ray Society

0361–803X/79/1325–0799 $0.00

TABLE 1

Effect of Iophendylate on the Polymerization of Cyanoacrylate

Mixture (%) Isobutyl-2-Cyanoacrylate/ Iophendylate	Polymerization Time* (average, sec)
10/90	167.0 ± 13.0
25/75	31.0 ± 2.6
33/66	8.4 ± 0.5
40/60	4.4 ± 0.5
50/50	3.2 ± 0.5
60/40	2.1 ± 0.2
66/33	1.2 ± 0.3
75/25	<1.0
100/0	<1.0

* Polymerization endpoint was arbitrarily chosen as the disappearance of the sheen on the liquid droplets that were placed on the citrated human blood. The average of five observations is given.

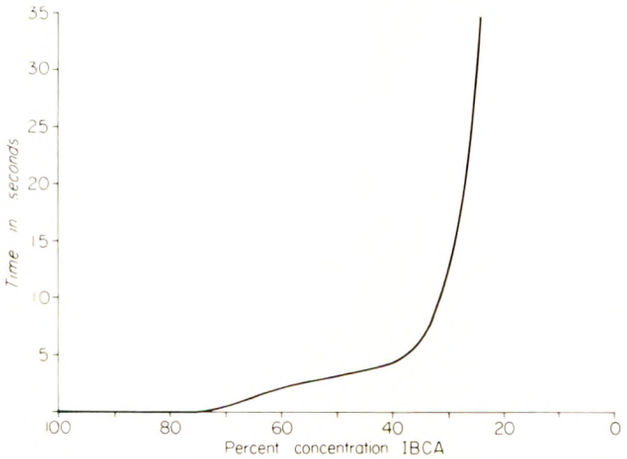


Fig. 1.—Polymerization concentration times plotted against various concentrations of iophendylate and cyanoacrylate (IBCA).

TABLE 2

Effect of Temperature on Polymerization Time

Mixture	Polymerization time* (average, sec)
Isobutyl-2-cyanoacrylate 66%/iophendylate 33%:	
7.6°C	8.0 ± 1.0
22.0°C	2.3 ± 0.2
Isobutyl-2-cyanoacrylate 50%/iophendylate 50%:	
7.6°C	22.2 ± 1.5
22.0°C	4.7 ± 0.2

Note.—Mixtures of cyanoacrylate and iophendylate greater than 1:2 were not studied because it takes several minutes for them to polymerize.

* Polymerization endpoint for studying the effects of temperature on the polymerization rate was taken to be formation of a rim on the droplet. The average of five observations is given.

particulate and settles out quickly. Unless the operator is experienced, the tantalum tends to fall to the bottom of the syringe giving poor opacification in only a few seconds, thus adding to the hazard of the procedure.

We began our studies with dextrose and water, since these materials do not initiate polymerization. We use dextrose 5% and water routinely to flush the ionic contrast agent and blood before introduction of the polymer. Our results show that dextrose 5% in varying concentrations has no appreciable effect on the polymerization of cyanoacrylate. However, increasing the quantity of dextrose makes an unstable emulsion that is impossible to control. We do not recommend its use at this time.

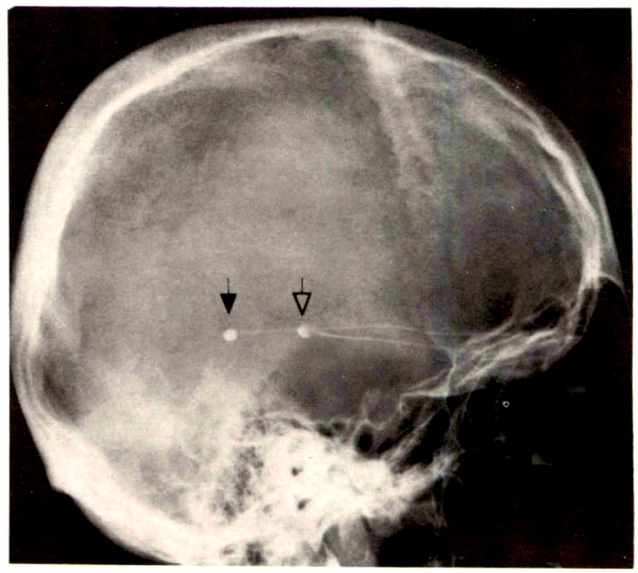
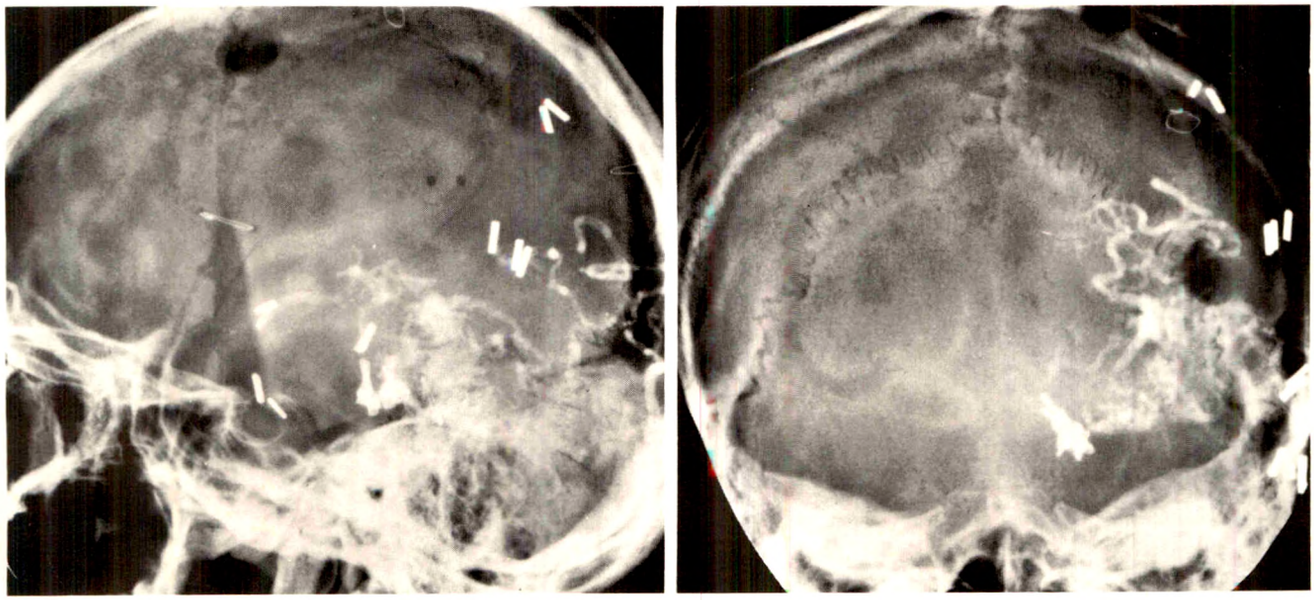


Fig. 2.—Kerber balloon catheters superimposed over patient's skull. More posteriorly located balloon (*closed arrow*) has 50% mixture of iophendylate and cyanoacrylate, and demonstrates even and useful opacification. More anteriorly situated balloon (*open arrow*) is filled with a mixture of 1 ml cyanoacrylate and 2 g tantalum. Cross-table horizontal beam in supine position demonstrates tantalum settling in dependent part of balloon.

On the other hand, iophendylate is quite useful. It allows wide range of polymerization times and it is radiopaque. Our observation of polymerization times are experimental and probably not directly transferable to humans. For reproducibility, we observed the beginning of polymerization. More experience will be necessary to determine the optimal concentration for use in low, high, and medium flow arteriovenous malformations. We found that opacification was satisfactory with the 50% iophendylate mixture. It is difficult, though, to have too much opacification. When lesser prolongation of the polymerization time is required, as with high flow shunts, we have increased the opacification by the addition of tantalum dust. It is our subjective impression that the addition of a small amount of iophendylate helps to suspend the tantalum dust, making embolization performance easier.

Although this material has worked satisfactorily in dogs in all instances (L. D. Cromwell, C. W. Kerber, P. C. Freeny, L. Kuntz, unpublished data), we have used it in too few humans to draw conclusions yet. Figure 3 shows an intraoperative treatment of an arteriovenous malformation with 50% iophendylate and 50% cyanoacrylate. As far as we are able to determine, admixture with iophendylate does not seem to reduce the strength of the polymer, nor does it render it more susceptible to earlier disintegration. In our experience, the iophendy-



A B

Fig. 3.—Anteroposterior (**A**) and lateral (**B**) skull films after intraoperative treatment of arteriovenous malformation. Malformation and blood vessels were opacified and obliterated with 50% mixture of iophendylate and cyanoacrylate. Mixture was plainly visible on standard C-arm fluoroscope during intraoperative injection.

late does not separate from the isobutyl-2-cyanoacrylate and does not result in a significant amount of inflammatory reaction either in the parenchyma or in the vessel walls (L. D. Cromwell, C. W. Kerber, P. C. Freeny, L. Kuntz, unpublished data).

REFERENCES

1. Kerber C: Balloon catheter with a calibrated leak. *Radiology* 120:547–550, 1976
2. Kerber C: Intracranial cyanoacrylate: a new catheter therapy for arteriovenous malformation. *Invest Radiol* 10:536–538, 1975
3. Zanetti P, Sherman F: Experimental evaluation of a tissue adhesive as an agent for the treatment of aneurysms and arteriovenous anomalies. *J Neurosurg* 36:72–79, 1972
4. Thelan VM, Bruhl P, Gerlach F, Biersac HJ: Catheter embolization of metastasizing renal carcinomas with isobutyl-cyanoacrylate. *ROEFO* 124:232–235, 1976
5. Doppman JL, Zapol W, Pierce J: Transcatheter embolization with a silicone rubber preparation. Experimental observations. *Invest Radiol* 6:304–309, 1971

Proficiency Examination of Physicians for Classifying Pneumoconiosis Chest Films

RUSSELL H. MORGAN[1]

An examination has been developed to test the proficiency of physicians classifying chest radiographs with pneumoconiosis in accordance with the classification system promulgated by the International Labor Office in Geneva. The examination, prepared by Johns Hopkins University under contract with the National Institute of Occupational Safety and Health, was commissioned to identify physicians qualified to serve in national pneumoconiosis programs directed both to epidemiological research and to the compensation of coal miners and others who suffer from dust-related illness.

The examination, consisting of 125 chest radiographs, includes examples of a broad range of disease extending from normal to far advanced pneumoconiosis. An examinee passes or fails by ability to classify the films, within prescribed limits, in the same manner as an expert panel of radiologists.

The examination is open to radiologists, chest physicians, occupational health specialists, and other physicians interested in pneumoconiosis. By the end of 1978, the examination had been given to 202 candidates, including 116 radiologists, 30 chest physicians, three candidates certified in preventive medicine, two family practicioners, and 51 others. Of the 202 candidates, 118 (58.4%) passed and 84 (41.6%) failed. Among the candidates taking the examination for the first time, 74 radiologists (63.8%) and 18 chest physicians (60%) received passing grades. Of the remainder, 21 physicians (37.5%) were successful. Early experience indicates the examination is quite successful in meeting its primary objectives, which suggests that this type of examination may be applicable in other situations to separate those who meet certain standards of performance in radiology from those who do not.

An examination has been developed under contract from the National Institute of Occupational Safety and Health to test the proficiency of physicians classifying chest radiographs with pneumoconiosis in accordance with the classification system promulgated by the International Labor Office (ILO) in Geneva [1, 2]. The examination consists of 125 films of individuals drawn largely from the underground mining industry; a few films have also been included of individuals who have been exposed to inorganic dusts in other occupations (e.g., asbestos, beryllium, and iron). A candidate taking the examination is required to classify all films on standardized report forms within the 8 hr allotted period. The candidate is permitted to use a set of ILO standard films illustrating various stages of coal workers' pneumoconiosis for assistance in classifying the films.

The examination* was commissioned to identify physicians qualified to serve as a pool of readers in national black lung programs. These programs include those directed to epidemiologic research on pneumoconiosis and those of government agencies processing compensation claims of miners who developed pneumoconiosis as a consequence of their work. The examination is open to radiologists, chest physicians, occupational health specialists, and other physicians interested in dust-related disease. Board certification is not a requirement. Failing candidates may be reexamined in 6 months.

The examination is administered by the National Institute of Occupational Safety and Health in Morgantown, West Virginia, and examination dates are arranged by its staff. Periodically, the examination is also given in conjunction with courses on pneumoconiosis sponsored by the American College of Radiology. By the end of 1978, 202 volunteer candidates had taken the examination a total of 213 times. Of these, 118 (58.4%) received passing grades and 84 (41.6%) failed. Nine failing candidates repeated the examination once, and a tenth twice; five were ultimately successful in passing.

ILO Classification System of Pneumoconiosis

In early stages of pneumoconiosis, radiographic changes characteristically include the presence of small rounded and/or irregular opacities variably distributed throughout one or both lung fields. If the subject's exposure to dust continues, the small opacities become more widespread until ultimately the lesions coalesce to form massive opacities that may replace much of the normal pulmonary architecture. Pleural changes also may occur, including the development of localized plaques and focal calcifications.

Radiologists interpreting chest radiographs that exhibit evidence of pneumoconiosis customarily report their findings in narrative form. This is satisfactory for most clinical purposes. However, physicians studying the epidemiology of pneumoconiosis require that the radiographic manifestations of the disease be recorded in a more systematic, quantitative manner. To fill this need, the ILO classification system was developed. The ILO system requires that small opacities be classified according to their shape (rounded and/or irregular), size, profusion (the number of opacities per unit area of the radiograph), and location. With respect to large opacities, the system requires that only their size and border sharpness be classified. All pleural changes,

Received November 27, 1978; accepted after revision February 1, 1979.
This work was supported by National Institute of Occupational Safety and Health contract 210-76-0114.
[1]Department of Radiology and Radiological Science, Johns Hopkins School of Medicine, Baltimore, Maryland 21205.

* This examination is often referred to as the "B" reader examination because of the practice followed by the National Institute of Occupational Safety and Health of dividing physicians who read chest radiographs under its pneumoconiosis program into "A" readers (physicians who have completed an introductory 2 day course on the ILO classification system given by the American College of Radiology) and "B" readers (physicians with more advanced training and experience in the use of the system).

© 1979 American Roentgen Ray Society

0361–803X/79/1325–0803 $0.00

including the presence of localized plaques and calcifications, must also be codified. Of the foregoing parameters, small opacity profusion is unquestionably the most important for it, more than any other, reflects the severity of disease from a radiographic standpoint.

With respect to small opacity shape, "rounded" applies to those lesions whose long and short dimensions are roughly similar. The size of these opacities is classified in one of the following three categories: (p) lesions up to 1.5 mm in maximum diameter; (q) lesions over 1.5 mm and up to 3 mm in maximum diameter; and (r) lesions over 3 mm in diameter and up to 10 mm in maximum diameter. "Irregular" refers to those lesions that might be described as linear, reticular, fibrotic, honeycombed, or blotchy. The size of these opacities is classified in one of the following three categories: (s) fine irregular, or linear, opacities; (t) medium irregular opacities; and (u) coarse or blotchy irregular opacities.

Regarding small opacity profusion, four categories were established originally. The first (category 0) was reserved for cases in which small opacities were either absent or so few in number that the case could be regarded as essentially normal. Categories 1, 2, and 3 were reserved for cases of increasing levels of profusion when small opacities were definitely present. In 1968, the system was revised with each of the four major profusion categories subdivided into three minor divisions. A 12 point scale or continuum was thereby created for the classification of small opacity profusion levels. The lowest three categories of the scale are used to reflect the profusion levels of the so-called normal chest. Although the presence of small opacities is not usually associated with the norm, such opacities do occur in individuals who have not been exposed to mineral dusts, particularly in those of advancing age and in those who are heavy cigarette smokers. The remaining nine categories of the scale have been reserved for the classification of cases of increasing small opacity profusion.

A special notation scheme has been devised to classify small opacity profusion with the 12 point scale. This scheme, (table I) denotes each profusion level in terms of a 2 digit code. The first digit indicates the major profusion category in which a case may be classified; the second digit indicates whether the profusion level is somewhat less than, equal to, or somewhat greater than is typical of the major category. For example, 1/0 indicates a profusion level that clearly falls within the scope of major category 1 but is slightly less than is typical of that category; 2/3 indicates a profusion level clearly within major category 2 but which is somewhat greater than is typical of that category.

Because of the overriding importance of small opacity profusion, ability to estimate this parameter in chest radiographs is the keystone on which the proficiency examination is based. Also, because the radiographic recording of small opacities is markedly affected by the technical quality of the radiograph, the examination also attempts to measure the ability of the examinee to evaluate this parameter.

TABLE 1

Codes for Designating Small Opacity Profusion Levels

Small Opacities/Unit Area	Profusion Notations		
Few or none	0/–	0/0	0/1
Few but definite	1/0	1/1	1/2
Moderate; lung markings visible	2/1	2/2	2/3
Many; lung markings obscured	3/2	3/3	3/4

Selection of Test Films

The 125 films used in the examination were selected principally from the files of the Social Security Administration and the National Institute of Occupational Safety and Health. Small numbers of additional films were provided by other agencies and institutions. The "correct" classification of each film was established and verified for small opacity profusion and for large opacity size by taking the means of the readings of an expert panel of 10 radiologists, each of whom read the films independent of colleagues.† No film was included in the examination unless the standard deviation of the panel's classification of small opacity profusion was equal to or less than ±1.50 minor categories (85% of the films), or unless in subsequent review of the film, the whole panel together unanimously agreed on the film's profusion level (15% of the films).

The expert panel also classified the films for technical quality on a 3 point scale, with category 1 representing films of excellent quality, category 2 representing films less satisfactory than those in category 1 but sufficiently good to permit classification of small opacity profusion with confidence, and category 3 representing films considered unreadable. Of the 125 films, the panel judged 74 to be in category 1, 46 in category 2, and five in category 3.

Of the 120 films in the technical quality categories 1 and 2, the expert panel classified 52 cases in the first two categories of small opacity profusion, 25 cases in the third and fourth categories, and 43 cases in the remaining eight categories. Although this distribution indicates that the examination includes a higher proportion of cases with pneumoconiosis than is encountered in a normal population of coal miners, it was adopted to provide the examinee with a sufficient number of pathologic cases to test his skill.

A majority of the expert panel classified 15 cases as exhibiting large opacities. Finally, the examination includes 10 cases demonstrating disease other than pneumoconiosis. Among these were four cases of lung carcinoma, three cases of active tuberculosis, one case each of sarcoid disease, rheumatoid lung, and chronic congestive failure.

† Panel members were chosen on the basis of their many years of experience in the use of the ILO classification system. All were diplomates of the American Board of Radiology. Seven were selected from the Task Force on Pneumoconiosis of the American College of Radiology. The other three were members of the faculty of Johns Hopkins Department of Radiology and Radiological Science.

Grading

The grading of the examination was designed to test a candidate for the following reading characteristics: (1) mean overreading or underreading tendency, based on the candidate's classification of small opacity profusion; (2) standard reading error, corrected for overreading/underreading tendency, again based on the candidate's classification of small opacity profusion; (3) false positive and false negative errors in the classification of small opacities (a radiograph is negative if placed in one of the lowest three profusion categories and positive if classified in one of the highest nine); (4) false positive and false negative errors in the detection of large opacities; (5) detection of clinical disease other than pneumoconiosis; and (6) proficiency in classifying the films in terms of their technical quality. A passing grade is 50 of a possible 100 points. The reading characteristics tested and the number of points assigned to each is given in table 2.

With respect to overreading/underreading, the mean value of all of the candidate's readings of small opacity profusion was calculated and the difference between this value and that recorded by the expert panel determined. The candidate was then given a number of points equal to 10 times the numerical value this difference is less than one minor category of profusion. For example, if the mean of a candidate's readings of small opacity profusion is 0.10 minor category greater than that of the panel, 9.0 points are given ([10(1.00 - 0.10)] = 9.0). A candidate receives maximum points (10) if his or her average reading is identical to that of the expert panel, half points if his or her average reading is 0.5 minor category greater or less than that of the panel, and no points if his or her average reading is one or more minor categories greater or less than that of the panel.

The standard error of a candidate's readings of small opacity profusion, calculated with reference to the readings of the expert panel, provides a measure of the candidate's reading consistency if such error is corrected for overreading/underreading tendency. This correction is required because a candidate might overread by 0.5 minor category of profusion, and yet in all other respects be consistent relative to the panel. Under these circumstances, an uncorrected standard error yields misleading information on the issue of consistency.

When the corrected standard error is calculated,‡ a candidate is given a number of points equal to 30 times the difference between 1.80 and the numerical value of the error. For example, a candidate whose error is ±0.80 minor profusion category receives 30 points (the maximum possible for this measure); a candidate with an error of ±1.30 minor categories receives 15 or half points; and a candidate with an error of ±1.80 or more minor categories receives no points. This grading scheme was adopted after early experience indicated that about half of the candidates were likely to have errors less than ±1.30 minor categories and no candidates less than ±0.80 minor category.

TABLE 2
Examination Grading Plan

Reading Characteristics	Points
Mean overreading/underreading tendency	10
Corrected standard reading error	30
Sum of false negative and false positive errors:	
Small opacities	20
Large opacities	20
Detection of clinical disease other than pneumoconiosis	10
Evaluation of radiographic technical quality	10
Total	100

For false positive and false negative errors in detecting small and large opacities, the candidate is given a score in each instance equal to 20 points less 0.4 times the total of the percentage false positive and false negative errors. Full points are given only when the total error is zero, half points (10) when the error is 25%, and no points when the error is 50% or more. This grading scheme was adopted because experience indicated that about half of the candidates were likely to have a total error of 25% or less when classifying either small or large opacities. For the 10 cases that illustrate pathologically proven disease other than pneumoconiosis, one point is given for each case correctly detected.

For proficiency in classifying films in terms of technical quality, the candidate is given a number of points equal to 10 times the ratio of the number of films correctly classified for technical quality to the total number of films in the examination; a maximum of 10 points is possible.

Reading Characteristics of Candidates

Table 3 illustrates the distribution of the 213 examinees with respect to overreading/underreading tendency. For comparison, the distribution of the individual members of the expert panel is also given. For the passing group, the mean overreading/underreading tendency was +0.11 minor category; that is, the passing candidates, on average, classified their films for small opacity profusion close to the expert panel members (slight overreading). Moreover, their values are distributed about the mean in a narrow symmetrical manner, with 86% of the candidates having values within the range of ±0.5 minor profusion category. For the failing group, the mean overreading/underreading tendency was +0.62 minor

‡ Corrected standard reading error is calculated from the formula:

$$\sigma_c = \sqrt{\frac{1}{n}\sum^{n}(x_{ic} - x_{ip})^2 - \left[\frac{1}{n}\sum^{n}(x_{ic} - x_{ip})\right]^2}$$

when n is the number of radiographs reported and x_{ic} and x_{ip} are the small opacity profusion levels classified by the candidate and expert panel respectively for the *ith* radiograph.

category, indicating that this group tended to overread its films. In addition, the values of overreading/underreading in this group were more broadly distributed (table 3). Clearly, the characteristics of the passing and failing groups were different.

Table 4 illustrates the distribution of the 213 examinees with respect to corrected standard reading error. The data are again separated into passing and failing candidates with comparable data provided for the expert panel. As might be expected, values for the passing group are distributed mainly below an error of ±1.3 minor profusion categories, with only 16% of the examinees having greater values. Quite the opposite is true for the failing group. Most of these values (83%) are distributed at and above ±1.3 minor categories. However, unlike the passing group whose values are concentrated in a relatively narrow range, generally similar to that of the expert panel, the failing group's are broadly distributed, extending upward to over ±2 minor categories.

Proficiency in the use of the ILO classification system for epidemiological purposes may be judged reasonably well by the overreading/underreading tendency and corrected standard reading error. However, use of the system for purposes of miner compensation requires that the examination include additional ways to evaluate proficiency. In the United States, a number of government agencies have organized their programs in a manner such that the boundary between the third and fourth small opacity profusion categories is a critical action point, with radiographs below the boundary regarded as negative and those above, as positive for pneumoconiosis. Moreover, the recording of one or more large opacities precipitates certain additional actions. Consequently, the grading system has also been designed to measure a candidate's ability to separate positive and negative radiographs in both the small and large opacity categories.

The division of cases into positives and negatives causes the examinee to make false positive and false negative errors as the radiographs are classified. Table 5 tabulates the sum of these errors for small opacity profusion. The data are classified separately for passing and failing candidates, and column 1 provides comparable data for the expert panel. For passing candidates, the mean total small opacity error was 22.4%; for those who failed, 40.4%. These values compare with a mean total error of 16.2% recorded by the expert panel. Interestingly, the distribution for those who passed is clearly peaked in a generally symmetrical manner about the mean whereas that of the failing examinees is quite broad with little evidence of peaking.

Table 6 tabulates the sum of false positive and false negative errors for large opacities. The mean total large opacity error for passing candidates was 23.6% and for failing examinees, 35.7%. The expert panel had an error of 19.3%. For this measure of reader proficiency, the distributions depart somewhat from previous ones. The data tend to be broadly distributed for *both* passing and failing groups, although not so much for passing as for failing.

It is noteworthy that of the 15 films in the examination in which a majority of the expert panel judged one or more large opacities to be present, all 10 of the panel members concurred in only six of these; there were three cases in which only nine of members agreed, two cases where only eight agreed, one case where only seven agreed, and three cases where only six agreed. Part of

TABLE 3

Distribution of Overreading/Underreading Tendency in Classification of Small Opacity Profusion

Deviation from Experts (minor profusion categories)	No. Expert Panel Members	No. Passing Examinees	No. Failing Examinees
> +1.59	0	0	4
+1.20 to +1.59	0	0	13
+0.80 to +1.19	0	2	13
+0.40 to +0.79	0	24	22
0.00 to +0.39	4	50	22
−0.01 to −0.40	5	35	7
−0.41 to −0.80	1	7	6
< −0.80	0	0	1

TABLE 4

Distribution of Corrected Standard Reading Error for Small Opacity Profusion

Error Class (minor profusion categories)	No. Expert Panel Members	No. Passing Examinees	No. Failing Examinees
< 0.90	3	2	0
0.90–1.09	1	32	0
1.10–1.29	5	65	16
1.30–1.49	1	18	33
1.50–1.69	0	1	23
1.70–1.89	0	0	14
1.90–2.09	0	0	6
> 2.09	0	0	3
Means	1.08mpc	1.17mpc	1.53mpc

TABLE 5

Distribution of Small Opacity Profusion Error (Total*)

Error Class (% Films Examined)	No. Expert Panel Members	No. Passing Examinees	No. Failing Examinees
0–10	1	3	. . .
11–20	7	44	5
21–30	2	58	20
31–40	. . .	12	30
41–50	. . .	1	15
>50	. . .	. . .	25
Mean (%)	16.2	22.4	40.4

* Sum of false positive and false negative errors.

TABLE 6

Distribution of Large Opacity Detection Error (Total*)

Error Class (% Films Examined)	No. Expert Panel Members	No. Passing Examinees	No. Failing Examinees
0–10	1	9	2
11–20	5	36	15
21–30	3	45	24
31–40	1	25	16
41–50	. . .	2	14
>50	. . .	1	24
Mean (%)	19.3	23.6	35.7

* Sum of false positive and false negative errors.

the disagreement encountered may be related to the fact that many disease processes other than pneumoconiosis can produce large opacities. Hence, disagreement among expert panel members may not indicate differences of opinion regarding the presence or absence of large opacities but disagreement over their cause, with positive readings given by some only when pneumoconiosis was considered the basis of the finding. In any case, this situation is conducive to broadening the distribution shown in table 6.

The 213 examinees who have taken the examination represent a total of 202 candidates. Of these, 116 are diplomates of the American Board of Radiology, 30 of the American Board of Internal Medicine, three of the American Board of Preventive Medicine, and two of the American Board of Family Practice; 51 are not identified with any medical specialty. The difference between the number of examinees and the number of candidates represents 10 individuals who, after failing on their first try, repeated the examination in an effort to raise their grades to passing levels. Five were successful, including one individual who repeated the examination twice.

The grade distribution of the 213 examinees, classified according to medical specialty are listed in table 7. Examinees who are diplomates of the American Boards of Preventive Medicine and Family Practice are grouped with those without specialty identification into a category designated as "other." It will be observed that the distribution of all examinees is skewed to the lower grades. Interestingly, the distribution of the "other" examinees appears to be bimodal, suggesting that they constitute two different populations, one with better training and preparation than the other. The radiologist distribution also suggests bimodality but to a less convincing degree.

The average grades of the examinees, classified according to medical specialty and divided into those passing and failing, are shown in table 8. It is noteworthy that the average grades of the passing examinees fell within a narrow range, largely independent of medical specialty.

The pass/fail performance of the examinees, classified according to medical specialty and expressed in terms of the numbers and percentages of the examinees passing and failing are listed in table 9. The radiologists appear to be the most successful, with the internists close behind. The remaining candidates performed poorly.

Table 10 provides information on the performance of those candidates who repeated the examination after failing on the first try. It is noteworthy that the candidates who passed on the second and third try allowed an average of 16 months to elapse between tests, whereas the candidates who failed on both attempts took the second test an average of only 6.5 months after the first. Apparently a failing candidate places himself or herself at a disadvantage when the examination is repeated at too short an interval. For this reason, the time for a reexamination will soon be increased to 12 months from the current 6.

When the examination was first placed in use, limited trials were carried out to determine the consistency of the grades obtained when candidates repeated the examination. Four candidates were given the examination twice, one candidate three times. The ratios of the candidates' grades on the second and third tests to those on the first were then calculated. The mean of these ratios was 1.03 (SD ± 0.11). Such values indicate that, on the average, there was little change in any candidate's grade from the first test to the second; moreover, the intracandidate variation between tests was quite small. These data are reassuring that the examination is reasonably consistent when repeated.

The examination has not been given to the expert panel. However, when the data generated at their reading trails are converted into test scores, a mean grade of 68.1 is obtained with all panelists passing. As might be expected, this grade is considerably higher than the means of the candidates who took and passed the examination.

TABLE 7

Grade Distribution of Examinees by Medical Specialty

Grade	No. Radiology Examinees	No. Internal Medicine Examinees	No. Others*	Totals
0–9.9	0	0	2	2
10–19.9	3	0	7	10
20–29.9	4	2	11	17
30–39.9	18	5	6	29
40–49.9	17	10	10	37
50–59.9	38	13	14	65
60–69.9	32	6	6	44
70–79.9	5	2	1	8
80–89.9	1	0	0	1

* Includes diplomates of the American Board of Preventive Medicine and the American Board of Family Practice.

TABLE 8

Average Grades of Examinees Classified by Specialty

Specialty	Passing Examinees	Failing Examinees	All Examinees
Radiology	60.6	37.5	52.4
Internal medicine	59.5	38.9	50.3
Preventive medicine	60.2	16.3	30.9
Family practice	...	23.0	23.0
No specialty	59.3	30.5	41.6
All examinees	60.2	32.9	48.8

TABLE 9

Pass/Fail Performance of Examinees Classified According to Specialty

Specialty	Passing Examinees		Failing Examinees	
	No.	%	No.	%
Radiology (N = 118)	76	64.4	42	35.6
Internal medicine (N = 38)	21	55.3	17	44.7
Preventive medicine (N = 3)	1	33.3	2	66.7
Family practice (N = 2)	0	0.0	2	100
No specialty (N = 52)	20	38.5	32	61.5
All Examinees (N = 213)	118	55.4	95	44.6

TABLE 10

Performance of Candidates Repeating Test After Failing First Time

Specialty	No. Passing Second Time	No. Failing Second Time
Radiology	2	...
Internal medicine	3*	4
No specialty	...	1

* Includes one candidate who passed on a second reexamination.

Discussion

It has been shown that candidates with formal training in radiology or internal medicine fare substantially better and score appreciably higher than physicians without this training. However, such backgrounds by no means guarantee success. A considerable number of candidates with specialty training failed the examination, and a sizable number without such training passed. This plus similar average grades of passing candidates suggest that other factors play a role in a candidate's performance. Almost certainly, one of these is specific training and experience in the use of the ILO classification system, as distinct from formal work in the specialties. The bimodal distribution of the grades observed in table 7 lends some support to this view.

Another factor likely to affect candidate performance is familiarity with ILO standard films and their use during the examination. Unfortunately, it is not yet possible to evaluate the influence of this factor because of ILO's difficulties in making these films widely available. Only a small number of the candidates taking the examination possessed these films, and hence insufficient data are available to test this variable. It is hoped that ILO will be able to provide the films without restriction within several months.

From the limited results obtained so far, the examination seems to be meeting its primary objective of identifying those individuals who are proficient in the use of the ILO classification system. The 118 candidates who successfully passed the examination appear to exhibit reading characteristics similar to those of expert radiologists, whereas those who failed did not. Because of its success, the examination is likely to be more widely used in the future.

Another question that may be raised is the usefulness of an examination of the type described in this paper in other phases of radiology. In recent years, increasing dissatisfaction has been expressed in a number of quarters with traditional examination processes. This has caused such organizations as the American Board of Radiology to reexamine their examination philosophies and methods. There is some reason to believe that the principles upon which the pneumoconiosis examination is based are transferable to other situations. It should be pointed out, however, that such a process will not always be easy and that much work may be necessary to develop examinations which clearly are able to separate individuals who meet prescribed standards of performance form those who do not. Nevertheless, the success of the pneumoconiosis examination suggests that its concepts and techniques should be explored for possibly broader application in radiology.

REFERENCES

1. *ILO U/C International Classification of Radiographs of Pneumoconiosis*. Occupational Safety and Health Service, revision 22, Geneva, International Labour Office, 1972
2. Jacobson G, Lainhart WS: ILO U/C 1971 international classification of radiographs of pneumoconiosis. *Med Radiogr Photogr* 48:67–110, 1972

Case Reports

Central Vertebral End-Plate Depression in Chronic Renal Disease: Report of Two Cases

FRED M. H. ZITER, JR.[1]

Steplike depressions in the central parts of the end-plates of vertebral bodies have been considered characteristic of sickle cell disease [1]. These unique deformities have recently been demonstrated to occur in patients with thalassemia major, homocystinuria, and Gaucher's disease [2–4]. This report describes similar vertebral distortion associated with chronic renal disease.

Case Reports

Case 1

A 33-year-old white woman with familial medullary cystic renal disease was first noted to have hypertension and albuminuria during a physical examination in 1960. Thyroid carcinoma was diagnosed and successfully treated 4 years later. During her first pregnancy in 1967, albuminuria and hypertension were again recorded and progressive deterioration in renal function continued to end-stage renal disease by age 29. Radiography in 1973 revealed spinal changes of renal osteodystrophy with sclerosis and indistinct trabeculae in the thoracic region and a "rugger-jersey" appearance of the lumbar spine. Central vertebral end-plate depressions were noted dorsally (fig. 1A). Hand films failed to show subperiosteal resorption, intracortical tunnelling, acral resorption, or soft tissue calcification. An iliac crest biopsy showed histologic findings compatible with renal osteodystrophy.

Hemodialysis was begun in September 1972 followed by bilateral nephrectomies 3 months later. Successful renal transplantation was performed subsequently from a living related donor. Localized avascular necrosis developed in the right femoral head after an orthopedic nailing procedure for a traumatic femoral fracture. The patient is active and well at this time.

Case 2

A 37-year-old black woman had polio as a child requiring the use of leg braces for several years. In 1963, she was evaluated for weakness at another hospital and found to be markedly hypertensive (210/130). Subsequent workup revealed atrophic kidneys and angiographic evidence of intrinsic renal disease. An open renal biopsy demonstrated chronic glomerulonephritis. Hemodialysis was begun in 1970 followed by bilateral nephrectomies 6 months later. Because two attempts at renal transplantation (1971 and 1972) resulted in rejection, maintenance hemodialysis was instituted. In 1973, hand radiographs demonstrated mild but definite subperiosteal resorption and 1+ intracortical tunnelling. Films of the thoracic spine showed central end-plate depression (fig. 1B.). Extremity films lacked evidence of aseptic necrosis, medullary infarction, or soft tissue calcification. Sickle cell preparations and hemoglobin electrophoresis failed to show evidence of sickle cell disease. The patient suffered numerous problems over the ensuing years and in 1975 succumbed of septic shock and pulmonary complications. No autopsy was performed.

Discussion

Pathologic *biconcave* depressions involving the upper and lower vertebral surfaces in man resemble the normal appearance of the vertebrae of fish. Such deformities, extending in a smooth continuous curve from one end of the vertebral end-plate to the other, occur in those conditions associated with weakened bones, (e.g., osteoporosis) and apparently result from mechanical compression.

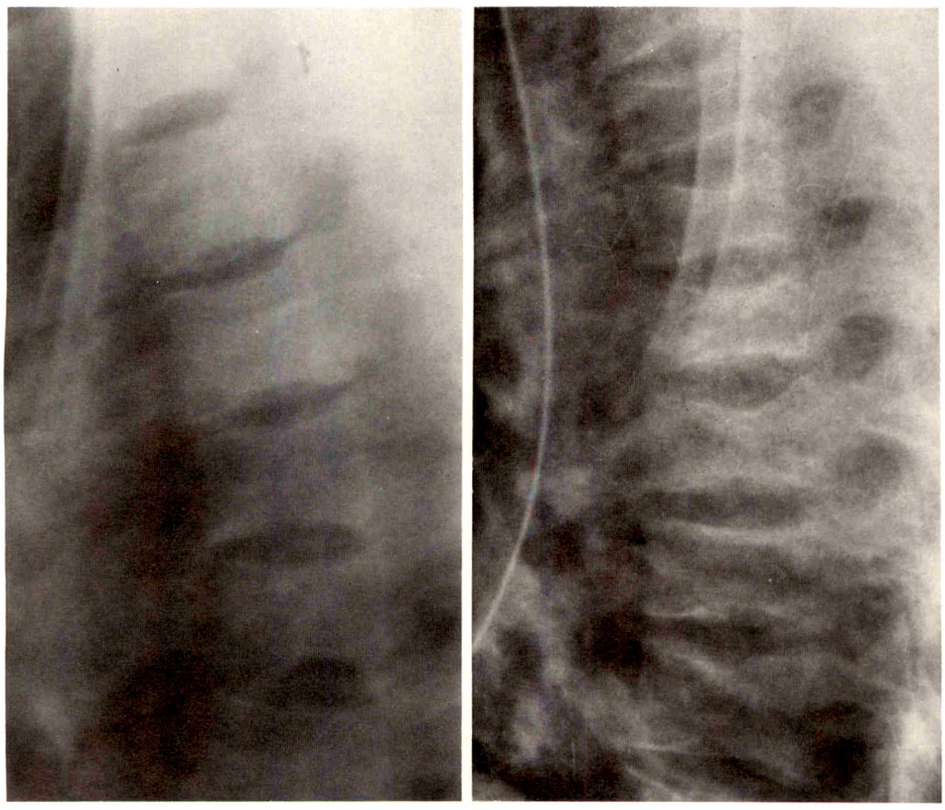
In 1966, Reynolds, [1] suggested that the term fish vertebra should not be applied to the sickle cell hemoglobinopathies. He described a separate and characteristic deformity which involved the central portions of the end-plate while sparing the periphery. This steplike deformity often affects several contiguous vertebral segments and, while most clearly defined in the thoracic region, may involve the cervical and lumbar areas as well. The floor of the depression is characteristically flat and sclerotic and the sides squared off. The margins may undergo modification in ensuing years to assume more rounded edges. These deep central defects described by Reynolds are usually easily differentiated from the 1–2 mm of end-plate depression commonly seen in normal individuals [5], and from Schmorl's nodes which are usually smaller, rounded, and asymmetric in position.

Although these vertebral depressions are most often associated with the sickle cell hemoglobinopathies, cases have been described in thalassemia major, homocystinuria, and Gaucher's disease [2–4]. The etiology of these depressions remains controversial, and both ischemia and mechanical compression have been implicated. Reynolds [1] suggests chronic ischemia during the growth period resulting from circulatory stasis as the etiology in sickle cell disease. The peculiarity of vertebral

Received May 12, 1978; accepted after revision January 30, 1979.
[1]Department of Radiology, Hartford Hospital, 80 Seymour Street, Hartford, Connecticut 06115.

© 1979 American Roentgen Ray Society

0361-803X/79/1325-0809 $0.00



A B

Fig. 1.—Case 1. **A**, Several thoracic vertebrae demonstrating sclerosis, trabecular indistinctness, and central end-plate depression. **B**, Case 2. Prominent central end-plate depressions.

blood supply is said to account for the central location with peripheral sparing. Patients with homocystinuria also have vasoocclusive changes caused by thrombosis and arterial wall fibrosis so that ischemia is plausible in this circumstance [3]. An ischemic etiology in Gaucher's disease is also easily understood [4]. The etiology in thalassemia is less clear since ischemia would have to be caused by vascular compression from marrow hyperplasia and Cassady et al. [2] suggested that mechanical compression might play an integral part.

The cause of vertebral deformity in chronic renal disease is unknown, but ischemia could play a role. Patients on prolonged maintenance hemodialysis are known to have accelerated atherosclerosis [6, 7]. This might impair vertebral blood supply resulting in growth disturbance or central aseptic necrosis. Both patients in this report received steroids during the course of their illnesses which could have caused ischemia either by altered coagulability or fat embolism [8, 9].

Recently, it has been shown that patients with renal osteodystrophy demonstrate subchondral bone resorption in the spine. Because of the resulting trabecular weakening, mechanical compression might play a role in the etiology of the radiographic changes of central end-plate depression [10]. Herniation of large portions of disk material into the weakened vertebral bodies seems unlikely as the primary event in these cases since it would be presumptuous to expect such changes to occur so centrally and symmetrically at so many successive levels [11]. Autopsy observation may eventually shed some light on this etiologic controversy, although the lack of physiologic information may be the ultimate limitation. Unfortunately, no documentation was possible of the point at which the vertebral deformities first appeared in my cases since the observation period was confined to the latter stages of the disease and the vertebrae were already abnormal. Because such defects have not been noted previously with chronic renal disease, they must be most unusual [12, 13].

ACKNOWLEDGMENTS

I thank Dr. Jack L. Westcott for his valuable suggestions and Christine M. Volzo for manuscript preparation.

REFERENCES

1. Reynolds J: A re-evaluation of the "fish-vertebra" sign in sickle cell hemoglobinopathy. *AJR* 97:693–707, 1966
2. Cassady JR, Berdon WE, Baker DH: The "typical" spine changes of sickle-cell anemia in a patient with thalassemia major (Cooley's anemia). *Radiology* 89:1065–1068, 1967
3. Westerman MP, Greenfield GB, Wong PWK: "Fish vertebrae", homocystinuria, and sickle cell anemia. *JAMA* 230: 261–262, 1974
4. Hansen GC, Gold RH: Central depression of multiple vertebral end-plates: a "pathognomonic" sign of sickle hemoglobinopathy in Gaucher's disease. *AJR* 129:343–344, 1977
5. Rohlfing BM: Vertebral end-plate depression: report of two patients without hemoglobinopathy. *AJR* 128:599–600, 1977
6. Lindner A, Charra B, Sherrard DJ, Scribner BH: Accelerated atherosclerosis in prolonged maintenance hemodialysis. *N*

Engl J Med 290:697–700, 1974
7. Friedman SA, Novack S, Thomson GE: Arterial calcification and gangrene in uremia. *N Engl J Med* 280:1392–1394, 1969
8. Cosgriff SW, Diefenbach AF, Vogt W Jr: Hypercoagulability of the blood associated with ACTH and cortisone therapy. *Am J Med* 9:752–756, 1950
9. Jones JP, Engelman EP, Steinbach HL, Murray WR, Rambo ON: Fat embolization as a possible mechanism producing avascular necrosis. *Arthritis Rheum* 8:449, 1965
10. Resnick D, Niwayama G: Subchondral resorption of bone in renal osteodystrophy. *Radiology* 118:315–321, 1976
11. Resnick D, Niwayama G: Intravertebral disk herniations: cartilaginous (Schmorl's) nodes. *Radiology* 126:57–65, 1978
12. Griffiths HJ, Ennis JT, Bailey G: Skeletal changes following renal translantation. *Radiology* 113:621–626, 1974
13. Levine E, Erken EH, Price HI, Meyers AM, Solomon L: Osteonecrosis following renal transplantation. *AJR* 128: 985–991, 1977

Unusual Case of Metastatic Pulmonary Calcification

M. E. BEIN,[1] D. B. N. LEE,[2] J. H. MINK,[1] AND J. DICKMEYER[2]

Metastatic calcification occurs when calcium salts are deposited in previously normal tissues [1–6]. It has been associated with chronic renal failure, primary parathyroid neoplasms, chronic destructive diseases of bone, hypervitaminosis-D, and excessive ingestion or intravenous administration of calcium salts [1–17]. The development of soft tissue calcification in patients with renal disease is usually attributed to an abnormal calcium-phosphorus ion product and the coexistence of secondary hyperparathyroidism [1, 2, 4, 5, 7]. We describe a case of chronic metastatic pulmonary calcification in a renal transplant patient in whom extensive calcification became radiographically apparent at a time when renal function was near normal, calcium-phosphorus ion product was not elevated, and all parathyroid tissue had been surgically removed.

Case Report

M. G., a white man, received a renal allograft at age 21; the underlying renal disease was membranoproliferative glomerulonephritis. Chest radiography 14 months later was normal. However, graft function subsequently deteriorated, and the patient developed muscle cramps, ischemic ulcerations of the skin, extensive vascular calcifications of the limbs and digits, and subperiosteal new bone formation. Creatinine clearance 19 months after renal allograft was 20 ml/min; serum calcium, 8.6 mg/dl; and serum phosphorus, 4.8 mg/dl. Chest radiography (fig. 1A) revealed poorly defined nodular densities in the upper lung zones. The patient was afebrile, had no respiratory symptoms, and sputum cultures were negative. There was no clinical suggestion of congestive heart failure. Presumptive diagnosis was metastatic pulmonary calcification. A subtotal parathyroidectomy was done and hemodialysis was begun 3 months later. Total parathyroidectomy and thyroidectomy were eventually performed after 2 more months and dialysis with a low calcium bath (3.0 mg/dl) was initiated.

The patient's second renal allograft was 4 years after the first, at which time the skin ulcers had healed and vascular calcification had resolved. The pulmonary densities had decreased in comparison with earlier radiographs. With resumption of renal function, the patient became hypocalcemic, with total serum calcium concentrations as low as 4.0 mg/dl. Calciferol (50,000 U) and an equivalent of 1 g of calcium in the form of calcium gluconate were given after transplant. Throughout the posttransplant period, serum calcium and phosphorus ranged between 8.0–9.5 mg/dl and 3.1–5.0 mg/dl. Serum immunoreactive parathyroid hormone concentration was 147 pg/ml (serum calcium concentration, 9.5 mg/dl), which was consistent with surgical or idiopathic hypoparathyroidism (C.D. Hawker, UpJohn, personal communication). Renal function has been well maintained with an average serum creatinine of 1.8 mg/dl and creatinine clearance of 50–60 ml/min. Immunosuppressive therapy consisted of Imuran 100 mg daily and prednisone 30 mg daily.

Chest radiography about 10 months after the second transplant was unchanged from the first posttransplant period. After about another 10 months, nodular densities were present throughout the middle and upper lung zones bilaterally (fig. 1B). Low kilovoltage grid radiography confirmed the suspicion of parenchymal calcification (fig. 1C). Renal function, serum calcium, and serum phosphorus were unchanged, and the patient remained entirely asymptomatic. Pulmonary function studies revealed a severe reduction in diffusing capacity consistent with a diffuse interstitial process. Renal function remained stable for about 15 months, at which time deterioration in graft function developed; hemodialysis was reinstituted about 4 months later. Chest radiography after 7 months showed slightly increased pulmonary calcification (fig. 1D); there has been no change since that time. Recent ^{99m}Tc-HEDSPA bone scan showed marked radionuclide activity in the lungs with increased blood pool activity (fig. 2), findings consistent with metastatic pulmonary calcification and renal failure. The patient has remained free of respiratory symptoms.

Discussion

Metastatic calcification is found principally in the peripheral vascular system, soft tissues, lung, kidney, stomach, and heart [2, 4, 6, 9]. The lung is the most frequent visceral site of calcification [5, 6]; there is a direct correlation between the occurrence of metastatic pulmonary calcification and other visceral calcification [7]. Pulmonary calcification has been found at autopsy in 60% of chronic dialysis patients [7]. The calcification occurs predominately in the alveolar walls, but it is also found in the walls of bronchi and blood vessels [1, 4, 7–12, 14, 15]. In all of the chronic dialysis cases studied by Conger et al. [7], the upper lobes showed slightly greater involvement than the lower lobes.

There is usually a marked disparity between the presence of histologic and radiographic pulmonary calcification, so that metastatic pulmonary calcification is rarely diagnosed on premortem chest radiography [2–4, 7, 9, 11]. The presence of calcification may be mistaken for or obscured by associated pulmonary edema or infection [1, 2, 4, 17]. Felson [18] alluded to the difficulty in distinguishing alveolar disease of water density from metastatic calcification. The frequent occurrence of cardiorenal complications in patients with chronic renal failure especially underscores this problem [4]. Alternatively, the calcification may simply not be visible on

Received July 14, 1978; accepted after revision January 8, 1979.
This work was supported in part by U.S. Public Health Service grant RR 865.
[1] Department of Radiological Sciences, UCLA Center for the Health Sciences, Los Angeles, California 90024. Address reprint requests to M. E. Bein.
[2] Renal Transplantation Center, Division of Nephrology, Department of Medicine, UCLA Center for the Health Sciences, Los Angeles, California 90024.

© 1979 American Roentgen Ray Society

0361-803X/79/1325-0812 $0.00

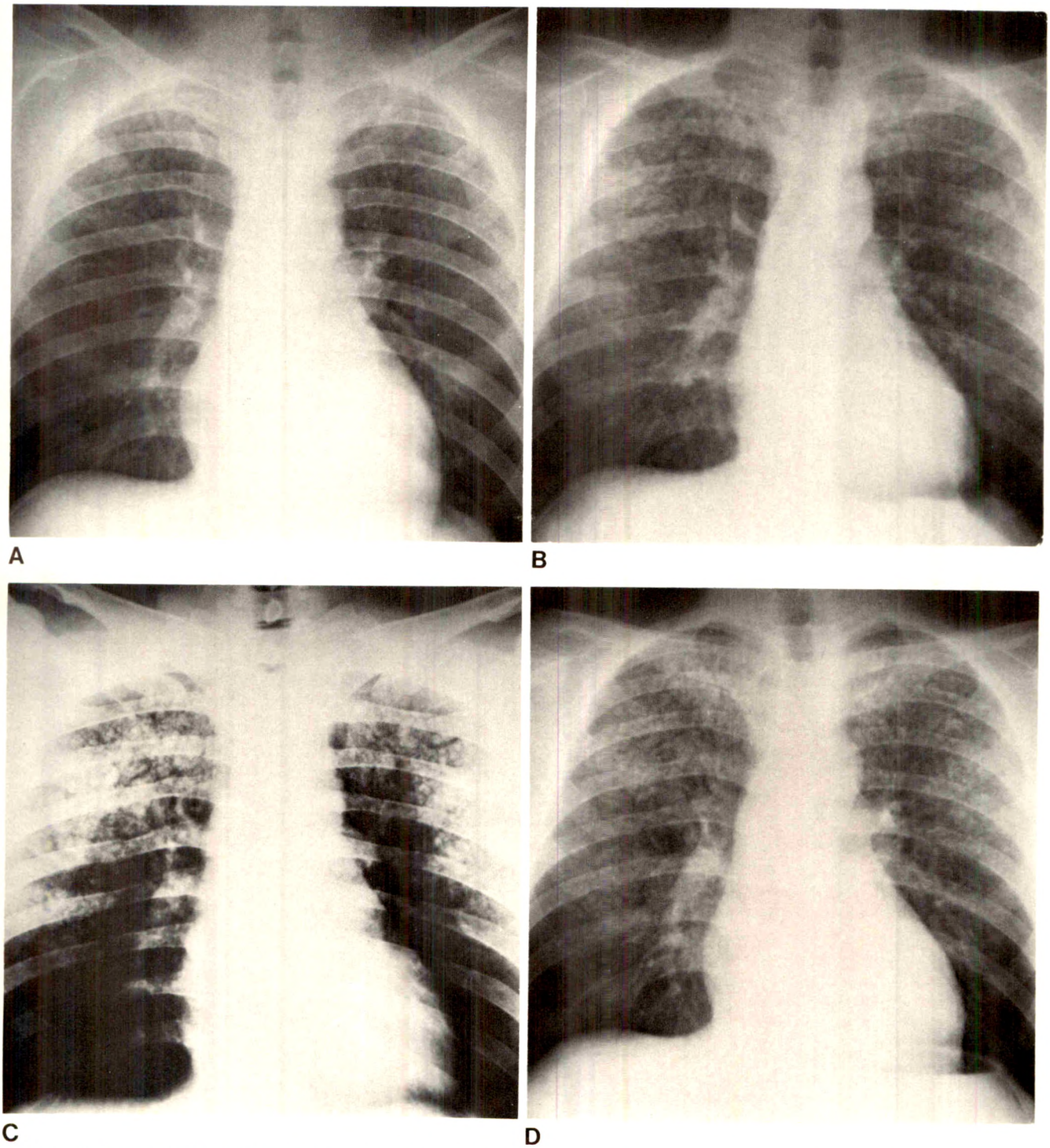


Fig. 1.—**A,** Poorly defined nodular densities in upper lung zone bilaterally. Presumptive diagnosis was metastatic pulmonary calcification. **B,** 4 years later, increased pulmonary calcification in middle and upper lung zones bilaterally. **C,** Low kilovoltage grid radiograph at same time demonstrates calcificatons. **D,** After 3 more years, further increase in parenchymal calcifications.

routine chest radiography because of very small foci (1–2 mm) scattered throughout the parenchyma [1, 4].

There have been numerous cases of radiologically evident metastatic pulmonary calcification, usually in association with chronic renal failure [1, 5, 8–10, 14–17]. Diffuse parenchymal involvement may occur in a pattern simulating interstitial or alveolar pulmonary edema [5, 8, 9, 14–17]. Localized densities in either the upper or lower lobes with wedge-shaped, infiltrative, or nodular appearances have also been described [1, 8, 10]. The calcification usually develops over a long period of time but it may occur relatively acutely in several weeks to months

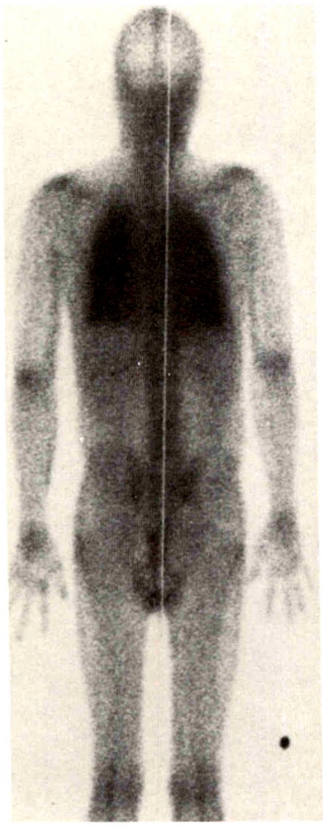


Fig. 2.—^{99m}Tc-HEDSPA bone scan 10 months after fig. 1D shows extensive radionuclide activity in lungs consistent with metastatic pulmonary calcification.

[1, 5, 9, 16]. Resolution of pulmonary calcification in chronic renal failure may occur after parathyroidectomy, renal transplantation, or dialysis [8].

The presence of punctate calcifications within radiographic densities may suggest the correct diagnosis of metastatic pulmonary calcification [8]. The diagnosis should also be suspected whenever there are radiographically stable opacities previously thought to represent pulmonary edema or infection, even if definite calcifications cannot be demonstrated [1, 8]. Low kilovoltage, grid, or tomographic examinations have been suggested to define the presence of calcification [1]. Finally, the diagnosis can be made by the presence of increased radionuclide activity in the lungs after administration of ^{99m}Tc bone scanning agents [16, 19, 20].

Patients with pulmonary calcification are usually relatively asymptomatic, although there have been cases of respiratory failure secondary to massive pulmonary involvement [7, 8]. Pulmonary function tests may show restrictive and diffusion defects even when chest radiography appears normal. Vital capacity has been inversely correlated with the histological severity of calcification [7].

Over a century ago, Virchow [22] postulated that calcium salts dissolved from the skeleton were transported by blood and deposited at some distant site forming calcium "metastases," a process analogous to neoplastic metastases. In 1947, Mulligan [6] reviewed 88 patients with metastatic calcification. He noted that the underlying pathologic process was neoplastic involvement of the skeleton in 35, uremia in 23, primary hyperparathyroidism in 21, and Vitamin D intoxication in nine. Interest in metastatic calcification escalated in the past 2 decades mainly as a result of its frequent occurrence in uremic patients treated by dialysis and/or renal transplant. [21, 23–25]. The prevalence in dialysis patients may be as high as 80% [25].

The most frequent association found in metastatic calcification is elevation of the plasma calcium and phosphorus product as a result of hypercalcemia and/or hyperphosphatemia. The product in normal subjects is about 40 mg^2/dl^2 (10 mg/dl × 4 mg/dl = 40 mg^2/dl^2). Precipitation of secondary calcium phosphate occurs in vitro when the product exceeds a critical level. In uremic patients with metastatic calcification, it usually exceeds 70 mg^2/dl^2 [21, 25, 26]. The predilection to extraosseous calcification in uremic patients has also been attributed to a number of other factors. Secondary hyperparathyroidism, in addition to its hyperphosphatemic effect in uremic patients [23], may cause calcification through a more direct mechanism [24]. It is also possible that uremia per se may alter the configuration of tissue proteins so as to render them more calcifiable. Eisenstein et al. [29] and Urist et al. [30, 31] developed the concept that metastatic calcification is first preceded by some physiochemical change in tissue protein. Therefore, it is interesting that alterations in protein [32] and collagen [33] metabolism have been demonstrated in uremic patients by some investigators.

Both experimental and clinical observations suggest parathyroid hormone as a possible pathogenetic agent in the development of extraosseous calcification. Parathyroid hormone administration to rats may induce a state of sensitization so that after an appropriate interval (the "critical period"), a challenger, usually the salt of a rare or heavy metal, can lead to calcification or the syndrome of calciphylaxis [34]. In man, metastatic calcification may develop in patients with primary hyperparathyroidism either with or without azotemia [6, 16, 35–38]. The association of azotemic (secondary) hyperparathyroidism with soft tissue calcification has already been discussed. When azotemia is corrected by renal transplantation, metastatic calcification may nonetheless develop [21]. A role of excess parathyroid hormone is suggested by healing of lesions attributed to soft tissue calcium deposition in some patients after parathyroidectomy.

Experimentally, vitamin D can also act as sensitizer in the syndrome of calciphylaxis [34]. In man, soft tissue calcification is seen in cases of vitamin D intoxication [6, 13, 24]. In such instances, the patients are usually also hypercalcemic and azotemic.

Our patient has a number of unusual features. Pulmonary calcification developed during a period when his renal function was only minimally compromised and he was neither hypercalcemic nor hyperphosphatemic. He also had virtually no circulating parathyroid hormone since he had previous total parathyroidectomy. It is

possible that our patient may be a human variant of the syndrome of experimental calciphylaxis [34]. In this context, he is certainly primed by glucocorticoid (used as an immunosuppressive drug for his kidney graft) and calciferol (used as a substitute for parathyroid hormone in maintaining normocalcemia) administration. However, the clinical course of his calcification is not similar to the experimentally described calciphylaxis in animals [32] and no clear calcifying challenger could be identified. We postulate that previous azotemia, and glucocorticoid and calciferol administration, either alone or in combination, has altered his tissue "resistance" to calcification, so that apparently normal levels of circulating calcium and phosphorus become supersaturating concentrations resulting in metastatic calcification. More recently, Kuzela et al. [25], in an extensive study on extraosseous calcification in chronic dialysis patients, also failed to demonstrate a correlation between presence and severity of soft tissue calcification and multiple factors, such as duration of dialysis, degree of parathyroid gland hyperplasia, and serum calcium and phosphorus concentrations and product. Such findings would lend credence to the postulated phenomenon of altered tissue 'resistance' to calcification.

ACKNOWLEDGMENTS

We thank Barbara LeBlanc and Judy Merit for secretarial assistance, and Paul Stout and Kim Willis for technical contributions.

REFERENCES

1. McLachlan MSF, Wallace M, Seveviratan C: Pulmonary calcification in renal failure. Report of three cases. *Br J Radiol* 41:99–106, 1968
2. Agus ZS, Goldberg M: Pathogenesis of uremic osteodystrophy. *Radiol Clin North Am* 10:545–556, 1972
3. Salzman E: *Lung Calcifications in X-Ray Diagnosis*. Springfield, Ill., Thomas, 1968, pp 56–57
4. Rubin EH, Siegelman SS: *The Lungs in Systemic Diseases*. Springfield, Ill., Thomas, 1969, pp 195–199
5. Neff M, Yalcin S, Gupda S, Berger H: Extensive metastatic calcification of the lung in an azotemic patient. *Am J Med* 56:103–109, 1974
6. Mulligan RM: Metastatic calcification. *Arch Pathol Lab Med* 43:177–230, 1947
7. Conger JD, Hammond WS, Alfrey AC, Contiguglia SR, Stanford RE, Huffer WE: Pulmonary calcification in chronic dialysis patients. Clinical and pathological studies. *Ann Intern Med* 83:330–336, 1975
8. Mootz JR, Sagel SF, Roberts TH: Roentgenographic manifestations of pulmonary calcifications. A rare cause of respiratory failure in chronic renal disease. *Radiology* 107: 55–60, 1973
9. Kaltreider HB, Baum GL, Bogaty G, McCoy MD, Tucker M: So-called "metastatic" calcification of the lung. *Am J Med* 46:188–196, 1969
10. Smith JC, Stanton LW, Kramer NC, Parrish AE: Nodular pulmonary calcification in renal failure. Report of a case. *Am Rev Respir Dis* 100:723–728, 1969
11. Burns WA, Matthews MJ: Pulmonary calcinosis: a clinical-pathological study of twelve cases. *Lab Invest* 28:404, 1973
12. Werner P, Kuschner M, Riley EA: Reversible metastatic calcification associated with excessive milk and alkali intake. *Am J Med* 14:108–115, 1953
13. Wilson CW, Wingfield WL, Toone EC Jr: Vitamin D poisoning with metastatic calcification. Report of a case and review of the mechanism of intoxication. *Am J Med* 14:116–123, 1953
14. Cooke CR, Hyland JW: Pathological calcification of the lungs following intravenous administration of calcium. *Am J Med* 29:363–368, 1960
15. Cabal EC: Case of the winter season. *Semin Roentgenol* 11: 15–16, 1976
16. Cohen AM, Maxon HR, Goldsmith RE, Schneider HJ, Wiot JF, London RG, Altemeier WA: Metastatic pulmonary calcification in primary hyperparathyroidism. *Arch Intern Med* 137:520–522, 1977
17. Firooznia H, Pudlowski R, Golimbu C, Rafii M, McCauley D: Diffuse interstitial calcification of the lungs in chronic renal failure mimicking pulmonary edema. *AJR* 129:1103–1105, 1977
18. Felson B: Thoracic calcifications. *Chest* 56:330–343, 1969
19. McLaughlin AF: Uptake of ^{99m}Tc bone scanning agent by lungs with metastatic calcification. *J Nucl Med* 16:322–323, 1975
20. Rosenthal DI, Chandler HL, Azizi F, Schneider PB: Uptake of bone imaging agents by diffuse pulmonary metastatic calcification. *AJR* 129:871–874, 1977
21. Gipstein RM, Coburn JW, Adams DA, Lee DBN, Khosrow PP, Sellers A, Suki WN, Massry SG: Calciphylaxis in man. A syndrome of tissue necrosis and vascular calcification in 11 patients with chronic renal failure. *Arch Intern Med* 136: 1273–1280, 1976
22. Virchow R: Kalk metastasen. *Virchows Arch [Pathol Anat]* 8:103–113, 1855
23. Massry SG, Coburn JW, Popovtzer MM, Shinaberger JH, Maxwell MH, Kleeman CR: Secondary hyperparathyroidism in chronic renal failure. The clinical spectrum in uremia during hemodialysis and after renal transplantation. *Arch Intern Med* 124:431–441, 1969
24. Parfitt AM: Soft tissue calcification in uremia. *Arch Intern Med* 124:544–556, 1969
25. Kuzela DC, Huffer WE, Conger JD, Winter SD, Hammond WS: Soft tissue calcification in chronic dialysis patients. *Am J Pathol* 86:403–417, 1977
26. Logan MA: Recent advances in the chemistry of calcification. *Physiol Rev* 20:522–560, 1940
27. Berlyne GM, Shaw AG: Red eyes in renal failure. *Lancet* 1: 4–7, 1967
28. Herbert FK, Miller HG, Richardson GO: Chronic renal disease, secondary parathyroid hyperplasia, decalcification of bone and metastatic calcification. *J Pathol Bacteriol* 53: 161–182, 1941
29. Eisenstein R, Truehart RE, Hass GM: Pathogenesis of abnormal tissue calcifications, in *Calcification in Biological Systems*, edited by Sognnaes RF, Washington DC, American Association for the Advancement of Science, 1960, pp 281–305
30. Urist MR, Moss MJ, Adams JM: Calcification of tendon: a triphasic local mechanism. *Arch Pathol* 77:594–608, 1964
31. Urist MR, Adams JM: Localization mechanism of calcification in transplants of aorta. *Ann Surg* 166:1–18, 1967
32. Shear L: Internal redistribution of tissue protein synthesis in uremia. *J Clin Invest* 48:1252–1257, 1969
33. Alvioli LV: Collagen metabolism, uremia and bone. *Kidney*

Int 4:105–115, 1973
34. Selye H, Berczi I: The present status of calciphylaxis and calcergy. *Clin Orthop* 69:28–54, 1970
35. Parson WB: Results of operations for hyperparathyroidism. *Bull N Y Acad Med* 25:285–297, 1949
36. Hanes FM: Hyperparathyroidism due to parathyroid adenoma with death from parathormone intoxication. *Am J Med Sci* 197:85–90, 1939
37. Rogers HM: Parathyroid adenoma and hypertrophy of parathyroid glands. *JAMA* 130:22–28, 1946
38. Ballin DE, Gershwin BS: Hyperparathyroidism with renal insufficiency. *Am J Med Sci* 190:519, 1935

Significance of Pneumomediastinum in Blunt Trauma to the Thorax

PRESTON R. LOTZ,[1,2] WILLIAM MARTEL,[1] JAY J. ROHWEDDER,[3] AND ROBERT A. GREEN[3]

Mediastinal and deep cervical emphysema are among the signs of tracheobronchial laceration [1–4]. According to Eijgelaar and van der Heide [5] and Kirsh et al. [1], either of these signs should prompt bronchoscopy to exclude a bronchial rupture. This concept has not been emphasized in the radiologic literature. Either of these findings in a patient who has not received positive-pressure ventilation is strongly suggestive of a tracheobronchial fracture.

Case Reports

Case 1

A 37-year-old man was brought to the emergency room of a nearby hospital after an automobile accident in which he sustained severe closed chest trauma. On arrival, he was acutely dyspneic with respirations of 32, pulse of 140, and systolic blood pressure of 80 mm Hg. Initial chest radiography showed fractures of the left first through fifth and right eighth through twelfth ribs, small extrapleural hematomas in relation to the bilateral rib fractures, extensive contusion of the right upper lobe, elevation of the left hemidiaphragm, and widening of the superior mediastinum. Pneumomediastinum or deep cervical emphysema was not evident. Respiratory arrest occurred 1 hr later and chest radiography (figs. 1A and 1B) showed bilateral pneumothorax and pneumomediastinum. The collapsed left lung appeared to fall away from its normal attachment to the mediastinum. Deep cervical emphysema was also present (fig. 1C). The significance of these findings was not appreciated. Chest tubes were inserted into each pleural space. The pulses in his left upper extremity, present 1 hr earlier, were no longer palpable. Angiography revealed a laceration of the left subclavian artery about 5 cm distal to its origin.

The patient was promptly transferred to University of Michigan Hospital, where surgical correction of the arterial damage was undertaken. At thoracotomy, complete transection of the left main bronchus 2 cm from the carina was found. The fractured bronchus was immediately repaired, and he was discharged after 2 months. He was readmitted 10 weeks later because of two episodes of pneumonia. Bronchoscopy at that time demonstrated complete obliteration of the lumen at the site of previous laceration. At thoracotomy, two abscesses were found in the atelectatic left lung. The stenotic segment of the bronchus was resected and an anastomosis was performed.

Case 2

A 34-year-old man with no history of pulmonary disease sustained blunt chest trauma during a motor vehicle accident. Physical examination in a hospital emergency room a few hours later showed extensive subcutaneous emphysema and the breath sounds over the posterior aspect of the right lung were diminished. Vital signs were satisfactory except for a systolic blood pressure recording of 90 mm Hg. Chest radiography (fig. 2A) revealed mediastinal emphysema and a small right pneumothorax. Tracheostomy and tube thoracostomy were performed. Chest radiography (fig. 2B) 6 days after injury demonstrated partial atelectasis of the right lower lobe; this was not appreciated and he was discharged after 10 days. Bronchoscopy was not performed.

A persistent cough developed shortly thereafter with recurrent episodes of right-side pneumonia. After an episode of pneumonia with production of foul sputum 15 months after original injury, a chest film demonstrated complete right lower lobe atelectasis. Bronchoscopy revealed moderate stenosis of the right main bronchus and considerable pus in the right lung. Bronchography showed complete atelectasis of the right lower lobe, and the lobe was removed 16 months after the original injury.

Subsequently, severe pneumonia developed in the right upper and middle lobes. When seen 30 months after the original trauma, he was producing up to 200 ml of purulent sputum daily. Review of earlier radiographs then led to the diagnosis of previous bronchial fracture. A perfusion isotope scan demonstrated no flow to the right lung, and an inhalation isotope scan showed little ventilation with gas trapping. Repeat bronchoscopy demonstrated further concentric narrowing of the right main bronchus just distal to the carina, with copious retained secretions.

It was believed that bronchoplasty would not restore function in the remaining right lung, so the right pneumonectomy was completed.

Discussion

Clinical and radiographic signs of tracheobronchial ruptures have been discussed [1, 6–9], as have the mechanisms producing such an injury [1, 6, 10]. Tracheobronchial lacerations usually affect the main bronchi, typically within 2.5 cm of the carina [6]. Davis and Hopkins [11] described two clinical presentations of this lesion. If the rent in the bronchus communicates freely with the pleural space, a large pneumothorax results (case 1), and the lung frequently fails to reexpand despite tube thoracostomy and appropriate suction. In the second type of clinical presentation, the pneumothorax is small or absent, depending on the size of the communication. In either situation, gas may escape through the bronchial wall and peribronchial connective tissues directly into the mediastinum.

However, in the second the peribronchial tissues remain sufficiently intact to permit at least some ventilation of the involved lung. Moreover, the mediastinal gas may be impossible to detect radiographically, and the fracture

Received September 5, 1978; accepted after revision January 3, 1979.

[1]Department of Radiology, University of Michigan Medical Center, Ann Arbor, Michigan 48109.

[2]Present address: Neuroradiology Division, Department of Radiology, University of Pittsburgh School of Medicine, Pittsburgh, Pennsylvania 15261. Address reprint requests to P. R. Lotz.

[3] Pulmonary Division, Department of Internal Medicine, University of Michigan Medical Center and Veterans Administration Hospital, Ann Arbor, Michigan 48105.

© 1979 American Roentgen Ray Society

0361-803X/79/1325-0817 $0.00

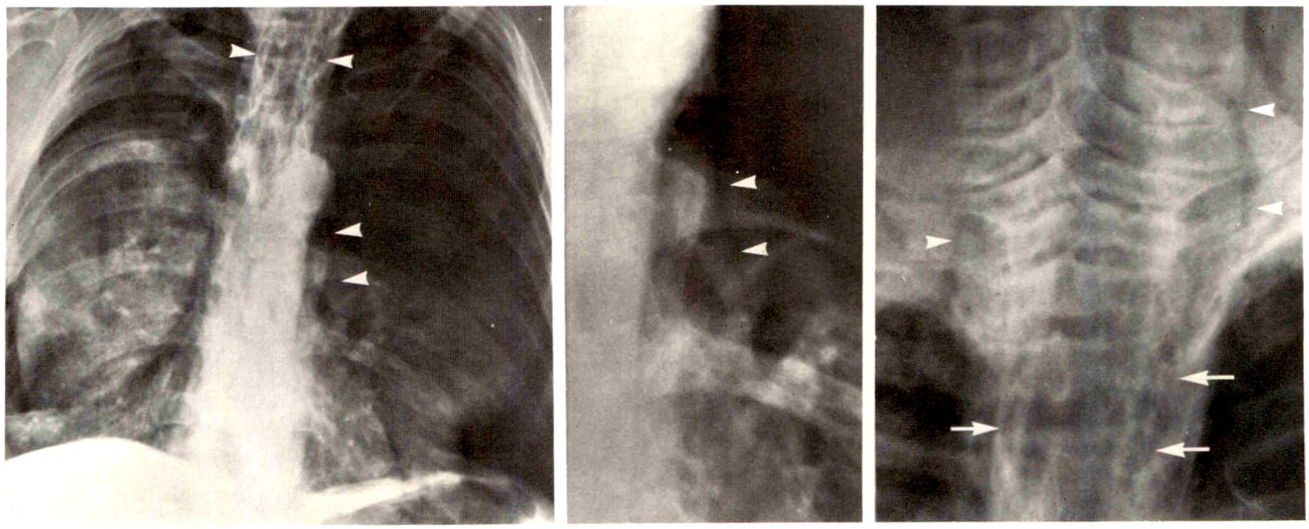


Fig. 1.—Case 1. **A**, In upright position within 3 hr after accident. Massive pneumothorax on left and lesser on right. Opacity of right lung reflects both contusion and atelectasis. Greatly collapsed left lung appears separated from normal point of attachment to mediastinum. Mediastinal emphysema (*arrowheads*) more apparent in enlarged view of left hilar region (**B**, *arrowheads*). **C**, Enlarged view of the cervical region. Deep cervical (*arrowheads*) and paratracheal (*arrows*) emphysema.

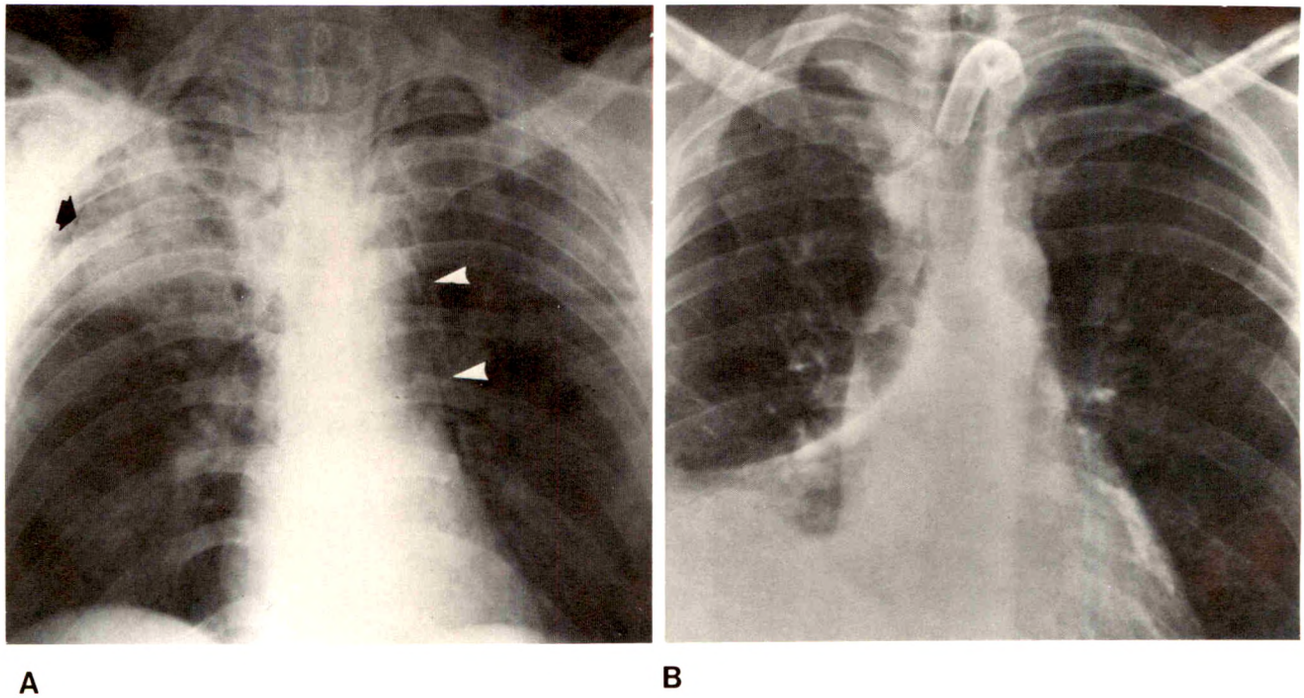


Fig. 2.—Case 2. **A**, In supine position within several hours of trauma. Mediastinal emphysema (*arrowheads*). Subcutaneous emphysema in neck, supraclavicular regions, and right lateral chest wall. Small pneumothorax on right (*arrow*). Right fourth rib fractured posterolaterally. **B**, Posteroanterior film of chest in upright position 6 days later. Partial atelectasis of right lower lobe.

is unsuspected until atelectasis and pulmonary infection develop distal to bronchial obstruction at the site of laceration. The obstruction develops from the accumulation of granulation tissue at the fracture site and may occur as early as 1 week after injury. In our case 2, the significance of the mediastinal and deep cervical emphysema was not appreciated and diagnosis was delayed until the right lung was no longer salvageable 30 months later.

After closed chest injury, in the absence of injury to

the airway in the neck, gas in the deep cervical fascial planes should be considered an extension of mediastinal emphysema, even if the mediastinal component is not radiographically apparent. Mediastinal gas ascends easily into the neck [5] and soft tissue cervical emphysema is often a clue to the correct diagnosis [1, 5]. In a literature review, Silbiger and Kushner [12] found mediastinal or subcutaneous emphysema in 61% of 66 cases of tracheobronchial laceration. Burke [7] stated that in 10% of such injuries there are no radiographic or physical findings to suggest the diagnosis. The yield of early diagnoses would certainly be improved by routine radiography of the cervical soft tissues in patients with severe closed chest trauma. It should be noted that the absence of gas in these locations does not exclude an airway fracture.

The pathway for the passage of gas from the pulmonary interstitium through the hilum to the mediastinum was demonstrated in cats by Macklin [13]. He stated that the amount of gas that accumulated in the pulmonary interstitium and mediastinum was directly dependent upon the pressure of injection of the gas through the intrabronchial cannula. He did not indicate the pressures used in the injections. A pulmonary laceration may permit gas to enter the pulmonary interstitium, but we believe that it would be very unusual for large amounts of gas to be forced into the mediastinum unless the patient has been subjected to positive-pressure ventilation.

Tension pneumothorax and subcutaneous emphysema may develop after rib fracture due to laceration of the visceral and parietal pleura. It is theoretically possible for the subcutaneous gas to dissect into the deep cervical and/or mediastinal fascial planes. However, such a pathway was not mentioned by Evans and Smalldon [14] in their review of mediastinal emphysema, and we are not aware that pneumomediastinum of this origin has ever been documented. Traumatic rupture of the esophagus may cause pneumomediastinum, but this is a rare lesion. Furthermore, in a severe blunt chest injury, a rigid structure such as the tracheobronchial tree is far more likely to rupture than a mobile and elastic one like the esophagus. An esophageal rupture should be sought when a tracheobronchial fracture cannot be demonstrated by bronchoscopy [15].

In some patients, mediastinal or deep cervical emphysema will be apparent on chest radiography only after artificial ventilation. In such instances, these signs are less reliable indicators of a bronchial fracture but that diagnosis should still be considered.

The presence of a pneumomediastinum or deep cervical emphysema in a patient who has sustained closed trauma to the chest and who has not been subjected to positive-pressure ventilation should arouse strong suspicion of a fracture of the tracheobronchial tree. Such fractures should be recognized promptly in order to avoid complications. Surgical repair, if attempted early, is usually successful.

REFERENCES

1. Kirsh MM, Orringer MB, Behrendt DM, Sloan H: Management of tracheobronchial disruption secondary to nonpenetrating trauma. *Ann Thorac Surg* 22:93–101, 1976
2. Mazzei EA, Mulder DG: Closed-chest injuries to the trachea and bronchus. *Arch Surg* 100:677–680, 1970
3. Eertelsen S, Howitz P: Injuries of the trachea and bronchi. *Thorax* 27:188–194, 1972
4. Guest JL Jr: Major airway injury in closed chest trauma. *Chest* 72:63–66, 1977
5. Eijgelaar A, van der Heide JNH: A reliable early symptom of bronchial or tracheal rupture. *Thorax* 25:120–125, 1970
6. Payne WS, DeRemee RA: Injuries of the trachea and major bronchi. *Postgrad Med* 49:152–158, 1971
7. Burke JF: Early diagnosis of traumatic rupture of the bronchus. *JAMA* 181:682–686, 1962
8. Hood RM, Sloan HE: Injuries of the trachea and major bronchi. *J Thorac Cardiovasc Surg* 38:458–480, 1959
9. Oh KS, Fleischner FG, Wyman SM: Characteristic pulmonary finding in traumatic complete transection of a mainstem bronchus. *Radiology* 92:371–372, 1969
10. Eastridge CE, Hughes FA Jr, Pate JW, Cole F, Richardson F: Tracheobronchial injury caused by blunt trauma. *Am Rev Respir Dis* 101:230–237, 1970
11. Davies D, Hopkins JS: Patterns in traumatic rupture of the bronchus. *Injury* 4:261–264, 1973
12. Silbiger ML, Kushner LN: Tracheobronchial perforation: its diagnosis and treatment. *Radiology* 85:242–246, 1965
13. Macklin CC: Pneumothorax with massive collapse from experimental local overinflation of the lung substance. *Can Med Assoc J* 36:414–420, 1937
14. Evans JA, Smalldon TR: Mediastinal emphysema. *AJR* 64: 375–390, 1950
15. Kirsh MM, Sloan H: *Blunt Chest Trauma: General Principles of Management*. Boston, Little, Brown, 1977, pp 122–123

Laryngeal Papillomatosis with Pulmonary Spread in a 69-Year-Old Man

GARY GLAZER[1] AND W. RICHARD WEBB[1]

Pulmonary involvement by laryngeal papillomatosis is rare. It typically occurs in children or young adults; only one prior case has been reported in a patient over 40 years of age [1]. We report a case of pulmonary involvement by laryngeal papillomatosis occurring in a 69-year-old man. Despite the rarity of this disease in adults, the correct diagnosis may be suggested by a characteristic combination of clinical and radiographic features.

Case Report

In 1967, a 62-year-old man was first evaluated for hoarseness. Laryngoscopy revealed several squamous papillomas of both vocal cords, extending locally into the left supraglottic region. He had no history of cervical irradiation or previous laryngeal papillomas. In 1969, tomograms demonstrated numerous endotracheal papillomas (fig. 1) and tracheostomy was performed which showed papillomas extending down the trachea to the carina and main bronchi. Between 1967 and 1973, the patient was hospitalized 37 times for excision of laryngeal and tracheal papillomas. Chest radiographs during this period remained normal (fig. 2A).

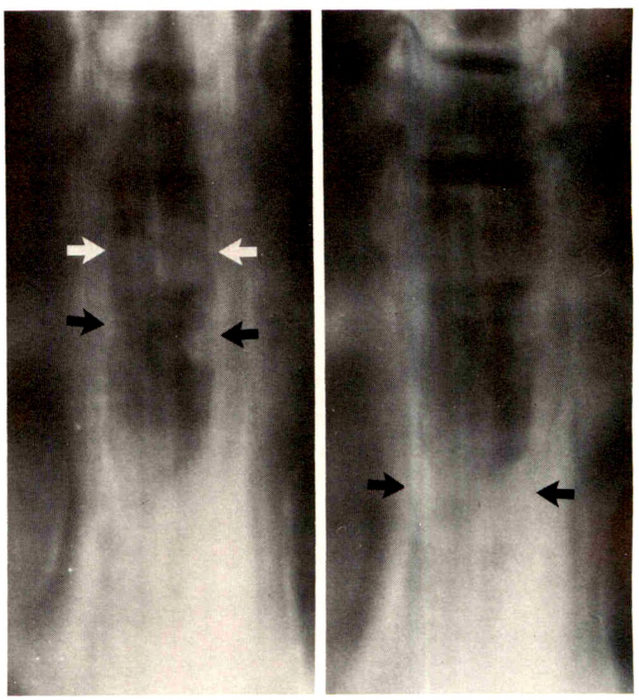
In 1974, chest radiographs showed multiple thin-walled lung cysts typical of pulmonary spread (fig. 2B). A single cyst in the left lower lobe contained an air-fluid level. No pathogens were cultured from his sputum and the left lower lobe fluid level resolved following penicillin treatment. During the next 4 years, pulmonary cysts and some associated nodular densities slowly enlarged (fig. 2C and 2D). By mid-1978, the patient had been hospitalized 54 times for removal of laryngeal and tracheal papillomas and continued to be disabled by this unusual condition.

Discussion

Squamous papilloma is the most common benign tumor of the larynx and histologically represents an abnormal proliferation of stratified squamous epithelium supported by a core of fibrovascular tissue. The etiology of laryngeal papilloma remains obscure although speculation has centered on viral causes since the classic experiment of Ullmann in 1923 [2]. He transplanted a laryngeal papilloma from a 6-year-old boy to his own arm, and then successfully implanted this onto canine vaginal mucosa. More recent indirect evidence of viral causation includes the increased incidence of skin warts in children with laryngeal papillomatosis. Also a retrospective study showed a high incidence of genital warts in mothers whose children had laryngeal papillomas [3].

Spread of laryngeal papillomas through the respiratory tract, termed "tracheobronchial papillomatosis," is rare and occurs in only 2% of patients with laryngeal papillomas. The trachea is most often involved when distal spread occurs [4]. Among a series of 26 patients with tracheobronchial papillomatosis surveyed by Caldarola et al. [5], the trachea alone was affected in 21 patients, the trachea and main bronchi in three, and the bronchi alone in two. Extension of papillomas to involve the distal bronchi, bronchioles, and lung parenchyma has been reported in only 11 prior instances [1, 6]. The natural history of laryngeal papillomas in adults is different than in children. In children, the typical course is one of extensive growth and rapid local recurrence. In adults, laryngeal papillomatosis is less aggressive and distal spread is distinctly unusual [7].

The mode of spread of laryngeal papillomas to involve the tracheobronchial tree is unknown. Peripheral seeding and multicentric origin of papillomas have been advanced as two possible explanations [8, 9]. Tracheostomy and surgical manipulation are thought to induce spread of papillomas to the distal respiratory tree [10]. In



A B

Fig. 1.—Tracheal tomograms in 1969. **A**, Shows multiple endotracheal papillomas. Two sessile masses (*arrows*) arise from lateral tracheal walls. Mass arising from anterior tracheal wall is seen less clearly (*white arrows*). **B**, 1 cm more posterior than **A** shows two additional papillomas arising from lateral tracheal walls at a lower level.

Received December 4, 1978; accepted after revision February 8, 1979.
[1]Department of Radiology, University of California, San Francisco, California 94143. Address reprint requests to W. R. Webb.

© 1979 American Roentgen Ray Society

0361-803X/79/1325-0820 $0.00

the airway in the neck, gas in the deep cervical fascial planes should be considered an extension of mediastinal emphysema, even if the mediastinal component is not radiographically apparent. Mediastinal gas ascends easily into the neck [5] and soft tissue cervical emphysema is often a clue to the correct diagnosis [1, 5]. In a literature review, Silbiger and Kushner [12] found mediastinal or subcutaneous emphysema in 61% of 66 cases of tracheobronchial laceration. Burke [7] stated that in 10% of such injuries there are no radiographic or physical findings to suggest the diagnosis. The yield of early diagnoses would certainly be improved by routine radiography of the cervical soft tissues in patients with severe closed chest trauma. It should be noted that the absence of gas in these locations does not exclude an airway fracture.

The pathway for the passage of gas from the pulmonary interstitium through the hilum to the mediastinum was demonstrated in cats by Macklin [13]. He stated that the amount of gas that accumulated in the pulmonary interstitium and mediastinum was directly dependent upon the pressure of injection of the gas through the intrabronchial cannula. He did not indicate the pressures used in the injections. A pulmonary laceration may permit gas to enter the pulmonary interstitium, but we believe that it would be very unusual for large amounts of gas to be forced into the mediastinum unless the patient has been subjected to positive-pressure ventilation.

Tension pneumothorax and subcutaneous emphysema may develop after rib fracture due to laceration of the visceral and parietal pleura. It is theoretically possible for the subcutaneous gas to dissect into the deep cervical and/or mediastinal fascial planes. However, such a pathway was not mentioned by Evans and Smalldon [14] in their review of mediastinal emphysema, and we are not aware that pneumomediastinum of this origin has ever been documented. Traumatic rupture of the esophagus may cause pneumomediastinum, but this is a rare lesion. Furthermore, in a severe blunt chest injury, a rigid structure such as the tracheobronchial tree is far more likely to rupture than a mobile and elastic one like the esophagus. An esophageal rupture should be sought when a tracheobronchial fracture cannot be demonstrated by bronchoscopy [15].

In some patients, mediastinal or deep cervical emphysema will be apparent on chest radiography only after artificial ventilation. In such instances, these signs are less reliable indicators of a bronchial fracture, but that diagnosis should still be considered.

The presence of a pneumomediastinum or deep cervical emphysema in a patient who has sustained closed trauma to the chest and who has not been subjected to positive-pressure ventilation should arouse strong suspicion of a fracture of the tracheobronchial tree. Such fractures should be recognized promptly in order to avoid complications. Surgical repair, if attempted early, is usually successful.

REFERENCES

1. Kirsh MM, Orringer MB, Behrendt DM, Sloan H: Management of tracheobronchial disruption secondary to nonpenetrating trauma. *Ann Thorac Surg* 22:93–101, 1976
2. Mazzei EA, Mulder DG: Closed-chest injuries to the trachea and bronchus. *Arch Surg* 100:677–680, 1970
3. Bertelsen S, Howitz P: Injuries of the trachea and bronchi. *Thorax* 27:188–194, 1972
4. Guest JL Jr: Major airway injury in closed chest trauma. *Chest* 72:63–66, 1977
5. Eijgelaar A, van der Heide JNH: A reliable early symptom of bronchial or tracheal rupture. *Thorax* 25:120–125, 1970
6. Payne WS, DeRemee RA: Injuries of the trachea and major bronchi. *Postgrad Med* 49:152–158, 1971
7. Burke JF: Early diagnosis of traumatic rupture of the bronchus. *JAMA* 181:682–686, 1962
8. Hood RM, Sloan HE: Injuries of the trachea and major bronchi. *J Thorac Cardiovasc Surg* 38:458–480, 1959
9. Oh KS, Fleischner FG, Wyman SM: Characteristic pulmonary finding in traumatic complete transection of a mainstem bronchus. *Radiology* 92:371–372, 1969
10. Eastridge CE, Hughes FA Jr, Pate JW, Cole F, Richardson R: Tracheobronchial injury caused by blunt trauma. *Am Rev Respir Dis* 101:230–237, 1970
11. Davies D, Hopkins JS: Patterns in traumatic rupture of the bronchus. *Injury* 4:261–264, 1973
12. Silbiger ML, Kushner LN: Tracheobronchial perforation: its diagnosis and treatment. *Radiology* 85:242–246, 1965
13. Macklin CC: Pneumothorax with massive collapse from experimental local overinflation of the lung substance. *Can Med Assoc J* 36:414–420, 1937
14. Evans JA, Smalldon TR: Mediastinal emphysema. *AJR* 64: 375–390, 1950
15. Kirsh MM, Sloan H: *Blunt Chest Trauma: General Principles of Management*. Boston, Little, Brown, 1977, pp 122–123

Laryngeal Papillomatosis with Pulmonary Spread in a 69-Year-Old Man

GARY GLAZER[1] AND W. RICHARD WEBB[1]

Pulmonary involvement by laryngeal papillomatosis is rare. It typically occurs in children or young adults; only one prior case has been reported in a patient over 40 years of age [1]. We report a case of pulmonary involvement by laryngeal papillomatosis occurring in a 69-year-old man. Despite the rarity of this disease in adults, the correct diagnosis may be suggested by a characteristic combination of clinical and radiographic features.

Case Report

In 1967, a 62-year-old man was first evaluated for hoarseness. Laryngoscopy revealed several squamous papillomas of both vocal cords, extending locally into the left supraglottic region. He had no history of cervical irradiation or previous laryngeal papillomas. In 1969, tomograms demonstrated numerous endotracheal papillomas (fig. 1) and tracheostomy was performed which showed papillomas extending down the trachea to the carina and main bronchi. Between 1967 and 1973, the patient was hospitalized 37 times for excision of laryngeal and tracheal papillomas. Chest radiographs during this period remained normal (fig. 2A).

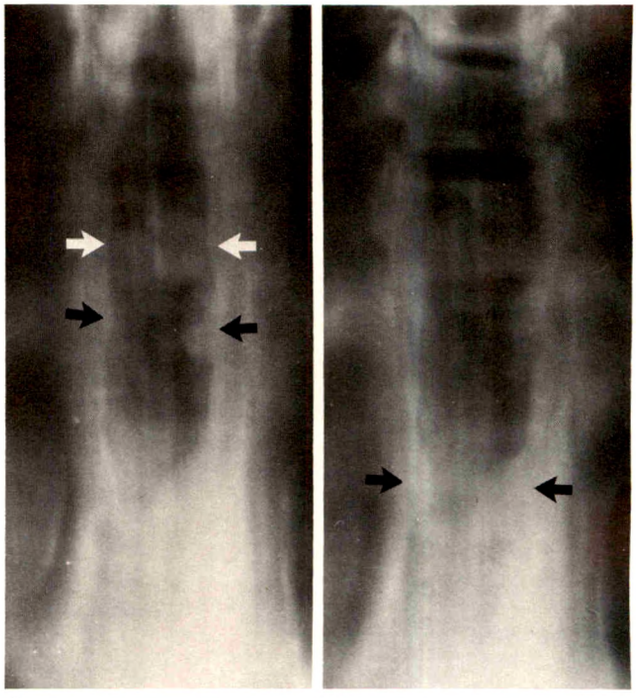
In 1974, chest radiographs showed multiple thin-walled lung cysts typical of pulmonary spread (fig. 2B). A single cyst in the left lower lobe contained an air-fluid level. No pathogens were cultured from his sputum and the left lower lobe fluid level resolved following penicillin treatment. During the next 4 years, pulmonary cysts and some associated nodular densities slowly enlarged (fig. 2C and 2D). By mid-1978, the patient had been hospitalized 54 times for removal of laryngeal and tracheal papillomas and continued to be disabled by this unusual condition.

Discussion

Squamous papilloma is the most common benign tumor of the larynx and histologically represents an abnormal proliferation of stratified squamous epithelium supported by a core of fibrovascular tissue. The etiology of laryngeal papilloma remains obscure although speculation has centered on viral causes since the classic experiment of Ullmann in 1923 [2]. He transplanted a laryngeal papilloma from a 6-year-old boy to his own arm, and then successfully implanted this onto canine vaginal mucosa. More recent indirect evidence of viral causation includes the increased incidence of skin warts in children with laryngeal papillomatosis. Also a retrospective study showed a high incidence of genital warts in mothers whose children had laryngeal papillomas [3].

Spread of laryngeal papillomas through the respiratory tract, termed "tracheobronchial papillomatosis," is rare and occurs in only 2% of patients with laryngeal papillomas. The trachea is most often involved when distal spread occurs [4]. Among a series of 26 patients with tracheobronchial papillomatosis surveyed by Caldarola et al. [5], the trachea alone was affected in 21 patients, the trachea and main bronchi in three, and the bronchi alone in two. Extension of papillomas to involve the distal bronchi, bronchioles, and lung parenchyma has been reported in only 11 prior instances [1, 6]. The natural history of laryngeal papillomas in adults is different than in children. In children, the typical course is one of extensive growth and rapid local recurrence. In adults, laryngeal papillomatosis is less aggressive and distal spread is distinctly unusual [7].

The mode of spread of laryngeal papillomas to involve the tracheobronchial tree is unknown. Peripheral seeding and multicentric origin of papillomas have been advanced as two possible explanations [8, 9]. Tracheostomy and surgical manipulation are thought to induce spread of papillomas to the distal respiratory tree [10]. In



A B

Fig. 1.—Tracheal tomograms in 1969. **A**, Shows multiple endotracheal papillomas. Two sessile masses (*arrows*) arise from lateral tracheal walls. Mass arising from anterior tracheal wall is seen less clearly (*white arrows*). **B**, 1 cm more posterior than **A** shows two additional papillomas arising from lateral tracheal walls at a lower level.

Received December 4, 1978; accepted after revision February 8, 1979.
[1]Department of Radiology, University of California, San Francisco, California 94143. Address reprint requests to W. R. Webb.

© 1979 American Roentgen Ray Society

0361-803X/79/1325-0820 $0.00

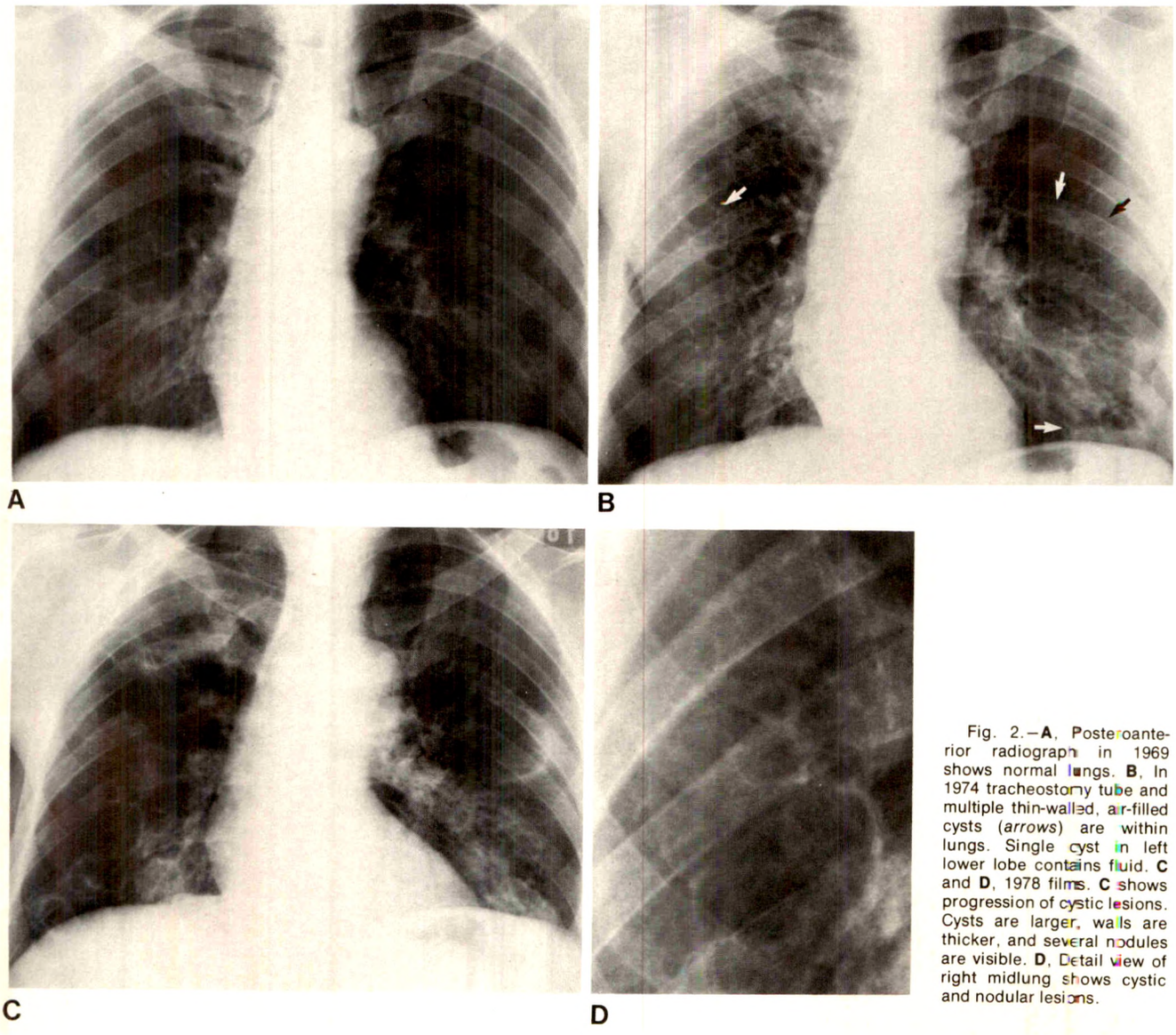


Fig. 2.—**A**, Posteroanterior radiograph in 1969 shows normal lungs. **B**, In 1974 tracheostomy tube and multiple thin-walled, air-filled cysts (*arrows*) are within lungs. Single cyst in left lower lobe contains fluid. **C** and **D**, 1978 films. **C** shows progression of cystic lesions. Cysts are larger, walls are thicker, and several nodules are visible. **D**, Detail view of right midlung shows cystic and nodular lesions.

fact, a review of published cases of pulmonary involvement in laryngeal papillomatosis shows that all patients but one [1] have had tracheostomy and multiple surgical procedures [4, 6, 8, 10, 11]. Hypomagnesemia, at one time felt to correlate with recurrence of papillomas (12), is no longer considered to be related to recurrence or spread.

In a collective review of 10 patients with pulmonary involvement by papillomas [6], nine had laryngeal lesions diagnosed by age 7. The tenth had his laryngeal papillomas discovered at the age of 22. Pulmonary involvement occurs an average of 15 years after laryngeal tumors appear and has ranged up to 36 years. Among the series of 10 patients reviewed by Smith and Gooding [6], the eldest patient was 32 years old when pulmonary spread was first detected. In the single case reported by Kaufman and Klopstock [1], pulmonary cysts and laryngeal papillomas were first diagnosed in a 47-year-old man. Our patient is, by far, the oldest patient yet described with pulmonary involvement by laryngeal papillomatosis, and is also somewhat unique in that his laryngeal papillomas developed at the age of 62. Occurrence of typical tracheal, bronchial, or pulmonary papillomas rarely occurs without evidence of prior laryngeal lesions. Elliott et al. [13] reported a 53-year-old man who developed a single papilomatous cyst in the left lung without evidence of a laryngeal lesion.

Radiographically, tracheal and bronchial papillomas are difficult to recognize without bronchograms or tomograms, and even tomograms may not clearly define endobronchial or endotracheal lesions. In patients with bronchial lesions, bronchial obstruction with recurrent obstructive pneumonias or bronchiectasis are often present. When pulmonary spread occurs, however, multiple thin-walled cystic lesions are typically seen. These are probably due to cavitation of papillomas or bronchial

obstruction by papillomas with distal airtrapping and pneumatocele formation. These cysts are characteristically lined by squamous epithelium. Occasionally large papillomas growing within cysts are visible radiographically as nodular densities within a cavity. Small lung nodules, representing pulmonary papillomas, are occasionally seen [6]. As in our case, fluid levels developing within pulmonary cysts are common and have been seen in five of 11 reported cases [1, 4, 8, 11, 14]. They probably represent bacterial superinfection within cysts and promptly respond to antibiotic therapy.

The radiographic differential diagnosis of thin-walled cysts includes metastatic tumor, fungal disease, tuberculosis, septic embolism and infarction, cystic bronchiectasis, rheumatoid nodules, amyloidosis, sarcoidosis, Wegener's granulomatosis, and hydatid cysts. However, the association of thin-walled cysts with laryngeal and tracheal lesions or upper airway obstruction as occurs in papillomatosis is more specific; this combination of findings could occur with metastatic laryngeal carcinoma, tuberculosis, occasional fungal infections, or amyloidosis. When, in addition, the slow progression of pulmonary cysts characteristic of patients with papillomatosis is also considered, this diagnosis becomes even more likely. More rapid progression would be expected to occur with metastatic tumor or infectious processes.

The treatment of laryngeal papillomatosis is difficult. The mainstay of therapy is surgical removal, but as in this case, recurrence is common. Large tracheobronchial papillomas require endoscopic surgical removal in order to avoid airway obstruction. Cystic pulmonary lesions, in themselves, are not symptomatic and require no treatment unless infected. Lobectomy or wedge resection for removal of pulmonary cysts is not recommended. Since pulmonary lesions are multiple and may recur, repeated surgical resections would leave the patient with little remaining pulmonary tissue.

The risk of malignancy in patients with pulmonary involvement by laryngeal papillomatosis is unknown. Complicating the issue is the fact that several patients with pulmonary papillomatosis have received therapeutic irradiation to the larynx. None of the children with pulmonary involvement by papillomas have developed malignancy, although follow-up has been short. The adult with lung and laryngeal papillomas reported by Buffmire et al. [14] died at age 48 from squamous cell carcinoma of the bronchus [15]. The patient reported by Greenfield and Herman [16] developed a squamous cell carcinoma of the lung with intrapulmonary lymph node metastases.

Pulmonary spread of laryngeal papillomatosis should be considered as the diagnosis of choice in the patient with known laryngeal papillomas and pulmonary cysts. This is particularly true if the patient has had a tracheostomy. Until the risk of malignancy in adults with pulmonary papillomatosis is better known, close follow-up is indicated.

REFERENCES

1. Kaufman G, Klopstock R: Papillomatosis of the respiratory tract. *Am Rev Respir Dis* 88:839–846, 1963
2. Ullmann EV: On the aetiology of the laryngeal papilloma. *Acta Otolaryngol* 5:317–334, 1923
3. Bone R, Feren A, Nahum A, Winkelhake B: Laryngeal papillomatosis: Immunologic and viral basis for therapy. *Laryngoscope* 86:341–348, 1976
4. Rosenbaum H, Alavi S, Bryant L: Pulmonary parenchymal spread of juvenile laryngeal papillomatosis. *Radiology* 90: 654–660, 1968
5. Caldarola VT, Harrison EG, Clagett OT, and Schmidt HW: Benign tumors and tumorlike conditions of the trachea and bronchi. *Ann Otol Rhinol Laryngol* 73:1042–1061, 1964
6. Smith L, Gooding C: Pulmonary involvement in laryngeal papillomatosis. *Pediatr Radiol* 2:161–166, 1974
7. Cook T, Brunschwig J, Butel J, Cohn A, Goepfert H, Rawls W: Laryngeal papilloma: Etiologic and therapeutic considerations. *Ann Otol Rhinol Laryngol* 82:649–655, 1973
8. Moore R, Lattes R: Papillomatosis of larynx and bronchi: case report with 34 year follow-up. *Cancer* 12:117–126, 1959
9. Hitz H, Oesterlin E: A case of multiple papillomata of the larynx with aerial metastases to lungs. *Am J Pathol* 8:333–338, 1932
10. Singer S, Greenberg S, Harrison G: Papillomatosis of the lung. *Am Rev Respir Dis* 94:777–781, 1966
11. Kirchner J: Papilloma of the larynx with extensive lung involvement. *Laryngoscope* 61:1022–1029, 1951
12. Hollinger P, Schild J, Maurizi D: Laryngeal papilloma: review of etiology and therapy. *Laryngoscope* 78:1462–1474, 1968
13. Elliott GB, Belkin A, Donald WAJ: Cystic bronchial papillomatosis. *Clin Radiol* 13:62–67, 1962
14. Buffmire D, Clage HO, McDonald J: Papillomas of the larynx, trachea, and bronchi: report of a case. *Mayo Clinic Proc* 25:595–600, 1950
15. Castleman B, Towne V: Case 43361. Case records of the Massachusetts General Hospital. *New Engl J Med* 257:465–471, 1957
16. Greenfield H, Herman P: Papillomatosis of the trachea and bronchi. *AJR* 89:45–50, 1963

Lymphomatoid Granulomatosis Involving the Central Nervous System: Radiologic-Pathologic Correlation

JOSEPH F. SACKETT,[1] GABRIELLE M. ZuRHEIN,[2] AND SULTAN M. BHIMANI[1]

Lymphomatoid granulomatosis was first described in 1972 by Liebow et al. [1] in their study of 40 cases. Certain features of lymphomatoid granulomatosis resemble lymphoma, while others resemble Wegener's granulomatosis. It does not involve the reticuloendothelial system. Lesions of the central nervous system were considered relatively common [1], and were detected clinically, by postmortem examination, or by both in 22.5% of the cases. The histopathology of lymphomatoid granulomatosis is focused on blood vessels. Arteries and veins are commonly infiltrated with numerous atypical mononuclear cells that may cause constriction of the lumen. Necrosis of vessels and a chiefly fibrinous thrombosis is also seen. In stages of healing, as can result from steroid therapy, fibrous thickening of vessel walls, focal loss of muscle tissue, and recanalization of thrombi may be observed [1].

Case Report

A 38-year-old woman was first seen for cough, fever, rash, weakness, and chest pain. Physical examination was normal except for fine rales in both lung bases. Routine laboratory studies, VDRL, and lupus erythematosus preparations were normal. Chest radiography showed several nodular densities. A lung biopsy was interpreted as lymphomatoid granulomatosis. Oral steroid therapy was started with a dose of 18 mg/day. This regimen was continued for 6 months, at which time the pulmonary lesions had cleared. When the steroid therapy was reduced 1 month later, the patient developed neurologic symptoms. She was readmitted 6 months after her first admission and lung biopsy because of headaches, weakness, numbness of the left hand, intermittent aphasia, episodes of vertigo, and memory loss. On physical examination, she was obtunded and had drift of the left upper extremity. Cerebrospinal fluid protein was 90 mg/100 ml and blood cell count showed 60 lymphocytes/mm^3. Cerebrospinal fluid pressure was 350 ml of water. Steroid therapy was increased. Her neurologic symptoms improved, and she was discharged. She was readmitted 2 months later with progression of neurologic signs. A ventriculoperitoneal shunt was performed. After this, she progressed into coma and died 10½ months after onset of pulmonary symptoms.

Findings

When the patient was readmitted with her first signs of neurologic symptoms, a radionuclide brain scan showed abnormal uptake in both temporal lobes and right parietal lobe. Computed tomography (CT) showed slight ventricular enlargement. After intravenous injection of contrast material, three lesions were defined on CT that had nonhomogeneous reduced density with central contrast enhancement (fig. 1A). On her final admission before dying, repeat CT showed progression of the previously described lesions, as well as an additional mass in the cerebellar vermis (fig. 1A). Repeat radionuclide scan had abnormal uptake in both temporal lobes, right parietal lobe, and cerebellar vermis (fig. 1B). Cerebral angiography confirmed the presence of an avascular mass in the cerebellar vermis. Sylvian segments of both middle cerebral arteries showed caliber variations: focal constriction adjacent to aneurysmal dilatation (fig. 2). Angiographic findings were interpreted as necrotizing vasculitis.

The autopsy permit was restricted to the brain. Three major lesions were found in the cerebrum and two in the cerebellum. Each consisted of a central area of necrosis and peripheral edema of variable extent (fig. 3). All cerebral lesions involved chiefly the cortex and extended into the pia-arachnoid and the subcortical white matter. Almost symmetric 2 × 3 cm necroses involved the perisylvian tissue in each hemisphere, especially the superior temporal gyri, frontal opercular gyri, and portions of insulae. Together with the collateral edema, the anteroposterior extent of these lesions was 8 cm. Blood vessels were conspicuous in the lesions, especially branches of the middle cerebral arteries in the sylvian cisterns or in sulci (fig. 3A). These vessels had stiff, thickened walls and showed aneurysmal dilatation of the lumina. The second lesion of the right hemisphere was located dorsolaterally within the frontoparietal lobes and was 3.5 cm, including collateral edema. It also contained an artery with aneruysmal dilatation with a total width of 2 mm and a lumen of 1.5 mm (fig. 4A). The larger of the cerebellar lesions, 4 cm, was associated with considerable recent hemorrhage. It involved the vermis and contiguous portion of the left cerebellar hemisphere. Another necrosis, 2 cm and nonhemorrhagic, extended along the periphery of the right cerebellar hemisphere.

By light microscopy, an extensive and variegated angiopathy of veins and arteries was present within the parenchyma and pia around the necroses. The arteries, which on gross inspection showed aneurysmal dilatation, were about twice the diameter of uninvolved pial arteries in the same location (figs. 4A and 4B). Their intima was greatly thickened by connective tissue of varying cellularity and collagen content. On occasion, cushionlike intimal projections into the lumen were

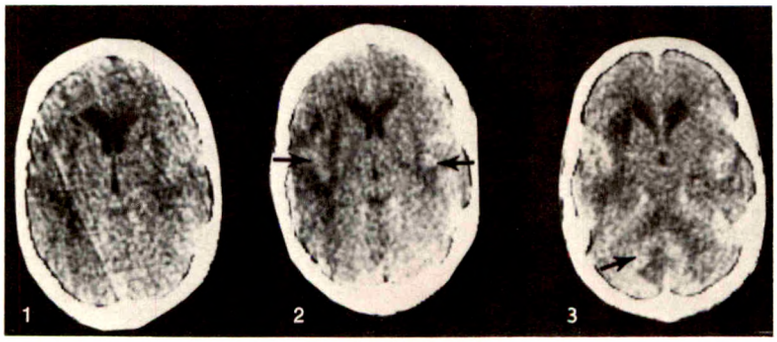
Received August 1, 1978; accepted after revision January 30, 1979.

[1]Department of Radiology, University of Wisconsin Medical Center, 1300 University Avenue, Madison, Wisconsin 53706. Address reprint requests to J. F. Sackett.

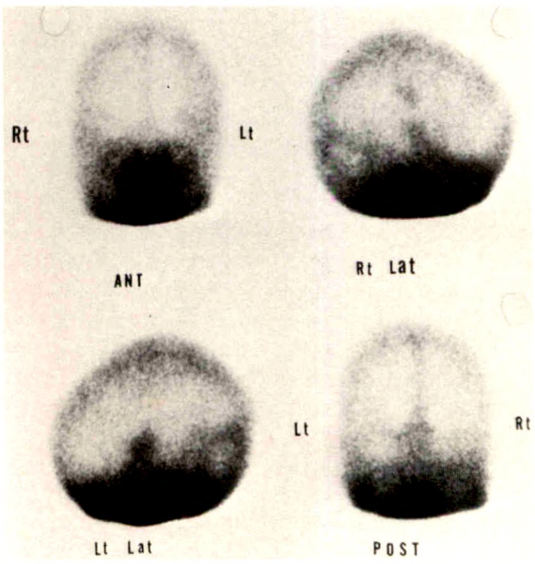
[2]Department of Pathology, University of Wisconsin Medical Center, Madison, Wisconsin 53706.

© 1979 American Roentgen Ray Society

0361–803X/79/1325–0823 $0.00



A



B

Fig. 1.—**A**, Serial CT. (1) Precontrast. Bilateral temporal lobe lesions of reduced density, poorly defined borders, and nonhomogeneous. (2) Postcontrast 4 days later. Centers of temporal lobe lesions enhance slightly with irregular margins (*arrows*). (3) Postcontrast 1 month later. Cerebellar vermis enhancing lesion (*arrow*) and more enhancement of temporal lobe lesions. **B**, Technetium pertechnetate brain scan. Four lesions identified: one in each temporal lobe, one in right frontoparietal lobes, and one in midline posterior fossa.

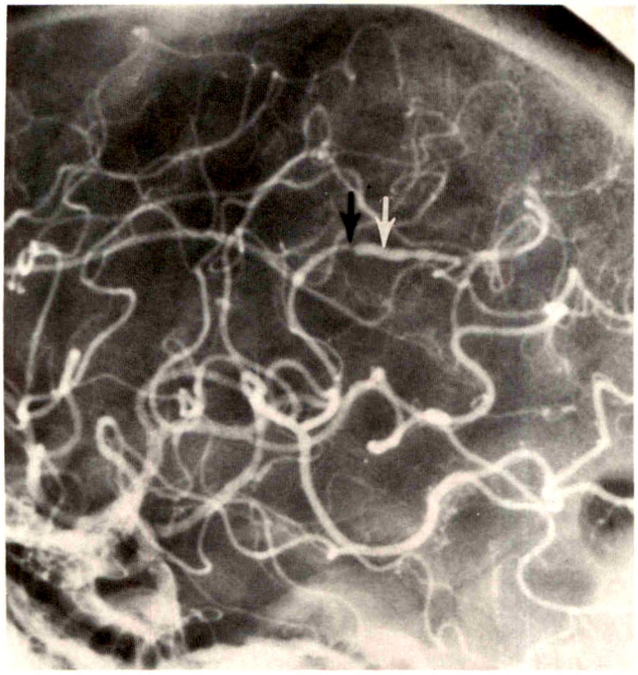


Fig. 2.—Right carotid arteriogram. Caliber variation of portions of middle cerebral artery, constriction of vessel (*black arrow*) and aneurysmal enlargement of vessel (*white arrow*).

suggestive of organized thrombotic material. Elastic membranes were interrupted and were lost in many areas, and there was fibrinoid necrosis of all wall layers and infiltration with lymphocytes, plasma cells, large immature mononuclear cells, and phagocytes. In some cross-sectioned vessels, the lumina were found drawn out toward the area of most advanced destructive change in the walls (fig. 4C).

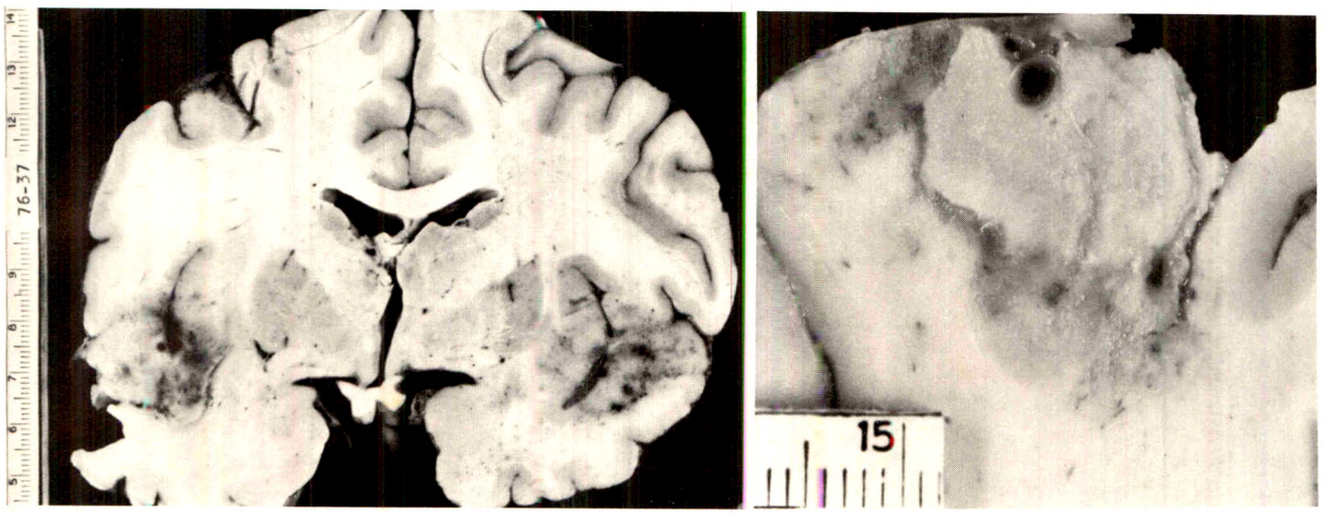
Most of the vessels showed expanded walls and constricted lumina as a result of proliferation of pleomorphic, often primitive-appearing mononuclear cells (fig. 4D). Mitoses were seen, especially in areas where severe infiltrates coalesced to form lymphomalike lesions. A smaller number of vessels had undergone fibrinoid necrosis of their walls. Thrombosis was a complication of all three types of vascular lesions.

Discussion

The central nervous system involvement with lymphomatoid granulomatosis developed while the patient's pulmonary disease was under control with steroid therapy. Technetium pertechnetate brain scan showed several regions of increased radionuclide uptake. This multifocal disturbance in blood-brain barrier is nonspecific, but suggests metastatic neoplasm, multiple cerebral infarcts with unusual distribution, or multiple inflammatory lesions. The CT scan had poorly defined areas of nonhomogeneous reduced density and slight ventricular enlargement. The center of these lesions enhanced with contrast material. Again, these findings are nonspecific and suggest the same differential diagnosis as the nuclide brain scan. Cerebral angiography showed marked aneurysmal dilatation and constriction of the sylvian segments of both middle cerebral arteries. These angiographic findings suggest infiltration and necrosis of major intracerebral arteries. Angiographic technique was direct serial ×2 magnification. The major intracerebral arteries that demonstrated the caliber variation were 1–2 mm. The resolution in this angiographic system allows good definition down to 0.2 mm vessel size [2].

The combination of radionuclide, CT, and angiographic findings indicates infiltration and necrosis of major arteries with subsequent intracerebral edema or encephalomalacia. The cause for the ventricular enlargement is uncertain, but may be secondary to the mass in the cerebellar vermis.

Gross autopsy findings in the brain confirmed the presence of thickened major blood vessel walls with



A B

Fig. 3.—Coronal sections. **A**, Formalin-fixed brain. Almost symmetrically placed lesions in insulae and neighboring frontotemporal gyri vascularity and necrosis. **B**, Necrotic lesion. Aneurysmally dilated artery in frontoparietal cortex and subcortex.

surrounding brain necrosis and edema. Microscopic findings also confirmed the radiographic findings of aneurysmal enlargement and breakdown of blood vessel walls, infiltration of blood vessels, and thrombosis. The CT and radionuclide scans were very sensitive for demonstrating the lesions, but the findings on these scans were nonspecific. Cerebral angiography demonstrated the necrotizing vasculitis. Leeds et al. [3] stated that segmental narrowing of vessels and vascular irregularities may occur in patients with cerebral lymphoma. They do not mention aneurysmal arterial dilatation.

Four cases of central nervous system involvement with lymphomatoid granulomatosis have recently been reported. Verity and Wolfson [4] reported two cases and Peña [5] reported one case with central nervous system involvement. Only two of these three cases had pathologic evidence of central nervous system involvement. Neither of these two cases with histologic confirmation had the vascular abnormalities discussed in our case. A case of Kokmen et al. [6] had no clinical extracerebral disease. At autopsy he had lymphomatoid granulomatosis at the base of the right lung and, chiefly, of the brain stem. Neuroradiologic workup, including left carotid and left vertebral angiography, isotope scan, and pneumoencephalography, demonstrated only slightly ventricular enlargement [6]. CT scan was not reported. The vascular changes seen in our case were not observed. If the small pontine arteries were involved with a necrotic infiltrating process similar to our case, it would be difficult to detect on usual vertebral angiography.

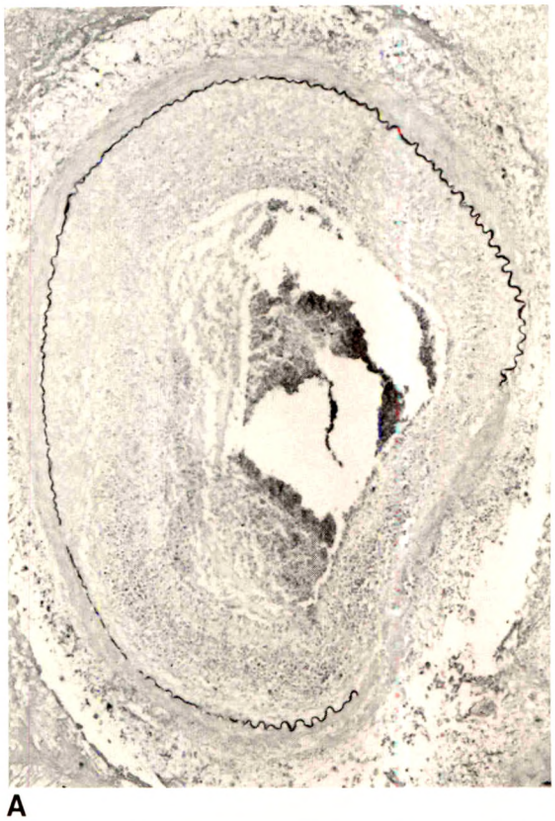
Aneurysmal dilatation in association with vasculopathy of lymphomatoid granulomatosis was not part of the original description of Liebow et al. [1]. Angiographic and histopathologic correlation in our case confirms that the necrotizing vasculopathy in lymphomatoid granulomatosis can result in aneurysm formation, as well as constriction of vessel lumina and thromboses.

ACKNOWLEDGMENTS

We thank Evelyn Ireland and John Blomquist for technical assistance in tissue preparation and photography, and Dr. V. H. Dahl, Mercy Medical Center, Oshkosh, Wisconsin for the lung biopsy.

REFERENCES

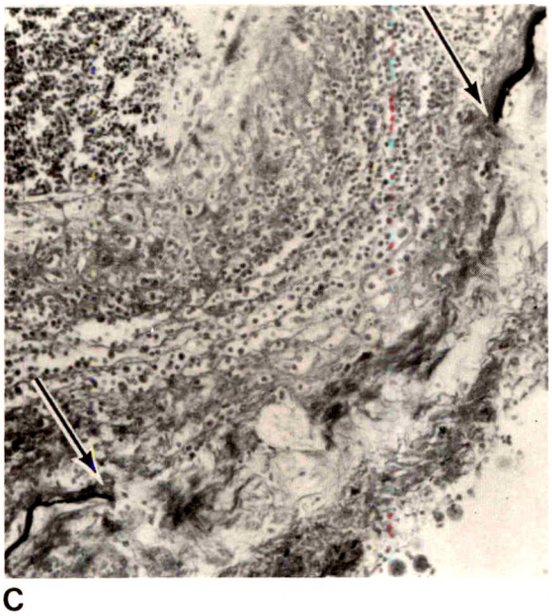
1. Liebow AA, Carrington CR, Friedman J: Lymphomatoid granulomatosis. *Hum Pathol* 3:457–558, 1972
2. Hale J, Mishkin MM: Serial direct magnification cerebral angiography. Theoretical aspects. *AJR* 107:616–621, 1969
3. Leeds NE, Rosenblatt R, Zimmerman HM: Focal angiographic changes of cerebral lymphoma with pathological correlations. *Radiology* 99:595–599, 1971
4. Verity MA, Wolfson WL: Cerebral lymphomatoid granulomatosis: a report of two cases, with disseminated necrotizing leukoencephalopathy in one. *Acta Neuropathol* (Berlin) 36:117–124, 1976.
5. Peña CE: Lymphomatoid granulomatosis with cerebral involvement: light and electron microscopic study of a case. *Acta Neuropathol* (Berlin) 37:193–197, 1977
6. Kokmen E, Billman JK, Abell MR: Lymphomatoid granulomatosis clinically confined to the CNS. *Arch Neurol* 34:782–784, 1977



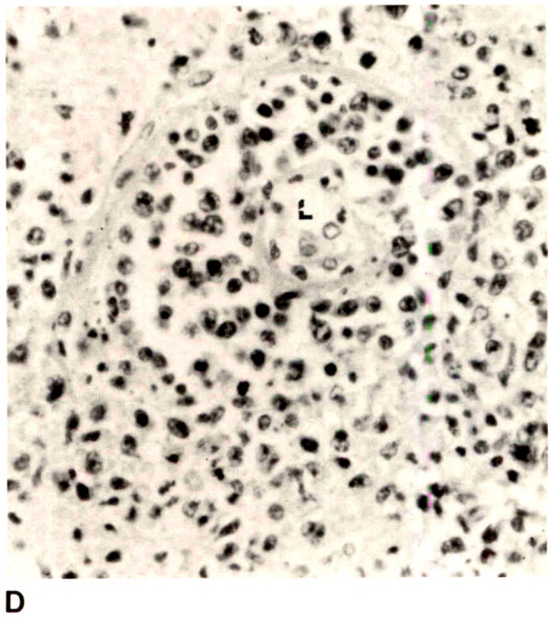
A



B



C



D

Fig. 4.—**A**, Aneurysmally dilated pial artery (see fig. 3B). Intimal thickening and thinning and focal necrosis of media and elastica (×45). **B**, Uninvolved pial artery (×45). **C**, Segment of anerysmally dilated pial artery. Focal herniation of infiltrated and thickened intima at site of media necrosis and disintegration of elastica (*arrows*). (Elastica and van Gieson × 120.) **D**, Vascular and perivascular infiltrates of various lymphoreticular cells with encroachment on lumen (L). (H and E × 320.)

Pseudo Thick-Walled Renal Cyst by CT

ARTHUR J. SEGAL[1] AND ROBERT M. SPITZER[1]

Wider application of abdominal computed tomography (CT) has resulted in its use to image a variety of renal masses. Sometimes the renal mass is the reason for the examination and sometimes its discovery is fortuitous. Conventional uroradiographic criteria for the differentiation of benign cysts from complex cysts and solid lesions have been applied to CT and are generally reliable. A notable exception may occur when the "beak" of renal parenchyma adjacent to a cyst wall is imaged in cross section. This gives the illusion of a thick-walled cyst and could lead to an erroneous diagnosis of malignancy.

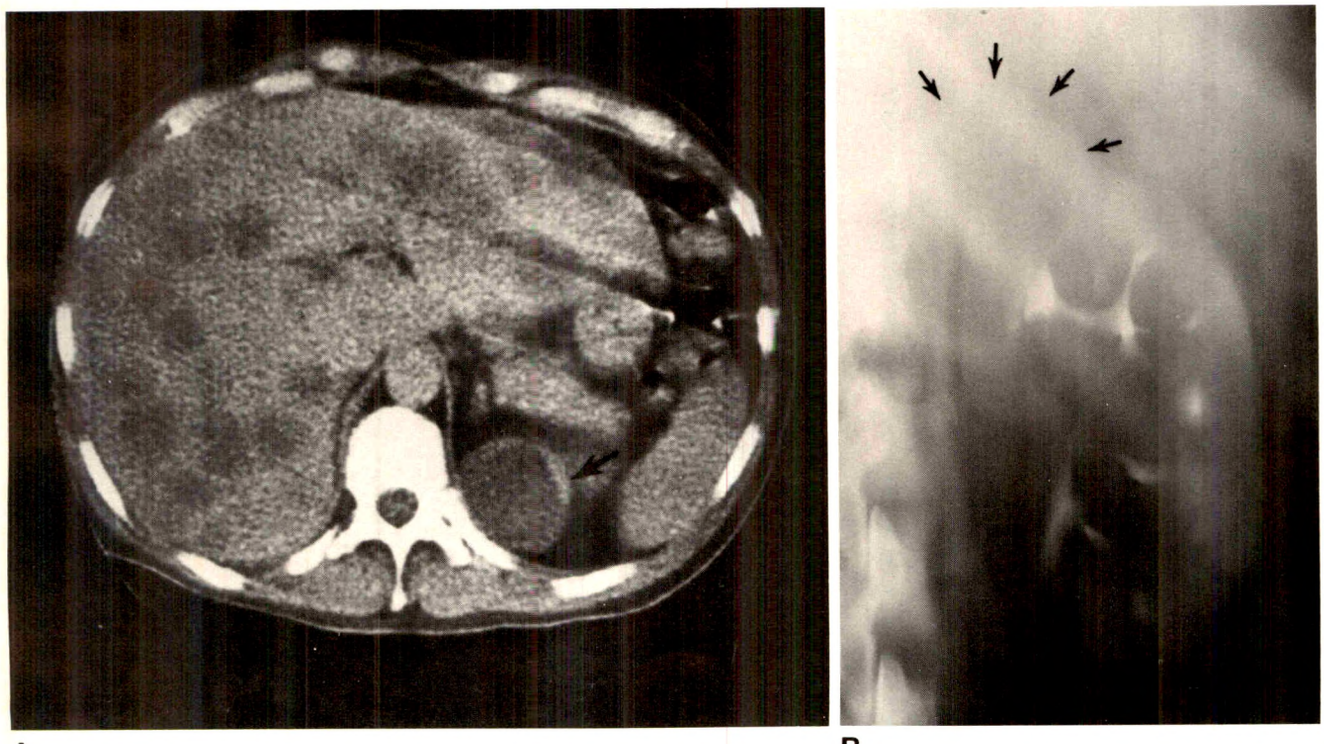
Case Report

E. D., a 56-year-old man with known metastatic lung carcinoma, had abdominal CT which confirmed liver metastases. In addition, a left upper pole renal mass was identified (fig. 1A). Because of a thick wall and the consequent possibility of neoplasm, the renal mass was further evaluated by excretory urography with nephrotomography (fig. 1B). A cyst puncture confirmed the urographic diagnosis of benign simple cyst.

Discussion

At excretory urography with nephrotomography, benign, simple renal cysts are sharply separated from surrounding renal parenchyma and their walls are thin and smooth. Cysts are homogeneous, appear relatively less dense than normal renal parenchyma, and, when located on the surface of the kidney, will often lift up a small rim of parenchyma ("beak") at the interface of the cyst and normal kidney (figs. 2A and 2B) [1–3].

Our experience indicates that most of these criteria for the diagnosis of a benign renal cyst established for nephrotomography also apply to CT. However, in a CT cross section through the "beak" of normal parenchyma (figs. 2B and 2D) adjacent to a renal cyst, the wall of the cyst will appear thick. This single finding should not lead to a diagnosis of complex cyst or malignancy, as in excretory urography [4]. Rather, in these selected cases, the CT examination should be evaluated in conjunction with more conventional examinations for the workup of



A B

Fig. 1.—**A**, Left upper pole renal mass with thick rim (*arrow*). **B**, Nephrotomogram. Thin peripheral margin (*arrows*), "beak," and relative mass lucency.

Received October 27, 1978; accepted after revision January 26, 1979.
[1]Department of Radiology, Rochester General Hospital, 1425 Portland Avenue, Rochester, New York 14621. Address reprint requests to A. J. Segal.

© 1979 American Roentgen Ray Society

0361-803X/79/1325-0827 $0.00

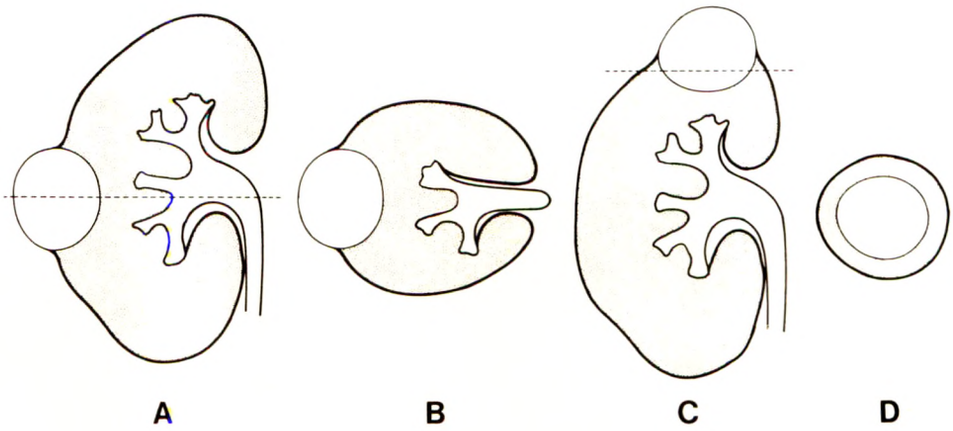


Fig. 2.—Kidney, benign cyst. **B**, Transverse section at level indicated in **A**. Rim is thin and well defined, "beak" clearly depicted, center of cyst is of water density (all classic signs of benign renal cyst). **C**, Relation of "beak" to adjacent normal renal parenchyma. **D**, Transverse section at level indicated in **C**. Rim appears too thick to be cyst by classic uroradiographic criteria.

renal masses to ascertain the true character of the lesion wall [3, 4].

REFERENCES

1. Chynn KY, Evans JA: Nephrotomography in the differentiation of renal cyst from neoplasm: a review of 500 cases. *J Urol* 83:21–24, 1960
2. Greene LF, Witten DM, Emmett JL: Nephrotomography in urologic diagnosis. *J Urol* 91:184–189, 1964
3. Witten DM, Myers GH Jr, Utz DC: *Emmett's Clinical Urography—An Atlas and Textbook of Roentgenologic Diagnosis*, 4th ed, Philadelphia, Saunders, 1977
4. Bosniak MA, Faegenburg C: The thick-wall sign: an important finding in nephrotomography. *Radiology* 84:692–697, 1965

Percutaneous CT-Guided Pancreatography and Pseudocystography

JOHN R. HAAGA,[1] L. M. HIGHMAN,[2] AVRAM V. COOPERMAN,[2] AND F. J. OWENS[3]

The diagnosis of pancreatic pseudocyst can be accomplished with a variety of techniques including gray scale ultrasound [1], computed tomography (CT) [2] and endoscopic retrograde pancreatography [3]. Traditionally ultrasound and CT have been the methods of choice for detection of pseudocysts within the pancreas while endoscopic retrograde cholangiopancreatography has been reserved to determine the anatomic configuration of the pancreatic duct and possible communication with a pseudocyst. We report a case which demonstrates the value of CT in diagnosis of a pancreatic pseudocyst when other methods had failed. In addition, this case reaffirms the usefulness of CT-guided aspiration procedures and illustrates a new technique for demonstration of communication between a pancreatic pseudocyst and the pancreatic duct.

Case Report

A 31-year-old black man was admitted for evaluation of chronic pancreatitis secondary to alcohol ingestion. Five months earlier, while hospitalized elsewhere, laboratory studies demonstrated elevation of the serum amylase and pseudocysts in the head and tail of the pancreas. His symptoms had abated for 4 months when he again experienced epigastric discomfort. A gray scale ultrasound scan demonstrated no abnormalities within the head and body of the pancreas. However, the tail of the pancreas was not seen. Computed tomography demonstrated a pseudocyst in the distal tail of the pancreas as well as dilatation of the pancreatic duct in the tail immediately adjacent to the pseudocyst (fig. 1A). Moreover, a small calcification in the body of the pancreas proximal to the area of dilatation in the pancreatic duct was noted. Endoscopic retrograde cholangiopancreatography was attempted but was unsuccessful. Serum amylase levels and amylase clearances were normal.

CT-guided puncture of the pancreatic pseudocyst was performed (fig. 1B). Before drainage was attempted, injected iso-osmolar contrast material opacified the pseudocyst and a dilated pancreatic duct indicating communication between them (fig. 1B and 1C). The fluid aspirated from the pancreatic pseudocyst contained 17,000 amylase units. A drainage catheter was left in place because of the communication with the pancreatic duct. Sequential serum amylase levels were slightly elevated immediately after the procedure but returned to normal within 24 hr. Because of the communication with the duct, internal drainage was chosen as the method of treatment.

One week later, laparotomy confirmed a pseudocyst involving the tail of the pancreas, spleen, and greater curvature of the stomach. A distal 60% pancreatectomy was performed along with a Roux-en-Y pancreaticojejunostomy.

Discussion

Pancreatic pseudocysts arise from disruption of pancreatic duct and acinar tissue as a result of inflammation, trauma, or tumor. Because of enzymes within the cyst fluid, there is a potential for pseudocyst rupture, hemorrhage, peritonitis, and sepsis; all of which have high associated morbidity and mortality. To avoid such com-

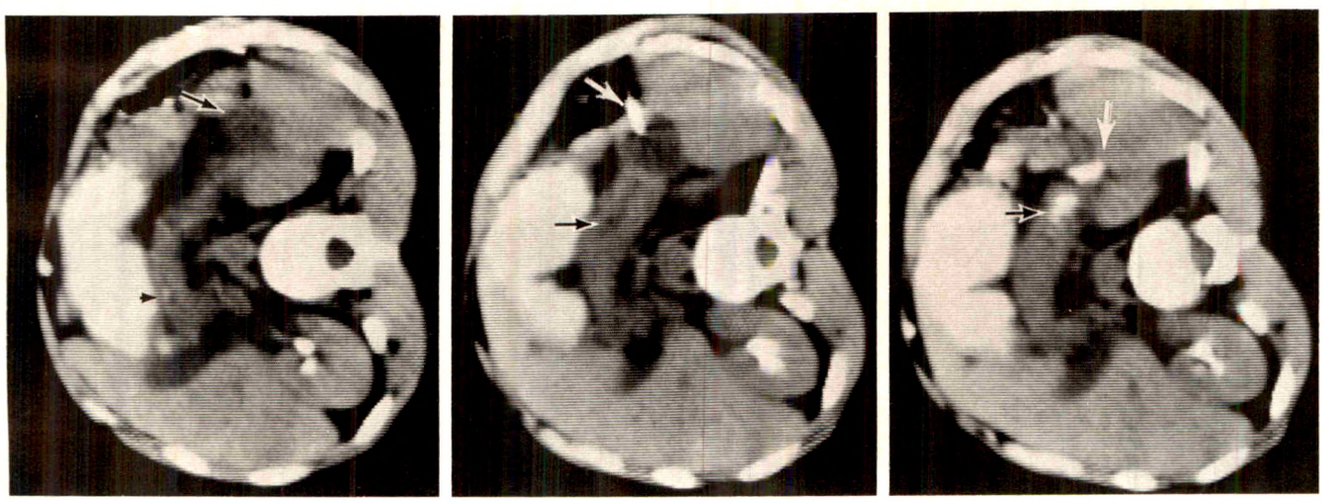


Fig. 1.—Scans with patient in right decubitus position. **A**, Cystic collection in hilum of spleen (*arrow*). Small calcification within body of pancreas (*arrowhead*). **B**, During CT aspiration of pancreatic pseudocyst. Needle is in pseudocyst (*white arrow*). Note dilatation of pancreatic duct (*arrow*). **C**, After injection of iso-osmolar contrast material. Contrast level in pancreatic pseudocyst is indicated by *white arrow*. Note contrast material filling dilated pancreatic duct (*arrow*).

Received August 1, 1978; accepted after revision January 3, 1979.
[1]Department of Radiology, Cleveland Clinic Foundation, 9500 Euclid Avenue, Cleveland, Ohio 44106. Address reprint requests to J. R. Haaga.
[2]Department of Surgery, Cleveland Clinic Foundation, Cleveland, Ohio 44106.
[3]Department of Gastroenterology, Cleveland Clinic Foundation, Cleveland, Ohio 44106.

© 1979 American Roentgen Ray Society

0361-803X/79/1325-0829 $0.00

plications, surgical intervention is desirable if spontaneous resolution does not occur within 6–8 weeks [4–11]. In cases in which the pancreatic pseudocyst does not communicate with the pancreatic duct, external drainage may be feasible either surgically or percutaneously. On the other hand, if there is communication between duct and cyst, internal drainage is the preferred treatment because of the lower morbidity and recurrence [4–11].

With the development of sophisticated cross-sectional imaging techniques, there has been renewed interest in percutaneous external drainage. In a previously reported series [12], ultrasonically guided puncture of pseudocysts was performed on 19 occasions in eight patients. Although the authors did not comment on the relation of pancreatic duct communication to recurrence, others have found that up to 34% of externally drained pseudocysts recur because of continued communication with the pancreatic duct [9]. For this reason, preoperative or operative pancreatography has been advocated to determine the most satisfactory treatment [11, 14]. Until now, endoscopic retrograde cholangiopancreatography has been the most useful method of determining the presence of pancreatic duct communication. However, for technical reasons, not all examinations are successful.

Although we report only a single case, we believe our technique is useful for obtaining information about potential communication of the pancreatic duct with a pancreatic pseudocyst. Either ultrasound or CT can be used when puncturing such pseudocysts [12, 15]; however, CT is capable of visualizing iodinated contrast material [15]. In our case, contrast material injection enabled demonstration of the communication of the pseudocyst with the pancreatic duct. Moreover, because of density sensitivity of CT, it was possible to use iso-osmolar contrast material. Although, to our knowledge, it has not been suggested that hypertenic contrast material causes or aggravates pancreatitis, we hesitate to use such contrast because of the possibility of producing hyperosmolar damage which might initiate or perpetuate pancreatitis. In this case we used iso-osmolar contrast, and intend to do so in similar cases in the future.

REFERENCES

1. Stuber JI, Templeton AW, Bishop K: Sonographic diagnosis of pancreatic lesions. *AJR* 116:406–412, 1972
2. Haaga JR, Alfidi RJ, Zelch MG, Meaney TF, Boller M, Gonzalez L, Jelden GL: Computed tomography of the pancreas. *Radiology* 120:589–595, 1976
3. Silvis SE, Vennes JA: Endoscopic pancreatography in the evaluation of patients with suspected pancreatic pseudocysts. *Am J Gastroenterol* 61:452–459, 1974
4. Rosenberg IK, Kahn JA, Walt AJ: Surgical experience with pancreatic pseudocysts. *Am J Surg.* 117:11–17, 1969
5. Murphy RF, Hinkamp JF: Pancreatic pseudocysts. *Arch Surg* 81:564–568, 1960
6. Thomford NR, Jesseph JE: Pseudocyst of the pancreas: A review of fifty cases. *Am J Surg* 118:86–94, 1969
7. Kaiser GC, King RD, Kilman J, Lempke RE, Shumacher HB: Pancreatic pseudocysts. *Arch Surg* 80:275–281, 1964
8. Tucker PC, Webster PD: Traumatic pseudocysts of the pancreas. *Arch Intern Med* 129:583–586, 1972
9. Becker WF, Pratt HS, Ganji H: Pseudocysts of the pancreas. *Surg Gynecol Obstet* 127:744–747, 1968
10. Karatzns GM: Pancreatic pseudocysts. *Br J Surg* 63:55–59, 1976
11. Gilman PK, Gibbons JC, Kaplan MS: Unusual diagnostic aspects and current management of pancreatic pseudocysts. *Am Surg* 40:326–334, 1974
12. Andersen BN, Hancke S, Neilsen SAD: The diagnosis of pancreatic cyst by endoscopic retrograde pancreatography and ultrasonic scanning. *Ann Surg* 185:286–289, 1977
13. Cooperman AM, Sivak MV, Sullivan BH: Endoscopic pancreatography. Its value in preoperative-postoperative assessment of pancreatic disease. *Am J Surg* 129:38–43, 1975
14. Bilbao MK, Dotter CT, Lee TG: Complications of endoscopic retrograde cholangiopancreatography (ERCP). *Gastroenterology* 70:314–320, 1976
15. Haaga JR, Reich NE, Havrilla TR, Alfidi RJ: Interventional CT scanning. *Radiol Clin North Am,* 15:449–456, 1977

Urachal Cyst in the Adult: Ultrasound Diagnosis

MARTIN E. MORIN,[1] ANTON TAN, DENNIS A. BAKER, AND HAK K. SUE

Urachal anomalies requiring clinical attention are rare, and most occur in early childhood [1]. Our review of the radiologic literature revealed no reports of urachal cysts in adulthood, and no gray scale ultrasound depictions of the lesion [2, 3]. Sanders et al. [2] reported one probable urachal cyst in an infant, and Han and Witten [3] described a urachal carcinoma. Both lesions were imaged with bistable equipment. We recently encountered a case in which the classic signs and symptoms were absent, the physical examination and conventional radiographs were normal, and the ultrasound examination was diagnostic.

Case Report

A 45-year-old white man had gross hematuria and dysuria associated with nausea and epigastric pain for 1 week. With the exception of voluntary guarding during palpation of the abdomen, the physical examination was normal. White blood cell count was 13,800/mm^3 with 59% neutrophils, 15% bands, and 26% lymphocytes. Urinalysis revealed many red blood cells and white blood cells. The remainder of the hemogram and the routine serum chemistries were normal. Urine cultures revealed no significant growth, and cultures for acid-fast bacilli were also negative.

Excretory urography was normal. Cystoscopy revealed a 2-cm-diam focal area of hyperemia at the bladder apex with a tiny central orifice draining purulent material. Repeated attempts to catheterize this orifice were unsuccessful. Transurethral biopsy of the hyperemic area showed acute inflammation of transitional mucosa. Urine cultures were again negative.

Barium examinations of the upper gastrointestinal tract, small bowel, and colon were normal. B-mode gray scale ultrasound scan showed a small mass compressing the bladder dome, and an even smaller cyst between the apex of the urinary bladder and the umbilicus (fig. 1). The findings were interpreted as representing a cystic lesion of the urachus, and surgery was performed.

A urachus coursed preperitoneally from the umbilicus to the apex of the urinary bladder. The umbilical portion of the urachus was a cordlike structure 1 cm thick. The central part was dilated to 2 cm diameter and contained a cavity filled with pus, while the urachus widened distally so that its vesical portion formed a tent-shaped attachment to the bladder apex. Both the central and vesical portions were surrounded by inflammatory changes. The urachus was excised, and segmental resection of the bladder apex was performed.

Microscopic examination revealed the urachus to be lined with transitional epithelium merging occasionally with small areas of columnar epithelium. The diagnosis was infected urachal cyst with spontaneous drainage to the urinary bladder.

Discussion

The fetal urinary bladder is formed when a septum develops dividing the common cloaca into an anterior bladder and a posterior rectum. Although this fetal bladder initially extends to the umbilicus, the superior half contracts into a cordlike structure, the urachus, while the inferior portion becomes the urinary bladder [4]. The normal adult urachus is a fibrous cord 3–5 cm long, and is functionally closed. It is located in the extraperitoneal tissue of the anterior abdominal wall in the midline between the umbilicus and the urinary bladder [5].

Incomplete regression of the urachus results in anomalies with the following classifications [5]. When the bladder is located inferior to the level of the umbilicus, and the urachus is a tube, these anomalies have been noted: (1) urachus is patent throughout (fig. 2A); (2) caudal part of the urachus is patent, opening into the urinary bladder—a vesicourachal diverticulum (fig. 2B); (3) cephalic part of the urachus is patent, opening at the umbilicus—a urachal sinus (fig. 2C); and (4) midportion of urachus is patent, with both the cephalic and the caudal ends closed—a urachal cyst (fig. 2D). An additional classification is when the bladder is located at the level of the umbilicus, and a widely patent umbilicovesical fistula is present (fig. 2E).

Unlike the other urachal anomalies, the urachal cyst typically remains clinically silent until infection supervenes in adulthood [1]. It is often manifested by uncharacteristic abdominal complaints, the classic sign of congenital urachal lesions (urine leakage from the umbilicus) either not present or not appreciated [6, 7]. It

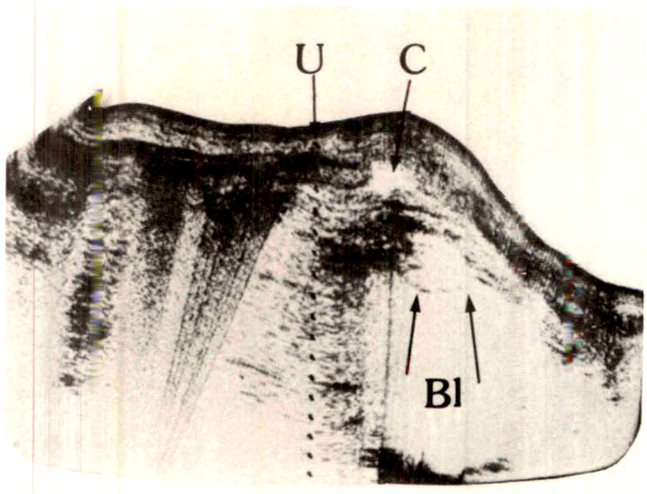


Fig. 1.—Midline longitudinal sonogram of pelvis shows 2 cm cyst between umbilicus and bladder apex. Associated submucosal-extravesical inflammatory mass compresses the bladder apex over 3 cm area (*arrows*). U = umbilicus; Bl = bladder; C = urachal cyst

Received October 27, 1978; accepted January 12, 1979.

[1]All authors: Department of Diagnostic Radiology, Veterans Administration Lakeside Hospital-Northwestern University, 333 East Huron Street, Chicago, Illinois 60611. Address reprint requests to M. E. Morin.

© 1979 American Roentgen Ray Society
0361-803X/79/1325-0831 $0.00

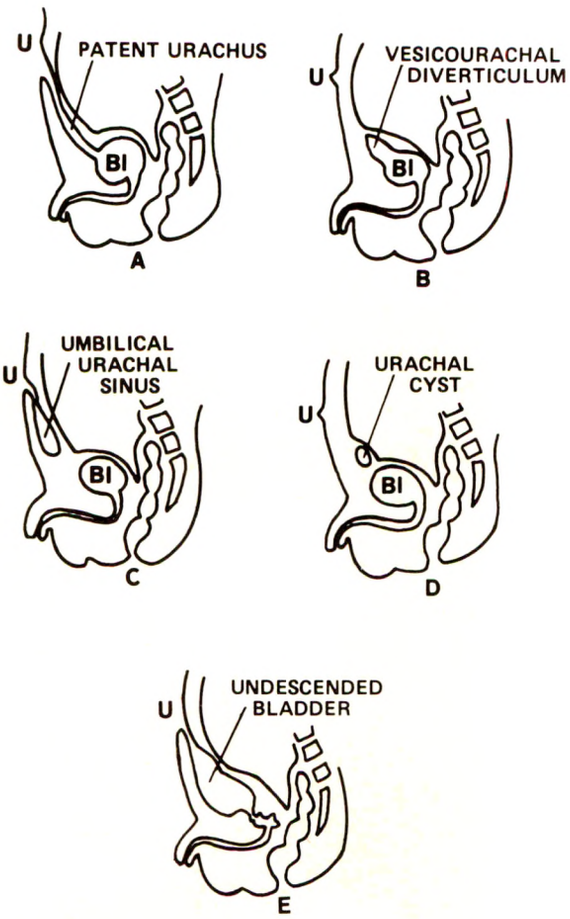


Fig. 2.—Types of urachal anomalies. U = umbilicus, Bl = urinary bladder

communicates with neither the umbilicus nor the urinary bladder, and therefore cannot be directly imaged by conventional radiography [8]. These factors, combined with the relative rarity of the lesion and until recently the lack of a satisfactory imaging method [2, 8], have long made preoperative diagnosis difficult in adults.

Urachal lesions are ideally suited for imaging by ultrasound since they are often cystic [3] and are located in the anterior abdominal wall away from the interference of intestinal gas [3]. Lesions as small as 2 cm can be detected. The diagnosis of infected urachal cyst is rarely considered in an adult. B-mode gray scale ultrasound scan may be the only imaging method able to detect the lesion.

REFERENCES

1. Bauer SB, Retik AB: Urachal anomalies and related umbilical disorders. *Urol Clin North Am* 5:196–211, 1978
2. Sanders RC, Oh KS, Dorst JP: B-scan ultrasound: positive and negative contrast material evaluation of congenital urachal anomaly. *AJR* 120:448–452, 1974
3. Han SY, Witten DM: Carcinoma of the urachus. *AJR* 127: 351–353, 1976
4. Thomford NR, Knight PR, Nusbaum JW: Urachal anomalies in the adult. *Am Surg* 37:405–407, 1971
5. Gray SW, Skandalakis JE: *Embyrology for Surgeons: The Embryological Basis for the Treatment of Congenital Defects*. Philadelphia, Saunders, 1972
6. Blichert-Toft M, Nielsen OV: Diseases of the urachus simulating intra-abdominal disorders. *Am J Surg* 122:123–128, 1971
7. Blichert-Toft M, Nielsen OV: Congenital patent urachus and acquired variants. *Acta Chir Scand* 137:807–814, 1971
8. Ney C, Friedenberg RM: Radiographic findings in anomalies of the urachus. *J Urol* 99:288–291, 1968

Isolation of the Left Innominate Artery, a Right Arch, and a Left Patent Ductus Arteriosus

E. C. MARTIN,[1, 2] Z. G. MESKO,[3] R. B. GRIEPP,[4] J. O. HALLER,[1] AND D. H. GORDON[1]

Abnormalities of the aortic arch attract an interest sometimes out of proportion to their clinical significance. We believe the anomaly reported here, an isolated innominate artery, has not previously been reported. The patient had a significant left-to-right shunt and presented as a patent ductus arteriosus.

Case Report

An asymptomatic 8½-year-old Puerto Rican girl, had a heart murmur apparently first heard at age 2 years. She had not otherwise previously been studied. On examination, her height and weight were at the tenth percentile. The pulses in the left carotid and the left brachial arteries were diminished, but all other pulses were equal. Blood pressure in her right arm was 110/60 mm Hg and in the left arm 50 mm Hg systolic. The left arm was otherwise normal. There was a left ventricular impulse and a grade 3/6 continuous murmur along the left sternal border. The second sound was normal. Electrocardiography showed a mean QRS axis of +45° and left ventricular hypertrophy. Chest radiography showed the heart at the upper limits of normal with pulmonary vascular prominence compatible with a left to right shunt and a right aortic arch. A barium swallow showed no evidence of a vascular ring. Clinical diagnosis was patent ductus arteriosus, but the pulse differences and the right aortic arch suggested additional abnormalities of fourth arch branching.

Right and left heart catheterization were performed percutaneously from the right groin. There was a significant step-up of oxygen tension at the ductal level with a calculated Qp/Qs of 2.2:1. The pulmonary artery pressure was 24/13 mm Hg.

Left ventriculography demonstrated a right arch with only two branches arising from it, the right subclavian artery and the right common carotid artery (fig. 1A). Late films in the series showed contrast material flowing down the left common carotid artery and the left vertebral artery to outline an isolated innominate trunk that communicated through a left patent ductus arteriosus with the pulmonary artery (fig. 1B). The left subclavian artery also filled late from the left innominate trunk. The intermediate films showed numerous collaterals around the upper mediastinum whose major arterial supply was the left supreme intercostal artery. Injection of contrast material in the left common carotid artery by passing the catheter from the main pulmonary artery through the left patent ductus confirmed these anatomic and hemodynamic relationships (fig. 1C). Injection of the left supreme intercostal artery resulted in late opacification of the left subclavian artery via several collateral vessels (figs. 1D and 1E).

It was postulated that the low pressure runoff through the patent ductus arteriosus caused a "physiologic" atresia distal to the left vertebral artery so the left subclavian artery filled only through collaterals. It was not known whether an anatomic atresia also existed at this site, and it was decided to resolve this point at surgery rather than jeopardize the left brachial artery in its resolution.

At operation, the anomaly was approached via a left thoracotomy. A large isolated left innominate artery gave off a somewhat enlarged left common carotid artery; a left subclavian artery appeared slightly smaller than normal. The innominate artery tapered slightly in its proximal part and then entered the superior aspect of the left pulmonary artery. The three upper left intercostal arteries were markedly dilated, as was the left internal mammary artery. The innominate, the proximal left common carotid, and the left subclavian arteries were all dissected free of the posterior mediastinum to achieve maximum mobility. The descending right thoracic aorta was approached by dissection posterior to the trachea and the esophagus. The innominate artery was then clamped where it joined the pulmonary artery and transected. The isolated innominate artery was passed posterior to the trachea and esophagus and anastomosed end-to-side to the aortic arch just distal to the takeoff of the right common carotid artery.

Immediately after surgery, pulses were stronger in the left carotid and left brachial arteries than preoperatively. Over the next 3 days, these gradually increased and strengthened until they were equivalent to those on the right side. Auscultatory blood pressures in both arms were identical 6 weeks after surgery.

Discussion

There has been no adequate explanation for the abnormalities of the embryonic fourth brachial arch, which result in aortic arch anomalies. However, in 1948, Edwards [1] described a theoretical model to which all anomalies have been found to conform [2, 3]. He proposed a double arch as the primitive precursor by which selective resorption of various parts could account for the normal configuration of the aorta, great vessels, and both common and uncommon anomalies (fig. 2). We believe our patient with a right arch had two interruptions, one in the left posterior arch distal to the left ductus arteriosus and the other in the left anterior arch proximal to the left common carotid artery (fig. 2).

Each of these breaks in the primitive double arch has been reported, but as isolated anomalies. A right arch with mirror-image branching (type 1, Shuford and Sybers

Received September 11, 1978; accepted after revision January 11, 1979.

[1]Department of Radiology, State University of New York, Downstate Medical Center, 450 Clarkson Avenue, Brooklyn, New York 11203.
[2]Present address: Department of Radiology, Columbia Presbyterian Medical Center, 622 West 168th Street, New York, New York 10032. Address reprint requests to E. C. Martin.
[3] Department of Pediatrics, State University of New York, Downstate Medical Center, Brooklyn, New York 11203.
[4] Department of Surgery, State University of New York, Downstate Medical Center, Brooklyn, New York 11203.

© 1979 American Roentgen Ray Society

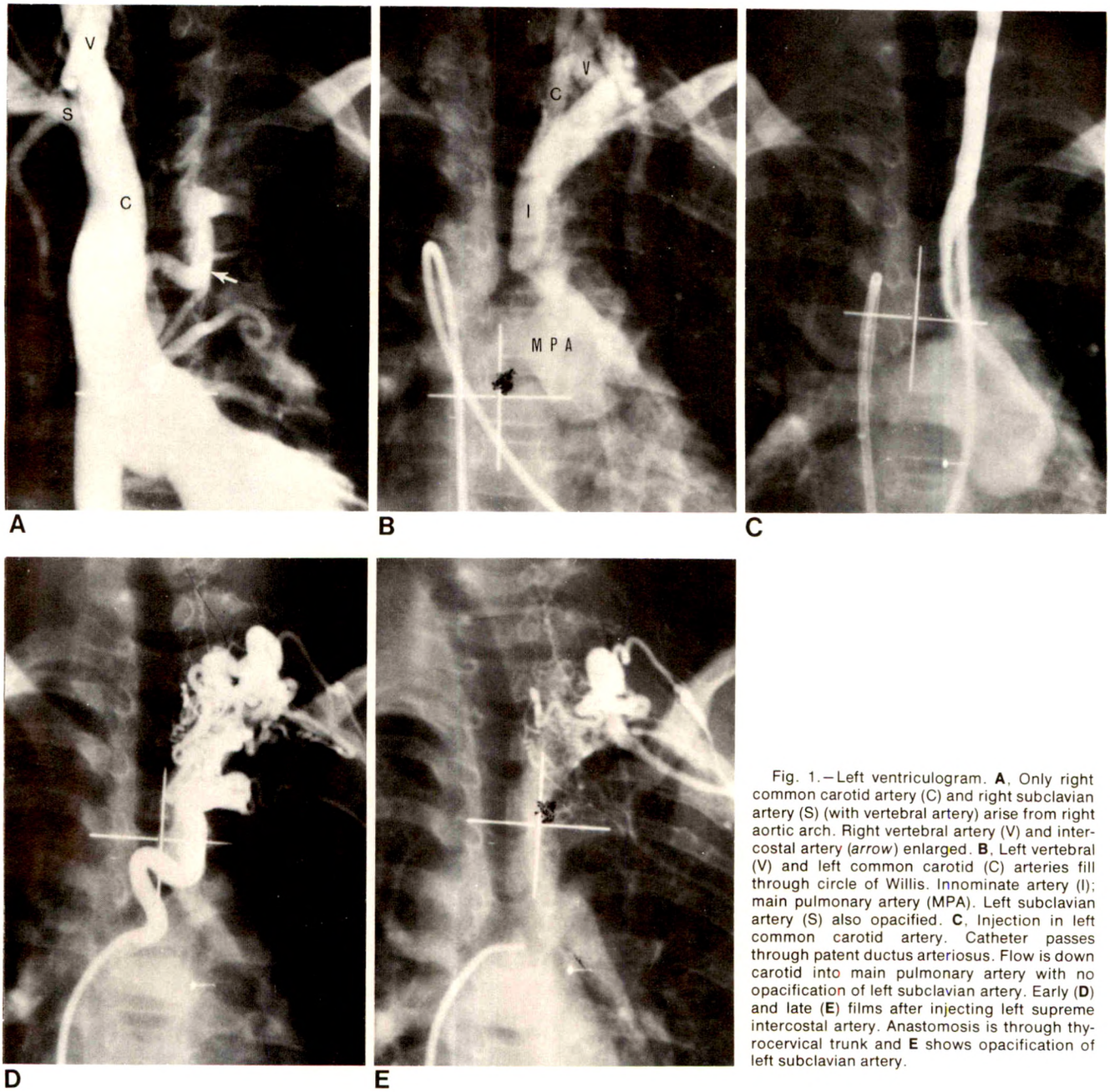


Fig. 1.—Left ventriculogram. **A**, Only right common carotid artery (C) and right subclavian artery (S) (with vertebral artery) arise from right aortic arch. Right vertebral artery (V) and intercostal artery (*arrow*) enlarged. **B**, Left vertebral (V) and left common carotid (C) arteries fill through circle of Willis. Innominate artery (I); main pulmonary artery (MPA). Left subclavian artery (S) also opacified. **C**, Injection in left common carotid artery. Catheter passes through patent ductus arteriosus. Flow is down carotid into main pulmonary artery with no opacification of left subclavian artery. Early (**D**) and late (**E**) films after injecting left supreme intercostal artery. Anastomosis is through thyrocervical trunk and **E** shows opacification of left subclavian artery.

[4]) is the most common arch anomaly, and derives from resorption of the proximal part of the left arch, creating a left innominate artery. There is a common association of congenital heart disease with this anomaly [3, 5] (fig. 2). An anterior aortic break (type 4 right arch [4]) is associated with a vascular ring because the innominate artery arises posteriorly as a third branch. Only a few cases of this rare anomaly have been reported [6]. In our case there was a combination of these two anomalies. Other "combination" lesions have been described. One, the isolated left subclavian artery [3, 7], is also very rare but seems to be associated with tetralogy of Fallot [8].

In our patient, the nonopacification of the left subclavian artery after injection of the left common carotid artery was confusing. We presume this was due to the low pressure runoff through the left patent ductus arteriosus. Hence, there was a need for a collateral supply to the distal left subclavian artery that occurred through the supreme intercostal artery to the thyrocervical trunk. Therefore, the patient exhibited both a pulmonary artery steal (from the carotid and vertebral arteries) and a "physiologic" subclavian occlusion with a supply from

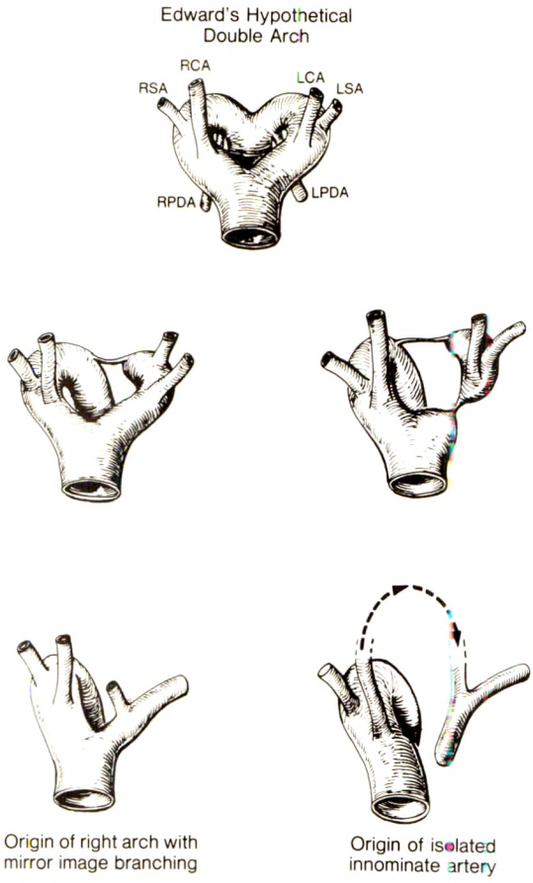


Fig. 2.—Left: development of most common right arch. Break occurring posteriorly on the left and resorption of free limb form innominate trunk. Right: postulated origin in our patient. Two breaks occurred both anteriorly and posteriorly with resorption into isolated innominate trunk. RCA = right carotid artery; LCA = left carotid artery; LSA = left subclavian artery; LPDA = left patent ductus arteriosus; RPDA = right patent ductus arteriosus; RSA = right subclavian artery.

aortic collaterals. Both were asymptomatic, but both had clear physical signs.

Apart from the unusual anatomy, this patient had two other interesting features. One was the significant shunt through the left patent ductus arteriosus, measured as 2.2:1. We are not aware of significant shunts being documented previously in aortic arch anomalies. As it took place through the circle of Willis, we felt that the combination of the shunt and the high cerebral blood flow justified surgery. The other was that as a result of the steal through the low pressure patent ductus arteriosus, the left arm was supplied through collaterals, particularly from the supreme intercostal artery to the costocervical trunk. This additional anomaly of a "physiologic," but nonanatomic, atresia is a combination not previously described.

REFERENCES

1. Edwards JE: Anomalies of the derivatives of the aortic arch system. *Med Clin North Am* 32:925–949, 1948
2. Blake HA, Manion WC: Thoracic arterial arch anomalies. *Circulation* 26:251–265, 1962
3. Stewart JR, Kincaid OW, Edwards JE: *An Atlas of Vascular Rings and Related Malformations of the Aortic Arch System*. Springfield, Ill. Thomas, 1964, pp 8–13, 124–219
4. Shuford WH, Sybers RG: *The Aortic Arch and its Malformations*. Springfield, Ill., Thomas, 1974
5. Shuford WH, Sybers RG, Edwards FK: The three types of right aortic arch. *AJR* 109:67–74, 1970
6. Grollman JH, Bedynek JC, Henderson HS, Hall RJ: Right aortic arch with an aberrant retroesophageal innominate artery angiographic diagnosis. *Radiology* 90:782–783, 1968
7. Shuford WH, Sybers RG, Schlant RC: Right aortic arch with isolation of the left subclavian artery. *AJR* 109:75–83, 1970
8. Ghon A: Uber eine selhene Entwicklungsstorung des Gefasssystems. *Verh Dtsch Ges Pathol* 12:242–247, 1908

Usefulness of the Prone Position for Aortography of Aortic Graft–Intestinal Fistulae

ERIK G. PINGOUD[1] AND S. OSHER PAIS[1]

Frontal and lateral supine aortography is sometimes nondiagnostic in patients with aortic graft–intestinal fistulae [1–4]. A case in which lateral prone aortography demonstrated the proximal end of an aortic graft duodenal fistula, undetected on anteroposterior and lateral supine aortograms, is reported. While the theoretical value of the lateral prone position has been discussed [1], we were unable to find a demonstrative case in the literature. Aortography in suspected cases of aortic graft–intestinal fistula may be improved with lateral prone projection, since failure to demonstrate rupture of the graft may lead to delay of surgical intervention and grave clinical consequences.

Case Report

A 56-year-old white man had received a Dacron aortic bifurcation graft because of a large abdominal aortic aneurysm. He did well for the next 5 weeks, but then developed abdominal pain and spiking temperatures. Workup including barium studies, ultrasonography, CT scanning, and biplane supine abdominal aortography (fig. 1) failed to reveal a source of infection. Blood cultures were negative. He improved on antibiotic and prednisone therapy and was discharged. He was readmitted 1 week later because of melena and hypotension.

Emergency frontal and lateral abdominal aortography in the supine position demonstrated an apparently normal aortic bifurcation graft (fig. 2). There was no apparent dehiscence. Lateral aortography with the patient prone demonstrated rupture involving the anterior surface of the proximal anastomotic graft site (fig. 3). Immediate surgery revealed a partially thrombosed fistula between the proximal anastomosis and the third part of the duodenum; a large abscess surrounding the proximal graft was identified. After placement of a left axillo-bifemoral Dacron bypass graft, the aortic bifurcation graft was excised and the duodenum oversewn. The patient gradually improved over the next 3 months after a stormy postoperative course, but then deteriorated rapidly and died from complications of widespread infection.

Discussion

Aortic graft–enteric fistula formation is a well known entity. Various radiographic manifestations have been described, but several reports indicate that diagnosis is difficult and radiographic studies often do not identify an abnormality suggesting graft rupture, particularly when bleeding is low grade or intermittent [1–4]. Since rupture of an aortic graft requires early surgical intervention, delay in diagnosis may result in disastrous consequences. The most frequent site of fistulization involves the proximal anastomosis and the third part of the duodenum [5]. Since rupture in this instance occurs on the anterior surface of the anastomosis, a lateral rather than frontal projection will better show discontinuity of the lumen. Thompson et al. [1] suggested that lateral filming with the patient prone rather than supine may optimize visualization of the rupture, although in none of their cases did this projection prove to be critical.

Contrast material, which is heavier than blood, will layer in the most dependent sections of the aorta. In the supine position, the posterior aspects of the aortic lumen are best outlined by contrast material; in the prone position the anterior aspects are best seen. Therefore, the lateral projection with the patient prone will maximize chances to detect discontinuity of the anastomosis at the anterior surface. Attention to this detail may be especially critical when the rupture is small or when much of the fistula contains thrombus, as it did in our case.

REFERENCES

1. Thompson WM, Jackson DC, Johnsrude IS: Aortoenteric and paraprosthetic-enteric fistulas: radiologic findings. *AJR* 127:235–242, 1976
2. Case records of the Massachusetts General Hospital (case 38-1971). *N Engl J Med* 285:739–745, 1971
3. Case records of the Massachusetts General Hospital (case 21-1974). *N Engl J Med* 290:1248–1253, 1974
4. Lise M, Yacoub MH: Aorto-duodenal fistula: a complication of abdominal aortic grafts. *J Cardiovasc Surg* (Torino) 10: 1196–1199, 1969
5. Humphries AW, Young JR, DeWolfe UG, Lefevre FA: Complications of abdominal aortic surgery. *Arch Surg* 86:43–50, 1963

Received August 21, 1978; accepted after revision January 12, 1979.
[1]Department of Diagnostic Radiology, Yale University School of Medicine, 333 Cedar Street, New Haven, Connecticut 06501. Address reprint requests to E. G. Pingoud.

AJR 132:836–837, May 1979
0361–803X/79/1325–0836 $0.00
© 1979 American Roentgen Ray Society

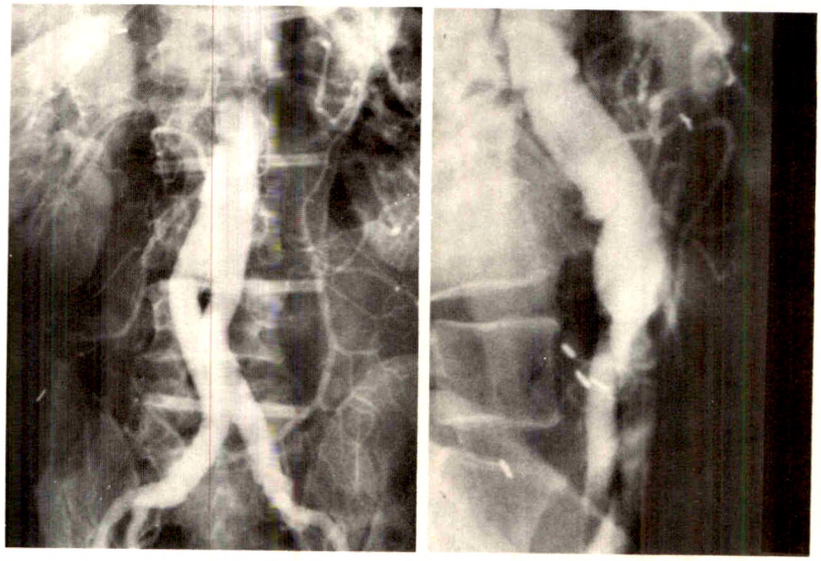


Fig. 1.—Transaxillary approach with patient supine. No evidence of rupture of graft in either frontal or lateral projection.

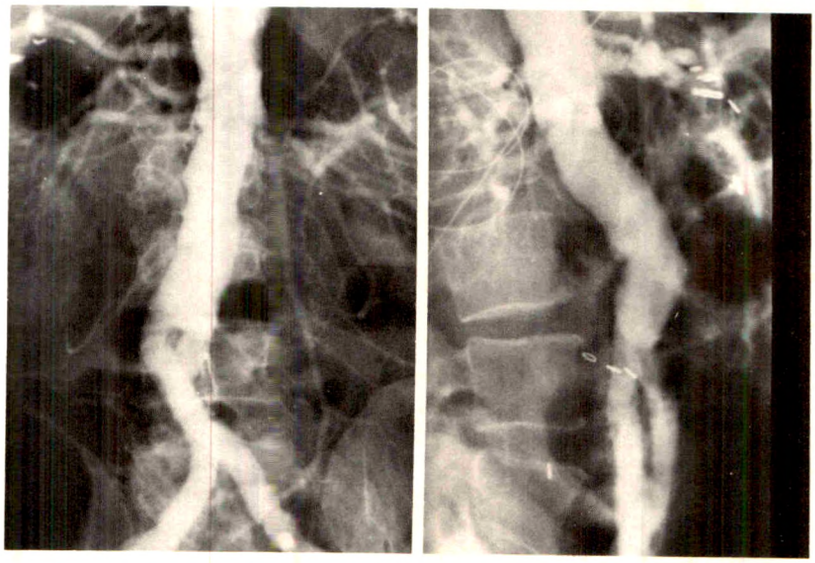


Fig. 2.—Transaxillary approach with patient supine 3 weeks after fig. 1. No evidence of graft rupture.

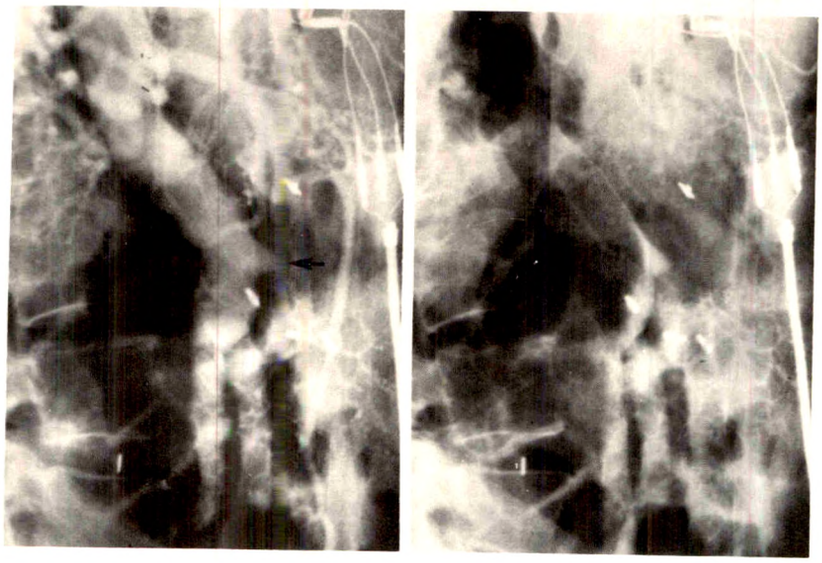


Fig. 3.—With patient prone, discontinuity of anterior aspect of proximal anastomotic site (*arrow*). Angiographically, this could represent either false aneurysm or partially thrombosed fistula. At surgery, fistula partly filled with thrombus between proximal anastomotic graft site and third part of duodenum was found.

Popliteal Vein Displacement by Popliteal Artery Aneurysms: Report of Two Cases

SEYMOUR SPRAYREGEN[1]

Venography is sometimes performed on patients with popliteal artery aneurysms because they have thrombophlebitis or a clinical picture resembling thrombophlebitis. Two cases are presented in which popliteal vein displacement was produced by such aneurysms.

Case Reports

Case 1

A 73-year-old hypertensive white man had right leg claudication. The pain began suddenly while walking and was associated with tenderness and induration of the right calf. At that time, he was considered to have thrombophlebitis and was anticoagulated. Venography was not performed.

When admitted 3 months later, pulses were normal except for a 4+ right popliteal pulse. Femoral arteriography revealed bilateral popliteal artery aneurysms. On the right (fig. 1A), the opacified lumen measured about 4 cm in diameter while on the left the diameter of the lumen of the aneurysm was about 1.5 cm. At operation, a large right aneurysm was identified. The popliteal vein was displaced laterally and posteriorly. The aneurysm was ligated proximally and distally but not excised and the excluded popliteal segment bypassed with a prosthetic graft.

On postoperative day 8, venous pulse volume recordings were questionably abnormal bilaterally. Right lower extremity venography showed lateral and posterior displacement of the popliteal vein by the aneurysm (figs. 1B and 1C). An area of thrombophlebitis in the thigh was also demonstrated. Left lower extremity venography was not performed. Treatment with anticoagulants resulted in improvement of symptoms.

Case 2

A 70-year-old white man had a 4-day history of right calf and ankle pain which began suddenly. He had a 1-year history of claudication on the right. Physical examination revealed right calf tenderness with a positive Homan's sign. Popliteal pulses were present bilaterally. Foot pulses were present on the left but absent on the right. Venography demonstrated slight lateral displacement of the popliteal vein and compression of a tributary (fig. 2B). Arteriography showed a popliteal artery aneurysm with thrombosis of the distal popliteal artery (fig. 2A). The angiographic findings were confirmed at surgery. The aneurysm was resected, popliteal thrombectomy performed, and a prosthetic bypass graft inserted. The patient made an uneventful recovery and was discharged 8 days after the operation.

Discussion

Patients with popliteal artery aneurysms may have signs and symptoms of thrombophlebitis. This may be related to compression of the popliteal vein leading to edema of the leg or, in some patients, to actual thrombosis of the popliteal or leg veins. Wychulis et al. [1] reported that venous occlusion occurred in 30 patients and popliteal thrombophlebitis in 11 patients in a series of 233 popliteal aneurysms (18%) [1]. Similarly venous compression or thrombosis was reported in 24 of 100 aneurysms by Gifford et al. [2], in 13 of 73 aneurysms (18%) by Friesen et al. [3], and in 11 of 48 aneurysms (23%) by Crichlow and Roberts [4]. In case 1 the patient experienced calf pain due to thrombophlebitis or expansion of the aneurysm simulating thrombophlebitis prior to the most recent admission, and also developed thrombophlebitis in the postoperative period. In case 2 thrombophlebitis was considered the sole cause, or an associated cause of the patient's symptoms, until venography excluded this possibility.

In addition to compression and thrombosis of the popliteal vein, popliteal aneurysms may produce a clinical picture simulating thrombophlebitis due to pressure on the tibial and peroneal nerves or inflammation of the aneurysm. Inflammation may be related to bacterial seeding of an aneurysm, erosion of the arterial wall by a popliteal abscess, or previous rupture of an aneurysm with inflammation due to infiltration of blood in the subcutaneous tissues [5]. Since popliteal aneurysms occur almost exclusively in males [1–4], the possibility of an aneurysm should be considered in any male patient in the arteriosclerotic age group who has signs and symptoms of thrombophlebitis.

The popliteal vein begins at the inferior aspect of the popliteal space, medial to the popliteal artery, crosses posterior to the artery and lies lateral to the artery in the superior aspect of the popliteal space. In my experience, most aneurysms occur in the upper two-thirds of the popliteal space. Aneurysms in this position will displace the popliteal vein laterally and/or posteriorly as seen in the two cases described. Although Britton [6] mentioned that the popliteal vein may be narrowed by a popliteal aneurysm, he did not illustrate or reference this finding. Giustra et al. [7] reported two patients with popliteal vein thrombosis secondary to aneurysm. In one case the popliteal vein was displaced laterally at the popliteal-femoral junction. In the other, a similar displacement was suggested. If the popliteal vein is completely occluded, displacement of the vein may be difficult or impossible to appreciate. Bergan and Trippel [8] showed venograms of two patients with large aneurysms in which the popliteal vein was not filled, due to compression in one case and presumably thrombosis in the other [8]. In one case the greater saphenous vein was displaced medially as well.

The main differential diagnosis for a displaced and

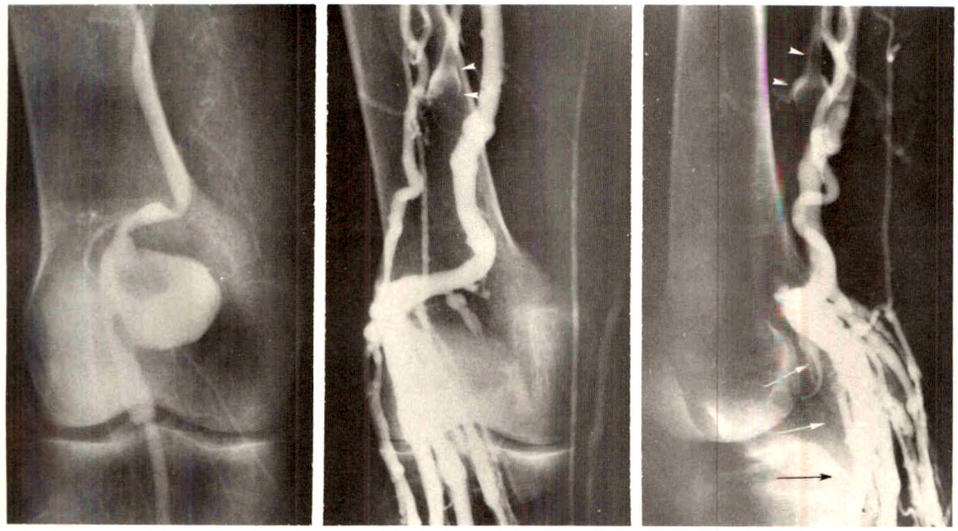
Received September 14, 1978; accepted after revision January 3, 1979.

[1] Department of Radiology, Albert Einstein College of Medicine and Montefiore Hospital and Medical Center, 111 East 210th Street, Bronx, New York 10467.

AJR 132:838–839, May 1979

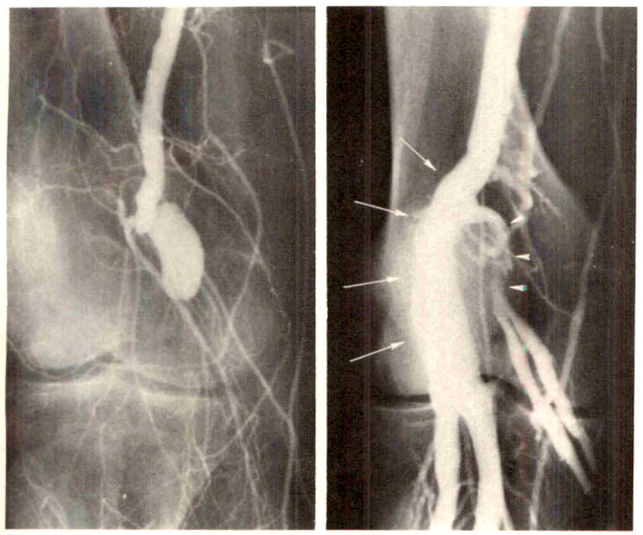
© 1979 American Roentgen Ray Society

0361–803X/79/1325–0838 $0.00



A B C

Fig. 1.—**A,** Anteroposterior arteriogram. Large popliteal artery aneurysm and lateral deviation of popliteal artery. **B,** Anteroposterior venogram. Lateral displacement without narrowing of popliteal vein. Thrombus is in vein in distal thigh (*arrowheads*). **C,** Lateral venogram. Posterior displacement of popliteal vein (*arrows*) and thrombus in distal thigh vein (*arrowheads*).



A B

Fig. 2.—**A,** Anteroposterior arteriogram. Popliteal artery aneurysm with thrombosis of distal popliteal artery. **B,** Anteroposterior venogram. Localized lateral deviation without narrowing of popliteal vein (*arrows*); also deviation and narrowing of popliteal tributary (*arrowheads*).

compressed popliteal vein is a popliteal cyst. Typically these cysts are associated with rheumatoid arthritis or meniscal tears. These patients also can have signs and symptoms suggestive of thrombophlebitis. Swett et al. [9] performed venography on four patients with popliteal cysts presenting as thrombophlebitis. In three patients in whom anteroposterior venograms were shown, lateral displacement of the popliteal vein was demonstrated. In the fourth patient, an oblique venogram showed narrowing of the popliteal vein. Thus, a similar type of displacement of the popliteal vein can be seen with aneurysms and cysts.

Venography should be performed with the knee slightly flexed. With the knee extended there may be compression of the popliteal vein by the surrounding muscles simulating extrinsic pressure on the vein by an abnormal mass [10]. At times this extrinsic compression may even result in nonfilling of the popliteal vein.

REFERENCES

1. Wychulis AR, Spittell JA Jr, Wallace RB: Popliteal aneurysms. *Surgery* 68:942–952, 1970
2. Gifford RW Jr, Hines EA Jr, Janes JM: An analysis and follow-up study of one hundred popliteal aneurysms. *Surgery* 33:284–293, 1953
3. Friesen G, Ivins JC, Janes JM: Popliteal aneurysms. *Surgery* 51:90–98, 1962
4. Crichlow RW, Roberts B: Treatment of popliteal aneurysms by restoration of continuity: review of 48 cases. *Ann Surg* 163:417–426, 1966
5. Gage M: Inflamed arterial popliteal aneurysm simulating acute abscess. *Ann Surg* 145:893–897, 1957
6. Britton RC: Roentgen anatomy (of lower extremity phlebography), in *Vascular Roentgenology*, edited by Schobinger RA, Ruzicka FF, New York, Macmillan, 1964, pp 658–661
7. Giustra PE, Root JA, Mason SE, Killoran PJ: Popliteal vein thrombosis secondary to popliteal artery aneurysm. *AJR* 130:25–27, 1978
8. Bergan JJ, Trippel OH: Management of giant popliteal aneurysms. *Arch Surg* 86:818–825, 1963
9. Swett HA, Jaffe RB, McIff EB: Popliteal cysts: presentation as thrombophlebitis. *Radiology* 115:613–615, 1975
10. Arkoff RS, Gilfillan RS, Burhenne HJ: A simple method for lower extremity phlebography-pseudo-obstruction of the popliteal vein. *Radiology* 90:66–69, 1968

Gallium Scan in Sternal Osteomyelitis

PHILIP W. SMITH,[1] RICHARD J. PETERSEN,[2] AND RANDOLPH M. FERLIC[3]

Sternal osteomyelitis may occur secondary to hematogenous spread from a distant site, local mediastinal infection, or as a complication of thoracic surgery. A case of sternal osteomyelitis after median sternotomy is described.

Case Report

A 59-year-old man was well until an abnormal treadmill exercise test led to discovery of two-vessel coronary artery disease. He underwent a left anterior descending coronary artery bypass. Postoperatively, he had chest pain in the region of his sternal incision. The pain continued after discharge and the patient was readmitted 1 month later. At that time, he had a second surgical procedure for repositioning of his sternotomy bands. However, the pain continued and the patient was readmitted after another month. He continued to have sternal pain and purulent discharge from his sternal wound. He had a low grade fever and an elevated white blood cell count. A wound culture grew *Pseudomonas aeruginosa*. Tomography of the chest wall 1 month later revealed advanced bony destruction. Gallium scan (fig. 1A) demonstrated marked uptake of ^{67}Ga in the sternum at 24 hr.

Diagnosis was sternal osteomyelitis, and the patient was begun on Tobramycin 60 mg every 8 hr and carbenicillin 4 g every 4 hr intravenously. The Tobramycin was discontinued after 5 days, and the patient was switched to gentamicin 60 mg intravenously every 8 hr. Adequate in vitro bacterial killing levels were achieved on the two drug regimen, and both antibiotics were continued until discharge. The patient had 26 days of effective antibiotic therapy.

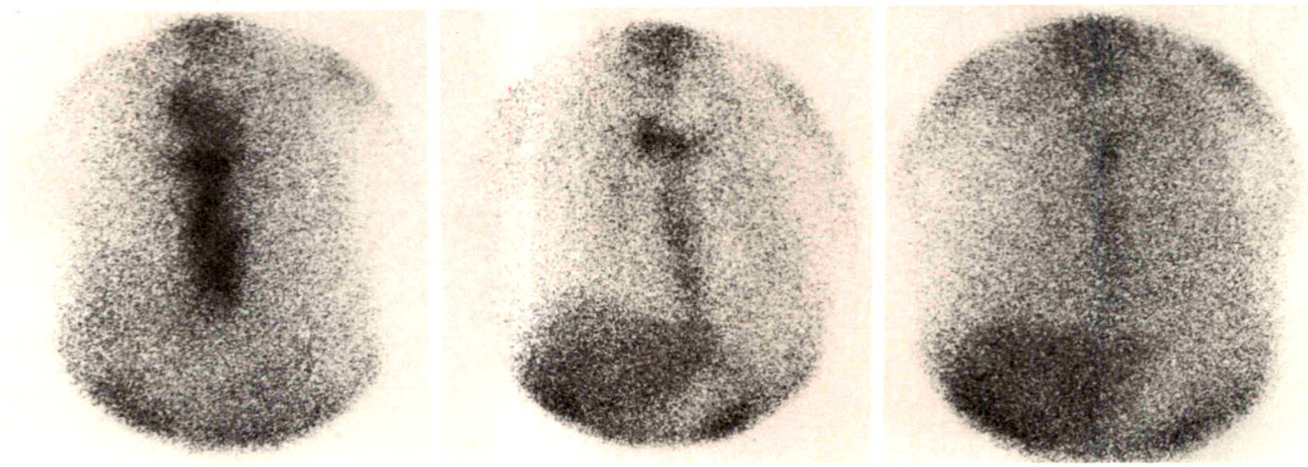
At the beginning of therapy, the infectious disease consultant suggested debridement of the sternum. However, the cardiovascular surgery consultant believed this was not indicated. Consequently, medical therapy alone was undertaken. The patient demonstrated significant clinical improvement on antibiotic therapy. He had been running a low grade fever of 37.2–38.3°C prior to therapy, but the fever rapidly disappeared after the institution of therapy. By day 7 of therapy, there was no purulent drainage seen in the region of the sternal wound. The patient continued to have mild sternal tenderness.

A follow-up ^{67}Ga scan (fig. 1B) demonstrated significant improvement, with the sternal uptake of ^{67}Ga estimated to be 20%–30% of the previous uptake. Other laboratory parameters were also consistent with the clinical and radiologic improvement. The white blood cell count had decreased from 17,500 to 8,500/mm^3. A third ^{67}Ga scan 3 months later demonstrated continued improvement (fig. 1C).

Discussion

Sternal osteomyelitis is an uncommon but serious complication of median sternotomy. *Pseudomonas* species and *Staphylococcus aureus* are the most common bacterial pathogens [1–3], with incidences reported as high as 5.9% [1].

Wray et al. [1] noted that routine radiographic exami-



A B C

Fig. 1.—Total body ^{67}Ga scans at 24 hr after administration of 5 mCi ^{67}Ga. **A**, Marked increased uptake throughout sternum during period of acute osteomyelitis. **B**, Markedly diminished activity during early healing phase. **C**, Essentially normal activity within bony sternum demonstrated on examination 3 months after therapy.

Received October 2, 1978; accepted after revision January 11, 1979.

[1]Department of Internal Medicine, Bishop Clarkson Memorial Hospital, Omaha, Nebraska 68105.

[2]Department of Radiology, Bishop Clarkson Memorial Hospital, 44th and Dewey Avenue, Omaha, Nebraska 68105. Address reprint requests to R. J. Petersen.

[3]Department of Surgery, Bishop Clarkson Memorial Hospital, Omaha, Nebraska 68105.

© 1979 American Roentgen Ray Society

0361-803X/79/1325-0840 $0.00

nation was not helpful, because it is often normal despite significant osteomyelitis. The ^{67}Ga has been shown to concentrate in inflamed bone. Lisbona and Rosenthall [4] studied ^{99m}Tc methylene diphosphonate and ^{67}Ga in osteomyelitis and found the ^{67}Ga scan was positive in 16 of 16 cases of active osteomyelitis. In addition, ^{67}Ga scans normalized earlier and paralleled clinical symptomatic responses better than ^{99m}Tc methylene diphosphonate scans.

In our case the ^{67}Ga scan was helpful in confirming the clinical impression of sternal osteomyelitis. Serial ^{67}Ga scans paralleled clinical response. It is of interest that the ^{67}Ga scan continued to improve even after antibiotic therapy was discontinued. Patients with sternal osteomyelitis frequently lack radiologic abnormalities and systemic symptoms [1] and often have a normal white blood cell count. Hence, the ^{67}Ga scan provides an objective and useful marker of response to therapy.

The ^{67}Ga scans may demonstrate concentration of the isotope in a recent incision site. However, the activity corresponds to the incision, is of uniform intensity, and is just slightly more intense than background [5]. Our experience is similar. Five ^{67}Ga scans performed on patients 3 days to 3 weeks after uncomplicated median sternotomy demonstrated virtually no increased uptake in the sternum. The increased uptake in our patient with osteomyelitis was in distinct contrast to normal postoperative ^{67}Ga scans.

REFERENCES

1. Wray TM, Bryant RE, Killen DA: Sternal osteomyelitis and costochondritis after median sternotomy. *J Thorac Cardiovasc Surg* 65:227–233, 1973
2. Sanfelippo PM, Danielson GK: Complications associated with median sternotomy. *J Thorac Cardiovasc Surg* 63:419–423, 1972
3. Weinstein RA, Ellis LJ, Schwarzmann SW, Hatcher CR: Sternal osteomyelitis after open-heart operation: pathogenesis and prevention. *Ann Thorac Surg* 21:442–444, 1976
4. Lisbona R, Rosenthall L: Observations on the sequential use of ^{99}Tc-phosphate complex and ^{67}Ga imaging in osteomyelitis, cellulitis, and septic arthritis. *Radiology* 123:123–129, 1977
5. Staab EV, McCartney WH: Role of gallium^{67} in inflammatory disease. *Semin Nucl Med* 8:219–234, 1978

Fat in the Intrahepatic Fissure

MICHAEL D. HALBER[1] AND RICHARD H. DAFFNER[1]

The radiologic evaluation of the patient with acute onset of abdominal pain uses the gamut of available imaging studies. Computed tomography (CT) is not often considered for a patient with the "acute abdomen." However, in certain circumstances in which a confusing clinical picture is associated with bizarre findings on "conventional" radiographic studies, the CT scan may provide the correct diagnosis. The following case illustrates a situation in which a normal anatomic structure not usually seen by conventional radiography produced confusing shadows on the plain film. CT was necessary to resolve the problem.

Case Report

A 53-year-old white man developed sharp midabdominal pain below the umbilicus 1 week before admission. The pain subsided after 24 hr only to return and migrate to the right flank. There was associated nausea and vomiting and mild dysuria. There was no gross hematuria. The medical history was significant for a high alcohol consumption. Physical examination showed an obese man in no acute distress. He was slightly febrile and mildly hypertensive. The abdominal examination revealed exquisite tenderness in the right upper quadrant just below the ribs, right flank, and right costovertebral angle. Significant laboratory values included blood urea nitrogen, 14; amylase, 660 U; bilirubin, 0.5; white blood cell count, 8,400 with a normal differential. The urine showed 2+ proteinuria, 10–15 red blood cells/high power field, 35–40 white blood cells/high power field and many Gram-positive rods and cocci.

An abdominal plain film revealed calcification over the right kidney and a linear lucency in the right upper quadrant that

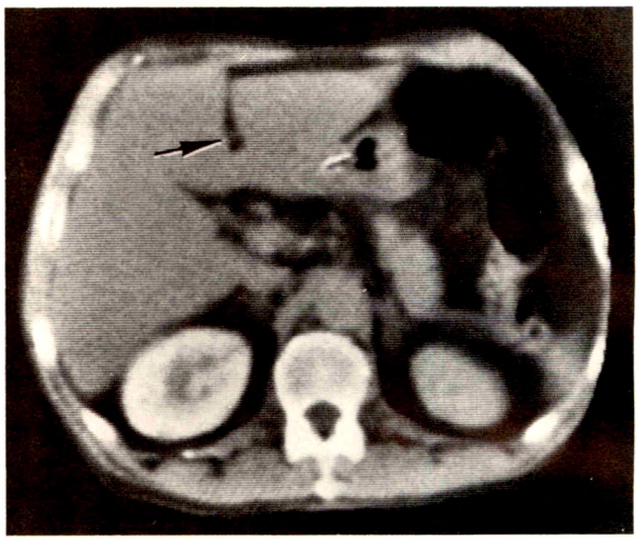
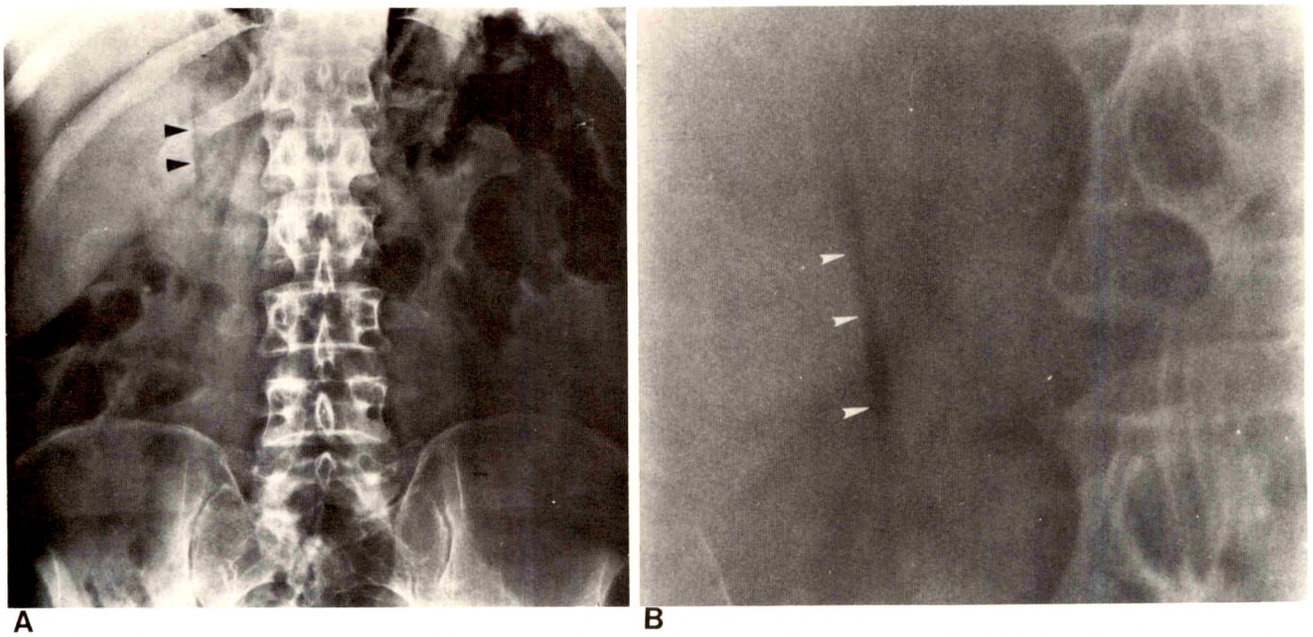


Fig. 2.—CT scan. Prominent interlobar fissure containing vessel in liver (*arrow*). Prominent nephrogram in right kidney from previous intravenous urogram, due to obstructing ureteral calculus.



A B

Fig. 1.—**A**, Plain film on admission. Vertical lucency (*arrowheads*) overlies hepatic shadow. Right renal calculus. **B**, Detail of right upper quadrant.

Received August 14, 1978; accepted after revision January 11, 1979.

[1] Department of Radiology, Veterans Administration Medical Center, Duke University Medical Center, Durham, North Carolina 27705. Address reprint requests to R. H. Daffner at VA.

© 1979 American Roentgen Ray Society

0361-803X/79/1325-0842 $0.00

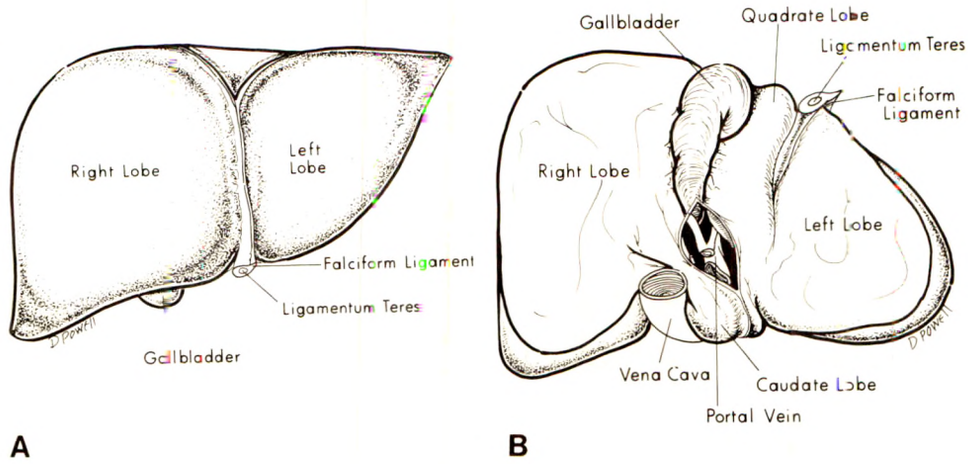


Fig. 3.—**A**, Anterior view of liver. Falciform ligament separates right and left lobes. Excess fat along border may occasionally be demonstrated radiographically. **B**, Posterior surface of liver from below. Relation of lobes.

looked like gas (fig. 1). This shadow could only be seen on the supine film. There was no evidence of extraluminal gas on upright abdominal films. Because of the initial suspicion that the patient had a right ureteral stone, excretory urography was performed; it revealed delayed function on the right with subsequent ureteropelvocaliectasis. However, the elevated amylase, abdominal pain, history of heavy alcohol consumption, and unusual lucency in the right upper quadrant were of additional concern. A ruptured viscus with free air, gallstone ileus, pancreatitis, cholecystitis, or cholangitis were considered possible. Fluoroscopy of the abdomen revealed the linear lucency in question to be anteriorly located. CT examination of the abdomen (fig. 2) showed the lucency to be fat between the lobes of the liver. The patient passed a ureteral calculus 24 hr after admission with dramatic relief of symptoms.

Discussion

The liver develops from a bud which also forms the descending limb of the duodenum. The liver is generally considered to be composed of four lobes—right, left, caudate, and quadrate. Some of the divisional landmarks, not well seen on conventional radiographic studies, may be well demonstrated with computed tomography (fig. 3). Of interest in our patient is the prominent fissure separating the left and quadrate lobes. This fissure containing the ligamentum teres, a remnant of the umbilical vein, is often overlapped by a tongue of hepatic tissue called the pons hepatis [1–3]. The ligament may be invested with fat which may be increased in the obese patient. In our patient, the fat apparently was increased enough to be seen on a plain abdominal film and was very easily demonstrated by CT.

Our patient had acute onset of right flank and abdominal pain with hematuria and was strongly suspected of having a ureteral or renal calculus. However, an unusual radiographic finding of fat in an intrahepatic fissure [4] was initially confused with a pathologic process and delayed an unequivocal diagnosis. Knowledge of this anatomic variation will prevent such mistakes.

REFERENCES

1. Goss CM: *Gray's Anatomy*. Philadelphia, Lea & Febiger, 1973, pp 1244–1253
2. Carter B, Morehead J, Wolpert SM, Hammerschlag SB, Griffiths HE, Kahn PC: *Cross Sectional Anatomy, Computed Tomography, and Ultrasound Correlation*. New York, Appleton-Century-Crofts, 1977, sections 27–31
3. Becker RF, Wilson JW, Gehweiler JA: *The Anatomical Basis of Medical Practice*. Baltimore, Williams & Wilkins, 1971, pp 601–602
4. Meyers MA: *Dynamic Radiology of the Abdomen: Normal and Pathologic Anatomy*. New York, Springer, 1976, p xxii

Pseudolymphoma in Two Immunodeficient Children

ROBERT C. BRASCH,[1] STUART ROYAL,[1] ARTHUR J. AMMANN,[2] AND JAMES CROWE[1, 3]

The development of malignancy, particularly lymphoproliferative tumors, in primary immunodeficient patients is well documented [1, 2]. An increased incidence of malignancy (from 2% to 10%) has been clearly demonstrated in several primary immunodeficient states, including Bruton type X-linked agammaglobulinemia, Wiskott-Aldrich syndrome, severe combined immunodeficiency, selective IgM deficiency, selective IgA deficiency, ataxia-telangiectasia, cellular immunodeficiency with abnormal immunoglobulin synthesis (Nezelof's syndrome), and common variable hypogammaglobulinemia disease [1, 3]. This tendency to develop malignancy has been attributed to a defect in immune surveillance for neoplastic cells (a function that the intact immune system normally provides), a susceptibility to recurrent viral infections, and an inability to repair damaged DNA [1, 4]. The radiologist aware of this risk must give careful attention for the first signs of tumor in the immunodeficient child.

Radiographic diagnosis of malignancy in immunodeficiency is complicated by the common occurrence of nonmalignant lymphoid enlargement in certain immunodeficient patients [5–7]. Benign lymphoid hyperplasia is frequently detected in the gastrointestinal tract where it characteristically appears as 2–5 mm centrally umbilicated nodules. Less commonly, lymphoid hyperplasia may appear as massive adenopathy and radiographically mimic malignant lymphoma.

Two children with primary immunodeficiency syndromes and massive retroperitoneal lymphadenopathy demonstrated by computed tomography (CT) are reported. The CT scans, obtained with a General Electric CT/T scanner, were falsely interpreted as demonstrating lymphoma. However, pathologic specimens from both patients revealed only benign lymphoid hyperplasia of the massive type. We wish to point out the increased occurrence of both benign and malignant lymphoproliferation in children with immunodeficiency and to emphasize that the two entities cannot be reliably differentiated by CT.

Case Reports

Case 1

M. V., a 10-year-old girl, has been seen at University of California Medical Center since infancy with a combined (T- and B-cell) immunodeficiency, hepatosplenomegaly, and peripheral adenopathy. Her first manifestations of disease were recurrent infections beginning at age 6 months, including episodes of otitis media, pneumonia, bronchitis, and pneumococcal sepsis. Hepatosplenomegaly and peripheral adenopathy in the neck and axillae were noted in early childhood. At age 3½ years, complete immunologic workup revealed increased serum immunoglobulins and a normal total lymphocyte count, but a decreased number of T-cell rosettes. Delayed hypersensitivity skin tests, including dinitrochlorobenzene, were all negative. No serum antibody response could be elicited after immunization to a variety of antigens. This combination of laboratory results indicated that the child had functional deficiencies of the T- and B-cell components of her immune system; hence, combined immunodeficiency. Her specific disease would best be categorized as cellular immunodeficiency with abnormal immunoglobulin synthesis (Nezelof's syndrome).

After unsatisfactory response from transfer factor therapy alone, at age 5 years, she received the first of four intraperitoneal fetal thymic transplants. This form of therapy plus monthly plasma infusions resulted in a decreased frequency of infections and improvement in her laboratory parameters of T-cell function.

The patient's clinical status remained stable for several years until, at age 10 years, chest radiography revealed a new mass in the gastric fundus. Subsequent barium upper gastrointestinal examination demonstrated an ulcerated fundic mass (fig. 1A). Also seen were numerous small centrally umbilicated nodules throughout the stomach, duodenum, and small bowel, diagnosed as lymphoid hyperplasia (fig. 1B). The large fundic mass was thought to be compatible with lymphoma, and a CT examination was performed to determine the extragastric extent of abdominal disease. CT revealed a large continuous, lobulated, retroperitoneal mass extending from the level of the renal pelvis cephalad to the gastric fundus (fig. 1C) with apparent invasion of the stomach. The suspected diagnosis remained lymphoma until laparotomy and pathologic examination of the biopsied lesion revealed benign reactive lymphadenitis without evidence of malignancy. At surgery, the extent of the adenopathy was impressive, surrounding the aorta and inferior vena cava, extending along the lesser curve of the stomach and into the small bowel mesentery. Microscopy of the nodal mass demonstrated loss of the normal corticomedullary junctions with extensive fibrosis, loss of germinal centers, and infiltration by eosinophils, histiocytes, and plasma cells. Cultures for virus, bacteria, and tuberculosis were negative.

After surgery, the patient received a fifth fetal thymic transplant, and her clinical status has remained unchanged without significant infection for over 1 year. No further adenopathy has appeared but her gastric mass remains evident on chest films.

Case 2

J. R., product of a normal pregnancy, labor, and delivery, was seen at age 5 months with a persistent upper respiratory infection and hepatosplenomegaly. Partial white blood cell count and differential were abnormal with 13,800/mm³ white blood cells and 80% lymphocytes. However, serum immuno-

Received October 13, 1978; accepted after revision January 25, 1979.
R. C. Brasch is a James Picker Foundation Scholar in Radiologic Research.
[1] Department of Radiology, University of California School of Medicine, San Francisco, California 94143. Address reprint requests to R. C. Brasch.
[2] Department of Pediatrics, University of California School of Medicine, San Francisco, California 94143.
[3] Present address: Department of Radiology, Bowman Gray Medical School, Winston-Salem, North Carolina 27103.

© 1979 American Roentgen Ray Society

0361-803X/79/1325-0844 $0.00

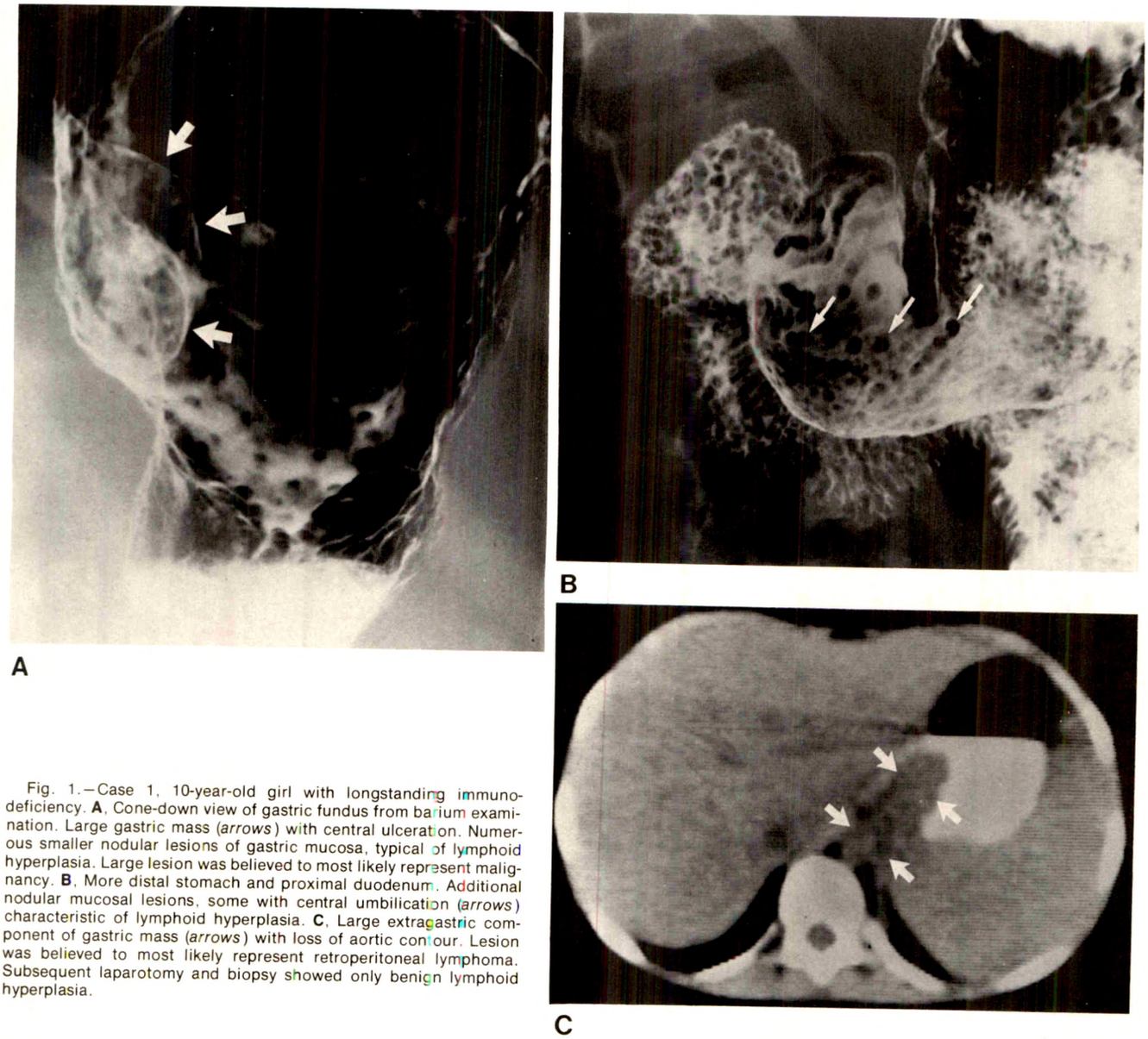


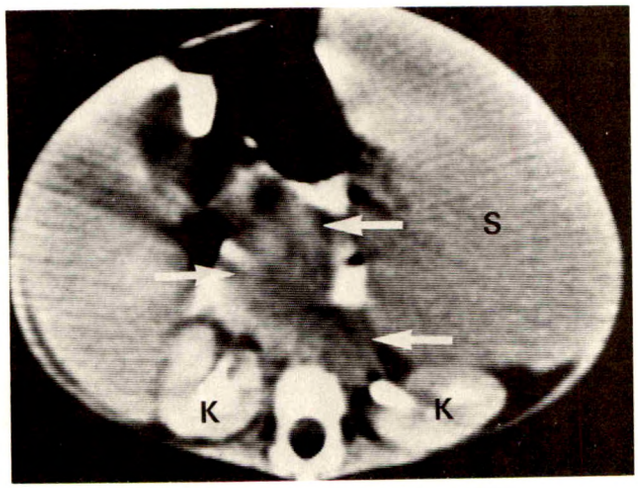
Fig. 1.—Case 1, 10-year-old girl with longstanding immunodeficiency. **A**, Cone-down view of gastric fundus from barium examination. Large gastric mass (*arrows*) with central ulceration. Numerous smaller nodular lesions of gastric mucosa, typical of lymphoid hyperplasia. Large lesion was believed to most likely represent malignancy. **B**, More distal stomach and proximal duodenum. Additional nodular mucosal lesions, some with central umbilication (*arrows*) characteristic of lymphoid hyperplasia. **C**, Large extragastric component of gastric mass (*arrows*) with loss of aortic contour. Lesion was believed to most likely represent retroperitoneal lymphoma. Subsequent laparotomy and biopsy showed only benign lymphoid hyperplasia.

globulins were normal on the basis of immunoelectrophoresis and quantitative immunoglobulins. Skin testing to diphtheria and tetanus antigens was positive. Biopsy of the enlarged liver revealed periportal inflammation compatible with persistent hepatitis. Testing for hepatitis-associated antigen was negative. At age 12 months, repeat liver biopsy demonstrated periportal fibrosis and inflammation with early bridging suggesting chronic active liver disease. Serum immunoglobulins were again normal and the patient was begun on prednisone therapy.

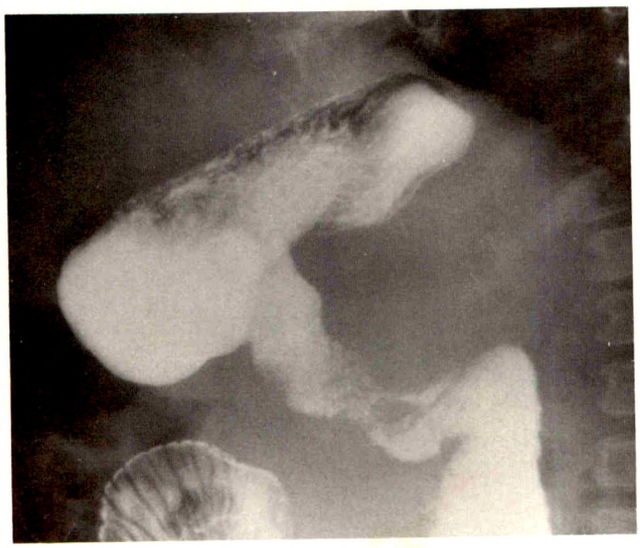
At age 16 months, J. R. was readmitted for evaluation of increasing hepatosplenomegaly, cutaneous petechia, and development of a Cushingoid state. Hypersplenism was diagnosed clinically. White blood cell count was initially 13,300/mm^3, but rose to 30,800/mm^3 with onset of fever during hospitalization. Repeat immunologic evaluation revealed an abnormality for the first time consisting of low levels of T-cell rosettes (3%) and appearance of a monoclonal IgM paraprotein on immunoelectrophoresis. Serum IgG levels were elevated and IgA levels were normal for age. The percentage of peripheral blood B-cells was normal. Other T-cell functions were abnormal, as evidenced by a depressed phytohemagglutination response and absent mixed lymphocyte culture reactivity of peripheral blood lymphocytes.

Abdominal CT to evaluate splenic size and search for possible abscess formation demonstrated an enormous spleen without macroscopic abscess formation. A large retroperitoneal lobulated mass, compatible with enlarged lymph nodes and a possible retroperitoneal neoplasm, was identified (fig. 2A). Subsequent upper gastrointestinal examination demonstrated anterior displacement of the stomach and second part of the duodenum by the retroperitoneal mass (fig. 2B).

The patient's clinical status deteriorated and serial chest radiography showed development of bilateral alveolar infiltrates. The patient was taken to surgery for splenectomy because of platelet sequestration and to obtain biopsies of the liver, lung, and retroperitoneal mass. Liver biopsy specimen again showed periportal inflammation. Samples from the lung



A



B

Fig. 2.—Case 2, 16-month-old boy with immunodeficiency. **A**, At level of kidneys (K), massively enlarged spleen (S) without evidence of abscess formation. Mass of retroperitoneal tissue (*arrows*) displaces several contrast-filled bowel loops. Retroperitoneal mass was believed to probably represent malignant lymphoma, but autopsy specimens showed only benign lymphoid proliferation. **B**, Lateral view from barium upper gastrointestinal examination. Anterior displacement of body of stomach and proximal duodenum indicates large retroperitoneal mass.

revealed *Pneumocystis carinii* infection. The biopsy specimen of the retroperitoneal nodal mass revealed reactive lymphoid hyperplasia without evidence of lymphoma, abscess, or granuloma.

Despite sulfamethoxazole and trimethoprim therapy, the patient died of overwhelming *Pneumocystis* pneumonia. Postmortem examination revealed mediastinal, retroperitoneal, and mesenteric lymphadenopathy, in addition to hepatitis and pulmonary *Pneumocystis carinii* infection. *M. tuberculosis* infection, unsuspected during life, was found at autopsy to have produced microabscesses within several abdominal organs, but no macroscopic foci were found. Subsequently, *M. tuberculosis* was identified within the splenic and lymphoid tissues.

Comment. The abnormal immunologic status of this child was not fully appreciated until the days just preceeding his death. The abnormal T-cell functions and paraprotein suggest the category of cellular immunodeficiency with abnormal immunoglobulin synthesis (Nezelof's syndrome). Such patients have been known to develop lymphadenopathy and splenomegaly and several have developed lymphoid malignancies [3]. Disseminated tuberculosis, not suspected during life, was probably secondary to the patient's depressed immunologic responses. Although the enlarged retroperitoneal lymph nodes contained acid-fast bacilli, they showed no granulomas typical of tuberculosis infection and the retroperitoneal lymph node enlargement was probably on the basis of benign reactive hyperplasia rather than infection.

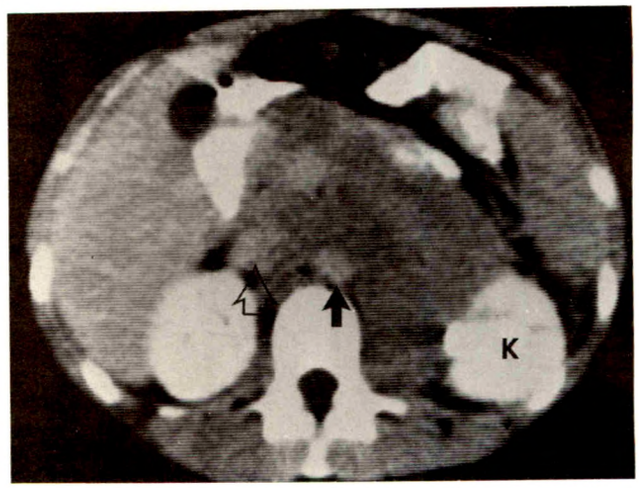


Fig. 3.—After intravenous contrast administration from child with known ataxia-telangiectasia. Mantle of retroperitoneal adenopathy causes displacement of bowel loops, lateral deviation of left kidney (K), and loss of aorta (*black arrow*) and inferior vena cava contours. Inferior vena cava (*open arrow*) displaced ventrally from normal anatomic position.

Discussion

Since the first report of eight patients by Hermans et al. [5], there have been many further reports of benign lymphoid hyperplasia in the immunodeficient patient [6–12]. However, a retroperitoneal location of massively enlarged lymph nodes has not been previously reported. The most frequently identified location of benign lymphoid hyperplasia has been the alimentary tract. The jejunum and ileum are the most common sites of involvement [6], but colonic [6, 7], duodenal [9], gastric [13], and total small bowel [10] distributions have also been reported. The classic radiographic appearance of benign lymphoid hyperplasia is well demonstrated in fig. 1B. Many of the reported patients with intestinal benign lymphoid hyperplasia may have had additional adenopathy in the retroperitoneum, but such retroperitoneal involvement has not been appreciated. Our two cases represent the first reported examples of massive retroperitoneal adenopathy in immunodeficiency. However, with the advent of CT scanning and its unique ability to image the retroperitoneum, we anticipate additional reports in the future.

No single pattern of immunodeficiency is linked to benign lymphoid hyperplasia, but the majority of patients

demonstrate some defect in gamma globulin synthesis, particularly low levels of serum IgA and IgM, with an often intact T-cell immune component. Precisely what proportion of immunodeficient patients demonstrate lymphoid hyperplasia is unknown. Conversely, nodular lymphoid hyperplasia should not always be taken as evidence of immunodeficiency, since it may appear in otherwise normal children [12].

Reports of CT findings in retroperitoneal adenopathy are now available [14–17]. Signs of the adenopathy include: (1) loss of the aorta and the inferior vena cava contours due to contiguous isodense adenopathy forming a mantle in an inverted "U" in the retroperitoneum; (2) identification of individually enlarged lymph nodes; and (3) displacement or distortion of the aorta, inferior vena cava, or other contiguous structures. However, there is no known method of differentiating benign from malignant lymphoproliferation on the basis of CT findings. Figure 3 is a CT section from a child with ataxia-telangiectasia who developed a true lymphoma. The section through the upper abdomen demonstrates a diffuse mantle of retroperitoneal adenopathy larger, but otherwise indistinguishable, from our two patients. Apparently even invasion of structures contiguous to the retroperitoneum (e.g., the stomach) does not reliably predict malignancy.

In conclusion, the radiologist faced with the observation of diffuse retroperitoneal lymph node enlargement in the immunodeficient patient should consider benign lymphoid hyperplasia and malignant lymphoma in the differential diagnosis. Reliance on gross anatomy demonstrated by CT for determination of malignancy is not sufficient, and histologic diagnosis is mandatory.

REFERENCES

1. Kersey JH, Specter BD, Good RA: Primary immunodeficiency diseases and cancer: the immunodeficiency-cancer registry. *Int J Cancer* 12:333–347, 1973
2. Shackelford G, McAlister WH: Primary immunodeficiency diseases and malignancy. *AJR* 123:144–153, 1975
3. Ammann AJ: T-cell and T-B cell immunodeficiency disorders. *Pediatr Clin North Am* 24:293–311, 1977
4. Paterson MC, Smith RP, Lohman PHM, Anderson AK, Fishman I: Defective excision repair of x-ray-damaged DNA in human (ataxia-telangiectasia) fibroblasts. *Nature* 260: 444–445, 1976
5. Hermans PE, Huizenga KA, Hoffman HN, Brown AL Jr, Markowitz H: Dysgammaglobulinemia associated with nodular lymphoid hyperplasia of the small intestine. *Am J Med* 40:78–89, 1966
6. Hodgson JR, Hoffman HN, Huizenga KA: Roentgenologic features of lymphoid hyperplasia of the small intestine associated with dysgammaglobulinemia. *Radiology* 88: 883–888, 1967
7. Bird DC, Jacobs JB, Silbiger M, Wolff SM: Hypogammaglobulinemia with nodular lymphoid hyperplasia of the intestine. *Radiology* 92:1535–1536, 1969
8. Grise JW: Dysgammaglobulinemia with nodular lymphoid hyperplasia of the small intestine. *Radiology* 90:579–580, 1968
9. Kirkpatrick CH, Waxman D, Smith OD, Schimke RN: Hypogammaglobulinemia with nodular lymphoid hyperplasia of the small bowel. *Arch Intern Med* 121:273–277, 1968
10. Goulston K, Stephen D: Nodular lymphoid hyperplasia of the small intestine associated with hypogammaglobulinemia. *Australas Radiol* 12:225–227, 1968
11. Ajdukiewicz AB, Youngs GR, Bouchier AD: Nodular lymphoid hyperplasia with hypogammaglobulinemia. *Gut* 13:589–595, 1972
12. Marshak RH, Hazzi C, Lindner AE, Maklansky D: Small bowel in immunoglobulin deficiency syndromes. *AJR* 122: 227–240, 1974
13. Bahk YU, Ahn JS, Choi HJ: Lymphoid hyperplasia of the stomach presenting as umbilicated polypoid lesions. *Radiology* 100:277–280, 1971
14. Callen PW, Korobkin M, Isherwood I: Computed tomographic evaluation of the retrocrural prevertebral space. *AJR* 129:907–910, 1977
15. Marshall WH Jr, Breiman RS, Harell GS, Glatstein E, Kaplan HS: Computed tomography of abdominal para-aortic lymph node disease: preliminary observations with a 6 second scanner. *AJR* 128:759–764, 1977
16. Kreel L: The EMI whole body scanner in the demonstration of lymph node enlargement. *Clin Radiol* 27:421–429, 1976
17. Redman HC, Glatstein E, Castellino RA, Federal WA: Computed tomography as an adjunct in the staging of Hodgkin's Disease and non-Hodgkin's lymphomas. *Radiology* 124: 381–385, 1977

Coincident Renal Cell Carcinoma and Renal Angiomyolipoma in Tuberous Sclerosis

OSCAR H. GUTIERREZ,[1] FRANCIS A. BURGENER,[1] AND STANLEY SCHWARTZ[2]

Renal angiomyolipomas occur in two distinctive clinical patterns. One type includes those associated with tuberous sclerosis, in which the renal involvement is usually bilateral and multifocal. It can occur as early as childhood and has an equal gender distribution [1]. The second type occurs predominantly in women 40–70 years old. These patients do not suffer from tuberous sclerosis and the renal lesion is usually unilateral and unifocal [1].

Renal angiomyolipomas are composed of three main tissues: (1) abnormal thick-walled blood vessels with a tendency to hemorrhage, (2) smooth muscle, and (3) fat [1]. It is generally believed that all three tissue components arise from embryonal cells in the kidney [1]. Since there are no documented cases of distant metastases, the general behavior of this tumor is that of a benign lesion although it is occasionally locally invasive [1].

The first case of a renal cell carcinoma and an angiomyolipoma occurring as two separate masses within the same kidney was recently reported in a patient without stigmata of tuberous sclerosis [2]. We report a patient with tuberous sclerosis in whom a renal cell carcinoma is superimposed on a kidney completely involved with angiomyolipomatosis, and demonstrate the diagnostic difficulties of this condition.

Case Report

A 24-year-old woman was first admitted to Strong Memorial Hospital for gross hematuria after a motor vehicle accident. Clinical history was remarkable for seizures since age 7 months, progressively developing sebaceous adenomas, a bowing deformity of the right forearm, and several intracranial calcifications.

At admission, there were bilateral palpable renal masses with bruits over the right side. On cystoscopy, blood was seen coming from the right ureteral orifice, and excretory urography revealed bilateral enlarged kidneys with deformed collecting systems. Bilateral renal arteriography did not identify a bleeding site, but showed angiographic features consistent with angiomyolipomas (figs. 1A and 1B). The patient was discharged after her urine cleared spontaneously.

The patient was readmitted 9 months later because of left flank pain, fever, nausea, and a rapidly falling hematocrit. Excretory urography revealed partial obstruction of the upper calyceal group by a large central mass on the left side. Repeat left renal arteriography (figs. 1C and 1D) showed significant further enlargement of the kidney caused by an avascular intrarenal mass considered to represent a large hematoma. A sizable intrarenal hematoma was evacuated during exploratory laparotomy, but no active bleeding point could be identified. Follow-up excretory urography demonstrated persistence of the partial obstruction in the left upper collecting system after evacuation of the hematoma.

At left nephrectomy 2 months later for recurrence of acute bleeding, the resected kidney measured 17 × 14 × 8 cm and weighed 1,350 g. On cross section, the lower pole was completely replaced by blood (hematoma). The rest of the kidney was composed of yellowish red nodules. No normal renal parenchyma was seen grossly. Two tumors were identified microscopically (fig. 2): (1) a typical renal cell carcinoma consisting of sheets and papillary structures of uniform clear cells and (2) an angiomyolipoma of the tuberous sclerosis complex. The latter was predominantly myomatous with a mixture of smooth muscle bundles, adipose tissue, and poorly formed blood vessels. The tumors were adjacent.

The patient showed marked clinical improvement after nephrectomy and remained asymptomatic until 1 year later, when she was readmitted because of a rapidly growing intrapelvic mass lesion. Angiography and liver scan revealed hypervascular metastases in the pelvis and liver involvement, the former confirmed by needle biopsy as metastases from the renal cell carcinoma. The patient died about 1 month after discharge. No autopsy was obtained.

Discussion

Angiomyolipomatosis of the tuberous sclerosis type with bilateral involvement of the kidneys can mimic adult polycystic disease on intravenous urography [3]. This was originally the case with our patient, who subsequently developed a hydronephrosis of the upper pole calyces of the kidney resulting probably from both intrarenal hemorrhage and renal cell carcinoma. It is of interest that this partial hydronephrosis persisted after surgical evacuation of the intrarenal hematoma. In the only other reported case in which an angiomyolipoma and a renal cell carcinoma coexisted in the same kidney [2], radiographic findings were similar. Although extrinsic filling defects in the collecting system due to tumors and hematomas are a common manifestation in renal angiomyolipomatosis, partial or complete hydronephrosis has to our knowledge not been reported in this entity. It remains to be determined whether this radiographic finding was purely coincidental or should have

→

Fig. 1.—Selective left renal arteriogram, early (**A**) and late (**B**) arterial phase. Kidney enlarged with numerous pathologic vessels throughout, a few saccular aneurysms, and no arteriovenous shunting. Circumferential peripheral vessels around tumor nodules in hilum and outer margin of left lower pole. "Onion peel" appearance suggested in nodule on outer margin of upper pole. Early (**C**) and late (**D**) arterial phase 9 months later. Further enlargement of kidney with central avascular mass (intrarenal hematoma) stretching and narrowing intrarenal branches. Coincident renal cell carcinoma cannot be diagnosed.

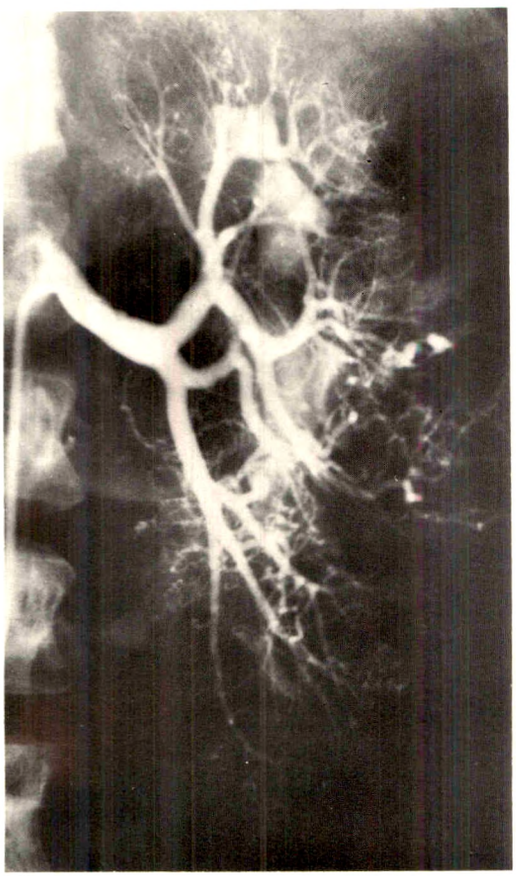
Received October 16, 1978; accepted after revision January 25, 1979.

[1]Department of Radiology, University of Rochester School of Medicine and Dentistry, Strong Memorial Hospital, 601 Elmwood Avenue, Rochester, New York 14642. Address reprint requests to O. H. Gutierrez.

[2]Department of Pathology, University of Rochester School of Medicine and Dentistry, Rochester, New York 14642.

© 1979 American Roentgen Ray Society

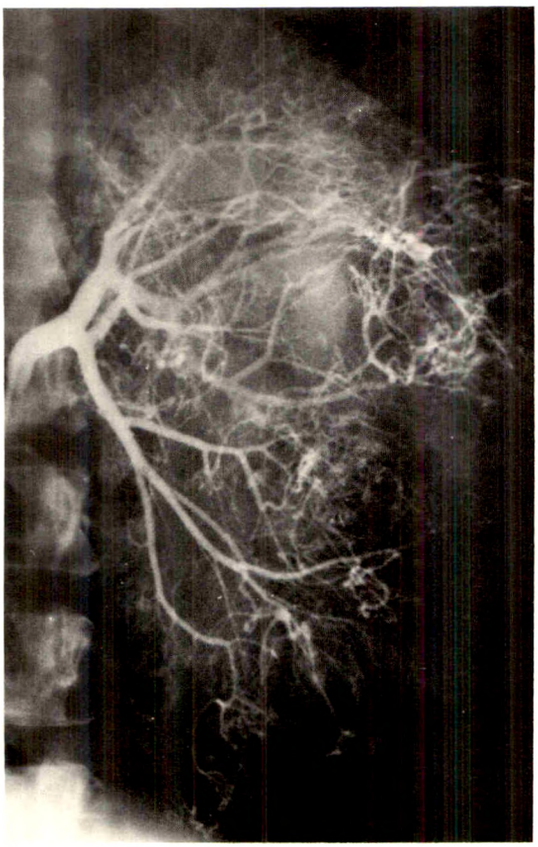
0361-803X/79/1325-0848 $0.00



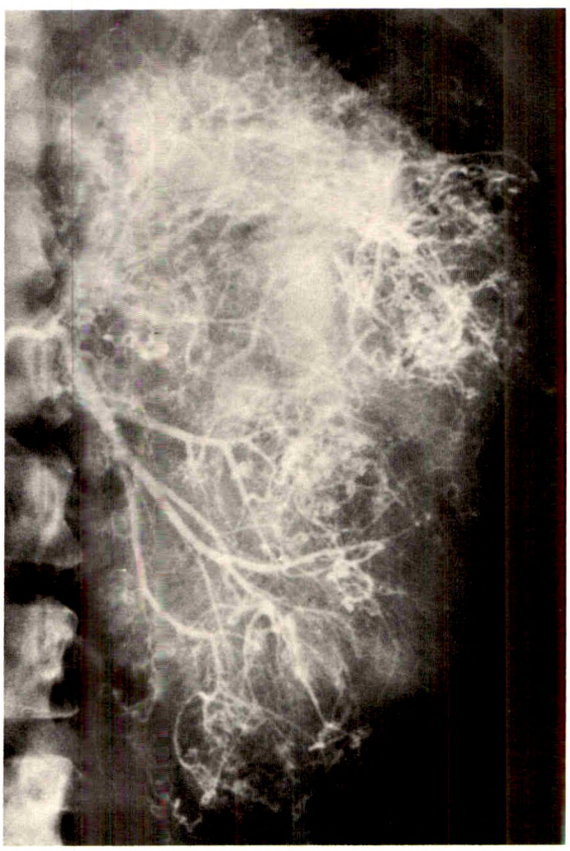
A



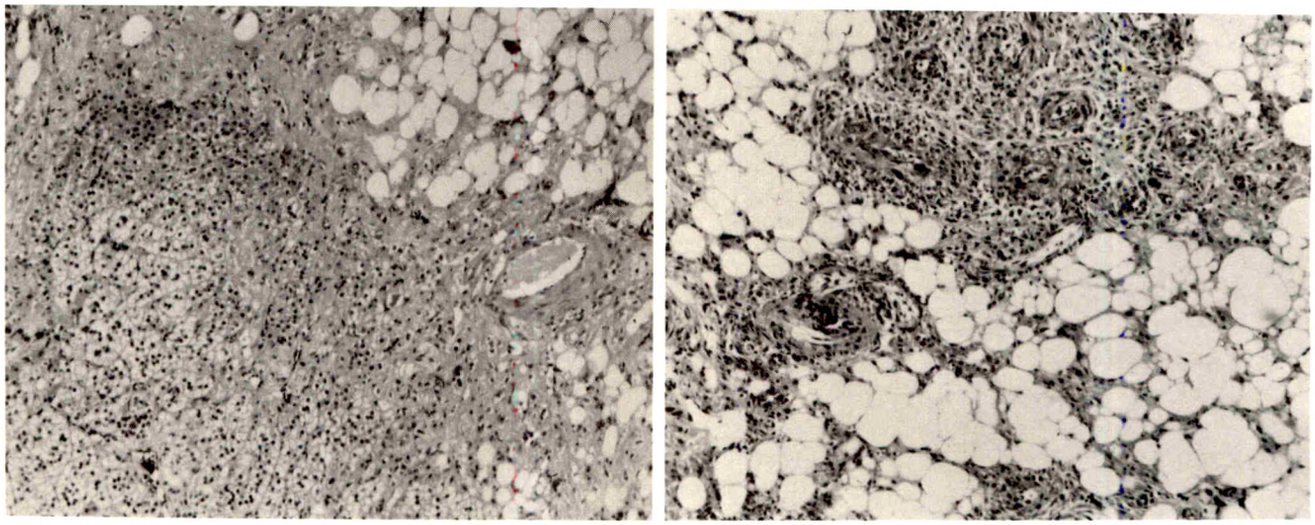
B



C



D



A B

Fig. 2.—Microscopic section. **A,** From boundary between renal carcinoma with large, clear cells arranged in cords and angiomyolipoma. **B,** Interlacing of smooth muscle bundles, fat, and atypical blood vessels. (H and E ×20).

raised the suspicion of a complicating malignancy, such as a renal cell carcinoma.

Arteriography has been used in the differentiation of angiomyolipomas from renal cell carcinomas. Angiographic findings shared by both tumors and, therefore, of no differential diagnostic value include: (1) tumor hypervascularity [1], (2) pathologic vessels of great tortuosity, abnormal distribution, and branching pattern [4], (3) parasitic lumbar arterial blood supply [5], (4) puddling of contrast material in the venous phase ("tumor stain"), and (5) no response of tumor vessels to epinephrine [6].

Other findings are reported to be more characteristic for an angiomyolipoma: (1) saccular aneurysmal dilatations of interlobar and interlobular arteries that look like a "cluster of grapes" [7], (2) circumferential peripheral tumors vessels [4], (3) "whorled onion peel" appearance in the nephrographic phase presumably related to the myomatous tissue present [8], (4) sharp delineation between the tumor and the normal kidney in the nephrographic phase [9], (5) thin radiolucent cleavage line around parts of the tumor peripherally [1], and (6) lack of arteriovenous shunt and early venous filling [4]. However, it must be realized that angiographic findings "typical" for an angiomyolipoma are present in well under half of histologically verified lesions [5] and are found with about equal frequency in tuberous sclerosis with diffuse lesions and individuals with a solitary renal tumor [4]. Furthermore, these findings are not diagnostic for angiomyolipomas since they can occasionally be found in renal cell carcinomas and other lesions [4, 10].

The correct angiographic diagnosis of renal angiolipomatosis complicated by hemorrhages and renal cell carcinoma cannot be made even retrospectively in our case, despite the fact that a baseline arteriogram, available for comparison, showed most of the described findings characteristic of renal angiomyolipomatosis. Therefore, follow-up arteriography seems of limited value for diagnosis of a coincident carcinoma when clinically suspected in a similar situation. Due to the large fat content of angiomyolipomas, computed tomography scanning represents a useful diagnostic approach; however, it is doubtful whether the coexistence of both pathologic entities could have been determined by this method, and it was not available to our patient at that time. Therefore, the correct diagnosis might only have been suggested with the radiographic demonstration of distant metastases not known to occur in uncomplicated renal angiomyolipomatosis.

REFERENCES

1. Bissada NK, White HJ, Sun NC, Smith PL, Barbour GL, Redman JF: Tuberous sclerosis complex and renal angiomyolipoma. Collective review. *Urology* 6:105–113, 1975
2. Kavaney PB, Fielding I: Angiomyolipoma and renal cell carcinoma in the same kidney. *Urology* 6:643–646, 1975
3. Taylor JM, Genters K: Renal angiomyolipoma and tuberous sclerosis. *J Urol* 79:685–696, 1958
4. Becker JA, Kinkhabwala M, Pollack H, Bosniak M: Angiomyolipoma (hamartoma) of the kidney. An angiographic review. *Acta Radiol [Diagn]* (Stockh) 14:561–568, 1975
5. Hyman RA, Bluestone P, Waldbaum RS, Naidich JB, Susin M: Parasitic lumbar arterial blood supply in renal angiomyolipoma. *Urology* 8:629–633, 1976
6. Silbiger ML, Peterson CC: Renal angiomyolipoma—its distinctive angiographic characteristics. *J Urol* 106:363–365, 1971
7. Viamonte M, Ravel R, Politano V, Bridges B: Angiographic findings in a patient with tuberous sclerosis. *AJR* 18:723–733, 1966
8. Khilnani MT, Abrams RM, Beranbaum ER: Angiographic features of hamartoma of the kidney. *Radiology* 90:999–1000, 1968
9. Love L, Frank SJ: Angiographic features of angiomyolipoma of the kidney. *AJR* 95:406–408, 1965
10. Brendler H, Maguire JW, Mitty HA: Angiographic characteristics of renal hamartoma. *Br J Urol* 43:674–678, 1971

Technical Notes

Convenient Method for Labeling Computed Tomographic Images

C. M. CITRIN[1]

Early dedicated head scanners and many subsequent scanners do not have the capability of either indicating patient position or of labeling the left or right side of the patient. This was not a problem in the past since CT scans were generally interpreted as viewing the patient from above. Although I advocate continued use of this convention, whole body scanners which can label either side of the image have enabled physicians to label cranial CT scans as if viewed from below. Surgical mistakes have been made and will continue in the future if a generally accepted labeling method is not adopted by all responsible for scan interpretation. Until that time, it is important that all scans be labeled, even those produced by scanners without the appropriate software. We have developed a simple method to indicate the appropriate side of the patient on our EMI CT 1005 scanner.

Technique

A small piece of transparent tape is placed on the roller of a typewriter. The bottom half of the strip of tape is aligned with the keys and the appropriate word (left, right, or both) is typed directly onto this portion of the tape. The upper part of the tape is not typed on to enable easier removal. After the tape is removed, the word is cut out, and this tiny piece of tape with the word is placed directly on either the screen from which a Polaroid picture will be obtained or on the cathode ray tube from which a transparency film image is generated. Since Polaroid pictures are obtained from a positive image, it is necessary to place the label over a white part of the screen, such as the scale. For the occasional coronal scan, the tape can be removed and either replaced with a fresh label on the opposite side or, if removed gently, can simply be moved over to the opposite side and then moved back after completion of the scan (fig. 1).

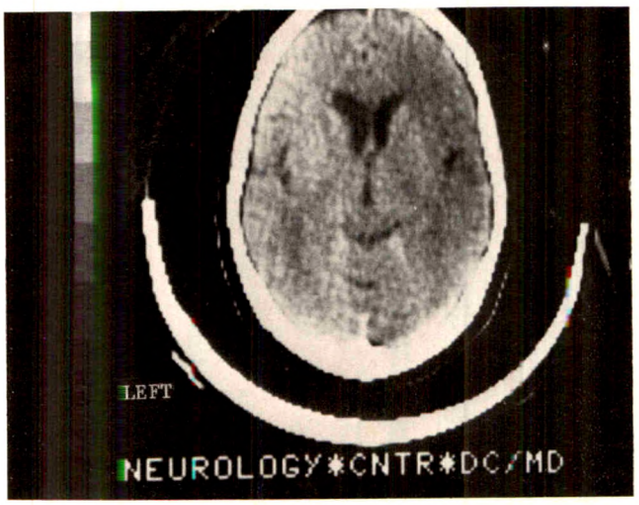


Fig. 1.—Image from transparency imager with patient's left side clearly labeled.

Received January 23, 1979; accepted January 29, 1979.
[1] Neurology Center, 5454 Wisconsin Avenue, Chevy Chase, Maryland 20015.

© 1979 American Roentgen Ray Society

0361-803X/79/1325-0851 $0.00

Catheter Angiography Through Aortofemoral Grafts: Inadvertent Catheterization of the Native Iliac Artery

RONALD L. EISENBERG,[1] CHARLES E. FISKE, AND MARCUS W. HEDGCOCK

Catheter angiography by direct puncture through aortofemoral bypass grafts has been demonstrated to be safe and the procedure of choice in the evaluation of graft patency [1]. Although two instances of catheter breakage have been reported with direct graft puncture, insertion of the guide wire before careful catheter withdrawal should eliminate this complication [2]. We report an inadvertent catheterization of the native iliac artery after direct puncture of an aortofemoral bypass graft and a simple technique to overcome this difficulty.

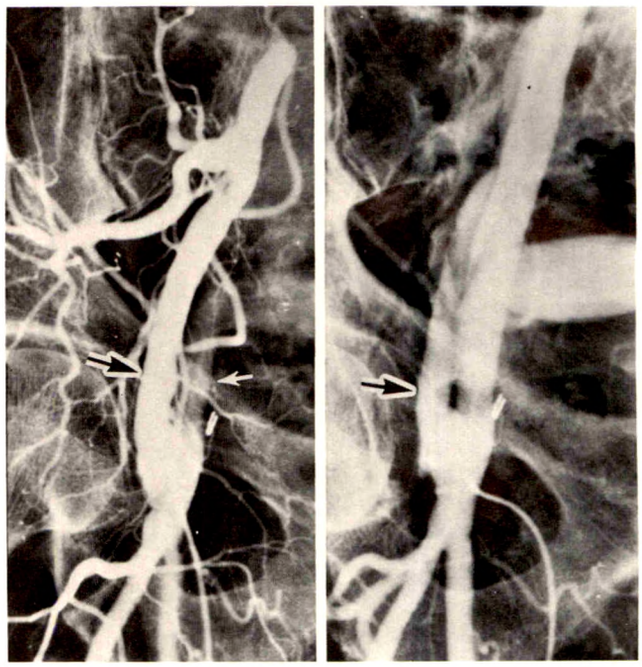
Case Report

A 55-year-old man, who had an aortobilateral femoral bypass graft placed 4 years before, was admitted for evaluation of bilateral rest pain in his legs of 1 year duration. Femoral pulses were strong bilaterally with no pulses distally. No femoral bruits were noted.

From an uncomplicated single wall puncture of the right limb of the bypass graft, excellent blood flow was obtained, and a guide wire was inserted. In the upper iliac region, there was an obstruction to further passage of the guide wire. A No. 5 French polyethylene catheter was inserted over the wire, and a contrast injection demonstrated the catheter inadvertently situated in the patient's native iliac artery, which was occluded proximally (fig. 1A). Reflux of contrast material into the bypass graft was noted. At this point, a new catheter with a short hockey stick tip was inserted and maneuvered to the level of anastomosis of the native iliac artery and the bypass graft. The tip of the catheter was positioned facing the graft, and the wire was reinserted and passed without difficulty into the right limb of the bypass graft. The rest of the examination was uneventful and demonstrated bilaterally patent aortofemoral grafts (fig. 1B), bilateral occlusions of the superficial femoral arteries with reconstitution at the level of the adductor canals, and excellent trifurcation runoff.

Discussion

No case of preferential catheterization of the native aorta has been reported after direct puncture of an aortofemoral bypass graft, although others have undoubtedly encountered this complication. In our case, this technical complication seems to have been caused by a puncture close to the end-to-side anastomosis and a lateral angulation of the needle. After direct puncture through an aortofemoral bypass graft, the inability to advance a guide wire through the graft into the aorta does not necessarily imply that the graft is occluded. As in our case, the wire may have inadvertently entered the patient's native iliac artery and, if this vessel were severely narrowed or occluded, it could prevent further passage of the wire. In either instance, a small catheter should be inserted over the wire and contrast injected. If the catheter is seen in the native vessel, simple maneuvering may successfully redirect the wire into the graft limb. This may obviate the need for an unnecessary repeat puncture of the aortofemoral bypass graft or a separate puncture of the axillary artery.



A B

Fig. 1.—Contrast injections. **A**, In native iliac artery (*black arrow*), proximal occlusion. Reflux into aortofemoral bypass graft (*white arrow*). **B**, Via catheter in distal aorta, patent right limb of aortofemoral bypass graft fills. Reflux into native iliac artery (*arrow*).

REFERENCES

1. Eisenberg RL, Mani RL, McDonald EJ Jr: The complication rate of catheter angiography by direct puncture through aortofemoral bypass grafts. *AJR* 126:814–816, 1976
2. Mani RL, Costin BS: Catheter angiography through aortofemoral grafts: prevention of catheter separation during withdrawal. *AJR* 128:328–329, 1977.

Received December 12, 1978; accepted February 6, 1979.

[1]All authors: Department of Radiology, Veterans Administration Medical Center, and University of California School of Medicine, 4150 Clement Street, San Francisco, California 94121. Address reprint requests to R. L. Eisenberg.

 0361-803X/79/1325-0852 $0.00

Simplified Method of Transcatheter Embolization with Polyvinyl Alcohol Foam (Ivalon)

STEPHEN L. KAUFMAN[1]

Polyvinyl alcohol (Ivalon) (Unipoint Industries, High Point, N.C.) is an inert biocompatible material capable of producing a permanent vascular occlusion after transcatheter embolization [1, 2]. A significant drawback inherent in its use as an embolic agent is the difficulty of introducing particles of this material from syringes into angiographic catheters [2, 3]. Several methods for overcoming this have been proposed, including preloading of polyvinyl alcohol plugs into polyethylene tubes [2] and the production of uniform suspensions of small polyvinyl alcohol particles before injection [3]. We recently developed a simple method for consistently successful embolization of polyvinyl alcohol using materials that are inexpensive and readily avialable in any angiographic laboratory.

Materials and Methods

Polyvinyl alcohol sponge is cut into about 1 × 1 × 10 mm strips, packaged, and gas-sterilized for future use. Packages of 10–15 strips are opened and immersed in flushing solution for several minutes immediately before use. At the time of embolization, from one to three strips are inserted with fine forceps into the tip of the male end of a K-50 extension tube (Pharmaseal, Inc., Toa Alta, P.R.) filled with dilute contrast material and the proximal end closed with a stopcock (fig. 1). The male end of the extension tube is then connected directly to the flange of the angiographic catheter and under fluoroscopic observation the particles are slowly flushed through the catheter using diluted contrast material. The process is repeated until the desired degree of embolic occlusion has been achieved. Direct connection of the extension tube to the catheter eliminates the possibility of the polyvinyl alcohol particles being caught in the stopcock and a wet hookup reduces the possibility of air embolization. The use of contrast material and fluoroscopic monitoring during embolization reduces the possibility of reflux and inadvertent embolization of circulations other than the one intended [4]. For repeated embolizations of angiomatous malformations, several K-50 extension tubes are used to shorten the length of the procedure.

Discussion

The choice of a transcatheter embolic agent in a given stiuation depends on the disease process involved and the size of the vessel to be occluded. Gelfoam is an effective, easy-to-use agent in the treatment of arterial hemorrhage from small vessels due to benign self-limited conditions, such as duodenal ulcers. Because Gelfoam does not result in permanent vascular occlusion [5] it is not always the agent of choice (such as in the transcatheter occlusion of small hemangiomas or in the therapy of neoplastic hemorrhage).

Polyvinyl alcohol is inert, nonresorbable, and results in permanent vascular occlusion [1, 2]. Unfortunately, its physical characteristics have heretofore made it difficult to inject through angiographic catheters. This method is simple and uses readily available materials. We have effectively used this method in several patients to occlude small vessels leading to angiomatous malformations, and we believe this means of polyvinyl alcohol embolization should be used when long term occlusion is desirable.

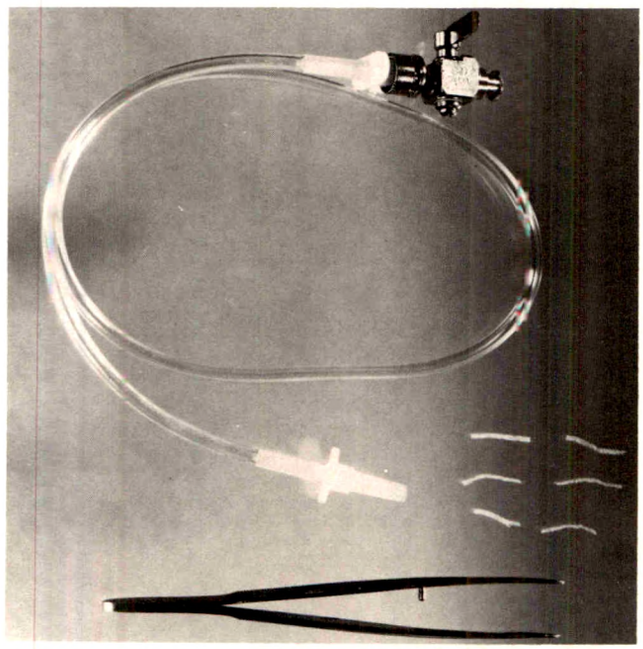


Fig. 1.—Apparatus for embolization. Strips of polyvinyl alcohol are inserted with fine forceps into tip of male end of K-50 extension tube filled with diluted contrast material.

ACKNOWLEDGMENT

I thank Dr. Robert I. White, Jr., for editing this manuscript.

REFERENCES

1. Tadavarthy SM, Moller JH, Amplatz K: Polyvinyl alcohol (Ivalon)—a new embolic material. *AJR* 125:609–616, 1975
2. White RI Jr, Strandberg JD, Gross GS, Barth KH: Therapeutic embolization with long term occluding agents and their effects on embolized tissues. *Radiology* 125:677–687, 1977
3. Kerber CW, Bank WO, Horton JA: Polyvinyl alcohol foam: prepackaged emboli for therapeutic embolization. *AJR* 130: 1193–1194, 1978
4. Kerber CW: Catheter therapy: fluoroscopic monitoring of deliberate embolic occlusion. *Radiology* 125:538–540, 1977
5. Barth KH, Strandberg JD, White RI Jr: Long term follow-up of transcatheter embolization with autologous clot, Oxycel and Gelfoam in domestic swine. *Invest Radiol* 12:273–280, 1977

Received December 19, 1978; accepted February 6, 1979.

[1] Russell H. Morgan Department of Radiology and Radiological Science, Johns Hopkins Medical Institutions, Baltimore, Maryland 21205.

© 1979 American Roentgen Ray Society

0361–803X/79/1325–0853 $0.00

Editorial

First Year Radiology Residents: PGI vs. PGII

As members of the University of North Carolina Department of Radiology Residency Selection Committee, we would like to address the issue of whether a clinically oriented year should be a prerequisite to proper diagnostic radiology training and whether training programs should admit residents with or without prior postgraduate experience. Our opinions derive from experience with two groups of trainees in the past 5 years, 16 residents who had varying degrees of postgraduate clinical training and 12 residents who came to us directly from medical school

Of the 16 with postgraduate experience, eight had 1 year of medicine, two had 2 years of medicine, three had 2–4 years of surgery training, two had 1 year of OB-GYN training and one had 1 year of pediatric training. Of the 12 residents coming directly from medical school, one had Ph.D. experience in nuclear engineering prior to medical school. The average age at the beginning of radiology residency training of the 16 residents with clinical experience was 27.7 years and the average age of the 12 residents coming from medical school was 27.0 (skewed somewhat by the one resident with Ph.D. experience who was 35). All the trainees in each group were rated in the upper half of their graduating classes or higher.

Historically, before the demise of the free-standing internship, *all* radiology residents had some clinical experience prior to their 3 years of training in radiology. There is no question that a clinical year was (and is) beneficial. Valuable experience in learning how to take care of patients and how to get along with one's peers was gained, not to mention the medical or surgical knowledge gained. One also matured as a person and, more importantly, as a physician.

Since free-standing internships have been abolished and all first postgraduate years are now part of residency training programs, the situation has drastically changed. The requirements for the American Board of Radiology for certification in Diagnostic Radiology require 4 postgraduate years, with 3 spent in diagnostic radiology. Now the graduating medical student who wishes to go into radiology has two options: doing a postgraduate (usually clinical) year followed by 3 years of radiology training or going directly into radiology and doing a 4 year residency (which may include some clinical training).

Our diagnostic radiology residency program includes both types of residents, both becoming Board eligible upon completion.The resident who has had one or more prior years in postgraduate training spends 3 years in diagnostic radiology.The graduating medical student spends 4 years in radiology training: 3 years in diagnostic radiology followed by an elective fourth year in which he obtains fellowship experience in general or subspecialty radiology. The 3 year period spent in diagnostic radiology is the same for the two groups—basic rotations through all the subspecialty and general areas of radiology; experience in neuroradiology and peripheral vascular angiography, CT, ultrasound, nuclear medicine, pathology, and physics; and elective time with opportunity for research experience.

What differences have we observed in our two types of residents? We have experienced no difference in the level of performance of the residents as judged by their peers, their attending staffs, or, more importantly, their clinical colleagues. The differences in residents are differences in personalities, not level of previous experience. Both types of residents do equally well on the Board examinations (all have passed successfully both parts I and II). In a limited sample (four PGIs and six PGIIs) in which scores on part I (written) of the Boards were available the PGIs scores averaged 67.7 percentile; the PGIIs averaged 53.5 percentile. (The PGII has one more year of radiology at the time of this examination.) Both types find postresidency positions (both private practice and academic) equally well. We have not trained enough residents yet to attach any statistical significance, but it would seem that more of the fourth year residents stay in academic radiology than the three year residents. This may be because those who specialize further with their fellowship experience tend to stay in academic centers. Yet, both perform equally well in either academic pursuits or private practice. In summary, both types of programs produce quality radiologists.

For the graduating medical student who knows he will enter radiology, but wants to do a clinical year first, the doors are usually closed to quality clinical training, since most programs accept only residents who are expected to finish the program. No longer are many "rotating" type internships available which give experience in multiple fields of medicine.Thus, a "general" clinical experience is now only available in the traditional medical school years. We feel that although a clinical year might be beneficial, it is not necessary as a prerequisite to the training process of radiologists. Therefore, we encourage medical students to go directly into radiology training if they have made a firm commitment to our specialty during the medical school years.

Conversely, we feel that residents with postgraduate experience should not be denied entrance into radiology. There are many medical schools where students are not exposed to radiology soon enough to make it a valid career choice. The national Intern/Residency Matching Process necessitates career choice after the third year of

© 1979 American Roentgen Ray Society

0361–803X/79/1325–0855 $0.00

medical school. Therefore, so as not to penalize residents who only are "turned on" to radiology some time after beginning clinical training, we will continue to offer both PGI (first postgraduate year residents directly from medical school) and PGII (second postgraduate year residents with prior postgraduate experience) positions for our first year residents.

Furthermore, we urge other training programs not to restrict their training programs to one type of resident. This limits the options available to the other type of resident and overburdens the residency selection process of other institutions who admit that type. We also urge the American Board of Radiology not to require a "clinical" year as a prerequisite to radiology training, thus forcing many residents to spend a year doing something in which they have no interest and which may not significantly benefit their education in radiology.

John T. Cuttino
James H. Scatliff
University of North Carolina
School of Medicine
Chapel Hill, North Carolina 27514

Letters

Sitting on the Fence in X-ray Reporting

"May be," "probably," "possibly," etc. are words seen too often in too many x-ray reports. In many cases these words replace "I do not know" or "I do not want to take the effort to look further, or consult a textbook or a colleague, but I am ready to take the money." I would like to see what these same radiologists would do if they went to purchase a shirt and found a sleeve missing. Sometimes a simple comparison with previous studies gives an answer. There is nothing wrong with reading previous reports to see what another radiologist thinks. There is no excuse for neglecting to look into the x-ray jacket, even if doing so cuts down the speed of our work.

Sometimes the clinician is at fault in not giving important clinical information. I know it is difficult to educate a clinician on whom we depend for our bread and butter. However, we can make his life miserable by giving him a long list of differential diagnoses, until he learns that only by giving us pertinent information will we be able to supply him with a concise and, hopefully, accurate answer.

There are, of course, gray areas—borderlands between normal and abnormal where even the best radiologist is not sure. In these cases, we can use "probably." I prefer sometimes to say, "The significance of this is not clear to me," or "I do not know the answer but I will give you one after the films are shown to Dr. ." A radiologist is a consultant and the clinician depends on his interpretation. We have to give as short and precise an answer as possible. If we like to give a long one, then it is our duty to at least give a *short* impression or conclusion at the end of the long report. Radiology is a profession that is involved in anatomy, pathology, medicine, and surgery. The radiologist should not try to escape involvement.*

Kenneth R. Kattan
Veterans Administration Medical Center
Dayton, Ohio 45428

Whole Body Opacification

Griscom's article [1] has again brought to our attention the useful technique of whole body opacification. Many radiologists (pediatric and otherwise) are under the impression that to achieve this effect the radiographs must be taken immediately after injection of contrast media. The technique is particularly useful in the young infant and, as pointed out in the article, the slow glomerular filtration rate in neonates makes the time flexible. We want to reinforce that statement. We have seen excellent visualization at 30 min (dose, 3-4 ml/kg) of avascular structures such as hydrocolops and adrenal hemorrhage pseudocysts, the latter being seen on tomography. We cannot say whether the technique is as effective at 30-40 min as at less than 10 min, but we suspect it may be. What we would like to note is that junior staff members should not neglect to take a later radiograph in neonates because an avascular lesion was not initially considered.

B. J. Cremin
Groote Schuur Hospital
Cape Town 7925, South Africa

REFERENCE

1. Griscom NT: Total body opacification. *AJR* 131:919–925, 1978

Another Look Around the Corner

The March 1978 *AJR* contains two interesting articles [1, 2] regarding pulmonary radiology. Based on the authority of the authors and on the great value of their papers, an editorial appeared in the same journal entitled "A Corner is Turned" [3]. In this, Figley states, "the static chest film cannot confidently predict the extent and location of respiratory surface destruction" and, further, "we may safely assume its story [static chest film] has been told."

In the above-mentioned articles, only maximum inspiration films were used. Milne [4] wrote, "It is surprising how few radiologists use expiratory chest films and yet will report—purely from an inspiratory film—that lung volumes are increased or that there is extensive fibrosis, when an expiratory film would reveal a large diaphragmatic excursion and no airtrapping whatsoever."

Based upon the visibility of the minor fissure on ±70% of chest films, we [5–8] derived a method for evaluating regional lung expansion on maximal inspiration-expiration pairs of chest radiographs in a zone above and below the horizontal fissure. In all situations studied, the linear regional craniocaudal lung expansion appeared larger in the zone below the horizontal fissure. Changes in regional lung expansions were shown in different body positions [5], young male smokers and nonsmokers [6], young males and females [8], and in females with and without left heart failure [7].

I believe this simple method allows the radiologist to have another look around the corner. That nuclear medicine procedures are more sensitive in assessing regional ventilation is beyond discussion. George Simon [9], who inspired me to investigate the challenges of pulmonary radiology, suggested we reevaluate our findings, "what you see, or think you see, is a pale reflection of physiological reality." This criticism is undoubtedly true, but in the clinical situation, the radiograph can indeed give a "pale reflection of such measurements and this may be all that is possible or needed in relation to the patient at a particular phase of his illness."

Paul Beeckman
Vrije Universiteit Brussel
1090 Brussels, Belgium

REFERENCES

1. Fazio F, Lavender JP, Steiner RE: ^{81m}Kr ventilation and ^{99m}Tc perfusion scans in chest disease: comparison with standard radiographs. *AJR* 130:421–428, 1978
2. Thurlbeck WM, Simon G: Radiographic appearances of the chest in emphysema. *AJR* 130:429–440, 1978
3. Figley MM: Editorial: a corner is turned. *AJR* 130:585, 1978
4. Milne E: Correlation of physiologic findings with chest roentgenology. *Radiol Clin North Am* 9:17–47, 1973

* The views expressed in this letter are solely the opinion of the writer and do not represent those of the Veterans Administration.

© 1979 American Roentgen Ray Society

0361-803X/79/1325-0857 $0.00

5. Beeckman P, Vanclooster R, Michels J, Silver D, van Damme E: A radiological study of the effects of body position and respiration on regional differences in the lung. *J Belge Radiol* 61:229–236, 1978
6. Beeckman P, Vanclooster R, Michels J, Silver D, van Damme E, van Damme W: A radiological study of the effects of smoking on regional differences in the lung. *J Belge Radiol* 61:241–245, 1978
7. Beeckman P, Vanclooster R, Michels J, Silver D: A radiological study of the effects of left heart failure on regional lung differences. *J Belge Radiol* 61:247–252, 1978
8. Beeckman P: *The Importance of the Minor Fissure in Assessing Regional Differences in the Lung*, edited by Beeckman P, Brussels, Vrije Universiteit, 1978, pp 80–91
9. Simon G: The plain radiograph in relation to lung physiology. *Radiol Clin North Am* 19:3–16, 1973

Reply

Dr. Beeckman has properly brought to my attention his interesting work on regional variations in ventilation that may be determined by the simple expedient of inspiration and expiration films using the minor fissure as a landmark in the right lung for separating the lung into apical and basal components. In publications to which he refers, he and his associates have documented the relatively larger inflation of the basal portion of the normal lung in erect posture and somewhat lesser inflation of this portion of the lung in supine 45°, head down, and lateral decubitus positions. Of special interest is the sensitivity of this simple technique in recognizing alterations with left heart failure and smoking. Heart failure selectively reduces the ventilation of the lung base below the horizontal fissure, while not appreciably altering the ventilation of the lung above the fissure. Smoking also lessens the ventilation of the lung bases, an effect more pronounced in older than young male smokers, but even in youth the effect of smoking is measurable.

As Dr. Beeckman acknowledges in his letter, the method is not a substitute for radionuclide scanning, but is more informative than the simple static film against which the authors of the papers to which he refers contrasted their scanning and pathologic observations. No doubt these authors would agree with Dr. Beeckman that the static film is more limited than the dynamic examinations he proposes. They would undoubtedly also be interested in correlations between his method and radionuclide scanning were it possible to obtain some information in groups of patients such as he has studied.

MMF

Positioning for Oblique Projection in Mammography

As a promotor of the oblique view at mammography, I was saddened to see the drawing I assume should illustrate its positioning in [1]. I sincerely hope that the authors have not actually used this positioning in the belief that they would be able to produce an acceptable oblique view (as I understand it). Unfortunately, it is not possible to describe how the real oblique view is positioned, but the accompanying photograph (fig. 1) should convey the basic idea. This photo appeared with an article to which the authors referred [2]. Usually it takes a couple of weeks of intensive training even for clever radiographers to acquire the skill needed for the proper adjustment of the x-ray unit to the patient's body, breast, axilla, and arm. The idea is to include the whole breast in this view, right into the chest wall. That is impossible if Hall and Berenberg's positioning [1] is used.

Unless two radiographers work together, it is also practically impossible to obtain acceptable oblique views if the x-ray unit lacks the motorized compression (an idea of mine) now available on Philips, Siemens, and CGR units, at least in Scandinavia. The compression plate is foot-maneuvered, leaving both hands free to position the patient.

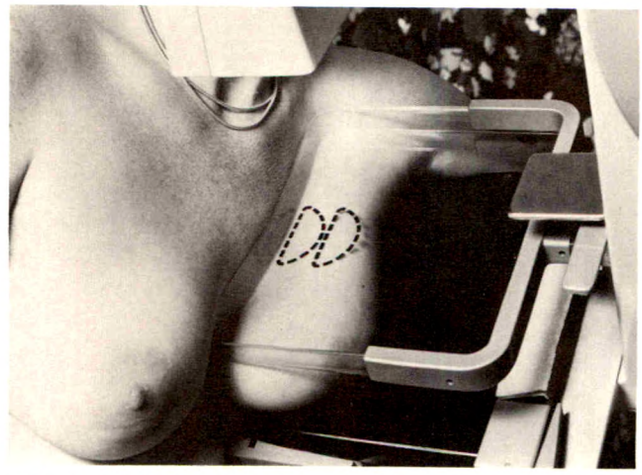


Fig. 1.—Positioning for oblique view at mammography. Patient's whole breast, right into the chest wall, is included in this view. (Reprinted from [2].)

It took us 5 years of rather indifferent work with the oblique view until we stumbled on the "real" way to do it, with a concomitant, quite remarkable improvement in image quality. Anyone wishing to learn the technique is very much welcome to visit us (for 1 or 2 weeks).

Bengt Lundgren
Gävle Hospital
Gävle 7, Sweden

REFERENCES

1. Hall FM, Berenberg AL: Selective use of the oblique projection in mammography. *AJR* 131:465–468, 1978
2. Lundgren B: The oblique view at mammography. *Br J Radiol* 50:626–628, 1976

Reply

We concur with the thrust of Dr. Lundgren's remarks concerning the difficulty in obtaining optimal oblique projections of the breast. Our diagramatic figure certainly does not convey the difficulty in positioning that Dr. Lundgren describes. We have been impressed with the lack of reproducibility of oblique views and our frequent inability to visualize as much of the breast parenchyma as obtained on standard lateral and craniocaudad projections. This probably relates in part to our examinations being performed by a single technician using a standard mammographic unit without motorized compression.

The technique of obtaining oblique mammographic projections described by Dr. Lundgren will enable a larger portion of the breast to be visualized than is possible on either the craniocaudad or lateral views alone. This technique is therefore extremely important when the oblique view is used routinely. However, this positioning for the oblique projection, although obviously desirable, is usually unnecessary for the purposes we describe in our article: distinguishing true masses from pseudolesions caused by superimposition of focal areas of normal or dysplastic breast tissue. The latter problem, arises relatively seldomly and can usually be resolved by slight changes in mammographic positioning.

Ferris M. Hall
Arnold L. Berenberg
Beth Israel Hospital
Harvard Medical School
Boston, Massachusetts 02215

Abstracts of Current Literature

Chest

Usual manifestations of pulmonary aspergillosis. Kipinski JK, Weisbrod GL, Sanders DE (Toronto General Hospital, University of Toronto, 101 College Street, Toronto, Ontario, Canada M5G 1L7). *J Can Assoc Radiol* 29:216–220, Dec 1978

Pulmonary aspergillosis is now seen more frequently. There are three main categories of this disease, these are: (1) noninvasive pulmonary aspergillosis; (2) allergic bronchopulmonary aspergillosis; and (3) invasive pulmonary aspergillosis. The latter can be associated with altered defense mechanisms or with overwhelming inhalation of aspergillus spores. The authors describe their experience with five cases of pulmonary aspergillosis, illustrating unusual features of each of these major groups.

In noninvasive pulmonary aspergillosis, the prerequisite chronic cavity may be due to virtually any cause. When there is interference to the drainage of this cavity, a suitable milieu arises for the growth of the mycetoma. The fairly typical "fungus ball" becomes apparent on the radiographs.

In allergic bronchopulmonary aspergillosis, the radiographic patterns are variable, the most common changes being transient migratory nonsegmented consolidation, mucoid impaction and proximal bronchiectasis.

Invasive aspergillosis most commonly occurs in the immunologically compromised host. The characteristic radiographic findings are a single or multiple area of consolidation with cavitation. These changes often are similar to those seen in the noninvasive form of the disease but follow-up films will often permit differentiation.

Jack M.A. Tishler

Leiomyosarcoma of the thorax. Carlson DH, Hanelin J (Newton-Wellesley Hospital, Newton Lower Falls, Massachusetts 02162). *J Can Assoc Radiol* 29:221–224, Dec 1978

Thoracic leiomyosarcoma is a rare neoplasm with fewer than 100 cases presented in the world literature. The vast majority of cases have occurred in middle aged males, with cough, chest pains, and hemoptysis the common presenting symptoms. The authors report their experience with three additional cases, one presenting with loss of volume of the right lower lobe secondary to an endobronchial leiomyosarcoma, diagnosed at bronchoscopic biopsy, the second with a right upper lung mass diagnosed as pulmonary leiomyosarcoma at surgery and the third patient presenting with a left upper extrapulmonary chest mass which eroded the adjacent rib. A chest wall leiomyosarcoma was resected at surgery. These lesions are very aggressive, all three patients had extensive metastases and none survived 1 year following surgery.

Jack M.A. Tishler

Diaphragmatic hernia simulating pleural effusion and complicating puerperim. Thind GS (Department of Tuberculosis and Chest Diseases, Medical College Hospital, Amritsar, India). *Australas Radiol* 21:325–327, Dec 1977

This case describes a 22-year-old female who developed a large paraesophageal hernia after the birth of her first child following a difficult labor. A large opacity in the left side of the thorax was initially thought to be a tuberculosis effusion and was treated accordingly. However, further investigations were prompted by continued mild symptoms. The subsequent chest radiograph suggested a diaphragmatic hernia. Barium examination was performed, revealing a large paraesophageal hernia with the stomach in organoaxial rotation. Surgery was refused and there was no change in her clinical condition at 4-year follow-up.

The author asserts that although small hiatus hernias are common in pregnancy, the paraesophageal variety, particularly if large, are rare. In this case it was felt to be related to the difficult labor. Attempted aspiration under the mistaken diagnosis of pleural effusion can cause chemical pleuritis and shock. Surgical repair of paraesophageal hernias should always be considered even in the absence of symptoms because of the possibility of strangulation occurring with small defects, and kinking and obstruction in the case of large defects.

J. A. Branson

Bronchiolitis. Wohl MEB, Chernick V *Am Rev Respir Dis* 118: 759–781, Oct 1978

This excellent "State of the Art" review details the clinical features, epidemiology, radiography, pathology, and pathogenesis of this common disease. The authors further review the association of bronchiolitis with the later development of unilateral hyperlucent lung or the Swyer-James syndrome.

W. Richard Webb

Percutaneous transthoracic aspiration needle biopsy. Sagel SS, Ferguson TB, Forrest JV, et al. (Mallinckrodt Institute of Radiology, Washington University School of Medicine, St. Louis, Missouri). *Ann Thorac Surg* 26:399–404, Nov 1978

Experience with transthoracic needle aspiration biopsy in 1,211 patients has shown this procedure to be valuable in the diagnosis of neoplastic lesions beyond the reach of the fiberoptic bronchoscope. In 896 patients with a malignant intrathoracic tumor, the needle aspirate found malignant cells in 96%, but multiple aspirations were sometimes necessary. Only 87% of malignancies were diagnosed during the first aspiration procedure consisting of one or more biopsies; a second procedure the same or the following day was performed when cancer was suspect clinically. A false positive diagnosis of carcinoma occurred in two patients with tuberculosis and squamous metaplasia.

The true negative rate (accuracy of a negative diagnosis) was only 87%; in other words, the biopsy finding of "no malignant cells" does not mean tumor is reliably absent. In 31 immunosuppressed patients in whom a focal pneumonic lesion was aspirated, 24 (77%) had positive cultures of the aspirate, and smear disclosed the causative organism in 11. Complications were relatively minor. No deaths resulted. Pneumothorax occurred in 292 (24%) and chest tube drainage was necessary in 167 (15%). Transient minor hemoptysis occurred in 73 patients (6%) with minor bleeding around the lesion visible radiographically in 48.

W. Richard Webb

Acute traumatic hemothorax. Griffith GL, Todd EP, McMillin RD, Zeok JV, Dillon ML, Utley JR, Griffin WO (University of Kentucky Medical Center, 800 Rose Street, MN 272 Lexington, Kentucky 40506). *Ann Thorac Surg* 26:204–207, Sept 1978

Over a 5-year-period, 107 patients with acute traumatic hemothorax were evaluated and treated. Fifty-two percent had penetrating trauma and 48% had associated abdominal injuries, usually to spleen, liver, or diaphragm. The large majority of hemothoraces result from rupture or laceration of low pressure pulmonary vessels and will spontaneously tamponade after evacuation of the pleural contents and reapposition of the

© 1979 American Roentgen Ray Society

0361–803X/79/1325–0859 $0.00

pleural surfaces. Eighty-eight patients were treated solely by tube thoracostomy; eight developed late complications (empyema or fibrothorax), but in all, tube placement was sufficient to control bleeding. Immediate or delayed thoracotomy was required to control bleeding in only 11 patients; four had mediastinal bleeding or pericardial tamponade, two had lacerated intercostal vessels, and three had continued hemorrhage from lung parenchyma.

W. Richard Webb

Blunt traumatic rupture of the diaphragm. Brooks JW (Department of Surgery, Medical College of Virginia, Virginia Commonwealth University, Richmond, Virginia 23298). *Ann Thorac Surg* 26:199–203, Sept 1978

During a 25-year period, 42 patients with blunt traumatic rupture of the diaphragm were studied. Patients often have multisystem injuries, and symptoms and physical findings of diaphragmatic rupture are frequently vague. Preoperative diagnosis of diaphragmatic rupture is usually made by chest radiography, showing an abnormal or obscured diaphragm or a herniated viscus in the chest. Among the 42 patients surveyed, 38 (90%) had left-sided ruptures; this is often associated with herniation of stomach into the left chest. Confirmation of the diagnosis often requires diagnostic pneumoperitoneum; the presence of air within the pleural space following this procedure indicates a ruptured diaphragm.

W. Richard Webb

Pulmonary function abnormalities in asymptomatic children after hydrocarbon pneumonitis. Gurwitz D, Kattan M, Levison H, Culham JAG (Hospital for Sick Children, 555 University Avenue, Toronto, Ontario M5G 1X8, Canada). *Pediatrics* 62: 789–794, 1978

Seventeen asymptomatic children were studied 8–14 years after hydrocarbon pneumonitis. Some 82% had abnormalities of pulmonary function which were thought to be due to small airway obstruction and/or loss of elastic recoil. The chest films at follow-up were normal in all but one patient who showed areas of scarring. The authors postulate that these children may be at risk in adult life for the development of chronic lung disease.

B. J. Wood

Cardiovascular

Hemodynamic and angiographic guidelines in selection of patients for femoro-femoral bypass. Flanigan DP, Pratt DG, Goodreau JJ, Burnham SJ, Yao JST, Bergan JJ (Northwestern University Medical School, Chicago, Illinois 60611). *Arch Surg* 113:1257–1262, Nov 1978

The femoro-femoral crossover graft is an alternative to aorto-femoral bypass procedures and is used in poor risk patients with unilateral claudication, rest pain, or gangrene due to unilateral iliac artery occlusive disease. Although crossover femoro-femoral grafts have had good long-term patency, early graft failure due either to thrombosis or hemodynamic factors occurs in 16%–26%. This study was undertaken to establish better guidelines for selection of patients for this procedure. Fifty-one of 80 graft procedures (74%) remained patent. The failures were predominately in two groups, those with greater than 50% stenosis of the donor iliac artery and those with severe recipient limb outflow occlusive disease. Patients with greater than 50% stenosis of the donor iliac artery uniformly had unsuccessful grafts. Patients with recipient limb outflow disease had only a 41% success rate, and if concomitant donor iliac artery stenosis (less than 50%) was present, the success rate dropped to 21%.

Reiley Kidd

Pseudotumoral angiographic patterns in cirrhosis of the liver (In Italian). Passariello R, Rossi P, Simonetti G, Ciolina A (Istituto di Radiologia, Policlinico Umberto I, I-00161 Roma, Italy). *Radiol Med* 64:516–523, 1978

In cirrhosis of the liver the angiographic findings are usually related to the stage of the pathologic process. In advanced stages, however, at times an angiographic pattern can simulate the presence of a neoplastic growth, either primary or secondary. The authors analyze the abnormal angiograms by these categories: (1) arterioportal fistulae; (2) stenosis of hilar or of intraparenchymal vascular branches; (3) areas of increased or diminished vascularization; and (4) changes in the course of intraparenchymal arterial branches. These abnormal angiographic findings were noted in 12 of 154 cases with hepatic cirrhosis. In eight, the angiograms simulated a malignant primary neoplasm of the liver and in four, disseminated metastases.

Antonio F. Govoni

Pericardiocentesis. Krikorian JG, Hancock EW (Cardiology Division, Stanford University School of Medicine, Stanford, California 94305). *Am J Med* 65:808–814, 1978

This article reviews 123 patients requiring pericardiocentesis between 1970–1976 at Stanford University Hospital. The study was conducted sufficiently recently so that most patients had echocardiographic evidence of a pericardial effusion before the tap was attempted. The disease processes diagnosed were varied and included neoplastic diseases, infections, and others. This review indicates that the larger the effusion the easier it is to tap, that pericardiocentesis yields a specific diagnosis about 25% of the time, that about 60% of the time cardiac tamponade can be managed by single or repeated pericardiocentesis, that most metastatic carcinomas except for lymphomas and mesotheliomas can be managed without surgery, that bacterial pericarditis, other than tuberculous pericarditis, usually requires surgery. Bleeding was found to be a problem in patients with platelet counts of less than 50,000/mm³. In the hands of an experienced physician, pericardiocentesis remains a useful diagnostic maneuver and this article is a very helpful review of this procedure.

David C. Dale
Department of Medicine
University of Washington

Bile duct cysts secondary to liver infarcts: report of a case and experimental production by small vessel hepatic artery occlusion. Doppman JL, Dunnick NR, Girton M, Fauci AS, Popovsky MA (NIH, Clinical Center, Building 10, Room 68211, Bethesda, Maryland 20014). *Radiology* 130:1–5, Jan 1979

Hepatic bile duct cysts were demonstrated on an abdominal CT scan and confirmed at autopsy in a patient with polyarteritis nodosa. The cysts developed in close proximity to hepatic artery aneurysms and occlusions visualized at hepatic arteriography and confirmed postmortem. The development of similar bile duct cysts following hepatic artery occlusion was demonstrated in 13 Rhesus monkeys.

Author Abstract

Role of angiography in cervicothoracic trauma. Thomas AN, Goodman PC, Roon AJ (San Francisco General Hospital, 1001 Portrero Avenue, San Francisco, California 94110). *J Thorac Cardiovasc Surg* 76:633–637, Nov 1978

During a period of more than 10 years, 376 patients with suspected vascular injuries from cervical or thoracic trauma were evaluated and treated. Retrospectively, these patients were divided into two groups; 72 who had operative treatment without angiography and 304 who had angiographic evaluation.

Among the 304 patients with angiography, 102 had penetrating cervical wounds; 71 had had penetrating thoracic wounds;

and 131 had blunt thoracic trauma. Sixty-six of these 304 patients had significant vascular injury, 30 with penetrating cervical wounds, and 36 with thoracic trauma. Multiple vascular lesions were found in about one-third. There were no major complications from angiography, and although one angiogram was interpreted falsely as positive, there were no false negatives. The authors conclude that angiography is safe and useful in selected patients with cervicothoracic trauma and when abnormal, aids in planning treatment.

W. Richard Webb

Age-dependent closure of the patent ductus arteriosus by indomethacin. McCarthy JS, Zies LG, Gelband H (Pediatric Cardiology, University of Miami School of Medicine, P.O. Box 520875, Miami, Florida 33152). *Pediatrics* 62:706–712, 1978

Indomethacin has been shown to be effective in closing a patent ductus arteriosus (PDA) in small premature infants. However, the age range over which this therapy is effective remains undetermined. Eighteen infants ranging in age from 4 to 45 days were studied. All had auscultatory and clinical findings indicative of PDA. Seventeen had roentgenographic evidence of cardiomegaly and/or increased pulmonary vascular markings, and eight had ECG evidence of ventricular hypertrophy. Indomethacin was administered to most patients in two doses of 0.1–0.3 mg/kg 24 hr apart. In eight of 12 patients, 3 weeks of age or younger, the PDA closed after indomethacin therapy. Two patients had a decrease in the intensity of murmur and improvement of congestive heart failure after treatment, but the PDA did not close completely. Only patients 33 weeks of age (actual age) or younger responded to indomethacin therapy with complete ductal closure. The condition of patients 34–36 weeks of age improved but there was not complete closure; in patients older than 36 weeks there was no response. The data suggest an age-related mechanism for PDA closure and that treatment with indomethacin before 33 weeks of age is probably required. A role for prostaglandin in ductal patency is postulated.

Author Abstract

Takayasu's arteritis in Thailand. Piyachon C (Faculty of Medicine, Chulalongkorn University of Chulalongkorn Hospital, Bangkok, Thailand). *Australas Radiol* 21:350–361, Dec 1977

The geographic differences of the sex incidence, anatomic distribution, and type of lesion has been observed in the past and this author reports 20 cases of Takayasu's disease in Thailand seen over a 6-year period. All patients were of Oriental descent and the sex ratio was three females to one male. The diagnosis was based on clinical, arteriographic and laboratory studies: four cases were studied at postmortem examination. Total angiography was performed in all cases, the arteriographic findings are described under the headings of aneurysm, dilatation, stenosis, occlusion, and irregular contour and are discussed in detail as well as summarized in table form.

The most common finding was dilatation of the ascending aorta. This agrees with other reports of the disease although in India the descending thoracic aorta was found to be most commonly involved while in China the ascending aorta is rarely involved. Of the branch vessels the brachio-cephalic arteries are the most commonly involved in this series and this correlates well with reports from other countries. Geographic variation and the types of vascular lesions found is described. It is stated that occlusive lesions are common in Japan, Europe, and the U.S. and aneurysms are rare, while in India, Thailand, and Africa aneurysms are common. The earliest detectable change in arteriography has been stated elsewhere to be a localized narrowing or irregularity of the aortic wall while the author finds that a long and diffuse narrowing is more common—being called the rat tail thoracic aorta.

I. V. Benn

Magnification pulmonary wedge angiography in the evaluation of children with congenital heart disease and pulmonary hypertension. Nihill MR, McNamara DG (Texas Children's Hospital, Houston, Texas 77030). *Circulation* 58:1094–1106, Dec 1978

Wedge arteriograms were produced by hand injection of 0.5–3 ml of contrast medium for the arterial phase and flushing with 5–10 mm of D5W for the venous phase. The image intensifier was raised 53 cm from the table top and the technique set at 60 to 70 KV, 10 mA, and 4 millisec for 30 frames/sec. One to five separate wedge arteriograms were performed on each examination, the most easily analyzed being obtained from the peripheral areas of the right lung or the left upper lobe. The projected image averaged 7.5 times actual size and muscular arteries 2 mm in diameter were studied. Normally there was even tapering, orderly branching, and an even capillary blush surrounding each small muscular artery. Increased vascular resistance produced dilatation and tortuosity of the elastic vessels and abrupt tapering of the muscular arteries. Reduction of branches of the distal muscular pulmonary arteries and an incomplete patchy capillary blush were signs of severe elevation of pulmonary vascular resistance. Pulmonary venous hypertension was associated with dilated veins, the diameter of the parallobular vein more than 1.3 times the central artery. The authors believe this technique provided a comprehensive assessment of pulmonary vascular disease in 155 infants and children undergoing cardiac catheterization.

Robert S. Frech

Gastrointestinal

Watery diarrhea syndrome with elevated levels of vasoactive intestinal polypeptide associated with pancreatitis and pancreatic pseudocyst. Burbige EJ, Manning RJ, Belber JP (Martinez Veterans Administration Hospital, University of California, Davis, California). *Am J Gastroenterol* 70:136–140, Aug 1978

The authors describe a case history of a 32-year-old black male who presented with recurrent pancreatitis, severe watery diarrhea, and elevated serum levels of vasoactive intestinal polypeptide (VIP). Ultrasound demonstrated a 5 × 3 cm cystic mass in the midabdomen, consistent with a pseudocyst, and endoscopic retrograde pancreatography showed complete obstruction of the pancreatic duct. The watery diarrhea syndrome has been described in association with pancreatic islet cell adenoma, nonbeta pancreatic islet cell hyperplasia, bronchogenic carcinoma, pheochromocytoma, ganglioneuroblastoma, and possibly medullary carcinoma of the thyroid. How pancreatitis or pancreatic pseudocyst can cause elevated levels of VIP remains speculative. It has been postulated that since VIP is present in high concentrations in normal intestine, inflammation of the bowel wall may cause increased secretion. The authors suggest that the inflammation associated with the patient's pancreatitis caused hyperplasia of the VIP secreting cells producing elevated blood levels and profuse watery diarrhea.

James M. Halls

Radiologic aspects of hepatic echinococcosis. Value of the intravenous viscerogram and computed tomography. Gonzalez LR, Marcos J, Illanas M, Hernandez-Mora M, Peña F, Picouto JP, Cienfuegos JA, Alvarez JLR (Servicio de Radiodiagnóstico, Clinica Puerta de Hierro, San Martín de Porres, 4, Madrid—35, Spain). *Radiology* 130:21–27, Jan 1979

Over five years, 105 patients with hepatic echinococcosis were studied. Plain radiographs of the hepatic area yielded the correct diagnosis in 35% of patients. Intravenous viscerograms were diagnostic in all but 14 of the patients (an accuracy of 83%). Computed tomography was performed in 15 cases and proved the most efficient of the techniques—it was diagnostic

in all 19 cases. The radiological signs of this entity are discussed.

Author Abstract

Association of pancreatitis and variant ductal anatomy. Heiss FW, Shea JA (Lahey Clinic Foundation, Boston, Massachusetts). *Am J Gastroenterol* 70:158–162, Aug 1978

Chronic alcohol abuse and cholelithiasis are the common causes of pancreatitis. Less often the disease is related to hyperlipidemia, hypercalcemia, trauma, adverse drug reactions, or hereditary pancreatitis. The authors describe four cases of cryptogenic pancreatitis in which congenital variants of the pancreatic duct were demonstrated by endoscopic retrograde cholangiopancreatography. The main pancreatic drainage was through the accessory papilla and the duct of Santorini. Injection of contrast medium through the easily cannulated major papilla demonstrated a short branching pancreatic ductular structure, typical of a ventral pancreas. The authors suggest that pancreatitis occurred in their four patients as a result of poor pancreatic drainage through an attenuated duct of Santorini.

James M. Halls

Superior mesenteric artery compression syndrome. Chung-Seng L, Mangla JC (Monroe Community Hospital and University of Rochester School of Medicine, Rochester, New York). *Am J Gastroenterol* 70:141–150, Aug 1978

The authors searched the records of their hospital and five affiliates over a 10-year period and found 17 patients with superior mesenteric artery compression syndrome. They found that the incidence in a chronic care hospital was significantly higher than in acute general hospitals. The etiology of the syndrome is obscure. Obstruction of the third portion of the duodenum is thought to be due to narrowing of the normal angle between the aorta and the superior mesenteric artery. A variety of factors are associated with narrowing of this angle, i.e., weight loss, prolonged bed rest, asthenic body build, and increased lumbar lordosis. Some patients benefit from conservative treatment, such as nasogastric suction, improved nutrition, chest-knee position, and physical exercise.

Duodenojejunostomy is the most commonly used surgical procedure when medical treatment fails. The authors described complications following gastrojejunostomy and lysis of the ligament of Treitz. Superior mesenteric artery syndrome is rare, but should be considered in any bedridden patient suffering from a wasting disease who develops upper abdominal distention and frequent vomiting.

James M. Halls

An unusual cause of radiologically demonstrable deformation of the duodenum. Callaghan B (Department of Anatomy and Histology, University of Adelaide, Australia). *Australas Radiol* 21:243–245, Sept 1977

A case of duodenal deformity is described that was caused by a grossly enlarged transverse colon but which mimicked carcinoma of the pancreas. The patient, a 77-year-old man, presented with several months history of anorexia, occasional vomiting, and recurrent diarrhea and constipation. Barium enema revealed a grossly and uniformly dilated colon thought to be due to chronic constipation and laxative use. Barium meal showed a duodenal diverticulum and marked anteroposterior compression, principally of the second part of the duodenum. There was also some widening of the duodenal loop. Following a period of colonic cleansing and advice regarding the management of his condition, he remained alive and well 12 years later.

Other possibilities that may have caused the duodenal deformity such as carcinoma of the pancreas, common bile and ampulla of Vater, and pancreatitis are discussed and excluded. The mechanism whereby the transverse colon causes the duodenal deformity is thought to be that the colon expands into the transverse mesocolon and compresses the duodenum. The compression is not great enough to compress the common bile duct, thus there is absence of jaundice.

I. V. Benn

Primary adenocarcinoma of the upper oesophagus. Danoff B, Cooper J, Klein M (Division of Radiation Oncology, New York University Medical Center, New York, New York 10016). *Clin Radiol* 29:519–522, Sept 1978

Adenocarcinoma of the upper one-third of the esophagus is an uncommon entity. A review of the literature reveals 20 reported cases. This paper reports an additional case. The lesion may arise from esophageal glands, foci of ectopic gastric mucosa, or a Barrett's esophagus. In contrast with squamous cell carcinomas submucosal spread is not prominent; however, transverse penetration through the esophageal wall is common. The prognosis is grave. Treatment modalities include supportive care, surgery alone, preoperative radiation therapy and surgery, and radiation therapy alone. Survival statistics provided by these various regimens are similar. There is little documented evidence for the radioresponsiveness of primary adenocarcinoma of the esophagus. The case described demonstrates marked tumor regression following a course of external radiotherapy as shown by serial esophagrams. Optimum treatment for adenocarcinoma of the upper esophagus remains to be determined. It is felt that the role of radiation therapy should be further evaluated.

Author Abstract

Colonscopic evaluation of rectal bleeding. Tedesco FJ, Waye JD, Raskin JB, Morris SJ, Greenwald RA (Division of Gastroenterology, Department of Medicine, University of Miami Medical Center, Miami, Florida). *Ann Intern Med* 89:907–909, 1978

A retrospective analysis of 258 patients with rectal bleeding was conducted in an attempt to determine the productivity of colonscopic evaluation of patients with rectal bleeding who have previously undergone proctosigmoidoscopy and barium enema. In this study, the finding of previously unrecognized lesions was surprisingly high. More than 10% of the patients (29 patients) had cancer, another 39 had polyps larger than 5 mm. Occult inflammatory bowel disease and other lesions were found in many others. This study suggests a very aggressive approach to rectal bleeding, especially in patients over 40. Although this study supports the widespread use of colonoscopy in any patient with rectal bleeding, more prospectively collected clinical information is needed to assist general physicians in determining the best management of this common problem.

David C. Dale
Department of Medicine
University of Washington

Bile duct obstruction in hepatocellular carcinoma (hepatoma)—clinical and cholangiographic characteristics. Report of 6 cases and review of the literature. vanSonnenberg E, Ferrucci, JT Jr (J. T. Ferrucci, Jr., Massachusetts General Hospital, Boston, Massachusetts 02114). *Radiology* 130:7–13, Jan 1979

Direct cholangiography revealed 6 cases of hepatoma where tumor growth within the bile ducts caused obstructive jaundice. Characteristic features included bulky obstructing intraluminal masses in the proximal extrahepatic ducts. Distal common duct defects usually signify hemobilia and clots as tumor complication. Review of the literature disclosed only 22 cases in which common duct involvement was a predominant clinical feature. Hepatoma should be included in the differential diagnosis of a cholangiographic filling defect in the proximal extrahepatic bile ducts. The recent widespread use of endoscopic and fine needle transhepatic cholangiography should aid in preoperative diagnosis.

Author Abstract

Perforation of duodenal ulcer during barium meal. Gillespie P, Riley J, Hunt J (Department of Gastroenterology, Royal North Shore Hospital, St. Leonards, N.S.W., Australia 2065). *Australas Radiol* 21:241–242, Sept 1977

Duodenal ulcer perforation is a rare occurrence during barium meal. This article describes three such perforations from a series of 10,250 examinations over a 13-year period. The cases are described in detail. All demonstrate several common features; an ulcer over 2 cm in diameter and situated on the anterior wall of the first part of the duodenum and partial pyloric obstruction. Routine manual palpation of the duodenal cap and air contrast techniques were used during each examination. The main presenting complaints were severe epigastric pain and tenderness and weight loss. The authors suggest that in patients with these symptoms that continuous naso-gastric suction be applied until there is a significant decrease in abdominal pain and naso-gastric aspirate.

I. V. Benn

The radiological and pathological features in a case of secondary amyloidosis involving the gastro-interstinal tract. Sage MR, Hall P, William DR, *Australas Radiol* 22:42–47, March 1978

Amyloid involvement of the gastrointestinal tract may lead to a wide variety of clinical and radiologic manifestations. This case report stresses the need to differentiate the radiologic appearance in the upper GI tract from other lesions of the esophagus and stomach. The patient, a 56-year-old male, had a past history of empyema and bronchiectasis and presented with a 1-year history of diarrhea, constipation, and colicky abdominal pains. Barium meals showed absence of the normal peristaltic waves in the esophagus together with dilation, and the stomach also showed absence of peristalsis with no delay in outflow. Endoscopy revealed atrophic gastric mucosa which showed amyloid deposits on biopsies. The patient died following pulmonary aspiration and at postmortem amyloid infiltration of the entire gastrointestinal system was present. The gastrointestinal tract is most commonly involved in both primary and secondary amyloid and mobility dysfunction is one of the most common radiologic findings—due to either muscular or neural replacement by amyloid material.

I. V. Benn

Transjugular cholangiography in the differential diagnosis of jaundice and exploration of the portal system. Teisseire R, Marty MH, Clanet J, Fourtanier G, Putois J (Service de Radiologie C.H.U. Toulouse Purpan, 31052 Toulouse, France). *J Radiol Electrol Med Nucl* 59:531–538, 1978

By means of the transjugular approach, cholangiography, liver biopsy, and a study of the hemodynamics of the liver, can be performed in a single examination. The chief indication for this procedure is the need to visualize the biliary tree in obstructive (surgical) jaundice. However in medical (hepatocellular) jaundice, catheterization of the papilla is the method of choice. The examination should not be performed on patients with a history of a recent acute infection of the biliary tract.

The authors report the results of the examination of 200 jaundiced patients by means of transjugular cholangiography. There were no complications due to catheterization of the right internal jugular vein. However, the examination could not be successfully performed in the presence of a cervical goiter, thrombosis of the internal jugular vein, dorsolumbar scoliosis, obstruction at the junction of the vena cava and the subhepatic vein due to compression by a large malignant tumor of the adrenal gland. Two patients experienced extrasystole during the passage of the catheter through the right heart. One patient had an accumulation of contrast material under the liver due to a subcapsular injection and although he experienced pain for about 2 hr, he had no further complaints.

The subhepatic veins were readily catheterized in 175 patients and a successful cholangiogram was obtained on 145 (85%). Dilated bile ducts are more readily visualized than normal ducts. Nonopacification of the bile ducts is a reasonable indication of the absence of obstruction. Portography was successfully performed in 31 of 37 patients (84%). Liver biopsy was attempted on 95 patients and was successful in 91 (96%). The pathologic findings demonstrated by this procedure, many of which are well illustrated by reproductions of excellent radiographs, include impacted calculi in the common bile duct, cirrhosis of the liver, carcinoma of the biliary tract, carcinoma of the head of the pancreas, portal hypertension, and esophageal varices.

William H. Shehadi

Transjugular cholangiography and liver biopsy in the diagnosis of cholestasis (in French). Teisseire R, Marty MH, Tournut R, Clanet J, Fourtanier G, Pascal JP (J-P Pascal Service de Gastroentérologie, C.H.U. Purpan, F-3100 Toulouse, France). *Gastroenterol Clin Biol* 2:797–804, 1978

Ninety-six patients with cholestasis were examined by transjugular cholangiography. Ages ranged from 35–90 years, with an average age of 62. Of the patients, 61 were males, 35 females. In the majority of cases, the reason for the examination was the demonstration and evaluation of the common bile duct. In six cases the procedure was performed only in order to obtain a liver biopsy because the classic percutaneous liver biopsy could not be performed.

The technique is presented in detail and consists of the positioning of a catheter at the level of the subhepatic vein via an internal jugular vein approach. Preferably, the slightly curved catheter should reach the main right subhepatic vein. Once the catheter is in position a special needle is passed into the catheter and is then pushed for about 2–3 cm into the liver parenchyma. If satisfactorily in situ, 20–80 cc of a water soluble contrast medium are injected through the catheter.

In those cases in which a biopsy is indicated, aspiration is performed when the needle penetrates into the parenchyma and the tissue passes into a syringe which contains an isotonic solution of sodium chloride.

A satisfactory cholangiogram was obtained in 71 patients. Of these, 54 showed dilated extrahepatic biliary ducts, while in 17 the ducts were within the normal limits. In 15 cases in which no opacification of the ducts could be obtained by endoscopic retograde cholangiopancreatography or at surgery, it was found that three cases had dilated ducts while in 12, these were normal.

Liver biopsy was performed in 46 patients and was successful in 42, demonstrating cholestasis in 12, metastases in two, chronic or acute hepatitis in 71, cirrhosis in 14, and normal hepatic parenchyma in seven.

The authors point to the simplicity of the procedure, to the lack of untoward complications, and to the possibility of performing a liver biopsy even though the procedure is successful only in about 40% of the cases in whom the biliary ducts are not dilated. The study should not be performed in cases with biliary infection, while in those cases in which the cholestasis is of medical origin, endoscopic retrograde cholangiopancreatography is preferable. When the cholestasis is of a nature which calls for surgical intervention and in cases of cirrhosis, the transjugular approach is preferred because it permits biopsy of the hepatic parenchyma.

Antonio F. Govoni

Genitourinary

Computed tomography in the evaluation of post-nephrectomy patients. Bernardino ME, deSantos LA, Johnson DE, Bracken RB (M. D. Anderson Hospital and Tumor Institute, University of Texas System Cancer Center, Houston, Texas 77030). *Radiology* 130:183–187, Jan 1979

Twenty-one CT examinations were performed in 19 patients who had undergone previous nephrectomy for renal carcinoma or retroperitoneal malignancy. Nine patients were free of disease and 10 had recurrence. Findings of recurrent disease included masses in the vacant renal fossa, inability to visualize

the inferior vena cava or aorta, and ipsilateral psoas muscle thickening. Possible pitfalls in diagnosis are discussed.

Author Abstract

Fibrous ureteral polyps. Banner MP, Pollack HM (Hospital of the University of Pennsylvania, Philadelphia, Pennsylvania 19104). *Radiology* 130:73–76, Jan 1979

Twelve cases of fibrous ureteral polyps are presented, illustrating their characteristic radiographic appearances. Two types—a long pedunculated mobile variety having a smooth surface, and a relatively shorter lesion covered with thin, finger-like projections—may be identified. Demonstration of the typical findings on excretory urography and/or retrograde ureterography establishes the diagnosis and permits surgical conservatism. Although no sex preponderance was noted, a wide sex-related age disparity was observed, the involved males being much younger than the females.

Author Abstract

Current concepts: the pursuit of the renal mass. Clayman RV, Williams RD, Fraley EE (Department of Urologic Surgery, Box 394 Mayo, University of Minnesota Health Sciences Center, Minneapolis Minnesota 55455). *N Engl J Med* 300:72–74, 1979

This is a noteworthy article that carefully reviews how to work up a renal mass. The article emphasizes the positive and negative benefits of a number of procedures as well as their costs. The basic tests: intravenous pyelography, nephrosonography, selective angiography plus puncture of a cyst and the analysis of its contents should lead to a diagnosis in more than 95% of all cases. The authors emphasize that the risk of spreading tumor from a needle aspiration of a cystic carcinoma is very small, there being only two reports over the last 15 years of tumors growing along the needle track. The authors emphasize that because the nonoperative evaluation of renal masses has become so good and because a surgical approach costs approximately 2½ times as much as a nonoperative approach and has 10 times the risk, surgery should now rarely be done to define a renal mass.

David C. Dale
Department of Medicine
University of Washington

Renal arteriography in Von Hippel-Lindau disease. Campbell DR, Mason WF, Standen JR (Victoria General Hospital, Halifax, Nova Scotia B3H 2Y9, Canada). *J Can Assoc Radiol* 29:243–246, Dec 1978

Since 1960, 17 patients with Von Hippel-Lindau disease have had cerebellar hemangioblastomas resected at Victoria General Hospital. The last four had renal angiograms as part of their clinical workup. One patient had both renal cysts and bilateral renal cell carcinomas, another patient had cysts in addition to multiple left renal carcinomas and a right pheochromocytoma, the third patient had a small renal cell carcinoma, and the fourth patient bilateral cystic disease. Three of the four had normal excretory urograms. The authors urge that all patients suspected of having Von Hippel-Lindau disease should have renal angiography regardless of the findings on the excretory urogram. This may permit earlier diagnosis of neoplasia in these patients and alter their overall medical and surgical management. Because of the high incidence of renal carcinoma in these patients, the authors suggest that follow-up arteriography is probably indicated in those patients who initially have relatively normal studies.

Jack M.A. Tishler

Medullary sponge kidney. Fon G, Sage MR (Flinders Medical Centre, Bedford Park, South Australia 5042). *Australas Radiol* 21:337, Dec 1977

This is a review of the clinical and radiological features of 13 patients with medullary sponge kidneys presenting over an 18 month period. The radiologic features following intravenous urography were first described in 1939 by Lenarduzzi and since then the condition has been found to be more common than initially thought. Pathologically the defect is seen as multiple cystic cavities in the pyramids of one or more kidneys while clinically the main presenting symptoms are renal colic and hematuria. Biochemically the patients were found to be normal.

Intravenous pyelography was performed in all 13 cases; renal sizes were all within normal range of Hodson's curves. The nephrogram was of normal density. A characteristic feature was the early filling of the papillary cavities before the calyces were opacified. Enlargement of the individual pyramids and of the corresponding calyces has been described by others; this was observed in only five of these cases. All the involved papilla except one showed at least two or more cavities, an important point in distinguishing the condition from papillary necrosis. Renal calcification in relation to the pyramids was recognized in seven of the cases.

I. V. Benn

Musculoskeletal

Involvement of the cervical spine in rheumatoid arthritis. Chevrot A, Correas G, Pallardy G (G. Pallardy, Service de Radiology, B, Hopital Cochin, 27 Rue Faubourg-Saint Jacques, E75674 Paris Cedex 14, France). *J Radiol Electrol Med Nucl* 59: 545–550, 1978

In a series of 577 patients with rheumatoid arthritis, 165 showed evidence of involvement of the cervical spine, an incidence of 28%. The examination revealed the following, in descending frequency: subluxation of C1–C2, basilar impression, erosion of the odontoid process, degeneration of the intervertebral discs at C2–C3, and C3–C4. Multiple lesions were present in approximately one-third of the patients. Neck pain was the presenting symptom.

The potential for neurologic complications should always be considered although the actual development of such a complication is infrequent. Dislocation up to 10 mm has been observed with minimal clinical symptoms. However, the possibility of neurologic complications, especially quadriplegia, occurring following slight trauma should not be ignored.

Rheumatoid arthritis occurs predominantly in the female, approximately four times as frequently as in the male. Involvement of the cervical spine may occur at any time during the course of the disease. Thus periodic examination of the cervical spine is strongly recommended. The authors stress the importance of obtaining lateral views of the cervical spine in flexion in addition to the routine standard projections.

William H. Shehadi

Soft tissue changes in early rheumatoid arthritis as seen on xeroradiography and nonscreen radiographs. Verow PW, Dippy J (Welsh National School of Medicine, Heath Park, Cardiff, Wales). *Clin Radiol* 29:585–590, Sept, 1978

Forty-seven patients with early or newly established rheumatoid arthritis were studied with nonscreen radiography and xerography. Estimations of soft tissue swelling, bone erosion, and cysts were made by two observers and the results compared between observers and the two types of imaging. The results indicate no significant advantage or disadvantage in xerographic imaging compared with nonscreen radiographs in the identification of superficial soft tissue swelling and bone erosions. More cysts were, however, identified on the radiographs. In a previous anatomical study of the dissected hand, xerogra-

phy showed definite advantages in the detection of certain features.

Author Abstract

Percutaneous needle biopsy in the management of solitary lesions of bone. Legge D, Ennis JT, Dempsy J (Mater Hospital, Dublin, Wales). *Clin Radiol* 29:497–500, Sept 1978

Needle biopsies under general anesthesia and fluoroscopic control were performed in 12 patients with solitary bone lesions using a simple 18 guage cutting needle as designed for transthoracic biopsy. Cytologic and histologic material sufficient for a reliable diagnosis was obtained from eight of the 12 patients, thereby avoiding open biopsy. No complications ensued. These authors suggest that if the initial biopsy is unsuccessful, a repeat biopsy is immediately performed, using a larger diameter instrument, such as trephine. Solitary or atypical lesions of bone may be produced by a variety of diseases and biopsy is required for a definitive diagnosis. In this small series, it was concluded that percutaneous needle biopsy of bone is a safe and simple procedure of value in the management of solitary bone lesions.

Noel K. Allan

Chondromyxoid fibroma of lumbar spine. Mayer B (University of Oregon Health Sciences Center, Veterans Administration Hospital, Portland, Oregon). *J Can Assoc Radiol* 29:271–272, Dec 1978

Chondromyxoid fibroma is a rare neoplasm seen in both tubular and flat bones. Only two chondromyxoid fibromas of spine were previously reported, one in the cervical and the other in the thoracic vertebra, both arising in the spinous process. The author adds another case, one involving the spinous process of the second lumbar vertebra. The patient presented for a preemployment lumbar spine radiographic examination. No unusual signs or symptoms were elicited. Radiographically, a well circumscribed cystic lesion was seen confined to the spinous process of L2. The edges of the lesion were scalloped and sclerotic and the lesion appeared to be benign. The lesion was resected and a histologic diagnosis of chondromyxoid fibroma made.

Jack M.A. Tishler

Unusual calcification in the region of the gluteus medius and minimus muscles. Callaghan BD (Department of Anatomy and Histology, University of Adelaide, Australia). *Australas Radiol* 21:362–366, Dec 1977

Calcification in the supraspinatus tendon is quite common, however, calcification in the gluteus minimus and medius muscles as a radiologic finding together with local symptoms and bilateral calcification in the supraspinatus tendons is unusual on review of the more recent literature. The patient, a 98 kg 38-year-old male, presented with right supraspinatus tendinitis with typical symptoms and radiologic changes. He then developed persistent deep seated pain in the left hip region aggravated by standing on the left foot and sitting for long intervals. X-rays revealed localized calcification in association with the attachments of the gluteus medius and minimus muscles and soon after the patient developed an acute left sided supraspinatus tendinitis.

The calcification in the gluteal muscles was in close proximity to the articular capsule of the hip and extended into the muscles. Welfing (1966) found that in patients suffering with supraspinatus calcification, periarticular hip calcification was found to coexist in 60%–65% and that this percentage was high when there was bilateral shoulder calcification. In this patient there was nothing to suggest the generalized disorder that may have caused the calcification and the author goes on to discuss mechanical similarities between the hip and the shoulder joint and the possibility of ischemia causing the calcification. It is thought that calcification in the hip muscles is a result of local damage possibly following heavy unaccustomed exercise.

I. V. Benn

Double-contrast arthrography of the elbow. Pavlov H, Ghelman B, Warren RF (Hospital for Special Surgery, 535 East 70th Street, New York, New York 10021.) *Radiology* 130:87–95, Jan 1979

Double-contrast arthrography using gravity provides more detail than single-contrast techniques. With gravity, air rises to the uppermost portion of the joint and the positive contrast material settles. The cartilagenous articular surfaces and the synovial lining of the elbow are coated with contrast material and highlighted by the intra-articular air. Cartilagenous intra-articular bodies can be identified and located and the size of cartilagenous encapsulated osseous bodies can be confirmed. This method is faster to perform and easier to interpret than single-contrast studies, exposes the patient less than a tomographic examination, and is helpful before surgical exploration.

Author Abstract

The angiographic findings in a haemophilic pseudotumour of bone. Thomas M, Walters HL (St. Thomas Hospital and Medical School, London, S.E.1. 7EH England). *Australas Radiol* 21:346–349, Dec 1977

The angiographic findings in a hemophilic pseudotumor are discussed, the findings having not previously been described. Pseudotumor was first described by Starker in 1918 and its estimated incidence is approximately 1%–2% in severe hemophiliacs. The incidence has increased recently with greater longevity of hemophiliacs. The patient was a 21-year-old hemophiliac Iraqui male who was admitted with a large firm nontender swelling over the medial aspect of the distal thigh which had gradually increased in size over many years. Radiographs showed a large soft tissue swelling with no calcification causing extensive destruction of the distal half of the femoral shaft extending to the subarticular margin above the knee joint. In view of the risk of pathologic fracture, surgery was thought to be necessary and, therefore, a femoral angiogram (under factor VIII cover) was performed to display the femoral artery. The distal femoral artery was shown to be displaced by an avascular mass with no evidence of pathologic circulation. It is thought that this is a safe procedure in a hemophiliac patient especially if the exact nature of the lesion is uncertain.

I. V. Benn

Nervous System

Computed tomography in the diagnosis of diseases of the paranasal sinuses. Forbes W St. C, Fawcitt RA, Isherwood I, Webb R, Farrington T (Stopford Building, Oxford Road, Manchester University, Manchester, England). *Clin Radiol* 29:501–511, Sept 1978

The authors investigated 31 patients suffering from benign and malignant lesions of the paranasal sinuses. Clinical, conventional radiological methods, and computed tomography were used. In benign lesions, CT added little significant information to that obtained by conventional radiologic methods. In malignant lesions, however, CT provides additional valuable information. It gives a clear picture of the posterior, superior, and orbital extent of paranasal tumors. It also shows the extent of the tumor into the infratemporal fossa.

Author Abstract

Meatocisternography with water-soluble contrast medium for the diagnosis of cerebellopontine angle tumors. Bocken-

heimer S, Schmidt CL (Psychiatrische und Nervenklinik der Universitaet Freiburg, Hauptstr. 5, D-7800 Freiburg/Br., Germany). *Radiologe* 18:316–319, 1978

Four patients underwent meatocisternography with metrizamide (Amipaque) for the evaluation of cerebellopontine angle tumors. With the patient prone in a 20° oblique position and his head in the Stenver position, 10 ml of metrizamide was instilled into the subarachnoid space via a lumbar puncture; its entry into the cerebellomedullary cisterns was followed fluoroscopically. Conventional radiographs and tomographic sections were obtained.

In two of the four patients, a cerebellopontine angle tumor could be detected, while in the other two patients such a tumor could be excluded because of complete filling of the cerebellomedullary cisterns and meatus acusticus internus without detection of a tumor mass. Except for transient nausea, no subjective side effects occurred. Electroencephalographic changes were not observed; the electronystagmogram showed a slight increase in eye movements without nystagmus.

In comparison with Pantopaque myelography, a relatively large volume is used with Amipaque myelography and the contrast of the water-soluble contrast medium is less than that of the oily medium. These actually are advantages. Because of its large volume, metrizamide flows around the entire tumor and allows complete visualization of even large tumors, and the low contrast of metrizamide facilitates topographic orientation since the osseous structures are not completely obscured.

Peter F. Winter

Techniques in transfemoral lumbar epidural phlebography. Wilmink JT, Penning L, Beks JWF (University Hospital, 59 Oostersingel, Groningen, Netherlands). *Neuroradiology* 15:273–286, Oct 2, 1978

The authors review the world's literature on lumbar epidural phlebography and describe their technique and experience in detail. They use No. 5 French catheters 50 cm in length. The catheter shape is a long radius C with a tight C at the tip which can then be altered by inserting the guide wire. They caution that the guide wire should not be passed through the catheter tip when the tip is in a wedged position in an ascending lumbar or intervertebral vein because of the risk of perforation. They prefer bilateral selective intervertebral vein cannulation and are successful on at least one side in about two-thirds of their cases. If a lateral sacral vein is used, the catheter tip is advanced through the sacral foramen if possible.

With these very selective catheter positions 25 cc of Meglumine ioxithalamate (Telebrix 30) is simultaneously injected in each catheter at a rate of 5 cc/sec. There is very good epidural venous filling including the intervertebral veins and attempts to slow caval flow are not necessary either by Valsalva maneuver, abdominal compression, or both. With less selective catheter position, impedance of caval flow to force contrast into the epidural venous plexus is necessary and the authors prefer a Valsalva maneuver rather than abdominal compression. If the catheter is in a small vein, the injection rate is slowed to 3–4 cc/sec. They also comment that catheter manipulation in an intervertebral vein next to a nerve root compressed by disc will frequently reproduce the patients complaint of radicular pain. Filming is carried out primarily in the anteroposterior projection with 8 films exposed at 1.8 sec intervals.

The authors feel the major disadvantage in epidural venography is the false positive diagnosis because of insufficient venous filling. They add that epidural venography demonstrates laterally placed disc prolapses better than myelography.

Paul M. Chikos

Orbitocranial asymmetry. Burrows EH (Wessex Neurological Centre, Southampton General Hospital, Southampton SO9 4XY, England). *Br J Radiol* 51:771–781, Oct 1978

Eleven cases illustrate the differential diagnosis of deforming lesions of the bony orbit and its vicinity, which cause unilateral proptosis or other craniofacial disfigurement. Three distinct varieties of orbitocranial neurofibromatosis are distinguished, and they are contrasted with other deforming lesions of childhood—unilateral craniosynostosis, chronic juvenile subdural hygroma of the temporal fossa, and congenital facial hemihypertrophy. Adult lesions are represented by intrinsic tumors of the orbit and paranasal sinuses, and by the commonest two processes deforming the sphenoid bone, meningioma and osseous fibrous dysplasia

Author Abstract

Persistent hypoglossal artery and persistent trigeminal artery presenting with posterior fossa transient ischemic attacks. Stern J, Correll JW, Bryan N (Neurological Institute 710 West 168th Street, New York, New York 10032). *J Neurosurg* 49:614–619, Oct 1978

The authors report two patients who presented with transient ischemic attacks in the distribution of the posterior fossa. The first case was a 68-year-old right handed hypertensive woman with an 8 month history of transient dizziness, vertigo, bilateral visual blurring, and periods of numbness and tingling involving the left lower extremity. Cerebral angiography demonstrated a persistent trigeminal artery supplying the distal basilar and posterior cerebral arteries with an ulcerated minimally stenotic lesion in the posterior wall of the proximal internal carotid artery. At operation a large ulcerated atheromatous plaque was removed from the proximal internal carotid artery and the patient had no further symptoms with 11 month follow up.

The other case was a 57-year-old hypertensive left handed woman with a 1-year history of transient episodes of nausea, vomiting, dizziness, and dysequilibrium. Cerebral angiography showed the posterior circulation was derived almost entirely from a persistent hypoglossal artery on the right. The posterior wall of the distal common carotid and contiguous hypoglossal artery showed evidence of irregularity and narrowing consistent with an atheromatous plaque and ulceration. Following endarterectomy the patient was asymptomatic at 14 month follow-up.

In a large angiographic series the relative frequency of these vascular anomalies is quite low, 0.1%–0.6% for the persistent trigeminal artery, and approximately 0.25% for the persistent hypoglossal artery. Carotid-basilar anastomosis should be kept in mind when evaluating a patient with posterior fossa ischemic episodes and small to absent vertebral arteries. The focus of attention should then be directed to the carotid system.

Paul M. Chikos

Asymmetries of the cerebral hemispheres on computed tomograms. LeMay M, Kido D (Massachusetts General Hospital, Fruit Street, Boston, Massachusetts 02114). *J Computer Assisted Tomography* 2:471–476, Sept 1978

Transverse scans of 165 patients were examined to determine the presence of asymmetry which could be evaluated by computed tomographic techniques. Patient handedness was determined. By CT techniques, the more obvious asymmetries are in the width and length of the parieto-occipital and frontal regions of the brain. The right frontal lobe and left occipito-parietal lobes were found to be larger in right handed individuals than their opposite side counterpart. The opposite asymmetry was seen in left handed individuals. Awareness of hemispheric asymmetry, particularly in the parieto-occipital region, appears to have significant clinical importance. CT scanning may offer a noninvasive method of studying this area, particularly after injury.

Michael J. Meagher

Lumbar phlebography in the diagnosis of disc herniations. Roland J, Treil J, Larde D, Picard L, Manelfe C (CHU Nancy, Case officielle No. 34, 54037 Nancy Cedex, France). *J Neurosurg* 49:544–550, Oct 1978

The authors report their experience with 240 cases of lumbar epidural venography in the diagnosis of disc herniation. They utilize bilateral selective catheterization of both ascending lum-

bar veins or an ascending lumbar vein and lateral sacral vein using No. 5 French catheters. Abdominal compression is used and contrast is injected at a rate of 4–6 ml/sec for 8 sec. Films were obtained over a 12 sec period, at the rate of one film/sec. Extravasation of contrast material is said to cause intense but temporary pain.

There were three incidences of a phlebitis occurring immediately after epidural venography. In one case, a patient with the previous history of venous thrombosis, the phlebitis was serious. The authors consider the previous history of thrombophlebitis as an absolute contraindication to lumbar phlebography.

The diagnosis of disc herniation is made by the displacement or obstruction of epidural veins. They still recommend myelography (with metrizamide) as the examination of choice in patients who have not undergone surgery. Patients are then selected for phlebography who have a large dural sac, large anterior epidural space, possible lateral disc herniation, arachnoiditis, or a technically inadequate myelogram. Following surgery the lumbar phlebogram cannot distinguish between disc herniation and scarring secondary to surgery. The usefulness of phlebography was demonstrated in 111 patients who had both studies preoperatively. Water soluble myelography was correct in 44 (40%) while 100 of 111 cases (90%) were correctly diagnosed by lumbar phlebography.

Paul M. Chikos

Computer assisted tomography and pneumoencephalography in non-hydrocephalic, non-tumorous head enlargement. Michels L, Benson J (Sacred Heart General Hospital, Eugene, Oregon 97401). *J Computer Assisted Tomography* 2:439–447, Sept 1978

Forty children with enlarged head size were evaluated, 17 by pneumoencephalography and 23 by CT scanning. Computed tomography showed a closer relationship between ventricular size and neurologic deficit than did pneumoencephalography. There was some difference in the groups within the study in that those children undergoing pneumoencephalography were significantly more impaired than those undergoing CT scans. It also was noted that the CT scan technique examines the ventricle in a "physiologic" state as opposed to a situation where the ventricle is under the stress of insufflated gas.

Michael J. Meagher

Miscellaneous

Computed-tomographic demonstration of intramuscular hematomas in hemophiliacs. Lackner K, Hofmann P, Grauthoff H, Brecht G, Thurn P (Radiologische Klinik der Universitaet Bonn, 5300 Bonn-Venusberg, Germany). *ROEFO* 129:298–302, 1978

In 21 of 30 patients with hemophilia A or B, hematomas could be demonstrated by computed tomography in various locations: subdural space, three patients; m. iliacus, 10 patients; m. psoas, five; abdominal wall, two, thigh, two and calf, one. The CT diagnosis could be verified surgically in six patients and confirmed by clinical findings and course in the remaining cases.

Whenever there was a clinical suspicion of an intramuscular hematoma (12 patients), a hematoma could be demonstrated by CT, whereas in five patients the clinically suspected location turned out to be wrong. In nine patients an unsuspected hematoma was detected by CT. In all cases CT allowed an exact determination of the extent and anatomic location of the hematoma.

Peter F.Winter

The effect of computed tomography viewer controls on anatomical measurements. Koehler PR, Anderson RE, Baxter B (University of Utah, Salt Lake City, Utah 84132). *Radiology* 130: 189–194, Jan 1979

Newer computed tomography (CT) scanners provide a means for direct measurement of the size of normal and abnormal body structures from the viewing screen. Because tissue densities within the brain tend to fall in a narrow range, viewer control settings (window width and window center) are used in a relatively stereotyped fashion when studying head scans. In contrast, CT body scan images usually include tissues of widely different densities and require much broader use of the control settings for complete examination. Studies of the effect of changing the control settings have uncovered wide differences in how these controls should be set when measuring structures directly from the CT scan.

Author Abstract

Computer-tomographic densitometry of liver, spleen, and kidneys with intravenous bolus injection of biliary contrast media. Huebner KH (Med. Strahleninsitut der Universitaet Tuebingen, Roentgenweg 11, 7400 Tuebingen, Germany). *ROEFO* 129:289–297, 1978

Computed tomography with densitometric measurements of liver, spleen and kidney, and serial determinations of serum iodine levels was performed on 21 patients following the intravenous bolus injection of biliary contrast media at a dose of 100 mg of iodine/kg body weight.

On the basis of computed tomographic determinations, the maximum concentration in the hepatic cells is reached 1 hour after the injection. The decline of the absorption values follows an exponential curve with a half life of 118 ± 20 min. The time dependent course of the absorption values of the hepatic metastases (six patients) shows a relatively flat, two peak curve. The difference of the absorption values between metastases and hepatic tissue increases by maximal 15 Hounsfield units, usually 30–90 min after the injection. The resulting contrast enhancement is less than that achieved with renal agents, yet sufficient to detect additional small metastases.

The densitometic pattern of the renal parenchyma, a well perfused tissue, shows a rapid initial rise of absorption values as the result of the high serum concentration, which is not followed by the rapid decline of absorption values found in the serum; this delayed decline is caused by the heterotopic excretion of the nonalbumin bound fraction of contrast medium. The spleen shows a rapid, perfusion related rise of absorption values, followed by a rapid decline, which is only slightly delayed in comparison with the serum values.

Peter F. Winter

Experience with xeroradiography in the maxillofacial region. Hardt N, Bally E (Zentrales Roentgeninstitut, Kantonsspital Luzern, Spitalstr., 6000 Luzern, Switzerland). *ROEFO* 129:330–334, 1978

The application of xeroradiography in the maxillofacial region is discussed on the basis of the authors' experience. Xeroradiography delineates facial fractures better than conventional radiography. In fractures of the orbital floor it can depict the dislocated bone fragments as well as the accompanying soft tissue changes. Xerotomography is the preferred method for the evaluation of complex fractures of the middle and upper level of the facial bones. Soft tissue tumors of the oro-nasopharyngeal region are also well seen on xeroradiographs; however, xeroradiography is inferior to conventional radiography for the evaluation of large destructive, infiltrating neoplasms.

Peter F. Winter

Xeroradiography of the larynx. Ting YM, Curran J, Maklad N (St. Joseph Mercy Hospital, 900 Woodward Avenue Pontiac, Michigan 48053). *Australas Radiol* 22:39–41, March 1978

The advantages of xeroradiography of the larynx are discussed. The authors performed 156 studies over a 3-year period. The detail and clarity is thought to approach that of positive contrast laryngography without the discomfort and morbidity of the latter. In all patients the lateral xeroradiograph of the neck was obtained first followed by xerotomography in the antero-

posterior projection at the desired levels. The radiation dose per xerographic tomogram is higher than that from conventional tomograms but less than that from positive contrast laryngography and fluoroscopy. Two cases are described in detail to illustrate the diagnostic value of laryngeal xeroradiography.

I. V. Benn

Xeroradiography of the pharynx. Thompson RI, Foley WD, Doust VL, Doust, BD (Medical College of Wisconsin, 8700 West Wisconsin Avenue, Milwaukee, Wisconsin 53226.) *Australas Radiol* 22:34–38, March 1978

A total of 75 cases of pharyngeal malignancy were reviewed to determine the place of xeroradiography in their management and to detemine the lesions to which xeroradiography was particularly adapted and to determine which of the techniques and views was the most convenient routine examination. Other radiographic techniques reviewed as part of the study included conventional x-rays, conventional tomography, and barium studies. Of the nine nasopharyngeal tumors, six were best demonstrated by xeroradiography while the other three were not demonstrated and were less than 1 cm in diameter. There were 48 oropharyngeal lesions which could be divided into those situated laterally and those in the midline. Most of the midline masses were readily seen on the plain lateral xeroradiographs. Barium swallow in the lateral projection was occasionally of value in the assessment of the small midline lesions. Of the 28 laterally placed masses anteroposterior tomography (either conventional or xerotomography) and barium studies were superior to lateral films. Retropharyngeal soft tissue tumors were readily demonstrated by plain lateral radiographs and were the easiest to delineate. The authors conclude that plain lateral xeroradiography is the single most useful examination for the midline masses while laterally placed masses are best seen in the anteroposterior tomographic techniques.

I. V. Benn

Ultrasound and computed tomography in abdominal diagnosis. Duffy P (14, Ethel Street, Eastwood, N.S.W. 2112, Australia). *Australas Radiol* 21:208–216 Sept 1977

The advantages and disadvantages of ultrasound and computed tomographic scanning are compared for conditions in the abdomen, although at this stage advances in each are so rapid that it is difficult to build up adequate numbers for comparison. The author describes the relative merits of each imaging system for all organs within the abdomen and concludes that the organ imaging modalities are complimentary for the soft tissues in the abdomen, conventional radiologic scintiscanning and ultrasound can diagnose most problems leaving the more difficult for CT or angiography in "tailored" programs.

I. V. Benn

Ultrasound as a screening test for adrenal tumors. Anderegg A (Service de Radiologie, C.H.U. Vaudois, 1011 Lausanne, Switzerland). *J. Radiol Electrol Med Nucl* 59:539–543, 1978

Ultrasound examination of the abdomen of 2,600 patients during a 1-year-period revealed the presence of 6 tumors of the adrenal gland including two carcinomas, two simple cysts, and two metastatic tumors from primary bronchogenic carcinoma. Details of the clinical history and findings are described. Intravenous urography, selective arteriography, and laparotomy confirmed the results of the ultrasound examination.

Computed tomography is an invasive procedure, costly and time consuming. Selective arteriography of the adrenal gland, also an invasive procedure, when preoperatively performed, gives pertinent information about the vascularity of the tumor. Retroperitoneal pneumography, long abandoned because of pain and low diagnostic accuracy, failed to give any information regarding the structure of the tumor. Intravenous urography obviously provides only limited information. The author recommends routine studies with ultrasound as the method of choice in the search for tumors of the adrenal glands.

William H. Shehadi

Radiation Oncology

Estrogen receptors and responses to chemotherapy and hormonal therapy in advanced breast cancer. Kiang DT, Frenning DH, Goldman AI, Ascensao VF, Kennedy BJ (Box 168, University Hospitals, Minneapolis, Minnesota 55455). *N Engl J Med* 299: 1330–1334, 1978

The authors have retrospectively reviewed their data regarding estrogen receptor-rich and estrogen receptor-poor tumors in the relationship to chemotherapy response in view of recent publications stating that 76% of receptor-poor tumors responded to chemotherapy, whereas only 12% of receptor-rich tumors responded.

The authors retrospectively analyzed the clinical data of 143 patients with advanced breast cancer. Patients were analyzed in three separate groups: 83 patients for the correlation of estrogen receptor and hormonal response; 86 patients for the correlation of estrogen receptor and response to chemotherapy; and 104 patients for the correlation between responses to hormonal therapy and chemotherapy. Of the 86 patients who had adequate chemotherapy and who had tumor estrogen-receptor assay, 38 had receptor-rich, and 48 receptor-poor tumors.

The response rate to chemotherapy was significantly higher in receptor-rich tumors (86%) than in receptor-poor tumors (36%) with a $P < .001$. Responses included complete and partial regression. The authors feel that recent publication demonstrating a low response rate to chemotherapy in patients with receptor-rich tumors was derived from a biased patient selection.

Herbert C. Berry

Carcinoma of the vagina. Marcus RB, Million RR, Daly JW (Division of Radiation Therapy, Box J-385, J. Hillis Miller Health Center, Gainesville, Florida 32610). *Cancer* 42:2507–2512, 1978

The results of irradiation for cure of 22 patients with stages I through IV primary epidermoid carcinomas of the vagina are reported. Most patients received whole pelvis irradiation in the 4,000–6,000 rad range plus at least one brachytherapy application. Most patients were in the stage II group. Two of 22 patients failed within the pelvis, one of whom also developed disseminated disease. NED 3-year survival for stage I was 100% (6/6), stage II was 70% (7/10), stage III was 100% (3/3), and it was 67% in stage IVA (2/3). Absolute survival NED for 2 years was 82% (18/22) and 67% at 5 years (8/12). Major complications appeared in two patients and were vaginal necroses and urethral fibrosis respectively.

The authors recommend 4,000–5,000 whole pelvis technique followed by a 2,000–3,000 rad interstitial implant or brachytherapy application for 6,000 rad mucosal surface dose in two applications for stage I and early stage II disease. For late stage II, stage III, and selected stage IV they recommend 5,000–6,000 rad whole pelvis followed by 2,500–3,500 rad interstitial implantation.

Herbert C. Berry

Midline pineal tumors and suprasellar germinomas: highly curable by irradiation. Sung D, Harisiadis L, Chang CH (Division of Radiotherapy, Columbia-Presbyterian Medical Center, 622 West 168th Street, New York, New York 10032). *Radiology* 128: 745–751, Sept 1978

Sixty-one patients with midline pineal tumors and 16 patients with suprasellar germinomas treated by irradiation are described. Twelve of the 61 midline pineal tumors and 11 of 16 suprasellar germinomas were verified histologically. The earliest and most frequent complaint of patients with midline pineal

tumors was headaches while diabetes insipidus was the most common presenting symptom in patients with suprasellar germinoma. The cerebrospinal fluid was examined in 50% of the patients. Of 12 patients with spinal subarachnoid space metastases, only three showed malignant cells on cytologic study.

All 61 patients with midline pineal tumors were shunted prior to radiotherapy. One of this group had gross total removal, six had subtotal removal, and four had biopsy only. One of the 16 patients with suprasellar germinoma had gross total removal of tumor, while six had subtotal and four had craniotomy and biopsy.

This study group comprising patients irradiated between 1950 and 1975 was treated with either a 200-kVp beam, ^{60}Co photons or 6-MeV linear accelarator photons. Of the 73 patients who completed irradiation, the entire brain was treated in 37%, and the entire spinal axis additionally in 15% of this group of 27. The authors' present policy is to deliver a tumor dose of 5,000–5,500 rads in 5 to 6½ weeks to the tumor with the remainder of the brain receiving 4,000 rads in 4 weeks and the spinal axis receiving 3,500 rads in 4 to 4½ weeks. No patients received chemotherapy.

The 5-year survival rate was 79% for midline pineal tumors and 77% for suprasellar germinomas, with the majority of patients followed for more than 5 years. Of the 40 patients given 5,000 to 5,500 rads in 5 to 6 weeks, only four (10%) demonstrated recurrent primary tumor. Of the 32 patients given 3,800 to 4,500 rads in 4 to 5 weeks, 15 (47%) showed recurrent tumor at the primary site. Ten percent of the midline pineal tumors and 37% of the suprasellar germinomas metastasized to the cerebral or spinal subarachnoid space following treatment. Eight of the 22 patients (36%) with histologically verified pineal tumors had spinal metastases. The authors recommend that the entire neural axis be irradiated for all locally extensive tumors, simultaneous pineal and hypothalamic lesions, and all biopsy-proven germinomas.

Herbert C. Berry

Postoperative irradiation of pterygia: ten more years of experience. Cooper JS (Division of Radiation Oncology, New York University Medical Center, 566 1st Avenue, New York, New York 10016). *Radiology* 128:753–756, Sept 1978

The experience of treating 526 pterygia in 403 patients with ^{90}Sr beta rays following "bare sclera" excision at Bellevue Hospital is reported. Most patients receive 3,000 reps divided into three equal fractions over 3 weeks. Follow-up was done solely by physician examination and was available for 221 patients (272 pterygia). Thirty-two pterygia of the total of 272 recurred with an additional 13 showing limited regrowth. Therefore, 227 pterygia remained without evidence of disease. Males demonstrated a disproportionately higher recurrence rate than females. Only three pterygia were not controlled by combined therapy. A third course of combined treatment is not recommended by the authors. Three of the 32 initial recurrences and one of the four ultimate failures involved lateral pterygia although temporal pterygia accounted for only 5% of the total cases.

Herbert C. Berry

Anatomical substages of stage III Hodgkin's disease. Stein RS, Hilborn RM, Flexner JM, Bolin M, Stroup S, Reynolds V, Krantz S (Section of Hematology, A3311, Vanderbilt University Hospital, Nashville, Tennessee 37232). *Cancer* 42:429–436, 1978

The authors describe 23 patients with pathologic stage III Hodgkin's disease broken down into stage III_1 (disease limited to the upper abdomen, i.e. spleen, splenic nodes, celiac node, and/or portal node) and stage III_2 (all other more extensive disease). The presence or absence of these symptoms and/or splenic involvement did not predict either disease-free survival or survival. Anatomical substage III_1 patients had a 100% 5-year survival while the III_2 patients had a 5-year survival of 65%. These survivals were not statistically significantly different however the disease-free survivals of 77% versus 13% for these respected stages were statistically significantly different at $p < .001$. The authors point out that studies which identify patients only as stage III may have limited clinical meaning and that it seems meaningless to consider all stage III patients as a single group. The possibility of revising the Ann Arbor staging classification is raised.

Herbert C. Berry

Weekly localization films and detection of field placement errors. Bynardt RW, Cox JD, Hornburg A, Liermann G (J. D. Cox, Division of Radiation Therapy, Medical College of Wisconsin, 8700 West Wisconsin Avenue, Milwaukee, Wisconsin 53226). *Int J Radiat Oncol Biol Phys* 4:881–887, Sept/Oct 1978

The authors have received the portal films of 337 male patients receiving x-ray therapy to establish a baseline rate of field placement errors. Deviations of more than 5 mm from the planning films were considered field placement errors. The overall error rate was 15% with pelvis and aero-digestive having the highest rates (27% and 17%). Some 19% of weekly beam films showed field placement errors while 9% of verification films showed such errors. Raising the threshold of error to 1.0 cm decreased these rates to 13% and 7.5% respectively. Localization films are recommended at intervals of from every 2–3 days to a minimum of once weekly.

Herbert C. Berry

The effect of pelvic irradiation on lactose absorption. Stryker JA, Mortel R, Hepner GW (Division of Radiotherapy, Hershey Medical Center, Pennsylvania State University, Hershey, Pennsylvania 17033). *Int J Radiat Oncol Biol Phys* 4:859–863, Sept/Oct 1978

Twenty-four patients undergoing pelvic irradiation for gynecologic malignancy were studied during their first and fifth weeks of treatment with $^{14}CO_2$ lactose breath tests to reflect gastrointestinal lactose absorptions of ^{14}C lactose. The difference at 1, 2, and 3 hr (1 week versus 5 weeks) was 1.7% versus 1.2% ($p < .02$), 4.5% versus 3.6% ($p < .05$) and 5.8% versus 4.7% ($p < .01$). A relationship between low $^{14}CO_2$ and the presence of nausea/diarrhea was recorded ($p < .05$). The authors suggest that patients undergoing radiotherapy to the abdomen and pelvis should not be encouraged to use lactose-containing products during the course of treatment.

Herbert C. Berry

Book Reviews

MGH Textbook of Emergency Medicine. Edited by Earle W. Wilkins, Jr., James J. Dineen, Ashby C. Moncure. Baltimore: Williams & Wilkins, 829 pp, 1978. $59.95

To paraphrase Madison Avenue, emergency medicine has come a long way in the last decade. Emergency Medicine residency programs, the formation of the American College of Emergency Physicians, applications for specialty approval all reflect the burgeoning interest in the field. Also indicative of the interest has been the publication of several textbooks of emergency medicine. The *MGH Textbook of Emergency Medicine* is among the best. The authors and editors have done a commendable job of covering a great deal of material and have done it in a manner neither superficial nor excessively detailed.

The first section deals with life support. The opening chapter is an excellent review of pathophysiologic principles. The next two sections cover medical and surgical emergencies. There are fine chapters on arrhythmias, pulmonary edema, endocrine emergencies, patients with rash and fever, neurosurgical emergencies, emergencies of the injured hand, to name but a few of the topics covered.

The fourth section deals with administrative matters and the last section presents in a clearly illustrated fashion emergency techniques such as subclavian catheter placement and culdocentesis. Of special merit are the good summary tables and figures throughout. Just one of many examples is the differential diagnosis of electrocardiographic features of tachycardia with wide QRS complexis.

An undertaking which attempts to codify all of emergency medicine can't help but have its faults. Some examples: the section on administrative matters is not appropriate in a textbook of this nature and I hope will be eliminated in the next edition. The section on how to draw blood cultures or how to streak agar plates is more appropriate for third year medical students, not practicing physicians. The section on drug abuse overdose is inexplicably found in the psychiatric emergency section rather than toxicologic emergencies. There should be separate sections on pediatric and obstetric/gynecologic emergencies. Despite these inevitable shortcomings, this book represents a commendable effort in advancing the state of emergency medicine.

Mickey Eisenberg
Emergency Medicine Service
University of Washington Hospital
Seattle, Washington 98195

Roentgenology of Fractures and Dislocations. A *Seminars in Roentgenology* reprint. Edited by Benjamin Felson. New York: Grune & Stratton, 179 pp, 1978

This book is a reprint of the *Seminars in Roentgenology* of January and April 1978. Different authors including some quite eminent in their field discuss varied aspects of fractures, dislocations, and related trauma. The skull, face, spine, bony thorax, shoulder, elbow, hand and wrist, pelvis and hips, knee, ankle, and foot are covered as well as pediatric fractures. An introductory chapter, The Radiologist, the Orthopedist, the Lawyer and the Fracture, discusses well the nomenclature of fractures and fracture healing but says much less about the Lawyer and the orthopedist than the title suggests. Material on epiphyseal fractures is somewhat redundantly covered in this chapter as well as that on pediatric fractures. Space limitation did restrict contributors, but the section on the skull, which covers fractures *and* intracranial injuries in 10 pages, was impacted the most. Other sections, such as the spine, are more successfully done. In this case discussion is restricted almost entirely to the cervical spine, the most important and most difficult area. The ankle is well suited to the abbreviated format and is probably the best chapter. The hip and pelvis is also well done.

The text is virtually free of errors. However, on page 13 the word "osteoblastic" has been used in place of "osteoclastic", in describing fracture remodeling. A few of the radiographs reproduced poorly. While I can see some difficulty in obtaining a technically good anterior oblique view of a dislocated hip (p. 123), a better base view for a depressed zygomatic arch (p. 44) should be available. Only a single arthrogram (shoulder) is reproduced, but arthrography does not appear to be within the province of this book. Six cerebral CT scans are included in the skull section, but there are no CT scans of the spine. Radioisotope scans are not shown or mentioned. Discussion of fracture management including acceptable position, complications, and internal fixation would have been of great interest, but perhaps it would be better to refer the reader to another book entirely, rather than to include so much additional material.

Considering the space limitations, this book is eminently successful. It is highly readable and well organized. While every general radiologist could benefit from reading this volume, it is ideally suited to the resident. This facile text should find its place next to the view box in every emergency room.

David H. Carlson
Newton-Wellesley Hospital
Newton Lower Falls, Massachusetts 02162

Myelography, Textbook and Atlas. By Ingar O. Skalpe and Ove Sortland. Oslo: Tanum-Norli, 104 pp, 1978. N. kr. 98

If you found this book on a shelf, you might pass it by because it is small and thin and the spine says simply "Myelography." It is, however, well worth examining. The authors appear uniquely qualified to write such a concise handbook on Amipaque myelography, which has only recently achieved widespread use in this country. Of 91 pages of text (with several unimportant typographical errors and illustrations of satisfactory quality) some 28 pages tell in detail how to use Amipaque in lumbar, thoracic, cervical, and total myelography and in some special situations (e.g., spinal stenosis, pediatric meylography). My only objection is to the authors' emphasis on the importance of horizontal beam fluoroscopy. Another 41 pages are devoted to interpretation while shorter sections discuss the development of the agent, its absorption and excretion, adverse effects, and patient preparation and follow-up. The bibliography contains 123 references to 1976; several are by the authors. I would recommend this book to anyone involved in myelography as a convenient, up-to-date manual which will not soon be supplanted.

Fred B. Ferguson, Jr.
4115 Sears Road
Columbus, Georgia 31907

© 1979 American Roentgen Ray Society

0361–803X/79/1325–0870 $0.00

Atlas of Roentgenographic Measurement, 4th ed. By Lee B. Lusted and Theodore E. Keats. Chicago: Year Book Medical Publishers, 354 pp, 1978. $39.85

This is the fourth edition of this familiar reference. The format is identical to previous editions and is arranged by organ systems. Original figures and radiographic reproductions remain much the same. Many of the charts and tables are again repeated. Some updates are incorporated along with newer measurements which have appeared in recent literature. The authors indicate the edition has more than 50 new entries with the largest numbers in pediatric radiology. In some areas, new information has been incorporated as it relates to the differences between male and female or between different ethnic groups. It is indicated that the newer imaging methods such as echocardiography, nuclear medicine, and computed tomography have enabled visualization of body parts not previously measurable such as the pancreas and fetal maturity. These have been inserted where appropriate. Other areas, e.g. the adrenal glands and spinal cord, which might have been included since the advent of CT, were omitted, perhaps because the book was compiled prior to evaluation of these areas in the literature.

The authors plea for continued measurements based on more than one imaging technique. They also comment that the newer imaging techniques, especially echocardiography and CT have actually corroborated the measurements obtained by older modalities such as cerebral ventricular size.

Some minor criticisms include the need for more illustrations to show the sites from which measurements for a given region were derived. The lack of these sometimes leads to confusion in translating the measurements from tables to actual radiographs. Some of the newer orthopedic devices and prostheses with their appropriate measurements might also be included. A few more comments relating to the clinical usefulness and degree of accuracy of the measurements would be helpful.

The book is a practical tool for the working radiologist and deserves to be in radiology departments.

Ronald D. Harris
Green Hospital of Scripps Clinic
La Jolla, California 92037

L'Angiographie Digestive. Chez L'Adulte et L'Enfant (in French). By D. Doyon, A. Roche, P. Chaumont. Paris: Masson, 204 pp, 1978. 192F

The translated title of this small French book is Angiography of the Digestive Tract in the Adult and the Child. Despite its size, this book is inclusive in discussing angiography of the digestive tract. The text is concise, lucid, and easy to follow. The book is clinically oriented as it deals with different disease entities—inflammatory as well as benign and malignant tumoral conditions. There is good correlation of the anatomic, pathologic, radiologic, and clinical material.

In the preface the authors state that in its early days angiography went through a period of exuberant enthusiasm and overutilization. As experience was gained the definite indications, limitations, and true value of this procedure became well recognized and its place in diagnostic radiology well established. The book is written from this point of view.

There are 10 chapters. The first eight deal with the anatomy of the vasculature of the digestive tract, including the liver, gallbladder, pancreas and spleen; technique of angiography including instrumentation; and avoidance of complications and treatment if they do occur. The appearance of the vasculature in various pathologic conditions is fully described and well illustrated. Included also is a chapter on portal hypertension. In the chapter on anatomy the point is made that there are numerous vascular anomalies and anatomic variations. These should be so recognized and not mistakenly considered as evidence of pathologic conditions. The value of emergency angiography is clearly brought out and the role of therapeutic angiography and embolization is discussed.

Chapter nine is an inclusive description of angiography of the digestive tract in children. It is the longest chapter and constitutes about one fourth of the book. Chapter 10, the final chapter, entitled Exercise, is a unique feature. Where feasible such a chapter would be a worthwhile addition to many books, greatly enhancing their value. This chapter consists of a series of case presentations, with questions and answers, pertinent radiographs, clinical history, and finally the diagnosis. This is similar to the "Case of the Day" presentations, a popular feature at radiologic meetings.

The profuse illustrations are of excellent quality and with good detail. There are several companion line drawings especially in the chapter on anatomy. The legends are brief but adequately descriptive.

Unlike European publications which have the "positive" or dark reproductions of radiographs, the illustrations in this book are in the conventional "negative" print to which the American reader is accustomed. The legends are clear and concise. Those unfamiliar with the French language need not deprive themselves of the use of this book since the illustrations are self explanatory and the legends are easy to follow.

A four page bibliography is at the end and references are grouped to correspond to each chapter.

William H. Shehadi
27 Byram Shore Road
Greenwich, Connecticut 06830

An Introduction to the Physics of Diagnostic Radiology, 2d ed. By Edward E. Christensen, Thomas S. Curry, and James E. Dowdey. Philadelphia: Lea & Febiger, 428 pp, 1978. $13

Radiology has always been one of the more technologically oriented of the clinical specialities. Consequently, the physics of radiology has long been a part of the diagnostic radiology curriculum. With the advent of new imaging modalities, physics has become an even more important part of the radiologist's training. Ultrasound requires an understanding of the generation, propagation, and detection of sound waves. Computed tomography adds the complex mathematics of image reconstruction with strange new words like pixel and voxel. Xeroradiography takes a radiologist into the realm of solid state physics. Intensifying and fluoroscopic screens, x-ray film, and image intensifiers now are produced with new technologies largely unheard of in radiology only a few years ago.

These new imaging methods can be described in varying degrees of exactness. This is evidenced by the spectrum of new textbooks now available for radiological physics. I believe the second edition of *An Introduction to the Physics of Diagnostic Radiology* comes the closest to meeting the needs of both the resident and the practicing radiologist. Extremely well written, with many new illustrations, this edition is a substantial improvement over the previous one. Major updating has been done on chapters dealing with x-ray screens, x-ray film, the

radiographic image, image intensifiers, and television. Chapters on magnification and cinefluoroscopy have been greatly expanded and now describe all pertinent physical concepts. New chapters dealing with xeroradiography, computed tomography, ultrasound, and radiologic protection have been added.

While this edition has incorporated much new material, the basic principles are still explained in a nonmathematical manner that avoids technical language and highly theoretical concepts. Consequently some presentations are simplified to the point of superficiality, and some are incomplete. Nevertheless, this book is recommended to radiology residents and radiologists, both as a text and refresher.

William E. Moore
University of Washington Hospital
Seattle, Washington 98195

Introduction to Clinical Radiology: A Correlative Approach to Diagnostic Imaging. By Richard H. Daffner. St. Louis: Mosby, 410 pp, 1978. $14.75

This reasonably priced text will be welcomed by the medical student for whom it is intended, and has much to offer the clinical house officer. It comprises all phases of modern diagnostic radiology including CT, ultrasound, and nuclear medicine. The indications for, application and hazards of each method is covered appropriately. The illustrations are numerous and for the most part excellent. The author has used them well; while sparing verbal description so prone to sedate the student reader. Each chapter on clinical application is followed by a few quiz cases wherein the reader may test his new found knowledge.

The text contains generalizations to which the experienced radiologist would take exception. The chapter on cardiovascular disorders correctly emphasizes vascularity as the key to diagnosis, but leaves the reader with the impression that this is a simple, straight forward evaluation, and that the assessment of specific chamber enlargement is usually accurate, even in complex congenital cardiac disorders. This approach is perhaps justified for the student reader who will in time learn that many patients "didn't read the book". These minor criticisms should not be construed as condemnation of the book as a whole. It is, in my opinion, a very fine, up-to-date and practical text that is written with care and enthusiasm by a teacher who obviously enjoys what he is doing.

J. H. Arndt
Baylor University Medical Center
Dallas, Texas 75246

Radiobiology for the Radiologist, 2d ed. By Eric J. Hall. Hagerstown, Md.: Harper and Row, 460 pp, 1978. $25

The second edition of this volume continues as a brief survey of parts of the field of radiation biology that are of special interest to radiologists. It will be a useful source for review by radiology residents preparing for board examinations. Each chapter is keyed to show which has relevance to diagnostic radiology and/or nuclear medicine and/or radiotherapy.

The book contains 21 chapters and covers radiobiology from the physics of energy absorption through cellular and organ responses, including the effects of *in utero* exposures. Radiosensitivity as a function of LET, mitotic cycle, and chemical modifiers are covered in separate chapters as are the effects of dose rate and repair mechanisms. The chapters on radiation carcinogenesis and genetic effects have been expanded and chapters on hyperthermia and risks versus the benefits of medical uses of ionizing radiation have been added. Radiologists will find this book a well organized survey of radiation biology as it pertains specifically to the practice of radiology, particularly radiotherapy.

Kenneth L. Jackson
University of Washington Hospital
Seattle, Washington 98195

Biological Effects of ^{224}RA. Benefit and Risk of Therapeutic Application. Edited by W. A. Müller and H. E. Ebert. The Hague: Martinus Nijhoff, 236 pp, 1978. 62.5 guilders

This book contains the proceedings of the Second Symposium on the Biological Effects of ^{224}Ra which was in Neuherberg, Germany in 1976; the proceedings of the first meeting held in Alta, Utah in 1974 have just been published. This small international meeting had 33 participants from seven countries (two from the United States). The texts of 22 of the 23 presented papers are included, together with a two-page abstract of one paper and verbatim records of round table discussions on risk evaluation of and clinical results of ankylosing spondylitis therapy. Three papers are in German; and one is in French.

The 2-day meeting was divided into five unnamed sessions. The first presented the clinical picture (Hartl, Germany), and the pathology and radiology (Schilling, Germany), of ankylosing spondylitis. There were six papers in the second session which was largely on ^{224}Ra in the treatment of ankylosing spondylitis. An exception to this theme was Windeyer's (U.K.) paper on x-ray therapy of this disorder. The other papers dealt with indications for the use of ^{224}Ra (Koch, Germany), a new epidemiological follow-up study (Schales, Germany), quantitative estimates of the risk to bone from *present* therapy (Mays, U.S.), radiochemical purity (Delikan, Germany), and therapeutic results in a follow-up study (Schmitt, Germany). On a personal note, it is sad to record that Dr. Fritz Schales died less than 3 weeks before the symposium; he was a victim of ankylosing spondylitis (he had even been treated with ^{224}Ra) and had been well known to me since 1961.

The four papers in Session III were a mixed bag. The first (Bahous, Switzerland) made no mention of ^{224}Ra, dealing mainly with the use of ^{90}Y in the local treatment of rheumatoid arthritis while Bertrand's (France) paper compared ^{224}Ra with other radionuclides in the treatment of the same disorder. Wallner (Germany) presented data on the injection of ^{224}Ra into the knee joints of animals while Koch (Germany) described the use of the radionuclide in the treatment of Paget's disease.

The theme of Session IV was essentially the late effects of ^{224}Ra, in man (Spiess, Germany) but mainly in mice (Dvorak, Czechoslovakia; Kofranek, Czechoslovakia; Luz, Germany; Marquart, Germany). Erfle (Germany) demonstrated the expression of virus particles in osteosarcomas caused by ^{224}Ra in mice.

In the final session, three papers (Mays, U.S.; Dolphin, U.K.; Groer, U.S.) related to risk of induction of osteosarcoma especially from ^{224}Ra, but also from ^{226}Ra and ^{239}Pu. Martin (France) proposed a protocol to permit soundly based epidemiologic

studies of the late effects of the continued use of ^{224}Ra. The final paper (Roux, France) more properly belonged in Session II.

The two aspects of the continued use of ^{224}Ra as a therapeutic agent in man (clinical usefulness and risk of late effects) were explored in the round table discussions. There seems to be no doubt that there is substantial subjective improvement (relief from pain); equally there is abundant unequivocal evidence of the carcinogenic properties of ^{224}Ra (Spiess reported 54 bone sarcomas in a follow-up of about 900 cases) when administered at higher doses than is current practice (up to 100 μCi/kg, compared to 280 μCi total now). Cataract has also been observed in juveniles. Mays' calculated risk of bone sarcoma of about 0.3% (based on a linear dose-response relation) from present ^{224}Ra therapy was the same as Windeyer's estimate of the risk of leukemia from x-ray therapy. Windeyer thought that this would be acceptable if he had ankylosing spondylitis.

Another important aspect of the effects of ^{224}Ra is the suggestion that it may be a radiocarcinogenic analogue for ^{239}Pu, because both are assumed to decay on bone surfaces, but Dolphin dismissed this as "altogether too simplistic to merit serious consideration." Certainly, dose-rate effects must be considered in such a comparison, since the radiation dose from ^{224}Ra is delivered in about a month, whereas that from ^{239}Pu is delivered chronically and at an essentially constant rate.

There was no indication that the use of ^{224}Ra as a therapeutic agent in the treatment of ankylosing spondylitis will be discontinued in Germany or France, and these papers constitute an interesting survey of a vexatious problem. The volume is well bound and the paper glossy, but the texts have been reproduced directly from typescript. Typographical errors abound (they are not the usual type of misprints), but most are obvious. Perhaps the most serious refers to "a few tenths of a microcurie" when what is meant is "a few tens of microcuries" (p. 83). This book will be a useful reference to all those who are concerned with the late effects of internal radioactive materials in man.

John Rundo
Argonne National Laboratory
Argonne, Illinois 60439

An International Neutron Dosimetry Intercomparison. ICRU Report 27. Washington, D.C.: International Commission on Radiation Units and Measurements, 54 pp., 1978

The International Neutron Dosimetry Intercomparison (INDI) was conducted to compare the results obtained by various individuals and/or groups: participants selected by the ICRU on the basis of their activity and competence in fast neutron dosimetry in performing absolute fast neutron dosimetry using various techniques in situations approximating those generally encountered in radiotherapy and radiobiology. This work was to provide information on the present adequacy of neutron dosimetry and on the advantages, diasdvantages, corrections, and systematic errors involved in the various methods used; its long-range goal was to identify the most accurate method(s) of performing fast neutron dosimetry.

The measurements were carried out at the Radiological Research Accelerator Facility of the Medical Research Center at Brookhaven National Laboratory. Fourteen groups of scientists from six countries participated at various times during six 2-week measurement sessions in 1973.

This report presents and discusses the INDI project in detail. It describes the procedures for carrying out the intercomparison, the methods of production, monitoring and stability of the radiation fields, the various dosimetry systems used, the important factors in the evaluation of dose, and the analysis of the results of the intercomparison.

Although these measurements were conducted 5 years ago, the presentation has significantly more than historical value. Preliminary reports of this effort have helped to improve the present state of absolute neutron dosimetry beyond that achieved during this intercomparison. A couple of the conclusions and recommendations of the committee bear repeating here. Namely, that for the case of homogeneous tissue-equivalent ionization chambers, which were and still are the predominant method employed, more emphasis is needed on improving the uniformity of the procedures and techniques for measuring chamber responses and for applying corrections appropriate to the radiation field. Also, adoption of uniform $\overline{W}$ ratios, kerma ratios, and mass stopping power ratios is desirable.

Because of increasing activity in the use of neutrons in radiotherapy, the report is recommended reading for all dosimetry physicists in the field.

Jüri Eenmaa
University of Washington Hospital
Seattle, Washington 98195

The Radiology of Joint Disease, 2d ed. By D. M. Forrester, J. C. Brown, and John W. Nesson. Philadelphia: Saunders, 626 pp., 1978. $34.50

The first edition of this book was published in 1973, as volume 2 of the Saunders series, Monographs in Clinical Radiology. Its well deserved success was based on logical organization, attractive writing style, and excellent illustrations. The second edition, in my opinion, is even better.

This book is about a third longer than the original, a result of augmentation of both text and illustrations. In the first four chapters the authors again provide explicit descriptions and illustrations of basic findings in arthritis as depicted in the hands and wrists. They emphasize a logical approach to analysis of films, with systematic evaluation of soft tissues, alignment, bone mineralization, and cartilage. In chapters five through 10, these principles are used again to detect and understand disease involving the foot and ankle, knee, hip, elbow, shoulder, and axial skeleton.

Internal structure and content of each chapter have been altered to reflect new concepts and developments. New diseases, variant manifestations of old ones and better examples of specific case findings have been added. In the thoracolumbar spine section for instance, the new edition now begins more appropriately with a clinically oriented overview of low back pain and only then moves into the specifics of infection, spondylitis, and degenerative disease.

Additional features of the first 10 chapters merit comment. Although most of the illustrations remain in the "excellent" category, they fall a little short of previous quality. In the copies

available to me, the images were slightly darker than in the first edition, enhancing some features but degrading others. A few were marred by printing artifacts, which would not necessarily recur in all copies.

Although the writing is very precise and descriptive, its effect nevertheless is one of informality. Quotes from the (nonmedical) literature, quips, and puns are tastefully incorporated as before and enhance interest and reader enthusiasm. In keeping with this informality the authors have continued to offer Suggested Reading at the end of each chapter rather than a specifically cited bibliography. Overall, the decision was probably a wise one. Occasionally however, tighter documentation would have been welcome. As one minor example of this, the authors assert that the "vacuum disc" is probably lipid rather than gas. They don't support that opinion in text or references and fail to comment on a previous paper (*AJR* 128:1056–1057, 1977) in which the gas has been collected and analyzed.

"Exercises," the diagnostic unknowns at the end of each chapter, have been dropped. While they added to the overall enjoyment and effectiveness of the original book, the authors have incorporated many of these cases into the logical flow of each chapter, and perhaps their impact is improved.

Finally, in a uniquely welcome addition, the new coauthor Dr. John C. Brown, offers a rheumatologist's differential diagnosis of arthritis. In a succinct but very readable 45 pages, he provides the reader with a background of structure and function of cartilage and synovium, as well as insights into the clinical and pathogenetic features of the arthritides. Organization into inflammatory, degenerative, and metabolic etiologies with their significant subcategories, provides excellent perspective and knowledgeable starting points for interaction by radiologist and clinician in arthritis problems.

I would strongly recommend this book for the libraries and personal shelves of clinical radiologists. Donate the original book to a young friend and acquire the new edition.

Rosalind H. Troupin
Hospital of the University of Pennsylvania
Philadelphia, Pennsylvania 19107

Books Received

Receipt of books is acknowledged as a courtesy to the sender. Books that appear of sufficient interest will be reviewed as space permits.

Evaluation of Liver Function. A Multifacted Approach to Clinical Diagnosis. Edited by L. M. Demers, L. M. Shaw. Baltimore: Urban & Schwarzenberg, 211 pp., 1978. $19.50

Chest Nuclear Medicine Case Studies. By M. Guter, A. N. Serafini. Garden City, N.Y.: Medical Examination Publishing, 170 pp., 1979. $12

Atlas of Nuclear Medicine, vol. 4. Bone. By P. E. Dibos, H. N. Wagner, Jr. Philadelphia: Saunders, 197 pp., 1978. $35

Why be Quantitative about Radiation Risk Estimates? By E. E. Pochin. DC: National Council on Radiation Protection and Measurements, 36 pp., 1978. $6

Atlas of Pediatric Nuclear Medicine. By P. O. Alderson, D. L. Gilday, H. N. Wagner, Jr. St. Louis: Mosby, 296 pp., 1978. $44.50

Radiology of the Heart and Great Vessels, 3d. ed. Golden's Diagnostic Radiology. By R. N. Cooley, M. H. Schreiber, L. B. Morettin. Baltimore: Williams & Wilkins, 673 pp., 1978. $65

Bone Dysplasias of Infancy. A Radiological Atlas. By B. J. Cremin, P. Beighton. Berlin: Springer-Verlag, 107 pp., 1978. $39

News

North Carolina Postgraduate Course

The faculty of the Duke University Medical Center will present a 6-day postgraduate course, July 30–August 4, at Atlantic Beach, North Carolina. C. E. Putman is program chairman. Scientific sessions will cover ultrasound, CT scanning, and nuclear medicine. A total of 30 hr AMA Category I credit is available. Registration fee is $250 ($125 for those in training with verification from department chairman). Direct inquiries to the program director, Dr. R. McLelland, Radiology—Box 3808, Duke University Medical Center, Durham, NC 27710; telephone (919) 684-4397.

Spanish American Medical Society Meeting

The Spanish American Medical Society, a 50-year-old organization of Spanish speaking physicians in the New York metropolitan area, will sponsor the third Interamerican Medical Congress, Oct. 5–8, in New York City. The course will carry 20 hr continuing education credit. For information, contact: Dr. R. F. Rodriguez, 37-21 75th St., Jackson Heights, NY 11372.

International Body Imaging Conference

The fourth annual International Body Imaging Conference will be Oct. 13–21 in Maui, Hawaii. The conference offers about 30 hr AMA Category I credit and will present a correlated approach to the principles, indications, uses, interpretation, and results obtained with computed tomography, ultrasound, and nuclear imaging. Conference faculty will be: G. Leopold, University of California, San Diego; M. Johnson, University of Colorado; L. Rosenthall, Montreal General Hospital; J. Haaga, Cleveland Clinic; P. Sheedy, Mayo Clinic; W. F. Sample, UCLA Medical Center; and S. Fierstien, University of California, Irvine. Registration is limited. Course fee is $295 ($225 for residents and technologists). Address inquiries to: Conference Secretary, Fourth Annual International Body Imaging Conference, West Park Hospital, Department of Radiology, 22141 Roscoe Blvd., Canaga Park, CA 91304.

Symposium on Intervention Radiology

The first International Symposium on Intervention Radiology will be May 29–June 2 in Algarve, Portugal. The European Society of Radiology is sponsor. Details may be obtained from the Secretariat: 123, 1.°-Esq., Av. Elias Garcia, Lisbon, Portugal.

Meeting and Course Review

For reader convenience, a summary of upcoming meetings and courses is provided. Detailed listings of these events appeared in journal issues indicated in parentheses.

XIII Interamerican Congress of Radiology, July–August 1979, Quito, Ecuador (October).

Noninvasive Imaging in Medicine, symposium, June 6–9, Lund, Sweden (October).

Conference on Medical and Biological Engineering and Medical Physics, Aug. 19–24, Jerusalem (October).

L. H. Gray Conference, Sept. 10–14, Cambridge, England (October).

Asian Oceanian Congress of Radiology, Oct. 28–Nov. 3, Singapore (October).

Abdominal Real Time Sonography Courses, June 11–15, July 16–20, Aug. 6–10, Dec. 9–13, 1979, Winston-Salem, N.C. (November).

Fleischner Society Ninth Symposium (and course), June 11–13, Stockholm, (November).

American Board of Radiology, oral and written examination dates and locations for 1979 and 1980 (December).

AFIP Diagnostic Radiology Seminars, series, August 27–31, November 12–16, Washington, D.C. (December).

Canadian Radiologists Annual Meeting, June 24–28, Vancouver (December).

Multidisciplinary Aspects of Brain Tumor Therapy, June 8–10, Lake Garda, Italy (December).

Symposium: Computerized Tomography of the Brain, Sept. 20–22, Bordeaux, France (January).

Diagnostic Ultrasound Training Programs, continuing weekly series, New York City (January).

Diagnostic Ultrasound Workshop, weekly postgraduate sessions through December 14, Houston (January).

Eighth Congress, European Society of Neuroradiology, Sept. 7 and 8, Strasbourg, France (January).

University of Pennsylvania Diagnostic Radiology Seminar, June 4–8, Philadelphia (February).

AAPM Summer School, July 22–28, Chapel Hill, N.C. (February).

Austrian Nuclear Medicine Meeting, Sept. 11–14, Innsbruck (February).

Irish-American Radiology Symposium, Sept. 15–21, Killarney, Ireland (March).

Diagnostic Ultrasound Courses, series of 2-week courses, Winnipeg, Canada (March).

Gastrointestinal Refresher Course, Oct. 11–14, Williamsburg, Virginia (March).

Diagnostic Ultrasound Course, Sept. 7–9, Ann Arbor, Michigan (April).

Preceptor Training Programs in Diagnostic Ultrasound, 1-month programs, San Diego (April).

Radiology of Signs and Symptoms, course, May 30–June 2, Cambridge, Massachusetts (April).

National Conference on Breast Cancer, Sept. 6–8, New York City (April).

Medical Imaging Meeting, July 28–Aug. 4, Mauna Kea Beach, Hawaii (April).

IV European Congress of Radiology, Sept. 4–8, Hamburg, West Germany (April).

Arthrography Course, June 7–9, New York City (April).

Uro-Radiology Seminar, Aug. 19–22, Lake Chapala, Mexico (April).

Ultrasound Annual Meeting, Aug. 27–31, Montreal (April).

Diagnostic Radiology Refresher Course, June 4–8, Cincinnati (April).

Asian Congress on Radiation Protection, Nov. 5–9, Manila (April).

© 1979 American Roentgen Ray Society

0361-803X/79/1325-0875 $0.00

American Roentgen Ray Society

President: Harry Z. Mellins
President Elect: Paul A. Riemenschneider
1st Vice-president: Joseph D. Calhoun
2nd Vice-president: Charles E. Bickham, Jr.
Secretary: James F. Martin
Treasurer: Harley C. Carlson

COMMITTEES 1977–1978

Executive Council: H. Z. Mellins, P. A. Riemenschneider, J. D. Calhoun, C. E. Bickham, Jr., J. F. Martin, H. C. Carlson, M. M. Figley, R. G. Evens, B. G. Brogdon, R. A. Gagliardi, E. Gedgaudas, G. A. Kling, T. F. Leigh, S. F. Ochsner, J. F. Wiot, R. E. Buenger, E. C. Klatte, J. P. Tampas, J. L. Gwinn, chairman

Finance and Budget: A. E. James, E. C. Klatte, R. McLeeland, J. P. Tampas, R. G. Evens, chairman

Publications: M. P. Capp, K. Ellis, F. F. Ruzicka, Jr., E. R. Heitzman, R. A. Gagliardi, chairman

Editorial Policy: M. M. Figley, E. F. Lang, R. H. Troupin, E. R. Heitzman, K. Ellis, F. F. Ruzicka, Jr., M. P. Capp, R. A. Gagliardi, chairman

Advisory Committee on Education and Research: J. E. Youker, G. Wilson, G. W. Hartman, L. F. Rogers, E. Gedgaudas, chairman

Scientific Exhibits: T. C. Beneventano, G. Dodd, B. G. Brogdon, chairman

Constitution and Bylaws: J. H. Walker, W. M. Whitehouse, J. P. Tampas, chairman

American Board of Radiology Representatives: J. F. Roach, R. W. McConnell, S. W. Nelson

Program Committee: H. Z. Mellins, J. F. Martin, J. L. Gwinn, M. M. Figley, R. A. Gagliardi, B. G. Brogdon, E. Gedgaudas, G. A. Kling, P. Riemenschneider, chairman

Instruction Courses: E. Gedgaudas, director; G. W. Hartman, associate director

American College of Radiology Board of Chancellors Representative: W. B. Seaman

Annual Meeting: March 25–30, 1979, Sheraton Centre, Toronto, Canada

Scientific Program: P. A. Riemenschneider, president elect, Cottage Hospital, Santa Barbara, California 93105

Manager Annual Meeting: George A. Kling, Harper Hospital, Detroit, Michigan 48201

Membership: John L. Gwinn, 4650 Sunset Blvd., Los Angeles, California 90027

Business Office: Keith W. Gundlach, comptroller, American College of Radiology, 20 North Wacker Drive, Chicago, Illinois 60606

American Radium Society

President: Frederick W. George, III
President Elect: Alfred S. Ketcham
1st Vice-president: Julian P. Smith
2d Vice-president: Edwin M. Jacobs
Secretary: Norah duV. Tapley
Treasurer: Simon Kramer

COMMITTEES 1978–1979

Executive: A. S. Ketcham, J. P. Smith, E. M. Jacobs, N. duV. Tapley, S. Kramer, L. W. Brady, R. H. Jesse, F. W. George, F. Rutledge, chairman

Public Relations: V. Marcial, J. Vaeth, C. Honaker, ex-officio, and F. George, chairman

Publication: K. L. Krabbenhoft, D. Hussey, A. Raventos, I. Fix, L. W. Brady, chairman

Scientific Program: R. Parker, J. Durant, A. S. Ketcham, M. S. Mitchell, G. Murphy, F. Rutledge, M. Griem, W. E. Powers, M. Apuzzo, F. George, chairman

Local Arrangements: L. Davis, J. Vaeth, J. Nolan, R. McKenna, J. Slater, J. Stein, J. Scallon, S. Kramer, J. Helsper, chairman

Constitution and Bylaws: A. S. Glicksman, P. J. DiSaia, K. L. Krabbenhoft, chairman

Audiovisual: C. R. Bogardus, J. Helsper, R. Schweitzer, R. H. Jesse, C. Perez, J. Glassburn, A. M. Nisar Syed, R. Young, B. Herrington, F. George, chairman

American Board of Radiology Representatives: J. J. Stein, R. E. King, N. duV. Tapley

American College of Radiology Board of Chancellors Representative: L. W. Brady

American College of Radiology Council Representative: J. del Regato

Editorial Board of AFCOS Newsletter Representative: J. Vaeth

National Council on Radiation Protection and Measurements Liaison Representative: L. W. Davis

Annual Meeting: March 4–8, Los Angeles, California

Scientific Program: F. W. George, III, University of Southern California School of Medicine, Los Angeles, California 90033

Local Arrangements: James Helsper, Pasadena, California

Membership: Norah duV. Tapley, secretary, M. D. Anderson Hospital, 6723 Bertner Avenue, Houston, Texas 77030

Business Office: N. V. Jordan, c/o R. H. Jesse, M. D. Anderson Hospital and Tumor Institute, 6723 Bertner Avenue, Houston, Texas 77030

Mailing note.—Mailing surcharges: U.S. and possessions, none; European countries, $25; Japan, $45; other, $10. European rates apply to Algeria, Austria, Belgium, Czechoslovakia, Denmark, Finland, France, Germany, Great Britain, Greece, Hungary, India, Iran, Ireland, Israel, Italy, Kenya, Luxembourg, Netherlands, Nigeria, Norway, Portugal, Romania, South Africa, Spain, Sweden, Switzerland, Turkey, Uganda, Yugoslavia. All subscriptions to Japan and European countries are delivered by air freight; there is no option for surface mail.

Cook County
Graduate School of Medicine

announces

REFRESHER COURSE IN DIAGNOSTIC RADIOLOGICAL PHYSICS

June 4–9, 1979

Write or call for information and registration.

Registrar
707 South Wood Street
Chicago, Illinois 60612
(312) 733-2800

RADIOLOGIST

Board Certified or Eligible

Immediate fulltime vacancy in 107 bed JCAH accredited community general hospital in an historic setting. Interested parties please send curriculum vitae in confidence to: Dr. Edward J. Baranski, Chairman of the Medical Staff, c/o Annie M. Warner Hospital, South Washington Street, Gettysburg, Pennsylvania 17325. Telephone 717-334-2121, Extention 129.

Index to Advertisers

In Alphabetical Order

Amrad
Body Imaging Conference
Boehringer Ingleheim
Dunn Instruments, Inc.
Eastman Kodak Company
Elema-Schonander, Inc.
Elscint Inc.
E-Z-EM Company
C. B. Fleet Company
Gammex, Inc.
General Electric
Guerbet Laboratories
Humanoid Systems
Imaging Systems
Lea & Febiger
Machlett Laboratories
Ohio Nuclear
Pfizer Medical Systems, Inc.
Philips Medical Systems, Inc.
Picker Corporation
Precise Optics
Purdue Frederick Company
Raytheon Medical Imaging
Siemens Corporation
Smith Kline & French Laboratories
E. R. Squibb & Sons
Toshiba Medical Systems
VAS Corporation

A Public Service of this magazine & The Advertising Council Ad Council



Your Business can be one, too.

Red Cross needs individual volunteers, and donors of blood and money, by the millions.

But we need even more help. We need the solid support of American Business. And we never needed it more.

If your business is already helping, by organizing blood drives, and by supporting payroll deductions—either directly for the Red Cross, or through the local combined fund drive—the whole community owes you thanks. And we thank you, too.

Last year, with help from our friends, we offered major aid at over 30,000 disasters—from typhoons, to local (but just as devastating) house fires.

We were able to help the elderly with practical programs, we helped veterans by the hundreds of thousands, we taught people by the millions to swim or swim better. And that's just the tip of the iceberg.

Think of America without The American Red Cross.

And you'll know why we need your business as a Red Cross Volunteer. In your community. And all across America. Contact your local Red Cross Chapter to see how your company can become a volunteer.

Red Cross. The Good Neighbor.

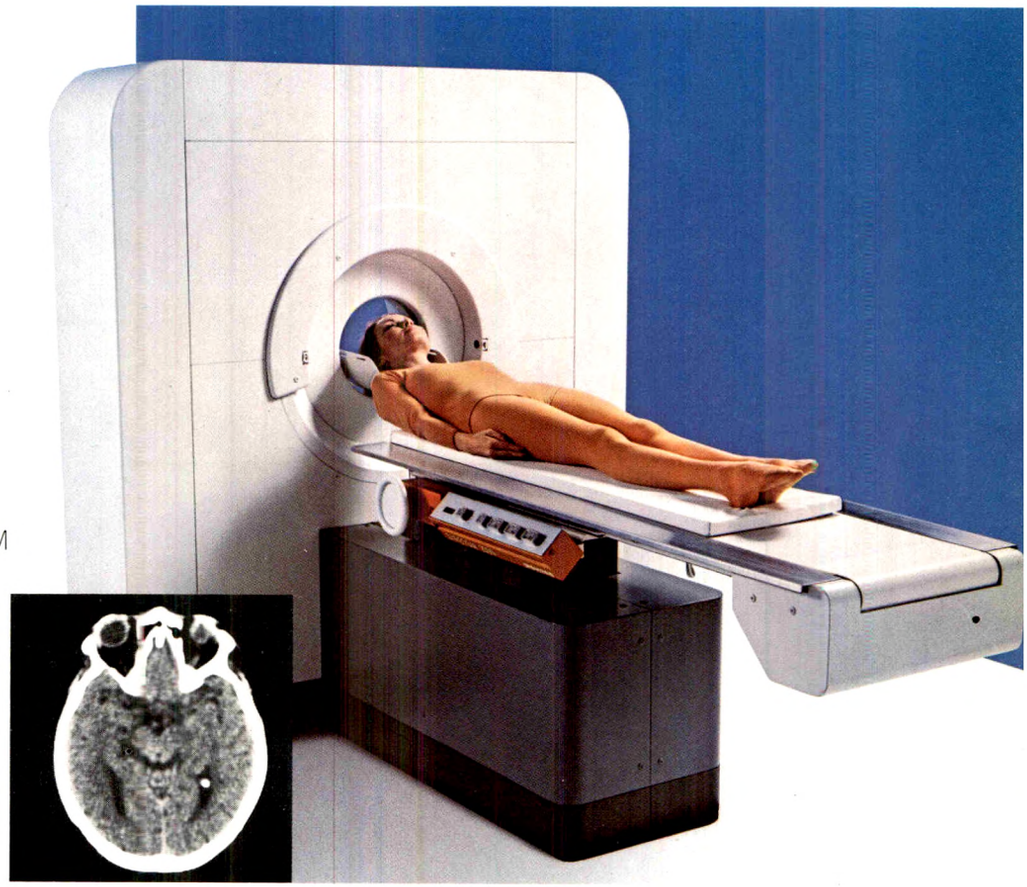
The Siemens Difference: Instantaneous image reconstruction

Immediate clinical evaluation

Delayed processing time is a thing of the past with Siemens computer tomographs, SIRETOM and SOMATOM. A specially designed high-speed computer reconstructs scanned images instantaneously. This permits immediate decisions as to diagnosis and course of treatment while providing for faster and smoother patient processing.

Reduced scan time

Scanning for both SIRETOM (head scanner) and SOMATOM (whole body scanner) is governed by the SCINTILLARC fan-beam solid-state detector array system. The result of this advanced engineering is evidenced by a dramatic reduction in setup and scan time along with unsurpassed quality tomograms achieved under clinical conditions.



Concepts... engineered to radiologic excellence

SIEMENS

The Siemens Difference: Advanced X-ray target and electron scattering foil systems

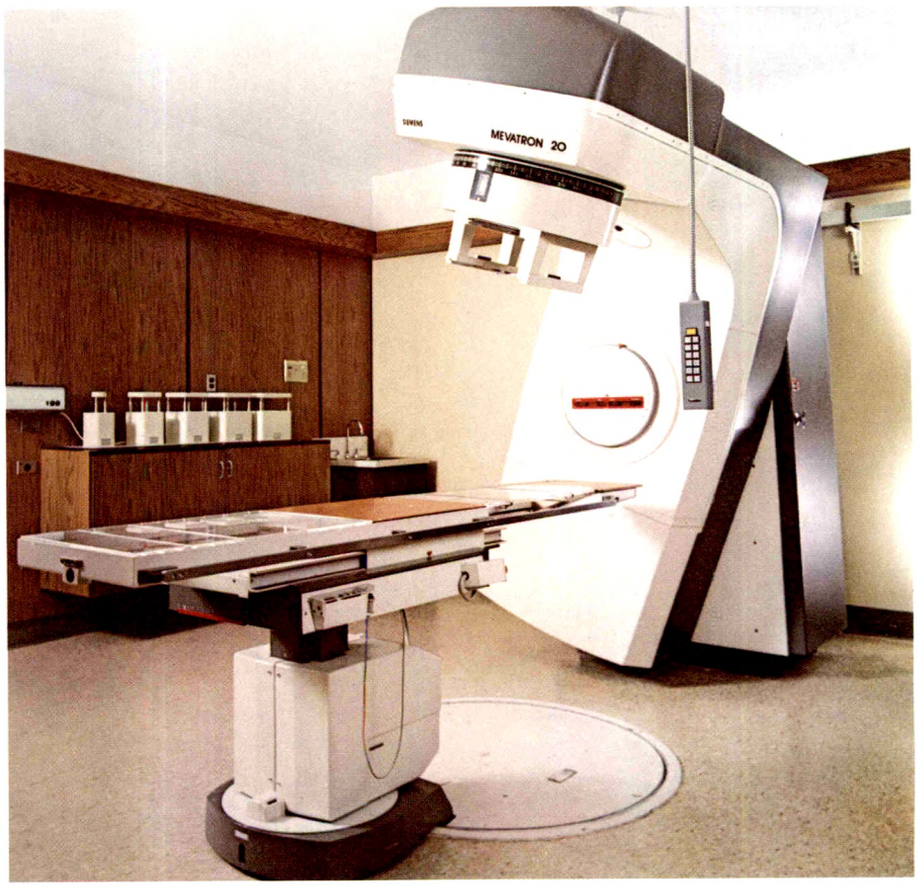
The MEVATRON-20

Siemens' newest accelerator, the MEVATRON-20, utilizes a multiple element X-ray target and a unique double-foil electron scattering system to produce outstanding beam quality. Additionally, it features an integral verification capability for error-free machine setup. And with the highly flexible "Z" patient table, it forms a truly integrated installation ideally suited for modern radiation therapy technique.

The MEVATRON series

Siemens' product selection also includes the MEVATRON-6 and MEVATRON-12 which,

- together with MEVATRON-20, cover the full spectrum of energy and modality requirements.



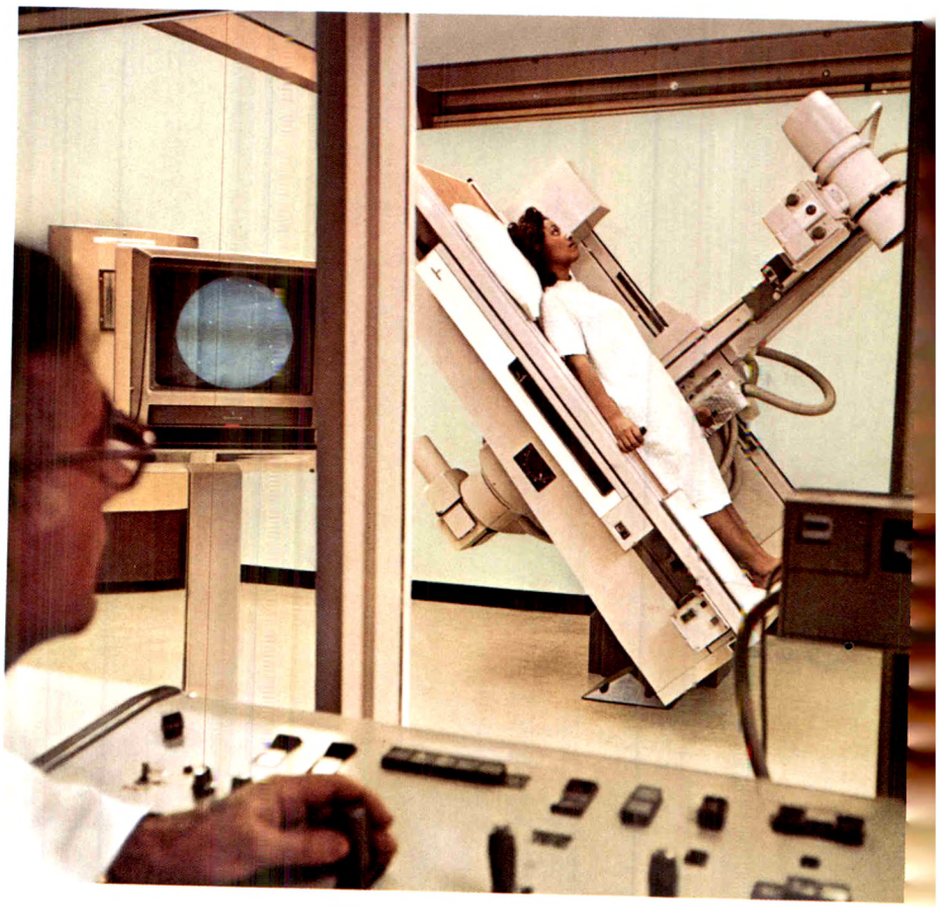
The Siemens Difference: Specific systems for specific needs

Versatile applications

Siemens responds to the varying needs of the radiologist with a full line of remote-controlled examination units – SIREGRAPH A, SIREGRAPH B, and SIREGRAPH II. Virtually every radiographic or fluoroscopic examination may be performed on a system from our wide selection of universal procedure or dedicated-purpose remote-controlled diagnostic products.

Individualized systems

Our systems were developed to meet the growing preference for remote examination tables and to meet the need for individual, custom-designed units that would satisfy different levels of requirements for versatility and application.



Concepts... engineered to radiologic excellence

SIEMENS

The Siemens Difference: Organ-related push-button programming

Simplicity of operation

Siemens has engineered operator time efficiency into diagnostic X-ray generators. Both OPTIMATIC and ORGANOMATIC generator series feature organ-related techniques which eliminate errors caused by miscalculation of exposure times and settings. One push button selects the examination units, kV, mAs, focal spot, and screen-type. The result is more efficient operational control and improved patient processing.



The Siemens Difference: Immediate automatic processing and printing of final reports

A new way of reporting

SIREP replaces the dictating machine and all other conventional methods of X-ray reporting with a computerized input terminal and a comprehensive radiological lexicon, RADLEX. Each RADLEX frame contains a vocabulary of diagnostic, anatomical, and radiologic terms from which the radiologist selects his findings. These are compiled in a logical manner by the radiologist to form a concise and accurate report emphasizing positive findings, degrees of certainty, statements of change, and advice for further study. Once the text has been completed and approved, the radiologist simply pushes a button to receive a perfectly typed copy of his final report.



Concepts... engineered to radiologic excellence

SIEMENS

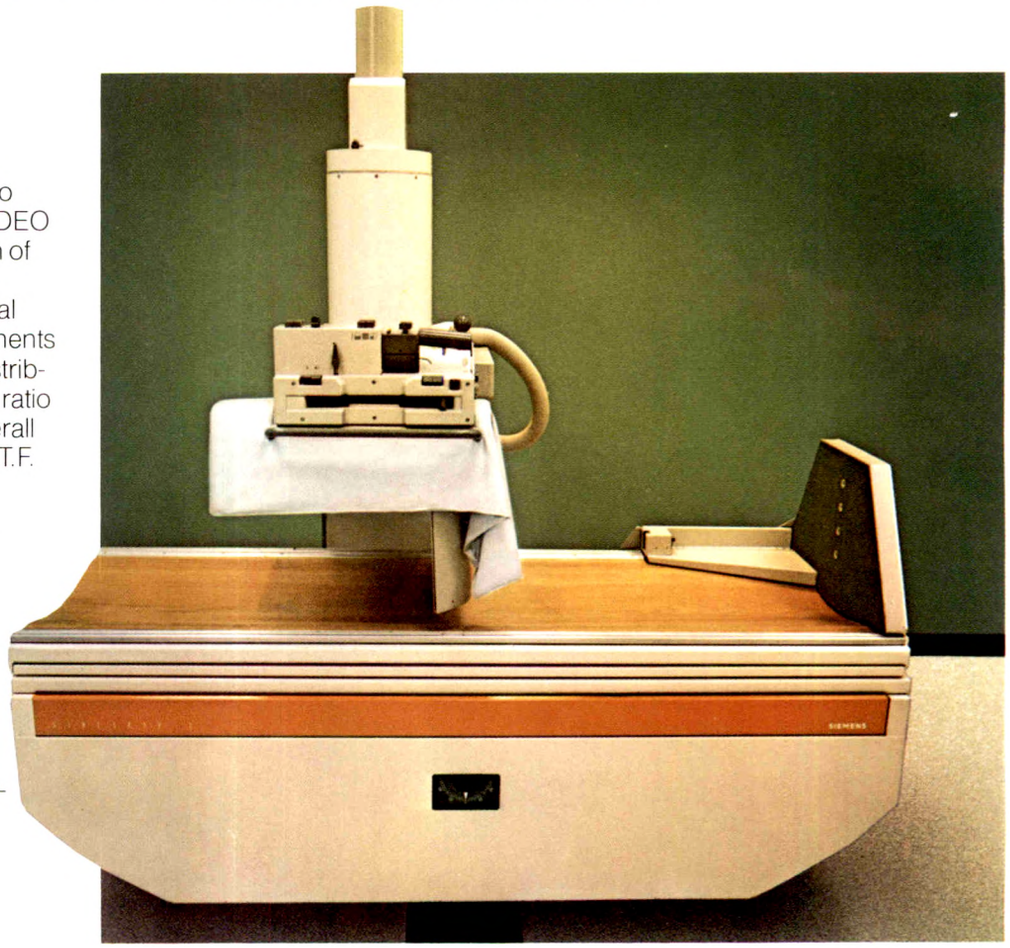
The Siemens Difference: Total electronic transfer of all available information

Improved image quality

Siemens has gone beyond doubling the line frequency to enhance the image of the VIDEO MED H. Electrical bandwidth of the video amplifier has been extended, resolution of optical and electron-optical components has been more uniformly distributed, and the signal-to-noise ratio has been increased. The overall result is improved system M.T.F.

Diagnose directly from the television display

The VIDEO MED H represents one of the truly great achievements in the use of X-ray television systems. Details of the fluoroscopic image maintain their sharpness, even with a high brightness level in the television display.



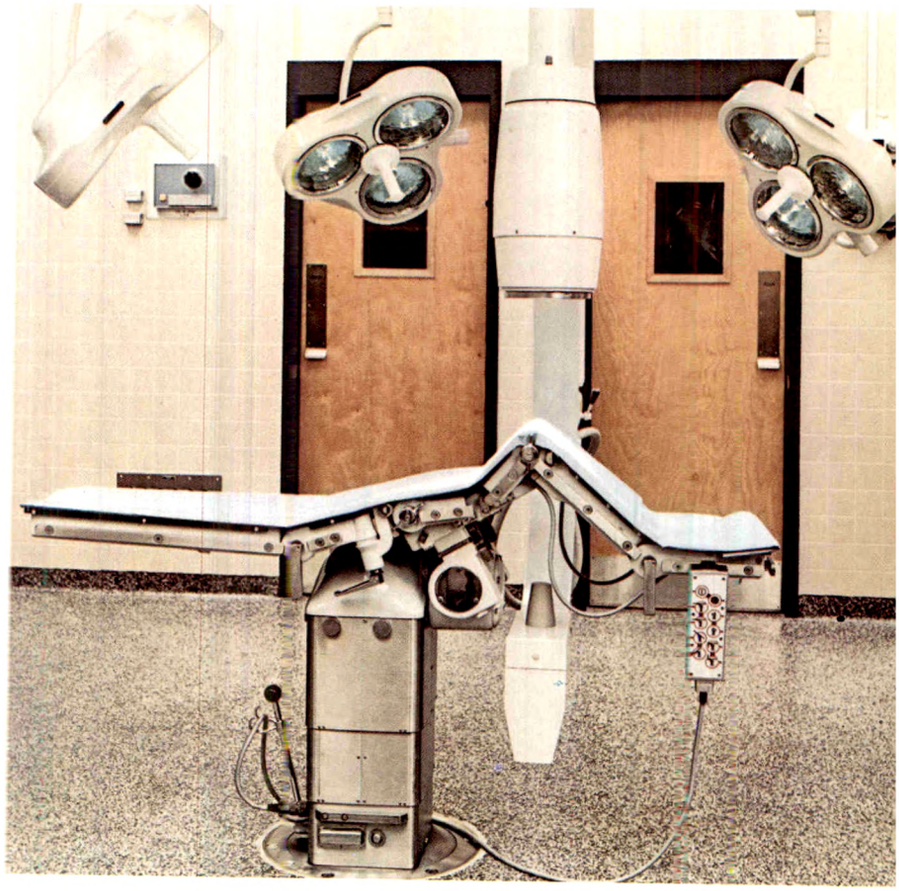
The Siemens Difference: Complete single-source O.R. systems

Total system planning

There is no room for error when it comes to planning something as complex and sophisticated as an operating room installation. Only Siemens offers an experienced approach that includes the designing, planning, installation, in-service training, financing, and servicing of a *total system* to meet your individual requirements.

Compatibility is engineered into the system

Because Siemens is a single-source supplier, system compatibility of all equipment is assured. Tables, lights, X-ray equipment, electrosurgical units, patient monitors, defibrillators—all are required to meet the high standard of Siemens' performance prior to system installation. Whenever you are planning an operating room, depend on Siemens.



Concepts... engineered to radiologic excellence

SIEMENS

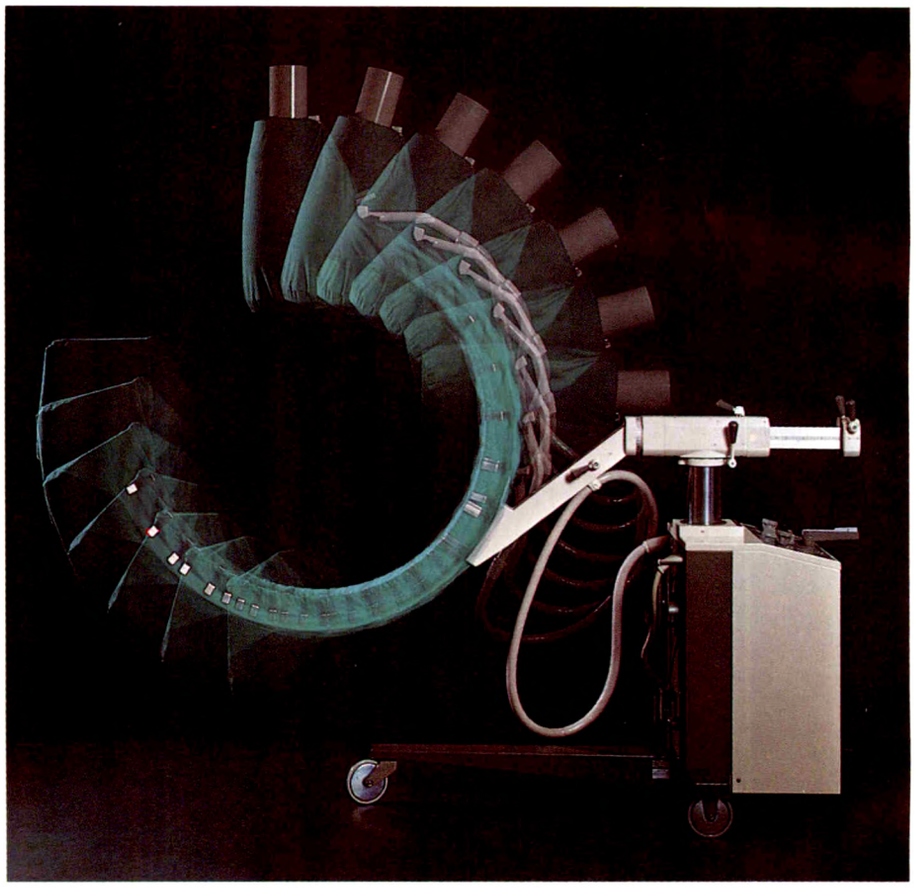
The Siemens Difference: Total maneuverability in aseptic procedures

No inhibition of mobility

Siemens has designed the SIREMOBIL 2U with the special requirements of the operating environment in mind. The C-arm is uniquely assembled to the horizontal support with a recessed slide track mechanism. Because there are no external gears, maneuverability remains unobstructed during surgical procedures.

Other system benefits

The unique operating capability of the SIREMOBIL 2U is exceptionally enhanced with the IMAGE STORE disc recorder which allows alternating comparison of previously stored and live fluoroscopy images.



For Total Imaging



TOSHIBA
MEDICAL SYSTEMS

At Toshiba, the concept has always been total imaging. It is the reason the world looks to us for all four types of imaging systems in use today.

From modular radiology and fluoroscopy systems, to the world's first super high resolution large field gamma camera, six decades as medicine's international imaging leader goes into every system we make.

Two things make Toshiba Medical Systems the image to look for, resolution and human engineering.

As an example, both have contributed equally to making Toshiba's Ultrasound Sonolayergraph series the finest available to modern clinical medicine.

Backing Toshiba Medical System's 60 years of medical imaging experience, is Toshiba Corporation's position as a leader in electronics and computer integrated systems of all types.

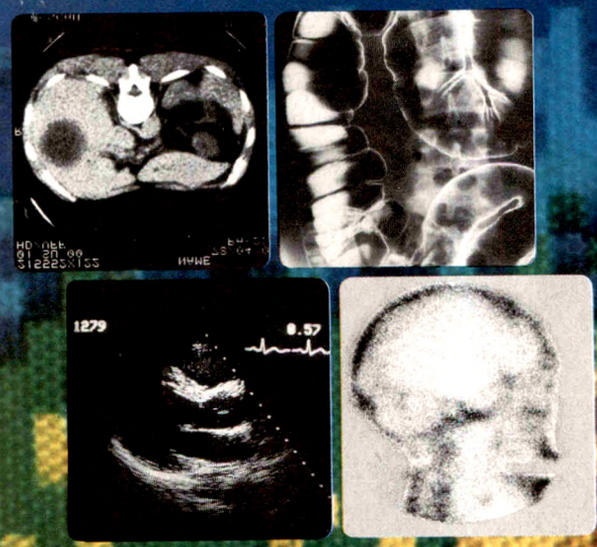
This kind of technical capability enabled Toshiba to incorporate the latest advances from a wide range of fields, to produce a new level of computer tomography with Toshiba's whole body CT scanner.

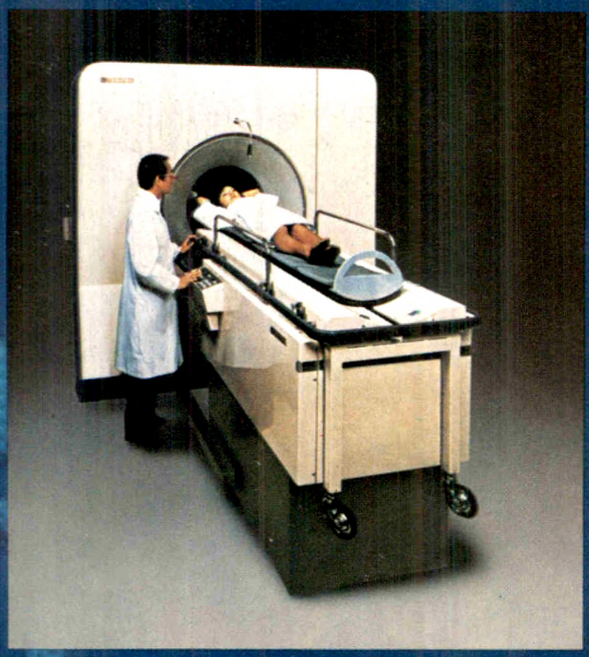
As medicine goes forward, you can be assured Toshiba Medical Systems will be there to give you the most useful diagnostic image you can get. That's because our commitment to giving you the finest imaging is as deep as your commitment to the good health of your patients.

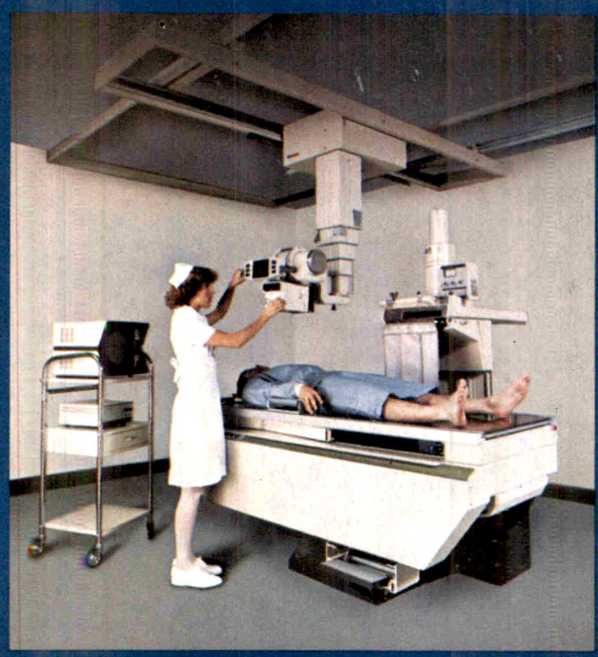
Look to us, we are your total imaging company.

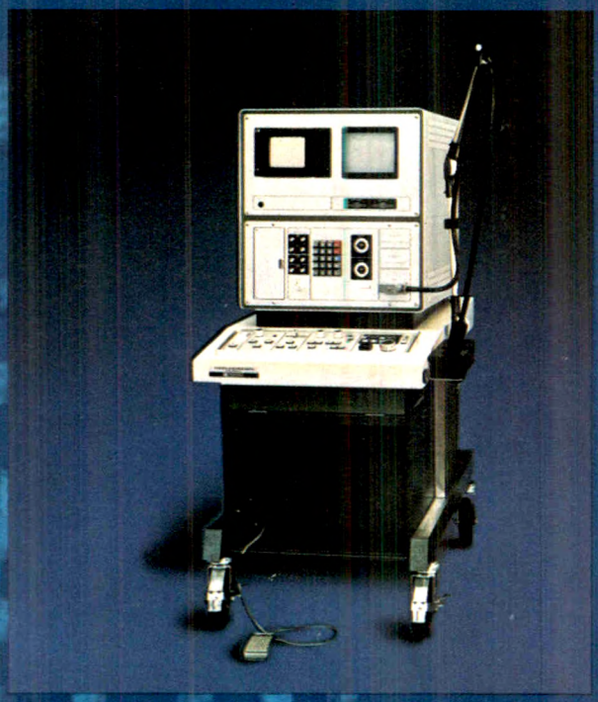
Toshiba is Your Total Image,

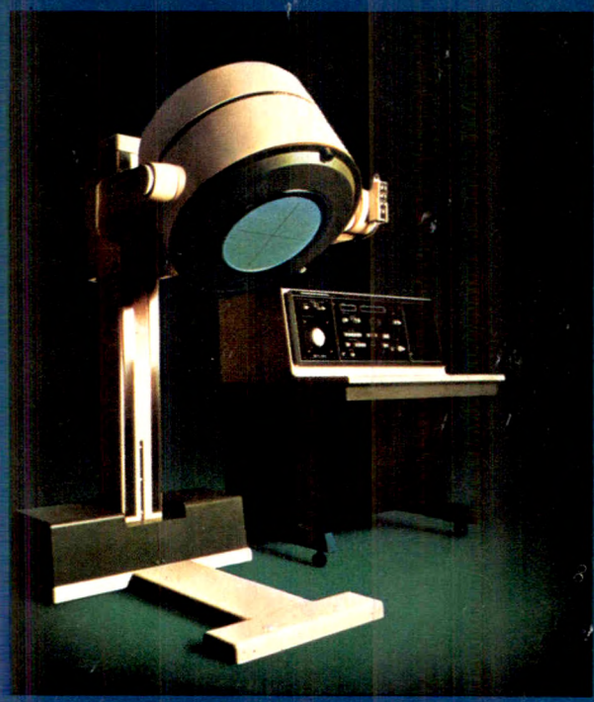
manufacturing the total gamut of imaging systems.











The ultimate in image clarity and human engineering for Radiology and Fluorcscopy, Ultrasound, Computer Tomography and Nuclear Medicine.

EXTENDED SERVICE PLANNING

Toshiba Medical Systems is also your total service company. With engineering personnel and logistics support that span the globe, Toshiba is committed to provide around the clock service and support anywhere in the world.

Toshiba Medical Systems sales and service headquarters around the world:

Argentina, Buenos Aires
Australia, Sydney
England, London
Hong Kong, Hong Kong
Iran, Teheran
Mexico, Mexico City
The Netherlands, Amsterdam
New Zealand, Wellington
Philippines, Manila
Republic of South Africa, Johannesburg
Taiwan, Taipei
Thailand, Bangkok
Venezuela, Caracas

Toshiba Medical Systems
Division of Toshiba International, Corporation,
U.S.A. — Los Angeles, California

Atlanta, Georgia
Boston, Massachusetts
Chicago, Illinois
Cincinnati, Ohio
Cleveland, Ohio
Dallas, Texas
Detroit, Michigan
Houston, Texas
Kansas City, Missouri
Los Angeles, California
Memphis, Tennessee
Miami, Florida
New Orleans, Louisiana
New York, New York
Philadelphia, Pennsylvania
Phoenix, Arizona
San Francisco, California
Seattle, Washington
Tampa, Florida
Washington, D.C.
Ontario, Canada

Toshiba Medical do Brasil, Ltda. — Sao Paulo, Brazil







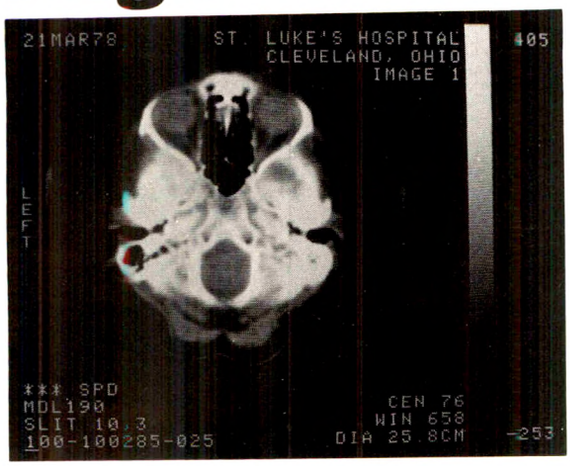


Toshiba

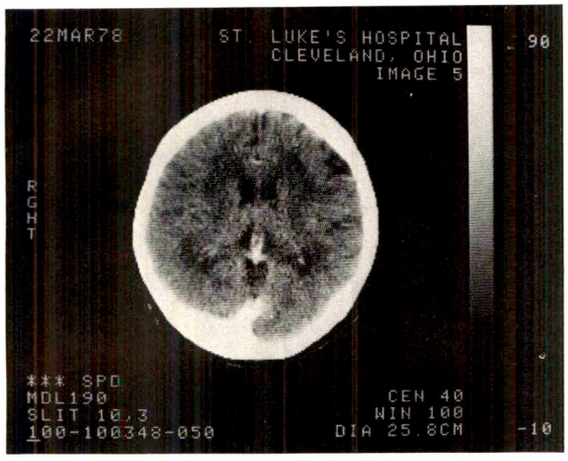
TOSHIBA

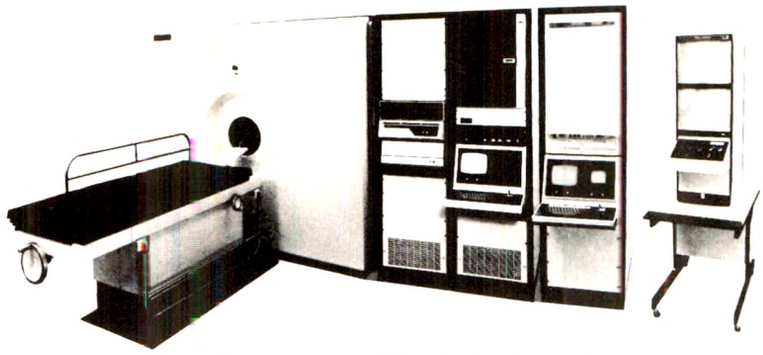
Toshiba Corporation, Tokyo, Japan

High-resolution,



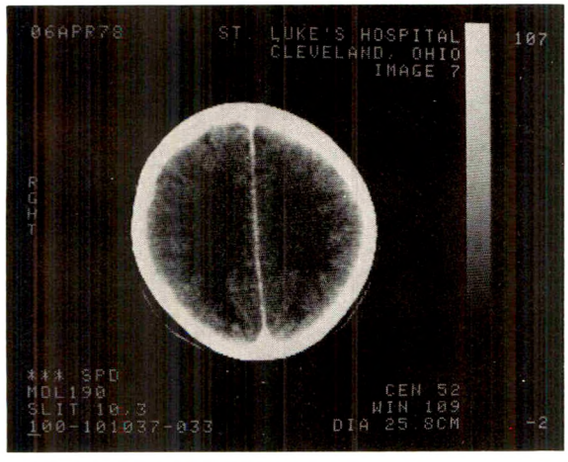
low-cost,





DeltaScan™ 100 Series.

neurological CT scanners



Computerized Tomography of the Brain, unquestionably the preferred modality in neurologic diagnosis, is now available at an economically feasible price.

The DeltaScan 100 Series scanners, starting at $96,500, combine uncompromised resolution with a uniquely compact, new design, resulting in affordable, clinically proven CT scanners which are ideally suited for smaller institutions with moderate patient throughput needs.

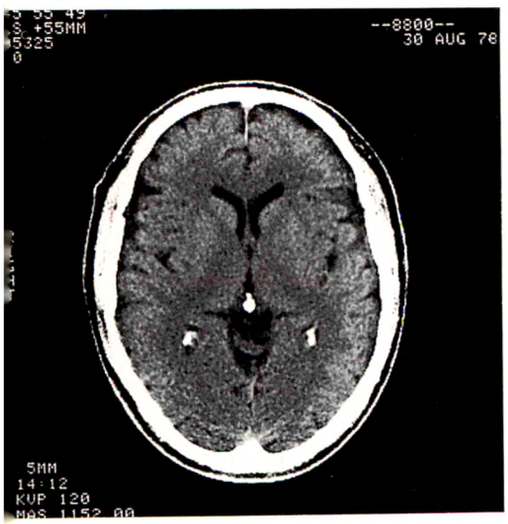
For additional information concerning cost and performance of the DeltaScan 100 Series scanners, contact Ohio-Nuclear, Inc.

from Ohio-Nuclear, Inc.

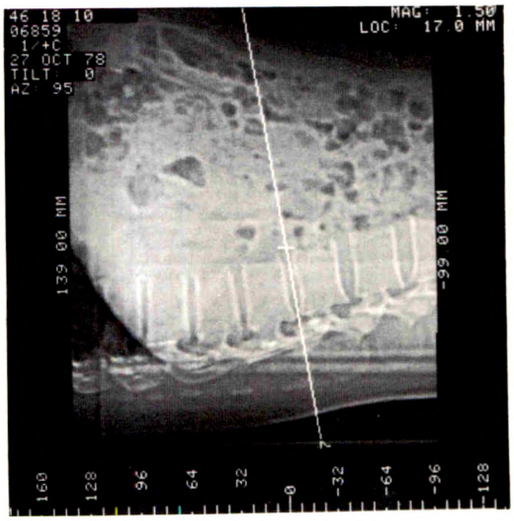
A subsidiary of Technicare Corporation

29100 Aurora Road, Solon, Ohio 44139
Phone: (216) 248-1800
TWX No. 810-427-2696

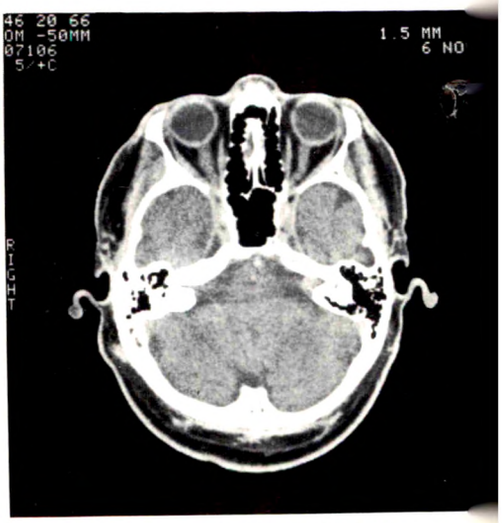
Simple addition.



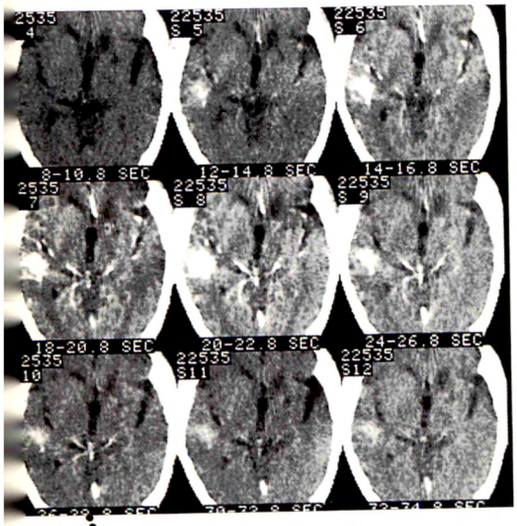
Ultra-high resolution X-2 detector
Optional on CT/T 7800, standard on CT/T 8800.



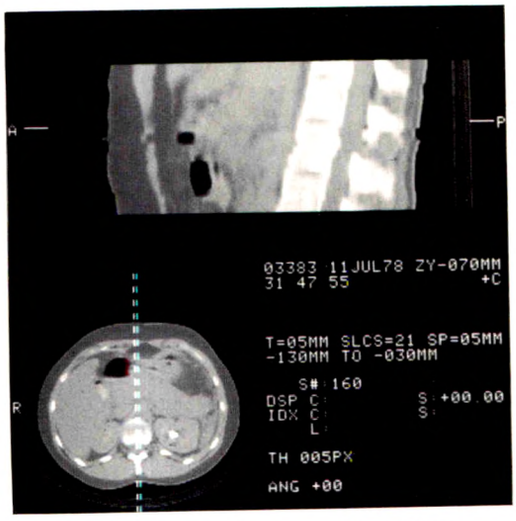
ScoutView localization
Included in Optional Diagnostic Capability package.



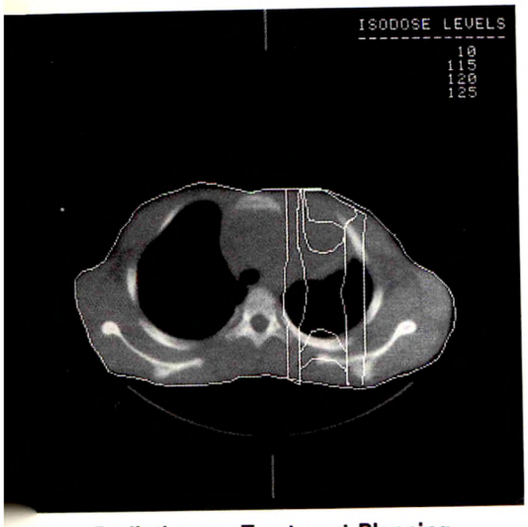
1.5 mm axial slice capability
Included in Optional Diagnostic Capability pack



Dynamic scanning
Optional.



Sagittal and coronal transformations
No added cost.



Radiotherapy Treatment Planning
No added cost.



These advanced capabilities can be added to any CT/T system, even the first one installed in 1976.

You'd expect it from GE

How would you like a CT system that resists obsolescence? One that lets you choose the capabilities that match your department... now and in the future?

That's the objective of General Electric's CT/T Continuum.

We've designed our scanner so that new functions can be added at minimum cost to any new or existing CT/T system. For example:

Ultra-high resolution X-2 detector (optional). Unprecedented image quality. Resolving power of 1.0 mm (AAPM pin phantom) and 4.0 mm resolution at 0.4% contrast (GE Mod I gray/white phantom) in one reconstruction. Standard on CT/T 8800 systems.

Optional Diagnostic Capability (ODC) with ScoutView localization. Improves throughput. ScoutView images are digitized radiographs in AP, PA, lateral or oblique planes. They allow the physician to develop a scan prescription for first and last slice locations and gantry angulation. Subsequent axial scans can visualize extremely small anatomy, with 1.5 mm contiguous slice capability to minimize partial volume effect.

Dynamic scanning (optional). Up to 12 rapic sequence scans can be made in 72 seconds, providing up to 24 images. These allow visualization of a contrast bolus passing through a designated anatomical slice (CT transit study).

Sagittal and coronal transformations (no added cost). Use axial scan data to reconstruct either sagittal or coronal images, which are ready for display in less than 15 seconds per axial slice. Selectable thickness from 1 to 320 pixels. Allows three-dimensional image analysis.

Radiotherapy Treatment Planning (no added cost). Lets the operator establish external outlines, target outline and internal inhomogeneity outlines; assign densities; plan beam positions; calculate depth dose; and display isodose contours, dose, beam or patient data. A complete plan in a few minutes.

And General Electric is now developing even more CT/T capabilities for you in the future. So when you're choosing a CT system, total up GE's advantages: best images, best value, best service and protection against obsolescence. It all adds up.

General Electric Medical Systems,
Milwaukee, Toronto, Madrid.



GENERAL ELECTRIC

Fourth Annual International Body Imaging Conference



Royal Lahaina Hotel · Maui, Hawaii

OCTOBER 13–21, 1979 • CATEGORY I AMA-CMA CREDITS

The Fourth Annual International Body Imaging Conference
will be held at the Royal Lahaina Hotel, Maui, Hawaii, October 13 through 21, 1979.
Formal sessions Oct. 14–18

The Conference offers approximately 30 Category I AMA-CMA credits and will present to the participant a correlated approach to the principles, indications, uses, interpretation, and results obtained with computed tomography, ultrasonography, and nuclear imaging. Course participation by practicing imaging physicians, residents, technologists, and corporate personnel is encouraged.

COURSE FACULTY:

George Leopold, UC San Diego, California
Michael Johnson, M.D., University of Colorado Medical Center, Denver, Colorado
Leonard Rosenthall, M.D., Montreal General Hospital, Montreal, Quebec
John Haaga, M.D., Cleveland Clinic, Cleveland, Ohio
Pat Sheedy, M.D., Mayo Clinic, Rochester, Minnesota
W. F. Sample, M.D., UCLA Medical Center, Los Angeles, California
Stephen Fierstien, M.D., University of California at Irvine, Irvine, California

Enrollment limited. Registration fee $295. Residents and Technologists $225 (with letter)

W. FREDERICK SAMPLE, M.D. — Faculty Coordinator
RONALD J. FRIEDMAN, M.D. — Conference Coordinator
MICHAEL R. TERK, M.D. — Conference Co-Coordinator

For enrollment or further information write: Conference Secretary
Fourth Annual International Body Imaging Conference
Department of Radiology, West Park Hospital
22141 Roscoe Boulevard, Canoga Park, California 91304
213 340-0580 ext. 248

NAME _____

ADDRESS _____

CITY _____ STATE _____ ZIP _____

PHONE (Home) _____ (Business) _____

SIEMENS

Angioskop

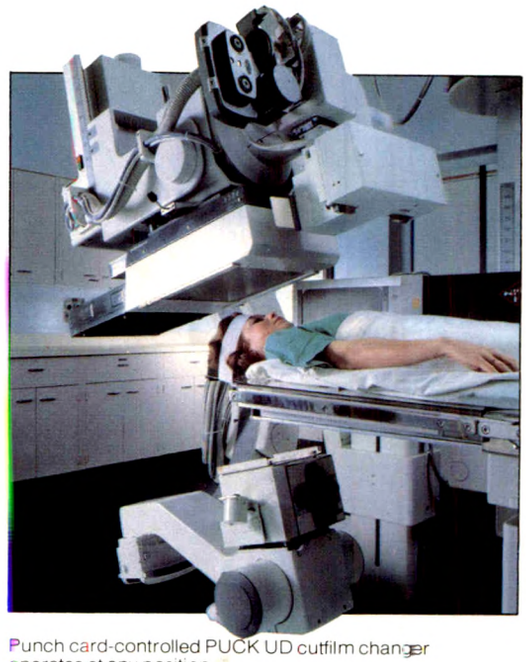
The most comprehensive angiographic system available

The versatility and sophistication of Siemens ANGIOSKOP is virtually unparalleled in modern angiography. It is a direct result of the freedom of beam direction, free access to the patient from all sides, free choice of magnification technique, and the freedom of recording methods which have all been uniquely engineered into this system.

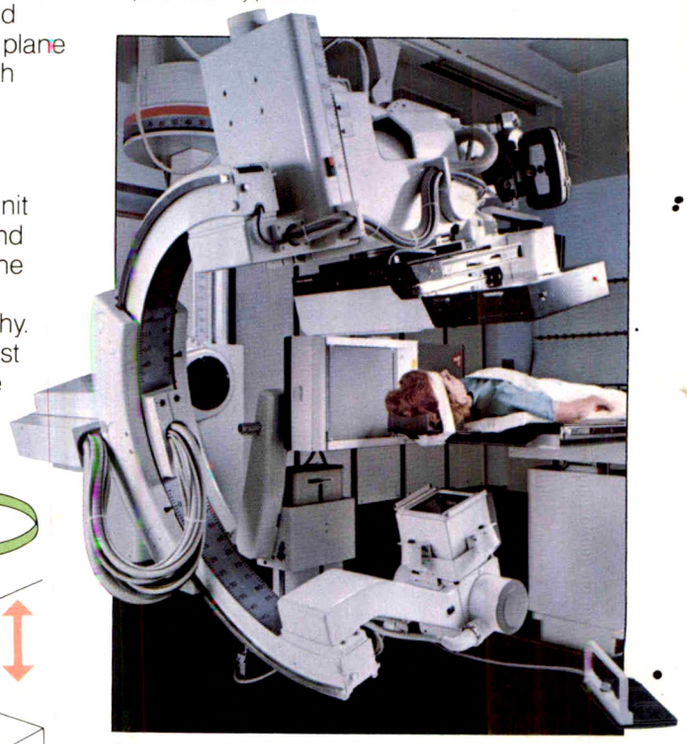
Unlike other angiography units, ANGIOSKOP has an imaging system mounted on an offset C-arm. This exclusive design allows the patient to remain isocentrically positioned while the ANGIOSKOP rotates unrestricted around him for a collision-free performance in all projections from any point of a sphere.

The offset C-arm construction lends itself extremely well to biplane operation. The overtable X-ray tube and free-standing PUCK film changer will form the lateral plane and can also be used separately in AP projections with the KOORDINAT ANGIO.

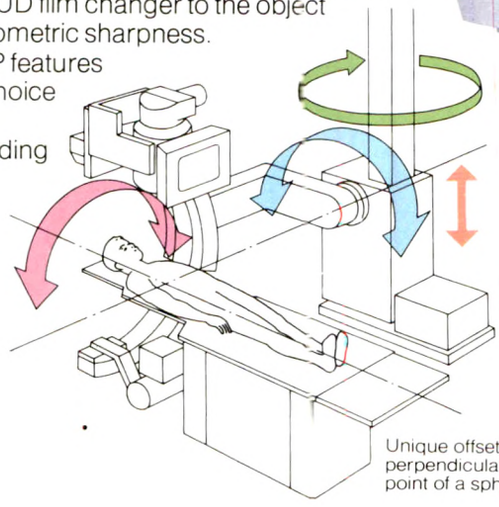
Conversion from fluoroscopy to radiography is accomplished with remarkable rapidity. This is made possible by the revolver mechanism of the receptor unit with the specially designed PUCK UD film changer and image intensifier. The changeover is so smooth that the centered position of the patient is not disturbed. The PUCK UD is particularly useful in cerebral angiography. By simply positioning the PUCK UD upside down, just above the patient's head, radiation to the eyes can be dramatically reduced. And the close proximity of the PUCK UD film changer to the object increases geometric sharpness. ANGIOSKOP features a complete choice of direct and indirect recording techniques.



Punch card-controlled PUCK UD cutfilm changer operates at any position



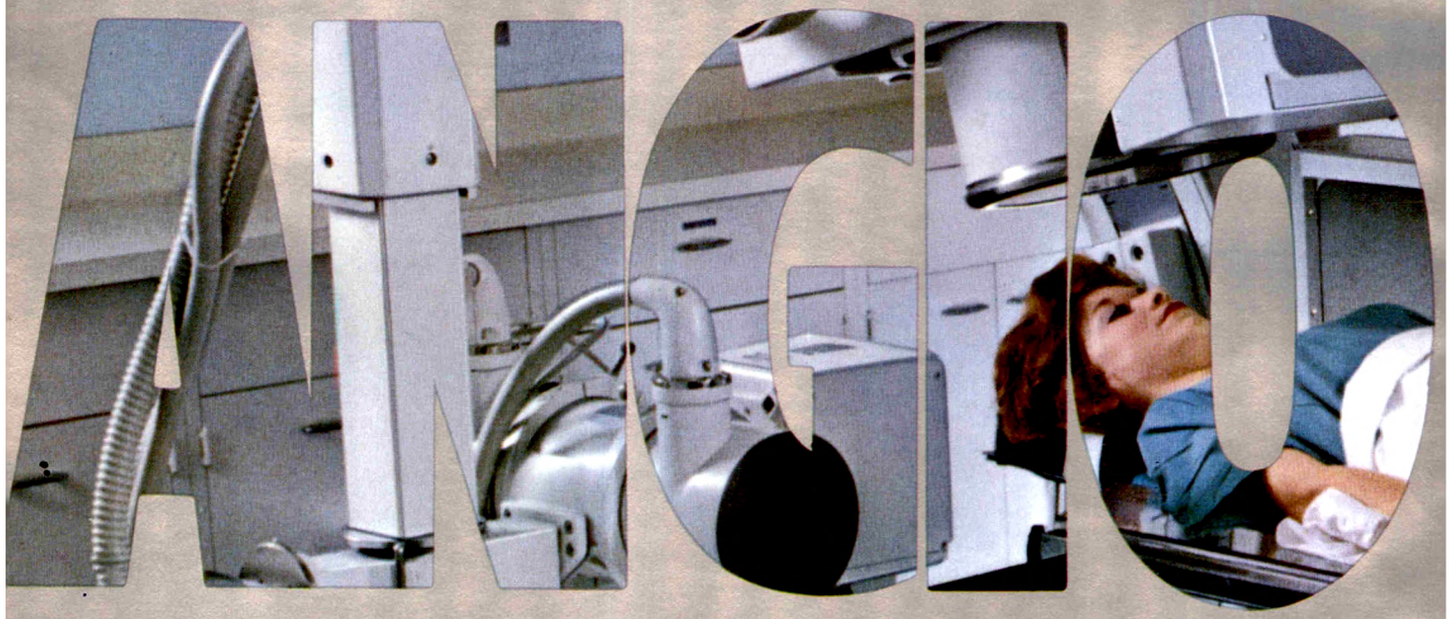
Conversion from fluoroscopy to radiography is quickly accomplished by the revolver mechanism of the receptor unit retaining perfect alignment



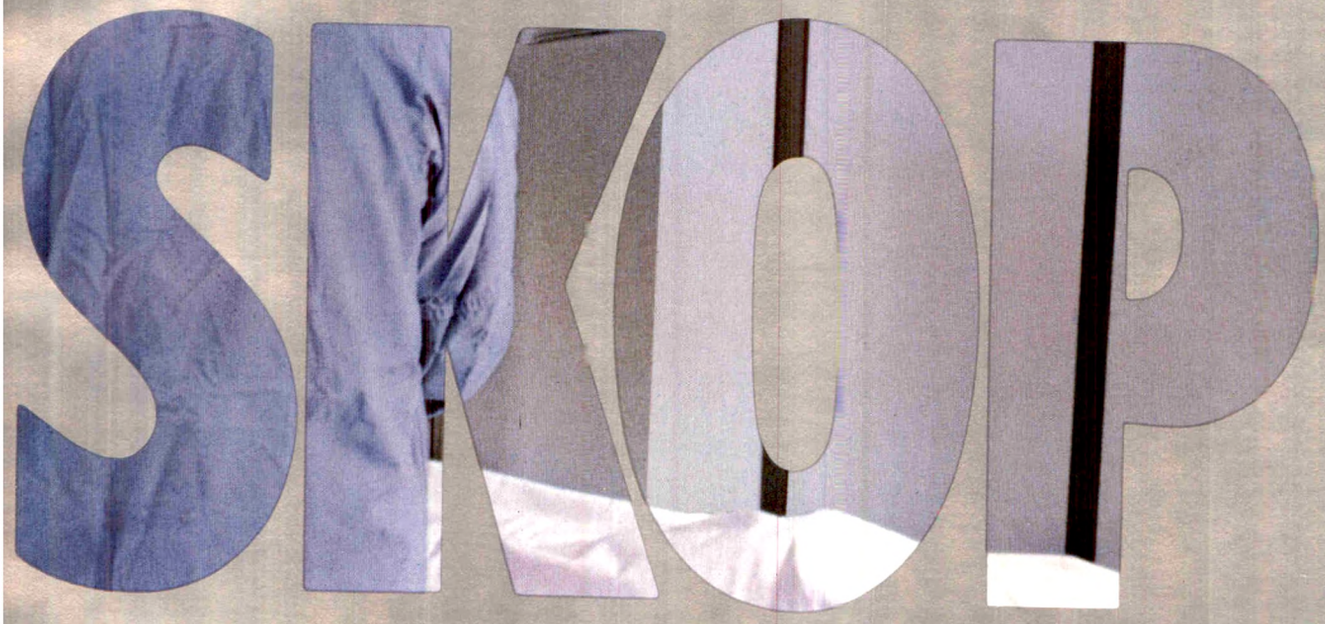
Unique offset mounting of C-arm permits perpendicular beam projection from any point of a sphere

SIEMENS

Ahead of its time...



ahead of its competition

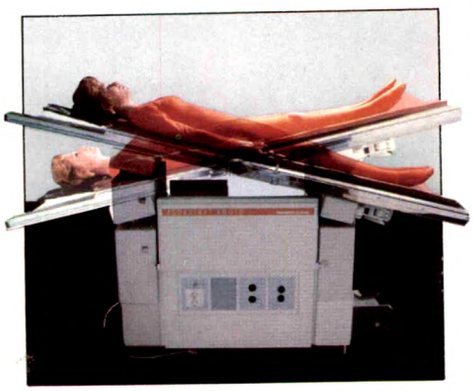


The only system versatile and sophisticated enough to permit:

- selective or super-selective cerebral angiography
- angiographic examination of the heart and the peripheral vessels
- selective renal angiography with or without magnification
- biopsies of deep tissues under fluoroscopic and radiographic control
- endoscopic examinations under fluoroscopic control
- precision-controlled therapeutic embolization
- bile duct and kidney pelvis drainage
- percutaneous coronary transluminal angioplasty

Koordinat Angio

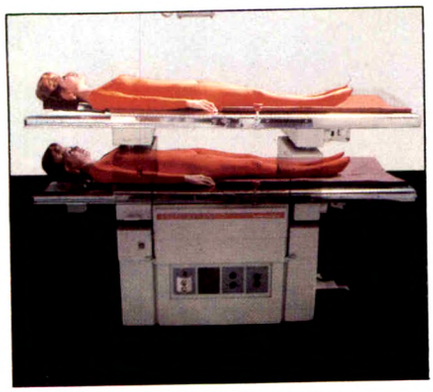
Extends the capabilities of angiography



Tabletop tilts 13° head up or head down for additional angulations and emergency trauma

Up, down, sideways, forward, backward, head up, head down. The KOORDINAT ANGIO is capable of assuming so complete a range of positions, when used with ANGIOSKOP, an overtable X-ray tube, and undertable PUCK film changer, that the patient can remain comfortably stationary while being examined from head to toe. And ease of positioning is just one feature which makes KOORDINAT ANGIO basic to any well-planned angiography system.

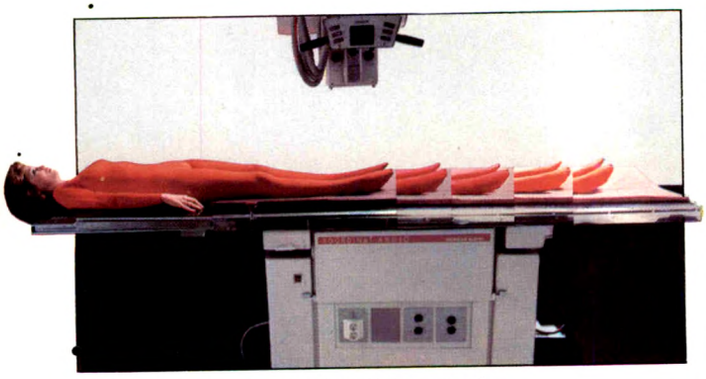
KOORDINAT ANGIO has been engineered with the safety of the patient and the needs of the radiologist and other medical specialists in mind. The shielded undertable X-ray tube minimizes the hazards of scattered radiation.



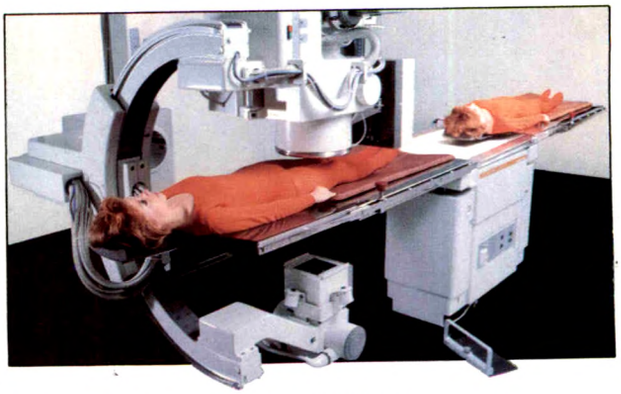
Motorized vertical adjustment of up to 40 cm. for magnification technique

Switchover from fluoroscopy to radiography is fast and easy. The patient is positioned above an undertable X-ray tube which activates an overtable image intensifier. Once the region of interest is isolated, the PUCK film changer is automatically shifted into the proper position for radiography; simultaneously, an overtable X-ray tube aligns with the PUCK. This makes the KOORDINAT ANGIO the ideal unit for all angiographic studies including abdominal and peripheral angiography.

KOORDINAT ANGIO, like the ANGIOSKOP, offers free choice of recording technique – 35 mm. cine and/or 100 mm. spotfilm camera, and/or 24 x 30 cm. or 35 x 35 cm. cutfilm changer.



Built-in motor drive for stepwise tabletop excursion, essential for peripheral angiography



Telescopic tabletop can be displaced 2340 mm. for head-to-toe examinations

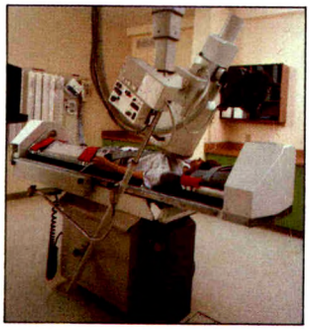
Concepts...
engineered to radiologic excellence.


ANGIOSKOP
SIEMENS-ELEMA
ANGIO
SIEMENS-ELEMA

SIEMENS

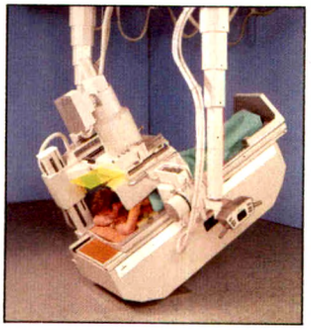
The Siemens difference...

A full line of angiographic units for every need and every budget



CCO attachment

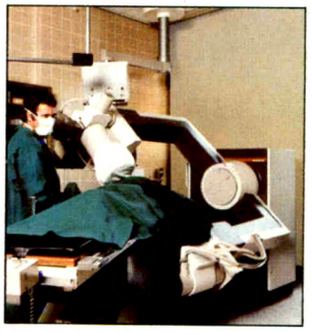
Not only is this system used for multipurpose angiography, but it can angulate to demonstrate the left coronary arteries as well. The CCO ATTACHMENT easily achieves cranio-caudal oblique projections of the heart. Just a simple coupling of the image intensifier to the X-ray tube permits angulation of the central beam along the longitudinal plane. And to ensure that the patient's heart remains within the image intensifier's field during angulation, the tabletop can also be attached to the coupling rod.



Sireskop 3N

Although designed primarily for biplane myelography, this special 90/90 RF table is invaluable for cerebral angiography. The simple addition of a cutfilm changer makes this extra application possible.

Another special feature of the SIRESKOP 3N is the EXPLORATOR 35 spotfilm device. The lateral X-ray tubes and image intensifier TV units can be coupled to this spotfilm device for perpendicular biplane alignment. This unique coupling connects both beam projections with the movements of the spotfilm device so that the object remains continuously centered for easy scanning of the spinal column.

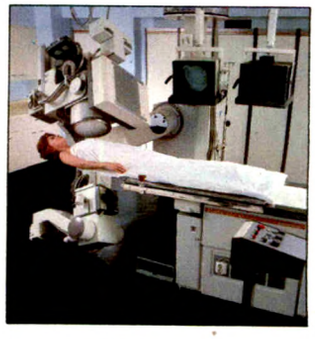


Cardoskop U

Complete and easy to operate, the CARDOSKOP U is a dedicated cardiac angiography unit. This unit has a sturdily constructed U-arm that moves about the patient isocentrically. The stability of the U-arm assures vibration-free and optimum quality cine and spotfilm camera images.

The CARDOSKOP U table comes equipped with a four-way floating tabletop which can be adjusted vertically for proper isocentric positioning. The table and U-arm share a common isocenter. And by swiveling the table about its isocentric pivot point and rotating the U-arm, any projection can be achieved around a sphere.

Should a cardiac emergency arise during examination, the table can be quickly swiveled out of range of the U-arm providing free access to the patient from any point.



Angioskop

This multidirectional, remote-controlled angiographic system permits perpendicular beam projections from any point on a sphere. Virtually any projection can be obtained without moving the patient.

Other special features of ANGIOSKOP include easy access to the patient, free choice of recording method, free choice of magnification technique, rapid changeover from fluoroscopy to radiography with exact alignment, and biplane capability.

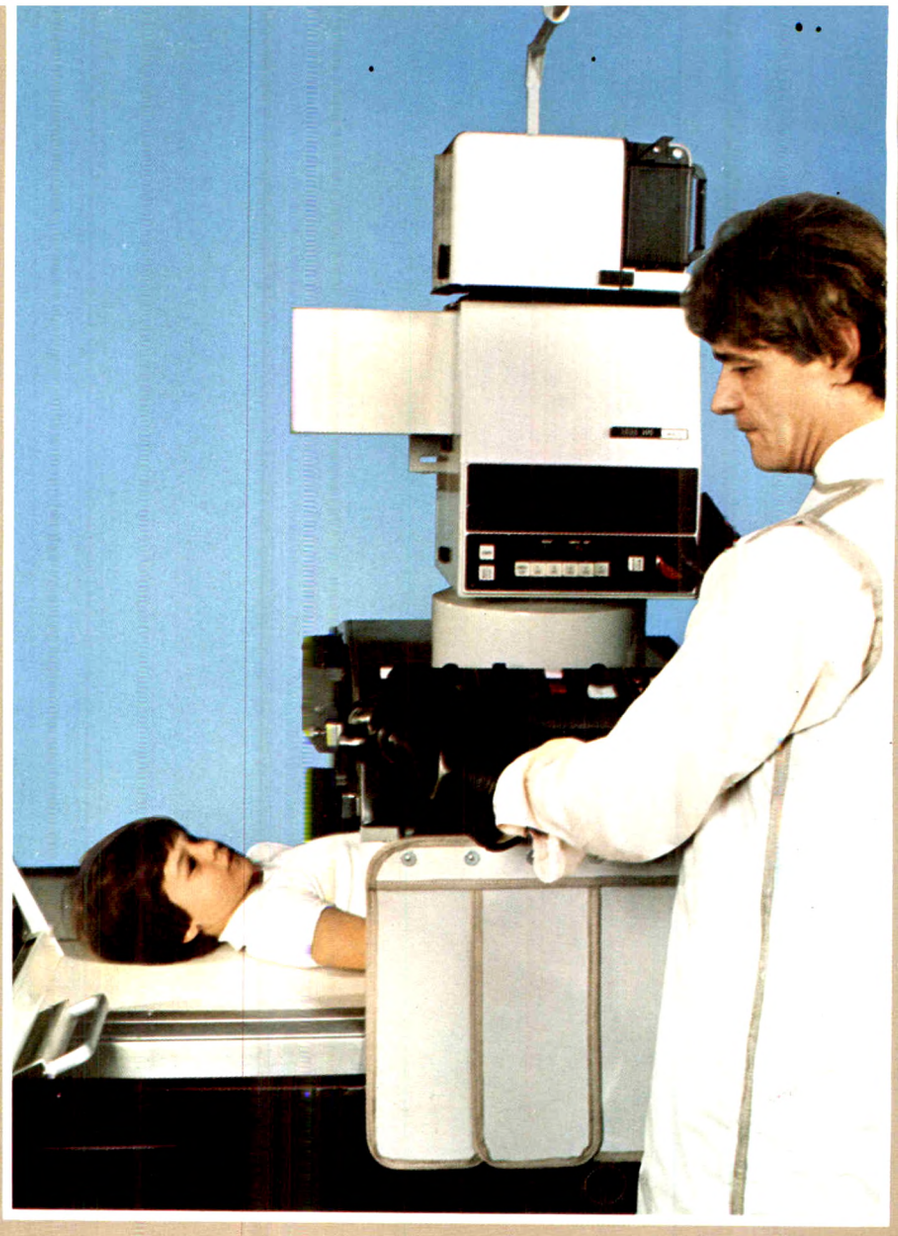
The newly designed PUCK UD film changer operates in the upside-down position to protect the patient's eyes from radiation during cerebral angiography. KOORDINAT ANGIO, an independent telescopic examination table complements the system.

Concepts... engineered to radiologic excellence.

For further information, contact your Siemens Representative or Siemens Corporation, Medical Systems Division, 186 Wood Avenue South, Iselin, New Jersey (201) 494-1000.

In Canada: Siemens Electric Limited, Medical Systems, P.O. Box 7300, Pointe Claire, Quebec H9R 4R6.

SIR-417



Now! All the advantages of Machlett's IRIS* system with a choice of 105mm roll film or 100mm cut film.

With its brilliant television fluoroscopy and its high-resolution, low-distortion spotfilming, the Machlett *Intensified Radiographic Imaging System — **IRIS 100** — has won wide clinical acceptance for dependability and value.

Now There Are Two

Now, in addition to **IRIS 100**, there is **IRIS 105**, for those who prefer 105mm roll film with exposure rates to 6-per-second, rather than 100mm cut film.

Both Offer These Advantages:

The television resolution you need. You choose the standard 525 lines or high resolution 875 or 1023-line systems.

The Dynascope Cesium Iodide image tube for brilliant, sharp images. Available with 17 cm (24% greater area than 6 inch) or 22 cm (9 inch) input with single or dual fields.

Machlett's exclusive sliding mirror optical distributor. Permits smooth switching from fluoro to film in 0.4 seconds. Straight-through light path to film, no mirror to cause distortion.

For new R/F rooms or modernization. Easy retrofit to most existing equipment. No need to change an entire room to get the benefits of IRIS.

For full details, contact your x-ray equipment dealer, or:

MACHLETT

Marketing Department
The Machlett Laboratories, Incorporated
1063 Hope Street
Stamford, Connecticut 06907
(203) 348-7511

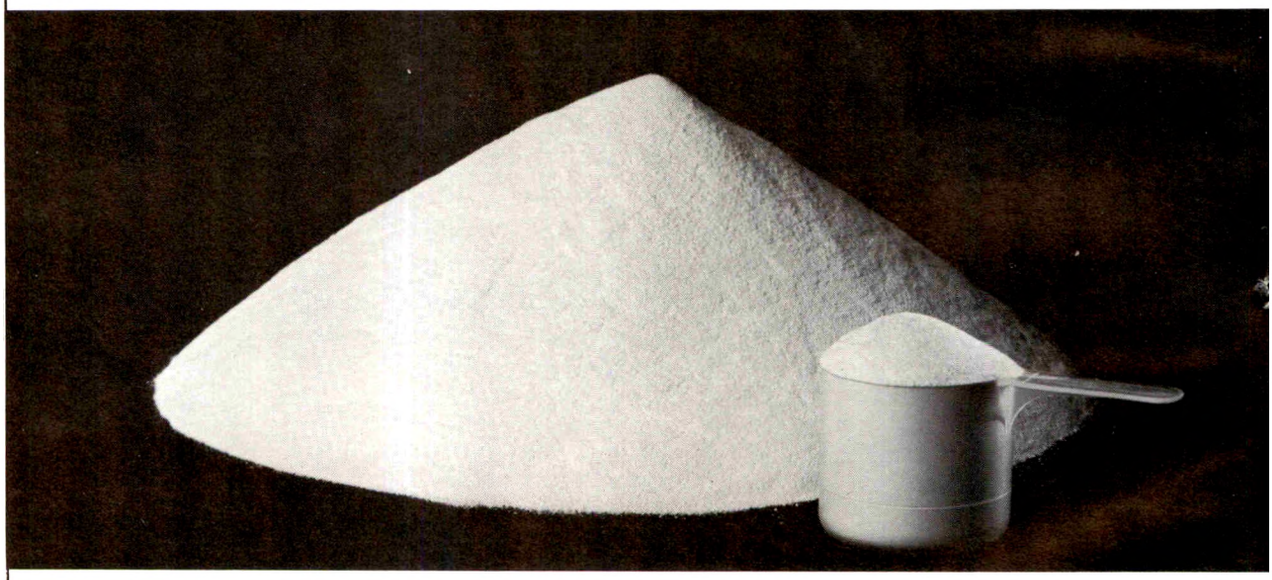
A Raytheon Company

ROUTINE BARIUM

NOT JUST WHAT YOU WANT...
BUT EXACTLY WHAT YOU WANT!

If you are not using an E-Z-EM Barium Enema System you are not using the best.

We know that as a professional, your requirements are very specific. And that's why we make available barium enema systems in virtually any configuration you specify. Our extensive range of barium sulfate formulations, bags, tips, and tubing lets you select exactly what you need. We then combine them into the customized system that's best for you. If you would like further details or assistance in creating your own particular "package", call an E-Z-EM distributor or contact us directly.

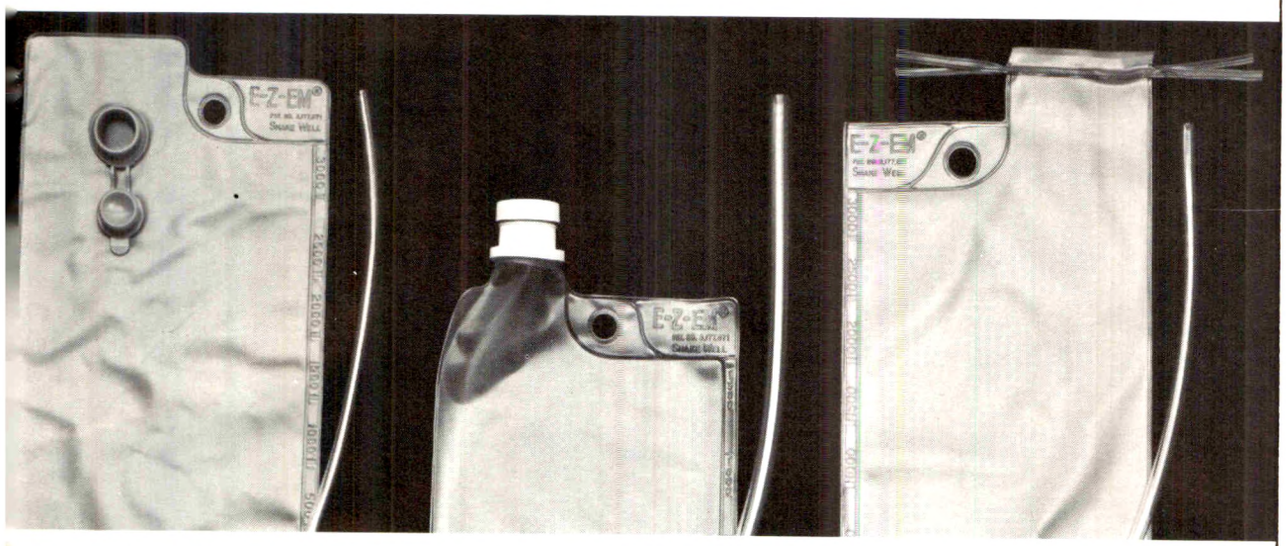


BARIUM

While most suppliers offer you a choice of only one barium sulfate formulation... we give you four distinct formulations... to fit your budgetary needs and give you greater working flexibility: Sol-o-Pake,™ Polibar™ Powder, E-Z-Paque,® and new ACB.™ Whichever you select, you can be sure of the highest quality radiographs... because they're all from E-Z-EM.

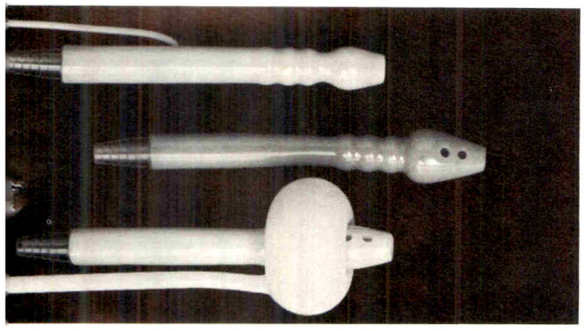
All E-Z-EM Barium systems offer density versatility from the lightest (12% w/w) for see through effect to 60% w/w for single stage air contrast.

ENEMA SYSTEMS.



BAGS

There's one to meet every preference ... all made of durable, non-crack, heavyweight vinyl. Our selection includes snap cap models... 1 and 2–piece rigid spout... retrograde fill... double tie wrap... and others, each crafted to our highest standards, and every enema bag is completely inspected to assure compliance with our rigorous quality control standards.

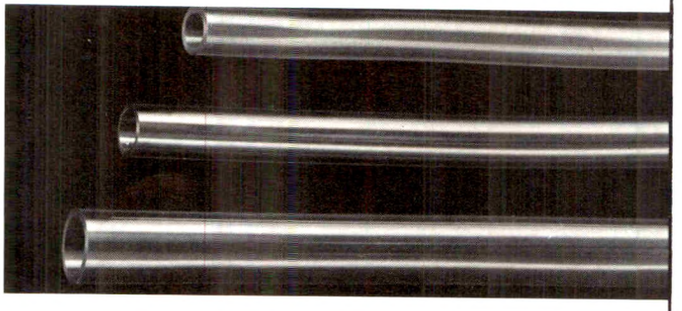


TIPS

Perhaps the largest selection anywhere. Choose from flexible tips... Miller air tips for double contrast, with and without cuffs... colostomy air contrast tips... pediatric tips and over 30 other specialized designs that make your work easier.

TUBING

We use only the finest grade of flexible vinyl... to be a perfect component of any E-Z-EM barium enema system you create. Available in either standard 5/16" lumen, 3/8" XL, and 1/2" Super XL.



Call today... we have the knowledge and the products!

E-Z-EM® 7 Portland Avenue, Westbury, New York 11590 (516) 333-8230

International Affiliates: E-Z-EM Rooster B. V., Infirmeriestraat 6-8, Rotterdam 16, Netherlands
E-Z-EM De Mexico, S. A. de C. V., Calz. Azcapotzalco La Villa No 882, Zona Industrial Vallejo, Mexico 16 D. F.

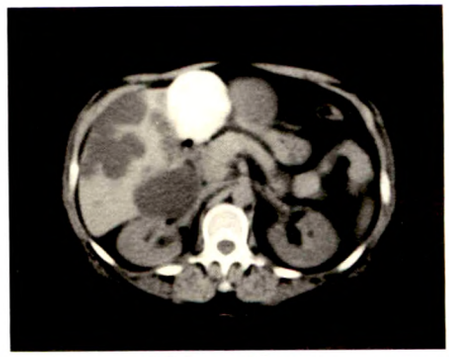
©1/79

For high-quality CT body scans,



1 Second Scan

The advantages of speed in body scanning are evident in the absence of artifacts due to physiological motion. Note the well-defined loops of bowel in the above scan. Other structures seen are the kidneys and the renal arteries.



3.3 Second Scan

The above image demonstrates polycystic disease of the liver. Note the clear delineation of the pancreas, superior mesenteric artery and renal arteries. In addition, the left colic or splenic flexure can be seen.



faster is better.

To achieve high-quality body scans, faster is better. Synerview is the fastest scanning CT system presently available. It can routinely perform high-quality scans, as fast as 1 second.

Because of the natural involuntary motions that occur within the human body, fast-scanning capabilities are necessary for clear images in body scans. The faster your CT scanning capabilities, the more you can minimize motion artifacts caused by peristaltic, muscular, respiratory, and cardiovascular actions.

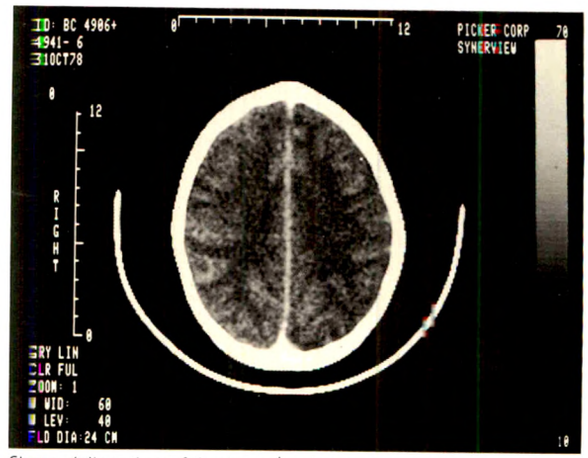
And for CT diagnosis to be effective for uncooperative, unconscious, pediatric or geriatric patients, you need 1-second scanning.

Ready to advance the state-of-the-art for CT. An investment in Synerview is the best way to obtain a high-quality CT scanner and minimize the obsolescence factor. Other manufacturers have reached the limit of their CT capabilities with the technology employed in their present systems. But Synerview, based on the proven Stationary Detector principle, has the potential to advance state-of-the-art for CT. Synerview is ready to expand its capabilities when new technology becomes available.

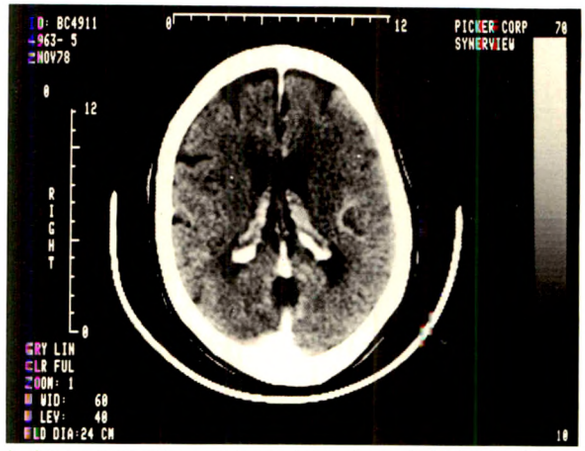
Synerview performance features. Synerview has features that help make CT operation fast and convenient. Our unique patient transport is one example. It lets you prepare a patient for scanning almost anywhere in the hospital. And to maximize your patient throughput, Synerview combines fast patient-data entry and scanning selection protocol with processing as fast as 25 seconds.

Superb software capabilities bring added dimensions to your CT operations. Synerview can display sagittal and coronal reconstructions in less than 5 seconds. Our bone correction software provides better visualization of the bone/brain interface. In addition, Synerview's optional therapy treatment planning feature can be supplied either for economical shared use, or for more versatile independent use.

And a field size of 48 cm means Synerview can perform body scans with even your larger patients.



Sharp delineation of the bone/brain interface is demonstrated in the above image. Note the white and gray matter separation.



In this contrast-enhanced image taken through the body of the lateral ventricles we see enhanced choroid plexus, torcula, and vein of galen. Note the white and gray matter differentiation as well as cortical sulci.

Head to head, there's no one better. We have the latest technology and the images to prove it.

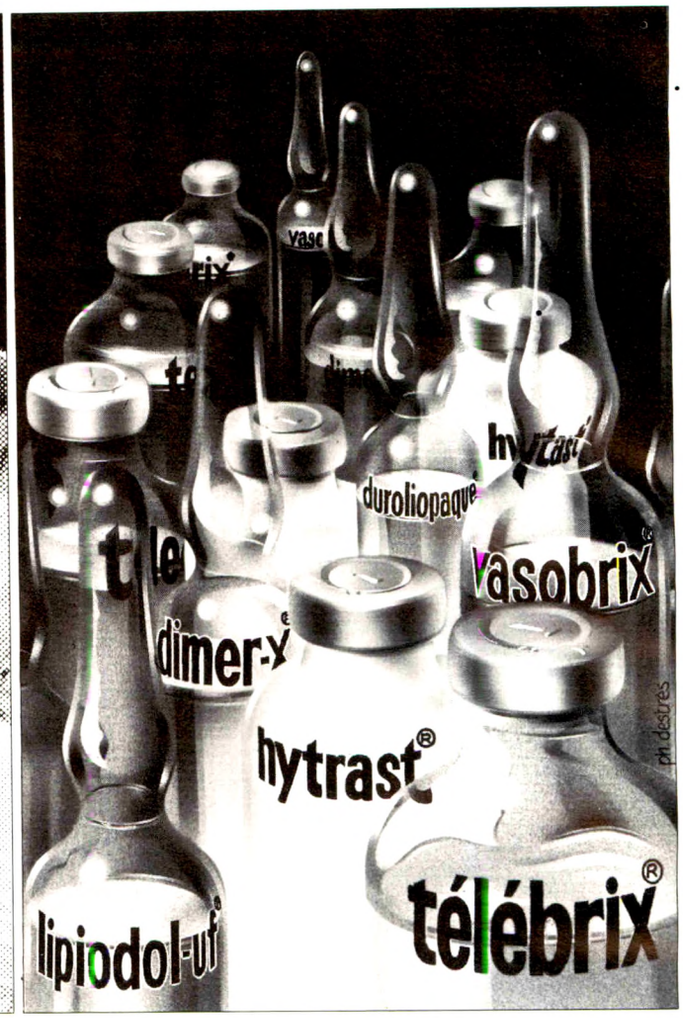
A large portion of any CT caseload involves head scans. It's of particular significance to know that Synerview brings you high-quality head scans in addition to high-quality body scans. It's also important that you can position your patient's head easily with Synerview. You can get the right scan — the first time. And, for accurate Towne's projections, Synerview's ultra-stable gantry can tilt ± 20 degrees.

For a free portfolio of Synerview head and body scans, contact your local Picker representative, or call collect 216/461-9100, CT Marketing, extension 332. Picker Corporation, 595 Miner Road, Cleveland, OH 44143.

PICKER®

ONE OF THE CIT COMPANIES





Research & development

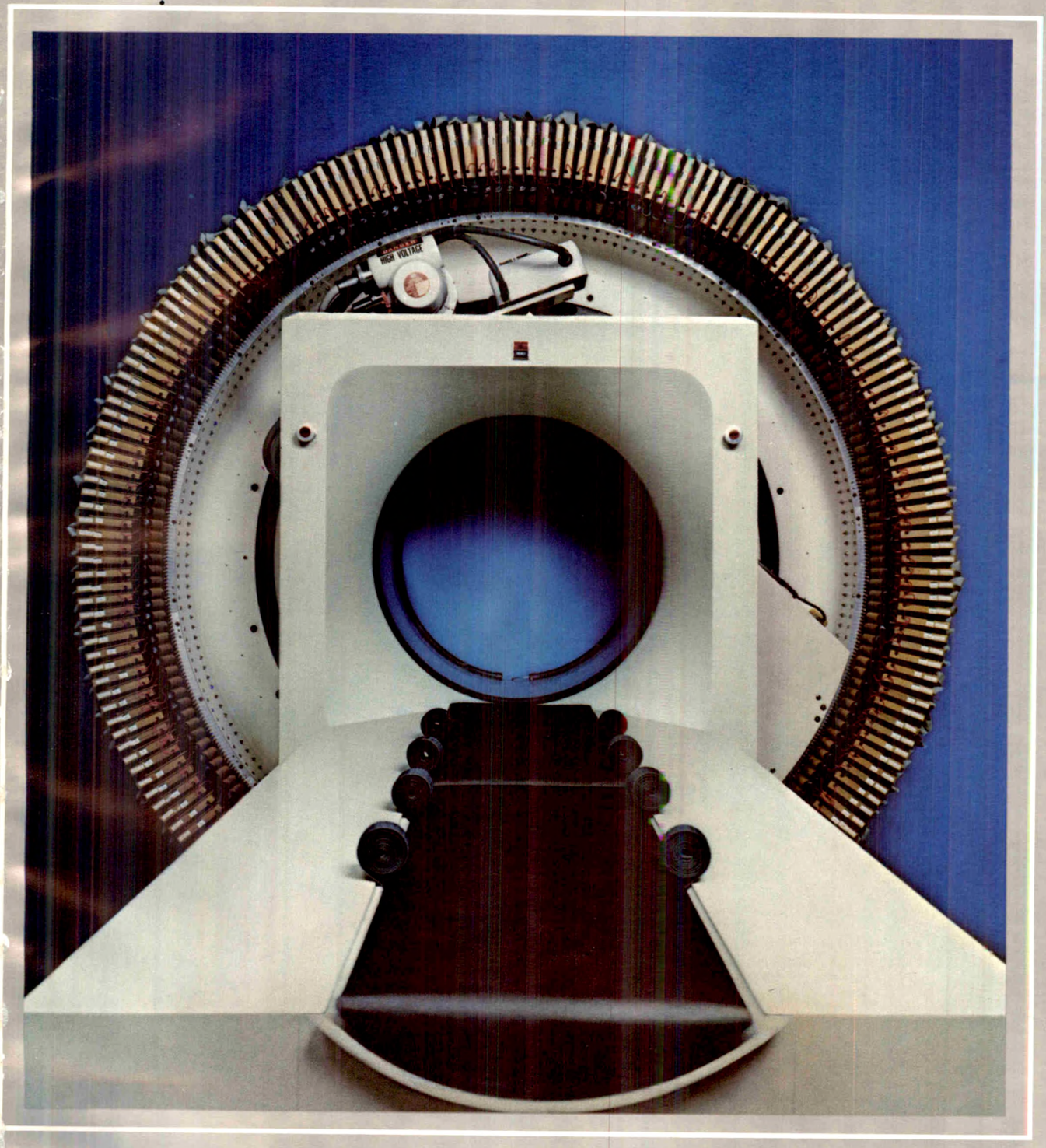
GUERBET

Better contrast media through research

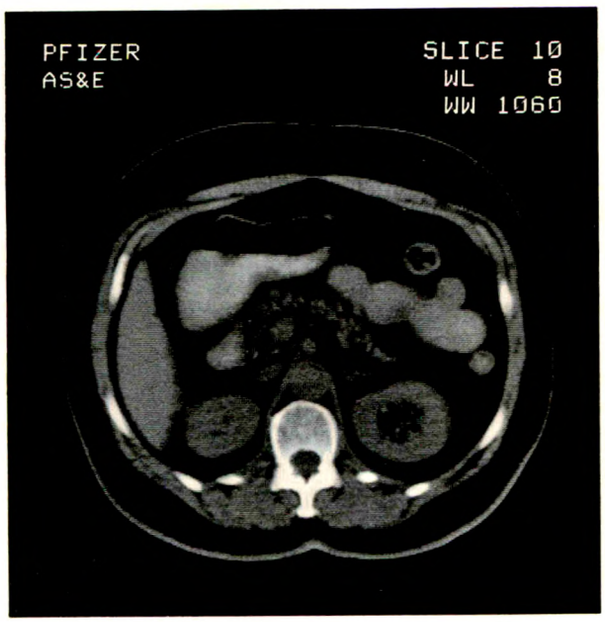
Laboratoire GUERBET
16-24, rue Jean Chaptal - 93609 Aulnay-sous-Bois - Cedex FRANCE
Tél. : 929.78.37 - Télex : 212382 F.

A new standard of accuracy in CT imaging

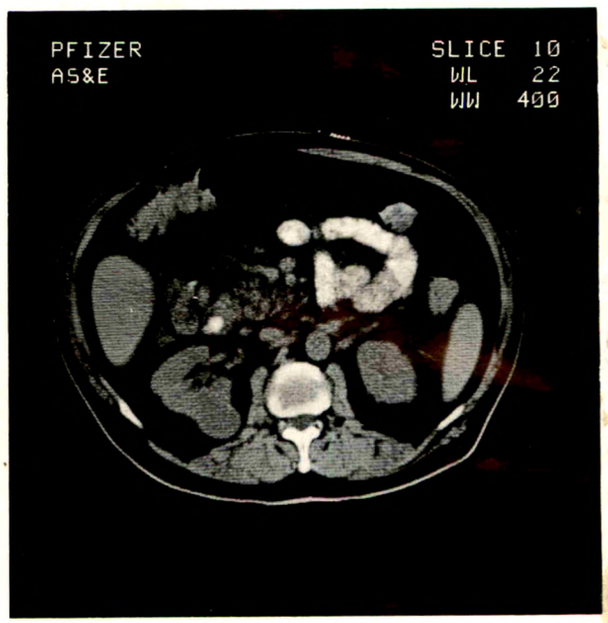
Pfizer/AS&E Generation IV



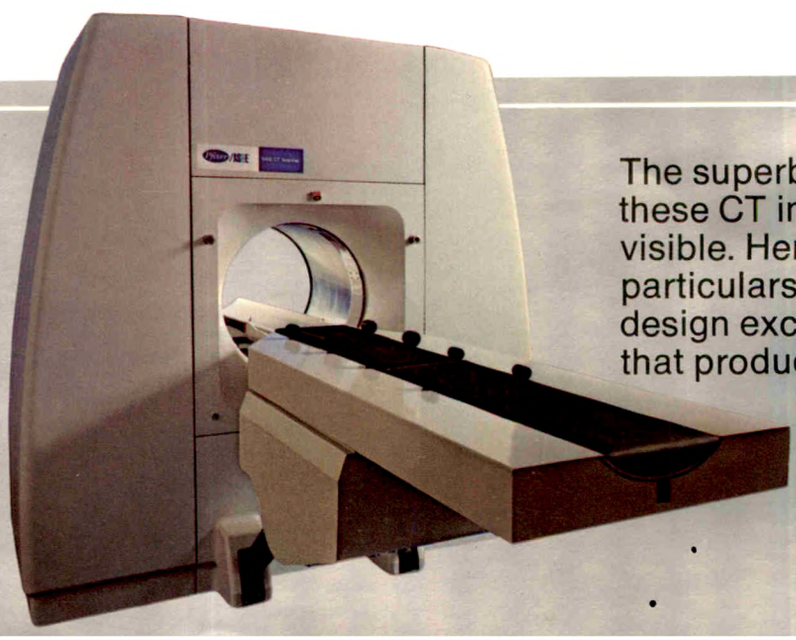
Superior scans from stationary detectors



CT scan of the abdomen. The inferior portion of the left adrenal gland is well visualized as is the vertical portion of the superior mesenteric artery anterior to the aorta.



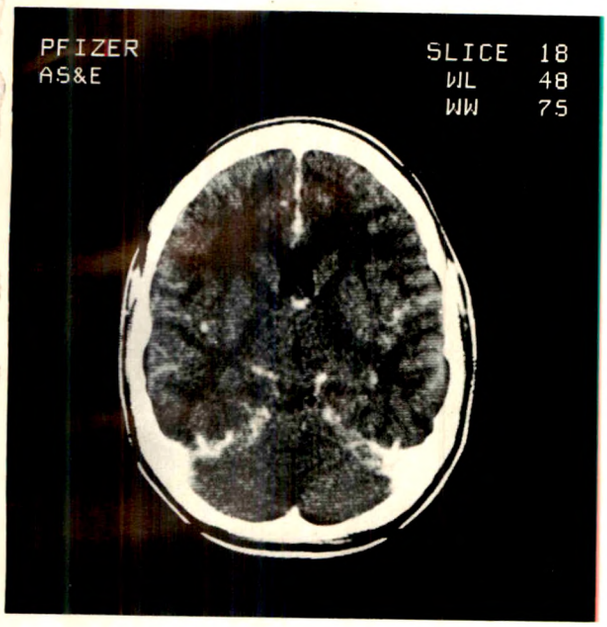
CT scan of the abdomen. The spinal cord and nerve roots are well demonstrated. Note the mass at the posterior medial aspect of the right kidney.



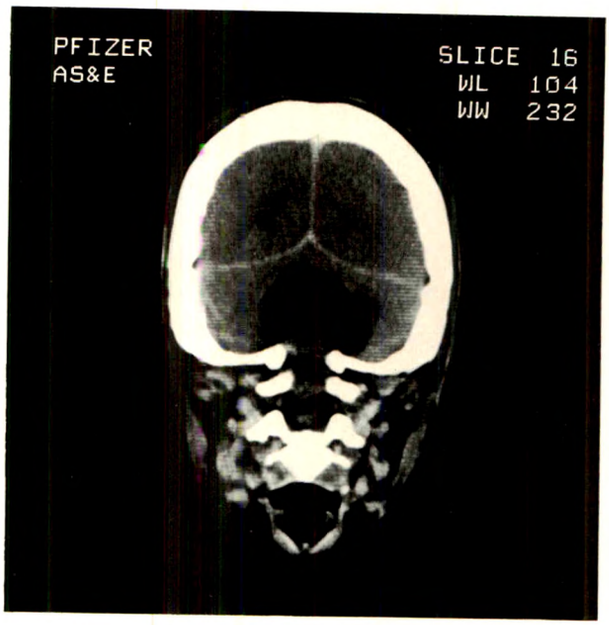
The superb quality of these CT images is clearly visible. Here are some particulars of the design excellence that produced them:

Pfizer/AS&E

0450



CT scan of the head. There is excellent separation of central white and gray matter. The caudate nucleus and basal ganglia are clearly seen.



CT scan of the head. Coronal view. Contrast enhanced tentorium demonstrated. There is a midline posterior fossa arachnoid cyst. Note the absence of artifacts.

Continuous detector calibration for the most accurate CT numbers and images available...

Pfizer/AS&E 0450. Generation IV. Only the x-ray tube rotates; the full circle of photon detectors is stationary. All attenuation data are continuously referenced to objects of known attenuation within, and immediately outside, the patient scan field. And each detector is calibrated on every scan—making possible DENSET, the precise CT number stabilization system which eliminates even potential errors in data acquisition. DENSET clearly provides a new dimension in CT diagnosis—reliable, repeatable imaging across the entire scan field.

...And freedom from artifacts

Pfizer/AS&E Generation IV. Where every detector reviews the entire scan field, not just a small portion. The classic image-degrading circular artifact caused by detectors viewing individual circles within the scan field simply cannot occur. 0450 Generation IV CT images are, by design, free from geometric defects.

Superior scans from advanced technology

More efficient detection—better dose utilization

The scintillation crystal/photomultiplier detectors used in the Pfizer/AS&E 0450 provide you and your patient with optimum dose utilization. Because we start with solid crystals, having twice the detector efficiency of comparable Xenon chambers at high pressures, over 98% of all x-ray photons striking the crystal are detected and contribute to the final image.

Less noise—better contrast resolution

Of all x-ray detectors, the solid scintillation photomultiplier tube combination provides the highest signal-to-noise ratio and widest dynamic range. Readings are not degraded by noise introduced with less sensitive detectors. Contrast resolution and range of dose utilization are superior by design.

Faster detector response—better spatial resolution

0450 detectors are sensitive, exhibit fast response, and do not become saturated. These properties allow data to be collected continuously instead of at the rate with which the x-ray source can be pulsed. The results: more data, faster scans and superb spatial resolution.

Full field resolution—image integrity

Tiny anatomical structures (1-1.5 mm) varying only slightly in density are faithfully resolved and displayed uniformly over the entire scan field even at *lowest dose settings.* This ultra-high fidelity is achieved by using a 640 x 512 matrix which is reconstructed from more than 700,000 data measurements—requiring no extensive "smoothing" software.

Pfizer/AS&E 0450

The superior CT scanning system you'll want to know more about



Write us for a detailed brochure:
Pfizer Medical Systems, Inc.
235 East 42nd Street, New York, N.Y. 10017

PFIZER MEDICAL SYSTEMS, INC.
A subsidiary of Pfizer Inc.
235 East 42nd Street, New York, N.Y. 10017
Telephone: (212) 573-2323
Telex: 234088 (RCA) 62422 (WUI) 420440 (ITT)

PRINTED IN U.S.A.

Th perfect s tup.

Laser-precise patient alignment.

Chest-A-Line system from Gammex makes chest exams faster and more accurate than ever.

Safe, precise laser beams project three ve tical lines: two define the lateral edges of the fi m, and the center beam aligns with the patient's spine.

Any lateral movement or twisting by the patient changes the contour of these lines and ale ts the technologist before the exposure is made. So you can get an accurately positioned exam every time. In fact, you'll probably eliminate enough retakes to pay for the system in about three months.

Gammex also offers laser systems for exact alignment of CT and tomography patients. Sensors that automatically detect excessive patient movement are available. And we can provide a complete laser alignment system for radiotherapy procedures.

For details on any of these time-saving cost-saving systems, call or write Gammex today.

Gammex, inc.
Patient Positioning Systems
6685 N. Sidney Pl., Milwaukee, WI 53209 • Phone (414) 228-7400

Tome-A-Line

Tome-A-Line/CT



American Journal of Roentgenology

Vol. 132 May 1979 No. 5

DIAGNOSTIC IMAGING

711 **Primary and Metastatic Scirrhous Carcinoma of the Rectum.** *Balthazar EJ, Rosenberg HD, Davidian MM*
717 **Radiology of the Continent Ileostomy.** *Stephens DH, Mantell BE, Kelly KA*
723 **Neonatal Gastric Volvulus.** *Campbell JB*
727 **Nonvisualized Gallbladder by Cholecystosonography.** *Harbin WP, Ferrucci JT Jr, Wittenberg J, Kirkpatrick RH*
729 **Ultrasonography of Biliary Tract Dilatation Without Jaundice.** *Weinstein DP, Weinstein BJ, Brodmerkel GJ*
735 **Clinical Comparison of Iocetamic Acid (Cholebrine) and Ipodate Sodium (Oragrafin).** *Neal RR, Harvey KG, Cantwell KG, Press HC Jr*
737 **Breast Cancer Missed by Mammography.** *Martin JE, Moskowitz M, Milbrath JR*
741 ***Pneumocystis carinii* Infection of the Lung: Radiologic and Pathologic Correlation.** *Dee P, Winn W, McKee K*
747 **Endometriosis: Clinical and Ultrasonic Correlation.** *Coleman BG, Arger PH, Mulhern CB Jr*
751 **Primary Renal Calculi: Anderson-Carr-Randall Progression?** *Bruwer A*
759 **CT Evaluation of Anomalies of the Inferior Vena Cava and Left Renal Vein.** *Royal SA, Callen PW*
765 **Accessory Renal Hilus.** *Stephenson TF, Paul GJ*
769 **Arterial Impressions on the Stomach.** *Childress MH, Cho KJ, Newlin N, Martel W*
773 **Suprarenal Aortic Occlusion.** *Sequeira JC, Beckmann CF, Levin DC*
777 **Partial Splenic Embolization in the Treatment of Hypersplenism.** *Spigos DG, Jonasson O, Mozes M, Capek V*
783 **Sinus Histiocytosis: Some Radiologic Observations.** *Siegel MJ, Shackelford GD, McAlister WH*
787 **Epidurography: Selective Catheter Technique and Review of 53 Cases.** *Roberson GH, Hatten HP Jr, Hesselink JH*
795 **Nontraumatic Intravasation of Myelographic Contrast Medium.** *Zito JL, Schellinger D*
799 **Modification of Cyanoacrylate for Therapeutic Embolization: Preliminary Experience.** *Cromwell LD, Kerber CW*
803 **Proficiency Examination of Physicians for Classifying Pneumoconiosis Chest Films.** *Morgan RH*

CASE REPORTS

809 **Central Vertebral End-Plate Depression in Chronic Renal Disease: Report of Two Cases.** *Ziter FMH Jr*
812 **Unusual Case of Metastatic Pulmonary Calcification.** *Bein ME, Lee DBN, Mink JH, Dickmeyer J*
817 **Significance of Pneumomediastinum in Blunt Trauma to the Thorax.** *Lotz PR, Martel W, Rohwedder JJ, Green RA*
820 **Laryngeal Papillomatosis with Pulmonary Spread in a 69-Year-Old Man.** *Glazer G, Webb WR*
823 **Lymphomatoid Granulomatosis Involving the Central Nervous System: Radiologic-Pathologic Correlation.** *Sackett JF, ZuRhein GM, Bhimani SM*
827 **Pseudo Thick-Walled Renal Cyst by CT.** *Segal AJ, Spitzer RM*
829 **Percutaneous CT-Guided Pancreatography and Pseudocystography.** *Haaga JR, Highman LM, Cooperman AV, Owens FJ*
831 **Urachal Cyst in the Adult: Ultrasound Diagnosis.** *Morin ME, Tan A, Baker DA, Sue HK*
833 **Isolation of the Left Innominate Artery, a Right Arch, and a Left Patent Ductus Arteriosus.** *Martin EC, Mesko ZG, Griepp RB, Haller JO, Gordon DH*
836 **Usefulness of the Prone Position for Aortography of Aortic Graft–Intestinal Fistulae.** *Pingoud EG, Pais SO*
838 **Popliteal Vein Displacement by Popliteal Artery Aneurysms: Report of Two Cases.** *Sprayregen S*
840 **Gallium Scan in Sternal Osteomyelitis.** *Smith PW, Petersen RJ, Ferlic RM*
842 **Fat in the Intrahepatic Fissure.** *Halber MD, Daffner RH*
844 **Pseudolymphoma in Two Immunodeficient Children.** *Brasch RC, Royal S, Ammann AJ, Crowe J*
848 **Coincident Renal Cell Carcinoma and Renal Angiomyolipoma in Tuberous Sclerosis.** *Gutierrez OH, Burgener FA, Schwartz S*

TECHNICAL NOTES

851 **Convenient Method for Labeling Computed Tomographic Images.** *Citrin CM*
852 **Catheter Angiography Through Aortofemoral Grafts: Inadvertent Catheterization of the Native Iliac Artery.** *Eisenberg RL, Fiske CE, Hedgcock MW*
853 **Simplified Method of Transcatheter Embolization with Polyvinyl Alcohol Foam (Ivalon).** *Kaufman SL*

855 **Editorial: First Year Radiology Residents: PGI vs. PGII.** *Cuttino JT, Scatliff JH*
857 **Letters**
859 **Abstracts of Current Literature**
870 **Book Reviews**
875 **News**
716 **Guidelines for Authors**